

Form 25
[Rule 5.34]

Clerk's Stamp

COURT FILE NUMBER	2001-14300
COURT	COURT OF QUEEN'S BENCH OF ALBERTA
JUDICIAL CENTRE	CALGARY
APPLICANT	REBECCA MARIE INGRAM, HEIGHTS BAPTIST CHURCH, NORTHSIDE BAPTIST CHURCH, ERIN BLACKLAWS and TORRY TANNER
RESPONDENTS	HER MAJESTY THE QUEEN IN RIGHT OF THE PROVINCE OF ALBERTA and THE CHIEF MEDICAL OFFICER OF HEALTH
DOCUMENT	EXPERT REPORT
ADDRESS FOR SERVICE AND CONTACT INFORMATION OF PARTY FILING THIS DOCUMENT	Alberta Justice, Constitutional and Aboriginal Law 10 th Floor, 102A Tower 10025 -102A Avenue Edmonton, Alberta T5J 2Z2 Attention: Nicholas Parker and Nicholas Trofimuk Tel: (780) 643-0853 Fax: (780) 643-0852

EXPERT REPORT OF DR JASON KINDRACHUK

1. My name is Dr Jason Kindrachuk. I am an Assistant Professor and the Canada Research Chair in emerging viruses in the Department of Medical Microbiology & Infectious Diseases at the University of Manitoba.
2. I have been asked by the Respondents to provide my opinion on some of the important issues regarding the virus SARS-CoV-2 and the disease it causes, namely COVID-19, in response to the expert report of Dr Jay Bhattacharya.
3. The substance of my opinion, including the information and assumptions upon which my opinion is based, is contained in **Schedule A**.
4. My qualifications and background are set out in my Curriculum Vitae, attached hereto as **Schedule B**, and the sources used in my report are attached hereto as **Schedule C**.

08 July 2021



Dr Jason Kindrachuk

Schedule A

Background

I am an Assistant Professor and Canada Research Chair in emerging viruses in the Department of Medical Microbiology & Infectious Diseases, University of Manitoba. My field of expertise is the investigation of emerging viruses, the infections they cause and their impact on global health. I am engaged in multiple international scientific outreach activities with regional partners across Africa including Sierra Leone, Gabon and Kenya. I was recently seconded to the Vaccine and Infectious Disease Organization, University of Saskatchewan, Canada, as part of a 12-month research partnership agreement where I lead and facilitated national COVID-19 research response efforts. I also serve as an Associate Professor in the College of Medicine and Allied Health Sciences at the University of Sierra Leone and as a Visiting Scientist at the Centre International de Recherches Medicales de Franceville in Gabon, one of two biosafety level 4 facilities in Africa. I have also served in a volunteer capacity as an infection prevention and control expert for Heart to Heart International, an international disaster response agency, throughout the Covid-19 pandemic. Heart to Heart International, founded in 1992, has shipped more than \$1.7 billion in humanitarian aid across more than 130 countries. It is a global humanitarian organization that focuses on improving public health and responding to the victims of disaster worldwide.

My education is as follows. I completed my undergraduate and graduate training at the University of Saskatchewan and completed my PhD in 2007 in the Department of Biochemistry. Following this, I participated in and led several projects as a postdoctoral fellow in Dr. Robert E.W. Hancock's laboratory, Centre for Microbial Diseases and Immunity Research, University of British Columbia. Here, my work focused on the design and development of novel anti-infective therapeutics and vaccine adjuvants, which are substances that are added to vaccine formulations to help amplify the immune response to the vaccine, for emerging pathogens. During this fellowship, the focus of my research was the investigation of emerging and re-emerging pathogens of importance to global public health, notably antibiotic resistant bacteria. These investigations fostered my commitment to both basic scientific research approaches and application of this research to public health in developed and developing nations. In 2009, I joined the National Institutes of Health (NIH) in Bethesda, MD, USA, as a Visiting Fellow to expand my expertise in the molecular mechanisms that underlie severe infections focusing on emerging and re-emerging viruses. Following this fellowship, I served in multiple senior scientific and leadership capacities, including Principal Research Scientist (NIH Integrated Research Facility-Frederick) and Staff Scientist (Critical Care Medicine Department, NIH). I also volunteered as a Scientific Lead in diagnostic support for the Centers for Disease Control/Department of Defense joint operations in Monrovia, Liberia during the 2014 Ebola virus disease outbreak.

Research History

My research has contributed to our understanding of the complex mechanisms underlying emerging viruses, their transmission and the infections they cause. Research in my laboratory focuses on the circulation, transmission and clinical aspects of emerging viruses that pose the greatest threat to global human and animal health. My current Covid-19 research includes:

- characterization of how SARS-CoV-2 manipulates human immune responses to cause severe disease in high-risk patient populations
- investigation of repurposed drugs as SARS-CoV-2 therapeutics through kinome analysis
- characterization of neurological and reproductive health complications in animal models of SARS-CoV-2 infections. Further, the animal models we are developing will allow us to inform how neurological manifestations associated with Covid-19 occur in humans.

Prior to my work on SARS-CoV-2 and Covid-19, my research focused on viruses that pose the greatest threat to global human and animal health. These included Ebola virus, Middle East respiratory syndrome

coronavirus (MERS-CoV) and influenza viruses. A summary of these research activities follows below.

1) Ebola virus research (basic and clinical) & support efforts. I have conducted extensive research into Ebola (Wahl-Jensen, Kurz et al. 2011, Kindrachuk, Wahl-Jensen et al. 2014, Falcinelli, Chertow et al. 2016, Barnes, Kindrachuk et al. 2017, Kash, Walters et al. 2017, Schindell, Webb et al. 2018, Khurana, Ravichandran et al. 2020) and received a 2018 National Institute of Allergy and Infectious Diseases (NIAID, NIH, Bethesda, MD, USA) Merit Award for my work. In 2014, I served as Scientific Diagnostics Lead in Liberia during the Ebola virus disease epidemic in West Africa. I provided daily situation reports and recommendations to local and international officials. I received a National Institutes of Health Director's Award in 2014 for these efforts. I have also recently received a five-year project grant from the Canadian Institutes for Health Research for my work on Ebola virus persistence, sexual transmission and long-term reproductive health impacts in Ebola virus disease survivors.

2) MERS-CoV efforts. My work on coronaviruses began in 2013 following the emergence of Middle East respiratory syndrome coronavirus. This work culminated in multiple peer reviewed publications on therapeutic screening and identification as well as characterization of molecular pathogenesis (Dyall et al. 2014; Dyall et al. 2017; Falcinelli, Chertow, and Kindrachuk 2016; Hart et al. 2014; Kindrachuk et al. 2015; Willman, Kobasa, and Kindrachuk 2019).

3) Variola virus and monkeypox virus pathogenesis. I developed and led collaborations with the US Centers for Disease Control and Prevention to investigate variola virus pathogenesis, the etiologic agent of human smallpox. This work demonstrated that kinome analysis could be used as a predictive drug repurposing tool for orthopoxviruses. Based on this, I was invited to serve as a member of the US delegation at the World Health Organization Advisory Committee of Variola Virus Research. Meeting reports, including overviews of my work, are publicly available ([WHO Advisory Committee on Variola Virus Research, 14th meeting](#); [WHO Advisory Committee on Variola Virus Research, 15th meeting](#)). My work on monkeypox virus was the first to identify how the West African and Congo Basin virus behave differently at the cellular level and may explain the differences in case fatality rates between the two clades (Kindrachuk et al. 2012).

4) Influenza viruses. I have investigated influenza virus pathogenesis extensively with a focus on influenza-bacterial co-infections (Chertow et al. 2016; Davis et al. 2016; Walters et al. 2016). This included pandemic and seasonal strains, including 1918 H1N1 virus. My work provided increased clarity regarding the mechanisms employed by pandemic and seasonal influenza viruses to infect cells as well as assessing the role of aerosol infection in acute respiratory distress during influenza virus infection in Rhesus macaques, with or without bacterial co-infection. Recently, my group published findings on 2009 pandemic H1N1-*Staphylococcus aureus* co-infections and provided perspectives on the 1918-1919 influenza pandemic (Nickol et al. 2019; Nickol and Kindrachuk 2019).

I have been actively engaged in emerging infectious disease research and response efforts throughout my research career. In 2014, I was as a Scientific Lead in diagnostic support for the Centers for Disease Control/Department of Defense joint operations in Monrovia, Liberia, during the West African Ebola virus disease outbreak. I continue to work with local communities and perform research on the African continent. I have an active research program in Sierra Leone where I am leading investigations that focus on the long-term reproductive health impacts found in Ebola virus disease survivors. Here, we are working with local survivor advocacy groups to identify complications that are faced by survivors through anonymous surveys. My research group is also collaborating with similar advocacy groups and researchers in Liberia on this work. I have also co-founded the Consortium for Intercepting Emerging Diseases in Africa (CIEDA) with Dr. Kris Forbes (University of Arkansas) which brings together partners from North America, Europe and Africa to increase surveillance and identification of emerging infectious diseases that could impact global human and animal health. This work began through my research partnership with the Interdisciplinary Centre of Medical Research of

Franceville, Gabon, where I am a Visiting Scientist. I also have emerging infectious disease collaborations at the University of Nairobi Institute for Tropical Infectious Diseases, Kenya, where I have led emerging virus training programs for trainees and staff.

Covid-19 and SARS-CoV-2 Grants, Reports and Committee Appointments

My research group is currently examining the effects of respiratory virus co-infection on disease outcome during SARS-CoV-2 infection in hamsters. I was a co-applicant on a grant funded by the Canadian Institutes for Health Research (CIHR) entitled “Animal models for SARS-CoV-2: vaccines and immune enhancement” in Spring, 2020. I have also received funding as a co- or lead-applicant for two additional grants: i) Scalable, Customizable, Digital Health Communication Materials to Help Canada Address the COVID19 Pandemic (CIHR); and ii) Broad Spectrum CoV Therapeutic; rhACE2 Immunoadhesin to treat COVID19 (MITACS Accelerate).

My work on SARS-CoV-2 began in early January of 2020 following the identification of the emergent virus in Wuhan, China, as a novel coronavirus. Following the emergence of SARS-CoV-2, I have been involved in various research investigations that have included development of animal models of infection, characterization of biological variables on disease severity, novel drug development and behavioral assessments of Covid-19 infection prevention and control messaging. In addition, I am currently investigating the differences in molecular pathogenesis in respiratory cells from patients with no underlying respiratory complications and those with chronic obstructive pulmonary disorder. My work on SARS-CoV-2 began in early January of 2020 when I co-authored a publication with other Canadian emerging virus experts on the emergence of a new virus (then called 2019-nCoV).

I have published two peer reviewed manuscripts on SARS-CoV-2, including as a co-author on a peer-reviewed clinical review of Covid-19 (Cevik et al. 2020; Ralph et al. 2020) and two recently accepted data manuscripts describing Covid-19 pathogenesis in hamsters (Accepted in *PLoS Pathogens*) and ferrets (Accepted in *Scientific Reports*). Two additional manuscripts are currently in revision at *Clinical Microbiology Reviews* and *BMC Infect Dis*. I have also been involved in two publicly available reports from national committees on Covid-19 transmission as well as multiple national and international Covid-19 committees. These are outlined below.

Published Reports on Covid-19 Transmission:

- 1) CIHR-PHAC-CADTH – Best Brains Exchange – Transmission Routes for COVID-19: Implications for Public Health. Canadian Institutes of Health Research (CIHR); 2020 October. <https://cihr-irsc.gc.ca/e/52238.html>
- 2) Heating, Ventilation and Air Conditioning Systems in Public Spaces. Ottawa: Canadian Agency for Drugs and Technologies in Health (CADTH); 2020 June. (CADTH technology review). [Heating, Ventilation, and Air Conditioning Systems in Public Spaces \(cadth.ca\)](https://www.cadth.ca/heating-ventilation-and-air-conditioning-systems-in-public-spaces)

National and International Covid-19 Committees:

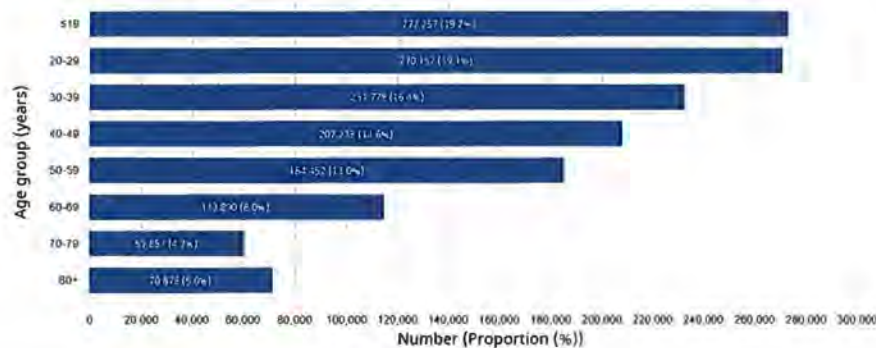
- 1) Panel Member – CIHR Institute of Infection and Immunity Consultation on Variant Strains of SARS-CoV-2
- 2) Panel Member – CIHR-PHAC-CADTH – Best Brains Exchange – Transmission Routes for COVID-19: Implications for Public Health. Canadian Institutes of Health Research (CIHR); 2020 October. <https://cihr-irsc.gc.ca/e/52238.html>
- 3) Panel Member – Heating, Ventilation and Air Conditioning Systems in Public Spaces. Ottawa: Canadian Agency for Drugs and Technologies in Health (CADTH); 2020 June. (CADTH technology review). [Heating, Ventilation, and Air Conditioning Systems in Public Spaces \(cadth.ca\)](https://www.cadth.ca/heating-ventilation-and-air-conditioning-systems-in-public-spaces)

- 4) Member – World Health Organization COVID-19 Solidarity Serology Study Group
- 5) Member – World Health Organization Ad Hoc Committee on COVID-19 Animal Models

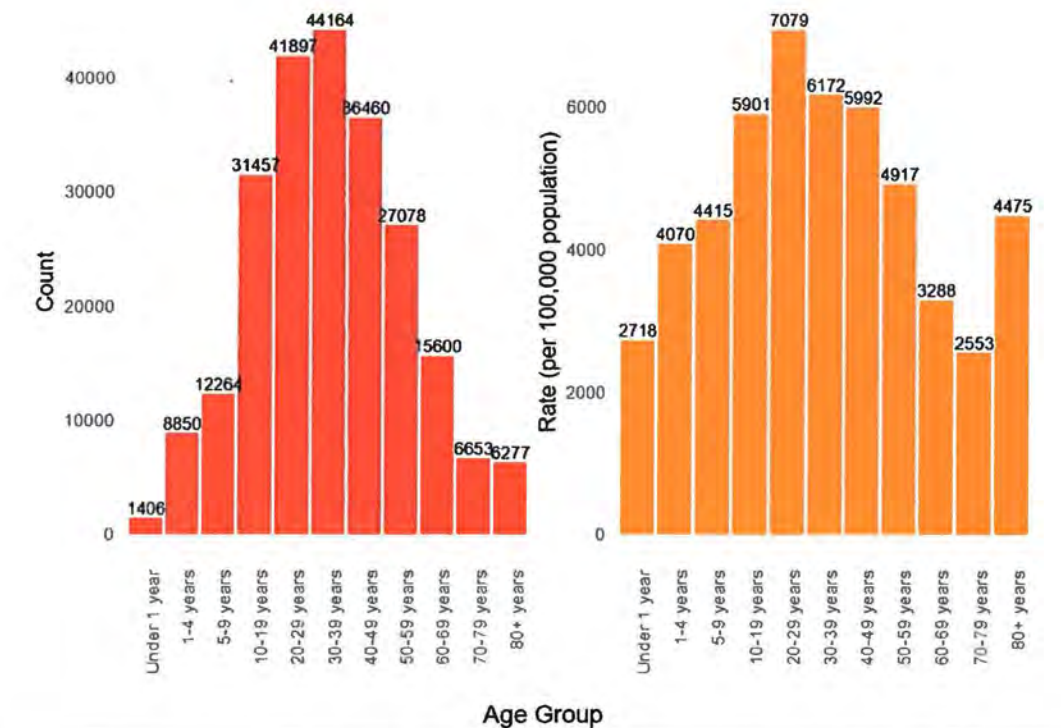
1. Current Knowledge of Covid-19 Cases and Disease Severity

There has been extensive investigation into the relation between biological risk factors and Covid-19 disease severity. Severe disease, including intensive care unit admission and fatal disease, are associated with older age, race/ethnicity, gender and socioeconomic status. The US Centers for Disease Control and Prevention outlined and ranked the risks for severe Covid-19 based on supportive published evidence including case series, cohort studies, cross-sectional studies, meta-analyses and systematic reviews (CDC 2021). While older age is convincingly linked to severe Covid-19, the outlined risks were not limited to those in high age groups. Factors strongly linked to severe disease in adults include cancer, chronic kidney disease, COPD, cardiovascular disease, obesity, pregnancy, sickle cell disease, smoking, organ transplantation and type 2 diabetes.

As of July 2, 2021, age distributions of Covid-19 cases in Canada show that both ≤ 19 years and 20-29 years represented the greatest proportion of all cases of infection and were nearly identical overall ([COVID-19 daily epidemiology update - Canada.ca](#)):

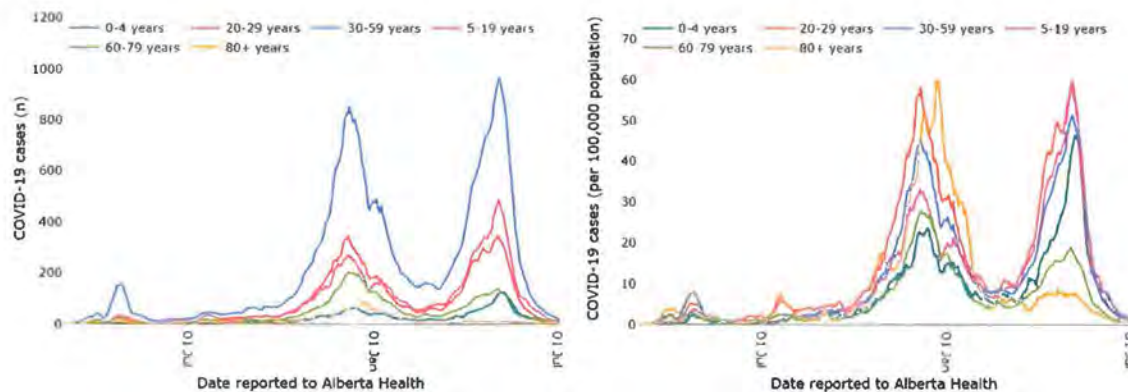


Alberta data is presented below ([COVID-19 Alberta statistics | alberta.ca](#)):

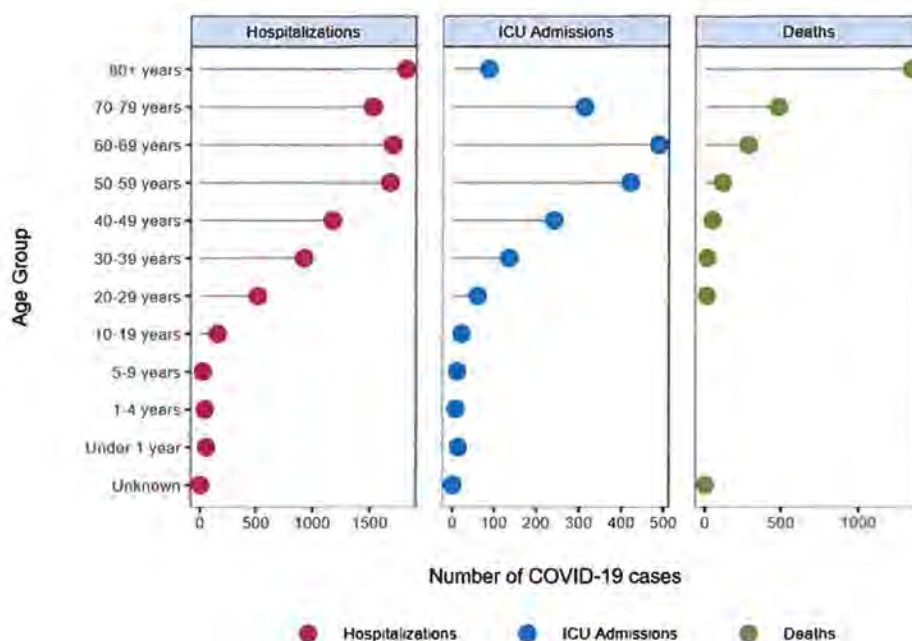


Temporal distribution of cases by age group in Alberta throughout the pandemic (A) and age distributions for severe outcomes (B):

A)



B)



In Alberta, total Covid-19 cases were highest in the ≤ 19 years age group with 53,977 cases (summation of all age groups from 0-19). This was followed by the 30-39, 20-29 and 40-49 year age groups, respectively. While hospitalizations were highest across all age groups ≥ 50 , ICU admissions highest in the 60-69 year age group followed by 50-59, 70-79 and 40-49 age groups, respectively. This data continues to demonstrate that younger age groups are susceptible to moderate or severe illness and at risk for hospitalization and intensive care unit admission.

Covid-19 clinical symptom onset and diversity

Covid-19 has a diverse range of clinical presentations that range from asymptomatic infections to severe and fatal disease. The presentation of symptoms is variable within increasing severity of illness associated with older age and/or underlying health complications. Symptom and wellness checks, including temperature screening, to identify have been employed to identify infected individuals. Malenfant and colleagues reported on the frequency of symptoms associated with Covid-19 in healthcare workers from March to April 2020 (Malenfant, Newhouse, and Kuo 2020). The authors demonstrated that Covid-19 presented with a broad spectrum of mild symptoms. While cough (51%), fever (41%), myalgia (38%) and headache (30%) were the most common initial symptoms reported, one-third of the respondents did not report fever or cough as one of their symptoms and nearly half (49%) continued to work while experiencing symptoms, some for several days. In an investigation of over 1,000 hospitalized patients, 44% of patients had fever upon admission though the half of these patients (22%) had very mild elevations in body temperature (37.6 to 38 °C) (Guan et al. 2020). Further, according to the Clinician Guide for Covid-19 signs, symptoms and severity of disease from the Government of Canada, clinical symptoms among older adults (≥ 65 years old) and those with underlying health conditions may be atypical or subtle (<https://www.canada.ca/en/public-health/services/diseases/2019-novel-coronavirus-infection/guidance-documents/signs-symptoms-severity.html>). Thus, it must be appreciated that symptoms are highly variable in regards to both type

and severity across infected individuals and thus screening alone as a measure of case identification would likely lead to many missed cases of infection.

Investigations of Covid-19 pathology suggest that there are similar pathologic findings and distribution of virus during infection. These reports suggest similarities across different geographic regions as well as similarities to prior observations from SARS and MERS patients. Deshmukh and colleagues published a systematic review demonstrating that SARS-CoV-2 infections in the lower respiratory tract correlated with more severe disease including pneumonia and organ failure (Deshmukh et al. 2021). The authors noted that many of the histopathological findings bore similarity to those described for severe acute respiratory syndrome (SARS) and Middle East respiratory syndrome (MERS). It should be appreciated that 15-30% of those who recovered from either SARS or MERS developed long-term lung complications including pulmonary fibrosis (Hui et al. 2005; Ooi et al. 2004; Das et al. 2017). Therefore, though further research will be required to determine the full extent, it is likely that some who recover from Covid-19 will continue to experience long-term negative health effects.

2. SARS-CoV-2 Transmission and High Risk Activities

While three coronaviruses have emerged over the past two decades with drastic public health consequences, SARS-CoV-2 is distinguished by a high degree of community transmission. Thus, it has been important to establish the infectious period for those that have been infected. This has been driven by investigations of viral loads (amount of virus) within the respiratory tract of infected patients as well as the duration of infectiousness, including during the pre- and post-symptomatic periods of infection. Investigations from the SARS epidemic and MERS outbreaks demonstrated limited community transmission with either coronavirus with transmission largely concentrated in healthcare settings through close contacts. Scientific evidence strongly supports that SARS-CoV-2 transmission is driven by respiratory droplets and aerosols. Respiratory droplets ($>5\text{--}10\text{ }\mu\text{m}$ in diameter) remain suspended for short periods of time and are transmitted over short distances though this can be dependent on airflow. Small-particle aerosols ($<5\text{ }\mu\text{m}$) can disperse quickly and remain airborne while traveling longer distances. Epidemiological data suggests that close contact, defined as anyone who has shared an indoor space with a case for a cumulative total of 15 minutes over a 24 hour period (Canada 2020), or enclosed settings is a major driver for SARS-CoV-2 transmission (Leclerc et al. 2020; Qian et al. 2020). Recent animal model investigations (Richard et al. 2020; Kim, Kim, et al. 2020; Sia et al. 2020; Chan et al. 2020) and epidemiological studies (Lu and Yang 2020; Park, Kim, et al. 2020; Jang, Han, and Rhee 2020; Cai et al. 2020) suggest that aerosol transmission can occur during prolonged exposure in enclosed settings with reduced ventilation.

There has been considerable scientific investigation into the role of presymptomatic (prior to onset of symptoms) and asymptomatic (no symptom development though infected) transmission for Covid-19. Of central focus has been characterizing how the viral load (amount of virus) within the respiratory tract of an infected individual changes throughout the course of infection, both prior to symptom onset and following symptom resolution. The presence (viral load) and duration (kinetics) of virus within the respiratory tract are important determinants for the duration of infectiousness and thus transmission. Cevik and colleagues recently published a systematic review that incorporated data from 5,340 individuals across 79 studies (Cevik et al. 2021). Prior assessments of viral loads in the respiratory

tract through repeated sampling suggests that peak viral loads occurred either just prior to (presymptomatic phase), or coincident with, symptom onset (Wolfel et al. 2020; Zou et al. 2020; Kim, Chin, et al. 2020). In the systematic review by Cevik et al., the authors identified 12 reports that provided temporal viral load data for individuals with asymptomatic infections. Viral loads in the reports were found to be similar to (four reports) or lower than (two reports) those from symptomatic patients. However, viral clearance appeared faster in asymptomatic patients based on observations from six reports. This review provided temporal evidence for viral accumulation and clearance in asymptomatic patients. These observations are in good agreement with prior contact tracing studies where the highest risk of transmission fell from a few days prior to symptom onset to five days post-onset.

The contributions of asymptomatic and presymptomatic infections to SARS-CoV-2 transmission have been broadly investigated. An early study in April 2020 by Kimball and colleagues investigated an outbreak of Covid-19 in a long-term care facility in King County, Washington, US (Kimball et al. 2020). Following the initial identification of a Covid-19 case in the facility, broad testing was employed 16 days later and demonstrated that rapid spread of the virus had occurred with positive tests found in 30.3% of residents. Early adoption of infection prevention and control measures had been instituted following the identification of the first case. Nearly half of the residents that had positive test results were not symptomatic at the time of testing and the authors concluded that the evidence suggested transmission from asymptomatic and presymptomatic residents may have contributed to spread. Wang and colleagues performed a retrospective cohort study of 335 people in 124 families and with at least one laboratory confirmed Covid-19 case and provide strong evidence for the importance of the pre-symptomatic transmission of SARS-CoV-2 (Wang et al. 2020). Further, they found that face mask use by the primary case and family contacts prior to symptom onset in the primary case was 79% effective in reducing transmission. In a prospective study, Cheng and colleagues demonstrated that secondary transmission was higher among individuals with initial exposures to index cases within 5 days of symptom onset as compared to day 6 or later (Cheng et al. 2020). This study also found that transmission was similar whether contacts only had presymptomatic or postsymptomatic exposure to index cases. In the four clusters for which the date of exposure could be determined, presymptomatic transmission occurred 1-3 days before symptom onset in the presymptomatic source case. Clinical and epidemiological assessment of 243 Covid-19 cases between January 23, 2020 - March 26, 2020 were reviewed to identify potential cases of presymptomatic transmission of SARS-CoV-2. Out of 243 cases, 157 were locally acquired (Wei et al. 2020). The authors found seven epidemiologic clusters where presymptomatic transmission likely occurred and ten of the cases within these clusters were attributed to presymptomatic transmission, accounting for 6.4% of the 157 locally acquired cases. Katelaris and colleagues recently provided epidemiological evidence for airborne transmission of SARS-CoV-2 among attendees of a religious service in the absence of close physical contact (Katelaris et al. 2021). Here, 12 secondary case-patients were identified among 508 attendees across four services where the index patient had sung for 1 hour per service from a choir loft 3.5 metres above the congregation. The authors concluded that singing likely resulted in more dissemination of droplets and aerosols than talking, that limitations to ventilation may have allowed for the concentration of infectious virus in shared air, and lastly that the index patient was likely near the peak of infectiousness with symptom onset occurring around the exposure date. The index patient performed during his infectious period starting from 48 hours prior to symptom onset (initially malaise and headache).

There have been a growing number of investigations that have focused on separating asymptomatic and presymptomatic infections to facilitate increased understanding of transmission risks throughout the infectious period. Johansson and colleagues employed a decision analytical model to examine virus transmission from presymptomatic, symptomatic and asymptomatic individuals (Johansson et al. 2021). Model assumptions were that peak viral transmission occurred at the median of symptom onset, 30% of infected individuals were true asymptomatic infections and were 75% as infectious as symptomatic individuals. The model suggested that 59% of all infections occurred from those without symptoms of disease where 35% were patients that were in the presymptomatic stage of disease and 24% had asymptomatic infections. Buitrago-Garcia and colleagues recently examined asymptomatic and presymptomatic SARS-CoV-2 infections and transmission through a systematic review (Buitrago-Garcia et al. 2020). Using data from 94 studies, the authors calculated the overall estimate of true asymptomatic infection was 20% with the balance of 80% being those with presymptomatic infections. Thus, approximately 1 in 5 infected individuals will remain truly asymptomatic throughout the course of infection. However, the authors also stated that most studies included in the review were not designed to estimate asymptomatic infection proportions and thus combination nonpharmaceutical interventions will continue to be needed to help curb virus transmission. These sentiments were also echoed by Byambasuren and colleagues in their recent systematic review of asymptomatic Covid-19 (Byambasuren O 2020). The authors reviewed 13 studies and the asymptomatic proportion of described cases ranged from 4-41% with a corresponding overall proportion of asymptomatic infections as 17% exclusive of presymptomatic infections based on their meta-analysis. The authors stated that this remained sufficient to warrant policy attention. In the systematic review from Buitrago-Garcia et al., asymptomatic infections rose to 31% in seven of the studies with defined populations (Buitrago-Garcia et al. 2020). The secondary attack rate, and thus indication of transmission potential, was lower for asymptomatic infection as compared to symptomatic infection with a relative risk ratio of 0.35, suggesting that there is greater risk for transmission from those with symptomatic disease; however, risk of transmission remains from those with asymptomatic infections. Interestingly, the authors also found that the relative risk ratio of presymptomatic transmission as compared to symptomatic transmission was 0.63, further demonstrating that transmission in the absence of symptoms presents a risk. Moreover, the authors state that based on the contributions of asymptomatic and symptomatic infections in virus transmission, “combination prevention measures, with enhanced hand hygiene, masks, testing tracing, and isolation strategies and social distancing, will continue to be needed”. A recent investigation by Li et al assessed household transmission rates in Wuhan through a retrospective observational study (Li et al. 2021). The authors assessed 29,578 primary cases, 27,101 households and 57,581 household contacts in their analysis. The odds ratio for infection from asymptomatic individuals was lower than from symptomatic cases (0.21), similar to those reported by Liu et al (Liu et al. 2020). Importantly, the odds ratio for infection from presymptomatic cases was higher than from post-symptom onset cases (1.42). Thus, while true asymptomatic transmission may occur less frequently than during symptomatic transmission, there was a greater likelihood of transmission before symptom onset (presymptomatic) than post-symptom onset. The authors concluded that presymptomatic cases were more infectious than symptomatic cases and individuals with asymptomatic infection less infectious than their symptomatic counterparts.

Cevik and colleagues recently published a systematic review that included data from 79 studies and

5,340 individuals (Cevik et al. 2021). Prior assessments of respiratory tract viral loads have suggested that peak loads occurred either just prior to (presymptomatic phase), or coincident with, symptom onset (Wolfel et al. 2020; Zou et al. 2020; Kim, Chin, et al. 2020). Cevik et al. identified 12 reports that for individuals with asymptomatic infections where viral loads were assessed throughout the course of infection. Viral loads in asymptomatic patients were similar to, or lower than, those from symptomatic patients in four reports and two reports, respectively. Viral clearance appeared to be faster in asymptomatic patients (six reports). Overall, the accumulated data across all studies suggested that highest risk of transmission fell from a few days prior to symptom onset to five days post-onset. Chung et al. recently provided a comparison of SARS-CoV-2 viral loads from upper respiratory tract samples in children and adults in a respiratory surveillance study (Chung et al. 2021). Assessments were carried out across 555 virus-positive participants (mean age 33.7 years) that included 432 adults (≥ 18 years) and 123 children. Higher viral loads were found in those with symptomatic infections as compared to their asymptomatic counterparts; however, there were no statistical differences in viral loads between adults and children within either group.

While SARS-CoV-2 transmission is likely lower from individuals with asymptomatic infections as compared to symptomatic cases, those in the presymptomatic phase of disease appear to be able to transmit the virus similarly to symptomatic individuals. Dr. Nathalie Dean, corresponding author for this study, has provided additional context on the quantitative generalizations that can be drawn from her team's study, including the direct limitation noted in the paper recognizing that few studies were used in their analysis of asymptomatic transmission (four studies) as compared to symptomatic transmission (27 studies). Further, on December 29, 2020, Dr. Dean highlighted on social media that her study could not separate out asymptomatic and presymptomatic disease cases and instead directed those questions to the data presented from Qiu et al. which did directly assess this (<https://twitter.com/nataliexdean/status/1343989533050867712?s=20>). Dr. Zachary Madewell also provided additional context and commentary on the JAMA analysis on February 17, 2021:

February 17, 2021

Comment from the authors

Zachary Madewell, PhD, MPH | University of Florida

Thank you for your interest in our paper. In this sub-analysis of the household studies from our main analysis, we separated papers reporting index cases identified as symptomatic versus asymptomatic/pre-symptomatic. We noted lower transmission from this latter group, though we state that there was much less data. For this reason, we view the qualitative result as noteworthy but requiring further exploration. Since we relied upon other studies in the literature, we were unable to separate out fully asymptomatic index cases (who never develop symptoms) from pre-symptomatic index cases. A more recent meta-analysis has focused directly on separating these two groups (<https://pubmed.ncbi.nlm.nih.gov/33484843/>). The growing literature indicates that, while individuals can be similarly infectious during the pre-symptomatic and symptomatic phases, individuals who are fully asymptomatic are less infectious to others (summary secondary attack rate of 1% from Qiu et al. 2021). This may explain the low secondary attack rate we observed in our sub-analysis.

Qiu et al. assessed available secondary attack rate data from individuals with asymptomatic, pre-symptomatic and symptomatic SARS-CoV-2 infection. Eighty studies were included for their analysis and in agreement with other investigations, secondary attack rates (defined as the probability that an infected individual will transmit the disease to a susceptible individual) from asymptomatic cases were found to be lower than symptomatic cases (Qiu et al. 2021). Importantly, their analysis demonstrated that secondary attack rates were similar between presymptomatic and symptomatic cases.

More recently, Bi et al. assessed household transmission from asymptomatic patients as compared to those with symptoms (Bi Q 2021). Using serology testing, the authors used a population serosurvey of 4,534 individuals (≥ 5 years of age) in Geneva, Switzerland, across 2,267 households from April-June 2020. The risk of infection was three times higher for household exposures as compared to those outside of the household. Here, asymptomatic infections accounted for 14.5% (95% CI, 7.2-22.7%) of all household infections and had 0.31 times the odd ratio of infecting another household member compared to those with symptomatic infections. As stated directly by the authors, “While asymptomatic individuals appear to be less than a third as likely to transmit, they cannot be dismissed as inconsequential to disease spread, and are responsible for one in six within-household transmissions in this study”. The authors also commented on the fact that while their study did not assess asymptomatic spread in community settings, it is plausible that those with asymptomatic infections could play an even larger role there in regards to transmission as symptomatic individuals would be more likely to stay home or seek care.

It must be appreciated that while presymptomatic transmission likely plays a larger role in community transmission than asymptomatic transmission, there is also a reliance on the recognition of clinical symptom onset by individuals once they enter into the symptomatic phase of disease. As highlighted previously, given the mild and broad nature of clinical presentation in mild disease, it should be appreciated that there is no single indicator of infection outside of testing and many reports describing transmission events are related to index patients that attended events just prior to, or coincident with, the onset of clinical symptoms of disease.

There have been numerous investigations on the relation between viral load, transmission and biological characteristics including age, sex and disease severity. A recent systematic review by Koopmans et al. reviewed data from 26 studies to determine the relation between viral load dynamics and Covid-19 severity, age and sex (Chen PZ 2021). Higher viral loads were found in those with severe disease as compared to those with non-severe infections. Interestingly, viral load within those with symptomatic infections was not altered by age or sex as children had similar viral loads following symptom onset as their non-severe adult counterparts. While severe Covid-19 has largely been linked to age and underlying health comorbidities, there is growing appreciation that children can be infected and transmit SARS-CoV-2. Recent reports have suggested that transmission is efficient in children ≥ 10 years old (Szablewski et al. 2020; Park, Choe, et al. 2020). In the conclusion of the analysis of SARS-CoV-2 transmission at the summer camp in Georgia (Szablewski et al. 2020), Szablewski et al suggested that asymptomatic infection was common amongst the cases and could have contributed to undetected transmission as suggested in additional studies (Team 2020; Dong et al. 2020; Gotzinger et al. 2020; Huang et al. 2020). More recently, a case report from Lopez and colleagues investigated Covid-19 outbreaks at childcare facilities in Utah (Lopez et al. 2020). Twelve children (mean age 7 years; range 0.2-16 years) were found to have acquired SARS-CoV-2 in the facilities and transmitted the virus to 12

of 46 non-facility contacts that were assessed. Importantly, three of 12 children had asymptomatic infection (25%) and two transmitted the virus. It must also be appreciated that reduced incidence of severe disease in children is not equivalent to the absence of severe disease risk. The US Centers for Disease Control and Prevention estimate that the prevalence of obesity in US children is ~19%, a comorbidity linked to higher risk of severe Covid-19 ([Childhood Obesity Facts | Overweight & Obesity | CDC](#)), and higher amongst minority populations, which have been disproportionately affected by Covid-19 (Abedi et al. 2021). In Canada, children ≤ 19 years have thus far accounted for 1.8% of Covid-19-related hospitalizations, in line with US estimations from the American Academy of Pediatrics of 1.3-3.1% ([COVID-19 and Age \(aap.org\)](#)).

Taken together, there is strong scientific evidence for SARS-CoV-2 transmission to primarily occur from a few days prior to symptom onset up to ~5 days post-onset. Direct assessments of viral loads and the kinetics of viral shedding, when virus is released from infected cells in the respiratory tract, are in agreement with this and contact tracing studies in household cohort studies provide direct evidence for asymptomatic and presymptomatic transmission of SARS-CoV-2. Further, additional epidemiological studies of SARS-CoV-2 suggest that similar patterns of asymptomatic and presymptomatic transmission likely occur within children as with adults.

In sum, it is clear that people who have SARS-Cov-2 but are not displaying any symptoms still can and do transmit the disease and infect others. Accordingly, relying on symptom checks alone would not be an effective way to control the spread of COVID-19 in group settings.

Transmission Related to Activities

Exposure risk guidance is primarily based on the relation between exposure time and SARS-CoV-2 infection. By Health Canada guidelines, a high risk exposure (close contact) includes anyone that has shared an indoor space with a positive Covid-19 case for a prolonged period (a period of 15 cumulative minutes over 24 hours) without adhering to appropriate mitigation measures (Canada 2020). This also includes anyone with a close-range contact with a positive Covid-19 case or anyone that has been in settings where that person engaged in singing, shouting or heavy breathing (including exercise). Given the role of aerosol exposure in transmission, the accumulation of virus-laden aerosol particles in the air of an enclosed setting could result in continued exposure of individuals to virus over a prolonged period.

There have been multiple superspreader events during the Covid-19 pandemic that have been linked to close contacts in enclosed settings, including faith-based settings or places of worship. Most notably, infection of 53 of 61 attendees (33 confirmed and 20 probable cases) from a single symptomatic individual occurred during a 2.5-hour choir practice in Skagit County, Washington, USA (Hamner et al. 2020). Three of those infected during the practice were hospitalized and two succumbed to infection. A similar superspreader event occurred in Arkansas where 35 of 92 church attendees were infected, three fatally, during a five-day period (March 6-11) (James et al. 2020). Additionally, contact tracing found at least 26 additional Covid-19 cases among community members that had reported contacts with church attendees and had likely been infected during those contacts, including a fatal disease case. The index cases, a husband (pastor at the church) and his spouse, were likely infected during a two-day period

(March 6-8) with potential presymptomatic transmission from the pastor to others during a group event on March 11. Of the 61 total identified cases (35 church attendees and 26 contacts), eight were hospitalized and four had fatal infections. These observations have not been limited to North America. A superspreading event linked to a service at Shinchunji Church of Jesus, Daegu, South Korea is postulated to have resulted in >3,900 secondary Covid-19 cases (Shim et al. 2020) and choir-related outbreaks have been reported in Berlin and Amsterdam (Bahl et al. 2020).

Alsved et al. recently examined exhaled respiratory particle generation during breathing, talking and singing (Alsved M 2020). The generation of aerosol particles, as determined by particle number emission rates, were highest from those singing loudly with exaggerated diction followed by loud singing alone, normal singing, loud talking, normal talking and breathing. Addition of a face mask to those singing loudly reduced particle emission rates to levels found during normal talking. The authors examined SARS-CoV-2 release from those with confirmed Covid-19 during singing and talking. While virus was not detected, the authors identified several limitations in the study including variations in patient viral loads, test positivity versus infectious virus presence in the respiratory tract, and dilution steps in the sample preparation method.

These observations are in line with prior studies looking at respiratory viruses and aerosol particle emission. Previously, Lindsley and colleagues examined the release of influenza virus in aerosol particles during coughing and exhalation (Lindsley et al. 2016). The authors collected aerosol particles produced during coughing or exhalation from 61 patients with influenza-like illness. Aerosol particles with infectious virus were collected from 28 (53%) patients while coughing and 22 (42%) patients from exhalation. These results demonstrated that normal exhalation can generate virus-laden infectious particles which could potentially lead to virus accumulation over extended periods of exposure in an enclosed setting.

Previous investigations have also assessed droplet and aerosol emission during common vocal activities. An investigation by Bahl et al. examined the spread of droplet and aerosol generation during singing (Bahl et al. 2020). This was done using a detailed flow visualization of aerosols and droplets emitted during singing of a major scale using an image-based flow diagnostic system. The authors found that droplets generated by singing did not settle rapidly suggesting high aerosol generation which could saturate the indoor environment in the absence of adequate ventilation. Further, the direction of the generated droplets suggested that they could pose a potential infectious risk for other members arranged in multiple adjacent and distant rows. Recommendations from the authors to reduce droplet and aerosol exposure included reduction in group numbers, greater physical distancing between members, softer singing and shorter duration, and the implementation of face masks. Of interest, prior investigations of particle emission patterns during normal speech by Asadi and colleagues demonstrated that particle emission during normal speech is correlated with the loudness of vocalization, is highly heterogeneous and could amplify respiratory pathogen transmission (Asadi et al. 2019). A similar study from Mürbe and colleagues assessed the release of aerosol emissions from adolescents: four boys and four girls aged 13-15 (Murbe et al. 2021). Overall, while the emission spectrum reflected that found in adults (highest during shouting followed by singing and speaking) the emission of aerosol particles was lower during singing than adults. However, particle emission was within the same order of magnitude between the two groups during speaking. In a retrospective study, Wang and colleagues found that face mask use by

the primary case and family contacts prior to symptom onset in the primary case was 79% effective in reducing transmission (Wang et al. 2020).

Taken together, there is accumulating evidence and historical data demonstrating that SARS-CoV-2 emission from infected individuals is likely positively correlated with vocal activities and increases with the volume and exaggeration of vocalizations. Importantly, the emission of aerosol particles is of particular importance given that they can accumulate in the air of enclosed spaces over time based on their physical characteristics and increasing the potential for infection beyond proximal contacts (at 2 m or less in distance away). This highlights the importance of reducing emissions through nonpharmaceutical interventions including masking and social distancing.

3. Non-pharmaceutical interventions reduce SARS-CoV-2 transmission

Non-pharmaceutical interventions (NPIs) are actions, apart from getting vaccinated and taking medicine, that people and communities can take to help slow the spread of illnesses. These can include a variety of different actions, such as wearing face masks and other personal protective equipment, washing hands, social distancing, restricting gatherings, and, in more serious situations, stay-at-home orders or lockdowns. NPIs continue to play a central role in disrupting SARS-CoV-2 transmission chains. It must be appreciated that Covid-19 control is not a decision between unrestricted transmission and lockdowns. Lockdowns and stay-at-home restrictions should continue to be a decision of last resort when community transmission can no longer be either controlled or monitored via testing and contact tracing. NPIs, including face masks, have been utilized as a mechanism to reduce transmission of SARS-CoV-2, including those that are infected prior to symptom onset (pre-symptomatic infections) as well as those that may have asymptomatic infections (no development of disease symptoms).

Brooks and Butler recently outlined the increasing data demonstrating that face masks are associated with reduced SARS-CoV-2 infections (Brooks and Butler 2021). The authors also highlighted recent work from Ruba and Pollak that assessed the ability of 81 racially-diverse children (7-13 years of age) to make accurate inferences regarding emotions when faces were partially occluded (Ruba and Pollak 2020). The authors concluded that the social interactions of children may be minimally impacted by face masks. Interestingly, Ruba and Pollak also demonstrated that the accuracy of children in identifying masked facial configurations did not significantly differ from those identified in facial configurations that wore sunglasses.

A recent investigation by Fischer et al. assessed relationships between adherence to mask wearing and Covid-19 case rates in the United States (Fischer et al. 2021). In their analysis, the authors used state-level data for the study. This investigation demonstrated that out of 15 states with no mask wearing policy, 14 had high monthly Covid case rates (>200 per 100,000 residents). Further, states with the lowest levels of mask adherence were most likely to have high Covid-19 case rates in the subsequent month, independent of either mask policy or demographics. Monthly case rates did not meet the high criteria across all eight states with $\geq 75\%$ mask adherence where case rates were 109.26 per 100,000 in the prior month as compared to 249.99 per 100,000 with lower mask adherence. Importantly, the authors noted that while there was strong supportive evidence for mask wearing reducing Covid-19 case rates, the relationship between mask policy and case rates was less stable. Thus, it is important to also consider the adherence and adoption to NPI recommendations rather than relying solely on mandated policies.

Similarly, Trauer and colleagues recently assessed the roles of NPIs and mobility restrictions on the trajectory of Covid-19 in the state of Victoria, Australia. Note that this is a preprint article that was posted to *medRxiv* on April 7, 2021 (Trauer JM 2021). The authors assessed the impact of these recommendations and policies on local Covid-19 cases in the southern hemisphere in Winter 2020. Through the authors' transmission model, the authors demonstrated that both face coverings (masks) and behavioral changes were associated with a significant reduction in transmission risk per contact. Importantly, masks had a considerably greater effect on reversing the epidemic, as stated by the authors. Pratt and colleagues assessed the implementation of community mitigation measures, which included stay-at-home orders and masking, on Covid-19 transmission in the Blackfoot Reservation, Montana, USA, from June to December 2020 (Pratt et al. 2021). Following the implementation of both stay-at-home orders and mask use, the incidence of Covid-19 decreased from 6.40 cases per 1,000 residents on October 5 to 0.19 cases per 1,000 residents on November 7. Of note, the average daily incidence was 0.10 in July and local campgrounds were opened following the expiration of prior mandatory stay-at-home orders. Daily incidence began to rise in August and while a recommended stay-at-home order was issued, incidence peaked at 6.40 on October 5, one week after the implementation and strict enforcement of a new stay-at-home order. Incidence decreased to 0.19 one month later.

An investigation by Flaxman and colleagues from June 2020 that was published in *Nature*, one of the top scientific journals in the world (2019 impact factor 42.779), analyzed mortality data from 11 European countries estimated lockdowns reduced the R_t of SARS-CoV-2 transmission by 81% (Flaxman et al. 2020). Further, the authors stated that while the rapid deployment of multiple NPIs made it difficult to characterize the individual effects of each intervention separately, the sole effect of lockdowns was identifiable. Lai and colleagues examined the effect of combined NPIs in SARS-CoV-2 transmission in China from early 2020 in *Nature* (Lai et al. 2020). The authors suggested that their data supported that both population movement and close contact were important drivers of virus transmission and that early detection and isolation of cases in tandem with social distancing were important for virus containment. Further, they estimated that without NPIs, the cases of SARS-CoV-2 infection in mainland China would have been 67-fold higher by the end of February. Cowling and colleagues used an observational study of SARS-CoV-2 and influenza infections in Hong Kong in early 2020 to reach similar conclusions - transmission can be contained through a combination of NPIs that included test, trace and isolate approaches, quarantining close contacts and behavioral changes (including social distancing and personal protective measures) (Cowling et al. 2020).

In sum, NPIs are extremely effective in reducing the spread of SARS-CoV-2 in a population, especially when used in combination, and are indeed necessary to limit exponential spread which could otherwise overwhelm healthcare resources.

4. SARS-CoV-2 Variant of Concern

The emergence of SARS-CoV-2 variants of concern, where mutations have resulted in phenotypic changes within the virus (including increased transmission and disease severity, reduced vaccine effectiveness, detection failure) have had deleterious health consequences in Canada and abroad. While variants emerge frequently within RNA viruses due to error-prone genome replication, including coronaviruses, these mutations often have negligible effects on viral behaviors or activities. In contrast, variants of concern have emerged infrequently throughout the pandemic but have resulted in devastating waves of Covid-19. It has been suggested that the selection of variants at the population level is likely not driven by host immunity because there are not sufficient numbers of immune individuals to push

evolution of the virus in a given direction (Lauring and Hodcroft 2021). Rather, there is supporting evidence to suggest that variants of concern may have emerged in chronically infected Covid-19 patients. A preliminary characterization of the Alpha variant, formerly B.1.1.7, by Rambaut and colleagues highlighted that the accumulation of 14 amino-acid replacements found within B.1.1.7 prior to the initial detection of this variant was thus far unprecedented in the pandemic. In contrast to this, the authors noted that most branches in the global SARS-CoV-2 phylogenetic tree had shown relatively few mutations with a fairly rate of accumulation over time (~1-2 nucleotide changes per month) (Rambaut A 2020). However, prior studies of chronic SARS-CoV-2 infections in immunodeficient or immunocompromised patients have demonstrated high rates of mutation accumulation over short periods of time (Choi et al. 2020; Avanzato et al. 2020). Thus, the evolutionary dynamics and selective pressures exerted upon the virus population within such patients are likely very different from those found during a typical infection. Kemp and colleagues characterized the evolution of SARS-CoV-2 in a chronically-infected immunocompromised patient following multiple therapeutic treatments (Kemp et al. 2021). Remdesivir treatment during the first 57 days had negligible effects on the viral population; however, convalescent plasma therapy resulted in large population shifts and the emergence of a dominant variant. This demonstrated a strong selection for viral variants with reduced susceptibility to neutralizing antibodies following treatment of an immunosuppressed individual with a chronic SARS-CoV-2 infection. Generally, there is relatively limited within-host variation reported for SARS-CoV-2 over the course of infection (Jary et al. 2020; Shen et al. 2020; Capobianchi et al. 2020). However, factors such as prolonged infection and immunodeficiencies could result in selective pressures not encountered within those that are immune-competent. Thus, the strongest evidence to date suggests that prolonged infections and compromised immune system functions likely exert selective pressures on SARS-CoV-2 resulting in a more extensive genetic changes than found during typical infections. More recently, a pre-print study from Niesen and colleagues posted on July 5, 2021, suggests that viral genomic diversity was reduced in patients that were vaccinated as compared to unvaccinated individuals (Niesen MJM 2021). Through a longitudinal analysis of more than 1.8 million viral genomes spanning 183 countries, the authors showed that SARS-CoV-2 diversity decreases at the country-level with increasing vaccination status and that breakthrough infections harbored viruses with lower diversity in B cell epitopes as compared to those found in unvaccinated patients. The recent emergence of SARS-CoV-2 variants of concern, which includes Alpha (first identified in the UK), Beta (first identified in South Africa) Gamma (first identified in Brazil), and Delta (first identified in India) has resulted in new concerns regarding the global burden of Covid-19. Concerningly, Alpha has increased transmissibility ranging from 30-70% over circulating non-variants of concern and has been associated with increased risk of severe and fatal disease in hospitalized patients (Horby P 2021). The emergence of Alpha in the UK resulted in the overtaking of circulating SARS-CoV-2 strains within a few months, a trend echoed in additional countries including Canada, and currently being repeated with Delta. The enhanced transmissibility associated with these variants have resulted in renewed public messaging regarding the importance of infection prevention and control measures, including mask use and social distancing, to curb community transmission of these variants of concern and others that may emerge. There have also been concerns regarding the potential for re-infections by VOCs due to their adoption of mutations associated with immune evasion and decreased ability for antibodies from convalescent Covid-19 patients or vaccinees to neutralize these variants. Thus, decreased community transmission will reduce the potential for additional emergence of variants of concern that could have better immune escape mechanisms that could have detrimental impacts on global vaccination programs.

5. Herd Immunity and Vaccinations

In Canada, variants of concern had deleterious effects on health and healthcare systems across many regions during the third wave of Covid-19 in early 2021. While the high mortality associated with individuals living in long-term care facilities and personal care homes were drastically reduced during the third wave, hospitalizations and ICU admissions pushed healthcare systems beyond their capacity in numerous jurisdictions. Notably, Manitoba transferred Covid-19 patients out of province for care to Ontario, Alberta and Saskatchewan due to ICU capacity limits. The Ontario Covid-19 Science Table released a report on March 29, 2021, detailing increasing trends in hospitalizations and ICU admissions as compared to late December 2020, during the second pandemic wave

(<https://doi.org/10.47326/ocsat.2021.02.18.1.0>). The authors noted that patients ≤ 59 years comprised 46% of all new COVID-19 ICU admissions to ICUs, compared with 30% just prior to the start of the province-wide lockdown in December 2020. Similar trends in other regions of the country during the third wave demonstrated that the view of younger age groups as being refractory to severe disease were flawed. Mass vaccination rollouts coupled with restrictions in regions with high rates of community have coincided with decreased cases and test positivity rates. Test positivity rates in Ontario have subsequently fallen from +10% in late April to 1.1% on July 6, 2021.

There have been rampant discussions regarding the potential of natural herd immunity, dictated by broad infections in the community, as a mechanism to curb global transmission of SARS-CoV-2. While focused protection has been raised as a mechanism to protect those at highest risk for severe disease while allowing the virus to transmit in the absence of broad employment of nonpharmaceutical interventions, there are serious concerns regarding the public health outcome of such a strategy. In particular, the resurgence of Covid-19 in Manaus, Brazil, provides a cautionary tale for a natural infection-based herd immunity-style approach. Manaus was devastated by the first wave of the pandemic with 4.5-fold excess mortality (Orellana et al. 2020). A serological assessment of antibodies in Manaus suggested that between 44-66% of the population was infected with SARS-CoV-2 by July 2020, which followed the epidemic peak (Buss et al. 2021). This rate rose to 76% by October 2020, surpassing the theoretical herd immunity threshold for Covid-19 of 67%. However, virus transmission continued with a devastating second surge of SARS-CoV-2 infections by mid-January 2021 (Sabino et al. 2021). The authors provided four potential explanations for their observations. First, attack rates could have been overestimated during the first wave. However, as the authors suggest, even with an upwards bias there should have still been a larger effect of population immunity given the breadth of the first wave in 2020. Second, the authors raised concerns regarding the potential impacts of waning immunity in those that were previously infected. Could decreasing protective immunity in individuals infected during the first wave have resulted in a resurgence of Covid-19 due to reinfections in this population? Such a phenomenon would be devastating for an infection-based herd immunity strategy as the threshold for sustained herd immunity to curb virus transmission would be impeded. Third, the emergence of virus variants that might evade immunity generated from prior SARS-CoV-2 infection. Two virus variants, P.1 and P.2, have been identified in Brazil that possess a mutation in the spike protein that has been associated with immune evasion. Reinfections have been identified in Brazil for both P.1 and P.2 (Naveca F 2021; Vasques Nonaka 2021; Resende PC 2021). And fourth, new SARS-CoV-2 variants circulating in Manaus may have higher transmissibility than currently circulating strains. The emergence of the VOCs have served as a continuing reminder that ongoing transmission of the virus results in mutations within the viral genome that could lead to increased rates of infection.

India experienced a devastating second wave of Covid-19 in 2021, with 414,188 new cases reported on May 7, the most reported during a 24 hour period throughout the pandemic ([india-situation-report-72.pdf \(who.int\)](#)). By the end of May, India had recorded more than 300,000 deaths due to Covid-19 with ~100,000 occurring the prior 26 days, including 50,000 deaths the prior 12 days (<https://timesofindia.indiatimes.com/india/indias-covid-toll-tops-3-lakh-50000-deaths-in-12-days/articleshow/82892432.cms>). This contrasted with opinions provided in *The Print* (Agarwal S 2021) suggesting that mathematical modelling demonstrated that “more than 50% of the Indian population may have developed immunity” and were corroborated by serological tests by Thyrocare. However, this data contrasted with data released on March 30, 2021, where IgG antibodies against either the N or S1-RBD virus proteins were found in 26% of samples (Murhekar MV 2021). High seroprevalence levels ($\geq 50\%$) would have been expected to reduce the toll of subsequent pandemic waves. This is also the case for the high seroprevalence data suggested in Brazil from investigations in Manaus, Brazil, where the country was also enveloped in a devastating wave of infections starting in early 2021.

Over-estimations of seroprevalence could ultimately have far reaching consequences if used to guide Covid-19 public health responses if assumptions are made regarding levels of immune protection within communities. In addition, herd immunity thresholds are fluid given the reliance on R_0 and shifts in this value due to the emergence of the more transmissible variants of concern, including the newly identified Delta variant (B.1.617.2) that was first identified during the second pandemic wave in India. The herd immunity threshold (HIT) can be calculated using the formula: $HIT = 1 - 1/R_0$, where R_0 (the basic reproduction number) represents the transmissibility of a virus. For the ancestral strain of SARS-CoV-2, this was estimated to be 2-4, so $HIT = 50-75\%$. However, the increased transmissibility of Alpha (~50% more transmissible than the ancestral strain) and Delta (~50% more transmissible than the Alpha variant) variants will result in higher R_0 values that drive up the HIT. Randolph and Barreiro also discussed additional considerations that must be appreciated when estimating HIT, “It relies on several key assumptions, including homogeneous mixing of individuals within a population and that all individuals develop sterilizing immunity—immunity that confers lifelong protection against reinfection—upon vaccination or natural infection. In real-world situations, these epidemiological and immunological assumptions are often not met, and the magnitude of indirect protection attributed to herd immunity will depend on variations in these assumptions” (Randolph and Barreiro 2020).

In sum, reaching herd immunity without vaccines would require somewhere between 50-90% of the population to get infected. At Alberta’s population of 4.4 million, this would equate to roughly 2.2-4 million people infected. Using a conservative death rate of 1% this would equate to 22,000-40,000 deaths. However, if SARS-Cov-2 was allowed to spread exponentially without NPIs, the real death toll would actually be much higher, as the death rate would necessarily increase for patients who cannot access healthcare resources.

As Randolph and Barreiro noted, “Particularly in the context of attaining herd immunity to SARS-CoV-2, a regard for finite healthcare resources cannot be overstated, as this policy inherently relies on allowing a large fraction of the population to become infected. Unchecked, the spread of SARS-CoV-2 will rapidly overwhelm healthcare systems. A depletion in healthcare resources will lead not only to elevated COVID-19 mortality but also to increased all-cause mortality. This effect will be especially devastating for countries in which hospitals have limited surge capacity, where minimal public health infrastructure exists, and among vulnerable communities, including prison and homeless populations”.

Krammer and colleagues recently investigated the effect of vaccines on previously infected individuals (Krammer et al. 2021). Their study involved 110 participants with or without pre-existing SARS-CoV-2 immunity. Vaccinees with pre-existing immunity developed antibody titers 10-45 times as high as those without pre-existing immunity at the same time point following the first vaccine dose. A second dose of vaccine in the Covid-19 survivors had no further enhancement on antibody titers. While vaccinees with pre-existing immunity had higher frequencies of local and systemic side effects, no severe adverse events were reported.

Following the emergence and global spread of the SARS-CoV-2 Delta variant, now considered a VOC, there has been an expeditious effort to define the transmissibility and sensitivity to immune responses for this variant. Transmissibility is now generally regarded as to be ~50% greater than the Alpha variant. A recent publication from Planas and colleagues suggests that sera from long-term convalescent patients had reduced capacity to neutralize the Delta variant (Planas D 2021). In contrast, vaccination of resulted in a strong humoral immune response within these individuals resulting in elevation of neutralizing antibodies well above the threshold of neutralization. The authors stated that vaccination of previously infected individuals would likely result in protection against SARS-CoV-2 variants.

6. Ongoing and Future Research

There are many aspects of Covid-19 that will need to be continually researched in both the short- and long-term. Notably, research into the further understanding of the specific host and viral factors that underlie transmission needs to continue (including the minimum infectious dose, virus concentrations and viability in indoor and outdoor settings). Thus, adherence to established nonpharmaceutical interventions should remain the focus of the global response pending further research. In addition, the paucity of frontline antiviral therapeutics for those that have symptomatic infections or are hospitalized are desperately needed. Lastly, detailed understanding of the role of social determinants in Covid-19 disease severity and transmission are desperately needed.

Long-term complications in Covid-19 recoverees

There is a growing appreciation that Covid-19 can result in extended health complications and abnormalities, independent of disease severity and age (Rubin 2020). These include extended fatigue, shortness of breath, joint and chest pain, and neurological complications. A recent study from Italy suggested that 44% of recovered patients reported a worsened quality of life post-Covid-19 (Carfi et al. 2020). A US study by Tenforde et al. reported that 35% of surveyed patients had not returned to their normal state of health two to three weeks following a positive Covid-19 test result with 20% of those surveyed being 18-34 years of age with no underlying chronic medical conditions at the time of survey (Tenforde et al. 2020).

Reproductive health concerns

Recent data has suggested that severe Covid-19 can result in reproductive tissue damage in males. An investigation by Ma et al. assessed pathology in the testes from males with fatal disease and found strong signs of germ cell damage and may indicate the potential for reproductive health impairment in severe disease (Ma et al. 2021). Yang and colleagues had similar observations for reproductive tissue damage in deceased male Covid-19 patients including seminiferous tubular injury, reduced Leydig cell populations and mild lymphocytic inflammation (Yang, Chen, et al. 2020). There have also been recent

insights regarding the potential for Covid-19-related complications during pregnancy. Yang et al. provide evidence that SARS-CoV-2 infection during late pregnancy is associated with increased risks of adverse birth outcomes (Yang, Mei, et al. 2020). Kotlyar et al. also recently provided evidence for vertical transmission of SARS-CoV-2 in the third trimester (Kotlyar et al. 2021). These data suggest that SARS-CoV-2 infections may have impacts on both reproductive health and pregnancy that could have detrimental impacts on younger populations.

In conclusion, data overwhelmingly suggests that both asymptomatic transmission and presymptomatic transmission contribute to SARS-CoV-2 transmission with increasing reports suggesting that presymptomatic transmission in particular plays an important role in these events. Given this, there is an inherent need to utilize nonpharmaceutical interventions including, but not limited to face masks, to reduce transmission events from those in our communities that are unaware that they are infected and contagious. Primary points of consideration include:

- **Morbidity and mortality:** while much of the pandemic has centered around the increasing fatalities nationally and globally, there has been less discussion regarding the effects of Covid-19 associated morbidity. Hospitalization data demonstrates that this disease can have health impacts on individuals across multiple age groups and adds significant stress on national healthcare systems and capacity.
- **SARS-CoV-2 transmission routes:** there is growing appreciation for the role of aerosols in SARS-CoV-2 transmission in addition to respiratory droplets. Aerosols have the potential for broader transmission within enclosed settings in the absence of multiple nonpharmaceutical interventions (including face masks, distancing, ventilation) and data demonstrates that aerosols may be an important factor in presymptomatic transmission of the virus.
- **Nonpharmaceutical interventions:** while there is strong evidence that face masks provide a benefit for reducing SARS-CoV-2 transmission they are not a single failsafe intervention measure. This requires a multi-faceted approach that includes multiple interventions due the synergistic effects these measures.
- **VOCs and herd immunity:** the recent emergence of SARS-CoV-2 variants of concern that have increased transmissibility and the immune evasion characteristics supports the need to curb transmission in the global community quickly prior to further variant emergence. VOCs may be able to circulate even in populations that have exceeded the proposed herd immunity threshold with potentially devastating public health consequences. Thus, approaches that combine nonpharmaceutical interventions in addition to expanding vaccination campaigns will have the greatest opportunity to curb community transmission of the virus expediently.

References

- Abedi, V., O. Olulana, V. Avula, D. Chaudhary, A. Khan, S. Shahjouei, J. Li, and R. Zand. 2021. 'Racial, Economic, and Health Inequality and COVID-19 Infection in the United States', *J Racial Ethn Health Disparities*, 8: 732-42.
- Agarwal S, Bhattacharya J. 2021. "Majority Indians have natural immunity. Vaccinating entire population can cause great harm." In *The Print*.
- Alsved M, Matamis A, Bohlin R, Richter M, Bengtsson P-E, Fraenkel C-J, Medstrand P, Londaal J. 2020. 'Exhaled respiratory particles during singing and talking', *Aerosol Sci Technol*, 54: 1245-48.
- Asadi, S., A. S. Wexler, C. D. Cappa, S. Barreda, N. M. Bouvier, and W. D. Ristenpart. 2019. 'Aerosol emission and superemission during human speech increase with voice loudness', *Sci Rep*, 9: 2348.
- Avanzato, V. A., M. J. Matson, S. N. Seifert, R. Pryce, B. N. Williamson, S. L. Anzick, K. Barbian, S. D. Judson, E. R. Fischer, C. Martens, T. A. Bowden, E. de Wit, F. X. Riedo, and V. J. Munster. 2020. 'Case Study: Prolonged Infectious SARS-CoV-2 Shedding from an Asymptomatic Immunocompromised Individual with Cancer', *Cell*, 183: 1901-12 e9.
- Bahl, P., C. de Silva, S. Bhattacharjee, H. Stone, C. Doolan, A. A. Chughtai, and C. R. MacIntyre. 2020. 'Droplets and Aerosols generated by singing and the risk of COVID-19 for choirs', *Clin Infect Dis*.
- Bi Q, Lessler J et al. 2021. 'Insights into household transmission of SARS-CoV-2 from a population-based serological survey', *Nat Commun*, 12: 3643.
- Brooks, J. T., and J. C. Butler. 2021. 'Effectiveness of Mask Wearing to Control Community Spread of SARS-CoV-2', *JAMA*, 325: 998-99.
- Buitrago-Garcia, D., D. Egli-Gany, M. J. Counotte, S. Hossmann, H. Imeri, A. M. Ipekci, G. Salanti, and N. Low. 2020. 'Occurrence and transmission potential of asymptomatic and presymptomatic SARS-CoV-2 infections: A living systematic review and meta-analysis', *PLoS Med*, 17: e1003346.
- Buss, L. F., C. A. Prete, Jr., C. M. M. Abraham, A. Mendrone, Jr., T. Salomon, C. de Almeida-Neto, R. F. O. Franca, M. C. Belotti, Mps Carvalho, A. G. Costa, M. A. E. Crispim, S. C. Ferreira, N. A. Fraiji, S. Gurzenda, C. Whittaker, L. T. Kamaura, P. L. Takecian, P. da Silva Peixoto, M. K. Oikawa, A. S. Nishiya, V. Rocha, N. A. Salles, A. A. de Souza Santos, M. A. da Silva, B. Custer, K. V. Parag, M. Barral-Netto, M. U. G. Kraemer, R. H. M. Pereira, O. G. Pybus, M. P. Busch, M. C. Castro, C. Dye, V. H. Nascimento, N. R. Faria, and E. C. Sabino. 2021. 'Three-quarters attack rate of SARS-CoV-2 in the Brazilian Amazon during a largely unmitigated epidemic', *Science*, 371: 288-92.
- Byambasuren O, Cardona M, Bell K, Clark J, McLaws M-L, Glasziou P. 2020. 'Estimating the extent of asymptomatic COVID-19 and its potential for community transmission: Systematic review and meta-analysis', *JAMMI*, 5: 223-34.
- Cai, J., W. Sun, J. Huang, M. Gamber, J. Wu, and G. He. 2020. 'Indirect Virus Transmission in Cluster of COVID-19 Cases, Wenzhou, China, 2020', *Emerg Infect Dis*, 26: 1343-45.
- Canada, Government of. 2020. 'Public health management of cases and contacts associated with COVID-19'. <https://www.canada.ca/en/public-health/services/diseases/2019-novel-coronavirus-infection/health-professionals/interim-guidance-cases-contacts.html>.
- Capobianchi, M. R., M. Rueca, F. Messina, E. Giombini, F. Carletti, F. Colavita, C. Castilletti, E. Lalle, L. Bordini, F. Vairo, E. Nicastri, G. Ippolito, C. E. M. Gruber, and B. Bartolini. 2020. 'Molecular characterization of SARS-CoV-2 from the first case of COVID-19 in Italy', *Clin Microbiol Infect*, 26: 954-56.
- Carfi, A., R. Bernabei, F. Landi, and Covid-Post-Acute Care Study Group Gemelli Against. 2020. 'Persistent Symptoms in Patients After Acute COVID-19', *JAMA*, 324: 603-05.
- CDC, US. 2021. 'Evidence used to update the list of underlying medical conditions that increase a person's risk of severe illness from COVID-19', US Centers for Disease Control and Prevention, Accessed 22 February. <https://www.cdc.gov/coronavirus/2019-ncov/need-extra-precautions/evidence-table.html>.

- Cevik, M., K. Kuppalli, J. Kindrachuk, and M. Peiris. 2020. 'Virology, transmission, and pathogenesis of SARS-CoV-2', *BMJ*, 371: m3862.
- Cevik, M., M. Tate, O. Lloyd, A. E. Maraolo, J. Schafers, and A. Ho. 2021. 'SARS-CoV-2, SARS-CoV, and MERS-CoV viral load dynamics, duration of viral shedding, and infectiousness: a systematic review and meta-analysis', *Lancet Microbe*, 2: e13-e22.
- Chan, J. F., S. Yuan, A. J. Zhang, V. K. Poon, C. C. Chan, A. C. Lee, Z. Fan, C. Li, R. Liang, J. Cao, K. Tang, C. Luo, V. C. Cheng, J. P. Cai, H. Chu, K. H. Chan, K. K. To, S. Sridhar, and K. Y. Yuen. 2020. 'Surgical Mask Partition Reduces the Risk of Noncontact Transmission in a Golden Syrian Hamster Model for Coronavirus Disease 2019 (COVID-19)', *Clin Infect Dis*, 71: 2139-49.
- Chen PZ, Bobrovitz N, Premji Z, Koopmans M, Fisman DN, Gu FX. 2021. 'SARS-CoV-2 Shedding Dynamics Across the Respiratory Tract, Sex, and Disease Severity for Adult and Pediatric COVID-19', *medRxiv*.
- Cheng, H. Y., S. W. Jian, D. P. Liu, T. C. Ng, W. T. Huang, H. H. Lin, and Covid-Outbreak Investigation Team Taiwan. 2020. 'Contact Tracing Assessment of COVID-19 Transmission Dynamics in Taiwan and Risk at Different Exposure Periods Before and After Symptom Onset', *JAMA Intern Med*, 180: 1156-63.
- Chertow, D. S., J. Kindrachuk, Z. M. Sheng, L. M. Pujanauskí, K. Cooper, D. Noguee, M. S. Claire, J. Solomon, D. Perry, P. Sayre, K. B. Janosko, M. G. Lackemeyer, J. K. Bohannon, J. C. Kash, P. B. Jahrling, and J. K. Taubenberger. 2016. 'Influenza A and methicillin-resistant *Staphylococcus aureus* co-infection in rhesus macaques - A model of severe pneumonia', *Antiviral Res*, 129: 120-29.
- Choi, B., M. C. Choudhary, J. Regan, J. A. Sparks, R. F. Padera, X. Qiu, I. H. Solomon, H. H. Kuo, J. Boucau, K. Bowman, U. D. Adhikari, M. L. Winkler, A. A. Mueller, T. Y. Hsu, M. Desjardins, L. R. Baden, B. T. Chan, B. D. Walker, M. Lichterfeld, M. Brigl, D. S. Kwon, S. Kanjilal, E. T. Richardson, A. H. Jonsson, G. Alter, A. K. Barczak, W. P. Hanage, X. G. Yu, G. D. Gaiha, M. S. Seaman, M. Cernadas, and J. Z. Li. 2020. 'Persistence and Evolution of SARS-CoV-2 in an Immunocompromised Host', *N Engl J Med*, 383: 2291-93.
- Chung, E., E. J. Chow, N. C. Wilcox, R. Burstein, E. Brandstetter, P. D. Han, K. Fay, B. Pfau, A. Adler, K. Lacombe, C. M. Lockwood, T. M. Uyeki, J. Shendure, J. S. Duchin, M. J. Rieder, D. A. Nickerson, M. Boeckh, M. Famulare, J. P. Hughes, L. M. Starita, T. Bedford, J. A. Englund, and H. Y. Chu. 2021. 'Comparison of Symptoms and RNA Levels in Children and Adults With SARS-CoV-2 Infection in the Community Setting', *JAMA Pediatr*.
- Cowling, B. J., S. T. Ali, T. W. Y. Ng, T. K. Tsang, J. C. M. Li, M. W. Fong, Q. Liao, M. Y. Kwan, S. L. Lee, S. S. Chiu, J. T. Wu, P. Wu, and G. M. Leung. 2020. 'Impact assessment of non-pharmaceutical interventions against coronavirus disease 2019 and influenza in Hong Kong: an observational study', *Lancet Public Health*, 5: e279-e88.
- Das, K. M., E. Y. Lee, R. Singh, M. A. Enani, K. Al Dossari, K. Van Gorkom, S. G. Larsson, and R. D. Langer. 2017. 'Follow-up chest radiographic findings in patients with MERS-CoV after recovery', *Indian J Radiol Imaging*, 27: 342-49.
- Davis, A. S., D. S. Chertow, J. Kindrachuk, L. Qi, L. M. Schwartzman, J. Suzich, S. Alsaaty, C. Logun, J. H. Shelhamer, and J. K. Taubenberger. 2016. '1918 Influenza receptor binding domain variants bind and replicate in primary human airway cells regardless of receptor specificity', *Virology*, 493: 238-46.
- Deshmukh, V., R. Motwani, A. Kumar, C. Kumari, and K. Raza. 2021. 'Histopathological observations in COVID-19: a systematic review', *J Clin Pathol*, 74: 76-83.
- Dong, Y., X. Mo, Y. Hu, X. Qi, F. Jiang, Z. Jiang, and S. Tong. 2020. 'Epidemiology of COVID-19 Among Children in China', *Pediatrics*, 145.
- Dyall, J., C. M. Coleman, B. J. Hart, T. Venkataraman, M. R. Holbrook, J. Kindrachuk, R. F. Johnson, G. G. Olinger, Jr., P. B. Jahrling, M. Laidlaw, L. M. Johansen, C. M. Lear-Rooney, P. J. Glass, L. E. Hensley, and M. B. Frieman. 2014. 'Repurposing of clinically developed drugs for treatment of Middle East respiratory syndrome coronavirus infection', *Antimicrob Agents Chemother*, 58: 4885-93.
- Dyall, J., R. Gross, J. Kindrachuk, R. F. Johnson, G. G. Olinger, Jr., L. E. Hensley, M. B. Frieman, and P. B. Jahrling. 2017. 'Middle East Respiratory Syndrome and Severe Acute Respiratory Syndrome: Current Therapeutic Options and Potential Targets for Novel Therapies', *Drugs*, 77: 1935-66.

- Falcinelli, S. D., D. S. Chertow, and J. Kindrachuk. 2016. 'Integration of Global Analyses of Host Molecular Responses with Clinical Data To Evaluate Pathogenesis and Advance Therapies for Emerging and Re-emerging Viral Infections', *ACS Infect Dis*, 2: 787-99.
- Fischer, C. B., N. Adrien, J. J. Silguero, J. J. Hopper, A. I. Chowdhury, and M. M. Werler. 2021. 'Mask adherence and rate of COVID-19 across the United States', *PLoS One*, 16: e0249891.
- Flaxman, S., S. Mishra, A. Gandy, H. J. T. Unwin, T. A. Mellan, H. Coupland, C. Whittaker, H. Zhu, T. Berah, J. W. Eaton, M. Monod, Covid-Response Team Imperial College, A. C. Ghani, C. A. Donnelly, S. Riley, M. A. C. Vollmer, N. M. Ferguson, L. C. Okell, and S. Bhatt. 2020. 'Estimating the effects of non-pharmaceutical interventions on COVID-19 in Europe', *Nature*, 584: 257-61.
- Gotzinger, F., B. Santiago-Garcia, A. Noguera-Julian, M. Lanaspá, L. Lancellata, F. I. Calo Carducci, N. Gabrovská, S. Velizarova, P. Prunk, V. Osterman, U. Krivec, A. Lo Vecchio, D. Shingadia, A. Soriano-Arandes, S. Melendo, M. Lanari, L. Pierantoni, N. Wagner, A. G. L'Huillier, U. Heininger, N. Ritz, S. Bandi, N. Krajcar, S. Roglic, M. Santos, C. Christiaens, M. Creuven, D. Buonsenso, S. B. Welch, M. Bogyi, F. Brinkmann, M. Tebruegge, and Covid-Study Group ptbnet. 2020. 'COVID-19 in children and adolescents in Europe: a multinational, multicentre cohort study', *Lancet Child Adolesc Health*, 4: 653-61.
- Guan, W. J., Z. Y. Ni, Y. Hu, W. H. Liang, C. Q. Ou, J. X. He, L. Liu, H. Shan, C. L. Lei, D. S. C. Hui, B. Du, L. J. Li, G. Zeng, K. Y. Yuen, R. C. Chen, C. L. Tang, T. Wang, P. Y. Chen, J. Xiang, S. Y. Li, J. L. Wang, Z. J. Liang, Y. X. Peng, L. Wei, Y. Liu, Y. H. Hu, P. Peng, J. M. Wang, J. Y. Liu, Z. Chen, G. Li, Z. J. Zheng, S. Q. Qiu, J. Luo, C. J. Ye, S. Y. Zhu, N. S. Zhong, and Covid China Medical Treatment Expert Group for. 2020. 'Clinical Characteristics of Coronavirus Disease 2019 in China', *N Engl J Med*, 382: 1708-20.
- Hamner, L., P. Dubbel, I. Capron, A. Ross, A. Jordan, J. Lee, J. Lynn, A. Ball, S. Narwal, S. Russell, D. Patrick, and H. Leibrand. 2020. 'High SARS-CoV-2 Attack Rate Following Exposure at a Choir Practice - Skagit County, Washington, March 2020', *MMWR Morb Mortal Wkly Rep*, 69: 606-10.
- Hart, B. J., J. Dyal, E. Postnikova, H. Zhou, J. Kindrachuk, R. F. Johnson, G. G. Olinger, M. B. Frieman, M. R. Holbrook, P. B. Jahrling, and L. Hensley. 2014. 'Interferon-beta and mycophenolic acid are potent inhibitors of Middle East respiratory syndrome coronavirus in cell-based assays', *J Gen Virol*, 95: 571-77.
- Horby P, Huntley C, Davies N, Edmunds J, Ferguson N, Medley G, Semple C. 2021. "NERVTAG paper on COVID-19 variant of concern B.1.1.7 " In.: New and Emerging Respiratory Virus Threats Advisory Group.
- Huang, L., X. Zhang, X. Zhang, Z. Wei, L. Zhang, J. Xu, P. Liang, Y. Xu, C. Zhang, and A. Xu. 2020. 'Rapid asymptomatic transmission of COVID-19 during the incubation period demonstrating strong infectivity in a cluster of youngsters aged 16-23 years outside Wuhan and characteristics of young patients with COVID-19: A prospective contact-tracing study', *J Infect*, 80: e1-e13.
- Hui, D. S., G. M. Joynt, K. T. Wong, C. D. Gomersall, T. S. Li, G. Antonio, F. W. Ko, M. C. Chan, D. P. Chan, M. W. Tong, T. H. Rainer, A. T. Ahuja, C. S. Cockram, and J. J. Sung. 2005. 'Impact of severe acute respiratory syndrome (SARS) on pulmonary function, functional capacity and quality of life in a cohort of survivors', *Thorax*, 60: 401-9.
- James, A., L. Eagle, C. Phillips, D. S. Hedges, C. Bodenhamer, R. Brown, J. G. Wheeler, and H. Kirking. 2020. 'High COVID-19 Attack Rate Among Attendees at Events at a Church - Arkansas, March 2020', *MMWR Morb Mortal Wkly Rep*, 69: 632-35.
- Jang, S., S. H. Han, and J. Y. Rhee. 2020. 'Cluster of Coronavirus Disease Associated with Fitness Dance Classes, South Korea', *Emerg Infect Dis*, 26: 1917-20.
- Jary, A., V. Leducq, I. Malet, S. Marot, E. Klement-Frutos, E. Teyssou, C. Soulie, B. Abdi, M. Wirten, V. Pourcher, E. Caumes, V. Calvez, S. Burrel, A. G. Marcelin, and D. Boutolleau. 2020. 'Evolution of viral quasiespecies during SARS-CoV-2 infection', *Clin Microbiol Infect*, 26: 1560 e1-60 e4.
- Johansson, M. A., T. M. Quandelacy, S. Kada, P. V. Prasad, M. Steele, J. T. Brooks, R. B. Slayton, M. Biggerstaff, and J. C. Butler. 2021. 'SARS-CoV-2 Transmission From People Without COVID-19 Symptoms', *JAMA Netw Open*, 4: e2035057.
- Katelaris, A. L., J. Wells, P. Clark, S. Norton, R. Rockett, A. Arnott, V. Sintchenko, S. Corbett, and S. K. Bag. 2021. 'Epidemiologic Evidence for Airborne Transmission of SARS-CoV-2 during Church Singing, Australia, 2020', *Emerg Infect Dis*, 27: 1677-80.

- Kemp, S. A., D. A. Collier, R. P. Datir, Iatm Ferreira, S. Gayed, A. Jahun, M. Hosmillo, C. Rees-Spear, P. Mlcochova, I. U. Lumb, D. J. Roberts, A. Chandra, N. Temperton, Citiid-Nihr BioResource COVID-19 Collaboration, Covid- Genomics UK Consortium, K. Sharrocks, E. Blane, Y. Modis, K. E. Leigh, J. A. G. Briggs, M. J. van Gils, K. G. C. Smith, J. R. Bradley, C. Smith, R. Doffinger, L. Ceron-Gutierrez, G. Barcenias-Morales, D. D. Pollock, R. A. Goldstein, A. Smielewska, J. P. Skittrall, T. Gouliouris, I. G. Goodfellow, E. Gkrania-Klotsas, C. J. R. Illingworth, L. E. McCoy, and R. K. Gupta. 2021. 'SARS-CoV-2 evolution during treatment of chronic infection', *Nature*, 592: 277-82.
- Kim, E. S., B. S. Chin, C. K. Kang, N. J. Kim, Y. M. Kang, J. P. Choi, D. H. Oh, J. H. Kim, B. Koh, S. E. Kim, N. R. Yun, J. H. Lee, J. Y. Kim, Y. Kim, J. H. Bang, K. H. Song, H. B. Kim, K. H. Chung, M. D. Oh, and Covid Korea National Committee for Clinical Management of. 2020. 'Clinical Course and Outcomes of Patients with Severe Acute Respiratory Syndrome Coronavirus 2 Infection: a Preliminary Report of the First 28 Patients from the Korean Cohort Study on COVID-19', *J Korean Med Sci*, 35: e142.
- Kim, Y. I., S. G. Kim, S. M. Kim, E. H. Kim, S. J. Park, K. M. Yu, J. H. Chang, E. J. Kim, S. Lee, M. A. B. Casel, J. Um, M. S. Song, H. W. Jeong, V. D. Lai, Y. Kim, B. S. Chin, J. S. Park, K. H. Chung, S. S. Foo, H. Poo, I. P. Mo, O. J. Lee, R. J. Webby, J. U. Jung, and Y. K. Choi. 2020. 'Infection and Rapid Transmission of SARS-CoV-2 in Ferrets', *Cell Host Microbe*, 27: 704-09 e2.
- Kimball, A., K. M. Hatfield, M. Arons, A. James, J. Taylor, K. Spicer, A. C. Bardossy, L. P. Oakley, S. Tanwar, Z. Chisty, J. M. Bell, M. Methner, J. Harney, J. R. Jacobs, C. M. Carlson, H. P. McLaughlin, N. Stone, S. Clark, C. Brostrom-Smith, L. C. Page, M. Kay, J. Lewis, D. Russell, B. Hiatt, J. Gant, J. S. Duchin, T. A. Clark, M. A. Honein, S. C. Reddy, J. A. Jernigan, Seattle Public Health, County King, and Cdc Covid- Investigation Team. 2020. 'Asymptomatic and Presymptomatic SARS-CoV-2 Infections in Residents of a Long-Term Care Skilled Nursing Facility - King County, Washington, March 2020', *MMWR Morb Mortal Wkly Rep*, 69: 377-81.
- Kindrachuk, J., R. Arsenault, A. Kusalik, K. N. Kindrachuk, B. Trost, S. Napper, P. B. Jahrling, and J. E. Blaney. 2012. 'Systems kinomics demonstrates Congo Basin monkeypox virus infection selectively modulates host cell signaling responses as compared to West African monkeypox virus', *Mol Cell Proteomics*, 11: M111 015701.
- Kindrachuk, J., B. Ork, B. J. Hart, S. Mazur, M. R. Holbrook, M. B. Frieman, D. Traynor, R. F. Johnson, J. Dyal, J. H. Kuhn, G. G. Olinger, L. E. Hensley, and P. B. Jahrling. 2015. 'Antiviral potential of ERK/MAPK and PI3K/AKT/mTOR signaling modulation for Middle East respiratory syndrome coronavirus infection as identified by temporal kinome analysis', *Antimicrob Agents Chemother*, 59: 1088-99.
- Kotlyar, A. M., O. Grechukhina, A. Chen, S. Popkhadze, A. Grimshaw, O. Tal, H. S. Taylor, and R. Tal. 2021. 'Vertical transmission of coronavirus disease 2019: a systematic review and meta-analysis', *Am J Obstet Gynecol*, 224: 35-53 e3.
- Krammer, F., K. Srivastava, H. Alshammary, A. A. Amoako, M. H. Awawda, K. F. Beach, M. C. Bermudez-Gonzalez, D. A. Bielak, J. M. Carreno, R. L. Chernet, L. Q. Eaker, E. D. Ferreri, D. L. Floda, C. R. Gleason, J. Z. Hamburger, K. Jiang, G. Kleiner, D. Jurczynszak, J. C. Matthews, W. A. Mendez, I. Nabeel, L. C. F. Mulder, A. J. Raskin, K. T. Russo, A. T. Salimbangon, M. Saksena, A. S. Shin, G. Singh, L. A. Sominsky, D. Stadlbauer, A. Wajnberg, and V. Simon. 2021. 'Antibody Responses in Seropositive Persons after a Single Dose of SARS-CoV-2 mRNA Vaccine', *N Engl J Med*, 384: 1372-74.
- Lai, S., N. W. Ruktanonchai, L. Zhou, O. Prosper, W. Luo, J. R. Floyd, A. Wesolowski, M. Santillana, C. Zhang, X. Du, H. Yu, and A. J. Tatem. 2020. 'Effect of non-pharmaceutical interventions to contain COVID-19 in China', *Nature*, 585: 410-13.
- Lauring, A. S., and E. B. Hodcroft. 2021. 'Genetic Variants of SARS-CoV-2-What Do They Mean?', *JAMA*, 325: 529-31.
- Leclerc, Q. J., N. M. Fuller, L. E. Knight, Cmmid Covid- Working Group, S. Funk, and G. M. Knight. 2020. 'What settings have been linked to SARS-CoV-2 transmission clusters?', *Wellcome Open Res*, 5: 83.
- Li, F., Y. Y. Li, M. J. Liu, L. Q. Fang, N. E. Dean, G. W. K. Wong, X. B. Yang, I. Longini, M. E. Halloran, H. J. Wang, P. L. Liu, Y. H. Pang, Y. Q. Yan, S. Liu, W. Xia, X. X. Lu, Q. Liu, Y. Yang, and S. Q. Xu. 2021. 'Household

- transmission of SARS-CoV-2 and risk factors for susceptibility and infectivity in Wuhan: a retrospective observational study', *Lancet Infect Dis*.
- Lindsley, W. G., F. M. Blachere, D. H. Beezhold, R. E. Thewlis, B. Noorbakhsh, S. Othumpangat, W. T. Goldsmith, C. M. McMillen, M. E. Andrew, C. N. Burrell, and J. D. Noti. 2016. 'Viable influenza A virus in airborne particles expelled during coughs versus exhalations', *Influenza Other Respir Viruses*, 10: 404-13.
- Liu, Z., R. Chu, L. Gong, B. Su, and J. Wu. 2020. 'The assessment of transmission efficiency and latent infection period in asymptomatic carriers of SARS-CoV-2 infection', *Int J Infect Dis*, 99: 325-27.
- Lopez, A. S., M. Hill, J. Antezano, D. Vilven, T. Rutner, L. Bogdanow, C. Claflin, I. T. Kracalik, V. L. Fields, A. Dunn, J. E. Tate, H. L. Kirking, T. Kiphibane, I. Risk, and C. H. Tran. 2020. 'Transmission Dynamics of COVID-19 Outbreaks Associated with Child Care Facilities - Salt Lake City, Utah, April-July 2020', *MMWR Morb Mortal Wkly Rep*, 69: 1319-23.
- Lu, J., and Z. Yang. 2020. 'COVID-19 Outbreak Associated with Air Conditioning in Restaurant, Guangzhou, China, 2020', *Emerg Infect Dis*, 26: 2791-93.
- Ma, X., C. Guan, R. Chen, Y. Wang, S. Feng, R. Wang, G. Qu, S. Zhao, F. Wang, X. Wang, D. Zhang, L. Liu, A. Liao, and S. Yuan. 2021. 'Pathological and molecular examinations of postmortem testis biopsies reveal SARS-CoV-2 infection in the testis and spermatogenesis damage in COVID-19 patients', *Cell Mol Immunol*, 18: 487-89.
- Malenfant, J. H., C. N. Newhouse, and A. A. Kuo. 2020. 'Frequency of coronavirus disease 2019 (COVID-19) symptoms in healthcare workers in a large health system', *Infect Control Hosp Epidemiol*: 1-2.
- Murbe, D., M. Kriegel, J. Lange, L. Schumann, A. Hartmann, and M. Fleischer. 2021. 'Aerosol emission of adolescents voices during speaking, singing and shouting', *PLoS One*, 16: e0246819.
- Murhekar MV, Bhatnagar T, Thangaraj JWV et al. 2021. 'SARS-CoV-2 Sero-Prevalence among General Population and Healthcare Workers in India, December 2020 - January 2021', *SSRN*.
- Naveca F, da Costa C, Nascimento V et al. 2021. 'SARS-CoV-2 reinfection by the new Variant of Concern (VOC) P.1 in Amazonas, Brazil'. <https://virological.org/t/sars-cov-2-reinfection-by-the-new-variant-of-concern-voc-p-1-in-amazonas-brazil/596>.
- Nickol, M. E., J. Ciric, S. D. Falcinelli, D. S. Chertow, and J. Kindrachuk. 2019. 'Characterization of Host and Bacterial Contributions to Lung Barrier Dysfunction Following Co-infection with 2009 Pandemic Influenza and Methicillin Resistant Staphylococcus aureus', *Viruses*, 11.
- Nickol, M. E., and J. Kindrachuk. 2019. 'A year of terror and a century of reflection: perspectives on the great influenza pandemic of 1918-1919', *BMC Infect Dis*, 19: 117.
- Niesen MJM, Anand P, Silvert E, Suratekar R, Pawlowski C, Ghosh P, Lenehan P, Hughes T, Zemmour D, O'Horo JC, Yao JD, Pritt BS, Norgan A, Hurt RT, Badley AD, Venkatakrishnan AJ, Soundararajan V. 2021. 'COVID-19 vaccines dampen genomic diversity of SARS-CoV-2: Unvaccinated patients exhibit more antigenic mutational variance', *medRxiv*.
- Ooi, G. C., P. L. Khong, N. L. Muller, W. C. Yiu, L. J. Zhou, J. C. Ho, B. Lam, S. Nicolaou, and K. W. Tsang. 2004. 'Severe acute respiratory syndrome: temporal lung changes at thin-section CT in 30 patients', *Radiology*, 230: 836-44.
- Orellana, J. D. Y., G. M. D. Cunha, L. Marrero, B. L. Horta, and I. D. C. Leite. 2020. 'Explosion in mortality in the Amazonian epicenter of the COVID-19 epidemic 19', *Cad Saude Publica*, 36: e00120020.
- Park, S. Y., Y. M. Kim, S. Yi, S. Lee, B. J. Na, C. B. Kim, J. I. Kim, H. S. Kim, Y. B. Kim, Y. Park, I. S. Huh, H. K. Kim, H. J. Yoon, H. Jang, K. Kim, Y. Chang, I. Kim, H. Lee, J. Gwack, S. S. Kim, M. Kim, S. Kweon, Y. J. Choe, O. Park, Y. J. Park, and E. K. Jeong. 2020. 'Coronavirus Disease Outbreak in Call Center, South Korea', *Emerg Infect Dis*, 26: 1666-70.
- Park, Y. J., Y. J. Choe, O. Park, S. Y. Park, Y. M. Kim, J. Kim, S. Kweon, Y. Woo, J. Gwack, S. S. Kim, J. Lee, J. Hyun, B. Ryu, Y. S. Jang, H. Kim, S. H. Shin, S. Yi, S. Lee, H. K. Kim, H. Lee, Y. Jin, E. Park, S. W. Choi, M. Kim, J. Song, S. W. Choi, D. Kim, B. H. Jeon, H. Yoo, E. K. Jeong, Epidemiology Covid-19 National Emergency Response Center, and Team Case Management. 2020. 'Contact Tracing during Coronavirus Disease Outbreak, South Korea, 2020', *Emerg Infect Dis*, 26: 2465-68.

- Planas D, Veyer D, Baidaliuk A et al. 2021. 'Reduced sensitivity of SARS-CoV-2 variant Delta to antibody neutralization', *Nature*.
- Pratt, C. Q., A. N. Chard, R. LaPine, K. W. Galbreath, C. Crawford, A. Plant, G. Stiffarm, N. S. Rhodes, L. Hannon, and T. H. Dinh. 2021. 'Use of Stay-at-Home Orders and Mask Mandates to Control COVID-19 Transmission - Blackfeet Tribal Reservation, Montana, June-December 2020', *MMWR Morb Mortal Wkly Rep*, 70: 514-18.
- Qian, H., T. Miao, L. Liu, X. Zheng, D. Luo, and Y. Li. 2020. 'Indoor transmission of SARS-CoV-2', *Indoor Air*.
- Qiu, X., A. I. Nergiz, A. E. Maraolo, Bogoch, II, N. Low, and M. Cevik. 2021. 'Defining the role of asymptomatic and pre-symptomatic SARS-CoV-2 transmission - a living systematic review', *Clin Microbiol Infect*.
- Ralph, R., J. Lew, T. Zeng, M. Francis, B. Xue, M. Roux, A. Toloue Ostadgavahi, S. Rubino, N. J. Dawe, M. N. Al-Ahdal, D. J. Kelvin, C. D. Richardson, J. Kindrachuk, D. Falzarano, and A. A. Kelvin. 2020. '2019-nCoV (Wuhan virus), a novel Coronavirus: human-to-human transmission, travel-related cases, and vaccine readiness', *J Infect Dev Ctries*, 14: 3-17.
- Rambaut A, Loman N, Pybus O, Barclay W, Barrett J, Carabelli A, Connor T, Peacock T, Robertson DL, Volz E, COVID-19 Genomics Consortium UK. 2020. 'Preliminary genomic characterisation of an emergent SARS-CoV-2 lineage in the UK defined by a novel set of spike mutations', *Virological*, Accessed 29 April 2021. <https://virological.org/t/preliminary-genomic-characterisation-of-an-emergent-sars-cov-2-lineage-in-the-uk-defined-by-a-novel-set-of-spike-mutations/563>.
- Randolph, H. E., and L. B. Barreiro. 2020. 'Herd Immunity: Understanding COVID-19', *Immunity*, 52: 737-41.
- Resende PC, Bezerra JF, de Vasconcelos RH et al. 2021. 'Spike E484K mutation in the first SARS-CoV-2 reinfection case confirmed in Brazil, 2020'. <https://virological.org/t/spike-e484k-mutation-in-the-first-sars-cov-2-reinfection-case-confirmed-in-brazil-2020/584>.
- Richard, M., A. Kok, D. de Meulder, T. M. Bestebroer, M. M. Lamers, N. M. A. Okba, M. Fentener van Vlissingen, B. Rockx, B. L. Haagmans, M. P. G. Koopmans, R. A. M. Fouchier, and S. Herfst. 2020. 'SARS-CoV-2 is transmitted via contact and via the air between ferrets', *Nat Commun*, 11: 3496.
- Ruba, A. L., and S. D. Pollak. 2020. 'Children's emotion inferences from masked faces: Implications for social interactions during COVID-19', *PLoS One*, 15: e0243708.
- Rubin, R. 2020. 'As Their Numbers Grow, COVID-19 "Long Haulers" Stump Experts', *JAMA*.
- Sabino, E. C., L. F. Buss, M. P. S. Carvalho, C. A. Prete, Jr., M. A. E. Crispim, N. A. Fraiji, R. H. M. Pereira, K. V. Parag, P. da Silva Peixoto, M. U. G. Kraemer, M. K. Oikawa, T. Salomon, Z. M. Cucunuba, M. C. Castro, A. A. de Souza Santos, V. H. Nascimento, H. S. Pereira, N. M. Ferguson, O. G. Pybus, A. Kucharski, M. P. Busch, C. Dye, and N. R. Faria. 2021. 'Resurgence of COVID-19 in Manaus, Brazil, despite high seroprevalence', *Lancet*, 397: 452-55.
- Shen, Z., Y. Xiao, L. Kang, W. Ma, L. Shi, L. Zhang, Z. Zhou, J. Yang, J. Zhong, D. Yang, L. Guo, G. Zhang, H. Li, Y. Xu, M. Chen, Z. Gao, J. Wang, L. Ren, and M. Li. 2020. 'Genomic Diversity of Severe Acute Respiratory Syndrome-Coronavirus 2 in Patients With Coronavirus Disease 2019', *Clin Infect Dis*, 71: 713-20.
- Shim, E., A. Tariq, W. Choi, Y. Lee, and G. Chowell. 2020. 'Transmission potential and severity of COVID-19 in South Korea', *Int J Infect Dis*, 93: 339-44.
- Sia, S. F., L. M. Yan, A. W. H. Chin, K. Fung, K. T. Choy, A. Y. L. Wong, P. Kaewpreedee, Rapm Perera, L. L. M. Poon, J. M. Nicholls, M. Peiris, and H. L. Yen. 2020. 'Pathogenesis and transmission of SARS-CoV-2 in golden hamsters', *Nature*, 583: 834-38.
- Szablewski, C. M., K. T. Chang, M. M. Brown, V. T. Chu, A. R. Yousaf, N. Anyalechi, P. A. Aryee, H. L. Kirking, M. Lumsden, E. Mayweather, C. J. McDaniel, R. Montierth, A. Mohammed, N. G. Schwartz, J. A. Shah, J. E. Tate, E. Dirlikov, C. Drenzek, T. M. Lanzieri, and R. J. Stewart. 2020. 'SARS-CoV-2 Transmission and Infection Among Attendees of an Overnight Camp - Georgia, June 2020', *MMWR Morb Mortal Wkly Rep*, 69: 1023-25.
- Team, Cdc Covid- Response. 2020. 'Coronavirus Disease 2019 in Children - United States, February 12-April 2, 2020', *MMWR Morb Mortal Wkly Rep*, 69: 422-26.
- Tenforde, M. W., S. S. Kim, C. J. Lindsell, E. Billig Rose, N. I. Shapiro, D. C. Files, K. W. Gibbs, H. L. Erickson, J. S. Steingrub, H. A. Smithline, M. N. Gong, M. S. Aboodi, M. C. Exline, D. J. Henning, J. G. Wilson, A. Khan, N.

- Qadir, S. M. Brown, I. D. Peltan, T. W. Rice, D. N. Hager, A. A. Ginde, W. B. Stubblefield, M. M. Patel, W. H. Self, L. R. Feldstein, I. V. Y. Network Investigators, Cdc Covid- Response Team, and I. V. Y. Network Investigators. 2020. 'Symptom Duration and Risk Factors for Delayed Return to Usual Health Among Outpatients with COVID-19 in a Multistate Health Care Systems Network - United States, March-June 2020', *MMWR Morb Mortal Wkly Rep*, 69: 993-98.
- Trauer JM, Lydeamore MJ, Dalton GW, Pilcher D, Meehan MT, McBryde ES, Cheng AC, Sutton B, Ragonnet R. 2021. 'Understanding how Victoria, Australia gained control of its second COVID-19 wave', *medRxiv*.
- Vasques Nonaka, C.K.; Miranda Franco, M.; Gräf, T.; Almeida Mendes, A.V.; Santana de Aguiar, R.; Giovanetti, M.; Solano de Freitas Souza, B. 2021. 'Genomic Evidence of a Sars-Cov-2 Reinfection Case With E484K Spike Mutation in Brazil', *Preprints*.
- Walters, K. A., F. D'Agnillo, Z. M. Sheng, J. Kindrachuk, L. M. Schwartzman, R. E. Kuestner, D. S. Chertow, B. T. Golding, J. K. Taubenberger, and J. C. Kash. 2016. '1918 pandemic influenza virus and Streptococcus pneumoniae co-infection results in activation of coagulation and widespread pulmonary thrombosis in mice and humans', *J Pathol*, 238: 85-97.
- Wang, Y., H. Tian, L. Zhang, M. Zhang, D. Guo, W. Wu, X. Zhang, G. L. Kan, L. Jia, D. Huo, B. Liu, X. Wang, Y. Sun, Q. Wang, P. Yang, and C. R. MacIntyre. 2020. 'Reduction of secondary transmission of SARS-CoV-2 in households by face mask use, disinfection and social distancing: a cohort study in Beijing, China', *BMJ Glob Health*, 5.
- Wei, W. E., Z. Li, C. J. Chiew, S. E. Yong, M. P. Toh, and V. J. Lee. 2020. 'Presymptomatic Transmission of SARS-CoV-2 - Singapore, January 23-March 16, 2020', *MMWR Morb Mortal Wkly Rep*, 69: 411-15.
- Willman, M., D. Kobasa, and J. Kindrachuk. 2019. 'A Comparative Analysis of Factors Influencing Two Outbreaks of Middle Eastern Respiratory Syndrome (MERS) in Saudi Arabia and South Korea', *Viruses*, 11.
- Wolfel, R., V. M. Corman, W. Guggemos, M. Seilmaier, S. Zange, M. A. Muller, D. Niemeyer, T. C. Jones, P. Vollmar, C. Rothe, M. Hoelscher, T. Bleicker, S. Brunink, J. Schneider, R. Ehmann, K. Zwirgmaier, C. Drosten, and C. Wendtner. 2020. 'Virological assessment of hospitalized patients with COVID-2019', *Nature*, 581: 465-69.
- Yang, M., S. Chen, B. Huang, J. M. Zhong, H. Su, Y. J. Chen, Q. Cao, L. Ma, J. He, X. F. Li, X. Li, J. J. Zhou, J. Fan, D. J. Luo, X. N. Chang, K. Arkun, M. Zhou, and X. Nie. 2020. 'Pathological Findings in the Testes of COVID-19 Patients: Clinical Implications', *Eur Urol Focus*, 6: 1124-29.
- Yang, R., H. Mei, T. Zheng, Q. Fu, Y. Zhang, S. Buka, X. Yao, Z. Tang, X. Zhang, L. Qiu, Y. Zhang, J. Zhou, J. Cao, Y. Wang, and A. Zhou. 2020. 'Pregnant women with COVID-19 and risk of adverse birth outcomes and maternal-fetal vertical transmission: a population-based cohort study in Wuhan, China', *BMC Med*, 18: 330.
- Zou, L., F. Ruan, M. Huang, L. Liang, H. Huang, Z. Hong, J. Yu, M. Kang, Y. Song, J. Xia, Q. Guo, T. Song, J. He, H. L. Yen, M. Peiris, and J. Wu. 2020. 'SARS-CoV-2 Viral Load in Upper Respiratory Specimens of Infected Patients', *N Engl J Med*, 382: 1177-79.

Schedule B

Jason Kindrachuk, PhD

Laboratory of Emerging and Re-emerging Viruses
 Department of Medical Microbiology & Infectious Diseases
 University of Manitoba
 Winnipeg, MB, Canada
 Tel: (204) 789-3807
 Email: Jason.Kindrachuk@umanitoba.ca

EDUCATION

- 2002-2007 **Ph.D., Department of Biochemistry**
 University of Saskatchewan, Saskatoon, SK, Canada
 Supervisor: Dr. Scott Napper
 Thesis Title: *Host and Pathogen Sensory Systems as Targets for Therapeutic Intervention*
- 1996-2001 **B.Sc. (Honors), Department of Biochemistry**
 University of Saskatchewan, Saskatoon, SK, Canada

PROFESSIONAL EXPERIENCE

- 2017-present **Assistant Professor**
Canada Research Chair
 Laboratory of Emerging and Re-Emerging Viruses
 Department of Medical Microbiology and Infectious Diseases
 University of Manitoba
 Winnipeg, MB
- Associate Professor**
 Department of Biochemistry
 College of Medicine and Allied Health Sciences
 University of Sierra Leone
 Freetown, Sierra Leone
- 2014-2016 **Staff Scientist**
 Critical Care Medicine Department
 Clinical Center
 National Institutes of Health, Bethesda, MD, USA
- Sept 2014 **Scientific Lead – Field Diagnostics**
 Ebola Virus Disease Outbreak Response Efforts
 Centers for Disease Control/Department of Defense Joint Operations
 Monrovia, Liberia
- 2013-2014 **Principal Research Scientist**
 Battelle Memorial Institute
 Integrated Research Facility
 National Institutes of Allergy and Infectious Diseases
 National Institutes of Health, Frederick, MD, USA

- 2009-2013 **Visiting Fellow**
Emerging Viral Pathogens Section
National Institutes of Allergy and Infectious Diseases
National Institutes of Health, Bethesda, MD, USA
- 2007-2009 **Postdoctoral Fellow**
Centre for Microbial Diseases and Immunity Research
Department of Microbiology and Immunology
University of British Columbia, Vancouver, BC, Canada

SCIENTIFIC AFFILIATIONS & COMMITTEE ACTIVITIES

Affiliations

- 2020-present **Visiting Scientist** – Vaccine and Infectious Disease Organization-International Vaccine Centre
- 2020-present **Science Contributor** – Forbes Media, LLC
- 2020-present **Volunteer, Regional Leader** – COVID-19 Resources Canada
- 2020-present **Volunteer, Infection Control Lead** – Heart to Heart International COVID-19 Preparedness and Response Efforts
- 2019-present **Visiting Researcher** – The International Center for Medical Research in Franceville, Gabon (CIRMF)
- 2018-present **Visiting Scientist** – Public Health Agency of Canada, Special Pathogens Section
- 2018-present **Visiting Scientist** – Canadian Food Inspection Agency, Special Pathogens Unit
- 2017-present **Investigator** – Children's Health Research Institute of Manitoba

Committees and Review Panels

- 2020 **Panel Member** – CIHR Institute of Infection and Immunity Consultation on Variant Strains of SARS-CoV-2
- 2020 **Member** – World Health Organization COVID-19 Solidarity Serology Study Group
- 2020 **Member** – World Health Organization Ad Hoc Committee on COVID-19 Animal Models
- 2020 **Session chair** – Tuberculosis and other Infectious Diseases, University of Nairobi HIV/AIDS Collaborative Conference
- 2019-present **Member** – Community for Emerging and Zoonotic Diseases, Canadian Network for Public Health Intelligence (CNPHI)
- 2019 **Member** – CIHR Strategic Planning Meeting
- 2019 **Review Panel Member** – New Frontiers in Research Fund Exploration Grant
- 2018-present **Director** – Canadian Society for Virology Executive Council
- 2018-present **Member** – CIHR College of Reviewers
- 2018 **Co-Chair** – Emerging Viral Diseases and Global Preparedness Symposium
- 2018 **Organizing Committee Member** – Canada's Role in Global Public Health Conference
- 2017-present **Review Panel** – American Association for the Advancement of Science (AAAS) Research Competitiveness Program

- 2017-present **Reviewer** – Manitoba Poster Competition of the Canadian Student Health Research Forum
- 2017-present **Review Panel** – Research Manitoba PhD Scholarship Competition
- 2016 **External Reviewer** – National Science Centre, Poland (Narodowe Centrum Nauki – NCN) PRELUDIUM Funding scheme
- 2014 **Reviewer** – Alberta Livestock and Meat Agency (ALMA)
- 2012-2013 **Scientific Advisor** – World Health Organization Advisory Committee on Variola Virus Research (ACVVR): Provided updates and participated in critical discussions regarding ongoing variola virus research as a member of the US delegation

AWARDS & HONOURS

- 2021 Ken Hughes Young Investigator's Award in Medical Research
- 2021 Campbell Outreach Award
- 2018 Department of Medical Microbiology Faculty Educator Award
- 2018 National Institutes of Allergy and Infectious Diseases Merit Award
- 2017 Tier 2 Canada Research Chair Award
- 2015 National Institutes of Health Director's Award
- 2015 National Institutes of Health Clinical Center Summer Internship Program Best Mentor Award
- 2013 University of Maryland Integrated Life Sciences Honors College Mentor Award
- 2010-2013 National Institutes of Health Visiting Fellow Intramural Research Training Award

SCIENTIFIC JOURNAL ADVISORY BOARDS

- 2019-present **Guest Editor** – Viruses (Pathogenesis of Emerging Viruses Special Issue)
- 2019-present **Associate Editor** – Viruses
- 2019-present **Associate Editor** – Frontiers in Microbiology
- 2016-present **Associate Editor** – BMC Infectious Diseases
- 2014-present **Associated Review Editor** – Frontiers in Veterinary Science

PROFESSIONAL ASSOCIATIONS & MEMBERSHIPS

- 2019-present **Member** – Infectious Diseases Society of America
- 2017-present **Member** – Canadian Society for Virology
- 2017-present **Member** – Canadian Society of Microbiologists
- 2014-present **Member** – American Society for Microbiology
- 2014-present **Member** – American Society for Virology

PUBLICATIONS

1. Carlson, C.J., Farrell, M.J., Grange, Z., Han, B.A., Mollentze, N., Phelan, A.L., Rasmussen, A.L., Albery, G.F., Brett-Major, D.M., Cohen, L.E., Dallas, T., Eskew, E.A., Fagre, A.C., Forbes, K., Gibb, R., Halabi, S., Hammer, C.C., **Kindrachuk, J.**, Nutter, F.B., Rourke, M., Ryan, S.J., Katz, R., Ross, N., Seifert, S.N., Sironen, T., Standley, C.J., Taylor, K., Olival, K.J., Venter, M. Zoonotic risk technology enters the viral emergence toolkit. *Phil Trans B*. [In Revision]
2. Escandón, K., **Kindrachuk, J.**, Lee, R.S. and Rasmussen, A.L. Face masks, SARS-CoV-2 inoculum, COVID-19 severity, and immunity: is there any evidence to support a link? *Ann Intern Med*. [In Submission]
3. Webb, A.L., Schindell, B., Soule, G., Siddik, A.B., Abrenica, B., Memon, H., Su, R., Safronetz, D. and **Kindrachuk, J.** Sertoli cells remain viable and inhibit viral replication during Ebola virus infection. *Sci Rep*. [In revision]
4. Francis, M.E., Richardson, B., McNeil, M., Rioux, M., Foley, M.K., Ge, A., Pechous, R.D., **Kindrachuk, J.**, Cameron, C.M., Richardson, C., Lew, J., Cameron, M.J., Gerdt, V., Falzarano, D. and Kelvin, A.A. Male sex and age biases viral burden, viral shedding, and type 1 and 2 interferon responses during SARS-CoV-2 infection in ferrets. *Sci Rep*. [Accepted]
5. Escandón, K., Rasmussen, A.L., Bogoch, I.I., Murray, E.J., Escandón, K. and **Kindrachuk, J.** (2020) COVID-19 and false dichotomies — a nuanced review of the evidence regarding public health, COVID-19 symptomatology, SARS-CoV-2 transmission, masks, and reinfection. *BMC Infect Dis*. [Accepted]
6. Francis, M.E., Goncin, U., Kroeker, A., Swan, C., Ralph, R., Lu, Y., Falzarano, D., Gerdt, V., Machtaler, S., **Kindrachuk, J.**, and Kelvin, A.A. SARS-CoV-2 infection in the Syrian hamster model causes inflammation as well as type I interferon dysregulation in both respiratory and non-respiratory tissues. *PLoS Path*. [Accepted]
7. Forbes, K.M., Anzala, O., Carlson, C.J., Kelvin, A.A., Kuppalli, K., Leroy, E.M., Maganga, G.D., Masika, M.M., Mombo, I.M., Mwaengo, D.M., Niama, R.F., Nziza, J., Ogola, J., Pickering, B.S., Rasmussen, A.L., Sironen, T., Vapalahti, O., Webala, P.W., and **Kindrachuk, J.** (2020) Towards a coordinated strategy for intercepting human disease emergence in Africa. *Lancet Microbe*. [Accepted]
8. Schindell, B.*, Allardice, M.*, Lockman, S. and **Kindrachuk, J.** (2020) Drug Identification and Repurposing During a Novel Viral Pandemic (Invited Perspective). *ACS Infect Dis*. [Accepted]
9. Nickol, M.E., Lyle, S.M., Dennehy, B. and **Kindrachuk, J.** (2020) Dysregulated Host Responses Underlie 2009 Pandemic Influenza-Methicillin Resistant Staphylococcus aureus Coinfection Pathogenesis at the Alveolar-Capillary Barrier. *Cells*. 9: 2472
10. Connelly, M., Swerczek, J., **Kindrachuk, J.**, Vannella, K., Ramos-Benitez, M., Sun, J., Dougherty, E., Danner, R., Moore, I., Herbert, R. and Chertow, D.S. (2020) A Model of Prolonged Human Intensive Care and Recovery in Rhesus Macaques. *Sci Rep*. [Accepted]
11. Pascoe, C.D., Jha, A., Ryu, M.H., Ragheb, M., Basu, S., Stelmack, G., **Kindrachuk, J.**, Gaurveau, G.M., O'Byrne, P.M., Ravandi, A., Carlsten, C. and Halayko, A.J. (2020) Oxidized phosphatidylcholine are produced in response to allergen inhalation and promote inflammation. *Eur Respir J*. 3: 2000839
12. Cevik, M., Kuppalli, K., **Kindrachuk, J.** and Peris, M. (2020) Transmission and risk factors for severe acute respiratory syndrome coronavirus 2. *BMJ*. 371: m3862
13. Rashid, M., Zahedi-Amiri, A., Glover, K.K.M., Ang, G., Nickol, M.E., **Kindrachuk, J.**, Wilkins, J.A. and Coombs, K.M. (2020) Zika virus dysregulates human sertoli cell proteins involved in spermatogenesis with little effect on blood-testes tight junctions. *PLoS Negl Trop Dis*. 14: e0008335

14. Vanella, K.M., Stein, S., Connelly, M., Swerczek, J., Amaro-Carambot, E., Coyle, E.M., Babyak, A., Winkler, C.W., Saturday, G., Gai, N.D., Hammoud, D.A., **Kindrachuk, J.**, Peterson, K.E., Brenchley, J.M., Whitehead, S.S., Khurana, S., Herbert, R. and Chertow, D.S. (2020) Nonhuman primates exposed to Zika virus *in utero* are not protected against viral re-challenge over one year postpartum. *Sci Trans Med*. 12: eaaz4997
15. Khurana, S., Ravichandran, S., Hahn, M., Coyle, E.M., Stonier, S.W., Zak, S.E., **Kindrachuk, J.**, Davey Jr., R.T., Dye, J.M. and Chertow, D.S. (2020) Longitudinal human antibody repertoire against complete viral proteome following acute Ebola virus infection reveals protective sites for vaccine design. *Cell Host Microbe*. 27: 262-276.e4
16. Ralph, R., Lew, J., Zeng, T., Francis, M., Bei, X., Roux, M., Toloue, M., Rubino, S., Daw, N., Al-Ahdal, M.N., Kelvin, D.J., Richardson, C., **Kindrachuk, J.**, Falzarano, D., and Kelvin, A.A. (2020) 2019-nCoV (Wuhan virus), A Novel Coronavirus, linked to Chinese Pneumonia Cases: Human-to-Human Transmission, Travel-Related Cases and Vaccine Readiness. *J Infect Dev Ctries*. 14: 3-17
17. Willman, M., Kobasa, D. and **Kindrachuk J[¶]**. (2019) A comparative analysis of factors influencing two outbreaks of Middle Eastern respiratory syndrome (MERS) in Saudi Arabia and South Korea. *Viruses*. 11: 1119.
18. Nickol, M.E., Ciric, J., Falcinelli, S.D., Chertow, D.S. and **Kindrachuk, J[¶]**. (2019) Characterization of Host and Bacterial Contributions to Lung Barrier Dysfunction Following 2009 Pandemic Influenza-Methicillin Resistant Staphylococcus aureus Co-infection. *Viruses*. 11: 116.
19. Schindell, B.G., Webb, A.L. and **Kindrachuk, J[¶]**. (2019) Persistence and Sexual Transmission of Filoviruses. *Viruses*. 10: 683.
*article highlighted in NBC News article "Ebola is back in the Congo — and America's Africa policies aren't helping contain its spread"
20. Nickol, M.E. and **Kindrachuk, J[¶]**. (2019) A Year of Terror and a Century of Reflection: Perspectives on the Great Influenza Pandemic of 1918-1919. *BMC Inf Dis*. 19: 117.
21. Kashem, M.A., Li, H., Toledo, N., Omange, R.W., Liang, B., Liu, L.R., Yuan, X., **Kindrachuk, J.**, Plummer, F.A. and Luo, M. (2019) Toll-like Interleukin 1 Receptor Regulator is an important modulator of inflammation responsive genes. *Front Immunol*. 10: 272.
22. Dyal, J., Gross, R., **Kindrachuk, J.**, Johnson, R.F., Olinger, G.G., Hensley, L.E., Frieman, M.B., and Jahrling, P.B. (2017) Middle East respiratory syndrome and severe acute respiratory syndrome: current therapeutic options and potential targets for novel therapies and vaccines. *Drugs*. 77: 1935-1966.
23. **Kindrachuk, J[¶]**. (2017) Invited Editorial: Selective Inhibition of Host Cell Signaling for Rotavirus Antivirals: PI3K/Akt/mTOR-Mediated Rotavirus Pathogenesis. *Virulence*. 9: 5-8.
24. Barnes, K.G.*, **Kindrachuk, J.***, Lin, A.E.*, Wohl, S., Qu, J., Tostenson, S.D., Dorman, W.R., Busby, M., Siddle, K.J., Matranga, C.B., Davey, R.T., Sabeti, P.C. and Chertow, D.S. (2017) Evidence for replication and high concentration of ebola virus in semen of a patient recovering from severe disease. *Clin Infect Dis*. 65: 1400-1403.
*Authors contributed equally to this work
25. Kash, J.C.*, Walters, K.A.*, **Kindrachuk, J.**, Baxter, D., Scherler, K., Janosko, K.B., Adams, R.D., Herbert, A.S., James, R.M., Stonier, S.W., Memoli, M.J., Dye, J.M., Davey, R.T., Chertow, D.S., and Taubenberger, J.K. (2017) Peripheral blood transcriptional analysis of a severe ebola virus disease patient reveals dramatic transitions during critical illness and recovery. *Sci Transl Med*. 9: eaai9321.
*Authors contributed equally to this work

26. Falcinelli, S.D., Chertow, D.S., and **Kindrachuk, J[¶]**. (2016) Integration of Global Analyses of Host Molecular Responses with Clinical Data to Evaluate Pathogenesis and Advance Therapies for Emerging and Re-Emerging Viral Infections. *ACS Infect Dis.* 2: 787-799.
27. Davis, S.A.*, Chertow, D.S.*, **Kindrachuk, J.**, Schwartzman, L.M., Suzich, J., Alsaaty, S., Logun, C., Shelhamer, J.H., and Taubenberger, J.K. (2016) 1918 Influenza Receptor Binding Domain Variants Bind and Replicate in Primary Human Airway Cells Regardless of Receptor Specificity. *Virology.* 493: 283-246.
*Authors contributed equally to this work
28. Chertow, D.S., **Kindrachuk, J.**, Sheng, Z.M., Pujanauski, L., Cooper, K., Nogee, D., St. Claire, M., Solomon, J., Perry, D., Sayre, P., Janosko, K.B., Lackemeyer, M.G., Bohannon, J.K., Hensley, L.E., Kash, J.C., Jahrling, P.B. and Taubenberger, J.K. (2016) An experimental model of lung injury in rhesus macaques following influenza and bacterial co-infection. *Antiviral Res.* 129: 120-9.
29. Walters, K.A., D'Agnillo, F., Sheng, Z.M., **Kindrachuk, J.**, Schwartzman, L.M., Keustner, R.E., Chertow, D.S., Golding, B., Taubenberger, J.K. and Kash, J.C. (2016) 1918 pandemic influenza virus and *Streptococcus pneumoniae* coinfection results in activation of coagulation and widespread pulmonary microvascular thrombosis in mice and humans. *J Pathol.* 238: 85-97.
30. Falcinelli, S., Gowen, B., Trost, B., Napper, S., Kusalik, A., Safronetz, D., Prescott, J., Johnson, R.F., Wahl-Jensen, V. Jahrling, P.B. and **Kindrachuk, J[¶]**. (2015) Characterization of the functional host response to Pichinde virus infection in the Syrian golden hamster. *Mol Cell Proteomics.* 14: 646-57.
31. **Kindrachuk, J.[¶]**, Ork, B., Hart, B., Holbrook, M., Frieman, M., Johnson, R.F., Dyal, J., Olinger, G.G., Hensley, L.E., Jahrling, P.B. (2015) Temporal kinome analysis demonstrates that MERS-CoV selectively modulates ERK/MAPK and PI3K/AKT/mTOR signaling. *Antimicrob Agents Chemother.* 59: 1088-99.
32. Kuhn, J.H., Andersen, K.G., Bào, Y., Bavari, S., Becker, S., Bennett, R.S., Bergman, N.H., Blinkova, O., Bradfute, S., Brister, J.R., Bukreyev, A., Chandran, K., Chepurinov, A.A., Davey, R.A., Dietzgen, R.G., Doggett, N.A., Dolnik, O., Dye, J.M., Enterlein, S., Fenimore, P.W., Formenty, P., Freiberg, A.N., Garry, R.F., Garza, N.L., Gire, S.K., Gonzalez, J.P., Griffiths, A., Hapji, C.T., Hensley, L.E., Herbert, A.S., Hevey, M.C., Hoenen, T., Honko, A.N., Ignatyev, G.M., Jahrling, P.B., Johnson, J.C., Johnson, K.M., **Kindrachuk, J.**, et al. (2014) Filovirus RefSeq entries: evaluation and selection of filovirus type variants, type sequences, and names. *Viruses.* 6: 3663-82.
33. **Kindrachuk, J.[¶]**, Wahl-Jensen, V.*, Safronetz, D., Arsenault, R., Hoenen, T., Traynor, D., Postnikova, E., Napper, S., Blaney, J.E., and Jahrling, P.B. (2014) Temporal systems kinomics demonstrates that Ebola virus infection selectively modulates transforming growth factor β signaling in hepatocytes. *J Virol.* 88: 9877-92.
*Authors contributed equally
34. Dyal, J., Coleman, C., Hart, B., Venkataraman, T., Holbrook, M., **Kindrachuk, J.**, Johnson, R.F., Olinger, G.G., Jahrling, P.B., Laidlaw, M., Johnson, L., Glass, P., Hensley, L.E., and Frieman, M. (2014) Discovery of FDA-approved inhibitors of Middle East respiratory syndrome coronavirus infection. *Antimicrob Agents Chemother.* 58: 4885-93.
35. Jahrling, P.B., Lauren, K., St. Claire, M., Johnson, R., Bollinger, L., Lackemeyer, M., Hensley, L., **Kindrachuk, J.**, and Kuhn, J.H. (2014) Medical management and imaging of animals infected with risk group 4 pathogens at the NIAID Integrated Research Facility at Fort Detrick, Maryland. *Pathog Dis.* 71: 213-9.
36. **Kindrachuk, J.[¶]**, Falcinelli, S., Wada, J., Kuhn, J.H., Hensley, L.E., and Jahrling, P.B. (2014) Systems kinomics: a new paradigm for characterizing host responses to high consequence

- pathogens at the NIH/NIAID Integrated Research Facility at Frederick, MD. *Pathog Dis.* 71: 190-98.
37. Lackemeyer, M.G., de Kok-Mercado, F., Wada, J., **Kindrachuk, J.**, Wahl-Jensen, V., Kuhn, J.H., and Jahrling, P.B. (2014) ABSL-4 aerobiology biosafety and technology at the NIH/NIAID Integrated Research Facility at Fort Detrick. *Viruses*. 6: 137-50.
 38. Hart, B.J., Dyal, J., Postnikova, E., Zhou, H., **Kindrachuk, J.**, Johnson, R.F., Olinger, G.G., Jahrling, P.B. and Hensley, L. (2014) Interferon-beta and mycophenolic acid are potent inhibitors of MERS-CoV in cell-based assays. *J Gen Virol.* 95: 571-7.
 39. Trost, B., **Kindrachuk, J.**, Maattanen, P., Napper, S., and Kusalik, A. (2013) PIKA 2: novel tools for the analysis of kinome microarray data. *PLoS ONE*. 8: e80837.
 40. Trost, B., **Kindrachuk, J.**, Scruten, E., Griebel, P., Kusalik, A. and Napper, S. (2013) Personalized profiles of cellular kinase activity: the kinotype. *BMC Genomics* 14: 854.
 41. **Kindrachuk, J.**, Jenssen, H., Elliott, M., Nijnik, A., Fang, Y., Pistolic, J., Pasupuleti, M., Thorson, L., Ma, S., Easton, D., Bains, M., Arnusch, C.J., Finlay, B., Sahl, H.G., Breukink, E. and Hancock, R.E.W. (2013) Manipulation of innate immunity by a bacterial secreted peptide; the lantibiotic nisin Z is selectively immunomodulatory. *Innate Immun.* 19: 315-27.
 42. Achtman, A.H., Pilat, S., Law, C.W., Lynn, D.J., Janot, L., Ma, S., **Kindrachuk, J.**, Finlay, B.B., Brinkman, F.S.L., Smyth, G.K., Hancock, R.E.W., and Schofield, L. (2012) Effective adjunctive therapy by an innate defense regulatory peptide in a preclinical model of severe malaria. *Sci Transl Med.* 4: 135ra64.
 43. Steintraesser, L., Hirsch, T., Schulte, M., Kueckelhaus, M., Jacobsen, F., Mersch, E., Al-Benna, S., Stricker, I., Afacan, N., Jenssen, H., Hancock, R.E. and **Kindrachuk, J.** (2012) Innate defense regulator peptide 1018 in wound healing and wound infection. *PLoS One*. 7: e39373.
 44. **Kindrachuk, J.**, Arsenault, R., Kusalik, T., Kindrachuk, K.N., Trost, B., Napper, S., Jahrling, P.B. and Blaney, J.E. (2012) Systems kinomics demonstrates Congo Basin Monkeypox virus infection selectively modulates host cell signaling responses as compared to West African Monkeypox virus. *Mol Cell Proteomics*. 11: M.111.015701.
 45. Gao, G.*, Cheng, J.T.*, **Kindrachuk, J.**, Hancock, R.E.W., Straus, S.K. and Kizhakkedathu, J. (2012) Biomembrane interactions reveal the mechanism of action of surface-immobilized host defense IDR-1010 peptide. *Chem Bio.* 19: 199-209.
*Authors contributed equally to this work
 46. Gao, G., Yu, K., **Kindrachuk, J.**, Brooks, D.E., Hancock, R.E.W., and Kizhakkedathu, J.N. (2011) Antibacterial surfaces based on polymer brushes: Investigation on the influence of brush properties on antimicrobial peptide immobilization and antimicrobial activity. *Biomacromolecules*. 32: 3899-909.
 47. Wahl-Jensen, V.*, Kurz, S.*, Buehler, L.K., **Kindrachuk, J.**, DeFilippis, V., da Silva, J., Fruh, K., Kuhn, J.H., Burton, D.R. and Feldmann, H. (2011) Ebola virion binding to and entry into human macrophages profoundly effects cellular gene expression prior to expression of virus proteins. *PLoS Negl Trop Dis*. 5: e1359.
*Authors contributed equally to this work
 48. Garlapati, S.*, Eng, N.F.*, Kiros, T., **Kindrachuk, J.**, Mutwiri, G.K., Hancock, R.E., Babiuk, L.A. and Gerdts, V. (2011) Immunization with PCEP microparticles containing pertussis toxoid, CpG ODN and a synthetic innate defense regulator peptide induces protective immunity against pertussis. *Vaccine*. 29: 6540-8.
*Authors contributed equally to this work
 49. McAndrew Lynn, M.A., **Kindrachuk, J.**, Jenssen, H., Pante, N., Elliott, M., Napper, S., Hancock,

- R.E.W., and McMaster, R. (2011) Effect of BMAP-28 antimicrobial peptides on *Leishmania* major promastigote and amastigote growth: role of leishmanolysin in parasite survival. *PLoS Negl Trop Dis*. 5: e1141.
50. Gao, G.*, Lange, D.*, Hilpert, K., **Kindrachuk, J.**, Zou, Y., Cheng, J.T., Kazemzadeh, M., Yu, K., Wang, R., Straus, S.K., Brooks, D.E., Chew, B.H., Hancock, R.E. and Kizhakkeedathu, J.N. (2011) The biocompatibility and biofilm resistance of implant coatings based on hydrophilic polymer brushes conjugated with antimicrobial peptides. *Biomaterials*. 32: 3899-909.
*Authors contributed equally to this work
 51. **Kindrachuk, J.**, Scruten, E., Attah-Poku, S., Bell, K., Potter, A., Babiuk, L.A., Griebel, P.J., and Napper, S. (2011) Stability, toxicity and biological activity of host defense peptide BMAP28 and its inversed and retro-inversed isomers. *Biopolymers*. 96: 14-24.
 52. Cheng, J.T., Hale, J.D., **Kindrachuk, J.**, Jenssen, H., Elliott, M., Hancock, R.E. and Straus, S.K. (2010) Importance of residue 13 and the C-terminus for the structure and activity of the antimicrobial Peptide aurein 2.2. *Biophys J*. 99: 2926-35.
 53. Kazemzadeh-Narbat, M., **Kindrachuk, J.**, Duan, K., Jenssen, H., Hancock, R.E., and Wang, R. (2010) Antimicrobial peptides on calcium phosphate-coated titanium for the prevention of implant-associated infections. *Biomaterials*. 31: 9519-26.
 54. **Kindrachuk, J.***, Jenssen, H.*, Wieczorek, M.*, Scott, W.R.P., Elliott, M., Hilpert, K., Cheng, J.T.J., Hancock, R.E.W., and Straus, S.K. (2010) Structural studies of a peptide with immune modulating and direct antimicrobial activity. *Chem Biol*. 17: 970-80.
*Authors contributed equally to this work
 55. Bommarius, B., Jenssen, H., Elliott, M., **Kindrachuk, J.**, Pasupuleti, M., Gieren, H., Jaeger, K.E., Hancock, R.E., and Kalman, D. (2010) Cost-effective expression and purification of antimicrobial and host defense peptides in *Escherichia coli*. *Peptides*. 31: 1957-65.
 56. **Kindrachuk, J.** and Napper, S. (2010) Structure-activity relationships of multifunctional host defense peptides. *Mini Rev Med Chem*. 10: 596-614.
 57. Scruten, E., Kovacs-Nolan, J., Griebel, P.J., Latimer, L., **Kindrachuk, J.**, Potter, A., Babiuk, L.A., Little-van den Hurk, S.D., and Napper, S. (2010) Retro-inversion enhances the adjuvant and CpG co-adjuvant activity of host defense peptide Bac2A. *Vaccine* 28: 2945-56.
 58. Nijnik, A., Madera, L., Ma, S., Waldbrook, M., Elliott, M.R., Easton, D.M., Mayer, M.L., Mullaly, S.C., **Kindrachuk, J.**, Jenssen, H., and Hancock, R.E. (2010) Synthetic cationic peptide IDR-1002 provides protection against bacterial infections through chemokine induction and enhanced leukocyte recruitment. *J Immunol*. 184: 2539-50.
 59. Mookherjee, N., Lippert, D.N.D., Hamill, P., Falsafi, R., Nijnik, A., **Kindrachuk, J.**, Pistolic, J., Gardy, J., Miri, P., Naseer, M., Foster, L.J., and Hancock, R.E.W. (2009) Intracellular receptor for human host defense peptide LL-37 in monocytes. *J Immunol*. 183: 2688-96.
 60. **Kindrachuk, J.**, Jenssen, H., Elliott, M., Townsend, R., Nijnik, A., Lee, S., Halperin, S., and Hancock, R.E.W. (2009) A novel vaccine adjuvant comprised of a synthetic innate defense regulator peptide and CpG oligonucleotide links innate and adaptive immunity. *Vaccine* 27: 4662-71.
 61. Hilpert, K., Elliott, M., Jenssen, H., **Kindrachuk, J.**, Fjell, C.D., Korner, J., Winkler, D.F.H., Weaver, L.L., Henklein, P., Ulrich, A.S., Chiang, S.H.Y., Farmer, S.W., Pante, N., Volkmer, R., and Hancock, R.E.W. (2008) Screening and characterization of surface-tethered cationic peptides for antimicrobial activity. *Chem Biol*. 16: 58-69.
 62. **Kindrachuk, J.**, Potter, J., Wilson, H.L., Griebel, P., Babiuk, L.A., and Napper, S. (2008) Activation and regulation of toll-like receptor 9: CpGs and beyond. *Mini Rev Med Chem*. 8: 590-

600.

63. **Kindrachuk, J.**, Paur, N., Reiman, C., Scruten, E., and Napper, S. (2007) The PhoQ-activating potential of antimicrobial peptides contributes to antimicrobial efficacy and is predictive of the induction of bacterial resistance. *Antimicrob Agents Chemother.* 51: 4374-81.
64. **Kindrachuk, J.**, Potter, J.E., Brownlie, R., Ficzyz, A.D., Griebel, P.J., Mookherjee, N., Mutwiri, G.K., Babiuk, L.A., and Napper, S. (2007) Nucleic acids exert a sequence-independent cooperative effect on sequence-dependent activation of toll-like receptor 9. *J Biol Chem.* 282: 13944-13953.
65. Jalal, S., **Kindrachuk, J.**, and Napper, S. (2007) Phosphoproteome and Kinome Analysis: Unique Perspectives on the Same Problem. *Curr Anal Chem.* 3: 1-15.
66. **Kindrachuk, J.**, Parent, J., Davies, G.F., Dinsmore, M., Attah-Poku, S., and Napper, S. (2003) Overexpression of L-isoaspartate O-methyltransferase in *Escherichia coli* increases heat shock survival by a mechanism independent of methyltransferase activity. *J Biol Chem.* 278: 50880-50886.
67. Napper, S., **Kindrachuk, J.**, Olson, D.J., Ambrose, S.J., Dereniowsky, C., Ross, A.R. (2003) Selective extraction and characterization of a histidine-phosphorylated peptide using immobilized copper (II) ion affinity chromatography and matrix-assisted laser desorption/ionization time-of-flight mass spectrometry. *Anal Chem.* 75: 1741-1747.
68. Napper, S., Wolanin, P.M., Webre, D.J., **Kindrachuk, J.**, Waygood, B., and Stock, J.B. (2003) Intramolecular rearrangements as a consequence of the dephosphorylation of phosphoaspartate residues in proteins. *FEBS Lett.* 538: 77-80.
69. Athmer, L., **Kindrachuk, J.**, Georges, F., and Napper, S. (2002) The influence of protein structure on the products emerging from succinimide hydrolysis. *J Biol Chem.* 277: 30502-30507.
70. Napper, S., Brokx, S.J., Pally, E., **Kindrachuk, J.**, Delbaere, L.T., and Waygood, E.B. (2001) Substitution of aspartate and glutamate for active center histidines in the *Escherichia coli* phosphoenolpyruvate:sugar phosphotransferase system maintain phosphotransfer potential. *J Biol Chem.* 276: 41588-41593.

BOOK CHAPTERS

1. Chertow, D.S. and **Kindrachuk, J.** (2019) Respiratory Viruses: Influenza, Measles, SARS, MERS, and Smallpox. In: *Highly Infectious Diseases in Critical Care: A Comprehensive Clinical Guide*. Springer New York.
2. Falcinelli, S.D., Ciric, J., **Kindrachuk, J.** (2018) Variola Virus: Clinical, Molecular and Bioterrorism Perspectives. In: *Defense Against Biological Attacks*. Springer New York.
3. Jahrling, P.B., Goff, A.J., Johnston, S.C., **Kindrachuk, J.**, Lin, K.L., Huggins, J.W., Ibrahim, S., Lawler, J.V., Martin, J.W. (2016) Chapter 11: Smallpox and Related Orthopoxviruses. In: *Textbooks of Military Medicine: Medical Aspects of Biological Warfare*.
4. **Kindrachuk, J.**, Kuhn, J.H. and Jahrling, P.B. (2015) The role of viral protein phosphorylation during filovirus infection. In: *Global Virology*. Springer New York.
5. **Kindrachuk, J.** and Napper, S. (2013) Sample Preparation and Profiling: Probing the kinome for biomarkers and therapeutic targets: peptide arrays for global phosphorylation-mediated signal transduction. In: *Comprehensive Biomarker Discover and Validation for Clinical Application*. Royal Society of Chemistry.
6. Petersen, P.D., **Kindrachuk, J.**, Jenssen, H. (2012) Immune modulation for treatment of herpes simplex virus. In: *Herpes Simplex Virus: Prevention, Recognition and Management*. In: *Advances*

in Medicine and Biology. Nova Science Publishers.

7. **Kindrachuk, J.**, Nijnik, A. and Hancock, R.E.W. (2009) Ch. 5.07 Host Defense Peptides: Bridging Antimicrobial and Immunomodulatory Activities. In: Mander, L., and Liu, H.W. *Comprehensive Natural Products Chemistry II*. Oxford: Elsevier.

NON-PEER REVIEWED PUBLICATIONS

1. COVID-19 Delta variant in Canada: FAQ on origins, hotspots and vaccine protection. *The Conversation*.
<https://theconversation.com/covid-19-delta-variant-in-canada-faq-on-origins-hotspots-and-vaccine-protection-162653>
2. Why Early Wins Over Covid-19 Do Not Mean Victory: Canada's Cautionary Tale. *Forbes*.
<https://www.forbes.com/sites/coronavirusfrontlines/2020/11/04/why-early-wins-over-covid-19-do-not-mean-victory-canadas-cautionary-tale/?sh=740b94722041>
3. The Realities of Biomedical Research During a Pandemic. *Forbes*.
<https://www.forbes.com/sites/coronavirusfrontlines/2020/09/17/a-virologist-explains-the-realities-of-biomedical-research-during-a-pandemic/#62d6a66111a2>
4. A Virologist Explains Why It Is Unlikely COVID-19 Escaped from A Lab. *Forbes*.
<https://www.forbes.com/sites/coronavirusfrontlines/2020/04/17/a-virologist-explains-why-it-is-unlikely-covid-19-escaped-from-a-lab/#58bd5fb63042>
5. How The Coronavirus Pandemic Has Impacted International Research Programs: A Personal Perspective. *Forbes*.
<https://www.forbes.com/sites/coronavirusfrontlines/2020/06/06/how-the-coronavirus-pandemic-has-impacted-international-research-programs-a-personal-perspective/#b10049750bbf>
6. Repurposing Drugs Is Key to Fighting the Coronavirus Pandemic, This Virologist Explains. *Forbes*.
<https://www.forbes.com/sites/coronavirusfrontlines/2020/05/08/repurposing-drugs-is-key-to-fighting-the-coronavirus-pandemic-this-virologist-explains/#5c9efd1217ce>
7. No Mercy for the Coronas. *La Liberté*.
<https://www.lalibertesciencesmagjunior.ca/>
8. The Value of Social Media Now. *New York Times*.
<https://www.nytimes.com/2020/03/27/opinion/letters/iran-sanctions.html>
9. How social media is changing research and reactions to coronavirus outbreak. *The Conversation*.
<http://theconversation.com/how-social-media-is-changing-research-and-reactions-to-coronavirus-outbreak-130748>
10. Ebola survivors can pass on the virus: we're trying to understand what role sex plays. *The Conversation Africa*.
<https://theconversation.com/ebola-survivors-can-pass-on-the-virus-were-trying-to-understand-what-role-sex-plays-124015>

REPORTS

1. CIHR-PHAC-CADTH – Best Brains Exchange – Transmission Routes for COVID-19: Implications for Public Health. Canadian Institutes of Health Research (CIHR); 2020 October. <https://cihr-irsc.gc.ca/e/52238.html>
2. Heating, Ventilation and Air Conditioning Systems in Public Spaces. Ottawa: Canadian Agency for Drugs and Technologies in Health (CADTH); 2020 June. (CADTH technology review).

3. Public statement for collaboration on COVID-19 vaccine development. World Health Organization. 13 April 2020. <https://www.who.int/news-room/detail/13-04-2020-public-statement-for-collaboration-on-covid-19-vaccine-development>
4. WHO Advisory Committee on Variola Virus Research, 15th Meeting. Report of the Fourteenth Meeting, Geneva, Switzerland, 24-24 September 2013. WHO/HSE/PED/CED/2013.2
5. WHO Advisory Committee on Variola Virus Research, 14th Meeting. Report of the Fourteenth Meeting, Geneva, Switzerland, 16-17 October 2012. WHO/HSE/PED/CED/2013.1

FUNDING

1. Tier 2 Canada Research Chair in the molecular pathogenesis of emerging and re-emerging viruses.
Funding Sources:
 2017-2022 Canada Research Chairs Program
 Total Funding – 500,000 (Canadian dollar)
 Principal Investigator
2. Identification of the molecular determinants underlying asymptomatic Ebola virus testicular infections and long-term effects on reproductive health
Funding Sources:
 2021-2026 Canadian Institutes of Health Research Project Grant
 Total Funding – 726,500 (Canadian dollar)
 Principal Investigator
3. Cryo-electron microscopy (cryo-EM) to guide rapid development of novel therapeutic strategies and improved diagnostics for COVID-19
Funding Sources:
 Canadian Foundation for Innovation
 Total Funding – 950,000 (Canadian dollar)
 Co-Applicant
4. Animal models for SARS-CoV-2: vaccines and immune enhancement
Funding Sources:
 2020-2022 Canadian Institutes of Health 2019 Novel Coronavirus (COVID-19) Rapid Research Funding
 Total Funding – 999,793 (Canadian dollar)
 Co-Applicant
5. Scalable, Customizable, Digital Health Communication Materials to Help Canada Address the COVID19 Pandemic
Funding Sources:
 2020-2021 Canadian Institutes of Health COVID-19 Rapid Research - Social Policy and Public Health Responses
 Total Funding – 311,296 (Canadian dollar)
 Co-Applicant
6. Broad Spectrum CoV Therapeutic; rhACE2 Immunoadhesin to treat COVID19
Funding Sources:
 2020-2021 MITACS Accelerate
 Total Funding – 90,000 (Canadian dollar)
 Principal Applicant
7. Prairie Infectious Immunology Network 2020
Funding Sources:

2020-2021 Canadian Institutes of Health Research Planning and Dissemination Grant

Total Funding – 10,000 (Canadian dollar)

Co-Principal Investigator

8. Characterization of the molecular pathogenesis of severe influenza and influenza-bacterial infections at the alveolar-capillary barrier

Funding Sources:

2018-2020 Research Manitoba New Investigator Operating Grant

Total Funding – 130,000 (Canadian dollar)

Principal Investigator

9. Investigation of kinase-mediated cell signaling pathway modulation at the vector pathogen-livestock interface in vector-borne livestock diseases

Funding Sources:

2018/4 - 2023/3 Natural Sciences and Engineering Research Council of Canada (NSERC) Discovery Grant

Total Funding - 165,000 (Canadian dollar)

Principal Investigator

10. Establishment of a high-throughput molecular dynamics facility

Co-applicant: Denice Bay

Funding Sources:

2017/11 - 2022/11 Canada Foundation for Innovation (CFI) John R. Evans Leaders Fund

Total Funding - 609,191 (Canadian dollar)

Principal Investigator

11. Deciphering the bat kinome by immunometabolic peptide kinome arrays: critical insights for emerging viral diseases

Funding Sources:

2018/7 - 2019/6 University of Manitoba Dr. Paul H. T. Thorlakson Foundation Fund

Total Funding - 30,000 (Canadian dollar)

Principal Investigator

12. Characterizing the molecular mechanisms of Ebola virus persistence at the blood-testis barrier

Funding Sources:

2018/8 - 2019/4 University of Manitoba Tri-Agency Bridge Funding

Total Funding - 60,000 (Canadian dollar)

Principal Investigator

13. Characterizing the molecular mechanisms of Ebola virus persistence in a 3D co-culture model of the blood-testis barrier

Funding Sources:

2018/3 - 2019/3 Manitoba Medical Service Foundation (MMSF) Operating Grant

Total Funding - 19,219 (Canadian dollar)

Principal Investigator

14. Capacity Building Projects in an Institution of Higher Learning in the Developing World

Funding Sources:

2018/1 - 2019/10 University of Manitoba International Program and Partnership Seed

Total Funding – 5,000 (Canadian dollar)

Principal Investigator

INVITED PRESENTATIONS

1. Universal coronavirus vaccines: How close are we? **American Thoracic Society Annual Meeting**. Virtual. 2021

2. What virus goes there? Emerging virus research from the field to the lab. Molecular Biology & Biochemistry Department. **Simon Fraser University**. Virtual. 2021
3. Covid-19 and vaccine safety. Bisons Athletics. **University of Manitoba**. Virtual. 2021
4. Covid Q&A Part II with Raman Dhaliwal and Dr. Jason Kindrachuk. **University of Manitoba**. Virtual. 2021
5. Current perspectives on Covid-19. **British Columbia Dental Association**. Virtual. 2021
6. Covid-19: Current state of knowledge. **Wastewater Epidemiology Group**. Public Health Agency of Canada. Virtual. 2021
7. Covid-19: Current state of knowledge. **Covid-19 Genome Sequencing Group**. Public Health Agency of Canada. Virtual. 2021
8. Vaccines & therapeutics for COVID-19. **Café Scientifique**. Virtual. 2021
9. Balancing science and disinformation during Covid-19. Stem Skills for the 21st Century. **Bioscience Association of Manitoba**. Virtual. 2021
10. Eleven Covid months equals one decade - Emerging virus research during a pandemic. **Quebec Centre for Advanced Materials (QCAM)**. Virtual. 2020
11. Emerging Virus Research in the Time of Covid. Global Health Seminar Series. **Tel Aviv University**. Virtual. 2020
12. COVID-19 Transmission: Current state of virology knowledge. **Community-based aerosol transmission of Covid-19 and HVAC systems**. Canadian Agency for Drugs and Technologies in Health (CADTH). Virtual. 2020
13. Transmission Routes for COVID-19: Implications for Public Health. **CIHR-PHAC-CADTH – Best Brains Exchange**. Canadian Institutes of Health Research (CIHR). Virtual. 2020
14. Heating, Ventilation and Air Conditioning Systems in Public Spaces. Ottawa: **Canadian Agency for Drugs and Technologies in Health (CADTH)**. Virtual. 2020
15. 2020 Fall Member Forum: What's Next? The Aftermath of the COVID-19 Crisis. **Western Transportation Advisory Council (WESTAC)**. Virtual. 2020
16. Basic, Translational and Public Health Research During a Novel Pandemic. **School of Public Health, University of Saskatchewan**. Virtual. 2020
17. Characterizing tissue-barrier specific pathogenesis of epidemic and pandemic emerging viruses. **Infectious Disease, Microbiome, and Public Health Conference**. Virtual. 2020
18. COVID-19: Early Assessments of the First Coronavirus Pandemic. **Value Partners Annual General Meeting**. Virtual. 2020
19. COVID-19 and infection, prevention and control. **Canadian Dental Association**. Virtual. 2020
20. COVID-19: The Emergence and Spread of a Pandemic in the Age of Social Media. **UM Learning for Life Program**. University of Manitoba. Virtual. 2020
21. COVID-19: Monitoring the Emergence and Pandemic Spread of SARS-CoV-2 in Real Time. **International Life Sciences Institute – North America**. Virtual. 2020
22. Characterizing Emerging Virus Circulation and Spillovers in West and Central Africa. **Society of Clinical Research Associates**. Winnipeg, Canada. 2020

23. The Real Hot Zone: Studying Emerging Virus Circulation and Spillover in the Lab and the Field. **Department of Microbiology, Immunology & Infectious Diseases, University of Calgary.** 2020
24. COVID-19: An Emerging Public Health and Economic Crisis. **Manitoba Young Presidents Organization.** Winnipeg, Canada. 2020
25. Characterizing emerging virus circulation and spillovers in West and Central Africa. **Annual University of Nairobi HIV/AIDS Collaborative Conference.** Nairobi, Kenya. 2020
26. Identifying the molecular determinants underlying Ebola virus persistence in incidental and reservoir hosts. **KAVI Institute for Clinical Research.** University of Nairobi, Nairobi, Kenya. 2020
27. Characterizing the molecular determinants underlying severe Ebola virus disease and post-recovery persistence. **International Infection, Immunity and Inflammation Conference (I4C),** Vancouver, Canada. 2019
28. Investigating the molecular pathogenesis of emerging and re-emerging viruses at the interface of basic and clinical research. **Manitoba Chemistry Symposium,** Winnipeg, Canada. 2018
29. Navigating the Storm: merging basic research with clinical information for (re)emerging infectious diseases. **Canadian Society of Microbiologists Annual Meeting,** Winnipeg, Canada. 2018
30. Are We Ready for the Next Pandemic? Reflections from the laboratory and the field. **CPD Medicine Program: Trends & Challenges in Virology,** Winnipeg, Canada. 2017
31. Investigating Interactions between the Host and High-Consequence Pathogens with Systems Kinomics. **University of Delaware Graduate Student Seminar Series.** University of Delaware, DE. 2015.
32. Characterizing High-Consequence Pathogens through Systems Kinome Analysis. **NICBR Exploring Careers in a Scientific Environment Symposium (NECSES).** Fort Detrick, Frederick, MD, 2014.
33. Species-Specific Kinome Analysis for the Investigation of the Molecular Pathogenesis of High-Consequence Pathogen and Identification of Novel Therapeutic Targets. **American Society of Virology.** Fort Collins, CO, 2014.
34. Temporal kinome analysis demonstrates Ebola virus selectively modulates transforming growth factor β signaling. **6th International Symposium on Filoviruses.** Galveston, TX, 2014.
35. Use of live variola virus in systems kinomics for identification of host targets for therapeutic intervention. **15th Meeting of the WHO Advisory Committee on Variola Virus Research.** Geneva, Switzerland, 2013.
36. Systems kinome analysis of differential host responses to variola virus and monkeypox virus. **US Delegation to WHO.** Eisenhower Office Building, Washington, DC, 2013.
37. Ebola virus selectively modulates transforming growth factor- β signaling as demonstrated by temporal kinome analysis. **American Society of Virology.** Pennsylvania State University, PA, 2013.
38. Investigating high-consequence viral pathogenesis under (negative) pressure. **Vaccine and Infectious Disease Organization (VIDO).** Saskatoon, SK, 2012.
39. Use of live variola virus in systems kinomics for identification of host targets for therapeutic intervention. **14th Meeting of the WHO Advisory Committee on Variola Virus Research.** Geneva, Switzerland, 2012.
40. Temporal kinome analysis of Ebola virus molecular pathogenesis. **Centers for Disease Control (CDC): Special Pathogens Branch.** Atlanta, GA, 2012.

41. Temporal systems kinomics analysis of host cell responses to Ebola virus. **Keystone Symposium: Cell Biology of Virus Entry, Replication and Pathogenesis (X7)**. Whistler, BC, 2012.
42. Kinome analysis reveals differential host cell responses to west african and congo basin monkeypox virus. **Gordon Research Conference – Chemical and Biological Terrorism Defense**. Ventura, CA, 2011.

CONSULTING

1. Covid-19 infection prevention and control procedures – Winnipeg Blue Bombers
2. Covid-19 expert advice – Young Presidents Organization (Winnipeg Chapter)
3. Covid-19 transmission – Manitoba Government

SELECTED MEDIA LINKS

News Articles

1. Tokyo Olympics: Can vaccines save the Games? *CNN*.
<https://www.cnn.com/2021/01/29/sport/tokyo-olympics-vaccines-cmd-spt-intl/index.html>
2. The Health 202: The pandemic intensified the tech censorship debate. *The Washington Post*.
<https://www.washingtonpost.com/politics/2021/06/07/health-202-pandemic-intensified-tech-censorship-debate/>
3. Yes, vaccines block most transmission of COVID-19. *National Geographic*.
<https://www.nationalgeographic.com/science/article/yes-vaccines-block-most-transmission-of-covid-19>
4. Inside the global race against COVID-19 mutations. *Macleans*.
<https://www.macleans.ca/society/science/covid-variants-vaccination-race/>
5. Canada could see COVID resurgence; only 4 percent of population have had both shots. *Newsweek*.
<https://www.newsweek.com/canada-covid-resurgence-1594280>
6. Province working on screening for 'Delta' variant that threatens fourth wave. *Winnipeg Sun*.
<https://winnipegssun.com/news/provincial/province-working-on-screening-for-delta-variant-that-threatens-fourth-wave>
7. ALDRICH: Reopening plan would be sign of hope, positivity. *Winnipeg Sun*.
<https://winnipegssun.com/opinion/columnists/aldrich-reopening-plan-would-be-sign-of-hope-positivity>
8. Manitoba expects to break record for intensive care demand as COVID-19 numbers rise. *Toronto Sun*.
<https://www.thestar.com/politics/2021/05/17/manitoba-expects-to-break-record-for-intensive-care-demand-as-covid-19-numbers-rise.html?rf>
9. Yankees outbreak spurs concern, but experts say breakthrough COVID-19 cases expected. *Toronto Sun*.
<https://www.thestar.com/sports/2021/05/18/yankees-outbreak-spurs-concern-but-experts-say-breakthrough-covid-19-cases-expected.html>
10. Opinion: Post-vaccination COVID numbers prove the miracle is real. *The National Post*.
<https://www.healthing.ca/diseases-and-conditions/coronavirus/opinion-post-vaccination-covid-numbers-prove-the-miracle-is-real>
11. How many COVID-19 vaccine doses could make the difference between a fourth wave in Canada and no wave at all? New models offer four scenarios. *The Globe and Mail*.
<https://www.theglobeandmail.com/canada/article-how-many-doses-will-make-the-difference-between-a-canadian-fourth-wave/>

12. Ramping up COVID-19 vaccine production is harder than it seems. *Popular Science*.
<https://www.popsci.com/story/health/mrna-covid-vaccine-ramp-up-production/>
13. What's important to know about the new COVID-19 variants? *CMAJ*.
<https://www.cmaj.ca/content/193/4/E141>
14. Bombshell analysis traces new Ebola outbreak to survivor of West Africa crisis. *STAT News*.
<https://www.statnews.com/2021/03/12/bombshell-analysis-traces-new-ebola-outbreak-to-survivor-of-west-africa-crisis/>
15. 'Breakthrough' COVID-19 cases: The possibility of infection after vaccination. *CTV News*.
<https://www.ctvnews.ca/health/coronavirus/breakthrough-covid-19-cases-the-possibility-of-infection-after-vaccination-1.5360944>
16. Canada surpasses 10 per cent COVID vaccination mark, but are we going fast enough? *Toronto Star*.
https://www.thestar.com/life/health_wellness/2021/03/25/canada-surpasses-10-per-cent-covid-vaccination-mark-but-are-we-going-fast-enough.html
17. Manitoba could see 3rd wave of COVID-19, experts say, as cases surge in other provinces. *CBC News*.
<https://www.cbc.ca/news/canada/manitoba/manitoba-third-wave-covid-1.5974214>
18. Patience a COVID virtue. *Winnipeg Free Press*.
<https://www.winnipegfreepress.com/special/coronavirus/patience-a-covid-virtue-574118032.html>
19. Blood survey suggests COVID-19 was more prevalent in Manitoba during second wave than previously believed. *CBC News*.
<https://www.cbc.ca/news/canada/manitoba/manitoba-seroprevalence-second-wave-1.5968324>
20. 1 death and 57 new cases of COVID-19 in Manitoba Saturday. *Global News*.
<https://globalnews.ca/news/7723521/manitoba-covid-19-update-march-27/>
21. A look at how much the government spends on tracking, studying viruses like COVID-19. *Global News*.
<https://globalnews.ca/news/7708921/canada-covid-19-research-funding/>
22. 'It's a forest fire': experts predict rise of COVID-19 variant cases, warn of 3rd wave. *Global News*.
<https://globalnews.ca/news/7639265/coronavirus-canada-third-wave/>
23. Congo suffers its fourth Ebola outbreak in three years - just three months since the disease was last quashed. *The Daily Mail*.
<https://www.dailymail.co.uk/news/article-9237389/Congo-suffers-fourth-Ebola-outbreak-three-years.html>
24. Congo working to stop new Ebola outbreak in country's east. *Associated Press*.
<https://abcnews.go.com/Health/wireStory/congo-working-stop-ebola-outbreak-countrys-east-75745874>
25. Ramping up COVID-19 vaccine production is harder than it seems. *Popular Science*.
<https://www.popsci.com/story/health/mrna-covid-vaccine-ramp-up-production/>
26. Vaccinated residents avoid serious illness during COVID-19 outbreak. *Winnipeg Free Press*.
<https://www.winnipegfreepress.com/special/coronavirus/vaccinated-residents-avoid-serious-illness-during-covid-19-outbreak-573856632.html>
27. AstraZeneca approval will speed up Manitoba vaccine rollout, task force head says. *CBC News*.
<https://www.cbc.ca/news/canada/manitoba/manitoba-vaccine-timeline-speeds-up-with-astrazeneca-approval-1.5929495>
28. This is shaping up to be the winter nobody got sick – unless you got COVID-19. *The Globe and Mail*.
<https://www.theglobeandmail.com/canada/article-this-is-shaping-up-to-be-the-winter-nobody-got-sick-unless-you-got/>
29. Saskatchewan estimates it has nearly 19,000 asymptomatic cases of COVID-19. *CTV News*.
<https://regina.ctvnews.ca/saskatchewan-estimates-it-has-nearly-19-000-asymptomatic-cases-of-covid-19-1.5304708>
30. COVID-19: Large increases in cases towards the end of February?. *Inspired Traveler*.

- <https://www.inspiredtraveler.ca/covid-19-large-increases-in-cases-towards-the-end-of-february/>
31. Manitoba detects COVID-19 variant first recorded in U.K. *CTV News*.
<https://winnipeg.ctvnews.ca/manitoba-detects-covid-19-variant-first-recorded-in-u-k-1.5301689>
 32. Infectious disease expert weighs in on new vaccines, effectiveness. *650 CKOM*.
<https://www.ckom.com/2021/03/01/infectious-disease-expert-weighs-in-on-new-vaccines-effectiveness/>
 33. Coronavirus: 7 probable cases of U.K. variant on Manitoba First Nation. *Global News*.
<https://globalnews.ca/news/7640192/coronavirus-u-k-variant-manitoba-first-nation/>
 34. Manitoba move to secure own vaccine supply 'a political statement': expert. *Winnipeg Free Press*.
<https://www.winnipegfreepress.com/special/coronavirus/manitoba-move-to-secure-own-vaccine-supply-a-political-statement-expert-573787812.html>
 35. Study offers 'promising' evidence that at least 1 COVID-19 vaccine may curb virus transmission. *CBC News*.
<https://www.cbc.ca/news/health/covid-vaccine-transmission-pfizer-1.5907459>
 36. Scott Moe says he didn't mean to disparage with work from home comment. *Global News*.
<https://globalnews.ca/news/7634266/saskatchewan-premier-scott-moe-covid-19-coronavirus-work-home/>
 37. 'Cautious' capacity limits confusing. *Toronto Star*.
<https://www.thestar.com/news/canada/2021/02/02/cautious-capacity-limits-confusing.html>
 38. Coronavirus: 7 probable cases of U.K. variant on Manitoba First Nation. *Global News*.
<https://globalnews.ca/news/7640192/coronavirus-u-k-variant-manitoba-first-nation/>
 39. Keeping virus variants out of Manitoba no easy task. *CBC News*.
<https://www.cbc.ca/news/canada/manitoba/covid19-variants-manitoba-wfp-cbc-wfp-1.5901854>
 40. 8 things to know about the coronavirus variant detected in Saskatchewan. *CBC News*.
<https://www.cbc.ca/news/canada/saskatchewan/covid-19-uk-variant-jason-kindrachuk-1.5900057>
 41. Johnson & Johnson's lower-immunity single-dose COVID vaccine might be just what the doctor ordered. *Fortune*.
<https://fortune.com/2021/02/01/johnson-johnsons-covid-vaccine/>
 42. Decoding the virus – what we know about Sars-CoV-2 a year on. *Chemistry World (Royal Society of Chemistry)*.
<https://www.chemistryworld.com/news/decoding-the-virus-what-we-know-about-sars-cov-2-a-year-on/4013076.article>
 43. Scientists Now Worried the UK Coronavirus Variant Is Deadlier. *Gizmodo*.
<https://gizmodo.com/scientists-now-worried-the-uk-coronavirus-variant-is-deadlier-1846112293>
 44. Some experts claim Covid-19 reinfections are 'not a huge problem' – but nobody's tracking the numbers. *Forbes*.
<https://www.forbes.com/sites/leahrosenbaum/2021/01/29/some-experts-claim-covid-19-reinfections-are-not-a-huge-problem-but-nobodys-tracking-the-numbers/?sh=750e330e1915>
 45. 'We're really in a bit of a time crunch': Infectious disease expert warns of COVID-19 variants in Canada. *CTV News*.
<https://saskatoon.ctvnews.ca/we-re-really-in-a-bit-of-a-time-crunch-infectious-disease-expert-warns-of-covid-19-variants-in-canada-1.5285277>
 46. Trudeau doubles down on promise of vaccines for all Canadians by fall. Is that still a realistic target? *CBC News*.
<https://www.cbc.ca/news/politics/trudeau-vaccine-covid-target-september-1.5888178?cmp=rss>
 47. 72 per cent of Manitobans want to be vaccinated at first opportunity: poll. *Winnipeg Free Press*.
<https://www.winnipegfreepress.com/special/coronavirus/72-per-cent-of-manitobans-want-to-be-vaccinated-at-first-opportunity-poll-573660332.html>
 48. What's important to know about the new COVID-19 variants? *Canadian Medical Association Journal*.
<https://www.cmaj.ca/content/193/4/E141>
 49. Boris Johnson warns U.K. variant may be deadlier, but experts say it's too soon to tell. *NBC News*.

- <https://www.nbcnews.com/health/health-news/boris-johnson-warns-u-k-variant-may-be-deadlier-experts-n1255353>
50. Tokyo Games chief expects decision by March on allowing spectators. *Reuters*.
<https://www.reuters.com/article/olympics-2020-spectators-int-idUSKBN29H1DP>
 51. Northern Sask. medical health officer calls for tighter restrictions on outdoor gatherings. *CTV News*.
<https://regina.ctvnews.ca/northern-sask-medical-health-officer-calls-for-tighter-restrictions-on-outdoor-gatherings-1.5271879>
 52. How the spread of coronavirus variants could completely change the pandemic in Canada. *CBC News*.
<https://www.cbc.ca/news/health/coronavirus-variants-canada-1.5875629>
 53. Workplaces were source of 25% of Manitoba's COVID-19 community-linked cases last fall. *CBC News*.
<https://www.cbc.ca/news/canada/manitoba/workplace-retail-covid19-manitoba-wfp-cbc-cbc-1.5868189>
 54. COVID-19 vs. school: We asked experts about transmission risks and what is needed to keep classrooms open. *CBC News*.
<https://www.cbc.ca/news/canada/covid-19-schools-newyear-1.5865427>
 55. Socializing after the vaccine: Experts say shot won't offer "free pass" right away. *The Canadian Press*.
https://www.thepeterboroughexaminer.com/ts/life/health_wellness/2021/01/08/socializing-after-the-vaccine-experts-say-shot-wont-offer-free-pass-right-away.html
 56. Immune but infectious: Can someone vaccinated against COVID-19 still spread the virus? *Global News*.
<https://globalnews.ca/news/7559408/health-matters-covid-19-vaccine-immune-but-infectious/>
 57. The fast-spreading mutant COVID-19 strain is a '2021 nightmare': researchers. *National Post*.
<https://nationalpost.com/news/the-fast-spreading-mutant-covid-19-strain-is-a-2021-nightmare-researchers>
 58. Quebec curfew 'sets the tone' for pandemic fight. *The Canadian Press*.
<https://www.simcoe.com/news-story/10303203-quebec-curfew-sets-the-tone-for-pandemic-fight/>
 59. Prescription for a smooth COVID-19 vaccination plan in Manitoba. *Winnipeg Free Press*.
<https://www.winnipegfreepress.com/special/coronavirus/prescription-for-a-smooth-covid-19-vaccination-plan-in-manitoba-573552322.html>
 60. Lessons from San Francisco's Experience of The Great Influenza. *SF Weekly*.
<https://www.sfweekly.com/news/lessons-san-francisco-great-influenza/>
 61. Families, experts question school reopening plans as COVID-19 cases remain high. *The Canadian Press*.
https://www.thestar.com/life/health_wellness/2021/01/06/families-experts-question-school-reopening-plans-as-covid-19-cases-remain-high.html?rf
 62. WHO predicts COVID-19 will become endemic, but some experts are less certain. *The Canadian Press*.
<https://www.ctvnews.ca/health/coronavirus/who-predicts-covid-19-will-become-endemic-but-some-experts-are-less-certain-1.5248847>
 63. Hopes for brave new/old world. *Winnipeg Free Press*.
<https://www.winnipegfreepress.com/special/coronavirus/hopes-for-brave-newold-world-573516872.html>
 64. Detection of U.K. variant of COVID-19 in Manitoba may only be a matter of time, experts warn. *CTV News*.
<https://winnipeg.ctvnews.ca/detection-of-u-k-variant-of-covid-19-in-manitoba-may-only-be-a-matter-of-time-experts-warn-1.5249194>
 65. What scientists still want to know about the new coronavirus variant in the U.K. *NBC News*.

- <https://www.nbcnews.com/health/health-news/what-scientists-still-want-know-about-new-coronavirus-variant-u-n1252122>
66. How The U.S. Government's Billion Dollar Bet On Moderna's Covid-19 Vaccine Paid Off. *Forbes*.
<https://www.forbes.com/sites/leahrosenbaum/2020/12/18/the-feds-risky-billion-dollar-bet-on-moderna-pays-off-as-fda-authorizes-its-covid-19-vaccine/?sh=a151fc565ad8>
 67. Coronaviruses and Vaccine Design – A Conversation With Jason Kindrachuk. *Technology Networks*.
<https://www.technologynetworks.com/tn/articles/coronaviruses-and-vaccine-design-a-conversation-with-jason-kindrachuk-342200>
 68. New COVID-19 strain dominating U.K. infections not yet found in Canada: Tam. *The Canadian Press*.
<https://www.ctvnews.ca/health/coronavirus/new-covid-19-strain-dominating-u-k-infections-not-yet-found-in-canada-tam-1.5241953>
 69. What's known, unknown about the coronavirus variant in Britain. *CBC News*.
<https://www.cbc.ca/news/health/coronavirus-variant-britain-explainer-1.5849905>
 70. Health officials in Canada monitoring for variant of virus identified in the U.K. *CTV News*.
<https://winnipeg.ctvnews.ca/health-officials-in-canada-monitoring-for-variant-of-virus-identified-in-the-u-k-1.5240567>
 71. Researchers propose process to detect and contain emerging diseases. *Science Daily*.
<https://www.sciencedaily.com/releases/2020/12/201218152727.htm>
 72. UA biologist working to help stop future diseases. *5 News Online*.
<https://www.5newsonline.com/article/news/local/ua-biologist-working-to-help-stop-future-diseases/527-60ad477b-c23c-408d-b538-6d6300b3616c>
 73. 'Expedited, not fast-tracked': Virologist explains the safety of the COVID-19 vaccine. *CTV News*.
<https://winnipeg.ctvnews.ca/expedited-not-fast-tracked-virologist-explains-the-safety-of-the-covid-19-vaccine-1.5232461>
 74. What you need to know as COVID-19 vaccinations begin in Alberta. *Global News*.
<https://globalnews.ca/news/7522076/alberta-covid-19-vaccinations/>
 75. Manitoba to start COVID-19 vaccinations Wednesday. *CTV News*.
<https://winnipeg.ctvnews.ca/manitoba-to-start-covid-19-vaccinations-wednesday-1.5228741>
 76. Great expectations, uncertain reality amidst COVID clampdown. *Winnipeg Free Press*.
<https://www.winnipegfreepress.com/special/coronavirus/great-expectations-uncertain-reality-amidst-covid-clampdown-573324781.html>
 77. Saskatoon mail processing facility sanitized after COVID-19 case confirmed: Canada Post. *CTV News*.
<https://saskatoon.ctvnews.ca/saskatoon-mail-processing-facility-sanitized-after-covid-19-case-confirmed-canada-post-1.5220655>
 78. Death of Manitoban boy under 10 a rare but sad reminder of reality of COVID-19, expert says. *CBC News*.
<https://www.cbc.ca/news/canada/manitoba/covid-19-manitoba-jason-kindrachuk-1.5821464>
 79. Saskatoon pharmacist experiences ongoing fatigue, gaps in memory months after contracting COVID-19. *CTV News*.
<https://saskatoon.ctvnews.ca/saskatoon-pharmacist-experiences-ongoing-fatigue-gaps-in-memory-months-after-contracting-covid-19-1.5206240>
 80. Sask. COVID-19 situation appears to be a 'carbon copy' of Manitoba: expert. *CTV News*.
<https://saskatoon.ctvnews.ca/sask-covid-19-situation-appears-to-be-a-carbon-copy-of-manitoba-expert-1.5202627>
 81. Winnipeg region slapped with code-red restrictions. *Winnipeg Free Press*.
<https://www.winnipegfreepress.com/special/coronavirus/code-red-for-winnipeg-572925971.html>
 82. Manitoba researchers bring range of expertise to front lines of COVID-19 fight. *Global News*.
<https://globalnews.ca/news/7438172/manitoba-researchers-coronavirus-fight/>

83. Doctors left bewildered after Health Minister dismisses their concerns. *Winnipeg Sun*.
<https://winnipegsun.com/news/news-news/doctors-left-bewildered-after-health-minister-dismisses-their-concerns>
84. How did COVID-19 get so bad in Manitoba and what can we learn from that? *CBC News*.
<https://www.cbc.ca/radio/whitecoat/how-did-covid-19-get-so-bad-in-manitoba-and-what-can-we-learn-from-that-1.5790488>
85. Amid Manitoba's COVID-19 surge, First Nations response team leads fight in hard-hit Indigenous communities. *CBC News*.
<https://www.cbc.ca/radio/whitecoat/amid-manitoba-s-covid-19-surge-first-nations-response-team-leads-fight-in-hard-hit-indigenous-communities-1.5789916>
86. Why COVID-19 cases are surging across Canada and what needs to be done. *CBC News*.
<https://www.cbc.ca/news/health/coronavirus-canada-surge-second-wave-1.5793753>
87. University of Manitoba lab gets funding boost to take extremely close look at COVID-19. *CBC News*.
<https://www.cbc.ca/news/canada/manitoba/covid19-university-manitoba-researchers-grant-1.5793474>
88. Flu season calls for added vigilance. *Winnipeg Free Press*.
<https://www.winnipegfreepress.com/arts-and-life/life/health/flu-season-calls-for-added-vigilance-573010681.html>
89. Virologist says Albertans should avoid all in-person socializing as COVID-19 cases rise. *Global News*.
<https://globalnews.ca/news/7463597/coronavirus-restaurant-restrictions-alberta-virologist/>
90. COVID Alert app could help identify Manitoba cases faster, expert says. *CTV Winnipeg*.
<https://winnipeg.ctvnews.ca/covid-alert-app-could-help-identify-manitoba-cases-faster-expert-says-1.5128271>
91. COVID Alert app is another tool to help in battle against virus, microbiologist says. *CBC Saskatchewan*.
<https://www.cbc.ca/news/canada/saskatoon/covid-alert-app-saskatchewan-jason-kindrachuk-university-of-manitoba-1.5750678>
92. Feds push downloads of COVID Alert app, while Alberta, B.C. drag their feet. *iPolitics*.
<https://ipolitics.ca/2020/10/16/feds-push-downloads-of-covid-alert-app-while-alberta-b-c-drag-their-feet/>
93. Using a jerry can of water on a wildfire: Contact tracing during Winnipeg's new COVID-19 wave. *CBC News*.
<https://www.cbc.ca/news/canada/manitoba/manitoba-contact-tracing-analysis-1.5772107>
94. Hospitals pushed to 'the brink'. *Winnipeg Free Press*.
<https://www.winnipegfreepress.com/special/coronavirus/hospitals-pushed-to-the-brink-572865531.html>
95. As Winnipeg pandemic concerns rise, Transit rolls on. *Winnipeg Free Press*.
<https://www.winnipegfreepress.com/special/coronavirus/as-winnipeg-pandemic-concerns-rise-transit-rolls-on-572915851.html>
96. Disease experts raising alarm about Manitoba's growing COVID-19 crisis. *Global News*.
<https://globalnews.ca/news/7430100/disease-experts-alarm-manitoba-coronavirus-covid-19-crisis/>
97. COVID-19 app needs Manitoba social media push, 'no app, no entry' strategy in bars, says expert. *CBC Manitoba*.
<https://www.cbc.ca/news/canada/manitoba/manitoba-canada-covid-alert-app-use-1.5742986>
98. A tale of two pandemic curves: COVID-19 and the 1918 flu in Winnipeg. *CBC News*.
<https://www.cbc.ca/news/canada/manitoba/winnipeg-covid-influenza-pandemics-1.5752150>
99. COVID cases skyrocket in Winnipeg, new daily record set Tuesday. *Winnipeg Free Press*.
<https://www.winnipegfreepress.com/special/coronavirus/covid-cases-skyrocket-in-winnipeg-new-daily-record-set-572733241.html>

100. COVID-19 deaths among young people 'exceedingly rare,' epidemiologist says after 40-year-old Manitoban dies. *CBC News*.
<https://www.cbc.ca/news/canada/manitoba/covid-19-manitoba-young-deaths-1.5761363>
101. The pros and cons of COVID-19 saliva tests, as Alberta explores testing method. *Global News*.
<https://globalnews.ca/news/7359436/alberta-health-covid-19-saliva-tests/>
102. 'I did not tell her I oppose masks': Saskatoon MLA Cheveldayoff says he supports masks in schools. *CTV Saskatoon*.
<https://saskatoon.ctvnews.ca/i-did-not-tell-her-i-oppose-masks-saskatoon-mla-cheveldayoff-says-he-supports-masks-in-schools-1.5118582>
103. Telegraph article describing the hypothesis that face masks can variolate a population receives mixed reviews on its scientific accuracy. *Health Feedback*.
<https://healthfeedback.org/evaluation/telegraph-article-describing-the-hypothesis-that-face-masks-can-variolate-a-population-receives-mixed-reviews-on-its-scientific-accuracy/>
104. Study Finds Just 1 in 5 People with Coronavirus Are Asymptomatic—Half What Fauci Estimated Earlier This Month. *Newsweek*.
<https://www.newsweek.com/study-percentage-asymptomatic-coronavirus-fauci-1533289>
105. Viruses that come to stay. *Knowable Magazine* (from Annual Reviews).
<https://www.knowablemagazine.org/article/health-disease/2020/viruses-come-stay>
106. Manitoba back-to-school good so far — but still much to learn, more to do about COVID-19 in schools: expert. *CBC News*.
<https://www.cbc.ca/news/canada/manitoba/back-to-school-manitoba-covid-19-1.5732609>
107. Manitoba behind the COVID-technology curve. *Winnipeg Free Press*.
<https://www.winnipegfreepress.com/special/coronavirus/manitoba-behind-the-covid-technology-curve-572456942.html>
108. Manitobans, health officials gearing up for unpredictable flu season. *Global News*.
<https://globalnews.ca/news/7333721/manitobans-health-officials-gearing-up-for-unpredictable-flu-season/>
109. Wearing a mask could protect you from COVID-19 in more ways than you think. *Popular Science*.
<https://www.popsoci.com/story/health/masks-covid-19-immunity/>
110. 'COVID-19 has inevitably changed our history'. *CBC News*.
<https://newsinteractives.cbc.ca/longform/looking-back-at-6-months-of-covid-19-in-manitoba>
111. Lockdowns and a second wave? What the coronavirus pandemic could look like this fall. *Global News*.
<https://globalnews.ca/news/7308087/face-masks-mandatory-starbucks-canada/>
112. Watching for symptoms and anxiety about the unknown: Manitoba's back-to-school. *Global News*.
<https://globalnews.ca/news/7324382/manitoba-back-to-school-issues/>
113. Fall season presents additional COVID-19 risks and a 'chaotic couple of months,' experts suggest. *Global News*.
<https://globalnews.ca/news/7325485/fall-season-coronavirus-risks-experts/>
114. Who is exempt from wearing masks in Manitoba schools? Your back-to-school COVID-19 questions answered. *CBC News*.
<https://www.cbc.ca/news/canada/manitoba/manitoba-covid-19-back-to-school-masks-questions-1.5708357>
115. What a virologist has to say about sending kids to school and asymptomatic carriers of COVID-19. *CTV News*.
<https://winnipeg.ctvnews.ca/what-a-virologist-has-to-say-about-sending-kids-to-school-and-asymptomatic-carriers-of-covid-19-1.5083762>
116. Letting it all air out: Deflating the idea ventilation can easily make schools safer. *CBC News*.
<https://www.cbc.ca/news/canada/manitoba/manitoba-schools-ventilation-covid-analysis-1.5693574>

117. Saliva tests could make spotting coronavirus easier: expert. *Global News*.
<https://globalnews.ca/news/7297186/saliva-coronavirus-test/>
118. Fact check: A coronavirus vaccine that makes everyone infertile has not been approved for use. *Reuters*.
<https://www.reuters.com/article/uk-factcheck-covid-vaccine-causing-infer/fact-check-a-coronavirus-vaccine-that-makes-everyone-infertile-has-not-been-approved-for-use-idUSKBN25H20G>
119. Manitoba students get ready to wear masks for the school year. *Global News*.
<https://globalnews.ca/news/7290229/manitoba-back-to-school-plan/>
120. Spike in home-schooling inquiries in Manitoba brought on by COVID-19 pandemic. *CBC News*.
<https://www.cbc.ca/news/canada/manitoba/manitoba-homeschool-covid-19-1.5671225>
121. Quebec students Grade 5 and up will be required to wear masks in hallways, but not classrooms. *CBC News*.
<https://www.cbc.ca/news/canada/montreal/jean-fran%C3%A7ois-roberge-announces-more-details-in-covid-19-school-plans-1.5680294>
122. Coronavirus: All Manitoba students to head back to classrooms this fall, says education minister. *Global News*.
<https://globalnews.ca/news/7234849/manitoba-coronavirus-back-to-school-plan/>
123. Looking for the COVID-19 hotspots? Ignore the countries seeing virus resurgences. *CTV News*.
<https://www.ctvnews.ca/health/coronavirus/looking-for-the-covid-19-hotspots-ignore-the-countries-seeing-virus-resurgences-1.5066461>
124. Why these Manitoba professors believe masks should be mandatory in schools. *CTV News*.
<https://winnipeg.ctvnews.ca/mobile/why-these-manitoba-professors-believe-masks-should-be-mandatory-in-schools-1.5052875>
125. Children may carry coronavirus at high levels, study finds. *New York Times*.
<https://www.nytimes.com/2020/07/30/health/coronavirus-children.html>
126. Where were you when the pandemic hit? *University Affairs*.
<https://www.universityaffairs.ca/features/feature-article/where-were-you-when-the-pandemic-hit/>
127. Benefits to hygiene theatre? Experts say all-encompassing approach needed. *The Chronicle Journal*.
https://www.chroniclejournal.com/life/health/benefits-to-hygiene-theatre-experts-say-all-encompassing-approach-needed/article_28f79683-46c7-595a-9001-db79a038d104.html
128. Anti-mask movement 'not based in reality', health expert says after Winnipeg protest. *Global News*.
<https://globalnews.ca/news/7195150/coronavirus-anti-mask-protest-health-expert/>
129. As other provinces mandate masks in schools, Manitoba still mulls over decision. *CBC News*.
<https://www.cbc.ca/news/canada/manitoba/as-other-province-mandates-masks-in-schools-manitoba-still-mulls-over-decision-1.5674583>
130. Even Asymptomatic People Carry the Coronavirus in High Amounts. *New York Times*.
<https://www.nytimes.com/2020/08/06/health/coronavirus-asymptomatic-transmission.html>
131. USask's VIDO-InterVac team collaborating with other universities to develop COVID-19 vaccine. *Global News*.
<https://globalnews.ca/news/7207363/covid-19-vaccine-usask-vido-intervacuuniversities/>
132. Canada's coronavirus performance hasn't been perfect. But it's done far better than the U.S. *Washington Post*.
https://www.washingtonpost.com/world/the_americas/coronavirus-canada-united-states/2020/07/14/0686330a-c14c-11ea-b4f6-cb39cd8940fb_story.html
133. Viral Voice. *RadyUM Magazine*.
<https://news.radyfhs.umanitoba.ca/viral-voice/>
134. How Manitobans can safely celebrate Canada Day during the pandemic. *CBC News*.

- <https://www.cbc.ca/news/canada/manitoba/canada-day-2020-pandemic-manitoba-1.5623544>
135. Canada's Coronavirus Outbreak Slows as Cases Top 50,000, but Long Fight Looms. *New York Times*.
<https://www.nytimes.com/reuters/2020/04/29/world/americas/29reuters-health-coronavirus-canada-cases.html>
 136. Olympics: Organisers must be flexible if coronavirus vaccine not ready in time, experts say. *Reuters*.
<https://www.reuters.com/article/us-health-coronavirus-olympics-vaccine/olympics-organisers-must-be-flexible-if-coronavirus-vaccine-not-ready-in-time-experts-say-idUSKBN2220OU>
 137. What the 2018 DRC Ebola epidemic taught us about outbreak response and experimental countermeasures. *Contagion Live*.
<https://www.contagionlive.com/publications/contagion/2020/april/what-the-2018-drc-ebola-epidemic-taught-us-about-outbreak-response-and-experimental-countermeasures>
 138. Higher flu vaccination rates could help expose new viruses like Covid-19 earlier, expert says. *The Guardian*.
<https://www.theguardian.com/world/2020/apr/10/higher-flu-vaccination-rates-could-help-expose-new-viruses-like-covid-19-earlier-expert-says>
 139. Early testing helps Canada's British Columbia fight coronavirus, cases elsewhere soar. *Reuters*.
<https://www.reuters.com/article/us-health-coronavirus-canada-british-col/early-testing-helps-canadas-british-columbia-fight-coronavirus-cases-elsewhere-soar-idUSKCN21R3DI>
 140. When COVID-19 Attacks, Patient's Cells Turn into Virus Factories. *VOA*.
<https://www.voanews.com/science-health/coronavirus-outbreak/when-covid-19-attacks-patients-cells-turn-virus-factories>
 141. How science is accelerating to try and catch up with COVID-19. *Macleans*.
<https://www.macleans.ca/society/health/how-science-is-accelerating-to-try-and-catch-up-with-covid-19/>
 142. This social media post on coronavirus is full of misinformation. *Euronews*.
<https://www.euronews.com/2020/04/08/this-social-media-post-on-coronavirus-is-full-of-misinformation>
 143. Can mosquitoes and black flies transmit COVID-19? *Cottage Life*.
<https://cottagelife.com/general/can-mosquitoes-and-black-flies-transmit-covid-19/>
 144. Sales of Winnipeg company's COVID-19 detection tests halted by Health Canada. *CBC News*.
<https://www.cbc.ca/news/canada/manitoba/covid19-tests-winnipeg-1.5519904>
 145. Super-spreading events linked to COVID-19 across the country. *CBC News*.
<https://www.cbc.ca/news/canada/edmonton/super-spreading-events-covid-19-edmonton-vancouver-1.5518697>
 146. Canada's top doc: 'Masks prevent COVID-19 spread'. *Healthing.ca*.
<https://www.healthing.ca/diseases-and-conditions/coronavirus/not-all-face-masks-are-created-equal-what-you-need-to-know-to-help-prevent-covid-19>
 147. Some labs facing backlog due to shortage of essential chemicals needed for COVID-19 test. *Globe and Mail*.
<https://www.theglobeandmail.com/canada/article-some-labs-facing-backlog-due-to-shortage-of-essential-chemicals-needed/>
 148. Canada has tested more than 50,000 people for Covid-19. Is that enough? *Politico*.
<https://www.politico.com/news/2020/03/19/canada-has-tested-more-than-50-000-people-for-covid-19-is-that-enough-137028>
 149. Coronavirus: Can Canadians expect another pandemic like COVID-19 in the future? *Global News*.
<https://globalnews.ca/news/6712312/coronavirus-outbreak-future-viruses/>
 150. Tap into Manitoba's scientific community for help during pandemic, scientist says. *CBC News*.

- <https://www.cbc.ca/news/canada/manitoba/manitoba-scientific-community-pandemic-covid-19-1.5512504>
151. 'A sinking feeling': Canadian experts on when coronavirus first felt like a serious risk. *Global News*.
<https://globalnews.ca/news/6750755/coronavirus-experts-look-back/>
 152. Manitobans quickly got the message to go home. Now, prepare to stay there. *CBC News*.
<https://www.cbc.ca/news/canada/manitoba/manitoba-covid19-analysis-pandemic-1.5506183>
 153. COVID-19: Bust the coronavirus like a medical microbiologist. *Ottawa Citizen*.
<https://ottawacitizen.com/health/busting-the-coronavirus/>
 154. "It's going to take time" says virus expert on getting through COVID-19 crisis. *Winnipeg Free Press*.
<https://www.winnipegfreepress.com/special/coronavirus/fight-against-covid-19-could-be-a-long-one-says-virus-expert-568882952.html>
 155. Coronavirus RNA detected on cruise ship 17 days after passengers left: CDC report. *Global News*.
<https://globalnews.ca/news/6723553/coronavirus-cruise-ship-surfaces-study/>
 156. America botched coronavirus testing. We're about to find out how badly. *The Daily Beast*.
<https://www.thedailybeast.com/america-botched-coronavirus-testing-were-about-to-find-out-just-how-badly?ref=scroll>
 157. How the provinces differ when it comes to messaging on COVID-19. *The Globe and Mail*.
<https://www.theglobeandmail.com/canada/article-how-the-provinces-differ-when-it-comes-to-messaging-on-covid-19/>
 158. Fight against COVID-19 could be a long one, says virus expert. *Winnipeg Free Press*.
<https://www.winnipegfreepress.com/special/coronavirus/fight-against-covid-19-could-be-a-long-one-says-virus-expert-568882952.html>
 159. Coronavirus: How long can Canadians expect to be social distancing? *Global News*.
<https://globalnews.ca/news/6695737/coronavirus-canadians-social-distancing/>
 160. Want to Help Others in This Crisis? Here Are Some Ideas. *The Tyee*.
<https://thetyee.ca/Solutions/2020/03/19/How-To-Support-Your-Neighbours-During-A-Pandemic/>
 161. Keep your distance: What social distancing means, and why you're being asked to do it. *CBC News*.
<https://www.cbc.ca/news/canada/manitoba/manitoba-coronavirus-covid-19-social-distancing-1.5497790>
 162. ACT FAST: We need to be '10 steps ahead,' says emerging viruses expert. *Winnipeg Sun*.
<https://winnipeg.sun.com/news/news-news/act-fast-we-need-to-be-10-steps-ahead-says-emerging-viruses-expert>
 163. The time is now to act': COVID-19 spreading in Canada with no known link to travel, previous cases. *CBC News*.
<https://www.cbc.ca/news/health/coronavirus-community-transmission-canada-1.5498804>
 164. Why an infectious disease expert thinks the NHL season won't resume soon. *The Athletic*.
<https://theathletic.com/1673842/2020/03/13/why-an-infectious-disease-expert-thinks-the-nhl-season-wont-resume-soon/>
 165. Coronavirus: Can patients get reinfected after recovery? Some reports say yes but experts are divided. *MEAWW*.
<https://meaww.com/coronavirus-reinfection-patients-recovery-japan-case-test-positive-negative-virus-sickness-symptoms>
 166. Overreacting in response to coronavirus pandemic 'just as harmful as underreacting': health expert. *CBC News*.
<https://www.cbc.ca/news/canada/manitoba/coronavirus-covid-19-manitoba-winnipeg-health-strategy-1.5495297>
 167. Oil companies move to prevent coronavirus outbreaks at remote lodges. *The Globe and Mail*.

- <https://www.theglobeandmail.com/canada/alberta/article-oil-companies-move-to-prevent-coronavirus-outbreaks-at-remote-lodges/>
168. Should You Be Sanitizing Your Phone to Avoid Getting Sick? *Livestrong*.
<https://www.livestrong.com/article/13725307-how-to-disinfect-phone/>
 169. Seattle Comic Con Just Got Postponed Because Coronavirus. *VICE News*.
https://www.vice.com/en_ca/article/m7qxp/seattle-comic-con-just-got-postponed-because-coronavirus
 170. Response in China slowed outbreak of coronavirus — but experts caution against extreme measures in Seattle. *The Seattle Times*.
<https://www.seattletimes.com/seattle-news/response-in-china-slowed-outbreak-of-coronavirus-but-experts-caution-against-extreme-measures-in-seattle/>
 171. Can an Algorithm Predict the Next Disease Outbreak? *Freethink*.
<https://www.freethink.com/articles/zoonotic-disease>
 172. Can Coronavirus Be Transmitted Through Food? Here's What You Should Know. *Huffington Post*.
https://www.huffingtonpost.ca/entry/coronavirus-food-what-to-know_15e600d6bc5b644545ea4913b
 173. COVID-19: What You Might Need If You're Quarantined at Home. *Consumer Reports*.
<https://www.consumerreports.org/coronavirus/covid-19-what-you-might-need-if-youre-quarantined-at-home/>
 174. Don't panic, don't stockpile food, Manitoba health minister urges as coronavirus fears ramp up. *CBC Manitoba*.
<https://www.cbc.ca/news/canada/manitoba/panic-food-cameron-friesen-health-minister-coronavirus-1.5483935>
 175. How contagious is COVID-19 compared to other viral diseases? *CTV News*.
<https://www.ctvnews.ca/health/coronavirus/how-contagious-is-covid-19-compared-to-other-viral-diseases-1.4836734>
 176. 'This will not be contained': Experts cast doubt that spread of COVID-19 can be stopped. *CBC World*.
<https://www.cbc.ca/news/world/coronavirus-covid-19-containment-who-1.5478766>
 177. COVID-19: How effective are household cleaners in fighting coronavirus? *Global News*.
<https://globalnews.ca/news/6617690/coronavirus-household-cleaners/>
 178. Canadian virus expert hopes to douse COVID-19 concerns. *Kitchener Today*.
<https://www.kitchenertoday.com/local-news/canadian-virus-expert-hopes-to-douse-covid-19-concerns-2141870>
 179. Coronavirus outbreak prompts Canadian officials to weigh asking all travelers from China to 'self-isolate'. *The Globe and Mail*.
<https://www.theglobeandmail.com/canada/article-coronavirus-outbreak-prompts-canadian-officials-to-weigh-asking-all/>
 180. Trump says COVID-19 will go away in April. Experts say it's too soon to tell. *Global News*.
<https://globalnews.ca/news/6535483/coronavirus-seasonal-virus-experts/>
 181. 'A perfect setup': Virus outbreaks common on cruise ships, experts say. *Global News*.
<https://globalnews.ca/news/6525470/coronavirus-cruise-ships/>
 182. The novel coronavirus has now killed more people than SARS. *The Daily Hive*.
<https://dailyhive.com/vancouver/coronavirus-more-deaths-sars>
 183. The novel coronavirus explained: Should I be worried? *The Daily Hive*.
<https://dailyhive.com/vancouver/coronavirus-outbreak-explained>
 184. What if China fails to contain the coronavirus outbreak? *CBC Health*.
<https://www.cbc.ca/news/health/coronavirus-china-quarantine-endemic-1.5456641>
 185. Canadian health officials urge travelers from Hubei to voluntarily quarantine themselves for 14 days. *The Globe and Mail*.

- <https://www.theglobeandmail.com/canada/article-canadian-health-officials-urge-visitors-from-hubei-to-voluntarily/>
186. What the Worst Case of a Coronavirus Pandemic Might Look Like. *The Daily Beast*.
<https://www.thedailybeast.com/coronavirus-pandemic-worst-case-scenario-is-ugly-experts-say>
 187. New coronavirus may be no more dangerous than the flu, despite worldwide alarm: experts. *National Post*.
<https://nationalpost.com/health/new-coronavirus-may-be-no-more-dangerous-than-the-flu-despite-worldwide-alarm-experts>
 188. Coronavirus: No scientific evidence airport screening measures work, experts say. *Global News*.
<https://globalnews.ca/news/6491615/coronavirus-airport-screening-effectiveness/>
 189. 'Watch and wait': More time needed to determine scope of the novel coronavirus, expert says. *CTV News*.
<https://winnipeg.ctvnews.ca/watch-and-wait-more-time-needed-to-determine-scope-of-the-novel-coronavirus-expert-says-1.4779124>
 190. U of M researcher urges sense of perspective on Wuhan coronavirus. *650 CKOM*.
<https://www.ckom.com/2020/01/23/u-of-m-researcher-urges-sense-of-perspective-on-wuhan-coronavirus/>
 191. Cured but still contagious: How mixed messages on sexual transmission and breastfeeding may help Ebola spread. *The New Humanitarian*.
<https://www.thenewhumanitarian.org/news/2019/11/28/Ebola-sexual-transmission-breastfeeding-women-children>
 192. U of M researchers head to West Africa to study how Ebola affects reproductive system. *CBC News*.
<https://www.cbc.ca/news/canada/manitoba/university-of-manitoba-researchers-ebola-reproductive-system-1.5328917>
 193. Ebola hasn't been cured yet, but two experimental drugs are showing significant progress. *Popular Science*.
<https://www.popsoci.com/experimental-ebola-drugs-improve-survival-rates/>
 194. Ebola is back in the Congo — and America's Africa policies aren't helping contain its spread. *NBC Think*.
<https://www.nbcnews.com/think/opinion/ebola-back-congo-america-s-africa-policies-aren-t-helping-ncna1045531>
 195. Confronting a Killer. *RadyUM Magazine*.
<http://news.radyfhs.umanitoba.ca/confronting-a-killer/>
 196. Kindrachuk Battling Bugs. *Winnipeg Free Press*.
<https://www.winnipegfreepress.com/our-communities/souwester/Kindrachuk-battling-the-bugs-425152084.html>
 197. NIH Study of Ebola Patient Traces Disease Progression and Recovery. *National Institutes of Allergy and Infectious Diseases Press Release*.
<https://www.nih.gov/news-events/news-releases/nih-study-ebola-patient-traces-disease-progression-recovery>
 198. Feature article: Using hamsters to study hemorrhagic fever. *American Society of Biochemistry and Molecular Biology Today*.
<http://www.asbmb.org/asbmbtoday/201504/JournalNews/MCPHamsters/>
 199. The fight on Ebola continues in the lab. *USAID*. October, 2014.
<https://blog.usaid.gov/2014/10/the-fight-on-ebola-continues-in-the-lab/>
 200. U of S alumnus and tech helping in fight against Ebola. *University of Saskatchewan Press Release*.
<http://words.usask.ca/news/2014/10/08/u-of-s-alumnus-and-tech-helping-in-fight-against-ebola/>
 201. Software helps Ebola Research. *University of Saskatchewan News Article*.
<http://words.usask.ca/news/2014/10/08/software-helps-ebola-research/>

202. Technology developed at U of S advancing research on Ebola. *CBC News*.
<http://www.cbc.ca/news/canada/saskatoon/technology-developed-at-u-of-s-advancing-research-on-ebola-1.2795980>
203. Man who grew up in Saskatchewan fighting Ebola. *650 CKOM News*.
<http://ckom.com/story/man-who-grew-sask-fighting-ebola-west-africa/418777>
204. Ebola: What you need to know. *The Sheaf*.
<https://thesheaf.com/2014/12/02/ebola-what-you-need-to-know/>
205. Perkin Elmer Featured Publication Notes:
http://cellularimaging.perkinelmer.com/pdfs/featured_notes/PublicationNoteJahrling.pdf

Radio, Podcast and Television Interviews

Recurring Appearances

1. Weekly guest – *CTV News Channel*
2. Weekly radio guest – COVID-19 updates. *Charles Adler Tonight*.
3. Weekly radio guest – COVID-19 updates. *Sunday Night Health Show* (with Maureen McGrath).
4. Weekly radio guest – *The News with Richard Cloutier and Julie Buckingham*.
5. Recurring guest – Ask an Expert. *Reuters*
6. Recurring guest – *Ottawa at Work with Leslie Roberts*. 580 CFRA
7. Recurring guest – *Jody Vance*. CKNW
8. Recurring guest – *Lynda Steele Show*. CKNW
9. Recurring guest – *CBC News Network*
10. Recurring radio guest – Hal Anderson. 680 CJOB
11. Recurring guest – COVID-19 updates. *Leading Britain's Conversation*
12. Recurring guest – COVID-19 safety restrictions and economic impacts. *Bloomberg News Network*.
13. Recurring guest – COVID-19 updates. *Viewpoints with Todd Vanderhayden*

Individual Appearances

14. The Covid Cruise. *The Nature of Things*
<https://www.cbc.ca/natureofthings/episodes/the-covid-cruise>
15. Covid-19 vaccine hesitancy. *CNN Newsroom* (with John Avlon)
<http://www.cnn.com/TRANSCRIPTS/2104/08/cnr.18.html>
16. COVID-19 Chapter 15: Disease, Take 2. *This Podcast Will Kill You*.
<https://podcasts.apple.com/gr/podcast/covid-19-chapter-15-disease-take-2/id1299915173?i=1000514995071>
17. Getting to the truth on vaccines with Dr. Jason Kindrachuk – Infectious disease expert at the University of Manitoba. *No Nonsense with Pamela Wallin*.
<http://pamelawallin.com/getting-to-the-truth-on-vaccines-with-dr-jason-kindrachuk-infectious-disease-expert-at-the-university-of-manitoba/>
18. Canada needs to be better prepared for the next pandemic, which can be very soon: Virologist. *Bloomberg News Network*.
<https://www.bnnbloomberg.ca/canada/video/canada-needs-to-be-better-prepared-for-the-next-pandemic-which-can-be-very-soon-virologist~2142993>
19. Covid-19 vaccines for Canadians. *The Morning Show*. 770 CHQR.
20. Covid-19 a year later. *The Mike Fawrell Show*. 570 News.
21. Covid-19 vaccines and variants. 580 CFRA.
22. Covid-19 in schools. *CBC Saskatchewan*.
23. Covid-19: variants and vaccination. *Alberta at Noon*.

24. 'We're really in a bit of a time crunch': Infectious disease expert warns of COVID-19 variants in Canada. *CTV News*.
<https://saskatoon.ctvnews.ca/we-re-really-in-a-bit-of-a-time-crunch-infectious-disease-expert-warns-of-covid-19-variants-in-canada-1.5285277>
25. Tracking the global race to vaccinate against COVID-19. *Global News*.
<https://globalnews.ca/video/7596856/tracking-the-global-race-to-vaccinate-against-covid-19/>
26. Manitoba premier amends interprovincial travel rules amid COVID-19 variant surge. *CTV News*.
<https://winnipeg.ctvnews.ca/manitoba-premier-amends-interprovincial-travel-rules-amid-covid-19-variant-surge-1.5282677?cache=yesclipId104062>
27. Immune but infectious: Can someone vaccinated against COVID-19 still spread the virus? *Global News*.
<https://globalnews.ca/news/7559408/health-matters-covid-19-vaccine-immune-but-infectious/>
28. Covid-19 variants and transmission. *BBC World*.
29. Detection of U.K. variant of COVID-19 in Manitoba may only be a matter of time, experts warn. *CTV News*.
<https://winnipeg.ctvnews.ca/detection-of-u-k-variant-of-covid-19-in-manitoba-may-only-be-a-matter-of-time-experts-warn-1.5249194>
30. Health officials in Canada monitoring for variant of virus identified in the U.K. *CTV News*.
<https://winnipeg.ctvnews.ca/health-officials-in-canada-monitoring-for-variant-of-virus-identified-in-the-u-k-1.5240567>
31. Covid-19 and the holidays. *RTE News*.
32. UA biologist working to help stop future diseases. *5 News Online*.
<https://www.5news.com/article/news/local/ua-biologist-working-to-help-stop-future-diseases/527-60ad477b-c23c-408d-b538-6d6300b3616c>
33. 'Expedited, not fast-tracked': Virologist explains the safety of the COVID-19 vaccine. *CTV News*.
<https://winnipeg.ctvnews.ca/expedited-not-fast-tracked-virologist-explains-the-safety-of-the-covid-19-vaccine-1.5232461>
34. What you need to know as COVID-19 vaccinations begin in Alberta. *Global News*.
<https://globalnews.ca/news/7522076/alberta-covid-19-vaccinations/>
35. Saskatoon mail processing facility sanitized after COVID-19 case confirmed: Canada Post. *CTV News*.
<https://saskatoon.ctvnews.ca/saskatoon-mail-processing-facility-sanitized-after-covid-19-case-confirmed-canada-post-1.5220655>
36. Saskatoon pharmacist experiences ongoing fatigue, gaps in memory months after contracting COVID-19. *CTV News*.
<https://saskatoon.ctvnews.ca/saskatoon-pharmacist-experiences-ongoing-fatigue-gaps-in-memory-months-after-contracting-covid-19-1.5206240>
37. How did COVID-19 get so bad in Manitoba and what can we learn from that? *The Dose*.
<https://www.cbc.ca/radio/whitecoat/how-did-covid-19-get-so-bad-in-manitoba-and-what-can-we-learn-from-that-1.5790488>
38. Flu shot recommended to ease pandemic burden on hospitals. *Global National*.
<https://globalnews.ca/video/7377951/flu-shot-recommended-to-ease-pandemic-burden-on-hospitals>
39. COVID-19 and COVID Alert. *CBC Morning Edition*.
40. COVID-19 and COVID Alert. *CBC Saskatoon Morning*.
41. Northern Sask. medical health officer calls for tighter restrictions on outdoor gatherings. *CTV News*.
<https://regina.ctvnews.ca/northern-sask-medical-health-officer-calls-for-tighter-restrictions-on-outdoor-gatherings-1.5271879>
42. Millions of coronavirus rapid tests won't arrive for months: Health Canada. *Global News*.
<https://globalnews.ca/news/7373108/coronavirus-rapid-tests-health-canada/>

43. Early identification is crucial in stopping transmission: Emerging viruses specialist. *Bloomberg News Network*.
<https://www.bnnbloomberg.ca/video/early-identification-is-crucial-in-stopping-transmission-emerging-viruses-specialist~2022493>
44. Inside Canada's race for a COVID-19 vaccine. *CBC Front Burner*.
<https://www.cbc.ca/radio/frontburner/inside-canada-s-race-for-a-covid-19-vaccine-1.5691393>
45. No Easy Answers. *CBC The Current*.
<https://www.cbc.ca/radio/thecurrent/the-current-for-aug-10-2020-1.5680419>
46. Coronavirus: Face coverings to be mandatory at all Starbucks Canada locations. *Global News*.
<https://globalnews.ca/news/7308087/face-masks-mandatory-starbucks-canada/>
47. Manitoba students get ready to wear masks for the school year. *Global News*.
<https://globalnews.ca/news/7290229/manitoba-back-to-school-plan/>
48. Ebola Survivors Face Stigma, Reproductive Health Impact. *Contagion Live*.
<https://www.contagionlive.com/news/supporting-african-nations-fight-against-ebola->
49. The West Block — Episode 32, Season 9. *Global News*.
<https://globalnews.ca/news/6809583/the-west-block-episode-32-season-9/>
50. Podcast. Blood Brothers #31: Is 5G network linked to the Coronavirus pandemic? *5 Pillars*.
<https://5pillarsuk.com/2020/04/10/blood-brothers-31-is-5g-network-linked-to-the-coronavirus-pandemic/>
51. Podcast. Understanding SARS-CoV-2 in an emerging virus context (3 parts). *Contagion Live*.
<https://www.contagionlive.com/news/jason-kindrachuk-phd-understanding-sarscov2-in-an-emerging-virus-context>
52. How to fight COVID-19 in Canada. *Marketplace*.
<https://www.cbc.ca/marketplace/episodes/2019-2020/how-to-fight-covid-19-in-canada>
53. Viewer questions answered about COVID-19. *CBC News*.
<https://www.msn.com/en-ca/news/world/viewer-questions-answered-about-covid-19/vi-BB12cwww>
54. Manitoba experts weigh in on wearing face masks amid COVID-19 pandemic. *Global News*.
<https://globalnews.ca/news/6777311/manitoba-experts-face-masks-coronavirus/>
55. Jason Kindrachuk studies emerging viruses. *CBC News*.
<https://www.cbc.ca/player/play/1714835523791>
56. Winnipeg's microbiology lab playing pivotal role in the fight against COVID-19. *Global News*.
<https://globalnews.ca/news/6720413/winnipegs-microbiology-lab-playing-pivotal-role-in-the-fight-against-covid-19/>
57. Medical expert discusses deal to close Canada-US border. *Cable Public Affairs Channel (CPAC)*.
<https://www.youtube.com/watch?v=TjLs8x6CPs8>
58. Coronavirus outbreak: we are not as prepared as we thought. *The West Block*.
<https://www.youtube.com/watch?v=gaughXPYXIU>
59. Fighting COVID-19 with the right information. *CTV Winnipeg*.
<https://winnipeg.ctvnews.ca/video?clipId=1923952>
60. Manitoba researchers working to crack Covid-19. *CTV Winnipeg*.
<https://winnipeg.ctvnews.ca/video?clipId=1923235>
61. Pandemic stalks but congress still fails to pass emergency legislation. *Loud & Clear Radio*.
<https://t.co/HK9nZia7yH?amp=1>
62. COVID-19 update. *CTV Winnipeg*.
<https://winnipeg.ctvnews.ca/video?clipId=1921542>
63. One step closer to a coronavirus vaccine. *Charles Adler Tonight*.
<https://omny.fm/shows/charles-adler-tonight/one-step-closer-to-a-coronavirus-vaccine>
64. The latest updates on COVID-19. *Charles Adler Tonight*.
<https://player.fm/series/series-2342436/full-show-the-latest-updates-on-covid-19>
65. Coronavirus shuts down the sports world - Part 1. *630 CHED Inside Sports*.
<https://omny.fm/shows/inside-sports/coronavirus-shuts-down-the-sports-world-part-1>
66. Why are so many countries better than the US at handling COVID-19? *Loud & Clear Radio*.

- <https://t.co/diVAO77XMe?amp=1>
67. Don't make your own hand sanitizer: infectious disease expert. *CBC National News*.
<https://www.cbc.ca/player/play/1707545667562>
 68. Radio Interview. COVID-19 preparation and responses. 630 CHED.
 69. Radio Interview. Canadian virus expert hopes to douse COVID-19 concerns. *Kitchener Today with Brian Bourke*.
 70. 'We're not gonna take a chance': travellers express concern as COVID-19 cases grow. *CTV Winnipeg*.
<https://winnipeg.ctvnews.ca/we-re-not-gonna-take-a-chance-travellers-express-concern-as-covid-19-cases-grow-1.4835954>
 71. 'Watch and wait': More time needed to determine scope of the novel coronavirus, expert says. *CTV News*.
<https://winnipeg.ctvnews.ca/watch-and-wait-more-time-needed-to-determine-scope-of-the-novel-coronavirus-expert-says-1.4779124>
 72. Radio Interview. COVID-19 transmission and spread. 640 Global News Radio.
 73. How contagious is COVID-19 compared to other viral diseases? *CTV National News*.
 74. Radio Interview nationwide spots. COVID-19. *CBC News Radio*.
 75. Podcast Interview. Coronavirus fears in Canada. *Spice Radio*.
 76. Podcast Interview. Ebola persistence and current situation in DRC. *Contagion Live*.
<https://www.contagionlive.com/news/contagion-connect-episode-5-ebola-past-present-future>
 77. Radio Interview. Coronavirus fears. 630 CHED.
 78. Radio Interview. Understanding emerging virus outbreaks. *Kitchener Today with Brian Bourke*.
 79. Radio Interview. Novel coronavirus epidemic. *CBC Blue Sky*.
 80. National radio interview. Coronavirus cases in Canada. *Evan Solomon Show*.
 81. Second presumptive coronavirus case in Canada. *CTV National News*.
<https://www.ctvnews.ca/video?clipId=1885463>
 82. Canada's first presumptive coronavirus case. *CTV National News*.
<https://www.ctvnews.ca/video?clipId=1885091>
 83. Radio Interview. Novel coronavirus outbreak situation update. *CBC Manitoba*.
 84. Radio Interview. Novel coronavirus outbreak. *Brent Loucks Show*. 650 CKOM.
 85. Radio Interview. Ebola virus persistence in West Africa. *CBC Up to Speed*.
 86. Fighting an Ebola Outbreak, *CTV Winnipeg*. 2019/06/19
<https://winnipeg.ctvnews.ca/video?clipId=1711335>
 87. Testicular persistence of Ebola virus. *CTV Winnipeg*. 2018/05/28
<https://winnipeg.ctvnews.ca/video?clipId=1404560>
 88. A firsthand Ebola experience. *CTV News*.
<http://saskatoon.ctvnews.ca/video?clipId=476855>
 89. Radio Interview. Ebola experiences in Liberia. *John Gormley Show*. 650 CKOM.
 90. Radio Interview. Saskatoon man fighting Ebola in Liberia. *Brent Loucks Show*. 650 CKOM.

PATENT SUBMISSIONS

1. Small Cationic Anti-biofilm and IDR Peptides.
United States. PCT/US2014/052993. 2014/08/27.
Patent Status: Pending
2. Combination adjuvant formulation.
United States. US9408908 B2. 2013/02/15.
Patent Status: Granted/Issued
Year Issued: 2016
3. Immunomodulatory compositions and methods for treating disease with modified host defense peptides.

United States. US9102754 B2. 2008/06/27.
Patent Status: Granted/Issued
Year Issued: 2015

Schedule C



Racial, Economic, and Health Inequality and COVID-19 Infection in the United States

Vida Abedi^{1,2} · Oluwaseyi Olulana³ · Venkatesh Avula¹ · Durgesh Chaudhary⁴ · Ayesha Khan⁴ · Shima Shahjouei⁴ · Jiang Li¹ · Ramin Zand⁴

Received: 4 May 2020 / Revised: 4 May 2020 / Accepted: 27 July 2020
 © W. Montague Cobb-NMA Health Institute 2020

Abstract

Objectives There is preliminary evidence of racial and social economic disparities in the population infected by and dying from COVID-19. The goal of this study is to report the associations of COVID-19 with respect to race, health, and economic inequality in the United States.

Methods We performed an ecological study of the associations between infection and mortality rate of COVID-19 and demographic, socioeconomic, and mobility variables from 369 counties (total population, 102,178,117 [median, 73,447; IQR, 30,761–256,098]) from the seven most affected states (Michigan, New York, New Jersey, Pennsylvania, California, Louisiana, Massachusetts).

Results The risk factors for infection and mortality are different. Our analysis shows that counties with more diverse demographics, higher population, education, income levels, and lower disability rates were at a higher risk of COVID-19 infection. However, counties with higher proportion with disability and poverty rates had a higher death rate. African Americans were more vulnerable to COVID-19 than other ethnic groups (1981 African American infected cases versus 658 Whites per million). Data on mobility changes corroborate the impact of social distancing.

Conclusion Our study provides evidence of racial, economic, and health inequality in the population infected by and dying from COVID-19. These observations might be due to the workforce of essential services, poverty, and access to care. Counties in more urban areas are probably better equipped at providing care. The lower rate of infection, but a higher death rate in counties with higher poverty and disability could be due to lower levels of mobility, but a higher rate of comorbidities and health care access.

Keywords Healthcare disparities · Health status disparities · Socioeconomic factors · COVID-19 · Economic inequality · Racial disparity · United States · Population-based analysis · Ecological-based study

Jiang Li and Ramin Zand are co-senior authors.

Electronic supplementary material The online version of this article (<https://doi.org/10.1007/s40615-020-00833-4>) contains supplementary material, which is available to authorized users.

✉ Ramin Zand
 rzand@geisinger.edu; ramin.zand@gmail.com

¹ Department of Molecular and Functional Genomics, Weis Center for Research, Geisinger Health System, Danville, PA, USA

² Biocomplexity Institute, Virginia Tech, Blacksburg, VA, USA

³ Geisinger Commonwealth School of Medicine, Scranton, PA, USA

⁴ Geisinger Neuroscience Institute, Geisinger Health System, Danville, PA, USA

Introduction

The complexity of managing patients with the coronavirus disease 2019 (COVID-19), a global pandemic [1] originated in China [2], has led to the widespread implementation of preventative measures such as social distancing and mask use [3] in many countries including the United States (US). As of April 14, 2020, there were over 1.9 million confirmed cases around the world with 601,000 cases and 24,129 deaths in the US alone [4]. It has been reported that age 65 and older, body mass index ≥ 40 , diabetes [5] immunosuppression, smoking, hypertension, and cardiovascular diseases are underlying conditions that increase the risk of death from COVID-19 [6, 7].

The most recent conundrum of this disease is ascribed to the preliminary evidence of racial disparities in the population infected and dying from COVID-19 [3]. In a recent study, the Centers for Disease Control and Prevention (CDC) reported

data from fourteen states and suggested that the US Black population may be disproportionately affected by COVID-19 [3]. This observation is consistent with the influenza A (H1N1) pandemic where other studies showed evidence of racial and ethnic disparities in the population affected both in exposure, severity, and mortality of the disease [8, 9]. As states release the racial and ethnic demographic data of COVID-19 cases, in addition to the increased spread of this disease to the central states, it is imperative that we understand the patterns of infection and death to reduce the risks, especially for high-risk population, and resolve issues that impede the provision of optimal care.

In this study, we conducted an ecological-based analysis to explore racial and economic inequality associated with the infection rate and risk of mortality due to COVID-19 in the US. The goal of the study was to provide evidence on the association of COVID-19 with respect to race, income level, poverty, education, and the impact of preventative measures such as social distancing. We trust that the decision making by the states' officials will be driven by data and based on their unique needs and population characteristics to help in combating this disease.

Methodology

The study was conducted at two levels: (1) analysis of population characteristics (44 variables) for 369 counties in seven states which had the highest rate of COVID-19 infection as of April 9, 2020, along with COVID-19 infection and mortality rates. The included states were California, Michigan, New York, New Jersey, Louisiana, Pennsylvania, and Massachusetts; (2) analysis of COVID-19-related infection and death rate across all the states in the US with race/ethnicity information on the affected subject when available.

Data Source, Outcomes, and Independent Variables: Data sources in this study include (1) publicly available data from USAfacts and the US Census Bureau for COVID-19 cases and county-level demographic data [10, 11], (2) COVID-19 data reported by each state on their department of health websites [10], (3) State Population by race/ethnicity data [12, 13], and (4) mobility data extracted from Google [14].

The variables used in this study include county-level information on total population, mobility, race, poverty level, median income, education, disability, and rate of the insured population. Mobility data were extracted from Google as reported on April 05, 2020. The state-level data were extracted on April 16, 2020. The outcome variables include the rate of COVID-19 infection and all COVID-19-related death as provided by each state's department of health as of April 09, 2020. The infection rate is based on the reported results from all the laboratories testing samples in each county/state. The

mortality data are reported by hospitals, nursing homes, and other health facilities. Table 1 summarizes the data elements used in this study. Only data provided by the states on their official websites were included in this study. Additionally, to compare the rate of COVID-19 cases and death, the population data for each ethnic/racial group affected were extracted from health department websites.

Statistical Analysis We summarized all continuous variables as mean \pm standard deviation or median with inter-quartile range [IQR] and categorical variables as percentages. Data from different sources were extracted and analyzed for outliers. Values not within three inter-quartiles were removed as part of the data pre-processing. Each continuous variable was centralized and z score transformed. Thus, the transformed variables passed the normality test and the correlation matrix was created. Bivariate, partial correlation, and regression were used to test hypotheses of association. The correlation coefficients between "death rate" and "infection rate" with independent variables were calculated by Pearson's correlation (R corr package). Partial correlation was further evaluated by Pearson's correlation (R ppcor package) to determine if the existing correlation was still valid after controlling the second independent variable. The Bonferroni correction for multiple testing of controlling variables was considered to adjust the p value of the correlation. Bivariate linear regression adjusted for "State" variables was utilized to test the association between "death rate" or "infection rate" with independent variables. The raw p value was present in the forest plot. False discovery rate (FDR) corrections for multiple testing were calculated using the Benjamin and Hochberg procedure. Statistical analyses were performed using R version 3.6.2 [16]. and IBM SPSS Statistics 26 [17].

Results

Population, Mobility, and Socioeconomic Determinants

We extracted data from four different sources on 369 counties from seven states, including five states from the East Coast (Michigan, New York, New Jersey, Pennsylvania, and Massachusetts), one state from the West Coast (California), and one state from the South (Louisiana) with the total population of 102,178,117 (median, 73,447; IQR, 30,761–256,098). The information on race, income, education level, insurance, poverty, and disability including the description of abbreviated variables is summarized in Table 1, (Supplemental Table S1 includes additional summary statistics of the dataset).

Our data show a significant association among different socioeconomic determinants, such as poverty level, education,

Table 1 Data elements, descriptions, reference to sources of data, and base statistics used in this study

Data elements	Description, source ref.	N (valid)	N missing/outlier)	Mean	Minimum	Maximum
Population	Total Population [15]	346	23 (0/23)	155,080	1129	918,702
Rate COVID	Rate of COVID in one In Million [10]	325	44 (38/6)	912.20	15.36	5093.99
Death rate	Rate of COVID related Death (percent) [10]	218	151(139/12)	4.13	0.31	15.79
Change in mobility						
Retail mobility	GOOGLE RETAIL RECREATION MOBILITY [14]	353	16 (14/2)	-0.47	-1.00	0.01
Grocery mobility	GOOGLE GROCERY PHARMACY MOBILITY [14]	354	15 (15/0)	-0.16	-0.67	0.31
Parks mobility	GOOGLE PARKS MOBILITY [14]	201	168 (168/0)	0.05	-0.87	1.80
Transit mobility	GOOGLE TRANSIT MOBILITY [14]	198	171 (169/2)	-0.48	-0.88	0.09
Work mobility	GOOGLE WORKPLACE MOBILITY [14]	356	13 (11/2)	-0.37	-0.60	-0.15
Resident mobility	GOOGLE RESIDENTIAL MOBILITY [14]	282	87 (87/0)	0.14	-0.02	0.32
Computer	Percent Has computer with broadband Internet subscription [11]	368	1 (0/1)	28.82	13.88	38.50
Race						
Black male	Percent BA (Black Alone) MALE [15]	359	10 (0/10)	4.66	0.00	23.04
Black female	Percent BA (Black Alone) FEMALE [15]	359	10 (0/10)	4.24	0.09	23.98
Asian male	Percent AA (Asian Alone) MALE [15]	349	20 (0/20)	1.00	0.00	5.71
Asian female	Percent AA (Asian Alone) FEMALE [15]	346	23 (0/23)	1.06	0.04	5.60
White male	Percent NHWA (non-Hispanic White Alone) MALE [15]	369	0 (0/0)	37.07	4.48	50.26
White female	Percent NHWA (non-Hispanic White Alone) FEMALE [15]	369	0 (0/0)	37.56	4.65	49.00
Hispanic male	Percent H (Hispanic) MALE [15]	348	21 (0/21)	3.83	0.40	17.75
Hispanic female	Percent H (Hispanic) FEMALE [15]	348	21 (0/21)	3.51	0.39	17.09
Income						
Median income	Median Family income; past 12 months 2018 [15]	364	5 (0/5)	68,969	30,717	131,554
Poverty	Percent below poverty level Population for whom poverty status is determined [15]	366	3 (0/3)	14.89	4.60	33.50
Poverty male	Percent below poverty level Population for whom poverty status is determined SEX Male [15]	367	2 (0/2)	13.64	4.20	33.20
Poverty female	Percent below poverty level Population for whom poverty status is determined SEX Female [15]	367	2 (0/2)	16.20	4.80	38.50
Poverty Black	Percent below poverty level Population for whom poverty status is determined RACE AND HISPANIC OR LATINO ORIGIN Black or African American alone [15]	368	1 (1/0)	32.30	0.60	100.00

Table 1 (continued)

Data elements	Description, source ref.	N (valid)	N missing/outlier	Mean	Minimum	Maximum
Poverty Asian	Percent below poverty level Population for whom poverty status is determined RACE AND HISPANIC OR LATINO ORIGIN Asian alone [15]	359	10 (5/5)	14.71	0.00	70.10
Poverty Hispanic	Percent bel poverty Pop for whom poverty is determined RACE AND HISPANIC OR LATINO ORIGIN Hispanic or Latino origin of any race [15]	365	4 (0/4)	24.00	0.00	68.70
Poverty White	Percent below poverty level Population for whom poverty status is determined RACE AND HISPANIC OR LATINO ORIGIN White alone not Hispanic or Latino [15]	369	0 (0/0)	11.82	3.20	26.40
Education						
High school	Percent below poverty level Population for whom poverty status is determined RACE AND HISPANIC OR LATINO ORIGIN White alone [15]	367	2 (0/2)	87.67	69.40	96.10
Bachelors	Percent Population 25 years and over Bachelors degree or higher [15]	369	0 (0/0)	24.64	7.40	60.80
High school White	Percent RACE AND HISPANIC OR LATINO ORIGIN BY EDUCATIONAL ATTAINMENT White alone not Hispanic or Latino High school graduate or higher [15]	369	0 (0/0)	90.78	76.20	98.30
Bachelors White	Percent RACE AND HISPANIC OR LATINO ORIGIN BY EDUCATIONAL ATTAINMENT White alone not Hispanic or Latino Bachelors degree or higher [15]	368	1 (0/1)	27.04	10.70	76.40
High school Black	Percent RACE AND HISPANIC OR LATINO ORIGIN BY EDUCATIONAL ATTAINMENT Black alone High school graduate or higher [15]	366	3 (0/3)	81.30	40.80	100.00
Bachelors Black	Percent RACE AND HISPANIC OR LATINO ORIGIN BY EDUCATIONAL ATTAINMENT Black alone Bachelors degree or higher [15]	369	0 (0/0)	16.21	0.00	69.60
High school Asian	Percent RACE AND HISPANIC OR LATINO ORIGIN BY EDUCATIONAL ATTAINMENT Asian alone High school graduate or higher [15]	356	13 (6/7)	85.48	52.10	100.00
Bachelors Asian	Percent RACE AND HISPANIC OR LATINO ORIGIN BY EDUCATIONAL ATTAINMENT Asian alone Bachelors degree or higher [15]	363	6 (6/0)	45.35	0.00	100.00

Table 1 (continued)

Data elements	Description, source ref.	N (valid)	N missing/outlier)	Mean	Minimum	Maximum
High school Hispanic	Percent RACE AND HISPANIC OR LATINO ORIGIN BY EDUCATIONAL ATTAINMENT Hispanic or Latino Origin High school graduate or higher [15]	368	1 (1/0)	72.91	22.20	100.00
Bachelors Hispanic	Percent RACE AND HISPANIC OR LATINO ORIGIN BY EDUCATIONAL ATTAINMENT Hispanic or Latino Origin Bachelors degree or higher [15]	368	1 (1/0)	15.36	0.00	50.30
Disability/insurance						
Disability	Percent with a disability Subject Total civilian noninstitutionalized population [15]	369	0 (0/0)	14.99	6.50	28.50
Insured male	Percent Insured Civilian noninstitutionalized population SEX Male [15]	368	1 (0/1)	91.53	80.50	97.50
Insured female	Percent Insured Civilian noninstitutionalized population SEX Female [15]	367	2 (0/2)	93.69	81.10	98.40
Insured Black	Percent Insured Civilian noninstitutionalized population RACE AND HISPANIC OR LATINO ORIGIN Black or African American alone [15]	365	4 (1/3)	91.64	71.40	100.00
Insured Asian	Percent Insured Civilian noninstitutionalized population RACE AND HISPANIC OR LATINO ORIGIN Asian alone [15]	347	22 (5/17)	92.45	67.00	100.00
Insured Hispanic	Percent Insured Civilian noninstitutionalized population RACE AND HISPANIC OR LATINO ORIGIN Hispanic or Latino of any race [15]	364	5 (0/5)	86.58	55.50	100.00
Insured White	Percent Insured Civilian noninstitutionalized population RACE AND HISPANIC OR LATINO ORIGIN White alone not Hispanic or Latino [15]	368	1 (0/1)	93.90	85.10	98.40
Medicaid	Percent Public Coverage Medicaid means tested public coverage alone or in combination [15]	369	0 (0/0)	23.23	6.90	48.40

and income (see Table S2). In particular, counties with a higher percentage of people below the poverty level had a significantly lower percentage of the population with higher education (Pearson correlation, -0.52 , $p < 0.005$ for Bachelor's degree; Pearson correlation, -0.61 , $p < 0.005$ for high school), as well as a lower percentage of people insured, but a higher percentage of people on Medicaid (Pearson correlation, 0.77 , $p < 0.005$) or on disability (Pearson correlation, 0.41 , $p < 0.005$; see Table S2 for more details). Counties with a higher percentage of residents below the poverty level had a higher percentage of Blacks (Pearson correlation, 0.52 , $p < 0.005$ for men; Pearson correlation, 0.50 , $p < 0.005$ for women) and a lower percentage of non-Hispanic Whites (Pearson correlation, -0.30 , $p < 0.005$ for men; Pearson correlation, -0.33 , $p < 0.005$ for women).

Counties with a Higher Total Population, More Diverse Demographics, Higher Education, and Income Level Are at a Higher Risk of COVID-19 Infection

The COVID-19 infection rate per one million (mean, 912.20 ± 1034.26) ranged from 15.36 to 5093.99 in different counties (Table 1 and S1). Figure 1 shows the map of Pennsylvania with total population for each county, rate of infection and death due to COVID-19 infection, as well as, median income in the counties and percentage of the population who are

identified as non-Hispanic Whites. The map of the other six states is provided as Supplemental Fig. S1-S6 for reference. The outliers were not removed in these figures.

The results of the bivariate linear regression (Fig. 2, Table S3) estimate effect sizes (regression coefficients) of a number of variables contributed to COVID-19 infection when controlled for states in the model. Counties with a higher population (est. 0.34 , 95% CI 0.24 , 0.44 , $q < 1.1E-08$), a higher median income (est. 0.36 , 95% CI 0.25 , 0.48 , $q < 2.3E-08$), and a more diverse population (higher percentage of Hispanics, Asians, and Blacks) have a higher rate of infection. More specifically, a higher percentage of Asians (est. 0.32 , 95% CI 0.20 , 0.44 , $q < 6.3E-07$, women; est. 0.32 , 95% CI 0.20 , 0.43 , $q < 4.5E-07$, men), Blacks (est. 0.47 , 95% CI 0.32 , 0.62 , $q < 2.3E-08$, women; est. 0.35 , 95% CI 0.20 , 0.51 , $q < 1.7E-05$, men), and Hispanics (est. 0.49 , 95% CI 0.34 , 0.64 , $q < 1.2E-08$, women; est. 0.46 , CI 0.31 , 0.62 , $q < 8.1E-08$, men) are associated with a higher rate of infection while a higher percentage of non-Hispanic Whites (est. -0.41 , 95% CI -0.55 , -0.26 , $q < 2.9E-07$, women; est. -0.44 , 95% CI -0.58 , -0.30 , $q < 4.2E-08$, men) is associated with a lower rate of COVID-19. Change in grocery mobility (est. -0.24 , 95% CI -0.36 , -0.13 , $q < 5.5E-05$), retail mobility (est. -0.26 , 95% CI -0.38 , -0.14 , $q < 4.5E-05$), and work mobility (est. -0.31 , 95% CI -0.43 , -0.20 , $q < 9.0E-07$) were associated with a lower rate of infection. Another protective factor in

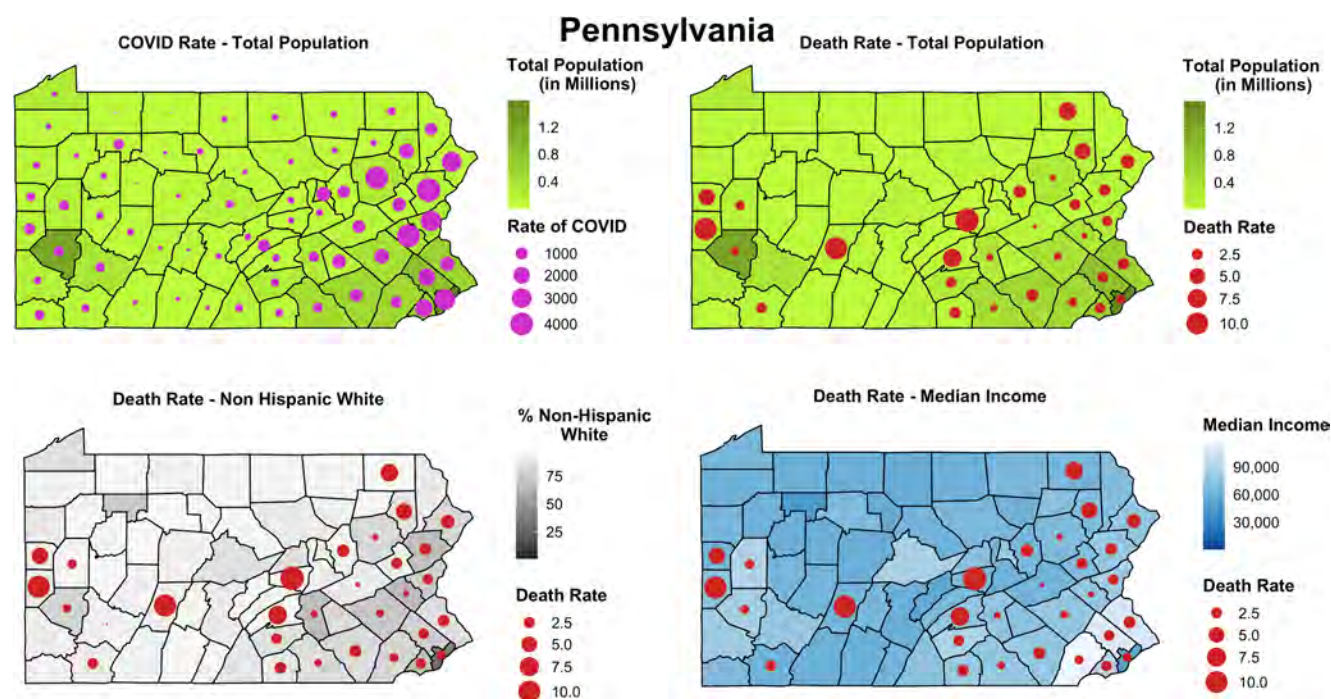


Fig. 1 Population count, non-Hispanic White, and Median Income and the rate of COVID-19 and related death in the counties of the state of Pennsylvania, as of April 9, 2020

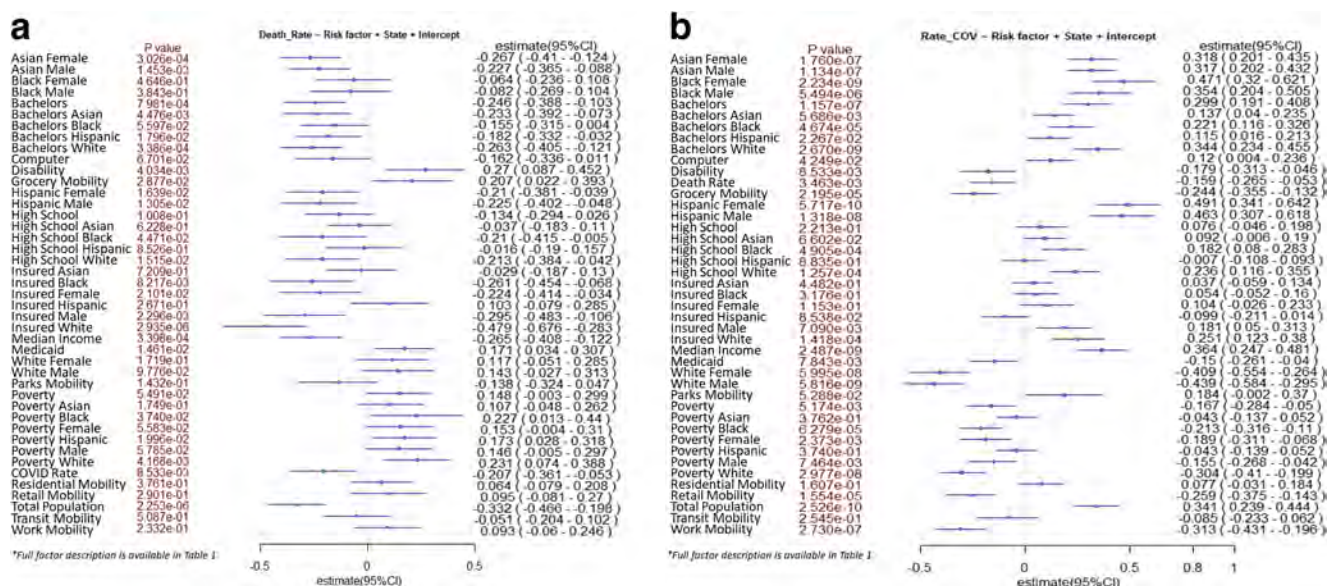


Fig. 2 a Bivariate analysis of factors for mortality due to COVID-19. b Bivariate analysis of factors for infection by COVID-19

terms of rate of infection for the counties analyzed was a higher percentage of disability (est. -0.159 , 95% CI $-0.265, -0.053$, $q < 0.006$). We also analyzed the rate of infection for counties with respect to their percentage of uninsured and found no significant association other than among men (est. 0.181 , 95% CI $0.05, 0.313$, $q < 1.2E-02$) and non-Hispanic Whites (est. 0.251 , 95% CI $0.123, 0.380$, $q < 3.1E-04$). Furthermore, in our stepwise regression model, minorities specifically Black and Hispanic women, poverty, and level of education among non-Hispanic Whites, disability, the total county population, and level of mobility are predictors of the rate of COVID-19 infection (Table S4).

Counties with a Smaller Population, Higher Poverty Levels, and Higher Disability Have a Higher Rate of Mortality

The COVID-19-related death (mean, $4.13\% \pm 2.70\%$; median, 3.40 ; IQR, $2.22-5.61$) varied among different counties (Table 1 and S1). Figure 2 and Table S5 show the results of the bivariate regression analysis estimating the odds of mortality due to COVID-19 infection (model corrected for states). Protective factors for the counties are a higher percentage of Asians (est. -0.27 , 95% CI $-0.41, -0.12$, $q < 0.003$, women; est. -0.23 , 95% CI $-0.37, -0.09$, $q < 0.009$, men) and education level with a bachelor's degree or higher with an odds ratio ranging from -0.41 to -0.03 across the various ethnicities (see Fig. 2). Other protective factors for counties include having a higher percentage of people insured (strongest indicator being for non-Hispanic White people with an estimate of

-0.48 , 95% CI $-0.68, -0.28$, $q < 6.0E-05$) and median income (est. -0.27 , 95% CI $-0.41, -0.12$, $q < 0.003$). The total population in the counties is also a major indicator (est. -0.33 , 95% CI $-0.43, -0.20$, $q < 6.0E-05$) of lower COVID-related death. We have also explored the association between total population and various confounding factors, such as mobility data when analyzing the death rate and found that the total population is still an important protective factor (see Table S6, Fig. S7 and S8). Factors significantly associated with higher mortality in the counties analyzed include a higher percentage of people under the poverty level (for all the races analyzed in this study), a higher percentage of people on Medicaid (est. 0.17 , 95% CI $0.03, 0.30$, $q < 0.04$), and a higher rate of people with disability in the county (est. 0.27 , 95% CI $0.09, 0.45$, $q < 0.02$). Grocery mobility was also highly associated with mortality (est. 0.21 , 95% CI $0.02, 0.39$, $q < 0.06$).

To better understand the characteristics of counties with higher or lower death rates, we performed a comparative analysis using ANOVA and found that, similar to the above, counties with more population diversity, higher income and education, a lower rate of disability, and a higher rate at the insured population have a significantly lower than the median death rate. Table 2 and Table S7 summarizes the population characteristics when counties are compared with death rate lower and higher than the median (median death rate is 3.4% across the counties in the seven states, Table S1). Park and retail mobility changes are significantly different between the two groups. The average number of Asians (both man and woman), as well as Hispanics (both man and woman), is significantly higher ($p < 0.05$) in group 1 (death rate ≤ 3.4). The

Table 2 ANOVA comparing counties with higher and lower than the median death rate

	<i>Covariates</i>	Total (N: 218)		Group 1: death rate ≤ 3.4 (N: 109)		Group 2: death rate > 3.4 (N: 109)		ANOVA—between groups Sig.
		Mean	Std. deviation	Mean	Std. deviation	Mean	Std. deviation	
Density	Population**	237,239.53	233,671.21	319,585.59	245,715.54	159,010.78	192,309.74	8.25E-07
Change in mobility	Rate of COVID**	1272.57	1142.34	1433.01	1166.21	1099.91	1096.27	4.37E-02
	Retail mobility**	−0.49	0.13	−0.51	0.12	−0.47	0.14	2.86E-02
	Grocery mobility	−0.18	0.13	−0.19	0.14	−0.17	0.13	1.37E-01
	Parks mobility**	0.13	0.60	0.21	0.60	0.00	0.59	3.65E-02
	Transit mobility	−0.50	0.16	−0.49	0.17	−0.50	0.16	7.98E-01
	Work mobility	−0.38	0.08	−0.39	0.07	−0.38	0.08	1.13E-01
PC	Resident mobility	0.15	0.05	0.14	0.04	0.15	0.06	6.62E-02
	Computer**	29.17	3.64	29.89	3.06	28.46	4.03	3.39E-03
Race	Black male	5.68	5.42	5.24	4.52	6.14	6.21	2.29E-01
	Black female	5.76	6.01	5.34	4.98	6.19	6.91	3.03E-01
	Asian male**	1.37	1.33	1.69	1.36	1.06	1.23	9.25E-04
	Asian female**	1.43	1.31	1.76	1.35	1.12	1.21	5.98E-04
	White male	33.99	10.08	33.55	9.38	34.42	10.76	5.28E-01
	White female	35.00	10.40	34.84	9.96	35.16	10.87	8.18E-01
	Hispanic male**	4.68	4.29	5.43	4.53	3.92	3.92	1.24E-02
	Hispanic female**	4.48	4.27	5.22	4.48	3.74	3.94	1.32E-02
Income	Median income**	74,817.20	18,918.79	81,488.08	19,201.41	68,083.38	16,103.69	1.00E-07
	Poverty**	14.35	5.43	12.87	4.72	15.83	5.70	4.21E-05
	Poverty male**	13.03	5.08	11.66	4.36	14.40	5.40	5.40E-05
	Poverty female**	15.60	5.82	14.01	5.12	17.19	6.07	4.18E-05
	Poverty Black**	27.42	11.81	24.46	9.80	30.38	12.91	1.76E-04
	Poverty Asian**	14.15	11.29	12.65	9.93	15.65	12.37	4.95E-02
	Poverty Hispanic**	23.55	10.23	21.74	7.60	25.37	12.08	8.49E-03
	Poverty White**	10.51	3.92	9.42	3.38	11.61	4.13	2.69E-05
Education	High school**	87.70	5.44	88.50	4.83	86.90	5.90	2.92E-02
	Bachelors**	28.06	11.32	31.31	10.97	24.80	10.75	1.53E-05
	High school White**	91.60	3.95	92.43	3.62	90.77	4.10	1.76E-03
	Bachelors White**	31.31	13.13	34.96	13.01	27.64	12.24	2.95E-05
	High school Black**	83.24	7.47	85.02	6.24	81.46	8.17	3.60E-04
	Bachelors Black**	18.98	9.90	20.75	9.19	17.21	10.29	8.00E-03
	High school Asian**	85.36	9.37	86.68	7.79	83.98	10.64	3.45E-02
	Bachelors Asian**	47.44	18.44	52.27	14.74	42.61	20.46	8.62E-05
	High school Hispanic	72.57	10.05	72.79	8.54	72.35	11.39	7.46E-01

Table 2 (continued)

Covariates	Total (N: 218)		Group 1: death rate ≤ 3.4 (N: 109)		Group 2: death rate > 3.4 (N: 109)		ANOVA—between groups Sig.
	Mean	Std. deviation	Mean	Std. deviation	Mean	Std. deviation	
Disability/insurance							
Bachelors Hispanic**	16.82	8.00	18.22	7.78	15.41	8.00	9.39E-03
Disability**	13.59	3.06	12.92	2.87	14.26	3.10	1.06E-03
Insured male**	91.75	3.15	92.45	3.03	91.05	3.13	9.59E-04
Insured female**	93.87	2.73	94.39	2.57	93.35	2.80	5.14E-03
Insured Black**	91.42	4.24	92.16	3.03	90.69	5.10	1.03E-02
Insured Asian	92.14	5.51	92.68	4.23	91.57	6.57	1.45E-01
Insured Hispanic	85.66	8.26	86.26	7.25	85.06	9.15	2.83E-01
Insured White**	94.50	2.43	95.21	2.09	93.80	2.55	1.33E-05
Medicaid**	22.44	7.01	20.88	6.36	24.00	7.30	9.23E-04

Full risk factor description is available in Table 1

**Denotes statistically significant

counties with higher death rates have lower median income and higher poverty levels across all the races. The group with a lower death rate has also a higher rate of the insured population and a lower rate of disability. The percentage of Medicaid is significantly higher in the group with a higher death rate.

COVID-19 Infection and Mortality Are Higher Among African Americans

We have also extracted data on all the states with respect to race distribution (see Table S8). As of April 16, 2020, we have observed that African Americans, as defined in the reports, have a higher rate of COVID-19 infection and a higher death rate. The number of African Americans infected by COVID-19 is 64,605 (1981 cases per million) with the number of deaths reaching 6181 (211 deaths per million), while the number of Whites, as defined in the reports, is 104,914 (658 cases per million) infected and 9806 (76 deaths per million) dead leading to a disproportional percentage of African Americans infected ($p < 0.0001$) by COVID-19 and dead ($p < 0.0001$) as the result. The number of infected Latinos and Asians per million, as defined in the reports, is 947 and 390, while the rate of mortality (per million) is 82 and 52 respectively.

Discussion

Our analysis highlights that counties with a higher total population, more diverse demographics, higher education, and income level are at a higher risk of COVID-19 infection; however, counties with a smaller population, higher disability rates, and higher poverty levels have a higher rate of mortality. The conflicting results for counties' population could be related to the population density, easier access to the high quality of healthcare, and more experience managing the COVID-19 infection due to the higher number of patients. One can argue that counties with fewer residents have a higher rural population. Studies have shown that there are significant differences in the overall healthcare assessment of rural populations as compared with urban populations [18]. Our observation is also aligned with a recent analysis of health differences in 3053 US counties, showing that rural areas are more likely to have poorer health outcomes [19]. The association of poverty and disability makes the conclusion of this study more complex and beyond the analysis of social determinants. By adding the interaction terms in the linear regression model (death rate~poverty + disability + poverty:disability) of death rate, we do not observe a significant interaction ($p = 0.469$), suggesting these two variables could be independent in their contribution to the risk of mortality. Populations with a higher disability [20] and lower median income [21] might be less mobile, have more comorbidities [22, 23], and also less likely

benefit from timely high-quality care [24] and high-quality nutrition; all of these factors could be equally important to combating this pandemic [25, 26]. Furthermore, our analysis of the preliminary data on mobility, given the recent social distancing guidelines, corroborate the impact of this intervention on lowering the infection rate and death.

Our findings highlight that race (especially Black) is a risk factor for the infection. To further our understanding of the impact of race, we performed an additional comparative analysis using ANOVA and found that counties with fewer than median non-Hispanic Whites (group 1: percentage of non-Hispanic Whites $\leq 39.7\%$) had a significantly lower total population ($p < 5.2\text{E-}15$) than counties with more than median non-Hispanic Whites (group 2: percentage of non-Hispanic Whites $> 39.7\%$); however, the rate of mortality is significantly higher ($p < 0.003$) while the rate of infection is significantly lower ($p < 4.4\text{E-}13$) in this group; Table S9 includes additional details. Finally, access to insurance was a protective factor in terms of mortality from COVID-19, but access to insurance did not significantly associate with the rate of infection. Comparison of counties with higher or lower than median death rates provided further evidence of the association of lower median income and higher poverty levels across all the races with mortality. The counties with a higher death rate also had a higher percentage of people on Medicaid. The latter is expected since Medicaid is significantly associated with the rate of poverty (Pearson correlation, 0.769, $p < 0.005$) as well as the rate of disability (Pearson correlation, 0.428, $p < 0.005$). Descriptive statistics of data from all the states also corroborates that African Americans might be disproportionally affected by this pandemic as of April 16, 2020. This observation is consistent with the H1N1 pandemic, where studies have shown evidence of racial and ethnic disparities in the population affected in terms of exposure, severity, and mortality of the disease [8, 9]. Finally, historical data have taught us that minorities and people of color tend to be more affected by different diseases [27–30].

This is the first systematic study on the racial, health, and economic disparity, as well as education, mobility, and COVID-19 infection in the US with the available data from the most severely impacted states. Our study had several limitations; the data was not granular, and we had missingness, especially for smaller and less populated counties. Access to the infected patient information and mortality data was not possible, and only aggregated data were used. Furthermore, many states claimed difficulties in reporting racial/ethnic demographic data due to patients opting out of providing their racial identification. The lack of clarity resulted in partially reported data for the death and case rate per million reported in this article, due to some states reporting on racial data for one, two, or all the racial variables specified in this study. The infection rate estimate may be underrepresented, as some individuals may have mild symptoms but lacked clinical validation of the infection. Finally, our in-depth analysis was

based on only seven states, leading to conclusions that may not be generalizable to other regions.

Conclusion

Implications of the results from this study highlight the value of the targeted interventions, as different counties, even within the same state, may have different characteristics and different needs. Furthermore, as the association between COVID-19-related fatality and infection is different among different race and health status, it is important to further study the impact of the immune system and immune-boosting strategies in the at-risk population (such as people with certain disabilities or those residing in elderly community centers), as preventive measure along with other measures based on social distancing guidelines and the ability to work from home.

Author's Contribution V.A. and R.Z. designed the study. O.O. and V.A. extracted and prepared the data for analysis. A.K. and D.C. performed data validation. J.L., R.Z., O.O., and V.A. performed the analysis. J.L., R.Z., O.O., S.S., and V.A. contributed to the interpretation of the results. V.A. and O.O. wrote the initial draft. All authors provided critical feedback and contributed to different sections of the manuscript. All authors reviewed and approved the final version of the manuscript. Authors would like to extend their thanks to Drs. Annemarie G. Hirsch, Melissa Poulsen, and Lester H. Kirchner for insightful comments.

Funding Information R.Z. and V.A. have funding support from the Geisinger Health Plan Quality Fund as well as the National Institute of Health R56HL116832 (sub-award) during the study period. The funders had no role in study design, data collection, and interpretation, or the decision to submit the work for publication.

Compliance with Ethical Standards

Conflict of Interest The authors declare that they have no conflict of interest.

References

1. Branswell H, Joseph A. WHO declares the coronavirus outbreak a pandemic. n.d. Retrieved April 14, 2020, from <https://www.statnews.com/2020/03/11/who-declares-the-coronavirus-outbreak-a-pandemic/>
2. Lake MA. What we know so far: COVID-19 current clinical knowledge and research. Clin Med. 2020;20(2):124–7.
3. Garg S, Kim L, Whitaker M, O'Halloran A, Cummings C, Holstein R, et al. Hospitalization Rates and Characteristics of Patients Hospitalized with. 2020. MMWR:Morbidity and Mortality Weekly Report. 69(15):458–64.
4. JHU. Coronavirus COVID-19 global cases by the center for systems science and engineering [Internet]. Johns Hopkins Univ. 2020; Available from: <https://coronavirus.jhu.edu/map.html>
5. Zhu L, She ZG, Cheng X, Qin JJ, Zhang XJ, Cai J, Lei F, Wang H, Xie J, Wang W, Li H. Association of Blood Glucose Control and Outcomes in Patients with COVID-19 and Pre-existing Type 2

- Diabetes. *Cell Metabolism*. 2020 May 1. [https://www.cell.com/cell-metabolism/pdfExtended/S1550-4131\(20\)30238-2](https://www.cell.com/cell-metabolism/pdfExtended/S1550-4131(20)30238-2).
6. Souch JM, Cossman JS. A commentary on rural-urban disparities in COVID-19 testing rates per 100,000 and risk factors. *J Rural Health*. 2020;9:1–6.
 7. Rothan HA, Byrareddy SN. The epidemiology and pathogenesis of coronavirus disease (COVID-19) outbreak. *J Autoimmun*. 2020;109:102433.
 8. Quinn SC, Kumar S, Freimuth VS, Musa D, Casteneda-Angarita N, Kidwell K. Racial disparities in exposure, susceptibility, and access to health care in the US H1N1 influenza pandemic. *Am J Public Health*. 2011;101(2):285–93.
 9. Placzek H, Madoff L. Effect of race/ethnicity and socioeconomic status on pandemic H1N1-related outcomes in Massachusetts. *Am J Public Health*. 2014;104(1).
 10. Coronavirus Locations: COVID-19 Map by County and State. n.d. Retrieved April 12, 2020, from <https://usafacts.org/visualizations/coronavirus-covid-19-spread-map/>
 11. U.S. Census Bureau. United States Census. Presence of A Computer And Internet Subscription. [Internet]. [cited 2020 Apr 12]; Available from: <https://data.census.gov/cedsci/table?q=Computer&tid=ACST1Y2018.S2801&t=Telephone,Computer,andInternetAccess>.
 12. State Population By Race, Ethnicity Data [Internet]. [cited 2020 Apr 12]; Available from: <https://www.governing.com/gov-data/census/state-minority-population-data-estimates.html>
 13. Black Population by State 2020. n.d. Retrieved April 12, 2020, from <https://worldpopulationreview.com/states/black-population-by-state/>
 14. Google. See how your community is moving around differently due to COVID-19 [Internet]. [cited 2020 Apr 12]; Available from: <https://www.google.com/covid19/mobility/>
 15. United States Census. Explore Census Data. <https://data.census.gov/cedsci/>. Accessed April 12, 2020.
 16. The R Foundation. The R Project for Statistical Computing. <http://www.R-ProjectOrg/> 2018;1–12.
 17. IBM. Downloading IBM SPSS Statistics 25 [Internet]. Ibm. 2020 [cited 2020 Apr 20]; Available from: <https://www.ibm.com/support/pages/downloading-ibm-spss-statistics-25>
 18. Spasojevic N, Vasilj I, Hrabac B, Celik D. Rural - urban differences in health care quality assessment. *Mater Socio Medica*. 2015;27(6):409–11.
 19. Anderson TJ, Saman DM, Lipsky MS, Lutfiyya MN. A cross-sectional study on health differences between rural and non-rural U.S. counties using the County Health Rankings. *BMC Health Serv Res*. 2015;15(1):1–8.
 20. Montez JK, Hayward MD, Wolf DA. Do U.S. states' socioeconomic and policy contexts shape adult disability? *Soc Sci Med [Internet]* 2017;178:115–26. Available from: <https://linkinghub.elsevier.com/retrieve/pii/S0277953617301016>
 21. Meyer BD, Mok WKC. Disability, earnings, income and consumption. *J Public Econ*. 2019;171:51–69 Available from: <https://linkinghub.elsevier.com/retrieve/pii/S0047272718301245>.
 22. Reichard A, Stolzle H, Fox MH. Health disparities among adults with physical disabilities or cognitive limitations compared to individuals with no disabilities in the United States. *Disabil Health J*. 2011;4(2):59–67.
 23. Havercamp SM, Scandlin D, Roth M. Health disparities among adults with developmental disabilities, adults with other disabilities, and adults not reporting disability in North Carolina. *Public Health Rep*. 2004;119(4):418–26.
 24. Swanson ME, Wall S, Kisker E, Peterson C. Health disparities in low-income families with infants and toddlers: needs and challenges related to disability. *J Child Heal Care*. 2011;15(1):25–38.
 25. Cena H, Chieppa M. Coronavirus disease (COVID-19 SARS-CoV-2) and nutrition: Is infection in Italy suggesting a connection? *Front Immunol*. 2020;11:944. <https://doi.org/10.3389/fimmu.2020.00944>.
 26. Sharma V, Sharma V, Khan A, et al. Malnutrition, health and the role of machine learning in clinical setting. *Front Nutr [Internet]*. 2020;7(April):1–9 Available from: <https://www.frontiersin.org/article/10.3389/fnut.2020.00044/full>.
 27. Crouse Quinn S, Jamison AM, Freimuth VS, An J, Hancock GR. Determinants of influenza vaccination among high-risk Black and White adults. *Vaccine*. 2017;35(51):7154–9.
 28. Anandappa M, Adjei Boakye E, Li W, Zeng W, Rebmann T, Chang JJ. Racial disparities in vaccination for seasonal influenza in early childhood. *Public Health*. 2018;158:1–8.
 29. Yoo BK, Hasebe T, Szilagyi PG. Decomposing racial/ethnic disparities in influenza vaccination among the elderly. *Vaccine*. 2015;33(26):2997–3002.
 30. Canedo JR, Miller ST, Schlundt D, Fadden MK, Sanderson M. Racial/ethnic disparities in diabetes quality of care: the role of healthcare access and socioeconomic status. *J Racial Ethn Health Disparities*. 2018;5:7–14.

Publisher's Note Springer Nature remains neutral with regard to jurisdictional claims in published maps and institutional affiliations.

Majority Indians have natural immunity. Vaccinating entire population can cause great harm

For recovered Covid patients, the vaccines provide no benefit and some harm. It is thus unethical to vaccinate them.



SANJIV AGARWAL and JAY BHATTACHARYA

11 January, 2021 11:34 am IST



Health workers prepare for the dry run of COVID-19 vaccine at a community centre, in Gurugram, on 7 January 2021 (representational image) | PTI Photo

Text Size: A- A+

As we start 2021, the Covid-19 epidemic in India has progressed to a point where a near majority of the population has **developed immunity** to the virus. Though too many have died, India's Covid death rate is, fortunately, lower than many other countries. With the vaccine roll-out imminent, there are reasons for optimism after a challenging year.

The primary question at hand for Indian Covid response policy planners is how best to use the vaccine — roll-out for which in India begins from **16 January** and will target three crore health staff — to minimise the harm from the disease until the end of the epidemic. Given the size of the population and the rate of production of the vaccine, it may take a considerable amount of time to vaccinate the entire population. So it will be necessary to choose who receives priority.

Despite the deployment of the vaccine, many countries – including the US and UK – continue to impose lockdowns as the primary means of controlling the virus's spread. The results have not been good, with both cases and deaths rising despite the shuttered businesses, schools, and places of worship. Indian policy planners should take full advantage of these bad examples and continue to avoid **lockdowns**



that have devastated the lives and livelihoods of millions of poor people throughout the country.

We know from the mortality statistics that the Covid infection poses the greatest risk to older populations. Worldwide, the **infection survival rate** for people under 70 is 99.95 per cent, while the analogous number for those aged 70 and over is 95 per cent. So, the only ethical choice requires offering the vaccine to people aged 70 and older first, as well as to the frontline health workers who care for Covid patients.

The problem is that, with 88 million elderly citizens in India, there will not be enough doses in the immediate future to vaccinate them all for months to come. We argue that inoculating only people who have not been previously infected provides an efficient way to target the vaccine at those who will benefit from it most.

Also read: *Russia's Sputnik V vaccine has no peer-reviewed data yet. Question is — would you take it*

Immunity after recovery from Covid

The scientific evidence is overwhelming that natural immunity attained after recovery from Covid infection **is effective and long lasting**. The immune system responds to infection by various mechanisms, including the production of specific antibodies, T-cells, and B-cells to protect nearly every recovered Covid patient from reinfection. After almost a year of pandemic, globally, only **34 cases and two deaths** have been definitively identified as reinfections at the time of writing, out of the **90 million** Covid cases and likely hundreds of millions of infections worldwide.

Vaccines cause the immune system of those inoculated to mimic the immune response that natural infection induces. While the immunity conferred by the Covid vaccines documented in the clinical trials is excellent, it is not as effective as the immunity conferred by natural infection.

Furthermore, those who have already developed immunity to Covid through natural infection are extremely unlikely to develop additional immunity from vaccination. For instance, in the **Pfizer randomised trial**, the vaccine was tested in previously infected patients to check for its safety in that group. But those same patients were excluded from the analysis of efficacy, presumably because the scientists understood that the vaccine would confer no additional benefit to them.

Every vaccine has some side effects, and though the approved Covid vaccines are safe, they are no exception. Most of the side effects are mild – soreness at the injection site, aches and pains from the immunological reaction – but very rarely, severe adverse events do occur. For recovered Covid patients, then, the vaccines provide no benefit and some harm. It is thus unethical to vaccinate them.

Also read: *How India's regulatory pitfalls helped Covishield and Covaxin get rapid approval*

India is reaching very high level of natural immunity

These considerations are not merely of theoretical interest because an enormous proportion of the Indian population has already been infected and recovered. While the officially reported figure of Covid cases in India is around **1.4 crore**, mathematical models imply that more than 50 per cent of the Indian population may have developed natural immunity to the virus.

This fact is corroborated by serological **tests for Covid antibodies carried out commercially on a large scale by Thyrocare**. The founder of Thyrocare, **Dr A. Velumani**, says that “nature... already has immunised, freely, silently 70% Indians”.

Though this may sound like bad news, since it implies that nearly a billion Indians have already been infected, the silver lining is that the vast majority have recovered from infection and have lasting immunity to reinfection. They will likely be better protected from Covid over a longer period of time than those who achieve immunity via vaccination since it is not clear **how long the vaccination-induced immunity lasts**.

Checking for previous infection is simple. Before vaccination, patients should be asked if they have been previously infected, and if the answer is no, an inexpensive test for antibodies should be administered. Only if that test is negative should the vaccine be administered. This procedure will not capture all previous infections **since antibodies fade after a few months**, and many infected people were never identified as cases. Still, this procedure will nevertheless spare a large number of people from unnecessary vaccination.

Thus, reserving vaccine doses for people who have not been previously infected could solve the problem of excess demand for the vaccine by the vulnerable in the early months of the vaccine roll out when not enough doses will be available for all.

Also read: *Vaccine maker IIL, other companies in touch with Moderna to bring its Covid vaccine to India*

Prioritise the vulnerable for vaccination

In a disease with high asymptomatic cases and low morbidity or infection fatality rate, the first goal of vaccination is to reach **herd immunity** and not 100 per cent eradication through universal vaccination — that would be simply impossible. The only human virus that has been entirely eradicated from the face of the earth is smallpox, and that effort took decades despite the availability of an excellent vaccine. Chasing this impossible goal would impose great harm to India.

By contrast, a swift, focused protection strategy of vaccine administration, which prioritises the most vulnerable who have not been previously been infected, would reduce death rates from Covid infection to nearly zero and is a far better strategy.

Once the vulnerable are protected, even while the vaccine is administered to the less vulnerable younger populations, the Disaster Management Act's lockdown restrictions should be lifted fully and forever. The economic, physical, and emotional harms from the lockdown far exceed the mortality and morbidity risks from Covid infection for less vulnerable people. Since either vaccine-induced or natural immunity would already protect the vulnerable, there would be no ethical reason for the remaining lockdown restrictions to be in place.

Sanjiv Agarwal is the founder of the Good Governance India Foundation, Mumbai. Jay Bhattacharya is Professor of Medicine at Stanford University. Views are personal.

Subscribe to our channels on [YouTube](#) & [Telegram](#)

Why news media is in crisis & How you can fix it

India needs free, fair, non-hyphenated and questioning journalism even more as it faces multiple crises.

But the news media is in a crisis of its own. There have been brutal layoffs and pay-cuts. The best of journalism is shrinking, yielding to crude prime-time spectacle.

ThePrint has the finest young reporters, columnists and editors working for it. Sustaining journalism of this quality needs smart and thinking people like you to pay for it. Whether you live in India or overseas, you can do it [here](#).

Support Our Journalism [➔](#)

Recommended Content by [theprint.in](#)



PTI challenges new digital media rules in HC, says would bring in 'era of surveillance & fear'

VIEW COMMENTS

New Cadillac's Finally On Sale

All Things Auto | Sponsored

See The Astonishing New Chevy Blazer SUV

Chevrolet Blazer | sponsored searches | Sponsored

Don't play this game if you are under 40 years old

Raid Shadow Legends | Sponsored

Play Now

Experts Say: This Tiny Device Can Practically Replace Your Ear

hear.com | Sponsored

Winnipeg Residents Are Choosing This \$89 Mini AC

This incredible portable AC will chill the air in any room faster than any other portable solution you've tried.

Gadget Guide | Sponsored

Casinos Hate This. But You Are 100% Allowed To Do It

Daily Pulse | Sponsored

Living in MANITOBA? Don't Buy a Hearing Aid Before Reading This

hear.com | Sponsored



Exhaled respiratory particles during singing and talking

M. Alsved, A. Matamis, R. Bohlin, M. Richter, P.-E. Bengtsson, C.-J. Fraenkel, P. Medstrand & J. Löndahl

To cite this article: M. Alsved, A. Matamis, R. Bohlin, M. Richter, P.-E. Bengtsson, C.-J. Fraenkel, P. Medstrand & J. Löndahl (2020) Exhaled respiratory particles during singing and talking, *Aerosol Science and Technology*, 54:11, 1245-1248, DOI: [10.1080/02786826.2020.1812502](https://doi.org/10.1080/02786826.2020.1812502)

To link to this article: <https://doi.org/10.1080/02786826.2020.1812502>



View supplementary material



Published online: 17 Sep 2020.



Submit your article to this journal



Article views: 44944



View related articles



View Crossmark data



Citing articles: 27 View citing articles



AEROSOL RESEARCH LETTER

Exhaled respiratory particles during singing and talking

M. Alsved^a , A. Matamis^b , R. Bohlin^c, M. Richter^b , P.-E. Bengtsson^b , C.-J. Fraenkel^d ,
P. Medstrand^e , and J. Löndahl^a

^aDepartment of Ergonomics and Aerosol Technology, Lund University, Lund, Sweden; ^bDepartment of Combustion Physics, Lund University, Lund, Sweden; ^cSan Francisco Symphony Chorus, San Francisco, CA, USA; ^dDepartment of Infection Control, Skåne University Hospital, SUS, Lund, Sweden; ^eDepartment of Translational Medicine, Lund University, Lund, Sweden

ARTICLE HISTORY Received 12 July 2020; Accepted 15 August 2020

EDITOR Tiina Reponen

Introduction

Choir singing has been suspended in many countries during the Covid-19 pandemic due to incidental reports of disease transmission (Hamner et al. 2020). The mode of transmission has been attributed to exhaled droplets, but with the exception of a study on tuberculosis from 1968, there is presently almost no scientific evidence of increased particle emissions from singing (Loudon and Roberts 1968). A substantial number of studies have, however, investigated aerosols emitted from breathing, talking, coughing and sneezing (e.g., Asadi et al. 2019; Johnson et al. 2011). It has also been shown that just normal breathing over time can generate more viable virus aerosol than coughing, since the latter is a less frequent activity (Lindsley et al. 2016).

Compared to talking, singing often involves continuous voicing, higher sound pressure, higher frequencies, deeper breaths, higher peak airflows and more articulated consonants. All these factors are likely to increase exhaled emissions.

The aim of this study was to investigate aerosol and droplet emissions during singing, as compared to talking and breathing. We also examined the presence of SARS-CoV-2 in the air from breathing, talking and singing, and the efficacy of face masks to reduce emissions. In this study we defined aerosol particles as having a dry size in the range 0.5–10 µm. Although debatable from an aerosol physics point of view, a cutoff diameter between 5 and 10 µm is normally used in medicine for classification of aerosol versus droplet route of transmission. Droplets are here defined as exhaled particles, from micron size with no upper size limit, and measured directly at the mouth before complete evaporation, thus partly in liquid phase.

Methods

Twelve volunteer singers were included in the study: 7 professional opera singers (2 basses, 1 baritone, 2 altos and 2 sopranos) and 5 amateurs (3 tenors, 2 altos). The singers were sitting or standing in an upright position. Measurements on the 12 singers were carried out in a 22 m³ airtight experimental chamber at room temperature around 22 °C and maximum 40% relative humidity. The chamber was ventilated by particle-free air with an air exchange rate of 3 h⁻¹. Both singers and researches were wearing clean air suits to minimize background particle concentrations. In addition, we analyzed SARS-CoV-2 in air samples collected close to two persons confirmed positive for Covid-19 while talking and singing.

A short consonant-rich text was repeated during eight exercises: talking normal (no set tone, 50–60 dBA measured at 1 m distance), talking loud (no set tone, 65–80 dBA), singing normal (A natural, man/woman: A3/A4, <70 dBA), singing loud (A natural, 70–90 dBA), singing loud with exaggerated diction (A natural, 70–90 dBA), singing loud at high pitch (man/woman: E4/E5) and singing loud wearing a surgical face mask (A natural). The singers had varied voice strength at the chosen pitches, and sound pressure values are thus approximate. Singing was carried out at a single pitch with a metronome set at 92 bpm to provide constant rhythm. Each exercise was performed for 2 min, which corresponded to 12 repetitions of the spoken or sung text. Particle concentrations reached a steady state after 10–15 s, after which the data were analyzed. For reference, we also detected particle emissions during normal breathing.

The size and concentration of aerosol particles in the range 0.5–10 µm were measured by an aerodynamic particle sizer (APS, Model 3321, TSI Inc.) at 5 s scan time.

CONTACT Jakob Löndahl jakob.londahl@design.lth.se Department of Design Sciences, Lund University, Box 188, SE 22100 Lund, Sweden.

Supplemental data for this article is available online at <https://doi.org/10.1080/02786826.2020.1812502>.

© 2020 American Association for Aerosol Research

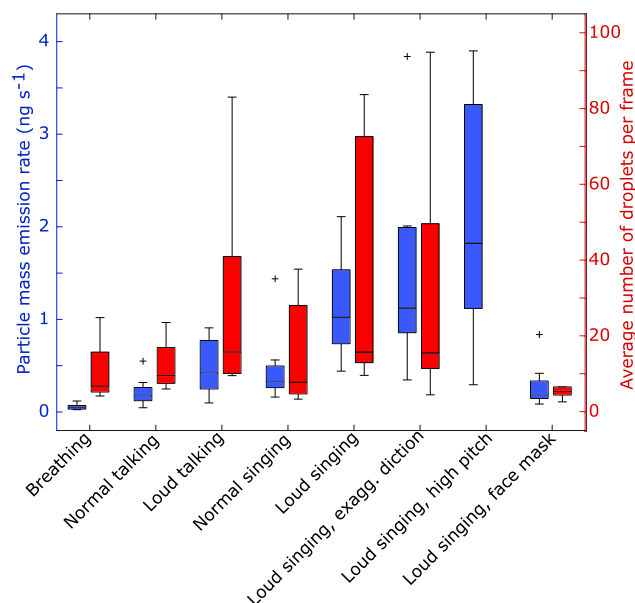


Figure 1. Aerosol particle mass emission rates during different exercises (dark blue, left y-axis), and the average number of droplets per frame (from image analysis, see Figure 3) in the exhaled air during the same exercises (red, right y-axis). Particle mass was measured in the range 0.5–10 μm . Each blue box represent data for 12 singers for aerosol particles and 5 singers for droplets. Two high values for loud singing not shown.

The aerosol was sampled from a 50 cm long horizontal anti-static metal funnel (volume 4.4 L) fitted around the face of the singers. A vacuum pump pulled a constant airflow of 15 L/min through the funnel in order to introduce fresh air for the singers, reduce deposition by limiting particle residence time, and decrease relative humidity to ensure measurement at particle dry size. It was not possible to achieve isokinetic and vertical sampling due to the varying flow rates from breathing and the preferable upright positioning of the singers. Emission rates were calculated with the assumption of zero particle losses in the funnel, and thus aerosol emissions may be somewhat underestimated. Between exercises, the aerosol particle concentration was left to decrease to background levels below 0.5 cm^{-3} .

For five of the singers, droplet emissions (non-evaporated particles with no upper size limit) were imaged with a high-speed camera (Photron FastCAM SA-X2) with an acquisition frequency of 125 frames per second and exposure time of 250 μs . A Nikon 50 mm prime lens was used with the aperture set at $f/2.8$ to balance adequate depth-of-field and low-light sensitivity. Particles were visualized by means of elastic light scattering, with light provided by ten 50 W narrow spread-angle reflector halogen lamps in a configuration of two overlapping racks of five lamps, resulting in a homogenous illumination profile with a rectangular cross section of 10x50 cm. This light profile was aimed in front of the participants, directed toward the camera at an angle

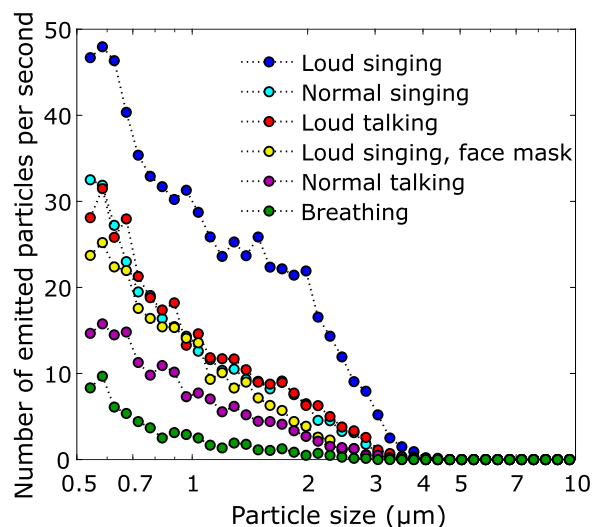


Figure 2. Median number of emitted particles in the size range 0.54–10 μm per second for the 12 singers.

approximately 30° off the detection axis, in order to utilize the forward scattering properties of micrometer sized particles. The detection limit of the setup was evaluated using glass beads with a MMAD of 4 μm ($\rho = 2 \text{ g/cm}^3$), which yielded high signals and clearly resolved particles. The images were analyzed with an in-house developed algorithm in Matlab to obtain the number of particles and visualize the temporal variation.

The SARS-CoV-2 virus in aerosols was investigated with a method previously validated for detection of airborne virus (Alsvéd et al. 2020). Samples were collected at a distance of 0.8 m in front of two persons with confirmed Covid-19 that were talking or singing (sitting position). Both were within two days of symptom onset. No precise quantitative information about viral loads in the airways could be obtained, but combined nasal/throat swabs analyzed for SARS-CoV-2 within 24 h of measurement had qPCR Ct values of 22–25, as reported by the hospital laboratory. Aerosols were collected into phosphate buffered saline by a cyclone (Coriolis μ , Bertin Technologies, flow rate 200 L/min) and on gelatin filters (MD8 airscan, Sartorius GmbH, flow rate 100 L/min). Sampling was performed for 10 min each for: (1) normal silent breathing, (2) reading a book loud, (3) singing, and (4) singing with a face mask. The samples were stored at 4°C . RNA was extracted with the viral RNA mini kit (QIAGEN) according to the protocol of the manufacturer and quantitative reverse transcription polymerase chain reaction (qRT-PCR) was performed using the SuperScriptTM III PlatinumTM One-Step qRT-PCR Kit (ThermoFisher Scientific) with primer and probes as described (Corman et al. 2020). Both positive (patient samples) and negative controls (blanks and sampling in virus-free environments) were made to validate the virus analysis. Approval was granted by the ethical review board in Sweden (2020-01396) for collecting air

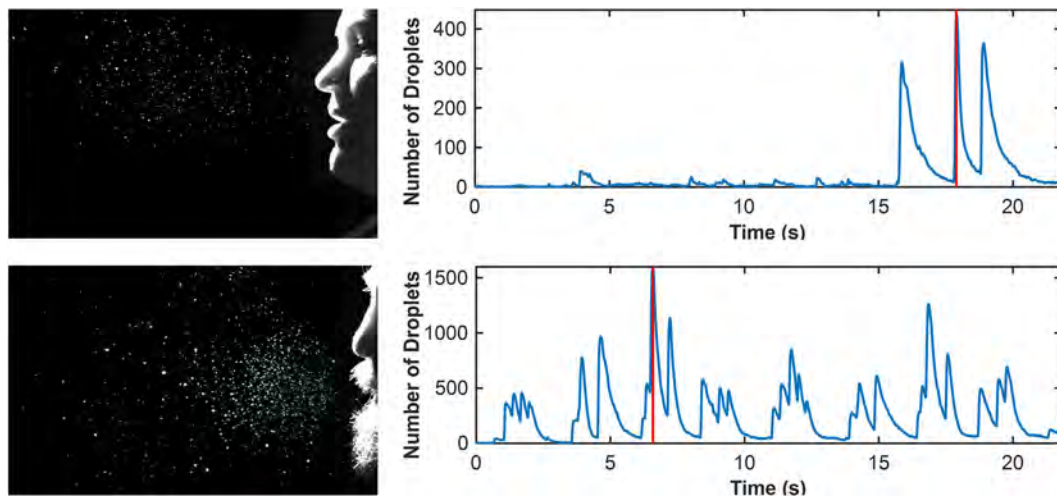


Figure 3. The number of droplets per picture frame generated during loud singing with exaggerated consonants by the professional opera singers. During the 20 s the same phrase is repeated twice. Videos are available in the [online supplementary information](#).

samples close to Covid-19 infected patients and for retrieving personal data about patient samples.

The Friedman test was used to evaluate if there were differences between all types of exercises and post hoc analysis with the Wilcoxon signed rank test was conducted for pairs of samples (SPSS version 26, IBM Inc.).

Results and discussion

As illustrated in [Figures 1](#) and [2](#), there were significant differences in particle emissions between breathing, talking and singing (Friedman test for emitted aerosol particle mass, $p < 0.0001$). Normal singing generated significantly more aerosol particles than normal talking ($p = 0.002$). Loud singing produced more particles than normal singing ($p = 0.002$). [Figure 1](#) illustrates mass emission rates. Median (range) aerosol particle number emission rates were ([Figure 2](#)): 135 (85–691) particles/s for breathing, 270 (120–1380) particles/s for normal talking, 570 (180–1760) particles/s for loud talking, 690 (320–2870) particles/s for normal singing, 980 (390–2870) particles/s for loud singing, and 1480 (500–2820) particles/s for loud singing with exaggerated diction. For loud singing with a face mask, the emission rate was 410 (200–1150) particles/s. Hence, a simple face mask reduced the amount of generated aerosol particles from singing to a level similar to normal talking (no significant difference, $p = 0.08$).

There was a trend toward increased aerosol emissions with higher pitched singing, but this could also be an effect of increased sound pressures achieved at especially high pitches. The professional singers in this study generated 2–3 times more aerosol particle mass when singing loud at high E compared to A natural. The professional singers produced about a factor two more aerosol particles than the amateur singers at perceived normal sound pressure (Mann-Whitney, $p = 0.03$).

From the high-speed camera droplet analysis we found that some consonants, for example ‘p’, ‘b’, ‘r’ and ‘t’, generated a high number of small to large droplets ([Figure 3](#), see also the videos provided in the [online supplementary information](#)). The singing of vowels does not provide high airflows for the dispersal of particles, but as shown in the video files, the articulation of consonants expels droplets with considerable forward velocity. Nevertheless, many of the largest droplets travel a limited distance (< 0.5 m) before their movement become vertical due to sedimentation.

There were substantial differences in emissions of droplets between singing and talking, but statistical significance could not be verified due to the limited group size for the video recordings ([Figures 1](#) and [3](#)). Mean (\pm SEM) droplet numbers per frame were 12 ± 3 for normal talking, 29 ± 14 for loud talking, 16 ± 7 for normal singing, 38 ± 16 for loud singing, and 5 ± 1 for loud singing with a face mask. Thus, for the droplet analysis a common face mask also appears to be very efficient in reducing emissions. Although not measured systematically, we noted that subject-reported sense of accumulation of saliva in the mouth coincided with increased droplet generation from articulation, which resulted in high variation also within the data from the same singer ([Figure 3](#), top diagram). When singing loud with a surgical mask, almost no droplets were detected with the camera. A warm-up exercise where one lets the lips vibrate during exhalation (without activating the vocal cords) generated immense amounts of droplets (data not shown).

SARS-CoV-2 could not be detected in the air samples collected while confirmed Covid-19 patients were singing and talking. This can be due to the low concentrations of viruses in the air, but could also be attributed to individual differences in viral loads in the parts of the respiratory tract where the droplets are produced, as well as dilution steps in the sample preparation method.

Singing generated more respiratory aerosol particles and droplets than talking. Exhaled aerosol particles and droplets increased with song loudness. The data also indicated that emissions might increase at high pitch. Wearing an ordinary surgical face mask reduced the amount of measured exhaled aerosol particles and droplets to levels comparable with normal talking. However, as surgical masks have a loose fit, some particles may have exited on the sides where we did not measure. Based on these results, singing in groups is likely to be an activity at risk of transmitting infection if not appropriate control and prevention measures are applied, such as distancing, hygiene, ventilation and shielding.

Acknowledgments

We want to express our gratitude to the singers who kindly and enthusiastically contributed with song for the aerosol detectors: foremost from Malmö Opera Choir but also from Malmö Limelight Chorus, Svanholm Singers, Lunds Student Singers and last, but not least, the two people who sang while having Covid-19.

Funding

This work was supported by Barbro Osher Pro Suecia Foundation, AFA insurance [grant numbers 180113, 200109] and the Swedish Research Council FORMAS [grant number 2017-00383].

ORCID

M. Alsved  <http://orcid.org/0000-0002-8407-8758>
 A. Matamis  <http://orcid.org/0000-0001-8072-599X>
 M. Richter  <http://orcid.org/0000-0002-9914-7218>

P.-E. Bengtsson  <http://orcid.org/0000-0002-3819-7465>
 C.-J. Fraenkel  <http://orcid.org/0000-0002-3086-5553>
 P. Medstrand  <http://orcid.org/0000-0003-4259-8744>
 J. Löndahl  <http://orcid.org/0000-0001-9379-592X>

References

- Alsved, M., C. J. Fraenkel, M. Bohgard, A. Widell, A. Soderlund-Strand, P. Lanbeck, T. Holmdahl, C. Isaxon, A. Gudmundsson, P. Medstrand, et al. 2020. Sources of airborne norovirus in hospital outbreaks. *Clin. Infect. Dis.* 70 (10):2023–2028. doi: 10.1093/cid/ciz584.
- Asadi, S., A. S. Wexler, C. D. Cappa, S. Barreda, N. M. Bouvier, and W. D. Ristenpart. 2019. Aerosol emission and superemission during human speech increase with voice loudness. *Sci. Rep.* 9 (1):2348. doi: 10.1038/s41598-019-38808-z.
- Corman, Victor M., Olfert Landt, Marco Kaiser, Richard Molenkamp, Adam Meijer, Daniel KW Chu, Tobias Bleicker et al. 2020. “Detection of 2019 novel coronavirus (2019-nCoV) by real-time RT-PCR.” *Eurosurveillance* 25 (3): 2000045.
- Hamner, L., P. Dubbel, I. Capron, A. Ross, A. Jordan, J. Lee, J. Lynn, A. Ball, S. Narwal, S. Russell, et al. 2020. High sars-cov-2 attack rate following exposure at a choir practice—skagit county, washington, march 2020. *Mmwr. Morb. Mortal. Wkly. Rep.* 69 (19):606–10., doi. doi: 10.15585/mmwr.mm6919e6.
- Johnson, G. R., L. Morawska, Z. D. Ristovski, M. Hargreaves, K. Mengersen, C. Y. H. Chao, M. P. Wan, Y. Li, X. Xie, D. Katoshevski, et al. 2011. Modality of human expired aerosol size distributions. *J. Aerosol Sci.* 42 (12):839–51. doi: 10.1016/j.jaerosci.2011.07.009.
- Lindsley, W. G., F. M. Blachere, D. H. Beezhold, R. E. Thewlis, B. Noorbakhsh, S. Othumpangat, W. T. Goldsmith, C. M. McMillen, M. E. Andrew, C. N. Burrell, et al. 2016. Viable influenza a virus in airborne particles expelled during coughs versus exhalations. *Influenza Other Respir Viruses* 10 (5):404–13. doi: 10.1111/irv.12390.
- Loudon, R. G., and R. M. Roberts. 1968. Singing and the dissemination of tuberculosis. *Am. Rev. Respir. Dis.* 98 (2):297–300. doi: 10.1164/arrd.1968.98.2.297.

SCIENTIFIC REPORTS

OPEN

Aerosol emission and superemission during human speech increase with voice loudness

Sima Asadi¹, Anthony S. Wexler^{2,3,4,5}, Christopher D. Cappa⁴, Santiago Barreda⁶, Nicole M. Bouvier^{7,8} & William D. Ristenpart¹

Mechanistic hypotheses about airborne infectious disease transmission have traditionally emphasized the role of coughing and sneezing, which are dramatic expiratory events that yield both easily visible droplets and large quantities of particles too small to see by eye. Nonetheless, it has long been known that normal speech also yields large quantities of particles that are too small to see by eye, but are large enough to carry a variety of communicable respiratory pathogens. Here we show that the rate of particle emission during normal human speech is positively correlated with the loudness (amplitude) of vocalization, ranging from approximately 1 to 50 particles per second (0.06 to 3 particles per cm³) for low to high amplitudes, regardless of the language spoken (English, Spanish, Mandarin, or Arabic). Furthermore, a small fraction of individuals behaves as “speech superemitters,” consistently releasing an order of magnitude more particles than their peers. Our data demonstrate that the phenomenon of speech superemission cannot be fully explained either by the phonic structures or the amplitude of the speech. These results suggest that other unknown physiological factors, varying dramatically among individuals, could affect the probability of respiratory infectious disease transmission, and also help explain the existence of superspreaders who are disproportionately responsible for outbreaks of airborne infectious disease.

It has long been recognized that particles expelled during human expiratory events, such as sneezing, coughing, talking, and breathing, serve as vehicles for respiratory pathogen transmission^{1–6}. The relative contribution of each expiratory activity in transmitting infectious microorganisms, however, remains unclear⁴. Much previous research has focused on coughing^{7–12} and sneezing^{11,13,14} activities that yield relatively large droplets (approximately 50 µm or larger) easily visible to the naked eye. Less noticeable, but arguably more infectious for some diseases, are the smaller particles emitted during sneezing and coughing as well as during breathing^{15–17} and talking^{16,18,19}. These small particles are believed to be generated during breathing and talking from the mucosal layers coating the respiratory tract via a combination of a “fluid-film burst” mechanism within the bronchioles and from vocal folds adduction and vibration within the larynx^{6,20,21}. The particles emitted during breathing and typical speech predominantly average only 1 µm in diameter^{15–17} and are thus too small to see without specialized equipment; most people outside of the community of bioaerosol researchers are less aware of them.

Despite their small size, however, these micron-scale particles are sufficiently large to carry a variety of respiratory pathogens such as measles virus (50–500 nm)²², influenza virus (100 nm–1 µm)²³, and *Mycobacterium tuberculosis* (1–3 µm)²⁴. Indeed, recent work by Yan *et al.* has confirmed that significant amounts of influenza viral RNA are present in small particles (<5 µm) emitted by influenza-infected individuals during natural breathing, without coughing or sneezing²⁵. These small particles are potentially more infectious than larger sneeze- or

¹Department of Chemical Engineering, University of California Davis, 1 Shields Ave, Davis, CA, 95616, USA.

²Department of Mechanical and Aerospace Engineering, University of California Davis, 1 Shields Ave, Davis, CA, 95616, USA. ³Air Quality Research Center, University of California Davis, 1 Shields Ave, Davis, CA, 95616, USA.

⁴Department of Civil and Environmental Engineering, University of California Davis, 1 Shields Ave, Davis, CA, 95616, USA.

⁵Department of Land, Air and Water Resources, University of California Davis, 1 Shields Ave, Davis, CA, 95616, USA. ⁶Department of Linguistics, University of California Davis, 1 Shields Ave, Davis, CA, 95616, USA.

⁷Department of Medicine, Div. of Infectious Diseases, Icahn School of Medicine at Mount Sinai, 1 Gustave Levy Place, New York, NY, 10029, USA. ⁸Department of Microbiology, Icahn School of Medicine at Mount Sinai, 1 Gustave Levy Place, New York, NY, 10029, USA.

Correspondence and requests for materials should be addressed to W.D.R. (email: wdristenpart@ucdavis.edu)

cough-generated droplets for several reasons. First, smaller particles persist in the air for longer time periods before settling by gravity, thus increasing the probability of inhalation by susceptible individuals²⁶. Second, smaller particles have a larger probability of penetrating further into the respiratory tract of a susceptible individual to initiate a lower respiratory tract infection⁴. Third, and perhaps most importantly, speech can release dramatically larger numbers of particles compared to coughing. Early work by Papineni and Rosenthal¹⁶ and Loudon and Roberts¹⁹ reported that speaking (as exemplified by counting aloud) releases about 2–10 times as many total particles as a single cough. Similarly, Loudon and Roberts investigated the role of singing in the spread of tuberculosis and showed that the percentage of airborne droplet nuclei generated by singing is 6 times more than that emitted during normal talking and approximately equivalent to that released by coughing²⁷. More recent work using advanced particle characterization techniques have yielded similar results^{21,28–30}. Chao *et al.*²⁸ used an interferometric imaging technique to obtain the size distribution of particles larger than 2 μm and found that counting aloud from 1 to 100 releases at least 6 times as many particles as an individual cough. Likewise, Morawska and coworkers^{21,29} reported that counting aloud for 10 seconds followed by 10 seconds of breathing, repeated over two minutes, releases half as many particles as 30 seconds of continual coughing, which in turn releases half as many particles as saying “aah” for 30 seconds. They also reported that more particles are released when speech is voiced, which involves vocal folds vibration, rather than whispered, which does not.

Despite the clear evidence that speech emits large quantities of potentially infectious particles, to date little is known about how particle emission is modulated by different types of speech. Notably, the above work measured neither the total duration nor the loudness of the vocalizations; it is also unclear whether counting aloud will have a distribution of phones (phonemes) that is representative of typical conversational speech. Many important questions remain unanswered. For example, does raising your voice cause an increase in particle emission, or alter the particle size distribution? Does it matter what language you speak? Do all individuals emit particles at similar rates?

To address these questions, we used an aerodynamic particle sizer (APS) placed in a laminar flow hood to characterize the number and size distribution of particles emitted by individual human volunteers while they performed various vocalizations and breathing activities. Using this approach, we found three key results:

- (1) The particle emission rate during speech is linearly correlated with the amplitude (loudness) of vocalization, for four different languages tested.
- (2) The particle size distribution is independent of vocalization loudness or language spoken.
- (3) Some individuals emit particles at a rate more than an order of magnitude larger than their peers, i.e., they behave as “speech superemitters.”

Taken together, the results strongly suggest that individual human speech patterns and speech-associated particle emissions are highly heterogeneous and thus might play a role in the transmission of some respiratory pathogens. Furthermore, the results suggest a new hypothesis: that speech superemitters might contribute to the phenomenon of superspreading, in which a relative few contagious individuals infect a disproportionately large number of secondary cases during infectious disease outbreaks³¹.

Results

Four separate types of experiments were performed. In the first experiment, participants said /a/ (the vowel sound in ‘saw’) for five seconds, followed by 15 seconds of nose breathing, repeated six times in succession. This procedure mimics previous experimental measurements of particle emission during vocalization²¹, but here the participants also systematically repeated the experiment at different voice amplitudes. Representative raw data for a single participant performing a series of six successive /a/ vocalizations, at approximately the same loudness, are shown in Fig. 1. The simultaneous microphone recording (Fig. 1A) and APS measurements (Fig. 1B) demonstrate that the dynamics of particle release are highly correlated with the vocalization. Prior to and between vocalizations, during nose breathing in which exhaled air is directed away from the APS, the particle count is negligible, as is expected for the HEPA filtered air inside the laminar flow hood. Shortly after the vocalization commences, the number of particles rapidly increases and peaks, then decreases back to zero as the participant resumes nose breathing; the process then repeats at the next five-second vocalization. The approximately two-second lag between onset of vocalization and the observed increase in particle count is due to the time necessary for the released particles to reach the sensor in the APS. We emphasize that by design an APS does not measure 100% of the particles drawn into it, so the particle emission rates reported here do not represent the absolute number of particles emitted by the participant; the emission rates are best understood in relative terms, or in terms of the equivalent instantaneous concentrations of particles sampled from the funnel. As shown in the secondary axis of Fig. 1B, the instantaneous concentration of particles for this particular experiment was approximately 2 per cm^3 of sampled air.

The six vocalizations shown in Fig. 1A were made, to the best of the participant’s ability, at the same loudness. Each participant then repeated a similar series of /a/ vocalizations at different self-regulated voice amplitudes. Representative results for a single participant (F4) show that the particle emission rate (N), defined as the total number of particles emitted during a single vocalization divided by the measured duration (in seconds) of that vocalization, also correlates with the root mean square amplitude (A_{rms}) of the vocalization (Fig. 2A). In our set-up $A_{\text{rms}} = 0.45$ corresponds to an extremely loud conversational voice, as loud as comfortable without yelling (~98 decibels measured 6.5 cm from the participant’s mouth, measured over background noise of approximately 65 decibels), while $A_{\text{rms}} = 0.02$ corresponds to a quiet vocalization just above whispering (~70 decibels; cf. Supplementary Fig. S1). As shown in Fig. 2A, the particle emission rate is linearly correlated with A_{rms} over this entire range of vocalization amplitudes, with the particle emission rate increasing from 6 to 53 particles per second at the quietest and loudest vocalizations respectively.

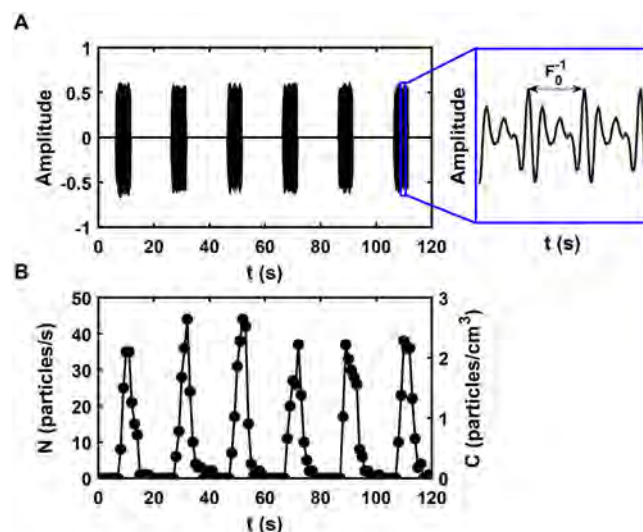


Figure 1. Representative raw data in which a participant (F4) said /a/ for 5 seconds, followed by 15 seconds of nose breathing, repeated 6 times at approximately the same loudness. (A) The amplitude (arb. units) recorded by the microphone versus time. Magnification shows 13 ms of the waveform with fundamental frequency of F_0 . (B) The corresponding number/concentration of particles measured by the APS versus time.

Although the particle emission rate increased with amplitude, the size distribution of the particles was not affected significantly (Fig. 2B), with the geometric mean particle diameter remaining near $1\ \mu\text{m}$ regardless of voice amplitude (Supplementary Fig. S2A). Because the particle size remains similar regardless of amplitude, the increased particle counts shown in Fig. 2 indicate that the total volume of emitted respiratory fluid (i.e., the proteinaceous liquid droplets aerosolized from the serous and mucoid layers lining the respiratory tract) increases considerably with the vocalization loudness. Note that the characteristic time scale for evaporative drying of 1-micron diameter droplets is on the order of 100 milliseconds²⁶, which is much less than the time required for the particles to move from the participant's mouth into the detection module within the APS, suggesting that the particles measured here had fully dried into droplet nuclei prior to measurement (see methods and Supplementary Fig. S3).

Experiments with multiple participants indicated that these trends are conserved over a larger sample size (Fig. 2C). The particle emission rate increased approximately linearly with A_{rms} for each of the study participants, although the absolute magnitude varied between individuals. One participant (F3) released as many as 200 particles per second at higher amplitudes; another (F2) released as few as 1 particle per second at lower amplitudes. Notably, the data with this cohort of non-elderly adults reveal no obvious trends with gender or age (Supplementary Figs S4A, B). Similarly, no clear correlation was observed with the body mass index (BMI) of the participants (Supplementary Figs S4C, D).

To more closely represent normal conversational speech, the participants read aloud a short passage of text in English at varied loudness (quiet, intermediate, or loud). Representative raw data for a single participant (F4) indicate that the particle emission rate also correlates with voice amplitude for normal speech (Fig. 3A,B). To quantify the loudness, we take A_{rms} here as the average over the entire approximately two-minute duration of the vocalization, excluding pauses between words. Aggregated data for 10 participants confirms that the particle emission rate for normal English speech correlates linearly with A_{rms} (Fig. 3C); speaking loudly yielded on average a 10-fold increase in the emission rate compared to speaking the same series of words quietly. Again, the size distributions (Fig. 3D) and geometric mean diameter of particles (Supplementary Fig. S2B) were insensitive to voice amplitude. The reading experiment also was repeated in different languages to test whether choice of language matters; the results (Supplementary Fig. S5) confirmed the increasing trend between particle emission rate and amplitude, but exhibited no significant difference in the particle emission rate among the languages tested (Supplementary Fig. S6). Likewise, we measured the temperature and humidity during the experiments, and found no significant impact of temperature or humidity on either the particle emission rate or the mean particle size (Supplementary Figs S7 and S8).

A key recurring feature of the data is that some individual participants emitted many more particles than others. Because all participants spoke at slightly different amplitudes, we used linear regressions of the particle emission rate versus amplitude for each individual (cf. Fig. 2A) to calculate a normalized particle emission rate at the loudness amplitude of 0.1 (approximately 85 dB). Using this approach, the results for 40 people show that the particle emission rate for different individuals follows a long-tailed distribution for both vocalization of /a/ (Fig. 4A) and reading of English text aloud (Fig. 4B). At this loudness, the normalized particle emission rates ranged from approximately 1 to 14 particles per second between different individuals, with an average of approximately 4 particles per second. Notably, the rates have a sizeable standard deviation well approximated by a lognormal fit (red curves in Fig. 4). In other words, although half of the participants emitted fewer than 3 particles per second, a small fraction of individuals (8 out of 40) emitted considerably more. These “speech superemitters,”

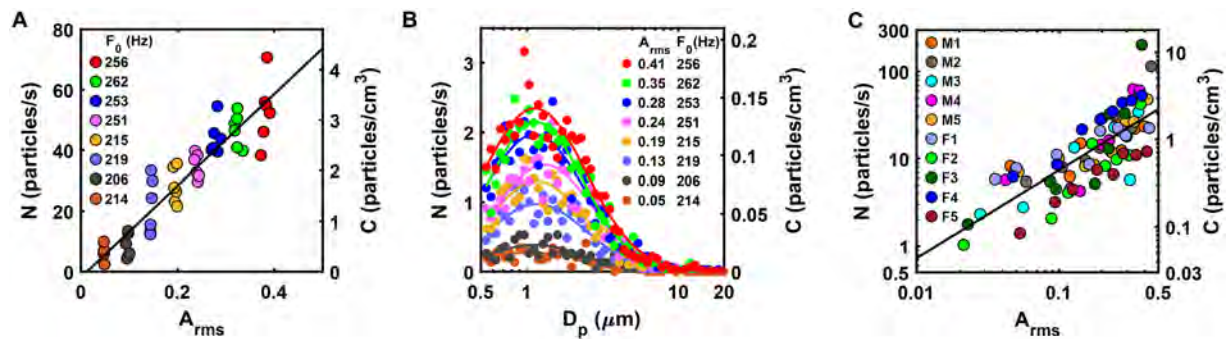


Figure 2. Particle emission rate/concentration while saying /a/ at 8 different amplitudes, repeated 6 times at each amplitude. (A) Particle emission rate/concentration versus root mean square amplitude, A_{rms} (arb. units) for a representative participant (F4). Solid line is the best linear fit, with correlation coefficient $r = 0.932$ and Pearson's p value $= 5.9 \times 10^{-22}$. (B) Corresponding particle size distribution for the data presented in (A). (C) Aggregated particle emission rate/concentration versus root mean square amplitude, A_{rms} (arb. units) for 10 participants, 5 males (denoted as M1 to M5) and 5 females (denoted as F1 to F5). There are 8 data points for each participant, each representing the average of repeating /a/ six times at approximately the same voice amplitude (cf. Fig. 1). Solid line is a power law fit with exponent 1.004, correlation coefficient $r = 0.774$ and Pearson's p value $= 3.8 \times 10^{-17}$.

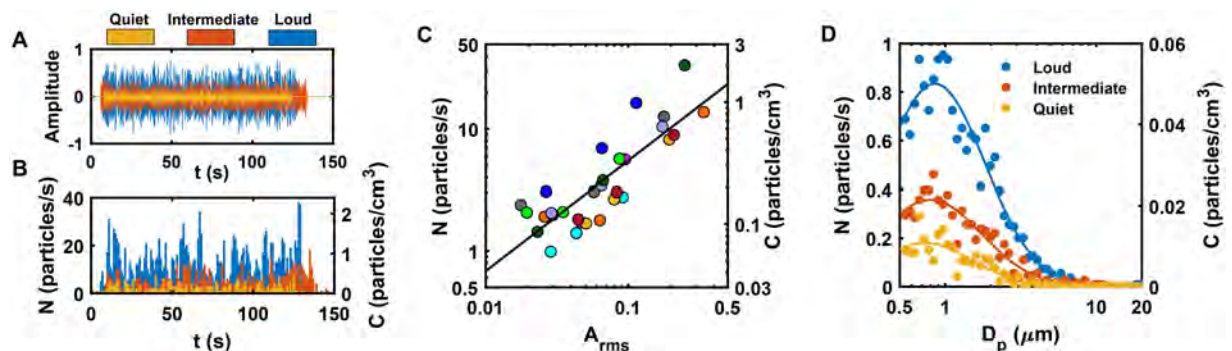


Figure 3. Particle emission rate/concentration while reading a passage of text aloud (the “Rainbow” passage), at three different loudness levels. (A) Superimposed representative recordings of amplitude (arb. units) for an individual (F4) reading the passage at three different voice amplitudes, and (B) the corresponding number/concentration of particles measured by the APS versus time. Color code same as in (A). (C) Particle emission rate/concentration as a function of root mean square amplitude, A_{rms} , for 10 participants. There are 3 points for each person, representing 3 voice amplitudes, color code same as Fig. 2C. Solid line is a power law fit with exponent 0.96, correlation coefficient $r = 0.865$ and Pearson's p value $= 6.8 \times 10^{-10}$. (D) Representative particle size distribution for the one individual (F4).

whose individual particle emission rate exceeded the group mean by one standard deviation or more, consistently released an order of magnitude more particles than their peers. For vocalizing /a/, Fig. 4A shows that 15% of the participants emitted 32% of the total particles, while Fig. 4B shows that, for reading aloud in English, 12.5% of the participants emitted 40% of the total particles. Supplementary Fig. S9A shows that 4 out of these 8 individuals are superemitters for both saying /a/ and passage reading activities, while 2 of them are only superemitters while saying /a/, and 2 of them are superemitters while reading a text passage. We repeated the passage reading experiment for two of the participants (M5 and F4) on three different days separated by several months (Supplementary Fig. S9B), and the results show that the particle emission rates remained almost unchanged for at least these two individuals (F4, a superemitter, and M5, a non-superemitter) despite the long time period between measurements.

To help interpret our findings we also compared the particle emission rates of four different types of breathing with speech at three levels of loudness using the same experimental set-up. The breathing experiments included nose breathing, mouth breathing, a “deep-fast” mode, and a “fast-deep” mode (see methods for details). The results show that the particle emission rate for speech is significantly higher than all types of breathing tested here (Fig. 5A). Furthermore, the corresponding geometric mean diameters of the particles generated during speech are slightly larger on average than those generated during breathing (Fig. 5B), consistent with prior work and the hypothesis that vocalization activates laryngeal particle generation²¹. Note that in Fig. 5A the speech outliers correspond to a single participant who is a speech superemitter (F4), but this individual was not also responsible

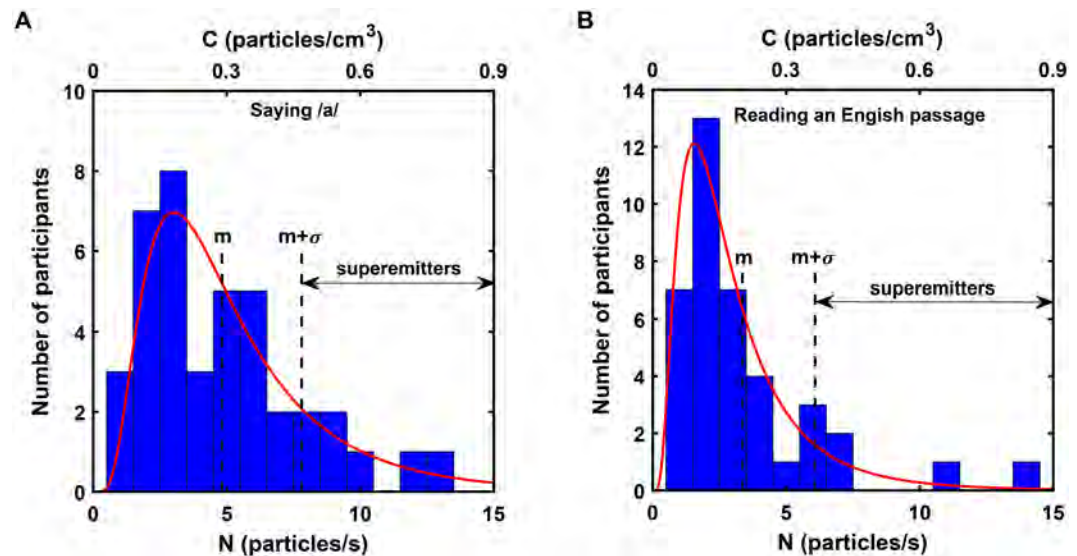


Figure 4. Histogram of particle emission rate/concentration at voice amplitude of 0.1 (approximately 85 dB). (A) For saying /a/, with median of $M = 4.3$ particles/s, mean of $m = 4.8$ particles/s and standard deviation of $\sigma = 3.0$ particles/s. (B) For reading an English passage (10 people read the “Rainbow” passage and 30 people read chapter 24 of “The Little Prince”) with median of $M = 2.5$ particles/s, mean of $m = 3.4$ particles/s and standard deviation of $\sigma = 2.7$ particles/s. Particle emission rates larger than $m + \sigma$ are labeled superemitters. Red curves are lognormal fits found via nonlinear regression.

for the observed outliers of “fast-deep” and “nose” breathing activities. In other words, the “breathing high producers” as defined by Edwards *et al.*¹⁵ are not necessarily also speech superemitters.

Discussion

Given that the results clearly indicate that particle emission rate is correlated with vocalization amplitude, a natural question is: why? The particles emitted during breathing and speech are hypothesized to be formed primarily by a “fluid-film burst” mechanism inside the small airways of the lungs and/or via vocal folds vibration and adduction at the larynx^{6,20,21}. During exhalation the elastic walls of the respiratory bronchioles contract, and the mucosal fluid on the lumen surface forms a continuous film that can completely fill the airway. During the subsequent inhalation, the bronchioles expand and the film ruptures, yielding particles that are drawn into the alveoli and subsequently exhaled. A similar mechanism is believed to occur in the larynx, as the vocal folds repeatedly close and open during vocalization²¹; when the vocal folds come into contact during adduction, fluid films that form between them can then rupture during their subsequent abduction. Our direct comparison of particles emitted during various types of breathing versus speech demonstrates that even quiet speech yields significantly more particles than normal breathing (Fig. 5A). Coupled with the observation that the particles generated during speech on average are slightly larger (Fig. 5B), the results suggest that laryngeal particle generation, which presumably does not occur during normal breathing, is at least partially responsible for the observed larger rates of particle emission. Indeed, the fundamental frequency or “pitch” of vocalization (i.e., the frequency at which the vocal folds open and close) increases slightly with amplitude (cf. Supplementary Fig. S11 and Gramming *et al.*³²), so the increased amplitude could reflect an increased opportunity for particles to form at the larynx.

Complicating matters, however, vocalization at a larger voice amplitude requires a larger exhalation flow rate^{33,34}. A possible interpretation of our observations is that the underlying physical mechanism of particle release hinges on the combination of laryngeal particle generation rate and the time integral of the exhalation flow rate during vocalization³⁵. If the volume of exhaled air is larger when the voice amplitude is higher, a larger fraction of particles formed in bronchiolar film rupture may escape from the lungs, with consequently more emitted particles, thus increasing the particle concentration in the exhaled air. Since our measurements only gauge the particle emission rate (and equivalent concentration), it is difficult to decouple the relative contributions of these two mechanisms. Fitting our particle size distributions to constrained bimodal lognormal distributions provides some evidence consistent with the interpretation presented by Johnson *et al.*²¹ that there are two modes, presumably due to bronchiolar versus laryngeal generation, but we do not find any significant difference in particle emission rates for the two modes as a function of vocalization amplitude (Supplementary Fig. S10 and cf. Fig. 5B). Furthermore, it is less understood how particles originating in the respiratory tract might deposit in more proximal regions instead of being emitted during exhalation. Particle deposition efficiency during nasal exhalation is known to depend on exhalation flow rate in a convoluted fashion, with Brownian diffusion, sedimentation, and inertial impaction all playing roles at different length and time scales within the respiratory tract³⁶. Nonetheless, our results strongly suggest that, in general, more particles escape the respiratory tract if the vocalization is louder.

Our results also clearly show that some participants release many more particles than others, for as-yet unclear reasons. It is known that the Rayleigh-Plateau instability that gives rise to small droplets during the “film burst” is

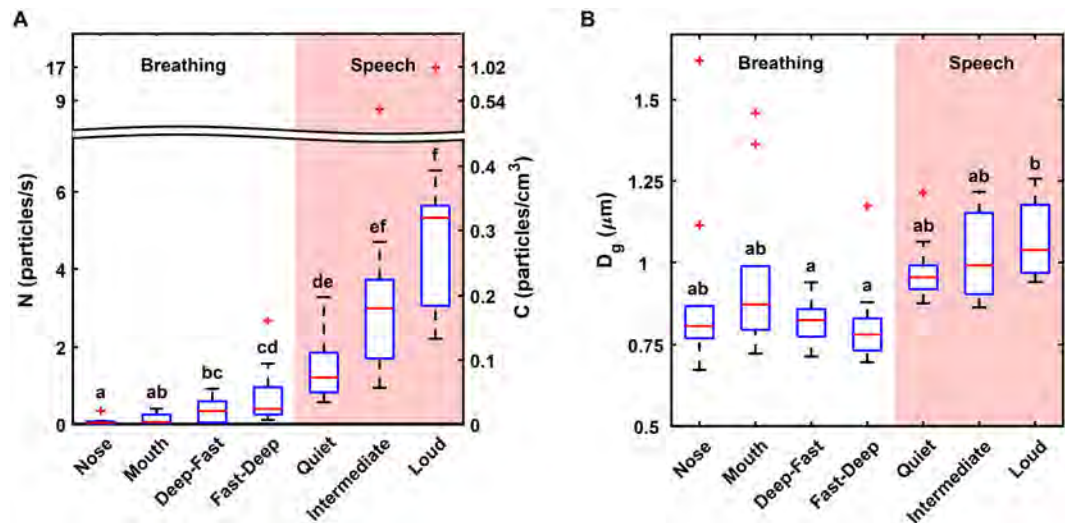


Figure 5. Comparison of (A) emission rate/concentration and (B) corresponding geometric mean diameters of particles emitted during various modes of breathing versus speech at different loudness levels. “Nose” denotes normal nasal breathing; “Mouth” denotes normal mouth breathing; “Deep-Fast” denotes deep, slow nasal inhalation followed by fast mouth exhalation; “Fast-Deep” denotes fast nasal inhalation followed by deep (i.e., slow and prolonged) mouth exhalation. “Quiet”, “Intermediate”, and “Loud” denote loudness levels while reading aloud a passage of text (“Rainbow” passage) at respective amplitudes. Red lines indicate medians, while bottom and top of blue boxes indicate the 25th and 75th percentiles respectively; sample size is $n = 10$. Outliers (defined as values that exceed 2.7 standard deviations) are indicated with red plus signs. Note that the 2 outliers for speech in (A) are a different individual (F4) than the two outliers observed for nose and fast-deep breathing (M24 and M5 respectively). Scheffé groups are indicated with letters; groups with no common letter are considered significantly different with $p < 0.05$, cf. Supplementary Table S1. Note that (A) has different scales above and below the break.

sensitive to the interfacial tension, density, and viscosity of the fluid³⁷, so one possible explanation is that the mucosal fluids in different people have different material properties and correspondingly generate more or fewer drops. Notably, different disease states are known to alter the physicochemical properties of the mucosal fluid lining the respiratory tract³⁸, so it is possible that infected individuals might generate markedly different quantities of particles than those emitted by the healthy individuals tested here. Intriguingly, Edwards *et al.*¹⁵ found that delivering nebulized isotonic saline to individuals decreased the number of particles exhaled during normal breathing for a few hours after inhalation of the saline; further tests are warranted with speech. Alternatively, it is possible that individual manners of articulation affect the amount of internal deposition of the particles before they manage to escape the mouth. Our tests of different languages yielded no significant differences, at odds with previous speculation that language spoken might have played a role in the epidemiology of SARS coronavirus transmission³⁹, and suggesting that some as yet unknown physiological factor causes the dramatic variation among individuals.

Regardless of the underlying physical mechanism, from an epidemiological perspective the existence of speech superemitters motivates consideration of a new hypothesis: that speech superemitters contribute to “superspreading” of infectious diseases transmitted by emitted airborne particles. A superspreader is a contagious individual who infects a disproportionately large number of susceptible contacts^{31,40,41}. To date, several airborne superspreading events have been documented, such as the MERS-CoV outbreak in South Korea in 2015 and the SARS-CoV outbreak in 2003, the latter being initiated in Hong Kong and spreading to Canada, Vietnam, and Singapore through travel^{40–43}. In the case of respiratory infectious diseases in particular, the underlying physiological and immunological factors that contribute to heterogeneity in individual infectiousness remain poorly understood, despite the epidemiological importance of respiratory superspreaders. Quantifying infectious pathogen loads in exhaled air is technically challenging, relative to other contagious substances like blood, urine, and feces. Many factors presumably affect the secondary attack rate attributable to any infectious individual, including the herd immunity status of others in proximity. Nonetheless, our results suggest that, for respiratory infections transmitted from person to person via airborne particles, the existence of speech superemitters might help explain the existence of superspreaders. A similar hypothesis was advanced by Edwards *et al.*¹⁵ in response to their observation of variability between individuals in the number of particles emitted during mouth breathing. Interestingly, our data show that speech superemitters are not necessarily breathing superemitters as well (Fig. 5A), suggesting that respiratory superemission during vocalized speech has a different underlying physiology than superemission during tidal breathing.

Our results indicate that speech is potentially of much greater concern than breathing for two reasons: the particles on average are larger, and thus could potentially carry a larger number of pathogens, and much greater quantities of particles are emitted compared to breathing, thus increasing the odds of infecting nearby susceptible individuals. Laryngeal particle generation during speech is also potentially important since some studies suggest that human influenza viruses attach more abundantly to the large airways of the upper respiratory tract than to

the bronchiolar and alveolar cells in the lower respiratory tract, while MERS-CoV and avian influenza viruses mainly cause lower respiratory tract infections due to the greater presence of these virus receptors deeper within the lung^{44–47}; likewise there is evidence that laryngeal tuberculosis is potentially more contagious than typical pulmonary tuberculosis⁴⁸.

A second key epidemiological implication of our results is that simply talking in a loud voice would increase the rate at which an infected individual releases pathogen-laden particles into the air, which in turn would increase the probability of transmission to susceptible individuals nearby⁴⁹. For example, an airborne infectious disease might spread more efficiently in a school cafeteria than a library, or in a noisy hospital waiting room than a quiet ward. Moreover, our data suggest a related hypothesis, that infected individuals could be transmitting significant numbers of respiratory pathogens via speech in the absence of overt clinical signs of illness like coughing or sneezing. More research is needed; however, the presence of asymptomatic or paucisymptomatic superspreaders would have important public health implications in the surveillance for and mitigation of infectious disease epidemics that are spread by airborne respiratory particles. The data presented here strongly suggest that further efforts to test these hypotheses are warranted.

Methods

Human subjects. The University of California Davis Institutional Review Board approved this study and all research was performed in accordance with relevant guidelines and regulations of the Institutional Review Board. We recruited 48 healthy volunteers (26 males and 22 females, ranging in age from 18 to 45 years old) by posting flyers at the University of California Davis campus over the time period May 2016 to March 2018. Informed consent was obtained from all participants prior to study participation. All participants completed a brief questionnaire including age, gender, weight, height, general health status, and smoking history. Only participants who self-reported as healthy non-smokers were included in the study. The subject in Supplementary Fig. S12 provided her written informed consent for the publication of identifying information/images in an online open-access publication.

Experimental set-up. A photograph of the experimental set-up is provided as Supplementary Fig. S12. An aerodynamic particle sizer (APS, TSI model 3321) operating at a total flow rate of 5 L/min (sheath flow rate \cong 4 L/min, sample flow rate \cong 1 L/min) was placed inside a HEPA filtered laminar flow hood that provided class 10 air. A plastic funnel (diameter = 10 cm) was connected to the APS sampling inlet via a conductive silicon tube (distance between funnel hole to APS inlet = 7.5 cm, tube inner diameter = 1.2 cm). During each experiment, participants sat at the laminar flow hood, in front of the APS, and spoke into the funnel. For the majority of speaking and breathing experiments, a nose rest across the funnel opening was used to position participants' mouths approximately 7.5 cm away from the funnel inlet (hole) and also to divert nasal exhalations away from the APS. During "nose-breathing" experiments, the nose rest was removed to allow nasal exhalations to be drawn into the APS. Note that participants' faces did not touch the funnel, so that air was free to move around the side of their faces; in this sense the cone was a semi-confined environment and not all expired particles were necessarily sampled by the APS. Also note that the sheath flow inside of an APS is filtered, so the particle emission rates sampled by the APS automatically remove 80% of the particles sampled from the funnel. Equivalent concentrations reported on the secondary axes in Figs 1 through 5 are determined from the raw particle counts using the sample flow rate, i.e., $C = \frac{\text{particles}}{\text{cm}^3} \times \frac{s}{\text{cm}^3} = \frac{\text{particles}}{\text{cm}^3}$. Also note that the APS measures the size distribution of particles larger than 0.5 μm , but only detects the presence of particles between 0.37 μm and 0.5 μm without providing precise size measurements. For this reason Figs 1–5 exclude the counts of particles smaller than 0.5 μm ; including them has little impact on the results since the vast majority of particles were larger than 0.5 microns.

A microphone (audio-technica PRO 37) and a decibel meter (Extech, 407760) were placed immediately on either side of the funnel to record the vocalizations. A computer screen with word prompts and a timer was placed behind the APS to guide participants in making requested vocalizations for the specified duration. The timing, duration, repetition, and order of vocalization and breathing experiments were coordinated by customized code written in LabVIEW (National Instruments). A digital hygrometer was used to measure the ambient temperature and relative humidity inside the laminar flow hood during all experiments. The participants were not allowed to drink or eat during the experiment, but they were free to rest between experiments for a few minutes as needed; data from each individual participant was gathered over an approximately 1-hour time period. We performed the experiments in an indoor (controlled) environment, so the ambient temperature varied only from approximately 20 to 25 °C, while the ambient relative humidity measured inside the laminar flow hood varied from a low of approximately 45% to a high of 80%. Control experiments indicate that the particle size distribution was independent of whether the particles were expired early or late during a sustained vocalization (Supplementary Fig. S3), indicating that transient fluctuations in the humidity inside the funnel due to exhalation had no impact on the final measured size distribution. Particles with initial diameter of less than 20 μm dry to approximately half of their initial diameter in less than 1 second^{49,50}. Different correction factors have been suggested in the literature that one can use to estimate the initial size of the particles^{49,51}; here we focus on the final size distribution because epidemiologically it is the final size distribution governs the deposition efficiency of the particles in the respiratory tract of nearby susceptible individuals⁵².

Vocalization experiments. *“/a/” experiments.* Participants (n = 10, 5 males, M1 to M5, and 5 females, F1 to F5) voiced /a/ (the vowel sound in ‘saw’) for five seconds, followed by 15 seconds of nose breathing, repeated six times in succession. The participant repeated the series of six /a/ vocalizations, to the best of the participant's ability, at the same amplitude. Each participant completed eight sets of /a/ experiments, each set performed at different, self-regulated voice amplitude. Timed prompts with directions for the requested vocalization appeared on the computer screen, which displayed a timer and an amplitude (loudness) gauge to help the participants regulate their voice amplitude. The requested amplitudes were presented to participants in a random order.

“Rainbow passage” experiments. Participants ($n = 10$, 5 males, M1 to M5, and 5 females, F1 to F5) read aloud a 330-word excerpt of text in English, known in linguistics research as the Rainbow passage⁵³. Participants were asked to read the Rainbow passage aloud three times, at a comfortable pace, over approximately 2 minutes per reading. Each of the three readings was performed at a different self-regulated amplitude: quiet, intermediate, and loud. Quiet was defined for participants as “just louder than a whisper,” intermediate as a “normal conversational voice,” and loud as “giving a loud lecture”.

“The Little Prince” experiments. Bilingual participants ($n = 30$) fluent in both English and either Spanish ($n = 10$, 5 males, M6 to M10, and 5 females, F6 to F10), Mandarin ($n = 10$, 5 males, M11 to M15, and 5 females, F11 to F15), or Arabic ($n = 10$, 6 males, M16 to M21, and 4 females, F16 to F19) read Chapter 24 of “The Little Prince”⁵⁴ aloud six times, three times in English translation, each time at a different amplitude (quiet, intermediate, and loud) and three times in their respective language, again at three loudness levels.

Breathing/speaking experiments. Participants ($n = 10$, 6 males, M5 and M22 to M26, and 4 females, F4 and F20 to F22) alternated four silent breathing patterns with vocalized speech at three amplitudes. For breathing measurements, the breathing patterns were designated as “nose” (both inhalation and exhalation through the nose), “mouth” (both inhalation and exhalation through the mouth), “deep-fast” (deep, slow inhalation for ~3 seconds through the nose, holding it for ~1 second, followed by fast exhalation through the mouth (~1 second)), and “fast-deep” (rapid inhalation through the nose (~1 second), holding it for ~1 second, followed by slow exhalation through the mouth for ~3 seconds). Each breathing experiment was performed over 2 minutes, and at a comfortable pace for the participants. Between performing different breathing patterns, participants were asked to read the Rainbow passage in a “quiet,” “intermediate,” or “loud” voice, as prompted by the computer in random order.

Statistical analysis. Data analysis was performed in MATLAB (MathWorks), with data fits performed as noted in figure legends. Pearson’s linear correlation coefficients and p values were calculated for linear fits. Lognormal fits were made via nonlinear regression, and median, mean, and standard deviation were calculated. Box-and-whisker plots show the median (red line), interquartile range (blue box), and range (black whiskers). To analyze the breathing/speaking experiments data presented in Fig. 5, Stata/SE 15.1 was used to perform general linear mixed model (GLMM) analysis to account for person-level correlations, and post hoc pairwise comparisons were performed and adjusted for multiple comparisons using Scheffe’s method.

Data Availability

All relevant data are available from the corresponding authors upon request.

References

1. Tellier, R. Review of aerosol transmission of influenza A virus. *Emerg. Infect. Dis* **12**, 1657–1662, <https://doi.org/10.3201/eid1211.060426> (2006).
2. Weber, T. P. & Stilianakis, N. I. Inactivation of influenza A viruses in the environment and modes of transmission: A critical review. *Journal of Infection* **57**, 361–373, <https://doi.org/10.1016/j.jinf.2008.08.013> (2008).
3. Tellier, R. Aerosol transmission of influenza A virus: a review of new studies. *Journal of the Royal Society Interface* **6**, S783–S790, <https://doi.org/10.1098/rsif.2009.0302.focus> (2009).
4. Gralton, J., Tovey, E., McLaws, M. L. & Rawlinson, W. D. The role of particle size in aerosolised pathogen transmission: a review. *Journal of Infection* **62**, 1–13, <https://doi.org/10.1016/j.jinf.2010.11.010> (2011).
5. Tang, J. W. Investigating the airborne transmission pathway - different approaches with the same objectives. *Indoor Air* **25**, 119–124, <https://doi.org/10.1111/ina.12175> (2015).
6. Wei, J. J. & Li, Y. G. Airborne spread of infectious agents in the indoor environment. *Am. J. Infect. Control* **44**, S102–S108, <https://doi.org/10.1016/j.ajic.2016.06.003> (2016).
7. Yang, S. H., Lee, G. W. M., Chen, C. M., Wu, C. C. & Yu, K. P. The size and concentration of droplets generated by coughing in human subjects. *Journal of Aerosol Medicine-Deposition Clearance and Effects in the Lung* **20**, 484–494, <https://doi.org/10.1089/jam.2007.0610> (2007).
8. Lindsley, W. G. *et al.* Quantity and size distribution of cough-generated aerosol particles produced by influenza patients during and after illness. *Journal of Occupational and Environmental Hygiene* **9**, 443–449, <https://doi.org/10.1080/15459624.2012.684582> (2012).
9. Lindsley, W. G., Reynolds, J. S., Szalajda, J. V., Noti, J. D. & Beezhold, D. H. A cough aerosol simulator for the study of disease transmission by human cough-generated aerosols. *Aerosol Sci. Technol.* **47**, 937–944, <https://doi.org/10.1080/02786826.2013.803019> (2013).
10. Lindsley, W. G. *et al.* Viable influenza A virus in airborne particles expelled during coughs versus exhalations. *Influenza and Other Respiratory Viruses* **10**, 404–413, <https://doi.org/10.1111/irv.12390> (2016).
11. Bourouiba, L., Dehandschoewercker, E. & Bush, J. W. M. Violent expiratory events: on coughing and sneezing. *Journal of Fluid Mechanics* **745**, 537–563, <https://doi.org/10.1017/jfm.2014.88> (2014).
12. Zayas, G. *et al.* Cough aerosol in healthy participants: fundamental knowledge to optimize droplet-spread infectious respiratory disease management. *Bmc Pulmonary Medicine* **12**, <https://doi.org/10.1186/1471-2466-12-11> (2012).
13. Scharfman, B. E., Tchet, A. H., Bush, J. W. M. & Bourouiba, L. Visualization of sneeze ejecta: steps of fluid fragmentation leading to respiratory droplets. *Experiments in Fluids* **57**, 9, <https://doi.org/10.1007/s00348-015-2078-4> (2016).
14. Han, Z. Y., Weng, W. G. & Huang, Q. Y. Characterizations of particle size distribution of the droplets exhaled by sneeze. *Journal of the Royal Society Interface* **10**, 1–11, <https://doi.org/10.1098/rsif.2013.0560> (2013).
15. Edwards, D. A. *et al.* Inhaling to mitigate exhaled bioaerosols. *Proceedings of the National Academy of Sciences of the United States of America* **101**, 17383–17388, <https://doi.org/10.1073/pnas.0408159101> (2004).
16. Papineni, R. S. & Rosenthal, F. S. The size distribution of droplets in the exhaled breath of healthy human subjects. *Journal of Aerosol Medicine and Pulmonary Drug Delivery* **10**, 105–116, <https://doi.org/10.1089/jam.1997.10.105> (1997).
17. Fabian, P. *et al.* Influenza virus in human exhaled breath: an observational study. *Plos One* **3**, <https://doi.org/10.1371/journal.pone.0002691> (2008).
18. Duguid, J. P. The size and the duration of air-carriage of respiratory droplets and droplet-nuclei. *Journal of Hygiene* **44**, 471–479 (1946).
19. Loudon, R. G. & Roberts, R. M. Droplet expulsion from the respiratory tract. *American Review of Respiratory Disease* **95**, 435–442, <https://doi.org/10.1164/arrd.1967.95.3.435> (1967).

20. Johnson, G. R. & Morawska, L. The mechanism of breath aerosol formation. *Journal of Aerosol Medicine and Pulmonary Drug Delivery* **22**, 229–237, <https://doi.org/10.1089/jamp.2008.0720> (2009).
21. Johnson, G. R. *et al.* Modality of human expired aerosol size distributions. *Journal of Aerosol Science* **42**, 839–851, <https://doi.org/10.1016/j.jaerosci.2011.07.009> (2011).
22. Liljeroos, L., Huiskonen, J. T., Ora, A., Susi, P. & Butcher, S. J. Electron cryotomography of measles virus reveals how matrix protein coats the ribonucleocapsid within intact virions. *Proceedings of the National Academy of Sciences of the United States of America* **108**, 18085–18090, <https://doi.org/10.1073/pnas.1105770108> (2011).
23. Rossman, J. S. & Lamb, R. A. Influenza virus assembly and budding. *Virology* **411**, 229–236, <https://doi.org/10.1016/j.virol.2010.12.003> (2011).
24. Fennelly, K. P. *et al.* Variability of infectious aerosols produced during coughing by patients with pulmonary tuberculosis. *American Journal of Respiratory and Critical Care Medicine* **186**, 450–457, <https://doi.org/10.1164/rccm.201203-0444OC> (2012).
25. Yan, J. *et al.* Infectious virus in exhaled breath of symptomatic seasonal influenza cases from a college community. *Proceedings of the National Academy of Sciences of the United States of America* **115**, 1081–1086, <https://doi.org/10.1073/pnas.1716561115> (2018).
26. Shaman, J. & Kohn, M. Absolute humidity modulates influenza survival, transmission, and seasonality. *Proceedings of the National Academy of Sciences of the United States of America* **106**, 3243–3248, <https://doi.org/10.1073/pnas.0806852106> (2009).
27. Loudon, R. G. & Roberts, M. R. Singing and the dissemination of tuberculosis. *American Review of Respiratory Disease* **98**, 297–300 (1968).
28. Chao, C. Y. H. *et al.* Characterization of expiration air jets and droplet size distributions immediately at the mouth opening. *Journal of Aerosol Science* **40**, 122–133, <https://doi.org/10.1016/j.jaerosci.2008.10.003> (2009).
29. Morawska, L. *et al.* Size distribution and sites of origin of droplets expelled from the human respiratory tract during expiratory activities. *Journal of Aerosol Science* **40**, 256–269, <https://doi.org/10.1016/j.jaerosci.2008.11.002> (2009).
30. Xie, X. J., Li, Y. G., Sun, H. Q. & Liu, L. Exhaled droplets due to talking and coughing. *Journal of the Royal Society Interface* **6**, S703–S714, <https://doi.org/10.1098/rsif.2009.0388.focus> (2009).
31. Lloyd-Smith, J. O., Schreiber, S. J., Kopp, P. E. & Getz, W. M. Superspreading and the effect of individual variation on disease emergence. *Nature* **438**, 355–359, <https://doi.org/10.1038/nature04153> (2005).
32. Gramming, P., Sundberg, J., Ternström, S., Leanderson, R. & Perkins, W. H. Relationship between changes in voice pitch and loudness. *Journal of Voice* **2**, 118–126, [https://doi.org/10.1016/S0892-1997\(88\)80067-5](https://doi.org/10.1016/S0892-1997(88)80067-5) (1988).
33. Titze, I. R. Phonation threshold pressure: A missing link in glottal aerodynamics. *J. Acoust. Soc. Am.* **91**, 2926–2935, <https://doi.org/10.1121/1.402928> (1992).
34. Titze, I. R. & Sundberg, J. Vocal intensity in speakers and singers. *J. Acoust. Soc. Am.* **91**, 2936–2946, <https://doi.org/10.1121/1.402929> (1992).
35. Gupta, J. K., Lin, C. H. & Chen, Q. Y. Characterizing exhaled airflow from breathing and talking. *Indoor Air* **20**, 31–39, <https://doi.org/10.1111/j.1600-0668.2009.00623.x> (2010).
36. Xi, J. X. & Longest, P. W. Characterization of submicrometer aerosol deposition in extrathoracic airways during nasal exhalation. *Aerosol Sci. Technol.* **43**, 808–827, <https://doi.org/10.1080/02786820902950887> (2009).
37. Eggers, J. Nonlinear dynamics and breakup of free-surface flows. *Reviews of Modern Physics* **69**, 865–929, <https://doi.org/10.1103/RevModPhys.69.865> (1997).
38. Girod, S., Zahm, J. M., Plotkowski, C., Beck, G. & Puchelle, E. Role of the physiochemical properties of mucus in the protection of the respiratory epithelium. *European Respiratory Journal* **5**, 477–487 (1992).
39. Inouye, S. SARS transmission: language and droplet production. *Lancet* **362**, 170–170, [https://doi.org/10.1016/S0140-6736\(03\)13874-3](https://doi.org/10.1016/S0140-6736(03)13874-3) (2003).
40. Wong, G. *et al.* MERS, SARS, and Ebola: The role of super-spreaders in infectious disease. *Cell Host & Microbe* **18**, 398–401, <https://doi.org/10.1016/j.chom.2015.09.013> (2015).
41. Lau, M. S. Y. *et al.* Spatial and temporal dynamics of superspreading events in the 2014–2015 West Africa Ebola epidemic. *Proceedings of the National Academy of Sciences of the United States of America* **114**, 2337–2342, <https://doi.org/10.1073/pnas.1614595114> (2017).
42. Stein, R. A. Super-spreaders in infectious diseases. *International Journal of Infectious Diseases* **15**, E510–E513, <https://doi.org/10.1016/j.ijid.2010.06.020> (2011).
43. Chun, B. C. Understanding and modeling the super-spreading events of the Middle East respiratory syndrome outbreak in Korea. *Infection and Chemotherapy* **48**, 147–149, <https://doi.org/10.3947/ic.2016.48.2.147> (2016).
44. van Riel, D. *et al.* Seasonal and pandemic human influenza viruses attach better to human upper respiratory tract epithelium than avian influenza viruses. *American Journal of Pathology* **176**, 1614–1618, <https://doi.org/10.2353/ajpath.2010.090949> (2010).
45. van Riel, D. *et al.* Human and avian influenza viruses target different cells in the lower respiratory tract of humans and other mammals. *American Journal of Pathology* **171**, 1215–1223, <https://doi.org/10.2353/ajpath.2007.070248> (2007).
46. Widagdo, W., Okba, N. M. A., Raj, V. S. & Haagmans, B. L. MERS-coronavirus: From discovery to intervention. *One Health* **3**, 11–16, <https://doi.org/10.1016/j.onehlt.2016.12.001> (2017).
47. Shinya, K. *et al.* Influenza virus receptors in the human airway. *Nature* **440**, 435, <https://doi.org/10.1038/440435a> (2006).
48. Sepkowitz, K. A. How contagious is tuberculosis? *Clinical Infectious Diseases* **23**, 954–962, <https://doi.org/10.1093/clinids/23.5.954> (1996).
49. Nicas, M., Nazaroff, W. W. & Hubbard, A. Toward understanding the risk of secondary airborne infection: Emission of respirable pathogens. *Journal of Occupational and Environmental Hygiene* **2**, 143–154, <https://doi.org/10.1080/15459620590918466> (2005).
50. Xie, X., Li, Y., Chwang, A. T. Y., Ho, P. L. & Seto, W. H. How far droplets can move in indoor environments - revisiting the Wells evaporation-falling curve. *Indoor Air* **17**, 211–225, <https://doi.org/10.1111/j.1600-0668.2006.00469.x> (2007).
51. Liu, L., Wei, J., Li, Y. & Ooi, A. Evaporation and dispersion of respiratory droplets from coughing. *Indoor Air* **27**, 179–190, <https://doi.org/10.1111/ina.12297> (2017).
52. Heyder, J., Gebhart, J., Rudolf, G., Schiller, C. F. & Stahlhofen, W. Deposition of particles in the human respiratory tract in the size range 0.005–15- μm . *Journal of Aerosol Science* **17**, 811–825, [https://doi.org/10.1016/0021-8502\(86\)90035-2](https://doi.org/10.1016/0021-8502(86)90035-2) (1986).
53. Fairbanks, G. *Voice and articulation drillbook*. (Harper, 1960).
54. Saint-Exupéry, A. Le Petit Prince, trans Woods K (Harcourt, Brace & World, New York) 1st ed., Chapter 24 (1943).

Acknowledgements

We thank the National Institute of Allergy and Infectious Diseases of the National Institutes of Health (NIAID/NIH), grant R01 AI110703, and the NIEHS UC Davis Core Centre, grant P30-ES023513, for supporting this research, and P. Dayal for assistance with statistical analysis.

Author Contributions

S.A., A.S.W., C.D.C., S. B., N.M.B. and W.D.R. designed research; S.A. performed experiments; S.A. and W.D.R. analysed the data; S.A. and W.D.R. wrote the manuscript, and all co-authors reviewed the manuscript.

Additional Information

Supplementary information accompanies this paper at <https://doi.org/10.1038/s41598-019-38808-z>.

Competing Interests: The authors declare no competing interests.

Publisher's note: Springer Nature remains neutral with regard to jurisdictional claims in published maps and institutional affiliations.



Open Access This article is licensed under a Creative Commons Attribution 4.0 International License, which permits use, sharing, adaptation, distribution and reproduction in any medium or format, as long as you give appropriate credit to the original author(s) and the source, provide a link to the Creative Commons license, and indicate if changes were made. The images or other third party material in this article are included in the article's Creative Commons license, unless indicated otherwise in a credit line to the material. If material is not included in the article's Creative Commons license and your intended use is not permitted by statutory regulation or exceeds the permitted use, you will need to obtain permission directly from the copyright holder. To view a copy of this license, visit <http://creativecommons.org/licenses/by/4.0/>.

© The Author(s) 2019

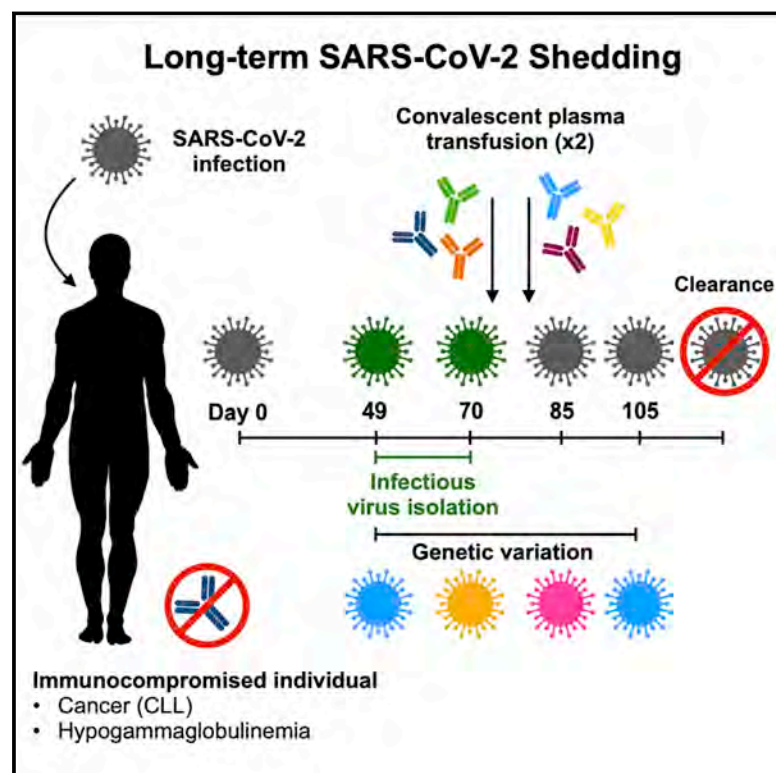


Since January 2020 Elsevier has created a COVID-19 resource centre with free information in English and Mandarin on the novel coronavirus COVID-19. The COVID-19 resource centre is hosted on Elsevier Connect, the company's public news and information website.

Elsevier hereby grants permission to make all its COVID-19-related research that is available on the COVID-19 resource centre - including this research content - immediately available in PubMed Central and other publicly funded repositories, such as the WHO COVID database with rights for unrestricted research re-use and analyses in any form or by any means with acknowledgement of the original source. These permissions are granted for free by Elsevier for as long as the COVID-19 resource centre remains active.

Case Study: Prolonged Infectious SARS-CoV-2 Shedding from an Asymptomatic Immunocompromised Individual with Cancer

Graphical Abstract



Authors

Victoria A. Avanzato,
M. Jeremiah Matson,
Stephanie N. Seifert, ..., Emmie de Wit,
Francis X. Riedo, Vincent J. Munster

Correspondence

fxriedo@evergreenhealthcare.org
(F.X.R.),
vincent.munster@nih.gov (V.J.M.)

In Brief

This case study describes a female immunocompromised individual with chronic lymphocytic leukemia and acquired hypogammaglobulinemia who became persistently infected with SARS-CoV-2. Although asymptomatic throughout the course of infection, she demonstrated prolonged shedding of infectious SARS-CoV-2 virus and RNA. This study demonstrates that certain individuals may remain infectious for prolonged periods of time and highlights the need for further studies to understand risk factors for prolonged infectious SARS-CoV-2 shedding.

Highlights

- Persistent SARS-CoV-2 infection and shedding in immunocompromised individual
- Infectious SARS-CoV-2 isolated up to 70 days after diagnosis
- Observed within-host genetic variation with continuous turnover of viral variants
- SARS-CoV-2 isolates from the individual do not display altered replication



Article

Case Study: Prolonged Infectious SARS-CoV-2 Shedding from an Asymptomatic Immunocompromised Individual with Cancer

Victoria A. Avanzato,^{1,2,7} M. Jeremiah Matson,^{1,3,7} Stephanie N. Seifert,^{1,7} Rhys Pryce,² Brandi N. Williamson,¹ Sarah L. Anzick,⁴ Kent Barbian,⁴ Seth D. Judson,⁵ Elizabeth R. Fischer,⁴ Craig Martens,⁴ Thomas A. Bowden,² Emmie de Wit,¹ Francis X. Riedo,^{6,*} and Vincent J. Munster^{1,8,*}

¹Laboratory of Virology, National Institute of Allergy and Infectious Diseases, National Institutes of Health, Hamilton, MT 59840, USA

²Division of Structural Biology, Wellcome Centre for Human Genetics, University of Oxford, Oxford OX3 7BN, UK

³Marshall University Joan C. Edwards School of Medicine, Huntington, WV 25701, USA

⁴Research Technologies Branch, National Institute of Allergy and Infectious Diseases, National Institutes of Health, Hamilton, MT 59840, USA

⁵Department of Medicine, University of Washington, Seattle, WA 98195, USA

⁶EvergreenHealth, Kirkland, WA 98034, USA

⁷These authors contributed equally

⁸Lead Contact

*Correspondence: fxriedo@evergreenhealthcare.org (F.X.R.), vincent.munster@nih.gov (V.J.M.)

<https://doi.org/10.1016/j.cell.2020.10.049>

SUMMARY

Long-term severe acute respiratory syndrome coronavirus 2 (SARS-CoV-2) shedding was observed from the upper respiratory tract of a female immunocompromised individual with chronic lymphocytic leukemia and acquired hypogammaglobulinemia. Shedding of infectious SARS-CoV-2 was observed up to 70 days, and of genomic and subgenomic RNA up to 105 days, after initial diagnosis. The infection was not cleared after the first treatment with convalescent plasma, suggesting a limited effect on SARS-CoV-2 in the upper respiratory tract of this individual. Several weeks after a second convalescent plasma transfusion, SARS-CoV-2 RNA was no longer detected. We observed marked within-host genomic evolution of SARS-CoV-2 with continuous turnover of dominant viral variants. However, replication kinetics in Vero E6 cells and primary human alveolar epithelial tissues were not affected. Our data indicate that certain immunocompromised individuals may shed infectious virus longer than previously recognized. Detection of subgenomic RNA is recommended in persistently SARS-CoV-2-positive individuals as a proxy for shedding of infectious virus.

INTRODUCTION

Severe acute respiratory syndrome coronavirus 2 (SARS-CoV-2) RNA can be detected at various sites, including samples obtained from the nares, nasopharynx, pharynx, bronchoalveolar lavage (BAL) fluid, feces, and blood (Wang et al., 2020a; Sun et al., 2020; Judson and Munster, 2020). The duration of SARS-CoV-2 RNA shedding is generally between 3 and 46 days after symptom onset (Fu et al., 2020; Qian et al., 2020; Liu et al., 2020c). Asymptomatic individuals shed SARS-CoV-2 RNA comparably with symptomatic individuals regarding duration and viral load (Lee et al., 2020; Long et al., 2020; Zou et al., 2020). Persistent SARS-CoV-2 RNA shedding has been documented, with patients remaining qRT-PCR-positive for up to 63 days (Li et al., 2020; Liu et al., 2020b). In addition, there are reports of symptomatic and asymptomatic individuals testing positive again after a period of negative testing (Lan et al., 2020; Hu et al., 2020). Because qRT-PCR detects viral RNA but does not confirm the presence of infectious SARS-

CoV-2, these observations raise questions about the duration of infectious SARS-CoV-2 shedding and transmission potential for symptomatic and asymptomatic individuals.

Estimates suggest that infectiousness begins 2.3 days prior to symptom onset and declines within 7 days of symptom onset (He et al., 2020b). Consistent with this, infectious SARS-CoV-2 has been isolated from patient samples taken up to 8 days after symptom onset but typically not thereafter (Wölfel et al., 2020; Bullard et al., 2020). In contrast to prolonged shedding of SARS-CoV-2 RNA, the longest detected shedding of infectious SARS-CoV-2 virus is up to 20 days after the initial positive test result (van Kampen et al., 2020; Liu et al., 2020b). The probability of isolating SARS-CoV-2 decreases with a lower viral load, when the duration of symptoms exceeds 15 days, and upon generation of detectable neutralizing antibodies (van Kampen et al., 2020).

On January 19, 2020, the first case of coronavirus disease 2019 (COVID-19) was identified in the United States, in Snohomish County, Washington, in a traveler returning from Wuhan,



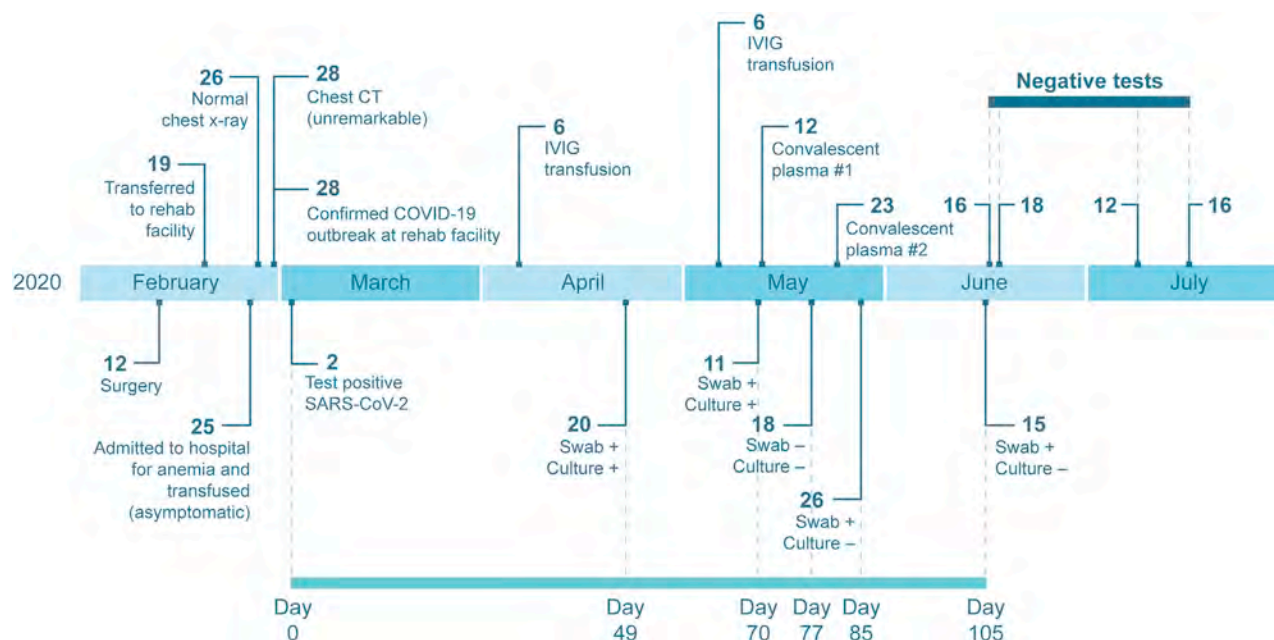


Figure 1. Timeline of Clinical Presentation, Diagnostic Tests, and Treatments of an Immunocompromised Individual with Long-Term Shedding of SARS-CoV-2

Dates of relevant clinical events, such as surgeries, therapies, and outcome of diagnostic tests, are shown. Diagnostic qRT-PCR-positive nasopharyngeal and oropharyngeal swabs taken 49, 70, 77, 85, and 105 days after the initial positive sample were sent to Rocky Mountain Laboratories, NIH, for further analysis. Serum and plasma samples pre- and post-transfusion as well as a sample from the donor plasma were also provided. See also [Tables S1–S3](#) for additional laboratory values and clinical information.

China. Community spread in the Seattle region became evident in late February of 2020 ([Bhatraju et al., 2020](#)), with extensive spread in a long-term care facility ([McMichael et al., 2020a](#)). Here we describe an asymptomatic, immunocompromised individual persistently testing positive for SARS-CoV-2 by qRT-PCR who was infected during the early phase of SARS-CoV-2 spread in the United States. Infectious SARS-CoV-2 was successfully isolated from nasopharyngeal swabs 49 days and 70 days after the initial positive qRT-PCR test. Convalescent plasma treatment was not immediately successful in clearing the infection, but evidence of SARS-CoV-2 RNA was eventually cleared after 105 days.

RESULTS

Clinical Presentation of an Immunocompromised Individual Persistently Infected with SARS-CoV-2

On February 12, 2020, a 71-year-old woman with a 10-year history of chronic lymphocytic leukemia (CLL), acquired hypogammaglobulinemia, anemia, and chronic leukocytosis presented to the emergency department with low back and lower extremity pain. She underwent surgery for a spinal fracture and stenosis related to her cancer on February 14, 2020 (biopsy results in [Table S1](#)) and was subsequently transferred to a rehabilitation facility on February 19, 2020. On February 25, 2020, she was re-hospitalized for anemia and underwent a chest X-ray the following day, which was normal. She could not return to her rehabilitation center because of a confirmed outbreak of COVID-19 at the facility ([McMichael et al., 2020a, 2020b](#)). Chest computed tomog-

raphy (CT), performed on February 28, 2020, was unremarkable. The patient had no respiratory or systemic symptoms during this time. Because she was residing in the rehabilitation facility around the time of the COVID-19 outbreak, she was tested and found positive for SARS-CoV-2 on March 2, 2020 ([Figure 1](#)). After the initial SARS-CoV-2 diagnosis, she was kept in an isolation ward in a single room with negative airflow. Attending medical staff were using full personal protective equipment comprised of powered air-purifying respirators (PAPR) or N95 respirators with goggles, gowns, and gloves. Over the course of the next 15 weeks, she was tested for SARS-CoV-2 another 14 times by several diagnostic companies and remained positive through June 15, 2020, 105 days since the initial positive test. Subsequently, she tested negative on four consecutive swabs from June 16 to July 16, indicating that her infection had cleared.

Because of acquired hypogammaglobulinemia caused by her CLL, the individual received intravenous immunoglobulin (IVIG) every 4–6 weeks as part of her treatment regimen. She received IVIG treatment on April 6 and May 6, 2020. The manufacture date of her specific lot of IVIG preceded January 1, 2020, the beginning of the COVID-19 pandemic, and therefore did not contribute to any SARS-CoV-2 serology results ([Table S2](#)). Because of the persistence of her SARS-CoV-2 infection, serum samples were tested for antibodies against the spike glycoprotein through a study at the NIH Clinical Center, and no spike-specific antibodies were detected ([Burbelo et al., 2020](#)). On May 12, 2020, she was transfused with 200 mL of SARS-CoV-2 convalescent plasma provided by Bloodworks Northwest under a US Food and Drug Administration (FDA) emergency investigational new drug

Table 1. Virus Neutralization Titers in Pre- and Post-transfusion Sera from the Individual and Convalescent Plasma Used for Transfusion

Serum	USA/WA1/2020	Day 49 Isolate	Day 70 Isolate
Day 49	<10	<10	<10
Day 71	<10	<10	<10
Day 71 after transfusion	<10	<10	<10
Day 77	<10	<10	<10
Day 82	< 10	10	<10
Day 82 after transfusion	10	10	15
Day 105	10	<10	<10
Convalescent plasma 1	60	40	40
Convalescent plasma 2	160	160	60

Virus neutralization assays were performed for all serum and plasma samples with SARS-CoV-2 strains USA/WA1/2020 and the day 49 and day 70 isolates from the individual. Each serum/plasma sample was tested in duplicate.

(eIND) protocol with a virus-neutralizing (VN) titer of 60 (Table 1). Her infection persisted, and on May 23, 2020, she received another 200-mL dose of convalescent plasma from a different donor with a VN titer of 160 under the same protocol (Table 1). Additional laboratory values are available in Table S3.

Long-Term Shedding of Genomic RNA, Subgenomic RNA, and Infectious SARS-CoV-2

SARS-CoV-2 shedding kinetics in the individual were monitored using detection of genomic RNA (gRNA), subgenomic RNA (sgRNA), and infectious SARS-CoV-2. RNA was extracted from nasopharyngeal and oropharyngeal swabs collected 49, 70, 77, 85, 105, and 136 days after the initial diagnosis and evaluated for the presence of viral gRNA (Corman et al., 2020) and sgRNA (Wölfel et al., 2020). gRNA and sgRNA were detected in nasopharyngeal swabs out to day 105, except for the swab taken on day 77 (Figure 2A), although the test through EvergreenHealth was positive at this time. None of the oropharyngeal swabs were positive for gRNA or sgRNA, suggesting that the infection was confined to the nasopharynx. Absolute quantification of gRNA and sgRNA on positive swabs was performed by droplet digital PCR (ddPCR) (Figure 2A). The highest viral load was detected in the day 70 swab, at 2.2×10^6 gRNA copies/mL (cycle threshold [Ct] 22.44) and 1.1×10^5 sgRNA copies/mL (Ct 29.05). Detection of sgRNA in swabs is indicative of active SARS-CoV-2 replication because only actively replicating SARS-CoV-2 initiates RNA synthesis, resulting in replication and transcription of sgRNAs (Wang et al., 2020b; Kim et al., 2020), and sgRNA, unlike gRNA, does not persist in the nasal cavity in the absence of virus replication (Speranza et al., 2020). Virus isolation was attempted on all qRT-PCR-positive samples. Infectious SARS-CoV-2 was successfully cultured from the nasopharyngeal swabs collected on day 49 and day 70. Scanning and transmission electron microscopy on SARS-CoV-2 cultured from the nasopharyngeal swabs collected on days 49 and 70 showed viral particles consistent with coronavirus morphology, supporting persistent SARS-CoV-2 infection with shedding of infectious virus in this individual (Figure 3).

Convalescent Plasma Treatment Did Not Clear SARS-CoV-2 from the Upper Respiratory Tract

In an attempt to treat the persistent SARS-CoV-2 infection, the individual received two doses of convalescent plasma therapy on days 71 and 82. Pre- and post-transfusion serum samples and the transfusion convalescent plasma samples were analyzed for the presence of full-length spike and spike receptor binding domain (RBD) antibodies by ELISA assay and of SARS-CoV-2-neutralizing antibodies in a VN assay (Figures 2B and 2C; Figures S1A and S1B; Table 1; Amanat et al., 2020; Wrapp et al., 2020). The first dose of convalescent plasma (convalescent plasma 1) had an immunoglobulin G (IgG) spike titer of 2,560, RBD titer of 3,840, and VN titer of 60. The second dose of convalescent plasma (convalescent plasma 2) had an IgG spike titer of 5,120, RBD titer of 5,120, and VN titer of 160 (Figure 2B; Figure S1A; Table 1). Prior to the first dose of plasma given on day 71, detectable spike and RBD IgG antibody titers were very low in serum collected from the individual, with IgG titers between 1:10 and 1:40 on days 49 and 71 pre transfusion; no VN titers were detected in these samples. Immediately after the first transfusion on day 71, the spike and RBD IgG antibody titers rose to 1:320 and then decreased to 1:80 and 1:160, respectively, on day 77. No VN titers were detected on days 71 and 77 (Figure 2C; Figure S1B; Table 1). Immediately after the second transfusion on day 82, the spike and RBD IgG titers increased to 1:320 and 1:640, respectively, and remained elevated by day 105 (Figure 2C; Figure S1B). Low neutralizing titers of 1:10 were observed on day 82 and 105 (Table 1).

Despite two transfusions of convalescent plasma, nasopharyngeal swabs on days 85 and 105 remained positive for gRNA and sgRNA, suggesting that the convalescent plasma therapy was not successful in rapidly clearing the infection from the upper respiratory tract in this individual. Although the presence of sgRNA at these time points suggests active viral replication, infectious SARS-CoV-2 could not be cultured after day 70.

Genetic Analysis of Patient Swab Samples Links Infection to the Primary Washington State Outbreak

SARS-CoV-2 full genome sequences were obtained from nasopharyngeal swabs collected on days 49, 70, 85, and 105 (Table S4). Full genomes were obtained by sequencing using the ARTIC primer set (<https://artic.network/>) and assembling reads to MN985325.1 (USA/WA1/2020) as the reference genome (Harcourt et al., 2020). The SARS-CoV-2 lineage was determined using Pangolin software (<https://pangolin.cog-uk.io/>), which placed the individual's viral genomes in lineage A.1, which consists of genomes originating from the primary outbreak in Washington state (Rambaut et al., 2020). A maximum-likelihood tree was generated using representative SARS-CoV-2 genomes from previously described lineages (Rambaut et al., 2020) obtained from the GISAID database (<https://www.gisaid.org/>; Shu and McCauley, 2017). The individual's SARS-CoV-2 full-length genomes cluster together within lineage A.1 (Figure 4A). This suggests that she was infected with a virus from the SARS-CoV-2 A.1 lineage, which circulated after the initial import from China, followed by exponential growth and local transmission in Washington state.

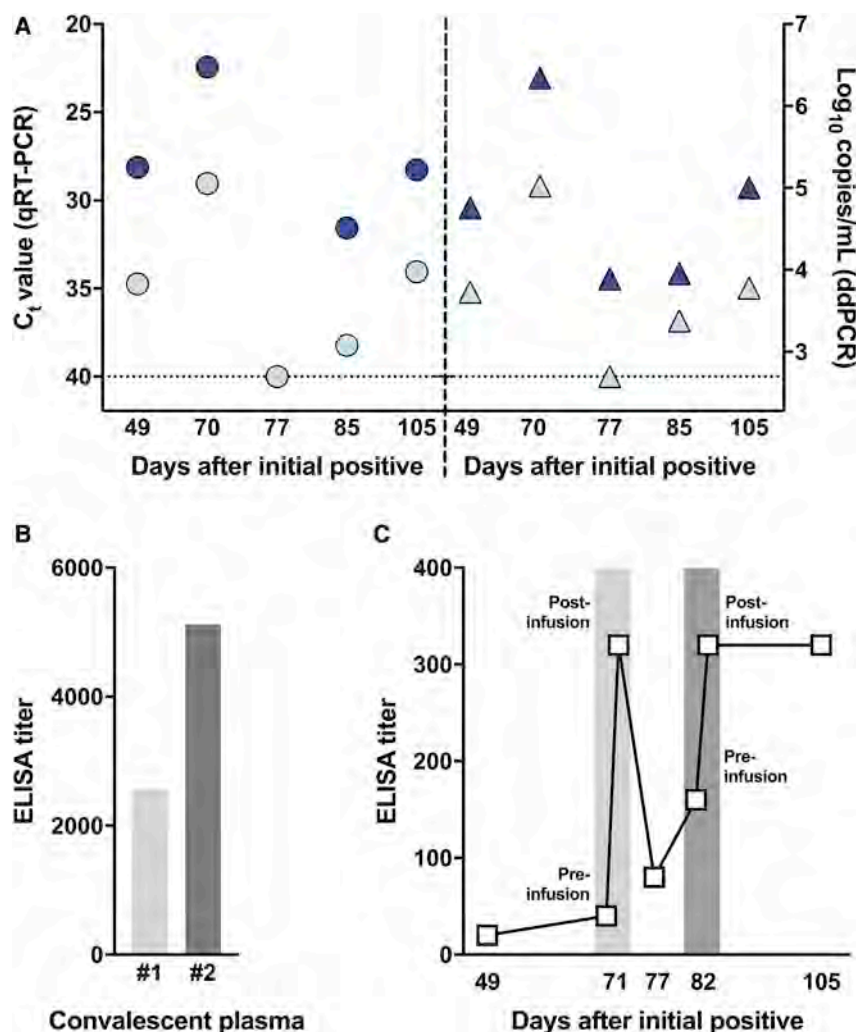


Figure 2. Assessment of Viral Load and Seroconversion in an Individual Persistently Infected with SARS-CoV-2 and Treated with Convalescent Plasma

(A) Viral loads were in nasopharyngeal swabs collected at different time points after the initial SARS-CoV-2 diagnosis. Viral RNA extracted from a nasopharyngeal swab was analyzed for the presence of genomic RNA (gRNA; dark blue) and sub-genomic RNA (sgRNA; light blue symbols) by qRT-PCR and reported as a cycle threshold (Ct) value (circles, left panel) and in ddPCR and reported as copy numbers (triangles, right panel).

(B) IgG titers against the full-length recombinant SARS-CoV-2 spike ectodomain were determined by ELISA in convalescent plasma used for transfusion. The light gray bar represents the IgG titer of the first donor (convalescent plasma 1), and the dark gray bar represents the second donor (convalescent plasma 2).

(C) IgG titers against the full-length recombinant SARS-CoV-2 spike ectodomain were determined by ELISA in patient serum collected at several time points, including immediately before and after transfusion with convalescent plasma on days 71 (light gray) and 82 (dark gray). Each serum/plasma sample was tested in duplicate.

See also Figure S1 for IgG titers against the SARS-CoV-2 receptor binding domain (RBD).

tween February 27 and March 31, 2020, within 90% of the marginal probability distribution. This is consistent with the timing of the individual's first positive test on March 2, 2020. To further evaluate the relationship between the SARS-CoV-2 genomes recovered from the patient swabs and other SARS-CoV-2 genomes circulating in Washington state at the times of sampling (April 20, May 11, May 26, and

To visualize the temporal relationships of the patient isolates, 44 full SARS-CoV-2 genome sequences from Washington state belonging to NextStrain clade 19B (<http://clades.nextstrain.org/>) were subsampled from the GISAID database (<https://www.gisaid.org/>; Shu and McCauley, 2017) representing strains collected in Washington state from February to May 2020. A full genome alignment was performed with four of the full genome sequences recovered from the persistently infected individual, the USA/WA1/2020 genome sequence, and the Wuhan-Hu-1/2019 genome sequence with MAFFT v.1.4 (Katoh and Standley, 2013; Katoh et al., 2002) implemented in Geneious Prime v.2020.1.2 (<https://www.geneious.com/>). A maximum-likelihood tree was reconstructed with PhyML v.3.1 (Guindon et al., 2010), and a tree showing temporal divergence (Figure 4B) was inferred in TreeTime v.0.7.6 (Sagulenko et al., 2018; Hadfield et al., 2018) using the HKY85 model of nucleotide substitution and a fixed molecular clock at 8×10^{-4} with a standard deviation of 4×10^{-4} , as implemented in the NextStrain pipeline (<https://nextstrain.org/sars-cov-2/>). Divergence dating estimates place the patient isolates sharing a most recent common ancestor be-

June 15, 2020), Washington SARS-CoV-2 genomes were downloaded from the GISAID database (Shu and McCauley, 2017). The quality of the sequences was determined by Nextclade v.0.7.5 (<https://nextstrain.org/ncov/global>), and 1,789 sequences on April 20, 385 sequences between April 20 and May 11, 268 sequences between May 11 and May 26, and 709 sequences between May 26 and June 15 were kept for further phylogenetic analysis. Maximum likelihood trees using the curated sets of sequences, the four patient genomes, and the USA/WA1/2020 genome were inferred using ModelFinder (Kalyaanamoorthy et al., 2017) and ultrafast bootstrap (Hoang et al., 2018) implemented in IQ-TREE v.1.6.12 (Nguyen et al., 2015). The phylogenetic trees show that the patient genomes in this study cluster as a monophyletic clade consistent with infection in late February/early March, followed by virus persistence (Figure S2).

Next, full genome sequences from the two SARS-CoV-2 isolates were obtained (Table S4), and the consensus level variants in the sequences obtained from nasopharyngeal swabs and SARS-CoV-2 isolates cultured from those swabs were

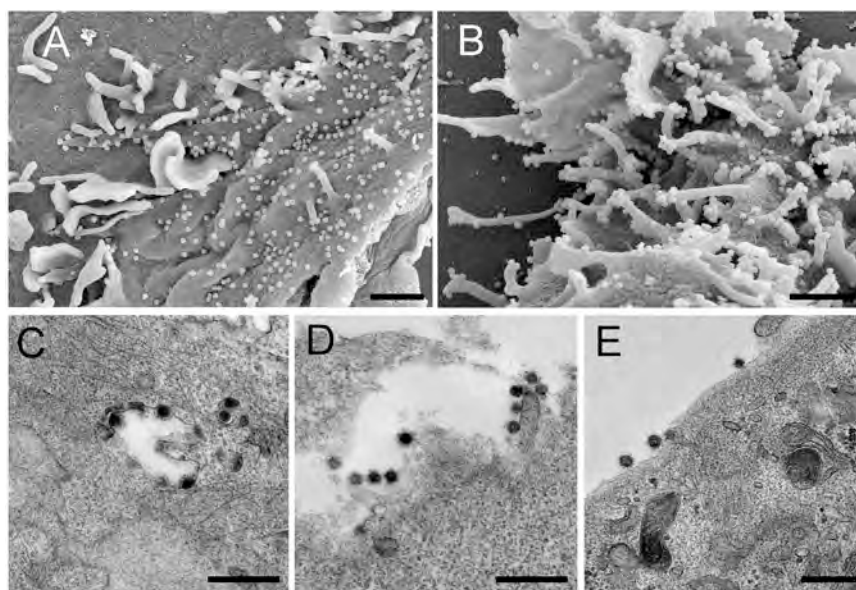


Figure 3. Electron Microscopy Confirms Isolation of Coronavirus from the Individual's Nasopharyngeal Swabs

SARS-CoV-2 cultured from the individual's nasopharyngeal swabs was used to inoculate Vero E6 cells for imaging by scanning and transmission electron microscopy (SEM and TEM, respectively).

(A and B) SEM images of the day 49 (A) and day 70 (B) isolates.

(C–E) TEM images of the day 49 (C) and day 70 (D and E) isolates.

SEM scale bars, 1 μ m; TEM scale bars, 0.5 μ m.

compared with the reference strain USA/WA1/2020 (MN985325.1) (Harcourt et al., 2020). Several single-nucleotide (nt) substitutions were observed within the ORF1ab, spike, M, and ORF8 coding sequence in the full-genome sequences obtained directly from the individual's swabs and the SARS-CoV-2 isolates. In addition, a 3-nt deletion leading to loss of a methionine residue was observed in nsp1 in day 49 and day 70 samples (Table 2). Within the genomes of the two SARS-CoV-2 isolates, two in-frame deletions were observed in the spike glycoprotein coding region. A 21-nt in-frame deletion (residues 21,975–21,995) was found in the N-terminal domain (NTD) of S1, leading to a 7-amino-acid deletion (amino acids [aa] 139–145) in the spike glycoprotein of the SARS-CoV-2 day 49 isolate. A smaller, 12-nt deletion (residues 21,982–21,993) was detected in the day 70 isolate, leading to a 4-aa deletion (aa 141–144) in the NTD, which falls within the 7-aa deletion found in the day 49 isolate (Figure 5A). These observed deletions in the spike glycoprotein map to a region in the NTD that is partially solvent exposed and forms a β strand in a compact conformation of the spike (Wrobel et al., 2020; Figures 5B and 5C). This region is unmodelled in other structures representing additional conformational states of the spike and, thus, is likely flexible (Wrapp et al., 2020; Walls et al., 2020). It is possible that the apparent plasticity in this region of the molecule may contribute to the structural permissibility of the identified deletions. The position of these deletions is distinct from those observed in other SARS-CoV-2 isolates, which locate to the S1/S2 and S2' cleavage sites (Andrés et al., 2020; Lau et al., 2020; Liu et al., 2020d).

Comparison of the full genome sequences obtained directly from the individual's samples with the genome data obtained from the two SARS-CoV-2 isolates showed that the 21-nt deletion was present in a minority of sequencing reads (1%) in the genome obtained from the individual's sample from day 49 (Table 2) and was selected for upon passage in cell culture. The 12-nt deletion on day 70 was present in 100% of the reads in the

clinical sample and tissue culture isolate. Notably, neither spike deletion was detected in the genome sequences from the day 85 and day 105 swabs (Table 2). It is possible that other minor variants exist at low levels that were undetected by the depth of sequencing coverage or were not reflected in the sampling at that time point. The variation observed

between the different full-length genomes obtained at various time points during the course of infection points to a quasispecies complex with continuous turnover of dominant viral species.

Growth Kinetics of SARS-CoV-2 Patient Isolates

The replication kinetics of the day 49 isolate SARS-CoV-2 were compared with those of the reference strain USA/WA1/2020 in Vero E6 cells. Despite the observed mutations in the day 49 isolate, no difference in replication kinetics were observed between the day 49 isolate and the reference strain (Figure 6A). To determine growth kinetics in a more functionally relevant cell type, growth curves were also performed on primary human alveolar epithelial tissues (EpiAlveolar; MatTek, Ashland, MA, USA). No significant differences were observed between the individual's isolate and the reference strain in these cells (Figure 6B).

DISCUSSION

In this report, we describe long-term SARS-CoV-2 shedding in an immunocompromised individual with CLL and acquired hypogammaglobulinemia out to 105 days after the initial positive test. Although the exact time point when the individual acquired SARS-CoV-2 is unknown, it is likely that the exposure occurred in the long-term care facility where she resided between February 19–25, 2020, shortly before a large COVID-19 outbreak was identified in that facility on February 28, 2020. The individual remained asymptomatic throughout the course of infection despite isolation of infectious SARS-CoV-2 49 and 70 days after the initial diagnosis, much longer than shedding of infectious virus up to day 20, as reported previously (van Kampen et al., 2020). The information available to date about SARS-CoV-2 infection in immunocompromised individuals, including those with cancers such as CLL, is limited and mostly focuses on disease severity and outcome (He et al., 2020a; Paneesha et al.,

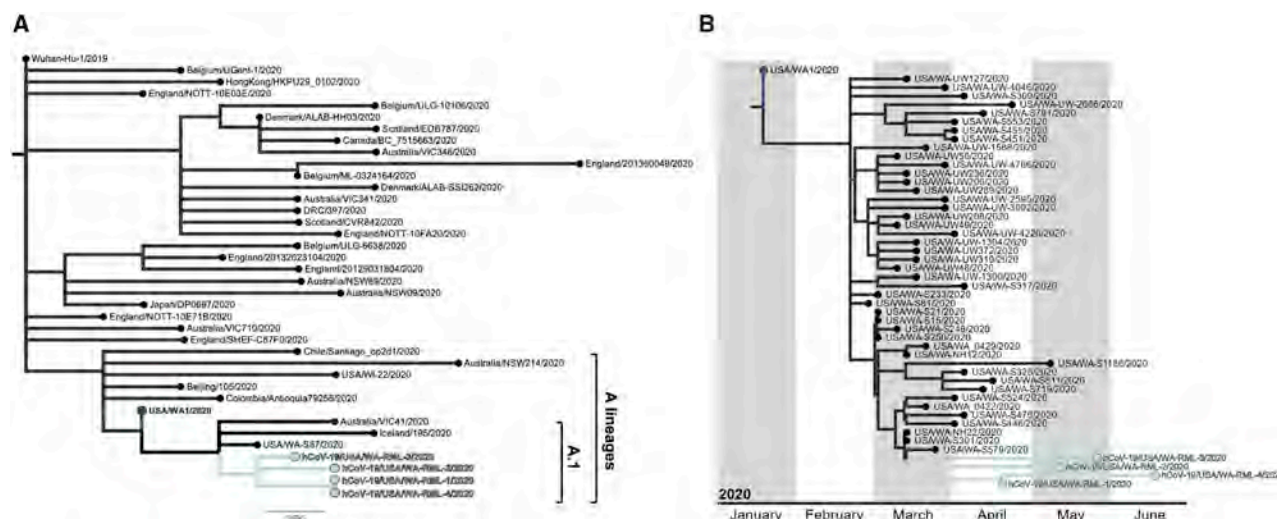


Figure 4. Phylogenomic Analyses of Described SARS-CoV-2 Strains in a Persistently Infected Individual

(A) Full-genome SARS-CoV-2 sequences representing previously described lineages (Rambaut et al., 2020) were downloaded from GISAID (Shu and McCauley, 2017). Lineages were then assigned using Pangolin v.2.0.3 (<https://pangolin.cog-uk.io/>). Using a representative genome from the assigned lineages and the four SARS-CoV-2 sequences from the individual, a maximum-likelihood tree was inferred using PhyML v.3.3.20180621 (Guindon et al., 2010) implemented in Geneious Prime v.2020.1.2 (<https://www.geneious.com/>) with a general time-reversible model of nucleotide substitution and rooted at the Wuhan-Hu-1/2019 SARS-CoV-2 strain. Sequences from the A and A.1 lineages are labeled, and the individual's SARS-CoV-2 sequences are shown in cyan. hCoV-19/USA/WA-RML-1, -2, -3, and -4 are the genome sequences derived from the individual from day 49, 70, 85, and 105 nasopharyngeal swabs, respectively.

(B) Full SARS-CoV-2 genomes were subsampled from Washington state, representing NextStrain clade 19B, including the four full-genome sequences recovered from the individual and the Wuhan-Hu-1/2019 sequence and aligned using MAFFT v.1.4 (Katoh and Standley, 2013; Katoh et al., 2002) implemented in Geneious Prime v.2020.1.2 (<https://www.geneious.com/>). A maximum-likelihood tree was then reconstructed with PhyML v.3.1 (Guindon et al., 2010), and a tree showing temporal divergence was inferred in TreeTime v.0.7.6 (Hadfield et al., 2018). The individual's SARS-CoV-2 sequences are shown in cyan, and hCoV-19/USA/WA-RML-1, -2, -3, and -4 are the genome sequences derived from the individual from day 49, 70, 85, and 105 nasopharyngeal swabs, respectively.

See also Figure S2.

2020; Baumann et al., 2020; Fürstenau et al., 2020; Jin et al., 2020; Soresina et al., 2020; Zhu et al., 2020; Fill et al., 2020). Although it is difficult to extrapolate from a single individual, our data suggest that long-term shedding of infectious virus may be a concern in certain immunocompromised people. Given that immunocompromised individuals could have prolonged shedding and may not have typical symptoms of COVID-19, symptom-based strategies for testing and discontinuing transmission-based precautions, as recommended by the Centers for Disease Control and Prevention (CDC) (CDC, 2020b), may fail to detect whether certain individuals are shedding infectious virus.

The individual eventually cleared the SARS-CoV-2 infection from the upper respiratory tract after developing low neutralizing antibody titers. How the virus was cleared and the effect of convalescent plasma on clearance of the virus is unknown. The initial administration of convalescent plasma was followed by a decreased viral load in nasal swabs, but viral loads subsequently increased, despite administration of a second dose of convalescent plasma comprising higher antibody titers. Therapeutic administration of convalescent plasma is focused on treatment of severe or life-threatening COVID-19. Several clinical trials are investigating the efficacy of convalescent plasma, but currently the effect of convalescent plasma therapy on COVID-19 outcome remains equivocal (Mira et al., 2020; Salazar et al., 2020). The limited effect of convalescent plasma treatment on

clearance of SARS-CoV-2 could be due to the fact that intravenously (i.v.) administered antibodies do not distribute well to the nasal epithelium (Ikegami et al., 2020) compared with the lower respiratory tract (Mira et al., 2020).

Throughout the course of infection, there was marked within-host genomic evolution of SARS-CoV-2. Deep sequencing revealed a continuously changing virus population structure with turnover in the relative frequency of the observed genotypes over the course of infection. With SARS-CoV-2, there is generally relatively limited within-host variation reported, and over the course of infection, the major SARS-CoV-2 population remains identical (Jary et al., 2020; Shen et al., 2020; Capobianchi et al., 2020). Potential factors contributing to the observed within-host evolution is prolonged infection and the compromised immune status of the host, possibly resulting in a different set of selective pressures compared with an immune-competent host. These differential selective pressures may have allowed a larger genetic diversity with continuous turnover of dominant viral species throughout the course of infection. Although some sequence variants remain consistent throughout the duration of infection, we also observed variants unique to individual time points, such as the spike deletions observed on day 49 and day 70. Previously reported spike deletions, distinct from those reported here, were observed at relatively low frequency in clinical samples but were enriched upon virus isolation (Andrés et al., 2020; Liu et al., 2020d). Similar to these reports, the spike

Table 2. Consensus Sequence Variants in Clinical Samples from the Individual and SARS-CoV-2 Isolates Compared with Reference USA/WA1/2020 (MN985325.1)

Position	Gene	Nucleotide Change	Protein Change	Day 49 Individual	Day 49 Isolate	Day 70 Individual	Day 70 Isolate	Day 85 Individual	Day 105 Individual
518–520	orf1ab	3-bp deletion	M → del	22% ^a	100%	100%	100%	–	–
2,113	orf1ab	C → T	none	–	–	100%	100%	–	–
4,084	orf1ab	C → T	none	87.5%	100%	–	–	–	97%
17,747	orf1ab	C → T	P → L	100%	100%	100%	100%	100%	100%
17,858	orf1ab	A → G	Y → C	100%	100%	100%	100%	100%	100%
19,420	orf1ab	T → C	S → P	72%	98%	–	–	–	92%
21,975–21,995	spike	21-bp deletion	DPFLGVYY → D	1% ^a	100%	–	–	–	–
21,982–21,993	spike	12-bp deletion	FLGVY → F	–	–	100%	100%	–	–
23,010	spike	T → C	V → A	100%	100%	100%	100%	100%	99%
23,616	spike	G → A	R → Q	–	–	–	95%	–	–
23,617	spike	T → A	–	–	–	–	95%	–	–
26,526	M	G → T	A → S	–	–	16% ^a	100%	–	–
27,899	orf8	A → T	K → N	–	–	100%	100%	–	–
29,308	N	T → A	N → K	–	–	–	–	56%	–
29,854	–	C → T	–	–	–	–	100%	–	–

^aMinor variants present in less than 50% of the reads were not included in the consensus, but these minor variants were included in the table to demonstrate their presence in clinical samples as well as the isolate.

deletion in the isolate on day 49 was observed as a minor variant in the individual's sample but was also selected for during passage upon virus isolation.

In contrast to the previously reported deletions at the cleavage sites, both spike deletions observed on day 49 and 70 in the individual are located in the NTD of S1, a region distal from the receptor binding site. These deleted residues are not modeled in a number of spike structures (Wrapp et al., 2020; Walls et al., 2020), suggesting that this region is conformationally labile. Although the NTD has been identified as an antigenic target (Brouwer et al., 2020; Chi et al., 2020; Liu et al., 2020a), no clear difference in virus neutralization was observed between the two patient isolates and the prototype USA/WA1/2020 SARS-CoV-2 isolate.

Despite genetic changes in the SARS-CoV-2 isolated from the individual, the replication kinetics did not change significantly compared with the USA/WA1/2020 virus in Vero E6 cells and primary human alveolar epithelial tissues. This indicates that, most likely, the infectious virus shed by the individual would still be able to establish productive infection in contacts upon transmission, assuming that viral growth kinetics *in vitro* are a suitable surrogate for virus fitness *in vivo*. Moreover, despite prolonged replication exclusively in the upper respiratory tract, the virus was still able to replicate in epithelial cells derived from the lower respiratory tract, suggesting that it could still cause pneumonia.

Many current infection control guidelines assume that persistently PCR-positive individuals are shedding residual RNA and not infectious virus, with immunocompromised people thought to remain infectious for no longer than 20 days after symptom onset (CDC, 2020a). Here we show that certain individuals may shed infectious, replication-competent virus for much longer

than previously recognized (van Kampen et al., 2020). Although infectious virus could be detected up to day 70, sgRNA, a molecular marker for active SARS-CoV-2 replication (Speranza et al., 2020), could be detected up until day 105. An immunocompromised state has been identified as a risk factor for development of severe disease and complications from COVID-19 (CDC, 2020b). A wide variety of conditions and treatments can alter the immune system and cause immunodeficiency, creating opportunities for prolonged viral replication and shedding of infectious SARS-CoV-2. Although this report focuses on long-term shedding of one immunocompromised individual, an estimated 3 million people in the United States have some form of immunocompromising condition, including individuals with HIV infection, solid organ transplant recipients, hematopoietic stem cell transplant recipients, and individuals receiving chemotherapy and corticosteroids (Kunisaki and Janoff, 2009). This transient or chronic immunocompromised population is at higher risk of respiratory disease complications with respiratory infections such as influenza A virus and SARS-CoV-2 (Kunisaki and Janoff, 2009). Prolonged shedding of pH1N1 was observed in immunocompromised individuals with a variety of immunocompromising conditions during the previous pandemic in 2009, such as people with cancer on chemotherapy and solid organ transplant recipients (van der Vries et al., 2013). For the SARS-CoV-2 related Middle East respiratory syndrome CoV (MERS-CoV), prolonged shedding up to 38 days was observed in individuals with myelodysplastic syndrome, autologous peripheral blood stem cell transplantation for treatment of large B cell lymphoma, and an individual with peripheral T cell lymphoma (Kim et al., 2017). MERS-CoV shedding was higher and longer in experimentally

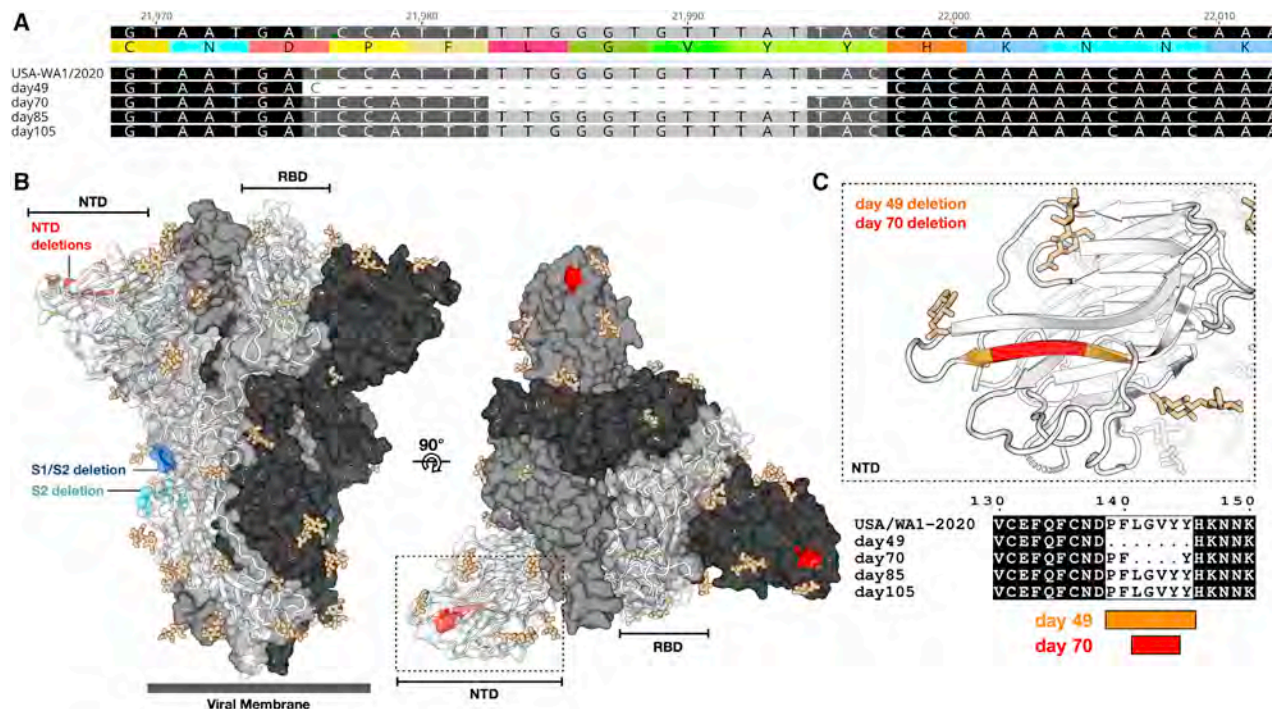


Figure 5. Deletions in the NTD of S1 of the Spike Protein

(A) Nucleotide and amino acid sequence alignment of the region of the spike gene of the four sequences from the individual and the reference USA/WA1/2020 genome sequence containing the deletions observed in the day 49 and day 70 samples. Alignment was generated with MAFFT v.1.4 (Kato and Standley, 2013; Kato et al., 2002) implemented in Geneious Prime 2020.1.2 (<https://www.geneious.com>).

(B) Amino acid residues removed by the day 49 (orange) and day 70 (red) spike deletions are highlighted on a SARS-CoV-2 spike trimer (PDB: 6zge; Wrobel et al., 2020). Each protomer of the trimer is shown in surface representation, colored in shades of gray. A single protomer is annotated, and its secondary structure is shown in cartoon representation. Glycans are shown as beige sticks. Previously reported spike deletions observed at the S1/S2 and S2' cleavage sites (Andrés et al., 2020; Lau et al., 2020; Liu et al., 2020d) are colored blue and cyan, respectively.

(C) Close-up view of the indicated region of (B) (dotted box) with the protein surface removed for clarity and accompanying amino acid sequence alignment, generated using Multalin (Corpet, 1988) and plotted with ESPrpt (Robert and Gouet, 2014).

infected non-human primates immunosuppressed with cyclophosphamide and dexamethasone, providing experimental support for the effect of immunosuppression on virus-host dynamics observed here (Prescott et al., 2018).

Limitations of Study

A limitation of the present study is that it comprises only a single case, making it difficult to draw general conclusions regarding use of convalescent plasma for clearance of the virus, potential alternative mechanisms involved in virus clearance, and the frequency of persistent SARS-CoV-2 infection and shedding in individuals with other immunocompromising conditions. Identification of additional cases of persistent infection and long-term shedding of infectious virus are needed so the infection dynamics can be studied in more detail in this diverse population. Understanding the mechanism of virus persistence and eventual clearance will be essential for providing appropriate treatment and preventing transmission of SARS-CoV-2 because persistent infection and prolonged shedding of infectious SARS-CoV-2 might occur more frequently. Because immunocompromised individuals are often cohorted in hospital settings, a more nuanced approach to testing these individuals is warranted, and the presence of persistently positive people by performing SARS-CoV-2

gRNA and sgRNA analyses on clinical samples should be investigated.

STAR★METHODS

Detailed methods are provided in the online version of this paper and include the following:

- **KEY RESOURCES TABLE**
- **RESOURCE AVAILABILITY**
 - Lead Contact
 - Materials Availability
 - Data Availability
- **EXPERIMENTAL MODEL AND SUBJECT DETAILS**
 - Human Patient
 - Cells
 - SARS-CoV-2 Virus
- **METHOD DETAILS**
 - Clinical Sample RNA Extraction and qRT-PCR
 - Virus Isolation
 - Growth kinetics of SARS-CoV-2 isolates
 - Expression and Purification of SARS-CoV-2 Spike and Receptor Binding Domain

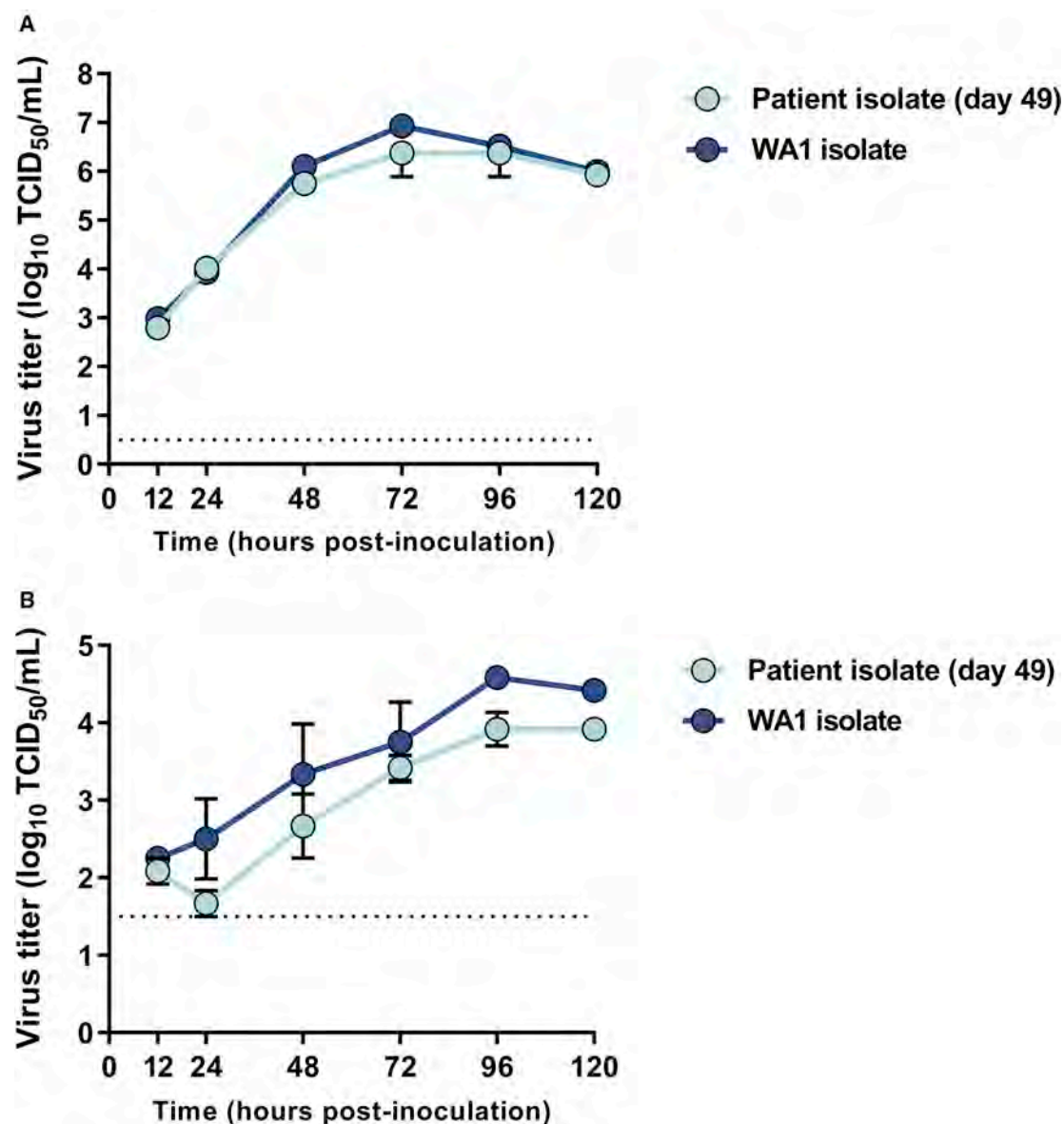


Figure 6. Growth Kinetics of the Day 49 Isolate from the Individual in Vero E6 Cells and Primary Human Alveolar Epithelial Tissues

(A) Vero E6 cells were inoculated with the day 49 patient isolate and the reference USA/WA1/2020 strain at a MOI of 0.01 in triplicate.

(B) Primary 3D human alveolar epithelial tissues grown in 3D Transwell culture were inoculated with the same isolates at a MOI of 0.1. Supernatant was harvested at designated time points for assessment of viable virus using endpoint titration.

Data shown are the mean and the standard error of the mean for three independent replicates. Statistical analysis using a 2-way ANOVA in GraphPad Prism shows no significant difference between the isolates at any of the time points.

- Enzyme-Linked Immunosorbent Assay (ELISA)
- Virus Neutralization assay
- Next generation sequencing of patient clinical samples and isolates
- Sequencing and bioinformatics
- Phylogenomic Analysis
- Electron Microscopy
- Scanning electron microscopy
- Transmission electron microscopy
- Structure Mapping

● QUANTIFICATION AND STATISTICAL ANALYSIS

SUPPLEMENTAL INFORMATION

Supplemental Information can be found online at <https://doi.org/10.1016/j.cell.2020.10.049>.

ACKNOWLEDGMENTS

We would like to thank Neeltje van Doremalen, Jonathan Schulz, Myndi Holbrook, Anita Mora, and Rose Perry for excellent technical assistance. We

would like to thank MatTek for providing the alveolar tissue culture system and technical support as well as all the originating and submitting laboratories and authors who deposited SARS-CoV-2 genomes to GISAID. We would also like to thank the health care workers and laboratorians at EvergreenHealth for selfless service to patients. Finally, we thank the individual described in this report for her gracious willingness to participate and contribute to these studies as we sought to understand this enigmatic infection. This work was supported by the Intramural Research Program of the National Institute of Allergy and Infectious Diseases (NIAID). T.A.B. is supported by the Medical Research Council UK (MR/S007555/1). The Wellcome Centre for Human Genetics is supported by Wellcome Centre grant 203141/Z/16Z.

AUTHOR CONTRIBUTIONS

Conceptualization, F.X.R. and V.J.M.; Resources, E.R.F., C.M., and F.X.R.; Methodology, V.A.A., M.J.M., S.N.S., B.N.W., E.R.F., C.M., T.A.B., and E.D.W.; Investigation, V.A.A., M.J.M., S.N.S., R.P., B.N.W., S.L.A., K.B., E.R.F., and E.D.W.; Writing – Original Draft, V.A.A., M.J.M., F.X.R., and V.J.M.; Writing – Review & Editing, S.N.S., S.D.J., C.M., T.A.B., and E.D.W.; Data Curation, C.M.; Supervision, T.A.B., E.D.W., F.X.R., and V.J.M.

DECLARATION OF INTERESTS

The authors declare no competing interests.

Received: September 20, 2020

Revised: October 13, 2020

Accepted: October 28, 2020

Published: November 4, 2020

REFERENCES

- Amanat, F., Stadlbauer, D., Strohmaier, S., Nguyen, T.H.O., Chromikova, V., McMahon, M., Jiang, K., Arunkumar, G.A., Jurchyszczak, D., Polanco, J., et al. (2020). A serological assay to detect SARS-CoV-2 seroconversion in humans. *Nat. Med.* 26, 1033–1036.
- Andrés, C., García-Cehic, D., Gregori, J., Piñana, M., Rodríguez-Frias, F., Guerrero-Murillo, M., Esperalba, J., Rando, A., Goterris, L., Codina, M.G., et al. (2020). Naturally occurring SARS-CoV-2 gene deletions close to the spike S1/S2 cleavage site in the viral quasispecies of COVID19 patients. *Emerg. Microbes Infect.* 9, 1900–1911.
- Baumann, T., Delgado, J., and Montserrat, E. (2020). CLL and COVID-19 at the Hospital Clinic of Barcelona: an interim report. *Leukemia* 34, 1954–1956.
- Bhatraju, P.K., Ghassemieh, B.J., Nichols, M., Kim, R., Jerome, K.R., Nalla, A.K., Greninger, A.L., Pipavath, S., Wurfel, M.M., Evans, L., et al. (2020). Covid-19 in Critically Ill Patients in the Seattle Region - Case Series. *N. Engl. J. Med.* 382, 2012–2022.
- Brouwer, P.J.M., Daniels, T.G., van der Straten, K., Snitselaar, J.L., Aldon, Y., Bangaru, S., Torres, J.L., Okba, N.M.A., Claireaux, M., Kerster, G., et al. (2020). Potent neutralizing antibodies from COVID-19 patients define multiple targets of vulnerability. *Science* 369, 643–650.
- Bullard, J., Dust, K., Funk, D., Strong, J.E., Alexander, D., Garnett, L., Boodman, C., Bello, A., Hedley, A., Schiffman, Z., et al. (2020). Predicting infectious SARS-CoV-2 from diagnostic samples. *Clin. Infect. Dis.*, ciaa638.
- Burbelo, P.D., Riedo, F.X., Morishima, C., Rawlings, S., Smith, D., Das, S., Strich, J.R., Chertow, D.S., Davey, R.T., Jr., and Cohen, J.I. (2020). Detection of Nucleocapsid Antibody to SARS-CoV-2 is More Sensitive than Antibody to Spike Protein in COVID-19 Patients. *medRxiv*, 2020.04.20.20071423.
- Capobianchi, M.R., Rueca, M., Messina, F., Giombini, E., Carletti, F., Colavita, F., Castilletti, C., Lalle, E., Bordin, L., Vairo, F., et al. (2020). Molecular characterization of SARS-CoV-2 from the first case of COVID-19 in Italy. *Clin. Microbiol. Infect.* 26, 954–956.
- CDC (2020a). Duration of Isolation and Precautions for Adults with COVID-19. <https://www.cdc.gov/coronavirus/2019-ncov/hcp/duration-isolation.html>.
- CDC (2020b). People with Certain Medical Conditions. <https://www.cdc.gov/coronavirus/2019-ncov/need-extra-precautions/people-with-medical-conditions.html>.
- Chi, X., Yan, R., Zhang, J., Zhang, G., Zhang, Y., Hao, M., Zhang, Z., Fan, P., Dong, Y., Yang, Y., et al. (2020). A neutralizing human antibody binds to the N-terminal domain of the Spike protein of SARS-CoV-2. *Science* 369, 650–655.
- Corman, V.M., Landt, O., Kaiser, M., Molenkamp, R., Meijer, A., Chu, D.K., Bleicker, T., Brünink, S., Schneider, J., Schmidt, M.L., et al. (2020). Detection of 2019 novel coronavirus (2019-nCoV) by real-time RT-PCR. *Euro Surveill.* 25, 2000045.
- Corpet, F. (1988). Multiple sequence alignment with hierarchical clustering. *Nucleic Acids Res.* 16, 10881–10890.
- Fill, L., Hadney, L., Graven, K., Persaud, R., and Hostoffer, R. (2020). The clinical observation of a patient with common variable immunodeficiency diagnosed as having coronavirus disease 2019. *Ann. Allergy Asthma Immunol.* 125, 112–114.
- Fu, Y., Han, P., Zhu, R., Bai, T., Yi, J., Zhao, X., Tao, M., Quan, R., Chen, C., Zhang, Y., et al. (2020). Risk factors for viral RNA shedding in COVID-19 patients. *Eur. Respir. J.* 56, 2001190.
- Fürstenau, M., Langerbeins, P., De Silva, N., Fink, A.M., Robrecht, S., von Tresckow, J., Simon, F., Hohloch, K., Droogendijk, J., van der Klift, M., et al. (2020). COVID-19 among fit patients with CLL treated with venetoclax-based combinations. *Leukemia* 34, 2225–2229.
- Gordon, A. (2018). FASTX-Toolkit. http://hannonlab.cshl.edu/fastx_toolkit/.
- Guindon, S., Dufayard, J.F., Lefort, V., Anisimova, M., Hordijk, W., and Gascuel, O. (2010). New algorithms and methods to estimate maximum-likelihood phylogenies: assessing the performance of PhyML 3.0. *Syst. Biol.* 59, 307–321.
- Hadfield, J., Megill, C., Bell, S.M., Huddleston, J., Potter, B., Callender, C., Sagulenko, P., Bedford, T., and Neher, R.A. (2018). Nextstrain: real-time tracking of pathogen evolution. *Bioinformatics* 34, 4121–4123.
- Harcourt, J., Tamin, A., Lu, X., Kamili, S., Sakthivel, S.K., Murray, J., Queen, K., Tao, Y., Paden, C.R., Zhang, J., et al. (2020). Severe Acute Respiratory Syndrome Coronavirus 2 from Patient with Coronavirus Disease, United States. *Emerg. Infect. Dis.* 26, 1266–1273.
- He, W., Chen, L., Chen, L., Yuan, G., Fang, Y., Chen, W., Wu, D., Liang, B., Lu, X., Ma, Y., et al. (2020a). COVID-19 in persons with haematological cancers. *Leukemia* 34, 1637–1645.
- He, X., Lau, E.H.Y., Wu, P., Deng, X., Wang, J., Hao, X., Lau, Y.C., Wong, J.Y., Guan, Y., Tan, X., et al. (2020b). Temporal dynamics in viral shedding and transmissibility of COVID-19. *Nat. Med.* 26, 672–675.
- Hoang, D.T., Chernomor, O., von Haeseler, A., Minh, B.Q., and Vinh, L.S. (2018). UFBBoot2: Improving the Ultrafast Bootstrap Approximation. *Mol. Biol. Evol.* 35, 518–522.
- Hu, Z., Song, C., Xu, C., Jin, G., Chen, Y., Xu, X., Ma, H., Chen, W., Lin, Y., Zheng, Y., et al. (2020). Clinical characteristics of 24 asymptomatic infections with COVID-19 screened among close contacts in Nanjing, China. *Sci. China Life Sci.* 63, 706–711.
- Ikegami, S., Benirschke, R., Flanagan, T., Tanna, N., Klein, T., Elue, R., De-bosz, P., Mallek, J., Wright, G., Guariglia, P., et al. (2020). Persistence of SARS-CoV-2 nasopharyngeal swab PCR positivity in COVID-19 convalescent plasma donors. *Transfusion*. Published online August 24, 2020. <https://doi.org/10.1111/trf.16015>.
- Broad Institute (2018). Picard Toolkit. <http://broadinstitute.github.io/picard>.
- Jary, A., Leducq, V., Malet, I., Marot, S., Klement-Frutos, E., Teyssou, E., Soulié, C., Abdi, B., Wirde, M., Pourcher, V., et al. (2020). Evolution of viral quasispecies during SARS-CoV-2 infection. *Clin. Microbiol. Infect.*, S1198-743X(20)30440-7.
- Jin, X.H., Zheng, K.I., Pan, K.H., Xie, Y.P., and Zheng, M.H. (2020). COVID-19 in a patient with chronic lymphocytic leukaemia. *Lancet Haematol.* 7, e351–e352.

- Judson, S.D., and Munster, V.J. (2020). A framework for nosocomial transmission of emerging coronaviruses. *Infect. Control Hosp. Epidemiol.*, 1–2.
- Kalyanamoorthy, S., Minh, B.Q., Wong, T.K.F., von Haeseler, A., and Jermini, L.S. (2017). ModelFinder: fast model selection for accurate phylogenetic estimates. *Nat. Methods* 14, 587–589.
- Katoh, K., and Standley, D.M. (2013). MAFFT multiple sequence alignment software version 7: improvements in performance and usability. *Mol. Biol. Evol.* 30, 772–780.
- Katoh, K., Misawa, K., Kuma, K., and Miyata, T. (2002). MAFFT: a novel method for rapid multiple sequence alignment based on fast Fourier transform. *Nucleic Acids Res.* 30, 3059–3066.
- Kim, S.H., Ko, J.H., Park, G.E., Cho, S.Y., Ha, Y.E., Kang, J.M., Kim, Y.J., Huh, H.J., Ki, C.S., Jeong, B.H., et al. (2017). Atypical presentations of MERS-CoV infection in immunocompromised hosts. *J. Infect. Chemother.* 23, 769–773.
- Kim, D., Lee, J.Y., Yang, J.S., Kim, J.W., Kim, V.N., and Chang, H. (2020). The Architecture of SARS-CoV-2 Transcriptome. *Cell* 181, 914–921.e10.
- Kunisaki, K.M., and Janoff, E.N. (2009). Influenza in immunosuppressed populations: a review of infection frequency, morbidity, mortality, and vaccine responses. *Lancet Infect. Dis.* 9, 493–504.
- Lan, L., Xu, D., Ye, G., Xia, C., Wang, S., Li, Y., and Xu, H. (2020). Positive RT-PCR Test Results in Patients Recovered From COVID-19. *JAMA* 323, 1502–1503.
- Langmead, B., and Salzberg, S.L. (2012). Fast gapped-read alignment with Bowtie 2. *Nat. Methods* 9, 357–359.
- Lau, S.Y., Wang, P., Mok, B.W., Zhang, A.J., Chu, H., Lee, A.C., Deng, S., Chen, P., Chan, K.H., Song, W., et al. (2020). Attenuated SARS-CoV-2 variants with deletions at the S1/S2 junction. *Emerg. Microbes Infect.* 9, 837–842.
- Lee, S., Kim, T., Lee, E., Lee, C., Kim, H., Rhee, H., Park, S.Y., Son, H.J., Yu, S., Park, J.W., et al. (2020). Clinical Course and Molecular Viral Shedding Among Asymptomatic and Symptomatic Patients With SARS-CoV-2 Infection in a Community Treatment Center in the Republic of Korea. *JAMA Intern. Med.* 180, 1–6.
- Li, H., Handsaker, B., Wysoker, A., Fennell, T., Ruan, J., Homer, N., Marth, G., Abecasis, G., and Durbin, R.; 1000 Genome Project Data Processing Subgroup (2009). The Sequence Alignment/Map format and SAMtools. *Bioinformatics* 25, 2078–2079.
- Li, J., Zhang, L., Liu, B., and Song, D. (2020). Case Report: Viral Shedding for 60 Days in a Woman with COVID-19. *Am. J. Trop. Med. Hyg.* 102, 1210–1213.
- Liu, L., Wang, P., Nair, M.S., Yu, J., Rapp, M., Wang, Q., Luo, Y., Chan, J.F., Sahi, V., Figueroa, A., et al. (2020a). Potent Neutralizing Monoclonal Antibodies Directed to Multiple Epitopes on the SARS-CoV-2 Spike. *bioRxiv*. <https://doi.org/10.1101/2020.06.17.153486>.
- Liu, W.D., Chang, S.Y., Wang, J.T., Tsai, M.J., Hung, C.C., Hsu, C.L., and Chang, S.C. (2020b). Prolonged virus shedding even after seroconversion in a patient with COVID-19. *J. Infect.* 81, 318–356.
- Liu, Y., Chen, X., Zou, X., and Luo, H. (2020c). A severe-type COVID-19 case with prolonged virus shedding. *J. Formos. Med. Assoc.* 119, 1555–1557.
- Liu, Z., Zheng, H., Lin, H., Li, M., Yuan, R., Peng, J., Xiong, Q., Sun, J., Li, B., Wu, J., et al. (2020d). Identification of common deletions in the spike protein of SARS-CoV-2. *J. Virol.* 94, e00790–20.
- Long, Q.X., Tang, X.J., Shi, Q.L., Li, Q., Deng, H.J., Yuan, J., Hu, J.L., Xu, W., Zhang, Y., Lv, F.J., et al. (2020). Clinical and immunological assessment of asymptomatic SARS-CoV-2 infections. *Nat. Med.* 26, 1200–1204.
- Martin, M. (2011). Cutadapt removes adapter sequences from high-throughput sequencing reads. *EMBnet. J.* 17, 10–12.
- McKenna, A., Hanna, M., Banks, E., Sivachenko, A., Cibulskis, K., Kernysky, A., Garimella, K., Altshuler, D., Gabriel, S., Daly, M., and DePristo, M.A. (2010). The Genome Analysis Toolkit: a MapReduce framework for analyzing next-generation DNA sequencing data. *Genome Res.* 20, 1297–1303.
- McMichael, T.M., Clark, S., Pogojans, S., Kay, M., Lewis, J., Baer, A., Kawakami, V., Lukoff, M.D., Ferro, J., Brostrom-Smith, C., et al. (2020a). COVID-19 in a Long-Term Care Facility - King County, Washington, February 27–March 9, 2020. *MMWR Morb. Mortal. Wkly. Rep.* 69, 339–342.
- McMichael, T.M., Currie, D.W., Clark, S., Pogojans, S., Kay, M., Schwartz, N.G., Lewis, J., Baer, A., Kawakami, V., Lukoff, M.D., et al.; Public Health–Seattle and King County, EvergreenHealth, and CDC COVID-19 Investigation Team (2020b). Epidemiology of Covid-19 in a Long-Term Care Facility in King County, Washington. *N. Engl. J. Med.* 382, 2005–2011.
- Mira, E., Yarce, O.A., Ortega, C., Fernández, S., Pascual, N.M., Gómez, C., Alvarez, M.A., Molina, I.J., Lama, R., and Santamaria, M. (2020). Rapid recovery of a SARS-CoV-2-infected X-linked agammaglobulinemia patient after infusion of COVID-19 convalescent plasma. *J. Allergy Clin. Immunol. Pract.* 8, 2793–2795.
- Nguyen, L.T., Schmidt, H.A., von Haeseler, A., and Minh, B.Q. (2015). IQ-TREE: a fast and effective stochastic algorithm for estimating maximum-likelihood phylogenies. *Mol. Biol. Evol.* 32, 268–274.
- Paneesha, S., Pratt, G., Parry, H., and Moss, P. (2020). Covid-19 infection in therapy-naïve patients with B-cell chronic lymphocytic leukemia. *Leuk. Res.* 93, 106366.
- Prescott, J., Falzarano, D., de Wit, E., Hardcastle, K., Feldmann, F., Haddock, E., Scott, D., Feldmann, H., and Munster, V.J. (2018). Pathogenicity and Viral Shedding of MERS-CoV in Immunocompromised Rhesus Macaques. *Front. Immunol.* 9, 205.
- Qian, G.Q., Chen, X.Q., Lv, D.F., Ma, A.H.Y., Wang, L.P., Yang, N.B., and Chen, X.M. (2020). Duration of SARS-CoV-2 viral shedding during COVID-19 infection. *Infect. Dis. (Lond.)* 52, 511–512.
- Rambaut, A., Holmes, E.C., O’Toole, Á., Hill, V., McCrone, J.T., Ruis, C., du Plessis, L., and Pybus, O.G. (2020). A dynamic nomenclature proposal for SARS-CoV-2 lineages to assist genomic epidemiology. *Nat. Microbiol.* 5, 1403–1407.
- Robert, X., and Gouet, P. (2014). Deciphering key features in protein structures with the new ENDscript server. *Nucleic Acids Res.* 42, W320–4.
- Robinson, J.T., Thorvaldsdóttir, H., Wenger, A.M., Zehir, A., and Mesirov, J.P. (2017). Variant Review with the Integrative Genomics Viewer. *Cancer Res.* 77, e31–e34.
- Sagunenko, P., Puller, V., and Neher, R.A. (2018). TreeTime: Maximum-likelihood phylodynamic analysis. *Virus Evol.* 4, vex042.
- Salazar, E., Perez, K.K., Ashraf, M., Chen, J., Castillo, B., Christensen, P.A., Eubank, T., Bernard, D.W., Eagar, T.N., Long, S.W., et al. (2020). Treatment of Coronavirus Disease 2019 (COVID-19) Patients with Convalescent Plasma. *Am. J. Pathol.* 190, 1680–1690.
- Schubert, M., Lindgreen, S., and Orlando, L. (2016). AdapterRemoval v2: rapid adapter trimming, identification, and read merging. *BMC Res. Notes* 9, 88.
- Shen, Z., Xiao, Y., Kang, L., Ma, W., Shi, L., Zhang, L., Zhou, Z., Yang, J., Zhong, J., Yang, D., et al. (2020). Genomic Diversity of Severe Acute Respiratory Syndrome-Coronavirus 2 in Patients With Coronavirus Disease 2019. *Clin. Infect. Dis.* 71, 713–720.
- Shu, Y., and McCauley, J. (2017). GISAID: Global initiative on sharing all influenza data - from vision to reality. *Euro Surveill.* 22, 30494.
- Soresina, A., Moratto, D., Chiarini, M., Paolillo, C., Baresi, G., Focà, E., Bezzi, M., Baronio, B., Giacomelli, M., and Badolati, R. (2020). Two X-linked agammaglobulinemia patients develop pneumonia as COVID-19 manifestation but recover. *Pediatr. Allergy Immunol.* 31, 565–569.
- Speranza, E., Williamson, B.N., Feldmann, F., Sturdevant, G.L., Pérez-Pérez, L., Mead-White, K., Smith, B.J., Lovaglio, J., Martens, C., Munster, V.J., et al. (2020). SARS-CoV-2 infection dynamics in lungs of African green monkeys. *bioRxiv*. <https://doi.org/10.1101/2020.08.20.258087>.
- Sun, J., Xiao, J., Sun, R., Tang, X., Liang, C., Lin, H., Zeng, L., Hu, J., Yuan, R., Zhou, P., et al. (2020). Prolonged Persistence of SARS-CoV-2 RNA in Body Fluids. *Emerg. Infect. Dis.* 26, 1834–1838.
- van der Vries, E., Stittelaar, K.J., van Amerongen, G., Veldhuis Kroeze, E.J., de Waal, L., Fraaij, P.L., Meesters, R.J., Luidert, T.M., van der Nagel, B., Koch, B., et al. (2013). Prolonged influenza virus shedding and emergence of antiviral

- resistance in immunocompromised patients and ferrets. *PLoS Pathog.* 9, e1003343.
- van Kampen, J.J.A., van de Vijver, D.A.M.C., Fraaij, P.L.A., Haagmans, B.L., Lamers, M.M., Okba, N., van den Akker, J.P.C., Endeman, H., Gommers, D.A.M.P.J., Cornelissen, J.J., et al. (2020). Shedding of infectious virus in hospitalized patients with coronavirus disease-2019 (COVID-19): duration and key determinants. *medRxiv*. <https://doi.org/10.1101/2020.06.08.20125310>.
- Walls, A.C., Park, Y.J., Tortorici, M.A., Wall, A., McGuire, A.T., and Veesler, D. (2020). Structure, Function, and Antigenicity of the SARS-CoV-2 Spike Glycoprotein. *Cell* 181, 281–292.e6.
- Wang, Y., Grunewald, M., and Perlman, S. (2020a). Coronaviruses: An Updated Overview of Their Replication and Pathogenesis. *Methods Mol. Biol.* 2203, 1–29.
- Wang, W., Xu, Y., Gao, R., Lu, R., Han, K., Wu, G., and Tan, W. (2020b). Detection of SARS-CoV-2 in Different Types of Clinical Specimens. *JAMA* 323, 1843–1844.
- Wölfel, R., Corman, V.M., Guggemos, W., Seilmaier, M., Zange, S., Müller, M.A., Niemeyer, D., Jones, T.C., Vollmar, P., Rothe, C., et al. (2020). Virological assessment of hospitalized patients with COVID-2019. *Nature* 581, 465–469.
- Wrapp, D., Wang, N., Corbett, K.S., Goldsmith, J.A., Hsieh, C.L., Abiona, O., Graham, B.S., and McLellan, J.S. (2020). Cryo-EM structure of the 2019-nCoV spike in the prefusion conformation. *Science* 367, 1260–1263.
- Wrobel, A.G., Benton, D.J., Xu, P., Roustan, C., Martin, S.R., Rosenthal, P.B., Skehel, J.J., and Gamblin, S.J. (2020). SARS-CoV-2 and bat RaTG13 spike glycoprotein structures inform on virus evolution and furin-cleavage effects. *Nat. Struct. Mol. Biol.* 27, 763–767.
- Zhu, L., Xu, X., Ma, K., Yang, J., Guan, H., Chen, S., Chen, Z., and Chen, G. (2020). Successful recovery of COVID-19 pneumonia in a renal transplant recipient with long-term immunosuppression. *Am. J. Transplant.* 20, 1859–1863.
- Zou, L., Ruan, F., Huang, M., Liang, L., Huang, H., Hong, Z., Yu, J., Kang, M., Song, Y., Xia, J., et al. (2020). SARS-CoV-2 Viral Load in Upper Respiratory Specimens of Infected Patients. *N. Engl. J. Med.* 382, 1177–1179.

STAR★METHODS

KEY RESOURCES TABLE

REAGENT or RESOURCE	SOURCE	IDENTIFIER
Antibodies		
Rabbit anti-Human IgG Fc fragment Secondary Antibody (HRP)	Novus biologicals	Cat# NBP1-73529; Lot 34900
Bacterial and Virus Strains		
hCoV-19/USA/WA1/2020	CDC, Atlanta, USA (Harcourt et al., 2020)	GenBank: MN985325.1
hCoV-19/USA/WA-RML-5/2020 (SARS-CoV-2 patient genome d49 isolate)	This paper	GenBank: MT982401
hCoV-19/USA/WA-RML-6/2020 (SARS-CoV-2 patient genome d70 isolate)	This paper	GenBank: MT982404
Biological Samples		
Patient nasopharyngeal swabs	This paper	EvergreenHealth
Patient oropharyngeal swabs	This paper	EvergreenHealth
Patient serum and plasma	This paper	EvergreenHealth
Donor convalescent plasma	This paper	EvergreenHealth
Chemicals, Peptides, and Recombinant Proteins		
SARS-CoV-2 spike protein	This paper (Wrapp et al., 2020)	N/A
SARS-CoV-2 receptor binding domain protein	This paper (Amanat et al., 2020)	N/A
PEI transfection reagent	Polysciences	Cat# 23966-1
Blocker Casein in PBS	ThermoFisher	Cat# 37528
TMB 2-Component Microwell Peroxidase Substrate Kit	SeraCare	Cat# 5120-0047
KPL TMB Stop Solution	SeraCare	Cat# 5150-0020
Trizol Reagent	Invitrogen	Cat# 15596026
Karnovsky's EM fixative	Electron Microscopy Sciences	Cat#15720
Sodium Cacodylate	Sigma	Cat#C4945-10G; CAS#6131-99-3
Osmium Tetroxide	Electron Microscopy Sciences	Cat#19190; CAS#20816-12-0
Potassium Ferrocyanide	Sigma	Cat#P-3289; CAS#14459-95-1
Uranyl Acetate	Ted Pella	Cat#19481; CAS#6159-44-0
Critical Commercial Assays		
PureLink RNA Mini Kit	Invitrogen	Cat# 12183018A
SuperScript IV First-Strand Synthesis System	Invitrogen	Cat# 18091050
Quantifast Probe RT-PCR Kit (for Rotorgene)	QIAGEN	Cat# 204556
ddPCR Supermix for Probes (no dUTP)	Biorad	Cat# 1863024
Q5 Hot Start High-Fidelity DNA Polymerase – 100U	New England Biolabs	Cat#M0493S
ARTIC nCoV-2019 V3 Panel, 500rxn	Integrated DNA Technologies	Cat#10006788
TruSeq DNA PCR-Free LT Library Prep	Illumina	Cat#20015962
TruSeq DNA Idx Kit Set A	Illumina	Cat#20015960
MiSeq Reagent Nano Kit, v2 (500 cycles) (1M)	Illumina	Cat#MS-103-1003
Deposited Data		
Data used to generate figures	This paper	Mendeley Data at https://dx.doi.org/10.17632/3n377gv8kb .
hCoV-19/USA/WA-RML-1/2020 (SARS-CoV-2 patient genome d49 NP swab)	This paper	GenBank: MT982403

(Continued on next page)

Continued

REAGENT or RESOURCE	SOURCE	IDENTIFIER
hCoV-19/USA/WA-RML-2/2020 (SARS-CoV-2 patient genome d70 NP swab)	This paper	GenBank: MT982402
hCoV-19/USA/WA-RML-3/2020 (SARS-CoV-2 patient genome d85 NP swab)	This paper	GenBank: MT982405
hCoV-19/USA/WA-RML-4/2020 (SARS-CoV-2 patient genome d105 NP swab)	This paper	GenBank: MT982406
hCoV-19/USA/WA-RML-5/2020 (SARS-CoV-2 patient genome d49 isolate)	This paper	GenBank: MT982401
hCoV-19/USA/WA-RML-6/2020 (SARS-CoV-2 patient genome d70 isolate)	This paper	GenBank: MT982404
Experimental Models: Cell Lines		
Freestyle 293-F	ThermoFisher	Cat# R79007; RRID CVCL_D603
VeroE6	Ralph Baric	ATCC CRL-1586
MatTek EpiAlveolar	MatTek Life Sciences (https://www.mattek.com/products/epialveolar/)	Cat# ALV-100-FT-PE12
Oligonucleotides		
Primer to E genomic (E_Sarbeco_F1) AACAGGTACGTTAATAGTTAATAGCGT	Corman et al., 2020; Integrated DNA Technologies	https://www.who.int/docs/default-source/coronaviruse/wuhan-virus-assay-v1991527e5122341d99287a1b17c111902.pdf
Primer to E subgenomic (sgLeadSARS2-F) CGATCTCTGTAGATCTGTCTCTC	Wölfel et al., 2020; Integrated DNA Technologies	N/A
Reverse primer to E (E_Sarbeco_R2) ATATTGCAGCAGTACGCACACA	Corman et al., 2020; Integrated DNA Technologies	https://www.who.int/docs/default-source/coronaviruse/wuhan-virus-assay-v1991527e5122341d99287a1b17c111902.pdf
Probe for E (E_Sarbeco_P1) FAM- ACACTAGCCATCCTTACTGCGCTTCG- ZEN-IBHQ	Corman et al., 2020; Integrated DNA Technologies	https://www.who.int/docs/default-source/coronaviruse/wuhan-virus-assay-v1991527e5122341d99287a1b17c111902.pdf
Recombinant DNA		
pzH SARS-CoV-2 spike plasmid	Kizzemekia Corbett and Barney GrahamVaccine Research Center, NIH, Bethesda, USA (Wrapp et al., 2020)	N/A
pCAGGS SARS-CoV-2 receptor binding domain plasmid	Florian KrammerIcahn School of Medicine at Mt. Sinai, New York, USA (Amanat et al., 2020)	N/A
Software and Algorithms		
MAFFT align	(Katoh and Standley, 2013 , Katoh et al., 2002)	Geneious Prime 2020.1.2 plugin
Multalin sequence alignment	(Corpet, 1988)	http://multalin.toulouse.inra.fr/multalin/
ESPrpt 3.0	(Robert and Gouet, 2014)	http://esprpt.ibcp.fr/ESPrpt/ESPrpt/
Geneious Prime 2020.1.2	Geneious	https://www.geneious.com
PhyML 3.320180621	Guindon et al., 2010	Geneious Prime 2020.1.2 plugin
FigTree v1.4.4	http://tree.bio.ed.ac.uk/software/figtree/	https://github.com/rambaut/figtree/
Pangolin COVID-19 Lineage Assigner	Rambaut et al., 2020	https://pangolin.cog-uk.io
Pymol Molecular Graphics System version 2.0.1	Schrödinger	https://www.schrodinger.com/pymol
Prism 8.2.0	GraphPad	https://www.graphpad.com:443/
NextClade v0.7.5	https://github.com/nextstrain/nextclade	https://nextstrain.org/ncov/global?c=region
ModelFinder	Kalyaanamoorthy et al., 2017	http://www.iqtree.org/
Ultrafast bootstrap	Hoang et al., 2018	http://www.iqtree.org/

(Continued on next page)

Continued

REAGENT or RESOURCE	SOURCE	IDENTIFIER
IQ-TREE v1.6.12	Nguyen et al., 2015	http://www.iqtree.org/
TreeTime v.0.7.6	Sagulenko et al., 2018	https://github.com/neherlab/treetime
BCFtools v1.10.2	Li et al., 2009	https://www.htslib.org
Bowtie2	Langmead and Salzberg, 2012	http://bowtie-bio.sourceforge.net/bowtie2/index.shtml
Samtools	Li et al., 2009	http://samtools.sourceforge.net/
AdapterRemoval v2.2.2	Schubert et al., 2016	https://github.com/MikkelSchubert/adapterremoval
Picard 2.18.7	Broad Institute, 2018	https://broadinstitute.github.io/picard/
GATK 4 v 4.1.2.0	McKenna et al., 2010	https://github.com/broadinstitute/gatk/releases

Other

Ni Sepharose 6 Fast Flow	GE Lifesciences	Cat# 17531802
NiNTA Agarose	QIAGEN	Cat# 30230
Phasemaker Tubes	Invitrogen	Cat# A33248
Thermanox coverslips	Ted Pella	Cat#26028
Silicon Chips	Ted Pella	Cat#16007
Aluminum specimen mounts	Ted Pella	Cat#16111
Double-sided carbon tape	Ted Pella	Cat#16084-1
Spurr's resin	Ted Pella	Cat#18300-4221
Iridium target	Electron Microscopy Sciences	Cat#3431
Bal-Tec Drier	Balzers, Liechtenstein	Cat#CPD 030
Quorum sputter coater	Electron Microscopy Sciences, Hatfield, PA	Cat#EMS300T D
Hitachi field emission scanning electron microscope	Hitachi, Tokyo, Japan	Model#SU-8000
Leica UC7 ultramicrotome	Leica Microsystems	N/A
FEI BT Tecnai transmission electron microscope	ThermoFisher/FEI	N/A
Gatan Rio camera	Gatan	N/A

RESOURCE AVAILABILITY**Lead Contact**

Further information and requests for resources and reagents should be directed to and will be fulfilled by the Lead Contact, Vincent Munster (Vincent.munster@nih.gov).

Materials Availability

This study did not generate new reagents.

Data Availability

The data and the Supplementary Tables from this study have been deposited to Mendeley Data at <https://dx.doi.org/10.17632/3n377gv8kb>.

Genome sequences have been deposited to GenBank: MT982403, MT982402, MT982405, MT982406, MT982401 and MT982404.

EXPERIMENTAL MODEL AND SUBJECT DETAILS**Human Patient**

The patient described in this case study is a 71 year old female with a 10 year history of chronic lymphocytic leukemia (CLL), acquired hypogammaglobulinemia, anemia, and chronic leukocytosis. The patient tested positive for SARS-CoV-2 on March 2, 2020, and

remained positive through June 15, 2020. During the course of the study, the patient was transfused with intravenous immunoglobulin (IVIG, 25 g) on April 6 and May 6, 2020, and convalescent plasma against SARS-CoV-2 on May 12 and May 23, 2020. After the initial SARS-CoV-2 diagnosis, the patient was kept in isolation in an isolation ward in a single room with negative airflow. Anonymized plasma, serum and swabs from a patient at EvergreenHealth, Kirkland, Washington were obtained under an NIH Institutional Review Board exemption. Verbal and signed consent were obtained from the patient to allow analyses of the samples.

Cells

Vero E6 is a female African green monkey kidney epithelial cell line. Vero E6 cells were maintained at 37°C and 5% CO₂ in DMEM supplemented with 10% fetal bovine serum, 1 mM L-glutamine, 50 U/mL penicillin and 50 µg/mL streptomycin. Vero E6 cells were provided by Dr. Ralph Baric. Cells were authenticated by cytochrome B sequencing. Mycoplasma testing was performed monthly, and no mycoplasma was detected.

FreeStyle 293-F (RRID: CVCL_D603) is a female human embryonic cell line adapted for growth in suspension culture. FreeStyle 293-F cells were grown in Freestyle 293 Expression Medium (GIBCO) at 37°C and 8% CO₂, shaking at 130 rpm. Cells were not authenticated in house. Mycoplasma testing was performed monthly, and no mycoplasma was detected.

MatTek EpiAlveolar is a 3D co-culture model of the air-blood barrier produced from primary human alveolar epithelial cells, pulmonary endothelial cells and fibroblasts, and maintained according to manufactures instructions (<https://www.mattek.com/products/epialveolar/>). Cells were not authenticated in house. Mycoplasma testing was performed monthly, and no mycoplasma was detected.

SARS-CoV-2 Virus

SARS-CoV-2 strain nCoV-WA1-2020 (MN985325.1) (Harcourt et al., 2020) was provided by CDC, Atlanta, USA. SARS-CoV-2 isolates were propagated on Vero E6 cells grown in DMEM supplemented with 2% fetal bovine serum (GIBCO), 1 mM L-glutamine (GIBCO), 50 U/mL penicillin and 50 µg/mL streptomycin (GIBCO) (virus isolation medium), at 37°C and 5% CO₂.

Infectious titer of SARS-CoV-2 virus stocks was determined by end-point titration and is reported as log₁₀ 50% tissue culture infective dose (TCID₅₀/mL). 1.5 × 10⁴ Vero E6 cells were seeded into each well in 96-well plates in DMEM supplemented with 10% fetal bovine serum, 1 mM L-glutamine, 50 U/mL penicillin and 50 µg/mL streptomycin and incubated overnight at 37°C and 5% CO₂. The following morning, when the cells were at approximately 90% confluency, the wells were inoculated with ten-fold serial dilutions of virus stock diluted in virus isolation medium (100 µL per well, with 10 replicate wells for each dilution). The plates were incubated at 37°C and 5% CO₂, and the cytopathic effect (CPE) was assessed for each well after 5 days. Wells that demonstrated CPE were counted, and the titer was determined by the method of Spearman and Kärber using 10 replicates as follows:

$$\text{Log}_{10}\text{TCID}_{50}/\text{mL} = (X - d/2 + [d \bullet S])$$

where X is log₁₀ of the lowest dilution with all wells positive for CPE, d is log₁₀ of the dilution factor (10 in these titrations), and S is the sum of the fraction of wells positive for CPE at all tested dilutions.

METHOD DETAILS

Clinical Sample RNA Extraction and qRT-PCR

Clinical samples were deidentified as part of their analyses. Nasopharyngeal and oropharyngeal swabs were shipped on wet ice in viral transport medium (VTM) to Rocky Mountain Laboratories (NIH). RNA was extracted using Trizol (Invitrogen), Phasemaker tubes (Invitrogen) and the PureLink RNA Mini Kit (Invitrogen) according to manufacturer's instructions and eluted in 100 µL RNase-free H₂O. First strand cDNA synthesis was performed with the SuperScript IV First Strand Synthesis System (Invitrogen), using 11 µL input RNA and random hexamers. qRT-PCR was performed using 5 µL of cDNA using the QuantiFast Probe kit (QIAGEN) using E gRNA (Corman et al., 2020) and sgRNA specific assays (Wölfel et al., 2020). To quantify viral load within the patient samples, 5 µL of cDNA was analyzed using droplet digital PCR (Biorad) using the same E gRNA and sgRNA assays. The SARS-CoV-2 testing through EvergreenHealth were performed by University of Washington, LabCrop, Cepheid, and GenMark. Kashi clinical laboratories and Magnolia diagnostics performed the negative tests taken at the care facilities.

Virus Isolation

Virus isolation of the clinical specimen was performed on Vero E6 cells in 96 well plates. In brief, media was removed from wells and replaced with 100 µL of undiluted swab sample, or swab sample diluted 1:10 in DMEM supplemented with 2% fetal bovine serum (GIBCO), 1 mM L-glutamine (GIBCO), 50 U/mL penicillin and 50 µg/mL streptomycin (GIBCO) (virus isolation medium). Diluted and undiluted samples were inoculated onto 7 wells. Spin inoculation was performed at 1000 x g for 1 hour at 35°C. Inoculum was removed and wells were washed twice with and replaced with 100 µL of virus isolation medium and incubated at 37°C and 5% CO₂. After 5 days, replicate wells were pooled, diluted 10x in virus isolation medium, and used to inoculate T25 flasks of Vero E6 cells in virus isolation medium and incubated at 37°C and 5% CO₂. Flasks were observed for cytopathic effect. RNA was extracted, as described above, for confirmation of SARS-CoV-2 by qRT-PCR and next generation sequencing.

Growth kinetics of SARS-CoV-2 isolates

Vero E6 cells were seeded in 6 well plates at a density of 4×10^5 cells/well in DMEM supplemented with 2% fetal bovine serum (GIBCO), 1 mM L-glutamine (GIBCO), 50 U/mL penicillin and 50 μ g/mL streptomycin (GIBCO) (virus isolation medium) and incubated overnight at 37°C and 5% CO₂. The following day, the media was removed from the wells and replaced with 1 mL of virus isolation medium containing virus at a MOI of 0.01. The patient day49 isolate and the USA/WA1/2020 strain were tested in triplicate, with mock control wells in triplicate. After a 1-hour incubation at 37°C and 5% CO₂, the inoculum was removed, and wells were washed 3x with PBS and replaced with a fresh 2 mL of virus isolation medium. Supernatant samples were taken at 0, 12, 24, 48, 72, 96, and 120 hours post inoculation. Titer of infectious virus from supernatant was determined by endpoint titration in Vero E6 cells, as described above, but using 4 replicates per sample to determine the TCID₅₀/mL using the Spearman-Kärber method. The EpiAlveolar cell growth kinetic experiment was set up similar to the Vero E6 cells but with the following differences. Cells were provided by MatTek with 2.5×10^5 cells/transwell insert. Cells were infected by adding 75 μ L of ALI medium containing virus at an MOI of 0.01 to the apical side of the transwell insert. After the above outlined incubation, the inoculum was removed, wells were washed 1x with PBS and replaced with 75 μ L of ALI medium upon the apical surface. During sampling of the EpiAlveolar cells, 500 μ L of DMEM medium was added to the apical side, gently pipetted to mix, removed, and 75 μ L of fresh ALI medium replaced on the apical surface.

Expression and Purification of SARS-CoV-2 Spike and Receptor Binding Domain

Expression plasmids encoding the codon optimized SARS-CoV-2 full length spike and receptor binding domain (RBD) were kindly provided Kizzmekia Corbett and Barney Graham (Vaccine Research Center, Bethesda, USA) and Florian Krammer (Icahn School of Medicine at Mt. Sinai, New York, USA), respectively (Wrapp et al., 2020; Amanat et al., 2020). Both plasmids were expressed in Freestyle 293-F cells (ThermoFisher), maintained in Freestyle 293 Expression Medium (GIBCO/ThermoFisher) at 37°C and 8% CO₂ in a humidified incubator shaking at 130 rpm. Cultures totaling 500 mL were transfected with PEI at a density of one million cells per mL. Supernatant was harvested 7 days post transfection, clarified by centrifugation and sterile filtered through a 0.22 μ m membrane. The protein was purified using Ni-NTA immobilized metal-affinity chromatography (IMAC) using Ni Sepharose 6 Fast Flow Resin (GE Lifesciences) or NiNTA Agarose (QIAGEN) and gravity flow. After elution the protein was buffer exchanged into 10 mM Tris pH8, 150 mM NaCl buffer before further use or frozen at –80°C for storage.

Enzyme-Linked Immunosorbent Assay (ELISA)

Purified SARS-CoV-2 full length spike or RBD protein was diluted to 1 μ g/mL in PBS. Maxisorp plates (Nunc) were coated with 100 μ L per well (100 ng protein per well) and incubated overnight at 4°C. Plates were washed 3x with PBST (0.1% Tween) and blocked with 100 μ L casein in PBS blocking buffer (ThermoFisher) for 1 hour at room temp. Plates were again washed 3x with PBST (0.1% Tween), and 100 μ L of serum samples, serially diluted 2 fold in casein in PBS blocking buffer, in duplicate, was added to the wells and incubated at room temperature for 1 hour. Plates were washed 4x with PBST (0.1% Tween), and 100 μ L secondary antibody, rabbit anti-human IgG Fc HRP (Novus Biologicals, NBP1-73529) diluted 1:4000 in casein in PBS blocking buffer, was added to the wells and incubated for 1 hour at room temperature. The wells were washed 5x with PBST (0.1% Tween) and developed with the KPL TMP 2-component peroxidase substrate kit (Seracare, 5120-0047). The reaction was stopped with KPL stop solution (Seracare, 5150-0020) and read at 450 nm. The threshold for positivity was calculated as the average plus 3 times the standard deviation of negative control sera. Reported titers are the reciprocal value of the highest dilution at which signal was observed above the calculated threshold.

Virus Neutralization assay

Serum and plasma samples were heat inactivated at 56°C for 30 minutes. Two-fold serial dilutions were prepared in DMEM supplemented with 2% FBS, with each sample diluted in duplicate in 96 well plate format. 100 TCID₅₀ of SARS-CoV-2, in virus isolation medium, was then added to each well. The virus-serum/plasma mixture was incubated at 37°C for 1 hour to allow for neutralization, then 100 μ L per well was added to Vero E6 cells in 96 well plates and incubated at 37°C and 5% CO₂. After 5 days, wells were observed for cytopathic effect. The virus neutralization titer is displayed as the reciprocal value of the highest dilution of serum/plasma that still inhibited virus replication at which no cytopathic effect was observed.

Next generation sequencing of patient clinical samples and isolates

Clinical Samples - Viral RNA was extracted from patient nasopharyngeal swabs using Trizol (Invitrogen) for use with the ARTIC nCoV-2019 sequencing protocol V.1 (Protocols.io; <https://www.protocols.io/view/ncov-2019-sequencing-protocol-bbmuik6w>). 30-35 PCR cycles were used to generate tiled-PCR amplicons. Primer pools consisted of the ARTIC nCoV-2019 v3 Panel (Integrated DNA Technologies, Belgium) and were diluted and used in PCR reactions following the instructions. Products from Pool 1 and Pool 2 were combined, AmPure XP cleaned, and quantitated as per the instructions – through step 16.18. Following assessment on a BioAnalyzer DNA Chip (Agilent Technologies, Santa Clara, CA), a volume consisting of 500 ng of product was taken directly into TruSeq DNA PCR-Free Library Preparation Guide, Revision D. (Illumina, San Diego, CA) beginning with the Repair Ends step (q.s. to 50 μ L with RSB) and subsequent cleanup consisted of a single 1:1 AmPure XP/reaction ratio. All downstream steps followed the manufacturer's instructions. Final libraries were visualized on a BioAnalyzer HS chip (Agilent Technologies, Santa Clara, CA) and quantified using KAPA Library Quant Kit (Illumina) Universal qPCR Mix (Kapa Biosystems, Wilmington, MA) on a CFX96 Real-Time System (BioRad, Hercules, CA).

Isolates - Viral RNA was extracted from clarified cell culture supernatant using Trizol (Invitrogen). Extracted RNA was depleted of rRNA using Ribo-Zero Gold H/M/R (Illumina, San Diego, CA) based on manufacturer's protocols. After Ampure RNAClean XP (Beckman Coulter, Brea, CA) purification, the enriched RNA was eluted in 6 μ L of water and assessed on a BioAnalyzer RNA Pico Chip (Agilent Technologies, Santa Clara, CA). Following the Truseq Stranded mRNA Library Preparation Guide, Revision E., (Illumina, San Diego, CA), the remaining RNA was added to Elute-Frag-Prime Buffer and continued through second-strand cDNA synthesis. The resulting double-stranded cDNAs were treated with a combined mixture of RiboShredder RNase Blend (Lucigen, Middleton, WI) and high concentration DNase-free RNase (Roche Diagnostics, Indianapolis, IN). After AMPure XP purification (Beckman Coulter, Brea, CA), samples were analyzed on a RNA Pico chip to confirm no remaining RNA. Library preparation continued with adenylation of ends following manufacturer's recommendations. All downstream steps followed the manufacturer's instructions. Final libraries were visualized on a BioAnalyzer DNA1000 chip (Agilent Technologies, Santa Clara, CA) and quantified using KAPA Library Quant Kit (Illumina) Universal qPCR Mix (Kapa Biosystems, Wilmington, MA) on a CFX96 Real-Time System (BioRad, Hercules, CA).

Sequencing and bioinformatics

Libraries were diluted to 2 nM stock, pooled together as needed in equimolar concentrations and sequenced on the MiSeq (Illumina, Inc, San Diego, CA) using on-board cluster generation and 2 \times 150 paired-end sequencing. Raw image files were converted to fastq files using bcl2fastq (v2.20.0.422, Illumina, Inc. San Diego, CA) and trimmed of adaptor sequences using cutadapt version 1.12 (Martin, 2011). Adaptor-trimmed reads were trimmed and filtered to remove low quality sequence using fastq_quality_trimmer and fastq_quality_filter tools from the FASTX Toolkit, v 0.0.14 (Gordon, 2018). Singletons were removed and quality filtered reads were coordinate-order sorted using a custom perl script.

Reads were filtered for repeat sequence, rRNA, and PhiX contaminants and then mapped to the SARS-CoV-2 isolate 2019-nCoV/USA_WA1 (MN985325.1) reference genome using bowtie2 with `-no-mixed -no-unal -X 1500` options (Langmead and Salzberg, 2012). Aligned SAM files were converted to BAM format, then sorted and indexed using SAMtools (Li et al., 2009). Duplicate reads were removed from the mapped reads using picard's MarkDuplicates tool (Broad Institute, 2018).

To process the ARTIC data a custom pipeline was developed. Fastq read pairs were first compared to a database of ARTIC primer pairs to identify read pairs that had correct, matching primers on each end. Once identified, the ARTIC primer sequence was trimmed off. Read pairs that did not have the correct ARTIC primer pairs were discarded. Remaining read pairs were collapsed into one sequence using AdapterRemoval (Schubert et al., 2016), requiring a minimum 25 base overlap and 300 base minimum length, generating ARTIC amplicon sequences. Identical amplicon sequences were removed and the unique amplicon sequences were then mapped to the SARS-CoV-2 genome (MN985325.1) using Bowtie2 (Langmead and Salzberg, 2012). Aligned SAM files were converted to BAM format, then sorted and indexed using SAMtools (Li et al., 2009).

Variant calling was performed using Genome Analysis Toolkit (GATK, version 4.1.2) HaplotypeCaller with ploidy set to 2 (McKenna et al., 2010). Single nucleotide polymorphic variants were filtered for QUAL > 200 and quality by depth (QD) > 20 and indels were filtered for QUAL > 500 and QD > 20 using the filter tool in bcftools, v1.9 (Li et al., 2009). The accuracy of the filtered variant calls was manually inspected in Broad's Integrative Genomics Viewer (IGV) (Robinson et al., 2017). Consensus sequences were generated using bcftools consensus (Li et al., 2009) and subsequently aligned using MAFFT (Katoh and Standley, 2013; Katoh et al., 2002) with 2,434 GISAID Washington SARS2 reference sequences in addition to the 2019-nCoV/USA_WA1 genome used for mapping.

Phylogenomic Analysis

Available SARS-CoV-2 full genome sequences were downloaded from the GISAID database (<https://gisaid.org/>; Shu and McCauley, 2017). The sequences were then assigned to previously described lineages (Rambaut et al., 2020) using Pangolin v2.0.3 (<https://pangolin.cog-uk.io/>), and aligned using MAFFT v. 1.4 (Katoh and Standley, 2013; Katoh et al., 2002). A maximum likelihood tree with the patient SARS-CoV-2 genomes, the Wuhan-Hu-1/2019 genome sequence, the USA/WA-1/2020 genome, and a representative genome from the assigned lineages was inferred using PhyML v.3.3.20180621 (Guindon et al., 2010) implemented in Geneious Prime v.2020.1.2 (<https://www.geneious.com/>) with a general time reversible model of nucleotide substitution and rooted at the Wuhan-Hu-1/2019 SARS-CoV-2 strain. The final figure was made using FigTree v.1.4.4 (<http://tree.bio.ed.ac.uk/software/figtree/>). For the time tree, full SARS-CoV-2 genomes were subsampled from Washington state representing NextStrain clade 19B, including the four patient genomes sequences and the Wuhan-Hu-1/2019 genome sequence. The sequences were aligned using MAFFT v. 1.4 (Katoh and Standley, 2013; Katoh et al., 2002) implemented in Geneious Prime v. 2020.1.2 (<https://www.geneious.com/>), a maximum likelihood tree reconstructed with PhyML v.3.1 (Guindon et al., 2010), and the time tree showing temporal divergence inferred in Tree-Time v.0.7.6 (Hadfield et al., 2018) using the HKY85 model of nucleotide substitution and a fixed molecular clock at 8e-4 with a standard deviation of 4e-4 as implemented in the NextStrain pipeline (<https://nextstrain.org/sars-cov-2/>).

To evaluate the relationship between the SARS-CoV-2 genomes recovered from the patient swabs with other SARS-CoV-2 genomes from Washington state, genomes at the times of sampling (April 20, May 11, May 26, and June 15, 2020) from Washington state were downloaded from the GISAID database (<https://gisaid.org/>; Shu and McCauley, 2017). The sequences were aligned by MAFFT (Katoh and Standley, 2013; Katoh et al., 2002). The sequences were analyzed by the Nextclade server v0.7.5 (<https://clades.nextstrain.org/>) for quality and sequences that were not of sufficient quality were discarded. 1,789 sequences at April 20, 385 sequences between April 20 and May 11, 268 sequences between May 11 and May 26, and 709 sequences between May 26 and June 15 were kept for further phylogenetic analysis. Maximum likelihood trees using the curated sets of genomes, the four patient

genomes, and the USA/WA1/2020 genome, were inferred using ModelFinder (Kalyaanamoorthy et al., 2017) and ultrafast bootstrap (Hoang et al., 2018) implemented in IQ-TREE (Nguyen et al., 2015), and rooted at USA/WA1/2020. Final figures were made using FigTree v.1.4.4 (<http://tree.bio.ed.ac.uk/software/figtree/>). A table of acknowledgments for the GISAID genome sequences used to within this work is available at Mendeley Data at <https://dx.doi.org/10.17632/3n377gv8kb>.

Electron Microscopy

Vero E6 cells cultured in DMEM supplemented with 10% fetal bovine serum, 1 mM L-glutamine, 50 U/mL penicillin and 50 µg/mL streptomycin were plated at 5×10^4 cells/well in 24 well plates containing Thermanox coverslips (Ted Pella, Redding, CA) for transmission electron microscopy or silicon chips (Ted Pella, Redding, CA) for scanning electron microscopy in the wells, and incubated overnight at 37°C and 5% CO₂. The next day, media was carefully aspirated from the wells and replaced with 1 mL of virus isolation medium containing SARS-CoV-2 virus at a MOI of 1 and incubated for 1 hour at 37°C and 5% CO₂. Wells were washed three times with PBS, then replaced with 1 mL fresh virus isolation medium and incubated at 37°C and 5% CO₂. At 24 and 48 hours post-infection, wells were washed three times with PBS, then fixed as described below.

Scanning electron microscopy

Cells were fixed with Karnovsky's formulation of 2% paraformaldehyde/2.5% glutaraldehyde in 0.1 M Sorenson's phosphate buffer, and then post-fixed with 1.0% osmium tetroxide/0.8% potassium ferrocyanide in 0.1 M sodium cacodylate buffer washed with 0.1 M sodium cacodylate buffer then stained with 1% tannic acid in dH₂O. After additional buffer washes, the samples were further osmicated with 2% osmium tetroxide in 0.1M sodium cacodylate, then washed with dH₂O. Specimens were dehydrated with a graded ethanol series from 50%, 75%, 100% x 3 for 5 minutes each, critical point dried under CO₂ in a Bal-Tec model CPD 030 Drier (Balzers, Liechtenstein), mounted with double sided carbon tape on aluminum specimen mounts (Ted Pella), and sputter coated with 35 Å of iridium in a Quorum EMS300T D sputter coater (Electron Microscopy Sciences, Hatfield, PA) prior to viewing at 5 kV in a Hitachi SU-8000 field emission scanning electron microscope (Hitachi, Tokyo, Japan).

Transmission electron microscopy

Specimens were fixed as described above for scanning electron microscopy and additionally stained overnight with 1% uranyl acetate at 4°C after the second osmium staining and then dehydrated with the same graded ethanol series and embedded in Spurr's resin. Thin sections were cut with a Leica UC7 ultramicrotome (Buffalo Grove, IL) prior to viewing at 120 kV on a FEI BT Tecnai transmission electron microscope (ThermoFisher/FEI, Hillsboro, OR). Digital images were acquired with a Gatan Rio camera (Gatan, Pleasanton, CA).

Structure Mapping

The Pymol Molecular Graphics System (<https://www.schrodinger.com/pymol>) was used to map the location of the observed deletions onto a SARS-CoV-2 spike structure (PDB: 6ZGE; Wrobel et al., 2020). Nucleotide sequence alignments were generated using MAAFT align (Kato and Standley, 2013; Kato et al., 2002) implemented in Geneious Prime v.2020.1.2 (<https://www.geneious.com>) and amino acid sequence alignments were generated with Multalin (Corpet, 1988) and plotted with ESPript (Robert and Gouet, 2014).

QUANTIFICATION AND STATISTICAL ANALYSIS

Data and statistical analysis was performed using GraphPad Prism 8.2.0. Replicates and statistical details can also be found in the methods and figure legends. For ELISA and virus neutralization assays, the serum/plasma samples were diluted and tested in duplicate. For the growth curves, both virus isolates (day 49 patient isolate and USA/WA1/2020) were tested in three replicate wells for both Vero E6 cells and the primary human alveolar epithelial cells. The growth curve data shown are the mean and standard error of the mean for the three independent replicates. The statistical analysis was performed using a 2-way ANOVA in Graphpad Prism 8.2.0. Further methods to determine whether the data met assumptions of the statistical approach were not relevant for these analyses.

Supplemental Figures

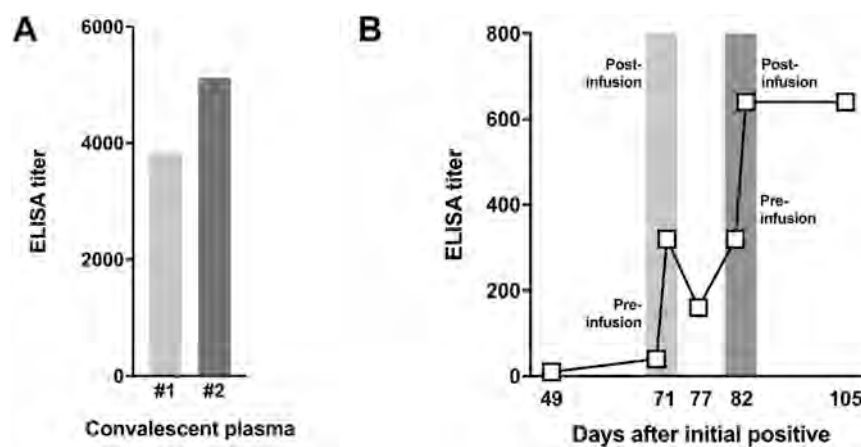


Figure S1. ELISA Titers against the SARS-CoV-2 RBD, Related to Figure 2

(A) IgG titers against SARS-CoV-2 receptor binding domain (RBD) were determined in ELISA on convalescent plasma used for transfusion. The light gray bar is the IgG titer of the first donor (convalescent plasma 1) and the dark gray is the second donor (convalescent plasma 2). (B) IgG titers against SARS-CoV-2 (RBD) were determined in ELISA on patient serum collected on several time points, including immediately before and after transfusion with convalescent plasma at day 71 (light gray) and day 82 (dark gray). Each serum/plasma sample was tested in duplicate.

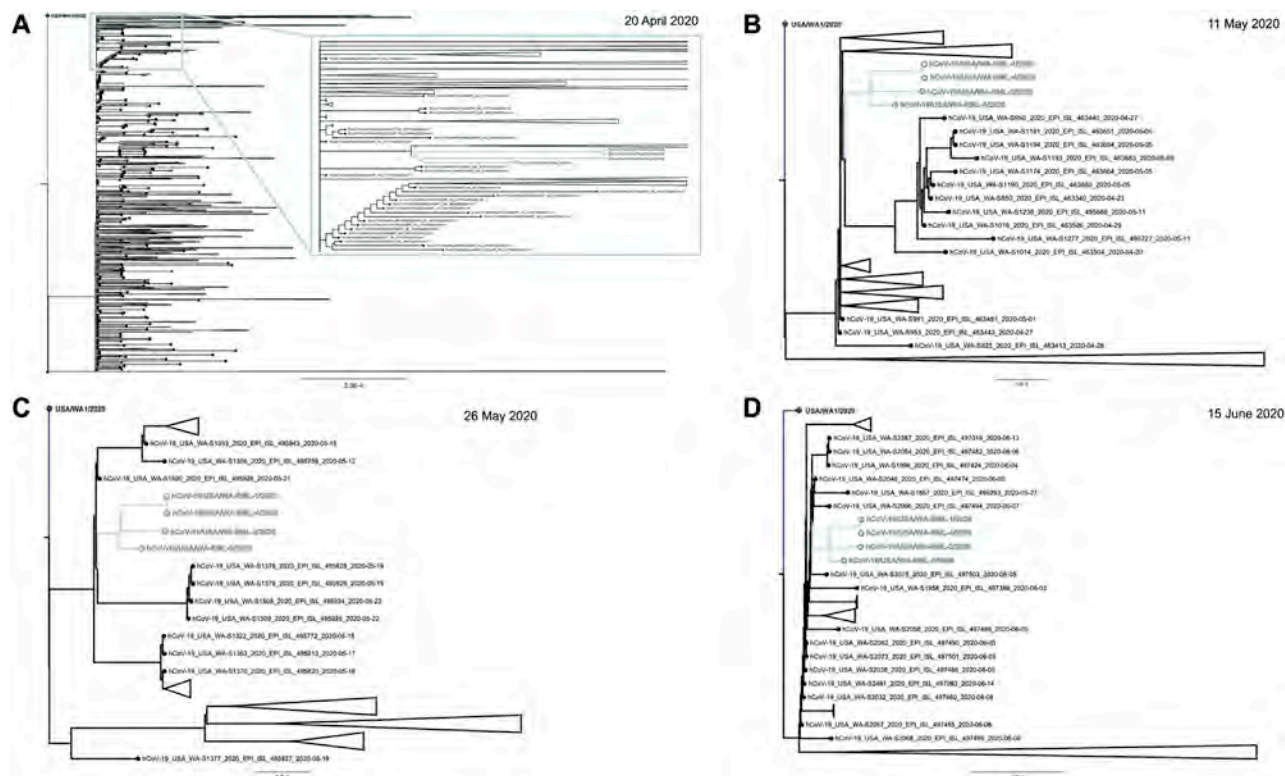


Figure S2. Maximum-Likelihood Trees of the Individual with SARS-CoV-2 with Other SARS-CoV-2 Genomes Circulating in Washington State at the Times of Sampling (April 20, May 11, May 26, and June 15, 2020), Related to Figure 4 and Table 2

(A) Maximum likelihood tree using 1789 full genome SARS-CoV-2 sequences deposited to GISAID until 20 April 2020. Inset shows a close up of the monophyletic clade of the genomes directly obtained from the patient samples (cyan). (B) Maximum likelihood tree using 385 full genome SARS-CoV-2 sequences deposited to GISAID between 20 April and 11 May, 2020. The monophyletic clade of the genomes directly obtained from the patient samples is shown in cyan. (C) Maximum likelihood tree using 268 full genome SARS-CoV-2 sequences deposited to GISAID between 11 May and 26 May, 2020. The monophyletic clade of the genomes directly obtained from the patient samples is shown in cyan. (D) Maximum likelihood tree using 709 full genome SARS-CoV-2 sequences deposited to GISAID between 26 May and 15 June, 2020. The monophyletic clade of the genomes directly obtained from the patient samples is shown in cyan.

Droplets and Aerosols generated by singing and the risk of COVID-19 for choirs.

Prateek Bahl^a, Charitha de Silva^a, Shovon Bhattacharjee^b, Haley Stone^c, Con Doolan^a, Abrar Ahmad Chughtai^c, C Raina MacIntyre^b

^a School of Mechanical and Manufacturing Engineering, UNSW Sydney, NSW 2052, Australia

^b The Kirby Institute, UNSW Sydney, NSW 2052, Australia

^c School of Public Health and Community Medicine, UNSW Sydney, NSW 2052, Australia

Corresponding Author

Prateek Bahl

School of Mechanical and Manufacturing Engineering,

UNSW Sydney, NSW 2052, Australia

Email: prateek.bahl@protonmail.com

Abstract

Choral singing has become a major risk during COVID-19 pandemic due to high infection rates. Our visualisation and velocimetry results reveal that majority of droplets expelled during singing follow the ambient airflow pattern. These results points toward the possibility of COVID-19 spread by small airborne droplets during singing.

Background

Singing in group settings has become an apparent risk for outbreaks of COVID-19 [1]. While social distancing is effective in normal social interactions, singing can produce a substantially larger number of respiratory droplets and aerosols than speaking, as it is louder and sustained for longer durations [2]. This may require further measures to be put into place to mitigate risks. In contained smaller spaces, the transmission risk may be higher, as respiratory aerosols may saturate the whole indoor environment [3]. Despite this, at present there is not a collective approach or response to the potential risks of group singing. Certain countries, including Germany and the Netherlands, have banned all group singing activities [4].

Choir-related outbreaks of COVID-19 in Berlin, Amsterdam, and Washington State had high attack rates of 75.6%, 78.5% and 86.9% respectively [1,4,5]. Since restrictions have eased globally, a rise in outbreaks related to singing has been reported [6]. A large proportion of these documented outbreaks associated with singing (approx. 69%), were reported from the United States resulting in over 544 cases [1].

COVID-19 is assumed to be transmitted through respiratory and contact routes; and transmission by respiratory droplets is believed to occur only in close contact (within 1-2 m) with someone who is infectious [7]. However, there is uncertainty about the dynamics of respiratory emissions during singing. Additionally, studies have shown that droplet and airborne transmission may not be mutually exclusive modes of transmission and exist as a continuum [8]. Hence, unravelling the spread of respiratory particles during singing, especially in closed environments, could inform infection control policy and practice.

Methods

To quantify and understand the spread of infection during singing we performed a detailed flow visualization of aerosols and droplets expelled during singing using an image-based flow diagnostic system. The visualisation technique employs a LED based light source (GS Vitec MultiLED PT) with a spherical lens to control the divergence of the light beam, along with a high-speed camera (nac MEMRECAM HX-7s) to capture the light scattered by the droplets expelled during singing. To capture the video, the head of the subject was adjusted in front of black backdrop/background and the light was positioned in a forward scatter arrangement to maximize the scattering from expelled droplets (Figure 1).

Once the position is adjusted, the subject was asked to sing a major scale using the solfège system and the high-speed video was captured with an exposure of 600 μ s per frame at a resolution of 2 Megapixels. In addition to singing, the subject also counted from 1 to 10 and coughed voluntarily. The horizontal field of view captured in the high-speed video, from the mouth of the subject, was 26 cm approximately. Frames obtained from the video were first calibrated and a 2-axis stabilisation was applied to subject's head (Further details on this procedure can be found in [9]). Thereafter, all the frames were processed with a hybrid Particle Tracking Velocimetry technique [10]. This technique first performs a Particle Image Velocimetry (PIV) procedure to estimate flow velocity and these estimates are subsequently refined using a particle tracking algorithm applied to each droplet. Specifically, for the PIV step we used a variable interrogation window with an initial size of 96×96 pixels and a final size of 48×48 pixels with an overlap of 75%. For particle tracking we used a correlation window of 64 pixels and particle size range of 2 to 100 pixels in order to cover the entire size range of visible droplets. The flow visualisation together with detailed particle tracking results are included in supplementary video.

Results and Discussion

The results of detailed particle tracking (in supplementary video) reveals that the maximum velocity of droplets expelled, specifically for certain syllables such as ‘do’, ‘fa’ and ‘ti’, is approx. 6 m/s, which is similar to the velocities reported for speaking [11]. Upon further examining the motion of droplets at a distance of 15 cm from the mouth, we observed that almost 90% of the droplets are moving at velocities less than 1 m/s (Figure 2a). The droplets moving with velocities greater than 1 m/s are moving in the direction between $120^\circ - 240^\circ$ ($\theta = 0^\circ$ towards subject (Figure 1)) and move away from the mouth. Moreover, approx. 75% of droplets observed are moving at velocities less than 0.5 m/s and the motion is equally distributed in all the directions, which implies that they do not settle rapidly and may follow the ambient airflow pattern. These results points toward high aerosol generation, as the behaviour of these droplets is like airborne particles [12]. Nevertheless, to accurately quantify the size, future work using particle counters, is essential to better understand the dynamics of these droplets.

Figure 2b shows the distribution of droplet velocities obtained at 15 cm from the mouth for syllable ‘fa’ and the direction in which these droplets are moving. Approximately 50% of the droplets are moving at velocities less than 0.5 m/s and more than 75% are moving away from mouth ($\theta = 120^\circ$ to 240°), which is also evident in the supplementary video. Figure 2c shows the velocity distribution of droplets that are visible while the subject was singing syllable ‘sol’ & ‘la’ and the direction in which these droplets are moving. It can be observed that all droplets are moving at velocities less than 0.5 m/s and are equally distributed in all directions. The direction in which these droplets are moving is important because it implies that for a normal choir configuration with multiple rows and heights, these droplets can pose a risk to those in the adjacent rows as well as to those in the distant rows.

Figure 2d and 2e shows the distribution for counting and coughing, respectively. In the case of coughing approximately 50% of the detected droplets were moving at velocities greater than 6 m/s whereas in case of speaking only 15% were moving at velocities greater than 6 m/s.

We note, the loudness measured during singing was within the range of 66 – 72 decibels. Further, it is also worth noting that some degree of variability is expected in the number of droplets expelled between different individuals, and due to other parameters, such as loudness, notes, consonants, and duration of each note sung. Nevertheless, the droplets observed do not appear to be settling down rapidly and without adequate ventilation, these droplets can potentially saturate the indoor environment which can likely explain the very high attack rates of COVID-19 seen in choirs in the US and Europe (almost 87% in Skagit County, Washington) [1].

We note the present study only provides visual evidence of the droplets and aerosols expelled during singing and compare the associated velocities and directions with speaking and coughing. However, these droplets have the capacity to potentially transmit viruses such as SARS-CoV-2. We only used a basic major scale for our experiments and during singing various other factors comes into play, such as pitch, rhythm, diction, etc. and it would be valuable to investigate all these aspects for future studies to have a better understanding of droplet and aerosol generation while singing. Nonetheless, the data presented combined with high infection rate among the choir members (60 – 90%) [1] points towards the possibility of airborne spread of COVID-19 during singing events, hence, should be considered when designing safety guidelines for public singing events.

These findings could inform safety guidelines for restarting choirs during and after the COVID-19 pandemic and other similar respiratory infection outbreaks. For example, rehearsals could be done with fewer people, greater physical distancing between singers, or face coverings and masks to reduce droplet and aerosol expulsion [13]. In addition to that either well ventilated large spaces or outdoor performances should be utilised to minimize the risk of infection.

Acknowledgements**Funding**

This research was supported by NHMRC Centre for Research Excellence (Grant Number 1107393), Integrated Systems for Epidemic Response. C. R. MacIntyre is supported by a NHMRC Principal Research Fellowship, grant number 1137582.

None of the authors has any potential conflicts to disclose.

References

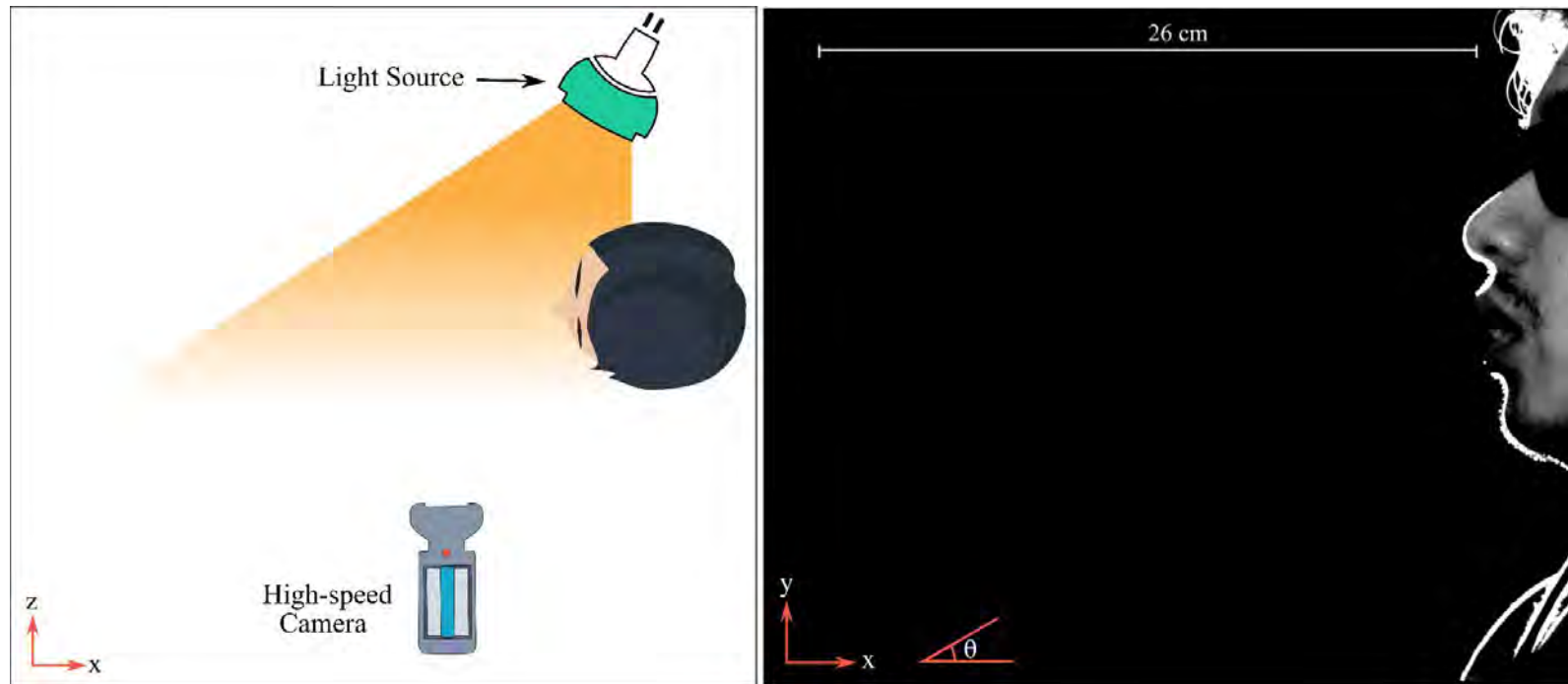
1. Hamner L, Dubbel P, Capron I, et al. High SARS-CoV-2 Attack Rate Following Exposure at a Choir Practice — Skagit County, Washington, March 2020. *MMWR* **2020**; 69:606–610.
2. Asadi S, Wexler AS, Cappa CD, Barreda S, Bouvier NM, Ristenpart WD. Aerosol emission and superemission during human speech increase with voice loudness. *Sci Rep* **2019**; 9.
3. Morawska L, Afshari A, Bae GN, et al. Indoor aerosols: from personal exposure to risk assessment. *Indoor Air* **2013**; 23:462–487. Available at: <http://doi.wiley.com/10.1111/ina.12044>.
4. Colborne F. German choirs silenced as singing branded virus risk. 2020. Available at: <https://au.news.yahoo.com/german-choirs-silenced-singing-branded-virus-risk-025930646--spt.html%0D>. Accessed 25 June 2020.
5. Lebrecht N. Concertgebouw chorus is devastated after pre-Covid Bach Passion. 2020. Available at: <https://slippedisc.com/2020/05/concertgebouw-chorus-is-devastated-after-pre-covid-bach-passion/>. Accessed 25 June 2020.
6. Porterfield C. Church-Related Coronavirus Outbreaks Reported As Trump Pushes For Reopening. 2020. Available at: <https://www.forbes.com/sites/carlieporterfield/2020/05/23/church-related-coronavirus-outbreaks-reported-as-trump-pushes-for-reopening/>. Accessed 20 June 2020.
7. WHO. Modes of transmission of virus causing COVID-19 : implications for IPC precaution recommendations. *Sci Br* **2020**; :1–3.
8. Bahl P, Doolan C, de Silva C, Chughtai AA, Bourouiba L, MacIntyre CR. Airborne or Droplet Precautions for Health Workers Treating Coronavirus Disease 2019? *J Infect Dis* **2020**; Available at: <https://academic.oup.com/jid/advance-article/doi/10.1093/infdis/jiaa189/5820886>.
9. Bahl P, de Silva CM, Chughtai AA, MacIntyre CR, Doolan C. An experimental framework to capture the flow dynamics of droplets expelled by a sneeze. *Exp Fluids* **2020**; 61:176. Available at: <http://link.springer.com/10.1007/s00348-020-03008-3>.
10. Cowen EA, Monismith SG, Cowen EA, Monismith SG. A hybrid digital particle tracking velocimetry technique. *Exp Fluids* **1997**; 22:199–211. Available at: <http://link.springer.com/10.1007/s003480050038>.
11. Chao CYH, Wan MP, Morawska L, et al. Characterization of expiration air jets and droplet size distributions immediately at the mouth opening. *J Aerosol Sci* **2009**; 40:122–133.
12. Hinds WC. *Aerosol technology: properties, behavior, and measurement of airborne particles*. John Wiley & Sons, 2012.
13. Bahl P, Bhattacharjee S, de Silva C, Chughtai AA, Doolan C, MacIntyre CR. Face coverings and mask to minimise droplet dispersion and aerosolisation: a video case study. *Thorax* **2020**; :thoraxjnl-2020-215748. Available at: <http://thorax.bmj.com/lookup/doi/10.1136/thoraxjnl-2020-215748>.

Figure Legends:

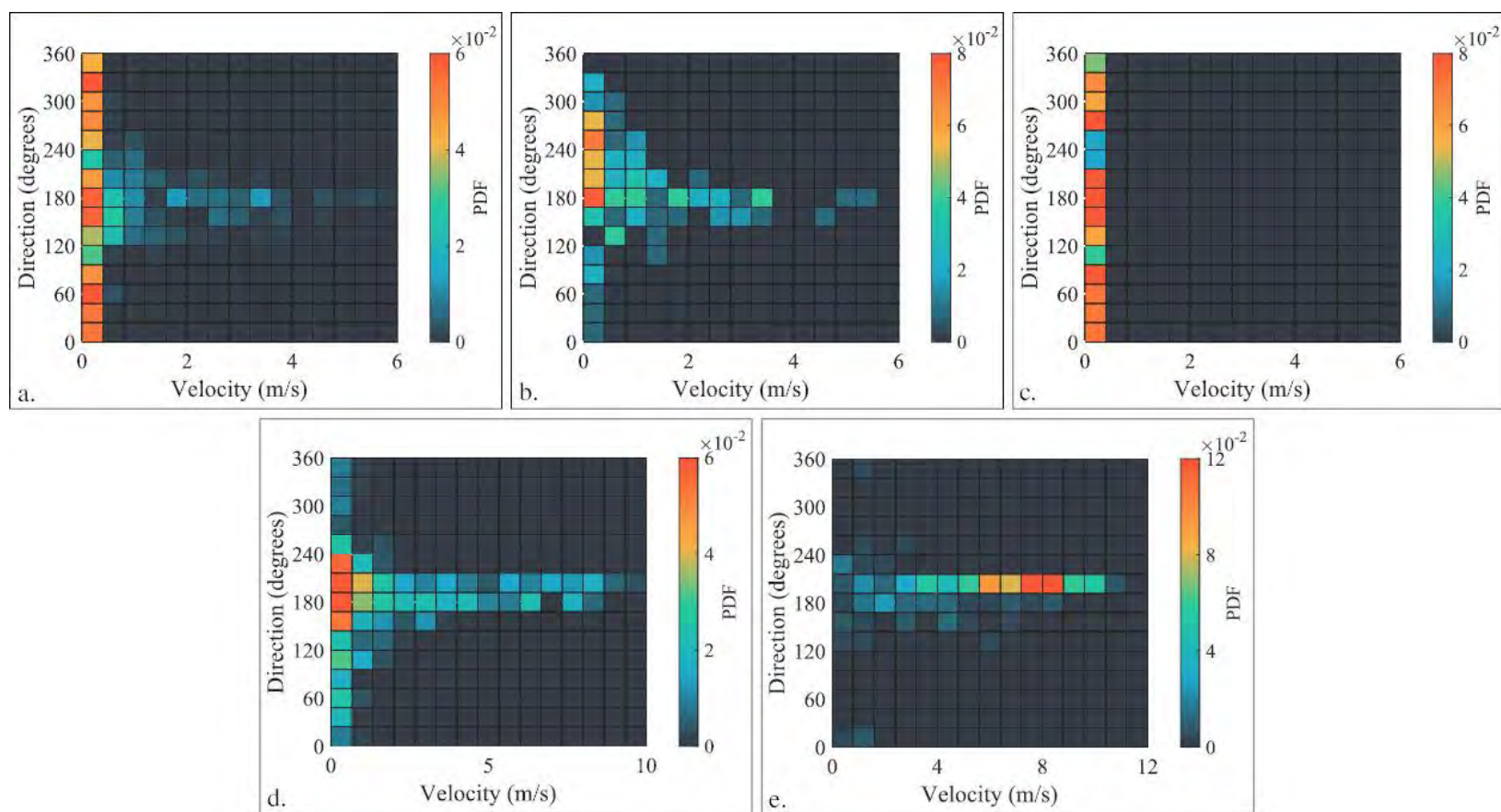
Figure 1: *Schematic of the setup to capture the droplets expelled during singing.*

Figure 2: *a. – Probability density function (PDF) of droplet velocities and direction of droplets measured at 15 cm from the mouth of the subject while singing a full major scale. b. – PDF of droplet velocities and direction of droplets measured at 15 cm from the mouth of the subject while singing syllable 'fa'. c. – PDF of droplet velocities and direction of droplets measured at 15 cm from the mouth of the subject while singing syllables 'sol' and 'la'. d. – PDF of droplet velocities and direction of droplets measured at 15 cm from the mouth of the subject while counting from 1 to 10. e. –PDF of droplet velocities and direction of droplets measured at 15 cm from the mouth of the subject while coughing.*

Figure_1



Figure_2



ARTICLE


<https://doi.org/10.1038/s41467-021-23733-5>

OPEN

Insights into household transmission of SARS-CoV-2 from a population-based serological survey

Qifang Bi¹, Justin Lessler^{1,2,4}, Isabella Eckerle^{2,3}, Stephen A. Lauer¹, Laurent Kaiser^{2,4,5}, Nicolas Vuilleumier^{5,6}, Derek A. T. Cummings^{7,8}, Antoine Flahault^{9,10,11}, Dusan Petrovic^{12,13,14}, Idris Guessous^{10,12}, Silvia Stringhini^{10,12,13}, Andrew S. Azman^{1,11,12,24}✉, SEROCO-V-POP Study Group*

Understanding the risk of infection from household- and community-exposures and the transmissibility of asymptomatic infections is critical to SARS-CoV-2 control. Limited previous evidence is based primarily on virologic testing, which disproportionately misses mild and asymptomatic infections. Serologic measures are more likely to capture all previously infected individuals. We apply household transmission models to data from a cross-sectional, household-based population serosurvey of 4,534 people ≥ 5 years from 2,267 households enrolled April-June 2020 in Geneva, Switzerland. We found that the risk of infection from exposure to a single infected household member aged ≥ 5 years (17.3%, 13.7–21.7) was more than three-times that of extra-household exposures over the first pandemic wave (5.1%, 4.5–5.8). Young children had a lower risk of infection from household members. Working-age adults had the highest extra-household infection risk. Seropositive asymptomatic household members had 69.4% lower odds (95%CrI, 31.8–88.8%) of infecting another household member compared to those reporting symptoms, accounting for 14.5% (95%CrI, 7.2–22.7%) of all household infections.

¹Department of Epidemiology, Johns Hopkins Bloomberg School of Public Health, Baltimore, MD, USA. ²Geneva Center for Emerging Viral Diseases and Laboratory of Virology, Geneva University Hospitals, Geneva, Switzerland. ³Department of Microbiology and Molecular Medicine, Faculty of Medicine, University of Geneva, Geneva, Switzerland. ⁴Division of Infectious Diseases, Geneva University Hospitals, Geneva, Switzerland. ⁵Department of Medicine, Faculty of Medicine, University of Geneva, Geneva, Switzerland. ⁶Division of Laboratory Medicine, Geneva University Hospitals, Geneva, Switzerland. ⁷Department of Biology, University of Florida, Gainesville, FL, USA. ⁸Emerging Pathogens Institute, University of Florida, Gainesville, FL, USA. ⁹Division of Tropical and Humanitarian Medicine, Geneva University Hospitals, Geneva, Switzerland. ¹⁰Department of Health and Community Medicine, Faculty of Medicine, University of Geneva, Geneva, Switzerland. ¹¹Institute of Global Health, Faculty of Medicine, University of Geneva, Geneva, Switzerland. ¹²Division of Primary Care Medicine, Geneva University Hospitals, Geneva, Switzerland. ¹³University Centre for General Medicine and Public Health, University of Lausanne, Lausanne, Switzerland. ¹⁴Centre for Environment and Health, School of Public Health, Department of Epidemiology and Biostatistics, Imperial College London, London, UK. ²⁴The authors contributed equally: Justin Lessler, Andrew S. Azman. *A list of authors and their affiliations appears at the end of the paper. ✉email: azman@jhu.edu

Household-centered studies provide an enumerable set of individuals known to be exposed to an infectious person, hence, they have played an important role for estimating key transmission properties of SARS-CoV-2. However, most published studies of SARS-CoV-2 household transmission rely on clinical disease (COVID-19), and/or PCR-based viral detection to identify infected individuals^{1,2}. Due to the narrow time window after exposure in which RT-PCR can be highly sensitive³, case ascertainment based on virologic testing may miss infections, especially those that are mild or asymptomatic⁴. This can lead to important biases and limit what can be studied, including underestimates of the importance of sub-clinical infections and household secondary attack rates⁴.

Serologic studies provide an alternative tool for understanding SARS-CoV-2 transmission. Serological tests remain sensitive to detecting past infections well beyond the period when the virus is detectable^{5–7}, thereby providing a measure of whether individuals have ever been infected.

Virologic and serologic studies have each provided important insights into SARS-CoV-2 transmission. These include estimates of the household secondary attack rate (e.g., 17% in a meta-analysis²) and evidence of reduced infection rates among young children^{2,8,9}. However, in general, these estimates do not distinguish between intra- and extra-household transmission nor do they provide an estimate of transmission risk from a single infected individual. A notable exception is a household study from Guangzhou, China¹⁰, but this PCR-based study suffered from the limitations of virologic testing noted above. Hence, a number of critical gaps in the evidence remain, including the relative role of transmission between household members, the frequency of viral introductions into households from the community, the infectiousness of asymptomatic individuals, and the effect of age on transmission.

To help fill these gaps, we apply household transmission models to data from a cross-sectional, household-based population serosurvey of 4534 people from 2267 households in Geneva, Switzerland (SEROCoV-POP). We provide a serology-based assessment of transmission between intra- and extra-household contacts, identify risk factors for infection and transmission and estimate the relative risk of asymptomatic transmission. By doing so, we provide important evidence for guiding the COVID-19 pandemic response.

Results

Between April 3rd and June 30th, during the first wave of the SARS-CoV-2 pandemic in Geneva, 8344 individuals coming from 4393 households were successfully enrolled in the SEROCov-POP study (Figs. 1 and S1)¹¹. The median enrollment date was May 22nd, 86 days after the first case was detected in Geneva (February 26th, 2020). In 2267 of these households, all members of the household were eligible, available, and provided a blood sample for detection of anti-SARS-CoV-2 IgG antibodies by ELISA (4354 individuals). The majority of these households were either one (37.9%, $n=860$) or two (39.2%, $n=889$) person households (Fig. S2, Table S1). The median household size in our study (2.0, interquartile range [IQR]=1,2) was similar to the general population in Geneva canton (median=2.0, IQR=1,3)¹².

The median age of participants was 53 years (IQR=34,65), and 53.6% were female. Compared with the general canton population, our study sample included more individuals 50 years and older and fewer 20–49 year olds. Individuals in older age groups were more likely to live in smaller households: 94.6% (1100/1163) of people who were 65 years and older lived alone or in two-person households versus 44.5% (588/1302) of those 20–49 years old (Table 1). Our study sample, like that of the original

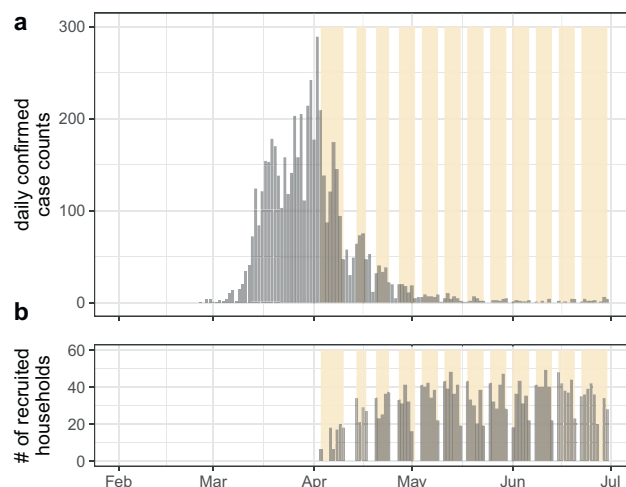


Fig. 1 Epidemic curve and recruitment period of household serosurvey.

a daily confirmed COVID-19 cases reported in Geneva up to July 1st, 2020. **b** Daily number of recruited households over the 12-week study period. First detected case in Geneva canton was reported on February 26th, and the first epidemic wave lasted about two months. Yellow bands indicate time periods of study enrollment for each week. This includes all 4438 households enrolled in the SEROCov-POP study, not restricted to the complete households used in these analyses for which serostatus of all household members were available.

SEROCoV-POP study, had a higher level of formal education than the general canton population with only 8.5% not having a high school degree or equivalent, compared with 23.5% in the general canton population (Table S5)¹³.

Overall, 6.6% (298/4534) of individuals tested positive for SARS-CoV-2 anti-S1 IgG antibodies by ELISA. Of the 2267 households included in the analyses, 222 (9.8%) had at least one seropositive household member. The proportion of households with seropositive members increased from 4.8% (41/860) in households of size one, to 17.0% (39/229) in households of size three, and was relatively constant in larger households (Fig. S2, Table 1, Fig. S3). Symptoms consistent with COVID-19 were reported by 69.5% (207/298) of seropositive individuals although this was significantly lower in young children (37.5%, 3/8), similar to the results of an early modeling study¹⁴.

We fit household transmission models and estimated that from the start of the epidemic in Geneva through the time of the serosurvey, the cumulative risk of infection from extra-household exposures was 5.1% (95% Credible Interval [CrI] 4.5–5.8%). The probability of being infected from a single infected household member was 17.3% (95% CrI 13.7–21.7%, Fig. 2).

The risk of being infected by a household member was the lowest among 5–9 years old and highest among those 65 years and older, with teenagers and working age adults sharing similar risks (Figs. 2, 3). Compared to 20–49 years olds, 5–9 years olds had less than half the odds of being infected by an infected household member (OR=0.4, 95%CrI 0.1–1.6), while those 65 years and older had nearly three times the odds (OR=2.7, 95%CrI 0.9–7.9). Though credible intervals on these estimates are wide, and both include the null value of 1, inclusion of age substantially improved model fit (Δ WAIC =14.8, Table S2). In contrast, the extra-household infection risk was the highest among working age adults (20–49 years olds). Compared to this group, 5–9 year olds (OR=0.5, 95%CrI 0.2–0.9) and those 65 years and older (OR=0.4, 95%CrI 0.3–0.6) had the lowest risk (Fig. 3, Tables S2 and S4). Models allowing for differential risk of transmission by

Table 1 Number of recruited and seropositive individuals by age-group, sex and household size of the households they reside in.

	HH Size 1 sero +/N % (95% CI)	HH Size 2 sero +/N % (95% CI)	HH Size 3 sero +/N % (95% CI)	HH Size 4 sero +/N % (95% CI)	HH Size 5 +sero+/N % (95% CI)	Overall sero +/N % (95% CI)	Odds ratio for being seropositive
HOUSEHOLDS							
0 seropositive	819/860 95% (94–96)	807/889 91% (89–93)	190/229 83% (78–87)	188/239 79% (73–83)	41/50 82% (69–90)	2045/2267 90% (89–91)	–
1 seropositive	41/860 5% (4–6)	52/889 6% (4–8)	29/229 13% (9–18)	38/230 16% (12–21)	5/50 10% (4–21)	165/2267 7% (6–8)	–
Over 1 seropositive	–	30/889 3% (2–5)	10/229 4% (2–8)	13/239 5% (3–9)	4/50 8% (3–19)	57/2267 3% (2–3)	–
INDIVIDUALS							
Age							
5–9	–	0/6 0% (0–39)	1/38 3% (0–13)	5/97 5% (2–12)	2/26 8% (2–24)	8/167 5% (2–9)	0.5 (0.2–1.0)
10–19	–	2/21 10% (3–29)	8/99 8% (4–15)	14/248 6% (3–9)	7/91 8% (4–15)	31/459 7% (5–9)	0.7 (0.5–1.1)
20–49	14/227 6% (4–10)	39/361 11% (8–14)	23/249 9% (6–13)	36/375 10% (7–13)	7/90 8% (4–15)	119/1302 9% (8–11)	Ref
50–64	17/316 5% (3–8)	38/607 6% (5–8)	18/253 7% (5–11)	22/224 10% (7–14)	1/43 2% (0–12)	96/1443 7% (5–8)	0.7 (0.5–0.9)
65+	10/317 3% (2–6)	33/783 4% (3–6)	1/48 2% (0–11)	0/12 0% (0–24)	0/3 0% (0–56)	44/1163 4% (3–5)	0.4 (0.3–0.6)
Sex							
Female	28/558 5% (3–7)	40/900 4% (3–6)	27/364 7% (5–11)	34/475 7% (5–10)	8/135 6% (3–11)	137/2432 6% (5–7)	Ref
Male	13/302 4% (3–7)	72/878 8% (7–10)	24/323 7% (5–11)	43/481 9% (7–12)	9/118 8% (4–14)	161/2102 8% (7–9)	1.4 (1.1–1.8)
Self-reported symptom							
Asymptomatic or seronegative	7/602 1% (1–2)	36/1277 3% (2–4)	19/449 4% (3–7)	24/643 4% (3–5)	5/176 3% (1–6)	91/3147 3% (2–4)	Ref
Symptomatic	34/258 13% (10–18)	76/501 15% (12–19)	32/238 13% (10–18)	53/313 17% (13–21)	12/77 15% (9–25)	207/1387 15% (13–17)	5.9 (4.6–7.6)
Reduced contact^a							
No	8/71 11% (6–21)	1/70 1% (0–8)	5/37 14% (6–28)	3/39 8% (3–20)	0/7 0% (0–35)	17/224 8% (5–12)	–
Yes	33/788 4% (3–6)	107/1672 6% (5–8)	40/569 7% (5–9)	63/707 9% (7–11)	11/178 6% (3–11)	254/3914 6% (6–7)	0.8 (0.5–1.5)
Missing Response	0/1 0% (0–95)	4/36 11% (4–25)	6/81 7% (3–15)	11/210 5% (3–9)	6/68 9% (4–18)	27/396 7% (5–10)	–
Number of extra-HH contacts/week^b							
0	3/64 5% (2–13)	14/188 7% (4–12)	7/72 10% (5–19)	5/88 6% (2–13)	1/12 8% (0–35)	30/424 7% (5–10)	0.9 (0.6–1.4)
1–2	10/207 5% (3–9)	26/375 7% (5–10)	7/134 5% (3–10)	15/180 8% (5–13)	2/49 4% (1–14)	60/945 6% (5–8)	0.8 (0.5–1.2)
3–5	12/283 4% (2–7)	32/563 6% (4–8)	7/158 4% (2–9)	12/152 8% (5–13)	3/47 6% (2–17)	66/1203 5% (4–7)	Ref
6–10	10/115 9% (5–15)	22/266 8% (6–12)	8/86 9% (5–17)	12/132 9% (5–15)	1/26 4% (0–10)	53/625 8% (7–11)	1.2 (0.8–2.0)
Over 10	6/190 3% (1–7)	14/350 4% (2–7)	16/156 10% (6–16)	22/194 11% (8–17)	4/51 8% (3–18)	62/941 7% (5–8)	0.9 (0.6–1.5)
Missing Response	0/1 0% (0–95)	4/36 11% (4–25)	6/81 7% (3–15)	11/210 5% (3–9)	6/68 9% (4–18)	27/396 7% (5–8)	–
Overall	41/860 5% (4–6)	112/1778 6% (5–8)	51/687 7% (6–10)	77/956 8% (6–10)	17/253 7% (4–10)	298/4534 7% (6–7)	–

^aA self-assessment of whether the participants have reduced the number of people they meet since the start of the epidemic.^bAverage number of people participants meet outside of the people they lived with since the start of the epidemic.

the age of the infector were not well supported by the data (Δ WAIC –15.5 to –24.7) and included no significant differences between ages (Table S2).

Males were more likely to be infected outside (OR=1.4, 95% CrI 1.0–2.0), and possibly inside the household (OR=1.4, 95% CrI 0.6–3.1), though the latter estimate is less strongly supported by the data (Fig. 3 and Table S2).

Seropositive household members not reporting symptoms had 0.31 times the odds (95%CrI: 0.11–0.68) of infecting another household member compared to those reporting symptoms consistent with COVID-19 (Fig. 3). This difference was larger (OR=0.24, 95%CrI 0.09–0.54) when only considering those who reported symptoms more than two weeks before blood draw as symptomatic infections (Table S6, Fig. S6).

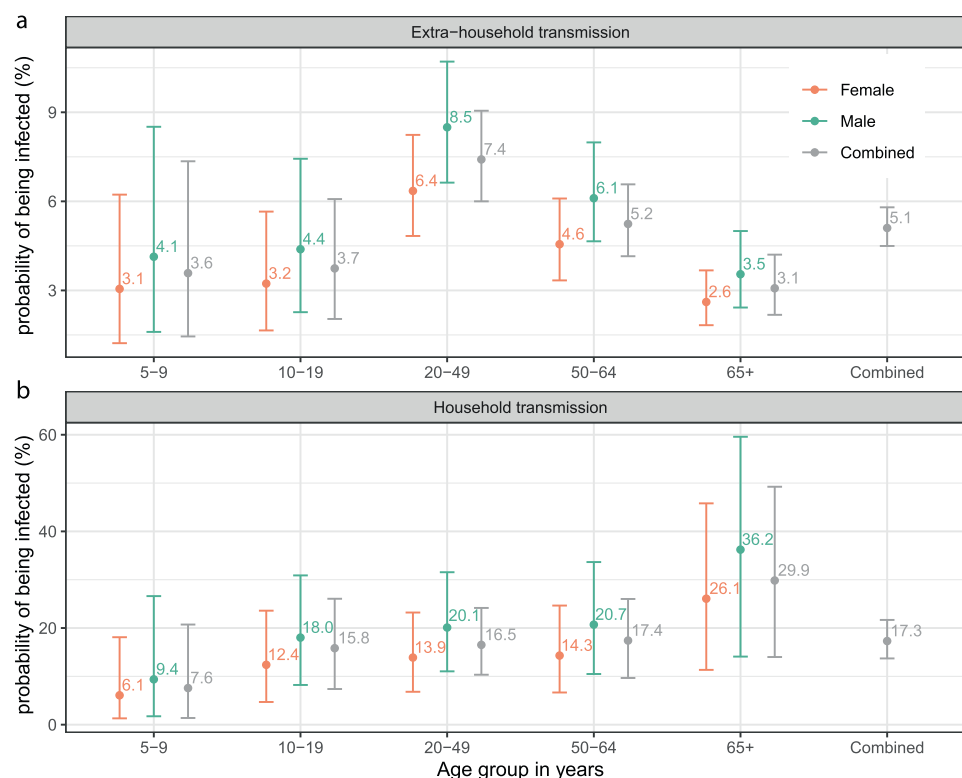


Fig. 2 Risk of extra-household transmission and within-household transmission from a single infected household member. a Estimated median probability of extra-household infection from the start of the epidemic in Geneva until the time of the serosurvey by age group and sex. **b** Estimated median probability of infection from a single infected household member by age group and sex. Dots and bars represent median and 95% credible intervals of the posterior distribution. Probabilities of being infected by sex and age group of the exposed individuals are estimated by a model only including age and sex of the exposed individuals (model 2, orange/green bars; see Table S2). Probabilities of being infected by the age group of the exposed individuals combining males and females (left four gray bars on both panels) are estimated with an age-only model (model 1). The overall probabilities of being infected (rightmost gray bar on both panels) are estimated with the null model (model 0).

Using posterior distributions of parameters, we simulated the source of infection for all individuals in the study. We estimate that 22.5% (95%CrI 20.1–24.2) of all infections were caused by another household member, with the proportion of infections attributable to household transmission increasing with household size (Table S3, Figs. S8 and S9). A larger proportion of infections were attributable to household transmission for those recruited after mid-May (last 6 weeks of the study, 27.8, 95%CrI 22.8–30.4) compared to those recruited in the first six weeks of the study (first 6 weeks: 20.5, 95%CrI 17.8, 22.4). In households with two individuals, 23.2% (95%CrI 19.6–25.9) of infections were between household members, increasing to 41.2% (95%CrI 29.4–47.1) in households of five people (Table S3). Of within-household infections, we estimate 14.5% (95%CrI 7.2–22.7) were due to individuals not reporting symptoms consistent with COVID-19.

Here we focus on the results of the best fitting models, but across the ten models considered (Table S2), estimates were qualitatively and quantitatively consistent with the primary findings. Similarly, we explored the sensitivity of our results to the ELISA seropositivity cutoff and found no qualitative differences in results (Fig. S4).

Discussion

The results presented here appropriately place symptomatic household transmission of SARS-CoV-2 in the context of community risk and asymptomatic spread. We show an approximate 1 in 6 risk (17.3%) of being infected by a single SARS-CoV-2 infected household member (Table S3). This contrasts with a 1 in 20 chance (5.1%) of being infected in the community over most of

the first epidemic wave in Geneva, a period of roughly 2 months. Despite the high risk of transmission from an infected household member, as in many cities in high-income nations, households are mostly small limiting opportunities for onward transmission. Thus, less than a quarter of cases could be attributed to transmission between household members. While asymptomatic individuals appear to be less than a third as likely to transmit, they cannot be dismissed as inconsequential to disease spread, and are responsible for one in six within-household transmissions in this study. Our results are suggestive of the dual roles of biology and social behavior in shaping age-specific infection patterns, with the age signature of risk within households indicative of lower biological susceptibility in the very young, and elevated susceptibility in the old; while extra-household risk seems more driven by behavior, with working age adults being at the highest risk.

It has long been thought that asymptomatic individuals are less likely to transmit than symptomatic ones, though studies have recovered similar concentrations of viral RNA from nasopharyngeal samples from these two groups¹⁵. By using serological data, we were able to show that those not reporting symptoms have one-third the odds of transmitting within households as symptomatic ones, similar to a study from Wuhan, China¹⁶, and ultimately caused about 15% of household infections. This reduced transmissibility may be due to reduced duration of viral shedding and reduced ability to mechanically spread virions (e.g., through coughs). We did not assess the role of asymptomatics in community spread, but it is plausible that they may play an even larger role there, as symptomatic

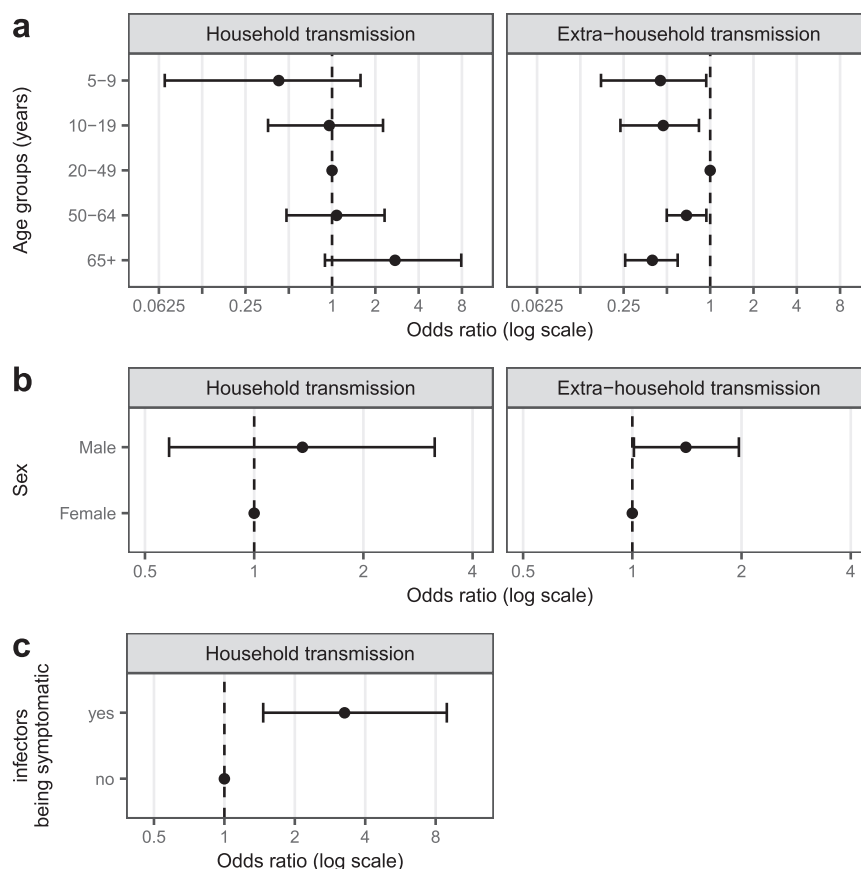


Fig. 3 Risk factors of SARS-CoV-2 infection and transmission. Relative odds of being infected outside the household and from a single infected household member by individual characteristics of the exposed individuals, **a** age group, **b** sex, and **c** potential infectors' symptom status. Odds ratios and credible intervals, shown on the log-scale, are estimates from model 4 (see Table S2).

individuals are more likely to stay home or take extra precautions to reduce exposures when sick.

As with previous studies of SARS-CoV-2 transmission among household members and other close contacts^{2,17,18}, we find evidence supporting a reduced risk of infection from household exposures among young children, and elevated risk of infection among those 65 or older. However, it is important to note that we only find this reduced risk among the youngest children in our study (5–9-year-olds), while 10–19 year olds have a similar risk profile to working age adults. The other PCR-based household study that reported per-exposure transmission did not report susceptibility results from this age group¹⁰. This is consistent with the hypothesis that young children may be biologically less susceptible to SARS-CoV-2 infection, though heterogeneity in social contact and other behaviors within households cannot be ruled out.

Patterns of extra-household infection suggest social factors dominate this risk, as both young children and older adults are at reduced risk of infection compared to working age adults. As children have returned to schools in Geneva (mid-May 2020), the social factors driving this pattern have likely changed significantly and we may see children become a more significant source of extra-household infections¹⁹, despite their apparently lower susceptibility. The risk that infected young children pose to their household members is unclear; the sample size was likely too low to detect small to moderate differences in risk. While there are mixed results in the literature on age-specific differences in infectiousness²⁰, a large study from Wuhan, China suggested that those less than 20 years old are more likely to infect others than adults 60 years and older, given the same amount of exposure¹⁶.

We did not find any significant relationship between the age of an infector and probability of transmission (nor did including these terms improve model fit), but children are less often symptomatic²¹ and we did find a strong relationship between symptoms and transmission.

Our study has a number of important limitations. Symptoms were self-reported and, given that the times of infection are unknown, they may not necessarily have been a result of the SARS-CoV-2 infection. We cannot exclude recall bias in symptom reports and other self-reported exposures. Further, we looked at only a narrow range of symptoms to increase specificity, which left out more general potentially SARS-CoV-2-related symptoms (e.g., nausea, diarrhea). We detected only eight seropositive children under the age of 10, leading to large uncertainty in age-specific risk estimates for this group. Although extra-household estimates are informed by data from all households, within-household estimates are only informed by data from households with at least one seropositive member (222/2267 households), thus limiting our statistical power. While validation data of the Euroimmun ELISA from across the world have confirmed its high specificity and sensitivity for detecting recent infections^{22–24}, most data are from adults, and it is possible that performance in young children may be different. Most of the participants in the study were recruited after the epidemic peak and it is possible that we did not fully capture all infections in each household due to insufficient time to mount a detectable response. Conversely, we may have also missed infections due to waning of responses. However, antibody responses appear to generally sustain over the first 4 months from infection, the plausible infection time window of participants in this study²⁵. When conducting stratified

analyses including households recruited early and late, we found few qualitative differences in the primary results (Figs. S5 and S7). We included only households where all household members provided blood samples in the main analysis, but sensitivity analyses of all enrolled individuals led to similar primary results (Table S6). Given the cross-sectional nature of our data, all transmission chains within households were equally likely within our modeling framework, which led to larger uncertainty than having prospectively collected data. However, collection of these data over thousands of households can be challenging, and we show that more commonly collected data from serosurveys can be leveraged to refine our understanding of transmission.

This study captures infections that occurred during the first wave of the pandemic in Geneva, a period of time when workplaces and schools were largely closed and peoples' social contacts were greatly reduced. In future phases of this pandemic, when social contact patterns change the proportion of transmission that occurs between household members and potentially age-sex specific risks could differ. While we found no evidence in previous analyses of these data for differences in seropositivity by neighborhood wealth or education²⁶, these and other indicators of wealth might be associated with transmission risk within Geneva or in other populations. Likewise, the general nature of the Geneva population and the control measures in place may limit the generalizability of our estimates of absolute risk of infection, attributable fraction, and extra-household risks. For example, the increasing importance of household transmission with increasing household size (Fig. S8) suggests household transmission would be far more important in settings with larger households. However, we believe our estimates of relative risks by age and symptom status within households, which are likely more biologically driven, should be generalizable to most settings; as should our general observations about how social and biological factors influence different types of transmission.

Our study highlights how biological and social factors might combine to shape the risk of SARS-CoV-2 infection. While we expect some differences across settings, we believe that the general trend in per-exposure infection risk by age and sex and increased infectiousness of symptomatic individuals are fundamental attributes of this pandemic. These differences have important implications for guiding patient care and public health policy. For example, increased susceptibility of the oldest individuals suggests that rapid and aggressive measures are needed to protect them as soon as there is any possibility that SARS-CoV-2 was introduced into their living environment. At the population level, quantifying the infectiousness of asymptomatics can help us understand the extent the pandemic is driven by asymptomatic infections. Our study provides a model for using cross-sectional serologic surveys to assess the relative contribution of household and community transmission. As countries continue to alter quarantine and self-isolation policies, disentangling the contribution of household and community transmission can help evaluate success of these intervention strategies. Continued serological and virologic monitoring of diverse populations with detailed analyses like those presented here are critical to the continued evidence-based response to this pandemic.

Methods

Study design, participants, and procedures. The SEROCov-POP study is a cross-sectional population-based survey of former participants of an annual survey of individuals 20–74 years old representative of the population of Geneva (Canton), Switzerland. The enrollment into the study occurred from April through June 2020 during the first wave of the SARS-CoV-2 pandemic in Geneva. First wave lockdown measures (including school closures) started in mid-March and largely

ended by the end of May. The full survey protocol is available online and a detailed description of the design and seroprevalence results were previously published^{11,26}.

The SEROCov-POP study invited all 10,587 participants of the previous annual surveys to participate in the study through email or post. Participants were invited to bring all members of their household aged 5 years and older to join the study. After providing informed written consent, participants either filled out a questionnaire online, in the days before their visit, or at the time of their visit at one of two enrollment locations (the main canton hospital and one satellite location) within Geneva. The questionnaire included questions about participants' demographics, household composition, symptoms since January 2020, details on the frequency of extra-household contacts and reduction in social interaction since the start of the pandemic. Only participants 14 years and older were asked about their frequency of extra-household contacts and changes in behavior. Despite this age cut off, we use more standard age cutoffs (10–19 years) in our analysis for comparability with other studies¹¹. We defined symptom presentation a priori as having reported any of: cough, fever, shortness of breath, or loss of smell or taste since January 2020 (symptoms reported in the 2-week prior to testing were excluded in a sensitivity analysis). We collected peripheral venous blood from each consenting participant. Households where all members provided blood samples were included in the present analysis (there was a 100% questionnaire response rate in this group). As blood was not collected from children under 5, all households with children in this age group were excluded. We conducted a sensitivity analysis with all households, regardless of whether all members provided blood samples, effectively treating household members outside the study as a community source of infection. All participants gave written informed consent before participation in the SEROCov-POP study. For individuals younger than 18 years, parents or a legal representative provided consent. The study was approved by the Cantonal Research Ethics Commission of Geneva, Switzerland (CER16-363).

Laboratory analysis. We assessed anti-SARS-CoV-2 IgG antibodies in each participant using an ELISA (Euroimmun; Lübeck, Germany #EI 2606-9601 G) targeting the S1 domain of the spike protein of SARS-CoV-2; sera diluted 1:101 were processed on a EuroLabWorkstation ELISA (Euroimmun). An in-house validation study found that the manufacturer's recommended cutoff for positivity (≥ 1.1) had a specificity of 99% and sensitivity of 93%, based on positive controls tested between 0 and 39 days after symptom onset²⁴. In our primary analyses we defined seropositivity based on the cutoff recommended by the manufacturer and explored a higher cut-off of 1.5 (>1.5) in sensitivity analyses²⁴. As the presence of antibodies has been shown to be a reliable marker of past infection, we use the term "infected" to refer to a seropositive individual.

Statistical analyses. We fit chain binomial transmission models to estimate two primary quantities; the average probability of extra-household infection from the start of the epidemic through the time of blood draw across Geneva (referred to also as "community infections" over the first epidemic wave) and the probability of being infected from a single infected household member over the course of his/her infectious period (referred to as "household exposures"; see supplemental text for model assumptions)^{27,28}. We assume that serologic status is a perfect marker of having been infected, that individuals cannot get reinfected, and that all individuals were susceptible at the start of the pandemic. When fitting these models we explicitly consider all possible sequences of viral introductions to each household and subsequent transmission events within the household. For example, in a household

with 2 seropositive individuals, both could have been infected outside of the household, or one could have been infected outside and then infected one other person within the household. We adapted models to estimate the within household and extra-household transmission risk according to the characteristics of potential infectees (age, sex, self-reported extra-household contact behavior) and, for within-household risk, those of the potential infectors (symptoms, age). As extra-household contact questions were only asked to those over 14 years old, we compared extra-household transmission by self-reported reduction or frequency in social contacts only for those 20 years and older. We imputed a small number of missing data (1%, 36/3908) related to extra-household contacts among those who were 20 years and older based on household averages (see supplement). We simulate the proportion of infections attributable to extra-household and within household exposures.

We built a series of ten models including different combinations of individual-level characteristics (e.g., age, sex, self-reported contacts, symptoms) and compared their fit using the widely applicable information criterion (WAIC)²⁹. We implemented the models in the Stan probabilistic programming language and used the *rstan* package (version 2.21.0) to sample from the posterior distribution and analyse outputs³⁰. We used weakly informative priors on all parameters to be normally distributed on the logit scale with mean of 0 and standard error of 1.5. We ran four chains of 1,000 iterations each with 250 warm-up iterations and assessed convergence visually and using the Gelman-Rubin Convergence Statistic (R-hat)³¹. All estimates are means of the posterior samples with the 2.5th and 97.5th percentiles of this distribution reported as the 95% credible interval. Full model and inference details are provided in the supplement and code needed to reproduce analyses are available at <https://github.com/HopkinsIDD/serocovpop-households> (<https://doi.org/10.5281/zenodo.4740044>).

Reporting summary. Further information on research design is available in the Nature Research Reporting Summary linked to this article.

Data availability

Data can be made available to share upon submission of a data request application to the investigators board via the corresponding author or S.S. (silvia.stringhini@hcuge.ch). Data needed for testing the code can be found at <https://github.com/HopkinsIDD/serocovpop-households> (<https://doi.org/10.5281/zenodo.4740044>).

Code availability

All relevant code can be found at <https://github.com/HopkinsIDD/serocovpop-households>.

Received: 10 February 2021; Accepted: 13 May 2021;

Published online: 15 June 2021

References

- Fung, H. F. et al. The household secondary attack rate of SARS-CoV-2: A rapid review. *Clin. Infect. Dis.* <https://doi.org/10.1093/cid/ciaa1558> (2020).
- Madewell, Z. J., Yang, Y., Longini, I. M. Jr, Halloran, M. E. & Dean, N. E. Household transmission of SARS-CoV-2: a systematic review and meta-analysis. *JAMA Netw. Open* **3**, e2031756 (2020).
- Kucirka, L. M., Lauer, S. A., Laeyendecker, O., Boon, D. & Lessler, J. Variation in false-negative rate of reverse transcriptase polymerase chain reaction-based SARS-CoV-2 tests by time since exposure. *Ann. Intern. Med.* <https://doi.org/10.7326/M20-1495> (2020).
- Zhang, Z. et al. Insights into the practical effectiveness of RT-PCR testing for SARS-CoV-2 from serologic data, a cohort study. *Lancet Microbe* **2**, E79–E87 (2021).
- Iyer, A. S. et al. Persistence and decay of human antibody responses to the receptor binding domain of SARS-CoV-2 spike protein in COVID-19 patients. *Sci Immunol* **5**, eabe0367 (2020).
- Rosado, J. et al. Multiplex assays for the identification of serological signatures of SARS-CoV-2 infection: an antibody-based diagnostic and machine learning study. *Lancet Microbe* [https://doi.org/10.1016/S2666-5247\(20\)30197-X](https://doi.org/10.1016/S2666-5247(20)30197-X) (2020).
- Ainsworth, M. et al. Performance characteristics of five immunoassays for SARS-CoV-2: a head-to-head benchmark comparison. *Lancet Infect. Dis.* **20**, 1390–1400 (2020).
- Li, W. et al. The characteristics of household transmission of COVID-19. *Clin. Infect. Dis.* <https://doi.org/10.1093/cid/ciaa450> (2020).
- Wang, Z., Ma, W., Zheng, X., Wu, G. & Zhang, R. Household transmission of SARS-CoV-2. *J. Infect.* **81**, 179–182 (2020).
- Jing, Q.-L. et al. Household secondary attack rate of COVID-19 and associated determinants in Guangzhou, China: a retrospective cohort study. *Lancet Infect. Dis.* [https://doi.org/10.1016/S1473-3099\(20\)30471-0](https://doi.org/10.1016/S1473-3099(20)30471-0) (2020).
- Stringhini, S. et al. Seroprevalence of anti-SARS-CoV-2 IgG antibodies in Geneva, Switzerland (SEROCoV-POP): a population-based study. *Lancet* **396**, 313–319 (2020).
- Office fédéral de la statistique. Ménages. <https://www.bfs.admin.ch/bfs/fr/home/statistiken/bevoelkerung/stand-entwicklung/haushalte.html>.
- Office fédéral de la statistique. Formation achevée la plus élevée selon le canton. <https://www.bfs.admin.ch/bfs/fr/home/statistiques/education-science/niveau-formation/niveau-formation-regional.assetdetail.15404054.html> (2021).
- Davies, N. G. et al. Age-dependent effects in the transmission and control of COVID-19 epidemics. *Nat. Med.* **26**, 1205–1211 (2020).
- Kissler, S. M. et al. Viral dynamics of SARS-CoV-2 infection and the predictive value of repeat testing. *Epidemiology*. <https://doi.org/10.1101/2020.11.20217042> (2020).
- Li, F. et al. Household transmission of SARS-CoV-2 and risk factors for susceptibility and infectivity in Wuhan: a retrospective observational study. *Lancet Infect. Dis.* [https://doi.org/10.1016/S1473-3099\(20\)30981-6](https://doi.org/10.1016/S1473-3099(20)30981-6) (2021).
- Viner, R. M. et al. Susceptibility to SARS-CoV-2 infection among children and adolescents compared with adults: a systematic review and meta-analysis. *JAMA Pediatr.* <https://doi.org/10.1001/jamapediatrics.2020.4573> (2020).
- Dattner, I. et al. The role of children in the spread of COVID-19: Using household data from Bnei Brak, Israel, to estimate the relative susceptibility and infectivity of children. *PLoS Comput. Biol.* **17**, e1008559 (2021).
- Flasche, S. & John Edmunds, W. The role of schools and school-aged children in SARS-CoV-2 transmission. *Lancet Infect. Dis.* [https://doi.org/10.1016/S1473-3099\(20\)30927-0](https://doi.org/10.1016/S1473-3099(20)30927-0) (2020).
- Goldstein, E., Lipsitch, M. & Cevik, M. On the effect of age on the transmission of SARS-CoV-2 in households, schools, and the community. *J. Infect. Dis.* **223**, 362–369 (2021).
- Salje, H. et al. Estimating the burden of SARS-CoV-2 in France. *Science* **369**, 208–211 (2020).
- Jääskeläinen, A. J. et al. Evaluation of commercial and automated SARS-CoV-2 IgG and IgA ELISAs using coronavirus disease (COVID-19) patient samples. *Euro Surveill.* **25**, 2000603 (2020).
- Weidner, L. et al. Quantification of SARS-CoV-2 antibodies with eight commercially available immunoassays. *J. Clin. Virol.* **129**, 104540 (2020).
- Meyer, B. et al. Validation of a commercially available SARS-CoV-2 serological immunoassay. *Clin. Microbiol. Infect.* <https://doi.org/10.1016/j.cmi.2020.06.024> (2020).
- Persistence and detection of anti-SARS-CoV-2 antibodies: immunoassay heterogeneity and implications for serosurveillance. Preprint at: <https://doi.org/10.1101/2021.03.16.21253710>.
- Richard, A. et al. Seroprevalence of anti-SARS-CoV-2 IgG antibodies, risk factors for infection and associated symptoms in Geneva, Switzerland: a population-based study. *medRxiv* <https://doi.org/10.1101/2020.12.16.20248180> (2020).
- Fraser, C., Cummings, D. A. T., Klinkenberg, D., Burke, D. S. & Ferguson, N. M. Influenza transmission in households during the 1918 pandemic. *Am. J. Epidemiol.* **174**, 505–514 (2011).
- Longini, I. M. Jr & Koopman, J. S. Household and community transmission parameters from final distributions of infections in households. *Biometrics* **38**, 115–126 (1982).
- Watanabe, S. & Oppen, M. Asymptotic equivalence of Bayes cross validation and widely applicable information criterion in singular learning theory. *J. Mach. Learn. Res.* **11**, 3571–3594 (2010).
- Carpenter, B. et al. Stan: A probabilistic programming language. *J. Stat. Softw.* <https://www.jstatsoft.org/article/view/v076i01> (2017).
- Gelman, A. & Rubin, D. B. Inference from iterative simulation using multiple sequences. *Stat. Sci.* **7**, 457–472 (1992).

Acknowledgements

Funding was provided by Swiss Federal Office of Public Health, Swiss School of Public Health (Corona Immunitas research program), Fondation de Bienfaisance du Groupe Pictet, Fondation Ancrage, Fondation Privée des Hôpitaux Universitaires de Genève, and Center for Emerging Viral Diseases.

JAMA Insights

Effectiveness of Mask Wearing to Control Community Spread of SARS-CoV-2

John T. Brooks, MD; Jay C. Butler, MD

Prior to the coronavirus disease 2019 (COVID-19) pandemic, the efficacy of community mask wearing to reduce the spread of respiratory infections was controversial because there were no solid relevant data to support their use. During the pandemic, the scientific evidence has increased. Compelling data now demonstrate that community mask wearing is an effective nonpharmacologic intervention to reduce the spread of this infection, especially as source control to prevent spread from infected persons, but also as protection to reduce wearers' exposure to infection.

COVID-19 spreads primarily through respiratory droplets exhaled when infected people breathe, talk, cough, sneeze, or sing. Most of these droplets are smaller than 10 μm in diameter, often referred to as *aerosols*. The amount of small droplets and particles increases with the rate and force of airflow during exhalation (eg, shouting, vigorous exercise). Exposure is greater the closer a person is to the source of exhalations. Larger droplets fall out of the air rapidly, but small droplets and the dried particles formed from them (ie, droplet nuclei) can remain suspended in the air. In circumstances with poor ventilation, typically indoor enclosed spaces where an infected person is present for an extended period, the concentrations of these small droplets and particles can build sufficiently to transmit infection.

Community mask wearing substantially reduces transmission of severe acute respiratory syndrome coronavirus 2 (SARS-CoV-2) in 2 ways. First, masks prevent infected persons from exposing others to SARS-CoV-2 by blocking exhalation of virus-containing droplets into the air (termed *source control*). This aspect of mask wearing is especially important because it is estimated that at least 50% or more of transmissions are from persons who never develop symptoms or those who are in the presymptomatic phase of COVID-19 illness.¹ In recent laboratory experiments, multilayer cloth masks were more effective than single-layer masks, blocking as much as 50% to 70% of exhaled small droplets and particles.^{2,3} In some cases, cloth masks have performed similar to surgical or procedure masks for source control. Second, masks protect uninfected wearers. Masks form a barrier to large respiratory droplets that could land on exposed mucous membranes of the eye, nose, and mouth. Masks can also partially filter out small droplets and particles from inhaled air. Multiple layers of fabric and fabrics with higher thread counts improve filtration. However, the observed effectiveness of cloth masks to protect the wearer is lower than their effectiveness for source control,³ and the filtration capacity of cloth masks can be highly dependent on design, fit, and materials used. Standards for cloth masks are needed to help consumers select marketed products.

Epidemiological investigations have helped quantify the benefit of mask wearing to prevent the spread of SARS-CoV-2 (Table; Supplement). At a hair salon in which all staff and clients were required to wear a mask under local ordinance and company policy, 2 symptomatic, infected stylists attended to 139 clients and no infections were observed in the 67 clients who were reached for interviewing and testing. During a COVID-19 outbreak on the USS Theodore Roosevelt,

persons who wore masks experienced a 70% lower risk of testing positive for SARS-CoV-2 infection.⁴ Similar reductions have been reported in case contact investigations when contacts were masked⁵ and in household clusters in which household members were masked.⁶

An increasing number of ecological studies have also provided persuasive evidence that universal mandatory mask wearing policies have been associated with reductions in the number or rate of infections and deaths (Table). These studies did not distinguish the types of masks (cloth, surgical, or N95) used in the community. This association is strengthened because, in many cases, other mitigation strategies (eg, school and workplace closures, recommendations for social distancing, hand hygiene) had already been deployed before enactment of mask wearing policies, after which the reductions were observed. A study that examined changes in growth rates for infections in 15 states and the District of Columbia before and after mask mandates showed that rates were growing before the mandates were enacted and slowed significantly after, with greater benefit the longer the mandates had been in place.⁷

Wearing a mask can become uncomfortable, particularly for long periods in warm environments, and covering the nose and mouth may inhibit verbal and nonverbal communication, particularly for children and deaf individuals. However, children aged 7 to 13 years have been shown to be able to make accurate inferences about the emotions of others with partially covered faces,⁸ and the US Food and Drug Administration recently approved a transparent surgical mask that may be useful in such circumstances. Concerns about reduced oxygen saturation and carbon dioxide retention when wearing a mask have not been supported by available data.⁹

The overall community benefit of wearing masks derives from their combined ability to limit both exhalation and inhalation of infectious virus. Similar to the principle of herd immunity for vaccination, the greater the extent to which the intervention—mask wearing in this case—is adopted by the community, the larger the benefit to each individual member. The prevalence of mask use in the community may be of greater importance than the type of mask worn. It merits noting that a recent study has been improperly characterized by some sources as showing that cloth or surgical masks offer no benefit. This randomized trial in Denmark was designed to detect at least a 50% reduction in risk for persons wearing surgical masks. Findings were inconclusive,¹⁰ most likely because the actual reduction in exposure these masks provided for the wearer was lower. More importantly, the study was far too small (ie, enrolled about 0.1% of the population) to assess the community benefit achieved when wearer protection is combined with reduced source transmission from mask wearers to others.

During past national crises, persons in the US have willingly united and endured temporary sacrifices for the common good. Recovery of the nation from the COVID-19 pandemic requires the combined efforts of families, friends, and neighbors working together in unified public health action. When masks are worn and combined with other recommended mitigation measures, they protect not only the wearer but also the greater community. Recommendations for masks will likely

 [Multimedia](#)

 [Supplemental content](#)

Table. Studies of the Effect of Mask Wearing on SARS-CoV-2 Infection Risk^a

Source	Location	Population studied	Intervention	Outcome
Hendrix et al	Hair salon in Springfield, Missouri	139 Patrons at a salon with 2 infected and symptomatic stylists	Universal mask wearing in salon (by local ordinance and company policy)	No COVID-19 infections among 67 patrons who were available for follow-up
Payne et al	USS Theodore Roosevelt, Guam	382 US Navy service members	Self-reported mask wearing	Mask wearing reduced risk of infection by 70% (unadjusted odds ratio, 0.30 [95% CI, 0.17-0.52])
Wang Y et al	Households in Beijing, China	124 Households of diagnosed cases comprising 335 people	Self-reported mask wearing by index cases or ≥1 household member prior to index case's diagnosis	Mask wearing reduced risk of secondary infection by 79% (adjusted odds ratio, 0.21 [95% CI, 0.06-0.79])
Doung-ngern et al	Bangkok, Thailand	839 Close contacts of 211 index cases	Self-reported mask wearing by contact at time of high-risk exposure to case	Always having used a mask reduced infection risk by 77% (adjusted odds ratio, 0.23 [95% CI, 0.09-0.60])
Gallaway et al	Arizona	State population	Mandatory mask wearing in public	Temporal association between institution of mask wearing policy and subsequent decline in new diagnoses
Rader et al	US	374 021 Persons who completed web-based surveys	Self-reported mask wearing in grocery stores and in the homes of family or friends	A 10% increase in mask wearing tripled the likelihood of stopping community transmission (adjusted odds ratio, 3.53 [95% CI, 2.03-6.43])
Wang X et al	Boston, Massachusetts	9850 Health care workers (HCWs)	Universal masking of HCWs and patients in the Mass General Brigham health care system	Estimated weekly decline in new diagnoses among HCWs of 3.4% after full implementation of the mask wearing policy
Mitze et al	Jena (Thuringia), Germany	City population aged ≥15 y	Mandatory mask wearing in public spaces (eg, public transport, shops)	Estimated daily decline in new diagnoses of 1.32% after implementation of the mask mandate
Van Dyke et al	Kansas	State population	Mandatory mask wearing in public spaces	Estimated case rate per 100 000 persons decreased by 0.08 in counties with mask mandates but increased by 0.11 in those without
Lyu and Wehby	15 US states and Washington, DC	State populations	Mandatory mask wearing in public	Estimated overall initial daily decline in new diagnoses of 0.9% grew to 2.0% at 21 days following mandates
Karaivanov et al	Canada	Country population	Mandatory mask wearing indoors	Estimated weekly 25%-40% decline in new diagnoses following mask mandates

^a See the Supplement for the complete table.

change as more is learned about various mask types and as the pandemic evolves. With the emergence of more transmissible SARS-CoV-2 variants, it is even more important to adopt widespread mask

wearing as well as to redouble efforts with use of all other nonpharmaceutical prevention measures until effective levels of vaccination are achieved nationally.

ARTICLE INFORMATION

Author Affiliations: Centers for Disease Control and Prevention, Atlanta, Georgia.

Corresponding Author: John T. Brooks, MD, Centers for Disease Control and Prevention, Division of HIV/AIDS Prevention, 1600 Clifton Rd, NE, Mailstop D-21, Atlanta, GA 30333 (zud4@cdc.gov).

Published Online: February 10, 2021. doi:10.1001/jama.2021.1505

Correction: This article was corrected on February 22, 2021, to correct a typo indicating that there were solid relevant data to support community mask wearing to reduce the spread of respiratory infections before the pandemic. This typo has been corrected.

Conflict of Interest Disclosures: None reported.

Additional Information: The science summarized in this article is reviewed in greater detail with a full set of references on the Centers for Disease Control and Prevention's COVID-19 website Scientific Brief: Community Use of Cloth Masks to Control the Spread of SARS-CoV-2 (<https://www.cdc.gov/coronavirus/2019-ncov/more/masking-science-sars-cov2.html>). This website and a public slide deck will be updated periodically.

REFERENCES

- Johansson MA, Quandelacy TM, Kada S, et al. SARS-CoV-2 transmission from people without COVID-19 symptoms. *JAMA Netw Open*. 2021;4(1):e2035057.
- Lindsley WG, Blachere FM, Law BF, Beezhold DH, Noti JD. Efficacy of face masks, neck gaiters and face shields for reducing the expulsion of simulated cough-generated aerosols. *Aerosol Sci Technol*. Published online January 7, 2021. doi:10.1080/02786826.2020.1862409
- Ueki H, Furusawa Y, Iwatsuki-Horimoto K, et al. Effectiveness of face masks in preventing airborne transmission of SARS-CoV-2. *mSphere*. 2020;5(5):e00637-20. doi:10.1128/mSphere.00637-20
- Payne DC, Smith-Jeffcoat SE, Nowak G, et al; CDC COVID-19 Surge Laboratory Group. SARS-CoV-2 infections and serologic responses from a sample of U.S. Navy Service Members: USS Theodore Roosevelt, April 2020. *MMWR Morb Mortal Wkly Rep*. 2020;69(23):714-721.
- Doung-ngern P, Suphanchaimat R, Panjangampathana A, et al. Case-control study of use of personal protective measures and risk for SARS-CoV 2 Infection, Thailand. *Emerg Infect Dis*. 2020;26(11):2607-2616. doi:10.3201/eid2611.203003
- Wang Y, Tian H, Zhang L, et al. Reduction of secondary transmission of SARS-CoV-2 in households by face mask use, disinfection and social distancing: a cohort study in Beijing, China. *BMJ Glob Health*. 2020;5(5):e002794.
- Lyu W, Wehby GL. Community use of face masks and COVID-19: evidence from a natural experiment of state mandates in the US. *Health Aff (Millwood)*. 2020;39(8):1419-1425.
- Ruba AL, Pollak SD. Children's emotion inferences from masked faces: Implications for social interactions during COVID-19. *PLoS One*. 2020;15(12):e0243708.
- Samannan R, Holt G, Calderon-Candelario R, Mirsaedi M, Campos M. Effect of face masks on gas exchange in healthy persons and patients with COPD. *Ann Am Thorac Soc*. Published online October 2, 2020. doi:10.1513/AnnalsATS.202007-812RL
- Bundgaard H, Bundgaard JS, Raaschou-Pedersen DET, et al. Effectiveness of adding a mask recommendation to other public health measures to prevent SARS-CoV-2 infection in danish mask wearers: a randomized controlled trial. *Ann Intern Med*. Published online November 18, 2020. doi:10.7326/M20-6817

RESEARCH ARTICLE

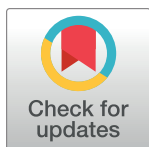
Occurrence and transmission potential of asymptomatic and presymptomatic SARS-CoV-2 infections: A living systematic review and meta-analysis

Diana Buitrago-Garcia^{1,2}, Dianne Egli-Gany¹, Michel J. Counotte¹, Stefanie Hossmann¹, Hira Imeri¹, Aziz Mert Ipekci¹, Georgia Salanti¹, Nicola Low^{1*}

1 Institute of Social and Preventive Medicine, University of Bern, Bern, Switzerland, **2** Graduate School of Health Sciences, University of Bern, Bern, Switzerland

☞ These authors contributed equally to this work.

* nicola.low@ispm.unibe.ch



OPEN ACCESS

Citation: Buitrago-Garcia D, Egli-Gany D, Counotte MJ, Hossmann S, Imeri H, Ipekci AM, et al. (2020) Occurrence and transmission potential of asymptomatic and presymptomatic SARS-CoV-2 infections: A living systematic review and meta-analysis. *PLoS Med* 17(9): e1003346. <https://doi.org/10.1371/journal.pmed.1003346>

Academic Editor: Nathan Ford, World Health Organization, SWITZERLAND

Received: June 11, 2020

Accepted: August 18, 2020

Published: September 22, 2020

Peer Review History: PLOS recognizes the benefits of transparency in the peer review process; therefore, we enable the publication of all of the content of peer review and author responses alongside final, published articles. The editorial history of this article is available here: <https://doi.org/10.1371/journal.pmed.1003346>

Copyright: © 2020 Buitrago-Garcia et al. This is an open access article distributed under the terms of the [Creative Commons Attribution License](https://creativecommons.org/licenses/by/4.0/), which permits unrestricted use, distribution, and reproduction in any medium, provided the original author and source are credited.

Data Availability Statement: The file listing all included studies and files used for all analyses are available from the Harvard Dataverse database.

Abstract

Background

There is disagreement about the level of asymptomatic severe acute respiratory syndrome coronavirus 2 (SARS-CoV-2) infection. We conducted a living systematic review and meta-analysis to address three questions: (1) Amongst people who become infected with SARS-CoV-2, what proportion does not experience symptoms at all during their infection? (2) Amongst people with SARS-CoV-2 infection who are asymptomatic when diagnosed, what proportion will develop symptoms later? (3) What proportion of SARS-CoV-2 transmission is accounted for by people who are either asymptomatic throughout infection or presymptomatic?

Methods and findings

We searched PubMed, Embase, bioRxiv, and medRxiv using a database of SARS-CoV-2 literature that is updated daily, on 25 March 2020, 20 April 2020, and 10 June 2020. Studies of people with SARS-CoV-2 diagnosed by reverse transcriptase PCR (RT-PCR) that documented follow-up and symptom status at the beginning and end of follow-up or modelling studies were included. One reviewer extracted data and a second verified the extraction, with disagreement resolved by discussion or a third reviewer. Risk of bias in empirical studies was assessed with an adapted checklist for case series, and the relevance and credibility of modelling studies were assessed using a published checklist. We included a total of 94 studies. The overall estimate of the proportion of people who become infected with SARS-CoV-2 and remain asymptomatic throughout infection was 20% (95% confidence interval [CI] 17–25) with a prediction interval of 3%–67% in 79 studies that addressed this review question. There was some evidence that biases in the selection of participants influence the estimate. In seven studies of defined populations screened for SARS-CoV-2 and then

<https://doi.org/10.7910/DVN/TZFXYO>, Harvard Dataverse, V2, UNF:6:nblmY3m4rXPJ/oD2d9Lo5A== [fileUNF].

Funding: Funding was received from the Swiss National Science Foundation (320030_176233, to NL), <http://www.snf.ch/en/Pages/default.aspx>; European Union Horizon 2020 research and innovation programme (101003688, to NL), <https://ec.europa.eu/programmes/horizon2020/en>; Swiss government excellence scholarship (2019.0774, to DB-G), <https://www.sbf.admin.ch/sbf/en/home/education/scholarships-and-grants/swiss-government-excellence-scholarships.html>; and the Swiss School of Public Health Global P3HS stipend (to DB-G), <https://ssphplus.ch/en/globalp3hs/>. The funders had no role in study design, data collection and analysis, decision to publish, or preparation of the manuscript.

Competing interests: I have read the journal's policy and the authors of this manuscript have the following competing interests: GS has participated in two scientific meetings for Merck and Biogen. NL is a member of the PLOS Medicine editorial board.

Abbreviations: CI, confidence interval; COVID-19, coronavirus disease 2019; CrI, credibility interval; E, number of secondary transmission events; F, female; GI, generation interval; IQR, interquartile range; M, male; NR, not reported; RT-PCR, reverse transcriptase PCR; SARS-CoV-2, severe acute respiratory syndrome coronavirus 2; USA, United States of America.

followed, 31% (95% CI 26%–37%, prediction interval 24%–38%) remained asymptomatic. The proportion of people that is presymptomatic could not be summarised, owing to heterogeneity. The secondary attack rate was lower in contacts of people with asymptomatic infection than those with symptomatic infection (relative risk 0.35, 95% CI 0.10–1.27). Modelling studies fit to data found a higher proportion of all SARS-CoV-2 infections resulting from transmission from presymptomatic individuals than from asymptomatic individuals. Limitations of the review include that most included studies were not designed to estimate the proportion of asymptomatic SARS-CoV-2 infections and were at risk of selection biases; we did not consider the possible impact of false negative RT-PCR results, which would underestimate the proportion of asymptomatic infections; and the database does not include all sources.

Conclusions

The findings of this living systematic review suggest that most people who become infected with SARS-CoV-2 will not remain asymptomatic throughout the course of the infection. The contribution of presymptomatic and asymptomatic infections to overall SARS-CoV-2 transmission means that combination prevention measures, with enhanced hand hygiene, masks, testing tracing, and isolation strategies and social distancing, will continue to be needed.

Author summary

Why was this study done?

- The proportion of people who will remain asymptomatic throughout the course of infection with severe acute respiratory syndrome coronavirus 2 (SARS-CoV-2), the cause of coronavirus disease 2019 (COVID-19), is not known.
- Studies that assess people at just one time point will overestimate the proportion of true asymptomatic infection because those who go on to develop COVID-19 symptoms will be wrongly classified as asymptomatic rather than presymptomatic.
- The amount, and infectiousness, of asymptomatic SARS-CoV-2 infection will determine what kind of measures will prevent transmission most effectively.

What did the researchers do and find?

- We did a living systematic review through 10 June 2020, using automated workflows that speed up the review processes and allow the review to be updated when relevant new evidence becomes available.
- Overall, in 79 studies in a range of different settings, 20% (95% confidence interval [CI] 17%–25%, prediction interval 3%–67%) of people with SARS-CoV-2 infection remained asymptomatic during follow-up, but biases in study designs limit the certainty of this estimate.
- In seven studies of defined populations screened for SARS-CoV-2 and then followed, 31% (95% CI 26%–37%, prediction interval 24%–38%) remained asymptomatic.

- We found some evidence that SARS-CoV-2 infection in contacts of people with asymptomatic infection is less likely than in contacts of people with symptomatic infection (relative risk 0.35, 95% CI 0.10–1.27).

What do these findings mean?

- The findings of this living systematic review suggest that most people who become infected with SARS-CoV-2 will not remain asymptomatic throughout the course of infection.
- Future studies should be designed specifically to determine the true proportion of asymptomatic SARS-CoV-2 infections, using methods to minimise biases in the selection of study participants and ascertainment of symptom status during follow-up.
- The contribution of presymptomatic and asymptomatic infections to overall SARS-CoV-2 transmission means that combination prevention measures, with enhanced hand hygiene, masks, testing tracing, and isolation strategies and social distancing, will continue to be needed.

Introduction

There is ongoing discussion about the level of asymptomatic severe acute respiratory syndrome coronavirus 2 (SARS-CoV-2) infection. The authors of a narrative review report a range of proportions of participants positive for SARS-CoV-2 but asymptomatic in different studies from 6% to 96% [1]. The discrepancy results, in part, from the interpretation of studies that report a proportion of asymptomatic people with SARS-CoV-2 detected at a single point. The studies cited include both people who will remain asymptomatic throughout and those, known as presymptomatic, who will develop symptoms of coronavirus disease 2019 (COVID-19) if followed up [2]. The full spectrum and distribution of COVID-19, from completely asymptomatic, to mild and nonspecific symptoms, viral pneumonia, respiratory distress syndrome, and death, are not yet known [3]. Without follow-up, however, the proportions of asymptomatic and presymptomatic infections cannot be determined.

Accurate estimates of the proportions of true asymptomatic and presymptomatic infections are needed urgently because their contribution to overall SARS-CoV-2 transmission at the population level will determine the appropriate balance of control measures [3]. If the predominant route of transmission is from people who have symptoms, then strategies should focus on testing, followed by isolation of infected individuals and quarantine of their contacts. If, however, most transmission is from people without symptoms, social distancing measures that reduce contact with people who might be infectious should be prioritised, enhanced by active case-finding through testing of asymptomatic people.

The objectives of this study were to address three questions: (1) Amongst people who become infected with SARS-CoV-2, what proportion do not experience symptoms at all during their infection? (2) Amongst people with SARS-CoV-2 infection who are asymptomatic when diagnosed, what proportion will develop symptoms later? (3) What proportion of SARS-CoV-2 transmission is accounted for by people who are either asymptomatic throughout infection or presymptomatic?

Methods

We conducted a living systematic review, a systematic review that provides an online summary of findings and is updated when relevant new evidence becomes available [4]. The review follows a published protocol (<https://osf.io/9ewys/>), which describes in detail the methods used to speed up review tasks [5] and to assess relevant evidence rapidly during a public health emergency [6]. The first two versions of the review have been published as preprints [7,8]. We report our findings according to the statement on preferred reporting items for systematic reviews and meta-analyses (S1 PRISMA Checklist) [9]. Ethics committee review was not required for this study. Box 1 shows our definitions of symptoms, asymptomatic infection, and presymptomatic status. We use the term asymptomatic SARS-CoV-2 infection for people without symptoms of COVID-19 who remain asymptomatic throughout the course of infection. We use the term presymptomatic for people who do not have symptoms of COVID-19 when enrolled in a study but who develop symptoms during adequate follow-up.

Box 1. Definitions of symptoms and symptom status in a person with SARS-CoV-2 infections

Symptoms: symptoms that a person experiences and reports. We used the authors' definitions. We searched included manuscripts for an explicit statement that the study participant did not report symptoms that they experienced. Some authors defined 'asymptomatic' as an absence of self-reported symptoms. We did not include clinical signs observed or elicited on examination.

Asymptomatic infection: a person with laboratory-confirmed SARS-CoV-2 infection, who has no symptoms, according to the authors' report, at the time of first clinical assessment and had no symptoms at the end of follow-up. The end of follow-up was defined as any of the following: virological cure, with one or more negative reverse transcriptase PCR (RT-PCR) test results; follow-up for 14 days or more after the last possible exposure to an index case; follow-up for 7 days or more after the first RT-PCR positive result.

Presymptomatic: a person with laboratory-confirmed SARS-CoV-2 infection, who has no symptoms, according to the authors' report, at the time of first clinical assessment but who developed symptoms by the end of follow-up. The end of follow-up was defined as any of the following: virological cure, with one or more negative RT-PCR test results; follow-up for 14 days or more after the last possible exposure to an index case; follow-up for 7 days or more after the first RT-PCR positive result.

Information sources and search

We conducted the first search on 25 March 2020 and updated it on 20 April and 10 June 2020. We searched the COVID-19 living evidence database [10], which is generated using automated workflow processes [5] to (1) provide daily updates of searches of four electronic databases (Medline PubMed, Ovid Embase, bioRxiv, and medRxiv), using medical subject headings and free-text keywords for SARS-CoV-2 infection and COVID-19; (2) de-duplicate the records; (3) tag records that are preprints; and (4) allow searches of titles and abstracts using Boolean operators. We used the search function to identify studies of asymptomatic or presymptomatic SARS-CoV-2 infection using a search string of medical subject headings and free-text

keywords ([S1 Text](#)). We also examined articles suggested by experts and the reference lists of retrieved mathematical modelling studies and systematic reviews. Reports from this living rapid systematic review will be updated at 3-monthly intervals, with continuously updated searches.

Eligibility criteria

We included studies in any language of people with SARS-CoV-2 diagnosed by RT-PCR that documented follow-up and symptom status at the beginning and end of follow-up or investigated the contribution to SARS-CoV-2 transmission of asymptomatic or presymptomatic infection. We included contact-tracing investigations, case series, cohort studies, case-control studies, and statistical and mathematical modelling studies. We excluded the following study types: case reports of a single patient and case series in which participants were not enrolled consecutively. When multiple records included data from the same study population, we linked the records and extracted data from the most complete report.

Study selection and data extraction

Reviewers worked in pairs to screen records using an application programming interface in the electronic data capture system (REDCap, Vanderbilt University, Nashville, TN, USA). One reviewer selected potentially eligible studies and a second reviewer verified all included and excluded studies. We reported the identification, exclusion, and inclusion of studies in a flow-chart ([S1 Fig](#)). The reviewers determined which of the three review questions each study addressed, using the definitions in [Box 1](#). One reviewer extracted data using a pre-piloted extraction form in REDCap, and a second reviewer verified the extracted data using the query system. A third reviewer adjudicated on disagreements that could not be resolved by discussion. We contacted study authors for clarification when the study description was insufficient to reach a decision on inclusion or if reported data in the manuscript were internally inconsistent. The extracted variables included, but were not limited to, study design, country and/or region, study setting, population, age, primary outcomes, and length of follow-up. From empirical studies, we extracted raw numbers of individuals with any outcome and its relevant denominator. From statistical and mathematical modelling studies, we extracted proportions and uncertainty intervals reported by the authors.

The primary outcomes for each review question were (1) proportion with asymptomatic SARS-CoV-2 infection who did not experience symptoms at all during follow-up; (2) proportion with SARS-CoV-2 infections who did not have symptoms at the time of testing but developed symptoms during follow-up; (3) estimated proportion (with uncertainty interval) of SARS-CoV-2 transmission accounted for by people who are asymptomatic or presymptomatic. A secondary outcome for review question 3 was the secondary attack rate from asymptomatic or presymptomatic index cases.

Risk of bias in included studies

Two authors independently assessed the risk of bias. A third reviewer resolved disagreements. For observational epidemiological studies, we adapted the Joanna Briggs Institute Critical Appraisal Checklist for Case Series [11]. The adapted tool included items about inclusion criteria, measurement of asymptomatic status, follow-up of course of disease, and statistical analysis. We added items about selection biases affecting the study population from a tool for the assessment of risk of bias in prevalence studies [12]. For mathematical modelling studies, we used a checklist for assessing relevance and credibility [13].

Synthesis of the evidence

We used the ‘metaprop’ and ‘metabin’ functions from the ‘meta’ package (version 4.11–0) [14] in R (version 3.5.1) to display the study findings in forest plots and synthesise their findings. The 95% confidence intervals (CIs) for each study are estimated using the Clopper-Pearson method [15]. We examined heterogeneity visually in forest plots. We stratified studies according to the methods used to identify people with asymptomatic SARS-CoV-2 infection and the study setting. To synthesise proportions from comparable studies, in terms of design and population, we used stratified random-effects meta-analysis. For the stratified and overall summary estimates, we calculated prediction intervals, to represent the likely range of proportions that would be obtained in subsequent studies conducted in similar settings [16]. We calculated the secondary attack rate as the number of cases among contacts as a proportion of all close contacts ascertained. We did not account for potential clustering of contacts because the included studies did not report the size of clusters. We compared the secondary attack rate from asymptomatic or presymptomatic index cases with that from symptomatic cases. If there were no events in a group, we added 0.5 to each cell in the 2×2 table. We used random-effects meta-analysis with the Mantel-Haenszel method to estimate a summary risk ratio (with 95% CI).

Results

The living evidence database contained a total of 25,538 records about SARS-CoV-2 or COVID-19 by 10 June 2020. The searches for studies about asymptomatic or presymptomatic SARS-CoV-2 on 25 March, 20 April, and 10 June resulted in 89, 230, and 688 records for screening (S1 Fig). In the first version of the review [7], 11 articles were eligible for inclusion [17–27], version 2 [8] identified another 26 eligible records [28–53], and version 3 identified another 61 eligible records [54–114]. After excluding four articles for which more recent data became available in a subsequent version [25,29,30,35], the total number of articles included was 94 (S1 Table) [17–24,26–28,31–34,36–114]. The types of evidence changed across the three versions of the review (S1 Table). In the first version, six of 11 studies were contact investigations of single-family clusters with a total of 39 people. In the next versions, study designs included larger investigations of contacts and outbreaks, screening of defined groups, and studies of hospitalised adults and children. Across all three review versions, data from 79 empirical observational studies were collected in 19 countries or territories (Tables 1 and 2) and included 6,832 people with SARS-CoV-2 infection. Forty-seven of the studies, including 3,802 infected people, were done in China (S2 Table). At the time of their inclusion in the review, 23 of the included records were preprints; six of these had been published in peer-reviewed journals by 17 July 2020 [19,20,27,81,82,106].

Proportion of people with asymptomatic SARS-CoV-2 infection

We included 79 studies that reported empirical data about 6,616 people with SARS-CoV-2 infection (1,287 defined as having asymptomatic infection) [17,18,21–23,26–28,31,32,34,36,39–45,47–50,52–54,56–62,64,66–68,70–77,79–90,92–112,114] and one statistical modelling study [24] (Table 1). The sex distribution of the people with asymptomatic infection was reported in 41/79 studies, and the median age was reported in 35/79 studies (Table 1). The results of the studies were heterogeneous (S2 Fig). We defined seven strata, according to the method of selection of asymptomatic status and study settings. Study findings within some of these strata were more consistent (Fig 1). We considered the statistical modelling study of passengers on the *Diamond Princess* cruise ship passengers [24] separately, because of the different

Table 1. Characteristics of studies reporting on proportion of asymptomatic SARS-CoV-2 infections.

Author	Country, location	Total SARS-CoV-2, <i>n</i>	Asymptomatic SARS-CoV-2, <i>n</i>	Sex of asymptomatic people	Age of asymptomatic people, years, median	Follow-up method ^a
Contact investigation, single						
Tong, ZD [44]	China, Zhejiang	5	3	2 F, 3 M	28 IQR 12–41	1, 3
Huang, R [74]	China, Suqian	2	1	1 F, 0 M	54	3
Jiang, XL [76]	China, Shandong	8	3	3 F, 0 M	35 IQR 0–53	3
Jiang, X [75]	China, Chongqing	3	1	1 F, 0 M	8	2
Liao, J [22]	China, Chongqing	12	3	NR	NR	1, 2
Hu, Z [21]	China, Nanjing	4	1	0 F, 1 M	64	2, 3
Luo, SH [23]	China, Anhui	4	1	1 F, 0 M	50	1, 2, 3
Chan, JF [18]	China, Guangdong	5	1	0 F, 1 M	10	1
Ye, F [49]	China, Sichuan	5	1	0 F, 1 M	28	1, 2
Bai, Y [17]	China, Anyang	6	1	1 F, 0 M	20	1
Luo, Y [85]	China, Wuhan	6	5	NR	37 IQR 7–62	1
Zhang, J [50]	China, Wuhan and Beijing	5	2	1 F, 1 M	NR	2
Zhang, B [110]	China, Guangdong	7	2	0 F, 2 M	13.5 IQR 13–14	3
Huang, L [73]	China, Gansu	7	2	2 F, 0 M	44 IQR 38.5–49.5	2
Qian, G [26]	China, Zhejiang	8	2	1 F, 1 M	30.5 IQR 1–60	1, 2
Gao, Y [70]	China, Wuxi	15	6	3 F, 3 M	50 IQR 48–51	1, 2
Contact investigation, aggregated						
Hijnen, D [72]	Germany	11	1	0 F, 1 M	49	1
Brandstetter, S [62]	Germany	36	2	NR	NR	2
Zhang, W2 [111]	China, Guiyang	12	4	NR	NR	1, 2, 3
Cheng, HY [66]	Taiwan	22	4	NR	NR	1
Wang, Z [47]	China, Wuhan	47	4	NR	NR	1
Wu, J [105]	China, Zhuhai	83	8	NR	NR	1, 2
Luo, L [36]	China, Guangzhou	129	8	NR	NR	1, 2, 3
Bi, Q [60]	China, Shenzhen	87	17	NR	NR	2, 3
Yang, R [108]	China, Wuhan	78	33	22 F, 11 M	37 IQR 26–45	3
Outbreak investigation						
Danis, K [32]	France	13	1	NR	NR	1, 2
Böhmer, MM [61]	Germany	16	1	NR	NR	1
Roxby, AC [94]	USA	6	3	NR	NR	1
Yang, N [48]	China, Xiaoshan	10	2	1 F, 1 M	NR	1, 2
Schwieerzeck, V [95]	Germany	12	2	NR	NR	2
Arons, MM [58]	USA	47	3	NR	NR	2
Park, SY [90]	South Korea	97	4	NR	NR	2
Dora, AV [68]	USA	19	6	0 F, 6 M	75 IQR 72–75	3
Tian, S [43]	China, Shandong	24	7	NR	NR	3
Solbach, W [97]	Germany	97	10	NR	NR	2
Graham, N [71]	United Kingdom	126	46	NR	NR	2

(Continued)

Table 1. (Continued)

Author	Country, location	Total SARS-CoV-2, <i>n</i>	Asymptomatic SARS-CoV-2, <i>n</i>	Sex of asymptomatic people	Age of asymptomatic people, years, median	Follow-up method ^a
Pham, TQ [100]	Vietnam	208	89	NR	31 IQR 23–45	2
Screening of defined population						
Hoehl, S [34]	Germany	2	1	0 F, 1 M	58	2
Chang, L [31]	China, Wuhan	4	2	0 F, 2 M	45 IQR 37–53	2
Arima, Y [28]	Japan	12	4	NR	NR	1, 2
Rivett, L [93]	United Kingdom	30	5	NR	NR	2
Treibel, TA [101]	United Kingdom	44	12	NR	NR	2
Lavezzo, E [81]	Italy	73	29	NR	NR	2
Lombardi, A [82]	Italy	138	41	NR	NR	3
Hospitalised adults						
Pongpirul, WA [39]	Thailand	11	1	1 F, 0 M	66	2, 3
Zou, L [53]	China, Zhuhai	18	1	1 M, 0 M	26	1
Qiu, C [92]	China, Hunan	104	5	NR	NR	2
Zhou, R [114]	China, Guangdong	31	9	NR	NR	3
Chang, MC [64]	South Korea	139	10	4 F, 6 M	NR	1, 2
Zhou, X [52]	China, Shanghai	328	10	NR	NR	1, 2, 3
Angelo Vaira, L [57]	Italy	345	10	NR	NR	3
Wang, X [45]	China, Wuhan	1012	14	NR	NR	1, 2
Wong, J [103]	Brunei	138	16	NR	NR	2, 3
Xu, T [107]	China, Jiangsu	342	15	5 F, 10 M	27 IQR 17–36	2, 3
London, V [83]	USA	68	22	22 F, 0 M	30.5 IQR 24.5–34.8	2
Tabata, S [27]	Japan ^b	104	33	18 F, 15 M	70 IQR 57–75	2
Andrikopoulou, M [56]	USA	158	46	46 F, 0 M	NR	1, 2
Noh, JY [89]	South Korea	199	53	NR	NR	3
Kumar, R [80]	India, New Delhi	231	108	18 F, 90 M	NR	2, 3
Hospitalised children						
See, KC [41]	Malaysia	4	1	0 F, 1 M	9	1, 2, 3
Tan, YP [42]	China, Changsha	10	2	1 F, 1 M	8	2, 3
Tan, X [99]	China, Changsha	13	2	2 F, 0 M	5 IQR 2–8	1, 2, 3
Melgosa, M [87]	Spain	16	3	NR	NR	1, 2
Wu, HP [104]	China, Jiangxi	23	3	NR	NR	3
Song, W [98]	China, Hubei	16	8	3 F, 5 M	11 IQR 7–12	1, 2
Bai, K [59]	China, Chongqing	25	8	NR	NR	3
Xu, H [106]	China, Guizhou	32	11	4 F, 7 M	NR	1, 2
Qiu, H [40]	China, Zhejiang	36	10	NR	NR	1, 2, 3
Lu, Y [84]	China, Wuhan	110	29	12 F, 17 M	7 IQR 6–11	2, 3
Hospitalised adults and children						
Merza, MA [88]	Iraqi Kurdistan	15	6	NR	NR	2, 3
Yongchen, Z [109]	China, Jiangsu	21	5	2 F, 3 M	25 IQR 14–54	1, 2, 3

(Continued)

Table 1. (Continued)

Author	Country, location	Total SARS-CoV-2, <i>n</i>	Asymptomatic SARS-CoV-2, <i>n</i>	Sex of asymptomatic people	Age of asymptomatic people, years, median	Follow-up method ^a
Ma, Y [86]	China, Shandong	47	11	5 F, 6 M	23 IQR NR	2
Kim, SE [77]	South Korea	71	10	6 F, 4 M	31 IQR 21–55	2
Choe, PG [67]	South Korea	113	15	17 F, 8 M	NR	3
Sharma, AK [96]	India, Jaipur	234	215	NR	NR	1, 2, 3
Zhang, W3 [112]	China, Guiyang	137	26	12 F, 14 M	24 IQR 12–36	1, 2
Alshami, AA [54]	Saudi Arabia	128	69	36 F, 33 M	NR	2, 3
Kong, W [79]	China, Sichuan	473	45	NR	NR	1, 2
Wang, Y2 [102]	China, Chongqing	279	63	29 F, 34 M	39 IQR 27–53	3

^aFollow-up according to protocol (1: 14 days after last possible exposure; 2: 7 days after diagnosis; 3: until negative RT-PCR result).

^bPeople of different nationalities taken from *Diamond Princess* cruise ship to a hospital in Japan.

Abbreviations: F, female; IQR, interquartile range; M, male; NR, not reported; RT-PCR, reverse transcriptase PCR; SARS-CoV-2, severe acute respiratory syndrome coronavirus 2; USA, United States of America

<https://doi.org/10.1371/journal.pmed.1003346.t001>

method of analysis and overlap with the study population reported by Tabata and colleagues [27].

The main risks of bias across all categories of empirical studies were in the selection and enrolment of people with asymptomatic infection and mismeasurement of asymptomatic status because of absent or incomplete definitions (S3 Fig). Sources of bias specific to studies in particular settings are discussed with the relevant results.

The overall estimate of the proportion of people who become infected with SARS-CoV-2 and remain asymptomatic throughout the course of infection was 20% (95% CI 17%–25%, 79 studies), with a prediction interval of 3%–67% (Fig 1). One statistical modelling study was based on data from all 634 passengers from the *Diamond Princess* cruise ship with RT-PCR positive test results [24]. The authors adjusted for the proportion of people who would develop symptoms (right censoring) in a Bayesian framework to estimate that, if all were followed up until the end of the incubation period, the probability of asymptomatic infections would be 17.9% (95% credibility interval [CrI] 15.5%–20.2%).

The summary estimates of the proportion of people with asymptomatic SARS-CoV-2 infection differed according to study setting, although prediction intervals for all groups overlapped. The first three strata in Fig 1 involve studies that reported on different types of contact investigation, which start with an identified COVID-19 case. The studies reporting on single-family clusters (21 estimates from 16 studies in China, *n* = 102 people with SARS-CoV-2) all included at least one asymptomatic person [17,18,21–23,26,44,49,50,70,73–76,85,110]. The summary estimate was 34% (95% CI 26%–44%, prediction interval 25%–45%). In nine studies that reported on close contacts of infected individuals and aggregated data from clusters of both asymptomatic and symptomatic people with SARS-CoV-2 the summary estimate was 14% (95% CI 8%–23%, prediction interval 2%–53%) [36,47,60,62,66,72,105,108,111]. We included 12 studies (*n* = 675 people) that reported on outbreak investigations arising from a single symptomatic person or from the country's first imported cases of people with COVID-19 [32,43,48,58,61,68,71,90,94,95,97,100]. Four of the outbreaks involved nursing homes [58,68,71,94] and four involved occupational settings [43,61,90,95]. The summary estimate of

Table 2. Characteristics of studies that measured the proportion of people with SARS-CoV-2 infection that develops symptoms.

Author	Country, location	Total asymptomatic SARS-CoV-2, <i>n</i>	Develop symptoms after testing, <i>n</i>	Sex of asymptomatic people at time of testing	Age of asymptomatic people at time of testing, years, median	Follow-up method ^a
Contact investigation, single						
Ye, F [49]	China, Sichuan	3	2	0 F, 3 M	28 IQR 23–50	1, 2
Zhang, B [110]	China, Guangdong	4	2	0 F, 4 M	34 IQR 33–35	3
Huang, L [73]	China, Gansu	4	2	3 F, 1 M	44.5 IQR 34.50–54.25	2
Jiang, XL [76]	China, Shandong	5	2	3 F, 2 M	35 IQR 35–37	3
Hu, Z [21]	China, Nanjing	24	5	NR	NR	2, 3
Contact investigation, aggregated						
Zhang, W2 [111]	China, Guangzhou	12	8	NR	NR	1, 2, 3
Outbreak investigation						
Schwierzeck, V [95]	Germany	6	4	NR	NR	2
Park, SY [90]	South Korea	8	4	NR	NR	2
Arons, MM [58]	USA	27	24	NR	NR	2
Dora, AV [68]	USA	14	8	0 F, 14 M	NR	3
Graham, N [71]	United Kingdom	54	8	NR	NR	1
Screening of defined population						
Hoehl, S [34]	Germany	2	1	1 F, 1 M	51	2
Rivett, L [93]	United Kingdom	6	1	NR	NR	2
Chang, L [31]	China, Wuhan	4	2	1 F, 3 M	39.5 IQR 29–47.5	2
Arima, Y [28]	Japan	5	2	NR	NR	1, 2
Lytras, T [37]	Greece	39	4	NR	NR	2
Lavezzo, E [81]	Italy	39	10	NR	NR	2
Hospitalised adults						
Al-Shamsi, HO [55]	United Arab Emirates	7	7	5 F, 2 M	51.6 IQR 40–76	3
Luo, SH [23]	China, Anhui	8	7	NR	NR	1, 2, 3
Zhou, X [52]	China, Shanghai	13	3	7 F, 6 M	NR	2, 3
Zhou, R [114]	China, Guangdong	31	22	NR	NR	3
Wang, X [45]	China, Wuhan	30	16	NR	NR	1, 2
Tabata, S [27]	Cruise Ship	43	10	24 F, 19 M	69 IQR 60.5–75	2
Wang, Y1 [46]	China, Shenzhen	55	43	NR	49 IQR 2–69	3
Meng, H [38]	China, Wuhan	58	16	NR	NR	2
Andrikopoulou, M [56]	USA	63	16	63 F, 0 M	NR	1, 2
Zhang, Z [113]	China, Shenzhen	56	33	33 F, 23 M	NR	2, 3
Wong, J [103]	Brunei	138	42	NR	NR	2, 3
Hospitalised children						

(Continued)

Table 2. (Continued)

Author	Country, location	Total asymptomatic SARS-CoV-2, <i>n</i>	Develop symptoms after testing, <i>n</i>	Sex of asymptomatic people at time of testing	Age of asymptomatic people at time of testing, years, median	Follow-up method ^a
See, KC [41]	Malaysia	2	1	0 F, 2 M	5 IQR 1–9	1, 2, 3
Hospitalised adults and children						
Kim, SE [77]	South Korea	13	3	7 F, 6 M	31 IQR 20.5–51.5	2
Choe, PG [67]	South Korea	54	39	32 F, 22 M	NR	3
Kong, W [79]	China, Sichuan	62	17	NR	NR	1

^aFollow-up according to protocol (1: 14 days after possible exposure; 2: 7 days after diagnosis; 3: until one or more negative RT-PCR result).

^bPeople of different nationalities taken from *Diamond Princess* cruise ship to a hospital in Japan.

^cUntil hospital discharge or negative RT-PCR.

Abbreviations: F, female; IQR, interquartile range; M, male; NR, not reported; RT-PCR, reverse transcriptase PCR; SARS-CoV-2, severe acute respiratory syndrome coronavirus 2; USA, United States of America

<https://doi.org/10.1371/journal.pmed.1003346.t002>

the proportion of asymptomatic SARS-CoV-2 infections was 18% (95% CI 10%–28%, prediction interval 2%–64%).

In seven studies, people with SARS-CoV-2 infection were detected through screening of all people in defined populations who were potentially exposed (303 infected people amongst 10,090 screened) [28,31,34,81,82,93,101]. The screened populations included healthcare workers [82,93,101]; people evacuated from a setting where SARS-CoV-2 transmission was confirmed, irrespective of symptom status [28,34]; the whole population of one village in Italy [81]; and blood donors [31]. In these studies, the summary estimate of the proportion asymptomatic was 31% (95% CI 26%–37%, prediction interval 24%–38%). There is a risk of selection bias in studies of certain groups, such as healthcare workers and blood donors, because people with symptoms are excluded [31,82,93,101], or from nonresponders in population-based screening [81]. Retrospective symptom ascertainment could also increase the proportion determined asymptomatic [81,82,101].

The remaining studies, in hospital settings, included adult patients only (15 studies, *n* = 3,228) [27,39,45,52,53,56,57,64,80,83,89,92,103,107,114], children only (10 studies, *n* = 285) [40–42,59,84,87,98,99,104,106], or adults and children (10 studies, *n* = 1,518) [54,67,77,79,86,88,96,102,109,112] (Table 1, Fig 1). The types of hospital and clinical severity of patients differed, including settings in which anyone with SARS-CoV-2 infection was admitted for isolation and traditional hospitals.

Proportion of presymptomatic SARS-CoV-2 infections

We included 31 studies in which the people with no symptoms of COVID-19 at enrolment were followed up, and the proportion that develops symptoms is defined as presymptomatic (Table 2, Fig 2) [21,27,28,31,34,37,38,41,45,46,49,52,55,56,58,67,68,71,73,76,77,79,81,90,93,95,103,110,111,113,114]. Four studies addressed only this review question [37,38,55,113]. The findings from the 31 studies were heterogeneous (S4 Fig), even when categorised according to the method of selection of asymptomatic participants, and we did not estimate a summary measure (Fig 2).

Additional analyses

We investigated heterogeneity in the estimates of the proportion of asymptomatic SARS-CoV-2 infections in subgroup analyses that were not specified in the original protocol. In studies of

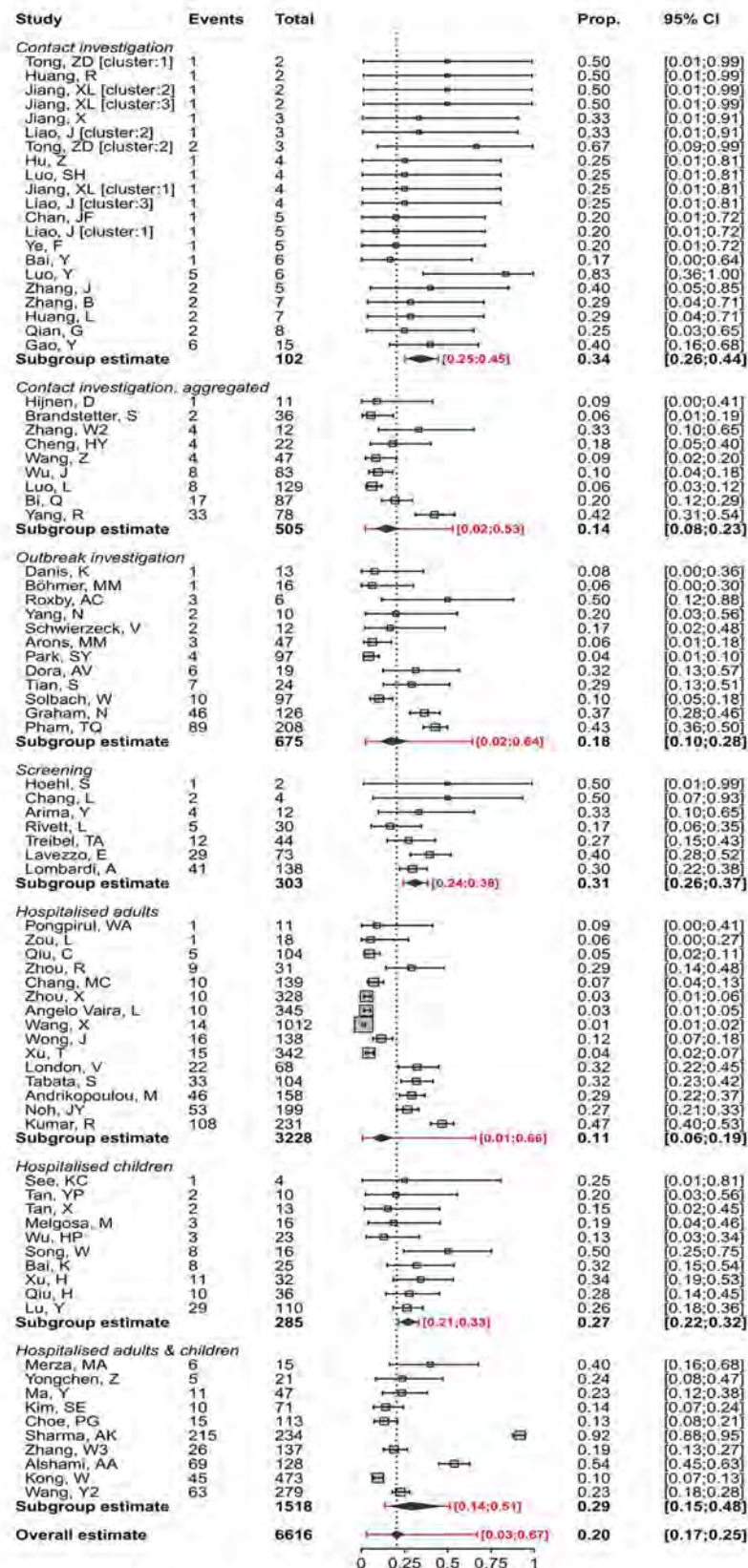


Fig 1. Forest plot of proportion ('Prop.') of people with asymptomatic SARS-CoV-2 infection, stratified by setting. In the setting 'Contact investigations', in which more than one cluster was reported, clusters are annotated with '[cluster]'. The diamond shows the summary estimate and its 95% CI. The red bar and red text show the prediction interval. CI, confidence interval; SARS-CoV-2, severe acute respiratory syndrome coronavirus 2.

<https://doi.org/10.1371/journal.pmed.1003346.g001>

hospitalised children, the point estimate was higher (27%, 95% CI 22%–32%, 10 studies) than in adults (11%, 95% CI 6%–19%, 15 studies) (Fig 1). The proportion of asymptomatic SARS-CoV-2 infection estimated in studies of hospitalised patients (35 studies, 19%, 95% CI 14%–25%) was similar to that in all other settings (44 studies, 22%, 95% CI 17%–29%, S5 Fig). To examine publication status, we conducted a sensitivity analysis, omitting studies that were identified as preprints at the time of data extraction (S6 Fig). The estimate of the proportion of asymptomatic infection in all settings (18%, 95% CI 14%–22%) and setting-specific estimates were very similar to the main analysis.

Contribution of asymptomatic and presymptomatic infection to SARS-CoV-2 to transmission

Five of the studies that conducted detailed contact investigations provided enough data to calculate a secondary attack rate according to the symptom status of the index cases (Fig 3) [36,65,66,90,111]. The summary risk ratio for asymptomatic compared with symptomatic was 0.35 (95% CI 0.1–1.27) and for presymptomatic compared with symptomatic people was 0.63 (95% CI 0.18–2.26) [66,90]. The risk of bias in ascertainment of contacts was judged to be low in all studies.

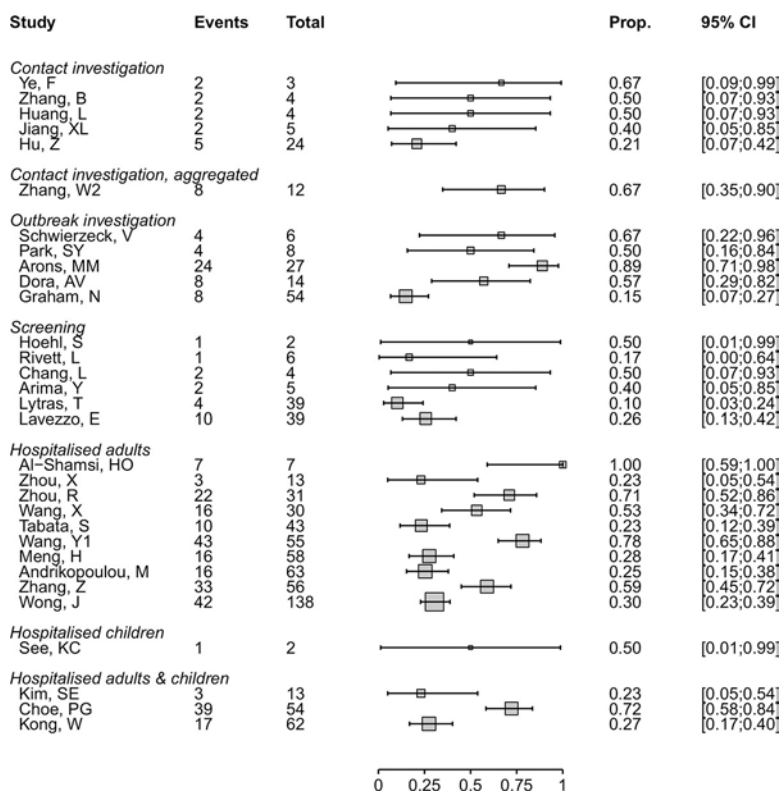


Fig 2. Forest plot of proportion ('Prop.') of people with presymptomatic SARS-CoV-2 infection, stratified by setting. CI, confidence interval; SARS-CoV-2, severe acute respiratory syndrome coronavirus 2.

<https://doi.org/10.1371/journal.pmed.1003346.g002>

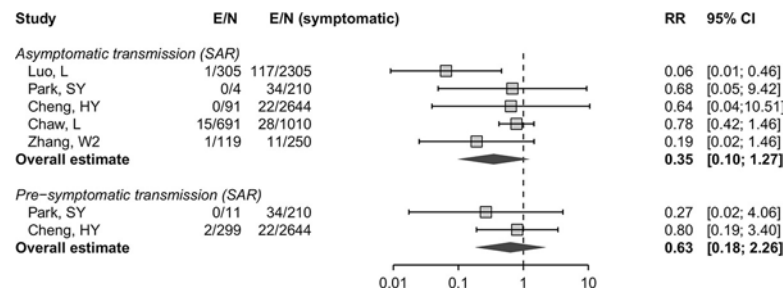


Fig 3. Forest plot of the RR and 95% CI of the SAR, comparing infections in contacts of asymptomatic and presymptomatic index cases with infections in contacts of symptomatic cases. The RR is on a logarithmic scale. CI, confidence interval; E, number of secondary transmission events; N, number of close contacts; RR, risk ratio; SAR, secondary attack rate.

<https://doi.org/10.1371/journal.pmed.1003346.g003>

We included eight mathematical modelling studies (Fig 4) [19,20,33,51,63,69,78,91]. The models in five studies were informed by analysis of data from contact investigations in China, South Korea, Singapore, and the *Diamond Princess* cruise ship, using data to estimate the serial interval or generation time [19,20,33,69,78], and in three studies the authors used previously published estimates [51,63,91].

Estimates of the contributions of both asymptomatic and presymptomatic infections SARS-CoV-2 transmission were very heterogeneous. In two studies, the contributions to SARS-CoV-2 transmission of asymptomatic infection were estimated to be 6% (95% CrI 0%–57%) [19] and 69% (95% CrI 20%–85%) [69] (Fig 4). The estimates have large uncertainty intervals and the disparate predictions result from differences in the proportion of asymptomatic infections and relative infectiousness of asymptomatic infection. Ferretti and colleagues provide an interactive web application [19] that shows how these parameters affect the model results.

Models of the contribution of presymptomatic transmission used different assumptions about the durations and distributions of infection parameters such as incubation period,

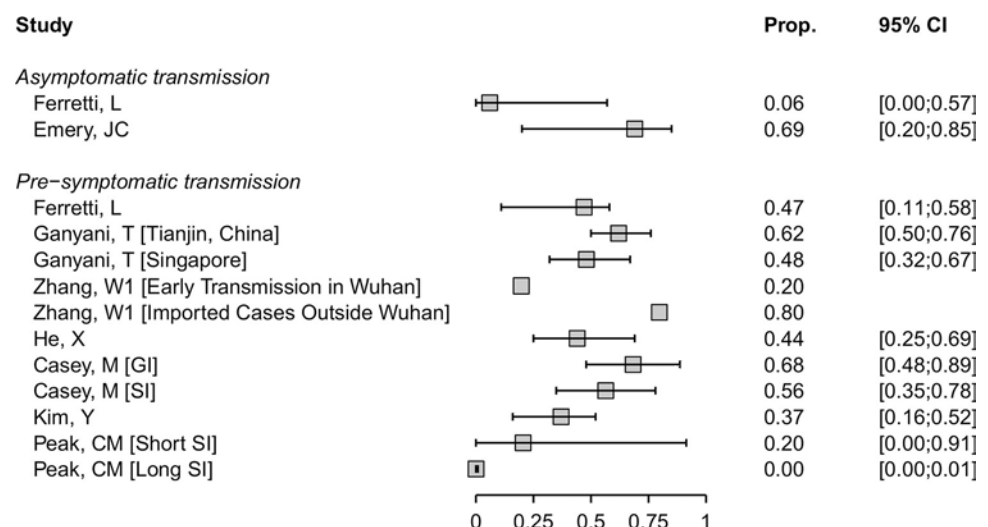


Fig 4. Forest plot of proportion ('Prop.') of SARS-CoV-2 infection resulting from asymptomatic or presymptomatic transmission. For studies that report outcomes in multiple settings, these are annotated in brackets. CI, confidence interval; GI, generation interval; SARS-CoV-2, severe acute respiratory syndrome coronavirus 2; SI, serial interval.

<https://doi.org/10.1371/journal.pmed.1003346.g004>

generation time, and serial interval [19,20,33,51,63,78,91]. In models that accounted for uncertainty appropriately, most estimates of the proportion of transmission resulting from people with SARS-CoV-2 who are presymptomatic ranged from 20% to 70%. In one study that estimated a contribution of <1% [91], the model-fitted serial interval was longer than observed in empirical studies [115]. The credibility of most modelling studies was limited by the absence of external validation. The data to which the models were fitted were generally from small samples (S7 Fig).

Discussion

Summary of main findings

The summary proportion of SARS-CoV-2 that is asymptomatic throughout the course of infection was estimated, across all study settings, to be 20% (95% CI 17%–25%, 79 studies), with a prediction interval of 3%–67%. In studies that identified SARS-CoV-2 infection through screening of defined populations, the proportion of asymptomatic infections was 31% (95% CI 26%–37%, 7 studies). In 31 studies reporting on people who are presymptomatic but who go on to develop symptoms, the results were too heterogeneous to combine. The secondary attack rate from asymptomatic infections may be lower than that from symptomatic infections (relative risk 0.35, 95% CI 0.1–1.27). Modelling studies estimated a wide range of the proportion of all SARS-CoV-2 infections that result from transmission from asymptomatic and presymptomatic individuals.

Strengths and weaknesses

A strength of this review is that we used clear definitions and separated review questions to distinguish between SARS-CoV-2 infections that remain asymptomatic throughout their course from those that become symptomatic and to separate proportions of people with infection from their contribution to transmission in a population. This living systematic review uses methods to minimise bias whilst increasing the speed of the review process [5,6] and will be updated regularly. We only included studies that provided information about follow-up through the course of infection, which allowed reliable assessment about the proportion of asymptomatic people in different settings. In the statistical synthesis of proportions, we used a method that accounts for the binary nature of the data and avoids the normality approximation (weighted logistic regression).

Limitations of the review are that most included studies were not designed to estimate the proportion of asymptomatic SARS-CoV-2 infection and definitions of asymptomatic status were often incomplete or absent. The risks of bias, particularly those affecting selection of participants, differed between studies and could result in both underestimation and overestimation of the true proportion of asymptomatic infections. Also, we did not consider the possible impact of false negative RT-PCR results, which might be more likely to occur in asymptomatic infections [116] and would underestimate the proportion of asymptomatic infections [117]. The four databases that we searched are not comprehensive, but they cover the majority of publications and we do not believe that we have missed studies that would change our conclusions.

Comparison with other reviews

We found narrative reviews that reported wide ranges (5%–96%) of infections that might be asymptomatic [1,118]. These reviews presented cross-sectional studies alongside longitudinal studies and did not distinguish between asymptomatic and presymptomatic infection. We found three systematic reviews, which reported similar summary estimates from meta-analysis

of studies published up to May [119–121]. In two reviews, authors applied inclusion criteria to reduce the risks of selection bias, with summary estimates of 11% (95% CI 4%–18%, 6 studies) [120] and 15% (95% CI 12%–18%, 9 studies) [121]. Our review includes all these studies, mostly in the categories of aggregated contact or outbreak investigations, with compatible summary estimates (Fig 1). We categorised one report [81] with other studies in which a defined population was screened. The summary estimate in the third systematic review (16%, 95% CI 10%–23%, 41 studies) [119] was similar to that of other systematic reviews, despite inclusion of studies with no information about follow-up. In comparison with other reviews, rather than restricting inclusion, we give a comprehensive overview of studies with adequate follow-up, with assessment of risks of bias and exploration of heterogeneity (S2–S7 Figs). The three versions of this review to date have shown how types of evidence change over time, from single-family investigations to large screening studies (S1 Table).

Interpretation

The findings from systematic reviews, including ours [119–121], do not support the claim that a large majority of SARS-CoV-2 infections are asymptomatic [122]. We estimated that, across all study settings, the proportion of SARS-CoV-2 infections that are asymptomatic throughout the course of infection is 20% (95% CI 17%–25%). The wider prediction interval reflects the heterogeneity between studies and indicates that future studies with similar study designs and in similar settings will estimate a proportion of asymptomatic infections from 3% to 67%. Studies that detect SARS-CoV-2 through screening of defined populations irrespective of infection status at enrolment should be less affected by selection biases. In this group of studies, the estimated proportion of asymptomatic infection was 31% (95% CI 26%–37%, prediction interval 24%–38%). This estimate suggests that other studies might have had an overrepresentation of participants diagnosed because of symptoms, but there were also potential selection biases in screening studies that might have overestimated the proportion of asymptomatic infections. Our knowledge to date is based on data collected during the acute phase of an international public health emergency, mostly for other purposes. To estimate the true proportion of asymptomatic SARS-CoV-2 infections, researchers need to design prospective longitudinal studies with clear definitions, methods that minimise selection and measurement biases, and transparent reporting. Serological tests, in combination with virological diagnostic methods, might improve ascertainment of SARS-CoV-2 infection in asymptomatic populations. Prospective documentation of symptom status would be required, and improvements in the performance of serological tests are still needed [123].

Our review adds to information about the relative contributions of asymptomatic and pre-symptomatic infection to overall SARS-CoV-2 transmission. Since all people infected with SARS-CoV-2 are initially asymptomatic, the proportion that will go on to develop symptoms can be derived by subtraction from the estimated proportion with true asymptomatic infections; from our review, we would estimate this fraction to be 80% (95% CI 75%–83%). Since SARS-CoV-2 can be transmitted a few days before the onset of symptoms [124], presymptomatic transmission likely contributes substantially to overall SARS-CoV-2 epidemics. The analysis of secondary attack rates provides some evidence of lower infectiousness of people with asymptomatic than symptomatic infection (Fig 3) [36,65,66,90,111], but more studies are needed to quantify this association more precisely. If both the proportion and transmissibility of asymptomatic infection are relatively low, people with asymptomatic SARS-CoV-2 infection should account for a smaller proportion of overall transmission than presymptomatic individuals. This is consistent with the findings of the only mathematical modelling study in our review that explored this question [19]. Uncertainties in estimates of the true proportion and

the relative infectiousness of asymptomatic SARS-CoV-2 infection and other infection parameters contributed to heterogeneous predictions about the proportion of presymptomatic transmission [20,33,51,63,78,91].

Implications and unanswered questions

Integration of evidence from epidemiological, clinical, and laboratory studies will help to clarify the relative infectiousness of asymptomatic SARS-CoV-2. Studies using viral culture as well as RNA detection are needed, since RT-PCR defined viral loads appear to be broadly similar in asymptomatic and symptomatic people [116,125]. Age might play a role as children appear more likely than adults to have an asymptomatic course of infection (Fig 1) [126]; age was poorly reported in studies included in this review (Table 1).

SARS-CoV-2 transmission from people who are either asymptomatic or presymptomatic has implications for prevention. Social distancing measures will need to be sustained at some level because droplet transmission from close contact with people with asymptomatic and presymptomatic infection occurs. Easing of restrictions will, however, only be possible with wide access to testing, contact tracing, and rapid isolation of infected individuals. Quarantine of close contacts is also essential to prevent onward transmission during asymptomatic or presymptomatic periods of those that have become infected. Digital, proximity tracing could supplement classical contact tracing to speed up detection of contacts to interrupt transmission during the presymptomatic phase if shown to be effective [19,127]. The findings of this systematic review of publications early in the pandemic suggests that most SARS-CoV-2 infections are not asymptomatic throughout the course of infection. The contribution of presymptomatic and asymptomatic infections to overall SARS-CoV-2 transmission means that combination prevention measures, with enhanced hand and respiratory hygiene, testing tracing, and isolation strategies and social distancing, will continue to be needed.

Supporting information

S1 PRISMA Checklist.

(DOCX)

S1 Text. Search strings.

(DOCX)

S1 Fig. Flowchart.

(PDF)

S2 Fig. Review question 1, forest plot of included studies, by study precision.

(PDF)

S3 Fig. Risk of bias in studies included in review question 1 and review question 2.

(PDF)

S4 Fig. Review question 2, forest plot of included studies, by study precision.

(PDF)

S5 Fig. Review question 1, subgroup analysis comparing studies of hospitalised patients with all other settings.

(PDF)

S6 Fig. Review question 1, sensitivity analysis, omitting studies that were preprints at the time of literature search.

(PDF)

S7 Fig. Assessment of credibility of mathematical modelling studies.

(PDF)

S1 Table. Types of study included in successive versions of the living systematic review, as of 10 June 2020.

(DOCX)

S2 Table. Location of studies contributing data to review questions 1 and 2.

(DOCX)

Author Contributions

Conceptualization: Diana Buitrago-Garcia, Dianne Egli-Gany, Nicola Low.

Data curation: Diana Buitrago-Garcia, Dianne Egli-Gany, Michel J. Counotte, Stefanie Hossmann, Hira Imeri, Nicola Low.

Formal analysis: Michel J. Counotte, Georgia Salanti.

Investigation: Aziz Mert Ipekci.

Methodology: Diana Buitrago-Garcia, Dianne Egli-Gany, Michel J. Counotte, Georgia Salanti, Nicola Low.

Project administration: Diana Buitrago-Garcia, Dianne Egli-Gany.

Supervision: Nicola Low.

Validation: Diana Buitrago-Garcia, Dianne Egli-Gany, Michel J. Counotte, Stefanie Hossmann, Hira Imeri, Aziz Mert Ipekci, Nicola Low.

Writing – original draft: Diana Buitrago-Garcia, Nicola Low.

Writing – review & editing: Diana Buitrago-Garcia, Dianne Egli-Gany, Michel J. Counotte, Stefanie Hossmann, Hira Imeri, Aziz Mert Ipekci, Georgia Salanti, Nicola Low.

References

- Oran DP, Topol EJ. Prevalence of Asymptomatic Sars-Cov-2 Infection: A Narrative Review. *Ann Intern Med*. 2020. Epub 2020/06/04. <https://doi.org/10.7326/M20-3012> PMID: 32491919.
- World Health Organization. Coronavirus Disease 2019 (Covid-19) Situation Report—73. Geneva: 2020.
- Lipsitch M, Swerdlow DL, Finelli L. Defining the Epidemiology of Covid-19—Studies Needed. *N Engl J Med*. 2020. Epub 2020/02/20. <https://doi.org/10.1056/NEJMp2002125> PMID: 32074416.
- Elliott JH, Turner T, Clavisi O, Thomas J, Higgins JP, Mavergames C, et al. Living Systematic Reviews: An Emerging Opportunity to Narrow the Evidence-Practice Gap. *PLoS Med*. 2014; 11(2): e1001603. <https://doi.org/10.1371/journal.pmed.1001603> PMID: 24558353; PubMed Central PMCID: PMC3928029.
- Thomas J, Noel-Storr A, Marshall I, Wallace B, McDonald S, Mavergames C, et al. Living Systematic Reviews: 2. Combining Human and Machine Effort. *J Clin Epidemiol*. 2017; 91:31–7. Epub 2017/09/16. <https://doi.org/10.1016/j.jclinepi.2017.08.011> PMID: 28912003.
- Rapid Reviews to Strengthen Health Policy and Systems: A Practical Guide. Geneva: World Health Organization; 2017 [cited 2020 Jul 27]. Available from: <https://apps.who.int/iris/bitstream/handle/10665/258698/9789241512763-eng.pdf;sequence=1>.
- Buitrago-Garcia D, Egli-Gany D, Counotte M, Hossmann S, Imeri H, Salanti G, et al. The Role of Asymptomatic Sars-Cov-2 Infections: Rapid Living Systematic Review and Meta-Analysis. Version 1. medRxiv [Preprint]. 2020 [cited 2020 Jul 27]. Available from: <https://doi.org/10.1101/2020.04.25.20079103>

8. Buitrago-Garcia D, Egli-Gany D, Counotte M, Hossmann S, Imeri H, Salanti G, et al. The Role of Asymptomatic Sars-Cov-2 Infections: Rapid Living Systematic Review and Meta-Analysis. Version 2. medRxiv [Preprint]. 2020 [cited 2020 Jul 27]. Available from: <https://doi.org/10.1101/2020.04.25.20079103>
9. Liberati A, Altman DG, Tetzlaff J, Mulrow C, Gotzsche PC, Ioannidis JP, et al. The Prisma Statement for Reporting Systematic Reviews and Meta-Analyses of Studies That Evaluate Health Care Interventions: Explanation and Elaboration. PLoS Med. 2009; 6(7):e1000100. <https://doi.org/10.1371/journal.pmed.1000100> PMID: 19621070
10. Counotte M, Imeri H, Ipekci M, Low N. Covid-19 Living Evidence. Bern: Institute of Social and Preventive Medicine, University of Bern; 2020 [cited 2020 May 9]. Available from: <https://ispmbern.github.io/covid-19/living-review/>
11. Joanna Briggs Institute. The Joanna Briggs Institute Critical Appraisal Tools for Use in JBI Systematic Reviews—Checklist for Case Series. 2017 [cited 2020 Aug 31]. Available from: https://joannabriggs.org/sites/default/files/2019-05/JBI_Critical_Appraisal-Checklist_for_Case_Series2017_0.pdf
12. Boyle MH. Guidelines for Evaluating Prevalence Studies. Evid Based Ment Health. 1998; 1(2):37–40.
13. Jaime Caro J, Eddy DM, Kan H, Kaltz C, Patel B, Eldessouki R, et al. Questionnaire to Assess Relevance and Credibility of Modeling Studies for Informing Health Care Decision Making: An Ispor-Amcp-Npc Good Practice Task Force Report. Value Health. 2014; 17(2):174–82. <https://doi.org/10.1016/j.jval.2014.01.003> PMID: 24636375.
14. Balduzzi S, Rucker G, Schwarzer G. How to Perform a Meta-Analysis with R: A Practical Tutorial. Evid Based Ment Health. 2019; 22(4):153–60. Epub 2019/09/30. <https://doi.org/10.1136/ebmental-2019-300117> PMID: 31563865.
15. Newcombe RG. Two-Sided Confidence Intervals for the Single Proportion: Comparison of Seven Methods. Stat Med. 1998; 17(8):857–72. [https://doi.org/10.1002/\(sici\)1097-0258\(19980430\)17:8<857::aid-sim777>3.0.co;2-e](https://doi.org/10.1002/(sici)1097-0258(19980430)17:8<857::aid-sim777>3.0.co;2-e) PMID: 9595616
16. Riley RD, Higgins JP, Deeks JJ. Interpretation of Random Effects Meta-Analyses. BMJ. 2011; 342:d549. <https://doi.org/10.1136/bmj.d549> PMID: 21310794
17. Bai Y, Yao L, Wei T, Tian F, Jin DY, Chen L, et al. Presumed Asymptomatic Carrier Transmission of Covid-19. JAMA. 2020; 54(0):E017. <https://doi.org/10.1001/jama.2020.2565> PMID: 32083643
18. Chan JF, Yuan S, Kok KH, To KK, Chu H, Yang J, et al. A Familial Cluster of Pneumonia Associated with the 2019 Novel Coronavirus Indicating Person-to-Person Transmission: A Study of a Family Cluster. Lancet. 2020; 395(10223):514–23. Epub 2020/01/28. [https://doi.org/10.1016/S0140-6736\(20\)30154-9](https://doi.org/10.1016/S0140-6736(20)30154-9) PMID: 31986261; PubMed Central PMCID: 7159286.
19. Ferretti L, Wymant C, Kendall M, Zhao L, Nurtay A, Abeler-Dörner L, et al. Quantifying Sars-Cov-2 Transmission Suggests Epidemic Control with Digital Contact Tracing. Science. 2020; 368(6491):2020.03.08.20032946. Epub 2020/04/03. <https://doi.org/10.1126/science.abb6936> PMID: 32234805; PubMed Central PMCID: 7164555.
20. Ganyani T, Kremer C, Chen D, Torneri A, Faes C, Wallinga J, et al. Estimating the Generation Interval for Coronavirus Disease (Covid-19) Based on Symptom Onset Data, March 2020. Euro Surveill. 2020; 25(17):2020.03.05.20031815. Epub 2020/05/07. <https://doi.org/10.2807/1560-7917.ES.2020.25.17.2000257> PMID: 32372755; PubMed Central PMCID: 7201952.
21. Hu Z, Song C, Xu C, Jin G, Chen Y, Xu X, et al. Clinical Characteristics of 24 Asymptomatic Infections with Covid-19 Screened among Close Contacts in Nanjing, China. Sci China Life Sci. 2020; 63(5):706–11. Epub 2020/03/09. <https://doi.org/10.1007/s11427-020-1661-4> PMID: 32146694; PubMed Central PMCID: 7088568.
22. Liao J, Fan S, Chen J, Wu J, Xu S, Guo Y, et al. Epidemiological and Clinical Characteristics of Covid-19 in Adolescents and Young Adults. medRxiv [Preprint]. 2020. Available from: <https://www.medrxiv.org/content/10.1101/2020.03.10.20032136v1>
23. Luo SH, Liu W, Liu ZJ, Zheng XY, Hong CX, Liu ZR, et al. A Confirmed Asymptomatic Carrier of 2019 Novel Coronavirus. Chin Med J (Engl). 2020; 133(9):1123–5. Epub 2020/03/10. <https://doi.org/10.1097/CM9.0000000000000798> PMID: 32149768.
24. Mizumoto K, Kagaya K, Zarebski A, Chowell G. Estimating the Asymptomatic Proportion of Coronavirus Disease 2019 (Covid-19) Cases on Board the Diamond Princess Cruise Ship, Yokohama, Japan, 2020. Euro Surveill. 2020; 25(10). Epub 2020/03/19. <https://doi.org/10.2807/1560-7917.ES.2020.25.10.2000180> PMID: 32183930; PubMed Central PMCID: 7078829.
25. Nishiura H, Kobayashi T, Suzuki A, Jung SM, Hayashi K, Kinoshita R, et al. Estimation of the Asymptomatic Ratio of Novel Coronavirus Infections (Covid-19). Int J Infect Dis. 2020. <https://doi.org/10.1016/j.ijid.2020.03.020> PMID: 32179137
26. Qian G, Yang N, Ma AHY, Wang L, Li G, Chen X, et al. A Covid-19 Transmission within a Family Cluster by Presymptomatic Infectors in China. Clin Infect Dis. 2020; 71(15):861–862. <https://doi.org/10.1093/cid/ciaa316> PMID: 32201889

27. Tabata S, Imai K, Kawano S, Ikeda M, Kodama T, Miyoshi K, et al. Non-Severe Vs Severe Symptomatic Covid-19: 104 Cases from the Outbreak on the Cruise Ship 'Diamond Princess' in Japan. medRxiv [Preprint]. 2020 [cited 2020 Jul 27]. <https://doi.org/10.1101/2020.03.18.20038125>
28. Arima Y, Shimada T, Suzuki M, Suzuki T, Kobayashi Y, Tsuchihashi Y, et al. Severe Acute Respiratory Syndrome Coronavirus 2 Infection among Returnees to Japan from Wuhan, China, 2020. *Emerg Infect Dis.* 2020; 26(7). Epub 2020/04/11. <https://doi.org/10.3201/eid2607.200994> PMID: 32275498.
29. Breslin N, Baptiste C, Gyamfi-Bannerman C, Miller R, Martinez R, Bernstein K, et al. Covid-19 Infection among Asymptomatic and Symptomatic Pregnant Women: Two Weeks of Confirmed Presentations to an Affiliated Pair of New York City Hospitals. *Am J Obstet Gynecol MFM.* 2020;100118. Epub 2020/04/16. <https://doi.org/10.1016/j.ajogmf.2020.100118> PMID: 32292903; PubMed Central PMCID: PMC7144599.
30. Le TQM, Takemura T, Moi ML, Nabeshima T, Nguyen LKH, Hoang VMP, et al. Severe Acute Respiratory Syndrome Coronavirus 2 Shedding by Travelers, Vietnam, 2020. *Emerg Infect Dis.* 2020. <https://doi.org/10.3201/eid2607.200591> PMID: 32240079
31. Chang L, Zhao L, Gong H, Wang L, Wang L. Severe Acute Respiratory Syndrome Coronavirus 2 Rna Detected in Blood Donations. *Emerg Infect Dis.* 2020; 26(7). Epub 2020/04/04. <https://doi.org/10.3201/eid2607.200839> PMID: 32243255.
32. Danis K, Epaulard O, Benet T, Gaymard A, Campoy S, Bothelo-Nevers E, et al. Cluster of Coronavirus Disease 2019 (Covid-19) in the French Alps, 2020. *Clin Infect Dis.* 2020. Epub 2020/04/12. <https://doi.org/10.1093/cid/ciaa424> PMID: 32277759; PubMed Central PMCID: 7184384.
33. He X, Lau EHY, Wu P, Deng X, Wang J, Hao X, et al. Temporal Dynamics in Viral Shedding and Transmissibility of Covid-19. *Nat Med.* 2020. Epub 2020/04/17. <https://doi.org/10.1038/s41591-020-0869-5> PMID: 32296168.
34. Hoehl S, Rabenau H, Berger A, Kortenbusch M, Cinatl J, Bojkova D, et al. Evidence of Sars-Cov-2 Infection in Returning Travelers from Wuhan, China. *N Engl J Med.* 2020; 382(13):1278–80. Epub 2020/02/19. <https://doi.org/10.1056/NEJMc2001899> PMID: 32069388; PubMed Central PMCID: 7121749.
35. Kimball A, Hatfield KM, Arons M, James A, Taylor J, Spicer K, et al. Asymptomatic and Presymptomatic Sars-Cov-2 Infections in Residents of a Long-Term Care Skilled Nursing Facility—King County, Washington, March 2020. *MMWR Morb Mortal Wkly Rep.* 2020; 69(13):377–81. Epub 2020/04/03. <https://doi.org/10.15585/mmwr.mm6913e1> PMID: 32240128; PubMed Central PMCID: PMC7119514
36. Luo L, Liu D, Liao X-I, Wu X-b, Jing Q-I, Zheng J-z, et al. Modes of Contact and Risk of Transmission in Covid-19 among Close Contacts. *bioRxiv* [Preprint]. 2020 [cited 2020 Jul 27]. Available from: <https://www.medrxiv.org/content/10.1101/2020.03.24.20042606v1>
37. Lytras T, Dellis G, Flountzi A, Hatzianastasiou S, Nikolopoulou G, Tsekou K, et al. High Prevalence of Sars-Cov-2 Infection in Repatriation Flights to Greece from Three European Countries. *J Travel Med.* 2020. Epub 2020/04/17. <https://doi.org/10.1093/jtm/taaa054> PMID: 32297940; PubMed Central PMCID: 7184451.
38. Meng H, Xiong R, He R, Lin W, Hao B, Zhang L, et al. Ct Imaging and Clinical Course of Asymptomatic Cases with Covid-19 Pneumonia at Admission in Wuhan, China. *J Infect.* 2020. Epub 2020/04/16. <https://doi.org/10.1016/j.jinf.2020.04.004> PMID: 32294504; PubMed Central PMCID: 7152865.
39. Pongpirul WA, Mott JA, Woodring JV, Uyeki TM, MacArthur JR, Vachiraphan A, et al. Clinical Characteristics of Patients Hospitalized with Coronavirus Disease, Thailand. *Emerg Infect Dis.* 2020; 26(7). Epub 2020/04/09. <https://doi.org/10.3201/eid2607.200598> PMID: 32267826.
40. Qiu H, Wu J, Hong L, Luo Y, Song Q, Chen D. Clinical and Epidemiological Features of 36 Children with Coronavirus Disease 2019 (Covid-19) in Zhejiang, China: An Observational Cohort Study. *Lancet Infect Dis.* 2020. Epub 2020/03/30. [https://doi.org/10.1016/S1473-3099\(20\)30198-5](https://doi.org/10.1016/S1473-3099(20)30198-5) PMID: 32220650; PubMed Central PMCID: PMC7158906.
41. See KC, Liew SM, Ng DCE, Chew EL, Khoo EM, Sam CH, et al. Covid-19: Four Paediatric Cases in Malaysia. *Int J Infect Dis.* 2020; 94:125–7. Epub 2020/04/19. <https://doi.org/10.1016/j.ijid.2020.03.049> PMID: 32304822; PubMed Central PMCID: PMC7158792.
42. Tan YP, Tan BY, Pan J, Wu J, Zeng SZ, Wei HY. Epidemiologic and Clinical Characteristics of 10 Children with Coronavirus Disease 2019 in Changsha, China. *J Clin Virol.* 2020; 127(NA):104353. Epub 2020/04/18. <https://doi.org/10.1016/j.jcv.2020.104353> PMID: 32302953; PubMed Central PMCID: PMC7195108.
43. Tian S, Wu M, Chang Z, Wang Y, Zhou G, Zhang W, et al. Epidemiological Investigation and Intergenerational Clinical Characteristics of 24 Covid-19 Patients Associated with Supermarket Cluster. *bioRxiv* [Preprint]. 2020 [cited 2020 Jul 27]. <https://doi.org/10.1101/2020.04.11.20058891>
44. Tong ZD, Tang A, Li KF, Li P, Wang HL, Yi JP, et al. Potential Presymptomatic Transmission of Sars-Cov-2, Zhejiang Province, China, 2020. *Emerg Infect Dis.* 2020; 26(5):1052–4. Epub 2020/02/25. <https://doi.org/10.3201/eid2605.200198> PMID: 32091386; PubMed Central PMCID: PMC7181913.

45. Wang X, Fang J, Zhu Y, Chen L, Ding F, Zhou R, et al. Clinical Characteristics of Non-Critically Ill Patients with Novel Coronavirus Infection (Covid-19) in a Fangcang Hospital. *Clin Microbiol Infect*. 2020. Epub 2020/04/07. <https://doi.org/10.1016/j.cmi.2020.03.032> PubMed Central PMCID: PMC7195539. PMID: 32251842
46. Wang Y, Liu Y, Liu L, Wang X, Luo N, Ling L. Clinical Outcome of 55 Asymptomatic Cases at the Time of Hospital Admission Infected with Sars-Coronavirus-2 in Shenzhen, China. *J Infect Dis*. 2020. Epub 2020/03/18. <https://doi.org/10.1093/infdis/jiaa119> PMID: 32179910; PubMed Central PMCID: PMC7184401.
47. Wang Z, Ma W, Zheng X, Wu G, Zhang R. Household Transmission of Sars-Cov-2. *J Infect*. 2020. Epub 2020/04/14. <https://doi.org/10.1016/j.jinf.2020.03.040> PMID: 32283139; PubMed Central PMCID: PMC7151261.
48. Yang N, Shen Y, Shi C, Ma AHY, Zhang X, Jian X, et al. In-Flight Transmission Cluster of Covid-19: A Retrospective Case Series. *bioRxiv [Preprint]*. 2020 [cited 2020 Jul 27]. <https://doi.org/10.1101/2020.03.28.20040097>
49. Ye F, Xu S, Rong Z, Xu R, Liu X, Deng P, et al. Delivery of Infection from Asymptomatic Carriers of Covid-19 in a Familial Cluster. *Int J Infect Dis*. 2020; 94:133–8. Epub 2020/04/06. <https://doi.org/10.1016/j.ijid.2020.03.042> PMID: 32247826; PubMed Central PMCID: PMC7129961.
50. Zhang J, Tian S, Lou J, Chen Y. Familial Cluster of Covid-19 Infection from an Asymptomatic. *Crit Care*. 2020. <https://doi.org/10.1186/s13054-020-2817-7> PMID: 32220236
51. Zhang W. Estimating the Presymptomatic Transmission of Covid19 Using Incubation Period and Serial Interval Data. *bioRxiv [Preprint]*. 2020 [cited 2020 Jul 27]. <https://doi.org/10.1101/2020.04.02.20051318>
52. Zhou X, Li Y, Li T, Zhang W. Follow-up of Asymptomatic Patients with Sars-Cov-2 Infection. *Clin Microbiol Infect*. 2020. Epub 2020/04/03. <https://doi.org/10.1016/j.cmi.2020.03.024> PMID: 32234453.
53. Zou L, Ruan F, Huang M, Liang L, Huang H, Hong Z, et al. Sars-Cov-2 Viral Load in Upper Respiratory Specimens of Infected Patients. *N Engl J Med*. 2020; 382(12):1177–9. Epub 2020/02/20. <https://doi.org/10.1056/NEJMc2001737> PMID: 32074444; PubMed Central PMCID: PMC7121626.
54. Alshami AA, Alattas RA, Anan HF, Al Qahtani HS, Al Mulhim MA, Alahilmi AA, et al. Silent Disease and Loss of Taste and Smell Are Common Manifestations of Sars-Cov-2 Infection in a Quarantine Facility: First Report from Saudi Arabia. *medRxiv [Preprint]*. 2020 [cited 2020 Jul 27]. <https://doi.org/10.1101/2020.05.13.20100222>
55. Al-Shamsi HO, Coomes EA, Alrawi S. Screening for Covid-19 in Asymptomatic Patients with Cancer in a Hospital in the United Arab Emirates. *JAMA Oncol*. 2020. <https://doi.org/10.1001/jamaoncol.2020.2548> PMID: 32459297
56. Andrikopoulou M, Madden N, Wen T, Aubey JJ, Aziz A, Baptiste CD, et al. Symptoms and Critical Illness among Obstetric Patients with Coronavirus Disease 2019 (Covid-19) Infection. *Obstet Gynecol*. 2020. <https://doi.org/10.1097/AOG.0000000000003996> PMID: 32459701
57. Angelo Vaira L, Hopkins C, Salzano G, Petrocelli M, Melis A, Cucurullo M, et al. Olfactory and Gustatory Function Impairment in Covid-19 Patients: Italian Objective Multicenter-Study. *Head Neck*. 2020. <https://doi.org/10.1002/hed.26269> PMID: 32437022
58. Arons MM, Hatfield KM, Reddy SC, Kimball A, James A, Jacobs JR, et al. Presymptomatic Sars-Cov-2 Infections and Transmission in a Skilled Nursing Facility. *N Engl J Med*. 2020. <https://doi.org/10.1056/NEJMoa2008457> PMID: 32329971
59. Bai K, Liu W, Liu C, Fu Y, Hu J, Qin Y, et al. Clinical Analysis of 25 Novel Coronavirus Infections in Children. *Pediatr Infect Dis J*. 2020. <https://doi.org/10.1097/INF.0000000000002740> PMID: 32520888
60. Bi Q, Wu Y, Mei S, Ye C, Zou X, Zhang Z, et al. Epidemiology and Transmission of Covid-19 in 391 Cases and 1286 of Their Close Contacts in Shenzhen, China: A Retrospective Cohort Study. *Lancet Infect Dis*. 2020. Epub 2020/05/01. [https://doi.org/10.1016/S1473-3099\(20\)30287-5](https://doi.org/10.1016/S1473-3099(20)30287-5) PMID: 32353347; PubMed Central PMCID: PMC7185944.
61. Bohmer MM, Buchholz U, Corman VM, Hoch M, Katz K, Marosevic DV, et al. Investigation of a Covid-19 Outbreak in Germany Resulting from a Single Travel-Associated Primary Case: A Case Series. *Lancet Infect Dis*. 2020. Epub 2020/05/19. [https://doi.org/10.1016/S1473-3099\(20\)30314-5](https://doi.org/10.1016/S1473-3099(20)30314-5) PMID: 32422201; PubMed Central PMCID: PMC7228725.
62. Brandstetter S, Roth S, Harner S, Buntrock-Döpke H, Toncheva A, Borchers N, et al. Symptoms and Immunoglobulin Development in Hospital Staff Exposed to a Sars-Cov-2 Outbreak. *Pediatr Allergy Immunol*. 2020. <https://doi.org/10.1111/pai.13278> PMID: 32413201
63. Casey M, Griffin J, McAloon CG, Byrne AW, Madden JM, McEvoy D, et al. Estimating Pre-Symptomatic Transmission of Covid-19: A Secondary Analysis Using Published Data. *medRxiv [Preprint]*. 2020 [cited 2020 Jul 27]. <https://doi.org/10.1101/2020.05.08.20094870>

64. Chang MC, Hur J, Park D. Chest Computed Tomography Findings in Asymptomatic Patients with Covid-19. medRxiv [Preprint]. 2020 [cited 2020 Jul 27]. <https://doi.org/10.1101/2020.05.09.20096370>
65. Chaw L, Koh WC, Jamaludin SA, Naing L, Alikhan MF, Wong J. Sars-Cov-2 Transmission in Different Settings: Analysis of Cases and Close Contacts from the Tablighi Cluster in Brunei Darussalam. medRxiv [Preprint]. 2020 [cited 2020 Jul 27]. <https://doi.org/10.1101/2020.05.04.20090043>
66. Cheng HY, Jian SW, Liu DP, Ng TC, Huang WT, Lin HH, et al. Contact Tracing Assessment of Covid-19 Transmission Dynamics in Taiwan and Risk at Different Exposure Periods before and after Symptom Onset. JAMA Intern Med. 2020. Epub 2020/05/02. <https://doi.org/10.1001/jamainternmed.2020.2020> PMID: 32356867; PubMed Central PMCID: PMC7195694.
67. Choe PG, Kang EK, Lee SY, Oh B, Im D, Lee HY, et al. Selecting Coronavirus Disease 2019 Patients with Negligible Risk of Progression: Early Experience from Non-Hospital Isolation Facility in Korea. Korean J Intern Med. 2020. <https://doi.org/10.3904/kjim.2020.159> PMID: 32460457
68. Dora AV, Winnett A, Jatt LP, Davar K, Watanabe M, Sohn L, et al. Universal and Serial Laboratory Testing for Sars-Cov-2 at a Long-Term Care Skilled Nursing Facility for Veterans—Los Angeles, California, 2020. MMWR Morb Mortal Wkly Rep. 2020. <https://doi.org/10.15585/mmwr.mm6921e1> PMID: 32463809
69. Emery JC, Russel TW, Liu Y, Hellewell J, Pearson CA, group Cnw, et al. The Contribution of Asymptomatic Sars-Cov-2 Infections to Transmission—a Model-Based Analysis of the Diamond Princess Outbreak. medRxiv [Preprint]. 2020 [cited 2020 Jul 27]. <https://doi.org/10.1101/2020.05.07.20093849>
70. Gao Y, Shi C, Chen Y, Shi P, Liu J, Xiao Y, et al. A Cluster of the Corona Virus Disease 2019 Caused by Incubation Period Transmission in Wuxi, China. J Infect. 2020. <https://doi.org/10.1016/j.jinf.2020.03.042> PMID: 32283165
71. Graham N, Junghans C, Downes R, Sendall C, Lai H, McKirdy A, et al. Sars-Cov-2 Infection, Clinical Features and Outcome of Covid-19 in United Kingdom Nursing Homes. J Infect. 2020. <https://doi.org/10.1016/j.jinf.2020.05.073> PMID: 32504743
72. Hijnen D, Marzano AV, Eyerich K, GeurtsvanKessel C, Giménez-Arnau AM, Joly P, et al. Sars-Cov-2 Transmission from Presymptomatic Meeting Attendee, Germany. Emerg Infect Dis. 2020. <https://doi.org/10.3201/eid2608.201235> PMID: 32392125
73. Huang L, Jiang J, Li X, Zhou Y, Xu M, Zhou J. Initial Ct Imaging Characters of an Imported Family Cluster of Covid-19. Clin Imaging. 2020. <https://doi.org/10.1016/j.clinimag.2020.04.010> PMID: 32361413
74. Huang R, Zhao H, Wang J, Yan X, Shao H, Wu C. A Family Cluster of Covid-19 Involving an Asymptomatic Case with Persistently Positive Sars-Cov-2 in Anal Swabs. Travel Med Infect Dis. 2020. <https://doi.org/10.1016/j.tmaid.2020.101745> PMID: 32425697
75. Jiang X, Luo M, Zou Z, Wang X, Chen C, Qiu J. Asymptomatic Sars-Cov-2 Infected Case with Viral Detection Positive in Stool but Negative in Nasopharyngeal Samples Lasts for 42 Days. J Med Virol. 2020. <https://doi.org/10.1002/jmv.25941> PMID: 32330309
76. Jiang XL, Zhang XL, Zhao XN, Li CB, Lei J, Kou ZQ, et al. Transmission Potential of Asymptomatic and Paucisymptomatic Sars-Cov-2 Infections: A Three-Family Cluster Study in China. J Infect Dis. 2020. <https://doi.org/10.1093/infdis/jiaa206> PMID: 32319519
77. Kim SE, Jeong HS, Yu Y, Shin SU, Kim S, Oh TH, et al. Viral Kinetics of Sars-Cov-2 in Asymptomatic Carriers and Presymptomatic Patients. Int J Infect Dis. 2020. <https://doi.org/10.1016/j.ijid.2020.04.083> PMID: 32376309
78. Kim Y, Chun JY, Baek G. Transmission Onset Distribution of Covid-19 in South Korea. medRxiv [Preprint]. 2020 [cited 2020 Jul 27]. <https://doi.org/10.1101/2020.05.13.20101246>
79. Kong W, Wang Y, Hu J, Chughtai A, Pu H. Comparison of Clinical and Epidemiological Characteristics of Asymptomatic and Symptomatic Sars-Cov-2 Infection: A Multi-Center Study in Sichuan Province, China. Travel Med Infect Dis. 2020. <https://doi.org/10.1016/j.tmaid.2020.101754> PMID: 32492485
80. Kumar R, Bhattacharya B, Meena VP, Aggarwal A, Tripathi M, Soneja M, et al. Management of Mild Covid-19: Policy Implications of Initial Experience in India. medRxiv [Preprint]. 2020 [cited 2020 Jul 27]. <https://doi.org/10.1101/2020.05.20.20107664>
81. Lavezzo E, Franchin E, Ciavarella C, Cuomo-Dannenburg G, Barzon L, Del Vecchio C, et al. Suppression of a Sars-Cov-2 Outbreak in the Italian Municipality of Vo'. Nature. 2020. Epub 2020/07/01. <https://doi.org/10.1038/s41586-020-2488-1> PMID: 32604404.
82. Lombardi A, Consonni D, Carugno M, Bozzi G, Mangioni D, Muscatello A, et al. Characteristics of 1,573 Healthcare Workers Who Underwent Nasopharyngeal Swab for Sars-Cov-2 in Milano, Lombardy, Italy. medRxiv [Preprint]. 2020 [cited 2020 Jul 27]. <https://doi.org/10.1101/2020.05.07.20094276>

83. London V, McLaren R, Atallah F, Cepeda C, McCalla S, Fisher N, et al. The Relationship between Status at Presentation and Outcomes among Pregnant Women with Covid-19. *Am J Perinatol*. 2020. <https://doi.org/10.1055/s-0040-1712164> PMID: 32428964
84. Lu Y, Li Y, Deng W, Liu M, He Y, Huang L, et al. Symptomatic Infection Is Associated with Prolonged Duration of Viral Shedding in Mild Coronavirus Disease 2019: A Retrospective Study of 110 Children in Wuhan. *Pediatr Infect Dis J*. 2020. <https://doi.org/10.1097/INF.0000000000002729> PMID: 32379191
85. Luo Y, Trevathan E, Qian Z, Li Y, Li J, Xiao W, et al. Asymptomatic Sars-Cov-2 Infection in Household Contacts of a Healthcare Provider, Wuhan, China. *Emerg Infect Dis*. 2020. <https://doi.org/10.3201/eid2608.201016> PMID: 32330112
86. Ma Y, Xu QN, Wang FL, Ma XM, Wang XY, Zhang XG, et al. Characteristics of Asymptomatic Patients with Sars-Cov-2 Infection in Jinan, China. *Microbes Infect*. 2020. <https://doi.org/10.1016/j.micinf.2020.04.011> PMID: 32387682
87. Melgosa M, Madrid A, Álvarez O, Lumberras J, Nieto F, Parada E, et al. Sars-Cov-2 Infection in Spanish Children with Chronic Kidney Pathologies. *Pediatr Nephrol*. 2020. <https://doi.org/10.1007/s00467-020-04597-1> PMID: 32435879
88. Merza MA, Haleem AI Mezori AA, Mohammed HM, Abdulah DM. Covid-19 Outbreak in Iraqi Kurdistan: The First Report Characterizing Epidemiological, Clinical, Laboratory, and Radiological Findings of the Disease. *Diabetes Metab Syndr Clin Res Rev*. 2020. <https://doi.org/10.1016/j.dsx.2020.04.047> PMID: 32408119
89. Noh JY, Yoon JG, Seong H, Choi WS, Sohn JW, Cheong HJ, et al. Asymptomatic Infection and Atypical Manifestations of Covid-19: Comparison of Viral Shedding Duration. *J Infect*. 2020. <https://doi.org/10.1016/j.jinf.2020.05.035> PMID: 32445728
90. Park SY, Kim YM, Yi S, Lee S, Na BJ, Kim CB, et al. Coronavirus Disease Outbreak in Call Center, South Korea. *Emerg Infect Dis*. 2020. <https://doi.org/10.3201/eid2608.201274> PMID: 32324530
91. Peak CM, Kahn R, Grad YH, Childs LM, Li R, Lipsitch M, et al. Individual Quarantine Versus Active Monitoring of Contacts for the Mitigation of Covid-19: A Modelling Study. *Lancet Infect Dis*. 2020. [https://doi.org/10.1016/S1473-3099\(20\)30361-3](https://doi.org/10.1016/S1473-3099(20)30361-3) PMID: 32445710
92. Qiu C, Deng Z, Xiao Q, Shu Y, Deng Y, Wang H, et al. Transmission and Clinical Characteristics of Coronavirus Disease 2019 in 104 Outside-Wuhan Patients, China. *J Med Virol*. 2020. <https://doi.org/10.1002/jmv.25975> PMID: 32369217
93. Rivett L, Sridhar S, Sparkes D, Routledge M, Jones NK, Forrest S, et al. Screening of Healthcare Workers for Sars-Cov-2 Highlights the Role of Asymptomatic Carriage in Covid-19 Transmission. *Elife*. 2020; 9. Epub 2020/05/12. <https://doi.org/10.7554/eLife.58728> PMID: 32392129.
94. Roxby AC, Greninger AL, Hatfield KM, Lynch JB, Dellit TH, James A, et al. Outbreak Investigation of Covid-19 among Residents and Staff of an Independent and Assisted Living Community for Older Adults in Seattle, Washington. *JAMA Intern Med*. 2020. <https://doi.org/10.1001/jamainternmed.2020.2233> PMID: 32437547
95. Schwierzeck V, König JC, Kühn J, Mellmann A, Correa-Martínez CL, Omran H, et al. First Reported Nosocomial Outbreak of Severe Acute Respiratory Syndrome Coronavirus 2 (Sars-Cov-2) in a Pediatric Dialysis Unit. *Clin Infect Dis*. 2020. <https://doi.org/10.1093/cid/ciaa491> PMID: 32337584
96. Sharma AK, Ahmed A, Baig VN, Dhakad P, Dalela G, Kacker S, et al. Characteristics and Outcomes of Hospitalized Young Adults with Mild to Moderate Covid-19 at a University Hospital in India. *medRxiv* [Preprint]. 2020 [cited 2020 Jul 27]. <https://doi.org/10.1101/2020.06.02.20106310>
97. Solbach W, Schiffner J, Backhaus I, Burger D, Staiger R, Tiemer B, et al. Antibody Profiling of Covid-19 Patients in an Urban Low-Incidence Region in Northern Germany. *medRxiv* [Preprint]. 2020 [cited 2020 Jul 27]. <https://doi.org/10.1101/2020.05.30.20111393>
98. Song W, Li J, Zou N, Guan W, Pan J, Xu W. Clinical Features of Pediatric Patients with Coronavirus Disease (Covid-19). *J Clin Virol*. 2020. <https://doi.org/10.1016/j.jcv.2020.104377> PMID: 32361323
99. Tan X, Huang J, Zhao F, Zhou Y, Li JQ, Wang XY. [Clinical Features of Children with Sars-Cov-2 Infection: An Analysis of 13 Cases from Changsha, China]. *Zhongguo Dang Dai Er Ke Za Zhi*. 2020. <https://doi.org/10.7499/j.issn.1008-8830.2003199> PMID: 32312364
100. Pham TQ, Rabaa MA, Duong LH, Dang TQ, Tran QD, Quach HL, et al. The First 100 Days of Sars-Cov-2 Control in Vietnam. *medRxiv* [Preprint]. 2020 [cited 2020 Jul 27]. <https://doi.org/10.1101/2020.05.12.20099242>
101. Treibel TA, Manisty C, Burton M, McKnight NA, Lambourne J, Augusto JB, et al. Covid-19: Pcr Screening of Asymptomatic Health-Care Workers at London Hospital. *Lancet*. 2020. [https://doi.org/10.1016/S0140-6736\(20\)31100-4](https://doi.org/10.1016/S0140-6736(20)31100-4) PMID: 32401714

102. Wang Y, Tong J, Qin Y, Xie T, Li J, Li J, et al. Characterization of an Asymptomatic Cohort of Sars-Cov-2 Infected Individuals Outside of Wuhan, China. *Clin Infect Dis*. 2020. <https://doi.org/10.1093/cid/ciaa629> PMID: 32442265
103. Wong J, Abdul Aziz ABZ, Chaw L, Mahamud A, Griffith MM, Ying-Ru LO, et al. High Proportion of Asymptomatic and Presymptomatic Covid-19 Infections in Travelers and Returning Residents to Brunei. *J Travel Med*. 2020. <https://doi.org/10.1093/jtm/taaa066> PMID: 32365178
104. Wu HP, Li BF, Chen X, Hu HZ, Jiang SA, Cheng H, et al. Clinical Features of Coronavirus Disease 2019 in Children Aged <18 Years in Jiangxi, China: An Analysis of 23 Cases. *Zhongguo Dang Dai Er Ke Za Zhi*. 2020; 22(5):419–424. <https://doi.org/10.7499/j.issn.1008-8830.2003202> PMID: 32434634
105. Wu J, Huang Y, Tu C, Bi C, Chen Z, Luo L, et al. Household Transmission of Sars-Cov-2, Zhuhai, China, 2020. *Clin Infect Dis*. 2020. <https://doi.org/10.1093/cid/ciaa557> PMID: 32392331
106. Xu H, Liu E, Xie J, Smyth R, Zhou Q, Zhao R, et al. A Follow-up Study of Children Infected with Sars-Cov-2 from Western China. *medRxiv* [Preprint]. 2020 [cited 2020 Jul 27]. <https://doi.org/10.1101/2020.04.20.20073288>
107. Xu T, Huang R, Zhu L, Wang J, Cheng J, Zhang B, et al. Epidemiological and Clinical Features of Asymptomatic Patients with Sars-Cov-2 Infection. *J Med Virol*. 2020. <https://doi.org/10.1002/jmv.25944> PMID: 32346873
108. Yang R, Gui X, Xiong Y. Comparison of Clinical Characteristics of Patients with Asymptomatic Vs Symptomatic Coronavirus Disease 2019 in Wuhan, China. *JAMA Netw Open*. 2020. <https://doi.org/10.1001/jamanetworkopen.2020.10182> PMID: 32459353
109. Yongchen Z, Shen H, Wang X, Shi X, Li Y, Yan J, et al. Different Longitudinal Patterns of Nucleic Acid and Serology Testing Results Based on Disease Severity of Covid-19 Patients. *Emerg Microbes Infect*. 2020. <https://doi.org/10.1080/22221751.2020.1756699> PMID: 32306864
110. Zhang B, Liu S, Dong Y, Zhang L, Zhong Q, Zou Y, et al. Positive Rectal Swabs in Young Patients Recovered from Coronavirus Disease 2019 (Covid-19). *J Infect*. 2020. <https://doi.org/10.1016/j.jinf.2020.04.023> PMID: 32335176
111. Zhang W, Cheng W, Luo L, Ma Y, Xu C, Qin P, et al. Secondary Transmission of Coronavirus Disease from Presymptomatic Persons, China. *Emerg Infect Dis*. 2020. <https://doi.org/10.3201/eid2608.201142> PMID: 32453686
112. Zhang W, Long Q, Huang Y, Chen C, Wu J, Hong Y, et al. Asymptomatic Covid-19 Have Longer Treatment Cycle Than Moderate Type of Confirmed Patients. *medRxiv* [Preprint]. 2020 [cited 2020 Jul 27]. <https://doi.org/10.1101/2020.05.16.20103796>
113. Zhang Z, Xiao T, Wang Y, Yuan J, Ye H, Wei L, et al. Early Viral Clearance and Antibody Kinetics of Covid-19 among Asymptomatic Carriers. *medRxiv* [Preprint]. 2020 [cited 2020 Jul 27]. <https://doi.org/10.1101/2020.04.28.20083139>
114. Zhou R, Li F, Chen F, Liu H, Zheng J, Lei C, et al. Viral Dynamics in Asymptomatic Patients with Covid-19. *Int J Infect Dis*. 2020. <https://doi.org/10.1016/j.ijid.2020.05.030> PMID: 32437933
115. Savvides C, Siegel R. Asymptomatic and Presymptomatic Transmission of Sars-Cov-2: A Systematic Review. *medRxiv* [Preprint]. 2020 [cited 2020 Jul 27]. <https://doi.org/10.1101/2020.06.11.20129072> PMID: 32587980.
116. Chau NVV, Thanh Lam V, Thanh Dung N, Yen LM, Minh NNQ, Hung LM, et al. The Natural History and Transmission Potential of Asymptomatic Sars-Cov-2 Infection. *Clin Infect Dis*. 2020. <https://doi.org/10.1093/cid/ciaa711> PMID: 32497212
117. Kucirka LM, Lauer SA, Laeyendecker O, Boon D, Lessler J. Variation in False-Negative Rate of Reverse Transcriptase Polymerase Chain Reaction-Based Sars-Cov-2 Tests by Time since Exposure. *Ann Intern Med*. 2020. Epub 2020/05/19. <https://doi.org/10.7326/M20-1495> PMID: 32422057; PubMed Central PMCID: PMC7240870.
118. Heneghan C, Brassey J, Jefferson T. Covid-19: What Proportion Are Asymptomatic? Oxford: Centre for Evidence Based Medicine; 2020 [cited 2020 Jul 27]. Available from: <https://www.cebm.net/covid-19/covid-19-what-proportion-are-asymptomatic/>.
119. He J, Guo Y, Mao R, Zhang J. Proportion of Asymptomatic Coronavirus Disease 2019 (Covid-19): A Systematic Review and Meta-Analysis. *J Med Virol*. 2020. Epub 2020/07/22. <https://doi.org/10.1002/jmv.26326> PMID: 32691881.
120. Beale S, Hayward A, Shallcross L, Aldridge RW, Fragaszy E. A Rapid Review of the Asymptomatic Proportion of Pcr-Confirmed Sars-Cov-2 Infections in Community Settings. *medRxiv* [Preprint]. 2020 [cited 2020 Jul 27]. <https://doi.org/10.1101/2020.05.20.20108183>
121. Byambasuren O, Cardona M, Bell K, Clark J, McLaws ML, Glasziou P. Estimating the Extent of True Asymptomatic Covid-19 and Its Potential for Community Transmission: Systematic Review and Meta-Analysis. *medRxiv* [Preprint]. 2020 [cited 2020 Jul 27]. <https://doi.org/10.1101/2020.05.10.20097543>

122. Day M. Covid-19: Four Fifths of Cases Are Asymptomatic, China Figures Indicate. *BMJ*. 2020; 369: m1375. Epub 2020/04/04. <https://doi.org/10.1136/bmj.m1375> PMID: 32241884.
123. Deeks JJ, Dinnes J, Takwoingi Y, Davenport C, Spijker R, Taylor-Phillips S, et al. Antibody Tests for Identification of Current and Past Infection with Sars-Cov-2. *Cochrane Database Syst Rev*. 2020; 6: CD013652. Epub 2020/06/26. <https://doi.org/10.1002/14651858.CD013652> PMID: 32584464.
124. Wei WE, Li Z, Chiew CJ, Yong SE, Toh MP, Lee VJ. Presymptomatic Transmission of Sars-Cov-2—Singapore, January 23–March 16, 2020. *MMWR Morb Mortal Wkly Rep*. 2020; 69(14):411–5. Epub 2020/04/10. <https://doi.org/10.15585/mmwr.mm6914e1> PMID: 32271722; PubMed Central PMCID: PMC7147908
125. Long QX, Tang XJ, Shi QL, Li Q, Deng HJ, Yuan J, et al. Clinical and Immunological Assessment of Asymptomatic Sars-Cov-2 Infections. *Nat Med*. 2020. Epub 2020/06/20. <https://doi.org/10.1038/s41591-020-0965-6> PMID: 32555424.
126. Ludvigsson JF. Systematic Review of Covid-19 in Children Shows Milder Cases and a Better Prognosis Than Adults. *Acta Paediatr*. 2020; 109(6):1088–95. Epub 2020/03/24. <https://doi.org/10.1111/apa.15270> PMID: 32202343; PubMed Central PMCID: PMC7228328.
127. von Wyl V, Bonhoeffer S, Bugnion E, Puhan MA, Salathe M, Stadler T, et al. A Research Agenda for Digital Proximity Tracing Apps. *Swiss Med Wkly*. 2020; 150:w20324. Epub 2020/07/17. <https://doi.org/10.4414/smww.2020.20324> PMID: 32672340.

CORONAVIRUS

Three-quarters attack rate of SARS-CoV-2 in the Brazilian Amazon during a largely unmitigated epidemic

Lewis F. Buss^{1*}, Carlos A. Prete Jr.^{2*}, Claudia M. M. Abraham^{3*}, Alfredo Mendrone Jr.^{4,5*}, Tassila Salomon^{6,7*}, Cesar de Almeida-Neto^{4,5}, Rafael F. O. França⁸, Maria C. Belotti², Maria P. S. S. Carvalho³, Allyson G. Costa³, Myuki A. E. Crispim³, Suzete C. Ferreira^{4,5}, Nelson A. Fraiji³, Susie Gurzenda⁹, Charles Whittaker¹⁰, Leonardo T. Kamaura¹¹, Pedro L. Takecian¹¹, Pedro da Silva Peixoto¹¹, Marcio K. Oikawa¹², Anna S. Nishiya^{4,5}, Vanderson Rocha^{4,5}, Nanci A. Salles⁴, Andreza Aruska de Souza Santos¹³, Martirene A. da Silva³, Brian Custer^{14,15}, Kris V. Parag¹⁶, Manoel Barral-Netto¹⁷, Moritz U. G. Kraemer¹⁸, Rafael H. M. Pereira¹⁹, Oliver G. Pybus¹⁸, Michael P. Busch^{14,15}, Márcia C. Castro⁹, Christopher Dye¹⁸, Vítor H. Nascimento², Nuno R. Faria^{1,16,18†}, Ester C. Sabino^{1†}

Severe acute respiratory syndrome coronavirus 2 (SARS-CoV-2) spread rapidly in Manaus, the capital of Amazonas state in northern Brazil. The attack rate there is an estimate of the final size of the largely unmitigated epidemic that occurred in Manaus. We use a convenience sample of blood donors to show that by June 2020, 1 month after the epidemic peak in Manaus, 44% of the population had detectable immunoglobulin G (IgG) antibodies. Correcting for cases without a detectable antibody response and for antibody waning, we estimate a 66% attack rate in June, rising to 76% in October. This is higher than in São Paulo, in southeastern Brazil, where the estimated attack rate in October was 29%. These results confirm that when poorly controlled, COVID-19 can infect a large proportion of the population, causing high mortality.

Brazil has experienced one of the world's most rapidly growing COVID-19 epidemics, with the Amazon being the worst-hit region (1). Manaus is the largest metropolis in the Amazon, with a population of more than 2 million and a population density of 158 inhabitants/km². The first severe acute respiratory syndrome coronavirus 2 (SARS-CoV-2) case in Manaus was confirmed on 13 March 2020 (2) and was followed by an explosive epidemic, peaking in early May with 4.5-fold excess mortality (3). This was followed by a sustained drop in new cases despite relaxation of nonpharmaceutical interventions (NPIs). The prevalence of antibodies to SARS-CoV-2 is an estimate of the attack rate in Manaus and provides a data-based estimate of the extent of COVID-19 spread in the absence of effective mitigation.

Given a basic reproduction number (R_0) of 2.5 to 3.0 for Amazonas state (4), the expected attack rate during an unmitigated epidemic in a homogeneously mixed population is 89 to 94% (5). When the percentage of infected people

exceeds the herd immunity threshold of 60 to 67%, or $100 \times [1 - (1/R_0)]$, each infection generates fewer than one secondary case (case reproduction number $R_t < 1$) and incidence declines. We sought to measure the SARS-CoV-2 attack rate in Manaus and to explore whether the epidemic was contained ($R_t < 1$) because infection reached the herd immunity threshold, or because of other factors such as behavioral changes and NPIs. We compared data from Manaus with findings from São Paulo, where the first Brazilian COVID-19 cases were detected (2, 6) and both the rise and fall in mortality were slower and more protracted.

We used a chemiluminescent microparticle immunoassay (CMIA; AdviseDx, Abbott) that detects immunoglobulin G (IgG) antibodies to the SARS-CoV-2 nucleocapsid (N) protein. To infer the attack rate from antibody test positivity, we need to account for the sensitivity and specificity of the test (7). The specificity of the CMIA is high (>99.0%) (8–10), but previous high (>90.0%) sensitivity estimates (8, 10) may not apply to blood donor screening (11, 12)

for two reasons. First, most SARS-CoV-2 infections in blood donors are asymptomatic, and weaker antibody responses in asymptomatic disease (13) may lead to a lower initial seroconversion rate (i.e., more “serosilent” infections). Second, as a result of antibody waning, sensitivity falls over time (14), such that test positivity increasingly underestimates the true attack rate.

We used a variety of clinical samples at different time points to gain insight into the dynamics of the anti-N IgG detected by the Abbott CMIA (Fig. 1). In samples from hospitalized COVID-19 patients collected at 20 to 33 days after symptom onset, reflecting high disease severity and optimal timing of blood collection, sensitivity was 91.8% [95% confidence interval (CI), 80.8% to 96.8%], which suggests that ~8% of severe convalescent cases do not develop detectable antibodies. Among a cohort of symptomatic cases with mild disease also tested in the early convalescent period, sensitivity fell to 84.5% (95% CI, 78.7% to 88.9%), indicating that initial seroconversion is lower in milder cases. In samples drawn later (50 to 131 days) from the same mild disease cohort, sensitivity was lower still (80.4%; 95% CI, 71.8% to 86.8%), reflecting antibody waning. Indeed, in a subset of 104 patients with two consecutive blood draws, the signal-to-cutoff (S/C) declined over the period observed (Fig. 1B) and among 88 individuals with a positive reading at the first time point, the mean rate of decay was $-0.9 \log_2$ S/C units every 100 days (95% CI, -1.1 to -0.75), equating to a half-life of 106 days (95% CI, 89 to 132 days) (Fig. 1C).

Finally, we tested 1000 blood donations given in São Paulo in July 2020 in parallel, using a second high-specificity [>99.0% (15)] immunoassay less prone to antibody waning (14) (Roche Elecsys). Of these, 103 samples were positive using the Abbott CMIA and an additional 30 were positive using the Roche assay. Assuming that all 133 samples were true positives, the sensitivity of the Abbott N IgG assay was 77.4% (95% CI, 69.6% to 83.7%) on asymptomatic blood donor samples. Samples in July were donated 4 months into the ongoing epidemic in São Paulo; accordingly, the false negatives using the Abbott assay include cases that did not initially seroconvert, as well as past infections that had subsequently seroreverted.

¹Departamento de Molestias Infecciosas e Parasitárias and Instituto de Medicina Tropical da Faculdade de Medicina da Universidade de São Paulo, São Paulo, Brazil. ²Departamento de Engenharia de Sistemas Eletrônicos, Escola Politécnica da Universidade de São Paulo, São Paulo, Brazil. ³Fundação Hospitalar de Hematologia e Hemoterapia do Amazonas, Manaus, Brazil. ⁴Fundação Pró-Sangue-Hemocentro de São Paulo, São Paulo, Brazil. ⁵Laboratório de Investigação Médica em Patogênese e Terapia dirigida em Onco-Imuno-Hematologia (LIM-31), Departamento de Hematologia, Hospital das Clínicas HCFMUSP, Faculdade de Medicina da Universidade de São Paulo, São Paulo, Brazil. ⁶Fundação Hemominas-Fundação Centro de Hematologia e Hemoterapia de Minas Gerais, Belo Horizonte, Brazil. ⁷Faculdade Ciências Médicas de Minas Gerais, Belo Horizonte, Brazil. ⁸Department of Virology and Experimental Therapy, Institute Aggeu Magalhães, Oswaldo Cruz Foundation, Recife, Brazil. ⁹Department of Global Health and Population, Harvard T. H. Chan School of Public Health, Boston, MA, USA. ¹⁰Department of Infectious Disease Epidemiology, School of Public Health, Imperial College London, London, UK. ¹¹Institute of Mathematics and Statistics, University of São Paulo, São Paulo, Brazil. ¹²Center of Mathematics, Computing and Cognition—Universidade Federal do ABC, São Paulo, Brazil. ¹³Oxford School of Global and Area Studies, Latin American Centre, University of Oxford, Oxford, UK. ¹⁴Vitalant Research Institute, San Francisco, CA, USA. ¹⁵University of California, San Francisco, CA, USA. ¹⁶MRC Centre for Global Infectious Disease Analysis, J-IDEA, Imperial College London, London, UK. ¹⁷Instituto Gonçalo Moniz—Fundação Oswaldo Cruz (Fiocruz), Salvador, Brazil. ¹⁸Department of Zoology, University of Oxford, Oxford, UK. ¹⁹Institute for Applied Economic Research—Ipea, Brasília, Brazil.

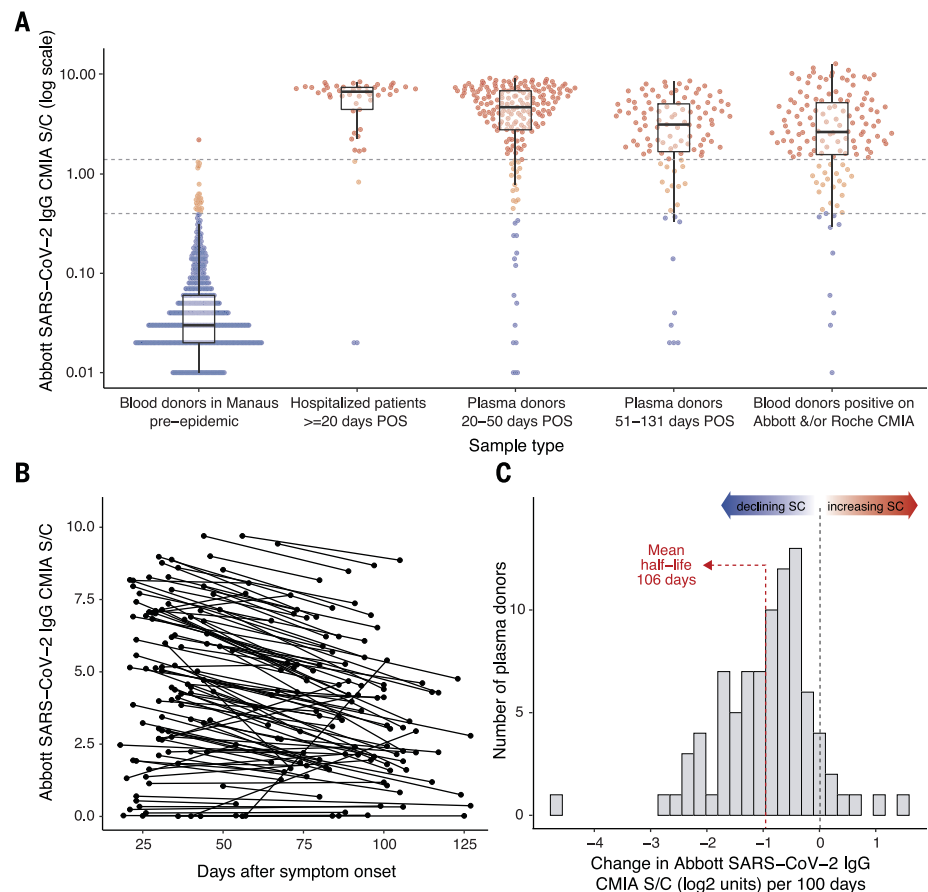
*These authors contributed equally to this work.

†Corresponding author. Email: sabinoec@usp.br (E.C.S.); nfaria@ic.ac.uk (N.R.F.)

Fig. 1. Abbott SARS-CoV-2 N IgG chemiluminescence assay performance and antibody dynamics in different clinical samples.

(A) Signal-to-cutoff (S/C) values using the Abbott chemiluminescence assay (CMIA) in the following clinical samples (from left to right): 821 routine blood donation samples from Manaus in February 2020, >1 month before the first notified case in the city; 49 samples collected at 20 to 33 days after symptom onset from SARS-CoV-2 PCR-positive patients in São Paulo requiring hospital care; 193 patients in São Paulo with PCR-confirmed symptomatic COVID-19 not requiring hospital care, with plasma donation samples taken in the early convalescent period; 107 samples from the same nonhospitalized plasma donor cohort from the late convalescent period; 133 samples that tested positive on either the Abbott CMIA or the Roche Elecsys assay out of 1000 routine blood donations collected in July 2020 and tested in parallel from the Fundação Pró-Sangue blood center (São Paulo). Upper dashed line denotes the manufacturer's threshold for positive result of 1.4 S/C; lower dashed line denotes an alternative threshold of 0.4 S/C. In the box plots of Abbott IgG CMIA S/C, the central line is the median; upper and lower hinges are the 25th and 75th centiles, respectively; whiskers show the range, extending to a maximum of 1.5 times the interquartile range from the hinge.

(B) S/C values of the Abbott CMIA for 104 convalescent plasma donors who were sampled at two different times. **(C)** Histogram of the slopes among 88 individuals shown in (B) who tested positive (>1.4 S/C) at the first time point. POS, post-onset of symptoms.



Because specificity was high, with only one false positive result in 821 pre-epidemic donations from Manaus (Fig. 1A), we also attempted to improve assay performance by reducing the threshold for a positive result from 1.4 S/C (as per the manufacturer) to 0.4 S/C. This resulted in 27 false positives and a specificity of 96.7% but substantially improved sensitivity at this threshold (Fig. 1A and table S1).

To estimate the proportion of the population with IgG antibodies to SARS-CoV-2, we used a convenience sample of routine blood donations made at the Fundação Pró-Sangue blood bank in São Paulo and the Fundação Hospitalar de Hematologia e Hemoterapia do Amazonas (HEMOAM) in Manaus. The monthly sample size and sampling dates, spanning February to October, are shown in table S2.

The prevalence of SARS-CoV-2 antibodies in February and March was low (<1%) in both São Paulo and Manaus. This is consistent with the timing of the first confirmed cases that were diagnosed on 13 March in Manaus and on 25 February in São Paulo (2). In Manaus, after adjustment for the sensitivity and specificity of the test (but not antibody waning) and reweighting for age and sex, the prevalence

of SARS-CoV-2 IgG antibodies was 4.8% (95% CI, 3.3% to 6.8%) in April and 44.5% (95% CI, 39.2% to 50.0%) in May, reaching a peak of 52.5% (47.6% to 57.5%) in June (Fig. 2 and table S2). The increasing seroprevalence closely followed the curve of cumulative deaths. In São Paulo, the prevalence of SARS-CoV-2 IgG in blood donors also increased steadily, reaching 13.6% (95% CI, 12.0% to 15.1%) in June.

Between June and October, the effect of seroreversion became apparent in both cities. In Manaus, after the peak antibody prevalence in June, the proportion of blood donors who tested positive fell steadily to 25.8% in October. Excluding extreme negative samples (<0.4 S/C), the median assay signal fell steadily from May: 3.9 (May), 3.5 (June), 2.3 (July), 1.7 (August), 1.4 (September), and 1.3 (October) (Fig. 2B). Similarly, in São Paulo, antibody prevalence remained stable between June and October while the number of daily COVID-19 deaths also remained relatively stable, reflecting a balance between antibody waning from infections earlier in the outbreak and seroconversions following recent infections (Fig. 2C).

In Manaus, the effect of antibody waning on apparent prevalence was partially ameliorated by reducing the threshold for a positive

result from 1.4 S/C to 0.4 S/C and correcting for the resulting increased false positive rate. However, the results in São Paulo were largely unchanged by this correction (Fig. 2 and table S2).

We further corrected for seroreversion with a model-based approach (see supplementary materials). Briefly, we assumed that the probability of an individual seroreverting exactly m months after recovery decays exponentially with m . We estimated the decay rate and the proportion of patients who seroreverted using the seroprevalence data from Manaus to find the decay rate that minimized the number of new cases in July and August while avoiding decreases in prevalence—that is, assuming there were few cases in Manaus in July and August and that changes in seroprevalence were due mainly to waning antibodies. The results of these corrections are shown in Fig. 2 and table S2. After adjusting for seroreversion, we find that cumulative incidence in Manaus may have reached as high as 66.2% (95% CI, 61.5% to 80.1%) in July and 76.0% (95% CI, 66.6% to 97.9%) in October. The reliability of this estimate depends on the validity of the exponential decay assumption, and in the absence of an accepted approach to account for

seroreversion, these results should be interpreted with caution.

To calculate infection fatality ratios (IFRs), we used the prevalence (adjusted for sensitivity and specificity, and reweighted for age and sex) in June, as this followed the epidemic peak in Manaus but preceded appreciable seroreversion. In Manaus, the IFRs were 0.17% and 0.28%, taking into consideration the numbers of polymerase chain reaction (PCR)-confirmed COVID-19 deaths and probable COVID-19 deaths based on syndromic identification, respectively. In São Paulo, the global IFRs were 0.46% and 0.72%, respectively. The difference may be explained by an older population structure in São Paulo (fig. S1A). Supporting this inference, the age-specific IFRs were similar in the two cities, and were similar to estimates based on data from China (16) (fig. S1B) and a recent systematic review (17). We also obtained similar age-specific IFRs using the seroreversion-corrected prevalence estimates from October (fig. S1).

Blood donors may not be representative of the wider population. In both cities, the eligible age range for blood donation in Brazil (16 to 69 years) and the sex distribution of donors are different from those of the under-

lying population (fig. S2). Reweighting our estimates for age and sex (Fig. 2 and table S2) resulted in a slight reduction in prevalence, particularly in Manaus, where men were overrepresented among donors and also had a higher seroprevalence (fig. S3). Self-reported ethnicity in donors was similar to that of the census populations (fig. S2). The median income in blood donors' census tracts of residence was marginally higher than a population-weighted average for both cities (fig. S4). Regarding the spatial distribution of donors, there was a similar antibody prevalence across different regions sampled in both cities (fig. S5), and we achieved good geographic coverage in both cities (see supplementary materials and fig. S5).

Because potential donors are deferred if they have a positive SARS-CoV-2 PCR test or clinical diagnosis of COVID-19, increasing access to testing might have reduced the pool of eligible donors through time. However, only 2.7% of residents in Manaus and 8.5% in São Paulo reported having a PCR test performed by September (fig. S6). As such, changing access to testing is unlikely to have been important. Considering these factors together,

we suggest that our results can be cautiously extrapolated to the population aged 16 to 69 years in Manaus and São Paulo. Within this group, studies of blood donors may underestimate the true exposure to SARS-CoV-2 because donors may have higher socioeconomic profiles and greater health awareness and engagement, and because symptomatic donors are deferred. However, it is likely that seroprevalence in children and older adults is lower.

Our results show that between 44% and 66% of the population of Manaus was infected with SARS-CoV-2 by July, following the epidemic peak there. The lower estimate does not account for false negative cases or antibody waning; the upper estimate accounts for both. R_t fell to <1 (fig. S7) in late April when cumulative infections were between 5% and 46% of the population. NPIs (table S3) were implemented in mid- to late March when physical distancing also increased (fig. S8). It is likely that these factors worked in tandem with growing population immunity to contain the epidemic. Transmission has since continued in Manaus, albeit to a lesser extent than in April and May (Fig. 2 and fig. S7). From the second

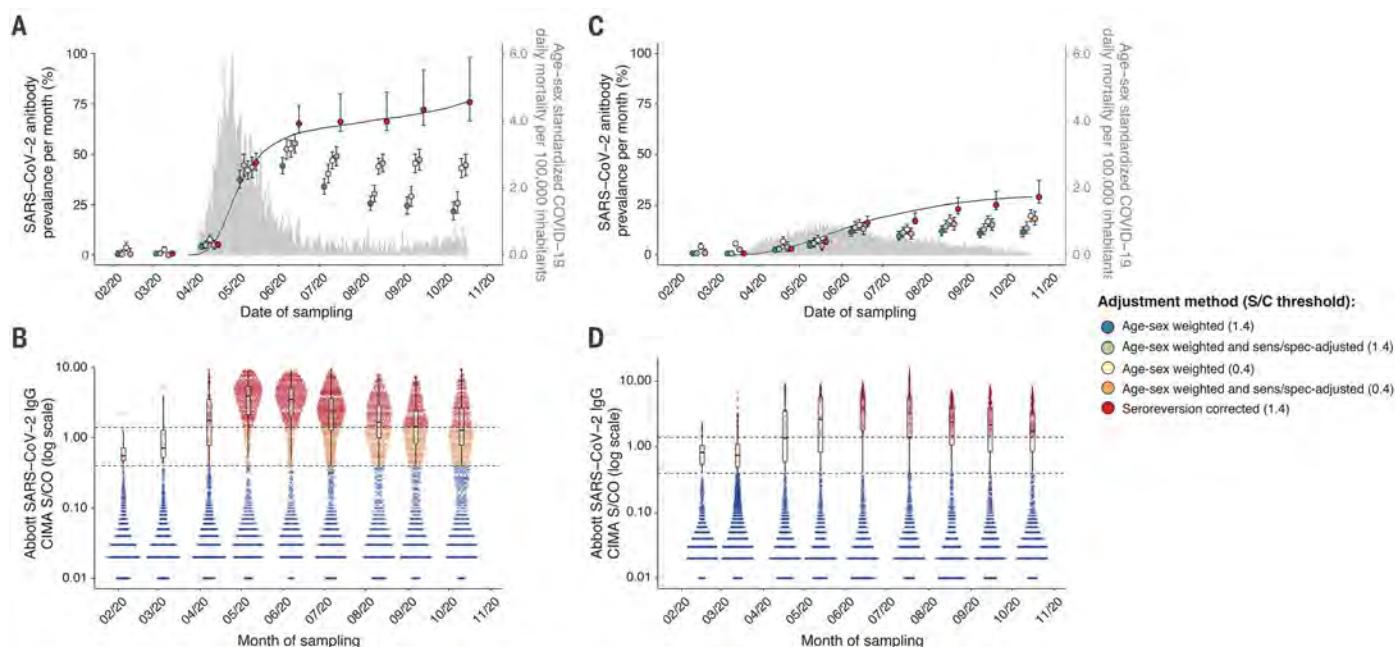


Fig. 2. Monthly antibody prevalence and signal-to-cutoff (S/C) reading in Manaus and São Paulo. (A and C) SARS-CoV-2 antibody prevalence estimates in Manaus (A) and São Paulo (C) with a range of corrections, from left to right: reweighting positive tests, at positivity threshold of 1.4 S/C, to the age and sex distribution of each city; further correcting for sensitivity and specificity at this assay threshold; reweighting positive tests for age and sex at a reduced threshold of 0.4 S/C; correcting for sensitivity and specificity at this threshold; and finally correcting for seroreversion. Error bars are 95% confidence intervals. Gray bars are standardized daily mortality using confirmed COVID-19 deaths from the SIVEP-Gripe (Sistema de Informação de Vigilância Epidemiológica da Gripe; <https://covid.saude.gov.br/>) notification system and standardized by the

direct method using the total projected Brazilian population for 2020 as reference. Black lines are rescaled cumulative deaths, such that the maximum is set to the maximum seroprevalence estimate for each city. Mortality data are plotted according to the date of death. (B and D) Distribution of S/C values over the nine monthly samples are shown for Manaus (B) and São Paulo (D). Each point represents the S/C reading for a single donation sample. Upper dashed line denotes the manufacturer's threshold (1.4 S/C units); lower dashed line denotes an alternative threshold (0.4 S/C units); black box plots show the median (central lines), interquartile range (hinges), and range extending to 1.5 times the interquartile range from each hinge (whiskers) of S/C values above 0.4 (i.e., excluding very low and likely true-negative values).

week of August there has been a small increase in the number of cases (18), which, at the time of writing, has begun to decline. Consequently, the attack rate rose to 76% in October. This remains lower than predicted in a homogeneously mixed population with no mitigation strategies (~90%). Homogeneous mixing is unlikely to be a valid assumption (19), and behavioral change and NPIs may explain why the estimated final epidemic size has not yet reached 89 to 94%, as expected for R_0 values between 2.5 and 3.0 (4).

By 1 October, Manaus recorded 2642 [1193/million inhabitants (mil)] COVID-19 confirmed deaths and 3789 (1710/mil) severe acute respiratory syndrome deaths; São Paulo recorded 12,988 (1070/mil) and 20,063 (1652/mil), respectively. The cumulative mortality proportions were similar in both cities and high relative to other locations such as the United Kingdom (620/mil), France (490/mil), or the United States (625/mil) as of 1 October (20). The different attack rates in Manaus and São Paulo (76% versus 29% of people infected), despite similar overall mortality rates, are due to the higher IFR in São Paulo. The age-standardized mortality ratio was 2.0 comparing observed deaths in Manaus to those expected from projecting the age-specific mortality in São Paulo onto the age structure of Manaus. The R_0 was similar in the two cities (fig. S7), but cases and deaths increased and then decreased more slowly in São Paulo than in Manaus where both the rise and fall were more abrupt (fig. S7). The lower attack rate in São Paulo is partly explained by the larger population size (2.2 million versus 12.2 million inhabitants). As population size increases, the time to reach a given attack rate also increases (21).

The attack rate in Manaus is higher than estimates based on seroprevalence studies conducted in Europe and North America (8, 22, 23) and on recent results from Kenyan blood donors (24). A similarly high seroprevalence (~50%) was observed in slums in Mumbai, India (25). In Brazil, one population-based serosurvey in São Paulo (26) found a prevalence similar to that in our study (26.2% versus 28.8% in blood donors, in October). In Manaus, a lower seroprevalence (14%, in June) was found in a random household sample of 250 people (1). But this study was not powered at the city level and used the lower-sensitivity Wondfo (27) rapid test. As such, the results are not directly comparable.

Future investigations should be conducted to determine what accounted for such extensive transmission of SARS-CoV-2 in Manaus. Possible explanations include socioeconomic conditions, household crowding (28), limited access to clean water, and reliance on boat travel (1) in which overcrowding results in accelerated contagion, similar to that seen

on cruise ships (29). The young mobile population with potentially low preexisting immunity to SARS-CoV-2 (30), as well as the early circulation of multiple virus lineages introduced from multiple locations, may have contributed to the large scale of the outbreak.

Our data show that >70% of the population had been infected in Manaus about 7 months after the virus first arrived in the city. This is above the theoretical herd immunity threshold. However, prior infection may not confer long-lasting immunity (30, 31). Indeed, we observed rapid antibody waning in Manaus, consistent with other reports that have shown signal waning on the Abbott IgG assay (14, 32). However, other commercial assays, with different designs or targeting different antigens, have more stable signal (14), and there is evidence for a robust neutralizing antibody response several months out from infection (33). Rare reports of reinfection have been confirmed (34), but the frequency of its occurrence remains an open question (35). Manaus represents a “sentinel” population, giving us a data-based indication of what may happen if SARS-CoV-2 is allowed to spread largely unmitigated. Further seroepidemiological, molecular, and genomic surveillance studies in the region are required urgently to determine the longevity of population immunity, the correlation with the observed antibody waning, and the diversity of circulating lineages. Monitoring of new cases and the ratio of local versus imported cases will also be vital to understand the extent to which population immunity might prevent future transmission, and the potential need for booster vaccinations to bolster protective immunity.

REFERENCES AND NOTES

1. P. C. Hallal et al., *Lancet Glob. Health* **8**, e1390–e1398 (2020).
2. D. da S. Candido et al., *Science* **369**, 1255–1260 (2020).
3. J. D. Y. Orellana, G. M. da Cunha, L. Marrero, B. L. Horta, I. da Costa Leite, *Cad. Saude Publica* **36**, e00120020 (2020).
4. W. M. de Souza et al., *Nat. Hum. Behav.* **4**, 856–865 (2020).
5. J. Ma, D. J. D. Earn, *Bull. Math. Biol.* **68**, 679–702 (2006).
6. J. G. de Jesus et al., *Rev. Inst. Med. Trop. São Paulo* **62**, e30 (2020).
7. F. I. Lewis, P. R. Torgerson, *Emerg. Themes Epidemiol.* **9**, 9 (2012).
8. A. Bryan et al., *J. Clin. Microbiol.* **58**, e00941-20 (2020).
9. Public Health England, “Evaluation of Abbott SARS-CoV-2 IgG assay for the detection of anti-SARS-CoV-2 antibodies” (2020); www.gov.uk/government/publications/covid-19-laboratory-evaluations-of-serological-assays.
10. D. L. Ng et al., *Nat. Commun.* **11**, 4698 (2020).
11. D. W. Eyre et al., medRxiv 20159038 [preprint]. 25 July 2020.
12. F. Hamilton et al., *J. Infect.* **10.1016/j.jinf.2020.07.031** (2020).
13. Q.-X. Long et al., *Nat. Med.* **26**, 1200–1204 (2020).
14. F. Muecksch et al., *J. Infect. Dis.* **jiaa659** (2020).
15. Public Health England, “Evaluation of Roche Elecsys Anti-SARS-CoV-2 serology assay for the detection of anti-SARS-CoV-2 antibodies” (2020); www.gov.uk/government/publications/covid-19-laboratory-evaluations-of-serological-assays.
16. R. Verity et al., *Lancet Infect. Dis.* **20**, 669–677 (2020).
17. N. Brazeau et al., “Report 34: COVID-19 infection fatality ratio: estimates from seroprevalence” (Imperial College London, 2020).
18. MAVE, Grupo de Métodos Analíticos em Vigilância Epidemiológica (PROCC/Fiocruz e EMAP/GFV), *Resumo do Boletim InfoGripe-Semana Epidemiológica (SE) 42*; <https://gitlab.procc.fiocruz.br/mave/repo/tree/master/Boletins%20do%20InfoGripe>.

19. T. Britton, F. Ball, P. Trapman, *Science* **369**, 846–849 (2020).
20. Our World in Data, “Coronavirus Pandemic (COVID-19)” (2020); <https://ourworldindata.org/coronavirus>.
21. B. Ridenhour, J. M. Kowalik, D. K. Shay, *Am. J. Public Health* **104**, e32–e41 (2014).
22. M. Pollán et al., *Lancet* **396**, 535–544 (2020).
23. S. Stringhini et al., *Lancet* **396**, 313–319 (2020).
24. S. Uyoga et al., *Science* **10.1126/science.abe1916** (2020).
25. A. Malani et al., *Lancet Glob. Health* **10.1016/S2214-109X(20)30467-8** (2020).
26. SoroEpi MSP: Serial seroepidemiological survey to monitor the prevalence of SARS-CoV-2 infection in the Municipality of São Paulo, SP, Brazil (2020); www.monitoramentocovid19.org/.
27. V. A. dos Santos, M. M. Rafael, E. C. Sabino, A. J. da S. Duarte, *Clinics* **75**, e2013 (2020).
28. B. Rader et al., *Nat. Med.* **10.1038/s41591-020-1104-0** (2020).
29. K. Mizumoto, K. Kagaya, A. Zarebski, G. Chowell, *Euro Surveill.* **25**, 2000180 (2020).
30. A. W. D. Edridge et al., *Nat. Med.* **26**, 1691–1693 (2020).
31. K. A. Callow, H. F. Parry, M. Sergeant, D. A. J. Tyrrell, *Epidemiol. Infect.* **105**, 435–446 (1990).
32. S. F. Lumley et al., medRxiv 20224824 [preprint]. 4 November 2020.
33. A. Wajnberg et al., *Science* **370**, 1227–1230 (2020).
34. K. K.-W. To et al., *Clin. Infect. Dis.* **ciaa1275** (2020).
35. J. Shaman, M. Galanti, *Science* **370**, 527–529 (2020).
36. Data and code for “Three-quarters attack rate of SARS-CoV-2 in the Brazilian Amazon during a largely unmitigated epidemic”; doi:doi.org/10.5061/dryad.c59zw3r5n.

ACKNOWLEDGMENTS

Funding: Supported by the Itau Unibanco “Todos pela Saude” program and by CADDE/FAPESP (MR/S0195/1 and FAPESP/18/14389-0) (<http://caddecentre.org/>); Wellcome Trust and Royal Society Sir Henry Dale Fellowship 204311/Z/16/Z (N.R.F.); the National Heart, Lung, and Blood Institute Recipient Epidemiology and Donor Evaluation Study (REDS, now in its fourth phase, REDS-IV-P) for providing the blood donor demographic and zip code data for analysis (grant HHSN268201100007); and the UK Medical Research Council under a concordat with the UK Department for International Development and Community Jameel and the NIHR Health Protection Research Unit in Modelling Methodology. **Author contributions:** Conception, M.B.-N., L.F.B., M.C., B.C., C.d.A.N., N.R.F., S.C.F., A.M.J., A.S.N., R.H.M.P., V.R., E.C.S., N.A.S., T.S., M.A.d.S., and C.W.; acquisition, A.C.M.M., M.P.S.S.C., A.G.C., M.A.E.C., C.d.A.N., A.A.d.S.S., N.R.F., S.C.F., N.A.F., P.L.T., A.M.J., M.K.O., N.V., R.H.M.P., V.R., E.C.S., N.A.S., T.S., P.d.S.P., and M.A.d.S.; analysis, L.F.B., C.d.A.N., R.H.M.P., C.W., E.C.S., C.A.P., K.V.P., V.H.N., and M.C.B.; interpretation, A.C.M.M., L.F.B., M.P.S.S.C., A.G.C., M.A.E.C., C.d.A.N., N.R.F., N.A.F., E.C.S., M.A.d.S., C.W., C.D., M.U.G.K., O.P., and V.H.N.; drafting, L.F.B. and E.C.S.; revising, all authors; funding, M.B.-N., A.G.C., B.C., N.R.F., N.A.F., E.C.S., and N.A.S. **Competing interests:** The authors declare no competing interests. **Data and materials availability:** The data and code required to reproduce the results in this article can be found on Dryad (36). This project was approved by the Brazilian national research ethics committee, CONEP CAAE - 30178220.3.1001.0068. This work is licensed under a Creative Commons Attribution 4.0 International (CC BY 4.0) license, which permits unrestricted use, distribution, and reproduction in any medium, provided the original work is properly cited. To view a copy of this license, visit <https://creativecommons.org/licenses/by/4.0/>. This license does not apply to figures/photos/artwork or other content included in the article that is credited to a third party; obtain authorization from the rights holder before using such material.



SUPPLEMENTARY MATERIALS

science.sciencemag.org/content/371/6526/288/suppl/DC1
Materials and Methods
Figs. S1 to S9
Tables S1 to S3
References (37–41)
MDAR Reproducibility Checklist

[View/request a protocol for this paper from Bio-protocol.](#)

28 September 2020; accepted 2 December 2020
Published online 8 December 2020
10.1126/science.abe9728

Estimating the extent of asymptomatic COVID-19 and its potential for community transmission: Systematic review and meta-analysis

Oyungerel Byambasuren MD¹ , Magnolia Cardona PhD¹ , Katy Bell PhD², Justin Clark BA¹, Mary-Louise McLaws PhD³, Paul Glasziou PhD¹

BACKGROUND: Knowing the prevalence of true asymptomatic coronavirus disease 2019 (COVID-19) cases is critical for designing mitigation measures against the pandemic. We aimed to synthesize all available research on asymptomatic cases and transmission rates. **METHODS:** We searched PubMed, Embase, Cochrane COVID-19 trials, and Europe PMC for primary studies on asymptomatic prevalence in which (1) the sample frame includes at-risk populations and (2) follow-up was sufficient to identify pre-symptomatic cases. Meta-analysis used fixed-effects and random-effects models. We assessed risk of bias by combination of questions adapted from risk of bias tools for prevalence and diagnostic accuracy studies. **RESULTS:** We screened 2,454 articles and included 13 low risk-of-bias studies from seven countries that tested 21,708 at-risk people, of which 663 were positive and 111 asymptomatic. Diagnosis in all studies was confirmed using a real-time reverse transcriptase–polymerase chain reaction test. The asymptomatic proportion ranged from 4% to 41%. Meta-analysis (fixed effects) found that the proportion of asymptomatic cases was 17% (95% CI 14% to 20%) overall and higher in aged care (20%; 95% CI 14% to 27%) than in non-aged care (16%; 95% CI 13% to 20%). The relative risk (RR) of asymptomatic transmission was 42% lower than that for symptomatic transmission (combined RR 0.58; 95% CI 0.34 to 0.99, $p = 0.047$). **CONCLUSIONS:** Our one-in-six estimate of the prevalence of asymptomatic COVID-19 cases and asymptomatic transmission rates is lower than those of many highly publicized studies but still sufficient to warrant policy attention. Further robust epidemiological evidence is urgently needed, including in subpopulations such as children, to better understand how asymptomatic cases contribute to the pandemic.

KEYWORDS: emerging or re-emerging diseases, epidemiology, evidence-based medicine, public health policy

HISTORIQUE : Il est essentiel de connaître la prévalence des véritables cas asymptomatiques de maladie à coronavirus 2019 (COVID-19) pour concevoir des mesures d'atténuation de la pandémie. Les chercheurs ont voulu synthétiser toutes les recherches disponibles sur les cas asymptomatiques et les taux de transmission. **MÉTHODOLOGIE :** Les chercheurs ont fouillé les bases de données PubMed, Embase, Cochrane pour trouver les études sur la COVID-19, et Europe PMC pour colliger les études primaires sur la prévalence des cas asymptomatiques dans lesquelles 1) le cadre d'échantillonnage incluait une population à risque et 2) le suivi était suffisant pour dépister les cas présymptomatiques. La méta-analyse a fait appel à des modèles d'effets fixes et d'effets aléatoires. Nous avons évalué le risque de biais par une combinaison de questions adaptées d'outils sur les risques de biais des études de prévalence et de précision diagnostique. **RÉSULTATS :** Les chercheurs ont extrait 2 454 articles, dont 13 études à faible risque de biais de sept pays dans lesquelles 21 708 personnes à risque ont subi le test de dépistage, soit 663 cas positifs et 111 cas asymptomatiques. Dans toutes les études, le diagnostic a été confirmé au moyen du test d'amplification en chaîne par polymérase après transcriptase inverse en temps réel. La proportion de cas asymptomatiques se situait entre 4 % et 41 %. La méta-analyse (à effets fixes) a établi que la proportion de cas asymptomatiques s'élevait à 17 % (IC à 95 %, 14 % à 20 %) dans l'ensemble, mais qu'elles étaient plus élevées dans les soins aux aînés (20 %; IC à 95 %, 14 % à 27 %) qu'auprès du reste de la population (16 %; IC à 95 %, 13 % à 20 %). Le risque relatif [RR] de transmission de cas asymptomatiques était plus faible de 42 % que celui de cas symptomatiques (RR combiné de 0,58; IC à 95 %, 0,34 à 0,99, $p = 0,047$). **CONCLUSIONS :** L'évaluation de la prévalence d'un sixième de cas asymptomatiques de COVID-19 et de taux de transmission de cas asymptomatiques est inférieure à celle de nombreuses études hautement publicisées, mais suffit tout de même pour justifier l'intérêt de la santé publique. D'autres données épidémiologiques solides s'imposent de toute urgence, y compris dans des sous-populations comme les enfants, pour mieux comprendre l'effet des cas asymptomatiques sur la pandémie.



MOTS-CLÉS : épidémiologie, maladie émergente ou réémergente, médecine fondée sur des données probantes, politique de santé publique

¹*Institute for Evidence-Based Healthcare, Bond University, Gold Coast, Queensland, Australia;* ²*School of Public Health, University of Sydney, Sydney, New South Wales, Australia;* ³*School of Public Health and Community Medicine, UNSW Sydney, Sydney, New South Wales, Australia*

Correspondence: Oyungerel Byambasuren, Institute for Evidence-Based Healthcare, Bond University, 14 University Drive, Robina, Gold Coast, Queensland 4229, Australia. E-mail: obyambas@bond.edu.au

INTRODUCTION

Asymptomatic cases of any infection are of considerable concern for public health policies to manage epidemics. Such asymptomatic cases complicate the tracking of an epidemic and prevent reliable estimates of transmission, tracing, and tracking strategies for containing an epidemic through isolation and quarantine. This has been a significant concern in the current coronavirus disease 2019 (COVID-19) pandemic (1).

The possibility of asymptomatic transmission of COVID-19 cases was first raised by a case report in China in which a traveller from Wuhan was presumed to have transmitted the infection to five other family members in other locations while she remained asymptomatic for the entire 21-day follow-up period (2). Subsequently, other reports confirmed not only the possibility of such transmission but began quantifying the potential proportions. For example, the outbreak on the Diamond Princess cruise ship included a substantial proportion of asymptomatic cases after widespread testing of those on board the ship (3). An early rapid review by the Centre for Evidence-Based Medicine in Oxford, United Kingdom, found that the estimated proportion of asymptomatic COVID-19 cases ranged from 5% to 80% (4). However, many of the identified studies were either poorly executed or poorly documented, making the validity of these estimates questionable.

We therefore sought to identify all studies that had attempted to estimate the proportion of asymptomatic COVID-19 cases, select those with low risk of bias, and synthesize them to provide an overall estimate and potential range. We also aimed to estimate the rate of forward transmission from asymptomatic cases if sufficient data were found.

METHODS

We conducted a systematic review and meta-analysis using enhanced processes with an initial report completed within 2 weeks and daily short team meetings to review progress, plan the next actions, and resolve discrepancies and other obstacles (5). We also used locally developed open access automation tools and programs such as the Polyglot Search Translator, SearchRefiner, and the SRA Helper to design, refine, and convert our search strategy for all the databases

we searched and to speed up the screening process (6). We searched the PROSPERO database to rule out the existence of a similar review and PubMed, Embase, and Cochrane COVID-19 trials for published studies and Europe PMC for pre-prints from January 2020 to July 20, 2020. A search string composed of MeSH terms and words was developed in PubMed and was translated to be run in other databases using the Polyglot Search Translator. The search strategies for all databases are presented in Supplemental Appendix 1. We also conducted forward and backward citation searches of the included studies in the Scopus citation database.

We restricted publication types to reports of primary data collection released in full (including pre-prints) with sufficient details to enable a risk-of-bias assessment, and we contacted authors for clarifications on follow-up times and sampling frames. We anticipated that cross-sectional prevalence surveys with follow-up and cohort studies would be the bulk of eligible reports. No restrictions on language were imposed. We excluded studies for the following reasons: sampling frame in part determined by presence or absence of symptoms; no or unclear follow-up; no data on asymptomatic cases; single case study or small cluster; modelling or simulation studies (but sources of real data were checked for possible inclusion); non-severe acute respiratory syndrome coronavirus 2 (SARS-CoV-2) studies; antiviral treatment studies; and study protocols, guidelines, editorials, or historical accounts without data to calculate primary outcomes.

Participants

We included studies of people of any age in which all those at risk of contracting SARS-CoV-2 were tested regardless of presence or absence of symptoms; diagnosis was confirmed by a positive result on a real-time reverse transcriptase-polymerase chain reaction (RT-PCR), and all cases had a follow-up period of at least 7 days to distinguish asymptomatic cases from pre-symptomatic cases (Figure 1).

Outcomes

Our primary outcome was the proportion of all people with SARS-Cov-2 infection who were completely asymptomatic at the time of the test and throughout the follow-up period, where the denominator included all tested individuals in the

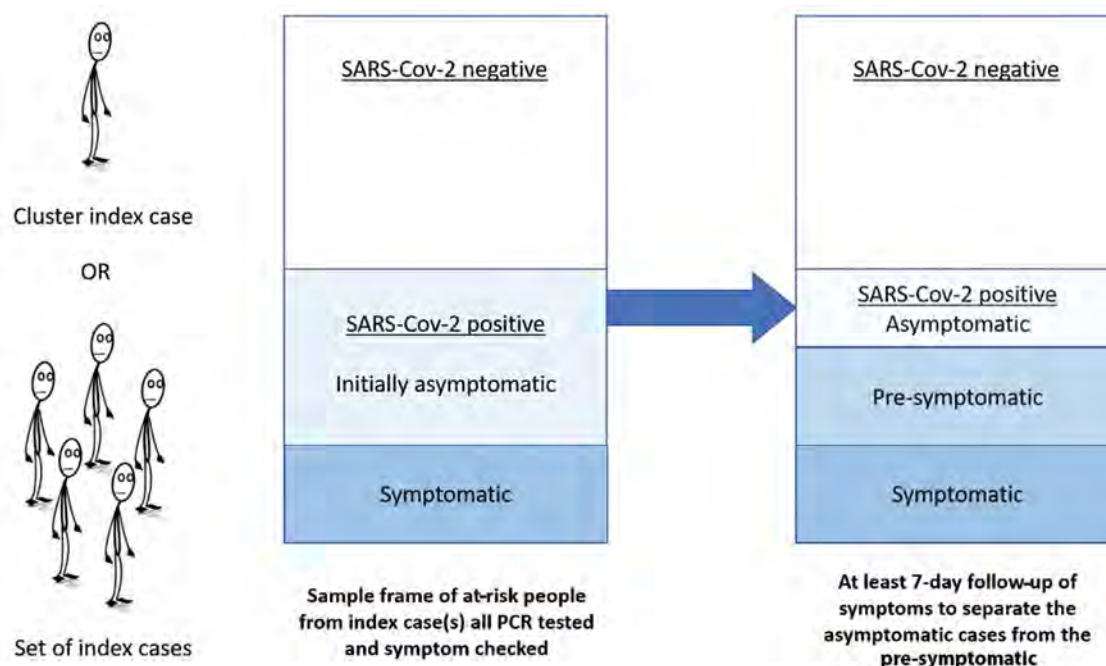


Figure 1: Depiction of ideal study flow and criteria used for study inclusion: (1) sample frame of at-risk people and (2) adequate follow-up on symptoms

SARS-Cov-2 = Severe acute respiratory syndrome coronavirus 2; PCR = Polymerase chain reaction

study sample whose result was positive, and the numerator included those who tested positive and had no symptoms. Our secondary outcome was estimate of onward transmission of the infection from asymptomatic cases.

Study selection and screening

Two authors (OB and MC) independently screened titles, abstracts, and full texts according to eligibility criteria. All discrepancies were resolved via group discussion with the other authors. Reasons for exclusion were documented for all full-text articles deemed ineligible (Supplemental Appendix 2); see the Preferred Reporting Information for Systematic Reviews and Meta-Analyses diagram (Figure 2).

Data extraction

Three authors (OB, MC, KB) used a Microsoft Excel spreadsheet to extract the following information:

1. Methods: study authors, year of publication, country, publication type, duration of study, duration of follow-up
2. Participants: sample size, age (mean or median, range), setting (community, province, aged care facility, hospital, screening clinic), presence or absence of symptoms, test results
3. History of illness and diagnosis: type of test; numerator (number of asymptomatic); denominator (sampling

frame); mildly symptomatic or symptomatic subjects; and number or proportion of people infected by the asymptomatic case.

4. Case definitions were as follows:

- Asymptomatic: confirmed via any testing specified earlier with report of no symptoms for the duration of sufficient follow-up to differentiate from pre-symptomatic cases.
- Exposure: contact with a confirmed case or potential contact with another pre-symptomatic person (e.g., came from an endemic area or linked with an infected traveller).

The World Health Organization recommends that “for confirmed asymptomatic cases, the period of contact is measured as the 2 days before through the 14 days after the date on which the sample was taken which led to confirmation” (7, p.11).

Risk-of-bias assessment

Three authors (OB, MC, KB) assessed the risk of bias of potentially includable studies. We used a combination of risk-of-bias tools for prevalence studies and diagnostic accuracy and adapted the key signaling questions on sampling frame, ascertainment of infectious disease status, acceptability of methods to identify denominators, case

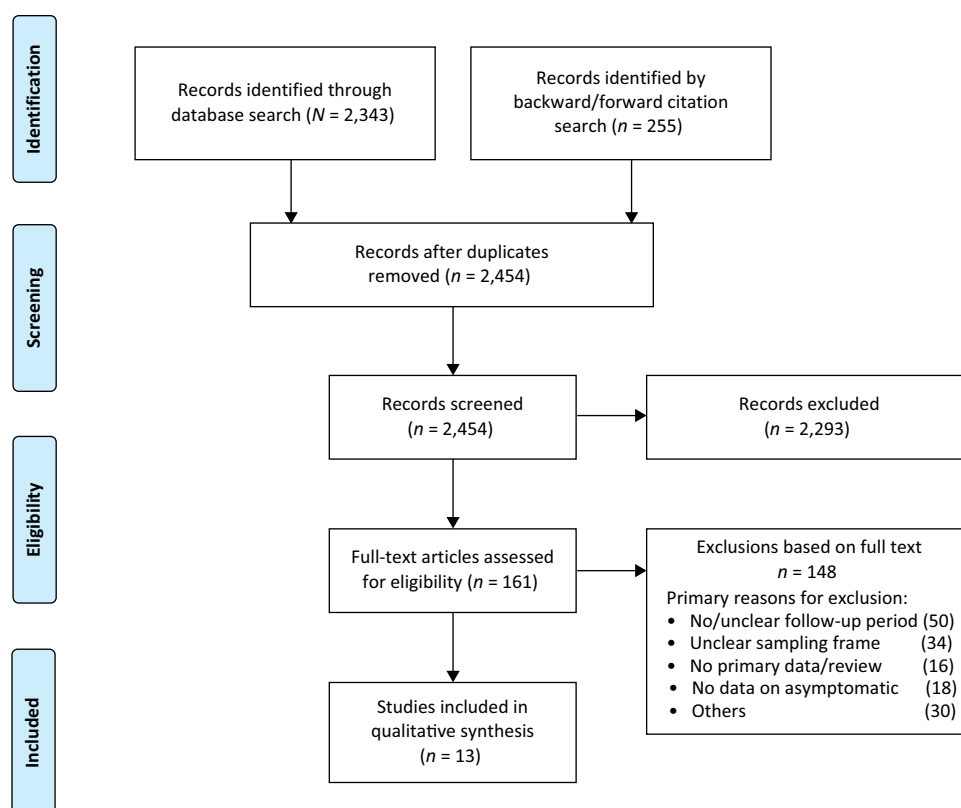


Figure 2: Screening and selection of articles

definition of *asymptomatic* for the numerator, and length of follow-up, as shown in Table 2 and in Supplemental Appendix 3 in full (8,9).

Data analysis

We estimated the proportion of COVID-19 cases who were asymptomatic for each included study population, assuming a binomial distribution and calculating exact Clopper–Pearson confidence intervals. We then pooled data from all included studies using (1) fixed-effects meta-analysis and (2) random-effects meta-analysis. All analyses were conducted using SAS version 9.4 (SAS Institute, Cary, NC); the FREQ procedure was used for individual studies and the fixed-effects meta-analysis; the NLMIXED procedure was used for the random-effects meta-analysis.

We also meta-analyzed the forward transmission rates from asymptomatic and symptomatic cases when there were sufficient data and report the pooled RR comparing the two. We planned to undertake subgroup analysis for age (between studies, and within studies when age was reported separately for asymptomatic and symptomatic cases). Because the analysis included only studies deemed to be of high quality on items

1 and 2 after risk-of-bias appraisal, no sensitivity analysis of high- versus low-quality studies was undertaken. Instead, we did a sensitivity analysis in which we omitted studies with a follow-up duration of less than 14 days.

RESULTS

A total of 2,454 articles were screened for title and abstract, and 161 full-text articles were assessed for inclusion (Figure 2). Major reasons for exclusion were inadequate sampling frame and insufficient follow-up time to accurately classify the asymptomatic cases. The full list of excluded studies with reasons is presented in Supplemental Appendix 2. Thirteen articles—nine published and four preprints—from seven countries (China, $n = 4$; United States, $n = 4$; Taiwan, $n = 1$; Brunei, $n = 1$; Korea, $n = 1$; France, $n = 1$; and Italy, $n = 1$) that tested 21,708 close contacts of at least 849 confirmed COVID-19 cases, of which 663 were positive and 111 were asymptomatic, met the eligibility criteria for the estimation of the primary outcome (10–22).

The sampling frames of the selected studies included residents of skilled nursing facilities (SNFs; 10, 12, 15, 19, 20); high-risk close contacts of confirmed COVID-19 cases

Table 1: Characteristics of included studies ($N = 13$)

Study (country) and publication status	Study population (sampling frame)	Sample size and age	Diagnostic testing and frequency	Length of follow-up for asymptomatic cases
Roxby et al (20) (United States) Published	Residents of independent and assisted living communities (Facility 1) in Seattle after two confirmed cases between 5 and 9 Mar	$N = 79$; mean age of cohort 86 y	Nasal swab, RT-PCR, twice, 1 wk apart	7 d
Patel et al (19) (United States) Published	Residents and staff of skilled nursing facility in Illinois on 15 Mar	$N = 126$; median age of cases 82 y.	Nasal swab, RT-PCR, once	30 d
Dora et al (15) (United States) Published	Residents of skilled nursing facility in Veterans Affairs Greater Los Angeles Healthcare System between 29 Mar and 23 Apr	$N = 99$; median age of cohort 75 y.	Nasal swab, RT-PCR, repeated every 10 d	At least 14 d
Blain et al (12) (France) Published	Nursing home residents in France tested weekly since early Mar	$N = 79$; mean age 86 y	Nasal swab, RT-PCR, repeated weekly	6 wk
Arons et al (10) (United States) Published	Residents of skilled nursing facility (Facility A) in Seattle after a confirmed case on 1 Mar	$N = 86$; mean age of cohort 77 y, mean age of cases 79 y.	Nasal swab, RT-PCR, twice, 1 wk apart	7 d
Zhang et al (22) (China) Published	Close contacts of confirmed cases between 28 Jan and 15 Mar in Guangzhou, China	$N = 369$; median age 35 y.	Nasal swab, RT-PCR, at least twice	14 d
Tian et al (21) (China) Preprint	Close contacts (coworkers, family members, customers) of a confirmed supermarket employee (super-spreader) in Liaocheng, China.	$N \approx 8,000$; mean age of cases 48 y	Nasal swab, RT-PCR, repeated every 2 days	16 ± 6.15 d
Cheng et al (14) (Taiwan) Published	High-risk close contacts (household members, HCWs) of first 100 cases in Taiwan	$N = 849$; mean age of cohort 42 y, mean age of cases 41 y	Nasal swab, RT-PCR, repeated during 14 d quarantine	14 d
Lavezzo et al (16) (Italy) Published	Majority of population of Italian town of Vò after a COVID-19 death on 21 Feb.	$N = 2,812$; mean age of cohort 47 y, mean age of cases 58 y	Nasal swab, RT-PCR, twice, 7–14 d apart	7–14 d
Bi et al (11) (China) Published	Close contacts of cases confirmed before 9 Feb in Shenzhen, China	$N = 1,286$; mean age of cohort 38 y, mean age of cases 43 y	Nasal swab, RT-PCR, repeated during 14 d quarantine	95% followed up for ≥ 12 d
Chaw et al (13) (Brunei) Preprint	Bruneian attendants of a religious event in Malaysia, where a confirmed case was present	$N = 1,830$; mean age of cohort 31 y, mean age of cases 33 y	Nasal swab, RT-PCR, repeated weekly	14 d

(Continued)

Table 1: Characteristics of included studies (*N* = 13) (*Continued*)

Study (country) and publication status	Study population (sampling frame)	Sample size and age	Diagnostic testing and frequency	Length of follow-up for asymptomatic cases
Luo et al (17) (China) Preprint	Close contacts of 347 confirmed COVID-19 patients identified between 13 Jan and 6 Mar in Guangzhou, China	<i>N</i> = 4,950; mean age of cohort 38 y, mean age of cases 44 y	Nasal swab, RT-PCR, repeated every 2 d	14 d
Park et al (18) (Korea) Published	Employees, residents, and visitors of a commercial and residential building where a confirmed case worked	<i>N</i> = 1,143; mean age of cohort 38 y	Nasal swab, RT-PCR, repeated during 14 d quarantine	14 d

RT-PCR = Reverse transcriptase–polymerase chain reaction; HCWs = Health care workers; COVID-19 = Coronavirus disease 2019

(11, 13, 14, 17, 18, 21); and a whole district surveillance program in Italy (16). The demographic characteristics (Table 1) indicate that most of the tested individuals were adults, with a mean age of more than 75 years in the five SNF studies and a mean age of more than 31 years in the non-aged care studies. The proportions of children and young people (0–20 years) ranged from 6% to 23.5%.

Diagnosis in all studies was confirmed via RT-PCR and in two cases was supplemented with radiological evidence (17, 21). Testing of individuals in the study sample varied across settings but was generally very high: all contacts regardless of symptoms (11, 13, 14, 17, 18, 21), more than 97% of SNF residents (10, 12, 15, 19, 20), and 85.9% of an entire town (16). The length of follow-up for monitored individuals in the SNF studies ranged from 7 to 30 days (10, 12, 15, 19, 20); 14 days for the Bruneian (13), Taiwanese (14), Korean (18), and Chinese close contacts (17, 22); 7–14 days in the Italian community (16); 12 days for 95% of all contacts in the Shenzhen community surveillance (11); and a mean of 16 (SD 6) days in Liaocheng, China (21).

The proportion of asymptomatic cases in the 13 included studies ranged from 4% (95% CI 1% to 10%) in Korea (18) to 40% in Vò, Italy (16) and in an aged care facility in the United States (20). Combining data from all 13 studies, we estimate that 17% of cases were asymptomatic (fixed effects 95% CI 14% to 20%); for the eight non-aged care studies, 16% (95% CI 13% to 19%); and for the five studies of SNFs, 20% (95% CI 14% to 27%) (Figure 3). The corresponding estimated proportions in the random-effects meta-analysis were, overall, 18% (95% CI 9% to 26%); non-aged care, 16% (95% CI 7% to 26%); and aged care, 21% (95% CI 5% to 36%). The 95% prediction interval was 4% to 52%. In the sensitivity analysis, which omitted studies in which length of follow-up was less than 14 days (10, 11, 16, 20), the overall estimate was modestly lower at 15% (fixed-effects 95% CI 12% to 18%)

or 17% (random-effects 95% CI 8 to 26%). Heterogeneity as expressed by I^2 was 84%.

Five studies reported data on secondary infection transmission from asymptomatic cases (Table 2). The asymptomatic transmission rates ranged from none to 2.2%, whereas symptomatic transmission rates ranged between 0.8% and 15.4%. Cycle threshold from real-time RT-PCR assays or the viral load did not differ between asymptomatic and symptomatic individuals in three of the studies (10, 14, 16). Overall, the RR of asymptomatic transmission was 42% lower than that of symptomatic transmission (pooled RR 0.58, fixed-effects 95% CI 0.335 to 0.994, p = 0.047; RR 0.38, random-effects 95% CI 0.13 to 1.083, p = 0.07; I^2 = 43.4%).

Risk of bias of included studies

Table 3 summarizes the overall risk-of-bias assessment of the nine included studies (the full list of risk-of-bias questions is in Supplemental Appendix 3). All of the studies were evaluated as low risk of bias for the sampling frame and length of follow-up domains (domains 1 and 5), which were part of the inclusion criteria. Two studies had potential non-response bias because not all of the eligible participants were tested (14% [463/3,275] of the target population was not tested in the Lavezzo et al study [16]) or results were not reported for all tested participants (87/98 cases were reported in the Bi et al study [11]; domain 2). Four studies either had not tested the study population at least twice during the follow-up period or had not provided clear information on testing (11, 13, 14, 21) (domain 3). Nine studies did not explicitly state the asymptomatic case definition they adhered to or had additional bias because of a high percentage of people in the SNFs with severe cognitive impairment (10–12, 14–16, 19–21) (domain 4).

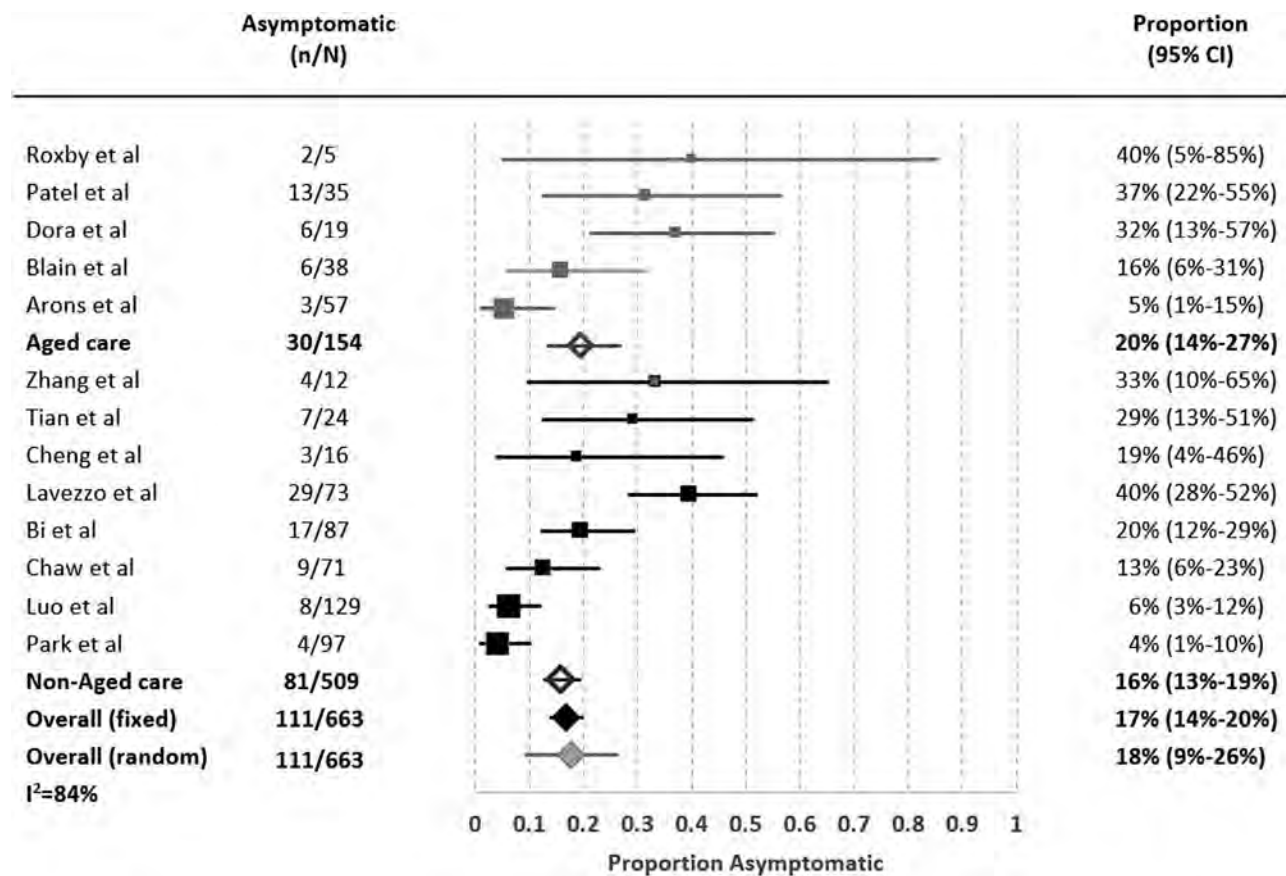


Figure 3: Pooled estimates of proportion of asymptomatic carriers by subpopulations
N = Positive cases; n = Asymptomatic cases

Table 2: Comparison of secondary transmission rates

Study	No./N (%)		Relative risk
	Asymptomatic transmission rate	Symptomatic transmission rate	
Zhang et al (22)	1/119 (0.8)	11/250 (4.4)	0.2
Cheng et al (14)	0/91 (0)	22/2644 (0.8)	0.66
Chaw et al (13)	15/691 (2.2)	28/1010 (2.8)	0.78
Luo et al (17)	1/305 (0.3)	117/2305 (5.1)	0.06
Park et al (18)	0/4 (0)	34/221 (15.4)	0.72


































































Excluded studies

Several well-publicized studies did not meet our inclusion criteria. The outbreak on the Diamond Princess cruise ship involved 3,711 passengers, of whom more than 600 acquired COVID-19 (3). Many of the positive cases were relocated to medical facilities in Japan without details of their clinical progression. To correct for the lack of follow-up, Mizumoto et al applied a statistical adjustment for the right censoring

and estimated that 17.9% (95% CI 15.5% to 20.2%) of positive cases were asymptomatic.

An open-invitation screening of the Icelandic population suggested that around 0.8% of the population were SARS-CoV-2 positive, with half classified as (initially) asymptomatic (2). However, because there was no follow-up, we cannot separate asymptomatic from pre-symptomatic individuals. Moreover, the study excluded symptomatic people undergoing

Table 3: Risk of bias in 13 included studies*

Included Studies	Risk-of-bias assessment questions				
	1. Was the sampling frame a true or close representation of the target population?	2. Was the likelihood of non-response bias among those at risk of infection minimal?	3. Is the reference standard used likely to correctly classify all SARS-CoV-2 infections?	4. Was an acceptable case definition used in the study?	5. Was the length of follow-up to define case definition appropriate?
Roxby et al					
Patel et al					
Dora et al					
Blain et al					
Arons et al					
Zhang et al					
Tian et al					
Chen et al					
Lavezzo et al					
Bi et al					
Chaw et al					
Luo et al					
Park et al					

SARS-CoV-2 = Severe acute respiratory syndrome coronavirus 2; Green smiley face = Low risk; Yellow straight face = moderate or unclear risk

targeted testing, which impeded estimation of an overall asymptomatic rate.

A study of 215 pregnant women in New York identified 33 SARS-CoV-2-positive women (23). On admission to the delivery unit, 4 of the 33 positive cases were symptomatic and 3 became symptomatic before postpartum discharge, suggesting an asymptomatic rate of 79% (26/33). However, the 2 days of follow-up were insufficient to meet our inclusion criteria.

A case report of a pre-symptomatic Chinese businessman transmitting COVID-19 to a German business partner was also excluded because despite three other people acquiring the infection from the infected German source, none of them was asymptomatic at follow-up (24). A 5-day point-prevalence testing of adults living in homeless shelters in Boston found 147 positive cases, of which the majority had mild or no symptoms (25). We excluded this study because no numeric estimate was included of those who were truly asymptomatic, and there was no follow-up assessment.

Two studies examined people repatriated from overseas to their home countries by plane. Neither study was clear on whether symptomatic people could board the plane and be included, and if they were excluded, the asymptomatic rates

would be overestimated. A study of 565 Japanese citizens repatriated from China (26) found 13 positives—4 asymptomatic and 9 symptomatic, based on screening on arrival. Another study of 383 Greek citizens repatriated from the United Kingdom, Spain, and Turkey (27) found 40 asymptomatic positive people on arrival, 4 of whom later self-reported symptoms. Again, the likely initial exclusion of symptomatic people and the lack of comprehensive follow-up would both result in overestimation of the asymptomatic rates.

DISCUSSION

Principal findings

Although the rate of asymptomatic COVID-19 cases has received considerable attention, we found only 13 studies that provided an adequate sample frame and follow-up to ascertain a valid estimate of the proportion of asymptomatic cases. The combined estimate of the asymptomatic proportion was 17% (95% CI 14% to 20%) but had considerable heterogeneity ($I^2 = 84\%$) and a 95% prediction interval that ranged from 4% to 52%. There was no clear difference in the proportions between aged care and non-aged care studies. Only 5 of the

13 studies provided data on transmission rates from asymptomatic cases. The transmission risk from asymptomatic cases appeared to be lower than that of symptomatic cases, but there was considerable uncertainty in the extent of this (RR 0.58; 95% CI 0.335 to 0.994, $p = 0.047$).

Strengths and weaknesses of the study

Strengths of our systematic review include achieving full methodological rigor within a much shorter time frame than traditional reviews using enhanced processes and automation tools (5). We also critically assessed the risk of bias of all full-text articles we screened to include studies with the least risk of bias in sampling frame and length of follow-up domains to be able to differentiate between asymptomatic and pre-symptomatic cases.

Our findings have several limitations. First, our search focused on published and pre-print articles, and we may have missed some public health reports that are either unpublished or only available on organisational websites. Second, the design and reporting of most of the studies had a number of important deficits that could affect their inclusion or our estimates. These deficits include poor reporting of the sample frame, testing and symptom check, and follow-up processes. Such reporting would have been considerably aided by including a flow chart of cases (as Lavezzo et al [16] did) with identification, testing, and follow-up, including missing data. A further important limitation was the poor reporting of symptoms, which was often simply dichotomised into symptomatic versus asymptomatic without clear definitions and details of possible mild symptoms. The included studies did not report sufficient data to examine the impact of age and underlying comorbidities on the asymptomatic rate. Finally, all included studies relied on RT-qPCR; hence, some cases might have been missed because of false-negative results, especially when study participants were only tested once (28). If the tests missed more asymptomatic cases, then the true proportion of asymptomatic cases could be higher than our estimates. However, false-positive results, which may occur when people without symptoms are tested in low-prevalence settings, would mean the true prevalence of asymptomatic cases was lower than our estimates.

Strengths and weaknesses compared with other studies

Several other non-systematic and systematic reviews have examined the proportion of asymptomatic cases. The non-systematic reviews estimated asymptomatic rates as between 5% and 80% (4, 29). However, they included only early cross-sectional reports and did not critically appraise the study design, nor did they attempt to pool the most valid studies. Five other systematic reviews reported pooled estimates of asymptomatic rate as between 8% and 16% (30–34). However,

these reviews included studies that we excluded because of high risk of bias in the sampling frame. Ongoing monitoring for new studies is warranted but should include robust methodological assessment, including ensuring included studies have a sufficient follow-up period to differentiate the asymptomatic from the pre-symptomatic cases. Our review currently also has a more recent search date than other reviews and includes sensitivity analysis by length of follow-up time. Our estimate of risk of transmission by asymptomatic cases was comparable to those reported in two other empirical reviews by Buitrago-Garcia et al (RR 0.35) and Koh et al (RR 0.39) (32, 34).

Meaning of the study

Estimates of the proportion of the cases that are asymptomatic and the risk of transmission are vital parameters for modelling studies. Our estimates of the proportion of asymptomatic cases and their risk of transmission suggest that asymptomatic spread is unlikely to be a major driver of clusters or community transmission of infection, but the extent of transmission risk for pre-symptomatic and minor symptomatic cases remains unknown. The generalisability of the overall estimate is unclear, and we observed considerable variation across the included studies, which had different settings, countries, and study design, reflected in the reasonably wide prediction interval.

Unanswered questions and future research

Many unanswered questions about asymptomatic cases remain. Only one of the more recent studies we included tested patients for immunoglobulin G antibodies to determine seroconversion among elderly individuals. Without repeated and widespread RT-PCR and antibody tests, it is difficult to accurately estimate the prevalence of COVID-19 infection and inform our infection prevention strategies (35). The role of viral load and virus shedding dynamics in asymptomatic and symptomatic cases will further help answer the question of forward transmission and disease length and severity. Other unknowns include whether there is a difference in the proportion of cases that are asymptomatic according to age (particularly children versus adults), sex, or underlying comorbidities, and whether asymptomatic cases develop long-term immunity to new infections. For most studies, the PCR (positive) cases were traced from the index cases, and the testing was carried out mostly at the beginning of the pandemic wave for the locale. So, for this review of inception cohorts, people with long-term persistent positive testing were unlikely to be misclassified as asymptomatic. The issue of persistent PCR positivity after a person has recovered from infection might be of concern to more recent studies conducted at some time after the first wave of the pandemic. In such

studies, researchers will need to ask about history of illness compatible with COVID-19 even if this occurred months ago, and PCR testing could be supplemented by other tests such as viral culture and anti-SARS-CoV-2 antibody tests.

Our recommendations for future research also include improved clearer reporting of methods, sampling frames, case definition of *asymptomatic*, extent of contact tracing, duration of follow-up periods, presentation of age distribution of asymptomatic cases, and separation of pre-symptomatic and mild cases from asymptomatic cases in results tables. Most studies used a limited definition of asymptomatic COVID-19 case, which could lead to mixing paucisymptomatic cases with asymptomatic cases. If that were a common issue, then the true prevalence of asymptomatic cases would be even lower than the current estimates. A reliable estimate of the proportion of asymptomatic cases and the burden of disease is imperative in understanding the infection transmission capacity of asymptomatic cases to inform public health measures for these individuals who, according to our findings, appear to pose lower risk of transmission. Until we have further immunological and epidemiological evidence, we advise that the importance of asymptomatic cases for driving the spread of pandemic to be considered with caution.

ACKNOWLEDGMENTS: The authors thank the authors of eligible articles for their replies to our queries.

CONTRIBUTORS: Conceptualization, OB, MC, KB, PG; Methodology, OB, MC, KB, JC, M-LM, PG; Software, JC; Formal Analysis, OB, MC, KB, PG; Data Curation, MC, KB, M-LM, PG; Writing – Original Draft, OB, MC, KB, JC, M-LM, PG; Writing – Review & Editing, OB, MC, KB, JC, M-LM, PG; Visualization, OB; Supervision, PG; Project Administration, OB.

FUNDING: OB is supported by National Health and Medical Research Council (NHMRC) grant APP1106452. PG is supported by NHMRC Australian Fellowship grant 1080042. KB is supported by NHMRC Investigator grant 1174523. All authors had full access to all data and agreed on the final manuscript submitted for publication. This study had no funding source.

DISCLOSURES: Mary-Louise McLaws is a member of the World Health Organization (WHO) Health Emergencies Program Experts Advisory Panel for Infection Prevention and Control (IPC) Preparedness, Readiness and Response to COVID-19 and WHO IPC Guidance Development Group for COVID-19.

PEER REVIEW: This article has been peer reviewed.

REFERENCES

1. Yuen K-S, Ye ZW, Fung S-Y, Chan C-P, Jin D-Y. SARS-CoV-2 and COVID-19: the most important research questions. *Cell Bioscience*. 2020;10(1):40. <https://doi.org/10.1186/s13578-020-00404-4>. Medline: 32190290
2. Bai Y, Yao L, Wei T, et al. Presumed asymptomatic carrier transmission of COVID-19. *JAMA*. 2020;323(14):1406–7. <https://doi.org/10.1001/jama.2020.2565>. Medline: 32083643
3. Mizumoto K, Kagaya K, Zarebski A, Chowell G. Estimating the asymptomatic proportion of coronavirus disease 2019 (COVID-19) cases on board the Diamond Princess cruise ship, Yokohama, Japan, 2020. *Euro Surveill*. 2020;25(10). <https://doi.org/10.2807/1560-7917.ES.2020.25.10.2000180>. Medline: 32183930
4. Heneghan C, Brassey J, Jefferson T. COVID-19: what proportion are asymptomatic? Centre for Evidence-Based Medicine, Oxford, UK. 2020. <https://www.cebm.net/covid-19/covid-19-what-proportion-are-asymptomatic/> (Accessed April 5, 2020).
5. Clark J, Glasziou P, Del Mar C, Bannach-Brown A, Stehlik P, Scott AM. A full systematic review was completed in 2 weeks using automation tools: a case study. *J Clin Epidemiol*. 2020;121:81–90. <https://doi.org/10.1016/j.jclinepi.2020.01.008>. Medline: 32004673
6. Clark JM, Sanders S, Carter M, et al. Improving the translation of search strategies using the Polyglot Search Translator: a randomized controlled trial. *J Med Libr Assoc*. 2020;108(2):195–207. <https://doi.org/10.5195/jmla.2020.834>. Medline: 32256231
7. World Health Organization. Coronavirus disease 2019 (COVID-19) Situation Report—66. 2020 26 March; Geneva, Switzerland.
8. Hoy D, Brooks P, Woolf A, et al. Assessing risk of bias in prevalence studies: modification of an existing tool and evidence of interrater agreement. *J Clin Epidemiol*. 2012;65(9):934–9. <https://doi.org/10.1016/j.jclinepi.2011.11.014>. Medline: 22742910
9. Whiting PF, Rutjes AW, Westwood ME, et al. QUADAS-2: a revised tool for the quality assessment of diagnostic accuracy studies. *Ann Intern Med*. 2011;155(8):529–36. <https://doi.org/10.7326/0003-4819-155-8-201110180-00009>. Medline: 22007046
10. Arons MM, Hatfield KM, Reddy SC, et al. Presymptomatic SARS-CoV-2 infections and transmission in a skilled nursing facility. *N Engl J Med*.

- 2020; 382:2081–90. <https://doi.org/10.1056/NEJMoa2008457>. Medline: 32329971
11. Bi Q, Wu Y, Mei S, et al. Epidemiology and transmission of COVID-19 in 391 cases and 1286 of their close contacts in Shenzhen, China: a retrospective cohort study. *Lancet Infectious Diseases*. 2020; 20(8):P911–9. [https://doi.org/10.1016/S1473-3099\(20\)30287-5](https://doi.org/10.1016/S1473-3099(20)30287-5).
 12. Blain H, Rolland Y, Tuaillon E, et al. Efficacy of a test-retest strategy in residents and health care personnel of a nursing home facing a COVID-19 outbreak. *J Am Med Dir Assoc*. 2020;21(7):933–6. <https://doi.org/10.1016/j.jamda.2020.06.013>. Medline: 32674822
 13. Chaw L, Koh WC, Jamaludin SA, Naing L, Alikhan MF, Wong J. SARS-CoV-2 transmission in different settings: analysis of cases and close contacts from the Tablighi cluster in Brunei Darussalam. *medRxiv*; 2020. <https://doi.org/10.1101/2020.05.04.20090043>.
 14. Cheng H-Y, Jian S-W, Liu D-P, Ng T-C, Huang W-T, Lin H-H. Contact tracing assessment of COVID-19 transmission dynamics in Taiwan and risk at different exposure periods before and after symptom onset. *JAMA Intern Med*. 2020; 180(9):1156–63 <https://doi.org/10.1001/jamainternmed.2020.2020>. Medline: 32356867
 15. Dora AV, Winnett A, Jatt LP, et al. Universal and serial laboratory testing for SARS-CoV-2 at a long-term care skilled nursing facility for veterans—Los Angeles, California, 2020. *MMWR Morb Mortal Wkly Rep*. 2020;69(21):651–5. <https://doi.org/10.15585/mmwr.mm6921e1>. Medline: 32463809
 16. Lavezzo E, Franchin E, Ciavarella C, et al. Suppression of a SARS-CoV-2 outbreak in the Italian municipality of Vo'. *Nature*. 2020; 584:425–9.
 17. Luo L, Liu D, Liao X-l, et al. Modes of contact and risk of transmission in COVID-19 among close contacts. *medRxiv*; 2020. <https://doi.org/10.1101/2020.03.24.20042606>.
 18. Park SY, Kim YM, Yi S, et al. Coronavirus disease outbreak in call center, South Korea. *Emerg Infect Dis*. 2020;26(8):1666–70. <https://doi.org/10.3201/eid2608.201274>. Medline: 32324530
 19. Patel MC, Chaisson LH, Borgetti S, et al. Asymptomatic SARS-CoV-2 infection and COVID-19 mortality during an outbreak investigation in a skilled nursing facility. *Clin Infect Dis*. 2020. (ePub Ahead of Print) <https://doi.org/10.1093/cid/ciaa763>. Medline: 32548628
 20. Roxby AC, Greninger AL, Hatfield KM, et al. Detection of SARS-CoV-2 among residents and staff members of an independent and assisted living community for older adults—Seattle, Washington, 2020. *MMWR Morb Mortal Wkly Rep*. 2020;69(14):416–8. <https://doi.org/10.15585/mmwr.mm6914e2>. Medline: 32271726
 21. Tian S, Wu M, Chang Z, et al. Epidemiological investigation and intergenerational clinical characteristics of 24 COVID-19 patients associated with supermarket cluster. *medRxiv*; 2020. <https://doi.org/10.1101/2020.04.11.20058891>.
 22. Zhang W, Cheng W, Luo L, et al. Secondary transmission of coronavirus disease from presymptomatic persons, China. *Emerg Infect Dis*. 2020;26(8). <https://doi.org/10.3201/eid2608.201142>. Medline: 32453686
 23. Sutton D, Fuchs K, D'Alton M, Goffman D. Universal screening for SARS-CoV-2 in women admitted for delivery (Lett). *New Engl J Med*. 2020;382:2163–4 <https://doi.org/10.1056/NEJMc2009316>. Medline: 32283004
 24. Rothe C, Schunk M, Sothmann P, et al. Transmission of 2019-nCoV infection from an asymptomatic contact in Germany. *N Engl J Med*. 2020;382(10):970–1. <https://doi.org/10.1056/NEJMc2001468>. Medline: 32003551
 25. Baggett TP, Keyes H, Sporn N, Gaeta JM. COVID-19 outbreak at a large homeless shelter in Boston: implications for universal testing. *medRxiv*. 2020. <https://doi.org/10.1101/2020.04.12.20059618>.
 26. Nishiura H, Kobayashi T, Suzuki A, et al. Estimation of the asymptomatic ratio of novel coronavirus infections (COVID-19) (Lett). *Int J Infect Dis*. 2020;9:P154–5. <https://doi.org/10.1016/j.ijid.2020.03.020>.
 27. Lytras T, Dellis G, Flountzi A, et al. High prevalence of SARS-CoV-2 infection in repatriation flights to Greece from three European countries. *J Travel Med*. 2020;27(3):taaa054. <https://doi.org/10.1093/jtm/taaa054>. Medline: 32297940
 28. Ai T, Yang Z, Hou H, et al. Correlation of chest CT and RT-PCR testing in coronavirus disease 2019 (COVID-19) in China: a report of 1014 cases. *Radiology*. 2020;296(2):200642. <https://doi.org/10.1148/radiol.20200642>. Medline: 32101510
 29. Oran D, Topol E. Prevalence of asymptomatic SARS-CoV-2 infection. *Ann Intern Med*. 2020;M20-3012. <https://doi.org/10.7326/M20-3012>. Medline: 32491919
 30. Al-Sadeq DW, Nasrallah GK. The incidence of the novel coronavirus SARS-CoV-2 among asymptomatic patients: a systematic review. *Int J Infect*

- Dis. 2020;98:372–80 <https://doi.org/10.1016/j.ijid.2020.06.098>. Medline: 32623083
31. Beale S, Hayward A, Shallcross L, Aldridge R, Fragaszy E. A rapid review of the asymptomatic proportion of PCR-confirmed SARS-CoV-2 infections in community settings. medRxiv; 2020. <https://doi.org/10.1101/2020.05.20.20108183>.
 32. Buitrago-Garcia DC, Egli-Gany D, Counotte MJ, et al. The role of asymptomatic SARS-CoV-2 infections: rapid living systematic review and meta-analysis. medRxiv. 2020. <https://doi.org/10.1101/2020.04.25.20079103>.
 33. He J, Guo Y, Mao R, Zhang J. Proportion of asymptomatic coronavirus disease 2019: a systematic review and meta-analysis. J Med Virology. 2020. (ePub Ahead of Print) <https://doi.org/10.1002/jmv.26326>. Medline: 32691881
 34. Koh WC, Naing L, Rosledzana MA, et al. What do we know about SARS-CoV-2 transmission? A systematic review and meta-analysis of the secondary attack rate, serial interval, and asymptomatic infection. medRxiv. 2020. <https://doi.org/10.1101/2020.05.21.20108746>.
 35. Byambasuren O, Dobler CC, Bell K, et al. Estimating the seroprevalence of SARS-CoV-2 infections: systematic review. medRxiv. 2020. <https://doi.org/10.1101/2020.07.13.20153163>.

- respiratory syndrome. *Science*. 2003;300:1966–70. <https://doi.org/10.1126/science.1086616>
6. Park SH, Kim Y-S, Jung Y, Choi SY, Cho N-H, Jeong HW, et al. Outbreaks of Middle East respiratory syndrome in two hospitals initiated by a single patient in Daejeon, South Korea. *Infect Chemother*. 2016;48:99–107. <https://doi.org/10.3947/ic.2016.48.2.99>
 7. Li Q, Guan X, Wu P, Wang X, Zhou L, Tong Y, et al. Early transmission dynamics in Wuhan, China, of novel coronavirus-infected pneumonia. *N Engl J Med*. 2020 Jan 29 [Epub ahead of print]. <https://doi.org/10.1056/NEJMoa2001316>
 8. Wu JT, Leung K, Leung GM. Nowcasting and forecasting the potential domestic and international spread of the 2019-nCoV outbreak originating in Wuhan, China: a modelling study. *Lancet*. 2020;395:689–97. [https://doi.org/10.1016/S0140-6736\(20\)30260-9](https://doi.org/10.1016/S0140-6736(20)30260-9)
 9. Kenah E, Lipsitch M, Robins JM. Generation interval contraction and epidemic data analysis. *Math Biosci*. 2008;213:71–9. <https://doi.org/10.1016/j.mbs.2008.02.007>

Address for correspondence: Lauren Ancel Meyers, J.T. Patterson Labs Bldg, University of Texas at Austin, 2415 Speedway, Austin, TX 78712, USA; email: laurenmeyers@austin.utexas.edu

Indirect Virus Transmission in Cluster of COVID-19 Cases, Wenzhou, China, 2020

Jing Cai,¹ Wenjie Sun,¹ Jianping Huang,¹ Michelle Gamber, Jing Wu, Guiqing He

Author affiliations: Wenzhou Sixth People's Hospital, Wenzhou Central Hospital Medical Group, Wenzhou, China (J. Cai, J. Huang, G. He); The Second Affiliated Hospital of Fujian Traditional Chinese Medical University, Fuzhou, China (W. Sun); Robert Stempel College of Public Health and Social Work, Florida International University, Miami, Florida, USA (W. Sun); Shenandoah University, Winchester, Virginia, USA (M. Gamber); Huashan Hospital, Fudan University, Shanghai, China (J. Wu)

DOI: <https://doi.org/10.3201/eid2606.200412>

To determine possible modes of virus transmission, we investigated a cluster of coronavirus disease cases associated with a shopping mall in Wenzhou, China. Data indicated that indirect transmission of the causative virus occurred, perhaps resulting from virus contamination of common objects, virus aerosolization in a confined space, or spread from asymptomatic infected persons.

¹These authors contributed equally to this article.

Severe acute respiratory syndrome coronavirus 2 (SARS-CoV-2), the causative agent of coronavirus disease (COVID-19), is presumed to spread primarily via respiratory droplets and close contact. However, these transmission modes do not explain all cases. To determine how the virus may have spread among a cluster of COVID-19 cases associated with a shopping mall in Wenzhou (a city with 8 million residents), China, we monitored and traced close contacts and hypothesized possible transmission modes. We analyzed clinical and laboratory data for cases by using real-time reverse transcription PCR (1). The study was approved with written consent from the Ethics Committee of Wenzhou Central Hospital and written informed consent from all case-patients.

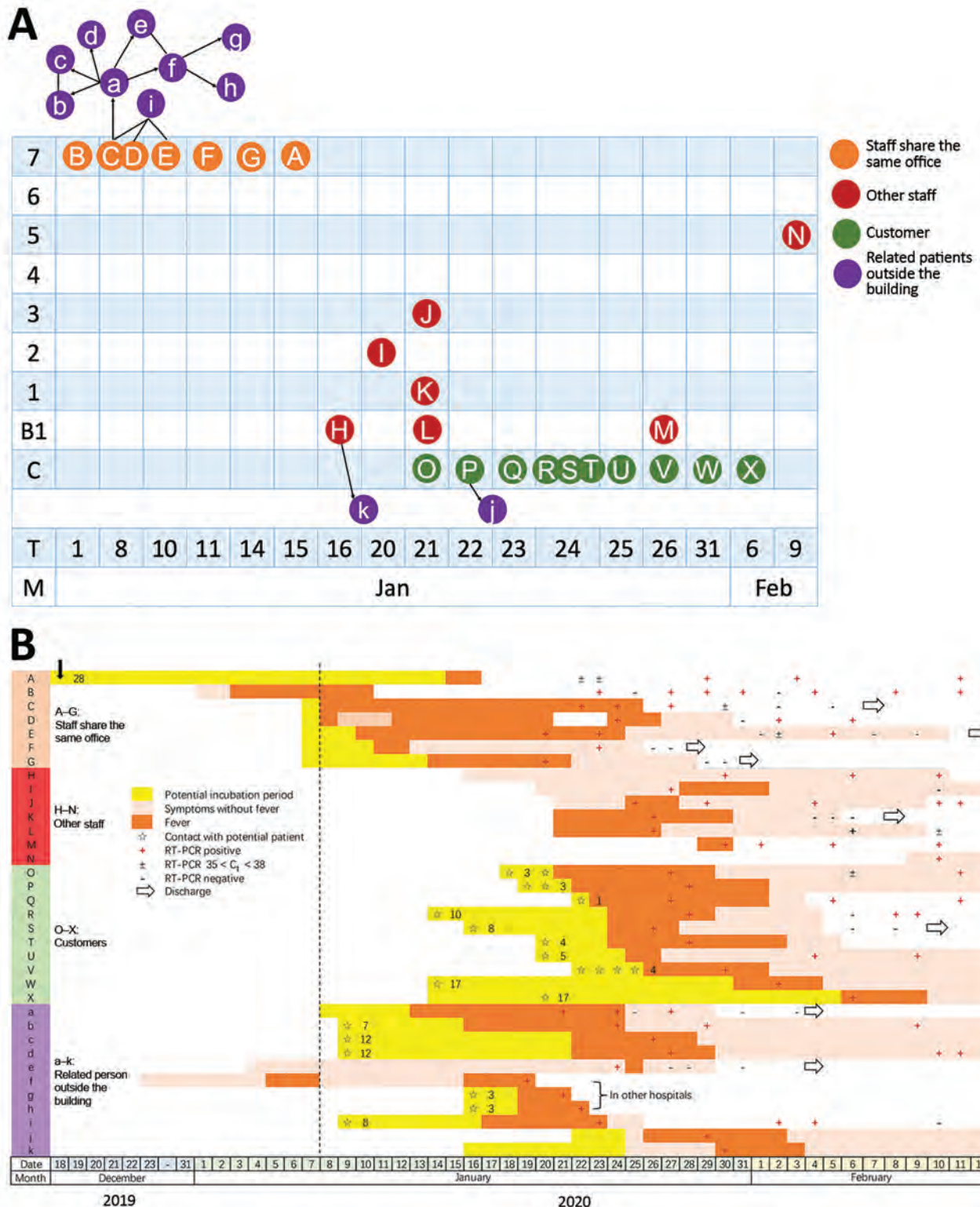
On January 20, 2020, a 23-year-old man (patient E) sought care at a hospital after 11 days of fever and headache. On January 21, COVID-19 was confirmed for patient E and his co-worker, patient G. The Wenzhou Center for Disease Control and Prevention traced and tested their contacts, and by January 28, COVID-19 was confirmed for 7 persons (patients A–G) from the same office (on floor 7).

Patient A, a 30-year-old woman, the only case-patient who indicated that she had been in Wuhan, China, returned from Wuhan on December 18, 2019. On January 15–16, 2020, she had a fever, but symptoms resolved without treatment. Despite symptom resolution, on January 30 she was confirmed to have SARS-CoV-2 infection. If patient A is the index patient, infected in Wuhan, her incubation period would have been 28 days, which would be extremely long, according to updated information (W.J. Guan et al., unpub. data, <https://www.medrxiv.org/content/10.1101/2020.02.06.20020974v1>). Asymptomatic carrier transmission has been reported for SARS-CoV-2 (2); hence, patient A could have been screened as a close contact during her incubation period and then hospitalized on the basis of a positive test (PCR) result only. However, her clinical symptoms did not appear until after hospitalization. Because persons with asymptomatic COVID-19 can spread the virus, patient A also could have been an asymptomatic carrier with a persistent infection (3).

On January 22, the mall was shut down. During January 19–February 9, COVID-19 was diagnosed for 7 mall staff from floors B1–3 and for 10 mall customers. Close contacts associated with the mall were traced, and COVID-19 was confirmed for 11 persons. Sixteen patients had had direct contact with other patients or had gone shopping in the mall. The average incubation period was 7.3 (range 1–17) days.

The mall has 8 floors above ground and several basement levels; floors B1 to 6 are commercial

RESEARCH LETTERS



shopping space, and floor 7 contains shopping and office space. We created an illustration showing the floors where the eventual COVID-19 case-patients worked or shopped, along with dates of symptom onset, potential incubation periods, symptom durations, confirmed times of positive diagnosis, and times of discharge (Figure 1, panel A).

Except for those who had been on floor 7, all other case-patients denied direct close contact with other case-patients. The possibility of customers being infected from other sources cannot be excluded. However, most customers reported early symptom onset in a concentrated time frame (Figure 1, panel B). We found no convincing evidence of definitive transmission pathways in this building. Patients A–G (Figure 1, panel A) worked in the same room on floor 7. Other case-patients who had been on other floors denied any direct contact with confirmed patients from floor 7, but they shared common building facilities (e.g., restrooms, elevators). Also, staff from floor 7 visited shops on other floors daily.

Until now, no evidence has shown that SARS-CoV-2 can survive outside the body for long. However, Middle East respiratory syndrome coronavirus demonstrates high robustness and a strong capability to survive outside the body and can remain infectious for up to 60 minutes after aerosolization (4). Hence, the rapid spread of SARS-CoV-2 in our study could have resulted from spread via fomites (e.g., elevator buttons or restroom taps) or virus aerosolization in a confined public space (e.g., restrooms or elevators). All case-patients other than those on floor 7 were female, including a restroom cleaner, so common restroom use could have been the infection source. For case-patients who were customers in the shopping mall but did not report using the restroom, the source of infection could have been the elevators. The Guangzhou Center for Disease Control and Prevention detected the nucleic acid of SARS-CoV-2 on a doorknob at a patient's house (5), but Wenzhou Center for Disease Control and Prevention test results for an environmental sample from the surface of a mall elevator wall and button were negative.

We cannot exclude the possibility of unknown infected persons (e.g., asymptomatic carriers) spreading

the virus. However, according to screening protocols implemented by the Wenzhou Center for Disease Control and Prevention, we traced all close contacts and included all patients with positive PCR results, including the asymptomatic carrier (patient A), in this study. Our findings appear to indicate that low intensity transmission occurred without prolonged close contact in this mall; that is, the virus spread by indirect transmission.

The work was supported by Major Project of Wenzhou Municipal Science and Technology Bureau (ZY202004).

About the Author

Dr. Cai is deputy chief physician and deputy director of the comprehensive internal medicine department. Her major research interest focuses on infectious diseases and gastrointestinal diseases.

References

1. National Microbiology Data Center. Novel Coronavirus National Science and Technology Resource Service System [cited 2020 Jan 30]. <http://nmcdc.cn/nCoV>
2. Bai Y, Yao L, Wei T, Tian F, Jin DY, Chen L, et al. Presumed asymptomatic carrier transmission of COVID-19. *JAMA*. 2020 Feb 21 [Epub ahead of print]. <https://doi.org/10.1001/jama.2020.2565>
3. Rothe C, Schunk M, Sothmann P, Bretzel G, Froeschl G, Wallrauch C, et al. Transmission of 2019-nCoV Infection from an asymptomatic contact in Germany. *N Engl J Med*. 2020;382:970–1. <https://doi.org/10.1056/NEJMc2001468>
4. Pyankov OV, Bodnev SA, Pyankova OG, Agranovski IE. Survival of aerosolized coronavirus in the ambient air. *Journal of Aerosol Science*. 2018;115:158–63.
5. Meiping G. Coronavirus detected on doorknob in S. China's Guangzhou. 2020 [cited 2020 Feb 3]. <https://news.cgtn.com/news/2020-02-03/Coronavirus-detected-on-doorknob-in-S-China-s-Guangzhou-NMualLcOWY/index.html>

Address for correspondence: Guiqing He, Department of Infectious Diseases, Infectious Diseases Laboratory, Wenzhou Sixth People's Hospital, Wenzhou Central Hospital Medical Group, Wenzhou, 325000 China; email: hegq123@126.com; Jing Wu, Department of Infectious Diseases, #5-504, Huashan Hospital, Fudan University, 12 Wulumuqizhong Rd, Jing'an District Shanghai 200040, China; email: jingee@fudan.edu.cn



Updated: Public health management of cases and contacts associated with COVID-19

Updated July 5, 2021

Note

This page is continually under review and updated as this situation evolves. Select updates have been made to the last version (April 22, 2021) in the following sections:

- Introductory content
- Contact management
- Persons possibly exposed through travel
- Contact tracing for airline passengers and flight crew

The updates in this version:

- Reflect emerging evidence regarding vaccine effectiveness and increasing vaccine coverage in the Canadian population
- Classify fully vaccinated contacts as low risk for the purposes of determining recommended public health authority (PHA) actions. This includes relaxation of quarantine recommendations for fully vaccinated contacts of cases (see Table 1), unless the risk assessment conducted by the PHA indicates otherwise
- Adjust quarantine period language to allow for flexibility in situations where a combination of testing and quarantine may be used
- Incorporate changes to reflect [border measures policies](#)

Please visit the [provincial and territorial resources for COVID-19](#) page for updated guidance specific to your province or territory

On this page

- [Case management](#)
- [Contact management](#)
 - [Table 1: Contact management recommendations by exposure risk level](#)
- [Appendix 1: Recommendations for isolation of COVID-19 cases in the community](#)
- [Appendix 2: Assessment of a suitable isolation location for a case of COVID-19](#)
- [Appendix 3: Recommended infection prevention and control precautions when caring for a case in the home or co-living setting](#)
- [Acknowledgments](#)
- [Footnotes](#)
- [References](#)

The Public Health Agency of Canada (PHAC), in collaboration with Canadian public health experts, has developed this guidance for federal/provincial/territorial (FPT) public health authorities (PHAs) to support the management of individuals infected with or who may have been infected with the SARS-CoV-2 virus (i.e., "cases") and contacts of

COVID-19 cases within their jurisdictions. *It is recognized that PHAs may adjust case and contact management recommendations based on a risk assessment that would include the local epidemiology, vaccination coverage in the community, vaccination status of the contacts, etc.*

The strategy outlined in this guidance focuses on case and contact management to mitigate the health impacts of COVID-19 on individuals in Canada¹. This guidance is set in the Canadian context and is based on the available scientific evidence and expert opinion. In interpreting and applying this guidance, it is important to recognize that the health, disability, economic, social, or other circumstances faced by some individuals and households may limit their ability to follow the recommended measures. This may necessitate adapted case management and contact responses by PHAs.

The response to the COVID-19 pandemic has been further strengthened by the availability of vaccines, but is further challenged by the emergence of variants of concern (VOC) within Canada and worldwide. Mutations in the SARS-CoV-2 virus that result in it being designated as a VOC are those which may cause increased transmissibility and/or potential changes in virulence and/or the possibility for immune escape. Monitoring for VOCs in general, particularly those with evidence of escape from natural/vaccine immunity, and those with increased transmissibility/severity is an important public health action to help inform case and contact management.

Evidence on the effectiveness of COVID-19 vaccines against asymptomatic infection in adults has begun to emerge from international post-marketing studies. Evidence suggests mRNA vaccines are moderately to highly effective against asymptomatic SARS-CoV-2 infection after a first dose (depending on time since vaccination as at least 2 weeks is needed for the immune response to develop) and highly effective against asymptomatic SARS-CoV-2 infection after a second dose. There are currently limited data specific to other COVID-19 vaccines, but studies are ongoing. Evidence on the effectiveness of COVID-19 vaccines authorized for use in Canada is summarized in the National Advisory Committee on Immunization's (NACI) Recommendations on the use of COVID-19 vaccines statement and is updated as evidence evolves.

Provincial and territorial (PT) PHAs continue to adjust restrictive community-based measures (CBMs) based on the epidemiology of COVID-19 and vaccination coverage in their jurisdictions, taking into consideration other important indicators, such as sufficient public health capacity to test, to trace, to isolate and to quarantine a high proportion of cases and contacts, respectively, sufficient health care capacity to respond to surges and risk reduction measures are in place for high-risk populations (i.e., those at higher risk of developing more severe disease or outcomes) and settings.

This guidance is subject to change as new information on transmissibility and epidemiology becomes available. It should be read in conjunction with relevant PT and local legislation, regulations and policies. Coronavirus disease (COVID-19) outbreak updates are available.

Case management

Reporting and notification

The national case definition for COVID-19 provides surveillance case definitions as well as associated surveillance reporting requirements.

It is important for frontline health care providers to notify PHAs of cases of COVID-19 in accordance with jurisdictional reporting requirements. PHAs need to provide overall co-ordination with health care providers and provincial laboratories for the management and reporting of cases, and to establish communication links with all involved health care providers for the full duration of illness. PHAs should report confirmed cases of COVID-19, as

well as probable cases where feasible, to PHAC within 24 hours of receipt of their own notification. [National surveillance for Coronavirus disease \(COVID-19\) guidance](#) is available. At the time of publication, a process for national reporting of VOCs has been approved, and provinces and territories are working closely with PHAC to implement and optimize this process to ensure national surveillance of VOCs.

In some instances, cases or contacts of cases are identified with epidemiological linkages that span two or more jurisdictions within and/or between provinces/territories. During case investigation, it may also be identified that the case acquired their infection, or was potentially exposed, in another jurisdiction. PHAs should use established inter-jurisdictional processes to enable timely case and contact management. Examples where this may be required include when a case travelled between jurisdictions during their communicable period; or when contacts reside in a different jurisdiction than a case.

Laboratory testing and screening

Laboratory testing strategies have evolved over time. Each PT has modified their approach (e.g., who is being tested and how) based on factors such as emerging evidence, new technology, laboratory capacity and local epidemiological circumstances. [Information is available](#) on the important roles that FPT governments play in COVID-19 testing.

At present, a [validated reverse transcription polymerase chain reaction \(RT-PCR\) test](#) on a clinically appropriate sample collected by a trained health care provider is the gold standard for the diagnosis of SARS-CoV-2 infection.

Appropriate laboratory testing for COVID-19 infection should be accessible by health care providers through community-based, hospital or reference laboratory services (e.g., a provincial public health laboratory (PHL) running a validated assay), or the National Microbiology Laboratory. In addition, PTs should have a process for screening and sequencing positive specimens for mutations common to VOCs. The establishment of screening assays looking for mutations specific to VOCs can provide results sooner than sequencing of virus samples and may be useful for informing timely public health action. However, not all VOCs will have common mutations so surveillance using partial or whole genome sequencing must be established by the PT. Although ideally, all positive specimens should be sequenced, when volumes preclude this, it is recommended that specimens from travelers, outbreaks and patients admitted to hospital should be prioritized and a subset of community-based specimens should also be selected for sequencing.

[Guidance for health professionals related to laboratory testing](#) is available. In addition, the Respiratory Virus Infections Working Group of the Canadian Public Health Laboratory Network has developed [laboratory testing best practices for COVID-19](#) and has updated its [protocol on microbiological investigation of emerging respiratory pathogens, including severe acute respiratory infections](#) ^{2 3}.

Rapid testing for COVID-19 using non-molecular assays has the potential to increase testing capacity; however, current data suggest that these methods are less sensitive than the current RT-PCR assays ⁴. The quick turn-around times and ease of use by a wide range of users allows rapid testing to be an important tool in a broader testing strategy (e.g., rapid testing of asymptomatic individuals in a cohort in which an outbreak is occurring or as part of a broader community-based testing strategy to help bring community transmission under control) ⁵. Interim guidance is available for use of the [nucleic acid-](#) and [antigen-based](#) rapid detection tests.

Re-infection

There is evidence that, although uncommon, individuals can become re-infected with SARS-CoV-2 ⁶. The dynamics, duration, and nature of immunity produced during infection with SARS-CoV-2 are still unclear, but there is good evidence of immunity for at least several months in the majority of individuals previously infected ⁷. The evidence will be monitored to determine if there is a higher risk of re-infection associated with VOCs, which may impact future guidance on testing. Refer to guidance for [laboratory testing for individuals suspected of being re-infected](#) for more information.

Clinical management/treatment

Clinical management of the case, whether in the home or in an acute care setting, is based on the case's condition and at the discretion of the case's health care provider. Refer to relevant guidance on [clinical management of patients with COVID-19](#).

Health care providers involved in home care for a case should follow interim guidance developed for [infection prevention and control in home care settings](#). Guidance for household members providing care for a case in the home, or occupants/staff in a co-living setting, are detailed in [Appendix 1](#).

Case management in the community

Epidemiologic evidence suggests that the majority of people with COVID-19 do not require care in a hospital ⁸.

When care in a hospital is not required, cases should isolate themselves as soon as possible. If they are isolating in the home or co-living setting (e.g., student residence, group home, shelter, etc.), they should isolate away from other household members or occupants, as directed by their PHA.

Those who live alone, or in a home where the members of the household are in isolation or quarantine, should identify community and social supports (e.g., family, friends, social services) where possible to assist with essential needs, including [care of pets](#) when required, or consult with their local PHA for information about additional community resources.

Appendices 1 and 2 provide information regarding recommendations for isolation and assessment of a suitable isolation location respectively.

Seeking medical care

In the event of a medical emergency, the case or their caregiver should contact emergency medical services (911) or the local emergency helpline for medical assistance, including transportation to the hospital or clinic if necessary. If using an ambulance to travel to a hospital or clinic, inform the dispatcher that the person requiring medical care has COVID-19. Public transportation should not be used to seek medical care (if possible).

If using a private vehicle to seek medical care:

- Call ahead to inform the hospital or clinic that the individual has COVID-19, and follow any directions provided;
- When traveling in a private vehicle:
 - minimize occupants in the vehicle (e.g., only the driver and case, if possible)
 - maximize distance between all occupants in the vehicle (e.g., case in the back seat, opposite to the driver in the car; or third row in larger vehicles)
 - open all windows if possible and safe to do so ⁹;
 - the case should be wearing a medical mask ^a, if no contraindications to doing so
 - all other occupants in the vehicle should wear medical masks ^a;

- The case and those assisting with transport should follow strict adherence to personal preventive practices to help reduce risk of transmission (e.g., frequent hand hygiene, respiratory etiquette).

Isolating in the community

When advising individuals to isolate in the community-at home or in a co-living setting-it is important that the risk of transmission from the case to other members of the household or occupants in the co-living setting be minimized as much as possible.

Guidance for isolating at home or in other co-living settings, as well as recommendations when strict adherence to isolation requirements may not be possible, are available in [Appendix 1](#).

Assessing suitability for isolation in the community

The PHA, in collaboration with the case and their health care provider, will determine the location where a case of COVID-19 isolates, as appropriate. It is important that cases who do not require hospital-level care convalesce in a suitable environment where effective isolation can be maintained and appropriate monitoring (e.g., for worsening of illness) can be provided.

Considerations for a suitable environment will depend on the individual and their living situation; and may vary depending on the sex, gender, or other socioeconomic or identity factors of the case. The vaccination status of other household members may also be taken into consideration. When feasible and as directed by the PHA, an alternate dwelling (e.g., hotel, self-containing unit) may be used for isolation of a case.

The PHA plays an important role in assessing the suitability of the case's isolation setting, and the considerations listed above are detailed in [Appendix 2](#).

Psychosocial considerations

PHAs should encourage individuals, families and communities to create a supportive environment for people who are isolating to take care of their mental health, and minimize stress and hardship associated with isolation as the financial, social, and psychological impact can be substantial.

Obtaining and maintaining public trust are key to successful implementation of these measures. Clear messages about isolation, including the criteria, rationale, justifications, and duration, as well as ways in which persons will be supported during the isolation period, will help to generate public trust. Messaging should also be sensitive and tailored to the needs of populations confronting social, economic, cultural or other vulnerabilities. Additional information on [the psychological impacts of COVID-19](#) is available.

For Indigenous Peoples, mandatory isolation away from home due to COVID-19 may trigger re-traumatization issues associated with experiences of forced removals in the past. There is also the potential for new trauma if their ability to be with their community, practice cultural and/or spiritual activities is limited. To avoid relocation of persons with COVID-19 to locations outside of their community, many Indigenous communities have re-purposed facilities or set up temporary structures to use as isolation sites so that community members may safely isolate in situations where their home setting is not suitable.

Public health monitoring of cases

Ideally, PHAs should provide or facilitate active daily monitoring of cases of COVID-19, including those infected with a VOC, as long as feasible based on available resources. If there are insufficient resources available to provide daily monitoring for all cases, PHAs should give consideration to prioritizing daily monitoring for cases infected with a VOC.

It is recognized that the frequency of monitoring of COVID-19 cases may vary by PHA and the local context, but generally, should include the following actions or advice:

- The ability to adhere to the standard isolation measures recommended;
- Appropriate information on infection prevention and control precautions, personal preventive practices, and environmental cleaning;
- Advice for self-monitoring for symptoms, including daily temperature checks;
- Steps to take if symptoms worsen, including instruction on self-care and how/when to access medical care; and
- When and where to access further diagnostic testing for COVID-19, if appropriate based on provincial/territorial testing strategies;
- Monitoring for symptom-onset in household contacts (if relevant) and/or identifying additional contacts.

PHAs should provide additional information about VOCs as required, such as when VOCs are circulating in the community or when a case has been diagnosed with a variant strain, including heightened vigilance for increased transmissibility if isolating at home or in a co-living setting with other household members or occupants.

Cases of COVID-19 should be monitored until they have met the criteria set by the PHA for discontinuing isolation.

Discontinuation of isolation for cases in the community

The PHA should direct the discontinuation of isolation of cases in the community (i.e., those not hospitalized or residents of long-term care facilities) ^b. Criteria may include:

- For symptomatic cases:
 - At least 10 days have passed since onset of first symptom.
 - The case is afebrile and has improved clinically.
 - Absence of anosmia or fatigue/tiredness should not be required.
 - Absence of cough should also not be required for those known to have chronic cough or for those who are experiencing reactive airways post infection.
- For asymptomatic cases:
 - At least 10 days have passed since the date their positive specimen was collected and the case remained asymptomatic.

In general, repeat laboratory testing (e.g., a negative test result) as the basis for discontinuing home isolation is not recommended. In most individuals with competent immune systems and those recovered from mild or moderate illness, prolonged or renewed RNA detection is not believed to reflect infectious virus, but rather non-infectious viral fragments, as viable virus has rarely been reported to persist for longer than 10 days in these populations. Additional information can be found in [Guidance for repeated PCR testing in individuals previously positive for COVID-19](#).

There may be exceptions to these criteria for which PHA and/or clinical care providers may determine a longer isolation period is warranted (e.g., immunocompromised individuals, those hospitalized due to COVID-19). Discontinuation of isolation is not related to clinical management of cases. In some cases, clinical management may continue to be required after discontinuation of isolation.

Contact management

Contact management for community-based cases of COVID is the responsibility of local and provincial public health authorities, and is evolving as vaccine coverage in Canada increases and cases of COVID-19 are lowering in many jurisdictions.

It is important to identify and manage the contacts of cases of COVID-19 to reduce ongoing transmission of the virus in the community¹⁰. Several objectives may be achieved through contact management activities by PHAs, including:

- To facilitate rapid identification of secondary cases of COVID-19 (or source cases, in the context of backward contact tracing);
- To facilitate early implementation of public health measures as appropriate, depending on the contacts' exposure risks; and
- To gain a better understanding of the epidemiology of COVID-19.

Early identification of contacts, and direction regarding diagnostic testing for COVID-19 based on existing PT testing strategies, is a key component of rapid case identification and management to reduce transmission of the coronavirus. With the many unknowns associated with VOCs, testing of vaccinated individuals will be an important consideration of contact management.

In an outbreak context, contact tracing and management also serves the purpose of active case finding during an investigation. Where an outbreak is suspected, the PHA may adopt a situation-specific definition for those at high risk of exposure (i.e., "close contact") to help efficiently target their contact investigation and case finding efforts. For example, all individuals at an event associated with a high risk of transmission could be evaluated as being at high risk of exposure (e.g., all guests at a wedding, or participants of an indoor fitness class). This approach may be considered when the outbreak setting results in a high risk of exposure for most participants, or where risk assessments for individuals are not feasible.

Outbreaks may have a greater impact on certain groups due to their social, economic, health, or other risk factors, such as older age, having chronic medical conditions, living in a remote and isolated community, or living in poverty or crowded settings.

PHAs should give consideration to engaging in more rigorous outbreak investigation activities when an outbreak involves a VOC. This may include backward contact tracing or mass asymptomatic testing of individuals with known or suspected close contact exposure to a case with a VOC.

Contact tracing

The public health approach to COVID-19 case and contact management to date has largely focused on interrupting chains of transmission through contact tracing by identifying individuals at risk of exposure to SARS-CoV-2 from an identified case. The primary goal of contact tracing is to identify and to quarantine, or to facilitate self-monitoring of, individuals who are potentially exposed to a case to stop future chains of transmission.

Contacts should be identified and managed as per the recommendations in this document, where feasible based on public health resources. The level and intensity of public health actions may vary among jurisdictions according to the local epidemiology of COVID-19 at a given time and the identification of VOCs. Alternative contact management strategies that PHAs may consider when resources are constrained are detailed below.

The risk assessment conducted by the PHA can help identify each contact's exposure risk level, determine the appropriate intervention for the individual (e.g., quarantine, self-monitoring) and PHA actions for the recommended monitoring period. If the contact has been vaccinated, the PHA risk assessment may consider

additional factors that could influence risk categorization and subsequent PHA actions. For example, these factors could include whether the contact has been partially or fully vaccinated, if the contact had been previously infected, if the contact is immune compromised, the time since last dose of vaccine or the potential risk of transmission to others, especially unvaccinated individuals who are at risk of more severe disease or outcomes from COVID-19. In addition, if there is significant spread of VOCs within the community or there is uncertainty about the risk assessment for a contact of a case infected with a VOC, PHAs may choose to adopt a more cautious approach when managing contacts as either high- or low-risk of exposure (see [Table 1](#) below).

Given that transmission of SARS-CoV-2 can occur from cases who are symptomatic, pre-symptomatic, or asymptomatic, contact tracing should include:

- Identifying people who were exposed to a symptomatic case in the period starting 48 hours prior to the case developing a symptom consistent with COVID-19, and until the case was no longer considered infectious (e.g., 10 days following symptom onset for a non-hospitalized case).
- Identifying people who were exposed to a laboratory confirmed asymptomatic case in the period starting 48 hours prior to the day their positive specimen was collected, and until the case was no longer considered infectious (e.g., 10 days after specimen collection date) ¹¹.

For operational purposes, a minimum period of 48 hours prior to symptom onset (or positive test result) should be considered by jurisdictions for contact tracing. Under certain circumstances (e.g., outbreak management, VOCs, backward contact tracing), and given that in some instances the infectious period of a COVID-19 case may be longer than 48 hours, jurisdictions may extend contact tracing greater than 48 hours when public health capacity and/or the risk assessment warrants it.

Table 1 provides guidance for classifying contacts as either high or low risk, depending on their exposure, for the purposes of determining recommended actions. Fully vaccinated in this context means at least 14 days have passed since the completion of the recommended number of doses of a Health Canada approved COVID-19 vaccine. The information provided in Table 1 is not intended to replace more personalized public health advice provided to contacts, based on comprehensive risk assessments conducted by PHAs.

Table 1: Contact management recommendations by exposure risk level

Note: All potential exposures described below are considered to have occurred when the case was communicable in determining exposure risk level.

Risk Level	Description	Recommendations for the contact
------------	-------------	---------------------------------

<p>High risk exposure (close contact)</p>	<ul style="list-style-type: none"> • HCW who is not fully vaccinated and who provided direct physical care to a case, or a laboratory worker handling COVID-19 specimens, without consistent and appropriate use of recommended PPE and infection prevention and control practices ^d. • Anyone who is not fully vaccinated and lives with a case, has direct physical contact with a case, or is exposed to their infectious body fluids, including the case's caregiver, intimate partner, child receiving care from the case, etc. • Anyone who is not fully vaccinated and has shared an indoor space (e.g., same room) with a case for a prolonged period of time ^d, including closed spaces and crowded places, (e.g., social gatherings, workplaces, etc.), without adhering to appropriate individual-level and setting-specific risk mitigation measures ^e. • Anyone who is not fully vaccinated and has had a close-range conversation with a case or has been in settings where a case engaged in singing, shouting, or heavy breathing (e.g., exercise), without adhering to appropriate individual-level and setting-specific risk mitigation measures ^e. 	<ol style="list-style-type: none"> 1. Quarantine at home for 14 days from last exposure or for the recommended period determined by the local PHA ^f. 2. Follow recommended <u>personal preventive practices</u>. If living with the case, avoid further exposure to the case and wear <u>medical mask</u> or a <u>well-constructed and well-fitting, non-medical mask</u> ^f when in a shared space (e.g., same room) with the case. 3. Follow PHA directions related to testing requirements ^g. 4. Self-monitor for the appearance of <u>symptoms consistent with COVID-19</u> for 14 days following their last exposure to the case. 5. Take and record temperature daily and avoid the use of fever-reducing medications (e.g., acetaminophen, ibuprofen) as much as possible. These medications could mask an early symptom of COVID-19; if these medications must be taken, advise the PHA ¹². 6. If symptoms occur, isolate away from others within the home or co-living setting as quickly as possible; put on a medical mask ^a and contact the PHA for further direction, which will include: <ul style="list-style-type: none"> ◦ where to go for care, ◦ appropriate mode of transportation to use, and ◦ IPC precautions to be followed. 7. Avoid in-person interactions with others, especially <u>those who are at risk for developing more severe disease or outcomes from COVID-19</u>. 8. Contacts who are <u>at risk for developing more severe disease or outcomes</u> should not provide care for the case and should stay elsewhere if feasible.
--	---	---

Low risk exposure	<ul style="list-style-type: none"> • HCW (regardless of vaccination status) who provided direct physical care to a case, or a laboratory worker handling COVID-19 specimens, with consistent and appropriate use of recommended PPE and infection prevention and control practices ^ε. • Anyone (regardless of vaccination status) who has shared an indoor space (e.g., same room) with a case, including closed spaces and crowded places (e.g., social gatherings, workplaces, etc.), with adherence to appropriate individual-level and setting-specific risk mitigation measures ^ε. • Anyone (regardless of vaccination status) who has had a close-range conversation with a case or has been in settings where a case engaged in singing, shouting, or heavy breathing (e.g., exercise), with adherence to appropriate individual-level and setting-specific risk mitigation measures ^ε. • Fully vaccinated individuals in the above-mentioned high-risk exposure (close contact) situations would be considered to have a low risk exposure and be managed accordingly. 	<ol style="list-style-type: none"> 1. Self-monitor for <u>symptoms</u> for 14 days following their last exposure. 2. If symptoms occur, isolate away from others as quickly as possible, put on a medical mask ^a and contact the PHA for further direction, which will include: <ul style="list-style-type: none"> ◦ where to go for care, ◦ appropriate mode of transportation to use, and ◦ IPC precautions to be followed. 3. Where possible avoid interactions with <u>individuals at higher risk for severe illness</u> (this may not apply to HCWs who are using PPE and following IPC practices appropriately in their workplace) ^ε. 4. Follow PHA directions related to testing requirements. 5. Follow recommended <u>personal preventive practices</u>.
Acronyms:		
<ul style="list-style-type: none"> • HCW: health care worker • PPE: personal protective equipment • IPC: infection prevention and control 		

Although transmission of SARS-CoV-2, including VOCs, may occur during brief exposures, transient interactions (e.g., walking by a case) have not been identified as high- or low-risk exposures in Table 1 because identifying such contacts is typically not feasible outside of digital contact tracing applications (see Alternative contact management strategies below).

Based on a risk assessment, PHAs may consider more robust approaches to contact management and quarantine specifications, particularly in the context of outbreak investigations involving VOCs. PHAs may also need to consider modifications to quarantine recommendations in some circumstances, such as the need for essential workers to maintain critical services. In these circumstances, jurisdictions may consider reducing quarantine with negative test results. At present, there is limited evidence to support this as a widespread approach, as there remains a residual risk of transmission ¹³.

The duration of contact management for a contact who develops symptoms compatible with COVID-19 within 14 days of last exposure to a case should be based on the following considerations:

- If laboratory testing is conducted and the test result is **negative** for SARS-CoV-2, consider continuing to manage the individual as a contact for the duration of the possible 14-day incubation period, based on a risk assessment. The contact may be considered for re-testing if they have a worsening or progression of symptoms, and management would depend on the results of the second test.
- If laboratory testing is **not** conducted, the contact who develops symptoms should be managed as a probable/suspect case as applicable, and they should complete at least 10 days of isolation. Since they are still

a contact of a case and not a laboratory confirmed case themselves, depending on the timing of symptom onset and last exposure to a case, this individual may need to quarantine after the isolation period, for 14 days from the last known exposure. In this situation, the PHA should complete a risk assessment to determine the appropriate quarantine period based on the individual's level of risk (see [Table 1](#)).

Alternative contact management strategies

To complement or accommodate limited local resources, PHAs may consider alternative approaches to traditional contact tracing, particularly when they are experiencing a local surge in cases¹⁴. These may include the following:

- Using well-trained non-public health staff and volunteers for certain contact tracing activities;
- Repurposing existing resources, such as call centres or hotlines;
- Reducing the intensity of follow-up of contacts based on risk assessment, for example, automated calls or text messages to low-risk contacts, or follow-up text messages instead of daily calls; and
- Leveraging available technology, such as contact tracing software, as well as web-based and mobile phone applications (e.g., [COVID Alert](#)).

During local peaks in COVID-19 activity and declared outbreaks, PHAs may also consider prioritizing contact tracing activities for specific settings where people gather (e.g., schools, events, workplaces, remote communities, etc.), and in particular, when epidemiologic features suggest a change in transmission dynamics (e.g., when a VOC is suspected or confirmed). PHAs may also consider prioritizing follow-up of contacts (e.g., those with vulnerabilities, those who work in high-risk settings, or those who provide care to someone with vulnerabilities, etc.)¹⁵.

PHAs may also consider alternative approaches where cases, employers, or event coordinators notify contacts (i.e., simple referral); or notify contacts and provide additional information related to infection prevention and control, quarantine, and symptom monitoring (i.e., enhanced referral)¹⁶.

Backward contact tracing

PHAs may also consider 'backward' contact tracing, which focuses on trying to determine where and when the case likely acquired their infection. Backward contact tracing is routinely done as part of case or outbreak investigations for communicable diseases of public health significance, when PHAs collect information on a case's potential acquisition history. In this guidance, backward contact tracing is proposed as a less intensive activity, and therefore potentially less resource intensive, compared to outbreak investigation.

While COVID-19 has been observed to spread steadily in the community, with one case infecting one or two other individuals on average, clusters have been identified where some individuals disproportionately infect a larger number of individuals. This represents a statistical concept called over-dispersion, where there is high individual-level variation in the distribution of the number of secondary transmissions. Clusters associated with these cases have been referred to as super-spreading events (SSEs).

Mutations in the genetic code of SARS-CoV-2 can also cause the virus to act in ways that have significant impacts on case and contact management (e.g., increases in disease spread or severity; its ability to become undetectable by tests; or the effectiveness of vaccines or treatments).

In these circumstances, 'backward' contact tracing may help to:

- Identify the source case;
- Find additional cases by focusing on the setting where a case's exposure likely took place; and
- Interrupt additional chains of transmission by then tracing contacts of the newly identified cases.

If the source case is identified through backward contact tracing, contact tracing to identify individuals who may have been exposed to a case should be employed as detailed above, and contacts managed based on their risk of exposure as described in [Table 1](#). Depending on a given situation, testing requirements and public health interventions may need to be scaled based on local epidemiology.

Backward contact tracing is considered to be most useful when localized outbreaks may be occurring in areas experiencing relatively low levels of transmission. It may also be considered for investigating outbreaks with an epidemiologic feature suggestive of change in transmission dynamics (e.g., where a VOC is implicated).

It is considerably more challenging when there is widespread community transmission, due to the volume of cases and uncertainty created by having multiple potential sources of transmission for any given case. Backward contact tracing may also be less useful during periods of restrictive public health measures, due to fewer events or localized settings where outbreaks or SSEs might occur ¹⁷. Employing backward contact tracing approaches may have significant resource implications, depending on the specific contact tracing strategies used, approaches to testing, and local epidemiology.

There is currently limited evidence regarding the effectiveness of backward tracing for COVID-19, so it is not possible to be definitive about when it would be most useful or how it would be best implemented. A limited number of countries have utilized this strategy, and beneficial impact was correlated with low incidence and limited community transmission ^{18 19}.

Provinces/territories (PTs) should consider the utility of backward contact tracing based on their individual circumstances and available resources and, if implemented, consider evaluating the effectiveness in order to contribute to the evidence base for this practice.

Persons possibly exposed during travel

In response to the COVID-19 pandemic, all travellers entering Canada are subject to the rules set out by the [emergency orders](#) under the *Quarantine Act*.

Current information regarding travel, testing, quarantine and borders requirements can be found at [COVID-19: Travel, testing, quarantine and borders](#).

History of travel should be considered by PHAs during a risk assessment during contact tracing. Potential [travel-related exposures on specific conveyances \(e.g., flights, trains, cruise ships\)](#) may be available.

Contact tracing for airplane passengers and flight crew

Potential exposure to SARS-CoV-2 among passengers and crew during air travel is a topic of concern; however, risk mitigation measures such as vaccination status, mandatory use of masks, physical distancing, reduced occupancy, ventilation, environmental cleaning, and hand hygiene, applied in a layered approach, can significantly reduce the likelihood of transmission ²⁰.

Decisions related to contact tracing individual airplane passengers and flight crew who may have been exposed to a confirmed case of COVID-19 on any flight should be made based on available resources and a risk assessment. Risk assessments should be conducted by the PHA to which the case is notified, considering the following:

- Type, severity, and onset date of symptoms for symptomatic cases, or specimen collection date for asymptomatic cases, in relation to the flight date;
- Current messaging to all international travellers, specifically with respect to any federally mandated testing, quarantine or isolation requirements;

- Current legislation, regulations and policies that may be imposed on domestic travellers by a PT upon arrival to that PT;
- Timing of notification and likelihood of getting sufficient passenger contact information within the recommended timeframe; and
- Incremental benefit of individual communication to those seated within 2 metres (or more) ^b of the case versus public communication of the flight number.

If the province/territory determines that notification to potential contacts is required, the PHA can follow local protocols for publicly communicating when a case has had a history of travel during their period of communicability. The information required is the flight number, flight date, departure/arrival locations, and affected rows of the flight. Additionally, flight exposure notifications received by PHAC's Inter-jurisdictional Notices (IJN) team can be posted on the [COVID-19: Passenger transport where you may have been exposed](#) webpage.

Appendix 1: Recommendations for isolation of COVID-19 cases in the community

When care in a hospital is not required, cases of COVID-19 should isolate themselves as soon as possible. If they are isolating in the home or co-living setting (e.g., shelter, group home, or student residence), they should isolate away from other household members or occupants, as directed by their PHA. It is recommended the case isolate in a separate room for sleeping with access to a separate washroom from other household members or occupants, if possible. When feasible and as directed by the PHA, cases could isolate in an alternate dwelling such a hotel or self-containing unit. They should isolate for a minimum of 10 days from the onset of symptoms for a symptomatic case, or the collection date of a positive specimen for an asymptomatic case.

During isolation, the case should not leave the isolation setting, whether it is their home, co-living setting, or an alternate setting identified by their PHA or health care provider. They should:

- Avoid in-person interactions with others, including members of their household, if possible;
- Not go out unless required or directed to seek medical care;
 - If a case must go out to seek medical care, they should wear a medical mask ^a.
- Not go to school, work, or other public places; and
- Not take public transportation to seek medical care, if possible.

Isolating in the community

When advising individuals to isolate at home or in a co-living setting, it is important that the risk of transmission from the case to other members of the household or occupants in the co-living setting be minimized as much as possible. Advice is available for [individuals who are required to isolate at home due to COVID-19](#).

As much as possible, the following strategies should be used during isolation in the community:

- A case should have their own room and a dedicated washroom.
 - When awake, the case should wear a medical mask ^a, when they are in a shared space (e.g., kitchen, washroom, hallway), regardless if other household members or occupants in the co-living setting are present, to avoid aerosol transmission and/or contaminating shared surfaces and objects.
- The case and other members of the household or co-living setting should avoid any activities that put them in a shared space (e.g., in the same room) with one another. This includes avoiding shared activities like watching television, congregate dining (e.g., family meals), playing games, etc.

- When other members of the household or co-living setting are unable to avoid sharing a space (e.g., the same room) with the case, they should wear a medical mask or a properly worn, well-constructed and well-fitting non-medical mask¹. If household members are at high risk of more severe disease or outcomes, a medical mask should be worn².
- If a member of the household or co-living setting needs to provide care to the case, they should wear a medical mask². The case should only access an outdoor setting if it is a private space (i.e., their private backyard or balcony). If household members are present in this outdoor space, all individuals present should continue to wear masks and practice physical distancing.
- The case should avoid sharing personal items with others, as much as possible (e.g., towels, bed linen, cigarettes, unwashed eating utensils, toothbrushes, etc.).
- In situations where childcare is shared between two homes, wherever possible consider having the child stay in one home for the duration of the isolation or quarantine period.
- If possible, shared spaces (e.g., kitchen, washroom, hallways) should be well ventilated (e.g., windows open, as weather permits), regardless if individuals are present or not.
- The case and all household members or occupants of the co-living setting should strictly follow the recommended personal preventive practices.
- A list of supplies to have on-hand while isolating is available.

Recommendations when strict isolation is not possible

Cases of COVID-19 who have been directed to isolate may not be able to strictly follow instructions for isolation in the home or co-living setting. This may be due to the isolation setting itself, for instance, there are not enough rooms in the home for the case to have a separate room or a dedicated washroom, or occupants in a shelter who must share space. It may also be difficult to isolate due to other factors; for example, if the case is a child, has child-/elder- care responsibilities, or lives in a multigenerational household.

When it is not possible to relocate the case, or members of the household or co-living setting, the following approaches may be considered:

- In overcrowded housing, or where a dedicated room and washroom are not available for isolation, consider having the case, household members, or other occupants relocate to another location so the case can be isolated.
- Take steps to bring fresh air into the space, by opening windows and doors to the outside if possible (e.g., depending on weather) and safe (e.g., no fall hazards, outdoor air quality); and ensuring the mechanical ventilation system (e.g., heating, ventilation and air conditioning (HVAC) system) is functioning properly and turned on continuously if possible.
- Although the effectiveness is limited due to possible transmission of SARS-CoV-2 via respiratory droplets and aerosols, consideration may be given to separating the case from others with dividers such as curtains in a shared space (e.g., home with limited rooms, sharing space for sleeping).
 - If other members of the home or co-living setting are sleeping in the same room as a case, it is important to maintain as much distance as possible from the case (ideally a minimum of 2 metres)¹. This may be accomplished by separating beds and having occupants sleep head-to-toe.
- If a separate washroom is not available, open the window, turn on the exhaust fan to improve ventilation, put the lid of the toilet down before flushing and, when possible, clean and disinfect surfaces touched by the case after each use²¹.

Appendix 2: Assessment of a suitable isolation location for a case of COVID-19

The location where a COVID-19 case will be isolated should be determined by the public health authority (PHA), in collaboration with the case and their health care provider, as applicable. It is important that cases who do not require hospital-level care convalesce in a suitable environment where effective isolation and appropriate monitoring (e.g., for worsening of illness) can be provided.

Considerations for a suitable environment will depend on the individual and their living situations, and may vary depending on the sex, gender, or other socioeconomic or identity factors of cases.

Factors to consider when determining the suitability of an isolation location:

Can the case's clinical condition be managed as an outpatient?

For isolation in the community, including the home or a co-living setting (e.g., shelter, group home, student residence, etc.), it must be possible to manage the case as an outpatient, taking into consideration their baseline health status and the presence of risk factors for more severe disease or outcomes. If hospitalization is required (e.g., worsening condition, health emergency, direction of health care provider), home isolation will no longer be feasible.

Is the case able to manage their own care?

Symptomatic and asymptomatic cases should be able to monitor themselves for new or worsening symptoms; take appropriate action as advised by the PHA or their health care provider, including self-care; properly wear a medical mask ^a; maintain appropriate personal preventive practices (e.g., maintain proper hygiene practices, clean and disinfect high-touch surfaces, etc.), and isolate away from others.

A case's ability to manage their own care may be impacted by various factors, including:

- Social and economic circumstances, such as lost income or poverty (e.g., unable to purchase necessary supplies, housing instability, etc.), unstable employment, inflexible working conditions, food insecurity, and domestic violence or abuse;
- Individual skills, abilities and vulnerabilities, such as difficulty reading, speaking, understanding or communicating; physical or psychological difficulty undertaking personal preventive practices; need for assistance with personal or medical care activities or supplies; or need for ongoing supervision. COVID-19 guidance on considerations for people with disabilities in Canada is available.
- Social or geographic isolation such as lacking family, friends, or community resources for support ²², or residing in an area with reduced access to services or supports; including mental health and addiction support, as well as telecommunications access.
- The ability for the case to access plain-language instructions in the appropriate languages related to proper personal hygiene practices, isolating away from others, self-monitoring for symptoms, and when to seek help. Note that male cases are more likely to live alone and may be less likely to seek help ^{23 24}.

Does the case require care? Is someone available to provide the care?

Some circumstances may require a household member to provide care to the case; for example, when the case is a child, an elderly relative who requires support, or a case who is very ill. When this occurs, the following should be considered:

- The caregiver should be willing and able to provide the necessary care and monitoring for the case.

- If possible, the caregiver should not be a person who is at risk for more severe disease or outcomes.
- The caregiver should reduce their risk of COVID-19 infection by wearing a medical mask ^awhen providing care to the case. They should also use appropriate eye protection while providing care to the case (see Appendix 3).
- Advice is available to support those caring for someone with COVID-19 at home:
 - How to care for a child with COVID-19 at home: Advice for caregivers
 - How to care for someone with COVID-19 at home
 - How to care for a person with COVID-19 at home: Advice for caregivers

What are the characteristics of the home or co-living configuration?

Cases may be in various household configurations that may hinder their ability to isolate themselves. For instance, the case may be a single-parent who must provide care to a child, or they may live in a multi-generational home with shared child- and elder-care responsibilities. If the case provides care to a child where childcare is shared between parents in two separate homes, consideration should be given to the most appropriate location for the child while the case is isolating.

If the case is isolating in their home or co-living setting, they should isolate away from others as soon as they are notified they have or may have COVID-19. Special consideration is also needed to support cases living in homes where it is difficult to separate from others (e.g., a one-bedroom apartment), or are living in co-living settings, such as student residence, shelters, and overcrowded housing,. The preferred option is to provide the case in these settings with a single room and a private washroom, which may require relocating the case, their roommates, or other household members to another location, (e.g., hotel, self-containing unit), if possible and as directed by the PHA. Relocation will be dependent on a variety of factors, including guidance from the jurisdiction's PHA, financial support, and availability of alternate spaces.

If it is not possible to provide the case with a single room and a private washroom in the co-living setting, or to relocate the case, efforts should be made to cohort confirmed cases together. For example, if two cases reside in a co-living setting and single rooms are not available, they could share a double room. Specific guidance has been developed on the considerations for people experiencing homelessness and for post-secondary institutions.

Are there others with greater risk of more severe disease or outcomes in the home or co-living setting?

Household members, or other occupants in co-living settings, who are at risk for more severe disease or outcomes from COVID-19 should not provide care to the case and alternative arrangements may be necessary. This could include temporarily relocating these individuals or the case outside of the home to a location determined by public health, such as a designated hotel.

Is the home or co-living setting suitable for isolation?

The PHA should determine if the home or co-living setting is suitable for isolation of the case. Cases may live in conditions where they lack available space to provide a dedicated room and private washroom for the case, such as an overcrowded house, student residence where the case has a roommate, or a homeless shelter. Housing conditions should also be assessed, including access to potable, running water, and the state of repair of the home. Safety of the setting should also be assessed in terms of the potential occurrence of gender-based or family violence or other abuse.

Can the case access adequate supplies and necessities?

Consider whether or not the case has access to supplies and necessities for the duration of isolation, such as food, running water, drinking water, supplies for infection control (e.g., masks), and cleaning supplies. A [list of supplies](#) to have on-hand while isolating is available. Those residing in [remote and isolated communities](#) may wish to consider stockpiling the needed supplies, as well as food and medications usually taken, if it is likely that the supply chain may be interrupted or unreliable.

A case who does not have access to adequate food or necessary supplies could contact local leadership, public health or organizations that provide direct support. Guidance is available for [hand washing in the absence of running or clean water](#).

If the home or co-living setting is inadequate for home isolation based on the assessment, PHAs should collaborate with the case and their health care provider, to determine a more suitable location. This may involve relocating the case to a more suitable community setting, hospitalizing the case, or accessing additional community supports and resources where available.

Appendix 3: Recommended infection prevention and control precautions when caring for a case in the home or co-living setting

Anyone who provides care to a case of COVID-19 should wear a medical mask ^a, as well as [eye protection](#) whenever providing care. Caregivers should also frequently [wash their hands](#), especially when in direct contact with the ill person or their environment, including soiled materials and surfaces.

Advice is available to support those caring for someone with COVID-19 at home:

- [How to care for a child with COVID-19 at home: Advice for caregivers](#)
- [How to care for someone with COVID-19 at home](#)
- [How to care for a person with COVID-19 at home: Advice for caregivers](#)

Additional information may be provided to caregivers in the home related to how to appropriately put on (don) and take off (doff) eye protection and gloves.

Eye protection

Eye protection is recommended to protect the mucous membranes of the caregiver's eyes while providing care to a case of COVID-19, or during any activities likely to generate splashes or sprays of bodily fluids, including respiratory secretions.

- Eye protection should be worn over prescription eyeglasses. Prescription eyeglasses alone are not adequate protection against respiratory droplets.
- Protective eye wear should be put on after putting on a mask.
- If using gloves, they should be donned (see below) after applying eye protection.
- To remove eye protection, first remove gloves and perform hand hygiene. Then remove the eye protection by handling the arms of goggles or sides or back of face shield. The front of the goggles or face shield is considered contaminated.
- Discard the eye protection into a plastic lined waste container. If the eye protection is not intended for single use, clean it with soap and water and then disinfect it with [approved hard-surface disinfectants](#) or, if not available, a diluted bleach solution, being mindful not to contaminate the environment with the eye protection. Refer to [Clean and disinfect all high-touch surfaces](#) for instructions on diluting bleach.
- Perform [hand hygiene](#).

Gloves

Caregivers do not have to wear disposable single-use gloves when caring for someone in the home setting. Frequent hand washing is preferred.

However, caregivers may still choose to wear disposable single use gloves, when in direct contact with the ill person, cleaning contaminated surfaces, and handling items soiled with bodily fluids, including dishes, cutlery, clothing, laundry, and waste for disposal.

Gloves are not a substitute for hand hygiene; caregivers must perform hand hygiene before and after putting on and taking off gloves.

- Gloves should be removed, hand hygiene performed, and new gloves applied when they become soiled or torn during care.
- To remove gloves safely, with one of your gloved hands pull off your glove for the opposite hand from the fingertips, as you are pulling, form your glove into a ball within the palm of your gloved hand. To remove your other glove, slide your ungloved hand in under the glove at the wrist and gently roll inside out, and away from your body. Avoid touching the outside of the gloves with your bare hands.
- Discard the gloves in a plastic-lined waste container.
- Perform hand hygiene.
- Double-gloving is not necessary.

Acknowledgments

The Public Health Measures (PHM) technical guidance is developed and approved in collaboration with federal, provincial and territorial partners, via the Technical Advisory Committee (TAC) and/or the Special Advisory Committee (SAC). In its guidance development process, PHM also works closely with: multilateral partners; other government departments; First Nations, Inuit and Métis stakeholders (through the Public Health Working Group on Remote and Isolated Communities); Sex and Gender-based Analysis (SGBA) experts at Public Health Agency of Canada; and other external stakeholders with a vested interest or a stake in the guidance.

This current iteration was prepared by: Lynn Cochrane, Lisa Paddle, Corey Green, Abraham Abood and Harunya Sivanesan

Previous iterations prepared by: Nicole Winters, Jill Sciberras, Jill Williams, Lynn Cochrane, Corey Green, Sharon E. Smith, Angela Sinilaite, Alexandra Nunn, Fanie Lalonde and Lisa Paddle

and supported by: Canadian Pandemic Influenza Preparedness (CPIP) Task Group Members, an external expert group: Bonnie Henry, Susy Hota, Brian Schwartz, Carolina Alfieri, Ian Gemmill, Kim Daly (ISC), Pamela Wolfe-Roberge, Todd Hatchette, Erin Henry, Nadine Sicard, Michelle Murti and Eleni Galanis

Footnotes

- a In situations where a medical mask is recommended but not available, the individual should properly wear a well-constructed and well-fitting non-medical mask.
- b COVID-19 guidance for acute care settings: <https://www.canada.ca/en/public-health/services/diseases/2019-novel-coronavirus-infection/health-professionals/infection-prevention-control-covid-19-second-interim-guidance.html> COVID-19 guidance for long-term care settings: <https://www.canada.ca/en/public-health/services/diseases/2019-novel-coronavirus-infection/prevention-control-covid-19-long-term-care-homes.html#a22>
- c This guidance is focused on community settings, and does not replace point-of-care risk assessments by health care providers in health care settings, or a risk assessment conducted by PHAs to determine the exposure risk for a health care worker (HCW).
Guidance related to the appropriate use of personal protective equipment (PPE) and infection prevention and control for HCWs and laboratory workers is available. See the following guidance documents:
- [Infection prevention and control for COVID-19: Second interim guidance for acute health care settings](#)
 - [Infection prevention and control for COVID-19: Interim guidance for home care settings](#)
 - [Infection prevention and control for COVID-19: Interim guidance for long term care homes](#)
 - [Routine practices and additional precautions for preventing the transmission of infection in health care settings](#)
 - Instructions on handling specimens: [Biosafety advisory: SARS-CoV-2 \(Severe acute respiratory syndrome-related coronavirus 2\)](#).
- d There is insufficient evidence available to define risk in terms of the length of exposure time required for transmission. For public health contact identification and management purposes only, a period of 15 cumulative minutes over 24 hours has been selected to distinguish between brief and prolonged exposure. This same period has been used in other countries ^{14 25 26}. This parameter should not replace the conclusions derived from a risk assessment, conducted by the public health authority, that addresses a variety of factors (i.e. infectiousness of the case at time of exposure, exposure is to a VOC, likely route of transmission, risk factors, etc.) that will more precisely inform risk.
- e The high and low risk exposure categories in Table 1 offer a simple guide for assessing a contact's risk of exposure to COVID-19 during contact tracing. In reality, there is a spectrum of risk, where adherence to public health risk mitigation measures helps to decrease the chance of infection. A risk assessment conducted by the PHA may further inform personalized recommendations.
Individual-level risk mitigation measures for consideration in the risk assessment include adherence to [personal preventive practices](#) (e.g., mask wearing, hand hygiene, physical distancing, etc.) by both the case and the contact. It should also include whether or not the contact avoids settings or activities where they may be exposed, including closed spaces and crowded places, as well as settings where these factors overlap and/or involve activities such as close-range conversations, singing, shouting, or heavy breathing. Setting-specific considerations include those places where a contact was potentially exposed, including whether the exposure was indoors (higher risk) or outdoors (lower risk), ventilation quality, the size and number of people in the setting, and risk mitigation measures in place in the setting (e.g., requirements for wearing masks, physical distancing, cleaning high-touch surfaces, etc.) ²⁷.
Although outdoor settings are not generally considered high risk, the potential for transmission still exists under certain circumstances, such as close conversations or rigorous exercise when participants are in close proximity and are not wearing masks; therefore, public health authorities should consider these risks when classifying contacts based on risk ²⁷.

- f The quarantine period typically aligns with the period of communicability. However, PTs may opt to implement a reduced quarantine period in combination with testing protocols, depending on the risk assessment and local circumstances.
- In general, quarantine means that a contact stays in their home and does not go out, and avoids in-person interactions with others, including their household members.
- A contact who does not live with a case should quarantine away from other household members or occupants, as directed by their PHA. It is recommended the contact quarantine in a separate room for sleeping with access to a separate washroom from other household members or occupants, if possible. When feasible and as directed by the PHA, a contact who does not live with the case could quarantine in an alternate dwelling such a hotel or self-containing unit.
- A contact who does not live with a case should wear a non-medical mask when in shared spaces (e.g., kitchen, washroom, hallway) in the home or co-living setting, regardless if others are present.
- For contacts in quarantine who are living with a case, it is recommended they wear a medical mask or a well-fitted, well-constructed and properly worn non-medical mask when in a shared space (e.g., the same room) as the case. Jurisdictions may adjust mask recommendations depending on local circumstances (e.g., if VOCs are circulating in the community; if the case and household contacts are living in a overcrowded or poorly ventilated setting).
- For contacts in quarantine who are living with a case, the PHA will determine when their quarantine period begins by assessing the characteristics of the setting. If it is determined that there is adequate separation between the case and their household members, the PHA may advise that household members' quarantine period begins the day the case goes into isolation. If there is inadequate separation (e.g., shared sleeping quarters, shared washroom, etc.), the PHA may require household members to quarantine for the duration of the case's isolation period, plus up to an additional 14 days afterwards.
- If additional members of a household with a case become ill, the PHA should assess whether other asymptomatic household members need to extend their period of quarantine based on their last exposure to the new case.
- g Jurisdictional specific testing policies/capacity could have implications on individual quarantine recommendations within that jurisdiction
- h The 2-metre parameter should not replace the conclusions derived from a risk assessment conducted by the PHA that addresses a variety of factors (e.g., infectiousness to the case at time of exposure, exposure is to a VOC, the likely route of transmission, increased risk of more severe disease or outcomes) that will more precisely inform risk.
- i For operational purposes, an appropriate physical distance is at least 2 metres. In general, if in-person interactions must take place, individuals should be encouraged to interact from the greatest distance possible, and with other personal preventive practices in place for a layered approach.

References

- 1 Public Health Agency of Canada, "Public health measures: Canadian Pandemic Influenza Preparedness: Planning Guidance for the Health Sector," 18 December 2018. [Online]. Available: <https://www.canada.ca/en/public-health/services/flu-influenza/canadian-pandemic-influenza-preparedness-planning-guidance-health-sector/public-health-measures.html#a354>. [Accessed 11 March 2021].
- 2 Respiratory Virus Infections Working Group, "Canadian Public Health Laboratory Network Best Practices for COVID-19," *Can Commun Dis Rep*, vol. 46, no. 5, pp. 113-120, 2020.
- 3 Respiratory Virus Infections Working Group, "The Canadian Public Health Laboratory Network protocol for microbiological investigations of emerging respiratory pathogens, including severe acute respiratory infections," *Can Commun Dis Rep*, vol. 46, no. 6, pp. 205-209, 2020.
- 4 Deeks, J., Dinnes, J., Takwoingi Y., et.al., "Diagnosis of SARS-CoV-2 infection and COVID-19: accuracy of signs and symptoms; molecular, antigen, and antibody tests; and routine laboratory markers," *Cochrane Database of Systematic Reviews*, no. 4, April 2020.
- 5 Testing and Screening Expert Advisory Panel., "Priority strategies to optimize testing and screening for COVID-19 in Canada: Report," Health Canada, January 2021. [Online]. Available: <https://www.canada.ca/en/health-canada/services/drugs-health-products/covid19-industry/medical-devices/testing-screening-advisory-panel/reports-summaries/priority-strategies.html>. [Accessed 11 March 2021].
- 6 Kang, Y. J., "South Korea's COVID-19 Infection Status: From the Perspective of Re-positive Test Results After Viral Clearance Evidenced by Negative Test Results," *Disaster Medicine and Public Health Preparedness*, pp. 1-3, 22 May 2020.
- 7 Jiang, X.L., Wang, G.L., Zhao, X.N. et al., "Lasting antibody and T cell responses to SARS-CoV-2 in COVID-19 patients three months after infection," *Nature Communications*, vol. 12, no. 1, p. 897, February 2021.
- 8 Government of Canada, "Coronavirus disease 2019 (COVID-19): Epidemiology update," 22 June 2020. [Online]. Available: <https://health-infobase.canada.ca/covid-19/epidemiological-summary-covid-19-cases.html>. [Accessed 11 March 2021].
- 9 Mathai, V., Das, A., Bailey, J. A., & Breuer, K., "Airflows inside passenger cars and implications for airborne disease transmission," *Science Advances*, vol. 7, no. 1, 2021.
- 10 Juneau, C., Briand, A., Pueyo, T., Collazzo, P., Potvin, L., "Effective Contact Tracing for COVID-19: A Systematic Review," *PrePrint: medRxiv*, 2020.
- 11 World Health Organization, "Contact tracing in the context of COVID-19," 1 February 2021. [Online]. Available: <https://www.who.int/publications/i/item/contact-tracing-in-the-context-of-covid-19>. [Accessed 11 March 2021].
- 12 Wahba, H., "The antipyretic effect of ibuprofen and acetaminophen in children," *Pharmacotherapy: The Journal of Human Pharmacology and Drug Therapy*, vol. 24, no. 2, pp. 280-284, February 2004.
- 13 A. Otten and L. Waddel, "Evidence breif of COVID-19 quarantine length and reduction strategies and effectiveness, Update 1".

- 14 European Centre for Disease Prevention and Control, "Contact tracing for COVID-19: current evidence, options for scale-up and an assessment of resources needed," 5 May 2020. [Online]. Available: <https://www.ecdc.europa.eu/en/publications-data/contact-tracing-covid-19-evidence-scale-up-assessment-resources>. [Accessed 11 March 2021].
- 15 European Centre for Disease Prevention and Control, "Contact tracing for COVID-19: current evidence, options for scale-up and an assessment of resources needed," 5 May 2020. [Online]. Available: <https://www.ecdc.europa.eu/en/publications-data/contact-tracing-covid-19-evidence-scale-up-assessment-resources>. [Accessed 11 March 2021].
- 16 Ferreira, A., Young, T., Methews, C., Zunza, M. and Low, N., "Strategies for partner notification for sexually transmitted infections, including HIV," *Cochrane Database of Systemic Reviews*, no. 10, 3 October 2013.
- 17 Rapid Investigation Team, Public Health England, "Preliminary investigation into COVID-19 exceedances in Leicester (June 2020)," 29 June 2020. [Online]. Available: https://assets.publishing.service.gov.uk/government/uploads/system/uploads/attachment_data/file/89712/19_activity_Leicester_Final-report_010720_v3.pdf.
- 18 Choi, H., Cho, W., Kim, M. H., and Hur, J.Y., "Public Health Emergency and Crisis Management: Case Study of SARS-CoV-2 Outbreak," *International Journal of Environmental Research and Public Health*, vol. 17, no. 11, p. 3984, June 2020.
- 19 Lee, V., Chiew, C., and Khong, W., "Interrupting transmission of COVID-19: lessons from containment efforts in Singapore," *Journal of Travel Medicine*, vol. 27, no. 3, p. taaa039, May 2020.
- 20 Marcus, L. and S. o. P. H. Harvard TH Chan, "Assessment of Risks of SARS-CoV-2 Transmission During Air Travel and Non-Pharmaceutical Interventions to Reduce Risk: Phase One Report: Gate-to-Gate Travel Onboard Aircraft," Harvard TH Chan School of Public Health, 2020.
- 21 Li, Y.Y., Wang, J.X., and Chen, X., "Can a toilet promote virus transmission? From a fluid dynamics perspective," *Physics of Fluids*, vol. 32, no. 6, June 2020.
- 22 Leigh-Hunt, N., Bagguley, D., Bash, K., Turner V., Turnbull, S., Valtorta, N., and Caan, W., "An overview of systematic reviews on the public health consequences of social isolation and loneliness," *Public Health*, vol. 152, pp. 157-171, November 2017.
- 23 Statistics Canada: Jackie Tang, Nora Galbraith and Johnny Truong, "Insights on Canadian Society: Living alone in Canada," 6 March 2019. [Online]. Available: <https://www150.statcan.gc.ca/n1/pub/75-006-x/2019001/article/00003-eng.htm>. [Accessed 11 March 2021].
- 24 Thompson A., Anisimowicz Y., Miedema B., Hogg, W., Wodchis, W., and Aubrey-Bassler, K., "The influence of gender and other patient characteristics on health care-seeking behaviour: a QUALICOPC study," *BMC Family Practice*, vol. 17, no. 38, March 2016.
- 25 US Centres for Disease Control, "Public Health Guidance for Community-Related Exposure," 1 March 2021. [Online]. Available: <https://www.cdc.gov/coronavirus/2019-ncov/php/public-health-recommendations.html>. [Accessed 11 March 2021].

- 26 World Health Organization, "Public Health Surveillance for COVID-19: Interim Guidance," 16 December 2020. [Online]. Available: [https://www.who.int/publications-detail/global-surveillance-for-human-infection-with-novel-coronavirus-\(2019-ncov\)](https://www.who.int/publications-detail/global-surveillance-for-human-infection-with-novel-coronavirus-(2019-ncov)). [Accessed 11 March 2021].
- 27 Jones, N., Qureshi, Z., Temple, R., et.al., "Two metres or one: what is the evidence for physical distancing in covid-19?," BMJ, vol. 370, p. m3223, 2020.
-

Date modified:

2021-07-05



Since January 2020 Elsevier has created a COVID-19 resource centre with free information in English and Mandarin on the novel coronavirus COVID-19. The COVID-19 resource centre is hosted on Elsevier Connect, the company's public news and information website.

Elsevier hereby grants permission to make all its COVID-19-related research that is available on the COVID-19 resource centre - including this research content - immediately available in PubMed Central and other publicly funded repositories, such as the WHO COVID database with rights for unrestricted research re-use and analyses in any form or by any means with acknowledgement of the original source. These permissions are granted for free by Elsevier for as long as the COVID-19 resource centre remains active.



Contents lists available at ScienceDirect

Clinical Microbiology and Infection

journal homepage: www.clinicalmicrobiologyandinfection.com

Letter to the Editor

Molecular characterization of SARS-CoV-2 from the first case of COVID-19 in Italy

M.R. Capobianchi, M. Rueca, F. Messina, E. Giombini, F. Carletti, F. Colavita, C. Castilletti, E. Lalle, L. Bordi, F. Vairo, E. Nicastri, G. Ippolito, C.E.M. Gruber*, B. Bartolini

National Institute for Infectious Diseases Lazzaro Spallanzani IRCCS, Rome, Italy

ARTICLE INFO

Article history:

Received 26 February 2020

Received in revised form

17 March 2020

Accepted 21 March 2020

Available online 27 March 2020

Editor: L. Leibovici

To the Editor,

On January 29, 2020, two Chinese spouses (patient 1, female; patient 2, male), coming to Italy as tourists from Hubei province, were hospitalized at the National Institute for Infectious Diseases “L. Spallanzani”, Rome, with fever and respiratory symptoms. SARS-CoV-2 diagnosis was accomplished using real-time RT-PCR [1] on a nasopharyngeal swab and sputum for patient 1 and on a nasopharyngeal swab for patient 2, collected 1 day after symptom onset. Partial sequencing confirmed both patients to be infected with SARS-CoV-2.

A virus isolate was obtained (in a Vero E6 cell line) from the sputum of patient 1, with cytopathic effects evident 24 h post-inoculation. At the time of writing, virus isolation from the nasopharyngeal swab sample collected from patient 2 was not successful, likely due to the lower viral load (higher cycle threshold value, 24.56 in the real-time RT-PCR), therefore no further analysis was performed on the virus detected in patient 2. Next-generation sequencing (NGS) was performed on the respiratory samples from patient 1 and on the primary isolate, prior to any further passage, by using the Ion Torrent S5 platform (ThermoFisher). The mean count of sequencing reads obtained per sample was 44 000 000 (minimum 41.6×10^6 to maximum 49.7×10^6). The reads from the

two respiratory samples of patient 1 were merged to obtain a better coverage along the virus genome, and in this paper are referred to as data from the clinical sample. Details of sequencing and bioinformatic analyses are available upon request.

The number of SARS-CoV-2 reads obtained varied from 4079 to $>14 \times 10^6$. By using *de novo* assembly, two contigs of 29 867 nt (mean coverage: 81 324 reads; range: 26–510 718 reads) and 29 792 nt (mean coverage: 80 reads; range: 5–599 reads) were obtained for the isolate and clinical sample of patient 1, respectively, and referred to as consensus sequences. Further analysis was dedicated to identifying the variants present at any nucleotide position for the variability analysis.

Considering the consensus sequences, two non-synonymous changes with respect to the Wuhan-Hu-1 NCBI Reference Genome (Accession number: MN908947.3) [2] were observed in the sequence from the clinical sample from patient 1: G11083T, leading to L3606F change in Orf1a, and G26144T, leading to G251V change in Orf3a. One additional synonymous substitution in Orf1a (A2269T) was detected in the isolate but not in the corresponding clinical sample. All variants were confirmed by Sanger sequencing.

Considering the analysis of genomic variability, several intra-sample variants were observed in both the isolate and the clinical sample, but only the positions with a minimum coverage of 20 reads were considered. Intra-sample assessment of overall virus genome variability resulted in 1.27×10^{-4} and 1.02×10^{-4} nucleotide substitutions per site for the isolate and the clinical sample, respectively. Only two variable positions were observed with a frequency $>10\%$ in the clinical sample, both in Orf1a: A2269T (13.73%, coverage: 51x), synonymous for amino acid A668, and G7388A (13.21%, coverage: 53x), leading to amino acid change (A2375T). Interestingly, the frequency of variants at position 2269 was different in the isolate, being T dominant over A in 72% of reads (coverage: 119 582x), accounting for the difference resulting in the consensus sequences.

For the phylogenetic analysis, 87 full-genome SARS-CoV-2 sequences were retrieved from the Global Initiative on Sharing All Influenza Data (GISAID), along with WH-01_MN908947.3 from GenBank. The G26144T substitution observed in the isolate from Italy was also present in five sequences from cases occurring

* Corresponding author. C.E.M. Gruber, Laboratory of Virology, INMI Lazzaro Spallanzani IRCCS, via Portuense 292, 00149, Roma, Italy.

E-mail address: cesare.gruber@inmi.it (C.E.M. Gruber).

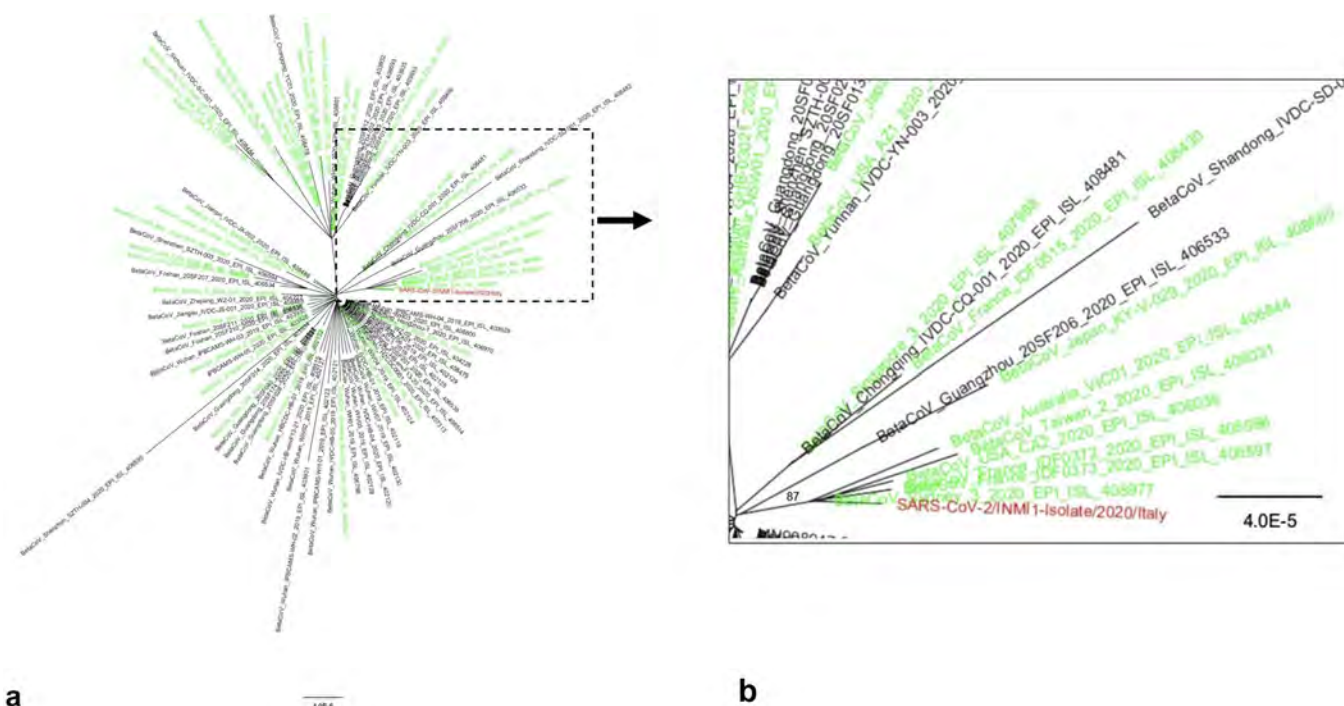


Fig. 1. (a) Unrooted phylogenetic tree based on SARS-CoV-2 full genome database from the Global Initiative on Sharing All Influenza Data (GISAID). Genomes collected outside China are highlighted in green. (b) Enlargement of clade reporting SARS-CoV-2/INMI1-Isolate/2020/Italy (in red). Maximum likelihood phylogeny was reconstructed under Hasegawa-Kishino-Yano plus proportion of invariable sites (HKY + I), inferred by model test function.

outside of China: EPI_ISL_406596 and EPI_ISL_406597 from France, EPI_ISL_406031 from Taiwan, EPI_ISL_406036 from USA, EPI_ISL_406844 and EPI_ISL_408977 from Australia. All the genomes carrying this mutation are included in a significant phylogenetic cluster (bootstrap 87%), suggesting a common origin (Fig. 1); in fact, the G251V substitution in Orf3a has recently been defined as the marker variant of the 'V' clade (GISAID).

The presence of quasispecies has previously been reported for SARS-CoV and MERS-CoV [3,4], suggesting that these betacoronaviruses may consist of complex and dynamic distributions of closely related variants *in vivo*, similarly to other RNA viruses. When applied to SARS-CoV-2 in this study, the analysis of sequence variability supported the presence of viral quasispecies in the clinical sample as well as in the primary isolate. Namely, two positions with variant frequency >10% were observed in the biological sample, both in Orf1a: A2269T, synonymous, and G7388A, corresponding to amino acid change A2375T. The synonymous variant A2269T, representing a minority variant in the clinical sample, was the dominant one in the isolate. Although low coverage may have affected the precise calculation of minority variant frequency in the clinical sample, the data are consistent with variant selection occurring during the isolation procedure, as previously shown for other respiratory viruses. In the respiratory sample neither mutations nor intra-sample variants were found at positions 8782 and 28 144, recently identified as hotspots of hypervariability (coverage: 61x and 76x respectively) [5].

Full-genome characterization of new viruses is instrumental for updating diagnostics and assessing viral evolution. On the other hand, virus variability, leading to the development of quasispecies within infected patients, may provide the background for virus evolution and adaptation to new hosts; more studies are necessary

to unravel the importance of intra-patient variability in the SARS-CoV-2 evolutionary trajectory.

Genome sequences described on this manuscript are available from GISAID and from GenBank (Acc. Numb: MT008022, MT008023, MT066156 and MT077125).

Author contributions

All authors contributed to the analysis and the writing of the final manuscript.

Transparency declaration

The authors declare that they have no conflicts of interest. This research was supported by funds to the National Institute for Infectious Diseases 'Lazzaro Spallanzani' IRCCS from the Ministero della Salute, Ricerca Corrente.

Acknowledgements

We gratefully acknowledge the contributors of genome sequences of the newly emerging coronavirus, i.e. the originating and submitting laboratories, for sharing their sequences and other metadata through the GISAID Initiative, on which this research is based.

References

- [1] Corman VM, Landt O, Kaiser M, Molenkamp R, Meijer A, Chu DK, et al. Detection of 2019 novel coronavirus (2019-nCoV) by real-time RT-PCR. *Euro Surveill* 2020;25. <https://doi.org/10.2807/1560-7917.ES.2020.25.3.2000045>. pii=2000045.

- [2] Wu F, Zhao S, Yu B, Chen YM, Wang W, Song ZG, et al. A new coronavirus associated with human respiratory disease in China. *Nature* 2020;579:265–9. <https://www.nature.com/articles/s41586-020-2008-3>.
- [3] Park D, Huh HJ, Kim YJ, Son DS, Jeon HJ, Im EH, et al. Analysis of inpatient heterogeneity uncovers the microevolution of Middle East respiratory syndrome coronavirus. *Cold Spring Harbor Mol Case Stud* 2016;2:a001214. <https://doi.org/10.1101/mcs.a001214>.
- [4] Xu D, Zhang Z, Wang FS. SARS-associated coronavirus quasispecies in individual patients. *New Engl J Med* 2004;350:1366–7. <https://doi.org/10.1056/NEJMc032421>.
- [5] Ceraolo C, Giorgi F. Genomic variance of the 2019-nCoV coronavirus. *J Med Virol* 2020;92:522–8. <https://doi.org/10.1002/jmv.25700>.



[JAMA](#). 2020 Aug 11; 324(6): 603–605.

PMCID: PMC7349096

Published online 2020 Jul 9. doi: 10.1001/jama.2020.12603: 10.1001/jama.2020.12603

PMID: [32644129](#)

Persistent Symptoms in Patients After Acute COVID-19

[Angelo Carfi](#), MD, ^{✉1} [Roberto Bernabei](#), MD,¹ and [Francesco Landi](#), MD, PhD¹, for the Gemelli Against COVID-19 Post-Acute Care Study Group

¹Geriatrics Department, Fondazione Policlinico Universitario Agostino Gemelli IRCCS, Rome, Italy

[✉]Corresponding author.

Article Information

Corresponding Author: Angelo Carfi, MD, Centro Medicina dell'Invecchiamento, Fondazione Policlinico Universitario Agostino Gemelli IRCCS, Largo Francesco Vito 1, 00168 Rome, Italy (angelo.carfi@policlinicogemelli.it).

Accepted for Publication: June 23, 2020.

Published Online: July 9, 2020. doi:10.1001/jama.2020.12603

Author Contributions: Drs Carfi and Landi had full access to all of the data in the study and take responsibility for the integrity of the data and the accuracy of the data analysis.

Concept and design: All authors.

Drafting of the manuscript: Carfi, Landi.

Critical revision of the manuscript for important intellectual content: Bernabei, Landi.

Statistical analysis: Carfi.

Supervision: Bernabei, Landi.

Conflict of Interest Disclosures: None reported.

Additional Information: The members of the Gemelli Against COVID-19 Post-Acute Care Study Group are listed in reference 5.

Received 2020 May 22; Accepted 2020 Jun 23.

[Copyright](#) 2020 American Medical Association. All Rights Reserved.

This case series describes COVID-19 symptoms persisting a mean of 60 days after onset among Italian patients previously discharged from COVID-19 hospitalization.

In Italy, a large proportion of patients with coronavirus disease 2019 (COVID-19) presented with symptoms (71.4% of 31 845 confirmed cases as of June 3, 2020).¹ Common symptoms include cough, fever, dyspnea, musculoskeletal symptoms (myalgia, joint pain, fatigue), gastrointestinal symptoms, and anosmia/dysgeusia.^{2,3,4} However, information is lacking on symptoms that persist after recovery. We assessed persistent symptoms in patients who were discharged from the hospital after recovery from COVID-19.

Methods

In the waning phase of the pandemic, beginning on April 21, 2020, the Fondazione Policlinico Universitario Agostino Gemelli IRCCS in Rome, Italy, established a postacute outpatient service for individuals discharged from the hospital after recovery from COVID-19. All patients who met World Health Organization criteria for discontinuation of quarantine (no fever for 3 consecutive days, improvement in other symptoms, and 2 negative test results for severe acute respiratory syndrome coronavirus 2 [SARS-CoV-2] 24 hours apart) were followed up. At enrollment in the study, real-time reverse transcriptase–polymerase chain reaction for SARS-CoV-2 was performed and patients with a negative test result were included.

Patients were offered a comprehensive medical assessment with detailed history and physical examination. Data on all clinical characteristics, including clinical and pharmacological history, lifestyle factors, vaccination status, and body measurements, were collected in a structured electronic data collection system. The COVID-19 postacute outpatient service is currently active, and further details about the patient evaluation protocol are described elsewhere.⁵

In particular, data on specific symptoms potentially correlated with COVID-19 were obtained using a standardized questionnaire administered at enrollment. Patients were asked to retrospectively recount the presence or absence of symptoms during the acute phase of COVID-19 and whether each symptom persisted at the time of the visit. More than 1 symptom could be reported. The EuroQol visual analog scale was used to ask patients to score their quality of life from 0 (worst imaginable health) to 100 (best imaginable health) before COVID-19 and at the time of the visit. A difference of 10 points defined worsened quality of life. All analyses were performed using R version 3.6.3 (R Foundation).

This study was approved by the Università Cattolica and Fondazione Policlinico Gemelli IRCCS Institutional Ethics Committee. Written informed consent was obtained from all participants.

Results

From April 21 to May 29, 2020, 179 patients were potentially eligible for the follow-up post-acute care assessment; 14 individuals (8%) refused to participate and 22 had a positive test result. Thus, 143 patients were included. The mean age was 56.5 (SD, 14.6) years (range, 19–84 years), and 53 (37%) were women. During hospitalization, 72.7% of participants had evidence of interstitial pneumonia. The mean length of hospital stay was 13.5 (SD, 9.7) days; 21 patients (15%) received noninvasive ventilation and 7 patients (5%) received invasive ventilation. The characteristics of the study population are summarized in the [Table](#).

Patients were assessed a mean of 60.3 (SD, 13.6) days after onset of the first COVID-19 symptom; at the time of the evaluation, only 18 (12.6%) were completely free of any COVID-19–related symptom, while 32% had 1 or 2 symptoms and 55% had 3 or more. None of the patients had fever or any signs or symptoms of acute illness. Worsened quality of life was observed among 44.1% of patients. The [Figure](#) shows that a high proportion of individuals still reported fatigue (53.1%), dyspnea (43.4%), joint pain, (27.3%) and chest pain (21.7%).

Discussion

This study found that in patients who had recovered from COVID-19, 87.4% reported persistence of at least 1 symptom, particularly fatigue and dyspnea. Limitations of the study include the lack of information on symptom history before acute COVID-19 illness and the lack of details on symptom severity. Furthermore, this is a single-center study with a relatively small number of patients and without a control group of patients discharged for other reasons. Patients with community-acquired pneumonia can also have persistent symptoms, suggesting that these findings may not be exclusive to COVID-19.⁶

Clinicians and researchers have focused on the acute phase of COVID-19, but continued monitoring after discharge for long-lasting effects is needed.

Notes

Section Editor: Jody W. Zylke, MD, Deputy Editor.

References

1. Istituto Superiore Sanità *Sorveglianza Integrata COVID-19 in Italia* Published 2020. Accessed June 8, 2020. https://www.epicentro.iss.it/coronavirus/bollettino/Infografica_3giugno%20ITA.pdf
2. Docherty AB, Harrison EM, Green CA, et al. ; ISARIC4C Investigators . Features of 20 133 UK patients in hospital with COVID-19 using the ISARIC WHO Clinical Characterisation Protocol: prospective observational cohort study. *BMJ*. 2020;369:m1985. doi:10.1136/bmj.m1985 [PMCID: PMC7243036] [PubMed: 32444460] [CrossRef: 10.1136/bmj.m1985]
3. Wang D, Hu B, Hu C, et al. . Clinical characteristics of 138 hospitalized patients with 2019 novel coronavirus–infected pneumonia in Wuhan, China. *JAMA*. 2020;323(13):1239-1242. doi:10.1001/jama.2020.1585 [PMCID: PMC7042881] [PubMed: 32031570] [CrossRef: 10.1001/jama.2020.1585]
4. Landi F, Barillaro C, Bellieni A, et al. . The new challenge of geriatrics: saving frail older people from the SARS-CoV-2 pandemic infection. *J Nutr Health Aging*. 2020;24(5):466-470. doi:10.1007/s12603-020-1356-x [PMCID: PMC7118362] [PubMed: 32346682] [CrossRef: 10.1007/s12603-020-1356-x]
5. Gemelli Against COVID-19 Post-Acute Care Study Group Post-COVID-19 global health strategies: the need for an interdisciplinary approach. *Aging Clin Exp Res*. Published online June 11, 2020. doi:10.1007/s40520-020-01616-x [PMCID: PMC7287410] [PubMed: 32529595] [CrossRef: 10.1007/s40520-020-01616-x]
6. Metlay JP, Fine MJ, Schulz R, et al. . Measuring symptomatic and functional recovery in patients with community-acquired pneumonia. *J Gen Intern Med*. 1997;12(7):423-430. doi:10.1046/j.1525-1497.1997.00074.x [PMCID: PMC1497132] [PubMed: 9229281] [CrossRef: 10.1046/j.1525-1497.1997.00074.x]

Figures and Tables

Table.
Demographic and Clinical Characteristics of the Study Sample (N = 143)



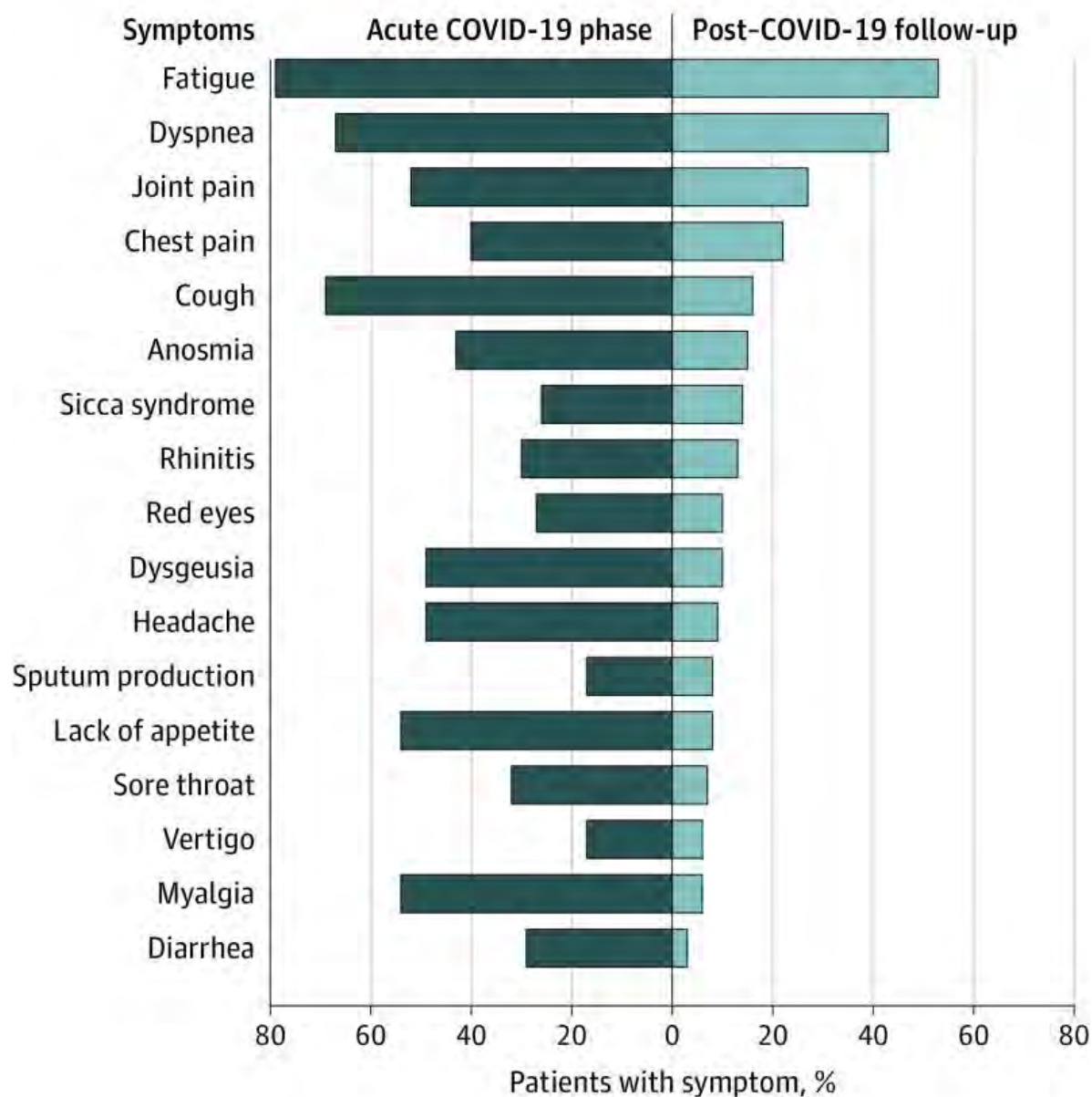
Characteristics	Value
Age, mean (SD), y	56.5 (14.6)
Female sex, No. (%)	53 (37.1)
Body mass index, mean (SD) ^a	26.3 (4.4)
Vaccination, No. (%)	
Seasonal influenza	32 (22.4)
Pneumococcus	13 (9.1)
Diagnoses, No. (%)	
Chronic heart disease	7 (4.9)
Atrial fibrillation	4 (2.8)
Heart failure	4 (2.8)
Stroke	2 (1.4)
Hypertension	50 (35)
Diabetes	10 (7)
Kidney failure	3 (2.1)
Thyroid disease	26 (18.2)
Chronic obstructive pulmonary disease	13 (9.1)
Active cancer	5 (3.5)
Immune disorders	16 (11.2)
Regular physical activity, No. (%)	90 (62.9)
Smoking status, No. (%)	
None	63 (44.1)
Active	15 (10.5)
Former	65 (45.4)
Acute COVID-19 characteristics, No. (%)	
Pneumonia diagnosed	104 (72.7)
Intensive care unit admission	18 (12.6)
Oxygen supplementation	
Oxygen therapy	77 (53.8)
Ventilation	
Noninvasive	21 (14.7)
Mechanical	7 (4.9)

[Open in a separate window](#)

Abbreviation: COVID-19, coronavirus disease 2019.

^aCalculated as weight in kilograms divided by height in meters squared.

^bQuality of life was assessed using the EuroQol visual analog scale, ranging from 0 (worst imaginable health) to 100 (best imaginable health). Worsened quality of life was defined by a 10-point difference in health status before COVID-19 vs at the time of the visit.

Figure.**COVID-19–Related Symptoms**

The figure shows percentages of patients presenting with specific coronavirus disease 2019 (COVID-19)–related symptoms during the acute phase of the disease (left) and at the time of the follow-up visit (right).

Coronavirus Disease 2019 in Children — United States, February 12–April 2, 2020

CDC COVID-19 Response Team

On April 6, 2020, this report was posted as an MMWR Early Release on the MMWR website (<https://www.cdc.gov/mmwr>).

As of April 2, 2020, the coronavirus disease 2019 (COVID-19) pandemic has resulted in >890,000 cases and >45,000 deaths worldwide, including 239,279 cases and 5,443 deaths in the United States (1,2). In the United States, 22% of the population is made up of infants, children, and adolescents aged <18 years (children) (3). Data from China suggest that pediatric COVID-19 cases might be less severe than cases in adults and that children might experience different symptoms than do adults (4,5); however, disease characteristics among pediatric patients in the United States have not been described. Data from 149,760 laboratory-confirmed COVID-19 cases in the United States occurring during February 12–April 2, 2020 were analyzed. Among 149,082 (99.6%) reported cases for which age was known, 2,572 (1.7%) were among children aged <18 years. Data were available for a small proportion of patients on many important variables, including symptoms (9.4%), underlying conditions (13%), and hospitalization status (33%). Among those with available information, 73% of pediatric patients had symptoms of fever, cough, or shortness of breath compared with 93% of adults aged 18–64 years during the same period; 5.7% of all pediatric patients, or 20% of those for whom hospitalization status was known, were hospitalized, lower than the percentages hospitalized among all adults aged 18–64 years (10%) or those with known hospitalization status (33%). Three deaths were reported among the pediatric cases included in this analysis. These data support previous findings that children with COVID-19 might not have reported fever or cough as often as do adults (4). Whereas most COVID-19 cases in children are not severe, serious COVID-19 illness resulting in hospitalization still occurs in this age group. Social distancing and everyday preventive behaviors remain important for all age groups as patients with less serious illness and those without symptoms likely play an important role in disease transmission (6,7).

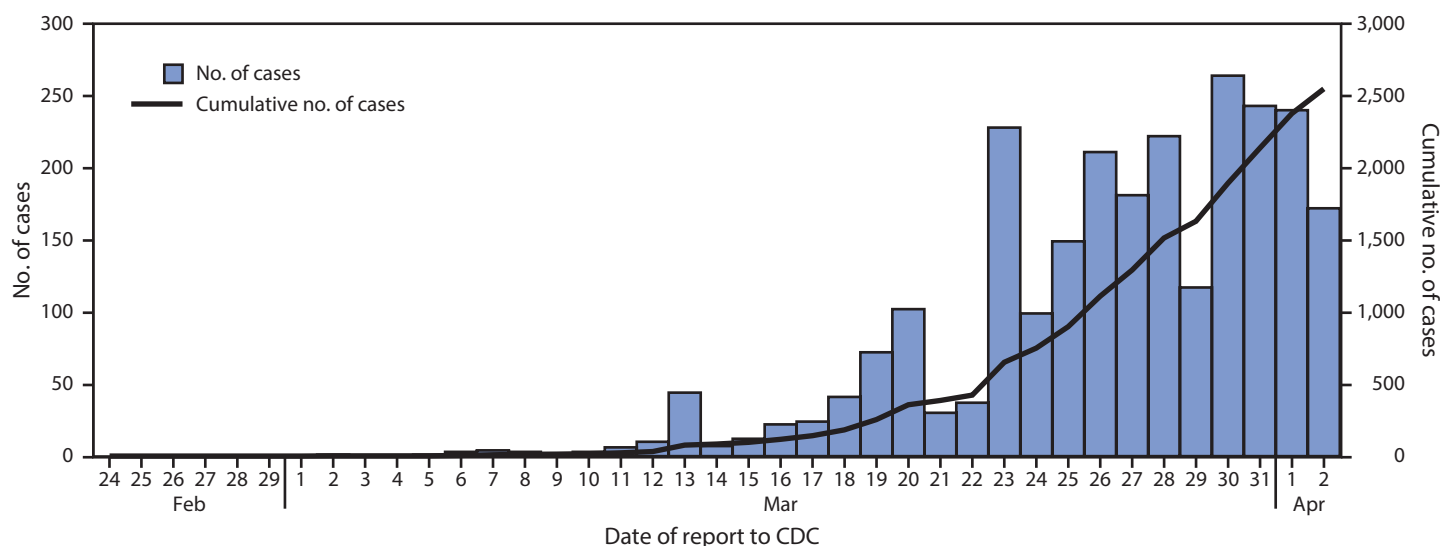
Data on COVID-19 cases were reported to CDC from 50 states, the District of Columbia, New York City, and four U.S. territories. Jurisdictions voluntarily report data on laboratory-confirmed cases using a standardized case report form.* Data on cases occurring during February 12–April 2, 2020 and submitted through an electronic case-based COVID-19

surveillance database were reviewed for this report. Data submitted to CDC are preliminary and can be updated by health departments as more data become available. At the time of this analysis, characteristics of interest were available for only a minority of cases, including hospitalization status (33%), presence of preexisting underlying medical conditions (13%), and symptoms (9.4%). Because of the high percentage of cases with missing data and because cases with severe outcomes are more likely to have hospitalization or intensive care unit (ICU) status reported, percentages of patients hospitalized, including those admitted to the ICU, were estimated as a range, for which the denominator for the lower bound included cases with both known and unknown hospitalization or ICU status, and the upper bound included only cases with known hospitalization or ICU status. For other characteristics, percentages were calculated from among the number of cases with known information for that characteristic. Demographics of COVID-19 cases were assessed among cases in children aged <18 years and adults aged ≥18 years. Because clinical severity of COVID-19 is higher among adults aged ≥65 years than in younger age groups (8), clinical features including symptoms and hospitalizations were assessed among adults aged 18–64 years and compared with those among the pediatric cases. Statistical comparisons were not performed because of the high percentage of missing data.

As of April 2, 2020, data on 149,760 laboratory-confirmed U.S. COVID-19 cases were available for analysis. Among 149,082 (99.6%) cases for which patient age was known, 2,572 (1.7%) occurred in children aged <18 years and 146,510 (98%) in adults aged ≥18 years, including 113,985 (76%) aged 18–64 years. Among the 2,572 pediatric cases, 850 (33%) were reported from New York City; 584 (23%) from the rest of New York state; 393 (15%) from New Jersey; and the remaining 745 (29%) from other jurisdictions. The distribution of reporting jurisdictions for pediatric cases was similar to that of reporting jurisdictions for cases among adults aged ≥18 years, except that a lower percentage of adult cases was reported from New York state (14%). The first pediatric U.S. COVID-19 case was reported to CDC on March 2, 2020; since March 5, pediatric cases have been reported daily (Figure 1).

Among all 2,572 COVID-19 cases in children aged <18 years, the median age was 11 years (range 0–17 years). Nearly one third of reported pediatric cases (813; 32%) occurred in children aged 15–17 years, followed by those in children aged 10–14 years (682; 27%). Among younger

* <https://www.cdc.gov/coronavirus/2019-ncov/downloads/pui-form.pdf>.

FIGURE 1. COVID-19 cases in children* aged <18 years, by date reported to CDC (N = 2,549)[†] — United States, February 24–April 2, 2020[§]

* Includes infants, children, and adolescents.

[†] Excludes 23 cases in children aged <18 years with missing report date.

[§] Date of report available starting February 24, 2020; reported cases include any with onset on or after February 12, 2020.

children, 398 (15%) occurred in children aged <1 year, 291 (11%) in children aged 1–4 years, and 388 (15%) in children aged 5–9 years. Among 2,490 pediatric COVID-19 cases for which sex was known, 1,408 (57%) occurred in males; among cases in adults aged ≥18 years for which sex was known, 53% (75,450 of 143,414) were in males. Among 184 (7.2%) cases in children aged <18 years with known exposure information, 16 (9%) were associated with travel and 168 (91%) had exposure to a COVID-19 patient in the household or community.

Data on signs and symptoms of COVID-19 were available for 291 of 2,572 (11%) pediatric cases and 10,944 of 113,985 (9.6%) cases among adults aged 18–64 years (Table). Whereas fever (subjective or documented), cough, and shortness of breath were commonly reported among adult patients aged 18–64 years (93% reported at least one of these), these signs and symptoms were less frequently reported among pediatric patients (73%). Among those with known information on each symptom, 56% of pediatric patients reported fever, 54% reported cough, and 13% reported shortness of breath, compared with 71%, 80%, and 43%, respectively, reporting these signs and symptoms among patients aged 18–64 years. Myalgia, sore throat, headache, and diarrhea were also less commonly reported by pediatric patients. Fifty-three (68%) of the 78 pediatric cases reported not to have fever, cough, or shortness of breath had no symptoms reported, but could not be classified as asymptomatic because of incomplete symptom information. One (1.3%) additional pediatric patient with a positive test result for SARS-CoV-2 was reported to be asymptomatic.

Information on hospitalization status was available for 745 (29%) cases in children aged <18 years and 35,061 (31%) cases in adults aged 18–64 years. Among children with COVID-19, 147 (estimated range = 5.7%–20%) were reported to be hospitalized, with 15 (0.58%–2.0%) admitted to an ICU (Figure 2). Among adults aged 18–64 years, the percentages of patients who were hospitalized (10%–33%), including those admitted to an ICU (1.4%–4.5%), were higher. Children aged <1 year accounted for the highest percentage (15%–62%) of hospitalization among pediatric patients with COVID-19. Among 95 children aged <1 year with known hospitalization status, 59 (62%) were hospitalized, including five who were admitted to an ICU. The percentage of patients hospitalized among those aged 1–17 years was lower (estimated range = 4.1%–14%), with little variation among age groups (Figure 2).

Among 345 pediatric cases with information on underlying conditions, 80 (23%) had at least one underlying condition. The most common underlying conditions were chronic lung disease (including asthma) (40), cardiovascular disease (25), and immunosuppression (10). Among the 295 pediatric cases for which information on both hospitalization status and underlying medical conditions was available, 28 of 37 (77%) hospitalized patients, including all six patients admitted to an ICU, had one or more underlying medical condition; among 258 patients who were not hospitalized, 30 (12%) patients had underlying conditions. Three deaths were reported among the pediatric cases included in this analysis; however, review of these cases is ongoing to confirm COVID-19 as the likely cause of death.

TABLE. Signs and symptoms among 291 pediatric (age <18 years) and 10,944 adult (age 18–64 years) patients* with laboratory-confirmed COVID-19 — United States, February 12–April 2, 2020

Sign/Symptom	No. (%) with sign/symptom	
	Pediatric	Adult
Fever, cough, or shortness of breath [†]	213 (73)	10,167 (93)
Fever [§]	163 (56)	7,794 (71)
Cough	158 (54)	8,775 (80)
Shortness of breath	39 (13)	4,674 (43)
Myalgia	66 (23)	6,713 (61)
Runny nose [¶]	21 (7.2)	757 (6.9)
Sore throat	71 (24)	3,795 (35)
Headache	81 (28)	6,335 (58)
Nausea/Vomiting	31 (11)	1,746 (16)
Abdominal pain [¶]	17 (5.8)	1,329 (12)
Diarrhea	37 (13)	3,353 (31)

* Cases were included in the denominator if they had a known symptom status for fever, cough, shortness of breath, nausea/vomiting, and diarrhea. Total number of patients by age group: <18 years (N = 2,572), 18–64 years (N = 113,985).

[†] Includes all cases with one or more of these symptoms.

[§] Patients were included if they had information for either measured or subjective fever variables and were considered to have a fever if “yes” was indicated for either variable.

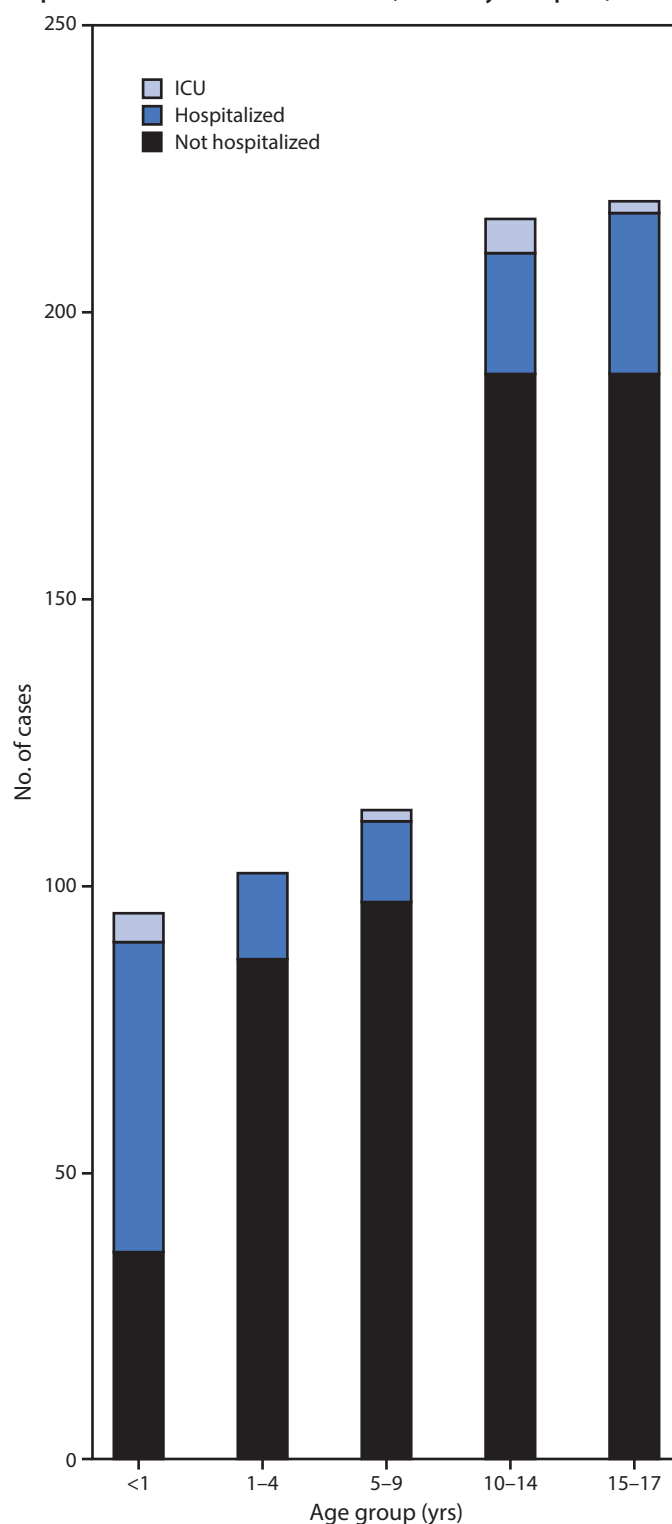
[¶] Runny nose and abdominal pain were less frequently completed than other symptoms; therefore, percentages with these symptoms are likely underestimates.

Discussion

Among 149,082 U.S. cases of COVID-19 reported as of April 2, 2020, for which age was known, 2,572 (1.7%) occurred in patients aged <18 years. In comparison, persons aged <18 years account for 22% of the U.S. population (3). Although infants <1 year accounted for 15% of pediatric COVID-19 cases, they remain underrepresented among COVID-19 cases in patients of all ages (393 of 149,082; 0.27%) compared with the percentage of the U.S. population aged <1 year (1.2%) (3). Relatively few pediatric COVID-19 cases were hospitalized (5.7%–20%; including 0.58%–2.0% admitted to an ICU), consistent with previous reports that COVID-19 illness often might have a mild course among younger patients (4,5). Hospitalization was most common among pediatric patients aged <1 year and those with underlying conditions. In addition, 73% of children for whom symptom information was known reported the characteristic COVID-19 signs and symptoms of fever, cough, or shortness of breath.

These findings are largely consistent with a report on pediatric COVID-19 patients aged <16 years in China, which found that only 41.5% of pediatric patients had fever, 48.5% had cough, and 1.8% were admitted to an ICU (4). A second report suggested that although pediatric COVID-19 patients infrequently have severe outcomes, the infection might be more severe among infants (5). In the current analysis, 59 of 147 pediatric hospitalizations, including five of 15 pediatric ICU admissions, were among children aged <1 year; however, most reported U.S. cases in infants had unknown hospitalization status.

FIGURE 2. COVID-19 cases among children* aged <18 years, among those with known hospitalization status (N = 745),[†] by age group and hospitalization status — United States, February 12–April 2, 2020



Abbreviation: ICU = intensive care unit.

* Includes infants, children, and adolescents.

[†] Number of children missing hospitalization status by age group: <1 year (303 of 398; 76%); 1–4 years (189 of 291; 65%); 5–9 years (275 of 388; 71%); 10–14 years (466 of 682; 68%); 15–17 years (594 of 813; 73%).

Summary

What is already known about this topic?

Data from China suggest that pediatric coronavirus disease 2019 (COVID-19) cases might be less severe than cases in adults and that children (persons aged <18 years) might experience different symptoms than adults.

What is added by this report?

In this preliminary description of pediatric U.S. COVID-19 cases, relatively few children with COVID-19 are hospitalized, and fewer children than adults experience fever, cough, or shortness of breath. Severe outcomes have been reported in children, including three deaths.

What are the implications for public health practice?

Pediatric COVID-19 patients might not have fever or cough. Social distancing and everyday preventive behaviors remain important for all age groups because patients with less serious illness and those without symptoms likely play an important role in disease transmission.

In this preliminary analysis of U.S. pediatric COVID-19 cases, a majority (57%) of patients were males. Several studies have reported a majority of COVID-19 cases among males (4,9), and an analysis of 44,000 COVID-19 cases in patients of all ages in China reported a higher case-fatality rate among men than among women (10). However, the same report, as well as a separate analysis of 2,143 pediatric COVID-19 cases from China, detected no substantial difference in the number of cases among males and females (5,10). Reasons for any potential difference in COVID-19 incidence or severity between males and females are unknown. In the present analysis, the predominance of males in all pediatric age groups, including patients aged <1 year, suggests that biologic factors might play a role in any differences in COVID-19 susceptibility by sex.

The findings in this report are subject to at least four limitations. First, because of the high workload associated with COVID-19 response activities on local, state, and territorial public health personnel, a majority of pediatric cases were missing data on disease symptoms, severity, or underlying conditions. Data for many variables are unlikely to be missing at random, and as such, these results must be interpreted with caution. Because of the high percentage of missing data, statistical comparisons could not be conducted. Second, because many cases occurred only days before publication of this report, the outcome for many patients is unknown, and this analysis might underestimate severity of disease or symptoms that manifested later in the course of illness. Third, COVID-19 testing practices differ across jurisdictions and might also differ across age groups. In many areas, prioritization of testing for severely

ill patients likely occurs, which would result in overestimation of the percentage of patients with COVID-19 infection who are hospitalized (including those treated in an ICU) among all age groups. Finally, this analysis compares clinical characteristics of pediatric cases (persons aged <18 years) with those of cases among adults aged 18–64 years. Severe COVID-19 disease appears to be more common among adults at the high end of this age range (6), and therefore cases in young adults might be more similar to those among children than suggested by the current analysis.

As the number of COVID-19 cases continues to increase in many parts of the United States, it will be important to adapt COVID-19 surveillance strategies to maintain collection of critical case information without overburdening jurisdiction health departments. National surveillance will increasingly be complemented by focused surveillance systems collecting comprehensive case information on a subset of cases across various health care settings. These systems will provide detailed information on the evolving COVID-19 incidence and risk factors for infection and severe disease. More systematic and detailed collection of underlying condition data among pediatric patients would be helpful to understand which children might be at highest risk for severe COVID-19 illness.

This preliminary examination of characteristics of COVID-19 disease among children in the United States suggests that children do not always have fever or cough as reported signs and symptoms. Although most cases reported among children to date have not been severe, clinicians should maintain a high index of suspicion for COVID-19 infection in children and monitor for progression of illness, particularly among infants and children with underlying conditions. However, these findings must be interpreted with caution because of the high percentage of cases missing data on important characteristics. Because persons with asymptomatic and mild disease, including children, are likely playing a role in transmission and spread of COVID-19 in the community, social distancing and everyday preventive behaviors are recommended for persons of all ages to slow the spread of the virus, protect the health care system from being overloaded, and protect older adults and persons of any age with serious underlying medical conditions. Recommendations for reducing the spread of COVID-19 by staying at home and practicing strategies such as respiratory hygiene, wearing cloth face coverings when around others, and others are available on CDC's coronavirus website at <https://www.cdc.gov/coronavirus/2019-ncov/prevent-getting-sick/prevention.html>.

Acknowledgments

State, local, and territorial health department personnel; U.S. clinical, public health, and emergency response staff members; Grace Appiah, Andrea Carmichael, Nancy Chow, Brian Emerson, Katie Forsberg, Alicia Fry, Aron Hall, Clinton McDaniel, Daniel C. Payne, Rachael Porter, Sarah Reagan-Steiner, Matt Ritchey, Katherine Roguski, Tom Shimabukuro, Ben Silk, Emily Ussery, Kate Woodworth, CDC.

CDC COVID-19 Response Team

Stephanie Bialek, CDC; Ryan Gierke, CDC; Michelle Hughes, CDC; Lucy A. McNamara, CDC; Tamara Pilishvili, CDC; Tami Skoff, CDC.

Corresponding author: Lucy A. McNamara for the CDC COVID-19 Response Team, eoevent294@cdc.gov, 770-488-7100.

All authors have completed and submitted the International Committee of Medical Journal Editors form for disclosure of potential conflicts of interest. No potential conflicts of interest were disclosed.

References

1. World Health Organization. Coronavirus disease 2019 (COVID-19) situation report – 73. Geneva, Switzerland: World Health Organization; 2020. <https://www.who.int/emergencies/diseases/novel-coronavirus-2019/situation-reports>
2. CDC. Coronavirus disease 2019 (COVID-19): cases in U.S. Atlanta, GA: US Department of Health and Human Services, CDC; 2020. <https://www.cdc.gov/coronavirus/2019-ncov/cases-updates/cases-in-us.html>
3. CDC. Bridged race population estimates. Atlanta, GA: US Department of Health and Human Services, CDC; 2020. <https://wonder.cdc.gov/bridged-race-population.html>
4. Lu X, Zhang L, Du H, et al.; Chinese Pediatric Novel Coronavirus Study Team. SARS-CoV-2 infection in children. *N Engl J Med* 2020. Epub March 18, 2020. <https://doi.org/10.1056/NEJMc2005073>
5. Dong Y, Mo X, Hu Y, et al. Epidemiological characteristics of 2143 pediatric patients with 2019 coronavirus disease in China. *Pediatrics* 2020. Epub March 16, 2020. <https://doi.org/10.1542/peds.2020-0702>
6. Hoehl S, Rabenau H, Berger A, et al. Evidence of SARS-CoV-2 infection in returning travelers from Wuhan, China. *N Engl J Med* 2020;382:1278–80. <https://doi.org/10.1056/NEJMc2001899>
7. Wei WE, Li Z, Chiew CJ, Yong SE, Toh MP, Lee VJ. Presymptomatic transmission of SARS-CoV-2—Singapore, January 23–March 16, 2020. *MMWR Morb Mortal Wkly Rep* 2020. Epub April 1, 2020.
8. Bialek S, Boundy E, Bowen V, et al.; CDC COVID-19 Response Team. Severe outcomes among patients with coronavirus disease 2019 (COVID-19)—United States, February 12–March 16, 2020. *MMWR Morb Mortal Wkly Rep* 2020;69:343–6. <https://doi.org/10.15585/mmwr.mm6912e2>
9. Ng Y, Li Z, Chua YX, et al. Evaluation of the effectiveness of surveillance and containment measures for the first 100 patients with COVID-19 in Singapore—January 2–February 29, 2020. *MMWR Morb Mortal Wkly Rep* 2020;69:307–11. <https://doi.org/10.15585/mmwr.mm6911e1>
10. The Novel Coronavirus Emergency Response Epidemiology Team. The epidemiological characteristics of an outbreak of 2019 novel coronavirus diseases (COVID-19)—China, 2020. *China CDC Weekly* 2020;2:113–22.



CLINICAL UPDATE

Virology, transmission, and pathogenesis of SARS-CoV-2

Muge Cevik,^{1,2} Krutika Kuppalli,³ Jason Kindrachuk,⁴ Malik Peiris⁵

What you need to know

- SARS-CoV-2 is genetically similar to SARS-CoV-1, but characteristics of SARS-CoV-2—eg, structural differences in its surface proteins and viral load kinetics—may help explain its enhanced rate of transmission
- In the respiratory tract, peak SARS-CoV-2 load is observed at the time of symptom onset or in the first week of illness, with subsequent decline thereafter, indicating the highest infectiousness potential just before or within the first five days of symptom onset
- Reverse transcription polymerase chain reaction (RT-PCR) tests can detect viral SARS-CoV-2 RNA in the upper respiratory tract for a mean of 17 days; however, detection of viral RNA does not necessarily equate to infectiousness, and viral culture from PCR positive upper respiratory tract samples has been rarely positive beyond nine days of illness
- Symptomatic and pre-symptomatic transmission (1–2 days before symptom onset), is likely to play a greater role in the spread of SARS-CoV-2 than asymptomatic transmission
- A wide range of virus-neutralising antibodies have been reported, and emerging evidence suggests that these may correlate with severity of illness but wane over time

Since the emergence of SARS-CoV-2 in December 2019, there has been an unparalleled global effort to characterise the virus and the clinical course of disease. Coronavirus disease 2019 (covid-19), caused by SARS-CoV-2, follows a biphasic pattern of illness that likely results from the combination of an early

viral response phase and an inflammatory second phase. Most clinical presentations are mild, and the typical pattern of covid-19 more resembles an influenza-like illness—which includes fever, cough, malaise, myalgia, headache, and taste and smell disturbance—rather than severe pneumonia (although emerging evidence about long term consequences is yet to be understood in detail).¹ In this review, we provide a broad update on the emerging understanding of SARS-CoV-2 pathophysiology, including virology, transmission dynamics, and the immune response to the virus. Any of the mechanisms and assumptions discussed in the article and in our understanding of covid-19 may be revised as further evidence emerges.

What we know about the virus

SARS-CoV-2 is an enveloped β -coronavirus, with a genetic sequence very similar to SARS-CoV-1 (80%) and bat coronavirus RaTG13 (96.2%).² The viral envelope is coated by spike (S) glycoprotein, envelope (E), and membrane (M) proteins (fig 1). Host cell binding and entry are mediated by the S protein. The first step in infection is virus binding to a host cell through its target receptor. The S1 sub-unit of the S protein contains the receptor binding domain that binds to the peptidase domain of angiotensin-converting enzyme 2 (ACE 2). In SARS-CoV-2 the S2 sub-unit is highly preserved and is considered a potential antiviral target. The virus structure and replication cycle are described in figure 1.

¹ Division of Infection and Global Health Research, School of Medicine, University of St Andrews, St Andrews, UK

² Specialist Virology Laboratory, Royal Infirmary of Edinburgh, Edinburgh, UK and Regional Infectious Diseases Unit, Western General Hospital, Edinburgh, UK

³ Division of Infectious Diseases, Medical University of South Carolina, Charleston, SC, USA

⁴ Laboratory of Emerging and Re-Emerging Viruses, Department of Medical Microbiology, University of Manitoba, Winnipeg, MB, Canada

⁵ School of Public Health, LKS Faculty of Medicine, The University of Hong Kong, Hong Kong Special Administrative Region, China

Correspondence to M Cevik mc349@st-andrews.ac.uk

Cite this as: *BMJ* 2020;371:m3862

<http://dx.doi.org/10.1136/bmj.m3862>

Published: 23 October 2020

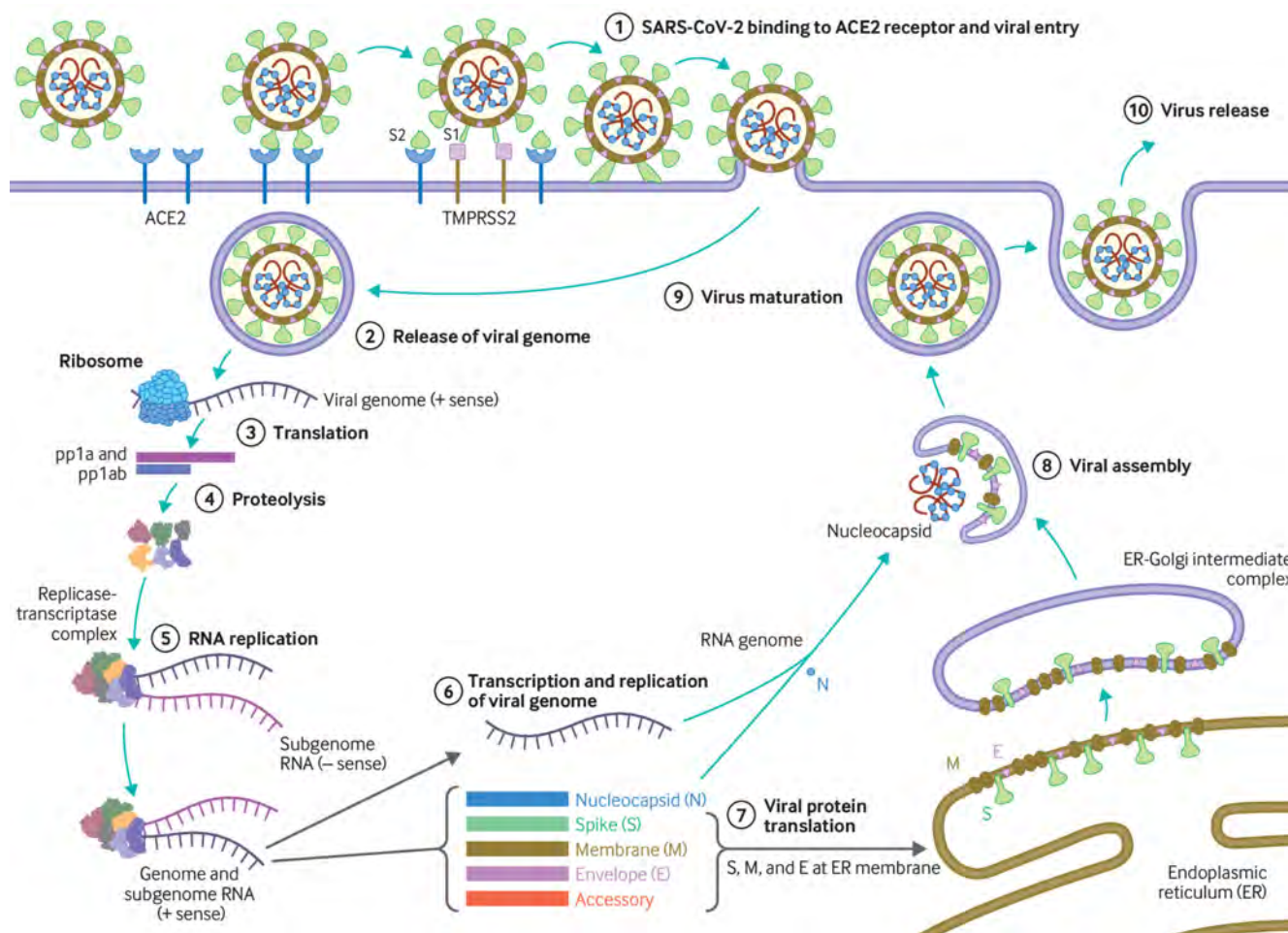


Fig 1 | (1) The virus binds to ACE 2 as the host target cell receptor in synergy with the host's transmembrane serine protease 2 (cell surface protein), which is principally expressed in the airway epithelial cells and vascular endothelial cells. This leads to membrane fusion and releases the viral genome into the host cytoplasm (2). Stages (3-7) show the remaining steps of viral replication, leading to viral assembly, maturation, and virus release

Coronaviruses have the capacity for proofreading during replication, and therefore mutation rates are lower than in other RNA viruses. As SARS-CoV-2 has spread globally it has, like other viruses, accumulated some mutations in the viral genome, which contains geographic signatures. Researchers have examined these mutations to study virus characterisation and understand epidemiology and transmission patterns. In general, the mutations have not been attributed to phenotypic changes affecting viral transmissibility or pathogenicity. The G614 variant in the S protein has been postulated to increase infectivity and transmissibility of the virus.³ Higher viral loads were reported in clinical samples with virus containing G614 than previously circulating variant D614, although no association was made with severity of illness as measured by hospitalisation outcomes.³ These findings have yet to be confirmed with regards to natural infection.

Why is SARS-CoV-2 more infectious than SARS-CoV-1?

SARS-CoV-2 has a higher reproductive number (R_0) than SARS-CoV-1, indicating much more efficient spread.¹ Several characteristics of SARS-CoV-2 may help explain this enhanced

transmission. While both SARS-CoV-1 and SARS-CoV-2 preferentially interact with the angiotensin-converting enzyme 2 (ACE 2) receptor, SARS-CoV-2 has structural differences in its surface proteins that enable stronger binding to the ACE 2 receptor⁴ and greater efficiency at invading host cells.¹ SARS-CoV-2 also has greater affinity (or bonding) for the upper respiratory tract and conjunctiva,⁵ thus can infect the upper respiratory tract and can conduct airways more easily.⁶

Viral load dynamics and duration of infectiousness

Viral load kinetics could also explain some of the differences between SARS-CoV-2 and SARS-CoV-1. In the respiratory tract, peak SARS-CoV-2 load is observed at the time of symptom onset or in the first week of illness, with subsequent decline thereafter, which indicates the highest infectiousness potential just before or within the first five days of symptom onset (fig 2).⁷ In contrast, in SARS-CoV-1 the highest viral loads were detected in the upper respiratory tract in the second week of illness, which explains its minimal contagiousness in the first week after symptom onset, enabling early case detection in the community.⁷

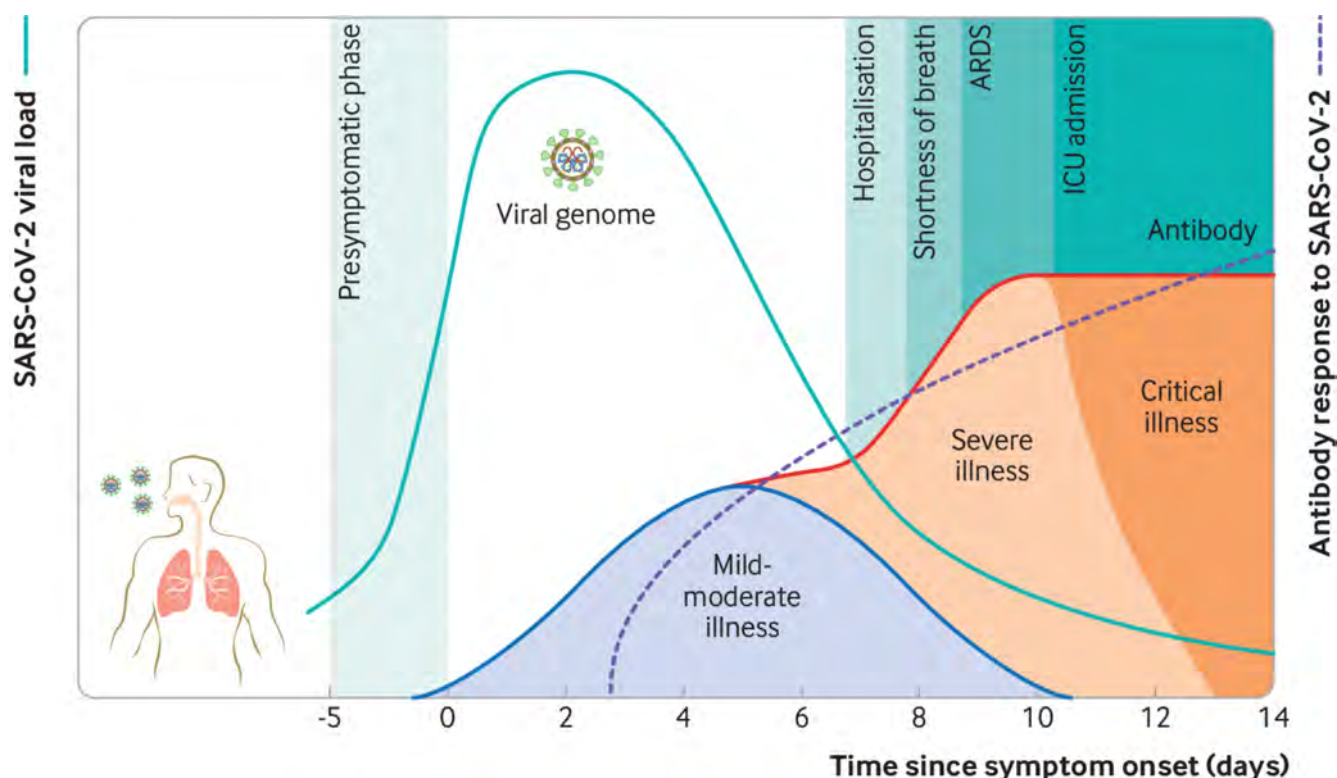


Fig 2 | After the initial exposure, patients typically develop symptoms within 5-6 days (incubation period). SARS-CoV-2 generates a diverse range of clinical manifestations, ranging from mild infection to severe disease accompanied by high mortality. In patients with mild infection, initial host immune response is capable of controlling the infection. In severe disease, excessive immune response leads to organ damage, intensive care admission, or death. The viral load peaks in the first week of infection, declines thereafter gradually, while the antibody response gradually increases and is often detectable by day 14 (figure adapted with permission from <https://www.sciencedirect.com/science/article/pii/S009286742030475X>; [https://www.thelancet.com/journals/lanres/article/PIIS2213-2600\(20\)30230-7/fulltext](https://www.thelancet.com/journals/lanres/article/PIIS2213-2600(20)30230-7/fulltext))

Quantitative reverse transcription polymerase chain reaction (qRT-PCR) technology can detect viral SARS-CoV-2 RNA in the upper respiratory tract for a mean of 17 days (maximum 83 days) after symptom onset.⁷ However, detection of viral RNA by qRT-PCR does not necessarily equate to infectiousness, and viral culture from PCR positive upper respiratory tract samples has been rarely positive beyond nine days of illness.⁵ This corresponds to what is known about transmission based on contact tracing studies, which is that transmission capacity is maximal in the first week of illness, and that transmission after this period has not been documented.⁸ Severely ill or immune-compromised patients may have relatively prolonged virus shedding, and some patients may have intermittent RNA shedding; however, low level results close to the detection limit may not constitute infectious viral particles. While asymptomatic individuals (those with no symptoms throughout the infection) can transmit the infection, their relative degree of infectiousness seems to be limited.⁹⁻¹¹ People with mild symptoms (paucisymptomatic) and those whose symptom have not yet appeared still carry large amounts of virus in the upper respiratory tract, which might contribute to the easy and rapid spread of SARS-CoV-2.⁷ Symptomatic and pre-symptomatic transmission (one to two days before symptom onset) is likely to play a greater role in the spread of SARS-CoV-2.^{10,12} A combination of preventive measures, such as physical distancing and testing, tracing, and self-isolation, continue to be needed.

Route of transmission and transmission dynamics

Like other coronaviruses, the primary mechanism of transmission of SARS-CoV-2 is via infected respiratory droplets, with viral

infection occurring by direct or indirect contact with nasal, conjunctival, or oral mucosa, when respiratory particles are inhaled or deposited on these mucous membranes.⁶ Target host receptors are found mainly in the human respiratory tract epithelium, including the oropharynx and upper airway. The conjunctiva and gastrointestinal tracts are also susceptible to infection and may serve as transmission portals.⁶

Transmission risk depends on factors such as contact pattern, environment, infectiousness of the host, and socioeconomic factors, as described elsewhere.¹² Most transmission occurs through close range contact (such as 15 minutes face to face and within 2 m),¹³ and spread is especially efficient within households and through gatherings of family and friends.¹² Household secondary attack rates (the proportion of susceptible individuals who become infected within a group of susceptible contacts with a primary case) ranges from 4% to 35%.¹² Sleeping in the same room as, or being a spouse of an infected individual increases the risk of infection, but isolation of the infected person away from the family is related to lower risk of infection.¹² Other activities identified as high risk include dining in close proximity with the infected person, sharing food, and taking part in group activities.¹² The risk of infection substantially increases in enclosed environments compared with outdoor settings.¹² For example, a systematic review of transmission clusters found that most superspreading events occurred indoors.¹¹ Aerosol transmission can still factor during prolonged stay in crowded, poorly ventilated indoor settings (meaning transmission could occur at a distance > 2 m).^{12,14-17}

The role of faecal shedding in SARS-CoV-2 transmission and the extent of fomite (through inanimate surfaces) transmission also remain to be fully understood. Both SARS-CoV-2 and SARS-CoV-1 remain viable for many days on smooth surfaces (stainless steel, plastic, glass) and at lower temperature and humidity (eg, air conditioned environments).^{18 19} Thus, transferring infection from contaminated surfaces to the mucosa of eyes, nose, and mouth via unwashed hands is a possible route of transmission. This route of transmission may contribute especially in facilities with communal areas, with increased likelihood of environmental contamination. However, both SARS-CoV-1 and SARS-CoV-2 are readily inactivated by commonly used disinfectants, emphasising the potential value of surface cleaning and handwashing. SARS-CoV-2 RNA has been found in stool samples and RNA shedding often persists for longer than in respiratory samples⁷; however, virus isolation has rarely been successful from the stool.^{5 7} No published reports describe faecal-oral transmission. In SARS-CoV-1, faecal-oral transmission was not considered to occur in most circumstances; but, one explosive outbreak was attributed to aerosolisation and spread of the virus across an apartment block via a faulty sewage system.²⁰ It remains to be seen if similar transmission may occur with SARS-CoV-2.

Pathogenesis

Viral entry and interaction with target cells

SARS-CoV-2 binds to ACE 2, the host target cell receptor.¹ Active replication and release of the virus in the lung cells lead to non-specific symptoms such as fever, myalgia, headache, and respiratory symptoms.¹ In an experimental hamster model, the virus causes transient damage to the cells in the olfactory epithelium, leading to olfactory dysfunction, which may explain temporary loss of taste and smell commonly seen in covid-19.²¹ The distribution of ACE 2 receptors in different tissues may explain the sites of infection and patient symptoms. For example, the ACE 2 receptor is found on the epithelium of other organs such as the intestine and endothelial cells in the kidney and blood vessels, which may explain gastrointestinal symptoms and cardiovascular complications.²² Lymphocytic endotheliitis has been observed in postmortem pathology examination of the lung, heart, kidney, and liver as well as liver cell necrosis and myocardial infarction in patients who died of covid-19.^{1 23} These findings indicate that the virus directly affects many organs, as was seen in SARS-CoV-1 and influenzae.

Much remains unknown. Are the pathological changes in the respiratory tract or endothelial dysfunction the result of direct viral infection, cytokine dysregulation, coagulopathy, or are they multifactorial? And does direct viral invasion or coagulopathy directly contribute to some of the ischaemic complications such as ischaemic infarcts? These and more, will require further work to elucidate.

Immune response and disease spectrum (figure 2)

After viral entry, the initial inflammatory response attracts virus-specific T cells to the site of infection, where the infected cells are eliminated before the virus spreads, leading to recovery in most people.²⁴ In patients who develop severe disease, SARS-CoV-2 elicits an aberrant host immune response.^{24 25} For example, postmortem histology of lung tissues of patients who died of covid-19 have confirmed the inflammatory nature of the injury, with features of bilateral diffuse alveolar damage, hyaline-membrane formation, interstitial mononuclear inflammatory infiltrates, and desquamation consistent with acute respiratory distress syndrome (ARDS), and is similar to the lung pathology seen in severe Middle East respiratory

syndrome (MERS) and severe acute respiratory syndrome (SARS).^{26 27} A distinctive feature of covid-19 is the presence of mucus plugs with fibrinous exudate in the respiratory tract, which may explain the severity of covid-19 even in young adults.²⁸ This is potentially caused by the overproduction of pro-inflammatory cytokines that accumulate in the lungs, eventually damaging the lung parenchyma.²⁴

Some patients also experience septic shock and multi-organ dysfunction.²⁴ For example, the cardiovascular system is often involved early in covid-19 disease and is reflected in the release of highly sensitive troponin and natriuretic peptides.²⁹ Consistent with the clinical context of coagulopathy, focal intra-alveolar haemorrhage and presence of platelet-fibrin thrombi in small arterial vessels is also seen.²⁷ Cytokines normally mediate and regulate immunity, inflammation, and haematopoiesis; however, further exacerbation of immune reaction and accumulation of cytokines in other organs in some patients may cause extensive tissue damage, or a cytokine release syndrome (cytokine storm), resulting in capillary leak, thrombus formation, and organ dysfunction.^{24 30}

Mechanisms underlying the diverse clinical outcomes

Clinical outcomes are influenced by host factors such as older age, male sex, and underlying medical conditions,¹ as well as factors related to the virus (such as viral load kinetics), host-immune response, and potential cross-reactive immune memory from previous exposure to seasonal coronaviruses (box 1).

Box 1: Risk factors associated with the development of severe disease, admission to intensive care unit, and mortality

Underlying condition

- Older age
- Hypertension
- Cardiovascular disease
- Chronic obstructive pulmonary disease
- Diabetes
- Obesity
- Malignancy

Presentation

- Higher fever ($\geq 39^{\circ}\text{C}$ on admission)
- Dyspnoea on admission
- Higher qSOFA score

Laboratory markers

- Neutrophilia/lymphopenia
- Raised lactate and lactate dehydrogenase
- Raised C reactive protein
- Raised ferritin
- Raised IL-6
- Raised ACE2
- D-dimer $>1 \mu\text{g/mL}$

Sex-related differences in immune response have been reported, revealing that men had higher plasma innate immune cytokines and chemokines at baseline than women.³¹ In contrast, women had notably more robust T cell activation than men, and among male participants T cell activation declined with age, which was sustained among female patients. These findings suggest that adaptive immune response may be important in defining the clinical outcome

as older age and male sex is associated with increased risk of severe disease and mortality.

Increased levels of pro-inflammatory cytokines correlate with severe pneumonia and increased ground glass opacities within the lungs.^{30 32} In people with severe illness, increased plasma concentrations of inflammatory cytokines and biomarkers were observed compared with people with non-severe illness.^{30 33 34}

Emerging evidence suggests a correlation between viral dynamics, the severity of illness, and disease outcome.⁷ Longitudinal characteristics of immune response show a correlation between the severity of illness, viral load, and IFN- α , IFN- γ , and TNF- α

response.³⁴ In the same study many interferons, cytokines, and chemokines were elevated early in disease for patients who had severe disease and higher viral loads. This emphasises that viral load may drive these cytokines and the possible pathological roles associated with the host defence factors. This is in keeping with the pathogenesis of influenza, SARS, and MERS whereby prolonged viral shedding was also associated with severity of illness.^{7 35}

Given the substantial role of the immune response in determining clinical outcomes, several immunosuppressive therapies aimed at limiting immune-mediated damage are currently in various phases of development (table 1).

Table 1 | Therapeutics currently under investigation

Entry to the cell	Viral replication	Host immune response
ACE receptor inhibitors	RNA polymerase inhibitors	Immunomodulators
Angiotensin II receptor blockers	Remdesivir	Tocilizumab
Fusion inhibitors	Ribavirin	Sarilumab
Uminefovir	Favipiravir	Adalimumab (TNF inhibitor)
Baricitinib	Protease inhibitors	IFN
Monoclonal antibodies	Lopinavir	Corticosteroids
	Darunavir	

Immune response to the virus and its role in protection

Covid-19 leads to an antibody response to a range of viral proteins, but the spike (S) protein and nucleocapsid are those most often used in serological diagnosis. Few antibodies are detectable in the first four days of illness, but patients progressively develop them, with most achieving a detectable response after four weeks.³⁶ A wide range of virus-neutralising antibodies have been reported, and emerging evidence suggests that these may correlate with severity but wane over time.³⁷ The duration and protectivity of antibody and T cell responses remain to be defined through studies with longer follow-up. CD-4 T cell responses to endemic human coronaviruses appear to manifest cross-reactivity with SARS-CoV-2, but their role in protection remains unclear.³⁸

Unanswered questions

Further understanding of the pathogenesis for SARS-CoV-2 will be vital in developing therapeutics, vaccines, and supportive care modalities in the treatment of covid-19. More data are needed to understand the determinants of healthy versus dysfunctional response and immune markers for protection and the severity of disease. Neutralising antibodies are potential correlates of protection, but other protective antibody mechanisms may exist. Similarly, the protective role of T cell immunity and duration of both antibody and T cell responses and the correlates of protection need to be defined. In addition, we need optimal testing systems and technologies to support and inform early detection and clinical management of infection. Greater understanding is needed regarding the long term consequences following acute illness and multisystem inflammatory disease, especially in children.

Education into practice

How would you describe SARS-CoV-2 transmission routes and ways to prevent infection?

How would you describe to a patient why cough, anosmia, and fever occur in covid-19?

Questions for future research

- What is the role of the cytokine storm and how could it inform the development of therapeutics, vaccines, and supportive care modalities?
- What is the window period when patients are most infectious?
- Why do some patients develop severe disease while others, especially children, remain mildly symptomatic or do not develop symptoms?
- What are the determinants of healthy versus dysfunctional response, and the biomarkers to define immune correlates of protection and disease severity for the effective triage of patients?
- What is the protective role of T cell immunity and duration of both antibody and T cell responses, and how would you define the correlates of protection?

How patients were involved in the creation of this article

No patients were directly involved in the creation of this article.

How this article was created

We searched PubMed from 2000 to 18 September 2020, limited to publications in English. Our search strategy used a combination of key words including "COVID-19," "SARS-CoV-2," "SARS," "MERS," "Coronavirus," "Novel Coronavirus," "Pathogenesis," "Transmission," "Cytokine Release," "immune response," "antibody response." These sources were supplemented with systematic reviews. We also reviewed technical documents produced by the Centers for Disease Control and Prevention and World Health Organization technical documents.

Author contributions: MC, KK, JK, MP drafted the first and subsequent versions of the manuscript and all authors provided critical feedback and contributed to the manuscript.

Competing interests: *The BMJ* has judged that there are no disqualifying financial ties to commercial companies. The authors declare the following other interests: none.

Further details of *The BMJ* policy on financial interests are here: <https://www.bmj.com/about-bmj/resources/authors/forms-policies-and-checklists/declaration-competing-interests>

Provenance and peer review: commissioned; externally peer reviewed.

- 1 Cevik M, Bamford CGG, Ho A. COVID-19 pandemic-a focused review for clinicians. *Clin Microbiol Infect* 2020;26:842-7. doi: 10.1016/j.cmi.2020.04.023 PMID: 32344166
- 2 Yan R, Zhang Y, Li Y, Xia L, Guo Y, Zhou Q. Structural basis for the recognition of SARS-CoV-2 by full-length human ACE2. *Science* 2020;367:1444-8. doi: 10.1126/science.abb2762 PMID: 32132184
- 3 Korber B, Fischer WM, Gnanakaran S, et al. Sheffield COVID-19 Genomics Group. Tracking changes in SARS-CoV-2 spike: evidence that D614G increases infectivity of the covid-19 virus. *Cell* 2020;182:812-827.e19. doi: 10.1016/j.cell.2020.06.043 PMID: 32697968
- 4 Wrapp D, Wang N, Corbett KS, et al. Cryo-EM structure of the 2019-nCoV spike in the prefusion conformation. *Science* 2020;367:1260-3. doi: 10.1126/science.abb2507 PMID: 32075877
- 5 Wölfel R, Corman VM, Guggemos W, et al. Virological assessment of hospitalized patients with COVID-2019. *Nature* 2020;581:465-9. doi: 10.1038/s41586-020-2196-x PMID: 32235945
- 6 Hui KPY, Cheung MC, Perera RAPM, et al. Tropism, replication competence, and innate immune responses of the coronavirus SARS-CoV-2 in human respiratory tract and conjunctiva: an analysis in ex-vivo and in-vitro cultures. *Lancet Respir Med* 2020;8:687-95. doi: 10.1016/S2213-2600(20)30193-4 PMID: 32386571
- 7 Cevik M, Tate M, Lloyd O, et al. SARS-CoV-2, SARS-CoV-1 and MERS-CoV viral load dynamics, duration of viral shedding and infectiousness: a living systematic review and meta-analysis. *Lancet Microbe* 2020; (forthcoming) doi: 10.1016/S2666-5247(20)30172-5.
- 8 Cheng H-Y, Jian S-W, Liu D-P, Ng TC, Huang WT, Lin HHT. Taiwan COVID-19 Outbreak Investigation Team. Contact tracing assessment of covid-19 transmission dynamics in Taiwan and risk at different exposure periods before and after symptom onset. *JAMA Intern Med* 2020;180:1156-63. doi: 10.1001/jamainternmed.2020.2020 PMID: 32356867
- 9 Meyerowitz E, Richterman A, Bogoch I, Low N, Cevik M. Towards an accurate and systematic characterization of persistently asymptomatic infection with SARS-CoV-2. *Lancet Infect Dis* 2020; (forthcoming).
- 10 Qiu X, Nergiz AI, Maraolo AE, et al. Defining the role of asymptomatic SARS-CoV-2 transmission: a living systematic review. *MedRxiv* [Preprint] 2020. doi: 10.1101/2020.09.01.20135194
- 11 Buitrago-Garcia D, Egli-Gany D, Counotte MJ, et al. Occurrence and transmission potential of asymptomatic and presymptomatic SARS-CoV-2 infections: a living systematic review and meta-analysis. *PLoS Med* 2020;17:e1003346. doi: 10.1371/journal.pmed.1003346 PMID: 32960881
- 12 Cevik M, Marcus J, Buckee C, Smith T. SARS-CoV-2 transmission dynamics should inform policy. *Clin Infect Dis*;2020. doi: 10.1093/cid/ciaa1442.
- 13 European Centre for Disease Prevention and Control. Surveillance definitions for COVID-19. 2020. <https://www.ecdc.europa.eu/en/covid-19/surveillance/surveillance-definitions>.
- 14 Klompas M, Baker MA, Rhee C. Airborne transmission of SARS-CoV-2: theoretical considerations and available evidence. *JAMA* 2020;324:441-2. doi: 10.1001/jama.2020.12458 PMID: 32749495
- 15 Centers for Disease Control and Prevention. How COVID-19 spreads. 2020. <https://www.cdc.gov/coronavirus/2019-ncov/prevent-getting-sick/how-covid-spreads.html>
- 16 Centers for Disease Control and Prevention. Scientific brief: SARS-CoV-2 and potential airborne transmission. 2020. <https://www.cdc.gov/coronavirus/2019-ncov/more/scientific-brief-sars-cov-2.html>
- 17 Yu IT, Li Y, Wong TW, et al. Evidence of airborne transmission of the severe acute respiratory syndrome virus. *N Engl J Med* 2004;350:1731-9. doi: 10.1056/NEJMoa032867 PMID: 15102999
- 18 Chin AWH, Chu JTS, Perera MRA, et al. Stability of SARS-CoV-2 in different environmental conditions. *Lancet Microbe* 2020;1:e10. doi: 10.1016/S2666-5247(20)30003-3 PMID: 32835322
- 19 van Doremalen N, Bushmaker T, Morris DH, et al. Aerosol and surface stability of SARS-CoV-2 as compared with SARS-CoV-1. *N Engl J Med* 2020;382:1564-7. doi: 10.1056/NEJMc2004973 PMID: 32182409
- 20 Kang M, Wei J, Yuan J, et al. Probable evidence of fecal aerosol transmission of SARS-CoV-2 in a high-rise building. *Ann Intern Med* 2020. . doi: 10.7326/M20-0928 PMID: 32870707
- 21 Sia SF, Yan LM, Chin AWH, et al. Pathogenesis and transmission of SARS-CoV-2 in golden hamsters. *Nature* 2020;583:834-8. doi: 10.1038/s41586-020-2342-5 PMID: 32408338
- 22 Monteil V, Kwon H, Prado P, et al. Inhibition of SARS-CoV-2 infections in engineered human tissues using clinical-grade soluble human ACE2. *Cell* 2020;181:905-913.e7. doi: 10.1016/j.cell.2020.04.004 PMID: 32333836
- 23 Varga Z, Flammer AJ, Steiger P, et al. Endothelial cell infection and endothelitis in COVID-19. *Lancet* 2020;395:1417-8. doi: 10.1016/S0140-6736(20)30937-5 PMID: 32325026
- 24 Mangalmurti N, Hunter CA. Cytokine Storms: understanding COVID-19. *Immunity* 2020;53:19-25. doi: 10.1016/j.immuni.2020.06.017 PMID: 32610079
- 25 Blanco-Melo D, Nilsson-Payant BE, Liu W-C, et al. Imbalanced host response to SARS-CoV-2 drives development of covid-19. *Cell* 2020;181:1036-1045.e9. doi: 10.1016/j.cell.2020.04.026 PMID: 32416070
- 26 Xu Z, Shi L, Wang Y, et al. Pathological findings of COVID-19 associated with acute respiratory distress syndrome. *Lancet Respir Med* 2020;8:420-2. doi: 10.1016/S2213-2600(20)30076-X PMID: 32085846
- 27 Carsana L, Sonzogni A, Nasr A, et al. Pulmonary post-mortem findings in a series of COVID-19 cases from northern Italy: a two-centre descriptive study. *Lancet Infect Dis* 2020;20:1135-40. doi: 10.1016/S1473-3099(20)30434-5 PMID: 32526193
- 28 Wang C, Xie J, Zhao L, et al. Alveolar macrophage dysfunction and cytokine storm in the pathogenesis of two severe COVID-19 patients. *EBioMedicine* 2020;57:102833. doi: 10.1016/j.ebiom.2020.102833 PMID: 32574956
- 29 Liu PP, Blet A, Smyth D, Li H. The science underlying covid-19: implications for the cardiovascular system. *Circulation* 2020;142:68-78. doi: 10.1161/CIRCULATIONAHA.120.047549 PMID: 32293910
- 30 Wu C, Chen X, Cai Y, et al. Risk factors associated with acute respiratory distress syndrome and death in patients with coronavirus disease 2019 pneumonia in Wuhan, China. *JAMA Intern Med* 2020;180:934-43. doi: 10.1001/jamainternmed.2020.0994 PMID: 32167524
- 31 Takahashi T, Ellingson MK, Wong P, et al. Sex differences in immune responses that underlie COVID-19 disease outcomes. *Nature* 2020. <https://pubmed.ncbi.nlm.nih.gov/32846427/>
- 32 Liu Y, Yan L-M, Wan L, et al. Viral dynamics in mild and severe cases of COVID-19. *Lancet Infect Dis* 2020;20:656-7. doi: 10.1016/S1473-3099(20)30232-2 PMID: 32199493
- 33 Huang C, Wang Y, Li X, et al. Clinical features of patients infected with 2019 novel coronavirus in Wuhan, China. *Lancet* 2020;395:497-506. doi: 10.1016/S0140-6736(20)30183-5 PMID: 31986264
- 34 Lucas C, Wong P, Klein J, et al. Yale IMPACT Team. Longitudinal analyses reveal immunological misfiring in severe COVID-19. *Nature* 2020;584:463-9. doi: 10.1038/s41586-020-2588-y PMID: 32717743
- 35 Wang Y, Guo Q, Yan Z, et al. CAP-China Network. Factors associated with prolonged viral shedding in patients with avian influenza A (H7N9) virus infection. *J Infect Dis* 2018;217:1708-17. doi: 10.1093/infdis/jiy115 PMID: 29648602
- 36 Perera RA, Mok CK, Tsang OT, et al. Serological assays for severe acute respiratory syndrome coronavirus 2 (SARS-CoV-2), March 2020. *Euro Surveill* 2020;25:2000421. doi: 10.2807/1560-7917.ES.2020.25.16.2000421 PMID: 32347204
- 37 Seow J, Graham C, Merrick B, et al. Longitudinal evaluation and decline of antibody responses in SARS-CoV-2 infection. *Nat Microbiol* 2020;doi: 10.1038/s41564-020-00813-8
- 38 Grifoni A, Weiskopf D, Ramirez SI, et al. Targets of T cell responses to SARS-CoV-2 coronavirus in humans with covid-19 disease and unexposed individuals. *Cell* 2020;181:1489-1501.e15. doi: 10.1016/j.cell.2020.05.015 PMID: 32473127

This article is made freely available for use in accordance with BMJ's website terms and conditions for the duration of the covid-19 pandemic or until otherwise determined by BMJ. You may use, download and print the article for any lawful, non-commercial purpose (including text and data mining) provided that all copyright notices and trade marks are retained.



Since January 2020 Elsevier has created a COVID-19 resource centre with free information in English and Mandarin on the novel coronavirus COVID-19. The COVID-19 resource centre is hosted on Elsevier Connect, the company's public news and information website.

Elsevier hereby grants permission to make all its COVID-19-related research that is available on the COVID-19 resource centre - including this research content - immediately available in PubMed Central and other publicly funded repositories, such as the WHO COVID database with rights for unrestricted research re-use and analyses in any form or by any means with acknowledgement of the original source. These permissions are granted for free by Elsevier for as long as the COVID-19 resource centre remains active.

SARS-CoV-2, SARS-CoV, and MERS-CoV viral load dynamics, duration of viral shedding, and infectiousness: a systematic review and meta-analysis



Muge Cevik, Matthew Tate, Ollie Lloyd, Alberto Enrico Maraolo, Jenna Schafers, Antonia Ho



Summary

Background Viral load kinetics and duration of viral shedding are important determinants for disease transmission. We aimed to characterise viral load dynamics, duration of viral RNA shedding, and viable virus shedding of severe acute respiratory syndrome coronavirus 2 (SARS-CoV-2) in various body fluids, and to compare SARS-CoV-2, SARS-CoV, and Middle East respiratory syndrome coronavirus (MERS-CoV) viral dynamics.

Methods In this systematic review and meta-analysis, we searched databases, including MEDLINE, Embase, Europe PubMed Central, *medRxiv*, and *bioRxiv*, and the grey literature, for research articles published between Jan 1, 2003, and June 6, 2020. We included case series (with five or more participants), cohort studies, and randomised controlled trials that reported SARS-CoV-2, SARS-CoV, or MERS-CoV infection, and reported viral load kinetics, duration of viral shedding, or viable virus. Two authors independently extracted data from published studies, or contacted authors to request data, and assessed study quality and risk of bias using the Joanna Briggs Institute Critical Appraisal Checklist tools. We calculated the mean duration of viral shedding and 95% CIs for every study included and applied the random-effects model to estimate a pooled effect size. We used a weighted meta-regression with an unrestricted maximum likelihood model to assess the effect of potential moderators on the pooled effect size. This study is registered with PROSPERO, CRD42020181914.

Findings 79 studies (5340 individuals) on SARS-CoV-2, eight studies (1858 individuals) on SARS-CoV, and 11 studies (799 individuals) on MERS-CoV were included. Mean duration of SARS-CoV-2 RNA shedding was 17·0 days (95% CI 15·5–18·6; 43 studies, 3229 individuals) in upper respiratory tract, 14·6 days (9·3–20·0; seven studies, 260 individuals) in lower respiratory tract, 17·2 days (14·4–20·1; 13 studies, 586 individuals) in stool, and 16·6 days (3·6–29·7; two studies, 108 individuals) in serum samples. Maximum shedding duration was 83 days in the upper respiratory tract, 59 days in the lower respiratory tract, 126 days in stools, and 60 days in serum. Pooled mean SARS-CoV-2 shedding duration was positively associated with age (slope 0·304 [95% CI 0·115–0·493]; $p=0·0016$). No study detected live virus beyond day 9 of illness, despite persistently high viral loads, which were inferred from cycle threshold values. SARS-CoV-2 viral load in the upper respiratory tract appeared to peak in the first week of illness, whereas that of SARS-CoV peaked at days 10–14 and that of MERS-CoV peaked at days 7–10.

Interpretation Although SARS-CoV-2 RNA shedding in respiratory and stool samples can be prolonged, duration of viable virus is relatively short-lived. SARS-CoV-2 titres in the upper respiratory tract peak in the first week of illness. Early case finding and isolation, and public education on the spectrum of illness and period of infectiousness are key to the effective containment of SARS-CoV-2.

Funding None.

Copyright © 2020 The Author(s). Published by Elsevier Ltd. This is an Open Access article under the CC BY-NC-ND 4.0 license.

Introduction

Viral load kinetics and the duration of viral shedding are important determinants for disease transmission. They determine the duration of infectiousness, which is a critical parameter to inform effective control measures and disease modelling. Although several studies have evaluated severe acute respiratory syndrome coronavirus 2 (SARS-CoV-2) shedding, viral load dynamics and duration of viral shedding reported across studies so far have been heterogeneous.¹ In several case series with serial respiratory sampling, peak viral load was observed just

before, or at the time of, symptom onset.^{2–4} Viral RNA shedding was reported to be persistent in the upper respiratory tract and in faeces for more than 1 month after illness onset.¹ However, the duration of SARS-CoV-2 RNA detection has not been well characterised. A comprehensive understanding of viral load dynamics, length of viral shedding, and how these measures relate to other factors, such as age and disease severity, is lacking.

We aimed to characterise the viral load dynamics of SARS-CoV-2, duration of viral RNA shedding by RT-PCR, and viable virus shedding in various body fluids,

Lancet Microbe 2021; 2: e13–22

Published Online

November 19, 2020

[https://doi.org/10.1016/S2666-5247\(20\)30172-5](https://doi.org/10.1016/S2666-5247(20)30172-5)

S2666-5247(20)30172-5

Division of Infection and Global Health Research, School of Medicine, University of St Andrews, Fife, UK (M Cevik MRC); NHS Lothian Infection Service, Regional Infectious Diseases Unit, Western General Hospital, Edinburgh, UK (M Cevik, O Lloyd MRC, J Schafers MRC); Respiratory Medicine, Queen Elizabeth University Hospital, Glasgow, UK (M Tate MRC); Edinburgh Medical School, College of Medicine and Veterinary Medicine, University of Edinburgh, Edinburgh, UK (O Lloyd); First Division of Infectious Diseases, Cotugno Hospital, AORN dei Colli, Naples, Italy (A E Maraolo MD); and MRC-University of Glasgow Centre for Virus Research, University of Glasgow, Glasgow, UK (A Ho PhD)

Correspondence to:

Dr Muge Cevik, Division of Infection and Global Health Research, School of Medicine, University of St Andrews, Fife KY16 9TF, UK
mc349@st-andrews.ac.uk

Research in context

Evidence before this study

Understanding when patients are most infectious and the duration of infectiousness are of critical importance to controlling the COVID-19 pandemic. The duration of RNA detection across human coronaviruses has not been well characterised, and comprehensive understanding about viral load dynamics and the duration of viral shedding in severe acute respiratory syndrome coronavirus 2 (SARS-CoV-2) is lacking. We retrieved all articles reporting the dynamics and the duration of SARS-CoV-2, SARS-CoV, and Middle East respiratory syndrome coronavirus (MERS-CoV) shedding in various specimens through systematic searches of major databases. Our research identified publications that included terms related to viral dynamics and viral shedding. We included case series, cohort studies, and randomised controlled trials in which the viral dynamics or the duration of viral shedding was reported. We excluded case reports, case series with fewer than five patients, and studies that did not have a clear time of symptom onset.

Added value of this study

To our knowledge, this is the first systematic review and meta-analysis that has examined and compared the viral dynamics of the three highly pathogenic human coronaviruses: SARS-CoV-2, SARS-CoV, and MERS-CoV. The results provide a comprehensive understanding regarding their viral kinetics and duration of shedding. Mean SARS-CoV-2 RNA shedding duration was 17.0 days (maximum shedding duration 83 days) in upper respiratory tract, 14.6 days (maximum 59 days) in lower respiratory tract, 17.2 days (maximum 35 days) in stool, and 16.6 days (maximum 60 days) in serum samples. Pooled mean SARS-CoV-2 shedding duration was positively associated with

age. No study detected live virus beyond day 9 of illness, despite persistently high viral loads. SARS-CoV-2 viral load in the upper respiratory tract appeared to peak in the first week of illness, whereas SARS-CoV and MERS-CoV peaked later. Several studies reported similar viral loads at the start of infection among asymptomatic and symptomatic patients infected with SARS-CoV-2; however, most studies demonstrated faster viral clearance in asymptomatic individuals, as also seen in MERS-CoV, suggesting a shorter infectious period but with similar potential transmissibility at the onset of infection.

Implications of all the available evidence

Our study shows that despite evidence of prolonged SARS-CoV-2 RNA shedding in respiratory and stool samples, viable virus appears to be short-lived. Therefore, RNA detection cannot be used to infer infectiousness. High titres of SARS-CoV-2 are detected early in the disease course, with an early peak observed at the time of symptom onset to day 5 of illness; this finding probably explains the efficient spread of SARS-CoV-2 compared with SARS-CoV and MERS-CoV. This has important implications for SARS-CoV-2 transmission in the community and hospital setting, emphasising the importance of early case finding and prompt isolation as well as public education about the spectrum of illness. Our study shows that isolation practices should be commenced with the start of first symptoms, which can include mild and atypical symptoms, preceding typical symptoms of COVID-19 such as cough and fever. However, given the potential delays in isolation of patients, even the early detection and isolation strategy might not be fully effective in containing SARS-CoV-2.

and to compare SARS-CoV-2 viral dynamics with those of SARS-CoV and Middle East respiratory syndrome coronavirus (MERS-CoV).

Methods

Search strategy and selection criteria

We retrieved all English-language research articles reporting viral dynamics or the duration of shedding of SARS-CoV-2, SARS-CoV, or MERS-CoV in various specimens through systematic searches of major databases, including MEDLINE, Embase, Europe PubMed Central, *medRxiv*, and *bioRxiv*, and the grey literature from Jan 1, 2003, to June 6, 2020, using medical subject headings terms (appendix p 14). We also manually screened the references of included original studies to obtain additional studies. Studies published before 2003 were excluded because the first recognised case of SARS-CoV was identified in March, 2003.

Studies were eligible if they met the following inclusion criteria: report on SARS-CoV-2, SARS-CoV, or MERS-CoV

infection, and report viral load kinetics, duration of viral shedding, or viable virus shedding. We excluded review papers; animal studies; studies on environmental sampling; case reports and case series with less than five participants, due to likely reporting bias; papers in which the starting point of viral shedding was not clear or reported from post hospital discharge; and modelling studies with no original data.

Data extraction

Two authors (MT and OL) screened and retrieved articles according to the eligibility criteria. Four reviewers (MT, OL, JS, and MC) reviewed full-text articles and selected articles to be included. From each study, the following variables were extracted as a minimum: name of first author, year of publication, city and country, sample size, median age, sex ratio, time from symptom onset to viral clearance detected by RT-PCR and culture in different specimens, and longest reported time to viral clearance. If these data were not reported, we also contacted the

See Online for appendix

authors to request the data. If available, we extracted data on peak viral load, clinical outcome, and reported factors associated with duration of viral shedding.

Two authors (OL and JS) independently assessed study quality and risk of bias using the Joanna Briggs Institute Critical Appraisal Checklist tools,⁵ which comprise standardised checklists, for the different study designs included in this review. Any disagreements regarding grading of quality were resolved through discussion with a third author (MC).

Data analysis

For every study included, we calculated the mean duration of viral shedding and 95% CIs. We applied the random-effects model to estimate a pooled effect size. We generated forest plots to show the detailed representation of all studies based on the effect size and 95% CI. If not reported, we derived means and SDs from sample size, and median, IQR, minimum, and maximum values.⁶ Heterogeneity between studies was quantified by the *I*² index and Cochran's *Q* test. We did not assess publication bias because usual appraisal methods are uninformative when meta-analysed studies do not include a test of significance. We used a weighted meta-regression with an unrestricted maximum likelihood model to assess the effect of potential moderators on the pooled effect size ($p < 0.05$ was considered to be significant). The eligibility criterion for meta-regression was the presence of at least ten studies (referring to one virus) for each covariate. All statistical analyses were done with Comprehensive Meta-Analysis (version 3) software (Biostat, Englewood, NJ, USA).

This systematic review is registered with PROSPERO, CRD42020181914, and will be updated periodically.

Role of the funding source

There was no funding source for this study. The corresponding author and senior author (AH) had full access to all the data in the study and had final responsibility for the decision to submit for publication.

Results

The systematic search identified 1486 potentially relevant articles. 350 articles were retrieved for full-text review. After reviewing the eligibility criteria, 79 studies (5340 individuals) on SARS-CoV-2,^{2,4,7–82} eight (1858 individuals) on SARS-CoV,^{83–90} and 11 (799 individuals) on MERS-CoV^{91–101} were included (figure 1).

Of the 79 papers included, 58 studies were done in China (appendix pp 1–4).^{2,10–12,14–17,19–21,23–28,35–41,43,44,48–50,52–63,65–73,75–82} 73 studies included only patients who were admitted to hospital.^{3,4,7–29,31,32,34–49,52–54,56–82} Six studies reported viral load dynamics exclusively in children (age younger than 16 years).^{7–12} Two additional studies included children, but data on viral load dynamics were presented in aggregate with adults.^{13,14}

61 studies reported median or maximum viral RNA shedding in at least one body fluid and were eligible

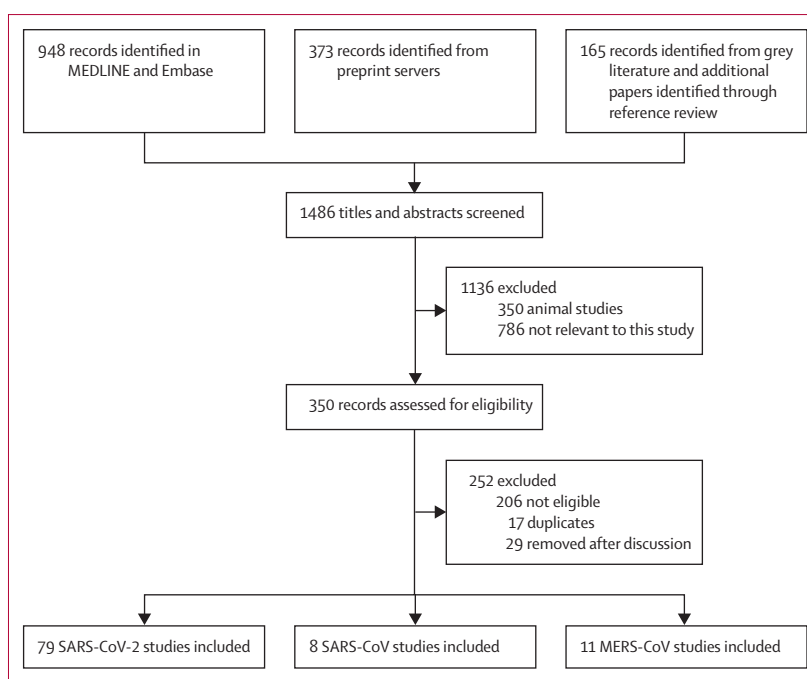


Figure 1: Study selection

MERS-CoV=Middle East respiratory syndrome coronavirus. SARS-CoV=severe acute respiratory syndrome coronavirus. SARS-CoV-2=severe acute respiratory syndrome coronavirus 2.

for quantitative analysis,^{3,4,7,9–12,14–17,19–22,24,25,27–30,34–43,45,47,48,50,51,53,54,57–65,}

^{67–76,78–80,82} and six studies provided duration of shedding stratified by illness severity only.^{13,39,52,55,77,81} Of those studies, 43 (including 3229 individuals) reported duration of shedding in the upper respiratory tract (mean viral shedding duration 17.0 days [95% CI 15.5–18.6]; figure 2), seven (260 individuals) in the lower respiratory tract (14.6 days [9.3–20.0]; appendix p 6), 13 (586 individuals) in stool samples (17.2 days [14.4–20.1]; appendix p 7), and two (108 individuals) in serum samples (16.6 days [3.6–29.7]; appendix p 6). Maximum duration of RNA shedding reported was 83 days in the upper respiratory tract,³⁵ 59 days in the lower respiratory tract,²⁷ 126 days in stool samples,⁸⁸ and 60 days in serum samples.⁷⁸

Studies reporting duration of viral shedding in upper respiratory tract and stool samples were eligible for meta-regression analysis. Pooled mean viral shedding duration was positively associated with age (slope 0.304 [95% CI 0.115–0.493]; $p=0.0016$), but not sex ($p=0.28$; appendix pp 7–8). When adjusted for the proportion of males in a multivariable analysis, mean age was positively associated with the mean duration of viral shedding in upper respiratory tract specimens ($p=0.0029$). There was a positive but non-significant association between mean age and duration of shedding in stool samples ($p=0.37$; appendix p 8).

Eight of 13 studies evaluating SARS-CoV-2 viral load in serial upper respiratory tract samples showed peak viral loads inferred from cycle threshold values within the first week of symptom onset.^{2–4,8,15–23} The highest viral loads were

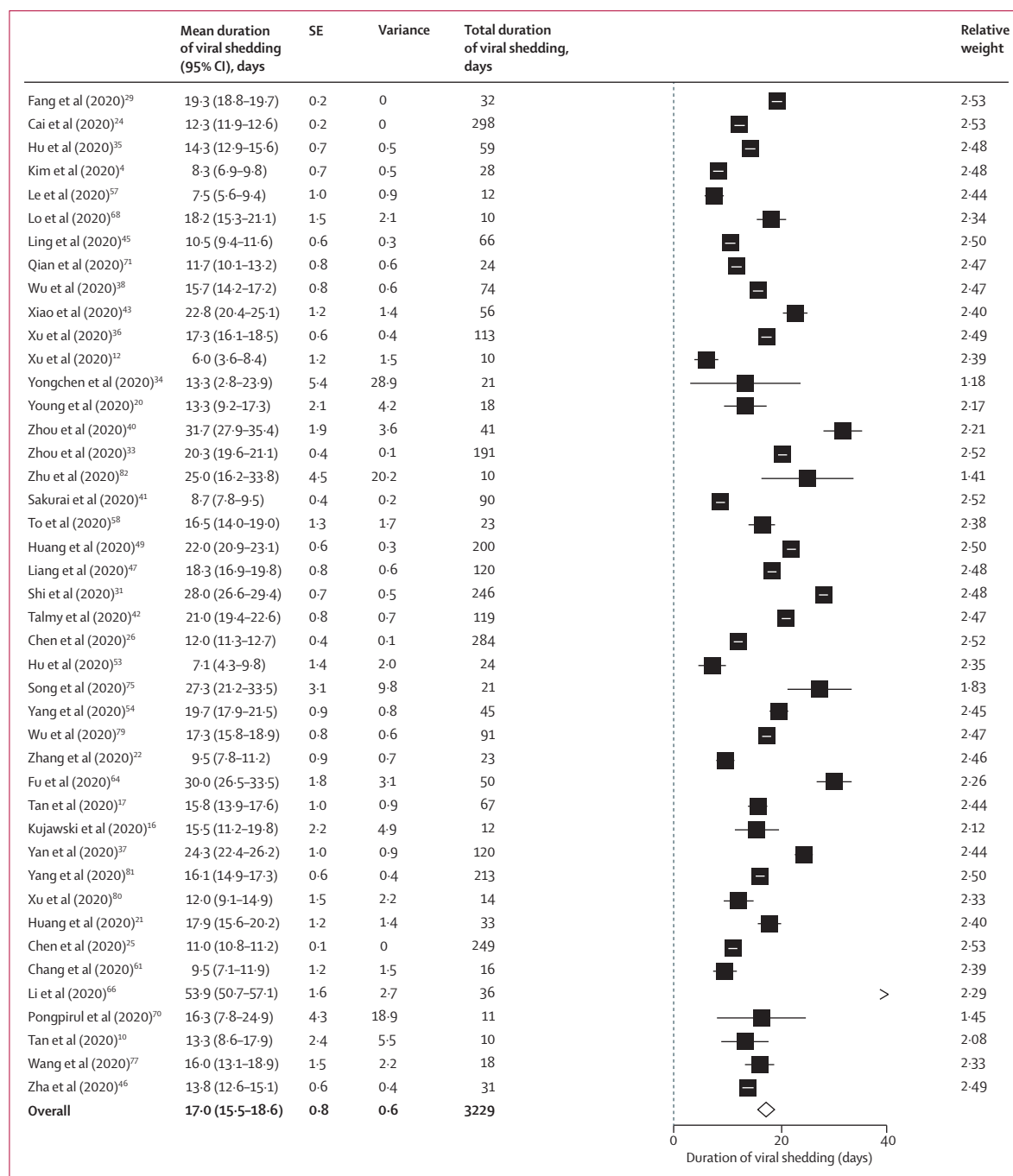


Figure 2: Pooled mean duration (days) of SARS-CoV-2 shedding from the upper respiratory tract (random-effects model)
SARS-CoV-2=severe acute respiratory syndrome coronavirus 2.

reported soon after or at the time of symptom onset,^{2,8,15,21,23} or at day 3–5 of illness,^{3,4,20} followed by a consistent decline.

Five studies that evaluated viral load dynamics in lower respiratory tract samples observed a peak viral load in the second week of illness.^{3,4,17,21,23} By contrast, the dynamics of SARS-CoV-2 shedding in stool samples was erratic, with highest viral loads reported on day 7,¹⁷ 2–3 weeks,^{22,23} and up

to 5–6 weeks after symptom onset.²¹ Although two studies reported significantly higher viral titres in stool samples than in respiratory samples,^{8,23} one study reported lower viral load in stool samples than in both lower and upper respiratory tract samples at the time of symptom onset.²¹

20 studies evaluated duration of viral RNA shedding based on disease severity. 13 of these studies reported

longer duration of viral shedding in patients with severe illness than in those with non-severe illness,^{17,23–34} whereas five studies in upper respiratory tract samples^{16,18,35–37} and one study in stool samples³⁸ reported similar shedding durations according to disease severity. One study reported shorter duration of viral shedding in moderate to severe illness than in mild to moderate illness.³⁹ Six studies compared viral shedding among individuals with severe illness versus non-severe illness:^{17,23,25,26,36,37} five studies showed significantly longer duration of shedding among those with severe illness than among those with non-severe illness,^{17,23,25,26,36} and one study observed no difference³⁷ (table 1).

All but one study⁴⁰ that examined the effect of age on SARS-CoV-2 shedding identified an association between older age (older than 60 years) and prolonged viral RNA shedding.^{23,24,26,31,35–37,41–43} Three studies identified age as an independent risk factor for delayed viral clearance.^{23,24,36} Male sex was also associated with prolonged shedding,^{23,36,44} and the association remained significant even when patients were stratified based on illness severity.^{23,36} Corticosteroid treatment was associated with delayed viral clearance in four studies,^{31,36,45,46} and one study that recruited 120 patients with critical illness found no difference between corticosteroid and control groups.⁴⁷

A randomised, placebo-controlled trial of remdesivir in adults with severe COVID-19 found a similar decline in viral load over time in remdesivir and control groups, as well as similar proportions of patients with undetectable viral RNA at 28 days.¹⁰² In a phase 2, open-label study evaluating interferon beta-1b, lopinavir–ritonavir, and ribavirin, a shorter duration of viral shedding was seen with combination treatment than with the control.⁴⁸ None of the antiviral regimens (chloroquine, oseltamivir, arbidol, and lopinavir–ritonavir) independently improved viral RNA clearance.^{26,49} In a retrospective study of 284 patients, lopinavir–ritonavir use was associated with delayed viral clearance even after adjusting for confounders.²⁶

12 studies reported viral load dynamics or duration of viral shedding among individuals with asymptomatic SARS-CoV-2 infection (table 2); two demonstrated lower viral loads among asymptomatic individuals than among symptomatic individuals,^{8,50} and four found similar initial viral loads.^{13,14,51,52} However, Chau and colleagues reported significantly lower viral load in asymptomatic individuals during the follow-up than in symptomatic individuals.⁵¹ Faster viral clearance was observed in asymptomatic individuals in five of six studies.^{13,26,51,53,54} The exception, Yongchen and colleagues, found longer shedding duration among asymptomatic cases, but the difference was not significant.³⁴

We identified 11 studies that attempted to isolate live virus. All eight studies that attempted virus isolation in respiratory samples successfully cultured viable virus within the first week of illness.^{3,9,16,52,55–58} No live virus was

	Classification of illness severity	Median (IQR)* duration of SARS-CoV-2 positivity in cohort, days	Viral dynamics in patients with severe illness vs those with non-severe illness	p value
Chen et al (2020) ³⁵	ICU vs non-ICU patients	11 (95% CI 10–12)	Median time to viral clearance significantly longer in ICU vs non-ICU patients (HR 3.17, 95% CI 2.29–4.37)	Only HR provided
Chen et al (2020) ³⁶	China CDC guideline (version 7)	12 (8–16)	Shedding duration varies by severity: asymptomatic 6 days; mild 10 days; moderate 12 days; serious 14 days; critical 32 days	<0.0001
Tan et al (2020) ³⁷	China CDC guideline (version 6)	Nasopharyngeal swab: 12 (range 3–38); any sample: 22 (range 3–38)	Viral shedding significantly longer in patients with severe illness: any sample 23 days vs 20 days (note that nasopharyngeal swab 14 vs 11 days was non-significant)	0.023 (any sample)
Xu et al (2020) ³⁸	WHO criteria	17 (13–32)	Higher proportion of patients with severe illness had shedding >15 days (34.2% vs 16.2%)	0.049
Yan et al (2020) ³⁹	China CDC guideline (version 6)	23 (18–32)	No difference in shedding duration (general illness 23 days vs severe illness 26 days vs critical illness 28 days)	0.51
Zheng et al (2020) ³³	China CDC guideline (version 6)	Respiratory sample: 18 (13–29)	Shedding duration significantly longer in patients with severe illness (21 vs 14 days) in respiratory samples; no difference in shedding duration in stool or serum samples	0.04

CDC=Center for Disease Control and Prevention. HR=hazard ratio. ICU=intensive care unit. SARS-CoV-2=severe acute respiratory syndrome coronavirus 2. *IQR unless otherwise stated.

Table 1: Severity of illness and viral dynamics

isolated from any respiratory samples taken after day 8 of symptoms in three studies,^{3,55,56} or beyond day 9 in two studies^{16,52} despite persistently high viral RNA loads. One study demonstrated the highest probability of positive culture on day 3 of symptoms.⁵⁵ Arons and colleagues cultured viable virus 6 days before typical symptom onset; however, onset of symptoms was unclear.⁵²

The success of viral isolation correlated with viral load quantified by RT-PCR. No successful viral culture was obtained from samples with a viral load below 1×10^6 copies per mL in one study,³ cycle threshold values higher than 24 in another study,⁵⁵ or higher than 34 in other studies,^{52,56} with culture positivity declining with increasing cycle threshold values.⁵⁶ Several other studies cultured live virus from RT-PCR-positive specimens; however, they did not correlate these results with viral load titres.^{9,57,58}

One study reported the duration of viable virus shedding in respiratory samples; time to clearance from symptom onset was 3–12 days in upper respiratory tract samples and 5–13 days in lower respiratory tract samples, and no positive viral culture was obtained after day 4 in upper respiratory tract infection and day 8 in lower respiratory tract infection.³ Arons and colleagues cultured viable virus from the respiratory tract in one of three asymptomatic cases.⁵²

Viral culture was successful in two of three RT-PCR-positive patients in one study, but the timepoints

	Median (IQR*) duration of SARS-CoV-2 positivity in asymptomatic individuals, days	Viral dynamics in asymptomatic vs symptomatic individuals	p value
Arons et al (2020) ⁵²	Not reported	No difference in viral load	Not reported
Chau et al (2020) ⁵¹	Not reported	Initial viral load similar; asymptomatic individuals had significantly lower viral load during follow-up and faster viral clearance than symptomatic individuals	0.027
Chen et al (2020) ²⁶	6 (4–10)	Significantly shorter duration of viral shedding among asymptomatic cases, with increasing shedding duration associated with increasing illness severity	<0.0001
Han et al (2020) ⁸	Not reported	Symptomatic children had higher initial RNA load in nasopharyngeal swab specimens than asymptomatic children (9.01 vs 6.32 log ₁₀ copies per mL)	0.048
Hu et al (2020) ⁵³	6 (2–12)	Asymptomatic individuals had shorter duration of viral shedding compared with pre-symptomatic individuals (median duration of viral shedding was 6 days [2–12] vs 12 days [12–14])	Not reported
Lavezzo et al (2020) ¹⁴	Not reported	No difference in viral load	p=0.62 (E gene); p=0.74 (RdRp gene)
Le et al (2020) ⁵⁷	9	Not reported	Not applicable
Sakurai et al (2020) ⁴¹	9 (6–11)	Not reported	Not applicable
Yang et al (2020) ⁵⁴	8 (3–12)	Significantly shorter duration of viral shedding from nasopharynx swabs was observed among asymptomatic vs symptomatic individuals	0.001
Yongchen et al (2020) ³⁴	18 (range 5–28)	Longer shedding duration among asymptomatic cases (median 18 days [range 5–28]) vs non-severe (10 days [2–21]) and severe (14 days [9–33]) cases	Not reported
Zhang et al (2020) ¹³	9.6	Initial viral load similar; viral clearance occurred earlier in the asymptomatic (9.6 days) and symptomatic individuals (9.7 days), vs pre-symptomatic group (13.6 days)	<0.05
Zhou et al (2020) ⁵⁰	Not reported	Significantly higher viral load in symptomatic (n=22) vs asymptomatic (n=9) individuals (median cycle threshold value 34.5 [IQR 37.5–39.5] vs 39.0 [32.2–37.0]), but duration of shedding was similar	Not reported

SARS-CoV-2=severe acute respiratory syndrome coronavirus 2. *IQR, if available, unless otherwise stated.

Table 2: SARS-CoV-2 viral dynamics in asymptomatic individuals compared with symptomatic individuals

from symptom onset were not reported.⁵⁹ Andersson and colleagues were unable to culture virus from 27 RT-PCR-positive serum samples.⁶⁰

Of eight studies on SARS-CoV, none reported mean or median duration of viral shedding and thus were not eligible for quantitative analysis. The maximum duration of viral shedding reported was 8 weeks in upper respiratory tract,^{83,84} 52 days in lower respiratory tract,^{83,85} 6–7 weeks in serum,⁸⁶ and 126 days in stool samples.^{83,85,87–89} Studies that evaluated SARS-CoV kinetics found low viral load in the initial days of illness, increasing after the

first week of illness in upper respiratory tract samples, peaking at day 10,⁹⁰ or days 12–14,⁸⁷ and declining after weeks 3–4.⁸⁴ High viral loads correlated with severity of illness and poor survival.⁸⁴ Although Chen and colleagues identified an association between younger age and lower viral titres,⁸⁴ Leong and colleagues found no difference.⁸⁹ Viable SARS-CoV was isolated from stool and respiratory samples up to 4 weeks, and urine specimens up to day 36 from symptom onset.^{83,86} All attempts to isolate virus from RT-PCR-positive stool specimens collected more than 6 weeks after disease onset failed.⁸⁵ The isolation probability for stool samples was approximately five to ten times lower than for respiratory specimens.⁸³

We identified 11 studies on MERS-CoV. Three studies (324 participants) reporting MERS-CoV shedding in the upper respiratory tract^{99–101} and four studies (93 participants) reporting MERS-CoV shedding in the lower respiratory tract^{91,92,96,101} were included in the quantitative analysis. The mean shedding duration was 15.3 days (95% CI 11.6–19.0) in the upper respiratory tract and 16.3 days (13.8–18.9) in the lower respiratory tract (figures 3, 4). Only one study reported duration of viral shedding in serum with a maximum of 34 days.⁹¹ In a small study, mortality was higher in patients with viraemia (viral RNA in blood).⁹² In upper and lower respiratory tract specimens, prolonged shedding was associated with illness severity^{93,94} and survival,⁹⁵ with the shortest duration observed in asymptomatic individuals.⁹³ Peak viral loads were observed between days 7 and 10, and higher viral loads were observed among patients with severe illness and fatal outcome.^{91,93,94,96,97} Differences in viral loads between survivors and fatal cases was more pronounced in the second week of illness (p=0.0006).⁹⁷ The proportion of successful viable culture was 6% in respiratory samples, with a viral load value below 1×10⁷ copies per mL.⁹⁸

All but 11 studies (six cohort studies, two cross-sectional studies, and one randomised controlled trial on SARS-CoV-2 and two cohort studies on MERS-CoV) were case series, the majority of which recruited non-consecutive patients and were therefore prone to possible selection bias (appendix pp 9–13).

Discussion

This systematic review and meta-analysis provides comprehensive data on the viral dynamics of SARS-CoV-2, including the duration of RNA shedding and viable virus isolation. Our findings suggest that, although patients with SARS-CoV-2 infection might have prolonged RNA shedding of up to 83 days in upper respiratory tract infection, no live virus was isolated from culture beyond day 9 of symptoms despite persistently high viral RNA loads. This finding is supported by several studies demonstrating an association between viral load and viability of virus, with no successful culture from samples below a certain viral load threshold. These findings indicate that, in clinical practice, repeat testing might not

be indicated to deem patients no longer infectious. Duration of infectiousness and subsequent isolation timelines could reflect viral load dynamics and could be counted from symptom onset for 10 days in non-severe cases.

SARS-CoV-2 viral load appeared to peak in the upper respiratory tract within the first week after symptom onset, and later in the lower respiratory tract. By contrast, the viral load of SARS-CoV peaked at days 10–14 of illness and that of MERS-CoV peaked at 7–10 days of illness. Combined with isolation of viable virus in respiratory samples primarily within the first week of illness, patients with SARS-CoV-2 infection are likely to be most infectious in the first week of illness, emphasising the importance of immediate isolation with symptom onset early in the course of illness. Several studies report viral load peaks during the prodromal phase of illness or at the time of symptom onset.^{2–4,8,15–21} providing a rationale for the efficient spread of SARS-CoV-2. This finding is supported by the observation in contact-tracing studies that the highest risk of transmission occurs very early in the disease course (a few days before and within the first 5 days after symptom onset).^{103,104} Although modelling studies estimated potential viral load peak before symptom onset, we did not identify any study that confirms pre-symptomatic viral load peak.¹⁵

Similar to SARS-CoV, SARS-CoV-2 can be detected in stool samples for prolonged periods, with high viral loads detected even after 3 weeks of illness. In SARS-CoV, RNA prevalence in stool samples was high, with almost all studies reporting shedding in stools. Although viable SARS-CoV was isolated during up to 4 weeks of illness, faecal–oral transmission was not considered to be a primary driver of infection. By contrast, none of the studies in MERS-CoV reported duration of viral shedding in stool samples and RNA detection was low.^{97,105} So far, only a few studies have demonstrated viable SARS-CoV-2 in stool samples.^{59,106} Thus, the role of faecal shedding in viral transmission remains unclear.

Viral loads appear to be similar between asymptomatic and symptomatic individuals infected with SARS-CoV-2. Nevertheless, most studies demonstrate faster viral clearance among asymptomatic individuals than those who are symptomatic. This finding is in keeping with viral kinetics observed with other respiratory viruses such as influenza and MERS-CoV, in which people with asymptomatic infection have a shorter duration of viral shedding than symptomatic individuals.^{93,107} However, data on the shedding of infectious virus in asymptomatic individuals are too scarce to quantify their transmission potential in order to inform policy on quarantine duration in the absence of testing.

To our knowledge, this is the first systematic review to comprehensively examine and compare SARS-CoV-2, SARS-CoV, and MERS-CoV viral dynamics, and the first meta-analysis of viral shedding duration. Our study has limitations. First, almost all patients in the included

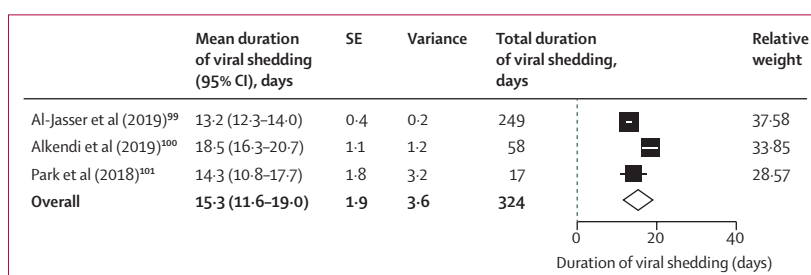


Figure 3: Pooled mean duration (days) of MERS-CoV shedding from the upper respiratory tract (random-effects model)

MERS-CoV=Middle East respiratory syndrome coronavirus.

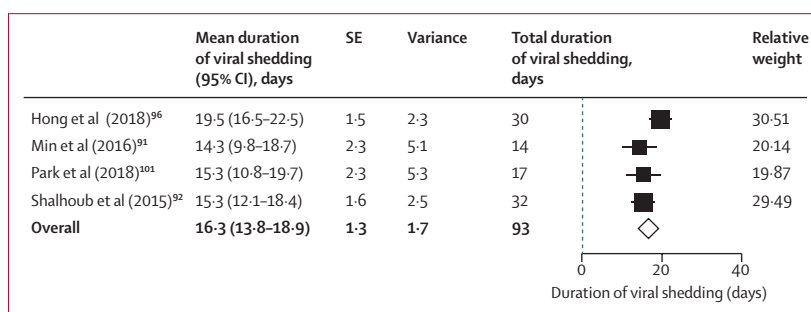


Figure 4: Pooled mean duration (days) of MERS-CoV shedding from the lower respiratory tract (random-effects model)

MERS-CoV=Middle East respiratory syndrome coronavirus.

studies received a range of treatments, which might have modified the shedding dynamics. Second, our meta-analysis identified substantial study heterogeneity, probably due to differences in study population, follow-up, and management approaches. Furthermore, shedding duration is reported as median with IQR for most studies, but meta-analysis necessitates conversion to mean with SD.⁶ The validity of this conversion is based on the assumption that duration of viral shedding is normally distributed, which might not apply to some studies. Last, although there is probably a broad overlap, the true clinical window of infectious shedding might not entirely align with viral culture duration.

We identified a systematic review of SARS-CoV-2 viral load kinetics that included studies published up until May 12, 2020.¹⁰⁸ This review included 26 case reports and 13 case series involving less than five individuals, which did not meet our eligibility criteria; these studies are prone to substantial selection bias, reporting atypical cases with prolonged viral shedding. Additionally, the review included studies that reported viral shedding duration from the time of hospital admission or initial PCR positivity. Furthermore, no meta-analysis of the duration of viral shedding was done.

This review provides detailed understanding about the evidence available so far on viral dynamics of SARS-CoV-2 and has implications for pandemic control strategies and infection control practices. Although SARS-CoV-2 RNA shedding can be prolonged in respiratory and stool

samples, viable virus is short-lived, with culture success associated with viral load levels. Most studies detected the SARS-CoV-2 viral load peak within the first week of illness. These findings highlight that isolation practices should be commenced with the start of first symptoms, including mild and atypical symptoms that precede more typical COVID-19 symptoms. However, given potential delays in the isolation of patients, effective containment of SARS-CoV-2 might be challenging even with an early detection and isolation strategy.¹⁰⁹

Contributors

MC was involved in conceptualisation, methodology, investigation, data curation, and writing of the original draft. MT was involved in investigation, data curation, and writing of the original draft. OL was involved in investigation, data curation, and review and editing of the manuscript. AEM was involved in formal analysis and writing of the original draft. JS was involved in investigation, data curation, and review and editing of the manuscript. AH was involved in conceptualisation, methodology, data curation, writing of the original draft, and supervision of the study.

Declaration of interests

We declare no competing interests.

Data sharing

Data used in this study are available upon request from the corresponding author.

Acknowledgments

We thank Vicki Cormie at the University of St Andrews (Fife, UK) for assistance with the search and obtaining papers not readily accessible.

References

- Cevik M, Bamford CCG, Ho A. COVID-19 pandemic—a focused review for clinicians. *Clin Microbiol Infect* 2020; **26**: 842–47.
- Zou L, Ruan F, Huang M, et al. SARS-CoV-2 viral load in upper respiratory specimens of infected patients. *N Engl J Med* 2020; **382**: 1177–79.
- Wölfel R, Corman VM, Guggemos W, et al. Virological assessment of hospitalized patients with COVID-19. *Nature* 2020; **581**: 465–69.
- Kim ES, Chin BS, Kang CK, et al. Clinical course and outcomes of patients with severe acute respiratory syndrome coronavirus 2 infection: a preliminary report of the first 28 patients from the Korean cohort study on COVID-19. *J Korean Med Sci* 2020; **35**: e142.
- The Joanna Briggs Institute. The Joanna Briggs Institute Critical Appraisal tools for use in JBI systematic reviews. Checklist for case series. 2017. https://joannabriggs.org/sites/default/files/2019-05/JBI_Critical_Appraisal-Checklist_for_Case_Series2017_0.pdf (accessed July 6, 2020).
- Wan X, Wang W, Liu J, Tong T. Estimating the sample mean and standard deviation from the sample size, median, range and/or interquartile range. *BMC Med Res Methodol* 2014; **14**: 135.
- Cai J, Xu J, Lin D, et al. A case series of children with 2019 novel coronavirus infection: clinical and epidemiological features. *Clin Infect Dis* 2020; **71**: 1547–51.
- Han MS, Seong M-W, Kim N, et al. Viral RNA load in mildly symptomatic and asymptomatic children with COVID-19, Seoul, South Korea. *Emerg Infect Dis* 2020; **26**: 2497–99.
- L'Huillier AG, Torriani G, Pigny F, Kaiser L, Eckerle I. Culture-competent SARS-CoV-2 in nasopharynx of symptomatic neonates, children, and adolescents. *Emerg Infect Dis* 2020; **26**: 2494–97.
- Tan YP, Tan BY, Pan J, Wu J, Zeng SZ, Wei HY. Epidemiologic and clinical characteristics of 10 children with coronavirus disease 2019 in Changsha, China. *J Clin Virol* 2020; **127**: 104353.
- Wu Q, Xing Y, Shi L, et al. Epidemiological and clinical characteristics of children with coronavirus disease 2019. *medRxiv* 2020; published online March 26. <https://doi.org/10.1101/2020.03.19.20027078> (preprint).
- Xu Y, Li X, Zhu B, et al. Characteristics of pediatric SARS-CoV-2 infection and potential evidence for persistent fecal viral shedding. *Nat Med* 2020; **26**: 502–05.
- Zhang Z, Xiao T, Wang Y, et al. Early viral clearance and antibody kinetics of COVID-19 among asymptomatic carriers. *medRxiv* 2020; published online May 2. <https://doi.org/10.1101/2020.04.28.20083139> (preprint).
- Lavezzo E, Franchin E, Ciavarella C, et al. Suppression of a SARS-CoV-2 outbreak in the Italian municipality of Vo'. *Nature* 2020; **584**: 425–29.
- He X, Lau EHY, Wu P, et al. Temporal dynamics in viral shedding and transmissibility of COVID-19. *Nat Med* 2020; **26**: 672–75.
- Kujawski SA, Wong KK, Collins JP, et al. Clinical and virologic characteristics of the first 12 patients with coronavirus disease 2019 (COVID-19) in the United States. *Nat Med* 2020; **26**: 861–68.
- Tan W, Lu Y, Zhang J, et al. Viral kinetics and antibody responses in patients with COVID-19. *medRxiv* 2020; published online March 26. <https://doi.org/10.1101/2020.03.24.20042382> (preprint).
- To KK-W, Tsang OT-Y, Leung W-S, et al. Temporal profiles of viral load in posterior oropharyngeal saliva samples and serum antibody responses during infection by SARS-CoV-2: an observational cohort study. *Lancet Infect Dis* 2020; **20**: 565–74.
- Wyllie AL, Fournier J, Casanovas-Massana A, et al. Saliva or nasopharyngeal swab specimens for detection of SARS-CoV-2. *N Engl J Med* 2020; **383**: 1283–86.
- Young BE, Ong SWX, Kalimuddin S, et al. Epidemiologic features and clinical course of patients infected with SARS-CoV-2 in Singapore. *JAMA* 2020; **323**: 1488–94.
- Huang J, Mao T, Li S, et al. Long period dynamics of viral load and antibodies for SARS-CoV-2 infection: an observational cohort study. *medRxiv* 2020; published online April 27. <https://doi.org/10.1101/2020.04.22.20071258> (preprint).
- Zhang N, Gong Y, Meng F, Bi Y, Yang P, Wang F. Virus shedding patterns in nasopharyngeal and fecal specimens of COVID-19 patients. *medRxiv* 2020; published online March 30. <https://doi.org/10.1101/2020.03.28.20043059> (preprint).
- Zheng S, Fan J, Yu F, et al. Viral load dynamics and disease severity in patients infected with SARS-CoV-2 in Zhejiang province, China, January–March 2020: retrospective cohort study. *BMJ* 2020; **369**: m1443.
- Cai Q, Huang D, Ou P, et al. COVID-19 in a designated infectious diseases hospital outside Hubei Province, China. *Allergy* 2020; **75**: 1742–52.
- Chen J, Qi T, Liu L, et al. Clinical progression of patients with COVID-19 in Shanghai, China. *J Infect* 2020; **80**: e1–6.
- Chen X, Zhu B, Hong W, et al. Associations of clinical characteristics and treatment regimens with the duration of viral RNA shedding in patients with COVID-19. *Int J Infect Dis* 2020; **98**: 252–60.
- Chen Y, Chen L, Deng Q, et al. The presence of SARS-CoV-2 RNA in the feces of COVID-19 patients. *J Med Virol* 2020; **92**: 833–40.
- Fan L, Liu C, Li N, et al. Medical treatment of 55 patients with COVID-19 from seven cities in northeast China who fully recovered: a single-center, retrospective, observational study. *medRxiv* 2020; published online March 30. <https://doi.org/10.1101/2020.03.28.20045955> (preprint).
- Fang Z, Zhang Y, Hang C, Ai J, Li S, Zhang W. Comparisons of viral shedding time of SARS-CoV-2 of different samples in ICU and non-ICU patients. *J Infect* 2020; **81**: 147–78.
- Liu Y, Yan L-M, Wan L, et al. Viral dynamics in mild and severe cases of COVID-19. *Lancet Infect Dis* 2020; **20**: 656–57.
- Shi J, Cheng C, Yu M, et al. Systemic inflammatory cytokines associate with SARS-CoV-2 viral shedding time in Covid-19 inpatients. *Res Sq* 2020; published online May 29. <https://doi.org/10.21203/rs.3.rs-31556/v1> (preprint).
- Tan L, Kang X, Ji X, et al. Validation of predictors of disease severity and outcomes in COVID-19 patients: a descriptive and retrospective study. *Med* 2020; published online May 19. <https://doi.org/10.1016%2Fj.medj.2020.05.002>.
- Zhou F, Yu T, Du R, et al. Clinical course and risk factors for mortality of adult inpatients with COVID-19 in Wuhan, China: a retrospective cohort study. *Lancet* 2020; **395**: 1054–62.
- Yongchen Z, Shen H, Wang X, et al. Different longitudinal patterns of nucleic acid and serology testing results based on disease severity of COVID-19 patients. *Emerg Microbes Infect* 2020; **9**: 833–36.
- Hu X, Xing Y, Jia J, et al. Factors associated with negative conversion of viral RNA in patients hospitalized with COVID-19. *Sci Total Environ* 2020; **728**: 138812.

- 36 Xu K, Chen Y, Yuan J, et al. Factors associated with prolonged viral RNA shedding in patients with coronavirus disease 2019 (COVID-19). *Clin Infect Dis* 2020; **71**: 799–806.
- 37 Yan D, Liu X-Y, Zhu YN, et al. Factors associated with prolonged viral shedding and impact of lopinavir/ritonavir treatment in hospitalised non-critically ill patients with SARS-CoV-2 infection. *Eur Respir J* 2020; **56**: 2000799.
- 38 Wu Y, Guo C, Tang L, et al. Prolonged presence of SARS-CoV-2 viral RNA in faecal samples. *Lancet Gastroenterol Hepatol* 2020; **5**: 434–35.
- 39 Tian D, Wang L, Wang X, et al. Clinical research and factors associated with prolonged duration of viral shedding in patients with COVID-19. *Res Sq* 2020; published online June 1. <https://doi.org/10.21203/rs.3.rs-29818/v1> (preprint).
- 40 Zhou B, She J, Wang Y, Ma X. The duration of viral shedding of discharged patients with severe COVID-19. *Clin Infect Dis* 2020; published online April 17. <https://doi.org/10.1093/cid/ciaa451>.
- 41 Sakurai A, Sasaki T, Kato S, et al. Natural history of asymptomatic SARS-CoV-2 infection. *N Engl J Med* 2020; **383**: 885–86.
- 42 Talmy T, Tsur A, Shabtay O. Duration of SARS-CoV-2 detection in Israel Defense Forces soldiers with mild COVID-19. *J Med Virol* 2020; published online July 30. <https://doi.org/10.1002/jmv.26374>.
- 43 Xiao AT, Tong YX, Zhang S. Profile of RT-PCR for SARS-CoV-2: a preliminary study from 56 COVID-19 patients. *Clin Infect Dis* 2020; published online April 19. <https://doi.org/10.1093/cid/ciaa460>.
- 44 Shastri A, Wheat J, Agrawal S, et al. Delayed clearance of SARS-CoV2 in male compared to female patients: high ACE2 expression in testes suggests possible existence of gender-specific viral reservoirs. *medRxiv* 2020; published online April 17. <https://doi.org/10.1101/2020.04.16.20060566> (preprint).
- 45 Ling Y, Xu S-B, Lin Y-X, et al. Persistence and clearance of viral RNA in 2019 novel coronavirus disease rehabilitation patients. *Chin Med J* 2020; **133**: 1039–43.
- 46 Zha L, Li S, Pan L, et al. Corticosteroid treatment of patients with coronavirus disease 2019 (COVID-19). *Med J Aust* 2020; **212**: 416–20.
- 47 Liang M, Chen P, He M, et al. Corticosteroid treatment in critically ill patients with COVID-19: a retrospective cohort study. *Res Sq* 2020; published online May 11. <https://doi.org/10.21203/rs.3.rs-27386/v1> (preprint).
- 48 Hung IFN, Lung KC, Tso EYK, et al. Triple combination of interferon beta-1b, lopinavir-ritonavir, and ribavirin in the treatment of patients admitted to hospital with COVID-19: an open-label, randomised, phase 2 trial. *Lancet* 2020; **395**: 1695–704.
- 49 Huang H, Guan L, Yang Y, et al. Chloroquine, arbidol (umifenovir) or lopinavir/ritonavir as the antiviral monotherapy for COVID-19 patients: a retrospective cohort study. *Res Sq* 2020; published online April 24. <https://doi.org/10.21203/rs.3.rs-24667/v1> (preprint).
- 50 Zhou R, Li F, Chen F, et al. Viral dynamics in asymptomatic patients with COVID-19. *Int J Infect Dis* 2020; **96**: 288–90.
- 51 Chau NVV, Thanh Lam V, Thanh Dung N, et al. The natural history and transmission potential of asymptomatic SARS-CoV-2 infection. *Clin Infect Dis* 2020; published online June 4. <https://doi.org/10.1093/cid/ciaa711>.
- 52 Arons MM, Hatfield KM, Reddy SC, et al. Presymptomatic SARS-CoV-2 infections and transmission in a skilled nursing facility. *N Engl J Med* 2020; **382**: 2081–90.
- 53 Hu Z, Song C, Xu C, et al. Clinical characteristics of 24 asymptomatic infections with COVID-19 screened among close contacts in Nanjing, China. *Sci China Life Sci* 2020; **63**: 706–11.
- 54 Yang R, Gui X, Xiong Y. Comparison of clinical characteristics of patients with asymptomatic vs symptomatic coronavirus disease 2019 in Wuhan, China. *JAMA New Open* 2020; **3**: e2010182.
- 55 Bullard J, Dust K, Funk D, et al. Predicting infectious severe acute respiratory syndrome coronavirus 2 from diagnostic samples. *Clin Infect Dis* 2020; published online May 22. <https://doi.org/10.1093/cid/ciaa638>.
- 56 La Scola B, Le Bideau M, Andreani J, et al. Viral RNA load as determined by cell culture as a management tool for discharge of SARS-CoV-2 patients from infectious disease wards. *Eur J Clin Microbiol Infect Dis* 2020; **39**: 1059–61.
- 57 Le TQM, Takemura T, Moi ML, et al. Severe acute respiratory syndrome coronavirus 2 shedding by travelers, Vietnam, 2020. *Emerg Infect Dis* 2020; **26**: 1624–26.
- 58 To KK-W, Tsang OT-Y, Yip CC-Y, et al. Consistent detection of 2019 novel coronavirus in saliva. *Clin Infect Dis* 2020; **71**: 841–43.
- 59 Xiao F, Sun J, Xu Y, et al. Infectious SARS-CoV-2 in feces of patient with severe COVID-19. *Emerg Infect Dis J* 2020; **26**: 1920–22.
- 60 Andersson M, Arancibia-Carcamo CV, Auckland K, et al. SARS-CoV-2 RNA detected in blood samples from patients with COVID-19 is not associated with infectious virus. *medRxiv* 2020; published online June 17. <https://doi.org/10.1101/2020.05.21.20105486> (preprint).
- 61 Chang D, Mo G, Yuan X, et al. Time kinetics of viral clearance and resolution of symptoms in novel coronavirus infection. *Am J Respir Crit Care Med* 2020; **201**: 1150–52.
- 62 Chen X, Ling J, Mo P, et al. Restoration of leukomonocyte counts is associated with viral clearance in COVID-19 hospitalized patients. *medRxiv* 2020; published online March 6. <https://doi.org/10.1101/2020.03.03.20030437> (preprint).
- 63 Corman VM, Rabenau HF, Adams O, et al. SARS-CoV-2 asymptomatic and symptomatic patients and risk for transfusion transmission. *Transfusion* 2020; **60**: 1119–22.
- 64 Fu S, Fu X, Song Y, et al. Virologic and clinical characteristics for prognosis of severe COVID-19: a retrospective observational study in Wuhan, China. *medRxiv* 2020; published online April 6. <https://doi.org/10.1101/2020.04.03.20051763> (preprint).
- 65 Huang L, Chen Z, Ni L, et al. Impact of angiotensin-converting enzyme inhibitors and angiotensin receptor blockers on inflammatory responses and viral clearance in COVID-19 patients: a multicenter retrospective cohort study. *Res Sq* 2020; published online May 8. <https://doi.org/10.21203/rs.3.rs-27366/v1> (preprint).
- 66 Li N, Wang X, Lv T. Prolonged SARS-CoV-2 RNA shedding: not a rare phenomenon. *J Med Virol* 2020; **92**: 2286–87.
- 67 Liu L, Liu W, Zheng Y, et al. A preliminary study on serological assay for severe acute respiratory syndrome coronavirus 2 (SARS-CoV-2) in 238 admitted hospital patients. *Microbes Infect* 2020; **22**: 206–11.
- 68 Lo IL, Lio CF, Cheong HH, et al. Evaluation of SARS-CoV-2 RNA shedding in clinical specimens and clinical characteristics of 10 patients with COVID-19 in Macau. *Int J Biol Sci* 2020; **16**: 1698–707.
- 69 Lou B, Li T-D, Zheng S-F, et al. Serology characteristics of SARS-CoV-2 infection after exposure and post-symptom onset. *Eur Respir J* 2020; **56**: 2000763.
- 70 Pongpirul WA, Mott JA, Woodring JV, et al. Clinical characteristics of patients hospitalized with coronavirus disease, Thailand. *Emerg Infect Dis* 2020; **26**: 1580–85.
- 71 Qian GQ, Chen XQ, Lv DF, et al. Duration of SARS-CoV-2 viral shedding during COVID-19 infection. *Infect Dis* 2020; **52**: 511–12.
- 72 Quan W, Zheng Q, Tian J, et al. No SARS-CoV-2 in expressed prostatic secretion of patients with coronavirus disease 2019: a descriptive multicentre study in China. *medRxiv* 2020; published online March 30. <https://doi.org/10.1101/2020.03.26.20044198> (preprint).
- 73 Seah IYJ, Anderson DE, Kang AEZ, et al. Assessing viral shedding and infectivity of tears in coronavirus disease 2019 (COVID-19) patients. *Ophthalmology* 2020; **127**: 977–79.
- 74 Song C, Wang Y, Li W, et al. Detection of 2019 novel coronavirus in semen and testicular biopsy specimen of COVID-19 patients. *medRxiv* 2020; published online April 10. <https://doi.org/10.1101/2020.03.31.20042333> (preprint).
- 75 Song R, Han B, Song M, et al. Clinical and epidemiological features of COVID-19 family clusters in Beijing, China. *J Infect* 2020; **81**: e26–30.
- 76 Tu Y-H, Wei Y-Y, Zhang D-W, Chen C-S, Hu X-W, Fei G. Analysis of factors affected the SARS-CoV-2 viral shedding time of COVID-19 patients in Anhui, China: a retrospective study. *Res Sq* 2020; published online April 6. <https://doi.org/10.21203/rs.3.rs-20954/v1> (preprint).
- 77 Wang L, Gao Y-h, Lou L-L, Zhang G-J. The clinical dynamics of 18 cases of COVID-19 outside of Wuhan, China. *Eur Respir J* 2020; **55**: 2000398.
- 78 Wang S, Tu J, Sheng Y. Clinical characteristics and fecal-oral transmission potential of patients with COVID-19. *medRxiv* 2020; published online May 6. <https://doi.org/10.1101/2020.05.02.20089094> (preprint).
- 79 Wu B, Lei Z-Y, Wu K-L, et al. Epidemiological and clinical features of imported and local patients with coronavirus disease 2019 (COVID-19) in Hainan, China. *SSRN* 2020; published online March 24. <https://doi.org/10.2139/ssrn.3555222> (preprint).

- 80 Xu L, Zhang X, Song W, et al. Conjunctival polymerase chain reaction-tests of 2019 novel coronavirus in patients in Shenyang, China. *medRxiv* 2020; published online Feb 25. <https://doi.org/10.1101/2020.02.23.20024935> (preprint).
- 81 Yang Y, Yang M, Shen C, et al. Evaluating the accuracy of different respiratory specimens in the laboratory diagnosis and monitoring the viral shedding of 2019-nCoV infections. *medRxiv* 2020; published online Feb 17. <https://doi.org/10.1101/2020.02.11.20021493> (preprint).
- 82 Zhu L, Gong N, Liu B, et al. Coronavirus disease 2019 pneumonia in immunosuppressed renal transplant recipients: a summary of 10 confirmed cases in Wuhan, China. *Eur Urol* 2020; **18**: 18.
- 83 Chan PK, To WK, Ng KC, et al. Laboratory diagnosis of SARS. *Emerg Infect Dis* 2004; **10**: 825–31.
- 84 Chen WJ, Yang JY, Lin JH, et al. Nasopharyngeal shedding of severe acute respiratory syndrome-associated coronavirus is associated with genetic polymorphisms. *Clin Infect Dis* 2006; **42**: 1561–69.
- 85 Liu W, Tang F, Fontanet A, et al. Long-term SARS coronavirus excretion from patient cohort, China. *Emerg Infect Dis* 2004; **10**: 1841–43.
- 86 Xu D, Zhang Z, Jin L, et al. Persistent shedding of viable SARS-CoV in urine and stool of SARS patients during the convalescent phase. *Eur J Clin Microbiol Infect Dis* 2005; **24**: 165–71.
- 87 Cheng PK, Wong DA, Tong LK, et al. Viral shedding patterns of coronavirus in patients with probable severe acute respiratory syndrome. *Lancet* 2004; **363**: 1699–700.
- 88 Kwan BC, Leung CB, Szeto CC, et al. Severe acute respiratory syndrome in dialysis patients. *J Am Soc Nephrol* 2004; **15**: 1883–88.
- 89 Leong HN, Chan KP, Khan AS, et al. Virus-specific RNA and antibody from convalescent-phase SARS patients discharged from hospital. *Emerg Infect Dis* 2004; **10**: 1745–50.
- 90 Peiris JSM, Chu CM, Cheng VCC, et al. Clinical progression and viral load in a community outbreak of coronavirus-associated SARS pneumonia: a prospective study. *Lancet* 2003; **361**: 1767–72.
- 91 Min CK, Cheon S, Ha NY, et al. Comparative and kinetic analysis of viral shedding and immunological responses in MERS patients representing a broad spectrum of disease severity. *Sci Rep* 2016; **6**: 25359.
- 92 Shalhoub S, Farahat F, Al-Jiffri A, et al. IFN- α 2a or IFN- β 1a in combination with ribavirin to treat Middle East respiratory syndrome coronavirus pneumonia: a retrospective study. *J Antimicrob Chemother* 2015; **70**: 2129–32.
- 93 Al Hosani FI, Pringle K, Al Mulla M, et al. Response to emergence of Middle East respiratory syndrome coronavirus, Abu Dhabi, United Arab Emirates, 2013–2014. *Emerg Infect Dis* 2016; **22**: 1162–68.
- 94 Oh MD, Park WB, Choe PG, et al. Viral load kinetics of MERS coronavirus infection. *N Engl J Med* 2016; **375**: 1303–05.
- 95 Arabi YM, Al-Omari A, Mandourah Y, et al. Critically ill patients with the Middle East respiratory syndrome: a multicenter retrospective cohort study. *Crit Care Med* 2017; **45**: 1683–95.
- 96 Hong KH, Choi JP, Hong SH, et al. Predictors of mortality in Middle East respiratory syndrome (MERS). *Thorax* 2018; **73**: 286–89.
- 97 Corman VM, Albarrak AM, Omrani AS, et al. Viral shedding and antibody response in 37 patients with Middle East respiratory syndrome coronavirus infection. *Clin Infect Dis* 2016; **62**: 477–83.
- 98 Muth D, Corman VM, Meyer B, et al. Infectious Middle East respiratory syndrome coronavirus excretion and serotype variability based on live virus isolates from patients in Saudi Arabia. *J Clin Microbiol* 2015; **53**: 2951–55.
- 99 Al-Jasser FS, Nouh RM, Youssef RM. Epidemiology and predictors of survival of MERS-CoV infections in Riyadh region, 2014–2015. *J Infect Public Health* 2019; **12**: 171–77.
- 100 Alkendi F, Nair SC, Hashmeyer R. Descriptive epidemiology, clinical characteristics and outcomes for Middle East respiratory syndrome coronavirus (MERS-CoV) infected patients in AlAin – Abu Dhabi Emirate. *J Infect Public Health* 2019; **12**: 137.
- 101 Park WB, Poon LLM, Choi SJ, et al. Replicative virus shedding in the respiratory tract of patients with Middle East respiratory syndrome coronavirus infection. *Int J Infect Dis* 2018; **72**: 8–10.
- 102 Wang Y, Zhang D, Du G, et al. Remdesivir in adults with severe COVID-19: a randomised, double-blind, placebo-controlled, multicentre trial. *Lancet* 2020; **395**: 1569–78.
- 103 Wang Y, Tian H, Zhang L, et al. Reduction of secondary transmission of SARS-CoV-2 in households by face mask use, disinfection and social distancing: a cohort study in Beijing, China. *BMJ Glob Health* 2020; **5**: e002794.
- 104 Cheng H-Y, Jian S-W, Liu D-P, Ng TC, Huang WT, Lin HH. Contact tracing assessment of COVID-19 transmission dynamics in Taiwan and risk at different exposure periods before and after symptom onset. *JAMA Intern Med* 2020; **180**: 1156–63.
- 105 Memish A. Viral shedding and antibody response in MERS. *Vox Sang* 2016; **111** (suppl 1): 48–49.
- 106 Wang W, Xu Y, Gao R, et al. Detection of SARS-CoV-2 in different types of clinical specimens. *JAMA* 2020; **323**: 1843–44.
- 107 Ip DKM, Lau LLH, Leung NHL, et al. Viral shedding and transmission potential of asymptomatic and paucisymptomatic influenza virus infections in the community. *Clin Infect Dis* 2017; **64**: 736–42.
- 108 Walsh KA, Jordan K, Clyne B, et al. SARS-CoV-2 detection, viral load and infectivity over the course of an infection. *J Infect* 2020; **81**: 357–71.
- 109 Kretzschmar ME, Rozhnova G, Bootsma MCJ, van Boven M, van de Wijgert JHHM, Bonten MJM. Impact of delays on effectiveness of contact tracing strategies for COVID-19: a modelling study. *Lancet Public Health* 2020; **5**: e452–59.

Surgical mask partition reduces the risk of non-contact transmission in a golden Syrian hamster model for Coronavirus Disease 2019 (COVID-19)

Jasper Fuk-Woo Chan^{1,2,3,a}, Shuofeng Yuan^{1,a}, Anna Jinxia Zhang^{1,a}, Vincent Kwok-Man Poon¹, Chris Chung-Sing Chan¹, Andrew Chak-Yiu Lee¹, Zhimeng Fan¹, Can Li¹, Ronghui Liang¹, Jianli Cao¹, Kaiming Tang¹, Cuiting Luo¹, Vincent Chi-Chung Cheng³, Jian-Piao Cai¹, Hin Chu¹, Kwok-Hung Chan¹, Kelvin Kai-Wang To^{1,2,3}, Siddharth Sridhar^{1,2,3}, Kwok-Yung Yuen^{1,2,3}

¹State Key Laboratory of Emerging Infectious Diseases, Carol Yu Centre for Infection, Department of Microbiology, Li Ka Shing Faculty of Medicine, The University of Hong Kong, Pokfulam, Hong Kong Special Administrative Region, China.

²Department of Clinical Microbiology and Infection Control, The University of Hong Kong-Shenzhen Hospital, Shenzhen, China.

³Department of Microbiology, Queen Mary Hospital, Pokfulam, Hong Kong Special Administrative Region, China.

^aJ.F.-W.C., S.Y., and A.J.Z. contributed equally to this work.

Correspondence: Kwok-Yung Yuen (kyyuen@hku.hk), State Key Laboratory of Emerging Infectious Diseases, Carol Yu Centre for Infection, Department of Microbiology, Li Ka Shing Faculty of Medicine, The University of Hong Kong, Pokfulam, Hong Kong Special Administrative Region, China. Tel: 852-22552402. Fax: 852-28551241.

Summary:

Non-contact transmission of SARS-CoV-2 was demonstrated in a Syrian hamster model. Surgical mask partition significantly reduced the transmission of SARS-CoV-2 from challenged index hamsters to the exposed naïve hamsters via respiratory droplets and/or airborne droplet nuclei.

Accepted Manuscript

ABSTRACT

Background. Coronavirus disease 2019 (COVID-19) caused by severe acute respiratory syndrome coronavirus 2 (SARS-CoV-2) is believed to be mostly transmitted by medium-to-large sized respiratory droplets although airborne transmission is theoretically possible in healthcare settings involving aerosol-generating procedures. Exposure to respiratory droplets can theoretically be reduced by surgical mask usage. However, there is a lack of experimental evidence supporting surgical mask usage for prevention of COVID-19.

Methods. We used a well-established golden Syrian hamster SARS-CoV-2 model. We placed SARS-CoV-2-challenged index hamsters and naïve hamsters into closed system units each comprising two different cages separated by a polyvinyl chloride air porous partition with unidirectional airflow within the isolator. The effect of a surgical mask partition placed in between the cages was investigated. Besides clinical scoring, hamster specimens were tested for viral load, histopathology, and viral nucleocapsid antigen expression.

Results. Non-contact transmission was found in 66.7% (10/15) of exposed naïve hamsters. Surgical mask partition for challenged index or naïve hamsters significantly reduced transmission to 25% (6/24, $P=0.018$). Surgical mask partition for challenged index hamsters significantly reduced transmission to only 16.7% (2/12, $P=0.019$) of exposed naïve hamsters. Unlike the severe COVID-19 manifestations of challenged hamsters, infected naïve hamsters had lower clinical scores, milder histopathological changes, and lower viral nucleocapsid antigen expression in respiratory tract tissues.

Conclusions. SARS-CoV-2 could be transmitted by respiratory droplets or airborne droplet nuclei in the hamster model. Such transmission could be reduced by surgical mask usage, especially when masks were worn by infected individuals.

Keywords: coronavirus; COVID-19; SARS-CoV-2; mask; transmission.

Accepted Manuscript

The source of the 2003 severe acute respiratory syndrome (SARS) epidemic was traced to civets in live animal markets, and ultimately to Chinese horseshoe bats in the wild.¹⁻³ The epidemiological significance of the large number of bat SARS-related coronaviruses subsequently found in horseshoe and other bat species was not fully appreciated for the last 17 years.^{4, 5} In late 2019, infection due to a novel *betacoronavirus* named severe acute respiratory syndrome coronavirus 2 (SARS-CoV-2), which is phylogenetically close to bat SARS-related coronaviruses, was reported in patients with epidemiological link to a market with wild mammal trade in Wuhan, China.⁶⁻⁸ SARS-CoV-2 infection causing Coronavirus Disease 2019 (COVID-19) was initially recognized as an acute febrile pneumonia with lymphopenia and multifocal peripheral ground glass changes on thoracic computerized tomography.⁹⁻¹¹ COVID-19 is often self-limiting, but may have severe manifestations such as silent (asymptomatic until sudden collapse) hypoxia, acute respiratory distress syndrome (ARDS), thrombocytopenia and disseminated intravascular coagulation with diffuse microvascular thrombosis, deep venous thrombosis with pulmonary embolism, and/or multi-organ failure.^{9, 10, 12, 13} Gastrointestinal manifestations such as diarrhea, neurological manifestations such as meningoencephalitis and Guillain-Barré syndrome, and Kawasaki syndrome-like multi-systemic inflammatory disorder in children have also been reported.¹⁴⁻¹⁶ However, most symptomatic patients have mild to moderate respiratory illness with manifestations such as rhinorrhea, sore throat, cough, conjunctivitis, anosmia, and ageusia.^{17, 18} Furthermore, a high proportion of patients with COVID-19 have subclinical infections, which is believed to enable efficient person-to-person transmission in both community and hospital settings. This renders symptom screening at borders ineffective, entails extensive testing and isolation of infected individuals, require labor-intensive contact tracing measures, and necessitates social distancing or lockdowns. As a result, the ongoing COVID-19

pandemic has already affected more than 4 million patients with over 280,000 deaths in just 5 months.¹⁹

Although COVID-19 is believed to be transmitted by respiratory droplet and direct or indirect contact, no clear experimental evidence for this has been reported. Based on *in silico* estimates of the binding affinity of angiotensin-converting enzyme 2 (ACE2) of common laboratory mammals and the receptor-binding domain of the surface spike protein of SARS-CoV-2, we recently established a golden Syrian hamster model for COVID-19.²⁰ SARS-CoV-2-infected hamsters developed clinical signs of rapid breathing, weight loss, and histopathological changes of ARDS.²⁰ Using this animal model, we showed that SARS-CoV-2-challenged index hamsters consistently infected co-housed naïve hamsters, confirming virus transmission by direct or indirect contact.²⁰ However, the controversies of whether there is transmission by respiratory droplets or airborne droplet nuclei, and whether the wearing of surgical mask by the virus shedder or by the susceptible individual is useful for the prevention of transmission, are still unsettled. In this study, using our hamster model for COVID-19, we confirmed non-contact transmission of SARS-CoV-2 which could potentially be prevented by surgical mask worn by the infected or by the susceptible host.

METHODS

Virus and biosafety

SARS-CoV-2 was isolated from the nasopharyngeal aspirate specimen of a laboratory-confirmed COVID-19 patient in Hong Kong.²¹ The plaque purified viral isolate was amplified by one additional passage in VeroE6 cells to make working stocks of the virus as described previously.²¹ All experiments involving live SARS-CoV-2 followed the approved standard operating procedures of the Biosafety Level (BSL)-3 facility of The University of Hong Kong (HKU).^{22, 23}

Animals

Approval was obtained from the HKU Committee on the Use of Live Animals in Teaching and Research. Male and female Syrian hamsters, aged 6-10 weeks old, were obtained from the Chinese University of Hong Kong Laboratory Animal Service Centre through the HKU Laboratory Animal Unit. The animals were kept in BSL-2 housing and given access to standard pellet feed and water ad libitum until virus challenge in our BSL-3 animal facility. The animal rooms were kept at 25°C and 50% humidity.

Non-contact transmission model set-up

To study the transmissibility of SARS-CoV-2 among hamsters through non-contact transmission, we housed SARS-CoV-2-challenged index hamsters and naïve hamsters together in closed systems. The closed systems were kept in isolators (Tecniplast SpA, Varese, Italy) to prevent leakage of contaminated air to the external environment (Figure 1A). Each closed system contained two cages (Marukan Co., Ltd., Osaka, Japan) separated by a polyvinyl chloride air porous partition with unidirectional airflow maintained by an electrically powered fan from the cage housing one SARS-CoV-2-challenged index hamster towards the cage housing three naïve hamsters (Figure 1B). Each system had either no surgical mask partition or a fully knitted layer of partition made of surgical mask (A. R. Medicom Inc. (Asia) Ltd., Hong Kong, China) fulfilling the ASTM F2100 Level 1 standard placed on the polyvinyl chloride air porous partition between the cages to assess the effect of the surgical mask partition in this hamster model (Figure 1C). There were two or three closed systems per isolator.

Animal challenge and transmission experiments

Three sets of experiments were conducted using our isolator non-contact transmission model. In the first experiment, no mask partition was placed between the two cages in each system to investigate whether non-contact transmission occurred among the hamsters (Figure 2). A total of five systems housing 20 hamsters were included in the first experiment. In the second experiment, to simulate the situation when surgical masks are worn by a SARS-CoV-2-infected person, a fully knitted partition layer using surgical mask was placed on the polyvinyl chloride air porous partition between the cages with the outer fluid-repellent layer (the blue side) facing the exposed-naïve hamsters to prevent emitted respiratory droplets containing SARS-CoV-2 from the challenged index hamster from reaching exposed naïve hamsters (Figure 3A). A total of four systems housing 16 hamsters were included in the second experiment. In the third experiment, to simulate the situation when close contacts of a SARS-CoV-2-infected person wear surgical masks, the surgical mask partition with the outer fluid-repellent layer (the blue side) facing the challenged index hamsters was placed on the polyvinyl chloride air porous partition between the cages to prevent droplets containing SARS-CoV-2 emitted by the challenged index hamster from reaching the exposed naïve hamsters (Figure 3B). A total of four systems housing 16 hamsters were included in the third experiment. The air velocities from the challenged index hamster's cage to the exposed naïve hamsters' cage in the three experiments were shown in Table 1.

At day 0, a challenge dose of 100µl of Dulbecco's Modified Eagle Medium (DMEM) containing 10^5 plaque-forming units of SARS-CoV-2 was intranasally inoculated to the index hamster in each system under intraperitoneal ketamine (200mg/kg) and xylazine (10mg/kg) anaesthesia as we described previously.²⁰ Twenty-four hours later, three naïve hamsters were transferred to the cage adjacent and exposed to the cage housing the virus-challenged index hamster per system. The animals were monitored daily for clinical signs of disease. Two of

the three exposed naïve hamsters in each system were sacrificed at 5 days post-inoculation (dpi) (4 days after exposure). The challenged index animal and remaining exposed naïve animal in each system were then sacrificed at 7dpi. The animals' organ tissues at necropsy were separated into two parts, one immediately fixed in 10% PBS-buffered formalin for histopathological analysis, and the other immediately frozen at -80°C until use for viral load studies as we described previously.^{20, 24, 25} Serum samples were used for neutralizing antibody detection as we described previously.²⁰ To compare the histopathological changes at 5dpi, an additional control SARS-CoV-2-challenged hamster was sacrificed at 5dpi.

Statistical analysis

All data were analysed with GraphPad Prism software (GraphPad Software, Inc). Fisher's exact test was used to compare the rate of infection between the different groups of hamsters with or without surgical mask partition. Student's t-test was used to determine significant differences in clinical scores and virus loads between different groups.²⁰ $P < 0.05$ was considered statistically significant.

RESULTS

Non-contact transmission of SARS-CoV-2 among hamsters

Consistent with our previous findings, all 13 (n=5, 4, and 4 for experiments 1, 2, and 3, respectively) SARS-CoV-2-challenged index hamsters developed clinical signs of lethargy, ruffled furs, hunched back posture, and rapid breathing starting at 2dpi, and had virological and histological evidence of infection.²⁰ In the first experiment, six of the ten (60%) exposed naïve hamsters sacrificed at 5dpi (4 days after exposure) also developed similar clinical signs. The overall mean clinical score of the 10 exposed naïve hamsters was 1.800 ± 1.687 (Table 2). The 6 naïve hamsters which developed clinical signs were confirmed to be infected with

SARS-CoV-2 as evidenced by positive RT-PCR results (Table 3). The viral loads ranged from around 0.1 to 1000 genome copies/ β -actin (nasal turbinate), 0.1 to 100 genome copies/ β -actin (trachea), and 0.02 to 10 genome copies/ β -actin (lung) (Figure 4A). At 7 dpi (6 days after exposure), the remaining 5 naïve hamsters had a mean clinical score of 2.400 ± 1.517 . Four of the five (80.0%) exposed naïve hamsters were found to be infected, with viral loads of around 100 to 1000 genome copies/ β -actin (nasal turbinate), 10 to 100 genome copies/ β -actin (trachea), and 0.1 to 100 genome copies/ β -actin (lung) (Figure 4B). None of the index and naïve hamsters died.

Non-contact transmission of SARS-CoV-2 among hamsters with surgical mask partition

Having demonstrated that non-contact transmission of SARS-CoV-2 occurred among the hamsters in our model, we next investigated the effectiveness of surgical mask partition to reduce the risk of non-contact transmission. Surgical mask partition between cages was installed with the external fluid-repelling surface facing the exposed naïve hamsters or the challenged index hamsters to mimic the situation of the mask being worn by index hamsters or by exposed naïve contact hamsters, respectively.

In the second experiment in which the external surface of the mask was facing the naïve hamsters, at 5 dpi (4 days after exposure), two of the three naïve hamsters in each system (n=8) were sacrificed. Only 1 out of 8 (12.5%) naïve hamsters was SARS-CoV-2 RT-PCR-positive (Table 3). The viral loads of this hamster were about 1 (nasal turbinate), 100 (trachea), and 10 (lung) genome copies/ β -actin (Figure 4A). At 7 dpi, the remaining exposed naïve hamster (n=4) and the SARS-CoV-2-challenged index hamster (n=4) in each system were also sacrificed. Only one of the four (25.0%) remaining naïve hamsters were RT-PCR-positive, with viral loads of around 0.5 (lung) to 100 (nasal turbinate) genome copies/ β -actin

(Figure 4B). This transmission rate (16.7%) was significantly ($P=0.019$) lower than that of the exposed naïve hamsters without surgical mask partition (66.7%).

In the third experiment, the external surface of the mask was facing the challenged index hamsters. At 5 dpi (4 days after exposure), two of the three naïve hamsters in each system ($n=8$) were sacrificed. Three out of 8 (37.5%) exposed naïve hamsters developed clinical signs and were SARS-CoV-2 RT-PCR positive (Table 3). The viral loads ranged from around 1 to 10 genome copies/ β -actin (nasal turbinate), 0.01 to 100 (trachea) genome copies/ β -actin, and 1 to 1000 genome copies/ β -actin (lung) (Figure 4A). At 7 dpi, the remaining exposed naïve hamster ($n=4$) and the challenged index hamster ($n=4$) in each system were also sacrificed. One of the four (25.0%) remaining naïve hamsters were RT-PCR positive, with viral loads of around 1 (lung) to 100 (nasal turbinate) genome copies/ β -actin (Figure 4B). This transmission rate (33.3%) was also lower than that of the exposed naïve hamsters without surgical mask partition (66.7%), although not reaching statistical significance ($P=0.128$).

Immunological response in hamsters infected by SARS-CoV-2 through non-contact transmission

At 7 dpi (6 days after exposure of the naïve hamsters to the challenged index hamsters), all challenged index hamsters ($n=13$) exhibited high titers of serum neutralizing antibodies, ranging from 1:320 to $\geq 1:640$, which is consistent with our previous observation (Figure 5). Interestingly, three of the five exposed (60%) naïve hamsters without surgical mask partition sacrificed at 7 dpi also developed serum neutralizing antibody titers of 1:160 to 1:640, which suggested that these three RT-PCR-positive infected naïve hamsters likely acquired the virus very early after exposure to the challenged index hamsters as it required 5 to 7 days before serum neutralizing antibodies were detectable in this animal model. In contrast, none of the 8

exposed naïve hamsters with surgical mask partition facing either side sacrificed at 7 dpi, including the two RT-PCR-positive hamsters, developed detectable serum neutralizing antibody (all $<1:20$). These results suggested that even though these two exposed naïve hamsters were infected, they likely acquired the virus much later than the infected naïve hamsters without protection by surgical mask partition.

Histological features of hamsters infected by SARS-CoV-2 through non-contact transmission

The representative histological and immunofluorescent staining findings of the infected naïve hamsters are shown in Figure 6. At 5dpi (4 days after exposure), the histopathological changes of the infected naïve hamsters in experiments 1, 2, and 3, were generally milder than those of the challenged control hamster (Figure 6A, a to d). In the infected naïve hamsters, the nasal turbinate only showed mild degree of epithelium cells swelling and submucosal infiltration, whereas there were severe epithelial cell death, desquamation, and massive submucosal infiltration in the challenged control hamster. Similarly, the histopathological changes in the trachea (Figure 6A, e to h) and lung (Figure 6A, i to l) of the challenged control hamster were generally more severe than the infected naïve hamsters in experiments 1, 2, and 3. This was corroborated by the viral N antigen expression pattern (Figure 6B).

DISCUSSION

Following up on the demonstration of SARS-CoV-2 transmission through direct or indirect contact in our hamster model, a non-contact transmission model inside isolators was established in this study.²⁰ We showed that non-contact transmission occurred in 66.7% of unprotected naïve hamsters after exposure to SARS-CoV-2-challenged hamsters for less than 96 hours. Despite documented transmission in the exposed naïve hamsters as evident by positive viral loads in the upper and lower respiratory tract at 4 days after exposure or serum neutralizing antibody titre at 6 days after exposure, these hamsters had less severe histopathological changes and lower amount of SARS-CoV-2-N antigen expression in the upper and lower respiratory tract compared to virus-challenged hamsters. Moreover, the use of surgical mask partition to prevent emission of respiratory droplets from SARS-CoV-2-challenged index hamsters significantly reduced the transmission rate to 16.7% ($P=0.019$). The use of surgical mask partition to protect naïve hamsters reduced the transmission rate to 33.3%, although this did not reach statistical significance, likely because of the relatively small number of animals ($P=0.128$). As expected, the histopathological changes and the amount of respiratory tract viral N antigen expression of these protected naïve hamsters were also significantly lower than those of the challenged index hamsters.

The finding of SARS-CoV-2 being transmitted by the non-contact route of respiratory droplets or airborne droplet nuclei is not unexpected as this is the case for other respiratory viruses. For seasonal influenza viruses, similar transmission has been demonstrated with Syrian hamster, ferret, and guinea pig models.²⁶⁻²⁸ Seasonal influenza viruses could be isolated by plaque assay from naïve hamsters by day 4 post-exposure, whereas SARS-CoV-2 could be detected by RT-PCR in our infected naïve hamsters as early as day 4 post-exposure.²⁶ However, in the case of Nipah virus which is more of a neurotropic than

respiratory virus, transmission in the Syrian hamster model was largely by direct contact, despite predominant virus shedding in nasal and oropharyngeal secretions.²⁹

The intensity of exposure may affect the severity of viral infections as has been demonstrated in outbreaks of chickenpox, measles, and poliomyelitis.³⁰⁻³² The effect of virus inoculum on the severity of COVID-19 is evident when the histopathological changes and amount of viral N antigen expression in the respiratory tracts of the infected naïve hamsters with or without protection by surgical mask partition was compared with those of the virus-challenged hamsters. Besides a virus inoculum of 10^5 plaque forming units in 100µl DMEM being instilled intranasally into the challenged hamsters, the inoculum might be aspirated directly into the lungs when the hamsters were under anaesthesia. Such large dose of deep exposure resulted in significantly more severe histopathological changes and higher amount of viral N antigen expression in the respiratory tract than the infected naïve hamsters after droplet and/or aerosol exposure. The protective effect of masking may not be just determined by the success or failure of SARS-CoV-2 transmission, but also by the severity of COVID-19 in the case of transmission. For example, in Hong Kong where the population has a mask-use compliance rate of 96.6% during local COVID-19 epidemic, both the incidence rate (1048 cases per 7.5 million population) and crude fatality rate (4 out of 1048, 0.4%) of COVID-19 were amongst the lowest in the world at the timing of writing.³³

Although we could not differentiate whether transmission occurred by respiratory droplets or airborne aerosols in this study, both types of non-contact transmission might have happened because surgical masks is most efficient in filtering out large respiratory droplets of more than 10µm, but not the airborne aerosol particles of less than 5µm. Therefore, non-contact transmission still occurred in our hamster model despite a reduction of transmission when the naïve hamsters were protected by mask partitioning. Alternatively, the filtration efficiency of the masks might have declined over time during the study period. Interestingly,

transmission to the exposed naïve hamsters was significantly reduced when surgical mask partition was placed to prevent emission from the challenged index hamsters. This was not completely unexpected because the masking of infectious patients with multidrug-resistant tuberculosis on a hospital ward in South Africa reduced airborne transmission by 56% from these patients to guinea pigs which were breathing the ward air, compared with the percentage of transmission to guinea pigs during periods when masks were not worn.³⁴ This report clearly showed that surgical masks could be partially effective in reducing the transmission of a well-known airborne pathogen *Mycobacterium tuberculosis* and corroborated with the masking experiments in our hamster model of non-contact transmission of SARS-CoV-2.

Unlike the use of surgical mask in healthcare setting, masking in the community remains controversial. The World Health Organization found no evidence that wearing a surgical mask by healthy persons can prevent acquisition of SARS-CoV-2. However, the US Centers for Disease Control and Prevention recommends the use of cloth face coverings in communities with significant community-based transmission. This shift of recommendation was based on the finding of pre-symptomatic shedding of SARS-CoV-2 and the presence of asymptomatic patients with high viral loads in the community. Face mask usage may serve as source control by preventing dispersal of droplets during talking, sneezing, and coughing, and also reduce the risk of environmental contamination by SARS-CoV-2. Our results showed that masking of the challenged index appeared to be more important than masking the exposed naïve, which is consistent with the findings in a systematic review on influenza transmission.³⁵ Masking is a continuous form of protection to stop the spreading of saliva and respiratory droplets to or from others, and to or from the environment to the susceptible individuals by hands through subconscious touching of their nose, mouth, and eyes. Hand hygiene is always the cornerstone to prevent transmission of SARS-CoV-2, but it is a one-off

discontinuous process where hand contamination may occur again easily between each episode of alcoholic hand rubbing or hand washing. Studies have also shown that wearing a mask with frequent hand hygiene significantly reduced transmission of seasonal influenza virus in the community setting.³⁶ But once the effect of the use of surgical mask was removed, the effect of hand hygiene became insignificant.³⁶

Containment public health interventions including border source control, extensive testing of cases and isolation, rapid contact tracing and quarantine, and mitigation measures of social distancing including school closures, home office, closure of food premises and public places to stop gatherings and even city lockdown, were used by every developed country at different time points and to different extents to control the COVID-19 pandemic. However, the presence of a significant proportion of asymptotically infected patients who were not aware of the need of testing, wearing mask, or isolation has markedly impaired these control measures. In the case of the Princess Diamond cruise outbreak, 6 out of 9 returnees were found to be asymptotically infected during the 14 days of quarantine and serial virological monitoring after returning to Hong Kong.³⁷ Our findings on the use of surgical mask partition for protection against non-contact transmission in this hamster model supported the use of community-wide masking to reduce the amount of virus shedding from the asymptotically infected patients and to protect susceptible individuals. This should be a reasonable approach for the epidemic control of a densely populated city like Hong Kong without resorting to city lockdown, and an important measure during the stepwise loosening of social distancing measures in the days ahead.

Our study had limitations. The speed of the unidirectional airflow could not be unified when the surgical mask partitions were installed, but that would also apply when surgical masks were worn by different individuals in real life, and this could indeed be a mechanism for protection during mask usage. We could not determine the exact timing of acquisition of

SARS-CoV-2 by the exposed naïve hamsters as we only started sampling them 4 days after exposure. Moreover, we could not determine if contact transmission has occurred among exposed naïve hamsters housed in the same cage. This might have resulted in an underestimation of the protective efficacy of masks, which would otherwise be even more significant. Further studies on the relative importance of large respiratory droplets and small airborne aerosols are warranted.

Accepted Manuscript

Notes

Author contributions. JF-WC, SY, AJZ, and K-YY had roles in the study design, data collection, data analysis, data interpretation, and writing of the manuscript. VK-MP and CC-SC had roles in the study design, experiments, data collection, data analysis, and data interpretation. AC-YL, ZF, CL, RL, JC, KT, CL, VC-CC, J-PC, HC, K-HC, KK-WT, and SS had roles in the experiments, data collection, data analysis, and/or data interpretation. All authors reviewed and approved the final version of the manuscript.

Disclaimer. The funding sources had no role in the study design, data collection, analysis, interpretation, or writing of the report.

Financial support. This study was partly supported by the donations of May Tam Mak Mei Yin, Richard Yu and Carol Yu, the Shaw Foundation Hong Kong, Michael Seak-Kan Tong, Respiratory Viral Research Foundation Limited, Hui Ming, Hui Hoy and Chow Sin Lan Charity Fund Limited, Chan Yin Chuen Memorial Charitable Foundation, Marina Man-Wai Lee, the Hong Kong Hainan Commercial Association South China Microbiology Research Fund, the Jessie & George Ho Charitable Foundation, Perfect Shape Medical Limited, and Kai Chong Tong; and funding from the Health and Medical Research Fund (grant no. COVID190121 and COVID190123), the Food and Health Bureau, The Government of the Hong Kong Special Administrative Region; the National Program on Key Research Project of China (grant no. 2020YFA0707500 and 2020YFA0707504); the Consultancy Service for Enhancing Laboratory Surveillance of Emerging Infectious Diseases and Research Capability on Antimicrobial Resistance for Department of Health of the Hong Kong Special Administrative Region Government; the Theme-Based Research Scheme (T11/707/15) of the Research Grants Council, Hong Kong Special Administrative Region; Sanming Project of

Medicine in Shenzhen, China (No. SZSM201911014); and the High Level-Hospital Program, Health Commission of Guangdong Province, China.

Potential conflicts of interests. We declare no competing interests.

Accepted Manuscript

References

1. Peiris JS, Lai ST, Poon LL, et al. Coronavirus as a possible cause of severe acute respiratory syndrome. *Lancet* 2003; **361**: 1319-25.
2. Lau SK, Woo PC, Li KS, et al. Severe acute respiratory syndrome coronavirus-like virus in Chinese horseshoe bats. *Proc Natl Acad Sci U S A* 2005; **102**: 14040-5.
3. Ge XY, Li JL, Yang XL, et al. Isolation and characterization of a bat SARS-like coronavirus that uses the ACE2 receptor. *Nature* 2013; **503**: 535-8.
4. Chan JF, To KK, Tse H, Jin DY, Yuen KY. Interspecies transmission and emergence of novel viruses: lessons from bats and birds. *Trends Microbiol* 2013; **21**: 544-55.
5. Chan JF, Lau SK, To KK, Cheng VC, Woo PC, Yuen KY. Middle East respiratory syndrome coronavirus: another zoonotic betacoronavirus causing SARS-like disease. *Clin Microbiol Rev* 2015; **28**: 465-522.
6. Zhu N, Zhang D, Wang W, et al. A Novel Coronavirus from Patients with Pneumonia in China, 2019. *N Engl J Med* 2020; **382**: 727-33.
7. Zhou P, Yang XL, Wang XG, et al. A pneumonia outbreak associated with a new coronavirus of probable bat origin. *Nature* 2020; **579**: 270-3.
8. Chan JF, Kok KH, Zhu Z, et al. Genomic characterization of the 2019 novel human-pathogenic coronavirus isolated from a patient with atypical pneumonia after visiting Wuhan. *Emerg Microbes Infect* 2020; **9**(1): 221-236.
9. Chan JF, Yuan S, Kok KH, et al. A familial cluster of pneumonia associated with the 2019 novel coronavirus indicating person-to-person transmission: a study of a family cluster. *Lancet* 2020; **395**: 514-523.
10. Huang C, Wang Y, Li X, et al. Clinical features of patients infected with 2019 novel coronavirus in Wuhan, China. *Lancet* 2020; **395**: 497-506.

11. To KK, Tsang OT, Leung WS, et al. Temporal profiles of viral load in posterior oropharyngeal saliva samples and serum antibody responses during infection by SARS-CoV-2: an observational cohort study. *Lancet Infect Dis* 2020; **20**: 565-74.
12. Wichmann D, Sperhake JP, Lutgehetmann M, et al. Autopsy Findings and Venous Thromboembolism in Patients With COVID-19: A Prospective Cohort Study. *Ann Intern Med* 2020; May 6. doi: 10.7326/M20-2003. [Epub ahead of print]
13. Connors JM, Levy JH. COVID-19 and its implications for thrombosis and anticoagulation. *Blood* 2020 Apr 27. pii: blood.2020006000. doi: 10.1182/blood.2020006000. [Epub ahead of print]
14. Cheung KS, Hung IF, Chan PP, et al. Gastrointestinal Manifestations of SARS-CoV-2 Infection and Virus Load in Fecal Samples from the Hong Kong Cohort and Systematic Review and Meta-analysis. *Gastroenterology* 2020 Apr 3. pii: S0016-5085(20)30448-0. doi: 10.1053/j.gastro.2020.03.065. [Epub ahead of print]
15. Jones VG, Mills M, Suarez D, et al. COVID-19 and Kawasaki Disease: Novel Virus and Novel Case. *Hosp Pediatr* 2020 Apr 7. pii: hpeds.2020-0123. doi: 10.1542/hpeds.2020-0123. [Epub ahead of print]
16. Toscano G, Palmerini F, Ravaglia S, et al. Guillain-Barre Syndrome Associated with SARS-CoV-2. *N Engl J Med* 2020 Apr 17. doi: 10.1056/NEJMc2009191. [Epub ahead of print]
17. Guan WJ, Ni ZY, Hu Y, et al. Clinical Characteristics of Coronavirus Disease 2019 in China. *N Engl J Med* 2020; **382**: 1708-20.
18. Vaira LA, Salzano G, Deiana G, De Riu G. Anosmia and Ageusia: Common Findings in COVID-19 Patients. *Laryngoscope* 2020 Apr 1. doi: 10.1002/lary.28692. [Epub ahead of print]

19. World Health Organization. Coronavirus disease (COVID-2019) situation reports: Situation report - 112. https://www.who.int/docs/default-source/coronaviruse/situation-reports/20200511-covid-19-sitrep-112.pdf?sfvrsn=813f2669_2. Accessed on 12 May, 2020.
20. Chan JF, Zhang AJ, Yuan S, et al. Simulation of the clinical and pathological manifestations of Coronavirus Disease 2019 (COVID-19) in golden Syrian hamster model: implications for disease pathogenesis and transmissibility. *Clin Infect Dis* 2020 Mar 26. pii: ciaa325. doi: 10.1093/cid/ciaa325. [Epub ahead of print]
21. Chu H, Chan JF, Yuen TT, et al. An observational study on the comparative tropism, replication kinetics, and cell damage profiling of SARS-CoV-2 and SARS-CoV: implications for clinical manifestations, transmissibility, and laboratory studies of COVID-19. *Lancet Microbe* 2020 April 21. doi: 10.1016/S2666-5247(20)30004-5.
22. Chan JF, Chan KH, Choi GK, et al. Differential cell line susceptibility to the emerging novel human betacoronavirus 2c EMC/2012: implications for disease pathogenesis and clinical manifestation. *J Infect Dis* 2013; **207**: 1743-52.
23. Zhou J, Chu H, Li C, et al. Active replication of Middle East respiratory syndrome coronavirus and aberrant induction of inflammatory cytokines and chemokines in human macrophages: implications for pathogenesis. *J Infect Dis* 2014; **209**: 1331-42.
24. Chu H, Chan JF, Wang Y, et al. Comparative replication and immune activation profiles of SARS-CoV-2 and SARS-CoV in human lungs: an ex vivo study with implications for the pathogenesis of COVID-19. *Clin Infect Dis* 2020 Apr 9. pii: ciaa410. doi: 10.1093/cid/ciaa410. [Epub ahead of print]
25. Chan JF, Yip CC, To KK, et al. Improved Molecular Diagnosis of COVID-19 by the Novel, Highly Sensitive and Specific COVID-19-RdRp/Hel Real-Time Reverse

- Transcription-PCR Assay Validated In Vitro and with Clinical Specimens. *J Clin Microbiol* 2020; **58**.
26. Iwatsuki-Horimoto K, Nakajima N, Ichiko Y, et al. Syrian Hamster as an Animal Model for the Study of Human Influenza Virus Infection. *J Virol* 2018; **92**.
 27. Jayaraman A, Pappas C, Raman R, et al. A single base-pair change in 2009 H1N1 hemagglutinin increases human receptor affinity and leads to efficient airborne viral transmission in ferrets. *PLoS One* 2011; **6**: e17616.
 28. Seibert CW, Rahmat S, Krause JC, et al. Recombinant IgA is sufficient to prevent influenza virus transmission in guinea pigs. *J Virol* 2013; **87**: 7793-804.
 29. de Wit E, Bushmaker T, Scott D, Feldmann H, Munster VJ. Nipah virus transmission in a hamster model. *PLoS Negl Trop Dis* 2011; **5**: e1432.
 30. Garenne M, Aaby P. Pattern of exposure and measles mortality in Senegal. *J Infect Dis* 1990; **161**: 1088-94.
 31. Poulsen A, Cabral F, Nielsen J, et al. Varicella zoster in Guinea-Bissau: intensity of exposure and severity of infection. *Pediatr Infect Dis J* 2005; **24**: 102-7.
 32. Nielsen NM, Aaby P, Wohlfahrt J, Pedersen JB, Melbye M, Molbak K. Intensive exposure as a risk factor for severe polio: a study of multiple family cases. *Scan J Infect Dis* 2001; **33**: 301-5.
 33. Cheng VC, Wong SC, Chuang VW, et al. The role of community-wide wearing of face mask for control of coronavirus disease 2019 (COVID-19) epidemic due to SARS-CoV-2. *J Infect* 2020 Apr 23. pii: S0163-4453(20)30235-8. doi: 10.1016/j.jinf.2020.04.024. [Epub ahead of print]
 34. Dharmadhikari AS, Mphahlele M, Stoltz A, et al. Surgical face masks worn by patients with multidrug-resistant tuberculosis: impact on infectivity of air on a hospital ward. *Am J Respir Crit Care Med* 2012; **185**: 1104-9.

35. Cowling BJ, Zhou Y, Ip DK, Leung GM, Aiello AE. Face masks to prevent transmission of influenza virus: a systematic review. *Epidemiol Infect* 2010; **138**: 449-56.
36. Wong VW, Cowling BJ, Aiello AE. Hand hygiene and risk of influenza virus infections in the community: a systematic review and meta-analysis. *Epidemiol Infect* 2014; **142**: 922-32.
37. Hung IF, Cheng VC, Li X, et al. COVID-19 in its making during quarantine after release from a cruise ship: a cohort study on SARS-CoV-2 shedding and seroconversion. *Lancet Infect Dis* 2020. [accepted and in press]

Figure legends

Figure 1. Non-contact transmission of SARS-CoV-2 in the Syrian hamster model. (A)

The closed systems housing the hamsters were placed in the isolator in a Biosafety Level-3 laboratory. **(B)** Enlarged view of the closed systems used in the non-contact transmission studies. Each system contained two cages (left and right) separated by a polyvinyl chloride air porous partition. An electrically powered fan was installed at the polyvinyl chloride air porous partition to ensure unidirectional airflow from the cage housing the challenged index hamsters to the cage housing the naïve hamsters. **(C)** Surgical mask partition with the blue external surface facing the challenged hamsters in experiment 3.

Figure 2. Non-contact transmission of SARS-CoV-2 from virus-challenged index hamsters to exposed naïve hamsters without surgical mask partition between the cages (experiment 1).

SARS-CoV-2 was intranasally inoculated to the index hamsters (n=5) at day 0. Twenty-four hours later, three naïve hamsters were transferred to the adjacent cage and exposed to the cage housing the virus-challenged index hamster. Two exposed naïve hamsters in each system were sacrificed at day 5 post-inoculation (4 days after exposure). The challenged index animal and the remaining exposed naïve animal in each system were then sacrificed at 7 dpi. A total of 5 systems (n=20) were included in experiment 1.

Figure 3. Non-contact transmission of SARS-CoV-2 from virus-challenged index hamsters to exposed naïve hamsters with surgical mask partition between the cages.

Surgical mask partition with the external surface facing (A) exposed naïve hamsters (experiment 2) to mimic the situation of the mask being worn by the challenged index hamster for preventing the emission of SARS-CoV-2 infected droplets, or (B) facing the challenged index hamsters to mimic the situation of the mask being worn by the exposed

naïve hamsters to prevent the reception of SARS-CoV-2-infected droplets from the challenged index hamsters. The timing of virus challenge and sacrifice of animals was the same as experiment 1. A total of 4 systems (n=16) were included in experiment 2 and another 4 systems (n=16) were included in experiment 3.

Figure 4. Viral loads in the respiratory tract tissues of the SARS-CoV-2 RT-PCR-positive naïve hamsters exposed to the challenged index hamsters. Naïve hamsters without surgical mask partition in experiment 1 (red squares), naïve hamsters exposed to masked challenged index hamsters in experiment 2 (black circles), and the masked naïve hamsters exposed to the challenged index hamsters in experiment 3 (blue triangles). Statistical comparison between the SARS-CoV-2 RT-PCR-positive naïve hamsters without surgical mask partition (experiment 1) and the SARS-CoV-2 RT-PCR-positive naïve hamsters with surgical mask partition (experiments 2 and 3) was performed using Student's t-test. n.s. = not significant and * = $P < 0.05$. LOD, limit of detection.

Figure 5. Reciprocal serum SARS-CoV-2-specific neutralizing antibody titers in the hamsters. The mean serum neutralizing antibody titers of the challenged index hamsters (n=13, orange diamonds), the naïve hamsters exposed to the challenged index hamsters without surgical mask partition in experiment 1 (n=5, red squares), the naïve hamsters exposed to masked challenged index hamsters in experiment 2 (n=4, black circles), and the masked naïve hamsters exposed to the challenged index hamsters in experiment 3 (n=4, blue triangles) at 7 days post-inoculation (6 days after exposure of the naïve hamsters to the index hamsters) are shown on a logarithmic scale. The dotted line indicates the lower limit of detection (<1:20). LOD, limit of detection.

Figure 6. Histopathological changes and SARS-CoV-2 nucleocapsid (N) protein expression in the upper and lower respiratory tissues of the hamsters.

(A) Hematoxylin and eosin-stained tissue sections. (a) to (d) Representative images of nasal turbinate tissue sections which showed pieces of epithelium desquamation (arrows) in all four groups of hamsters. The tissue damage was generally more severe in the challenged control hamster which exhibited massive secretion mixed with detached epithelial cells in the nasal cavity (empty arrow). (e) to (h) Representative images of the tracheal tissue sections showing various degrees of epithelial desquamation (arrows) and submucosal infiltration which was also more prominent in the challenged control hamster (empty arrows). (i) to (l) Representative images of the lung sections. (i) The lung of the challenged control hamster at 5 dpi showed bronchiolar epithelial cell death, luminal secretion and cell debris (arrow), severe alveolar infiltration, exudation and hemorrhage (empty arrows). Two blood vessels showed perivascular and intra-endothelial infiltration (arrowheads). (j) The lung of the infected naïve hamster from experiment 1 showed bronchiolar epithelial desquamation (arrows), patchy alveolar wall thickening and blood vessel congestion (arrowhead). (k) The lung of the infected naïve hamster from experiment 2 showed no apparent alveolar damage, but with bronchiolar epithelial desquamation (arrow) and mild perivascular infiltration (arrowhead). (l) The lung of the infected naïve hamster from experiment 3 showed mild alveolar wall thickening with blood vessel congestion.

(B) Immunofluorescence-stained viral N protein (green) expression in hamster respiratory tissues. (a) to (d) Representative images of the nasal turbinate of the hamsters, showing more abundant viral N antigen expression in the challenged control hamster than the infected naïve hamsters in experiments 1, 2, and 3. Viral N antigen-positive cells located in the epithelium (arrows) and viral N antigens associated with detached cells (solid arrows). (e) to (h) The tracheal tissue of the challenged control hamster showed more intense epithelial viral N

antigen expression (arrows) than the infected naïve hamsters in experiments 1, 2, and 3. (i) to (l) Viral N antigen expression in the lung tissues. The lung sections of the challenged control hamster showed diffuse viral N antigen expression in alveolar cells compared to scanty expression in the bronchiolar epithelium (thin arrows) and alveoli (solid arrows) of the infected naïve hamsters in experiments 1, 2, and 3.

Accepted Manuscript

Table 1. Air velocity from the challenged index hamsters' cages to the exposed naïve hamsters' cages with or without surgical mask partition

Group	Air velocity from the challenged index hamster's cage to the exposed naïve hamsters' cage (meters per second)^a
Experiment 1: No mask	0.676 ± 0.107
Experiment 2: Masked index	0.335 ± 0.070
Experiment 3: Masked naïve	0.428 ± 0.028

^aThe values represent the mean air velocity ± standard deviations.

Accepted Manuscript

Table 2. Clinical scores of exposed naïve hamsters with or without surgical mask partition

Group	5 dpi ^a	<i>P</i> -value ^b	7 dpi ^a	<i>P</i> -value ^b
Naïve (no mask)	1.800 ± 1.687		2.400 ± 1.517	
Naïve (any mask)	0.313 ± 0.793	0.036	0.375 ± 0.744	0.008
Naïve (masked index)	0.000 ± 0.000	0.008	0.250 ± 0.500	0.031
Naïve (masked naïve)	0.625 ± 1.061	0.107	0.500 ± 1.000	0.069

^aA score of 1 was given to each of the following clinical signs: lethargy, ruffled fur, hunchback posture, and rapid breathing.

^b*P*-values represent comparison between the naïve (no mask) group with the other groups (Student's *t*-test). The values represent the mean clinical scores ± standard deviations.

Table 3. Non-contact transmission rate from challenged hamsters to exposed naïve hamsters with or without surgical mask partition^a

Group	5 dpi	<i>P</i> -value ^a	7 dpi	<i>P</i> -value ^a	Total	<i>P</i> -value ^a
Naïve (no mask)	6/10 (60.0%)		4/5 (80.0%)		10/15 (66.7%)	
Naïve (any mask)	4/16 (25.0%)	0.109	2/8 (25.0%)	0.103	6/24 (25.0%)	0.018
Naïve (masked index)	1/8 (12.5%)	0.066	1/4 (25.0%)	0.206	2/12 (16.7%)	0.019
Naïve (masked naïve)	3/8 (37.5%)	0.637	1/4 (25.0%)	0.206	4/12 (33.3%)	0.128

^a*P*-values represent comparison between the naïve (no mask) group with the other groups (Fisher's exact test).

Figure 1

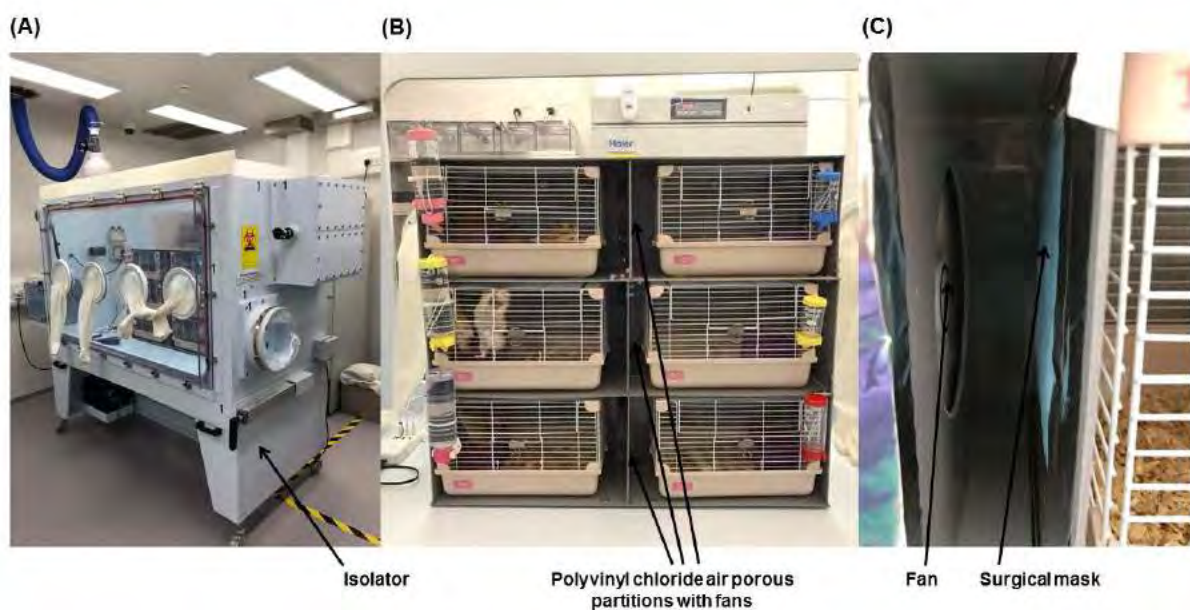


Figure 2

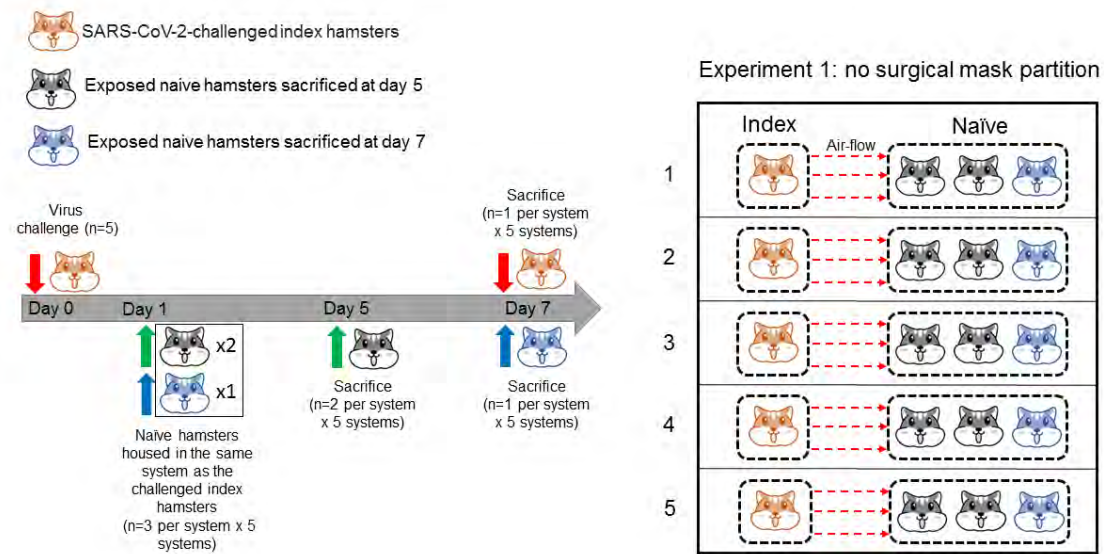


Figure 3A

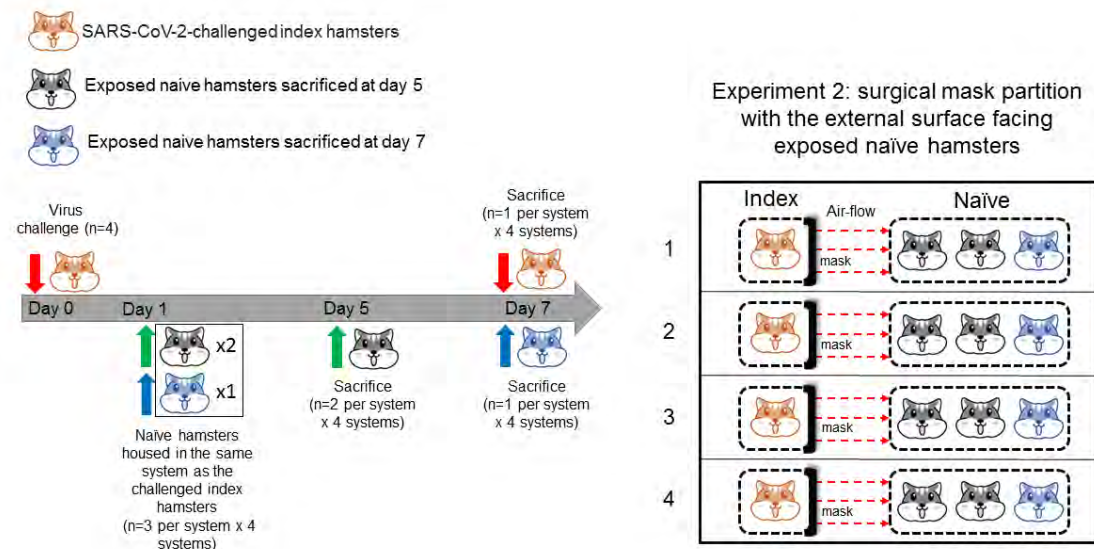


Figure 3B

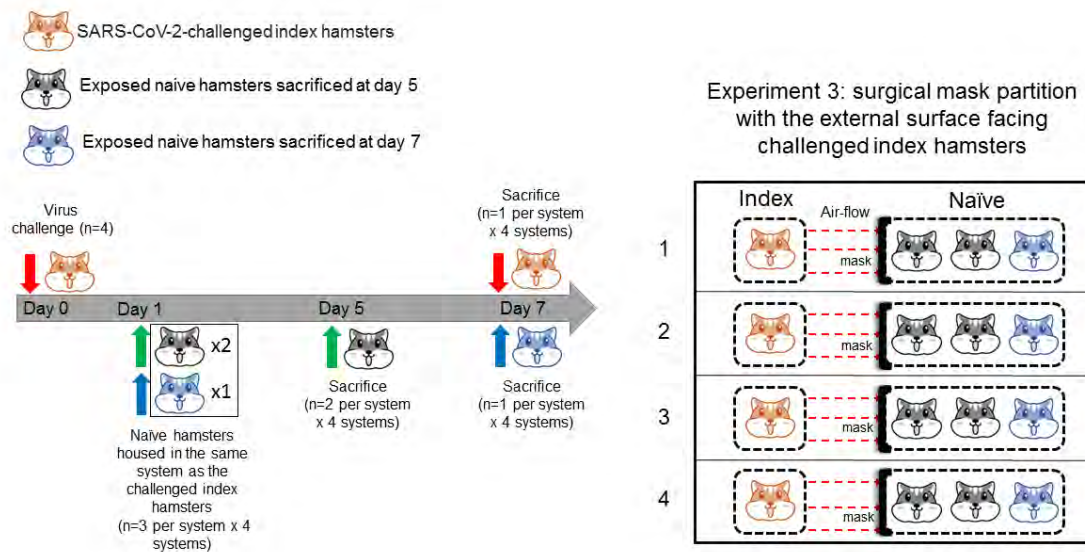
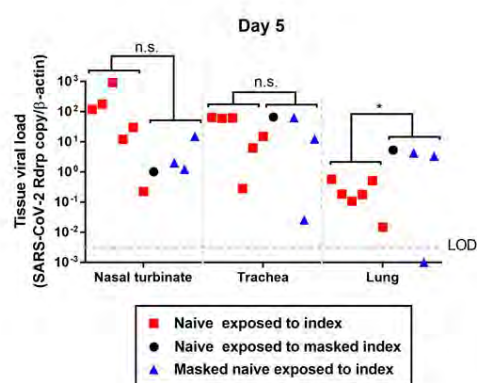


Figure 4

(A)



(B)

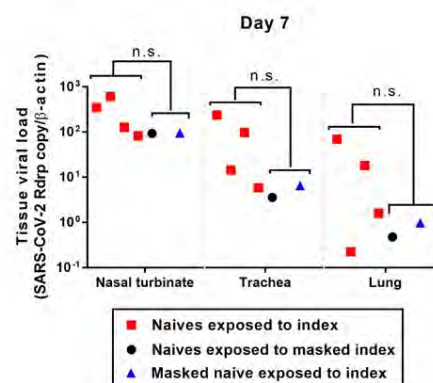


Figure 5

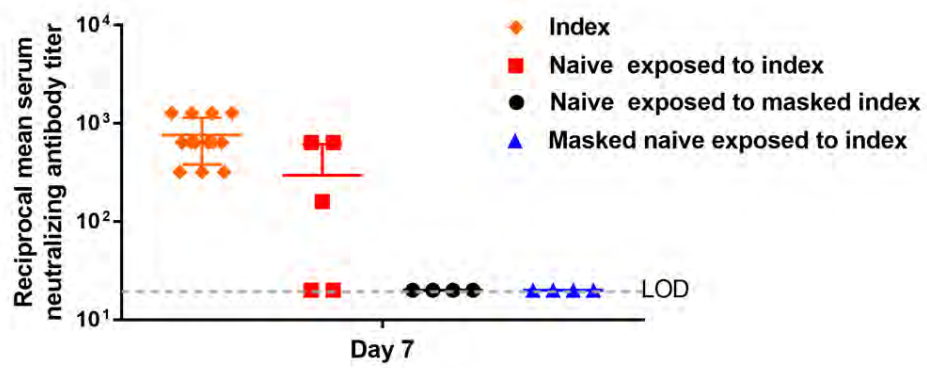


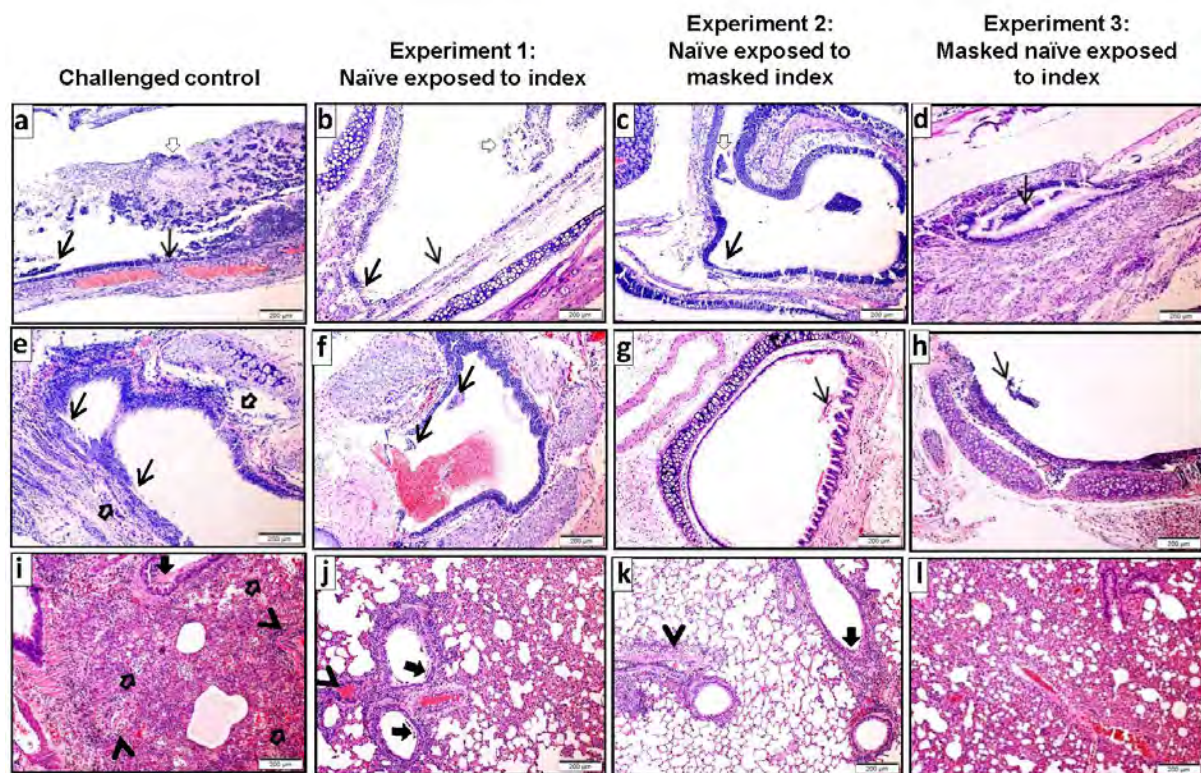
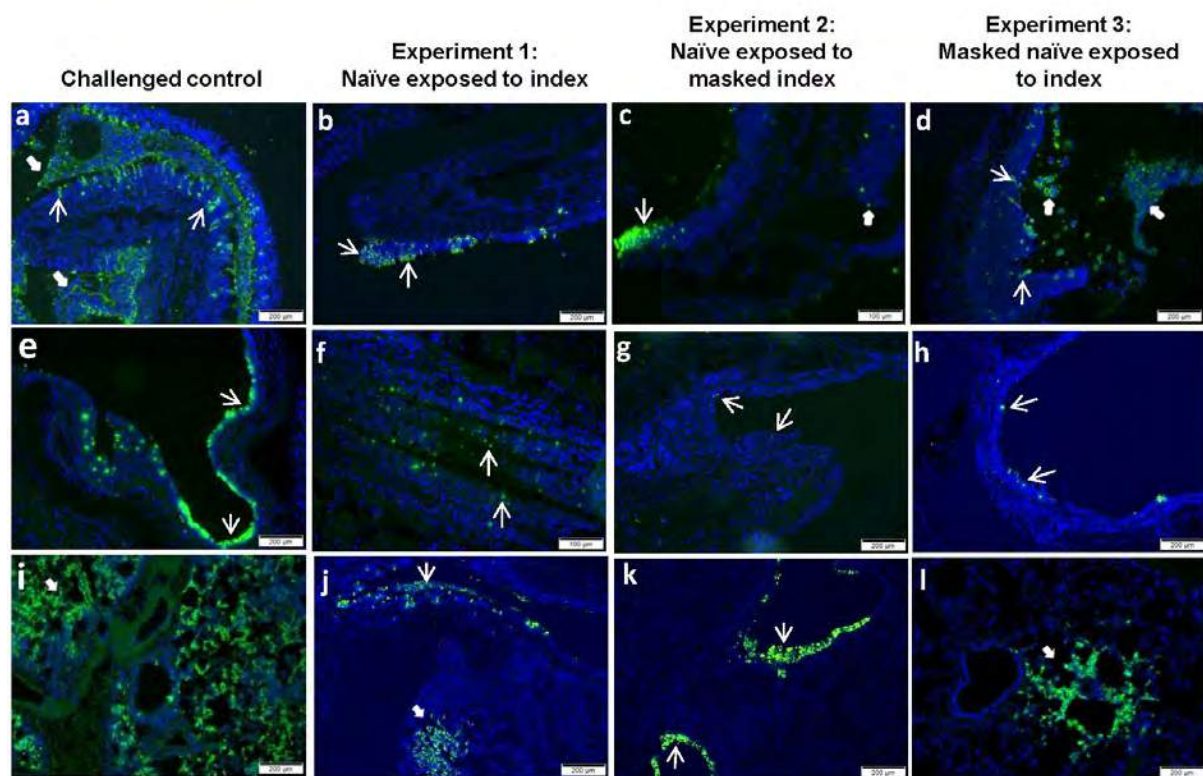
Figure 6A

Figure 6B

SARS-CoV-2 Shedding Dynamics Across the Respiratory Tract, Sex, and Disease Severity for Adult and Pediatric COVID-19

Paul Z. Chen, BAsC¹, Niklas Bobrovitz, DPhil, MSc^{1,2}, Zahra Premji, PhD, MLIS², Marion
Koopmans, DVM, PhD³, David N. Fisman, MD, MPH¹, Frank X. Gu, PhD^{1*}

¹University of Toronto, Toronto, Ontario, Canada

²University of Calgary, Calgary, Alberta, Canada

³Erasmus University Medical Center, Rotterdam, Netherlands

Corresponding author: Frank X. Gu, PhD, University of Toronto, 200 College St., Toronto,

ON M5S 3E5, Canada; e-mail, f.gu@utoronto.ca

Word count (abstract): 273 words

Word count (text only): 3,500 words

Background: SARS-CoV-2 shedding dynamics in the upper (URT) and lower respiratory tract (LRT) remain unclear.

Objective: To analyze SARS-CoV-2 shedding dynamics across COVID-19 severity, the respiratory tract, sex and age cohorts (aged 0 to 17 years, 18 to 59 years, and 60 years or older).

Design: Systematic review and pooled analyses.

Setting: MEDLINE, EMBASE, CENTRAL, Web of Science Core Collection, medRxiv and bioRxiv were searched up to 20 November 2020.

Participants: The systematic dataset included 1,266 adults and 136 children with COVID-19.

Measurements: Case characteristics (COVID-19 severity, age and sex) and quantitative respiratory viral loads (rVLs).

Results: In the URT, adults with severe COVID-19 had higher rVLs at 1 DFSO than adults ($P = 0.005$) or children ($P = 0.017$) with nonsevere illness. Between 1-10 DFSO, severe adults had comparable rates of SARS-CoV-2 clearance from the URT as nonsevere adults ($P = 0.479$) and nonsevere children ($P = 0.863$). In the LRT, severe adults showed higher post-symptom-onset rVLs than nonsevere adults ($P = 0.006$). In the analyzed period (4-10 DFSO), severely affected adults had no significant trend in SARS-CoV-2 clearance from LRT ($P = 0.105$), whereas

nonsevere adults showed a clear trend ($P < 0.001$). After stratifying for disease severity, sex and age (including child vs. adult) were not predictive of the duration of respiratory shedding.

Limitation: Limited data on case comorbidities and few samples in some cohorts.

Conclusion: High, persistent LRT shedding of SARS-CoV-2 characterized severe COVID-19 in adults. After symptom onset, severe cases tended to have higher URT shedding than their nonsevere counterparts. Disease severity, rather than age or sex, predicted SARS-CoV-2 kinetics. LRT specimens should more accurately prognosticate COVID-19 severity than URT specimens.

Primary Funding Source: Natural Sciences and Engineering Research Council.

INTRODUCTION

As of 17 February 2021, the coronavirus disease 2019 (COVID-19) pandemic has caused more than 109 million infections and 2.4 million deaths globally (1). The clinical spectrum of COVID-19, caused by severe acute respiratory syndrome coronavirus 2 (SARS-CoV-2), is wide, ranging from asymptomatic infection to fatal disease. Risk factors for severe illness and death include age, sex, smoking and comorbidities, such as obesity, hypertension, diabetes and cardiovascular disease (2-4). Emerging evidence indicates that age and sex differences in innate, cross-reactive and adaptive immunity facilitate the higher risks in older and male cases (5-8). Robust immune responses putatively mediate nonsevere illness, in part, by controlling the replication of SARS-CoV-2 (9).

As SARS-CoV-2 is a respiratory virus, its shedding dynamics in the upper (URT) and lower respiratory tract (LRT) provide insight into clinical and epidemiological factors. URT viral load has been associated with transmission risk, duration of infectiousness, disease severity and mortality (10-16). Key questions, however, remain. While chest computed tomography (CT) evidence of viral pneumonitis suggests pulmonary replication in most symptomatic cases (17), the LRT kinetics of SARS-CoV-2, especially as related to disease severity, remain unknown. The relationships between sex, age and disease severity on respiratory shedding are unclear. Moreover, whether children clear SARS-CoV-2 at similar rates as adults, and if this correlates the age-based differences in disease severity, is unknown.

For insight into these questions, we conducted a systematic review on SARS-CoV-2 quantitation from respiratory specimens and developed a large, diverse dataset of respiratory viral loads (rVLs) and individual case characteristics. Stratified pooled analyses then assessed SARS-CoV-2 shedding dynamics across the respiratory tract, age, sex and COVID-19 severity.

73

74 **METHODS**

75 Our systematic review identified studies reporting SARS-CoV-2 quantitation in respiratory
76 specimens taken during the estimated infectious period (-3 to 10 days from symptom onset
77 [DFS0]) (15, 18). The systematic review protocol was based on our previous study (19) and was
78 prospectively registered on PROSPERO (registration number, CRD42020204637). The
79 systematic review was conducted according to Cochrane methods guidance (20). Other than the
80 title of this study, we have followed PRISMA reporting guidelines (21).

81

82 **Data Sources and Searches**

83 Up to 20 November 2020, we searched, without the use of filters or language restrictions,
84 the following sources: MEDLINE (Ovid), EMBASE (Ovid), Cochrane Central Register of
85 Controlled Trials (CENTRAL, Ovid), Web of Science Core Collection, and medRxiv and
86 bioRxiv (both searched through Google Scholar via the Publish or Perish program). We also
87 gathered studies by searching through the reference lists of review articles identified by the
88 database search, by searching through the reference lists of included articles, through expert
89 recommendation (by Epic J. Topol and Akiko Iwasaki on Twitter) and by hand-searching
90 through journals. A comprehensive search was developed by a librarian (Z.P.). Additional details
91 on the search are included in the **Supplement**.

92

93 **Study selection**

94 Studies that reported SARS-CoV-2 quantitation in individual URT (nasopharyngeal swab
95 [NPS], nasopharyngeal aspirate [NPA], oropharyngeal swab [OPS] or posterior oropharyngeal

saliva [POS]) or LRT (endotracheal aspirate [ETA] or sputum [Spu]) specimens taken during the estimated infectious period (-3 to 10 DFSO) in humans were included (additional details in the **Supplement**). As semiquantitative metrics (cycle threshold [Ct] values) cannot be compared on an absolute scale between studies based on instrument and batch variation (22), studies reporting specimen measurements as Ct values, without quantitative calibration, were excluded. Two authors (P.Z.C. and N.B.) independently screened titles and abstracts and reviewed full texts. At the full-text stage, reference lists were reviewed for study inclusion. Inconsistencies were resolved by discussion and consensus.

Data Extraction and Risk-of-Bias Assessment

Two authors (P.Z.C. and N.B.) independently collected data (specimen measurements taken between -3 and 10 DFSO, specimen type, volume of transport media and case characteristics, including age, sex and disease severity) from contributing studies and assessed risk of bias using a modified Joanna Briggs Institute (JBI) critical appraisal checklist (described in the **Supplement** and shown in **Supplement Table 6**). Data were collected for individually reported specimens of known type, with known DFSO, and for COVID-19 cases with known age, sex or severity. Case characteristics were collected directly from contributing studies when reported individually or obtained via data request from the authors. Data from serially sampled asymptomatic cases were included, and the day of laboratory diagnosis was referenced as 0 DFSO (15, 23). Based on the modified JBI checklist, studies were considered to have low risk of bias if they met the majority of items and included item 1 (representative sample). Discrepancies were resolved by discussion and consensus.

Respiratory Viral Load

For analyses based on rVL (viral RNA concentration in the respiratory tract) and to account for interstudy variation in the volumes of viral transport media (VTM) used, the rVL for each collected sample was estimated based on the specimen concentration (viral RNA concentration in the specimen) and dilution factor in VTM. Typically, swabbed specimens (NPS and OPS) report the viral RNA concentration in VTM. Based on the VTM volume reported in the study along with the expected uptake volume for swabs (0.128 ± 0.031 ml, mean \pm SD) (24), we calculated the dilution factor for each respiratory specimen and then estimated the rVL. Similarly, liquid specimens (ETA, POS and Spu) are often diluted in VTM, and the rVL was estimated based on the reported collection and VTM volumes. If the diluent volume was not reported, then VTM volumes of 1 ml (NPS and OPS) or 2 ml (POS and ETA) were assumed (23, 25). Unless dilution was reported, Spu specimens were taken as undiluted (15). The non-reporting of VTM volume was noted as an element increasing risk of bias in the modified JBI critical appraisal checklist. For laboratory-confirmed COVID-19 cases, negative specimen measurements were taken at the reported assay detection limit in the respective study.

Case Definitions

As severity in the clinical manifestations of COVID-19 and case-fatality rates tend to increase among children (aged 0-17 y), younger adults (aged 18-59 y) and older adults (aged 60 y or older) (4, 26), the data were delineated based on these three age cohorts. Cases were also categorized by sex.

U.S. National Institutes of Health guidance was used to categorize disease severity as nonsevere or severe (27). The nonsevere cohort included those with asymptomatic infection

(individuals who test positive via a molecular test for SARS-CoV-2 and report no symptoms consistent with COVID-19); mild illness (individuals who report any signs or symptoms of COVID-19, including fever, cough, sore throat, malaise, headache, muscle pain, nausea, vomiting, diarrhea, loss of taste and smell, but who do not have dyspnea or abnormal chest imaging); and moderate illness (individuals with clinical or radiographic evidence of LRT disease, fever $>39.4^{\circ}\text{C}$ or $\text{SpO}_2 \geq 94\%$ on room air) disease. The severe cohort included those with severe illness (individuals who have $\text{SpO}_2 < 94\%$ on room air, $[\text{PaO}_2/\text{FiO}_2] < 300$ mmHg, respiratory rate > 30 breaths/min or lung infiltrates $> 50\%$) and critical illness (respiratory failure, septic shock or multiple organ dysfunction).

Statistical Analysis

We used regression analysis to assess the respiratory shedding of SARS-CoV-2 and compare age, sex or severity cohorts. In COVID-19 cases, rVL tends to diminish exponentially after 1 DFSO in the URT, whereas it tends to do so after 4 DFSO in the LRT (15, 17, 19). Hence, rVLs (in units of \log_{10} copies/ml) between 1-10 DFSO for the URT, or 4-10 DFSO for the LRT, were fitted using general linear regression with interaction:

$$V = \alpha + \beta_1 X_1 + \beta_2 X_2 + \beta_3 X_1 X_2, \quad (1)$$

where V represents the rVL, α represents the estimated mean rVL (at 1 DFSO for URT or 4 DFSO for LRT) for the reference cohort, X_1 represents DFSO for the reference cohort, X_2 represents the comparison cohort, β_1 represents the effect of DFSO on rVL for the reference cohort, β_2 represents the effect of the comparison cohort on the intercept and β_3 represents the interaction between DFSO and cohorts. Regression analyses were offset by DFSO such that mean rVLs at 1 DFSO for URT, or 4 DFSO for LRT, were compared between cohorts by the

effect on the intercept (regression t -test for β_2). Shedding dynamics were compared between cohorts by interaction (regression t -test for β_3). The statistical significance of viral clearance for each cohort was analyzed using simple linear regression (regression t -test on the slope). Regression models were extrapolated (to 0 log₁₀ copies/ml, rather than an assay detection limit) to estimate the duration of shedding.

To assess heterogeneity in shedding, rVL data were fitted to Weibull distributions (19), and the rVL at a case percentile was estimated using the Weibull quantile function. Each cohort in statistical analyses included all rVLs for which the relevant characteristic (LRT or URT, age cohort, sex or disease severity) was ascertained at the individual level. Cohorts with small sample sizes were not compared, as these analyses are more sensitive to potential sampling error. Statistical analyses were performed using OriginPro 2019b (OriginLab) and the General Linear regression app or Matlab R2019b (MathWorks) and the Distribution Fitter app. P values below 0.05 were considered statistically significant.

Role of the Funding Source

This study was funded by the Natural Science Research Council of Canada (NSERC). The funder had no role in study design, collection or interpretation of the data, preparation of the manuscript, or the decision to submit the manuscript for publication.

RESULTS

Overview of Contributing Studies

After screening and full-text review, 26 studies met the inclusion criteria and contributed to the systematic dataset (**Figure 1**) (15, 16, 23, 25, 26, 28-48). We collected 1,915 quantitative

specimen measurements of SARS-CoV-2 from 1,402 COVID-19 cases (**Table 1**, rVL data summarized in **Appendix Figure**). For pediatric cases, the search found only nonsevere infections and URT specimen measurements. **Appendix Table 1** summarizes the characteristics of contributing studies, of which 18 had low risk of bias according to the modified JBI critical appraisal checklist. Studies at high or unclear risk of bias typically included samples that were not representative of the target population; did not report the VTM volume used; had non-consecutive inclusion for case series and cohort studies or did not use probability-based sampling for cross-sectional studies; and did not report the response rate (**Appendix Table 2**).

URT Shedding of SARS-CoV-2 for Adult COVID-19

In the adult URT, regression analysis showed that, at 1 DFSO, the mean rVL for severe COVID-19 (8.28 [95% CI, 7.71-8.84] log₁₀ copies/ml) was significantly greater (*P* for intercept = 0.005) than that of nonsevere COVID-19 (7.45 [95% CI, 7.26-7.65] log₁₀ copies/ml) (**Figure 2A**). Meanwhile, these cohorts showed comparable rates of SARS-CoV-2 clearance from the URT (*P* for interaction = 0.479). For severe cases, the estimated mean duration of URT shedding (down to 0 log₁₀ copies/ml) was 27.5 (95% CI, 21.2-33.8) DFSO; it was 27.9 (95% CI, 24.4-31.3) DFSO for nonsevere cases.

While regression analysis compared mean shedding levels and dynamics, we fitted rVLs to Weibull distributions to assess heterogeneity in shedding. Both severe and nonsevere adult COVID-19 showed comparably broad heterogeneity in URT shedding throughout disease course (**Figure 2B**). For severe disease, the standard deviation (SD) of rVL was 1.86, 2.34, 1.89 and 1.90 log₁₀ copies/ml at 2, 4, 7 and 10 DFSO, respectively. For nonsevere illness, these SDs were 2.08, 1.90, 1.89 and 1.96 log₁₀ copies/ml, respectively.

Based on our data, the distinction in rVL between severity cohorts was greater near symptom onset. Based on distribution fitting (**Figure 2B**), at 2 DFSO, the estimated rVL at the 80th case percentile (cp) for severe disease was 9.54 (95% CI, 8.78-10.4) log₁₀ copies/ml, while it was 8.84 (95% CI, 8.49-9.20) log₁₀ copies/ml for nonsevere illness. By 10 DFSO, this difference reduced: the 80th-cp estimates were 6.86 (95% CI, 6.20-7.59) and 6.45 (95% CI, 5.91-7.04) log₁₀ copies/ml for severe and nonsevere disease, respectively.

After stratifying adults for disease severity, our analyses showed nonsignificant differences in URT shedding based on sex and age. For nonsevere illness, male and female cases had no significant difference in mean rVL at 1 DFSO (P for intercept = 0.085) or rate of viral clearance (P for interaction = 0.644) (**Figure 2C**). Similarly, for severe disease, male and female cases had comparable mean rVLs at 1 DFSO (P for intercept = 0.326) and URT dynamics (P for interaction = 0.280) (**Figure 2D**). For nonsevere illness, younger and older adults had no significant difference in URT shedding levels at 1 DFSO (P for intercept = 0.294) or post-symptom-onset dynamics (P for interaction = 0.100) (**Figure 2E**). For severe disease, the adult age cohorts showed similar mean rVLs at 1 DFSO (P for intercept = 0.915) and rates of viral clearance (P for interaction = 0.359) (**Figure 2F**).

LRT Shedding of SARS-CoV-2 for Adult COVID-19

Our analyses showed that high, persistent LRT shedding of SARS-CoV-2 was associated with severe COVID-19, but not nonsevere illness, in adults (**Figure 3A**). At the initial day in our analyzed period (4 DFSO), the mean rVL in the LRT of severe cases (8.42 [95% CI, 7.67-9.17] log₁₀ copies/ml) was significantly greater (P for intercept = 0.006) than that of nonsevere cases (6.82 [95% CI, 5.95-7.69] log₁₀ copies/ml). Between severities, the difference in LRT clearance

rates was marginally above the threshold for statistical significance (P for interaction = 0.053). However, severe cases had persistent LRT shedding, with no significant trend in SARS-CoV-2 clearance in the analyzed period (-0.14 [95% CI, -0.32 to 0.030] \log_{10} copies/ml day⁻¹, P = 0.105), whereas nonsevere cases rapidly cleared the virus from the LRT (-0.41 [95% CI, -0.64 to -0.19] \log_{10} copies/ml day⁻¹, P < 0.001). For nonsevere cases, the estimated mean duration of LRT shedding (down to 0 \log_{10} copies/ml) was 20.4 (95% CI, 13.2-27.7) DFSO.

Accordingly, the distributions of severe and nonsevere LRT shedding bifurcated along disease course (**Figure 3B**). At 6 DFSO, the 80th cp estimate of LRT rVL was 9.40 (95% CI, 8.67-10.20) \log_{10} copies/ml for severe COVID-19, while it was 7.66 (95% CI, 6.65-8.83) \log_{10} copies/ml for nonsevere illness. At 10 DFSO, the difference between 80th-cp estimates expanded, as they were 8.63 (95% CI, 8.04-9.26) and 6.01 (95% CI, 4.65-7.78) \log_{10} copies/ml for severe and nonsevere disease, respectively.

Our data indicated that nonsevere illness yielded greater skewing in LRT shedding than severe disease in the analyzed period (**Figure 3B**). For nonsevere COVID-19, the SD of rVL was 1.92, 2.01 and 2.09 \log_{10} copies/ml at 6, 8 and 10 DFSO, respectively. For severe disease, it was lesser 1.25, 1.37 and 1.61 \log_{10} copies/ml at 6, 8 and 10 DFSO, respectively.

For severe COVID-19, regression analysis showed, in the LRT, comparable mean rVLs at 4 DFSO between younger and older adults (P for intercept = 0.745) (**Figure 3C**). Both severe age cohorts also showed persistent LRT shedding in the analyzed period: younger adults (-0.20 [95% CI, -0.32 to 0.042] \log_{10} copies/ml day⁻¹, P = 0.105) and older adults (-0.13 [95% CI, -0.39 to 0.13] \log_{10} copies/ml day⁻¹, P = 0.316) both had no significant trend in SARS-CoV-2 clearance. Likewise, severely affected male cases had no significant trend in LRT shedding (0.001 [95%

CI, -0.16 to 0.19] \log_{10} copies/ml day⁻¹, $P = 0.988$). The female cohort included few samples, and statistically analyses were not conducted (**Appendix Table 3**).

Interestingly, nonsevere cases showed similar SARS-CoV-2 shedding between the URT and LRT, whereas severe cases shed greater and longer in the LRT than the URT (**Figure 3, D and E**). At 4 DFSO, the URT rVL of nonsevere adults was 6.62 (95% CI, 6.50-6.74) \log_{10} copies/ml, which was not different from the LRT rVL of nonsevere adults (P for intercept = 0.651). In contrast, at 4 DFSO, the URT rVL of severe adults (7.34 [95% CI, 7.01-7.68] \log_{10} copies/ml) was significantly lower than the LRT rVL of severe adults (P for intercept = 0.031).

Comparison of URT Shedding between Adult and Pediatric COVID-19

For the pediatric cohort, regression estimated, in the URT, the mean rVL at 1 DFSO to be 7.32 (95% CI, 6.78-7.86) \log_{10} copies/ml and SARS-CoV-2 clearance rate as -0.32 (95% CI, -0.42 to -0.22) \log_{10} copies/ml day⁻¹ (**Figure 4A**). Both estimates were comparable between the sexes for children (**Figure 4D**). The estimated mean duration of URT shedding (down to 0 \log_{10} copies/ml) was 22.6 (95% CI, 17.0-28.1) DFSO for children with COVID-19.

Between pediatric cases, who had nonsevere illness in our dataset, and adults with nonsevere illness, both URT shedding at 1 DFSO (P for intercept = 0.653) and URT dynamics (P for interaction = 0.400) were similar (**Figure 4A**). Distributions of rVL were also comparable between these cohorts (**Figure 4B**). Conversely, URT shedding at 1 DFSO was greater for severely affected adults when compared to nonsevere pediatric cases (P for intercept = 0.017), but URT dynamics remained similar (P for interaction = 0.863) (**Figure 4C**).

DISCUSSION

Our study systematically developed a dataset of COVID-19 case characteristics and rVLs and conducted stratified analyses on SARS-CoV-2 shedding post-symptom onset. In the URT, we found that adults with severe COVID-19 showed higher rVLs shortly after symptom onset, but similar SARS-CoV-2 clearance rates, when compared with their nonsevere counterparts. In the LRT, we found that high, persistent shedding was associated with severe COVID-19, but not nonsevere illness, in adults. Interestingly, in the analyzed periods, adults with severe disease tended to have higher rVLs in the LRT than the URT.

After stratifying for disease severity, we found that sex and age had nonsignificant effects on post-symptom-onset SARS-CoV-2 shedding levels and dynamics for each included analysis (summarized in **Table 2**). Thus, while sex and age influence the tendency to develop severe COVID-19 (2-4), we find no such sex dimorphism or age distinction in URT shedding among cases of similar severity. This includes children, who had nonsevere illness in our study and show similar URT shedding post-symptom onset as adults with nonsevere illness.

Notably, our analyses indicate that high, persistent LRT shedding of SARS-CoV-2 characterizes severe COVID-19 in adults. This suggests that the effective immune responses associated with milder COVID-19, including innate, cross-reactive and coordinated adaptive immunity (5-9), do not significantly inhibit early, or prolonged, SARS-CoV-2 replication in the LRT of severely affected adults. Hence, uncontrolled LRT replication tends to continue, at least, to 10 DFSO, coinciding with the timing of clinical deterioration (median, 10 DFSO) (2, 49). Furthermore, the bifurcated profiles of LRT shedding concur with the observed severity-associated differences in lung pathology, in which severe cases show hyperinflammation and progressive loss of epithelial-endothelial integrity (50-52).

Our results suggest that rVL may be a key prognostic indicator in SARS-CoV-2 infection. They reinforce that severe COVID-19 is associated with greater rVLs than nonsevere illness (12-14), and suggest that sex and age may not significantly influence prognostic thresholds. In the URT, both nonsevere and severe cases tend to clear SARS-CoV-2 at comparable rates. Thus, time course of disease (e.g., DFSO) should be considered alongside rVL, rather than simply employing rVL at admission. LRT shedding, however, bifurcates considerably between nonsevere and severe COVID-19, meaning that SARS-CoV-2 quantitation from the LRT may more accurately predict severity. While URT specimens are typically used to diagnose COVID-19, LRT specimens (our study predominantly analyzed sputum) may be collected from high-risk patients for severity prognostication.

While our analyses did not account for virus infectivity, higher SARS-CoV-2 rVL is associated with a higher likelihood of culture positivity, from adults (15, 16) as well as children (36), and higher transmission risk (10). Hence, our results suggest that infectiousness increases with COVID-19 severity, concurring with epidemiological analyses (53, 54). They also suggest that adult and pediatric infections of similar severity have comparable infectiousness, reflecting epidemiological findings on age-based infectiousness (54-56). Moreover, since respiratory aerosols are typically produced from the LRT (57), severe SARS-CoV-2 infections may have increased, and extended, risk for aerosol transmission. As severe cases tend to be hospitalized, this provides one possible explanation for the elevated risk of COVID-19 among healthcare workers in inpatient settings (58); airborne precautions, such as the use of N95 or air-purifying respirators, should be implemented around patients with COVID-19.

Our study has limitations. First, while our study design systematically developed a large, diverse dataset, there were few severe female cases with LRT specimens and no severe pediatric

cases included. Statistical comparisons involving these cohorts were not conducted based on increased sensitivity to sampling bias, as COVID-19 presents broad heterogeneity in rVL. Additional studies should permit these remaining comparisons. Second, our analyses did not assess the influence of therapies or additional case characteristics, including comorbidities. While the relationships between some comorbidities and SARS-CoV-2 kinetics remain unclear, recent studies indicate many potential therapies (e.g., remdesivir, hydroxychloroquine, lopinavir, ritonavir, low-dose monoclonal antibodies and ivermectin) have no significant anti-SARS-CoV-2 effects in patients (59-64). Third, the systematic dataset consisted largely of hospitalized patients, and our results may not generalize to asymptomatic infections.

In summary, our findings provide insight into SARS-CoV-2 kinetics and describe virological factors that distinguish severe COVID-19 from nonsevere illness. They show that high, persistent LRT shedding characterizes severe disease in adults, highlighting the potential prognostic utility of SARS-CoV-2 quantitation from LRT specimens. Lastly, each study identified by our systematic review collected specimens before October 2020. As widespread transmission of the emerging variants of concern likely occurred after this date (65, 66), our study presents a quantitative resource to assess the effects of their mutations on respiratory shedding levels and dynamics.

Acknowledgement: The authors thank S. Fafi-Kremer, PharmD, PhD (Strasbourg University Hospital); Y. Hirotsu, PhD (Yamanashi Central Hospital); M.S. Kelly, MD, MPH (Duke University); E. Lavezzo, PhD, and A. Crisanti, MD, PhD (University of Padova); J.Z. Li, MD, MMSc (Brigham & Women's Hospital); Cédric Laouénan, MD, PhD, and Yazdan Yazdanpanah, MD, PhD (Bichat-Claude Bernard University Hospital); N.K. Shrestha, MD (Cleveland Clinic); T. Teshima, MD, PhD (Hokkaido University); S. Trouillet-Assant, PhD (Université Hospital of Lyon); J.J.A. van Kampen, MD, PhD (Erasmus University Medical Center); A. Wyllie, PhD, N. Grubaugh, PhD, and A. Ko, MD (Yale School of Public Health); and A. Yilmaz, MD, PhD (Sahlgrenska University Hospital) for responses to data inquiries.

Financial support: This study was supported by NSERC. Mr. Chen was supported by the NSERC Vanier Canada Graduate Scholarship (608544). Dr. Fisman was supported by the Canadian Institutes of Health Research (Canadian COVID-19 Rapid Research Fund, OV4-170360). Dr. Gu was supported by the NSERC Senior Industrial Research Chair.

Disclosures: Dr. Fisman has received honoraria related to work with Pfizer, Astra Zeneca and Seqirus on vaccines for respiratory viruses.

Reproducible Research Statement: *Study protocol, statistical code and data set:* Available from Dr. Gu (e-mail, f.gu@utoronto.ca).

Corresponding Author: Frank X. Gu, PhD, University of Toronto, 200 College St., Toronto, ON M5S 3E5, Canada; e-mail, f.gu@utoronto.ca.

References

1. Dong E, Du H, Gardner L. An interactive web-based dashboard to track COVID-19 in real time. *Lancet Infect Dis.* 2020;20(5):533-4. [PMID: 32087114] doi:10.1016/S1473-3099(20)30120-1
2. Zhou F, Yu T, Du R, et al. Clinical course and risk factors for mortality of adult inpatients with COVID-19 in Wuhan, China: a retrospective cohort study. *Lancet.* 2020;395(10229):1054-62. [PMID: 32171076] doi:10.1016/S0140-6736(20)30566-3
3. Tartof SY, Qian L, Hong V, et al. Obesity and mortality among patients diagnosed with COVID-19: results from an integrated health care organization. *Ann Intern Med.* 2020;173(10):773-81. [PMID: 32783686] doi:10.7326/M20-3742
4. Onder G, Rezza G, Brusaferro S. Case-fatality rate and characteristics of patients dying in relation to COVID-19 in Italy. *JAMA.* 2020;323(18):1775-6. [PMID: 32203977] doi:10.1001/jama.2020.4683
5. Takahashi T, Ellingson MK, Wong P, et al. Sex differences in immune responses that underlie COVID-19 disease outcomes. *Nature.* 2020;588(7837):315-20. [PMID: 32846427] doi:10.1038/s41586-020-2700-3
6. Pierce CA, Preston-Hurlburt P, Dai Y, et al. Immune responses to SARS-CoV-2 infection in hospitalized pediatric and adult patients. *Sci Transl Med.* 2020;12(564). [PMID: 32958614] doi:10.1126/scitranslmed.abd5487
7. Rydzynski MC, Ramirez SI, Dan JM, et al. Antigen-specific adaptive immunity to SARS-CoV-2 in acute COVID-19 and associations with age and disease severity. *Cell.* 2020;183(4):996-1012 e19. [PMID: 33010815] doi:10.1016/j.cell.2020.09.038
8. Ng KW, Faulkner N, Cornish GH, et al. Preexisting and de novo humoral immunity to SARS-CoV-2 in humans. *Science.* 2020;370(6522):1339-43. [PMID: 33159009] doi:10.1126/science.abe1107
9. Lucas C, Wong P, Klein J, et al. Longitudinal analyses reveal immunological misfiring in severe COVID-19. *Nature.* 2020;584(7821):463-9. [PMID: 32717743] doi:10.1038/s41586-020-2588-y
10. Marks M, Millat-Martinez P, Ouchi D, et al. Transmission of COVID-19 in 282 clusters in Catalonia, Spain: a cohort study. *Lancet Infect Dis.* 2021. [PMID: 33545090] doi:10.1016/S1473-3099(20)30985-3
11. Fu Y, Li Y, Guo E, et al. Dynamics and correlation among viral positivity, seroconversion, and disease severity in COVID-19: a retrospective study. *Ann Intern Med.* 2020. [PMID: 33284684] doi:10.7326/M20-3337
12. Pujadas E, Chaudhry F, McBride R, et al. SARS-CoV-2 viral load predicts COVID-19 mortality. *Lancet Respir Med.* 2020;8(9):e70. [PMID: 32771081] doi:10.1016/S2213-2600(20)30354-4
13. Westblade LF, Brar G, Pinheiro LC, et al. SARS-CoV-2 viral load predicts mortality in patients with and without cancer who are hospitalized with COVID-19. *Cancer Cell.* 2020;38(5):661-71 e2. [PMID: 32997958] doi:10.1016/j.ccell.2020.09.007
14. Magleby R, Westblade LF, Trzebucki A, et al. Impact of SARS-CoV-2 viral load on risk of intubation and mortality among hospitalized patients with coronavirus disease 2019. *Clin Infect Dis.* 2020. [PMID: 32603425] doi:10.1093/cid/ciaa851
15. Wolfel R, Corman VM, Guggemos W, et al. Virological assessment of hospitalized patients with COVID-2019. *Nature.* 2020;581(7809):465-9. [PMID: 32235945] doi:10.1038/s41586-020-2196-x
16. van Kampen JJA, van de Vijver D, Fraaij PLA, et al. Duration and key determinants of infectious virus shedding in hospitalized patients with coronavirus disease-2019 (COVID-19). *Nat Commun.* 2021;12(1):267. [PMID: 33431879] doi:10.1038/s41467-020-20568-4
17. Bernheim A, Mei X, Huang M, et al. Chest CT findings in coronavirus disease-19 (COVID-19): relationship to duration of infection. *Radiology.* 2020;295(3):200463. [PMID: 32077789] doi:10.1148/radiol.2020200463
18. He X, Lau EHY, Wu P, et al. Temporal dynamics in viral shedding and transmissibility of COVID-19. *Nat Med.* 2020;26(5):672-5. [PMID: 32296168] doi:10.1038/s41591-020-0869-5
19. Chen PZ, Bobrovitz N, Premji Z, et al. Heterogeneity in transmissibility and shedding SARS-CoV-2 via droplets and aerosols. *medRxiv.* Preprint posted online 2 December 2020. doi:10.1101/2020.10.13.20212233
20. Higgins JPT, Thomas J, Chandler J, et al. *Cochrane handbook for systematic reviews of interventions.* Cochrane book series. 2nd ed. Chichester (UK): John Wiley & Sons; 2019.

21. Moher D, Liberati A, Tetzlaff J, et al. Preferred reporting items for systematic reviews and meta-analyses: the PRISMA statement. *PLOS Med*. 2009;6(7):e1000097. [PMID: 19621072] doi:10.1371/journal.pmed.1000097
22. Han MS, Byun JH, Cho Y, et al. RT-PCR for SARS-CoV-2: quantitative versus qualitative. *Lancet Infect Dis*. 2021;21(2):165. [PMID: 32445709] doi:10.1016/S1473-3099(20)30424-2
23. Lavezzo E, Franchin E, Ciavarella C, et al. Suppression of a SARS-CoV-2 outbreak in the Italian municipality of Vo'. *Nature*. 2020;584(7821):425-9. [PMID: 32604404] doi:10.1038/s41586-020-2488-1
24. Warnke P, Warning L, Podbielski A. Some are more equal - a comparative study on swab uptake and release of bacterial suspensions. *PLOS One*. 2014;9(7):e102215. [PMID: 25010422] doi:10.1371/journal.pone.0102215
25. To KK, Tsang OT, Leung WS, et al. Temporal profiles of viral load in posterior oropharyngeal saliva samples and serum antibody responses during infection by SARS-CoV-2: an observational cohort study. *Lancet Infect Dis*. 2020;20(5):565-74. [PMID: 32213337] doi:10.1016/S1473-3099(20)30196-1
26. Zheng SF, Fan J, Yu F, et al. Viral load dynamics and disease severity in patients infected with SARS-CoV-2 in Zhejiang province, China, January-March 2020: retrospective cohort study. *BMJ*. 2020;369:m1443. [PMID: 32317267] doi:10.1136/bmj.m1443
27. National Institutes of Health. Clinical spectrum of SARS-CoV-2 infection. Accessed at <https://www.covid19treatmentguidelines.nih.gov/overview/clinical-spectrum> on 1 February 2020.
28. Bal A, Brengel-Pesce K, Gaymard A, et al. Clinical and microbiological assessments of COVID-19 in healthcare workers: a prospective longitudinal study. *medRxiv*. Preprint posted online 6 November 2020. doi:10.1101/2020.11.04.20225862
29. Benotmane I, Gautier-Vargas G, Wendling MJ, et al. In-depth virological assessment of kidney transplant recipients with COVID-19. *Am J Transplant*. 2020;20(11):3162-72. [PMID: 32777130] doi:10.1111/ajt.16251
30. Biguenet A, Bouiller K, Marty-Quinnet S, et al. SARS-CoV-2 respiratory viral loads and association with clinical and biological features. *J Med Virol*. 2020. [PMID: 32889755] doi:10.1002/jmv.26489
31. Fajnzylber J, Regan J, Coxen K, et al. SARS-CoV-2 viral load is associated with increased disease severity and mortality. *Nat Commun*. 2020;11(1):5493. [PMID: 33127906] doi:10.1038/s41467-020-19057-5
32. Han MS, Seong MW, Kim N, et al. Viral RNA load in mildly symptomatic and asymptomatic children with COVID-19, Seoul, South Korea. *Emerg Infect Dis*. 2020;26(10):2497-9. [PMID: 32497001] doi:10.3201/eid2610.202449
33. Hirotsu Y, Maejima M, Shibusawa M, et al. Comparison of automated SARS-CoV-2 antigen test for COVID-19 infection with quantitative RT-PCR using 313 nasopharyngeal swabs, including from seven serially followed patients. *Int J Infect Dis*. 2020;99:397-402. [PMID: 32800855] doi:10.1016/j.ijid.2020.08.029
34. Hurst JH, Heston SM, Chambers HN, et al. SARS-CoV-2 infections among children in the biospecimens from respiratory virus-exposed kids (BRAVE Kids) study. *Clin Infect Dis*. 2020. [PMID: 33141180] doi:10.1093/cid/ciaa1693
35. Iwasaki S, Fujisawa S, Nakakubo S, et al. Comparison of SARS-CoV-2 detection in nasopharyngeal swab and saliva. *J Infect*. 2020;81(2):e145-e7. [PMID: 32504740] doi:10.1016/j.jinf.2020.05.071
36. L'Huillier AG, Torriani G, Pigny F, et al. Culture-competent SARS-CoV-2 in nasopharynx of symptomatic neonates, children, and adolescents. *Emerg Infect Dis*. 2020;26(10):2494-7. [PMID: 32603290] doi:10.3201/eid2610.202403
37. Pan Y, Zhang D, Yang P, et al. Viral load of SARS-CoV-2 in clinical samples. *Lancet Infect Dis*. 2020;20(4):411-2. [PMID: 32105638] doi:10.1016/S1473-3099(20)30113-4
38. Peng L, Liu J, Xu WX, et al. SARS-CoV-2 can be detected in urine, blood, anal swabs, and oropharyngeal swabs specimens. *J Med Virol*. 2020;92(9):1676-80. [PMID: 32330305] doi:10.1002/jmv.25936
39. Shrestha NK, Marco Canosa F, Nowacki AS, et al. Distribution of transmission potential during nonsevere COVID-19 illness. *Clin Infect Dis*. 2020;71(11):2927-32. [PMID: 32594116] doi:10.1093/cid/ciaa886

40. Sun J, Tang X, Bai R, et al. The kinetics of viral load and antibodies to SARS-CoV-2. *Clin Microbiol Infect.* 2020;26(12):1690 e1- e4. [PMID: 32898715] doi:10.1016/j.cmi.2020.08.043
41. Vetter P, Eberhardt CS, Meyer B, et al. Daily viral kinetics and innate and adaptive immune response assessment in COVID-19: a case series. *mSphere.* 2020;5(6). [PMID: 33177214] doi:10.1128/mSphere.00827-20
42. Wyllie AL, Fournier J, Casanovas-Massana A, et al. Saliva or nasopharyngeal swab specimens for detection of SARS-CoV-2. *N Engl J Med.* 2020;383(13):1283-6. [PMID: 32857487] doi:10.1056/NEJMc2016359
43. Xu Y, Li X, Zhu B, et al. Characteristics of pediatric SARS-CoV-2 infection and potential evidence for persistent fecal viral shedding. *Nat Med.* 2020;26(4):502-5. [PMID: 32284613] doi:10.1038/s41591-020-0817-4
44. Yazdanpanah Y, French COVID cohort investigators and study group. Impact on disease mortality of clinical, biological, and virological characteristics at hospital admission and overtime in COVID-19 patients. *J Med Virol.* 2020. [PMID: 33058220] doi:10.1002/jmv.26601
45. Yilmaz A, Marklund E, Andersson M, et al. Upper respiratory tract levels of Severe Acute Respiratory Syndrome Coronavirus 2 RNA and duration of viral RNA shedding do not differ between patients with mild and severe/critical Coronavirus Disease 2019. *J Infect Dis.* 2021;223(1):15-8. [PMID: 33020822] doi:10.1093/infdis/jiaa632
46. Yonker LM, Neilan AM, Bartsch Y, et al. Pediatric severe acute respiratory syndrome coronavirus 2 (SARS-CoV-2): clinical presentation, infectivity, and immune responses. *J Pediatr.* 2020;227:45-52. [PMID: 32827525] doi:10.1016/j.jpeds.2020.08.037
47. Zhang N, Gong YH, Meng FP, et al. Comparative study on virus shedding patterns in nasopharyngeal and fecal specimens of COVID-19 patients. *Sci China Life Sci.* 2020. [PMID: 32778998] doi:10.1007/s11427-020-1783-9
48. Zou L, Ruan F, Huang M, et al. SARS-CoV-2 viral load in upper respiratory specimens of infected patients. *N Engl J Med.* 2020;382(12):1177-9. [PMID: 32074444] doi:10.1056/NEJMc2001737
49. Berlin DA, Gulick RM, Martinez FJ. Severe Covid-19. *N Engl J Med.* 2020;383(25):2451-60. [PMID: 32412710] doi:10.1056/NEJMcp2009575
50. Matheson NJ, Lehner PJ. How does SARS-CoV-2 cause COVID-19? *Science.* 2020;369(6503):510-1. [PMID: 32732413] doi:10.1126/science.abc6156
51. Magro C, Mulvey JJ, Berlin D, et al. Complement associated microvascular injury and thrombosis in the pathogenesis of severe COVID-19 infection: A report of five cases. *Transl Res.* 2020;220:1-13. [PMID: 32299776] doi:10.1016/j.trsl.2020.04.007
52. Xu Z, Shi L, Wang Y, et al. Pathological findings of COVID-19 associated with acute respiratory distress syndrome. *Lancet Respir Med.* 2020;8(4):420-2. [PMID: 32085846] doi:10.1016/S2213-2600(20)30076-X
53. Sayampanathan AA, Heng CS, Pin PH, et al. Infectivity of asymptomatic versus symptomatic COVID-19. *Lancet.* 2021;397(10269):93-4. [PMID: 33347812] doi:10.1016/S0140-6736(20)32651-9
54. Li F, Li YY, Liu MJ, et al. Household transmission of SARS-CoV-2 and risk factors for susceptibility and infectivity in Wuhan: a retrospective observational study. *Lancet Infect Dis.* 2021. [PMID: 33476567] doi:10.1016/S1473-3099(20)30981-6
55. Sun K, Wang W, Gao L, et al. Transmission heterogeneities, kinetics, and controllability of SARS-CoV-2. *Science.* 2021;371(6526). [PMID: 33234698] doi:10.1126/science.abe2424
56. Laxminarayan R, Wahl B, Dudala SR, et al. Epidemiology and transmission dynamics of COVID-19 in two Indian states. *Science.* 2020;370(6517):691-7. [PMID: 33154136] doi:10.1126/science.abd7672
57. Johnson GR, Morawska L, Ristovski ZD, et al. Modality of human expired aerosol size distributions. *J Aerosol Sci.* 2011;42(12):839-51. [PMID: 20923611] doi:10.1016/j.jaerosci.2011.07.009
58. Nguyen LH, Drew DA, Graham MS, et al. Risk of COVID-19 among front-line health-care workers and the general community: a prospective cohort study. *Lancet Public Health.* 2020;5(9):E475-E83. [PMID: 32745512] doi:10.1016/S2468-2667(20)30164-X
59. Wang Y, Zhang D, Du G, et al. Remdesivir in adults with severe COVID-19: a randomised, double-blind, placebo-controlled, multicentre trial. *Lancet.* 2020;395(10236):1569-78. [PMID: 32423584] doi:10.1016/S0140-6736(20)31022-9

60. Lyngbakken MN, Berdal JE, Eskesen A, et al. A pragmatic randomized controlled trial reports lack of efficacy of hydroxychloroquine on coronavirus disease 2019 viral kinetics. *Nat Commun.* 2020;11(1):5284. [PMID: 33082342] doi:10.1038/s41467-020-19056-6
61. Chen P, Nirula A, Heller B, et al. SARS-CoV-2 neutralizing antibody LY-CoV555 in outpatients with Covid-19. *N Engl J Med.* 2021;384(3):229-37. [PMID: 33113295] doi:10.1056/NEJMoa2029849
62. Chaccour C, Casellas A, Blanco-Di Matteo A, et al. The effect of early treatment with ivermectin on viral load, symptoms and humoral response in patients with non-severe COVID-19: a pilot, double-blind, placebo-controlled, randomized clinical trial. *EClinicalMedicine.* 2021:100720. [PMID: 33495752] doi:10.1016/j.eclinm.2020.100720
63. Cao B, Wang Y, Wen D, et al. A trial of lopinavir-ritonavir in adults hospitalized with severe Covid-19. *N Engl J Med.* 2020;382(19):1787-99. [PMID: 32187464] doi:10.1056/NEJMoa2001282
64. World Health Organization Solidarity Trial Consortium. Repurposed antiviral drugs for Covid-19 - interim WHO Solidarity trial results. *N Engl J Med.* 2021;384(6):497-511. [PMID: 33264556] doi:10.1056/NEJMoa2023184
65. Davies NG, Abbott S, Barnard RC, et al. Estimated transmissibility and severity of novel SARS-CoV-2 variant of concern 202012/01 in England. *medRxiv.* Preprint posted online 7 February 2021. doi:10.1101/2020.12.24.20248822
66. Tegally H, Wilkinson E, Giovanetti M, et al. Emergence and rapid spread of a new severe acute respiratory syndrome-related coronavirus 2 (SARS-CoV-2) lineage with multiple spike mutations in South Africa. *medRxiv.* Preprint posted online 22 December 2020. doi:10.1101/2020.12.21.20248640

541 **Table 1.** Characteristics of adult and pediatric COVID-19 cases

	Adult	Pediatric
Cases, <i>n</i>	1 266	136
URT specimens, <i>n</i>	1 513	192
LRT specimens, <i>n</i>	210	0
Mean age (SD), <i>y</i>	51.8 (18.0)	8.7 (5.3)
Male, <i>n</i> (%)	528 (44.0)	63 (52.5)
Disease severity, <i>n</i> (%)		
Asymptomatic	2 (0.2)	5 (3.7)
Mild	710 (57.5)	112 (83.6)
Moderate	178 (14.4)	17 (12.7)
Severe	167 (13.5)	0 (0.0)
Critical	178 (14.4)	0 (0.0)

542 LRT = lower respiratory tract; URT = upper respiratory tract.

543 The table summarizes collected case characteristics in the systematic dataset. Adult cases were

544 those aged 18 y or older, while pediatric cases were those aged younger than 18 y.

Table 2. Summary of statistical comparisons on SARS-CoV-2 shedding, across the respiratory tract, COVID-19 severity, sex and age cohorts

Group 1	Group 2	P value*	
		Intercept†	Interaction‡
URT, ≥18 y			
Nonsevere	Severe	0.005*	0.479
Female (nonsevere)	Male (nonsevere)	0.085	0.644
Female (severe)	Male (severe)	0.326	0.280
Nonsevere (18-59 y)	Nonsevere (≥60 y)	0.294	0.100
Severe (18-59 y)	Severe (≥60 y)	0.915	0.359
LRT, ≥18 y §			
Nonsevere	Severe	0.006*	0.053
Severe (18-59 y)	Severe (≥60 y)	0.745	0.716
URT vs. LRT, ≥18 y			
Nonsevere (URT, ≥18 y)	Nonsevere (LRT, ≥18 y)	0.651	0.231
Severe (URT, ≥18 y)	Severe (LRT, ≥18 y)	0.031*	0.151
URT, 0-17 y			
Nonsevere (0-17 y)	Nonsevere (≥18 y)	0.653	0.400
Nonsevere (0-17 y)	Severe (≥18 y)	0.017*	0.863
Female (nonsevere)	Male (nonsevere)	0.667	0.333

COVID-19 = coronavirus disease 2019; DFSO = days from symptom onset; LRT = lower

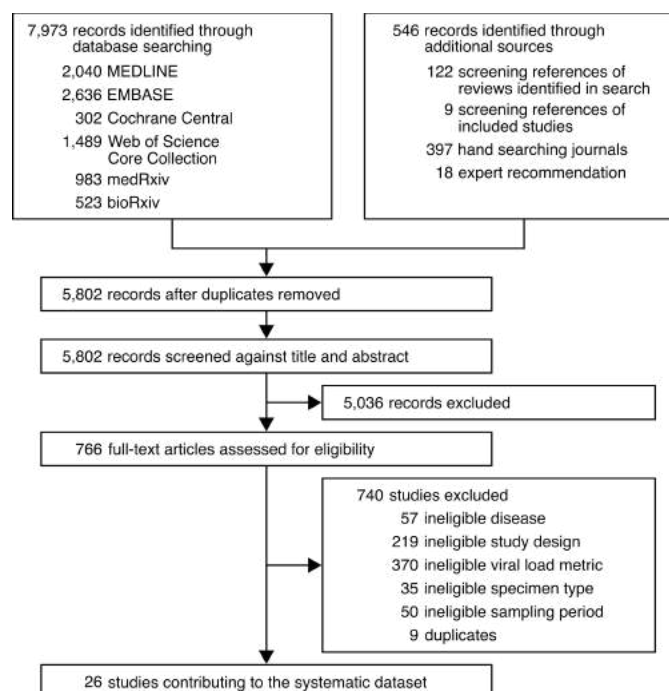
respiratory tract; nonsevere = asymptomatic, mild and moderate COVID-19; rVL = respiratory viral load; severe = severe and critical COVID-19; URT = upper respiratory tract.

* $P < 0.05$. Each regression analysis was shown in **Figures 2 to 4**.

† P value for the intercept in regression analysis compares the mean rVLs at 1 DFSO for the URT or, for any analyses including the LRT, at 4 DFSO.

‡ P value for interaction in regression analysis describes the difference in respiratory shedding dynamics along the time course of disease.

§ There were small sample sizes in the nonsevere cohorts and female (LRT, severe, ≥18 y) cohort, and these analyses were not included.



558

559 **Figure 1.** Study selection.

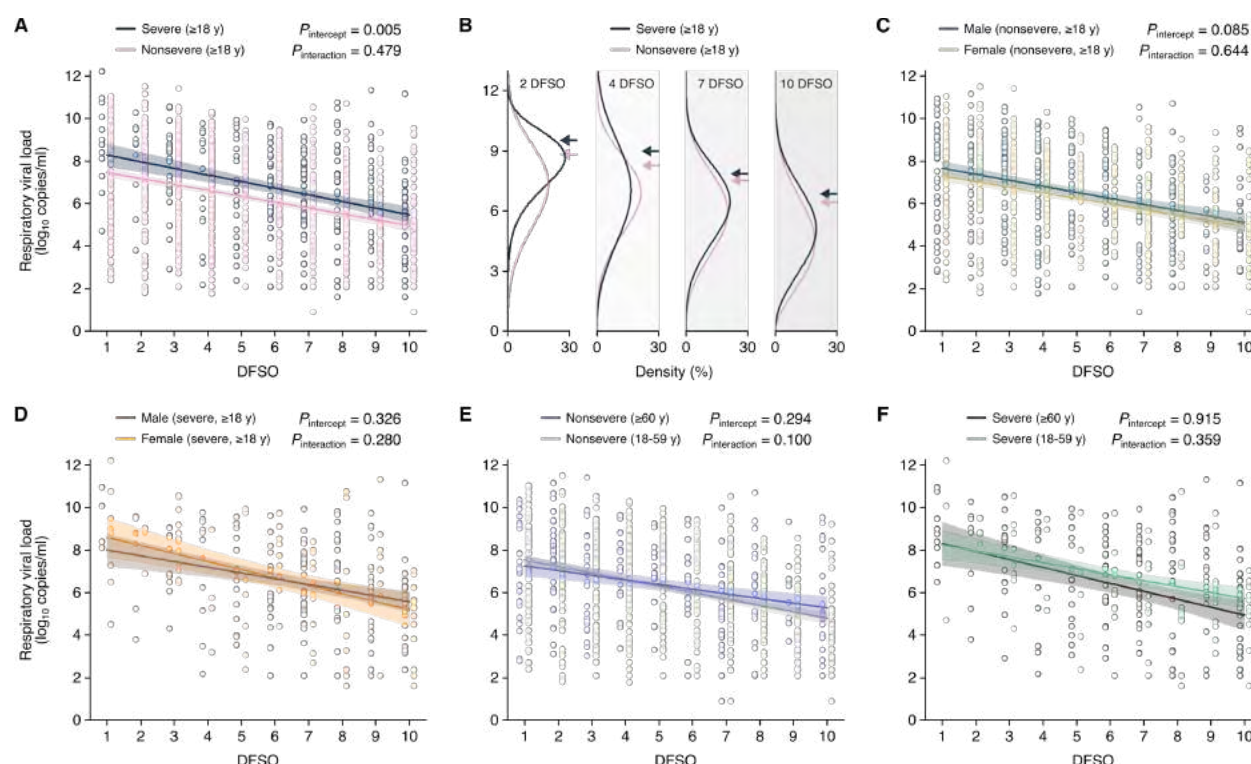


Figure 2. Comparison of SARS-CoV-2 shedding in the adult URT, across disease severity, sex and age cohorts.

COVID-19 = coronavirus disease 2019; DFSO = days from symptom onset; nonsevere = asymptomatic, mild and moderate COVID-19; rVL = respiratory viral load; SARS-CoV-2 = severe acute respiratory syndrome coronavirus 2; severe = severe and critical COVID-19; URT = upper respiratory tract.

A and B. Regression analysis (A) and estimated distributions at 2, 4, 7 and 10 DFSO (B) of URT shedding for severe and nonsevere adult (aged 18 y or older) COVID-19. Arrows denote rVLs for the 80th case percentiles, in terms of rVL, for each age group. **C and D.** Regression analyses comparing URT shedding between sexes for nonsevere (C) and severe (D) adult COVID-19. **E and F.** Regression analyses comparing URT shedding between age cohorts (aged 18-59 y and 60

574 y or older) for nonsevere (E) and severe (F) adult COVID-19. Open circles represent rVL data
 575 and were offset from their DFSO for visualization. Lines and bands show regressions and their
 576 95% CIs, respectively. *P* values for the intercept compare the rVLs at 1 DFSO. *P* values for
 577 interaction compare shedding dynamics.

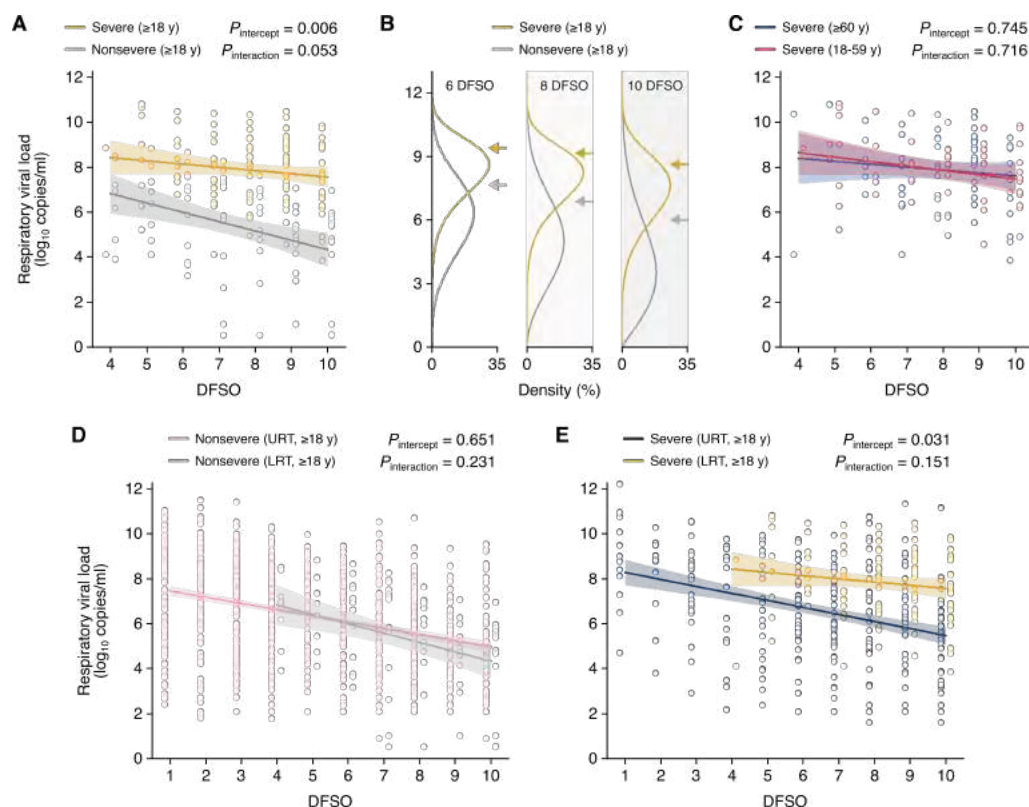


Figure 3. Comparison of SARS-CoV-2 shedding in the adult LRT, across disease severity, age and with shedding in the adult URT.

COVID-19 = coronavirus disease 2019; DFSO = days from symptom onset; LRT = lower respiratory tract; nonsevere = asymptomatic, mild and moderate COVID-19; rVL = respiratory viral load; SARS-CoV-2 = severe acute respiratory syndrome coronavirus 2; severe = severe and critical COVID-19; URT = upper respiratory tract.

A and B. Regression analysis (A) and estimated distributions at 6, 8 and 10 DFSO (B) of LRT shedding for severe and nonsevere adult (aged 18 y or older) COVID-19. Arrows denote rVLs for the 80th case percentiles, in terms of rVL, for each age group. **C.** Regression analyses comparing LRT shedding between age cohorts (aged 18-59 y and 60 y or older) for severe adult

591 COVID-19. **D** and **E**. Regression analyses comparing URT and LRT shedding for nonsevere (D)
 592 and severe (E) adult COVID-19. Open circles represent rVL data and were offset from their
 593 DFSO for visualization. Lines and bands show regressions and their 95% CIs, respectively. *P*
 594 values for the intercept compare the rVLs at 4 DFSO. *P* values for interaction compare shedding
 595 dynamics.

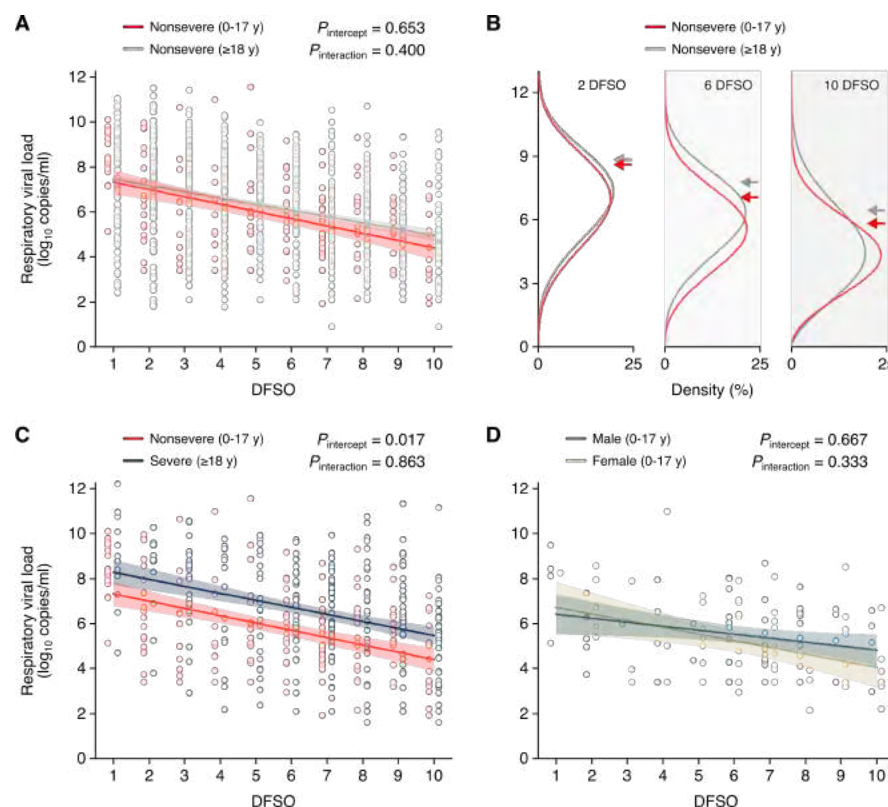


Figure 4. URT shedding of SARS-CoV-2 in pediatric COVID-19, compared with adults and across sex.

COVID-19 = coronavirus disease 2019; DFSO = days from symptom onset; nonsevere = asymptomatic, mild and moderate COVID-19; rVL = respiratory viral load; SARS-CoV-2 = severe acute respiratory syndrome coronavirus 2; severe = severe and critical COVID-19; URT = upper respiratory tract.

A and B. Regression analysis (A) and estimated distributions at 2, 6, and 10 DFSO (B) of URT shedding for children (aged 0-17 y) with nonsevere COVID-19 and adults (aged 18 y or older) with nonsevere illness. Arrows denote rVLs for the 80th case percentiles, in terms of rVL, for each cohort. **C.** Regression analysis comparing URT shedding between nonsevere pediatric and

609 severe adult COVID-19. **D.** Regression analysis comparing URT shedding between sexes for
 610 pediatric cases. Open circles represent rVL data and were offset from their DFSO for
 611 visualization. Lines and bands show regressions and their 95% CIs, respectively. *P* values for the
 612 intercept compare the rVLs at 1 DFSO. *P* values for interaction compare shedding dynamics.



[JAMA Intern Med.](#) 2020 Sep; 180(9): 1156–1163.

PMCID: PMC7195694

Published online 2020 May 1.

PMID: [32356867](#)

doi: 10.1001/jamainternmed.2020.2020: 10.1001/jamainternmed.2020.2020

Contact Tracing Assessment of COVID-19 Transmission Dynamics in Taiwan and Risk at Different Exposure Periods Before and After Symptom Onset

[Hao-Yuan Cheng](#), MD, MSc,¹ [Shu-Wan Jian](#), DVM, MPH,¹ [Ding-Ping Liu](#), PhD,¹ [Ta-Chou Ng](#), BSc,² [Wan-Ting Huang](#), MD,³ and [Hsien-Ho Lin](#), MD, ScD^{1,2,4}, for the Taiwan COVID-19 Outbreak Investigation Team

¹Epidemic Intelligence Center, Taiwan Centers for Disease Control, Taipei, Taiwan

²Institute of Epidemiology and Preventive Medicine, National Taiwan University College of Public Health, Taipei, Taiwan

³Office of Preventive Medicine, Taiwan Centers for Disease Control, Taipei, Taiwan

⁴Global Health Program, National Taiwan University College of Public Health, Taipei, Taiwan

 Corresponding author.

Article Information

Group Information: A complete list of the members of the Taiwan COVID-19 Outbreak Investigation Team appears at the end of this article.

Accepted for Publication: April 21, 2020.

Published Online: May 1, 2020. doi:10.1001/jamainternmed.2020.2020

Correction: This article was corrected on September 8, 2020, to fix transposed numbers of men and women study participants in the Abstract and in the Results section; an error in the definition of serial interval in the Introduction; the misspelling of 2 names in the Group Information section; and typographical data errors in the Supplement.

Open Access: This is an open access article distributed under the terms of the [CC-BY License](#). © 2020 Cheng H-Y et al. *JAMA Internal Medicine*.

Corresponding Author: Hsien-Ho Lin, MD, ScD, National Taiwan University, 17 Xuzhou Rd, Taipei 100, Taiwan (hsienho@ntu.edu.tw).

Author Contributions: Drs Cheng and Lin had full access to all of the data in the study and take responsibility for the integrity of the data and the accuracy of the data analysis.

Concept and design: Cheng, Jian, Huang, Lin.

Acquisition, analysis, or interpretation of data: All authors.

Drafting of the manuscript: Cheng, Jian, Ng, Lin.

Critical revision of the manuscript for important intellectual content: Cheng, Jian, Liu, Huang, Lin.

Statistical analysis: Cheng, Jian, Ng, Lin.

Obtained funding: Lin.

Administrative, technical, or material support: Jian, Liu, Ng, Huang, Lin.

Supervision: Liu, Huang, Lin.

Conflict of Interest Disclosures: None reported.

Funding/Support: The study was funded by Taiwan Ministry of Science and Technology (MOST 107-2314-B-002-187-MY2 and MOST 108-2628-B-002-022).

Role of the Funder/Sponsor: The funder had no role in the design and conduct of the study; collection, management, analysis, and interpretation of the data; preparation, review, or approval of the manuscript; and decision to submit the manuscript for publication.

Group Information: The Taiwan COVID-19 Outbreak Investigation Team members include the following: Taiwan CDC: Office of Preventive Medicine and Taiwan Field Epidemiology Training Program: Wan-Ting Huang, Wan-Chin Chen, Angela Song-En Huang, Chia-Ping Su, Pin-Hui Lee, Pei-Chun Chan, Hao-Hsin Wu, Shih-Tse Huang, Tsung-Pei Tsou, Ying-Shih Su, and Yang Li. Taipei Regional Control Center: Hsin-Yi Wei, Meng-Yu Chen, Shiao-Ping Tung, Yu-Fang Tsai, Xiang-Ting Huang, and Chien-Yu Chou. North Regional Control Center: Pei-Yuan Wu, Fang-Tzu Chang, Chia-Ying Yen, Hsueh-Mei Chiang, Ju-Hui Lin, and Ming-Chu Tai. Central Regional Control Center: Kung-Chin Wang, Ching-Fen Ko, Pei-Fang Lai, Du-Ling Lin, Min-Tsung Lin, and Zhi-Jie Ding. South Regional Control Center: Huai-Te Tsai, Ping-Jung Liu, Pei-Yi Lin, Shu-Chen Chang, and Yi-Ying Lin. Kao-Ping Regional Control Center: Hsin-Chun Lee, Chi-Nan Hung, Ching-Li Lin, Chi-Mei Lai, and Hsiao-Mei Liu.

Additional Contributions: We thank the Taiwan COVID-19 Outbreak Investigation Team, the staffs of regional control centers of the Taiwan Centers for Disease Control (CDC), and partners from other public health bureaus (Taipei City, New Taipei City, Taoyuan City, Taichung City, Tainan City, Kaohsiung City, Changhua, Nantou, Hsinchu, Miaoli, Yunlin, and Ilan County) for their dedicated outbreak investigation and meticulous data collection. Our study could not have been done without their efforts. We also thank Chia-Lin Lee, MSc, and Yu-Lun Liu, MD, MSc, for the development of electronic contact tracing system (Epidemic Intelligence Center, Taiwan CDC); Ching-Hung Wang (TonyQ) for the consultation of system development; Angela Song-En Huang, MD, MPH (Office of Preventive Medicine, Taiwan CDC), for writing assistance. They did not receive compensation outside of their salary.

Received 2020 Apr 10; Accepted 2020 Apr 21.

[Copyright](#) 2020 Cheng H-Y et al. *JAMA Internal Medicine*.

This is an open access article distributed under the terms of the CC-BY License.

Key Points

Question

What is the transmissibility of coronavirus disease 2019 (COVID-19) to close contacts?

Findings

In this case-ascertained study of 100 cases of confirmed COVID-19 and 2761 close contacts, the overall secondary clinical attack rate was 0.7%. The attack rate was higher among contacts whose exposure to the index case started within 5 days of symptom onset than those who were exposed later.

Meaning

High transmissibility of COVID-19 before and immediately after symptom onset suggests that finding and isolating symptomatic patients alone may not suffice to interrupt transmission, and that more generalized measures might be required, such as social distancing.

Abstract

Importance

The dynamics of coronavirus disease 2019 (COVID-19) transmissibility are yet to be fully understood. Better understanding of the transmission dynamics is important for the development and evaluation of effective control policies.

Objective

To delineate the transmission dynamics of COVID-19 and evaluate the transmission risk at different exposure window periods before and after symptom onset.

Design, Setting, and Participants

This prospective case-ascertained study in Taiwan included laboratory-confirmed cases of COVID-19 and their contacts. The study period was from January 15 to March 18, 2020. All close contacts were quarantined at home for 14 days after their last exposure to the index case. During the quarantine period, any relevant symptoms (fever, cough, or other respiratory symptoms) of contacts triggered a COVID-19 test. The final follow-up date was April 2, 2020.

Main Outcomes and Measures

Secondary clinical attack rate (considering symptomatic cases only) for different exposure time windows of the index cases and for different exposure settings (such as household, family, and health care).

Results

We enrolled 100 confirmed patients, with a median age of 44 years (range, 11-88 years), including 44 men and 56 women. Among their 2761 close contacts, there were 22 paired index-secondary cases. The overall secondary clinical attack rate was 0.7% (95% CI, 0.4%-1.0%). The attack rate was higher among the 1818 contacts whose exposure to index cases started within 5 days of symptom onset (1.0% [95% CI, 0.6%-1.6%]) compared with those who were exposed later (0 cases from 852 contacts; 95% CI, 0%-0.4%). The 299 contacts with exclusive presymptomatic exposures were also at risk (attack rate, 0.7% [95% CI, 0.2%-2.4%]). The attack rate was higher among household (4.6% [95% CI, 2.3%-9.3%]) and nonhousehold (5.3% [95% CI, 2.1%-12.8%]) family contacts than that in health care or other settings. The attack rates were higher among those aged 40 to 59 years (1.1% [95% CI, 0.6%-2.1%]) and those aged 60 years and older (0.9% [95% CI, 0.3%-2.6%]).

Conclusions and Relevance

In this study, high transmissibility of COVID-19 before and immediately after symptom onset suggests that finding and isolating symptomatic patients alone may not suffice to contain the epidemic, and more generalized measures may be required, such as social distancing.

Introduction

The coronavirus disease 2019 (COVID-19) outbreak that originated in Wuhan, China, spread to more than 100 countries within 2 months of when the severe acute respiratory syndrome coronavirus 2 (SARS-CoV-2) was identified in January 2020.^{1,2} Following the Wuhan lockdown and other extreme social-distancing

measures conducted by the Chinese government, several countries with widespread outbreaks implemented similar measures, including shutting down entire cities or communities, banning international or domestic travel, conducting border control with symptom screening, and implementing isolation and quarantine.

The unknown epidemiologic characteristics and transmission dynamics of a novel pathogen, such as SARS-CoV-2, complicate the development and evaluation of effective control policies.³ The serial interval of COVID-19, defined as the interval between the symptom onset of the index case and that of the secondary case, was found to be short (4-5 days) and was similar to the estimated incubation period.⁴ The short serial interval of COVID-19 and results from viral shedding studies suggested that most transmission occurred near or even before the time of symptom onset.^{4,5,6} On the other hand, prolonged viral shedding raised concerns about prolonged infectiousness of patients and the need for extended isolation. A few preliminary contact-tracing studies showed that the highest-risk exposure setting of COVID-19 transmission was the household.^{7,8,9} Nevertheless, it is not known when and how long a patient with COVID-19 should be isolated or whether close contacts should be quarantined. Additional information is needed about the transmission risk at different time points before and after symptom onset and with different types of exposures, such as through the household or a health care facility.

In Taiwan, the first COVID-19 case was confirmed on January 21, 2020.¹⁰ With proactive containment efforts and comprehensive contact tracing, the number of COVID-19 cases remained low, as compared with other countries that had widespread outbreaks.^{11,12} Using the contact tracing data in Taiwan, we aimed to delineate the transmission dynamics of COVID-19, evaluate the infection risk at different exposure windows, and estimate the infectious period.

Methods

Study Population

On January 15, 2020, in response to the outbreak in Wuhan, the Taiwan Centers for Disease Control (Taiwan CDC) made COVID-19 a notifiable disease. We conducted a prospective case-ascertained study that enrolled all the initial 100 confirmed cases in Taiwan between January 15 and March 18, 2020, and their close contacts. All contacts were followed up until 14 days after the last exposure to the index case. The last follow-up date was April 2, 2020.

The study followed the Strengthening the Reporting of Observational Studies in Epidemiology (STROBE) reporting guideline.¹³ Information was collected according to the pronouncement of the Central Epidemic Command Center and in accordance with Article 17 of the Communicable Disease Control Act.¹⁴ As part of the public health response functions of the Central Epidemic Command Center for surveillance purposes, institutional review board approval of this study and informed consent were waived. Prior to analysis, the data were deidentified.

Ascertainment of Cases

A confirmed case met the criteria of notification for COVID-19 in Taiwan and tested positive by real-time reverse transcriptase–polymerase chain reaction (RT-PCR) test.¹⁵ Detailed information, including demographic and clinical data, was reported to the National Notifiable Disease Surveillance System.¹⁶ The investigation team determined the clinical severity of the confirmed patients following the World Health Organization (WHO) interim guidance.¹⁷

Contact Tracing for COVID-19

When a patient was laboratory-confirmed to have SARS-CoV-2 infection, a thorough epidemiological investigation, including contact tracing, was implemented by the outbreak investigation team of the Taiwan CDC and local health authorities. The period of investigation started at the date at symptom onset (and could be extended to up to 4 days before symptom onset when epidemiologically indicated) and ended at the date at COVID-19 confirmation. For asymptomatic confirmed cases, the period of investigation was based on the date at confirmation (instead of date at onset) and was determined according to epidemiological investigation. The definition of a close contact was a person who did not wear appropriate personal protection equipment (PPE) while having face-to-face contact with a confirmed case for more than 15 minutes during the investigation period. A contact was listed as a household contact if he or she lived in the same household with the index case. Those listed as family contacts were family members not living in the same household.

For health care settings, medical staff, hospital workers, and other patients in the same setting were included; close contact was defined by contacting an index case within 2 m without appropriate PPE and without a minimal requirement of exposure time. Whether the PPE was regarded as “appropriate” depended on the exposure setting and the procedures performed. For example, for physicians who performed aerosol-generating procedures, such as intubation, an N95 respirator was required. For such procedures, a surgical mask would not be appropriate PPE. Accordingly, the medical staff would be listed as a close contact.

All close contacts were quarantined at home for 14 days after their last exposure to the index case. During the quarantine period, any relevant symptoms (fever, cough, or other respiratory symptoms) of close contacts would trigger RT-PCR testing for COVID-19. For high-risk populations, including household and hospital contacts, RT-PCR was performed regardless of symptoms. Essentially, these high-risk contacts were tested once when they were listed as a close contact. If the initial COVID-19 test result was negative, further testing would only be performed if a close contact developed symptoms during quarantine. The Taiwan CDC used an electronic tracing system (Infectious Disease Contact Tracing Platform and Management System) to follow and record the daily health status of those quarantined contacts.¹⁸ The information collected included age, sex, the index case, date at exposure, and the exposure setting.

Data Processing and Analysis

Paired data of index case and close contacts were extracted from the contact tracing database and outbreak investigation reports. For a family cluster, the index case was determined based on the temporality of symptom onset and review of the epidemiological link. A secondary case was excluded from the paired data if the beginning of exposure was after symptom onset of the secondary case (only applied when the secondary case was symptomatic). For health care contacts, the date at exposure would be the date at admission of the case if the exact date at exposure was not recorded.

Incubation period and serial interval were estimated using the contact tracing data in Taiwan and publicly available data sets globally (eMethods in the [Supplement](#)). We used the Bayesian hierarchical model to increase the stability in small-sample estimation. The exposure window period was defined as the period between the first and last day of reported exposure to the index case based on contact investigation. Following the WHO, we defined the secondary clinical attack rate as the ratio of symptomatic confirmed cases among the close contacts.¹⁹ We analyzed the dynamic change of secondary clinical attack rate in relation to symptom onset of the index case (days <0, 0-3, 4-5, 6-7, 8-9, or >9).

The percentage of missing information was small (7.0% for age, 6.1% for sex, and 3.3% for time from onset to exposure; [Table 1](#)). In the univariable analysis of secondary clinical attack rate by different exposure characteristics (eg, age), close contacts with missing information in that particular exposure

attribute were excluded. All statistical tests were 2-sided with an α level of .05. All confidence intervals (CIs) were 95%. R software (R Foundation for Statistical Computing) and RStan (Stan Development Team) were used for data management and analysis.

Results

As of March 18, 2020, there were 100 patients with laboratory-confirmed COVID-19 in Taiwan, including 10 clusters of patients and 9 asymptomatic patients. The median age of the 100 patients was 44 years old (range, 11-88 years); 44 were men and 56 were women. Of the 2761 close contacts that were identified, 5.5% were household contacts, 2.8% were non-household family contacts, and 25.3% were health care contacts ([Table 1](#)). Through contact tracing, 23 secondary cases were found. One of the 23 cases was excluded from subsequent transmission-pair analysis because the documented day at exposure occurred after symptom onset of the secondary case. None of the 9 asymptomatic case patients transmitted a secondary case. Using the data on the 22 paired cases, we estimated that the median incubation period was 4.1 days (95% credible interval [CrI], 0.4-15.8), and the median serial interval was 4.1 days (95% CrI, 0.1-27.8) (eTables 1-5 and eFigures 1-5 in the [Supplement](#)).

Among the 2761 close contacts, 22 secondary cases of COVID-19 infection (including 4 asymptomatic infections) were detected, with an infection risk of 0.8% (95% CI, 0.5%-1.2%). The secondary clinical attack rate was 18 of 2761, or 0.7% (95% CI, 0.4%-1.0%). [Figure 1](#) shows the exposure window of all contacts. All of the 22 secondary cases had their first exposure before the sixth day of the index case's symptom onset. By comparison, only 68% of noncase contacts had their first exposure before day 6 ([Table 1](#)). The secondary clinical attack rate was higher among those whose initial exposure to the index case was within 5 days of symptom onset than those who were exposed after day 6 (zero transmission of 852 contacts [95% CI, 0%-0.4%]) ([Table 2](#) and [Figure 2A](#)). The 735 contacts whose initial exposure occurred before symptom onset of the index case were also at risk, with a secondary clinical attack rate of 1.0% (95% CI, 0.5%-2.0%). A subgroup of 299 contacts with exclusive presymptomatic exposures were also at risk (secondary clinical attack rate, 0.7% [95% CI, 0.2%-2.4%]).

The secondary clinical attack rate was 4.6% (95% CI, 2.3%-9.3%) among 151 household contacts and 5.3% (95% CI, 2.1%-12.8%) in 76 nonhousehold family contacts ([Table 2](#)). The high attack rate from early exposure remained when the analysis was restricted to household and nonhousehold family contacts ([Table 3](#) and [Figure 2B](#)). The attack rates were higher among those aged 40 to 59 years (1.1% [95% CI, 0.6%-2.1%]) and those aged 60 years and older (0.9% [95% CI, 0.3%-2.6%]). The 786 close contacts of the 6 confirmed cases presenting with severe disease were at a higher risk compared with the 1097 close contacts of the 56 cases presenting with mild disease (risk ratio, 3.76 [95% CI, 1.10-12.76] and 3.99 [95% CI, 1.00-15.84] for severe pneumonia and acute respiratory distress syndrome/sepsis, respectively). Among the 91 close contacts of the 9 asymptomatic cases, no secondary transmission was observed. The secondary attack rate among contacts of cases with infection acquired in Taiwan was higher than that among contacts of cases with infection acquired outside of Taiwan ([Table 2](#)).

Discussion

Our analysis of close contacts to confirmed COVID-19 cases revealed a relatively short infectious period of COVID-19 and a higher transmission risk around the time of symptom onset of the index case, followed by a lower transmission risk at the later stage of disease. The observed decreasing transmission risk over time for COVID-19 was in striking contrast to the transmission pattern of severe acute respiratory syndrome (SARS), in which the transmission risk remained low until after day 5 of symptom onset in the index cases.²⁰ Our study and the study by Nishiura et al⁴ revealed a short serial interval of COVID-19, with a median of 4 to 5 days. In contrast, the mean serial interval of SARS was estimated to be 8.4 days in Singapore.²⁰ The present contact tracing analysis suggested that the shorter serial interval of COVID-19 was due to the combination of early-stage transmission and a short period of infectiousness.

The observed pattern of the secondary clinical attack rate over time was also consistent with the quantitative data of the SARS-CoV-2 viral shedding in upper respiratory specimens, which has been found in China to be a high viral load around the time of symptom onset, followed by a gradual decrease in viral shedding to a low level after 10 days.⁵ The viral load was similar among asymptomatic, minimally symptomatic, and symptomatic patients. Another virological study in patients with COVID-19 in Germany also found no viable isolates of the virus after the first week of symptoms.²¹ Our findings agree with the virological data on high transmissibility of COVID-19 in the first week after the onset of symptoms and decreased risk afterwards.²¹ We also documented and quantified the transmission potential of COVID-19 in a subgroup of contacts whose exposure occurred exclusively during the presymptomatic period of the index case. Our analysis revealed a similar clinical attack rate between the contacts who only had presymptomatic exposure and those who had postsymptomatic exposure.

To summarize the evidence, the decreasing risk for secondary infection over time in our study, the observed short serial interval, and the trend of decreasing viral shedding and viability after symptom onset strongly suggested high transmissibility of the disease near or even before the day of symptom onset. Because the onset of overt clinical symptoms, such as fever, dyspnea, and signs of pneumonia, usually occurred 5 to 7 days after initial symptom onset, the infection might well have been transmitted at or before the time of detection.^{22,23} This characteristic makes containment efforts challenging. In a modeling study, Hellewell et al²⁴ found that the possibility of controlling COVID-19 through isolation and contact tracing decreased with increasing proportion of transmission that occurred before symptom onset. The findings of this modeling study, when viewed in the context of our findings, might help to explain the difficult situation in such areas and countries as China, South Korea, Iran, and Italy. Aggressive social distancing and proactive contact tracing might be necessary to block the transmission chain of COVID-19 and to keep presumptive patients away from susceptible populations with a high risk for severe disease.

The observed short duration of infectiousness with lower risk of transmission 1 week after symptom onset has important implications for redirecting the efforts to control COVID-19. Given the nonspecific and mostly mild symptoms of COVID-19 at presentation, patients are often identified and hospitalized at a later stage of disease when the transmissibility of infection has started to decrease. In this case, hospitalization would not be helpful for isolation and reducing transmission, and should be only for patients whose clinical course is sufficiently severe. When the number of confirmed cases rapidly increases, home care for patients with mild illness may be preferred.²⁵ In Taiwan (where patients with COVID-19 have been routinely hospitalized), the most prolonged duration of hospital isolation for the 100 confirmed cases was more than 2 months. If every patient with mild illness is to be isolated in the hospital or other isolation facilities for such a prolonged period during a large epidemic, the health care system would soon be overwhelmed, and the case-fatality rate may increase, as observed in Wuhan.^{26,27} Similarly, better understanding of the potential duration of transmission could help direct containment strategies. For example, contact tracing could focus on the contacts near or even before symptom onset of the index cases when the number of index cases or contacts is too large for all contacts to be traced, given the available resources.

Several patients in our study were initially considered to have pneumonia of unknown etiology and had multiple contacts in the health care setting before being diagnosed. However, the number of health care contacts that led to nosocomial transmission was low. Besides the basic PPE used by medical staffs, this finding might be due to the late admissions of these patients and their lower risk of transmitting COVID-19 by the time of hospitalization. This pattern is compatible with the observations in China and Hong Kong. In China, the number of nosocomial infections might be lower than reported because some health care workers acquired infections in their households rather than in the health care facility.⁹ In Hong Kong, most hospitalization was also delayed to at least 5 days after disease onset.²⁸ In closed settings such as a hospital or a cruise ship,^{29,30} fomite transmission might play an important role, amplifying the risk of

transmission and making the temporality of transmission less identifiable.^{30,31,32} Better understanding of the dynamic change of transmissibility of COVID-19 over time and how health care workers are most likely to be infected could allow for better targeting of control measures, including the use of appropriate PPE.

In the contact tracing cohort, we observed a relatively low transmission rate of COVID-19. During the study period (January to early March 2020), the major containment measures in Taiwan were travel alerts with restriction to affected countries (principally China), home quarantine for travelers entering Taiwan, and comprehensive contact tracing for confirmed cases.¹¹ In response to a possible shortage of face masks, the government proactively initiated a name-based rationing system for mask purchase and boosted the production of face masks to ensure the availability for both N95 respirators and face masks to both health care professionals and the general public. A general recommendation on social distancing from the government was not in place, but spontaneous behavioral changes that reduced community mobility were observed.³³

Limitations

Our study has limitations. First, we did not completely examine contacts before the symptom onset of the index cases. Therefore, we might have underestimated the importance of early transmission. Thus, the actual contribution of early transmission to new infections could be greater than our estimates suggests. Our findings agree with the recommendation from the WHO to use 4 days before symptom onset as the starting date for contact tracing.¹⁹ This modification may help to further understand the pattern of early transmission in COVID-19. Second, we could not completely separate out the effect of close household contact and early contact given the strong correlation of the 2. The increased transmissibility in the early stage of COVID-19 may be partially attributed to the effect of household and nonhousehold family contacts rather than increased infectiousness at the early stage. When we stratified by type of exposure, however, the pattern of early transmission remained.

Conclusions

In summary, the findings of this study suggest that most transmission of COVID-19 occurred at the very early stage of the disease or even before the onset of symptoms, and the secondary clinical attack rate among contacts decreased over time as symptoms developed and progressed. The pattern of high transmissibility near and before symptom onset and the likely short infectious period of the virus could inform control strategies for COVID-19, as well as additional studies to fully elucidate the transmission dynamics of the virus.

Notes

Supplement.

eMethods. Serial interval and incubation period distribution

eTable 1. The estimated distribution parameters of the serial interval for each exposure setting (household, community, and others)

eTable 2. The estimated distribution parameters of the serial interval for each region (Taiwan, Mainland China, and others)

eTable 3. The estimated distribution parameters of the serial interval (overall countries and settings)

eTable 4. The estimated distribution parameters of the incubation period for each region (Taiwan, Mainland China, and others)

eTable 5. The estimated distribution parameters of the incubation period (overall countries and settings)

eFigure 1. The estimated serial interval distributions for each exposure setting (household, community, and others)

eFigure 2. The estimated serial interval distributions for each region (Taiwan, Mainland China, and others)

eFigure 3. The estimated serial interval distribution (overall countries and settings)

eFigure 4. The estimated incubation period distributions for each region (Taiwan, Mainland China, and others)

eFigure 5. The estimated incubation period distribution (overall countries and settings)

eReferences

References

1. Zhu N, Zhang D, Wang W, et al. ; China Novel Coronavirus Investigating and Research Team . A novel coronavirus from patients with pneumonia in China, 2019. *N Engl J Med.* 2020;382(8):727-733. doi:10.1056/NEJMoa2001017 [PMCID: PMC7092803] [PubMed: 31978945] [CrossRef: 10.1056/NEJMoa2001017]
2. World Health Organization Coronavirus disease 2019 (COVID-19) situation report—48. Published March 8, 2020. Accessed April 5, 2020. https://www.who.int/docs/default-source/coronaviruse/situation-reports/20200308-sitrep-48-covid-19.pdf?sfvrsn=16f7ccef_4
3. Lipsitch M, Swerdlow DL, Finelli L. Defining the epidemiology of Covid-19—studies needed. *N Engl J Med.* 2020;382(13):1194-1196. doi:10.1056/NEJMp2002125 [PubMed: 32074416] [CrossRef: 10.1056/NEJMp2002125]
4. Nishiura H, Linton NM, Akhmetzhanov AR. Serial interval of novel coronavirus (COVID-19) infections. *Int J Infect Dis.* 2020;93:284-286. doi:10.1016/j.ijid.2020.02.060 [PMCID: PMC7128842] [PubMed: 32145466] [CrossRef: 10.1016/j.ijid.2020.02.060]
5. Zou L, Ruan F, Huang M, et al. . SARS-CoV-2 viral load in upper respiratory specimens of infected patients. *N Engl J Med.* 2020;382(12):1177-1179. doi:10.1056/NEJMc2001737 [PMCID: PMC7121626] [PubMed: 32074444] [CrossRef: 10.1056/NEJMc2001737]
6. Pan Y, Zhang D, Yang P, Poon LLM, Wang Q. Viral load of SARS-CoV-2 in clinical samples. *Lancet Infect Dis.* 2020;20(4):411-412. doi:10.1016/S1473-3099(20)30113-4 [PMCID: PMC7128099] [PubMed: 32105638] [CrossRef: 10.1016/S1473-3099(20)30113-4]
7. Liu J, Liao X, Qian S, et al. . Community transmission of severe acute respiratory syndrome coronavirus 2, Shenzhen, China, 2020. *Emerg Infect Dis.* 2020;26(6):507. doi:10.3201/eid2606.200239 [PMCID: PMC7258448] [PubMed: 32125269] [CrossRef: 10.3201/eid2606.200239]
8. Patel A, Jernigan DB, Abdirizak F, et al. ; 2019-nCoV CDC Response Team . Initial public health response and interim clinical guidance for the 2019 novel coronavirus outbreak—United States, December 31, 2019–February 4, 2020. *MMWR Morb Mortal Wkly Rep.* 2020;69(5):140-146.

doi:10.15585/mmwr.mm6905e1 [PMCID: PMC7004396] [PubMed: 32027631] [CrossRef: 10.15585/mmwr.mm6905e1]

9. World Health Organization Report of the WHO-China joint mission on coronavirus disease 2019 (COVID-19). Published February 28, 2020. Accessed April 5, 2020. <https://www.who.int/docs/default-source/coronaviruse/who-china-joint-mission-on-covid-19-final-report.pdf>
10. Cheng S-C, Chang Y-C, Fan Chiang YL, et al. . First case of coronavirus disease 2019 (COVID-19) pneumonia in Taiwan. *J Formos Med Assoc.* 2020;119(3):747-751. doi:10.1016/j.jfma.2020.02.007 [PMCID: PMC7127252] [PubMed: 32113824] [CrossRef: 10.1016/j.jfma.2020.02.007]
11. Cheng H-Y, Li S-Y, Yang C-H. Initial rapid and proactive response for the COVID-19 outbreak—Taiwan's experience. *J Formos Med Assoc.* 2020;119(4):771-773. doi:10.1016/j.jfma.2020.03.007 [PMCID: PMC7118675] [PubMed: 3222336] [CrossRef: 10.1016/j.jfma.2020.03.007]
12. Wang CJ, Ng CY, Brook RH. Response to COVID-19 in Taiwan. *JAMA.* 2020;323(14):1341-1342. doi:10.1001/jama.2020.3151 [PubMed: 32125371] [CrossRef: 10.1001/jama.2020.3151]
13. von Elm E, Altman DG, Egger M, Pocock SJ, Gøtzsche PC, Vandenbroucke JP; STROBE Initiative . The Strengthening the Reporting of Observational Studies in Epidemiology (STROBE) statement: guidelines for reporting observational studies. *Lancet.* 2007;370(9596):1453-1457. doi:10.1016/S0140-6736(07)61602-X [PubMed: 18064739] [CrossRef: 10.1016/S0140-6736(07)61602-X]
14. Taiwan Legislative Yuan. The Communicable Disease Control Act. Accessed April 18, 2020. <https://law.moj.gov.tw/ENG/LawClass/LawAll.aspx?pcode=L0050001>
15. Corman VM, Landt O, Kaiser M, et al. . Detection of 2019 novel coronavirus (2019-nCoV) by real-time RT-PCR. *Euro Surveill.* 2020;25(3):2000045. doi:10.2807/1560-7917.ES.2020.25.3.2000045 [PMCID: PMC6988269] [PubMed: 31992387] [CrossRef: 10.2807/1560-7917.ES.2020.25.3.2000045]
16. Jian S-W, Chen C-M, Lee C-Y, Liu D-P. Real-time surveillance of infectious diseases: Taiwan's experience. *Health Secur.* 2017;15(2):144-153. doi:10.1089/hs.2016.0107 [PMCID: PMC5404256] [PubMed: 28418738] [CrossRef: 10.1089/hs.2016.0107]
17. World Health Organization Clinical management of severe acute respiratory infection when COVID-19 is suspected. Published March 13, 2020. Accessed April 5, 2020. [https://www.who.int/publications-detail/clinical-management-of-severe-acute-respiratory-infection-when-novel-coronavirus-\(ncov\)-infection-is-suspected](https://www.who.int/publications-detail/clinical-management-of-severe-acute-respiratory-infection-when-novel-coronavirus-(ncov)-infection-is-suspected)
18. Taiwan Centers for Disease Control Infectious disease contact tracing platform and management system. Accessed April 18, 2020. https://www.cdc.gov.tw/Professional/ProgramResultInfo/LeYn5b0UwF_lgvjR5rhT-A?programResultId=I2JMxghoGbL10LOSGB3h5Q
19. World Health Organization The First Few X (FFX) Cases and contact investigation protocol for 2019-novel coronavirus (2019-nCoV) infection. Published January 29, 2020. Accessed April 5, 2020. [https://www.who.int/publications-detail/the-first-few-x-\(ffx\)-cases-and-contact-investigation-protocol-for-2019-novel-coronavirus-\(2019-ncov\)-infection](https://www.who.int/publications-detail/the-first-few-x-(ffx)-cases-and-contact-investigation-protocol-for-2019-novel-coronavirus-(2019-ncov)-infection)
20. Lipsitch M, Cohen T, Cooper B, et al. . Transmission dynamics and control of severe acute respiratory syndrome. *Science.* 2003;300(5627):1966-1970. doi:10.1126/science.1086616 [PMCID: PMC2760158] [PubMed: 12766207] [CrossRef: 10.1126/science.1086616]
21. Wölfel R, Corman VM, Guggemos W, et al. . Virological assessment of hospitalized patients with COVID-2019. *Nature.* Published online April 1, 2020. doi:10.1038/s41586-020-2196-x [PubMed: 32235945] [CrossRef: 10.1038/s41586-020-2196-x]

22. Huang C, Wang Y, Li X, et al. . Clinical features of patients infected with 2019 novel coronavirus in Wuhan, China. *Lancet*. 2020;395(10223):497-506. doi:10.1016/S0140-6736(20)30183-5 [PMCID: PMC7159299] [PubMed: 31986264] [CrossRef: 10.1016/S0140-6736(20)30183-5]
23. Wang D, Hu B, Hu C, et al. . Clinical characteristics of 138 hospitalized patients with 2019 novel coronavirus-infected pneumonia in Wuhan, China. *JAMA*. 2020;323(11). doi:10.1001/jama.2020.1585 [PMCID: PMC7042881] [PubMed: 32031570] [CrossRef: 10.1001/jama.2020.1585]
24. Hellewell J, Abbott S, Gimma A, et al. ; Centre for the Mathematical Modelling of Infectious Diseases COVID-19 Working Group . Feasibility of controlling COVID-19 outbreaks by isolation of cases and contacts. *Lancet Glob Health*. 2020;8(4):e488-e496. doi:10.1016/S2214-109X(20)30074-7 [PMCID: PMC7097845] [PubMed: 32119825] [CrossRef: 10.1016/S2214-109X(20)30074-7]
25. World Health Organization Home care for patients with COVID-19 presenting with mild symptoms and management of their contacts. Published March 17, 2020. Assessed April 5, 2020. [https://www.who.int/publications-detail/home-care-for-patients-with-suspected-novel-coronavirus-\(ncov\)-infection-presenting-with-mild-symptoms-and-management-of-contacts](https://www.who.int/publications-detail/home-care-for-patients-with-suspected-novel-coronavirus-(ncov)-infection-presenting-with-mild-symptoms-and-management-of-contacts)
26. Wu Z, McGoogan JM. Characteristics of and important lessons from the coronavirus disease 2019 (COVID-19) outbreak in China: summary of a report of 72 314 cases from the Chinese Center for Disease Control and Prevention. *JAMA*. 2020;323(13). doi:10.1001/jama.2020.2648 [PubMed: 32091533] [CrossRef: 10.1001/jama.2020.2648]
27. Ji Y, Ma Z, Peppelenbosch MP, Pan Q. Potential association between COVID-19 mortality and health-care resource availability. *Lancet Glob Health*. 2020;8(4):e480. doi:10.1016/S2214-109X(20)30068-1 [PMCID: PMC7128131] [PubMed: 32109372] [CrossRef: 10.1016/S2214-109X(20)30068-1]
28. Li Q, Guan X, Wu P, et al. . Early transmission dynamics in Wuhan, China, of novel coronavirus-infected pneumonia. *N Engl J Med*. 2020;382(13):1199-1207. doi:10.1056/NEJMoa2001316 [PMCID: PMC7121484] [PubMed: 31995857] [CrossRef: 10.1056/NEJMoa2001316]
29. Nishiura H. Backcalculating the incidence of infection with COVID-19 on the Diamond Princess. *J Clin Med*. 2020;9(3):657. doi:10.3390/jcm9030657 [PMCID: PMC7141332] [PubMed: 32121356] [CrossRef: 10.3390/jcm9030657]
30. Ong SWX, Tan YK, Chia PY, et al. . Air, surface environmental, and personal protective equipment contamination by severe acute respiratory syndrome coronavirus 2 (SARS-CoV-2) from a symptomatic patient. *JAMA*. 2020;323(16). doi:10.1001/jama.2020.3227 [PMCID: PMC7057172] [PubMed: 32129805] [CrossRef: 10.1001/jama.2020.3227]
31. Bin SY, Heo JY, Song M-S, et al. . Environmental contamination and viral shedding in MERS patients during MERS-CoV outbreak in South Korea. *Clin Infect Dis*. 2016;62(6):755-760. doi:10.1093/cid/civ1020 [PMCID: PMC7108026] [PubMed: 26679623] [CrossRef: 10.1093/cid/civ1020]
32. Kim S-H, Chang SY, Sung M, et al. . Extensive viable Middle East Respiratory Syndrome (MERS) coronavirus contamination in air and surrounding environment in MERS isolation wards. *Clin Infect Dis*. 2016;63(3):363-369. doi:10.1093/cid/ciw239 [PMCID: PMC7108054] [PubMed: 27090992] [CrossRef: 10.1093/cid/ciw239]
33. Google COVID-19 community mobility reports. Accessed April 16, 2020. <https://www.google.com/covid19/mobility/>

Figures and Tables

Table 1.
Characteristics of the 2761 Close Contacts by Different Exposure Settings

	Exposure, No. (%)			
	Household (n = 151)	Family (n = 76)	Health care (n = 698)	Others (n = 1836) ^a
Age, median (range), y	33 (1-96)	45 (0-88)	39 (0-92)	35 (0-89)
Age group, y				
0-19	24 (16)	14 (18)	29 (4)	214 (12)
20-39	55 (36)	16 (21)	281 (40)	809 (44)
40-59	38 (25)	24 (32)	175 (25)	557 (30)
≥60	26 (17)	11 (14)	119 (17)	175 (10)
Unknown	8 (5)	11 (14)	94 (13)	81 (4)
Sex				
Female	70 (46)	41 (54)	454 (65)	872 (47)
Male	81 (54)	30 (39)	228 (33)	816 (44)
Unknown	0	5 (7)	16 (2)	148 (8)
Time from onset to exposure, median (range), d ^b	−4 (−4 to 9)	6 (−4 to 26)	1 (−4 to 23)	2 (−4 to 26)
Time from onset to exposure, d ^b				
<0	100 (66)	10 (13)	236 (34)	389 (21)
0-3	39 (26)	15 (20)	150 (21)	663 (36)
4-5	6 (4)	6 (8)	38 (5)	166 (9)
6-7	4 (3)	10 (13)	17 (2)	88 (5)
8-9	2 (1)	3 (4)	110 (16)	334 (18)
>9	0	24 (32)	146 (21)	114 (6)
Unknown	0	8 (11)	1 (0.1)	82 (5)

[Open in a separate window](#)

^aOthers include friends, airline crew members and passengers, and other casual contacts.

^bDefined as the elapsed time between the date at symptom onset of the index case and the first date at exposure. For example, people from the group “<0 days” had their first contact with the index case before the case had any symptoms.

Figure 1.**Exposure Window Period Among Secondary Cases and Noncase Contacts**

The exposure time was defined as the period from the first day of exposure to the index case to the last day of exposure. Time zero indicates the day of symptom onset of the index case.

Table 2.
Secondary Clinical Attack Rate for COVID-19 Among the 2761 Close Contacts by Different Exposure Settings, Times, and Characteristics

	No. of secondary cases (asymptomatic case)	No. of contacts	Secondary clinical attack rate, % (95% CI)	Risk ratio (95% CI)
Exposure setting				
Household	10 (3)	151	4.6 (2.3-9.3)	1 [Reference]
Nonhousehold family	5 (1)	76	5.3 (2.1-12.8)	1.14 (0.34- 3.76)
Health care	6 (0)	698	0.9 (0.4-1.9)	0.19 (0.06- 0.54)
Others ^a	1 (0)	1836	0.1 (0-0.3)	0.01 (0-0.09)
Time from onset to exposure, d ^b				
<0	10 (3)	735	1.0 (0.5-2.0)	1 [Reference]
0-3	9 (1)	867	0.9 (0.5-1.8)	0.97 (0.35- 2.66)
4-5	3 (0)	216	1.4 (0.5-4.0)	1.46 (0.38- 5.59)
6-7	0	119	0 (0-3.1)	0
8-9	0	449	0 (0-0.9)	0
>9	0	284	0 (0-1.3)	0
Exclusively presymptomatic exposure ^c				
No	20 (4)	2371	0.7 (0.4-1.1)	1 [Reference]
Yes	2 (0)	299	0.7 (0.2-2.4)	0.99 (0.23- 4.29)
Age of close contacts, y				
0-19	1 (1)	281	0 (0-1.4)	0
20-39	8 (2)	1161	0.5 (0.2- 1.1)	1 [Reference]
40-59	10 (1)	794	1.1 (0.6-2.1)	2.19 (0.78- 6.14)

[Open in a separate window](#)

Abbreviations: ARDS, acute respiratory distress syndrome; COVID-19, coronavirus disease 2019.

^aOthers include friends, airline crew members and passengers, and other casual contacts.

^bDefined as the elapsed time between the date at symptom onset of the index case and the first date at exposure. For example, people from the group “<0 days” had their first contact with the index case before the case had any symptoms.

^cAll the reported exposures occurred during the presymptomatic period of the index case.

Figure 2.

Number of Contacts, Secondary Cases, and Secondary Clinical Attack Rate by the Time of First Exposure

Table 3.

Risk for Symptomatic COVID-19 Infection Among the 2761 Close Contacts, Simultaneously Stratified by Exposure Setting and Time From Symptom Onset of the Index Case to First Day of Exposure

First day of exposure, d	Household		Nonhousehold family		Health care		Others ^a	
	Case/contact, No.	Attack rate, % (95% CI) ^b	Case/contact, No.	Attack rate, % (95% CI) ^b	Case/contact, No.	Attack rate, % (95% CI) ^b	Case/contact, No.	Attack rate, % (95% CI) ^b
<0	4/100	4.0 (1.6-9.8)	1/10	10.0 (1.8-40.4)	2/236	0.8 (0.2-3.0)	0/389	0 (0-1.0)
0-3	2/39	5.1 (1.4-16.9)	3/15	20.0 (7.0-45.2)	3/150	2.0 (0.7-5.7)	0/663	0 (0-0.6)
4-5	1/6	16.7 (3.0-56.4)	0/6	0 (0-39.0)	1/38	2.6 (0.5-13.5)	1/166	0.6 (0.1-3.3)
6-7	0/4	0 (0-49.0)	0/10	0 (0-27.8)	0/17	0 (0-18.4)	0/88	0 (0-4.2)
8-9	0/2	0 (0-65.7)	0/3	0 (0-56.1)	0/110	0 (0-3.3)	0/334	0 (0-1.1)
>9	0/0	NC	0/24	0 (0-13.8)	0/146	0 (0-2.6)	0/114	0 (0-3.3)

Abbreviations: COVID-19, coronavirus disease 2019; NC, not calculable.

^aOthers include friends, airline crew members and passengers, and other casual contacts.

^bSecondary clinical attack rate.



Published in final edited form as:

Antiviral Res. 2016 May ; 129: 120–129. doi:10.1016/j.antiviral.2016.02.013.

Influenza A and methicillin-resistant *Staphylococcus aureus* co-infection in rhesus macaques – A model of severe pneumonia

Daniel S. Chertow^{a,c,*}, Jason Kindrachuk^{a,b}, Zong-Mei Sheng^c, Lindsey M. Pujanauski^c, Kurt Cooper^b, Daniel Noguee^{a,c}, Marisa St. Claire^b, Jeffrey Solomon^d, Donna Perry^b, Philip Sayre^b, Krisztina B. Janosko^b, Matthew G. Lackemeyer^b, Jordan K. Bohannon^b, John C. Kash^c, Peter B. Jahrling^b, and Jeffery K. Taubenberger^c

^aCritical Care Medicine Department, Clinical Center, National Institutes of Health, Bethesda, MD, USA

^bIntegrated Research Facility-Frederick, National Institutes of Health, Frederick, MD, USA

^cViral Pathogenesis and Evolution Section, Laboratory of Infectious Diseases, National Institute of Allergy and Infectious Diseases, National Institutes of Health, Bethesda, MD, USA

^dCenter for Infectious Disease Imaging, RAD&IS, Clinical Center, National Institutes of Health, Bethesda, MD, USA

Abstract

Background: Influenza results in up to 500,000 deaths annually. Seasonal influenza vaccines have an estimated 60% effectiveness, but provide little or no protection against novel subtypes, and may be less protective in high-risk groups. Neuraminidase inhibitors are recommended for the treatment of severe influenza infection, but are not proven to reduce mortality in severe disease. Preclinical models of severe influenza infection that closely correlate to human disease are needed to assess efficacy of new vaccines and therapeutics.

Methods: We developed a nonhuman primate model of influenza and bacterial co-infection that re-capitulates severe pneumonia in humans. Animals were infected with influenza A virus via intra-bronchial or small-particle aerosol inoculation, methicillin-resistant *Staphylococcus aureus*, or co-infected with influenza and methicillin-resistant *S. aureus* combined. We assessed the severity of disease in animals over the course of our study using tools available to evaluate critically ill human patients including high-resolution computed tomography imaging of the lungs, arterial blood gas analyses, and bronchoalveolar lavage.

Results: Using an intra-bronchial route of inoculation we successfully induced severe pneumonia following influenza infection alone and following influenza and bacterial co-infection. Peak illness was observed at day 6 post-influenza infection, manifested by bilateral pulmonary infiltrates and

This is an open access article under the CC BY-NC-ND license (<http://creativecommons.org/licenses/by-nc-nd/4.0/>).

*Corresponding author. Critical Care Medicine Department, Clinical Center, NIH, 10 Center Drive, Room 2C-145, Bethesda, MD 20892-1662, USA. chertowd@cc.nih.gov (D.S. Chertow).

Appendix A. Supplementary data

Supplementary data related to this article can be found at <http://dx.doi.org/10.1016/j.antiviral.2016.02.013>.

hypoxemia. The timing of radiographic and physiologic manifestations of disease in our model closely match those observed in severe human influenza infection.

Discussion: This was the first nonhuman primate study of influenza and bacterial co-infection where high-resolution computed tomography scanning of the lungs was used to quantitatively assess pneumonia over the course of illness and where hypoxemia was correlated with pneumonia severity. With additional validation this model may serve as a pathway for regulatory approval of vaccines and therapeutics for the prevention and treatment of severe influenza pneumonia.

Keywords

Influenza; Co-infection; Pneumonia; Vaccines; Therapies

1. Introduction

An estimated 5–10% of adults and 20–30% of children are infected with influenza globally each year. Severe illness occurs predominantly in high-risk groups (the very young, elderly, and those with premorbid conditions) affecting an estimated 3–5 million people resulting in an estimated 250,000–500,000 deaths annually (World Health Organization, 2015). The 1918 influenza pandemic caused an estimated 50 million deaths worldwide, disproportionately affecting young adults (World Health Organization, 2015). Zoonotic avian influenza (e.g., H5N1 and H7N9) causes infrequent although highly lethal human infections and poses risk for a severe pandemic (Su et al., 2015).

Seasonal influenza vaccines have an estimated 60% effectiveness, but provide little or no protection against novel influenza subtypes, and may be less protective in high-risk groups. Neuraminidase inhibitors (NAIs) are recommended for the treatment of severe influenza infection, but are not proven to reduce mortality in severe disease. Recent meta-analysis of observational data suggest early initiation of NAI therapy, within 5-days of symptom onset, is associated with reduced mortality (Muthuri et al., 2014). However, patients with severe influenza infection typically present to the hospital after 5-days of symptoms and experience high case-fatality (Rice et al., 2012).

New vaccines and therapies are needed to prevent and treat severe influenza illness. Efficacy of interventions must be assessed accounting for the impact of bacterial co-infection that commonly contributes to mortality (Morens et al., 2008). Clinical trials of influenza vaccine or therapeutic efficacy do not typically evaluate severe disease as a clinical endpoint, largely due to the expense required to adequately power such studies. Highly pathogenic strains of influenza and severe disease cannot be assessed in human challenge experiments for obvious ethical reasons. Preclinical models of severe influenza infection that closely correlate with the natural history of disease in humans are needed to assess efficacy of vaccines and therapeutics. Showing benefit of interventions in permissive small animals (mice and ferrets) that are genetically and phenotypically distinct from humans may not adequately translate to benefit in humans.

Nonhuman primates are naturally, and may be experimentally, infected with human influenza viruses (Davis et al., 2015). Seasonal influenza infection in most nonhuman

primate species results in mild or subclinical illness, reflective of self-limited disease observed in otherwise healthy humans. Inoculation of influenza into the lower airways of nonhuman primates induces more severe disease than upper airway inoculation or exposure via small particle aerosol (Davis et al., 2015). Bacterial infection following intra-tracheal influenza infection has been evaluated in four nonhuman primate studies since 1954 (Berendt, 1974; Berendt et al., 1975; Kobayashi et al., 2013; Miyake et al., 2010). In three of the four studies co-infection resulted in more severe bronchopneumonia than viral infection alone.

We sought to develop a nonhuman primate model of influenza and bacterial co-infection that recapitulates severe disease in humans. Severe influenza infection in humans is typically manifested by bilateral bronchopneumonia resulting in hypoxemia. Animals were infected with influenza inoculated directly into bilateral main-stem bronchi, to maximize lower respiratory tract disease. Decades of experimental observations show that intra-nasal inoculation induces only mild illness in both otherwise healthy nonhuman primate and human subjects. Co-infected animals were inoculated with bacteria into the lower airways at four days post-influenza infection. The timing of co-infection in our study closely approximates estimated timing of co-infection in human cases of severe influenza infection (Rice et al., 2012). Influenza A/Swine/Iowa/31 (Sw31) was selected as a surrogate for the 1918 pandemic influenza virus in this study based on close genetic homology and similar pathogenesis in mice and ferrets (Memoli et al., 2009). Methicillin-resistant *Staphylococcus aureus* (MRSA) was selected as a clinically relevant bacterial co-pathogen.

We also evaluated the role of aerosolized influenza with and without bacterial co-infection in this study. Few historical data exist to inform the impact of aerosolized influenza on the development of severe pneumonia in the setting of bacterial co-infection. We sought to fill this knowledge gap. We assessed the severity of disease in animals over the course of our study using tools available to evaluate critically ill human patients. These included high-resolution computed tomography (CT) imaging of the lungs, arterial blood gas analyses, and bronchoalveolar lavage (BAL).

2. Methods

2.1. Inoculations

Eighteen male juvenile rhesus macaques (4–8 kg) of Indian origin without detectable pre-existing influenza A antibody titers were randomly assigned to one of six study groups (see Table 1, Supplementary Table 1). Staff that assigned animals to groups were blinded to the intervention (i.e., pathogen and inoculation route) designated for that group. Viral stocks of Influenza A/Swine/Iowa/31 (Sw31) were grown in Madin–Darby canine kidney (MDCK) cells, harvested, purified on a sucrose cushion, and stored at -80°C . Viral titers were assessed by plaque assay technique (Qi et al., 2009). MRSA (strain USA300) was grown in tryptic soy broth (TSB) from frozen glycerol stocks until mid-log phase growth was achieved. The desired number of bacteria were pelleted, washed, and diluted in 4 mL of sterile saline immediately prior to inoculation. Bacterial titers were confirmed by serial dilution of samples on TSB agar plates Table 1.

Intra-bronchial (IB) inoculations were performed under ketamine anesthesia using a pediatric bronchoscope advanced into the airway of seated upright animals (see experimental timeline, Fig. 1). A target IB viral inoculum of 5×10^6 plaque forming units (pfu) was diluted in 4 mL of saline and administered in equal proportions into the right and left main stem bronchus. A target IB bacterial inoculum of 1×10^9 colony forming units (cfu) was similarly administered. A target aerosol viral inoculum of 5×10^6 pfu was administered as previously described (Johnson et al., 2015). All animal procedures were approved by the National Institute of Allergy and Infectious Diseases (NIAID) Division of Clinical Research Animal Care and Use Committee, and adhered to National Institutes of Health (NIH) policies. The experiments were carried out at the NIAID Integrated Research Facility, an AAALAC and AALAS accredited facility.

2.2. Procedures

Physical exams, vital sign measurements, and venous and arterial blood draws were performed every other day and BALs were performed every fourth day under ketamine anesthesia. Arterial blood was collected by puncture of the femoral artery under direct ultrasound guidance at atmospheric pressure and samples were immediately loaded onto the iSTAT® (Abbott laboratories) for bedside blood gas analysis. BALs were performed by advancing a sterile pediatric bronchoscope into the right lower lobe of an upright animal, instilling four 10 mL aliquots (40 mL total) of sterile saline into the distal lung segment, and aspirating BAL fluid into a sterile trap.

2.3. Laboratory testing

Complete blood counts (CBC) with differentials and comprehensive blood chemistries were performed on venous blood samples collected in ethylenediaminetetraacetic acid (EDTA)-coated blood tubes using a Sysmex XT2000V™ (Sysmex America, IL USA) and the Piccolo Xpress® (Abbott laboratories).

Quantitative real-time PCR (RT-PCR) was used to determine the viral copy numbers in BAL samples from all groups. Total RNA was extracted from 100 µL aliquots of BAL using standard TRIzol chloroform extraction. Reverse transcription of total RNA was performed with primers specific for swine H1N1 HA sequence using the Superscript III first-strand cDNA synthesis kit (Invitrogen, Carlsbad, CA). TaqMan primers and probes were designed using Primer Express 3.0 software (Applied Biosystems, Foster City, CA) and generated the following primers and probe: Swine-691F, 5' CAGGAGGTTCACTCCAGAAATAG 3'; Swine-787R, 5' GTGTCTCCGGTCTAGTAATG 3'; Probe, 5' FAM-AGGTCAGGCAGGGAGGATGAACTA-TAMRA 3'. RT-PCR was performed on an Applied Biosystems QuantStudio 6 Flex Real-Time PCR System and each sample was run in duplicate with TaqMan 2X PCR Universal Master Mix (Applied Biosystems) and a 25 µL total reaction volume. Quantification of viral copy number was accomplished by comparison of RT-PCR results to an established external standard of viral copy number.

Cells from BAL were pelleted by centrifugation and re-suspended in 100 µl phosphate buffered saline (PBS) + 2% fetal bovine serum (FBS). Cell aliquots were exposed to a myeloid or lymphoid antibody panel. The myeloid panel contained markers for CD14, Live/

Dead Fixable Yellow dead cell stain (Thermo Fisher Scientific, MA, USA), CD3, CD45, HLA-DR, CD11c (BD Biosciences, CA, USA), CD20 (eBioscience Inc. CA, USA), CD66abce (Miltenyi Biotech Inc. CA, USA), and CD163 (Biolegend, CA, USA). The lymphoid panel contained markers for CD3, CD8, CD20, CD16 (BD Biosciences, CA, USA), CD4 (Biolegend, CA, USA), CD14, Live/Dead Fixable Yellow dead cell stain (Thermo Fisher Scientific, MA, USA) and CD 159(NKG2a) (Beckman Coulter, CA, USA). Samples were then fixed and permeabilized using BD Cytotfix/Cytoperm solution (BD Biosciences CA, USA) and analyzed on the BD LSR II Fortessa Flow Cytometer. Data were analyzed using FlowJo Software (FlowJo LLC, OR, USA). All cells were gated first as live cells (viability dye negative) and CD45⁺ and then analyzed further. Myeloid cells were gated by forward and side scatter and monocytes were defined as CD3⁻CD20⁻HLA-DR⁺CD163⁺. CD3⁻CD20⁻CD163⁻ cells were separated by CD66abce⁺ (neutrophils) or CD11c⁺ (dendritic cells). Lymphoid cells were gated by forward and side scatter and CD14⁻. B cells were defined as CD3⁻CD20⁺ and NK cells were defined as CD3⁻NKG2a⁺. T cells were defined as CD20⁻ and CD4⁺CD8⁻ or CD4⁻CD8⁺. Percentage of each cell type was determined based on all live CD45⁺ cells.

2.4. High-resolution computed tomography scanning

Animal were intubated, deeply sedated with propofol, and mechanically ventilated on an assist-control volume-cycled ventilator mode. A standard breath-hold maneuver normalizing tidal volume to 8 cc/kg actual body weight was performed immediately prior to CT imaging of lungs using a Philips Gemini 16 slice PET/CT scanner. Lung hyper-intensity and percent change from baseline over time was determined using previously published methods (Solomon et al., 2014).

2.5. Pathology

Detailed necropsies were performed on all animals following euthanasia. Tissues were collected from major organs including multiple lung lobes, preserved in 10% normal-buffered formalin, embedded in paraffin, and 5-μm sections applied to positively charged slides for hematoxylin and eosin staining. Lung lobes were sampled for a qualitative assessment of histopathology. Both “affected” and “unaffected” regions, based upon gross pathologic evaluation, were sampled.

2.6. Statistical analysis

GraphPad Prism 6 was used for all statistical analysis including mean and standard error of the mean (SEM) calculations. Two-way ANOVA was used to detect differences in dependent variables between groups on multiple study days. Tukey’s test was used to assess for significant differences between means with $p < 0.05$, $p < 0.01$, $p < 0.001$, or $p < 0.0001$.

3. Results

3.1. Influenza and MRSA infection induced mild clinical or subclinical illness

Animals were inoculated with Sw31 or saline on day 0 and MRSA or saline on day +4 (Fig. 1). Viral and bacterial inoculation doses were confirmed by back-titration (Table 1). Group 3 (Sw31 IB) animals had the highest peak viral RNA in lung-lining fluid at day +2 that

significantly declined by day +6 (Fig. 1). MRSA was cultured from lung-lining fluid of all 3 animals from Group 4 (Sw31 IB + MRSA) on day +6 but not at later time-points and not from animals in other MRSA-infected groups (Groups 2 and 6).

Clinical scoring to quantify disease severity and early euthanasia criteria are summarized in Supplementary Tables 2 and 3. Animals in groups 3 (Sw31 IB), 4 (Sw31 IB + MRSA), and 6 (Sw31 aero + MRSA) developed self-limited fever to greater $>39.7^{\circ}\text{C}$. One animal each from Groups 3 and 4 developed mild cough on day +6 and +7 and two animals from Group 4 developed mild depressed activity on day +6. Less than 5% weight loss was observed in all animals. No clinically significant abnormalities were observed in CBC with differentials or serum chemistries.

3.2. CT imaging of lungs characterized timing and extent of influenza or MRSA pneumonia

Radiographic evidence of pneumonia with focal or multifocal infiltrates was observed in all infected animals in Groups 2 (MRSA), 3 (Sw31 IB), 4 (Sw31 IB + MRSA), and 6 (Sw31 aero + MRSA) but not in animals from Groups 1 (saline IB) or 5 (Sw31 aero) (Fig. 2A). No statistically significant difference was observed in density of radiographic infiltrates on day +2, as measured by percent change in lung hyper-intensity (PCLH) between groups (Fig. 2B). On day +6, PCLH was significantly increased in Group 4 animals (Sw31 IB + MRSA) relative to animals in all other groups, and in group 3 (Sw31 IB) and 6 (Sw31 aero + MRSA) animals relative to animals in Groups 1 (saline) and 5 (Sw31 aero) (Fig. 2B). On day +10, PCLH was significantly increased in Group 4 animals (SW31 IB + MRSA) relative to animals in Groups 1 (saline), 2 (MRSA), and 5 (Sw31 aero) (Fig. 2B). No statistically significant differences in PCLH were observed between groups on day +14 (Fig. 2B).

3.3. IB influenza with or without MRSA co-infection induced acute lung injury by clinical criteria

The clinical criteria for acute lung injury (ALI) include an arterial partial pressure of oxygen to fraction of inspired oxygen (P: F) ratio <300 in the setting of bilateral pulmonary infiltrates (Bernard et al., 1994). Three animals from Group 3 (Sw31 IB) and two animals from Group 4 (Sw31 IB + MRSA) met clinical criteria for ALI on day +6 (Fig. 2C). Clinical criteria for ALI were not met on other study days or in other groups. Timing of ALI in animals from Groups 3 and 4 correlated with timing of peak radiographic infiltrates (Fig. 2B and C).

3.4. Cellular immune responses in BAL were distinct between groups

Animals from Group 1 (saline) had no significant changes in the number or distribution of immune cell populations in BAL (Figs. 3 and 4 A–G) over the course of the study. Group 2 (MRSA) animals had significant elevations of NK cells ($\text{CD14}^{-}\text{CD3}^{-}\text{NKG2A}^{+}$), dendritic cells ($\text{CD3}^{-}\text{CD20}^{-}\text{CD163}^{-}\text{CD66}^{-}\text{HLA-DR}^{+/-}\text{CD11c}^{+}$), neutrophils ($\text{CD3}^{-}\text{CD20}^{-}\text{CD163}^{-}\text{CD11c}^{-}\text{CD66}^{+}$), monocytes ($\text{CD3}^{-}\text{CD20}^{-}\text{HLA-DR}^{+}\text{CD163}^{+}$), and B-cells ($\text{CD14}^{-}\text{CD3}^{-}\text{CD20}^{+}$) (Fig. 4A, C, D, E, and G) on day +6 and all cell populations returned to baseline by day +10. Group 3 (Sw31 IB) animals showed significant elevation of neutrophils on day +6 (Fig. 4D) and cytotoxic T-cells ($\text{CD14}^{-}\text{CD20}^{-}\text{CD3}^{+}\text{CD4}^{-}\text{CD8}^{+}$) and

dendritic cells on day +14 (Fig. 4 B and C). Group 4 (Sw31 IB + MRSA) animals had significant elevations of neutrophils, monocytes, and B-cells on day +6 (Fig. 4D, E, and G) and significant elevations of cytotoxic T-cells and dendritic cells on day +10 (Fig. 4B and C). CD4⁺ T-cell populations (CD14⁻CD20⁻CD3⁺CD8⁻CD4⁺) were significantly elevated on day +6 and +10 (Fig. 4F). Group 5 (SW31 aero) animals had significant elevation in NK cells on day +6 (Fig. 4A). Group 6 (Sw31 aero + MRSA) animals had significant elevations of NK cells on days +2, +6, and +10 (Fig. 4A); of neutrophils on days +2 and +6 (Fig. 4D); of monocytes on days +6 and +10 (Fig. 4E); of B-cells on day +6 (Fig. 4G); and of cytotoxic T-cells, dendritic cells, and CD4⁺ T-cells on day +10 (Fig. 4B, C, and F).

3.5. Pneumonia and pathologic lung injury were most severe following IB influenza and MRSA co-infection

Histopathologic examination was performed on tissues sampled on day +14. Group 1 (saline) animals had no abnormal histopathology in the respiratory epithelium of the trachea, main-stem bronchi (Fig. 5A), bronchioles (Fig. 5B), or lung parenchyma (Fig. 5C). Group 2 (MRSA) animals had focal chronic bronchiolitis (Fig. 5D), often with reparative changes (Fig. 5E), and very rarely with bacteria morphologically consistent with *Staphylococcus* associated with small amounts of necrotic luminal debris (Fig. 5F; arrow). Group 3 (Sw31 IB) animals had few foci of acute exudative DAD (Fig. 5G; left half) characterized by prominent alveolar edema and vascular congestion (Fig. 5H), surrounded by multifocal areas of proliferative organizing DAD (Fig. 5G; right half) characterized by interstitial fibrosis (Fig. 5I; arrow) and type II alveolar cell hyperplasia (Fig. 5J; arrow). Multifocal chronic bronchiolitis was also observed (Fig. 5K; arrow) with several foci of bronchiolitis obliterans (Fig. 5L, arrow). Group 4 (Sw31 IB + MRSA) animals had extensive pathology with widespread consolidation in most lung lobes. Organizing pneumonia with extensive organizing DAD (Fig. 6A–C), with multifocal bronchiolitis obliterans (Fig. 6A–C arrows), chronic bronchiolitis with transmural infiltrates of inflammatory cells and loss of epithelial cell integrity (Fig. 6D) were observed. The key features of the areas of organizing DAD included interstitial fibrosis (Fig. 6E; arrows) and type II alveolar cell hyperplasia (Fig. 6F; arrow). Group 5 (Sw31 aerosol) (Fig. 6G–I) and 6 (Sw31 aero + MRSA) (Fig. 6J–L) animals had similar histopathology features with multifocal areas of interstitial inflammatory infiltrates producing an interstitial pneumonia pattern (Fig. 6G and J) with multifocal areas of chronic bronchiolitis often with prominent submucosal lymphoid nodules (Fig. 6H & KL; arrows). Areas with organizing DAD features were noted (Fig. 6I) with interstitial fibrosis and type II hyperplasia (Fig. 6L) but were much less prominent than observed in groups 3 and 4.

4. Discussion

We developed a model of severe pneumonia following influenza and bacterial co-infection in nonhuman primates. This was the first nonhuman primate study of influenza and bacterial co-infection where high-resolution CT scanning of the lungs was used to quantitatively assess pneumonia over the course of illness and where hypoxemia was correlated with pneumonia severity. This was also the first nonhuman primate study of influenza and bacterial co-infection where immune cell responses in BAL were serially evaluated in

animals over the course of illness. Using an IB route of inoculation we successfully induced severe pneumonia following influenza infection alone and following influenza and bacterial co-infection. Peak illness was observed at day 6 post-influenza infection, manifested by bilateral pulmonary infiltrates and hypoxemia. The timing of radiographic and physiologic manifestations of disease in our model closely match those observed in severe human influenza infection (Chertow, 2012).

We observed that influenza and bacterial co-infection resulted in more severe lung histopathology than influenza infection alone. This same observation has been made in three of four prior nonhuman primate studies of influenza and bacterial co-infection where influenza was inoculated into the lower airways (Berendt, 1974; Berendt et al., 1975; Kobayashi et al., 2013; Miyake et al., 2010). In the most recent study by Kobayashi et al., no difference in lung histopathology was observed following influenza infection alone versus influenza and bacterial co-infection (Kobayashi et al., 2013). However, the MRSA inoculating dose employed by these authors was 1×10^6 CFU, 3 logs lower than the dose used in our study and lung histopathology was assessed at day 9 post-influenza infection, likely past the peak of illness.

Pneumonia in our model did not progress to refractory hypoxic respiratory failure or death. We postulate that the underlying normal health status of the animals protected them from more severe disease, similar to most healthy humans infected with influenza. A recent influenza A challenge study in humans showed that a dose of 10^7 tissue culture infectious dose 50 was needed to induce mild illness in 69% of individuals (Memoli et al., 2015). These data suggest that high-dose influenza A exposure is likely needed to induce more than mild illness in healthy hosts. Despite this, development of pneumonia was reproducible in our model. Severity of influenza pneumonia is dependent upon the viral and bacterial strain used, pathogen dose, and route of infection. We selected Sw31 because it is well characterized in mice and ferrets to cause severe pneumonia, and is genetically similar to 1918 influenza, that causes severe pneumonia in nonhuman primates (Kobasa et al., 2007). Viral dose of 5×10^6 pfu was selected as the highest dose that could be reasonably achieved and matched across routes of delivery. MRSA was selected given its high prevalence among adult and pediatric patients with severe influenza infection (Rice et al., 2012; Randolph et al., 2011). While MRSA is known to induce pneumonia in nonhuman primates, Pantone-Valentine leukocidin (PVL) does not appear to significantly contribute to pathogenesis (Olsen et al., 2010). While PVL is known to be a *S. aureus* virulence molecule *in vitro*, its contribution to pneumonia pathogenesis in humans remains controversial. While the route of infection we studied does not mirror natural infection, our intention was not to evaluate the natural history of mild influenza infection. This can be best accomplished in human challenge experiments or natural history studies. Our intention was to model severe influenza pneumonia as observed in humans.

To expand the relevance of our findings and establish the utility of this model for assessing efficacy of vaccines and therapies for the prevention and treatment of severe influenza pneumonia, additional experiments are needed. Future studies should assess reproducibility of our findings with other relevant seasonal and high-path avian influenza strains with pandemic potential. *Streptococcus pneumoniae*, another clinically relevant bacterial co-

pathogen, should also be evaluated. Dose response studies are also needed. Quantitative assessment of lung histopathology correlated to CT findings at peak illness (day 6) will also strengthen the validity of this model. Interestingly aerosolized influenza alone induced only subclinical disease despite presence of interstitial pneumonia on lung histopathology. This was made only moderately worse with bacterial co-infection. Some variation in delivered inoculum was observed, primarily across routes of delivery. This is likely attributable to methodological differences required to deliver virus IB versus aerosol. Also, the design of the aerosol chamber, where not all inoculum is delivered into the airway, likely resulted in a dose reduction in the influenza aerosol groups. However, diffuse interstitial pneumonia observed on histopathology in these groups, and robust immune response in BAL suggest that aerosol exposure to influenza results in a distinct and more mild clinic-pathological phenotype.

Nonhuman primate models of influenza infection will not and should not replace mice and ferret studies for the preclinical assessment of influenza vaccines and therapies. Relevant small animal models will always be needed for initial higher throughput evaluation of interventions. However, nonhuman primate models provide an important adjunct for validating findings in small animal models and may more closely predict vaccine and therapeutic efficacy for severe disease in humans. Lung immune cell responses in nonhuman primates likely correlate better to those of humans than those of more genetically distant animals. Characterization of lung immune cell responses in nonhuman primates following influenza infection may facilitate discovery of improved correlates of influenza immunity in humans, needed for better vaccine design. Additionally, characterization of lung immune responses contributing to progression and resolution of lung injury may lead to discovery of novel therapeutic targets within the host to improve severe pneumonia outcomes.

In summary, we report a nonhuman primate model of IB influenza and MRSA co-infection that induced severe pneumonia similar to that observed in humans. With additional validation this model may serve as a pathway for regulatory approval of vaccines and therapeutics for the prevention and treatment of severe influenza pneumonia. This will be particularly useful for high-path avian influenza strains with pandemic potential that cause sporadic infections and are thus not easily amenable to large clinical trials of vaccine and therapeutic efficacy.

Supplementary Material

Refer to Web version on PubMed Central for supplementary material.

Acknowledgments

The Intramural Research Program of NIAID, NIH supported this work. We are grateful to Lisa E. Hensley, Russell Byrum, Dan Ragland, Dawn Traynor, Catherine Jett and the entire IRF team for their contributions to these studies. The content of this publication does not necessarily reflect the views or policies of the US Department of Health and Human Services (DHHS) or of the institutions and companies affiliated with the authors. This work was funded in part through Battelle Memorial Institute's prime contract with NIAID under Contract no. HHSN272200700016I. J.K.B. and K.B.J. performed this work as employees of Battelle Memorial Institute. Subcontractors to Battelle Memorial Institute who performed this work are: M.G.L., an employee of Lovelace Respiratory Research Institute; and P.S., an employee of MEDRelief.

References

- Berendt RF, 1974 Simian model for the evaluation of immunity to influenza. *Infect. Immun.* 9,101–105. [PubMed: 4202882]
- Berendt RF, Long GG, Walker JS, 1975 Influenza alone and in sequence with pneumonia due to *Streptococcus pneumoniae* in the squirrel monkey. *J. Infect. Dis.* 132, 689–693. [PubMed: 811714]
- Bernard GR, Artigas A, Brigham KL, Carlet J, Falke K, Hudson L, Lamy M, LeGall JR, Morris A, Spragg R, 1994 Report of the American-European consensus conference on ARDS: definitions, mechanisms, relevant outcomes and clinical trial coordination. *The Consensus Committee Intensive Care Med.* 20, 225–232. [PubMed: 8014293]
- Chertow DS, 2012 Contribution of bacterial coinfection to severe influenza infection. *Crit. Care Med.* 40, 1664–1665. [PubMed: 22511151]
- Davis AS, Taubenberger JK, Bray M, 2015 The use of nonhuman primates in research on seasonal, pandemic and avian influenza, 1893–2014. *Antivir. Res.* 117, 75–98. [PubMed: 25746173]
- Johnson RF, Hammoud DA, Lackemeyer MG, Yellayi S, Solomon J, Bohannon JK, Janosko KB, Jett C, Cooper K, Blaney JE, Jahrling PB, 2015 Small particle aerosol inoculation of cowpox Brighton Red in rhesus monkeys results in a severe respiratory disease. *Virology* 481,124–135. [PubMed: 25776759]
- Kobasa D, Jones SM, Shinya K, Kash JC, Copps J, Ebihara H, Hatta Y, Kim JH, Halfmann P, Hatta M, Feldmann F, Alimonti JB, Fernando L, Li Y, Katze MG, Feldmann H, Kawaoka Y, 2007 Aberrant innate immune response in lethal infection of macaques with the 1918 influenza virus. *Nature* 445, 319–323. [PubMed: 17230189]
- Kobayashi SD, Olsen RJ, LaCasse RA, Safronetz D, Ashraf M, Porter AR, Braughton KR, Feldmann F, Clifton DR, Kash JC, Bailey JR, Gardner DJ, Otto M, Brining DL, Kreiswirth BN, Taubenberger JK, Parnell MJ, Feldmann H, Musser JM, DeLeo FR, 2013 Seasonal H3N2 influenza A virus fails to enhance *Staphylococcus aureus* co-infection in a non-human primate respiratory tract infection model. *Virulence* 4, 707–715. [PubMed: 24104465]
- Memoli MJ, Tumpey TM, Jagger BW, Dugan VG, Sheng ZM, Qi L, Kash JC, Taubenberger JK, 2009 An early ‘classical’ swine H1N1 influenza virus shows similar pathogenicity to the 1918 pandemic virus in ferrets and mice. *Virology* 393, 338–345. [PubMed: 19733889]
- Memoli MJ, Czajkowski L, Reed S, Athota R, Bristol T, Proudfoot K, Fargis S, Stein M, Dunfee RL, Shaw PA, Davey RT, Taubenberger JK, 2015 Validation of the wild-type influenza A human challenge model H1N1pdMIST: an A(H1N1)pdm09 dose-finding investigational new drug study. *Clin. Infect. Dis.* 60, 693–702. [PubMed: 25416753]
- Miyake T, Soda K, Itoh Y, Sakoda Y, Ishigaki H, Nagata T, Ishida H, Nakayama M, Ozaki H, Tsuchiya H, Torii R, Kida H, Ogasawara K, 2010 Amelioration of pneumonia with *Streptococcus pneumoniae* infection by inoculation with a vaccine against highly pathogenic avian influenza virus in a non-human primate mixed infection model. *J. Med. Primatol.* 39, 58–70. [PubMed: 19900170]
- Morens DM, Taubenberger JK, Fauci AS, 2008 Predominant role of bacterial pneumonia as a cause of death in pandemic influenza: implications for pandemic influenza preparedness. *J. Infect. Dis.* 198, 962–970. [PubMed: 18710327]
- Muthuri SG, Venkatesan S, Myles PR, Leonardi-Bee J, Al Khuwaitir TS, Al Mamun A, Anovadiya AP, Azziz-Baumgartner E, Baez C, Bassetti M, Beovic B, Bertisch B, Bonmarin I, Booy R, Borja-Aburto VH, Burgmann H, Cao B, Carratala J, Denholm JT, Dominguez SR, Duarte PA, Dubnov-Raz G, Echavarria M, Fanella S, Gao Z, Gerardin P, Giannella M, Gubbels S, Herberg J, Iglesias AL, Hoger PH, Hu X, Islam QT, Jimenez MF, Kandeel A, Keijzers G, Khalili H, Knight M, Kudo K, Kuszniarz G, Kuzman I, Kwan AM, Amine IL, Langenegger E, Lankarani KB, Leo YS, Linko R, Liu P, Madanat F, Mayo-Montero E, McGeer A, Memish Z, Metan G, Mickiene A, Mikic D, Mohn KG, Moradi A, Nymadawa P, Oliva ME, Ozkan M, Parekh D, Paul M, Polack FP, Rath BA, Rodriguez AH, Sarrouf EB, Seale AC, Sertogullarindan B, Siqueira MM, Skret-Magierlo J, Stephan F, Talarek E, Tang JW, To KK, Torres A, Torun SH, Tran D, Uyeki TM, Van Zwol A, Vaudry W, Vidmar T, Yokota RT, Zarogoulidis P, Investigators PC, Nguyen-Van-Tam JS, 2014 Effectiveness of neuraminidase inhibitors in reducing mortality in patients admitted to hospital

with influenza A H1N1pdm09 virus infection: a meta-analysis of individual participant data. *Lancet Respir. Med.* 2, 395–404. [PubMed: 24815805]

Olsen RJ, Kobayashi SD, Ayeras AA, Ashraf M, Graves SF, Ragasa W, Humbird T, Greaver JL, Cantu C, Swain JL, Jenkins L, Blasdel T, Cagle PT, Gardner DJ, DeLeo FR, Musser JM, 2010 Lack of a major role of *Staphylococcus aureus* Panton-Valentine leukocidin in lower respiratory tract infection in nonhuman primates. *Am. J. Pathol.* 176, 1346–1354. [PubMed: 20093487]

Qi L, Kash JC, Dugan VG, Wang R, Jin G, Cunningham RE, Taubenberger JK, 2009 Role of sialic acid binding specificity of the 1918 influenza virus hemagglutinin protein in virulence and pathogenesis for mice. *J. Virol.* 83, 3754–3761. [PubMed: 19211766]

Randolph AG, Vaughn F, Sullivan R, Rubinson L, Thompson BT, Yoon G, Smoot E, Rice TW, Loftis LL, Helfaer M, Doctor A, Paden M, Flori H, Babbitt C, Graciano AL, Gedeit R, Sanders RC, Giuliano JS, Zimmerman J, Uyeki TM, Pediatric Acute Lung I, Sepsis Investigator's N, the National Heart L, Blood Institute ACTN, 2011 Critically ill children during the 2009–2010 influenza pandemic in the United States. *Pediatrics* 128, e1450–1458. [PubMed: 22065262]

Rice TW, Rubinson L, Uyeki TM, Vaughn FL, John BB, Miller RR 3rd, Higgs E, Randolph AG, Smoot BE, Thompson BT, Network NA, 2012 Critical illness from 2009 pandemic influenza A virus and bacterial coinfection in the United States. *Crit. Care Med.* 40, 1487–1498. [PubMed: 22511131]

Solomon J, Johnson RF, Douglas D, Hammoud D, 2014. New image analysis technique for quantitative longitudinal assessment of lung pathology on CT in infected rhesus macaques. In: 27th International Symposium on Computer-based Medical Systems (CBMS), 2014 IEEE, pp. 169–172.

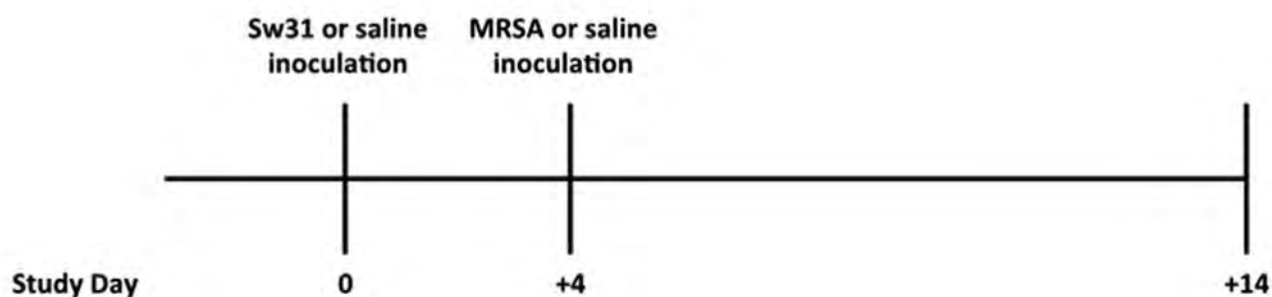
Su S, Bi Y, Wong G, Gray GC, Gao GF, Li S, 2015 Epidemiology, evolution, and recent outbreaks of avian influenza virus in China. *J. Virol.* 89, 8671–8676. [PubMed: 26063419]

World Health Organization, 2015, November 25. Influenza, Seasonal. Retrieved from. <http://www.who.int/mediacentre/factsheets/fs211/en/>.

Further reading

Taubenberger JK, Morens DM, 2006 1918 influenza: the mother of all pandemics. *Emerg. Infect. Dis.* 12, 15–22. [PubMed: 16494711]

A.



B.

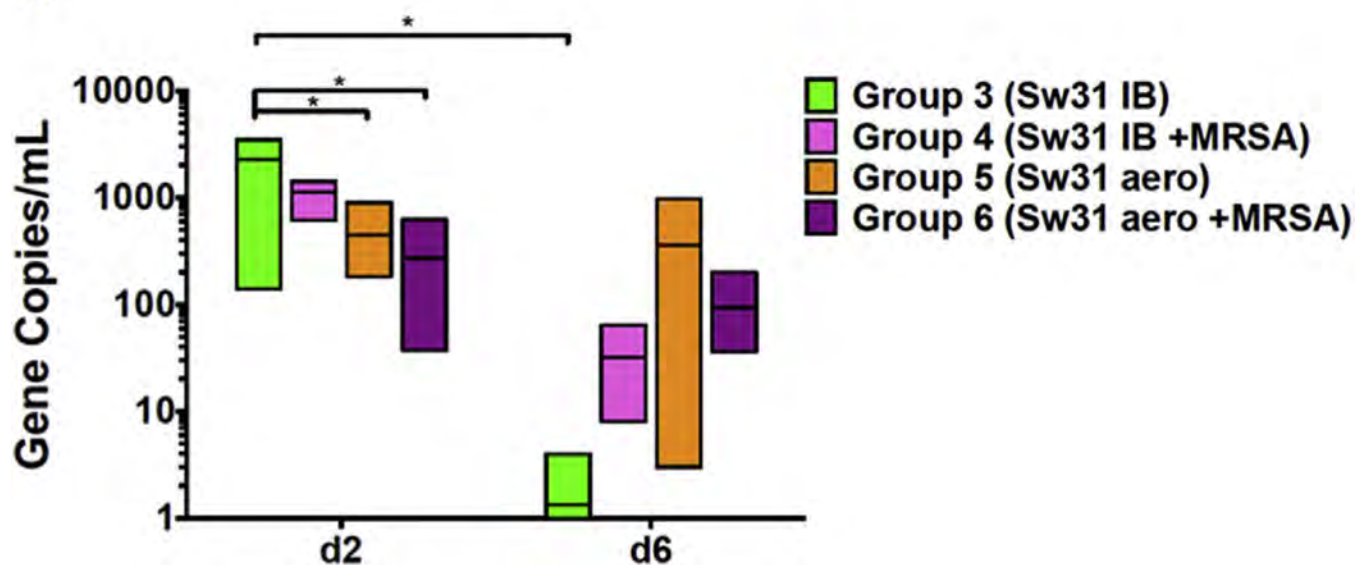


Fig. 1. Study timeline and viral RNA copy number in bronchoalveolar lavage.

A) Inoculation schedule. B) Viral RNA copy number in bronchoalveolar lavage from influenza inoculated groups. Data are represented as box plots showing median values (bar) and range (box). Comparison between groups was assessed by two-way ANOVA and significance testing by Tukey's test, * $p < 0.05$.

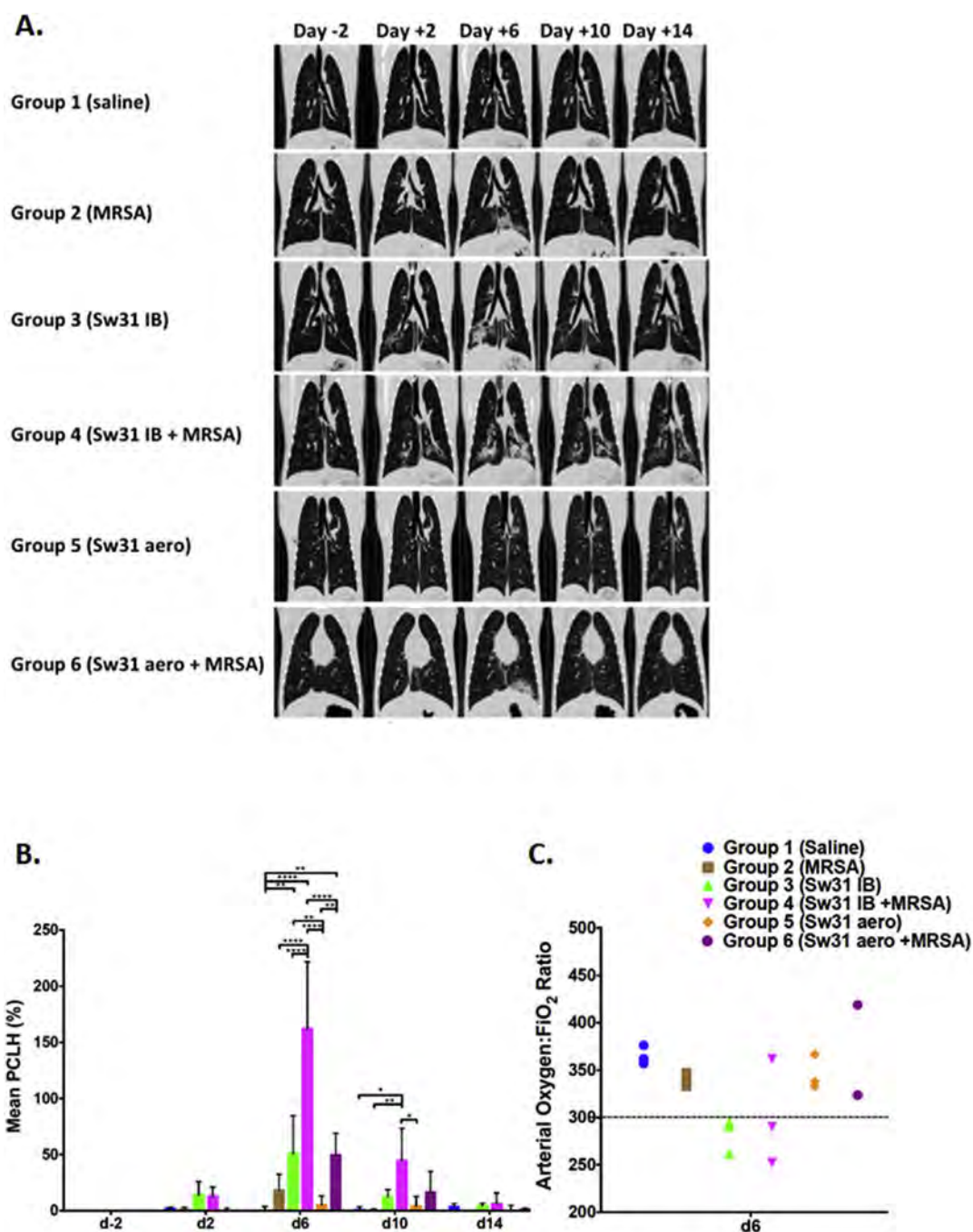


Fig. 2. High resolution computed tomography imaging of lungs; percent change in lung hyper-intensity over time; and animals that met clinical criteria for acute lung injury.

A) Representative sagittal lung images of animals from each group over time. B) Percent change in lung hyper-intensity for all animals in each group over time. Bar graphs represent group means and SEMs. Comparison between groups was assessed by two-way ANOVA and significance testing by Tukey's test, * $p < 0.05$, ** $p < 0.01$, and **** $p < 0.0001$. C) Animals (individuals dots) that met clinical criteria acute lung injury including arterial partial pressure of oxygen to fraction of inspired oxygen (P:F) ratio < 300 (below dotted line) and bilateral radiographic infiltrates.

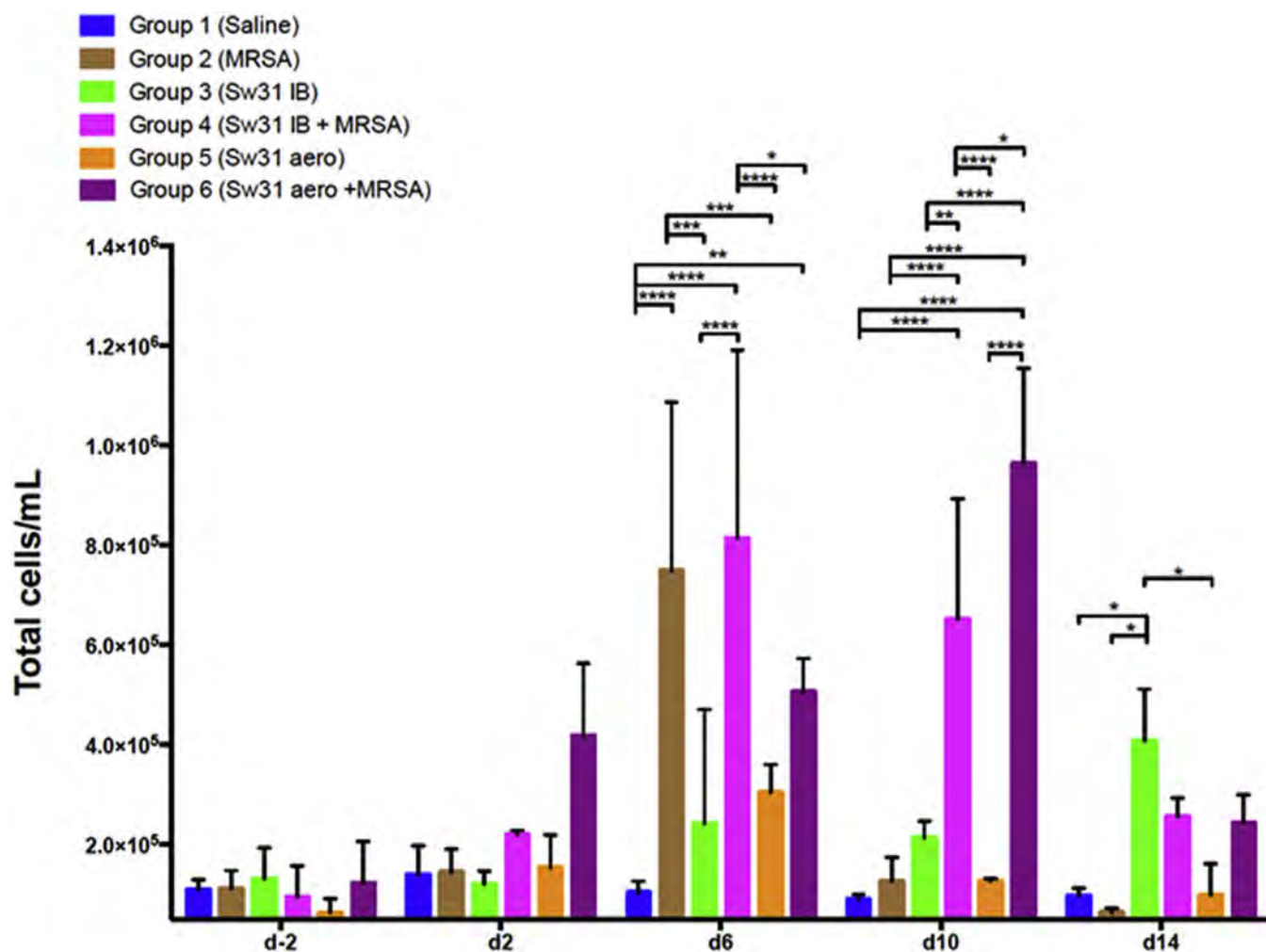


Fig. 3. Total CD45+ cells in bronchoalveolar lavage by group over time.

Bar graphs represent group means and SEMs. Comparison between groups was assessed by two-way ANOVA and significance testing by Tukey's test, * $p < 0.05$, ** $p < 0.01$, *** $p < 0.001$, and **** $p < 0.0001$.

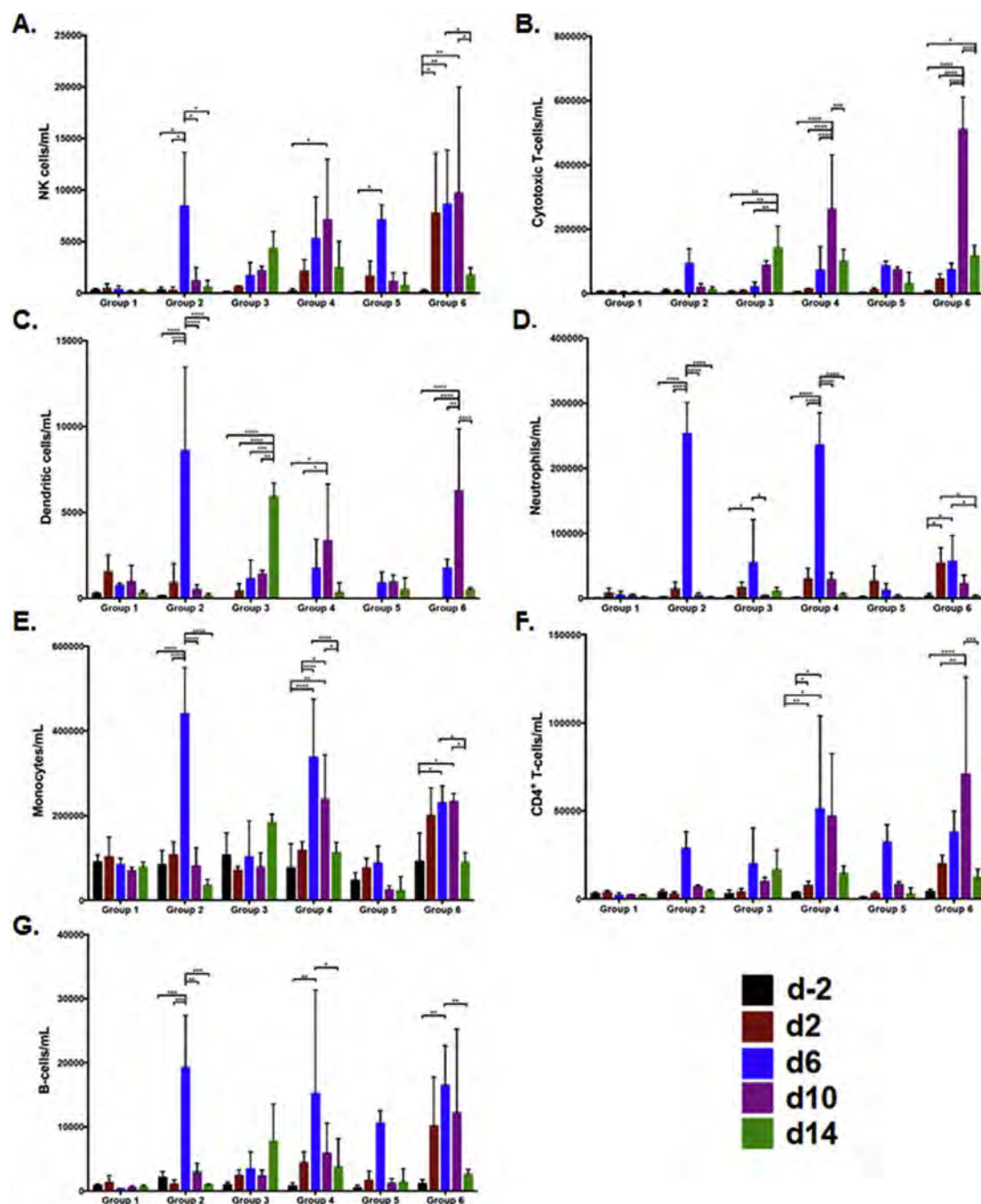


Fig. 4. Immunophenotypes of CD45+ cells from bronchoalveolar lavage by group overtime. A) NK cells; B) Cytotoxic T-cells; C) Dendritic cells; D) Neutrophils; E) Monocytes; F) CD4+ cells; G) B-cells. Bar graphs represent group means and SEMs. Comparison between groups was assessed by two-way ANOVA and significance testing by Tukey's test, * $p < 0.05$, ** $p < 0.01$, *** $p < 0.001$, and **** $p < 0.0001$.

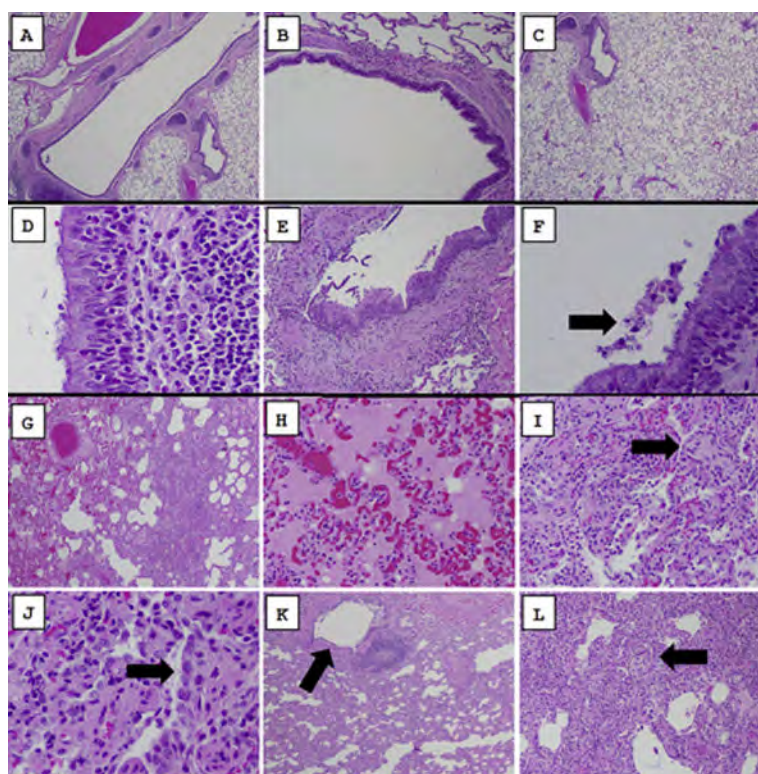


Fig. 5. Day +14 histopathology of lungs from Sw31 and/or MRSA infected animals (Groups 1 to 3).

A–C) Group 1 saline: No significant histopathological changes were noted in the tracheobronchial tree (A & B) or in the lung parenchyma (C); D–F) Group 2 MRSA: sections demonstrated foci of chronic bronchiolitis (D) with evidence of repair (E), and rare, foci of luminal bacteria (F, arrow); G–L) Group 3 Sw31 IB: sections showed multifocal areas of acute DAD (G) with alveolar edema and capillary congestion (H) admixed with multifocal areas of organizing DAD with interstitial fibrosis (I, arrow) and type II alveolar hyperplasia (J, arrow), focal chronic bronchiolitis (K, arrow), and focal bronchiolitis obliterans (L, arrow). Original magnifications are as follows: (A) 20×, (B) 100×, (C) 20×, (D) 400×, (E) 100×, (F) 400×, (G) 40×, (H) 200×, (I) 200×, (J) 400×, (K) 40×, (L) 100×.

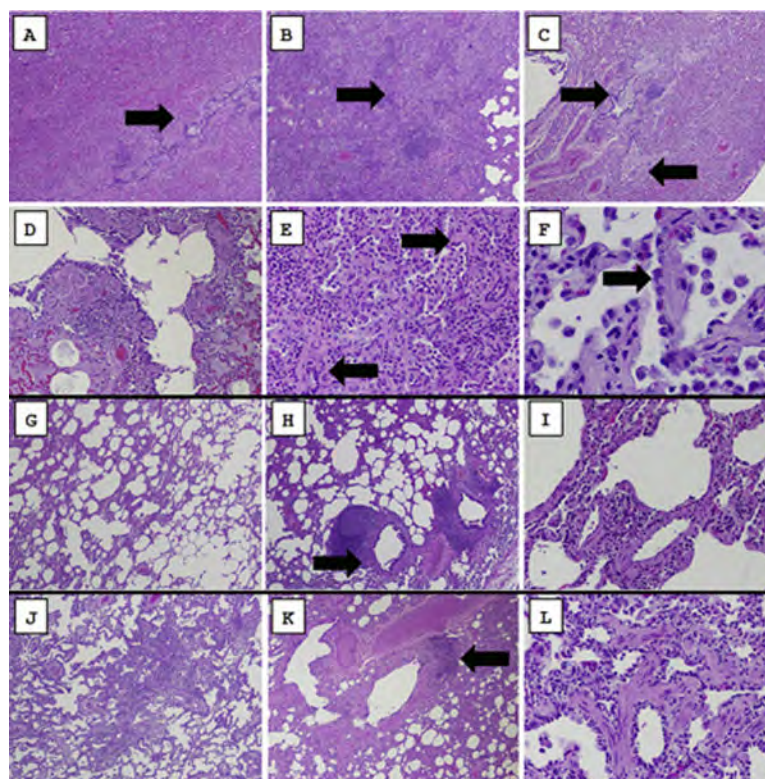


Fig. 6. Day +14 histopathology of lungs from Sw31 and/or MRSA infected animals (Groups 4 to 6).

A–F) Group 4 Sw31 IB + MRSA: multifocal areas of organizing pneumonia (A–C) with acute DAD with alveolar edema and capillary congestion admixed focal chronic bronchiolitis (D) and bronchiolitis obliterans (A–C, arrows), with multifocal areas of organizing DAD with interstitial fibrosis (E, arrows) and type II alveolar hyperplasia (F, arrow); G–I) Group 5 Sw31 aero: multifocal areas of interstitial pneumonia (G), focal chronic bronchiolitis with prominent submucosal lymphoid nodules (H, arrow), and multifocal areas of organizing DAD (I); J–L) Group 6 Sw31 aero + MRSA: multifocal areas of interstitial pneumonia (J), focal chronic bronchiolitis with prominent submucosal lymphoid nodules (K, arrow), and multifocal areas of organizing DAD, with interstitial fibrosis and type II alveolar hyperplasia (L). Original magnifications are as follows: (A) 40×, (B) 40×, (C) 40×, (D) 100×, (E) 200×, (F) 400×, (G) 40×, (H) 40×, (I) 200×, (J) 40×, (K) 40×, (L) 200×.

Table 1

Back-titration results for influenza and bacterial challenge inoculum.

Experimental group	Delivered inoculum (mean \pm standard deviation)	
	Sw31 (PFU/animal)	MRSA (CFU/animal)
1: Saline	X	X
2: MRSA	X	$1.20 \times 10^9 \pm 4.00 \times 10^8$
3: Sw31 IB	$2.06 \times 10^6 \pm 1.30 \times 10^6$	X
4: Sw31 IB + MRSA	$2.11 \times 10^6 \pm 3.15 \times 10^5$	$1.33 \times 10^9 \pm 3.8 \times 10^8$
5: Sw31 aero	$6.15 \times 10^6 \pm 4.86 \times 10^5$	X
6: Sw31 aero + MRSA	$6.21 \times 10^6 \pm 3.85 \times 10^6$	$8.88 \times 10^8 \pm 1.25 \times 10^8$

CORRESPONDENCE

Persistence and Evolution of SARS-CoV-2 in an Immunocompromised Host

TO THE EDITOR: A 45-year-old man with severe antiphospholipid syndrome complicated by diffuse alveolar hemorrhage,¹ who was receiving anticoagulation therapy, glucocorticoids, cyclophosphamide, and intermittent rituximab and eculizumab, was admitted to the hospital with fever (Fig. S1 in the Supplementary Appendix, available with the full text of this letter at NEJM.org). On day 0, Covid-19 was diagnosed by SARS-CoV-2 reverse-transcriptase–polymerase-chain-reaction (RT-PCR) assay of a nasopharyngeal swab specimen, and the patient received a 5-day course of remdesivir (Fig. S2). Glucocorticoid doses were increased because of suspected diffuse alveolar hemorrhage. He was discharged on day 5 without a need for supplemental oxygen.

From day 6 through day 68, the patient quarantined alone at home, but during the quarantine period, he was hospitalized three times for abdominal pain and once for fatigue and dyspnea. The admissions were complicated by hypoxemia that caused concern for recurrent diffuse alveolar hemorrhage and was treated with increased doses of glucocorticoids. SARS-CoV-2 RT-PCR cycle threshold (Ct) values increased to 37.8 on day 39, which suggested resolving infection (Table S1).^{2,3}

On day 72 (4 days into another hospital admission for hypoxemia), RT-PCR assay of a nasopharyngeal swab was positive, with a Ct value of 27.6, causing concern for a recurrence of Covid-19. The patient again received remdesivir (a 10-day course), and subsequent RT-PCR assays were negative.

On day 105, the patient was admitted for cellulitis. On day 111, hypoxemia developed, ultimately requiring treatment with high-flow oxygen. Given the concern for recurrent diffuse alveolar hemorrhage, the patient's immunosuppression was escalated (Figs. S1 through S3). On day 128, the RT-PCR Ct value was 32.7, which caused concern for a second Covid-19 recurrence,

and the patient was given another 5-day course of remdesivir. A subsequent RT-PCR assay was negative. Given continued respiratory decline and concern for ongoing diffuse alveolar hemorrhage, the patient was treated with intravenous immunoglobulin, intravenous cyclophosphamide, and daily ruxolitinib, in addition to glucocorticoids.

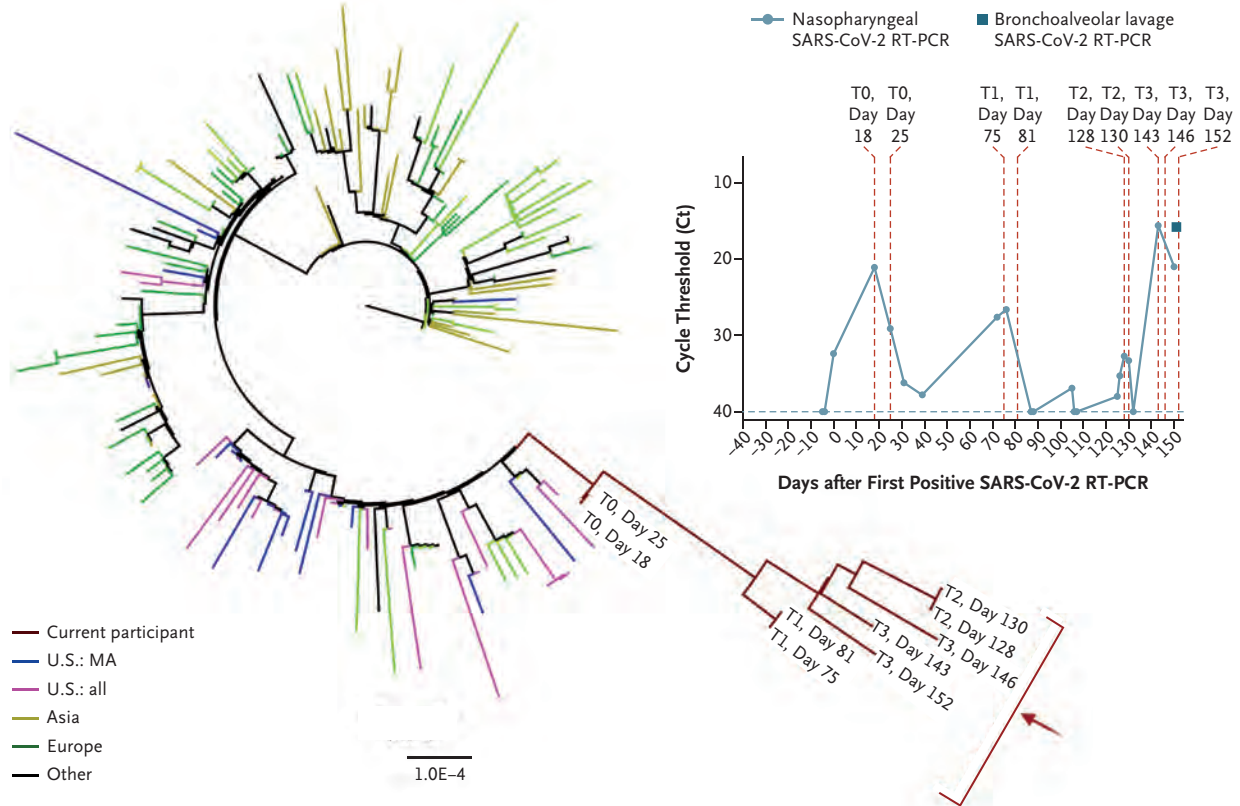
On day 143, the RT-PCR Ct value was 15.6, which caused concern for a third recurrence of Covid-19. The patient received a SARS-CoV-2 antibody cocktail against the SARS-CoV-2 spike protein (Regeneron).⁴ On day 150, he underwent endotracheal intubation because of hypoxemia. A bronchoalveolar-lavage specimen on day 151 revealed an RT-PCR Ct value of 15.8 and grew *Aspergillus fumigatus*. The patient received remdesivir and antifungal agents. On day 154, he died from shock and respiratory failure.

We performed quantitative SARS-CoV-2 viral load assays in respiratory samples (nasopharyngeal and sputum) and in plasma, and the results were concordant with RT-PCR Ct values, peaking at 8.9 log₁₀ copies per milliliter (Fig. S2 and Table S1). Tissue studies showed the highest SARS-CoV-2 RNA levels in the lungs and spleen (Figs. S4 and S5).

Phylogenetic analysis was consistent with persistent infection and accelerated viral evolution (Figs. 1A and S6). Amino acid changes were predominantly in the spike gene and the receptor-binding domain, which make up 13% and 2% of the viral genome, respectively, but harbored 57% and 38% of the observed changes (Fig. 1B). Viral infectivity studies confirmed infectious virus in nasopharyngeal samples from days 75 and 143 (Fig. S7). Immunophenotyping and SARS-CoV-2–specific B-cell and T-cell responses are shown in Table S2 and Figures S8 through S11.

Although most immunocompromised persons effectively clear SARS-CoV-2 infection, this case

A Global and Patient SARS-CoV-2 Sequences



B Locations of SARS-CoV-2 Sequence Polymorphisms over Time

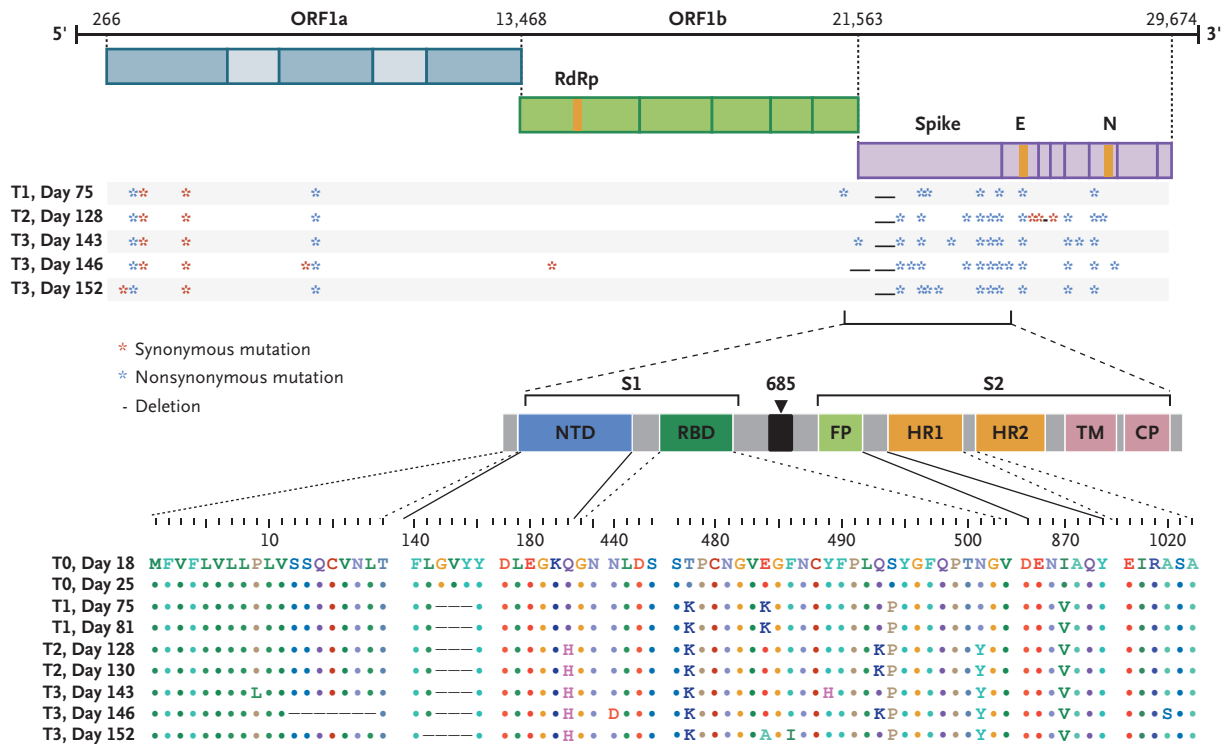


Figure 1 (facing page). SARS-CoV-2 Whole-Genome Viral Sequencing from Longitudinally Collected Nasopharyngeal Swabs.

Shown in Panel A is a maximum-likelihood phylogenetic tree with patient sequences (red arrow) at four time points with high levels of SARS-CoV-2 viral loads (T0 denotes days 18 and 25; T1 days 75 and 81; T2 days 128 and 130; and T3 days 143, 146, and 152), along with representative sequences from the state (U.S.: MA), country (U.S.: all), Asia, Europe, and Other (Africa, South America, and Canada). The scale represents 0.0001 nucleotide substitutions per site. The inset shows nasopharyngeal and bronchoalveolar-lavage SARS-CoV-2 RT-PCR cycle threshold (Ct) values; the horizontal dashed line represents the cutoff for positivity at 40, and vertical red dashed lines represent days of viral sequencing (days 18, 25, 75, 81, 128, 130, 143, 146, and 152). Shown in Panel B are the locations of deletions and synonymous and nonsynonymous mutations in the patient at T1, T2, and T3 as compared with T0. CP denotes cytoplasmic domain, E envelope, FP fusion peptide, HR1 heptad repeat 1, HR2 heptad repeat 2, N nucleocapsid, NTD N-terminal domain, ORF open reading frame, RBD receptor-binding domain, RdRp RNA-dependent RNA polymerase, S1 subunit 1, S2 subunit 2, and TM transmembrane domain.

highlights the potential for persistent infection⁵ and accelerated viral evolution associated with an immunocompromised state.

Bina Choi, M.D.

Manish C. Choudhary, Ph.D.

James Regan, B.S.

Jeffrey A. Sparks, M.D.

Robert F. Padera, M.D., Ph.D.

Brigham and Women's Hospital
Boston, MA

Xueting Qiu, Ph.D.

Harvard T.H. Chan School of Public Health
Boston, MA

Isaac H. Solomon, M.D., Ph.D.

Brigham and Women's Hospital
Boston, MA

Hsiao-Hsuan Kuo, Ph.D.

Julie Boucau, Ph.D.

Kathryn Bowman, M.D.

U. Das Adhikari, Ph.D.

Ragon Institute of MGH, MIT, and Harvard
Cambridge, MA

Marisa L. Winkler, M.D., Ph.D.

Alisa A. Mueller, M.D., Ph.D.

Tiffany Y.-T. Hsu, M.D., Ph.D.

Michaël Desjardins, M.D.

Lindsey R. Baden, M.D.

Brian T. Chan, M.D., M.P.H.

Brigham and Women's Hospital
Boston, MA

Bruce D. Walker, M.D.

Ragon Institute of MGH, MIT, and Harvard
Cambridge, MA

Mathias Lichterfeld, M.D., Ph.D.

Manfred Brigl, M.D.

Brigham and Women's Hospital
Boston, MA

Douglas S. Kwon, M.D., Ph.D.

Ragon Institute of MGH, MIT, and Harvard
Cambridge, MA

Sanjat Kanjilal, M.D., M.P.H.

Brigham and Women's Hospital
Boston, MA

Eugene T. Richardson, M.D., Ph.D.

Harvard Medical School
Boston, MA

A. Helena Jonsson, M.D., Ph.D.

Brigham and Women's Hospital
Boston, MA

Galit Alter, Ph.D.

Amy K. Barczak, M.D.

Ragon Institute of MGH, MIT and Harvard
Cambridge, MA

William P. Hanage, Ph.D.

Harvard T.H. Chan School of Public Health
Boston, MA

Xu G. Yu, M.D.

Gaurav D. Gaiha, M.D., D.Phil.

Ragon Institute of MGH, MIT and Harvard
Cambridge, MA

Michael S. Seaman, Ph.D.

Beth Israel Deaconess Medical Center
Boston, MA

Manuela Cernadas, M.D.

Jonathan Z. Li, M.D.

Brigham and Women's Hospital
Boston, MA

Drs. Choi and Choudhary and Drs. Cernadas and Li contributed equally to this letter.

Supported in part by the Massachusetts Consortium for Pathogen Readiness through grants from the Evergrande Fund; Mark, Lisa, and Enid Schwartz; the Harvard University Center for AIDS Research (NIAID 5P30AI060354); Brigham and Women's Hospital; and a grant (1UL1TR001102) from the National Center for Advancing Translational Sciences to the Harvard Clinical and Translational Science Center.

Disclosure forms provided by the authors are available with the full text of this letter at NEJM.org.

This letter was published on November 11, 2020, at NEJM.org.

1. Deane KD, West SG. Antiphospholipid antibodies as a cause of pulmonary capillaritis and diffuse alveolar hemorrhage: a case series and literature review. *Semin Arthritis Rheum* 2005; 35:154-65.
2. Wölfel R, Corman VM, Guggemos W, et al. Virological assessment of hospitalized patients with COVID-2019. *Nature* 2020;581:465-9.
3. He X, Lau EHY, Wu P, et al. Temporal dynamics in viral shedding and transmissibility of COVID-19. *Nat Med* 2020;26: 672-5.
4. Baum A, Fulton BO, Wloga E, et al. Antibody cocktail to SARS-CoV-2 spike protein prevents rapid mutational escape seen with individual antibodies. *Science* 2020;369:1014-8.
5. Helleberg M, Utoft Niemann C, Sommerlund Moestrup K, et al. Persistent COVID-19 in an immunocompromised patient temporarily responsive to two courses of remdesivir therapy. *J Infect Dis* 2020;222:1103-7.

DOI: 10.1056/NEJMc2031364

Correspondence Copyright © 2020 Massachusetts Medical Society.

Comparison of Symptoms and RNA Levels in Children and Adults With SARS-CoV-2 Infection in the Community Setting

Erin Chung, MD; Eric J. Chow, MD, MS, MPH; Naomi C. Wilcox, MPH; Roy Burstein, PhD; Elisabeth Brandstetter, MPH; Peter D. Han, MS; Kairsten Fay, BS; Brian Pfau, BS; Amanda Adler, MS; Kirsten Lacombe, RN, MSN; Christina M. Lockwood, PhD; Timothy M. Uyeki, MD, MPH, MPP; Jay Shendure, MD, PhD; Jeffrey S. Duchin, MD; Mark J. Rieder, PhD; Deborah A. Nickerson, PhD; Michael Boeckh, MD, PhD; Michael Famulare, PhD; James P. Hughes, PhD; Lea M. Starita, PhD; Trevor Bedford, PhD; Janet A. Englund, MD; Helen Y. Chu, MD, MPH

IMPORTANCE The association between COVID-19 symptoms and SARS-CoV-2 viral levels in children living in the community is not well understood.

OBJECTIVE To characterize symptoms of pediatric COVID-19 in the community and analyze the association between symptoms and SARS-CoV-2 RNA levels, as approximated by cycle threshold (Ct) values, in children and adults.

DESIGN, SETTING, AND PARTICIPANTS This cross-sectional study used a respiratory virus surveillance platform in persons of all ages to detect community COVID-19 cases from March 23 to November 9, 2020. A population-based convenience sample of children younger than 18 years and adults in King County, Washington, who enrolled online for home self-collection of upper respiratory samples for SARS-CoV-2 testing were included.

EXPOSURES Detection of SARS-CoV-2 RNA by reverse transcription-polymerase chain reaction (RT-PCR) from participant-collected samples.

MAIN OUTCOMES AND MEASURES RT-PCR-confirmed SARS-CoV-2 infection, with Ct values stratified by age and symptoms.

RESULTS Among 555 SARS-CoV-2-positive participants (mean [SD] age, 33.7 [20.1] years; 320 were female [57.7%]), 47 of 123 children (38.2%) were asymptomatic compared with 31 of 432 adults (7.2%). When symptomatic, fewer symptoms were reported in children compared with adults (mean [SD], 1.6 [2.0] vs 4.5 [3.1]). Symptomatic individuals had lower Ct values (which corresponded to higher viral RNA levels) than asymptomatic individuals (adjusted estimate for children, −3.0; 95% CI, −5.5 to −0.6; $P = .02$; adjusted estimate for adults, −2.9; 95% CI, −5.2 to −0.6; $P = .01$). The difference in mean Ct values was neither statistically significant between symptomatic children and symptomatic adults (adjusted estimate, −0.7; 95% CI, −2.2 to 0.9; $P = .41$) nor between asymptomatic children and asymptomatic adults (adjusted estimate, −0.6; 95% CI, −4.0 to 2.8; $P = .74$).

CONCLUSIONS AND RELEVANCE In this community-based cross-sectional study, SARS-CoV-2 RNA levels, as determined by Ct values, were significantly higher in symptomatic individuals than in asymptomatic individuals and no significant age-related differences were found. Further research is needed to understand the role of SARS-CoV-2 RNA levels and viral transmission.

JAMA Pediatr. doi:10.1001/jamapediatrics.2021.2025
Published online June 11, 2021.

[+ Editorial](#)

[+ Supplemental content](#)

Author Affiliations: Author affiliations are listed at the end of this article.

Corresponding Author: Erin Chung, MD, University of Washington School of Medicine, Box 358061, 750 Republican St, Room E691, Seattle, WA 98109 (ec72@uw.edu).

The COVID-19 pandemic caused by SARS-CoV-2 has resulted in substantial morbidity and mortality worldwide. Early public health interventions, including the closure of schools, were implemented to prevent the spread of SARS-CoV-2. However, the role of children in community SARS-CoV-2 transmission remains poorly understood as most children with SARS-CoV-2 infection are asymptomatic¹ or experience mild disease.^{2,3} There have been few community-based studies of pediatric COVID-19 cases, and thus there are limited data on the role of children in the transmission of COVID-19.⁴

One potential driver of SARS-CoV-2 transmissibility is respiratory tract viral load, approximated by quantification of viral RNA levels via reverse transcription-polymerase chain reaction (RT-PCR) cycle threshold (Ct) values. Studies have shown a strong association between lower Ct values (higher RNA levels) and successful isolation of SARS-CoV-2 in culture.⁵⁻⁷ Early case reports showed that asymptomatic individuals had levels of detectable SARS-CoV-2 RNA comparable with symptomatic individuals,⁸⁻¹⁰ and this observation has been supported by a growing body of evidence from larger community-based studies in predominantly adult populations.¹¹⁻¹⁴ Studies examining SARS-CoV-2 RNA levels in children, which have generally involved small sample sizes and relied on sampling associated with presentation at medical care facilities or community-based contact tracing, have shown conflicting results¹⁵⁻¹⁸ and comparison of community-derived pediatric and adult data has been limited.¹⁹

In this study, using data from a novel countywide respiratory virus surveillance platform, we described the association between SARS-CoV-2 Ct values and symptoms in SARS-CoV-2-positive children in King County, Washington. We also compared these findings between children and adults with SARS-CoV-2 infection.

Methods

Study Platform and Setting

This is a cross-sectional population-based analysis of data collected as part of the Seattle Coronavirus Assessment Network (SCAN). SCAN launched on March 23, 2020, to evaluate the feasibility of testing individuals both with and without COVID-19-like illness via unsupervised home self-collected nasal swabs for detection of SARS-CoV-2 and other respiratory pathogens.²⁰ The network was originally established in November 2018 as the Seattle Flu Study (SFS),²¹ which focused on the community transmission of influenza and other respiratory viruses. SCAN was limited to residents of King County, Washington. We split the county into 16 groupings, defined roughly by the 16 public use microdata areas defined by the US Census Bureau. The proportion of individuals relative to the county population in each grouping dictated the proportion of daily test kits allotted to each public use microdata area. Individuals of all ages, whether they had any COVID-19 symptoms or not, were eligible to enroll on the study website.²⁰ The website and study materials were translated into 11 non-English languages and translation services were avail-

Key Points

Question How is the presence of symptoms associated with SARS-CoV-2 RNA levels in children vs adults in the community?

Findings In this cross-sectional study of 555 children and adults with SARS-CoV-2 confirmed by reverse transcription-polymerase chain reaction, symptomatic individuals had higher SARS-CoV-2 RNA levels (as indicated by lower mean cycle threshold values) compared with asymptomatic individuals. No significant differences in RNA levels were found between asymptomatic children and asymptomatic adults or between symptomatic children and symptomatic adults.

Meaning Regardless of age, in this community-based study, SARS-CoV-2 RNA levels were higher in symptomatic individuals.

able. This study was approved by the University of Washington Institutional Review Board. This study followed the Strengthening the Reporting of Observational Studies in Epidemiology (STROBE) reporting guideline.²⁹ All patients who enrolled online provided written informed consent.

Data and Sample Collection

After signing an electronic consent form, all participants, or parents or guardians for participants younger than 18 years, completed an electronic questionnaire to collect data on sociodemographic and clinical characteristics, exposures, and health-related behaviors. Race and ethnicity were self-classified by participants using provided standard race and ethnic categories.²² Race and ethnicity data were collected to examine disparities between racial/ethnic groups in study participation as well as in outcomes, such as SARS-CoV-2 positivity. Study data were collected and managed using REDCap Electronic Data Capture version 10.9.2 (Vanderbilt University) hosted at the University of Washington.^{23,24} Within 24 hours of enrollment, sample collection kits were delivered using a private courier for contactless receipt at the participants' homes. Samples were self-collected by participants 13 years and older via unsupervised middle turbinate (MTB) or anterior nares (AN) swabs.²⁵ Parents or guardians performed swab collection for children younger than 13 years. Swab collection instructions were included with the swab kit (eFigure 1 in the Supplement) and were available on the study website.^{26,27} Swab samples were returned to the laboratory within 48 hours via private courier.

This study included participants who enrolled in SCAN from March 23 to November 9, 2020, and who collected at home a nasal swab that tested positive for SARS-CoV-2 by RT-PCR. Repeated samples from individuals were excluded from analysis. Children were defined as participants younger than 18 years. For privacy, all adults older than 85 years were classified as aged 85 years. Symptomatic participants reported at least 1 symptom (ie, runny or stuffy nose, fever, headache, cough, fatigue, sore throat, muscle or body aches, chills, sweats, loss of smell or taste, diarrhea, eye pain, nausea or vomiting, trouble breathing, ear pain or discharge, or rash) within 7 days prior to study enrollment. Asymptomatic participants were

those who reported no symptoms in this time frame. Per guidelines from the US Centers for Disease Control and Prevention at the time of the study, close contact was defined as an encounter in the past 2 weeks in which the individual spent at least 10 minutes within 6 feet of a person who tested positive for SARS-CoV-2.

Laboratory Analyses

From March 23 to July 23, 2020, MTB swabs (Copan) were returned in 3-mL tubes of BD universal viral transport media (Becton, Dickinson and Company) or viral transport media (Brainbits) at room temperature, and aliquoted and stored at 4° C prior to testing. After July 23, 2020, AN swabs (US Cotton #3) were used by participants and returned in empty transport tubes. AN swabs were rehydrated and eluted in 1 mL of either phosphate-buffered saline or Tris-EDTA buffer. All samples were processed, including rehydration, within 48 hours of collection. Stability studies have shown consistent SARS-CoV-2 Ct values at 4° C and 40° C for both AN and MTB swabs up to 3 days²⁸ and 9 days,²¹ respectively. Laboratory testing was performed at the Brotman Baty Institute for Precision Medicine, Seattle, Washington, and the Northwest Genomics Center, Seattle, Washington. Total nucleic acids were extracted (before October 18, 2020, MagNA Pure 96, Roche; on or after October 18, 2020, KingFisher, Thermo Fisher) and tested for the presence of SARS-CoV-2 and the human marker ribonuclease P (RNase P) using a Clinical Laboratory Improvement Amendments-compliant laboratory developed test. RNase P Ct values were used as an extraction and sample collection control. The laboratory developed test consisted of 2 unique multiplexed assays run in duplicate for a total of 4 RT-PCR reactions; each multiplex reaction included a target for SARS-CoV-2 and RNase P. One assay targeted Orf1b with FAM fluor (Life Technologies 4332079 assay #APGZJKF) and was multiplexed with an RNase P probe set with VIC or HEX fluor (Life Technologies A30064 or Integrated DNA Technologies) on a QuantStudio 6 (Applied Biosystems), and the other targeted the S gene (Life Technologies 4332079 assay #APXGVC4) and was also multiplexed with RNase P-VIC or RNase P-HEX assay. Standard curves demonstrated a linear association with mean Ct values and logarithm of SARS-CoV-2 RNA copy numbers for each primer set and from each collection method (MTB vs AN) (eFigure 2 in the [Supplement](#)). At least 3 replicates for RNase P had to be detected for a valid test result. For a positive result, 3 or more SARS-CoV-2 targets must have had a Ct value of less than 40. Most samples were also tested for the presence of 24 respiratory pathogens by TaqMan RT-PCR on the OpenArray platform (Thermo Fisher).

Statistical Analyses

Mean SARS-CoV-2 Ct values were obtained using the 2 Ct values for the Orf1b gene primer. Results were not affected by the primer used (eFigure 3 in the [Supplement](#)) but we excluded analysis by S gene because of better Orf1b sensitivity and reproducibility. Analysis by RNase P Ct values did not show evidence of confounding by age or symptom status (eFigure 4 in the [Supplement](#)). We generated descriptive statistics for all variables. Proportions of missing data were reported. Data analy-

ses were performed using R version 4.0.5 (The R Foundation). Statistical comparisons between groups were determined using χ^2 tests, Welch *t* test, and multiple linear regression. Two-tailed tests were used for all comparisons and statistical significance was defined as $P < .05$. AN swabs were used in the later portion of the study when rates of positivity in children, many of whom were asymptomatic, increased. Therefore, because swab type is a confounder of the association between age and SARS-CoV-2 RNA levels, we used multiple linear regression to adjust individual Ct values to the average swab type in the study. This ensured that our figures would show an unconfounded comparison of ages and symptom status, while preserving the mean Ct value across the sample. Although 2 different nucleic acid extraction platforms were used, multiple linear regression analysis showed that the extraction platform used did not have statistically significant or clinically meaningful associations with our results.

Results

From March 23 to November 9, 2020, 37 067 samples were tested for SARS-CoV-2 via SCAN. Overall, 673 samples (1.8%) had positive results (493 of 31 664 [1.6%] of adult samples and 180 of 5356 [3.4%] of child samples; 47 positive samples did not have age data). Of these positive samples, 180 samples (26.7%) were from children younger than 18 years and 493 (73.3%) were from adults. We excluded 118 samples: 42 that represented repeated positive testing in SCAN and 76 that were missing clinical information.

Of the 555 participants with SARS-CoV-2-positive results, 123 (22.2%) were children and 432 (77.8%) were adults (**Table 1**), ranging in age from 73 days to 85 years. The mean (SD) age was 33.7 (20.1) years: 7.5 (5.3) years for children and 41.2 (16.0) years for adults. Among 123 SARS-CoV-2-positive children in this study, 50 (40.7%) were younger than 5 years, 45 (36.6%) were aged 5 to 11 years, and 28 (22.8%) were aged 12 to 17 years. Of the total positive sample, 320 (57.7%) were female. Of 123 SARS-CoV-2-positive children, 64 (52.0%) were female, 55 (44.7%) were White, and 30 (24.4%) were Hispanic or Latino. The most common underlying conditions among SARS-CoV-2-positive children included seasonal allergies (9 [7.3%]) and asthma (5 [4.1%]), but most children reported no previous underlying medical conditions (106 [86.2%]). Compared with the mean King County household size of 2.4 people,³⁰ people of all ages with SARS-CoV-2-positive results reported larger mean (SD) household sizes (3.8 [1.6]). Most children (91 [74.0%]) resided in households of 4 or more people. Most children (98 [79.7%]) had at least 1 known SARS-CoV-2-positive contact, and most contacts (84 [68.3%]) were in the same household. In contrast, only 179 of 432 SARS-CoV-2-positive adults (41.4%) reported any known positive contact.

Fewer children were symptomatic compared with adults (76 of 123 children [61.8%] vs 401 of 432 adults [92.8%]; $P < .001$) (**Table 2**). When symptomatic, fewer symptoms were reported in children compared with adults (mean [SD], 1.6 [2.0] vs 4.5 [3.1]) (**Figure 1**). Symptomatic children reported a mean

Table 1. Demographic Characteristics of SARS-CoV-2-Positive Children and Adults in Seattle Coronavirus Assessment Network (SCAN) From March 23 to November 9, 2020

Characteristic	No. (%)		
	Total sample	Children	Adults
Total, No.	555	123	432
Sex			
Female	320 (57.7)	64 (52.0)	256 (59.3)
Male	235 (42.2)	59 (48.0)	176 (40.7)
Race/ethnicity ^a			
American Indian or Alaskan Native	1 (0.2)	0	1 (0.2)
Asian	75 (13.5)	13 (10.6)	62 (14.4)
Black or African American	35 (6.3)	10 (8.1)	25 (5.8)
Native Hawaiian or other Pacific Islander	11 (2.0)	2 (1.6)	9 (2.1)
White	283 (51.0)	55 (44.7)	228 (52.8)
Other ^b	76 (13.7)	17 (13.8)	59 (13.7)
Multiple races	42 (7.6)	19 (15.4)	23 (5.3)
Not reported	32 (5.8)	7 (5.7)	25 (5.8)
Hispanic or Latino ethnicity			
Yes	118 (21.3)	30 (24.4)	88 (20.4)
No	414 (74.6)	89 (72.4)	325 (75.2)
Not reported	23 (4.1)	4 (3.3)	19 (4.4)
Age, y			
0-4	50 (9.0)	50 (40.7)	NA
5-11	45 (8.1)	45 (36.6)	NA
12-17	28 (5.0)	28 (22.8)	NA
18-49	305 (55.0)	NA	305 (70.6)
50-64	93 (16.7)	NA	93 (21.5)
65-85 ^c	34 (6.1)	NA	34 (7.9)
Mean (SD)	33.7 (20.1)	7.5 (5.3)	41.2 (16)
Comorbidity			
None	394 (71.0)	106 (86.2)	288 (66.7)
Allergy	77 (13.8)	9 (7.3)	68 (15.7)
Asthma	41 (7.4)	5 (4.1)	36 (8.3)
Cardiovascular disease	9 (1.6)	0	9 (2.1)
Cancer	2 (0.4)	0	2 (0.5)
Chronic lung disease, not asthma	3 (0.5)	0	3 (0.7)
Diabetes	24 (4.3)	0	24 (5.6)
Hypertension	42 (7.5)	1 (0.8)	41 (9.5)
Unknown/not reported	16 (2.9)	2 (1.6)	14 (3.2)
Household size (including participant)			
1	36 (6.5)	0	33 (7.6)
2	116 (20.9)	21 (17.1)	95 (22.0)
3	83 (15.0)	11 (8.9)	72 (16.7)
4	123 (22.0)	38 (30.9)	88 (20.4)
5	95 (17.1)	30 (24.4)	65 (15.0)
≥6 ^d	102 (18.4)	23 (18.7)	79 (18.3)
Mean (SD)	3.8 (1.6)	4.1 (1.4)	3.7 (1.6)
SARS-CoV-2-positive close contacts ^e			
None	69 (12.4)	10 (8.1)	59 (13.7)
Any positive contact	277 (49.9)	98 (79.7)	179 (41.4)
Household	225 (40.5)	84 (68.3)	141 (32.6)
Friend	45 (8.1)	14 (11.4)	31 (7.2)
Coworker	16 (2.9)	0	16 (3.7)
Unsure/not reported	209 (37.7)	15 (12.2)	194 (44.9)

Abbreviation: NA, not applicable.

^a Race/ethnicity categories were treated as mutually exclusive groups; multiple races was defined as 2 or more of the above groups.

^b This included unlisted races not specified by participant.

^c For privacy, all adults older than 85 years were classified as aged 85 years.

^d For the purpose of analysis, we assumed a household size of 6 for individuals who reported 6 or more household members.

^e Close contact was defined as an encounter in the past 2 weeks in which the individual spent at least 10 minutes within 6 feet of a person who tested positive for SARS-CoV-2.

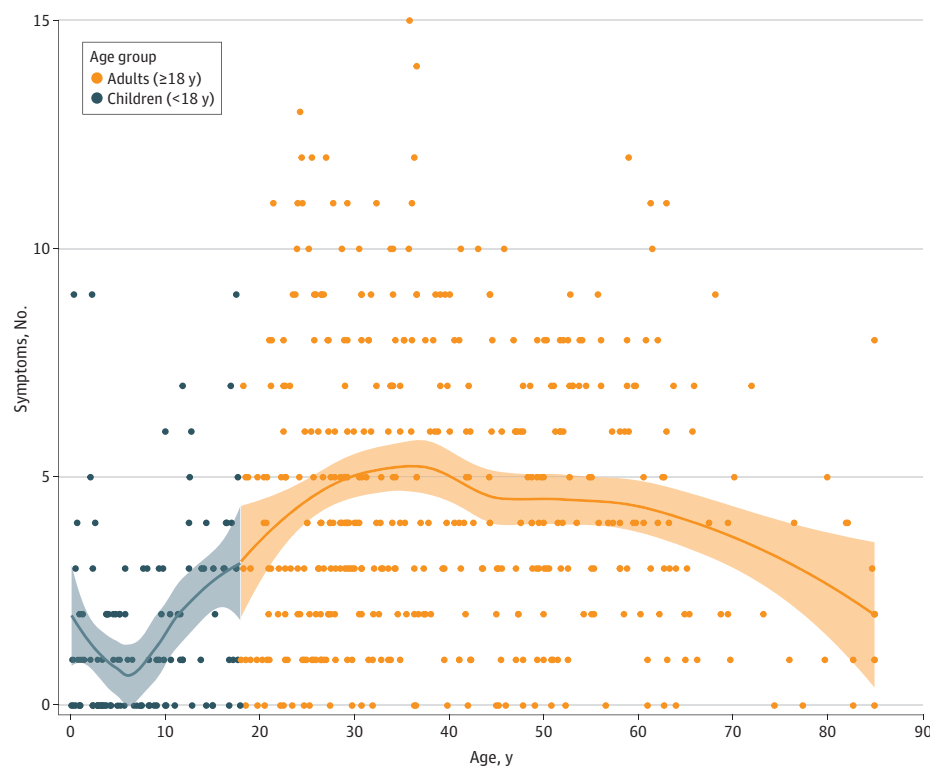
Table 2. Reported Signs and Symptoms and Duration in SARS-CoV-2-Positive Children and Adults at Enrollment

Sign or symptom ^a	No (%)			P value	
	Children Aged ≤4 y (n = 50)	Aged 5-17 y (n = 73)	Adults (n = 432)	Children aged ≤4 y vs children aged 5-17 y	All children vs adults
No symptoms	23 (46.0)	24 (32.9)	31 (7.2)		
Any symptom	27 (54.0)	49 (67.1)	401 (92.8)	.20	<.001
Runny or stuffy nose	14 (28.0)	22 (30.1)	192 (47.9)	.97	.004
Fever	11 (22.0)	15 (20.5)	161 (40.1)	>.99	.001
Headache	5 (10.0)	19 (26.0)	247 (57.2)	.05	<.001
Cough	12 (24.0)	12 (16.4)	235 (58.6)	.42	<.001
Fatigue	5 (10.0)	14 (19.2)	213 (53.1)	.26	<.001
Sore throat	4 (8.0)	14 (19.2)	169 (42.1)	.14	<.001
Muscle or body aches	3 (6.0)	10 (13.7)	197 (49.1)	.29	<.001
Chills	2 (4.0)	8 (11.0)	130 (32.4)	.29	<.001
Sweats	2 (4.0)	4 (5.5)	96 (23.9)	>.99	<.001
Loss of smell or taste	0	6 (8.2)	81 (20.2)	.10	<.001
Diarrhea	4 (8.0)	2 (2.7)	70 (17.5)	.37	.002
Eye pain	2 (4.0)	3 (4.1)	46 (11.5)	>.99	.04
Nausea or vomiting	0	4 (5.5)	49 (12.2)	.24	.01
Trouble breathing	1 (2.0)	0	47 (11.7)	.85	<.001
Ear pain or discharge	0	1 (1.4)	23 (5.7)	>.99	.06
Rash	0	0	3 (7.5)	NA	.80
No. of symptoms, mean (SD)	1.3 (2.0)	1.8 (2.0)	4.5 (3.1)	.15	<.001
Symptom duration, mean (SD), d ^b	4.1 (5.3)	3.6 (2.6)	4.9 (4.1)	.28	.03

Abbreviation: NA, not applicable.

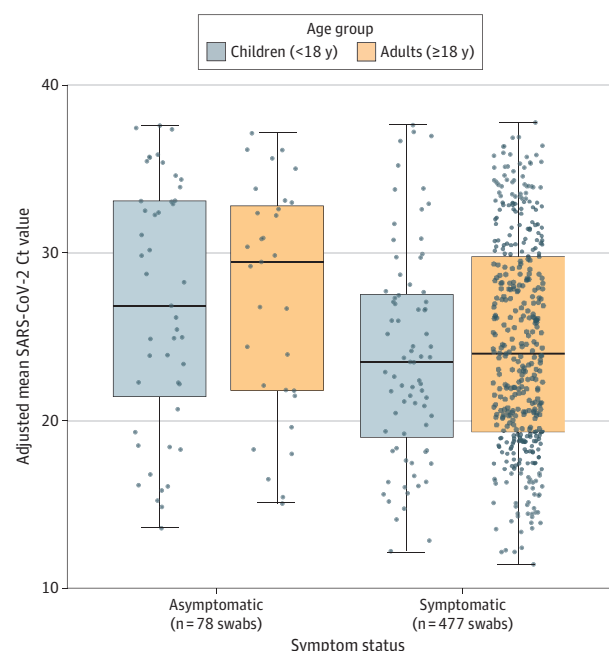
^a Signs and symptoms reported at enrollment.^b Number of days between participant-reported date of symptom onset and swab collection date. Symptom duration was limited to 10 or fewer days. Date of symptom onset was not reported by 392 participants (327 adults and 65 children).

Figure 1. Number of COVID-19 Signs and Symptoms Reported by Participants at Enrollment by Age



The total number of signs and symptoms at enrollment are shown by age group with individual locally estimated scatterplot smoothing regression lines plotted for each age group. Data points represent SARS-CoV-2-positive individuals. Shaded areas represent 95% CIs.

Figure 2. Adjusted Mean SARS-CoV-2 Orf1b Cycle Threshold (Ct) Values by Age Group, Grouped by Symptom Status



Boxes range from the first to third quartiles. Midlines represent median values. Error bars represent the minimum and maximum values. Individual points represent SARS-CoV-2-positive individuals. There were 47 asymptomatic children, 31 asymptomatic adults, 76 symptomatic children, and 401 symptomatic adults. Ct values are adjusted for swab type.

(SD) of 3.8 (3.8) days of symptoms compared with 4.9 (4.1) days in symptomatic adults. The most common signs or symptoms reported in children were runny or stuffy nose, fever, headache, and cough, while adults most frequently reported headache, cough, and fatigue (eFigure 5 in the [Supplement](#)).

Asymptomatic children were younger than symptomatic children (mean [SD] age, 6.2 [4.5] years compared with 8.3 [5.7] years; $P < .001$). Although there were differences in percentage symptomatic and symptoms reported between children younger than 5 years and children aged 5 to 17 years, these differences were not statistically significant. No comorbidities were reported for asymptomatic children. A higher proportion of asymptomatic children than symptomatic children reported any SARS-CoV-2-positive contact (41 of 47 [87.2%] vs 57 of 76 [75.0%]), most of whom were household contacts (36 of 47 [76.6%] vs 48 of 76 [63.2%]).

Of the 555 SARS-CoV-2-positive swabs, 487 were tested for 24 respiratory pathogens by RT-PCR. Only 3 of 108 children (2.8%) tested for other respiratory pathogens had another virus detected by RT-PCR. Rhinovirus was detected in 2 children and adenovirus in 1 child. Ten of 379 adults (2.6%) tested by respiratory pathogen RT-PCR had another virus identified, with rhinovirus predominantly detected (7 of 10); adenovirus (1 of 10), enterovirus (1 of 10), and influenza virus (1 of 10) were also detected.

MTB swabs were used by 176 participants (18 children and 158 adults) and AN swabs were used by 379 participants (105

children and 274 adults). Multiple linear regression of mean SARS-CoV-2 Ct value by age group and swab type showed that MTB swabs were associated with a 4.0-point higher mean Ct value compared with AN swabs ($P < .001$) (eFigure 6 in the [Supplement](#)).

Mean SARS-CoV-2 Ct values between children and adults were not significantly different (adjusted estimate for difference in mean Ct values, 0.3; 95% CI, -1.1 to 1.6; $P = .67$) after adjusting for swab type (**Figure 2**). Subgroup analyses showed that symptomatic individuals had consistently lower Ct values than asymptomatic individuals, regardless of age, after adjusting for swab type (adjusted estimate for children, -3.0; 95% CI, -5.5 to -0.6; $P = .02$; adjusted estimate for adults, -2.9; 95% CI, -5.2 to -0.6; $P = .01$) (eTable in the [Supplement](#)). The difference in mean Ct value between symptomatic children and adults was not significant (adjusted estimate, -0.7; 95% CI, -2.2 to 0.9; $P = .41$). Among 399 symptomatic individuals who reported a symptom onset date, the difference in mean Ct values between symptomatic children and symptomatic adults remained not significant after adjusting for swab type and for the number of days between symptom onset and swab collection (adjusted estimate, 0.5; 95% CI, -1.0 to 2.0; $P = .50$). The difference in mean Ct value between asymptomatic children and adults was also not significant (adjusted estimate, -0.6; 95% CI, -4.0 to 2.8; $P = .74$). No evidence of interaction by age and symptom status was found. Mean SARS-CoV-2 Ct values (as a continuous variable) did not vary significantly across age, even when adjusted for swab type (**Figure 3**).

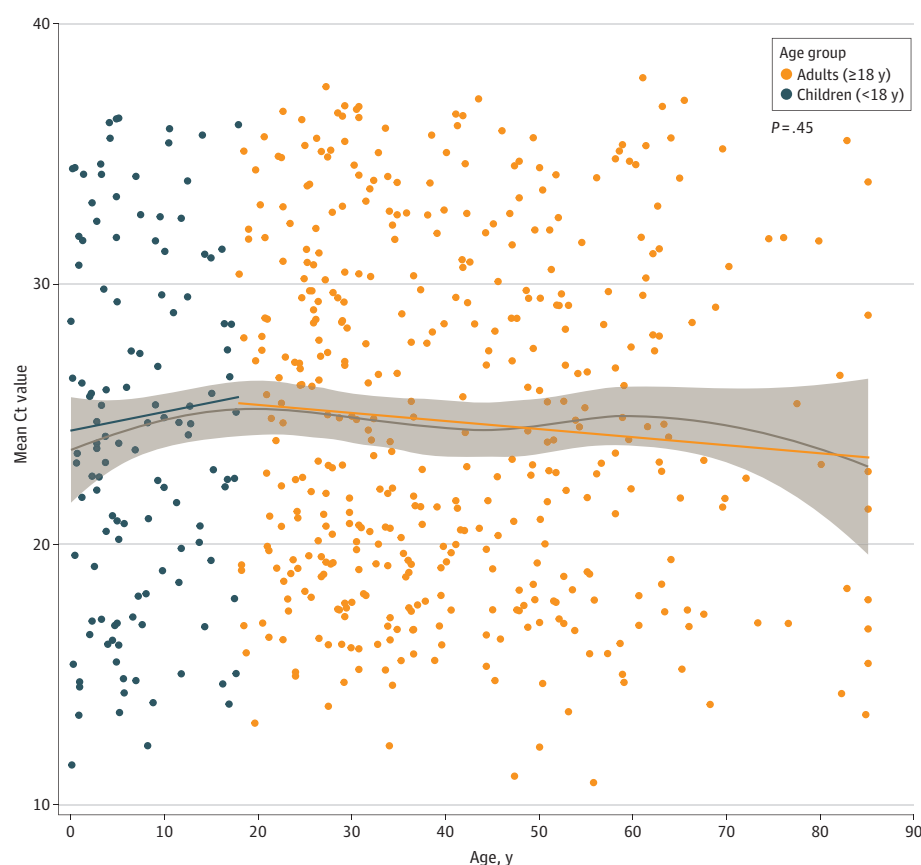
There was a nonsignificant association of lower mean Ct values with an increase in the number of symptoms reported (eFigure 7 in the [Supplement](#)). Longer time since symptom onset to date of swab collection was associated with higher Ct values. There was not a significant difference between children and adults in this association (eFigure 8 in the [Supplement](#)).

Discussion

This countywide community-based study of SARS-CoV-2 infection in King County, Washington, showed that symptomatic individuals had lower Ct values than those who were asymptomatic. Ct values did not differ significantly between asymptomatic children vs asymptomatic adults or in symptomatic children vs symptomatic adults. This study was unique in that participant-driven community-wide surveillance was instituted in a large metropolitan area using methods without direct participant contact and directed at persons who were not actively seeking medical care or follow-up.

Overall, children with documented SARS-CoV-2 infection in our study were younger, with 40% younger than 5 years, than in other community-based studies.¹⁷⁻¹⁹ A variety of signs and symptoms were reported by SARS-CoV-2-positive children or their caregivers, with runny nose documented in nearly half of the children, followed by fever, headache, and cough. The predominance of rhinorrhea contrasts with other studies, which have shown fever and cough to be more common symptoms.^{17,31,32} The variation in symptoms and lack of predictive value of specific symptoms have been suggested as rea-

Figure 3. Mean SARS-CoV-2 Orf1b Cycle Threshold (Ct) Values by Age



The scatterplot depicts Ct values adjusted by swab type. The gray line represents the locally estimated scatterplot smoothing curve using unadjusted Ct values. Linear regression lines per age group (orange indicates adults; blue indicates children) are adjusted by swab type. Data points represent SARS-CoV-2-positive individuals. Shaded areas represent 95% CIs.

sons for failure of symptom-based testing when screening children for COVID-19.³³

This study was not designed to measure the prevalence of asymptomatic SARS-CoV-2 infection. The high proportion of asymptomatic infection we observed in children is within the upper limit of the asymptomatic ranges of 40% to 45% estimated in other studies.^{34,35} The high proportion of asymptomatic infection we observed in children might be attributed to household enrollment of children following interest in study participation from adults with symptoms. The true frequency of asymptomatic SARS-CoV-2 infection might be closer to 16% to 22%, as suggested by other pediatric studies.^{16,32,35,36}

Because we only assessed symptoms at one point before specimen collection, it is possible that we misclassified some participants who were presymptomatic (who would be expected to have low Ct values) as asymptomatic. Regardless, we were able to show a significant difference in Ct values between symptomatic and asymptomatic groups. Our findings of higher SARS-CoV-2 Ct values in asymptomatic children corroborate results from a small study of asymptomatic and mildly symptomatic SARS-CoV-2-positive children in South Korea¹⁶ and a large study of asymptomatic and symptomatic SARS-CoV-2-positive children from 9 US pediatric hospital testing programs.¹⁵ Two large community-based studies found similar SARS-CoV-2 Ct values in symptomatic and asymptomatic children.^{17,18} In these studies, children were tested as part of contact tracing, and both asymptomatic and sympto-

matic children might have had similarly low Ct values because of recent exposures to infected individuals. In contrast to early studies, which suggested that symptomatic children might have lower Ct values than symptomatic adults,^{37,38} we did not find a significant difference in SARS-CoV-2 Ct values between symptomatic children and symptomatic adults. As these prior studies included participants who sought medical attention, they likely involved more acutely ill children who might have had higher SARS-CoV-2 RNA levels corresponding to lower Ct values. For both symptomatic and asymptomatic individuals, SARS-CoV-2 Ct values did not vary by age when compared as a continuous or categorical variable (ie, children and adults), corroborating studies that examined viral loads and age.^{1,19,39,40} However, the comparison of SARS-CoV-2 Ct values between children and adults depends on the proportion of symptomatic vs asymptomatic individuals in each group and might differ in other settings.

The mechanisms of how SARS-CoV-2 RNA levels might influence transmission have yet to be fully delineated. One large retrospective cohort study suggested that children and adolescents were more likely to transmit SARS-CoV-2 in households.⁴¹ In contrast, multiple studies of household infections have suggested that children are not the key drivers of SARS-CoV-2 transmission.^{18,42-44} It could be that lack of symptoms is associated with decreased viral transmission; studies have found lower relative risks of SARS-CoV-2 transmission from asymptomatic infected household members^{35,41,45} and close contacts.⁴⁶

Another explanation is that asymptomatic infected individuals have lower levels of transmissible SARS-CoV-2 owing to their ability to rapidly clear the virus.^{47,48} In regards to disease acquisition, most transmission studies suggest that children might be less susceptible to SARS-CoV-2 infection.^{41,44,45,49} In contrast, a household seroprevalence study suggests that children are at equal risk as adults for SARS-CoV-2 infection.^{50,51} Current epidemiologic tracing methods might not be detecting asymptomatic infections or infections associated with brief windows of viral detection. Transmission studies have focused on household transmission and even those studies might have been confounded by school and daycare closures, which precluded evaluation of transmission within school or daycare settings. In the King County, Washington, region, public schools were closed for in-person learning during the study period. This may have decreased the number of SARS-CoV-2-positive children and our data may be reflective of secondary SARS-CoV-2 infections transmitted primarily from adult household members. As a result, studies completed thus far might not have fully identified the potential transmission risks by children. To confirm whether there are age-dependent factors associated with SARS-CoV-2 transmissibility, more epidemiological studies are needed.

Limitations

Our study had limitations. First, enrollment in the study relied on individuals to self-request home-collection kits. Individuals needed to be familiar with the study and to have had access to a device with internet capabilities. Therefore, while our study aimed to sample from across various demographic categories (eg, age, race/ethnicity, residence, and household income), our study findings might not be representative of the county population as a whole or completely generalize to other US counties. Second,

demographic and illness-related information were self-reported and therefore subject to response bias. Although the study accepted both asymptomatic and symptomatic individuals, individual self-reporting of symptoms might have been biased by participant-perceived eligibility criteria. Third, the exact duration of symptoms prior to obtaining a swab were self-reported and not independently verified. Fourth, the number of children enrolled increased in the later part of the study when we switched to using AN swabs because of supply chain disruptions. Because AN swabs had higher yield of viral RNA compared with MTB swabs, likely because of increased comfort and ease of swabbing, we adjusted for the different types of swabs in our analysis. Fifth, this study relied on Ct values from semiquantitative RT-PCRs as proxies for viral RNA levels; more studies using quantitative RT-PCRs to generate direct viral RNA levels are needed. Sixth, the cross-sectional design of this study in addition to brief delays between symptom reporting and swab collection might have led to misclassification of asymptomatic and presymptomatic individuals at the time of sample collection. Characteristics, including Ct values, might differ between these 2 groups.

Conclusions

In this community-based cross-sectional study, SARS-CoV-2 RNA levels, as determined by RT-PCR Cts, were significantly higher in symptomatic individuals than in asymptomatic individuals. There were no significant differences in RNA levels in asymptomatic children vs asymptomatic adults or in symptomatic children vs symptomatic adults. Further research is needed to understand the role of SARS-CoV-2 RNA levels in transmission among children and adults.

ARTICLE INFORMATION

Accepted for Publication: May 10, 2021.

Published Online: June 11, 2021.

doi:10.1001/jamapediatrics.2021.2025

Author Affiliations: Department of Pediatrics, University of Washington, Seattle Children's Hospital, Seattle (Chung); Division of Allergy and Infectious Diseases, Department of Medicine, University of Washington, Seattle (Chow, Wilcox, Brandstetter, Duchin, Boeckh, Chu); Institute for Disease Modeling, Seattle, Washington (Burstein, Famulare); Brotman Baty Institute for Precision Medicine, Seattle, Washington (Brandstetter, Han, Pfau, Lockwood, Shendure, Rieder, Nickerson, Starita, Bedford); Department of Genome Sciences, University of Washington, Seattle (Han, Pfau, Shendure, Rieder, Nickerson, Starita, Bedford); Vaccine and Infectious Disease Division, Fred Hutchinson Cancer Research Center, Seattle, Washington (Fay, Boeckh, Bedford); Seattle Children's Research Institute, Seattle, Washington (Adler, Lacombe, England); Department of Laboratory Medicine and Pathology, University of Washington, Seattle (Lockwood); Influenza Division, Centers for Disease Control and Prevention, Atlanta, Georgia (Uyeki); Howard Hughes Medical Institute, Seattle, Washington (Shendure); Public Health—Seattle & King County, Seattle, Washington (Duchin); Department of

Biostatistics, University of Washington, Seattle (Hughes).

Author Contributions: Dr Chung had full access to all of the data in the study and takes responsibility for the integrity of the data and the accuracy of the data analysis.

Concept and design: Chung, Chow, Wilcox, Brandstetter, Adler, Lacombe, Rieder, Starita, Bedford, England, Chu.

Acquisition, analysis, or interpretation of data: Chung, Chow, Wilcox, Burstein, Brandstetter, Han, Fay, Pfau, Adler, Lacombe, Lockwood, Uyeki, Shendure, Duchin, Nickerson, Boeckh, Famulare, Hughes, Starita, Bedford, England, Chu.

Drafting of the manuscript: Chung, Chow, Wilcox, Brandstetter, Rieder, England, Chu.

Critical revision of the manuscript for important intellectual content: Chung, Chow, Wilcox, Burstein, Brandstetter, Han, Fay, Pfau, Adler, Lacombe, Lockwood, Uyeki, Shendure, Duchin, Nickerson, Boeckh, Famulare, Hughes, Starita, Bedford, England, Chu.

Statistical analysis: Wilcox, Pfau, Famulare, Hughes, Starita.

Obtained funding: Lacombe, Nickerson, Famulare, Starita, Bedford, England, Chu.

Administrative, technical, or material support: Burstein, Han, Fay, Adler, Lacombe, Lockwood, Shendure, Duchin, Rieder, Nickerson, Starita, England, Chu.

Supervision: Brandstetter, Lacombe, Boeckh, Starita, Bedford, England, Chu.

Conflict of Interest Disclosures: Drs Adler and Lockwood and Ms Lacombe report grants from the Bill and Melinda Gates Foundation during the conduct of the study. Dr Shendure is a consultant with Guardant Health, Maze Therapeutics, Camp4 Therapeutics, Nanostring, Phase Genomics, Adaptive Biotechnologies, and Stratos Genomics; and has a research collaboration with Illumina. Dr Boeckh is a consultant for Moderna, VirBio, and Merck; has received research support from Regeneron, Ridgeback, Merck, and VirBio outside the submitted work; and has received research support from the Bill and Melinda Gates Foundation during the conduct of the study. Dr Hughes reports grants from the Bill and Melinda Gates Foundation during the conduct of the study and National Institutes of Health outside the submitted work. Dr Bedford reports grants from the Bill and Melinda Gates Foundation, The Pew Charitable Trusts, and the National Institute of General Medical Sciences during the conduct of the study. Dr England receives research support paid to her institution from AstraZeneca, the Bill and Melinda Gates Foundation, Chimerix, GlaxoSmithKline, Novavax, Merck, and Pfizer; and is a consultant for Sanofi Pasteur and Meissa Vaccines. Dr Chu has served as a consultant with Ellume, Pfizer, the Bill and Melinda Gates Foundation, GlaxoSmithKline, and

Merck; and has received research funding from Sanofi Pasteur and support and reagents from Ellume and Cepheid outside of the submitted work. No other disclosures were reported.

Funding/Support: This work was funded by the Bill and Melinda Gates Foundation. This work was supported in part by the National Institutes of Health (grant T32HD007233 to Dr Chung). Dr Bedford is a Pew Biomedical Scholar and is supported by National Institutes of Health grant R35 GM119774-01.

Role of the Funder/Sponsor: The funders had no role in the design and conduct of the study; collection, management, analysis, and interpretation of the data; preparation, review, or approval of the manuscript; and decision to submit the manuscript for publication.

Disclaimer: The findings and conclusions in this report are those of the authors and do not necessarily represent the official position of the Centers for Disease Control and Prevention or the funder.

Additional Contributions: We thank the study participants for their contribution of samples.

REFERENCES

- He J, Guo Y, Mao R, Zhang J. Proportion of asymptomatic coronavirus disease 2019: a systematic review and meta-analysis. *J Med Virol*. 2021;93(2):820-830. doi:10.1002/jmv.26326
- Dong Y, Mo X, Hu Y, et al. Epidemiology of COVID-19 among children in China. *Pediatrics*. 2020;145(6):e20200702. doi:10.1542/peds.2020-0702
- Ludvigsson JF. Systematic review of COVID-19 in children shows milder cases and a better prognosis than adults. *Acta Paediatr*. 2020;109(6):1088-1095. doi:10.1111/apa.15270
- Shane AL, Sato AI, Kao C, et al. A pediatric infectious diseases perspective of severe acute respiratory syndrome coronavirus 2 (SARS-CoV-2) and novel coronavirus disease 2019 (COVID-19) in children. *J Pediatric Infect Dis Soc*. 2020;9(5):596-608. doi:10.1093/jpids/piaa099
- Wölfel R, Corman VM, Guggemos W, et al. Virological assessment of hospitalized patients with COVID-2019. *Nature*. 2020;581(7809):465-469. doi:10.1038/s41586-020-2196-x
- Bullard J, Dust K, Funk D, et al. Predicting infectious severe acute respiratory syndrome coronavirus 2 from diagnostic samples. *Clin Infect Dis*. 2020;71(10):2663-2666. doi:10.1093/cid/ciaa638
- L'Huillier AG, Torriani G, Pigny F, Kaiser L, Eckerle I. Culture-competent SARS-CoV-2 in nasopharynx of symptomatic neonates, children, and adolescents. *Emerg Infect Dis*. 2020;26(10):2494-2497. doi:10.3201/eid2610.202403
- Singanayagam A, Patel M, Charlett A, et al. Duration of infectiousness and correlation with RT-PCR cycle threshold values in cases of COVID-19, England, January to May 2020. *Euro Surveill*. 2020;25(32). doi:10.2807/1560-7917.ES.2020.25.32.2001483
- Arons MM, Hatfield KM, Reddy SC, et al; Public Health–Seattle and King County and CDC COVID-19 Investigation Team. Presymptomatic SARS-CoV-2 infections and transmission in a skilled nursing facility. *N Engl J Med*. 2020;382(22):2081-2090. doi:10.1056/NEJMoa2008457
- Zou L, Ruan F, Huang M, et al. SARS-CoV-2 viral load in upper respiratory specimens of infected patients. *N Engl J Med*. 2020;382(12):1177-1179. doi:10.1056/NEJMc2001737
- Lavezzo E, Franchin E, Ciavarella C, et al; Imperial College COVID-19 Response Team; Imperial College COVID-19 Response Team. Suppression of a SARS-CoV-2 outbreak in the Italian municipality of Vo'. *Nature*. 2020;584(7821):425-429. doi:10.1038/s41586-020-2488-1
- Lee S, Kim T, Lee E, et al. Clinical course and molecular viral shedding among asymptomatic and symptomatic patients with SARS-CoV-2 infection in a community treatment center in the Republic of Korea. *JAMA Intern Med*. 2020;180(11):1447-1452. doi:10.1001/jamainternmed.2020.3862
- Cereda D, Tirani M, Rovida F, et al. The early phase of the COVID-19 outbreak in Lombardy, Italy. arXiv. Preprint posted online March 2020. <https://ui.adsabs.harvard.edu/abs/2020arXiv200309320C>
- Salvatore PP, Dawson P, Wadhwa A, et al. Epidemiological correlates of PCR cycle threshold values in the detection of SARS-CoV-2. *Clin Infect Dis*. 2020;ciaa1469. doi:10.1093/cid/ciaa1469
- Kocielek LK, Muller WJ, Yee R, et al. Comparison of upper respiratory viral load distributions in asymptomatic and symptomatic children diagnosed with SARS-CoV-2 infection in pediatric hospital testing programs. *J Clin Microbiol*. 2020;59(1):e02593-20. doi:10.1128/JCM.02593-20
- Han MS, Seong MW, Kim N, et al. Viral RNA load in mildly symptomatic and asymptomatic children with COVID-19, Seoul, South Korea. *Emerg Infect Dis*. 2020;26(10):2497-2499. doi:10.3201/eid2610.202449
- Hurst JH, Heston SM, Chambers HN, et al. SARS-CoV-2 infections among children in the Biospecimens from Respiratory Virus-Exposed Kids (BRAVE Kids) study. *Clin Infect Dis*. 2020;ciaa1693. doi:10.1093/cid/ciaa1693
- Maltezou HC, Magaziotou I, Dedoukou X, et al; Greek Study Group on SARS-CoV-2 Infections in Children. Children and adolescents with SARS-CoV-2 infection: epidemiology, clinical course and viral loads. *Pediatr Infect Dis J*. 2020;39(12):e388-e392. doi:10.1097/INF.0000000000002899
- Madera S, Crawford E, Langelier C, et al. Nasopharyngeal SARS-CoV-2 viral loads in young children do not differ significantly from those in older children and adults. *Sci Rep*. 2021;11(1):3044. doi:10.1038/s41598-021-81934-w
- Greater Seattle Coronavirus Assessment Network Study. Helping researchers and public health leaders track the spread of coronavirus. Accessed December 22, 2020. <http://www.scanpublichealth.org>
- Chu HY, Englund JA, Starita LM, et al; Seattle Flu Study Investigators. Early detection of COVID-19 through a citywide pandemic surveillance platform. *N Engl J Med*. 2020;383(2):185-187. doi:10.1056/NEJMc2008646
- Revisions to the Standards for the Classification of Federal Data on Race and Ethnicity. Office of Management and Budget. Accessed May 26, 2021. https://obamawhitehouse.archives.gov/omb/fedreg_1997standards
- Harris PA, Taylor R, Thielke R, Payne J, Gonzalez N, Conde JG. Research Electronic Data Capture (REDCap)—a metadata-driven methodology and workflow process for providing translational research informatics support. *J Biomed Inform*. 2009;42(2):377-381. doi:10.1016/j.jbi.2008.08.010
- Harris PA, Taylor R, Minor BL, et al; REDCap Consortium. The REDCap consortium: building an international community of software platform partners. *J Biomed Inform*. 2019;95:103208. doi:10.1016/j.jbi.2019.103208
- McCulloch DJ, Kim AE, Wilcox NC, et al. Comparison of unsupervised home self-collected midnasal swabs with clinician-collected nasopharyngeal swabs for detection of SARS-CoV-2 infection. *JAMA Netw Open*. 2020;3(7):e2016382. doi:10.1001/jamanetworkopen.2020.16382
- Kim AE, Brandstetter E, Wilcox N, et al. Evaluating specimen quality and results from a community-wide, home-based respiratory surveillance study. *J Clin Microbiol*. 2021;59(5):e02934-20. doi:10.1128/JCM.02934-20
- Greater Seattle Coronavirus Assessment Network. How to use a SCAN kit. Accessed April 28, 2021. <https://scanpublichealth.org/how-to-use-a-scan-kit>
- Padgett LR, Kennington LA, Ahls CL, et al. Polyester nasal swabs collected in a dry tube are a robust and inexpensive, minimal self-collection kit for SARS-CoV-2 testing. *PLoS One*. 2021;16(4):e0245423. doi:10.1371/journal.pone.0245423
- von Elm E, Altman DG, Egger M, Pocock SJ, Gøtzsche PC, Vandenbroucke JP; STROBE Initiative. The Strengthening of Reporting of Observational Studies in Epidemiology (STROBE) statement: guidelines for reporting observational studies. *Ann Intern Med*. 2007;147(8):573-577. doi:10.7326/0003-4819-147-8-200710160-00010
- US Census Bureau. American community survey 1-year estimates. Accessed May 1, 2021. <http://censusreporter.org/profiles/05000US53033-king-county-wa/>
- CDC COVID-19 Response Team. Coronavirus disease 2019 in children—United States, February 12–April 2, 2020. *MMWR Morb Mortal Wkly Rep*. 2020;69(14):422-426. doi:10.15585/mmwr.mm6914e4
- Assaker R, Colas AE, Julien-Marsollier F, et al. Presenting symptoms of COVID-19 in children: a meta-analysis of published studies. *Br J Anaesth*. 2020;125(3):e330-e332. doi:10.1016/j.bja.2020.05.026
- Poline J, Gaschignard J, Leblanc C, et al. Systematic SARS-CoV-2 screening at hospital admission in children: a French prospective multicenter study. *Clin Infect Dis*. 2020;ciaa1044. doi:10.1093/cid/ciaa1044
- Oran DP, Topol EJ. Prevalence of asymptomatic SARS-CoV-2 infection: a narrative review. *Ann Intern Med*. 2020;173(5):362-367. doi:10.7326/M20-3012
- Byambasuren O, Cardona M, Bell K, Clark J, McLaws M-L, Glasziou P. Estimating the extent of asymptomatic COVID-19 and its potential for community transmission: systematic review and meta-analysis. *JAMMI*. 2020;5(4):223-234. doi:10.3138/jammi-2020-0030
- Hoang A, Chorath K, Moreira A, et al. COVID-19 in 7780 pediatric patients: a systematic review. *EClinicalMedicine*. 2020;24:100433. doi:10.1016/j.eclinm.2020.100433

38. Heald-Sargent T, Muller WJ, Zheng X, Rippe J, Patel AB, Kocielek LK. Age-related differences in nasopharyngeal severe acute respiratory syndrome coronavirus 2 (SARS-CoV-2) levels in patients with mild to moderate coronavirus disease 2019 (COVID-19). *JAMA Pediatr*. 2020;174(9):902-903. doi:10.1001/jamapediatrics.2020.3651
39. Yonker LM, Neilan AM, Bartsch Y, et al. Pediatric severe acute respiratory syndrome coronavirus 2 (SARS-CoV-2): clinical presentation, infectivity, and immune responses. *J Pediatr*. 2020; 227:45-52.e5. doi:10.1016/j.jpeds.2020.08.037
40. Baggio S, L'Huillier AG, Yerly S, et al. SARS-CoV-2 viral load in the upper respiratory tract of children and adults with early acute COVID-19. *Clin Infect Dis*. 2020;ciaa1157. doi:10.1093/cid/ciaa1157
41. Jones TC, Mühlemann B, Veith T, et al. An analysis of SARS-CoV-2 viral load by patient age. *medRxiv*. Preprint posted online June 9, 2020. doi:10.1101/2020.06.08.20125484
42. Li F, Li Y-Y, Liu M-J, et al. Household transmission of SARS-CoV-2 and risk factors for susceptibility and infectivity in Wuhan: a retrospective observational study. *Lancet Infect Dis*. 2021;21(5):617-628. doi:10.1016/S1473-3099(20)30981-6
43. Li X, Xu W, Dozier M, He Y, Kirolos A, Theodoratou E; Usher Network for COVID-19 Evidence Reviews (UNCOVER). The role of children in transmission of SARS-CoV-2: a rapid review. *J Glob Health*. 2020;10(1):011101. doi:10.7189/jogh.10.011101
44. Lee B, Raszka WV Jr. COVID-19 transmission and children: the child is not to blame. *Pediatrics*. 2020;146(2):e2020004879. doi:10.1542/peds.2020-004879
45. Zhu Y, Bloxham CJ, Hulme KD, et al. A meta-analysis on the role of children in SARS-CoV-2 in household transmission clusters. *Clin Infect Dis*. 2020;ciaa1825. doi:10.1093/cid/ciaa1825
46. Madewell ZJ, Yang Y, Longini IM Jr, Halloran ME, Dean NE. Household transmission of SARS-CoV-2: a systematic review and meta-analysis. *JAMA Netw Open*. 2020;3(12):e2031756. doi:10.1001/jamanetworkopen.2020.31756
47. Sayampanathan AA, Heng CS, Pin PH, Pang J, Leong TY, Lee VJ. Infectivity of asymptomatic versus symptomatic COVID-19. *Lancet*. 2021;397(10269):93-94. doi:10.1016/S0140-6736(20)32651-9
48. Kissler SM, Fauver JR, Mack C, et al. SARS-CoV-2 viral dynamics in acute infections. *medRxiv*. Preprint posted online December 1, 2020. doi:10.1101/2020.10.21.20217042
49. Cevik M, Tate M, Lloyd O, Maraolo AE, Schafers J, Ho A. SARS-CoV-2, SARS-CoV, and MERS-CoV viral load dynamics, duration of viral shedding, and infectiousness: a systematic review and meta-analysis. *Lancet Microbe*. 2021;2(1):e13-e22. doi:10.1016/S2666-5247(20)30172-5
50. Viner RM, Mytton OT, Bonell C, et al. Susceptibility to SARS-CoV-2 infection among children and adolescents compared with adults: a systematic review and meta-analysis. *JAMA Pediatr*. 2021;175(2):143-156. doi:10.1001/jamapediatrics.2020.4573
51. Brotons P, Launes C, Buetas E, et al. Susceptibility to Sars-COV-2 infection among children and adults: a seroprevalence study of family households in the Barcelona Metropolitan Region, Spain. *Clin Infect Dis*. 2020;ciaa1721. doi:10.1093/cid/ciaa1721
52. Lewis NM, Chu VT, Ye D, et al. Household transmission of SARS-CoV-2 in the United States. *Clin Infect Dis*. 2020;ciaa1166. doi:10.1093/cid/ciaa1166



Since January 2020 Elsevier has created a COVID-19 resource centre with free information in English and Mandarin on the novel coronavirus COVID-19. The COVID-19 resource centre is hosted on Elsevier Connect, the company's public news and information website.

Elsevier hereby grants permission to make all its COVID-19-related research that is available on the COVID-19 resource centre - including this research content - immediately available in PubMed Central and other publicly funded repositories, such as the WHO COVID database with rights for unrestricted research re-use and analyses in any form or by any means with acknowledgement of the original source. These permissions are granted for free by Elsevier for as long as the COVID-19 resource centre remains active.

Impact assessment of non-pharmaceutical interventions against coronavirus disease 2019 and influenza in Hong Kong: an observational study

Benjamin J Cowling*, Sheikh Taslim Ali*, Tiffany W Y Ng*, Tim K Tsang, Julian C M Li, Min Whui Fong, Qiuyan Liao, Mike YW Kwan, So Lun Lee, Susan S Chiu, Joseph T Wu, Peng Wu, Gabriel M Leung



Summary

Background A range of public health measures have been implemented to suppress local transmission of coronavirus disease 2019 (COVID-19) in Hong Kong. We examined the effect of these interventions and behavioural changes of the public on the incidence of COVID-19, as well as on influenza virus infections, which might share some aspects of transmission dynamics with COVID-19.

Methods We analysed data on laboratory-confirmed COVID-19 cases, influenza surveillance data in outpatients of all ages, and influenza hospitalisations in children. We estimated the daily effective reproduction number (R_t) for COVID-19 and influenza A H1N1 to estimate changes in transmissibility over time. Attitudes towards COVID-19 and changes in population behaviours were reviewed through three telephone surveys done on Jan 20–23, Feb 11–14, and March 10–13, 2020.

Findings COVID-19 transmissibility measured by R_t has remained at approximately 1 for 8 weeks in Hong Kong. Influenza transmission declined substantially after the implementation of social distancing measures and changes in population behaviours in late January, with a 44% (95% CI 34–53%) reduction in transmissibility in the community, from an estimated R_t of 1.28 (95% CI 1.26–1.30) before the start of the school closures to 0.72 (0.70–0.74) during the closure weeks. Similarly, a 33% (24–43%) reduction in transmissibility was seen based on paediatric hospitalisation rates, from an R_t of 1.10 (1.06–1.12) before the start of the school closures to 0.73 (0.68–0.77) after school closures. Among respondents to the surveys, 74.5%, 97.5%, and 98.8% reported wearing masks when going out, and 61.3%, 90.2%, and 85.1% reported avoiding crowded places in surveys 1 ($n=1008$), 2 ($n=1000$), and 3 ($n=1005$), respectively.

Interpretation Our study shows that non-pharmaceutical interventions (including border restrictions, quarantine and isolation, distancing, and changes in population behaviour) were associated with reduced transmission of COVID-19 in Hong Kong, and are also likely to have substantially reduced influenza transmission in early February, 2020.

Funding Health and Medical Research Fund, Hong Kong.

Copyright © 2020 The Author(s). Published by Elsevier Ltd. This is an Open Access article under the CC BY 4.0 license.

Introduction

The first wave of coronavirus disease 2019 (COVID-19) in China, outside of Hubei province, was addressed with the implementation of aggressive public health measures.¹ These measures relied heavily on massive mobility restrictions, universal fever screening in all settings, and neighbourhood-based, household-focused social distancing that was enforced by large teams of community workers, as well as pervasive deployment of artificial intelligence-based social media applications and the use of big data.² Whether some or all of these measures would be acceptable and feasible in settings outside of mainland China has been questioned.³

Hong Kong is a Special Administrative Region of China that operates with a large degree of autonomy. It is located outside the mainland on the southern coast of China, neighbouring Guangdong province—which has recorded the largest number of confirmed cases of COVID-19 (1490 cases as of March 31, 2020) outside of Hubei. Having

been one of the most heavily affected epicentres during the severe acute respiratory syndrome (SARS) epidemic in 2003, the community in Hong Kong has been prepared to respond to emerging infectious diseases. A range of public health measures have been implemented to delay and reduce local transmission of COVID-19, and there have been major changes in population behaviour.

The initial containment or current suppression measures used to control COVID-19 in Hong Kong include intense surveillance for infections, not only in incoming travellers but also in the local community, with around 400 outpatients and 600 inpatients tested each day in early March, 2020. Once individuals are identified to be positive for COVID-19, they are isolated in hospital until they recover and cease virus shedding. Their close contacts are traced (from 2 days before illness onset) and quarantined in special facilities, including holiday camps and newly constructed housing estates. Because not every infected person will be identified, containment measures only work if social distancing

Lancet Public Health 2020;
5: e279–88

Published Online
April 17, 2020
[https://doi.org/10.1016/S2468-2667\(20\)30090-6](https://doi.org/10.1016/S2468-2667(20)30090-6)

*Co-first authors

WHO Collaborating Centre for
Infectious Disease
Epidemiology and Control,
School of Public Health, Li Ka
Shing Faculty of Medicine,
University of Hong Kong,
Hong Kong Special

Administrative Region, China
(Prof B J Cowling PhD, S T Ali PhD,
T W Y Ng PhD, T K Tsang PhD,
J C M Li BSc, M W Fong MPH,
Q Liao PhD, Prof J T Wu PhD,
P Wu PhD, Prof G M Leung MD);
Department of Paediatrics and
Adolescent Medicine, Princess
Margaret Hospital, Hong Kong
Special Administrative Region,
China (M Y W Kwan MBBS); and
Department of Paediatrics and
Adolescent Medicine, Queen
Mary Hospital and Li Ka Shing
Faculty of Medicine, The
University of Hong Kong,
Hong Kong Special
Administrative Region, China
(S L Lee MPH, S S Chiu MD)

Correspondence to:
Dr Peng Wu, School of Public
Health, Li Ka Shing Faculty of
Medicine, University of
Hong Kong, Hong Kong Special
Administrative Region,
Hong Kong, China
pengwu@hku.hk

Research in context

Evidence before this study

Coronavirus disease 2019 (COVID-19) was first identified in late December 2019, in a cluster of cases of atypical pneumonia in Wuhan. Infections increased through January until the implementation of a lockdown of Wuhan and other affected cities. Since January, 2020, COVID-19 cases have been reported outside China in increasing numbers, with many countries not taking strong control measures, such as lockdowns, until relatively larger numbers of cases had been reported. In Hong Kong, Singapore, and Taiwan public health measures to prevent community epidemics were quickly implemented and were able to avoid the need for complete lockdowns. We searched PubMed on March 31, 2020, for studies reporting the impact of alternative public health measures against COVID-19 using keywords including "COVID-19", "2019-nCoV", "novel coronavirus-infected pneumonia", "SARS-CoV-2", "lockdown", "social distancing", "isolation", "contact tracing", and "quarantine". We scanned 227 published studies and found six that estimated the impact of public health measures in Wuhan or elsewhere in mainland China, one study that described the early application of testing and contact tracing in Singapore,

and one study reporting the impact of quarantine on transmission on the Diamond Princess cruise ship.

Added value of this study

We estimated the effective reproduction number of COVID-19 in Hong Kong as a measure of transmissibility over time and found that it has remained at approximately 1 for the past 8 weeks. We described the public health measures that have been introduced to contain COVID-19 transmission and the behavioural changes reported by the population, and found that distancing measures and changes in behaviour were associated with rapid declines in influenza activity. The speed of decline in influenza activity in 2020 was quicker than in previous years in which school closures were implemented but there were no other social distancing measures or voluntary changes in behaviour.

Implications of all the available evidence

The experience in Hong Kong indicates that COVID-19 transmission can be contained with a combination of testing and isolating cases, plus tracing and quarantining their close contacts, along with some degree of social distancing to reduce community transmission from unidentified cases.

measures or behavioural changes also reduce so-called silent transmission in the community as a whole.

Hong Kong offers an opportunity to study the impact of public health interventions and population behavioural changes that could be rolled out in resource-sufficient settings in other countries. We aimed to quantify the effect of containment measures on COVID-19. In addition, to identify whether social distancing and behavioural changes have been associated with reducing silent transmission of COVID-19, we analysed data on influenza activity as a proxy for potential changes in transmission of infection in line with the interventions implemented, assuming a similar mode and efficiency of spread of influenza and COVID-19. The specific objective of this study was to quantify population behavioural changes in Hong Kong during the COVID-19 outbreak, and to describe the likely impact of the behavioural changes and public health measures on COVID-19 transmission and influenza transmission in the community.

Methods

Data collection

Data on laboratory-confirmed COVID-19 cases were obtained from the Hong Kong Centre for Health Protection, which provides daily updates with individual case data on a dedicated webpage.

We obtained sentinel surveillance data on influenza-like illnesses in a network of around 60 general outpatient clinics from the Centre for Health Protection. These include weekly reports on the proportion of outpatient consultations that were in patients with influenza-like

illness, defined as fever plus cough or sore throat. We obtained laboratory surveillance data from the Public Health Laboratory Services on influenza testing results on specimens from public hospitals and sentinel surveillance sites, including the weekly number of specimens tested and the number testing positive for influenza by type and subtype. Data on the current population of Hong Kong by age and sex were obtained from the Census and Statistics Department of the Hong Kong Government. We obtained the daily hospitalisation rates for influenza-positive cases among children in Hong Kong using the daily hospital admissions for influenza to the paediatric departments of two large hospitals in Hong Kong and the relevant catchment populations.⁴

We did three cross-sectional telephone surveys among the general adult population in Hong Kong, on Jan 20–23, Feb 11–14, and March 10–13, 2020. The methods and survey instruments used were similar to those used for surveys during the SARS epidemic in 2003,^{5,6} the influenza A H1N1 pandemic in 2009,⁷ and the influenza A H7N9 outbreak in China in 2013.⁸ Participants were recruited using random-digit dialling of both landline and mobile telephone numbers. Telephone numbers were randomly generated by a computer system. Calls were made during both working and non-working hours by trained interviewers to avoid over-representation of non-working groups. Respondents were required to be at least 18 years old and able to speak Cantonese Chinese or English. New respondents were recruited for each survey round. Within each household, an eligible household member with the nearest birthday was invited to participate in the survey,

which was not necessarily the person that initially answered the telephone. Survey items included measures of risk perception, attitudes towards COVID-19, and behaviours taken against contracting COVID-19, including hygiene, face masks, and reduction of social contact. In the second and third surveys, respondents who were parents of school-age children were asked to answer additional questions about social contact patterns of their children because schools were closed at the time of the interviews. Ethical approval for this study was obtained from the Institutional Review Board of the University of Hong Kong. All participants gave verbal informed consent.

Statistical analysis

Means and proportions of survey responses were directly weighted by sex and age to the general population. Categorical variables with ordinal Likert-type response scales, including risk perception and attitudes towards COVID-19, were first dichotomised as either above or below a threshold. Responses to perceived susceptibility were dichotomised as 1 (likely, very likely, or certain) versus 0 (never, very unlikely, unlikely, or even chance); responses to perceived severity were dichotomised as 1 (serious or very serious) versus 0 (very mild, mild, or moderate); responses about worry were dichotomised as 1 (moderately worried or very worried) versus 0 (not at all worried or slightly worried); responses about attitudes towards COVID-19 were dichotomised as 1 (agree or strongly agree) versus 0 (strongly disagree, disagree, or neutral).

We estimated changes in COVID-19 transmissibility over time via the effective reproduction number (R_t), which represents the mean number of secondary infections that result from a primary case of infection at time t . Values of R_t exceeding 1 indicate that the epidemic will tend to grow, whereas values below 1 indicate that the epidemic will tend to decline. We estimated the time-varying reproduction numbers from serial intervals and incidence of COVID-19 cases over time,^{9,10} assuming a serial interval of 7.5 days.¹¹ We extended the approach used by Thompson and colleagues¹⁰ to allow for undetected cases due to censoring and imperfect detection of local cases. We assumed that 99% of imported cases and 80% of local cases would be detected. We developed a data-augmented Markov chain Monte Carlo algorithm to jointly estimate the time-varying reproduction number, the delay distribution from onset to reporting which can be used to inform censoring and undetected cases. Time-varying estimates of reproduction numbers were made with a 7-day sliding window.

To measure changes in influenza transmissibility over time, we first calculated the influenza proxy^{12,13} for influenza A H1N1 during the 2019–20 winter by multiplying the weekly influenza-like illness consultation rates by the weekly proportions of specimens positive for influenza A H1N1, which was the predominant strain. This influenza proxy is a better correlate of the incidence

of influenza virus infections in the community than either influenza-like illness rates or laboratory detection rates alone.¹³ We interpolated daily influenza proxy values from the weekly influenza proxy values with use of flexible cubic splines.¹⁴

Using the daily influenza proxy, we estimated daily transmissibility via the daily effective reproduction number, R_t . We used a simple branching process model for epidemic spread to estimate the time-varying intensity of transmission.¹⁵ We assumed the serial interval distribution for influenza followed a gamma distribution with a mean of 2.85 days and SD of 0.93 days.¹⁶ We repeated these analyses for the daily influenza A H1N1 hospitalisation rates among children in two large local hospitals (Queen Mary Hospital and Princess Margaret Hospital). We evaluated the changes in transmissibility by comparing the R_t values during the 2 weeks before and after the start of the school closures (including the Chinese New Year holidays) for the 2019–20 winter influenza season. The 95% CIs for the change in R_t were calculated using Fieller's theorem.¹⁷ We compared the reductions in 2019–20 with reductions in previous years when the Chinese New Year holidays occurred during influenza epidemics. All analyses were done with R version 3.6.2.

Role of the funding source

The funder of the study had no role in study design, data collection, data analysis, data interpretation, or writing of the report. The corresponding author had full access to all the data in the study and had final responsibility for the decision to submit for publication.

Results

As of March 31, 2020, Hong Kong had confirmed 715 cases of SARS coronavirus 2 (SARS-CoV-2) infection, including 386 individuals that were presumed to have acquired infection outside of Hong Kong (imported cases), 142 cases that could not be linked to any other case (unlinked local cases), and 187 cases that were linked to the other known cases (secondary cases; appendix p 1). Among these 715 cases of SARS-CoV-2 infection, 94 were asymptomatic infections and 621 were symptomatic infections. Figure 1 shows the timeline of interventions that were implemented by the government in Hong Kong, including travel restrictions and bans, flexible working arrangements, and school closures from kindergartens up to tertiary and post-tertiary institutions, including tutorial centres. Some religious organisations cancelled services from Feb 13 onwards, and many conferences and other local mass gatherings have been cancelled. Quarantine orders have been issued to the close contacts of individuals with confirmed infection, as well as travellers arriving from affected countries (figure 1).

Although unlinked COVID-19 cases have been detected in increasing numbers since early March, transmissibility (R_t) remains around the critical threshold of 1 (figure 2). Increases in local cases could be attributed to the

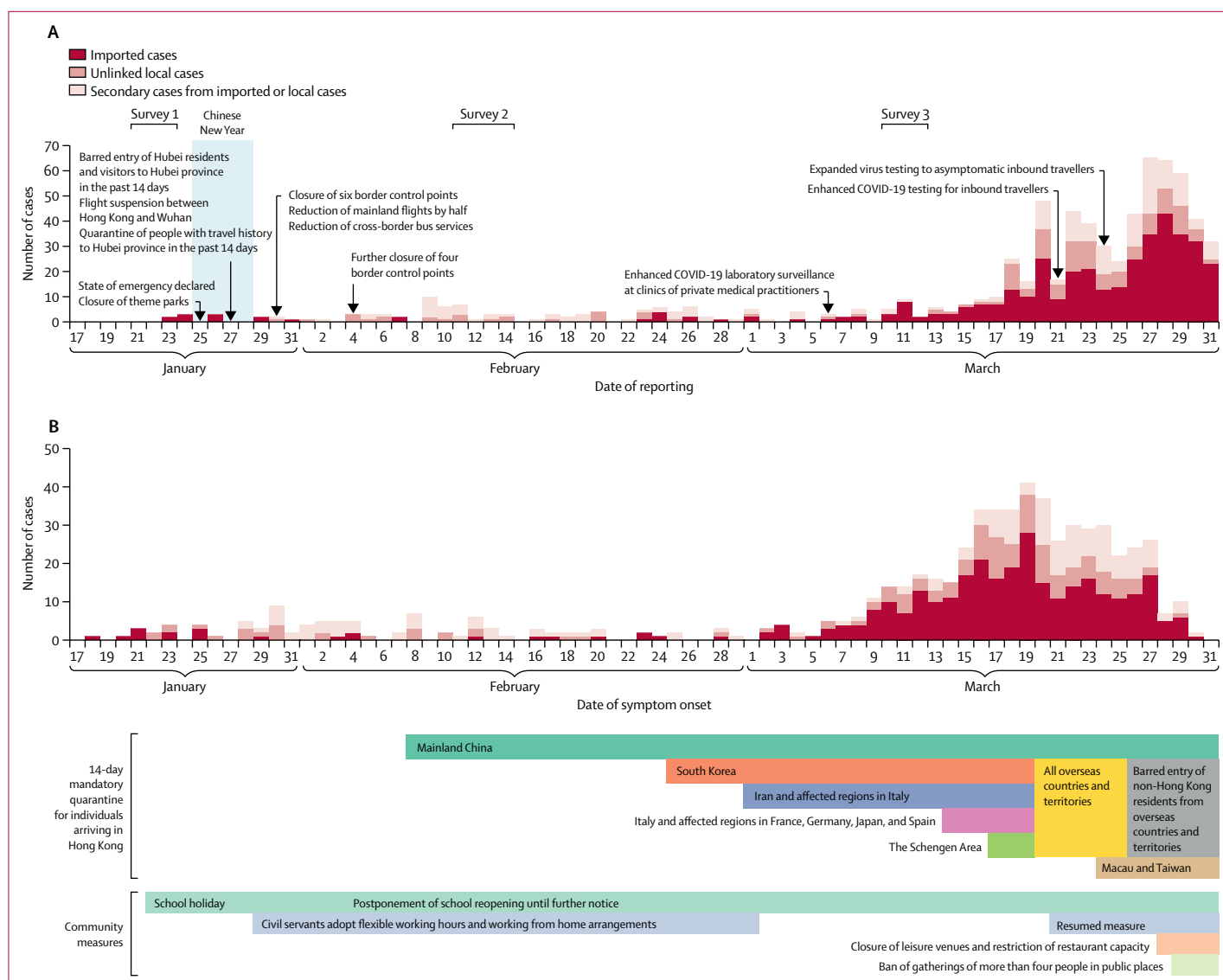


Figure 1: COVID-19 cases in Hong Kong by date of reporting (A) and date of symptom onset (B)

The Chinese New Year, a major winter festival in Hong Kong, was on Jan 25, and there were public holidays on Jan 25–28. Most schools started holidays on Jan 22 and were scheduled to resume on Feb 3. The Hong Kong Government has deferred class resumption several times and closures are now until further notice without an expected resumption date. 94 asymptomatic cases are not shown in panel B. All dates are in 2020. COVID-19=coronavirus disease 2019.

transmission of infections into the community, resulting from an increasing number of imported infections since early March. With a local effective reproduction number of 1, a gradual increase in the incidence of local infections would be expected.

Data on influenza activity based on the community influenza proxy were consistent with the rate of hospitalisation of children with influenza A H1N1 in Hong Kong (figure 3A, B). Influenza incidence peaked in the third week of January, with influenza A H1N1 predominating, and declined to low levels by the second week of February. The R_t for influenza A H1N1 gradually declined from the second week of January but was

greater than 1 before the start of the school closures and Chinese New Year. The R_t then declined to less than 1 shortly after the school closures and continued to decrease until early February (figure 3C, D). The estimated R_t was 1.28 (95% CI 1.26–1.30) during the 2-week period before the start of the school closures and 0.72 (0.70–0.74) during the first 2 weeks of school closures, corresponding to a 44% (34–53%) reduction in transmissibility (figure 3C). Similarly, the R_t calculated from hospitalisation data was 1.10 (1.06–1.12) before the start of the school closures and reduced to 0.73 (0.68–0.77) after school closures, corresponding to a 33% (24–43%) reduction in transmissibility (figure 3D).

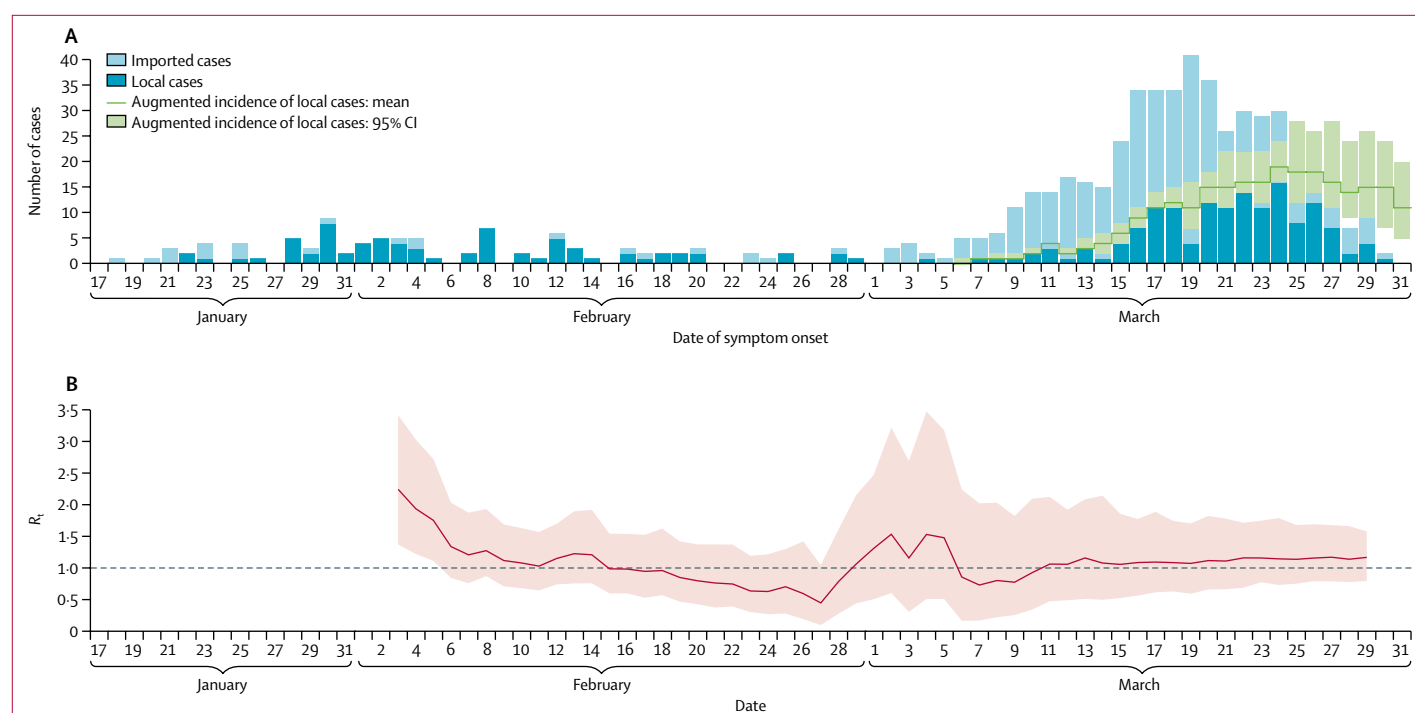


Figure 2: Incidence and transmissibility of COVID-19 in Hong Kong

(A) Incidence of local COVID-19 cases in Hong Kong (dark blue bars) and cases infected overseas but detected locally (light blue bars). Augmented incidence includes estimated additional cases that have occurred but have not yet been identified due to reporting delays. (B) Estimates of the daily R_t of COVID-19 over time. The pink shaded area indicates 95% CIs. The dashed line indicates the critical threshold of $R_t=1$. All dates are in 2020. COVID-19=coronavirus disease 2019. R_t =effective reproduction number.

In comparison, during the 2010–11 winter, we estimated the reduction in transmissibility of influenza associated with the Chinese New Year holidays to be 15% (95% CI 11–19%), declining from an R_t of 1.10 (1.08–1.13) in the 11-day period before the start of the school holidays to 0.95 (0.92–0.96) during the 11-day school holiday (figure 4). In the 2014–15 winter, the reduction in transmissibility associated with the Chinese New Year holidays was 14% (7–22%), declining from an R_t of 0.94 (0.93–0.96) in the 11-day period before the start of the school holidays to 0.81 (0.75–0.86) during the 11-day school holiday.

We interviewed 1008 participants on Jan 20–23 (22% response rate), 1000 participants on Feb 11–14 (23% response rate), and 1005 participants on March 10–13 (response rate 15%; appendix p 3). Respondents included a broad cross-section of the adult population of Hong Kong (appendix p 2). Respondents perceived that they had similar susceptibility to COVID-19 as they did to seasonal influenza, but that COVID-19 was a much more serious infection, and around half of the respondents reported worrying about being infected with COVID-19 compared with around a third of respondents for seasonal influenza (table). In survey 2, 76.4% of respondents agreed with the statement that complete border closure would be effective in preventing the spread of COVID-19 to Hong Kong,

84.1% were worried about the availability of medical supplies, including face masks, but only 27.7% were worried about the availability of living supplies, including food and household goods, in Hong Kong (table).

We identified considerable increases in the use of preventive measures in response to the threat of COVID-19. In recent years, face masks have mainly been used by individuals in the general community who are ill and by those who feel particularly susceptible to infection and want to protect themselves. We found that 74.5%, 97.5%, and 98.8% of respondents wore masks when going out; 61.3%, 90.2%, and 85.1% avoided going to crowded places; and 71.1%, 92.5%, and 93.0% reported washing or sanitising their hands more often, in surveys 1, 2, and 3, respectively (table). In surveys 2 and 3, 88.0% and 83.8% reported staying at home as much as possible.

In surveys 2 and 3, we asked the subset of respondents who were parents of school-age children about their support for school closures and the activities of their children during the school closures. Among respondents who were parents, 249 (95.4%) of 261 and 192 (93.7%) of 205 agreed or strongly agreed that school closure was needed as a control measure for COVID-19 in Hong Kong, and 209 (80.1%) of 261 and 141 (68.8%) of 205 responded that their children had no contact with people other than their household members on the preceding day.

See Online for appendix

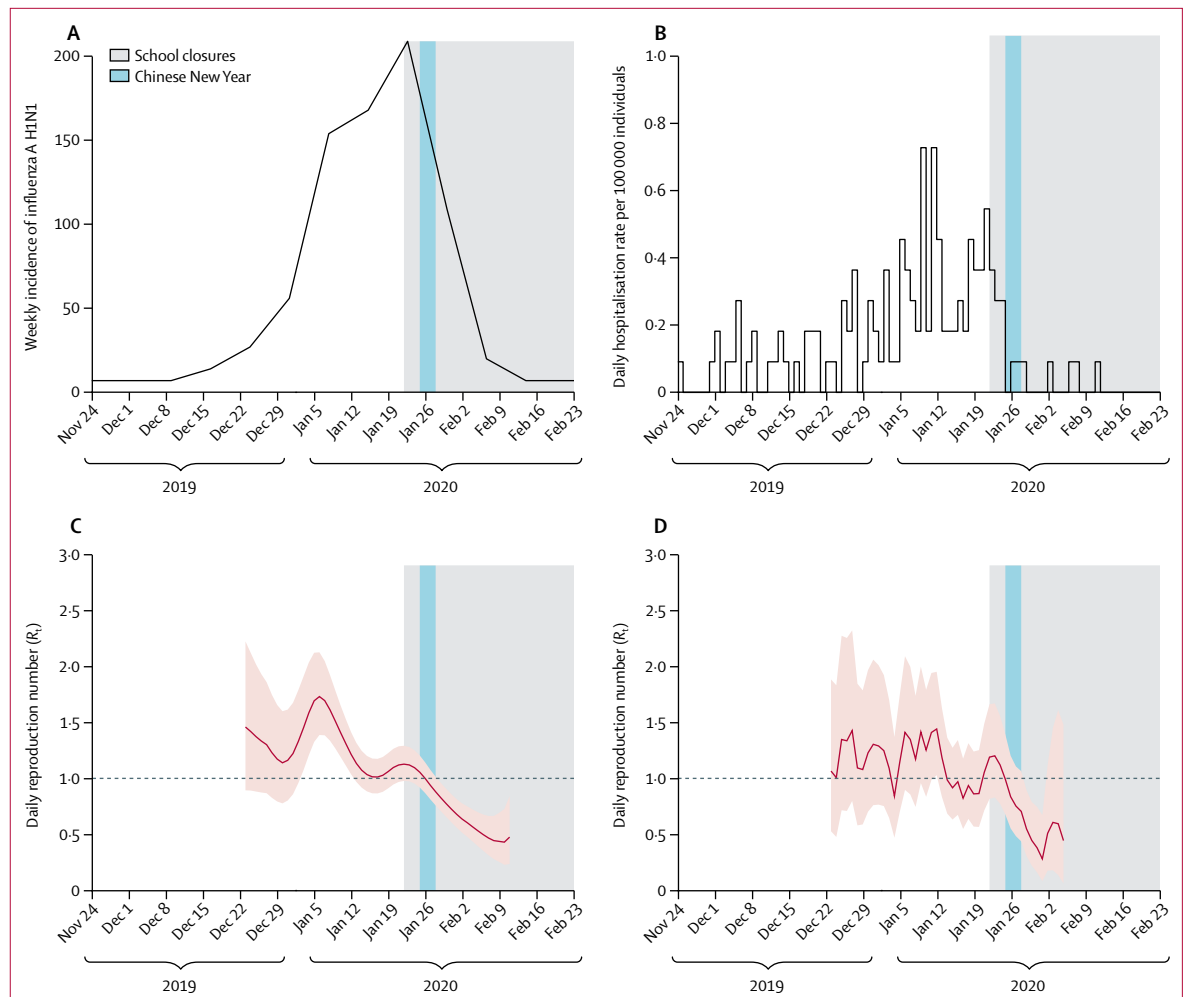


Figure 3: Incidence, hospitalisation rate, and R_t of influenza A (H1N1) in 2019–20

(A) Weekly incidence, calculated as the weekly consultation rate multiplied by the proportion of laboratory specimens testing positive for influenza A (H1N1). (B) Daily hospitalisation rate with influenza A (H1N1) in children in two large hospitals in Hong Kong. (C) Estimated R_t in Hong Kong based on the influenza proxy data, with 95% CIs indicated by the pink shaded region. (D) Estimated R_t in Hong Kong based on the hospitalisation data, with 95% CIs indicated by the pink shaded region. We stopped estimating R_t when the local epidemic ended, indicated by a reduction in influenza proxy to very low levels and no further influenza hospitalisations in children. Dashed lines indicate the critical threshold of $R_t=1$. Shaded bars show the dates of Chinese New Year (light blue) and school closures (grey). R_t =effective reproduction number.

Discussion

Our findings suggest that the package of public health interventions (including border entry restrictions, quarantine and isolation of cases and contacts, and population behaviour changes, such as social distancing and personal protective measures) that Hong Kong has implemented since late January, 2020, is associated with reduced spread of COVID-19. In the 10 weeks (corresponding to about ten generation times) since the first known individual with COVID-19 in Hong Kong began to show symptoms, there has been little sustained, local transmission of the disease. Our findings strongly suggest that social distancing and population behavioural changes—that have a social and economic impact that is less disruptive than total lockdown—can meaningfully control COVID-19.

The increasing number of imported infections in March poses a challenge to suppression efforts. This increase has occurred at the same time as relaxation of some voluntary avoidance behaviours in the general community. Without a strengthening of social distancing measures, local infections are likely to continue to occur, given that the effective reproduction number is approximately 1 or slightly higher than 1. Travel measures and testing, tracing, and treating efforts are particularly important in maintaining suppression, although these measures will be increasingly difficult to implement as case numbers increase.

In addition to the identification of cases with isolation, contact tracing, and quarantine, social distancing has also likely played an important role in suppressing transmission. We found that control measures and changes in population behaviour coincided with a substantial reduction in

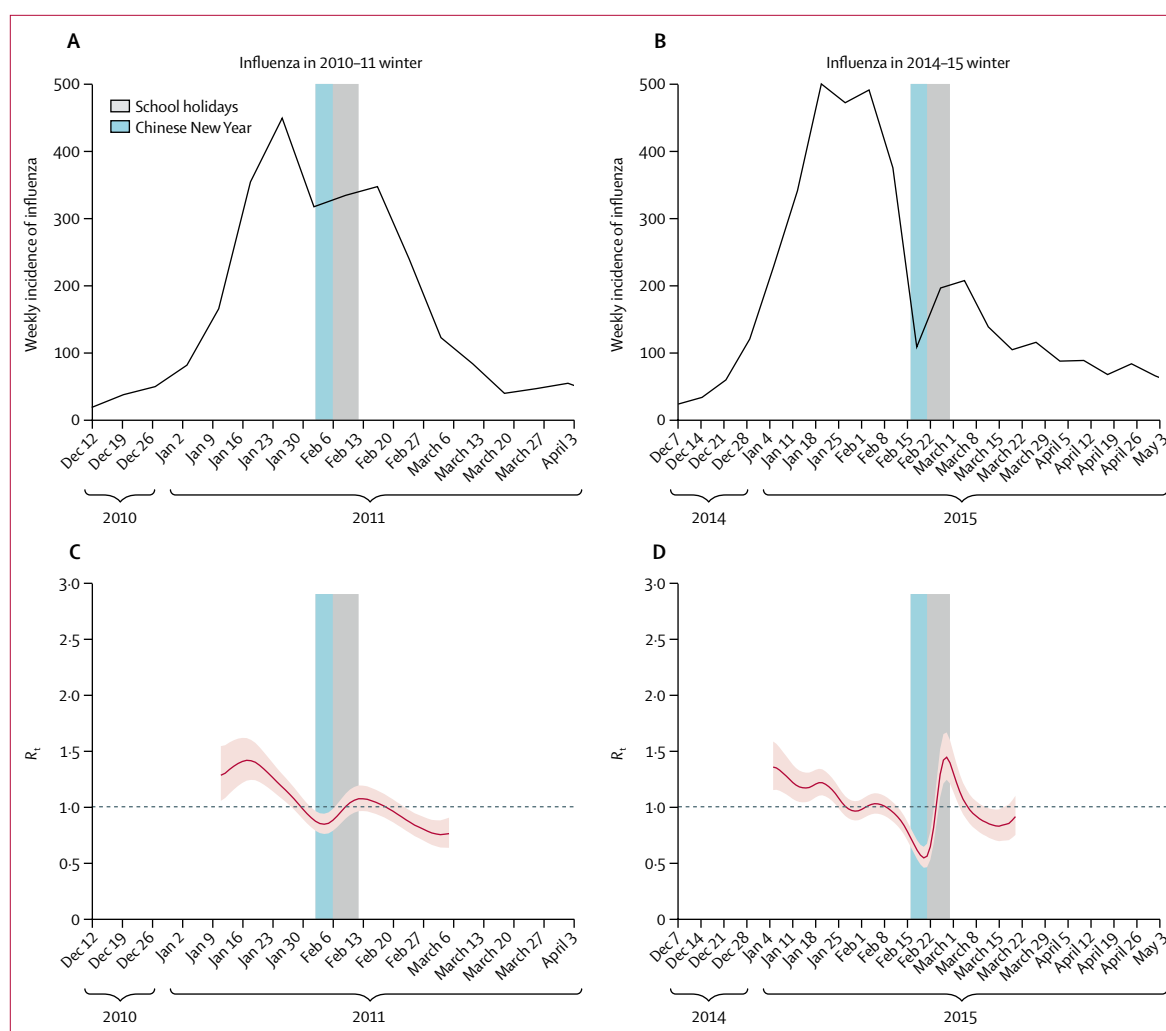


Figure 4: Incidence and R_t of influenza in 2010–11 and 2014–15

Weekly incidence of influenza (all type and subtypes) was calculated as the weekly consultation rate multiplied by the proportion of laboratory specimens testing positive for influenza in the winter influenza season of 2010–11 (A) and 2014–15 (B). R_t in Hong Kong was estimated based on the influenza proxy data, with 95% CIs indicated by the pink shaded region, for the winter influenza season of 2010–11 (C) and 2014–15 (D). Dashed lines indicate the critical threshold of $R_t=1$. Shaded bars show the dates of Chinese New Year (light blue) and school holidays (grey). R_t =effective reproduction number.

influenza transmission in early February, 2020. This observation suggests that the same measures would also have affected COVID-19 transmission in the community, because there will be some similarities—as well as some differences—in the modes of transmission of influenza and COVID-19. The potentially higher basic reproduction number for COVID-19 indicates that it might be more difficult to control than influenza.¹¹ Because a variety of measures were used simultaneously, we were not able to disentangle the specific effects of each one, although this may become possible in the future if some measures are strengthened or relaxed locally, or with use of cross-national or subnational comparisons of the differential application of these measures.

The estimated 44% reduction in influenza transmission in the general community in February, 2020, was

much greater than the estimated 10–15% reduction in transmission associated with school closures alone during the 2009 pandemic,¹⁸ and the 16% reduction in transmission of influenza B associated with school closures during the 2017–18 winter in Hong Kong.¹⁹ We therefore estimate that the other social distancing measures and avoidance behaviours have had a substantial effect on influenza transmission in addition to the effect of school closures. However, if the basic reproduction number of COVID-19 in Hong Kong exceeds 2, (it was 2.2 in Wuhan),¹¹ we would need more than a 44% reduction in COVID-19 transmission to completely avert a local epidemic. A reduction of this magnitude could, however, substantially flatten the peak of and area under the epidemic curve, thus reducing the risk of exceeding the capacity of the health-care system,

	Survey 1, Jan 20–23 (n=1008)	Survey 2, Feb 11–14 (n=1000)	Survey 3, March 10–13 (n=1005)
Risk perception of COVID-19			
Perceived susceptibility to COVID-19*	186 (18.9%; 16.0–21.9)	185 (17.4%; 14.8–20.1)	140 (15.2%; 12.6–17.8)
Perceived severity of COVID-19†	916 (89.6%; 85.8–93.3)	902 (90.5%; 86.4–94.7)	829 (82.0%; 78.6–85.4)
Worried about being infected with COVID-19‡	551 (52.5%; 48.7–56.3)	558 (53.9%; 49.9–57.9)	471 (46.5%; 42.9–50.0)
Risk perception of seasonal influenza			
Perceived susceptibility to seasonal influenza*	260 (25.1%; 22.0–28.3)	231 (22.5%; 19.4–25.6)	NA
Perceived severity of seasonal influenza†	406 (42.3%; 38.4–46.3)	311 (32.7%; 28.9–36.6)	NA
Worried about being infected with seasonal influenza‡	370 (36.5%; 32.9–40.0)	283 (30.3%; 26.6–33.9)	NA
Attitudes towards COVID-19§			
I'm confident that I can take measures to protect myself against COVID-19	518 (50.5%; 46.6–54.4)	594 (59.2%; 54.9–63.5)	679 (68.0%; 64.3–71.7)
I believe that the Hong Kong Government can take effective measures to control the spread of COVID-19 in Hong Kong	338 (33.5%; 29.9–37.1)	271 (31.8%; 27.8–35.8)	336 (35.8%; 32.2–39.3)
I believe that the Central Chinese Government can take effective measures to control COVID-19	308 (31.7%; 28.1–35.3)	352 (39.0%; 34.8–43.2)	NA
I believe that complete border closure is an effective measure to prevent COVID-19 spreading from mainland China to Hong Kong	NA	784 (76.4%; 72.3–80.5)	NA
Complete border closure will seriously affect the life of citizens	NA	298 (33.2%; 29.2–37.1)	NA
I worry about medical supplies, such as face masks, in Hong Kong	NA	860 (84.1%; 80.0–88.2)	NA
I worry about the living supplies in Hong Kong due to border closure	NA	244 (27.7%; 24.0–31.4)	NA
Preventive measures taken against COVID-19¶			
Avoided going to crowded places	627 (61.3%; 57.2–65.4)	920 (90.2%; 86.2–94.2)	860 (85.1%; 81.7–88.4)
Avoided visiting mainland China	800 (78.1%; 73.9–82.2)	NA	NA
Avoided contact with people with respiratory symptoms	687 (66.8%; 62.7–70.9)	834 (80.0%; 76.0–84.0)	806 (78.7%; 75.3–82.1)
Used face masks	778 (74.5%; 70.4–78.6)	976 (97.5%; 93.5–100.0)	992 (98.8%; 96.0–100.0)
Washed hands more often (including using hand sanitiser)	726 (71.1%; 67.0–75.2)	938 (92.5%; 88.6–96.5)	941 (93.0%; 90.0–96.0)
Avoided touching public objects or used protective measures when touching public objects (eg, use tissue)	387 (36.4%; 32.3–40.5)	767 (73.8%; 69.8–77.9)	746 (73.1%; 69.6–76.7)
House disinfection	NA	897 (89.3%; 85.2–93.4)	899 (89.6%; 86.4–92.8)
Used serving utensils when eating	NA	686 (66.0%; 61.9–70.1)	692 (67.7%; 64.1–71.3)
Stayed at home as much as possible	NA	894 (88.0%; 83.9–92.1)	868 (83.8%; 80.5–87.1)
Avoided going to health-care facilities	NA	832 (81.0%; 77.0–85.1)	759 (74.7%; 71.1–78.3)
Data are n (%; 95% CI). Proportions were weighted by age and sex to the adult population in Hong Kong. All dates are in 2020. NA=not applicable (question was not asked in the survey). COVID-19=coronavirus disease 2019. *Numbers and proportions represent respondents that answered likely, very likely, or certain, rather than never, very unlikely, unlikely, or even chance. †Numbers and proportions represent respondents that answered serious or very serious, rather than very mild, mild, or moderate. ‡Numbers and proportions represent respondents that answered moderately worried or very worried, rather than not at all worried or slightly worried. §Numbers and proportions represent respondents that answered agree or strongly agree to these statements, rather than strongly disagree, disagree, or neutral. ¶Numbers and proportions represent respondents who had taken the measure in the previous 7 days to prevent contracting COVID-19.			

Table: Public attitudes, risk perceptions, and behavioural responses towards COVID-19 and seasonal influenza in three telephone surveys in Hong Kong

and potentially saving many lives, especially among older adults.

The postponement of class resumption in local schools in Hong Kong after the Chinese New Year holiday is technically a class dismissal or suspension rather than a school closure, because most teachers are still required to go to school premises to plan e-learning activities and set homework. Full school closures have been implemented locally in previous years, including during the SARS epidemic in 2003,⁶ during the influenza pandemic in 2009,¹⁸ and to control seasonal influenza epidemics in 2008 and 2018.^{19,20} Although school closures can have considerable effects on influenza transmission, their role in reducing COVID-19 transmission would depend on the susceptibility of children to infection and their infectiousness if infected. Both of these factors are

major unanswered questions at present.^{21,22} Despite this acknowledged uncertainty, our surveys revealed considerable local support for school closures.

Individual behaviours in the Hong Kong population have changed in response to the threat of COVID-19. People have been choosing to stay at home, and in our most recent survey, 85% of respondents reported avoiding crowded places and 99% reported wearing face masks when leaving home. Using similar surveys, face mask use during the SARS outbreak in 2003 was 79%,⁵ and it reached a maximum of 10% during the influenza A (H1N1) pandemic in 2009.⁷ These changes in behaviour indicate the level of concern among the population about this particular infection, and the extent of voluntary social distancing in addition to the distancing created by school closures. However, we did identify evidence of

reductions in voluntary social distancing behaviours in our third survey in March, perhaps indicating some fatigue with these measures.

Our study has some limitations. First, we could not identify which measure was potentially the most effective and whether border restrictions, quarantine and isolation, social distancing, or behavioural changes are most important in suppressing COVID-19 transmission. It is likely that each plays a part. Unlinked cases have been identified in the community and will continue to be identified, indicating that not every chain of transmission has been identified by contact tracing from known cases. Although we have noted major effects of control measures and behavioural changes on influenza transmission, the effects could be of a different magnitude for COVID-19 because of differences in transmission dynamics. Second, our surveys of population behaviours could have been affected by response bias, because we relied on self-reported data. They also could have been affected by selection bias away from working adults, although this should have been reduced by conducting surveys in non-working as well as working hours—we were unable to assess potential selection bias. Without a baseline survey before Jan 23, 2020, we could not compare changes in behaviours, although the results of similar surveys from previous epidemics can be used for comparison.^{6–8,11} Finally, although we identified reductions in the incidence of influenza virus infections in outpatients and paediatric inpatients, it is possible that these time series were affected by reduced health-care-seeking behaviours and limited health-care access that probably resulted from private clinic closure, which occurred around the period of the Chinese New Year holiday.

In conclusion, our study suggests that measures taken to control the spread of COVID-19 have been effective and have also had a substantial impact on influenza transmission in Hong Kong. Although the transmission dynamics and modes of transmission of COVID-19 have not been precisely elucidated, they are likely to share at least some characteristics with influenza virus transmission, because both viruses are directly transmissible respiratory pathogens with similar viral shedding dynamics.²³ The measures implemented in Hong Kong are less drastic than those used to contain transmission in mainland China, and are probably more feasible in many other locations worldwide. If these measures and population responses can be sustained, avoiding fatigue among the general population, they could meaningfully mitigate the impact of a local epidemic of COVID-19.

Contributors

BJC and GML designed the study. STA, TWYN, MWF, QL, MYWK, SLL, and SSC collected the data. STA, TWYN, TKT, JCML, and MWF analysed the data. BJC, STA, TWYN, PW, and GML interpreted the data. BJC wrote the first draft. All authors contributed to the final draft.

Declaration of interests

BJC reports honoraria from Sanofi Pasteur and Roche. All other authors declare no competing interests.

Data sharing

Data on the incidence of coronavirus disease 2019 and influenza activity are freely available from the Centre for Health Protection website (<https://www.chp.gov.hk/en/index.html>). Survey data are available from the corresponding author on request.

Acknowledgments

This project was supported by a commissioned grant from the Health and Medical Research Fund, Food and Health Bureau, Government of the Hong Kong Special Administrative Region.

Editorial note: The *Lancet* Group takes a neutral position with respect to territorial claims in published maps and institutional affiliations.

References

- 1 Leung K, Wu JT, Liu D, Leung GM. First-wave COVID-19 transmissibility and severity in China outside Hubei after control measures and second-wave scenario planning: a modelling impact assessment. *Lancet* 2020; published online April 8. [https://doi.org/10.1016/S0140-6736\(20\)30746-7](https://doi.org/10.1016/S0140-6736(20)30746-7).
- 2 Zhong R, Mosur P. To tame coronavirus, Mao-style social control blankets China. Feb 20, 2020. <https://www.nytimes.com/2020/02/15/business/china-coronavirus-lockdown.html> (accessed Feb 25, 2020).
- 3 Kavanagh MM. Authoritarianism, outbreaks, and information politics. *Lancet Public Health* 2020; 5: 135–36.
- 4 Chiu SS, Kwan MY, Feng S, et al. Early season estimate of influenza vaccination effectiveness against influenza hospitalisation in children, Hong Kong, winter influenza season 2018/19. *Euro Surveill* 2019; 24: 1900056.
- 5 Leung GM, Quah S, Ho LM, et al. A tale of two cities: community psychobehavioral surveillance and related impact on outbreak control in Hong Kong and Singapore during the severe acute respiratory syndrome epidemic. *Infect Control Hosp Epidemiol* 2004; 25: 1033–41.
- 6 Leung GM, Ho LM, Chan SK, et al. Longitudinal assessment of community psychobehavioral responses during and after the 2003 outbreak of severe acute respiratory syndrome in Hong Kong. *Clin Infect Dis* 2005; 40: 1713–20.
- 7 Cowling BJ, Ng DM, Ip DK, et al. Community psychological and behavioral responses through the first wave of the 2009 influenza A(H1N1) pandemic in Hong Kong. *J Infect Dis* 2010; 202: 867–76.
- 8 Wu P, Fang VJ, Liao Q, et al. Responses to threat of influenza A(H7N9) and support for live poultry markets, Hong Kong, 2013. *Emerg Infect Dis* 2014; 20: 882–86.
- 9 Cori A. EpiEstim: estimate time varying reproduction numbers from epidemic curves. 2019. <https://CRAN.R-project.org/package=EpiEstim> (accessed March 31, 2020).
- 10 Thompson RN, Stockwin JE, van Gaalen RD, et al. Improved inference of time-varying reproduction numbers during infectious disease outbreaks. *Epidemics* 2019; 29: 100356.
- 11 Li Q, Guan X, Wu P, et al. Early transmission dynamics in Wuhan, China, of novel coronavirus-infected pneumonia. *N Engl J Med* 2020; 382: 1199–207.
- 12 Goldstein E, Viboud C, Charu V, Lipsitch M. Improving the estimation of influenza-related mortality over a seasonal baseline. *Epidemiology* 2012; 23: 829–38.
- 13 Wong JY, Wu P, Nishiura H, et al. Infection fatality risk of the pandemic A(H1N1)2009 virus in Hong Kong. *Am J Epidemiol* 2013; 177: 834–40.
- 14 Ali ST, Wu P, Cauchemez S, et al. Ambient ozone and influenza transmissibility in Hong Kong. *Eur Respir J* 2018; 51: 1800369.
- 15 Cori A, Ferguson NM, Fraser C, Cauchemez S. A new framework and software to estimate time-varying reproduction numbers during epidemics. *Am J Epidemiol* 2013; 178: 1505–12.
- 16 Wallinga J, Lipsitch M. How generation intervals shape the relationship between growth rates and reproductive numbers. *Proc Biol Sci* 2007; 274: 599–604.
- 17 Fieller EC. Some problems in interval estimation. *J R Stat Soc B* 1954; 16: 175–85.
- 18 Wu JT, Leung K, Perera RA, et al. Inferring influenza infection attack rate from seroprevalence data. *PLoS Pathog* 2014; 10: e1004054.

- 19 Ali ST, Cowling BJ, Lau EHY, Fang VJ, Leung GM. Mitigation of influenza B epidemic with school closures, Hong Kong, 2018. *Emerg Infect Dis* 2018; **24**: 2071–73.
- 20 Cowling BJ, Ho LM, Leung GM. Effectiveness of control measures during the SARS epidemic in Beijing: a comparison of the Rt curve and the epidemic curve. *Epidemiol Infect* 2008; **136**: 562–66.
- 21 Cowling BJ, Leung GM. Epidemiological research priorities for public health control of the ongoing global novel coronavirus (2019-nCoV) outbreak. *Euro Surveill* 2020; **25**: 2000110.
- 22 Lipsitch M, Swerdlow DL, Finelli L. Defining the epidemiology of COVID-19—studies needed. *N Engl J Med* 2020; **382**: 1194–96.
- 23 Zou L, Ruan F, Huang M, et al. SARS-CoV-2 viral load in upper respiratory specimens of infected patients. *N Engl J Med* 2020; **382**: 1177–79.



[Indian J Radiol Imaging](#). 2017 Jul-Sep; 27(3): 342–349.

PMCID: PMC5644332

doi: 10.4103/ijri.IJRI_469_16: 10.4103/ijri.IJRI_469_16

PMID: [29089687](#)

Follow-up chest radiographic findings in patients with MERS-CoV after recovery

[Karuna M Das](#),^{1,2} [Edward Y Lee](#),³ [Rajvir Singh](#),⁴ [Mushira A Enani](#),⁵ [Khalid Al Dossari](#),² [Klaus Van Gorkom](#),¹ [Sven G Larsson](#),² and [Ruth D Langer](#)¹

¹Department of Radiology, College of Medicine and Health Sciences, United Arab Emirates University, Al-Ain, UAE

²Department of Medical Imaging, King Fahad Medical City, Riyadh, KSA

³Department of Radiology and Medicine, Pulmonary Division, Boston Children's Hospital and Harvard Medical School, Boston, Massachusetts, USA

⁴Department of Cardiology and Biostatistics, Hamad Medical Corporation, Doha, Qatar

⁵Department of Medicine (Infectious Disease), King Fahad Medical City, Riyadh, KSA

Correspondence: Dr. Karuna M Das, Department of Radiology, College of Medicine and Health Sciences, United Arab Emirates University, Al-Ain-17666, UAE. E-mail: daskmoy@gmail.com

Copyright : © 2017 Indian Journal of Radiology and Imaging

This is an open access article distributed under the terms of the Creative Commons Attribution-NonCommercial-ShareAlike 3.0 License, which allows others to remix, tweak, and build upon the work non-commercially, as long as the author is credited and the new creations are licensed under the identical terms.

Abstract

Purpose:

To evaluate the follow-up chest radiographic findings in patients with Middle East respiratory syndrome coronavirus (MERS-CoV) who were discharged from the hospital following improved clinical symptoms.

Materials and Methods:

Thirty-six consecutive patients (9 men, 27 women; age range 21–73 years, mean \pm SD 42.5 \pm 14.5 years) with confirmed MERS-CoV underwent follow-up chest radiographs after recovery from MERS-CoV. The 36 chest radiographs were obtained at 32 to 230 days with a median follow-up of 43 days. The reviewers systemically evaluated the follow-up chest radiographs from 36 patients for lung parenchymal, airway, pleural, hilar and mediastinal abnormalities. Lung parenchyma and airways were assessed for consolidation, ground-glass opacity (GGO), nodular opacity and reticular opacity (i.e., fibrosis). Follow-up chest radiographs were also evaluated for pleural thickening, pleural effusion, pneumothorax and lymphadenopathy. Patients were categorized into two groups: group 1 (no evidence of lung fibrosis) and group 2 (chest radiographic evidence of lung fibrosis) for comparative analysis. Patient demographics, length of ventilations days, number of intensive care unit (ICU) admission days, chest radiographic score, chest radiographic deterioration pattern (Types 1-4) and peak lactate dehydrogenase level were compared between the two groups using the student *t*-test, Mann-Whitney *U* test and Fisher's exact test.

Results:

Follow-up chest radiographs were normal in 23 out of 36 (64%) patients. Among the patients with abnormal chest radiographs (13/36, 36%), the following were found: lung fibrosis in 12 (33%) patients GGO in 2 (5.5%) patients, and pleural thickening in 2 (5.5%) patients. Patients with lung fibrosis had significantly greater number of ICU admission days (19 ± 8.7 days; P value = 0.001), older age (50.6 ± 12.6 years; P value = 0.02), higher chest radiographic scores [10 (0-15.3); P value = 0.04] and higher peak lactate dehydrogenase levels (315-370 U/L; P value = 0.001) when compared to patients without lung fibrosis.

Conclusion:

Lung fibrosis may develop in a substantial number of patients who have recovered from Middle East respiratory syndrome coronavirus (MERS-CoV). Significantly greater number of ICU admission days, older age, higher chest radiographic scores, chest radiographic deterioration patterns and peak lactate dehydrogenase levels were noted in the patients with lung fibrosis on follow-up chest radiographs after recovery from MERS-CoV.

Keywords: Lung fibrosis, MERS-CoV, Chest radiograph

Introduction

Outbreaks of infection of the Middle East respiratory syndrome coronavirus (MERS-CoV) are an emerging global health crisis.[1] Until recently, most cases (1,223 with 520 deaths) have occurred in Saudi Arabia and exhibit a case fatality of approximately 43%.[2] The morbidity and mortality caused by MERS-CoV are particularly alarming. The majority of affected patients typically present with a severe respiratory illness that requires hospitalization; the mortality rate approaches 60%.[3]

Chest radiography is found to be useful in the diagnosis of MERS-CoV by demonstrating lung abnormalities and in the evaluation of the progress of disease and its response to treatment.[4] Two recently published studies reported MERS-CoV chest radiographic findings and showed that sequential chest radiographs were valuable in the evaluation of the early diagnosis and monitoring of the radiographic progression of the disease.[5,6,7] Approximately 55% of MERS-CoV patients require ICU admission for respiratory failure and adult respiratory distress syndrome (ARDS).[5,6,7] Survivors of ARDS have a clinically significant reduction in health-related quality of life and varied radiological changes.[8,9,10] In the present study, we focused on investigating the lung parenchymal, airway, pleural, hilar and mediastinal abnormalities which can be present on short- and medium-term follow-up chest radiographs during the recovery period; this may have important clinical implications for understanding the sequelae of the disease and contribute to the future management of affected patients.

Therefore, the purpose of this study is to evaluate the follow-up chest radiographic findings in MERS-CoV patients who were discharged from the hospital following improved clinical symptoms.

Materials and Methods

Participants

This retrospective study was approved by the institutional review board with a waiver of informed consent. Our study ran from August 10, 2014 to September 02, 2015 and included 36 patients who were discharged from the hospital following recovery from the MERS-CoV infection. The final study population consisted of nine male and 27 female patients. Patient age ranged from 21 years to 73 years (mean \pm SD, 42.5 ± 14.5 years).

In our study population, MERS-CoV diagnosis was based on the World Health Organization (WHO) criteria.[11] At our institution, the treatment protocol for non-ICU patients suspected of having MERS-CoV was empiric treatment with oseltamivir (Tamiflu) until screening for respiratory viruses excluded

influenza A and H1N1. In addition, antibiotics (ceftriaxone and azithromycin) were started to manage the potential of bacterial pneumonia. For ICU patients, the same patient management policy was followed, but the choice of antibiotics was broader, such as piperacillin-tazobactam (Zosyn) with or without vancomycin (Vancocin). All 36 patients were discharged from the hospital after the following: 1) complete recovery from their current illness, 2) complete resolution of respiratory symptoms and oxygen dependency, 3) improved radiological parameters based upon serial radiographs and 4) improved laboratory parameters. All these patients fulfilled above mentioned criterion before discharge from the hospital.

The chest radiographic findings and computed tomographic findings of 36 out of 55 patients obtained during the active phase of the infection that are included in this report have previously been published. [5,6,7] The current study focused on the retrospective analysis of follow-up chest radiographic findings of the 36 patients after they had recovered from MERS-CoV as this had not been previously investigated.

Imaging technique

Digital radiography equipment (Mobilett Plus; Siemens, Erlangen, Germany) was used to obtain anteroposterior (AP) projection radiographs with standardized parameters [65 kV, 4–8 mAs according to body mass index (BMI) and focus-film distance of 100 cm. Non-portable radiography equipment (Philips Medical Systems, Hamburg, Germany) was used to obtain anteroposterior (PA) and lateral projection radiographs with standard techniques at a 180-cm focus-film distance.

Among the 36 follow-up chest radiographs from the 36 patients, 31 (86%) were obtained with a portable one-view technique (AP projection radiographs), while the remaining five (14%) radiographs were obtained with standard chest two-view techniques (PA and lateral projection radiographs).

Chest radiograph review

Two thoracic radiologists with 20 (K.M.D) and 8 (K.D.) years of experience of interpreting chest radiographs independently reviewed all chest radiographs which had been randomized prior to the evaluation process. The reviewers reached a decision on the final interpretation by consensus. Although the two reviewers were aware of the MERS-CoV infection diagnosis in our study population, other information, such as clinical information, laboratory results, prior imaging or non-imaging studies, original radiologic interpretation of chest radiographs and the group into which each of the patients were categorized, was blinded to decrease potential reviewer bias. For the studies with interpretation discrepancies from the two initial reviewers, a third reviewer (S.G.L., with 40 years of experience) served as the arbitrator and made the final decision after independently reviewing the chest radiographs.

A dedicated radiology picture archiving and communication system (PACS) workstation (Centricity 2.1.2.1; GE Healthcare, Milwaukee, WI, USA) that is available in our department was used for the evaluation of the chest radiographs from our study population. During the evaluation, reviewers could manually alter the degree of radiodensity settings and zoom into areas of interest to achieve a complete and detailed assessment.

Chest radiograph evaluation

Initially, all chest radiographs were categorized into two groups, normal or abnormal, based on lung parenchymal, airway, pleural, hilar and mediastinal findings on follow-up chest radiographs. Abnormal follow-up chest radiographs were subsequently assessed by established criteria as detailed in the following sections.

Lung parenchyma and airways were evaluated for the following: 1) consolidation, 2) ground-glass opacity (GGO), 3) nodular opacity, and 4) reticular opacity (i.e., fibrosis). [12,13,14,15,16,17,18] A diagnosis of consolidation was made when there was an area of increased opacity present that obscured the vessel margin and airway walls, with or without an air bronchogram. [14] GGO was defined as an area of

increased lung opacity within which margins of pulmonary vessels may be indistinct.[14] A diagnosis of nodular opacity was considered when an opacity was focal and round in shape. Reticular opacity which signals fibrosis, was defined as linear opacities forming a mesh-like pattern.[12,13,14,15,16,17,18] Follow-up chest radiographs were also evaluated for the presence of pleural thickening, effusion, or pneumothorax. Additionally, the hilar and mediastinum were assessed for lymphadenopathy. A hilar lymphadenopathy was considered to be present when there was an increase in the size and opacity of the hilum with a lobulated hilar contour and obscuration of the interlobular artery.[18,19] Mediastinal lymphadenopathy was defined as the presence of the widening of one or more mediastinal contours at known anatomic lymph node sites.[19]

Furthermore, if any other thoracic abnormalities not included in the aforementioned categories during the evaluation process were detected on follow-up chest radiographs, the reviewers were instructed to record them.

Comparison of chest radiograph findings and clinical parameters

Patient demographics, length of ventilations days, number of ICU admission days, chest radiographic score, chest radiographic deterioration pattern (Types 1–4)[5,6,7] and peak lactate dehydrogenase level[20,21] were compared between the cohort's two study groups[5,6,7] in order to evaluate the association with the presence of lung fibrosis seen on follow-up chest radiographs.

The chest radiographic score of MERS-CoV infection can be obtained by first dividing each lung into three zones and evaluating the levels of involvement in each zone.[22] The development of MERS-CoV lesions within each lung zone is then scored as follows: 0 = normal; 4 = complete involvement of one zone; or, 24 = complete involvement of all six zones.[5] The scores for all six zones per chest radiograph are added together to yield a cumulative chest radiographic score ranging from 0 to 24, depending upon the involvement of the lung parenchyma.

Chest radiographic deterioration during disease progression can be classified into four types.[1,2,3,4] Type 1 disease progression represents initial radiographic deterioration followed by improvement.[12,13] Type 2 disease progression is defined as static radiographic changes with no discernible radiographic peak or a change in overall mean lung involvement of less than 25%. Type 3 disease progression is represented by fluctuating radiographic changes with at least two radiographic peaks separated by a period of mild remission (remission is defined as a level of mean lung parenchyma involvement that differs from the peak level by >25%). Type 4 progression is defined as progressive radiographic deterioration.

Statistical analysis

Descriptive statistics in the form of mean, standard deviation, median and range as appropriate for age, length of ventilations days, number of ICU admission days, chest radiographic score, chest radiographic deterioration pattern, peak lactate dehydrogenase (LDH) level and frequency, with percentages for categorical variables, were calculated separately for the group of patients with lung fibrosis and without. The student *t*-test for normally distributed data and the Mann-Whitney *U*-test for non-normal distributed data were applied to assess statistically significant differences between with and without evidence of lung fibrosis groups. Fisher's exact tests were used to evaluate associations for categorical variables. A *P* value 0.05 (two-tailed) was considered for the statistically significant level. The IBM SPSS version 21.0 (IBM, Armonk, NY, USA) statistical package was used for the analysis of the study.

Results

Study cohort

There were no significant gender differences between the two groups ($p = 0.41$). However, group 2 patients with evidence of lung fibrosis were significantly older ($p = 0.02$) than group 1 patients and had a significantly greater number of ICU admission days ($p = 0.001$). The mean \pm SD, median, and range of follow-up of the 36 chest radiographs were 64.8 ± 85 days, 43 days, and 32–230 days, respectively. The mean \pm SD, median and range of lung fibrosis development of 12 patients were 82.4 ± 66 days, 44 days, and 32–230 days, respectively.

Chest radiograph findings

Two reviewers (K.M.D., K.D.) were able to reach a consensus on all abnormal findings detected on follow-up chest radiographs. The follow-up chest radiographs were normal in 23 of 36 (64%) patients. Abnormal chest radiographic findings were detected in 13 of 36 (36%) patients and are shown in Tables [1](#), [2](#) and [3](#).

The most frequent abnormality found on follow-up chest radiographs in MERS-CoV patients who recovered was lung fibrosis which was seen in 12 of 36 (33%) patients. Lung fibrosis was confined to one lobe in the 10 patients, including the right upper lobe in three (8%) patients, left lower lobe in three (8%) patients, right middle lobe in two (5.5%) patients and lingula in two (5.5%) patients [[Figure 1](#)]. The remaining lung fibrosis involved multiple zones in two (5.5%) patients [[Figures 2](#) and [3](#)]. GGO was the next most frequently detected abnormality on follow-up chest radiographs as seen in two (5.5%) patients and it was located in the lingula [[Figure 4](#)] in one patient and in the left lower lobe in one patient, respectively. No consolidation or nodular opacity was detected on follow-up chest radiographs.

In regard to pleural abnormality detected on follow-up chest radiographs in our study population, pleural thickening was seen in two patients and it was located in the right lower and left lower lobes, respectively [[Figure 5](#)]. No pleural effusion or pneumothorax was identified.

None of the patients had hilar and/or mediastinal lymphadenopathy. No other additional thoracic abnormalities were observed on follow-up chest radiographs in our study population.

Comparison of chest radiograph findings and clinical parameters

With regard to the extent of lung parenchymal involvement (chest radiographic score) during the course of the disease, the patients with evidence of lung fibrosis were associated with a significantly higher number of chest radiographic score ($P = 0.04$) [[Table 2](#)].

The association of lung fibrosis was highest (67%) in the Type 2 radiographic deterioration pattern, followed by the Type 3 (25%, $P = 0.01$) radiographic deterioration pattern [[Table 3](#)]. The association with the Type 4 radiographic deterioration pattern could not be ascertained due to lack of follow-up following the highest number of deaths in this group [[Table 3](#)].

The peak lactate dehydrogenase level was also higher in group 2 than in group 1 [315 (0–370 U/L) vs. 0 (0–310 U/L)] [[Table 2](#)]. The normal range of lactate dehydrogenase level at our institution is 121–214 U/L.

Discussion

The results of our study show that a substantial portion (33%) of the follow-up chest radiographs obtained from the MERS-CoV patients who recovered is abnormal. In our study population, the chest radiographic abnormalities are characterized by the presence of lung fibrosis, GGOs, and pleural thickening.

We believe that our finding of potentially permanent damage, such as lung fibrosis and pleural thickening, seen in a substantial portion of our MERS-CoV patients who recovered is important because typical viral pneumonia usually results in a complete recovery without any significant radiological consequences.[\[23\]](#) The results of our study suggest that MERS-CoV may be a novel, more aggressive type of lung infection than other viral lung infections and that it may be associated with more significant morbidity in affected

patients. In fact, our study also shows that lung fibrosis developed rather rapidly in the study population with a mean \pm SD, median and range of lung fibrosis development of 82.4 ± 66 days 44 days, and 32–230 days, respectively, after discharge from the hospital.

Lung fibrosis has been detected on follow-up imaging studies in patients who recovered from relatively new pulmonary infections such as swine influenza (i.e. H1N1) pneumonia[24] and severe acute respiratory syndrome (SARS).[25] We found that the incidence (33%) of lung fibrosis seen in our study population is higher than the rate (10%) of lung fibrosis seen in patients who recovered from swine influenza pneumonia.[24] However, the incidence (33%) of lung fibrosis seen in patients who recovered from MERS-CoV is similar to the incidence (38%) of lung fibrosis detected in patients who recovered from SARS.[25] Given that the presence of pulmonary fibrosis was evaluated based on follow-up chest radiographs in our study population, in comparison to the chest computed tomography (CT) used in another study that focused on detecting lung fibrosis in patients who recovered from SARS, we believe that the presence of lung fibrosis would be much higher if lung fibrosis was evaluated on chest CT rather than on chest radiographs as in our study population. Unfortunately, most of our patients underwent chest radiographs rather than chest CT for a follow-up evaluation after MERS-CoV recovery, which prevented us from investigating pulmonary fibrosis with chest CT. A future study using chest CT for the detection of lung abnormalities in our study population would be helpful to gain a more precise evaluation as CT is more sensitive than chest radiographs for accurately detecting such abnormalities.

In our study, direct comparison of the follow-up chest radiographic findings with clinical data revealed several significant differences between patients with follow-up chest radiographic evidence of lung fibrosis and those without evidence of lung fibrosis. We found that patients with lung fibrosis detected on follow-up chest radiographs were associated with a greater number of ICU admission days, older age, higher chest radiographic score and higher peak lactate dehydrogenase level. In other words, we believe that these are the underlying risk factors and/or predictors for developing lung fibrosis in MERS-CoV patients who recovered. It is understandable that lung fibrosis develops in patients who have been more severely infected with MERS-CoV (i.e. higher chest radiographic score) and who experience a longer infection period (i.e., greater number of ICU admission days). In addition, older patients with already aged lungs and decreased immune systems may not be able to completely recover from MERS-CoV and may be prone to develop viral-induced lung fibrosis.[26]

The exact triggers which initiate the lung fibrotic process remain unknown. Infectious agents, including both viruses and bacteria, have the capacity to cause alveolar epithelial cell injury and apoptosis.[24,27,28] Presumably, because of the similar reaction, a considerable number of the patients in our cohort with MERS-CoV have developed pulmonary fibrosis. If infection plays a causal role in the process of pulmonary fibrosis, then it is possible that therapeutic strategies, utilizing currently available antiviral or antibiotic drugs, may be effective in modifying the course of this dreadful condition.[27,28]

In regard to our finding of the association between the presence of lung fibrosis on follow-up chest radiographs and higher peak lactate dehydrogenase level, we believe that this can be explained because the higher peak of lactate dehydrogenase level may indicate underlying lung tissue destruction (i.e. lung fibrosis). This finding of the higher peak of lactate dehydrogenase level has been seen in patients affected with SARS and shown to be a good independent predictor of a worse clinical outcome.[20,21] Future studies focusing on understanding the underlying pathophysiology of developing lung fibrosis in this patient population would be valuable to better elucidate the direct underlying risk factors and their consequences.

This study has some limitations. First, some of the patients in our study had only frontal radiographs. Although we believe that this did not have a significant effect on our findings, we acknowledge that there may have been a limitation regarding the complete assessment of subtle retrocardiac abnormalities and small pleural effusions that can be better seen on lateral radiographs. However, we would like to

emphasize that the reason for obtaining a single view (i.e. frontal radiograph only) was primarily due to our concerted effort to reduce the radiation exposure of our patient population. Second, as we have briefly mentioned in the discussion section, CT has better sensitivity than chest radiography in the diagnosis of lung fibrosis. Thus, the frequency of imaging findings such as lung fibrosis may have been underestimated in our study. A future study focusing on follow-up CT findings in patients who have recovered from MERS-CoV would be valuable in this regard. Lastly, our study focused on short- and intermediate-term follow-up imaging findings in our study population. A future study focusing on a long-term follow-up would be helpful for understanding the full spectrum of the sequelae of this new lung infection.

In conclusion, it is alarming that a substantial portion of the follow-up chest radiographs from the MERS-CoV patients who recovered are abnormal and characterized by potentially permanent lung damage such as lung fibrosis. Based on the observations made in our study, we believe that the greater number of higher ICU admission days, older age, higher chest radiographic score and higher peak lactate dehydrogenase level may have value in the prediction of lung fibrosis development in patients who have recovered from MERS-CoV. However, we wish to stress that our findings are based on short- and intermediate-term follow-up evaluation. Future studies consisting of a larger patient population with a longer follow-up period would be necessary in order to confirm our findings and better determine the long-term outcomes of patients who recovered from MERS-CoV.

Financial support and sponsorship

Nil.

Conflicts of interest

There are no conflicts of interest.

References

1. Zaki AM, Van Boheemen S, Bestebroer TM, Osterhaus AD, Fouchier RA. Isolation of a novel coronavirus from a man with pneumonia in Saudi Arabia. *N Engl J Med*. 2012;367:1814–20. [PubMed: 23075143]
2. MERS-an uncertain future, Editorial review. *Lancet Infect Dis*. 2015;15:1115. [PMCID: PMC7129319] [PubMed: 26461936]
3. World Health Organization. Global Alert and Response (GAR). Corona virus infections. http://www.who.int/uml.idm.oclc.org/csr/disease/coronavirus_infections/en/
4. World Health Organization. Preliminary clinical description of severe acute respiratory syndrome. [Accessed 2003 March 21]. www.who.int/csr/sars/clinical/en/
5. Das KM, Lee EY, Jawder SE, Enani MA, Singh R, Skakni L, et al. Acute Middle East Respiratory Syndrome Coronavirus: Temporal Lung Changes Observed on the Chest Radiographs of 55 Patients. *AJR Am J Roentgenol*. 2015;205:W267–74. [PubMed: 26102309]
6. Das KM, Lee EY, Enani MA, Jawder SE, Enani MA, Singh R, Skakni L, et al. CT correlation with outcomes in 15 patients with acute Middle East respiratory syndrome corona virus. *AJR Am J Roentgenol*. 2015;204:736–42. [PubMed: 25615627]
7. Das KM, Lee EY, Langer RD, Larsson SG. Middle East Respiratory Syndrome Coronavirus: What Does a Radiologist Need to Know? *AJR Am J Roentgenol*. 2015;206:1193–01. [PubMed: 26998804]

8. Davidson TA, Caldwell ES, Curtis JR, Hudson LD, Steinberg KP. Reduced quality of life in survivors of acute respiratory distress syndrome compared with critically ill control patients. *JAMA*. 1999;281:354–60. [PubMed: 9929089]
9. Howling SJ, Evans TW, Hansell DM. The significance of bronchial dilatation on CT in patients with adult respiratory distress syndrome. *Clin Radiol*. 1998;53:105–9. [PubMed: 9502085]
10. Zapol WM, Trelstad RL, Coffey JW, Tsai I, Salvador RA. Pulmonary fibrosis in severe acute respiratory failure. *Am Rev Respir Dis*. 1979;119:547–54. [PubMed: 443627]
11. The Who Mers-Cov Research Group. State of Knowledge and Data Gaps of Middle East Respiratory Syndrome Coronavirus (MERS-Cov) in Humans. *PLoS Curr*. 2013;12:5. [PMCID: PMC3828229] [PubMed: 24270606]
12. Wong KT, Antonio GE, Hui DS, Lee N, Yuen EH, Wu A, et al. Severe acute respiratory syndrome: Radiographic appearances and pattern of progression in 138 patients. *Radiology*. 2003;228:401–6. [PubMed: 12759474]
13. Wong KT, Antonio GE, Hui DS, Lee N, Yuen EH, Wu A, et al. Thin-section CT of severe acute respiratory syndrome: Evaluation of 73 patients exposed to or with the disease. *Radiology*. 2003;228:395–400. [PubMed: 12738877]
14. Hansell DM, Bankier AA, MacMahon H, McLoud TC, Müller NL, Remy J. Fleischner Society: Glossary of terms for thoracic imaging. *Radiology*. 2008;246:697–722. [PubMed: 18195376]
15. Ooi GC, Daqing M. SARS: Radiological features. *Respirology*. 2003;8:S15–9. [PMCID: PMC7169195] [PubMed: 15018128]
16. Austin JH, Müller NL, Friedman PJ, Hansell DM, Naidich DP, Remy-Jardin M, et al. Glossary of terms for CT of the lungs: Recommendations of the Nomenclature Committee of the Fleischner Society. *Radiology*. 1996;200:327–31. [PubMed: 8685321]
17. Collins J, Stern EJ. *Chest radiology: The essentials*. Philadelphia: Wolters Kluwer Health/Lippincott Williams & Wilkins; 2008. pp. 34–47.
18. Copley S, Hansell DM, Kanne JP. *Thoracic imaging*. CRC Press; 2014. pp. 158–9.
19. Muller NL, Silva CIS. Mediastinum. In: Muller NL, Silva CIS, editors. *Imaging of the chest*. Philadelphia, Pa: Elsevier Saunders; 2008. pp. 1447–572.
20. Lee N, Hui D, Wu A, Chan P, Cameron P, Joynt GM, et al. A major outbreak of severe acute respiratory syndrome in Hong Kong. *N Engl J Med*. 2003;348:1986–94. [PubMed: 12682352]
21. Chiang CH, Shih JF, Su WJ, Perng RP. Eight-month prospective study of 14 patients with hospital-acquired severe acute respiratory syndrome. *Mayo Clin Proc*. 2004;79:1372–79. [PMCID: PMC7094584] [PubMed: 15544014]
22. Ooi GC, Khong PL, Müller NL, Yiu WC, Zhou LJ, Ho JC, et al. Severe acute respiratory syndrome: Temporal lung changes at thin-section CT in 30 patients. *Radiology*. 2004;230:836–44. [PubMed: 14990845]
23. Razer RS, Muller NL, Colman N, Pare PD. *Fraser and Pare's diagnosis of diseases of the chest*. 4th ed. Philadelphia, PA: Saunders; 1999. Viruses, mycoplasmas, chlamydiae, and rickettsiae; pp. 979–1032.
24. Mineo G, Ciccarese F, Modolon C, Landini MP, Valentino M, Zompatori M. Post-ARDS lung fibrosis in patients with H1N1 pneumonia: Role of follow-up CT. *Radiol Med*. 2012;117:185–200. [PMCID: PMC7102178] [PubMed: 22020433]

25. Antonio GE, Wong KT, Hui DS, Wu A, Lee N, Yuen EH, et al. Thin-section CT in patients with severe acute respiratory syndrome following hospital discharge: Preliminary experience. *Radiology*. 2003;228:810–5. [PubMed: 12805557]
26. Naik PK, Moore BB. Viral infection and aging as cofactors for the development of lung fibrosis. *Expert Rev Respir Med*. 2010;4:759–71. [PMCID: PMC3028433] [PubMed: 21128751]
27. Moore BB, Moore TA. Viruses in Idiopathic Pulmonary Fibrosis. Etiology and Exacerbation. *Ann Am Thorac Soc*. 2015;12:S186–92. [PMCID: PMC4722834] [PubMed: 26595738]
28. Molyneaux PL, Cox MJ, Willis-Owen SA, Mallia A, Russell KE, Russell AM, et al. The role of bacteria in the pathogenesis and progression of idiopathic pulmonary fibrosis. *Am J Respir Crit Care Med*. 2014;190:906–13. [PMCID: PMC4299577] [PubMed: 25184687]

Figures and Tables

Table 1

Distribution of radiological findings noted in 13/36 patients with abnormal chest radiographs

Table 2

Distribution of different clinical parameters with and without lung fibrosis in 36 Patients of MERS-CoV

Table 3

Association of type radiographic deterioration and fibrosis in 36 patients of MERS-CoV

Figure 1 (A-C)

A 58-year-old male with Middle East respiratory syndrome coronavirus (MERS-CoV), serial radiographs showing irregular reticular lines of fibrosis (A) Frontal chest radiograph obtained on two days before illness shows a normal chest radiograph. (B) A follow-up frontal chest radiograph obtained at day 5, shows ground-glass opacities in the right lower zone and left mid and lower zones. (C) A follow-up frontal chest radiograph obtained at day 33 shows unilateral multiple irregular reticular lines of fibrosis in the right lower and left mid zones

Figure 2 (A-C)

A 33-year-old female with Middle East respiratory syndrome coronavirus (MERS-CoV), serial radiographs showing multiple irregular reticular lines of fibrosis on follow-up chest radiographs. The rest of the lung is completely free of any irregular reticular lines of fibrosis (A) Frontal chest radiograph obtained on the initial presentation shows the area of ground-glass opacity at the right cardio-phrenic angle. (B) A follow-up frontal chest radiograph obtained at day 20, shows bilateral diffuse ground-glass opacities with occasional airspace consolidations. (C) A follow-up frontal chest radiograph obtained at day 230, shows bilateral multiple irregular reticular lines of fibrosis (arrows)

Figure 3 (A-C)

A 73-year-old female with Middle East respiratory syndrome coronavirus (MERS-CoV), serial radiographs showing multiple thick reticular lines of fibrosis and sub-pleural reticular opacities on follow-up chest radiographs. (A) A frontal chest radiograph obtained on day 3, of the initial presentation, shows bilateral ill-defined ground-glass opacities with air space disease at both lung bases. (B) A follow-up frontal chest radiograph obtained at day 19, shows bilateral sub-pleural ground-glass opacities with occasional air space consolidations. (C) A follow-up frontal chest radiograph obtained at day 130, shows unilateral thick multiple linear fibrotic parenchymal bands (arrows) in the right side along with sub-pleural reticulations, pleural thickening, and bilateral ground-glass opacities

Figure 4 (A and B)

A 24-year-old female with Middle East respiratory syndrome coronavirus (MERS-CoV), serial radiographs showing ground-glass opacities on follow-up chest radiographs. (A) A frontal chest radiograph obtained on the second day of the presentation shows the area of air space consolidation involving the lingual and left lower lobe. (B) Follow-up frontal chest radiograph obtained at 210 days shows only a small area of ground-glass opacity obscuring the left cardiac border

Figure 5

A 52-year-old female with Middle East respiratory syndrome coronavirus (MERS-CoV). A frontal chest radiograph obtained at day 168, shows bilateral multiple irregular reticular lines of fibrosis along with obscured lateral aspect of the right hemidiaphragm and costo-phrenic angle in the same side due to pleural thickening

Articles from The Indian Journal of Radiology & Imaging are provided here courtesy of **Wolters Kluwer -- Medknow Publications**



Published in final edited form as:

Virology. 2016 June ; 493: 238–246. doi:10.1016/j.virol.2016.03.025.

1918 Influenza Receptor Binding Domain Variants Bind and Replicate in Primary Human Airway Cells Regardless of Receptor Specificity

A. Sally Davis^{a,b,1}, Daniel S. Chertow^{a,c,1}, Jason Kindrachuk^{a,c}, Li Qi^a, Louis M. Schwartzman^a, Jon Suzich^{a,c}, Sara Alsaaty^c, Carolea Logun^c, James H. Shelhamer^c, and Jeffery K. Taubenberger^{a,*}

^aViral Pathogenesis and Evolution Section, National Institute of Allergy and Infectious Diseases (NIAID), National Institutes of Health (NIH), Bethesda, MD

^bDiagnostic Medicine and Pathobiology, Kansas State University College of Veterinary Medicine, Manhattan, KS

^cCritical Care Medicine Department, Clinical Center, NIH, Bethesda, MD

Abstract

The 1918 influenza pandemic caused ~50 million deaths. Many questions remain regarding the origin, pathogenicity, and mechanisms of human adaptation of this virus. Avian-adapted influenza A viruses preferentially bind α 2,3-linked sialic acids (Sia) while human-adapted viruses preferentially bind α 2,6-linked Sia. A change in Sia preference from α 2,3 to α 2,6 is thought to be a requirement for human adaptation of avian influenza viruses. Autopsy data from 1918 cases, however, suggest that factors other than Sia preference played a role in viral binding and entry to human airway cells. Here, we evaluated binding and entry of five 1918 influenza receptor binding domain variants in a primary human airway cell model along with control avian and human influenza viruses. We observed that all five variants bound and entered cells efficiently and that Sia preference did not predict entry of influenza A virus to primary human airway cells evaluated in this model.

Keywords

Influenza A virus; Pandemic; Receptor binding; hemagglutinin

*Corresponding author. Jeffery K. Taubenberger, M.D., Ph.D., NIAID, 33 North Dr., MSC 3203, Bethesda, MD 20892; Phone: (301) 443-5960; Fax: (301) 480-1696; taubenbergerj@niaid.nih.gov.

¹These authors contributed equally to this manuscript.

Publisher's Disclaimer: This is a PDF file of an unedited manuscript that has been accepted for publication. As a service to our customers we are providing this early version of the manuscript. The manuscript will undergo copyediting, typesetting, and review of the resulting proof before it is published in its final citable form. Please note that during the production process errors may be discovered which could affect the content, and all legal disclaimers that apply to the journal pertain.

INTRODUCTION

Influenza A viruses cause acute respiratory viral disease in humans in both annual epidemics and in infrequent pandemics (1). The 1918 “Spanish” influenza pandemic resulted in approximately 50 million deaths globally and is the most severe influenza pandemic on record (2, 3). Many questions remain regarding the origin, pathogenicity, and mechanisms of human host adaptation of this deadly virus (4). Influenza A viruses bind to terminal sialic acids (Sia) on target cell glycans and it is hypothesized that changes in the influenza A virus hemagglutinin (HA) protein receptor-binding domain (RBD) are important in the process of host adaptation, specifically allowing avian-origin influenza A viruses to adapt to humans.

The 1918 HA gene has been sequenced from multiple postmortem human lung samples, and several naturally occurring 1918 HA RBD sequence variants have been reported (5–7). These include A/South Carolina/1/1918 (SC), which has an aspartic acid at both positions 187 and 222 in HA1 (H1 subtype numbering) (5) conferring an $\alpha 2,6$ Sia receptor-binding specificity and A/NY/1/1918 (NY), which differs from SC by a single amino acid, encoding a glycine at position 222 that confers a mixed $\alpha 2,3/\alpha 2,6$ binding specificity (8–10). Sheng et al., 2011 reported two 1918 HA sequences with new RBD variants with yet to be confirmed binding specificities (Table 1). The HA RBD of A/Virginia/1/1918 (VA), which, in addition to aspartic acids at positions 187 and 222 has a change from glutamine to arginine at position 189 in the HA1 domain, may have an enhanced $\alpha 2,6$ binding specificity based on computational modeling (7, 9). No binding specificity data is available for the A/New York/3/1918 (NY3), although deep sequencing revealed a predominance of asparagine rather than glycine at position 222 (11). Finally, the ‘avianized’ laboratory-produced variant of the 1918 virus HA (AV), in which the aspartic acid at position 187 in NY was mutagenized back to the avian influenza virus consensus glycine, is reported to be exclusively $\alpha 2,3$ Sia binding (8–10).

It is not yet fully clear how influenza A virus Sia preferences, as predicted by *in vitro* glycan array analysis with limited numbers of synthetic oligosaccharides, relate to binding and entry of influenza viruses into the human respiratory tract, including the epithelium of the distal trachea and bronchi. Review of 1918 autopsy material, including correlative analyses of histopathology, distribution of influenza viral antigen by immunohistochemistry, and 1918 HA RBD variant gene sequencing, demonstrated no difference in cell tropism between the four naturally occurring 1918 RBD variants outlined above (7). Autopsy sections demonstrated that the 1918 virus, regardless of HA RBD sequence, infected the entirety of the respiratory tract, including ciliated cells and goblet cells of the tracheobronchial tree and of the bronchiolar epithelium, and alveolar lining type I and type II cells. Based on lectin histochemistry, however, the upper airway and distal trachea in humans is reported to display predominantly $\alpha 2,6$ Sia on apical epithelial cell surfaces (12–14). Mouse models of 1918 influenza viral infection also suggested that factors other than Sia preference play a role in influenza binding and entry to airway cells (15). Histopathological changes, cell tropism, and viral antigen distribution in lungs of mice infected with the 1918 RBD variants SC, NY, and AV were similar across viral variants and correlated with human autopsy findings.

Normal human bronchial epithelial (NHBE) cells, are primary human airway cells, and are variably reported to display exclusively $\alpha 2,6$ Sia or a mixture of $\alpha 2,3/\alpha 2,6$ Sia on their cell surfaces (14, 16–20). This laboratory has previously characterized the Sia distribution on a single lot of NHBE cells harvested from a healthy female donor and showed that this lot displays near exclusively $\alpha 2,6$ Sia on goblet and ciliated cell surfaces and rarely displays $\alpha 2,3$ Sia on goblet cell surfaces (14). Additionally it was shown that this lot of cells readily supports both human- and avian-adapted influenza virus growth to peak titers of 10^4 -to- 10^6 viral plaque forming units (pfu)/mL (14, 21). , Experiments described here were conducted to evaluate the binding, entry, and peak replication of 1918 HA RBD variants, utilizing this lot of well-characterized NHBE cells, and to compare their binding and entry to human-adapted and avian H1 subtype influenza virus controls. Prevailing hypotheses suggest that variants with $\alpha 2,6$ Sia preferences would bind and enter human airway epithelial cells more efficiently than those the $\alpha 2,3$ Sia or mixed $\alpha 2,3/\alpha 2,6$ Sia preferences. Here NHBE cells were infected at a constant multiplicity of infection (MOI). In multiple experiments binding and entry was examined by immunofluorescence at 5- and 20-minutes post-addition of virus and quantification of cell-associated virus was performed by quantitative reverse transcriptase polymerase chain reaction (qRT-PCR). Viral replication was assessed at 12, 24, and 36-hours post-infection in a subset of viruses representing the a range of Sia binding preference (AV $\alpha 2,3$; NY mixed $\alpha 2,3$ and 2,6; and SC $\alpha 2,6$).

MATERIALS AND METHODS

Growth and differentiation of cells

Primary Normal Human Bronchial/Tracheal Epithelial (NHBE) cells (CC-2541, Lonza; Walkersville, MD) from a single donor were grown as per manufacturer's instructions as described in detail previously (14). Briefly, NHBE cells were grown submerged in vendor-supplied medium on transwell-clear membrane supports coated with rat-tail collagen until fully confluent, at which point the apical medium was removed, creating an air-liquid interface and the media type was changed. Cells were then grown until they formed a mature pseudostratified epithelium, ~28 days total time.

Construction and rescue of chimeric viruses

Five variants of 1918 influenza A HA RBD virus were generated including four previously reported and a fully avianized version (5, 7, 8). Table 1 shows the amino acid sequences of each HA RBD variant's critical amino acid mutations, its hemagglutinin Sia binding preference (if known), and the abbreviated name as used in this study. In summary, all viruses but AV encode an aspartic acid (D) at position 187 [H1 numbering used throughout]; AV was engineered to encode the avian H1 influenza virus consensus glutamic acid (E) at this position. At position 222, SC and VA have D, NY and AV have glycine (G), and the HA of NY3 encodes an asparagine (N) (7). VA encodes a D at positions 187 and 222 as does SC but additionally encodes an arginine (R) at position 189 instead of the consensus glutamine (Q).

The fully reconstructed 1918 H1N1 influenza viruses were isogenic except for the above HA RBD polymorphisms, and were prepared by reverse genetics as previously described (15).

RBD mutations in the 1918 HA gene for each of the other viruses were generated with a site-directed mutagenesis kit following the manufacturer's instructions (Stratagene; La Jolla, CA). All rescued viruses were propagated in Madin-Darby canine kidney (MDCK) cells (ATCC; Manassas, VA). The genomic sequence of each rescued virus was then confirmed by sequence analysis of the inoculum prior to performing the experiments. All viruses and infectious samples were handled under BSL3+ conditions in accordance with the Select Agent guidelines of the National Institutes of Health (NIH) and the Centers for Disease Control and Prevention under the supervision of the NIH Select Agent and Biosurety Programs and the NIH Department of Health and Safety.

Hemagglutination Assay

Viral stocks were titrated by plaque assay as previously described (15) and NHBE infections were normalized by multiplicity of infection (MOI). Given a primary experimental focus on viral binding and entry, viral stocks were also quantitated by hemagglutinin units using a standard hemagglutination assay for influenza A virus with turkey red blood cells (22).

Viral infections

Uninfected histologic control inserts were immersed in 10% neutral buffered formalin (NBF) prior to transporting the rest of the cells into the select agent suite where infections were conducted. In order to examine variation in binding and entry patterns of the five 1918 viruses, infections were initially conducted as a single experiment with MOIs of 1.0 and 3.0 in triplicate for all five viruses (three inserts per MOI/virus combination). Following aspiration of mucus from each well, adherent mucus was solubilized by incubation in 200 μ L of PBS for 1 hr, removed by aspiration, and then infected with 100 μ L virus at the appropriate MOI (diluted in sterile PBS). Cells were incubated with virus for 20 min at 37 °C in an atmosphere of 5% CO₂, followed by aspiration of the virus supernatant from the apical aspect of the upper chamber. Cells were then washed once with sterile PBS, and inserts were placed in NBF. After 48 hr, fixed noninfectious inserts were removed from the Select Agent suite. Subsequent experiments were conducted as above but with variations to the MOI and incubation times. These experimental conditions included infections with MOIs of 0.1 and 0.01 for a 20 min incubation period, and infections with MOIs of 1.0, 0.1, and 0.01 for a 5 min period.

Quantitative reverse transcriptase PCR on cell lysates

We determined viral load (intracytoplasmic and plasma membrane bound) by qRT-PCR for the influenza A virus matrix protein 1 (M1) gene using RNA isolated from cell lysates from parallel experiments with all 5 1918 RBD variants at MOI of 0.1 and 0.01 for both 5- and 20- minute incubation time periods, conducted in triplicate. Further, we compared 1918 RBD variants AV, NY, and SC to a set of control influenza viruses, including human seasonal influenza A/New York/312/2001 (H1N1) [NY312] (14), 2009 H1N1 pandemic influenza A/Mexico/4108/09 (H1N1) [Mex09] (23), and low-pathogenic avian influenza A/mallard/Ohio/265/1987 (H1N9) (24) [LPAI]. These infections were performed at an MOI of 0.01 at 5 and 20 minutes incubations in sextuplicate. Briefly, total RNA was isolated from individual infected NHBE samples and their viral loads estimated as previously described (23). Results were graphed as a threshold cycle threshold (C_T) ratio of the human

housekeeping gene glyceraldehyde-3-phosphate-dehydrogenase (GAPDH) over influenza A viral gene Matrix. Two-way ANOVAs with Tukey's Multiple Comparison Tests were used for statistical analysis of both cell lysate real-time PCR data and replication kinetics and with alpha set to 0.05. Graphs and analyses were performed in Prism 6.0c (GraphPad; La Jolla, CA) and graphs further annotated in Adobe Illustrator CC 2014 (Adobe; San Jose, CA).

Viral replication kinetics

Replication kinetics including the 12, 24, and 36-hour time-points were determined for the AV, SC, and NY 1918 viruses. These viruses were selected to represent the range of known Sia binding preferences (AV α 2,3; NY mixed α 2,3 and 2,6; and SC α 2,6). Timepoints were selected to cover peak viral infection as seen in prior experiments with human and avian influenza A viruses in this lot of NHBE cells (14, 21). These experiments had also indicated that live-virus could not be detected in cell supernatants prior to 8 hours post-infection and that cell viability drops off between 24 and 48 hours post-viral infection (14, 21). Cells were infected with 100 μ L of virus at an MOI of 0.1 and wells were cultured at 37°C in an atmosphere of 5% CO₂ until each time-point was reached. This experiment was conducted in triplicate for each time-point/virus combination. Apical media was collected at the appropriate time for each infected insert by addition of 400 μ L PBS (200 μ L X 2) to each biological replicate and then collecting all fluid at the apical aspect. The remaining insert was placed into NBF. All supernatants were stored individually in cryovials at -80 °C for subsequent evaluation of viral titers by standard influenza A virus plaque assays (15).

Immunofluorescence (IF)

Fixed, differentiated infected and uninfected cells on their transwell membranes were individually embedded on edge in paraffin. Approximately 5 μ m thick cross sections of differentiated cells were cut and placed on positively charged slides, two sections per slide (NC State University College of Veterinary Medicine Histopathology Lab; Raleigh, NC). Each slide included two serial sections from a given well. In order to determine which epithelial cell types facilitated binding and entry of the influenza A viruses, sections for each MOI/virus combination were labeled using immunofluorescence for influenza A antigen as well as NHBE ciliated, goblet, and basal epithelial cell types as previously described (14) with the following changes. The donkey serum block was reduced to 5% strength as the lot of the anti-influenza antibody lacked the background issues documented in Davis et al., 2015 (14). Goblet cells were detected with 2 μ g/mL biotinylated Jacalin (B-1155, Vector Labs; Burlingame, CA) and visualized with 10 μ g/ml of Streptavidin Alexa Fluor-488 conjugate (S-11223, Molecular Probes; Eugene, OR), instead of fluorochrome conjugated Jacalin. Ciliated and basal cells were detected as before but visualized with Dylight-549 AffiniPure Donkey Anti-Mouse (discontinued, Jackson ImmunoResearch (JI); West Grove, PA) and Dylight-649 AffiniPure Donkey Anti-Rabbit (discontinued, JI) respectively. Sia distribution by lectin histochemistry was not repeated in this experiment given prior detailed characterization of this in the same NHBE donor and cell lot (14).

Immunofluorescence for endocytic pathway markers was used to determine the cellular compartment in which the influenza antigen signal was located. Slides were prepared for

antibody application as described previously (14). Dual labels were prepared with influenza A virus antibody, and an early endosome marker, rabbit polyclonal Anti-Rab5 antibody (ab13253, Abcam; Cambridge, MA), or the lysosome marker mouse monoclonal antibody Anti-LAMP1 [H4A3] (ab25630, Abcam). Additionally, a triple label was prepared with both endosome markers and influenza A virus antibody. Rab5 was applied at a 1:50 dilution and Lamp1 at 2 ug/mL, with both dilutions made in TBS. Appropriate secondary antibody pairings were selected for each of the markers in accordance with the previously described immunofluorescence work (14). All slides were mounted in Prolong Gold (P36930, Life Technologies; Grand Island, NY) as per vendor instructions. Slides were visualized and images captured on a Leica TCS SP5 X White Light Laser confocal system (Leica Microsystems; Buffalo Grove, IL) configured with Argon laser, 405 nm diode and photomultiplier tube detectors.

Image capture and analysis

Individual confocal sessions focused on an entire batch, defined as a single MOI/incubation time. In this manner, intra-batch image capture conditions were as constant as possible. Also, settings were reused between sessions, re-checking the thresholding of the influenza antigen signal against batch-specific uninfected control slides at each session start. Slides from the first experiment, MOI 3.0 and 1.0 with 20 min incubation, were reviewed manually with representative images taken for each virus/MOI combination.

For the second experiment, each well for each virus/MOI combination was reviewed manually for all virus/MOI combinations, visually scanning both strips of cells on the slide. Minimally, three representative 63x oil objective at zoom 1, 1024 x 1024 pixels full-thickness z-stacks were taken. Additionally, a 63x oil objective at zoom 2.5, 1024 x 1024 pixels representative full-thickness z-stack was captured for each virus/MOI combination was taken. As there was little difference between MOI 0.1 and 0.01, subsequent analyses focused on infections at an MOI of 0.01 at the 5 minute time point.

Image post-processing and analysis were done with the Leica Application Suite (Leica Microsystems) and Imaris 7.6.3 (Bitplane; Zurich, Switzerland). Maximum projected fluorescent images for influenza antigen with and without cell type markers were created. Within an experimental batch, intensity levels were adjusted consistently across all samples. Additionally, the differential interference contrast (DIC) slice, wherein ciliated and goblet cells were near equivalently in focus for the largest number of cells, was selected from each z-stack and merged with a max projected image of multi-label fluorescence. These images were reviewed for presence of influenza A virus antigen by cell type. Final figure compilation was done in Adobe Photoshop CS6 Extended (Adobe).

RESULTS

1918 RBD variants bound and entered NHBE cells efficiently

Infections at all MOI and incubation time combinations resulted in binding and entry of influenza virus in all samples. Immunofluorescence (IF) analysis of virus infections at MOI 3.0 or 1.0 incubated for 20 minutes demonstrated intracytoplasmic influenza antigen from

nearly every apical epithelial cell (data not shown). To look for more subtle differences between the 1918 virus RBD variants (Table 1), experiments with lower MOI and shorter incubation periods were performed. Variance in the virus entry patterns at MOI 0.1, especially for the 5 min incubation time, was noted. The results from the MOI 0.01, 5 min incubation time combination reinforced these findings. Therefore the main focus of the subsequent detailed analyses were infections at MOI 0.01 for 5 min along with cross checks with the 20 min incubations from the same MOI and the MOI 0.1 triplicates. Representative images for each 1918 virus at MOI 0.01 at the 5 min timepoint are shown in Figure 1.

1918 Influenza viral antigen was intracytoplasmic as well as bound to the apical epithelial surface of both goblet and ciliated cells. The relative intensity of influenza antigen labeling across the entire epithelium of the NHBE cells was highest for AV (Figure 1A), lowest for SC (Figure 1B), and intermediary for the other three viruses (Figure 1C–E; no virus control shown in Figure 1F). For each of the 1918 variants examined, intracytoplasmic influenza viral antigen signal was more prominent in goblet cells than in ciliated cells. Overall, patterns of 1918 viral antigen in NHBE cells at MOI 0.01 after incubation for 5 minutes were very similar for the naturally occurring 1918 RBD variants (Figure 1B–E), with more prominent labeling with the AV variant (Figure 1A). When the intracytoplasmic location of the influenza antigen was explored using endosomal markers (Fig. 2), there was occasional co-localization with early, Rab5 (Fig. 2D, yellow color), and more co-localization with late, Lamp1 (Fig. 2D, white), endosomal markers as well as a noticeable portion of intracytoplasmic influenza antigen signal that failed to co-localize with either marker (Fig. 2D, green color), suggesting that the majority of intracytoplasmic influenza virus was not present in endosomes at 20 minutes.

Evaluation of hemagglutination by three 1918 RBD variant viruses

We selected the 1918 viral variants AV, NY, and SC, representing the diversity of Sia preferences and conducted hemagglutination assays in order to determine if HA binding capacity varied across viral stocks. AV viral stock titer by plaque assay and HA units were approximately 4 times lower than those of NY and SC. After adjusting for differences in viral stock titer, however, HA units were equivalent across the three viruses (Table 2).

Quantitative reverse transcriptase PCR for viral RNA in NHBE cells

1918 RBD variant viral RNA was detected in lysates from cells infected at MOIs of 0.1 and 0.01 following 5 and 20 min incubations. The relative amounts of viral RNA were not statistically different across all viruses when infections were performed at an MOI of 0.1 for either incubation time (data not shown). When performed at an MOI of 0.01 at 5 minutes, AV viral RNA was present in statistically significantly higher amounts than the other four viral variants at 5 minutes ($p < 0.05$) (Figure 3). At 20 min after MOI 0.01 infection, AV viral RNA was still present in statistically significantly higher amounts than NY ($p < 0.05$) and SC ($p < 0.05$), but not as compared to NY3 or VA (Figure 3).

To determine the significance of these observations an additional experiment was performed comparing 1918 AV, NY, and SC RBD variant binding and entry to a set of control influenza viruses, including human seasonal influenza A/New York/312/2001 (H1N1) [NY312] (14),

2009 H1N1 pandemic influenza A/Mexico/4108/09 (H1N1) [Mex09] (23), and low-pathogenic avian influenza A/mallard/Ohio/265/1987 (H1N9) (24) [LPAI] as described above. At 5 and 20 minutes after addition of virus, the relative amounts of cell-associated viral RNA were generally comparable between human seasonal, pandemic, and avian H1 subtype influenza viruses with the seasonal H1N1 strain NY312 showing the highest amount of cell-associated viral RNA at both time points ($p < 0.05$). Otherwise, viral RNA levels were comparable between the different 1918 RBD strains, Mex09, and LPAI H1 viruses (Figure 4).

Viral replication of selected 1918 viral variants

Viral replication was measured in NHBE cells at 12, 24, and 36 hours following infection with the 1918 SC, NY, and AV viruses (Fig. 5). There was no statistical difference between viral titers among these groups at 12 hours, but at 24 and 36 hours, the AV variant replicated to slightly higher titers as compared to NY and SC ($p < 0.05$), with AV replicating $\sim 1 \log_{10}$ pfu/mL higher than SC and NY.

DISCUSSION

In this study we evaluated whether 1918 influenza viral variants with polymorphisms in their HA RBD differed in binding and entry to primary human airway cells from a single donor source. During preliminary studies performed at high MOIs (3.0 and 1.0), it was observed that the majority of luminal NHBE cells were positive for intracytoplasmic influenza antigen by IF labeling. Consequently we decreased MOIs to 0.1 and 0.01 in an effort to detect subtle differences in viral binding and entry under more discerning conditions. Following a 20-minute incubation at these lower MOIs, no difference in viral binding and entry could be detected by IF. At an MOI of 0.01 and 5-minute incubation, the “avianized” 1918 virus AV, with an $\alpha 2,3$ Sia receptor-binding specificity, was found to bind and enter NHBE cells more efficiently than the other four variants as assessed by IF (Figure 1).

The extent of antigen signal by IF was greater than predicted for MOIs of 0.1 (i.e., 1 viral particle per 10 cells) and 0.01 (i.e., 1 viral particle per 100 cells) for all viruses. Replication competent virus is believed to compose only a small fraction of viral stocks, which are otherwise largely composed of replication incompetent viral-like particles (25). Given this we sought to confirm that the proportion of HA binding particles did not vary significantly across viral stocks. We performed HA assays on AV, SC and NY, representing the range of binding configurations, and after adjusting for baseline viral stock titers, we confirmed that these infections were performed with equivalent HA units (Table 2). Additionally, we sequence-confirmed all rescued viral variants to rule out the possibility that observed differences in viral binding and entry might be attributable to human error during viral rescue or viral mutations during cell passage.

The observation that AV infections at MOI 0.01 following a 5-minute incubation resulted in slightly enhanced binding and entry to NHBE cells as compared with the four other 1918 RBD variants was further assessed by qRT-PCR for cell-associated viral RNA. In independent parallel experiments performed at MOI 0.01, we observed that cell-associated AV viral RNA was detected in slightly greater proportions than the 4 other RBD variants

following both a 5- and a 20-minute incubation (Figure 3). To further validate these results an additional experiment was performed comparing a seasonal H1N1 virus [NY312], a 2009 pandemic H1N1 virus [Mex09], and a low-pathogenic avian influenza H1N9 virus [LPAI] to three 1918 RBD variants - AV, NY, and SC (Figure 4). As shown, all viruses tested bound and entered NHBE cells, including an avian H1 virus with an $\alpha 2,3$ Sia preference. These data support the primary observation that avian viruses with an $\alpha 2,3$ Sia preference bound and entered NHBE cells in our system efficiently.

All five 1918 RBD variants were detected on the apical surface and within the cytoplasm of both ciliated and goblet cells with no discernable qualitative or quantitative difference in cell-type tropism between viruses. The potential for subtle quantitative differences in cell-type tropism between variants exists and could be evaluated in future work. While we did not repeat lectin histochemical analysis of cell surface Sia distribution in this study, prior detailed studies of the same NHBE cell donor and lot grown in the same conditions indicate that $\alpha 2,6$ Sia are predominantly displayed on ciliated and goblet cell surfaces and rarely $\alpha 2,3$ Sia are displayed on goblet cell surfaces (14). Similarly, we did not repeat glycan-binding arrays on the 1918 RBD variants AV, NY, and SC given that these have been previously well characterized and that we sequence-confirmed the 1918 RBD variants used in these experiments. Consequently in the present study cell surface Sia distribution did not predict binding and entry or cell-type preference of the five 1918 RBD variants in the primary human airway epithelial cells examined here.

Previously published data support that influenza viruses with $\alpha 2,3$ Sia preferences successfully infect NHBE cells. Oshansky et al., 2011 showed that low pathogenic avian influenza viruses with $\alpha 2,3$ binding preference infected differentiated NHBE cells displaying only $\alpha 2,6$ Sia receptors (26). Similar findings have been observed in *ex vivo* human respiratory tissue using an H5N1 avian virus (26–28). Our data fit with these prior observations. Sia-independent pathways for influenza viral entry into airway cells likely exist (29, 30). For example, when NHBE cells are treated with neuraminidase to remove the Sia, it has been observed that both avian and human influenza viruses readily infect them (26, 28). Mice lacking the enzyme ST6Gal I sialyltransferase, and thus unable to attach $\alpha 2,6$ Sia to cell surface N-linked glycoproteins, had similar viral titers in lung tissue as wild-type mice following influenza infection (31).

In an effort to discern intracellular location of influenza virus in our study, immunohistochemistry multi-labeling analysis for both viral antigen with early (Rab5) and late (Lamp1) endosomal markers was employed. Influenza viral antigen co-localized with early and late endosomal markers but was predominantly observed independent of endosomes within the cytoplasm (Fig 2). Influenza viruses are thought capable of entering cells through a variety of mechanisms including macropinocytosis, calveolar entry, clathrin-mediated endocytosis, as well as a non-calveolar, non-clathrin dependent pathways (32, 33). In this study, while co-localization of virus with early and late endosomal markers supports viral entry via endocytosis, the preponderance of virus independent of endosomes also suggests a non-endocytic entry (Figure 2). Future studies in primary human airway cell lines may further characterize mechanisms of influenza A viral binding and entry.

Finally at 24 and 36 hours post-infection, 1918 AV with $\alpha 2,3$ Sia-preference, replicated to higher titers than NY with mixed $\alpha 2,3/\alpha 2,6$ preference and SC with $\alpha 2,6$ preference. It was previously shown that seasonal and pandemic H1N1 influenza viruses replicated to peak viral titers of $\sim 10^4$ pfu/mL following MOI 0.1 infection in this NHBE cell lot (14) and multiple avian influenza viruses following MOI 1.0 infection replicate to peak titers between 10^4 and 10^5 pfu/mL at similar time-points post-infection (21). Similar to these prior observations, in this study two naturally occurring human 1918 influenza A RBD variants NY and SC replicated to peak titers of 10^4 pfu/mL while the avianized variant AV replicated to peak titers of $\sim 10^5$ pfu/mL.

Understanding viral and host factors contributing to influenza virus infection of human airway cells is necessary to elucidate the process of host-switch events and thus pandemic viral emergence. While cell surface Sia specificity may be important, it is conceivable that influenza viruses with $\alpha 2,6$ Sia receptor-binding specificity are better adapted to humans not due to an advantage in viral binding and entry at the cell surface but due to an advantage in evading decoy receptors present in mucus lining the human airway. Mucus is known to be rich in O-linked $\alpha 2,3$ sialic acids that efficiently bind influenza viruses with an $\alpha 2,3$ Sia binding preference (34). In our NHBE model, mucus was systematically solubilized and removed from the NHBE cell surfaces prior to infection so as not to interfere with viral infection. This process may have eliminated any selective advantage of influenza variants with $\alpha 2,6$ Sia receptor-binding specificity exposing subtle binding and entry advantages of the AV virus.

It is worth noting that *in vitro* glycan array hybridization has been relied upon to predict *in vivo* influenza virus Sia preference. However, *in vitro* glycan arrays likely do not reproduce the spectrum of Sia receptors present on human airway epithelia. A spectrum of Sia receptors on the human airway was recently characterized by mass spectrometry, confirming a wide variety of both N- and O-linked glycans, both $\alpha 2,3$ and $\alpha 2,6$, that correlated poorly with those found on the glycan arrays currently employed to determine viral binding preferences (35). Consequently Sia preference as predicted by glycan array hybridization may not accurately predict Sia preference *in vivo*. Additionally, the variability of airway Sia receptors with co-factors such as age, co-morbid medical conditions, etc. remains unknown. Host factors that result in differential expression of Sia receptors on cell surfaces may in part account for observed variability in host susceptibility to respiratory viral infections. Finally, plant lectins, which have been used to characterize the distribution of $\alpha 2,3$ Sia versus $\alpha 2,6$ Sia receptors on cell surfaces, have variable sensitivity and specificity. It is possible that in our model AV preferentially bound $\alpha 2,3$ Sia receptors distributed on NHBE cell surfaces not detected by standard lectins previously employed (14).

The primary limitation of this work is that all experiments were performed using a single NHBE cell donor and lot and a limited subset of viruses. Generalizability of our observations to other primary human airway cell lines and viruses would need to be evaluated in future work. Additionally *in vitro* models, even with primary human airway cell lines, cannot replicate the full spectrum of pathogen-host interactions that influence viral binding and entry *in vivo*. The strength of utilizing a single lot of NHBE cells in this study, however, relates to our prior detailed characterization of $\alpha 2,3$ versus $\alpha 2,6$ Sia distribution

over multiple experiments from this donor and cell lot (14). Despite a clear predominance of $\alpha 2,6$ Sia on cell surfaces we have shown that 1918 influenza viral variants with $\alpha 2,3$ and mixed $\alpha 2,3/\alpha 2,6$ Sia preferences readily bind, enter, and replicate within primary human airway cells. These findings suggest that predicted Sia preferences alone do not dictate influenza A viral binding and entry to human airway cells.

In summary, five 1918 RBD influenza viral variants efficiently bound and infected primary human airway cells comparably to control human and avian influenza A viruses. The experimental findings in this study correlated with the post-mortem observations of lung specimens from fatal 1918 influenza infections, which show no differences in viral distribution along the airway for the four naturally occurring 1918 RBD viral variants studied here (7). Taken together, these observations support that viral and host factors unrelated to Sia binding preference likely contribute to influenza binding and entry into human tracheobronchial airway epithelial cells, or perhaps Sia preferences restrict $\alpha 2,3$ Sia binding and entry in the nasopharyngeal epithelium. Further probing of these factors is needed to unravel the complexities of host switch events, the essential first step in the initiation of a pandemic.

Acknowledgments

The authors would like to acknowledge the staff at the NIAID RTB Bioimaging Section for their assistance with confocal microscopy and image post-processing. We thank Sandra Horton and her staff at the North Carolina State University College of Veterinary Medicine Histopathology Laboratory for their preparation of tissue and embedded NHBE cell sections for immunofluorescence and histological analysis. This work was supported by the Intramural Research Program of the National Institute of Allergy and Infectious Diseases, National Institute of Health. ASD and JKT are further thankful for the support of the NIH Comparative Molecular Pathology Research Training Program. This work was done in partial fulfillment of A. Sally Davis' dissertation work towards a Ph.D. in Comparative Biomedical Sciences at the North Carolina State University College of Veterinary Medicine.

References

1. Wright PFNG, Kawaoka Y. Orthomyxoviruses. *Fields virology* (5). 2007; 2:1691–1740.
2. Johnson NP, Mueller J. Updating the accounts: global mortality of the 1918–1920 "Spanish" influenza pandemic. *Bull Hist Med*. 2002; 76:105–115. [PubMed: 11875246]
3. Taubenberger JK, Morens DM. 1918 Influenza: the mother of all pandemics. *Emerg Infect Dis*. 2006; 12:15–22. [PubMed: 16494711]
4. Taubenberger JK, Kash JC. Insights on influenza pathogenesis from the grave. *Virus Res*. 2011; 162:2–7. [PubMed: 21925551]
5. Reid AH, Fanning TG, Hultin JV, Taubenberger JK. Origin and evolution of the 1918 "Spanish" influenza virus hemagglutinin gene. *Proc Natl Acad Sci U S A*. 1999; 96:1651–1656. [PubMed: 9990079]
6. Reid AH, Janczewski TA, Lourens RM, Elliot AJ, Daniels RS, Berry CL, Oxford JS, Taubenberger JK. 1918 influenza pandemic caused by highly conserved viruses with two receptor-binding variants. *Emerg Infect Dis*. 2003; 9:1249–1253. [PubMed: 14609459]
7. Sheng ZM, Chertow DS, Ambroggio X, McCall S, Przygodzki RM, Cunningham RE, Maximova OA, Kash JC, Morens DM, Taubenberger JK. Autopsy series of 68 cases dying before and during the 1918 influenza pandemic peak. *Proc Natl Acad Sci U S A*. 2011; 108:16416–16421. [PubMed: 21930918]
8. Glaser L, Stevens J, Zamarin D, Wilson IA, Garcia-Sastre A, Tumpey TM, Basler CF, Taubenberger JK, Palese P. A single amino acid substitution in 1918 influenza virus hemagglutinin changes receptor binding specificity. *J Virol*. 2005; 79:11533–11536. [PubMed: 16103207]

9. Stevens J, Blixt O, Glaser L, Taubenberger JK, Palese P, Paulson JC, Wilson IA. Glycan microarray analysis of the hemagglutinins from modern and pandemic influenza viruses reveals different receptor specificities. *J Mol Biol.* 2006; 355:1143–1155. [PubMed: 16343533]
10. Stevens J, Corper AL, Basler CF, Taubenberger JK, Palese P, Wilson IA. Structure of the uncleaved human H1 hemagglutinin from the extinct 1918 influenza virus. *Science.* 2004; 303:1866–1870. [PubMed: 14764887]
11. Xiao YL, Kash JC, Beres SB, Sheng ZM, Musser JM, Taubenberger JK. High-throughput RNA sequencing of a formalin-fixed, paraffin-embedded autopsy lung tissue sample from the 1918 influenza pandemic. *J Pathol.* 2013; 229:535–545. [PubMed: 23180419]
12. Shinya K, Ebina M, Yamada S, Ono M, Kasai N, Kawaoka Y. Influenza virus receptors in the human airway. *Nature.* 2006; 440:435–436. [PubMed: 16554799]
13. Nicholls JM, Chan RWY, Russell RJ, Air GM, Peiris JSM. Evolving complexities of influenza virus and its receptors. *Trends in Microbiology.* 2008; 16:149–157. [PubMed: 18375125]
14. Davis AS, Chertow DS, Moyer JE, Suzich J, Sandouk A, Dorward DW, Logun C, Shelhamer JH, Taubenberger JK. Validation of Normal Human Bronchial Epithelial Cells as a Model for Influenza A Infections in Human Distal Trachea. *J Histochem Cytochem.* 2015; doi: 10.1369/0022155415570968
15. Qi L, Kash JC, Dugan VG, Wang R, Jin G, Cunningham RE, Taubenberger JK. Role of sialic acid binding specificity of the 1918 influenza virus hemagglutinin protein in virulence and pathogenesis for mice. *J Virol.* 2009; 83:3754–3761. [PubMed: 19211766]
16. Matrosovich MN, Matrosovich TY, Gray T, Roberts NA, Klenk HD. Human and avian influenza viruses target different cell types in cultures of human airway epithelium. *Proc Natl Acad Sci U S A.* 2004; 101:4620–4624. [PubMed: 15070767]
17. Ibricevic A, Pekosz A, Walter MJ, Newby C, Battaile JT, Brown EG, Holtzman MJ, Brody SL. Influenza virus receptor specificity and cell tropism in mouse and human airway epithelial cells. *J Virol.* 2006; 80:7469–7480. [PubMed: 16840327]
18. Chan RW, Yuen KM, Yu WC, Ho CC, Nicholls JM, Peiris JS, Chan MC. Influenza H5N1 and H1N1 virus replication and innate immune responses in bronchial epithelial cells are influenced by the state of differentiation. *PLoS One.* 2010; 5:e8713. [PubMed: 20090947]
19. Chan RW, Chan MC, Nicholls JM, Malik Peiris JS. Use of *ex vivo* and *in vitro* cultures of the human respiratory tract to study the tropism and host responses of highly pathogenic avian influenza A (H5N1) and other influenza viruses. *Virus Res.* 2013; 178:133–145. [PubMed: 23684848]
20. Kogure T, Suzuki T, Takahashi T, Miyamoto D, Hidari KI, Guo CT, Ito T, Kawaoka Y, Suzuki Y. Human trachea primary epithelial cells express both sialyl(alpha2-3)Gal receptor for human parainfluenza virus type 1 and avian influenza viruses, and sialyl(alpha2-6)Gal receptor for human influenza viruses. *Glycoconj J.* 2006; 23:101–106. [PubMed: 16575527]
21. Qi L, Pujanauski LM, Davis AS, Schwartzman LM, Chertow DS, Baxter D, Scherler K, Hartshorn KL, Slemons RD, Walters KA, Kash JC, Taubenberger JK. Contemporary avian influenza A virus subtype H1, H6, H7, H10, and H15 hemagglutinin genes encode a mammalian virulence factor similar to the 1918 pandemic virus H1 hemagglutinin. *MBio.* 2014; 5:e02116. [PubMed: 25406382]
22. Hirst GK. The Quantitative Determination of Influenza Virus and Antibodies by means of Red Cell Agglutination. *J Exp Med.* 1942; 75:49–64. [PubMed: 19871167]
23. Kash JC, Walters KA, Davis AS, Sandouk A, Schwartzman LM, Jagger BW, Chertow DS, Li Q, Kuestner RE, Ozinsky A, Taubenberger JK. Lethal synergism of 2009 pandemic H1N1 influenza virus and *Streptococcus pneumoniae* coinfection is associated with loss of murine lung repair responses. *mBio.* 2011; 2:e00172–11. [PubMed: 21933918]
24. Qi L, Davis SA, Jagger BW, Schwartzman LM, Dunham EJ, Kash JC, Taubenberger JK. Analysis by Single-Gene Reassortment Demonstrates that the 1918 Influenza Virus Is Functionally Compatible with a Low-Pathogenicity Avian Influenza Virus in Mice. *J Virol.* 2012; 86:9211–9220. [PubMed: 22718825]
25. Marriott AC, Dimmock NJ. Defective interfering viruses and their potential as antiviral agents. *Rev Med Virol.* 2010; 20:51–62. [PubMed: 20041441]

26. Oshansky CM, Pickens JA, Bradley KC, Jones LP, Saavedra-Ebner GM, Barber JP, Crabtree JM, Steinhauer DA, Tompkins SM, Tripp RA. Avian influenza viruses infect primary human bronchial epithelial cells unconstrained by sialic acid alpha2,3 residues. *PLoS One*. 2011; 6:e21183. [PubMed: 21731666]
27. Nicholls JM, Chan MC, Chan WY, Wong HK, Cheung CY, Kwong DL, Wong MP, Chui WH, Poon LL, Tsao SW, Guan Y, Peiris JS. Tropism of avian influenza A (H5N1) in the upper and lower respiratory tract. *Nat Med*. 2007; 13:147–149. [PubMed: 17206149]
28. Thompson CI, Barclay WS, Zambon MC, Pickles RJ. Infection of human airway epithelium by human and avian strains of influenza A virus. *J Virol*. 2006; 80:8060–8068. [PubMed: 16873262]
29. de Vries E, de Vries RP, Wienholts MJ, Floris CE, Jacobs MS, van den Heuvel A, Rottier PJ, de Haan CA. Influenza A virus entry into cells lacking sialylated N-glycans. *Proc Natl Acad Sci U S A*. 2012; 109:7457–7462. [PubMed: 22529385]
30. Chu VC, Whittaker GR. Influenza virus entry and infection require host cell N-linked glycoprotein. *Proc Natl Acad Sci U S A*. 2004; 101:18153–18158. [PubMed: 15601777]
31. Glaser L, Conenello G, Paulson J, Palese P. Effective replication of human influenza viruses in mice lacking a major alpha2,6 sialyltransferase. *Virus Res*. 2007; 126:9–18. [PubMed: 17313986]
32. Sieczkarski SB, Whittaker GR. Influenza virus can enter and infect cells in the absence of clathrin-mediated endocytosis. *J Virol*. 2002; 76:10455–10464. [PubMed: 12239322]
33. de Vries E, Tscherne DM, Wienholts MJ, Cobos-Jimenez V, Scholte F, Garcia-Sastre A, Rottier PJ, de Haan CA. Dissection of the influenza A virus endocytic routes reveals macropinocytosis as an alternative entry pathway. *PLoS Pathog*. 2011; 7:e1001329. [PubMed: 21483486]
34. Baum LG, Paulson JC. Sialyloligosaccharides of the respiratory epithelium in the selection of human influenza virus receptor specificity. *Acta Histochem Suppl*. 1990; 40:35–38. [PubMed: 2091044]
35. Walther T, Karamanska R, Chan RW, Chan MC, Jia N, Air G, Hopton C, Wong MP, Dell A, Malik Peiris JS, Haslam SM, Nicholls JM. Glycomic analysis of human respiratory tract tissues and correlation with influenza virus infection. *PLoS Pathog*. 2013; 9:e1003223. [PubMed: 23516363]

Highlights

- 1918 influenza viral receptor-binding variants all bound and entered primary human airway cells.
- All 1918 variants were detected on the apical surface and cytoplasm of ciliated and goblet cells.
- Viral RNA levels in cells were comparable between human, pandemic, and avian influenza viruses.
- Sialic acid preference predicted by glycan array may not accurately predict preference *in vivo*.

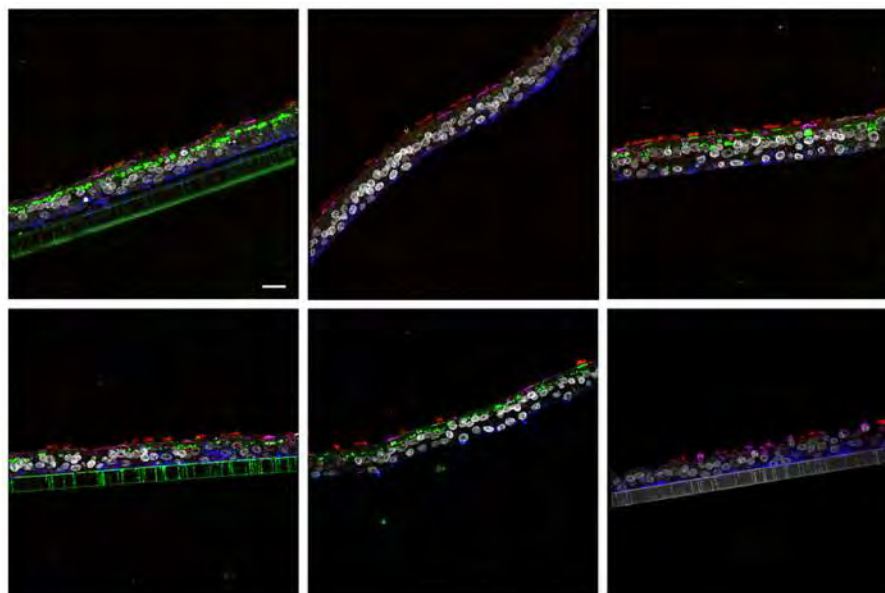


Figure 1.

Comparison of influenza viral antigen distribution by cell type for 1918 receptor binding domain variants. Leica SP5 white light laser confocal maximum projection images of full thickness zstacks of immunofluorescence labeled formalin-fixed paraffin embedded NHBE cells. All imaging was done with a 63x oil objective at zoom 1, 1024 x 1024 pixels. (A) 1918 AV, (B) 1918 SC, (C) 1918 NY, (D) 1918 NY3, (E) 1918 VA and (F) media control (no virus); all were 5 min incubations with virus at MOI 0.01. The pseudo-colors are influenza viral antigen (green), goblet cells (magenta), ciliated cells (red), basal cells (blue), and nuclei (gray). Presented images are representative of the relative influenza viral antigen intensity across three individually infected wells for each virus and where there was inter- or intra-well variance in influenza antigen intensity, a field representative of the median relative intensity was selected. The influenza antigen signal in SC (B) is less than the other viruses and AV (A) has the strongest signal. Scale, 20 μ m.

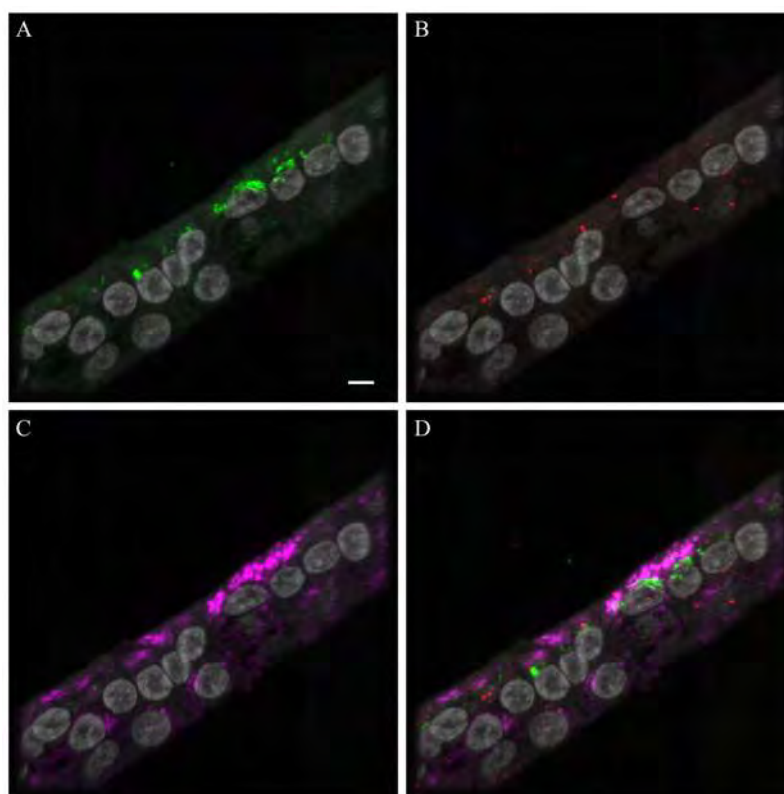


Figure 2.

Endosomal markers with influenza antigen. Leica SP5 white light laser confocal maximum projection images of full thickness zstacks of immunofluorescence labeled formalin-fixed paraffin embedded NHBE cells infected with AV at MOI 1.0 for 20 min. All imaging was done with a 63x oil objective at zoom 3.5, 1024 x 1024 pixels. All images have nuclei (gray): (A) influenza viral antigen (green), (B) early endosomal marker Rab5 (red), (C) late endosomal marker Lamp1 (magenta), and (D) the fluorescence merge. Yellow or orange indicates colocalization of influenza viral antigen with the early endosomal marker Rab5. White indicates co-localization of influenza antigen with late endosomal marker LAMP1. Bar = 5 μ m.

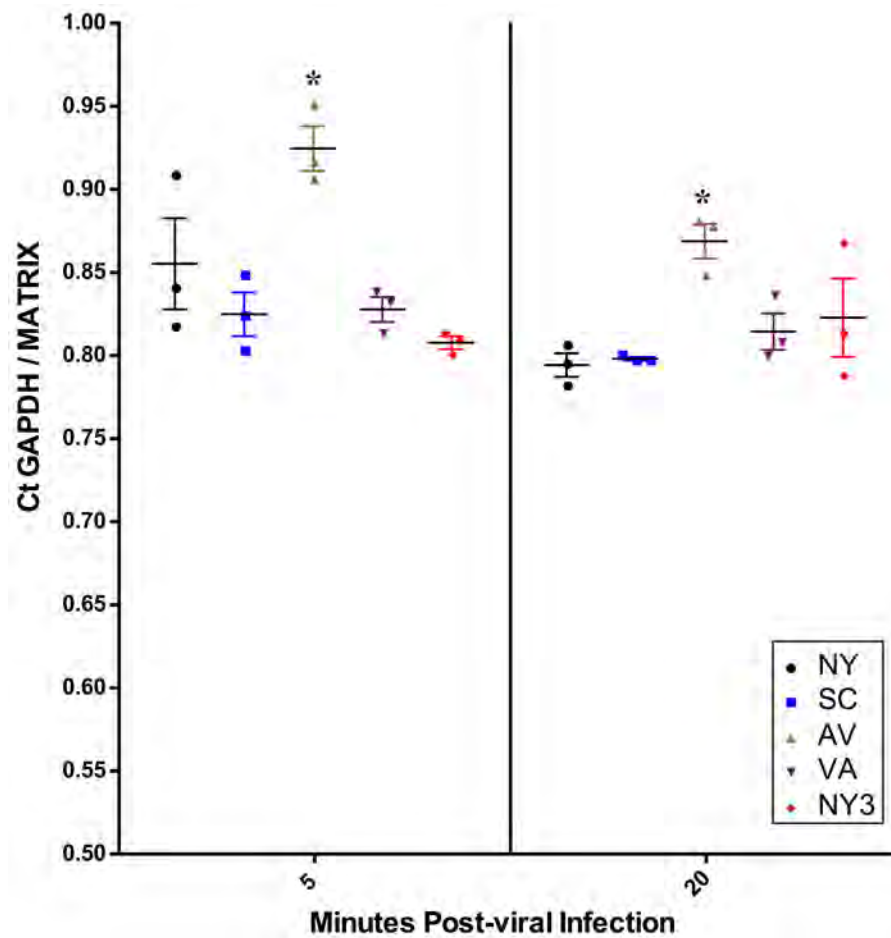


Figure 3.

Real-time PCR results for all five viruses at a multiplicity of infection of 0.01. Real-time PCR data for MOI 0.01 both 5 min (left side) and 20 min (right side) post-viral infection. The data are presented as GAPDH cycle time (C_T)/Influenza viral Matrix C_T as previously described (23). At 5 min (*) denotes AV cell associated viral RNA level is significantly higher as compared to all other viruses and at 20 min is significantly higher than SC and NY by ANOVA with an alpha of 0.05.

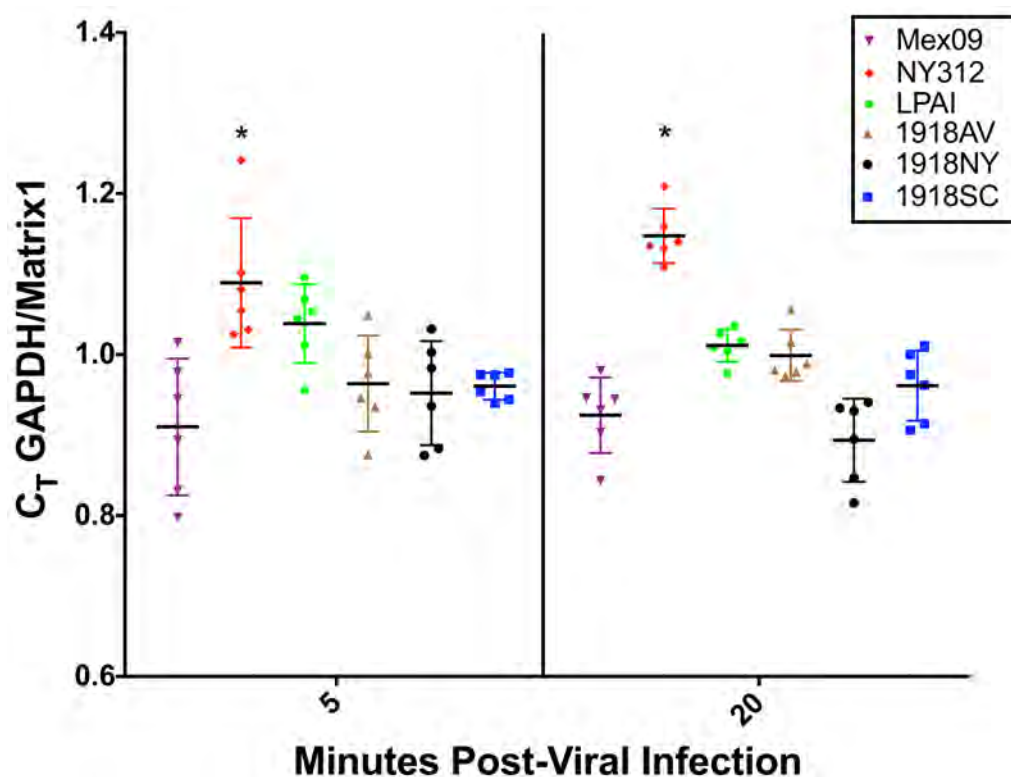


Figure 4.

Real-time PCR results for Mex09, NY312, LPAI virus and three 1918 RBD variants AV, NY, SC. Real-time PCR data for MOI 0.01 both 5 minutes (left panel) and 20 minutes (right panel) post-viral infection. The data are presented as GAPDH cycle time (C_T)/Influenza viral Matrix C_T as previously described (23). At 5 min (*) denotes NY312 cell-associated viral RNA level is significantly higher as compared to all other viruses, except the LPAI virus. At 20 min (*) denotes NY312 cell-associated viral RNA level is significantly higher as compared to all other viruses by ANOVA with an alpha of 0.05.

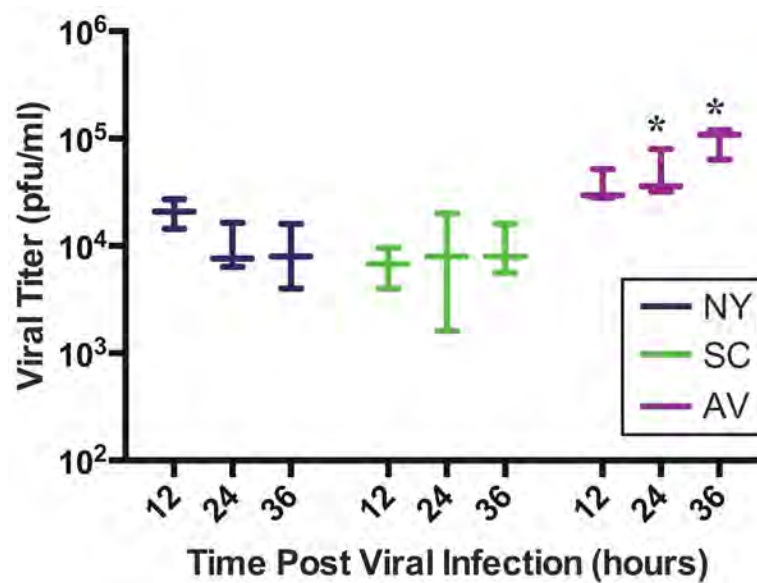


Figure 5.

Replications kinetics for viruses AV, NY and SC. Plaque forming units at 12-, 24- and 36-hours post-infection with MOI 0.1 of NY, SC and AV. (*) denotes that AV is significantly different than both NY and SC at both 24 and 36 hours post-viral infection by ANOVA with an alpha of 0.05.

1918 Pandemic Influenza HA Receptor Binding Domain Variants Amino Acid Sequences

Table 1

Virus (Reference)	Abbreviation	Residue at HA1 domain			Binding
		187	189	222	
A/South Carolina/1/1918 (5)	SC	D	Q	D	$\alpha 2,6$
A/New York/1/1918 (5)	NY	D	Q	G	$\alpha 2,3 > \alpha 2,6$
A/New York/3/1918 (7)	NY3	D	Q	N	Unknown
A/Virginia/1/1918 (7)	VA	D	R	D	$\alpha 2,6$ (modeled)
„Avianized“ 1918 (8, 9)	AV	E	Q	G	$\alpha 2,3$

Table 2

Hemagglutination assay results for AV, NY, and SC

Virus	Titer of viral stock by plaque assay (pfu/ml)	HA unit (measured)	HA unit (adjusted for viral stock titer)
SC	7.6×10^7	1:256	1:256
NY	8.0×10^7	1:256	1:256
AV	2.0×10^7	1:64	1:256

Histopathological observations in COVID-19: a systematic review

Vishwajit Deshmukh,¹ Rohini Motwani ,² Ashutosh Kumar ,³ Chiman Kumari,⁴ Khursheed Raza⁵

► Additional material is published online only. To view please visit the journal online (<http://dx.doi.org/10.1136/jclinpath-2020-206995>).

¹Department of Anatomy, All India Institute of Medical Sciences (AIIMS), Nagpur, Maharashtra, India

²Department of Anatomy, ESIC Medical College and Hospital, Sanathnagar, Hyderabad, Telangana, India

³Department of Anatomy, All India Institute of Medical Sciences (AIIMS), Patna, Bihar, India

⁴Department of Anatomy, Post Graduate Institute of Medical Education & Research (PGIMER), Chandigarh, India

⁵Department of Anatomy, All India Institute of Medical Sciences (AIIMS), Deogarh, Jharkhand, India

Correspondence to

Dr Rohini Motwani, Department of Anatomy, ESIC Medical College and Hospital, Sanathnagar, Hyderabad, Telangana, India; rohini-motwani@gmail.com

AK, CK and KR contributed equally.

Received 29 July 2020

Accepted 31 July 2020

Published Online First

18 August 2020



© Author(s) (or their employer(s)) 2021. No commercial re-use. See rights and permissions. Published by BMJ.

To cite: Deshmukh V, Motwani R, Kumar A, et al. *J Clin Pathol* 2021;**74**:76–83.

ABSTRACT

Background Coronavirus disease-2019 (COVID-19) has caused a great global threat to public health. The World Health Organization (WHO) has declared COVID-19 disease as a pandemic, affecting the human respiratory and other body systems, which urgently demands for better understanding of COVID-19 histopathogenesis.

Objective Data on pathological changes in different organs are still scarce, thus we aim to review and summarise the latest histopathological changes in different organs observed after autopsy of COVID-19 cases.

Materials and methods Over the period of 3 months, authors performed vast review of the articles. The search engines included were PubMed, Medline (EBSCO & Ovid), Google Scholar, Science Direct, Scopus and Bio-Medical. Search terms used were 'Histopathology in COVID-19', 'COVID-19', 'Pathological changes in different organs in COVID-19' or 'SARS-CoV-2'. Preferred Reporting Items for Systematic Reviews and Meta-Analyses (PRISMA) 2009 guidelines were used for review writing.

Result We identified various articles related to the histopathology of various organs in COVID-19 positive patients. Overall, 45 articles were identified as full articles to be included in our study. Histopathological findings observed are summarised according to the systems involved.

Conclusion Although COVID-19 mainly affects respiratory and immune systems, but other systems like cardiovascular, urinary, gastrointestinal tract, reproductive system, nervous system and integumentary system are not spared, especially in elderly cases and those with comorbidity. This review would help clinicians and researchers to understand the tissue pathology, which can help in better planning of the management and avoiding future risks.

INTRODUCTION

Coronavirus disease 2019 (COVID-19), which is zoonotic in origin and most commonly spread through respiratory droplets or aerosol transmission, has caused a big threat to mankind.¹ The disease was originated in the seafood market of Wuhan, Hubei, China, in early December 2019 with clinical presentations greatly resembling viral pneumonia.² This disease has affected most of the countries in the period of 2 months itself. The outbreak of COVID-19 has been declared a pandemic by World Health Organization (WHO)

and presents a great challenge for the healthcare communities across the globe.

The presently identified causative agent for COVID-19, severe acute respiratory syndrome coronavirus-2 (SARS-CoV-2), has shared 82% genome sequence similarity to previously identified SARS-CoV-1, which also originated in China in 2002.^{3,4} The structure of the enveloped single-stranded RNA virus consists of spike protein, which is mainly responsible for the pathogenesis in the human species. The spike protein of the virus, through its receptor binding domain (RBD) gets attached to a human cell surface receptor protein Angiotensin Converting Enzyme -2 (ACE-2), encoded by the ACE2 gene, followed by its priming through auxiliary protein TMPRSS2 (transmembrane protease, serine 2), a cell-surface protein that is expressed by epithelial cells of specific tissues including those in the aerodigestive tract. ACE-2, which acts as a viral host cell entry receptor, has ubiquitous distribution on the organs, therefore SARS-CoV-2 in severe cases causes a systemic disease, with possible involvement of the kidneys, the heart and blood vessels, the liver, the pancreas and also regulates alterations in circulating lymphocytes and the immune system.^{5–7} The maximum expression of the ACE-2 receptors according to the consensus dataset from the human protein atlas is found in small intestine, duodenum and colon followed by kidney, testis, gall bladder, heart, thyroid gland, adipose tissue, rectum and lungs.⁸

The lungs are affected the most, with patients presenting symptoms related to the respiratory system such as sore throat, fever, malaise, and respiratory distress, and in worst cases may proceed to respiratory failure. Mice-related studies show that there is no gender difference in ACE-2 activity in lungs and heart but an expression of ACE-2 is more in male kidneys as compared with female kidneys, making the males more prone to kidney-related disorders, due to SARS infection.⁹

The entry of virus in the host cells induces immune response with wide secretion of inflammatory cytokines and chemokines. Because SARS-CoV-1 and SARS-CoV-2 have the same mechanism of action, both can cause rapid production of multiple cytokines in body fluids following infection, leading to acute respiratory distress and multiple organ failure. This also explains why most patients with COVID-19 have mild symptoms at the onset of the disease, while conditions of a few affected patients are suddenly worsened

Table 1 Important histopathological findings of systems/organs observed by authors in different studies

S.N.	Histopathological findings	Authors
Respiratory system: Lung		
1.	<ul style="list-style-type: none"> ▶ Alveoli: Damaged or atypical enlarged pneumocytes with large nuclei, type II pneumocyte hyperplasia, diffuse alveolar damage (DAD), focal sloughing, hyaline membrane formation, intra-alveolar haemorrhage, intra-alveolar neutrophil infiltration, amphophilic granular cytoplasm and prominent nucleoli characteristic of viral cytopathic-like changes. ▶ Vessels: Oedematous and congested vessels, plug formation, fibrinoid necrosis of the small vasculature, hyaline thrombi in microvessels. Significant deposits of complements—C5b-9 (membrane attack complex), C4d, and mannose binding lectin (MBL)-associated serine protease (MASP)-2, in the microvasculature. ▶ Cellular components: Presence of syncytial giant cells, focal infiltration of immune and inflammatory (lymphocytes and monocytes) and increased stromal cells. ▶ Ultrastructural changes: Viral particles in bronchial mucosal epithelia and type II alveolar epithelia. 	Tian <i>et al</i> , Barton <i>et al</i> , Xu <i>et al</i> , Luo <i>et al</i> , Yao, Magroet <i>et al</i> , Bradley <i>et al</i>
Urinary system: Kidney		
2.	<ul style="list-style-type: none"> ▶ Glomerulus: Ischaemic changes, podocyte vacuolation, focal segmental glomerulosclerosis, accumulation of plasma in Bowman's space. ▶ Renal tubules: Loss of brush border in proximal tubule, non-isometric vacuolar degeneration, and necrosis, oedematous epithelial cells. ▶ Vessels: Erythrocyte aggregates obstructing the lumen of capillaries without platelet or fibrinoid material with occasional hemosiderin granules and pigmented casts, hyalinosis of arteriole, arteriosclerosis of medium sized arteries, fibrin thrombus, shrinkage of capillary loops in glomeruli. ▶ Ultrastructural changes: Clusters of viral particles with distinctive spikes in the tubular epithelium and podocytes. 	Yao <i>et al</i> , Su <i>et al</i> , Tietäväinen <i>et al</i> , Grimes <i>et al</i> , Bradley <i>et al</i>
Gastrointestinal system		
3.	<ul style="list-style-type: none"> ▶ Liver: Focal macrovesicular steatosis, nuclear glycogen accumulation in hepatocytes, dense atypical small lymphocytes in portal tracts. Regenerative nodules and thick fibrous bands, mild zone 3 sinusoidal dilatation, mild lobular lymphocytic infiltration. Patchy hepatic necrosis in the periportal and centrilobular areas. Hepatic cell degeneration and focal necrosis, biliary plugs in the small bile duct. ▶ Oesophagus: Occasional lymphocytic infiltration in the oesophageal squamous epithelium. ▶ Stomach: Partial epithelial degeneration, necrosis and shedding of the gastric mucosa. Dilatation and congestion of small blood vessels and oedema of lamina propria and submucosa with infiltration of immune cells (as lymphocytes, monocytes and plasma cells). ▶ Intestine: Stenosis of the small intestine and segmental dilatation. Numerous infiltrating plasma cells and lymphocytes with interstitial oedema in the lamina propria. ▶ Pancreas: Degeneration of the cells of islets. 	Tian <i>et al</i> , Yao <i>et al</i> , Liu <i>et al</i> , Xiao <i>et al</i>
Cardiovascular system		
4.	<ul style="list-style-type: none"> ▶ Foci of lymphocytic inflammation. ▶ Acute myocyte necrosis. ▶ Presence of inflammatory cells and apoptotic bodies. ▶ Ultrastructural observation: Viral inclusion bodies in vascular endothelial cells. ▶ Immunohistochemistry: Presence of CD61+ megakaryocytes in purpuric papulovesicular. 	Tian <i>et al</i> , Bradley <i>et al</i> , Wichmann <i>et al</i> , Tavazzi <i>et al</i> , Yao <i>et al</i> , Varga <i>et al</i> , Fox <i>et al</i> , Gianotti <i>et al</i> , Kolivras <i>et al</i> , Varga <i>et al</i>
Reproductive system		
5.	<ul style="list-style-type: none"> ▶ Thickened basement membrane with peritubular fibrosis and vascular congestion. ▶ Leucocyte infiltration. ▶ Extensive germ cell destruction. ▶ TUNEL assay: Increased apoptotic spermatogenic cells. 	Jian Xu <i>et al</i> , Chen <i>et al</i>
Nervous system		
6.	<ul style="list-style-type: none"> ▶ Acute hypoxic ischaemic injury, hyperaemia, oedema and neuronal degeneration. ▶ CT, MRI: Ischaemia and/or haemorrhage, and enhanced cortical/subcortical grey matter and fibre tracts. ▶ SARS-CoV-2 RNA was detected in the brain tissue and cerebrospinal fluid in some patients. 	Solomon <i>et al</i> , Mahammedi <i>et al</i> , Moriguchi <i>et al</i>
Histopathological findings (skin)		
7.	<ul style="list-style-type: none"> ▶ Vessels: Perivascular inflammatory cells, intraluminal thrombi. ▶ Epidermis: Parakeratosis, acanthosis, dyskeratotic keratinocytes, necrotic keratinocytes, acantholytic clefts, lymphocyte satellitosis and pseudoherpetic. ▶ Immunohistochemistry: ACE-2 positivity in basal layer of cells in hair follicle, sebaceous glands, smooth muscle cells. 	Hamming <i>et al</i> , Gianotti <i>et al</i> , Kolivras <i>et al</i>

after being diagnosed in hospital, which may be related to the body producing excessive cytokines after the disease, leading to 'cytokine storm' in the body.¹⁰ The association of viral infection with any comorbid conditions such as hypertension, diabetes and renal failure has shown more severe form of clinical presentations such as respiratory failure to multiple organ failure.^{8,9} To understand the effects, presenting symptoms and the pathophysiology of SARS-CoV-2 on various organs, it is of utmost need to understand the pathological findings related to the coronavirus disease, depending on the localisation of the ACE-2 receptors in various organs.

MATERIALS AND METHODS

Objective

Data on histopathological changes in different organs are still scarce, thus we aim to review and summarise the latest histopathological findings observed in different organs related to the infection following autopsy of patient's corpse who died following SARS-CoV-2 infection.

Information sources and search strategy

Over the period of 3 months, the authors performed vast review of the articles. The search engines used included PubMed,

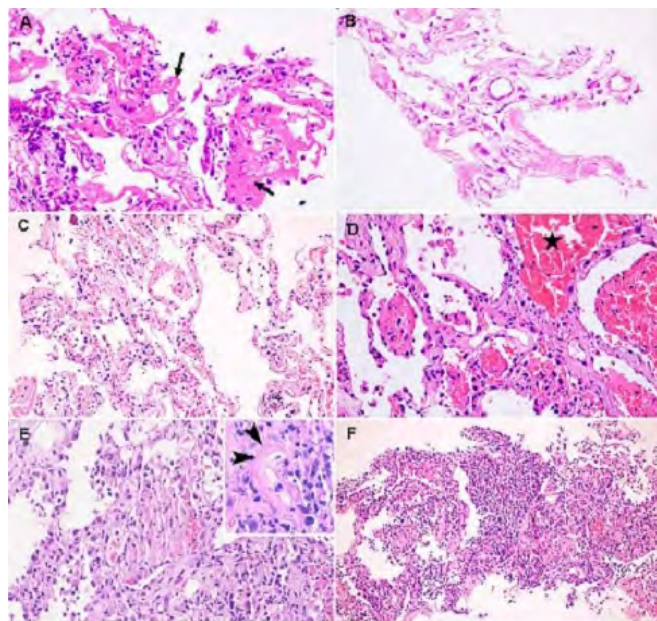


Figure 1 Histopathological changes in lungs of COVID-19 patients. (A) Infiltration of lung tissue by mononuclear inflammatory cells, along with desquamation of alveolar epithelium and formation of hyaline membrane (arrow). (B) Hyaline membrane formation with no signs of inflammatory cell infiltrate. (C) Interstitial thickening with hyperplasia of type II alveolar epithelium. (D) Red blood cells present in alveolar lumen (asterisk) along with formation of fibrin plugs. (E) Diffuse hyperplasia of type II alveolar epithelium and presence of fibrinoid vascular necrosis (inset). (F) Infiltration of inflammatory cells, predominantly neutrophils into the alveolar lumen, indicative of broncho-pneumonia. (Courtesy: Tian S, Xiong Y, Liu H, Niu L, Guo J, Liao M, et al. *Pathological study of the 2019 novel coronavirus disease (COVID) through postmortem core biopsies. Mod Pathol.* 2020 Apr 14;1–8.)

Medline (EBSCO & Ovid), Google Scholar, Science Direct, Scopus and Bio Medical. Search terms used were 'Histopathology in COVID-19', 'COVID-19', 'Coronavirus', 'Pathological changes in different organs in COVID-19' or 'SARS-CoV-2', 'Lung pathology in COVID-19', 'Liver pathology in COVID-19', 'Cardiac involvement in COVID-19', 'Kidney pathology in COVID-19', 'Neuropathology in COVID-19', 'Endothelium and COVID-19' and so on. All the authors were asked to take one system and to extract all the data related to that particular system. Titles and abstracts were screened independently and reviewed with inclusion/exclusion criteria. After data extraction, findings were summarised and reported in [table 1](#) according to the objective of the study.

Protocol followed

Systematic review writing was performed using the Preferred Reporting Items for Systematic Reviews and Meta-Analyses (PRISMA) 2009 guidelines (online supplementary table).

Inclusion and exclusion criteria

Articles (original, review, case series, case reports, published and preprints) that reported histopathological findings of organs in patients with COVID-19 after autopsy or endoscopic biopsy, from 31 December 2019 to 15 June 2020, were included in the study. Exclusive articles of SARS and MERS related to histopathological findings and a very few studies on animal models related to the topic were also included. Articles that did not

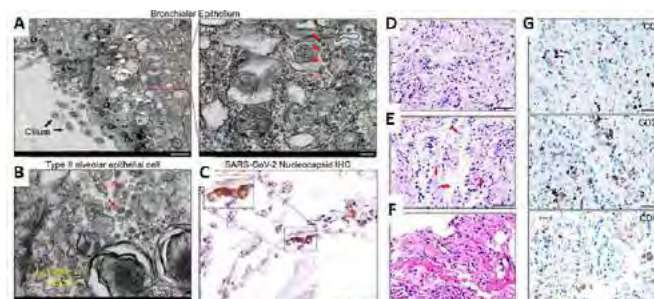


Figure 2 Histopathological changes in lungs of COVID-19 patients. (A) Ultrastructure of an epithelial cell of a bronchiole. Left panel shows organelle within epithelial cell while right panel shows viral particles. (B) Ultrastructure of a type II pneumocyte shows presence of organelle (yellow arrow) and viral particles (red arrows). (C) Positive (dark brown signals) SARS-CoV-2 nucleocapsid (N) in pulmonary tissue, confirmed by immunohistochemistry (IHC) and nuclei counter stained with hematoxylin. Inset shows magnified selected area. (D) Enlarged epithelial cells with areas of desquamation, stained with H & E. (E) Alveoli shows signs of exudation and infiltration by macrophages along with monocytes. (F) Formation of hyaline membrane within the lung tissue. (G) Infiltration of lung tissue with immune cells, which, immunohistochemically detected as CD68+ macrophages, CD20+ B cells, and CD8+ T cells. Scale bar: 50 μ m. (Courtesy: Yao X-H, He Z-C, Li T-Y, Zhang H-R, Wang Y, Mou H, et al. *Pathological evidence for residual SARS-CoV-2 in pulmonary tissues of a ready-for-discharge patient. Cell Res.* 2020;30(6):541–3.)

mention about histopathology of organs, unavailable full text, no target observations and other article types (letters, comments, news and so on) as well as studies reporting cases with incomplete information were excluded. As the study was a systematic review of the literature, institutional ethical committee approval and informed consent were not obtained as we limited our study to published information and human subjects were not involved directly.

RESULTS AND DISCUSSION

In this review, authors identified various articles related to the histopathology of different organs in COVID-19 positive patients. Overall, 45 articles were identified using different databases as full articles to be included in our study. Histopathological findings observed are summarised according to the systems involved.

Pathological features

The early pathological findings identified in the COVID-19 suggested that SARS-CoV-2 can widely spread in the epithelial lining of the respiratory tract, digestive tract, distal convoluted tubules of the kidney, the sweat glands of the skin and testicular epithelium including spermatogonia and sertoli cells. Now, it has been found that, in addition to respiratory transmission, the virus might also be transmitted through faeces, urine and skin. The new findings have also necessitated new ways to prevent the transmission of disease. Many studies on epidemiology and clinical characteristics of COVID-19 have been published but data on pathological changes in different organs are still scanty.¹¹ Hence, the histopathological findings in details have been described below according to the body systems involved.

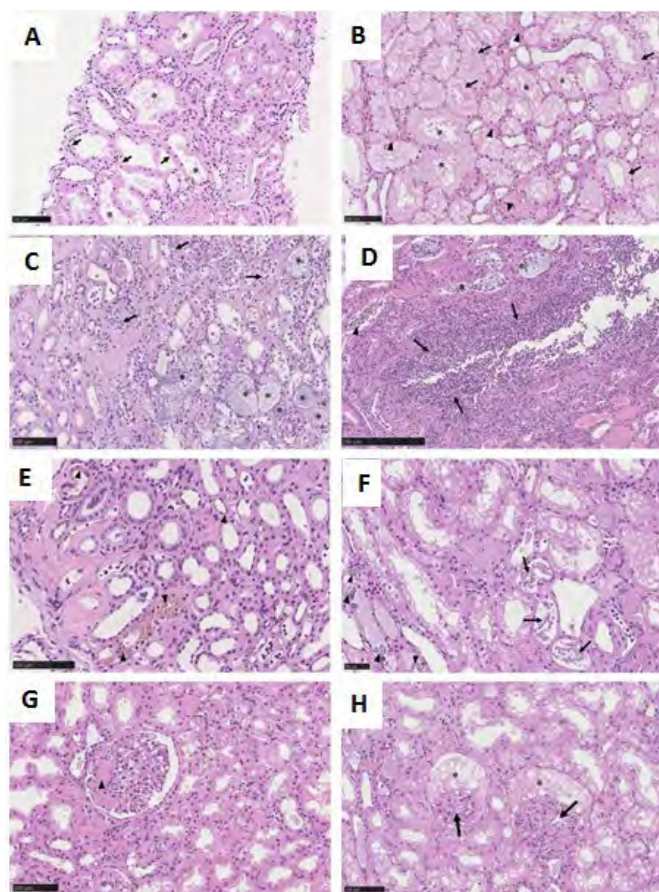


Figure 3 Histopathological changes in kidneys of COVID-19 patients (A) Epithelium of proximal convoluted tubules shows decreased/loss of the brush border. (B) Tubular epithelial cells show vacuolar degeneration (arrows), leading to collection of necrotic debris in the lumen (asterisks). Blocked peritubular capillaries due to erythrocytic aggregates (arrowheads). (C,D) Inflammatory cells (arrowhead) infiltrate the tubules and arcuate artery (arrows). Bacterial foci (asterisks) is also observed. (E,F) Tubular deposition of hemosiderin granules, calcium deposits (arrowhead) and pigmented cast (arrow). (G,H) Glomeruli show ischaemic contraction (arrows) and fibrin thrombi (arrowhead). Bowman's space show presence of leaked accumulated plasma; hematoxylin and eosin. Bars = (F) 50 μ m, (A–C, E, G, H) 100 μ m, and (D) 250 μ m. (Courtesy: Su H, Yang M, Wan C, Yi L-X, Tang F, Zhu H-Y, et al. *Renal histopathological analysis of 26 postmortem findings of patients with COVID-19 in China*. *Kidney Int*. 2020 Jul;98(1):219–2.)

Histopathological findings in respiratory system

Patients with affected upper respiratory tract usually present with mild to moderate symptoms but patients with lower respiratory tract infection show features of pneumonia and land up with organ failure. The severity increases with presence of comorbidities like hypertension, chronic kidney disease, obstructive sleep apnoea and metabolic diseases like diabetes and obesity,^{11,12} and the pathological changes may even vary between right and left lung.¹¹ Macroscopically, lungs appear congestive, with patches of haemorrhagic necrosis.¹¹ Alveolitis with atrophy, vacuolar degeneration, proliferation, desquamation and squamous metaplasia of alveolar epithelial cells (figure 1A), with presence of exudative monocytes and macrophages (figure 2E) are prominent features microscopically. There may be presence of massive fibrinous exudate, multinucleate giant cells and intracytoplasmic viral inclusion bodies and presence of epithelial

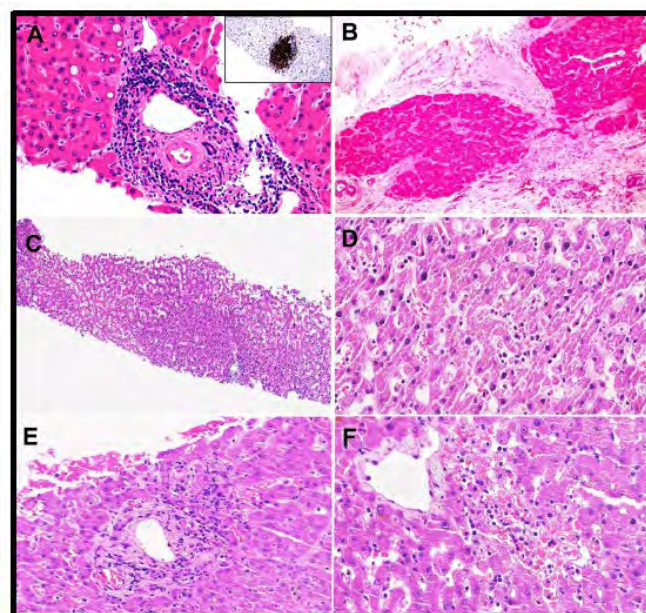


Figure 4 (A) Hepatocytes showing glycogenated nuclei and atypical small lymphocytes densely infiltrating the area of portal triad and showing CD20 positivity (inset). Dense portal infiltration by atypical small lymphocytes (inset: CD20 immunostaining) and focal glycogenated nuclei in hepatocytes have also been observed. (B) Hepatic nodules showing fibrosis, indicative of cirrhosis. Cirrhotic nodules with thick fibrosis. (C) Hepatic sinusoids are dilated and filled with lymphocytes. Mild sinusoidal dilatation with increased lymphocytic infiltration. (D) High power view showing sinusoidal lymphocytes. (E,F) Periportal and centrilobular areas show necrosis, indicative of injury. (Courtesy: Tian S, Xiong Y, Liu H, Niu L, Guo J, Liao M, et al. *Pathological study of the 2019 novel coronavirus disease (COVID) through postmortem core biopsies*. *Mod Pathol*. 2020 Apr 14;1–8.)

cells in the lumen suggesting necrotic changes (necrotising bronchiolitis).¹¹ There may be presence of diffuse alveolar damage (DAD), hyaline membrane formation and vascular congestion with occasional inflammatory cells, damaged pneumocytes with focal sloughing and formation of syncytial giant cells, along with focal infiltration of immune cells in the form of lymphocytes, monocytes and increased stromal cells (figure 1A).¹² Additional findings included intra-alveolar haemorrhages, cluster or plug formation due to the accumulated fibrin (figure 1D) and degraded hyaline membrane remnants in some of the alveoli, type II pneumocyte hyperplasia, fibrinoid necrosis of the small vasculature and abundant intra-alveolar neutrophil infiltration (suggestive of superimposed bacterial infection) leading to bronchopneumonia (figure 1F).⁵ There may be presence of patchy and sparse chronic inflammation, composed mainly of lymphocytes, along with thrombi in branches of pulmonary artery and focal areas of congestion in alveolar septal capillaries along with septal capillary injury with mural and luminal fibrin deposition.^{10,13} Inflammatory oedema in the respiratory mucosa⁶ along with CD3+, CD4+ T cells, CD20+ B-lymphocytes and presence of CD68+ macrophages highlight the presence of inflammatory changes.¹³ There is also evidence of significant deposits of terminal complement components C5b-9 (membrane attack complex), C4d, and mannose binding lectin (MBL)-associated serine protease (MASP)-2, in the microvasculature, consistent with sustained, systemic activation of the alternative and lectin-based complement pathways.¹⁴ Pneumocytes may contain the

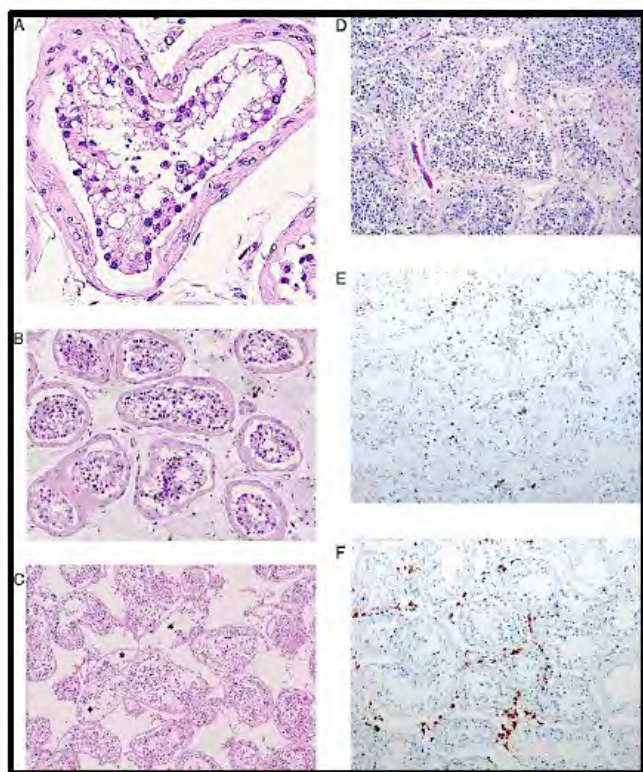


Figure 5 Pathological changes observed in testes from patients with COVID-19. (A,B) Defoliated and oedematous sertoli cells with vacuoles along with reduced spermatogenesis and scattered Leydig cells (arrow). (C) Tubular cells shows sloughing into the lumen (asterisks) indicative of injury. There is marked interstitial oedema. (D) Non-Covid testis with protracted disease showing interstitial edema with infiltration of inflammatory cells. (E) Immunohistochemical findings showing CD3-positive+T lymphocytes and (F) CD68-positive+ histiocytes. (Courtesy: Yang M, Chen S, Huang B, Zhong J-M, Su H, Chen Y-J, et al. *Pathological Findings in the Testes of COVID-19 Patients: Clinical Implications. Eur Urol Focus.*2020 May 31; pp 1–6.)

virus within the cytoplasm and may show nucleomegaly and prominent nucleoli with small basophilic and larger eosinophilic cytoplasmic inclusions. Ultrastructural examination can reveal more details regarding the viral particles. Type II pneumocytes harbour numerous autophagosomes, characterised by double membranes and presence of organelles, in the cytoplasm (figure 2). These autophagosomes which contain viral aggregates, may also be present in tracheal epithelial cells and within the extracellular mucus in the tracheal lumen.⁵ Presence of virus particles has been shown by immunohistochemical staining using monoclonal antibody against SARS-CoV-2 nucleocapsid protein (figure 2C).¹⁵

Most of the histopathological findings are similar to those described in severe acute respiratory syndrome corona virus-1 (SARS-CoV-1) and Middle East respiratory syndrome coronavirus (MERS-CoV).¹⁶ These data suggest similarities in the pathogenesis and the mechanisms of tissue damage in lung tissue and inflammatory response to coronavirus infections, highlighting that the successful methodology in managing SARS and MERS could be referred to patients with COVID-19. Microscopic study of the COVID-19 lung tissue raises a possibility that nasopharyngeal swab showing negative result might not reflect the actual viral load in lung tissue.¹³ This study is important for the clinicians and virologists dealing with patients with COVID-19

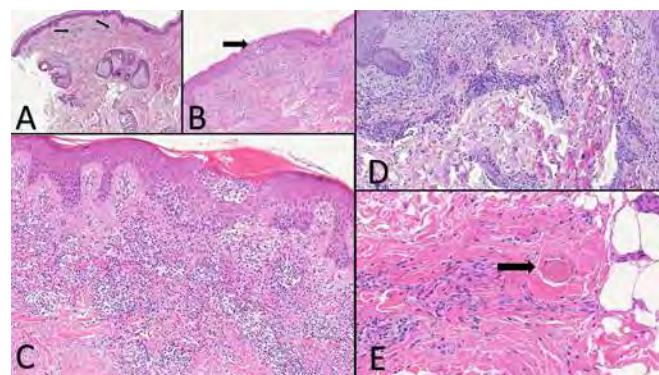


Figure 6 Histopathological changes in skin of COVID-19 patients. (A) Arrow showing telangiectatic blood vessels in early exanthematous rash. (B) Epidermis (arrow) showing groups of Langerhans cells in the laterphase of exanthematous rash. Superficial dermis also shows perivascularinfiltration of lymphocytes. (C) An intraepidermal group of Langerhans cell seen in apapulovescicular rash. (D) Micrographic feature in a Maculo-papular eruption. (E) Capillary thrombosis (arrow) along with diffusehaemorrhage in an exanthemous (Courtesy: Raffaele Gianotti, *Clinical and histopathological study of skin dermatoses in patients affected by COVID-19 infection in the Northern part of Italy. Letter to the Editor. Journal of Dermatological Science.* G Model DESC 3594 No. of Pages 3.)

as this study provides the pathological evidence for residual virus in the lungs for a patient with three consecutive negative PCR test results for the virus. Hence, PCR detection of SARS-CoV-2 nucleic acid on bronchoalveolar lavage fluid, extension of quarantine time and timely follow-up medical examination on discharged patients, especially older or immunocompromised patients, should be preferred.

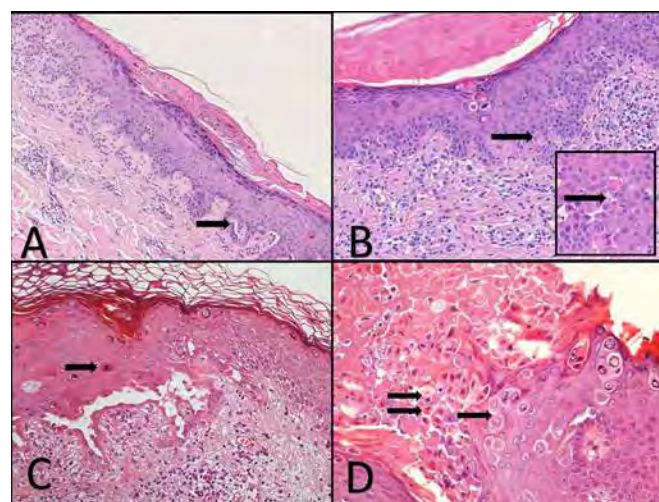


Figure 7 Histopathological changes in skin of COVID-19 patients(A) Acanthosis with presence of cleft (arrow) observed in skin of COVID-19 patients. Parakeratosis is also observed along with abnormal keratinization. (B) Localized necrotic keratinocytes (arrow) with abnormal keratinization InsetInset, with lymphocytic infiltration (arrow). (C) Acantholytic cleft with an adjacent apoptotic keratinocyte (arrow). (D) Pseudoherpetic features (arrow) along with apoptotic keratinocytes (double arrow). (Courtesy: Raffaele Gianotti, *Clinical and histopathological study of skin dermatoses in patients affected by COVID-19 infection in the Northern part of Italy. Letter to the Editor. Journal of Dermatological Science.* G Model DESC 3594 No. of Pages 3.)

Histopathological findings in urinary system (kidney)

ACE-2 is found to be upregulated in patients with COVID-19, and immunostaining with SARS-CoV-2 nucleoprotein antibody is positive in tubules. In addition to the direct virulence of SARS-CoV-2, factors contributing to acute kidney injury (AKI) includes systemic hypoxia, abnormal coagulation and possible drug or hyperventilation-relevant rhabdomyolysis.¹⁷ In some patients, pigmented casts is observed to be associated with high creatine phosphokinase levels possibly representing rhabdomyolysis.¹⁸

Clinically, the incidence of AKI in COVID-19 varies from 0.9% to 29%¹² with new onset proteinuria. Microscopic changes in adult may range from diffuse proximal tubule injury with loss of brush border, non-isometric vacuolar degeneration to even frank necrosis.¹⁷ Other changes seen are swollen glomerular endothelial cells with small amount of protein exudate in the balloon cavity, and presence of thrombus in the capillaries, tubular epithelial cell oedema, vacuolar degeneration (figure 3A,B),¹⁸ with occasional cellular swelling and oedematous expansion of the interstitial spaces in distal collecting tubules and collecting ducts.¹⁵ Non-specific fibrosis along with lymphocytic infiltrates may be found beneath the renal capsule.¹⁵ Absence of interstitial haemorrhage or vasculitis differentiates this type of tissue injury from other causative factors like Hanta virus or injury by anti-neutrophil cytoplasmic antibodies.^{15 16} There can be presence of prominent erythrocyte aggregates, obstructing the lumen of capillaries, without platelet or fibrinoid material, with occasional hemosiderin granules and pigmented casts (figure 3E,F). Electron microscopic (EM) examination shows clusters of viral particles with distinctive spikes, in the tubular epithelium and podocytes.¹⁴

Microscopic changes associated with the comorbid conditions such as diabetes and hypertension show characteristic findings in glomeruli, which include nodular mesangial expansion and hyalinosis of arterioles (associated with diabetic nephropathy) and arteriosclerosis of medium-sized arteries with ischaemic glomeruli.¹⁷ Occasional findings include segmental fibrin thrombus, podocyte vacuolation, focal segmental glomerulosclerosis and shrinkage of capillary loops with accumulation of plasma in Bowman's space (ischaemic changes)(figure 3G,H).¹⁸

Histopathological findings in digestive system (liver)

Although microscopic changes of hepatic tissue in COVID-19 have not been reported much, hepatic injuries cannot be ignored as the ACE-2 receptors have also been detected in the hepatobiliary system where cholangiocytes (59.7%) showed higher expression of ACE-2 cell surface receptor compared to hepatocytes (2.6%).¹⁹ Considering the fact that cholangiocytes expressed ACE-2 in the same manner as the type-2 alveolar cells, there is every possibility for the liver to be a potential target for SARS-CoV-2.¹⁹ Besides, concomitant use of medications also has effect on the hepatobiliary system. Hepatic injury mostly occurs in those with moderate to severe illness.²⁰

Hepatic cell degeneration and focal necrosis in addition to presence of some biliary plugs in the small bile duct²¹ has been observed in light microscopic study. Although endothelial cells show positive ACE-2 expression, the endothelial lining of the liver sinusoids may be negative for ACE-2 along with Kupffer cells and hepatocytes.²² However, it cannot be denied that apart from the SARS-CoV-2 infection, parallel use of hepatotoxic drugs, pre-existing chronic liver disease and COVID-19 related hyperinflammatory conditions can lead to hepatic injury, particularly when the patient is in hypoxic state.

Microscopically, a liver, injured due to SARS-CoV-2 infection, may show signs of cirrhosis and regeneration with macrovesicular steatosis and glycogen accumulation in the liver cells along with atypical lymphocytic infiltration in the portal tract (figure 4A,B). Sinusoidal dilatation in zone 3, mild lymphocytic infiltration and patchy hepatic necrosis have also been observed in the area of portal triad and centrilobular areas²⁰ (figure 4E,F).

Histopathological findings in other parts of digestive system (gastrointestinal tract)

Common gastrointestinal symptoms with which COVID-19 positive patients presented were diarrhoea, decreased appetite, nausea, vomiting, abdominal pain and gastrointestinal bleeding during the onset and subsequent hospitalisation.¹²

There are pieces of evidence of stenosis of the small intestine and segmental dilatation along with varying degrees of degeneration, necrosis and shedding in the gastrointestinal mucosa.²³ Gastric tissue may show epithelial degeneration, necrosis and shedding of the mucosa with the presence of dilated and congested small blood vessels in lamina propria and submucosa along with infiltration of lymphocytes, monocytes and plasma cells. Endocrine pancreas may show evidence of tissue degradation.²¹ However, mucosal epithelial cells of the gastrointestinal tract may be apparently normal with occasional inflammatory infiltrates.²⁴

Histopathological findings in cardiovascular system

Cardiac pathology

Viral infections being one of the most common causes of infectious myocarditis, cardiac involvement by SARS-CoV-2 cannot be ruled out.²⁵ Endomyocardial biopsy from a 69-year-old COVID-19 positive patient, who died of septic shock, depicted low-grade myocardial inflammation and viral particles in the myocardial interstitial cells but not in cardiomyocytes or endothelial cells.²⁶ However, involvement of cardiomyocytes cannot be ruled out as there are reports of hypertrophied cardiomyocytes along with inflammatory infiltrates, focal oedema, interstitial hyperplasia, fibrosis, degeneration, necrosis and signs of lymphocytic myocarditis.¹⁸ Besides ultrastructural changes like swelling of myocardial fibres, myocardium also shows presence of CD4 Tcells along with other inflammatory infiltrates. However, pre-existing morbidity cannot be ruled out like hypertension-associated myocardial hypertrophy and past ischaemic injury.^{5 9 21}

Endomyocardial biopsy from non-ischaemic heart showed endocarditis and inflammation of interstitial tissue and viral particles have been observed in interstitial cells with damaged cell membrane, but myocytes were apparently normal with no viral particles.²⁶ Viral particles may be absent while other signs of inflammation may be present within the cardiac tissue like leucocyte infiltration and presence of CD4+ Tcells^{22 23} indicating indirect injury to the cells by the virus.

Blood vessels

Due to the presence of ACE-2 receptor in the vascular endothelial cells, these are easy target for the SARS-CoV-2 virus.²² Studies show presence of viral inclusions along with inflammatory cells and apoptotic bodies in the endothelial cells.²⁴ There are pieces of evidence of oedematous changes in alveolar capillaries and small vessels with the presence of fibrin thrombi, neutrophils and CD61+ megakaryocytes.²⁷ Histological findings in purpuric papulovesicular rash of skin showed dense perivascular lymphocytic infiltration around the swollen blood vessels

with extravasation of red blood cells.²⁸ While punch biopsy from a case showed plump endothelial cells in lymphoplasmacytic infiltrate surrounded venules without intraluminal thrombi.²⁹

Histopathological findings in nervous system

Neurological symptoms in COVID-19 have been frequently reported; however, the histopathological studies that investigated central nervous system (CNS) lesions are currently very limited.¹⁰ Dizziness and headache were most common CNS manifestations, while taste and smell impairment were the most common peripheral nervous system symptoms.³⁰ Stroke, acute encephalopathy, convulsions, ataxia or nerve demyelination symptoms were occasional neurological presentations in some patients.³¹ Based on the analysis of spectrum of neurological symptoms, possible routes of CNS entry for SARS-CoV-2 virus have been proposed through the hematogenous route by breaching blood-brain barrier or retrograde neuronal spread involving olfactory nerves.³¹ Olfactory route of viral entry into CNS were shown in mice models of SARS-CoV-1 and MERS-CoV which also showed widespread brain lesions following olfactory inoculation of the virus; however, no such evidence is specifically available at present for SARS-CoV-2.^{32,33} A recent postmortem examination study in patients with COVID-19 who displayed neurological symptoms showed widespread brain lesions.³⁴ Autopsied brain tissue showed signs of acute hypoxic ischaemic injury like hyperaemia, oedema and neuronal degeneration.^{31,33} Neuroimaging scans (CT and MRI) for patients with COVID-19 presenting with acute neurological symptoms showed signs of ischaemia and/or haemorrhage, and enhanced cortical/subcortical grey matter and fibre tracts.³⁵ SARS-CoV-2 RNA was detected in the brain tissue and cerebrospinal fluid of some autopsied patients with COVID-19 who had presented with neurological symptoms.^{36,37}

Histopathological findings in genital system (testis)

Evidence has been found between the association of coronavirus family and orchitis in humans.³⁸ ACE2 is present in seminiferous tubules, leydig cells, sertoli cells and spermatogonia.³⁹ Binding of the virus with the testicular cells expressing ACE2 receptors not only damages the testicular tissue but also forms a potential safehouse for the virus. These hidden hotbeds for the virus may form an important cause for infertility worldwide.

Studies show that sertoli cells are more susceptible than germ cells as more than 90% of the sertoli cells expressed ACE-2 receptors. Also, spermatogonia stem cells show higher expression of TMPRSS2 but lower expression of ACE-2, while the sertoli cells show higher expression of ACE-2 but lower expression of TMPRSS2, suggesting the mutual role of spermatogonia and somatic cells or sertoli cells for the invasion of the virus.⁴⁰

All SARS-infected testes demonstrate histological findings with extensive germ cell destruction and decreased spermatogenesis in the seminiferous tubules. The basement membrane gets thickened with peritubular fibrosis along with leucocyte infiltration and vascular congestion in the interstitial tissue. Sertoli cells show swelling, vacuolation and cytoplasmic rarefaction (figure 5A,B). TUNEL assay shows increased apoptosis in the spermatogenic cells and leydig cells of the SARS patients' testes.⁴⁰ One of the evident phenomena in the COVID-19 testis is leucocyte infiltration (figure 5D). These cells could affect the function of leydig cells and thus responsible for decreased production of testosterone (figure 5C). These infiltrated cells especially the lymphocytes and histiocytes, also damage the blood-testis barrier and destroy the seminiferous tubules directly (figure 5E,F).⁴¹

Similar to other viruses like HIV, mumps and hepatitis B virus, SARS-CoV-2 also may lead to activation of inflammatory cytokines, which may potentiate the autoimmune response. They may cause orchitis by several mechanisms, which may result in the testicular damage leading to infertility and sterility, which may further increase the chances of testicular tumours.³⁸ Hence, it is a point of concern for patients suffering from testicular cancers with superadded SARS-CoV-2 infection. According to Song *et al*, no positive RT-PCR result was found in the semen or testicular biopsy specimen, hence suggesting that possibly it will not be transmitted through the sexual route.⁴²

Histopathological findings in skin

The virus reaches the cutaneous tissue through the blood vessels. Since the endothelium abundantly expresses ACE-2, it can easily bind to the viral spike protein and facilitate viral invasion into the skin tissue thus initiating the pathogenesis. Inflammatory response caused by the viral invasion leads to inflammatory cell infiltrates, giving the pathological feature of vasculitis. Immune response leads to activation of Langerhans cells causing a cascade of reactions.⁴³ With the usual common manifestations in COVID-19 positive cases, the dermatological manifestations may go unnoticed and a person may be a source of infection without his or her knowledge. As any other viral infection, the skin manifestations of a COVID-19 positive person may also show signs of erythematous rash, dermatitis, urticaria, chicken pox-like vesicles purpuric papulovesicular rash which may even be painful, pseudo-chilblains on fingertips and toes, macular/maculopapular exanthems, livedo reticularis lesions, petechiae and so on (figure 6). Since there is no correlation with disease severity or duration,⁴⁴ an apparently normal person with positive test may come with only dermatological complaints, with the dermatological lesions mostly in trunk, hands and feet, as they are the most exposed regions of the body.⁴⁵ Most of the skin lesions heal without any residual signs.⁴⁵ Knowledge of skin manifestation may aid in early diagnosis of an asymptomatic COVID-19 patient.

In the epidermis of the skin, the ACE-2 expression is observed in the stratum basale. ACE-2 expression has also been identified in smooth muscle cells of the skin along with the cells around the hair follicle.²² Although not very strong, the cytoplasm of the cells of sebaceous glands also expresses ACE-2 along with its strong expression in the cells of eccrine glands.²² Dense perivascular lymphocytic and plasmacytic infiltration has also been observed around the swollen blood vessels with extravasation of red blood cells and intraluminal thrombi.^{28,29} Parakeratosis, acanthosis, dyskeratotic keratinocytes, necrotic keratinocytes, acantholytic clefts along with lymphocytes satellitisms have also been observed in biopsy samples of COVID-19 positive patients (figure 7).²⁸ Presence of COVID-19 cutaneous manifestations may not be specific to SARS-CoV-2, but may be secondary to the various chains of events taking place due to the viral invasion. But keeping the features in mind will be a good approach towards determining the clinical value of the medical examinations required.

CONCLUSIONS

Information regarding the pathological findings in COVID-19 is limited, although the virus mainly affects respiratory and immune systems, but other systems like cardiovascular, urinary (kidneys), gastrointestinal tract, reproductive (testes), and nervous system are not spared, especially in elderly patients, more often if comorbidities are also present. This review would definitely help

clinicians and researchers to understand the tissue pathology, which can further help in better planning of the disease management and avoiding future health risks.

Take home messages

- COVID-19 mainly affects respiratory and immune systems.
- Other systems like cardiovascular, urinary, gastrointestinal tract, reproductive, nervous and integumentary systems are also not spared, indicating that it is a multi-system disease.
- The elderly and those with comorbidities are affected more severely.

Handling editor Runjan Chetty.

Contributors RM: Contribution in writing abstract, tables and histopathology of respiratory system and gastrointestinal system, and image collection. VD: Contribution in writing abstract, tables and histopathology of genital system, and arrangement of references using software. AK, CK and KR: Equally contributed in writing of histopathology of cardiovascular system, nervous system and skin, and contributed to tables and images of respective system. Final review is done by all authors individually.

Funding The authors have not declared a specific grant for this research from any funding agency in the public, commercial or not-for-profit sectors.

Competing interests None declared.

Patient consent for publication Not required.

Provenance and peer review Not commissioned; internally peer reviewed.

This article is made freely available for use in accordance with BMJ's website terms and conditions for the duration of the covid-19 pandemic or until otherwise determined by BMJ. You may use, download and print the article for any lawful, non-commercial purpose (including text and data mining) provided that all copyright notices and trade marks are retained.

ORCID iDs

Rohini Motwani <http://orcid.org/0000-0002-2002-5198>

Ashutosh Kumar <http://orcid.org/0000-0003-1589-9568>

REFERENCES

- 1 Wang W, Yoneda M. Determination of the optimal penetration factor for evaluating the invasion process of aerosols from a confined source space to an uncontaminated area. *Sci Total Environ* 2020;740:140113.
- 2 WHO. Coronavirus. Available: <https://www.who.int/emergencies/diseases/novel-coronavirus-2019> [Accessed 5 Jun 2020].
- 3 Zhang C, Shi L, Wang F-S. Liver injury in COVID-19: management and challenges. *Lancet Gastroenterol Hepatol* 2020;5:428–30.
- 4 Lu R, Zhao X, Li J, et al. Genomic characterisation and epidemiology of 2019 novel coronavirus: implications for virus origins and receptor binding. *Lancet* 2020;395:565–74.
- 5 Huang C, Wang Y, Li X, et al. Clinical features of patients infected with 2019 novel coronavirus in Wuhan, China. *Lancet* 2020;395:497–506.
- 6 Xu Z, Shi L, Wang Y, et al. Pathological findings of COVID-19 associated with acute respiratory distress syndrome. *Lancet Respir Med* 2020;8:420–2.
- 7 Mehta P, McAuley DF, Brown M, et al. COVID-19: consider cytokine storm syndromes and immunosuppression. *Lancet* 2020;395:1033–4.
- 8 The Human Protein Atlas. Tissue expression of ACE2 - Summary. Available: <https://www.proteinatlas.org/ENSG00000130234-ACE2/tissue> [Accessed 21 Jun 2020].
- 9 Warner FJ, Guy JL, Lambert DW, et al. Angiotensin converting enzyme-2 (ACE2) and its possible roles in hypertension, diabetes and cardiac function. *Int J Pept Res Ther* 2003;10:377–85.
- 10 Yaqian M, Lin W, Wen J, et al. Clinical and pathological characteristics of 2019 novel coronavirus disease (COVID-19): a systematic review. *medRxiv* 2020.
- 11 Zhu N, Zhang D, Wang W, et al. A novel coronavirus from patients with pneumonia in China, 2019. *N Engl J Med* 2020;382:727–33.
- 12 Tian S, Xiong Y, Liu H, et al. Pathological study of the 2019 novel coronavirus disease (COVID-19) through postmortem core biopsies. *Mod Pathol* 2020;33:1007–14.
- 13 Barton LM, Duval EJ, Stroberg E, et al. COVID-19 autopsies, Oklahoma, USA. *Am J Clin Pathol* 2020;153:725–33.
- 14 Magro C, Mulvey JJ, Berlin D, et al. Complement associated microvascular injury and thrombosis in the pathogenesis of severe COVID-19 infection: a report of five cases. *Transl Res* 2020;220:1–13.
- 15 Yao X-H, He Z-C, Li T-Y, et al. Pathological evidence for residual SARS-CoV-2 in pulmonary tissues of a ready-for-discharge patient. *Cell Res* 2020;30:541–3.
- 16 Alsaad KO, Hajeer AH, Al Balwi M, et al. Histopathology of Middle East respiratory syndrome coronavirus (MERS-CoV) infection - clinicopathological and ultrastructural study. *Histopathology* 2018;72:516–24.
- 17 Su H, Yang M, Wan C, et al. Renal histopathological analysis of 26 postmortem findings of patients with COVID-19 in China. *Kidney Int* 2020;98:219–27.
- 18 Yao X-H, He Z-C, Li T-Y, et al. Pathological evidence for residual SARS-CoV-2 in pulmonary tissues of a ready-for-discharge patient. *Cell Res* 2020;30:541–3.
- 19 Chai X, Hu L, Zhang Y, et al. Specific ACE2 expression in cholangiocytes may cause liver damage after 2019-nCoV infection. *bioRxiv* 2020.
- 20 Li Y, Xiao S-Y. Hepatic involvement in COVID-19 patients: pathology, pathogenesis, and clinical implications. *J Med Virol* 2020. doi:10.1002/jmv.25973. [Epub ahead of print: 05 May 2020].
- 21 Yao XH, Li TY, He ZC, et al. [A pathological report of three COVID-19 cases by minimal invasive autopsies]. *Zhonghua Bing Li Xue Za Zhi* 2020;49:411–7.
- 22 Hamming I, Timens W, Bulthuis MLC, et al. Tissue distribution of ACE2 protein, the functional receptor for SARS coronavirus. A first step in understanding SARS pathogenesis. *J Pathol* 2004;203:631–7.
- 23 State Council. The state council of the people's republic of China. Available: <http://english.www.gov.cn/> [Accessed 26 Jul 2020].
- 24 Xiao F, Tang M, Zheng X, et al. Evidence for gastrointestinal infection of SARS-CoV-2. *Gastroenterology* 2020;158:1831–3.
- 25 Fung G, Luo H, Qiu Y, et al. Myocarditis. *Circ Res* 2016;118:496–514.
- 26 Tavazzi G, Pellegrini C, Maurelli M, et al. Myocardial localization of coronavirus in COVID-19 cardiogenic shock. *Eur J Heart Fail* 2020;22:911–5.
- 27 Fox SE, Akmatbekov A, Harbert JL, et al. Pulmonary and cardiac pathology in Covid-19: the first autopsy series from new Orleans. *medRxiv* 2020.
- 28 Gianotti R, Zerbi P, Dodiuk-Gad RP. Clinical and histopathological study of skin dermatoses in patients affected by COVID-19 infection in the Northern part of Italy. *J Dermatol Sci* 2020;98:141–3.
- 29 Kolivras A, Dehavy F, Delplace D, et al. Coronavirus (COVID-19) infection-induced chilblains: a case report with histopathologic findings. *JAAD Case Rep* 2020. doi:10.1016/j.jidcr.2020.04.011. [Epub ahead of print: 18 Apr 2020].
- 30 Mao L, Jin H, Wang M, et al. Neurologic manifestations of hospitalized patients with coronavirus disease 2019 in Wuhan, China. *JAMA Neurol* 2020. doi:10.1001/jamaneurol.2020.1127. [Epub ahead of print: 10 Apr 2020].
- 31 Zubair AS, McAlpine LS, Gardin T, et al. Neuropathogenesis and neurologic manifestations of the coronaviruses in the age of coronavirus disease 2019: a review. *JAMA Neurol* 2020. doi:10.1001/jamaneurol.2020.2065. [Epub ahead of print: 29 May 2020].
- 32 Agrawal AS, Garron T, Tao X, et al. Generation of a transgenic mouse model of middle East respiratory syndrome coronavirus infection and disease. *J Virol* 2015;89:3659–70.
- 33 Solomon IH, Normandin E, Bhattacharyya S, et al. Neuropathological features of Covid-19. *N Engl J Med* 2020.
- 34 Rimmelin M, Mendoca RD, D'Haene N, et al. Unspecific post-mortem findings despite multiorgan 1 viral spread in COVID-19 patients. *medRxiv*.
- 35 Mahammed A, Saba L, Vagal A, et al. Imaging in neurological disease of hospitalized COVID-19 patients: an Italian multicenter retrospective observational study. *Radiology* 2020;201933:201933.
- 36 Moriguchi T, Harii N, Goto J, et al. A first case of meningitis/encephalitis associated with SARS-Coronavirus-2. *Int J Infect Dis* 2020;94:55–8.
- 37 Zhou L, Zhang M, Wang J, et al. Sars-Cov-2: underestimated damage to nervous system. *Travel Med Infect Dis* 2020;101642:101642.
- 38 Xu J, Qi L, Chi X, et al. Orchitis: a complication of severe acute respiratory syndrome (SARS). *Biol Reprod* 2006;74:410–6.
- 39 Li M-Y, Li L, Zhang Y, et al. Expression of the SARS-CoV-2 cell receptor gene ACE2 in a wide variety of human tissues. *Infect Dis Poverty* 2020;9:45.
- 40 Wang Z, Xu X. scRNA-Seq profiling of human testes reveals the presence of the ACE2 receptor, a target for SARS-CoV-2 infection in spermatogonia, Leydig and Sertoli cells. *Cells* 2020;9. doi:10.3390/cells9040920. [Epub ahead of print: 09 Apr 2020].
- 41 Shen Q, Xiao X, Aierken A, et al. The ACE2 expression in Sertoli cells and germ cells may cause male reproductive disorder after SARS-CoV-2 infection. *J Cell Mol Med* 2020;130.
- 42 Song C, Wang Y, Li W, et al. Absence of 2019 novel coronavirus in semen and testes of COVID-19 patients†. *Biol Reprod* 2020;103:4–6.
- 43 Sungnak W, Huang N, Bécavin C, et al. SARS-CoV-2 entry factors are highly expressed in nasal epithelial cells together with innate immune genes. *Nat Med* 2020;26:681–7.
- 44 Recalcati S. Cutaneous manifestations in COVID-19: a first perspective. *J Eur Acad Dermatol Venereol* 2020;34:e212–3.
- 45 Sachdeva M, Gianotti R, Shah M, et al. Cutaneous manifestations of COVID-19: report of three cases and a review of literature. *J Dermatol Sci* 2020;98:75–81.

Epidemiology of COVID-19 Among Children in China

Yuanyuan Dong, MD,^{a,b,*} Xi Mo, PhD,^{a,*} Yabin Hu, MD,^a Xin Qi, PhD,^c Fan Jiang, MD, PhD,^a Zhongyi Jiang, MD,^{a,b} Shilu Tong, MD, PhD^{a,d,e}

OBJECTIVE: To identify the epidemiological characteristics and transmission patterns of pediatric patients with the 2019 novel coronavirus disease (COVID-19) in China. abstract

METHODS: Nationwide case series of 2135 pediatric patients with COVID-19 reported to the Chinese Center for Disease Control and Prevention from January 16, 2020, to February 8, 2020, were included. The epidemic curves were constructed by key dates of disease onset and case diagnosis. Onset-to-diagnosis curves were constructed by fitting a log-normal distribution to data on both onset and diagnosis dates.

RESULTS: There were 728 (34.1%) laboratory-confirmed cases and 1407 (65.9%) suspected cases. The median age of all patients was 7 years (interquartile range: 2–13 years), and 1208 case patients (56.6%) were boys. More than 90% of all patients had asymptomatic, mild, or moderate cases. The median time from illness onset to diagnoses was 2 days (range: 0–42 days). There was a rapid increase of disease at the early stage of the epidemic, and then there was a gradual and steady decrease. The disease rapidly spread from Hubei province to surrounding provinces over time. More children were infected in Hubei province than any other province.

CONCLUSIONS: Children of all ages appeared susceptible to COVID-19, and there was no significant sex difference. Although clinical manifestations of children's COVID-19 cases were generally less severe than those of adult patients, young children, particularly infants, were vulnerable to infection. The distribution of children's COVID-19 cases varied with time and space, and most of the cases were concentrated in Hubei province and surrounding areas. Furthermore, this study provides strong evidence of human-to-human transmission.



^aShanghai Children's Medical Center, Shanghai Jiao Tong University School of Medicine, Shanghai, China; ^bChild Health Advocacy Institute, China Hospital Development Institute, Shanghai Jiao Tong University, Shanghai, China; ^cSchools of Public Health and Medicine, Xian Jiaotong University, Xian, China; ^dInstitute of Environment and Population Health, School of Public Health, Anhui Medical University, Hefei, China; and ^eSchool of Public Health, Nanjing Medical University, Nanjing, China

*Contributed equally as co-first authors

Prof Tong conceptualized and designed the study, collected data, drafted the initial manuscript, obtained the funding, and reviewed and revised the manuscript; Ms Dong and Dr Mo conducted the initial analyses, drafted the initial manuscript, and reviewed and revised the manuscript; Dr Qi, Mr Hu, and Profs Jiang and Jiang critically reviewed the manuscript for important intellectual content; and all authors approved the final manuscript as submitted and agree to be accountable for all aspects of the work.

DOI: <https://doi.org/10.1542/peds.2020-0702>

Accepted for publication Mar 13, 2020

Address correspondence to Shilu Tong, Shanghai Children's Medical Center, Shanghai Jiao Tong University School of Medicine, Shanghai 200127, China. E-mail: tongshilu@scmc.com.cn

WHAT'S KNOWN ON THIS SUBJECT: A growing number of studies have focused on the 2019 novel coronavirus disease (COVID-19) since its outbreak, but few data are available on epidemiological features and transmission patterns in children with COVID-19.

WHAT THIS STUDY ADDS: Children of all ages were susceptible to COVID-19, but no significant sex difference was found. Clinical manifestations of pediatric patients were generally less severe than those of adult patients. However, young children, particularly infants, were vulnerable to 2019 novel coronavirus infection.

To cite: Dong Y, Mo X, Hu Y, et al. Epidemiology of COVID-19 Among Children in China. *Pediatrics*. 2020;145(6):e20200702

In early December 2019, a number of pneumonia cases of unknown origin emerged in Wuhan, Hubei province, China.^{1,2} Most of these patients reported exposure to the Huanan Seafood Wholesale Market selling many species of live animals. The disease rapidly spread, domestically, to other parts of China, and globally to many countries across 6 continents. On January 3, 2020, a novel member of enveloped RNA coronavirus was identified in samples of bronchoalveolar lavage fluid from a patient in Wuhan and subsequently confirmed as the cause of this disease by the Chinese Center for Disease Control and Prevention (CDC).^{3–5} On January 7, 2020, the World Health Organization (WHO) named it the 2019 novel coronavirus (2019-nCoV). On February 11, 2020, the WHO named the illness associated with 2019-nCoV the 2019 novel coronavirus disease (COVID-19).

Emergence of 2019-nCoV has attracted global attention, and the WHO has declared the COVID-19 a public health emergency of international concern (PHEIC).⁶ Since the outbreak of severe acute respiratory syndrome in Guangdong, China, in 2003, the WHO has declared 5 PHEICs: H1N1 (2009), polio (2014), Ebola in West Africa (2014), Zika (2016), and Ebola in the Democratic Republic of the Congo (2019). Declaring a PHEIC is an urgent call, at the highest level, for the international community to launch a global coordinated effort to stop the outbreak, which requires a strong public health response, high-level political commitment, and sufficient funding. As of March 2, 2020, a total of 80 174 COVID-19 cases in China and 8774 cases in 64 countries (and regions) have been confirmed.⁷ Despite the worldwide spread, the epidemiological and clinical patterns of COVID-19 remain largely unclear, particularly among children. In this study, we explored the

epidemiological characteristics and transmission patterns of 2135 pediatric patients with COVID-19 in mainland China.

METHODS

Data Sources

We conducted a retrospective study on the epidemiological characteristics of 2135 pediatric patients with COVID-19. Children were defined as being <18 years old.

The cases were initially diagnosed on the basis of clinical manifestations and exposure history.^{8,9} Within the last 2 weeks, if a child was exposed to a COVID-19 case patient or lived in an epidemic area (ie, Hubei province), a community where a COVID-19 case (or cases) was reported, or a nonepidemic area where no COVID-19 case(s) was reported, she or he was defined as having high, medium, or low risk, respectively, on the basis

of the possibility of contracting the disease. Suspected cases were identified if a child at high risk had 2 of the following conditions: (1) fever, respiratory, digestive symptoms (eg, vomiting, nausea, and diarrhea), or fatigue; (2) laboratory test white blood cell count was normal, decreased, or had a lymphocyte count or increased level of C-reactive protein; or (3) abnormal chest radiograph imaging result. For a child at medium or low risk, similar diagnostic criteria were applied after excluding influenza and other common respiratory infections. Suspected cases that met any one of the following criteria were defined as confirmed cases:

1. Nasal and pharyngeal swab specimens or blood samples tested positive for 2019-nCoV nucleic acid by using real-time reverse-transcriptase polymerase chain reaction assay.

TABLE 1 Characteristics of Children's COVID-19 Cases in China

Characteristics	All Cases	Category		P
		Confirmed	Suspected	
Age, median (interquartile range)	7 (2–13)	10 (4–15)	6 (2–12)	<.001
Age group, n (%)				
<1	379 (17.6)	85 (11.7)	291 (20.7)	<.001
1–5	491 (23.0)	137 (18.8)	354 (25.2)	
6–10	522 (24.5)	170 (23.4)	352 (25.0)	
11–15	412 (19.3)	180 (24.7)	232 (16.5)	
>15	334 (15.6)	156 (21.4)	178 (12.6)	
Sex, n (%)				
Male	1208 (56.6)	418 (57.4)	790 (56.1)	.575
Female	927 (43.4)	310 (42.6)	617 (43.9)	
Severity of illness, n (%)				
Asymptomatic	94 (4.4)	94 (12.9)	0 (0.0)	<.001
Mild	1088 (51.0)	314 (43.1)	774 (55.0)	
Moderate	826 (38.7)	298 (40.9)	528 (37.5)	
Severe	112 (5.2)	18 (2.5)	94 (6.7)	
Critical	13 (0.6)	3 (0.4)	10 (0.7)	
Missing	2 (0.1)	1 (0.2)	1 (0.1)	
Days from symptom onset to diagnosis				
Median (interquartile range)	2 (1–5)	3 (1–5)	2 (0–4)	<.001
Range	0–42	0–42	0–36	—
Province, n (%)				
Hubei	981 (46.0)	229 (31.5)	752 (53.4)	<.001
Surrounding areas ^a	396 (18.5)	154 (21.1)	242 (17.2)	
Other	758 (35.5)	345 (47.4)	413 (29.4)	
Total	2135	728 (34.1)	1407 (65.9)	—

—, not applicable.

^a Surrounding areas are the provinces and municipality bordering Hubei; they are Anhui, Henan, Hunan, Jiangxi, Shaanxi, and Chongqing.

TABLE 2 Different Severity of Illness by Age Group

Age Group, y ^a	Asymptomatic, n (%)	Mild, n (%)	Moderate, n (%)	Severe, n (%)	Critical, n (%)	Total, n
<1	7 (1.9)	204 (54.2)	125 (33.2)	33 (8.8)	7 (1.9)	376
1–5	15 (3.1)	245 (49.9)	195 (39.7)	34 (6.9)	2 (0.4)	491
6–10	30 (5.8)	277 (53.3)	191 (36.7)	22 (4.2)	0 (0.0)	520
11–15	27 (6.5)	198 (48.1)	170 (41.3)	14 (3.4)	3 (0.7)	412
>15	15 (4.5)	164 (49.1)	145 (43.4)	9 (2.7)	1 (0.3)	334
Total	94 (4.4)	1088 (51.0)	826 (38.7)	112 (5.3)	13 (0.6)	2133

See also Supplemental Table 3.

^a Two cases had missing values.

2. Genetic sequencing of respiratory tract or blood samples is highly homologous with 2019-nCoV.

The severity of COVID-19 was defined on the basis of the clinical features, laboratory testing, and chest radiograph imaging, including asymptomatic infection, as mild, moderate, severe, or critical. The diagnostic criteria were as follows.⁸

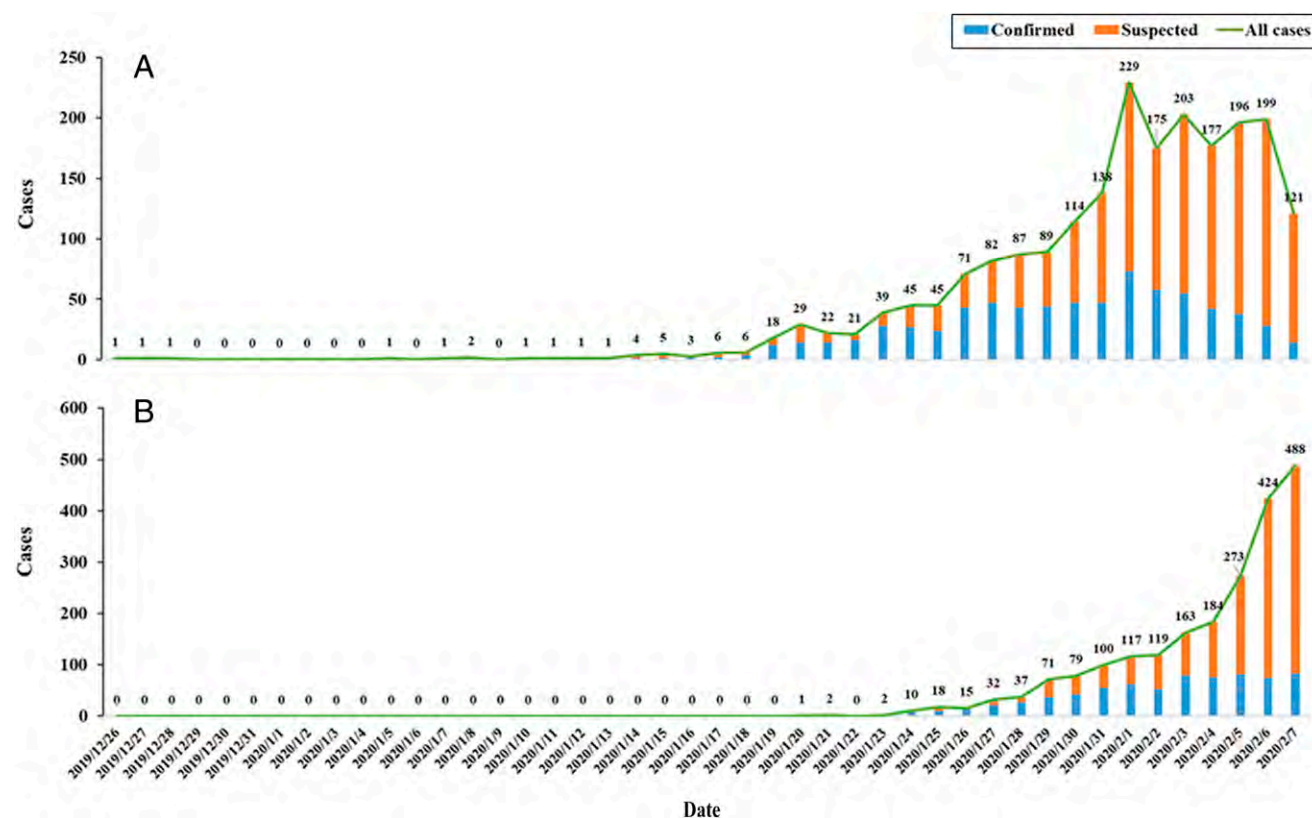
1. Asymptomatic infection: without any clinical symptoms and signs, and the chest imaging results

normal, whereas the 2019-nCoV nucleic acid test result is positive.

2. Mild: symptoms of acute upper respiratory tract infection, including fever, fatigue, myalgia, cough, sore throat, runny nose, and sneezing. Physical examination shows congestion of the pharynx and no auscultatory abnormalities. Some cases may have no fever or have only digestive symptoms, such as nausea, vomiting, abdominal pain, and diarrhea.

3. Moderate: with pneumonia, frequent fever, and cough (mostly dry cough, followed by productive cough); some may have wheezing, but no obvious hypoxemia such as shortness of breath, and lungs can hear sputum or dry and/or wet snoring. Some cases may have no clinical signs and symptoms, but chest computed tomography shows lung lesions, which are subclinical.

4. Severe: early respiratory symptoms, such as fever and

**FIGURE 1**

Onset and diagnosis dates of 2135 children's COVID-19 cases in China. A, Onset date. B, Diagnosis date.

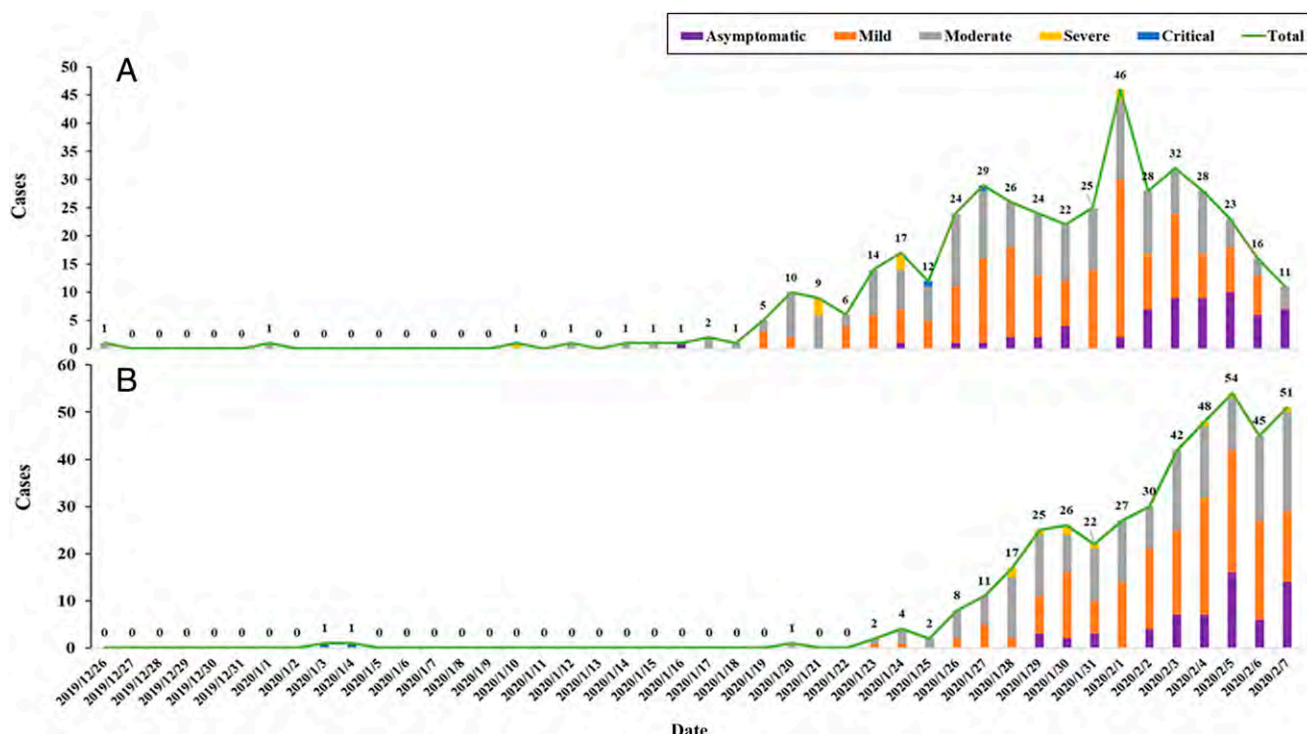


FIGURE 2
Onset and diagnosis dates of 418 confirmed male children's COVID-19 cases in China. A, Onset date. B, Diagnosis date.

cough, may be accompanied by gastrointestinal symptoms, such as diarrhea. The disease usually progresses at ~1 week, and dyspnea occurs with central cyanosis. Oxygen saturation is <92% with other hypoxia manifestations.

5. Critical: children can quickly progress to acute respiratory distress syndrome or respiratory failure and may also have shock, encephalopathy, myocardial injury or heart failure, coagulation dysfunction, and acute kidney injury. Organ dysfunction can be life-threatening.

Both the laboratory-confirmed and suspected cases were included in the analysis. The data sets were extracted from the National Notifiable Infectious Disease Surveillance System at the Chinese CDC. Data were entered into a computer and secured with a password at Shanghai Children's Medical Center.

Cross-check and data cleaning were performed before the data analysis.

Statistical Analysis

We first described case characteristics, including age, sex, dates of disease onset and diagnosis, and location where the case was notified. χ^2 tests and Fisher's exact tests were used for categorical variables as appropriate, and the Mann-Whitney *U* test was used for comparing median values of nonnormally distributed variables. The epidemic curves were constructed by key dates of disease onset and case diagnosis. Because of the data unavailability (ie, no detailed exposure data), we were unable to estimate the incubation period. Onset-to-diagnosis curves were constructed by fitting a log-normal distribution to data on both the onset and diagnosis dates. All analyses were conducted with the use of SPSS 22.0 software (IBM SPSS Statistics, IBM Corporation), and distribution maps

were plotted by using ArcGIS version 10.2.

Ethics

Because of the nature of aggregated data and the ongoing public health response to control the outbreak, as well as the importance of sharing the research findings and bridging the knowledge gaps, an ethical approval was waived by institutional review board.

RESULTS

By February 8, 2020, 2135 pediatric patients with COVID-19 were reported to the Chinese CDC (Table 1). Of the patients, 728 (34.1%) were identified as laboratory-confirmed cases, and 1407 (65.9%) were suspected cases. The median age of all patients was 7 years (interquartile range: 2–13 years). Among those patients, 1208 cases (56.6%) were boys, and there was no statistically significant difference in the number of pediatric patients

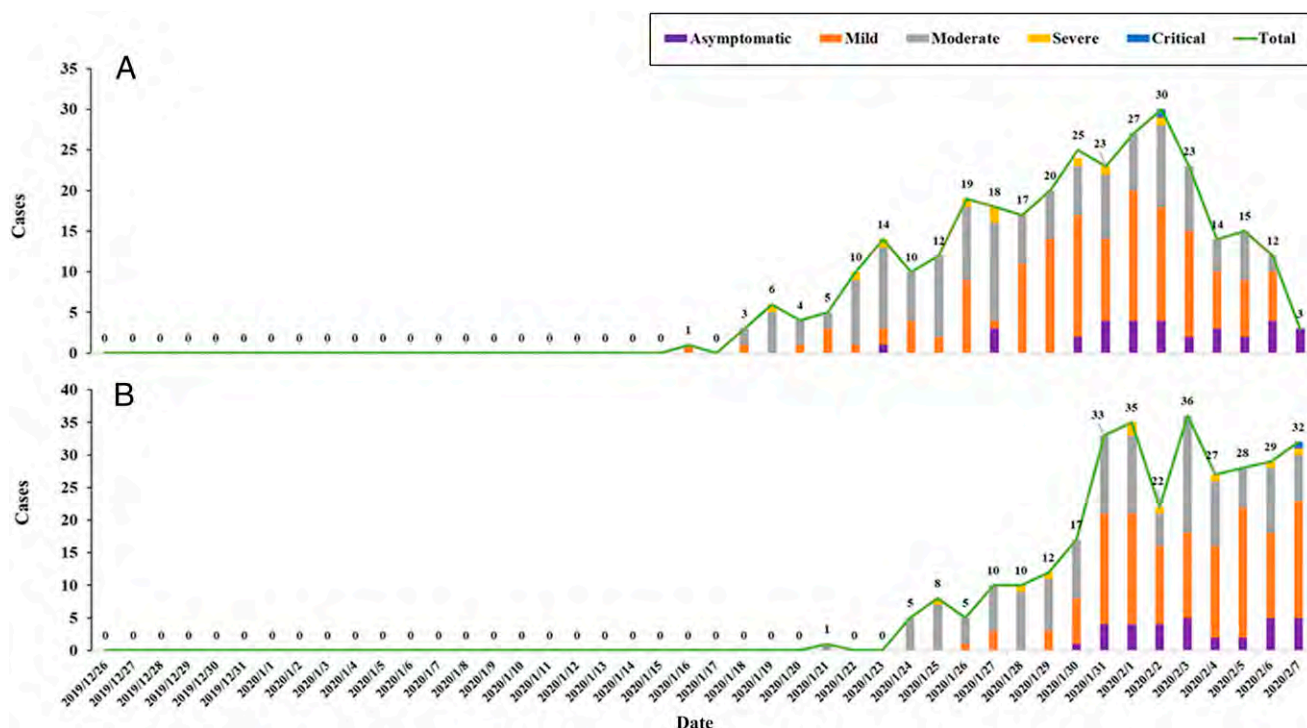


FIGURE 3 Onset and diagnosis dates of 310 confirmed female children's COVID-19 cases in China. A, Onset date. B, Diagnosis date.

between boys and girls. Regarding the severity (including both confirmed and suspected cases), 94 (4.4%), 1088 (51.0%), and 826 (38.7%) cases were diagnosed as asymptomatic, mild, or moderate, respectively; and totally accounted for 94.1% of all cases. Approximately half of the patients were from Hubei province (981; 46.0%), whereas 396 (18.5%) case patients were from Anhui, Henan, Hunan, Jiangxi, Shanxi and

Chongqing, which border Hubei province.

Table 2 shows the severity of illness by age and reveals that young children, particularly infants, were vulnerable to 2019-nCoV infection. The proportions of severe and critical cases were 10.6%, 7.3%, 4.2%, 4.1%, and 3.0% for the age groups <1, 1 to 5, 6 to 10, 11 to 15, and ≥ 16 years, respectively. A 14-year-old boy from

Hubei province died on February 7, 2020.

In the temporal distribution, among the 2135 pediatric patients, there was a trend of rapid increase of disease onset in the early stage of the epidemic and then a gradual and steady decrease (Fig 1). The total number of pediatric patients increased remarkably between mid-January and early February, peaked around February 1, and then has declined since early February 2020. The number of diagnoses had been rising every day from January 20, when the first case was diagnosed. Similar trends of onset and diagnoses were found in confirmed cases (Figs 2 and 3) and suspected cases (Supplemental Figs 6 and 7). The earliest date of illness onset was December 26, 2019, whereas the earliest date of diagnosis was January 20, 2020. The median number of days from illness onset to diagnosis was 2 days (range: 0–42 days). Figure 4 shows that most cases were

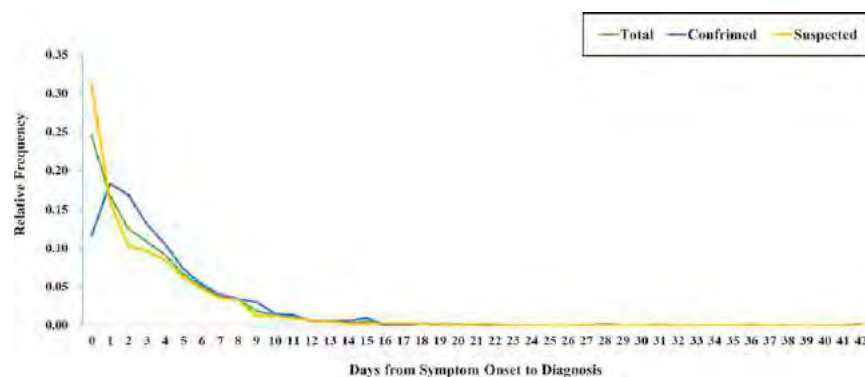


FIGURE 4 Relative frequency of days from symptom onset to diagnosis.

diagnosed in the first week after illness onset occurred.

In the spatial distribution, there was a clear trend that disease spread rapidly from Hubei province to surrounding provinces and cities over time. There were more children infected in the areas around Hubei province than in areas farther away except for Heilongjiang province (Fig 5).

DISCUSSION

To the best of our knowledge, this is the first retrospective study on the epidemiological characteristics and transmission dynamics of children's COVID-19 in China. Because most of these children were likely to expose themselves to family members and/or other children with COVID-19, it clearly indicates person-to-person transmission. Supportive evidence of such a transmission pathway has also been reported from studies on adult

patients.^{10–12} As of February 8, 2020, of the 2135 pediatric patients included in this study, only 1 child died and most cases were mild, with much fewer being severe and critical cases (5.8%) than in adult patients (18.5%).¹³ The evidence suggests that, compared with adult patients, clinical manifestations of children's COVID-19 may be less severe.

Coronaviruses are large, enveloped, positive-strand RNA viruses that can be divided into 4 genera, α , β , δ , and γ , of which α and β coronaviruses are known to infect humans, which are called human coronaviruses (HCoVs).¹⁴ Four HCoVs (HCoV 229E, NL63, OC43, and HKU1) are endemic globally and account for 10% to 30% of upper respiratory tract infections in adults.¹⁵ Although HCoVs have long been regarded as inconsequential pathogens because of their mild phenotypes in humans, in the early 21st century, 2 large-scale epidemics with alarming morbidity and

mortality (ie, severe acute respiratory syndrome coronavirus [SARS-CoV] and Middle East respiratory syndrome coronavirus), have changed that view. From December 2019 to March 25, 2020, 2019-nCoV, another highly pathogenic HCoV, caused 81285 confirmed cases of illnesses and 3287 deaths.¹⁶ The epidemic is ongoing and rapidly evolving, and the ultimate scope and impact of this event is still unclear.

Genomic analyses suggest that the 2019-nCoV may originally come from bats because of the similarity of its genetic sequence to those of other known coronaviruses, but the pathogen was probably transmitted to humans by other animals that may serve as intermediate hosts, facilitating recombination and mutation events with the expansion of genetic diversity.^{3–5} On February 7, 2020, researchers in Guangzhou, China, identified the pangolin as one of the potential sources of 2019-nCoV



FIGURE 5

Spatial distribution of children's COVID-19 cases diagnosed in different time periods. A, January 20, 2020, to January 24, 2020. B, January 25, 2020, to January 31, 2020. C, February 1, 2020, February 7, 2020. D, January 20, 2020, to February 7, 2020.



FIGURE 5
Continued.

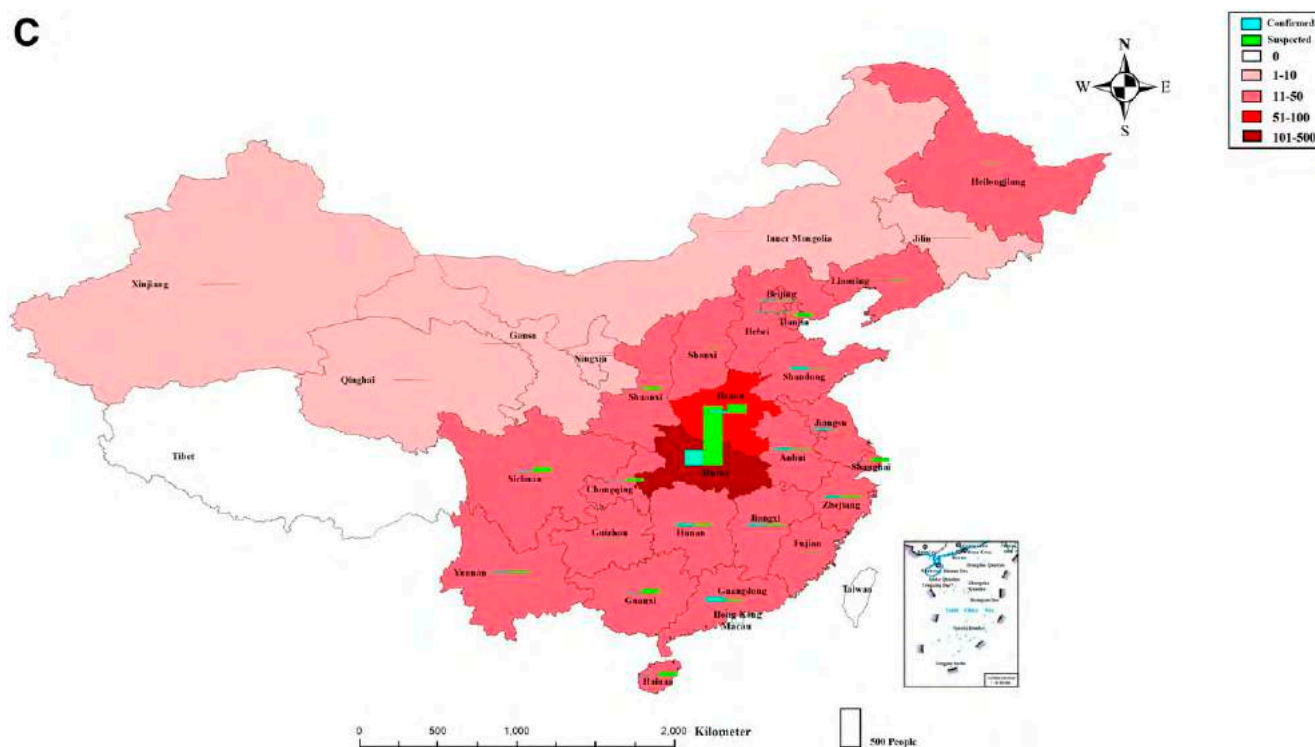


FIGURE 5
Continued.

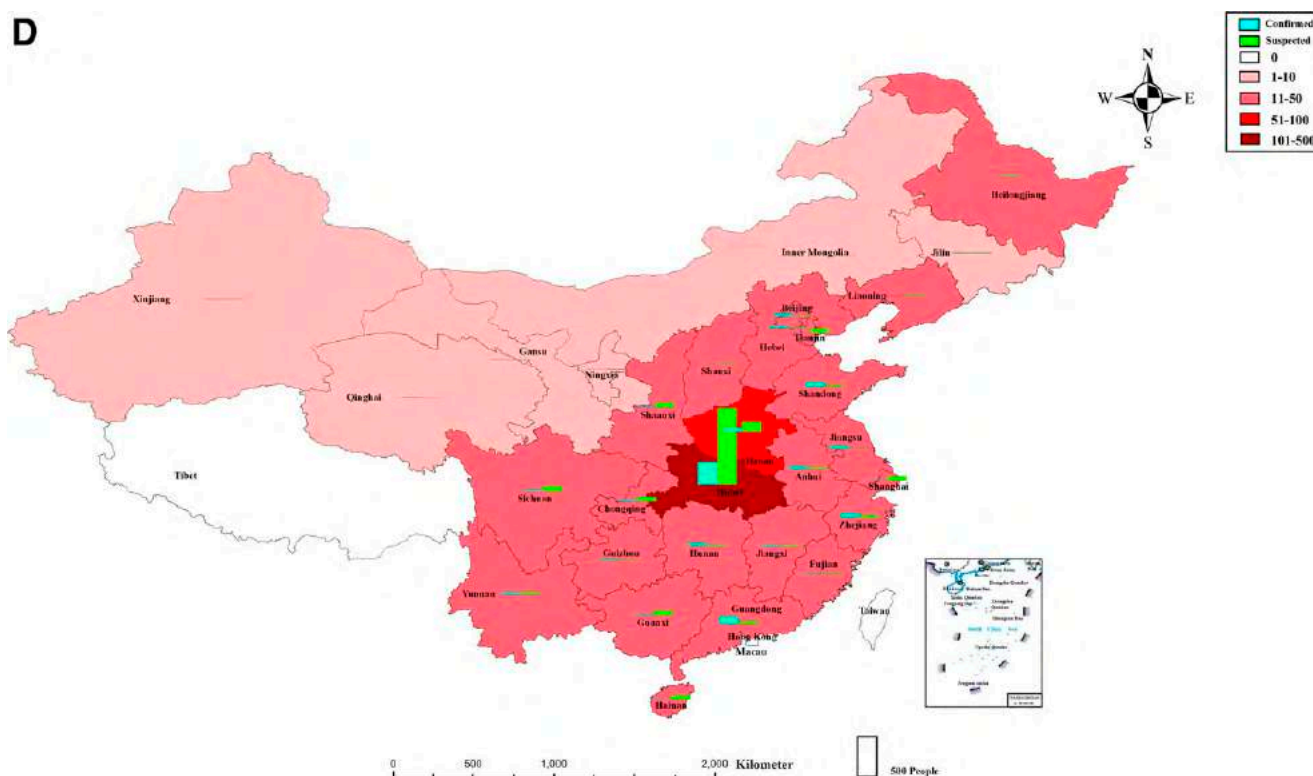


FIGURE 5

Continued.

on the basis of a genetic comparison of CoVs in the samples taken from the animals and from humans who were infected in the outbreak and other findings.^{17,18} Genetic sequences of viruses that were isolated from the scaly animals are 99% similar to that of the circulating virus.

Why most of the children's COVID-19 cases were less severe than adult cases is puzzling. This may be related to both exposure and host factors. Children were usually well cared for at home and might have relatively fewer opportunities to expose themselves to pathogens and/or patients who are sick. Angiotensin-converting enzyme II (ACE2) was known as a cell receptor for SARS-CoV.¹⁹ 2019-nCoV has some amino acid homology to SARS-CoV and may be able to use ACE2 as a receptor. Recent evidence indicates that ACE2 is also likely the cell receptor of 2019-nCoV.^{20,21} It is speculated that children were less sensitive to

2019-nCoV because the maturity and function (eg, binding ability) of ACE2 in children may be lower than in adults.²² Additionally, children often experience respiratory infections (eg, respiratory syncytial virus [RSV]) in winter and may have higher levels of antibody against virus than adults. Furthermore, children's immune systems are still developing and may respond to pathogens differently from adult immune systems. However, we found that the proportion of severe and critical cases was 10.6%, 7.3%, 4.2%, 4.1%, and 3.0% for the age groups <1, 1 to 5, 6 to 10, 11 to 15, and >15 years, respectively. These results suggest that young children, particularly infants, were vulnerable to 2019-nCoV infection. Therefore, the mechanisms for the difference in clinical manifestations between children and adults remains to be determined.

There were more severe and critical cases in the suspected than confirmed

category in this study. However, it remains to be determined if these severe and critical cases in the suspected group were caused by 2019-nCoV or other pathogens (eg, RSV). It may become clearer because the epidemic is quickly unfolding.

We observed slightly more boys than girls (56.6% vs 43.4%) being affected in the COVID-19 outbreak, which is similar to the 2 recent epidemiological studies.^{13,23} However, no significant sex difference was observed in this study. The median age of all children's COVID-19 cases was 7 years (interquartile range: 2–13), but ages ranged from 1 day to 18 years. This finding suggests that all ages of childhood were susceptible to 2019-nCoV.

Temporal distribution of children's COVID-19 cases shows that, in the early stage of the epidemic (ie, between December 2019 and early February 2020), there was a trend of rapid increase of disease onset. Since

early February 2020, the number of children's COVID-19 cases has been declining. This finding indicates that the disease control measures implemented by the government were effective, and it is likely that this epidemic will continue to decline and finally stop in the near future unless sustained human-to-human transmissions occur. Most of the children's COVID-19 cases were concentrated in Wuhan but spread to other areas of Hubei province and farther to other areas of China. It seems that the closer to Wuhan, the more cases in that area, which suggests that population mobility is an important factor of the spread of 2019-nCoV. Heilongjiang province is an exception, which may be because many visitors went there, including those from Wuhan, because of the Ice and Snow Sculpture Festival in Harbin, the provincial capital.

This study has several strengths. First, this is the first nationwide study, to date, with a major focus on the epidemiological characteristics and transmission dynamics of children's COVID-19 in China. It shows that, compared with the adult cases, the severity of children's COVID-19 cases was milder, and the case fatality rate was much lower.^{13,23} Second, the large number of children's COVID-19 cases enabled us to conduct detailed stratified analyses on sex, age, and spatiotemporal distribution. Finally, we included both

confirmed and suspected COVID-19 cases, and it may reveal a comprehensive picture of pediatric patients with COVID-19 in China.

This study also has a number of limitations. First, we were unable to assess clinical characteristics of children's COVID-19 because these data were unavailable at the time of analysis. As an important and urgent issue, clinical features of children's COVID-19 need to be analyzed in further research. It appeared to have more severe and critical cases in the suspected than in the confirmed group (Table 1), which suggests that some suspected cases might be caused by other respiratory infections (eg, RSV). Second, we did not have information on children's exposure history, and thus, the incubation period was not examined in this study. Finally, because the epidemic of COVID-19 is ongoing and rapidly evolving, many children who are affected still remain hospitalized. To gain a better understanding of children's COVID-19, more detailed patient information, particularly clinical outcomes (eg, discharge, transfer to ICU, or death), should be collected in future studies.

CONCLUSIONS

Children of all ages were sensitive to COVID-19, and there was no significant sex difference. Clinical manifestations of children's COVID-19 cases were less severe than those of

adult patients. However, young children, particularly infants, were vulnerable to 2019-nCoV infection. The distribution of children's COVID-19 cases varied with time and space, and most of the cases were concentrated in Wuhan and surrounding areas. Furthermore, the results of this study provide strong evidence for human-to-human transmission because children were unlikely to visit the Huanan Seafood Wholesale Market, where the early adult patients were reported to have obtained 2019-nCoV.

ACKNOWLEDGMENT

We are grateful for the support provided by the Chinese CDC.

ABBREVIATIONS

2019-nCoV:	2019 novel coronavirus
ACE2:	angiotensin-converting enzyme II
CDC:	Center for Disease Control and Prevention
COVID-19:	2019 novel coronavirus disease
HCoV:	human coronavirus
PHEIC:	public health emergency of international concern
RSV:	respiratory syncytial virus
SARS-CoV:	severe acute respiratory syndrome coronavirus
WHO:	World Health Organization

REFERENCES

- Li Q, Guan X, Wu P, et al. Early transmission dynamics in Wuhan, China, of novel coronavirus-infected pneumonia. *N Engl J Med*. 2020;382(13):1199–1207
- Huang C, Wang Y, Li X, et al. Clinical features of patients infected with 2019 novel coronavirus in Wuhan, China [published correction appears in *Lancet*. 2020;395(10223):496]. *Lancet*. 2020;395(10223):497–506
- Tan WJ, Zhao X, Ma XJ, et al. A novel coronavirus genome identified in a cluster of pneumonia cases — Wuhan, China 2019–2020. *China CDC Weekly*. 2020;2:61–62
- Lu R, Zhao X, Li J, et al. Genomic characterisation and epidemiology of 2019 novel coronavirus: implications for virus origins and receptor binding. *Lancet*. 2020;395(10224):565–574
- Zhu N, Zhang D, Wang W, et al; China Novel Coronavirus Investigating and Research Team. A novel coronavirus from patients with pneumonia in China, 2019. *N Engl J Med*. 2020;382(8):727–733
- WHO. WHO director-general's statement on IHR Emergency Committee on Novel Coronavirus (2019-nCoV). Available at: [https://www.who.int/dg/speeches/detail/who-director-general-s-statement-on-ihc-emergency-committee-on-novel-coronavirus-\(2019-ncov\)](https://www.who.int/dg/speeches/detail/who-director-general-s-statement-on-ihc-emergency-committee-on-novel-coronavirus-(2019-ncov)). Accessed March 3, 2020
- WHO. Coronavirus disease 2019 (COVID-19): situation report – 42. Available at: https://www.who.int/docs/default-source/coronavirus/20200302-sitrep-42-covid-19.pdf?sfvrsn=d863e045_2. Accessed March 3, 2020
- Fang F, Zhao D, Chen Y, et al. Recommendations for the diagnosis, prevention and control of the 2019 novel coronavirus infection in children (first interim edition). *Zhonghua Er Ke Zhi*. 2020;145(6):e20200834
- Shen K, Yang Y, Wang T, et al; China National Clinical Research Center for Respiratory Diseases; National Center for Children's Health, Beijing, China; Group of Respiratory, Chinese Pediatric Society, Chinese Medical Association; Chinese Medical Doctor Association Committee on Respiratory Pediatrics; China Medicine Education Association Committee on Pediatrics; Chinese Research Hospital Association Committee on Pediatrics; Chinese Non-government Medical Institutions Association Committee on Pediatrics; China Association of Traditional Chinese Medicine, Committee on Children's Health and Medicine Research; China News of Drug Information Association, Committee on Children's Safety Medication; Global Pediatric Pulmonology Alliance. Diagnosis, treatment, and prevention of 2019 novel coronavirus infection in children: experts' consensus statement. *World J Pediatr*. 2020. doi:10.1007/s12519-020-00343-7
- Chan JF, Yuan S, Kok KH, et al. A familial cluster of pneumonia associated with the 2019 novel coronavirus indicating person-to-person transmission: a study of a family cluster. *Lancet*. 2020;395(10223):514–523
- Wang D, Hu B, Hu C, et al. Clinical characteristics of 138 hospitalized patients with 2019 novel coronavirus-infected pneumonia in Wuhan, China. *JAMA*. 2020. doi:10.1001/jama.2020.1585
- Phan LT, Nguyen TV, Luong QC, et al. Importation and human-to-human transmission of a novel coronavirus in Vietnam. *N Engl J Med*. 2020;382(9):872–874
- The Novel Coronavirus Pneumonia Emergency Response Epidemiology Team. The epidemiological characteristics of an outbreak of 2019 novel coronavirus diseases (COVID-19) -China, 2020. *China CDC Weekly*. 2020;2(8):113–122
- de Wilde AH, Snijder EJ, Kikkert M, van Hemert MJ. Host factors in coronavirus replication. *Curr Top Microbiol Immunol*. 2018;419:1–42
- Paules CI, Marston HD, Fauci AS. Coronavirus infections—more than just the common cold. *JAMA*. 2020. doi:10.1001/jama.2020.0757
- National Health Commission of the People's Republic of China. Update on COVID-19 epidemic situation as of 24:00 on March 25. Available at: <http://www.nhc.gov.cn/xcs/yqtb/202003/f01fc26a8a7b48debe194bd1277fdb3.shtml>. Accessed March 26, 2020
- South China Agricultural University. South China Agricultural University finds pangolin may be a potential intermediate host for a new coronavirus. Available at: <https://scau.edu.cn/2020/0207/c1300a219015/page.htm>. Accessed March 3, 2020
- Cyranoski D. Did pangolins spread the China coronavirus to people? [published online ahead of print February 7, 2020]. *Nature*. doi:10.1038/d41586-020-00364-2
- Li W, Moore MJ, Vasilieva N, et al. Angiotensin-converting enzyme 2 is a functional receptor for the SARS coronavirus. *Nature*. 2003;426(6965):450–454
- Zhou P, Yang XL, Wang XG, et al. A pneumonia outbreak associated with a new coronavirus of probable bat origin. *Nature*. 2020;579(7798):270–273
- Wrapp D, Wang N, Corbett KS, et al. Cryo-EM structure of the 2019-nCoV spike in the prefusion conformation. *Science*. 2020;367(6483):1260–1263
- Fang F, Lu X. Facing the pandemic of 2019 novel coronavirus infections: the pediatric perspectives [published online ahead of print February 2, 2020]. *Zhonghua Er Ke Zhi*. 2020;58(0):E001
- Guan WJ, Ni ZY, Hu Y, et al; China Medical Treatment Expert Group for COVID-19. Clinical characteristics of coronavirus disease 2019 in China [published online ahead of print February 28, 2020]. *N Engl J Med*. doi:10.1056/NEJMoa2002032

Epidemiology of COVID-19 Among Children in China

Yuanyuan Dong, Xi Mo, Yabin Hu, Xin Qi, Fan Jiang, Zhongyi Jiang and Shilu Tong

Pediatrics 2020;145;

DOI: 10.1542/peds.2020-0702 originally published online March 16, 2020;

Updated Information & Services	including high resolution figures, can be found at: http://pediatrics.aappublications.org/content/145/6/e20200702
References	This article cites 17 articles, 1 of which you can access for free at: http://pediatrics.aappublications.org/content/145/6/e20200702#BIBL
Subspecialty Collections	This article, along with others on similar topics, appears in the following collection(s): Infectious Disease http://www.aappublications.org/cgi/collection/infectious_diseases_sub Epidemiology http://www.aappublications.org/cgi/collection/epidemiology_sub Pulmonology http://www.aappublications.org/cgi/collection/pulmonology_sub
Permissions & Licensing	Information about reproducing this article in parts (figures, tables) or in its entirety can be found online at: http://www.aappublications.org/site/misc/Permissions.xhtml
Reprints	Information about ordering reprints can be found online: http://www.aappublications.org/site/misc/reprints.xhtml

American Academy of Pediatrics

DEDICATED TO THE HEALTH OF ALL CHILDREN®



PEDIATRICS®

OFFICIAL JOURNAL OF THE AMERICAN ACADEMY OF PEDIATRICS

Epidemiology of COVID-19 Among Children in China

Yuanyuan Dong, Xi Mo, Yabin Hu, Xin Qi, Fan Jiang, Zhongyi Jiang and Shilu Tong

Pediatrics 2020;145;

DOI: 10.1542/peds.2020-0702 originally published online March 16, 2020;

The online version of this article, along with updated information and services, is located on the World Wide Web at:

<http://pediatrics.aappublications.org/content/145/6/e20200702>

Data Supplement at:

<http://pediatrics.aappublications.org/content/suppl/2020/04/08/peds.2020-0702.DCSupplemental>

Pediatrics is the official journal of the American Academy of Pediatrics. A monthly publication, it has been published continuously since 1948. Pediatrics is owned, published, and trademarked by the American Academy of Pediatrics, 345 Park Avenue, Itasca, Illinois, 60143. Copyright © 2020 by the American Academy of Pediatrics. All rights reserved. Print ISSN: 1073-0397.

American Academy of Pediatrics

DEDICATED TO THE HEALTH OF ALL CHILDREN®



Repurposing of Clinically Developed Drugs for Treatment of Middle East Respiratory Syndrome Coronavirus Infection

Julie Dyall,^a Christopher M. Coleman,^b Brit J. Hart,^a Thiagarajan Venkataraman,^b Michael R. Holbrook,^a Jason Kindrachuk,^a Reed F. Johnson,^c Gene G. Olinger, Jr.,^a Peter B. Jahrling,^{a,c} Monique Laidlaw,^d Lisa M. Johansen,^d Calli M. Lear-Rooney,^e Pamela J. Glass,^e Lisa E. Hensley,^a Matthew B. Frieman^b

Integrated Research Facility, National Institute of Allergy and Infectious Diseases, National Institutes of Health, Frederick, Maryland, USA^a; Department of Microbiology and Immunology, University of Maryland School of Medicine, Baltimore, Maryland, USA^b; Emerging Viral Pathogens Section, National Institute of Allergy and Infectious Diseases, National Institutes of Health, Frederick, Maryland, USA^c; Zalicus Inc., Cambridge, Massachusetts, USA^d; United States Army Medical Research Institute of Infectious Diseases, Frederick, Maryland, USA^e

Outbreaks of emerging infections present health professionals with the unique challenge of trying to select appropriate pharmacologic treatments in the clinic with little time available for drug testing and development. Typically, clinicians are left with general supportive care and often untested convalescent-phase plasma as available treatment options. Repurposing of approved pharmaceutical drugs for new indications presents an attractive alternative to clinicians, researchers, public health agencies, drug developers, and funding agencies. Given the development times and manufacturing requirements for new products, repurposing of existing drugs is likely the only solution for outbreaks due to emerging viruses. In the studies described here, a library of 290 compounds was screened for antiviral activity against Middle East respiratory syndrome coronavirus (MERS-CoV) and severe acute respiratory syndrome coronavirus (SARS-CoV). Selection of compounds for inclusion in the library was dependent on current or previous FDA approval or advanced clinical development. Some drugs that had a well-defined cellular pathway as target were included. In total, 27 compounds with activity against both MERS-CoV and SARS-CoV were identified. The compounds belong to 13 different classes of pharmaceuticals, including inhibitors of estrogen receptors used for cancer treatment and inhibitors of dopamine receptor used as antipsychotics. The drugs identified in these screens provide new targets for *in vivo* studies as well as incorporation into ongoing clinical studies.

Middle East respiratory syndrome coronavirus (MERS-CoV) is an emerging virus, and to date no antiviral or therapeutic has been approved for treating patients. Since September 2012, 206 cases, including 86 deaths, have been attributed to infection with MERS-CoV. Currently, supportive care remains the only available treatment option. As the number of cases continues to rise and the geographic range of the virus increases, there is a growing urgency for candidate interventions.

Prior to 2002, coronaviruses were not considered to be significant human pathogens. Other human coronaviruses such as HCoV-229E and HCoV-OC43 resulted in only mild respiratory infections in healthy adults. This perception was shattered in 2002, when severe acute respiratory syndrome coronavirus (SARS-CoV) emerged in Guangdong Province, China. This virus rapidly spread to 29 different countries, resulting in 8,273 confirmed cases and 775 (9%) deaths (1). While SARS-CoV predominantly impacted Southeast Asia, with significant outbreaks throughout China, Hong Kong, Taiwan, Singapore, and Vietnam, the virus was carried outside the region. Importation of the virus into Canada resulted in 251 confirmed cases and 44 deaths (1). The implementation of infection control measures was able to bring the epidemic to an end in 2003.

In 2012, a novel coronavirus, Middle East respiratory syndrome coronavirus (MERS-CoV), was detected in a patient with severe respiratory disease in the kingdom of Saudi Arabia. To date, 636 laboratory-confirmed cases of MERS-CoV infection have been reported, including 193 deaths, across nine countries (WHO Global Outbreak Alert & Response Network, 28 May 2014; <http://www.who.int/csr/outbreaknetwork/en/>). The clinical features of MERS-CoV infection in humans range from asymptomatic to

very severe pneumonia with the potential development of acute respiratory distress syndrome, septic shock, and multiorgan failure resulting in death. Since the first case of MERS-CoV infection was reported in September 2012 and the virus was isolated, significant progress has been made toward understanding the epidemiology, ecology, and biology of the virus (2). Several assays for the detection of acute infection with MERS-CoV by real-time reverse transcription (RT)-PCR have been developed and are now in widespread use (3). Over 30 whole- or partial-genome sequences from different MERS-CoV-infected patients have been posted to GenBank, and phylogenetic trees have been published by several groups (3). Dipeptidyl peptidase 4 (also known as CD26) has been identified as the functional cellular receptor for MERS-CoV (4, 5). Ecological studies have suggested that the virus is of animal origin and is most closely related to coronaviruses found in a number of species of bats, with MERS-CoV viral sequences now found in camels in Saudi Arabia (6–9). Interestingly, a subset of MERS-CoV patients reported close contact with camels. Camels may

Received 10 April 2014 Returned for modification 2 May 2014

Accepted 14 May 2014

Published ahead of print 19 May 2014

Address correspondence to Matthew B. Frieman, MFrieman@som.umaryland.edu. J.D. and C.M.C. contributed equally to this work.

Supplemental material for this article may be found at <http://dx.doi.org/10.1128/AAC.03036-14>.

Copyright © 2014, American Society for Microbiology. All Rights Reserved. doi:10.1128/AAC.03036-14

constitute an intermediate animal host, since camel serum samples collected in 2003 and 2013 had antibodies to MERS-CoV, indicating that MERS-CoV circulates in camels (10–12). The recent development of an animal model for MERS-CoV with adenovirus vectored human DPP4 in mice will now allow for further pathogenesis studies with various MERS-CoV strains (13).

The emergences of both SARS-CoV and MERS-CoV have demonstrated the importance of coronaviruses as potential emerging human pathogens and highlighted the necessity and value of effective communications within the international science community to facilitate rapid responses to emerging infectious diseases. In July 2013, the International Severe Acute Respiratory & Emerging Infection Consortium (ISARIC) compiled a list of drugs available to clinicians for treatment of MERS-CoV infection based on recent experience in treating SARS-CoV infection and pandemic influenza (14). The most promising and clinically available drugs were ribavirin and interferon (IFN), or a combination of the two, since they demonstrated efficacy in an *in vivo* model for MERS-CoV infection (15, 16). This combination has failed to demonstrate benefit in the small number of severely ill MERS-CoV patients treated (17). Outside ribavirin and IFN, the ISARIC recommendations had few alternatives for treating clinicians. It should be noted that these recommendations are meant to be fluid and based on the best available information at the time. As new data become available, these recommendations may change. Recently, we have shown mycophenolic acid (MPA) and IFN- β to be highly effective against MERS-CoV infection *in vitro*. Interestingly, the activity of MPA was specific to MERS-CoV, with little activity observed against SARS-CoV infection (18, 19).

In the work described here, we took the approach of screening a unique panel of both approved drugs and drugs with a well-defined cellular pathway for *in vitro* efficacy against MERS-CoV infection. This subset was identified previously as having antiviral activity against a series of other viruses (P. J. Glass, G. G. Olinger, Jr., and L. M. Johansen, unpublished data). A subset of drugs was also screened against SARS-CoV with the objective to identify drugs with broad activity against coronaviruses in preparedness for potential future emerging coronaviruses. We utilized this approach with the rationale that drugs that have been approved for use in humans would be more readily accepted as potential therapeutic options for MERS-CoV infection if shown to have antiviral activity. The screening of approved drugs to identify therapeutics for drug repurposing is a valid approach, and several approved drugs have been identified as having activity against many viral diseases (20–22). Here we found that 66 of the screened drugs were effective at inhibiting either MERS-CoV or SARS-CoV infection *in vitro* and that 27 of these compounds were effective against both MERS-CoV and SARS-CoV. These data demonstrate the efficiency of screening approved or clinically developed drugs for identification of potential therapeutic options for emerging viral diseases and also provide an expedited approach for supporting off-label use of approved therapeutics.

MATERIALS AND METHODS

Cell lines and virus. Vero E6 cell line (ATCC 1568; Manassas, VA) was maintained at the Integrated Research Facility (IRF, Frederick, MD) in Dulbecco's modified Eagle's medium (DMEM; Corning, Manassas, VA) plus 10% fetal bovine serum (FBS). The Jordan strain of MERS-CoV (GenBank accession no. [KC776174.1](#), MERS-CoV-Hu/Jordan-N3/2012

[23]), kindly provided by Kanta Subbarao (National Institutes of Health, Bethesda, MD) and Gabriel Defang (Naval Medical Research Unit-3, Cairo, Egypt), was amplified in Vero E6 cells at a multiplicity of infection (MOI) of 0.01. On day 4 after infection, when the cytopathic effect (CPE) was visible, virus-containing supernatants were collected and clarified by centrifugation. The MERS-CoV titers on Vero E6 cells were determined by plaque assay. All procedures using live MERS-CoV were performed under biosafety level 3 conditions at the IRF.

The Vero E6 cell line (ATCC 1568; Manassas, VA) at the University of Maryland, Baltimore (UMB), was maintained in minimal essential medium (MEM; Corning, Manassas, VA) supplemented with 10% FBS (SAFC, Bioscience, Lenexa, KS), 1% penicillin-streptomycin (Gemini Bio-products, West Sacramento, CA), and 1% L-glutamine (Life Technologies, Grand Island, NY). Mouse adapted SARS-CoV (MA15) has been described previously (24). SARS-CoV was amplified in Vero E6 cells for 2 days, when the CPE was visible. SARS-CoV-containing supernatants were collected and clarified by centrifugation. Titers of SARS-CoV on Vero E6 cells were determined by plaque assay. All procedures using live SARS-CoV were performed under biosafety level 3 conditions at UMB.

Reagents. Chlorpromazine hydrochloride (CAS 69-09-0) was purchased from Sigma-Aldrich, St. Louis, MO. Imatinib mesylate (CAS 220127-57-1), gemcitabine hydrochloride (CAS 122111-03-9), and toremifene citrate (CAS 89778-27-8) were purchased from Sequoia Research Products, Pangbourne, United Kingdom. Trifluoromazine hydrochloride (CAS 1098-60-8) was purchased from the U.S. Pharmacopeia, Rockville, MD. Dasatinib (CAS 302962-49-8) was purchased from Toronto Research Chemicals Inc., Toronto, Canada. Dimethyl sulfoxide (DMSO) was used as a solvent for the high-throughput screening assay described below.

Drug library and compound plate preparation. A library of approved drugs, including some drugs with a well-defined cellular target, was assembled and has been previously described (25). A subset of 290 compounds was selected for screening against MERS-CoV and SARS-CoV based on the antiviral activity observed in screens against other RNA viruses (21). For the MERS-CoV and SARS-CoV screens, compounds were added to compound plates using an acoustic compound dispenser (Echo 555; Labcyte, Sunnyvale, CA). The compounds were shot in nanoliter volumes directly onto 96-well plates from master stock solutions. Following addition of compound, 200 μ l of DMEM was added to plates, and plates were frozen at -80°C for a minimum of 24 h prior to shipment to the IRF and UMB investigators. Compound plates were thawed prior to the addition of compound to the infectivity assays described below at the IRF and UMB. For the MERS screen, compounds were plated in 200 μ l of media at 4 times the final concentrations such that the addition of 50 μ l to assay plates resulted in the appropriate final concentration (200- μ l final assay volume). For the SARS screens, drugs were plated in 200 μ l of media at 2 times the final concentrations such that the addition of 50 μ l resulted in the appropriate final concentration (100- μ l final assay volume). All drug plates were blinded to those performing the infectivity assays.

Cell-based ELISA screen for MERS-CoV antiviral agents. For cell-based enzyme-linked immunosorbent assay (ELISA) screen, Vero E6 cells were seeded at 40,000 cells in 100 μ l DMEM plus 10% FBS per well in black-, opaque-, or clear-bottom 96 well-plates. After 24 h, test drugs were transferred from compound plates and added to 3 cell plates in 50 μ l using a 96-well liquidator (Rainin Instrument LLC, Oakland, CA). The DMSO concentration was kept at 0.05% or lower. Duplicate Vero E6 seeded plates were used for detecting inhibition of MERS-CoV, and one plate was used for determining the cytotoxicity of compounds. For infection, duplicate plates were pretreated with drugs for 1 h before the plates were transferred into the containment laboratory to add MERS-CoV strain Hu/Jordan-N3/2012 at an MOI of 0.1 in 50 μ l of DMEM plus 10% FBS. After 48 h, plates were fixed with 10% neutral buffered formalin and removed from biocontainment. MERS-CoV infection was detected with a rabbit polyclonal antibody to the HCoV-EMC/2012 Spike protein (number 40069-RP02; Sino Biological Inc., Beijing, CN) followed by staining

with Alexa Fluor 594 goat anti-rabbit IgG (H+L) antibody (Life Technologies, Grand Island, NY). Fluorescence was quantified on a plate reader (Infinite M1000 Pro; Tecan US, Morrisville, NC) with an excitation wavelength of 590 nm and emission wavelength of 617 nm. The drugs with >50% inhibition of Spike expression and <30% toxicity were then screened with SARS-CoV as described below.

To detect cellular toxicity of drugs in the MERS-CoV screen, one of the three plates that received the test drugs was used to evaluate the cytotoxicity of drugs and was not infected with virus. At 48 h after drug addition, cell plates were analyzed using the CellTiter Glo luminescent cell viability assay kit according to the manufacturer's directions (Promega, Madison, WI), and luminescence was read on the Infinite M1000 Pro plate reader.

SARS-CoV cytopathic effect inhibition assay. For the SARS-CoV screen, 174 of the 290 drugs were screened against SARS-CoV, including all the hits that blocked MERS-CoV (72 drugs). The assay used to screen for inhibition of SARS-CoV replication was different from the one used for MERS-CoV replication due to differences in equipment for analysis at UMB and IRF/NIAID. For the SARS-CoV inhibitor screen at UMB, duplicate Vero E6 cells were seeded into white opaque 96-well plates (Corning Costar) at 1×10^4 cells per well and cultured overnight at 37°C. Cells were treated with the drugs for 2 h at 37°C and then mock infected or infected with SARS-CoV (MA15) at an MOI of 1. Cells were cultured at 37°C for 48 h and then analyzed for cell survival using the CellTiterGlo luminescent cell viability assay (Promega, Madison, WI) according to the manufacturer's instructions and read on a SpectraMax M5 plate reader (Molecular Devices, Sunnyvale, CA). A third identical drug compound plate was used to assess drug toxicity in the absence of SARS-CoV using the same Cell-Titer Glo assay (Promega) as above, with cells incubated in the presence of the drug for 48 h before being assayed.

Data analysis. For the MERS-CoV screen, a minimum of four replicates were performed on two separate days. For the SARS-CoV screen, a minimum of two replicates were performed on two separate days. Outlier data points were defined as values that were greater than the median plus 3 standard errors (σ) and were excluded from calculations.

For MERS screening, raw phenotype measurements (T) from each treated well were converted to normalized fractional inhibition, I , by the formula $I = 1 - (T/V)$, relative to the median, V , of vehicle-treated wells arranged around the plate. For SARS screening with a CPE endpoint, the calculation used to measure the antiviral activity of the compounds was the Percent Normal. The Percent Normal monitors the reduction in cytolysis of cells due to the presence of compound treatment and is determined as follows: Percent Normal = $(T - V)/(N - V)$, where T represents the number of cells infected with SARS-CoV and treated with compound, V represents the number of cells infected with SARS-CoV but vehicle treated, and N represents the number of the normal control cells that are neither infected nor treated with compound.

After normalization, average activity values were calculated between replicate measurements at the same treatment doses along with σ_1 , the accompanying standard error estimates. Drug response curves were represented by a logistic sigmoidal function with a maximal effect level (A_{\max}), the concentration at half-maximal activity of the compound (EC_{50}), and a Hill coefficient representing the sigmoidal transition. We used the fitted curve parameters to calculate the concentration at which the drug response reached an absolute inhibition of 50% (EC_{50}), limited to the maximum tested concentration for inactive compounds.

Compounds were considered active if the antiviral activity observed was >50% I (or Percent Normal) with no or low corresponding cytotoxicity (<30% I).

RESULTS

Overview of screening process. A primary screen of 290 compounds containing both approved drugs and developmental drugs with defined cellular targets was performed with three-point dose-response curves to identify compounds with activity against MERS-CoV using a cell-based ELISA (Fig. 1). The analysis

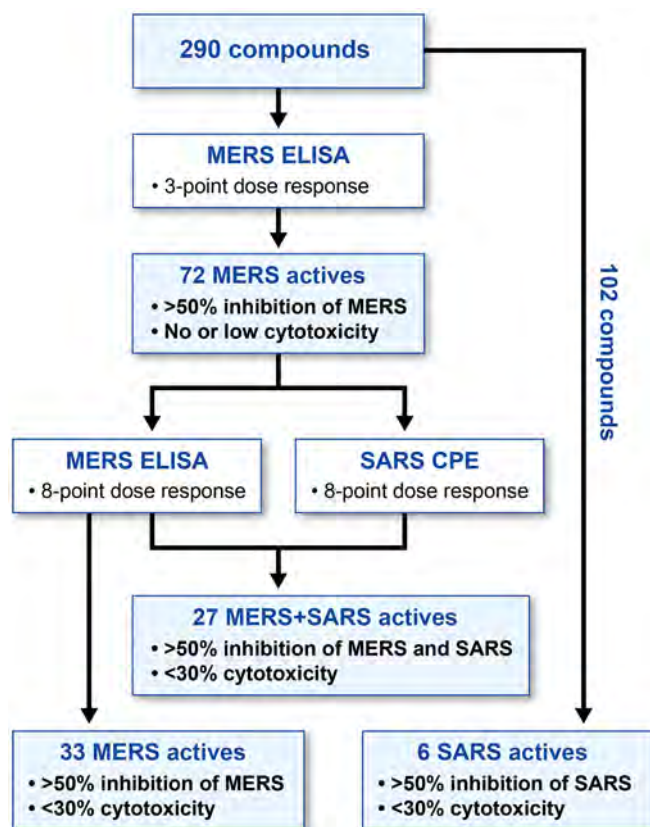


FIG 1 Flowchart of screening procedure. A library of 290 compounds was screened at three doses for activity against MERS-CoV. Seventy-two compounds that had activity against MERS-CoV were subsequently screened against both MERS-CoV and SARS-CoV. Twenty-seven compounds showed activity (>50% inhibition) against both viruses, while 33 compounds were active against only MERS-CoV. A 102-compound subset was screened against SARS-CoV, leading to 6 compounds that were active against only SARS-CoV.

of the raw screening data indicated that 72 compounds were active against MERS-CoV (>50% inhibition) with no or low cytotoxicity (<30% toxicity). In the secondary screen, the 72 compounds were plated at eight doses for confirmation of antiviral activity against MERS-CoV as well as to determine EC_{50} s in the MERS-CoV ELISA. The 72 compounds were also evaluated for their antiviral activity against SARS-CoV using a cytopathic effect (CPE) inhibition assay. An independent screen using a subset of 102 compounds against SARS-CoV infection identified 6 unique compounds with activity against SARS-CoV.

Overview of drugs active against SARS-CoV, MERS-CoV, or both. Analysis of data from all screening activities resulted in a list of 66 compounds that were active against SARS-CoV, MERS-CoV, or both. In summary, we found six drugs that were active against SARS-CoV only, 33 drugs that were active against MERS-CoV only, and 27 drugs that were active against both SARS-CoV and MERS-CoV. These drugs were grouped based upon their recognized mechanism of action into 13 different therapeutic classes that were active against SARS-CoV, MERS-CoV, or both (Table 1). The high hit rates of 21% (60 of 290) for MERS-CoV inhibitors and 19% (33 of 174) for SARS-CoV inhibitors can be explained by the fact that the library was enriched for compounds that have shown antiviral activity against other viruses (Glass et al., unpublished).

TABLE 1 Compounds with activity against MERS-CoV and/or SARS-CoV^a

Pharmaceutical class	No. of compounds with activity against:			Total no. of drugs for class
	SARS-CoV only	MERS-CoV only	SARS-CoV and MERS-CoV	
Antibacterial agents		1	1	2
Antiparasitic agents		2	4	6
Neurotransmitter inhibitors	2	3	11	16
Estrogen receptor inhibitors		3	2	5
DNA inhibitors		3	1	4
Protein-processing inhibitors		1	3	4
Signaling kinase inhibitors	1		2	3
Cytoskeleton inhibitors		8		8
Lipid, sterol metabolism inhibitors		2	2	4
Anti-inflammatory agents	3			3
Ion channel inhibitors		9		9
Apoptosis inhibitors		1		1
Cathepsin inhibitors			1	1
Total	6	33	27	66

^a Drugs showed inhibition (>50%) against the virus(es) and low cytotoxicity (<30%).

Pharmaceuticals that inhibited both coronaviruses included neurotransmitter inhibitors, estrogen receptor antagonists, kinase signaling inhibitors, inhibitors of lipid or sterol metabolism, protein-processing inhibitors, and inhibitors of DNA synthesis/repair. Antiparasitics or antibacterials were two classes of pharma-

ceuticals in which function was not obviously linked to coronaviruses, or viruses in general, but showed antiviral activity against SARS-CoV and MERS-CoV. We also found that a cathepsin inhibitor, E-64-D, blocked both SARS-CoV and MERS-CoV, though this was not surprising since it is known that cathepsins are important for the fusion step during virus entry of coronaviruses (26).

Interestingly, classes of drugs that seem to inhibit only SARS-CoV or MERS-CoV, but not both, were discovered. Though we identified only a small number of SARS-CoV-only inhibitors, they are primarily anti-inflammatories, which interfere with cell signaling associated with the immune response to virus infection. MERS-CoV was specifically blocked by inhibitors of ion transport, the cytoskeleton (specifically tubulin), and apoptosis.

Specific drugs. Twenty-seven specific drugs inhibited both MERS-CoV and SARS-CoV infection (Table 2; see also Fig. S1 and S2 in the supplemental material). We present a selection of drugs in Fig. 2, 3, and 4 that are particularly interesting because they have similar structures or similar mechanisms of action or have been tested against other viruses. Data on antiviral activity and cytotoxicity for the remaining compounds that inhibit MERS-CoV and SARS-CoV are provided in the supplemental material.

In total, 16 neurotransmitter antagonists were found to have activity against one or both of the coronaviruses (Table 1). Eleven of these antagonists were active against both MERS-CoV and SARS-CoV, two against only SARS-CoV, and three against only MERS-CoV. Two of the neurotransmitter inhibitors that inhibit both MERS-CoV and SARS-CoV are chlorpromazine hydrochloride and trifluorpromazine hydrochloride (Table 2). Both of these drugs inhibit the dopamine receptor, and they have similar chem-

TABLE 2 Specific compounds with activity against MERS-CoV and SARS-CoV

Compound	Pharmaceutical class	MERS-CoV EC ₅₀	SARS-CoV EC ₅₀
Emetine dihydrochloride hydrate	Antibacterial agent	0.014	0.051
Chloroquine diphosphate	Antiparasitic agent	6.275	6.538
Hydroxychloroquine sulfate	Antiparasitic agent	8.279	7.966
Mefloquine	Antiparasitic agent	7.416	15.553
Amodiaquine dihydrochloride dihydrate	Antiparasitic agent	6.212	1.274
E-64-D	Cathepsin inhibitor	1.275	0.760
Gemcitabine hydrochloride	DNA metabolism inhibitor	1.216	4.957
Tamoxifen citrate	Estrogen receptor inhibitor	10.117	92.886
Toremifene citrate	Estrogen receptor inhibitor	12.915	11.969
Terconazole	Sterol metabolism inhibitor	12.203	15.327
Triparanol	Sterol metabolism inhibitor	5.283	
Anisomycin	Protein-processing inhibitor	0.003	0.191
Cycloheximide	Protein-processing inhibitor	0.189	0.043
Homoharringtonine	Protein-processing inhibitor	0.0718	
Benztrapine mesylate	Neurotransmitter inhibitor	16.627	21.611
Fluspirilene	Neurotransmitter inhibitor	7.477	5.963
Thiothixene	Neurotransmitter inhibitor	9.297	5.316
Fluphenazine hydrochloride	Neurotransmitter inhibitor	5.868	21.431
Promethazine hydrochloride	Neurotransmitter inhibitor	11.802	7.545
Astemizole	Neurotransmitter inhibitor	4.884	5.591
Chlorphenoxamine hydrochloride	Neurotransmitter inhibitor	12.646	20.031
Chlorpromazine hydrochloride	Neurotransmitter inhibitor	9.514	12.971
Thiethylperazine maleate	Neurotransmitter inhibitor	7.865	
Trifluorpromazine hydrochloride	Neurotransmitter inhibitor	5.758	6.398
Clomipramine hydrochloride	Neurotransmitter inhibitor	9.332	13.238
Imatinib mesylate	Kinase signaling inhibitor	17.689	9.823
Dasatinib	Kinase signaling inhibitor	5.468	2.100

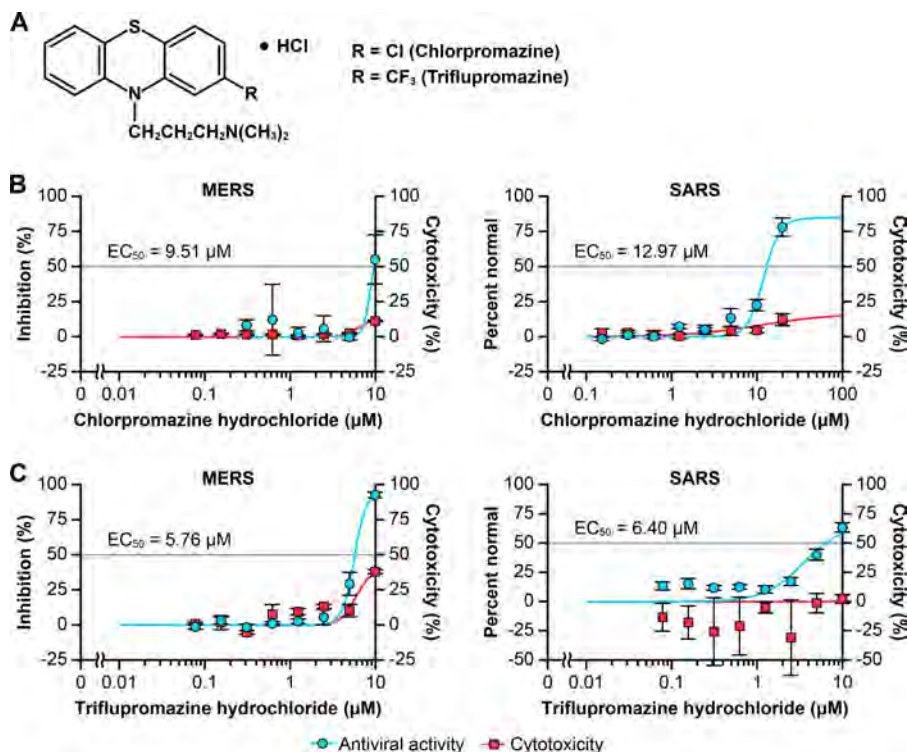


FIG 2 Antiviral activity of chlorpromazine hydrochloride and triflupromazine hydrochloride. (A) Chemical structures of the compounds. Vero E6 cells were infected with MERS-CoV or SARS-CoV at an MOI of 0.1 or 1, respectively, and treated for 48 h with eight doses of chlorpromazine hydrochloride (B) or triflupromazine hydrochloride (C). Antiviral activity is shown in blue, and cytotoxicity is shown in red. EC₅₀s are indicated. Results are representative of one experiment (means \pm standard error of the means [SEM]; $n = 2$).

ical structures (Fig. 2A), sharing the same core structure, with the only difference being the nature of the halide group: chlorpromazine hydrochloride has a single chlorine, while triflupromazine hydrochloride has three fluorine atoms surrounding a carbon.

Both chlorpromazine hydrochloride and triflupromazine hydrochloride strongly inhibit MERS-CoV and SARS-CoV, with micromolar EC₅₀s (range, 5.76 μM to 12.9 μM) and low toxicity (Fig. 2B and C). No significant difference was observed between the effects

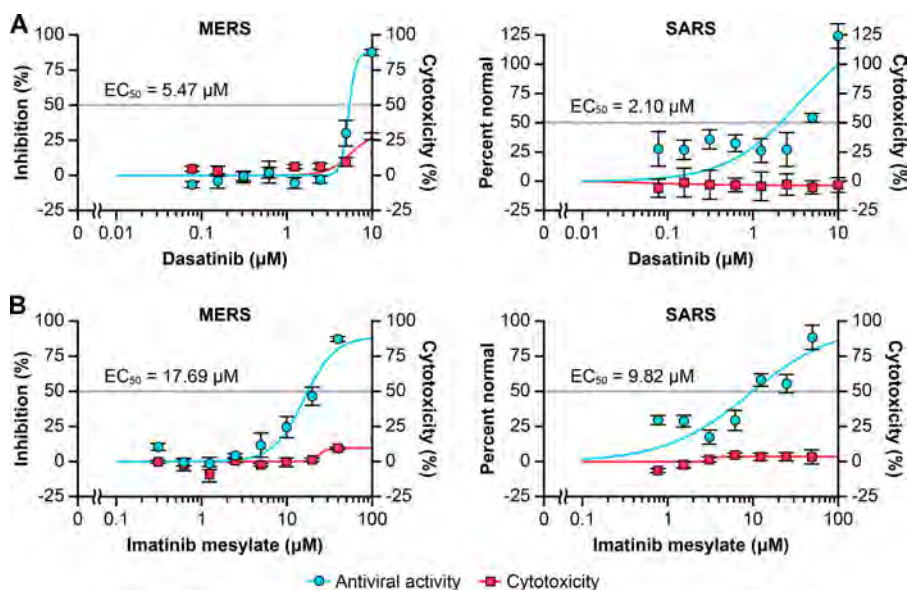


FIG 3 Antiviral activity of dasatinib and imatinib mesylate. Vero E6 cells were infected with MERS-CoV or SARS-CoV at an MOI of 0.1 or 1, respectively, and treated for 48 h with eight doses of dasatinib (A) or imatinib mesylate (B). Antiviral activity is shown in blue, and cytotoxicity is shown in red. EC₅₀s are indicated. Results are representative of one experiment (means \pm SEM; $n = 2$).

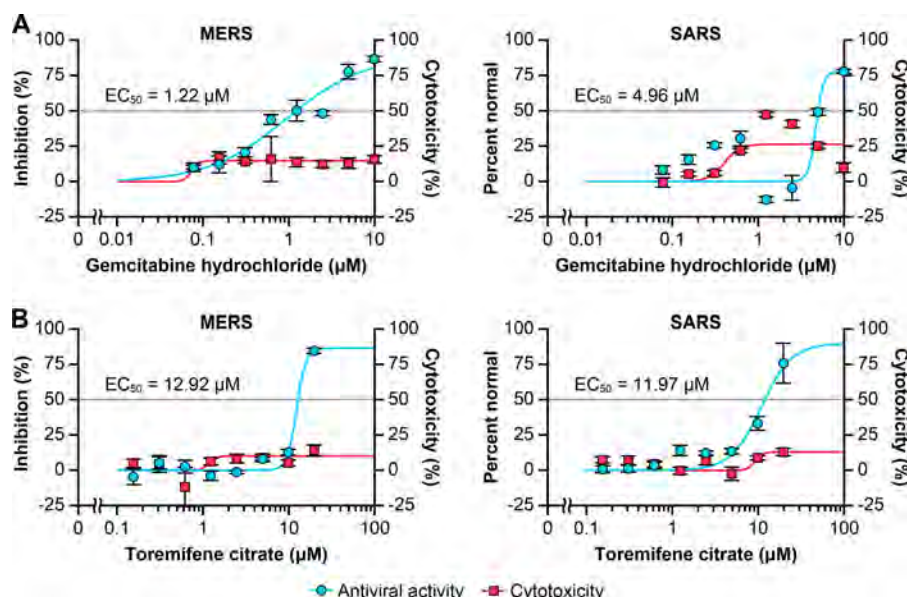


FIG 4 Antiviral activity of gemcitabine hydrochloride and toremifene citrate. Vero E6 cells were infected with MERS-CoV or SARS-CoV at an MOI of 0.1 or 1, respectively, and treated for 48 h with eight doses of gemcitabine hydrochloride (A) or toremifene citrate (B). Antiviral activity is shown in blue, and cytotoxicity is shown in red. EC_{50} s are indicated. Results are representative of one experiment (means \pm SEM; $n = 2$).

of these drugs on MERS-CoV and SARS-CoV; for example, triflupromazine hydrochloride inhibits both MERS-CoV and SARS-CoV with approximately the same EC_{50} (5.76 μ M and 6.39 μ M, respectively [Fig. 2C]). The similarity in the structures of chlorpromazine hydrochloride and triflupromazine hydrochloride would suggest that they inhibit MERS-CoV and SARS-CoV using the same mechanism of action. Chlorpromazine hydrochloride has been used to study virus entry by clathrin-mediated endocytosis of several viruses, including West Nile virus (WNV) and influenza virus (27–31). SARS-CoV also utilizes the clathrin-mediated endocytosis pathway for entry (32), suggesting that this drug may act similarly on MERS-CoV and SARS-CoV and have potential as a broad-spectrum coronavirus inhibitor.

We identified three inhibitors of the kinase signaling pathway, two (imatinib mesylate and dasatinib) that are active against both MERS-CoV and SARS-CoV, and one (nilotinib) that inhibits SARS-CoV only. Imatinib mesylate and dasatinib are known inhibitors of the Abelson murine leukemia viral oncogene homolog 1 (ABL1) pathway. The ABL1 pathway is a signaling pathway involved in cell differentiation, cell adhesion, and the cellular stress response. Overactivation of the ABL1 pathway can lead to chronic myelogenous leukemia. Both imatinib mesylate and dasatinib were developed and approved as inhibitors of this pathway for treating human cancers, including chronic myelogenous leukemia (33, 34). Both imatinib mesylate and dasatinib inhibit SARS-CoV and MERS-CoV with micromolar EC_{50} s (range, 2.1 to 17.6 μ M) and low toxicity (Fig. 3A and B). SARS-CoV does appear to be more sensitive to both ABL1 inhibitors; for example, the EC_{50} of dasatinib against SARS-CoV is 2.1 μ M, whereas for MERS-CoV the EC_{50} is 5.4 μ M (Fig. 3A). A third ABL1 inhibitor, nilotinib, was also used in this study. Nilotinib is able to inhibit SARS-CoV with a micromolar EC_{50} and low toxicity (data not shown) but does not significantly inhibit MERS-CoV, with the maximum inhibition of MERS-CoV being 39% at the highest dose tested (data not shown). However, the fact that nilotinib is able to inhibit SARS-

CoV and partially inhibit MERS-CoV further points to the importance of the ABL1 pathway in coronavirus replication. Imatinib mesylate has been shown to block egress of Ebola virus and of poxviruses and entry of coxsackievirus (20, 35, 36). These data suggest that the ABL1 pathway may be important for replication of many different virus families and, therefore, inhibitors of this pathway have the potential to be broad-spectrum antivirals.

Gemcitabine hydrochloride is a deoxycytidine analog that inhibits DNA synthesis and repair. Gemcitabine hydrochloride inhibits both MERS-CoV and SARS-CoV with micromolar EC_{50} s (1.2 μ M and 4.9 μ M, respectively) and low toxicity (Fig. 4A). Interestingly, we identified four DNA synthesis inhibitors that were active against at least one coronavirus (Table 1), suggesting that these drugs have potential as antivirals for coronaviruses. These data also demonstrate the importance of screening large drug sets, rather than targeted screens of suspected inhibitors, as it may not have been immediately obvious that a DNA synthesis inhibitor would have any effect on the replication of an RNA virus.

Toremifene citrate is an estrogen receptor 1 antagonist that inhibits both MERS-CoV and SARS-CoV with micromolar EC_{50} s (12.9 μ M and 11.97 μ M, respectively) and low toxicity (Fig. 4B). Toremifene citrate has been tested against several filoviruses and was shown to block filovirus entry (21, 37). In the screens described here, there were five estrogen receptor inhibitors that blocked at least one coronavirus (Table 1), and two of these blocked both MERS-CoV and SARS-CoV with micromolar EC_{50} s (Table 2) and low toxicity. While the antiviral mechanism against MERS-CoV and SARS-CoV is unknown, these results suggest that estrogen receptor 1 inhibitors have the potential for broad-spectrum antiviral activity.

DISCUSSION

In order to prevent the emergence of a novel virus from growing into a pandemic or established human pathogen, it is critical that public health officials and clinicians be able to diagnose the infec-

tion, control its spread, and treat those afflicted. First and foremost, we need more countermeasures that can be used for the early phase of an epidemic to provide an immediate treatment response while more-appropriate therapies are being developed. Given the time and costs associated with licensure of novel therapeutics, one feasible and rapid response is through repurposing of existing clinically developed products. Repurposing of approved drugs has several advantages, including known safety/tolerability profiles, availability, lower cost, and familiarity of clinicians in working with these drugs. Supplying the international community with robust sets of *in vitro* and *in vivo* data on potential drugs for treatment of emerging viral diseases continues to be a high priority, as it will allow clinicians to make educated decisions on clinically available drugs for testing in intervention trials.

Here we report that screening of a library of 290 drugs either clinically developed or with a well-defined cellular pathway identified 27 compounds with activity against MERS-CoV and SARS-CoV, 33 compounds with activity against MERS-CoV alone, and 6 compounds with activity against SARS-CoV alone. Overall, we have demonstrated that libraries of approved compounds can be used to screen for inhibitors of viruses and have identified a number of potential antivirals with activity against coronaviruses.

The drugs identified here belong to 13 different classes of pharmaceutical drugs. For two of the classes, kinase signaling inhibitors and estrogen receptor antagonists, previous work with other viruses has given insight into how these drugs may affect viral infections. Three tyrosine kinase inhibitors, imatinib mesylate (Gleevec), nilotinib (Tasigna), and dasatinib, were developed to treat human cancers and were later shown to have activity against several viruses, including poxviruses and Ebola virus (20, 36). Mechanism of action studies revealed that Abl1 tyrosine kinase regulates budding or release of poxviruses and Ebola virus, demonstrating that the c-Abl1 kinase signaling pathways play an important role in the egress of these viruses. Here we show that kinase signaling may also be important for replication of two members of the *Coronaviridae* family. Imatinib mesylate and dasatinib inhibit MERS-CoV and SARS-CoV, while nilotinib inhibits only SARS-CoV. The step in viral replication in which these kinases are involved will need to be investigated further. *In vivo* studies performed in the mouse model of vaccinia virus infection showed that imatinib mesylate was more effective than dasatinib in blocking dissemination of the virus, and this was attributed to the immunosuppressive effect of dasatinib (36). Nevertheless, dasatinib may have value for treating coronaviral infections if a dosing regimen that minimizes immunotoxicity while still blocking viral replication can be defined. Imatinib mesylate (Gleevec) and nilotinib (Tasigna) are FDA-approved oral cancer medicines and are considered promising candidates for development into antivirals against poxviruses (38).

Estrogen receptor modulators represent another class of FDA-approved drugs that have potential as antivirals in the clinic. Toremifene citrate, which we have shown blocks both MERS-CoV and SARS-CoV, has previously been shown to inhibit filoviruses (21). Mechanism of action studies showed that the drug acts at a late step of virus entry and may inhibit trafficking of the virus to the late endosome or triggering of fusion for filoviruses (21, 37). Interestingly, the estrogen signaling pathway is not involved in the virus entry step, indicating that these drugs may have off-target effects or the estrogen signaling pathway plays an as-yet-undiscovered

role in filovirus biology. Toremifene citrate also showed activity in the mouse model of Ebola virus infection (21).

Our screen also identified antiviral actives in the pharmaceutical class of neurotransmitter receptor antagonists. These antagonists have been developed for psychiatric care as antipsychotics, antiemetics, anticholinergics, and antidepressants and predominantly act by blocking the dopamine receptor or H₁ receptor (antihistamine). Chlorpromazine was shown to inhibit clathrin-mediated endocytosis of several viruses by preventing the formation of clathrin-coated pits at the plasma membrane (27). This drug is currently approved by the FDA as an antipsychotic and for the treatment of nausea (39) and is occasionally used for short-term use as off-label treatment of severe migraine (40), making it a promising candidate for testing as a broad-spectrum antiviral. Astemizole, an antihistamine that was identified in our screen, is a strong antagonist of the H₁ receptor (see Fig. S1 and S2 in the supplemental material). Interestingly, it has been reported that astemizole is an inhibitor of malaria and showed efficacy in two animal models of malaria with a mechanism of action similar to that of chloroquine (41). Although astemizole was withdrawn from the U.S. market in 1999, it may be worthwhile to reexamine this drug or existing analogs for short-term use in an acute infection. Previous work on chloroquine in coronavirus infections by Barnard et al. has found that while the drug inhibits viral replication *in vitro*, chloroquine did not show efficacy in reducing SARS-CoV virus titers in a nonlethal mouse model (42). Protection studies using a mouse-adapted SARS-CoV will be performed to identify the *in vivo* efficacy of targeted drugs from our screen.

While development of drugs with broad activity against a virus family or even unrelated viruses is advantageous for several reasons such as immediate availability, lower costs, and recycling of products from the strategic national stockpile, drug classes that are more selective in their activity and affect either MERS-CoV or SARS-CoV should also be further investigated. Our screen identified 33 MERS-CoV actives (Table 1), and the two largest classes were cytoskeleton inhibitors (8 drugs) and ion channel inhibitors (11 drugs). Drugs targeting the cytoskeleton specifically interfere with microtubule polymerization and are antimicrotubule developed for treatment of cancer. Some of them, such as nocodazole, have also been used in cell biology labs to synchronize the cell division cycle. Nocodazole's ability to depolymerize microtubules has been used to investigate the entry pathway of WNV, and results show that an intact microtubule network is necessary for trafficking of internalized WNV from early to late endosomes (27). This drug had high activity against MERS-CoV but had no activity against SARS-CoV, suggesting that, in addition to the application as therapeutics, these drugs may also have value in further elucidating differences in the virus replication cycle of MERS-CoV and SARS-CoV.

Two of the 9 ion channel inhibitors, monensin and salinomycin sodium, with activity against MERS-CoV, represent polyether ionophores that are currently well-recognized candidates for anticancer drugs (43, 44). Studies on the mechanism of anticancer activity have shown that these compounds affect cancer cells by increasing their sensitivity to chemotherapy and reversing multidrug resistance (monensin) in human carcinoma. Furthermore, ionophore antibiotics also inhibit chemoresistant cancer cells by increasing apoptosis, and salinomycin was specifically shown to be able to kill human cancer stem cells (45). Interestingly, these compounds affected MERS-CoV but not SARS-CoV, indicating

that MERS-CoV is uniquely susceptible to ionophore activities. Monensin has also been reported to inhibit La Crosse virus and Uukuniemi virus infection by blocking the formation and egress of virus particles (46, 47). Further studies will reveal if these drugs act at a similar step during MERS-CoV infection.

Overall, we identified several pharmaceutical classes of drugs that could be beneficial for treatment of coronaviral infections. Interestingly, chlorpromazine hydrochloride and chloroquine diphosphate were also identified in a similar but independent study described in the accompanying paper by A. H. de Wilde et al. (48). These drugs appear to target host factors rather than viral proteins specifically, and treatment of viral infections in patients aimed at host factors could reconfigure overt manifestations of viral pathogenesis into a less virulent subclinical infection and lower adverse disease outcome (38). The targets identified in this paper provide new candidates for future research studies and clinical intervention protocols.

ACKNOWLEDGMENTS

We thank Laura Pierce, Anatoly Myaskovsky, Kelly DeRoche, and Crag Markwood at Zalicus Inc. for compound plate preparation and data integration. We thank Yingyun Cai and Cindy Allan for outstanding assistance in the development of the drug screen protocol. We thank the IRF Cell Culture staff in preparing the cells used in this study. In addition, we acknowledge Laura Bollinger and Jiro Wada at the IRF for technical writing services and figure preparation for the manuscript.

This work was supported by the Division of Intramural Research of the National Institute of Allergy and Infectious Diseases (NIAID), the Integrated Research Facility (NIAID, Division of Clinical Research), the Battelle Memorial Institute's prime contract with NIAID (contract number HHSN2722007000161) and NIH grant R01AI1095569 (to M.B.F.), and a subcontract (W81XWH-12-2-0064) awarded to L.M.J. from the U.S. Army Research Institute of Infectious Diseases (USAMRIID).


L.M.J. was employed at Zalicus Inc. during the time the research was performed. M.L. is currently employed at Zalicus Inc. No other authors have conflicts of interest.

REFERENCES

- WHO. 2003. Summary of probable SARS cases with onset of illness from 1 November 2002 to 31 July 2003. http://www.who.int/csr/sars/country/table2004_04_21/en/index.html.
- Zaki AM, van Boheemen S, Bestebroer TM, Osterhaus AD, Fouchier RA. 2012. Isolation of a novel coronavirus from a man with pneumonia in Saudi Arabia. *N. Engl. J. Med.* 367:1814–1820. <http://dx.doi.org/10.1056/NEJMoa1211721>.
- The WHO MERS-Cov Research Group. 12 November 2013. State of knowledge and data gaps of Middle East respiratory syndrome coronavirus (MERS-CoV) in humans. *PLoS Curr.* 5:pii=ecurrents.outbreaks.0bf719e352e7478f7478ad7485fa30127ddb30128. <http://dx.doi.org/10.1371/currents.outbreaks.0bf719e352e7478f7478ad7485fa30127ddb30128>.
- Lu G, Hu Y, Wang Q, Qi J, Gao F, Li Y, Zhang Y, Zhang W, Yuan Y, Bao J, Zhang B, Shi Y, Yan J, Gao GF. 2013. Molecular basis of binding between novel human coronavirus MERS-CoV and its receptor CD26. *Nature* 500:227–231. <http://dx.doi.org/10.1038/nature12328>.
- Raj VS, Mou H, Smits SL, Dekkers DH, Muller MA, Dijkman R, Muth D, Demmers JA, Zaki A, Fouchier RA, Thiel V, Drosten C, Rottier PJ, Osterhaus AD, Bosch BJ, Haagmans BL. 2013. Dipeptidyl peptidase 4 is a functional receptor for the emerging human coronavirus-EMC. *Nature* 495:251–254. <http://dx.doi.org/10.1038/nature12005>.
- Alagaili AN, Briesse T, Mishra N, Kapoor V, Sameroff SC, de Wit E, Munster VJ, Hensley LE, Zalmout IS, Kapoor A, Epstein JH, Karesh WB, Daszak P, Mohammed OB, Lipkin WI. 2014. Middle East respiratory syndrome coronavirus infection in dromedary camels in Saudi Arabia. *mBio* 5:e00884-14. <http://dx.doi.org/10.1128/mBio.00884-14>.
- Annan A, Baldwin HJ, Corman VM, Klose SM, Owusu M, Nkrumah EE, Badu EK, Anti P, Agbenyega O, Meyer B, Oppong S, Sarkodie YA, Kalko EK, Lina PH, Godlevska EV, Reusken C, Seebens A, Gloza-Rausch F, Vallo P, Tschapka M, Drosten C, Drexler JF. 2013. Human betacoronavirus 2c EMC/2012-related viruses in bats, Ghana and Europe. *Emerg. Infect. Dis.* 19:456–459. <http://dx.doi.org/10.3201/eid1903.121503>.
- Ithete NL, Stoffberg S, Corman VM, Cottontail VM, Richards LR, Schoeman MC, Drosten C, Drexler JF, Preiser W. 2013. Close relative of human Middle East respiratory syndrome coronavirus in bat, South Africa. *Emerg. Infect. Dis.* 19:1697–1699. <http://dx.doi.org/10.3201/eid1910.130946>.
- Memish ZA, Mishra N, Olival KJ, Fagbo SF, Kapoor V, Epstein JH, Alhakeem R, Durosinioun A, Al Asmari M, Islam A, Kapoor A, Briesse T, Daszak P, Al Rabeeah AA, Lipkin WI. 2013. Middle East respiratory syndrome coronavirus in bats, Saudi Arabia. *Emerg. Infect. Dis.* 19:1819–1823. <http://dx.doi.org/10.3201/eid1911.131172>.
- Meyer B, Müller MA, Corman VM, Reusken CB, Ritz D, Godeke G-J, Lattwein E, Kallies S, Siemens A, van Beek J, Drexler JF, Muth D, Bosch B-J, Wernery U, Koopmans MP, Wernery R, Drosten C. 2014. Antibodies against MERS coronavirus in dromedary camels, United Arab Emirates, 2003 and 2013. *Emerg. Infect. Dis.* 20:552–559. <http://dx.doi.org/10.3201/eid2004.131746>.
- Perera RA, Wang P, Gomaa MR, El-Shesheny R, Kandeil A, Bagato O, Siu LY, Shehata MM, Kaye AS, Moatasim Y, Li M, Poon LL, Guan Y, Webby RJ, Ali MA, Peiris JS, Kayali G. 2013. Seroepidemiology for MERS coronavirus using microneutralisation and pseudoparticle virus neutralisation assays reveal a high prevalence of antibody in dromedary camels in Egypt, June 2013. *Euro Surveill.* 18:pii=20574. <http://www.eurosurveillance.org/ViewArticle.aspx?ArticleId=20574>.
- Reusken CB, Haagmans BL, Muller MA, Gutierrez C, Godeke GJ, Meyer B, Muth D, Raj VS, Smits-De Vries L, Corman VM, Drexler JF, Smits SL, El Tahir YE, De Sousa R, van Beek J, Nowotny N, van Maanen K, Hidalgo-Hermoso E, Bosch BJ, Rottier P, Osterhaus A, Gortazar-Schmidt C, Drosten C, Koopmans MP. 2013. Middle East respiratory syndrome coronavirus neutralising serum antibodies in dromedary camels: a comparative serological study. *Lancet Infect. Dis.* 13:859–866. [http://dx.doi.org/10.1016/S1473-3099\(13\)70164-6](http://dx.doi.org/10.1016/S1473-3099(13)70164-6).
- Zhao J, Li K, Wohlford-Lenane C, Agnihothram SS, Fett C, Zhao J, Gale MJ, Jr, Baric RS, Enjuanes L, Gallagher T, McCray PB, Jr, Perlman S. 2014. Rapid generation of a mouse model for Middle East respiratory syndrome. *Proc. Natl. Acad. Sci. U. S. A.* 111:4970–4975. <http://dx.doi.org/10.1073/pnas.1323279111>.
- Brown C, Carson G, Chand M, Zambon M. 2013 July 29. Treatment of MERS-CoV: Decision Support Tool. Clinical decision making tool for the treatment of MERS-CoV v. 1.1. International Severe Acute Respiratory and Emerging Infection Consortium, Oxford, United Kingdom. http://isaric.tghn.org/site_media/media/articles/Decision_Support_Document_v1_1_20130729.pdf. Accessed 23 Jan 2014.
- Falzarano D, de Wit E, Martellaro C, Callison J, Munster VJ, Feldmann H. 2013. Inhibition of novel beta coronavirus replication by a combination of interferon-alpha2b and ribavirin. *Sci. Rep.* 3:1686. <http://dx.doi.org/10.1038/srep01686>.
- Falzarano D, de Wit E, Rasmussen AL, Feldmann F, Okumura A, Scott DP, Brining D, Bushmaker T, Martellaro C, Baseler L, Benecke AG, Katze MG, Munster VJ, Feldmann H. 2013. Treatment with interferon-alpha2b and ribavirin improves outcome in MERS-CoV-infected rhesus macaques. *Nat. Med.* 19:1313–1317. <http://dx.doi.org/10.1038/nm.3362>.
- Al-Tawfiq JA, Momattin H, Dib J, Memish ZA. 2014. Ribavirin and interferon therapy in patients infected with the Middle East respiratory syndrome coronavirus: an observational study. *Int. J. Infect. Dis.* pii: S1201-9712(13)00376-7. <http://dx.doi.org/10.1016/j.ijid.2013.12.003>.
- Chan JF, Chan KH, Kao RY, To KK, Zheng BJ, Li CP, Li PT, Dai J, Mok FK, Chen H, Hayden FG, Yuen KY. 2013. Broad-spectrum antivirals for the emerging Middle East respiratory syndrome coronavirus. *J. Infect.* 67:606–616. <http://dx.doi.org/10.1016/j.jinf.2013.09.029>.
- Hart BJ, Dyall J, Postnikova E, Zhou H, Kindrachuk J, Johnson RF, Olinger GG, Jr, Frieman MB, Holbrook MR, Jahrling PB, Hensley L. 9 December 2013. Interferon-beta and mycophenolic acid are potent inhibitors of Middle East respiratory syndrome coronavirus in cell-based assays. *J. Gen. Virol.* <http://dx.doi.org/10.1099/vir.0.061911-0>.
- Garcia M, Cooper A, Shi W, Bornmann W, Carrion R, Kalman D, Nabel GJ. 2012. Productive replication of Ebola virus is regulated by the c-Ab1 tyrosine kinase. *Sci. Transl. Med.* 4:123ra24. <http://dx.doi.org/10.1126/scitranslmed.3003500>.
- Johansen LM, Brannan JM, Delos SE, Shoemaker CJ, Stossel A, Lear C,

- Hoffstrom BG, Dewald LE, Schornberg KL, Scully C, Lehar J, Hensley LE, White JM, Olinger GG. 2013. FDA-approved selective estrogen receptor modulators inhibit Ebola virus infection. *Sci. Transl. Med.* 5:190ra179. <http://dx.doi.org/10.1126/scitranslmed.3005471>.
22. Madrid PB, Chopra S, Manger ID, Gilfillan L, Keepers TR, Shurtleff AC, Green CE, Iyer LV, Dilks HH, Davey RA, Kolokoltsov AA, Carrion R, Jr, Patterson JL, Bavari S, Panchal RG, Warren TK, Wells JB, Moos WH, Burke RL, Tanga MJ. 2013. A systematic screen of FDA-approved drugs for inhibitors of biological threat agents. *PLoS One* 8:e60579. <http://dx.doi.org/10.1371/journal.pone.0060579>.
 23. de Groot RJ, Baker SC, Baric RS, Brown CS, Drosten C, Enjuanes L, Fouchier RA, Galiano M, Gorbalenya AE, Memish ZA, Perlman S, Poon LL, Snijder EJ, Stephens GM, Woo PC, Zaki AM, Zambon M, Ziebuhr J. 2013. Middle East respiratory syndrome coronavirus (MERS-CoV): announcement of the Coronavirus Study Group. *J. Virol.* 87:7790–7792. <http://dx.doi.org/10.1128/JVI.01244-13>.
 24. Roberts A, Deming D, Paddock CD, Cheng A, Yount B, Vogel L, Herman BD, Sheahan T, Heise M, Genrich GL, Zaki SR, Baric R, Subbarao K. 2007. A mouse-adapted SARS-coronavirus causes disease and mortality in BALB/c mice. *PLoS Pathog.* 3:e5. <http://dx.doi.org/10.1371/journal.ppat.0030005>.
 25. Lehar J, Krueger AS, Avery W, Heilbut AM, Johansen LM, Price ER, Rickles RJ, Short GF, III, Staunton JE, Jin X, Lee MS, Zimmermann GR, Borisy AA. 2009. Synergistic drug combinations tend to improve therapeutically relevant selectivity. *Nat. Biotechnol.* 27:659–666. <http://dx.doi.org/10.1038/nbt.1549>.
 26. Bosch BJ, Bartelink W, Rottier PJ. 2008. Cathepsin L functionally cleaves the severe acute respiratory syndrome coronavirus class I fusion protein upstream of rather than adjacent to the fusion peptide. *J. Virol.* 82:8887–8890. <http://dx.doi.org/10.1128/JVI.00415-08>.
 27. Chu JJ, Ng ML. 2004. Infectious entry of West Nile virus occurs through a clathrin-mediated endocytic pathway. *J. Virol.* 78:10543–10555. <http://dx.doi.org/10.1128/JVI.78.19.10543-10555.2004>.
 28. Joki-Korpela P, Marjomaki V, Krogerus C, Heino J, Hyypia T. 2001. Entry of human parechovirus 1. *J. Virol.* 75:1958–1967. <http://dx.doi.org/10.1128/JVI.75.4.1958-1967.2001>.
 29. Krizanov O, Ciampor F, Veber P. 1982. Influence of chlorpromazine on the replication of influenza virus in chick embryo cells. *Acta Virol.* 26: 209–216.
 30. Nawa M, Takasaki T, Yamada K, Kurane I, Akatsuka T. 2003. Interference in Japanese encephalitis virus infection of Vero cells by a cationic amphiphilic drug, chlorpromazine. *J. Gen. Virol.* 84:1737–1741. <http://dx.doi.org/10.1099/vir.0.18883-0>.
 31. Pho MT, Ashok A, Atwood WJ. 2000. JC virus enters human glial cells by clathrin-dependent receptor-mediated endocytosis. *J. Virol.* 74:2288–2292. <http://dx.doi.org/10.1128/JVI.74.5.2288-2292.2000>.
 32. Inoue Y, Tanaka N, Tanaka Y, Inoue S, Morita K, Zhuang M, Hattori T, Sugamura K. 2007. Clathrin-dependent entry of severe acute respiratory syndrome coronavirus into target cells expressing ACE2 with the cytoplasmic tail deleted. *J. Virol.* 81:8722–8729. <http://dx.doi.org/10.1128/JVI.00253-07>.
 33. Tolomeo M, Dieli F, Gebbia N, Simoni D. 2009. Tyrosine kinase inhibitors for the treatment of chronic myeloid leukemia. *Anticancer Agents Med. Chem.* 9:853–863. <http://dx.doi.org/10.2174/187152009789124637>.
 34. Wolf D, Rumpold H. 2009. A benefit-risk assessment of imatinib in chronic myeloid leukaemia and gastrointestinal stromal tumours. *Drug Saf.* 32:1001–1015. <http://dx.doi.org/10.2165/11314600-000000000-00000>.
 35. Coyne CB, Bergelson JM. 2006. Virus-induced Abl and Fyn kinase signals permit coxsackievirus entry through epithelial tight junctions. *Cell* 124: 119–131. <http://dx.doi.org/10.1016/j.cell.2005.10.035>.
 36. Reeves PM, Smith SK, Olson VA, Thorne SH, Bornmann W, Damon IK, Kalman D. 2011. Variola and monkeypox viruses utilize conserved mechanisms of virion motility and release that depend on abl and SRC family tyrosine kinases. *J. Virol.* 85:21–31. <http://dx.doi.org/10.1128/JVI.01814-10>.
 37. Shoemaker CJ, Schornberg KL, Delos SE, Scully C, Pajouhesh H, Olinger GG, Johansen LM, White JM. 2013. Multiple cationic amphiphiles induce a Niemann-Pick C phenotype and inhibit Ebola virus entry and infection. *PLoS One* 8:e56265. <http://dx.doi.org/10.1371/journal.pone.0056265>.
 38. McFadden G. 2005. Gleevec casts a pox on poxviruses. *Nat. Med.* 11:711–712. <http://dx.doi.org/10.1038/nm0705-711>.
 39. American Society of Health-System Pharmacists. 2014. Chlorpromazine. Chlorpromazine hydrochloride. In McEvoy GK (ed), AHFS drug information. American Society of Health-System Pharmacists, Bethesda, MD.
 40. Logan P, Lewis D. 2007. Towards evidence based emergency medicine: best BETs from the Manchester Royal Infirmary. Chlorpromazine in migraine. *Emerg. Med. J.* 24:297–300. <http://dx.doi.org/10.1136/emj.2007.047860>.
 41. Chong CR, Chen X, Shi L, Liu JO, Sullivan DJ, Jr. 2006. A clinical drug library screen identifies astemizole as an antimalarial agent. *Nat. Chem. Biol.* 2:415–416. <http://dx.doi.org/10.1038/nchembio806>.
 42. Barnard DL, Day CW, Bailey K, Heiner M, Montgomery R, Lauridsen L, Chan PK, Sidwell RW. 2006. Evaluation of immunomodulators, interferons and known in vitro SARS-CoV inhibitors for inhibition of SARS-CoV replication in BALB/c mice. *Antivir. Chem. Chemother.* 17:275–284. <http://dx.doi.org/10.1016/j.antiviral.2011.02.003>.
 43. Gupta PB, Onder TT, Jiang G, Tao K, Kuperwasser C, Weinberg RA, Lander ES. 2009. Identification of selective inhibitors of cancer stem cells by high-throughput screening. *Cell* 138:645–659. <http://dx.doi.org/10.1016/j.cell.2009.06.034>.
 44. Huczynski A. 2012. Polyether ionophores-promising bioactive molecules for cancer therapy. *Bioorg. Med. Chem. Lett.* 22:7002–7010. <http://dx.doi.org/10.1016/j.bmcl.2012.09.046>.
 45. Koo KH, Kim H, Bae YK, Kim K, Park BK, Lee CH, Kim YN. 2013. Salinomycin induces cell death via inactivation of Stat3 and downregulation of Skp2. *Cell Death Dis.* 4:e693. <http://dx.doi.org/10.1038/cddis.2013.223>.
 46. Cash P. 1982. Inhibition of La Crosse virus replication by monensin, monovalent ionophore. *J. Gen. Virol.* 59:193–196. <http://dx.doi.org/10.1099/0022-1317-59-1-193>.
 47. Kuismäen E, Saraste J, Pettersson RF. 1985. Effect of monensin on the assembly of Uukuniemi virus in the Golgi complex. *J. Virol.* 55:813–822.
 48. de Wilde AH, Jochmans D, Posthuma CC, Zevenhoven-Dobbe JC, van Nieuwkoop S, Bestebroer TM, van den Hoogen BG, Neyts J, Snijder EJ. 2014. Screening of an FDA-approved compound library identifies four small-molecule inhibitors of Middle East respiratory syndrome coronavirus replication in cell culture. *Antimicrob. Agents Chemother.* 58:4875–4884. <http://dx.doi.org/10.1128/AAC.03011-14>.

Middle East Respiratory Syndrome and Severe Acute Respiratory Syndrome: Current Therapeutic Options and Potential Targets for Novel Therapies

Julie Dyall¹  · Robin Gross¹ · Jason Kindrachuk² · Reed F. Johnson³ · Gene G. Olinger Jr.⁴ · Lisa E. Hensley¹ · Matthew B. Frieman⁵ · Peter B. Jahrling^{1,3}

Published online: 15 November 2017
© Springer International Publishing AG 2017

Abstract No specific antivirals are currently available for two emerging infectious diseases, Middle East respiratory syndrome (MERS) and severe acute respiratory syndrome (SARS). A literature search was performed covering pathogenesis, clinical features and therapeutics, clinically developed drugs for repurposing and novel drug targets. This review presents current knowledge on the epidemiology, pathogenesis and clinical features of the SARS and MERS coronaviruses. The rationale for and outcomes with treatments used for SARS and MERS is discussed. The main focus of the review is on drug development and the potential that drugs approved for other indications provide for repurposing. The drugs we discuss belong to a wide range of different drug classes, such as cancer therapeutics, antipsychotics, and antimalarials. In addition to their activity against MERS and SARS coronaviruses, many of these approved drugs have broad-spectrum potential and have already been in clinical use for treating other viral infections. A wealth of knowledge is available for these drugs. However, the information in this review is not meant

to guide clinical decisions, and any therapeutic described here should only be used in context of a clinical trial. Potential targets for novel antivirals and antibodies are discussed as well as lessons learned from treatment development for other RNA viruses. The article concludes with a discussion of the gaps in our knowledge and areas for future research on emerging coronaviruses.

Key Points

The outbreaks of Middle East respiratory syndrome (MERS) and severe acute respiratory syndrome (SARS) were caused by emerging coronaviruses.

A variety of approaches for developing therapeutics are discussed with emphasis on drugs that have been approved for other indications and could be repurposed for treating emerging coronaviral infections.

The recent MERS and SARS outbreaks highlight the importance of a panel of well-characterized broad-spectrum antivirals for treating emerging viral infections

✉ Julie Dyall
dyallj@niaid.nih.gov

¹ Integrated Research Facility, Division of Clinical Research, National Institute of Allergy and Infectious Diseases, National Institutes of Health, Frederick, MD, USA

² Department of Medical Microbiology, University of Manitoba, Winnipeg, MN, Canada

³ Emerging Viral Pathogens Section, National Institute of Allergy and Infectious Diseases, National Institutes of Health, Frederick, MD, USA

⁴ University of Boston, Boston, MA, USA

⁵ Department of Microbiology and Immunology, University of Maryland, School of Medicine, Baltimore, MD, USA

1 Introduction

An electronic literature search for countermeasures against Middle East respiratory syndrome coronavirus (MERS-CoV) and severe acute respiratory syndrome coronavirus (SARS-CoV) was performed using PubMed and Google

Scholar from 2000 through April 17, 2017. The search (key words: Middle East Respiratory Syndrome, Severe Acute Respiratory Syndrome, inhibitors, antivirals, therapeutics, FDA-approved) produced 1677 citations. References selected discussed (1) pathogenesis and history of disease, (2) clinical countermeasures used during the 2003 SARS and 2012 MERS outbreaks and outcomes, and (3) the efficacy of countermeasures targeting viral components and cellular targets of MERS-CoV and SARS-CoV. The main emphasis was on references for drug repurposing as an alternative to the costly development of novel drugs for emerging coronaviral infections.

1.1 Epidemiology of MERS and SARS

Since 2003, two human coronaviruses, SARS-CoV and MERS-CoV, emerged as global public health threats. SARS-CoV was first identified in February 2003 in Guangdong Province, Peoples Republic of China and was transmitted to humans from infected civets, likely infected from bats [1, 2]. SARS-CoV spread to 29 additional countries and was associated with high morbidity in humans (e.g. atypical pneumonia). Ultimately, SARS was contained in 2004 following a highly effective public health response but resulted in 8098 confirmed cases and 774 deaths (Fig. 1a) [3]. In 2012, MERS emerged in The Kingdom of Saudi Arabia and presented as a severe respiratory disease, with frequent gastrointestinal and renal complications. MERS-CoV, the causative agent of MERS, was later identified as a coronavirus. MERS-CoV has subsequently spread to 27 additional countries (Fig. 1B) [4]. As of September 12, 2017, 2080 confirmed cases of MERS and 722 deaths were reported [5].

Coronaviruses are enveloped, single-stranded, positive-sense RNA viruses (Fig. 2). They are members of the *Coronavirinae* subfamily of viruses and together with the *Torovirinae* subfamily comprise the *Coronaviridae* virus family (order *Nidovirales*). *Coronavirinae* is divided into four genera: alpha coronavirus, beta coronavirus, gamma coronavirus, and delta coronavirus. The coronaviruses share a similar genome organization. The open reading frame 1a and 1b comprise nearly 2/3 of the genome and encode the nonstructural proteins. The multiple structural proteins, including spike, nucleocapsid, envelope, and membrane proteins are encoded by downstream open reading frames (Fig. 2) [6–8]. SARS-CoV and MERS-CoV belong to the beta coronavirus genus. However, SARS-CoV belongs to lineage B, and MERS-CoV belongs to lineage C along with bat coronaviruses HKU4 and HKU5. As MERS-CoV and bat coronaviruses are part of lineage C and MERS-CoV RNA was found in a bat sample in The Kingdom of Saudi Arabia, researchers hypothesize that bats may be a natural reservoir for MERS-CoV [9, 10].

Results from a recent study support that bats may be a reservoir for MERS-CoV; however, camels and goats are thought to be intermediate hosts [11]. In this study, MERS-CoV was isolated from nasal secretions of MERS-CoV-infected dromedary camels that had a short, mild disease progression.

The suspected reservoir for SARS-CoV is the Chinese horseshoe bat [2]. However, the mechanism of emergence and adaptation to make the virus zoonotic is still not definitely understood [2]. SARS-CoV-like isolates from these bats have up to 95% sequence similarity to human and civet SARS-CoV. During the initial outbreak, SARS-CoV was originally isolated from palm civets found in a Chinese market; but, SARS-CoV was not found in the wild palm civet population [12]. Bats harbor many coronaviruses and are considered the main reservoir for later infections in an intermediate host, such as civets or camels, which spread the disease to humans [2]. Human-to-human transmission has been most commonly associated with health-care workers and those with close, unprotected contact with infected patients [13, 14].

1.2 Clinical Features

The clinical features of MERS and SARS are similar and can range from asymptomatic or mild disease to severe pneumonia with acute respiratory distress syndrome (ARDS) and multi-organ failure [15]. Although MERS and SARS are clinically similar, the MERS mortality rate is 40% and SARS's mortality rate is 10% [16]. Approximately 75% of MERS cases were associated with underlying comorbidities with a 60% mortality rate in this subgroup (including cardiopulmonary abnormalities, obesity, and diabetes). In contrast, 10–30% of patients with SARS have comorbidities with a mortality rate of 46% within this subgroup [15, 16].

The development of symptomatic MERS and SARS mostly occurs in adults (median age of 50 years; 40 years for SARS). MERS and SARS symptoms typically follow a mean incubation time of ~ 5 days (range 2–13 and 2–14 days, respectively) and include fever, chills, cough (some associated with blood), shortness of breath, myalgia, headache, nausea, vomiting, diarrhea, sore throat, and malaise [15–17]. Progression from mild to severe disease is more rapid with MERS as compared to SARS with means of 7 and 11 days, respectively [15]. Secondary bacterial infections have occurred in patients with severe MERS; however, the role of these coinfections in MERS pathogenesis has yet to be determined [18–20]. Laboratory abnormalities associated with MERS and SARS patients include elevated lactate dehydrogenase, elevated liver enzymes; thrombocytopenia; lymphopenia and leukopenia [21–23].

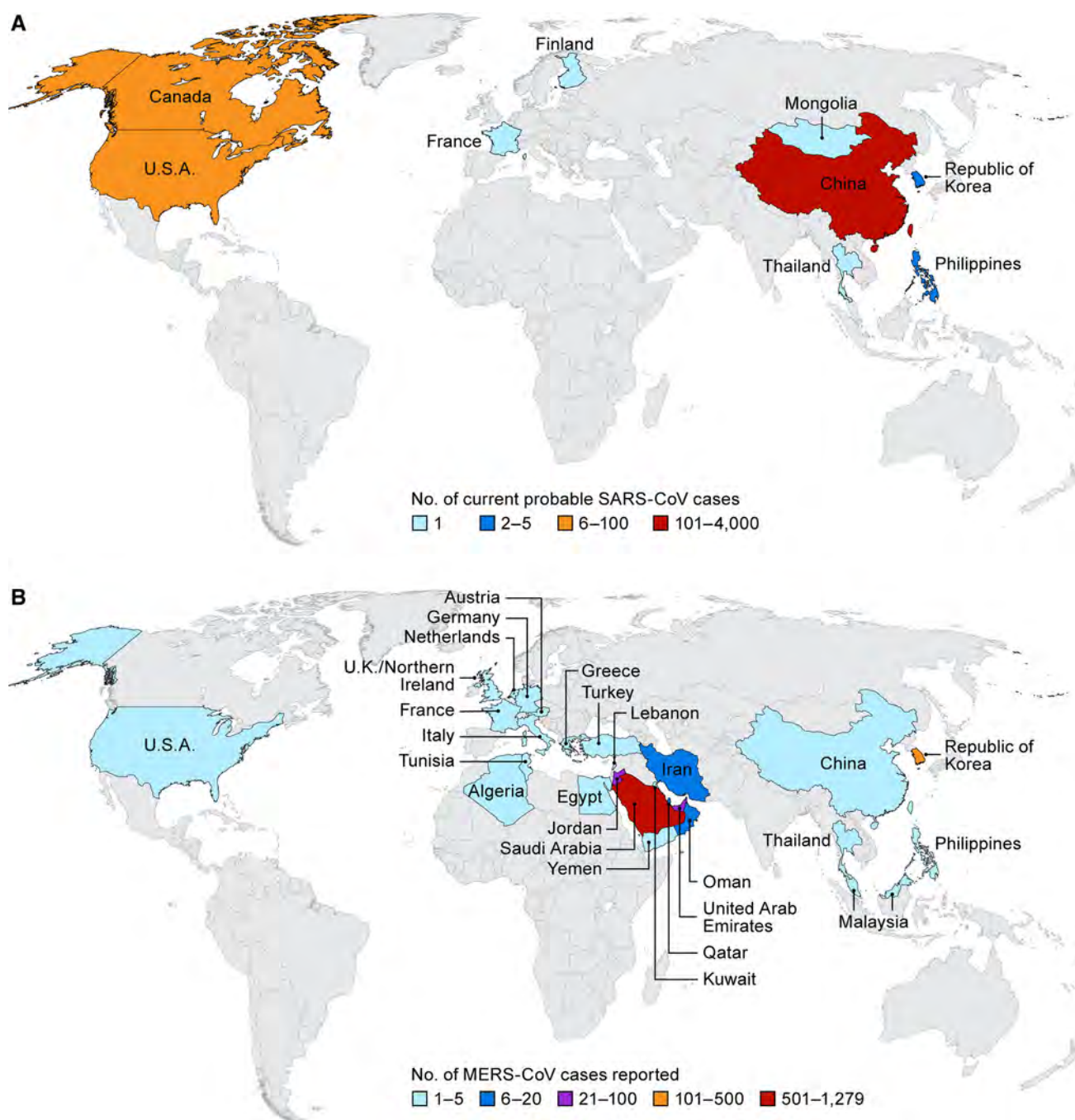


Fig. 1 Maps of the severe acute respiratory syndrome (SARS) (a) and Middle East respiratory syndrome (MERS) (b) outbreaks with confirmed case numbers

Radiographic abnormalities consistent with viral pneumonitis and ARDS are common in MERS and SARS. Radiographic progression in the lower lobes has been reported to be more rapid for MERS than SARS [21–23]. For SARS, disease in the lower lobes mimics pneumonia, radiographic progression includes ground-glass opacification and lobe thickening [17]. MERS-CoV (intact virus or

viral genome) is found at higher concentrations in the lower respiratory tract than in the upper respiratory tract in MERS patients and this may account for inefficient inter-human transmission [15, 24]. Currently, no approved therapeutics for patients with MERS or SARS are available, and clinical management has relied primarily on supportive care.

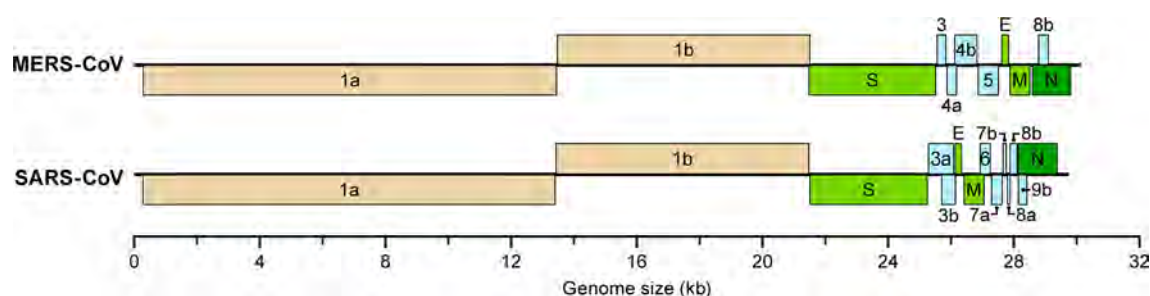


Fig. 2 Genomes of Middle East respiratory syndrome coronavirus (MERS-CoV) and severe acute respiratory syndrome coronavirus (SARS-CoV) indicating the open reading frames for nonstructural (1a

and 1b) and structural proteins (numbered 3–9, and E, M, N, S). *E* envelope, *M* membrane, *N* nucleocapsid, *S* Spike

2 Therapeutic Agents

2.1 Clinical Usage

2.1.1 Treatment of SARS

Effectiveness of antiviral treatments used during the SARS epidemic has been mainly based on case studies and retrospective analysis of patient cohorts. Few randomized, blinded, clinical trials of anti-SARS treatments were performed, which adds complexity when interpreting the available data (Table 1). Ribavirin, a nucleoside analog that prevents RNA and DNA virus replication, was initially used in the treatment of SARS due to its broad-spectrum efficacy. For example, in a Taiwanese study, 51 SARS patients were treated daily with fluoroquinolone antibiotics, [levofloxacin (500 mg) or moxifloxacin (400 mg)] following diagnosis. Out of 51 patients, 44 SARS patients were also treated intravenously (IV) with 2000 mg of ribavirin then orally daily with 1200 mg while 7 SARS patients did not receive ribavirin. Corticosteroids, IV methylprednisolone, or oral prednisolone were administered as needed to treat worsening lung infiltrates and fever [25]. Ribavirin treatment led to hypoxia and anemia and increased risk for death in SARS patients. In a retrospective analysis, a cohort of 229 patients from Hong Kong, Singapore, and Toronto were treated with ribavirin in conjunction with corticosteroids, immunoglobulins, and/or antibiotics [26]; ribavirin did not demonstrate efficacy. Patients in Hong Kong and Singapore were treated with ribavirin at 1200 mg orally at diagnosis, followed by oral treatments with 2400 mg daily, or continual IV ribavirin therapy [8 mg/kg every 8 h (h)]. In Toronto, patients received ribavirin IV treatment with 2000 mg, followed by 1000 mg every 6 h for 4 days, and 300 mg every 8 h for 3 days. Unfortunately, fatality rates were similar between the ribavirin-treated and control groups. Later, researchers demonstrated that the ribavirin dosage required to be effective against SARS-CoV in vitro was not clinically achievable [27]. Ribavirin treatment also resulted in

Table 1 Drug regimens used in the treatment of SARS

Treatment plan	Treatment outcome
Ribavirin (oral/IV)	No increased positive outcome with ribavirin compared to controls [25, 26]
Antibiotics	
± corticosteroids	Increased risk of anemia, hypomagnesemia, hypoxia, or bradycardia with ribavirin compared to ribavirin-naïve patients [25, 246]
± immunoglobulin	
Ribavirin (oral/IV)	Fatality or acute respiratory distress syndrome (ARDS) was reduced significantly from 28.8 to 2.4% [27]
Lopinavir/ritonavir	
± corticosteroids	
IFN- α con-1	Increased oxygen saturation
± corticosteroids	Increased clearance of lung abnormalities
± antibiotics	Slight increase in creatinine kinase concentrations [29, 247]
Fluoroquinolone (IV)	No increased positive outcome [248]
Azithromycin (IV)	
IFN- α (IM)	
± corticosteroids	
± Immunoglobulins	
± thymic peptides/proteins	
Quinolone (IV)	No increased positive outcome [248]
Azithromycin (IV)	
± IFN- α	
± corticosteroids	
Levofloxacin	Increased survival
Azithromycin	Increased clearance of lung abnormalities [248]
± IFN- α	
± corticosteroids	

IFN interferon, *IM* intramuscular, *IV* intravenous, *SARS* severe acute respiratory syndrome

adverse effects including anemia, hypoxemia and decreased hemoglobin levels, and did not improve patient outcome [26]. Due to the increasing adverse effects and lack of efficacy, Health Canada stopped permitting the use of ribavirin for SARS [25].

Additional studies tested the efficacy of ribavirin in conjunction with lopinavir, an anti-retroviral agent. Lopinavir demonstrated in vitro activity against SARS-CoV [28]. In a non-randomized, open-enrollment trial of 152 suspected SARS patients [27], all patients were treated with ribavirin and corticosteroids similar to the previously described studies. In addition, 41 of the confirmed SARS patients were also treated with a combination of lopinavir (400 mg) and ritonavir (100 mg). Mean viral loads in nasopharyngeal swabs within this treatment group decreased to undetectable levels by day 10. Overall, SARS-related symptoms subsided, disease progression was milder, and no adverse effects were reported as compared to the historical control group.

In an open-label, non-randomized study of 22 SARS patients, 9 patients who received subcutaneous (SC) injections of interferon (IFN) α , alfacon-1, for 10 days at an initial dose of 9 μ g/day for 2 days increasing to 15 μ g/day with disease progression. All 9 patients survived with minor adverse effects [29].

2.1.2 Treatment of MERS

The evaluation of treatments in MERS patients has been hampered as high-quality clinical data from randomized clinical trials are limited. Ribavirin (with or without IFN, or corticosteroids) was the primary treatment during the MERS outbreak. In a retrospective analysis, a cohort of 20 patients was treated with oral ribavirin and SC pegylated IFN- α 2a at a dose of 180 μ g/week for 2 weeks (Table 2) [30]. The initial dose of ribavirin was 2000 mg, followed by a 200–1200 mg dose depending on creatinine clearance.

Table 2 Drug regimens used in the treatment of MERS

Treatment plan	Treatment outcome
Ribavirin (oral/IV)	Late treatment administration. Disease progression delayed—all patients died [249]
IFN- α 2b	
Corticosteroids	
Ribavirin (oral/IV)	Treatment initiated 0–8 days after diagnosis
PEGylated IFN- α 2a (IV)	Adverse effects: significant decreases in hemoglobin and absolute neutrophil count (baseline count lower in treatment group) [30]
\pm corticosteroids	
Ribavirin (oral/IV)	No detectable viral RNA in serum after 2 days of therapy
Lopinavir/ritonavir	Adverse effects: ribavirin discontinued due to jaundice, hyperbilirubinemia
IFN- α 2b	Died of septic shock 2 months, 19 days after diagnosis [31]

IFN interferon, IV intravenous, MERS Middle East respiratory syndrome

A group of 24 patients that received supportive care and corticosteroids were considered the control group. At 14 days after confirmed diagnosis of MERS, survival was increased in the treated group (70%) compared to the control group (29%). By 28 days post-diagnosis, 30% of treated subjects survived versus 17% of the control group [30]. In an additional case study, a 69-year-old Greek patient who contracted MERS in Jeddah was treated with oral lopinavir/ritonavir (400/100 mg twice daily), pegylated IFN (180 μ g SC once per week for 12 weeks), and ribavirin (2000 mg initial dose; 1200 mg every 8 h for 8 days, initiated on day 13 post-diagnosis). Two days after treatment initiation, viremia could not be detected; however, viral RNA was detected in several patient samples (feces, respiratory secretions, and serum) up to 14 weeks post-diagnosis. Despite prolonged survival, the patient succumbed from septic shock 2 months post-diagnosis [31]. An ongoing randomized clinical trial in Saudi Arabia is evaluating treatment of MERS patients with IFN- β 1b in combination with lopinavir/ritonavir [32].

2.2 Drugs with Repurposing Potential for Treatment of Coronaviral Infections

Drug repurposing is an attractive alternative drug discovery strategy because it eliminates many steps usually required at the early phase of drug development. Over the past decade, interest in drug repurposing has increased as pharmaceutical companies are challenged with decreasing product pipelines, high costs associated with de novo drug discovery, and the imminent expiration of many drug patents. Some examples for successfully repurposed drugs include Viagra (Pfizer) for erectile dysfunction (original indication: angina) and raloxifene (Eli Lilly) for treatment of invasive breast cancer (original indication: osteoporosis).

The time required for traditional drug development is often discordant with the urgent need for novel therapies for emerging infectious diseases such as SARS and MERS. Outbreaks can occur anywhere in the world and frequently in resource-limited settings. Commonly, the treatment strategies that are available for emerging infectious diseases are less than adequate to improve patient outcome. Although specific antivirals for MERS-CoV and SARS-CoV are in development, drug repurposing could present an important arm in generating additional therapeutics for future coronaviruses. First, if these drugs are confirmed to have beneficial effects in vitro and in animal studies, they could be used to build a panel of approved drugs for use as a first-line of defense for newly emerging coronaviruses. Second, these drugs could be made accessible relatively quickly to patients under Emergency Use Authorization. Extending the choices of treatment by generating a panel of

broad-spectrum antivirals would provide a real improvement to healthcare communities struggling to cope during an outbreak of emerging infections. A great example of how repurposing can benefit in the search of treatments for emerging infections is the drug zidovudine. Zidovudine was originally developed in 1964 as a cancer drug. In 1985, zidovudine was found to be active against human immunodeficiency virus (HIV), and 2 years later it became the first drug to be approved for the treatment of acquired immunodeficiency syndrome (AIDS) [33].

A number of research groups have identified and investigated the usefulness of approved drugs for the treatment of viral infections including coronaviruses. Below, we summarize several drug classes with antiviral activity against MERS-CoV and SARS-CoV that have repurposing potential (Fig. 3, Table 3). Some of the drugs described have activity against other virus families indicating potential broad-spectrum applications and have already been in clinical use for treating other viral infections. We would like to emphasize that none of the therapeutics described in this section are recommended for clinical use outside a clinical trial setting.

2.2.1 Antidiarrheal Agents

Loperamide, an approved anti-diarrheal agent, is on the World Health Organization (WHO) Model List of Essential Medicines and is available in many countries. The drug acts on the opioid receptor and reduces intestinal motility [34]. Results from pharmacokinetic (PK) studies show that oral loperamide is well absorbed from the gut with less than 1% of the drug entering systemic circulation [35]. Loperamide demonstrated anti-MERS-CoV, anti-SARS, and anti-HCoV229E activity in an in vitro screen of approved drugs [36], although the mechanism of action is unknown. Interestingly, loperamide was suggested for limiting gastrointestinal fluid and electrolyte losses in patients with Ebola virus disease (EVD) [37].

2.2.2 Antimalarial Agents

The antimalarial agents, chloroquine (CQ), amodiaquine, and mefloquine have activity against SARS-CoV and MERS-CoV in vitro [36, 38, 39]. CQ is a U.S. Food and Drug Administration (FDA)-approved antimalarial agent that is also used to treat autoimmune disease such as rheumatoid arthritis due to its anti-inflammatory effects [40]. CQ has activity against a number of viruses in vitro and in vivo including flaviviruses [dengue virus (DENV)], Togaviruses [chikungunya virus (CHIKV)], paramyxoviruses (Hendra, Nipah virus), influenza viruses, HIV, and filoviruses [Ebola virus (EBOV)] [41–47].

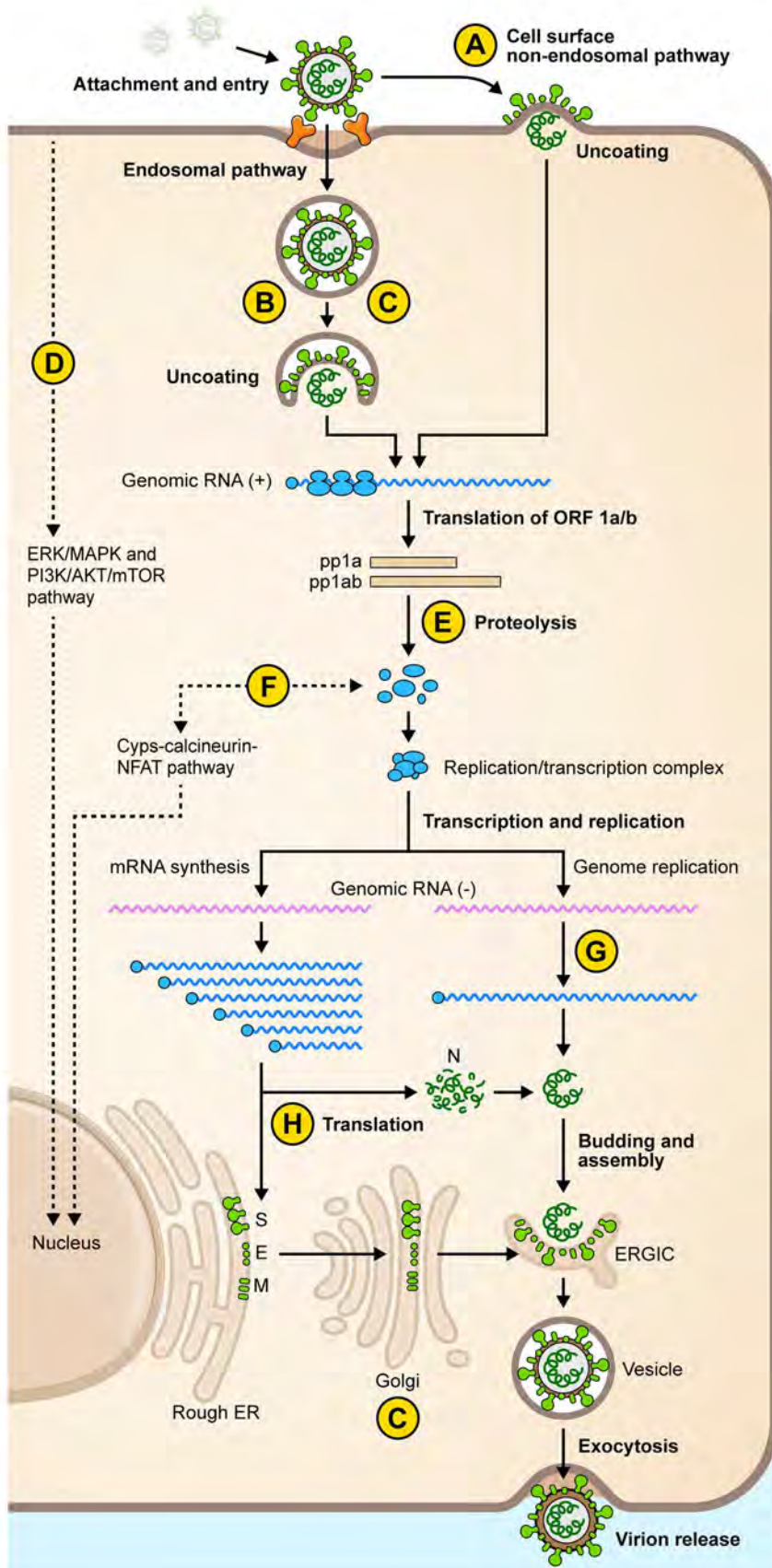
Fig. 3 Candidate drugs for repurposing for coronaviral infections. Several drug classes (A through I) have been studied, and the steps/processes of the viral replication cycle that they most likely target are indicated. *AKT* serine/threonine kinase, *CAD* cationic amphiphilic drug, *Cyp*s cytochrome P-450s, *E* envelope, *ER* endoplasmic reticulum, *ERGIC* ER–Golgi intermediate compartment, *ERK* extracellular signal-reduction kinase, *IFN* interferon, *MAPK* mitogen-activated protein kinase, *M* membrane, *MPA* mycophenolic acid, *mTOR* mechanistic target of rapamycin, *N* nucleocapsid, *NEFAT* nuclear factor of activated T cells, *ORF* open reading frame, *PI3K* phosphoinositide 3-kinase, *S* Spike

Several mechanisms of action have been identified for the antiviral effect of CQ and suggest that the drug acts nonspecifically at virus entry or at the later stages of virus production. CQ accumulates within acidic organelles such as endosomes, Golgi vesicles, and lysosomes, where the drug is protonated resulting in increased pH within the vesicle [48]. Viruses depend on these acidic organelles for entry, viral replication, and maturation of virus progeny. Similarly, MERS-CoV entry into cells depends on several proteases. Dipeptidyl peptidase 4 (DPP4) acts as functional virus receptor [49], and cellular proteases [e.g. type II transmembrane serine protease (TMPRSS2) and members of the cathepsin family] activate the viral spike (S) glycoprotein [50]. CQ may have an effect on any of these proteases. CQ also affects the glycosylation step within the Golgi that directs trafficking and maturation of viral proteins [51–53]. For SARS-CoV, the antiviral activity of CQ has also been attributed to a deficit in glycosylation of the receptor angiotensin-converting enzyme 2 (ACE2) [54].

The broad-spectrum antiviral activity makes CQ an attractive antiviral for repurposing and treating coronaviral and other emerging viral infections. In vivo activity of CQ in MERS or SARS animal models has not yet been reported. However, the antiviral activity of the drug has been evaluated against other viruses in preclinical and clinical studies with mixed results. CQ plasma steady state concentrations in mice are similar to those reported for humans (10 μ M) and are within range of the EC₅₀ values determined for MERS-CoV (3.6 μ M) and SARS-CoV (2.3 μ M) [43, 55]. Preclinical studies with CQ in mice against other viruses have shown survival benefits for influenza and EBOV infections.

In clinical studies, CQ was effective at reducing viral loads in asymptomatic HIV patients [56, 57], but results of CQ treatment of CHIKV and DENV infections were mixed [58, 59].

In summary, CQ has broad-spectrum potential and the information gained from studies on other viruses can be used to plan the most appropriate strategies for evaluating its specific clinical value for treating for MERS-CoV and SARS-CoV infections. CQ has several advantages including rapid absorption from gastrointestinal tract, low cost,



Candidate antiviral agents

- A** | **Host protease inhibitors**
 - camostat mesylate, K1177
- B** | **Host protease inhibitors**
 - E-64-D
- C** | **CADs**
 - toremifene, tamoxifen, chlorpromazine, fluphenazine, terconazole, triparanol
- D** | **Kinase inhibitors**
 - miltefosine, everolimus, selumetinib, trametinib, dabrafenib, sorafenib
- E** | **Virus protease inhibitors**
 - lopinavir
- F** | **Cyclophilin inhibitors**
 - cyclosporine A
- G** | **Nucleic acid synthesis inhibitors**
 - MPA & ribavirin
- H** | **Protein synthesis inhibitors**
 - emetine, anisomycin, omacetaxin
- I** | **Exogenous IFN- α or - β**
 - betaferon



and very effective biodistribution. CQ may be an excellent candidate for combinatorial treatments with other antivirals. However, considerable challenges remain for the treatment of viral infections including increased understanding of the pharmacodynamics of CQ, achievement of sufficient plasma concentrations in patients, and toxicity concerns [60]. Importantly, hydroxychloroquine, a CQ derivate, may provide an alternative due to lower toxicity and similar pharmacology profile [55].

A related antimalarial drug, amodiaquine, also has activity in vitro against MERS-CoV and SARS-CoV [38]. Previous investigations have demonstrated that amodiaquine inhibits filovirus replication, and the mechanism of action is hypothesized to be similar to that of CQ [43]. Amodiaquine is well tolerated and is commonly used for malaria treatments in many countries. Further, amodiaquine in combination with artesunate was administered to EVD patients during the 2013–2016 epidemic, and the resulting decrease in fatality rates may have been associated with the use of amodiaquine as an antimalarial agent [61]. Nonhuman primate (NHP) studies are currently underway to investigate the effect of amodiaquine treatment on EVD [62].

Mefloquine, a synthetic analog of quinine, is another antimalarial drug with activity against MERS-CoV and SARS-CoV [38]. It belongs to the WHO Model List of Essential Medicines. Mefloquine is known to penetrate the blood-brain barrier and was found to inhibit JC virus infection and replication at concentrations generally achieved in the brains of patients given mefloquine for malaria [63] leading to the clinical evaluation of this drug for the treatment of progressive multifocal leukoencephalopathy [64, 65]. In 2013, the FDA added a boxed warning to the US label of mefloquine regarding the potential for neuropsychiatric side effects. Additional investigations are warranted to determine if amodiaquine or mefloquine have value for repurposing for treatment of MERS or SARS.

2.2.3 Cyclophilin Inhibitors

Cyclophilins are ubiquitous host proteins believed to have multiple roles in trafficking, protein folding and T cell activation [66]. Cyclosporine A (CysA), forms a complex with cyclophilin A, thereby blocking T cell activation. CysA is licensed for use in organ transplantation to suppress the immune response. CysA has also been shown to inhibit coronaviruses including SARS-CoV and MERS-CoV effectively in cell culture [67, 68]; however, the mechanism has yet to be determined. There is increasing evidence that cyclophilins are involved in viral replication of RNA viruses such as hepatitis C virus (HCV) and West Nile virus, and this may also apply to coronaviruses [69].

Although the immunosuppressive properties of CysA are considered a risk for treating viral infections in patients, nonimmunosuppressive analogs of CysA that bind to cyclophilins with higher affinity have been developed and some are in clinical trials as HCV therapeutics [70–72].

2.2.4 Interferons

Interferons (IFNs) are approved by the FDA for other indications such as hepatitis C. Although IFN- α reduced SARS-CoV replication in mice and NHPs [73, 74], efficacy of IFN- α treatment in SARS patients was mixed (see Sect. 2.1.1). From in vitro studies, another type I interferon, IFN- β 1a, may be more effective than IFN- α either alone or in combination with IFN- γ [75–77]. Combinations of IFN- β and - γ were synergistic against SARS-CoV in vitro [77].

With regards to MERS, in vitro and in vivo preclinical studies have indicated that IFN- α 2b alone or in combination with ribavirin, may have a therapeutic effect if given early in disease [78, 79]. In clinical trials, however, IFN- α 2b (given in combination with other treatments) did not lead to a significant benefit to patients (see Sect. 2.1.2). IFN- β 1a ($EC_{50} = 1.37$ IU/mL) was superior in activity against MERS-CoV infection in vitro compared to IFN- α 2a, IFN- α 2b, and IFN- γ ; these IFNs had EC_{50} values of 160.8, 21.4, and 56.5 IU/mL, respectively [80]. IFN- β 1b is currently under evaluation for MERS-CoV in a randomized clinical trial (in combination with lopinavir/ritonavir) [32]. Investigating the IFN- β subtypes (1a and 1b) in combination with other antivirals may be worthwhile as potential synergistic combinations could reduce the effective drug dosage and IFN-associated adverse effects.

2.2.5 Kinase Inhibitors

Many cellular processes are regulated independently of changes in transcription or translation through kinase-mediated cell signaling pathways. As a testament to the biological importance of kinases, there have been over 500 kinases identified along with more than 900 genes encoding proteins with kinase activity [81, 82]. As of April 2015, 28 kinase inhibitors have been granted approval by the US FDA with over half gaining approval from 2012–2015. Further, kinases are the most frequently targeted gene class in cancer therapy, second only to the G protein-coupled receptors as therapeutic targets [83, 84].

The therapeutic potential for host-targeted immunomodulatory agents in viral infections has received considerable attention [85–87]. Recently, Dyall et al. identified two Abelson (Abl) kinase inhibitors (imatinib and dasatinib) that inhibited MERS-CoV and SARS-CoV infection through a cell-screening assay [38]. Both

Table 3 Clinically developed drugs with activity against MERS-CoV and SARS-CoV

Drug class members	Activity against coronaviruses ^a	Activity against other viruses	Clinical status	Known safety issues	Comments
Antidiarrheal agents					
Loperamide hydrochloride	MERS-CoV: 4.8 μ M [36] SARS-CoV: 5.9 μ M HCoV-229E-GFP: 4 μ M [36]		Approved for treatment of diarrhea	Well tolerated, commonly used	WHO list of essential medicines
Antimalaria agents					
Amodiaquine hydrochloride	MERS-CoV: 6.2 μ M [38] SARS-CoV: 1.3 μ M [38]	EBOV [43]; MARV [43]; DENV [250]	Approved for treatment of malaria	Well tolerated, commonly used	
Chloroquine diphosphate	MERS-CoV: 3–6.3 μ M [36, 38] SARS-CoV: 4.1–8.8 μ M [36, 38, 39]	In vitro: CHIKV [251, 252]; DENV [42, 47]; HeV, NiV [46]; HIV-1 [41]; FLUAV [44]; EBOV, MARV [43]; SFV, SINV [45] In vivo: Mixed data on efficacy against EBOV in mice [43, 60]; no efficacy against EBOV in hamsters, guinea pigs [60]; FLUAV : 70% survival in mice [253] In vitro: DENV [42]; HIV-1 [255]; JCV [63]	Approved for treatment of malaria Clinical trials for treatment of CHIKV, DENV, FLUAV, and FLUBV infections showed no impact on disease [58, 59, 254]	Well tolerated, commonly use	WHO list of essential medicines; WHO list of potential EVD treatments; dosing, formulation need to be optimized for treatment of viral infections [54]
Hydroxychloroquine sulfate	MERS-CoV: 8.3 μ M [38] SARS-CoV: 8.0 μ M [38]		Approved for treatment of malaria	Well tolerated, commonly used	WHO list of essential medicines
Mefloquine	MERS-CoV: 7.4 μ M [38] SARS-CoV: 15.6 μ M [38]		Approved for treatment of malaria Clinical trials for treatment of JCV infection: mixed results [64, 65]	Black box warning: potential neuropsychiatric side effects	WHO list of essential medicines
Cyclophilin inhibitors					
Cyclosporin A	MERS-CoV [67] SARS-CoV [68]	HCV [256]; WNV [257]; JEV [258] VSV [259]; HIV-1 [260]	Approved for immunosuppression during organ transplantation	Immunosuppression undesirable for infectious diseases	WHO list of essential medicines; non-immunosuppressive analogs are available [70–72]
Interferons					
IFN- α 2a	MERS-CoV: 160.8 U/mL [80]		Approved for treatment of hepatitis B and C	Well tolerated	

Table 3 continued

Drug class members	Activity against coronaviruses ^a	Activity against other viruses	Clinical status	Known safety issues	Comments
IFN- α 2b	MERS-CoV: 21.4 U/mL [80] SARS-CoV: 6500–4950 U/mL [75]		Approved for treatment of melanoma		
IFN- β 1a, 1b	MERS-CoV: 1.4 U/mL [80] SARS-CoV: 95–105 U/mL [75]		Approved for treatment of multiple sclerosis		
IFN- γ	MERS-CoV: 56.5 U/mL [80] SARS-CoV: 1700–2500 U/mL [115]		Approved for treatment of chronic granulomatous disease		
Kinase inhibitors					
Dabrafenib	MERS-CoV: 45% inhibition at 10 μ M [89]		Approved for treatment of cancers	Well tolerated	
Dasatinib	MERS-CoV: 5.5 μ M [38] SARS-CoV: 2.1 μ M [38]	In vitro: BKPvV [261]; EBOV [100]; HIV-1 [262]; DENV [263] In vivo: VACV: no activity in mice [264] DENV, CPXV, RSV, FLUAV [265]	Approved for treatment of cancers	Well tolerated	ABL1 inhibitor, CAD Immunosuppressive effects in vivo may preclude use as anti-infective
Everolimus	MERS-CoV: 56% inhibition at 10 μ M [89]		Approved immunosuppressant for cancer treatment and prevention of organ rejection; reduced incidence of HHV-5 in cardiac and renal transplant patients [266]	Well tolerated	mTOR inhibitor [267]
Imatinib mesylate	MERS-CoV: 17.7 μ M [38] SARS-CoV: 9.8 μ M [38]	In vitro: BKPvV [261]; HHV [268]; HCV [149]; MPXV, VACV, VARV [264] In vivo: VACV: 100% survival in mice [264] HSV-2 [269]	Approved for treatment of cancers	Well tolerated	ABL1 inhibitor
Miltefosine	MERS-CoV: 28% at 10 μ M [89]		Antimicrobial approved for treatment of leishmaniasis; investigational drug for treatment of amoeba infections	Well tolerated	Akt inhibitor WHO list of essential medicines

Table 3 continued

Drug class members	Activity against coronaviruses ^a	Activity against other viruses	Clinical status	Known safety issues	Comments
Nilotinib	MERS-CoV: 5.5 μ M [38] SARS-CoV: 2.1 μ M [38]				
Selumetinib sulfate	MERS-CoV: \geq 95% inhibition at 10 μ M [89]		In Phase II/III trials for cancer treatment	Well tolerated	MEK inhibitor
Sirolimus	MERS-CoV: 61% inhibition at 10 μ M [89]	HIV-1 [270]; HHV-5 [271]	Approved immunosuppressant in transplant; reduced viral replication in HIV- or HCV-positive transplant patients [272–274]	Well tolerated	mTOR inhibitor
Sorafenib	MERS-CoV: 93% inhibition at 10 μ M [89]	BKPyV [261]; HHV [275]; EV71 [276]; RVFV [277]	Approved for treatment of cancers	Well tolerated	
Trametinib	MERS-CoV: \geq 95% inhibition at 0.1 μ M [89]		Approved for treatment of cancers	Well tolerated	
Wortmannin	MERS-CoV: 40% inhibition at 10 μ M [89]	HSV-2 [269]; HIV-1 [278]	In development for treatment of cancer	Toxicity issues. Derivatives are in Phase I clinical trials	
Neurotransmitter inhibitors					
Astemizole	MERS-CoV: 4.9 μ M [38] SARS-CoV: 5.6 μ M [38]		Previously approved antihistamine	Withdrawn in 1999 because of rare arrhythmias	
Benztropine mesylate	MERS-CoV: 16.6 μ M [38] SARS-CoV: 21.6 μ M [38]	HCV [102], EBOV, MARV [100, 101, 104]	Approved anticholinergic for treatment of Parkinson's disease	Well tolerated	
Chlorphenoxamine	MERS-CoV: 12.7 μ M [38] SARS-CoV: 20.0 μ M [38]		Approved antihistamine and anticholinergic for treatment of Parkinson's Disease	Well tolerated	
Chlorpromazine hydrochloride	MERS-CoV: 4.9–9.5 μ M [36, 38] SARS-CoV: 8.8–13.0 μ M [36, 38]	EBOV [96]; JUNV [94]; SV40 [279]	Approved for treatment of schizophrenia	Well tolerated	CAD

Table 3 continued

Drug class members	Activity against coronaviruses ^a	Activity against other viruses	Clinical status	Known safety issues	Comments
Clomipramine hydrochloride	MERS-CoV: 9.3 μ M [38]; SARS-CoV: 13.2 μ M [38]	EBOV [100]	Approved for treatment of depression	Well tolerated	WHO list of essential medicines
Fluphenazine hydrochloride	MERS-CoV: 5.9 μ M [38]; SARS-CoV: 21.4 μ M [38]	HCV [149]; EBOV [100]	Approved for treatment of chronic psychoses	Well tolerated	WHO list of essential medicines; CAD
Fluspirilene	MERS-CoV: 7.5 μ M [38]; SARS-CoV: 5.9 μ M [38]		Approved for treatment of schizophrenia	Well tolerated	
Promethazine hydrochloride	MERS-CoV: 11.8 μ M [38]; SARS-CoV: 7.5 μ M [38]		Antipsychotic approved for sedation	Well tolerated	
Thiothixene	MERS-CoV: 9.3 μ M [38]; SARS-CoV: 5.3 μ M [38]		Antipsychotic approved for treatment of schizophrenia	Well tolerated	
Triethylperazine maleate	MERS-CoV: 7.8 μ M [38]	SFV [45], CHIKV [45, 99]	Approved antiemetic	Well tolerated	
Triflupromazine hydrochloride	MERS-CoV: 5.8 μ M [38]; SARS-CoV: 6.4 μ M [38]		Approved antipsychotic	Serious side effects include akathisia.	CAD
Nucleic acid synthesis inhibitors					
Gemcitabine hydrochloride	MERS-CoV: 1.2 μ M [38]	In vitro: FLUAV [125] In vivo: Mice MuLV [124] HCV [123]; BVDV [280]	Approved for treatment of cancers	Well tolerated	WHO list of essential medicines
Mizoribine	SARS-CoV: 3.5-16 μ g/mL [114] or > 40 μ M [111]		Approved immunosuppressant in organ transplantation and rheumatic diseases.	Well tolerated	
Mycophenolic acid	MERS-CoV: 0.17 μ g/mL [112] or 2.87 μ M [80] SARS-CoV: > 30 μ M [111]	DENV [118]; CHIKV [252]; FLUAV [112]; SFV, SINV [45]	Approved immunosuppressant in organ transplantation	FDA alert: risk of activation of latent herpes infections	

Table 3 continued

Drug class members	Activity against coronaviruses ^a	Activity against other viruses	Clinical status	Known safety issues	Comments
Protease inhibitors					
Lopinavir	In vitro: MERS-CoV: 8 μ M [36] SARS-CoV: 24.4 μ M [36] In vivo: 67% survival in MERS-infected NHPs [121]	HIV-1 [136] HPV [281]	Approved for treatment of HIV infections Clinical trial for topical treatment of cervical cancer Clinical trial in SARS patients [27]	Well tolerated	Lopinavir/ritonavir: WHO list of essential medicines
E-64-D	MERS-CoV: 1.27 μ M [38]; SARS-CoV: 0.76 μ M [38]	EBOV [134, 135]	Cysteine protease inhibitor Phase III for treatment of muscular dystrophy	Well tolerated	
K1177	MERS-CoV, SARS-CoV, HCoV-229E (VLP) [133]	EBOV, MARV, NiV (VLP) [133]	Cysteine protease inhibitor In clinical development for treatment of Chagas disease	Well tolerated	
Camostat mesylate	In vitro: MERS-CoV [132], SARS- CoV [132] In vivo: SARS: activity in mice [133]	In vitro: FLUAV, FLUBV [130]; no inhibition of EBOV [133]	Cellular serine protease inhibitor In clinical development for chronic pancreatitis	Well tolerated	SARS-CoV spread is driven by serine protease rather than cysteine protease [133]
Protein synthesis inhibitors					
Anisomycin	MERS-CoV: 0.003 μ M [38] SARS-CoV: 0.19 μ M [38]	PV [147]; EMCV [146]	Antibiotic in clinical development for treatment of amoebiasis		
Emetine hydrochloride	MERS-CoV: 0.014 μ M [38] SARS-CoV: 0.05 μ M [38]	FLUAV [112]; EMCV [146]	Approved antibiotic for treatment of amoebiasis in some countries	Side effects include nausea; derivatives with less side effects available	
Omacetaxine mepesuccinate	MERS-CoV: 9.07 μ M [38] MHV: 0.012 μ M [139]	HBV [148]	Approved for chronic myeloid leukemia	Well tolerated	

Table 3 continued

Drug class members	Activity against coronaviruses ^a	Activity against other viruses	Clinical status	Known safety issues	Comments
Selective estrogen response modulator					
Tamoxifen citrate	MERS-CoV: 10.1 µM [38]; SARS-CoV: 92.9 µM [38]	HCV [282]; HSV-1 [283]	Approved for treatment of breast cancer	Black box warning: uterine cancer, blood clots, stroke	WHO list of essential medicines; CAD
Toremifene citrate	MERS-CoV: 12.9 µM; SARS-CoV: 12 µM [38]	In vitro: HCV [149]; EBOV [100, 151]; SUDV; RAVV; MARV [151] In vivo: EBOV: 50% survival in mice [151]	Approved for treatment of breast cancer.	Black box warning: cardiac effect (QT prolongation) in patients with hypokalemia	WHO list of potential EVD treatments; CAD
Sterol metabolism inhibitors					
Terconazole	MERS-CoV: 12.2 µM [38]; SARS-CoV: 15.3 µM [38]	EBOV-VLP [152]; EVD [100]	Approved topical antifungal for treatment of vaginal yeast infections	Would require IND for oral use	CAD
Triparanol	MERS-CoV 5.3 µM [38]	EBOV-VLP [152]	Developed for lowering serum cholesterol; withdrawn	Acute cataract formation	CAD

ABL1 abelson murine leukemia viral oncogene homolog 1, *Akt* protein kinase B, *BKPyV* BK polyomavirus, *BVDV* Bovine viral diarrhoea virus, *CAD* cationic amphiphilic drug, *CHIK* Chikungunya virus, *CPXV* Cowpox virus, *CVs* Coxsackie viruses, *DENV-1* Dengue virus-1, *DENV-2* Dengue virus-2, *EBOV* Ebola virus, *EC₅₀* effective concentration 50, *EMCV* Encephalomyocarditis virus, *EV71* Enterovirus 71, *FCoV* Feline coronavirus, *FDA* Food and Drug Administration, *FLUAV* Influenza A virus, *FLUBV* Influenza B virus, *HBV* Hepatitis B virus, *HCV* hepatitis C virus, *HeV* Hendra virus, *HHV-1* Human herpesvirus-1 (herpes simplex virus-1), *HHV-2* human herpesvirus-2 (herpes simplex virus-2), *HHV-5* Human herpesvirus-5 (cytomegalovirus), *HIV-1* Human immunodeficiency virus-1, *HIV-2* Human immunodeficiency virus-2, *HPV* Human papilloma virus, *HRV*'s Human rhinoviruses, *IND* Investigational new drug, *JCV* John Cunningham virus, *JUNV* Junin virus, *MARV* Marburg virus, *MEK* MAPK/ERK kinase, *MERS-CoV* Middle East respiratory syndrome coronavirus, *MHV* Mouse hepatitis virus, *MPXV* Monkeypox virus, *mTOR* mechanistic target of rapamycin, *MuLV* Murine leukemia virus, *NiV* Nipah virus, *PV* Poliovirus, *RAVV* Ravn virus; *RSV* Respiratory syncytial virus, *RVFV* Rift Valley fever virus, *SARS-CoV* Severe acute respiratory syndrome coronavirus, *SFV* Semliki forest virus, *SFTSV* Severe fever with thrombocytopenia syndrome virus, *SINV* Sindbis virus, *SUDV* Sudan virus, *SV40* Simian virus 40; *VACV* Vaccinia virus, *VARV* Variola virus, *VLP* virus-like particles, *WHO* World Health Organization

^aAntiviral activity is expressed in terms of EC₅₀ unless otherwise noted

compounds significantly inhibited MERS-CoV and SARS-CoV with micromolar EC_{50} values and low cytotoxicity. Abl2 has been identified as critical for MERS-CoV and SARS-CoV virus entry, and may be the target that imatinib inhibits to block entry of both viruses [88]. A recent systems kinome analysis investigation of in vitro MERS-CoV infection suggested that ERK/MAPK and PI3 K/Akt/mTOR signaling pathways were specifically modulated during infection [89]. Subsequent analysis of licensed kinase inhibitors targeting these pathways demonstrated that kinase inhibitors targeting the ERK/MAPK signal pathway (selumetinib and trametinib) inhibited MERS-CoV infection by $\geq 95\%$ when added pre- or post-infection [89]. Further, trametinib demonstrated significantly stronger inhibitory activity against MERS-CoV than selumetinib suggesting that specific intermediates of the ERK/MAPK signaling pathway may represent crucial foci during early (viral entry) and late (viral replication) events in the viral life cycle. In contrast, sorafenib, an inhibitor of Raf-1 and B-Raf, components of the ERK/MAPK signaling pathway, and vascular endothelial growth factor receptor 2 (VEGFR2), inhibited MERS-CoV infection by $>90\%$ when added to cells prior to infection; however, the inhibitory activity was reduced to $<30\%$ when added post-infection suggesting Raf kinases were primarily involved in early viral life cycle events. In addition, the inhibitory activity dabrafenib, a Raf kinase inhibitor, was also largely ablated when added post-infection. Miltefosine, an alkyl phospholipid, considered to be an inhibitor of protein kinase B (Akt), garnered FDA approval for infectious disease-related treatments (cutaneous or mucosal leishmaniasis) [90]. In 2013, miltefosine became directly available from the US Centers for Diseases Control and Prevention for the treatment of free-living amoeba infections [91]. Pre-treatment of cells with miltefosine reduced MERS-CoV infection by 28%, but had no effect when added post-infection [89]. In contrast, inhibition of mTOR with sirolimus or everolimus reduced MERS-CoV infection by $\sim 60\%$ when added prior pre- or post-infection suggesting a critical role for mTOR in MERS-CoV infection. A recent clinical investigation by Wang et al. [92] evaluated sirolimus and corticosteroids in addition to standard antiviral treatment in a randomized controlled trial in patients with severe H1N1 pneumonia and acute respiratory failure [92]. Importantly, the addition of sirolimus was associated with improved patient outcomes including decreased hypoxia and multi-organ dysfunction, reduced mean times for liberation from mechanical ventilation, and increased clearance of virus. Thus, it may be prudent to extend the study of repurposed kinase inhibitors beyond stand-alone therapeutic investigations and also consider their potential as adjunctive therapies.

2.2.6 Neurotransmitter Inhibitors

Numerous neurotransmitter receptors inhibitors showed activity against MERS-CoV and SARS-CoV infection [38]. These drugs were initially developed as antipsychotics, antihistamines, and sedatives. Five neurotransmitter receptor antagonists belong to the chemical class of phenothiazines: chlorpromazine, trifluorpromazine, thiethylperazine, promethazine and fluphenazine. Phenothiazines were breakthrough medications developed in the 1950s for treating mental health patients and reduced episodes of bizarre behavior, hallucinations, and irrational thoughts [93]. Although phenothiazines primarily block dopamine receptors, they also have anticholinergic, antihistamine, and antiemetic effects.

The phenothiazines, chlorpromazine and trifluorpromazine, are approved antipsychotics. Chlorpromazine has been used off-label for short-term treatment of nausea and migraines. Trifluorpromazine is used to treat severe emesis, but the drug has more serious side effects than chlorpromazine including akathisia and tardive dyskinesia. The antiviral effect of chlorpromazine has been extensively studied, and the drug interferes with clathrin-mediated endocytosis, a process that many viruses exploit for host cell entry. Chlorpromazine inhibits entry of Junin virus [94], West Nile virus [95], EBOV [96], HCV [97], and Japanese encephalitis virus [98] suggesting broad-spectrum activity that could be exploited early during a novel virus outbreak. Chlorpromazine may have similar effects on coronaviruses as the drug effectively inhibits MERS-CoV, SARS-CoV, and human coronavirus 229E expressing green fluorescent protein [36, 38]. However, time-of-addition studies indicate that the inhibitory activity against MERS-CoV is retained whether added pre- or post-infection suggesting that there are additional effects to clathrin-mediated entry impairment [36].

Thiethylperazine is an approved antiemetic. Both chlorpromazine and thiethylperazine have been shown to inhibit alphaviruses, Semliki forest virus (SFV) and chikungunya virus (CHIKV) [45, 99]. As these drugs cross the brain-blood barrier, use of these drugs could be beneficial in the treatment of CHIKV, including common neurologic complications. Promethazine is an antihistamine used as a sedative in many countries under different brand names, but also acts as a weak anti-psychotic activity. Fluphenazine is a common antipsychotic used to treat chronic psychoses (primarily schizophrenia) and belongs to the WHO Model List of Essential Medicines. Promethazine and fluphenazine have shown in vitro activity against MERS-CoV and SARS-CoV and may have value as candidates for repurposing for coronaviral infections [38].

Benztrapine mesylate, an approved anticholinergic used to treat Parkinson's, had activity against MERS-CoV and

SARS-CoV [38]. Benztropine was also identified in other screens of clinically approved drugs for antiviral activities against HCV and EBOV [100–102]. Although the detailed mechanism of action is unknown, HCV studies indicate that benztropine inhibits at a virus entry step, while not interfering with viral genome replication, transcription or production of viral progeny or virus production of viral progeny [102]. It has been argued that a virus entry inhibitor may have value in decreasing the incidence of relapse in chronic HCV patients that receive liver transplants [102]. However, the peak plasma concentrations of benztropine may be too low to be effective for treating an acute infection [103]. Benztropine was also independently identified in two drug screens for EBOV antivirals [100, 101]. A recent report suggests that a step after virus attachment, but prior to viral/cell membrane fusion is targeted by benztropine [104].

Clomipramine, a tricyclic antidepressant, and thiothixene, a thioxanthene antipsychotic, have also been shown to inhibit MERS-CoV and SARS-CoV infection in vitro [38]. In addition, they were found to inhibit EVD VLP entry [101]. Both are approved clinically, and clomipramine belongs to the WHO Model List of Essential Medicines.

Several other neurotransmitter inhibitors, astemizole, promethazine, chlorphenoxamine, and fluspirilene, were active against MERS-CoV and SARS-CoV in cell culture, but we were not able to find reports on activity against other viruses [38]. Astemizole is an H1-histamine receptor antagonist for treating allergic rhinitis that was withdrawn from the market. Cardiac adverse events due to drug overdose have been reported, but are extremely rare [105]. Recently, astemizole has gained renewed interest as an anticancer and antimalarial drug [106, 107].

Chlorphenoxamine is an antihistamine and anticholinergic that is currently in preclinical trials for malaria. Fluspirilene is an approved antipsychotic for treatment of schizophrenia. It is a known autophagy inducer [108]. Autophagy is a cellular degradative pathway that viruses exploit for their propagation [109]. Modulators of autophagy may perturb MERS-CoV or SARS-CoV infection, and investigation of their broad-spectrum potential for the treatment of coronaviral infections would be interesting [110].

2.2.7 Nucleic Acid Synthesis Inhibitors

Several RNA/DNA synthesis inhibitors have broad-spectrum activity against viruses including SARS-CoV and MERS-CoV [38, 80, 111–114]. Inosine monophosphate dehydrogenase (IMPDH) inhibitors such as ribavirin, mycophenolic acid, and mizoribine inhibit an important step in de novo synthesis of nucleic acids although the potency of these drugs against viruses varies. Ribavirin has

been used in combination with IFN in the clinic for treatment of viral infections such as hepatitis C. Treatment regimens with ribavirin are well characterized and have been used in SARS and MERS patients with mixed results (see 2.1). Ribavirin weakly inhibits MERS-CoV in vitro, and conflicting data have been reported for the activity of ribavirin against SARS-CoV [80, 111, 115]. Many of the studies on ribavirin were performed in Vero cells that reportedly have a defect in ribonucleoside uptake, which could explain lack of activity for ribavirin in these cells [116]. Another coronavirus, mouse hepatitis virus (MHV), becomes sensitive to ribavirin when its exoribonuclease activity is inactivated. In presence of exoribonuclease, ribavirin does not inhibit MHV replication [117]. The MHV exoribonuclease has been suggested to function as a ‘proofreading’ viral enzyme that is necessary for high-fidelity replication of MHV. Similarly, the exoribonuclease activity of MERS-CoV and SARS-CoV could possibly counteract inhibitory activity of ribavirin.

Mycophenolic acid (MPA), an immunosuppressant used to prevent organ rejection, has broad-spectrum antiviral activities, and antifungal, antibacterial, anticancer, and antipsoriatic properties [45, 118, 119]. Although MPA has weak inhibitory activity against SARS-CoV in vitro, it has promising activity against MERS-CoV [80, 112]. A potential alternative to MPA, the prodrug mycophenolate mofetil, has improved oral bioavailability [120]. Mycophenolate mofetil evaluated in the common marmoset model of MERS did not reduce disease manifestations compared to that observed in control subjects [121]. However, the MERS marmoset model does not recapitulate human disease due to its rapid onset and pathology associated with exposure methods [122]. Mizoribine, an approved immunosuppressant in organ transplantation with limited adverse side effects, has shown in vitro activity against HCV and bovine viral diarrhoea virus (BVDV), and was considered as an alternative to ribavirin/IFN combinations for treatment of HCV infections [123]. In vivo analysis of ribavirin and other IMPDH inhibitors in SARS-CoV-infected mice have suggested that these agents would be of limited benefit [111].

The chemotherapeutic gemcitabine, has shown in vitro activity against MERS-CoV and SARS-CoV [38]. The drug’s anti-cancer mechanism is attributed to its ability to inhibit ribonucleotide reductase essential for de novo pyrimidine biosynthesis. Gemcitabine has been shown to suppress influenza virus RNA transcription and replication by targeting ribonucleotide reductase and showed anti-retroviral activity in vivo in the mouse model for murine leukemia virus [124, 125].

2.2.8 Protease Inhibitors

MERS-CoV and SARS-CoV require activation of their envelope glycoproteins by host proteases for cell entry by the endosomal or the non-endosomal pathways. Inhibitors of host cell proteases are being investigated as possible antivirals [126]. The serine protease TMPRSS2 mediates entry via the non-endosomal pathway for both MERS-CoV and SARS-CoV [50, 127–129]. Camostat mesylate, which has been used in the treatment of chronic pancreatitis, inhibits TMPRSS2-mediated glycoprotein activation of MERS-CoV, SARS-CoV, and influenza virus [126, 130–132]. K11777, a cysteine protease inhibitor, is in clinical development for treating parasitic infections. K11777 has broad-spectrum activity against coronaviruses (MERS-CoV, SARS-CoV, HCoV-229E), filoviruses (EBOV, Marburg virus), and paramyxoviruses (Nipah virus) [133]. Interestingly, Zhou et al. [133] demonstrated that Camostat and K11777 had inhibitory activity against SARS-CoV whereas EBOV was only inhibited by K11777, suggesting differential host protease requirements for these viruses [133]. E-64-D, an inhibitor of an endosomal cysteine protease currently in Phase III trials for the treatment of muscular dystrophy, inhibits both MERS-CoV and SARS-CoV in vitro [38]. E-64-D also inhibits filovirus cell entry [134, 135]. The dependency of viruses for specific serine or cysteine host proteases must be considered in the selection of protease inhibitors for antiviral therapeutic applications. Therefore, an increased understanding of the relationship between host proteases and viral pathogenesis will determine the most effective treatment options for viral infections.

Lopinavir was identified as an inhibitor of MERS-CoV and SARS-CoV in vitro, and time-of-addition experiments indicate that the drug acts at an early stage of viral entry [36]. Lopinavir, an inhibitor of the HIV protease, is used clinically for the treatment of HIV infections [136]. It is given in combination with ritonavir, an inhibitor of cytochrome P450 3A4, to increase blood concentrations because of the low bioavailability of lopinavir [136]. Lopinavir also inhibits human papilloma virus and is currently under development for the topical treatment of cervical cancer [137]. Treatment with lopinavir/ritonavir resulted in reduced mortality in a NHP model of MERS [121]. Lopinavir has been shown to target the main protease (M^{pro}) of SARS-CoV [138]. However, lopinavir has also been shown to act on other intracellular processes that are involved in coronavirus replication. Additional studies are needed to fully understand the mechanism of action of lopinavir involving cellular proteases. During the 2003 SARS outbreak, patients in open clinical trials were treated with lopinavir/ritonavir in combination with ribavirin had a

milder disease course and reduction in fatality rate compared to that observed with historical controls [27, 28].

2.2.9 Protein Synthesis Inhibitors

Three protein synthesis inhibitors with activity against coronaviruses were identified, emetine, anisomycin and omacetaxine mepesuccinate [38, 139]. Emetine, a natural plant alkaloid, and anisomycin, an antibiotic, both inhibit protein elongation and were identified as anti-protozoals [140, 141]. While emetine is approved for amoebiasis treatment, anisomycin did not move beyond clinical trials [141, 142]. Dehydroemetine, a synthetic emetine derivative, has fewer side effects and is available as an investigational new drug [143, 144]. Anisomycin was originally discovered as a peptidyl transferase inhibitor, but also activates the MAP kinase signaling pathway [145]. In addition to activity against MERS-CoV and SARS-CoV, emetine and anisomycin inhibit the animal picornavirus encephalomyocarditis virus [146]. Anisomycin has in vitro activity against poliovirus [147]. Omacetaxine mepesuccinate, a plant-derived alkaloid, is an anticancer therapeutic that received FDA approval in 2012 for the treatment of chronic myeloid leukemia. Omacetaxine inhibits MERS-CoV, bovine coronavirus, human enteric coronavirus and hepatitis B virus [139, 148]. In spite of omacetaxine broad spectrum anti-coronavirus activity, the drug had no activity against SARS-CoV [38]. Drugs that inhibit coronaviruses by targeting protein synthesis may have potential in the development of combination therapies with drugs that target other antiviral pathways.

2.2.10 Selective Estrogen Receptor Modulators

Recent investigations have demonstrated the potential of estrogen receptor (ER) antagonists for repurposing as anti-coronavirus compounds [38]. For example, toremifene citrate and tamoxifen citrate with activity against SARS-CoV and MERS-CoV were developed and approved as anticancer therapeutics. Both drugs have shown activity against HCV replication in vitro [149, 150]. Mechanistic studies revealed that the ER is functionally associated with HCV replication [150]. ER promotes the interaction between the HCV replication complex and the HCV polymerase NS5B. ER-mediated regulation of HCV genome replication is abrogated by tamoxifen.

Toremifene and tamoxifen also effectively inhibit EBOV infection in vitro [151]. However, in contrast to HCV, mechanistic studies have shown that toremifene-mediated EBOV inhibition is independent of the ER pathway as toremifene was still active against EBOV in cells that did not express ER [151, 152]. Toremifene acts at a late step of virus entry after internalization of EBOV and

may prevent fusion between the viral and endosomal membranes [151–153]. Based on the chemical structure, toremifene is a cationic amphiphilic drug (CAD) that is known to be lysosomotropic and could affect endosomal processes during virus entry [151, 154]. Treatment with toremifene led to 50% survival of EBOV-infected mice confirming that this drug has an effect in vivo as well [151].

In terms of clinical application, toremifene and tamoxifen have good bioavailability, safety and tolerability profiles combined with a long history of use in the clinic. However, prolongation of the QT interval has been noted for toremifene and should not be prescribed to patients with congenital or acquired long QT syndrome, uncorrected hypokalemia or uncorrected hypomagnesemia [155]. Tamoxifen can increase uterine malignancies, stroke and pulmonary embolism in women with ductal carcinoma in situ or at high risk for breast cancer [156]. Despite these side effects, the drugs may have substantial value for short-term treatment of acute coronavirus infections. Advanced patient studies and careful evaluation of the pharmacokinetic profiles may facilitate dosing strategies that limit the risk of adverse events.

2.2.11 Sterol Metabolism Inhibitors

Two sterol synthesis inhibitors, terconazole and triparanol, have shown activity against MERS-CoV and SARS-CoV [38]. Studies with virus-like particles (VLPs) have demonstrated that terconazole inhibits coronavirus cell entry, including MERS-CoV and SARS-CoV. The sterol synthesis pathway has been shown to be required for infection by several viruses including HCV [157, 158]. Terconazole, approved for vaginal yeast infections, can be administered orally, topically or by suppository. Triparanol was approved for lowering plasma cholesterol, but was withdrawn due to numerous side effects. Both are CADs that induce accumulation of cholesterol in late endosomes and have been shown to inhibit EBOV entry [152].

2.3 Drugs in Development

2.3.1 Potential Targets for Inhibition of MERS-CoV and SARS-CoV

In addition to drug repurposing, development of novel antiviral countermeasures is needed for emerging coronaviruses. To this end, design or development strategies have targeted the viral replication cycle and host pathways essential for viral replication (Table 4). Two nucleoside inhibitors of viral RNA-dependent RNA polymerases, GS-5734 and BCX4430, have potential as broad-spectrum

antivirals [159, 160]. Both drugs are active against MERS-CoV and SARS-CoV in cell culture, but in vivo efficacy remains to be investigated. In addition, a new class of nucleosides with a flexible purine base has anti-coronaviral activity, and further optimization could generate potent inhibitors of the coronaviral polymerase [161]. The surface glycoprotein (S) of SARS-CoV and MERS-CoV and other coronaviruses consists of two domains: S1, containing the receptor-binding domain (RBD) needed for extracellular binding; and S2, containing the fusion peptide needed for membrane fusion and release. Endocytosis of SARS-CoV is facilitated by the binding of RBD with the angiotensin converting enzyme 2 (ACE2) receptor on host cells. Membrane-bound cathepsin L cleaves the S protein revealing the S2 fusion protein, which fuses with the membrane and releases the viral RNA. Inhibitors of cathepsin L, the ACE2–SARS–S1 complex, or the S2 fusion peptide could be suitable targets to inhibit SARS-CoV entry [162]. Results from recent studies have identified inhibitors of viral entry, viral proteases, and helicases that potently inhibit both MERS-CoV and SARS-CoV [162]. Proteases, such as papain-like protease and 3C-like protease, could also be useful as antiviral targets for drug development as they are required for cleaving non-structural proteins for viral maturation. Most protease inhibitors are “suicide” protease inhibitors that bind to the target irreversibly. However, reversible protease inhibitors may have greater potential as they are less toxic and better tolerated [113]. Recent studies with helicase inhibitors show that three domain targets, N-terminal metal binding domain, a hinge domain, and a NTP/helicase domain, have potential for the development of new drugs [163].

2.3.2 RNA Interference

Directed RNA interference (RNAi) presents a powerful approach for the development of novel virus-specific therapeutics based on gene silencing [164]. Recent studies have shown that small interfering RNAs (siRNAs) or short hairpin RNAs can inhibit expression of viral genes and thereby block the replication of SARS-CoV in cultured cells [165–172]. Intranasal delivery of a combination of small interfering RNA (siSC2-5) targeting SARS-CoV open reading frame 1 and S protein decreased SARS pathogenesis in NHPs [173]. Potential RNAi candidates identified through computational modeling for MERS-CoV require further in vitro and preclinical investigation [174]. Several RNAi therapeutics for the treatment of viral infections have entered clinical trials including TKM-Ebola, a siRNA/lipid nanoparticle platform targeting EBOV [164, 175, 176]. This technology has great potential for therapeutics for emerging viruses as viral genome

Table 4 Drugs in development for the treatment of Middle East respiratory syndrome (MERS) or severe acute respiratory syndrome (SARS)

Viral/cellular target	Drug class	Drug
MERS-CoV		
3C-like protease	Benzotriazole esters	CE-5 [284]
Papain-like protease	Thiopurines	6-Thioguanine, 6-mercaptopurine [113]
Helicase	Triazole	SSYA10-001 [162]
RNA-dependent RNA polymerase	Nucleotide prodrug	GS-5734 [159]
RNA-dependent RNA polymerase	Nucleoside analog	BCX4430 [160]
Membrane-bound RNA synthesis	Small molecule inhibitor	K22 [285]
Furin inhibitor	Small molecule inhibitor	Decanoyl-RVCR [286]
SARS-CoV		
3C-like protease	Benzotriazole esters	CE-5 [284]
3C-like protease	Anilides	Peptide nitroanilides [287]
3C-like protease	C ₂ -symmetric inhibitors containing diol cores	TL-3 [288]
3C-like protease	Pyrazole analogs	Pyrazolones [289]
3C-like protease	Serine inhibitor	Trifluoromethyl ketones [290]
3C-like protease	Serotonin receptor antagonist	Cinanserin [291]
3C-like protease	Zinc-conjugated inhibitor	JMF 1586 [292]
Papain-like protease	Thiopurines	6-Thioguanine, 6-mercaptopurine [113]
Helicase	Triazole	SSYA10-001 [162]
Helicase	Bananin derivatives	Vanillinbananin, Idobananin [163]
NTPase/Helicase	Aryl diketoacids Dihydroxychromone and hydroxychromone derivatives	ADK analogs [293]; 2-(3-iodobenzyloxy)-6-(3-chlorobenzyloxy)-5-hydroxychromone [294]
RNA-dependent RNA polymerase	Nucleoside analogs	BCX4430 [160], 4-aza-7,9-dideazaadenosine C-nucleosides [295], fleximer nucleoside analogs [161]
Cathepsin L cellular protease	Small molecule inhibitor	Oxocarbamate [296], SSAA09E1 [297]
ACE2–SARS–S1 complex	Small molecule inhibitor	SSAA09E2 [297]
S2-cell membrane fusion	Small molecule inhibitor	SSAA09E3 [297]
ACE2–SARS–S1 complex	Small molecule inhibitor	NAAE [298]

ACE2 angiotensin converting enzyme, *MERS-CoV* Middle East respiratory syndrome coronavirus, *S1* spike protein 1 domain, *S2* Spike protein 2 domain

sequencing can now be completed in a very short time frame that is crucial in situations when an epidemic of a novel emerging viral infection unfolds. The main obstacle for RNAi strategies lies in the identification of suitable viral targets and in the delivery efficiency of nucleic acids to target cells in vivo.

2.3.3 Peptide Entry Inhibitors

Peptides share common physicochemical properties with CADs that facilitate interaction with cell membranes and interference with the fusion of cellular and viral membranes during virus entry. Researchers are making progress

in defining the mechanism of action of peptide entry inhibitors of enveloped viruses such as enfuvirtide, an approved HIV inhibitor [177]. Enfuvirtide is a 36-residue peptide derived from the amphipathic loop/C-helix heptad repeat domain of HIV gp41. A rational approach based on scanning fusion protein sequences for amphipathic sequences has led to the discovery of additional peptide inhibitors for other viruses including MERS-CoV and SARS-CoV [178–180]. Chemical modifications of peptides have increased their in vivo stability and bioavailability, improving their potential for clinical applications as novel broad-spectrum viral entry inhibitors [181–183].

2.4 Antibody Therapy

The success of palivizumab for treatment of respiratory syncytial virus infection has reinvigorated efforts to develop monoclonal antibody-based therapeutics for infectious diseases [184]. ZMapp, a monoclonal antibody cocktail targeting EBOV, has been tested in NHPs with success and was moved to Phase I and II clinical trials in humans during the EVD epidemic [185, 186]. Similarly, a monoclonal antibody against Hendra virus has been administered to humans on a “compassionate use” basis [187–189]. These examples demonstrate the potential for antibody therapy to combat emerging/re-emerging viruses, and similar strategies have been pursued by multiple groups for development of antibodies to MERS-CoV [190–197]. Monoclonal antibodies to MERS-CoV have been sourced from humanized mice libraries or human antibody libraries [192, 194, 197, 198]. Antibodies target the S RBD, S1, or S2 subunits, and have demonstrated efficacy in animal models as reviewed in Ying et al. [199]. Monoclonal antibody therapy can impart a selective pressure for generation of resistant viruses. Although mutants escaping monoclonal antibody pressure tend to be less fit, analysis of the emergence of mutations that confer resistance to the monoclonal antibody will need to be performed.

An alternative to monoclonal antibody therapy is polyclonal antibody therapy using convalescent sera (sera sourced from a nonhuman or humanized animal). Polyclonal antibodies provide an advantage over monoclonal antibodies in that escape mutants are less likely to emerge [200, 201]. Convalescent sera have been recommended for MERS, and a Phase II interventional clinical trial is ongoing to determine efficacy [198]. However, the availability of a suitable donor subject presents a significant complication for this approach. Nonhuman animal sera has been considered, but safety concerns limit this option. Fractionation of nonhuman sera is an alternative; however, antibody-mediated clearance can be limited due to failure of the human Fc receptors to recognize the antibody heavy chain.

An alternative is de-speciating the antibodies by using only the Fab antibody fragment; however, cost and sufficient material may make mass production of Fab fragments difficult. The use of sera from humanized mice or other small laboratory animals is complicated by sample acquisition/volume restraints. Larger laboratory animals may provide a potential alternative. SAB Biotherapeutics has developed a trans-chromosomal bovine platform for the generation of human IgG antibodies [201]. Vaccination of trans-chromosomal cattle with S protein nanoparticles or inactivated, whole virus generated fully humanized

polyclonal antibodies that demonstrated efficacy in the Ad-DPP4 murine model of MERS.

3 Lessons Learned

One of the most important lessons regarding antiviral drug development is that both highly specific and broad-spectrum antivirals bring unique advantages to the table. Antiviral agents can fall anywhere in the spectrum between “broad-spectrum” and “highly specific” [202]. A drug that targets a specific virus or virus family will have narrow activity, high potency, and low toxicity; however, such a drug may also promote resistance [202]. In contrast, broad-spectrum antivirals typically target a host factor or pathway, and often these agents have higher toxicities, lower potencies, and delayed treatment effects. However, the selective pressure for resistance is often lower with broad-spectrum agents.

A large part of our knowledge on antiviral development stems from the studies of chronic viral infections. Antiviral development strategies for DNA viruses have been successful in identifying a single drug that specifically targets a viral protein. This strategy has been less successful for RNA viruses. RNA viruses mutate at a higher rate than DNA viruses resulting in enhanced development of drug resistance.

3.1 AIDS

Despite extensive efforts over the past 30 years, a therapeutic or prophylactic HIV vaccine has remained elusive. Antiviral agents are the only available treatments for AIDS. Over 25 antivirals belonging to 6 different drug classes targeting different stages of viral replication are available (e.g. reverse transcriptase, protease, fusion, entry, integrase) [203]. Combination treatments with 2 to 3 drugs are effective and result in a sustained virologic response [204]. Two aspects have been found to be important for avoiding resistance: (1) selecting drugs with at least two different targets, and (2) selecting drugs that belong to different chemical classes. These considerations may also apply for drug combinations with synergistic effects against MERS- and SARS-CoV.

3.2 Hepatitis C

Broad-spectrum antiviral therapies can be of great value for treating emerging infections when it takes time to develop direct-acting antivirals. For treatment of chronic hepatitis C, clinicians have depended on IFN and ribavirin for a number of years [205]. Eventually, IFN and ribavirin combination was replaced by very effective fixed-

combination therapies using direct-acting antivirals that target multiple steps of the HCV life cycle [206]. IFN and ribavirin contribute significantly to the treatment of viral infections for which no direct-acting antivirals exist. However, they have major side effects [207]. More options for broad-spectrum antivirals with improved safety profiles would be beneficial for use for emerging coronavirus infections.

3.3 Influenza

Influenza viruses are characterized by a high mutation rate of the RNA genome. As available vaccines may not be protective against a novel pandemic strain, antiviral agents are considered an essential component for preparedness. Combinations of direct-acting antivirals are under evaluation for additive or synergistic effects and prevention of resistance [208, 209]. One triple combination (oseltamivir, amantadine and ribavirin) is synergistic and prevents resistance in vivo [210, 211], highlighting the potential of combinatorial therapy.

3.4 Ebola Virus Disease

The recent epidemic of EVD in Western Africa has renewed the urgency for development of treatments against emerging viruses. Although vaccines and direct-acting antiviral treatment are under investigation, none are approved for clinical use [212–216]. The WHO prioritized a panel of drugs approved for other indications that were considered for repurposing under FDA's Emergency Use Authorization [62]. Two of these drugs also have activity against MERS-CoV and SARS-CoV, amodiaquine (antimalarial agent) and toremifene citrate (breast cancer treatment).

Additional broad-spectrum antiviral agents (including repurposed drugs) should be a top priority for future emerging infections including coronavirus infections. A panel of broad-spectrum drugs that have been carefully validated for efficacy and safety and that could be used in combination would supply a minimum of protection for patients and healthcare workers at outbreak locations. This panel of drugs could be used in situations of a known re-emerging pathogen for which specific antiviral agents and vaccines has not been approved or of an unknown novel pathogen that could arise.

4 Gaps in Knowledge and Future Outlook

4.1 Animal Models of MERS and SARS

Effective development of countermeasures depends on developing appropriate animal models that uniformly

recapitulate human disease progression and severity of pathological manifestations. As with most animal models of human disease, no one animal model fully reflects SARS or MERS, therefore researchers are faced with exploring several small animal models or choosing the “best-fit” model. To date, animal models do not fully recapitulate human disease, thus animal models of MERS and SARS need further refinement. Many small animal models have been evaluated as potential MERS and SARS models including mice, hamsters, and ferrets for MERS and Syrian hamsters, and guinea pigs for SARS [217–219]. Four murine models have been reported for MERS. The first model that demonstrated promise involved transduction of the respiratory tract with the putative MERS-CoV receptor, human DPP4 (or CD26) [220]. The major indicator of disease in this model is viral load in the lung at 4 days post-inoculation. Although clinical signs of disease, including weight loss, were limited in this model, it has been used for pathogenesis countermeasure studies [221, 222]. Lethal, disseminated MERS infection has been demonstrated in transgenic mice expressing human DPP4 [223]. Inflammatory processes were observed in the brains of these mice in contrast to human disease in which CNS involvement has not been reported. A transgenic mouse MERS model was developed in which the mouse DPP4 gene was replaced by the human DPP4 gene under control of the endogenous mouse DPP4 promoter. Using this model, MERS-CoV-infected mice developed lung pathology [194]. In addition, administration of human monoclonal antibodies against the spike protein in these transgenic mice provided protection against MERS-CoV infection [194]. Clustered regularly interspaced short palindromic repeat-CRISPR-associated protein 9 (CRISPR-CAS9) gene editing technology was used to modify the mouse DPP4 to match human DPP4 by altering amino acids at positions 288 and 330. Interestingly, wild type virus infection of these mice did not result in an improved model of MERS. However, serial passage of MERS-CoV resulted in MERS-CoV-15. Intranasal exposure of MERS-CoV-15 in 288/330, mice led to weight loss and a severe respiratory disease that included ARDS-like signs and reduced pulmonary function [224].

MERS-CoV infection of rabbits has also been evaluated as a model for MERS. Haagmans et al. [225] demonstrated that MERS-CoV infected rabbits did not develop obvious clinical signs, but infectious virus could be detected in the upper respiratory tract [225]. Furthermore, epithelial cells of the bronchioles and terminal bronchioles respiratory tract were positive for MERS-CoV by immunohistochemistry and in-situ hybridization, which reflects tissue tropism in human disease [225]. Using the rabbit model, Houser et al. [191] demonstrated that human monoclonal antibody 336 given pre-exposure reduced viral RNA lung titer at

3 days post-exposure, but not when given post-exposure [191].

Due to phylogenetic similarities with humans, NHP models of disease have long been considered as necessary for evaluation of countermeasures to infectious diseases. Rhesus monkey and common marmoset have been evaluated as potential models for MERS. Following intratracheal instillation of MERS-CoV in rhesus monkey models, lung pathology was observed [122, 226–228]. Experiments using rhesus monkeys have indicated that they develop limited systemic disease and a transient respiratory disease. Radiologic evaluations have indicated inflammatory infiltrates that develop shortly after exposure. Analysis of lung tissues by reverse transcriptase-quantitative polymerase chain reaction indicated virus replication in the lung.

Similar to MERS, African green monkeys (AGMs), rhesus monkeys, cynomolgus monkeys, and common marmosets have been identified as potential models for SARS [229]. Smits et al. [230] compared SARS CoV infection in young AGMs to cynomolgus monkeys, they observed that neither species developed clinical signs during a 4-day experiment [230]. Gross pathology indicated multi-focal pulmonary consolidation with consolidated grey-red firm lungs. These lesions affected 30% of the lungs in one subject. By comparison, the cynomolgus monkeys developed small patchy macroscopic lesions. Similar to MERS-CoV infection of NHPs, viral load decreases from exposure day to day 4. A comparison between AGMs, rhesus monkeys, and cynomolgus monkeys further support AGMs as the best available NHP model for SARS [231]. AGMs developed the highest viral load and most disease when compared to cynomolgus and rhesus monkeys. Lethal disease was not observed in any of these species; therefore, further development of the SARS model is warranted since lethal respiratory tract disease was the hallmark of SARS.

As an alternative to Old World NHPs, many groups have employed marmosets as models of human infectious disease [232–234]. Common marmosets have been evaluated as a MERS model [121, 122, 235]. These studies have demonstrated that common marmosets develop disease following exposure to MERS-CoV as shown by histopathological analysis, radiological analysis, and RT-qPCR. However, variable results have been reported, and exposure methodology can impact disease progression. Therefore, mock-infected groups must be included to account for pathological artifacts. The virus-specific pathology could be quantified using computed tomography, and future experiments using large group sizes could be used for countermeasure evaluation. Greenough et al. [236] performed a serial euthanasia study of SARS-CoV infected marmosets [236]. Subjects were intratracheally exposed with SARS-CoV. They observed mild inconsistent clinical

signs of disease. Viral loads peaked at day 4 post-infection. Histopathology indicated interstitial pneumonitis with multinucleated syncytia that were described as mild and not observed in all late time-point subjects. Overall, further research is needed to develop animal models of SARS that reflect human disease presentation.

4.2 Combinations with Synergy

Drugs with repurposing potential discussed here (Table 3) have the advantage of easy access, availability and decreased cost of development and provide a wide array of options for combination studies. The pharmacological knowledge available for such compounds may also reduce concerns regarding adverse effects in patients. The generation of a translational database encompassing pharmacodynamics data and infectious disease biology data has been proposed and would greatly facilitate decision making to pursue new drug combinations [237]. Many of the drugs have potential for broad-spectrum antiviral activity and have already been in clinical use for treating other viral infections. As novel drugs in development move from the pre-clinical to clinical phase, they also become available for combination therapy. Care should be taken with the pharmacological evaluation of each combination to avoid possible contraindications of the drugs with regards to disease or adverse effects. Novel broad-spectrum replication inhibitors, such as GS-5734 (Gilead Sciences, in Phase I clinical trial), immunomodulators (nitazoxanide; steroids; statins) along with direct-acting antiviral agents for coronaviruses that are in development represent interesting partners for combinations. Combinations can involve broad-spectrum versus specific antiviral agents; drugs with different mechanism of action; or drugs that target different steps of the viral life cycle. Identifying one or more potent combinations with activity in an animal model would greatly increase preparedness for the next coronavirus outbreak.

4.3 Structure-Based Drug Design

Elucidation of the crystal structure of viral proteins has led to novel approaches for rational drug design. Rational design investigations using protein structure information and *in silico* screening for affinity to active sites of viral proteins holds promise. HIV-1 protease inhibitors have been one of the big successes of rational drug design. Only 6 years after the publication of the HIV-1 protease structure, saquinavir was developed in record time from bench to bedside and was licensed for use against AIDS in 1995 [238–240]. In total, six antivirals against the HIV-1 protease were designed and approved between 1995 and 2000. Similarly, for HCV, computer-aided approaches based on

the known crystal structure of a viral protein have successfully guided the design and synthesis of inhibitors for the HCV NS3/NS4A proteases such as the peptidomimetics, telaprevir and boceprevir [241–243].

Due to the power of computational modeling using crystal structures from known coronaviruses, the crystal structures for the viral proteases, M^{pro} and PL^{pro}, of SARS-CoV and MERS-CoV were determined relatively quickly [244]. These structures have already been used for the discovery of inhibitors with high binding affinity to the active site of the proteases. The structures of additional MERS-CoV or SARS-CoV viral proteins have yet to be determined and would offer additional viral targets for drug discovery.

Structural design can help with development of inhibitors in preparing for future outbreaks of yet unknown emerging coronaviruses. Based on the potential of zoonotic transmission of coronaviruses from bats to humans, crystal structures for the main protease (M^{pro}) of different bat coronavirus families have been proposed for screening and identifying broad-spectrum antiviral agents [244]. Proof-of-principle was shown for the novel protease inhibitor SG85, which inhibits the bat coronavirus HKU4 [244]. In 2012, SG85 was quickly identified as an inhibitor of MERS-CoV through *in silico* docking studies with the M^{pro} of MERS-CoV and the bat coronavirus HKU4.

4.4 Cationic Amphiphilic Drugs: A Novel Class of Antiviral Agents?

Several drugs (e.g. toremifene citrate, terconazole, Fig. 3) belong to a group of compounds termed cationic amphiphilic drugs (CADs) [100, 151, 152, 154, 245]. Phenothiazines (e.g. fluphenazine chlorpromazine, Fig. 3) are CADs that have been shown to inhibit HCV entry at virus-host cell fusion by intercalating into the cholesterol-rich domains of the host cell membrane and increasing membrane fluidity [97]. Drugs that act through this mechanism may present an interesting new class of broad-spectrum antivirals. CADs are known to be lysomotropic and accumulate in acidic compartments where their tertiary amine groups are protonated. The compounds act as mild bases and can neutralize the low pH of the acidic environment of endo/lysosomes. CADs can intercalate into membranes, alter the biophysical properties of membranes and thereby could potentially interfere with fusion of virus with the endo/lysosomal membrane. The concept of interfering with virus entry and budding through physicochemical properties of drugs is intriguing. Many viruses would be susceptible to this type of inhibition and CADs could be used as broad-spectrum antiviral agents. Detailed structure-activity

relationship studies on CADs will be required to determine the chemical core structures and physicochemical properties important for this type of antiviral agent. Future investigations regarding the conservation of this mechanism of action to coronaviruses, as well as other emerging viruses, are warranted.

4.5 Analogs of Developed Drugs

Approved drugs with activity against MERS-CoV or SARS-CoV could be used as lead compounds for further antiviral drug development. Pharmaceuticals usually have undergone multiple rounds of structure-activity relationship studies generating analogs to improve drug activity against the original indication or target. The analogs of drugs with activity against MERS-CoV and SARS-CoV may still be available and could be screened to identify other analogs with increased antiviral activity. Although drug analogs would have to go through the full licensure process, there would be little to no added initial cost associated with producing the structure-activity relationship compounds. Recycling old analogs is one approach that may have value for developing novel drugs for viral infections.

5 Conclusion

A more streamlined process is needed for development of effective treatment measures for emerging and re-emerging pathogens. The availability of a panel of approved broad-spectrum drugs would clearly be beneficial as they could be used for treating disease symptoms and reducing morbidity until more specific acting antivirals and vaccines are developed.

A large number of potential drugs and therapeutics for the treatment of MERS and SARS have been discussed. The greatest challenge will be how best to down-select and evaluate the different approaches. As we have learned from drug development for AIDS and hepatitis, alleviating disease symptoms and increasing life span may be a more achievable goal rather than looking for a treatment that will provide complete recovery. Broad-spectrum antivirals, specific antivirals, and immune modulators each have an important role in treating viral infections either individually or in combination. Effective communication between the different institute partners (government, industry, academic; national, and international partners) is essential. Combining these drug discovery efforts will increase the chance of having one or more potential therapeutic agents at an advanced development stage by the time another outbreak of an emerging coronavirus occurs.

Acknowledgements The authors thank Laura Bollinger and Jiro Wada for providing technical writing services and graphical support, respectively.

Compliance with Ethical Standards

The content of this publication does not necessarily reflect the views or policies of the US Department of Health and Human Services (DHHS) or of the institutions and companies affiliated with the authors.

Funding This work was supported in part by the Division of Intramural Research and Division of Clinical Research, National Institute of Allergy and Infectious Diseases. This work was funded in part through Battelle Memorial Institute's prime contract with the US National Institute of Allergy and Infectious Diseases (NIAID) under Contract No. HHSN272200700016I. J.D. performed this work as employee of Tunnell Government Services, Inc., subcontractor to Battelle Memorial Institute (BMI). R.G. performed this work as employee of BMI. G.G.O. performed this work as employee of MRI Global, subcontractor to BMI.

Conflict of interest The authors have declared that they have no conflict of interest.

References

- Li W, Shi Z, Yu M, Ren W, Smith C, Epstein JH, et al. Bats are natural reservoirs of SARS-like coronaviruses. *Science*. 2005;310(5748):676–9.
- Lau SK, Woo PC, Li KS, Huang Y, Tsoi HW, Wong BH, et al. Severe acute respiratory syndrome coronavirus-like virus in Chinese horseshoe bats. *Proc Natl Acad Sci USA*. 2005;102(39):14040–5.
- Revised US. surveillance case definition for severe acute respiratory syndrome (SARS) and update on SARS cases—United States and worldwide, December 2003. *MMWR Morb Mortal Wkly Rep*. 2003;52(49):1202–6.
- World Health Organization. Middle East respiratory syndrome coronavirus (MERS-CoV)—Saudi Arabia. Disease outbreak news. 2017. <http://www.who.int/csr/don/17-january-2017-mers-saudi-arabia/en/>. Accessed 24 Jan 2017.
- World Health Organization. Middle East respiratory syndrome coronavirus (MERS-CoV). Fact sheet. 2017.
- Fehr AR, Perlman S. Coronaviruses: an overview of their replication and pathogenesis. *Methods Mol Biol*. 2015;1282:1–23.
- Pasternak AO, Spaan WJ, Snijder EJ. Nidovirus transcription: how to make sense...? *J Gen Virol*. 2006;87(Pt 6):1403–21.
- Perlman S, Netland J. Coronaviruses post-SARS: update on replication and pathogenesis. *Nat Rev Microbiol*. 2009;7(6):439–50.
- Eckerle I, Corman VM, Muller MA, Lenk M, Ulrich RG, Drosten C. Replicative capacity of MERS coronavirus in live-stock cell lines. *Emerg Infect Dis*. 2014;20(2):276–9.
- Memish ZA, Mishra N, Olival KJ, Fagbo SF, Kapoor V, Epstein JH, et al. Middle East respiratory syndrome coronavirus in bats, Saudi Arabia. *Emerg Infect Dis*. 2013;19(11):1819–23.
- Adney DR, van Doremalen N, Brown VR, Bushmaker T, Scott D, de Wit E, et al. Replication and shedding of MERS-CoV in upper respiratory tract of inoculated dromedary camels. *Emerg Infect Dis*. 2014;20(12):1999–2005.
- Wang LF, Shi Z, Zhang S, Field H, Daszak P, Eaton BT. Review of bats and SARS. *Emerg Infect Dis*. 2006;12(12):1834–40.
- Chowell G, Abdirizak F, Lee S, Lee J, Jung E, Nishiura H, et al. Transmission characteristics of MERS and SARS in the healthcare setting: a comparative study. *BMC Med*. 2015;13:210.
- Hunter JC, Nguyen D, Aden B, Al Bandar Z, Al Dhaheri W, Abu Elkheir K, et al. Transmission of Middle East respiratory syndrome coronavirus infections in healthcare settings, Abu Dhabi. *Emerg Infect Dis*. 2016;22(4):647–56.
- Zumla A, Hui DS, Perlman S. Middle East respiratory syndrome. *Lancet*. 2015;386(9997):995–1007.
- Rasmussen SA, Watson AK, Swardlow DL. Middle East respiratory syndrome (MERS). *Microbiol Spectr*. 2016;4(3):1–23.
- Chan PK, Tang JW, Hui DS. SARS: clinical presentation, transmission, pathogenesis and treatment options. *Clin Sci (Lond)*. 2006;110(2):193–204.
- Zaki AM, van Boheemen S, Bestebroer TM, Osterhaus AD, Fouchier RA. Isolation of a novel coronavirus from a man with pneumonia in Saudi Arabia. *N Engl J Med*. 2012;367(19):1814–20.
- Guery B, Poissy J, el Mansouf L, Sejourne C, Ettahar N, Lemaire X, et al. Clinical features and viral diagnosis of two cases of infection with Middle East Respiratory Syndrome coronavirus: a report of nosocomial transmission. *Lancet*. 2013;381(9885):2265–72.
- WHO Mers-Cov Research Group. State of knowledge and data gaps of Middle East respiratory syndrome coronavirus (MERS-CoV) in humans. *PLoS Curr*. 2013;5.
- Arabi YM, Arifi AA, Balkhy HH, Najm H, Aldawood AS, Ghabashi A, et al. Clinical course and outcomes of critically ill patients with Middle East respiratory syndrome coronavirus infection. *Ann Intern Med*. 2014;160(6):389–97.
- Assiri A, Al-Tawfiq JA, Al-Rabeah AA, Al-Rabiah FA, Al-Hajjar S, Al-Barrak A, et al. Epidemiological, demographic, and clinical characteristics of 47 cases of Middle East respiratory syndrome coronavirus disease from Saudi Arabia: a descriptive study. *Lancet Infect Dis*. 2013;13(9):752–61.
- Ajlan AM, Ahyad RA, Jamjoom LG, Alharthy A, Madani TA. Middle East respiratory syndrome coronavirus (MERS-CoV) infection: chest CT findings. *AJR Am J Roentgenol*. 2014;203(4):782–7.
- Memish ZA, Al-Tawfiq JA, Makhdoom HQ, Assiri A, Alhakeem RF, Albarrak A, et al. Respiratory tract samples, viral load, and genome fraction yield in patients with Middle East respiratory syndrome. *J Infect Dis*. 2014;210(10):1590–4.
- Chiou HE, Liu CL, Buttrey MJ, Kuo HP, Liu HW, Kuo HT, et al. Adverse effects of ribavirin and outcome in severe acute respiratory syndrome: experience in two medical centers. *Chest*. 2005;128(1):263–72.
- Leong HN, Ang B, Earnest A, Teoh C, Xu W, Leo YS. Investigational use of ribavirin in the treatment of severe acute respiratory syndrome, Singapore, 2003. *Trop Med Int Health*. 2004;9(8):923–7.
- Chu CM, Cheng VC, Hung IF, Wong MM, Chan KH, Chan KS, et al. Role of lopinavir/ritonavir in the treatment of SARS: initial virological and clinical findings. *Thorax*. 2004;59(3):252–6.
- Chan KS, Lai ST, Chu CM, Tsui E, Tam CY, Wong MM, et al. Treatment of severe acute respiratory syndrome with lopinavir/ritonavir: a multicentre retrospective matched cohort study. *Hong Kong Med J*. 2003;9(6):399–406.
- Loutfy MR, Blatt LM, Siminovich KA, Ward S, Wolff B, Lho H, et al. Interferon alfacon-1 plus corticosteroids in severe acute respiratory syndrome: a preliminary study. *JAMA*. 2003;290(24):3222–8.
- Omrani AS, Saad MM, Baig K, Bahloul A, Abdul-Matin M, Alaidaroos AY, et al. Ribavirin and interferon alfa-2a for severe Middle East respiratory syndrome coronavirus infection: a retrospective cohort study. *Lancet Infect Dis*. 2014;14(11):1090–5.

31. Spanakis N, Tsiodras S, Haagmans BL, Raj VS, Pontikis K, Koutsoukou A, et al. Virological and serological analysis of a recent Middle East respiratory syndrome coronavirus infection case on a triple combination antiviral regimen. *Int J Antimicrob Agents*. 2014;44(6):528–32.
32. King Abdullah International Medical Research Center. MERS-CoV infection treated with a combination of lopinavir /ritonavir and interferon beta-1b (MIRACLE). Bethesda: National Institutes of Health; 2017. <https://clinicaltrials.gov/ct2/show/NCT02845843>. Accessed 12 July 2017.
33. Ashburn TT, Thor KB. Drug repositioning: identifying and developing new uses for existing drugs. *Nat Rev Drug Discov*. 2004;3(8):673–83.
34. Regnard C, Twycross R, Mihalyo M, Wilcock A. Loperamide. *J Pain Symptom Manag*. 2011;42(2):319–23.
35. Awouters F, Niemegeers CJ, Janssen PA. Pharmacology of antidiarrheal drugs. *Annu Rev Pharmacol Toxicol*. 1983;23:279–301.
36. de Wilde AH, Jochmans D, Posthuma CC, Zevenhoven-Dobbe JC, van Nieuwkoop S, Bestebroer TM, et al. Screening of an FDA-approved compound library identifies four small-molecule inhibitors of Middle East respiratory syndrome coronavirus replication in cell culture. *Antimicrob Agents Chemother*. 2014;58(8):4875–84.
37. Chertow DS, Uyeki TM, DuPont HL. Loperamide therapy for voluminous diarrhea in Ebola virus disease. *J Infect Dis*. 2015;211(7):1036–7.
38. Dyall J, Coleman CM, Hart BJ, Venkataraman T, Holbrook MR, Kindrachuk J, et al. Repurposing of clinically developed drugs for treatment of Middle East respiratory syndrome coronavirus infection. *Antimicrob Agents Chemother*. 2014;58(8):4885–93.
39. Keyaerts E, Vijgen L, Maes P, Neyts J, Van Ranst M. In vitro inhibition of severe acute respiratory syndrome coronavirus by chloroquine. *Biochem Biophys Res Commun*. 2004;323(1):264–8.
40. Thome R, Lopes SC, Costa FT, Verinaud L. Chloroquine: modes of action of an undervalued drug. *Immunol Lett*. 2013;153(1–2):50–7.
41. Brouwers J, Vermeire K, Schols D, Augustijns P. Development and in vitro evaluation of chloroquine gels as microbicides against HIV-1 infection. *Virology*. 2008;378(2):306–10.
42. Farias KJ, Machado PR, da Fonseca BA. Chloroquine inhibits dengue virus type 2 replication in Vero cells but not in C6/36 cells. *Sci World J*. 2013;2013:282734.
43. Madrid PB, Chopra S, Manger ID, Gilfillan L, Keepers TR, Shurtleff AC, et al. A systematic screen of FDA-approved drugs for inhibitors of biological threat agents. *PLoS One*. 2013;8(4):e60579.
44. Ooi EE, Chew JS, Loh JP, Chua RC. In vitro inhibition of human influenza A virus replication by chloroquine. *Viol J*. 2006;3:39.
45. Pohjala L, Utt A, Varjak M, Lulla A, Merits A, Ahola T, et al. Inhibitors of alphavirus entry and replication identified with a stable Chikungunya replicon cell line and virus-based assays. *PLoS One*. 2011;6(12):e28923.
46. Porotto M, Orefice G, Yokoyama CC, Mungall BA, Realubit R, Sganga ML, et al. Simulating henipavirus multicycle replication in a screening assay leads to identification of a promising candidate for therapy. *J Virol*. 2009;83(10):5148–55.
47. Randolph VB, Winkler G, Stollar V. Acidotropic amines inhibit proteolytic processing of flavivirus prM protein. *Virology*. 1990;174(2):450–8.
48. Savarino A, Boelaert JR, Cassone A, Majori G, Cauda R. Effects of chloroquine on viral infections: an old drug against today's diseases? *Lancet Infect Dis*. 2003;3(11):722–7.
49. Raj VS, Mou H, Smits SL, Dekkers DH, Muller MA, Dijkman R, et al. Dipeptidyl peptidase 4 is a functional receptor for the emerging human coronavirus-EMC. *Nature*. 2013;495(7440):251–4.
50. Gierer S, Bertram S, Kaup F, Wrensch F, Heurich A, Kramer-Kuhl A, et al. The spike protein of the emerging betacoronavirus EMC uses a novel coronavirus receptor for entry, can be activated by TMPRSS2, and is targeted by neutralizing antibodies. *J Virol*. 2013;87(10):5502–11.
51. Di Trani L, Savarino A, Campitelli L, Norelli S, Puzelli S, D'Ostilio D, et al. Different pH requirements are associated with divergent inhibitory effects of chloroquine on human and avian influenza A viruses. *Viol J*. 2007;4:39.
52. Marzi A, Moller P, Hanna SL, Harrer T, Eisemann J, Steinkasserer A, et al. Analysis of the interaction of Ebola virus glycoprotein with DC-SIGN (dendritic cell-specific intercellular adhesion molecule 3-grabbing nonintegrin) and its homologue DC-SIGNR. *J Infect Dis*. 2007;196(Suppl 2):S237–46.
53. Savarino A, Lucia MB, Rastrelli E, Rutella S, Golotta C, Morra E, et al. Anti-HIV effects of chloroquine: inhibition of viral particle glycosylation and synergism with protease inhibitors. *J Acquir Immune Defic Syndr*. 2004;35(3):223–32.
54. Vincent MJ, Bergeron E, Benjannet S, Erickson BR, Rollin PE, Ksiazek TG, et al. Chloroquine is a potent inhibitor of SARS coronavirus infection and spread. *Viol J*. 2005;2:69.
55. Browning DJ. Toxicology of hydroxychloroquine and chloroquine and the pathology of the retinopathy they cause. In: Browning DJ, editor. *Hydroxychloroquine and chloroquine retinopathy*. New York: Springer Science + Business Media; 2014. p. 65–83.
56. Sperber K, Chiang G, Chen H, Ross W, Chusid E, Gonchar M, et al. Comparison of hydroxychloroquine with zidovudine in asymptomatic patients infected with human immunodeficiency virus type 1. *Clin Ther*. 1997;19(5):913–23.
57. Sperber K, Louie M, Kraus T, Proner J, Sapira E, Lin S, et al. Hydroxychloroquine treatment of patients with human immunodeficiency virus type 1. *Clin Ther*. 1995;17(4):622–36.
58. De Lamballerie X, Boisson V, Reynier JC, Enault S, Charrel RN, Flahault A, et al. On chikungunya acute infection and chloroquine treatment. *Vector Borne Zoonotic Dis*. 2008;8(6):837–9.
59. Tricou V, Minh NN, Van TP, Lee SJ, Farrar J, Wills B, et al. A randomized controlled trial of chloroquine for the treatment of dengue in Vietnamese adults. *PLoS Negl Trop Dis*. 2010;4(8):e785.
60. Falzarano D, Safronetz D, Prescott J, Marzi A, Feldmann F, Feldmann H. Lack of protection against ebola virus from chloroquine in mice and hamsters. *Emerg Infect Dis*. 2015;21(6):1065–7.
61. Gignoux E, Azman AS, de Smet M, Azuma P, Massaquoi M, Job D, et al. Effect of artesunate-amodiaquine on mortality related to Ebola virus disease. *N Engl J Med*. 2016;374(1):23–32.
62. World Health Organization. Categorization and prioritization of drugs for consideration for testing or use in patients infected with Ebola. 2015. http://www.who.int/medicines/ebola-treatment/2015_0703TablesEbolaDrugs.pdf?ua=1. Accessed 13 Oct 2016.
63. Brickelmaier M, Lugovskoy A, Kartikeyan R, Reviriego-Mendoza MM, Allaire N, Simon K, et al. Identification and characterization of mefloquine efficacy against JC virus in vitro. *Antimicrob Agents Chemother*. 2009;53(5):1840–9.
64. Clifford DB, Nath A, Cinque P, Brew BJ, Zivadinov R, Gorelik L, et al. A study of mefloquine treatment for progressive multifocal leukoencephalopathy: results and exploration of predictors of PML outcomes. *J Neurovirol*. 2013;19(4):351–8.

65. Gofton TE, Al-Khotani A, O'Farrell B, Ang LC, McLachlan RS. Mefloquine in the treatment of progressive multifocal leukoencephalopathy. *J Neurol Neurosurg Psychiatry*. 2011;82(4):452–5.
66. Stamnes MA, Rutherford SL, Zuker CS. Cyclophilins: a new family of proteins involved in intracellular folding. *Trends Cell Biol*. 1992;2(9):272–6.
67. de Wilde AH, Raj VS, Oudshoorn D, Bestebroer TM, van Nieuwkoop S, Limpens RW, et al. MERS-coronavirus replication induces severe in vitro cytopathology and is strongly inhibited by cyclosporin A or interferon-alpha treatment. *J Gen Virol*. 2013;94(Pt 8):1749–60.
68. de Wilde AH, Zevenhoven-Dobbe JC, van der Meer Y, Thiel V, Narayanan K, Makino S, et al. Cyclosporin A inhibits the replication of diverse coronaviruses. *J Gen Virol*. 2011;92(Pt 11):2542–8.
69. Nagy PD, Wang RY, Pogany J, Hafren A, Makinen K. Emerging picture of host chaperone and cyclophilin roles in RNA virus replication. *Virology*. 2011;411(2):374–82.
70. Flisiak R, Horban A, Gally P, Bobardt M, Selvarajah S, Wiercinska-Drapalo A, et al. The cyclophilin inhibitor Debio-025 shows potent anti-hepatitis C effect in patients coinfecting with hepatitis C and human immunodeficiency virus. *Hepatology*. 2008;47(3):817–26.
71. Hopkins S, DiMassimo B, Rusnak P, Heuman D, Lalezari J, Sluder A, et al. The cyclophilin inhibitor SCY-635 suppresses viral replication and induces endogenous interferons in patients with chronic HCV genotype 1 infection. *J Hepatol*. 2012;57(1):47–54.
72. Lawitz E, Godofsky E, Rouzier R, Marbury T, Nguyen T, Ke J, et al. Safety, pharmacokinetics, and antiviral activity of the cyclophilin inhibitor NIM811 alone or in combination with pegylated interferon in HCV-infected patients receiving 14 days of therapy. *Antivir Res*. 2011;89(3):238–45.
73. Barnard DL, Day CW, Bailey K, Heiner M, Montgomery R, Lauridsen L, et al. Evaluation of immunomodulators, interferons and known in vitro SARS-CoV inhibitors for inhibition of SARS-CoV replication in BALB/c mice. *Antivir Chem Chemother*. 2006;17(5):275–84.
74. Haagmans BL, Kuiken T, Martina BE, Fouchier RA, Rimmelzwaan GF, van Amerongen G, et al. Pegylated interferon-alpha protects type 1 pneumocytes against SARS coronavirus infection in macaques. *Nat Med*. 2004;10(3):290–3.
75. Cinatl J, Morgenstern B, Bauer G, Chandra P, Rabenau H, Doerr HW. Treatment of SARS with human interferons. *Lancet*. 2003;362(9380):293–4.
76. Hensley LE, Fritz LE, Jahrling PB, Karp CL, Huggins JW, Geisbert TW. Interferon-beta 1a and SARS coronavirus replication. *Emerg Infect Dis*. 2004;10(2):317–9.
77. Sainz B Jr, Mossel EC, Peters CJ, Garry RF. Interferon-beta and interferon-gamma synergistically inhibit the replication of severe acute respiratory syndrome-associated coronavirus (SARS-CoV). *Virology*. 2004;329(1):11–7.
78. Falzarano D, de Wit E, Martellaro C, Callison J, Munster VJ, Feldmann H. Inhibition of novel beta coronavirus replication by a combination of interferon-alpha2b and ribavirin. *Sci Rep*. 2013;3:1686.
79. Falzarano D, de Wit E, Rasmussen AL, Feldmann F, Okumura A, Scott DP, et al. Treatment with interferon-alpha2b and ribavirin improves outcome in MERS-CoV-infected rhesus macaques. *Nat Med*. 2013;19(10):1313–7.
80. Hart BJ, Dyall J, Postnikova E, Zhou H, Kindrachuk J, Johnson RF, et al. Interferon-beta and mycophenolic acid are potent inhibitors of Middle East respiratory syndrome coronavirus in cell-based assays. *J Gen Virol*. 2014;95(Pt 3):571–7.
81. Wu P, Nielsen TE, Clausen MH. FDA-approved small-molecule kinase inhibitors. *Trends Pharmacol Sci*. 2015;36(7):422–39.
82. Hunter T. Protein kinases and phosphatases: the yin and yang of protein phosphorylation and signaling. *Cell*. 1995;80(2):225–36.
83. Cohen P. Protein kinases—the major drug targets of the twenty-first century? *Nat Rev Drug Discov*. 2002;1(4):309–15.
84. Hopkins AL, Groom CR. The druggable genome. *Nat Rev Drug Discov*. 2002;1(9):727–30.
85. Josset L, Menachery VD, Gralinski LE, Agnihotram S, Sova P, Carter VS, et al. Cell host response to infection with novel human coronavirus EMC predicts potential antivirals and important differences with SARS coronavirus. *MBio*. 2013;4(3):e00165–13.
86. Ludwig S. Disruption of virus-host cell interactions and cell signaling pathways as an anti-viral approach against influenza virus infections. *Biol Chem*. 2011;392(10):837–47.
87. Tisoncik JR, Korth MJ, Simmons CP, Farrar J, Martin TR, Katze MG. Into the eye of the cytokine storm. *Microbiol Mol Biol Rev*. 2012;76(1):16–32.
88. Coleman CM, Sisk JM, Mingo RM, Nelson EA, White JM, Frieman MB. Abelson kinase inhibitors are potent inhibitors of severe acute respiratory syndrome coronavirus and Middle East respiratory syndrome coronavirus fusion. *J Virol*. 2016;90(19):8924–33.
89. Kindrachuk J, Ork B, Hart BJ, Mazur S, Holbrook MR, Frieman MB, et al. Antiviral potential of ERK/MAPK and PI3 K/AKT/mTOR signaling modulation for Middle East respiratory syndrome coronavirus infection as identified by temporal kinase analysis. *Antimicrob Agents Chemother*. 2015;59(2):1088–99.
90. Paladin Therapeutics. Impavido (Miltefosine) capsules, for oral use prescribing information. Wilmington: Paladin Therapeutics; 2014. <https://dailymed.nlm.nih.gov/dailymed/fda/fdaDrugXsl.cfm?setid=d6658aeb-7bc1-4eeef-ad0d-0a873ddbcecf5&type=display>. Accessed 13 July 2017.
91. Centers for Disease Control and Prevention. Investigational drug available directly from CDC for the treatment of infections with free-living amoebae. *MMWR Morb Mortal Wkly Rep*. 2013;62(33):666.
92. Wang CH, Chung FT, Lin SM, Huang SY, Chou CL, Lee KY, et al. Adjuvant treatment with a mammalian target of rapamycin inhibitor, sirolimus, and steroids improves outcomes in patients with severe H1N1 pneumonia and acute respiratory failure. *Crit Care Med*. 2014;42(2):313–21.
93. Ohlow MJ, Moosmann B. Phenothiazine: the seven lives of pharmacology's first lead structure. *Drug Discov Today*. 2011;16(3–4):119–31.
94. Candurra NA, Maskin L, Damonte EB. Inhibition of arenavirus multiplication in vitro by phenothiazines. *Antivir Res*. 1996;31(3):149–58.
95. Chu JJ, Ng ML. Infectious entry of West Nile virus occurs through a clathrin-mediated endocytic pathway. *J Virol*. 2004;78(19):10543–55.
96. Bhattacharyya S, Warfield KL, Ruthel G, Bavari S, Aman MJ, Hope TJ. Ebola virus uses clathrin-mediated endocytosis as an entry pathway. *Virology*. 2010;401(1):18–28.
97. Chamoun-Emanuelli AM, Pecheur EI, Simeon RL, Huang D, Cremer PS, Chen Z. Phenothiazines inhibit hepatitis C virus entry, likely by increasing the fluidity of cholesterol-rich membranes. *Antimicrob Agents Chemother*. 2013;57(6):2571–81.
98. Nawa M, Takasaki T, Yamada K, Kurane I, Akatsuka T. Interference in Japanese encephalitis virus infection of Vero cells by a cationic amphiphilic drug, chlorpromazine. *J Gen Virol*. 2003;84(Pt 7):1737–41.
99. Kaur P, Chu JJ. Chikungunya virus: an update on antiviral development and challenges. *Drug Discov Today*. 2013;18(19–20):969–83.

100. Johansen LM, DeWald LE, Shoemaker CJ, Hoffstrom BG, Lear-Rooney CM, Stossel A, et al. A screen of approved drugs and molecular probes identifies therapeutics with anti-Ebola virus activity. *Sci Transl Med*. 2015;7(290):290ra89.
101. Kouznetsova J, Sun W, Martinez-Romero C, Tawa G, Shinn P, Chen CZ, et al. Identification of 53 compounds that block Ebola virus-like particle entry via a repurposing screen of approved drugs. *Emerg Microbes Infect*. 2014;3(12):e84.
102. Mingorance L, Friesland M, Coto-Llerena M, Perez-del-Pulgar S, Boix L, Lopez-Oliva JM, et al. Selective inhibition of hepatitis C virus infection by hydroxyzine and benztropine. *Antimicrob Agents Chemother*. 2014;58(6):3451–60.
103. Carranza M, Snyder MR, Shaw JD, Zesiewicz TA. Parkinson's disease. A guide to medical treatment. Turin: SEEd Medical Publishers; 2013.
104. Cheng H, Lear-Rooney CM, Johansen L, Varhegyi E, Chen ZW, Olinger GG, et al. Inhibition of Ebola and Marburg virus entry by G protein-coupled receptor antagonists. *J Virol*. 2015;89(19):9932–8.
105. Lindquist M, Edwards IR. Risks of non-sedating antihistamines. *Lancet*. 1997;349(9061):1322.
106. Chong CR, Chen X, Shi L, Liu JO, Sullivan DJ Jr. A clinical drug library screen identifies astemizole as an antimalarial agent. *Nat Chem Biol*. 2006;2(8):415–6.
107. Garcia-Quiroz J, Camacho J. Astemizole: an old anti-histamine as a new promising anti-cancer drug. *Anticancer Agents Med Chem*. 2011;11(3):307–14.
108. Zhang L, Yu J, Pan H, Hu P, Hao Y, Cai W, et al. Small molecule regulators of autophagy identified by an image-based high-throughput screen. *Proc Natl Acad Sci USA*. 2007;104(48):19023–8.
109. Chiramel AI, Brady NR, Bartenschlager R. Divergent roles of autophagy in virus infection. *Cells*. 2013;2(1):83–104.
110. Shoji-Kawata S, Sumpter R, Leveno M, Campbell GR, Zou Z, Kinch L, et al. Identification of a candidate therapeutic autophagy-inducing peptide. *Nature*. 2013;494(7436):201–6.
111. Barnard DL, Day CW, Bailey K, Heiner M, Montgomery R, Lauridsen L, et al. Enhancement of the infectivity of SARS-CoV in BALB/c mice by IMP dehydrogenase inhibitors, including ribavirin. *Antivir Res*. 2006;71(1):53–63.
112. Chan JF, Chan KH, Kao RY, To KK, Zheng BJ, Li CP, et al. Broad-spectrum antivirals for the emerging Middle East respiratory syndrome coronavirus. *J Infect*. 2013;67(6):606–16.
113. Cheng KW, Cheng SC, Chen WY, Lin MH, Chuang SJ, Cheng IH, et al. Thiopurine analogs and mycophenolic acid synergistically inhibit the papain-like protease of Middle East respiratory syndrome coronavirus. *Antivir Res*. 2015;115:9–16.
114. Saijo M, Morikawa S, Fukushima S, Mizutani T, Hasegawa H, Nagata N, et al. Inhibitory effect of mizoribine and ribavirin on the replication of severe acute respiratory syndrome (SARS)-associated coronavirus. *Antivir Res*. 2005;66(2–3):159–63.
115. Cinatl J Jr, Michaelis M, Hoever G, Preiser W, Doerr HW. Development of antiviral therapy for severe acute respiratory syndrome. *Antivir Res*. 2005;66(2–3):81–97.
116. Ibarra KD, Pfeiffer JK. Reduced ribavirin antiviral efficacy via nucleoside transporter-mediated drug resistance. *J Virol*. 2009;83(9):4538–47.
117. Smith EC, Denison MR. Coronaviruses as DNA wannabes: a new model for the regulation of RNA virus replication fidelity. *PLoS Pathog*. 2013;9(12):e1003760.
118. Diamond MS, Zachariah M, Harris E. Mycophenolic acid inhibits dengue virus infection by preventing replication of viral RNA. *Virology*. 2002;304(2):211–21.
119. Kitchin JE, Pomeranz MK, Pak G, Washenik K, Shupack JL. Rediscovering mycophenolic acid: a review of its mechanism, side effects, and potential uses. *J Am Acad Dermatol*. 1997;37(3 Pt 1):445–9.
120. Armstrong VW, Tenderich G, Shipkova M, Parsa A, Koerfer R, Schroder H, et al. Pharmacokinetics and bioavailability of mycophenolic acid after intravenous administration and oral administration of mycophenolate mofetil to heart transplant recipients. *Ther Drug Monit*. 2005;27(3):315–21.
121. Chan JF, Yao Y, Yeung ML, Deng W, Bao L, Jia L, et al. Treatment with lopinavir/ritonavir or interferon-beta1b improves outcome of MERS-CoV infection in a nonhuman primate model of common marmoset. *J Infect Dis*. 2015;212(12):1904–13.
122. Johnson RF, Via LE, Kumar MR, Cornish JP, Yellayi S, Huzella L, et al. Intratracheal exposure of common marmosets to MERS-CoV Jordan-n3/2012 or MERS-CoV EMC/2012 isolates does not result in lethal disease. *Virology*. 2015;485:422–30.
123. Naka K, Ikeda M, Abe K, Dansako H, Kato N. Mizoribine inhibits hepatitis C virus RNA replication: effect of combination with interferon-alpha. *Biochem Biophys Res Commun*. 2005;330(3):871–9.
124. Clouser CL, Holtz CM, Mullett M, Crankshaw DL, Briggs JE, Chauhan J, et al. Analysis of the ex vivo and in vivo antiretroviral activity of gemcitabine. *PLoS One*. 2011;6(1):e15840.
125. Denisova OV, Kakkola L, Feng L, Stenman J, Nagaraj A, Lampe J, et al. Obatoclox, saliphenylhalamide, and gemcitabine inhibit influenza A virus infection. *J Biol Chem*. 2012;287(42):35324–32.
126. Simmons G, Zmora P, Gierer S, Heurich A, Pohlmann S. Proteolytic activation of the SARS-coronavirus spike protein: cutting enzymes at the cutting edge of antiviral research. *Antivir Res*. 2013;100(3):605–14.
127. Glowacka I, Bertram S, Muller MA, Allen P, Soilleux E, Pfefferle S, et al. Evidence that TMPRSS2 activates the severe acute respiratory syndrome coronavirus spike protein for membrane fusion and reduces viral control by the humoral immune response. *J Virol*. 2011;85(9):4122–34.
128. Matsuyama S, Nagata N, Shirato K, Kawase M, Takeda M, Taguchi F. Efficient activation of the severe acute respiratory syndrome coronavirus spike protein by the transmembrane protease TMPRSS2. *J Virol*. 2010;84(24):12658–64.
129. Shulla A, Heald-Sargent T, Subramanya G, Zhao J, Perlman S, Gallagher T. A transmembrane serine protease is linked to the severe acute respiratory syndrome coronavirus receptor and activates virus entry. *J Virol*. 2011;85(2):873–82.
130. Hosoya M, Matsuyama S, Baba M, Suzuki H, Shigeta S. Effects of protease inhibitors on replication of various myxoviruses. *Antimicrob Agents Chemother*. 1992;36(7):1432–6.
131. Kawase M, Shirato K, van der Hoek L, Taguchi F, Matsuyama S. Simultaneous treatment of human bronchial epithelial cells with serine and cysteine protease inhibitors prevents severe acute respiratory syndrome coronavirus entry. *J Virol*. 2012;86(12):6537–45.
132. Shirato K, Kawase M, Matsuyama S. Middle East respiratory syndrome coronavirus infection mediated by the transmembrane serine protease TMPRSS2. *J Virol*. 2013;87(23):12552–61.
133. Zhou Y, Vedantham P, Lu K, Agudelo J, Carrion R Jr, Nunneley JW, et al. Protease inhibitors targeting coronavirus and filovirus entry. *Antivir Res*. 2015;116:76–84.
134. Chandran K, Sullivan NJ, Felbor U, Whelan SP, Cunningham JM. Endosomal proteolysis of the Ebola virus glycoprotein is necessary for infection. *Science*. 2005;308(5728):1643–5.
135. Schornberg K, Matsuyama S, Kabsch K, Delos S, Bouton A, White J. Role of endosomal cathepsins in entry mediated by the Ebola virus glycoprotein. *J Virol*. 2006;80(8):4174–8.

136. Sham HL, Kempf DJ, Molla A, Marsh KC, Kumar GN, Chen CM, et al. ABT-378, a highly potent inhibitor of the human immunodeficiency virus protease. *Antimicrob Agents Chemother.* 1998;42(12):3218–24.
137. Hampson L, Maranga IO, Masinde MS, Oliver AW, Batman G, He X, et al. A single-arm, proof-of-concept trial of lopimmune (lopinavir/ritonavir) as a treatment for HPV-related pre-invasive cervical disease. *PLoS One.* 2016;11(1):e0147917.
138. Wu CY, Jan JT, Ma SH, Kuo CJ, Juan HF, Cheng YS, et al. Small molecules targeting severe acute respiratory syndrome human coronavirus. *Proc Natl Acad Sci USA.* 2004;101(27):10012–7.
139. Cao J, Forrest JC, Zhang X. A screen of the NIH Clinical Collection small molecule library identifies potential anti-coronavirus drugs. *Antivir Res.* 2015;114:1–10.
140. Sobin BA, Tanner Jr. FW. Anisomycin, a new anti-protozoan antibiotic. *J Am Chem Soc.* 1954;76:4053.
141. Akinboye ES, Brennen WN, Rosen DM, Bakare O, Denmeade SR. Iterative design of emetine-based prodrug targeting fibroblast activation protein (FAP) and dipeptidyl peptidase IV DPPIV using a tandem enzymatic activation strategy. *Prostate.* 2016;76(8):703–14.
142. Gonzalez Constandse R. Anisomycin in intestinal amebiasis; study of 30 clinical cases. *Prensa Med Mex.* 1956;21(7–10):114–5.
143. Conte JE. *Manual of antibiotics and infectious diseases: Treatment and prevention.* 9th ed. Philadelphia: Lippincott Williams & Wilkins; 2001.
144. Gupta RS, Krepinsky JJ, Siminovitsh L. Structural determinants responsible for the biological activity of (–)-emetine, (–)-cryptopleurine, and (–)-tylocrebrine: structure-activity relationship among related compounds. *Mol Pharmacol.* 1980;18(1):136–43.
145. Zinck R, Cahill MA, Kracht M, Sachsenmaier C, Hipskind RA, Nordheim A. Protein synthesis inhibitors reveal differential regulation of mitogen-activated protein kinase and stress-activated protein kinase pathways that converge on Elk-1. *Mol Cell Biol.* 1995;15(9):4930–8.
146. Ramabhadran TV, Thach RE. Specificity of protein synthesis inhibitors in the inhibition of encephalomyocarditis virus replication. *J Virol.* 1980;34(1):293–6.
147. Hwang YC, Chu JJ, Yang PL, Chen W, Yates MV. Rapid identification of inhibitors that interfere with poliovirus replication using a cell-based assay. *Antivir Res.* 2008;77(3):232–6.
148. Romero MR, Serrano MA, Efferth T, Alvarez M, Marin JJ. Effect of cantharidin, cephalotaxine and homoharringtonine on “in vitro” models of hepatitis B virus (HBV) and bovine viral diarrhoea virus (BVDV) replication. *Planta Med.* 2007;73(6):552–8.
149. Gastaminza P, Whitten-Bauer C, Chisari FV. Unbiased probing of the entire hepatitis C virus life cycle identifies clinical compounds that target multiple aspects of the infection. *Proc Natl Acad Sci USA.* 2010;107(1):291–6.
150. Watashi K, Inoue D, Hijikata M, Goto K, Aly HH, Shimotohno K. Anti-hepatitis C virus activity of tamoxifen reveals the functional association of estrogen receptor with viral RNA polymerase NS5B. *J Biol Chem.* 2007;282(45):32765–72.
151. Johansen LM, Brannan JM, Delos SE, Shoemaker CJ, Stossel A, Lear C, et al. FDA-approved selective estrogen receptor modulators inhibit Ebola virus infection. *Sci Transl Med.* 2013;5(190):190ra79.
152. Shoemaker CJ, Schornberg KL, Delos SE, Scully C, Pajouhesh H, Olinger GG, et al. Multiple cationic amphiphiles induce a Niemann-Pick C phenotype and inhibit Ebola virus entry and infection. *PLoS One.* 2013;8(2):e56265.
153. Zhao Y, Ren J, Harlos K, Jones DM, Zeltina A, Bowden TA, et al. Toremifene interacts with and destabilizes the Ebola virus glycoprotein. *Nature.* 2016;535(7610):169–72.
154. Kaufmann AM, Krise JP. Lysosomal sequestration of amine-containing drugs: analysis and therapeutic implications. *J Pharm Sci.* 2007;96(4):729–46.
155. Pharma Orion. FARESTON® (toremifene citrate) tablets prescribing information. Memphis: GTx, Distributor; 2011.
156. AstraZeneca. NOLVADEX® tamoxifen citrate tablets prescribing information. Wilmington: AstraZeneca; 2006.
157. Blanc M, Hsieh WY, Robertson KA, Watterson S, Shui G, Lacaze P, et al. Host defense against viral infection involves interferon mediated down-regulation of sterol biosynthesis. *PLoS Biol.* 2011;9(3):e1000598.
158. Owens CM, Mawhinney C, Grenier JM, Altmeyer R, Lee MS, Borisy AA, et al. Chemical combinations elucidate pathway interactions and regulation relevant to Hepatitis C replication. *Mol Syst Biol.* 2010;8(6):375.
159. Warren TK, Jordan R, Lo MK, Ray AS, Mackman RL, Soloveva V, et al. Therapeutic efficacy of the small molecule GS-5734 against Ebola virus in rhesus monkeys. *Nature.* 2016;531(7594):381–5.
160. Warren TK, Wells J, Panchal RG, Stuthman KS, Garza NL, Van Tongeren SA, et al. Protection against filovirus diseases by a novel broad-spectrum nucleoside analogue BCX4430. *Nature.* 2014;508(7496):402–5.
161. Peters HL, Jochmans D, de Wilde AH, Posthuma CC, Snijder EJ, Neyts J, et al. Design, synthesis and evaluation of a series of acyclic fleximer nucleoside analogues with anti-coronavirus activity. *Bioorg Med Chem Lett.* 2015;25(15):2923–6.
162. Adedeji AO, Sarafianos SG. Antiviral drugs specific for coronaviruses in preclinical development. *Curr Opin Virol.* 2014;8:45–53.
163. Tanner JA, Zheng BJ, Zhou J, Watt RM, Jiang JQ, Wong KL, et al. The adamantane-derived bananins are potent inhibitors of the helicase activities and replication of SARS coronavirus. *Chem Biol.* 2005;12(3):303–11.
164. Leonard JN, Schaffer DV. Antiviral RNAi therapy: emerging approaches for hitting a moving target. *Gene Ther.* 2006;13(6):532–40.
165. He ML, Zheng B, Peng Y, Peiris JS, Poon LL, Yuen KY, et al. Inhibition of SARS-associated coronavirus infection and replication by RNA interference. *JAMA.* 2003;290(20):2665–6.
166. He ML, Zheng BJ, Chen Y, Wong KL, Huang JD, Lin MC, et al. Development of interfering RNA agents to inhibit SARS-associated coronavirus infection and replication. *Hong Kong Med J.* 2009;15(3 Suppl 4):28–31.
167. Lu A, Zhang H, Zhang X, Wang H, Hu Q, Shen L, et al. Attenuation of SARS coronavirus by a short hairpin RNA expression plasmid targeting RNA-dependent RNA polymerase. *Virology.* 2004;324(1):84–9.
168. Wang Z, Ren L, Zhao X, Hung T, Meng A, Wang J, et al. Inhibition of severe acute respiratory syndrome virus replication by small interfering RNAs in mammalian cells. *J Virol.* 2004;78(14):7523–7.
169. Zheng BJ, Guan Y, Tang Q, Du C, Xie FY, He ML, et al. Prophylactic and therapeutic effects of small interfering RNA targeting SARS-coronavirus. *Antivir Ther.* 2004;9(3):365–74.
170. Zhang Y, Li T, Fu L, Yu C, Li Y, Xu X, et al. Silencing SARS-CoV spike protein expression in cultured cells by RNA interference. *FEBS Lett.* 2004;560(1–3):141–6.
171. Wu CJ, Huang HW, Liu CY, Hong CF, Chan YL. Inhibition of SARS-CoV replication by siRNA. *Antivir Res.* 2005;65(1):45–8.
172. Akerstrom S, Mirazimi A, Tan YJ. Inhibition of SARS-CoV replication cycle by small interference RNAs silencing specific

- SARS proteins, 7a/7b, 3a/3b and S. *Antivir Res.* 2007;73(3):219–27.
173. Li BJ, Tang Q, Cheng D, Qin C, Xie FY, Wei Q, et al. Using siRNA in prophylactic and therapeutic regimens against SARS coronavirus in rhesus macaque. *Nat Med.* 2005;11(9):944–51.
 174. Hasan MM, Akter R, Ullah MS, Abedin MJ, Ullah GM, Hossain MZ. A computational approach for predicting role of human microRNAs in MERS-CoV genome. *Adv Bioinform.* 2014;2014:967946.
 175. Thi EP, Mire CE, Lee AC, Geisbert JB, Zhou JZ, Agans KN, et al. Lipid nanoparticle siRNA treatment of Ebola-virus-Makona-infected nonhuman primates. *Nature.* 2015;521(7552):362–5.
 176. Dunning J, Sahr F, Rojek A, Gannon F, Carson G, Idriss B, et al. Experimental treatment of Ebola virus disease with TKM-130803: a single-arm phase 2 clinical trial. *PLoS Med.* 2016;13(4):e1001997.
 177. Badani H, Garry RF, Wimley WC. Peptide entry inhibitors of enveloped viruses: the importance of interfacial hydrophobicity. *Biochim Biophys Acta.* 2014;1838(9):2180–97.
 178. Lu L, Liu Q, Zhu Y, Chan KH, Qin L, Li Y, et al. Structure-based discovery of Middle East respiratory syndrome coronavirus fusion inhibitor. *Nat Commun.* 2014;5:3067.
 179. Sainz B Jr, Mossel EC, Gallaher WR, Wimley WC, Peters CJ, Wilson RB, et al. Inhibition of severe acute respiratory syndrome-associated coronavirus (SARS-CoV) infectivity by peptides analogous to the viral spike protein. *Virus Res.* 2006;120(1–2):146–55.
 180. Sainz B Jr, Rausch JM, Gallaher WR, Garry RF, Wimley WC. Identification and characterization of the putative fusion peptide of the severe acute respiratory syndrome-associated coronavirus spike protein. *J Virol.* 2005;79(11):7195–206.
 181. Bird GH, Madani N, Perry AF, Princiotta AM, Supko JG, He X, et al. Hydrocarbon double-stapling remedies the proteolytic instability of a lengthy peptide therapeutic. *Proc Natl Acad Sci USA.* 2010;107(32):14093–8.
 182. Kindrachuk J, Scruten E, Attah-Poku S, Bell K, Potter A, Babiuk LA, et al. Stability, toxicity, and biological activity of host defense peptide BMAP28 and its inversed and retro-inversed isomers. *Biopolymers.* 2011;96(1):14–24.
 183. Walensky LD, Bird GH. Hydrocarbon-stapled peptides: principles, practice, and progress. *J Med Chem.* 2014;57(15):6275–88.
 184. Shadman KA, Wald ER. A review of palivizumab and emerging therapies for respiratory syncytial virus. *Expert Opin Biol Ther.* 2011;11(11):1455–67.
 185. Qiu X, Wong G, Audet J, Bello A, Fernando L, Alimonti JB, et al. Reversion of advanced Ebola virus disease in nonhuman primates with ZMapp. *Nature.* 2014;514(7520):47–53.
 186. PREVAIL II Writing Group for the Multinational PREVAIL Study Team. A randomized, controlled trial of ZMapp for Ebola virus infection. *N Engl J Med.* 2016;375(15):1448–56.
 187. Bossart KN, Zhu Z, Middleton D, Klippel J, Cramer G, Bingham J, et al. A neutralizing human monoclonal antibody protects against lethal disease in a new ferret model of acute nipah virus infection. *PLoS Pathog.* 2009;5(10):e1000642.
 188. Zhu Z, Dimitrov AS, Bossart KN, Cramer G, Bishop KA, Choudhry V, et al. Potent neutralization of Hendra and Nipah viruses by human monoclonal antibodies. *J Virol.* 2006;80(2):891–9.
 189. Bossart KN, Geisbert TW, Feldmann H, Zhu Z, Feldmann F, Geisbert JB, et al. A neutralizing human monoclonal antibody protects African green monkeys from hendra virus challenge. *Sci Transl Med.* 2011;3(105):105ra3.
 190. Corti D, Zhao J, Pedotti M, Simonelli L, Agnihothram S, Fett C, et al. Prophylactic and postexposure efficacy of a potent human monoclonal antibody against MERS coronavirus. *Proc Natl Acad Sci USA.* 2015;112(33):10473–8.
 191. Houser KV, Gretebeck L, Ying T, Wang Y, Vogel L, Lamirande EW, et al. Prophylaxis with a Middle East respiratory syndrome coronavirus (MERS-CoV)-specific human monoclonal antibody protects rabbits from MERS-CoV infection. *J Infect Dis.* 2016;213(10):1557–61.
 192. Jiang L, Wang N, Zuo T, Shi X, Poon KM, Wu Y, et al. Potent neutralization of MERS-CoV by human neutralizing monoclonal antibodies to the viral spike glycoprotein. *Sci Transl Med.* 2014;6(234):234ra59.
 193. Johnson RF, Bagci U, Keith L, Tang X, Mollura DJ, Zeitlin L, et al. 3B11-N, a monoclonal antibody against MERS-CoV, reduces lung pathology in rhesus monkeys following intratracheal inoculation of MERS-CoV Jordan-n3/2012. *Virology.* 2016;490:49–58.
 194. Pascal KE, Coleman CM, Mujica AO, Kamat V, Badithe A, Fairhurst J, et al. Pre- and postexposure efficacy of fully human antibodies against Spike protein in a novel humanized mouse model of MERS-CoV infection. *Proc Natl Acad Sci USA.* 2015;112(28):8738–43.
 195. Qiu H, Sun S, Xiao H, Feng J, Guo Y, Tai W, et al. Single-dose treatment with a humanized neutralizing antibody affords full protection of a human transgenic mouse model from lethal Middle East respiratory syndrome (MERS)-coronavirus infection. *Antivir Res.* 2016;14(132):141–8.
 196. Tang XC, Agnihothram SS, Jiao Y, Stanhope J, Graham RL, Peterson EC, et al. Identification of human neutralizing antibodies against MERS-CoV and their role in virus adaptive evolution. *Proc Natl Acad Sci USA.* 2014;111(19):E2018–26.
 197. Ying T, Du L, Ju TW, Prabakaran P, Lau CC, Lu L, et al. Exceptionally potent neutralization of Middle East respiratory syndrome coronavirus by human monoclonal antibodies. *J Virol.* 2014;88(14):7796–805.
 198. Mair-Jenkins J, Saavedra-Campos M, Baillie JK, Cleary P, Khaw FM, Lim WS, et al. The effectiveness of convalescent plasma and hyperimmune immunoglobulin for the treatment of severe acute respiratory infections of viral etiology: a systematic review and exploratory meta-analysis. *J Infect Dis.* 2015;211(1):80–90.
 199. Ying T, Li H, Lu L, Dimitrov DS, Jiang S. Development of human neutralizing monoclonal antibodies for prevention and therapy of MERS-CoV infections. *Microbes Infect.* 2015;17(2):142–8.
 200. Berry JD, Gaudet RG. Antibodies in infectious diseases: polyclonals, monoclonals and niche biotechnology. *New Biotechnol.* 2011;28(5):489–501.
 201. Luke T, Wu H, Zhao J, Channappanavar R, Coleman CM, Jiao JA, et al. Human polyclonal immunoglobulin G from transchromosomal bovines inhibits MERS-CoV in vivo. *Sci Transl Med.* 2016;8(326):326ra21.
 202. De Clercq E. Strategies in the design of antiviral drugs. *Nat Rev Drug Discov.* 2002;1(1):13–25.
 203. AIDSinfo. HIV treatment. FDA-approved HIV medicines. 2016. <https://aidsinfo.nih.gov/education-materials/fact-sheets/21/58/fda-approved-hiv-medicines>. Accessed 13 Oct 2016.
 204. World Health Organization. Consolidated guidelines for the use of antiretroviral drugs for treating and preventing HIV infection. Recommendations for a public health approach, 2nd edn. 2016. <http://www.who.int/hiv/pub/arv/arv-2016/en/>. Accessed 13 Oct 2016.
 205. American Association for the Study of Liver Diseases, Infectious Diseases Society of America. HCV guidance: recommendations for testing, managing, and treating hepatitis C. 2017. <http://www.hcvguidelines.org/sites/default/files/full-guidance->

- pdf/HCVGuidance_April_12_2017_b.pdf. Accessed 28 July 2017.
206. Kohli A, Shaffer A, Sherman A, Kotttilil S. Treatment of hepatitis C: a systematic review. *JAMA*. 2014;312(6):631–40.
 207. Ogawa E, Furusyo N, Kajiwara E, Takahashi K, Nomura H, Tanabe Y, et al. Evaluation of the adverse effect of premature discontinuation of pegylated interferon alpha-2b and ribavirin treatment for chronic hepatitis C virus infection: results from Kyushu University liver disease study. *J Gastroenterol Hepatol*. 2012;27(7):1233–40.
 208. Govorkova EA, McCullers JA. Therapeutics against influenza. *Curr Top Microbiol Immunol*. 2013;370:273–300.
 209. Dunning J, Baillie JK, Cao B, Hayden FG. International Severe Acute Respiratory Emerging Infection Consortium. Antiviral combinations for severe influenza. *Lancet Infect Dis*. 2014;14(12):1259–70.
 210. Hayden FG. Advances in antivirals for non-influenza respiratory virus infections. *Influenza Other Respir Viruses*. 2013;7(Suppl 3):36–43.
 211. Seo S, Englund JA, Nguyen JT, Pukrittayakamee S, Lindegardh N, Tarning J, et al. Combination therapy with amantadine, oseltamivir and ribavirin for influenza A infection: safety and pharmacokinetics. *Antivir Ther*. 2013;18(3):377–86.
 212. Agnandji ST, Huttner A, Zinser ME, Njuguna P, Dahlke C, Fernandes JF, et al. Phase 1 Trials of rVSV Ebola Vaccine in Africa and Europe. *N Engl J Med*. 2016;374(17):1647–60.
 213. Ewer K, Rampling T, Venkatraman N, Bowyer G, Wright D, Lambe T, et al. A monovalent chimpanzee adenovirus Ebola vaccine boosted with MVA. *N Engl J Med*. 2016;374(17):1635–46.
 214. Ledgerwood JE, DeZure AD, Stanley DA, Coates EE, Novik L, Enama ME, et al. Chimpanzee adenovirus vector Ebola vaccine. *N Engl J Med*. 2017; 376(10):928–38.
 215. Regules JA, Beigel JH, Paolino KM, Voell J, Castellano AR, Hu Z, et al. A recombinant vesicular stomatitis virus Ebola vaccine. *N Engl J Med*. 2017;376(4):330–41.
 216. Henao-Restrepo AM, Longini IM, Egger M, Dean NE, Edmunds WJ, Camacho A, et al. Efficacy and effectiveness of an rVSV-vectored vaccine expressing Ebola surface glycoprotein: interim results from the Guinea ring vaccination cluster-randomised trial. *Lancet*. 2015;386(9996):857–66.
 217. Baseler L, de Wit E, Feldmann H. A comparative review of animal models of Middle East respiratory syndrome coronavirus infection. *Vet Pathol*. 2016;53(3):521–31.
 218. Sutton TC, Subbarao K. Development of animal models against emerging coronaviruses: from SARS to MERS coronavirus. *Virology*. 2015;479–480:247–58.
 219. van Doremalen N, Munster VJ. Animal models of Middle East respiratory syndrome coronavirus infection. *Antivir Res*. 2015;122:28–38.
 220. Zhao J, Li K, Wohlford-Lenane C, Agnihothram SS, Fett C, Zhao J, et al. Rapid generation of a mouse model for Middle East respiratory syndrome. *Proc Natl Acad Sci USA*. 2014;111(13):4970–5.
 221. Channappanavar R, Fett C, Zhao J, Meyerholz DK, Perlman S. Virus-specific memory CD8 T cells provide substantial protection from lethal severe acute respiratory syndrome coronavirus infection. *J Virol*. 2014;88(19):11034–44.
 222. Channappanavar R, Zhao J, Perlman S. T cell-mediated immune response to respiratory coronaviruses. *Immunol Res*. 2014;59(1–3):118–28.
 223. Agrawal AS, Garron T, Tao X, Peng BH, Wakamiya M, Chan TS, et al. Generation of a transgenic mouse model of Middle East respiratory syndrome coronavirus infection and disease. *J Virol*. 2015;89(7):3659–70.
 224. Cockrell AS, Yount BL, Scobey T, Jensen K, Douglas M, Beall A, et al. A mouse model for MERS coronavirus-induced acute respiratory distress syndrome. *Nat Microbiol*. 2016;28(2):16226.
 225. Haagmans BL, van den Brand JM, Provacia LB, Raj VS, Stittelaar KJ, Getu S, et al. Asymptomatic Middle East respiratory syndrome coronavirus infection in rabbits. *J Virol*. 2015;89(11):6131–5.
 226. de Wit E, Rasmussen AL, Falzarano D, Bushmaker T, Feldmann F, Brining DL, et al. Middle East respiratory syndrome coronavirus (MERS-CoV) causes transient lower respiratory tract infection in rhesus macaques. *Proc Natl Acad Sci USA*. 2013;110(41):16598–603.
 227. Munster VJ, de Wit E, Feldmann H. Pneumonia from human coronavirus in a macaque model. *N Engl J Med*. 2013;368(16):1560–2.
 228. Yao Y, Bao L, Deng W, Xu L, Li F, Lv Q, et al. An animal model of MERS produced by infection of rhesus macaques with MERS coronavirus. *J Infect Dis*. 2014;209(2):236–42.
 229. Clay CC, Donart N, Fomukong N, Knight JB, Overheim K, Tipper J, et al. Severe acute respiratory syndrome-coronavirus infection in aged nonhuman primates is associated with modulated pulmonary and systemic immune responses. *Immun Ageing*. 2014;11(1):4.
 230. Smits SL, van den Brand JM, de Lang A, Leijten LM, van Ijcken WF, van Amerongen G, et al. Distinct severe acute respiratory syndrome coronavirus-induced acute lung injury pathways in two different nonhuman primate species. *J Virol*. 2011;85(9):4234–45.
 231. McAuliffe J, Vogel L, Roberts A, Fahle G, Fischer S, Shieh WJ, et al. Replication of SARS coronavirus administered into the respiratory tract of African green, rhesus and cynomolgus monkeys. *Virology*. 2004;330(1):8–15.
 232. Hartman AL, Powell DS, Bethel LM, Caroline AL, Schmid RJ, Oury T, et al. Aerosolized Rift Valley fever virus causes fatal encephalitis in African green monkeys and common marmosets. *J Virol*. 2014;88(4):2235–45.
 233. Kramski M, Matz-Rensing K, Stahl-Hennig C, Kaup FJ, Nitsche A, Pauli G, et al. A novel highly reproducible and lethal non-human primate model for orthopox virus infection. *PLoS One*. 2010;5(4):e10412.
 234. Mucker EM, Chapman J, Huzella LM, Huggins JW, Shamblin J, Robinson CG, et al. Susceptibility of marmosets (*Callithrix jacchus*) to monkeypox virus: a low dose prospective model for monkeypox and smallpox disease. *PLoS One*. 2015;10(7):e0131742.
 235. Falzarano D, de Wit E, Feldmann F, Rasmussen AL, Okumura A, Peng X, et al. Infection with MERS-CoV causes lethal pneumonia in the common marmoset. *PLoS Pathog*. 2014;10(8):e1004250.
 236. Greenough TC, Carville A, Coderre J, Somasundaran M, Sullivan JL, Luzuriaga K, et al. Pneumonitis and multi-organ system disease in common marmosets (*Callithrix jacchus*) infected with the severe acute respiratory syndrome-associated coronavirus. *Am J Pathol*. 2005;167(2):455–63.
 237. Bai JP. Pharmacodynamics and systems pharmacology approaches to repurposing drugs in the wake of global health burden. *J Pharm Sci*. 2016;105(10):3007–12.
 238. Brik A, Wong CH. HIV-1 protease: mechanism and drug discovery. *Org Biomol Chem*. 2003;1(1):5–14.
 239. Navia MA, Fitzgerald PM, McKeever BM, Leu CT, Heimbach JC, Herber WK, et al. Three-dimensional structure of aspartyl protease from human immunodeficiency virus HIV-1. *Nature*. 1989;337(6208):615–20.
 240. Wlodawer A, Miller M, Jaskolski M, Sathyanarayana BK, Baldwin E, Weber IT, et al. Conserved folding in retroviral

- proteases: crystal structure of a synthetic HIV-1 protease. *Science*. 1989;245(4918):616–21.
241. Gotte M, Feld JJ. Direct-acting antiviral agents for hepatitis C: structural and mechanistic insights. *Nat Rev Gastroenterol Hepatol*. 2016;13(6):338–51.
 242. Hazuda DJ, Burroughs M, Howe AY, Wahl J, Venkatraman S. Development of boceprevir: a first-in-class direct antiviral treatment for chronic hepatitis C infection. *Ann N Y Acad Sci*. 2013;1291:69–76.
 243. Kwong AD, Kauffman RS, Hurter P, Mueller P. Discovery and development of telaprevir: an NS3-4A protease inhibitor for treating genotype 1 chronic hepatitis C virus. *Nat Biotechnol*. 2011;29(11):993–1003.
 244. Hilgenfeld R. From SARS to MERS: crystallographic studies on coronaviral proteases enable antiviral drug design. *FEBS J*. 2014;281(18):4085–96.
 245. Miller ME, Adhikary S, Kolokoltsov AA, Davey RA. Ebola-virus requires acid sphingomyelinase activity and plasma membrane sphingomyelin for infection. *J Virol*. 2012;86(14):7473–83.
 246. Muller MP, Dresser L, Raboud J, McGeer A, Rea E, Richardson SE, et al. Adverse events associated with high-dose ribavirin: evidence from the Toronto outbreak of severe acute respiratory syndrome. *Pharmacotherapy*. 2007;27(4):494–503.
 247. Ward SE, Loutfy MR, Blatt LM, Siminovich KA, Chen J, Hinek A, et al. Dynamic changes in clinical features and cytokine/chemokine responses in SARS patients treated with interferon alfacon-1 plus corticosteroids. *Antivir Ther*. 2005;10(2):263–75.
 248. Zhao Z, Zhang F, Xu M, Huang K, Zhong W, Cai W, et al. Description and clinical treatment of an early outbreak of severe acute respiratory syndrome (SARS) in Guangzhou, PR China. *J Med Microbiol*. 2003;52(Pt 8):715–20.
 249. Al-Tawfiq JA, Momattin H, Dib J, Memish ZA. Ribavirin and interferon therapy in patients infected with the Middle East respiratory syndrome coronavirus: an observational study. *Int J Infect Dis*. 2014;20:42–6.
 250. Boonyasuppayakorn S, Reichert ED, Manzano M, Nagarajan K, Padmanabhan R. Amodiaquine, an antimalarial drug, inhibits dengue virus type 2 replication and infectivity. *Antivir Res*. 2014;106:125–34.
 251. Bassetto M, De Burghgraeve T, Delang L, Massarotti A, Coluccia A, Zonta N, et al. Computer-aided identification, design and synthesis of a novel series of compounds with selective antiviral activity against chikungunya virus. *Antivir Res*. 2013;98(1):12–8.
 252. Cruz DJ, Bonotto RM, Gomes RG, da Silva CT, Taniguchi JB, No JH, et al. Identification of novel compounds inhibiting chikungunya virus-induced cell death by high throughput screening of a kinase inhibitor library. *PLoS Negl Trop Dis*. 2013;7(10):e2471.
 253. Yan Y, Zou Z, Sun Y, Li X, Xu KF, Wei Y, et al. Anti-malaria drug chloroquine is highly effective in treating avian influenza A H5N1 virus infection in an animal model. *Cell Res*. 2013;23(2):300–2.
 254. Paton NI, Lee L, Xu Y, Ooi EE, Cheung YB, Archuleta S, et al. Chloroquine for influenza prevention: a randomised, double-blind, placebo controlled trial. *Lancet Infect Dis*. 2011;11(9):677–83.
 255. Romanelli F, Smith KM, Hoven AD. Chloroquine and hydroxychloroquine as inhibitors of human immunodeficiency virus (HIV-1) activity. *Curr Pharm Des*. 2004;10(21):2643–8.
 256. Nakagawa M, Sakamoto N, Tanabe Y, Koyama T, Itsui Y, Takeda Y, et al. Suppression of hepatitis C virus replication by cyclosporin A is mediated by blockade of cyclophilins. *Gastroenterology*. 2005;129(3):1031–41.
 257. Qing M, Yang F, Zhang B, Zou G, Robida JM, Yuan Z, et al. Cyclosporine inhibits flavivirus replication through blocking the interaction between host cyclophilins and viral NS5 protein. *Antimicrob Agents Chemother*. 2009;53(8):3226–35.
 258. Kambara H, Tani H, Mori Y, Abe T, Katoh H, Fukuhara T, et al. Involvement of cyclophilin B in the replication of Japanese encephalitis virus. *Virology*. 2011;412(1):211–9.
 259. Bose S, Mathur M, Bates P, Joshi N, Banerjee AK. Requirement for cyclophilin A for the replication of vesicular stomatitis virus New Jersey serotype. *J Gen Virol*. 2003;84(Pt 7):1687–99.
 260. Briggs CJ, Ott DE, Coren LV, Oroszlan S, Tozser J. Comparison of the effect of FK506 and cyclosporin A on virus production in H9 cells chronically and newly infected by HIV-1. *Arch Virol*. 1999;144(11):2151–60.
 261. Randhawa PS, Farasati NA, Huang Y, Mapara MY, Shapiro R. Viral drug sensitivity testing using quantitative PCR: effect of tyrosine kinase inhibitors on polyomavirus BK replication. *Am J Clin Pathol*. 2010;134(6):916–20.
 262. Pogliaghi M, Papagno L, Lambert S, Calin R, Calvez V, Katlama C, et al. The tyrosine kinase inhibitor Dasatinib blocks in-vitro HIV-1 production by primary CD4+ T cells from HIV-1 infected patients. *AIDS*. 2014;28(2):278–81.
 263. de Wispelaere M, LaCroix AJ, Yang PL. The small molecules AZD0530 and dasatinib inhibit dengue virus RNA replication via Fyn kinase. *J Virol*. 2013;87(13):7367–81.
 264. Reeves PM, Smith SK, Olson VA, Thorne SH, Bornmann W, Damon IK, et al. Variola and monkeypox viruses utilize conserved mechanisms of virion motility and release that depend on ABL and SRC family tyrosine kinases. *J Virol*. 2011;85(1):21–31.
 265. Murray JL, McDonald NJ, Sheng J, Shaw MW, Hodge TW, Rubin DH, et al. Inhibition of influenza A virus replication by antagonism of a PI3 K-AKT-mTOR pathway member identified by gene-trap insertional mutagenesis. *Antivir Chem Chemother*. 2012;22(5):205–15.
 266. Brennan DC, Legendre C, Patel D, Mange K, Wiland A, McCague K, et al. Cytomegalovirus incidence between everolimus versus mycophenolate in de novo renal transplants: pooled analysis of three clinical trials. *Am J Transplant*. 2011;11(11):2453–62.
 267. Kobashigawa J, Ross H, Bara C, Delgado JF, Dengler T, Lehmkuhl HB, et al. Everolimus is associated with a reduced incidence of cytomegalovirus infection following de novo cardiac transplantation. *Transpl Infect Dis*. 2013;15(2):150–62.
 268. Hutterer C, Wandinger SK, Wagner S, Muller R, Stamminger T, Zeittrager I, et al. Profiling of the kinome of cytomegalovirus-infected cells reveals the functional importance of host kinases Aurora A, ABL and AMPK. *Antivir Res*. 2013;99(2):139–48.
 269. Cheshenko N, Trepanier JB, Stefanidou M, Buckley N, Gonzalez P, Jacobs W, et al. HSV activates Akt to trigger calcium release and promote viral entry: novel candidate target for treatment and suppression. *FASEB J*. 2013;27(7):2584–99.
 270. Heredia A, Gilliam B, Latinovic O, Le N, Bamba D, Devico A, et al. Rapamycin reduces CCR5 density levels on CD4 T cells, and this effect results in potentiation of enfuvirtide (T-20) against R5 strains of human immunodeficiency virus type 1 in vitro. *Antimicrob Agents Chemother*. 2007;51(7):2489–96.
 271. Kudchodkar SB, Yu Y, Maguire TG, Alwine JC. Human cytomegalovirus infection alters the substrate specificities and rapamycin sensitivities of raptor- and rictor-containing complexes. *Proc Natl Acad Sci USA*. 2006;103(38):14182–7.
 272. Di Benedetto F, Di Sandro S, De Ruvo N, Montalti R, Ballarin R, Guerrini GP, et al. First report on a series of HIV patients undergoing rapamycin monotherapy after liver transplantation. *Transplantation*. 2010;89(6):733–8.

273. Ghassemieh B, Ahya VN, Baz MA, Valentine VG, Arcasoy SM, Love RB, et al. Decreased incidence of cytomegalovirus infection with sirolimus in a post hoc randomized, multicenter study in lung transplantation. *J Heart Lung Transplant*. 2013;32(7):701–6.
274. Soliman A, Fathy A, Khashab S, Shaheen N, Soliman M. Sirolimus conversion may suppress viral replication in hepatitis C virus-positive renal transplant candidates. *Exp Clin Transplant*. 2013;11(5):408–11.
275. Michaelis M, Paulus C, Loschmann N, Dauth S, Stange E, Doerr HW, et al. The multi-targeted kinase inhibitor sorafenib inhibits human cytomegalovirus replication. *Cell Mol Life Sci*. 2011;68(6):1079–90.
276. Gao M, Duan H, Liu J, Zhang H, Wang X, Zhu M, et al. The multi-targeted kinase inhibitor sorafenib inhibits enterovirus 71 replication by regulating IRES-dependent translation of viral proteins. *Antivir Res*. 2014;106:80–5.
277. Benedict A, Bansal N, Senina S, Hooper I, Lundberg L, de la Fuente C, et al. Repurposing FDA-approved drugs as therapeutics to treat Rift Valley fever virus infection. *Front Microbiol*. 2015;6:676.
278. Sasaki H, Nakamura M, Ohno T, Matsuda Y, Yuda Y, Nonomura Y. Myosin-actin interaction plays an important role in human immunodeficiency virus type 1 release from host cells. *Proc Natl Acad Sci USA*. 1995;92(6):2026–30.
279. Hirai H, Takeda S, Natori S, Sekimizu K. Inhibition of SV40 DNA replication in vitro by chlorpromazine. *Biol Pharm Bull*. 1993;16(6):565–7.
280. Yanagida K, Baba C, Baba M. Inhibition of bovine viral diarrhoea virus (BVDV) by mizoribine: synergistic effect of combination with interferon-alpha. *Antivir Res*. 2004;64(3):195–201.
281. Batman G, Oliver AW, Zehbe I, Richard C, Hampson L, Hampson IN. Lopinavir up-regulates expression of the antiviral protein ribonuclease L in human papillomavirus-positive cervical carcinoma cells. *Antivir Ther*. 2011;16(4):515–25.
282. Murakami Y, Fukasawa M, Kaneko Y, Suzuki T, Wakita T, Fukazawa H. Selective estrogen receptor modulators inhibit hepatitis C virus infection at multiple steps of the virus life cycle. *Microbes Infect*. 2013;15(1):45–55.
283. Zheng K, Chen M, Xiang Y, Ma K, Jin F, Wang X, et al. Inhibition of herpes simplex virus type 1 entry by chloride channel inhibitors tamoxifen and NPPB. *Biochem Biophys Res Commun*. 2014;446(4):990–6.
284. Kilianski A, Mielech AM, Deng X, Baker SC. Assessing activity and inhibition of Middle East respiratory syndrome coronavirus papain-like and 3C-like proteases using luciferase-based biosensors. *J Virol*. 2013;87(21):11955–62.
285. Lundin A, Dijkman R, Bergstrom T, Kann N, Adamiak B, Hannoun C, et al. Targeting membrane-bound viral RNA synthesis reveals potent inhibition of diverse coronaviruses including the Middle East respiratory syndrome virus. *PLoS Pathog*. 2014;10(5):e1004166.
286. Millet JK, Whittaker GR. Host cell entry of Middle East respiratory syndrome coronavirus after two-step, furin-mediated activation of the spike protein. *Proc Natl Acad Sci USA*. 2014;111(42):15214–9.
287. Shie JJ, Fang JM, Kuo CJ, Kuo TH, Liang PH, Huang HJ, et al. Discovery of potent anilide inhibitors against the severe acute respiratory syndrome 3CL protease. *J Med Chem*. 2005;48(13):4469–73.
288. Shao YM, Yang WB, Peng HP, Hsu MF, Tsai KC, Kuo TH, et al. Structure-based design and synthesis of highly potent SARS-CoV 3CL protease inhibitors. *ChemBioChem*. 2007;8(14):1654–7.
289. Ramajayam R, Tan KP, Liu HG, Liang PH. Synthesis and evaluation of pyrazolone compounds as SARS-coronavirus 3C-like protease inhibitors. *Bioorg Med Chem*. 2010;18(22):7849–54.
290. Shao YM, Yang WB, Kuo TH, Tsai KC, Lin CH, Yang AS, et al. Design, synthesis, and evaluation of trifluoromethyl ketones as inhibitors of SARS-CoV 3CL protease. *Bioorg Med Chem*. 2008;16(8):4652–60.
291. Chen L, Gui C, Luo X, Yang Q, Gunther S, Scandella E, et al. Cinanserin is an inhibitor of the 3C-like proteinase of severe acute respiratory syndrome coronavirus and strongly reduces virus replication in vitro. *J Virol*. 2005;79(11):7095–103.
292. Lee CC, Kuo CJ, Hsu MF, Liang PH, Fang JM, Shie JJ, et al. Structural basis of mercury- and zinc-conjugated complexes as SARS-CoV 3C-like protease inhibitors. *FEBS Lett*. 2007;581(28):5454–8.
293. Lee C, Lee JM, Lee NR, Kim DE, Jeong YJ, Chong Y. Investigation of the pharmacophore space of severe acute respiratory syndrome coronavirus (SARS-CoV) NTPase/helicase by dihydroxychromone derivatives. *Bioorg Med Chem Lett*. 2009;19(16):4538–41.
294. Kim MK, Yu MS, Park HR, Kim KB, Lee C, Cho SY, et al. 2,6-Bis-arylmethoxy-5-hydroxychromones with antiviral activity against both hepatitis C virus (HCV) and SARS-associated coronavirus (SCV). *Eur J Med Chem*. 2011;46(11):5698–704.
295. Cho A, Saunders OL, Butler T, Zhang L, Xu J, Vela JE, et al. Synthesis and antiviral activity of a series of 1'-substituted 4-aza-7,9-dideazaadenosine C-nucleosides. *Bioorg Med Chem Lett*. 2012;22(8):2705–7.
296. Shah PP, Wang T, Kaletsky RL, Myers MC, Purvis JE, Jing H, et al. A small-molecule oxocarbazate inhibitor of human cathepsin L blocks severe acute respiratory syndrome and Ebola pseudotype virus infection into human embryonic kidney 293T cells. *Mol Pharmacol*. 2010;78(2):319–24.
297. Adedeji AO, Severson W, Jonsson C, Singh K, Weiss SR, Sarafianos SG. Novel inhibitors of severe acute respiratory syndrome coronavirus entry that act by three distinct mechanisms. *J Virol*. 2013;87(14):8017–28.
298. Huentelman MJ, Zubcevic J, Hernandez Prada JA, Xiao X, Dimitrov DS, Raizada MK, et al. Structure-based discovery of a novel angiotensin-converting enzyme 2 inhibitor. *Hypertension*. 2004;44(6):903–6.

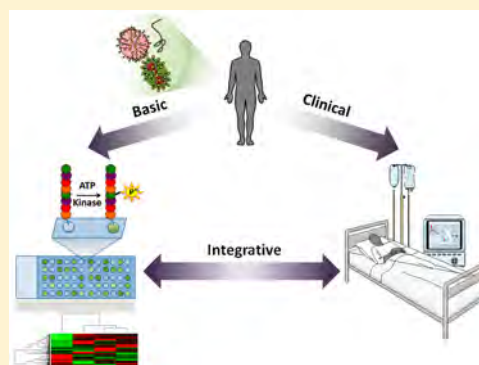
Integration of Global Analyses of Host Molecular Responses with Clinical Data To Evaluate Pathogenesis and Advance Therapies for Emerging and Re-emerging Viral Infections

Shane D. Falcinelli,[†] Daniel S. Chertow,[†] and Jason Kindrachuk^{*,†}

[†]Critical Care Medicine Department, Clinical Center, National Institutes of Health, Bethesda, Maryland 20814, United States

ABSTRACT: Outbreaks associated with emerging and re-emerging viral pathogens continue to increase in frequency and are associated with an increasing burden to global health. In light of this, there is a need to integrate basic and clinical research for investigating the connections between molecular and clinical pathogenesis and for therapeutic development strategies. Here, we will discuss this approach with a focus on the emerging viral pathogens Middle East respiratory syndrome coronavirus (MERS-CoV), Ebola virus (EBOV), and monkeypox virus (MPXV) from the context of clinical presentation, immunological and molecular features of the diseases, and OMICS-based analyses of pathogenesis. Furthermore, we will highlight the role of global investigations of host kinases, the kinome, for investigating emerging and re-emerging viral pathogens from the context of characterizing cellular responses and identifying novel therapeutic targets. Lastly, we will address how increased integration of clinical and basic research will assist treatment and prevention efforts for emerging pathogens.

KEYWORDS: emerging pathogens, kinomics, cell signaling, virology, kinases, high-consequence pathogens



Emerging and re-emerging viruses pose a significant threat to public health and global economies. Moreover, outbreaks caused by emerging and re-emerging viruses continue to increase in frequency as a result of changing socio-economic, environmental, and ecological factors.¹ Notably, the zoonotic viral pathogens, severe acute respiratory syndrome coronavirus (SARS-CoV), Middle East respiratory syndrome coronavirus (MERS-CoV), Ebola virus, chikungunya virus, and Zika virus, have emerged on a global scale in recent years; although less widely publicized, other emerging viral pathogens such as monkeypox virus and Andes virus have led to smaller recurrent outbreaks. A critical challenge for combating these outbreaks is often the discordant relationship between the economic status of outbreak “hotspots” and resource distribution or control capacity within these regions. In addition, the development and delivery of therapeutics for combating such outbreaks have been complicated by both the associated costs in design and development for novel anti-infective therapeutics and the requirements for regulatory approval and licensure.² Importantly, emerging infectious diseases present the additional inherent challenge that they are only “emerging”, and thus limited resources are made available for research until they present a significant risk. For many emerging viral pathogens, the requirement for high-containment facilities has further impeded widespread research. From the perspective of drug development, the limited knowledge and understanding of molecular pathogenesis for these agents is a daunting challenge to overcome when outbreaks emerge.

In the face of an increasing burden of emerging and re-emerging pathogens, it is necessary to overcome the barriers imposed by a paucity of information regarding molecular pathogenesis for these agents. OMICS-based approaches present a mechanism to rapidly generate large amounts of data in regard to host responses and assist in target identification for drug development efforts. In addition, OMICS-based analyses allow for the characterization of molecular events that mitigate cellular responses to viral pathogens from a global perspective across multiple levels of cellular complexity (individual cell types < tissues < organs). High-throughput global analyses of host gene expression, including microarrays and RNA-Seq, provide important information regarding transcriptional responses during infection. Although these validated approaches are among the most widespread of the OMICS-based technologies for infectious disease investigations, they do not provide a direct measure of the activation status of the cell signaling pathways that regulate underlying cellular responses. In contrast, global investigations of cellular kinase activities (the kinome) are able to provide insight into the activation status of cell signaling networks (including those that mediate pathogen recognition and innate immune activation, cell cycle activities, metabolic status, wound healing and repair, and cell death) at the level of

Special Issue: Host-Pathogen Interactions

Received: June 10, 2016

Published: July 29, 2016

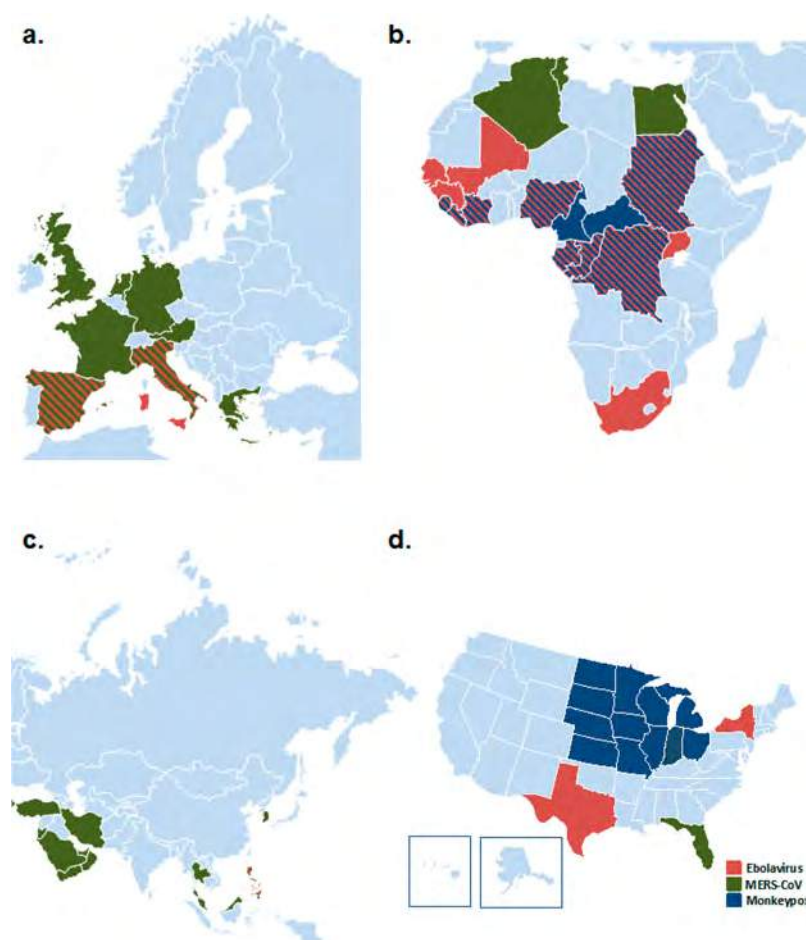


Figure 1. Global outbreaks of Ebola virus, MERS-CoV, and monkeypox: (a) Europe; (b) Africa; (c) Asia; (d) United States. Data include all transmission-related infections that have been documented. Laboratory accident-related infections and medical evacuations are not included.

individual kinase-mediated phosphorylation events. In addition, kinome investigations allow for potential identification of kinase drug targets. Kinases are currently one of the top targets for drug design and development, and there is potential for repurposing of kinase inhibitors with existing regulatory approval.

As emerging viral infections often result in severe illness including respiratory failure [severe acute respiratory syndrome (SARS), Middle East respiratory syndrome (MERS), and influenza] and multiorgan failure [Ebola virus disease (EVD)], understanding complex pathogenesis of these infections is required for effective vaccine and therapeutic design and for improved patient care. Healthcare providers caring for patients with severe emerging viral infections are generally focused on clinical care and biosafety as compared to the complex molecular events that underlie pathogenesis. In contrast, basic researchers typically focus on discrete aspects of pathogenesis through a variety of *in vitro* and *in vivo* analyses rather than the complex interplay between these events and the clinical, physiologic, and pathologic abnormalities observed by the clinician. Integrating basic and clinical research is needed to accelerate the translation of knowledge for emerging infections toward vaccine development and therapeutic discovery. Specifically, detailed natural history studies merging multiple data streams including OMICS approaches (high-throughput gene expression and kinomics) and focused translational investigations utilizing relevant models that can be validated

to human disease are needed to clarify disease pathogenesis, advance therapeutic discovery, and facilitate regulatory approval.

Although an integrated approach between basic and clinical research is ideal for investigating the connections between molecular and clinical pathogenesis, there has been a paucity of investigations for which this has been undertaken. Here, we will discuss emerging pathogens for which there is available information regarding the clinical course of disease, host immune responses during natural infection, and molecular information regarding the global cellular responses to infection, with particular attention on host kinome investigations. In this regard we will focus on the emerging viral pathogens MERS-CoV, Ebola virus (EBOV), and monkeypox virus (MPXV) (Figure 1). We will review the clinical presentation and immunological and molecular features of the diseases and summarize available OMICS data informing pathogenesis of these pathogens. Lastly, we will discuss the benefit of improved integration of available clinical knowledge or data regarding the pathologic manifestations of disease with basic research investigations to advance treatment and prevention of severe emerging viral infections.

■ INVESTIGATING MOLECULAR PATHOGENESIS THROUGH KINOME ANALYSIS

Global gene expression investigations have provided information regarding host response to emerging and re-emerging

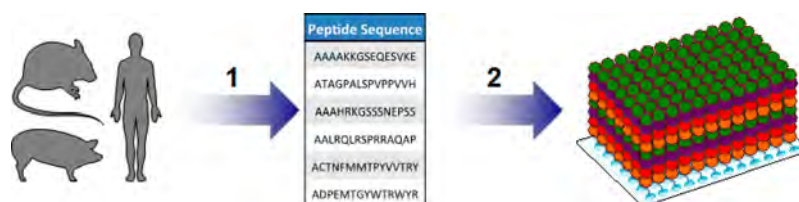


Figure 2. Generation of kinome peptide array targets and kinome peptide arrays: (1) species-specific proteomic or genomic information from a diverse range of species can be used to identify kinase recognition motifs that are composed of a central phosphorylation target and the surrounding amino acids (normally +4 and −4 amino acids from the central phosphorylated residue); (2) peptides that comprise the kinase recognition motifs identified in (1) are synthesized and covalently linked to a glass surface. Peptide targets are spotted in replicates of three to nine spots on each array to account for intra-array variability. Individual amino acids of the peptides are represented by orange, red, purple, and green spheres.

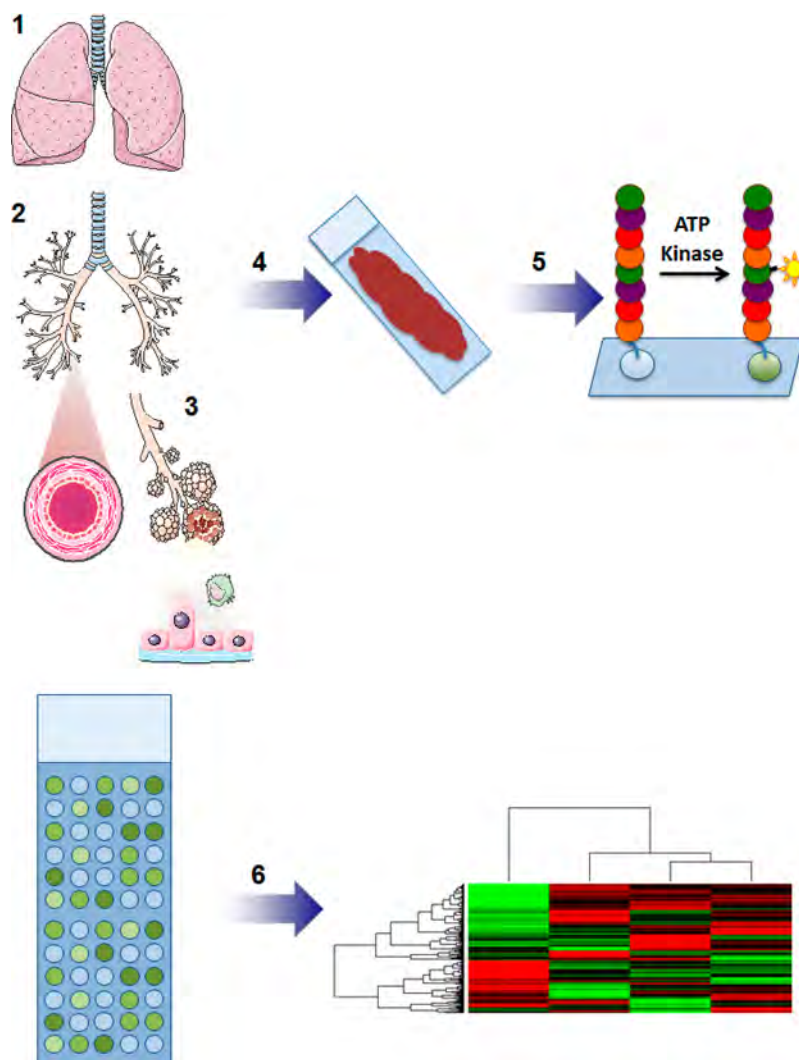


Figure 3. Kinome analysis of biological samples. Biological samples for kinome analysis can encompass (1) complex biological tissues (lung), (2) focused tissue sections (bronchioles), or (3) individual cell types associated with a particular tissue (alveolar epithelial cells or alveolar macrophages). (4) Biological samples are processed to generate cell lysates that are activated with ATP and applied to the kinome peptide array. (5) Following the application of the cell lysate, activated kinases in the cell lysate will recognize their respective kinase recognition motifs and phosphorylate the central phosphorylated residue of the peptide. (6) Kinome peptide arrays are subsequently stained with a phospho-specific fluorescent stain and imaged followed by comparative bioinformatics analyses. Tissue and cell images were derived and/or modified from Servier Medical Arts under a Creative Commons Attribution 3.0 Unported License.

pathogens at the level of individual genes or gene clusters. However, there is a paucity of information regarding the relationship of cell signaling networks, and in particular their activation status, with the biological/pathological events that occur throughout infection.

It has been well established that many biological processes can be regulated independent of transcriptional or translational changes through post-translational modification (PTM) events. Indeed, kinase-mediated phosphorylation of proteins, in which kinases catalyze the transfer of the γ phosphate group from ATP to the hydroxyl group of a specific Ser, Thr, Tyr residue, is

among the most thoroughly characterized PTM. Virtually all cell signal transduction events are regulated by kinases independent of biological complexity of the host (i.e., prokaryotes and eukaryotes).³ Lending further credence to the biological importance of kinases, >500 kinases have been identified in the human genome, and ~30% of the human proteome is modulated by kinase-mediated phosphorylation events.^{4,5} Thus, considering the central role of kinases in a broad range of cellular processes (including growth and development, metabolism, and immune responses), it has been postulated that the activities of individual kinases may represent more reliable predictors of cellular phenotypes than transcriptional or translational changes.⁶ Indeed, transcriptional or translational-based OMICS approaches are often unable to account for regulatory events including gene silencing, mRNA stability, translational efficiencies, protein turnover, enzyme/substrate subcellular sequestration, or protein activation/repression PTMs.⁷ Given the central role of kinases in the regulation of biological processes, kinases are a logical drug target. As a testament to this, 33 kinase inhibitors have been granted licensure by the U.S. Food and Drug Administration (FDA) for a broad range of malignancies, and there are a continually increasing number of kinase inhibitors that are in various stages of preclinical trials. Furthermore, kinases are the second most frequently targeted gene class in cancer therapy after the G protein coupled receptors.^{8,9} The recent prioritization for the repurposing of approved therapeutics for alternative malignancies by the National Institutes of Health Center for Advancing Translational Sciences (NCATS)^{10,11} also provides considerable impetus for the investigation of licensed kinase inhibitors as infectious disease therapeutics. Concerns exist regarding the therapeutic application of kinase inhibitors as novel therapeutics for infectious disease, in particular to the potential immunosuppressive effects following prolonged treatment. However, it should be appreciated that the application of kinase inhibitors in such cases would need to be targeted in terms of timing and dose, with appropriate molecular biomarkers guiding initiation and cessation. It should also be appreciated that the clinical symptoms associated with many emerging and re-emerging pathogens have been associated with dysregulated host immune responses (in particular pro-inflammatory responses).

Thus, the global analysis of the activation state of host kinases (the kinome) can provide critical insight into the specific activation state of individual kinases, cell signaling pathways, or larger biological networks. In addition, kinome investigations may offer important, and predictive, insight into the cellular mechanisms that regulate phenotypic changes within cells.⁷ As many kinases recognize a particular phosphorylation motif composed of the central phosphoacceptor site and the amino acids +4 and -4 residues from the central phosphorylation site,¹² peptides representing this kinase target motif can be synthesized with relatively high efficiency and low expense. Indeed, kinase target motif peptides have been shown to be appropriate substrates for their respective kinases with V_{\max} and K_m values approaching those of the full-length protein.¹³ Thus, peptide kinome arrays can be constructed in an analogous manner to traditional DNA microarrays where kinase target motif peptides are spotted onto a glass slide representing hundreds to thousands of unique peptide targets for kinases (Figure 2). Following this, samples in the form of cellular lysates from whole organs, tissues, or individual cell types can be applied to the kinome peptide

arrays, allowing for the phosphorylation of specific peptide targets by kinases within the lysate (Figure 3). The development of kinome-specific bioinformatics analysis software, including the Platform for Intelligent, Integrated Kinome Analysis (PIIKA), has provided a mechanism to identify the complex patterns of kinase-mediated phosphorylation events and quantitate the differences between compared conditions.^{14,15}

■ INTEGRATING KINOMICS WITH CLINICAL AND MOLECULAR PATHOGENESIS INVESTIGATIONS FOR EMERGING AND RE-EMERGING PATHOGENS

Middle East Respiratory Syndrome Coronavirus (MERS-CoV). Human coronaviruses are the causative agents of an estimated 30% of upper and lower respiratory tract infections in humans resulting in rhinitis, pharyngitis, sinusitis, bronchiolitis, and pneumonia.^{16,17} Coronaviruses are members of the Coronavirinae subfamily of viruses and together with the Torovirinae subfamily comprise the Coronaviridae virus family (order Nidovirales). Multiple coronavirus family members, including OC43 and 229E, can be found across the globe and largely result in mild illness with more-severe illness limited to children and the elderly.^{18–20} Since the emergence of SARS in 2003 and MERS in 2012, there is increased interest in coronaviruses as global public health threats.

SARS-CoV was first identified in China before spreading to 37 countries resulting in more than 8000 confirmed cases and 775 deaths. No additional cases have been reported since 2004.²¹ In 2012, MERS emerged in Saudi Arabia as a severe respiratory disease with gastrointestinal and renal complications.²² MERS-CoV has subsequently spread to 26 countries (WHO), resulting in 1733 confirmed cases and 628 deaths as of June 2016 (<http://www.who.int/emergencies/mers-cov/en/>). MERS may have emerged from a bat reservoir, likely spilling into humans via dromedary intermediate hosts. Human-to-human spread occurs primarily within healthcare settings, often leading to severe disease. No licensed vaccines or targeted therapies are available.

Clinical Findings during MERS-CoV Infection. Syndromic case-definition for MERS infection requires a compatible clinical syndrome and an epidemiologic risk factor including travel to an affected region or contact with a known or suspected case. Initial symptoms of MERS-CoV infection include fever, chills, cough, shortness of breath, myalgia, and malaise following a mean incubation period of 5 days, which can range from 2 to 14 days.²³ Mildly symptomatic or possibly asymptomatic infections have been reported, and progression to severe disease is associated with pre-existing medical conditions including cardiopulmonary disease, obesity, and diabetes. Most (98%) of reported MERS cases are among adults, with a median age of 50 years. In severe cases respiratory failure requiring mechanical ventilation typically occurs within 7 days of symptom onset.²² Laboratory abnormalities include lymphopenia, leukopenia, thrombocytopenia, elevated serum creatinine levels consistent with acute kidney injury, and elevated liver enzymes.^{23–27} High lactate levels and consumptive coagulopathy have also been reported.^{24,28} Chest radiographic abnormalities are observed in most cases consistent with viral pneumonitis, secondary bacterial pneumonia, or acute respiratory distress syndrome.^{22–24,27,29}

Soluble Immune Mediators Associated with MERS-CoV Infections. Data characterizing immune responses during MERS-CoV infection are limited. Faure et al. evaluated

cytokine levels in serum and bronchoalveolar lavage (BAL) from two MERS patients, one with fatal disease and one who survived.³⁰ Higher levels of retinoic acid-inducible gene 1 (RIG-1), melanoma differentiation-associated protein 5 (MDA5), interferon regulatory factor (IRF)-3 and -7, interleukin (IL) 17A, and IL-23 and lower levels of IL-12 and IFN γ were observed in the fatal case compared with the survivor. More recently, Min et al. performed a temporal analysis of cytokine, chemokine, and growth factor blood levels from 14 patients during the recent outbreak of MERS in South Korea.³¹ The patients were subcategorized into four groups on the basis of disease severity: Group I patients developed fever and recovered. Group II patients developed mild pneumonia without hypoxemia. Group III patients had prolonged and severe pneumonia. Group IV patients had severe pneumonia and acute respiratory distress syndrome. Group IV patients included five fatal cases of MERS; all patients in groups I–III fully recovered from illness. IFN α was elevated in all groups and largely peaked during the second week of illness. Granulocyte-colony stimulating factor (G-CSF) and granulocyte macrophage (GM)-CSF were similarly elevated across all patient groups; however, patients with fatal disease had reduced GM-CSF responses following antiviral treatment as compared to patients that recovered. Patients with pneumonia had relative elevations of IL-1, tumor necrosis factor (TNF)- α , IL-6, and IL-10 during the second and third weeks of illness. Elevated IL-6 and IL-10 appeared to trend positively with the severity of illness. A robust induction of multiple chemokines was found in most patients. Notably, eotaxin and regulated on activation, normal T expressed and secreted (RANTES) was elevated in all patients. In contrast, IL-8, monocyte chemotactic protein (MCP)-3 and macrophage inflammatory protein (MIP)-1 β were more prominent in groups II and III as compared to groups I and IV. Furthermore, elevated interferon gamma induced protein (IP)-10 correlated with the development of pneumonia (groups I–III). Multiple growth factors, including epidermal growth factor (EGF), fibroblast growth factor (FGF)-2, vascular endothelial growth factor (VEGF), and TGF- α , were significantly elevated across all patients; however, EGF was significantly higher in patients that recovered from disease as compared to the fatal cases. Further evaluations are needed to characterize the natural history of immune response during acute MERS-CoV infection and recovery.

Transcriptome Analyses of MERS-CoV. In an effort to better characterize MERS-CoV pathogenesis in the absence of available samples from human patients and, in particular, address pathologic changes associated with infection, multiple animal species have been employed in MERS-CoV investigations. While multiple small animals are not susceptible to MERS-CoV infection,³² rhesus macaques and marmosets develop mild to severe lung pathology following experimental infection. Transcriptome analysis in MERS-CoV-infected rhesus macaques revealed that genes related to antiviral immunity, chemotaxis, and inflammation were overexpressed in lesional versus grossly normal lung tissue at 3 days postinfection.³³ A significantly smaller number of differentially expressed genes was found on day 6 postinfection with no obvious trends following pathway enrichment analysis. Significant changes in the transcriptome profiles of peripheral blood mononuclear cells (PBMCs) were observed at only day 1 postinfection. This global analysis suggests a key role for an initial rapid innate immune and inflammatory response (through pattern recognition receptors) followed by rapid

resolution.³³ A study of MERS-CoV-infected marmosets evaluated lung lesions by RNaseq at days 3–6 postinfection.³⁴ Pathway analyses demonstrated that chemotaxis and cell migration, cell cycle progression, and cell proliferation and fibrogenesis were highly over-represented relative to uninfected controls. To a lesser degree, pathways associated with inflammation, vascularization, endothelial activation, proliferation of smooth muscle, and tissue repair were also over-represented in infected animals. Differences were most significant on days 4 and 6 postinfection during illness progression relative to day 3.

Recently, Menachery and colleagues examined the interaction between MERS-CoV EMC/2012 and the host IFN-stimulated gene (ISG) response by transcriptomics.³⁵ ISG responses in MERS-CoV infected Calu3 cells, a lung adenocarcinoma cell line, had no discernible induction initially upon infection but were up-regulated by 12 h postinfection.³⁵ Down-regulation of a subset of ISGs resulted in altered histone modifications, a potential epigenetic contributor to early impairment of antiviral cellular defenses. In a separate analysis genetically distinct MERS-CoV strains, MERS-CoV SA1 and MERS-CoV Eng1, produced distinct gene expression profiles in Calu-3 cells.³⁶ These analyses may better inform early host-cell antiviral responses and the impact of viral evolution on these and other complex biological responses. Proteomics analysis corroborated these transcriptional data with induction of ISGs observed 18 h postinfection. Significantly reduced levels of STAT1 and PKR compared with uninfected controls were also noted. Differential host transcriptome responses to MERS-CoV SA1 and MERS-CoV Eng1 highlight both the propensity of emerging viral pathogens to evolve rapidly and the importance of additional host response analyses for augmenting and clarifying such complex biological responses.

Kinome Analyses of MERS-CoV Infection. Host responses to MERS-CoV infection through kinome analysis were recently assessed using Huh-7 cells, an immortalized human hepatocyte cell line, that are highly permissive to MERS-CoV infection.³⁷ Temporal analysis of kinome responses by peptide arrays revealed selective modulation of extracellular signal-regulated kinases (ERK)/mitogen-activated protein kinases (MAPK) and phosphatidylinositol-3-kinases (PI3K)/AKT (also known as protein kinase B)/mechanistic target of rapamycin (mTOR) signaling responses. Over-representation analysis (ORA) revealed ERK/MAPK and PI3K/AKT/mTOR signaling responses were consistently up-regulated during infection. Multiple ERK/MAPK family members formed central components of functional networks and signaling pathways throughout infection. Similar results were observed for intermediates of the PI3K/AKT/mTOR signaling pathway at 1 and 24 h postinfection, suggesting that modulation of ERK/MAPK and PI3K/AKT/mTOR signaling may be important for productive MERS-CoV infection.

Downstream analysis of the phosphorylation patterns of pathway intermediates from the ERK/MAPK and PI3K/AKT/mTOR signaling supported observations from the kinome analysis. Both investigations demonstrated that nuclear factor kappa-light-chain-enhancer of activated B cells (NF κ B)-regulated family members were important mediators of MERS-CoV infection.³⁸ IL8- and IFN-mediated signalings were also modulated during MERS-CoV infection, consistent with prior analyses.^{39,40} These results were also in agreement with in vitro transcriptional analysis of MERS-CoV infection.³⁸ Prophylactic or therapeutic addition of FDA-licensed kinase

inhibitors targeting activated kinases in MERS-CoV infection impaired viral replication. These hypothesis-generating data may inform directed investigations into MERS-CoV pathogenesis and, importantly, demonstrate the potential to identify novel host-centric therapeutic targets.

Ebolaviruses. The Filoviridae family of viruses consists of three genera: Ebolavirus, Marburgvirus, and the newly identified Cuevavirus. Structurally, filoviruses have a pleomorphic enveloped, filamentous virion particle that encapsulates a negative-sense single-stranded RNA genome. Ebolaviruses were first described in 1976 following disease outbreaks in the Democratic Republic of Congo and Sudan and are composed of five viral species, including Ebola virus (EBOV), Sudan virus (SUDV), Bundibugyo virus (BDBV), Tai Forest virus (TAFV), and Reston virus (RESTV). Sporadic outbreaks of EBOV, SUDV, BDBV, and TAFV have occurred throughout central Africa for more than three decades, resulting in thousands of infections. Case fatality rates during these outbreaks have routinely exceeded 50%.⁴¹ Isolated outbreaks of RESTV have occurred outside Africa in nonhuman primate facilities in the United States, Italy, and the Philippines, and infection results in high morbidity and mortality in nonhuman primates; however, RESTV has only been associated with asymptomatic infections in humans.⁴² Although ebolaviruses have been historically associated with isolated outbreaks involving small cohorts of infected patients (<500), an outbreak of EVD in West Africa beginning in 2014 has resulted in 28,616 cases and 11,310 deaths (40% CFR) as of June 2016 (<http://www.who.int/csr/disease/ebola/en/>). Although virus transmission has greatly decreased in West Africa, surveillance for sporadic infections continues.

Clinical Findings in EVD. EBOV transmission occurs through exposure of infected body fluids or tissues to mucous membranes or nonintact skin.⁴³ The mean incubation period is 6–10 days, ranging from 2 to 21 days.⁴³ Initial signs and symptoms are nonspecific including fever, myalgia, and malaise and cannot be reliably distinguished from other endemic illnesses in Africa including malaria and enteric infections.⁴³ Whereas mild illness has been described, most patients develop severe disease within days of symptom onset. Massive gastrointestinal fluid losses of up to 5–10 L per day due to vomiting and watery diarrhea may result in progressive dehydration and hypovolemic shock. Even in the setting of adequate fluid and electrolyte replacement, sequential multi-organ failure may occur. EBOV infects multiple organs and cell types throughout the body with the notable exception of lymphocytes that are indirectly depleted early during infection. Organ injury due to direct viral or indirect host-mediated responses results in severe complications including meningo-encephalitis, uveitis, respiratory failure, secretory diarrhea, disordered coagulation, renal failure, hepatic necrosis, and myositis. The clinical presentation, laboratory values, viral kinetics, and clinical management of EVD patients in West Africa, Europe, and the United States during the 2014–2015 outbreak have been recently well-characterized.⁴⁴

Soluble Immune Mediators Associated with EBOV Infections. There is a paucity of information regarding EBOV pathogenesis in humans primarily due to the limited frequency of EVD outbreaks prior to 2014 and limitations presented by sample acquisition from infected patients in the field as well as the overall size of patient cohorts. Largely contradictory findings regarding the immune responses in those who survive or succumb to EVD have further confounded the under-

standing of EBOV pathogenesis in human patients. For example, Villinger et al. reported that serum cytokine concentrations (including IFN α , IFN γ , TNF- α , IL-2, and IL-4) were elevated in patients with fatal infections in comparison to survivors.⁴⁵ In contrast, additional studies have suggested that fatal infections were instead related to general immunosuppression including IFN γ , IL-2, and IL-4.^{46–49} An investigation of SUDV infection in humans by Sanchez et al. demonstrated limited changes in the expression levels of cytokines, Fas antigen, and Fas ligand in PBMCs from infected patients relative to those found for uninfected patients.⁵⁰ Furthermore, an investigation of 42 fatally infected EVD patients by Wauquier et al. has further confounded the role of host immune responses in fatal EVD as hypersecretion of multiple cytokines and growth factors and decreased secretion of T lymphocyte-derived cytokines were associated with fatal disease.⁵¹

Transcriptome Analyses of Ebola Virus Infection. To date, no investigations of host gene expression in EBOV-infected patients have been reported, although limited data are available from animal models of infection or from in vitro investigations.

In a study of PBMCs from EBOV-infected crab-eating macaques, Rubins et al. found few notable changes in the early stages of infection (1–2 days); however, broad changes were observed over days 4–6 post-infection. Pro-inflammatory cytokines (IL-1 β , IL-6, IL-8, and TNF- α) and chemokines (MIP-1 α and MCP1–4) were up-regulated at days 4–6 postinfection relative to healthy controls.⁵² Multiple genes related to apoptosis including Bcl-2 family members, multiple caspases, Fas-associated death domain protein, and TNF superfamily member 10 were also up-regulated at late time points. IFN-regulated genes were up-regulated by day 2 postinfection and remained so through study day 6.

Yan et al. investigated PBMC gene expression in EBOV-infected rhesus macaques with or without anticoagulant administration. Untreated animals displayed up-regulation of immune response genes, B cell receptor signaling intermediates, NK cell mediated cytotoxicity, leukocyte activation, and lymphocyte activation compared with anticoagulant-treated animals during the early stages of infection. The expression levels of these gene clusters fell to pre-infection levels at the late-stage of infection. In contrast, genes related to defense responses, apoptosis, wounding, inflammation, coagulation, and leukocyte activation remained elevated during early- and late-stage infection.

Following the isolation of RESTV from pigs,⁵³ subsequent investigations have demonstrated that pigs were susceptible to both RESTV and EBOV infection with preferential targeting of macrophages in the lungs. Recently, Nfon et al. demonstrated that EBOV infection in pigs resulted in up-regulation of chemokine expression beginning on day 3 postinfection as compared to mock-infected pigs.⁵⁴ The most pronounced changes in gene expression were found on days 5 and 7 postinfection and included the up-regulation of a broad set of cytokines (IL-5, IL-6, IL-8, IL-10, IL-22, IL-26, IL-27, resistin), chemokines (CCL2, CCL10, CCL19, CCL20, AMCF-II, CCL3L1, CCL4), cell adhesion protein (selectin), antimicrobial protein, palate, lung, and nasal epithelium clone proteins, and pro-apoptotic molecules (multiple caspases, caspase recruitment domain-containing protein 6 (CARD), apoptosis-associated tyrosine kinase (AATK), Fas, Fas-associated protein with death domain (FADD), TNF receptor-associated factor 3 (TRAF3), TNF α -induced protein 3-interacting protein 1

(TNIP1)). In addition, expression of multiple genes related to microbial sensing (pattern recognition receptors) or antiviral responses (ISGs) was up-regulated in the lungs of infected animals. Although the localization of the cytokine response of pigs and humans or NHPs differs during the course of EBOV infection (localized responses in the lungs of pigs versus a predominantly systemic response in humans and NHPs), the cytokine profiles of pigs, humans, and NHPs were quite similar. For example, comparison of NHP⁵² and porcine responses⁵⁴ during EBOV infection demonstrated multiple gene expression similarities between the two species (i.e., IL-6, IL-8, caspase family members). It is also likely that direct comparison of both data sets would likely yield many common gene signatures that are conserved in their identity as well as their directionality (up-regulation vs down-regulation).

Macrophages are an early target of EBOV infection and support high-level viral replication. EBOV attachment and entry into human macrophages in vitro induces pro-inflammatory mediators including IL-6, IL-8, and TNF- α as early as 1 h postinfection.⁵⁵ Noncardiogenic pulmonary edema is a recognized complication of EVD, and human autopsy data support that alveolar macrophages are a target of EBOV infection. EBOV infection of alveolar macrophages in vitro resulted in an early, transient increase in cytokine and chemokine expression,⁵⁶ supporting that paracrine-soluble mediators of inflammation may contribute to vascular leakage in the lungs. Gene expression responses of EBOV- and MARV-infected Huh7 cells resulted in the global suppression of antiviral responses, including Toll-like receptor (TLR), IRF3, and protein kinase R (PKR)-mediated pathways.⁵⁷ However, signal transducers and activators of transcription (STAT) phosphorylation in EBOV- and MARV-infected cells were differentially modulated. EBOV-mediated IFN inhibition has been well characterized and is thought to be attributable to EBOV proteins VP24 and VP35.⁵⁸ Interestingly, RESTV infection, which does not induce clinical illness in humans, resulted in the activation of >20% of the IFN-stimulated genes (ISGs).

Kinome Analysis of Ebola Virus. Hepatocytes are an early target of EBOV infection, directly contributing to diffuse hepatic necrosis observed in fatal cases. EBOV infection of Huh7 cells has been evaluated by kinome analyses, shedding light on liver pathogenesis in EVD.⁵⁹ EBOV infection of Huh-7 cells resulted in temporal modulation of the TGF- β signaling pathway as compared to mock-infected cells. Pathway ORA demonstrated that multiple TGF- β -mediated signaling pathways were up-regulated at 1 and 24 h post EBOV infection. Furthermore, these responses were associated with changes in the expression patterns of multiple cellular proteins associated with a mesenchyme-like transition. These included the up-regulation of matrix metalloproteinase 9, N-cadherin, and fibronectin and down-regulation of E-cadherin and claudin 1. In this process cells lose polarity and cell-to-cell adhesion transforming into mesenchymal stem cells that contribute to wound healing or organ fibrosis; however, the role of these events in EBOV infection remains to be elucidated. Additional analysis demonstrated that inhibition of PI3K/AKT, ERK/MAPK, or PKC pathways with kinase inhibitors reduced EBOV replication when administered prophylactically or therapeutically. Supporting this observation, a subset of kinase inhibitors administered to EBOV-infected mice reduced lethality. Defining mechanisms by which kinase inhibitors show benefit

in these models will better clarify their role as potential therapeutics.

Monkeypox Virus. MPXV, a member of the genus *Orthopoxvirus*, causes zoonotic infections with a case fatality rate of ~11%.⁶⁰ MPXV, vaccinia virus (VACV), cowpox virus (CPXV), ectromelia virus, and variola virus (VARV), the etiologic agent of human smallpox, comprise the Orthopoxviridae family of viruses. MPXV was first isolated in 1958 from cynomolgus macaques in Denmark; however, human MPXV infections were not recognized until 1970 following the isolation of the virus from a suspected case of smallpox infection in the Democratic Republic of Congo.⁶¹ MPXV is composed of two distinct clades that are genetically, clinically, and geographically distinct. The Congo Basin MPXV (Central African MPXV) clade is considered to have both higher lethality and morbidity than the West African MPXV clade as demonstrated from comparative infection models in various animal species (including nonhuman primates, mice, prairie dogs, and ground squirrels) and as well natural infection in humans.^{61–63} Fifty-four cases of human MPXV disease were recorded in West and Central Africa from 1970 to 1979. Although no fatalities were reported in West African cases (including Liberia, Nigeria, Ivory Coast, and Sierra Leone), 21% of cases from the Democratic Republic of Congo resulted in fatal disease.⁶¹ Furthermore, West African MPXV was responsible for the 2003 MPXV outbreak in the United States that resulted in 69 diagnosed cases of MPXV and no associated fatalities.⁶⁴ Although human MPXV infections have been recorded in West Africa, the majority of human MPXV infections have occurred in the Congo Basin region of Central Africa, largely in the Democratic Republic of Congo.⁶⁰

Clinical Findings in MPXV Infections. Clinical and epidemiological information regarding human MPXV disease has been derived from enhanced surveillance campaigns in the Congo Basin.⁶¹ From this work, it has been demonstrated that human MPXV infection and illness largely mirror those of discrete, ordinary smallpox.⁶¹ The incubation period for both viruses (VARV and MPXV) is 7–17 days with an initial febrile prodromal period of 1–4 days. This prodromal period is normally accompanied by fever, headache, backache, malaise, and prostration.⁶¹ The rash period for both smallpox and MPXV (including lesion appearance and desquamation) normally occurs 14–28 days postinfection with highly similar appearance, distribution, and progression of lesions.^{60,61} As with smallpox, MPXV-associated rash progresses through macular, papular, vesicular, and pustular phases. A second febrile period occurs when the lesions become pustular and is often associated with deteriorating conditions in the patient. Lymphadenopathy (maxillary, cervical, or inguinal) is often associated with MPXV infections prior to, or concomitant with, rash development but is absent in VARV infections. It has been postulated that this reflects the effective generation of host immune responses during MPXV infection as compared to VARV; however, this has yet to be validated.^{60,61} Severe complications have been noted late in the course of MPXV infection, including pulmonary distress or bronchopneumonia, corneal scarring and permanent vision loss, and encephalitis.⁶⁰ Severe dehydration due to excessive vomiting or diarrhea may also occur. Long-term sequelae in survivors are most commonly associated with pitted scarring.

Soluble Immune Mediators Associated with MPXV Infections. Although MPXV infections in humans have been recorded for over four decades, there has been little information

regarding host immune responses during the course of natural infection. As disease presentation is highly similar during MPXV and VARV infections, it has been postulated that immune responses would likely be highly conserved. Recently, Johnston et al. provided the first empirical evidence for a relationship between cytokine responses and disease severity during MPXV infection.⁶⁵ Serum cytokines were analyzed from 19 patients with confirmed MPXV infections ranging from mild to severe as assessed by the WHO smallpox lesion scoring system.^{66,67} Serum concentrations of IL-1 β , IL-1RA, IL-2R, IL-4, IL-5, IL-6, IL-8, IL-13, IL-15, IL-17, MCP-1, and RANTES were elevated in all disease groups (mild to severe) as compared to normal serum concentrations. IL-10 concentrations were also elevated in all disease groups and were proportional to disease severity. However, patients with serious MPXV disease had significantly higher concentrations of IL-10 compared to all other disease groups. MPXV infection resulted in elevated MIP-1 α and MIP-1 β ; mild cases had significantly elevated levels above the moderate or severe disease groups. Serum concentrations of IL-2R were elevated across all disease groups; however, patients with serious disease had significantly higher IL-2R serum levels than those with mild to severe MPXV disease. GM-CSF levels were significantly elevated only in those with serious MPXV disease as compared to normal serum ranges. On the basis of these observations, MPXV infection resulted in prominent T helper 2 (Th2) and dampened Th1 responses.

Transcriptome Analyses in MPXV Infection. Transcriptome analyses have largely been employed for the in vitro investigation of the molecular pathogenesis of MPXV infection. Alkhalil et al. investigated the host transcriptome responses to MPXV infection during the first cycle of viral replication (3 and 7 h postinfection) in rhesus macaque kidney epithelial cells.⁶⁸ Interestingly, MPXV infection resulted in a strong down-regulation of host transcriptional responses. Of the transcripts that met the authors' criteria for significance, 89% of the transcripts were found to be down-regulated at both post-infection time points. Comparative functional analysis from both time points suggested that the primary biological functions associated with these down-regulated transcriptional responses were largely related to cell morphology, cell development, metabolic responses, and post-translational modifications. Canonical pathway analysis demonstrated a general conservation in the identities of over-represented pathways at both time points including multiple growth factor signaling pathways, p53 signaling, and cell cycle-related pathways. More recently, Bourquain et al. investigated host transcriptome responses in MPXV-infected HeLa cells, a cervical epithelial cell line.⁶⁹ At 6 h post-MPXV infection, only 1.1% of the transcripts analyzed were found to have >2-fold changes in gene expression. In contrast to Alkhalil et al., the majority of these transcripts (~68%) were found to be up-regulated as compared to mock-infected controls. Functional analysis of all transcripts with >2-fold changes in gene expression demonstrated a strong over-representation of genes involved in the negative regulation of MAPK signaling and the intracellular protein cascade. Positive regulation of pathways related to Toll-like receptor signaling, chemotaxis, and regulation of leukocyte migration was also predicted from the data. An investigation by Rubins et al. compared the temporal host transcriptome response to MPXV in multiple human cells targeted by MPXV including primary macrophages, primary fibroblasts, and HeLa cells.⁷⁰ The transcriptome of

MPXV-infected fibroblasts was found to have the most significant changes where MPXV infection resulted in the depletion of ~2000 genes by a factor of ≥ 3 . Interestingly, MPXV infection resulted in the broad repression of many transcripts related to innate immune responses in all cell types tested. In contrast, inactivated MPXV resulted in strong up-regulation of innate immune responses in all of the cell types. It was also noted that MPXV infection resulted in strong cytopathic effects across all of the cell types in contrast to an almost universal repression of innate immune responses.

Kinome Analyses in MPXV Infection. Human MPXV infections and infection models of MPXV in various animal species have demonstrated that the Congo Basin MPXV clade is more virulent than the West African MPXV clade. However, there has been a paucity of information regarding the underlying molecular mechanisms mitigating these virulence differences. Furthermore, previous investigations focusing on gene expression or proteomic changes during MPXV infection have focused solely on Congo Basin MPXV. To address this, host kinome analysis was performed on Congo Basin and West African MPXV-infected human monocytes, a host cell targeted by orthopoxviruses.⁷¹ As the genomes of both MPXV clades demonstrate considerable diversity in the regions coding host response modifier proteins, and in particular in genes associated with anti-apoptotic activities, it was postulated that the virulence differences of the two MPXV clades may be related to differential modulation of host cellular responses. Hierarchical clustering of the kinome data sets suggested limited similarities at the level of host kinase modulation between the two MPXV clades. The Congo Basin MPXV kinome data set clustered most strongly with the kinome data set from CPXV-infected monocytes and moderately with the VACV-infected monocyte data set. Both CPXV and VACV can cause serious disease in humans. The pathway ORA of the kinome data demonstrated that Congo Basin MPXV infection resulted in strong down-regulation of a large proportion of host cell responses, most notably apoptosis, in comparison to West African MPXV. Biological validation through fluorescence-activated cell sorting (FACS) and caspase 3 activity analyses confirmed this phenomenon. From the perspective of individual phosphorylation events, the kinome data also suggested that AKT phosphorylation at Ser473 was increased in Congo Basin MPXV-infected cells as compared to West African MPXV-infected cells. Pharmacologic inhibition of AKT phosphorylation at Ser473 resulted in a >250-fold inhibition of Congo Basin MPXV virus yields, whereas those for West African MPXV were unaffected. Prior investigations with CPXV and VACV demonstrated that pharmacological inhibition of AKT resulted in decreased viral yields for both viruses.⁷² Overall, this investigation provided significant insight into the host cellular response differences between the two MPXV clades.

■ CONCLUSIONS

Emerging and re-emerging pathogens are a continual threat to global health. In recent years, disease outbreaks associated with SARS and the 2009 influenza pandemic have also demonstrated that these pathogens can have considerable effects on local, national, and international economies. As a consequence, regional outbreaks of emerging and re-emerging pathogens can have deleterious effects on global stability. Thus, it is prudent that a concerted effort is employed to assimilate data that bridge both clinical and molecular information in investigations

Table 1. Kinase Inhibitors Tested against EBOV, MERS-CoV, or MPXV

kinase inhibitor	host target	impact of inhibitor on viral replication (reduction in viral replication considered to be >40% inhibition)	impact of inhibitor on animal survival	reference
MERS-CoV				
Rapamycin	mTOR	in vitro reduction in viral replication with prophylatic and therapeutic treatment	no data available	37
GF109203X	PKC	in vitro reduction in viral replication with prophylatic and therapeutic treatment	no data available	37
Ro-31-8220	PKC	in vitro reduction in viral replication with prophylatic and therapeutic treatment	no data available	37
U0126	MEK1, MEK2	in vitro reduction in viral replication with prophylatic treatment	no data available	37
Wortmannin	PI3K	in vitro reduction in viral replication with prophylatic treatment	no data available	37
GW5074	c-Raf1	in vitro reduction in viral replication with prophylatic treatment	no data available	37
Imatinib	c-Abl1 family	in vitro reduction in viral replication with prophylatic treatment	no data available	79
SB203580	p38 MAPK	in vitro reduction in viral replication with prophylatic treatment	no data available	37, 38
Dasatinib (BMS-354825)	Src, Abl family kinases	in vitro reduction in viral replication with prophylatic treatment	no data available	79
PP2	Src family kinases	no significant inhibition of viral replication	no data available	37
Bay 11-7082	IKB α	no significant inhibition of viral replication	no data available	37
PKC-412	PKC	no significant inhibition of viral replication	no data available	37
AG490	EGFR; ERBB2	no significant inhibition of viral replication	no data available	37
L-NAME	nitric oxide synthase	no significant inhibition of viral replication	no data available	37
EBOV				
AG879	ErbB2 and FLK-1 (VEGF receptor)	in vitro reduction in viral replication with prophylatic and therapeutic treatment	improvement in mouse survival	59
LY294002	PI3K	in vitro reduction in viral replication with prophylatic and therapeutic treatment	improvement in mouse survival	59, 80
SB431542	activin receptor-like kinase receptors, ALK5, ALK4 and ALK7	in vitro reduction in viral replication with prophylatic and therapeutic treatment	improvement in mouse survival	59
SU1498	VEGF receptor 2	no significant inhibition of viral replication	improvement in mouse survival	59
Rottlerin	PKC	in vitro reduction in viral replication with prophylatic and therapeutic treatment	improvement in mouse survival	59
Wortmannin	PI3K	in vitro reduction in viral replication with prophylatic and therapeutic treatment	no data available	59
Indirubin-3-monoxamine	glycogen synthase kinase 3 β	in vitro reduction in viral replication with prophylatic and therapeutic treatment	no data available	59
SP600125	JNK	in vitro reduction in viral replication with prophylatic and therapeutic treatment	no data available	59
GF109203X	PKC	in vitro reduction in viral replication with prophylatic and therapeutic treatment	no data available	59
Genistein	EGFR	in vitro inhibition of vsv-ebov pseudotype transduction with prophylatic treatment	no data available	81
Tyrphostin	tyrosine kinases	in vitro inhibition of vsv-ebov pseudotype transduction with prophylatic treatment	no data available	81
KN-93	CAMK2	in vitro reduction in infectivity	no data available	80
U0126	MEK1, MEK2	in vitro reduction in viral replication with prophylatic treatment	no data available	59
Nilotinib	c-Abl1 family	in vitro reduction in viral replication with therapeutic treatment	no data available	82
Imatinib	c-Abl1 family	in vitro reduction in viral replication with therapeutic treatment	no data available	82
p38inK II	p38 MAPK	in vitro reduction of viral entry	no data available	83
SB202190	p38 MAPK	In vitro reduction of viral entry	no data available	83
AG1024	insulin-like growth factor 1 receptor	no significant inhibition of viral replication	no data available	59
Tricirbine	Akt	no significant inhibition of viral replication	no data available	59
GW5074	c-Raf1	no significant inhibition of viral replication	no data available	59
ZM336372	c-Raf1	no significant inhibition of viral replication	no data available	59
HBDDDE	PKC	no significant inhibition of viral replication	no data available	59
MPXV				
Dasatinib (BMS-354825)	Src, Abl family kinases	in vitro reduction in viral replication with prophylatic and therapeutic treatment (Congo Basin and West African clades)	no data available	84
Staurosporine	nonspecific kinase inhibitor	in vitro reduction in viral replication with prophylatic treatment (Congo Basin and West African clades)	no data available	71
SB202190	p38 MAPK	in vitro reduction in viral replication with prophylatic treatment (Congo Basin and West African clades)	no data available	71
BML-257	Akt	in vitro reduction in viral replication with prophylatic treatment (Congo Basin and West African clades)	no data available	71
LY294002	PI3K	in vitro reduction in viral replication with prophylatic treatment (Congo Basin clade only)	no data available	71

Table 1. continued

kinase inhibitor	host target	impact of inhibitor on viral replication (reduction in viral replication considered to be >40% inhibition)	impact of inhibitor on animal survival	reference
MPXV				
Akt-X	Akt	in vitro reduction in viral replication with prophylactic treatment (Congo Basin clade only)	no data available	71
Nutlin 3	MDM-2	no significant inhibition of viral replication	no data available	71

of these pathogens. These efforts will not only provide considerable context in regard to the molecular events that potentiate clinical manifestations of pathogenesis but also better inform the design and implementation of novel therapeutics. To this end, global analyses of host molecular responses can provide considerable insight into the complex molecular events that underlie cellular responses. Indeed, transcriptome analyses have provided important information regarding host transcriptional responses during emerging and re-emerging pathogen infection. These investigations often provide critical insight into the kinetics of host immune responses during the course of infection as well as mechanistic information regarding the cellular intermediates involved in these processes. However, the role of PTMs in the regulation of these events cannot be captured by traditional transcriptome technologies. In particular, the role of kinase-mediated regulation of cell signaling pathways has remained poorly understood. Given the central role of kinases in the regulation of cellular processes (e.g., homeostasis, metabolism, proliferation, and stress responses), it is of inherent importance that future investigations also address the role of the kinome in the cellular response to pathogen insult. Furthermore, kinomics also provides a mechanism for the identification of novel therapeutic targets based on the direct assessment of the activation state of cell signaling pathways. For example, pro-inflammatory responses during early stages of infection, and in particular the dysregulation of specific cytokines or cell signaling events that contribute to these, may represent potential therapeutic targets in the early stages of high-consequence viral pathogen infection. However, the selection of immunomodulatory therapeutics that target these dysregulated host responses is complicated by the regulatory events (i.e., kinase-mediated cell signaling events) that occur upstream of changes in gene expression. In addition, mRNA is subject to a variety of regulatory processes (including gene silencing, mRNA stability, translational efficiencies, protein turnover, enzyme/substrate subcellular sequestration, and/or protein activation/repression PTMs). Thus, from the standpoint of therapeutic discovery, the sole reliance on technologies for the global investigations of host responses that do not account for these regulatory processes or the role of PTMs in the modulation of cellular responses could impede the identification of efficacious therapeutics.

To this end, kinome analysis may also facilitate the identification of immunomodulatory therapeutics that have gained licensure through analysis of a quantifiable biological event (kinase-mediated phosphorylation) or for identifying novel host therapeutic targets for which therapeutics could be designed/developed. Furthermore, kinase inhibitors may serve as primary or adjunctive therapies for emerging infectious diseases. In addition, preclinical data and the increasing number of kinase inhibitors that have gained regulatory approval for cancer and other maladies suggest this approach is feasible and efficacious. From the perspective of this review, kinome investigations have identified several therapeutic targets and

licensed kinase inhibitors that have impaired viral replication in vitro and reduced the severity of disease in vivo (Table 1). For example, it has been demonstrated that the ERK/MAPK and PI3K/AKT/mTOR signaling pathways have a role in viral propagation during MERS-CoV infection.³⁷ Indeed, licensed kinase inhibitors that targeted these pathways (i.e., everolimus, selumetinib, and trametinib) resulted in decreased viral replication in vitro when added prior to, or following, infection. Furthermore, the pharmacologic inhibition of PI3K and PKC following EBOV infection provided partial protection in a lethal model of EVD in mice.⁵⁹ It should be noted that although the modulation of an individual kinase may have suppressive effects on infection (i.e., viral replication), this might not provide the level of inhibition required to completely negate viral escape. In addition, given the ability of many cell signaling pathways to signal through both canonical and noncanonical mechanisms, inhibition at a single intermediary point within a pathway may not provide the overall level of inhibition required to negate a deleterious response (i.e., viral replication, changes in cellular phenotypes, etc.). Thus, although previous investigations have demonstrated that individual kinases or cell signaling pathways may represent novel targets for anti-infective therapies, it is prudent that future investigations also examine combinations of inhibitors for efficacy and anti-infective activities. Furthermore, the targeting of cell signaling pathways at or near the origin point for the cell signaling cascade should also be examined as these likely represent stronger inhibitory targets given the generally reduced branching of cell signaling networks at or near the cell receptor.

In addition to host-directed therapeutic targeting, kinomics also confers the ability to identify novel inhibitors of pathogens through detailed characterization of the viral life cycle. Host-mediated PTMs, and in particular kinase-mediated phosphorylation, have been implicated in the viral life cycle and pathogenesis for several members of the order Mononegavirales, including EBOV.^{73–75} Thus, therapeutic targeting of kinases may represent a novel therapeutic strategy that can be employed to modulate host-centric or pathogen-centric molecular events during infection. For example, in silico prediction of viral protein phosphorylation sites provides a mechanism for the construction and, ultimately, the annotation of viral protein PTMs that are critical to the viral life cycle. Furthermore, the use of kinome peptide arrays has extended beyond the human kinome and now extends to a variety of animal species.^{76–78} It has been suggested that the interspecies phenotypic variability may reflect differences in phosphorylation sites found within the proteome.⁷⁸ Thus, the development of species-specific kinome peptide arrays provides additional utility for kinome analysis as peptide arrays representing traditional laboratory animal species (mouse, guinea pig, nonhuman primate) can be employed to detail the species-specific host response. The results from such analyses, and the overlap between these and those described previously from the analysis of human infections, may inform

the selection of appropriate animal models that meet regulatory approval through the FDA Animal Efficacy Rule.²⁹

Taken together, it is of inherent importance that future investigations of emerging and re-emerging pathogens address the complex nature of biological responses. Thus, molecular investigations of pathogenesis should be guided by available knowledge regarding the clinical and pathologic manifestations of disease. Indeed, technologies that provide further granularity into the precise molecular events that potentiate cellular responses during the course of infection will assist investigations of emerging and re-emerging pathogens and the identification of novel therapeutic targets. To this end, kinomics-based analyses of host responses provide a mechanism to directly address the cellular events at the level of specific cell signaling phenomena that underlie the biological responses and, ultimately, the clinical presentation of disease for emerging infectious pathogens.

AUTHOR INFORMATION

Corresponding Author

*(J.K.) Postal address: Critical Care Medicine Department, Clinical Center, National Institutes of Health, 10 Center Drive, Bethesda, MD 20814, USA. Phone: (301) 443-5961. E-mail: kindrachuk.kenneth@nih.gov.

Notes

The authors declare no competing financial interest.

ACKNOWLEDGMENTS

The Intramural Research Programs of National Institute of Health (Clinical Center, Critical Care Medicine Department) supported this work. The content of this publication does not necessarily reflect the views or policies of the U.S. Department of Health and Human Services, nor does mention of trade names, commercial products, or organizations imply endorsement by the U.S. government.

REFERENCES

- (1) Jones, K. E., Patel, N. G., Levy, M. A., Storeygard, A., Balk, D., Gittleman, J. L., and Daszak, P. (2008) Global trends in emerging infectious diseases. *Nature* 451, 990–993.
- (2) Arias, C. A., and Murray, B. E. (2015) A new antibiotic and the evolution of resistance. *N. Engl. J. Med.* 372, 1168–1170.
- (3) Hunter, T. (2000) Signaling – 2000 and beyond. *Cell* 100, 113–127.
- (4) Hunter, T. (1995) Protein kinases and phosphatases: the yin and yang of protein phosphorylation and signaling. *Cell* 80, 225–236.
- (5) Manning, G., Whyte, D. B., Martinez, R., Hunter, T., and Sudarsanam, S. (2002) The protein kinase complement of the human genome. *Science* 298, 1912–1934.
- (6) Kindrachuk, J., and Napper, S. (2013) Sample preparation and profiling: probing the kinome for biomarkers and therapeutic targets: peptide arrays for global phosphorylation mediated signal transduction. In *Comprehensive Biomarker Discovery and Validation for Clinical Application* (Horvatovich, P., and Bischoff, R., Eds.), pp 162–195, Royal Society of Chemistry, Cambridge, UK.
- (7) Arsenault, R., Griebel, P., and Napper, S. (2011) Peptide arrays for kinome analysis: new opportunities and remaining challenges. *Proteomics* 11, 4595–4609.
- (8) Cohen, P. (2002) Protein kinases – the major drug targets of the twenty-first century? *Nat. Rev. Drug Discovery* 1, 309–315.
- (9) Hopkins, A. L., and Groom, C. R. (2002) The druggable genome. *Nat. Rev. Drug Discovery* 1, 727–730.
- (10) Allison, M. (2012) NCATS launches drug repurposing program. *Nat. Biotechnol.* 30, 571–572.
- (11) Strittmatter, S. M. (2014) Overcoming drug development bottlenecks with repurposing: old drugs learn new tricks. *Nat. Med.* 20, 590–591.
- (12) Kreegipuu, A., Blom, N., Brunak, S., and Jarv, J. (1998) Statistical analysis of protein kinase specificity determinants. *FEBS Lett.* 430, 45–50.
- (13) Zhu, H., Klemic, J. F., Chang, S., Bertone, P., Casamayor, A., Klemic, K. G., Smith, D., Gerstein, M., Reed, M. A., and Snyder, M. (2000) Analysis of yeast protein kinases using protein chips. *Nat. Genet.* 26, 283–289.
- (14) Li, Y., Arsenault, R. J., Trost, B., Slind, J., Griebel, P. J., Napper, S., and Kusalik, A. (2012) A systematic approach for analysis of peptide array kinome data. *Sci. Signaling* 5, pl2.
- (15) Trost, B., Kindrachuk, J., Maattanen, P., Napper, S., and Kusalik, A. (2013) PIKA 2: an expanded, web-based platform for analysis of kinome microarray data. *PLoS One* 8, e80837.
- (16) Canducci, F., Debiaggi, M., Sampaolo, M., Marinozzi, M. C., Berre, S., Terulla, C., Gargantini, G., Cambieri, P., Romero, E., and Clementi, M. (2008) Two-year prospective study of single infections and co-infections by respiratory syncytial virus and viruses identified recently in infants with acute respiratory disease. *J. Med. Virol.* 80, 716–723.
- (17) Jevnsnik, M., Ursic, T., Zigon, N., Lusa, L., Krivec, U., and Petrovec, M. (2012) Coronavirus infections in hospitalized pediatric patients with acute respiratory tract disease. *BMC Infect. Dis.* 12, 365.
- (18) Birch, C. J., Clothier, H. J., Secclull, A., Tran, T., Catton, M. C., Lambert, S. B., and Druce, J. D. (1999) Human coronavirus OC43 causes influenza-like illness in residents and staff of aged-care facilities in Melbourne, Australia. *Epidemiol. Infect.* 133, 273–277.
- (19) El-Sahly, H. M., Atmar, R. L., Glezen, W. P., and Greenberg, S. B. (2000) Spectrum of clinical illness in hospitalized patients with “common cold” virus infections. *Clin. Infect. Dis.* 31, 96–100.
- (20) Vabret, A., Mourez, T., Gouarin, S., Petitjean, J., and Freymuth, F. (2003) An outbreak of coronavirus OC43 respiratory infection in Normandy, France. *Clin. Infect. Dis.* 36, 985–989.
- (21) Chinese, S. M. E. C. (2004) Molecular evolution of the SARS coronavirus during the course of the SARS epidemic in China. *Science* 303, 1666–1669.
- (22) Zumla, A., Hui, D. S., and Perlman, S. (2015) Middle East respiratory syndrome. *Lancet* 386, 995–1007.
- (23) Assiri, A., Al-Tawfiq, J. A., Al-Rabeeah, A. A., Al-Rabiah, F. A., Al-Hajjar, S., Al-Barrak, A., Flemman, H., Al-Nassir, W. N., Balkhy, H. H., Al-Hakeem, R. F., Makhdoom, H. Q., Zumla, A. I., and Memish, Z. A. (2013) Epidemiological, demographic, and clinical characteristics of 47 cases of Middle East respiratory syndrome coronavirus disease from Saudi Arabia: a descriptive study. *Lancet Infect. Dis.* 13, 752–761.
- (24) Arabi, Y. M., Arifi, A. A., Balkhy, H. H., Najm, H., Aldawood, A. S., Ghabashi, A., Hawa, H., Alothman, A., Khaldi, A., and Al Raiy, B. (2014) Clinical course and outcomes of critically ill patients with Middle East respiratory syndrome coronavirus infection. *Ann. Intern. Med.* 160, 389–397.
- (25) Guery, B., Poissy, J., el Mansouf, L., Sejourne, C., Ettahar, N., Lemaire, X., Vuotto, F., Goffard, A., Behillil, S., Enouf, V., Caro, V., Mailles, A., Che, D., Manuguerra, J. C., Mathieu, D., Fontanet, A., van der Werf, S., and MERS-CoV study group. (2013) Clinical features and viral diagnosis of two cases of infection with Middle East Respiratory Syndrome coronavirus: a report of nosocomial transmission. *Lancet* 381, 2265–2272.
- (26) Memish, Z. A., Zumla, A. I., Al-Hakeem, R. F., Al-Rabeeah, A. A., and Stephens, G. M. (2013) Family cluster of Middle East respiratory syndrome coronavirus infections. *N. Engl. J. Med.* 368, 2487–2494.
- (27) Zaki, A. M., van Boheemen, S., Bestebroer, T. M., Osterhaus, A. D., and Fouchier, R. A. (2012) Isolation of a novel coronavirus from a man with pneumonia in Saudi Arabia. *N. Engl. J. Med.* 367, 1814–1820.
- (28) Al-Tawfiq, J. A., Hinedi, K., Ghandour, J., Khairalla, H., Musleh, S., Ujayli, A., and Memish, Z. A. (2014) Middle East respiratory

syndrome coronavirus: a case-control study of hospitalized patients. *Clin. Infect. Dis.* 59, 160–165.

(29) Ajlan, A. M., Ahyad, R. A., Jamjoom, L. G., Alharthy, A., and Madani, T. A. (2014) Middle East respiratory syndrome coronavirus (MERS-CoV) infection: chest CT findings. *AJR, Am. J. Roentgenol.* 203, 782–787.

(30) Faure, E., Poissy, J., Goffard, A., Fournier, C., Kipnis, E., Titecat, M., Bortolotti, P., Martinez, L., Dubucquoi, S., Dessein, R., Gosset, P., Mathieu, D., and Guery, B. (2014) Distinct immune response in two MERS-CoV-infected patients: can we go from bench to bedside? *PLoS One* 9, e88716.

(31) Min, C. K., Cheon, S., Ha, N. Y., Sohn, K. M., Kim, Y., Aigerim, A., Shin, H. M., Choi, J. Y., Inn, K. S., Kim, J. H., Moon, J. Y., Choi, M. S., Cho, N. H., and Kim, Y. S. (2016) Comparative and kinetic analysis of viral shedding and immunological responses in MERS patients representing a broad spectrum of disease severity. *Sci. Rep.* 6, 25359.

(32) van Doremalen, N., and Munster, V. J. (2015) Animal models of Middle East respiratory syndrome coronavirus infection. *Antiviral Res.* 122, 28–38.

(33) de Wit, E., Rasmussen, A. L., Falzarano, D., Bushmaker, T., Feldmann, F., Brining, D. L., Fischer, E. R., Martellaro, C., Okumura, A., Chang, J., Scott, D., Benecke, A. G., Katze, M. G., Feldmann, H., and Munster, V. J. (2013) Middle East respiratory syndrome coronavirus (MERS-CoV) causes transient lower respiratory tract infection in rhesus macaques. *Proc. Natl. Acad. Sci. U. S. A.* 110, 16598–16603.

(34) Falzarano, D., de Wit, E., Feldmann, F., Rasmussen, A. L., Okumura, A., Peng, X., Thomas, M. J., van Doremalen, N., Haddock, E., Nagy, L., LaCasse, R., Liu, T., Zhu, J., McLellan, J. S., Scott, D. P., Katze, M. G., Feldmann, H., and Munster, V. J. (2014) Infection with MERS-CoV causes lethal pneumonia in the common marmoset. *PLoS Pathog.* 10, e1004250.

(35) Menachery, V. D., Eisfeld, A. J., Schafer, A., Josset, L., Sims, A. C., Prohl, S., Fan, S., Li, C., Neumann, G., Tilton, S. C., Chang, J., Gralinski, L. E., Long, C., Green, R., Williams, C. M., Weiss, J., Matzke, M. M., Webb-Robertson, B. J., Schepmoes, A. A., Shukla, A. K., Metz, T. O., Smith, R. D., Waters, K. M., Katze, M. G., Kawaoka, Y., and Baric, R. S. (2014) Pathogenic influenza viruses and coronaviruses utilize similar and contrasting approaches to control interferon-stimulated gene responses. *mBio* 5, e01174.

(36) Selinger, C., Tisoncik-Go, J., Menachery, V. D., Agnihothram, S., Law, G. L., Chang, J., Kelly, S. M., Sova, P., Baric, R. S., and Katze, M. G. (2014) Cytokine systems approach demonstrates differences in innate and pro-inflammatory host responses between genetically distinct MERS-CoV isolates. *BMC Genomics* 15, 1161.

(37) Kindrachuk, J., Ork, B., Hart, B. J., Mazur, S., Holbrook, M. R., Frieman, M. B., Traynor, D., Johnson, R. F., Dyall, J., Kuhn, J. H., Olinger, G. G., Hensley, L. E., and Jahrling, P. B. (2015) Antiviral potential of ERK/MAPK and PI3K/AKT/mTOR signaling modulation for Middle East respiratory syndrome coronavirus infection as identified by temporal kinome analysis. *Antimicrob. Agents Chemother.* 59, 1088–1099.

(38) Josset, L., Menachery, V. D., Gralinski, L. E., Agnihothram, S., Sova, P., Carter, V. S., Yount, B. L., Graham, R. L., Baric, R. S., and Katze, M. G. (2013) Cell host response to infection with novel human coronavirus EMC predicts potential antivirals and important differences with SARS coronavirus. *mBio* 4, e00165.

(39) Hart, B. J., Dyall, J., Postnikova, E., Zhou, H., Kindrachuk, J., Johnson, R. F., Olinger, G. G., Jr., Frieman, M. B., Holbrook, M. R., Jahrling, P. B., and Hensley, L. (2014) Interferon-beta and mycophenolic acid are potent inhibitors of Middle East respiratory syndrome coronavirus in cell-based assays. *J. Gen. Virol.* 95, 571–577.

(40) Loutfy, M. R., Blatt, L. M., Siminovich, K. A., Ward, S., Wolff, B., Lho, H., Pham, D. H., Deif, H., LaMere, E. A., Chang, M., Kain, K. C., Farcas, G. A., Ferguson, P., Latchford, M., Levy, G., Dennis, J. W., Lai, E. K., and Fish, E. N. (2003) Interferon alfacon-1 plus corticosteroids in severe acute respiratory syndrome: a preliminary study. *JAMA, J. Am. Med. Assoc.* 290, 3222–3228.

(41) Hartman, A. L., Towner, J. S., and Nichol, S. T. (2010) Ebola and Marburg hemorrhagic fever. *Clin. Lab. Med.* 30, 161–177.

(42) Miranda, M. E., and Miranda, N. L. (2011) Reston ebolavirus in humans and animals in the Philippines: a review. *J. Infect. Dis.* 204 (Suppl. 3), S757–S760.

(43) Ansari, A. A. (2014) Clinical features and pathobiology of Ebolavirus infection. *J. Autoimmun.* 55, 1–9.

(44) Uyeki, T. M., Mehta, A. K., Davey, R. T., Jr., Liddell, A. M., Wolf, T., Vetter, P., Schmiedel, S., Grunewald, T., Jacobs, M., Arribas, J. R., Evans, L., Hewlett, A. L., Brantsaeter, A. B., Ippolito, G., Rapp, C., Hoepelman, A. I., Gutman, J., and Working Group of the U.S.–European Clinical Network on Clinical Management of Ebola Virus Diseases Patients in the U.S. and Europe. (2016) Clinical Management of Ebola Virus Disease in the United States and Europe. *N. Engl. J. Med.* 374, 636–646.

(45) Villinger, F., Rollin, P. E., Brar, S. S., Chikkala, N. F., Winter, J., Sundstrom, J. B., Zaki, S. R., Swanepoel, R., Ansari, A. A., and Peters, C. J. (1999) Markedly elevated levels of interferon (IFN)-gamma, IFN-alpha, interleukin (IL)-2, IL-10, and tumor necrosis factor-alpha associated with fatal Ebola virus infection. *J. Infect. Dis.* 179 (Suppl. 1), S188–S191.

(46) Baize, S., Leroy, E. M., Georges, A. J., Georges-Courbot, M. C., Capron, M., Bedjabaga, I., Lansoud-Soukate, J., and Mavoungou, E. (2002) Inflammatory responses in Ebola virus-infected patients. *Clin. Exp. Immunol.* 128, 163–168.

(47) Baize, S., Leroy, E. M., Georges-Courbot, M. C., Capron, M., Lansoud-Soukate, J., Debre, P., Fisher-Hoch, S. P., McCormick, J. B., and Georges, A. J. (1999) Defective humoral responses and extensive intravascular apoptosis are associated with fatal outcome in Ebola virus-infected patients. *Nat. Med.* 5, 423–426.

(48) Leroy, E. M., Baize, S., Debre, P., Lansoud-Soukate, J., and Mavoungou, E. (2001) Early immune responses accompanying human asymptomatic Ebola infections. *Clin. Exp. Immunol.* 124, 453–460.

(49) Leroy, E. M., Baize, S., Volchkov, V. E., Fisher-Hoch, S. P., Georges-Courbot, M. C., Lansoud-Soukate, J., Capron, M., Debre, P., McCormick, J. B., and Georges, A. J. (2000) Human asymptomatic Ebola infection and strong inflammatory response. *Lancet* 355, 2210–2215.

(50) Sanchez, A., Lukwiya, M., Bausch, D., Mahanty, S., Sanchez, A. J., Wagoner, K. D., and Rollin, P. E. (2004) Analysis of human peripheral blood samples from fatal and nonfatal cases of Ebola (Sudan) hemorrhagic fever: cellular responses, virus load, and nitric oxide levels. *J. Virol.* 78, 10370–10377.

(51) Wauquier, N., Becquart, P., Padilla, C., Baize, S., and Leroy, E. M. (2010) Human fatal zaire ebola virus infection is associated with an aberrant innate immunity and with massive lymphocyte apoptosis. *PLoS Neglected Trop. Dis.* 4, e83710.1371/journal.pntd.0000837

(52) Rubins, K. H., Hensley, L. E., Wahl-Jensen, V., Daddario DiCaprio, K. M., Young, H. A., Reed, D. S., Jahrling, P. B., Brown, P. O., Relman, D. A., and Geisbert, T. W. (2007) The temporal program of peripheral blood gene expression in the response of nonhuman primates to Ebola hemorrhagic fever. *Genome Biol.* 8, R174.

(53) Barrette, R. W., Metwally, S. A., Rowland, J. M., Xu, L., Zaki, S. R., Nichol, S. T., Rollin, P. E., Towner, J. S., Shieh, W. J., Batten, B., Sealy, T. K., Carrillo, C., Moran, K. E., Bracht, A. J., Mayr, G. A., Sirios-Cruz, M., Catbagan, D. P., Lautner, E. A., Ksiazek, T. G., White, W. R., and McIntosh, M. T. (2009) Discovery of swine as a host for the Reston ebolavirus. *Science* 325, 204–206.

(54) Nfon, C. K., Leung, A., Smith, G., Embury-Hyatt, C., Kobinger, G., and Weingartl, H. M. (2013) Immunopathogenesis of severe acute respiratory disease in Zaire ebolavirus-infected pigs. *PLoS One* 8, e61904.

(55) Wahl-Jensen, V., Kurz, S., Feldmann, F., Buehler, L. K., Kindrachuk, J., DeFilippis, V., da Silva Correia, J., Fruh, K., Kuhn, J. H., Burton, D. R., and Feldmann, H. (2011) Ebola virion attachment and entry into human macrophages profoundly effects early cellular gene expression. *PLoS Neglected Trop. Dis.* 5, e1359.

(56) Gibb, T. R., Norwood, D. A., Jr., Woollen, N., and Henchal, E. A. (2002) Viral replication and host gene expression in alveolar

macrophages infected with Ebola virus (Zaire strain). *Clin. Diagn. Lab. Immunol.* 9, 19–27.

(57) Kash, J. C., Muhlberger, E., Carter, V., Grosch, M., Perwitasari, O., Prohl, S. C., Thomas, M. J., Weber, F., Klenk, H. D., and Katze, M. G. (2006) Global suppression of the host antiviral response by Ebola- and Marburgviruses: increased antagonism of the type I interferon response is associated with enhanced virulence. *J. Virol.* 80, 3009–3020.

(58) Dunham, E. C., Banadyga, L., Groseth, A., Chiramel, A. I., Best, S. M., Ebihara, H., Feldmann, H., and Hoenen, T. (2015) Assessing the contribution of interferon antagonism to the virulence of West African Ebola viruses. *Nat. Commun.* 6, 8000.

(59) Kindrachuk, J., Wahl-Jensen, V., Safronetz, D., Trost, B., Hoenen, T., Arsenault, R., Feldmann, F., Traynor, D., Postnikova, E., Kusalik, A., Napper, S., Blaney, J. E., Feldmann, H., and Jahrling, P. B. (2014) Ebola virus modulates transforming growth factor beta signaling and cellular markers of mesenchyme-like transition in hepatocytes. *J. Virol.* 88, 9877–9892.

(60) McCollum, A. M., and Damon, I. K. (2014) Human monkeypox. *Clin. Infect. Dis.* 58, 260–267.

(61) Damon, I. K. (2011) Status of human monkeypox: clinical disease, epidemiology and research. *Vaccine* 29 (Suppl. 4), D54–D59.

(62) Likos, A. M., Sammons, S. A., Olson, V. A., Frace, A. M., Li, Y., Olsen-Rasmussen, M., Davidson, W., Galloway, R., Khristova, M. L., Reynolds, M. G., Zhao, H., Carroll, D. S., Curns, A., Formenty, P., Esposito, J. J., Regnery, R. L., and Damon, I. K. (2005) A tale of two clades: monkeypox viruses. *J. Gen. Virol.* 86, 2661–2672.

(63) Saijo, M., Ami, Y., Suzuki, Y., Nagata, N., Iwata, N., Hasegawa, H., Iizuka, I., Shiota, T., Sakai, K., Ogata, M., Fukushima, S., Mizutani, T., Sata, T., Kurata, T., Kurane, I., and Morikawa, S. (2009) Virulence and pathophysiology of the Congo Basin and West African strains of monkeypox virus in non-human primates. *J. Gen. Virol.* 90, 2266–2271.

(64) Reynolds, M. G., Yorita, K. L., Kuehnert, M. J., Davidson, W. B., Huhn, G. D., Holman, R. C., and Damon, I. K. (2006) Clinical manifestations of human monkeypox influenced by route of infection. *J. Infect. Dis.* 194, 773–780.

(65) Johnston, S. C., Johnson, J. C., Stonier, S. W., Lin, K. L., Kisalu, N. K., Hensley, L. E., and Rimoin, A. W. (2015) Cytokine modulation correlates with severity of monkeypox disease in humans. *J. Clin. Virol.* 63, 42–45.

(66) Hooper, J. W., Thompson, E., Wilhelmsen, C., Zimmerman, M., Ichou, M. A., Steffen, S. E., Schmaljohn, C. S., Schmaljohn, A. L., and Jahrling, P. B. (2004) Smallpox DNA vaccine protects nonhuman primates against lethal monkeypox. *J. Virol.* 78, 4433–4443.

(67) Kugelman, J. R., Johnston, S. C., Mulembakani, P. M., Kisalu, N., Lee, M. S., Koroleva, G., McCarthy, S. E., Gestole, M. C., Wolfe, N. D., Fair, J. N., Schneider, B. S., Wright, L. L., Huggins, J., Whitehouse, C. A., Wemakoy, E. O., Muyembe-Tamfum, J. J., Hensley, L. E., Palacios, G. F., and Rimoin, A. W. (2014) Genomic variability of monkeypox virus among humans, Democratic Republic of the Congo. *Emerging Infect. Dis.* 20, 232–239.

(68) Alkhalil, A., Hammamieh, R., Hardick, J., Ichou, M. A., Jett, M., and Ibrahim, S. (2010) Gene expression profiling of monkeypox virus-infected cells reveals novel interfaces for host-virus interactions. *Virol. J.* 7, 173.

(69) Bourquain, D., Dabrowski, P. W., and Nitsche, A. (2013) Comparison of host cell gene expression in cowpox, monkeypox or vaccinia virus-infected cells reveals viral-specific regulation of immune responses. *Virol. J.* 10, 61.

(70) Rubins, K. H., Hensley, L. E., Relman, D. A., and Brown, P. O. (2011) Stunned silence: gene expression programs in human cells infected with monkeypox or vaccinia virus. *PLoS One* 6, e15615.

(71) Kindrachuk, J., Arsenault, R., Kusalik, A., Kindrachuk, K. N., Trost, B., Napper, S., Jahrling, P. B., and Blaney, J. E. (2012) Systems kinomics demonstrates Congo Basin monkeypox virus infection selectively modulates host cell signaling responses as compared to West African monkeypox virus. *Mol. Cell. Proteomics* 11, M111.015701.

(72) Soares, J. A., Leite, F. G., Andrade, L. G., Torres, A. A., De Sousa, L. P., Barcelos, L. S., Teixeira, M. M., Ferreira, P. C., Kroon, E. G., Souto-Adron, T., and Bonjardim, C. A. (2009) Activation of the PI3K/Akt pathway early during vaccinia and cowpox virus infections is required for both host survival and viral replication. *J. Virol.* 83, 6883–6899.

(73) Biedenkopf, N., Lier, C., and Becker, S. (2016) Dynamic phosphorylation of VP30 is essential for Ebola virus life cycle. *J. Virol.* 90, 4914.

(74) Cuesta, I., Geng, X., Asenjo, A., and Villanueva, N. (2000) Structural phosphoprotein M2-1 of the human respiratory syncytial virus is an RNA binding protein. *J. Virol.* 74, 9858–9867.

(75) Saikia, P., Gopinath, M., and Shaila, M. S. (2008) Phosphorylation status of the phosphoprotein P of rinderpest virus modulates transcription and replication of the genome. *Arch. Virol.* 153, 615–626.

(76) Arsenault, R. J., Trost, B., and Kogut, M. H. (2014) A comparison of the chicken and turkey proteomes and phosphoproteomes in the development of poultry-specific immuno-metabolism kinome peptide arrays. *Front. Vet. Sci.* 1, 22.

(77) Falcinelli, S., Gowen, B. B., Trost, B., Napper, S., Kusalik, A., Johnson, R. F., Safronetz, D., Prescott, J., Wahl-Jensen, V., Jahrling, P. B., and Kindrachuk, J. (2015) Characterization of the host response to pichinde virus infection in the Syrian golden hamster by species-specific kinome analysis. *Mol. Cell. Proteomics* 14, 646–657.

(78) Trost, B., Kusalik, A., and Napper, S. (2016) Computational analysis of the predicted evolutionary conservation of human phosphorylation sites. *PLoS One* 11, e0152809.

(79) Dyall, J., Coleman, C. M., Hart, B. J., Venkataraman, T., Holbrook, M. R., Kindrachuk, J., Johnson, R. F., Olinger, G. G., Jr., Jahrling, P. B., Laidlaw, M., Johansen, L. M., Lear-Rooney, C. M., Glass, P. J., Hensley, L. E., and Frieman, M. B. (2014) Repurposing of clinically developed drugs for treatment of Middle East respiratory syndrome coronavirus infection. *Antimicrob. Agents Chemother.* 58, 4885–4893.

(80) Kolokoltsov, A. A., Saeed, M. F., Freiberg, A. N., Holbrook, M. R., and Davey, R. A. (2009) Identification of novel cellular targets for therapeutic intervention against Ebola virus infection by siRNA screening. *Drug Dev. Res.* 70, 255–265.

(81) Kolokoltsov, A. A., Adhikary, S., Garver, J., Johnson, L., Davey, R. A., and Vela, E. M. (2012) Inhibition of Lassa virus and Ebola virus infection in host cells treated with the kinase inhibitors genistein and tyrphostin. *Arch. Virol.* 157, 121–127.

(82) Garcia, M., Cooper, A., Shi, W., Bornmann, W., Carrion, R., Kalman, D., and Nabel, G. J. (2012) Productive replication of Ebola virus is regulated by the c-Abl tyrosine kinase. *Sci. Transl. Med.* 4, 123ra124.

(83) Johnson, J. C., Martinez, O., Honko, A. N., Hensley, L. E., Olinger, G. G., and Basler, C. F. (2014) Pyridinyl imidazole inhibitors of p38 MAP kinase impair viral entry and reduce cytokine induction by Zaire ebolavirus in human dendritic cells. *Antiviral Res.* 107, 102–109.

(84) Reeves, P. M., Smith, S. K., Olson, V. A., Thorne, S. H., Bornmann, W., Damon, I. K., and Kalman, D. (2011) Variola and monkeypox viruses utilize conserved mechanisms of virion motility and release that depend on abl and SRC family tyrosine kinases. *J. Virol.* 85, 21–31.

RESEARCH ARTICLE

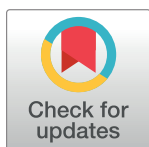
Mask adherence and rate of COVID-19 across the United States

Charlie B. Fischer[✉], Nedghie Adrien[✉], Jeremiah J. Silguero, Julianne J. Hopper, Abir I. Chowdhury, Martha M. Werler^{✉*}

Boston University School of Public Health, Boston, MA, United States of America

✉ These authors contributed equally to this work.

* werler@bu.edu



Abstract

Mask wearing has been advocated by public health officials as a way to reduce the spread of COVID-19. In the United States, policies on mask wearing have varied from state to state over the course of the pandemic. Even as more and more states encourage or even mandate mask wearing, many citizens still resist the notion. Our research examines mask wearing policy and adherence in association with COVID-19 case rates. We used state-level data on mask wearing policy for the general public and on proportion of residents who stated they always wear masks in public. For all 50 states and the District of Columbia (DC), these data were abstracted by month for April – September 2020 to measure their impact on COVID-19 rates in the subsequent month (May – October 2020). Monthly COVID-19 case rates (number of cases per capita over two weeks) >200 per 100,000 residents were considered high. Fourteen of the 15 states with no mask wearing policy for the general public through September reported a high COVID-19 rate. Of the 8 states with at least 75% mask adherence, none reported a high COVID-19 rate. States with the lowest levels of mask adherence were most likely to have high COVID-19 rates in the subsequent month, independent of mask policy or demographic factors. Mean COVID-19 rates for states with at least 75% mask adherence in the preceding month was 109.26 per 100,000 compared to 249.99 per 100,000 for those with less adherence. Our analysis suggests high adherence to mask wearing could be a key factor in reducing the spread of COVID-19. This association between high mask adherence and reduced COVID-19 rates should influence policy makers and public health officials to focus on ways to improve mask adherence across the population in order to mitigate the spread of COVID-19.

OPEN ACCESS

Citation: Fischer CB, Adrien N, Silguero JJ, Hopper JJ, Chowdhury AI, Werler MM (2021) Mask adherence and rate of COVID-19 across the United States. PLoS ONE 16(4): e0249891. <https://doi.org/10.1371/journal.pone.0249891>

Editor: Wen-Jun Tu, Chinese Academy of Medical Sciences and Peking Union Medical College, CHINA

Received: January 12, 2021

Accepted: March 26, 2021

Published: April 14, 2021

Peer Review History: PLOS recognizes the benefits of transparency in the peer review process; therefore, we enable the publication of all of the content of peer review and author responses alongside final, published articles. The editorial history of this article is available here: <https://doi.org/10.1371/journal.pone.0249891>

Copyright: © 2021 Fischer et al. This is an open access article distributed under the terms of the [Creative Commons Attribution License](https://creativecommons.org/licenses/by/4.0/), which permits unrestricted use, distribution, and reproduction in any medium, provided the original author and source are credited.

Data Availability Statement: Data are available in the paper and its [Supporting Information](#) file.

Funding: The authors received no specific funding for this work.

Introduction

The global pandemic of SARS-CoV-2 has overwhelmed health care systems, marked by peak numbers of hospital and intensive care unit admissions and deaths [1,2]. Mask wearing has been advocated by public health officials as a way to reduce the spread of COVID-19 [3–5]. In the United States, policies on mask wearing have varied from state to state over the course of the pandemic [6]. For the period of April 1 through October 31, 2020, less than half of states

Competing interests: The authors have declared that no competing interests exist.

had issued a mandate for mask wearing in public and nearly a third had not made any recommendation. Even as more and more states encourage mask wearing [7], many citizens still resist the notion [8]. Individuals' mask wearing behaviors are not only influenced by recommendations and mandates issued by state leaders, but also by print, televised, and social media [9]. Thus, adherence to mask wearing in public remains a challenge for mitigating the spread of COVID-19.

Public health policy-making requires navigating the balance of public good and individual rights [10]. The adoption of universal masking policies is increasingly polarized and politicized, demanding that public health authorities balance the values of health and individual liberty. Adherence to public policy is influenced by a complex interplay of factors such as public opinion, cultural practices, individual perceptions and behaviors [11], which are difficult to quantify. The politicization of COVID-19 epidemiology [9,12] has further complicated policy-making, messaging, and uptake. Nevertheless, adherence is essential for policy effectiveness. Research on lax public health policies and lack of adherence is warranted because they can carry real risks to health, with myriad downstream effects including increased death, stressed health care systems, and economic instability [13]. We examined the impact of state-based mask wearing policy and adherence on COVID-19 case rates during the summer and early fall of 2020 in order to quantify this effect.

Methods

For all 50 states and D.C., data on mask wearing and physical distance policies, mask adherence, COVID-19 cases, and demographics were abstracted from publicly available sources. We utilized the COVID-19 US State Policy Database, created by Dr. Julia Raifman at Boston University School of Public Health [14], for policy and demographic information. We abstracted data on whether the state issued a mandate of mask use by all individuals in public spaces, and if so, the dates of implementation and whether the mandate was enforced by fines or criminal charge/citation(s). For policies on physical distancing, we recorded whether a stay-at-home order was issued and, if so, when. For mask adherence levels, we utilized the Institute of Health Metrics and Evaluation (IHME) COVID-19 Projections online database [15], which holds data collected by Facebook Global in partnership with the University of Maryland Social Data Science Center [16]. We abstracted daily percentages of the population who say they always wear a mask in public. To calculate monthly COVID-19 case rates, we abstracted the number of new cases reported by the U.S. Centers for Disease Control and Prevention (CDC) [17] and state population sizes in 2019 [18].

Mask wearing policy

We categorized the existence of a mask policy as “None” if there was no requirement for face coverings in public spaces, “Recommended” if required in all public spaces without consequences, and “Strict” if required in all public spaces with consequences in the form of fine(s) or citation(s). We combined the Recommended and Strict groups into “Any” policy. States and D.C. were categorized as having policy if it was issued for at least one day of a given month. Although Hawaii's governor did not issue a mask wearing policy until after October 2020, we considered that state to have a policy because mayors of the four populous counties had mandated mask wearing earlier in the pandemic.

Mask wearing adherence

We calculated the average mask use percentage by month for April–September, 2020. For each month, the distributions of mask adherence across all 50 states and D.C. were categorized into

quartiles, meaning the cut-off values for each quartile may be different from one month to another. Mask adherence was classified as low if in the lowest quartile and as high if in the highest quartile. We also identified states with average mask adherence $\geq 75\%$ in a given month.

COVID-19 rates

We calculated the number of new cases in each month, for each state and D.C. Rates were the number of new cases divided by the population in 2019. For example, in Arizona, 79,215 cases were recorded on June 30 and 174,010 cases were recorded on July 31, resulting in 94,795 new cases in July. We divided the monthly number by 2.2 to obtain the number in a two-week period (43,088). The 2-week rate in July in Arizona = 43,088 cases/7,278,717 population in 2019 = 0.00592 or 592 per 100,000. We classified a state and D.C. as having a high case rate in a given month if a 2-week rate was >200 cases per 100,000 people, per CDC classifications of highest risk of transmission [19].

Covariates

Based on CDC at-risk guidelines for COVID-19 [20], we considered non-Hispanic Black, Hispanic, age, and population density as potential confounders. Data on population distributions from the COVID-19 US State Policy Database [13] came from the US Census. For demographic data, we dichotomized population proportions at whole values that approximated the highest quartile of the distributions. Specifically, we created the following categories: $>15\%$ non-Hispanic Black, $>15\%$ Hispanic, median age >40 years, and population density >200 people per square mile, which corresponded to 74.5%, 78.4%, 82.4%, and 78.4% of the distributions, respectively. Policy data on physical distancing were dichotomized as any versus no stay-at-home order during the April 1 to October 31, 2020 interval.

Statistical analysis

Our analyses took into consideration the delayed effect of mask wearing and policies on COVID-19 health outcomes. Thus, policy and adherence levels in a given month were contrasted with lagged COVID-19 case rates in the subsequent month. Both mask policy and mask adherence for states and D.C. were cross-tabulated with high case rates in the subsequent month. Logistic regression models were used to estimate the odds ratio and 95% confidence intervals for high case rates in the subsequent month associated with average mask adherence (as a continuous variable). Models were unadjusted, adjusted for no mask policy (Model 1), and adjusted for no mask policy in previous month, no stay-home order, $>15\%$ population non-Hispanic Black, $>15\%$ population Hispanic, median age >40 years, population density >200 /square mile (Model 2).

Results and discussion

States in COVID-19 high-risk categories are listed in Table 1. Because stay-at-home order, mask wearing policy, mask adherence, and COVID-19 rates can vary from month to month, we listed those states with consistent classifications across the period April through September (or May through October for COVID-19 rates). Eleven states had no stay-at-home order, 15 had no mask policy, and four states had low adherence throughout this six-month period.

The list of states with high COVID-19 rates by month shows the initial wave in northeastern states in May, followed by a wave in southern states, and then spreading across the U.S. over the next four months (Table 2). Of the 15 states with no mask policy from April through

Table 1. States with high COVID-19 population risk characteristics.

High risk category	States
>15% non-Hispanic Black	AL, AR, DC, DE, FL, GA, HI, LA, MD, MS, NC, SC, TN, VA
>15% Hispanic	AZ, CA, CO, CT, FL, IL, NJ, NM, NV, NY, RI, TX
Median age >40 years	CT, DE, FL, ME, MT, NH, NJ, PA, RI, VT, WV
Pop. density > 200/mile ²	CA, CT, DC, DE, FL, HI, MA, MD, NH, NY, OH, PA, RI
No stay at home order	AR, CT, IA, KY, ND, NE, OK, SD, TX, UT, WY
No mask policy Apr-Sep	AZ, FL, GA, IA, ID, MO, MT, ND, NE, NH, OK, SC, SD, TN, WY
<25%ile mask adherence Apr-Sep	IA, KS, ND, SD

<https://doi.org/10.1371/journal.pone.0249891.t001>

September, 14 reported high COVID-19 rates in at least one month from May to October. Because high COVID rates were reported by only eight states in May and four states in June, we did not examine mask adherence or policy in the preceding April or May. Thus, subsequent comparisons of states with high COVID-19 rates by month focused on July, August, September and October. Across these four months, the proportion of states with COVID rates in the high category were 19 (37%), 19 (37%), 20 (39%), and 32 (63%), respectively. Eight states were reported to have at least 75% mask adherence in any month between June and September (AZ, CT, HI, MA, NY, RI, VT, VA); none reported a high COVID-19 rate in the subsequent month.

For mask adherence, the cut-off values for the low and high quartiles were 31% and 46% in June, 53% and 72% in July, 55% and 71% in August, and 55% and 68% in September. The proportions of states with high COVID-19 rates are shown for those in the low and high quartiles of mask adherence in the preceding month (Fig 1). Most states in the low quartile had high COVID-19 rates in the subsequent month. Indeed all 13 states in the low mask adherence group in September had high COVID-19 rates in October. In contrast, just one state in July, August, and September and three in October in the high quartile had high COVID-19 rates in the subsequent month. When we looked at states with $\geq 75\%$ mask adherence (Arizona, Connecticut, Hawaii, Massachusetts, Michigan, New York, Rhode Island, Vermont), we found none had experienced a high COVID-19 rate in the subsequent month. Mean COVID-19 rates for states with $\geq 75\%$ mask adherence in the preceding month was 109.26 per 100,000 compared to 249.99 per 100,000 for those with less adherence.

The proportions of states and D.C. with high COVID-19 rates were greatest for those with no mask wearing policy for the general public in the preceding month (Fig 2). Among states and D.C. with no mask wearing policy, 50 to 73% had high COVID-19 rates in the subsequent month. In contrast, 25% or fewer states with a mask wearing policy had high COVID-19 rates,

Table 2. States with high COVID-19 rates.

COVID-19 >200 cases /100,000	States
May	DC, DE, IL, MA, MD, NE, NJ, RI
June	AR, AZ, FL, SC
July	AL, AR, AZ, CA, FL, GA, ID, IA, KS, LA, MO, MS, NC, NV, OK, SC, TN, TX, UT
August	AL, AR, CA, FL, GA, ID, IA, IL, KS, LA, MO, MS, ND, NV, OK, SC, SD, TN, TX
September	AL, AR, GA, ID, IA, IL, KS, KY, MO, MS, MT, NE, ND, OK, SC, SD, TN, TX, UT, WI
October	AL, AK, AR, CO, DE, ID, IA, IL, IN, KS, KY, MI, MN, MO, MS, MT, NC, NE, ND, NM, NV, OH, OK, RI, SC, SD, TN, TX, UT, WI, WV, WY
Jul, Aug, Sep or Oct and no mask policy Jun-Sep	AZ, FL, GA, IA, ID, MO, MT, ND, NH, OK, SC, SD, TN, WY

<https://doi.org/10.1371/journal.pone.0249891.t002>

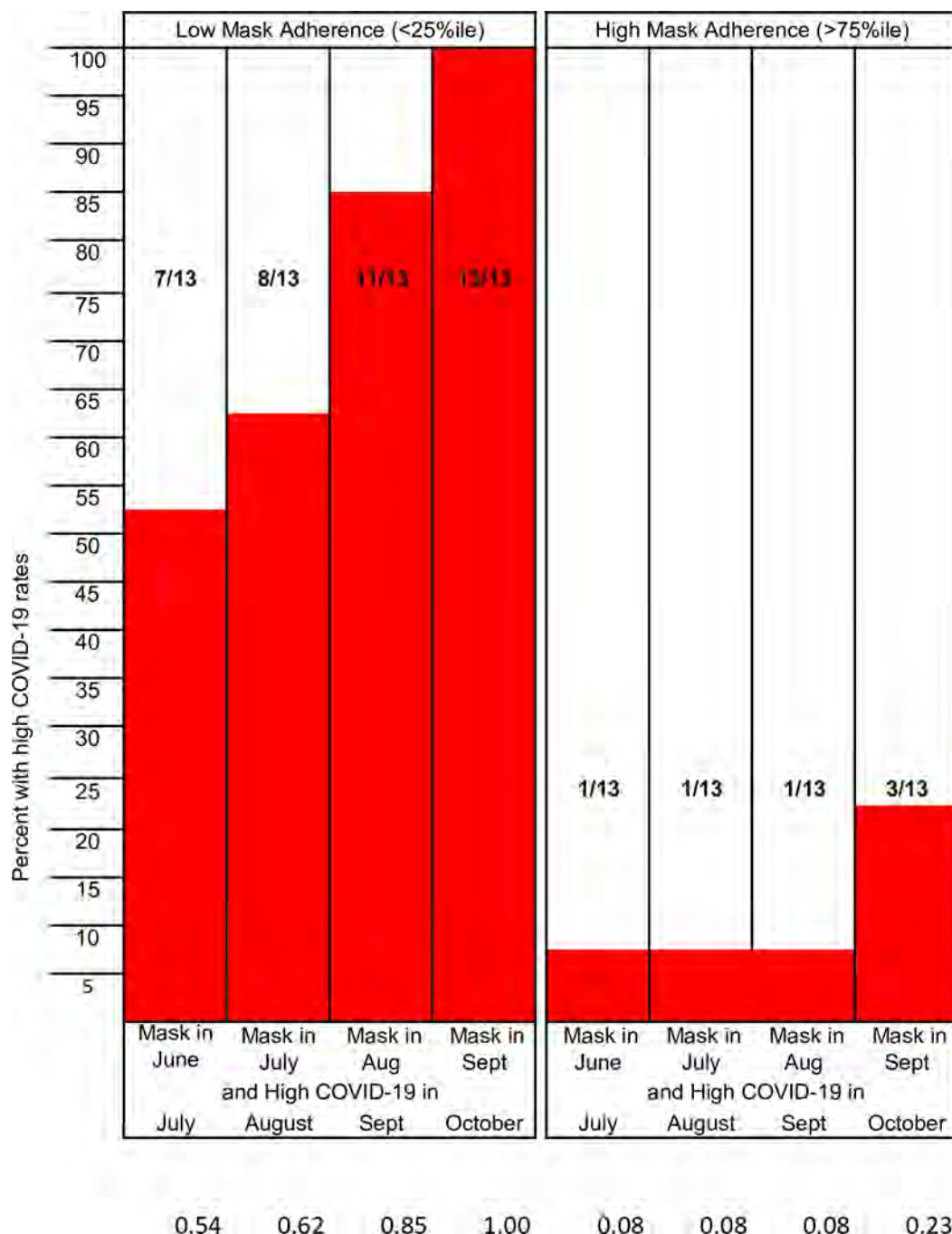


Fig 1. Proportion of states with high COVID-19 rates among those in the low and high mask adherence quartiles in the preceding month.

<https://doi.org/10.1371/journal.pone.0249891.g001>

except in September when over half experienced high rates. Fourteen of the 15 states with no mask wearing policy for the general public for the entire four month period (June through September) reported a high COVID-19 rate. High COVID-rates were less frequent in states and D.C. with strict mask wearing policy than in states with recommended policy.

Looking more closely at October when COVID-19 rates increased across the US, we found average adherence was only 47% in September for the 11 states without a mask policy and high

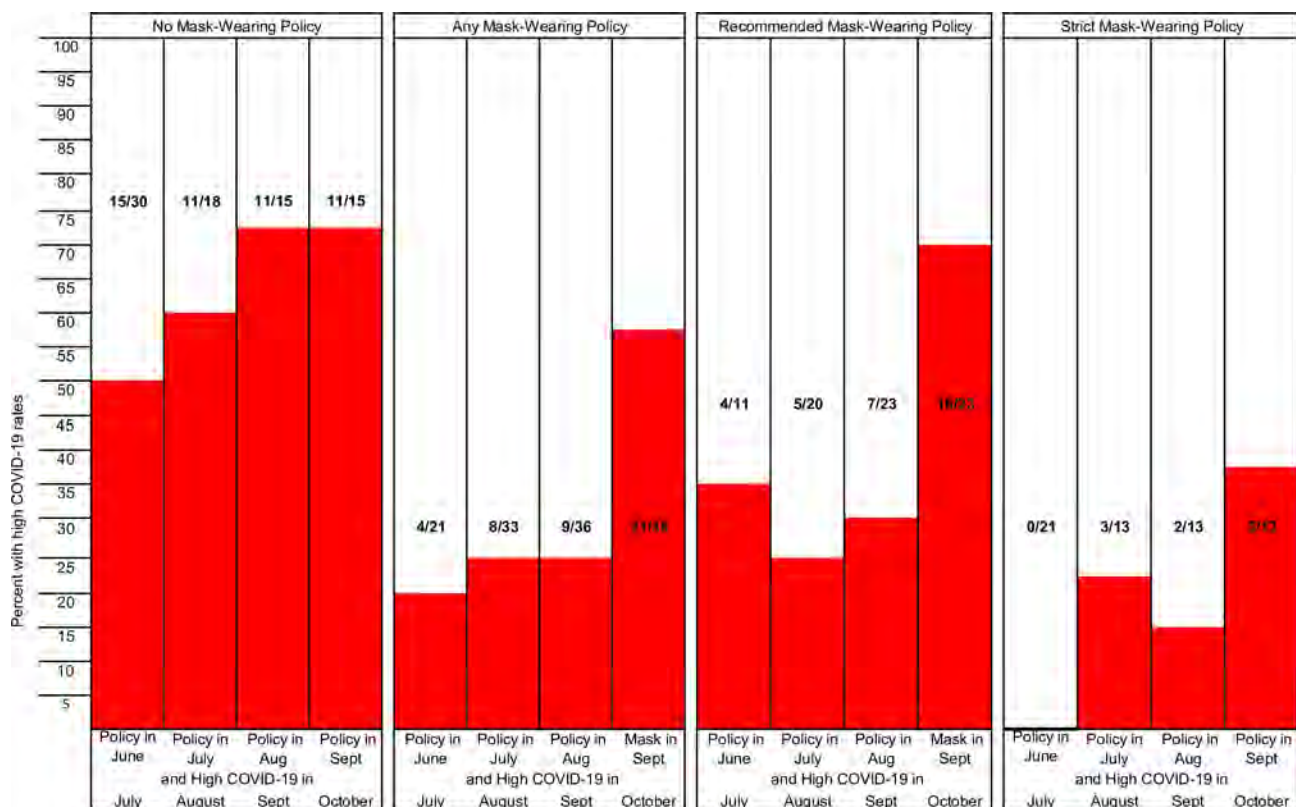


Fig 2. Proportion of states with high COVID-19 rates among those no, any, strict, and recommended mask wearing policy in the preceding month.

<https://doi.org/10.1371/journal.pone.0249891.g002>

October COVID-19 rates. In contrast, average adherence was 68% in the 15 states with lower COVID-19 rates in October and any mask policy in September. Of note, there were no states with $\geq 75\%$ in September.

Odds ratios and 95% confidence intervals for average mask adherence and mask policy for the general public are associated with high COVID-19 rates in the subsequent month (Table 3). Mask adherence was associated with lower odds of high COVID-19 rates, even after

Table 3. State-level odds ratios and 95% confidence intervals (CI) for high versus lower COVID-19 rates in the subsequent month.

		Unadjusted			Model 1*			Model 2**		
		OR	95% CI		OR	95% CI		OR	95% CI	
June	Mask adherence, avg	0.91	0.85,	0.98	0.93	0.86,	1.00	0.95	0.83,	1.08
	Any mask policy	0.24	0.06,	0.87	0.42	0.10,	1.78	0.19	0.03,	1.41
July	Mask adherence, avg	0.91	0.86,	0.97	0.93	0.87,	0.99	0.87	0.77,	0.99
	Any mask policy	0.20	0.06,	0.70	0.41	0.10,	1.70	0.22	0.03,	1.63
August	Mask adherence, avg	0.88	0.81,	0.95	0.90	0.83,	0.98	0.94	0.85,	1.03
	Any mask policy	0.12	0.03,	0.48	0.23	0.05,	1.18	0.21	0.03,	1.57
September	Mask adherence, avg	0.81	0.72,	0.92	0.78	0.68,	0.90	0.74	0.59,	0.93
	Any mask policy	0.41	0.11,	1.52	3.52	0.49,	25.41	6.28	0.61,	64.85

*Model 1, includes average mask adherence and any mask policy.

** Model 2, includes Model 1 and adjusted for no stay-home order, >15% population non-Hispanic Black, >15% population Hispanic, median age >40 years, population density > 200/mile².

<https://doi.org/10.1371/journal.pone.0249891.t003>

adjustment for mask policy and for demographic factors. For every 1% increase in average adherence in June, the fully adjusted odds ratios for high COVID-19 in July was 0.95, indicating a protective effect against high COVID-19 rates. Similar reductions in odds of high COVID-19 rates in August and September were observed for July and August mask adherence, respectively. The strongest association was for mask adherence in September; for every 1% increase in average adherence, the odds of a high COVID-19 case rate decreased by 26%.

Crude and adjusted odds ratios for any mask policy in relation to high COVID-19 rates in the subsequent month were below 1.0; but confidence intervals were wide. For mask policy and adherence in September in relation to high COVID-19 rates in October, collinearity caused the odds ratio to flip.

We were not able to measure statistical interactions between mask policy and adherence due to instability arising from small numbers. We did estimate odds ratios for mask adherence within subgroups of states with and without mask policy. Odds ratios indicating protection against high COVID-19 rates remained for all months and policy subgroups, ranging from 0.82 to 0.93 for states with any policy and from 0.60 to 0.95 for states with no policy.

Interpretation

We show supporting evidence for reducing the spread of COVID-19 through mask wearing. This protective effect of mask wearing was evident across four months of the pandemic, even after adjusting the associations for mask policy, distance policy, and demographic factors. We observed some benefit of mask policy on COVID-19 rates, but the findings were unstable. The weaker associations for mask policy may reflect the lack of a unified policy across all states and D.C. and the inconsistent messaging by the media and government leaders. Indeed, issuing such a policy is not the same as successfully implementing it. Our observed associations should influence policy-makers and contribute to public health messaging by government officials and the media that mask wearing is a key component of COVID-19 mitigation.

Our observation that states with mask adherence by $\geq 75\%$ of the population was associated with lower COVID-19 rates in the subsequent month suggests that states should strive to meet this threshold. The difference in mean COVID-19 rates between states with $\geq 75\%$ and $< 75\%$ mask adherence was 140 cases per 100,000. It is worth noting that no states achieved this level of mask adherence in September, which might account in part for the spike in COVID-19 rates in October. Of course, many other factors could be at play, like the possibility of cooler weather driving non-adherent persons to indoor gatherings.

Our study accounted for temporality by staggering COVID-19 outcome data after adherence measures. Nevertheless, it is possible that average mask adherence in a given month does not capture the most effective time period that influences COVID-19 rates. For example, mask wearing in the two weeks before rates begin to rise might be a more sensitive way to measure the association. If this is true, we would expect associations between mask adherence and high COVID-19 rates to be even stronger. It is also possible that survey respondents misreported their mask wearing adherence; whether they would be more or less likely to over or under-report is open to speculation, but residents in states with mask wearing policy might over-report adherence to appear compliant. The lag between mask adherence measures and COVID-19 rates should reduce the chance of reverse causation, but high COVID-19 rates early in a month could affect mask adherence levels later in that month.

It is important to note that state level distributions of demographic factors do not account for concentrations or sparsity of populations within a given state. Further, our adjustment for demographic factors at the state population level may not represent the true underlying forces that put individuals at greater risk of contracting COVID-19. Though demographic factors

were measured as proportions of the population, even if they were considered to be indicators for individual level characteristics, they do not denote an inherent biologic association with the outcome and more likely reflect structural inequities that lead to higher rates of infection in minoritized populations. Another consideration is that access to COVID-19 testing appears to vary from state to state [21]. Our study was also limited by the lack of information on accessibility of COVID-19 testing; if less accessible testing is associated with less mask adherence, the associations we report here may be under-estimates.

Our analysis of state and D.C.-level data does not account for variations in policy, adherence, and demographic factors at smaller geographic levels, such as county-levels. Further analyses of more granular geographic regions would be a logical next step. Indeed, associations between mask policy, adherence and other factors may be obscured in states with many high density and low density areas.

Conclusions

In conclusion, we show that mask wearing adherence, regardless of mask wearing policy, may curb the spread of COVID-19 infections. We recommend renewed efforts be employed to improve adherence to mask wearing.

Supporting information

S1 File.
(CSV)

Acknowledgments

We thank Dr. Julia Raifman Boston University School of Public Health for developing, maintaining, and providing open access to the COVID-19 US State Policy Database. We thank Drs. Eleanor J. Murray and Jennifer Weuve and the Boston University School of Public Health Epidemiology COVID-19 Response Corps for bringing together students and faculty for this project.

Author Contributions

Conceptualization: Charlie B. Fischer, Jeremiah J. Silguero, Julianne J. Hopper, Abir I. Chowdhury, Martha M. Werler.

Data curation: Charlie B. Fischer, Jeremiah J. Silguero, Julianne J. Hopper, Abir I. Chowdhury.

Formal analysis: Martha M. Werler.

Investigation: Charlie B. Fischer, Nedghie Adrien, Jeremiah J. Silguero, Julianne J. Hopper, Abir I. Chowdhury, Martha M. Werler.

Methodology: Charlie B. Fischer, Nedghie Adrien, Jeremiah J. Silguero, Julianne J. Hopper, Abir I. Chowdhury, Martha M. Werler.

Visualization: Charlie B. Fischer, Jeremiah J. Silguero, Julianne J. Hopper, Abir I. Chowdhury, Martha M. Werler.

Writing – original draft: Charlie B. Fischer, Jeremiah J. Silguero, Julianne J. Hopper, Abir I. Chowdhury, Martha M. Werler.

Writing – review & editing: Charlie B. Fischer, Nedghie Adrien, Jeremiah J. Silguero, Julianne J. Hopper, Abir I. Chowdhury.

References

- Centers for Disease Control and Prevention. Covid data tracker. <https://covid.cdc.gov/covid-data-tracker/#new-hospital-admissions>, accessed March 18, 2021.
- Cao J, T W-J, Cheng W, Yu L, Liu Y-K, Hu X, et al. Clinical Features and Short-term Outcomes of 102 Patients with Corona Virus Disease 2019 in Wuhan, China. *Clinical Infectious Diseases*, 71(15):748–755. <https://doi.org/10.1093/cid/ciaa243> PMID: 32239127
- Lerner AM, Folders GK, Fauci AS. Preventing the spread of SARS-CoV-2 with masks and other “low-tech” interventions. *Journal of American Medical Association*. 2020; 324: 1935–36. <https://doi.org/10.1001/jama.2020.21946> PMID: 33104157
- Leung CC, Cheng KK, Lam TH, Migliori GB. Mask wearing to complement social distancing and saving lives during COVID-19. *Int J Tuberc Lung Dis*. 2020; 24:556–58. <https://doi.org/10.5588/ijtld.20.0244> PMID: 32553007
- Centers for Disease Control and Prevention. Scientific brief: community use of cloth masks to control the spread of SARS-CoV-2. <https://www.cdc.gov/coronavirus/2019-ncov/more/masking-science-sars-cov2.html>, accessed December 28, 2020.
- Lyu W, Wehby GL. Community use of face masks and COVID-19: Evidence from a natural experiment of state mandates in the US. *Health Aff (Millwood)*. 2020; 39: 1419–25. <https://doi.org/10.1377/hlthaff.2020.00818> PMID: 32543923
- Hubbard K. These states have COVID-19 mask mandates. *US News & World Report*; Dec. 2, 2020. <https://www.usnews.com/news/best-states/articles/these-are-the-states-with-mask-mandates>, accessed December 28, 2020.
- Kasting ML, Head KJ, Hartsock JA, Sturm L, Zimet GD. Public perceptions of the effectiveness of recommended non-pharmaceutical intervention behaviors to mitigate the spread of SARS-CoV-2. *PLoS One*. 2020 Nov 4; 15(11):e0241662. <https://doi.org/10.1371/journal.pone.0241662> PMID: 33147261
- Havey N.F. Partisan public health: how does political ideology influence support for COVID-19 related misinformation?. *J Comput Soc Sc* 3, 319–342 (2020). <https://doi.org/10.1007/s42001-020-00089-2> PMID: 33163686
- Chia T, Oyeniran OI. Human health versus human rights: an emerging ethical dilemma arising from coronavirus disease pandemic. *Ethics Med Public Health*. 2020; 14: 100511. <https://doi.org/10.1016/j.jemep.2020.100511> PMID: 32292811
- Al-Hasan A, Yim D, Khuntia J. Citizens' adherence to COVID-19 mitigation recommendations by the government: a 3-country comparative evaluation using web-based cross-sectional survey data. *J Med Internet Res*. 2020; 22:e20634. <https://doi.org/10.2196/20634> PMID: 32716896
- Jefferson T, Heneghan C. Masking lack of evidence with politics. *Center for Evidence-Based Medicine*. <https://www.cebm.net/covid-19/masking-lack-of-evidence-with-politics/>.
- Rothert J, Brady R, Insler M. The Fragmented United States of America: The impact of scattered lockdown policies on country-wide infections. *Covid Economics* 2020; 43: 42–94. <https://cepr.org/sites/default/files/CovidEconomics43.pdf>.
- Raifman J, Nocka K, Jones D, Bor J, Lipson S, Jay J, et al. COVID-19 US state policy database. 2020. Available at: www.tinyurl.com/statepolicies, accessed December 28, 2020.
- The Institute for Health Metrics and Evaluation (IHME). <https://covid19.healthdata.org/united-states-of-america?view=mask-use&tab=trend>, accessed December 28, 2020.
- Kreuter F, Barkay N, Bilinski A, Bradford A, Chiu S, Eliat R, et al. Partnering with a global platform to inform research and public policy making. *Survey Research Methods* 2020; 14(2). <https://doi.org/10.18148/srm/2020.v14i2.7761>.
- Centers for Disease Control and Prevention. United States COVID-19 Cases and Deaths by State over Time [Data Set]. Retrieved from <https://data.cdc.gov/Case-Surveillance/United-States-COVID-19-Cases-and-Deaths-by-State-o/9mfq-cb36/data>, accessed December 28, 2020.
- USDA Economic Research Service. (2020). Population estimates for the U.S., States, and counties, 2010–19 [Data Set]. Retrieved from <https://www.ers.usda.gov/data-products/county-level-data-sets/download-data/>, accessed December 28, 2020.
- Centers for Disease Control and Prevention. CDC indicators and thresholds for risk of introduction and transmission of COVID-19 in schools. <https://www.cdc.gov/coronavirus/2019-ncov/community/schools-childcare/indicators.html#thresholds>, accessed December 28, 2020.

20. Centers for Disease Control and Prevention. COVID-19. People at increased risk. https://www.cdc.gov/coronavirus/2019-ncov/need-extra-precautions/index.html?CDC_AA_refVal=https%3A%2F%2Fwww.cdc.gov%2Fcoronavirus%2F2019-ncov%2Fneed-extra-precautions%2Fpeople-at-increased-risk.html, accessed December 28, 2020.
21. Rader B, Astley CM, Sy KTL, Kraemer MUG. Geographic access to United States SARS-CoV-2 testing sites highlights healthcare disparities and may bias transmission estimates. *J Travel Medicine*; 2020; 27(7), October 2020, taaa076, <https://doi.org/10.1093/jtm/taaa076> PMID: 32412064

Estimating the effects of non-pharmaceutical interventions on COVID-19 in Europe

<https://doi.org/10.1038/s41586-020-2405-7>

Received: 30 March 2020

Accepted: 22 May 2020

Published online: 8 June 2020

 Check for updates

Seth Flaxman^{1,7}, Swapnil Mishra^{2,7}, Axel Gandy^{1,7}, H. Juliette T. Unwin², Thomas A. Mellan², Helen Coupland², Charles Whittaker², Harrison Zhu¹, Tresnia Berah¹, Jeffrey W. Eaton², Mélodie Monod¹, Imperial College COVID-19 Response Team*, Azra C. Ghani², Christl A. Donnelly^{2,3}, Steven Riley², Michaela A. C. Vollmer², Neil M. Ferguson², Lucy C. Okell² & Samir Bhatt^{2,7}✉

Following the detection of the new coronavirus¹ severe acute respiratory syndrome coronavirus 2 (SARS-CoV-2) and its spread outside of China, Europe has experienced large epidemics of coronavirus disease 2019 (COVID-19). In response, many European countries have implemented non-pharmaceutical interventions, such as the closure of schools and national lockdowns. Here we study the effect of major interventions across 11 European countries for the period from the start of the COVID-19 epidemics in February 2020 until 4 May 2020, when lockdowns started to be lifted. Our model calculates backwards from observed deaths to estimate transmission that occurred several weeks previously, allowing for the time lag between infection and death. We use partial pooling of information between countries, with both individual and shared effects on the time-varying reproduction number (R_t). Pooling allows for more information to be used, helps to overcome idiosyncrasies in the data and enables more-timely estimates. Our model relies on fixed estimates of some epidemiological parameters (such as the infection fatality rate), does not include importation or subnational variation and assumes that changes in R_t are an immediate response to interventions rather than gradual changes in behaviour. Amidst the ongoing pandemic, we rely on death data that are incomplete, show systematic biases in reporting and are subject to future consolidation. We estimate that—for all of the countries we consider here—current interventions have been sufficient to drive R_t below 1 (probability $R_t < 1.0$ is greater than 99%) and achieve control of the epidemic. We estimate that across all 11 countries combined, between 12 and 15 million individuals were infected with SARS-CoV-2 up to 4 May 2020, representing between 3.2% and 4.0% of the population. Our results show that major non-pharmaceutical interventions—and lockdowns in particular—have had a large effect on reducing transmission. Continued intervention should be considered to keep transmission of SARS-CoV-2 under control.

Following the identification of the new coronavirus SARS-CoV-2 in Wuhan (China) in December 2019 and its global spread, large epidemics of COVID-19 have ensued in Europe. In response to the rising numbers of cases and deaths and to preserve health systems, European countries—as with those in Asia—have implemented measures to control their epidemics. These large-scale non-pharmaceutical interventions vary between countries, but include social distancing (such as banning large gatherings), border closures, school closures, measures to isolate symptomatic individuals and their contacts, and large-scale lockdowns of populations with all but essential internal travel banned. Understanding whether these interventions have had the desired effect of controlling

the epidemic, and which interventions are necessary to maintain control, is critical given their large economic and social costs. The key aim of these interventions is to reduce R_t , a fundamental epidemiological quantity that represents the average number of infections generated at time t by each infected case over the course of their infection.

In China, strict movement restrictions and other measures (including case isolation and quarantine) began to be introduced from 23 January 2020, which achieved a downward trend in the number of confirmed new cases during February and resulted in zero new confirmed indigenous cases in Wuhan by 19 March 2020. Studies have estimated how the values of R_t changed during this time in different

¹Department of Mathematics, Imperial College London, London, UK. ²MRC Centre for Global Infectious Disease Analysis, Jameel Institute for Disease and Emergency Analytics, Imperial College London, London, UK. ³Department of Statistics, University of Oxford, Oxford, UK. ⁷These authors contributed equally: Seth Flaxman, Swapnil Mishra, Axel Gandy, Samir Bhatt. *A list of members and their affiliations appears at the end of the paper. ✉e-mail: s.bhatt@imperial.ac.uk

Article

areas of China, from around 2–4 during the uncontrolled epidemic to below 1 (refs. ^{1,2}).

Estimating R_t for SARS-CoV-2 presents challenges, owing to the high proportion of infections that are not detected by health systems^{1,3,4} and to the regular changes in testing policies, which resulted in different proportions of infections being detected over time and between countries. Initially, most countries had the capacity to test only a small proportion of suspected cases and reserved tests for severely ill patients or for high-risk groups (for example, the contacts of positively tested individuals).

An alternative way to estimate the course of the epidemic is to calculate backwards from observed deaths to the number of infections. We introduce a Bayesian mechanistic model linking the infection cycle to observed deaths, inferring the total population infected (attack rates) as well as R_t . We assess whether there is evidence that interventions have so far been successful at reducing R_t to values below 1. We simulate a hypothetical counterfactual scenario in which R_t remains at starting levels to estimate the deaths that would have occurred without interventions.

Reported deaths are likely to be far more reliable than case data—although reported death data still have limitations. First, early deaths attributable to COVID-19 may have been missed. Second, there is variation in the reporting of deaths by country and over time. Third, reporting delays are expected and can be both systematic and random in nature. We attempt to overcome these data limitations by using a consolidated data source, incorporating noise in our observational model, partially pooling of information between countries and performing a sensitivity analysis under scenarios of underreporting to test our conclusions (Supplementary Information).

Our model relies on fixed estimates of some epidemiological parameters, such as the onset-to-death distribution, the infection fatality rate and the generation distribution, that are based on previous work^{5,6}; we perform a sensitivity analysis on these parameters. Our parametric form of R_t assumes that changes in R_t are an immediate response to interventions rather than gradual changes in behaviour, and it does not include importation or subnational variation. We assume that individual interventions have a similar effect in different countries, and that the efficacy of these interventions remains constant over time. Our framework infers R_t from mortality data, while accounting for time lags since infections occurred. As a result, even with perfect data and partial pooling, we cannot perfectly predict the current value of R_t . However, the credible intervals on R_t show the self-consistent behaviour that is a hallmark of a fully Bayesian analysis throughout the entire period we study, exhibiting appropriate shrinkage as more data become available (Supplementary Videos 1–3).

Italy was the first European country to begin major non-pharmaceutical interventions, and other countries followed soon afterwards (Extended Data Fig. 4). The onset of interventions ranged between 2 March and 29 March 2020. We analysed data on mortality from COVID-19 in 11 European countries until 4 May 2020, at which point lockdowns were relaxed in Italy and Spain. For each country, we model the number of infections, the number of deaths and R_t (Fig. 1). R_t is modelled as a piecewise constant function that changes only when an intervention occurs. Each country has its own individual starting R_t before interventions took place. For all countries, interventions are assumed to have the same relative effect on R_t and are informed by mortality data across all countries. The only exception is that we use partial pooling to introduce country-specific effects of the effectiveness of the last intervention introduced in the study period in a country (which is usually lockdown).

Estimated infections, R_t and effect sizes

In all countries, we estimate there are orders-of-magnitude fewer infections detected (Fig. 1, Extended Data Figs. 1, 2) than true infections, most

likely owing to mild and asymptomatic infections as well as limited testing capacities and changes in testing policy. In Italy, our results suggest that—cumulatively—2.8 (2.2–3.5) million people (all parenthetical ranges refer to 95% credible intervals) have been infected as of 4 May 2020, which gives an attack rate of 4.6% (3.6–5.8%) of the population (Table 1). In Spain (which has also experienced a large number of deaths), we estimate that 5.5% of the population (2.6 (2.1–3.3) million people) have been infected to date. Germany, the most populous country in our study, is estimated to have one of the lowest attack rates at 0.85% with 710,000 (550,000–930,000) people infected. Belgium has the highest estimated attack rates of 8%, followed by Spain with 5.5%. Although there have been few reliable national serological studies⁷, initial small-scale surveys in Austria⁸ and Denmark⁹ closely align with our estimates. A much larger study in Spain is very closely aligned with our estimates¹⁰. To some extent, these initial results validate our choice of infection fatality rate.

Averaged across all countries, we estimate the initial R_t to be 3.8 (2.4–5.6), consistent with previous analyses¹¹. These estimates are informed by our choice of generation-interval distribution and the initial growth rate of observed deaths. A shorter assumed generation time results in lower starting R_t (Supplementary Discussion 3). The initial values of R_t are also uncertain, owing to (a) importation (rather than local transmission) being the dominant source of new infections in the early period of the epidemic and (b) possible under-ascertainment in deaths, particularly before testing became widespread. We perform sensitivity analyses around these parameters (Supplementary Discussions 10, 11).

We estimate large reductions in R_t in response to the combined non-pharmaceutical interventions. Our results—which are driven more by countries with advanced epidemics and larger numbers of deaths—suggest that these interventions have together had a substantial effect on transmission, as measured by changes in the estimated R_t . At the time of this study, we find current estimates of R_t to range from a posterior mean of 0.44 (0.26–0.61) for Norway to a posterior mean of 0.82 (0.73–0.93) for Belgium, with an average of 0.66 across the 11 countries—an 82% reduction compared to the pre-intervention values. For all countries, we find that current interventions have been sufficient to drive R_t below 1 (probability $R_t < 1.0$ is greater than 99% across all countries we consider) and achieve control of the epidemic. These conclusions are corroborated by studies from individual countries—France¹², Spain¹³, Germany¹⁴ and the UK¹⁵—over a similar period, which arrive at very similar estimates despite different methodologies and data. For example, a previous study¹² estimates an R_t of 0.67 for France using hospitalization records (we estimate 0.68); for Germany, the Robert Koch Institute reports R_t of 0.76 using electronically notified cases¹⁴ (we estimate 0.71). The retrospective stability of our model (Supplementary Videos 1–3) is variable when the implementations of interventions are very dissimilar; an example of this is seen in Sweden, where interventions were dissimilar to other countries and led initially to large uncertainty. Our model uncertainty is also dependent on the magnitude of R_t ; this occurs because infections are a nonlinear function of R_t and are sensitive to small increases. Uncertainty shrinks greatly when R_t is reduced. Examples of this effect are seen in all countries, but it is most pronounced in Belgium and France; these countries show large uncertainties in the number of infections in the early period of the epidemic. Our choice of parameterizing R_t using piecewise constant functions means that we cannot capture the fine-scale variation that could be achieved by using additional covariates.

Lockdown has an identifiable large effect on transmission (81% (75–87%) reduction) (Fig. 2). The close spacing of interventions in time (Extended Data Fig. 4) means that the individual effects of the other interventions are not identifiable (Fig. 2). Our partial pooling model requires only one country to provide a signal for the effect of a given intervention, and this effect is then shared across all countries. Although this sharing can potentially lead to initial over- or under-estimation of the effect of an intervention, it also means that a

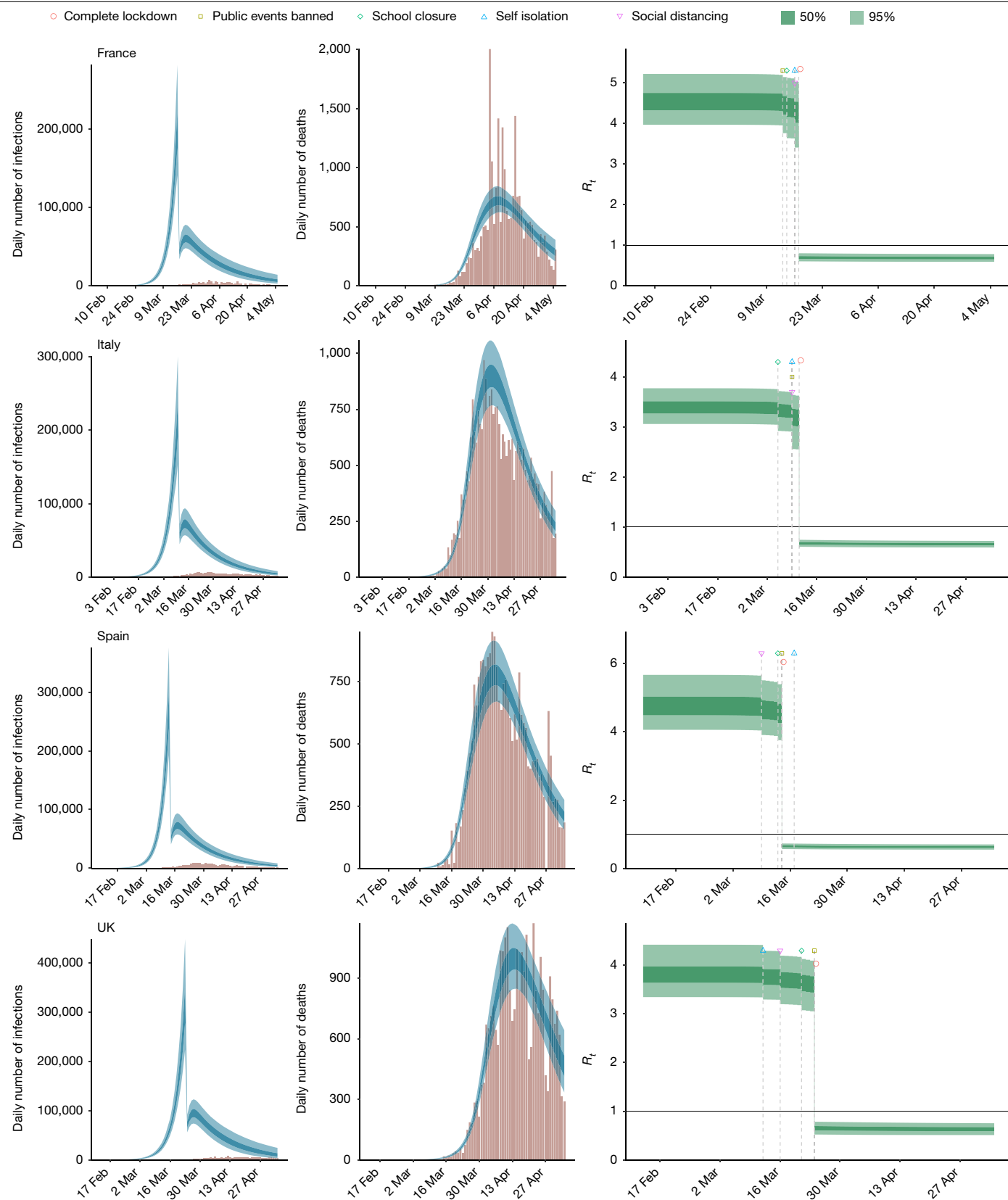


Fig. 1 | Country-level estimates of infections, deaths and R_t for France, Italy, Spain and the UK. Left, daily number of infections. Brown bars are reported infections; blue bands are predicted infections; dark blue, 50% credible interval; light blue 95% credible interval. The number of daily infections estimated by our model drops immediately after an intervention, as we assume that all infected people become immediately less infectious through the

intervention. Afterwards, if R_t is above 1, the number of infections will start growing again. Middle, daily number of deaths. Brown bars are reported deaths; blue bands are predicted deaths; credible intervals are as in the left plot. Right, R_t . Dark green, 50% credible interval; light green, 95% credible interval. Icons are interventions, shown at the time at which they occurred.

Table 1 | Total population infected by country

Country	Percentage of total population infected (mean (95% credible interval))
Austria	0.76% (0.59–0.98%)
Belgium	8% (6.1–11%)
Denmark	1.0% (0.81–1.4%)
France	3.4% (2.7–4.3%)
Germany	0.85% (0.66–1.1%)
Italy	4.6% (3.6–5.8%)
Norway	0.46% (0.34–0.61%)
Spain	5.5% (4.4–7.0%)
Sweden	3.7% (2.8–5.1%)
Switzerland	1.9% (1.5–2.4%)
UK	5.1% (4.0–6.5%)

Posterior model estimates of the attack rate by country (percentage of total population infected) as of 4 May 2020. Results are derived from a model representing 11 countries with a total population of 375 million and 128,928 reported COVID-19-related deaths up to 4 May 2020.

consistent signal for all countries can be estimated before that signal is present in data from an individual country¹⁶. Therefore, this sharing is potentially useful for generating early warnings, by leveraging what happened in countries with earlier epidemics to inform countries with more-recent epidemics.

Estimated effect of interventions on deaths

Extended Data Table 1 shows total deaths forecast from the beginning of the epidemic up to and including 4 May 2020 under our fitted model and under the counterfactual model, which predicts what would have happened if no interventions were implemented (and $R_t = R_0$; that is, the initial R_t estimated before interventions came into effect).

By comparing the deaths predicted under the model with no interventions to the deaths predicted in our intervention model, we calculated the total deaths averted in our study period. We find that across 11 countries 3.1 (2.8–3.5) million deaths have been averted owing to interventions since the beginning of the epidemic; Extended Data Fig. 5 compares the actual total deaths to the counterfactual total deaths. The counterfactual model without interventions is illustrative only, and reflects the assumptions of our model. We do not account for changes in behaviour; in reality, even in the absence of government interventions we would expect R_t to decrease and therefore would overestimate deaths in the no-intervention model. Conversely, we do not consider the effect on the infection fatality rate as a result of an overwhelmed health system in which patients may not be able to access critical care facilities, which would underestimate the number of counterfactual deaths. In the Supplementary Information, we show further counterfactual estimates under differing assumptions of the generation distribution and onset-to-death distribution and all scenarios broadly show the same trends. Given this agreement across differing scenarios, we believe our estimates for the counterfactual deaths averted to be plausible.

Discussion

During the ongoing transmission of SARS-CoV-2 in Europe, we analyse trends in the numbers of deaths to assess the extent to which transmission has been reduced. Representing the infection process associated with COVID-19 using a semi-mechanistic, joint Bayesian hierarchical model, we can reproduce trends observed in the data relating to deaths and produce empirically driven predictions that are valid over short time horizons.

We estimate that there have been many more infections than are currently reported. The high level of under-ascertainment of infections

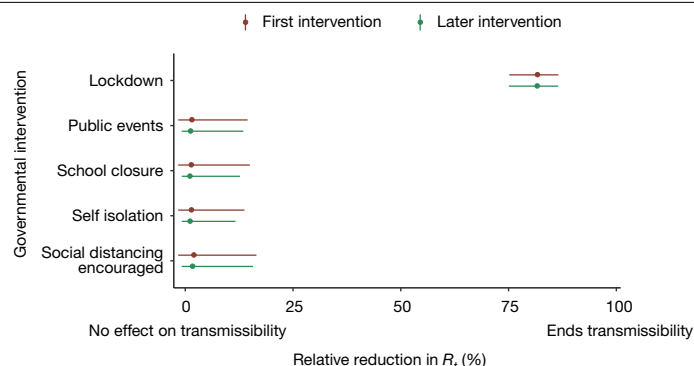


Fig. 2 | Effectiveness of interventions on R_t . Our model includes five covariates for governmental interventions, adjusting for whether the intervention was the first one undertaken by the government in response to COVID-19 (red) or was subsequent to other interventions (green). Mean relative percentage reduction in R_t is shown with 95% posterior credible intervals. If 100% reduction is achieved, $R_t = 0$ and there is no more transmission of COVID-19. Lockdown is significantly different from the other interventions; the other interventions are not significantly different from each other, probably owing to the fact that many interventions occurred on the same day or within days of each other (as shown in Extended Data Fig. 4). Results are derived from a model that represents 11 countries with a total population of 375 million and 128,928 reported COVID-19-related deaths up to 4 May 2020.

that we estimate here is probably due to the focus on testing in hospital settings, which misses milder or asymptomatic cases in the community. Despite this, we estimate that only a relatively small minority of individuals in each country have been infected (Table 1). Our estimates imply that the populations in Europe are not close to herd immunity (about 70% if R_0 is 3.8)¹⁷. Furthermore, with values of R_t below 1 in all countries, the rate of acquisition of herd immunity will slow down rapidly. Our estimates for attack rates during our study period are consistent with those reported from national serological studies⁷. Similarly, comparable studies estimating R_t all agree that the number as of 4 May 2020 is less than 1.

To our knowledge, our modelling approach is unique in pooling information from multiple countries at once. Using this approach means that we require a central consolidated data source (such as data from the European Centre of Disease Control (ECDC)), and also that trends in some countries will be affected by those countries with more data. We argue that this effect is beneficial, in that it helps to minimize idiosyncrasies in the data¹⁶, as well as to improve consistency of estimates over time. Although our qualitative conclusions surrounding the effect of interventions and the finding that R_t is less than 1 are robust to our choice of whether to incorporate pooling or not, the ability to use a greater extent of available data and share information across countries in a statistically principled manner markedly improves the consistency of model predictions across the study period (Supplementary Videos 1–3).

Most interventions were implemented in rapid succession in many countries, and as such it is difficult to disentangle the individual effect sizes of each intervention. In our analysis, we find that only the effect of lockdown is identifiable, and that it has a substantial effect (81% (75–87%) reduction in R_t). Taking into account country-specific effects, the effect size of lockdown remains large across all countries (Supplementary Fig. 29).

We acknowledge the limitations of existing mortality data relating to COVID-19—in particular, deaths outside hospitals may be underreported. However, by using the ECDC data, we rely on a comprehensive data source that is refined and updated each day in a systematic process. Our sensitivity analysis of underreporting and statistical-measurement noise suggests that we may slightly

underestimate the attack rates in some countries, but this does not change our overall conclusions pertaining to R_t . However, even if the data were complete, our method cannot surmount the time lag between infections and deaths and can only fully identify trends in infections 2–3 weeks earlier. Extensions of our model could use case, hospitalization or intensive care data, but reconciling the different biases inherent in these sources while ensuring parsimony is challenging and would require additional assumptions.

The modern understanding of infectious disease, combined with a global publicized response, has meant that nationwide interventions could be implemented with widespread adherence and support. Given the observed infection fatality ratios and the epidemiology of COVID-19, major non-pharmaceutical interventions have had an effect in reducing transmission in all of the countries we have considered. In all countries in this study, we find that these interventions have reduced R_t below 1, and have contained their epidemics at the current time. When looking at simplistic counterfactual models over the whole epidemic, the number of potential deaths averted is substantial. We cannot say for certain that the current measures will continue to control the epidemic in Europe; however, if current trends continue there is reason for optimism.

Online content

Any methods, additional references, Nature Research reporting summaries, source data, extended data, supplementary information, acknowledgements, peer review information; details of author contributions and competing interests; and statements of data and code availability are available at <https://doi.org/10.1038/s41586-020-2405-7>.

- Li, R. et al. Substantial undocumented infection facilitates the rapid dissemination of novel coronavirus (SARS-CoV-2). *Science* **368**, 489–493 (2020).
- Zhang, J. et al. Patterns of human social contact and contact with animals in Shanghai, China. *Sci. Rep.* **9**, 15141 (2019).
- Zhao, A. J. et al. Antibody responses to SARS-CoV-2 in patients of novel coronavirus disease 2019. *Clin. Infect. Dis.* ciaa344 <https://doi.org/10.1093/cid/ciaa344> (2020).
- Jombart, T. et al. Inferring the number of COVID-19 cases from recently reported deaths. *Wellcome Open Research* **5**, 78 (2020).
- Verity, R. et al. Estimates of the severity of coronavirus disease 2019: a model-based analysis. *Lancet* **20**, 669–677 (2020).
- Bi, Q. et al. Epidemiology and transmission of COVID-19 in 391 cases and 1286 of their close contacts in Shenzhen, China: a retrospective cohort study. *Lancet Infect. Dis.* [https://doi.org/10.1016/S1473-3099\(20\)30287-5](https://doi.org/10.1016/S1473-3099(20)30287-5) (2020).

- Bobrovitz, N. et al. Lessons from a rapid systematic review of early SARS-CoV-2 serosurveys. Preprint at medRxiv <https://doi.org/10.1101/2020.05.10.20097451> (2020).
- Statistics Austria. COVID-19 Prevalence Study: Maximum 0.15% of Austrian Population Infected with SARS-CoV-2 (Statistics Austria, 2020).
- Erikstrup, C. et al. Estimation of SARS-CoV-2 infection fatality rate by real-time antibody screening of blood donors. *Clin. Infect. Dis.* ciaa849 <https://doi.org/10.1093/cid/ciaa849> (2020).
- Pollán, M. et al. Prevalence of SARS-CoV-2 in Spain (ENE-COVID): a nationwide, population-based seroepidemiological study. *Lancet* [https://doi.org/10.1016/S0140-6736\(20\)31483-5](https://doi.org/10.1016/S0140-6736(20)31483-5) (2020).
- Zhang, J. et al. Age profile of susceptibility, mixing, and social distancing shape the dynamics of the novel coronavirus disease 2019 outbreak in China. Preprint at medRxiv <https://doi.org/10.1101/2020.03.19.20039107> (2020).
- Salje, H. et al. Estimating the burden of SARS-CoV-2 in France. *Science* **369**, 208–211 (2020).
- Hyafil, A. & Morina, D. Analysis of the impact of lockdown on the reproduction number of the SARS-Cov-2 in Spain. *Gac. Sanit.* <https://doi.org/10.1016/j.gaceta.2020.05.003> (2020).
- Robert Koch Institute. Coronavirus Disease 2019 (COVID-19) Daily Situation Report of the Robert Koch Institute (Robert Koch Institute, 2020).
- Davies, N. G., Kucharski, A. J., Eggo, R. M., Gimma, A. & Edmunds, W. J. The effect of non-pharmaceutical interventions on COVID-19 cases, deaths and demand for hospital services in the UK: a modelling study. *Lancet* **5**, E375–E385 (2020).
- Gelman, A. & Hill, J. *Data Analysis using Regression and Multilevel/Hierarchical Models* (Cambridge Univ. Press, 2006).
- Miller, J. C. A note on the derivation of epidemic final sizes. *Bull. Math. Biol.* **74**, 2125–2141 (2012).

Publisher's note Springer Nature remains neutral with regard to jurisdictional claims in published maps and institutional affiliations.

© The Author(s), under exclusive licence to Springer Nature Limited 2020

Imperial College COVID-19 Response Team

Pablo N. Perez-Guzman², Nora Schmit², Lucia Cilloni², Kylie E. C. Ainslie², Marc Baguelin², Adhiratha Boonyasiri⁴, Olivia Boyd², Lorenzo Cattarino², Laura V. Cooper², Zulma Cucunubá², Gina Cuomo-Dannenburg², Amy Dighe², Bimandra Djaafara², Ilaria Dorigatti², Sabine L. van Elsland², Richard G. FitzJohn², Katy A. M. Gaythorpe², Lily Geidelberg², Nicholas C. Grassly², William D. Green², Timothy Hallett², Arran Hamlet², Wes Hinsley², Ben Jeffrey², Edward Knock², Daniel J. Laydon², Gemma Nedjati-Gilani², Pierre Nouvellet^{2,5}, Kris V. Parag², Igor Siveroni², Hayley A. Thompson², Robert Verity², Erik Volz², Caroline E. Walters², Haowei Wang², Yuanrong Wang², Oliver J. Watson^{2,6}, Peter Winskill², Xiaoyue Xi¹ & Patrick G. T. Walker²

⁴NIHR Health Protection Research Unit in Healthcare Associated Infections and Antimicrobial Resistance, Imperial College London, London, UK. ⁵School of Life Sciences, University of Sussex, Brighton, UK. ⁶Department of Laboratory Medicine and Pathology, Brown University, Providence, RI, USA.

Methods

Data

Our model uses daily consolidated death data from the ECDC for 11 European countries currently experiencing the COVID-19 epidemic: Austria, Belgium, Denmark, France, Germany, Italy, Norway, Spain, Sweden, Switzerland and the UK. The ECDC provides information on confirmed cases and deaths attributable to COVID-19. For population counts, we use the United Nations Population Division age-stratified counts¹⁸.

We also catalogue data on the nature and type of major non-pharmaceutical interventions. We looked at the government webpages from each country as well as their official public health webpages to identify the latest advice or laws being issued by the government and public health authorities. We collected the following: school closure ordered; case-based measures; public events banned; social distancing encouraged; lockdown decreed; and the time of the first and last intervention. A full list of the timing of these interventions and the sources we have used is provided in the Supplementary Notes, Supplementary Table 2.

By using the ECDC data, we rely on a consolidated data source compiled by the ECDC, who include many sources of data each day, constantly refining and updating data using a comprehensive and systematic process. However, despite the rigorous protocols, countries may vary in the specifics of the data that they report to the ECDC. For example, there is variation in reporting (that is, community versus hospital) and time lags. Despite these issues, we use ECDC data to ensure as much consistency as possible across all countries.

Model

A visual summary of our model is presented in Extended Data Fig. 3; details are provided in the Supplementary Methods.

We fit our model to observed deaths according to ECDC data from 11 European countries. The modelled deaths are informed by an infection-to-death distribution (Supplementary Fig. 1; derived from assumptions about the time from infection to the onset of symptoms and about the time from the onset of symptoms to death), and the population-averaged infection fatality ratio (adjusted for the age structure and contact patterns of each country, as discussed in the Supplementary Methods, Supplementary Table 3).

Given these distributions and ratios, modelled deaths are a function of the number of infections. The number of infections is modelled as the product of R_t with a discrete convolution of the previous infections. Individual components of this convolution sum are weighted by the generation time distribution (the average time from the infection of one person to the time at which they infect another; Supplementary Fig. 2). In our work, we approximate the generation time distribution using the serial interval distribution. R_t is a function of the initial R_t before interventions and the effect sizes from interventions, in which interventions are modelled as piecewise constant functions.

Following the Bayesian hierarchy from bottom to top gives us a full framework to see how interventions affect infections, which can result in deaths. A schematic of our model is shown in Extended Data Fig. 3. To maximize the ability to observe the effect of interventions on deaths, we fit our model jointly for all 11 European countries, and use partial pooling of information between countries with both individual and shared effects on R_t . Partial pooling operates on the last intervention, which is—in most cases—lockdown. The effect of partial pooling can be seen in Supplementary Discussion 12, Supplementary Fig. 29. We chose a balanced prior that encodes the prior belief that interventions have an equal chance of having an effect or not, and ensure a uniform prior on the joint effect of all interventions (Supplementary Fig. 3). We evaluate the effect of our Bayesian prior distribution choices and evaluate our Bayesian posterior calibration to ensure our results are statistically robust.

We perform extensive model validation and sensitivity analyses. We validate our model by cross-validation over a 14-day period (Supplementary Discussion 1, Supplementary Table 1) and we show the fits for holdout samples in Supplementary Figs. 5–15. We check the convergence of the Markov chain Monte Carlo sampler (Supplementary Fig. 4). We consider the sensitivity of our estimates of R_t to the mean of the generation distribution (Supplementary Discussion 3, Supplementary Figs. 16, 17). We further show that the choice of generation distribution does not change our counterfactual conclusions (Supplementary Fig. 18). Using univariate analyses and uninformative priors, we find (Supplementary Fig. 19) that all effects on their own serve to decrease R_t (Supplementary Discussion 4). We compare our model to a non-parametric Gaussian Process model (Supplementary Discussion 5). To assess the effect of individual countries on the results, we perform a ‘leave one country out’ sensitivity analysis (Supplementary Discussion 6, Supplementary Figs. 20, 21). To validate our starting values of R_t , we compare our model against an exponential-growth linear model (Supplementary Discussion 7, Supplementary Fig. 22). Instead of a joint analysis, we consider fits of our model to individual countries (Supplementary Discussion 8, Supplementary Figs. 23–26). We perform a sensitivity analysis with respect to the onset-to-death distribution (Supplementary Discussion 9, Supplementary Fig. 27). We validate our probabilistic seeding scheme through an importance-sampling leave-one-out cross-validation (Supplementary Discussion 10). We consider a model extension with a constant, probabilistic under-reporting (Supplementary Discussion 11), finding that R_t does not change substantially (Supplementary Fig. 28).

Our model is different to other approaches (such as EpiEstim¹⁹) that use the discrete renewal equation. We use the renewal equation as a latent process to model infections and propose a generative mechanism to connect these infections to death data. Simply applying the renewal equation directly to death data requires positing a mechanism in which deaths in the past can cause future deaths (see, for example, ref.²⁰). In addition, for R_t , we are able to use a functional relationship in which non-pharmaceutical interventions can have a direct effect on R_t .

Reporting summary

Further information on research design is available in the Nature Research Reporting Summary linked to this paper.

Data availability

Death counts for the 11 European countries for the time period in our study and the full set of posterior draws from our model are available at <https://reshare.ukdataservice.ac.uk/854380/>.

Code availability

All source code and data necessary for the replication of our results and figures are available at <https://github.com/ImperialCollegeLondon/covid19model>. An R package based on our method is available at <https://imperialcollegelondon.github.io/epidemia/>.

18. United Nations, Department of Economic and Social Affairs, Population Division. *World Population Prospects 2019: Data Booklet*, ST/ESA/SER.A/424. (United Nations, 2019).

19. Cori, A., Ferguson, N. M., Fraser, C. & Cauchemez, S. A new framework and software to estimate time-varying reproduction numbers during epidemics. *Am. J. Epidemiol.* **178**, 1505–1512 (2013).

20. Goldstein, E. et al. Reconstructing influenza incidence by deconvolution of daily mortality time series. *Proc. Natl Acad. Sci. USA* **106**, 21825–21829 (2009).

Acknowledgements S.B. acknowledges the NIHR BRC Imperial College NHS Trust Infection and COVID themes, the Academy of Medical Sciences Springboard award and the Bill and Melinda Gates Foundation. L.C.O. acknowledges funding from a UK Royal Society fellowship. Initial research on covariates in Supplementary Table 2 was crowdsourced; we thank a number of people across the world for help with this. This work was supported by Centre funding from the UK Medical Research Council under a concordat with the UK Department for International Development, the NIHR Health Protection Research Unit in Modelling Methodology and Community Jameel. We thank F. Valka for creating our website, and A. Gelman and the Stan

team for helpful discussions. We acknowledge the resources provided by Cirrus UK National Tier-2 HPC Service at EPCC (<http://www.cirrus.ac.uk>) funded by the University of Edinburgh and EPSRC (EP/P020267/1), and cloud compute time donated by Microsoft and Amazon.

Author contributions S.B., S.F., S.M. and A.G. conceived and designed the study. S.B., S.F., S.M., A.G., H.C., H.J.T.U., T.A.M., M.A.C.V., J.W.E. and N.M.F. performed analysis. L.C.O., S.B., S.F., A.G., A.C.G., C.A.D., S.R. and N.M.F. wrote the first draft of the paper. S.B., S.F., H.C., C.W., P.W., T.B., P.N.P.G., N.S., L. Cilloni, M.A.C.V. and H.C. collected data. All authors discussed the results and contributed to the revision of the final manuscript.

Competing interests The authors declare no competing interests.

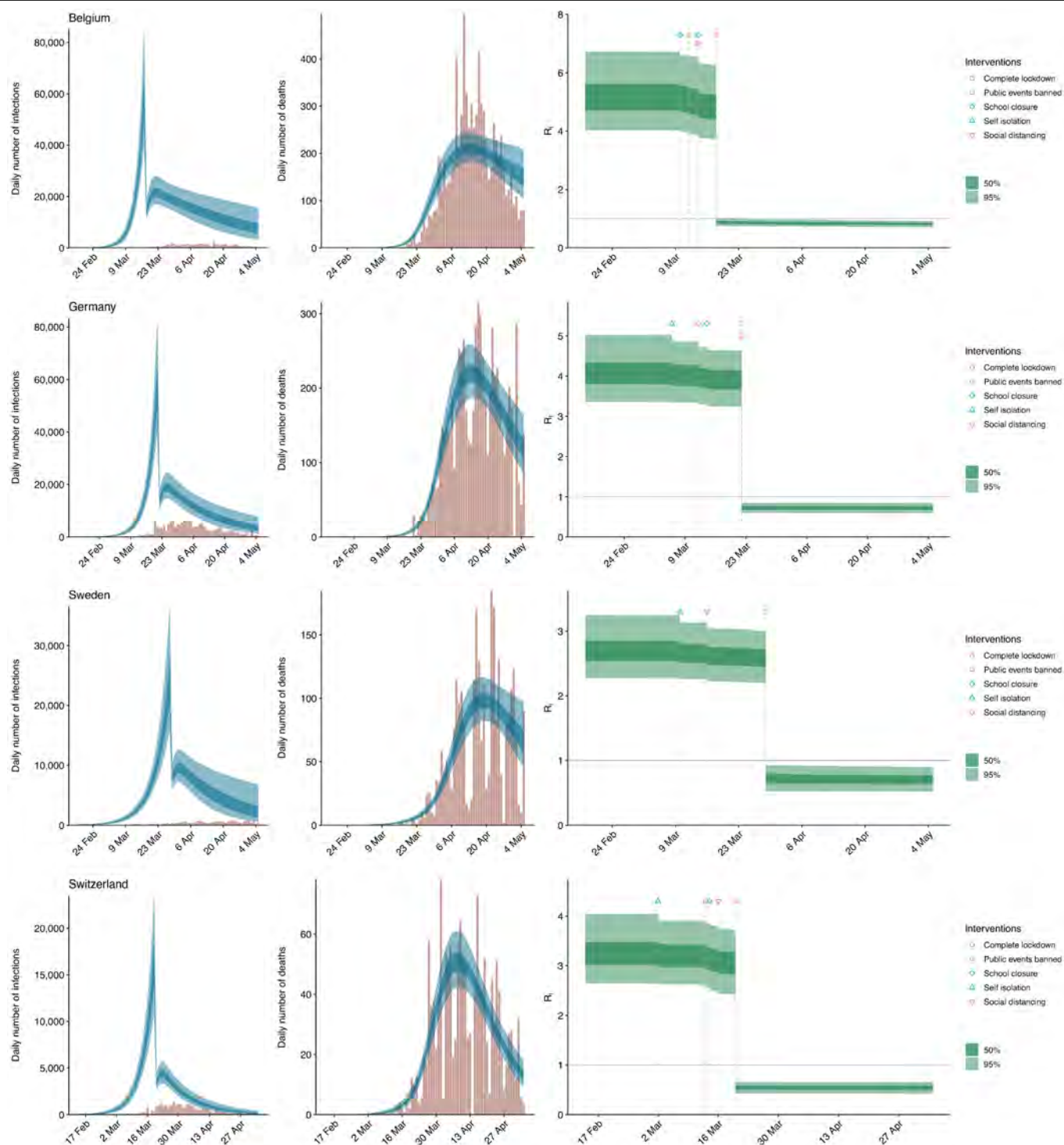
Additional information

Supplementary information is available for this paper at <https://doi.org/10.1038/s41586-020-2405-7>.

Correspondence and requests for materials should be addressed to S.B.

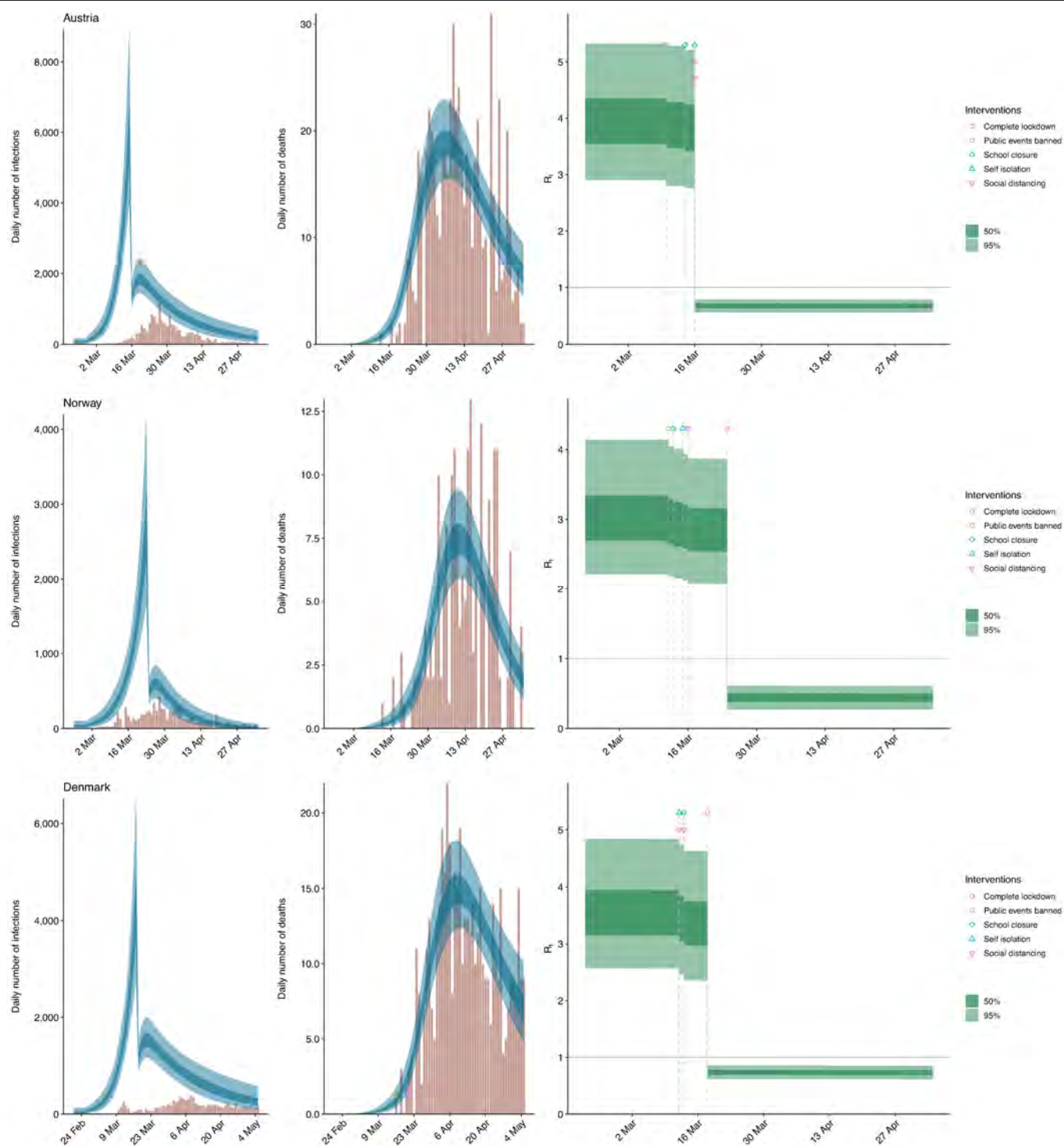
Peer review information *Nature* thanks David Earn and the other, anonymous, reviewer(s) for their contribution to the peer review of this work. Peer reviewer reports are available.

Reprints and permissions information is available at <http://www.nature.com/reprints>.



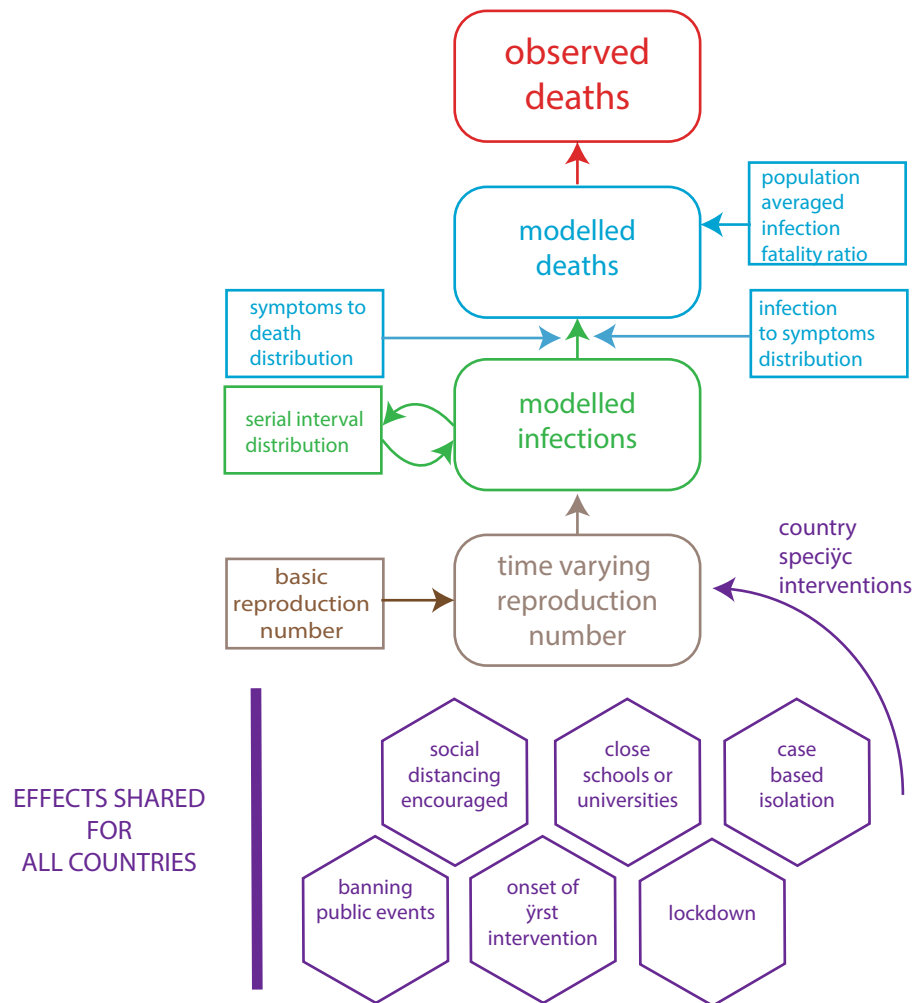
Extended Data Fig. 1 | Country-level estimates of infections, deaths and R_t for Belgium, Germany, Sweden and Switzerland. Left, daily number of infections. Brown bars are reported infections; blue bands are predicted infections; dark blue, 50% credible interval; light blue, 95% credible interval. The number of daily infections estimated by our model drops immediately after an intervention, as we assume that all infected people become

immediately less infectious through the intervention. Afterwards, if R_t is above 1, the number of infections will start growing again. Middle, daily number of deaths. Brown bars are reported deaths; blue bands are predicted deaths; credible intervals are as in the left plot. Right, R_t . Dark green, 50% credible interval; light green, 95% credible interval. Icons are interventions, shown at the time at which they occurred.

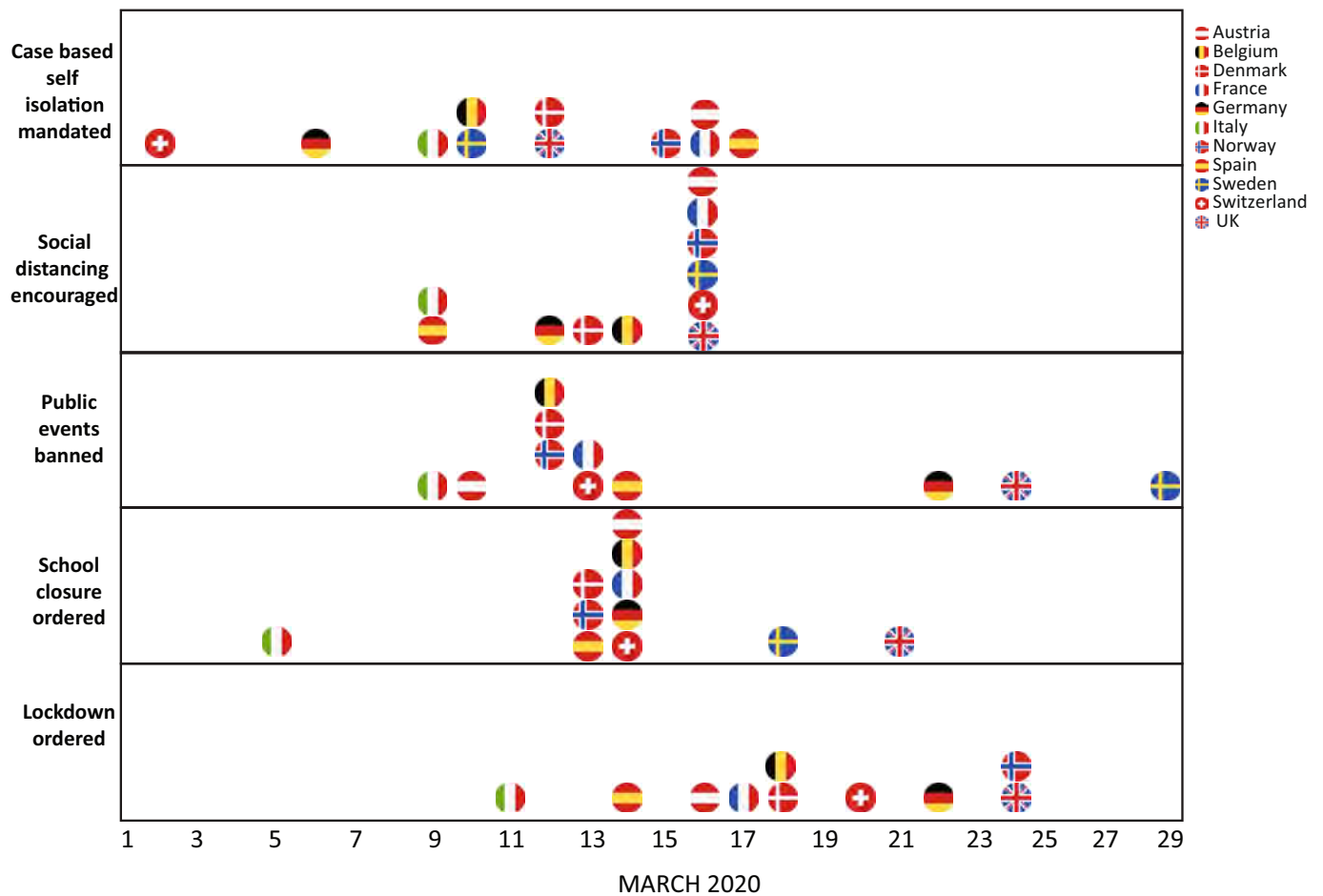


Extended Data Fig. 2 | Country-level estimates of infections, deaths and R_t for Austria, Norway and Denmark. Left, daily number of infections. Brown bars are reported infections; blue bands are predicted infections; dark blue, 50% credible interval; light blue, 95% credible interval. The number of daily infections estimated by our model drops immediately after an intervention, as we assume that all infected people become immediately less infectious

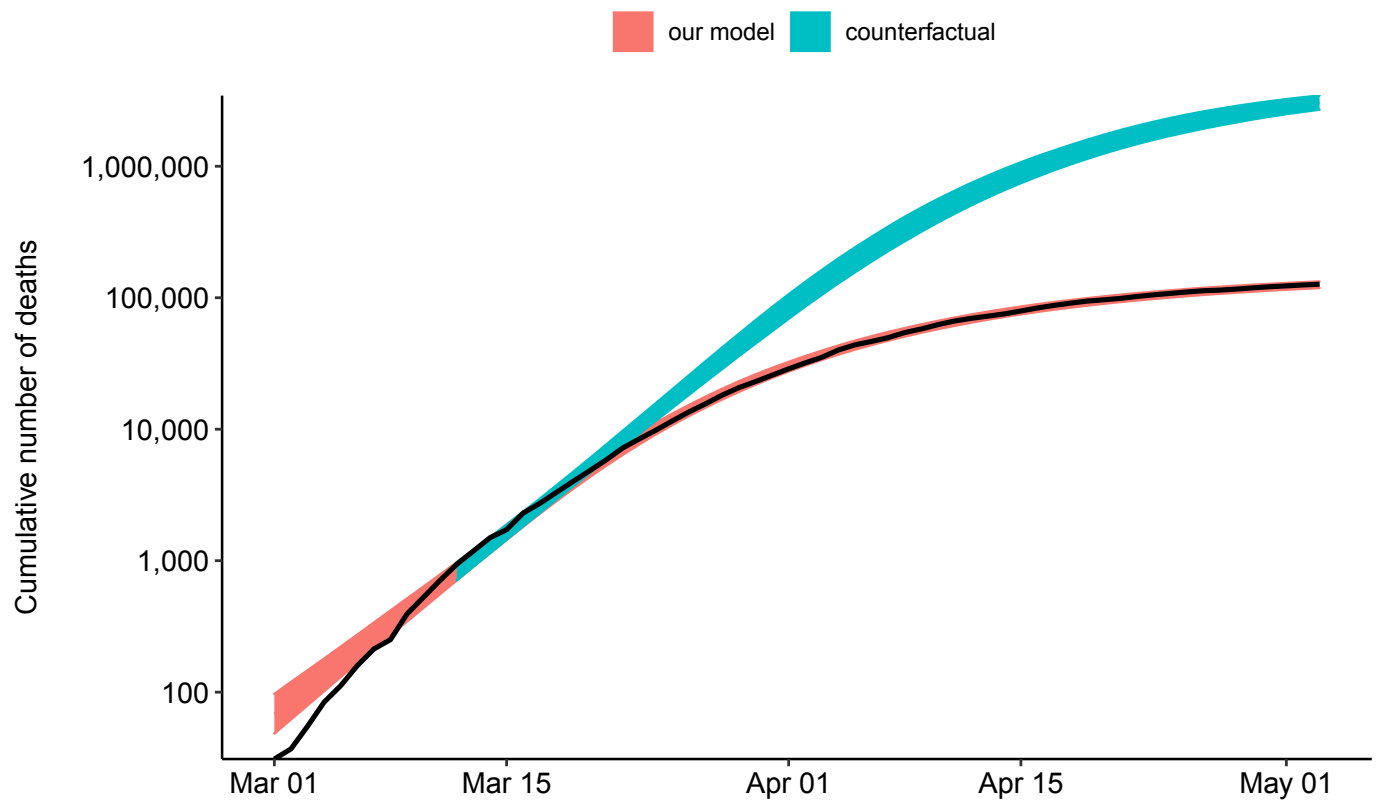
through the intervention. Afterwards, if R_t is above 1, the number of infections will start growing again. Middle, daily number of deaths. Brown bars are reported deaths; blue bands are predicted deaths; credible intervals are as in the left plot. Right, R_t . Dark green, 50% CI; light green, 95% CI. Icons are interventions, shown at the time at which they occurred.



Extended Data Fig. 3 | Model summary. This figure shows a summary of the components of our model.



Extended Data Fig. 4 | Timings of interventions. Timings of interventions for the 11 European countries included in our analysis. For further details, see the Supplementary Information.



Extended Data Fig. 5 | Deaths averted owing to interventions. Lower and upper credible interval for the cumulative number of deaths for the 11 European countries in our model with interventions (pink) and the no-interventions counterfactual model (blue). Reported deaths are shown as a thick black line.

Extended Data Table 1 | Total forecasted deaths since the beginning of the epidemic up to 4 May 2020 in our model and in a counterfactual model that assumes no interventions had taken place

Forecasted deaths since the beginning of the epidemic up to 4th May in our model vs. a counterfactual model assuming no interventions had taken place

Country	Observed Deaths up to 4th May (observed)	Model estimated deaths up to 4th May (our model)	Model estimated deaths up to 4th May (counterfactual model assuming no interventions have occurred)	Model deaths averted up to 4th May (difference between counterfactual and actual)
Austria	600	620 [520 - 720]	66,000 [40,000 - 86,000]	65,000 [40,000 - 85,000]
Belgium	7,924	7,300 [6,400 - 8,400]	120,000 [93,000 - 140,000]	110,000 [86,000 - 130,000]
Denmark	493	500 [430 - 590]	34,000 [17,000 - 50,000]	34,000 [17,000 - 49,000]
France	25,201	23,000 [21,000 - 27,000]	720,000 [590,000 - 850,000]	690,000 [570,000 - 820,000]
Germany	6,831	6,800 [6,000 - 7,900]	570,000 [370,000 - 780,000]	560,000 [370,000 - 770,000]
Italy	29,079	31,000 [27,000 - 35,000]	670,000 [540,000 - 800,000]	630,000 [510,000 - 760,000]
Norway	208	210 [170 - 250]	12,000 [3,400 - 24,000]	12,000 [3,200 - 23,000]
Spain	25,613	25,000 [22,000 - 28,000]	470,000 [390,000 - 560,000]	450,000 [360,000 - 540,000]
Sweden	2,769	2,800 [2,500 - 3,300]	28,000 [15,000 - 49,000]	26,000 [12,000 - 46,000]
Switzerland	1,476	1,500 [1,300 - 1,800]	54,000 [36,000 - 73,000]	52,000 [34,000 - 71,000]
United Kingdom	28,734	29,000 [25,000 - 34,000]	500,000 [400,000 - 610,000]	470,000 [370,000 - 580,000]
All	128,928	130,000 [120,000 - 140,000]	3,200,000 [2,900,000 - 3,600,000]	3,100,000 [2,800,000 - 3,500,000]

Estimated averted deaths over this time period as a result of the interventions. Numbers in brackets are 95% credible intervals.

Reporting Summary

Nature Research wishes to improve the reproducibility of the work that we publish. This form provides structure for consistency and transparency in reporting. For further information on Nature Research policies, see our [Editorial Policies](#) and the [Editorial Policy Checklist](#).

Statistics

For all statistical analyses, confirm that the following items are present in the figure legend, table legend, main text, or Methods section.

n/a Confirmed

- ☐ ☒ The exact sample size (n) for each experimental group/condition, given as a discrete number and unit of measurement
- ☐ ☒ A statement on whether measurements were taken from distinct samples or whether the same sample was measured repeatedly
- ☐ ☒ The statistical test(s) used AND whether they are one- or two-sided
Only common tests should be described solely by name; describe more complex techniques in the Methods section.
- ☐ ☒ A description of all covariates tested
- ☐ ☒ A description of any assumptions or corrections, such as tests of normality and adjustment for multiple comparisons
- ☐ ☒ A full description of the statistical parameters including central tendency (e.g. means) or other basic estimates (e.g. regression coefficient) AND variation (e.g. standard deviation) or associated estimates of uncertainty (e.g. confidence intervals)
- ☒ ☐ For null hypothesis testing, the test statistic (e.g. F , t , r) with confidence intervals, effect sizes, degrees of freedom and P value noted
Give P values as exact values whenever suitable.
- ☐ ☒ For Bayesian analysis, information on the choice of priors and Markov chain Monte Carlo settings
- ☐ ☒ For hierarchical and complex designs, identification of the appropriate level for tests and full reporting of outcomes
- ☒ ☐ Estimates of effect sizes (e.g. Cohen's d , Pearson's r), indicating how they were calculated

Our web collection on [statistics for biologists](#) contains articles on many of the points above.

Software and code

Policy information about [availability of computer code](#)

Data collection No such software was used

Data analysis RStan version 2.19.3 was used within R version 3.6.3

For manuscripts utilizing custom algorithms or software that are central to the research but not yet described in published literature, software must be made available to editors and reviewers. We strongly encourage code deposition in a community repository (e.g. GitHub). See the Nature Research [guidelines for submitting code & software](#) for further information.

Data

Policy information about [availability of data](#)

All manuscripts must include a [data availability statement](#). This statement should provide the following information, where applicable:

- Accession codes, unique identifiers, or web links for publicly available datasets
- A list of figures that have associated raw data
- A description of any restrictions on data availability

All source code and data necessary for the replication of our results is available at <https://github.com/ImperialCollegeLondon/covid19model>
The full set of posterior draws from our model are available at <https://reshare.ukdataservice.ac.uk/854380/>

Field-specific reporting

Please select the one below that is the best fit for your research. If you are not sure, read the appropriate sections before making your selection.

☒ Life sciences ☐ Behavioural & social sciences ☐ Ecological, evolutionary & environmental sciences

For a reference copy of the document with all sections, see [nature.com/documents/nr-reporting-summary-flat.pdf](https://www.nature.com/documents/nr-reporting-summary-flat.pdf)

Life sciences study design

All studies must disclose on these points even when the disclosure is negative.

Sample size	No samples were collected; data on the count of COVID-19-related deaths over time in 11 European countries was used.
Data exclusions	No data was excluded.
Replication	n/a
Randomization	n/a
Blinding	n/a

Reporting for specific materials, systems and methods

We require information from authors about some types of materials, experimental systems and methods used in many studies. Here, indicate whether each material, system or method listed is relevant to your study. If you are not sure if a list item applies to your research, read the appropriate section before selecting a response.

Materials & experimental systems

n/a	Involved in the study
<input checked="" type="checkbox"/>	<input type="checkbox"/> Antibodies
<input checked="" type="checkbox"/>	<input type="checkbox"/> Eukaryotic cell lines
<input checked="" type="checkbox"/>	<input type="checkbox"/> Palaeontology and archaeology
<input checked="" type="checkbox"/>	<input type="checkbox"/> Animals and other organisms
<input checked="" type="checkbox"/>	<input type="checkbox"/> Human research participants
<input checked="" type="checkbox"/>	<input type="checkbox"/> Clinical data
<input checked="" type="checkbox"/>	<input type="checkbox"/> Dual use research of concern

Methods

n/a	Involved in the study
<input checked="" type="checkbox"/>	<input type="checkbox"/> ChIP-seq
<input checked="" type="checkbox"/>	<input type="checkbox"/> Flow cytometry
<input checked="" type="checkbox"/>	<input type="checkbox"/> MRI-based neuroimaging



Since January 2020 Elsevier has created a COVID-19 resource centre with free information in English and Mandarin on the novel coronavirus COVID-19. The COVID-19 resource centre is hosted on Elsevier Connect, the company's public news and information website.

Elsevier hereby grants permission to make all its COVID-19-related research that is available on the COVID-19 resource centre - including this research content - immediately available in PubMed Central and other publicly funded repositories, such as the WHO COVID database with rights for unrestricted research re-use and analyses in any form or by any means with acknowledgement of the original source. These permissions are granted for free by Elsevier for as long as the COVID-19 resource centre remains active.

COVID-19 in children and adolescents in Europe: a multinational, multicentre cohort study



Florian Göttinger*, Begoña Santiago-García*, Antoni Noguera-Julián, Miguel Lanaspá, Laura Lancella, Francesca I Calò Carducci, Natalia Gabrovská, Svetlana Velizarova, Petra Prunk, Veronika Osterman, Uros Krivec, Andrea Lo Vecchio, Delane Shingadia, Antoni Soriano-Arandes, Susana Melendo, Marcello Lanari, Luca Pierantoni, Noémie Wagner, Arnaud G L'Huillier, Ulrich Heininger, Nicole Ritz, Srinil Bandi, Nina Krajcar, Srđan Roglić, Mar Santos, Christelle Christiaens, Marine Creuven, Danilo Buonsenso, Steven B Welch, Matthias Bogyi, Folke Brinkmann, Marc Tebrügge, on behalf of the ptbnet COVID-19 Study Group†

Summary

Background To date, few data on paediatric COVID-19 have been published, and most reports originate from China. This study aimed to capture key data on children and adolescents with severe acute respiratory syndrome coronavirus 2 (SARS-CoV-2) infection across Europe to inform physicians and health-care service planning during the ongoing pandemic.

Methods This multicentre cohort study involved 82 participating health-care institutions across 25 European countries, using a well established research network—the Paediatric Tuberculosis Network European Trials Group (ptbnet)—that mainly comprises paediatric infectious diseases specialists and paediatric pulmonologists. We included all individuals aged 18 years or younger with confirmed SARS-CoV-2 infection, detected at any anatomical site by RT-PCR, between April 1 and April 24, 2020, during the initial peak of the European COVID-19 pandemic. We explored factors associated with need for intensive care unit (ICU) admission and initiation of drug treatment for COVID-19 using univariable analysis, and applied multivariable logistic regression with backwards stepwise analysis to further explore those factors significantly associated with ICU admission.

Findings 582 individuals with PCR-confirmed SARS-CoV-2 infection were included, with a median age of 5·0 years (IQR 0·5–12·0) and a sex ratio of 1·15 males per female. 145 (25%) had pre-existing medical conditions. 363 (62%) individuals were admitted to hospital. 48 (8%) individuals required ICU admission, 25 (4%) mechanical ventilation (median duration 7 days, IQR 2–11, range 1–34), 19 (3%) inotropic support, and one (<1%) extracorporeal membrane oxygenation. Significant risk factors for requiring ICU admission in multivariable analyses were being younger than 1 month (odds ratio 5·06, 95% CI 1·72–14·87; $p=0·0035$), male sex (2·12, 1·06–4·21; $p=0·033$), pre-existing medical conditions (3·27, 1·67–6·42; $p=0·0015$), and presence of lower respiratory tract infection signs or symptoms at presentation (10·46, 5·16–21·23; $p<0·0001$). The most frequently used drug with antiviral activity was hydroxychloroquine (40 [7%] patients), followed by remdesivir (17 [3%] patients), lopinavir–ritonavir (six [1%] patients), and oseltamivir (three [1%] patients). Immunomodulatory medication used included corticosteroids (22 [4%] patients), intravenous immunoglobulin (seven [1%] patients), tocilizumab (four [1%] patients), anakinra (three [1%] patients), and siltuximab (one [1%] patient). Four children died (case-fatality rate 0·69%, 95% CI 0·20–1·82); at study end, the remaining 578 were alive and only 25 (4%) were still symptomatic or requiring respiratory support.

Interpretation COVID-19 is generally a mild disease in children, including infants. However, a small proportion develop severe disease requiring ICU admission and prolonged ventilation, although fatal outcome is overall rare. The data also reflect the current uncertainties regarding specific treatment options, highlighting that additional data on antiviral and immunomodulatory drugs are urgently needed.

Funding ptbnet is supported by Deutsche Gesellschaft für Internationale Zusammenarbeit.

Copyright © 2020 Elsevier Ltd. All rights reserved.

Introduction

In late December, 2019, WHO was notified of an unusual cluster of pneumonia cases in Wuhan, China. The disease, later termed COVID-19, spread quickly beyond the borders of China, with the first cases in Europe being recorded on Jan 25, 2020.¹

Subsequent investigations identified a novel beta-coronavirus now designated as severe acute respiratory syndrome coronavirus 2 (SARS-CoV-2).² Currently, there

are no antiviral treatment options with proven efficacy, but several randomised controlled trials are investigating agents such as hydroxychloroquine, lopinavir–ritonavir, favipiravir, and remdesivir (eg, NCT04336904, NCT04328285, and NCT04280705). Other trials are focusing on immunomodulators, including tocilizumab and anakinra (eg, NCT04317092 and NCT04330638).

To date, data on COVID-19 in children and adolescents remain scarce, despite the number of confirmed COVID-19

Lancet Child Adolesc Health
2020; 4: 653–61

Published Online
June 25, 2020
[https://doi.org/10.1016/S2352-4642\(20\)30177-2](https://doi.org/10.1016/S2352-4642(20)30177-2)

*Contributed equally

†Members are listed at the end of the Article

Department of Paediatric and Adolescent Medicine, National Reference Centre for Childhood Tuberculosis, Wilhelminenspital, Vienna, Austria (F Göttinger MD, M Bogyi MD); Department of Paediatric Infectious Diseases, University Hospital Gregorio Marañón and Gregorio Marañón Research Institute, Madrid, Spain

(B Santiago-García PhD, M Santos MD); Department of Infectious and Respiratory Inflammatory Systemic in Pediatrics, Unitat d'Infeccions, Servei de Pediatria, Institut de Recerca Pediàtrica Hospital Sant Joan de Déu, Barcelona, Spain (M Lanaspá PhD, Prof A Noguera-Julián PhD); Departament de Pediatria, Universitat de Barcelona, Barcelona, Spain (Prof A Noguera-Julián); Centro de Investigación Biomédica en Red de Epidemiología y Salud Pública, Madrid, Spain (Prof A Noguera-Julián); Red de Investigación Translacional en Infectología Pediátrica, Madrid, Spain (B Santiago-García, Prof A Noguera-Julián, M Santos); Academic Department of Paediatrics, Bambino Gesù Children's Hospital, Rome, Italy

(L Lancella PhD, F I Calò Carducci PhD); Children's Clinic, Department of Pulmonary Diseases, MHATLD "St Sofia", Medical University Sofia, Sofia, Bulgaria (N Gabrovská PhD, S Velizarova PhD); Department of Infectious Diseases

(P Prunk MD, V Osterman MD) and Department of Paediatric Pulmonology (U Krivec MD), University Medical Centre Ljubljana, Ljubljana, Slovenia; Section of Paediatrics, Department of Translational Medical Sciences, University of Naples Federico II, Naples, Italy (A Lo Vecchio MD); Department of Paediatric Infectious Diseases, Great Ormond Street Hospital, London, UK (D Shingadia FRCPCH); Department of Infection, Immunity and Inflammation, UCL Great Ormond Street Institute of Child Health, University College London, London, UK (D Shingadia, M Tebruegge PhD); Paediatric Infectious Diseases and Immunodeficiencies Unit, Hospital Universitari Vall d'Hebron, Vall d'Hebron Research Institute, Barcelona, Spain (A Soriano-Arandes PhD, S Melendo MD); Medical and Surgical Science Department, S Orsola University Hospital, Bologna, Italy (M Lanari PhD, L Pierantoni MD); Paediatric Infectious Diseases Unit, Geneva University Hospitals and Faculty of Medicine, Geneva, Switzerland (N Wagner MD, A G L'Huillier MD); Department of Paediatric Infectious Diseases and Vaccinology, University of Basel Children's Hospital, Basel, Switzerland (Prof U Heininger MD, N Ritz PhD); Department of Paediatrics, Royal Children's Hospital Melbourne, University of Melbourne, Melbourne, Australia (N Ritz, M Tebruegge); Department of Paediatrics, Leicester Children's Hospital, Leicester, UK (S Bandi MD); Department of Paediatric Infectious Diseases, University Hospital for Infectious Diseases, Zagreb, Croatia (N Krajcar MD, S Roglic PhD); Department of Paediatric Infectious Diseases, CHC Montlegia, Liège, Belgium (C Christiaens MD, M Creuven MD); Department of Woman and Child Health and Public Health, Fondazione Policlinico Universitario A Gemelli IRCCS, Rome, Italy (D Buonsenso MD); Birmingham Chest Clinic and Heartlands Hospital, University Hospitals Birmingham, Birmingham, UK (S B Welch FRCPCH); Department of Paediatric

Research in context

Evidence before this study

We searched MEDLINE on May 7, 2020, through the PubMed interface to identify publications describing clinical studies in children with COVID-19. To ensure a broad search, the search terms used were "(child OR children OR pediatric OR paediatric) AND COVID-19". No additional limits were set. This search yielded 809 papers: 104 case reports or case series; 38 epidemiological reports; 66 guidelines and consensus statements; 184 reviews, perspectives, or editorials without original data; and 53 letters; 332 were unrelated to children with COVID-19. 22 papers presented original data, but exclusively in adults. Only ten papers reported clinical studies in children with COVID-19: eight papers originated from China, one from Spain, and one from Italy. The study by Tagarro and colleagues was reported in letter format, and only included 41 children with confirmed severe acute respiratory syndrome coronavirus 2 (SARS-CoV-2) infection in Madrid. The study from Italy by Parri and colleagues was also reported as a letter and included 100 cases across several Italian hospitals. However, the study only featured a single patient who required mechanical ventilation, and consequently very few data on children with COVID-19 at the severe end of the disease spectrum.

Added value of this study

To our knowledge, this study is the first multinational, multicentre study in children with COVID-19, and provides a detailed overview on SARS-CoV-2 infection in children in

Europe during the initial peak of the pandemic, which was facilitated by a collaboration of 82 units across 25 European countries. The study has several key findings. First, the data show that COVID-19 is generally a mild disease in children, including infants. Second, the study found that a substantial proportion (8%) of children develop severe disease, requiring intensive care support and prolonged ventilation. Several predisposing factors for requiring intensive care support were identified. Third, the study confirms that fatal outcome is rare in children. There was considerable variability in the use of drugs with antiviral activity as well as immunomodulatory medication, reflecting current uncertainties regarding specific treatment options.

Implications of all the available evidence

This study confirms previous reports from China suggesting that the case-fatality rate of COVID-19 in children is substantially lower than in older adult patients. However, some children develop severe disease and require prolonged intensive care support, which should be accounted for in the planning of health-care services and allocation of resources during the ongoing pandemic. Finally, the findings highlight that data on antiviral and immunomodulatory drugs are urgently needed from well designed, randomised controlled trials in children, to enable paediatricians to make evidence-based decisions regarding treatment choices for children with severe COVID-19.

cases now exceeding 8 million globally.^{3,4} Most published data originate from China, which cannot necessarily be extrapolated to children in Europe and elsewhere.⁵⁻¹² Also, existing papers from China contain very few clinical data on children, and most lack details regarding supportive measures required by children with COVID-19. Similarly, recent epidemiological reports from Europe and North America contain little clinically relevant information.^{13,14} Determining the level of support required by children is essential for paediatric service planning during the ongoing COVID-19 pandemic.

By use of a well established research network, predominately comprising paediatric infectious diseases specialists and paediatric pulmonologists, the aim of this study was to rapidly capture key data on COVID-19 in children in Europe on a large scale, to aid physicians in Europe and in other geographical locations with service planning and allocation of resources.

Methods

Study design and participants

For this cohort study, European members of the Paediatric Tuberculosis Network European Trials Group (ptbnet)—which currently includes 304 clinicians and researchers, most of whom are based at tertiary or quaternary paediatric infectious diseases or paediatric

pulmonology units, across 128 paediatric health-care institutions in 31 European countries¹⁵⁻²⁰—were invited to contribute cases of confirmed SARS-CoV-2 infection that had been managed at or managed remotely by their health-care institution (including individuals admitted to other hospitals or identified during community screening) before or during the study period. Any individual aged 18 years or younger with SARS-CoV-2 infection confirmed by RT-PCR was eligible for inclusion. A standardised data collection spreadsheet was used by collaborators to record data from their centre. All data were reviewed by three of the investigators (FG, BS-G, and MT), and any inconsistencies and other data queries were clarified with the reporting collaborators. Units that did not see any cases before or during the study period were asked to report the absence of cases fulfilling the inclusion criteria at the end of the study period. The study was done over a 3·5-week period, from April 1 to April 24, 2020.

The study was reviewed and approved by the ptbnet steering committee, and the human research ethics committees of the University of Bochum, Germany (19-6545-BR), the Hospital Gregorio Marañón, Spain (CEIM HGUGM-177/20), and the city of Vienna, Austria (EK 20-071-VK). The study was conducted in accordance with the Declaration of Helsinki and its subsequent

amendments. No personal or identifiable data were collected during the conduct of this study.

Study definitions

A confirmed case was defined as a patient in whom SARS-CoV-2 was detected in any clinical sample (respiratory tract, blood, stool, or cerebrospinal fluid) by RT-PCR. PCR testing was done as part of routine clinical care, and therefore done according to local testing guidelines in place at the time. Date of symptom onset was defined as the day when the first symptom or sign occurred, and date of diagnosis as the day when SARS-CoV-2 was first detected. Pyrexia was defined as a body temperature at least 38·0°C. The index case was defined as the most likely source case based on history; if multiple family members were affected, the person who displayed symptoms first was recorded. Diagnosis of upper respiratory tract infection was based on clinical signs and symptoms, encompassing any of the following: coryza, pharyngitis, tonsillitis, otitis media, or sinusitis. Lower respiratory tract infection was based on clinical signs and auscultation findings. Inotropic support was defined as administration of dopamine, dobutamine, epinephrine, or norepinephrine by continuous infusion.

Statistical analysis

Non-parametric two-tailed Mann-Whitney *U* tests were used to compare continuous variables and χ^2 or Fisher's exact tests to compare categorical variables, as appropriate. In children younger than 2 years, age was calculated as fraction of a whole year (365 days); from 2 years of age, age was rounded to the nearest year. The 95% CI around the case-fatality rate (CFR) was calculated with the Wald method. Normality of data distribution was assessed with the Shapiro-Wilk test. The clinical endpoint was the need for admission to an intensive care unit (ICU; either neonatal or paediatric intensive care). The association of baseline characteristics and clinical findings with ICU admission was initially evaluated using univariable logistic regression. Subsequently, multivariable logistic regression analysis with the backward stepwise method was used to explore variables that were independently associated with ICU admission. Only variables that were significant in univariable analyses were introduced into the model. Factors associated with drug treatment for COVID-19 were also explored with univariable analysis. All probabilities are two tailed. $p < 0.05$ was considered statistically significant. All analyses were done with Prism (version 8.0; GraphPad, La Jolla, CA, USA) and SPSS (version 25.0; IBM, Armonk, NY, USA).

Role of the funding source

The funders had no role in the study design, data collection, data analysis, data interpretation, or writing of the manuscript. The corresponding author had full access to all the data and had the final responsibility for the decision to submit for publication.

Results

585 cases of SARS-CoV-2 infection were reported from 77 health-care institutions located in 21 European countries: Austria, Belgium, Bulgaria, Croatia, Denmark, Estonia, Germany, Greece, Hungary, Ireland, Italy, Lithuania, Norway, Portugal, Slovakia, Slovenia, Spain, Sweden, Switzerland, Turkey, and the UK (figure 1). Three cases did not meet the inclusion criteria (one 21-year-old individual and two individuals diagnosed with COVID-19 based on serological testing, but PCR negative). Five participating units in the Netherlands, Moldova, Ukraine, and Russia reported not having encountered any cases.

582 individuals with PCR-confirmed SARS-CoV-2 infection were included in the final analyses. 454 (78%) were contributed by tertiary or quaternary health-care institutions, whereas 54 (9%) had been diagnosed in secondary and 74 (13%) in primary health-care settings.

The median age of the study population was 5·0 years (IQR 0·5–12·0), ranging from 3 days to 18 years (table). Age was non-normally distributed ($W=0.8710$; $p<0.0001$), with 170 (29%) participants younger than 12 months (figure 2). The sex ratio was 1·15 males to every female. The most common source of infection was a parent, considered the index case in 324 (56%) individuals; for 24 (4%) individuals, the most probable index case was a sibling. In the remaining 234 (40%) individuals, the

Pulmonology, Ruhr University Bochum, Bochum, Germany (F Brinkmann PhD); and Department of Paediatric Infectious Diseases & Immunology, Evelina London Children's Hospital, Guy's and St Thomas' NHS Foundation Trust, London, UK (M Tebruegge)

Correspondence to: Dr Marc Tebruegge, Department of Infection, Immunity and Inflammation, UCL Great Ormond Street Institute of Child Health, University College London, London WC1N 1EH, UK. m.tebruegge@ucl.ac.uk

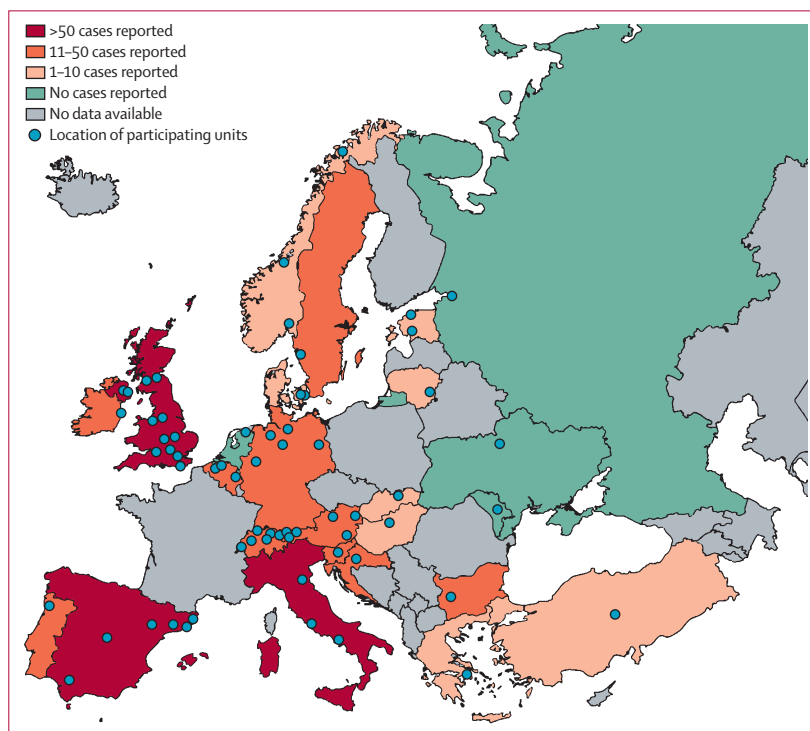


Figure 1: Location of participating units and number of paediatric cases reported by country 82 participating units are shown; cities with more than one participating unit are represented by a single dot only (London [four units], Antwerp [n=3], Madrid [n=3], Vienna [n=3], Barcelona [n=2], Berlin [n=2], Girona [n=2], Manchester [n=2], Rome [n=2], Tallinn [n=2], and Zagreb [n=2]).

	Entire cohort (n=582)	Not admitted to ICU (n=534)	Admitted to ICU (n=48)	p value	Odds ratio (95%CI)
Age, years	5.0 (0.5–12.0)	5.5 (0.6–12.0)	4.0 (0.3–11.0)	0.20	0.9 (0.9–1.0)
<2	230 (40%)	207 (39%)	23 (48%)	..	1.4 (0.8–2.6)
2–5	62 (11%)	60 (11%)	2 (4%)	..	0.3 (0.1–1.4)
5–10	94 (16%)	86 (16%)	8 (17%)	..	1.0 (0.4–2.3)
>10	196 (34%)	181 (34%)	15 (31%)	..	0.8 (0.4–1.6)
Age <1 month	40 (7%)	33 (6%)	7 (15%)	0.027	2.5 (1.0–6.2)
Sex					
Female	271 (47%)	256 (48%)	15 (31%)	..	1 (ref)
Male	311 (53%)	278 (52%)	33 (69%)	0.026	2.2 (1.0–3.8)
Pre-existing medical conditions					
Any	145 (25%)	120 (22%)	25 (52%)	<0.0001	3.7 (2.0–6.8)
Chromosomal abnormality	10 (2%)	8 (1%)	2 (4%)	0.19	2.8 (0.5–13.8)
Chronic kidney disease	9 (2%)	7 (1%)	2 (4%)	0.16	3.2 (0.6–16.2)
Chronic pulmonary disease	29 (5%)	23 (4%)	6 (13%)	0.012	3.1 (1.2–8.2)
Congenital heart disease	25 (4%)	20 (4%)	5 (10%)	0.029	2.9 (1.0–8.4)
Malignancy	27 (5%)	22 (4%)	5 (10%)	0.047	2.7 (0.9–7.5)
Neurological disorders	26 (4%)	21 (4%)	5 (10%)	0.037	2.8 (1.0–7.9)
Other	35 (6%)	29 (5%)	6 (13%)	0.048	2.4 (0.9–6.3)
Immunosuppressive therapy*	29 (5%)	26 (5%)	3 (6%)	0.72	1.3 (0.3–4.4)
Known immunodeficiency	3 (1%)	3 (1%)	0	1.00	..
Chemotherapy in past 6 months	25 (4%)	23 (4%)	2 (4%)	1.00	0.9 (0.2–4.2)
Signs and symptoms at presentation					
Asymptomatic	92 (16%)	90 (17%)	2 (4%)	0.021	0.2 (0.1–0.9)
Pyrexia	379 (65%)	339 (63%)	40 (83%)	0.0065	2.8 (1.3–6.2)
Upper respiratory tract infection	313 (54%)	288 (54%)	25 (52%)	0.80	0.9 (0.5–1.6)
Lower respiratory tract infection	143 (25%)	108 (20%)	35 (73%)	<0.0001	10.6 (5.4–20.7)
Gastrointestinal	128 (22%)	113 (21%)	15 (31%)	0.10	1.6 (0.8–3.2)
Headache†	70/255 (28%)	64/236 (27%)	6/19 (32%)	0.67	1.2 (0.4–3.4)
Radiological findings					
Suggestive of pneumonia	93/198 (47%)	65/156 (42%)	28/42 (67%)	0.0045	2.8 (1.3–5.7)
Suggestive of ARDS	10/198 (5%)	0/156	10/42 (24%)	<0.0001	..
Viral co-infection	29 (5%)	22 (4%)	7 (15%)	0.0015	3.9 (1.6–9.8)

Data are n (%), n/N (%), or median (IQR), unless stated otherwise. p values shown are based on univariable analyses, and calculated separately to the odds ratios. Odds ratios refer to the likelihood of admission to ICU, and were not calculated where one of the required values is zero. ICU=intensive care unit. ARDS=acute respiratory distress syndrome. *At diagnosis of COVID-19. †Only includes children aged 5 years or older in whom those data were recorded.

Table: Baseline characteristics in the entire cohort and by requirement of ICU admission

index case was a person outside of the immediate family or unknown. 363 (62%) individuals were admitted to hospital and 48 (8%) required admission to an ICU for additional support, corresponding to 13% of those admitted to hospital.

437 (75%) individuals had no pre-existing medical conditions. Among the remaining 145 (25%) individuals,

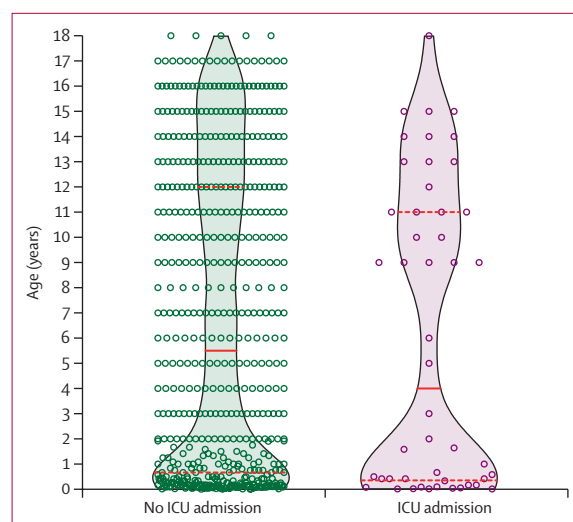


Figure 2: Violin plots showing the age distribution of patients by requirement of ICU support
Each circle represents a patient. The solid lines represent the medians and dashed lines represent IQRs. ICU=intensive care unit.

the most common conditions were chronic pulmonary disease (29 individuals, of whom 16 had asthma and six bronchopulmonary dysplasia), followed by malignancy (27 individuals, of whom 14 had leukaemia or lymphoma and 11 had solid tumours), neurological disorders (26 individuals, of whom nine had epilepsy and eight had cerebral palsy), congenital heart disease (25 individuals), chromosomal abnormalities (ten individuals, of whom eight had trisomy 21), and chronic kidney disease (nine individuals; table). 17 (3%) individuals had two or more pre-existing medical conditions.

29 (5%) individuals were receiving immunosuppressive medication at the time of COVID-19 diagnosis (table). Three (1%) had a previously diagnosed immunodeficiency, comprising common variable immunodeficiency, congenital neutropenia, and Schimke immuno-osseous dysplasia. 25 (4%) individuals were receiving chemotherapy at the time of their diagnosis or had received chemotherapy in the preceding 6 months. Three (1%) had previously undergone human stem cell transplant.

Pyrexia was the most common sign at presentation, observed in 379 (65%) individuals (table). Approximately half had signs or symptoms of upper respiratory tract infection and approximately a quarter had evidence of lower respiratory tract infection; 128 (22%) had gastrointestinal symptoms. 40 (7%) individuals with gastrointestinal symptoms had no respiratory symptoms; the majority (65%; n=26) of these individuals had pyrexia. 92 (16%) individuals were asymptomatic.

Dates when SARS-CoV-2 infection was confirmed by RT-PCR in the study population are summarised in figure 3. The median interval between symptom onset and diagnosis was 2 days (IQR 1–4; range 0–23); in the

majority (n=391; 67%) of cases, the interval was no more than 3 days. In eight cases, SARS-CoV-2 infection was confirmed before any signs or symptoms were present—mainly neonates born to SARS-CoV-2-positive mothers and household members of symptomatic adults with confirmed COVID-19.

A chest x-ray was done in 198 (34%) patients. Of those, 93 (47%) had changes consistent with pneumonia (table). Ten (5%) had changes suggestive of acute respiratory distress syndrome (ARDS), all of whom required mechanical ventilation. In 29 (5%) patients, additional viruses were detected in respiratory samples, comprising enterovirus or rhinovirus (n=18), influenza virus (n=5), parainfluenza virus (n=3), adenovirus (n=3), respiratory syncytial virus (RSV; n=2), bocavirus (n=2), and coronavirus NL63, coronavirus HKU1, coronavirus OC43, and human metapneumovirus (n=1 each). In 22 patients one virus was detected in addition to SARS-CoV-2; in six patients, two additional viruses were detected simultaneously; and in one patient, three were detected. Patients with one or more viral co-infections were more likely to have signs or symptoms of upper or lower respiratory tract infection at presentation compared with those in whom no additional viral agent was identified (appendix p 1). Furthermore, individuals with viral co-infection were significantly more likely to require ICU admission, respiratory support, or inotropic support.

507 (87%) individuals did not require respiratory support at any stage. 75 (13%) patients required oxygen support: 31 (5%) were started on continuous positive airway pressure (CPAP) and 25 (4%) on mechanical ventilation (including 14 who had been managed with CPAP initially). The median duration of mechanical ventilation was 7 days (IQR 2–11; range 1–34). One (<1%) patient was started on extracorporeal membrane oxygenation. 19 (3%) patients required support with inotropes.

When comparing individuals by their requirement of ICU admission, we found that patients who required ICU admission were younger than those who did not (ie, individuals in the community and those admitted to hospital but not needing ICU support), but this was not statistically significant (table; figure 2). In univariable analysis, being younger than 1 month of age, male sex, pre-existing medical conditions, pyrexia, signs or symptoms of lower respiratory tract infection, radiological changes suggestive of pneumonia or ARDS, and viral co-infection were associated with ICU admission (table). In multivariable analysis, the factors that remained associated with ICU admission were being younger than 1 month (odds ratio [OR] 5.06, 95% CI 1.72–14.87; p=0.0035), male sex (2.12, 1.06–4.21; p=0.033), signs or symptoms of lower respiratory tract infection at presentation (10.46, 5.16–21.23; p<0.0001), and presence of pre-existing medical conditions (3.27, 1.67–6.42; p=0.0015).

The most commonly used drug with antiviral activity was hydroxychloroquine, used in 40 (7%) patients, followed

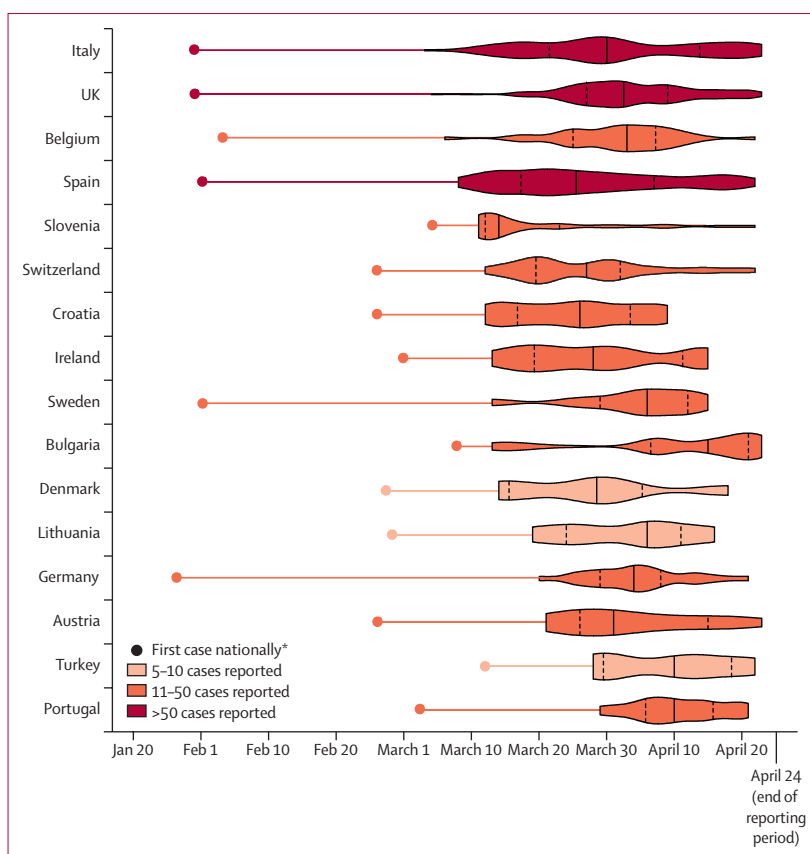


Figure 3: Violin plot illustrating the dates SARS-CoV-2 infection was confirmed by RT-PCR in the study population, by country

Countries with fewer than five paediatric cases reported are not shown. Solid lines represent the medians and dashed lines represent IQRs. The date of the first case in each country is based on data reported by the European Centre for Disease Prevention and Control. SARS-CoV-2=severe acute respiratory syndrome coronavirus 2.

*First case of any age.

by remdesivir, which was used in 17 (3%) patients. Lopinavir–ritonavir was used in six (1%) patients and oseltamivir in three (1%), two of whom had influenza virus co-infection. Three (1%) patients received two drugs with antiviral activity and one (<1%) patient received three; all four patients had ARDS on chest x-ray. No patient received chloroquine, favipiravir, zanamivir, or ribavirin. With regard to immunomodulatory medication, 22 (4%) patients received systemic corticosteroids, seven (1%) intravenous immunoglobulin, four (1%) tocilizumab, three (1%) anakinra, and one (<1%) siltuximab. In univariable analysis, factors associated with treatment initiation of drugs with antiviral or immunomodulatory activity comprised pre-existing malignancy (OR 6.3, 95% CI 2.8–14.2), cardiac disease (4.2, 1.8–10.0), or respiratory disease (6.5, 3.0–14.2); immunosuppressive therapy at presentation (6.5, 3.0–14.2) or recent chemotherapy (6.1, 2.6–14.1); radiological findings suggestive of pneumonia (4.5, 2.3–8.6) or ARDS (22.3, 2.7–180.5); and viral co-infection (5.5, 2.5–12.2; all p<0.0001; appendix p 2).

Four patients, all older than 10 years, had a fatal outcome (CFR 0.69%, 95% CI 0.20–1.82), with death

See Online for appendix

For the European Centre for Disease Prevention and Control COVID-19 data see <https://ecdc.europa.eu/public/extensions/COVID-19/COVID-19.html>

occurring at 3, 9, 11, and 17 days after symptom onset. Two patients had no known pre-existing medical conditions; one had a cardiorespiratory arrest before arrival at the hospital and resuscitation was unsuccessful and the other died while being mechanically ventilated in ICU. The third patient had undergone human stem cell transplant 15 months earlier. The fourth patient was managed palliatively (without intubation), due to the severity of their pre-existing medical conditions. The remaining 578 patients were alive when the study closed. 93 (16%) individuals never developed clinical symptoms. In 460 (80%) individuals, all symptoms had resolved without apparent sequelae, whereas 25 (4%) were still symptomatic or were requiring respiratory support when the study closed.

Discussion

To our knowledge, this is the first multinational, multicentre study on paediatric COVID-19, and also the largest clinical study in children outside of China to date. The inclusion of such a substantial number of cases was made possible by involving a large number of specialist centres across Europe via a well established collaborative paediatric tuberculosis research network, allowing this study to provide one of the most detailed accounts of COVID-19 in children and adolescents published to date.

It is important to highlight that this study has primarily captured data from children and adolescents who were seen or managed within the hospital setting, and that the majority of participating units were part of tertiary or quaternary health-care institutions. Consequently, the study population is likely to primarily represent individuals at the more severe end of the disease spectrum. Notably, a recent letter summarising 171 PCR-confirmed cases in Wuhan suggests that close to 20% of children and adolescents with SARS-CoV-2 infection are asymptomatic.¹⁰ At the time our study was conducted, testing capacity for SARS-CoV-2 in many European countries was lower than clinical demand, and therefore many children with symptoms consistent with COVID-19 in the community were not tested and consequently not diagnosed. Nevertheless, our data indicate that children and adolescents are overall less severely affected by COVID-19 than adults, particularly older patients. Previous, large-scale data suggest that the CFR in adults older than 70 years is close to 10%,⁶ potentially due to immunosenescence.²¹ It is reassuring that our data show that severe COVID-19 is uncommon in young children, including infants, despite their immune maturation being incomplete,^{22,23} with only few requiring mechanical ventilation. It was striking that all children who died in our cohort were older than 10 years.

The Centers for Disease Control and Prevention (CDC) reported 2572 confirmed cases of COVID-19 in individuals younger than 18 years in the USA as of April 2, 2020, representing only 1.7% of the total number of recorded cases ($n=149\,760$).¹⁴ The Australian Health Protection Agency has reported that children accounted for only 4%

of confirmed COVID-19 cases in Australia.²⁴ Unfortunately, in the CDC report, clinical data were only available in a small proportion of patients ($n=291$; 11%). In concordance with our observations, fever and cough were the predominant clinical features at presentation (present in 56% and 54% of individuals, respectively), with similar rates observed in a study from Italy.²⁵ In our cohort almost a quarter of patients had gastrointestinal symptoms, some of whom had no respiratory symptoms, and a substantial proportion of children were entirely asymptomatic.

The CDC report also mentions three deaths,¹⁴ but it is unclear how many patients were still hospitalised by the time of publication, so it is difficult to come to firm conclusions regarding the CFR in US children. Our data indicate that the CFR in children and adolescents across Europe is less than 1%. Considering that many children with mild disease will never have been brought to medical attention, and therefore not diagnosed, it is highly probable that the true CFR is substantially lower than the figure of 0.69% observed in our cohort. This hypothesis is further supported by an epidemiological study from China, in which the CFR in individuals aged 19 years or younger was only 0.1% (one death in 965 confirmed cases).⁶ Furthermore, our data indicate that sequelae related to COVID-19 are likely to be rare in children and adolescents. However, after the closure of our study, reports of a hyperinflammatory syndrome affecting children that is temporally, and potentially causally, associated with SARS-CoV-2 infection have emerged, which has subsequently been named paediatric inflammatory multisystem syndrome temporally associated with SARS-CoV-2 (PIMS-TS; sometimes known as MIC-S).^{26,27} Further research will be required to characterise this emerging disease entity in detail, and determine the long-term outcome of affected children.

Importantly, our data show that severe COVID-19 can occur both in young children and in adolescents, and that a significant proportion of those patients require ICU support, frequently including mechanical ventilation. A small study from Madrid also found that four (10%) of 41 children with SARS-CoV-2 infection required admission to ICU.²⁸ In our cohort, being younger than 1 month, male sex, presence of lower respiratory tract infection signs or symptoms at presentation, and presence of a pre-existing medical condition were associated with increased likelihood of requiring ICU admission. Our results also show that the majority of children who are intubated due to respiratory failure require prolonged ventilation, often for 1 week or more. This contrasts with observations in children with RSV infection who, on average, only require mechanical ventilation for 5–7 days,²⁹ but is not dissimilar to observations in children with influenza.³⁰ This has important implications for service planning, as although the overall demand for ICU support might be lower in children than in adults, each patient is likely to occupy ICU space for an extended period of time. At this time of intense strain on health-care services worldwide, it is vital

that adequate resources are allocated to paediatric services to sustain the provision of high-quality care for children.

The observation that, in our study, individuals with viral co-infection (ie, infected with SARS-CoV-2 and one or more other viral agents) were more likely to require ICU support than those in whom SARS-CoV-2 was the only viral agent identified might have implications for the winter period 2020–21, when the incidence of other viral respiratory tract infections, including RSV and influenza virus infections, is bound to increase. This could result in a greater proportion of paediatric patients with COVID-19 requiring ICU support than in the cohort described here, as the influenza season 2019–20 was already over in Europe before the study commenced.

Our data also reflect the uncertainties regarding drug treatment options for COVID-19. In some countries, including Spain and Italy, national guidelines were encouraging the use of hydroxychloroquine for selected cases, as reflected in our data, while in other countries, recommendations were more guarded regarding the use of antiviral agents in the absence of robust human data. An expert consensus statement from the USA has emphasised that antiviral treatment should be reserved for patients at the severe end of the disease spectrum, ideally within a clinical trial.³¹ Overall, the expert panel appeared to favour the use of remdesivir over other agents, based on the currently available data from in-vitro and animal studies, including in non-human primates, and recent data from compassionate use in humans.^{32,33} The panel members' opinion was split regarding the use of lopinavir–ritonavir, given the disappointing results of a recently published randomised controlled trial.³⁴

The main limitation of this study relates to the number of variables for which data were collected. In the context of the ongoing COVID-19 pandemic, to ensure high levels of participation and avoid diverting substantial time away from clinical front-line duties, a decision was made not to collect detailed data on laboratory parameters or ICU interventions. A further limitation was that a variety of in-house and commercial PCR assays were used across different participating centres, precluding an assessment of diagnostic test performance. Also, the number of children receiving antiviral or immunomodulatory treatment was too small to draw meaningful conclusions regarding their effectiveness, which will be addressed by the aforementioned randomised trials. A further limitation is that different countries were using different thresholds to screen for SARS-CoV-2 at the time the study was done, with some recommending screening of all children admitted to hospital or conducting community screening, whereas others were using more selective testing strategies. Despite those limitations, to our knowledge, this study provides the most comprehensive overview on COVID-19 in children and adolescents to date.

In conclusion, our data, originating from a large number of specialist centres across Europe, show that COVID-19 is

usually a mild disease in children, including infants. Nevertheless, a small proportion of children and adolescents develop severe disease and require ICU support, frequently needing prolonged ventilatory support. However, fatal outcome is rare overall. Our data also reflect the current uncertainties regarding specific treatment options, highlighting that more robust data on antiviral and immunomodulatory drugs are urgently needed.

Contributors

MT conceived of the study. FG, BS-G, SBW, MB, FB, and MT designed the study. FG, BS-G, and MT cleaned and analysed the data, constructed the figures, and wrote the first draft of the manuscript. All authors contributed data to the study, contributed to the data interpretation, critically reviewed the manuscript, and approved the final manuscript for submission.

ptbnet COVID-19 Study Group

Jasmin Pfefferle and Angela Zacharasiewicz (Wilhelminenspital, Vienna, Austria), Angelika Berger (Medical University Vienna, Vienna, Austria), Roland Berger (St Josef Hospital, Vienna, Austria), Volker Strenger and Daniela S Kohlfürst (Department of Paediatrics and Adolescent Medicine, Medical University of Graz, Graz, Austria), Anna Zschocke and Benoît Bernar (Department of Pediatrics, Medical University Innsbruck, Innsbruck, Austria), Burkhard Simma (Landeskrankenhaus Feldkirch, Feldkirch, Austria), Edda Haberlandt (Krankenhaus Dornbirn, Dornbirn, Austria), Christina Thir and Ariane Biebl (Kepler University Hospital, Linz, Austria), Koen Vanden Driessche and Tine Boiy (Antwerp University Hospital, Antwerp, Belgium), Daan Van Brusselen (GZA Hospitals Antwerp, Antwerp, Belgium), An Bael (ZNA Paola Children's Hospital Antwerp & University of Antwerp, Antwerp, Belgium), Sara Debulpaep and Petra Schelstraete (Gent University Hospital, Gent, Belgium), Ivan Pavić (Children's Hospital Zagreb, Zagreb, Croatia), Ulrikka Nygaard (Copenhagen University Hospital, Denmark), Jonathan Peter Glenthøj (Nordsjællands Hospital, Hillerød, Denmark), Lise Heilmann Jensen (Zealand University Hospital, Roskilde, Denmark), Ilona Lind (Pärnu Hospital, Pärnu, Estonia), Mihail Tistsenko (West-Tallinn Central Hospital, Tallinn, Estonia), Ülle Uustalu (Tallinn Children's Hospital, Tallinn, Estonia), Laura Buchtala (Klinikum Bremen-Mitte, Bremen, Germany), Stephanie Thee (Charité Universitätsmedizin, Berlin, Germany), Robin Kobbe and Cornelius Rau (University Children's Hospital, University Medical Center Hamburg-Eppendorf, Hamburg, Germany), Nicolaus Schwerk (Hannover Medical School, Hannover, Germany), Michael Barker (Helios Klinikum Emil von Behring, Berlin, Germany), Maria Tsolia and Irini Eleftheriou (2nd Department of Paediatrics, National & Kapodistrian University of Athens, P & A Kyriakou Children's Hospital, Greece), Patrick Gavin and Oksana Kozdoba (Children's Health Ireland at Crumlin and Temple Street, Dublin, Ireland), Borbála Zsigmond (Heim Pal Children's Hospital, Budapest, Hungary), Piero Valentini (Fondazione Policlinico Universitario A Gemelli IRCCS, Rome, Italy), Inga Ivaškevičienė and Rimvydas Ivaškevičius (Clinic of Children's Diseases, Institute of Clinical Medicine, Vilnius University, Vilnius, Lithuania), Valentina Vilc (Institute of Phthisiopneumology, Chisinau, Moldova), Elisabeth Schölvinc (Beatrix Children's Hospital University Medical Centre Groningen, Groningen, The Netherlands), Astrid Rojahn (Oslo University Hospital, Oslo, Norway), Anastasios Smyrniaos (St Olavs University Hospital, Trondheim, Norway), Claus Klingenberg (University Hospital of North Norway, Tromsø, Norway), Isabel Carvalho and Andreia Ribeiro (Hospital Center of Vila Nova de Gaia/Espinho, Porto, Portugal), Anna Starshinova (Almazov National Medical Research Centre, St Petersburg, Russia), Ivan Solovic (National Institute for Tuberculosis, Lung Diseases and Thoracic Surgery, Vysne Hagy, Slovakia), Lola Falcón and Olaf Neth (Hospital Infantil Virgen del Rocío, Sevilla, Spain), Mario Pérez-Butragueño (Hospital Universitario Infanta Leonor, Madrid, Spain), Laura Minguell (Hospital Universitari Arnau de Vilanova, Lleida, Spain), Matilde Bustillo and Aida María Gutiérrez-Sánchez (Miguel Servet University Hospital,

For more on influenza seasons in Europe see <https://flunewseurope.org>

Zaragoza, Spain), Borja Guarch Ibáñez (Hospital Universitari de Girona Dr Josep Trueta, Girona, Spain), Francesc Ripoll (Hospital Santa Caterina, Girona, Spain), Beatriz Soto (Hospital Universitario de Getafe, Madrid, Spain), Karsten Kötz (Queen Silvia Children's Hospital, Gothenburg, Sweden), Petra Zimmermann (Hôpital Fribourgeois, Fribourg, Switzerland), Hanna Schmid (University Children's Hospital Basel, Basel, Switzerland), Franziska Zucol (Kantonsspital Winterthur, Winterthur, Switzerland), Anita Niederer (Children's Hospital of Eastern Switzerland, St Gallen, Switzerland), Michael Buettcher (Lucerne Children's Hospital, Lucerne Cantonal Hospital, Lucerne, Switzerland), Benhur Sirvan Cetin (Erciyes University Hospital, Kayseri, Turkey), Olga Bilogortseva (National Institute of Phthisiology and Pulmonology, Kiev, Ukraine), Vera Chechenyeva (National Specialised Children's Centre for HIV & AIDS, Kiev, Ukraine), Alicia Demirjian (Evelina London Children's Hospital, Guy's and St Thomas' NHS Foundation Trust, London, UK), Fiona Shackley (Sheffield Children's Hospital, UK), Lynne McFetridge (Antrim Area Hospital, Antrim, UK), Lynne Speirs (Royal Belfast Hospital for Sick Children, Belfast, UK), Conor Doherty (Royal Hospital for Children, Glasgow, UK), Laura Jones (Royal Hospital for Sick Children, Edinburgh, UK), Paddy McMaster (North Manchester Care Organisation, Manchester, UK), Clare Murray and Frances Child (Royal Manchester Children's Hospital, Manchester University NHS Foundation Trust, Manchester, UK), Yvonne Beuvink and Nick Makwana (City and Sandwell Hospitals Birmingham, Birmingham, UK), Elisabeth Whittaker (St Mary's Hospital Paddington, London, UK), Amanda Williams (London North West University Healthcare NHS Trust, Harrow, UK), Katy Fidler (Royal Alexandra Children's Hospital, Brighton, UK), Jolanta Bernatoniene (Bristol Royal Hospital for Children, Bristol, UK), Rinn Song and Zoe Oliver (Oxford Children's Hospital, Oxford, UK), Andrew Riordan (Alder Hey Children's Hospital, Liverpool, UK).

Declaration of interests

FG has received funding from Gilead for research related to hepatitis E. BS-G and MT have received assays free of charge from Cepheid for tuberculosis diagnostics projects. MT has received assays at reduced pricing or free of charge from Cellestis/Qiagen for tuberculosis diagnostics projects, has received support for conference attendance from Cepheid, and is currently receiving funding from bioMérieux as an investigator of an ongoing tuberculosis diagnostics study. UH reports personal fees from CEPI for being a member of the SPEAC-CEPI Meta-Data safety monitoring board for COVID-19 vaccine trials, outside of the submitted work. The other authors declare no competing interests.

Acknowledgments

We express our gratitude to all colleagues and research personnel involved in the data collection for this study, as well as the members of the human research ethics committees and institutional review boards that have kindly fast-tracked this study. We are also grateful for the kind support of the Clinical Microbiology & Infectious Diseases Department and the COVID-19 Group at Hospital General Universitario Gregorio Marañón, Madrid, Spain. This project did not receive specific funding. ptbnet is supported by the Deutsche Gesellschaft für Internationale Zusammenarbeit. BS-G is funded by the Spanish Ministry of Health—Instituto de Salud Carlos III and co-funded by the European Union (FEDER; Contrato Juan Rodés, Grant JR16/00036). AN-J was supported by “Subvencions per a la Intensificació de Facultatius Especialistes”—Departament de Salut de la Generalitat de Catalunya, Programa PERIS 2016–2020 (SLT008/18/00193).

Editorial note: the *Lancet* Group takes a neutral position with respect to territorial claims in published maps and institutional affiliations.

References

- WHO. Novel coronavirus (2019-nCoV) situation report 5. https://www.who.int/docs/default-source/coronaviruse/situation-reports/20200125-sitrep-5-2019-ncov.pdf?sfvrsn=429b143d_8 (accessed June 16, 2020).
- Coronaviridae Study Group of the International Committee on Taxonomy of Viruses. The species severe acute respiratory syndrome-related coronavirus: classifying 2019-nCoV and naming it SARS-CoV-2. *Nat Microbiol* 2020; 5: 536–44.
- WHO. Novel coronavirus (2019-nCoV) situation report 148. https://www.who.int/docs/default-source/coronaviruse/situation-reports/20200616-covid-19-sitrep-148-draft.pdf?sfvrsn=9b2015e9_2 (accessed June 16, 2020).
- Zimmermann P, Goetzinger F, Ritz N. Severe and fatal COVID-19 occurs in young children. *JAMA Pediatrics* (in press).
- Xu Y, Li X, Zhu B, et al. Characteristics of pediatric SARS-CoV-2 infection and potential evidence for persistent fecal viral shedding. *Nat Med* 2020; 26: 502–05.
- Novel Coronavirus Pneumonia Emergency Response Epidemiology Team. The epidemiological characteristics of an outbreak of 2019 novel coronavirus diseases (COVID-19) in China. *Zhonghua Liu Xing Bing Xue Za Zhi* 2020; 41: 145–51.
- Chen H, Guo J, Wang C, et al. Clinical characteristics and intrauterine vertical transmission potential of COVID-19 infection in nine pregnant women: a retrospective review of medical records. *Lancet* 2020; 395: 809–15.
- Zhu L, Wang J, Huang R, et al. Clinical characteristics of a case series of children with coronavirus disease 2019. *Pediatr Pulmonol* 2020; 55: 1430–32.
- Castagnoli R, Votto M, Licari A, et al. Severe acute respiratory syndrome coronavirus 2 (SARS-CoV-2) infection in children and adolescents: a systematic review. *JAMA Pediatr* 2020; published online April 20. DOI:10.1001/jamapediatrics.2020.1467.
- Lu X, Zhang L, Du H, et al. SARS-CoV-2 infection in children. *N Engl J Med* 2020; 382: 1663–65.
- Dong Y, Mo X, Hu Y, et al. Epidemiology of COVID-19 among children in China. *Pediatrics* 2020; 145: e20200702.
- Liu W, Zhang Q, Chen J, et al. Detection of Covid-19 in children in early January 2020 in Wuhan, China. *N Engl J Med* 2020; 382: 1370–71.
- Gudbjartsson DF, Helgason A, Jonsson H, et al. Spread of SARS-CoV-2 in the Icelandic population. *N Engl J Med* 2020; published online April 14. DOI:10.1056/NEJMoa2006100.
- CDC COVID-19 Response Team. Coronavirus disease 2019 in children—United States, February 12–April 2, 2020. *MMWR Morb Mortal Wkly Rep* 2020; 69: 422–26.
- Basu Roy R, Thee S, Blazquez-Gamero D, et al. Performance of immune-based and microbiological tests in children with TB meningitis in Europe—a multi-center Paediatric Tuberculosis Network European Trials Group (ptbnet) study. *Eur Respir J* 2020; published online April 16. DOI:10.1183/13993003.02004-2019.
- Noguera-Julian A, Calzada-Hernandez J, Brinkmann F, et al. Tuberculosis disease in children and adolescents on therapy with anti-tumor necrosis factor-alpha agents: a collaborative, multi-centre ptbnet study. *Clin Infect Dis* 2019; published online Dec 4. DOI:10.1093/cid/ciz1138.
- Villanueva P, Neth O, Ritz N, Tebruegge M, Paediatric Tuberculosis Network European Trials Group. Use of Xpert MTB/RIF Ultra assays among paediatric tuberculosis experts in Europe. *Eur Respir J* 2018; 5: 1800346.
- Tebruegge M, Ritz N, Koetz K, et al. Availability and use of molecular microbiological and immunological tests for the diagnosis of tuberculosis in Europe. *PLoS One* 2014; 9: e99129.
- Tebruegge M, Buonsenso D, Brinkmann F, et al. European shortage of purified protein derivative and its impact on tuberculosis screening practices. *Int J Tuberc Lung Dis* 2016; 20: 1293–99.
- Tebruegge M, Bogyi M, Soriano-Arandes A, Kampmann B, Paediatric Tuberculosis Network European Trials Group. Shortage of purified protein derivative for tuberculosis testing. *Lancet* 2014; 384: 2026.
- Malaguarnera L, Ferlito L, Imbesi RM, et al. Immunosenescence: a review. *Arch Gerontol Geriatr* 2001; 32: 1–14.
- Kollmann TR, Kampmann B, Mazmanian SK, Marchant A, Levy O. Protecting the newborn and young infant from infectious diseases: lessons from immune ontogeny. *Immunity* 2017; 46: 350–63.
- Kollmann TR, Crabtree J, Rein-Weston A, et al. Neonatal innate TLR-mediated responses are distinct from those of adults. *J Immunol* 2009; 183: 7150–60.
- COVID-19 National Incident Room Surveillance Team. COVID-19, Australia: epidemiology report 11 (reporting week 12 April 2020). *Commun Dis Intell* 2020; 44.
- Parri N, Lenge M, Buonsenso D. Children with COVID-19 in pediatric emergency departments in Italy. *N Engl J Med* 2020; published online May 1. DOI:10.1056/NEJMc2007617.

- 26 Riphagen S, Gomez X, Gonzalez-Martinez C, Wilkinson N, Theocharis P. Hyperinflammatory shock in children during COVID-19 pandemic. *Lancet* 2020; **395**: 1607–08.
- 27 European Centre for Disease Prevention and Control. Rapid risk assessment: paediatric inflammatory multisystem syndrome and SARS-CoV-2 infection in children. May 15, 2020. <https://www.ecdc.europa.eu/en/publications-data/paediatric-inflammatory-multisystem-syndrome-and-sars-cov-2-rapid-risk-assessment> (accessed June 24, 2020).
- 28 Tagarro A, Epalza C, Santos M, et al. Screening and severity of coronavirus disease 2019 (COVID-19) in children in Madrid, Spain. *JAMA Pediatr* 2020; published online April 8. DOI:10.1001/jamapediatrics.2020.1346.
- 29 McKiernan C, Chua LC, Visintainer PF, Allen H. High flow nasal cannulae therapy in infants with bronchiolitis. *J Pediatr* 2010; **156**: 634–38.
- 30 von der Beck D, Seeger W, Herold S, Gunther A, Loh B. Characteristics and outcomes of a cohort hospitalized for pandemic and seasonal influenza in Germany based on nationwide inpatient data. *PLoS One* 2017; **12**: e0180920.
- 31 Chiotos K, Hayes M, Kimberlin DW, et al. Multicenter initial guidance on use of antivirals for children with COVID-19/SARS-CoV-2. *J Ped Infect Dis Soc* 2020; published online April 22. DOI:10.1093/jpids/piaa045.
- 32 Grein J, Ohmagari N, Shin D, et al. Compassionate use of remdesivir for patients with severe COVID-19. *N Engl J Med* 2020; published online April 10. DOI:10.1056/NEJMoa2007016.
- 33 Li G, De Clercq E. Therapeutic options for the 2019 novel coronavirus (2019-nCoV). *Nat Rev Drug Discov* 2020; **19**: 149–50.
- 34 Cao B, Wang Y, Wen D, et al. A trial of lopinavir-ritonavir in adults hospitalized with severe COVID-19. *N Engl J Med* 2020; **382**: 1787–99.

ORIGINAL ARTICLE

Clinical Characteristics of Coronavirus Disease 2019 in China

W. Guan, Z. Ni, Yu Hu, W. Liang, C. Ou, J. He, L. Liu, H. Shan, C. Lei, D.S.C. Hui, B. Du, L. Li, G. Zeng, K.-Y. Yuen, R. Chen, C. Tang, T. Wang, P. Chen, J. Xiang, S. Li, Jin-lin Wang, Z. Liang, Y. Peng, L. Wei, Y. Liu, Ya-hua Hu, P. Peng, Jian-ming Wang, J. Liu, Z. Chen, G. Li, Z. Zheng, S. Qiu, J. Luo, C. Ye, S. Zhu, and N. Zhong, for the China Medical Treatment Expert Group for Covid-19*

ABSTRACT

BACKGROUND

Since December 2019, when coronavirus disease 2019 (Covid-19) emerged in Wuhan city and rapidly spread throughout China, data have been needed on the clinical characteristics of the affected patients.

METHODS

We extracted data regarding 1099 patients with laboratory-confirmed Covid-19 from 552 hospitals in 30 provinces, autonomous regions, and municipalities in mainland China through January 29, 2020. The primary composite end point was admission to an intensive care unit (ICU), the use of mechanical ventilation, or death.

RESULTS

The median age of the patients was 47 years; 41.9% of the patients were female. The primary composite end point occurred in 67 patients (6.1%), including 5.0% who were admitted to the ICU, 2.3% who underwent invasive mechanical ventilation, and 1.4% who died. Only 1.9% of the patients had a history of direct contact with wildlife. Among nonresidents of Wuhan, 72.3% had contact with residents of Wuhan, including 31.3% who had visited the city. The most common symptoms were fever (43.8% on admission and 88.7% during hospitalization) and cough (67.8%). Diarrhea was uncommon (3.8%). The median incubation period was 4 days (interquartile range, 2 to 7). On admission, ground-glass opacity was the most common radiologic finding on chest computed tomography (CT) (56.4%). No radiographic or CT abnormality was found in 157 of 877 patients (17.9%) with nonsevere disease and in 5 of 173 patients (2.9%) with severe disease. Lymphocytopenia was present in 83.2% of the patients on admission.

CONCLUSIONS

During the first 2 months of the current outbreak, Covid-19 spread rapidly throughout China and caused varying degrees of illness. Patients often presented without fever, and many did not have abnormal radiologic findings. (Funded by the National Health Commission of China and others.)

The authors' full names, academic degrees, and affiliations are listed in the Appendix. Address reprint requests to Dr. Zhong at the State Key Laboratory of Respiratory Disease, National Clinical Research Center for Respiratory Disease, Guangzhou Institute of Respiratory Health, First Affiliated Hospital of Guangzhou Medical University, 151 Yanjiang Rd., Guangzhou, Guangdong, China, or at nanshan@vip.163.com.

*A list of investigators in the China Medical Treatment Expert Group for Covid-19 study is provided in the Supplementary Appendix, available at NEJM.org.

Drs. Guan, Ni, Yu Hu, W. Liang, Ou, He, L. Liu, Shan, Lei, Hui, Du, L. Li, Zeng, and Yuen contributed equally to this article.

This article was published on February 28, 2020, and last updated on March 6, 2020, at NEJM.org.

DOI: 10.1056/NEJMoa2002032

Copyright © 2020 Massachusetts Medical Society.

IN EARLY DECEMBER 2019, THE FIRST PNEUMONIA cases of unknown origin were identified in Wuhan, the capital city of Hubei province.¹ The pathogen has been identified as a novel enveloped RNA betacoronavirus² that has currently been named severe acute respiratory syndrome coronavirus 2 (SARS-CoV-2), which has a phylogenetic similarity to SARS-CoV.³ Patients with the infection have been documented both in hospitals and in family settings.⁴⁻⁸

The World Health Organization (WHO) has recently declared coronavirus disease 2019 (Covid-19) a public health emergency of international concern.⁹ As of February 25, 2020, a total of 81,109 laboratory-confirmed cases had been documented globally.^{5,6,9-11} In recent studies, the severity of some cases of Covid-19 mimicked that of SARS-CoV.^{1,12,13} Given the rapid spread of Covid-19, we determined that an updated analysis of cases throughout mainland China might help identify the defining clinical characteristics and severity of the disease. Here, we describe the results of our analysis of the clinical characteristics of Covid-19 in a selected cohort of patients throughout China.

METHODS

STUDY OVERSIGHT

The study was supported by National Health Commission of China and designed by the investigators. The study was approved by the institutional review board of the National Health Commission. Written informed consent was waived in light of the urgent need to collect data. Data were analyzed and interpreted by the authors. All the authors reviewed the manuscript and vouch for the accuracy and completeness of the data and for the adherence of the study to the protocol, available with the full text of this article at NEJM.org.

DATA SOURCES

We obtained the medical records and compiled data for hospitalized patients and outpatients with laboratory-confirmed Covid-19, as reported to the National Health Commission between December 11, 2019, and January 29, 2020; the data cutoff for the study was January 31, 2020. Covid-19 was diagnosed on the basis of the WHO interim guidance.¹⁴ A confirmed case of Covid-19 was defined as a positive result on high-

throughput sequencing or real-time reverse-transcriptase–polymerase-chain-reaction (RT-PCR) assay of nasal and pharyngeal swab specimens.¹ Only laboratory-confirmed cases were included in the analysis.

We obtained data regarding cases outside Hubei province from the National Health Commission. Because of the high workload of clinicians, three outside experts from Guangzhou performed raw data extraction at Wuhan Jinyintan Hospital, where many of the patients with Covid-19 in Wuhan were being treated.

We extracted the recent exposure history, clinical symptoms or signs, and laboratory findings on admission from electronic medical records. Radiologic assessments included chest radiography or computed tomography (CT), and all laboratory testing was performed according to the clinical care needs of the patient. We determined the presence of a radiologic abnormality on the basis of the documentation or description in medical charts; if imaging scans were available, they were reviewed by attending physicians in respiratory medicine who extracted the data. Major disagreement between two reviewers was resolved by consultation with a third reviewer. Laboratory assessments consisted of a complete blood count, blood chemical analysis, coagulation testing, assessment of liver and renal function, and measures of electrolytes, C-reactive protein, procalcitonin, lactate dehydrogenase, and creatine kinase. We defined the degree of severity of Covid-19 (severe vs. nonsevere) at the time of admission using the American Thoracic Society guidelines for community-acquired pneumonia.¹⁵

All medical records were copied and sent to the data-processing center in Guangzhou, under the coordination of the National Health Commission. A team of experienced respiratory clinicians reviewed and abstracted the data. Data were entered into a computerized database and cross-checked. If the core data were missing, requests for clarification were sent to the coordinators, who subsequently contacted the attending clinicians.

STUDY OUTCOMES

The primary composite end point was admission to an intensive care unit (ICU), the use of mechanical ventilation, or death. These outcomes

were used in a previous study to assess the severity of other serious infectious diseases, such as H7N9 infection.¹⁶ Secondary end points were the rate of death and the time from symptom onset until the composite end point and until each component of the composite end point.

STUDY DEFINITIONS

The incubation period was defined as the interval between the potential earliest date of contact of the transmission source (wildlife or person with suspected or confirmed case) and the potential earliest date of symptom onset (i.e., cough, fever, fatigue, or myalgia). We excluded incubation periods of less than 1 day because some patients had continuous exposure to contamination sources; in these cases, the latest date of exposure was recorded. The summary statistics of incubation periods were calculated on the basis of 291 patients who had clear information regarding the specific date of exposure.

Fever was defined as an axillary temperature of 37.5°C or higher. Lymphocytopenia was defined as a lymphocyte count of less than 1500 cells per cubic millimeter. Thrombocytopenia was defined as a platelet count of less than 150,000 per cubic millimeter. Additional definitions — including exposure to wildlife, acute respiratory distress syndrome (ARDS), pneumonia, acute kidney failure, acute heart failure, and rhabdomyolysis — are provided in the Supplementary Appendix, available at NEJM.org.

LABORATORY CONFIRMATION

Laboratory confirmation of SARS-CoV-2 was performed at the Chinese Center for Disease Prevention and Control before January 23, 2020, and subsequently in certified tertiary care hospitals. RT-PCR assays were performed in accordance with the protocol established by the WHO.¹⁷ Details regarding laboratory confirmation processes are provided in the Supplementary Appendix.

STATISTICAL ANALYSIS

Continuous variables were expressed as medians and interquartile ranges or simple ranges, as appropriate. Categorical variables were summarized as counts and percentages. No imputation was made for missing data. Because the cohort of patients in our study was not derived from random selection, all statistics are deemed to be

descriptive only. We used ArcGIS, version 10.2.2, to plot the numbers of patients with reportedly confirmed cases on a map. All the analyses were performed with the use of R software, version 3.6.2 (R Foundation for Statistical Computing).

RESULTS

DEMOGRAPHIC AND CLINICAL CHARACTERISTICS

Of the 7736 patients with Covid-19 who had been hospitalized at 552 sites as of January 29, 2020, we obtained data regarding clinical symptoms and outcomes for 1099 patients (14.2%). The largest number of patients (132) had been admitted to Wuhan Jinyintan Hospital. The hospitals that were included in this study accounted for 29.7% of the 1856 designated hospitals where patients with Covid-19 could be admitted in 30 provinces, autonomous regions, or municipalities across China (Fig. 1).

The demographic and clinical characteristics of the patients are shown in Table 1. A total of 3.5% were health care workers, and a history of contact with wildlife was documented in 1.9%; 483 patients (43.9%) were residents of Wuhan. Among the patients who lived outside Wuhan, 72.3% had contact with residents of Wuhan, including 31.3% who had visited the city; 25.9% of nonresidents had neither visited the city nor had contact with Wuhan residents.

The median incubation period was 4 days (interquartile range, 2 to 7). The median age of the patients was 47 years (interquartile range, 35 to 58); 0.9% of the patients were younger than 15 years of age. A total of 41.9% were female. Fever was present in 43.8% of the patients on admission but developed in 88.7% during hospitalization. The second most common symptom was cough (67.8%); nausea or vomiting (5.0%) and diarrhea (3.8%) were uncommon. Among the overall population, 23.7% had at least one coexisting illness (e.g., hypertension and chronic obstructive pulmonary disease).

On admission, the degree of severity of Covid-19 was categorized as nonsevere in 926 patients and severe in 173 patients. Patients with severe disease were older than those with nonsevere disease by a median of 7 years. Moreover, the presence of any coexisting illness was more common among patients with severe disease than among those with nonsevere disease (38.7% vs.

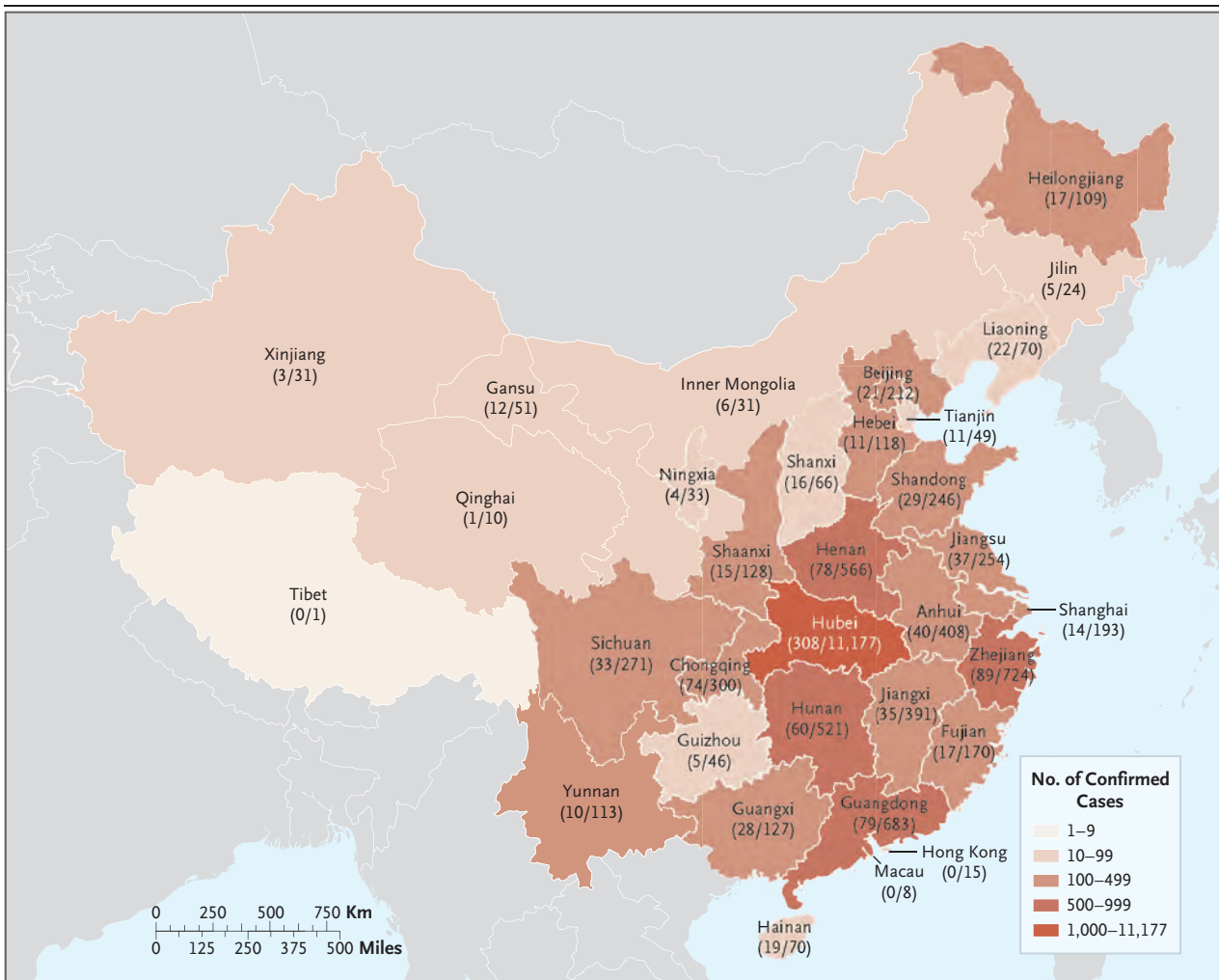


Figure 1. Distribution of Patients with Covid-19 across Mainland China.

Shown are the official statistics of all documented, laboratory-confirmed cases of coronavirus disease 2019 (Covid-19) throughout China, according to the National Health Commission as of February 4, 2020. The numerator denotes the number of patients who were included in the study cohort and the denominator denotes the number of laboratory-confirmed cases for each province, autonomous region, or provincial municipality, as reported by the National Health Commission.

21.0%). However, the exposure history between the two groups of disease severity was similar.

RADIOLOGIC AND LABORATORY FINDINGS

Table 2 shows the radiologic and laboratory findings on admission. Of 975 CT scans that were performed at the time of admission, 86.2% revealed abnormal results. The most common patterns on chest CT were ground-glass opacity (56.4%) and bilateral patchy shadowing (51.8%). Representative radiologic findings in two patients with nonsevere Covid-19 and in another

two patients with severe Covid-19 are provided in Figure S1 in the Supplementary Appendix. No radiographic or CT abnormality was found in 157 of 877 patients (17.9%) with nonsevere disease and in 5 of 173 patients (2.9%) with severe disease.

On admission, lymphocytopenia was present in 83.2% of the patients, thrombocytopenia in 36.2%, and leukopenia in 33.7%. Most of the patients had elevated levels of C-reactive protein; less common were elevated levels of alanine aminotransferase, aspartate aminotransferase,

creatinine kinase, and D-dimer. Patients with severe disease had more prominent laboratory abnormalities (including lymphocytopenia and leukopenia) than those with nonsevere disease.

CLINICAL OUTCOMES

None of the 1099 patients were lost to follow-up during the study. A primary composite end-point event occurred in 67 patients (6.1%), including 5.0% who were admitted to the ICU, 2.3% who underwent invasive mechanical ventilation, and 1.4% who died (Table 3). Among the 173 patients with severe disease, a primary composite end-point event occurred in 43 patients (24.9%). Among all the patients, the cumulative risk of the composite end point was 3.6%; among those with severe disease, the cumulative risk was 20.6%.

TREATMENT AND COMPLICATIONS

A majority of the patients (58.0%) received intravenous antibiotic therapy, and 35.8% received oseltamivir therapy; oxygen therapy was administered in 41.3% and mechanical ventilation in 6.1%; higher percentages of patients with severe disease received these therapies (Table 3). Mechanical ventilation was initiated in more patients with severe disease than in those with nonsevere disease (noninvasive ventilation, 32.4% vs. 0%; invasive ventilation, 14.5% vs. 0%). Systemic glucocorticoids were given to 204 patients (18.6%), with a higher percentage among those with severe disease than nonsevere disease (44.5% vs. 13.7%). Of these 204 patients, 33 (16.2%) were admitted to the ICU, 17 (8.3%) underwent invasive ventilation, and 5 (2.5%) died. Extracorporeal membrane oxygenation was performed in 5 patients (0.5%) with severe disease.

The median duration of hospitalization was 12.0 days (mean, 12.8). During hospital admission, most of the patients received a diagnosis of pneumonia from a physician (91.1%), followed by ARDS (3.4%) and shock (1.1%). Patients with severe disease had a higher incidence of physician-diagnosed pneumonia than those with nonsevere disease (99.4% vs. 89.5%).

DISCUSSION

During the initial phase of the Covid-19 outbreak, the diagnosis of the disease was complicated by the diversity in symptoms and imaging

findings and in the severity of disease at the time of presentation. Fever was identified in 43.8% of the patients on presentation but developed in 88.7% after hospitalization. Severe illness occurred in 15.7% of the patients after admission to a hospital. No radiologic abnormalities were noted on initial presentation in 2.9% of the patients with severe disease and in 17.9% of those with nonsevere disease. Despite the number of deaths associated with Covid-19, SARS-CoV-2 appears to have a lower case fatality rate than either SARS-CoV or Middle East respiratory syndrome-related coronavirus (MERS-CoV). Compromised respiratory status on admission (the primary driver of disease severity) was associated with worse outcomes.

Approximately 2% of the patients had a history of direct contact with wildlife, whereas more than three quarters were either residents of Wuhan, had visited the city, or had contact with city residents. These findings echo the latest reports, including the outbreak of a family cluster,⁴ transmission from an asymptomatic patient,⁶ and the three-phase outbreak patterns.⁸ Our study cannot preclude the presence of patients who have been termed “super-spreaders.”

Conventional routes of transmission of SARS-CoV, MERS-CoV, and highly pathogenic influenza consist of respiratory droplets and direct contact,¹⁸⁻²⁰ mechanisms that probably occur with SARS-CoV-2 as well. Because SARS-CoV-2 can be detected in the gastrointestinal tract, saliva, and urine, these routes of potential transmission need to be investigated²¹ (Tables S1 and S2).

The term Covid-19 has been applied to patients who have laboratory-confirmed symptomatic cases without apparent radiologic manifestations. A better understanding of the spectrum of the disease is needed, since in 8.9% of the patients, SARS-CoV-2 infection was detected before the development of viral pneumonia or viral pneumonia did not develop.

In concert with recent studies,^{1,8,12} we found that the clinical characteristics of Covid-19 mimic those of SARS-CoV. Fever and cough were the dominant symptoms and gastrointestinal symptoms were uncommon, which suggests a difference in viral tropism as compared with SARS-CoV, MERS-CoV, and seasonal influenza.^{22,23} The absence of fever in Covid-19 is more frequent than in SARS-CoV (1%) and MERS-CoV infection

Table 1. Clinical Characteristics of the Study Patients, According to Disease Severity and the Presence or Absence of the Primary Composite End Point.*

Characteristic	All Patients (N=1099)	Disease Severity		Presence of Primary Composite End Point†‡	
		Nonsevere (N = 926)	Severe (N = 173)	Yes (N = 67)	No (N = 1032)
Age					
Median (IQR) — yr	47.0 (35.0–58.0)	45.0 (34.0–57.0)	52.0 (40.0–65.0)	63.0 (53.0–71.0)	46.0 (35.0–57.0)
Distribution — no./total no. (%)					
0–14 yr	9/1011 (0.9)	8/848 (0.9)	1/163 (0.6)	0	9/946 (1.0)
15–49 yr	557/1011 (55.1)	490/848 (57.8)	67/163 (41.1)	12/65 (18.5)	545/946 (57.6)
50–64 yr	292/1011 (28.9)	241/848 (28.4)	51/163 (31.3)	21/65 (32.3)	271/946 (28.6)
≥65 yr	153/1011 (15.1)	109/848 (12.9)	44/163 (27.0)	32/65 (49.2)	121/946 (12.8)
Female sex — no./total no. (%)	459/1096 (41.9)	386/923 (41.8)	73/173 (42.2)	22/67 (32.8)	437/1029 (42.5)
Smoking history — no./total no. (%)					
Never smoked	927/1085 (85.4)	793/913 (86.9)	134/172 (77.9)	44/66 (66.7)	883/1019 (86.7)
Former smoker	21/1085 (1.9)	12/913 (1.3)	9/172 (5.2)	5/66 (7.6)	16/1019 (1.6)
Current smoker	137/1085 (12.6)	108/913 (11.8)	29/172 (16.9)	17/66 (25.8)	120/1019 (11.8)
Exposure to source of transmission within past 14 days — no./total no.					
Living in Wuhan	483/1099 (43.9)	400/926 (43.2)	83/173 (48.0)	39/67 (58.2)	444/1032 (43.0)
Contact with wildlife	13/687 (1.9)	10/559 (1.8)	3/128 (2.3)	1/41 (2.4)	12/646 (1.9)
Recently visited Wuhan‡	193/616 (31.3)	166/526 (31.6)	27/90 (30.0)	10/28 (35.7)	183/588 (31.1)
Had contact with Wuhan residents‡	442/611 (72.3)	376/522 (72.0)	66/89 (74.2)	19/28 (67.9)	423/583 (72.6)
Median incubation period (IQR) — days§	4.0 (2.0–7.0)	4.0 (2.8–7.0)	4.0 (2.0–7.0)	4.0 (1.0–7.5)	4.0 (2.0–7.0)
Fever on admission					
Patients — no./total no. (%)	473/1081 (43.8)	391/910 (43.0)	82/171 (48.0)	24/66 (36.4)	449/1015 (44.2)
Median temperature (IQR) — °C	37.3 (36.7–38.0)	37.3 (36.7–38.0)	37.4 (36.7–38.1)	36.8 (36.3–37.8)	37.3 (36.7–38.0)
Distribution of temperature — no./total no. (%)					
<37.5°C	608/1081 (56.2)	519/910 (57.0)	89/171 (52.0)	42/66 (63.6)	566/1015 (55.8)
37.5–38.0°C	238/1081 (22.0)	201/910 (22.1)	37/171 (21.6)	10/66 (15.2)	228/1015 (22.5)
38.1–39.0°C	197/1081 (18.2)	160/910 (17.6)	37/171 (21.6)	11/66 (16.7)	186/1015 (18.3)
>39.0°C	38/1081 (3.5)	30/910 (3.3)	8/171 (4.7)	3/66 (4.5)	35/1015 (3.4)
Fever during hospitalization					
Patients — no./total no. (%)	975/1099 (88.7)	816/926 (88.1)	159/173 (91.9)	59/67 (88.1)	916/1032 (88.8)
Median highest temperature (IQR) — °C	38.3 (37.8–38.9)	38.3 (37.8–38.9)	38.5 (38.0–39.0)	38.5 (38.0–39.0)	38.3 (37.8–38.9)
<37.5°C	92/926 (9.9)	79/774 (10.2)	13/152 (8.6)	3/54 (5.6)	89/872 (10.2)
37.5–38.0°C	286/926 (30.9)	251/774 (32.4)	35/152 (23.0)	20/54 (37.0)	266/872 (30.5)
38.1–39.0°C	434/926 (46.9)	356/774 (46.0)	78/152 (51.3)	21/54 (38.9)	413/872 (47.4)
>39.0°C	114/926 (12.3)	88/774 (11.4)	26/152 (17.1)	10/54 (18.5)	104/872 (11.9)

Symptoms — no. (%)	9 (0.8)	5 (0.5)	4 (2.3)	0	9 (0.9)
Conjunctival congestion	53 (4.8)	47 (5.1)	6 (3.5)	2 (3.0)	51 (4.9)
Nasal congestion	150 (13.6)	124 (13.4)	26 (15.0)	8 (11.9)	142 (13.8)
Headache	745 (67.8)	623 (67.3)	122 (70.5)	46 (68.7)	699 (67.7)
Cough	153 (13.9)	130 (14.0)	23 (13.3)	6 (9.0)	147 (14.2)
Sore throat	370 (33.7)	309 (33.4)	61 (35.3)	20 (29.9)	350 (33.9)
Sputum production	419 (38.1)	350 (37.8)	69 (39.9)	22 (32.8)	397 (38.5)
Fatigue	10 (0.9)	6 (0.6)	4 (2.3)	2 (3.0)	8 (0.8)
Hemoptysis	205 (18.7)	140 (15.1)	65 (37.6)	36 (53.7)	169 (16.4)
Shortness of breath	55 (5.0)	43 (4.6)	12 (6.9)	3 (4.5)	52 (5.0)
Nausea or vomiting	42 (3.8)	32 (3.5)	10 (5.8)	4 (6.0)	38 (3.7)
Diarrhea	164 (14.9)	134 (14.5)	30 (17.3)	6 (9.0)	158 (15.3)
Myalgia or arthralgia	126 (11.5)	100 (10.8)	26 (15.0)	8 (11.9)	118 (11.4)
Chills					
Signs of infection — no. (%)					
Throat congestion	19 (1.7)	17 (1.8)	2 (1.2)	0	19 (1.8)
Tonsil swelling	23 (2.1)	17 (1.8)	6 (3.5)	1 (1.5)	22 (2.1)
Enlargement of lymph nodes	2 (0.2)	1 (0.1)	1 (0.6)	1 (1.5)	1 (0.1)
Rash	2 (0.2)	0	2 (1.2)	0	2 (0.2)
Coexisting disorder — no. (%)					
Any	261 (23.7)	194 (21.0)	67 (38.7)	39 (58.2)	222 (21.5)
Chronic obstructive pulmonary disease	12 (1.1)	6 (0.6)	6 (3.5)	7 (10.4)	5 (0.5)
Diabetes	81 (7.4)	53 (5.7)	28 (16.2)	18 (26.9)	63 (6.1)
Hypertension	165 (15.0)	124 (13.4)	41 (23.7)	24 (35.8)	141 (13.7)
Coronary heart disease	27 (2.5)	17 (1.8)	10 (5.8)	6 (9.0)	21 (2.0)
Cerebrovascular disease	15 (1.4)	11 (1.2)	4 (2.3)	4 (6.0)	11 (1.1)
Hepatitis B infection¶	23 (2.1)	22 (2.4)	1 (0.6)	1 (1.5)	22 (2.1)
Cancer	10 (0.9)	7 (0.8)	3 (1.7)	1 (1.5)	9 (0.9)
Chronic renal disease	8 (0.7)	5 (0.5)	3 (1.7)	2 (3.0)	6 (0.6)
Immunodeficiency	2 (0.2)	2 (0.2)	0	0	2 (0.2)

* The denominators of patients who were included in the analysis are provided if they differed from the overall numbers in the group. Percentages may not total 100 because of rounding. Covid-19 denotes coronavirus disease 2019, and IQR interquartile range.

† The primary composite end point was admission to an intensive care unit, the use of mechanical ventilation, or death.

‡ These patients were not residents of Wuhan.

§ Data regarding the incubation period were missing for 808 patients (73.5%).

¶ The presence of hepatitis B infection was defined as a positive result on testing for hepatitis B surface antigen with or without elevated levels of alanine or aspartate aminotransferase.

|| Included in this category is any type of cancer.

Table 2. Radiographic and Laboratory Findings.*

Table 2. Radiographic and Laboratory Findings.*					
Variable	All Patients (N = 1099)	Disease Severity		Presence of Composite Primary End Point	
		Nonsevere (N = 926)	Severe (N = 173)	Yes (N = 67)	No (N = 1032)
Radiologic findings					
Abnormalities on chest radiograph — no./total no. (%)	162/274 (59.1)	116/214 (54.2)	46/60 (76.7)	30/39 (76.9)	132/235 (56.2)
Ground-glass opacity	55/274 (20.1)	37/214 (17.3)	18/60 (30.0)	9/39 (23.1)	46/235 (19.6)
Local patchy shadowing	77/274 (28.1)	56/214 (26.2)	21/60 (35.0)	13/39 (33.3)	64/235 (27.2)
Bilateral patchy shadowing	100/274 (36.5)	65/214 (30.4)	35/60 (58.3)	27/39 (69.2)	73/235 (31.1)
Interstitial abnormalities	12/274 (4.4)	7/214 (3.3)	5/60 (8.3)	6/39 (15.4)	6/235 (2.6)
Abnormalities on chest CT — no./total no. (%)	840/975 (86.2)	682/808 (84.4)	158/167 (94.6)	50/57 (87.7)	790/918 (86.1)
Ground-glass opacity	550/975 (56.4)	449/808 (55.6)	101/167 (60.5)	30/57 (52.6)	520/918 (56.6)
Local patchy shadowing	409/975 (41.9)	317/808 (39.2)	92/167 (55.1)	22/57 (38.6)	387/918 (42.2)
Bilateral patchy shadowing	505/975 (51.8)	368/808 (45.5)	137/167 (82.0)	40/57 (70.2)	465/918 (50.7)
Interstitial abnormalities	143/975 (14.7)	99/808 (12.3)	44/167 (26.3)	15/57 (26.3)	128/918 (13.9)
Laboratory findings					
Median Pao ₂ :Fio ₂ ratio (IQR) †	3.9 (2.9–4.7)	3.9 (2.9–4.5)	4.0 (2.8–5.2)	2.9 (2.2–5.4)	4.0 (3.1–4.6)
White-cell count					
Median (IQR) — per mm ³	4700 (3500–6000)	4900 (3800–6000)	3700 (3000–6200)	6100 (4900–11,100)	4700 (3500–5900)
Distribution — no./total no. (%)					
>10,000 per mm ³	58/978 (5.9)	39/811 (4.8)	19/167 (11.4)	15/58 (25.9)	43/920 (4.7)
<4000 per mm ³	330/978 (33.7)	228/811 (28.1)	102/167 (61.1)	8/58 (13.8)	322/920 (35.0)
Lymphocyte count					
Median (IQR) — per mm ³	1000 (700–1300)	1000 (800–1400)	800 (600–1000)	700 (600–900)	1000 (700–1300)
Distribution — no./total no. (%)					
<1500 per mm ³	731/879 (83.2)	584/726 (80.4)	147/153 (96.1)	50/54 (92.6)	681/825 (82.5)

Platelet count					
Median (IQR) — per mm ³	168,000 (132,000–207,000)	172,000 (139,000–212,000)	137,500 (99,000–179,500)	156,500 (114,200–195,000)	169,000 (133,000–207,000)
Distribution — no./total no. (%)					
<150,000 per mm ³	315/869 (36.2)	225/713 (31.6)	90/156 (57.7)	27/58 (46.6)	288/811 (35.5)
Median hemoglobin (IQR) — g/dl‡	13.4. (11.9–14.8)	13.5 (12.0–14.8)	12.8 (11.2–14.1)	12.5 (10.5–14.0)	13.4 (12.0–14.8)
Distribution of other findings — no./total no. (%)					
C-reactive protein ≥10 mg/liter	481/793 (60.7)	371/658 (56.4)	110/135 (81.5)	41/45 (91.1)	440/748 (58.8)
Procalcitonin ≥0.5 ng/ml	35/633 (5.5)	19/516 (3.7)	16/117 (13.7)	12/50 (24.0)	23/583 (3.9)
Lactate dehydrogenase ≥250 U/liter	277/675 (41.0)	205/551 (37.2)	72/124 (58.1)	31/44 (70.5)	246/631 (39.0)
Aspartate aminotransferase >40 U/liter	168/757 (22.2)	112/615 (18.2)	56/142 (39.4)	26/52 (50.0)	142/705 (20.1)
Alanine aminotransferase >40 U/liter	158/741 (21.3)	120/606 (19.8)	38/135 (28.1)	20/49 (40.8)	138/692 (19.9)
Total bilirubin >17.1 μmol/liter	76/722 (10.5)	59/594 (9.9)	17/128 (13.3)	10/48 (20.8)	66/674 (9.8)
Creatine kinase ≥200 U/liter	90/657 (13.7)	67/536 (12.5)	23/121 (19.0)	12/46 (26.1)	78/611 (12.8)
Creatinine ≥133 μmol/liter	12/752 (1.6)	6/614 (1.0)	6/138 (4.3)	5/52 (9.6)	7/700 (1.0)
D-dimer ≥0.5 mg/liter	260/560 (46.4)	195/451 (43.2)	65/109 (59.6)	34/49 (69.4)	226/511 (44.2)
Minerals§					
Median sodium (IQR) — mmol/liter	138.2 (136.1–140.3)	138.4 (136.6–140.4)	138.0 (136.0–140.0)	138.3 (135.0–141.2)	138.2 (136.1–140.2)
Median potassium (IQR) — mmol/liter	3.8 (3.5–4.2)	3.9 (3.6–4.2)	3.8 (3.5–4.1)	3.9 (3.6–4.1)	3.8 (3.5–4.2)
Median chloride (IQR) — mmol/liter	102.9 (99.7–105.6)	102.7 (99.7–105.3)	103.1 (99.8–106.0)	103.8 (100.8–107.0)	102.8 (99.6–105.3)

* Lymphocytopenia was defined as a lymphocyte count of less than 1500 per cubic millimeter. Thrombocytopenia was defined as a platelet count of less than 150,000 per cubic millimeter. To convert the values for creatinine to milligrams per deciliter, divide by 88.4.

† Data regarding the ratio of the partial pressure of arterial oxygen to the fraction of inspired oxygen (PaO₂:Fio₂) were missing for 894 patients (81.3%).

‡ Data regarding hemoglobin were missing for 226 patients (20.6%).

§ Data were missing for the measurement of sodium in 363 patients (33.0%), for potassium in 349 patients (31.8%), and for chloride in 392 patients (35.7%).

Table 3. Complications, Treatments, and Clinical Outcomes.

Variable	All Patients (N = 1099)	Disease Severity			Presence of Composite Primary End Point	
		Nonsevere (N = 926)	Severe (N = 173)		Yes (N = 67)	No (N = 1032)
Complications						
Septic shock — no. (%)	12 (1.1)	1 (0.1)	11 (6.4)		9 (13.4)	3 (0.3)
Acute respiratory distress syndrome — no. (%)	37 (3.4)	10 (1.1)	27 (15.6)		27 (40.3)	10 (1.0)
Acute kidney injury — no. (%)	6 (0.5)	1 (0.1)	5 (2.9)		4 (6.0)	2 (0.2)
Disseminated intravascular coagulation — no. (%)	1 (0.1)	0	1 (0.6)		1 (1.5)	0
Rhabdomyolysis — no. (%)	2 (0.2)	2 (0.2)	0		0	2 (0.2)
Physician-diagnosed pneumonia — no./total no. (%)	972/1067 (91.1)	800/894 (89.5)	172/173 (99.4)		63/66 (95.5)	909/1001 (90.8)
Median time until development of pneumonia (IQR) — days*						
After initial Covid-19 diagnosis	0.0 (0.0–1.0)	0.0 (0.0–1.0)	0.0 (0.0–2.0)		0.0 (0.0–3.5)	0.0 (0.0–1.0)
After onset of Covid-19 symptoms	3.0 (1.0–6.0)	3.0 (1.0–6.0)	5.0 (2.0–7.0)		4.0 (0.0–7.0)	3.0 (1.0–6.0)
Treatments						
Intravenous antibiotics — no. (%)	637 (58.0)	498 (53.8)	139 (80.3)		60 (89.6)	577 (55.9)
Oseltamivir — no. (%)	393 (35.8)	313 (33.8)	80 (46.2)		36 (53.7)	357 (34.6)
Antifungal medication — no. (%)	31 (2.8)	18 (1.9)	13 (7.5)		8 (11.9)	23 (2.2)
Systemic glucocorticoids — no. (%)	204 (18.6)	127 (13.7)	77 (44.5)		35 (52.2)	169 (16.4)
Oxygen therapy — no. (%)	454 (41.3)	331 (35.7)	123 (71.1)		59 (88.1)	395 (38.3)
Mechanical ventilation — no. (%)	67 (6.1)	0	67 (38.7)		40 (59.7)	27 (2.6)
Invasive	25 (2.3)	0	25 (14.5)		25 (37.3)	0
Noninvasive	56 (5.1)	0	56 (32.4)		29 (43.3)	27 (2.6)
Use of extracorporeal membrane oxygenation — no. (%)	5 (0.5)	0	5 (2.9)		5 (7.5)	0
Use of continuous renal-replacement therapy — no. (%)	9 (0.8)	0	9 (5.2)		8 (11.9)	1 (0.1)
Use of intravenous immune globulin — no. (%)	144 (13.1)	86 (9.3)	58 (33.5)		27 (40.3)	117 (11.3)
Admission to intensive care unit — no. (%)	55 (5.0)	22 (2.4)	33 (19.1)		55 (82.1)	0
Median length of hospital stay (IQR) — days†	12.0 (10.0–14.0)	11.0 (10.0–13.0)	13.0 (11.5–17.0)		14.5 (11.0–19.0)	12.0 (10.0–13.0)

Clinical outcomes at data cutoff — no. (%)					
Discharge from hospital	55 (5.0)	50 (5.4)	5 (2.9)	1 (1.5)	54 (5.2)
Death	15 (1.4)	1 (0.1)	14 (8.1)	15 (22.4)	0
Recovery	9 (0.8)	7 (0.8)	2 (1.2)	0	9 (0.9)
Hospitalization	1029 (93.6)	875 (94.5)	154 (89.0)	51 (76.1)	978 (94.8)

* For the development of pneumonia, data were missing for 347 patients (31.6%) regarding the time since the initial diagnosis and for 161 patients (14.6%) regarding the time since symptom onset.

† Data regarding the median length of hospital stay were missing for 136 patients (12.4%).

(2%),²⁰ so afebrile patients may be missed if the surveillance case definition focuses on fever detection.¹⁴ Lymphocytopenia was common and, in some cases, severe, a finding that was consistent with the results of two recent reports.^{1,12} We found a lower case fatality rate (1.4%) than the rate that was recently reportedly,^{1,12} probably because of the difference in sample sizes and case inclusion criteria. Our findings were more similar to the national official statistics, which showed a rate of death of 3.2% among 51,857 cases of Covid-19 as of February 16, 2020.^{11,24} Since patients who were mildly ill and who did not seek medical attention were not included in our study, the case fatality rate in a real-world scenario might be even lower. Early isolation, early diagnosis, and early management might have collectively contributed to the reduction in mortality in Guangdong.

Despite the phylogenetic homogeneity between SARS-CoV-2 and SARS-CoV, there are some clinical characteristics that differentiate Covid-19 from SARS-CoV, MERS-CoV, and seasonal influenza infections. (For example, seasonal influenza has been more common in respiratory outpatient clinics and wards.) Some additional characteristics that are unique to Covid-19 are detailed in Table S3.

Our study has some notable limitations. First, some cases had incomplete documentation of the exposure history and laboratory testing, given the variation in the structure of electronic databases among different participating sites and the urgent timeline for data extraction. Some cases were diagnosed in outpatient settings where medical information was briefly documented and incomplete laboratory testing was performed, along with a shortage of infrastructure and training of medical staff in non-specialty hospitals. Second, we could estimate the incubation period in only 291 of the study patients who had documented information. The uncertainty of the exact dates (recall bias) might have inevitably affected our assessment. Third, because many patients remained in the hospital and the outcomes were unknown at the time of data cutoff, we censored the data regarding their clinical outcomes as of the time of our analysis. Fourth, we no doubt missed patients who were asymptomatic or had mild cases and who were treated at home, so our study cohort may represent the more severe end of Covid-19. Fifth,

many patients did not undergo sputum bacteriologic or fungal assessment on admission because, in some hospitals, medical resources were overwhelmed. Sixth, data generation was clinically driven and not systematic.

Covid-19 has spread rapidly since it was first identified in Wuhan and has been shown to have a wide spectrum of severity. Some patients with Covid-19 do not have fever or radiologic abnormalities on initial presentation, which has complicated the diagnosis.

Supported by the National Health Commission of China, the National Natural Science Foundation, and the Department of Science and Technology of Guangdong Province.

Disclosure forms provided by the authors are available with the full text of this article at NEJM.org.

We thank all the hospital staff members (see Supplementary Appendix for a full list of the staff) for their efforts in collecting the information that was used in this study; Zong-jiu Zhang, Ya-hui Jiao, Xin-qiang Gao, and Tao Wei (National Health Commission), Yu-fei Duan and Zhi-ling Zhao (Health Commission of

Guangdong Province), and Yi-min Li, Nuo-fu Zhang, Qing-hui Huang, Wen-xi Huang, and Ming Li (Guangzhou Institute of Respiratory Health) for facilitating the collection of patients' data; the statistical team members Zheng Chen, Dong Han, Li Li, Zhi-ying Zhan, Jin-jian Chen, Li-jun Xu, and Xiao-han Xu (State Key Laboratory of Organ Failure Research, Department of Biostatistics, Guangdong Provincial Key Laboratory of Tropical Disease Research, School of Public Health, and Southern Medical University, respectively); Li-qiang Wang, Wei-peng Cai, Zi-sheng Chen (the Sixth Affiliated Hospital of Guangzhou Medical University) and Chang-xing Ou, Xiao-min Peng, Si-ni Cui, Yuan Wang, Mou Zeng, Xin Hao, Qi-hua He, Jing-pei Li, Xu-kai Li, Wei Wang, Li-min Ou, Ya-lei Zhang, Jing-wei Liu, Xin-guo Xiong, Wei-juna Shi, San-mei Yu, Run-dong Qin, Si-yang Yao, Bo-meng Zhang, Xiao-hong Xie, Zhan-hong Xie, Wan-di Wang, Xiao-xian Zhang, Hui-yin Xu, Zi-qing Zhou, Ying Jiang, Ni Liu, Jing-jing Yuan, Zheng Zhu, Jie-xia Zhang, Hong-hao Li, Wei-hua Huang, Lu-lin Wang, Jie-ying Li, Li-fen Gao, Cai-chen Li, Xue-wei Chen, Jia-bo Gao, Ming-shan Xue, Shou-xie Huang, Jia-man Tang, and Wei-li Gu (Guangzhou Institute of Respiratory Health) for their dedication to data entry and verification; Tencent (Internet-services company) for providing the number of hospitals certified to admit patients with Covid-19 throughout China; and all the patients who consented to donate their data for analysis and the medical staff members who are on the front line of caring for patients.

APPENDIX

The authors' full names and academic degrees are as follows: Wei-jie Guan, Ph.D., Zheng-yi Ni, M.D., Yu Hu, M.D., Wen-hua Liang, Ph.D., Chun-quan Ou, Ph.D., Jian-xing He, M.D., Lei Liu, M.D., Hong Shan, M.D., Chun-liang Lei, M.D., David S.C. Hui, M.D., Bin Du, M.D., Lan-juan Li, M.D., Guang Zeng, M.Sc., Kwok-Yung Yuen, Ph.D., Ru-chong Chen, M.D., Chun-li Tang, M.D., Tao Wang, M.D., Ping-yan Chen, M.D., Jie Xiang, M.D., Shi-yue Li, M.D., Jin-lin Wang, M.D., Zi-jing Liang, M.D., Yi-xiang Peng, M.D., Li Wei, M.D., Yong Liu, M.D., Ya-hua Hu, M.D., Peng Peng, M.D., Jian-ming Wang, M.D., Ji-yang Liu, M.D., Zhong Chen, M.D., Gang Li, M.D., Zhi-jian Zheng, M.D., Shao-qin Qiu, M.D., Jie Luo, M.D., Chang-jiang Ye, M.D., Shao-yong Zhu, M.D., and Nan-shan Zhong, M.D.

The authors' affiliations are as follows: the State Key Laboratory of Respiratory Disease, National Clinical Research Center for Respiratory Disease, Guangzhou Institute of Respiratory Health, First Affiliated Hospital of Guangzhou Medical University (W.G., W.L., J.H., R.C., C.T., T.W., S.L., Jin-lin Wang, N.Z., J.H., W.L.), the Departments of Thoracic Oncology (W.L.), Thoracic Surgery and Oncology (J.H.), and Emergency Medicine (Z.L.), First Affiliated Hospital of Guangzhou Medical University, and Guangzhou Eighth People's Hospital, Guangzhou Medical University (C.L.), and the State Key Laboratory of Organ Failure Research, Department of Biostatistics, Guangdong Provincial Key Laboratory of Tropical Disease Research, School of Public Health, Southern Medical University (C.O., P.C.), Guangzhou, Wuhan Jinyintan Hospital (Z.N., J.X.), Union Hospital, Tongji Medical College, Huazhong University of Science and Technology (Yu Hu), the Central Hospital of Wuhan (Y.P.), Wuhan No. 1 Hospital, Wuhan Hospital of Traditional Chinese and Western Medicine (L.W.), Wuhan Pulmonary Hospital (P.P.), Tianyou Hospital Affiliated to Wuhan University of Science and Technology (Jian-ming Wang), and the People's Hospital of Huangpi District (S.Z.), Wuhan, Shenzhen Third People's Hospital and the Second Affiliated Hospital of Southern University of Science and Technology, National Clinical Research Center for Infectious Diseases (L. Liu), and the Department of Clinical Microbiology and Infection Control, University of Hong Kong-Shenzhen Hospital (K.-Y.Y.), Shenzhen, the Fifth Affiliated Hospital of Sun Yat-sen University, Zhuhai (H.S.), the Department of Medicine and Therapeutics, Chinese University of Hong Kong, Shatin (D.S.C.H.), and the Department of Microbiology and the Carol Yu Center for Infection, Li Ka Shing Faculty of Medicine, University of Hong Kong, Pok Fu Lam (K.-Y.Y.), Hong Kong, Medical ICU, Peking Union Medical College Hospital, Peking Union Medical College and Chinese Academy of Medical Sciences (B.D.), and the Chinese Center for Disease Control and Prevention (G.Z.), Beijing, the State Key Laboratory for Diagnosis and Treatment of Infectious Diseases, National Clinical Research Center for Infectious Diseases, First Affiliated Hospital, College of Medicine, Zhejiang University, Hangzhou (L. Li), Chengdu Public Health Clinical Medical Center, Chengdu (Y.L.), Huangshi Central Hospital of Edong Healthcare Group, Affiliated Hospital of Hubei Polytechnic University, Huangshi (Ya-hua Hu), the First Hospital of Changsha, Changsha (J. Liu), the Third People's Hospital of Hainan Province, Sanya (Z.C.), Huanggang Central Hospital, Huanggang (G.L.), Wenling First People's Hospital, Wenling (Z.Z.), the Third People's Hospital of Yichang, Yichang (S.Q.), Affiliated Taihe Hospital of Hubei University of Medicine, Shiyan (J. Luo), and Xiantao First People's Hospital, Xiantao (C.Y.) — all in China.

REFERENCES

- Huang C, Wang Y, Li X, et al. Clinical features of patients infected with 2019 novel coronavirus in Wuhan, China. *Lancet* 2020;395:497-506.
- Lu R, Zhao X, Li J, et al. Genomic characterisation and epidemiology of 2019 novel coronavirus: implications for virus origins and receptor binding. *Lancet* 2020; 395:565-74.
- Zhu N, Zhang D, Wang W, et al. A novel coronavirus from patients with pneumonia in China, 2019. *N Engl J Med* 2020; 382:727-33.
- Chan JF, Yuan S, Kok KH, et al. A familial cluster of pneumonia associated with

- the 2019 novel coronavirus indicating person-to-person transmission: a study of a family cluster. *Lancet* 2020;395:514-23.
5. Phan LT, Nguyen TV, Luong QC, et al. Importation and human-to-human transmission of a novel coronavirus in Vietnam. *N Engl J Med*. DOI:10.1056/NEJMc2001272.
 6. Rothe C, Schunk M, Sothmann P, et al. Transmission of 2019-nCoV infection from an asymptomatic contact in Germany. *N Engl J Med*. DOI:10.1056/NEJMc2001468.
 7. Wu JT, Leung K, Leung GM. Nowcasting and forecasting the potential domestic and international spread of the 2019-nCoV outbreak originating in Wuhan, China: a modelling study. *Lancet* 2020 January 31 (Epub ahead of print).
 8. Li Q, Guan X, Wu P, et al. Early transmission dynamics in Wuhan, China, of novel coronavirus-infected pneumonia. *N Engl J Med*. DOI:10.1056/NEJMoa2001316.
 9. World Health Organization. Coronavirus disease (COVID-19) outbreak (<https://www.who.int>).
 10. Holshue ML, DeBolt C, Lindquist S, et al. First case of 2019 novel coronavirus in the United States. *N Engl J Med*. DOI:10.1056/NEJMoa2001191.
 11. National Health Commission of the People's Republic of China home page (<http://www.nhc.gov.cn>).
 12. Chen N, Zhou M, Dong X, et al. Epidemiological and clinical characteristics of 99 cases of 2019 novel coronavirus pneumonia in Wuhan, China: a descriptive study. *Lancet* 2020;395:507-13.
 13. Wang D, Hu B, Hu C, et al. Clinical characteristics of 138 hospitalized patients with 2019 novel coronavirus-infected pneumonia in Wuhan, China. *JAMA* 2020 February 7 (Epub ahead of print).
 14. World Health Organization. Clinical management of severe acute respiratory infection when novel coronavirus (2019-nCoV) infection is suspected: interim guidance. January 28, 2020 (<https://www.who.int/docs/default-source/coronaviruse/clinical-management-of-novel-cov.pdf>).
 15. Metlay JP, Waterer GW, Long AC, et al. Diagnosis and treatment of adults with community-acquired pneumonia: an official clinical practice guideline of the American Thoracic Society and Infectious Disease Society of America. *Am J Respir Crit Care Med* 2019;200(7):e45-e67.
 16. Gao H-N, Lu H-Z, Cao B, et al. Clinical findings in 111 cases of influenza A (H7N9) virus infection. *N Engl J Med* 2013;368:2277-85.
 17. World Health Organization. Coronavirus disease (COVID-19) technical guidance: laboratory testing for 2019-nCoV in humans (<https://www.who.int/emergencies/diseases/novel-coronavirus-2019/technical-guidance/laboratory-guidance>).
 18. Lei H, Li Y, Xiao S, et al. Routes of transmission of influenza A H1N1, SARS CoV, and norovirus in air cabin: comparative analyses. *Indoor Air* 2018;28:394-403.
 19. Otter JA, Donskey C, Yezli S, Douthwaite S, Goldenberg SD, Weber DJ. Transmission of SARS and MERS coronaviruses and influenza virus in healthcare settings: the possible role of dry surface contamination. *J Hosp Infect* 2016;92:235-50.
 20. Zumla A, Hui DS, Perlman S. Middle East respiratory syndrome. *Lancet* 2015;386:995-1007.
 21. Minodier L, Charrel RN, Ceccaldi PE, et al. Prevalence of gastrointestinal symptoms in patients with influenza, clinical significance, and pathophysiology of human influenza viruses in faecal samples: what do we know? *Virol J* 2015;12:215.
 22. Leung WK, To KF, Chan PK, et al. Enteric involvement of severe acute respiratory syndrome-associated coronavirus infection. *Gastroenterology* 2003;125:1011-7.
 23. Assiri A, McGeer A, Perl TM, et al. Hospital outbreak of Middle East respiratory syndrome coronavirus. *N Engl J Med* 2013;369:407-16.
 24. World Health Organization. Coronavirus disease (COVID-2019) situation reports (<https://www.who.int/emergencies/diseases/novel-coronavirus-2019/situation-reports/>).

Copyright © 2020 Massachusetts Medical Society.

High SARS-CoV-2 Attack Rate Following Exposure at a Choir Practice — Skagit County, Washington, March 2020

Lea Hamner, MPH¹; Polly Dubbel, MPH¹; Ian Capron¹; Andy Ross, MPH¹; Amber Jordan, MPH¹; Jaxon Lee, MPH¹; Joanne Lynn¹; Amelia Ball¹; Simranjit Narwal, MSc¹; Sam Russell¹; Dale Patrick¹; Howard Leibrand, MD¹

On May 12, 2020, this report was posted as an MMWR Early Release on the MMWR website (<https://www.cdc.gov/mmwr>).

On March 17, 2020, a member of a Skagit County, Washington, choir informed Skagit County Public Health (SCPH) that several members of the 122-member choir had become ill. Three persons, two from Skagit County and one from another area, had test results positive for SARS-CoV-2, the virus that causes coronavirus disease 2019 (COVID-19). Another 25 persons had compatible symptoms. SCPH obtained the choir's member list and began an investigation on March 18. Among 61 persons who attended a March 10 choir practice at which one person was known to be symptomatic, 53 cases were identified, including 33 confirmed and 20 probable cases (secondary attack rates of 53.3% among confirmed cases and 86.7% among all cases). Three of the 53 persons who became ill were hospitalized (5.7%), and two died (3.7%). The 2.5-hour singing practice provided several opportunities for droplet and fomite transmission, including members sitting close to one another, sharing snacks, and stacking chairs at the end of the practice. The act of singing, itself, might have contributed to transmission through emission of aerosols, which is affected by loudness of vocalization (1). Certain persons, known as superemitters, who release more aerosol particles during speech than do their peers, might have contributed to this and previously reported COVID-19 superspreading events (2–5). These data demonstrate the high transmissibility of SARS-CoV-2 and the possibility of superemitters contributing to broad transmission in certain unique activities and circumstances. It is recommended that persons avoid face-to-face contact with others, not gather in groups, avoid crowded places, maintain physical distancing of at least 6 feet to reduce transmission, and wear cloth face coverings in public settings where other social distancing measures are difficult to maintain.

Investigation and Findings

The choir, which included 122 members, met for a 2.5-hour practice every Tuesday evening through March 10. On March 15, the choir director e-mailed the group members to inform them that on March 11 or 12 at least six members had developed fever and that two members had been tested for SARS-CoV-2 and were awaiting results. On March 16, test results for three members were positive for SARS-CoV-2

and were reported to two respective local health jurisdictions, without indication of a common source of exposure. On March 17, the choir director sent a second e-mail stating that 24 members reported that they had developed influenza-like symptoms since March 11, and at least one had received test results positive for SARS-CoV-2. The email emphasized the importance of social distancing and awareness of symptoms suggestive of COVID-19. These two emails led many members to self-isolate or quarantine before a delegated member of the choir notified SCPH on March 17.

All 122 members were interviewed by telephone either during initial investigation of the cluster (March 18–20; 115 members) or a follow-up interview (April 7–10; 117); most persons participated in both interviews. Interviews focused on attendance at practices on March 3 and March 10, as well as attendance at any other events with members during March, other potential exposures, and symptoms of COVID-19. SCPH used Council of State and Territorial Epidemiologists case definitions to classify confirmed and probable cases of COVID-19 (6). Persons who did not have symptoms at the initial interview were instructed to quarantine for 14 days from the last practice they had attended. The odds of becoming ill after attending each practice were computed to ascertain the likelihood of a point-source exposure event.

No choir member reported having had symptoms at the March 3 practice. One person at the March 10 practice had cold-like symptoms beginning March 7. This person, who had also attended the March 3 practice, had a positive laboratory result for SARS-CoV-2 by reverse transcription–polymerase chain reaction (RT-PCR) testing.

In total, 78 members attended the March 3 practice, and 61 attended the March 10 practice (Table 1). Overall, 51 (65.4%) of the March 3 practice attendees became ill; all but one of these persons also attended the March 10 practice. Among 60 attendees at the March 10 practice (excluding the patient who became ill March 7, who also attended), 52 (86.7%) choir members subsequently became ill. Some members exclusively attended one practice; among 21 members who only attended March 3, one became ill and was not tested (4.8%), and among three members who only attended March 10, two became ill (66.7%), with one COVID-19 case being laboratory-confirmed.

Summary

What is already known about this topic?

Superspreading events involving SARS-CoV-2, the virus that causes COVID-19, have been reported.

What is added by this report?

Following a 2.5-hour choir practice attended by 61 persons, including a symptomatic index patient, 32 confirmed and 20 probable secondary COVID-19 cases occurred (attack rate = 53.3% to 86.7%); three patients were hospitalized, and two died. Transmission was likely facilitated by close proximity (within 6 feet) during practice and augmented by the act of singing.

What are the implications for public health practice?

The potential for superspreader events underscores the importance of physical distancing, including avoiding gathering in large groups, to control spread of COVID-19. Enhancing community awareness can encourage symptomatic persons and contacts of ill persons to isolate or self-quarantine to prevent ongoing transmission.

Because illness onset for 49 (92.5%) patients began during March 11–15 (Figure), a point-source exposure event seemed likely. The median interval from the March 3 practice to symptom onset was 10 days (range = 4–19 days), and from the March 10 practice to symptom onset was 3 days (range = 1–12 days). The odds of becoming ill after the March 3 practice were 17.0 times higher for practice attendees than for those who did not attend (95% confidence interval [CI] = 5.5–52.8), and after the March 10 practice, the odds were 125.7 times greater (95% CI = 31.7–498.9). The clustering of symptom onsets, odds of becoming ill according to practice attendance, and known presence of a symptomatic contagious case at the March 10 practice strongly suggest that date as the more likely point-source exposure event. Therefore, that practice was the focus of the rest of the investigation. Probable cases were defined as persons who attended the March 10 practice and developed clinically compatible COVID-19 symptoms, as defined by Council of State and Territorial Epidemiologists (6). The choir member who was ill beginning March 7 was considered the index patient.

The March 10 choir rehearsal lasted from 6:30 to 9:00 p.m. Several members arrived early to set up chairs in a large multipurpose room. Chairs were arranged in six rows of 20 chairs each, spaced 6–10 inches apart with a center aisle dividing left and right stages. Most choir members sat in their usual rehearsal seats. Sixty-one of the 122 members attended that evening, leaving some members sitting next to empty seats. Attendees practiced together for 40 minutes, then split into two smaller groups for an additional 50-minute practice, with one of the groups moving to a smaller room. At that

time, members in the larger room moved to seats next to one another, and members in the smaller room sat next to one another on benches. Attendees then had a 15-minute break, during which cookies and oranges were available at the back of the large room, although many members reported not eating the snacks. The group then reconvened for a final 45-minute session in their original seats. At the end of practice, each member returned their own chair, and in the process congregated around the chair racks. Most attendees left the practice immediately after it concluded. No one reported physical contact between attendees. SCPH assembled a seating chart of the all-choir portion of the March 10 practice (not reported here because of concerns about patient privacy).

Among the 61 choir members who attended the March 10 practice, the median age was 69 years (range = 31–83 years); 84% were women. Median age of those who became ill was 69 years, and 85% of cases occurred in women. Excluding the laboratory-confirmed index patient, 52 (86.7%) of 60 attendees became ill; 32 (61.5%) of these cases were confirmed by RT-PCR testing and 20 (38.5%) persons were considered to have probable infections. These figures correspond to secondary attack rates of 53.3% and 86.7% among confirmed and all cases, respectively. Attendees developed symptoms 1 to 12 days after the practice (median = 3 days). The first SARS-CoV-2 test was performed on March 13. The last person was tested on March 26.

Three of the 53 patients were hospitalized (5.7%), including two who died (3.8%). The mean interval from illness onset to hospitalization was 12 days. The intervals from onset to death were 14 and 15 days for the two patients who died.

SCPH collected information about patient signs and symptoms from patient interviews and hospital records (Table 2). Among persons with confirmed infections, the most common signs and symptoms reported at illness onset and at any time during the course of illness were cough (54.5% and 90.9%, respectively), fever (45.5%, 75.8%), myalgia (27.3%, 75.0%), and headache (21.2%, 60.6%). Several patients later developed gastrointestinal symptoms, including diarrhea (18.8%), nausea (9.4%), and abdominal cramps or pain (6.3%). One person experienced only loss of smell and taste. The most severe complications reported were viral pneumonia (18.2%) and severe hypoxemic respiratory failure (9.1%).

Among the recognized risk factors for severe illness, the most common was age, with 75.5% of patients aged ≥65 years. Most patients (67.9%) did not report any underlying medical conditions, 9.4% had one underlying medical condition, and 22.6% had two or more underlying medical conditions. All three hospitalized patients had two or more underlying medical conditions.

TABLE 1. Number of choir members with and without COVID-19-compatible symptoms (N = 122)* and members' choir practice attendance† — Skagit County, Washington, March 3 and 10, 2020

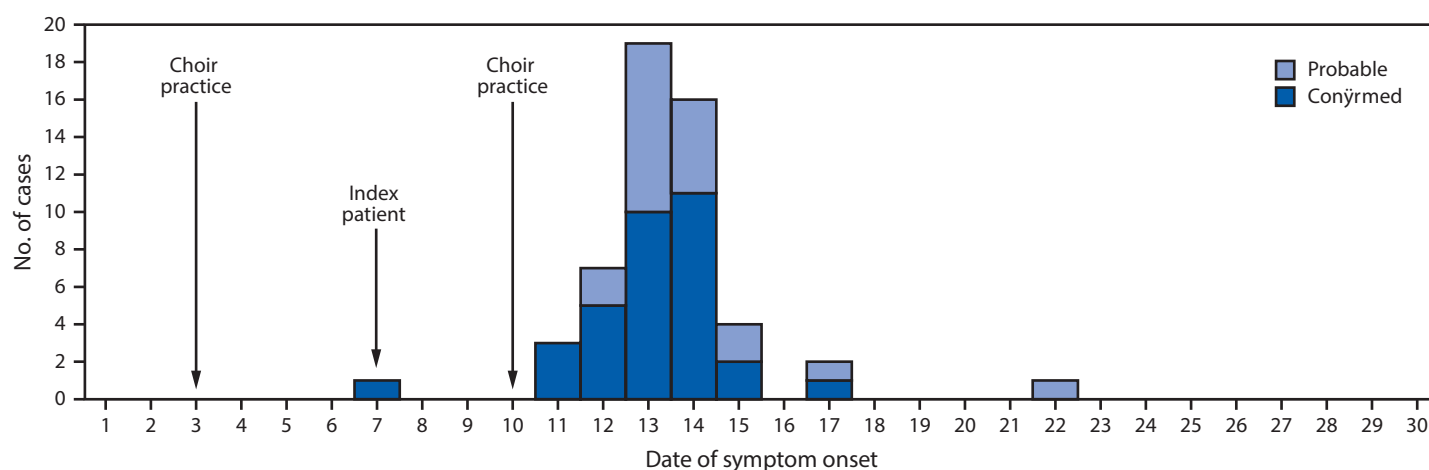
Attendance	No. (row %)					
	March 3 practice			March 10 practice		
	Total	Symptomatic	Asymptomatic	Total	Symptomatic	Asymptomatic
Attended	78	51 (65.4)	27 (34.6)	61	53 [§] (86.9)	8 (13.1)
Did not attend	40	4 (10.0)	36 (90.0)	61	3 (4.9)	58 (95.1)
Attendance information missing	4	1 (25.0)	3 (75.0)	0	0 (—)	0 (—)
Attended only one practice	21	1 (4.8)	20 (95.2)	3	2 (66.7)	1 (33.3)

Abbreviation: COVID-19 = coronavirus disease 2019.

* No choir members were symptomatic at the March 3 practice.

† Thirty-seven choir members attended neither practice; two developed symptoms, and 35 remained asymptomatic.

§ Includes index patient; if the index patient excluded, 52 secondary cases occurred among the other 60 attendees (attack rate = 86.7%).

FIGURE. Confirmed* and probable† cases of COVID-19 associated with two choir practices, by date of symptom onset (N = 53) — Skagit County, Washington, March 2020

Abbreviation: COVID-19 = coronavirus disease 2019.

* Positive reverse transcription-polymerase chain reaction test result.

† Attendance at the March 10 practice and clinically compatible symptoms as defined by the Council of State and Territorial Epidemiologists, Interim-20-ID-01: Standardized surveillance case definition and national notification for 2019 novel coronavirus disease (COVID-19). https://cdn.ymaws.com/www.cste.org/resource/resmgr/2020ps/interim-20-id-01_covid-19.pdf.

Public Health Response

SCPH provided March 10 practice attendees with isolation and quarantine instructions by telephone, email, and postal mail. Contacts of patients were traced and notified of isolation and quarantine guidelines. At initial contact, 15 attendees were quarantined, five of whom developed symptoms during quarantine and notified SCPH.

Before detection of this cluster on March 17, Skagit County had reported seven confirmed COVID-19 cases (5.4 cases per 100,000 population). At the time, SCPH informed residents that likely more community transmission had occurred than indicated by the low case counts.* On March 21, SCPH issued a press release to describe the outbreak and raise awareness about community transmission.† The press release emphasized

the highly contagious nature of COVID-19 and the importance of following social distancing guidelines to control the spread of the virus.

Discussion

Multiple reports have documented events involving super-spreading of COVID-19 (2–5); however, few have documented a community-based point-source exposure (5). This cluster of 52 secondary cases of COVID-19 presents a unique opportunity for understanding SARS-CoV-2 transmission following a likely point-source exposure event. Persons infected with SARS-CoV-2 are most infectious from 2 days before through 7 days after symptom onset (7). The index patient developed symptoms on March 7, which could have placed the patient within this infectious period during the March 10 practice. Choir members who developed symptoms on March 11 (three) and March 12 (seven) attended both the March 3

* Skagit County, updated social distancing information. <https://skagitcounty.net/departments/home/press/031620.htm>.

† Skagit County, public health investigating cluster of related COVID-19 cases. <https://skagitcounty.net/departments/home/press/032120.htm>.

TABLE 2. Signs and symptoms reported at the onset of COVID-19 illness and during the course of illness among persons infected at a choir practice (N = 53)* — Skagit County, Washington, March 2020

Sign or symptom	No. (%)		no./No. (%)	
	Reported at onset of illness		Reported during course of illness	
	All cases (N = 53)	Confirmed cases (N = 33)	All cases (N = 53)	Confirmed cases (N = 33)
Cough	27 (50.9)	18 (54.5)	47/53 (88.7)	30/33 (90.9)
Fever	28 (52.8)	15 (45.5)	36/53 (67.9)	25/33 (75.8)
Myalgia	13 (24.5)	9 (27.3)	34/52 (65.4)	24/32 (75.0)
Headache	10 (18.9)	7 (21.2)	32/53 (60.4)	20/33 (60.6)
Chills or rigors	7 (13.2)	6 (18.2)	23/51 (45.1)	16/31 (51.6)
Congestion	4 (7.5)	2 (6.1)	25/52 (48.1)	15/32 (46.9)
Pharyngitis	2 (3.8)	2 (6.1)	12/52 (23.1)	8/32 (25.0)
Lethargy	4 (7.5)	2 (6.1)	5/52 (9.6)	3/32 (9.4)
Fatigue	3 (5.7)	1 (3.0)	24/52 (46.2)	15/32 (46.9)
Agusia (loss of taste)	1 (1.9)	1 (3.0)	11/48 (22.9)	5/28 (17.9)
Anosmia (loss of smell)	1 (1.9)	1 (3.0)	10/48 (20.8)	5/28 (17.9)
Chest congestion or tightness	1 (1.9)	1 (3.0)	5/52 (9.6)	4/32 (12.5)
Weakness	1 (1.9)	1 (3.0)	3/52 (5.8)	2/32 (6.3)
Eye ache	1 (1.9)	1 (3.0)	1/52 (1.9)	1/32 (3.1)
Dyspnea	0 (—)	0 (—)	8/51 (15.7)	8/31 (25.8)
Diarrhea	0 (—)	0 (—)	8/52 (15.4)	6/32 (18.8)
Pneumonia	0 (—)	0 (—)	6/53 (11.3)	6/33 (18.2)
Nausea	0 (—)	0 (—)	3/52 (5.8)	3/32 (9.4)
Acute hypoxemic respiratory failure	0 (—)	0 (—)	3/53 (5.7)	3/33 (9.1)
Abdominal pain or cramps	0 (—)	0 (—)	2/52 (3.8)	2/32 (6.3)
Malaise	1 (1.9)	0 (—)	1/52 (1.9)	0/32 (—)
Anorexia	0 (—)	0 (—)	1/52 (1.9)	0/32 (—)
Vomiting	0 (—)	0 (—)	0/52 (—)	0/32 (—)

Abbreviation: COVID-19 = coronavirus disease 19.

* Including the index patient.

and March 10 practices and thus could have been infected earlier and might have been infectious in the 2 days preceding symptom onset (i.e., as early as March 9). The attack rate in this group (53.3% and 86.7% among confirmed cases and all cases, respectively) was higher than that seen in other clusters, and the March 10 practice could be considered a superspreading event (3,4). The median incubation period of COVID-19 is estimated to be 5.1 days (8). The median interval from exposure during the March 10 practice to onset of illness was 3 days, indicating a more rapid onset.

Choir practice attendees had multiple opportunities for droplet transmission from close contact or fomite transmission (9), and the act of singing itself might have contributed to SARS-CoV-2 transmission. Aerosol emission during speech has been correlated with loudness of vocalization, and certain persons, who release an order of magnitude more particles than their peers, have been referred to as superemitters and have been hypothesized to contribute to superspreading events (1). Members had an intense and prolonged exposure, singing while sitting 6–10 inches from one another, possibly emitting aerosols.

The findings in this report are subject to at least two limitations. First, the seating chart was not reported because of concerns about patient privacy. However, with attack rates of 53.3% and 86.7% among confirmed and all cases, respectively,

and one hour of the practice occurring outside of the seating arrangement, the seating chart does not add substantive additional information. Second, the 19 choir members classified as having probable cases did not seek testing to confirm their illness. One person classified as having probable COVID-19 did seek testing 10 days after symptom onset and received a negative test result. It is possible that persons designated as having probable cases had another illness.

This outbreak of COVID-19 with a high secondary attack rate indicates that SARS-CoV-2 might be highly transmissible in certain settings, including group singing events. This underscores the importance of physical distancing, including maintaining at least 6 feet between persons, avoiding group gatherings and crowded places, and wearing cloth face coverings in public settings where other social distancing measures are difficult to maintain during this pandemic. The choir mitigated further spread by quickly communicating to its members and notifying SCPH of a cluster of cases on March 18. When first contacted by SCPH during March 18–20, nearly all persons who attended the practice reported they were already self-isolating or quarantining. Current CDC recommendations, including maintaining physical distancing of at least 6 feet and wearing cloth face coverings if this is not feasible, washing hands often, covering coughs and sneezes, staying home when ill, and frequently cleaning and disinfecting

high-touch surfaces, remain critical to reducing transmission. Additional information is available at <https://www.cdc.gov/coronavirus/2019-ncov/prevent-getting-sick/prevention.html>.

Acknowledgments

Patients described in this report; health care personnel who cared for them; Skagit County Public Health staff members and leaders, particularly the Communicable Disease investigators; Washington State Department of Health.

Corresponding author: Lea Hamner, leah@co.skagit.wa.us, 360-416-1500.

¹Skagit County Public Health, Mount Vernon, Washington.

All authors have completed and submitted the International Committee of Medical Journal Editors form for disclosure of potential conflicts of interest. All authors report receipt of funding through Public Health Emergency Preparedness grant from the Washington State Department of Health during the conduct of the study. No other potential conflicts of interest were disclosed.

References

1. Asadi S, Wexler AS, Cappa CD, Barreda S, Bouvier NM, Ristenpart WD. Aerosol emission and superemission during human speech increase with voice loudness. *Sci Rep* 2019;9:2348. <https://doi.org/10.1038/s41598-019-38808-z>
2. Wang D, Hu B, Hu C, et al. Clinical characteristics of 138 hospitalized patients with 2019 novel coronavirus-infected pneumonia in Wuhan, China. *JAMA* 2020;323:1061–9. <https://doi.org/10.1001/jama.2020.1585>
3. McMichael TM, Currie DW, Clark S, et al. Epidemiology of COVID-19 in a long-term care facility in King County, Washington. *N Engl J Med* 2020;NEJMoa2005412. <https://doi.org/10.1056/NEJMoa2005412>
4. Ghinai I, Woods S, Ritger KA, et al. Community transmission of SARS-CoV-2 at two family gatherings—Chicago, Illinois, February–March 2020. *MMWR Morb Mortal Wkly Rep* 2020;69:446–50. <https://doi.org/10.15585/mmwr.mm6915e1>
5. South Korean city on high alert as coronavirus cases soar at ‘cult’ church. *The Guardian*, US Edition. February 20, 2020. <https://www.theguardian.com/world/2020/feb/20/south-korean-city-daegu-lockdown-coronavirus-outbreak-cases-soar-at-church-cult-cluster>
6. Council of State and Territorial Epidemiologists. Interim-20-ID-01: standardized surveillance case definition and national notification for 2019 novel coronavirus disease (COVID-19). Atlanta, GA: Council of State and Territorial Epidemiologists; 2020. https://cdn.ymaws.com/www.cste.org/resource/resmgr/2020ps/interim-20-id-01_covid-19.pdf
7. He X, Lau EHY, Wu P, et al. Temporal dynamics in viral shedding and transmissibility of COVID-19. *Nat Med* 2020;26:672–5.
8. Lauer SA, Grantz KH, Bi Q, et al. The incubation period of coronavirus disease 2019 (COVID-19) from publicly reported confirmed cases: estimation and application. *Ann Intern Med* 2020;172:577. <https://doi.org/10.7326/M20-0504>
9. van Doremalen N, Bushmaker T, Morris DH, et al. Aerosol and surface stability of SARS-CoV-2 as compared with SARS-CoV-1. *N Engl J Med* 2020;382:1564–7. <https://doi.org/10.1056/NEJMc2004973>

Interferon- β and mycophenolic acid are potent inhibitors of Middle East respiratory syndrome coronavirus in cell-based assays

Brit J. Hart,¹ Julie Dyall,¹ Elena Postnikova,¹ Huanying Zhou,¹ Jason Kindrachuk,¹ Reed F. Johnson,² Gene G. Olinger, Jr,¹ Matthew B. Frieman,³ Michael R. Holbrook,¹ Peter B. Jahrling^{1,2} and Lisa Hensley¹

Correspondence

Peter B. Jahrling
jahrlingp@niaid.nih.gov

¹Integrated Research Facility, National Institute of Allergy and Infectious Diseases, National Institutes of Health, Frederick, MD, USA

²Emerging Viral Pathogens Section, National Institute of Allergy and Infectious Diseases, National Institutes of Health, Frederick, MD, USA

³Department of Microbiology and Immunology, University of Maryland School of Medicine, Baltimore, MD, USA

The Middle East respiratory syndrome coronavirus (MERS-CoV) presents a novel emerging threat to public health worldwide. Several treatments for infected individuals have been suggested including IFN, ribavirin and passive immunotherapy with convalescent plasma. Administration of IFN- α 2b and ribavirin has improved outcomes of MERS-CoV infection in rhesus macaques when administered within 8 h post-challenge. However, detailed and systematic evidence on the activity of other clinically available drugs is limited. Here we compared the susceptibility of MERS-CoV with different IFN products (IFN- α 2b, IFN- γ , IFN-universal, IFN- α 2a and IFN- β), as well as with two antivirals, ribavirin and mycophenolic acid (MPA), against MERS-CoV (Hu/Jordan-N3/2012) *in vitro*. Of all the IFNs tested, IFN- β showed the strongest inhibition of MERS-CoV *in vitro*, with an IC₅₀ of 1.37 U ml⁻¹, 41 times lower than the previously reported IC₅₀ (56.08 U ml⁻¹) of IFN- α 2b. IFN- β inhibition was confirmed in the virus yield reduction assay, with an IC₉₀ of 38.8 U ml⁻¹. Ribavirin did not inhibit viral replication *in vitro* at a dose that would be applicable to current treatment protocols in humans. In contrast, MPA showed strong inhibition, with an IC₅₀ of 2.87 μ M. This drug has not been previously tested against MERS-CoV and may provide an alternative to ribavirin for treatment of MERS-CoV. In conclusion, IFN- β , MPA or a combination of the two may be beneficial in the treatment of MERS-CoV or as a post-exposure intervention in high-risk patients with known exposures to MERS-CoV.

Received 4 December 2013

Accepted 5 December 2013

INTRODUCTION

In June 2012, a novel betacoronavirus was isolated from a fatal case of pneumonia with renal failure (Zaki *et al.*, 2012). Owing to the genetic similarities as well as the development of respiratory disease, the new virus was commonly referred to as severe respiratory syndrome coronavirus (SARS)-like virus. The virus was later renamed Middle East respiratory syndrome coronavirus (MERS-CoV). MERS-CoV has been confirmed in 150 cases with 64 deaths to date (as of 4 November 2013; World Health Organization, 2013). Whilst the majority of the cases have occurred in the Kingdom of Saudi Arabia, cases have been identified across the Arabian Peninsula (Qatar, Jordan and United Arab Emirates). Imported cases have also been identified in the UK, Italy, Spain, Germany and Tunisia. Importantly, there are no approved medical countermeasures

for MERS-CoV disease, and thus case management has relied on supportive care, contact tracing, monitoring of close contacts and appropriate infection control (ISARIC, 2013).

Appreciable efforts have been made to identify novel antiviral therapeutics for MERS-CoV. It has been demonstrated that compounds targeting host effectors can be beneficial when administered alone or in combination with antivirals during the course of viral infection (Josset *et al.*, 2010; Ludwig, 2011; Tisoncik *et al.*, 2012). Falzarano *et al.* (2013a, b) recently reported that the administration of IFN- α 2b and ribavirin resulted in synergistic antiviral activities both *in vitro* and *in vivo* in rhesus macaques.

This paper expands on reported studies to evaluate the efficacy of a variety of IFNs and mycophenolic acid (MPA)

for the inhibition of MERS-CoV infection *in vitro* (Chan *et al.*, 2013a, 2013b; de Wilde *et al.*, 2013; Kindler *et al.*, 2013). Similar to ribavirin, MPA has broad antiviral activities. Whilst the mechanism of action for MPA remains under debate, data suggest that it may have both direct antiviral activity and indirect activity through modulation of IFN response activities (Henry *et al.*, 2006; Khan *et al.*, 2011; Leyssen *et al.*, 2005; Morrey *et al.*, 2002; Pan *et al.*, 2012; Smee *et al.*, 2001). Here, we applied a cell-based ELISA screen to test the activity of MPA and the IFN products and compared them with ribavirin and IFN- α 2b *in vitro*.

RESULTS

A cell-based ELISA was developed to screen candidate antivirals for MERS-CoV. To optimize this assay, Vero E6 cells were inoculated with MERS-CoV (Hu/Jordan-N3/2012) at an m.o.i. of 0.03, 0.1 or 0.3 for 48 h. Viral antigen was detected with an antibody specific to the MERS-CoV viral spike protein S and with an Alexa Fluor 594-conjugated secondary antibody. Data from over 10 experiments indicated that an m.o.i. of 0.1 consistently demonstrated a robust fluorescent signal with signal-to-noise ratios in the range of 6–16 with no visible cell death at 48 h (Fig. 1). Based on these results, an m.o.i. of 0.1 was used in all subsequent MERS-CoV ELISA drug screens.

The MERS-CoV ELISA screen was first used to evaluate four compounds, MPA, ribavirin, IFN- α 2a and IFN- β . Subsequently, a set of different IFNs (IFN- α 2b, IFN- γ , IFN-universal, IFN- α 2a and IFN- β) was compared in the MERS-CoV ELISA screen. Vero E6 cells were treated with threefold dilutions of MPA, ribavirin, IFN- α 2a or IFN- β approximately 1 h prior to infection with MERS-CoV. Following 48 h incubation, the cells were fixed and stained, and nine image fields per well were acquired with an Operetta high-content imaging platform (Fig. 2). Use of

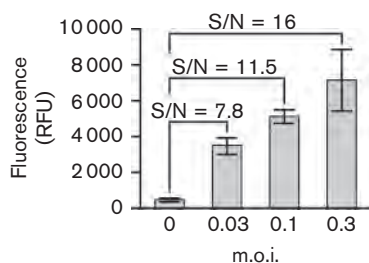


Fig. 1. Optimization of the cell-based ELISA screen for MERS antivirals. Vero E6 cells were infected at the indicated m.o.i. to optimize the relative fluorescence signal intensity in arbitrary relative fluorescence units (RFU) at 48 h. Signal-to-noise ratios (S/N) between mock-infected cells (noise; m.o.i. 0) and infected cells (signal; m.o.i. 0.03, 0.1, or 0.3) are shown for the indicated m.o.i. Results shown are representative of one experiment (mean \pm SD, $n=4$) out of at least 10 experiments.

the Operetta provides the advantage of monitoring different fluorescence parameters within the same well. Hoechst 33342 nuclei staining was used to determine cell numbers in each well to quantify the cytotoxic effect, and Alexa Fluor 594-conjugated secondary antibody bound to a MERS-CoV S protein-specific primary antibody was used to determine the percentage of infected cells per well. In the wells containing virus alone, 46–66 % of the cells were positive for viral antigen when left untreated (Fig. 2a, left column). MPA treatment had a significant inhibitory effect on MERS-CoV replication, whilst ribavirin did not show inhibition at the tested concentrations (Figs 2b and 3). Further analysis at lower concentrations confirmed strong inhibition of MERS-CoV replication with MPA at an IC_{50} of 2.87 μ M (Fig. 4). Ribavirin exhibited activity only at concentrations of 250 μ M or higher (Fig. 4). This inhibition of MERS-CoV with MPA is in contrast to the reported inability of MPA to inhibit SARS-CoV infection with MPA (Barnard *et al.*, 2006).

Strong anti-MERS-CoV activity was observed in the lower dose range (starting at 5 U ml^{-1} , Figs 2b and 3). A detailed comparison of various IFN products demonstrated that antiviral activity of IFN- β ($IC_{50}=1.37$ U ml^{-1}) was 16-, 41-, 83- and 117-fold higher than those of IFN- α 2b, IFN- γ , IFN-universal type 1 and IFN- α 2a, respectively (Fig. 5). The ability of IFN- β to inhibit MERS-CoV growth was confirmed in a virus yield reduction assay (Fig. 6). Vero E6 cells were infected at an m.o.i. of 0.1 and incubated in the presence of IFN- β (10–1000 U ml^{-1}) for 48 or 72 h. IFN- β reduced MERS-CoV yield very effectively with an IC_{90} and IC_{99} of 39 and 426 U ml^{-1} , respectively, at 48 h, approximately ten and four times lower, respectively, than previously reported for IFN- α 2b (Falzarano *et al.*, 2013b). At 72 h, IFN- β retained the ability to reduce MERS-CoV yield up to 99.9 % at the higher concentrations (100–1000 U ml^{-1}) tested.

DISCUSSION

Since the emergence of MERS, several potential treatments for clinical patients have been reviewed and recommended by the International Severe Acute Respiratory and Emerging Infection Consortium (Brown *et al.*, 2013). Whilst neutralizing antibody-based treatments such as convalescent plasma are considered to have the most probable beneficial effect, such plasma is limited in availability. The repurposing of Food and Drug Administration (FDA)-approved drugs typically provides the most viable treatment option during emergency situations if efficacy can be demonstrated. Previous *in vitro* and *in vivo* studies have indicated that IFN- α 2b alone, or in combination with ribavirin, could have a clinical effect if given early in the disease course (de Wilde *et al.*, 2013; Falzarano *et al.*, 2013a, b). Here, we demonstrated that IFN- β showed even higher (16 times) biological activity against MERS-CoV infection *in vitro* than IFN- α 2b. In addition, we also demonstrated that another broad-spectrum antiviral,

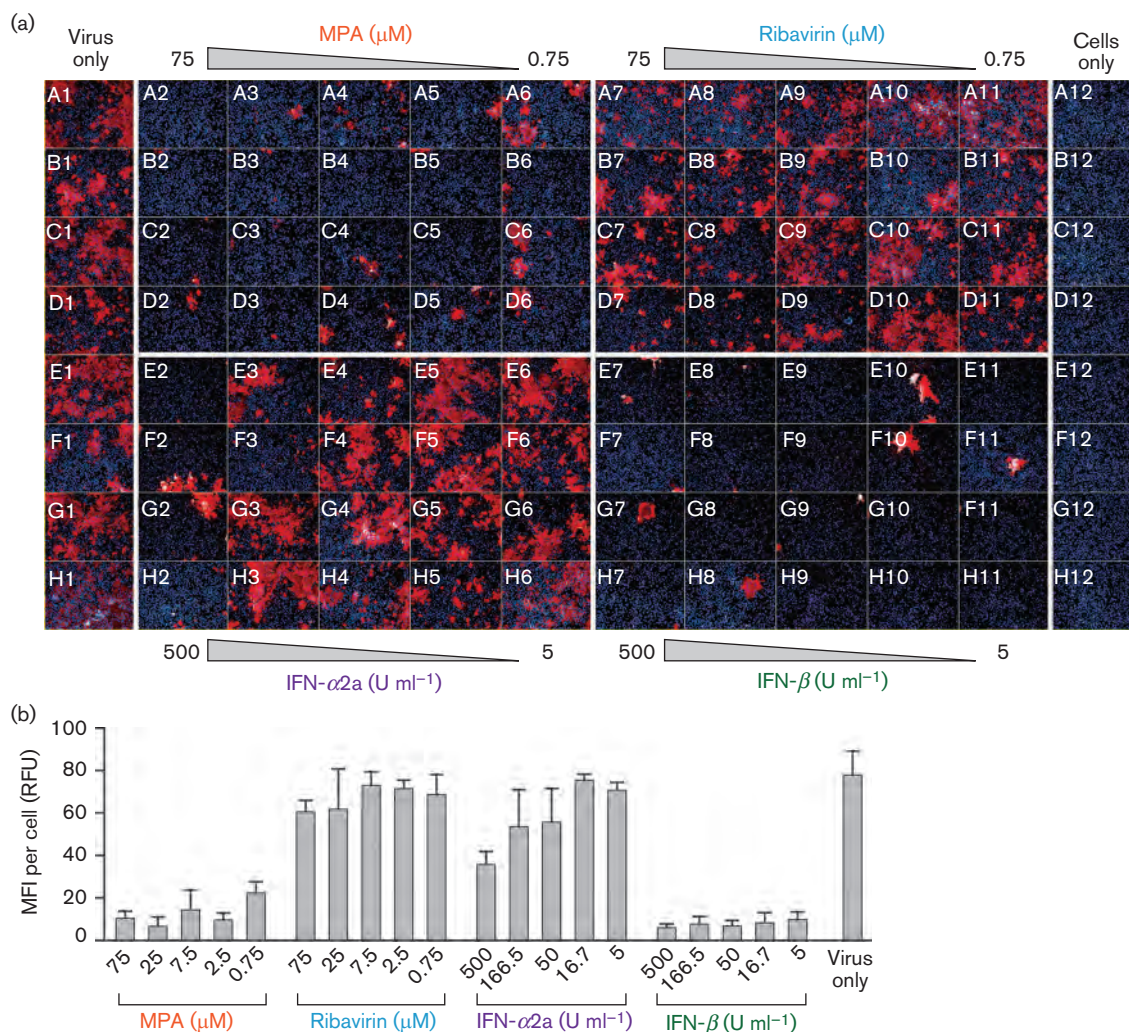


Fig. 2. High content imaging of the MPA, ribavirin, IFN- α 2a and IFN- β dose-response in MERS-CoV-infected Vero E6 cells. Vero E6 cells were treated with threefold dilutions of MPA and ribavirin (0.75–75 μ M), and threefold dilutions of IFN- α 2a and IFN- β (5–500 U ml⁻¹), and subsequently infected at an m.o.i. of 0.1 with MERS-CoV. (a) At 48 h post-inoculation, cells were fixed and stained with antibody to MERS-CoV S protein and Alexa Fluor 594-conjugated secondary antibody. High content imaging analysis (Operetta, Harmony 3.1) was performed to determine the percentage of infected cells per well, and Hoechst 33342 staining was used to determine the number of viable cells in each well. One out of nine acquired fields per well is shown. The left-hand column shows the positive control of cells infected with MERS-CoV without drug treatment. The right-hand column shows the negative control of uninfected viable cells without drug treatment. (b) Quantification of relative fluorescence intensity from fluorescence microscopic images shown in (a). Mean fluorescence intensity (MFI) was measured in relative fluorescence units (RFU) and normalized to the number of cells per well. Results are representative of one experiment (mean \pm SD, $n=4$). The experiment was repeated at least twice.

MPA, was effective against MERS-CoV infection *in vitro*. Furthermore, MERS-CoV was susceptible to MPA inhibition with an $IC_{50}=2.87 \mu$ M. Importantly, both IFN- β and MPA have been approved by the FDA for other indications and currently are in use. As a result, both of these drugs are readily available and can be used off label at the discretion of the clinician. There are also data in the literature to indicate that improved efficacy and potential synergy can be achieved when these drugs are combined.

Similar to ribavirin, there have been a number of proposed mechanisms of action for MPA. Previously, MPA treatment was shown to induce the expression of IFN-stimulated genes, including IFN regulatory factor 1, suggesting that the antiviral activity of MPA is dependent on the modulation of both inosine 5'-monophosphate dehydrogenase activity and IFN-stimulated gene expression (Pan *et al.*, 2012). These data also support the hypothesis that MPA may increase the responsiveness of cells to

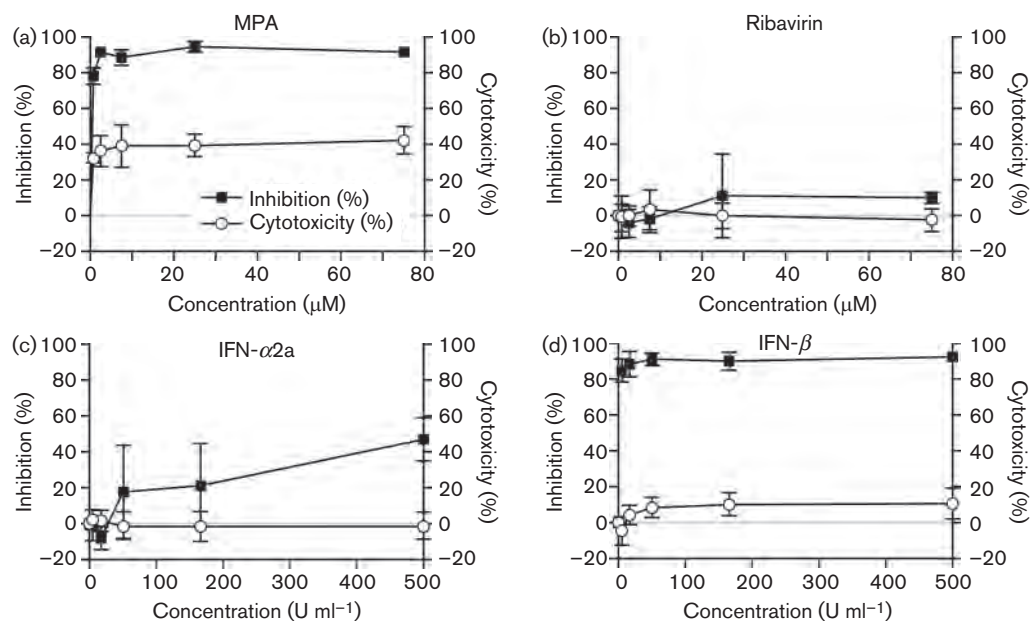


Fig. 3. Comparison of test compounds MPA (a), ribavirin (b), IFN- α 2a (c) and IFN- β (d) for inhibition of viral replication and cell cytotoxic effects. The MERS-CoV screen was performed as described in Fig. 2. The MFI of infected cells was determined using Harmony 3.1 software and the percentage inhibition of treated wells was normalized to uninfected control wells and measured relative to untreated wells. Viable cell numbers were used to determine the percentage cytotoxic effect in infected/treated wells relative to uninfected/untreated wells. Results are representative of one experiment (mean \pm SD, $n=4$). The experiment was repeated at least twice.

IFN treatment and, when combined with IFN, may act synergistically to reduce viral loads. To account for this possibility, the initial screens presented in this paper were performed in Vero cells. Vero cells, whilst responsive to IFN, cannot produce IFN. As such, the data here suggested that the observed MPA activity is not through induction or sensitization of cells to IFN. Future analysis will assess the mechanism of action for the MPA inhibitory effect on

MERS-CoV infection and possible additive or synergistic effects when combined with IFN.

In conclusion, the data presented here demonstrated that IFN- β and MPA, or a combination of the two drugs, should be considered for the treatment of MERS-CoV-infected patients. Previously published reports demonstrating IFN antagonist activity of MERS-CoV support

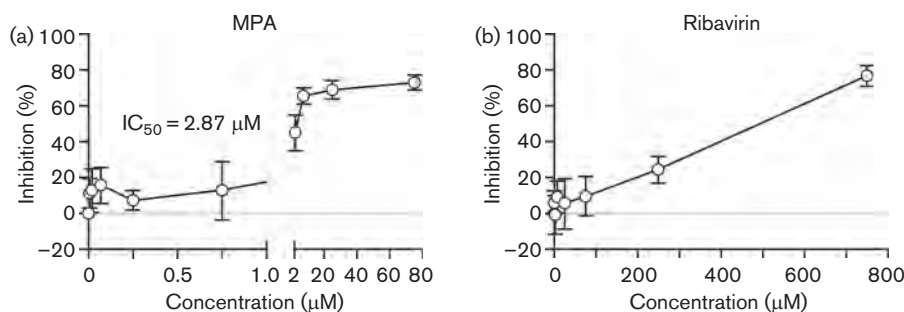


Fig. 4. Antiviral activity of MPA and ribavirin. Vero E6 cells were treated with threefold dilutions of MPA (0–75 μM) (a) or ribavirin (0–750 μM) (b) and subsequently infected at an m.o.i. of 0.1 with MERS-CoV. At 48 h post-inoculation, cells were fixed and stained with antibody to MERS-CoV S protein and Alexa Fluor 594-conjugated secondary antibody. Fluorescence was quantified on a plate reader and the percentage inhibition of treated wells was normalized to uninfected control wells and measured relative to untreated wells. Results are representative of one experiment (mean \pm SD, $n=4$). The experiment was repeated at least twice.

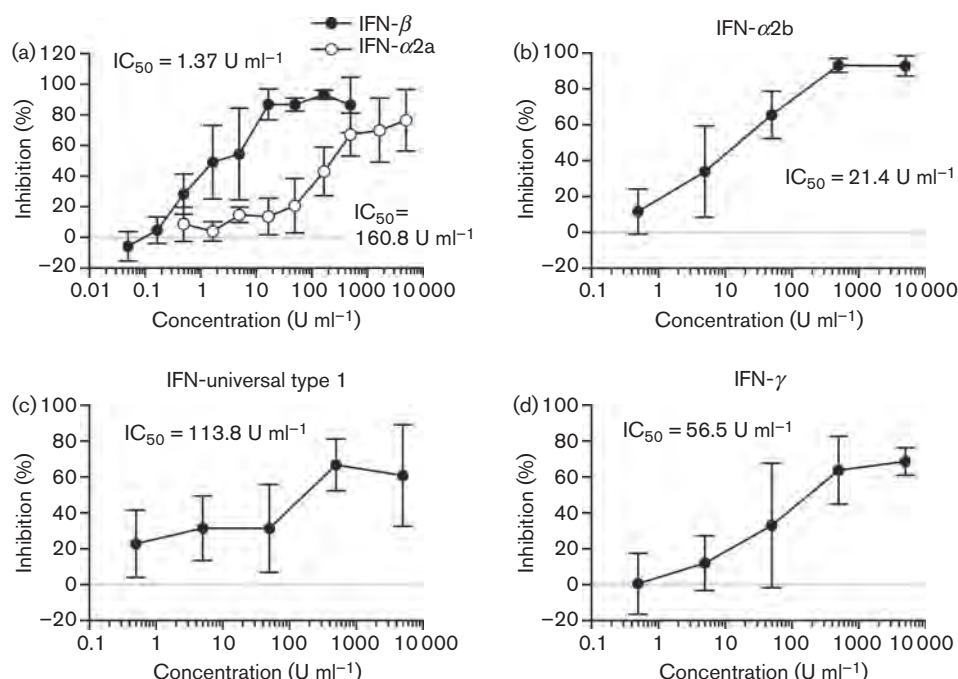


Fig. 5. Antiviral activity by various IFN types. Vero E6 cells were treated at indicated concentrations of IFN- β and IFN- α 2a (a), IFN- α 2b (b), IFN-universal (c) or IFN- γ (d) and subsequently infected at an m.o.i. of 0.1 with MERS-CoV. At 48 h post-inoculation, cells were fixed and stained with antibody to MERS-CoV S protein and Alexa Fluor 594-conjugated secondary antibody. The percentage inhibition of treated wells was normalized to uninfected control wells and measured relative to untreated wells. Results are representative of one experiment (mean \pm SD, $n=4$). The experiment was repeated at least twice.

the hypothesis that control of the host innate immune response, in particular the IFN response, is critical for survival of the virus. Early intervention with the use of exogenous IFNs alone or in combination with direct antivirals prior to complete subversion of the host's

immune response may provide a viable treatment option. In addition, the data presented here, in combination with the current state of knowledge of MERS-CoV, suggest that exogenous IFNs may also provide an option for intervention in high-risk individuals with known exposure to MERS-CoV.

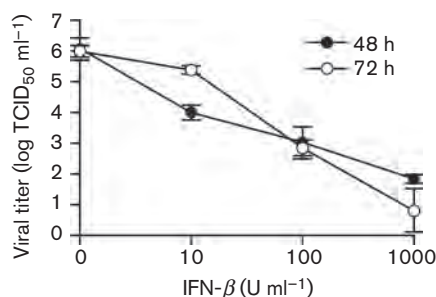


Fig. 6. Reduction in virus yield by IFN- β . Vero E6 cells were infected at an m.o.i. of 0.1 with MERS-CoV. At 1 h after inoculation, inoculum was removed, and cells washed and treated with the indicated concentrations of IFN. At 48 and 72 h, supernatants were titrated in the infectivity assay. Results are representative of one experiment (mean \pm SD, $n=3$). The experiment was repeated at least twice.

METHODS

Cell lines and virus. Vero E6 cell line (ATCC 1568) was maintained in Dulbecco's modified Eagle's medium (DMEM) plus 10 % FBS. The Jordan strain of MERS-CoV (Hu/Jordan-N3/2012, GenBank accession no. KC776174.1; de Groot *et al.*, 2013), kindly provided by Drs Kanta Subbarao (National Institutes of Health, Bethesda, MD, USA) and Gabriel Defang [Naval Medical Research Unit 3 (NAMRU-3), Cairo, Egypt], was amplified in Vero E6 cells at an m.o.i. of 0.01. On day 4 after infection, when a cytopathic effect was visible, virus-containing supernatants were collected and clarified by centrifugation. MERS-CoV was titrated on Vero E6 cells by plaque assay.

Cell-based ELISA screen for MERS antiviral agents. Vero E6 cells were seeded using 40 000 cells in 100 μ l DMEM plus 10 % FBS per well in black-, opaque- or clear-bottomed 96-well plates. Test compounds MPA and ribavirin were obtained from Sigma-Aldrich, and IFN- β , IFN- α 2a, IFN- α 2b, IFN- γ and a recombinant product based on the consensus sequence of the IFN- α subtypes designated 'universal type 1 IFN' were obtained from PBL. After 24 h, five dilutions of test compounds were added to the cells in 50 μ l using

a 96-well liquidator (Rainin Instrument). The cell plates were transferred to the containment laboratory to add MERS-CoV (Hu/Jordan-N3/2012) at an m.o.i. of 0.1 in 50 µl DMEM plus 10% FBS approximately 1 h after the addition of the drugs. After 48 h, plates were fixed with 10% neutral-buffered formalin and removed from biocontainment. MERS-CoV was detected with a rabbit polyclonal antibody to the HCoV-EMC/2012 S protein (Sino Biological) followed by staining with Alexa Fluor 594-conjugated goat anti-rabbit IgG (H+L) antibody (Life Technologies). Nuclei were detected with the Hoechst 33342 dye, which stains DNA. For Alexa Fluor 594, fluorescence was quantified on a plate reader (Infinite M1000 Pro; Tecan US) with an excitation wavelength of 590 nm and an emission wavelength of 617 nm. The Operetta high content imaging system (PerkinElmer) and analysis software (Harmony 3.1) was used to quantify fluorescence of both dyes, Alexa Fluor 594 and Hoechst 33342. Wavelengths of 360–400 and 560–580 nm were used to excite Hoechst 33342 dye and Alexa Fluor 594 dye, respectively. Emission wavelengths of 410–480 and 590–640 nm were used to detect Hoechst 33342 and Alexa Fluor 594 fluorescence, respectively. Operetta software was used to set the threshold for background versus MERS-CoV-positive cells and determine the mean fluorescence intensity (MFI) of MERS-CoV-positive cells in nine fields per well at $\times 20$ magnification. MFI per cell was determined by normalizing the MFI to the total cell number in each well. The percentage inhibition of treated wells (TREAT) compared with untreated wells (UNTR) was determined using the formula: % inhibition = $[1 - (\text{TREAT} - \text{normal}) / (\text{UNTR} - \text{normal})] \times 100$. The signal from treated wells was normalized to uninfected control wells (normal) and measured (as a %) relative to untreated wells. Non-linear regression analysis was performed to calculate IC_{50} values (GraphPad Software). The MERS-CoV ELISA drug screen was carried out with four replicates for each drug concentration and the assay was repeated at least twice for confirmation. Error bars for dose-response curves represent the SD of four replicates.

Cytotoxicity assay. To evaluate the cytotoxicity of the drugs, Vero E6 cells were plated and treated with the drugs at the same concentrations used for detection of MERS-CoV replication inhibition, as described above for the cell-based MERS-CoV ELISA drug screen, but were not infected with virus. At 48 h after drug addition, the plates were analysed using a CellTiter Glo luminescent cell viability assay kit (Promega), and luminescence was read on an Infinite M1000 Pro plate reader. Alternatively, the fluorescent stain Hoechst 33342 (Life Technologies) was used to determine cell numbers in each well to quantify the cytotoxic effect.

Virus yield reduction assay. Vero E6 cells were seeded in 12-well plates at 200 000 cells per well. After overnight incubation, the cells were infected in triplicate with MERS-CoV strain Hu/Jordan-N3/2012 at an m.o.i. of 0.1 and incubated at 37 °C for 1 h with shaking every 15 min. The inoculum was removed, the cells were washed with PBS and fresh medium was added containing 10-fold dilutions of IFN- β (10–1000 U ml⁻¹) for 48 and 72 h. Supernatants were collected and titrated using the infectivity assay. The assay was carried out with three replicates for each drug concentration and was repeated at least twice for confirmation. Error bars of dose-response curves represent the SD of three replicates.

Infectivity assay. Vero E6 cells were infected in eight replicates with 10-fold dilutions of supernatants from the virus yield reduction assay. MERS-CoV was absorbed for 1 h, and then removed and replaced with DMEM plus 10% FBS. Cells were incubated at 37 °C, 5% CO₂, in a humidified environment for 6 days. The cytopathic effect in wells was scored by fixing and staining the cells with crystal violet. The TCID₅₀ was calculated with Microsoft Excel as described by Reed & Muench (1938).

ACKNOWLEDGEMENTS

We thank Calli Lear, Yingyun Cai and Cindy Allan for outstanding assistance in development of the drug screen protocol and Cindy Allan for implementation of protocols in the biocontainment suite. We thank cell culture staff in preparing the cells used in this study. In addition, we acknowledge Laura Bollinger for technical writing services in preparation of this manuscript and Jiro Wada for figure preparation. This work was supported by the Division of Intramural Research of the National Institute of Allergy and Infectious Diseases (NIAID), Integrated Research Facility (NIAID, Division of Clinical Research) and Battelle Memorial Institute's prime contract with NIAID (contract no. HHSN2722007000161). The content of this publication does not necessarily reflect the views or policies of the US Department of Health and Human Services or of the institutions and companies affiliated with the authors. B.J.H., J.D. and E.P. performed this work as employees of Tunnell Consulting, Inc., a subcontractor to Battelle Memorial Institute; H.Z. performed this work as an employee of Loveless Commercial Contracting, Inc., a subcontractor to Battelle Memorial Institute; G.G.O., Jr performed this work as an employee of Midwest Research Institute, a subcontractor to Battelle Memorial Institute; and J.K. and M.R.H. performed this work as employees of Battelle Memorial Institute, all under its prime contract with NIAID, under contract no. HHSN2722007000161.

REFERENCES

- Barnard, D. L., Day, C. W., Bailey, K., Heiner, M., Montgomery, R., Lauridsen, L., Winslow, S., Hoopes, J., Li, J. K. & other authors (2006). Enhancement of the infectivity of SARS-CoV in BALB/c mice by IMP dehydrogenase inhibitors, including ribavirin. *Antiviral Res* 71, 53–63.
- Brown, C., Carson, G., Chand, M. & Zambon, M. for Public Health England and International Severe Acute Respiratory & Emerging Infection Consortium (2013). Treatment of MERS-CoV: decision support tool. Clinical decision making tool for the treatment of MERS-CoV v.1.1, 29 July 2013. Available at: http://isaric.tghn.org/site_media/media/articles/Decision_Support_Document_v1_1_20130729.pdf. Accessed 5 October 2013.
- Chan, J. F., Chan, K. H., Kao, R. Y., To, K. K., Zheng, B. J., Li, C. P., Li, P. T., Dai, J., Mok, F. K. & other authors (2013a). Broad-spectrum antivirals for the emerging Middle East respiratory syndrome coronavirus. *J Infect* 67, 606–616.
- Chan, R. W., Chan, M. C., Agnihothram, S., Chan, L. L., Kuok, D. I., Fong, J. H., Guan, Y., Poon, L. L., Baric, R. S. & other authors (2013b). Tropism of and innate immune responses to the novel human betacoronavirus lineage C virus in human ex vivo respiratory organ cultures. *J Virol* 87, 6604–6614.
- de Groot, R. J., Baker, S. C., Baric, R. S., Brown, C. S., Drosten, C., Enjuanes, L., Fouchier, R. A., Galiano, M., Gorbalenya, A. E. & other authors (2013). Middle East respiratory syndrome coronavirus (MERS-CoV): announcement of the Coronavirus Study Group. *J Virol* 87, 7790–7792.
- de Wilde, A. H., Raj, V. S., Oudshoorn, D., Bestebroer, T. M., van Nieuwkoop, S., Limpens, R. W., Posthuma, C. C., van der Meer, Y., Bárcena, M. & other authors (2013). MERS-coronavirus replication induces severe in vitro cytopathology and is strongly inhibited by cyclosporin A or interferon- α treatment. *J Gen Virol* 94, 1749–1760.
- Falzarano, D., de Wit, E., Martellaro, C., Callison, J., Munster, V. J. & Feldmann, H. (2013a). Inhibition of novel β coronavirus replication by a combination of interferon- α 2b and ribavirin. *Sci Rep* 3, 1686.

- Falzarano, D., de Wit, E., Rasmussen, A. L., Feldmann, F., Okumura, A., Scott, D. P., Brining, D., Bushmaker, T., Martellaro, C. & other authors (2013b). Treatment with interferon- α 2b and ribavirin improves outcome in MERS-CoV-infected rhesus macaques. *Nat Med* **19**, 1313–1317.
- Henry, S. D., Metselaar, H. J., Lonsdale, R. C., Kok, A., Haagmans, B. L., Tilanus, H. W. & van der Laan, L. J. (2006). Mycophenolic acid inhibits hepatitis C virus replication and acts in synergy with cyclosporin A and interferon- α . *Gastroenterology* **131**, 1452–1462.
- ISARIC (2013). Clinical Decision Making Tool for Treatment of MERS-CoV v.1.1 (29 July). International Severe Acute Respiratory & Emerging Infection Consortium (ISARIC). Available at: <http://isaric.tghn.org/articles/pheisarc-decision-support-document/> Accessed August 5, 2013.
- Josset, L., Textoris, J., Llorid, B., Ferraris, O., Moules, V., Lina, B., N'guyen, C., Diaz, J. J. & Rosa-Calatrava, M. (2010). Gene expression signature-based screening identifies new broadly effective influenza A antivirals. *PLoS ONE* **5**, e13169.
- Khan, M., Dhanwani, R., Patro, I. K., Rao, P. V. & Parida, M. M. (2011). Cellular IMPDH enzyme activity is a potential target for the inhibition of Chikungunya virus replication and virus induced apoptosis in cultured mammalian cells. *Antiviral Res* **89**, 1–8.
- Kindler, E., Jónsdóttir, H. R., Muth, D., Hamming, O. J., Hartmann, R., Rodriguez, R., Geffers, R., Fouchier, R. A., Drosten, C. & other authors (2013). Efficient replication of the novel human betacoronavirus EMC on primary human epithelium highlights its zoonotic potential. *mBio* **4**, e00611.
- Leyssen, P., Balzarini, J., De Clercq, E. & Neyts, J. (2005). The predominant mechanism by which ribavirin exerts its antiviral activity in vitro against flaviviruses and paramyxoviruses is mediated by inhibition of IMP dehydrogenase. *J Virol* **79**, 1943–1947.
- Ludwig, S. (2011). Disruption of virus–host cell interactions and cell signaling pathways as an anti-viral approach against influenza virus infections. *Biol Chem* **392**, 837–847.
- Morrey, J. D., Smee, D. F., Sidwell, R. W. & Tseng, C. (2002). Identification of active antiviral compounds against a New York isolate of West Nile virus. *Antiviral Res* **55**, 107–116.
- Pan, Q., de Ruiter, P. E., Metselaar, H. J., Kwekkeboom, J., de Jonge, J., Tilanus, H. W., Janssen, H. L. & van der Laan, L. J. (2012). Mycophenolic acid augments interferon-stimulated gene expression and inhibits hepatitis C virus infection in vitro and in vivo. *Hepatology* **55**, 1673–1683.
- Reed, L. J. & Muench, H. (1938). A simple method of estimating fifty per cent endpoints. *Am J Epidemiol* **27**, 493–497.
- Smee, D. F., Bray, M. & Huggins, J. W. (2001). Antiviral activity and mode of action studies of ribavirin and mycophenolic acid against orthopoxviruses in vitro. *Antivir Chem Chemother* **12**, 327–335.
- Tisoncik, J. R., Simmons, C. P., Farrar, J., Martin, T. R. & Katze, M. G. (2012). Into the eye of the cytokine storm. *Microbiol Mol Biol Rev* **76**, 16–32.
- World Health Organization (2013). Global Alert and Response (GAR). Middle East respiratory syndrome coronavirus (MERS-CoV) – update. Available: http://www.who.int/csr/don/2013_09_20/en/. Accessed 5 October 2013.
- Zaki, A. M., Van Boheemen, S., Bestebroer, T. M., Osterhaus, A. D. M. E. & Fouchier, R. A. M. (2012). Isolation of a novel coronavirus from a man with pneumonia in Saudi Arabia. *N Engl J Med* **367**, 1814–1820.

NERVTAG

Presented to SAGE on 21/1/21

Authors - Peter Horby, Catherine Huntley, Nick Davies, John Edmunds, Neil Ferguson, Graham Medley, Calum Semple

Summary

1. The variant of concern (VOC) B.1.1.7 appears to have substantially increased transmissibility compared to other variants and has grown quickly to become the dominant variant in much of the UK.
2. Initial assessment by PHE of disease severity through a matched case-control study reported no significant difference in the risk of hospitalisation or death in people infected with confirmed B.1.1.7 infection versus infection with other variants. [1]
3. Several new analyses are however consistent in reporting increased disease severity in people infected with VOC B.1.1.7 compared to people infected with non-VOC virus variants.
4. There have been several independent analyses of SGTF and non-SGTF cases identified through Pillar 2 testing linked to the PHE COVID-19 deaths line list:
 - a. LSHTM: reported that the relative hazard of death within 28 days of test for VOC-infected individuals compared to non-VOC was 1.35 (95%CI 1.08-1.68).
 - b. Imperial College London: mean ratio of CFR for VOC-infected individuals compared to non-VOC was 1.36 (95%CI 1.18-1.56) by a case-control weighting method, 1.29 (95%CI 1.07-1.54) by a standardised CFR method.
 - c. University of Exeter: mortality hazard ratio for VOC-infected individuals compared to non-VOC was 1.91 (1.35 - 2.71).
 - d. These analyses were all adjusted in various ways for age, location, time and other variables.
5. An updated PHE matched cohort analysis has reported a death risk ratio for VOC-infected individuals compared to non-VOC of 1.65 (95%CI 1.21-2.25).
6. There are several limitations to these datasets including representativeness of death data (<10% of all deaths are included in some datasets), power, potential biases in case ascertainment and transmission setting.
7. **Based on these analyses, there is a realistic possibility that infection with VOC B.1.1.7 is associated with an increased risk of death compared to infection with non-VOC viruses.**
8. It should be noted that the absolute risk of death per infection remains low.
9. An analysis of CO-CIN data has not identified an increased risk of death in hospitalised VOC B.1.1.7 cases. However, increased severity may not necessarily be reflected by increased in-hospital death risk.

10. Since the time lag from infection to hospitalisation and death is relatively long, data will accrue in coming weeks, at which time the analyses will become more definitive.

Full text

11. Previously, preliminary results from a matched-cohort study conducted by PHE reported no statistically significant increased risk of hospitalisation or death in VOC-infected individuals compared to non-VOC [1].
12. On Friday 15th January NERVTAG was presented with two papers that reported an increased case fatality rate in subjects with s-gene target failure (SGTF, a proxy for variant B.1.1.7).
13. Both papers used the same core dataset of SGTF cases identified through Pillar 2 testing linked to the PHE COVID-19 deaths line list: a paper from LSHTM [2] and a paper from Imperial College London [3].
14. The LSHTM paper used a Cox proportional hazards model to estimate change in risk of death within 28 days of test for individuals infected with the VOC [2].
 - a. The study was based on 2,583 deaths among 1.2 million tested individuals. 384 deaths were among SGTF individuals.
 - b. Results were controlled for age, sex, index of multiple deprivation, and Upper Tier Local Authority (UTLA).
 - c. The relative hazard of death within 28 days of test was 1.35 (95%CI 1.08-1.68) for VOC-infected individuals, compared to non-VOC, with adjustment made for misclassification of SGTF.
 - d. Focusing only on individuals with SGTF after 1 November 2020 (no adjustment for SGTF misclassification), the relative hazard of death is 1.28 (95%CI 1.06-1.56).
 - e. Relative increases in CFR appeared to be consistent across age groups
 - f. Sensitivity analyses including further hospital pressure covariates (proportion of beds capable of mechanical ventilation occupied; proportion of beds capable of non-invasive ventilation occupied; number of staff absences per bed among medical staff; and number of staff absences per bed among nursing staff) did not substantially change the measure of effect.
15. The Imperial Paper reported the results of a non-parametric analysis of fatal outcomes associated with B1.1.7 [3].
 - a. Two methods were used to evaluate the differences in mortality between VOC and non-VOC cases: case-control-weighting, and standardised CFR. In each case, the ratio of s-gene positive to s-gene negative case fatality ratios (CFRs) is calculated.
 - b. The study considers data from all of England and includes specimen dates in the epidemiological week range 46-54 (54 being week 1 of 2021) inclusive. Estimates are adjusted for NHS STP area, epidemiological week, ethnicity

code, and age band.

- c. Across all specimens, the mean ratio of CFRs is 1.36 (95%CI 1.18-1.56) by the case-control weighting method, and 1.29 (95%CI 1.07-1.54) by the standardised CFR method. This estimate includes a correction for the probability over time that a specimen with SGTF is the VOC.
 - d. Relative increases in CFR appeared to be consistent across age groups.
 - e. Subsequent correction for possible differences in PCR cycle threshold values (ct) between VOC and non-VOC cases was included by restricting both groups only to those samples with ct <30. This adjustment made no meaningful difference.
16. A PHE retrospective matched cohort study was also reported [4]:
- a. 23 November 2020 – 4 January 2021 study period (period when >90% of sequenced SGTF samples confirmed to be VOC202012/01). Matching based on 10-year age bands, sex, week of test and lower-tier local authority.
 - b. 92,207 SGTF cases and corresponding comparators were included in the matched cohort (n = 184,414), although routine hospitalisation data is subject to reporting delays and this should be considered preliminary.
 - c. The odds of SGTF cases being admitted was not significantly different to non-SGTF cases (OR = 1.07, 95% CI 0.86 – 1.33).
 - d. Initial analysis identified 152 deaths following a first positive SARS-CoV-2 test, n = 86 (0.09%) SGTF cases and n = 66 (0.07%) comparator cases. It was noted that 0.07% to 0.09% represents a 28% relative increase in the risk of death, which is compatible with the results from LSHTM and Imperial.
 - e. Initial analysis of 14,939 SGTF cases and 15,555 comparators who had at least 28 days between specimen date and the study period end date. There were 25 deaths (0.17%) in SGTF cases and 26 deaths (0.17%) in comparators (RR 1.00, 95% CI 0.58 – 1.73).
 - f. Updated linkage of deaths data to the same matched cohort on 19/01/2021 identified there were 65 deaths among non-SGTF cases (0.1%) and 104 deaths among SGTF cases (0.2%), within 28 days of specimen date. With this increased time for follow-up and ascertainment of deaths, the risk ratio increased to 1.65 (95%CI 1.21-2.25).
17. There are potential limitations in these datasets:
- a. The dataset used in the LSHTM, Imperial, Exeter and PHE analyses is based on a limited subset of the total deaths. This includes approximately 8% of the total deaths occurring during the study period. Of all coronavirus deaths, approximately 26% occur in individuals who have had a Pillar 2 test, and only 30% of these have S-gene data. The results of all studies may therefore not be representative of the total population.
 - b. Restriction of analysis in the PHE matched cohort to people with a full 28 days follow up at the first analysis reduced statistical power and removed the

excess death signal. However, the LSHTM analysis show an increasing divergence in CFR between VOC and non-COV with time since diagnosis. A later update of the PHE analysis with additional follow-up time identified an increased risk ratio for 28-day case fatality.

- c. Some laboratories only report SGTF if the PCR cycle threshold (ct) value is <30, since target gene failure can occur with low viral loads. For the LSHTM paper, no such ct threshold was applied to non-SGTF positive samples.
 - i. A sensitivity analysis of the Imperial study produced a CFR ratio estimate where the cycle threshold was limited to <30 for both SGTF and non-SGTF samples. The estimate was 1.37 (95%CI 1.19-1.56) by the case-control weighting method, and 1.30 (95%CI 1.08-1.57) by the standardised CFR method. These results were similar to those obtained without this restriction.
 - d. The increased transmissibility of VOC B.1.1.7 compared to non-VOC variants might lead to differences in the context in which cases are occurring. For example, if institutional outbreaks are more likely with B1.1.7 compared to non-VOC, then an age matched analysis might be comparing frail elderly people in nursing home outbreaks of B.1.1.7 with healthier elderly people infected with the non-VOC virus in the community. However, both the Imperial and the LSHTM analyses showed increased CFRs across all age groups. This potential bias could therefore not explain the increased CFR in younger age groups.
 - e. If there is an increase in the severity of infection with VOC B1.1.7, we would also expect to see an increase in the risk of hospitalisation. Currently, we do not have evidence of an increased risk of hospitalisation in individuals with VOC B1.1.7 but data are limited due to lags in the availability of hospitalisation data.
18. A rapid analysis of CO-CIN data during the period in which VOC B1.1.7 emerged was reported [5]:
- a. Across the whole CO-CIN cohort, there is no observed increase in hospital case fatality in the period during which VOC emerged in England, after adjusting for period of admission, age, sex, deprivation, and ethnicity.
 - b. Compared to March 2020, hospital CFR continues to be lower and has been stable in September through December.
 - c. Data return from CO-CIN is currently reduced and unevenly distributed, which will impact on the representativeness of findings. Importantly there are a substantial number of outcomes missing from cases admitted in late December, when the impact of VOC emergence would start to be apparent in hospital data.
 - d. A sub-analysis included linked data from 21,882 cases (21,596 non-VOC and 286 VOC) from across the whole CO-CIN cohort. VOC in this sub-study was robustly determined by COG sequence lineage, rather than assumed by

SGTF. Outcome data was available for only 143 VOC cases. However; 32 VOC cases were identified at one trust with good data quality returns throughout the period of study.

- e. Restricting the analysis to a trust with high proportion of proven VOC which has maintained good quality data returns, and after adjusting for age and sex, found no statistically significant change in hospital CFR comparing proven VOC (n=32) with non-VOC (n=184) (OR 0.63, 95%CI 0.20 – 1.69).
 - f. An increase in case fatality rates would not necessarily manifest as an increase in case fatality rates amongst those hospitalised. Rather, it may increase the proportion of cases who are ill enough to meet the severity threshold for hospitalisation, but not affect the likelihood of death amongst those who are sick enough to be admitted.
19. A subsequent independent case control analysis of Pillar 2 data linked to the death line list by Exeter University, matched on age, specimen time, location, ethnicity, gender and index of multiple deprivation, reported a mortality hazard ratio for VOC-infected individuals compared to non-VOC was 1.91 (1.35 - 2.71).

Summary

- 20. There is evidence from analysis of Pillar 2 testing data linked to COVID-19 deaths that infection with VOC B.1.1.7 is associated with an increased case fatality rate compared to infection with non-VOC viruses. The relative increase in CFR appears to be apparent across age groups.
- 21. An initial retrospective matched cohort study from PHE (also based on linked testing and mortality data) found no evidence of a significant difference in risk of hospitalisation or death between individuals with VOC and individuals with non-VOC when analysis was restricted to those with completed 28 days follow up, but had insufficient statistical power to assess this accurately. A later update of the analysis with additional follow-up time, has now also identified an increased risk ratio for 28-day case fatality.
- 22. CO-CIN has not found evidence of an increase in hospital case fatality rate associated with VOC B.1.1.7, both across the whole cohort and in a single trust with a high rate of good quality data using sequence determined lineage. However, increased severity may not necessarily be reflected by increased in-hospital death risk.
- 23. There are limitations in all datasets that it may not be possible to resolve but as more data accrue the analyses will become more definitive.

Conclusion

- 24. **There is a realistic possibility that VOC B.1.1.7 is associated with an increased risk of death compared to non-VOC viruses.**

Recommendations

25. PHE to review if cases associated with care homes can be flagged in Pillar 2 data for an analysis adjusted for care home status.
26. ONS should assess if it is possible to link ONS survey participants to SUS data on hospitalisations and to deaths. This dataset would suffer from less ascertainment bias since participants are a random selection and ascertainment of cases is not dependent on symptoms or on seeking a test from the Test and Trace. This analysis will be limited in power, so analyses comparing ONS estimates of the proportion of the population infected over time, with the number of hospitalisations and deaths over time, stratified by age and region, could also provide insight as to whether case fatality rates have changed during the period of emergence of the virus.
27. Co-CIN to stratify analyses by region to assess whether in hospital mortality time trends differ in those regions affected by the VOC earliest.
28. ISARIC CCP-UK / CO-CIN to be re-prioritised as Tier 1 UPH study.

References

1. Public Health England, 2020. *Variant Of Concern 202012/01: Technical Briefing 2*. Investigation of novel SARS-CoV-2 variant. [online] Available at: <https://assets.publishing.service.gov.uk/government/uploads/system/uploads/attachment_data/file/949639/Technical_Briefing_VOC202012-2_Briefing_2_FINAL.pdf> [Accessed 13 January 2021].
2. Ferguson, N. 2021. Non-parametric analysis of fatal outcomes associated with B.1.1.7. Imperial College London - unpublished analysis.
3. Davies, N., Diaz-Ordaz, K., Keogh, R. 2021. Relative fatality hazard in Pillar 2 tested individuals with VOC. LSHTM – unpublished analysis.
4. PHE, 2021. Unpublished analysis.
5. Docherty A., Harrison, E., Semple, C. 2021. Hospital case fatality and emergence of variant of concern B.1.1.7, rapid CO-CIN report to NERVTAG and SAGE. Unpublished analysis.

Annex.

Data table – preliminary results

Paper	Method	Sample	Outcome	Estimate of Effect	95%CI
Imperial	Non-parametric analysis: case-control weighting	All samples, corrected for probability that S-gene negative samples are the VOC	Ratio of S-negative to S-positive case fatality ratios	1.36	1.18-1.56
Imperial	Non-parametric analysis: standardised CFR	All samples, corrected for probability that S-gene negative samples are the VOC	Ratio of S-negative to S-positive case fatality ratios	1.29	1.07-1.54
LSHTM	Cox proportional hazards model	All samples, adjusted for misclassification of SGTF	Hazard ratio for death VOC-infected individuals to non-VOC infected individuals	1.35	1.08-1.68
LSHTM	Cox proportional hazards model	All samples, after 01.11.20 (not adjusted for misclassification of SGTF)	Hazard ratio death for VOC-infected individuals to non-VOC infected individuals	1.28	1.06-1.56
Exeter	Matched case control study	Samples since 01 October, various adjustments	Hazard ratio death for VOC-infected individuals to non-VOC infected individuals	1.91	1.35-2.71
CO-CIN	Multinomial model	CO-CIN data from a single trust	Odds ratio of death in hospitalised VOC-infected individuals to non-VOC infected individuals	0.63	0.20-1.69
PHE	Retrospective matched cohort study (initial analysis)	Cases and comparators <u>with at least 28 days</u> between specimen date and study end date	Odds ratio of hospital admission in SGTF cases vs non-SGTF cases	1.07	0.86-1.33
PHE	Retrospective matched cohort study (initial analysis)	Whole cohort	Relative risk of death in SGTF cases vs non-SGTF cases within 28 days of a +ve result	1.3	0.95-1.79
PHE	Retrospective matched cohort study (initial analysis)	Cases and comparators <u>with at least 28 days</u> between specimen date and study end date	Relative risk of death in SGTF cases vs non-SGTF cases within 28 days of a +ve result	1.00	0.58-1.73
PHE	Retrospective matched cohort study (updated analysis 19/01)	Whole cohort	Relative risk of death in SGTF cases vs non-SGTF cases within 28 days of a +ve result	1.65	1.21-2.25



Since January 2020 Elsevier has created a COVID-19 resource centre with free information in English and Mandarin on the novel coronavirus COVID-19. The COVID-19 resource centre is hosted on Elsevier Connect, the company's public news and information website.

Elsevier hereby grants permission to make all its COVID-19-related research that is available on the COVID-19 resource centre - including this research content - immediately available in PubMed Central and other publicly funded repositories, such as the WHO COVID database with rights for unrestricted research re-use and analyses in any form or by any means with acknowledgement of the original source. These permissions are granted for free by Elsevier for as long as the COVID-19 resource centre remains active.



Contents lists available at ScienceDirect

Journal of Infection

journal homepage: www.elsevier.com/locate/jinf

Rapid asymptomatic transmission of COVID-19 during the incubation period demonstrating strong infectivity in a cluster of youngsters aged 16–23 years outside Wuhan and characteristics of young patients with COVID-19: A prospective contact-tracing study

Lei Huang^{a,1,**}, Xiuwen Zhang^{b,c,1}, Xinyue Zhang^{d,1}, Zhijian Wei^{e,1}, Lingli Zhang^b, Jingjing Xu^b, Peipei Liang^f, Yuanhong Xu^{g,**}, Chengyuan Zhang^{h,**}, Aman Xu^{e,*}

^a Department of General Surgery, the First Affiliated Hospital of Anhui Medical University, Hefei 230022, Anhui Province, China

^b Department of Quarantine Ward, East District of First Affiliated Hospital of Anhui Medical University (Feidong People's Hospital), Hefei, Anhui Province, China

^c Graduate School, Soochow University, Suzhou, Jiangsu Province, China

^d Department of Academic Research, The First People's Hospital of Hefei, Hefei, Anhui Province, China

^e Department of General Surgery, the First Affiliated Hospital of Anhui Medical University, Hefei 230022, Anhui Province, China

^f Department of Emergency Medicine, the First Affiliated Hospital of Anhui Medical University, Hefei, Anhui Province, China

^g Department of Clinical Laboratory Medicine, the First Affiliated Hospital of Anhui Medical University, Hefei 230022, Anhui Province, China

^h Department of Respiratory and Critical Care Medicine, East District of First Affiliated Hospital of Anhui Medical University (Feidong People's Hospital), Hefei 231600, Anhui Province, China

ARTICLE INFO

Article history:

Accepted 3 March 2020

Available online 10 April 2020

Keywords:

COVID-19

Rapid transmission

Incubation period

Infectivity

Characteristics

Cluster of youngsters

Outside Wuhan

Prospective contact-tracing study

SUMMARY

Background: The outbreak of coronavirus-disease-2019 (COVID-19) has rapidly spread to many places outside Wuhan. Previous studies on COVID-19 mostly included older hospitalized-adults. Little information on infectivity among and characteristics of youngsters with COVID-19 is available.

Methods: A cluster of 22 close-contacts of a 22-year-old male (Patient-Index) including youngsters with laboratory-confirmed COVID-19 and hospitalized close-contacts testing negative for severe-acute-respiratory-syndrome-coronavirus-2 (SARS-CoV-2) in Anhui Province, China was prospectively-traced.

Results: Since January 23, 2020, we enrolled a cluster of eight youngsters with COVID-19 (median age [range], 22 [16–23] years; six males) originating from Patient-Index returning from Wuhan to Hefei on January 19. Patient-Index visited his 16-year-old female cousin in the evening on his return, and met 15 previous classmates in a get-together on January 21. He reported being totally asymptomatic and were described by all his contacts as healthy on January 19–21. His very first symptoms were itchy eyes and fever developed at noon and in the afternoon on January 22, respectively. Seven youngsters (his cousin and six classmates) became infected with COVID-19 after a few-hour-contact with Patient-Index. None of the patients and contacts had visited Wuhan (except Patient-Index), or had any exposure to wet-markets, wild-animals, or medical-institutes within three months. For affected youngsters, the median incubation-period was 2 days (range, 1–4). The median serial-interval was 1 day (range, 0–4). Half or more of the eight COVID-19-infected youngsters had fever, cough, sputum production, nasal congestion, and fatigue on admission. All patients had mild conditions. Six patients developed pneumonia (all mild; one bilateral) on admission. As of February 20, four patients were discharged.

Conclusions: SARS-CoV-2-infection presented strong infectivity during the incubation-period with rapid transmission in this cluster of youngsters outside Wuhan. COVID-19 developed in these youngsters had fast onset and various nonspecific atypical manifestations, and were much milder than in older patients as previously reported.

© 2020 The British Infection Association. Published by Elsevier Ltd. All rights reserved.

* Corresponding author at: Department of General Surgery, the First Affiliated Hospital of Anhui Medical University, Hefei 230022, Anhui Province, China (Aman Xu); Department of Respiratory and Critical Care Medicine, East District of First Affiliated Hospital of Anhui Medical University (Feidong People's Hospital), Hefei 231600, Anhui Province, China (Chengyuan Zhang); Department of Clinical Laboratory Medicine, the First Affiliated Hospital of Anhui Medical University, Hefei 230022, Anhui Province, China (Yuanhong Xu); Department of General Surgery, the First Affiliated Hospital of Anhui Medical University, Hefei 230022, Anhui Province, China (Lei Huang).

** Corresponding authors.

E-mail addresses: huangleizhenting@126.com (L. Huang), xyhong1964@163.com (Y. Xu), 2396476405@qq.com (C. Zhang), amanxu@163.com (A. Xu).

¹ These authors contributed equally to this article.

<https://doi.org/10.1016/j.jinf.2020.03.006>

0163-4453/© 2020 The British Infection Association. Published by Elsevier Ltd. All rights reserved.

Introduction

The outbreak of the 2019-novel-coronavirus-disease (COVID-19) caused by severe-acute-respiratory-syndrome-coronavirus-2 (SARS-CoV-2) emerging from Wuhan in December 2019 has been arousing great global health concern, with many unknowns regarding the transmission dynamics and spectrum of illness to be answered.^{1–3} SARS-CoV-2 has rapidly spread to many places outside Wuhan, where imported cases with ascertained COVID-19 among travelers returning from Wuhan without direct exposure to any wet-markets or wild-animals have been reported.^{2–4} Current epidemiologic data indicate that human-to-human transmission of SARS-CoV-2 has been rapidly occurring.^{2,5,6}

The great number of COVID-19 infections may be attributable to the late identification of sources-of-infection and the ability of the host to shed the infection while asymptomatic.^{1,7} While a study⁸ suggests that transmission may occur during the incubation-period, the validity was questioned by *Science* because the evidence was not directly obtained from the infectious-patient, who actually had developed symptoms, which were controlled by a fever-lowering agent, before disease transmission to others.⁹

Published reports^{2,10,11} focused on hospitalized older patients in Wuhan, many of whom had a history of exposure to the Huanan-Seafood-Wholesale-Market, and suggested that COVID-19 mainly affected older adults with frequent chronic comorbidities, and that many of them developed severe pneumonia, for whom organ dysfunction and failure and death can occur. However, the characteristics and infectivity of COVID-19 among youngsters have been rarely reported, and information on SARS-CoV-2-negative close-contacts, patients with mild infections, or those with infections outside Wuhan remains limited.

We collected and analyzed detailed data from a cluster of youngsters aged 16–23 years with laboratory-confirmed COVID-19 in Hefei, China, originating from a 22-year-old youngster (Patient-Index) returning from Wuhan who rapidly transmitted COVID-19 to seven other youngsters of similar ages without recent travel to Wuhan, where rapid transmission had occurred during the incubation-period of illness in Patient-Index. We also identified all the SARS-CoV-2-negative close-contacts of Patient-Index, and further compared them with the SARS-CoV-2-positive patients. We carefully examined the infectivity and transmission dynamics by obtaining valid information directly from the patients and contacts themselves. We are herein describing the demographic, epidemiological, clinical, radiological, and laboratory features, management, and outcomes of the cluster of youngsters with COVID-19 and also the SARS-CoV-2-negative close-contacts.

Methods

Participants

On January 23, 2020, we initially enrolled a 22-year-old male (Patient-Index/1) returning from Wuhan who initially presented to Feidong People's Hospital (Hospital-1; the eastern branch of First Affiliated Hospital of Anhui Medical University [Hospital-2]) in Hefei, with fever, productive cough, myalgia, and lung infiltrates on chest-computed-tomography (CT)-scan. He was suspected to be infected with COVID-19. We immediately formed an expert investigation-team prospectively following-up and tracing all the contacts.

Subsequently, from January 25 through 27, seven young symptomatic close-contacts of Patient-Index (his cousin and six classmates) also presented to hospital (**Table 1**; **Fig. S1**) for management of relevant manifestations and assessment of health-conditions after having learned about the COVID-19 outbreak in Wuhan and the human-to-human-transmission. All

the eight patients tested positive for SARS-CoV-2 using real-time-reverse-transcriptase-polymerase-chain-reaction (rRT-PCR), confirming COVID-19. Starting from January 27, the other contacts of Patient-Index were admitted to Hospital-1 for quarantine (nine; Contacts-1-9) if residing in Feidong, a county >400 kilometers northeast of Wuhan, or directly isolated at home and home-visited by local healthcare-authorities if living in other parts of Hefei (two), and they all tested negative for SARS-CoV-2. This study was approved by the Ethics Committee of Hospital 1. Informed consent was obtained from all patients and contacts.

We prospectively collected information on the demographic, epidemiological, clinical, radiological, and laboratory characteristics and management and outcomes for all the eight youngsters with laboratory-confirmed COVID-19 and the nine admitted SARS-CoV-2-negative contacts of Patient-Index. All data were collected into a standardized and customized data-collection form, and validated by a trained team of physician-scientists. At least two investigators independently reviewed the collected information to double-check the data and verify the accuracy. Follow-up was until February 20.

We directly communicated with and interviewed all SARS-CoV-2-positive patients and SARS-CoV-2-negative contacts themselves, and their family-members, relatives, classmates, friends, and healthcare-workers when necessary, to collect and ascertain all medical-history, epidemiological (exposure-history, timelines of events, close-contact identification, etc.), and symptom data, which were cross-checked with information from multiple sources. We determined exposure-histories during the three months before illness-onset or hospital-admission, including the dates, time, frequencies, and patterns of contacts with any person who had fever, respiratory-symptoms, or other relevant symptoms, with any wild-animals, or with any relevant environments such as any wet-markets or medical-institutes. Information on history of travel to Wuhan and direct contact with people returning from Wuhan within three months before symptom-onset or hospital-admission was also included.

The definitions and management of all suspected and ascertained COVID-19 cases enrolled were according to the World Health Organization (WHO) guidance¹² and the New Coronavirus Pneumonia Prevention and Control Program by the China National Health Commission,¹³ and pathogen examinations are detailed in *Supplementary methods*.

Statistics

The incubation-period was defined as days from infection/exposure to illness-onset was estimated. The serial-interval was defined as the time delay between illness-onset dates in successive cases in a transmission-chain.

Continuous variables were shown as median (range), and categorical variables as count (percentage). Blood laboratory-examination findings were illustrated using boxplots, assessed regarding whether the measurements were outside the reference-range, and compared between SARS-CoV-2-positive patients and SARS-CoV-2-negative contacts using the Mann-Whitney-Wilcoxon-test for unpaired samples. Considering the potential type-I-error, the findings should be interpreted as exploratory.

A two-sided *p*-value of <0.05 was considered statistically-significant. Statistical-analyses were performed using the R 3.6.2 software (<https://www.r-project.org/>).

Results

Patient-Index/1 is a 22-year-old overweight otherwise-healthy male-nonsmoker and a Wuhan company-employee. He took the high-speed-rail leaving Wuhan in the morning on January 19,

Table 1

Demographic and baseline characteristics of the eight young patients with confirmed 2019 novel coronavirus disease as of February 17, 2020

Characteristics	Patient 1	Patient 2	Patient 3	Patient 4	Patient 5	Patient 6	Patient 7	Patient 8	Summary ¹
Relationship with Patient 1	Index	Younger cousin	Previous classmate	Previous classmate	Previous classmate	Previous classmate	Previous classmate	Previous classmate	-
Age (years)	22	16	22	22	22	21	21	23	22 (16-23)
Male sex	Y	N	Y	Y	N	Y	Y	Y	6/8 (75%)
Height (cm)	170	167	180	175	160	170	180	180	173 (160-180)
Weight (kg)	82	60	77	65	48	85	70	85	74 (48-85)
Body mass index (kg/m ²)	28.4 ↑	21.5	23.8	21.2	18.6	29.4 ↑	21.6	26.2 ↑	22.7 (18.6-29.4)
Current smoker	N	N	N	Y	N	N	N	Y	2/8 (25%)
Comorbidity	None	None	None	None	Chronic gastritis	Fatty liver	Chronic gastritis	None	-
Travel to or passage through Wuhan or other potential epidemic places	Y (Wuhan)	N	N	N	N	N	N	N	1/8 (13%)
Days from exposure to illness onset	≥ 4	3 or 7	3	1	4	2	2	1	2 (1-4) ²
Days of serial interval	-	4	2	0	3	1	1	0	1 (0-4) ³
Days from illness onset to first admission	2	1	2	3	2	3	2	3	2 (1-3)
Days from admission of Patient 1 to admission of the underlying patient	-	3	2	1	3	2	1	1	2 (1-3) ³
Days from illness onset to first respiratory sample collection	4	1	2	4	2	3	2	3	3 (1-4)
Days from illness onset to first blood sample collection	4	2	2	4	3	5	2	3	3 (2-5)
Days from illness onset to first positive rRT-PCR test for SARS-CoV-2	4	1	2	4	2	3	2	3	3 (1-4)
Days from illness onset to diagnosis by two positive rRT-PCR tests for SARS-CoV-2	5	2	3	5	3	4	3	4	4 (2-5)
Days from first admission to transfer	5	3	3	4	3	2	-	-	3 (2-5) ⁴
Days from first admission to discharge	-	16	18	-	-	-	21	17	18 (16-21) ⁵

¹ Described for continuous and categorical variables, and expressed as median (range) and count/total number of patients with available data (percentage), respectively.² For Patients 3-8.³ For Patients 2-8.⁴ For Patients 1-6; the other patients have not been transferred.⁵ For Patients 2, 3, and 8; the other patients remain in hospital. Values shown in bold indicate abnormal ones. ↑, above the upper limit of the normal range; ↓, below the lower limit of the normal range; -, not applicable; Y, Yes; N, No; rRT-PCR, real-time reverse-transcriptase polymerase-chain-reaction.

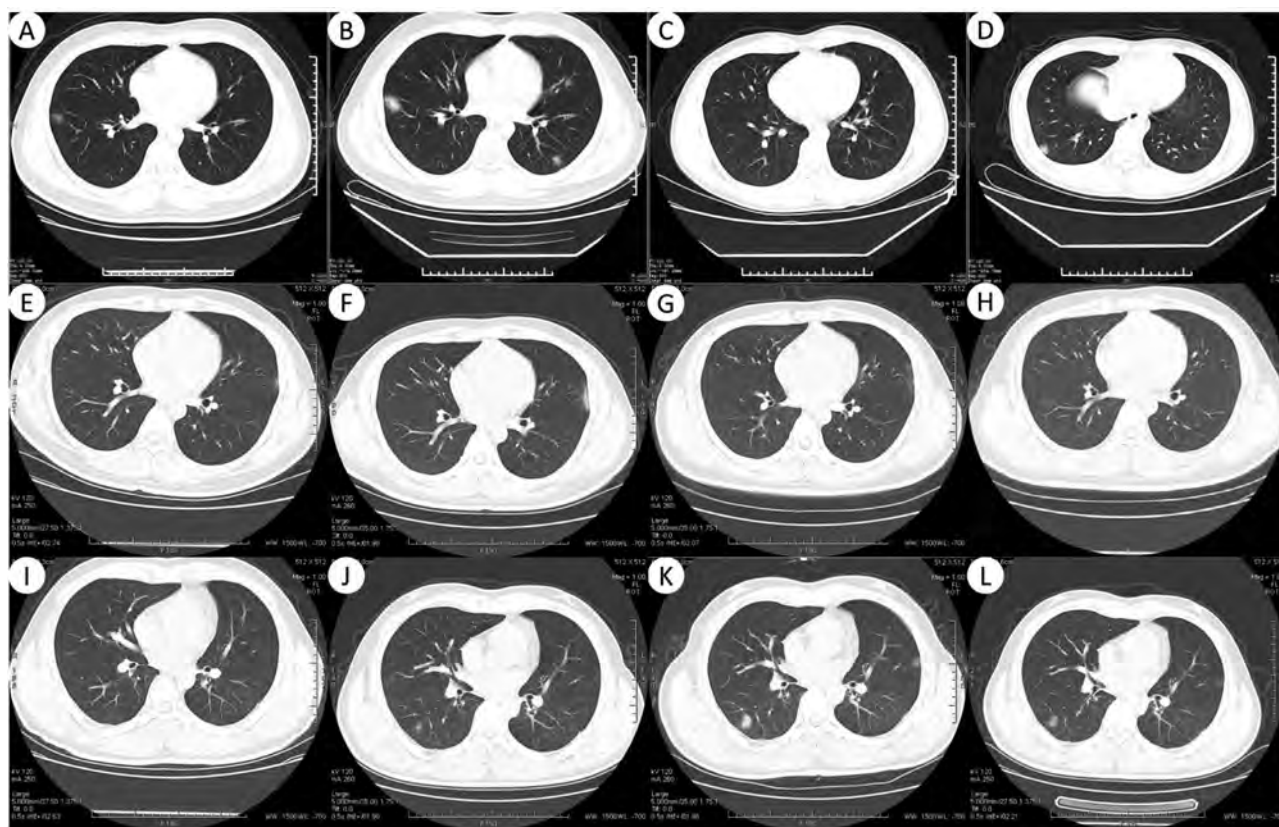


Fig. 1. Representative transverse chest computed tomography scan images. (A) Day 1 after illness onset for Patient Index. A few infiltrates (slight slice-like shadow with increased density) in the lower lobe of the right lung were seen. (B) Day 3 after illness onset for Patient Index. In the peripheral zones of both lungs, scattered ground-glass opacities with fuzzy edges were seen, suggesting bilateral pneumonia with highly likely viral nature. (C) Day 2 after illness onset for Patient 3. A few infiltrates and ground-glass opacities were detected in the lower lobe of left lung. (D) Day 3 after illness onset for Patient 4. Ground-glass opacities and infiltrates in the right lung were observed. (E) Day 2 after illness onset for Patient 7. Small patchy and mottling high-density sub-pleural shadows were seen in the upper lobe of left lung. (F) Day 5 after illness onset for Patient 7. The left upper lung lesion progressed. Antiviral therapy started. (G) Day 13 after illness onset for Patient 7. Patchy blurring infiltrates in the peripheral parts of the left lung with obscure boundary remained. (H) Day 21 after illness onset for Patient 7. The patchy ground-glass density shadows and infiltrates with fuzzy edges in the left lung had been obviously absorbed. (I) Day 3 after illness onset for Patient 8. Few strip-like shadows with uneven density were seen in both lungs. (J) Day 6 after illness onset for Patient 8. Multifocal ground-glass density shadows and opacities in the peripheral parts of both lungs were observed. Antiviral therapy started. (K) Day 14 after illness onset for Patient 8. The multiple patchy high-density shadows consistent with novel coronavirus pneumonia with unclear boundary seen in the peripheral parts of both lungs progressed. (L) Day 18 after illness onset for Patient 8. Absorption of pneumonia lesions in both lungs was observed compared to the previous scan.

2020, four days before the “lockdown” of Wuhan, and arrived at his hometown in Feidong in the afternoon for the China Spring-Festival (Fig. 1). In the evening on January 19, he went to visit (talk and have supper with) his cousin, a 16-year-old otherwise-healthy female (Patient-2) and his uncle (Contact-1; later excluded from infection), in their apartment for about 0.5 hours without air-conditioning or wearing a mask. Further exposure and contact details are shown in Supplementary results and Table S1.

At noon on January 20, he met and ate hotpot with a female (Contact-2; later excluded from infection), sitting face-to-face for about one hour, and went shopping together afterwards. The following day on January 21, he took part in a classmate-get-together in Feidong where he had dinner in a restaurant-room with air-conditioning and also windows open at about 11:30–14:00 and afterwards sang Karaoke in a confined-room at about 14:00–16:30 with air-conditioning and with some fruits shared, with 15 of his previous classmates whose hometowns are all in Hefei. Further details on the get-together are shown in Supplementary results, Table S1, and Figs. S1 and S4. Afterwards, he had supper with a 22-year-old otherwise-healthy male (Patient-4) while the others went right back home. Nobody found him unhealthy that day. He reported that he was totally asymptomatic and well before and on January 21. Among his classmates he contacted, six (Patients-3–8) were later confirmed with COVID-19, and the person who first ex-

perienced any relevant symptoms was Patients-4 and 8 (both on January 22).

Patient-Index reported that the very first symptom that he experienced was itchy eyes at noon on January 22 (Fig. S1). In the afternoon, he felt dizzy with a fever of 37.5°C developed (measured by himself), and he (starting to wear a mask) attended a local outpatient-clinic in Feidong and was prescribed amoxicillin capsules, paracetamol and amantadine compound capsules, and ambroxol dispersible-tablets, after taking which his temperature returned to normal (36.5°C). On the same day, he also developed mild nasal-congestion and rhinorrhea, both lasting 2 days. On January 23, his body temperature was normal in the morning but rose again to 37.5°C at noon, which was again temporarily controlled by the drugs; however, in the evening he had fever again. On the same day before the onset of fever, Patient-2 went to visit Patient-Index, and brought him some home-made food. They ate and chatted together in his room which was tightly confined with no doors or windows open and without air-conditioning for about 0.5 h. Patient-2 later became infected. Having learned about the COVID-19 emergence in Wuhan and the possible human-to-human-transmission from Internet at noon on January 22, he decided to go to Hospital-1 for further assessment and management in the evening on January 23. Virus-RNA detection using respiratory-samples taken on January 26 and 27 both revealed

positive results on rRT-PCR assays, confirming the SARS-CoV-2 infection (Fig. 1). Assays to detect other pathogens were all negative. Further descriptions of the disease-course and management of Patient-Index are detailed in *Supplementary results*.

Tracing of the contacts of Patient-Index started immediately after his admission to hospital. Before illness onset, he closely contacted 22 people (15 classmates and seven family-members). 16 of the contacts were admitted to hospital under isolation: seven (Patients-2–8) developed COVID-19-relevant symptoms, and were later identified to have laboratory-confirmed SARS-CoV-2-infection, and nine (Contacts-1–9) tested negative for SARS-CoV-2 and had normal CT-scan findings, and were discharged to home-isolation 4–5 days after admission. The other six contacts were quarantined and isolated at home, and closely watched by healthcare-workers; they all tested negative for SARS-CoV-2.

None of the contacts had visited any wet-markets or hospitals, contacted any wild-animals, or eaten any game-meat within three months (Tables S1). None of them had resided in, traveled to, or passed Wuhan, other cities in Hubei, or any region where SARS-CoV-2-transmission was known to be occurring within three months. They reported no contacts with any individual recently returning from such a region, with anyone having any suspicious symptoms (e.g., fever, cough, or other respiratory or relevant digestive symptoms), or with anybody later developing relevant symptoms or confirmed with COVID-19 except Patient-Index within three months (this was ascertained by an investigation by the healthcare-authority in Hefei). They did not have any infected family-members or members having visited Wuhan. None of the contacts had any symptom of illness during exposure.

Patients-2–8 were admitted to hospital under isolation 1–3 days after the admission of Patient-Index on February 25–27. The respiratory-samples of all patients tested positive for SARS-CoV-2 for at least two times. Five of the classmates Patient-Index contacted in the get-together initially tested positive for SARS-CoV-2 on January 26, and another classmate and Patient-Index's cousin initially on January 27. We did not find any evidence of co-infection with other known respiratory viral, bacterial, or fungal pathogens in any of the patients on microbiological-testing.

Of all the eight infected youngsters, the median-age was 22 years (range, 16–23; Table 1), and six were male. Three were company-employees, four university-students, and Patient-2 a senior-high-school-student. Three were overweight. Patients-4 and 8 were current-smokers. Three had mild comorbidities (Patients-5 and 7, chronic gastritis; Patient 6, fatty-liver). While Patient-3 initially reported no coexisting medical-conditions, his blood-pressure was measured to be 150/94 mm Hg on admission. They all immediately wore masks and paid special attention to hand-hygiene after illness-onset.

The median incubation-period for Patients-3–8 was two days (range, 1–4; Table 1). The median serial-interval in the young-cluster was one day (range, 0–4; Patients-4 and 8 had symptom onset on the same day as Patient-Index). Among the eight youngsters with COVID-19, the median duration from illness-onset to first-hospital-admission was two days (range, 1–3). The median interval between illness-onset and second positive-test for SARS-CoV-2 which ascertained the COVID-19 diagnosis was four days (range, 2–5).

The presentations of the eight young-patients are shown in Table 2 and Fig. S2. Because manifestations acquired after hospitalization may be influenced by the hospital-environment and drug-use, we primarily describe those developed before or on admission. We did not identify any patients asymptomatic on admission but testing positive for SARS-CoV-2. All patients had mild clinical-conditions, and developed ≥ 2 symptoms and/or signs before or on admission. Most youngsters (seven) developed fever

(except Patient-6). The median body-temperature on admission was 37.5°C (range, 37.0–38.2), and the median highest temperature during disease-course was 38.5°C (range, 37.1–38.9). None had a high fever (temperature $>39^\circ\text{C}$). The fever of Patients-Index, 2, and 5 showed an intermittent pattern, and Patients-3–5 experienced chills. Four patients had productive-cough, and Patients-6 and 7 had dry-cough. Five patients had both fever and cough. Four youngsters experienced fatigue, and three myalgia. Patients-2 and 7 reported experiencing no upper-respiratory-tract-infection symptoms (sore-throat, nasal-congestion, rhinorrhea, and/or sneezing), while five youngsters had more than two such symptoms. Patient-7 reported shortness of breath for two days on admission. None of the youngsters developed dyspnea, or chest-discomfort or pain. Three patients had headache, and Patient-Index reported dizziness. Eye-discomfort was noted in Patients-Index and 3, and backache in Patient-3. Two patients had anorexia, and three nausea, but vomiting did not develop in any of them before or on admission. Only Patient-8 developed diarrhea, and Patient-5 reported abdominal-discomfort. Nobody only presented with digestive-symptoms. Patient-2, the youngest patient (16 years), had only two presentations on admission: intermittent fever for two days and headache for one day, while the others reported 4–11 symptoms. The symptoms on illness onset are described in *Supplementary results*.

On admission, abnormalities in chest-CT-images suggesting viral-pneumonia were detected in six (all males; 22–23 years) of the eight youngsters confirmed with COVID-19 (Table 2; Fig. 1). None of the conditions were severe. Of the six pneumonia-patients, five had unilateral-involvement, and Patient-8 had bilateral-pneumonia on admission; four had involvement of the lower-lobe, and the other two of the middle-lobe. Of the five patients with unilateral-disease, pneumonia was located in the right-lung in four patients, and in the left-lung in Patient-3. The typical-findings on chest-CT-scan, multifocal-mottling, patchy-shadows, and/or ground-glass-opacities,² which were mostly around the peripheral-parts of the lungs and which were compatible with abnormalities seen in viral-pneumonia, were detected in the pneumonia-patients on admission. Patient-Index's pneumonia progressed to bilateral-pneumonia two days after the initial scan. For the youngest patient (Patient-2; 16 years), while no abnormalities were detected the next day after illness-onset, a few infiltrates were noticed in the lower-lobe of left-lung six days later.

The blood-routine tests of the seven youngsters with available information on admission showed leucopenia and substantial neutropenia in Patients-2 and 4 (Table 3). Patient-8 had increased neutrophils, but decreased lymphocytes. Patient-7 also had lymphopenia. Patients-1 and 3 had both red-blood-cell count and hemoglobin above the normal-range. Patient-2 had slightly shortened prothrombin-time, while Patient-4 showed mildly extended activated-partial-thromboplastin-time, and Patient-8 slightly increased international-normalized-ratio. Patient-3 had elevation of creatine-kinase and lactate-dehydrogenase reaching the upper-limit of reference-range. Regarding the infection-index, procalcitonin was above the normal-range in Patient-4. Patient-1 had an elevated level of C-reactive-protein. Most patients had normal serum levels of procalcitonin on admission (five of six youngsters with available information).

While testing negative for SARS-CoV-2, Contacts-1–9 also showed some changes in blood-examinations (Table 4; *Supplementary results*). When comparing the laboratory-findings between Patients-1–5 ascertained with COVID-19 with Contacts-1–9 with negative SARS-CoV-2-tests (Fig. S3), all of whom were initially admitted to Hospital-1, lymphocyte-count on admission was lower in the SARS-CoV-2-positive patients than the SARS-CoV-2-negative contacts ($p=0.042$). Initial fibrinogen-concentrations were higher in the patients ($p=0.019$). Levels of sodium were lower in the

Table 2

Symptoms, signs, radiological findings, treatment, and outcomes of the young cluster infected with the 2019 novel coronavirus disease.

Characteristics	Patient 1	Patient 2	Patient 3	Patient 4	Patient 5	Patient 6	Patient 7	Patient 8	Summary ¹
Symptoms and signs									
Fever	Y1 (3 d)	Y1 (2 d)	Y (1 d)	Y1 (3 d)	Y1 (3 d)	N	Y1 (2 d)	Y1 (4 d)	6; 7, 3 (1-4); 0, 0
Body temperature on admission (°C)	38.0	37.2	37.0	37.6	38.2	37.0	37.4	37.7	37.5 (37.0-38.2)
Highest body temperature (°C)	38.4	38.5	37.7	38.5	38.2	37.1	38.0	38.9	38.5 (37.1-38.9)
Intermittent fever	Y	Y	N	N	Y	N	N	N	3/8 (38%)
With chills	N	N	Y	Y	Y	N	N	N	3/8 (38%)
Fatigue	N	N	Y1 (3 d)	Y (1 d)	<u>Y</u>	N	Y1 (2 d)	Y (3 d)	2; 4, 3 (1-3); 1, 0
Myalgia	Y (2 d)	N	Y1 (3 d)	N	<u>Y</u>	N	N	Y (2 d)	1; 3, 2 (2-3); 1, 0
Cough	Y (2 d)	N	Y1 (3 d)	Y (2 d)	<u>Y</u>	Y1 (4 d)	Y1 (2 d)	Y (3 d)	3; 6, 3 (2-4); 1, 0
Sputum production	Y (2 d)	N	Y (1 d)	Y (2 d)	N	N	N	Y (3 d)	0; 4, 2 (1-3); 0, 0
Hemoptysis	<u>Y</u>	N	N	N	N	N	N	N	0; 0; 1, 0
Sore throat	N	N	Y1 (3 d)	N	Y1 (3 d)	N	N	Y1 (4 d)	3; 3, 3 (3-4); 0, 0
Nasal congestion	Y1 (3 d)	N	Y (1 d)	Y (3 d)	<u>Y</u>	Y (2 d)	N	Y1 (4 d)	2; 5, 3 (1-4); 1, 0
Rhinorrhea	Y1 (3 d)	<u>Y</u>	N	N	N	Y (2 d)	N	Y1 (4 d)	2; 3, 3 (2-4); 1, 0
Sneezing	N	<u>Y</u>	<u>Y</u>	Y (2 d)	N	Y (1 d)	N	Y (2 d)	0; 3, 2 (1-2); 2, 0
Shortness of breath	<u>Y</u>	N	N	N	N	<u>Y</u>	Y1 (2 d)	N	1; 1, 2 (2-2); 2, 1
Chest discomfort	<u>Y</u>	N	N	<u>Y</u>	<u>Y</u>	<u>Y</u>	N	<u>Y</u>	0; 0; 5, 2
Chest pain	<u>Y</u>	N	N	N	<u>Y</u>	N	N	N	0; 0; 2, 0
Headache	N	Y (1 d)	N	Y (1 d)	Y (2 d)	N	N	N	0; 3, 1 (1-2); 0, 0
Dizziness	Y1 (2 d)	N	N	N	N	N	N	N	1; 1, 2 (2-2); 0, 0
Eye discomfort	Y1 (3 d)	N	Y (2 d)	N	N	N	N	N	1; 2, 3 (2-3); 0, 0
Backache	N	N	Y1 (3 d)	N	N	N	N	N	1; 1, 3 (3-3); 0, 0
Anorexia	N	N	N	N	Y (1 d)	Y (1 d)	N	<u>Y</u>	0; 2, 1 (1-1); 1, 0
Nausea	<u>Y</u>	N	<u>Y</u>	<u>Y</u>	Y (1 d)	Y (1 d)	N	Y (1 d)	0; 3, 1 (1-1); 3, 1
Vomiting	<u>Y</u>	N	N	<u>Y</u> (1 time/d)	<u>Y</u> (up to 4 times/d)	<u>Y</u>	N	N	0; 0; 4, 3
Diarrhea	<u>Y</u> (up to 6 times/d)	<u>Y</u> (up to 6 times/d)	<u>Y</u> (2 times/d)	<u>Y</u> (1 time/d)	<u>Y</u> (up to 4 times/d)	N	N	Y (up to 3 times/d, 3 d)	0; 1, 3 (3-3); 5, 3
Abdominal discomfort	<u>Y</u>	N	N	N	Y (1 d)	N	N	N	0; 1, 1; 1, 0
≥2 upper respiratory infection symptoms before/on admission	Y	N	Y	Y	N	Y	N	Y	5/8 (63%)
≥1 digestive symptom before/on admission	N	N	N	N	Y	Y	N	Y	3/8 (38%)
Both fever and cough before/on admission	Y	N	Y	Y	N	N	Y	Y	5/8 (63%)
No. of symptoms on illness onset	5	1	5	1	2	1	4	4	3 (1-5)
No. of symptoms before/on admission	8	2	9	7	6	6	4	11	6 (2-11)
Respiratory rate on admission (breaths/min)	20	20	22 ↑	20	18	18	18	20	20 (18-22)
Oximetry saturation on admission (%)	97	97	98	97	96	97	98	98	97 (96-98)
Heart rate on admission (beats/min)	86	82	90	90	94	86	94	92	90 (82-94)
Systolic pressure on admission (mm Hg)	120	120	150 ↑	125	131	124	120	118	122 (118-150)
Diastolic pressure on admission (mm Hg)	80	74	94 ↑	76	89	78	74	75	77 (74-94)

(continued on next page)

Table 2 (continued)

Characteristics	Patient 1	Patient 2	Patient 3	Patient 4	Patient 5	Patient 6	Patient 7	Patient 8	Summary ¹
First chest CT findings on admission									
Pneumonia	Y (mild)	N	Y (mild)	Y (mild)	N	Y (mild)	Y (mild)	Y (mild)	6/8 (75%)
Multifocal mottling, patchy shadows, and/or ground-glass opacities	Y	N	Y	Y	N	Y	Y	Y	6/8 (75%)
Location of pneumonia	Lower lobe of right lung	-	Lower lobe of left lung	Middle and lower lobes of right lung	-	Lower lobe of right lung	Lower lobe of right lung	Middle lobe of both lungs	-
Bilateral lung involvement	N	-	N	N	-	N	N	Y	1/6 (17%)
Treatment									
Recombinant human interferon	Y (α -1b; α -2b)	Y (α -1b)	Y (α -1b; α -2b)	Y (α -1b; α -2b)	Y (α -1b)	N	Y	Y	7/8 (88%)
Lopinavir	Y	N	Y	Y	Y	Y	Y	Y	7/8 (88%)
Ritonavir	Y	N	Y	Y	Y	Y	Y	Y	7/8 (88%)
Other antiviral therapy	Y (adenosine monophosphate)	Y (ribavirin; oseltamivir)	N	N	N	N	Y (arbidol; ribavirin)	N	3/8 (38%)
Any antiviral therapy	Y	Y	Y	Y	Y	Y	Y	Y	8/8 (100%)
Levofloxacin	Y	N	Y	Y	N	N	N	N	4/8 (50%)
Moxifloxacin	N	Y	N	N	Y	Y	N	Y	3/8 (38%)
Other antibiotic therapy	N	N	N	Y (ceftazidime)	N	N	N	N	1/8 (13%)
Any antibiotic therapy	Y	Y	Y	Y	Y	Y	N	Y	7/8 (88%)
Outcomes									
Recovered	N	Y	Y	N	N	N	Y	Y	4/8 (50%)
Discharged	N	Y	Y	N	N	N	Y	Y	4/8 (50%)

¹ For symptom variables, it is shown as: number of patients with the symptom presenting on date of illness onset; number of patients with the symptom presenting before or on date of hospital admission, median (range) of the days from onset of the symptom to admission; number of patients with the symptom presenting after admission; number of patients with the symptom whose association with drug use could not be excluded; for the other variables, it is described for continuous and categorical variables, and expressed as median (range) and count/total number of patients with available data (percentage), respectively. -, not applicable; ↑, above the upper limit of the normal range; ↓, below the lower limit of the normal range; Y, Yes (symptom developed before or on admission; days from onset of the symptom through admission are shown in brackets); Y1, Yes (symptom developed on date of illness onset; days from onset of the symptom through admission are shown in brackets); Y2, Yes (symptom developed after admission); Y1, (symptom developed after admission; association with drug use could not be excluded).

Table 3Laboratory findings of the young cluster with the 2019 novel coronavirus disease, on admission to hospital¹.

Measure	Reference range	Patient 1	Patient 2	Patient 3	Patient 4	Patient 5	Patient 7	Patient 8	Summary ²
First admitted hospital	FDCPH; FAHAMU	FDCPH	FDCPH	FDCPH	FDCPH	FDCPH	FAHAMU	FAHAMU	-
Blood routine									
White blood cell count ($\times 10^9$ cells/L)	4.00-10.00; 3.50-9.50	4.77	2.92 ↓	5.26	3.82 ↓	4.02	7.79	9.48	↓, 2/7 (29%)
Absolute neutrophil count ($\times 10^9$ cells/L)	2.00-7.00; 1.80-6.30	3.10	1.20 ↓	3.60	1.40 ↓	2.10	6.64	7.89 ↑	↓, 2/7 (29%); ↑, 1/7 (14%)
Absolute lymphocyte count ($\times 10^9$ cells/L)	0.84-4.00; 1.10-3.20	1.23	1.27	1.04	1.75	1.46	0.77 ↓	0.86 ↓	↓, 2/7 (29%)
Red blood cell count ($\times 10^{12}$ cells/L)	3.50-5.50; 4.30-5.80	5.97 ↑	4.71	5.76 ↑	4.91	4.32	5.20	5.20	↑, 2/7 (29%)
Hemoglobin (g/L)	110-160; 130-175	162 ↑	132	166 ↑	151	125	152	159	↑, 2/7 (29%)
Hematocrit (%)	37.0-50.0; 40.0-50.0	49.3	42.4	49.2	45.5	38.5	46.6	46.8	AN
Platelet count ($\times 10^9$ cells/L)	100-300; 125-350	217	209	218	132	246	165	219	AN
Coagulation function									
Prothrombin time (sec)	10.5-14.5; 11.0-16.0	10.9	10.4 ↓	11.2	12.0	11.7	13.9	15.0	↓, 1/7 (14%)
Activated partial thromboplastin time (sec)	20.0-40.0; 28.0-42.0	26.0	21.8	28.4	42.2 ↑	25.4	40.5	39.5	↑, 1/7 (14%)
International normalized ratio	0.80-1.20; 0.85-1.15	0.94	0.89	0.96	1.04	1.01	1.06	1.16 ↑	↑, 1/7 (14%)
Fibrinogen (g/L)	2.00-4.00; 2.00-4.00	3.76	2.38	2.95	2.59	2.41	3.83	3.47	AN
D-dimer (μ g/L)	0.00-0.55; 0.00-0.50	-	-	-	0.19	0.19	0.20	0.27	AN
Blood biochemistry									
Total protein (g/L)	65.0-85.0; 63.0-82.0	80.9	65.6	78.0	65.6	69.4	71.2	82.0	AN
Albumin (g/L)	40.0-55.0; 35.0-50.0	53.6	43.4	53.3	40.4	42.8	45.5	47.2	AN
Pre-albumin (mg/L)	200-400; -	261	281	257	150 ↓	147 ↓	-	-	↓, 2/5 (40%)
Alanine aminotransferase (U/L)	5-50; 21-72	30	14	20	12	11	27	20 ↓	↓, 1/7 (14%)
Aspartate aminotransferase (U/L)	13-40; 17-59	29	22	24	16	18	24	29	AN
Alkaline phosphatase (U/L)	40-130; 38-126	84	79	104	78	71	51	78	AN
Total bilirubin (μ mol/L)	5.0-20.0; 3.0-22.0	9.0	7.4	10.5	7.8	12.2	12.2	25.8 ↑	↑, 1/7 (14%)
Direct bilirubin (μ mol/L)	0.0-7.0; -	2.1	1.6	2.1	2.1	3.2	-	-	AN
Serum creatinine (μ mol/L)	44.0-106.0; 58.0-110.0	69.0	69.6	69.6	83.9	57.7	78.8	104.5	AN
Blood urea nitrogen (mmol/L)	2.76-8.07; 3.20-7.10	4.79	3.84	5.19	3.07	3.51	4.10	4.80	AN
Creatine kinase (U/L)	38-174; 55-170	95	58	234 ↑	104	74	52 ↓	66	↓, 1/7 (14%); ↑, 1/7 (14%)
Lactate dehydrogenase (U/L)	110-240; -	224	163	240	111	151	-	-	AN
Hypersensitive troponin I (ng/mL)	-; 0.000-0.034	-	-	-	-	-	0.01	0.01	AN
Myoglobin (ng/mL)	-; 10-46	-	-	-	-	-	8 ↓	14	↓, 1/2 (50%)
Potassium (mmol/L)	3.50-5.30; 3.50-5.10	4.88	4.50	4.44	4.68	4.08	4.16	4.17	AN
Sodium (mmol/L)	137.0-147.0; 137.0-145.0	141.2	140.4	140.9	141.5	141.8	138.8	137.4	AN
Calcium (mmol/L)	2.15-2.75; 2.10-2.55	2.40	2.23	2.38	2.23	2.28	2.40	2.33	AN
Chloride (mmol/L)	96.0-110.0; 98.0-107.0	107.6	101.0	103.9	103.0	101.5	101.3	95.2 ↓	↓, 1/7 (14%)
Infection-associated biomarkers									
C-reactive protein (mg/L)	0.00-7.44; 0.00-10.00	8.01 ↑	-	4.61	2.59	6.18	2.65	1.04	↑, 1/6 (17%)
Procalcitonin (ng/mL)	0.000-0.046; 0.000-0.050	< 0.010	0.032	< 0.010	0.051 ↑	0.039	-	0.05	↑, 1/6 (17%)
Erythrocyte sedimentation rate (mm/h)	0-15; -	19 ↑	-	6	20 ↑	7	-	-	↑, 1/4 (25%)

¹ Laboratory findings for Patient 6 whose blood was initially examined in the Hefei City Infectious Disease Hospital have not been obtained.² Summary data are count/total number of patients with available data (percentage) for abnormal values. -, not available; ↑, value above the upper limit of the normal range; ↓, value below the lower limit of the normal range; AN, all measured values were within normal range; FDCPH, Feidong County People's Hospital; FAHAMU, First Affiliated Hospital of Anhui Medical University.

Table 4

Close contacts of the index patient admitted to hospital and testing negative for SARS-CoV-2 on rRT-PCR for at least two times.

Variable	Contact 1	Contact 2	Contact 3	Contact 4	Contact 5	Contact 6	Contact 7	Contact 8	Contact 9
Baseline characteristics									
Relationship with index patient	Uncle	Classmate	Classmate	Classmate	Classmate	Classmate	Classmate	Classmate	Classmate
Male sex	Y	N	Y	Y	Y	Y	Y	Y	Y
Age (years)	43	23	23	21	23	21	23	23	24
Current smoker	Y	N	N	N	N	N	N	N	N
Exposure									
Date of exposure	Jan 19	Jan 20	Jan 21	Jan 21	Jan 21	Jan 21	Jan 21	Jan 21	Jan 21
Exposure place	Apartment in Feidong	Hotpot restaurant in Feidong	Restaurant & Karaoke room with shared toilet in Feidong	Restaurant & Karaoke room with shared toilet in Feidong	Restaurant & Karaoke room with shared toilet in Feidong	Restaurant & Karaoke room with shared toilet in Feidong	Restaurant & Karaoke room with shared toilet in Feidong	Restaurant & Karaoke room with shared toilet in Feidong	Restaurant & Karaoke room with shared toilet in Feidong
Description of exposure place	Confined room without air conditioning	Room with air conditioning	Room with window open and air conditioning	Room with window open and air conditioning	Room with window open and air conditioning	Room with window open and air conditioning	Room with window open and air conditioning	Room with window open and air conditioning	Room with window open and air conditioning
Exposure duration	1.5 h	1 h	5 h	5 h	5 h	5 h	5 h	5 h	5 h
Clinical characteristics									
Fever	Y (0.5 d; Jan 27; subjective)	Y (0.5 d; Jan 26)	N	N	N	N	N	N	Y (5 h; Jan 26)
Body temperature on admission (°C)	36.6	36.6	36.7	36.2	36.8	36.7	36.6	36.7	36.5
Highest body temperature (°C)	-	37.6 (Jan 26; self-measured)	-	-	-	-	-	-	37.3 (Jan 26; self-measured)
Signs on admission									
Respiratory rate (breaths/min)	20	20	20	20	20	20	20	19	18
Oximetry saturation (%)	98	97	97	97	97	97	96	98	98
Heart rate (beats/min)	80	80	90	76	78	88	78	99	90
Systolic pressure (mm Hg)	127	127	140	120	137	115	125	141 ↑	120
Diastolic pressure (mm Hg)	81	81	96 ↑	80	77	83	84	81	80
Laboratory findings on admission									
White blood cell count ($\times 10^9$ cells/L)	4.62	4.08	5.99	3.84 ↓	8.19	6.55	5.99	3.76 ↓	8.99
Neutrophil count ($\times 10^9$ cells/L)	2.90	1.50 ↓	3.60	1.90 ↓	5.00	3.40	3.30	1.60 ↓	4.80
Lymphocyte count ($\times 10^9$ cells/L)	1.06	2.04	1.77	1.35	2.57	2.49	2.19	1.54	2.68
Red blood cell count ($\times 10^{12}$ cells/L)	4.81	3.91	5.58 ↑	4.65	5.54 ↑	5.22	5.57 ↑	5.02	4.77

(continued on next page)

Table 4 (continued)

Variable	Contact 1	Contact 2	Contact 3	Contact 4	Contact 5	Contact 6	Contact 7	Contact 8	Contact 9
Hemoglobin (g/dL)	151.0	121.0	168.0 ↑	148.0	155.0	141.0	157.0	145.0	141.0
Hematocrit (%)	45.70	36.30 ↓	49.50	43.60	47.20	44.10	48.00	45.30	43.00
Platelet count ($\times 10^9$ cells/L)	177	200	219	192	203	234	191	206	226
Prothrombin time (s)	9.10 ↓	11.30	12.20	12.20	12.10	12.00	10.60	12.10	11.00
Activated partial thromboplastin time (s)	23.90	28.20	30.40	34.80	26.40	26.20	25.40	22.90	25.30
International normalized ratio	0.78 ↓	0.97	1.05	1.05	1.04	1.04	0.91	1.04	0.95
Fibrinogen (g/L)	2.08	1.65 ↓	2.00	1.86 ↓	2.02	2.67	1.93 ↓	2.52	2.10
Total protein (g/L)	66.1	67.2	-	69.3	74.1	75.0	63.9 ↓	76.4	72.0
Albumin (g/L)	45.5	44.1	-	46.8	48.1	48.1	44.4	46.6	49.9
Pre-albumin (mg/L)	392	164 ↓	-	285	230	245	284	258	317
Alanine aminotransferase (U/L)	19	6	-	9	32	22	43	19	38
Aspartate aminotransferase (U/L)	20	20	34	14	28	21	32	20	28
Alkaline phosphatase (U/L)	55	50	-	90	93	49	104	52	97
Total bilirubin (μ mol/L)	11.3	13.6	-	12.6	18.7	14.1	11.9	9.6	5.0
Direct bilirubin (μ mol/L)	1.9	2.8	-	2.8	4.0	3.0	2.5	1.8	0.7
Serum creatinine (μ mol/L)	66.5	57.3	82.3	57.6	80.4	88.1	67.6	76.5	91.9
Blood urea nitrogen (mmol/L)	3.38	2.87	4.71	4.60	5.31	6.10	2.46 ↓	5.13	6.36
Creatine kinase (U/L)	60	105	64	61	104	59	89	58	240 ↑
Lactate dehydrogenase (U/L)	134	136	159	123	149	115	154	144	176
Potassium (mmol/L)	3.94	3.82	4.76	4.01	4.19	3.96	5.34 ↑	4.27	4.76
Sodium (mmol/L)	145.5	144.7	144.1	142.4	144.7	140.7	145.1	143.3	142.8
Calcium (mmol/L)	2.31	2.36	2.47	2.37	2.49	2.40	2.39	2.49	2.53
Chloride (mmol/L)	105.0	109.3	102.6	100.0	101.3	105.9	102.6	102.3	102.3
C-reactive protein (mg/L)	-	-	0.60	0.31	1.67	-	0.23	-	0.91
Procalcitonin (ng/mL)	0.044	0.046	0.039	-	0.074 ↑	0.055 ↑	0.033	0.055 ↑	< 0.01
Erythrocyte sedimentation rate (mm/h)	-	8	3	4	6	11	8	37 ↑	2
SARS-CoV-2 testing									
1 st sampling date	Jan 27	Jan 27	Jan 27	Jan 27	Jan 27	Jan 27	Jan 27	Jan 27	Jan 28
1 st sampling result	Negative	Negative	Negative	Negative	Negative	Negative	Negative	Negative	Negative
2 nd sampling date	Jan 28	Jan 28	Jan 28	Jan 28	Jan 28	Jan 28	Jan 28	Jan 28	Jan 29
2 nd sampling result	Negative	Negative	Negative	Negative	Negative	Negative	Negative	Negative	Negative
Date of discharged to home isolation	Jan 31	Feb 1	Feb 1	Jan 31	Jan 31	Jan 31	Feb 1	Jan 31	Jan 31

-, not available; ↑, above normal range; ↓, below normal range; Y, Yes; N, No; rRT-PCR, real-time reverse-transcriptase polymerase-chain-reaction.

patients ($p=0.016$). Plasma-concentrations of C-reactive-protein were markedly higher in SARS-CoV-2-positive patients ($p=0.016$).

Management and outcomes of the eight youngsters with laboratory-confirmed COVID-19, and description of all the other contacts are detailed in *Supplementary results*.

Discussion

Currently, our understanding of the spectrum and natural-history of SARS-CoV-2-infection remains limited. We herein provide an assessment of the infectivity, transmission dynamics, and other characteristics of a cluster of eight young-patients aged 16–23 years confirmed with SARS-CoV-2 on rRT-PCR originating from Patient-Index returning from Wuhan who rapidly transmitted COVID-19 when totally asymptomatic, and compare them to the other nine close-contacts of Patient-Index testing negative for SARS-CoV-2. The disease was transmitted outside Wuhan and all patients were diagnosed and managed in Hefei. The young patients admitted with COVID-19 had fast illness-onset and symptoms somehow resembling a common-cold, which were much milder than those of older hospitalized adults with COVID-19 as recently-reported.^{1,2,10} While patchy-shadows and ground-glass-opacity on CT-scan were common, they were much less severe than the older patients.^{2,10} Not all patients had radiological-changes indicating viral-pneumonia on admission.

Notably, our findings provide valid evidence demonstrating efficient local human-to-human-transmission with strong infectivity of SARS-CoV-2 within this cluster of youngsters during the incubation-period and asymptomatic-phase of COVID-19. SARS-CoV-2 tested positive in six of the 15 young classmates Patient-Index contacted in the get-together when he was totally asymptomatic, with the minimal exposure-duration of only two hours. The attack-rate is high (40%). The symptoms of Patients-4 and 8 developed on the same day as that of Patient-Index. We carefully had interviews directly with both Patient-Index himself and all the other contacts to confirm the absence of any symptoms of Patient-Index before and during the contacts, thus ascertaining the transmission during asymptomatic-phase. We may need to pay special attention to preventing COVID-19 transmission from people looking asymptomatic but with exposure-history. The incubation-period and serial-interval in this young cluster were much shorter than previously-reported for majorly older patients at the earlier stage of the epidemic.¹

Infected-youngsters may act as important sources-of-infection. Notably, Patient-6 remained afebrile throughout the disease-course. These cryptic cases of walking-SARS-CoV-2-infection might act as potential sources to propagate the epidemic. Since it is difficult to differentiate and screen patients during the incubation-period, further studies on the popularity of this transmission-pattern and the epidemiological-significance of cases with null or mild symptoms are warranted, which would help make relevant control-measures to prevent the future spread of infection. It may be needed to commit sufficient resources to examination in outpatient-clinics and emergency-departments for proactive case-identification, both as part of the containment-strategy in locations without local-spread yet and to permit earlier clinical-management of infected-individuals.

The most likely transmission-scenario is that Patient-Index acquired the SARS-CoV-2-infection in Wuhan, and then transmitted the virus to Patient-2 after two contacts and Patients-3–8 during get-together on January 21 after returning to Feidong on January 19. Patient-2 more likely acquired the infection during the second contact on January 23 with an incubation-period of three days rather than on January 19, since Contacts-1 and 2, with whom Patient-Index had close-contacts in the evening on January 19 and on January 20, respectively, did not develop the infection. These

indicate the relatively weak infectivity up till January 20, and the possibility of dynamic changes in infectivity, which possibly became strong enough to enable the disease to affect others sometime on January 20 or 21, still during the incubation-period of Patient-Index. Further studies on the diverse infectivity during different stages of disease and the corresponding time-points are warranted.

Almost half of the previously-reported cases were in adults aged ≥ 60 years.¹ Younger patients were thought to be less likely infected.¹ Few reports exist on younger patients aged 15–25 years. Delays from illness-onset to admission were generally short in these eight youngsters with COVID-19 in our study, with five hospitalized within two days of illness-onset. The symptoms of these youngsters were all mild and largely-nonspecific, which may be hardly clinically-distinguishable from many other common infectious-diseases, particularly in winter.

The first three most common symptoms on illness-onset were fever, cough, and sore-throat. None initially presented with a digestive-symptom. On admission, half or more of the youngsters with COVID-19 presented with fever, cough, sputum-production, nasal-congestion, and fatigue, which are much milder than previous reports including majorly older hospitalized-patients with frequent comorbidities, who may have lower immune-function than younger people.^{2,10} Fever developed in seven of the eight youngsters, with six having fever on illness-onset. Three youngsters developed one or more digestive-manifestations before or on admission, which are more frequent than the previous report on older hospitalized-patients.^{2,10} Patient-8 developed diarrhea before admission. About 11% of SARS-CoV¹⁴ and 30% of MERS-CoV patients¹⁵ also had diarrhea. None of the abovementioned symptoms was present in all youngsters. Notably, two youngsters presented with eye-discomfort on admission (one had itchy-eyes as the very initial symptom) and one with backache at illness-onset, which appears to not have been observed in older patients.^{2,10}

For the six youngsters showing pneumonia on admission, multifocal ground-glass opacities typical of viral-pneumonia on chest-CT-scans were frequently seen, while their lung-involvement was much milder and more local and limited than older patients.^{2,10} Unlike older patients typically having bilateral-pneumonia,^{2,10} the pneumonia youngsters mostly had showed unilateral lung-involvement on admission.

Regarding laboratory-examinations, two patients had leucopenia. The absolute neutrophil-counts were reduced in the same two patients, while they were elevated in another patient. Furthermore, lymphopenia occurred in two patients, and two youngsters had both elevated red-blood-cell-count and hemoglobin level. These changes were not consistent with the previous report on older patients with more severe conditions.¹⁰ These may suggest diverse immune-status against the virus. Neutrophilia may be related to cytokine-storm induced by SARS-CoV-2 invasion. Compared with SARS-CoV-2-negative contacts, SARS-CoV-2-positive patients had fewer lymphocytes and higher fibrinogen and C-reactive-protein levels. These suggest that SARS-CoV-2-infection may be associated with deficiency in immune-function and activation of coagulation, which could have been related to inflammatory-response.

As of February 20, 2020, none of the eight young patients had dyspnea, developed any severe clinical-conditions, complications, or adverse-outcomes, were admitted to an intensive-care-unit, required machine-ventilation, or died, which is largely different from the findings in older patients.^{2,3,10} They mostly remained stable during hospitalization. These suggest that age, comorbidity, and symptoms on illness-onset or admission may be important prognostic factors.

Our study has some limitations. First, the case number is limited, which necessitates the cautious interpretation of the generalizability of our findings. Collection of data for a larger

cohort would help to enable a more comprehensive understanding of COVID-19 among youngsters. Second, the route of transmission was not totally clear. While the most likely one was via droplets or aerosol or airborne, we did not collect urine or fecal samples, which prevented us from analyzing whether COVID-19 could be transmitted through the fecal-oral pathway. Third, the relative-risk of infection among youngsters compared to older individuals and the association of timing or mode of manifestations and CT and laboratory findings with disease-course, outcomes, and spread need to be further evaluated. Fourth, the serum of patients and contacts was not obtained to evaluate possible viremia. Respiratory-tract samples were used to diagnose COVID-19 through rRT-PCR according to the guidelines,^{1,16–19} and they have a higher positive rate than blood and other samples and are more clinically and epidemiologically relevant.²⁰ There could have been transient viremia in the SARS-CoV-2-negative contacts, which was not captured on admission. The corresponding epidemiological and clinical significances need to be further clarified.

Conclusion

We provide valid evidence supporting efficient asymptomatic human-to-human transmission of SARS-CoV-2 showing strong infectivity based on a cluster of youngsters aged 16–23 years in a local community setting outside Wuhan. COVID-19 was rapidly transmitted by the index patient during the (late) incubation-period to other seven youngsters, demonstrating strong infectivity. The symptoms of the youngsters with COVID-19 had fast-onset, and were generally mild, nonspecific, atypical, and diverse.

Declaration of Competing Interest

None reported.

Author contributions

Drs Lei Huang, Xiuwen Zhang, Xinyue Zhang, and Zhijian Wei contributed equally to this article. LH, XWZ, CYZ, and AMX had the idea for the study and full access to all data in the study and take responsibility for the integrity of the data and the accuracy of the data analysis. LH is an epidemiologist and physician scientist with clinical epidemiology as the major subject and public health and statistics as subjects during his PhD, XWZ is an infectious disease specialist with rich work experience in isolation ward, XYZ is a statistician, ZJW is a physician scientist, LLX and JJX have rich experience in clinical communication and data collection, PPL is an emergency medicine specialist, YHX is a professor of laboratory medicine, CYZ is a respiratory medicine and critical care medicine specialist, and AMX is a physician scientist with interest in clinical epidemiology and public health. LH, XWZ, ZYZ, ZJW, CYZ, and AMX played roles in the literature search, study conception and design, patient recruitment, clinical management, sample collection, data collection, analysis, and interpretation, and writing of the report. LLZ, JJX, and YHX played roles in the laboratory assays, data collection, analysis, interpretation, and confirmation and critical revision of the report. PPL played roles in recruitment, clinical management, data collection, and critical revision of the report. All authors reviewed and approved the final version of the manuscript. AMX is the guarantor. The corresponding authors attest that all listed authors meet authorship criteria and that no others meeting the criteria have been omitted.

Funding/support

This work was supported by the Emergency Scientific Research Projects of Anhui Medical University (YJGG202002), National Natural Science Foundation of China (81572350), Hefei Key Medical

Specialty Construction Project, Fifth Round (2016256), and Feidong People's Hospital Key Specialty Project, First Round (201911).

Role of the funders/sponsors

None of the funders had any role in the study design and the collection, analysis, and interpretation of data or in the writing of the article and the decision to submit it for publication. The researchers confirm their independence from funders.

Data sharing

The data that support the findings of this study are all included in the manuscript, with no additional data available.

Acknowledgments

We would like to thank the patients and contacts; all healthcare workers and hospitals who provide care for patients with COVID-19 and are involved in the diagnosis and treatment of COVID-19 patients and those who trace and quarantine the contacts; staff at the local, city, and province healthcare departments; members of the COVID-19 response teams at the local, city, province, and national levels; Feidong Center for Disease Control and Prevention (CDC) and medical institutions in Hefei for assistance with field investigation administration and data collection; the Feidong CDC for coordinating data collection for patients with COVID-19; and the Anhui Province CDC and Hefei City CDC for assistance with laboratory testing.

Supplementary materials

Supplementary material associated with this article can be found, in the online version, at doi:[10.1016/j.jinf.2020.03.006](https://doi.org/10.1016/j.jinf.2020.03.006).

References

- Li Q, Guan X, Wu P, et al. Early transmission dynamics in wuhan, china, of novel coronavirus-infected pneumonia. *New Engl J Med* 2020. doi:[10.1056/NEJMoa2001316](https://doi.org/10.1056/NEJMoa2001316).
- Huang C, Wang Y, Li X, et al. Clinical features of patients infected with 2019 novel coronavirus in Wuhan, China. *Lancet* 2020 (London, England)S0140-6736(20)30183-5.
- Zhu N, Zhang D, Wang W, et al. A novel coronavirus from patients with pneumonia in china, 2019. *New Engl J Med* 2020. doi:[10.1056/NEJMoa2001017](https://doi.org/10.1056/NEJMoa2001017).
- Guan W-J, Ni Z-Y, Hu Y, et al. Clinical characteristics of coronavirus disease 2019 in china. *New Engl J Med* 2020. doi:[10.1056/NEJMoa2002032](https://doi.org/10.1056/NEJMoa2002032).
- Chan JF-W, Yuan S, Kok K-H, et al. A familial cluster of pneumonia associated with the 2019 novel coronavirus indicating person-to-person transmission: A study of a family cluster. *Lancet* 2020 (London, England)S0140-6736(20)30154-9.
- Phan LT, Nguyen TV, Luong QC, et al. Importation and human-to-human transmission of a novel coronavirus in vietnam. *New Engl J Med* 2020. doi:[10.1056/NEJMc2001272](https://doi.org/10.1056/NEJMc2001272).
- Chang D, Lin M, Wei L, et al. Epidemiologic and clinical characteristics of novel coronavirus infections involving 13 patients outside Wuhan, China. *JAMA* 2020. doi:[10.1001/jama.2020.1623](https://doi.org/10.1001/jama.2020.1623).
- Rothe C, Schunk M, Sothmann P, et al. Transmission of 2019-ncov infection from an asymptomatic contact in Germany. *New Engl J Med* 2020. doi:[10.1056/NEJMc2001468](https://doi.org/10.1056/NEJMc2001468).
- Kupferschmidt K. Study claiming new coronavirus can be transmitted by people without symptoms was flawed. 2020. <https://www.sciencemag.org/news/2020/02/paper-non-symptomatic-patient-transmitting-coronavirus-wrong> accessed on Feb 20, 2020.
- Chen N, Zhou M, Dong X, et al. Epidemiological and clinical characteristics of 99 cases of 2019 novel coronavirus pneumonia in Wuhan, China: A descriptive study. *Lancet* 2020 (London, England)S0140-6736(20)30211-7.
- Wang D, Hu B, Hu C, et al. Clinical characteristics of 138 hospitalized patients with 2019 novel coronavirus-infected pneumonia in Wuhan, China. *JAMA* 2020. doi:[10.1001/jama.2020.1585](https://doi.org/10.1001/jama.2020.1585).
- World Health Organization. Clinical management of severe acute respiratory infection when novel coronavirus (nCoV) infection is suspected: interim guidance. 2020. [https://www.who.int/publications-detail/clinical-management-of-severe-acute-respiratory-infection-when-novel-coronavirus-\(ncov\)-infection-is-suspected](https://www.who.int/publications-detail/clinical-management-of-severe-acute-respiratory-infection-when-novel-coronavirus-(ncov)-infection-is-suspected) accessed on Feb 20, 2020.

13. China National Health Commission. New coronavirus pneumonia prevention and control program (4th edition). 2020. <http://www.gov.cn/zhengce/zhengceku/2020-01/28/5472673/files/0f96c10cc09d4d36a6f9a9f0b42d972b.pdf> accessed on Feb 20, 2020.
14. Cheng VCC, Hung IFN, Tang BSF, et al. Viral replication in the nasopharynx is associated with diarrhea in patients with severe acute respiratory syndrome. *Clin Infect Dis Offic Publ Infect Diseases Soc Am* 2004;**38**(4):467–75.
15. Chan JFW, Lau SKP, To KKW, et al. Middle east respiratory syndrome coronavirus: Another zoonotic betacoronavirus causing sars-like disease. *Clin Microbiol Rev* 2015;**28**(2):465–522.
16. World Health Organization. Laboratory testing for 2019 novel coronavirus (2019-nCoV) in suspected human cases. Interim guidance. 2020. <https://www.who.int/publications-detail/laboratory-testing-for-2019-novel-coronavirus-in-suspected-human-cases-20200117> accessed on Feb 20, 2020.
17. Corman VM, Landt O, Kaiser M, et al. Detection of 2019 novel coronavirus (2019-ncov) by real-time RT-PCR. *Euro Surveill Bull Eur Sur Les Maladies Transmissibles Eur Commun Disease Bull* 2020;**25**(3):2000045.
18. Center for Disease Control and Prevention. Interim guidelines for collecting, handling, and testing clinical specimens from patients under investigation (PUIs) for 2019 novel coronavirus (2019-nCoV). 2020. <https://www.cdc.gov/coronavirus/2019-nCoV/guidelines-clinical-specimens.html> accessed on Feb 20, 2020.
19. CfDCa Prevention Information for laboratories. *Novel Coronavirus 2020 Wuhan, China*.
20. Chan JF-W, Yuan S, Kok K-H, et al. A familial cluster of pneumonia associated with the 2019 novel coronavirus indicating person-to-person transmission: A study of a family cluster. *Lancet* 2020;**395**(10223):514–23 (London, England).

RESPIRATORY INFECTION

Impact of severe acute respiratory syndrome (SARS) on pulmonary function, functional capacity and quality of life in a cohort of survivors

D S Hui, G M Joynt, K T Wong, C D Gomersall, T S Li, G Antonio, F W Ko, M C Chan, D P Chan, M W Tong, T H Rainer, A T Ahuja, C S Cockram, J J Y Sung

Thorax 2005;60:401–409. doi: 10.1136/thx.2004.030205

See end of article for authors' affiliations

Correspondence to:
Dr D S Hui, Department of
Medicine and
Therapeutics, Chinese
University of Hong Kong,
Prince of Wales Hospital,
30–32 Ngan Shing Str,
Shatin, NT, Hong Kong;
dschui@cuhk.edu.hk

Received 15 June 2004
Accepted 19 October 2004

Objective: To examine the impact of severe acute respiratory syndrome (SARS) on pulmonary function, exercise capacity, and health-related quality of life (HRQoL) among survivors.

Methods: 110 survivors with confirmed SARS were evaluated at the Prince of Wales Hospital, HK at the end of 3 and 6 months after symptom onset. The assessment included lung volumes (TLC, VC, RV, FRC), spirometry (FVC, FEV₁), carbon monoxide transfer factor (TlCO adjusted for haemoglobin), inspiratory and expiratory respiratory muscle strength (Pimax and Pemax), 6 minute walk distance (6MWD), chest radiographs, and HRQoL by SF-36 questionnaire.

Results: There were 44 men and 66 women with a mean (SD) age of 35.6 (9.8) years and body mass index of 23.1 (4.8) kg/m². Seventy (64%) were healthcare workers. At 6 months 33 subjects (30%) had abnormal chest radiographs; four (3.6%), eight (7.4%), and 17 (15.5%) patients had FVC, TLC, and TlCO below 80% of predicted values; and 15 (13.9%) and 24 (22.2%) had Pimax and Pemax values below 80 cm H₂O, respectively. The 6MWD increased from a mean (SD) of 464 (83) m at 3 months to 502 (95) m (95% CI 22 to 54 m, $p < 0.001$), but the results were lower than normal controls in the same age groups. There was impairment of HRQoL at 6 months. Patients who required ICU admission ($n = 31$) had significantly lower FVC, TLC, and TlCO than those who did not.

Conclusion: The exercise capacity and health status of SARS survivors was considerably lower than that of a normal population at 6 months. Significant impairment in surface area for gas exchange was noted in 15.5% of survivors. The functional disability appears out of proportion to the degree of lung function impairment and may be related to additional factors such as muscle deconditioning and steroid myopathy.

Severe acute respiratory syndrome (SARS) is a recently emerged infectious disease caused by a SARS coronavirus (CoV).^{1–3} From 1 November 2002 to 31 July 2003, 8098 probable cases were reported worldwide with a death toll of 774.⁴ The clinical course of SARS is characterised by fever, myalgia, and other systemic symptoms that generally improve after a few days, followed by a second phase with recurrence of fever, oxygen desaturation, and radiological progression of pneumonia.⁵ The majority of patients improve with treatment, but 20–36% require intensive care unit (ICU) admission and 13–26% progress into acute respiratory distress syndrome (ARDS) necessitating invasive ventilatory support.^{5–8} The lung pathology of fatal SARS cases was dominated by diffuse alveolar damage, epithelial cell proliferation, an increase in macrophages in the lung, and extensive consolidation,^{9–11} but features of bronchiolitis obliterans organising pneumonia were also noted.¹² Previous studies on survivors of acute lung injury (ALI)¹³ and ARDS^{14–17} unrelated to SARS have shown variable degrees of residual abnormalities in pulmonary function, exercise capacity, and impairment in health-related quality of life (HRQoL).

During the global outbreak of SARS in 2003, healthcare workers were particularly vulnerable as the viral load increased to peak levels around day 10 from symptom onset.^{5–8 18 19} In a major outbreak of SARS at our hospital, over half of those infected were previously healthy healthcare workers.⁶ High resolution computed tomography (HRCT) performed at 5 weeks after discharge selectively on 24 outpatients with residual opacities revealed multiple patchy

ground glass appearance and interstitial thickening ($n = 9$, 38%) whereas CT evidence of fibrotic changes was noted in 15 patients (62%).²⁰ It is possible that ongoing active alveolitis—probably as a result of an uncontrolled host immune response triggered by the viral antigen—may lead to pulmonary fibrosis in some patients. It is thus important to follow these patients to detect and manage pulmonary sequelae and functional impairment.

We report the short to medium term outcome of a prospective follow up study of our cohort which was epidemiologically linked to a single index case during a major hospital outbreak in 2003.^{6 21} Serial lung function, exercise capacity, chest radiographs, and HRQoL were examined at 3 and 6 months after illness onset. In addition, SARS survivors who had required ICU admissions were compared with those who were treated on the medical wards with reference to the same outcome parameters.

METHODS

Subjects

This is a prospective longitudinal follow up study of patients with SARS who were discharged from our hospital after

Abbreviations: BMI, body mass index; CRP, C-reactive protein; FEV₁, forced expiratory volume in 1 second; FRC, functional residual capacity; FVC, forced vital capacity; HRQoL, health-related quality of life; LDH, lactate dehydrogenase; LOS, length of stay; 6MWD, 6 minute walk distance; 6MWT, 6 minute walk test; Pimax, Pemax, maximum static inspiratory and expiratory pressures; RV, residual volume; SARS, severe acute respiratory syndrome; TLC, total lung capacity; TlCO, carbon monoxide transfer factor

surviving the major outbreak in 2003. The patients came from our previously reported cohort⁶ recruited over a period of 2 weeks from 11 March to 25 March 2003. The diagnosis of SARS was based on the CDC criteria at the time,²² and all patients had subsequent laboratory confirmation of SARS.²³ The treatment and outcome of these patients during hospitalisation has been reported in detail elsewhere.²³ This prospective outcome study of SARS survivors was approved by the ethics committee of the Chinese University of Hong Kong.

Assessment

Following discharge from hospital, patients were evaluated in the lung function laboratory at the end of 3 and 6 months after disease onset. During the visit, subjects were interviewed and underwent a physical examination, pulmonary function testing, respiratory muscle strength measurement, postero-anterior chest radiography, resting oximetry, and a standardised 6 minute walk test (6MWT).^{24–25} In addition, they completed the Medical Outcomes Study 36-item Short-Form General Health Survey (SF-36) to measure HRQoL.²⁶

6 minute walk test (6MWT)

This provides a standardised, objective, integrated assessment of cardiopulmonary and musculoskeletal function that is relevant to daily activities.^{24–25} The self-paced 6MWT assesses the sub-maximal level of functional capacity²⁵ and has been applied in a long term follow up study of survivors of ARDS.¹⁴ The 6 minute walk distances (6MWD) were compared with the normative reference data collected from a population survey of 538 normal healthy subjects in 2004 by the Coordinating Committee in Physiotherapy, HK Hospital Authority, on two separate days. The mean (SD) 6MWD of the controls ($n = 538$) on days 1 and 2 of assessment were 598.4 (98.7) m and 609.2 (100.4) m, respectively, with an intra-class correlation coefficient of 0.87 (95% CI 0.84 to 0.89), standard error of measurement 35.3 m, minimum detectable change 97.8 m, and limits of agreement 10.8 (95% CI –87.1 to 108.6) m. The 6MWD data stratified into different age groups are available for comparison with the SARS patients, although we have no access to individual data of this population survey.

SF-36

This includes eight multiple item domains that assess physical functioning (PF), social functioning (SF), role limitation due to physical problems (RP), role limitation due to emotional problems (RE), mental health (MH), bodily pain (BP), vitality (VT), and general health (GH).²⁶ Scores for each aspect can range from 0 (worst) to 100 (best) with higher scores indicating better HRQoL. The validated Chinese (HK) version of the SF-36²⁷ was used for this study and the results were compared with the HK normative data collected from a random telephone survey of 2410 Chinese adults aged 18 years or above.²⁸ Based on this survey, SF-36 domain scores stratified into two age groups (18–40 years and 41–64 years) are available²⁸ for comparison with those of our SARS survivors.

Lung function testing

Lung volumes (total lung capacity (TLC), vital capacity (VC), residual volume (RV), functional residual capacity (FRC) using the nitrogen washout method), spirometric parameters (pre and post bronchodilator forced vital capacity (FVC), forced expiratory volume in 1 second (FEV₁), FEV₁/FVC ratio), and surface area for gas exchange (carbon monoxide transfer factor adjusted for haemoglobin (Tlco) and carbon monoxide transfer coefficient (Kco)) were measured using the SensorMedic Vmax System, USA. Tlco was determined

by the single breath carbon monoxide technique using an infrared analyser. Spirometric tests (FEV₁ and FVC pre and post bronchodilator) were performed according to the standards of the American Thoracic Society.²⁹ After the pre-bronchodilator measurement, salbutamol 400 µg was given via a metered dose inhaler with a spacer. Spirometric testing was repeated 10 minutes later. An increase in FEV₁ of more than 12% and more than 0.2 l was regarded as a positive bronchodilator response.³⁰ The results were compared with the normative data³¹ which have been widely adopted as the reference data in HK.

Measurement of the maximum static inspiratory pressure that a subject can generate at the mouth (Pimax) or the maximum static expiratory pressure (Pemax) is a simple way to gauge inspiratory and expiratory muscle strength.^{32–33} Since respiratory muscle weakness may lead to a restrictive pattern on lung function testing, Pimax and Pemax were assessed with a mouth pressure meter via a flanged mouthpiece³⁴ after full lung function testing. In a study of 24 normal subjects (23 Chinese and one Indian of mean age 29.2 years) in Singapore, the mean (SD) maximal static inspiratory effort from residual volume (Pdi Pimax) for the group was 83.5 (35.5) cm H₂O.³⁵ A Pimax of –80 cm H₂O or a Pemax of +80 cm H₂O generally excludes clinically significant weakness of the inspiratory or expiratory muscles.³⁶

To protect lung function laboratory staff, extra exhaust fans were installed in the lung function room and staff wore personal protective equipment including N95 respirators, protective goggles, gloves, and gowns. In addition, a disposable viral and bacterial filter (Spiroguard 2800/01, USA) was used for each patient during each visit.

Radiographic assessment

Frontal chest radiographs were performed at 3 and 6 months using standardised techniques with computed radiography equipment as reported during the major hospital outbreak.⁶ The images were assessed using a PACs system (Siemens Magicview Version VA22E, Germany) viewer (Siemens 2K monitor). Each lung was divided into three zones (upper, middle and lower) on the frontal radiograph. The observers assessed the presence, appearances (airspace opacities or reticular opacities), distribution, and size of lung parenchymal abnormalities on each chest radiograph of all patients. The size of the lesion was assessed by visually estimating the percentage area occupied in each zone on each side. The overall percentage of involvement was obtained by averaging the percentage involvement of the six lung zones. The frontal chest radiograph closest to the date of the lung function test was assessed by two radiologists, both blinded to the clinical information. Agreement was reached by consensus. The assessment method was as described in our previous study.³⁷

Analysis of data

Statistical analysis was performed using Statistical Package for Social Science (SPSS) Version 11.0. Cumulative steroid dosage during inpatient treatment and outpatient follow up was converted into hydrocortisone (mg) to facilitate analysis of the study. Continuous variables were compared using an independent sample *t* test and the Mann-Whitney U test was used for non-parametric data. Categorical variables were compared using the χ^2 test. All statistical tests were two tailed. Statistical significance was taken as $p < 0.05$. Univariate analyses were performed to evaluate the potential determinants of exercise capacity expressed as the 6MWD. Variables significant in the univariate analyses ($p < 0.1$) were included in the multivariate analysis. Age and sex were included in the final multivariable models because they are independent determinants of the 6MWD.³⁸

Table 1 Results of serial pulmonary function tests and respiratory muscle strength among SARS survivors (n = 110)

Parameter	3 months	6 months
FVC (% of predicted)	104.5 (95.0–114.0)	104.5 (95.0–113.0)
FEV ₁ (% of predicted)	108.0 (99.0–118.5)	106.0 (97.8–116.0)
TLC (% of predicted)	104.0 (93.3–115.8)	108.0 (98.0–117.0)
VC (% of predicted)	105.0 (95.0–115.5)	105.5 (95.0–113.5)
RV (% of predicted)	108.0 (70.5–140.8)	115.0 (84.0–139.8)
TlCO (% of predicted)	98.0 (88.5–107.0)	95.5 (85.0–106.0)
Kco (% of predicted)	106.0 (98.0–115.5)	110.5 (100.0–119.0)*
Pimax (% of predicted)	104.0 (88.0–127.0)	101.0 (87.5–125.0)
Pemax (% of predicted)	74.0 (62.0–86.0)	77.0 (59.0–86.0)

TLC, total lung capacity; VC, vital capacity; FVC, forced vital capacity; FEV₁, forced expiratory volume in 1 second; RV, residual volume; TlCO, carbon monoxide transfer factor adjusted for haemoglobin; Kco, transfer coefficient (transfer factor per alveolar volume); Pimax, Pemax, maximum static inspiratory and expiratory pressures.

Values are expressed as median (interquartile range).

*p < 0.01, Kco at 3 months v 6 months. No statistically significant differences were noted between other lung function parameters at 3 and 6 months.

RESULTS

Of the first 138 patients infected with SARS in March 2003, 15 (10.9%) died.²³ Among the 123 survivors, 13 (10.6%) did not attend for follow up (three returned overseas and 10 refused to participate in the study). A total of 110 were therefore available for analysis, 70 (64%) of whom were healthcare workers (doctors, nurses, ward assistants, and medical students). Sixty six (60%) patients were women. The mean (SD) age was 35.6 (9.8) years and the body mass index (BMI) was 23.1 (4.8) kg/m² during the visit at 3 months from illness onset. The mean (SD) length of stay (LOS) in hospital for the group was 22.0 (13.9) days. There were only three smokers (2.7%) among the whole group.

Seventeen patients had medical co-morbidities which included chronic obstructive pulmonary disease (COPD; n = 1 (0.9%)), ischaemic heart disease (IHD; n = 1 (0.9%)), ischaemic stroke (n = 1 (0.9%)), breast cancer stable on tamoxifen (n = 1 (0.9%)), diabetes mellitus (n = 3 (2.7%)), cirrhosis (n = 1 (0.9%)), hypertension (n = 4 (3.6%)), and five asymptomatic hepatitis B carriers (4.5%).

Among the 110 patients, 31 (28.2%; 17 men and 14 women) had required admission to the ICU with a mean (SD) LOS of 13.5 (15.6) days (median 7, range 2–64); six (5.5%) required invasive mechanical ventilation. Based on our ICU admission criteria,²³ all the 31 patients would have a Pao₂/Fio₂ ratio <300 mm Hg while the six patients who were intubated had a Pao₂/Fio₂ ratio <200 mm Hg. Among these 31 patients, six had medical co-morbidities (one IHD, one diabetes mellitus, two hypertension, and two asymptomatic hepatitis B carriers), but none had any history of smoking or pulmonary disease.

Lung function tests and respiratory muscle strength

An overview of the serial lung function test and respiratory muscle strength results for the group is shown in table 1. At 3 months 89 patients (80.9%) had an FEV₁/FVC ratio of >80% while one patient with COPD (0.9%) had an FEV₁/FVC ratio of <70%. Overall, the lung volume parameters and surface area for exchange were well preserved at 3 and 6 months. A significant proportion of patients appeared to have increased RV at 3 and 6 months (median (interquartile range, IQR) 108 (71–141)% and 115 (84–140)%, respectively. Although none complained of symptoms of asthma, seven (6.4%) had a significant bronchodilator response with increments of FEV₁ >200 ml after inhalation of salbutamol at 3 months. 22 (20.6%) and eight (7.5%) patients, respectively, had Pimax and Pemax values below 80 cm H₂O.

At 6 months 79 (71.8%) had an FEV₁/FVC ratio of >80% while the same patient with COPD had an FEV₁/FVC ratio of <70%. None had a significant bronchodilator response after inhalation of salbutamol. 15 (13.9%) and 24 (22.2%) subjects, respectively, had Pimax and Pemax values below 80 cm H₂O. There was a slight increase in Kco but no change in other lung function parameters at 6 months compared with 3 months (table 1).

The frequency of lung function parameters below 80% of predicted values in SARS survivors is shown in table 2. Seventeen patients (15.5%) had impaired TlCO while up to 7.3% of patients had reduced lung volume measurements at 6 months.

6MWD

The 6MWD of the SARS survivors at 3 and 6 months, compared with normative data, is shown in table 3. The mean 6MWD increased significantly from 464 m at 3 months to 502 m at 6 months (95% CI of difference 22 to 54, p < 0.01). When the subjects were stratified into different age groups and compared with the corresponding normative values, their exercise capacity was significantly lower than the normal subjects (table 3). There was no difference in oxygen saturation after exercise at 3 and 6 months (97.8 (2.6)% v 97.4 (8.8)%, p = 0.61). Two patients and one patient, respectively, had Sao₂ <88% after 6MWT at 3 and 6 months.

Univariate analysis was performed to look for factors associated with 6MWD. At 3 months, age (β coefficient −2.48 (SE 0.79), p = 0.002), female sex (β coefficient −43.33 (15.82), p = 0.007), and hospital LOS (β coefficient −1.72 (0.55), p = 0.002) were significant negative predictors of 6MWD whereas total dose of steroid (β coefficient 0.00 (0.00), p = 0.86), ICU admission (β coefficient −8.27 (17.81), p = 0.64), baseline lactate dehydrogenase (LDH) (β coefficient −0.02 (0.05), p = 0.69), peak LDH (β coefficient −0.01 (−0.02), p = 0.848), BMI (β coefficient −2.16 (1.66), p = 0.20), and peak CRP (β coefficient 0.25 (0.17), p = 0.143) were not. Following multivariate analysis (adjusted R² = 0.17), the independent negative predictors

Table 2 Frequency of lung function parameters below normal range in SARS patients

	N <60% predicted value		N <70% predicted value		N <80% predicted value	
	3 months	6 months	3 months	6 months	3 months	6 months
FEV ₁	0	0	2 (1.8%)	1 (0.9%)	3 (2.7%)	4 (3.6%)
FVC	1 (0.9%)	1 (0.9%)	1 (0.9%)	1 (0.9%)	6 (5.5%)	4 (3.6%)
VC	1 (0.9%)	2 (1.8%)	2 (1.8%)	3 (2.7%)	6 (5.5%)	5 (4.5%)
TLC	0	0	3 (2.7%)	2 (1.8%)	7 (6.4%)	8 (7.3%)
TlCO	2 (1.8%)	7 (6.4%)	7 (6.4%)	9 (8.2%)	14 (12.7%)	17 (15.5%)
Kco	0	0	0	0	2 (1.8%)	1 (0.9%)

TLC, total lung capacity; VC, vital capacity; FVC, forced vital capacity; FEV₁, forced expiratory volume in 1 second; TlCO, carbon monoxide transfer factor adjusted for haemoglobin; Kco, transfer coefficient (transfer factor per alveolar volume).

Table 3 Six minute walking distance (6MWD) among SARS survivors (n = 110) at 3 and 6 months after the onset of illness compared with Hong Kong normative data

Outcome		Normal	3 months	6 months	p value†
All survivors (n = 110*)			464 (83)	502 (95)	**
Age group (years)					
21–30 (n = 37)					0.01
Men	Mean (SD)	651 (105), (n = 80)	487 (58), (n = 17)	549 (73), (n = 17)	
	Mean difference (95% CI)		–164 (–201 to –127)**	–102 (–155 to –49)**	
	Mean (SD)	600 (84), (n = 85)	461 (75), (n = 20)	493 (92), (n = 20)	0.13
Women	Mean difference (95% CI)		–139 (–180 to –98)**	–107 (–149 to –65)**	
	Mean (SD)	645 (93), (n = 78)	513 (80), (n = 19)	551 (98), (n = 19)	0.06
	Mean difference (95% CI)		–132 (–178 to –86)**	–94 (–141 to 46)**	
31–40 (n = 40)					0.11
Men	Mean (SD)	606 (86), (n = 108)	476 (71), (n = 22)	502 (53), (n = 22)	
	Mean difference (95% CI)		–130 (–169 to 91)**	–101 (–139 to –63)**	
	Mean (SD)	623 (80), (n = 38)	477 (82), (n = 7)	543 (112), (n = 7)	0.09
Women	Mean difference (95% CI)		–146 (–212 to –79)**	–80 (–151 to –9), p = 0.03	
	Mean (SD)	541 (67), (n = 79)	404 (83), (n = 14)	473 (76), (n = 14)	**
	Mean difference (95% CI)		–137 (–177 to –97)**	–68 (–107 to –29)**	
41–50 (n = 21)					0.18
Men	Mean (SD)	588 (68), (n = 23)	331 (83), (n = 2)	405 (89), (n = 2)	
	Mean difference (95% CI)		–257 (–361 to –152)**	–183 (–288 to –78)**	
	Mean (SD)	534 (89), (n = 33)	399 (92), (n = 9)	371 (99), (n = 9)	0.67
Women	Mean difference (95% CI)		–135 (–203 to –67)**	–163 (–232 to –94)**	
	Mean (SD)				
	Mean difference (95% CI)				

*Including one woman aged 61 years with 6MWD 492 m and 465 m at 3 and 6 months, respectively.

**p < 0.01.

†6 months v 3 months.

for 6MWD were female sex (β coefficient -38.02 (15.18), $p = 0.014$) and hospital LOS (β coefficient -1.28 (0.57), $p = 0.028$), with a trend for age being a negative predictor (β coefficient -1.54 (0.82), $p = 0.063$). Based on this model, the mean (SE) difference in 6MWD between women and men after adjusting for hospital LOS was -34.0 (14.8) m (95% CI -63.5 to -4.6), $p = 0.024$.

At 6 months, age (β coefficient -3.31 (SE 0.88), $p < 0.001$), female sex (β coefficient -67.62 (17.41), $p < 0.001$), and hospital LOS (β coefficient -1.39 (0.65), $p = 0.036$) were significant negative predictors of 6MWD whereas total dose of steroid (β coefficient 0.00 (0.00), $p = 0.66$), ICU admission (β coefficient 28.17 (20.37), $p = 0.17$), baseline LDH (β coefficient 0.06 (0.06), $p = 0.31$), peak LDH (β coefficient 0.07 (0.13), $p = 0.19$), BMI (β coefficient -2.59 (2.04), $p = 0.21$), and peak CRP (β coefficient 0.26 (0.21), $p = 0.20$) were not. Following multivariate analysis (adjusted $R^2 = 0.20$), the independent negative predictors for 6MWD

were age (β coefficient -2.53 (0.91), $p = 0.006$) and female sex (β coefficient -60.11 (16.74), $p < 0.001$) whereas hospital LOS was no longer a factor (β coefficient -0.71 (0.63), $p = 0.264$). Based on this model, the adjusted mean (SE) difference in 6MWD between women and men was -55.3 (16.3) m, (95% CI -87.6 to -30.0), $p = 0.001$.

Chest radiographs and correlations with lung function and 6MWD

Thirty eight patients (35.8%) had abnormal total chest radiographic scores at 3 months involving a mean (SD) of 3.9 (3.5)% (range 0.5–15) of the total lung fields. These included eight patients with abnormal scores in both airspace opacity and reticular shadows, 16 with an abnormal airspace score, and 14 with an abnormal reticular score. At 6 months 33 subjects (30%) still had abnormal chest radiographic scores involving 3.1 (3.3)% (range 0.8–15) of the lung fields. These included three patients with abnormalities in both

Table 4 Comparison of demographic characteristics, biochemical markers, and steroid dosage in SARS survivors who required ICU care versus those treated on medical wards

	ICU (n = 31)	Non-ICU (n = 79)	95% CI	p value
Age (years)	38.4 (9.8)	33.9 (9.4)	–8.6 to –0.5	0.03*
Male sex	17/31	26/79	1	0.05
BMI (kg/m ²), 3 months	24.0 (3.8)	22.6 (5.1)	–3.4 to 0.6	0.17
BMI (kg/m ²), 6 months	24.3 (3.8)	23.0 (4.7)	–3.1 to 0.7	0.20
Hospital LOS (days)	32.4 (19.8)	17.9 (7.7)	–29.8 to –7.3	<0.01*
CRP baseline (mg/dl)	26.4 (28.1)	23.2 (32.1)	–17.1 to 10.8	0.65
CRP peak (mg/dl)	77.1 (61.6)	36.4 (39.2)	–65.6 to –15.8	<0.01*
LDH baseline (U/l)	357.8 (201.3)	274.6 (155.9)	–167.6 to 1.4	0.05
LDH peak (U/l)	522.3 (157.0)	349.4 (165.5)	–244.7 to –101.1	<0.01*
Cumulative steroid dosage (hydrocortisone, mg)	18881 (11425)	8217 (5874)	–15044 to –6284	<0.01*
Radiographic total score (%), 6 months	1.9 (3.7)	0.6 (1.3)	–2.7 to 0.1	0.06

Values are expressed as mean (SD).

BMI, body mass index; CRP, C-reactive protein; LOS, length of stay; LDH, lactate dehydrogenase; 95% CI, 95% confidence interval of the difference between groups.

*Statistically significant.

Table 5 Comparison of lung function indices, respiratory muscle strength, and 6MWD in SARS survivors who had required ICU care (n=31) versus those treated on the wards (n=79)

	3 months	6 months	Mean (SE) difference 6–3 months
FVC (% of predicted)			
Mean (SD)	94.3 (14.0) v 107.6 (12.1)	98.6 (15.8) v 106.1 (13.5)	4.3 (1.7) v -1.6 (1.0)
95% CI	7.9 to 18.7	1.5 to 13.5	-9.6 to -2.1
p value	p<0.01*	p=0.02*	p<0.01*
FEV ₁ (% of predicted)			
Mean (SD)	102.0 (13.1) v 111.1 (14.7)	103.8 (12.7) v 108.2 (15.4)	1.8 (1.2) v -2.9 (1.3)
95% CI	3.0 to 15.1	-1.8 to 10.6	-9.0 to -0.4
p value	p<0.01*	p=0.17	p=0.03*
VC (% of predicted)			
Mean (SD)	94.7 (15.1) v 107.9 (12.5)	98.4 (16.4) v 105.0 (17.9)	3.7 (1.4) v -2.8 (1.4)
95% CI	7.4 to 18.9	-0.9 to 14.1	-11.3 to -1.8
p value	p<0.01*	p=0.08	p=0.01*
TLC (% of predicted)			
Mean (SD)	94.6 (16.1) v 110.3 (16.4)	98.2 (19.3) v 110.1 (14.1)	3.6 (3.9) v -0.2 (1.9)
95% CI	8.7 to 22.7	4.0 to 19.7	-11.6 to 4.0
p value	p<0.01*	p<0.01*	p=0.33
RV (% of predicted)			
Mean (SD)	96.7 (39.4) v 115.7 (49.7)	99.9 (51.6) v 118.6 (38.5)	3.2 (12.3) v 2.9 (6.2)
95% CI	-1.2 to 39.2	-2.4 to 39.7	-25.0 to 24.3
p value	p=0.06	p=0.08	p=0.98
TlCO (% of predicted)			
Mean (SD)	84.3 (17.5) v 101.4 (13.4)	87.7 (21.0) v 98.3 (16.6)	3.4 (2.2) v -2.9 (1.6)
95% CI	10.9 to 23.4	3.0 to 18.2	-11.9 to -0.6
p value	p<0.01*	P=0.01*	p=0.03*
Kco (% of predicted)			
Mean (SD)	104.9 (13.5) v 107.4 (13.7)	109.4 (15.3) v 110.1 (13.6)	4.5(1.7) vs 2.6(1.3)
95% CI	-3.4 to 8.2	-5.3 to 6.7	-6.5 to 2.7
p value	p=0.41	P=0.83	p=0.42
Pimax (% of predicted)			
Mean (SD)	104.2 (29.1) v 108.5 (29.8)	105.6 (30.6) v 105.8 (25.8)	0.6 (5.6) v -2.6 (2.7)
95% CI	-8.5 to 17.0	-11.4 to 11.8	-14.0 to 7.6
p value	p=0.51	P=0.97	p=0.56
Pemax (% of predicted)			
Mean (SD)	75.7 (14.9) v 73.2 (18.9)	74.5 (19.1) v 71.5 (21.4)	-1.8 (2.8) v -1.5 (2.1)
95% CI	-10.2 to 5.2	-11.9 to 5.8	-7.1 to 7.6
p value	p=0.52	P=0.49	p=0.94
6MWD (m)			
Mean (SD)	458.2 (86.8) v 466.4 (80.7)	519.7 (101.4) v 491.5 (92.9)	64.5 (14.5) v 25.1 (9.7)
95% CI	-27.1 to 43.6	-11.4 to 11.8	-74.9 to -4.0
p value	p=0.64	P=0.97	p=0.03*

FVC, forced vital capacity; FEV₁, forced expiratory volume in 1 second; VC, vital capacity; TLC, total lung capacity; RV, residual volume; TlCO, carbon monoxide transfer factor adjusted for haemoglobin; Kco, transfer coefficient (transfer factor per alveolar volume); Pimax, Pemax, maximum static inspiratory and expiratory pressures; 6MWD, 6 minute walk distance.

Values are shown as mean (SD) ICU v non-ICU with 95% CI of difference and p values.

*Statistically significant.

airspace and reticular shadows, 16 with abnormal airspace shadows, and 14 with abnormal reticular shadows.

Correlations between the extent of radiographic abnormality and cumulative steroid dosage, lung function parameters, and 6MWD at 6 months were examined. There was a significant positive correlation between the extent of radiographic abnormalities (% of lung fields) and the cumulative hydrocortisone dosage ($r = 0.38$, $p < 0.01$), and a significant

negative correlation between the extent (%) of radiographic abnormalities and FVC ($r = -0.23$, $p = 0.02$), TLC ($r = -0.22$, $p = 0.02$), TlCO ($r = -0.29$, $p < 0.01$), and Kco ($r = -0.22$, $p = 0.02$) with a trend towards a negative correlation with VC ($r = -0.17$, $p = 0.07$). However, no significant correlations were noted between the extent of radiographic abnormalities and 6MWD ($r = -0.14$, $p = 0.15$), FEV₁ ($r = -0.12$, $p = 0.20$), RV ($r = -0.11$, $p = 0.25$), Pimax ($r = 0.10$, $p = 0.29$), and

Table 6 Correlations between pulmonary function and HRQoL at 6 months (n = 110)

SF-36	FVC	FEV ₁	VC	TLC	Tlco*
PF	0.31*	0.40*	0.42*	0.19	0.30*
RP	0.31*	0.39*	0.35*	0.18	0.34*
BP	0.16	0.29*	0.27*	0.03	0.17
GH	0.29*	0.32*	0.29*	0.11	0.32*
VT	0.16	0.23†	0.12	0.01	0.13
SF	0.24‡	0.39*	0.24‡	0.13	0.27‡
RE	0.15	0.22†	0.22†	-0.01	0.22†
MH	0.13	0.22†	0.09	0.02	0.26‡

PF, physical functioning; SF, social functioning; RP, role limitation due to physical problems; RE, role limitation due to emotional problems; MH, mental health; BP, bodily pain; VT, vitality; GH, general health.

Values shown are Pearson's correlation coefficients (r).

* $p < 0.01$; † $p < 0.05$; ‡ $p = 0.05$.

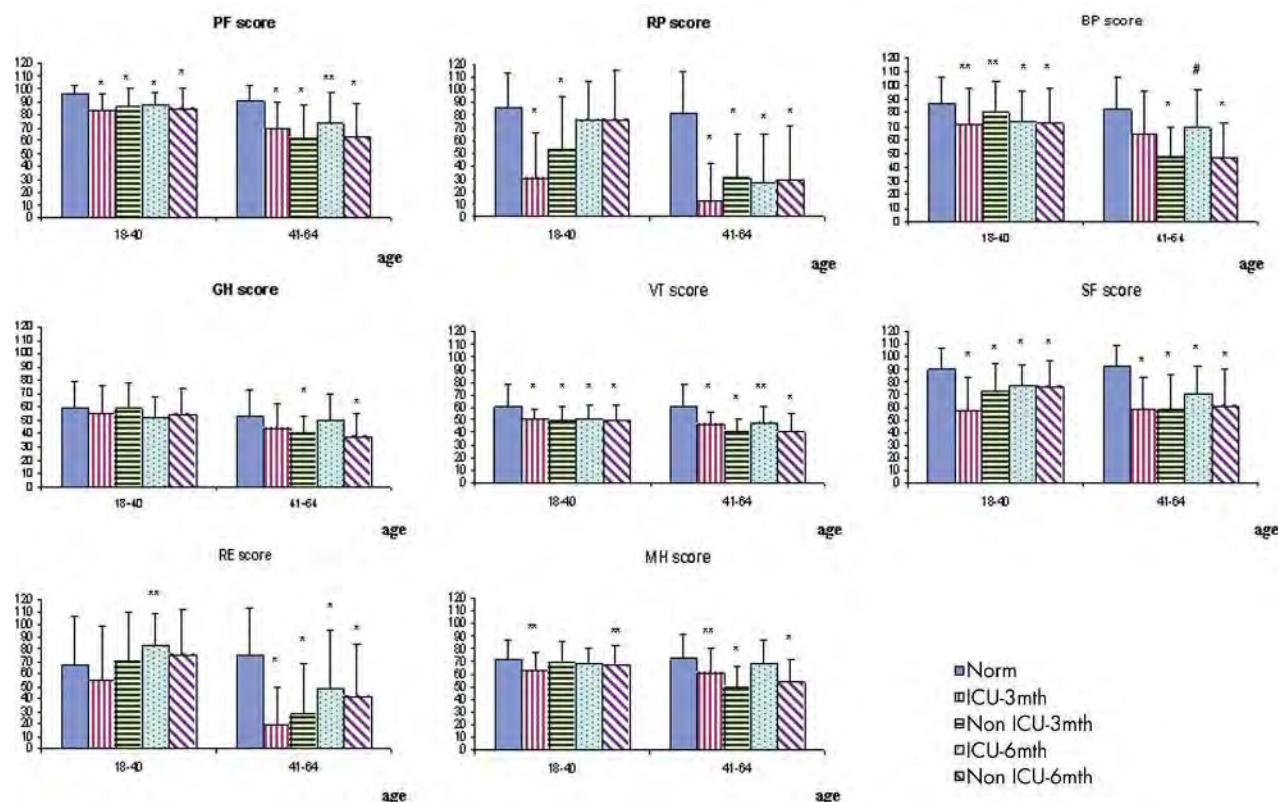


Figure 1 Health-related quality of life (SF-36) among SARS survivors at 3 and 6 months after illness onset compared with Hong Kong normative data stratified into different age groups.²⁸ The vertical axis represents mean (SD) SF-36 domain scores from 0 (minimum) to 100 (maximum) and the horizontal axis defines age groups in years. Based on the study by Lam *et al*²⁸ there were 1244 and 695 normal subjects in the age groups 18–40 years and 41–64 years, respectively. There were 19 and 12 SARS survivors who had required ICU support in the age groups 18–40 years and 41–64 years, and 60 and 19 SARS survivors, respectively, who did not require ICU support in the two age groups. PF, physical functioning; SF, social functioning; RP, role limitation due to physical problems; RE, role limitation due to emotional problems; MH, mental health; BP, bodily pain; VT, vitality; GH, general health. * $p < 0.01$; ** $p < 0.03$; # $p < 0.05$.

Pemax ($r = 0.12$, $p = 0.21$). These data are shown in a supplementary file available on the *Thorax* website at <http://www.thoraxjnl.com/supplemental>.

Comparison of patients requiring ICU support with those treated on the wards

Patients who had required ICU admission ($n = 31$, 17 men and 14 women) were older with a higher peak LDH, a longer hospital LOS, and received a significantly higher total steroid dosage than those who did not require ICU care (table 4). The lung function tests at 6 months showed significantly lower FVC, TLC, and Tlco in survivors who had required ICU support than those who were treated on medical wards, although no significant differences were noted in 6MWD and respiratory muscle strength between the two groups (table 5).

HRQoL among SARS survivors and its correlation with lung function parameters

Correlations between lung function parameters and SF-36 domains at 6 months are shown in table 6. In general there were significant positive correlations between lung function parameters (FVC, VC, FEV₁, and Tlco) and several SF-36 domains (PF, RP, GH, and SF).

SF-36 domain scores at 3 and 6 months after illness onset of patients who did and did not require ICU support during the acute illness compared with normative data are shown in fig 1 (more data are available in supplemental tables 2a and b on the *Thorax* website <http://www.thoraxjnl.com/>

supplemental). There was significant impairment of HRQoL among the SARS survivors at 6 months.

When those who had required ICU admissions were directly compared with those treated on the medical wards there was a significantly lower score in RP ($p = 0.026$) and SF ($p = 0.02$) for those aged 18–40 years who had required ICU support ($n = 19$) but no significant difference in any domain for those aged 41–64 years ($n = 12$) at 3 months. There was no significant difference in SF-36 domains between the two groups at 6 months apart from a lower score in BP ($p = 0.021$) for those aged 41–64 years who had required ICU support ($n = 12$).

In comparing the 25 patients who did not require intubation in the ICU with those who had required intubation ($n = 6$), the latter had more severe lung injury as reflected by a higher peak LDH level (median 466.0 (IR 259.0) v 652.0 (124.5) U/L, $p = 0.02$). There was, however, no statistically significant difference with regard to age (36.0 (15.5) v 36.5 (17.5) years, $p = 0.87$) and 6MWD (507.7 (163.9) v 449.0 (129.3) m, $p = 0.18$) at 6 months. In addition, there were no significant differences between the two groups with regard to lung function indices and SF-36 domain scores at 6 months (data available in supplemental table 3 on the *Thorax* website <http://www.thoraxjnl.com/supplemental>).

DISCUSSION

During the global outbreak of SARS in 2003 there was an enormous demand on ICU support for patients who developed severe respiratory failure.^{5–8 18 19} Although the use of

pulse methylprednisolone during clinical progression was associated with favourable clinical improvement in most of our patients with resolution of fever and improvement of lung opacities within 2 weeks.^{6, 23, 39, 40} Our preliminary follow up study with HRCT scanning has revealed multiple patchy ground glass appearance and interstitial thickening in nine patients and CT evidence of fibrotic changes in 15 out of 24 patients with residual radiographic opacities.²⁰ This has raised concern that some patients with SARS may have ongoing immune mediated alveolitis which has the potential to lead to significant parenchymal fibrosis and lung function impairment. A recent report by Ng *et al*⁴¹ has indicated that residual abnormalities of pulmonary function were still observed in three quarters of their cohort ($n = 57$), mostly consisting of isolated reductions in Tlco, while an abnormal HRCT score was detected in 75.4% of SARS patients at 6 months after admission to hospital.

This prospective cohort study has shown that most of the SARS survivors had relatively well preserved lung function at 6 months after symptom onset. Up to 15.5% of patients had significant impairment of lung function, as reflected by reduced Tlco with well preserved Kco. These results suggest an increase in the intra-alveolar diffusion pathway which may be the result of diffuse alveolar damage and/or bronchiolitis obliterans organising pneumonia in the acute stage,⁹⁻¹² followed by post-inflammatory changes such as atelectasis, ongoing alveolitis, and parenchymal fibrosis later in the course of the disease. Several studies on ARDS survivors have shown that their pulmonary function generally returns to normal or near normal by 6-12 months,⁴²⁻⁴⁴ but Tlco may remain abnormal in up to 80% of patients at 1 year after recovery.¹⁶

The self-paced 6MWT was performed to evaluate the global and integrated responses to exercise, and these would include cardiorespiratory systems, systemic and peripheral circulation, blood, neuromuscular units, and muscle metabolism. However, the 6MWT does not provide specific information on the function of individual organs and systems.²⁵ The 6MWD was substantially reduced for all age groups at 3 and 6 months compared with controls. Two previous studies have shown that 6MWD was substantially lower among ARDS survivors than controls 1-2 years after mechanical ventilation^{14, 45} while the absence of systemic steroid treatment, the absence of illness acquired and rapid resolution of lung injury, and rapid resolution of lung injury during ICU stay were important factors associated with a longer 6MWD at 3, 6, and 12 months, respectively.¹⁴ In contrast, our analysis has shown that a longer hospital stay and female sex were independent factors associated with lower 6MWD at 3 months whereas age and female sex were negative predictors for 6MWD at 6 months. During hospitalisation for an average of 3 weeks, most of our patients were on bed rest because of respiratory failure. Given the relatively well preserved lung function in the majority of our SARS survivors, the poor performance in 6MWT in all age groups could be due to additional factors such as muscle wasting, steroid myopathy, and possibly cardiac diastolic dysfunction.⁴⁶ In a study of the physical profile of SARS survivors ($n = 171$ and including the current cohort) at 3 months after illness onset, Lau *et al*⁴⁷ noted that muscle strength and endurance were more impaired in proximal than in distal muscles. This was reflected by "average" handgrip measured by a hand-held dynamometer and "below average" to "poor" performance for curl-up and push-up testing compared with the normative Hong Kong data. Ong *et al*⁴⁸ have recently reported that 18 of 44 SARS survivors in Singapore had reduced exercise capacity at 3 months after hospital discharge that could not be accounted for by impairment of pulmonary function. Their results suggest that the inability to

exercise in recovered SARS patients is primarily due to extrapulmonary disease and is probably caused by myopathy or physical deconditioning.⁴⁸

In addition, at 6 months there was significant impairment in HRQoL as measured by the Chinese version of the SF-36 questionnaire^{27, 28} in most domains. There were significant and positive correlations between lung function parameters (VC, FVC, FEV₁, and Tlco) and SF-36 domains such as PF, RP, GH, and SF. The results are not surprising as, in addition to the physical impairment, the long period of isolation and extreme uncertainty during the SARS illness had created tremendous psychological and mood disturbances. Other contributing factors included intense media attention, bereavement, phobia, and rejection of SARS survivors by some members of the general public (particularly in the initial phase of the outbreak), and fear of transmission of SARS to others.⁴⁰ Other studies on ALI or ARDS survivors unrelated to SARS have reported impaired HRQoL at 1-5 years after recovery,¹³⁻¹⁶ whereas pulmonary function abnormalities, especially Tlco, were correlated with SF-36 domains.^{15, 16}

Herridge *et al*¹⁴ reported that 20% of their ARDS survivors had minor abnormalities on the chest radiograph at 1 year. Our study has shown that 33 subjects (30%) still had abnormal radiographic scores at 6 months. The positive correlation between the extent of residual radiographic abnormalities and the cumulative steroid dosage used for SARS was not surprising as the former was an indication on the treatment protocol for more systemic steroid during the outbreak.^{5, 6, 23} The negative correlation between residual radiographic abnormalities and lung volume parameters (FVC, TLC) and parameters of surface area for gas exchange (Tlco and Kco) reflected the physiological effects of parenchymal inflammation and fibrosis. Patients with more severe disease (as reflected by higher peak LDH)^{6, 23, 39} who had required ICU support during the acute illness tended to have more residual opacities on the chest radiograph at 6 months. In addition, they had more extensive pulmonary injury and fibrosis as reflected by significantly lower lung volume parameters (FVC and TLC) and transfer factor (Tlco) at 6 months than those treated on the general wards. There were, however, no significant differences in 6MWD and HRQoL between the two groups at 6 months. In addition, there were no differences in any functional parameters between mechanically ventilated and non-ventilated ICU patients. It is interesting that, in those patients surviving to the chronic phase of SARS related ARDS, HRCT scanning showed no visible differences between the patients who had been mechanically ventilated and those who had not.³⁹

A significant proportion of SARS patients had evidence of respiratory muscle weakness, as reflected by decreased Pimax and Pemax values below 80 cm H₂O in 15 (13.9%) and 24 (22.2%), respectively, at 6 months. Weakness of the expiratory muscles (abdominal and intercostal muscles) could lead to air trapping (as reflected by increased RV above 120% of predicted in some patients), whereas inspiratory muscle weakness may lead to atelectasis. There are many possible causes for respiratory muscle weakness among SARS survivors. Many patients complained of myalgia with elevation of creatinine kinase suggestive of viral induced myositis at initial presentation.⁶ At least 40% of patients suffered from acute respiratory failure requiring supplemental oxygen and bed rest during the second phase of the disease.^{5-8, 23} The long period of bed rest could lead to muscle wasting and deconditioning, while the use of systemic corticosteroids to suppress immune mediated lung injury⁵⁻⁸ could contribute to myopathy. In 13 patients given high dose steroids for acute lung transplant rejection over 5 days, about 45% developed acute generalised muscle weakness which

took about 2 months to recover.⁵⁰ Similarly, myopathy has been observed in patients with status asthmaticus treated with high dose corticosteroid.^{51–52} Corticosteroids are thought to produce adverse effects on muscles through several mechanisms: altered electrical excitability of muscle fibres, loss of thick filaments, and/or inhibition of protein synthesis.^{53–56}

Interestingly, seven patients (6.4%) without any past history of airway disease had a significant bronchodilator response to salbutamol³⁰ with increments of FEV₁ of at least 12% and over 200 ml from baseline at 3 months, but the positive response was no longer present at 6 months. Although these patients had neither wheeze nor persistent cough at follow up, the bronchodilator response suggested that transient bronchial hyperresponsiveness might develop after SARS. Although we did not perform bronchial challenge in our patients, bronchial reactivity has been observed in some survivors of ARDS.⁴² Viral respiratory infections may cause increased airway responsiveness which can be observed in response to inhalation of histamine, methacholine, citric acid, or allergen.^{57–60}

There are several limitations to this study. Firstly, we assessed inspiratory and expiratory muscle strength with mouth pressure, but low P_{max} values do not always indicate expiratory muscle weakness and might result from technical difficulties such as mouth leakage. However, it is a well established simple test^{32–33} and none of our patients suffered from facial muscle or bulbar weakness. Cough gastric pressure provides a useful complementary test for the assessment of expiratory muscle strength but it involves insertion of a gastric balloon catheter and cough.⁶¹ At the time of planning this study there was still some concern among our lung function staff about potential infectivity via respiratory secretion of SARS survivors even though published data suggested this to be unlikely.⁵ It was therefore decided not to involve any invasive procedure. Lastly, although full lung function tests and 6 MWT were conducted in our patients, we did not perform cardiopulmonary exercise testing as most of our patients were complaining of generalised muscle weakness on follow up. In addition, cardiopulmonary exercise testing would be too labour intensive for the large cohort of SARS survivors. Nevertheless, reduced pulmonary gas exchange can be detected with cardiopulmonary exercise testing in many survivors of SARS at 3 months⁴⁸ and other causes of ARDS¹⁷ with normal Tl_{CO}.

In summary, this study has shown significant impairment of surface area for gas exchange in 15.5% of SARS survivors, while their functional ability and health status were significantly lower than the general population at 6 months after illness onset. The functional disability appears out of proportion to the degree of lung function impairment and may be due to additional factors such as muscle deconditioning and steroid myopathy. Long term follow up is needed to determine whether these deficits persist.

ACKNOWLEDGEMENTS

The authors would like to thank the following colleagues who have offered tremendous help in this ongoing study: PY Chan RN, MS Cheng RN, TY Cheong RN, MY Leung EN, Erica Lee (clerk) and Catherine Ho (research assistant). They would also like to acknowledge the Coordinating Committee in Physiotherapy, HK Hospital Authority, for collecting the updated normative data on 6 minute walk distances. They also thank Dr CC Szeto for his statistical advice on the data analysis.



Further data are given in a supplementary file available on the *Thorax* website at <http://www.thoraxjnl.com/supplemental>.

Authors' affiliations

D S Hui, C S Cockram, J J Y Sung, Center for Emerging Infectious Diseases, Chinese University of Hong Kong, Prince of Wales Hospital, Shatin, NT, Hong Kong
D S Hui, F W Ko, M C Chan, D P Chan, M W Tong, C S Cockram, J J Y Sung, Department of Medicine and Therapeutics, Chinese University of Hong Kong, Prince of Wales Hospital, Shatin, NT, Hong Kong
G M Joynt, C D Gomersall, T S Li, Department of Anaesthesia and Intensive Care, Chinese University of Hong Kong, Prince of Wales Hospital, Shatin, NT, Hong Kong
K T Wong, G Antonio, A T Ahuja, Department of Diagnostic Radiology and Organ Imaging, Chinese University of Hong Kong, Prince of Wales Hospital, Shatin, NT, Hong Kong
T H Rainer, Accident and Emergency, Chinese University of Hong Kong, Prince of Wales Hospital, Shatin, NT, Hong Kong

Source of funding: Research Fund for the Control of Infectious Diseases (Health, Welfare and Food Bureau, HKSAR).

REFERENCES

- Kuiken T**, Fouchier RA, Schutten M, *et al*. Newly discovered coronavirus as the primary cause of severe acute respiratory syndrome. *Lancet* 2003;**362**:263–70.
- Drosten C**, Gunther S, Preiser W, *et al*. Identification of a novel coronavirus in patients with severe acute respiratory syndrome. *N Engl J Med* 2003;**348**:1967–76.
- Ksiazek TG**, Erdman D, Goldsmith CS, *et al*. A novel coronavirus associated with severe acute respiratory syndrome. *N Engl J Med* 2003;**348**:1953–66.
- World Health Organization**. Summary of probable SARS cases with onset of illness from 1 November 2002 to 31 July 2003. http://www.who.int/csr/sars/country/table2003_09_23/en (accessed 10 September 2003).
- Peiris JSM**, Chu CM, Cheng VCC, *et al*. Clinical progression and viral load in a community outbreak of coronavirus-associated SARS pneumonia: a prospective study. *Lancet* 2003;**361**:1767–72.
- Lee N**, Hui DS, Wu A, *et al*. A major outbreak of severe acute respiratory syndrome in Hong Kong. *N Engl J Med* 2003;**348**:1986–94.
- Chan JW**, Ng CK, Chan YH, *et al*. Short term outcome and risk factors for adverse clinical outcomes in adults with severe acute respiratory syndrome (SARS). *Thorax* 2003;**58**:686–9.
- Tsui PT**, Kwok ML, Yuen H, *et al*. Severe acute respiratory syndrome: Clinical outcome and prognostic correlates. *Emerg Infect Dis* 2003;**9**:1064–9.
- Nicholls JM**, Poon LLM, Lee KC, *et al*. Lung pathology of fatal severe acute respiratory syndrome. *Lancet* 2003;**361**:1773–8.
- Ding Y**, Wang H, Shen H, *et al*. The clinical pathology of severe acute respiratory syndrome (SARS): a report from China. *J Pathol* 2003;**200**:282–9.
- Franks TJ**, Chong PY, Chui P, *et al*. Lung pathology of severe acute respiratory syndrome (SARS). A study of 8 autopsy cases from Singapore. *Hum Pathol* 2003;**34**:743–8.
- Tse GM**, To KF, Chan PK, *et al*. Pulmonary pathological features in coronavirus associated severe acute respiratory syndrome (SARS). *J Clin Pathol* 2004;**57**:260–5.
- Weinert CR**, Gross CR, Kangas JR, *et al*. Health-related quality of life after acute lung injury. *Am J Respir Crit Care Med* 1997;**156**:1120–8.
- Herridge MS**, Cheung AM, Tansey CM, *et al*. One-year outcomes in survivors of the acute respiratory distress syndrome. *N Engl J Med* 2003;**348**:683–93.
- Schelling G**, Stoll C, Vogelmeier C, *et al*. Pulmonary function and health-related quality of life in a sample of long-term survivors of the acute respiratory distress syndrome. *Intensive Care Med* 2000;**26**:1304–11.
- Orme J Jr**, Romney JS, Hopkins RO, *et al*. Pulmonary function and health-related quality of life in survivors of acute respiratory distress syndrome. *Am J Respir Crit Care Med* 2003;**167**:690–4.
- Neff TA**, Stocker R, Frey HR, *et al*. Long-term assessment of lung function in survivors of severe ARDS. *Chest* 2003;**123**:845–53.
- Booth CM**, Matukas LM, Tomlinson GA, *et al*. Clinical features and short-term outcomes of 144 patients with SARS in the Greater Toronto area. *JAMA* 2003;**289**:2801–9.
- Hsu LY**, Lee CC, Green JA, *et al*. Severe acute respiratory syndrome in Singapore: clinical features of index patient and initial contacts. *Emerg Infect Dis* 2003;**9**:713–7.
- Antonio GE**, Wong KT, Hui DS, *et al*. Thin-section CT in patients with severe acute respiratory syndrome following hospital discharge: preliminary experience. *Radiology* 2003;**228**:810–5.
- Wong RS**, Hui DS. Index patient and SARS outbreak in Hong Kong. *Emerg Infect Dis* 2004;**10**:339–41.
- Centers for Disease Control and Prevention**. Severe acute respiratory syndrome (SARS) updated interim US case definition. <http://www.cdc.gov/ncidod/sars/casedefinition.htm> (accessed 20 April 2003).
- Sung JJ**, Wu A, Joynt GM, *et al*. Severe acute respiratory syndrome: report of treatment and outcome after a major outbreak. *Thorax* 2004;**59**:414–20.
- Weisman IM**, Zeballos RJ. Clinical exercise testing. *Clin Chest Med* 2001;**22**:679–701.
- American Thoracic Society**. Statement: Guidelines for the six-minute walk test. *Am J Respir Crit Care Med* 2002;**166**:111–7.
- McHorney CA**, Ware JE Jr, Lu JF, *et al*. The MOS 36-item Short-Form Health Survey (SF 36). III. Tests of data quality, scaling assumptions, and reliability across diverse patient groups. *Med Care* 1994;**32**:40–66.

- 27 **Lam CL**, Gandek B, Ren XS, *et al*. Tests of scaling assumptions and construct validity of the Chinese (HK) version of the SF 36 health survey. *J Clin Epidemiol* 1998;**51**:1139–47.
- 28 **Lam CL**, Launder IJ, Lam TP, *et al*. Population based norming of the Chinese (HK) version of the SF 36 health survey. *Hong Kong Practitioner* 1999;**21**:460–70.
- 29 **American Thoracic Society**. Standardization of spirometry: 1994 update. *Am J Respir Crit Care Med* 1995;**152**:1107–36.
- 30 **American Thoracic Society**. Lung function testing: selection of reference values and interpretative strategies. *Am Rev Respir Dis* 1991;**144**:1202–18.
- 31 **Da Costa JL**. Pulmonary function studies in healthy Chinese adults in Singapore. *Am Rev Respir Dis* 1971;**104**:128–31.
- 32 **Black LF**, Hyatt RE. Maximal respiratory pressures: normal values and relationships to age and sex. *Am Rev Respir Dis* 1969;**99**:698–702.
- 33 **ATS/ERS**. Statement on respiratory muscle testing. *Am J Respir Crit Care Med* 2002;**166**:518–624.
- 34 **Koulouris N**, Mulvey DA, Larache CM, *et al*. Comparison of two different mouthpieces for the measurement of Pimax and Pemax in normal and weak subjects. *Eur Respir J* 1988;**1**:863–7.
- 35 **Chan CC**, Cheong TH, Wang YT, *et al*. Transdiaphragmatic pressure in young adult Singaporean subjects: normal values and a comparison between different respiratory manoeuvres. *Aust NZ J Med* 1996;**26**:75–81.
- 36 **Moxham J**. Respiratory muscles. In: Hughes JM, Pride NB, eds. *Lung function tests. Physiological principles and clinical applications*. 1st ed. London: WB Saunders, 2000:57–72.
- 37 **Wong KT**, Antonio GE, Hui DS, *et al*. Severe acute respiratory syndrome: radiographic appearances and pattern of progression in 138 patients. *Radiology* 2003;**228**:401–6.
- 38 **Enright PL**, Sherrill DL. Reference equations for the six-minute walk in healthy adults. *Am J Respir Crit Care Med* 1998;**158**:1384–7.
- 39 **Hui DS**, Sung JJ. Severe acute respiratory syndrome (editorial). *Chest* 2003;**124**:12–5.
- 40 **Wong GW**, Hui DS. Severe acute respiratory syndrome: epidemiology, diagnosis and treatment. *Thorax* 2003;**58**:558–60.
- 41 **Ng CK**, Chan JW, Kwan TL, *et al*. Six month radiological and physiological outcomes in severe acute respiratory syndrome (SARS) survivors. *Thorax* 2004;**59**:889–91.
- 42 **Simpson DL**, Goodman M, Spector SL, *et al*. Long-term follow-up and bronchial reactivity testing in survivors of the adult respiratory distress syndrome. *Am Rev Respir Dis* 1978;**117**:449–54.
- 43 **Lakshminarayan S**, Hudson LD. Pulmonary function following the adult respiratory distress syndrome. *Chest* 1978;**74**:489–90.
- 44 **Peters JL**, Bell RC, Prihoda TJ, *et al*. Clinical determinants of abnormalities in pulmonary functions in survivors of the adult respiratory distress syndrome. *Am Rev Respir Dis* 1989;**139**:1163–8.
- 45 **Cooper AB**, Ferguson ND, Hanly PJ, *et al*. Long-term follow-up of survivors of acute lung injury: lack of effect of a ventilation strategy to prevent barotraumas. *Crit Care Med* 1999;**27**:2616–21.
- 46 **Li SS**, Cheng CW, Fu CL, *et al*. Left ventricular performance in patients with severe acute respiratory syndrome. A 30 day echocardiographic follow-up study. *Circulation* 2003;**108**:r93–8.
- 47 **Lau HM**, Lee EW, Siu EH, *et al*. The impact of severe acute respiratory syndrome on the physical profile and quality of life in a cohort of survivors. *Arch Phys Med Rehab* 2005 (in press).
- 48 **Ong KC**, Ng AW, Lee LS, *et al*. Pulmonary function and exercise capacity in survivors of severe acute respiratory syndrome. *Eur Respir J* 2004;**24**:436–42.
- 49 **Joynt GM**, Antonio GE, Lam P, *et al*. Late-stage adult respiratory distress syndrome caused by severe acute respiratory syndrome: abnormal findings at thin-section CT. *Radiology* 2004;**230**:339–46.
- 50 **Nava S**, Fracchia G, Callegari G, *et al*. Weakness of respiratory and skeletal muscles after a short course of steroids in patients with acute lung rejection. *Eur Respir J* 2002;**20**:497–9.
- 51 **Kaplan PW**, Rocha W, Sanders DB, *et al*. Acute steroid-induced tetraplegia following status asthmaticus. *Paediatrics* 1986;**78**:121–3.
- 52 **Polsonetti BW**, Joy SD, Laos LF. Steroid-induced myopathy in the ICU. *Ann Pharmacother* 2002;**36**:1741–4.
- 53 **Mitch WE**, Goldberg AL. Mechanisms of muscle wasting: the role of the ubiquitin-proteasome pathway. *N Engl J Med* 1996;**335**:1897–905.
- 54 **Hund E**. Myopathy in critically ill patients. *Crit Care Med* 1999;**27**:2544–7.
- 55 **Larsson L**, Li X, Edstrom L, *et al*. Acute quadriplegia and loss of muscle myosin in patients treated with nondepolarizing neuromuscular blocking agents and corticosteroids: mechanisms at the cellular and molecular levels. *Crit Care Med* 2000;**28**:34–45.
- 56 **Dekhuijzen PH**, Decramer M. Steroid-induced myopathy and its significance to respiratory disease: a known disease rediscovered. *Eur Respir J* 1992;**5**:997–1003.
- 57 **Fraenkel DJ**, Bardin PG, Sanderson G, *et al*. Lower airway inflammation during rhinovirus colds in normal and in asthmatic subjects. *Am J Respir Crit Care Med* 1995;**151**:879–86.
- 58 **Sterk PJ**. Virus-induced airway hyperresponsiveness in man. *Eur Respir J* 1993;**6**:894–902.
- 59 **Laitinen LA**, Elkin RB, Empey DW, *et al*. Bronchial hyperresponsiveness in normal subjects during attenuated influenza virus infection. *Am Rev Respir Dis* 1991;**143**:358–61.
- 60 **Trigg CJ**, Nicholson KG, Wang JH, *et al*. Bronchial inflammation and the common cold: a comparison of atopic and non-atopic individuals. *Clin Exp Allergy* 1996;**26**:665–76.
- 61 **Man WD**, Kyroussis D, Fleming TA, *et al*. Cough gastric pressure and maximum expiratory mouth pressure in humans. *Am J Respir Crit Care Med* 2003;**168**:714–7.

LUNG ALERT

Molecular techniques improve organism identification from pleural fluid in empyema

▲ Saglani S, Harris KA, Wallis C, Hartley JC. Empyema: the use of broad range 16S rDNA PCR for pathogen detection. *Arch Dis Child* 2005;**90**:70–3

This study compares a broad range molecular technique with bacterial culture for the detection of organisms from pleural fluid in 32 children with empyema. The concordance of organisms identified and influence of prior antibiotic treatment was also investigated. There was a median duration of 8 (1–42) days antibiotic therapy before pleural fluid aspiration.

The molecular assay is an established and validated broad range 16S rDNA PCR technique. This is based on bacterial ribosomal (r)DNA with sequencing of the PCR product to reveal the source organism. Significant organisms were detected in 19% of cases by culture, whilst 69% of cases were PCR positive. Of the six culture positive samples, five were PCR positive and the organism identified was identical using both techniques. The organism not detected by PCR was grown only after enrichment culture and was present at levels below the PCR detection limit. The presence of organisms detected by PCR but not culture was probably because of prior antibiotic treatment. The PCR negative cases had also all received antibiotic therapy, causing organism death and DNA degradation.

Molecular (non-culture) techniques improve organism identification from pleural fluid in children with empyema, even after commencement of antibiotics, but should be considered complementary to culture. This assay produces a result in 48 hours, allowing appropriate alterations in management soon within the inpatient stay.

T H Chapman

Senior Clinical Fellow, Royal Free Hospital, London, UK; timothy.chapman@royalfree.nhs.uk

High COVID-19 Attack Rate Among Attendees at Events at a Church — Arkansas, March 2020

Allison James, DVM, PhD^{1,2}; Lesli Eagle¹; Cassandra Phillips¹; D. Stephen Hedges, MPH¹; Cathie Bodenhamer¹; Robin Brown, MPAS, MPH¹; J. Gary Wheeler, MD¹; Hannah Kirking, MD³

On May 19, 2020, this report was posted as an MMWR Early Release on the MMWR website (<https://www.cdc.gov/mmwr>).

On March 16, 2020, the day that national social distancing guidelines were released (1), the Arkansas Department of Health (ADH) was notified of two cases of coronavirus disease 2019 (COVID-19) from a rural county of approximately 25,000 persons; these cases were the first identified in this county. The two cases occurred in a husband and wife; the husband is the pastor at a local church (church A). The couple (the index cases) attended church-related events during March 6–8, and developed nonspecific respiratory symptoms and fever on March 10 (wife) and 11 (husband). Before his symptoms had developed, the husband attended a Bible study group on March 11. Including the index cases, 35 confirmed COVID-19 cases occurred among 92 (38%) persons who attended events held at church A during March 6–11; three patients died. The age-specific attack rates among persons aged ≤18 years, 19–64 years, and ≥65 years were 6.3%, 59.4%, and 50.0%, respectively. During contact tracing, at least 26 additional persons with confirmed COVID-19 cases were identified among community members who reported contact with church A attendees and likely were infected by them; one of the additional persons was hospitalized and subsequently died. This outbreak highlights the potential for widespread transmission of SARS-CoV-2, the virus that causes COVID-19, both at group gatherings during church events and within the broader community. These findings underscore the opportunity for faith-based organizations to prevent COVID-19 by following local authorities' guidance and the U.S. Government's Guidelines: Opening Up America Again (2) regarding modification of activities to prevent virus transmission during the COVID-19 pandemic.

On March 10 and 11, the wife of the church pastor, aged 56 years, and the pastor, aged 57 years, developed fever and cough. On March 12, the pastor, after becoming aware of similar nonspecific respiratory symptoms among members of their congregation, closed church A indefinitely. Because of fever, cough, and increasing shortness of breath, the couple sought testing for SARS-CoV-2 on March 13; both were notified of positive results by reverse transcription–polymerase chain reaction testing on March 16. The same day, ADH staff members began an investigation to identify how the couple had been exposed and to trace persons with whom they had been in contact. Based on their activities and onset dates, they likely were infected at

church A events during March 6–8, and the husband might have then exposed others while presymptomatic during a Bible study event held on March 11.

During March and April 2020, all persons in Arkansas who received testing for SARS-CoV-2 at any laboratory were entered into a database (Research Electronic Data Capture [REDCap]; version 8.8.0; Vanderbilt University) managed by ADH. Using a standardized questionnaire, ADH staff members interviewed persons who had positive test results to ascertain symptoms, onset date, and potential exposure information, including epidemiologic linkages to other COVID-19 patients; this information was stored in the database. Close contacts of patients with laboratory-confirmed cases of COVID-19 were interviewed and enrolled in active symptom monitoring; those who developed symptoms were tested and their information was also entered into the database. Church A–associated cases were defined as those in 1) persons who had laboratory results positive for SARS-CoV-2 who identified contact with church A attendees as a source of exposure and 2) actively monitored contacts of church attendees who had a test result positive for SARS-CoV-2 after becoming symptomatic.

The public health investigation focused on the transmission of SARS-CoV-2 among persons who attended church A events during March 6–11. To facilitate the investigation, the pastor and his wife generated a list of 94 church members and guests who had registered for, or who, based on the couple's recollection, might have attended these events.

During March 6–8, church A hosted a 3-day children's event which consisted of two separate 1.5-hour indoor sessions (one on March 6 and one on March 7) and two, 1-hour indoor sessions during normal church services on March 8. This event was led by two guests from another state. During each session, children participated in competitions to collect offerings by hand from adults, resulting in brief close contact among nearly all children and attending adults. On March 7, food prepared by church members was served buffet-style. A separate Bible study event was held March 11; the pastor reported most attendees sat apart from one another in a large room at this event. Most children and some adults participated in singing during the children's event; no singing occurred during the March 11 Bible study. Among all 94 persons who might have attended any of the events, 19 (20%) attended both the children's event and Bible study.

Summary**What is already known about this topic?**

Large gatherings pose a risk for SARS-CoV-2 transmission.

What is added by this report?

Among 92 attendees at a rural Arkansas church during March 6–11, 35 (38%) developed laboratory-confirmed COVID-19, and three persons died. Highest attack rates were in persons aged 19–64 years (59%) and ≥65 years (50%). An additional 26 cases linked to the church occurred in the community, including one death.

What are the implications for public health practice?

Faith-based organizations should work with local health officials to determine how to implement the U.S. Government guidelines for modifying activities during the COVID-19 pandemic to prevent transmission of the virus to their members and their communities.

The husband and wife were the first to be recognized by ADH among the 35 patients with laboratory-confirmed COVID-19 associated with church A attendance identified through April 22; their illnesses represent the index cases. During the investigation, two persons who were symptomatic (not the husband and wife) during March 6–8 were identified; these are considered the primary cases because they likely initiated the chain of transmission among church attendees. Additional cases included those in persons who attended any church A events during March 6–11, but whose symptom onset occurred on or after March 8, which was 2 days after the earliest possible church A exposure. One asymptomatic attendee who sought testing after household members became ill was included among these additional cases.

Consistent with CDC recommendations for laboratory testing at that time (3), clinical criteria for testing included cough, fever, or shortness of breath; asymptomatic persons were not routinely tested. To account for this limitation when calculating attack rates, upper and lower boundaries for the attack rates were estimated by dividing the total number of persons with laboratory-confirmed COVID-19 by the number of persons tested for SARS-CoV-2 and by the number of persons who attended church A during March 6–11, respectively. All analyses were performed using R statistical software (version 4.0.0; The R Foundation). Risk ratios were calculated to compare attack rates by age, sex, and attendance dates. Fisher's exact test was used to calculate two-sided p-values; p-values <0.05 were considered statistically significant.

Overall, 94 persons attended church A events during March 6–11 and might have been exposed to the index patients or to another infectious patient at the same event; among these persons, 92 were successfully contacted and are included in the analysis. Similar proportions of church A attendees were

aged ≤18 years (35%), 19–64 years (35%), and ≥65 years (30%) (Table 1). However, a higher proportion of adults aged 19–64 years and ≥65 years were tested (72% and 50%, respectively), and received positive test results (59% and 50%), than did younger persons. Forty-five persons were tested for SARS-CoV-2, among whom 35 (77.8%) received positive test results (Table 2).

During the investigation, two church A participants who attended the March 6–8 children's event were found to have had onset of symptoms on March 6 and 7; these represent the primary cases and likely were the source of infection of other church A attendees (Figure). The two out-of-state guests developed respiratory symptoms during March 9–10 and later received diagnoses of laboratory-confirmed COVID-19, suggesting that exposure to the primary cases resulted in their infections. The two primary cases were not linked except through the church; the persons lived locally and reported no travel and had no known contact with a traveler or anyone with confirmed COVID-19. Patient interviews revealed no additional common exposures among church attendees.

The estimated attack rate ranged from 38% (35 cases among all 92 church A event attendees) to 78% (35 cases among 45 church A event attendees who were tested for SARS-CoV-2). When stratified by age, attack rates were significantly lower among persons aged ≤18 years (6.3%–25.0%) than among adults aged 19–64 years (59.4%–82.6%) ($p<0.01$). The risk ratios for persons aged ≤18 years compared with those for persons aged 19–64 years were 0.1–0.3. No severe illnesses occurred in children. Among the 35 persons with laboratory-confirmed COVID-19, seven (20%) were hospitalized; three (9%) patients died.

At least 26 additional confirmed COVID-19 cases were identified among community members who, during contact tracing, reported contact with one or more of the 35 church A members with COVID-19 as an exposure. These persons likely were infected by church A attendees. Among these 26 persons, one was hospitalized and subsequently died. Thus, as of April 22, 61 confirmed cases (including eight [13%] hospitalizations and four [7%] deaths) had been identified in persons directly and indirectly associated with church A events.

Discussion

This investigation identified 35 confirmed COVID-19 cases among 92 attendees at church A events during March 6–11; estimated attack rates ranged from 38% to 78%. Despite canceling in-person church activities and closing the church as soon as it was recognized that several members of the congregation had become ill, widespread transmission within church A and within the surrounding community occurred. The primary patients had no known COVID-19 exposures in

TABLE 1. Demographic characteristics, church A event attendance, and SARS-CoV-2 testing status of persons who attended church A events where persons with confirmed COVID-19 (N = 92) also attended — Arkansas, March 2020

Characteristic	All attendees No. (%) [*]	No. (%) tested [†]	p-value [§]	No. (%) who tested positive [†]	p-value [§]
Total	92 (100)	45 (49)	—	35 (38)	—
Age group (yrs)					
≤18	32 (35)	8 (25)	0.001	2 (6)	0.004
18–64	32 (35)	23 (72)		19 (59)	
≥65	28 (30)	14 (50)		14 (50)	
Sex					
Male	44 (48)	22 (50)	1.0	17 (39)	1.0
Female	48 (52)	23 (48)		18 (38)	
Church A event attendance					
Weekend only (Mar 6–8)	64 (70)	33 (52)	0.28	28 (44)	0.16
Bible study only (Mar 11)	9 (10)	2 (22)		1 (11)	
Both weekend and Bible study	19 (21)	10 (53)		6 (32)	

Abbreviation: COVID-19 = coronavirus disease 2019.

^{*} Includes all persons who were confirmed to have attended church A events during March 6–11; percentages are column percentages.

[†] Percentage of attendees (row percentages).

[§] Calculated with Fisher's exact test.

TABLE 2. Estimated attack rates of COVID-19 among attendees at church A events — Arkansas, March 6–11, 2020

Characteristic	All Mar 6–11 church A attendees (lower bound)			All tested Mar 6–11 church A attendees (upper bound)		
	No. of cases/no. exposed (%)	Risk ratio (95% CI)	p-value	No. of cases/no. tested (%)	Risk ratio (95% CI)	p-value
Overall	35/92 (38.0)	—	—	35/45 (77.8)	—	—
Age group (yrs)						
≤18	2/32 (6.3)	0.1 (0.03–0.4)	<0.001	2/8 (25.0)	0.3 (0.1–1.0)	0.003
19–64	19/32 (59.4)	Referent	—	19/23 (82.6)	Referent	—
≥65	14/28 (50.0)	0.8 (0.5–1.3)	0.47	14/14 (100.0)	1.2 (1.0–1.5)	0.10
Sex						
Male	17/44 (38.6)	1.0 (0.6–1.7)	0.91	17/22 (77.3)	1.0 (0.7–1.3)	0.94
Female	18/48 (37.5)	Referent	—	18/23 (78.3)	Referent	—
Church A event attendance						
Weekend only (Mar 6–8)	28/64 (43.8)	1.4 (0.7–2.8)	0.3	28/33 (84.8)	1.4 (0.8–2.4)	0.09
Bible study only (Mar 11)	1/9 (11.1)	0.4 (0.05–2.5)	0.25	1/2 (50.0)	1.7 (0.4–6.8)	0.21
Both weekend and Bible study	6/19 (31.6)	Referent	—	6/10 (60.0)	Referent	—

Abbreviations: CI = confidence interval; COVID-19 = coronavirus disease 2019.

the 14 days preceding their symptom onset dates, suggesting that local transmission was occurring before case detection.

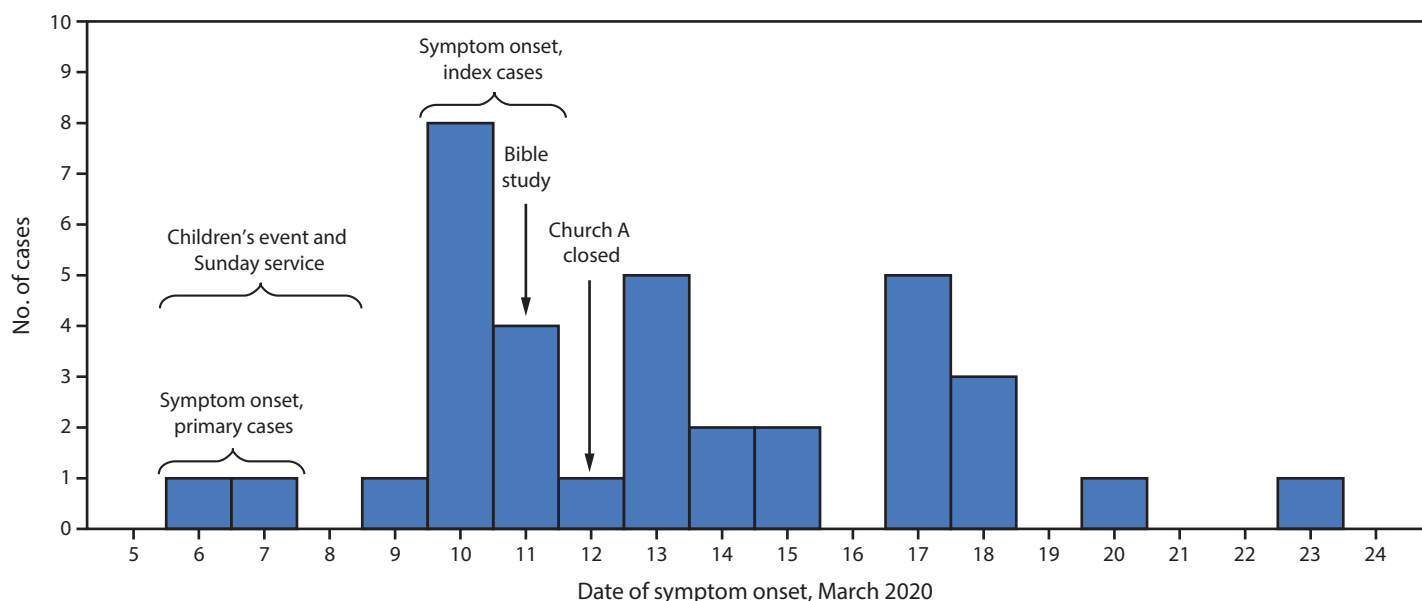
Children represented 35% of all church A attendees but accounted for only 18% of persons who received testing and 6% of confirmed cases. These findings are consistent with those from other reports suggesting that many children with COVID-19 experience more asymptomatic infections or milder symptoms and have lower hospitalization rates than do adults (4,5). The role of asymptomatic or mildly symptomatic children in SARS-CoV-2 transmission remains unknown and represents a critical knowledge gap as officials consider reopening public places.

The risk for symptomatic infection among adults aged ≥65 years was not higher than that among adults aged 19–64 years. However, six of the seven hospitalized persons and all three deaths occurred in persons aged ≥65 years, consistent with other U.S. data indicating a higher risk for

COVID-19–associated hospitalization and death among persons aged ≥65 years (6).

The findings in this report are subject to at least four limitations. First, some infected persons might have been missed because they did not seek testing, were ineligible for testing based on criteria at the time, or were unable to access testing. Second, although no previous cases had been reported from this county, undetected low-level community transmission was likely, and some patients in this cluster might have had exposures outside the church. Third, risk of exposure likely varied among attendees but could not be characterized because data regarding individual behaviors (e.g., shaking hands or hugging) were not collected. Finally, the number of cases beyond the cohort of church attendees likely is undercounted because tracking out-of-state transmission was not possible, and patients might not have identified church members as their source of exposure.

FIGURE. Date of symptom onset* among persons with laboratory-confirmed cases of COVID-19 (N = 35) who attended March 6–11 church A events — Arkansas, March 6–23, 2020



Abbreviation: COVID-19 = coronavirus disease 2019.

* One asymptomatic person who had a positive test result is included on the date of specimen collection (March 18).

High transmission rates of SARS-CoV-2 have been reported from hospitals (7), long-term care facilities (8), family gatherings (9), a choir practice (10), and, in this report, church events. Faith-based organizations that are operating or planning to resume in-person operations, including regular services, funerals, or other events, should be aware of the potential for high rates of transmission of SARS-CoV-2. These organizations should work with local health officials to determine how to implement the U.S. Government's guidelines for modifying activities during the COVID-19 pandemic to prevent transmission of the virus to their members and their communities (2).

Acknowledgments

Members of the congregation of church A, including the pastor and his wife; Arkansas Department of Health; Suzanne Beavers, CDC; Laura Rothfeldt, Arkansas Department of Health; state and local health departments where out-of-state visitors resided.

Corresponding author: Allison E. James, hwj7@cdc.gov, 501-614-5278.

¹Arkansas Department of Health; ²Epidemic Intelligence Service, CDC; ³COVID-19 Response Team, CDC.

All authors have completed and submitted the International Committee of Medical Journal Editors form for disclosure of potential conflicts of interest. No potential conflicts of interest were disclosed.

References

1. Office of the President of the United States. Coronavirus guidelines for America. Washington, DC: Office of the President of the United States; 2020. <https://www.whitehouse.gov/briefings-statements/coronavirus-guidelines-america/>

2. Office of the President of the United States. Guidelines: opening up America again. Washington, DC: Office of the President of the United States; 2020. <https://www.whitehouse.gov/openingamerica/>
3. CDC. Health Alert Network: update and interim guidance on outbreak of coronavirus disease 2019 (COVID-19). Atlanta, GA: US Department of Health and Human Services, CDC; 2020. <https://emergency.cdc.gov/han/2020/HAN00428.asp>
4. Bialek S, Gierke R, Hughes M, McNamara LA, Pilishvili T, Skoff T; CDC COVID-19 Response Team. Coronavirus disease 2019 in children—United States, February 12–April 2, 2020. *MMWR Morb Mortal Wkly Rep* 2020;69:422–6. <https://doi.org/10.15585/mmwr.mm6914e4>
5. Dong Y, Mo X, Hu Y, et al. Epidemiology of COVID-19 among children in China. *Pediatrics* 2020. Epub March 16, 2020. <https://doi.org/10.1542/peds.2020-0702>
6. Bialek S, Boundy E, Bowen V, et al.; CDC COVID-19 Response Team. Severe outcomes among patients with coronavirus disease 2019 (COVID-19)—United States, February 12–March 16, 2020. *MMWR Morb Mortal Wkly Rep* 2020;69:343–6. <https://doi.org/10.15585/mmwr.mm6912e2>
7. Heinzerling A, Stuckey MJ, Scheuer T, et al. Transmission of COVID-19 to health care personnel during exposures to a hospitalized patient—Solano County, California, February 2020. *MMWR Morb Mortal Wkly Rep* 2020;69:472–6. <https://doi.org/10.15585/mmwr.mm6915e5>
8. McMichael TM, Currie DW, Clark S, et al. Epidemiology of Covid-19 in a long-term care facility in King County, Washington. *N Engl J Med* 2020. Epub March 27, 2020. <https://doi.org/10.1056/NEJMoa2005412>
9. Ghinai I, Woods S, Ritger KA, et al. Community transmission of SARS-CoV-2 at two family gatherings—Chicago, Illinois, February–March 2020. *MMWR Morb Mortal Wkly Rep* 2020;69:446–50. <https://doi.org/10.15585/mmwr.mm6915e1>
10. Hamner L, Dubbel P, Capron I, et al. High SARS-CoV-2 attack rate following exposure at a choir practice—Skagit County, Washington, March 2020. *MMWR Morb Mortal Wkly Rep* 2020;69:606–10. <https://doi.org/10.15585/mmwr.mm6919e6>

About the Authors

Ms. Muniz-Rodriguez is a doctoral student in epidemiology and Dr. Fung is an associate professor of epidemiology at Jiann-Ping Hsu College of Public Health, Georgia Southern University. Their research interests include infectious disease epidemiology, digital health, and disaster emergency responses.

References

1. Wood G. Coronavirus could break Iranian society [cited 2020 Feb 29]. <https://www.theatlantic.com/ideas/archive/2020/02/iran-cannot-handle-coronavirus/607150/>
2. Viboud C, Simonsen L, Chowell G. A generalized-growth model to characterize the early ascending phase of infectious disease outbreaks. *Epidemics*. 2016;15:27–37. <https://doi.org/10.1016/j.epidem.2016.01.002>
3. Banks HT, Hu S, Thompson WC. Modeling and inverse problems in the presence of uncertainty: CRC Press; 2014.
4. Chowell G, Ammon CE, Hengartner NW, Hyman JM. Transmission dynamics of the great influenza pandemic of 1918 in Geneva, Switzerland: assessing the effects of hypothetical interventions. *J Theor Biol*. 2006;241:193–204. <https://doi.org/10.1016/j.jtbi.2005.11.026>
5. Chowell G, Shim E, Brauer F, Diaz-Dueñas P, Hyman JM, Castillo-Chavez C. Modelling the transmission dynamics of acute haemorrhagic conjunctivitis: application to the 2003 outbreak in Mexico. *Stat Med*. 2006;25:1840–57. <https://doi.org/10.1002/sim.2352>
6. Vynnycky E, White RG. An introduction to infectious disease modelling. Oxford (UK): Oxford University Press; 2010.
7. Nishiura H, Linton NM, Akhmetzhanov AR. Serial interval of novel coronavirus (COVID-19) infections. *Int J Infect Dis*. 2020;93:284–6. <https://doi.org/10.1016/j.ijid.2020.02.060>
8. Tuite AR, Bogoch II, Sherbo R, Watts A, Fisman D, Khan K. Estimation of coronavirus disease 2019 (COVID-19) burden and potential for international dissemination of infection from Iran. *Ann Intern Med*. 2020. <https://doi.org/10.7326/M20-0696>

Address for correspondence: Isaac Chun-Hai Fung, Department of Biostatistics, Epidemiology and Environmental Health Sciences, Jiann-Ping Hsu College of Public Health, Georgia Southern University, PO Box 7989, Statesboro, GA 30460-7989 USA; email: cfung@georgiasouthern.edu; or Gerardo Chowell, Department of Population Health Sciences, School of Public Health, Georgia State University, Suite 662, Office 640B, Atlanta, GA 30303, USA; email: gchowell@gsu.edu.

Cluster of Coronavirus Disease Associated with Fitness Dance Classes, South Korea

Sukbin Jang, Si Hyun Han, Ji-Young Rhee

Author affiliation: Dankook University Hospital, Dankook University College of Medicine, Cheonan, South Korea

DOI: <https://doi.org/10.3201/eid2608.200633>

During 24 days in Cheonan, South Korea, 112 persons were infected with severe acute respiratory syndrome coronavirus 2 associated with fitness dance classes at 12 sports facilities. Intense physical exercise in densely populated sports facilities could increase risk for infection. Vigorous exercise in confined spaces should be minimized during outbreaks.

By April 30, 2020, South Korea had reported 10,765 cases of coronavirus disease (COVID-19) (1); ≈76.2% of cases were from Daegu and North Gyeongsang provinces. On February 25, a COVID-19 case was detected in Cheonan, a city ≈200 km from Daegu. In response, public health and government officials from Cheonan and South Chungcheong Province activated the emergency response system. We began active surveillance and focused on identifying possible COVID-19 cases and contacts. We interviewed consecutive confirmed cases and found all had participated in a fitness dance class. We traced contacts back to a nationwide fitness dance instructor workshop that was held on February 15 in Cheonan.

Fitness dance classes set to Latin rhythms have gained popularity in South Korea because of the high aerobic intensity (2). At the February 15 workshop, instructors trained intensely for 4 hours. Among 27 instructors who participated in the workshop, 8 had positive real-time reverse transcription PCR (RT-PCR) results for severe acute respiratory syndrome coronavirus 2, which causes COVID-19; 6 were from Cheonan and 1 was from Daegu, which had the most reported COVID-19 cases in South Korea. All were asymptomatic on the day of the workshop.

By March 9, we identified 112 COVID-19 cases associated with fitness dance classes in 12 different sports facilities in Cheonan (Figure). All cases were confirmed by RT-PCR; 82 (73.2%) were symptomatic and 30 (26.8%) were asymptomatic at the time of laboratory confirmation. Instructors with very mild symptoms, such as coughs, taught classes for ≈1 week after attending the workshop

RESEARCH LETTERS

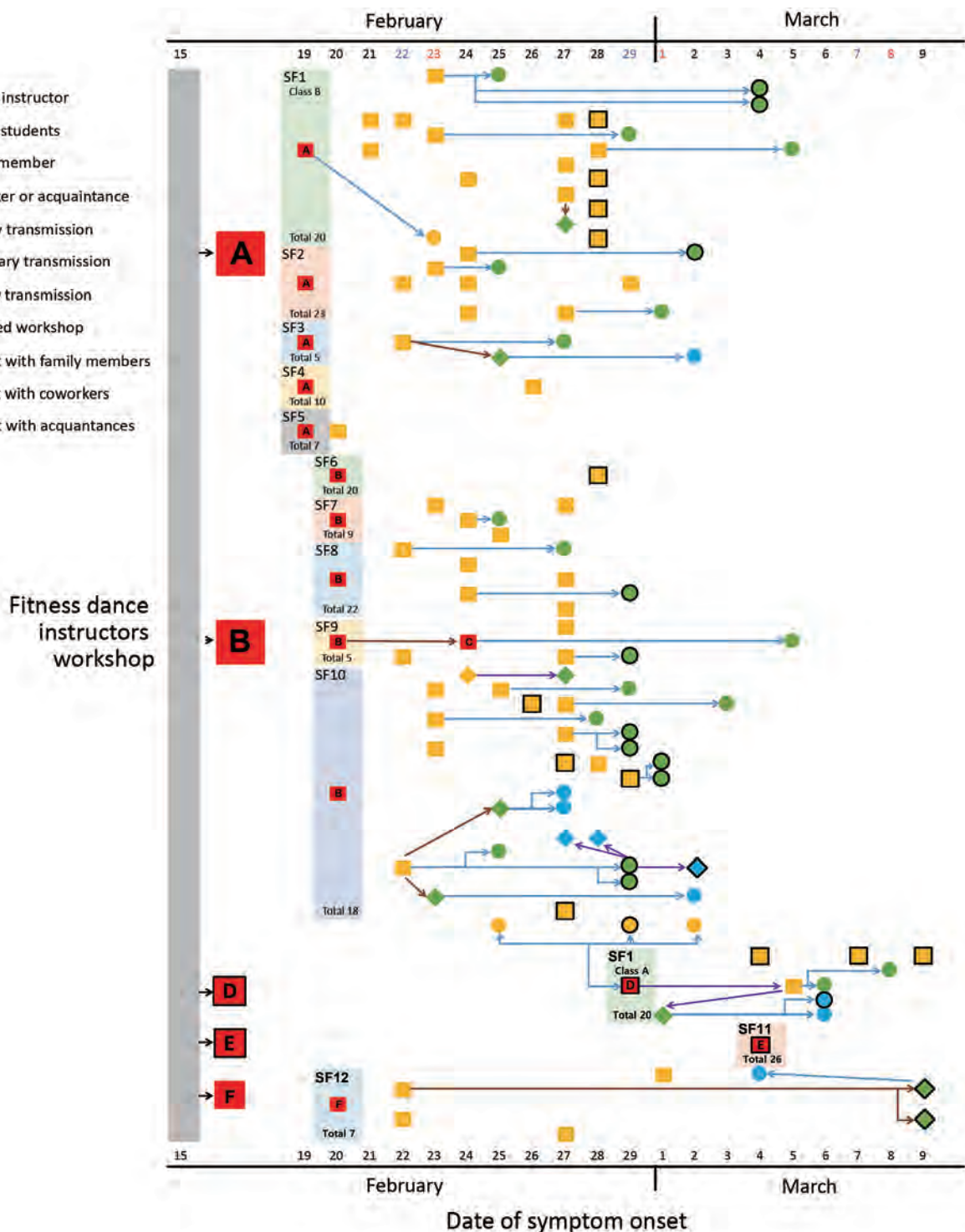


Figure. Case map of confirmed coronavirus disease (COVID-19) cases associated with fitness dance classes in Cheonan, South Korea, by date of symptom onset and relationship. Instructors outside of Cheonan are excluded. In 7 cases, transmission was suspected in the presymptomatic phase and the longest period before symptom onset was 5 days. None of the instructors had COVID-19 symptoms on the day of the workshop, but instructors from Daegu, which recently had a large outbreak, developed symptoms 3 days after the workshop. Sports facilities are represented by bars on the left with the number of students per class included. Bold outlines indicate a positive test for COVID-19 in a person in the presymptomatic phase.

(Appendix Figure 1, <https://wwwnc.cdc.gov/EID/article/26/8/20-0633.App1.pdf>). The instructors and students met only during classes, which lasted for 50 minutes 2 times per week, and did not have contact outside of class. On average, students developed symptoms 3.5 days after participating in a fitness dance class (3). Most (50.9%) cases were the result of transmission from instructors to fitness class participants; 38 cases (33.9%) were in-family transmission from instructors and students; and 17 cases (15.2%) were from transmission during meetings with co-workers or acquaintances.

Among 54 fitness class students with confirmed COVID-19, the median age was 42, all were women, and 10 (18.5%) had preexisting medical conditions (Appendix Table 1). The most common symptom at the time of admission for isolation was cough in 44.4% (24/54) of cases; 17 (31.5%) case-patients had pneumonia. The median time to discharge or end of isolation was 27.6 (range 13–66) days after symptom onset.

Before sports facilities were closed, a total of 217 students were exposed in 12 facilities, an attack rate of 26.3% (95% CI 20.9%–32.5%) (Appendix Table 2). Including family and coworkers, transmissions from the instructors accounted for 63 cases (Appendix Figure 2). We followed up on 830 close contacts of fitness instructors and students and identified 34 cases of COVID-19, translating to a secondary attack rate of 4.10% (95% CI 2.95%–5.67%). We identified 418 close contacts of 34 tertiary transmissions before the quarantine and confirmed 10 quaternary cases from the tertiary cases, translating to a tertiary attack rate of 2.39% (95% CI 1.30%–4.35%).

The instructor from Daegu who attended the February 15 workshop had symptoms develop on February 18 and might have been presymptomatic during the workshop. Evidence of transmission from presymptomatic persons has been shown in epidemiologic investigations of COVID-19 (4,5).

Characteristics that might have led to transmission from the instructors in Cheonan include large class sizes, small spaces, and intensity of the workouts. The moist, warm atmosphere in a sports facility coupled with turbulent air flow generated by intense physical exercise can cause more dense transmission of isolated droplets (6,7). Classes from which secondary COVID-19 cases were identified included 5–22 students in a room ≈ 60 m² during 50 minutes of intense exercise. We did not identify cases among classes with <5 participants in the same space. Of note, instructor C taught Pilates and yoga for classes of 7–8 students in the same facility

at the same time as instructor B (Figure; Appendix Table 2), but none of her students tested positive for the virus. We hypothesize that the lower intensity of Pilates and yoga did not cause the same transmission effects as those of the more intense fitness dance classes.

A limitation of our study is the unavailability of a complete roster of visitors to the sports facilities, which might have meant we missed infections among students during surveillance and investigation efforts. Discovery of outbreak cases centered on exercise facilities led to a survey of instructors who participated in a fitness dance workshop and provided clues to identifying additional cases among students. Early identification of asymptomatic persons with RT-PCR-confirmed infections helped block further transmissions. Because of the increased possibility of infection through droplets, vigorous exercise in closely confined spaces should be avoided (8) during the current outbreak, as should public gatherings, even in small groups (9,10).

Acknowledgments

We thank the state, local, and territorial health department personnel for providing the reported coronavirus disease data; patients in Dankook University Hospital participating in interviews and providing data; and the Dankook University College of Medicine for their support. We also thank Editage (<http://www.editage.co.kr>) for English language editing.

About the Author

Dr. Jang is a clinical assistant professor in the Division of Infectious Diseases, Department of Medicine, Dankook University Hospital. His research interests include ecology of infectious disease, hospital infection control, and trauma related infections.

References

1. Korea Centers for Disease Control and Prevention. Current status of the coronavirus disease 2019 (COVID-19) outbreak in Republic of Korea [in Korean] [cited 2020 Apr 30]. <http://ncov.mohw.go.kr>
2. Vendramin B, Bergamin M, Gobbo S, Cugusi L, Duregon F, Bullo V, et al. Health benefits of Zumba fitness training: a systematic review. *PM R*. 2016;8:1181–200. <https://doi.org/10.1016/j.pmrj.2016.06.010>
3. Korea Centers for Disease Control and Prevention. Updates on COVID-19 in Korea as of 5 March 2020 [cited 2020 Mar 5]. <https://www.cdc.go.kr/board/board.es?mid=a30402000000&bid=0030>
4. Tong ZD, Tang A, Li KF, Li P, Wang HL, Yi JP, et al. Potential presymptomatic transmission of SARS-CoV-2, Zhejiang Province, China, 2020. *Emerg Infect Dis*. 2020;26:1052–4. <https://doi.org/10.3201/eid2605.200198>

RESEARCH LETTERS

5. Arons MM, Hatfield KM, Reddy SC, Kimball A, James A, Jacobs JR, et al. Presymptomatic SARS-CoV-2 infections and transmission in a skilled nursing facility. *N Engl J Med*. 2020 Apr 24 [Epub ahead of print]. <https://doi.org/10.1056/NEJMoa2008457>
6. Bourouiba L. Turbulent gas clouds and respiratory pathogen emission: potential implications for reducing transmission of COVID-19. *JAMA*. 2020 Mar 26 [Epub ahead of print]. <https://doi.org/10.1001/jama.2020.4756>
7. van Doremalen N, Bushmaker T, Morris DH, Holbrook MG, Gamble A, Williamson BN, et al. Aerosol and surface stability of SARS-CoV-2 as compared with SARS-CoV-1. *N Engl J Med*. 2020;382:1564-7. <https://doi.org/10.1056/NEJMc2004973>
8. Andrade A, Dominski FH, Pereira ML, de Liz CM, Buonanno G. Infection risk in gyms during physical exercise. *Environ Sci Pollut Res Int*. 2018;25:19675-86. <https://doi.org/10.1007/s11356-018-1822-8>
9. Musher DM. How contagious are common respiratory tract infections? *N Engl J Med*. 2003;348:1256-66. <https://doi.org/10.1056/NEJMra021771>
10. Ebrahim SH, Memish ZA. COVID-19 - the role of mass gatherings. *Travel Med Infect Dis*. 2020 Mar 9 [Epub ahead of print]. <https://doi.org/10.1016/j.tmaid.2020.101617>

Address for correspondence: Ji-Young Rhee, Division of Infectious Diseases, Department of Medicine, Dankook University Hospital, Dankook University College of Medicine, 201 Manghang-ro, Dongnam-ku, Chungcheongnam-do, South Korea; email: pluripotent@naver.com

Infectious SARS-CoV-2 in Feces of Patient with Severe COVID-19

Fei Xiao,¹ Jing Sun,¹ Yonghao Xu,¹ Fang Li,¹ Xiaofang Huang,¹ Heying Li, Jingxian Zhao, Jicheng Huang, Jincun Zhao

Author affiliations: Sun Yat-sen University, Zhuhai, China (F. Xiao); Guangzhou Medical University, Guangzhou, China (J. Sun, Y. Xu, F. Li, X. Huang, Jingxian Zhao, Jincun Zhao); Chinese Academy of Sciences, Guangzhou (H. Li); Guangzhou Customs District Technology Center, Guangzhou (J. Huang)

DOI: <https://doi.org/10.3201/eid2608.200681>

¹These authors contributed equally to this article.

Severe acute respiratory syndrome coronavirus 2 was isolated from feces of a patient in China with coronavirus disease who died. Confirmation of infectious virus in feces affirms the potential for fecal-oral or fecal-respiratory transmission and warrants further study.

Severe acute respiratory syndrome coronavirus 2 (SARS-CoV-2) recently emerged in China, causing a major outbreak of severe pneumonia and spreading to >200 other countries (1). As of May 5, 2020, a total of 3,517,345 cases of coronavirus disease (COVID-2019) and 243,401 deaths had been reported to the World Health Organization (https://www.who.int/docs/default-source/coronaviruse/situation-reports/20200505covid-19-sitrep-106.pdf?sfvrsn=47090f63_2). The virus is believed to be spread by direct contact, fomites, respiratory droplets, and possibly aerosols (2). Viral RNA has been detected in feces and urine of some patients (3-7). Infectious virus was also isolated from urine of a patient with severe COVID-19 (8). However, it is unclear whether the virus in feces is infectious and might be an additional source for transmission.

This study was approved by the Health Commission of Guangdong Province and the Ethics Committees of Guangzhou Medical University to use patient and healthy donor sample specimens. On January 17, 2020, a 78-year-old man who had a history of recent travel to Wuhan, China, was admitted to the Fifth Affiliated Hospital of Sun Yat-Sen University because of a cough for 7 days and intermittent fever (Appendix Figure 1, panel A, <https://wwwnc.cdc.gov/EID/article/26/8/20-0681-App1.pdf>). Computed tomography of his chest showed multiple, ground-glass opacities (Appendix Figure 2). Nasopharyngeal and oropharyngeal swab specimens were positive for SARS-CoV-2 RNA by quantitative reverse transcription PCR (qRT-PCR).

On January 22, the patient's condition deteriorated and he was intubated. Ventilator-assisted breathing was instituted. The first feces specimen was collected on January 27 and was positive for viral RNA by qRT-PCR. Serial feces samples were collected on January 29, February 1, and February 7. All samples were positive for viral RNA (Appendix Figure 1, panel A). Viral antigen was also detected in gastrointestinal epithelial cells of a biopsy sample, as reported (9). The patient died on February 20.

We collected fecal specimens on January 29 to inoculate Vero E6 cells. Cycle threshold values for the fecal sample were 23.34 for the open reading frame 1lab gene and 20.82 for the nucleoprotein gene. A



Since January 2020 Elsevier has created a COVID-19 resource centre with free information in English and Mandarin on the novel coronavirus COVID-19. The COVID-19 resource centre is hosted on Elsevier Connect, the company's public news and information website.

Elsevier hereby grants permission to make all its COVID-19-related research that is available on the COVID-19 resource centre - including this research content - immediately available in PubMed Central and other publicly funded repositories, such as the WHO COVID database with rights for unrestricted research re-use and analyses in any form or by any means with acknowledgement of the original source. These permissions are granted for free by Elsevier for as long as the COVID-19 resource centre remains active.



Contents lists available at ScienceDirect

Clinical Microbiology and Infection

journal homepage: www.clinicalmicrobiologyandinfection.com

Research note

Evolution of viral quasispecies during SARS-CoV-2 infection

Aude Jary^{1,*}, Valentin Leducq¹, Isabelle Malet¹, Stéphane Marot¹, Elise Klement-Frutos², Elisa Teyssou¹, Cathia Soulié¹, Basma Abdi¹, Marc Wirten¹, Valérie Pourcher², Eric Caumes², Vincent Calvez¹, Sonia Burrel¹, Anne-Geneviève Marcelin¹, David Boutolleau¹

¹ Sorbonne Université, INSERM, Institut Pierre Louis d'Epidémiologie et de Santé Publique (iPLESP), AP-HP, Hôpital Pitié Salpêtrière, Service de Virologie, Paris, France

² Sorbonne Université, INSERM, Institut Pierre Louis d'Epidémiologie et de Santé Publique (iPLESP), AP-HP, Hôpital Pitié Salpêtrière, Service de Maladie Infectieuses et Tropicales, Paris, France

ARTICLE INFO

Article history:

Received 8 June 2020

Received in revised form

9 July 2020

Accepted 21 July 2020

Available online 24 July 2020

Editor: L. Kaiser

Keywords:

Infection follow-up

Minority variants

NGS

Quasispecies

SARS-CoV-2

ABSTRACT

Objectives: Studies are needed to better understand the genomic evolution of the recently emerged severe acute respiratory syndrome coronavirus 2 (SARS-CoV-2). This study aimed to describe genomic diversity of SARS-CoV-2 by next-generation sequencing (NGS) in a patient with longitudinal follow-up for SARS-CoV-2 infection.

Methods: Sequential samples collected between January 29th and February 4th, 2020, from a patient infected by SARS-CoV-2 were used to perform amplification of two genome fragments—including genes encoding spike, envelope, membrane and nucleocapsid proteins—and NGS was carried out with Illumina® technology. Phylogenetic analysis was performed with PhyML and viral variant identification with VarScan.

Results: Majority consensus sequences were identical in most of the samples (5/7) and differed in one synonymous mutation from the Wuhan reference sequence. We identified 233 variants; each sample harboured in median 38 different minority variants, and only four were shared by different samples. The frequency of mutation was similar between genes and correlated with the length of the gene ($r = 0.93$, $p = 0.0002$). Most of mutations were substitution variations ($n = 217$, 93.1%) and about 50% had moderate or high impact on gene expression. Viral variants also differed between lower and upper respiratory tract samples collected on the same day, suggesting independent sites of replication of SARS-CoV-2.

Conclusions: We report for the first time minority viral populations representing up to 1% during the course of SARS-CoV-2 infection. Quasispecies were different from one day to the next, as well as between anatomical sites, suggesting that *in vivo* this new coronavirus appears as a complex and dynamic distributions of variants. **Aude Jary, Clin Microbiol Infect 2020;26:1560.e1–1560.e4**

© 2020 European Society of Clinical Microbiology and Infectious Diseases. Published by Elsevier Ltd. All rights reserved.

Introduction

The genome organization in severe acute respiratory syndrome coronavirus 2 (SARS-CoV-2) is similar to that in the other beta-coronaviruses, with the open reading frame (ORF) 1a/b encoding non-structural proteins at the 5'-end, and structural proteins as follows: spike (S)—envelope (E)—membrane (M)—nucleocapsid

(NC)—3'-end [1]. Since the spike surface glycoprotein plays a major role in infection of the host cell, genomic variations may impact the interaction with the host receptor but also viral pathogenesis, transmissibility and infectivity [2].

As intra-host variants in a transversal study or from the same patient by nanopore sequencing have already been reported [3,4], this study aimed to describe genomic diversity of SARS-CoV-2 by

* Corresponding author. Aude Jary, 47–83 Boulevard de l'Hôpital, 75013, Paris, France.
E-mail address: aude.jary@aphp.fr (A. Jary).

next-generation sequencing (NGS) in a patient with longitudinal follow-up for SARS-CoV-2 infection.

Methods

The first patient diagnosed with SARS-CoV-2 infection in Pitié-Salpêtrière Hospital, Paris, France, was followed daily for SARS-CoV-2 by RT-PCR of respiratory samples; viral genome could be detected between January 29th and February 10th, 2020 [5]. This patient, hospitalized on day 2 of a mild form of coronavirus disease 2019 (Covid-19), did not receive any antiviral or immunomodulation treatment during the entire study period.

Two fragments of about 4000 nucleotides (nt) were amplified by nested PCR (Supplementary Material Table S1), and NGS was performed with paired-end reads (MiSeq v3, 2 x 300 bp) on the MiSeq Illumina® system. Reads were trimmed using Trimmomatic, then mapped on SARS-CoV-2 reference sequence (NC_045512.2) with Geneious Prime software and finally assembled *de novo* with SPAdes 3.12.0 [6] to generate majority consensus sequences.

Multiple alignment was performed with Mafft7 [7] and phylogenetic analysis of S, E, M and NC genes with PhyML3.0 [8] and GTR substitution model with 1000 bootstraps resampling.

Intra-host variants were called using VarScan [9] with the following requirements: sequencing depth ≥ 1000 , minor allele frequency $\geq 1\%$ and found at least 100 times. Intra-sample viral variants were studied by comparing each consensus sequence with

all cleaned reads generated from the same sample and viral variants during follow-up by comparing consensus sequence of the first nasopharyngeal sample (01292020_NP) with all reads generated from the different samples. Synonymous mutations were identified as having a low impact, missense mutations and insertions with conservative inframe as having a moderate impact, and acquisition or loss of stop codon as well as frameshift as having a high impact on gene expression.

The Spearman rank correlation test was performed on GraphPad.

Results

The sequencing was effective for the first seven samples (one induced sputum and six nasopharyngeal swabs) from January 29th to February 4th, 2020, with a Ct value of SARS-CoV-2 RT-PCR < 30 . A full-length fragment of 8257 nt was generated with a median (IQR) of 45 523 (41 014–46 023) depth sequencing per sample (Supplementary Material Table S2).

Phylogenetic analysis

Compared to the NC_045512.2 reference sequence, our majority consensus sequences differed in the S gene by only four variations. They all harboured the synonymous mutation 3591T > C, whereas a non-synonymous mutation (859G > A) was found only in sample

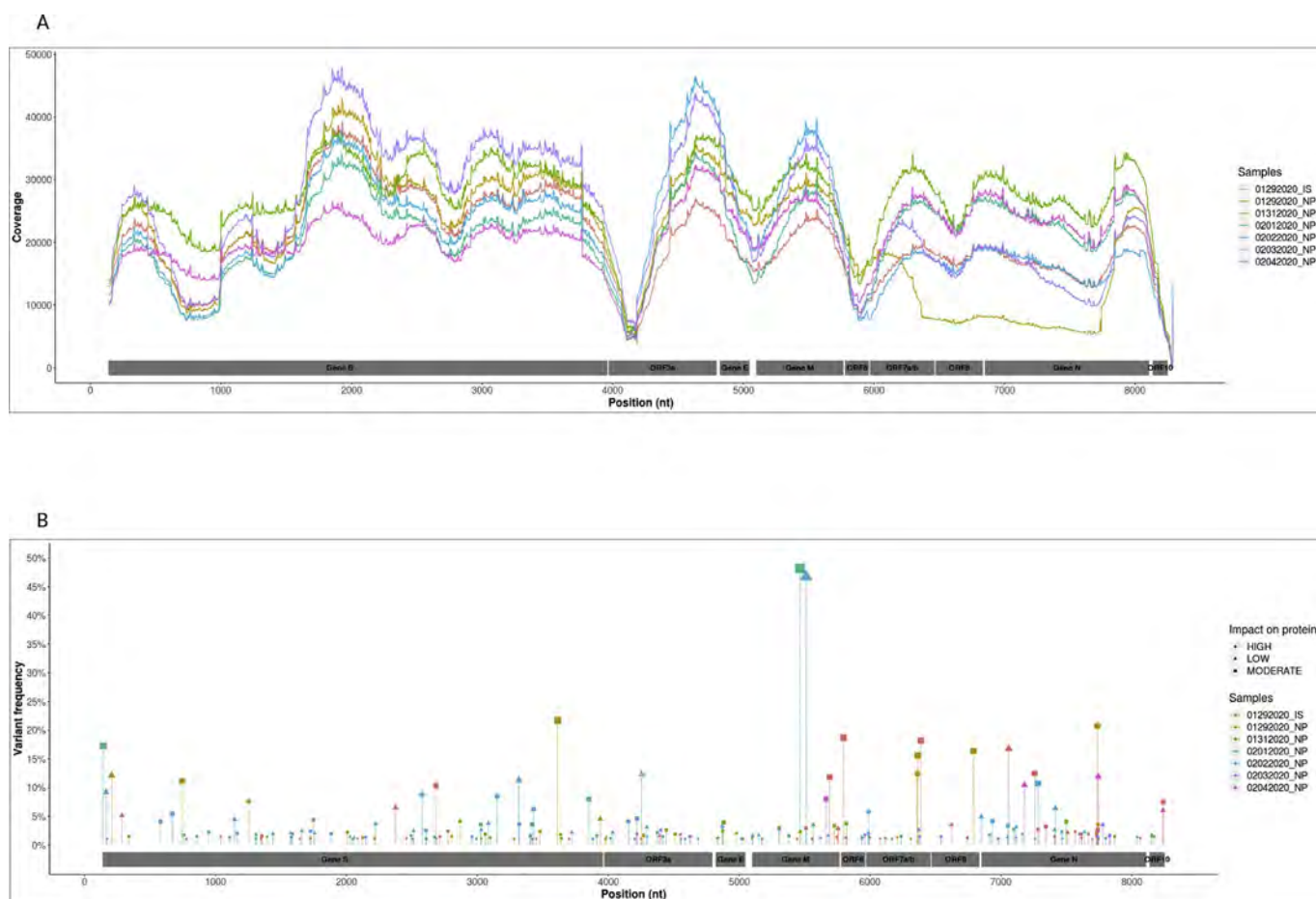


Fig. 1. The severe acute respiratory syndrome coronavirus 2 (SARS-CoV-2) genome diversity during infection. (A) Genome coverage (y axis) according to nucleotide position (x axis). (B) Distribution (x axis) and frequency (y axis) of the 233 intra-sample viral variants identified. Each sample is represented by the same colour in (A) and (B), and the impact of mutations on gene expression is represented by a different symbol (low: a rhombus, moderate: a square, high: a circle).

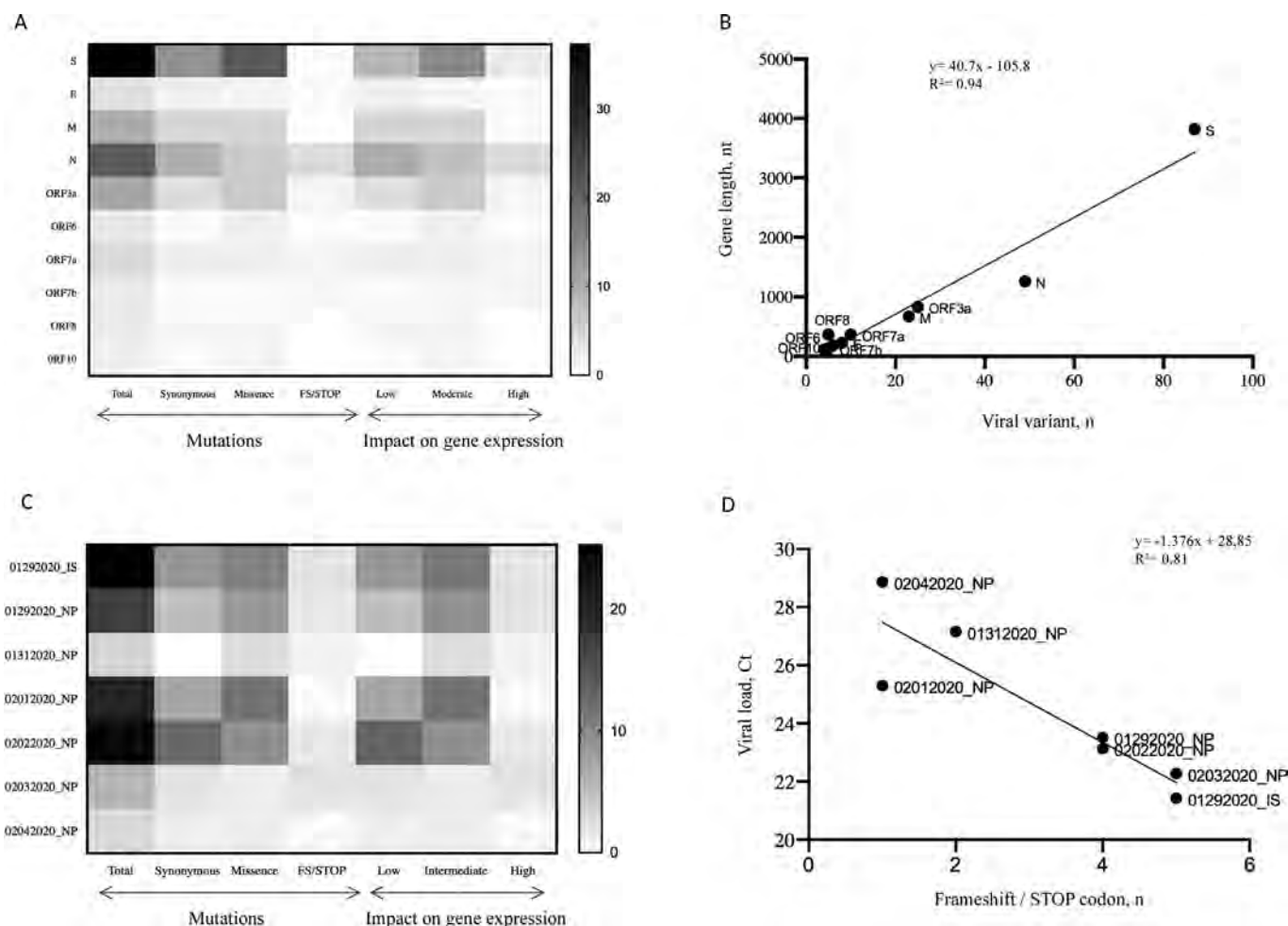


Fig. 2. Distribution of mutation frequency and correlation with gene length or viral load. (A) HeatMap representing the frequency and distribution of the mutations and their impact on gene expression between the different genes. (B) Linear regression line between the number of viral variant (x axis) and the gene length (y axis). (C) HeatMap representing the frequency and distribution of the mutations and their impact on gene expression between the different samples. (D) Linear regression line between the number of frameshift and stop codons (x axis) and the viral load expressed in cycle threshold (Ct) value (y axis). Viral variants by gene: S, $n = 87$; N, $n = 49$; ORF3a, $n = 25$; M, $n = 23$; ORF7a, $n = 10$; E, $n = 8$; ORF6, $n = 6$; ORF7b, $n = 5$; ORF8, $n = 5$; ORF10, $n = 4$. Scale on the right of (A) and (C) represents the frequency in percentages, with the largest value in dark and the lowest value in light.

02012020_NP. In sample 01312020_NP, a deletion of one nucleotide led to the appearance of a premature stop codon and a non-synonymous substitution at position 3554.

By phylogenetic analysis of the four structural genes, our sequences clustered with all the SARS-CoV-2 reference sequences issued from the NCBI database, and were distinct from the other human coronaviruses (Supplementary Material Fig. S1).

Intra-sample viral variant diversity

We identified 233 viral variants, and the number of variants per sample was not correlated with the depth sequencing ($r = 0.23$, $p = 0.28$).

Each sample harboured in median 38 (11–51.5) minority variants (<20%). Only 4/233 identical minority variants were common between two specimens, and 6/233 other mutations were identified at the same position in two samples but induced different variants (Supplementary Material Table S3). Although majority consensus sequences of the two specimens collected on January 29th were strictly identical, each one harboured their specific viral population with 59 variants identified in the induced sputum and 40 in the nasopharyngeal specimens (Fig. 1).

Nucleotide variations occurred in decreasing order in the S gene, N gene, ORF3a, M gene, ORF7a, E gene, ORF6, ORF7b and ORF8, and finally ORF10 (Fig. 2A). However, according to gene length, the frequency of mutation was similar and correlated with the length of the gene ($r = 0.93$, $p = 0.0002$) (Fig. 2B).

Most of the mutations were substitution variations (217/233), including 87/233 synonymous mutations and 107/233 missense mutations. According to gene expression, 88/233 variants had a low impact, 111/233 an intermediate impact, and 23/233 a high impact (Fig. 1). Between samples, only the frequencies of frameshift and stop codons were significantly and strongly correlated with the viral load ($r = 0.92$, $p = 0.0095$) (Fig. 2D).

Follow-up of viral variant diversity

By comparing with the consensus sequence collected on January 29th from the nasopharyngeal site, we found the same viral quasi-species in each sample as reported above. However, three majority variants emerged in the S gene obtained from the nasopharyngeal samples collected on January 31st and February 1st, corresponding to the three mutations described previously in the consensus sequences. None of them were found in the previous

and following samples as majority or minority variants (Supplementary Material Table S4).

Discussion

The virus identified in this patient was almost identical to the reference sequence from Wuhan [1]. This result was expected, as the patient was a general practitioner presumably infected by tourists from Wuhan and their guide who was later diagnosed SARS-CoV-2-positive [5].

Quasispecies in RNA viruses have previously been reported for SARS-CoV and MERS-CoV [10,11], as well as within individuals during SARS-CoV-2 infection [3,12]. The present study, allowing the analysis of SARS-CoV-2 minority variants at 1%, supports the previous finding. Indeed, we found a median of 38 different viral variants per sample during the follow-up of a single patient, with almost no common variant from one day to the next. More than half of the variants had an intermediate or high impact on gene expression and may explain the lack of persistence over time. Among the different types of mutations, the number of mutations inducing frameshift and stop codons were highly correlated with the viral load, reflecting the loss of fitness in variants harbouring deleterious mutations during intensive viral replication [13]. Otherwise, the viral variant population was also different between samples from the lower (induced sputum) and upper (nasopharyngeal swab) respiratory tract collected on the same day, suggesting independent replication of SARS-CoV-2, as previously reported [14].

Contrary to a previous study which identified a hotspot in ORF8 [15], the mutations identified in this study appeared to be spread fairly evenly throughout the sequenced fragment. Indeed, a limited number of viral variants was shared by two samples, the remainder (97%) being specific to each sample and occurring in different genomic sites, and a strong correlation was found between the number of variants and the length of each gene.

The main limitation of this study is that a fragment of only about 8000 nt was studied, in only one patient, and during a short period of follow-up because of low viral load in samples collected after February 5th. However, our results highlighted that during the first week of infection the major viral population remained identical (5/7), with several specific minority variants which did not seem to persist over time. Larger studies are needed to explore the entire intra-patient variability during the course of the infection, and in different clinical situations, to better understand the impact of the minority viral population on SARS-CoV-2 evolution, physiopathology and transmission.

Author contributions

DB, AGM, SB, VC planned the research; EKF, VP and EC collected the clinical data; VL, IM, ET and CS performed the experiments; AJ, VL, BA and MW analysed the data; AJ, SM, SB and DB wrote the paper. All the authors read and corrected the manuscript and approved the final version.

Transparency declaration

All the authors declare no competing interests. This study was funded by the Agence Nationale de Recherche sur le SIDA et les Hépatites Virales (ANRS, AC43), the Agence National de la Recherche (ANR) and Sorbonne Université.

Ethics

The study was carried out in accordance with the Declaration of Helsinki. It was a retrospective non-interventional study with no addition to standard care procedures. Reclassification of biological remnants into research material after completion of the ordered virological tests was approved by the local interventional review board of Pitié-Salpêtrière Hospital. According to the French Public Health Code (CSP Article L.1121-1.1) such protocols are exempted from individual informed consent.

Acknowledgements

We thank the SMIT PSL COVID cohort Team for its support.

Appendix A. Supplementary data

Supplementary data to this article can be found online at <https://doi.org/10.1016/j.cmi.2020.07.032>.

References

- [1] Chan JF-W, Kok K-H, Zhu Z, Chu H, To KK-W, Yuan S, et al. Genomic characterization of the 2019 novel human-pathogenic coronavirus isolated from a patient with atypical pneumonia after visiting Wuhan. *Emerg Microbe. Infect* 2020;9:221–36. <https://doi.org/10.1080/22221751.2020.1719902>.
- [2] Fung TS, Liu DX. Human coronavirus: host–pathogen interaction. *Annu Rev Microbiol* 2019;73:529–57. <https://doi.org/10.1146/annurev-micro-020518-115759>.
- [3] Shen Z, Xiao Y, Kang L, Ma W, Shi L, Zhang L, et al. Genomic diversity of SARS-CoV-2 in coronavirus disease 2019 patients. *Clin Infect Dis* 2020. <https://doi.org/10.1093/cid/ciaa203>.
- [4] To KK-W, Tsang OT-Y, Leung W-S, Tam AR, Wu T-C, Lung DC, et al. Temporal profiles of viral load in posterior oropharyngeal saliva samples and serum antibody responses during infection by SARS-CoV-2: an observational cohort study. *Lancet Infect Dis* 2020;20:565–74. [https://doi.org/10.1016/S1473-3099\(20\)30196-1](https://doi.org/10.1016/S1473-3099(20)30196-1).
- [5] Klement E, Godefroy N, Burrell S, Kornblum D, Monsel G, Bleibtreu A, et al. The first locally acquired novel case of 2019-nCoV infection in a healthcare worker in the Paris area. *Clin Infect Dis* 2020. <https://doi.org/10.1093/cid/ciaa171>.
- [6] Bankevich A, Nurk S, Antipov D, Gurevich AA, Dvorkin M, Kulikov AS, et al. SPAdes: a new genome assembly algorithm and its applications to single-cell sequencing. *J Comput Biol* 2012;19:455–77. <https://doi.org/10.1089/cmb.2012.0021>.
- [7] Katoh K, Standley DM. MAFFT multiple sequence alignment software version 7: improvements in performance and usability. *Mol Biol Evol* 2013;30:772–80. <https://doi.org/10.1093/molbev/mst010>.
- [8] Guindon S, Dufayard J-F, Lefort V, Anisimova M, Hordijk W, Gascuel O. New algorithms and methods to estimate maximum-likelihood phylogenies: assessing the performance of PhyML 3.0. *Syst Biol* 2010;59:307–21. <https://doi.org/10.1093/sysbio/syq010>.
- [9] Koboldt DC, Zhang Q, Larson DE, Shen D, McLellan MD, Lin L, et al. VarScan 2: somatic mutation and copy number alteration discovery in cancer by exome sequencing. *Genome Res* 2012;22:568–76. <https://doi.org/10.1101/gr.129684.111>.
- [10] Xu D, Zhang Z, Wang F-S. SARS-associated coronavirus quasispecies in individual patients. *N Engl J Med* 2004;350:1366–7. <https://doi.org/10.1056/NEJMc032421>.
- [11] Park D, Huh HJ, Kim YJ, Son D-S, Jeon H-J, Im E-H, et al. Analysis of inpatient heterogeneity uncovers the microevolution of Middle East respiratory syndrome coronavirus. *Cold Spring Harb Mol Case Stud* 2016;2:a001214. <https://doi.org/10.1101/mcs.a001214>.
- [12] Capobianchi MR, Rueca M, Messina F, Giombini E, Carletti F, Colavita F, et al. Molecular characterization of SARS-CoV-2 from the first case of COVID-19 in Italy. *Clin Microbiol Infect* 2020;26:954–6. <https://doi.org/10.1016/j.cmi.2020.03.025>.
- [13] Domingo E, Holland JJ. RNA virus mutations and fitness for survival. *Annu Rev Microbiol* 1997;51:151–78. <https://doi.org/10.1146/annurev.micro.51.1.151>.
- [14] Wölfel R, Corman VM, Guggemos W, Seilmaier M, Zange S, Müller MA, et al. Virological assessment of hospitalized patients with COVID-2019. *Nature* 2020. <https://doi.org/10.1038/s41586-020-2196-x>.
- [15] Ceraolo C, Giorgi FM. Genomic variance of the 2019-nCoV coronavirus. *J Med Virol* 2020;92:522–8. <https://doi.org/10.1002/jmv.25700>.



JAMA Netw Open. 2021 Jan; 4(1): e2035057.


PMCID: PMC7791354

Published online 2021 Jan 7.

PMID: 33410879

doi: 10.1001/jamanetworkopen.2020.35057: 10.1001/jamanetworkopen.2020.35057

SARS-CoV-2 Transmission From People Without COVID-19 Symptoms

[Michael A. Johansson](#), PhD,^{1,2} [Talia M. Quandelacy](#), PhD, MPH,¹ [Sarah Kada](#), PhD,¹ [Pragati Venkata Prasad](#), MPH,¹ [Molly Steele](#), PhD, MPH,¹ [John T. Brooks](#), MD,¹ [Rachel B. Slayton](#), PhD, MPH,^{1,2} [Matthew Biggerstaff](#), ScD, MPH,^{1,2} and [Jay C. Butler](#), MD² 

¹COVID-19 Response, US Centers for Disease Control and Prevention, Atlanta, Georgia

²Office of the Deputy Directory for Infectious Diseases, US Centers for Disease Control and Prevention, Atlanta, Georgia

 Corresponding author.

Article Information

Accepted for Publication: December 7, 2020.

Published: January 7, 2021. doi:10.1001/jamanetworkopen.2020.35057

Open Access: This is an open access article distributed under the terms of the [CC-BY License](#). © 2021 Johansson MA et al. *JAMA Network Open*.

Corresponding Author: Jay C. Butler, MD, Office of the Deputy Director for Infectious Diseases, US Centers for Disease Control and Prevention, 1600 Clifton Rd, Mailstop H24-12, Atlanta, GA 30329 (jcb3@cdc.gov).

Author Contributions: Dr Johansson had full access to all of the data in the study and takes responsibility for the integrity of the data and the accuracy of the data analysis.

Concept and design: Johansson, Quandelacy, Kada, Brooks, Slayton, Butler.

Acquisition, analysis, or interpretation of data: All authors.

Drafting of the manuscript: Johansson, Quandelacy, Brooks, Biggerstaff, Butler.

Critical revision of the manuscript for important intellectual content: Johansson, Kada, Prasad, Steele, Brooks, Slayton, Biggerstaff, Butler.

Statistical analysis: Johansson, Quandelacy, Kada.

Administrative, technical, or material support: Prasad, Steele, Brooks, Biggerstaff, Butler.

Supervision: Johansson, Butler.

Conflict of Interest Disclosures: None reported.

Funding/Support: This work was performed as part of the US Centers for Disease Control and Prevention's coronavirus disease 2019 response and was supported solely by federal base and response funding.

Role of the Funder/Sponsor: The funder had no role in the design and conduct of the study; collection, management, analysis, and interpretation of the data; preparation, review, or approval of the manuscript; and decision to submit the manuscript for publication.

Disclaimer: The findings and conclusions in this report are those of the authors and do not necessarily represent the views of the Centers for Disease Control and Prevention.

Received 2020 Oct 26; Accepted 2020 Dec 7.

[Copyright](#) 2021 Johansson MA et al. *JAMA Network Open*.

This is an open access article distributed under the terms of the CC-BY License.

Key Points

Question

What proportion of coronavirus disease 2019 (COVID-19) spread is associated with transmission of severe acute respiratory syndrome coronavirus 2 (SARS-CoV-2) from persons with no symptoms?

Findings

In this decision analytical model assessing multiple scenarios for the infectious period and the proportion of transmission from individuals who never have COVID-19 symptoms, transmission from asymptomatic individuals was estimated to account for more than half of all transmission.

Meaning

The findings of this study suggest that the identification and isolation of persons with symptomatic COVID-19 alone will not control the ongoing spread of SARS-CoV-2.

Abstract

Importance

Severe acute respiratory syndrome coronavirus 2 (SARS-CoV-2), the etiology of coronavirus disease 2019 (COVID-19), is readily transmitted person to person. Optimal control of COVID-19 depends on directing resources and health messaging to mitigation efforts that are most likely to prevent transmission, but the relative importance of such measures has been disputed.

Objective

To assess the proportion of SARS-CoV-2 transmissions in the community that likely occur from persons without symptoms.

Design, Setting, and Participants

This decision analytical model assessed the relative amount of transmission from presymptomatic, never symptomatic, and symptomatic individuals across a range of scenarios in which the proportion of transmission from people who never develop symptoms (ie, remain asymptomatic) and the infectious period were varied according to published best estimates. For all estimates, data from a meta-analysis was used to set the incubation period at a median of 5 days. The infectious period duration was maintained at 10 days, and peak infectiousness was varied between 3 and 7 days (−2 and +2 days relative to the median incubation period). The overall proportion of SARS-CoV-2 was varied between 0% and 70% to assess a wide range of possible proportions.

Main Outcomes and Measures

Level of transmission of SARS-CoV-2 from presymptomatic, never symptomatic, and symptomatic individuals.

Results

The baseline assumptions for the model were that peak infectiousness occurred at the median of symptom onset and that 30% of individuals with infection never develop symptoms and are 75% as infectious as those who do develop symptoms. Combined, these baseline assumptions imply that persons with infection who never develop symptoms may account for approximately 24% of all transmission. In this base case, 59% of all transmission came from asymptomatic transmission, comprising 35% from presymptomatic individuals and 24% from individuals who never develop symptoms. Under a broad range of values for each of these assumptions, at least 50% of new SARS-CoV-2 infections was estimated to have originated from exposure to individuals with infection but without symptoms.

Conclusions and Relevance

In this decision analytical model of multiple scenarios of proportions of asymptomatic individuals with COVID-19 and infectious periods, transmission from asymptomatic individuals was estimated to account for more than half of all transmissions. In addition to identification and isolation of persons with symptomatic COVID-19, effective control of spread will require reducing the risk of transmission from people with infection who do not have symptoms. These findings suggest that measures such as wearing masks, hand hygiene, social distancing, and strategic testing of people who are not ill will be foundational to slowing the spread of COVID-19 until safe and effective vaccines are available and widely used.

Introduction

As severe acute respiratory syndrome coronavirus 2 (SARS-CoV-2), the novel coronavirus that causes coronavirus disease 2019 (COVID-19), began to spread globally, it became apparent that the virus, unlike the closely related SARS-CoV in the 2003 outbreak, could not be contained by symptom-based screening alone. Asymptomatic and clinically mild infections were uncommon during the 2003 SARS-CoV outbreak, and there were no reported instances of transmission from persons before the onset of symptoms.¹ SARS-CoV-2 spread faster than SARS-CoV, and accumulating evidence showed that SARS-CoV-2, unlike SARS-CoV, is transmitted from persons without symptoms. However, measures to reduce transmission from individuals who do not have COVID-19 symptoms have become controversial and politicized and have likely had negative effects on the economy and many societal activities. Optimal control of COVID-19 depends on directing resources and health messaging to mitigation efforts that are most likely to prevent transmission. The relative importance of mitigation measures that prevent transmission from persons without symptoms has been disputed. Determining the proportion of SARS-CoV-2 transmission that occurs from persons without symptoms is foundational to prioritizing control practices and policies.

Transmission by persons who are infected but do not have any symptoms can arise from 2 different infection states: presymptomatic individuals (who are infectious before developing symptoms) and individuals who never experience symptoms (asymptomatic infections, which we will refer to as never symptomatic). Early modeling studies of COVID-19 case data found that the generation interval of SARS-CoV-2 was shorter than the serial interval, indicating that the average time between 1 person being infected and that person infecting someone else was shorter than the average time between 1 person developing symptoms and the person they infected developing symptoms.^{2,3,4,5} This finding meant that the epidemic was growing faster than would be expected if transmission were limited to the period of illness during which individuals were symptomatic. By the time a second generation of individuals was developing

symptoms, a third generation was already being infected. Epidemiological data from early in the pandemic also suggested the possibility of presymptomatic transmission,^{6,7} and laboratory studies confirmed that levels of viral RNA in respiratory secretions were already high at the time of symptom onset.^{8,9,10}

Asymptomatic SARS-CoV-2 transmission also occurs because of individuals with infection who are never symptomatic (or who experience very mild or almost unrecognizable symptoms). The proportion of individuals with infection who never have apparent symptoms is difficult to quantify because it requires intensive prospective clinical sampling and symptom screening from a representative sample of individuals with and without infection. Nonetheless, evidence from household contact studies indicates that asymptomatic or very mild symptomatic infections occur,^{11,12,13,14} and laboratory and epidemiological evidence suggests that individuals who never develop symptoms may be as likely as individuals with symptoms to transmit SARS-CoV-2 to others.^{9,15,16}

Methods

The Centers for Disease Control and Prevention determined that this decision analytical study, which involved no enrollment of human subjects, did not require institutional review board approval. We used a simple model to assess the proportion of transmission from presymptomatic (ie, infectious before symptom onset), never symptomatic, and symptomatic individuals across a range of scenarios in which we varied the timing of the infectious period to assess different contributions of presymptomatic transmission and the proportion of transmission from individuals who never develop symptoms (ie, remain asymptomatic).

For all estimates we used data from a meta-analysis of 8 studies from China to set the incubation period at a median of 5 days with 95% of symptomatic individuals developing symptoms by day 12.¹⁷ Therefore the daily (t) probability of symptom onset (p_{so}) for individuals who develop symptoms was:

$$p_{so}(t) = F_{Log-Normal}(t, \logmean = 1.63, \logsd = 0.5).$$

To approximate a distribution of the infectious period, we made a baseline assumption that peak infectiousness occurs on average at the same time as the median incubation period, such that infectiousness begins prior to symptom onset (Table).^{9,12,14,15,16,18,20} We then assumed that infectiousness (I) over time can be approximated by a γ density function and that the average person is infectious for as long as approximately 10 days (ie, 98% of transmission happens within a 10-day period)¹¹:

$$I(t) = f_{\gamma}(t, \text{mode} = 5, \text{interval} = 10).$$

For all estimates, we maintained the infectious period duration as 10 days, but varied the mode between 3 and 7 days (−2 and +2 days relative to the median incubation period).

Uncertainty also remains about the proportion of individuals with infection who are never symptomatic (p_{ns}) and the relative contribution of these infections to transmission (r_{ns}). Estimates of p_{ns} range from single digits to more than 50%, many with potential biases related to the study population (eg, age, prevalence of comorbidities) and the extent of long-term follow-up^{12,13,14,19,20} (Table). We made a baseline assumption that 30% of individuals with infection are never symptomatic and then assessed higher or lower assumptions. We also made a baseline assumption that individuals with asymptomatic infections are on average 75% as infectious as those with symptomatic infections.^{9,15,16} Combined, these baseline assumptions imply that persons with infection who never develop symptoms may account for approximately 24% of all transmission (T):

$$T_{ns} = p_{ns} \times r_{ns} / (p_{ns} \times r_{ns} + [1 - p_{ns}]).$$

We varied this overall proportion, T_{ns} , between 0% and 70% to assess a wide range of possible proportions. The daily proportion of transmission from individuals after symptom onset (T_s) was therefore:

$$T_s(t) = (1 - T_{ns}) \times p_{so}(t) \times I(t),$$

and the daily proportion of transmission from presymptomatic (T_{ps}) individuals, ie, those who develop symptoms but become infectious prior to symptom onset, is:

$$T_{ps}(t) = 1 - T_s(t) - T_{ns}.$$

We modified baseline assumptions to consider the relative importance of different levels of never symptomatic and presymptomatic transmission. Code is available in the eAppendix in the [Supplement](#).

Statistical Analysis

All analyses were conducted in R version 4.0.1 (R Project for Statistical Computing). No statistical testing was conducted, so no prespecified level of significance was set.

Results

Under baseline assumptions, approximately 59% of all transmission came from asymptomatic transmission: 35% from presymptomatic individuals and 24% from individuals who are never symptomatic ([Figure 1](#)). Because each component is uncertain, we assessed different timings of peak infectiousness relative to illness onset and different proportions of transmission from individuals who never have symptoms. Maintaining the 24% of transmission from individuals who never have symptoms, but shifting peak infectiousness 1 day earlier (to day 4) increased presymptomatic transmission to 43% and all asymptomatic transmission to 67% ([Figure 1A](#)). A later peak (ie, day 6) decreased presymptomatic to 27% and all asymptomatic transmission to 51% ([Figure 1C](#)).

Holding the day of peak infectiousness constant at day 5 and decreasing the proportion of transmission from individuals who are never symptomatic to 10% with a relative infectiousness of 75% (baseline assumption), the proportion of all transmission from those who are never symptomatic decreased to 8%, presymptomatic transmission increased to 42%, and combined asymptomatic transmission was 50% of all transmission ([Figure 1D](#)). In contrast, if the proportion of those who ever develop symptoms was 30% and their relative infectiousness increased to 100%, they contributed 30% of all transmission, presymptomatic transmission was 32%, and combined asymptomatic transmission was 62% of all transmission ([Figure 1F](#)).

Uncertainty remains regarding the magnitude of both presymptomatic and never symptomatic transmission. Therefore, we analyzed a wider range of each of these components, with peak infectiousness varying between 2 days before (more presymptomatic transmission) to 2 days after (less presymptomatic transmission) median symptom onset and with never symptomatic transmission ranging from 0% to 70% ([Figure 2](#)). Under this broader range of scenarios, most combined assumptions of peak infectiousness timing and transmission from individuals who never have symptoms indicated that at least 50% of new SARS-CoV-2 infections likely originated from individuals without symptoms at the time of transmission. If more than 30% of transmission was from individuals who never have symptoms, total asymptomatic transmission was higher than 50% with any value of peak infectiousness, up to 2 days after the median time of symptom onset. If peak infectiousness was at any point approximately 6 hours before median symptom onset time, more than 50% of transmission was from individuals without symptoms, regardless

of the proportion from those who never have symptoms. Even a very conservative assumption of peak infectiousness 2 days post–median onset and 0% never symptomatic transmission still resulted in more than 25% of transmission from asymptomatic individuals.

Discussion

The findings presented here complement an earlier assessment²¹ and reinforce the importance of asymptomatic transmission: across a range of plausible scenarios, at least 50% of transmission was estimated to have occurred from persons without symptoms. This overall proportion of transmission from presymptomatic and never symptomatic individuals is key to identifying mitigation measures that may be able to control SARS-CoV-2. For example, if the reproduction number (R) in a given setting is 2.0, then at least a 50% reduction in transmission is needed to drive the reproductive number below 1.0. Given that in some settings R is likely much greater than 2 and more than half of transmissions may come from individuals who are asymptomatic at the time of transmission, effective control must mitigate transmission risk from people without symptoms.

Limitations

This study has limitations. First, we used a simplistic model to represent a complex phenomenon, ie, the average infectiousness of SARS-CoV-2 infections over time. We used this model deliberately to test assumptions about the timing of peak infectiousness and transmission among asymptomatic individuals so that we could vary only these 2 critical parameters and assess their relative effects. Therefore, these results lack quantitative precision, but they demonstrate the qualitative roles of these 2 components and show that across broad ranges of possible assumptions, the finding that asymptomatic transmission is a critical component of SARS-CoV-2 transmission dynamics remains constant.

As discussed here, the exact proportions of presymptomatic and never symptomatic transmission are not known. This also applies to the incubation period estimates, which are based on individual exposure and onset windows that are difficult to observe with precision and therefore include substantial uncertainty even when leveraging estimates across multiple studies. Moreover, they likely vary substantially in different populations. For example, older individuals are more likely than younger persons to experience symptoms,²⁰ so in populations of older individuals, never asymptomatic transmission may be less important. However, specific age groups are rarely exclusively isolated from other age groups, so asymptomatic transmission risk is still important in those groups and even more so in younger age groups, in which transmission may be even more dominated by asymptomatic transmission.²⁰

Real-world transmission dynamics are also not entirely dependent on the individual-level dynamics of infectiousness over time. Now that COVID-19 is widely recognized, individuals with COVID-19 symptoms are more likely to isolate themselves and further reduce the proportion of transmission from symptomatic individuals, shifting a greater proportion of transmission to those who do not have symptoms. In this sense, the estimates here represent the lower end of the proportion of asymptomatic transmission in the presence of interventions to reduce symptomatic transmission.

Conclusions

Under a range of assumptions of presymptomatic transmission and transmission from individuals with infection who never develop symptoms, the model presented here estimated that more than half of transmission comes from asymptomatic individuals. In the absence of effective and widespread use of therapeutics or vaccines that can shorten or eliminate infectivity, successful control of SARS-CoV-2 cannot rely solely on identifying and isolating symptomatic cases; even if implemented effectively, this strategy would be insufficient. These findings suggest that effective control also requires reducing the risk of transmission from people with infection who do not have symptoms. Measures such as mask wearing

and social distancing empower individuals to protect themselves and, if infected, to reduce risk to their communities.²¹ These measures can also be supplemented by strategic testing of people who are not ill, such as those who have exposures to known cases (eg, contact tracing) or are at high risk of exposing others (eg, congregate facility staff, those with frequent contact with the public). Multiple measures that effectively address transmission risk in the absence of symptoms are imperative to control SARS-CoV-2.

Notes

Supplement.

eAppendix. Code for Analysis

References

1. Peiris JS, Yuen KY, Osterhaus AD, Stöhr K. The severe acute respiratory syndrome. *N Engl J Med*. 2003;349(25):2431-2441. doi:10.1056/NEJMra032498 [PubMed: 14681510] [CrossRef: 10.1056/NEJMra032498]
2. Tindale LC, Stockdale JE, Coombe M, et al. . Evidence for transmission of COVID-19 prior to symptom onset. *Elife*. 2020;9:e57149. doi:10.7554/eLife.57149 [PMCID: PMC7386904] [PubMed: 32568070] [CrossRef: 10.7554/eLife.57149]
3. Nishiura H, Linton NM, Akhmetzhanov AR. Serial interval of novel coronavirus (COVID-19) infections. *Int J Infect Dis*. 2020;93:284-286. doi:10.1016/j.ijid.2020.02.060 [PMCID: PMC7128842] [PubMed: 32145466] [CrossRef: 10.1016/j.ijid.2020.02.060]
4. Zhao S, Gao D, Zhuang Z, et al. . Estimating the serial interval of the novel coronavirus disease (COVID-19): a statistical analysis using the public data in Hong Kong from January 16 to February 15, 2020. *Front Phys*. Published online September 17, 2020. doi:10.3389/fphy.2020.00347 [CrossRef: 10.3389/fphy.2020.00347]
5. Du Z, Xu X, Wu Y, Wang L, Cowling BJ, Meyers LA. Serial interval of COVID-19 among publicly reported confirmed cases. *Emerg Infect Dis*. 2020;26(6):1341-1343. doi:10.3201/eid2606.200357 [PMCID: PMC7258488] [PubMed: 32191173] [CrossRef: 10.3201/eid2606.200357]
6. Wei WE, Li Z, Chiew CJ, Yong SE, Toh MP, Lee VJ. Presymptomatic transmission of SARS-CoV-2—Singapore, January 23–March 16, 2020. *MMWR Morb Mortal Wkly Rep*. 2020;69(14):411-415. doi:10.15585/mmwr.mm6914e1 [PMCID: PMC7147908] [PubMed: 32271722] [CrossRef: 10.15585/mmwr.mm6914e1]
7. Tong Z-D, Tang A, Li K-F, et al. . Potential presymptomatic transmission of SARS-CoV-2, Zhejiang Province, China, 2020. *Emerg Infect Dis*. 2020;26(5):1052-1054. doi:10.3201/eid2605.200198 [PMCID: PMC7181913] [PubMed: 32091386] [CrossRef: 10.3201/eid2605.200198]
8. He X, Lau EHY, Wu P, et al. . Temporal dynamics in viral shedding and transmissibility of COVID-19. *Nat Med*. 2020;26(5):672-675. doi:10.1038/s41591-020-0869-5 [PubMed: 32296168] [CrossRef: 10.1038/s41591-020-0869-5]
9. Lee S, Kim T, Lee E, et al. . Clinical course and molecular viral shedding among asymptomatic and symptomatic patients with SARS-CoV-2 infection in a community treatment center in the Republic of Korea. *JAMA Intern Med*. 2020. doi:10.1001/jamainternmed.2020.3862 [PMCID: PMC7411944] [PubMed: 32780793] [CrossRef: 10.1001/jamainternmed.2020.3862]

10. Benefield AE, Skrip LA, Clement A, Althouse RA, Chang S, Althouse BM. SARS-CoV-2 viral load peaks prior to symptom onset: a systematic review and individual-pooled analysis of coronavirus viral load from 66 studies. *medRxiv*. Preprint published online September 30, 2020. doi:10.1101/2020.09.28.20202028 [CrossRef: 10.1101/2020.09.28.20202028]
11. Byrne AW, McEvoy D, Collins AB, et al. . Inferred duration of infectious period of SARS-CoV-2: rapid scoping review and analysis of available evidence for asymptomatic and symptomatic COVID-19 cases. *BMJ Open*. 2020;10(8):e039856. doi:10.1136/bmjopen-2020-039856 [PMCID: PMC7409948] [PubMed: 32759252] [CrossRef: 10.1136/bmjopen-2020-039856]
12. Oran DP, Topol EJ. Prevalence of asymptomatic SARS-CoV-2 infection : a narrative review. *Ann Intern Med*. 2020;173(5):362-367. doi:10.7326/M20-3012 [PMCID: PMC7281624] [PubMed: 32491919] [CrossRef: 10.7326/M20-3012]
13. Poletti P, Tirani M, Cereda D, et al. . Probability of symptoms and critical disease after SARS-CoV-2 infection. *arXiv*. Preprint published online June 22, 2020. Accessed December 10, 2020. <https://arxiv.org/abs/2006.08471>
14. Buitrago-Garcia D, Egli-Gany D, Counotte MJ, et al. . Occurrence and transmission potential of asymptomatic and presymptomatic SARS-CoV-2 infections: a living systematic review and meta-analysis. *PLoS Med*. 2020;17(9):e1003346. doi:10.1371/journal.pmed.1003346 [PMCID: PMC7508369] [PubMed: 32960881] [CrossRef: 10.1371/journal.pmed.1003346]
15. Chaw L, Koh WC, Jamaludin SA, Naing L, Alikhan MF, Wong J. Analysis of SARS-CoV-2 transmission in different settings, Brunei. *Emerg Infect Dis*. 2020;26(11):2598-2606. doi:10.3201/eid2611.202263 [PMCID: PMC7588541] [PubMed: 33035448] [CrossRef: 10.3201/eid2611.202263]
16. Mc Evoy D, McAloon CG, Collins AB, et al. . The relative infectiousness of asymptomatic SARS-CoV-2 infected persons compared with symptomatic individuals: a rapid scoping review. *medRxiv*. Preprint published online August 1, 2020. doi:10.1101/2020.07.30.20165084 [CrossRef: 10.1101/2020.07.30.20165084]
17. McAloon C, Collins Á, Hunt K, et al. . Incubation period of COVID-19: a rapid systematic review and meta-analysis of observational research. *BMJ Open*. 2020;10(8):e039652. doi:10.1136/bmjopen-2020-039652 [PMCID: PMC7430485] [PubMed: 32801208] [CrossRef: 10.1136/bmjopen-2020-039652]
18. Casey M, Griffin J, McAloon CG, et al. . Pre-symptomatic transmission of SARS-CoV-2 infection: a secondary analysis using published data. *medRxiv*. Preprint published online June 11, 2020. doi:10.1101/2020.05.08.20094870 [CrossRef: 10.1101/2020.05.08.20094870]
19. Byambasuren O, Dobler CC, Bell K, et al. . Comparison of seroprevalence of SARS-CoV-2 infections with cumulative and imputed COVID-19 cases: systematic review. *medRxiv*. Preprint published online October 22, 2020. doi:10.1101/2020.07.13.20153163 [CrossRef: 10.1101/2020.07.13.20153163]
20. Davies NG, Klepac P, Liu Y, Prem K, Jit M, Eggo RM; CMMID COVID-19 working group . Age-dependent effects in the transmission and control of COVID-19 epidemics. *Nat Med*. 2020;26(8):1205-1211. doi:10.1038/s41591-020-0962-9 [PubMed: 32546824] [CrossRef: 10.1038/s41591-020-0962-9]
21. US Centers for Disease Control and Prevention Things to know about the COVID-19 pandemic. Updated December 4, 2020. Accessed December 10, 2020. <https://www-cdc.gov.uml.idm.oclc.org/coronavirus/2019-ncov/your-health/need-to-know.html>

Figures and Tables

Table.**Key Assumptions and Evidence Informing Those Assumptions**

Source	Evidence base	Estimate or assumption
Assumptions for presymptomatic transmission		
Peak infectiousness relative to onset, d		
Casey et al, 2020 ¹⁸	Range, 17 studies	−3 to 1.2 d
Assumed baseline	NA	0 d
Assumed range	NA	−2 to 2 d
Assumptions for never symptomatic transmission		
Proportion never symptomatic		
Oran et al, 2020 ¹²	Inferred range, 16 studies	30% to 45%
Buitrago-Garcia et al, 2020 ¹⁴	Meta-estimate, 7 studies	26% to 37%
Davies et al, 2020 ²⁰	Age-dependent estimate, 6 studies	20% to 70%
Assumed baseline	NA	30%
Relative infectiousness of individuals who never have symptoms		
Lee et al, 2020 ⁹	303 patients, assessment of viral shedding	Approximately 100%
Chaw et al, 2020 ¹⁵	1701 secondary contacts	40% to 140%
Mc Evoy et al, 2020 ¹⁶	Inferred range, 6 studies	40% to 70%
Assumed baseline		75%
Overall proportion of individuals who never have symptoms transmission		
Assumed range	NA	0% to 70%

Abbreviation: NA, not applicable.

Figure 1.**The Contribution of Asymptomatic Transmission Under Different Infection Profiles**

The top curve in each panel represents the average relative hourly infectiousness, such that while the lower curves change under different assumptions, the total hourly infectiousness equals 1 in all cases. Within each curve, the colored area indicates the proportion of transmission from each class of individuals. The portion attributed to individuals with symptoms (light blue) can also be interpreted as the maximum proportion of transmission that can be controlled by immediate isolation of all symptomatic cases. Panels A, B, and C show different levels of presymptomatic transmission. We calibrated infectiousness to peak at day 4 (A), 5 (B; median incubation period), or 6 (C) days. Panels D, E, and F show different proportions of transmission from individuals who are never symptomatic: 8% (C; eg, 10% never symptomatic and 75% relative infectivity), 24% (D; baseline, 30% never symptomatic and 75% relative infectivity), and 30% (E; eg, 30% never symptomatic and 100% relative infectivity).

Figure 2.**Combined Transmission From Individuals Who Are Presymptomatic and Those Who Never Have Symptoms**

Colors indicate the proportion of transmission due to all individuals without symptoms at the time of transmission, including presymptomatic transmission (x-axis, the timing of peak infectiousness relative to symptom onset) and transmission from individuals who are never symptomatic (y-axis). For example, peak infectiousness at the same time as median symptom onset (0 days difference) with 10% of transmission from individuals who never have symptoms would mean that approximately 51% of transmission is from asymptomatic individuals.

Epidemiologic Evidence for Airborne Transmission of SARS-CoV-2 during Church Singing, Australia, 2020

Anthea L. Katelaris, Jessica Wells, Penelope Clark, Sophie Norton, Rebecca Rockett, Alicia Arnott, Vitali Sintchenko, Stephen Corbett, Shopna K. Bag

An outbreak of severe acute respiratory syndrome coronavirus 2 infection occurred among church attendees after an infectious chorister sang at multiple services. We detected 12 secondary case-patients. Video recordings of the services showed that case-patients were seated in the same section, up to 15 m from the primary case-patient, without close physical contact, suggesting airborne transmission.

The circumstances under which airborne transmission of severe acute respiratory syndrome coronavirus 2 (SARS-CoV-2) might occur are uncertain (1,2). Previous cluster reports have suggested involvement of airborne transmission (3,4), but clear epidemiologic evidence is lacking. We investigated a SARS-CoV-2 outbreak in a church in Sydney, New South Wales, Australia, and reviewed the epidemiologic and environmental findings to assess the possibility of airborne transmission of SARS-CoV-2.

The Study

On July 18, 2020, the Western Sydney Public Health Unit was notified of a positive SARS-CoV-2 test result for an 18-year-old man (PCR cycle threshold [C_t] values: envelope gene 14.5, nucleocapsid gene 16.8). He had sought testing the day before, after learning of a SARS-CoV-2 exposure at a venue he attended on July 11. He reported symptom onset of malaise and headache on July 16 and cough and fever on July 17. He

was a church chorist and, during his infectious period (from 48 hours before onset), had sung at four 1-hour services, 1 each on July 15 and 16 and 2 on July 17.

The case-patient had sung from a choir loft, elevated 3.5 m above the congregation, which he entered before and left after the service. He denied touching objects in the church or mixing with the general congregation. Video recordings of the services corroborated this history. We identified close contacts according to the national coronavirus disease (COVID-19) control guidelines at the time (5): anyone who had spent >15 min face-to-face or shared a closed space for 2 hours with a case-patient during the infectious period of the case-patient. Initially, 10 other chorists and staff were classified as close contacts and required to quarantine (5).

On July 18, the church informed the community about the case-patient, prompting testing among members. On July 20, the Western Sydney Public Health Unit was notified of 2 additional case-patients who reported attendance on July 15 and 16. Neither was known by the primary case-patient.

Because transmission was deemed likely to have occurred at these services, we classified all attendees of the 4 services as close contacts, required to quarantine, and requested to seek baseline SARS-CoV-2 testing regardless of symptoms (in addition to if symptoms developed). Public health staff telephoned attendees (identified by mandatory service sign-in records), released alerts through the church and media, and established a testing clinic on-site. Close contacts were contacted every 2–3 days to inquire about symptoms and advised to retest if symptoms developed.

We identified 508 close contacts across the 4 services (Table), of which 434 (85%) were recorded as having a test within 17 days after exposure. Most contacts were tested 2–7 days after exposure (Appendix Figure 1,

Author affiliations: Western Sydney Local Health District, Sydney, New South Wales, Australia (A. Katelaris, J. Wells, P. Clark, S. Norton, S. Corbett, S.K. Bag); The University of Sydney, Sydney (S. Norton, R. Rockett, A. Arnott, V. Sintchenko, S. Corbett, S.K. Bag); New South Wales Health Pathology, Westmead, New South Wales, Australia (R. Rockett, A. Arnott, V. Sintchenko)

DOI: <https://doi.org/10.3201/eid2706.210465>

Table. Number of SARS-CoV-2 close contacts and case-patients in an outbreak in a church, by service date, Australia, 2020*

Date of service, July	No. contacts†	No. tested‡	Proportion tested, %	No. cases	Secondary attack rate, %
15	215	169	79	5	2.3
16	120	108	90	7§	5.8
17 (2 services)	173	157	91	(1§)	NC
Total	508	434	85	12	2.4

*SARS-CoV-2, severe acute respiratory syndrome coronavirus 2; NC, not calculated.

†Contacts identified through church service sign-in records and staff lists. This procedure might slightly underestimate the number of contacts because some persons might not have signed in and some telephone numbers were illegible or invalid.

‡Contacts were tested within 17 d (14-d incubation period plus 3 d) of the last exposure date. Pathology providers in New South Wales, Australia, routinely report SARS-CoV-2 test results (positive or negative) to public health authorities. This number would not include tests performed under a different name or spelling to that on the sign-in records.

§One case-patient attended 2 services on July 16 and 17. Because of the absence of additional case-patients on July 17, we have attributed exposure of this case-patient to have been on July 16.

<https://wwwnc.cdc.gov/EID/article/27/6/21-0465-App1.pdf>.

We detected 12 secondary case-patients among 508 service attendees, yielding an overall secondary attack rate (SAR) of 2.4% across the 4 services (Table). Five case-patients attended only the service on July 15 (SAR 5/215, 2.3%), and 7 attended only on July 16 (SAR 7/120, 5.8%). One case-patient who attended on July 16 also attended on July 17; however, no case-patients were identified who attended only a service on July 17. Secondary case-patients showed development of symptoms 2–12 days after exposure (Figure 1). Five of the secondary case-patients were from the same households as earlier cluster case-patients. Thus, these case-patients might have been infected within the household rather than the church. No secondary case-patients reported other SARS-CoV-2 exposures outside these services. There were no deaths, although 3 case-patients were hospitalized, including 2 who required intensive care.

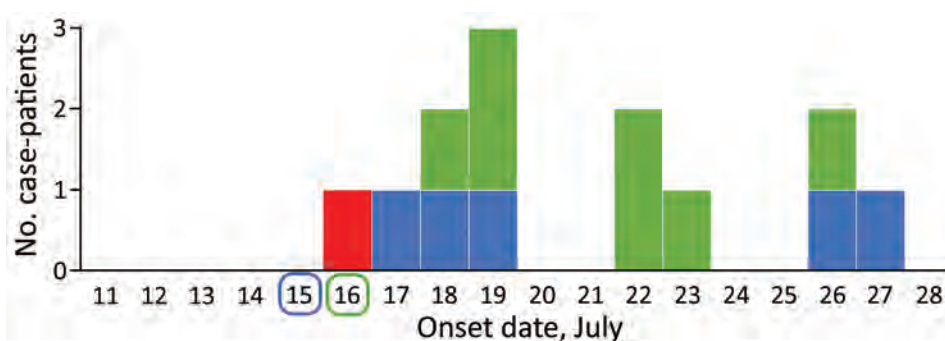
SARS-CoV-2 genome sequencing was performed for the primary case-patient and 10 secondary case-patients (6). These case-patients formed a single genomic cluster with a maximum of 2 nt changes from the SARS-CoV-2 genome of the primary case-patient (Appendix Figure 2). High C_t values for the remaining 2 case-patients prohibited sequencing.

To further characterize exposures, we determined the seating positions of secondary case-patients within the church. We asked case-patients to describe where they sat, and the video recordings of the services were reviewed, jointly with the case-patients where possible, to confirm locations.

The church was round, and pews were located circumferentially. We were able to locate the exact location of 10 of the 12 secondary case-patients by using the recordings. The remaining 2 case-patients (case-patients 3 and 4) were unable to review the recordings but described the section and row in which they sat. All secondary case-patients sat within a 70° section, below and 1–15 m from the primary case-patient (Figure 2). The primary case-patient faced away from this area, and used a microphone. Cases were not detected in attendees seated in other sections, and the spatial clustering remains if the 5 potentially household-acquired case-patients are excluded (case-patients 7, 8, 10, 12, and 13). None of the other choristers showed symptoms or tested positive for SARS-CoV-2. Use of masks was not in place.

To understand the ventilation, we conducted 2 site visits with the building manager. The church had a high conical roof, and the ventilation system at the apex was not in operating during the services. The doors and windows were largely closed, except

Figure 1. Epidemiologic curve of an outbreak of infection with severe acute respiratory syndrome coronavirus 2 in a church, Australia, 2020. Red indicates symptom onset date for the index case-patient, who sang at 4 services on July 15–17; secondary case-patient symptom onset dates are color coded by date of service attendance as indicated along baseline (1 secondary case-patient attended services on July 16 and 17). The 5 case-patients with onsets of July 22–26 also had exposures to earlier outbreak case-patients in their households.



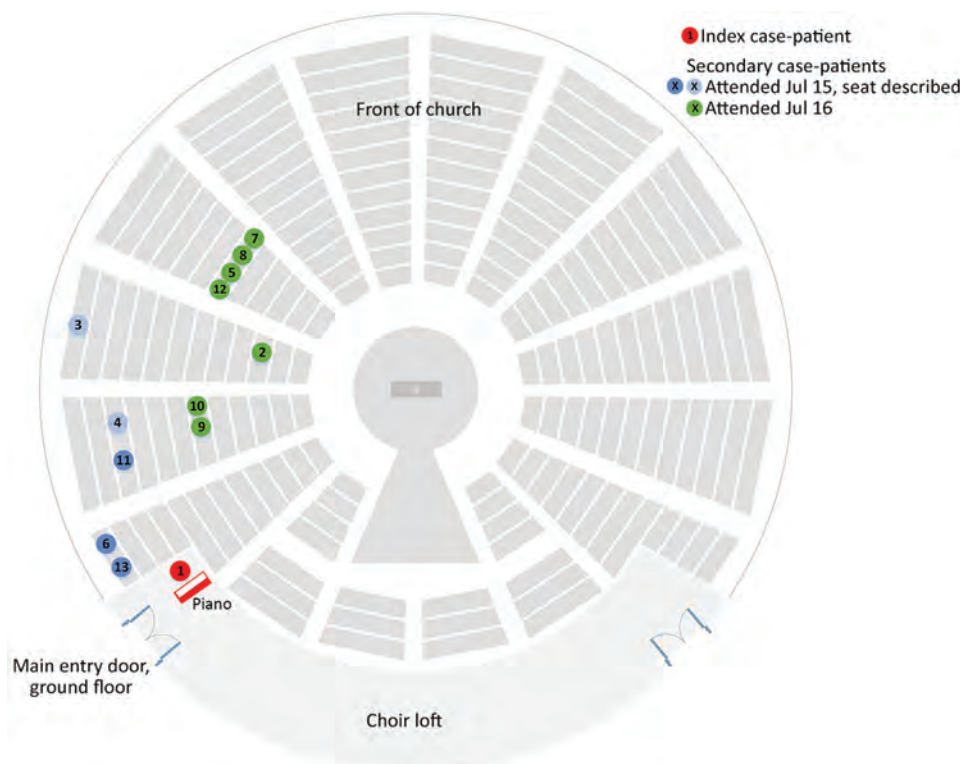


Figure 2. Schematic diagram of church layout showing seating locations of primary and secondary case-patients during an outbreak of infection with severe acute respiratory syndrome coronavirus 2, Australia, 2020. Case numbers are based on order of notification received by the Public Health Unit. Location of case-patients indicated in green and dark blue were confirmed on video recordings; the 2 case-patients indicated in light blue described their locations. The primary case-patient was located in an elevated loft ≈ 3 m above ground level. He was singing and playing the piano throughout the services and faced toward the piano. Other members of the congregation were seated throughout all sections of the church during the 4 services. Relatively more persons were seated in the front area of the church than in the sides or back.

as persons entered and exited, and the wall fans were off, meaning there was minimal ventilation.

Conclusions

We detected 12 secondary case-patients linked to an infectious case-patient at church services on 2 days. Secondary case-patients were seated in the same area of the church, up to 15 m from the primary case-patient, with whom there was no evidence of close physical contact. We believe that transmission during this outbreak is best explained by airborne spread, potentially the result of 3 factors. First, singing has been demonstrated to generate more respiratory aerosol particles and droplets than talking (7). Second, minimal ventilation might have enabled respiratory particles to accumulate in the air, and convection currents might have carried particles toward the pews where secondary case-patients were seated. Third, the primary case-patient was likely near the peak of infectiousness on the basis of low C_t values (8) and symptom onset occurring around the exposure dates (9). Although we cannot completely exclude fomite transmission, this transmission would not explain the spatial clustering of case-patients within the church over 2 days.

Strengths of our investigation include detailed case and contact follow-up, availability of video recordings of the services to confirm movements and

locations of case-patients, high uptake of testing by contacts, and that SARS-CoV-2 genome sequencing provided supportive evidence that case-patients were closely related genomically. In addition, the New South Wales context of low community transmission (10) and high estimated case ascertainment (11) makes it unlikely that case-patients acquired infection outside this cluster.

A limitation was that most contacts were tested within a week of exposure, which could have been too early to detect some asymptomatic infections. Second, this investigation only provides circumstantial evidence of airborne transmission, and does not help elucidate the exact mechanism of spread. Finally, we are unsure why transmission did not occur at the services on July 17 (except in 1 possible instance); reasons might be related to altered air flow, the primary case-patient being past peak infectiousness, or that cases that did occur went undetected.

This cluster occurred despite adherence to guidelines requiring microphone use and a 3-m cordon around singers. Guidelines for places of worship were tightened after this cluster was detected, including increasing the distance required around a singer to 5 m. However additional mitigation measures might be necessary to prevent airborne infection during church services and singing, including increased natural or artificial ventilation (12) or moving activities outdoors.

Acknowledgments

We thank the case-patients, church management, and wider church community for their participation and support during the outbreak management and investigations; Jennifer Paterson, Jennifer Lampard, Stephen Crone, and the Public Health Unit surge team for assistance with case and contact tracing; Kate Ward, Duleepa Jayasundara, and the Institute of Clinical Pathology and Medical Research, New South Wales Health Pathology for their contributions to the study; Aneliese Goodwin, Clement Lee, Carl Banting, Connie Lam, Karen-Ann Gray, Eby Sim, Elena Martinez, Mailie Gall, Jenny Draper, Rosemarie Sadsad, Andrew Ginn, and Qinning Wang for performing genome sequencing and bioinformatic analysis; and the New South Wales Ministry of Health Public Health Response Branch for its participation in the study.

About the Author

Dr. Katelaris is a public health physician and field epidemiologist in the Western Sydney Local Health District Public Health Unit, Sydney, New South Wales, Australia. Her primary research interests include communicable disease control, infectious disease epidemiology, and outbreak investigation.

References

- Centers for Disease Control and Prevention. Scientific brief: SARS-CoV-2 and potential airborne transmission; 2020 [cited 2020 Dec 19]. <https://www.cdc.gov/coronavirus/2019-ncov/more/scientific-brief-sars-cov-2.html>
- Wilson N, Corbett S, Tovey E. Airborne transmission of covid-19. *BMJ*. 2020;370:m3206. <https://doi.org/10.1136/bmj.m3206>
- Lu J, Yang Z. COVID-19 outbreak associated with air conditioning in restaurant, Guangzhou, China, 2020. *Emerg Infect Dis*. 2020;26:2791–3. <https://doi.org/10.3201/eid2611.203774>
- Hamner L, Dubbel P, Capron I, Ross A, Jordan A, Lee J, et al. High SARS-CoV-2 attack rate following exposure at a choir practice – Skagit County, Washington, March 2020. *MMWR Morb Mortal Wkly Rep*. 2020;69:606–10. <https://doi.org/10.15585/mmwr.mm6919e6>
- Australian Government Department of Health. Coronavirus disease 2019 (COVID-19) communicable diseases network Australia (CDNA) national guidelines interim advice to public health units, COVID-19, version 3.4. Canberra, 2020 [cited 2021 Mar 30]. <https://www1.health.gov.au/internet/main/publishing.nsf/Content/cdna-song-novel-coronavirus.htm>
- Rockett RJ, Arnott A, Lam C, Sadsad R, Timms V, Gray KA, et al. Revealing COVID-19 transmission in Australia by SARS-CoV-2 genome sequencing and agent-based modeling. *Nat Med*. 2020;26:1398–404. <https://doi.org/10.1038/s41591-020-1000-7>
- Alsved M, Matamis A, Bohlin R, Richter M, Bengtsson P, Fraenkel C, et al. Exhaled respiratory particles during singing and talking. *Aerosol Sci Technol*. 2020;54:1245–8. <https://doi.org/10.1080/02786826.2020.1812502>
- Singanayagam A, Patel M, Charlett A, Lopez Bernal J, Saliba V, Ellis J, et al. Duration of infectiousness and correlation with RT-PCR cycle threshold values in cases of COVID-19, England, January to May 2020. *Euro Surveill*. 2020;25. <https://doi.org/10.2807/1560-7917.ES.2020.25.32.2001483>
- Cheng HY, Jian SW, Liu DP, Ng TC, Huang WT, Lin HH; Taiwan COVID-19 Outbreak Investigation Team. Contact tracing assessment of COVID-19 transmission dynamics in Taiwan and risk at different exposure periods before and after symptom onset. *JAMA Intern Med*. 2020;180:1156–63. <https://doi.org/10.1001/jamainternmed.2020.2020>
- Health New South Wales. COVID-19 weekly surveillance in NSW, epidemiological week 29, ending 18 July 2020. NSW Government, 2020 [cited 2021 Mar 29]. <https://www.health.nsw.gov.au/Infectious/covid-19/Documents/covid-19-surveillance-180720.pdf>
- Price DJ, Shearer FM, Meehan M, McBryde E, Golding N, McVernon J, et al. Estimating the case detection rate and temporal variation in transmission of COVID-19 in Australia. Technical report, 2020. [cited 2020 Apr 14]. <https://www.apprise.org.au/publication/estimating-the-case-detection-rate-and-temporal-variation-in-transmission-of-covid-19-in-australia/>
- Morawska L, Tang JW, Bahnfleth W, Bluyssen PM, Boerstra A, Buonanno G, et al. How can airborne transmission of COVID-19 indoors be minimised? *Environ Int*. 2020;142:105832. <https://doi.org/10.1016/j.envint.2020.105832>

Address for correspondence: Anthea L. Katelaris, Centre for Population Health, Locked Bag 7118, Parramatta BC 2124, NSW, Australia; email: anthea.katelaris@health.nsw.gov.au

Published in final edited form as:

Nature. 2021 April 01; 592(7853): 277–282. doi:10.1038/s41586-021-03291-y.

SARS-CoV-2 evolution during treatment of chronic infection

Steven A Kemp^{#1}, Dami A Collier^{#1,2,3}, Rawlings P Datir^{#2,3}, Isabella ATM Ferreira^{2,3}, Salma Gayed⁴, Aminu Jahun⁵, Myra Hosmillo⁵, Chloe Rees-Spear¹, Petra Mlcochova^{2,3}, Ines Ushiro Lumb⁶, David J Roberts⁶, Anita Chandra^{2,3}, Nigel Temperton⁷, The CITIID-NIHR BioResource COVID-19 Collaboration

Stephen Baker^{2,3} [Principal Investigators], Gordon Dougan^{2,3} [Principal Investigators], Christoph Hess^{2,3,26,27} [Principal Investigators], Nathalie Kingston^{20,12} [Principal Investigators], Paul J. Lehner^{2,3} [Principal Investigators], Paul A. Lyons^{2,3} [Principal Investigators], Nicholas J. Matheson^{2,3} [Principal Investigators], Willem H. Owehand²⁰ [Principal Investigators], Caroline Saunders¹⁹ [Principal Investigators], Charlotte Summers^{3,24,25,28} [Principal Investigators], James E.D. Thaventhiran^{2,3,22} [Principal Investigators], Mark Toshner^{3,24,25} [Principal Investigators], Michael P. Weekes² [Principal Investigators], Ashlea Bucke¹⁹ [CRF and Volunteer Research Nurses], Jo Calder¹⁹ [CRF and Volunteer Research Nurses], Laura Canna¹⁹ [CRF and Volunteer Research Nurses], Jason Domingo¹⁹ [CRF and Volunteer Research Nurses], Anne Elmer¹⁹ [CRF and Volunteer Research Nurses], Stewart Fuller¹⁹ [CRF and Volunteer Research Nurses], Julie Harris⁴¹ [CRF and Volunteer Research Nurses], Sarah Hewitt¹⁹ [CRF and Volunteer Research Nurses], Jane Kennet¹⁹ [CRF and Volunteer Research Nurses], Sherly Jose¹⁹ [CRF and Volunteer Research Nurses], Jenny Kourampa¹⁹ [CRF and Volunteer Research Nurses], Anne Meadows¹⁹ [CRF and Volunteer Research Nurses], Criona O'Brien⁴¹ [CRF and Volunteer Research Nurses], Jane Price¹⁹ [CRF and Volunteer Research Nurses], Cherry Publico¹⁹ [CRF and Volunteer Research Nurses], Rebecca Rastall¹⁹ [CRF and Volunteer Research Nurses], Carla Ribeiro¹⁹ [CRF and Volunteer Research Nurses], Jane Rowlands¹⁹ [CRF and Volunteer Research Nurses], Valentina Ruffolo¹⁹ [CRF and Volunteer Research Nurses], Hugo Tordesillas¹⁹ [CRF and Volunteer Research Nurses], Ben Bullman² [Sample Logistics], Benjamin J Dunmore³ [Sample Logistics], Stuart Fawke³⁰ [Sample Logistics], Stefan Gräf^{3,12,20} [Sample Logistics], Josh Hodgson³ [Sample Logistics], Christopher Huang³ [Sample Logistics], Kelvin Hunter^{2,3} [Sample Logistics], Emma Jones²⁹ [Sample

Users may view, print, copy, and download text and data-mine the content in such documents, for the purposes of academic research, subject always to the full Conditions of use:http://www.nature.com/authors/editorial_policies/license.html#terms

Address for correspondence: Ravindra K. Gupta, Cambridge Institute for Therapeutic Immunology and Infectious Diseases, Jeffrey Cheah Biomedical Centre, Puddicombe Way, Cambridge CB2 0AW, UK; Tel: +44 1223 331491, rkg20@cam.ac.uk.

Competing interests: the authors declare no competing interests

Ethics

The study was approved by the East of England – Cambridge Central Research Ethics Committee (17/EE/0025). Written informed consent was obtained from both the patient and family. Additional controls with COVID-19 were enrolled to the NIHR BioResource Centre Cambridge under ethics review board (17/EE/0025).

Author contributions

Conceived study: RKG, SAK, DAC, AS, TG, EGK

Designed experiments: RKG, SAK, DAC, LEM, JAGB, EGK, AC, NT, AC, CS, RD, RG, DDP, YM

Performed experiments: SAK, DAC, LEM, RD, CRS, AJ, IATMF, KS, TG, CJRI, BB, JS, MJvG, LGC, GBM, LK

Interpreted data: RKG, SAK, DAC, PM, LEM, JAGB, PM, SG, KS, TG, JB, KGCS, IG, CJRI, JAGB, IUL, DR, JS, BB, RAG, DDP, RD, LCG, GBM

Logistics], Ekaterina Legchenko³ [Sample Logistics], Cecilia Matara³ [Sample Logistics], Jennifer Martin³ [Sample Logistics], Federica Mescia^{2,3} [Sample Logistics], Ciara O'Donnell³ [Sample Logistics], Linda Pointon³ [Sample Logistics], Nicole Pond^{2,3} [Sample Logistics], Joy Shih³ [Sample Logistics], Rachel Sutcliffe³ [Sample Logistics], Tobias Tilly³ [Sample Logistics], Carmen Treacy³ [Sample Logistics], Zhen Tong³ [Sample Logistics], Jennifer Wood³ [Sample Logistics], Marta Wylot³⁶ [Sample Logistics], Laura Bergamaschi^{2,3} [Sample Processing and Data Acquisition], Ariana Betancourt^{2,3} [Sample Processing and Data Acquisition], Georgie Bower^{2,3} [Sample Processing and Data Acquisition], Chiara Cossetti^{2,3} [Sample Processing and Data Acquisition], Aloka De Sa³ [Sample Processing and Data Acquisition], Madeline Epping^{2,3} [Sample Processing and Data Acquisition], Stuart Fawke³² [Sample Processing and Data Acquisition], Nick Gleadall²⁰ [Sample Processing and Data Acquisition], Richard Grenfell³¹ [Sample Processing and Data Acquisition], Andrew Hinch^{2,3} [Sample Processing and Data Acquisition], Oisin Huhn³² [Sample Processing and Data Acquisition], Sarah Jackson³ [Sample Processing and Data Acquisition], Isobel Jarvis³ [Sample Processing and Data Acquisition], Daniel Lewis³ [Sample Processing and Data Acquisition], Joe Marsden³ [Sample Processing and Data Acquisition], Francesca Nice³⁹ [Sample Processing and Data Acquisition], Georgina Okecha³ [Sample Processing and Data Acquisition], Omar Omarjee³ [Sample Processing and Data Acquisition], Marianne Perera³ [Sample Processing and Data Acquisition], Nathan Richoz³ [Sample Processing and Data Acquisition], Veronika Romashova^{2,3} [Sample Processing and Data Acquisition], Natalia Savinykh Yarkoni³ [Sample Processing and Data Acquisition], Rahul Sharma³ [Sample Processing and Data Acquisition], Luca Stefanucci²⁰ [Sample Processing and Data Acquisition], Jonathan Stephens²⁰ [Sample Processing and Data Acquisition], Mateusz Strezlecki³¹ [Sample Processing and Data Acquisition], Lori Turner^{2,3} [Sample Processing and Data Acquisition], Eckart M.D.D. De Bie³ [Clinical Data Collection], Katherine Bunclark³ [Clinical Data Collection], Masa Josipovic⁴⁰ [Clinical Data Collection], Michael Mackay³ [Clinical Data Collection], Federica Mescia^{2,3} [Clinical Data Collection], Alice Michael²⁵ [Clinical Data Collection], Sabrina Rossi³⁵ [Clinical Data Collection], Mayurun Selvan³ [Clinical Data Collection], Sarah Spencer¹⁵ [Clinical Data Collection], Cissy Yong³⁵ [Clinical Data Collection], Ali Ansaripour²⁵ [Royal Papworth Hospital ICU], Alice Michael²⁵ [Royal Papworth Hospital ICU], Lucy Mwaura²⁵ [Royal Papworth Hospital ICU], Caroline Patterson²⁵ [Royal Papworth Hospital ICU], Gary Polwarth²⁵ [Royal Papworth Hospital ICU], Petra Polgarova²⁸ [Addenbrooke's Hospital ICU], Giovanni di Stefano²⁸ [Addenbrooke's Hospital ICU], Codie Fahey³⁴ [Cambridge and Peterborough Foundation Trust], Rachel Michel³⁴ [Cambridge and Peterborough Foundation Trust], Sze-How Bong²¹ [ANPC and Centre for Molecular Medicine and Innovative Therapeutics], Jerome D. Coudert³³ [ANPC and Centre for Molecular Medicine and Innovative Therapeutics], Elaine Holmes³⁷ [ANPC and Centre for Molecular Medicine and Innovative Therapeutics], John Allison^{20,12} [NIHR BioResource], Helen Butcher^{12,38} [NIHR BioResource], Daniela Caputo^{12,38} [NIHR BioResource], Debbie Clapham-Riley^{12,38} [NIHR BioResource], Eleanor Dewhurst^{12,38} [NIHR BioResource], Anita Furlong^{12,38} [NIHR BioResource], Barbara Graves^{12,38} [NIHR BioResource], Jennifer Gray^{12,38} [NIHR BioResource], Tasmin Ivers^{12,38} [NIHR BioResource], Mary Kasanicki^{12,28} [NIHR BioResource], Emma Le Gresley^{12,38} [NIHR BioResource], Rachel Linger^{12,38} [NIHR BioResource], Sarah Meloy^{12,38} [NIHR

BioResource], Francesca Muldoon^{12,38} [NIHR BioResource], Nigel Ovington^{12,20} [NIHR BioResource], Sofia Papadia^{12,38} [NIHR BioResource], Isabel Phelan^{12,38} [NIHR BioResource], Hannah Stark^{12,38} [NIHR BioResource], Kathleen E Stirrups^{12,20} [NIHR BioResource], Paul Townsend^{12,20} [NIHR BioResource], Neil Walker^{12,20} [NIHR BioResource], Jennifer Webster^{12,38} [NIHR BioResource]

¹⁹Cambridge Clinical Research Centre, NIHR Clinical Research Facility, Cambridge University Hospitals NHS Foundation Trust, Addenbrooke's Hospital, Cambridge CB2 0QQ, UK ²⁰Department of Haematology, University of Cambridge, Cambridge Biomedical Campus, Cambridge CB2 0QQ, UK ²¹Australian National Phenome Centre, Murdoch University, Murdoch, Western Australia WA 6150, Australia ²²MRC Toxicology Unit, School of Biological Sciences, University of Cambridge, Cambridge CB2 1QR, UK ²³R&D Department, Hycult Biotech, 5405 PD Uden, The Netherlands ²⁴Heart and Lung Research Institute, Cambridge Biomedical Campus, Cambridge CB2 0QQ, UK ²⁵Royal Papworth Hospital NHS Foundation Trust, Cambridge Biomedical Campus, Cambridge CB2 0QQ, UK ²⁶Department of Biomedicine, University and University Hospital Basel, 4031 Basel, Switzerland ²⁷Botnar Research Centre for Child Health (BRCC) University Basel & ETH Zurich, 4058 Basel, Switzerland ²⁸Addenbrooke's Hospital, Cambridge CB2 0QQ, UK ²⁹Department of Veterinary Medicine, Madingley Road, Cambridge, CB3 0ES, UK ³⁰Cambridge Institute for Medical Research, Cambridge Biomedical Campus, Cambridge CB2 0XY, UK ³¹Cancer Research UK, Cambridge Institute, University of Cambridge CB2 0RE, UK ³²Department of Obstetrics & Gynaecology, The Rosie Maternity Hospital, Robinson Way, Cambridge CB2 0SW, UK ³³Centre for Molecular Medicine and Innovative Therapeutics, Health Futures Institute, Murdoch University, Perth, WA, Australia ³⁴Cambridge and Peterborough Foundation Trust, Fulbourn Hospital, Fulbourn, Cambridge CB21 5EF, UK ³⁵Department of Surgery, Addenbrooke's Hospital, Cambridge CB2 0QQ, UK ³⁶Department of Biochemistry, University of Cambridge, Cambridge, CB2 1QW, UK ³⁷Centre of Computational and Systems Medicine, Health Futures Institute, Murdoch University, Harry Perkins Building, Perth, WA 6150, Australia ³⁸Department of Public Health and Primary Care, School of Clinical Medicine, University of Cambridge, Cambridge Biomedical Campus, Cambridge, UK ³⁹Cancer Molecular Diagnostics Laboratory, Department of Oncology, University of Cambridge, Cambridge CB2 0AH, UK ⁴⁰Metabolic Research Laboratories, Wellcome Trust-Medical Research Council Institute of Metabolic Science, University of Cambridge, Cambridge CB2 0QQ, UK ⁴¹Department of Paediatrics, University of Cambridge, Cambridge Biomedical Campus, Cambridge, CB2 0QQ, UK

, The COVID-19 Genomics UK (COG-UK) Consortium

Samuel C Robson⁵⁴ [Funding acquisition, Leadership and supervision, Metadata curation, Project administration, Samples and logistics, Sequencing and analysis, Software and analysis tools, and Visualisation], Nicholas J Loman⁸², Thomas R Connor^{51,110} [Funding acquisition, Leadership and supervision, Metadata curation, Project administration, Samples and logistics, Sequencing and analysis, and Software and analysis tools], Tanya Golubchik⁴⁶ [Leadership and supervision, Metadata curation, Project administration, Samples and logistics, Sequencing and analysis, Software and analysis tools, and Visualisation], Rocio T Martinez Nunez⁸³ [Funding acquisition, Metadata curation, Samples

and logistics, Sequencing and analysis, Software and analysis tools, and Visualisation], Catherine Ludden¹²⁹ [Funding acquisition, Leadership and supervision, Metadata curation, Project administration, and Samples and logistics], Sally Corden¹¹⁰ [Funding acquisition, Leadership and supervision, Metadata curation, Samples and logistics, and Sequencing and analysis], Ian Johnston¹⁴⁰, David Bonsall⁴⁶ [Funding acquisition, Leadership and supervision, Project administration, Samples and logistics, and Sequencing and analysis], Colin P Smith¹²⁸, Ali R Awan⁶⁹ [Funding acquisition, Leadership and supervision, Sequencing and analysis, Software and analysis tools, and Visualisation], Giselda Bucca¹²⁸ [Funding acquisition, Samples and logistics, Sequencing and analysis, Software and analysis tools, and Visualisation], M. Estee Torok^{63,142} [Leadership and supervision, Metadata curation, Project administration, Samples and logistics, and Sequencing and analysis], Kordo Saeed^{122,151} [Leadership and supervision, Metadata curation, Project administration, Samples and logistics, and Visualisation], Jacqui A Prieto^{124,150} [Leadership and supervision, Metadata curation, Project administration, Samples and logistics, and Visualisation], David K Jackson¹⁴⁰ [Leadership and supervision, Metadata curation, Project administration, Sequencing and analysis, and Software and analysis tools], William L Hamilton⁶³ [Metadata curation, Project administration, Samples and logistics, Sequencing and analysis, and Software and analysis tools], Luke B Snell⁵² [Metadata curation, Project administration, Samples and logistics, Sequencing and analysis, and Visualisation], Catherine Moore¹¹⁰ [Funding acquisition, Leadership and supervision, Metadata curation, and Samples and logistics], Ewan M Harrison^{129,140} [Funding acquisition, Leadership and supervision, Project administration, and Samples and logistics], Sonia Goncalves¹⁴⁰ [Leadership and supervision, Metadata curation, Project administration, and Samples and logistics], Derek J Fairley^{44,113} [Leadership and supervision, Metadata curation, Samples and logistics, and Sequencing and analysis], Matthew W Loose⁵⁹ [Leadership and supervision, Metadata curation, Samples and logistics, and Sequencing and analysis], Joanne Watkins¹¹⁰ [Leadership and supervision, Metadata curation, Samples and logistics, and Sequencing and analysis], Rich Livett¹⁴⁰ [Leadership and supervision, Metadata curation, Samples and logistics, and Software and analysis tools], Samuel Moses^{66,147} [Leadership and supervision, Metadata curation, Samples and logistics, and Visualisation], Roberto Amato¹⁴⁰ [Leadership and supervision, Metadata curation, Sequencing and analysis, and Software and analysis tools], Sam Nicholls⁸² [Leadership and supervision, Metadata curation, Sequencing and analysis, and Software and analysis tools], Matthew Bull¹¹⁰ [Leadership and supervision, Metadata curation, Sequencing and analysis, and Software and analysis tools], Darren L Smith^{1,99,146} [Leadership and supervision, Project administration, Samples and logistics, and Sequencing and analysis], Jeff Barrett¹⁴⁰ [Leadership and supervision, Sequencing and analysis, Software and analysis tools, and Visualisation], David M Aanensen⁵⁵ [Leadership and supervision, Sequencing and analysis, Software and analysis tools, and Visualisation], Martin D Curran¹⁰⁶ [Metadata curation, Project administration, Samples and logistics, and Sequencing and analysis], Surendra Parmar¹⁰⁶ [Metadata curation, Project administration, Samples and logistics, and Sequencing and analysis], Dinesh Aggarwal^{1,140,105} [Metadata curation, Project administration, Samples and logistics, and Sequencing and analysis], James G Shepherd⁸⁹ [Metadata curation, Project administration, Samples and logistics, and Sequencing and analysis], Matthew D Parker¹³⁴

[Metadata curation, Project administration, Sequencing and analysis, and Software and analysis tools], Sharon Glaysher¹⁰² [Metadata curation, Samples and logistics, Sequencing and analysis, and Visualisation], Matthew Bashton^{78,99} [Metadata curation, Sequencing and analysis, Software and analysis tools, and Visualisation], Anthony P Underwood⁵⁵ [Metadata curation, Sequencing and analysis, Software and analysis tools, and Visualisation], Nicole Pacchiarini¹¹⁰ [Metadata curation, Sequencing and analysis, Software and analysis tools, and Visualisation], Katie F Loveson¹¹⁸ [Metadata curation, Sequencing and analysis, Software and analysis tools, and Visualisation], Alessandro M Carabelli¹²⁹ [Project administration, Sequencing and analysis, Software and analysis tools, and Visualisation], Kate E Templeton^{94,131} [Funding acquisition, Leadership and supervision, and Metadata curation], Cordelia F Langford¹⁴⁰ [Funding acquisition, Leadership and supervision, and Project administration], John Sillitoe¹⁴⁰ [Funding acquisition, Leadership and supervision, and Project administration], Thushan I de Silva¹³⁴ [Funding acquisition, Leadership and supervision, and Project administration], Dennis Wang¹³⁴ [Funding acquisition, Leadership and supervision, and Project administration], Dominic Kwiatkowski^{140,148} [Funding acquisition, Leadership and supervision, and Sequencing and analysis], Andrew Rambaut¹³¹ [Funding acquisition, Leadership and supervision, and Sequencing and analysis], Justin O'Grady^{111,130} [Funding acquisition, Leadership and supervision, and Sequencing and analysis], Simon Cottrell¹¹⁰ [Funding acquisition, Leadership and supervision, and Sequencing and analysis], Matthew T.G. Holden¹⁰⁹ [Leadership and supervision, Metadata curation, and Sequencing and analysis], Emma C Thomson⁸⁹ [Leadership and supervision, Metadata curation, and Sequencing and analysis], Husam Osman^{77,105} [Leadership and supervision, Project administration, and Samples and logistics], Monique Andersson¹⁰⁰ [Leadership and supervision, Project administration, and Samples and logistics], Anoop J Chauhan¹⁰² [Leadership and supervision, Project administration, and Samples and logistics], Mohammed O Hassan-Ibrahim⁴⁷ [Leadership and supervision, Project administration, and Samples and logistics], Mara Lawniczak¹⁴⁰ [Leadership and supervision, Project administration, and Sequencing and analysis], Alex Alderton¹⁴⁰ [Leadership and supervision, Samples and logistics, and Sequencing and analysis], Meera Chand¹⁰⁷ [Leadership and supervision, Samples and logistics, and Sequencing and analysis], Chrystala Constantinidou¹³⁵ [Leadership and supervision, Samples and logistics, and Sequencing and analysis], Meera Unnikrishnan¹³⁵ [Leadership and supervision, Samples and logistics, and Sequencing and analysis], Alistair C Darby¹³³ [Leadership and supervision, Samples and logistics, and Sequencing and analysis], Julian A Hiscox¹³³ [Leadership and supervision, Samples and logistics, and Sequencing and analysis], Steve Paterson¹³³ [Leadership and supervision, Samples and logistics, and Sequencing and analysis], Inigo Martincorena¹⁴⁰ [Leadership and supervision, Sequencing and analysis, and Software and analysis tools], David L Robertson⁸⁹ [Leadership and supervision, Sequencing and analysis, and Software and analysis tools], Erik M Volz⁸⁰ [Leadership and supervision, Sequencing and analysis, and Software and analysis tools], Andrew J Page¹¹¹ [Leadership and supervision, Sequencing and analysis, and Software and analysis tools], Oliver G Pybus⁶⁴ [Leadership and supervision, Sequencing and analysis, and Software and analysis tools], Andrew R Bassett¹⁴⁰ [Leadership and supervision, Sequencing and analysis, and Visualisation], Cristina V Ariani¹⁴⁰ [Metadata curation,

Project administration, and Samples and logistics], Michael H Spencer Chapman^{129,140} [Metadata curation, Project administration, and Samples and logistics], Kathy K Li⁸⁹ [Metadata curation, Project administration, and Samples and logistics], Rajiv N Shah⁸⁹ [Metadata curation, Project administration, and Samples and logistics], Natasha G Jesudason⁸⁹ [Metadata curation, Project administration, and Samples and logistics], Yusri Taha⁹¹ [Metadata curation, Project administration, and Samples and logistics], Martin P McHugh⁹⁴ [Metadata curation, Project administration, and Sequencing and analysis], Rebecca Dewar⁹⁴ [Metadata curation, Project administration, and Sequencing and analysis], Aminu S Jahun⁶⁵ [Metadata curation, Samples and logistics, and Sequencing and analysis], Claire McMurray⁸² [Metadata curation, Samples and logistics, and Sequencing and analysis], Sarojini Pandey¹²⁵ [Metadata curation, Samples and logistics, and Sequencing and analysis], James P McKenna⁴⁴ [Metadata curation, Samples and logistics, and Sequencing and analysis], Andrew Nelson^{99,146} [Metadata curation, Samples and logistics, and Sequencing and analysis], Gregory R Young^{78,99} [Metadata curation, Samples and logistics, and Sequencing and analysis], Clare M McCann^{99,146} [Metadata curation, Samples and logistics, and Sequencing and analysis], Scott Elliott¹⁰² [Metadata curation, Samples and logistics, and Sequencing and analysis], Hannah Lowe⁶⁶ [Metadata curation, Samples and logistics, and Visualisation], Ben Temperton¹³² [Metadata curation, Sequencing and analysis, and Software and analysis tools], Sunando Roy¹²³ [Metadata curation, Sequencing and analysis, and Software and analysis tools], Anna Price⁵¹ [Metadata curation, Sequencing and analysis, and Software and analysis tools], Sara Rey¹¹⁰ [Metadata curation, Sequencing and analysis, and Software and analysis tools], Matthew Wyles¹³⁴ [Metadata curation, Sequencing and analysis, and Software and analysis tools], Stefan Rooke¹³¹ [Metadata curation, Sequencing and analysis, and Visualisation], Sharif Shaaban¹⁰⁹ [Metadata curation, Sequencing and analysis, and Visualisation], Mariateresa de Cesare¹³⁹ [Project administration, Samples and logistics, Sequencing and analysis], Laura Letchford¹⁴⁰ [Project administration, Samples and logistics, and Software and analysis tools], Siona Silveira¹²² [Project administration, Samples and logistics, and Visualisation], Emanuela Pelosi¹²² [Project administration, Samples and logistics, and Visualisation], Eleri Wilson-Davies¹²² [Project administration, Samples and logistics, and Visualisation], Myra Hosmillo⁶⁵ [Samples and logistics, Sequencing and analysis, and Software and analysis tools], Áine O'Toole¹³¹ [Sequencing and analysis, Software and analysis tools, and Visualisation], Andrew R Hesketh¹²⁸ [Sequencing and analysis, Software and analysis tools, and Visualisation], Richard Stark¹³⁵ [Sequencing and analysis, Software and analysis tools, and Visualisation], Louis du Plessis⁶⁴ [Sequencing and analysis, Software and analysis tools, and Visualisation], Chris Ruis¹²⁹ [Sequencing and analysis, Software and analysis tools, and Visualisation], Helen Adams⁴⁵ [Sequencing and analysis, Software and analysis tools, and Visualisation], Yann Bourgeois¹¹⁷ [Sequencing and analysis, Software and analysis tools, and Visualisation], Stephen L Michell¹³² [Funding acquisition, and Leadership and supervision], Dimitris Gramatopoulos^{125,153} [Funding acquisition, and Leadership and supervision], Jonathan Edgeworth⁵³ [Funding acquisition, and Leadership and supervision], Judith Breuer^{71,123} [Funding acquisition, and Leadership and supervision], John A Todd¹³⁹ [Funding acquisition, and Leadership and supervision], Christophe Fraser⁴⁶ [Funding acquisition, and Leadership and supervision], David Buck¹³⁹ [Funding

acquisition, and Project administration], Michaela John⁵⁰ [Funding acquisition, and Project administration], Gemma L Kay¹¹¹ [Leadership and supervision, and Metadata curation], Steve Palmer¹⁴⁰ [Leadership and supervision, and Project administration], Sharon J Peacock^{129,105} [Leadership and supervision, and Project administration], David Heyburn¹¹⁰ [Leadership and supervision, and Project administration], Danni Weldon¹⁴⁰ [Leadership and supervision, and Samples and logistics], Esther Robinson^{105,77} [Leadership and supervision, and Samples and logistics], Alan McNally^{82,127} [Leadership and supervision, and Samples and logistics], Peter Muir¹⁰⁵ [Leadership and supervision, and Samples and logistics], Ian B Vipond¹⁰⁵ [Leadership and supervision, and Samples and logistics], John BoYes⁷⁰ [Leadership and supervision, and Samples and logistics], Venkat Sivaprakasam⁸⁷ [Leadership and supervision, and Samples and logistics], Tranprit Salluja¹¹⁶ [Leadership and supervision, and Samples and logistics], Samir Dervisevic⁹⁵ [Leadership and supervision, and Samples and logistics], Emma J Meader⁹⁵ [Leadership and supervision, and Samples and logistics], Naomi R Park¹⁴⁰ [Leadership and supervision, and Sequencing and analysis], Karen Oliver¹⁴⁰ [Leadership and supervision, and Sequencing and analysis], Aaron R Jeffries¹³² [Leadership and supervision, and Sequencing and analysis], Sascha Ott¹³⁵ [Leadership and supervision, and Sequencing and analysis], Ana da Silva Filipe⁸⁹ [Leadership and supervision, and Sequencing and analysis], David A Simpson¹¹³ [Leadership and supervision, and Sequencing and analysis], Chris Williams¹¹⁰ [Leadership and supervision, and Sequencing and analysis], Jane AH Masoli^{114,132} [Leadership and supervision, and Visualisation], Bridget A Knight^{114,132} [Metadata curation, and Samples and logistics], Christopher R Jones^{114,132} [Metadata curation, and Samples and logistics], Cherian Koshy⁴² [Metadata curation, and Samples and logistics], Amy Ash⁴² [Metadata curation, and Samples and logistics], Anna Casey¹¹² [Metadata curation, and Samples and logistics], Andrew Bosworth^{105,77} [Metadata curation, and Samples and logistics], Liz Ratcliffe¹¹² [Metadata curation, and Samples and logistics], Li Xu-McCrae⁷⁷ [Metadata curation, and Samples and logistics], Hannah M Pymont¹⁰⁵ [Metadata curation, and Samples and logistics], Stephanie Hutchings¹⁰⁵ [Metadata curation, and Samples and logistics], Lisa Berry¹²⁵ [Metadata curation, and Samples and logistics], Katie Jones¹²⁵ [Metadata curation, and Samples and logistics], Fenella Halstead⁸⁷ [Metadata curation, and Samples and logistics], Thomas Davis⁶² [Metadata curation, and Samples and logistics], Christopher Holmes⁵⁷ [Metadata curation, and Samples and logistics], Miren Iturriza-Gomara¹³³ [Metadata curation, and Samples and logistics], Anita O Lucaci¹³³ [Metadata curation, and Samples and logistics], Paul Anthony Randell^{79,145} [Metadata curation, and Samples and logistics], Alison Cox^{79,145} [Metadata curation, and Samples and logistics], Pinglawathee Madona^{79,145} [Metadata curation, and Samples and logistics], Kathryn Ann Harris⁷¹ [Metadata curation, and Samples and logistics], Julianne Rose Brown⁷¹ [Metadata curation, and Samples and logistics], Tabitha W Mahungu¹¹⁵ [Metadata curation, and Samples and logistics], Dianne Irish-Tavares¹¹⁵ [Metadata curation, and Samples and logistics], Tanzina Haque¹¹⁵ [Metadata curation, and Samples and logistics], Jennifer Hart¹¹⁵ [Metadata curation, and Samples and logistics], Eric Witele¹¹⁵ [Metadata curation, and Samples and logistics], Melisa Louise Fenton¹¹⁶ [Metadata curation, and Samples and logistics], Steven Liggett¹²⁰ [Metadata curation, and Samples and logistics], Clive Graham⁹⁷ [Metadata curation, and Samples and logistics], Emma Swindells⁹⁸ [Metadata curation, and Samples and logistics], Jennifer Collins⁹¹

[Metadata curation, and Samples and logistics], Gary Eltringham⁹¹ [Metadata curation, and Samples and logistics], Sharon Campbell⁵⁸ [Metadata curation, and Samples and logistics], Patrick C McClure¹³⁸ [Metadata curation, and Samples and logistics], Gemma Clark⁵⁶ [Metadata curation, and Samples and logistics], Tim J Sloan¹⁰¹ [Metadata curation, and Samples and logistics], Carl Jones⁵⁶ [Metadata curation, and Samples and logistics], Jessica Lynch^{43,152} [Metadata curation, and Samples and logistics], Ben Warne⁴⁹ [Metadata curation, and Sequencing and analysis], Steven Leonard¹⁴⁰ [Metadata curation, and Sequencing and analysis], Jillian Durham¹⁴⁰ [Metadata curation, and Sequencing and analysis], Thomas Williams¹³¹ [Metadata curation, and Sequencing and analysis], Sam T Haldenby¹³³ [Metadata curation, and Sequencing and analysis], Nathaniel Storey⁷¹ [Metadata curation, and Sequencing and analysis], Nabil-Fareed Alikhan¹¹¹ [Metadata curation, and Sequencing and analysis], Nadine Holmes⁵⁹ [Metadata curation, and Sequencing and analysis], Christopher Moore⁵⁹ [Metadata curation, and Sequencing and analysis], Matthew Carlile⁵⁹ [Metadata curation, and Sequencing and analysis], Malorie Perry¹¹⁰ [Metadata curation, and Sequencing and analysis], Noel Craine¹⁴⁰ [Metadata curation, and Sequencing and analysis], Ronan A Lyons¹⁴⁰ [Metadata curation, and Sequencing and analysis], Angela H Beckett⁵⁴ [Metadata curation, and Sequencing and analysis], Salman Goudarzi¹¹⁸ [Metadata curation, and Sequencing and analysis], Christopher Fearn¹¹⁸ [Metadata curation, and Sequencing and analysis], Kate Cook¹¹⁸ [Metadata curation, and Sequencing and analysis], Hannah Dent¹¹⁸ [Metadata curation, and Sequencing and analysis], Hannah Paul¹¹⁸ [Metadata curation, and Sequencing and analysis], Robert Davies¹⁴⁰ [Metadata curation, and Software and analysis tools], Beth Blane¹⁴⁰ [Project administration, and Samples and logistics], Sophia T Girgis¹⁴⁰ [Project administration, and Samples and logistics], Mathew A Beale¹⁴⁰ [Project administration, and Samples and logistics], Katherine L Bellis^{140,129} [Project administration, and Samples and logistics], Matthew J Dorman¹⁴⁰ [Project administration, and Samples and logistics], Eleanor Drury¹⁴⁰ [Project administration, and Samples and logistics], Leanne Kane¹⁴⁰ [Project administration, and Samples and logistics], Sally Kay¹⁴⁰ [Project administration, and Samples and logistics], Samantha McGuigan¹⁴⁰ [Project administration, and Samples and logistics], Rachel Nelson¹⁴⁰ [Project administration, and Samples and logistics], Liam Prestwood¹⁴⁰ [Project administration, and Samples and logistics], Shavanthi Rajatileka¹⁴⁰ [Project administration, and Samples and logistics], Rahul Batra¹⁴⁰ [Project administration, and Samples and logistics], Rachel J Williams¹²³ [Project administration, and Samples and logistics], Mark Kristiansen¹²³ [Project administration, and Samples and logistics], Angie Green¹³⁹ [Project administration, and Samples and logistics], Anita Justice¹⁴⁰ [Project administration, and Samples and logistics], Adhyana I.K Mahanama^{122,143} [Project administration, and Samples and logistics], Buddhini Samaraweera^{122,143} [Project administration, and Samples and logistics], Nazreen F Hadjirin¹²⁹ [Project administration, and Sequencing and analysis], Joshua Quick⁸² [Project administration, and Sequencing and analysis], Radoslaw Poplawski⁸² [Project administration, and Software and analysis tools], Leanne M Kermack¹²⁹ [Samples and logistics, and Sequencing and analysis], Nicola Reynolds⁴⁸ [Samples and logistics, and Sequencing and analysis], Grant Hall⁶⁵ [Samples and logistics, and Sequencing and analysis], Yasmin Chaudhry¹⁴⁰ [Samples and logistics, and Sequencing and analysis], Malte L Pinckert⁶⁵ [Samples and logistics, and Sequencing and analysis], Iliana

Georgana¹⁴⁰ [Samples and logistics, and Sequencing and analysis], Robin J Moll¹⁴⁰ [Samples and logistics, and Sequencing and analysis], Alicia Thornton¹⁰⁷ [Samples and logistics, and Sequencing and analysis], Richard Myers¹⁰⁷ [Samples and logistics, and Sequencing and analysis], Joanne Stockton¹⁴⁰ [Samples and logistics, and Sequencing and analysis], Charlotte A Williams¹⁴⁰ [Samples and logistics, and Sequencing and analysis], Wen C Yew¹⁴⁰ [Samples and logistics, and Sequencing and analysis], Alexander J Trotter¹¹¹ [Samples and logistics, and Sequencing and analysis], Amy Trebes¹⁴⁰ [Samples and logistics, and Sequencing and analysis], George MacIntyre-Cockett¹³⁹ [Samples and logistics, and Sequencing and analysis], Alec Birchley¹¹⁰ [Samples and logistics, and Sequencing and analysis], Alexander Adams¹¹⁰ [Samples and logistics, and Sequencing and analysis], Amy Plimmer¹⁴⁰ [Samples and logistics, and Sequencing and analysis], Bree Gatica-Wilcox¹¹⁰ [Samples and logistics, and Sequencing and analysis], Caoimhe McKerr¹¹⁰ [Samples and logistics, and Sequencing and analysis], Ember Hilvers¹¹⁰ [Samples and logistics, and Sequencing and analysis], Hannah Jones¹¹⁰ [Samples and logistics, and Sequencing and analysis], Hibo Asad¹¹⁰ [Samples and logistics, and Sequencing and analysis], Jason Coombes¹⁴⁰ [Samples and logistics, and Sequencing and analysis], Johnathan M Evans¹¹⁰ [Samples and logistics, and Sequencing and analysis], Laia Fina¹¹⁰ [Samples and logistics, and Sequencing and analysis], Lauren Gilbert¹¹⁰ [Samples and logistics, and Sequencing and analysis], Lee Graham¹¹⁰ [Samples and logistics, and Sequencing and analysis], Michelle Cronin¹⁴⁰ [Samples and logistics, and Sequencing and analysis], Sara Kumziene-SummerhaYes¹¹⁰ [Samples and logistics, and Sequencing and analysis], Sarah Taylor¹¹⁰ [Samples and logistics, and Sequencing and analysis], Sophie Jones¹⁴⁰ [Samples and logistics, and Sequencing and analysis], Danielle C Groves¹³⁴ [Samples and logistics, and Sequencing and analysis], Peijun Zhang¹³⁴ [Samples and logistics, and Sequencing and analysis], Marta Gallis¹³⁴ [Samples and logistics, and Sequencing and analysis], Stavroula F Louka¹³⁴ [Samples and logistics, and Sequencing and analysis], Igor Starinskiy⁸⁹ [Samples and logistics, and Software and analysis tools], Chris Jackson⁸⁸ [Sequencing and analysis, and Software and analysis tools], Marina Gourtovaia¹⁴⁰ [Sequencing and analysis, and Software and analysis tools], Gerry Tonkin-Hill¹⁴⁰ [Sequencing and analysis, and Software and analysis tools], Kevin Lewis¹⁴⁰ [Sequencing and analysis, and Software and analysis tools], Jaime M Tovar-Corona¹⁴⁰ [Sequencing and analysis, and Software and analysis tools], Keith James¹⁴⁰ [Sequencing and analysis, and Software and analysis tools], Laura Baxter¹³⁵ [Sequencing and analysis, and Software and analysis tools], Mohammad T Alam¹⁴⁰ [Sequencing and analysis, and Software and analysis tools], Richard J Orton⁸⁹ [Sequencing and analysis, and Software and analysis tools], Joseph Hughes⁸⁹ [Sequencing and analysis, and Software and analysis tools], Sreenu Vattipally¹⁴⁰ [Sequencing and analysis, and Software and analysis tools], Manon Ragonnet-Cronin⁸⁰ [Sequencing and analysis, and Software and analysis tools], Fabricia F Nascimento⁸⁰ [Sequencing and analysis, and Software and analysis tools], David Jorgensen⁸⁰ [Sequencing and analysis, and Software and analysis tools], Olivia Boyd⁸⁰ [Sequencing and analysis, and Software and analysis tools], Lily Geidelberg¹⁴⁰ [Sequencing and analysis, and Software and analysis tools], Alex E Zarebski⁶⁴ [Sequencing and analysis, and Software and analysis tools], Jayna Raghwani¹⁴⁰ [Sequencing and analysis, and Software and analysis tools], Moritz UG Kraemer⁶⁴ [Sequencing and analysis, and Software and analysis tools], Joel

Southgate^{51,110} [Sequencing and analysis, and Software and analysis tools], Benjamin B Lindsey¹³⁴ [Sequencing and analysis, and Software and analysis tools], Timothy M Freeman¹³⁴ [Sequencing and analysis, and Software and analysis tools], Jon-Paul Keatley¹⁴⁰ [Software and analysis tools, and Visualisation], Joshua B Singer¹⁴⁰ [Software and analysis tools, and Visualisation], Leonardo de Oliveira Martins¹⁴⁰ [Software and analysis tools, and Visualisation], Corin A Yeats⁵⁵ [Software and analysis tools, and Visualisation], Khalil Abudahab^{140,140} [Software and analysis tools, and Visualisation], Ben EW Taylor¹⁴⁰ [Software and analysis tools, and Visualisation], Mirko Menegazzo⁵⁵ [Software and analysis tools, and Visualisation], John Danesh¹⁴⁰ [Leadership and supervision], Wendy Hogsden⁸⁷ [Leadership and supervision], Sahar Eldirdiri⁶² [Leadership and supervision], Anita Kenyon⁶² [Leadership and supervision], Jenifer Mason¹⁴⁰ [Leadership and supervision], Trevor I Robinson⁸⁴ [Leadership and supervision], Alison Holmes^{140,144} [Leadership and supervision], James Price^{140,140} [Leadership and supervision], John A Hartley¹²³ [Leadership and supervision], Tanya Curran¹⁴⁰ [Leadership and supervision], Alison E Mather¹¹¹ [Leadership and supervision], Giri Shankar¹¹⁰ [Leadership and supervision], Rachel Jones¹¹⁰ [Leadership and supervision], Robin Howe¹¹⁰ [Leadership and supervision], Sian Morgan⁵⁰ [Leadership and supervision], Elizabeth Wastenge¹⁴⁰ [Metadata curation], Michael R Chapman^{1,129,140} [Metadata curation], Siddharth Mookerjee^{79,144} [Metadata curation], Rachael Stanley⁹⁵ [Metadata curation], Wendy Smith⁵⁶ [Metadata curation], Timothy Peto¹⁰⁰ [Metadata curation], David Eyre¹⁰⁰ [Metadata curation], Derrick Crook¹⁰⁰ [Metadata curation], Gabrielle Vernet⁷⁴ [Metadata curation], Christine Kitchen⁵¹ [Metadata curation], Huw Gulliver⁵¹ [Metadata curation], Ian Merrick⁵¹ [Metadata curation], Martyn Guest⁵¹ [Metadata curation], Robert Munn¹⁴⁰ [Metadata curation], Declan T Bradley^{140,113} [Metadata curation], Tim Wyatt¹⁰⁴ [Metadata curation], Charlotte Beaver¹⁴⁰ [Project administration], Luke Foulser¹⁴⁰ [Project administration], Sophie Palmer¹⁴⁰ [Project administration], Carol M Churcher¹²⁹ [Project administration], Ellena Brooks¹⁴⁰ [Project administration], Kim S Smith¹²⁹ [Project administration], Katerina Galai¹⁴⁰ [Project administration], Georgina M McManus¹²⁹ [Project administration], Frances Bolt^{79,144} [Project administration], Francesc Coll⁶⁰ [Project administration], Lizzie Meadows¹⁴⁰ [Project administration], Stephen W Attwood⁶⁴ [Project administration], Alisha Davies¹⁴⁰ [Project administration], Elen De Lacy¹¹⁰ [Project administration], Fatima Downing¹¹⁰ [Project administration], Sue Edwards¹⁴⁰ [Project administration], Garry P Scarlett¹¹⁷ [Project administration], Sarah Jeremiah¹²⁴ [Project administration], Nikki Smith¹³⁴ [Project administration], Danielle Leek¹²⁹ [Samples and logistics], Sushmita Sridhar^{140,140} [Samples and logistics], Sally Forrest¹²⁹ [Samples and logistics], Claire Cormie¹⁴⁰ [Samples and logistics], Harmeet K Gill¹²⁹ [Samples and logistics], Joana Dias¹⁴⁰ [Samples and logistics], Ellen E Higginson¹²⁹ [Samples and logistics], Mailis Maes¹²⁹ [Samples and logistics], Jamie Young¹²⁹ [Samples and logistics], Michelle Wantoch¹⁴⁰ [Samples and logistics], Sanger Covid Team¹⁴⁰ [Samples and logistics], Dorota Jamroz¹⁴⁰ [Samples and logistics], Stephanie Lo¹⁴⁰ [Samples and logistics], Minal Patel¹⁴⁰ [Samples and logistics], Verity Hill¹⁴⁰ [Samples and logistics], Claire M Bewshea¹³² [Samples and logistics], Sian Ellard^{114,132} [Samples and logistics], Cressida Auckland¹¹⁴ [Samples and logistics], Ian Harrison¹⁰⁷ [Samples and logistics], Chloe Bishop¹⁰⁷ [Samples and logistics], Vicki Chalker¹⁰⁷ [Samples and logistics], Alex Richter¹²⁶ [Samples and logistics], Andrew

Beggs¹²⁶ [Samples and logistics], Angus Best¹²⁷ [Samples and logistics], Benita Percival¹²⁷ [Samples and logistics], Jeremy Mirza¹²⁷ [Samples and logistics], Oliver Megram¹²⁷ [Samples and logistics], Megan Mayhew¹²⁷ [Samples and logistics], Liam Crawford¹²⁷ [Samples and logistics], Fiona Ashcroft¹⁴⁰ [Samples and logistics], Emma Moles-Garcia¹²⁷ [Samples and logistics], Nicola Cumley¹²⁷ [Samples and logistics], Richard Hopes¹⁰⁵ [Samples and logistics], Patawee Asamaphan¹⁴⁰ [Samples and logistics], Marc O Niebel¹⁴⁰ [Samples and logistics], Rory N Gunson¹⁴¹ [Samples and logistics], Amanda Bradley⁹³ [Samples and logistics], Alasdair Maclean⁹³ [Samples and logistics], Guy Mollett⁹³ [Samples and logistics], Rachel Blacow⁹³ [Samples and logistics], Paul Bird⁵⁷ [Samples and logistics], Thomas Helmer⁵⁷ [Samples and logistics], Karlie Fallon⁵⁷ [Samples and logistics], Julian Tang¹⁴⁰ [Samples and logistics], Antony D Hale¹⁴⁰ [Samples and logistics], Louissa R Macfarlane-Smith¹⁴⁰ [Samples and logistics], Katherine L Harper⁹⁰ [Samples and logistics], Holli Carden¹⁴⁰ [Samples and logistics], Nicholas W Machin^{86,105} [Samples and logistics], Kathryn A Jackson¹³³ [Samples and logistics], Shazaad SY Ahmad^{86,105} [Samples and logistics], Ryan P George⁸⁶ [Samples and logistics], Lance Turtle¹⁴⁰ [Samples and logistics], Elaine O'Toole⁸⁴ [Samples and logistics], Joanne Watts⁸⁴ [Samples and logistics], Cassie Breen⁸⁴ [Samples and logistics], Angela Cowell¹⁴⁰ [Samples and logistics], Adela Alcolea-Medina^{73,137} [Samples and logistics], Themoula Charalampous^{140,83} [Samples and logistics], Amita Patel¹⁴⁰ [Samples and logistics], Lisa J Levett⁷⁶ [Samples and logistics], Judith Heaney⁷⁶ [Samples and logistics], Aileen Rowan¹⁴⁰ [Samples and logistics], Graham P Taylor⁸⁰ [Samples and logistics], Divya Shah⁷¹ [Samples and logistics], Laura Atkinson¹⁴⁰ [Samples and logistics], Jack CD Lee¹⁴⁰ [Samples and logistics], Adam P Westhorpe¹²³ [Samples and logistics], Riaz Jannoo¹⁴⁰ [Samples and logistics], Helen L Lowe¹²³ [Samples and logistics], Angeliki Karamani¹²³ [Samples and logistics], Leah Ensell¹²³ [Samples and logistics], Wendy Chatterton⁷⁶, Monika Pusok⁷⁶ [Samples and logistics], Ashok Dadrah¹¹⁶ [Samples and logistics], Amanda Symmonds¹¹⁶ [Samples and logistics], Graciela Sluga⁸⁵ [Samples and logistics], Zoltan Molnar¹¹³ [Samples and logistics], Paul Baker¹²⁰ [Samples and logistics], Stephen Bonner¹²⁰ [Samples and logistics], Sarah Essex¹²⁰ [Samples and logistics], Edward Barton⁹⁷ [Samples and logistics], Debra Padgett⁹⁷ [Samples and logistics], Garren Scott⁹⁷ [Samples and logistics], Jane Greenaway¹⁴⁰ [Samples and logistics], Brendan Al Payne¹⁴⁰ [Samples and logistics], Shirelle Burton-Fanning⁹¹ [Samples and logistics], Sheila Waugh⁹¹ [Samples and logistics], Veena Raviprakash⁵⁸ [Samples and logistics], Nicola Sheriff⁵⁸ [Samples and logistics], Victoria Blakey¹⁴⁰ [Samples and logistics], Lesley-Anne Williams⁵⁸ [Samples and logistics], Jonathan Moore⁶⁸ [Samples and logistics], Susanne Stonehouse⁶⁸ [Samples and logistics], Louise Smith¹⁴⁰ [Samples and logistics], Rose K Davidson¹³⁰ [Samples and logistics], Luke Bedford⁶⁷ [Samples and logistics], Lindsay Coupland⁹⁵ [Samples and logistics], Victoria Wright¹⁴⁰ [Samples and logistics], Joseph G Chappell¹³⁸ [Samples and logistics], Theocharis Tsoleridis¹³⁸ [Samples and logistics], Jonathan Ball¹³⁸ [Samples and logistics], Manjinder Khakh¹⁴⁰ [Samples and logistics], Vicki M Fleming¹⁴⁰ [Samples and logistics], Michelle M Lister¹⁴⁰ [Samples and logistics], Hannah C Howson-Wells⁵⁶ [Samples and logistics], Louise Berry⁵⁶ [Samples and logistics], Tim Boswell⁵⁶ [Samples and logistics], Amelia Joseph⁵⁶ [Samples and logistics], Iona Willingham⁵⁶ [Samples and logistics], Nichola Duckworth¹⁰¹ [Samples and logistics], Sarah Walsh¹⁰¹ [Samples and

logistics], Emma Wise^{140,152} [Samples and logistics], Nathan Moore^{140,152} [Samples and logistics], Matilde Mori^{140,140,152} [Samples and logistics], Nick Cortes^{140,152} [Samples and logistics], Stephen Kidd^{140,152} [Samples and logistics], Rebecca Williams⁷⁴ [Samples and logistics], Laura Gifford¹¹⁰ [Samples and logistics], Kelly Bicknell¹⁰² [Samples and logistics], Sarah Wyllie¹⁰² [Samples and logistics], Allyson Lloyd¹⁰² [Samples and logistics], Robert Impey¹⁴⁰ [Samples and logistics], Cassandra S Malone¹⁴⁰ [Samples and logistics], Benjamin J Cogger⁴⁷ [Samples and logistics], Nick Levene¹⁰³ [Samples and logistics], Lynn Monaghan¹⁴⁰ [Samples and logistics], Alexander J Keeley¹⁴⁰ [Samples and logistics], David G Partridge^{140,134} [Samples and logistics], Mohammad Raza^{119,134} [Samples and logistics], Cariad Evans^{140,134} [Samples and logistics], Kate Johnson^{119,134} [Samples and logistics], Emma Betteridge¹⁴⁰ [Sequencing and analysis], Ben W Farr¹⁴⁰ [Sequencing and analysis], Scott Goodwin¹⁴⁰ [Sequencing and analysis], Michael A Quail¹⁴⁰ [Sequencing and analysis], Carol Scott¹⁴⁰ [Sequencing and analysis], Lesley Shirley¹⁴⁰ [Sequencing and analysis], Scott AJ Thurston¹⁴⁰ [Sequencing and analysis], Diana Rajan¹⁴⁰ [Sequencing and analysis], Iraad F Bronner¹⁴⁰ [Sequencing and analysis], Louise Aigrain¹⁴⁰ [Sequencing and analysis], Nicholas M Redshaw¹⁴⁰ [Sequencing and analysis], Stefanie V Lensing¹⁴⁰ [Sequencing and analysis], Shane McCarthy¹⁴⁰ [Sequencing and analysis], Alex Makunin¹⁴⁰ [Sequencing and analysis], Carlos E Balcazar¹⁴⁰ [Sequencing and analysis], Michael D Gallagher¹⁴⁰ [Sequencing and analysis], Kathleen A Williamson¹⁴⁰ [Sequencing and analysis], Thomas D Stanton¹⁴⁰ [Sequencing and analysis], Michelle L Michelsen¹⁴⁰ [Sequencing and analysis], Joanna Warwick-Dugdale¹³² [Sequencing and analysis], Robin Manley¹³² [Sequencing and analysis], Audrey Farbos¹⁴⁰ [Sequencing and analysis], James W Harrison¹⁴⁰ [Sequencing and analysis], Christine M Sambles¹⁴⁰ [Sequencing and analysis], David J Studholme¹³² [Sequencing and analysis], Angie Lackenby¹⁰⁷ [Sequencing and analysis], Tamyo Mbisa¹⁰⁷ [Sequencing and analysis], Steven Platt¹⁰⁷ [Sequencing and analysis], Shahjahan Miah¹⁰⁷ [Sequencing and analysis], David Bibby¹⁰⁷ [Sequencing and analysis], Carmen Manso¹⁰⁷ [Sequencing and analysis], Jonathan Hubb¹⁰⁷ [Sequencing and analysis], Gavin Dabrera¹⁰⁷ [Sequencing and analysis], Mary Ramsay¹⁰⁷ [Sequencing and analysis], Daniel Bradshaw¹⁰⁷ [Sequencing and analysis], Ulf Schaefer¹⁰⁷ [Sequencing and analysis], Natalie Groves¹⁰⁷ [Sequencing and analysis], Eileen Gallagher¹⁰⁷ [Sequencing and analysis], David Lee¹⁰⁷ [Sequencing and analysis], David Williams¹⁰⁷ [Sequencing and analysis], Nicholas Ellaby¹⁰⁷ [Sequencing and analysis], Hassan Hartman¹⁰⁷ [Sequencing and analysis], Nikos Manesis¹⁰⁷ [Sequencing and analysis], Vineet Patel¹⁰⁷ [Sequencing and analysis], Juan Ledesma¹⁴⁰ [Sequencing and analysis], Katherine A Twohig¹⁰⁸ [Sequencing and analysis], Elias Allara^{140,129} [Sequencing and analysis], Clare Pearson^{140,140} [Sequencing and analysis], Jeffrey K. J. Cheng¹³⁵ [Sequencing and analysis], Hannah E Bridgewater¹³⁵ [Sequencing and analysis], Lucy R Frost¹⁴⁰ [Sequencing and analysis], Grace Taylor-Joyce¹⁴⁰ [Sequencing and analysis], Paul E Brown¹³⁵ [Sequencing and analysis], Lily Tong⁸⁹ [Sequencing and analysis], Alice Broos⁸⁹ [Sequencing and analysis], Daniel Mair⁸⁹ [Sequencing and analysis], Jenna Nichols¹⁴⁰ [Sequencing and analysis], Stephen N Carmichael¹⁴⁰ [Sequencing and analysis], Katherine L Smollett⁸¹ [Sequencing and analysis], Kyriaki Nomikou¹⁴⁰ [Sequencing and analysis], Elihu Aranday-Cortes⁸⁹ [Sequencing and analysis], Natasha Johnson⁸⁹ [Sequencing and analysis], Seema Nickbakhsh^{140,140} [Sequencing and analysis], Edith E Vamos¹³³

[Sequencing and analysis], Margaret Hughes¹³³ [Sequencing and analysis], Lucille Rainbow¹³³ [Sequencing and analysis], Richard Eccles¹³³ [Sequencing and analysis], Charlotte Nelson¹³³ [Sequencing and analysis], Mark Whitehead¹³³ [Sequencing and analysis], Richard Gregory¹³³ [Sequencing and analysis], Matthew Gemmell¹³³ [Sequencing and analysis], Claudia Wierzbicki¹⁴⁰ [Sequencing and analysis], Hermione J Webster¹⁴⁰ [Sequencing and analysis], Chloe L Fisher¹⁴⁰ [Sequencing and analysis], Adrian W Signell⁶¹ [Sequencing and analysis], Gilberto Betancor¹⁴⁰ [Sequencing and analysis], Harry D Wilson⁶¹ [Sequencing and analysis], Gaia Nebbia⁵³ [Sequencing and analysis], Flavia Flaviani¹⁴⁰ [Sequencing and analysis], Alberto C Cerda¹⁴⁰ [Sequencing and analysis], Tammy V Merrill¹⁴⁰ [Sequencing and analysis], Rebekah E Wilson¹³⁷ [Sequencing and analysis], Marius Cotic¹²³ [Sequencing and analysis], Nadua Bayzid¹²³ [Sequencing and analysis], Thomas Thompson¹¹³ [Sequencing and analysis], Erwan Acheson¹¹³ [Sequencing and analysis], Steven Rushton¹⁴⁰ [Sequencing and analysis], Sarah O'Brien¹⁴⁰ [Sequencing and analysis], David J Baker¹¹¹ [Sequencing and analysis], Steven Rudder¹¹¹ [Sequencing and analysis], Alp Aydin¹¹¹ [Sequencing and analysis], Fei Sang⁵⁹ [Sequencing and analysis], Johnny Debebe⁵⁹ [Sequencing and analysis], Sarah Francois¹⁴⁰ [Sequencing and analysis], Tetyana I Vasylyeva¹⁴⁰ [Sequencing and analysis], Marina Escalera Zamudio⁶⁴ [Sequencing and analysis], Bernardo Gutierrez⁶⁴ [Sequencing and analysis], Angela Marchbank⁵¹ [Sequencing and analysis], Joshua Maksimovic⁵⁰ [Sequencing and analysis], Karla Spellman⁵⁰ [Sequencing and analysis], Kathryn McCluggage⁵⁰ [Sequencing and analysis], Mari Morgan¹¹⁰ [Sequencing and analysis], Robert Beer⁵⁰ [Sequencing and analysis], Safiah Afifi⁵⁰ [Sequencing and analysis], Trudy Workman⁵¹ [Sequencing and analysis], William Fuller⁵¹ [Sequencing and analysis], Catherine Bresner⁵¹ [Sequencing and analysis], Adrienn Angyal¹⁴⁰ [Sequencing and analysis], Luke R Green¹⁴⁰ [Sequencing and analysis], Paul J Parsons¹⁴⁰ [Sequencing and analysis], Rachel M Tucker¹³⁴ [Sequencing and analysis], Rebecca Brown¹³⁴ [Sequencing and analysis], Max Whiteley¹³⁴ [Sequencing and analysis], James Bonfield¹⁴⁰ [Software and analysis tools], Christoph Puethel¹⁴⁰ [Software and analysis tools], Andrew Whitwham¹⁴⁰ [Software and analysis tools], Jennifer Liddle¹⁴⁰ [Software and analysis tools], Will Rowe⁸² [Software and analysis tools], Igor Siveroni¹⁴⁰ [Software and analysis tools], Thanh Le-Viet¹⁴⁰ [Software and analysis tools], Amy Gaskin¹¹⁰ [Software and analysis tools], Rob Johnson⁸⁰ [Visualisation]

⁴²Barking, Havering and Redbridge University Hospitals NHS Trust, Barking, United Kingdom ⁴³Basingstoke Hospital, Basingstoke, United Kingdom ⁴⁴Belfast Health & Social Care Trust, Belfast, United Kingdom ⁴⁵Betsi Cadwaladr University Health Board, Betsi Cadwaladr, United Kingdom ⁴⁶Big Data Institute, Nuffield Department of Medicine, University of Oxford, Oxford, United Kingdom ⁴⁷Brighton and Sussex University Hospitals NHS Trust, Brighton & Sussex, United Kingdom ⁴⁸Cambridge Stem Cell Institute, University of Cambridge, Cambridge, United Kingdom ⁴⁹Cambridge University Hospitals NHS Foundation Trust, Cambridge, United Kingdom ⁵⁰Cardiff and Vale University Health Board, Cardiff, United Kingdom ⁵¹Cardiff University, Cardiff, United Kingdom ⁵²Centre for Clinical Infection & Diagnostics Research, St. Thomas' Hospital and Kings College London, London, United Kingdom ⁵³Centre for Clinical Infection and Diagnostics Research, Department of Infectious Diseases, Guy's and St Thomas' NHS Foundation

Trust, London, United Kingdom ⁵⁴Centre for Enzyme Innovation, University of Portsmouth (PORT), Portsmouth, United Kingdom ⁵⁵Centre for Genomic Pathogen Surveillance, University of Oxford, Oxford, United Kingdom ⁵⁶Clinical Microbiology Department, Queens Medical Centre, Nottingham, United Kingdom ⁵⁷Clinical Microbiology, University Hospitals of Leicester NHS Trust, Leicester, United Kingdom ⁵⁸County Durham and Darlington NHS Foundation Trust, Durham, United Kingdom ⁵⁹Deep Seq, School of Life Sciences, Queens Medical Centre, University of Nottingham, Nottingham, United Kingdom ⁶⁰Department of Infection Biology, Faculty of Infectious & Tropical Diseases, London School of Hygiene & Tropical Medicine, London, United Kingdom ⁶¹Department of Infectious Diseases, King's College London, London, United Kingdom ⁶²Department of Microbiology, Kettering General Hospital, Kettering, United Kingdom ⁶³Departments of Infectious Diseases and Microbiology, Cambridge University Hospitals NHS Foundation Trust; Cambridge, UK, Cambridge, United Kingdom ⁶⁴Department of Zoology, University of Oxford, Oxford, United Kingdom ⁶⁵Division of Virology, Department of Pathology, University of Cambridge, Cambridge, United Kingdom ⁶⁶East Kent Hospitals University NHS Foundation Trust, Kent, United Kingdom ⁶⁷East Suffolk and North Essex NHS Foundation Trust, Suffolk, United Kingdom ⁶⁸Gateshead Health NHS Foundation Trust, Gateshead, United Kingdom ⁶⁹Genomics Innovation Unit, Guy's and St. Thomas' NHS Foundation Trust, London, United Kingdom ⁷⁰Gloucestershire Hospitals NHS Foundation Trust, Gloucester, United Kingdom ⁷¹Great Ormond Street Hospital for Children NHS Foundation Trust, London, United Kingdom ⁷²Guy's and St. Thomas' BRC, London, United Kingdom ⁷³Guy's and St. Thomas' Hospitals, London, United Kingdom ⁷⁴Hampshire Hospitals NHS Foundation Trust, Hampshire, United Kingdom ⁷⁵Health Data Research UK Cambridge, Cambridge, United Kingdom ⁷⁶Health Services Laboratories, London, United Kingdom ⁷⁷Heartlands Hospital, Birmingham, Birmingham, United Kingdom ⁷⁸Hub for Biotechnology in the Built Environment, Northumbria University, Northumbria, United Kingdom ⁷⁹Imperial College Hospitals NHS Trust, London, United Kingdom ⁸⁰Imperial College London, London, United Kingdom ⁸¹Institute of Biodiversity, Animal Health & Comparative Medicine, Glasgow, United Kingdom ⁸²Institute of Microbiology and Infection, University of Birmingham, Birmingham, United Kingdom ⁸³King's College London, London, United Kingdom ⁸⁴Liverpool Clinical Laboratories, Liverpool, United Kingdom ⁸⁵Maidstone and Tunbridge Wells NHS Trust, Maidstone, United Kingdom ⁸⁶Manchester University NHS Foundation Trust, Manchester, United Kingdom ⁸⁷Microbiology Department, Wye Valley NHS Trust, Hereford, United Kingdom ⁸⁸MRC Biostatistics Unit, University of Cambridge, Cambridge, United Kingdom ⁸⁹MRC-University of Glasgow Centre for Virus Research, Glasgow, United Kingdom ⁹⁰National Infection Service, PHE and Leeds Teaching Hospitals Trust, Leeds, United Kingdom ⁹¹Newcastle Hospitals NHS Foundation Trust, Newcastle, United Kingdom ⁹²Newcastle University, Newcastle, United Kingdom ⁹³NHS Greater Glasgow and Clyde, Glasgow, United Kingdom ⁹⁴NHS Lothian, Edinburgh, United Kingdom ⁹⁵Norfolk and Norwich University Hospital, Norfolk, United Kingdom ⁹⁶Norfolk County Council, Norfolk, United Kingdom ⁹⁷North Cumbria Integrated Care NHS Foundation Trust, Carlisle, United Kingdom ⁹⁸North Tees and Hartlepool NHS Foundation Trust, Stockton-on-Tees, United Kingdom ⁹⁹Northumbria University, Northumbria, United Kingdom ¹⁰⁰Oxford University Hospitals NHS Foundation Trust, Oxford, United Kingdom ¹⁰¹PathLinks, Northern

Lincolnshire & Goole NHS Foundation Trust, Lincolnshire, United Kingdom ¹⁰²Portsmouth Hospitals University NHS Trust, Portsmouth, United Kingdom ¹⁰³Princess Alexandra Hospital Microbiology Dept., Harlow, United Kingdom ¹⁰⁴Public Health Agency, London, United Kingdom ¹⁰⁵Public Health England, London, United Kingdom ¹⁰⁶Public Health England, Clinical Microbiology and Public Health Laboratory, Cambridge, United Kingdom ¹⁰⁷Public Health England, Colindale, London, United Kingdom ¹⁰⁸Public Health England, Colindale, London, United Kingdom ¹⁰⁹Public Health Scotland, Glasgow, United Kingdom ¹¹⁰Public Health Wales NHS Trust, Cardiff, United Kingdom ¹¹¹Quadram Institute Bioscience, Norwich, United Kingdom ¹¹²Queen Elizabeth Hospital, Birmingham, United Kingdom ¹¹³Queen's University Belfast, Belfast, United Kingdom ¹¹⁴Royal Devon and Exeter NHS Foundation Trust, Devon, United Kingdom ¹¹⁵Royal Free NHS Trust, London, United Kingdom ¹¹⁶Sandwell and West Birmingham NHS Trust, Sandwell, United Kingdom ¹¹⁷School of Biological Sciences, University of Portsmouth (PORT), Portsmouth, United Kingdom ¹¹⁸School of Pharmacy and Biomedical Sciences, University of Portsmouth (PORT), Portsmouth, United Kingdom ¹¹⁹Sheffield Teaching Hospitals, Sheffield, United Kingdom ¹²⁰South Tees Hospitals NHS Foundation Trust, Newcastle, United Kingdom ¹²¹Swansea University, Swansea, United Kingdom ¹²²University Hospitals Southampton NHS Foundation Trust, Southampton, United Kingdom ¹²³University College London, London, United Kingdom ¹²⁴University Hospital Southampton NHS Foundation Trust, Southampton, United Kingdom ¹²⁵University Hospitals Coventry and Warwickshire, Coventry, United Kingdom ¹²⁶University of Birmingham, Birmingham, United Kingdom ¹²⁷University of Birmingham Turnkey Laboratory, Birmingham, United Kingdom ¹²⁸University of Brighton, Brighton, United Kingdom ¹²⁹University of Cambridge, Cambridge, United Kingdom ¹³⁰University of East Anglia, East Anglia, United Kingdom ¹³¹University of Edinburgh, Edinburgh, United Kingdom ¹³²University of Exeter, Exeter, United Kingdom ¹³³University of Liverpool, Liverpool, United Kingdom ¹³⁴University of Sheffield, Sheffield, United Kingdom ¹³⁵University of Warwick, Warwick, United Kingdom ¹³⁶University of Cambridge, Cambridge, United Kingdom ¹³⁷Viapath, Guy's and St Thomas' NHS Foundation Trust, and King's College Hospital NHS Foundation Trust, London, United Kingdom ¹³⁸Virology, School of Life Sciences, Queens Medical Centre, University of Nottingham, Nottingham, United Kingdom ¹³⁹Wellcome Centre for Human Genetics, Nuffield Department of Medicine, University of Oxford, Oxford, United Kingdom ¹⁴⁰Wellcome Sanger Institute, London, United Kingdom ¹⁴¹West of Scotland Specialist Virology Centre, NHS Greater Glasgow and Clyde, Glasgow, United Kingdom ¹⁴²Department of Medicine, University of Cambridge, Cambridge, United Kingdom ¹⁴³Ministry of Health, Colombo, Sri Lanka ¹⁴⁴NIHR Health Protection Research Unit in HCAI and AMR, Imperial College London, London, United Kingdom ¹⁴⁵North West London Pathology, London, United Kingdom ¹⁴⁶NU-OMICS, Northumbria University, Northumbria, United Kingdom ¹⁴⁷University of Kent, Kent, United Kingdom ¹⁴⁸University of Oxford, Oxford, United Kingdom ¹⁴⁹University of Southampton, Southampton, United Kingdom ¹⁵⁰University of Southampton School of Health Sciences, Southampton, United Kingdom ¹⁵¹University of Southampton School of Medicine, Southampton, United Kingdom ¹⁵²University of Surrey, Guildford, United Kingdom ¹⁵³Warwick Medical School and Institute of Precision Diagnostics, Pathology, UHCW NHS Trust, Warwick, United Kingdom

, Katherine Sharrocks⁴, Elizabeth Blane³, Yorgo Modis⁸, Kendra Leigh⁸, John Briggs⁸, Marit van Gils⁹, Kenneth GC Smith^{2,3}, John R Bradley^{3,10}, Chris Smith¹¹, Rainer Doffinger¹³, Lourdes Ceron-Gutierrez¹³, Gabriela Barcenas-Morales^{13,14}, David D Pollock¹⁵, Richard A Goldstein¹, Anna Smielewska^{5,11}, Jordan P Skittrall^{4,12,16}, Theodore Gouliouris⁴, Ian G Goodfellow⁵, Effrossyni Gkrania-Klotsas⁴, Christopher JR Illingworth^{12,17}, Laura E McCoy¹, Ravindra K Gupta^{2,3,18}

¹Division of Infection and Immunity, University College London, London, UK ² Cambridge Institute of Therapeutic Immunology & Infectious Disease (CITIID), Cambridge, UK ³Department of Medicine, University of Cambridge, Cambridge, UK ⁴Department of Infectious Diseases, Cambridge University NHS Hospitals Foundation Trust, Cambridge, UK ⁵Department of Pathology, University of Cambridge, Cambridge ⁶ NHS Blood and Transplant, Oxford and BRC Haematology Theme, University of Oxford, UK ⁷Viral Pseudotype Unit, Medway School of Pharmacy, University of Kent, UK ⁸Medical Research Council Laboratory of Molecular Biology, Cambridge, UK ⁹Department of Medical Microbiology, Academic Medical Center, University of Amsterdam, Amsterdam Institute for Infection and Immunity, Amsterdam, Netherlands ¹⁰ NIHR Cambridge Clinical Research Facility, Cambridge, UK ¹¹Department of Virology, Cambridge University NHS Hospitals Foundation Trust ¹²Department of Applied Mathematics and Theoretical Physics, University of Cambridge, UK ¹³ Department of Clinical Biochemistry and Immunology, Addenbrookes Hospital ¹⁴ FES-Cuautitlán, UNAM, Mexico ¹⁵Biochemistry and Molecular Genetics, University of Colorado School of Medicine, Aurora, Colorado, USA; ¹⁶Clinical Microbiology and Public Health Laboratory, Addenbrookes' Hospital, Cambridge, UK ¹⁷ MRC Biostatistics Unit, University of Cambridge, Cambridge, UK ¹⁸Africa Health Research Institute, Durban, South Africa

These authors contributed equally to this work.

Summary

SARS-CoV-2 Spike protein is critical for virus infection via engagement of ACE2¹, and is a major antibody target. Here we report chronic SARS-CoV-2 with reduced sensitivity to neutralising antibodies in an immune suppressed individual treated with convalescent plasma, generating whole genome ultradeep sequences over 23 time points spanning 101 days. Little change was observed in the overall viral population structure following two courses of remdesivir over the first 57 days. However, following convalescent plasma therapy we observed large, dynamic virus population shifts, with the emergence of a dominant viral strain bearing D796H in S2 and H69/V70 in the S1 N-terminal domain NTD of the Spike protein. As passively transferred serum antibodies diminished, viruses with the escape genotype diminished in frequency, before returning during a final, unsuccessful course of convalescent plasma. *In vitro*, the Spike escape double mutant bearing H69/V70 and D796H conferred modestly decreased sensitivity to convalescent plasma, whilst maintaining infectivity similar to wild type. D796H appeared to be the main contributor to decreased susceptibility but incurred an infectivity defect. The H69/V70 single mutant had two-fold higher infectivity compared to wild type, possibly compensating for the reduced infectivity of D796H. These data reveal strong selection on SARS-CoV-2 during convalescent plasma therapy associated with emergence of viral variants with evidence of reduced susceptibility to neutralising antibodies.

As passively transferred serum antibodies diminished, viruses with the escape genotype diminished in frequency, before returning during a final, unsuccessful course of convalescent plasma. *In vitro*, the Spike escape double mutant bearing H69/V70 and D796H conferred modestly decreased sensitivity to convalescent plasma, whilst maintaining infectivity similar to wild type. D796H appeared to be the main contributor to decreased susceptibility but incurred an infectivity defect. The H69/V70 single mutant had two-fold higher infectivity compared to wild type, possibly compensating for the reduced infectivity of D796H. These data reveal strong selection on SARS-CoV-2 during convalescent plasma therapy associated with emergence of viral variants with evidence of reduced susceptibility to neutralising antibodies.

Keywords

SARS-CoV-2; COVID-19; antibody escape, Convalescent plasma; neutralising antibodies; mutation; evasion; resistance; immune suppression

Clinical case history of SARS-CoV-2 infection in setting of immune-compromised host

A septuagenarian male was admitted to a tertiary hospital in summer of 2020 and had tested positive for SARS-CoV-2 RT-PCR 35 days previously on a nasopharyngeal swab (Day 1) at a local hospital (Extended data 1 and 2). His past medical history was significant for marginal B cell lymphoma diagnosed in 2012, with previous chemotherapy including vincristine, prednisolone, cyclophosphamide and anti-CD20 B cell depletion with rituximab. It is likely that both chemotherapy and underlying lymphoma contributed to B and T cell combined immunodeficiency (Extended data 2 and 3, Supplementary Table 1). Computed tomography (CT) of the chest showed widespread abnormalities consistent with COVID-19 pneumonia (Supplementary Figure 1). Treatment included two 10-day courses of remdesivir with a five day gap in between (Extended data 1). Two units of convalescent plasma were administered on days 63 and 65 (Extended data 3). Following clinical deterioration, remdesivir and a unit of convalescent plasma were administered on day 95, but the individual unfortunately died on day 102 (Supplementary text).

Virus genomic comparative analysis of 23 sequential respiratory samples over 101 days

The majority of samples were respiratory samples from nose and throat or endotracheal aspirates during the period of intubation (Supplementary Table 3). Ct values ranged from 16-34 and all 23 respiratory samples were successfully sequenced by standard single molecule sequencing approach as per the ARTIC protocol implemented by COG-UK; of these 20 additionally underwent short-read deep sequencing using the Illumina platform (Supplementary table 4). There was general agreement between the two methods (Extended data 4). However due to the higher reliability of Illumina for low frequency variants, this was used for formal analysis^{2,3}. Additionally, single genome amplification and sequencing of Spike using extracted RNA from respiratory samples was used as an independent method to detect mutations observed (Extended data 4). Finally, we detected no evidence of recombination, based on two independent methods.

Maximum likelihood analysis of patient-derived whole genome consensus sequences demonstrated clustering with other local sequences from the same region (Figure 1). The infecting strain was assigned to lineage 20B bearing the D614G Spike variant. Environmental sampling showed evidence of virus on surfaces such as telephone and call bell. Sequencing of these surface viruses showed clustering with those derived from the respiratory tract (Extended data 2). All samples were consistent with having arisen from a single underlying viral population. In our phylogenetic analysis, we included sequential sequences from three other local patients identified with persistent viral RNA shedding over

a period of 4 weeks or more as well as two long term immunosuppressed SARS-CoV-2 ‘shedders’ recently reported^{4,5}, (Extended data 2, Supplementary Table 2). While the sequences from the three local patients as well as from Avanzato et al⁵ showed little divergence with no amino acid changes in Spike over time, the case patient showed significant diversification. The Choi et al report⁴ showed similar degree of diversification as the case patient. Further investigation of the sequence data suggested the existence of an underlying structure to the viral population in our patient, with samples collected at days 93 and 95 being rooted within, but significantly divergent from the original population (Extended data 5 and 6). The relationship of the divergent samples to those at earlier time points argues against superinfection.

SARS-CoV-2 viral diversity

All samples tested positive by RT-PCR and there was no sustained change in Ct values throughout the 101 days following the first two courses of remdesivir (days 41 and 54), or the first two units of convalescent plasma with polyclonal antibodies (days 63 and 65, Extended data 3). Of note we were not able to culture virus from stored swab samples. Consensus sequences from short read deep sequence Illumina data revealed dynamic population changes after day 65, as shown by a highlighter plot (Extended data 6). In addition, we were also able to follow the dynamics of virus populations down to low frequencies during the entire period (Figure 2, Supplementary Table 4). Following remdesivir at day 41 the low frequency variant analysis allowed us to observe transient amino acid changes in populations at below 50% abundance in Orf 1b, 3a and Spike, with a T39I (C27509T) mutation in ORF7a reaching 79% on day 45 (Figure 2, pink, supplementary information). At day 66 we noted I513T in NSP2 (T2343C) and V157L (G13936T) in RdRp had emerged from undetectable at day 54 to almost 100% frequency (Figure 2, red and green dashed lines), with the polymerase being the more plausible candidate for driving this sweep. Notably, spike variant N501Y, which can increase the ACE2 receptor affinity⁶, and which is present in the new UK B.1.1.7 lineage⁷, was observed on day 55 at 33% frequency, but was eliminated by the sweep of the NSP2/RdRp variant.

In contrast to the early period of infection, between days 66 and 82, following the first two administrations of convalescent sera, a shift in the virus population was observed, with a variant bearing D796H in S2 and H69/ V70 in the S1 N-terminal domain (NTD) becoming the dominant population at day 82. This was identified in a nose and throat swab sample with high viral load as indicated by Ct of 23 (Figure 3A). The deletion was detected transiently at baseline according to short read deep sequencing. H69/ V70 was due to an out of frame six nucleotide deletion resulting in the sequence of codon 68 changing from ATA to ATC.

On Days 86 and 89, viruses obtained from upper respiratory tract samples were characterised by the Spike mutations Y200H and T240I, with the deletion/mutation pair observed on day 82 having fallen to frequencies of 10% or less (Figure 2 and 3). The Spike mutations Y200H and T240I were accompanied at high frequency by two other non-synonymous variants with similar allele frequencies, coding for I513T in NSP2, V157L in RdRp and N177S in NSP15 (Figure 2A). Both of these were also previously observed at

>98% frequency in the sample on day 66 (Figure 2A, red and green lines), arguing that this new lineage emerged out of a previously existing population.

Sequencing of a nose and throat swab sample at day 93 identified viruses characterised by Spike mutations P330S at the edge of the RBD and W64G in S1 NTD at close to 100% abundance, with D796H along with H69/ V70 at <1% abundance and the variants Y200H and T240I at frequencies of <2%. Viruses with the P330S variant were detected in two independent samples from different sampling sites, arguing against the possibility of contamination. The divergence of these samples from the remainder of the population (Figure 2, 3B and Extended data 5 and 6) suggests the possibility that they represent a compartmentalised subpopulation.

Patterns in the variant frequencies suggest competition between virus populations carrying different mutations, viruses with the D796H/ H69/ V70 deletion/mutation pair rising to high frequency during CP therapy, then being outcompeted by another population in the absence of therapy. Specifically, these data are consistent with a lineage of viruses with the NSP2 I513T and RdRp V157L variant, dominant on day 66, being outcompeted during therapy by the mutation/deletion variant. With the lapse in therapy, the original strain, having acquired NSP15 N1773S and the Spike mutations Y200H and T240I, regained dominance, followed by the emergence of a separate population with the W64G and P330S mutations.

In a final attempt to reduce the viral load, a third course of remdesivir (day 93) and third dose of CP (day 95) were administered. We observed a re-emergence of the D796H + H69/ V70 viral population (Figure 2, 3). The inferred linkage of D796H and H69/ V70 was maintained as evidenced by the highly similar frequencies of the two variants, suggesting that the third unit of CP led to the re-emergence of this population under renewed positive selection. In further support of our proposed idea of competition, noted above, frequencies of these two variants appeared to mirror changes in the NSP2 I513T mutation (Figure 2), suggesting these as markers of opposing clades in the viral population. Ct values remained low throughout this period with hyperinflammation, eventually leading to multi-organ failure and death at day 102. The repeated increase in frequency of the viral population with CP therapy strongly supports the hypothesis that the deletion/mutation combination conferred selective advantage.

Spike mutants emerging post convalescent plasma impair neutralising antibody potency

Using lentiviral pseudotyping we generated wild type, H69/ V70 + D796H and single mutant Spike proteins in enveloped virions in order to measure neutralisation activity of CP against these viruses (Figure 4). This system has been shown to give generally similar results to replication competent virus^{8,9}. Spike protein from each mutant was detected in pelleted virions (Figure 4A). We also probed with an HIV-1 p24 antibody to monitor levels of lentiviral particle production (Figure 4A, Supplementary Figure 2). We then measured infectivity of the pseudoviruses, correcting for virus input using reverse transcriptase activity measurement, and found that H69/ V70 appeared to have two-fold higher infectivity over

a single round of infection compared to wild type (Figure 4B, Extended data 7). By contrast, the D796H single mutant had significantly lower infectivity as compared to wild type and double mutant had similar infectivity to wild type (Figure 4B, Extended data 7).

We found that D796H alone and the D796H + H69/ V70 double mutant were less sensitive to neutralisation by convalescent plasma samples (Figure 4C-E, Extended data 7). By contrast the H69/ V70 single mutant did not reduce neutralisation sensitivity. In addition, patient derived serum from days 64 and 66 (one day either side of CP2 infusion) similarly showed lower potency against the D796H + H69/ V70 mutants (Figure 4F, G).

A panel of nineteen monoclonal antibodies (mAbs) isolated from three donors was previously identified to neutralize SARS-CoV-2. To establish if the mutations incurring *in vivo* (D796H and H69/ V70) resulted in a global change in neutralization sensitivity we tested neutralising mAbs targeting the seven major epitope clusters previously described (excluding non-neutralising clusters II, V and small [$n \leq 2$] neutralising clusters IV, X). The eight RBD-specific mAbs (Extended data 8) exhibited no major change in neutralisation potency and non-RBD specific COVA1-21 showing 3-5 fold reduction in potency against H69/ V70+D796H and H69/ V70, but not D796H alone⁹ (Extended data 8). We observed no differences in neutralisation between single/double mutants and wild type, suggesting that the mechanism of escape was likely outside these epitopes in the RBD. These data confirm the specificity of the findings from convalescent plasma and suggest that mutations observed are related to antibodies targeting regions outside the RBD. Interestingly, H69/ V70 containing viruses showed reduced neutralisation sensitivity to the mAb COVA1-21, targeting an as yet undefined epitope outside the RBD.¹⁰

To understand how the H69/ V70 and D796H might confer antibody resistance, we assessed how they might affect the Spike structure (Extended data 9). We based this analysis primarily on a structure lacking stabilising modifications (PDB 6xr8)¹¹, but also referred to stabilised structures determined at different pH values¹². H69/ V70 is located in a disordered, glycosylated loop at the distal surface of the NTD, near the binding site of polyclonal antibodies derived from COV57 plasma^{13,14} (Extended data 9). As this loop is flexible and highly accessible, H69/V70 could in principle affect antibody binding in this region. D796 is located near the base of Spike, in a surface loop that is structurally somewhat disordered in the prefusion conformation and becomes part of a large disordered region in the post fusion S2 trimer¹¹ (Extended data 9). The loop containing residue 796 is proposed to be targeted by antibodies¹⁵, despite mutations at position 796 being relatively uncommon (Extended data 9). In the RBD-down Spike structures^{11,12}, D796 forms contacts with residues in the neighbouring protomer, including the glycosylated residue N709 (Extended data 9).

Discussion

Here we have documented a repeated evolutionary response by SARS-CoV-2 in the presence of antibody therapy during the course of a persistent infection in an immunocompromised host. The observation of potential selection for specific variants coinciding with the presence of antibodies from convalescent plasma is supported by the experimental finding of two-fold

reduced susceptibility of these viruses to convalescent plasma containing polyclonal antibodies. In this case the emergence of the variant was not the primary reason for treatment failure. We have noted in our analysis signs of compartmentalised viral replication based on the sequences recovered in upper respiratory tract samples. Both population genetic and small animal studies have shown a lack of reassortment between influenza viruses within a single host during an infection, suggesting that acute respiratory viral infection may be characterised by spatially distinct viral populations^{16,17}. In the analysis of data, it is important to distinguish genetic changes which occur in the primary viral population from apparent changes that arise from the stochastic observation of spatially distinct subpopulations in the host. While the samples we observe on days 93 and 95 of infection are genetically distinct from the others, the remaining samples are consistent with arising from a consistent viral population. We note that Choi et al reported the detection in post-mortem tissue of viral RNA not only in lung tissue, but also in the spleen, liver, and heart⁴. Mixing of virus from different compartments, for example via blood, or movement of secretions from lower to upper respiratory tract, could lead to fluctuations in viral populations at particular sampling sites.

This is a single case report and therefore limited conclusions can be drawn about generalisability.

An important limitation is that the data were derived from sampling from the upper respiratory tract and not the lower tract, thus limiting the inferences that can be drawn regarding viral populations in this single case.

In addition to documenting the emergence of SARS-CoV-2 Spike H69/ V70 *in vivo*, we show that this mutation modestly increases infectivity of the Spike protein in a pseudotyping assay. The deletion was observed contemporaneously with the rare S2 mutation D796H after two separate courses of CP, with other viral populations emerging. D796H, but not H69/ V70, conferred reduction in susceptibility to polyclonal antibodies in the units of CP administered, though we cannot speculate as to their individual impacts on sera from other individuals. It is intriguing that the H69/ V70 + D796H double mutant diminished in between CP courses, suggesting that there were other selective forces at play in the intervening period, possibly driven by the inflammation observed in the individual. This includes the possibility that the haplotype with H69/ V70 + D796H may have carried mutations in other regions deleterious during that intervening period. Although H69/V70 is expanding at a high rate¹⁸, D796 mutations are also increasing. D796H has been documented in 0.02% of global sequences and D796Y appears in 0.05% of global sequences (Extended data 9).

The effects of CP on virus evolution seen here are unlikely to apply in immune competent hosts where viral diversity is likely to be lower due to better immune control. Our data highlight that infection control measures may need to be tailored to the needs of immunocompromised patients and also caution in interpretation of CDC guidelines that recommend 20 days as the upper limit of infection prevention precautions in immune compromised patients who are afebrile¹⁹. Due to the difficulty with culturing clinical isolates, use of surrogates are warranted²⁰. However, where detection of ongoing viral

evolution is possible, this serves as a clear proxy for the existence of infectious virus. In our case we detected environmental contamination whilst in a single occupancy room and the patient was moved to a negative-pressure high air-change infectious disease isolation room.

Clinical efficacy of convalescent plasma in severe COVID-19 has not been demonstrated²¹, and its use in different stages of infection and disease remains experimental; as such, we suggest that it should be reserved for use within clinical trials, with rigorous monitoring of clinical and virological parameters. The data from this single case report might warrant caution in use of convalescent plasma in patients with immune suppression of both T cell and B cell arms; in such cases, the antibodies administered have little support from cytotoxic T cells, thereby reducing chances of clearance and theoretically raising the potential for escape mutations. Whilst we await further data, where clinical trial enrolment is not possible, convalescent plasma administered for clinical need in immune suppression should ideally only be considered as part of observational studies, undertaken preferably in single occupancy rooms with enhanced infection control precautions, including SARS-CoV-2 environmental sampling and real-time sequencing. Understanding of viral dynamics and characterisation of viral evolution in response to different selection pressures in the immunocompromised host is necessary not only for improved patient management but also for public health benefit.

Methods

Clinical Sample Collection and Next generation sequencing

Serial samples were collected from the patient periodically from the lower respiratory tract (sputum or endotracheal aspirate), upper respiratory tract (throat and nasal swab), and from stool. Nucleic acid extraction was done from 500µl of sample with a dilution of MS2 bacteriophage to act as an internal control, using the easyMAG platform (Biomerieux, Marcy-l'Étoile) according to the manufacturers' instructions. All samples were tested for presence of SARS-CoV-2 with a validated one-step RT q-PCR assay developed in conjunction with the Public Health England Clinical Microbiology²². Amplification reaction were all performed on a Rotorgene™ PCR instrument. Samples which generated a CT of 36 were considered to be positive.

Sera from recovered patients in the COVIDx study²³ were used for testing of neutralisation activity by SARS-CoV-2 mutants.

SARS-CoV-2 serology by multiplex particle-based flow cytometry (Luminex)

Recombinant SARS-CoV-2 N, S and RBD were covalently coupled to distinct carboxylated bead sets (Luminex; Netherlands) to form a 3-plex and analyzed as previously described (Xiong et al. 2020). Specific binding was reported as mean fluorescence intensities (MFI).

Whole blood T cell and innate stimulation assay

Whole blood was diluted 1:5 in RPMI into 96-well F plates (Corning) and activated by single stimulation with phytohemagglutinin (PHA; 10 µg/ml; Sigma-Aldrich), or LPS (1 µg/ml, List Biochemicals) or by co-stimulating with anti-CD3 (MEM57, Abcam, 200 ng/ml,

1:1000) and IL-2 (Immunotools, 1430U/ml, 1:1000). Supernatants were taken after 24 hours. Levels (pg/ml) are shown for IFN γ , IL17, IL2, TNF α , IL6, IL1 β and IL10. Cytokines were measured by multiplexed particle based Flow cytometry on a Luminex analyzer (Bio-Plex, Bio-Rad, UK) using an R&D Systems custom kit (R&D Systems, UK).

For viral genomic sequencing, total RNA was extracted from samples as described. Samples were sequenced using MinION flow cells version 9.4.1 (Oxford Nanopore Technologies) following the ARTICnetwork V3 protocol (<https://dx.doi.org/10.17504/protocols.io.bbmuik6w>) and BAM files assembled using the ARTICnetwork assembly pipeline (<https://artic.network/ncov-2019/ncov2019-bioinformatics-sop.html>). A representative set of 10 sequences were selected and also sequenced using the Illumina MiSeq platform. Amplicons were diluted to 2 ng/ μ l and 25 μ l (50 ng) were used as input for each library preparation reaction. The library preparation used KAPA Hyper Prep kit (Roche) according to manufacturer's instructions. Briefly, amplicons were end-repaired and had A-overhang added; these were then ligated with 15mM of NEXTflex DNA Barcodes (Bio Scientific, Texas, USA). Post-ligation products were cleaned using AMPure beads and eluted in 25 μ l. Then, 20 μ l were used for library amplification by 5 cycles of PCR. For the negative controls, 1ng was used for ligation-based library preparation. All libraries were assayed using TapeStation (Agilent Technologies, California, USA) to assess fragment size and quantified by QPCR. All libraries were then pooled in equimolar accordingly. Libraries were loaded at 15nM and spiked in 5% PhiX (Illumina, California, USA) and sequenced on one MiSeq 500 cycle using a Miseq Nano v2 with 2x 250 paired-end sequencing. A minimum of ten reads were required for a variant call.

Bioinformatics Processes

For long-read sequencing, genomes were assembled with reference-based assembly and a curated bioinformatics pipeline with 20x minimum coverage across the whole-genome²⁴. For short-read sequencing, FASTQs were downloaded, poor-quality reads were identified and removed, and both Illumina and PHiX adapters were removed using TrimGalore v0.6.6²⁵. Trimmed paired-end reads were mapped to the National Center for Biotechnology Information SARS-CoV-2 reference sequence MN908947.3 using MiniMap2-2.17 with arguments -ax and sr²⁶. BAM files were then sorted and indexed with samtools v1.11 and PCR optical duplicates removed using Picard (<http://broadinstitute.github.io/picard>). A consensus sequences of nucleic acids with a minimum whole-genome coverage of at least 20 \times were generated with BCFtools using a 0% majority threshold.

Variant calling

Variant frequencies were validated using custom code as part of the *AnCovMulti* package (github.com/PollockLaboratory/AnCovMulti). The main idea behind this validation was to identify and remove consistent potential amplification errors and mutability near the end of Illumina reads. Furthermore, stringent filtering was applied to remove biased amplification of early laboratory-induced mutations or very low copy variations.

Filtering consisted of requiring exact initiation at a primer within two bp of the start of a read, a minimum of 247 bp length read, fewer than four well-separated sites divergent from

the reference sequence, a maximum insertion size of three nucleotides, a maximum deletion size of 11 bp, and resolution of conflicting signal from different primers.

Single Genome Amplification and sequencing

Viral RNA extracts were reverse transcribed from each sample to sufficiently capture the diversity of the viral population without introducing resampling bias. SuperScript IV (ThermoFisher Scientific) and the gene specific primers were used for reverse transcription. Template RNA was degraded with RNase H (ThermoFisher Scientific). All primers used were 'in-house' primers designed using the multiple sequence alignment of the patient's consensus NGS sequences. Partial Spike (amino acids 21-800) was amplified as 1 continuous length of DNA (Spike ~ 1.8 kb) by nested PCR. Terminally diluted cDNA was PCR-amplified using Platinum® Taq DNA Polymerase High Fidelity (Invitrogen, Carlsbad, CA) so that 30% of reactions were positive²⁷. By Poisson statistics, sequences were deemed 80% likely to be derived from HIV-1 single genomes. We obtained between 20–60 single genomes at each sample time point to achieve 90% confidence of detecting variants present at 8% of the viral population in vivo^{28,29}. Partial spike amplicons obtained from terminal dilution PCR amplification were Sanger sequenced to form a contiguous sequence using another set of 8 in-house primers. Sanger sequencing was provided by Genewiz UK and manual sequence editing was performed using DNA Dynamo software (Blue Tractor Software Ltd, UK).

Phylogenetic Analysis

All available full-genome SARS-CoV-2 sequences were downloaded from the GISAID database (<http://gisaid.org/>)³⁰ on 16th December. Duplicate and low-quality sequences (>5% N regions) were removed, leaving a dataset of 212,297 sequences with a length of >29,000bp. All sequences were sorted by name and only sequences sequenced with United Kingdom / England identifiers were retained. From this dataset, sequences were de-duplicated and where background sequences were required in figures, randomly subsampled using seqtk (<https://github.com/lh3/seqtk>). All sequences were aligned to the SARS-CoV-2 reference strain MN908947.3, using MAFFT v7.475 with automatic flavour selection³¹. Major SARS-CoV-2 clade memberships were assigned to all sequences using both the Nextclade server v0.9 (<https://clades.nextstrain.org/>) and Phylogenetic Assignment Of Named Global Outbreak Lineages (pangolin)³².

Maximum likelihood phylogenetic trees were produced using the above curated dataset using IQ-TREE v2.1.2³³. Evolutionary model selection for trees were inferred using ModelFinder³⁴ and trees were estimated using the GTR+F+I model with 1000 ultrafast bootstrap replicates³⁵. All trees were visualised with Figtree v.1.4.4 (<http://tree.bio.ed.ac.uk/software/figtree/>), rooted on the SARS-CoV-2 reference sequence and nodes arranged in descending order. Nodes with bootstraps values of <50 were collapsed using an in-house script.

In-depth allele frequency variant calling

The SAMFIRE package version 1.06³⁶ was used to call allele frequency trajectories from BAM file data. Reads were included in this analysis if they had a median PHRED score of at

least 30, trimming the ends of reads to achieve this if necessary. Nucleotides were then filtered to have a PHRED score of at least 30; reads with fewer than 30 such reads were discarded. Distances between sequences, accounting for low-frequency variant information, was also conducted using SAMFIRE. The sequence distance metric, described in an earlier paper³⁷, combines allele frequencies across the whole genome. Where L is the length of the genome, we define $q(t)$ as a $4 \times L$ element vector describing the frequencies of each of the nucleotides A, C, G, and T at each locus in the viral genome sampled at time t . For any given locus i in the genome we calculate the change in allele frequencies between the times t_1 and t_2 via a generalisation of the Hamming distance

$$d(q_i(t_1), q_i(t_2)) = \frac{1}{2} \sum_{a \in \{A, C, G, T\}} |q_i^a(t_1) - q_i^a(t_2)|$$

where the vertical lines indicate the absolute value of the difference. These statistics were then combined across the genome to generate the pairwise sequence distance metric

$$D(q(t_1), q(t_2)) = \sum_i d(q_i(t_1), q_i(t_2))$$

The Mathematica software package was used to conduct a regression analysis of pairwise sequence distances against time, leading to an estimate of a mean rate of within-host sequence evolution. In contrast to the phylogenetic analysis, this approach assumed the samples collected on days 93 and 95 to arise via stochastic emission from a spatially separated subpopulation within the host, leading to a lower inferred rate of viral evolution for the bulk of the viral population.

All variants were independently validated using custom code as part of the AnCovMulti package, found at <https://github.com/PollockLaboratory/AnCovMulti>.

Western blot analysis

Forty-eight hours after transfection of cells with plasmid preparations, the culture supernatant was harvested and passed through a 0.45- μ m-pore-size filter to remove cellular debris. The filtrate was centrifuged at 15,000 rpm for 120 min to pellet virions. The pelleted virions were lysed in Laemmli reducing buffer (1 M Tris-HCl [pH 6.8], SDS, 100% glycerol, β -mercaptoethanol, and bromophenol blue). Pelleted virions were subjected to electrophoresis on SDS–4 to 12% bis-Tris protein gels (Thermo Fisher Scientific) under reducing conditions. This was followed by electroblotting onto polyvinylidene difluoride (PVDF) membranes. The SARS-CoV-2 Spike proteins were visualized by a ChemiDoc^{MP} imaging system (Biorad) using anti-Spike S2 (Invitrogen at 1:1000 dilution) and anti-p24 Gag antibodies (NIH AIDS Reagents 1:1000 dilution).

Recombination Detection

All sequences were tested for potential recombination, as this would impact on evolutionary estimates. Potential recombination events were explored with nine algorithms (RDP, MaxChi, SisScan, GeneConv, Bootscan, PhylPro, Chimera, LARD and 3SEQ), implemented

in RDP5 with default settings³⁸. To corroborate any findings, ClonalFrameML v1.12³⁹ was also used to infer recombination breakpoints. Neither programs indicated evidence of recombination in our data.

Structural Viewing

The Pymol Molecular Graphics System v2.4.0 (<https://github.com/schrodinger/pymol-open-source/releases>) was used to map the location of the four spike mutations of interest onto a SARS-CoV-2 spike structure visualised by Wrobel et al (PDB: 6ZGE)⁴⁰.

Testing of convalescent plasma for antibody titres

The Anti-SARS-CoV-2 ELISA (IgG) assay used to test CP for *antibody titres* was Euroimmun Medizinische Labordiagnostika AG. This indirect ELISA based assay uses a recombinant structural spike 1 (S1) protein of SARS-CoV-2 expressed in the human cell line HEK 293 for the detection of SARS-CoV2 IgG.

Generation of Spike mutants

Amino acid substitutions were introduced into the D614G pCDNA_SARS-CoV-2_Spike plasmid as previously described⁴¹ using the QuikChange Lightning Site-Directed Mutagenesis kit, following the manufacturer's instructions (Agilent Technologies, Inc., Santa Clara, CA).

Pseudotype virus preparation

Viral vectors were prepared by transfection of 293T cells by using Fugene HD transfection reagent (Promega). 293T cells were transfected with a mixture of 11ul of Fugene HD, 1µg of pCDNAp19Spike-HA, 1ug of p8.91 HIV-1 gag-pol expression vector^{42,43}, and 1.5µg of pCSFLW (expressing the firefly luciferase reporter gene with the HIV-1 packaging signal). Viral supernatant was collected at 48 and 72h after transfection, filtered through 0.45um filter and stored at -8°C. The 50% tissue culture infectious dose (TCID50) of SARS-CoV-2 pseudovirus was determined using Steady-Glo Luciferase assay system (Promega).

Standardisation of virus input by SYBR Green-based product-enhanced PCR assay (SG-PERT)

The reverse transcriptase activity of virus preparations was determined by qPCR using a SYBR Green-based product-enhanced PCR assay (SG-PERT) as previously described⁴⁴. Briefly, 10-fold dilutions of virus supernatant were lysed in a 1:1 ratio in a 2x lysis solution (made up of 40% glycerol v/v 0.25% Triton X-100 v/v 100mM KCl, RNase inhibitor 0.8 U/ml, TrisHCL 100mM, buffered to pH7.4) for 10 minutes at room temperature.

12µl of each sample lysate was added to thirteen 13µl of a SYBR Green master mix (containing 0.5µM of MS2-RNA Fwd and Rev primers, 3.5pmol/ml of MS2-RNA, and 0.125U/µl of Ribolock RNase inhibitor and cycled in a QuantStudio. Relative amounts of reverse transcriptase activity were determined as the rate of transcription of bacteriophage MS2 RNA, with absolute RT activity calculated by comparing the relative amounts of RT to an RT standard of known activity.

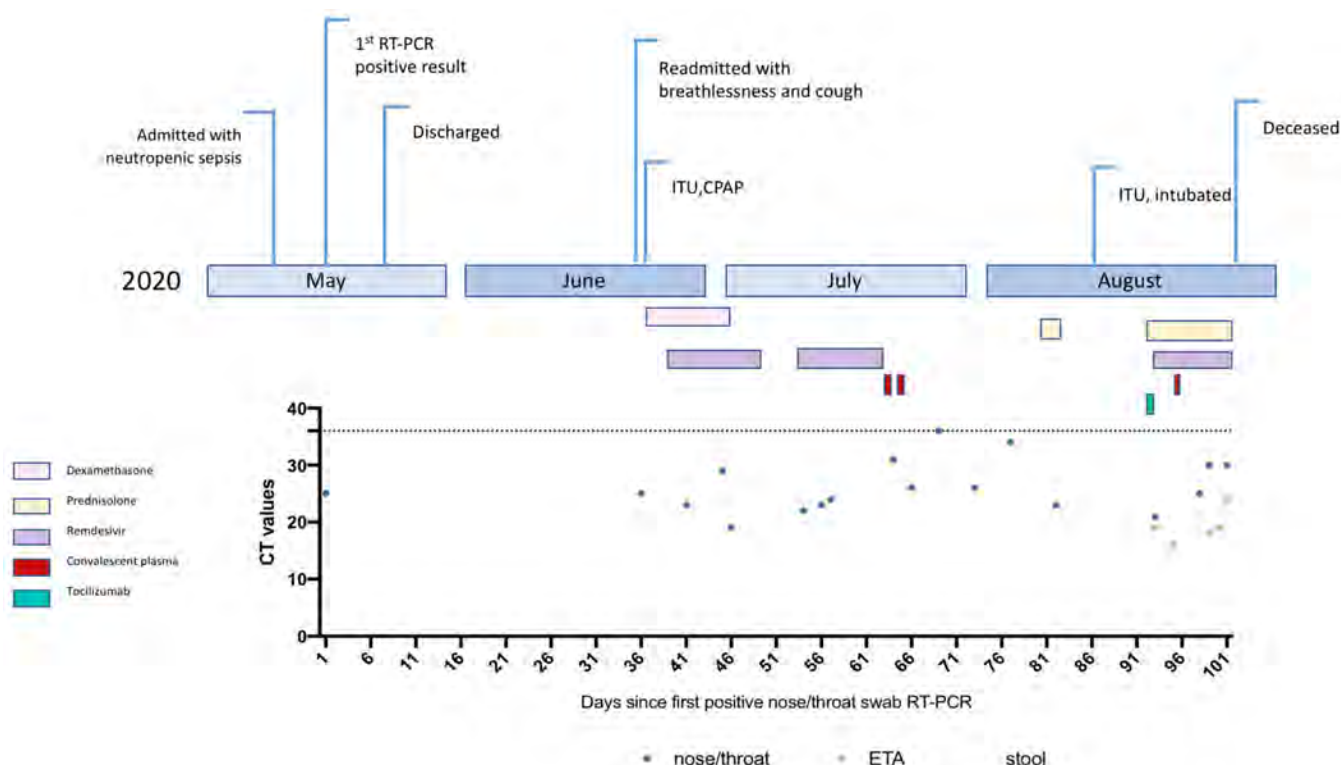
Serum/plasma pseudotype neutralization assay

Spike pseudotype assays have been shown to have similar characteristics as neutralisation testing using fully infectious wild type SARS-CoV-2⁸. Virus neutralisation assays were performed on 293T cell transiently transfected with ACE2 and TMPRSS2 using SARS-CoV-2 Spike pseudotyped virus expressing luciferase⁴⁵. Pseudotyped virus was incubated with serial dilution of heat inactivated human serum samples or convalescent plasma in duplicate for 1h at 37°C. Virus and cell only controls were also included. Then, freshly trypsinized 293T ACE2/TMPRSS2 expressing cells were added to each well. Following 48h incubation in a 5% CO₂ environment at 37°C, the luminescence was measured using Steady-Glo Luciferase assay system (Promega).

mAb pseudotype neutralisation assay

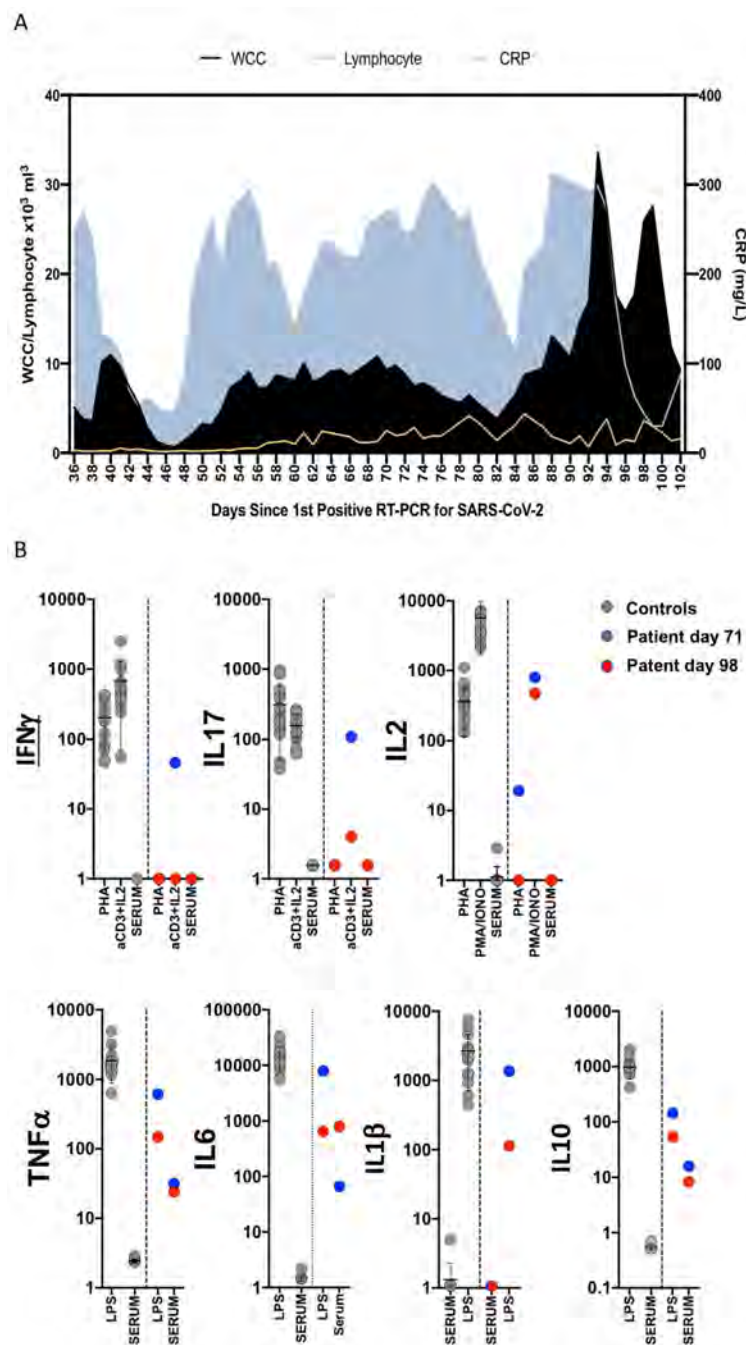
Virus neutralisation assays were performed on HeLa cells stably expressing ACE2 and using SARS-CoV-2 Spike pseudotyped virus expressing luciferase as previously described⁴⁶. Pseudotyped virus was incubated with serial dilution of purified mAbs⁹ in duplicate for 1h at 37°C. Then, freshly trypsinized HeLa ACE2-expressing cells were added to each well. Following 48h incubation in a 5% CO₂ environment at 37°C, the luminescence was measured using Bright-Glo Luciferase assay system (Promega) and neutralization calculated relative to virus only controls. IC₅₀ values were calculated in GraphPad Prism.

Extended Data



Extended Data Figure 1.

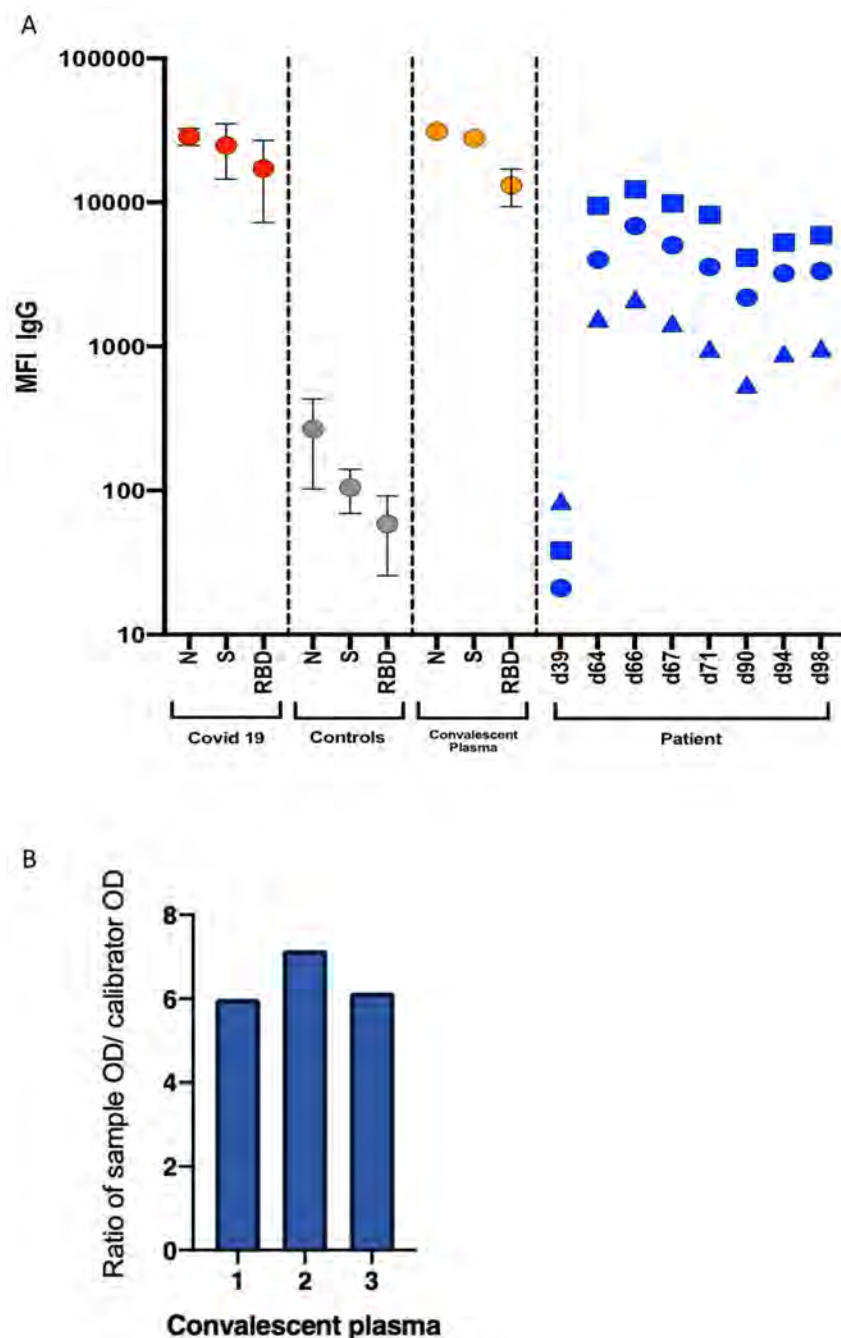
Clinical time line of events with longitudinal respiratory sample CT values. CT – cycle threshold.



Extended data 2.

A. Blood parameters over time in patient case: White cell count (WCC) and lymphocyte counts are expressed as $\times 10^3 \text{ Cells/mm}^3$. CRP: C reactive protein. **B. Assessment of T cell and innate function.** Whole blood cytokines were measured in whole blood after 24 hours stimulation either after T-cell stimulation with PHA or anti CD3/IL2 or innate stimulation

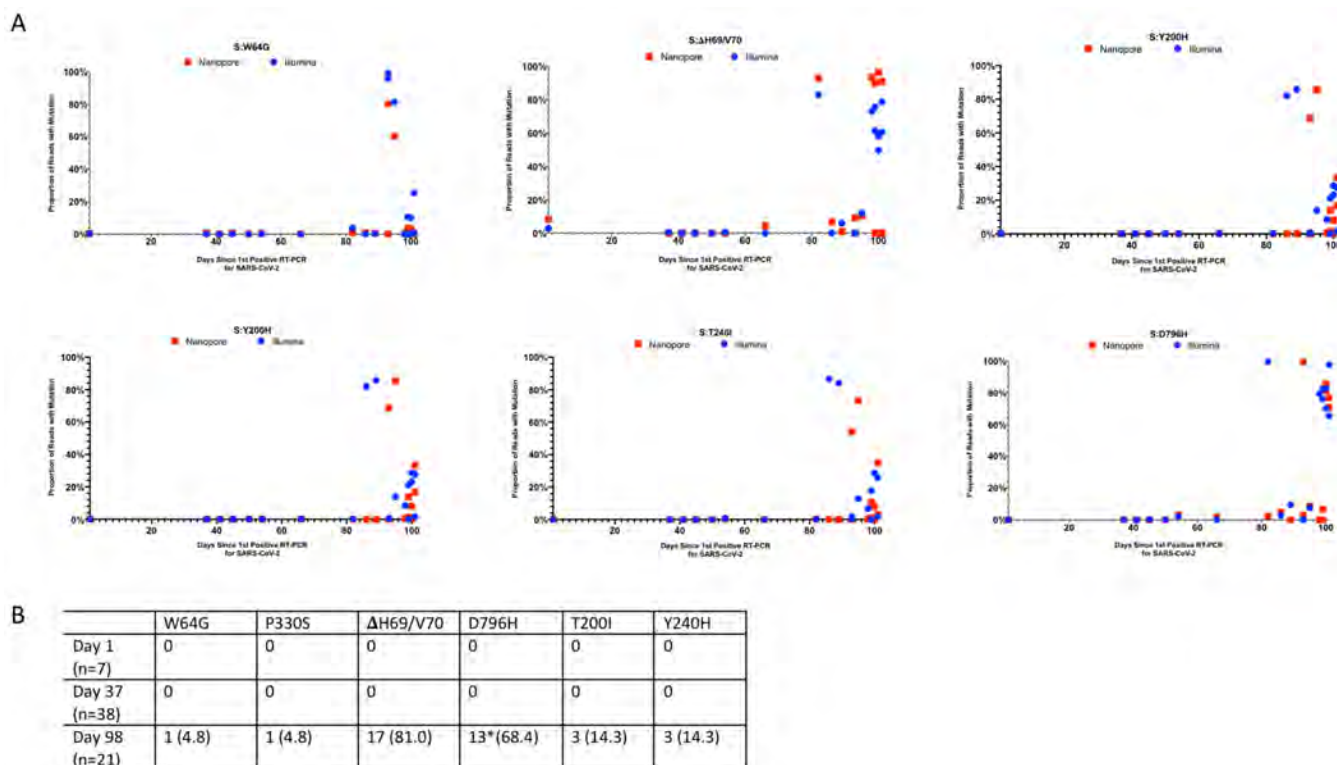
with LPS. Healthy controls are shown as grey circles (N=15), Patient at d71 and d98 is shown as blue circles or red circles respectively. Cytokine levels are shown as pg/ml stimulation. Mean is shown by line and whiskers representing standard deviation.



Extended Data Figure 3.

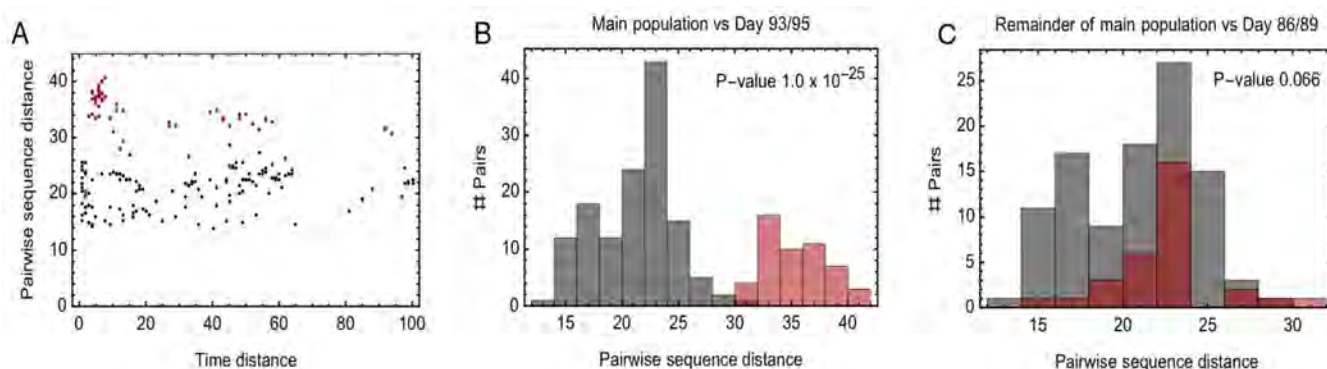
A. Serum SARS-CoV-2 antibody levels and virus population changes in chronic SARS-CoV-2 infection. Anti SARS-CoV2 IgG antibodies in patient and pre/post convalescent plasma compared to RNA+ Covid19 patients and pre-pandemic healthy controls: Red,

grey and gold: IgG antibodies to SARS-CoV2 nucleocapsid protein (N), trimeric S protein (S) and the receptor binding domain (RBD) were measured by multiplexed particle based flow cytometry (Luminex) in RNA+ COVID-19 patients (N=20, red dots), Pre-pandemic healthy controls (N=20, grey dots) and in the convalescent donor plasma (orange dots); Results are shown as mean fluorescent intensity (MFI) +/- SD. **Patient sera over time in blue:** Anti SARS-CoV2 IgG to N (blue squares), S (blue circles) and RBD (blue triangles). Timing of CP units is also shown. **B. SARS-CoV-2 antibody titres in patient and in convalescent plasma.** Measurement of SARS-CoV-2 specific IgG antibody titres in three units of convalescent plasma (CP) by Euroimmun assay.



Extended data 4. Comparison between short-read (Illumina) and long-read single molecule (Oxford Nanopore) sequencing methods for the six observed Spike mutations.

Concordance was generally good between the majority of timepoints, however due to large discrepancies in a number of timepoints, we suggest that due to the high base calling error rate, Nanopore is not yet suitable for calling minority variants. As such, all figures in the main paper were produced using Illumina data only. **B. Single genome sequencing (SGS) data from respiratory samples at indicated days.** Indicated are the number of single genomes obtained at each time point with the mutations of interest (identified by deep sequencing). *denominator is 19 as for 2 samples the primer reads were poor quality at amino acid 796 at day 98. Amino acid variant and corresponding nucleotide position: S:W64G = 21752, S: 69 = 21765-21770, S:Y200H = 22160, S:T240I = 22281, S:P330S = 22550, S:D795H = 23948



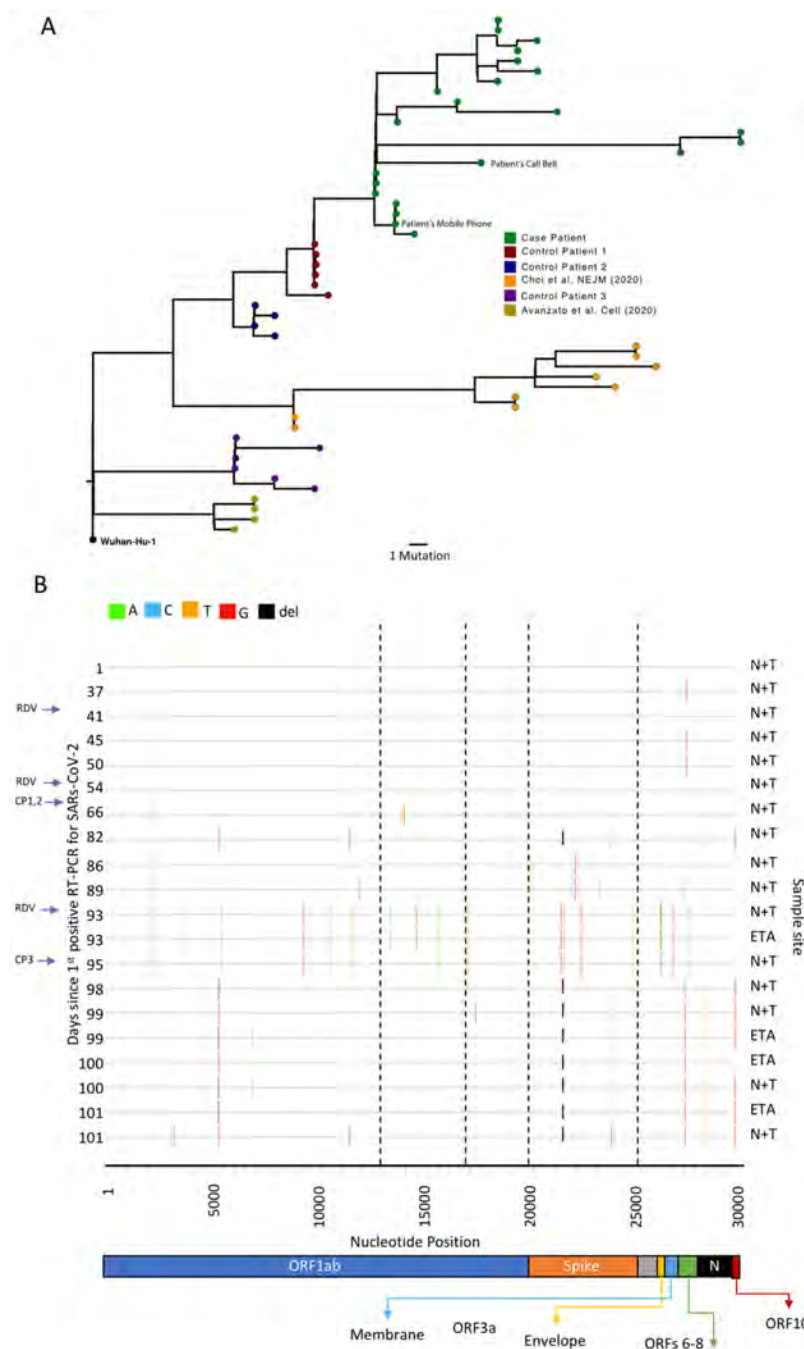
Extended Data Figure 5. Evidence for within-host cladal structure.

A. Pairwise distances between samples measured using the all-locus distance metric plotted against pairwise distances in time (measured in days) between samples being collected.

Internal distances between samples in the proposed main clade are shown in black, distances between samples in the main clade and samples collected on days 93 and 95 are shown in red, and internal distances between samples collected on days 93 and 95 are shown in green.

B. Pairwise distances between samples in the larger clade (black) and between these samples and those collected on days 93 and 95 (red). The median values of the distributions of these values are significantly different according to a Mann Whitney test. **C.** Pairwise distances between samples in the main clade, once those collected on days 86, 89, 93, 95 have been removed (black) and between these samples and those collected on days 86 and 89 (red).

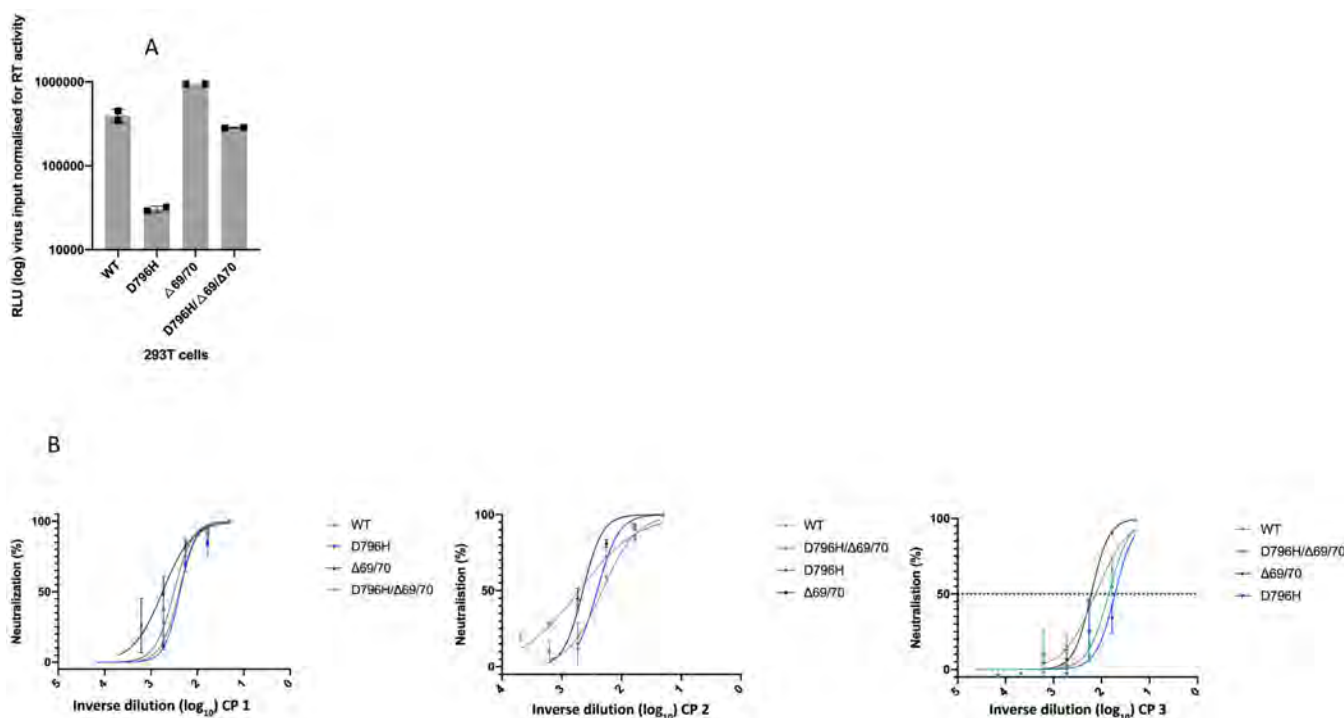
The median values of the distributions of these values are not significantly different at the 5 level according to a Mann Whitney test.



Extended Data Figure 6.

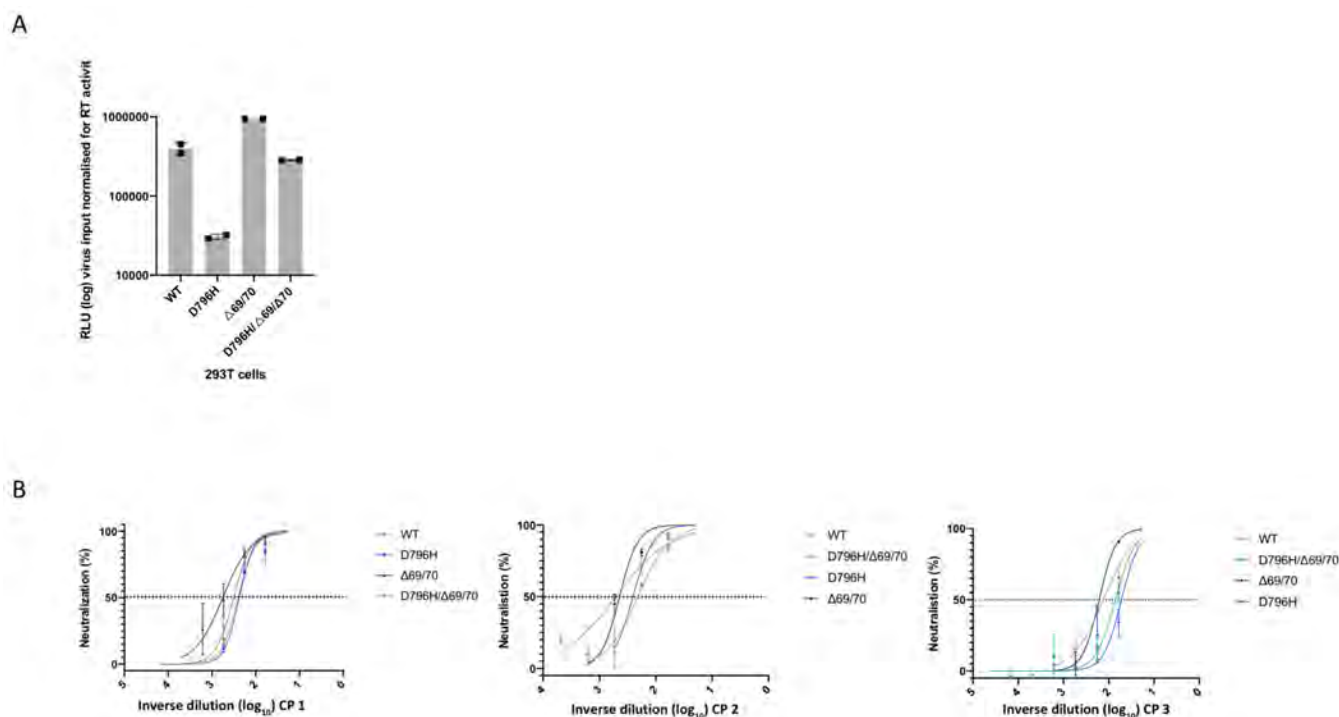
A. Close-view maximum-likelihood phylogenetic tree indicating the diversity of the case patient and three other long-term shedders from the local area (red, blue and purple), compared to recently published sequences from Choi et al (orange) and Avanzato et al (gold). Control patients generally showed limited diversity temporally, though the Choi et al sequences were highly divergent. Environmental samples (patient's call bell, and patient's mobile phone) are indicated. Tree branched have been collapsed where bootstrap support was <60.

B. Highlighter plot indicating nucleotide changes at consensus level in sequential respiratory samples compared to the consensus sequence at first diagnosis of COVID-19. Each row indicates the timepoint the sample was collected (number of days from first positive SARS-CoV-2 RT-PCR). Black dashed lines indicate the RNA-dependent RNA polymerase (RdRp) and Spike regions of the genome. There were few nucleotide substitutions between days 1-54, despite the patient receiving two courses of remdesivir. The first major changes in the spike genome occurred on day 82, following convalescent plasma given on days 63 and 65. The amino acid deletion in S1, H69/V70 is indicated by the black lines. Sites: Endotracheal aspirate (ETA) or Nose/throat swabs (N+T).



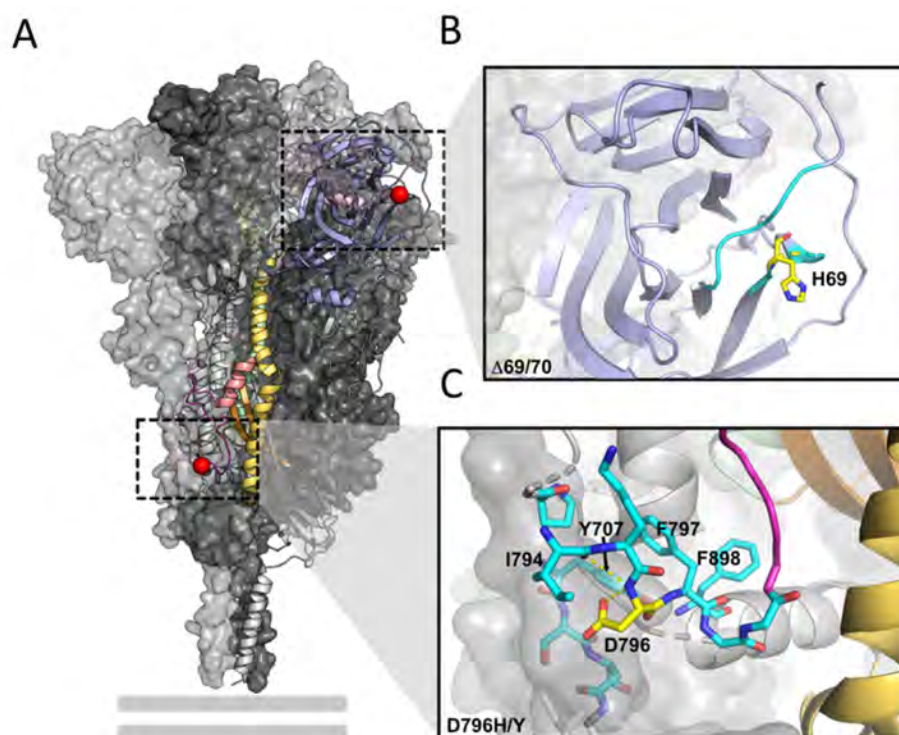
Extended Data 7. In vitro infectivity and neutralisation sensitivity of Spike pseudotyped lentiviruses.

A. infection of target 293T cells expressing TMPRSS2 and ACE2 receptors using equal amounts of virus as determined by reverse transcriptase activity. Data points represent technical replicates (n=2), with mean shown with error bars representing standard deviation. Data are representative of n=2 independent experiments (n=2). **B.** Representative Inverse dilution plots for Spike variants against convalescent plasma units 1-3. Data points represent mean neutralisation of technical replicates and error bars represent standard error of the mean of replicates. Data are representative of two independent experiments (n=2).



Extended Data Figure 8.

A. Neutralization potency of a panel of monoclonal antibodies targeting the RBD is not impacted by Spike mutations D796H or H69/V70. Lentivirus pseudotyped with SARS-CoV-2 Spike protein: WT (D614G background), D796H, H69/V70, D796H+ H69/V70 were produced in 293T cells and used to infect target Hela cells stably expressing ACE2 in the presence of serial dilutions of indicated monoclonal antibodies. Data are means of technical replicates with error bars representing SD. Data are representative of at least two independent experiments. RBD: receptor binding domain. **B. Classes of RBD binding antibodies and fold changes for Spike mutations D796H or H69/V70** are indicated based Bouwer et al. Clusters II, V contain only non-neutralising mAbs, smaller neutralising mAb clusters IV (n=2) and X (n=1) were not tested. Red indicates significant fold changes.



Mutation	Number of Sequences	Global Prevalence (%)
W64G	0	0.00
Δ H69/V70	12883	4.32
Y200H	7	<0.01
T240I	77	0.02
P330S	167	0.06
D796H	65	0.02
D796Y	141	0.05

Extended Data 9. Location of Spike mutations H69/Y70 and D796H.

A. The SARS-CoV-2 spike trimer (PDB ID: 6xr8) with two protomers represented as surfaces and one protomer represented as a ribbon. The NTD is coloured in light blue, the RBD in light pink, the fusion peptide in dark pink, the HR1 domain in yellow, the CH domain in pale green, and the CD domain in brown. The location of D796 and H69 are indicated by red spheres. The loop connecting D796 to the fusion peptide is coloured magenta to improve visibility. The double grey lines provide orientation relative to the membrane. **B.** A close-up of the region defined by the box around H69 in panel A. H69 is highlighted in yellow. Residues containing atoms that are within 6 Å of H69 are highlighted in cyan. **C.** A close-up of the region defined by the box around D796 in panel A. D796 is

highlighted in yellow. Residues containing atoms that are within 6 Å of D796 are highlighted in cyan. Hydrogen bonds are indicated by dashed yellow lines. Hydrophobic residues in the vicinity of D796 have been labelled. Y707 is from the neighbouring protomer. **D. Global prevalence of selected spike mutations detailed in this paper.** All high coverage sequences were downloaded from the GISAID database on 6th January and aligned using MAFFT; as of this date there were 298254 sequences available. The global prevalence of each of the six spike mutations W64G, H69/V70, Y200H, T240I, P330S and D796H were assessed by viewing the multiple sequence alignment in AliView, sorting by the column of interest, and counting the number of mutations.

Supplementary Material

Refer to Web version on PubMed Central for supplementary material.

Authors

Steven A Kemp^{#1}, Dami A Collier^{#1,2,3}, Rawlings P Datir^{#2,3}, Isabella ATM Ferreira^{2,3}, Salma Gayed⁴, Aminu Jahun⁵, Myra Hosmillo⁵, Chloe Rees-Spear¹, Petra Mlcochova^{2,3}, Ines Ushiro Lumb⁶, David J Roberts⁶, Anita Chandra^{2,3}, Nigel Temperton⁷, The CITIID-NIHR BioResource COVID-19 Collaboration Stephen Baker^{2,3} [Principal Investigators], Gordon Dougan^{2,3} [Principal Investigators], Christoph Hess^{2,3,26,27} [Principal Investigators], Nathalie Kingston^{20,12} [Principal Investigators], Paul J. Lehner^{2,3} [Principal Investigators], Paul A. Lyons^{2,3} [Principal Investigators], Nicholas J. Matheson^{2,3} [Principal Investigators], Willem H. Owehand²⁰ [Principal Investigators], Caroline Saunders¹⁹ [Principal Investigators], Charlotte Summers^{3,24,25,28} [Principal Investigators], James E.D. Thaventhiran^{2,3,22} [Principal Investigators], Mark Toshner^{3,24,25} [Principal Investigators], Michael P. Weekes² [Principal Investigators], Ashlea Bucke¹⁹ [CRF and Volunteer Research Nurses], Jo Calder¹⁹ [CRF and Volunteer Research Nurses], Laura Canna¹⁹ [CRF and Volunteer Research Nurses], Jason Domingo¹⁹ [CRF and Volunteer Research Nurses], Anne Elmer¹⁹ [CRF and Volunteer Research Nurses], Stewart Fuller¹⁹ [CRF and Volunteer Research Nurses], Julie Harris⁴¹ [CRF and Volunteer Research Nurses], Sarah Hewitt¹⁹ [CRF and Volunteer Research Nurses], Jane Kennet¹⁹ [CRF and Volunteer Research Nurses], Sherly Jose¹⁹ [CRF and Volunteer Research Nurses], Jenny Kourampa¹⁹ [CRF and Volunteer Research Nurses], Anne Meadows¹⁹ [CRF and Volunteer Research Nurses], Criona O'Brien⁴¹ [CRF and Volunteer Research Nurses], Jane Price¹⁹ [CRF and Volunteer Research Nurses], Cherry Publico¹⁹ [CRF and Volunteer Research Nurses], Rebecca Rastall¹⁹ [CRF and Volunteer Research Nurses], Carla Ribeiro¹⁹ [CRF and Volunteer Research Nurses], Jane Rowlands¹⁹ [CRF and Volunteer Research Nurses], Valentina Ruffolo¹⁹ [CRF and Volunteer Research Nurses], Hugo Tordesillas¹⁹ [CRF and Volunteer Research Nurses], Ben Bullman² [Sample Logistics], Benjamin J Dunmore³ [Sample Logistics], Stuart Fawke³⁰ [Sample Logistics], Stefan Gräf^{3,12,20} [Sample Logistics], Josh Hodgson³ [Sample Logistics], Christopher Huang³

[Sample Logistics], Kelvin Hunter^{2,3} [Sample Logistics], Emma Jones²⁹
 [Sample Logistics], Ekaterina Legchenko³ [Sample Logistics], Cecilia Matara³
 [Sample Logistics], Jennifer Martin³ [Sample Logistics], Federica Mescia^{2,3}
 [Sample Logistics], Ciara O'Donnell³ [Sample Logistics], Linda Pointon³
 [Sample Logistics], Nicole Pond^{2,3} [Sample Logistics], Joy Shih³ [Sample
 Logistics], Rachel Sutcliffe³ [Sample Logistics], Tobias Tilly³ [Sample
 Logistics], Carmen Treacy³ [Sample Logistics], Zhen Tong³ [Sample
 Logistics], Jennifer Wood³ [Sample Logistics], Marta Wylot³⁶ [Sample
 Logistics], Laura Bergamaschi^{2,3} [Sample Processing and Data Acquisition],
 Ariana Betancourt^{2,3} [Sample Processing and Data Acquisition], Georgie
 Bower^{2,3} [Sample Processing and Data Acquisition], Chiara Cossetti^{2,3}
 [Sample Processing and Data Acquisition], Aloka De Sa³ [Sample Processing
 and Data Acquisition], Madeline Epping^{2,3} [Sample Processing and Data
 Acquisition], Stuart Fawke³² [Sample Processing and Data Acquisition], Nick
 Gleadall²⁰ [Sample Processing and Data Acquisition], Richard Grenfell³¹
 [Sample Processing and Data Acquisition], Andrew Hinch^{2,3} [Sample
 Processing and Data Acquisition], Oisin Huhn³² [Sample Processing and Data
 Acquisition], Sarah Jackson³ [Sample Processing and Data Acquisition],
 Isobel Jarvis³ [Sample Processing and Data Acquisition], Daniel Lewis³
 [Sample Processing and Data Acquisition], Joe Marsden³ [Sample Processing
 and Data Acquisition], Francesca Nice³⁹ [Sample Processing and Data
 Acquisition], Georgina Okecha³ [Sample Processing and Data Acquisition],
 Ommar Omarjee³ [Sample Processing and Data Acquisition], Marianne
 Perera³ [Sample Processing and Data Acquisition], Nathan Richoz³ [Sample
 Processing and Data Acquisition], Veronika Romashova^{2,3} [Sample
 Processing and Data Acquisition], Natalia Savinykh Yarkoni³ [Sample
 Processing and Data Acquisition], Rahul Sharma³ [Sample Processing and
 Data Acquisition], Luca Stefanucci²⁰ [Sample Processing and Data
 Acquisition], Jonathan Stephens²⁰ [Sample Processing and Data Acquisition],
 Mateusz Strezlecki³¹ [Sample Processing and Data Acquisition], Lori Turner^{2,3}
 [Sample Processing and Data Acquisition], Eckart M.D.D. De Bie³ [Clinical
 Data Collection], Katherine Bunclark³ [Clinical Data Collection], Masa
 Josipovic⁴⁰ [Clinical Data Collection], Michael Mackay³ [Clinical Data
 Collection], Federica Mescia^{2,3} [Clinical Data Collection], Alice Michael²⁵
 [Clinical Data Collection], Sabrina Rossi³⁵ [Clinical Data Collection], Mayurun
 Selvan³ [Clinical Data Collection], Sarah Spencer¹⁵ [Clinical Data Collection],
 Cissy Yong³⁵ [Clinical Data Collection], Ali Ansari pour²⁵ [Royal Papworth
 Hospital ICU], Alice Michael²⁵ [Royal Papworth Hospital ICU], Lucy Mwaura²⁵
 [Royal Papworth Hospital ICU], Caroline Patterson²⁵ [Royal Papworth Hospital
 ICU], Gary Polwarth²⁵ [Royal Papworth Hospital ICU], Petra Polgarova²⁸
 [Addenbrooke's Hospital ICU], Giovanni di Stefano²⁸ [Addenbrooke's Hospital
 ICU], Codie Fahey³⁴ [Cambridge and Peterborough Foundation Trust], Rachel
 Michel³⁴ [Cambridge and Peterborough Foundation Trust], Sze-How Bong²¹
 [ANPC and Centre for Molecular Medicine and Innovative Therapeutics],
 Jerome D. Coudert³³ [ANPC and Centre for Molecular Medicine and Innovative

Therapeutics], Elaine Holmes³⁷ [ANPC and Centre for Molecular Medicine and Innovative Therapeutics], John Allison^{20,12} [NIHR BioResource], Helen Butcher^{12,38} [NIHR BioResource], Daniela Caputo^{12,38} [NIHR BioResource], Debbie Clapham-Riley^{12,38} [NIHR BioResource], Eleanor Dewhurst^{12,38} [NIHR BioResource], Anita Furlong^{12,38} [NIHR BioResource], Barbara Graves^{12,38} [NIHR BioResource], Jennifer Gray^{12,38} [NIHR BioResource], Tasmin Ivers^{12,38} [NIHR BioResource], Mary Kasanicki^{12,28} [NIHR BioResource], Emma Le Gresley^{12,38} [NIHR BioResource], Rachel Linger^{12,38} [NIHR BioResource], Sarah Meloy^{12,38} [NIHR BioResource], Francesca Muldoon^{12,38} [NIHR BioResource], Nigel Ovington^{12,20} [NIHR BioResource], Sofia Papadia^{12,38} [NIHR BioResource], Isabel Phelan^{12,38} [NIHR BioResource], Hannah Stark^{12,38} [NIHR BioResource], Kathleen E Stirrups^{12,20} [NIHR BioResource], Paul Townsend^{12,20} [NIHR BioResource], Neil Walker^{12,20} [NIHR BioResource], Jennifer Webster^{12,38} [NIHR BioResource]

¹⁹Cambridge Clinical Research Centre, NIHR Clinical Research Facility, Cambridge University Hospitals NHS Foundation Trust, Addenbrooke's Hospital, Cambridge CB2 0QQ, UK ²⁰Department of Haematology, University of Cambridge, Cambridge Biomedical Campus, Cambridge CB2 0QQ, UK ²¹Australian National Phenome Centre, Murdoch University, Murdoch, Western Australia WA 6150, Australia ²²MRC Toxicology Unit, School of Biological Sciences, University of Cambridge, Cambridge CB2 1QR, UK ²³R&D Department, Hycult Biotech, 5405 PD Uden, The Netherlands ²⁴Heart and Lung Research Institute, Cambridge Biomedical Campus, Cambridge CB2 0QQ, UK ²⁵Royal Papworth Hospital NHS Foundation Trust, Cambridge Biomedical Campus, Cambridge CB2 0QQ, UK ²⁶Department of Biomedicine, University and University Hospital Basel, 4031Basel, Switzerland ²⁷Botnar Research Centre for Child Health (BRCCH) University Basel & ETH Zurich, 4058 Basel, Switzerland ²⁸Addenbrooke's Hospital, Cambridge CB2 0QQ, UK ²⁹Department of Veterinary Medicine, Madingley Road, Cambridge, CB3 0ES, UK ³⁰Cambridge Institute for Medical Research, Cambridge Biomedical Campus, Cambridge CB2 0XY, UK ³¹Cancer Research UK, Cambridge Institute, University of Cambridge CB2 0RE, UK ³²Department of Obstetrics & Gynaecology, The Rosie Maternity Hospital, Robinson Way, Cambridge CB2 0SW, UK ³³Centre for Molecular Medicine and Innovative Therapeutics, Health Futures Institute, Murdoch University, Perth, WA, Australia ³⁴Cambridge and Peterborough Foundation Trust, Fulbourn Hospital, Fulbourn, Cambridge CB21 5EF, UK ³⁵Department of Surgery, Addenbrooke's Hospital, Cambridge CB2 0QQ, UK ³⁶Department of Biochemistry, University of Cambridge, Cambridge, CB2 1QW, UK ³⁷Centre of Computational and Systems Medicine, Health Futures Institute, Murdoch University, Harry Perkins Building, Perth, WA 6150, Australia ³⁸Department of Public Health and Primary Care, School of Clinical Medicine, University of Cambridge, Cambridge Biomedical Campus, Cambridge, UK ³⁹Cancer Molecular Diagnostics Laboratory, Department of Oncology, University of Cambridge, Cambridge CB2 0AH, UK ⁴⁰Metabolic

Research Laboratories, Wellcome Trust-Medical Research Council Institute of Metabolic Science, University of Cambridge, Cambridge CB2 0QQ, UK

⁴¹Department of Paediatrics, University of Cambridge, Cambridge Biomedical Campus, Cambridge, CB2 0QQ, UK

, The COVID-19 Genomics UK (COG-UK) Consortium

Samuel C Robson⁵⁴ [Funding acquisition, Leadership and supervision, Metadata curation, Project administration, Samples and logistics, Sequencing and analysis, Software and analysis tools, and Visualisation], Nicholas J Loman⁸², Thomas R Connor^{51,110} [Funding acquisition, Leadership and supervision, Metadata curation, Project administration, Samples and logistics, Sequencing and analysis, and Software and analysis tools], Tanya Golubchik⁴⁶ [Leadership and supervision, Metadata curation, Project administration, Samples and logistics, Sequencing and analysis, Software and analysis tools, and Visualisation], Rocio T Martinez Nunez⁸³ [Funding acquisition, Metadata curation, Samples and logistics, Sequencing and analysis, Software and analysis tools, and Visualisation], Catherine Ludden¹²⁹ [Funding acquisition, Leadership and supervision, Metadata curation, Project administration, and Samples and logistics], Sally Corden¹¹⁰ [Funding acquisition, Leadership and supervision, Metadata curation, Samples and logistics, and Sequencing and analysis], Ian Johnston¹⁴⁰, David Bonsall⁴⁶ [Funding acquisition, Leadership and supervision, Project administration, Samples and logistics, and Sequencing and analysis], Colin P Smith¹²⁸, Ali R Awan⁶⁹ [Funding acquisition, Leadership and supervision, Sequencing and analysis, Software and analysis tools, and Visualisation], Giselda Bucca¹²⁸ [Funding acquisition, Samples and logistics, Sequencing and analysis, Software and analysis tools, and Visualisation], M. Estee Torok^{63,142} [Leadership and supervision, Metadata curation, Project administration, Samples and logistics, and Sequencing and analysis], Kordo Saeed^{122,151} [Leadership and supervision, Metadata curation, Project administration, Samples and logistics, and Visualisation], Jacqui A Prieto^{124,150} [Leadership and supervision, Metadata curation, Project administration, Samples and logistics, and Visualisation], David K Jackson¹⁴⁰ [Leadership and supervision, Metadata curation, Project administration, Sequencing and analysis, and Software and analysis tools], William L Hamilton⁶³ [Metadata curation, Project administration, Samples and logistics, Sequencing and analysis, and Software and analysis tools], Luke B Snell⁵² [Metadata curation, Project administration, Samples and logistics, Sequencing and analysis, and Visualisation], Catherine Moore¹¹⁰ [Funding acquisition, Leadership and supervision, Metadata curation, and Samples and logistics], Ewan M Harrison^{129,140} [Funding acquisition, Leadership and supervision, Project administration, and Samples and logistics], Sonia Goncalves¹⁴⁰ [Leadership and supervision, Metadata curation, Project administration, and Samples and logistics], Derek J Fairley^{44,113} [Leadership and supervision, Metadata

curation, Samples and logistics, and Sequencing and analysis], Matthew W Loose⁵⁹ [Leadership and supervision, Metadata curation, Samples and logistics, and Sequencing and analysis], Joanne Watkins¹¹⁰ [Leadership and supervision, Metadata curation, Samples and logistics, and Sequencing and analysis], Rich Livett¹⁴⁰ [Leadership and supervision, Metadata curation, Samples and logistics, and Software and analysis tools], Samuel Moses^{66,147} [Leadership and supervision, Metadata curation, Samples and logistics, and Visualisation], Roberto Amato¹⁴⁰ [Leadership and supervision, Metadata curation, Sequencing and analysis, and Software and analysis tools], Sam Nicholls⁸² [Leadership and supervision, Metadata curation, Sequencing and analysis, and Software and analysis tools], Matthew Bull¹¹⁰ [Leadership and supervision, Metadata curation, Sequencing and analysis, and Software and analysis tools], Darren L Smith^{1,99,146} [Leadership and supervision, Project administration, Samples and logistics, and Sequencing and analysis], Jeff Barrett¹⁴⁰ [Leadership and supervision, Sequencing and analysis, Software and analysis tools, and Visualisation], David M Aanensen⁵⁵ [Leadership and supervision, Sequencing and analysis, Software and analysis tools, and Visualisation], Martin D Curran¹⁰⁶ [Metadata curation, Project administration, Samples and logistics, and Sequencing and analysis], Surendra Parmar¹⁰⁶ [Metadata curation, Project administration, Samples and logistics, and Sequencing and analysis], Dinesh Aggarwal^{1,140,105} [Metadata curation, Project administration, Samples and logistics, and Sequencing and analysis], James G Shepherd⁸⁹ [Metadata curation, Project administration, Samples and logistics, and Sequencing and analysis], Matthew D Parker¹³⁴ [Metadata curation, Project administration, Sequencing and analysis, and Software and analysis tools], Sharon Glaysher¹⁰² [Metadata curation, Samples and logistics, Sequencing and analysis, and Visualisation], Matthew Bashton^{78,99} [Metadata curation, Sequencing and analysis, Software and analysis tools, and Visualisation], Anthony P Underwood⁵⁵ [Metadata curation, Sequencing and analysis, Software and analysis tools, and Visualisation], Nicole Pacchiarini¹¹⁰ [Metadata curation, Sequencing and analysis, Software and analysis tools, and Visualisation], Katie F Loveson¹¹⁸ [Metadata curation, Sequencing and analysis, Software and analysis tools, and Visualisation], Alessandro M Carabelli¹²⁹ [Project administration, Sequencing and analysis, Software and analysis tools, and Visualisation], Kate E Templeton^{94,131} [Funding acquisition, Leadership and supervision, and Metadata curation], Cordelia F Langford¹⁴⁰ [Funding acquisition, Leadership and supervision, and Project administration], John Sillitoe¹⁴⁰ [Funding acquisition, Leadership and supervision, and Project administration], Thushan I de Silva¹³⁴ [Funding acquisition, Leadership and supervision, and Project administration], Dennis Wang¹³⁴ [Funding acquisition, Leadership and supervision, and Project administration], Dominic Kwiatkowski^{140,148} [Funding acquisition, Leadership and supervision, and Sequencing and analysis], Andrew Rambaut¹³¹ [Funding acquisition, Leadership and supervision, and Sequencing and analysis], Justin O'Grady^{111,130} [Funding acquisition, Leadership and

supervision, and Sequencing and analysis], Simon Cottrell¹¹⁰ [Funding acquisition, Leadership and supervision, and Sequencing and analysis], Matthew T.G. Holden¹⁰⁹ [Leadership and supervision, Metadata curation, and Sequencing and analysis], Emma C Thomson⁸⁹ [Leadership and supervision, Metadata curation, and Sequencing and analysis], Husam Osman^{77,105} [Leadership and supervision, Project administration, and Samples and logistics], Monique Andersson¹⁰⁰ [Leadership and supervision, Project administration, and Samples and logistics], Anoop J Chauhan¹⁰² [Leadership and supervision, Project administration, and Samples and logistics], Mohammed O Hassan-Ibrahim⁴⁷ [Leadership and supervision, Project administration, and Samples and logistics], Mara Lawniczak¹⁴⁰ [Leadership and supervision, Project administration, and Sequencing and analysis], Alex Alderton¹⁴⁰ [Leadership and supervision, Samples and logistics, and Sequencing and analysis], Meera Chand¹⁰⁷ [Leadership and supervision, Samples and logistics, and Sequencing and analysis], Chrystala Constantinidou¹³⁵ [Leadership and supervision, Samples and logistics, and Sequencing and analysis], Meera Unnikrishnan¹³⁵ [Leadership and supervision, Samples and logistics, and Sequencing and analysis], Alistair C Darby¹³³ [Leadership and supervision, Samples and logistics, and Sequencing and analysis], Julian A Hiscox¹³³ [Leadership and supervision, Samples and logistics, and Sequencing and analysis], Steve Paterson¹³³ [Leadership and supervision, Samples and logistics, and Sequencing and analysis], Inigo Martincorena¹⁴⁰ [Leadership and supervision, Sequencing and analysis, and Software and analysis tools], David L Robertson⁸⁹ [Leadership and supervision, Sequencing and analysis, and Software and analysis tools], Erik M Volz⁸⁰ [Leadership and supervision, Sequencing and analysis, and Software and analysis tools], Andrew J Page¹¹¹ [Leadership and supervision, Sequencing and analysis, and Software and analysis tools], Oliver G Pybus⁶⁴ [Leadership and supervision, Sequencing and analysis, and Software and analysis tools], Andrew R Bassett¹⁴⁰ [Leadership and supervision, Sequencing and analysis, and Visualisation], Cristina V Ariani¹⁴⁰ [Metadata curation, Project administration, and Samples and logistics], Michael H Spencer Chapman^{129,140} [Metadata curation, Project administration, and Samples and logistics], Kathy K Li⁸⁹ [Metadata curation, Project administration, and Samples and logistics], Rajiv N Shah⁸⁹ [Metadata curation, Project administration, and Samples and logistics], Natasha G Jesudason⁸⁹ [Metadata curation, Project administration, and Samples and logistics], Yusri Taha⁹¹ [Metadata curation, Project administration, and Samples and logistics], Martin P McHugh⁹⁴ [Metadata curation, Project administration, and Sequencing and analysis], Rebecca Dewar⁹⁴ [Metadata curation, Project administration, and Sequencing and analysis], Aminu S Jahun⁶⁵ [Metadata curation, Samples and logistics, and Sequencing and analysis], Claire McMurray⁸² [Metadata curation, Samples and logistics, and Sequencing and analysis], Sarojini Pandey¹²⁵ [Metadata curation, Samples and logistics, and Sequencing and analysis], James P McKenna⁴⁴ [Metadata

curation, Samples and logistics, and Sequencing and analysis], Andrew Nelson^{99,146} [Metadata curation, Samples and logistics, and Sequencing and analysis], Gregory R Young^{78,99} [Metadata curation, Samples and logistics, and Sequencing and analysis], Clare M McCann^{99,146} [Metadata curation, Samples and logistics, and Sequencing and analysis], Scott Elliott¹⁰² [Metadata curation, Samples and logistics, and Sequencing and analysis], Hannah Lowe⁶⁶ [Metadata curation, Samples and logistics, and Visualisation], Ben Temperton¹³² [Metadata curation, Sequencing and analysis, and Software and analysis tools], Sunando Roy¹²³ [Metadata curation, Sequencing and analysis, and Software and analysis tools], Anna Price⁵¹ [Metadata curation, Sequencing and analysis, and Software and analysis tools], Sara Rey¹¹⁰ [Metadata curation, Sequencing and analysis, and Software and analysis tools], Matthew Wyles¹³⁴ [Metadata curation, Sequencing and analysis, and Software and analysis tools], Stefan Rooke¹³¹ [Metadata curation, Sequencing and analysis, and Visualisation], Sharif Shaaban¹⁰⁹ [Metadata curation, Sequencing and analysis, and Visualisation], Mariateresa de Cesare¹³⁹ [Project administration, Samples and logistics, Sequencing and analysis], Laura Letchford¹⁴⁰ [Project administration, Samples and logistics, and Software and analysis tools], Siona Silveira¹²² [Project administration, Samples and logistics, and Visualisation], Emanuela Pelosi¹²² [Project administration, Samples and logistics, and Visualisation], Eleri Wilson-Davies¹²² [Project administration, Samples and logistics, and Visualisation], Myra Hosmillo⁶⁵ [Samples and logistics, Sequencing and analysis, and Software and analysis tools], Áine O'Toole¹³¹ [Sequencing and analysis, Software and analysis tools, and Visualisation], Andrew R Hesketh¹²⁸ [Sequencing and analysis, Software and analysis tools, and Visualisation], Richard Stark¹³⁵ [Sequencing and analysis, Software and analysis tools, and Visualisation], Louis du Plessis⁶⁴ [Sequencing and analysis, Software and analysis tools, and Visualisation], Chris Ruis¹²⁹ [Sequencing and analysis, Software and analysis tools, and Visualisation], Helen Adams⁴⁵ [Sequencing and analysis, Software and analysis tools, and Visualisation], Yann Bourgeois¹¹⁷ [Sequencing and analysis, Software and analysis tools, and Visualisation], Stephen L Michell¹³² [Funding acquisition, and Leadership and supervision], Dimitris Gramatopoulos^{125,153} [Funding acquisition, and Leadership and supervision], Jonathan Edgeworth⁵³ [Funding acquisition, and Leadership and supervision], Judith Breuer^{71,123} [Funding acquisition, and Leadership and supervision], John A Todd¹³⁹ [Funding acquisition, and Leadership and supervision], Christophe Fraser⁴⁶ [Funding acquisition, and Leadership and supervision], David Buck¹³⁹ [Funding acquisition, and Project administration], Michaela John⁵⁰ [Funding acquisition, and Project administration], Gemma L Kay¹¹¹ [Leadership and supervision, and Metadata curation], Steve Palmer¹⁴⁰ [Leadership and supervision, and Project administration], Sharon J Peacock^{129,105} [Leadership and supervision, and Project administration], David Heyburn¹¹⁰ [Leadership and supervision, and Project administration], Danni Weldon¹⁴⁰ [Leadership and supervision, and

Samples and logistics], Esther Robinson^{105,77} [Leadership and supervision, and Samples and logistics], Alan McNally^{82,127} [Leadership and supervision, and Samples and logistics], Peter Muir¹⁰⁵ [Leadership and supervision, and Samples and logistics], Ian B Vipond¹⁰⁵ [Leadership and supervision, and Samples and logistics], John BoYes⁷⁰ [Leadership and supervision, and Samples and logistics], Venkat Sivaprakasam⁸⁷ [Leadership and supervision, and Samples and logistics], Tranprit Salluja¹¹⁶ [Leadership and supervision, and Samples and logistics], Samir Dervisevic⁹⁵ [Leadership and supervision, and Samples and logistics], Emma J Meader⁹⁵ [Leadership and supervision, and Samples and logistics], Naomi R Park¹⁴⁰ [Leadership and supervision, and Sequencing and analysis], Karen Oliver¹⁴⁰ [Leadership and supervision, and Sequencing and analysis], Aaron R Jeffries¹³² [Leadership and supervision, and Sequencing and analysis], Sascha Ott¹³⁵ [Leadership and supervision, and Sequencing and analysis], Ana da Silva Filipe⁸⁹ [Leadership and supervision, and Sequencing and analysis], David A Simpson¹¹³ [Leadership and supervision, and Sequencing and analysis], Chris Williams¹¹⁰ [Leadership and supervision, and Sequencing and analysis], Jane AH Masoli^{114,132} [Leadership and supervision, and Visualisation], Bridget A Knight^{114,132} [Metadata curation, and Samples and logistics], Christopher R Jones^{114,132} [Metadata curation, and Samples and logistics], Cherian Koshy⁴² [Metadata curation, and Samples and logistics], Amy Ash⁴² [Metadata curation, and Samples and logistics], Anna Casey¹¹² [Metadata curation, and Samples and logistics], Andrew Bosworth^{105,77} [Metadata curation, and Samples and logistics], Liz Ratcliffe¹¹² [Metadata curation, and Samples and logistics], Li Xu-McCrae⁷⁷ [Metadata curation, and Samples and logistics], Hannah M Pymont¹⁰⁵ [Metadata curation, and Samples and logistics], Stephanie Hutchings¹⁰⁵ [Metadata curation, and Samples and logistics], Lisa Berry¹²⁵ [Metadata curation, and Samples and logistics], Katie Jones¹²⁵ [Metadata curation, and Samples and logistics], Fenella Halstead⁸⁷ [Metadata curation, and Samples and logistics], Thomas Davis⁶² [Metadata curation, and Samples and logistics], Christopher Holmes⁵⁷ [Metadata curation, and Samples and logistics], Miren Iturriza-Gomara¹³³ [Metadata curation, and Samples and logistics], Anita O Lucaci¹³³ [Metadata curation, and Samples and logistics], Paul Anthony Randell^{79,145} [Metadata curation, and Samples and logistics], Alison Cox^{79,145} [Metadata curation, and Samples and logistics], Pinglawathee Madona^{79,145} [Metadata curation, and Samples and logistics], Kathryn Ann Harris⁷¹ [Metadata curation, and Samples and logistics], Julianne Rose Brown⁷¹ [Metadata curation, and Samples and logistics], Tabitha W Mahungu¹¹⁵ [Metadata curation, and Samples and logistics], Dianne Irish-Tavares¹¹⁵ [Metadata curation, and Samples and logistics], Tanzina Haque¹¹⁵ [Metadata curation, and Samples and logistics], Jennifer Hart¹¹⁵ [Metadata curation, and Samples and logistics], Eric Witele¹¹⁵ [Metadata curation, and Samples and logistics], Melisa Louise Fenton¹¹⁶ [Metadata curation, and Samples and logistics], Steven Liggett¹²⁰ [Metadata curation, and Samples and logistics], Clive Graham⁹⁷ [Metadata curation, and

Samples and logistics], Emma Swindells⁹⁸ [Metadata curation, and Samples and logistics], Jennifer Collins⁹¹ [Metadata curation, and Samples and logistics], Gary Eltringham⁹¹ [Metadata curation, and Samples and logistics], Sharon Campbell⁵⁸ [Metadata curation, and Samples and logistics], Patrick C McClure¹³⁸ [Metadata curation, and Samples and logistics], Gemma Clark⁵⁶ [Metadata curation, and Samples and logistics], Tim J Sloan¹⁰¹ [Metadata curation, and Samples and logistics], Carl Jones⁵⁶ [Metadata curation, and Samples and logistics], Jessica Lynch^{43,152} [Metadata curation, and Samples and logistics], Ben Warne⁴⁹ [Metadata curation, and Sequencing and analysis], Steven Leonard¹⁴⁰ [Metadata curation, and Sequencing and analysis], Jillian Durham¹⁴⁰ [Metadata curation, and Sequencing and analysis], Thomas Williams¹³¹ [Metadata curation, and Sequencing and analysis], Sam T Haldenby¹³³ [Metadata curation, and Sequencing and analysis], Nathaniel Storey⁷¹ [Metadata curation, and Sequencing and analysis], Nabil-Fareed Alikhan¹¹¹ [Metadata curation, and Sequencing and analysis], Nadine Holmes⁵⁹ [Metadata curation, and Sequencing and analysis], Christopher Moore⁵⁹ [Metadata curation, and Sequencing and analysis], Matthew Carlile⁵⁹ [Metadata curation, and Sequencing and analysis], Malorie Perry¹¹⁰ [Metadata curation, and Sequencing and analysis], Noel Craine¹⁴⁰ [Metadata curation, and Sequencing and analysis], Ronan A Lyons¹⁴⁰ [Metadata curation, and Sequencing and analysis], Angela H Beckett⁵⁴ [Metadata curation, and Sequencing and analysis], Salman Goudarzi¹¹⁸ [Metadata curation, and Sequencing and analysis], Christopher Fearn¹¹⁸ [Metadata curation, and Sequencing and analysis], Kate Cook¹¹⁸ [Metadata curation, and Sequencing and analysis], Hannah Dent¹¹⁸ [Metadata curation, and Sequencing and analysis], Hannah Paul¹¹⁸ [Metadata curation, and Sequencing and analysis], Robert Davies¹⁴⁰ [Metadata curation, and Software and analysis tools], Beth Blane¹⁴⁰ [Project administration, and Samples and logistics], Sophia T Girgis¹⁴⁰ [Project administration, and Samples and logistics], Mathew A Beale¹⁴⁰ [Project administration, and Samples and logistics], Katherine L Bellis^{140,129} [Project administration, and Samples and logistics], Matthew J Dorman¹⁴⁰ [Project administration, and Samples and logistics], Eleanor Drury¹⁴⁰ [Project administration, and Samples and logistics], Leanne Kane¹⁴⁰ [Project administration, and Samples and logistics], Sally Kay¹⁴⁰ [Project administration, and Samples and logistics], Samantha McGuigan¹⁴⁰ [Project administration, and Samples and logistics], Rachel Nelson¹⁴⁰ [Project administration, and Samples and logistics], Liam Prestwood¹⁴⁰ [Project administration, and Samples and logistics], Shavanthi Rajatileka¹⁴⁰ [Project administration, and Samples and logistics], Rahul Batra¹⁴⁰ [Project administration, and Samples and logistics], Rachel J Williams¹²³ [Project administration, and Samples and logistics], Mark Kristiansen¹²³ [Project administration, and Samples and logistics], Angie Green¹³⁹ [Project administration, and Samples and logistics], Anita Justice¹⁴⁰ [Project administration, and Samples and logistics], Adhyana I.K Mahanama^{122,143} [Project administration, and Samples and logistics],

Buddhini Samaraweera^{122,143} [Project administration, and Samples and logistics], Nazreen F Hadjirin¹²⁹ [Project administration, and Sequencing and analysis], Joshua Quick⁸² [Project administration, and Sequencing and analysis], Radoslaw Poplawski⁸² [Project administration, and Software and analysis tools], Leanne M Kermack¹²⁹ [Samples and logistics, and Sequencing and analysis], Nicola Reynolds⁴⁸ [Samples and logistics, and Sequencing and analysis], Grant Hall⁶⁵ [Samples and logistics, and Sequencing and analysis], Yasmin Chaudhry¹⁴⁰ [Samples and logistics, and Sequencing and analysis], Malte L Pinckert⁶⁵ [Samples and logistics, and Sequencing and analysis], Iliana Georgana¹⁴⁰ [Samples and logistics, and Sequencing and analysis], Robin J Moll¹⁴⁰ [Samples and logistics, and Sequencing and analysis], Alicia Thornton¹⁰⁷ [Samples and logistics, and Sequencing and analysis], Richard Myers¹⁰⁷ [Samples and logistics, and Sequencing and analysis], Joanne Stockton¹⁴⁰ [Samples and logistics, and Sequencing and analysis], Charlotte A Williams¹⁴⁰ [Samples and logistics, and Sequencing and analysis], Wen C Yew¹⁴⁰ [Samples and logistics, and Sequencing and analysis], Alexander J Trotter¹¹¹ [Samples and logistics, and Sequencing and analysis], Amy Trebes¹⁴⁰ [Samples and logistics, and Sequencing and analysis], George MacIntyre-Cockett¹³⁹ [Samples and logistics, and Sequencing and analysis], Alec Birchley¹¹⁰ [Samples and logistics, and Sequencing and analysis], Alexander Adams¹¹⁰ [Samples and logistics, and Sequencing and analysis], Amy Plimmer¹⁴⁰ [Samples and logistics, and Sequencing and analysis], Bree Gatica-Wilcox¹¹⁰ [Samples and logistics, and Sequencing and analysis], Caoimhe McKerr¹¹⁰ [Samples and logistics, and Sequencing and analysis], Ember Hilvers¹¹⁰ [Samples and logistics, and Sequencing and analysis], Hannah Jones¹¹⁰ [Samples and logistics, and Sequencing and analysis], Hibo Asad¹¹⁰ [Samples and logistics, and Sequencing and analysis], Jason Coombes¹⁴⁰ [Samples and logistics, and Sequencing and analysis], Johnathan M Evans¹¹⁰ [Samples and logistics, and Sequencing and analysis], Laia Fina¹¹⁰ [Samples and logistics, and Sequencing and analysis], Lauren Gilbert¹¹⁰ [Samples and logistics, and Sequencing and analysis], Lee Graham¹¹⁰ [Samples and logistics, and Sequencing and analysis], Michelle Cronin¹⁴⁰ [Samples and logistics, and Sequencing and analysis], Sara Kumziene-SummerhaYes¹¹⁰ [Samples and logistics, and Sequencing and analysis], Sarah Taylor¹¹⁰ [Samples and logistics, and Sequencing and analysis], Sophie Jones¹⁴⁰ [Samples and logistics, and Sequencing and analysis], Danielle C Groves¹³⁴ [Samples and logistics, and Sequencing and analysis], Peijun Zhang¹³⁴ [Samples and logistics, and Sequencing and analysis], Marta Gallis¹³⁴ [Samples and logistics, and Sequencing and analysis], Stavroula F Louka¹³⁴ [Samples and logistics, and Sequencing and analysis], Igor Starinskij⁸⁹ [Samples and logistics, and Software and analysis tools], Chris Jackson⁸⁸ [Sequencing and analysis, and Software and analysis tools], Marina Gourtovaia¹⁴⁰ [Sequencing and analysis, and Software and analysis tools], Gerry Tonkin-Hill¹⁴⁰ [Sequencing and analysis, and Software and analysis tools], Kevin Lewis¹⁴⁰

[Sequencing and analysis, and Software and analysis tools], Jaime M Tovar-Corona¹⁴⁰ [Sequencing and analysis, and Software and analysis tools], Keith James¹⁴⁰ [Sequencing and analysis, and Software and analysis tools], Laura Baxter¹³⁵ [Sequencing and analysis, and Software and analysis tools], Mohammad T Alam¹⁴⁰ [Sequencing and analysis, and Software and analysis tools], Richard J Orton⁸⁹ [Sequencing and analysis, and Software and analysis tools], Joseph Hughes⁸⁹ [Sequencing and analysis, and Software and analysis tools], Sreenu Vattipally¹⁴⁰ [Sequencing and analysis, and Software and analysis tools], Manon Ragonnet-Cronin⁸⁰ [Sequencing and analysis, and Software and analysis tools], Fabricia F Nascimento⁸⁰ [Sequencing and analysis, and Software and analysis tools], David Jorgensen⁸⁰ [Sequencing and analysis, and Software and analysis tools], Olivia Boyd⁸⁰ [Sequencing and analysis, and Software and analysis tools], Lily Geidelberg¹⁴⁰ [Sequencing and analysis, and Software and analysis tools], Alex E Zarebski⁶⁴ [Sequencing and analysis, and Software and analysis tools], Jayna Raghwan¹⁴⁰ [Sequencing and analysis, and Software and analysis tools], Moritz UG Kraemer⁶⁴ [Sequencing and analysis, and Software and analysis tools], Joel Southgate^{51,110} [Sequencing and analysis, and Software and analysis tools], Benjamin B Lindsey¹³⁴ [Sequencing and analysis, and Software and analysis tools], Timothy M Freeman¹³⁴ [Sequencing and analysis, and Software and analysis tools], Jon-Paul Keatley¹⁴⁰ [Software and analysis tools, and Visualisation], Joshua B Singer¹⁴⁰ [Software and analysis tools, and Visualisation], Leonardo de Oliveira Martins¹⁴⁰ [Software and analysis tools, and Visualisation], Corin A Yeats⁵⁵ [Software and analysis tools, and Visualisation], Khalil Abudahab^{140,140} [Software and analysis tools, and Visualisation], Ben EW Taylor¹⁴⁰ [Software and analysis tools, and Visualisation], Mirko Menegazzo⁵⁵ [Software and analysis tools, and Visualisation], John Danesh¹⁴⁰ [Leadership and supervision], Wendy Hogsden⁸⁷ [Leadership and supervision], Sahar Eldirdi⁶² [Leadership and supervision], Anita Kenyon⁶² [Leadership and supervision], Jenifer Mason¹⁴⁰ [Leadership and supervision], Trevor I Robinson⁸⁴ [Leadership and supervision], Alison Holmes^{140,144} [Leadership and supervision], James Price^{140,140} [Leadership and supervision], John A Hartley¹²³ [Leadership and supervision], Tanya Curran¹⁴⁰ [Leadership and supervision], Alison E Mather¹¹¹ [Leadership and supervision], Giri Shankar¹¹⁰ [Leadership and supervision], Rachel Jones¹¹⁰ [Leadership and supervision], Robin Howe¹¹⁰ [Leadership and supervision], Sian Morgan⁵⁰ [Leadership and supervision], Elizabeth Wastenge¹⁴⁰ [Metadata curation], Michael R Chapman^{1,129,140} [Metadata curation], Siddharth Mookerjee^{79,144} [Metadata curation], Rachael Stanley⁹⁵ [Metadata curation], Wendy Smith⁵⁶ [Metadata curation], Timothy Peto¹⁰⁰ [Metadata curation], David Eyre¹⁰⁰ [Metadata curation], Derrick Crook¹⁰⁰ [Metadata curation], Gabrielle Vernet⁷⁴ [Metadata curation], Christine Kitchen⁵¹ [Metadata curation], Huw Gulliver⁵¹ [Metadata curation], Ian Merrick⁵¹ [Metadata curation], Martyn Guest⁵¹ [Metadata curation], Robert Munn¹⁴⁰ [Metadata curation], Declan T

Bradley^{140,113} [Metadata curation], Tim Wyatt¹⁰⁴ [Metadata curation], Charlotte Beaver¹⁴⁰ [Project administration], Luke Foulser¹⁴⁰ [Project administration], Sophie Palmer¹⁴⁰ [Project administration], Carol M Churcher¹²⁹ [Project administration], Ellena Brooks¹⁴⁰ [Project administration], Kim S Smith¹²⁹ [Project administration], Katerina Galai¹⁴⁰ [Project administration], Georgina M McManus¹²⁹ [Project administration], Frances Bolt^{79,144} [Project administration], Francesc Coll⁶⁰ [Project administration], Lizzie Meadows¹⁴⁰ [Project administration], Stephen W Attwood⁶⁴ [Project administration], Alisha Davies¹⁴⁰ [Project administration], Elen De Lacy¹¹⁰ [Project administration], Fatima Downing¹¹⁰ [Project administration], Sue Edwards¹⁴⁰ [Project administration], Garry P Scarlett¹¹⁷ [Project administration], Sarah Jeremiah¹²⁴ [Project administration], Nikki Smith¹³⁴ [Project administration], Danielle Leek¹²⁹ [Samples and logistics], Sushmita Sridhar^{140,140} [Samples and logistics], Sally Forrest¹²⁹ [Samples and logistics], Claire Cormie¹⁴⁰ [Samples and logistics], Harmeet K Gill¹²⁹ [Samples and logistics], Joana Dias¹⁴⁰ [Samples and logistics], Ellen E Higginson¹²⁹ [Samples and logistics], Mailis Maes¹²⁹ [Samples and logistics], Jamie Young¹²⁹ [Samples and logistics], Michelle Wantoch¹⁴⁰ [Samples and logistics], Sanger Covid Team¹⁴⁰ [Samples and logistics], Dorota Jamroz¹⁴⁰ [Samples and logistics], Stephanie Lo¹⁴⁰ [Samples and logistics], Minal Patel¹⁴⁰ [Samples and logistics], Verity Hill¹⁴⁰ [Samples and logistics], Claire M Bewshea¹³² [Samples and logistics], Sian Ellard^{114,132} [Samples and logistics], Cressida Auckland¹¹⁴ [Samples and logistics], Ian Harrison¹⁰⁷ [Samples and logistics], Chloe Bishop¹⁰⁷ [Samples and logistics], Vicki Chalker¹⁰⁷ [Samples and logistics], Alex Richter¹²⁶ [Samples and logistics], Andrew Beggs¹²⁶ [Samples and logistics], Angus Best¹²⁷ [Samples and logistics], Benita Percival¹²⁷ [Samples and logistics], Jeremy Mirza¹²⁷ [Samples and logistics], Oliver Megram¹²⁷ [Samples and logistics], Megan Mayhew¹²⁷ [Samples and logistics], Liam Crawford¹²⁷ [Samples and logistics], Fiona Ashcroft¹⁴⁰ [Samples and logistics], Emma Moles-Garcia¹²⁷ [Samples and logistics], Nicola Cumley¹²⁷ [Samples and logistics], Richard Hopes¹⁰⁵ [Samples and logistics], Patawee Asamaphan¹⁴⁰ [Samples and logistics], Marc O Niebel¹⁴⁰ [Samples and logistics], Rory N Gunson¹⁴¹ [Samples and logistics], Amanda Bradley⁹³ [Samples and logistics], Alasdair Maclean⁹³ [Samples and logistics], Guy Mollett⁹³ [Samples and logistics], Rachel Blacow⁹³ [Samples and logistics], Paul Bird⁵⁷ [Samples and logistics], Thomas Helmer⁵⁷ [Samples and logistics], Karlie Fallon⁵⁷ [Samples and logistics], Julian Tang¹⁴⁰ [Samples and logistics], Antony D Hale¹⁴⁰ [Samples and logistics], Louissa R Macfarlane-Smith¹⁴⁰ [Samples and logistics], Katherine L Harper⁹⁰ [Samples and logistics], Holli Carden¹⁴⁰ [Samples and logistics], Nicholas W Machin^{86,105} [Samples and logistics], Kathryn A Jackson¹³³ [Samples and logistics], Shazaad SY Ahmad^{86,105} [Samples and logistics], Ryan P George⁸⁶ [Samples and logistics], Lance Turtle¹⁴⁰ [Samples and logistics], Elaine O'Toole⁸⁴ [Samples and logistics], Joanne Watts⁸⁴ [Samples and logistics], Cassie Breen⁸⁴ [Samples and logistics], Angela Cowell¹⁴⁰ [Samples and

logistics], Adela Alcolea-Medina^{73,137} [Samples and logistics], Themoula Charalampous^{140,83} [Samples and logistics], Amita Patel¹⁴⁰ [Samples and logistics], Lisa J Levett⁷⁶ [Samples and logistics], Judith Heaney⁷⁶ [Samples and logistics], Aileen Rowan¹⁴⁰ [Samples and logistics], Graham P Taylor⁸⁰ [Samples and logistics], Divya Shah⁷¹ [Samples and logistics], Laura Atkinson¹⁴⁰ [Samples and logistics], Jack CD Lee¹⁴⁰ [Samples and logistics], Adam P Westhorpe¹²³ [Samples and logistics], Riaz Jannoo¹⁴⁰ [Samples and logistics], Helen L Lowe¹²³ [Samples and logistics], Angeliki Karamani¹²³ [Samples and logistics], Leah Ensell¹²³ [Samples and logistics], Wendy Chatterton⁷⁶, Monika Pusok⁷⁶ [Samples and logistics], Ashok Dadrah¹¹⁶ [Samples and logistics], Amanda Symmonds¹¹⁶ [Samples and logistics], Graciela Sluga⁸⁵ [Samples and logistics], Zoltan Molnar¹¹³ [Samples and logistics], Paul Baker¹²⁰ [Samples and logistics], Stephen Bonner¹²⁰ [Samples and logistics], Sarah Essex¹²⁰ [Samples and logistics], Edward Barton⁹⁷ [Samples and logistics], Debra Padgett⁹⁷ [Samples and logistics], Garren Scott⁹⁷ [Samples and logistics], Jane Greenaway¹⁴⁰ [Samples and logistics], Brendan Al Payne¹⁴⁰ [Samples and logistics], Shirelle Burton-Fanning⁹¹ [Samples and logistics], Sheila Waugh⁹¹ [Samples and logistics], Veena Raviprakash⁵⁸ [Samples and logistics], Nicola Sheriff⁵⁸ [Samples and logistics], Victoria Blakey¹⁴⁰ [Samples and logistics], Lesley-Anne Williams⁵⁸ [Samples and logistics], Jonathan Moore⁶⁸ [Samples and logistics], Susanne Stonehouse⁶⁸ [Samples and logistics], Louise Smith¹⁴⁰ [Samples and logistics], Rose K Davidson¹³⁰ [Samples and logistics], Luke Bedford⁶⁷ [Samples and logistics], Lindsay Coupland⁹⁵ [Samples and logistics], Victoria Wright¹⁴⁰ [Samples and logistics], Joseph G Chappell¹³⁸ [Samples and logistics], Theocharis Tsoleridis¹³⁸ [Samples and logistics], Jonathan Ball¹³⁸ [Samples and logistics], Manjinder Khakh¹⁴⁰ [Samples and logistics], Vicki M Fleming¹⁴⁰ [Samples and logistics], Michelle M Lister¹⁴⁰ [Samples and logistics], Hannah C Howson-Wells⁵⁶ [Samples and logistics], Louise Berry⁵⁶ [Samples and logistics], Tim Boswell⁵⁶ [Samples and logistics], Amelia Joseph⁵⁶ [Samples and logistics], Iona Willingham⁵⁶ [Samples and logistics], Nichola Duckworth¹⁰¹ [Samples and logistics], Sarah Walsh¹⁰¹ [Samples and logistics], Emma Wise^{140,152} [Samples and logistics], Nathan Moore^{140,152} [Samples and logistics], Matilde Mori^{140,140,152} [Samples and logistics], Nick Cortes^{140,152} [Samples and logistics], Stephen Kidd^{140,152} [Samples and logistics], Rebecca Williams⁷⁴ [Samples and logistics], Laura Gifford¹¹⁰ [Samples and logistics], Kelly Bicknell¹⁰² [Samples and logistics], Sarah Wyllie¹⁰² [Samples and logistics], Allyson Lloyd¹⁰² [Samples and logistics], Robert Impey¹⁴⁰ [Samples and logistics], Cassandra S Malone¹⁴⁰ [Samples and logistics], Benjamin J Cogger⁴⁷ [Samples and logistics], Nick Levene¹⁰³ [Samples and logistics], Lynn Monaghan¹⁴⁰ [Samples and logistics], Alexander J Keeley¹⁴⁰ [Samples and logistics], David G Partridge^{140,134} [Samples and logistics], Mohammad Raza^{119,134} [Samples and logistics], Cariad Evans^{140,134} [Samples and logistics], Kate Johnson^{119,134} [Samples and logistics], Emma Betteridge¹⁴⁰ [Sequencing and analysis], Ben W Farr¹⁴⁰

[Sequencing and analysis], Scott Goodwin¹⁴⁰ [Sequencing and analysis], Michael A Quail¹⁴⁰ [Sequencing and analysis], Carol Scott¹⁴⁰ [Sequencing and analysis], Lesley Shirley¹⁴⁰ [Sequencing and analysis], Scott AJ Thurston¹⁴⁰ [Sequencing and analysis], Diana Rajan¹⁴⁰ [Sequencing and analysis], Iraad F Bronner¹⁴⁰ [Sequencing and analysis], Louise Aigrain¹⁴⁰ [Sequencing and analysis], Nicholas M Redshaw¹⁴⁰ [Sequencing and analysis], Stefanie V Lensing¹⁴⁰ [Sequencing and analysis], Shane McCarthy¹⁴⁰ [Sequencing and analysis], Alex Makunin¹⁴⁰ [Sequencing and analysis], Carlos E Balcazar¹⁴⁰ [Sequencing and analysis], Michael D Gallagher¹⁴⁰ [Sequencing and analysis], Kathleen A Williamson¹⁴⁰ [Sequencing and analysis], Thomas D Stanton¹⁴⁰ [Sequencing and analysis], Michelle L Michelsen¹⁴⁰ [Sequencing and analysis], Joanna Warwick-Dugdale¹³² [Sequencing and analysis], Robin Manley¹³² [Sequencing and analysis], Audrey Farbos¹⁴⁰ [Sequencing and analysis], James W Harrison¹⁴⁰ [Sequencing and analysis], Christine M Sambles¹⁴⁰ [Sequencing and analysis], David J Studholme¹³² [Sequencing and analysis], Angie Lackenby¹⁰⁷ [Sequencing and analysis], Tamyo Mbisa¹⁰⁷ [Sequencing and analysis], Steven Platt¹⁰⁷ [Sequencing and analysis], Shahjahan Miah¹⁰⁷ [Sequencing and analysis], David Bibby¹⁰⁷ [Sequencing and analysis], Carmen Manso¹⁰⁷ [Sequencing and analysis], Jonathan Hubb¹⁰⁷ [Sequencing and analysis], Gavin Dabrera¹⁰⁷ [Sequencing and analysis], Mary Ramsay¹⁰⁷ [Sequencing and analysis], Daniel Bradshaw¹⁰⁷ [Sequencing and analysis], Ulf Schaefer¹⁰⁷ [Sequencing and analysis], Natalie Groves¹⁰⁷ [Sequencing and analysis], Eileen Gallagher¹⁰⁷ [Sequencing and analysis], David Lee¹⁰⁷ [Sequencing and analysis], David Williams¹⁰⁷ [Sequencing and analysis], Nicholas Ellaby¹⁰⁷ [Sequencing and analysis], Hassan Hartman¹⁰⁷ [Sequencing and analysis], Nikos Manesis¹⁰⁷ [Sequencing and analysis], Vineet Patel¹⁰⁷ [Sequencing and analysis], Juan Ledesma¹⁴⁰ [Sequencing and analysis], Katherine A Twohig¹⁰⁸ [Sequencing and analysis], Elias Allara^{140,129} [Sequencing and analysis], Clare Pearson^{140,140} [Sequencing and analysis], Jeffrey K. J. Cheng¹³⁵ [Sequencing and analysis], Hannah E Bridgewater¹³⁵ [Sequencing and analysis], Lucy R Frost¹⁴⁰ [Sequencing and analysis], Grace Taylor-Joyce¹⁴⁰ [Sequencing and analysis], Paul E Brown¹³⁵ [Sequencing and analysis], Lily Tong⁸⁹ [Sequencing and analysis], Alice Broos⁸⁹ [Sequencing and analysis], Daniel Mair⁸⁹ [Sequencing and analysis], Jenna Nichols¹⁴⁰ [Sequencing and analysis], Stephen N Carmichael¹⁴⁰ [Sequencing and analysis], Katherine L Smollett⁸¹ [Sequencing and analysis], Kyriaki Nomikou¹⁴⁰ [Sequencing and analysis], Elihu Aranday-Cortes⁸⁹ [Sequencing and analysis], Natasha Johnson⁸⁹ [Sequencing and analysis], Seema Nickbakhsh^{140,140} [Sequencing and analysis], Edith E Vamos¹³³ [Sequencing and analysis], Margaret Hughes¹³³ [Sequencing and analysis], Lucille Rainbow¹³³ [Sequencing and analysis], Richard Eccles¹³³ [Sequencing and analysis], Charlotte Nelson¹³³ [Sequencing and analysis], Mark Whitehead¹³³ [Sequencing and analysis], Richard Gregory¹³³ [Sequencing and analysis], Matthew Gemmell¹³³ [Sequencing and analysis], Claudia Wierzbicki¹⁴⁰ [Sequencing and analysis],

Hermione J Webster¹⁴⁰ [Sequencing and analysis], Chloe L Fisher¹⁴⁰ [Sequencing and analysis], Adrian W Signell⁶¹ [Sequencing and analysis], Gilberto Betancor¹⁴⁰ [Sequencing and analysis], Harry D Wilson⁶¹ [Sequencing and analysis], Gaia Nebbia⁵³ [Sequencing and analysis], Flavia Flaviani¹⁴⁰ [Sequencing and analysis], Alberto C Cerda¹⁴⁰ [Sequencing and analysis], Tammy V Merrill¹⁴⁰ [Sequencing and analysis], Rebekah E Wilson¹³⁷ [Sequencing and analysis], Marius Cotic¹²³ [Sequencing and analysis], Nadua Bayzid¹²³ [Sequencing and analysis], Thomas Thompson¹¹³ [Sequencing and analysis], Erwan Acheson¹¹³ [Sequencing and analysis], Steven Rushton¹⁴⁰ [Sequencing and analysis], Sarah O'Brien¹⁴⁰ [Sequencing and analysis], David J Baker¹¹¹ [Sequencing and analysis], Steven Rudder¹¹¹ [Sequencing and analysis], Alp Aydin¹¹¹ [Sequencing and analysis], Fei Sang⁵⁹ [Sequencing and analysis], Johnny Debebe⁵⁹ [Sequencing and analysis], Sarah Francois¹⁴⁰ [Sequencing and analysis], Tetyana I Vasylyeva¹⁴⁰ [Sequencing and analysis], Marina Escalera Zamudio⁶⁴ [Sequencing and analysis], Bernardo Gutierrez⁶⁴ [Sequencing and analysis], Angela Marchbank⁵¹ [Sequencing and analysis], Joshua Maksimovic⁵⁰ [Sequencing and analysis], Karla Spellman⁵⁰ [Sequencing and analysis], Kathryn McCluggage⁵⁰ [Sequencing and analysis], Mari Morgan¹¹⁰ [Sequencing and analysis], Robert Beer⁵⁰ [Sequencing and analysis], Safiah Afifi⁵⁰ [Sequencing and analysis], Trudy Workman⁵¹ [Sequencing and analysis], William Fuller⁵¹ [Sequencing and analysis], Catherine Bresner⁵¹ [Sequencing and analysis], Adrienn Angyal¹⁴⁰ [Sequencing and analysis], Luke R Green¹⁴⁰ [Sequencing and analysis], Paul J Parsons¹⁴⁰ [Sequencing and analysis], Rachel M Tucker¹³⁴ [Sequencing and analysis], Rebecca Brown¹³⁴ [Sequencing and analysis], Max Whiteley¹³⁴ [Sequencing and analysis], James Bonfield¹⁴⁰ [Software and analysis tools], Christoph Puethe¹⁴⁰ [Software and analysis tools], Andrew Whitwham¹⁴⁰ [Software and analysis tools], Jennifer Liddle¹⁴⁰ [Software and analysis tools], Will Rowe⁸² [Software and analysis tools], Igor Siveroni¹⁴⁰ [Software and analysis tools], Thanh Le-Viet¹⁴⁰ [Software and analysis tools], Amy Gaskin¹¹⁰ [Software and analysis tools], Rob Johnson⁸⁰ [Visualisation]

⁴²Barking, Havering and Redbridge University Hospitals NHS Trust, Barking, United Kingdom ⁴³Basingstoke Hospital, Basingstoke, United Kingdom

⁴⁴Belfast Health & Social Care Trust, Belfast, United Kingdom ⁴⁵Betsi Cadwaladr University Health Board, Betsi Cadwaladr, United Kingdom ⁴⁶Big Data Institute, Nuffield Department of Medicine, University of Oxford, Oxford, United Kingdom ⁴⁷Brighton and Sussex University Hospitals NHS Trust, Brighton & Sussex, United Kingdom ⁴⁸Cambridge Stem Cell Institute, University of Cambridge, Cambridge, United Kingdom ⁴⁹Cambridge University Hospitals NHS Foundation Trust, Cambridge, United Kingdom ⁵⁰Cardiff and Vale University Health Board, Cardiff, United Kingdom ⁵¹Cardiff University, Cardiff, United Kingdom ⁵²Centre for Clinical Infection & Diagnostics Research, St. Thomas' Hospital and Kings College London, London, United

Kingdom ⁵³Centre for Clinical Infection and Diagnostics Research, Department of Infectious Diseases, Guy's and St Thomas' NHS Foundation Trust, London, United Kingdom ⁵⁴Centre for Enzyme Innovation, University of Portsmouth (PORT), Portsmouth, United Kingdom ⁵⁵Centre for Genomic Pathogen Surveillance, University of Oxford, Oxford, United Kingdom ⁵⁶Clinical Microbiology Department, Queens Medical Centre, Nottingham, United Kingdom ⁵⁷Clinical Microbiology, University Hospitals of Leicester NHS Trust, Leicester, United Kingdom ⁵⁸County Durham and Darlington NHS Foundation Trust, Durham, United Kingdom ⁵⁹Deep Seq, School of Life Sciences, Queens Medical Centre, University of Nottingham, Nottingham, United Kingdom ⁶⁰Department of Infection Biology, Faculty of Infectious & Tropical Diseases, London School of Hygiene & Tropical Medicine, London, United Kingdom ⁶¹Department of Infectious Diseases, King's College London, London, United Kingdom ⁶²Department of Microbiology, Kettering General Hospital, Kettering, United Kingdom ⁶³Departments of Infectious Diseases and Microbiology, Cambridge University Hospitals NHS Foundation Trust; Cambridge, UK, Cambridge, United Kingdom ⁶⁴Department of Zoology, University of Oxford, Oxford, United Kingdom ⁶⁵Division of Virology, Department of Pathology, University of Cambridge, Cambridge, United Kingdom ⁶⁶East Kent Hospitals University NHS Foundation Trust, Kent, United Kingdom ⁶⁷East Suffolk and North Essex NHS Foundation Trust, Suffolk, United Kingdom ⁶⁸Gateshead Health NHS Foundation Trust, Gateshead, United Kingdom ⁶⁹Genomics Innovation Unit, Guy's and St. Thomas' NHS Foundation Trust, London, United Kingdom ⁷⁰Gloucestershire Hospitals NHS Foundation Trust, Gloucester, United Kingdom ⁷¹Great Ormond Street Hospital for Children NHS Foundation Trust, London, United Kingdom ⁷²Guy's and St. Thomas' BRC, London, United Kingdom ⁷³Guy's and St. Thomas' Hospitals, London, United Kingdom ⁷⁴Hampshire Hospitals NHS Foundation Trust, Hampshire, United Kingdom ⁷⁵Health Data Research UK Cambridge, Cambridge, United Kingdom ⁷⁶Health Services Laboratories, London, United Kingdom ⁷⁷Heartlands Hospital, Birmingham, Birmingham, United Kingdom ⁷⁸Hub for Biotechnology in the Built Environment, Northumbria University, Northumbria, United Kingdom ⁷⁹Imperial College Hospitals NHS Trust, London, United Kingdom ⁸⁰Imperial College London, London, United Kingdom ⁸¹Institute of Biodiversity, Animal Health & Comparative Medicine, Glasgow, United Kingdom ⁸²Institute of Microbiology and Infection, University of Birmingham, Birmingham, United Kingdom ⁸³King's College London, London, United Kingdom ⁸⁴Liverpool Clinical Laboratories, Liverpool, United Kingdom ⁸⁵Maidstone and Tunbridge Wells NHS Trust, Maidstone, United Kingdom ⁸⁶Manchester University NHS Foundation Trust, Manchester, United Kingdom ⁸⁷Microbiology Department, Wye Valley NHS Trust, Hereford, United Kingdom ⁸⁸MRC Biostatistics Unit, University of Cambridge, Cambridge, United Kingdom ⁸⁹MRC-University of Glasgow Centre for Virus Research, Glasgow, United Kingdom ⁹⁰National Infection Service, PHE and Leeds Teaching

Hospitals Trust, Leeds, United Kingdom ⁹¹Newcastle Hospitals NHS Foundation Trust, Newcastle, United Kingdom ⁹²Newcastle University, Newcastle, United Kingdom ⁹³NHS Greater Glasgow and Clyde, Glasgow, United Kingdom ⁹⁴NHS Lothian, Edinburgh, United Kingdom ⁹⁵Norfolk and Norwich University Hospital, Norfolk, United Kingdom ⁹⁶Norfolk County Council, Norfolk, United Kingdom ⁹⁷North Cumbria Integrated Care NHS Foundation Trust, Carlisle, United Kingdom ⁹⁸North Tees and Hartlepool NHS Foundation Trust, Stockton-on-Tees, United Kingdom ⁹⁹Northumbria University, Northumbria, United Kingdom ¹⁰⁰Oxford University Hospitals NHS Foundation Trust, Oxford, United Kingdom ¹⁰¹PathLinks, Northern Lincolnshire & Goole NHS Foundation Trust, Lincolnshire, United Kingdom ¹⁰²Portsmouth Hospitals University NHS Trust, Portsmouth, United Kingdom ¹⁰³Princess Alexandra Hospital Microbiology Dept., Harlow, United Kingdom ¹⁰⁴Public Health Agency, London, United Kingdom ¹⁰⁵Public Health England, London, United Kingdom ¹⁰⁶Public Health England, Clinical Microbiology and Public Health Laboratory, Cambridge, United Kingdom ¹⁰⁷Public Health England, Colindale, London, United Kingdom ¹⁰⁸Public Health England, Colindale, London, United Kingdom ¹⁰⁹Public Health Scotland, Glasgow, United Kingdom ¹¹⁰Public Health Wales NHS Trust, Cardiff, United Kingdom ¹¹¹Quadram Institute Bioscience, Norwich, United Kingdom ¹¹²Queen Elizabeth Hospital, Birmingham, United Kingdom ¹¹³Queen's University Belfast, Belfast, United Kingdom ¹¹⁴Royal Devon and Exeter NHS Foundation Trust, Devon, United Kingdom ¹¹⁵Royal Free NHS Trust, London, United Kingdom ¹¹⁶Sandwell and West Birmingham NHS Trust, Sandwell, United Kingdom ¹¹⁷School of Biological Sciences, University of Portsmouth (PORT), Portsmouth, United Kingdom ¹¹⁸School of Pharmacy and Biomedical Sciences, University of Portsmouth (PORT), Portsmouth, United Kingdom ¹¹⁹Sheffield Teaching Hospitals, Sheffield, United Kingdom ¹²⁰South Tees Hospitals NHS Foundation Trust, Newcastle, United Kingdom ¹²¹Swansea University, Swansea, United Kingdom ¹²²University Hospitals Southampton NHS Foundation Trust, Southampton, United Kingdom ¹²³University College London, London, United Kingdom ¹²⁴University Hospital Southampton NHS Foundation Trust, Southampton, United Kingdom ¹²⁵University Hospitals Coventry and Warwickshire, Coventry, United Kingdom ¹²⁶University of Birmingham, Birmingham, United Kingdom ¹²⁷University of Birmingham Turnkey Laboratory, Birmingham, United Kingdom ¹²⁸University of Brighton, Brighton, United Kingdom ¹²⁹University of Cambridge, Cambridge, United Kingdom ¹³⁰University of East Anglia, East Anglia, United Kingdom ¹³¹University of Edinburgh, Edinburgh, United Kingdom ¹³²University of Exeter, Exeter, United Kingdom ¹³³University of Liverpool, Liverpool, United Kingdom ¹³⁴University of Sheffield, Sheffield, United Kingdom ¹³⁵University of Warwick, Warwick, United Kingdom ¹³⁶University of Cambridge, Cambridge, United Kingdom ¹³⁷Viapath, Guy's and St Thomas' NHS Foundation Trust, and King's College Hospital NHS Foundation Trust, London, United Kingdom

¹³⁸Virology, School of Life Sciences, Queens Medical Centre, University of Nottingham, Nottingham, United Kingdom ¹³⁹Wellcome Centre for Human Genetics, Nuffield Department of Medicine, University of Oxford, Oxford, United Kingdom ¹⁴⁰Wellcome Sanger Institute, London, United Kingdom ¹⁴¹West of Scotland Specialist Virology Centre, NHS Greater Glasgow and Clyde, Glasgow, United Kingdom ¹⁴²Department of Medicine, University of Cambridge, Cambridge, United Kingdom ¹⁴³Ministry of Health, Colombo, Sri Lanka ¹⁴⁴NIHR Health Protection Research Unit in HCAI and AMR, Imperial College London, London, United Kingdom ¹⁴⁵North West London Pathology, London, United Kingdom ¹⁴⁶NU-OMICS, Northumbria University, Northumbria, United Kingdom ¹⁴⁷University of Kent, Kent, United Kingdom ¹⁴⁸University of Oxford, Oxford, United Kingdom ¹⁴⁹University of Southampton, Southampton, United Kingdom ¹⁵⁰University of Southampton School of Health Sciences, Southampton, United Kingdom ¹⁵¹University of Southampton School of Medicine, Southampton, United Kingdom ¹⁵²University of Surrey, Guildford, United Kingdom ¹⁵³Warwick Medical School and Institute of Precision Diagnostics, Pathology, UHCW NHS Trust, Warwick, United Kingdom

, Katherine Sharrocks⁴, Elizabeth Blane³, Yorgo Modis⁸, Kendra Leigh⁸, John Briggs⁸, Marit van Gils⁹, Kenneth GC Smith^{2,3}, John R Bradley^{3,10}, Chris Smith¹¹, Rainer Doffinger¹³, Lourdes Ceron-Gutierrez¹³, Gabriela Barcenas-Morales^{13,14}, David D Pollock¹⁵, Richard A Goldstein¹, Anna Smielewska^{5,11}, Jordan P Skittrall^{4,12,16}, Theodore Gouliouris⁴, Ian G Goodfellow⁵, Effrossyni Gkrania-Klotsas⁴, Christopher JR Illingworth^{12,17}, Laura E McCoy¹, Ravindra K Gupta^{2,3,18}

Stephen Baker^{2,3} [Principal Investigators], Gordon Dougan^{2,3} [Principal Investigators], Christoph Hess^{2,3,26,27} [Principal Investigators], Nathalie Kingston^{20,12} [Principal Investigators], Paul J. Lehner^{2,3} [Principal Investigators], Paul A. Lyons^{2,3} [Principal Investigators], Nicholas J. Matheson^{2,3} [Principal Investigators], Willem H. Owehand²⁰ [Principal Investigators], Caroline Saunders¹⁹ [Principal Investigators], Charlotte Summers^{3,24,25,28} [Principal Investigators], James E.D. Thaventhiran^{2,3,22} [Principal Investigators], Mark Toshner^{3,24,25} [Principal Investigators], Michael P. Weekes² [Principal Investigators], Ashlea Bucke¹⁹ [CRF and Volunteer Research Nurses], Jo Calder¹⁹ [CRF and Volunteer Research Nurses], Laura Canna¹⁹ [CRF and Volunteer Research Nurses], Jason Domingo¹⁹ [CRF and Volunteer Research Nurses], Anne Elmer¹⁹ [CRF and Volunteer Research Nurses], Stewart Fuller¹⁹ [CRF and Volunteer Research Nurses], Julie Harris⁴¹ [CRF and Volunteer Research Nurses], Sarah Hewitt¹⁹ [CRF and Volunteer Research Nurses], Jane Kennet¹⁹ [CRF and Volunteer Research Nurses], Sherly Jose¹⁹ [CRF and Volunteer Research Nurses], Jenny Kourampa¹⁹ [CRF and Volunteer Research Nurses], Anne Meadows¹⁹ [CRF and Volunteer Research Nurses], Criona O'Brien⁴¹ [CRF and Volunteer Research Nurses], Jane Price¹⁹ [CRF and Volunteer Research Nurses], Cherry Publico¹⁹ [CRF and Volunteer Research

Nurses], Rebecca Rastall¹⁹ [**CRF and Volunteer Research Nurses**], Carla Ribeiro¹⁹ [**CRF and Volunteer Research Nurses**], Jane Rowlands¹⁹ [**CRF and Volunteer Research Nurses**], Valentina Ruffolo¹⁹ [**CRF and Volunteer Research Nurses**], Hugo Tordesillas¹⁹ [**CRF and Volunteer Research Nurses**], Ben Bullman² [**Sample Logistics**], Benjamin J Dunmore³ [**Sample Logistics**], Stuart Fawke³⁰ [**Sample Logistics**], Stefan Gräf^{3,12,20} [**Sample Logistics**], Josh Hodgson³ [**Sample Logistics**], Christopher Huang³ [**Sample Logistics**], Kelvin Hunter^{2,3} [**Sample Logistics**], Emma Jones²⁹ [**Sample Logistics**], Ekaterina Legchenko³ [**Sample Logistics**], Cecilia Matara³ [**Sample Logistics**], Jennifer Martin³ [**Sample Logistics**], Federica Mescia^{2,3} [**Sample Logistics**], Ciara O'Donnell³ [**Sample Logistics**], Linda Pointon³ [**Sample Logistics**], Nicole Pond^{2,3} [**Sample Logistics**], Joy Shih³ [**Sample Logistics**], Rachel Sutcliffe³ [**Sample Logistics**], Tobias Tilly³ [**Sample Logistics**], Carmen Treacy³ [**Sample Logistics**], Zhen Tong³ [**Sample Logistics**], Jennifer Wood³ [**Sample Logistics**], Marta Wylot³⁶ [**Sample Logistics**], Laura Bergamaschi^{2,3} [**Sample Processing and Data Acquisition**], Ariana Betancourt^{2,3} [**Sample Processing and Data Acquisition**], Georgie Bower^{2,3} [**Sample Processing and Data Acquisition**], Chiara Cossetti^{2,3} [**Sample Processing and Data Acquisition**], Aloka De Sa³ [**Sample Processing and Data Acquisition**], Madeline Epping^{2,3} [**Sample Processing and Data Acquisition**], Stuart Fawke³² [**Sample Processing and Data Acquisition**], Nick Gleadall²⁰ [**Sample Processing and Data Acquisition**], Richard Grenfell³¹ [**Sample Processing and Data Acquisition**], Andrew Hinch^{2,3} [**Sample Processing and Data Acquisition**], Oisín Huhn³² [**Sample Processing and Data Acquisition**], Sarah Jackson³ [**Sample Processing and Data Acquisition**], Isobel Jarvis³ [**Sample Processing and Data Acquisition**], Daniel Lewis³ [**Sample Processing and Data Acquisition**], Joe Marsden³ [**Sample Processing and Data Acquisition**], Francesca Nice³⁹ [**Sample Processing and Data Acquisition**], Georgina Okecha³ [**Sample Processing and Data Acquisition**], Ommar Omarjee³ [**Sample Processing and Data Acquisition**], Marianne Perera³ [**Sample Processing and Data Acquisition**], Nathan Richoz³ [**Sample Processing and Data Acquisition**], Veronika Romashova^{2,3} [**Sample Processing and Data Acquisition**], Natalia Savinykh Yarkoni³ [**Sample Processing and Data Acquisition**], Rahul Sharma³ [**Sample Processing and Data Acquisition**], Luca Stefanucci²⁰ [**Sample Processing and Data Acquisition**], Jonathan Stephens²⁰ [**Sample Processing and Data Acquisition**], Mateusz Strezlecki³¹ [**Sample Processing and Data Acquisition**], Lori Turner^{2,3} [**Sample Processing and Data Acquisition**], Eckart M.D.D. De Bie³ [**Clinical Data Collection**], Katherine Bunclark³ [**Clinical Data Collection**], Masa Josipovic⁴⁰ [**Clinical Data Collection**], Michael Mackay³ [**Clinical Data Collection**], Federica Mescia^{2,3} [**Clinical Data Collection**], Alice Michael²⁵ [**Clinical Data Collection**], Sabrina Rossi³⁵ [**Clinical Data Collection**], Mayurun Selvan³ [**Clinical Data Collection**], Sarah Spencer¹⁵ [**Clinical Data Collection**], Cissy Yong³⁵ [**Clinical Data Collection**], Ali Ansari-pour²⁵ [**Royal Papworth Hospital ICU**], Alice Michael²⁵ [**Royal Papworth Hospital ICU**], Lucy Mwaura²⁵ [**Royal Papworth**

Hospital ICU], Caroline Patterson²⁵ [**Royal Papworth Hospital ICU**], Gary Polwarth²⁵ [**Royal Papworth Hospital ICU**], Petra Polgarova²⁸ [**Addenbrooke's Hospital ICU**], Giovanni di Stefano²⁸ [**Addenbrooke's Hospital ICU**], Codie Fahey³⁴ [**Cambridge and Peterborough Foundation Trust**], Rachel Michel³⁴ [**Cambridge and Peterborough Foundation Trust**], Sze-How Bong²¹ [**ANPC and Centre for Molecular Medicine and Innovative Therapeutics**], Jerome D. Coudert³³ [**ANPC and Centre for Molecular Medicine and Innovative Therapeutics**], Elaine Holmes³⁷ [**ANPC and Centre for Molecular Medicine and Innovative Therapeutics**], John Allison^{20,12} [**NIHR BioResource**], Helen Butcher^{12,38} [**NIHR BioResource**], Daniela Caputo^{12,38} [**NIHR BioResource**], Debbie Clapham-Riley^{12,38} [**NIHR BioResource**], Eleanor Dewhurst^{12,38} [**NIHR BioResource**], Anita Furlong^{12,38} [**NIHR BioResource**], Barbara Graves^{12,38} [**NIHR BioResource**], Jennifer Gray^{12,38} [**NIHR BioResource**], Tasmin Ivers^{12,38} [**NIHR BioResource**], Mary Kasanicki^{12,28} [**NIHR BioResource**], Emma Le Gresley^{12,38} [**NIHR BioResource**], Rachel Linger^{12,38} [**NIHR BioResource**], Sarah Meloy^{12,38} [**NIHR BioResource**], Francesca Muldoon^{12,38} [**NIHR BioResource**], Nigel Ovington^{12,20} [**NIHR BioResource**], Sofia Papadia^{12,38} [**NIHR BioResource**], Isabel Phelan^{12,38} [**NIHR BioResource**], Hannah Stark^{12,38} [**NIHR BioResource**], Kathleen E Stirrups^{12,20} [**NIHR BioResource**], Paul Townsend^{12,20} [**NIHR BioResource**], Neil Walker^{12,20} [**NIHR BioResource**], Jennifer Webster^{12,38} [**NIHR BioResource**]

Samuel C Robson⁵⁴ [**Funding acquisition, Leadership and supervision, Metadata curation, Project administration, Samples and logistics, Sequencing and analysis, Software and analysis tools, and Visualisation**], Nicholas J Loman⁸², Thomas R Connor^{51,110} [**Funding acquisition, Leadership and supervision, Metadata curation, Project administration, Samples and logistics, Sequencing and analysis, and Software and analysis tools**], Tanya Golubchik⁴⁶ [**Leadership and supervision, Metadata curation, Project administration, Samples and logistics, Sequencing and analysis, Software and analysis tools, and Visualisation**], Rocio T Martinez Nunez⁸³ [**Funding acquisition, Metadata curation, Samples and logistics, Sequencing and analysis, Software and analysis tools, and Visualisation**], Catherine Ludden¹²⁹ [**Funding acquisition, Leadership and supervision, Metadata curation, Project administration, and Samples and logistics**], Sally Corden¹¹⁰ [**Funding acquisition, Leadership and supervision, Metadata curation, Samples and logistics, and Sequencing and analysis**], Ian Johnston¹⁴⁰, David Bonsall⁴⁶ [**Funding acquisition, Leadership and supervision, Project administration, Samples and logistics, and Sequencing and analysis**], Colin P Smith¹²⁸, Ali R Awan⁶⁹ [**Funding acquisition, Leadership and supervision, Sequencing and analysis, Software and analysis tools, and Visualisation**], Giselda Bucca¹²⁸ [**Funding acquisition, Samples and logistics, Sequencing and analysis, Software and analysis tools, and Visualisation**], M. Estee Torok^{63,142} [**Leadership and supervision, Metadata curation, Project administration, Samples and logistics, and Sequencing and analysis**], Kordo Saeed^{122,151} [**Leadership and supervision, Metadata curation,**

Project administration, Samples and logistics, and Visualisation], Jacqui A Prieto^{124,150} **[Leadership and supervision, Metadata curation, Project administration, Samples and logistics, and Visualisation]**, David K Jackson¹⁴⁰ **[Leadership and supervision, Metadata curation, Project administration, Sequencing and analysis, and Software and analysis tools]**, William L Hamilton⁶³ **[Metadata curation, Project administration, Samples and logistics, Sequencing and analysis, and Software and analysis tools]**, Luke B Snell⁵² **[Metadata curation, Project administration, Samples and logistics, Sequencing and analysis, and Visualisation]**, Catherine Moore¹¹⁰ **[Funding acquisition, Leadership and supervision, Metadata curation, and Samples and logistics]**, Ewan M Harrison^{129,140} **[Funding acquisition, Leadership and supervision, Project administration, and Samples and logistics]**, Sonia Goncalves¹⁴⁰ **[Leadership and supervision, Metadata curation, Project administration, and Samples and logistics]**, Derek J Fairley^{44,113} **[Leadership and supervision, Metadata curation, Samples and logistics, and Sequencing and analysis]**, Matthew W Loose⁵⁹ **[Leadership and supervision, Metadata curation, Samples and logistics, and Sequencing and analysis]**, Joanne Watkins¹¹⁰ **[Leadership and supervision, Metadata curation, Samples and logistics, and Sequencing and analysis]**, Rich Livett¹⁴⁰ **[Leadership and supervision, Metadata curation, Samples and logistics, and Software and analysis tools]**, Samuel Moses^{66,147} **[Leadership and supervision, Metadata curation, Samples and logistics, and Visualisation]**, Roberto Amato¹⁴⁰ **[Leadership and supervision, Metadata curation, Sequencing and analysis, and Software and analysis tools]**, Sam Nicholls⁸² **[Leadership and supervision, Metadata curation, Sequencing and analysis, and Software and analysis tools]**, Matthew Bull¹¹⁰ **[Leadership and supervision, Metadata curation, Sequencing and analysis, and Software and analysis tools]**, Darren L Smith^{1,99,146} **[Leadership and supervision, Project administration, Samples and logistics, and Sequencing and analysis]**, Jeff Barrett¹⁴⁰ **[Leadership and supervision, Sequencing and analysis, Software and analysis tools, and Visualisation]**, David M Aanensen⁵⁵ **[Leadership and supervision, Sequencing and analysis, Software and analysis tools, and Visualisation]**, Martin D Curran¹⁰⁶ **[Metadata curation, Project administration, Samples and logistics, and Sequencing and analysis]**, Surendra Parmar¹⁰⁶ **[Metadata curation, Project administration, Samples and logistics, and Sequencing and analysis]**, Dinesh Aggarwal^{1,140,105} **[Metadata curation, Project administration, Samples and logistics, and Sequencing and analysis]**, James G Shepherd⁸⁹ **[Metadata curation, Project administration, Samples and logistics, and Sequencing and analysis]**, Matthew D Parker¹³⁴ **[Metadata curation, Project administration, Sequencing and analysis, and Software and analysis tools]**, Sharon Glaysher¹⁰² **[Metadata curation, Samples and logistics, Sequencing and analysis, and Visualisation]**, Matthew Bashton^{78,99} **[Metadata curation, Sequencing and analysis, Software and analysis tools, and Visualisation]**, Anthony P Underwood⁵⁵ **[Metadata curation, Sequencing and analysis, Software and analysis tools, and Visualisation]**, Nicole Pacchiarini¹¹⁰ **[Metadata**

curation, Sequencing and analysis, Software and analysis tools, and Visualisation], Katie F Loveson¹¹⁸ [Metadata curation, Sequencing and analysis, Software and analysis tools, and Visualisation], Alessandro M Carabelli¹²⁹ [Project administration, Sequencing and analysis, Software and analysis tools, and Visualisation], Kate E Templeton^{94,131} [Funding acquisition, Leadership and supervision, and Metadata curation], Cordelia F Langford¹⁴⁰ [Funding acquisition, Leadership and supervision, and Project administration], John Sillitoe¹⁴⁰ [Funding acquisition, Leadership and supervision, and Project administration], Thushan I de Silva¹³⁴ [Funding acquisition, Leadership and supervision, and Project administration], Dennis Wang¹³⁴ [Funding acquisition, Leadership and supervision, and Project administration], Dominic Kwiatkowski^{140,148} [Funding acquisition, Leadership and supervision, and Sequencing and analysis], Andrew Rambaut¹³¹ [Funding acquisition, Leadership and supervision, and Sequencing and analysis], Justin O'Grady^{111,130} [Funding acquisition, Leadership and supervision, and Sequencing and analysis], Simon Cottrell¹¹⁰ [Funding acquisition, Leadership and supervision, and Sequencing and analysis], Matthew T.G. Holden¹⁰⁹ [Leadership and supervision, Metadata curation, and Sequencing and analysis], Emma C Thomson⁸⁹ [Leadership and supervision, Metadata curation, and Sequencing and analysis], Husam Osman^{77,105} [Leadership and supervision, Project administration, and Samples and logistics], Monique Andersson¹⁰⁰ [Leadership and supervision, Project administration, and Samples and logistics], Anoop J Chauhan¹⁰² [Leadership and supervision, Project administration, and Samples and logistics], Mohammed O Hassan-Ibrahim⁴⁷ [Leadership and supervision, Project administration, and Samples and logistics], Mara Lawniczak¹⁴⁰ [Leadership and supervision, Project administration, and Sequencing and analysis], Alex Alderton¹⁴⁰ [Leadership and supervision, Samples and logistics, and Sequencing and analysis], Meera Chand¹⁰⁷ [Leadership and supervision, Samples and logistics, and Sequencing and analysis], Chrystala Constantinidou¹³⁵ [Leadership and supervision, Samples and logistics, and Sequencing and analysis], Meera Unnikrishnan¹³⁵ [Leadership and supervision, Samples and logistics, and Sequencing and analysis], Alistair C Darby¹³³ [Leadership and supervision, Samples and logistics, and Sequencing and analysis], Julian A Hiscox¹³³ [Leadership and supervision, Samples and logistics, and Sequencing and analysis], Steve Paterson¹³³ [Leadership and supervision, Samples and logistics, and Sequencing and analysis], Inigo Martincorena¹⁴⁰ [Leadership and supervision, Sequencing and analysis, and Software and analysis tools], David L Robertson⁸⁹ [Leadership and supervision, Sequencing and analysis, and Software and analysis tools], Erik M Volz⁸⁰ [Leadership and supervision, Sequencing and analysis, and Software and analysis tools], Andrew J Page¹¹¹ [Leadership and supervision, Sequencing and analysis, and Software and analysis tools], Oliver G Pybus⁶⁴ [Leadership and supervision, Sequencing and analysis, and Software and analysis tools], Andrew R Bassett¹⁴⁰ [Leadership and supervision, Sequencing and analysis, and Visualisation],

Cristina V Ariani¹⁴⁰ [Metadata curation, Project administration, and Samples and logistics], Michael H Spencer Chapman^{129,140} [Metadata curation, Project administration, and Samples and logistics], Kathy K Li⁸⁹ [Metadata curation, Project administration, and Samples and logistics], Rajiv N Shah⁸⁹ [Metadata curation, Project administration, and Samples and logistics], Natasha G Jesudason⁸⁹ [Metadata curation, Project administration, and Samples and logistics], Yusri Taha⁹¹ [Metadata curation, Project administration, and Samples and logistics], Martin P McHugh⁹⁴ [Metadata curation, Project administration, and Sequencing and analysis], Rebecca Dewar⁹⁴ [Metadata curation, Project administration, and Sequencing and analysis], Aminu S Jahun⁶⁵ [Metadata curation, Samples and logistics, and Sequencing and analysis], Claire McMurray⁸² [Metadata curation, Samples and logistics, and Sequencing and analysis], Sarojini Pandey¹²⁵ [Metadata curation, Samples and logistics, and Sequencing and analysis], James P McKenna⁴⁴ [Metadata curation, Samples and logistics, and Sequencing and analysis], Andrew Nelson^{99,146} [Metadata curation, Samples and logistics, and Sequencing and analysis], Gregory R Young^{78,99} [Metadata curation, Samples and logistics, and Sequencing and analysis], Clare M McCann^{99,146} [Metadata curation, Samples and logistics, and Sequencing and analysis], Scott Elliott¹⁰² [Metadata curation, Samples and logistics, and Sequencing and analysis], Hannah Lowe⁶⁶ [Metadata curation, Samples and logistics, and Visualisation], Ben Temperton¹³² [Metadata curation, Sequencing and analysis, and Software and analysis tools], Sunando Roy¹²³ [Metadata curation, Sequencing and analysis, and Software and analysis tools], Anna Price⁵¹ [Metadata curation, Sequencing and analysis, and Software and analysis tools], Sara Rey¹¹⁰ [Metadata curation, Sequencing and analysis, and Software and analysis tools], Matthew Wyles¹³⁴ [Metadata curation, Sequencing and analysis, and Software and analysis tools], Stefan Rooke¹³¹ [Metadata curation, Sequencing and analysis, and Visualisation], Sharif Shaaban¹⁰⁹ [Metadata curation, Sequencing and analysis, and Visualisation], Mariateresa de Cesare¹³⁹ [Project administration, Samples and logistics, Sequencing and analysis], Laura Letchford¹⁴⁰ [Project administration, Samples and logistics, and Software and analysis tools], Siona Silveira¹²² [Project administration, Samples and logistics, and Visualisation], Emanuela Pelosi¹²² [Project administration, Samples and logistics, and Visualisation], Eleri Wilson-Davies¹²² [Project administration, Samples and logistics, and Visualisation], Myra Hosmillo⁶⁵ [Samples and logistics, Sequencing and analysis, and Software and analysis tools], Áine O'Toole¹³¹ [Sequencing and analysis, Software and analysis tools, and Visualisation], Andrew R Hesketh¹²⁸ [Sequencing and analysis, Software and analysis tools, and Visualisation], Richard Stark¹³⁵ [Sequencing and analysis, Software and analysis tools, and Visualisation], Louis du Plessis⁶⁴ [Sequencing and analysis, Software and analysis tools, and Visualisation], Chris Ruis¹²⁹ [Sequencing and analysis, Software and analysis tools, and Visualisation], Helen Adams⁴⁵ [Sequencing and analysis, Software and

analysis tools, and Visualisation], Yann Bourgeois¹¹⁷ [Sequencing and analysis, Software and analysis tools, and Visualisation], Stephen L Michell¹³² [Funding acquisition, and Leadership and supervision], Dimitris Gramatopoulos^{125,153} [Funding acquisition, and Leadership and supervision], Jonathan Edgeworth⁵³ [Funding acquisition, and Leadership and supervision], Judith Breuer^{71,123} [Funding acquisition, and Leadership and supervision], John A Todd¹³⁹ [Funding acquisition, and Leadership and supervision], Christophe Fraser⁴⁶ [Funding acquisition, and Leadership and supervision], David Buck¹³⁹ [Funding acquisition, and Project administration], Michaela John⁵⁰ [Funding acquisition, and Project administration], Gemma L Kay¹¹¹ [Leadership and supervision, and Metadata curation], Steve Palmer¹⁴⁰ [Leadership and supervision, and Project administration], Sharon J Peacock^{129,105} [Leadership and supervision, and Project administration], David Heyburn¹¹⁰ [Leadership and supervision, and Project administration], Danni Weldon¹⁴⁰ [Leadership and supervision, and Samples and logistics], Esther Robinson^{105,77} [Leadership and supervision, and Samples and logistics], Alan McNally^{82,127} [Leadership and supervision, and Samples and logistics], Peter Muir¹⁰⁵ [Leadership and supervision, and Samples and logistics], Ian B Vipond¹⁰⁵ [Leadership and supervision, and Samples and logistics], John BoYes⁷⁰ [Leadership and supervision, and Samples and logistics], Venkat Sivaprakasam⁸⁷ [Leadership and supervision, and Samples and logistics], Tranpritt Salluja¹¹⁶ [Leadership and supervision, and Samples and logistics], Samir Dervisevic⁹⁵ [Leadership and supervision, and Samples and logistics], Emma J Meader⁹⁵ [Leadership and supervision, and Samples and logistics], Naomi R Park¹⁴⁰ [Leadership and supervision, and Sequencing and analysis], Karen Oliver¹⁴⁰ [Leadership and supervision, and Sequencing and analysis], Aaron R Jeffries¹³² [Leadership and supervision, and Sequencing and analysis], Sascha Ott¹³⁵ [Leadership and supervision, and Sequencing and analysis], Ana da Silva Filipe⁸⁹ [Leadership and supervision, and Sequencing and analysis], David A Simpson¹¹³ [Leadership and supervision, and Sequencing and analysis], Chris Williams¹¹⁰ [Leadership and supervision, and Sequencing and analysis], Jane AH Masoli^{114,132} [Leadership and supervision, and Visualisation], Bridget A Knight^{114,132} [Metadata curation, and Samples and logistics], Christopher R Jones^{114,132} [Metadata curation, and Samples and logistics], Cherian Koshy⁴² [Metadata curation, and Samples and logistics], Amy Ash⁴² [Metadata curation, and Samples and logistics], Anna Casey¹¹² [Metadata curation, and Samples and logistics], Andrew Bosworth^{105,77} [Metadata curation, and Samples and logistics], Liz Ratcliffe¹¹² [Metadata curation, and Samples and logistics], Li Xu-McCrae⁷⁷ [Metadata curation, and Samples and logistics], Hannah M Pymont¹⁰⁵ [Metadata curation, and Samples and logistics], Stephanie Hutchings¹⁰⁵ [Metadata curation, and Samples and logistics], Lisa Berry¹²⁵ [Metadata curation, and Samples and logistics], Katie Jones¹²⁵ [Metadata curation, and Samples and logistics], Fenella Halstead⁸⁷ [Metadata curation, and Samples and logistics], Thomas Davis⁶² [Metadata

curation, and Samples and logistics], Christopher Holmes⁵⁷ [Metadata curation, and Samples and logistics], Miren Iturriza-Gomara¹³³ [Metadata curation, and Samples and logistics], Anita O Lucaci¹³³ [Metadata curation, and Samples and logistics], Paul Anthony Randell^{79,145} [Metadata curation, and Samples and logistics], Alison Cox^{79,145} [Metadata curation, and Samples and logistics], Pinglawathee Madona^{79,145} [Metadata curation, and Samples and logistics], Kathryn Ann Harris⁷¹ [Metadata curation, and Samples and logistics], Julianne Rose Brown⁷¹ [Metadata curation, and Samples and logistics], Tabitha W Mahungu¹¹⁵ [Metadata curation, and Samples and logistics], Dianne Irish-Tavares¹¹⁵ [Metadata curation, and Samples and logistics], Tanzina Haque¹¹⁵ [Metadata curation, and Samples and logistics], Jennifer Hart¹¹⁵ [Metadata curation, and Samples and logistics], Eric Witele¹¹⁵ [Metadata curation, and Samples and logistics], Melisa Louise Fenton¹¹⁶ [Metadata curation, and Samples and logistics], Steven Liggett¹²⁰ [Metadata curation, and Samples and logistics], Clive Graham⁹⁷ [Metadata curation, and Samples and logistics], Emma Swindells⁹⁸ [Metadata curation, and Samples and logistics], Jennifer Collins⁹¹ [Metadata curation, and Samples and logistics], Gary Eltringham⁹¹ [Metadata curation, and Samples and logistics], Sharon Campbell⁵⁸ [Metadata curation, and Samples and logistics], Patrick C McClure¹³⁸ [Metadata curation, and Samples and logistics], Gemma Clark⁵⁶ [Metadata curation, and Samples and logistics], Tim J Sloan¹⁰¹ [Metadata curation, and Samples and logistics], Carl Jones⁵⁶ [Metadata curation, and Samples and logistics], Jessica Lynch^{43,152} [Metadata curation, and Samples and logistics], Ben Warne⁴⁹ [Metadata curation, and Sequencing and analysis], Steven Leonard¹⁴⁰ [Metadata curation, and Sequencing and analysis], Jillian Durham¹⁴⁰ [Metadata curation, and Sequencing and analysis], Thomas Williams¹³¹ [Metadata curation, and Sequencing and analysis], Sam T Haldenby¹³³ [Metadata curation, and Sequencing and analysis], Nathaniel Storey⁷¹ [Metadata curation, and Sequencing and analysis], Nabil-Fareed Alikhan¹¹¹ [Metadata curation, and Sequencing and analysis], Nadine Holmes⁵⁹ [Metadata curation, and Sequencing and analysis], Christopher Moore⁵⁹ [Metadata curation, and Sequencing and analysis], Matthew Carlile⁵⁹ [Metadata curation, and Sequencing and analysis], Malorie Perry¹¹⁰ [Metadata curation, and Sequencing and analysis], Noel Craine¹⁴⁰ [Metadata curation, and Sequencing and analysis], Ronan A Lyons¹⁴⁰ [Metadata curation, and Sequencing and analysis], Angela H Beckett⁵⁴ [Metadata curation, and Sequencing and analysis], Salman Goudarzi¹¹⁸ [Metadata curation, and Sequencing and analysis], Christopher Fearn¹¹⁸ [Metadata curation, and Sequencing and analysis], Kate Cook¹¹⁸ [Metadata curation, and Sequencing and analysis], Hannah Dent¹¹⁸ [Metadata curation, and Sequencing and analysis], Hannah Paul¹¹⁸ [Metadata curation, and Sequencing and analysis], Robert Davies¹⁴⁰ [Metadata curation, and Software and analysis tools], Beth Blane¹⁴⁰ [Project administration, and Samples and logistics], Sophia T Girgis¹⁴⁰ [Project administration, and Samples and logistics], Mathew A Beale¹⁴⁰ [Project

administration, and Samples and logistics], Katherine L Bellis^{140,129} [Project administration, and Samples and logistics], Matthew J Dorman¹⁴⁰ [Project administration, and Samples and logistics], Eleanor Drury¹⁴⁰ [Project administration, and Samples and logistics], Leanne Kane¹⁴⁰ [Project administration, and Samples and logistics], Sally Kay¹⁴⁰ [Project administration, and Samples and logistics], Samantha McGuigan¹⁴⁰ [Project administration, and Samples and logistics], Rachel Nelson¹⁴⁰ [Project administration, and Samples and logistics], Liam Prestwood¹⁴⁰ [Project administration, and Samples and logistics], Shavanthi Rajatileka¹⁴⁰ [Project administration, and Samples and logistics], Rahul Batra¹⁴⁰ [Project administration, and Samples and logistics], Rachel J Williams¹²³ [Project administration, and Samples and logistics], Mark Kristiansen¹²³ [Project administration, and Samples and logistics], Angie Green¹³⁹ [Project administration, and Samples and logistics], Anita Justice¹⁴⁰ [Project administration, and Samples and logistics], Adhyana I.K Mahanama^{122,143} [Project administration, and Samples and logistics], Buddhini Samaraweera^{122,143} [Project administration, and Samples and logistics], Nazreen F Hadjirin¹²⁹ [Project administration, and Sequencing and analysis], Joshua Quick⁸² [Project administration, and Sequencing and analysis], Radoslaw Poplawski⁸² [Project administration, and Software and analysis tools], Leanne M Kermack¹²⁹ [Samples and logistics, and Sequencing and analysis], Nicola Reynolds⁴⁸ [Samples and logistics, and Sequencing and analysis], Grant Hall⁶⁵ [Samples and logistics, and Sequencing and analysis], Yasmin Chaudhry¹⁴⁰ [Samples and logistics, and Sequencing and analysis], Malte L Pinckert⁶⁵ [Samples and logistics, and Sequencing and analysis], Iliana Georgana¹⁴⁰ [Samples and logistics, and Sequencing and analysis], Robin J Moll¹⁴⁰ [Samples and logistics, and Sequencing and analysis], Alicia Thornton¹⁰⁷ [Samples and logistics, and Sequencing and analysis], Richard Myers¹⁰⁷ [Samples and logistics, and Sequencing and analysis], Joanne Stockton¹⁴⁰ [Samples and logistics, and Sequencing and analysis], Charlotte A Williams¹⁴⁰ [Samples and logistics, and Sequencing and analysis], Wen C Yew¹⁴⁰ [Samples and logistics, and Sequencing and analysis], Alexander J Trotter¹¹¹ [Samples and logistics, and Sequencing and analysis], Amy Trebes¹⁴⁰ [Samples and logistics, and Sequencing and analysis], George MacIntyre-Cockett¹³⁹ [Samples and logistics, and Sequencing and analysis], Alec Birchley¹¹⁰ [Samples and logistics, and Sequencing and analysis], Alexander Adams¹¹⁰ [Samples and logistics, and Sequencing and analysis], Amy Plimmer¹⁴⁰ [Samples and logistics, and Sequencing and analysis], Bree Gatica-Wilcox¹¹⁰ [Samples and logistics, and Sequencing and analysis], Caoimhe McKerr¹¹⁰ [Samples and logistics, and Sequencing and analysis], Ember Hilvers¹¹⁰ [Samples and logistics, and Sequencing and analysis], Hannah Jones¹¹⁰ [Samples and logistics, and Sequencing and analysis], Hibo Asad¹¹⁰ [Samples and logistics, and Sequencing and analysis], Jason Coombes¹⁴⁰ [Samples and logistics, and Sequencing and analysis], Johnathan

M Evans¹¹⁰ [Samples and logistics, and Sequencing and analysis], Laia Fina¹¹⁰ [Samples and logistics, and Sequencing and analysis], Lauren Gilbert¹¹⁰ [Samples and logistics, and Sequencing and analysis], Lee Graham¹¹⁰ [Samples and logistics, and Sequencing and analysis], Michelle Cronin¹⁴⁰ [Samples and logistics, and Sequencing and analysis], Sara Kumziene-SummerhaYes¹¹⁰ [Samples and logistics, and Sequencing and analysis], Sarah Taylor¹¹⁰ [Samples and logistics, and Sequencing and analysis], Sophie Jones¹⁴⁰ [Samples and logistics, and Sequencing and analysis], Danielle C Groves¹³⁴ [Samples and logistics, and Sequencing and analysis], Peijun Zhang¹³⁴ [Samples and logistics, and Sequencing and analysis], Marta Gallis¹³⁴ [Samples and logistics, and Sequencing and analysis], Stavroula F Louka¹³⁴ [Samples and logistics, and Sequencing and analysis], Igor Starinskij⁸⁹ [Samples and logistics, and Software and analysis tools], Chris Jackson⁸⁸ [Sequencing and analysis, and Software and analysis tools], Marina Gourtovaia¹⁴⁰ [Sequencing and analysis, and Software and analysis tools], Gerry Tonkin-Hill¹⁴⁰ [Sequencing and analysis, and Software and analysis tools], Kevin Lewis¹⁴⁰ [Sequencing and analysis, and Software and analysis tools], Jaime M Tovar-Corona¹⁴⁰ [Sequencing and analysis, and Software and analysis tools], Keith James¹⁴⁰ [Sequencing and analysis, and Software and analysis tools], Laura Baxter¹³⁵ [Sequencing and analysis, and Software and analysis tools], Mohammad T Alam¹⁴⁰ [Sequencing and analysis, and Software and analysis tools], Richard J Orton⁸⁹ [Sequencing and analysis, and Software and analysis tools], Joseph Hughes⁸⁹ [Sequencing and analysis, and Software and analysis tools], Sreenu Vattipally¹⁴⁰ [Sequencing and analysis, and Software and analysis tools], Manon Ragonnet-Cronin⁸⁰ [Sequencing and analysis, and Software and analysis tools], Fabricia F Nascimento⁸⁰ [Sequencing and analysis, and Software and analysis tools], David Jorgensen⁸⁰ [Sequencing and analysis, and Software and analysis tools], Olivia Boyd⁸⁰ [Sequencing and analysis, and Software and analysis tools], Lily Geidelberg¹⁴⁰ [Sequencing and analysis, and Software and analysis tools], Alex E Zarebski⁶⁴ [Sequencing and analysis, and Software and analysis tools], Jayna Raghwan¹⁴⁰ [Sequencing and analysis, and Software and analysis tools], Moritz UG Kraemer⁶⁴ [Sequencing and analysis, and Software and analysis tools], Joel Southgate^{51,110} [Sequencing and analysis, and Software and analysis tools], Benjamin B Lindsey¹³⁴ [Sequencing and analysis, and Software and analysis tools], Timothy M Freeman¹³⁴ [Sequencing and analysis, and Software and analysis tools], Jon-Paul Keatley¹⁴⁰ [Software and analysis tools, and Visualisation], Joshua B Singer¹⁴⁰ [Software and analysis tools, and Visualisation], Leonardo de Oliveira Martins¹⁴⁰ [Software and analysis tools, and Visualisation], Corin A Yeats⁵⁵ [Software and analysis tools, and Visualisation], Khalil Abudahab^{140,140} [Software and analysis tools, and Visualisation], Ben EW Taylor¹⁴⁰ [Software and analysis tools, and Visualisation], Mirko Menegazzo⁵⁵ [Software and analysis tools, and Visualisation], John Danesh¹⁴⁰ [Leadership and supervision], Wendy

Hogsden⁸⁷ [Leadership and supervision], Sahar Eldirdiri⁶² [Leadership and supervision], Anita Kenyon⁶² [Leadership and supervision], Jenifer Mason¹⁴⁰ [Leadership and supervision], Trevor I Robinson⁸⁴ [Leadership and supervision], Alison Holmes^{140,144} [Leadership and supervision], James Price^{140,140} [Leadership and supervision], John A Hartley¹²³ [Leadership and supervision], Tanya Curran¹⁴⁰ [Leadership and supervision], Alison E Mather¹¹¹ [Leadership and supervision], Giri Shankar¹¹⁰ [Leadership and supervision], Rachel Jones¹¹⁰ [Leadership and supervision], Robin Howe¹¹⁰ [Leadership and supervision], Sian Morgan⁵⁰ [Leadership and supervision], Elizabeth Wastenge¹⁴⁰ [Metadata curation], Michael R Chapman^{1,129,140} [Metadata curation], Siddharth Mookerjee^{79,144} [Metadata curation], Rachael Stanley⁹⁵ [Metadata curation], Wendy Smith⁵⁶ [Metadata curation], Timothy Peto¹⁰⁰ [Metadata curation], David Eyre¹⁰⁰ [Metadata curation], Derrick Crook¹⁰⁰ [Metadata curation], Gabrielle Vernet⁷⁴ [Metadata curation], Christine Kitchen⁵¹ [Metadata curation], Huw Gulliver⁵¹ [Metadata curation], Ian Merrick⁵¹ [Metadata curation], Martyn Guest⁵¹ [Metadata curation], Robert Munn¹⁴⁰ [Metadata curation], Declan T Bradley^{140,113} [Metadata curation], Tim Wyatt¹⁰⁴ [Metadata curation], Charlotte Beaver¹⁴⁰ [Project administration], Luke Foulser¹⁴⁰ [Project administration], Sophie Palmer¹⁴⁰ [Project administration], Carol M Churcher¹²⁹ [Project administration], Ellena Brooks¹⁴⁰ [Project administration], Kim S Smith¹²⁹ [Project administration], Katerina Galai¹⁴⁰ [Project administration], Georgina M McManus¹²⁹ [Project administration], Frances Bolt^{79,144} [Project administration], Francesc Coll⁶⁰ [Project administration], Lizzie Meadows¹⁴⁰ [Project administration], Stephen W Attwood⁶⁴ [Project administration], Alisha Davies¹⁴⁰ [Project administration], Elen De Lacy¹¹⁰ [Project administration], Fatima Downing¹¹⁰ [Project administration], Sue Edwards¹⁴⁰ [Project administration], Garry P Scarlett¹¹⁷ [Project administration], Sarah Jeremiah¹²⁴ [Project administration], Nikki Smith¹³⁴ [Project administration], Danielle Leek¹²⁹ [Samples and logistics], Sushmita Sridhar^{140,140} [Samples and logistics], Sally Forrest¹²⁹ [Samples and logistics], Claire Cormie¹⁴⁰ [Samples and logistics], Harmeet K Gill¹²⁹ [Samples and logistics], Joana Dias¹⁴⁰ [Samples and logistics], Ellen E Higginson¹²⁹ [Samples and logistics], Mailis Maes¹²⁹ [Samples and logistics], Jamie Young¹²⁹ [Samples and logistics], Michelle Wantoch¹⁴⁰ [Samples and logistics], Sanger Covid Team¹⁴⁰ [Samples and logistics], Dorota Jamroz¹⁴⁰ [Samples and logistics], Stephanie Lo¹⁴⁰ [Samples and logistics], Minal Patel¹⁴⁰ [Samples and logistics], Verity Hill¹⁴⁰ [Samples and logistics], Claire M Bewshea¹³² [Samples and logistics], Sian Ellard^{114,132} [Samples and logistics], Cressida Auckland¹¹⁴ [Samples and logistics], Ian Harrison¹⁰⁷ [Samples and logistics], Chloe Bishop¹⁰⁷ [Samples and logistics], Vicki Chalker¹⁰⁷ [Samples and logistics], Alex Richter¹²⁶ [Samples and logistics], Andrew Beggs¹²⁶ [Samples and logistics], Angus Best¹²⁷ [Samples and logistics], Benita Percival¹²⁷ [Samples and logistics], Jeremy Mirza¹²⁷ [Samples and logistics], Oliver Megram¹²⁷ [Samples and logistics], Megan Mayhew¹²⁷ [Samples and logistics], Liam Crawford¹²⁷

[Samples and logistics], Fiona Ashcroft¹⁴⁰ [Samples and logistics], Emma Moles-Garcia¹²⁷ [Samples and logistics], Nicola Cumley¹²⁷ [Samples and logistics], Richard Hopes¹⁰⁵ [Samples and logistics], Patawee Asamaphan¹⁴⁰ [Samples and logistics], Marc O Niebel¹⁴⁰ [Samples and logistics], Rory N Gunson¹⁴¹ [Samples and logistics], Amanda Bradley⁹³ [Samples and logistics], Alasdair Maclean⁹³ [Samples and logistics], Guy Mollett⁹³ [Samples and logistics], Rachel Blacow⁹³ [Samples and logistics], Paul Bird⁵⁷ [Samples and logistics], Thomas Helmer⁵⁷ [Samples and logistics], Karlie Fallon⁵⁷ [Samples and logistics], Julian Tang¹⁴⁰ [Samples and logistics], Antony D Hale¹⁴⁰ [Samples and logistics], Louissa R Macfarlane-Smith¹⁴⁰ [Samples and logistics], Katherine L Harper⁹⁰ [Samples and logistics], Holli Carden¹⁴⁰ [Samples and logistics], Nicholas W Machin^{86,105} [Samples and logistics], Kathryn A Jackson¹³³ [Samples and logistics], Shazaad SY Ahmad^{86,105} [Samples and logistics], Ryan P George⁸⁶ [Samples and logistics], Lance Turtle¹⁴⁰ [Samples and logistics], Elaine O'Toole⁸⁴ [Samples and logistics], Joanne Watts⁸⁴ [Samples and logistics], Cassie Breen⁸⁴ [Samples and logistics], Angela Cowell¹⁴⁰ [Samples and logistics], Adela Alcolea-Medina^{73,137} [Samples and logistics], Themoula Charalampous^{140,83} [Samples and logistics], Amita Patel¹⁴⁰ [Samples and logistics], Lisa J Levett⁷⁶ [Samples and logistics], Judith Heaney⁷⁶ [Samples and logistics], Aileen Rowan¹⁴⁰ [Samples and logistics], Graham P Taylor⁸⁰ [Samples and logistics], Divya Shah⁷¹ [Samples and logistics], Laura Atkinson¹⁴⁰ [Samples and logistics], Jack CD Lee¹⁴⁰ [Samples and logistics], Adam P Westhorpe¹²³ [Samples and logistics], Riaz Jannoo¹⁴⁰ [Samples and logistics], Helen L Lowe¹²³ [Samples and logistics], Angeliki Karamani¹²³ [Samples and logistics], Leah Ensell¹²³ [Samples and logistics], Wendy Chatterton⁷⁶, Monika Pusok⁷⁶ [Samples and logistics], Ashok Dadrah¹¹⁶ [Samples and logistics], Amanda Symmonds¹¹⁶ [Samples and logistics], Graciela Sluga⁸⁵ [Samples and logistics], Zoltan Molnar¹¹³ [Samples and logistics], Paul Baker¹²⁰ [Samples and logistics], Stephen Bonner¹²⁰ [Samples and logistics], Sarah Essex¹²⁰ [Samples and logistics], Edward Barton⁹⁷ [Samples and logistics], Debra Padgett⁹⁷ [Samples and logistics], Garren Scott⁹⁷ [Samples and logistics], Jane Greenaway¹⁴⁰ [Samples and logistics], Brendan Al Payne¹⁴⁰ [Samples and logistics], Shirelle Burton-Fanning⁹¹ [Samples and logistics], Sheila Waugh⁹¹ [Samples and logistics], Veena Raviprakash⁵⁸ [Samples and logistics], Nicola Sheriff⁵⁸ [Samples and logistics], Victoria Blakey¹⁴⁰ [Samples and logistics], Lesley-Anne Williams⁵⁸ [Samples and logistics], Jonathan Moore⁶⁸ [Samples and logistics], Susanne Stonehouse⁶⁸ [Samples and logistics], Louise Smith¹⁴⁰ [Samples and logistics], Rose K Davidson¹³⁰ [Samples and logistics], Luke Bedford⁶⁷ [Samples and logistics], Lindsay Coupland⁹⁵ [Samples and logistics], Victoria Wright¹⁴⁰ [Samples and logistics], Joseph G Chappell¹³⁸ [Samples and logistics], Theocharis Tsoleridis¹³⁸ [Samples and logistics], Jonathan Ball¹³⁸ [Samples and logistics], Manjinder Khakh¹⁴⁰ [Samples and logistics], Vicki M Fleming¹⁴⁰ [Samples and logistics], Michelle M Lister¹⁴⁰ [Samples and logistics], Hannah C

Howson-Wells⁵⁶ [Samples and logistics], Louise Berry⁵⁶ [Samples and logistics], Tim Boswell⁵⁶ [Samples and logistics], Amelia Joseph⁵⁶ [Samples and logistics], Iona Willingham⁵⁶ [Samples and logistics], Nichola Duckworth¹⁰¹ [Samples and logistics], Sarah Walsh¹⁰¹ [Samples and logistics], Emma Wise^{140,152} [Samples and logistics], Nathan Moore^{140,152} [Samples and logistics], Matilde Mori^{140,140,152} [Samples and logistics], Nick Cortes^{140,152} [Samples and logistics], Stephen Kidd^{140,152} [Samples and logistics], Rebecca Williams⁷⁴ [Samples and logistics], Laura Gifford¹¹⁰ [Samples and logistics], Kelly Bicknell¹⁰² [Samples and logistics], Sarah Wyllie¹⁰² [Samples and logistics], Allyson Lloyd¹⁰² [Samples and logistics], Robert Impey¹⁴⁰ [Samples and logistics], Cassandra S Malone¹⁴⁰ [Samples and logistics], Benjamin J Cogger⁴⁷ [Samples and logistics], Nick Levene¹⁰³ [Samples and logistics], Lynn Monaghan¹⁴⁰ [Samples and logistics], Alexander J Keeley¹⁴⁰ [Samples and logistics], David G Partridge^{140,134} [Samples and logistics], Mohammad Raza^{119,134} [Samples and logistics], Cariad Evans^{140,134} [Samples and logistics], Kate Johnson^{119,134} [Samples and logistics], Emma Betteridge¹⁴⁰ [Sequencing and analysis], Ben W Farr¹⁴⁰ [Sequencing and analysis], Scott Goodwin¹⁴⁰ [Sequencing and analysis], Michael A Quail¹⁴⁰ [Sequencing and analysis], Carol Scott¹⁴⁰ [Sequencing and analysis], Lesley Shirley¹⁴⁰ [Sequencing and analysis], Scott AJ Thurston¹⁴⁰ [Sequencing and analysis], Diana Rajan¹⁴⁰ [Sequencing and analysis], Iraad F Bronner¹⁴⁰ [Sequencing and analysis], Louise Aigrain¹⁴⁰ [Sequencing and analysis], Nicholas M Redshaw¹⁴⁰ [Sequencing and analysis], Stefanie V Lensing¹⁴⁰ [Sequencing and analysis], Shane McCarthy¹⁴⁰ [Sequencing and analysis], Alex Makunin¹⁴⁰ [Sequencing and analysis], Carlos E Balcazar¹⁴⁰ [Sequencing and analysis], Michael D Gallagher¹⁴⁰ [Sequencing and analysis], Kathleen A Williamson¹⁴⁰ [Sequencing and analysis], Thomas D Stanton¹⁴⁰ [Sequencing and analysis], Michelle L Michelsen¹⁴⁰ [Sequencing and analysis], Joanna Warwick-Dugdale¹³² [Sequencing and analysis], Robin Manley¹³² [Sequencing and analysis], Audrey Farbos¹⁴⁰ [Sequencing and analysis], James W Harrison¹⁴⁰ [Sequencing and analysis], Christine M Sambles¹⁴⁰ [Sequencing and analysis], David J Studholme¹³² [Sequencing and analysis], Angie Lackenby¹⁰⁷ [Sequencing and analysis], Tamyo Mbisa¹⁰⁷ [Sequencing and analysis], Steven Platt¹⁰⁷ [Sequencing and analysis], Shahjahan Miah¹⁰⁷ [Sequencing and analysis], David Bibby¹⁰⁷ [Sequencing and analysis], Carmen Manso¹⁰⁷ [Sequencing and analysis], Jonathan Hubb¹⁰⁷ [Sequencing and analysis], Gavin Dabrera¹⁰⁷ [Sequencing and analysis], Mary Ramsay¹⁰⁷ [Sequencing and analysis], Daniel Bradshaw¹⁰⁷ [Sequencing and analysis], Ulf Schaefer¹⁰⁷ [Sequencing and analysis], Natalie Groves¹⁰⁷ [Sequencing and analysis], Eileen Gallagher¹⁰⁷ [Sequencing and analysis], David Lee¹⁰⁷ [Sequencing and analysis], David Williams¹⁰⁷ [Sequencing and analysis], Nicholas Ellaby¹⁰⁷ [Sequencing and analysis], Hassan Hartman¹⁰⁷ [Sequencing and analysis], Nikos Manesis¹⁰⁷ [Sequencing and analysis], Vineet Patel¹⁰⁷ [Sequencing and analysis], Juan Ledesma¹⁴⁰ [Sequencing and analysis], Katherine A Twohig¹⁰⁸ [Sequencing and

analysis], Elias Allara^{140,129} [Sequencing and analysis], Clare Pearson^{140,140} [Sequencing and analysis], Jeffrey K. J. Cheng¹³⁵ [Sequencing and analysis], Hannah E Bridgewater¹³⁵ [Sequencing and analysis], Lucy R Frost¹⁴⁰ [Sequencing and analysis], Grace Taylor-Joyce¹⁴⁰ [Sequencing and analysis], Paul E Brown¹³⁵ [Sequencing and analysis], Lily Tong⁸⁹ [Sequencing and analysis], Alice Broos⁸⁹ [Sequencing and analysis], Daniel Mair⁸⁹ [Sequencing and analysis], Jenna Nichols¹⁴⁰ [Sequencing and analysis], Stephen N Carmichael¹⁴⁰ [Sequencing and analysis], Katherine L Smollett⁸¹ [Sequencing and analysis], Kyriaki Nomikou¹⁴⁰ [Sequencing and analysis], Elihu Aranday-Cortes⁸⁹ [Sequencing and analysis], Natasha Johnson⁸⁹ [Sequencing and analysis], Seema Nickbakhsh^{140,140} [Sequencing and analysis], Edith E Vamos¹³³ [Sequencing and analysis], Margaret Hughes¹³³ [Sequencing and analysis], Lucille Rainbow¹³³ [Sequencing and analysis], Richard Eccles¹³³ [Sequencing and analysis], Charlotte Nelson¹³³ [Sequencing and analysis], Mark Whitehead¹³³ [Sequencing and analysis], Richard Gregory¹³³ [Sequencing and analysis], Matthew Gemmell¹³³ [Sequencing and analysis], Claudia Wierzbicki¹⁴⁰ [Sequencing and analysis], Hermione J Webster¹⁴⁰ [Sequencing and analysis], Chloe L Fisher¹⁴⁰ [Sequencing and analysis], Adrian W Signell⁶¹ [Sequencing and analysis], Gilberto Betancor¹⁴⁰ [Sequencing and analysis], Harry D Wilson⁶¹ [Sequencing and analysis], Gaia Nebbia⁵³ [Sequencing and analysis], Flavia Flaviani¹⁴⁰ [Sequencing and analysis], Alberto C Cerda¹⁴⁰ [Sequencing and analysis], Tammy V Merrill¹⁴⁰ [Sequencing and analysis], Rebekah E Wilson¹³⁷ [Sequencing and analysis], Marius Cotic¹²³ [Sequencing and analysis], Nadua Bayzid¹²³ [Sequencing and analysis], Thomas Thompson¹¹³ [Sequencing and analysis], Erwan Acheson¹¹³ [Sequencing and analysis], Steven Rushton¹⁴⁰ [Sequencing and analysis], Sarah O'Brien¹⁴⁰ [Sequencing and analysis], David J Baker¹¹¹ [Sequencing and analysis], Steven Rudder¹¹¹ [Sequencing and analysis], Alp Aydin¹¹¹ [Sequencing and analysis], Fei Sang⁵⁹ [Sequencing and analysis], Johnny Debebe⁵⁹ [Sequencing and analysis], Sarah Francois¹⁴⁰ [Sequencing and analysis], Tetyana I Vasylyeva¹⁴⁰ [Sequencing and analysis], Marina Escalera Zamudio⁶⁴ [Sequencing and analysis], Bernardo Gutierrez⁶⁴ [Sequencing and analysis], Angela Marchbank⁵¹ [Sequencing and analysis], Joshua Maksimovic⁵⁰ [Sequencing and analysis], Karla Spellman⁵⁰ [Sequencing and analysis], Kathryn McCluggage⁵⁰ [Sequencing and analysis], Mari Morgan¹¹⁰ [Sequencing and analysis], Robert Beer⁵⁰ [Sequencing and analysis], Safiah Affi⁵⁰ [Sequencing and analysis], Trudy Workman⁵¹ [Sequencing and analysis], William Fuller⁵¹ [Sequencing and analysis], Catherine Bresner⁵¹ [Sequencing and analysis], Adrienn Angyal¹⁴⁰ [Sequencing and analysis], Luke R Green¹⁴⁰ [Sequencing and analysis], Paul J Parsons¹⁴⁰ [Sequencing and analysis], Rachel M Tucker¹³⁴ [Sequencing and analysis], Rebecca Brown¹³⁴ [Sequencing and analysis], Max Whiteley¹³⁴ [Sequencing and analysis], James Bonfield¹⁴⁰ [Software and analysis tools], Christoph Pueth¹⁴⁰ [Software and analysis tools], Andrew Whitwham¹⁴⁰ [Software and analysis tools], Jennifer Liddle¹⁴⁰ [Software and analysis tools],

Will Rowe⁸² [Software and analysis tools], Igor Siveroni¹⁴⁰ [Software and analysis tools], Thanh Le-Viet¹⁴⁰ [Software and analysis tools], Amy Gaskin¹¹⁰ [Software and analysis tools], Rob Johnson⁸⁰ [Visualisation]

Affiliations

¹⁹Cambridge Clinical Research Centre, NIHR Clinical Research Facility, Cambridge University Hospitals NHS Foundation Trust, Addenbrooke's Hospital, Cambridge CB2 0QQ, UK ²⁰Department of Haematology, University of Cambridge, Cambridge Biomedical Campus, Cambridge CB2 0QQ, UK ²¹Australian National Phenome Centre, Murdoch University, Murdoch, Western Australia WA 6150, Australia ²²MRC Toxicology Unit, School of Biological Sciences, University of Cambridge, Cambridge CB2 1QR, UK ²³R&D Department, Hycult Biotech, 5405 PD Uden, The Netherlands ²⁴Heart and Lung Research Institute, Cambridge Biomedical Campus, Cambridge CB2 0QQ, UK ²⁵Royal Papworth Hospital NHS Foundation Trust, Cambridge Biomedical Campus, Cambridge CB2 0QQ, UK ²⁶Department of Biomedicine, University and University Hospital Basel, 4031 Basel, Switzerland ²⁷Botnar Research Centre for Child Health (BRCC) University Basel & ETH Zurich, 4058 Basel, Switzerland ²⁸Addenbrooke's Hospital, Cambridge CB2 0QQ, UK ²⁹Department of Veterinary Medicine, Madingley Road, Cambridge, CB3 0ES, UK ³⁰Cambridge Institute for Medical Research, Cambridge Biomedical Campus, Cambridge CB2 0XY, UK ³¹Cancer Research UK, Cambridge Institute, University of Cambridge CB2 0RE, UK ³²Department of Obstetrics & Gynaecology, The Rosie Maternity Hospital, Robinson Way, Cambridge CB2 0SW, UK ³³Centre for Molecular Medicine and Innovative Therapeutics, Health Futures Institute, Murdoch University, Perth, WA, Australia ³⁴Cambridge and Peterborough Foundation Trust, Fulbourn Hospital, Fulbourn, Cambridge CB21 5EF, UK ³⁵Department of Surgery, Addenbrooke's Hospital, Cambridge CB2 0QQ, UK ³⁶Department of Biochemistry, University of Cambridge, Cambridge, CB2 1QW, UK ³⁷Centre of Computational and Systems Medicine, Health Futures Institute, Murdoch University, Harry Perkins Building, Perth, WA 6150, Australia ³⁸Department of Public Health and Primary Care, School of Clinical Medicine, University of Cambridge, Cambridge Biomedical Campus, Cambridge, UK ³⁹Cancer Molecular Diagnostics Laboratory, Department of Oncology, University of Cambridge, Cambridge CB2 0AH, UK ⁴⁰Metabolic Research Laboratories, Wellcome Trust-Medical Research Council Institute of Metabolic Science, University of Cambridge, Cambridge CB2 0QQ, UK ⁴¹Department of Paediatrics, University of Cambridge, Cambridge Biomedical Campus, Cambridge, CB2 0QQ, UK

⁴²Barking, Havering and Redbridge University Hospitals NHS Trust, Barking, United Kingdom ⁴³Basingstoke Hospital, Basingstoke, United Kingdom ⁴⁴Belfast Health & Social Care Trust, Belfast, United Kingdom ⁴⁵Betsi Cadwaladr University Health Board, Betsi Cadwaladr, United Kingdom ⁴⁶Big Data Institute, Nuffield Department of Medicine, University of Oxford, Oxford, United Kingdom ⁴⁷Brighton and Sussex University Hospitals NHS Trust, Brighton & Sussex, United Kingdom ⁴⁸Cambridge Stem Cell Institute, University of Cambridge, Cambridge, United Kingdom

⁴⁹Cambridge University Hospitals NHS Foundation Trust, Cambridge, United Kingdom ⁵⁰Cardiff and Vale University Health Board, Cardiff, United Kingdom ⁵¹Cardiff University, Cardiff, United Kingdom ⁵²Centre for Clinical Infection & Diagnostics Research, St. Thomas' Hospital and Kings College London, London, United Kingdom ⁵³Centre for Clinical Infection and Diagnostics Research, Department of Infectious Diseases, Guy's and St Thomas' NHS Foundation Trust, London, United Kingdom ⁵⁴Centre for Enzyme Innovation, University of Portsmouth (PORT), Portsmouth, United Kingdom ⁵⁵Centre for Genomic Pathogen Surveillance, University of Oxford, Oxford, United Kingdom ⁵⁶Clinical Microbiology Department, Queens Medical Centre, Nottingham, United Kingdom ⁵⁷Clinical Microbiology, University Hospitals of Leicester NHS Trust, Leicester, United Kingdom ⁵⁸County Durham and Darlington NHS Foundation Trust, Durham, United Kingdom ⁵⁹Deep Seq, School of Life Sciences, Queens Medical Centre, University of Nottingham, Nottingham, United Kingdom ⁶⁰Department of Infection Biology, Faculty of Infectious & Tropical Diseases, London School of Hygiene & Tropical Medicine, London, United Kingdom ⁶¹Department of Infectious Diseases, King's College London, London, United Kingdom ⁶²Department of Microbiology, Kettering General Hospital, Kettering, United Kingdom ⁶³Departments of Infectious Diseases and Microbiology, Cambridge University Hospitals NHS Foundation Trust; Cambridge, UK, Cambridge, United Kingdom ⁶⁴Department of Zoology, University of Oxford, Oxford, United Kingdom ⁶⁵Division of Virology, Department of Pathology, University of Cambridge, Cambridge, United Kingdom ⁶⁶East Kent Hospitals University NHS Foundation Trust, Kent, United Kingdom ⁶⁷East Suffolk and North Essex NHS Foundation Trust, Suffolk, United Kingdom ⁶⁸Gateshead Health NHS Foundation Trust, Gateshead, United Kingdom ⁶⁹Genomics Innovation Unit, Guy's and St. Thomas' NHS Foundation Trust, London, United Kingdom ⁷⁰Gloucestershire Hospitals NHS Foundation Trust, Gloucester, United Kingdom ⁷¹Great Ormond Street Hospital for Children NHS Foundation Trust, London, United Kingdom ⁷²Guy's and St. Thomas' BRC, London, United Kingdom ⁷³Guy's and St. Thomas' Hospitals, London, United Kingdom ⁷⁴Hampshire Hospitals NHS Foundation Trust, Hampshire, United Kingdom ⁷⁵Health Data Research UK Cambridge, Cambridge, United Kingdom ⁷⁶Health Services Laboratories, London, United Kingdom ⁷⁷Heartlands Hospital, Birmingham, Birmingham, United Kingdom ⁷⁸Hub for Biotechnology in the Built Environment, Northumbria University, Northumbria, United Kingdom ⁷⁹Imperial College Hospitals NHS Trust, London, United Kingdom ⁸⁰Imperial College London, London, United Kingdom ⁸¹Institute of Biodiversity, Animal Health & Comparative Medicine, Glasgow, United Kingdom ⁸²Institute of Microbiology and Infection, University of Birmingham, Birmingham, United Kingdom ⁸³King's College London, London, United Kingdom ⁸⁴Liverpool Clinical Laboratories, Liverpool, United Kingdom ⁸⁵Maidstone and Tunbridge Wells NHS Trust, Maidstone, United Kingdom ⁸⁶Manchester University NHS Foundation Trust, Manchester, United Kingdom ⁸⁷Microbiology Department, Wye Valley NHS Trust, Hereford, United Kingdom ⁸⁸MRC Biostatistics Unit, University of Cambridge, Cambridge, United Kingdom ⁸⁹MRC-University of Glasgow Centre for Virus Research, Glasgow, United Kingdom

⁹⁰National Infection Service, PHE and Leeds Teaching Hospitals Trust, Leeds, United Kingdom ⁹¹Newcastle Hospitals NHS Foundation Trust, Newcastle, United Kingdom ⁹²Newcastle University, Newcastle, United Kingdom ⁹³NHS Greater Glasgow and Clyde, Glasgow, United Kingdom ⁹⁴NHS Lothian, Edinburgh, United Kingdom ⁹⁵Norfolk and Norwich University Hospital, Norfolk, United Kingdom ⁹⁶Norfolk County Council, Norfolk, United Kingdom ⁹⁷North Cumbria Integrated Care NHS Foundation Trust, Carlisle, United Kingdom ⁹⁸North Tees and Hartlepool NHS Foundation Trust, Stockton-on-Tees, United Kingdom ⁹⁹Northumbria University, Northumbria, United Kingdom ¹⁰⁰Oxford University Hospitals NHS Foundation Trust, Oxford, United Kingdom ¹⁰¹PathLinks, Northern Lincolnshire & Goole NHS Foundation Trust, Lincolnshire, United Kingdom ¹⁰²Portsmouth Hospitals University NHS Trust, Portsmouth, United Kingdom ¹⁰³Princess Alexandra Hospital Microbiology Dept., Harlow, United Kingdom ¹⁰⁴Public Health Agency, London, United Kingdom ¹⁰⁵Public Health England, London, United Kingdom ¹⁰⁶Public Health England, Clinical Microbiology and Public Health Laboratory, Cambridge, United Kingdom ¹⁰⁷Public Health England, Colindale, London, United Kingdom ¹⁰⁸Public Health England, Colindale, London, United Kingdom ¹⁰⁹Public Health Scotland, Glasgow, United Kingdom ¹¹⁰Public Health Wales NHS Trust, Cardiff, United Kingdom ¹¹¹Quadram Institute Bioscience, Norwich, United Kingdom ¹¹²Queen Elizabeth Hospital, Birmingham, United Kingdom ¹¹³Queen's University Belfast, Belfast, United Kingdom ¹¹⁴Royal Devon and Exeter NHS Foundation Trust, Devon, United Kingdom ¹¹⁵Royal Free NHS Trust, London, United Kingdom ¹¹⁶Sandwell and West Birmingham NHS Trust, Sandwell, United Kingdom ¹¹⁷School of Biological Sciences, University of Portsmouth (PORT), Portsmouth, United Kingdom ¹¹⁸School of Pharmacy and Biomedical Sciences, University of Portsmouth (PORT), Portsmouth, United Kingdom ¹¹⁹Sheffield Teaching Hospitals, Sheffield, United Kingdom ¹²⁰South Tees Hospitals NHS Foundation Trust, Newcastle, United Kingdom ¹²¹Swansea University, Swansea, United Kingdom ¹²²University Hospitals Southampton NHS Foundation Trust, Southampton, United Kingdom ¹²³University College London, London, United Kingdom ¹²⁴University Hospital Southampton NHS Foundation Trust, Southampton, United Kingdom ¹²⁵University Hospitals Coventry and Warwickshire, Coventry, United Kingdom ¹²⁶University of Birmingham, Birmingham, United Kingdom ¹²⁷University of Birmingham Turnkey Laboratory, Birmingham, United Kingdom ¹²⁸University of Brighton, Brighton, United Kingdom ¹²⁹University of Cambridge, Cambridge, United Kingdom ¹³⁰University of East Anglia, East Anglia, United Kingdom ¹³¹University of Edinburgh, Edinburgh, United Kingdom ¹³²University of Exeter, Exeter, United Kingdom ¹³³University of Liverpool, Liverpool, United Kingdom ¹³⁴University of Sheffield, Sheffield, United Kingdom ¹³⁵University of Warwick, Warwick, United Kingdom ¹³⁶University of Cambridge, Cambridge, United Kingdom ¹³⁷Viapath, Guy's and St Thomas' NHS Foundation Trust, and King's College Hospital NHS Foundation Trust, London, United Kingdom ¹³⁸Virology, School of Life Sciences, Queens Medical Centre, University of Nottingham, Nottingham, United Kingdom ¹³⁹Wellcome Centre for Human Genetics, Nuffield Department of Medicine,

University of Oxford, Oxford, United Kingdom ¹⁴⁰Wellcome Sanger Institute, London, United Kingdom ¹⁴¹West of Scotland Specialist Virology Centre, NHS Greater Glasgow and Clyde, Glasgow, United Kingdom ¹⁴²Department of Medicine, University of Cambridge, Cambridge, United Kingdom ¹⁴³Ministry of Health, Colombo, Sri Lanka ¹⁴⁴NIHR Health Protection Research Unit in HCAI and AMR, Imperial College London, London, United Kingdom ¹⁴⁵North West London Pathology, London, United Kingdom ¹⁴⁶NU-OMICS, Northumbria University, Northumbria, United Kingdom ¹⁴⁷University of Kent, Kent, United Kingdom ¹⁴⁸University of Oxford, Oxford, United Kingdom ¹⁴⁹University of Southampton, Southampton, United Kingdom ¹⁵⁰University of Southampton School of Health Sciences, Southampton, United Kingdom ¹⁵¹University of Southampton School of Medicine, Southampton, United Kingdom ¹⁵²University of Surrey, Guildford, United Kingdom ¹⁵³Warwick Medical School and Institute of Precision Diagnostics, Pathology, UHCW NHS Trust, Warwick, United Kingdom

¹Division of Infection and Immunity, University College London, London, UK ²Cambridge Institute of Therapeutic Immunology & Infectious Disease (CITIID), Cambridge, UK ³Department of Medicine, University of Cambridge, Cambridge, UK ⁴Department of Infectious Diseases, Cambridge University NHS Hospitals Foundation Trust, Cambridge, UK ⁵Department of Pathology, University of Cambridge, Cambridge ⁶NHS Blood and Transplant, Oxford and BRC Haematology Theme, University of Oxford, UK ⁷Viral Pseudotype Unit, Medway School of Pharmacy, University of Kent, UK ⁸Medical Research Council Laboratory of Molecular Biology, Cambridge, UK ⁹Department of Medical Microbiology, Academic Medical Center, University of Amsterdam, Amsterdam Institute for Infection and Immunity, Amsterdam, Netherlands ¹⁰NIHR Cambridge Clinical Research Facility, Cambridge, UK ¹¹Department of Virology, Cambridge University NHS Hospitals Foundation Trust ¹²Department of Applied Mathematics and Theoretical Physics, University of Cambridge, UK ¹³Department of Clinical Biochemistry and Immunology, Addenbrookes Hospital ¹⁴FES-Cuautitlán, UNAM, Mexico ¹⁵Biochemistry and Molecular Genetics, University of Colorado School of Medicine, Aurora, Colorado, USA; ¹⁶Clinical Microbiology and Public Health Laboratory, Addenbrookes' Hospital, Cambridge, UK ¹⁷MRC Biostatistics Unit, University of Cambridge, Cambridge, UK ¹⁸Africa Health Research Institute, Durban, South Africa

Acknowledgements

We are immensely grateful to the patient and his family. We would also like to thank the staff at CUH and the NIHR Cambridge Clinical Research Facility. We would like to thank Dr Ruthiran Kugathasan and Professor Wendy Barclay for helpful discussions and Dr Martin Curran, Dr William Hamilton, and Dr. Dominic Sparkes. We would like to thank Prof Andres Floto and Prof Ferdia Gallagher. We thank Dr James Voss for the kind gift of HeLa cells stably expressing ACE2. We would like to thank James Nathan for RBD protein and Leo James for N protein. COG-UK is supported by funding from the Medical Research Council (MRC) part of UK Research & Innovation (UKRI), the National Institute of Health Research (NIHR) and Genome Research Limited, operating as the Wellcome Sanger Institute. RKG is supported by a Wellcome Trust Senior Fellowship in Clinical Science (WT108082AIA). LEM is supported by a Medical Research Council Career Development Award (MR/R008698/1).

SAK is supported by the Bill and Melinda Gates Foundation via PANGAEA grant: OPP1175094. DAC is supported by a Wellcome Trust Clinical PhD Research Fellowship. CJRI acknowledges MRC funding (ref: MC_UU_00002/11). This research was supported by the National Institute for Health Research (NIHR) Cambridge Biomedical Research Centre, the Cambridge Clinical Trials Unit (CCTU) and by the UCL Coronavirus Response Fund and made possible through generous donations from UCL's supporters, alumni, and friends (LEM). JAGB is supported by the Medical Research Council (MC_UP_1201/16). IG is a Wellcome Senior Fellow and supported by the Wellcome Trust (207498/Z/17/Z). DDP is supported by NIH GM083127.

Data Availability

Long-read sequencing data that support the findings of this study have been deposited in the NCBI SRA database with the accession codes SAMN16976824 - SAMN16976846 under BioProject PRJNA682013 (<https://www.ncbi.nlm.nih.gov/bioproject/PRJNA682013>). Short reads and data used to construct figures were deposited at https://github.com/Steven-Kemp/sequence_files. All data are also available from the corresponding author.

Code Availability

The SAMFIRE package Version 1.06 was used for filtering and calling variants from the Illumina data. It is available at <https://github.com/cjri/samfire/> for review. Additional code was used to validate the variant frequencies and can be found at <https://github.com/PollockLaboratory/AnCovMulti>.

References

- Hoffmann M, et al. SARS-CoV-2 Cell Entry Depends on ACE2 and TMPRSS2 and Is Blocked by a Clinically Proven Protease Inhibitor. *Cell*. 2020; 181:271–280 e278. DOI: 10.1016/j.cell.2020.02.052 [PubMed: 32142651]
- Kim KW, et al. Respiratory viral co-infections among SARS-CoV-2 cases confirmed by virome capture sequencing. 2020
- Bull RA, et al. Analytical validity of nanopore sequencing for rapid SARS-CoV-2 genome analysis. *Nat Commun*. 2020; 11:6272.doi: 10.1038/s41467-020-20075-6 [PubMed: 33298935]
- Choi B, et al. Persistence and Evolution of SARS-CoV-2 in an Immunocompromised Host. *The New England journal of medicine*. 2020; 383:2291–2293. DOI: 10.1056/NEJMc2031364 [PubMed: 33176080]
- Avanzato VA, et al. Case Study: Prolonged infectious SARS-CoV-2 shedding from an asymptomatic immunocompromised cancer patient. *Cell*. 2020
- Starr TN, et al. Deep Mutational Scanning of SARS-CoV-2 Receptor Binding Domain Reveals Constraints on Folding and ACE2 Binding. *Cell*. 2020; 182:1295–1310 e1220. DOI: 10.1016/j.cell.2020.08.012 [PubMed: 32841599]
- Rambaut ALN, Pybus O, Barclay W, Carabelli AC, Connor T, Peacock T, Robertson DL, Volz E, COVID-19 Genomics Consortium UK (CoG-UK). Preliminary genomic characterisation of an emergent SARS-CoV-2 lineage in the UK defined by a novel set of spike mutations. 2020
- Schmidt F, et al. Measuring SARS-CoV-2 neutralizing antibody activity using pseudotyped and chimeric viruses. *bioRxiv*. 2020; doi: 10.1101/2020.06.08.140871
- Brouwer PJM, et al. Potent neutralizing antibodies from COVID-19 patients define multiple targets of vulnerability. *Science*. 2020; 369:643–650. DOI: 10.1126/science.abc5902 [PubMed: 32540902]
- Zussman ME, Bagby M, Benson DW, Gupta R, Hirsch R. Pulmonary vascular resistance in repaired congenital diaphragmatic hernia vs. age-matched controls. *Pediatr Res*. 2012; 71:697–700. DOI: 10.1038/pr.2012.16 [PubMed: 22456633]
- Cai Y, et al. Distinct conformational states of SARS-CoV-2 spike protein. *Science*. 2020; doi: 10.1126/science.abd4251

12. Zhou T, et al. Cryo-EM Structures of SARS-CoV-2 Spike without and with ACE2 Reveal a pH-Dependent Switch to Mediate Endosomal Positioning of Receptor-Binding Domains. *Cell Host & Microbe*. 2020; 28:867–879.e865. DOI: 10.1016/j.chom.2020.11.004 [PubMed: 33271067]
13. Robbani DF, et al. Convergent antibody responses to SARS-CoV-2 in convalescent individuals. *Nature*. 2020; 584:437–442. DOI: 10.1038/s41586-020-2456-9 [PubMed: 32555388]
14. Barnes CO, et al. Structures of Human Antibodies Bound to SARS-CoV-2 Spike Reveal Common Epitopes and Recurrent Features of Antibodies. *Cell*. 2020; 182:828–842 e816. DOI: 10.1016/j.cell.2020.06.025 [PubMed: 32645326]
15. Shrock E, et al. Viral epitope profiling of COVID-19 patients reveals cross-reactivity and correlates of severity. *Science*. 2020; doi: 10.1126/science.abd4250
16. Sobel Leonard A, et al. The effective rate of influenza reassortment is limited during human infection. *PLoS Pathog*. 2017; 13:e1006203.doi: 10.1371/journal.ppat.1006203 [PubMed: 28170438]
17. Richard M, Herfst S, Tao H, Jacobs NT, Lowen AC. Influenza A Virus Reassortment Is Limited by Anatomical Compartmentalization following Coinfection via Distinct Routes. *J Virol*. 2018; 92doi: 10.1128/JVI.02063-17
18. Kemp S, et al. Recurrent emergence and transmission of a SARS-CoV-2 Spike deletion H69/V70. *bioRxiv*. 2021; doi: 10.1101/2020.12.14.422555
19. CDC. Discontinuation of Transmission-Based Precautions and Disposition of Patients with COVID-19 in Healthcare Settings (Interim Guidance). 2020. <<https://www.cdc.gov/coronavirus/2019-ncov/hcp/disposition-hospitalized-patients.html>>
20. Boshier FAT, et al. Remdesivir induced viral RNA and subgenomic RNA suppression, and evolution of viral variants in SARS-CoV-2 infected patients. *medRxiv*. 2020; doi: 10.1101/2020.11.18.20230599
21. Simonovich VA, et al. A Randomized Trial of Convalescent Plasma in Covid-19 Severe Pneumonia. *N Engl J Med*. 2020; doi: 10.1056/NEJMoa2031304
22. Meredith LW, et al. Rapid implementation of SARS-CoV-2 sequencing to investigate cases of health-care associated COVID-19: a prospective genomic surveillance study. *The Lancet Infectious Diseases*. 2020; 20:1263–1272. DOI: 10.1016/S1473-3099(20)30562-4 [PubMed: 32679081]
23. Collier DA, et al. Point of Care Nucleic Acid Testing for SARS-CoV-2 in Hospitalized Patients: A Clinical Validation Trial and Implementation Study. *Cell Rep Med*. 2020; doi: 10.1016/j.xcrm.2020.100062
24. Loman N, Rowe W, Rambaut A. 2020
25. Martin M. Cutadapt removes adapter sequences from high-throughput sequencing reads. *EMBnet journal*. 2011; 17:10–12.
26. Li H. Minimap2: pairwise alignment for nucleotide sequences. *Bioinformatics (Oxford, England)*. 2018; 34:3094–3100. DOI: 10.1093/bioinformatics/bty191
27. Jordan MR, et al. Comparison of standard PCR/cloning to single genome sequencing for analysis of HIV-1 populations. *J Virol Methods*. 2010; 168:114–120. DOI: 10.1016/j.jviromet.2010.04.030 [PubMed: 20451557]
28. Palmer S, et al. Multiple, linked human immunodeficiency virus type 1 drug resistance mutations in treatment-experienced patients are missed by standard genotype analysis. *Journal of clinical microbiology*. 2005; 43:406–413. DOI: 10.1128/JCM.43.1.406-413.2005 [PubMed: 15635002]
29. Keele BF, et al. Identification and characterization of transmitted and early founder virus envelopes in primary HIV-1 infection. *Proceedings of the National Academy of Sciences of the United States of America*. 2008; 105:7552–7557. [PubMed: 18490657]
30. Shu Y, McCauley J. GISAID: Global initiative on sharing all influenza data - from vision to reality. *Euro surveillance: bulletin European sur les maladies transmissibles = European communicable disease bulletin*. 2017; 22:30494.doi: 10.2807/1560-7917.ES.2017.22.13.30494 [PubMed: 28382917]
31. Katoh K, Standley DM. MAFFT Multiple Sequence Alignment Software Version-7-Improvements in Performance and Usability. *Molecular Biology and Evolution*. 2013; 30:772–780. DOI: 10.1093/molbev/mst010 [PubMed: 23329690]

32. Rambaut A, et al. A dynamic nomenclature proposal for SARS-CoV-2 lineages to assist genomic epidemiology. *Nature Microbiology*. 2020; 5:1403–1407. DOI: 10.1038/s41564-020-0770-5
33. Minh BQ, et al. IQ-TREE 2: New Models and Efficient Methods for Phylogenetic Inference in the Genomic Era. *Molecular Biology and Evolution*. 2020; 37:1530–1534. DOI: 10.1093/molbev/msaa015 [PubMed: 32011700]
34. Kalyaanamoorthy S, Minh BQ, Wong TKF, von Haeseler A, Jermini LS. ModelFinder: fast model selection for accurate phylogenetic estimates. *Nature Methods*. 2017; 14:587–589. DOI: 10.1038/nmeth.4285 [PubMed: 28481363]
35. Minh BQ, Nguyen MA, von Haeseler A. Ultrafast approximation for phylogenetic bootstrap. *Mol Biol Evol*. 2013; 30:1188–1195. DOI: 10.1093/molbev/mst024 [PubMed: 23418397]
36. Illingworth CJ. SAMFIRE: multi-locus variant calling for time-resolved sequence data. *Bioinformatics*. 2016; 32:2208–2209. DOI: 10.1093/bioinformatics/btw205 [PubMed: 27153641]
37. Lumby CK, Zhao L, Breuer J, Illingworth CJ. A large effective population size for established within-host influenza virus infection. *Elife*. 2020; 9doi: 10.7554/eLife.56915
38. Martin DP, Murrell B, Golden M, Khoosal A, Muhire B. RDP4: Detection and analysis of recombination patterns in virus genomes. *Virus evolution*. 2015; 1
39. Didelot X, Wilson DJ. ClonalFrameML: efficient inference of recombination in whole bacterial genomes. *PLoS Comput Biol*. 2015; 11:e1004041. [PubMed: 25675341]
40. Wrobel AG, et al. SARS-CoV-2 and bat RaTG13 spike glycoprotein structures inform on virus evolution and furin-cleavage effects. *Nature Structural & Molecular Biology*. 2020; 27:763–767. DOI: 10.1038/s41594-020-0468-7
41. Gregson J, et al. HIV-1 viral load is elevated in individuals with reverse transcriptase mutation M184V/I during virological failure of first line antiretroviral therapy and is associated with compensatory mutation L74I. *Journal of Infectious Diseases*. 2019
42. Naldini L, Blomer U, Gage FH, Trono D, Verma IM. Efficient transfer, integration, and sustained long-term expression of the transgene in adult rat brains injected with a lentiviral vector. *Proc Natl Acad Sci U S A*. 1996; 93:11382–11388. DOI: 10.1073/pnas.93.21.11382 [PubMed: 8876144]
43. Gupta RK, et al. Full length HIV-1 gag determines protease inhibitor susceptibility within in vitro assays. *AIDS*. 2010; 24:1651. [PubMed: 20597164]
44. Vermeire J, et al. Quantification of reverse transcriptase activity by real-time PCR as a fast and accurate method for titration of HIV, lenti- and retroviral vectors. *PloS one*. 2012; 7:e50859–e50859. DOI: 10.1371/journal.pone.0050859 [PubMed: 23227216]
45. Mlcochova P, et al. Combined point of care nucleic acid and antibody testing for SARS-CoV-2 following emergence of D614G Spike Variant. *Cell Rep Med*. 2020; doi: 10.1016/j.xcrm.2020.100099
46. Seow J, et al. Longitudinal observation and decline of neutralizing antibody responses in the three months following SARS-CoV-2 infection in humans. *Nat Microbiol*. 2020; 5:1598–1607. DOI: 10.1038/s41564-020-00813-8 [PubMed: 33106674]

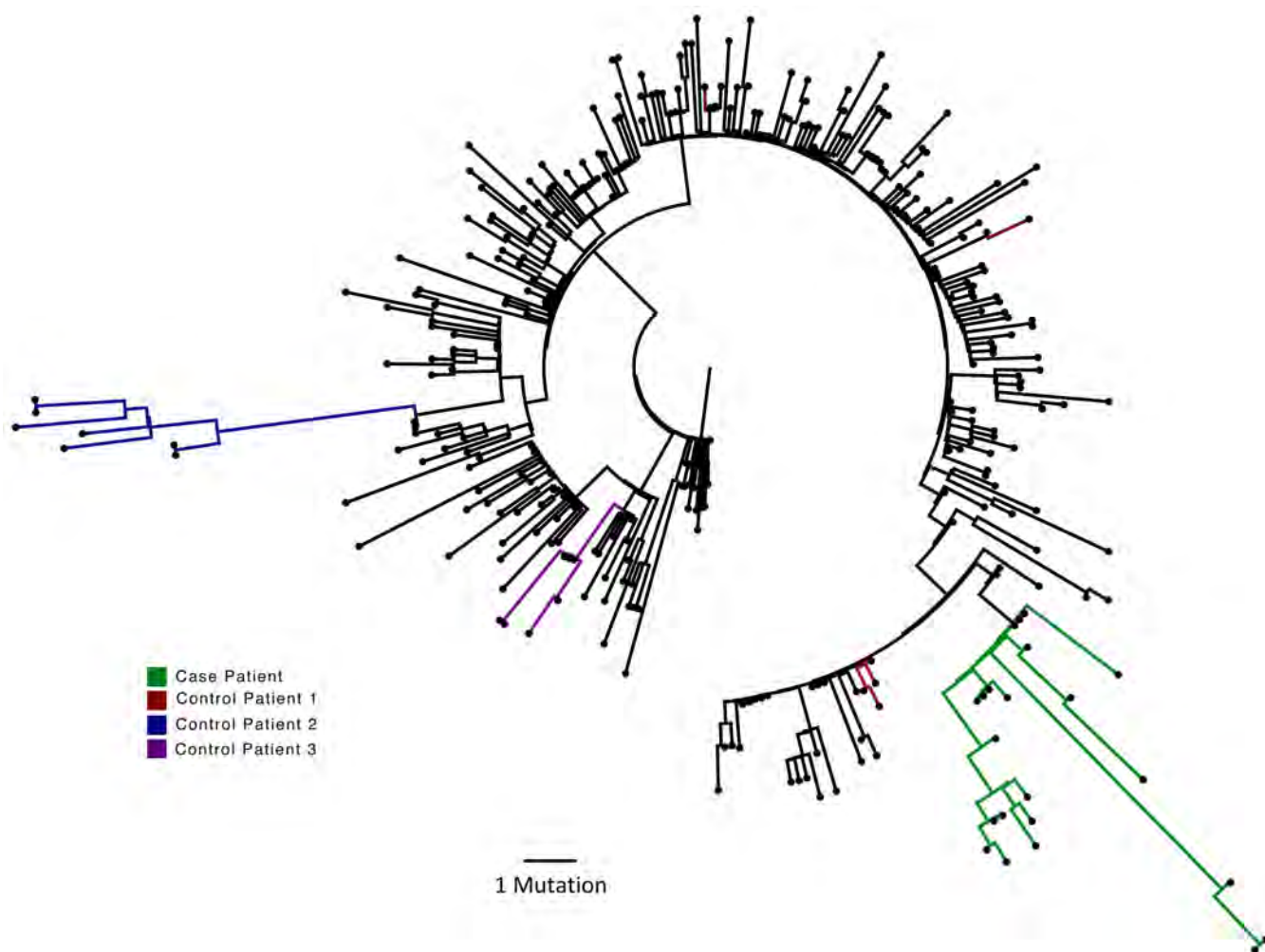


Figure 1.

Analysis of 23 Patient derived whole SARS-CoV-2 genome sequences in context of local sequences and other cases of chronic SARS-CoV-2 shedding. Circularised maximum-likelihood phylogenetic tree rooted on the Wuhan-Hu-1 reference sequence, showing a subset of 250 local SARS-CoV-2 genomes from GISAID. This diagram highlights significant diversity of the case patient (green) compared to three other local patients with prolonged shedding (blue, red and purple sequences). All “United Kingdom / English” SARS-CoV-2 genomes were downloaded from the GISAID database and a random subset of 250 selected as background.

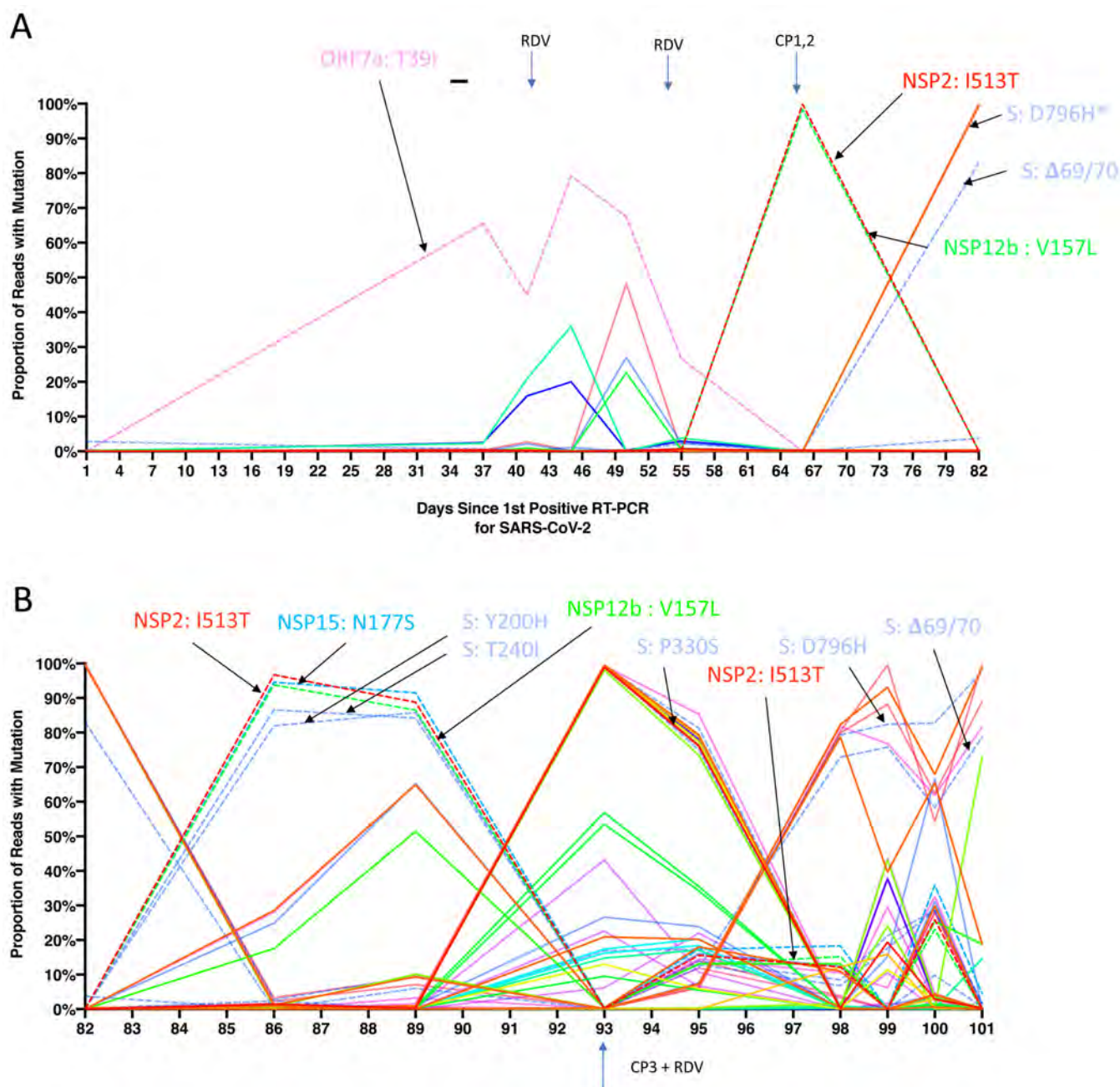


Figure 2. Whole genome variant trajectories showing amino acids and relationship to treatments. Data based on Illumina short read ultra deep sequencing at 1000x coverage. Variants shown reached a frequency of at least 10% in at least 2 samples. Treatments indicated are convalescent plasma (CP) and Remdesivir (RDV). Variants described in the text are designated by labels using the same colouring as the position in the genome. Variants labelled are represented by dashed lines. **A.** Variants detected in the patient from days 1-82. *D796H (light blue) is at the same frequency as NSP3 K902N (orange) therefore it is hidden beneath **B.** Variants detected in the patient from days 82-101.

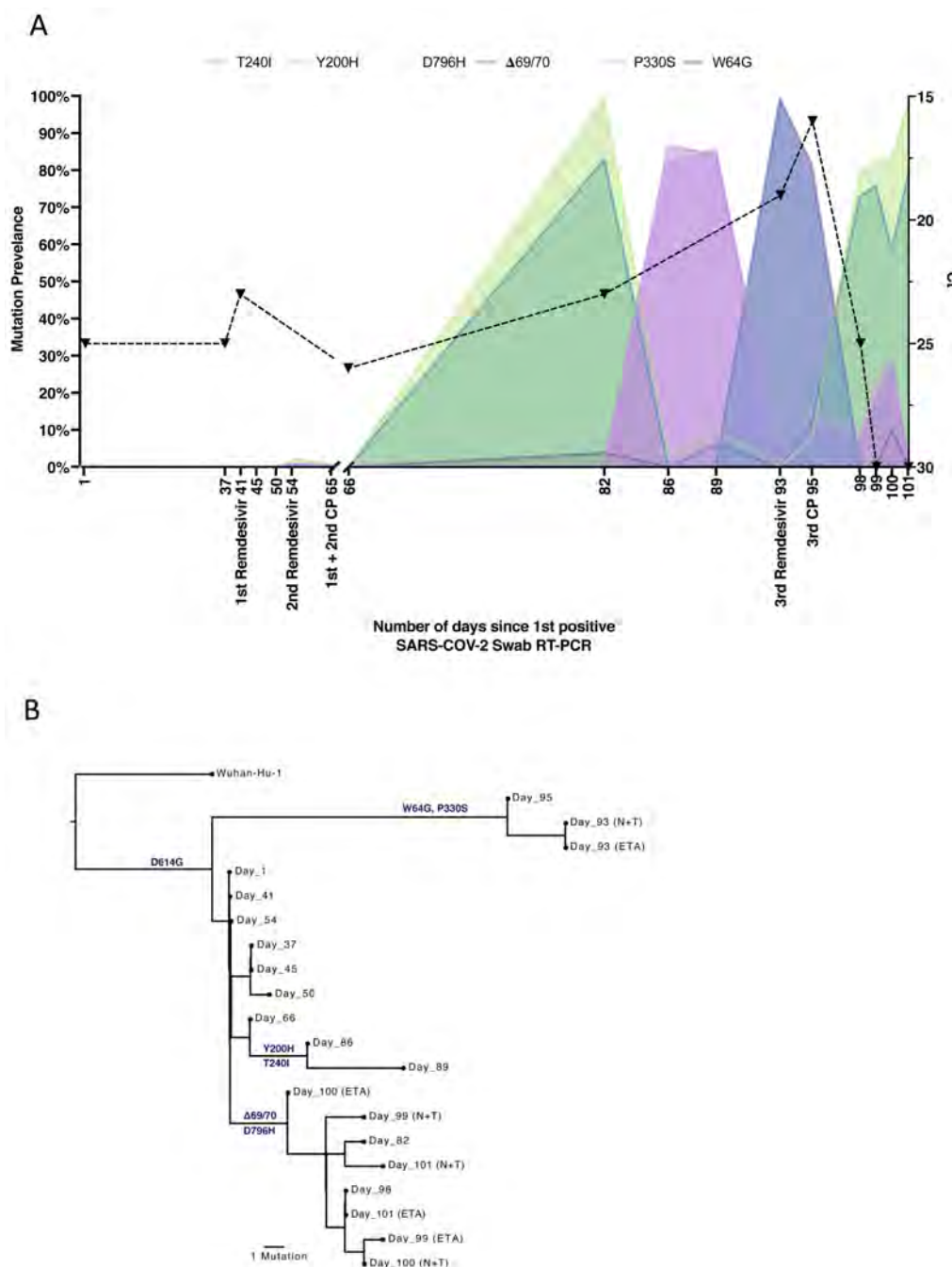


Figure 3. Longitudinal variant frequencies and phylogenetic relationships for virus populations bearing six Spike (S) mutations

A. At baseline, all six S variants (Illumina sequencing) except for H69/V70 were absent (<1% and <20 reads). Approximately two weeks after receiving two units of convalescent plasma (CP), viral populations carrying H69/V70 and D796H mutants rose to frequencies >80% but decreased significantly four days later. This population was replaced by a population bearing Y200H and T240I, detected in two samples over a period of 6 days. These viral populations were then replaced by virus carrying W64G and P330S mutations in

Spike, which both dominated at day 93. Following a 3rd course of remdesivir and an additional unit of convalescent plasma, the H69/V70 and D796H virus population re-emerged to become the dominant viral strain reaching variant frequencies of >75%. Pairs of mutations arose and disappeared simultaneously indicating linkage on the same viral haplotype. CT values from respiratory samples are indicated on the right y-axis (black dashed line and triangles). Where there were duplicate readings on the same day, to remain consistent, N+T samples were plotted **B**. Maximum likelihood phylogenetic tree of the case patient with day of sampling indicated. Spike mutations defining each of the clades are shown ancestrally on the branches on which they arose. On dates where multiple samples were collected, these are indicated as endotracheal aspirate (ETA) and Nose + throat swabs (N+T).

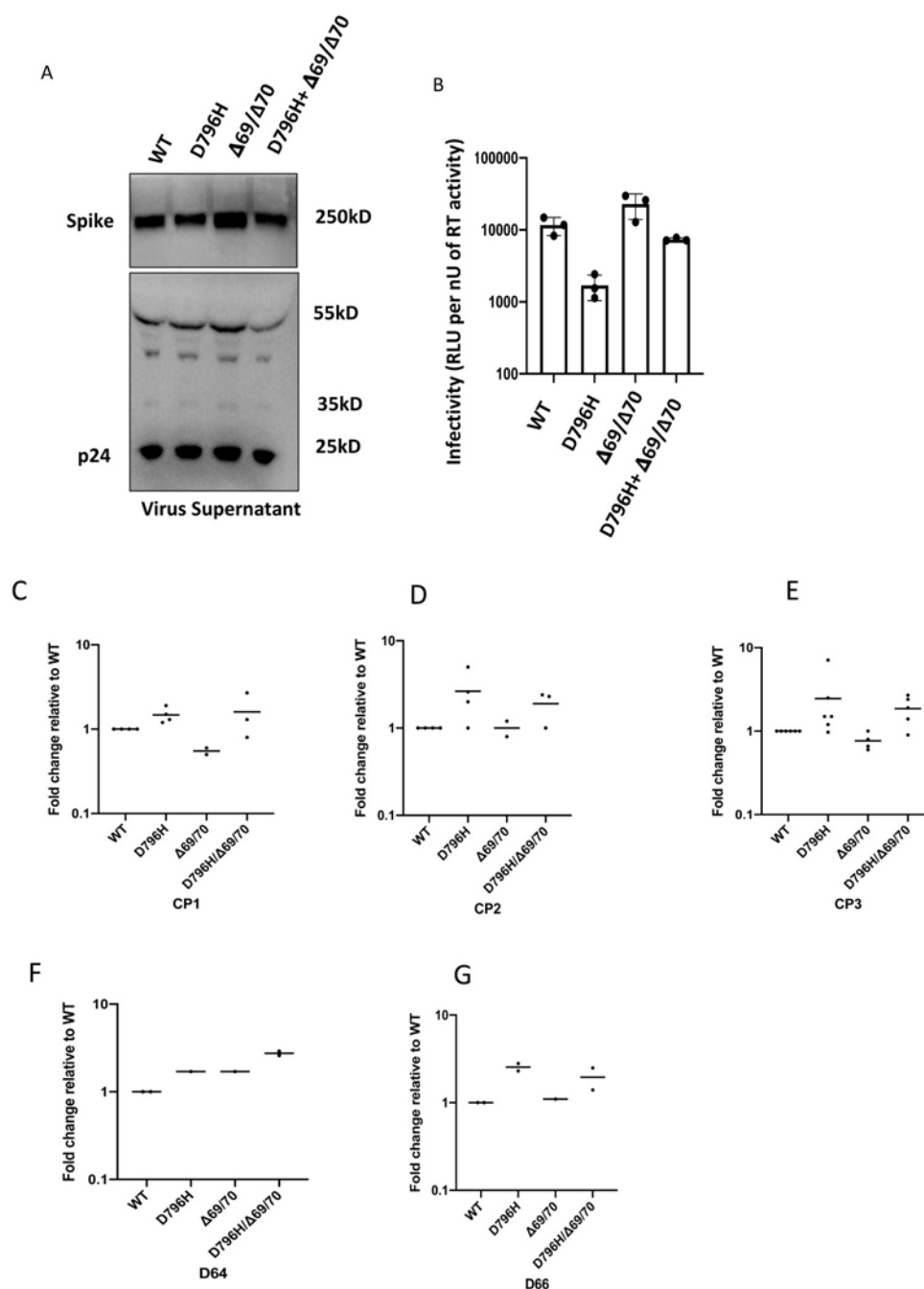


Figure 4. Spike mutant D796H + H69/V70 infectivity and sensitivity convalescent plasma (CP).

A. western blot of virus pellets after centrifugation of supernatants from cells transfected with lentiviral pseudotyping plasmids including Spike protein. Blots are representative of two independent transfections. **B.** Single round Infectivity of luciferase expressing lentivirus pseudotyped with SARS-CoV-2 Spike protein (WT versus mutant) on 293T cells co-transfected with ACE2 and TMPRSS2 plasmids. Infectivity is corrected for reverse transcriptase activity in virus supernatant as measured by real time PCR. Data points represent technical replicates (n=3) with mean and error bars representing standard error of

mean; data are representative of two independent experiments **C-E**. convalescent plasma (CP units 1-3) neutralization potency against pseudovirus virus bearing Spike mutants D796H, H69/V70 and D796H + H69/V70 **F, G** patient serum neutralisation potency against pseudovirus virus bearing Spike mutants D796H, H69/V70 and D796H + H69/V70. Patient serum was taken at indicated Day (D). Indicated is serum dilution required to inhibit 50% of virus infection (ID₅₀), expressed as fold change relative to WT. Data points represent means of technical replicates and each data point is an independent experiment (n=2-6). Mean of data points in C-G is shown by horizontal bars.

Original Article

Infectious Diseases,
Microbiology & Parasitology



Clinical Course and Outcomes of Patients with Severe Acute Respiratory Syndrome Coronavirus 2 Infection: a Preliminary Report of the First 28 Patients from the Korean Cohort Study on COVID-19

OPEN ACCESS

Received: Mar 12, 2020

Accepted: Mar 27, 2020

Address for Correspondence:

Myoung-don Oh, MD, PhD

Department of Internal Medicine, Seoul National University College of Medicine, 103 Daehak-ro, Jongno-gu, Seoul 03080, Korea.
E-mail: mdohmd@snu.ac.kr

*Eu Suk Kim and Bum Sik Chin contributed equally to this work.

© 2020 The Korean Academy of Medical Sciences.

This is an Open Access article distributed under the terms of the Creative Commons Attribution Non-Commercial License (<https://creativecommons.org/licenses/by-nc/4.0/>) which permits unrestricted non-commercial use, distribution, and reproduction in any medium, provided the original work is properly cited.

ORCID iDs

Eu Suk Kim ,
<https://orcid.org/0000-0001-7132-0157>
Bum Sik Chin ,
<https://orcid.org/0000-0003-3021-1434>
Chang Kyung Kang ,
<https://orcid.org/0000-0003-1952-072X>
Nam Joong Kim ,
<https://orcid.org/0000-0001-6793-9467>
Yu Min Kang ,
<https://orcid.org/0000-0002-4368-9878>
Jae-Phil Choi ,
<https://orcid.org/0000-0003-4805-7930>
Dong Hyun Oh ,
<https://orcid.org/0000-0002-9990-6042>
Jeong-Han Kim ,
<https://orcid.org/0000-0001-5117-4893>

Eu Suk Kim ^{1*}, Bum Sik Chin ^{2*}, Chang Kyung Kang ³, Nam Joong Kim ³, Yu Min Kang ⁴, Jae-Phil Choi ⁵, Dong Hyun Oh ⁵, Jeong-Han Kim ⁶, Boram Koh ⁷, Seong Eun Kim ⁸, Na Ra Yun ⁹, Jae-Hoon Lee ¹⁰, Jin Yong Kim ¹¹, Yeonjae Kim ¹², Ji Hwan Bang ¹², Kyoung-Ho Song ¹, Hong Bin Kim ¹, Ki-hyun Chung ¹³, Myoung-don Oh ³, and on behalf of the Korea National Committee for Clinical Management of COVID-19

¹Department of Internal Medicine, Seoul National University Bundang Hospital, Seoul National University College of Medicine, Seongnam, Korea

²Division of Infectious Diseases, Department of Internal Medicine, National Medical Center, Seoul, Korea

³Department of Internal Medicine, Seoul National University College of Medicine, Seoul, Korea

⁴Department of Infectious Diseases, Myongji Hospital, Goyang, Korea

⁵Department of Internal Medicine, Seoul Medical Center, Seoul, Korea

⁶Division of Infectious Diseases, Department of Internal Medicine, Armed Forces Capital Hospital, Seongnam, Korea

⁷Department of Internal Medicine, Gyeonggi Provincial Medical Center Ansong Hospital, Anseong, Korea

⁸Department of Infectious Diseases, Chonnam National University Medical School, Gwangju, Korea

⁹Department of Internal Medicine, College of Medicine, Chosun University, Gwangju, Korea

¹⁰Department of Internal Medicine, Wonkwang University School of Medicine, Iksan, Korea

¹¹Division of Infectious Diseases, Department of Internal Medicine, Incheon Medical Center, Incheon, Korea

¹²Division of Infectious Diseases, Seoul Metropolitan Government-Seoul National University Boramae Medical Center, Seoul, Korea

¹³Department of Pediatrics, National Medical Center, Seoul, Korea

ABSTRACT

Background: Severe acute respiratory syndrome coronavirus 2 (SARS-CoV-2)-infected pneumonia emerged in Wuhan, China in December 2019. In this retrospective multicenter study, we investigated the clinical course and outcomes of novel coronavirus disease 2019 (COVID-19) from early cases in Republic of Korea.

Methods: All of the cases confirmed by real time polymerase chain reaction were enrolled from the 1st to the 28th patient nationwide. Clinical data were collected and analyzed for changes in clinical severity including laboratory, radiological, and virologic dynamics during the progression of illness.

Results: The median age was 40 years (range, 20–73 years) and 15 (53.6%) patients were male. The most common symptoms were cough (28.6%) and sore throat (28.6%), followed by fever (25.0%). Diarrhea was not common (10.7%). Two patients had no symptoms. Initial chest X-ray (CXR) showed infiltration in 46.4% of the patients, but computed tomography scan confirmed pneumonia in 88.9% (16/18) of the patients. Six patients (21.4%) required

Boram Koh 
<https://orcid.org/0000-0002-8810-1417>
Seong Eun Kim 
<https://orcid.org/0000-0003-0162-6155>
Na Ra Yun 
<https://orcid.org/0000-0002-4219-0127>
Jae-Hoon Lee 
<https://orcid.org/0000-0002-0897-2838>
Jin Yong Kim 
<https://orcid.org/0000-0002-4306-1597>
Yeonjae Kim 
<https://orcid.org/0000-0003-4144-9077>
Ji Hwan Bang 
<https://orcid.org/0000-0002-7628-1182>
Kyoung-Ho Song 
<https://orcid.org/0000-0002-4517-3840>
Hong Bin Kim 
<https://orcid.org/0000-0001-6262-372X>
Ki-hyun Chung 
<https://orcid.org/0000-0002-7100-2519>
Myoung-don Oh 
<https://orcid.org/0000-0002-2344-7695>

Funding

This study was supported by National Health Promotion Fund (#2740-309-320-01) of Ministry of Health and Welfare.

Disclosure

The authors have no potential conflicts of interest to disclose.

Author Contributions

Conceptualization: Kim ES, Chin BS, Oh M.
Data curation: Kim ES, Chin BS, Kang CK, Kang YM, Choi JP, Oh DH, Kim JH, Koh B, Kim SE, Yun NR, Lee JH, Kim JY, Kim Y. Formal analysis: Kang CK, Kim NJ, Song KH, Kim HB, Oh M. Project administration: Bang JH, Chung KH. Writing - original draft: Kim ES, Chin BS, Oh M. Writing - review & editing: Kim ES, Oh M.

supplemental oxygen therapy, but no one needed mechanical ventilation. Lymphopenia was more common in severe cases. Higher level of C-reactive protein and worsening of chest radiographic score was observed during the 5–7 day period after symptom onset. Viral shedding was high from day 1 of illness, especially from the upper respiratory tract (URT).

Conclusion: The prodromal symptoms of COVID-19 were mild and most patients did not have limitations of daily activity. Viral shedding from URT was high from the prodromal phase. Radiological pneumonia was common from the early days of illness, but it was frequently not evident in simple CXR. These findings could be plausible explanations for the easy and rapid spread of SARS-CoV-2 in the community.

Keywords: COVID-19; SARS-CoV-2; Viral Pneumonia; Prognosis; Cohort Study; Republic of Korea

INTRODUCTION

Severe acute respiratory syndrome coronavirus 2 (SARS-CoV-2)-infected pneumonia has been initially identified in Wuhan, China since December 2019.¹ A total number of 693,224 laboratory-confirmed cases have been documented globally as of March 30th, 2020, including 33,106 deaths.² After experiencing the largest outbreak of Middle East respiratory syndrome (MERS) outside the Arabian Peninsula in 2015,³ the Korean government has maintained a strong quarantine system for emerging infectious diseases imported from foreign countries. The first novel coronavirus disease 2019 (COVID-19) case in Korea was a traveler from Wuhan, China in January 19th, 2020.⁴ While the spread of COVID-19 was limited before February 20,^{5,6} a huge outbreak occurred among a religious group in the southern part of Korea, Daegu, and the number of COVID-19 cases in Korea reached 6,593 on March 6th, 2020.^{7,8}

While clinical and epidemiological features of COVID-19 have been described in China by several investigations,⁹⁻¹⁴ most of them focused on SARS-CoV-2-infected pneumonia in China. There is still uncertainty about the clinical course and outcomes of COVID-19, especially outside of China where patients can be detected in the early course of disease by the quarantine system. Recently, the Korea Centers for Disease Control and Prevention (KCDC) reported epidemiological features of the earliest 28 COVID-19 cases in Republic of Korea.¹⁵ We performed this study to describe the clinical characteristics of COVID-19 in Republic of Korea, including radiological and virologic dynamics during the progression of illness.

METHODS

Study design and participants

Korea National Committee for Clinical Management of COVID-19 (KNCCMC) was organized in early February 2020 and consisted of infectious disease specialists or physicians of each hospital who took care of the confirmed COVID-19 patients. KNCCMC developed a standardized clinical record form (CRF) which was modified from the World Health Organization Global 2019-novel coronavirus clinical characterization CRF.¹⁶ Individual cases were reviewed and treatment and discharge plans were discussed during regular video conference calls three times a week. All of cases nationwide were enrolled in this study from the 1st to the 28th patient. Participating hospitals were as follows: Seoul National University Hospital, National Medical Center, and Seoul Medical Center, Seoul; Incheon Medical

Center, Incheon; Seoul National University Bundang Hospital and Armed Forces Capital Hospital, Seongnam; Myongji Hospital, Goyang; Gyeonggi Provincial Medical Center Ansong Hospital, Anseong; Wonkwang University Hospital, Iksan; Chonnam National University Hospital and Chosun University Hospital, Gwangju, Republic of Korea.

Case definitions

According to the definition of the KCDC,⁷ a suspected COVID-19 patient was defined as someone fulfilling both of the following criteria: 1) a presence of at least one condition among fever; respiratory symptoms such as cough, sore throat, or dyspnea; or radiographic evidence of pneumonia, 2) a recent visit to countries where SARS-CoV-2 transmission in the community has been reported including Wuhan city, China or recent close contact with a confirmed COVID-19 patient within 14 days before illness onset. A confirmed case was defined as a patient with positive results by real time reverse transcription polymerase chain reaction (RT-PCR) assay for SARS-CoV-2 in upper respiratory specimen (nasopharyngeal and oropharyngeal swab), with or without lower respiratory specimen (sputum). The patients who had no symptoms but had been screened for COVID-19 due to a strong epidemiologic link were also enrolled when they were laboratory-confirmed.

Viral diagnostic methods

Respiratory samples from the patients were sent to the KCDC and RT-PCR for detecting SARS-CoV-2 was performed as in previous study.¹⁷ In brief, RNA was extracted from clinical samples with a QIAamp® viral RNA mini kit (QIAGEN, Hilden, Germany). The primer and probe sequences used for RNA-dependent RNA polymerase gene detection were: 5'-GTGARATGGTCATGTGTGGCGG-3' (Forward), 5'-CARATGTAAASACACTATTAGCATA-3' (Reverse) and 5'-CAGGTGGAACCTCATCAGGAGATGC-3' (Probe in 5-FAM/3'-BHQ format) and the primer and probe sequences used for *E* gene detection were: 5'-ACAGGTACGTTAATAGTTAATAGCGT-3' (Forward), 5'-ATATTGCAGCAGTACGCACACA-3' (Reverse) and 5'-ACACTAGCCATCCTTACTGCGCTTCG-3' (Probe in 5-FAM/3'-BHQ format). Reverse transcription was performed at 50°C for 30 minutes, followed by inactivation of the reverse transcriptase at 95°C for 10 minutes. PCR amplification was performed with 40 cycles at 95°C for 15 seconds and 60°C for 1 minute using an ABI 7500 Fast instrument (Thermo Fisher Scientific, Waltham, MA, USA).

Clinical data collection and severity evaluation

Primary physicians from each participating hospital retrospectively collected clinical medical record data then two infectious disease physicians from KNCCMC reassessed the accuracy of the raw data. Patients were hospitalized in the isolation units in each hospital from January 19th, 2020, with final follow-up for the study on February 17th, 2020. Epidemiologic, demographic, and clinical information including laboratory and radiologic findings were obtained. Clinical severity and changes according to days after first symptom onset were assessed as follows: 1, no limit of daily activity; 2, limit of daily activity but no need for supplemental O₂ therapy; 3, need for supplemental O₂ therapy via nasal prong; 4, need for supplemental O₂ therapy via facial mask; 5, need for high flow supplemental O₂ therapy or non-invasive ventilation; 6, need for invasive ventilation; 7, multi-organ failure or need for extracorporeal membrane oxygenation (ECMO) therapy; 8, death.

Chest radiograph scoring was performed as described in a previous study¹⁸; in brief, serial chest radiographs were retrospectively reviewed in consensus by four physicians who were

unaware of the clinical conditions of the patients. Each lung was divided into the upper, middle, and lower zone, and infiltrations on each zone were scored from 0 to 4, with a total range of 0 to 24.

Ethics statement

The Institutional Review Board (IRB) at Seoul National University Hospital reviewed and approved the study protocol (IRB registration No. H-2002-042-1100). After that, the IRB at each participating hospital approved it. The board waived the requirement for written consent.

RESULTS

Patients and clinical characteristics

The study population included 28 hospitalized patients with confirmed COVID-19. The median age of the 28 patients was 40 years (interquartile range, 28–54; range, 20–73), and 15 (53.6%) were men. Of the 28 patients, five (17.9%) had one or more coexisting medical condition and diabetes was most common (**Table 1**). The most common symptoms at the time of admission for isolation were cough (8, 28.6%) and sore throat (8, 28.6%), followed by fever, myalgia, and headache (7, 25.0%). Diarrhea was present in three patients (10.7%) among initial symptoms. Two cases were asymptomatic when they were confirmed as COVID-19.

Clinical course and outcomes

During the hospitalization, six patients (21.4%) required oxygen supplement therapy: four with nasal cannula and two with face mask. No one required mechanical ventilator or ECMO therapy. Nineteen patients (67.9%) received lopinavir/ritonavir for antiviral therapy. Ultimately, pneumonia was present in 22 patients (78.5%) and the proportion of pneumonia was 91.3% (21/23) among the patients who received a CT scan (**Table 2**). Seventeen patients (60.7%) developed fever and became afebrile during the hospitalization and the median day of defervescence was 9 days (range, 3–18) after symptom onset (**Supplementary Fig. 1**). By February 17, 10 patients were off isolation or discharged, and the median day of off-isolation/discharge was 18.5 days after symptom onset (range, 11–27).

Chronological changes of COVID-19

Except for 2 patients who showed no symptoms, six among 26 patients showed clinical deterioration during the hospitalization and needed supplemental oxygen therapy (**Supplementary Fig. 2**). The others showed little limitation in daily activity during the hospitalization.

While neutrophilia or neutropenia was not common regardless of clinical severity (**Fig. 1A and B**), lymphopenia (defined as $\leq 1.0 \times 10^9/L$) was more common in severe cases (33.3%, 2/6) than mild cases (18.2%, 4/22) during the clinical course (**Fig. 1C and D**). High levels of C-reactive protein in the blood were more frequently observed in severe cases (**Fig. 1E and F**) as the clinical course became worse during the 5–7 day period after symptom onset.

We could evaluate viral kinetics by serial RT-PCR of respiratory specimens from 9 patients from the early course of illness. Viral shedding from upper respiratory tract (URT) and lower respiratory tract (LRT) was shown in **Fig. 2A and B** as cycle threshold (Ct) value, respectively (**Supplementary Table 1**). Viral shedding was high during the first 5 days of illness and higher in URT than LRT. It decreased after day 7 of illness.

Table 1. Clinical characteristics of 28 patients with COVID-19 at the time of admission for isolation

Characteristics	Values
Age, yr	42.6 ± 13.4
Sex	
Male	15 (53.6)
Female	13 (46.4)
Comorbidity	
Hypertension	0
Dyslipidemia	0
Diabetes without complication	2 (7.1)
Chronic cardiac disease	0
Chronic kidney disease	0
Chronic obstructive pulmonary disease	0
Asthma	1 (3.6)
Liver disease, mild	1 (3.6)
Malignancy	1 (3.6)
HIV/AIDS	0
Obesity (body mass index > 30 kg/m ²)	5 (17.9)
Smoking	5/27 (18.5)
Symptom onset to isolation	
0–1 day	6/26 (23.1)
2–3 days	7/26 (26.9)
4–5 days	7/26 (26.9)
≥ 6 days	6/26 (23.1)
Symptoms on admission day	
Fever (> 37.5°C)	7 (25.0)
Cough	8 (28.6)
Sputum	6 (21.4)
Sore throat	8 (28.6)
Rhinorrhea	2 (7.1)
Myalgia	7 (25.0)
Fatigue	3 (10.7)
Shortness of breath	1 (3.6)
Headache	7 (25.0)
Abdominal pain	1 (3.6)
Diarrhea	3 (10.7)
Blood leukocyte count	
≤ 4.0 × 10 ⁹ /L	7 (25.0)
> 4.0 × 10 ⁹ /L	21 (75.0)
Lymphocyte count, 10 ⁹ /L	1.563 ± 0.864
Lymphopenia (≤ 1.0 × 10 ⁹ /L)	7 (25.0)
Platelet count	
≤ 150 × 10 ⁹ /L	15 (53.6)
> 150 × 10 ⁹ /L	13 (46.4)
Haemoglobin level, g/dL	15.5 ± 5.0
C-reactive protein level ≥ 10 mg/L	11/27 (40.7)
Procalcitonin level ≥ 0.5 ng/mL	0/11
Lactate dehydrogenase ≥ 250 U/L	11/26 (42.3)
Creatinine ≥ 133 μmol/L	0
Alanine aminotransferase > 40 U/L	6 (21.4)
Infiltration in chest X-ray	
None	15 (53.6)
Unilateral	7 (25.0)
Bilateral	6 (21.4)
Infiltration in computed tomography	
None	2/18 (11.1)
Unilateral	8/18 (44.4)
Bilateral	8/18 (44.4)

Data are shown as mean ± standard deviation or number (%).

COVID-19 = coronavirus disease 2019, HIV = human immunodeficiency viruses, AIDS = acquired immunodeficiency syndrome.

Table 2. Clinical course and outcomes of 28 patients with COVID-19

Case No.	Risk factor	Maximum pneumonia extent	Radiology modality	Oxygen supplement by ID	Maximal oxygen (L/min)	Antiviral therapy	Outcome on Feb 17
1	Obesity	Bilateral	CXR/CT	2–15	Mask, 10	LPV/r	Discharge/off isolation on ID 20
2	Age ≥ 55	Bilateral	CXR/CT	-	-	LPV/r	Discharge/off isolation on ID 27
3	-	Bilateral	CXR/CT	11–19	Nasal, 2	LPV/r	Discharge/off isolation on ID 22
4	Age ≥ 55, obesity, smoking	Bilateral	CXR/CT	5–11	Nasal, 6	LPV/r	Discharge/off isolation on ID 19
5	Asthma	Bilateral	CT only	-	-	LPV/r	Isolation without oxygen
6	Age ≥ 55, DM	Bilateral	CT only	-	-	No	Isolation without oxygen
7	-	Unilateral	CXR/CT	-	-	LPV/r	Discharge/off isolation on ID 22
8	Age ≥ 55	Bilateral	CXR/CT	-	-	LPV/r	Discharge/off isolation on ID 18
9	-	Bilateral	CXR/CT	-	-	LPV/r	Isolation without oxygen
10	-	Bilateral	CT only	-	-	No	Isolation without oxygen
11	-	Unilateral	CXR/CT	-	-	No	Discharge/off isolation on ID 13
12	Obesity, smoking	Bilateral	CXR/CT	-	-	LPV/r	Isolation without oxygen
13	-	Bilateral	CT only	-	-	No	Isolation without oxygen
14	-	Bilateral	CT only	-	-	LPV/r	Isolation without oxygen
15	Obesity, smoking	None	CXR ^a	-	-	No	Isolation without oxygen
16	Malignancy	Bilateral	CXR/CT	7–8	Nasal, 3	LPV/r	Isolation without oxygen
17	-	Unilateral	CT only	-	-	No	Discharge/off isolation on ID 18
18	Obesity	None	CXR ^a	-	-	LPV/r	Isolation without oxygen
19	Obesity	Bilateral	CXR/CT	-	-	LPV/r	Isolation without oxygen
20	Smoking	Unilateral	CXR ^a	6–12	Nasal, 5	LPV/r	Isolation with oxygen nasal cannula
21	Age ≥ 55, DM	Bilateral	CT only	-	-	No	Isolation without oxygen
22	Obesity	Unilateral	CXR/CT	-	-	LPV/r	Discharge/off isolation on ID 11
23	Age ≥ 55	Bilateral	CXR/CT	7–15	Mask, 6	LPV/r	Isolation with oxygen facial mask
24	-	None	CXR/CT	-	-	LPV/r	Isolation without oxygen
25	Age ≥ 55	Unilateral	CT only	-	-	LPV/r	Isolation without oxygen
26	Smoking	None	CXR ^a	-	-	LPV/r	Isolation without oxygen
27	Obesity	None	CXR ^a	-	-	No	Isolation without oxygen
28	-	None	CXR/CT	-	-	No	Discharge/off isolation on Feb 17

COVID-19 = coronavirus disease 2019, ID = illness day, CT = computed tomography, CXR = chest X-ray, LPV/r = lopinavir/ritonavir, DM = diabetes mellitus.

^aOnly CXRs were performed.

Infiltration on initial chest X-ray was observed in 13 patients (46.4%), but pneumonia was confirmed in most patients who underwent computed tomography (CT) scan initially (16/18, 88.9%) (Table 1). The chest radiographic scores remained relatively stable during the first week of illness. However, around day 7 of illness, the scores began to increase in some patients, suggesting progression of pneumonia (Fig. 2C).

DISCUSSION

We report the clinical course and outcomes of the first 28 patients with COVID-19 in Republic of Korea. The clinical severity was mild symptomatic or asymptomatic in 78.6% (22/28) of the patients. The most common prodromal symptoms were sore throat, cough, fever, and myalgia, which was suggestive of common cold. Although radiological pneumonia was detected in the majority (22/28, 78.6%) of the patients, only 27.3% (6/22) of them required supplemental oxygen therapy. Radiological pneumonia was detected as early as from the 1st day of illness onset, and was even identified in patients who did not have any symptoms of the LRT infection, such as cough, sputum, chest pain, or dyspnea. Although they had radiological pneumonia, they did not feel unwell and were able to carry on their daily activities as usual (“walking pneumonia”). The titers of SARS-CoV-2 shedding from the URT were very high from the prodromal phase of illness until day 5 of illness.

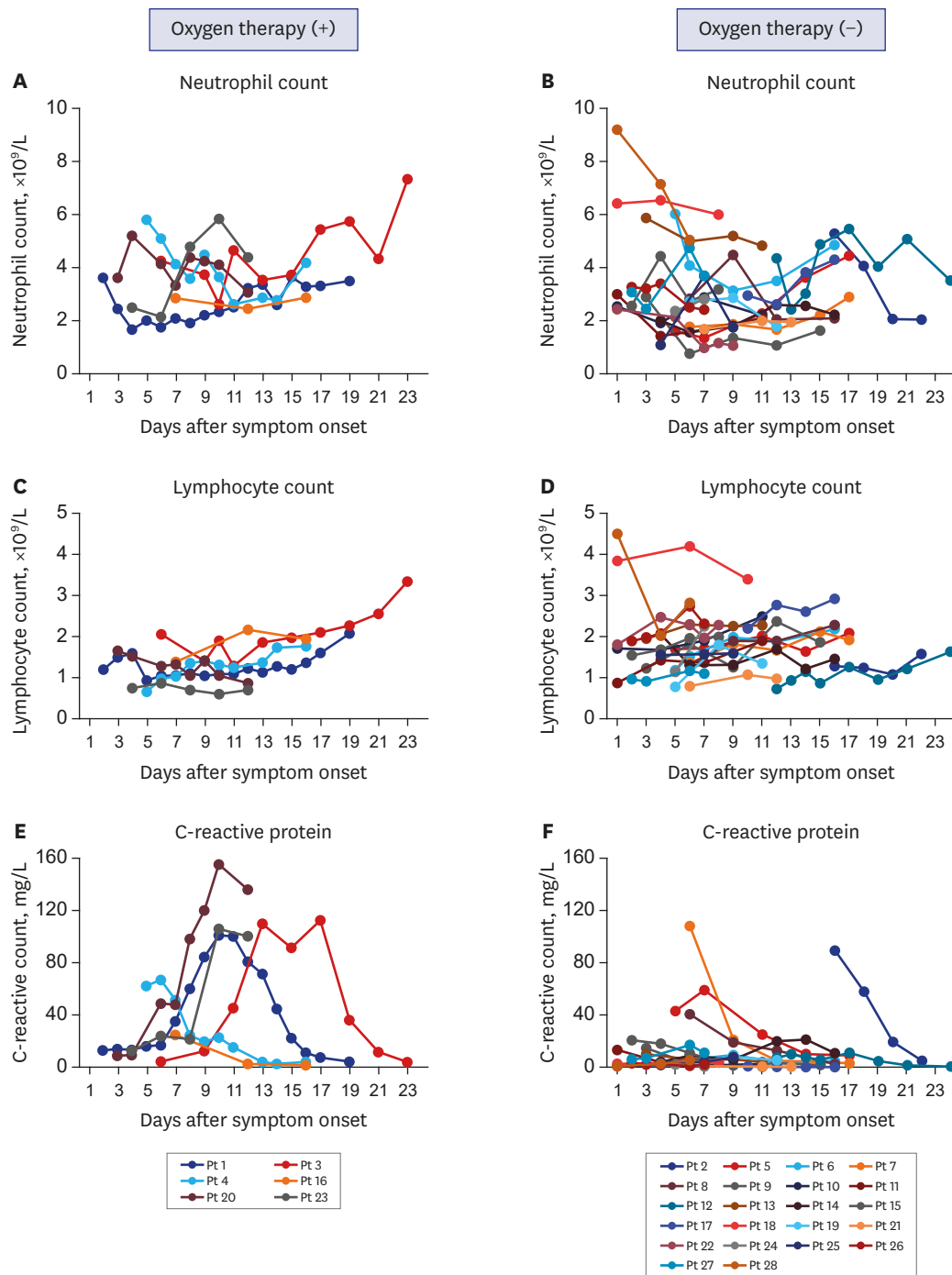


Fig. 1. Changes in laboratory data according to severity over time in 28 patients with COVID-19. Changes in peripheral blood neutrophil counts is shown in (A) and (B) according to requirement of O_2 therapy, respectively. Changes in peripheral blood lymphocyte counts is shown in (C) and (D). Changes in CRP is shown in (E) and (F).

COVID-19 = coronavirus disease 2019, CRP = C-reactive protein, Pt = patient.

In our patient cohort, the clinical features of COVID-19 during the prodromal phase were insidious and mild. Fever was absent in 75.0% of the patients at the time of admission. Throat symptoms, such as pain, discomfort and globus sensation and cough were ranked as relatively common, but only 1/3 had these symptoms. As the prodromal symptoms were

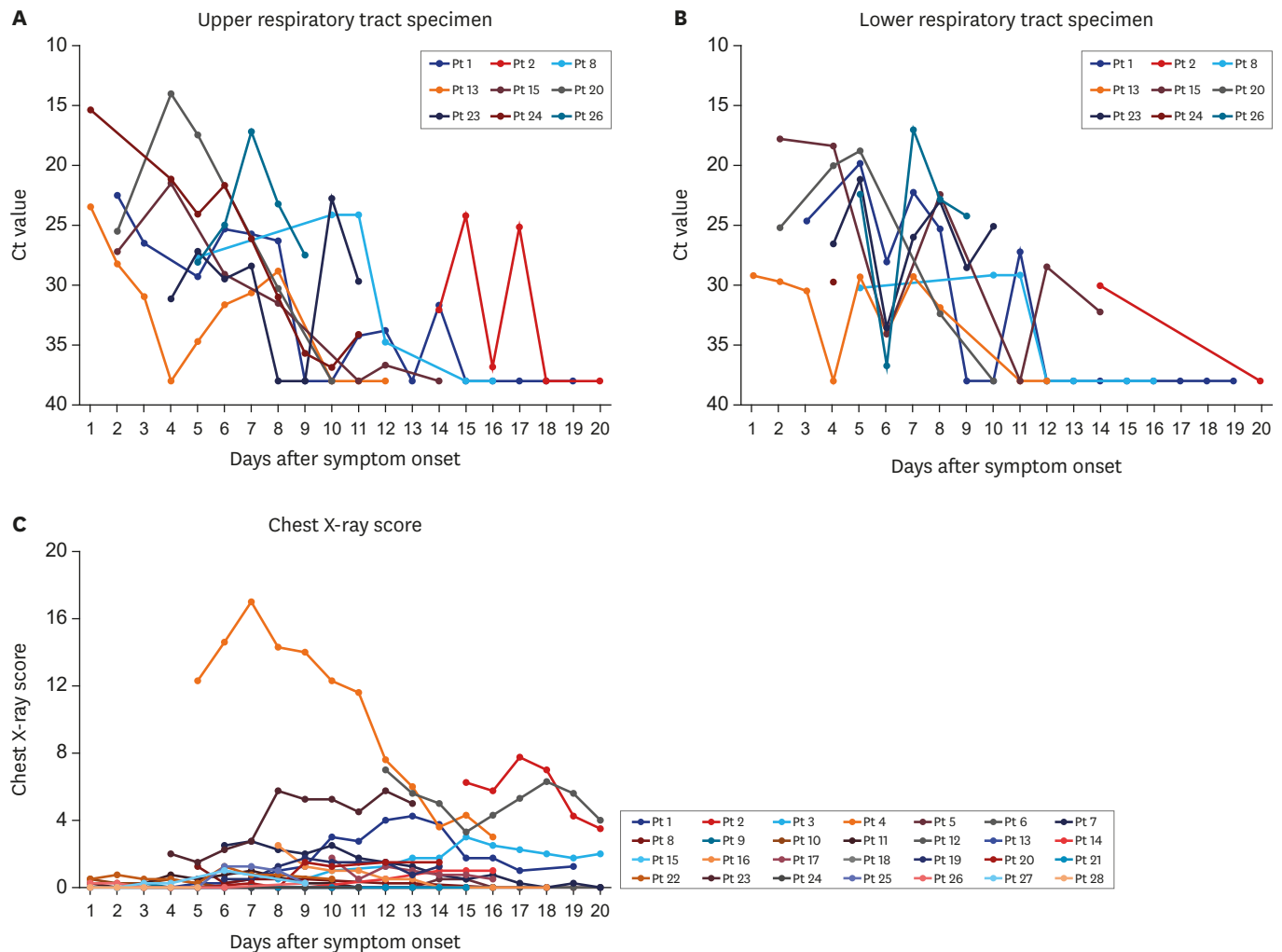


Fig. 2. Changes in SARS-CoV-2 Ct value of RT-PCR in respiratory specimens and radiologic features over time. Changes of Ct value of SARS-CoV-2 RNA (envelope gene, E) in nasopharyngeal with or without oropharyngeal specimen is shown in (A) in 9 patients with COVID-19. Changes of Ct value of SARS-CoV-2 RNA (E) in lower respiratory specimen (expectorate sputum) is shown in (B). Progression of pneumonia in 28 patients is shown in (C). Each lung was divided into the upper, middle, and lower zones, and infiltrates on each zone were scored from 0 to 4 (maximum CXR score, 24). SARS-CoV-2 = severe acute respiratory syndrome coronavirus 2, Ct = cycle threshold, RT-PCR = real time reverse transcription polymerase chain reaction, COVID-19 = coronavirus disease 2019, Pt = patient, CXR = chest X-ray.

mild and did not begin abruptly, most of the patients were not able to tell exactly when they had become ill. And because of this benign nature of the prodromal symptoms, they did not realize that they had been infected with SARS-CoV-2, and went out to carry on usual activities, while spreading the virus inadvertently.

The defining clinical characteristic of COVID-19 was an early development of radiological pneumonia. During the prodromal phase, only 1/3 of our patients developed any clinical features suggesting pneumonia, such as cough, sputum, or chest discomfort. Chest radiographs on hospitalization did not reveal any infiltrates in more than 50% of patients. However, chest CT scans, which were performed on hospitalization or within 1–2 days, showed infiltrates in the lungs suggesting viral pneumonia in 16/18 (88.9%) patients (Table 1). If we had not taken CT scans of the lungs, we would have easily missed the pneumonia diagnosis.⁴ The radiological pneumonia from CT scan was detected as early as day 1 of illness onset. The

most common findings of CT scans were bilateral, ground-glass opacity in the periphery of the lungs as described in previous studies.^{9,11,12} Despite radiological pneumonia, the patients were clinically stable and mobile during the first week of illness (“walking pneumonia”). We assessed the progression of COVID-19 pneumonia using the chest radiograph scoring, and it remained stable during the first week of illness, but increased around the day 7 of illness. This pattern of pneumonia progression was also noted in patients with MERS-CoV infection.¹⁸ The early onset of the lung infiltrates and few clinical manifestations of LRT infection may suggest that the virus can invade into the LRT, evading innate immune mechanisms and replicate before adaptive immune response begins to play a role. A tissue biopsy and immunohistopathological studies of the lungs may elucidate this unique and interesting clinical feature of SARS-CoV-2 infection.

Gastrointestinal manifestations were relatively uncommon in our patient cohort. While 10% of the patients had diarrhea, 3% had vomiting, and 3% had abdominal pain at presentation, all of them revealed other common symptoms of acute respiratory illness. Overall, diarrhea was present in 39% (11/28) of patients during hospitalization from the admission in this study. As diarrhea is an adverse effect of lopinavir/ritonavir, we reassessed the frequency of diarrhea according to the patients being treated with lopinavir/ritonavir or not, and 53% (10/19) and 11% (1/9) of our patients had diarrhea, respectively (data not shown). In Chinese patients, the frequency of diarrhea ranged 2%–10%.^{9,11,12} It is important to note that receptor binding is a major determinant of tissue tropism for a coronavirus.¹⁹ A recent study showed that SARS-CoV-2 used angiotensin converting enzyme II as a cellular entry receptor,^{20,21} as SARS-CoV.¹⁹ Therefore, it is plausible that SARS-CoV-2 may be able to replicate in the gastrointestinal epithelial cells and be excreted in the stool. Recently, China CDC reported that they isolated SARS-CoV-2 from a stool sample taken 15 days after illness onset of a laboratory confirmed patient.²² The possibilities of fecal-to-oral transmission and opportunistic aerosol transmission of SARS-CoV-2 remain to be determined.²³

It is important to note that the virus titers in the respiratory specimens peaked on early days after illness onset (**Fig. 2A and B**). Of the seven infectors of our cohort, two transmitted the virus on the first day of illness, one on the 8th day of illness, and 4 via household transmission. The Ct values of the URT specimens ranged from 18–25 in the 4 infectors within the 5 days of illness: 18.74, 18.33, 25.12, and 21.5 for each patient. Our data suggest that the viral shedding from the URT may reach its peak during the first 3–5 days after illness onset. A recent study on virus shedding kinetics is also in line with our finding.²⁴ This “shift to the left” pattern of virus shedding kinetics is strikingly different from that of SARS-CoV, which shows an inverted V pattern, with its peak at day 10 of illness.²⁵ Also of note is that 57.1% (4/7) of infectors had cough or sputum, in contrast to only 23.8% (5/21) of non-infectors having cough. These findings suggest that the transmissions of SARS-CoV-2 may occur easily and begin from the prodromal phase of illness, just like common cold or influenza viruses. Considering that the median time from symptom onset to isolation of the patients was 3 days, and that high titers of virus shedding began from day 1 of illness with the peak around day 3–5 of illness, early detection and isolation strategy may be relatively less effective in containing the virus in COVID-19.

The clinical outcomes of most patients in this study were not complicated. As of 17 February 2020, no patient required supplemental oxygen therapy with mechanical ventilation nor any organ-supporting treatments in intensive care unit. A total of 10 cases have fully recovered

from the infection and have been discharged from hospital. Of the 18 confirmed cases who are still in hospital, most are stable or improving.

There are some limitations in our study. Only 28 patients from our cohort were included in this study. However, we gathered and analyzed the detailed clinical information about all of the first 28 cases nationwide in Republic of Korea. Moreover, some cases were confirmed during the surveillance test for COVID-19 after exposure to SARS-CoV-2. The proportion of elderly patients and frequency of underlying conditions were small, and therefore the first 28 patients from the early phase of the COVID-19 outbreak in Korea had relatively favorable outcomes.²⁶ Most of the enrolled patients would be healthier than the population of recent larger outbreaks showing worse outcomes, mostly in the elderly group. The results regarding outcomes in this study should be interpreted cautiously. In most cases, we did not perform virologic tests for coinfection of other respiratory viruses such as influenza.

Our study suggests that (1) the prodromal symptoms of SARS-CoV-2 infection were mild, (2) radiological pneumonia was very common, and developed from the early days of illness, (3) pneumonia may progress at day 7 of illness, (4) high titers of the virus shed from the URT during the prodromal phase (5), and the median time from symptom onset to defervescence was 10 days and to off-isolation 18.5 days.

ACKNOWLEDGMENTS

We thank Yu Mi Jung MS (Medical Record Team, National Medical Center) who designed the case record form to collect data.

SUPPLEMENTARY MATERIALS

Supplementary Table 1

Cutoff threshold values of SARS-CoV-2 RNA (envelope gene, *E*) in nasopharyngeal with or without oropharyngeal specimen and in lower respiratory specimen in 9 patients with COVID-19

[Click here to view](#)

Supplementary Fig. 1

Changes of peak body temperature (°C) of 17 patients with COVID-19 during hospitalization.

[Click here to view](#)

Supplementary Fig. 2

Changes in clinical severity over time in 6 patients with COVID-19 who required supplemental oxygen therapy. Changes in clinical severity scores are as follows: 1, no limit of daily activity; 2, limit of daily activity but no need for O₂ therapy; 3, O₂ therapy via nasal prong; 4, O₂ therapy via facial mask; 5, high flow O₂ therapy or non-invasive ventilation; 6, invasive ventilation; 7, multi-organ failure or extracorporeal membrane oxygenation therapy; 8, death.

[Click here to view](#)

REFERENCES

1. Zhu N, Zhang D, Wang W, Li X, Yang B, Song J, et al. A novel coronavirus from patients with pneumonia in China, 2019. *N Engl J Med* 2020;382(8):727-33.
[PUBMED](#) | [CROSSREF](#)
2. World Health Organization main website. <https://www.who.int>. Updated 2020. Accessed March 31, 2020.
3. Choi WS, Kang CI, Kim Y, Choi JP, Joh JS, Shin HS, et al. Clinical presentation and outcomes of Middle East respiratory syndrome in the Republic of Korea. *Infect Chemother* 2016;48(2):118-26.
[PUBMED](#) | [CROSSREF](#)
4. Kim JY, Choe PG, Oh Y, Oh KJ, Kim J, Park SJ, et al. The first case of 2019 novel coronavirus pneumonia imported into Korea from Wuhan, China: implication for infection prevention and control measures. *J Korean Med Sci* 2020;35(5):e61.
[PUBMED](#) | [CROSSREF](#)
5. Kim JY, Ko JH, Kim Y, Kim YJ, Kim JM, Chung YS, et al. Viral load kinetics of SARS-CoV-2 infection in first two patients in Korea. *J Korean Med Sci* 2020;35(7):e86.
[PUBMED](#) | [CROSSREF](#)
6. Lim J, Jeon S, Shin HY, Kim MJ, Seong YM, Lee WJ, et al. Case of the index patient who caused tertiary transmission of COVID-19 infection in Korea: the application of lopinavir/ritonavir for the treatment of COVID-19 infected pneumonia monitored by quantitative RT-PCR. *J Korean Med Sci* 2020;35(6):e79.
[PUBMED](#) | [CROSSREF](#)
7. The Korea Centers for Disease Control and Prevention. http://ncov.mohw.go.kr/index_main.jsp. Updated 2020. Accessed February 14, 2020.
8. Korean Society of Infectious Diseases; Korean Society of Pediatric Infectious Diseases; Korean Society of Epidemiology; Korean Society for Antimicrobial Therapy; Korean Society for Healthcare-associated Infection Control and Prevention; Korea Centers for Disease Control and Prevention. Report on the epidemiological features of coronavirus disease 2019 (COVID-19) outbreak in the Republic of Korea from January 19 to March 2, 2020. *J Korean Med Sci* 2020;35(10):e112.
[PUBMED](#) | [CROSSREF](#)
9. Huang C, Wang Y, Li X, Ren L, Zhao J, Hu Y, et al. Clinical features of patients infected with 2019 novel coronavirus in Wuhan, China. *Lancet* 2020;395(10223):497-506.
[PUBMED](#) | [CROSSREF](#)
10. Chan JF, Yuan S, Kok KH, To KK, Chu H, Yang J, et al. A familial cluster of pneumonia associated with the 2019 novel coronavirus indicating person-to-person transmission: a study of a family cluster. *Lancet* 2020;395(10223):514-23.
[PUBMED](#) | [CROSSREF](#)
11. Chen N, Zhou M, Dong X, Qu J, Gong F, Han Y, et al. Epidemiological and clinical characteristics of 99 cases of 2019 novel coronavirus pneumonia in Wuhan, China: a descriptive study. *Lancet* 2020;395(10223):507-13.
[PUBMED](#) | [CROSSREF](#)
12. Wang D, Hu B, Hu C, Zhu F, Liu X, Zhang J, et al. Clinical characteristics of 138 hospitalized patients with 2019 novel coronavirus-infected pneumonia in Wuhan, China. *JAMA* 2020. DOI: 10.1001/jama.2020.1585.
[PUBMED](#) | [CROSSREF](#)
13. Chang, Lin M, Wei L, Xie L, Zhu G, Dela Cruz CS, et al. Epidemiologic and clinical characteristics of novel coronavirus infections involving 13 patients outside Wuhan, China. *JAMA* 2020. DOI: 10.1001/jama.2020.1623.
[PUBMED](#) | [CROSSREF](#)
14. Li Q, Guan X, Wu P, Wang X, Zhou L, Tong Y, et al. Early transmission dynamics in Wuhan, China, of novel coronavirus-infected pneumonia. *N Engl J Med* 2020;382(13):1199-207.
[PUBMED](#) | [CROSSREF](#)
15. COVID-19 National Emergency Response Center, Epidemiology and Case Management Team, Korea Centers for Disease Control and Prevention. Early epidemiological and clinical characteristics of 28 cases of coronavirus disease in South Korea. *Osong Public Health Res Perspect* 2020;11(1):8-14.
[PUBMED](#) | [CROSSREF](#)
16. World Health Organization. *Global COVID-19 Clinical Characterization Case Record Form*. Geneva: World Health Organization; 2020.
17. Kim JM, Chung YS, Jo HJ, Lee NJ, Kim MS, Woo SH, et al. Identification of coronavirus isolated from a patient in Korea with COVID-19. *Osong Public Health Res Perspect* 2020;11(1):3-7.
[PUBMED](#) | [CROSSREF](#)

18. Oh MD, Park WB, Choe PG, Choi SJ, Kim JI, Chae J, et al. Viral load kinetics of MERS coronavirus infection. *N Engl J Med* 2016;375(13):1303-5.
[PUBMED](#) | [CROSSREF](#)
19. Fung TS, Liu DX. Human coronavirus: host-pathogen interaction. *Annu Rev Microbiol* 2019;73(1):529-57.
[PUBMED](#) | [CROSSREF](#)
20. Zhou P, Yang XL, Wang XG, Hu B, Zhang L, Zhang W, et al. A pneumonia outbreak associated with a new coronavirus of probable bat origin. *Nature* 2020;579(7798):270-3.
[PUBMED](#) | [CROSSREF](#)
21. Lu R, Zhao X, Li J, Niu P, Yang B, Wu H, et al. Genomic characterisation and epidemiology of 2019 novel coronavirus: implications for virus origins and receptor binding. *Lancet* 2020;395(10224):565-74.
[PUBMED](#) | [CROSSREF](#)
22. Zhang Y, Chen C, Zhu S, Shu C, Wang D, Song J, et al. Isolation of 2019-nCoV from a stool specimen of a laboratory-confirmed case of the coronavirus disease 2019 (COVID-19). *China CDC Wkly* 2020;8:123-4.
23. Yeo C, Kaushal S, Yeo D. Enteric involvement of coronaviruses: is faecal-oral transmission of SARS-CoV-2 possible? *Lancet Gastroenterol Hepatol* 2020;5(4):335-7.
[PUBMED](#) | [CROSSREF](#)
24. Zou L, Ruan F, Huang M, Liang L, Huang H, Hong Z, et al. SARS-CoV-2 viral load in upper respiratory specimens of infected patients. *N Engl J Med* 2020;382(12):1177-9.
[PUBMED](#) | [CROSSREF](#)
25. Peiris JS, Chu CM, Cheng VC, Chan KS, Hung IF, Poon LL, et al. Clinical progression and viral load in a community outbreak of coronavirus-associated SARS pneumonia: a prospective study. *Lancet* 2003;361(9371):1767-72.
[PUBMED](#) | [CROSSREF](#)
26. Cowling BJ, Leung GM. Epidemiological research priorities for public health control of the ongoing global novel coronavirus (2019-nCoV) outbreak. *Euro Surveill* 2020;25(6):2000110.
[PUBMED](#) | [CROSSREF](#)



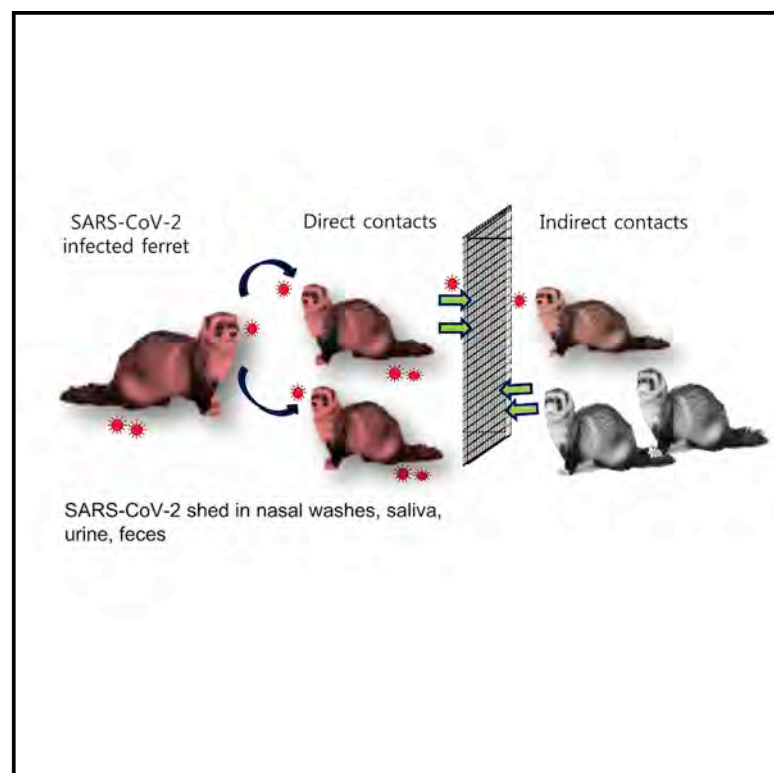
Since January 2020 Elsevier has created a COVID-19 resource centre with free information in English and Mandarin on the novel coronavirus COVID-19. The COVID-19 resource centre is hosted on Elsevier Connect, the company's public news and information website.

Elsevier hereby grants permission to make all its COVID-19-related research that is available on the COVID-19 resource centre - including this research content - immediately available in PubMed Central and other publicly funded repositories, such as the WHO COVID database with rights for unrestricted research re-use and analyses in any form or by any means with acknowledgement of the original source. These permissions are granted for free by Elsevier for as long as the COVID-19 resource centre remains active.

Cell Host & Microbe

Infection and Rapid Transmission of SARS-CoV-2 in Ferrets

Graphical Abstract



Authors

Young-Il Kim, Seong-Gyu Kim, Se-Mi Kim, ..., Richard J. Webby, Jae U. Jung, Young Ki Choi

Correspondence

jaeujung@med.usc.edu (J.U.J.), choiki55@chungbuk.ac.kr (Y.K.C.)

In Brief

The outbreak of coronavirus disease 2019 (COVID-19) caused by severe acute respiratory syndrome coronavirus 2 (SARS-CoV-2) rapidly spreads, leading to a pandemic infection. Kim et al. show that ferrets are highly susceptible to SARS-CoV-2 infection and effectively transmit the virus by direct or indirect contact, recapitulating human infection and transmission.

Highlights

- SARS-CoV-2-infected ferrets exhibit elevated body temperature and virus replication
- SARS-CoV-2 is shed in nasal washes, saliva, urine and feces
- SARS-CoV-2 is effectively transmitted to naive ferrets by direct contact
- SARS-CoV-2 infection leads acute bronchiolitis in infected ferrets



Brief Report

Infection and Rapid Transmission of SARS-CoV-2 in Ferrets

Young-Il Kim,^{1,2} Seong-Gyu Kim,¹ Se-Mi Kim,¹ Eun-Ha Kim,^{1,2} Su-Jin Park,^{1,2} Kwang-Min Yu,^{1,2} Jae-Hyung Chang,¹ Eun Ji Kim,¹ Seunghun Lee,¹ Mark Anthony B. Casel,^{1,2} Jihye Um,⁴ Min-Suk Song,^{1,2} Hye Won Jeong,¹ Van Dam Lai,³ Yeonjae Kim,⁴ Bum Sik Chin,⁴ Jun-Sun Park,⁴ Ki-Hyun Chung,⁴ Suan-Sin Foo,⁵ Haryoung Poo,⁶ In-Pil Mo,³ Ok-Jun Lee,¹ Richard J. Webby,⁷ Jae U. Jung,^{5,*} and Young Ki Choi^{1,2,8,*}

¹College of Medicine and Medical Research Institute, Chungbuk National University, Cheongju, Republic of Korea

²Zoonotic Infectious Diseases Research Center, Chungbuk National University, Cheongju, Republic of Korea

³College of Veterinary Medicine, Chungbuk National University, Cheongju, Republic of Korea

⁴Research Institute of Public Health, National Medical Center, Seoul, Republic of Korea

⁵Department of Molecular Microbiology and Immunology, Keck School of Medicine, University of Southern California, Los Angeles, CA 90033, USA

⁶Infectious Disease Research Center, Korea Research Institute of Bioscience and Biotechnology, University of Science and Technology, Daejeon, Republic of Korea

⁷Division of Virology, Department of Infectious Diseases, St. Jude Children's Research Hospital, Memphis, TN 38105, USA

⁸Lead Contact

*Correspondence: jaeujung@med.usc.edu (J.U.J.), choiki55@chungbuk.ac.kr (Y.K.C.)

<https://doi.org/10.1016/j.chom.2020.03.023>

SUMMARY

The outbreak of coronavirus disease 2019 (COVID-19) caused by severe acute respiratory syndrome coronavirus 2 (SARS-CoV-2) emerged in China and rapidly spread worldwide. To prevent SARS-CoV-2 dissemination, understanding the *in vivo* characteristics of SARS-CoV-2 is a high priority. We report a ferret model of SARS-CoV-2 infection and transmission that recapitulates aspects of human disease. SARS-CoV-2-infected ferrets exhibit elevated body temperatures and virus replication. Although fatalities were not observed, SARS-CoV-2-infected ferrets shed virus in nasal washes, saliva, urine, and feces up to 8 days post-infection. At 2 days post-contact, SARS-CoV-2 was detected in all naive direct contact ferrets. Furthermore, a few naive indirect contact ferrets were positive for viral RNA, suggesting airborne transmission. Viral antigens were detected in nasal turbinate, trachea, lungs, and intestine with acute bronchiolitis present in infected lungs. Thus, ferrets represent an infection and transmission animal model of COVID-19 that may facilitate development of SARS-CoV-2 therapeutics and vaccines.

Coronaviruses (CoVs) are a large family of viruses that cause respiratory and intestinal infections in animals and humans (Masters and Perlman, 2013). Of the four genera—alphacoronavirus, betacoronavirus, gammacoronavirus, and deltacoronavirus—alphacoronavirus and betacoronavirus are commonly associated with respiratory illness in humans and gastroenteritis in animals (Cui et al., 2019). CoVs were not typically considered to be highly pathogenic in humans until the outbreaks of Severe Acute Respiratory Syndrome CoV (SARS-CoV) (Zhong et al., 2003), Middle East Respiratory Syndrome CoV (MERS-CoV) (Zaki et al., 2012), and more recently, severe acute respiratory syndrome coronavirus 2 (SARS-CoV-2).

In late December of 2019, a novel coronavirus disease (COVID-19) was identified in Wuhan City, Hubei Province, China from patients with severe pneumonia (Zhu et al., 2020). Deep sequencing analysis of lower respiratory tract samples revealed the identity of the causative agent as a newly emerged strain of betacoronavirus, temporarily named 2019 novel coronavirus (2019-nCoV) and later renamed as severe acute respiratory syndrome coronavirus 2 (SARS-CoV-2) by the International Committee on Taxonomy of Viruses (ICTV) (ICTV, 2020). As of March 23, there have

been approximately 81,601 confirmed cases of COVID-19 in China with over 3,276 deaths (WHO, 2020b). The SARS-CoV-2 has been found to have high human-to-human transmission through close contact with infected patients, leading to rapid global spread by infected travelers from China. As of March 23, 2020, SARS-CoV-2 cases have been confirmed in at least 171 countries with a steady increase in the number of laboratory confirmed cases (251,329 cases) outside of China suggesting that non-pharmaceutical intervention strategies have not ultimately been successful in limiting spread. Therefore, an animal model that recapitulates the COVID-19 clinical symptoms in human infection is urgently needed in order to decipher the transmission routes and pathobiology of this virus and to allow testing of pharmaceutical interventions.

Given that SARS-CoV-2 shares higher sequence homology with SARS-CoV (79% homology) than with MERS-CoV (50% homology), the entry receptor for SARS-CoV, human Angiotensin-converting enzyme 2 (hACE2), was considered as a receptor candidate for SARS-CoV-2 (Lu et al., 2020). Correspondingly, Bao et al. (2020) reported weight loss and virus replication in lungs of hACE2 transgenic mice following SARS-CoV-2



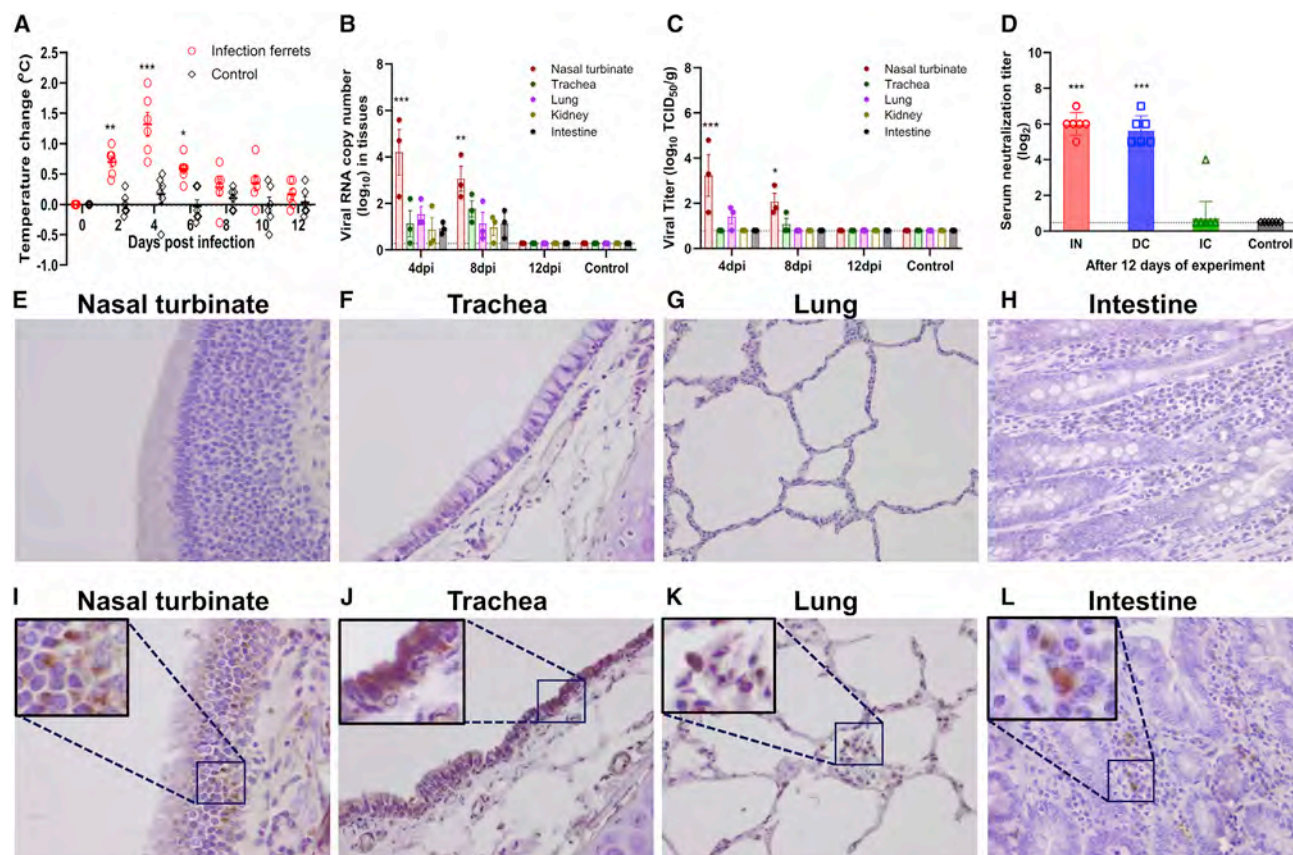


Figure 1. Temperature Changes, Weight Loss, Survival, Viral Shedding, and Immunohistochemistry of Tissues of NMC-nCoV02-Infected Ferrets

(A–C) Six ferrets were inoculated intranasally with $10^{5.5}$ TCID₅₀ of virus. (A) Temperature changes, (B) number of viral RNA copies, and (C) infectious virus titers were measured in tissues of NMC-nCoV02-infected ferrets ($n = 6$ /group). Each tissue ($n = 3$ per group) was collected at 4, 8, and 12 dpi. Viral loads in nasal turbinate, trachea, lung, kidney, and intestine were titrated using quantitative real-time PCR and TCID₅₀. Data are presented as mean \pm SEM.

(D) Serum neutralizing (SN) antibody titers (GMT) against NMC-nCoV02 (100 TCID₅₀) were measured onto Vero cells after 12 days of experiment ($n = 6$ per group). Data are presented as geometric mean \pm SD. Tissues were harvested on day 4 after inoculation and immunohistochemistry was performed with a mouse polyclonal antibody.

(E–H) Tissues of PBS control ferrets; (E) nasal turbinate, (F) trachea, (G) lung, and (H) intestine.

(I–L) Tissues of NMC-nCoV02 infected ferrets: (I) Nasal turbinate, (J) Trachea, (K) lung, and (L) Intestine.

The presence of NMC-nCoV02 antigen was determined by IHC with mouse polyclonal antibody. Magnification $\times 400$. Asterisks indicate statistical significance compared with PBS control group by the two-way ANOVA with Sidak's multiple comparisons test (A), the two way ANOVA with Dunnett's multiple comparisons test (B and C), or one-way ANOVA Dunnett's multiple comparisons test (* indicates $p < 0.05$, ** indicates $p < 0.001$, and *** indicates $p < 0.0001$).

infection; however, no other clinical symptoms such as cough or fever were observed. In order to understand the rapid spreading characteristics of SARS-CoV-2, additional animal models that mimic high human-to-human transmission of SARS-CoV-2 infections are warranted. Given that ferret ACE2 has been shown to contain critical SARS-CoV binding residues (Wan et al., 2020), we performed infection and direct and indirect contact transmission studies using a ferret model previously developed for influenza virus infections (Park et al., 2018; Bouvier, 2015).

To demonstrate ferret-to-ferret transmission in an experimental setting, ferrets ($n = 2$) were inoculated via the intranasal (IN) route with $10^{5.5}$ TCID₅₀ of NMC-nCoV02, a strain that was isolated from a COVID-19-confirmed patient in South Korea in February of 2020. To evaluate the transmission mode of the virus, naive ferrets ($n = 2$ /group) were placed in direct contact (DC) (co-housed) or indirect contact (IC) (housed in cages with a

permeable partition separating them from infected ferrets) with infected ferrets two days after the primary infection. Clinical features of SARS-CoV-2 infections were recorded. This study was repeated in three independent trials (total $n = 24$; direct infection [$n = 6$], DC [$n = 6$], IC [$n = 6$], and PBS control [$n = 6$] ferrets).

NMC-nCoV02-infected ferrets had elevated body temperatures, from 38.1°C to 40.3°C, between 2 and 8 dpi; these returned to normal by 8 dpi (Figure 1A). While reduced activity was observed in NMC-nCoV02-infected ferrets between 2 and 6 dpi with occasional coughs, there was no detectable body weight loss, nor were there any fatalities during the experimental period. Interestingly, all six DC ferrets showed increased body temperatures ($\sim 39^\circ\text{C}$) with reduced activity between 4 and 6 days post contact (dpc) and no detectable body weight loss (Figures S1A and S1B). However, none of the IC ferrets showed increased body temperature or weight loss over the 12 days of the studies (Figures S1C

Table 1. Quantitation of Viral RNA in Specimens (Serum, Feces, Nasal Wash, Saliva, and Urine) from Each Group of Ferrets

Route	Ferret groups	Days post treatment; log ₁₀ copies/mL (log ₁₀ TCID ₅₀ /mL) ^a					
		2	4	6	8	10	12
Serum	Infected	0.35 ± 0.08	0.35 ± 0.08	-	-	-	-
	DC	-	-	-	-	-	-
	IC	-	-	-	-	-	-
	Naive	-	-	-	-	-	-
Nasal washes	Infected	2.67 ± 1.01** (2.17 ± 0.94*)	3.83 ± 0.94*** (2.88 ± 0.84***)	2.67 ± 0.63** (1.83 ± 0.63*)	1.40 ± 1.06	-	-
	DC	0.67 ± 0.34*	3.27 ± 1.31 (2.40 ± 1.17)	1.48 ± 0.23 (1.00 ± 0.25)	1.38 ± 1.00	-	-
	IC	-	0.53 ± 0.36	0.39 ± 0.17*	0.38 ± 0.16	-	-
	Naive	-	-	-	-	-	-
Saliva	Infected	1.73 ± 0.54** (0.92 ± 0.38)	1.67 ± 0.94* (0.82 ± 0.62)	0.60 ± 0.47	0.50 ± 0.49	-	-
	DC	0.52 ± 0.33	0.85 ± 0.48*	0.53 ± 0.21	0.38 ± 0.2	-	-
	IC	-	-	-	-	-	-
	Naive	-	-	-	-	-	-
Urine	Infected	0.81 ± 0.56	0.87 ± 0.53 (2/3) ^b	0.52 ± 0.40	0.35 ± 0.12	-	-
	DC	0.72 ± 0.42	1.08 ± 0.81 (2/3)	-	-	-	-
	IC	-	-	-	-	-	-
	Naive	-	-	-	-	-	-
Fecal	Infected	1.37 ± 0.38*	1.51 ± 0.52** (2/3)	0.77 ± 0.73	0.53 ± 0.38	-	-
	DC	0.42 ± 0.10	1.40 ± 0.51* (2/3)	0.92 ± 1.04	0.80 ± 0.80	-	-
	IC	-	0.52 ± 0.44 (0/3)	1.08 ± 0.73*	-	-	-
	Naive	-	-	-	-	-	-

Infected: NMC-nCoV2 infected group; DC, directly contacted group; IC, indirectly infected group. Asterisks indicate statistical significance compared with naive sample by the Ordinary one-way ANOVA with Dunnett's multiple comparisons test (* indicates $p < 0.05$, ** indicates $p < 0.001$, and *** indicates $p < 0.0001$).

^aVirus spike RNA gene detection limit and viral titer limit were 0.3 log₁₀ copies/mL and 0.8 log₁₀ TCID₅₀/mL, respectively.

^bIsolated viruses from nasal wash samples inoculated in ferrets.

and S1D). These data indicate that the efficient establishment of COVID-19 clinical features in ferrets exposed to infected animals requires direct contact, recapitulating human-to-human transmission.

To investigate SARS-CoV-2 replication and shedding in each group of ferrets, we collected blood, nasal washes, saliva, urine, and fecal specimens every other day for 12 days. Collected ferret secretions were resuspended in cold phosphate-buffered saline (PBS) containing antibiotics (5% penicillin/streptomycin; GIBCO). For virus titration, total RNA was extracted from the collected samples using the RNeasy Mini kit (QIAGEN, Hilden, Germany) according to the manufacturer's instructions (QIAGEN, 2012) and cDNA was synthesized with a cDNA synthesis kit (Omniscrypt Reverse Transcriptase; QIAGEN, Hilden, Germany). To quantitate viral RNA copy number, quantitative real-time RT-PCR (qRT-PCR) was performed targeting the spike (Table 1) and ORF1a (Table S1) genes as previously described (Zhu et al., 2020) using the SYBR Green kit (iQTM SYBR Green supermix kit, Bio-Rad, Hercules, CA, USA). The number of viral RNA copies was calculated by comparison to the number of copies of a standard control. In the NMC-nCoV2 infected group, viral spike RNA was detected in all specimens at 2 dpi. The highest amount of viral RNA was detected in nasal washes and peaked at 4 dpi (3.83 log₁₀ copies/mL), persisting until 8 dpi before dropping below detection limits at 10 dpi (Table 1).

The virus was also detected in saliva specimens from 2 dpi (1.73 log₁₀ copies/mL) through 8 dpi. Although viral spike RNA was detected in sera of infected ferrets, the viral copy number was low (peaked titer 0.35 log₁₀ copies/mL) and dropped below detection limits earlier than in nasal wash and saliva specimens. To evaluate the infectious virus titer in each specimen, collected nasal washes and saliva specimens were inoculated onto Vero cells for virus isolation. In IN infected ferret group, NMC-nCoV2 was isolated from both saliva and nasal washes specimens as early as 2 dpi and persisted until 4 and 6 dpi, respectively (Table 1). Nasal washes specimens showed higher virus titers (1.83–2.88 log₁₀ TCID₅₀/mL) than saliva specimens (0.82–0.92 log₁₀ TCID₅₀/mL). In DC ferret group, virus was isolated from the nasal washes at 4 dpc (2.4 log₁₀ TCID₅₀/mL) and 6 dpc (1.0 log₁₀ TCID₅₀/mL) but not in saliva specimens (Table 1). Because gastrointestinal involvement is a characteristic of coronavirus infections of animals and humans (Leung et al., 2003), we also collected fecal and urine specimens. Viral RNA was detected in a majority of collected specimens in both IN-infected and DC groups as early as 2 dpc (Table 1). Similarly to the IN infected group, the DC group had the highest virus copy numbers (3.27 log₁₀ copies/mL) in nasal washes, with RNA detected through 8 dpc. In addition, viral RNA was detected in saliva and fecal specimens of the DC group for 8 days, whereas the urine

specimens contained detectable viral RNA until 4 dpc. For the IC group, 2 out of 6 ferrets were positive for viral RNA in nasal washes and fecal specimens at 4 dpc, although viral RNA copy numbers were lower (0.53 and 0.52 log₁₀ copies/mL, respectively) than in DC ferrets. Due to the cytotoxicity of urine and fecal specimens of ferrets, we could not assess virus isolation and titer in Vero cells. To evaluate the presence of infectious NMC-nCoV2 in urine and fecal specimens, urine or fecal specimens (at 4 dpi) of IN-infected DC or IC ferrets were centrifuged to remove the debris, and the supernatants were inoculated into naive ferrets (n = 3) per each specimen. Nasal washes from specimen-inoculated ferrets were collected at 2, 4, and 6 dpi and infected onto Vero cells for virus isolation. Noticeably, NMC-nCoV2 was isolated from the nasal wash specimens of 2 out of 3 urine-specimen-treated or fecal-specimen-treated ferrets (Table 1). However, we failed to re-isolate virus from the ferrets infected with the fecal specimens of IC ferrets. These results indicate that ferret is highly susceptible for the infection of SARS-CoV-2 derived from body fluids, and infectious SARS-CoV-2 sheds through urine and fecal specimens of infected ferrets.

To assess the replication of SARS-CoV-2 in ferret organs, an additional 12 ferrets were infected with NMC-nCoV2 or PBS via the IN route and 3 ferrets were sacrificed at 4, 8, and 12 dpi. Nasal turbinate, trachea, lung, kidney, and intestine tissues were collected using individual scissors to avoid cross contamination. The highest viral RNA levels were detected in nasal turbinate (4.2 log₁₀ copies/g) and lung tissue (1.53 log₁₀ copies/g) at 4 dpi. Viral RNA was also detected in intestine (0.93 log₁₀ copies/g) and kidney (0.87 log₁₀ copies/g) at 4 dpi. At 8 dpi, viral RNA was still detected in nasal turbinate, trachea, lungs, kidney, and intestine (Figure 1B). In correlation with viral RNA copy numbers (Figure 1B), the highest infectious virus titer was detected in nasal turbinate (3.23 log₁₀ TCID₅₀/g) and lung tissue (1.4 log₁₀ TCID₅₀/g) at 4 dpi, whereas infectious virus recovery failed from trachea, kidney, and intestine tissues, which carried less than 1.13 log₁₀ viral RNA copies/g (Figure 1C). Finally, infectious NMC-nCoV2 was isolated from nasal turbinate (2.07 log₁₀ TCID₅₀/g) and trachea (1.07 log₁₀ TCID₅₀/g) at 8 dpi but not from other tissues at 8 dpi (Figure 1C). However, both viral RNA detection and virus recovery failed in all tested tissues at 12 dpi. These results suggest that virus isolation from infected tissues is closely related to viral RNA copy number.

To further confirm viral replication in infected ferrets, immunohistochemistry (IHC) and histopathological examinations were conducted (Figure 1 and Figure S2). Briefly, tissue samples were collected from NMC-nCoV2 infected or PBS-treated ferrets at 4 dpi and incubated in 10% neutral-buffered formalin for virus inactivation and tissue fixation before they were embedded in paraffin. The embedded tissues were sectioned and dried for 3 days at room temperature. To detect the viral antigens by IHC, mouse polyclonal antibody raised by the immunization of mice with inactivated NMC-nCoV2 virions was used as a primary antibody. Slides were viewed using the Olympus BX53 (Olympus, Tokyo, Japan) microscope with DP controller software to capture images. IHC analyses showed that a number of cells in the nasal turbinate, trachea, lung, and intestine sections of NMC-nCoV2-infected ferrets (Figures 1I–1L), but not

PBS-treated control ferrets (Figures 1E–1H), were positive for SARS-CoV-2 antigen. Further, the lung histopathology showed that, compared with PBS-treated ferrets, NMC-nCoV2-infected ferrets at 4 dpi showed increased immune infiltration and cell debris in the alveolar wall, bronchial epithelium, and bronchial lumen (Figure S2), evidencing acute bronchiolitis by NMC-nCoV2 infection.

After 12 days of infection, all remaining ferrets, including IN infection (n = 6), DC (n = 6), and IC (n = 6), had returned to normal ranges of body temperature and body weight, and all specimens were negative for viral RNA. To evaluate the seroconversion rate of each group, sera were collected from all remaining ferrets and a serum-neutralizing (SN) antibody assay against NMC-nCoV2 (100 TCID₅₀) was conducted on Vero cells. Although IN infection group showed the highest mean SN titers compared the other groups, the SN titers of both IN infection and DC groups ranged between 32 and 128 (Figure 1D). On the other hand, only 1 of 6 IC ferrets showed a positive SN titer of 16. Taken together, this demonstrates the presence of SARS-CoV-2 in multiple sources from infected ferrets, potentially explaining the rapid transmission to naive hosts in close contact with the infected hosts.

Given the rapid geographical spread of COVID-19, the WHO declared the SARS-CoV-2 outbreak a public health emergency of international concern (PHEIC) on the 30th of January, 2020 (WHO, 2020a) and labeled the COVID-19 outbreak a pandemic by the 12th of March, 2020 (WHO, 2020). Most confirmed COVID-19 patients at this time reported close epidemiological association (direct or indirect) with other COVID-19 patients. Interestingly, a growing number of individuals with no travel history to China and no direct contact with infected patients have become infected (Lim et al., 2020). To understand how this virus rapidly spreads within a community, and to inform infection control messaging, it is essential to develop an experimental animal model that can support the active infection, shedding, and transmission of SARS-CoV-2 to sentinel animals. In this study, we established an infection and transmission ferret animal model for COVID-19. The SARS-CoV-2 was found to efficiently infect ferrets and induce moderate increases in body temperature (~38.5–40.3°C). Moreover, we were able to detect viral RNA in blood (for 4 dpi), nasal washes (for 8 dpi), urine (for 8 dpi), and fecal (for 8 dpi) specimens. Findings suggest that SARS-CoV-2 can be shed through multiple routes of body discharge specimens, with these potentially serving as sources for viral transmission to those in close contact with infected individuals.

Interestingly, ferrets in direct contact with SARS-CoV-2-infected ferrets were positive for SARS-CoV-2 infection as early as 2 dpc, suggesting that rapid transmission occurred even prior to infected ferrets reaching their highest viral RNA copy numbers in nasal washes at 4 dpi. Transmission also occurred prior to peak body temperature and body weight loss in infected animals, which is consistent with the infectiousness of individuals during asymptomatic periods. With regard to potential airborne transmission of SARS-CoV-2, viral RNA was detected in nasal washes and fecal specimens in IC ferrets and persisted for 4 days after indirect contact; only one of the two positive animals seroconverted. These data show that airborne transmission is likely but is considerably less robust than direct contact transmission.

Following the fortuitous discovery of the natural susceptibility of ferrets to human influenza viruses, ferret models were found to highly reproduce the human disease manifestation of several respiratory viruses, including respiratory syncytial virus, parainfluenzaviruses, and SARS-CoV-1 (Capraro et al., 2008; Chan et al., 2018; Enkirch and von Messling, 2015; Park et al., 2018). In addition to the presence of the respective viral receptors, the anatomic proportions of the ferret upper and lower respiratory tracts, the density of submucosal glands in the bronchial wall, and the number of generations of terminal bronchioles all reproduce the condition in the human respiratory tract (Enkirch and von Messling, 2015). This further supports the significance of ferrets as animal model for human respiratory viral infection. We demonstrated that SARS-CoV-2-infected ferrets showed high virus titers in upper respiratory tracts (nasal washes) and consequently transmitted to naive ferrets by direct contact at high efficiency, suggesting that SARS-CoV-2 ferret model recapitulates aspects of human infection and transmission. Further, as suspected in recent COVID-19 patients (Kim et al., 2020; Xu et al., 2020), we detected the infectious viruses in urine and fecal specimens of virus-infected ferrets. However, there are also limitations in the SARS-CoV-2 ferret model, as SARS-CoV-2 infected ferrets showed only mild clinical symptoms and relatively lower virus titers in lungs of infected animals than SARS-CoV-1-infected or MERS-CoV-infected hACE2 or hDPP4 transgenic mice (Glass et al., 2004 and Li et al., 2017). On the other hand, it is also possible that SARS-CoV-2 replicates weaker but persists longer *in vivo* than SARS-CoV-1, ultimately leading an asymptomatic carrier with a persistent infection to effectively spread the virus. Therefore, given the rapid spreading characteristics of SARS-CoV-2 in humans, ferret model would be a useful tool to evaluate the efficacy of prophylactic anti-virals and preventive vaccines.

STAR★METHODS

Detailed methods are provided in the online version of this paper and include the following:

- **KEY RESOURCES TABLE**
- **RESOURCE AVAILABILITY**
 - Lead Contact
 - Materials Availability
 - Data Code and Availability
- **EXPERIMENTAL MODEL AND SUBJECT DETAILS**
 - Experimental Animals
 - Growth and Isolation of Virus
- **METHOD DETAILS**
 - Study Design for Animal-to-Animal Transmission
 - Quantitative Real-Time RT-PCR (qRT-PCR) to Detect SARS-CoV-2 RNA
 - Immunohistochemistry (IHC)
- **QUANTIFICATION AND STATISTICAL ANALYSIS**
 - Statistical Analysis

SUPPLEMENTAL INFORMATION

Supplemental Information can be found online at <https://doi.org/10.1016/j.chom.2020.03.023>.

ACKNOWLEDGEMENT

All animal experiments were approved by the Medical Research Institute, a member of the Laboratory Animal Research Center of Chungbuk National University (LARC) (approval number CBNUA-1352-20-02), and were conducted in strict accordance and adherence to relevant policies regarding animal handling as mandated under the Guidelines for Animal Use and Care of the Korea Center for Disease Control (K-CDC). Viruses were handled in an enhanced biosafety level 3 (BSL3) containment laboratory as approved by the Korean Centers for Disease Control and Prevention (KCDC-14-3-07).

This work was supported by National Research Foundation of Korea (NRF-2018M3A9H4056536, 2020R1A2C 3008339), the Korea Research Institute of Bioscience and Biotechnology (KRIBB) Research Initiative Program (KGM9942011), the National Institute of Health (AI140705, AI140718, AI152190, and AI116585), and the National Institute of Allergy and Infectious Diseases (Centers of Excellence for Influenza Research and Surveillance [CEIRS] contract number HHSN272201400006C).

AUTHOR CONTRIBUTIONS

Conceptualization: Y.I. Kim, S.J. Park, R.J. Webby, J.U. Jung, and Y.K. Choi; Investigation: Y.I. Kim, S.G. Kim, S.M. Kim, E.H. Kim, S.J. Park, K.M. Yu, J.H. Chang, E.J. Kim, M.A.B. Casel, V.D. Lai, S.H. Lee, J. Um, Y. Kim, B.S. Chin, J.S. Park, H.W. Jeong, S.S. Foo, H. Poo, I.P. Mo, O.J. Lee, M.S. Song, and Y.K. Choi; Writing: Y.I. Kim, S.J. Park, R.J. Webby, J.U. Jung, Y.K. Choi.

DECLARATION OF INTERESTS

Jae U. Jung is a scientific advisor of the Vaccine Stabilization Institute, a California corporation.

Received: February 27, 2020

Revised: March 16, 2020

Accepted: March 27, 2020

Published: April 6, 2020

REFERENCES

- Bao, L., Deng, W., Huang, B., Gao, H., Ren, L., Wei, Q., Yu, P., Xu, Y., Liu, J., and Qi, F. (2020). The Pathogenicity of 2019 Novel Coronavirus in hACE2 Transgenic Mice. *bioRxiv*.
- Bouvier, N.M. (2015). Animal models for influenza virus transmission studies: a historical perspective. *Curr. Opin. Virol.* 13, 101–108.
- Capraro, G.A., Johnson, J.B., Kock, N.D., and Parks, G.D. (2008). Virus growth and antibody responses following respiratory tract infection of ferrets and mice with WT and P/V mutants of the paramyxovirus Simian Virus 5. *Virology* 376, 416–428.
- Chan, K.F., Carolan, L.A., Korenkov, D., Druce, J., McCaw, J., Reading, P.C., Barr, I.G., and Laurie, K.L. (2018). Investigating viral interference between influenza A virus and human respiratory syncytial virus in a ferret model of infection. *J. Infect. Dis.* 218, 406–417.
- Cui, J., Li, F., and Shi, Z.-L. (2019). Origin and evolution of pathogenic coronaviruses. *Nat. Rev. Microbiol.* 17, 181–192.
- El-Duah, P., Meyer, B., Sylverken, A., Owusu, M., Gottula, L.T., Yeboah, R., Lamptey, J., Frimpong, Y.O., Burimuah, V., Folitse, R., et al. (2019). Development of a whole-virus ELISA for serological evaluation of domestic livestock as possible hosts of human coronavirus NL63. *Viruses* 11, 43.
- Enkirch, T., and von Messling, V. (2015). Ferret models of viral pathogenesis. *Virology* 479–480, 259–270.
- Glass, W.G., Subbarao, K., Murphy, B., and Murphy, P.M. (2004). Mechanisms of host defense following severe acute respiratory syndrome-coronavirus (SARS-CoV) pulmonary infection of mice. *J. Immunol.* 173, 4030–4039.
- ICTV (2020). Naming the 2019 Coronavirus.
- Kim, J.Y., Ko, J.-H., Kim, Y., Kim, Y.-J., Kim, J.-M., Chung, Y.-S., Kim, H.M., Han, M.-G., Kim, S.Y., and Chin, B.S. (2020). Viral Load Kinetics of SARS-CoV-2 Infection in First Two Patients in Korea. *J. Korean Med. Sci.* 35, e86.

- Leung, W.K., To, K.F., Chan, P.K., Chan, H.L., Wu, A.K., Lee, N., Yuen, K.Y., and Sung, J.J. (2003). Enteric involvement of severe acute respiratory syndrome-associated coronavirus infection. *Gastroenterology* 125, 1011–1017.
- Li, K., Wohlford-Lenane, C.L., Channappanavar, R., Park, J.-E., Earnest, J.T., Bair, T.B., Bates, A.M., Brogden, K.A., Flaherty, H.A., Gallagher, T., et al. (2017). Mouse-adapted MERS coronavirus causes lethal lung disease in human DPP4 knockin mice. *Proc. Natl. Acad. Sci. USA* 114, E3119–E3128.
- Lim, J., Jeon, S., Shin, H.-Y., Kim, M.J., Seong, Y.M., Lee, W.J., Choe, K.-W., Kang, Y.M., Lee, B., and Park, S.-J. (2020). Case of the Index Patient Who Caused Tertiary Transmission of COVID-19 Infection in Korea: the Application of Lopinavir/Ritonavir for the Treatment of COVID-19 Infected Pneumonia Monitored by Quantitative RT-PCR. *J. Korean Med. Sci.* 35, e79.
- Lu, R., Zhao, X., Li, J., Niu, P., Yang, B., Wu, H., Wang, W., Song, H., Huang, B., Zhu, N., et al. (2020). Genomic characterisation and epidemiology of 2019 novel coronavirus: implications for virus origins and receptor binding. *Lancet* 395, 565–574.
- Masters, P.S., and Perlman, S. (2013). Coronaviridae. In *Fields Virology*, pp. 825–858.
- Park, S.-J., Kim, E.-H., Pascua, P.N.Q., Kwon, H.-I., Lim, G.-J., Decano, A., Kim, S.M., Song, M.K., Shin, E.-C., and Choi, Y.-K. (2014). Evaluation of heterosubtypic cross-protection against highly pathogenic H5N1 by active infection with human seasonal influenza A virus or trivalent inactivated vaccine immunization in ferret models. *J. Gen. Virol.* 95, 793–798.
- Park, S.-J., Kim, E.-H., Kwon, H.-I., Song, M.-S., Kim, S.M., Kim, Y.-I., Si, Y.-J., Lee, I.-W., Nguyen, H.D., Shin, O.S., et al. (2018). Altered virulence of Highly Pathogenic Avian Influenza (HPAI) H5N8 reassortant viruses in mammalian models. *Virulence* 9, 133–148.
- QIAGEN. (2012). RNeasy Mini Handbook.
- Wan, Y., Shang, J., Graham, R., Baric, R.S., and Li, F. (2020). Receptor recognition by the novel coronavirus from Wuhan: An analysis based on decade-long structural studies of SARS Coronavirus. *J. Virol.* 94, e00127–20.
- WHO (2020). WHO Director-General's opening remarks at the media briefing on COVID-19, <https://www.who.int/dg/speeches/detail/who-director-general-s-opening-remarks-at-the-media-briefing-on-covid-19-11-march-2020>.
- WHO (2020a). 2019-nCoV outbreak is an emergency of international concern. <http://www.euro.who.int/en/health-topics/health-emergencies/coronavirus-covid-19/news/news/2020/01/2019-ncov-outbreak-is-an-emergency-of-international-concern>.
- WHO (2020b). Coronavirus disease 2019 (COVID-19) Situation Report – 63. https://www.who.int/docs/default-source/coronaviruse/situation-reports/20200323-sitrep-63-covid-19.pdf?sfvrsn=d97cb6dd_2.
- Woo, P.C., Lau, S.K., Wong, B.H., Tsoi, H.W., Fung, A.M., Kao, R.Y., Chan, K.H., Peiris, J.S., and Yuen, K.Y. (2005). Differential sensitivities of severe acute respiratory syndrome (SARS) coronavirus spike polypeptide enzyme-linked immunosorbent assay (ELISA) and SARS coronavirus nucleocapsid protein ELISA for serodiagnosis of SARS coronavirus pneumonia. *J. Clin. Microbiol.* 43, 3054–3058.
- Xu, Y., Li, X., Zhu, B., Liang, H., Fang, C., Gong, Y., Guo, Q., Sun, X., Zhao, D., and Shen, J. (2020). Characteristics of pediatric SARS-CoV-2 infection and potential evidence for persistent fecal viral shedding. *Nat. Med.* <https://doi.org/10.1038/s41591-020-0817-4>.
- Zaki, A.M., Van Boheemen, S., Bestebroer, T.M., Osterhaus, A.D., and Fouchier, R.A. (2012). Isolation of a novel coronavirus from a man with pneumonia in Saudi Arabia. *New England Journal of Medicine* 367, 1814–1820.
- Zhong, N.S., Zheng, B.J., Li, Y.M., Poon, L., Xie, Z.H., Chan, K.H., Li, P.H., Tan, S.Y., Chang, Q., Xie, J.P., et al. (2003). Epidemiology and cause of severe acute respiratory syndrome (SARS) in Guangdong, People's Republic of China, in February, 2003. *Lancet* 362, 1353–1358.
- Zhu, N., Zhang, D., Wang, W., Li, X., Yang, B., Song, J., Zhao, X., Huang, B., Shi, W., and Lu, R. (2020). A novel coronavirus from patients with pneumonia in China, 2019. *N. Engl. J. Med.* <https://doi.org/10.1056/NEJMoa2001017>.

STAR★METHODS

KEY RESOURCES TABLE

REAGENT or RESOURCE	SOURCE	IDENTIFIER
Antibodies		
In-house mouse polyclonal antibody	This study	N/A
Bacterial and Virus Strains		
SARS-CoV-2; NMC-nCoV02	This study	N/A
Biological Samples		
Ferret nasal wash samples	This study	See Table 1
Ferret blood samples	This study	See Table 1
Ferret saliva samples	This study	See Table 1
Ferret urine samples	This study	See Table 1
Ferret fecal samples	This study	See Table 1
Chemicals, Peptides, and Recombinant Proteins		
Trypsin	Thermo Fisher Scientific	Cat#15090-046
Carbo-free blocking Solution	VECTOR	Cat#SP-5040
iQ SYBR green supermix	Biorad	Cat#1708882
Penicillin-Streptomycin	GIBCO	Cat#15140-122
Critical Commercial Assays		
Omniscript RT kit	QIAGEN	Cat#205113
RNeasy mini kit	QIAGEN	Cat#74106
Vecstain ABC kit	VECTOR	Cat#PK-6102
DAB substrate kit, peroxidase	VECTOR	Cat#SK-4100
Experimental Models: Cell Lines		
African green monkey: Vero cells	ATCC	Cat#ATCC CCL-81; RRID: CVCL_0059
Experimental Models: Organisms/Strains		
Ferret (<i>Mustela putorius furo</i>)	ID BIO	N/A
Oligonucleotides		
SARS-CoV-2 S F: attcaagactcactttctccaca	This study	See Table 1
SARS-CoV-2 S R: tggttaaagctgtgcattttggtgacc	This study	See Table 1
SARS-CoV-2 ORF1a F: ccctgtgggtttacactaa	This study	See Table S1
SARS-CoV-2 S ORF1a R: tcagctgatgcacaatcgt	This study	See Table S1
Software and Algorithms		
GraphPad Prism 8.3.1	N/A	https://www.graphpad.com/

RESOURCE AVAILABILITY

Lead Contact

Further information and requests for resources and reagents should be directed to and will be fulfilled by the Lead Contact, Young Ki Choi (choiki55@chungbuk.ac.kr).

Materials Availability

All unique/stable reagents generated in this study are available from the Lead Contact with a completed Materials Transfer Agreement.

Data Code and Availability

This study did not generate any unique datasets or code.

EXPERIMENTAL MODEL AND SUBJECT DETAILS

Experimental Animals

Male and female ferrets, 12- to 20- month old and sero-negative for influenza A viruses, MERS-CoV, and SARS-CoV (ID Bio Corporation) were maintained in the isolator (woori IB Corporation) in BSL3 of Chungbuk National University. All ferrets were group housed with a 12 h light/dark cycle and allowed access to diet and water. All animal studies were carried out in accordance with protocols approved by the Institutional Animal Care and Use Committee (IACUC) in Chungbuk National University.

Growth and Isolation of Virus

Virus was isolated from an isolate of SARS-CoV-2 from a COVID-19 confirmed patient in Korea. To infect the animal, viruses were propagated on the Vero cells in the DMEM medium (GIBCO) supplemented with 1% penicillin/streptomycin (GIBCO) and TPCK trypsin (0.5ug/mL; Worthington Biochemical) at 37°C for 72 h. Propagated viruses were stored at –80°C freezer for future usage.

METHOD DETAILS

Study Design for Animal-to-Animal Transmission

12–24 month old male and female ferrets, which were confirmed as Influenza A (H1N1, H3N1), MERS-CoV, and SARS-CoV antibody free ferrets by the standard enzyme-linked immunosorbent assay (ELISA) previously described elsewhere (El-Duah et al., 2019; Park et al., 2014; Woo et al., 2005), were infected through intranasal (IN) route with NMC2019-nCoV02 virus, an isolate of SARS-CoV-2 from a COVID-19 confirmed patient in Korea, 2020 February, at a dose of $10^{5.5}$ TCID₅₀ per ferrets (n = 2). At one-day post-infection, one naive direct contact (DC) and indirect contact (IC) ferrets were introduced into the cage, while IC ferrets were separated from inoculated animals with a partition, which allowed air to move, and without direct contact between animals. This study was conducted with three independent trials. Blood, fecal, nasal wash, saliva, and urine specimens were collected every other day for 12 days from each group of ferrets to detect SARS-CoV-2. Further, to investigate whether each collected specimen contained infectious live virus, we inoculated it onto Vero cells.

To access the replication of the virus in ferrets following SARS-CoV-2 infection in various organs, additional 9 ferrets were infected with SARS-CoV-2 by IN route. Three ferrets were sacrificed at 4, 8 and 12 dpi were and their lung, liver, spleen, kidney, and intestinal tissues were collected with individual scissors to avoid cross contamination.

Quantitative Real-Time RT-PCR (qRT-PCR) to Detect SARS-CoV-2 RNA

Collected ferret secretions were resuspended with cold phosphate-buffered saline (PBS) containing antibiotics (5% penicillin/streptomycin; GIBCO). For virus titration, total RNA was extracted from the collected samples using the RNeasy Mini® kit (QIAGEN, Hilden, Germany) according to the manufacturer's instructions. A cDNA synthesis kit (Omniscript Reverse Transcriptase; QIAGEN, Hilden, Germany) was used to synthesize single strand cDNA using total viral RNA. To quantify viral RNA and viral copy number, quantitative real-time RT-PCR (qRT-PCR) was performed for the partial Spike gene (Table 1) and ORF1a (Table S1) with the SYBR Green kit (iQ™ SYBR Green supermix kit, Bio-Rad, Hercules, CA, USA), and the number of viral RNA copies was calculated and compared to the number of copies of the standard control.

Immunohistochemistry (IHC)

Tissue samples were collected from PBS control and NMC-nCoV02 infected ferrets and incubated in 10% neutral-buffered formalin for fixation before they were embedded in paraffin based to standard procedures. The embedded tissues were sectioned and dried for 3 days at room temperature. To detect the viral antigen by immunohistochemistry, mouse polyclonal antibody developed by inactivated NMC-nCoV02 was used as the primary antibody. Antigen was visualized using the biotin-avidin system (Vector Labs). Slides were viewed using the Olympus IX 71 (Olympus, Tokyo, Japan) microscope with DP controller software to capture images.

QUANTIFICATION AND STATISTICAL ANALYSIS

Statistical Analysis

The statistical significance of infected and contact samples compared with naive sample was assessed by two-way ANOVA with Sidaks multiple comparisons test and one way ANOVA Dunnett's multiple comparisons test. While for the comparison of the significance of viral copy number or titer among samples, we use the two-way ANOVA with Dunnett's multiple comparisons test.

Data plotting, interpolation and statistical analysis were performed using GraphPad Prism 8.2 (GraphPad Software, La Jolla, CA). Statistical details of experiments are described in the figure legends. A p value less than 0.05 is considered statistically significant.

Asymptomatic and Presymptomatic SARS-CoV-2 Infections in Residents of a Long-Term Care Skilled Nursing Facility — King County, Washington, March 2020

Anne Kimball, MD^{1,2}; Kelly M. Hatfield, MSPH¹; Melissa Arons, MSc^{1,2}; Allison James, PhD^{1,2}; Joanne Taylor, PhD^{1,2}; Kevin Spicer, MD¹; Ana C. Bardossy, MD^{1,2}; Lisa P. Oakley, PhD^{1,2}; Sukarma Tanwar, MMed^{1,2}; Zeshan Chisty, MPH¹; Jeneita M. Bell, MD¹; Mark Methner, PhD¹; Josh Harney, MS¹; Jessica R. Jacobs, PhD^{1,3}; Christina M. Carlson, PhD^{1,3}; Heather P. McLaughlin, PhD¹; Nimalie Stone, MD¹; Shauna Clark⁴; Claire Brostrom-Smith, MSN⁴; Libby C. Page, MPH⁴; Meagan Kay, DVM⁴; James Lewis, MD⁴; Denny Russell⁵; Brian Hiatt⁵; Jessica Gant, MS⁵; Jeffrey S. Duchin, MD⁴; Thomas A. Clark, MD¹; Margaret A. Honein, PhD¹; Sujana C. Reddy, MD¹; John A. Jernigan, MD¹; Public Health – Seattle & King County; CDC COVID-19 Investigation Team

On March 27, 2020, this report was posted as an MMWR Early Release on the MMWR website (<https://www.cdc.gov/mmwr>).

Older adults are susceptible to severe coronavirus disease 2019 (COVID-19) outcomes as a consequence of their age and, in some cases, underlying health conditions (1). A COVID-19 outbreak in a long-term care skilled nursing facility (SNF) in King County, Washington that was first identified on February 28, 2020, highlighted the potential for rapid spread among residents of these types of facilities (2). On March 1, a health care provider at a second long-term care skilled nursing facility (facility A) in King County, Washington, had a positive test result for SARS-CoV-2, the novel coronavirus that causes COVID-19, after working while symptomatic on February 26 and 28. By March 6, seven residents of this second facility were symptomatic and had positive test results for SARS-CoV-2. On March 13, CDC performed symptom assessments and SARS-CoV-2 testing for 76 (93%) of the 82 facility A residents to evaluate the utility of symptom screening for identification of COVID-19 in SNF residents. Residents were categorized as asymptomatic or symptomatic at the time of testing, based on the absence or presence of fever, cough, shortness of breath, or other symptoms on the day of testing or during the preceding 14 days. Among 23 (30%) residents with positive test results, 10 (43%) had symptoms on the date of testing, and 13 (57%) were asymptomatic. Seven days after testing, 10 of these 13 previously asymptomatic residents had developed symptoms and were recategorized as presymptomatic at the time of testing. The reverse transcription–polymerase chain reaction (RT-PCR) testing cycle threshold (Ct) values indicated large quantities of viral RNA in asymptomatic, presymptomatic, and symptomatic residents, suggesting the potential for transmission regardless of symptoms. Symptom-based screening in SNFs could fail to identify approximately half of residents with COVID-19. Long-term care facilities should take proactive steps to prevent introduction of SARS-CoV-2 (3). Once a confirmed case is identified in an SNF, all residents should be placed on isolation precautions if possible (3), with considerations for extended use or reuse of personal protective equipment (PPE) as needed (4).

Immediately upon identification of the index case in facility A on March 1, nursing and administrative leadership instituted visitor restrictions, twice-daily assessments of COVID-19 signs and symptoms among residents, and fever screening of all health care personnel at the start of each shift. On March 6, Public Health – Seattle and King County, in collaboration with CDC, recommended infection prevention and control measures, including isolation of all symptomatic residents and use of gowns, gloves, eye protection, facemasks, and hand hygiene for health care personnel entering symptomatic residents' rooms. A data collection tool was developed to ascertain symptom status and underlying medical conditions for all residents.

On March 13, the symptom assessment tool was completed by facility A's nursing staff members by reviewing screening records of residents for the preceding 14 days and by clinician interview of residents at the time of specimen collection. For residents with significant cognitive impairment, symptoms were obtained solely from screening records. A follow-up symptom assessment was completed 7 days later by nursing staff members. Nasopharyngeal swabs were obtained from all 76 residents who agreed to testing and were present in the facility at the time; oropharyngeal swabs were also collected from most residents, depending upon their cooperation. The Washington State Public Health Laboratory performed one-step real-time RT-PCR assay on all specimens using the SARS-CoV-2 CDC assay protocol, which determines the presence of the virus through identification of two genetic markers, the N1 and N2 nucleocapsid protein gene regions (5). The Ct, the cycle number during RT-PCR testing when detection of viral amplicons occurs, is inversely correlated with the amount of RNA present; a Ct value <40 cycles denotes a positive result for SARS-CoV-2, with a lower value indicating a larger amount of viral RNA.

Residents were assessed for stable chronic symptoms (e.g., chronic, unchanged cough) as well as typical and atypical signs and symptoms of COVID-19. Typical COVID-19 signs and symptoms include fever, cough, and shortness of breath (3); potential atypical symptoms assessed included sore throat,

Summary

What is already known about this topic?

Once SARS-CoV-2 is introduced in a long-term care skilled nursing facility (SNF), rapid transmission can occur.

What is added by this report?

Following identification of a case of coronavirus disease 2019 (COVID-19) in a health care worker, 76 of 82 residents of an SNF were tested for SARS-CoV-2; 23 (30.3%) had positive test results, approximately half of whom were asymptomatic or presymptomatic on the day of testing.

What are the implications for public health practice?

Symptom-based screening of SNF residents might fail to identify all SARS-CoV-2 infections. Asymptomatic and presymptomatic SNF residents might contribute to SARS-CoV-2 transmission. Once a facility has confirmed a COVID-19 case, all residents should be cared for using CDC-recommended personal protective equipment (PPE), with considerations for extended use or reuse of PPE as needed.

chills, increased confusion, rhinorrhea or nasal congestion, myalgia, dizziness, malaise, headache, nausea, and diarrhea. Residents were categorized as asymptomatic (no symptoms or only stable chronic symptoms) or symptomatic (at least one new or worsened typical or atypical symptom of COVID-19) on the day of testing or during the preceding 14 days. Residents with positive test results and were asymptomatic at time of testing were reevaluated 1 week later to ascertain whether any symptoms had developed in the interim. Those who developed new symptoms were recategorized as presymptomatic. Ct values were compared for the recategorized symptom groups using one-way analysis of variance (ANOVA) for all residents with positive test results for SARS-CoV-2. Analyses were conducted using SAS statistical software (version 9.4; SAS Institute).

On March 13, among the 82 residents in facility A; 76 (92.7%) underwent symptom assessment and testing; three (3.7%) refused testing, two (2.4%) who had COVID-19 symptoms were transferred to a hospital before testing, and one (1.2%) was unavailable. Among the 76 tested residents, 23 (30.3%) had positive test results.

Demographic characteristics were similar among the 53 (69.7%) residents with negative test results and the 23 (30.3%) with positive test results (Table 1). Among the 23 residents with positive test results, 10 (43.5%) were symptomatic, and 13 (56.5%) were asymptomatic. Eight symptomatic residents had typical COVID-19 symptoms, and two had only atypical symptoms; the most common atypical symptoms reported were malaise (four residents) and nausea (three). Thirteen (24.5%) residents who had negative test results also reported typical and atypical COVID-19 symptoms during the 14 days preceding testing.

One week after testing, the 13 residents who had positive test results and were asymptomatic on the date of testing were reassessed; 10 had developed symptoms and were recategorized as presymptomatic at the time of testing (Table 2). The most common signs and symptoms that developed were fever (eight residents), malaise (six), and cough (five). The mean interval from testing to symptom onset in the presymptomatic residents was 3 days. Three residents with positive test results remained asymptomatic.

Real-time RT-PCR Ct values for both genetic markers among residents with positive test results for SARS-CoV-2 ranged from 18.6 to 29.2 (symptomatic [typical symptoms]), 24.3 to 26.3 (symptomatic [atypical symptoms only]), 15.3 to 37.9 (presymptomatic), and 21.9 to 31.0 (asymptomatic) (Figure). There were no significant differences between the mean Ct values in the four symptom status groups ($p = 0.3$).

Discussion

Sixteen days after introduction of SARS-CoV-2 into facility A, facility-wide testing identified a 30.3% prevalence of infection among residents, indicating very rapid spread, despite early adoption of infection prevention and control measures. Approximately half of all residents with positive test results did not have any symptoms at the time of testing, suggesting that transmission from asymptomatic and presymptomatic residents, who were not recognized as having SARS-CoV-2 infection and therefore not isolated, might have contributed to further spread. Similarly, studies have shown that influenza in the elderly, including those living in SNFs, often manifests as few or atypical symptoms, delaying diagnosis and contributing to transmission (6–8). These findings have important implications for infection control. Current interventions for preventing SARS-CoV-2 transmission primarily rely on presence of signs and symptoms to identify and isolate residents or patients who might have COVID-19. If asymptomatic or presymptomatic residents play an important role in transmission in this population at high risk, additional prevention measures merit consideration, including using testing to guide cohorting strategies or using transmission-based precautions for all residents of a facility after introduction of SARS-CoV-2. Limitations in availability of tests might necessitate taking the latter approach at this time.

Although these findings do not quantify the relative contributions of asymptomatic or presymptomatic residents to SARS-CoV-2 transmission in facility A, they suggest that these residents have the potential for substantial viral shedding. Low Ct values, which indicate large quantities of viral RNA, were identified for most of these residents, and there was no statistically significant difference in distribution of Ct values among the symptom status groups. Similar Ct values were reported in asymptomatic adults in China who were known to

TABLE 1. Demographics and reported symptoms for residents of a long-term care skilled nursing facility at time of testing* (N = 76), by SARS-CoV-2 test results — facility A, King County, Washington, March 2020

Characteristic	Initial SARS-CoV-2 test results	
	Negative, no. (%)	Positive, no. (%)
Overall	53 (100)	23 (100)
Women	32 (60.4)	16 (69.6)
Age, mean (SD)	75.1 (10.9)	80.7 (8.4)
Current smoker†	7 (13.2)	1 (4.4)
Long-term admission type to facility A	35 (66.0)	15 (65.2)
Length of stay in facility A before test date, days, median (IQR)	94 (40–455)	70 (21–504)
Symptoms in last 14 days		
Symptomatic	13 (24.5)	10 (43.5)
At least one typical COVID-19 symptom§	9 (17.0)	8 (34.8)
Only atypical COVID-19 symptoms¶	4 (7.5)	2 (8.7)
Asymptomatic	40 (75.5)	13 (56.5)
No symptoms	32 (60.4)	8 (34.8)
Only stable, chronic symptoms	8 (15.1)	5 (21.7)
Specific signs and symptoms reported as new or worse in last 14 days		
Typical symptoms		
Fever	3 (5.7)	1 (4.3)
Cough	6 (11.3)	7 (30.4)
Shortness of breath	0 (0)	1 (4.4)
Atypical symptoms		
Malaise	1 (1.9)	4 (17.4)
Nausea	0 (0)	3 (13.0)
Sore throat	2 (3.8)	2 (8.7)
Confusion	2 (3.8)	1 (4.4)
Dizziness	1 (1.9)	1 (4.4)
Diarrhea	3 (5.7)	1 (4.4)
Rhinorrhea/Congestion	1 (1.9)	0 (0)
Myalgia	0 (0)	0 (0)
Headache	0 (0)	0 (0)
Chills	0 (0)	0 (0)
Any preexisting medical condition listed	53 (100)	22 (95.7)
Specific conditions**		
Chronic lung disease	16 (30.2)	10 (43.5)
Diabetes	20 (37.7)	9 (39.1)
Cardiovascular disease	36 (67.9)	20 (87.0)
Cerebrovascular accident	19 (35.9)	8 (34.8)
Renal disease	18 (34.0)	9 (39.1)
Received hemodialysis	2 (3.8)	2 (8.7)
Cognitive Impairment	28 (52.8)	13 (56.5)
Obesity	11 (20.8)	6 (26.1)

Abbreviations: COVID-19 = coronavirus disease 2019; IQR = interquartile range, SD = standard deviation.

* Testing performed on March 13, 2020.

† Unknown for one resident with negative test results.

§ Typical symptoms include fever, cough, and shortness of breath.

¶ Atypical symptoms include chills, malaise, sore throat, increased confusion, rhinorrhea or nasal congestion, myalgia, dizziness, headache, nausea, and diarrhea.

** Residents might have multiple conditions.

transmit SARS-CoV-2 (9). Studies to determine the presence of viable virus from these specimens are currently under way.

SNFs have additional infection prevention and control challenges compared with those of assisted living or independent living long-term care facilities. For example, SNF residents might be in shared rooms rather than individual apartments, and there is often prolonged and close contact between residents and health care providers related to the residents' medical conditions and cognitive function. The index patient in this outbreak was a health care provider, which might have contributed to rapid spread in the facility. In addition, health care personnel in all types

of long-term care facilities might have limited experience with proper use of PPE. Symptom ascertainment and room isolation can be exceptionally challenging in elderly residents with neurologic conditions, including dementia. In addition, symptoms of COVID-19 are common and might have multiple etiologies in this population; 24.5% of facility A residents with negative test results for SARS-CoV-2 reported typical or atypical symptoms.

The findings in this report are subject to at least two limitations. First, accurate symptom ascertainment in persons with cognitive impairment and other disabilities is challenging; however, this limitation is estimated to be representative of

TABLE 2. Follow-up symptom assessment 1 week after testing for SARS-CoV-2 among 13 residents of a long-term care skilled nursing facility who were asymptomatic on March 13, 2020 (date of testing) and had positive test results — facility A, King County, Washington, March 2020

Symptom status 1 week after testing	No. (%)
Asymptomatic	3 (23.1)
Developed new symptoms	10 (76.7)
Fever	8 (61.5)
Malaise	6 (46.1)
Cough	5 (38.4)
Confusion	4 (30.8)
Rhinorrhea/Congestion	4 (30.8)
Shortness of breath	3 (23.1)
Diarrhea	3 (23.1)
Sore throat	1 (7.7)
Nausea	1 (7.7)
Dizziness	1 (7.7)

symptom data collected in most SNFs, and thus, these findings might be generalizable. Second, because this analysis was conducted among residents of an SNF, it is not known whether findings apply to the general population, including younger persons, those without underlying medical conditions, or similarly aged populations in the general community.

This analysis suggests that symptom screening could initially fail to identify approximately one half of SNF residents with SARS-CoV-2 infection. Unrecognized asymptomatic and presymptomatic infections might contribute to transmission in these settings. During the current COVID-19 pandemic, SNFs and all long-term care facilities should take proactive steps to prevent introduction of SARS-CoV-2, including restricting visitors except in compassionate care situations, restricting nonessential personnel from entering the building, asking staff members to monitor themselves for fever and other symptoms, screening all staff members at the beginning of their shift for fever and other symptoms, and supporting staff member sick leave, including for those with mild symptoms (3). Once a facility has a case of COVID-19, broad strategies should be implemented to prevent transmission, including restriction of resident-to-resident interactions, universal use of facemasks for all health care personnel while in the facility, and if possible, use of CDC-recommended PPE for the care of all residents (i.e., gown, gloves, eye protection, N95 respirator, or, if not available, a face mask) (3). In settings where PPE supplies are limited, strategies for extended PPE use and limited reuse should be employed (4). As testing availability improves, consideration might be given to test-based strategies for identifying residents with SARS-CoV-2 infection for the purpose of cohorting, either in designated units within a facility or in a separate facility designated for residents with COVID-19. During the COVID-19 pandemic, collaborative efforts are crucial to protecting the most vulnerable populations.

Acknowledgments

Nursing and administrative leaders at facility A; Washington State Public Health Laboratory's SARS-CoV-2 testing team.

Public Health – Seattle & King County

Atar Baer, Public Health – Seattle & King County; Leslie M. Barnard, Public Health – Seattle & King County; Eileen Benoliel, Public Health – Seattle & King County; Meaghan S. Fagalde, Public Health – Seattle & King County; Jessica Ferro, Public Health – Seattle & King County; Hal Garcia Smith, Public Health – Seattle & King County; Elysia Gonzales, Public Health – Seattle & King County; Noel Hatley, Public Health – Seattle & King County; Grace Hatt, Public Health – Seattle & King County; Michaela Hope, Public Health – Seattle & King County; Melinda Huntington-Frazier, Public Health – Seattle & King County; Vance Kawakami, Public Health – Seattle & King County; Jennifer L. Lenahan, Public Health – Seattle & King County; Margaret D. Lukoff, Public Health – Seattle & King County; Emily B. Maier, Public Health – Seattle & King County; Shelly McKeirnan, Public Health – Seattle & King County; Patricia Montgomery, Public Health – Seattle & King County; Jennifer L. Morgan, Public Health – Seattle & King County; Laura A. Mummert, Public Health – Seattle & King County; Sargis Pogojans, Public Health – Seattle & King County; Francis X. Riedo, Public Health – Seattle & King County; Leilani Schwarcz, Public Health – Seattle & King County; Daniel Smith, Public Health – Seattle & King County; Steve Stearns, Public Health – Seattle & King County; Kaitlyn J. Sykes, Public Health – Seattle & King County; Holly Whitney, Public Health – Seattle & King County.

CDC COVID-19 Investigation Team

Hammad Ali, CDC; Michelle Banks, CDC; Arun Balajee, CDC; Eric J. Chow, CDC; Barbara Cooper, CDC; Dustin W. Currie, CDC; Jonathan Dyal, CDC; Jessica Healy, CDC; Michael Hughes, CDC; Temet M. McMichael, CDC; Leisha Nolen, CDC; Christine Olson, CDC; Agam K. Rao, CDC; Kristine Schmit, CDC; Noah G. Schwartz, CDC; Farrell Tobolowsky, CDC; Rachael Zacks, CDC; Suzanne Zane, CDC.

Corresponding author: Anne Kimball, opu7@cdc.gov, 770-488-7100.

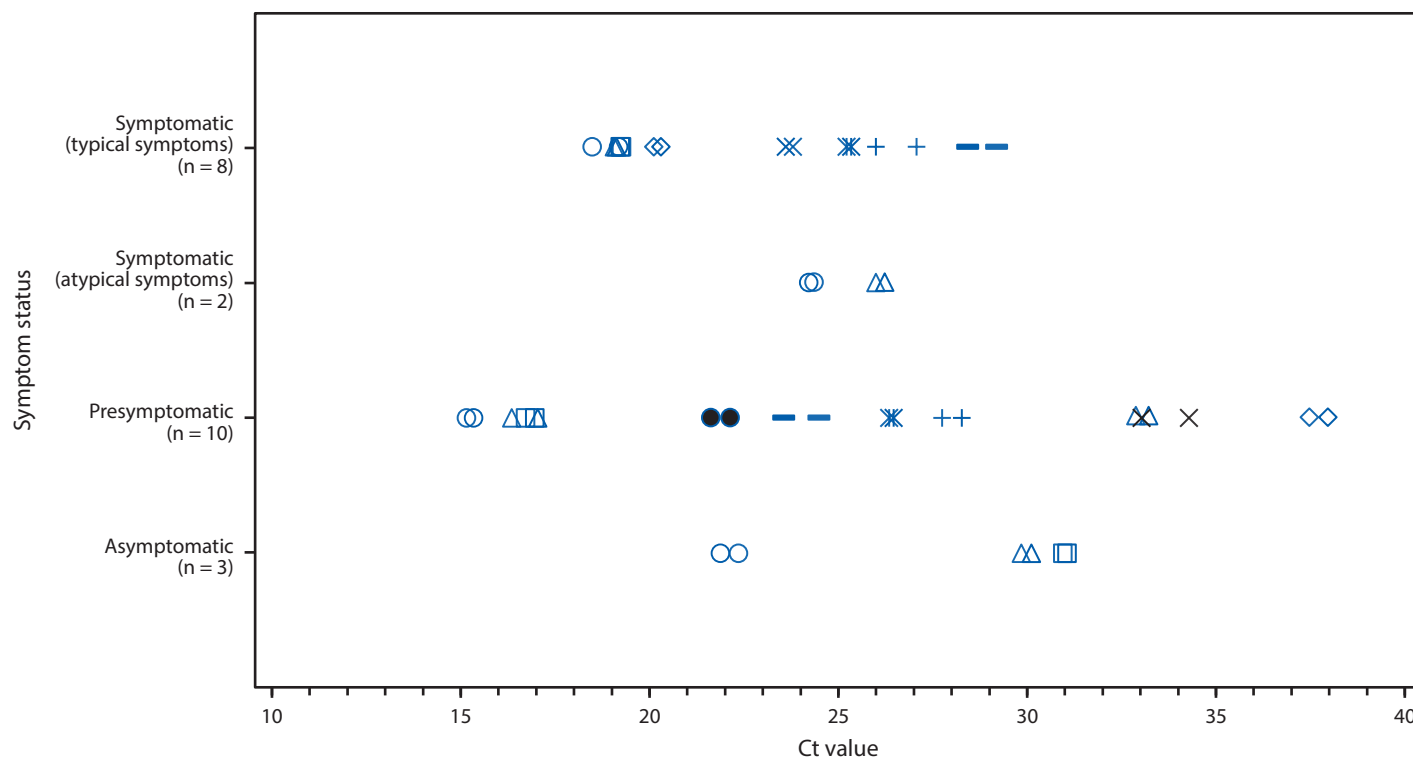
¹CDC COVID-19 Investigation Team; ²Epidemic Intelligence Service, CDC; ³Laboratory Leadership Service, CDC; ⁴Public Health – Seattle & King County; ⁵Washington State Public Health Laboratory.

All authors have completed and submitted the International Committee of Medical Journal Editors form for disclosure of potential conflicts of interest. No potential conflicts of interest were disclosed.

References

1. CDC COVID-19 Response Team. Severe outcomes among patients with coronavirus disease 2019 (COVID-19)—United States, February 12–March 16, 2020. *MMWR Morb Mortal Wkly Rep* 2020;69:343–6. <https://dx.doi.org/10.15585/mmwr.mm6912e2>
2. McMichael TM, Clark S, Pogojans S, et al. COVID-19 in a long-term care facility—King County, Washington, February 27–March 9, 2020. *MMWR Morb Mortal Wkly Rep* 2020;69:339–42. <https://dx.doi.org/10.15585/mmwr.mm6912e1>

FIGURE. Cycle threshold (Ct) values* for residents of a long-term care skilled nursing facility with positive test results for SARS-CoV-2 by real-time reverse transcription–polymerase chain reaction on March 13, 2020 (n = 23), by symptom status^{†,§} at time of test — facility A, King County, Washington



* Ct values are the number of cycles needed for detection of each genetic marker identified by real-time reverse transcription–polymerase chain reaction testing. A lower Ct value indicates a higher amount of viral RNA. Paired values for each resident are depicted using a different shape. Each resident has two Ct values for the two genetic markers (N1 and N2 nucleocapsid protein gene regions).

[†] Typical symptoms include fever, cough, and shortness of breath.

[§] Atypical symptoms include chills, malaise, sore throat, increased confusion, rhinorrhea or nasal congestion, myalgia, dizziness, headache, nausea, and diarrhea.

3. CDC. Preparing for COVID-19: long-term care facilities, nursing homes. Atlanta, GA: US Department of Health and Human Services, CDC; 2020. <https://www.cdc.gov/coronavirus/2019-ncov/healthcare-facilities/prevent-spread-in-long-term-care-facilities.html>

4. CDC. Strategies for optimizing the supply of PPE. Atlanta, GA: US Department of Health and Human Services, CDC; 2020. <https://www.cdc.gov/coronavirus/2019-ncov/hcp/ppe-strategy/index.html>

5. CDC. Interim guidelines for collecting, handling, and testing clinical specimens from persons for coronavirus disease 2019 (COVID-19). Atlanta, GA: US Department of Health and Human Services, CDC; 2020. <https://www.cdc.gov/coronavirus/2019-nCoV/lab/guidelines-clinical-specimens.html>

6. Lam PP, Coleman BL, Green K, et al. Predictors of influenza among older adults in the emergency department. *BMC Infect Dis* 2016;16:615. <https://doi.org/10.1186/s12879-016-1966-4>

7. Lansbury LE, Brown CS, Nguyen-Van-Tam JS. Influenza in long-term care facilities. *Influenza Other Respir Viruses* 2017;11:356–66. <https://doi.org/10.1111/irv.12464>

8. Sayers G, Igoe D, Carr M, et al. High morbidity and mortality associated with an outbreak of influenza A(H3N2) in a psycho-geriatric facility. *Epidemiol Infect* 2013;141:357–65. <https://doi.org/10.1017/S0950268812000659>

9. Zou L, Ruan F, Huang M, et al. SARS-CoV-2 viral load in upper respiratory specimens of infected patients. *N Engl J Med* 2020;382:1177–9. <https://doi.org/10.1056/NEJMc2001737>

Antiviral Potential of ERK/MAPK and PI3K/AKT/mTOR Signaling Modulation for Middle East Respiratory Syndrome Coronavirus Infection as Identified by Temporal Kinome Analysis

Jason Kindrachuk,^a Britini Ork,^a Brit J. Hart,^a  Steven Mazur,^a Michael R. Holbrook,^a Matthew B. Frieman,^b Dawn Traynor,^a Reed F. Johnson,^c Julie Dyall,^a  Jens H. Kuhn,^a Gene G. Olinger,^a Lisa E. Hensley,^a  Peter B. Jahrling^{a,c}

Integrated Research Facility, National Institute of Allergy and Infectious Diseases, National Institutes of Health, Frederick, Maryland, USA^a; Department of Microbiology and Immunology, University of Maryland at Baltimore, Baltimore, Maryland, USA^b; Emerging Viral Pathogens Section, National Institute of Allergy and Infectious Diseases, National Institutes of Health, Frederick, Maryland, USA^c

Middle East respiratory syndrome coronavirus (MERS-CoV) is a lineage C betacoronavirus, and infections with this virus can result in acute respiratory syndrome with renal failure. Globally, MERS-CoV has been responsible for 877 laboratory-confirmed infections, including 317 deaths, since September 2012. As there is a paucity of information regarding the molecular pathogenesis associated with this virus or the identities of novel antiviral drug targets, we performed temporal kinome analysis on human hepatocytes infected with the Erasmus isolate of MERS-CoV with peptide kinome arrays. bioinformatics analysis of our kinome data, including pathway overrepresentation analysis (ORA) and functional network analysis, suggested that extracellular signal-regulated kinase (ERK)/mitogen-activated protein kinase (MAPK) and phosphoinositol 3-kinase (PI3K)/serine-threonine kinase (AKT)/mammalian target of rapamycin (mTOR) signaling responses were specifically modulated in response to MERS-CoV infection *in vitro* throughout the course of infection. The overrepresentation of specific intermediates within these pathways determined by pathway and functional network analysis of our kinome data correlated with similar patterns of phosphorylation determined through Western blot array analysis. In addition, analysis of the effects of specific kinase inhibitors on MERS-CoV infection in tissue culture models confirmed these cellular response observations. Further, we have demonstrated that a subset of licensed kinase inhibitors targeting the ERK/MAPK and PI3K/AKT/mTOR pathways significantly inhibited MERS-CoV replication *in vitro* whether they were added before or after viral infection. Taken together, our data suggest that ERK/MAPK and PI3K/AKT/mTOR signaling responses play important roles in MERS-CoV infection and may represent novel drug targets for therapeutic intervention strategies.

Middle East respiratory syndrome (MERS) is a viral respiratory disease that results from infection with the MERS coronavirus (MERS-CoV) and was first identified in a patient with acute pneumonia and renal failure in Jeddah, Kingdom of Saudi Arabia, in June 2012 (1). Subsequently, there have been 877 laboratory-confirmed MERS-CoV infections to date, including 317 deaths (<http://www.who.int/csr/don/16-october-2014-mers/en/>), resulting in a case fatality rate of 30%, with all cases directly or indirectly being linked to the Middle East region (2). Recent announcements of laboratory-confirmed cases of MERS-CoV infection in patients in the United States and the Netherlands have further exacerbated concerns regarding the global evolution of this epidemic (3).

MERS-CoV belongs to the same genus (*Betacoronavirus*) as severe acute respiratory syndrome (SARS) coronavirus (SARS-CoV), which was responsible for the global SARS pandemic of 2002 and 2003 that affected more than 8,000 people (4), and the human coronaviruses (HCoVs) HKU1 and OC43, which cause mild to moderate respiratory disease (5). Further, MERS-CoV is the first lineage 2c betacoronavirus shown to infect humans (6, 7). Although the natural reservoir for MERS-CoV has yet to be determined, it has been suggested that bats are a likely candidate, given the similarity of MERS-CoV to bat coronaviruses (8). Recent evidence has also suggested that dromedary camels may act as an intermediate host for MERS-CoV, as supported by serological, genetic, and epidemiological evidence as well as the recent isolation of the virus (9, 10). Animal-to-human transmission has

largely been suspected to be the primary contributor to the recent outbreaks of MERS-CoV. Although human-to-human transmission has been reported in several case clusters, there is currently no evidence for sustained community transmission (11). MERS-CoV infections have been associated with severe lower respiratory tract infections, including acute respiratory syndrome with renal failure. Interestingly, the severity of disease presentation appears to be related to underlying comorbidities, as MERS-CoV infections in healthy individuals appear to result primarily in mild to asymptomatic disease (1, 12, 13).

Though appreciable efforts have been made to identify novel

Received 17 June 2014. Returned for modification 22 July 2014.

Accepted 29 October 2014.

Accepted manuscript posted online 8 December 2014.

Citation Kindrachuk J, Ork B, Hart BJ, Mazur S, Holbrook MR, Frieman MB, Traynor D, Johnson RF, Dyall J, Kuhn JH, Olinger GG, Hensley LE, Jahrling PB. 2015. Antiviral potential of ERK/MAPK and PI3K/AKT/mTOR signaling modulation for Middle East respiratory syndrome coronavirus infection as identified by temporal kinome analysis. *Antimicrob Agents Chemother* 59:1088–1099. doi:10.1128/AAC.03659-14.

Address correspondence to Jason Kindrachuk, kindrachuk.kenneth@nih.gov.

Supplemental material for this article may be found at <http://dx.doi.org/10.1128/AAC.03659-14>.

Copyright © 2015, American Society for Microbiology. All Rights Reserved. doi:10.1128/AAC.03659-14

antiviral therapeutics for MERS-CoV, there are currently no approved therapeutic interventions available, and treatment is based on supportive care (14). Initial investigations of interferon (IFN) demonstrated that alpha interferon (IFN- α), IFN- γ , and IFN- β were able to inhibit MERS-CoV replication (15, 16). Subsequent studies demonstrated that among the different interferons, IFN- β had the strongest inhibitory activity against MERS-CoV (17). Mycophenolic acid, IFN- β , and ribavirin have been demonstrated to have strong inhibitory activities against MERS-CoV *in vitro* (17, 18), and Falzarano et al. demonstrated that the administration of IFN- α 2b and ribavirin resulted in synergistic antiviral activities both *in vitro* and *in vivo* in rhesus macaques (19). Josset and colleagues employed systems-level gene expression analysis of MERS-CoV infection *in vitro* and identified that IFN- α 5 and IFN- β were specifically upregulated by MERS-CoV infection (20).

Surveys of the host response to infection through either genomic or proteomic technologies have previously been employed to characterize microbial pathogenesis and identify novel therapeutic targets (21–24). The incorporation of systems-level analysis to such investigations provides a unique opportunity to identify specific host or pathogen responses that are modulated during the course of infection. A global transcriptome analysis of host responses to MERS-CoV and SARS-CoV infection suggested that MERS-CoV modulated transcriptional changes in the host differently from the way in which SARS-CoV did, although viral replication kinetics were similar for both viruses (20). Subsequent systems-level analysis of the transcriptome data suggested that changes in the host transcriptome in response to either MERS-CoV or SARS-CoV may be related to the activation state of cell signaling networks. Further, the authors demonstrated that the identification of specific cellular intermediates through upstream regulator analysis could be used to predict potential host targets for therapeutic intervention. However, many cellular processes are regulated independently of changes in transcriptional or translational regulation through kinase-mediated modulation of cell signaling networks. Characterization of the activation state of cellular host kinases, or the kinome, provides a mechanism to identify the individual kinases and/or signaling networks that are of central importance to disease progression or resolution. Previously, we demonstrated the utility of species-specific kinome analysis with peptide kinome arrays for characterizing the modulation of host cell signaling networks, including responses to infection (25, 26).

Here, we have characterized the temporal host kinome response of human hepatocytes to infection with MERS-CoV isolate HCoV-EMC/2012 (MERS-CoV) and identified specific cell signaling networks and kinases that are modulated during the course of infection and may represent novel antiviral targets. As it has previously been demonstrated that Huh7 hepatocytes are highly permissive to MERS-CoV (27) and it is postulated that targets found to be overrepresented in our data sets would potentially represent conserved targets across multiple permissive cell types, we have focused on these cells for our analysis. Subsequent systems biology approaches, including pathway overrepresentation analysis (ORA) and functional network analysis (FNA), were used to identify and compare the specific kinome and cell signaling responses that were modulated throughout the course of MERS-CoV infection. Analysis of our kinome data suggested that extracellular signal-regulated kinase (ERK)/mitogen-activated protein kinase (MAPK) and phosphoinositol 3-kinase (PI3K)/ser-

ine-threonine kinase (AKT)/mammalian target of rapamycin (mTOR) signaling responses were specifically modulated in response to MERS-CoV infection *in vitro*. The phosphorylation patterns of specific intermediates within these pathways in the kinome array data correlated with the phosphorylation patterns from Western blot dot arrays. In addition, we confirmed these cellular responses through analysis of the effects of inhibition of these pathways or their intermediates on MERS-CoV infection in tissue culture models. Further, we have demonstrated that a subset of the licensed kinase inhibitors targeting the ERK/MAPK and PI3K/AKT/mTOR pathways significantly inhibited MERS-CoV propagation *in vitro* whether they were added before or after viral infection. Taken together, our investigation demonstrates that ERK/MAPK and PI3K/AKT/mTOR signaling responses play a critical role in MERS-CoV pathogenesis and may be potential targets for therapeutic intervention strategies.

MATERIALS AND METHODS

Cells and virus. Huh7 is a hepatocyte-derived epithelial-like cell line, and Huh7 cells were maintained in Dulbecco's minimal essential medium (DMEM; Sigma-Aldrich) supplemented with 10% (vol/vol) heat-inactivated fetal bovine serum (FBS) in a 37°C humidified incubator with 5% (vol/vol) CO₂. MERS-CoV isolate HCoV-EMC/2012 (MERS-CoV), kindly provided by Rocky Mountain Laboratories (NIH/NIHAIID) and the Viroscience Laboratory, Erasmus Medical Center (Rotterdam, Netherlands), was used for all experiments and propagated as reported previously (28).

Chemical inhibitors. The United States Food and Drug Administration (FDA)-licensed drugs tested (sorafenib, everolimus, dabrafenib, cabozantinib, afatinib, selumetinib, trametinib, and miltefosine) were purchased from Selleck Chemicals. Additional kinase inhibitors tested included AG490, PKC-412, GF109203X, SB203580, wortmannin, Bay 11-7082, GW5074, PP2, and rapamycin (sirolimus), as well as an inhibitor of nitric oxide synthase 2 (NOS2), L-nitro-arginine methyl ester (L-NAME). All were purchased from Enzo Scientific. The inhibitors were reconstituted according to the manufacturers' recommendations in either water or dimethyl sulfoxide (DMSO).

Viral infections for kinome analysis. Huh7 cells were plated in 6-well plates in fresh DMEM supplemented with 2% (vol/vol) FBS and rested for 24 h prior to infection. Cells were infected with MERS-CoV at a multiplicity of infection (MOI) of 0.05 for 1 h at 37°C in 5% CO₂ with periodic rocking. Following incubation, Huh7 cells were washed twice with phosphate-buffered saline (PBS) to remove unbound virus, replenished with fresh DMEM supplemented with 2% (vol/vol) FBS, and incubated at 37°C in 5% CO₂. MERS-CoV-infected and mock-infected cells and cell culture supernatant were harvested at identified time points (1, 6, and 24 h postinfection [p.i.]) for subsequent kinome analysis. Plaque assays were performed on Vero E6 cells as reported previously (17).

Kinome analysis with peptide arrays. The design, construction, and application of peptide arrays were based upon a previously reported protocol (29). Briefly, MERS-CoV-infected and mock-infected Huh7 cells were scraped and pelleted at 1, 6, and 24 h p.i. Following this, the cell supernatants were discarded and the cell pellets were lysed with 100 μ l of lysis buffer (20 mM Tris-HCl, pH 7.5, 150 mM NaCl, 1 mM EDTA, 1 mM EGTA, 1% Triton X-100, 2.5 mM sodium pyrophosphate, 1 mM Na₂VO₄, 1 mM NaF, 1 μ g/ml leupeptin, 1 μ g/ml aprotinin, 1 mM phenylmethylsulfonyl fluoride) and incubated on ice for 10 min, followed by centrifugation to remove cell debris. Cell lysates were transferred to fresh microcentrifuge tubes, and the total protein from the cell lysates was measured using a bicinchoninic acid (BCA) assay (Pierce) to calculate cell lysate volumes to ensure the loading of equal amounts of total protein onto the arrays. Activation mix (50% glycerol, 50 μ M ATP, 60 mM MgCl₂, 0.05% Brij 35, 0.25 mg/ml bovine serum albumin) was added to the cell lysate fractions, the mixture was spotted onto human kinome arrays (JPT Tech-

nologies), and the arrays were incubated for 2 h at 37°C as described previously (22). The kinome arrays were subsequently washed once with PBS containing 1% Triton X-100, followed by a single wash in deionized H₂O. The peptide arrays were held on dry ice and subjected to gamma irradiation (5 Mrd) to inactivate any residual virus following removal from biocontainment. Kinome arrays were submerged in PRO-Q Diamond phosphoprotein stain (Invitrogen) with gentle agitation in the dark for 1 h. Following staining, the arrays were washed in destain (20% acetonitrile, 50 mM sodium acetate, pH 4.0 [Sigma-Aldrich]) 3 times for 10 min per wash, with the addition of fresh destain each time. A final wash was performed with deionized H₂O, and the arrays were placed in 50-ml conical tubes to air dry for 20 min. The remaining moisture was removed by centrifugation of the arrays at 300 × *g* for 3 min. Array images were acquired using a PowerScanner microarray scanner (Tecan) at 532 to 560 nm with a 580-nm filter to detect dye fluorescence. Images were collected using GenePix (version 6.0) software (MDS). Signal intensity values were collected using GenePix (version 6.0) software (MDS). All data processing and subsequent analysis were performed using Platform for Integrated, Intelligent Kinome Analysis (PIIKA) software (<http://sapphire.usask.ca/sapphire/piika>) (29, 30) as described previously (22).

Pathway overrepresentation analysis and functional network analysis. Pathway overrepresentation analysis of differentially phosphorylated proteins was performed using InnateDB software, a publically available resource that predicts biological pathways on the basis of experimental fold change data sets in humans, mice, and bovines (31). Pathways are assigned a probability (*P*) value on the basis of the number of genes present for a particular pathway as well as the degree to which they are differentially expressed or modified relative to their expression under a control condition. For our investigation, input data were limited to peptides that demonstrated consistent responses across the biological replicates (*P* < 0.05) as well as statistically significant changes in expression from that under the control condition (*P* < 0.20), as reported previously (29). Additionally, functional networks were created using Ingenuity Pathway Analysis (IPA) software (Ingenuity Systems, Redwood City, CA). Protein identifiers and the respective phosphorylation fold change values and *P* values were uploaded and mapped to their corresponding protein objects in the IPA knowledge base. Networks of these proteins were algorithmically generated on the basis of their connectivity and assigned a score. Proteins are represented as nodes, and the biological relationship between two nodes is represented as an edge (a solid line for direct relationships and a dotted line for indirect relationships). The intensity of the node color indicates the degree of upregulation (red) or downregulation (green) of phosphorylation. Proteins in uncolored nodes were not identified as being differentially expressed in our experiment and were integrated into the computationally generated networks on the basis of the evidence stored in the IPA knowledge database indicating a relevance to this network.

Western blot array analysis of protein phosphorylation. Huh7 cells were infected with MERS-CoV or mock infected, as described above. Cells from infected or mock-infected cells were harvested at 1, 6, or 24 h p.i., lysed in SDS loading buffer without bromophenol blue (200 mM Tris-HCl, pH 6.8, 8% SDS, 40% glycerol, 4% β-mercaptoethanol, 50 mM EDTA), and boiled for 20 min at 95°C to inactivate remaining virus (as approved within facility-specific standard operating procedures). Following inactivation, supernatants were removed from biocontainment and boiled again for 20 min at 95°C for subsequent analysis. The protein concentration was determined using a BCA protein assay kit (Pierce), according to the manufacturer's instructions. Equal amounts of protein from mock-infected or MERS-CoV-infected samples were loaded onto PathScan intracellular signaling antibody array membranes (Cell Signaling Technologies) and analyzed according to the manufacturer's instructions. Images were acquired using a Syngene G:Box Chemi system (Syngene), and quantification of antibody spot intensities was performed using the ImageJ software suite (32).

Cytotoxicity assays. Kinase inhibitor cytotoxicity was determined using the Cytotox colorimetric assay, which measures the amount of lactate dehydrogenase (LDH; Promega) released from treated cells, following the manufacturer's instructions. Huh7 cells were incubated with each of the drugs for 24 h in a 37°C incubator with 5% CO₂ using the inhibitory concentrations used in the assays below. The cell culture supernatants were then used in the Cytotox 96-well assay, and the absorbance at 490 nm was read with a M1000 Tecan plate reader.

Cell-based ELISA for analysis of inhibition of MERS-CoV infection by kinase inhibitors. Huh7 cells were plated in black, opaque-bottom 96-well plates and allowed to rest for 24 h prior to infection and treatments. The cells were pretreated for either 1 h prior to infection or 2 h postinfection with kinase inhibitors at final concentrations of 0.1, 1, and 10 μM. The final concentration of DMSO was 0.1% for all experimental conditions. Cells were infected with MERS-CoV at an MOI of 0.05 and allowed to incubate for 48 h at 37°C in 5% CO₂ prior to fixation. After 48 h, the cells were fixed with 10% neutral buffered formalin (NBF) for 30 min, the NBF was changed, and the cells were fixed for an additional 24 h at 4°C to ensure viral inactivation following facility-specific standard operating procedures. Viral inhibition was then determined utilizing a cell-based enzyme-linked immunosorbent assay (ELISA) as described by Hart et al. (17).

Plaque reduction assay for analysis of inhibition of MERS-CoV infection by kinase inhibitors. To determine the antiviral activity of the kinase inhibitors, Huh7 cells were incubated with select kinase inhibitors (10 μM) for 1 h prior to infection with MERS-CoV. Cells were infected with MERS-CoV at an MOI of 0.05 for 1 h at 37°C in 5% CO₂ with periodic rocking. Following incubation, Huh7 cells were washed twice with PBS to remove unbound virus, replenished with fresh DMEM supplemented with 2% (vol/vol) FBS, and incubated at 37°C in 5% CO₂ with or without readministration of the same kinase inhibitor (10 μM). Cell supernatants from the infected and mock-infected cells were harvested 48 h p.i., and the inhibitory activity of the kinase inhibitor-treated cells was assessed by plaque reduction assay as described previously (17).

RESULTS

Temporal kinome analysis of MERS-CoV-infected hepatocytes.

To gain insight into potential host signaling networks or kinases that are modulated during MERS-CoV infection and that may represent novel therapeutic targets, we performed temporal kinome analysis of MERS-CoV-infected Huh7 human hepatocytes. Previously, de Wilde et al. demonstrated that Huh7 cells were highly permissive to MERS-CoV infection (27), and we postulated that host signaling networks or individual proteins identified by our analysis may be broadly conserved across multiple cell types targeted by MERS-CoV. In addition, we employed a low multiplicity of infection (MOI = 0.01) to identify host signaling networks or intermediates in an effort to recapitulate circumstances in which host cells would encounter small amounts of virus (i.e., during the initial phases of natural infection). Cells were harvested at multiple time points (1, 6, and 24 h) postinfection (p.i.) alongside time-matched, mock-infected control cells. Kinome analysis with peptide arrays relies on the phosphorylation of specific kinase targets (immobilized peptides) on the arrays by active kinases in a cell lysate (22). Our arrays contained 340 unique peptides representing key phosphorylation events from a broad spectrum of cell signaling pathways and processes. The kinome data were extracted from the arrays and analyzed using the PIIKA software tool (29, 30). Hierarchical clustering analysis demonstrated that the MERS-CoV-infected sample harvested at 1 h p.i. clustered between the mock-infected samples, whereas the MERS-CoV samples harvested at 6 h and 24 h p.i. clustered outside the mock-infected samples, suggesting an increased diversity in the host

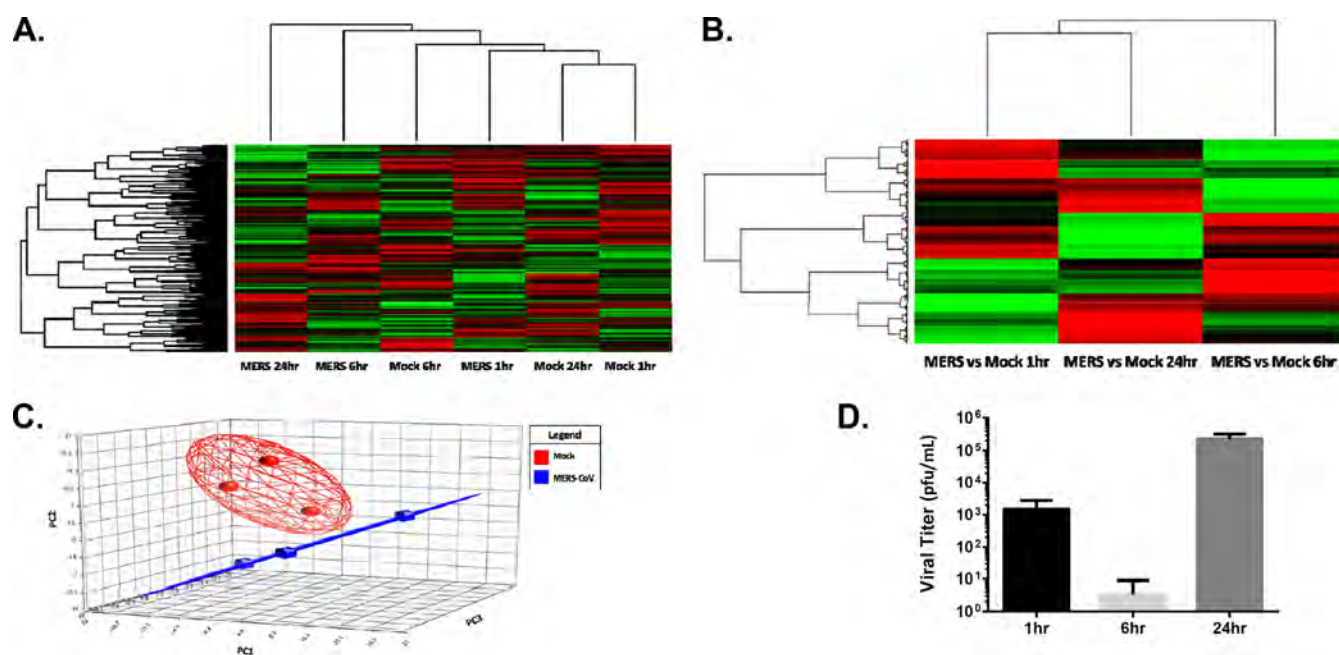


FIG 1 Heat maps and hierarchical clustering of host kinome responses to MERS-CoV infection. Peptide phosphorylation was assessed by densitometry. The results were scaled and normalized using GeneSpring (version 6.0) software. For hierarchical clustering, $1 -$ Pearson correlation coefficient was used as the distance metric and the McQuitty method was used as the linkage method. (A) Hierarchical clustering of the MERS-CoV-infected kinome data sets alongside the mock-infected control data sets. (B) Cluster analysis of the MERS-CoV-infected kinome data sets following background subtraction of the time-matched mock-infected control data sets. Spots demonstrating a significant differential phosphorylation between the MERS-CoV-infected and mock-infected control were compiled into a data set for each time point for comparative analysis. The lines at the top of the heat maps indicate the relative similarity between the conditions listed along the bottom edge of the heat maps. Line length indicates the degree of similarity, with shorter lines equating to stronger similarity. The lines on the left side of the heat maps indicate the relative similarity of the signal between the 300 individual peptide targets on the arrays. Red indicates increased phosphorylation; green indicates decreased phosphorylation. (C) Principal component analysis of the mock- and MERS-CoV-infected kinome data sets. (D) MERS-CoV titers from infected cells at each time point during the experiment.

response compared with that of the mock-infected samples at these time points (Fig. 1A). The results of clustering analysis of the kinome data following biological subtraction of the time-matched mock-infected kinome data sets from their MERS-CoV-infected counterparts are presented in Fig. 1B. Further, principal component analysis (PCA) of the kinome data for the mock- and MERS-CoV-infected samples demonstrated complete separation of the data sets into two individual clusters (Fig. 1C). Titration of cell culture supernatants from our kinome analysis by plaque assay also demonstrated that these cells were productively infected during the course of our analysis (Fig. 1D). It should be noted that the viral titers determined at 1 h p.i. represent the amount of virus remaining in the supernatant at this time point prior to washing of the cells.

Systems analysis of temporal kinome data. To gain biological insight into the molecular host response to MERS-CoV infection, we employed pathway overrepresentation analysis (ORA) with both the InnateDB and the IPA software suites. Pathway overrepresentation analysis with InnateDB was performed in an effort to identify specific signaling pathways that were modulated throughout the course of MERS-CoV infection. Analysis of the upregulated signaling pathways at all time points demonstrated that MERS-CoV infection modulated a broad range of cellular functions (see Table S1 in the supplemental material). Pathway ORA demonstrated that infection resulted in the modulation of host signaling pathways at 1 h p.i. Notably, multiple cell signaling pathways related to cell proliferation (cancer/carcinoma, growth fac-

tor signaling) and cell growth and differentiation (p53 effectors, Wnt signaling) were upregulated, while multiple proinflammatory signaling pathways (tumor necrosis factor alpha [TNF- α] and interleukin-1 [IL-1]) and innate immune response signaling pathways (Toll-like receptor [TLR] signaling) were downregulated at this time point. The signaling pathways identified to be modulated at 6 h and 24 h p.i. decreased in overall breadth and complexity compared to the breadth and complexity of the pathways identified to be modulated at the 1-h time point (see Table S1 in the supplemental material). In particular, by the 24-h time point the majority of upregulated signaling pathways were related to cell junctions (adherens junction and tight junction pathways) and Wnt-, transforming growth factor β -, or PI3K/AKT/mTOR-mediated signaling responses, with the concomitant downregulation of multiple innate immune response-related signaling pathways, including interleukin-, interferon- and TLR-related signaling pathways (see Table S1 in the supplemental material). We also observed specific trends within the signaling pathway data sets for each of the three time points. Pathways at the 1-h-p.i. time point had an overrepresentation of PI3K/AKT/mTOR pathway intermediates (including AKT1, mTOR, PDPK1, PIK3R1, PIK3R2, and RPS6KB1), ERK/MAPK pathway intermediates (including MAP2K1, MAPK3, and MAPK14), and NF- κ B pathway intermediates (IKBKB, IKBKG, and NFKB1) within many of the signaling pathways identified. These trends also appeared to be largely conserved in both the 6-h-p.i. and 24-h-p.i. signaling pathway data, suggesting a potentially critical role for these pathways

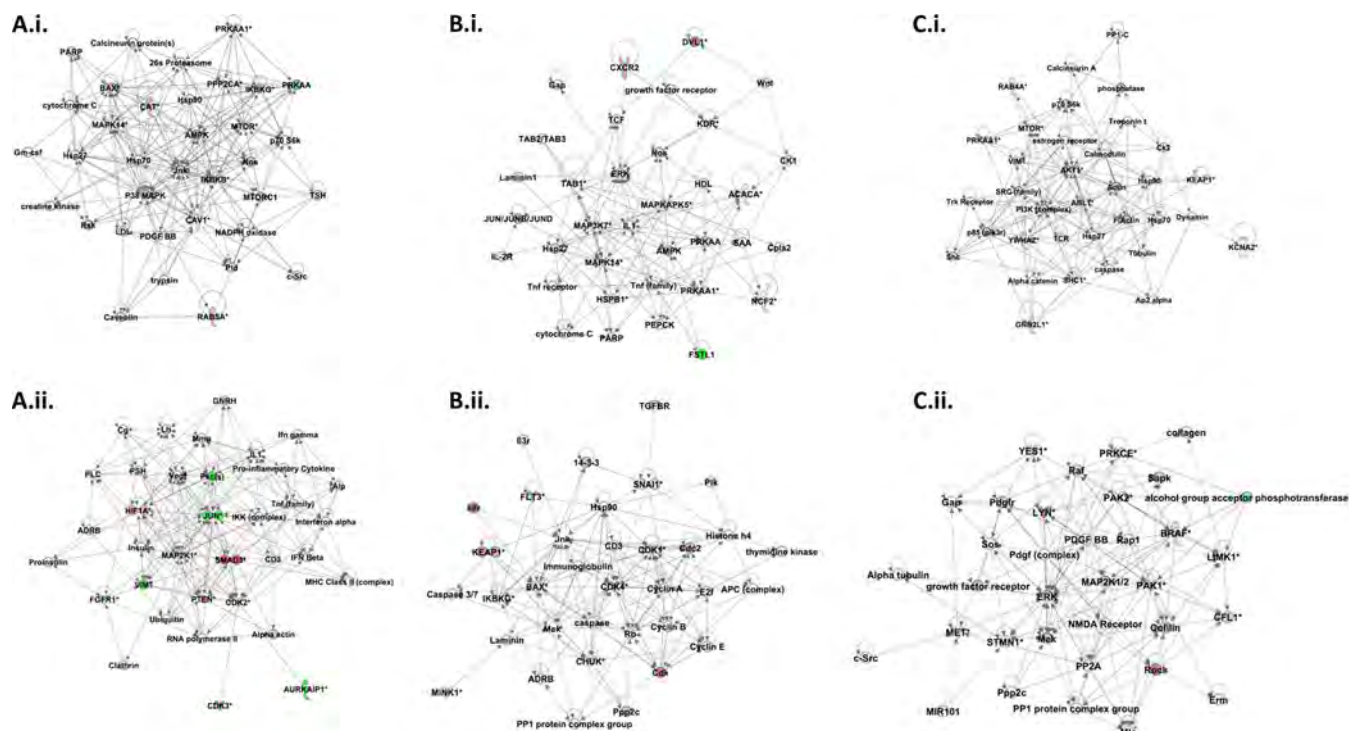


FIG 2 Functional network analysis of temporal kinase responses to MERS-CoV infection in Huh7 cells. Following PIKA, kinase data sets comparing MERS-CoV-infected cells to mock-infected cells were uploaded to IPA for functional network analysis to identify kinases of potential pharmacological interest. The top two functional networks from each time point are presented. (A) Results at 1 h postinfection. (i) Network 1 (cell morphology, cellular function and maintenance, and carbohydrate metabolism); (ii) network 2 (embryonic development, organ development, organismal development). (B) Results at 6 h postinfection. (i) Network 1 (gene expression, RNA damage and repair, RNA posttranscriptional modification); (ii) network 2 (cell morphology, cellular function and maintenance, cell cycle). (C) Results at 24 h postinfection. (i) Network 1 (cancer, hematological disease, cell death and survival); (ii) network 2 (posttranslational modification, cell morphology, cellular assembly and organization). Red nodes, upregulation of phosphorylation; green nodes, downregulation of phosphorylation; PARP, procytic acidic repetitive protein; CAT, chloramphenicol acetyltransferase; Cm-csf, granulocyte-macrophage colony-stimulating factor; LDL, low-density lipoprotein; PDGF BB, platelet-derived growth factor with two B chains; GNRH, gonadotropin-releasing hormone; PLC, phospholipase C; FSH, follicle-stimulating hormone; Vegf, vascular endothelial growth factor; IKK, I κ B kinase; MHC, major histocompatibility complex; CDK2, cyclin-dependent kinase 2; TCF, T cell factor; HDL, high-density lipoprotein; IL2R, interleukin-2 receptor; PEPCK, phosphoenolpyruvate carboxykinase; FSTL1, follistatin-like 1; PP1C, phosphatase 1 catalytic subunit; TCR, T cell receptor; Pdgfr, platelet-derived growth factor receptor; NMDA, *N*-methyl-D-aspartate. Solid lines represent direct interactions between proteins, and dashed lines represent indirect interactions.

and intermediates in MERS-CoV infection. These signaling pathway trends were also confirmed by kinome analysis at 24 h p.i. in MRC5 cells, providing further evidence for a central role for PI3K/AKT/mTOR and ERK/MAPK signaling intermediates (data not shown).

Although these pathway identities were informative, we sought further insight into a broader biological role for these intermediates through functional network analysis (FNA) using the Ingenuity Pathway Analysis software suite. FNA does not limit genes or proteins to specific signaling pathways and instead provides predicted biological networks in which signaling intermediates are grouped on the basis of similarities in overall cellular responses and direct or indirect molecular interactions. The top two functional networks for each time point are presented in Fig. 2. FNA demonstrated that multiple intermediates within the ERK/MAPK signaling pathway (including ERK1 [MAP2K1], p38 [MAPK14], and MEK) and the PI3K/AKT/mTOR signaling pathway were conserved across multiple time points (Fig. 2A to C). It was also noted that ERK1/2 formed central nodes at both 1 h (Fig. 2Aii) and 24 h (Fig. 2Cii) postinfection, while AKT, PI3K, and mTOR formed a central core of the top network found at 24 h postinfection (Fig. 2Ci).

Comparative analysis of the significantly modulated phosphorylation events from our MERS-CoV kinome data by Venn analysis demonstrated that 14 kinases were conserved among data sets from the three p.i. time points (see Table S2 and Fig. S1A in the supplemental material). Interestingly, FNA of this peptide list resulted in multiple ERK/MAPK and PI3K/AKT/mTOR signaling pathway intermediates forming central components of the network, further suggesting that these pathways may be important components of the cellular events that accompany MERS-CoV infection (see Fig. S1B in the supplemental material). The associated biological functions of this network were identified to be cellular movement, cell death and survival, and the cell cycle.

Based on the trends discovered in our systems analysis of the kinome data, we chose to focus primarily on those signaling pathways or intermediates that were identified as being broadly conserved across our kinome analysis. Western blot analysis with Western blot arrays of protein phosphorylation demonstrated that MERS-CoV infection resulted in the modulation of ERK1/2 phosphorylation in a pattern that matched that found on the kinome arrays. The pattern of mTOR and AKT phosphorylation also matched that found from our kinome analysis. Further, the phosphorylation of downstream targets of mTOR, including S6

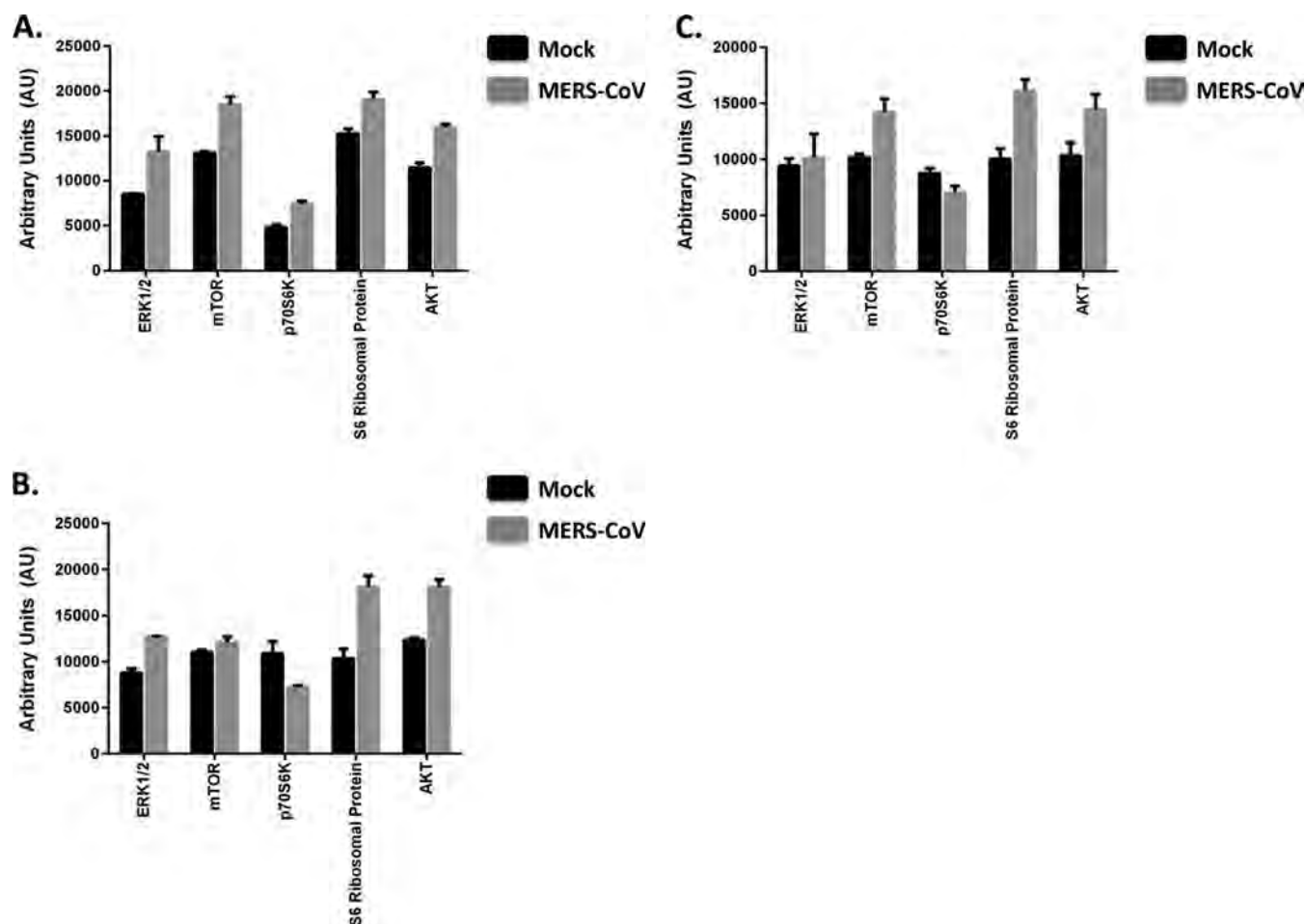


FIG 3 Western blot array analysis of select phosphorylation events in MERS-CoV-infected and mock-infected cells. Pixel intensities for selected spots on the array (in arbitrary units) are presented on the y axis. Results are presented as the mean \pm SD. (A) Results at 1 h postinfection; (B) results at 6 h postinfection; (C) results at 24 h postinfection. The results represent those from one experiment (mean \pm SD, $n = 3$), and the experiment was repeated twice.

ribosomal protein (S6RP) and p70S6 kinase (P70S6K), was also upregulated in a pattern that largely matched that of mTOR phosphorylation (Fig. 3A to C). Importantly, this type of phosphorylation analysis is largely qualitative rather than quantitative; however, the overall trends from our kinome analysis were in agreement with the trends found in our Western blot array analysis.

Kinase inhibitors targeting PI3K/AKT/mTOR and ERK/MAPK signaling inhibit MERS-CoV infection. Following our bioinformatics analysis of the kinome data, we sought further insight into the relationship between the host kinases or signaling networks that were overrepresented in our kinome data. As ERK/MAPK and PI3K/AKT/mTOR formed central components of multiple functional networks and signaling pathways within our analysis, we assessed the effect of selective inhibition of these kinases on MERS-CoV infection through a modified ELISA. Using our modified ELISA, we previously demonstrated that inhibition of MERS-CoV correlated with decreased viral titers through traditional plaque reduction assays (17). Thus, we chose to assess the effect of select kinase inhibitors targeting the PI3/AKT and ERK/MAPK pathways against MERS-CoV infection through this assay. We also selected inhibitors for specific kinases or signaling path-

ways identified from individual time points in our analysis (including protein kinase C [PKC]-, NF- κ B-, nitric oxide synthase [NOS]-, and Src-mediated signaling responses). These host components either were found within the functional networks formed from our kinome data or were present within signaling pathways found in our pathway ORA. Importantly, at the highest concentration of kinase inhibitors tested (10 μ M), all kinase inhibitors, with the exception of PKC-412 and Ro 31-8220 (20% and 23% cytotoxicity, respectively), had negligible (<10%) cytotoxic effects, as assessed by measurement of the level of lactate dehydrogenase, which is released during cell lysis (data not shown). For our analysis, we first examined the effects of kinase inhibitors when added 1 h prior to MERS-CoV infection *in vitro* using the same MOI used for the generation of the kinome data (MOI = 0.05). Inhibition of PI3K/AKT signaling with wortmannin resulted in 40% inhibition of MERS-CoV infection at the highest concentration tested, and inhibition decreased to 22% at submicromolar concentrations (Fig. 4A). In addition, treatment of cells with rapamycin, an inhibitor of mTOR, inhibited MERS-CoV infection by 61% at 10 μ M and 24% at the lowest concentration tested (0.1 μ M). Inhibitors for additional kinases that did not form critical components of signaling and/or the functional net-

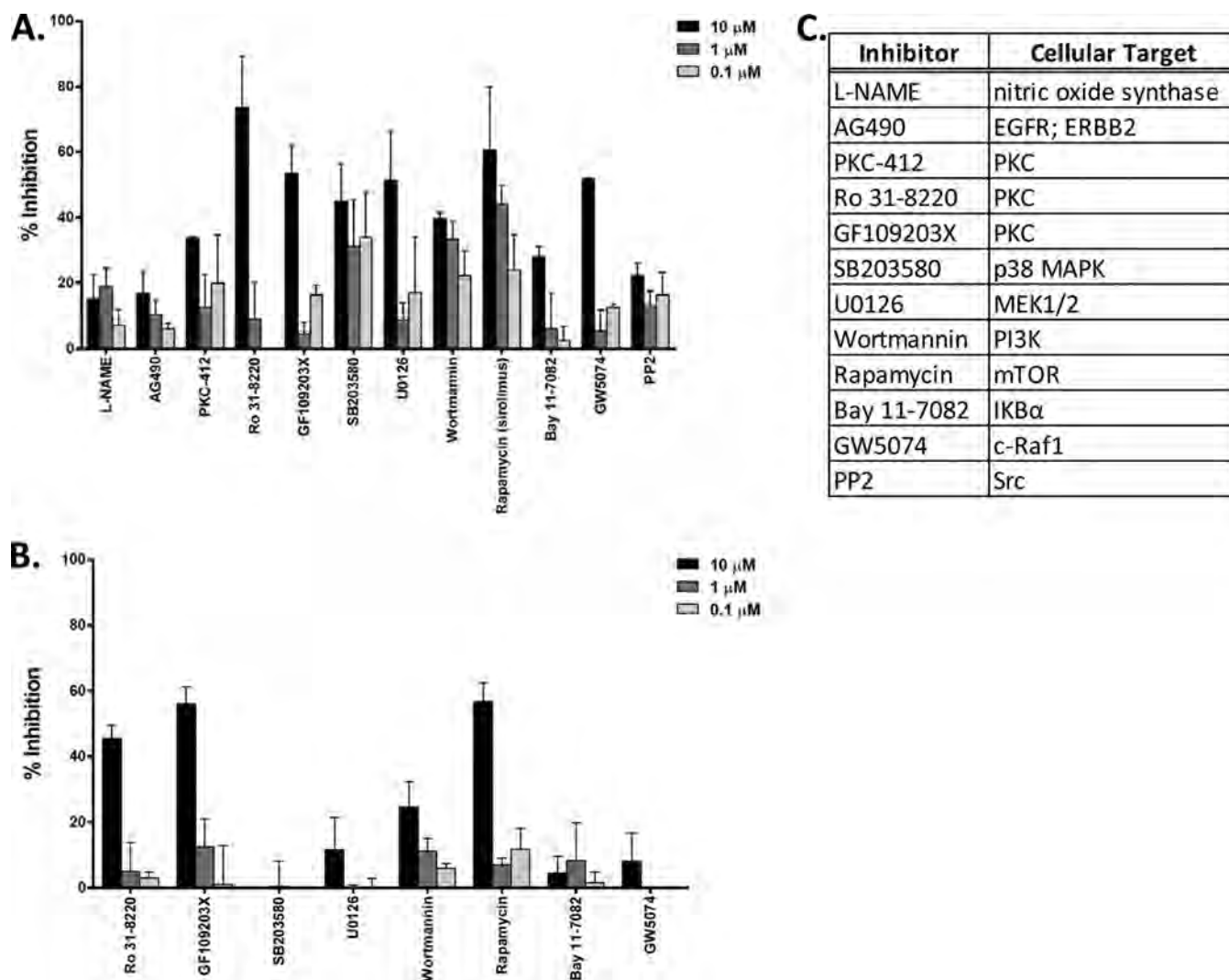


FIG 4 Inhibition of MERS-CoV infection by kinase inhibitors. Kinase inhibitors were added either preinfection (-1 h) or postinfection ($+2$ h) at the concentrations listed. Results are presented as the mean \pm SD. (A) Preinfection addition of kinase inhibitors targeting signaling pathways/kinases identified from bioinformatics analysis of temporal kinome data; (B) postinfection addition of kinase inhibitors selected from panel A. The cytotoxicities for all compounds at the highest concentration tested (10 μ M) were $<10\%$, with the exception of those of PKC-412 and Ro 31-8220 (20% and 23%, respectively). (C) Kinase inhibitor targets from this analysis. The results represent those from three experimental repeats (mean \pm SD, $n = 3$), with two technological repeats being performed in each experiment. EGFR, epidermal growth factor receptor.

work were also examined and had negligible effects on MERS-CoV infection. Taken together, these data provide further support for a role for the PI3K/AKT/mTOR signaling pathway during MERS-CoV infection.

Next, we examined the effects of ERK/MAPK pathway inhibitors. Pretreatment of cells with inhibitors of ERK/MAPK signaling resulted in the inhibition of MERS-CoV infection: SB203580 (p38 MAPK) and U0126 (MEK1/2) had similar inhibitory activities against MERS-CoV at 10 μ M (45% and 51% inhibition, respectively). Pretreatment of cells with 10 μ M GW5074, an inhibitor of Raf, a kinase that is involved in the ERK/MAPK signaling transduction cascade and was present in multiple signaling pathways identified from the kinome array data from 6 h and 24 h p.i., inhibited MERS-CoV by 52%. This also supported the findings from the analysis of the kinome data in regard to the modulation of ERK/MAPK signaling during MERS-CoV infection.

Inhibition of PKC prior to viral infection also resulted in inhibition of MERS-CoV (Fig. 3A). The PKC inhibitors PKC-412, GF109203X, and Ro 31-8220 inhibited MERS-CoV infection by 37%, 54%, and 74%, respectively, suggesting that PKC also plays an important role during infection. Inhibition of MERS-CoV infection by Ro 31-8220 and GF109203X was significantly greater than that by PKC-412 ($P < 0.1$). To examine the role for NF- κ B signaling in MERS-CoV infection, cells were also pretreated with Bay 11-7082, an inhibitor of NF- κ B DNA binding and tumor necrosis factor alpha (TNF- α)-induced I κ B α phosphorylation that inhibited MERS-CoV infection by 28%. MERS-CoV was largely insensitive ($<25\%$ inhibition) to pretreatment of cells with inhibitors for Src (PP2), epidermal growth factor receptor (AG490), or NOS2 (L-NAME) (Fig. 4A).

To further assess the role for these kinases or signaling pathways in MERS-CoV infection, we selected inhibitors from our

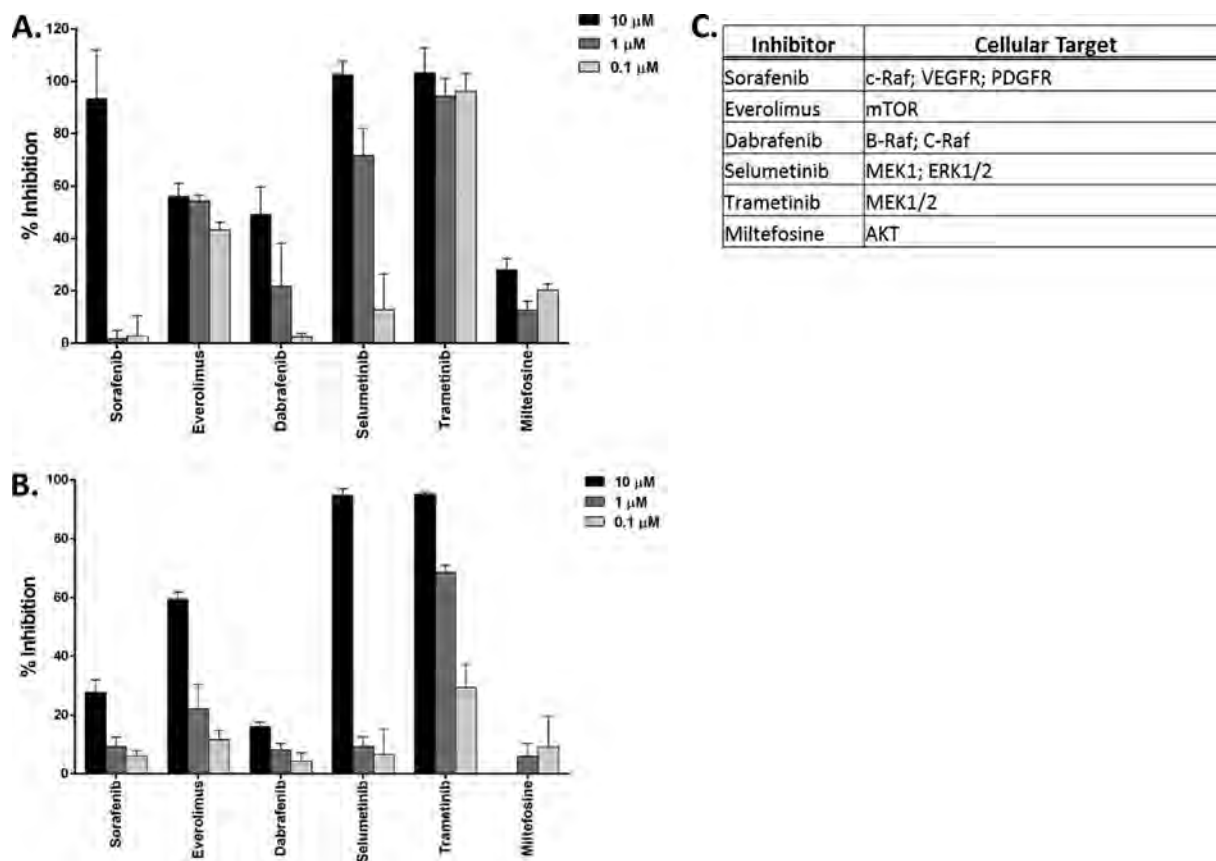


FIG 5 Inhibitory activity of FDA-licensed kinase inhibitors targeting ERK/MAPK or PI3K/AKT signaling added before or after MERS-CoV infection. Kinase inhibitors were added before (-1 h) or after ($+2$ h) MERS-CoV infection at the concentrations listed. Results are presented as the mean \pm SD. (A) Preinfection addition of kinase inhibitors targeting signaling pathways/kinases identified from bioinformatics analysis of temporal kinome data. (B) Postinfection addition of kinase inhibitors. The cytotoxicities for all compounds tested were $<10\%$. (C) Kinase inhibitor targets from this analysis. The results represent those from three experimental repeats (mean \pm SD, $n = 3$), with two technological repeats performed in each experiment. For the pretreatment experiments, trametinib was significantly more inhibitory than selumetinib at $0.1 \mu\text{M}$ ($P < 0.05$). For the postaddition experiments, trametinib was significantly more inhibitory than selumetinib at $1 \mu\text{M}$ ($P < 0.005$). VEGFR, vascular endothelial growth factor receptor; PDGFR, platelet-derived growth factor receptor.

pretreatment experiments with inhibitory activities of $\geq 40\%$ to examine the retention of these activities when added to the cells at 2 h p.i. Inhibitors that fit into this classification included inhibitors of PI3K (wortmannin), mTOR (rapamycin), MEK1/2 (U0126), PKC (Ro 31-8220, GF109203X), and c-Raf1 (GW5074). Addition of inhibitors from this subset to the cells at 2 h p.i. largely resulted in decreased inhibitory activity against MERS-CoV infection compared to that obtained with preinfection treatments. Postinfection treatment of cells with rapamycin (mTOR; 57%) had a significantly stronger inhibitory effect on infection than postinfection treatment of cells with wortmannin (PI3K; 25%), suggesting a more central role for mTOR than for PI3K during MERS-CoV infection ($P < 0.05$). Postinfection treatment of infected cells with Ro 31-8220 resulted in a modest conservation of inhibitory activity (46%) which was similar to that achieved with GF109203X (56%) and rapamycin (Fig. 3B).

As these analyses provided further support for the role of the ERK/MAPK and PI3K/AKT/mTOR signaling pathways initially identified from our kinome analysis, we postulated that licensed therapeutics targeting the same pathways would also have inhibitory activity against MERS-CoV infections. Here, we selected inhibitors targeting AKT (miltefosine), mTOR (everolimus),

ERK/MAPK (selumetinib, trametinib), and Raf (dabrafenib, sorafenib). Cells were treated with inhibitors prior to (1 h) or following (2 h) MERS-CoV infection. For kinase inhibitors targeting the ERK/MAPK signal pathway, selumetinib (MEK1, ERK1/2) and trametinib (MEK1/2) had the strongest inhibitory activities of all the inhibitors tested ($\geq 95\%$), including non-ERK/MAPK inhibitors, whether they were added prior to (-1 h; Fig. 5A) or following ($+2$ h; Fig. 5B) infection. Interestingly, trametinib demonstrated significantly stronger inhibitory activity against MERS-CoV than selumetinib at the lowest concentration tested when the inhibitors were added prior to infection ($P < 0.05$) or when a postinfection treatment concentration of $10 \mu\text{M}$ was used ($P < 0.05$). This suggests that these specific nodes of the ERK/MAPK signaling pathway (MEK1/2 and ERK1/2) may represent critical nodes of the biological responses of the host during MERS-CoV infection and may be the most logical targets for therapeutic intervention. We also examined inhibitors of Raf, a MAP3K found downstream of the Ras family of membrane GTPases, as Raf was found to be an intermediate in upregulated signaling pathways at all time points in our analysis and treatment of cells with GW5074 inhibited MERS-CoV infection (Fig. 3A). Pretreatment with sorafenib strongly inhibited MERS-CoV infection (93%), provid-

ing further support for a role for the ERK/MAPK signaling pathway during viral infection. The inhibitory activity was reduced when sorafenib was added to cells at 2 h following infection (<30% inhibition at the highest concentration tested), suggesting that the role for Raf may be related primarily to processes early in the viral life cycle (viral entry, uptake or uncoating of virions) rather than viral replication processes. Dabrafenib, an inhibitor that also targets Raf, had reduced inhibitory activity against MERS-CoV compared to the activity of sorafenib (45%) when added to cells prior to MERS-CoV infection. As with sorafenib, the inhibitory activity of dabrafenib against MERS-CoV was largely negated when added to cells postinfection (Fig. 5B), providing further mechanistic evidence for a role for Raf primarily in early viral entry or postentry events.

From the perspective of PI3K/AKT/mTOR signaling, we also investigated licensed inhibitors that targeted AKT or mTOR. Everolimus, an inhibitor of mTOR, largely retained inhibitory activity against MERS-CoV whether it was added pre- or postinfection (56% and 59% inhibition, respectively, at 10 μ M) (Fig. 5A). These results were very similar to those for rapamycin (sirolimus; Fig. 3A and B) and provide strong evidence for a critical role for mTOR in MERS-CoV infection. In contrast, miltefosine, an inhibitor of AKT approved for use for the treatment of leishmanial infection (33), had minimal inhibitory activity against MERS-CoV (28%) at the highest concentration tested when added preinfection. The activity was completely abrogated when added postinfection (Fig. 4B). As the inhibitory activity of everolimus was significantly greater than that of miltefosine at all concentrations tested ($P < 0.05$), this provided further support for a critical role for mTOR within the PI3K/AKT/mTOR signaling pathway in the exacerbation of MERS-CoV infection. The results for selumetinib, trametinib, and everolimus were also confirmed by traditional plaque reduction assays. Huh7 cells were pretreated for 1 h with each of the three inhibitors (10 μ M) and then infected at an MOI of 0.05, as in the initial kinome experiments. Following infection, cells were washed and then medium alone was added (see Fig. S2A in the supplemental material) or medium plus the inhibitor at the same concentration used in the preinfection treatments was added (see Fig. S2B in the supplemental material). A single preinfection addition of either selumetinib or trametinib resulted in a significant decrease in viral titers, and the readministration of inhibitor following infection (similar to the conditions for the cell-based ELISAs) resulted in significant inhibition of viral replication for all three inhibitors.

DISCUSSION

Concerns regarding the potential global implications of MERS-CoV as an emerging pathogen have been raised. As a result of this, there has been great interest in both increasing our understanding of the molecular pathogenesis associated with MERS-CoV infections and identifying potential therapeutic treatment options. Further, there is great interest in characterizing the molecular events that underlie host responses to MERS-CoV and the relation of these to disease pathogenesis and severity.

We and others have demonstrated the utility of kinome analysis for characterizing the molecular host response to viral infection through the identification of cell signaling networks or individual kinases that are uniquely modulated during these events (22, 34). Kinases are of critical importance to many biological processes and form an important mechanism for the regulation of

these processes independent of changes in transcription or translation. As the dysregulation of cellular kinases has been implicated in numerous human malignancies (35), kinases have become an important target for the design and development of novel therapeutics (25, 26). There are currently 26 kinase inhibitors with FDA licensure and a continually increasing number at various stages of clinical development. It should also be appreciated that the escalating costs of moving a new drug from bench to bedside (estimated at more than \$1 billion) have prompted calls for the investigation and potential repurposing of licensed therapeutics for alternative uses. Thus, kinome analysis provides a unique opportunity to characterize the molecular host response in the investigation of viral infections, including those caused by high-consequence pathogens. Here, we employed systems kinome analysis with peptide arrays to characterize the host response to MERS-CoV infection in Huh7 cells, a human hepatoma cell line that is highly permissive to MERS-CoV infection (27).

Our kinome analysis and subsequent pathway and functional network analyses demonstrated that MERS-CoV infection resulted in the selective modulation of the ERK/MAPK and PI3K/AKT/mTOR signaling responses throughout the course of infection. Recently, Josset et al. used an inverse genomic signature approach in their transcriptome analysis of MERS-CoV infection *in vitro* for the identification of potential drug targets (20). Our results complement those recently reported by Josset et al. in regard to the potential of kinase inhibitors to be novel treatments for MERS-CoV infection (20). The transcriptome analysis performed by the authors resulted in the prediction of two kinase inhibitors, LY294002 (PI3K) and SB203580 (p38 MAPK), to be potential modulators of MERS-CoV infection. Here, we have employed kinome analysis to provide critical data regarding the functional response of the host to viral infection through the analysis of the activation states of host kinases and cell signaling networks. Further, we have utilized this information for the logical prediction of host kinases that may serve as novel therapeutic targets for MERS-CoV infection. However, our analysis has expanded on these observations by providing functional evidence for the temporal roles of these signaling pathways in the host response during MERS-CoV infection (20).

We have demonstrated through systems-level analysis of our kinome data that multiple ERK/MAPK and PI3K/AKT/mTOR family members formed central components of functional networks and signaling pathways throughout the course of our investigation. In addition, ERK/MAPK and PI3K/AKT/mTOR signaling responses, including the functional network derived from the kinases that were conserved across all of the time points examined in our investigation, were overrepresented in our pathway and network analyses (see Fig. S1 in the supplemental material). The ERK/MAPK and PI3K/AKT/mTOR signaling networks are critical regulatory pathways for many cell regulatory responses, including cell proliferation and apoptosis, and have been demonstrated to be targeted by a broad range of viral pathogens (36–38). This would suggest that both ERK/MAPK and PI3K/AKT/mTOR signaling responses play important roles in the host response to MERS-CoV infection. Our kinome data and data from subsequent pathway and functional network analyses were corroborated by the phosphorylation patterns of specific members of these pathways obtained by Western blot array analysis. Further, the activation of mTOR-regulated intracellular kinases, including S6RP and p70S6K, lends further credence to our pathway and

functional network data. In addition to these findings, our analyses also suggested that PKC-mediated signaling also formed important components of the host response to MERS-CoV infection, as PKC formed components of both the functional and signaling pathway networks found in our investigation and the inhibition of PKC-mediated signaling responses resulted in decreased MERS-CoV infection whether it was added pre- or postinfection. As PKC can activate ERK/MAPK signaling (39), these results may provide additional information regarding the mechanism whereby MERS-CoV modulates ERK/MAPK signaling. A prior analysis of MERS-CoV infection also suggested that IFN responses and, in particular, those of IFN- β play important roles during the course of infection (17). Our analysis demonstrated that IFN-related signaling responses related to IFN signaling were found within the functional networks found at the 1-h-p.i. time point and, as well, were found in the downregulated signaling pathways at the 24-h-p.i. time point. These observations lend further credence to the growing evidence for a specific attenuation of IFN responses during MERS-CoV infection (17, 18, 40).

There has been considerable analysis of the therapeutic potential for host-targeted immunomodulatory agents in viral infections (20, 41, 42). Previous work has demonstrated that viruses modulate host cell signaling networks, including those involving PI3K/AKT/mTOR and ERK/MAPK. Human papillomavirus (HPV) is able to maintain an activated AKT, resulting in activated mTORC1, and it has been postulated that this may be required for the initiation of viral replication (43). A similar requirement for activated PI3K/AKT/mTOR signaling in viral replication has also been demonstrated for myxoma virus (44). Qin et al. have also demonstrated that herpes simplex virus 1 infection stimulated both the PI3K/AKT and ERK/MAPK signaling pathways (45), and the role of ERK/MAPK signaling modulation in viral infection has also been noted for reovirus (46), rabies virus (47), and hepatitis B virus (48), among others. We demonstrated that multiple licensed kinase inhibitors targeting the ERK/MAPK or PI3K/AKT/mTOR signaling pathway inhibited MERS-CoV infection *in vitro* when added prior to or following viral infection. Inhibitors of MEK1/2 (trametinib) and/or ERK1/2 (selumetinib) had the strongest and most conserved inhibitory activities, suggesting that MEK1/2 and ERK1/2 may have unique capabilities as stand-alone or combinatorial therapies for MERS-CoV infections. Further, across all time points, both ERK/MAPK intermediates were represented in signaling pathways or functional networks that were derived from our kinome analysis. These analyses also suggested that mTOR was highly overrepresented within our kinome data. Inhibitors of mTOR (rapamycin and everolimus) had reduced inhibitory activities against MERS-CoV compared to the activities of trametinib and selumetinib. However, the conservation of these activities following treatment pre- or postinfection also suggests that mTOR plays a critical role in MERS-CoV infections beyond viral entry. Although our kinome data suggested that PI3K could be an attractive therapeutic target for MERS-CoV and treatment of cells with wortmannin, a selective PI3K inhibitor, inhibited MERS-CoV infection, the administration of miltefosine (an AKT inhibitor licensed for use as an antileishmanial agent [33]) had minimal inhibitory activity in our analysis. These results suggest that in addition to ERK/MAPK intermediates, as targeted by trametinib and selumetinib, mTOR may also be a logical therapeutic target for MERS-CoV infections. These results were further validated by the significant reduction in viral titers demonstrated by a plaque

reduction assay when cells were treated for only 1 h prior to infection (trametinib and selumetinib) or when inhibitors were replenished following infection (trametinib, selumetinib, and everolimus). The specific mechanism(s) of inhibition for these inhibitors remains to be determined. Though it is postulated that this inhibitory effect is mitigated through the direct inactivation of the primary targets of these inhibitors, it is appreciated that many licensed kinase inhibitors have off-site targets that could contribute to the overall antiviral activities reported here. Specific inhibition of intermediates from the ERK/MAPK and PI3K/AKT/mTOR signaling pathways through approaches that use, for example, small interfering RNA knockdown or gene knockout will help shed light on this question. Although it is tempting to speculate that these compounds may have the potential to be used for the treatment of MERS-CoV infections in the future, their use will require additional investigations of their associated pharmacokinetics and the correlation of these with the levels required for antiviral activity *in vivo*. Future investigations will expand on these findings to determine the precise mechanism of action for these inhibitors in the MERS-CoV viral life cycle (i.e., inhibition of viral replication, viral assembly, or viral egress).

Using kinome analysis, we have demonstrated that MERS-CoV infection resulted in the selective modulation of the ERK/MAPK and PI3K/AKT/mTOR signaling responses in the host and confirmed this through biological validation experiments with kinase inhibitors. Further, we have also demonstrated the utility of temporal kinome analysis for characterizing host responses to infection and for the subsequent selection of therapeutics that may provide resolution of the infection. Taken together, we provide critical information regarding the molecular host response to MERS-CoV infection and evidence for the potential of kinase inhibitor therapeutics with preexisting licensure to be novel strategies for the treatment of MERS-CoV infections.

ACKNOWLEDGMENTS

This study was supported in part by the NIAID Division of Intramural Research.

B.J.H., J.D., and J.H.K. performed this work as employees of Tunnell Consulting, Inc., and D.T. and S.M. performed this work as employees of MRI Global. Tunnell Consulting, Inc., and MRI Global are subcontractors to Battelle Memorial Institute. J.K., B.O., and M.H. performed this work as employees of Battelle Memorial Institute. All work was performed under the Battelle Memorial Institute prime contract with NIAID (contract no. HHSN272200700016I).

The content of this publication does not necessarily reflect the views or policies of the U.S. Department of Health and Human Services or of the institutions and companies affiliated with the authors.

REFERENCES

1. Zaki AM, van Boheemen S, Bestebroer TM, Osterhaus AD, Fouchier RA. 2012. Isolation of a novel coronavirus from a man with pneumonia in Saudi Arabia. *N Engl J Med* 367:1814–1820. <http://dx.doi.org/10.1056/NEJMoa1211721>.
2. Raj VS, Osterhaus AD, Fouchier RA, Haagmans BL. 2014. MERS: emergence of a novel human coronavirus. *Curr Opin Virol* 5:58–62. <http://dx.doi.org/10.1016/j.coviro.2014.01.010>.
3. Bialek SR, Allen D, Alvarado-Ramy F, Arthur R, Balajee A, Bell D, Best S, Blackmore C, Breakwell L, Cannons A, Brown C, Cetron M, Chea N, Chommanard C, Cohen N, Conover C, Crespo A, Creviston J, Curns AT, Dahl R, Dearth S, DeMaria A, Echols F, Erdman DD, Feikin D, Frias M, Gerber SI, Gulati R, Hale C, Haynes LM, Heberlein-Larson L, Holton K, Ijaz K, Kapoor M, Kohl K, Kuhar DT, Kumar AM, Kundich M, Lippold S, Liu L, Lovchik JC, Madoff L, Martell S, Matthews S,

- Moore J, Murray LR, Onofrey S, Pallansch MA, Pesik N, Pham H, et al. 2014. First confirmed cases of Middle East respiratory syndrome coronavirus (MERS-CoV) infection in the United States, updated information on the epidemiology of MERS-CoV infection, and guidance for the public, clinicians, and public health authorities—May 2014. *MMWR Morb Mortal Wkly Rep* 63:431–436.
4. Peiris JS, Yuen KY, Osterhaus AD, Stohr K. 2003. The severe acute respiratory syndrome. *N Engl J Med* 349:2431–2441. <http://dx.doi.org/10.1056/NEJMra032498>.
5. Pyrc K, Sims AC, Dijkman R, Jebbink M, Long C, Deming D, Donaldson E, Vabret A, Baric R, van der Hoek L, Pickles R. 2010. Culturing the unculturable: human coronavirus HKU1 infects, replicates, and produces progeny virions in human ciliated airway epithelial cell cultures. *J Virol* 84:11255–11263. <http://dx.doi.org/10.1128/JVI.00947-10>.
6. Lau SK, Li KS, Tsang AK, Lam CS, Ahmed S, Chen H, Chan KH, Woo PC, Yuen KY. 2013. Genetic characterization of *Betacoronavirus* lineage C viruses in bats reveals marked sequence divergence in the spike protein of *Pipistrellus* bat coronavirus HKU5 in Japanese pipistrelle: implications for the origin of the novel Middle East respiratory syndrome coronavirus. *J Virol* 87:8638–8650. <http://dx.doi.org/10.1128/JVI.01055-13>.
7. van Boheemen S, de Graaf M, Lauber C, Bestebroer TM, Raj VS, Zaki AM, Osterhaus AD, Haagmans BL, Gorbalenya AE, Snijder EJ, Fouchier RA. 2012. Genomic characterization of a newly discovered coronavirus associated with acute respiratory distress syndrome in humans. *mBio* 3(6):e00473–12. <http://dx.doi.org/10.1128/mBio.00473-12>.
8. Coleman CM, Frieman MB. 2013. Emergence of the Middle East respiratory syndrome coronavirus. *PLoS Pathog* 9:e1003595. <http://dx.doi.org/10.1371/journal.ppat.1003595>.
9. Alagaili AN, Briesse T, Mishra N, Kapoor V, Sameroff SC, de Wit E, Munster VJ, Hensley LE, Zalmout IS, Kapoor A, Epstein JH, Karesh WB, Daszak P, Mohammed OB, Lipkin WI. 2014. Middle East respiratory syndrome coronavirus infection in dromedary camels in Saudi Arabia. *mBio* 5(2):e00884–14. <http://dx.doi.org/10.1128/mBio.00884-14>.
10. Ferguson NM, Van Kerkhove MD. 2014. Identification of MERS-CoV in dromedary camels. *Lancet Infect Dis* 14:93–94. [http://dx.doi.org/10.1016/S1473-3099\(13\)70691-1](http://dx.doi.org/10.1016/S1473-3099(13)70691-1).
11. Zumla AI, Memish ZA. 2014. Middle East respiratory syndrome coronavirus: epidemic potential or a storm in a teacup? *Eur Respir J* 43:1243–1248. <http://dx.doi.org/10.1183/09031936.00227213>.
12. Bermingham A, Chand MA, Brown CS, Aarons E, Tong C, Langrish C, Hoschler K, Brown K, Galiano M, Myers R, Pebody RG, Green HK, Boddington NL, Gopal R, Price N, Newsholme W, Drosten C, Fouchier RA, Zambon M. 2012. Severe respiratory illness caused by a novel coronavirus, in a patient transferred to the United Kingdom from the Middle East, September 2012. *Euro Surveill* 17(40):pii=20290. <http://www.eurosurveillance.org/ViewArticle.aspx?ArticleId=20290>.
13. Geng H, Tan W. 2013. A novel human coronavirus: Middle East respiratory syndrome human coronavirus. *Sci China Life Sci* 56:683–687. <http://dx.doi.org/10.1007/s11427-013-4519-8>.
14. Al-Tawfiq JA, Memish ZA. 2014. What are our pharmacotherapeutic options for MERS-CoV? *Expert Rev Clin Pharmacol* 7:235–238. <http://dx.doi.org/10.1586/17512433.2014.890515>.
15. Zieleski F, Weber M, Eickmann M, Spiegelberg L, Zaki AM, Matrosovich M, Becker S, Weber F. 2013. Human cell tropism and innate immune system interactions of human respiratory coronavirus EMC compared to those of severe acute respiratory syndrome coronavirus. *J Virol* 87:5300–5304. <http://dx.doi.org/10.1128/JVI.03496-12>.
16. Kindler E, Jonsdottir HR, Muth D, Hamming OJ, Hartmann R, Rodriguez R, Geffers R, Fouchier RA, Drosten C, Muller MA, Dijkman R, Thiel V. 2013. Efficient replication of the novel human betacoronavirus EMC on primary human epithelium highlights its zoonotic potential. *mBio* 4(1):e00611–12. <http://dx.doi.org/10.1128/mBio.00611-12>.
17. Hart BJ, Dyall J, Postnikova E, Zhou H, Kindrachuk J, Johnson RF, Olinger GG, Jr, Frieman MB, Holbrook MR, Jahrling PB, Hensley L. 2014. Interferon-beta and mycophenolic acid are potent inhibitors of Middle East respiratory syndrome coronavirus in cell-based assays. *J Gen Virol* 95:571–577. <http://dx.doi.org/10.1099/vir.0.061911-0>.
18. Chan JF, Chan KH, Kao RY, To KK, Zheng BJ, Li CP, Li PT, Dai J, Mok FK, Chen H, Hayden FG, Yuen KY. 2013. Broad-spectrum antivirals for the emerging Middle East respiratory syndrome coronavirus. *J Infect* 67:606–616. <http://dx.doi.org/10.1016/j.jinf.2013.09.029>.
19. Falzarano D, de Wit E, Martellaro C, Callison J, Munster VJ, Feldmann H. 2013. Inhibition of novel β coronavirus replication by a combination of interferon- α 2b and ribavirin. *Sci Rep* 3:1686. <http://dx.doi.org/10.1038/srep01686>.
20. Josset L, Menachery VD, Gralinski LE, Agnihothram S, Sova P, Carter VS, Yount BL, Graham RL, Baric RS, Katze MG. 2013. Cell host response to infection with novel human coronavirus EMC predicts potential antivirals and important differences with SARS coronavirus. *mBio* 4(3):e00165–13. <http://dx.doi.org/10.1128/mBio.00165-13>.
21. Clarke P, Leser JS, Bowen RA, Tyler KL. 2014. Virus-induced transcriptional changes in the brain include the differential expression of genes associated with interferon, apoptosis, interleukin 17 receptor A, and glutamate signaling as well as flavivirus-specific upregulation of tRNA synthetases. *mBio* 5(2):e00902–14. <http://dx.doi.org/10.1128/mBio.00902-14>.
22. Kindrachuk J, Arsenault R, Kusalik A, Kindrachuk KN, Trost B, Napper S, Jahrling PB, Blaney JE. 2012. Systems kinomics demonstrates Congo Basin monkeypox virus infection selectively modulates host cell signaling responses as compared to West African monkeypox virus. *Mol Cell Proteomics* 11:M111.015701. <http://dx.doi.org/10.1074/mcp.M111.015701>.
23. Maattanen P, Trost B, Scruten E, Potter A, Kusalik A, Griebel P, Napper S. 2013. Divergent immune responses to *Mycobacterium avium* subsp. *paratuberculosis* infection correlate with kinome responses at the site of intestinal infection. *Infect Immun* 81:2861–2872. <http://dx.doi.org/10.1128/IAI.00339-13>.
24. Mulongo M, Pryslak T, Scruten E, Napper S, Perez-Casal J. 2014. In vitro infection of bovine monocytes with *Mycoplasma bovis* delays apoptosis and suppresses production of gamma interferon and tumor necrosis factor alpha but not interleukin-10. *Infect Immun* 82:62–71. <http://dx.doi.org/10.1128/IAI.00961-13>.
25. Cohen P. 2002. Protein kinases—the major drug targets of the twenty-first century? *Nat Rev Drug Discov* 1:309–315. <http://dx.doi.org/10.1038/nrd773>.
26. Hopkins AL, Groom CR. 2002. The druggable genome. *Nat Rev Drug Discov* 1:727–730. <http://dx.doi.org/10.1038/nrd892>.
27. de Wilde AH, Raj VS, Oudshoorn D, Bestebroer TM, van Nieuwkoop S, Limpens RW, Posthuma CC, van der Meer Y, Barcena M, Haagmans BL, Snijder EJ, van den Hoogen BG. 2013. MERS-coronavirus replication induces severe in vitro cytopathology and is strongly inhibited by cyclosporin A or interferon-alpha treatment. *J Gen Virol* 94:1749–1760. <http://dx.doi.org/10.1099/vir.0.052910-0>.
28. de Wit E, Rasmussen AL, Falzarano D, Bushmaker T, Feldmann F, Brining DL, Fischer ER, Martellaro C, Okumura A, Chang J, Scott D, Benecke AG, Katze MG, Feldmann H, Munster VJ. 2013. Middle East respiratory syndrome coronavirus (MERS-CoV) causes transient lower respiratory tract infection in rhesus macaques. *Proc Natl Acad Sci U S A* 110:16598–16603. <http://dx.doi.org/10.1073/pnas.1310744110>.
29. Li Y, Arsenault RJ, Trost B, Slind J, Griebel PJ, Napper S, Kusalik A. 2012. A systematic approach for analysis of peptide array kinome data. *Sci Signal* 5:pl2. <http://dx.doi.org/10.1126/scisignal.2002429>.
30. Trost B, Kindrachuk J, Maattanen P, Napper S, Kusalik A. 2013. PIKA 2: an expanded, web-based platform for analysis of kinome microarray data. *PLoS One* 8:e80837. <http://dx.doi.org/10.1371/journal.pone.0080837>.
31. Lynn DJ, Winsor GL, Chan C, Richard N, Laird MR, Barsky A, Gardy JL, Roche FM, Chan TH, Shah N, Lo R, Naseer M, Que J, Yau M, Acab M, Tulpan D, Whiteside MD, Chikatarla A, Mah B, Munzner T, Hokamp K, Hancock RE, Brinkman FS. 2008. InnateDB: facilitating systems-level analyses of the mammalian innate immune response. *Mol Syst Biol* 4:218. <http://dx.doi.org/10.1038/msb.2008.55>.
32. Schneider CA, Rasband WS, Eliceiri KW. 2012. NIH Image to ImageJ: 25 years of image analysis. *Nat Methods* 9:671–675. <http://dx.doi.org/10.1038/nmeth.2089>.
33. Dorlo TP, Balasegaram M, Beijnen JH, de Vries PJ. 2012. Miltefosine: a review of its pharmacology and therapeutic efficacy in the treatment of leishmaniasis. *J Antimicrob Chemother* 67:2576–2597. <http://dx.doi.org/10.1093/jac/dks275>.
34. Bowick GC, Fennelwald SM, Scott EP, Zhang L, Elsom BL, Aronson JF, Spratt HM, Luxon BA, Gorenstein DG, Herzog NK. 2007. Identification of differentially activated cell-signaling networks associated with pichinde virus pathogenesis by using systems kinomics. *J Virol* 81:1923–1933. <http://dx.doi.org/10.1128/JVI.02199-06>.
35. Knuutila S, Bjorkqvist AM, Autio K, Tarkkanen M, Wolf M, Monni O, Szymanska J, Larramendy ML, Tapper J, Pere H, El-Rifai W, Hemmer S, Wasenius VM, Vidgren V, Zhu Y. 1998. DNA copy number amplifications in human neoplasms: review of comparative genomic hybridization studies. *Am J Pathol* 152:1107–1123.

36. Ji WT, Liu HJ. 2008. PI3K-Akt signaling and viral infection. *Recent Pat Biotechnol* 2:218–226. <http://dx.doi.org/10.2174/187220808786241042>.
37. Ehrhardt C, Ludwig S. 2009. A new player in a deadly game: influenza viruses and the PI3K/Akt signalling pathway. *Cell Microbiol* 11:863–871. <http://dx.doi.org/10.1111/j.1462-5822.2009.01309.x>.
38. Pleschka S. 2008. RNA viruses and the mitogenic Raf/MEK/ERK signal transduction cascade. *Biol Chem* 389:1273–1282. <http://dx.doi.org/10.1515/BC.2008.145>.
39. Ueda Y, Hirai S, Osada S, Suzuki A, Mizuno K, Ohno S. 1996. Protein kinase C activates the MEK-ERK pathway in a manner independent of Ras and dependent on Raf. *J Biol Chem* 271:23512–23519. <http://dx.doi.org/10.1074/jbc.271.38.23512>.
40. Falzarano D, de Wit E, Rasmussen AL, Feldmann F, Okumura A, Scott DP, Brining D, Bushmaker T, Martellaro C, Baseler L, Benecke AG, Katze MG, Munster VJ, Feldmann H. 2013. Treatment with interferon-alpha2b and ribavirin improves outcome in MERS-CoV-infected rhesus macaques. *Nat Med* 19:1313–1317. <http://dx.doi.org/10.1038/nm.3362>.
41. Ludwig S. 2011. Disruption of virus-host cell interactions and cell signaling pathways as an anti-viral approach against influenza virus infections. *Biol Chem* 392:837–847. <http://dx.doi.org/10.1515/BC.2011.121>.
42. Tisoncik JR, Korth MJ, Simmons CP, Farrar J, Martin TR, Katze MG. 2012. Into the eye of the cytokine storm. *Microbiol Mol Biol Rev* 76:16–32. <http://dx.doi.org/10.1128/MMBR.05015-11>.
43. Buchkovich NJ, Yu Y, Zampieri CA, Alwine JC. 2008. The TORrid affairs of viruses: effects of mammalian DNA viruses on the PI3K-Akt-mTOR signalling pathway. *Nat Rev Microbiol* 6:266–275. <http://dx.doi.org/10.1038/nrmicro1855>.
44. Wang G, Barrett JW, Stanford M, Werden SJ, Johnston JB, Gao X, Sun M, Cheng JQ, McFadden G. 2006. Infection of human cancer cells with myxoma virus requires Akt activation via interaction with a viral ankyrin-repeat host range factor. *Proc Natl Acad Sci U S A* 103:4640–4645. <http://dx.doi.org/10.1073/pnas.0509341103>.
45. Qin D, Feng N, Fan W, Ma X, Yan Q, Lv Z, Zeng Y, Zhu J, Lu C. 2011. Activation of PI3K/AKT and ERK MAPK signal pathways is required for the induction of lytic cycle replication of Kaposi's sarcoma-associated herpesvirus by herpes simplex virus type 1. *BMC Microbiol* 11:240. <http://dx.doi.org/10.1186/1471-2180-11-240>.
46. Norman KL, Hirasawa K, Yang AD, Shields MA, Lee PW. 2004. Reovirus oncolysis: the Ras/RalGEF/p38 pathway dictates host cell permissiveness to reovirus infection. *Proc Natl Acad Sci U S A* 101:11099–11104. <http://dx.doi.org/10.1073/pnas.0404310101>.
47. Nakamichi K, Inoue S, Takasaki T, Morimoto K, Kurane I. 2004. Rabies virus stimulates nitric oxide production and CXC chemokine ligand 10 expression in macrophages through activation of extracellular signal-regulated kinases 1 and 2. *J Virol* 78:9376–9388. <http://dx.doi.org/10.1128/JVI.78.17.9376-9388.2004>.
48. Chung TW, Lee YC, Kim CH. 2004. Hepatitis B viral HBx induces matrix metalloproteinase-9 gene expression through activation of ERK and PI3K/AKT pathways: involvement of invasive potential. *FASEB J* 18:1123–1125. <http://dx.doi.org/10.1096/fj.03-1429fje>.

Systems Kinomics Demonstrates Congo Basin Monkeypox Virus Infection Selectively Modulates Host Cell Signaling Responses as Compared to West African Monkeypox Virus*[§]

Jason Kindrachuk^{‡§§}, Ryan Arsenault^{§¶}, Anthony Kusalik^{||}, Kristen N. Kindrachuk^{**}, Brett Trost^{||}, Scott Napper^{§¶}, Peter B. Jahrling^{‡‡}, and Joseph E. Blaney[‡]

Monkeypox virus (MPXV) is comprised of two clades: Congo Basin MPXV, with an associated case fatality rate of 10%, and Western African MPXV, which is associated with less severe infection and minimal lethality. We thus postulated that Congo Basin and West African MPXV would differentially modulate host cell responses and, as many host responses are regulated through phosphorylation independent of transcription or translation, we employed systems kinomics with peptide arrays to investigate these functional host responses. Using this approach we have demonstrated that Congo Basin MPXV infection selectively down-regulates host responses as compared with West African MPXV, including growth factor- and apoptosis-related responses. These results were confirmed using fluorescence-activated cell sorting analysis demonstrating that West African MPXV infection resulted in a significant increase in apoptosis in human monocytes as compared with Congo Basin MPXV. Further, differentially phosphorylated kinases were identified through comparison of our MPXV data sets and validated as potential targets for pharmacological inhibition of Congo Basin MPXV infection, including increased Akt S473 phosphorylation and decreased p53 S15 phosphorylation. Inhibition of Akt S473 phosphorylation resulted in a significant decrease in Congo Basin MPXV virus yield (261-fold) but did not affect West African MPXV. In addition, treatment with staurosporine, an apoptosis acti-

vator resulted in a 49-fold greater decrease in Congo Basin MPXV yields as compared with West African MPXV. Thus, using a systems kinomics approach, our investigation demonstrates that West African and Congo Basin MPXV differentially modulate host cell responses and has identified potential host targets of therapeutic interest. *Molecular & Cellular Proteomics* 11: 10.1074/mcp.M111.015701, 1–12, 2012.

Monkeypox virus (MPXV)¹ is a member of the genus *Orthopoxvirus*, which also includes vaccinia virus (VACV), ectromelia virus, cowpox virus (CPXV), and variola virus (VARV), the causative agent of smallpox. MPXV causes zoonotic disease that manifests similarly to smallpox with associated case fatality rates of ~10% (1). Although MPXV was first isolated from cynomolgus macaques in 1958 in Denmark (2) there was limited scientific interest in the virus until it was demonstrated in the 1970s that MPXV could cause lethal infection in humans (3). Following the cessation of smallpox vaccination there has been a dramatic increase in MPXV incidence in the Democratic Republic of the Congo over the past 30 years (4) and it is estimated that ~50% of the general population is not protected against MPXV or VARV (4). These concerns have been compounded by the first reported incidence of MPXV outside of the African continent following the accidental introduction of MPXV in the Midwestern United States in 2003 (5). Further concerns have also been raised regarding the potential use of MPXV as a bioterrorism agent thus resulting in its classification as a Class C Select Agent (1, 6).

Monkeypox virus is comprised of two distinct clades that are genetically, clinically, and geographically distinct. Congo Basin MPXV, also known as Central African MPXV, has associated case fatality rates of ~10% in non-vaccinated individ-

From the [‡]Emerging Viral Pathogens Section, National Institute of Allergy and Infectious Diseases, National Institutes of Health, Bethesda, Maryland 20892; [§]Department of Biochemistry, University of Saskatchewan, Saskatoon, Saskatchewan, Canada, S7N 5E5; [¶]Vaccine and Infectious Disease Organization, University of Saskatchewan, Saskatoon, Saskatchewan, Canada, S7N 5E3; ^{||}Department of Computer Science, University of Saskatchewan, Saskatoon, Saskatchewan, Canada, S7N 5C9; ^{**}Laboratory of Parasitic Diseases, National Institute of Allergy and Infectious Diseases, National Institutes of Health, Bethesda, Maryland 20892; ^{‡‡}Integrated Research Facility, National Institute of Allergy and Infectious Diseases, National Institutes of Health, Frederick, Maryland 21702

Received November 9, 2011, and in revised form, December 19, 2011

Published, MCP Papers in Press, December 28, 2011, DOI 10.1074/mcp.M111.015701

¹ The abbreviations used are: MPXV, Monkeypox virus; CPXV, Cowpox virus; FBS, Fetal bovine serum; FGF, Fibroblast growth factor; HSV, Herpes simplex virus; IGF1, Insulin-like growth factor 1; MAPK, Mitogen activated protein kinase; ORA, Over-representation analysis; PTEN, Phosphatase and tensin homolog; TLR, Toll-like receptor; VACV, Vaccinia virus; VARV, Variola virus.

uals as compared with the minimal lethality associated with the less-virulent West African MPXV clade (7). Lending further support, comparative infection models in non-human primates (8), mice (9, 10), prairie dogs (11, 12) and ground squirrels (13) have all demonstrated greater lethality or morbidity associated with Congo Basin MPXV infection when compared with West African MPXV. Additionally, an outbreak of West African MPXV in the U.S. in 2003 following importation of MPXV-infected rodents from Ghana resulted in 69 diagnosed MPXV cases; however, disease severity was relatively mild with no fatalities (5). Although these reports have demonstrated a definitive difference in virulence between the two MPXV clades, there is a paucity of information regarding the virus or host factors that mediate the divergent pathogenesis. Recently, investigations of the global gene expression programs of both the host and virus during Congo Basin MPXV infection have provided insight into the underlying mechanisms of MPXV disease pathogenesis. In particular, independent investigations of host responses to Congo Basin MPXV infection by Rubins *et al.* (14) and Alkhalil *et al.* (15) have demonstrated global suppression of host gene expression programs following viral infection. Interestingly, these included the modulation of such diverse host responses as the regulation of histone expression, cytoskeletal rearrangement, cell cycle progression, and interferon-associated gene expression (14, 15). This is perhaps unsurprising as it was demonstrated that the host response modifier genes of Congo Basin MPXV are transcribed at steady-state levels throughout the course of infection (16). Corresponding investigations for West African MPXV have not been reported.

Although studies of global gene expression have been informative, it is increasingly appreciated that many cellular processes are regulated independently of changes in transcription or translation through post-translational modifications of host proteins. For example, phosphorylation is one of the most pivotal biological mechanisms for regulation of cellular processes with 518 annotated human kinase genes and ~100,000 human phosphorylation sites identified to date (17, 18). As virtually all cell signaling processes are regulated by phosphotransfer reactions, and aberrant kinase activity has been implicated in a variety of diseases, kinases are an attractive target for therapeutic intervention (19, 20). The priority that has been placed on the development of kinase inhibitors for the treatment of a variety of human diseases such as cancer has resulted in the development of tremendous libraries of potential inhibitors that may have other applications for treatment of infectious diseases.

Kinome profiling through global analysis of kinase abundance, activity, phosphorylation status, and substrate specificity provides a novel mechanism for investigating disease pathogenesis through the activation or repression of host cell signal transduction pathways (20). For example, a recent investigation by Bowick *et al.* utilized kinome peptide arrays to identify host cell signaling nodes of interest that were differ-

entially modulated by two variants of Pichinde virus producing either lethal or self-limiting disease (21). In addition, numerous pathogens, including poxviruses, have been shown to target host cellular processes as a part of their pathogenic mechanism through host protein mimicry (22, 23), including through production of eukaryotic-like kinases (24–26). Such pathogen-encoded effectors may be equally attractive therapeutic targets as their host-encoded counterparts. Thus, systems kinomics with kinome peptide arrays represents a novel methodology for investigating host responses to clinically relevant infectious diseases and identification of potential therapeutic targets.

As direct comparison of the genomes of West African and Congo Basin MPXV demonstrate significant variability in the regions coding for host response modifier proteins, we postulated that the differential virulence of the two MPXV clades is related to the differential modulation of host cell signaling pathways following infection (27, 28). Thus, we sought to investigate host signaling pathway responses to West African and Congo Basin MPXV insult with peptide arrays comprised of human kinase targets for cell growth and differentiation, stress responses, and innate immunity. Host kinome responses to CPXV and VACV were also included for comparison of host response conservation across the *orthopoxvirus* genus. In the hierarchical clustering analysis Congo Basin MPXV demonstrated similar target phosphorylation patterns to CPXV and moderately to VACV; however, there was limited similarity between West African and Congo Basin MPXV-induced phosphorylation patterns. Congo Basin MPXV infection resulted in a significant down-regulation of host cell responses as compared with infection with West African MPXV as demonstrated through pathway over-representation analysis (ORA) with InnateDB. The down-regulated pathways were related primarily to growth and proliferation, apoptosis, and immune surveillance. The biological relevance of the differential pathways identified was demonstrated through flow cytometry and cell proliferation assays as West African MPXV-infected monocytes had significantly increased apoptotic and cell proliferative responses. Further, pharmacological inhibition of selected host targets differentially phosphorylated following infection by the two MPXV clades validated our systems kinomics results. Thus, we have employed systems kinomics for the investigation of host responses to MPXV infection, and demonstrate for the first time that West African and Congo Basin MPXV induce significantly different host cell signaling pathway activities following viral infection.

MATERIALS AND METHODS

Cell and Virus Conditions—MPXV Zaire 79 and MPXV Sierra Leone 70 strains were propagated in BSC-1 cells at a MOI of 0.1 for 4 days. BSC-1 cells were maintained in MEM supplemented with 10% fetal calf serum and 1% penicillin and streptomycin. Virus stocks were prepared by disruption of BSC-1 cells by successive freeze thaw followed by purification using sucrose gradients. Virus was quantified in a standard plaque assay on either Vero E6 or BSC-1 cells as

described previously (19). VACV Western Reserve and CPXV Brighton Red were generated in a similar fashion. Human THP-1 monocytes (ATCC TIB-202R) were maintained in RPMI 1640 medium supplemented with 10% (v/v) heat inactivated fetal bovine serum, 2 mM L-glutamine and 1 mM sodium pyruvate. All cultures were maintained at 37 °C in a humidified 5% (v/v) CO₂ incubator.

Viral Infection—Cells were plated in six-well plates and rested for 24 h prior to infection. Cells were infected with either Congo Basin MPXV or West African MPXV at a MOI of 3 or mock infected with an equivalent fraction of culture medium free of any virus. All viral infections were performed at the National Institutes of Health at Biosafety Level 3 in accordance with NIH/CDC Biosafety in Microbiological and Biomedical Laboratories guidelines, as well as in accordance with CDC Select Agent regulations. Virus was incubated with host cells for 1 h at 37 °C with periodic rocking. Following incubation, monocytes were washed twice with phosphate-buffered saline (PBS), resuspended with fresh RPMI 1640 media with 2% (v/v) fetal bovine serum and incubated for 24 h.

Kinome Analysis—Design, construction and application of the peptide arrays were based upon a previously reported protocol with the following modifications (56). Virus-infected and mock-infected THP-1 monocytes were pelleted following incubation and cell lysate was prepared and incubated with human kinome arrays (JPT Technologies, Berlin, Germany). Briefly, cell pellets were lysed with 100 µl of lysis buffer (20 mM Tris-HCl, pH 7.5, 150 mM NaCl, 1 mM ethylenediamine tetraacetic acid, 1 mM ethylene glycol tetraacetic acid, 1% Triton-X100, 2.5 mM sodium pyrophosphate, 1 mM Na₃VO₄, 1 mM NaF, 1 µg/ml leupeptin, 1 µg/ml aprotinin, 1 mM phenylmethylsulfonyl fluoride) and incubated on ice for 10 min. Following incubation, cell lysates were filtered through Amicon 100K filters (Millipore) for 15 min at 4 °C to remove intact viral particles. Subsequent peptide array processing was performed under BSL2 conditions. A 70 µl aliquot of the supernatant was mixed with 10 µl of the activation mix (50% glycerol, 50 µM ATP, 60 mM MgCl₂, 0.05% Brij-35 and 0.25 mg/ml bovine serum albumin) and incubated on a peptide array for 2 h at 37 °C. Arrays were subsequently washed once with PBS containing 1% Triton X-100 and submerged in PRO-Q Diamond Phosphoprotein Stain (Invitrogen, Carlsbad, CA) with gentle agitation in the dark for 1 h. Following staining, arrays were washed in destain [20% acetonitrile, 50 mM sodium acetate, pH 4.0 (Sigma)] 3X for 10 min/wash with the addition of fresh destain each time. A final wash was performed with dH₂O and placed in 50 ml conical tubes and air-dried for 20 min. Remaining moisture on the arrays was removed by centrifugation of the arrays at 300 × g for 3 min. Array images were acquired using an Axon 4000B microarray scanner at 532–560 nm with a 580 nm filter to detect dye fluorescence. Images were collected using the GenePix 6.0 software (MDS, Foster City, CA). Signal intensity values were collected using the GenePix 6.0 Software (MDS) with the following settings: scanner saturation level 65535, background calculation done using local feature background, signal mean and background mean intensity values used for analysis, local background features excludes 2 pixels, and width of background set to 3 feature diameters. Intensity values for the spots and background were collected for each array.

Kinome Data Preprocessing—The specific responses of each peptide were calculated by subtracting background intensity from foreground intensity. The resulting data were transformed using the variance stabilization model (57), previously trained by a larger MAP kinome data set, to bring all the transformed data onto the same scale while alleviating variance-mean-dependence. In addition, for each of the 300 peptides in a single treatment, the intensities induced by the treatments were subtracted by the intensities from the biological control (i.e. THP-1 + control media) and test statistics calculated. Average intensities were then taken over the three transformed rep-

licate intensities and these values subjected to hierarchical clustering analysis. The R package variance stabilization was used for the transformation (58).

Treatment-Treatment Variability Analysis—Peptide phosphorylations were subjected to paired t-tests to compare their signal intensities under a treatment condition with those under the control condition. Four tests were done for each peptide. Specifically, the tests were Congo Basin MPXV versus THP-1, West African MPXV versus THP-1, CPXV BR versus THP-1, and VACV WR versus THP-1. The *p* value cutoff was chosen to be 0.20. Formally, the test statistic (TS) was calculated as:

$$TS = \frac{D}{S_D \sqrt{n}}$$

where *D* is the mean of the differences between responses for the same peptides induced by two different treatments, *S_D* the standard deviation of the differences, and *n* is the number of replicates for that peptide in each treatment (i.e. 3 in our data set). Finally, the *p* values for the phosphorylation and dephosphorylation events were calculated as $P[TS > t^{(n-1)}]$ and $P[TS < t^{(n-1)}]$, respectively (i.e. one-sided *t* test). Peptides with significant (*p* < 0.20) changes in phosphorylation were selected using PERL and BASH scripts. The paired *t* test was done using R built-in function *t.test* with *paired* = *True*.

Hierarchical Clustering Analysis—The preprocessed data was subjected to hierarchical clustering and principle component analysis (PCA) to cluster treatments based on their kinome profiles. Specifically, for hierarchical clustering, McQuitty + (1 - Pearson Correlation) was used. Briefly, each treatment vector was considered as a singleton (i.e. a cluster with a single element) at the initial stage of the clustering. This method uses (1 - Pearson correlation) to calculate the distances between any two vectors of treatment, say *X* and *Y*. Formally, the Pearson correlation is computed as:

$$V_{xy} = \frac{300}{300} \frac{\sum_{i=1}^{300} x_i - x(y_i - y)}{\sum_{i=1}^{300} (x_i - x) \sum_{j=1}^{300} (y_j - y)}$$

and,

$$\text{dist}(\mathbf{X}, \mathbf{Y}) = 1 - v_{xy}$$

In addition, the McQuitty method updates the distance between the two clusters in such a way that upon merging cluster *C_x* and cluster *C_y* into a new cluster *C_{xy}*, the distance between *C_{xy}* and each of the remaining clusters, say *C_R*, is calculated in concern with the sizes of *C_x* and *C_y*. Mathematically, let the size of *C_x* be *nX* and size of *C_y* be *nY*, then:

$$D(C_{xy}, C_R) = \frac{nX \times D(C_x, C_R) + nY \times D(C_y, C_R)}{nX + nY}$$

The hierarchical clustering was augmented by a heatmap which is also generated using the R function *heatmap.2*. The function converts the intensity values to statistical z-scores, and then the z-scores are encoded as color (green/red) intensities. Green usually means a value lower than the mean; red a value higher.

Pathway Analysis of Differentially Phosphorylated Peptides—InnateDb (www.innatedb.com) is a publicly available resource which, based on levels of either differential expression or phosphorylation, predicts biological pathways based on experiment fold change datasets. Pathways are assigned a probability value (*p*) based on the number of proteins present for a particular pathway as well as the degree to which they are differentially expressed or modified relative

to a control condition. For our investigation input data was limited to peptides which showed consistent responses across the biological replicates ($p < 0.05$) as well as statistically significant changes from the control condition ($p < 0.10$).

WST-1 Cell Proliferation Assay—Cell proliferation in the MPXV-infected and mock-infected THP-1 monocytes was performed using the WST-1 proliferation assay (Millipore). Briefly, THP-1s (2×10^4 cells) were plated and rested overnight followed by 24 h MPXV infection as described above. WST-1/ECS solution was then added at a ratio of 1:10 and incubated at 37 °C for 2 h. Absorbance readings were acquired on a plate reader at a wavelength of 450 nm. Independent experiments were done in duplicate or triplicate and were repeated at least three times.

Apoptosis Assays—Induction of apoptosis in MPXV-infected THP-1 monocytes was determined using the ApoAlert Annexin V assay (Clontech) according to the manufacturer's instructions. Briefly, THP-1 monocytes were infected as described above. Following 24 h infection, cells were rinsed and resuspended with 1X binding buffer followed by the addition of 500 ng of Annexin V-FITC and Propidium iodide and incubated at room temperature in the dark for 10 min. Cells were subsequently washed with 1X binding buffer, incubated in fixative solution for 1 h at room temperature (PBS, 4% formaldehyde, 1% pluronic acid), and finally washed and resuspended in 1X binding buffer. Percentage of apoptotic cells was determined by BD[®] FACS analysis. Independent experiments were done in duplicate or triplicate and were repeated at least three times.

Caspase-3 activity was assessed using the EnzChek Caspase-3 Assay Kit (Invitrogen) according to the manufacturer's instructions. Briefly, MPXV-infected and mock-infected THP-1 monocytes were harvested by centrifugation 24 h postinfection and washed with PBS. Cell pellets were resuspended in 1X cell lysis buffer for 30 min on ice and centrifuged to remove cellular debris. Z-DEVD-AMC substrate was subsequently added and samples were incubated at room temperature for 30 min and fluorescence was measured at 441 nm on a standard plate reader.

Met PhosphoELISAS—THP-1 monocytes were infected or mock-infected as described above. At 24 h post-infection cells were harvested by centrifugation, washed with PBS, and lysed on ice for 10 min with 1X lysis buffer (20 mM Tris-HCl, pH 7.5, 150 mM NaCl, 1 mM ethylenediamine tetraacetic acid, 1 mM ethylene glycol tetraacetic acid, 1% Triton-X100, 2.5 mM sodium pyrophosphate, 1 mM Na_3VO_4 , 1 mM NaF, 1 $\mu\text{g}/\text{ml}$ leupeptin, 1 $\mu\text{g}/\text{ml}$ aprotinin, 1 mM phenylmethylsulfonyl fluoride). Phosphorylated c-Met was measured using the PathScan Phospho-Met (Tyr1234/1235) enzyme-linked immunosorbent assay (ELISA) Assay Kit (Cell Signaling) following the manufacturer's instructions. Experiments were done in duplicate were repeated independently at least three times.

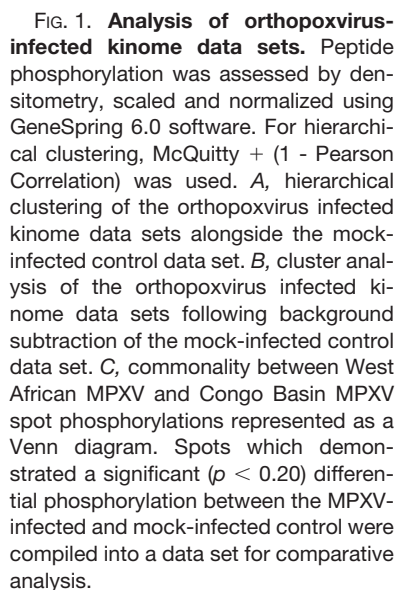
Pathway Inhibitor Assays—For the inhibitor studies THP-1 monocytes were pretreated for 30 min with LY29002 (20 μM ; Sigma Aldrich), Akt-X (15 μM ; EMD Biosciences, San Diego, CA) nutlin 3 (10 μM ; Sigma Aldrich), Met Kinase Inhibitor (1 μM or 10 μM ; Santa Cruz Biotechnology, Santa Cruz, CA), staurosporine (10 μM ; Enzo Lifesciences, Farmingdale, NY), SB-202190 (10 μM ; Enzo Lifesciences) or BML-257 (10 μM ; Enzo Lifesciences). Control cells were also employed in the absence of inhibitors. Cells were subsequently infected as described above in the continued presence or absence of inhibitor and harvested by centrifugation at 24 h post-infection followed by washing with cold PBS. Cells were subsequently disrupted by freezing and thawing and virus was collected from the supernatant of centrifuged cells and assayed for infectivity as described previously (19). Each experiment was run in duplicate and the results are reported as average values. The data was confirmed by at least three independent experiments with identical results.

RESULTS

West African and Congo Basin MPXV Induce Differential Host Target Phosphorylation—We postulated that the virulence differences associated with West African and Congo Basin MPXV may be attributed to the differential modulation of host cell signaling pathways following infection. Thus, we employed systems kinomics (20, 29, 30) with high-throughput human kinome peptide arrays to study the global activation state of host kinases, the kinome, following West African or Congo Basin MPXV infection. The resultant kinome data sets were subjected to hierarchical cluster analysis for comparative analysis and visualization of changes to host cell phosphorylation following infection. Conserved patterns of host kinome responses across the orthopoxvirus genus were also compared by the incorporation of CPXV BR and VACV WR. Interestingly, West African and Congo Basin MPXV demonstrated weak patterns of clustering independent of subtraction of the mock infected control (Figs. 1A, 1B). Further, Congo Basin MPXV-induced host phosphorylations clustered strongly with those induced by CPXV BR and VACV WR. Pairwise comparison of the MPXV data sets using Student's *t* test revealed a number of differential phosphorylations between either of the MPXV clades and the mock-infected condition or between the two MPXV clades directly. The commonality of peptide phosphorylations between West African and Congo Basin MPXV is presented in Fig. 1C. Of the peptide phosphorylations that displayed high technical reproducibility (as described in the materials and methods), 129 and 130 peptides were differentially phosphorylated relative to the mock-infected control for Congo Basin and West African MPXV, respectively. Approximately one-third of the differentially phosphorylated peptides were conserved in both identity and direction of phosphorylation changes (Fig. 1C). This is not unanticipated as the limited amino acid sequence variability between the MPXV clades (27) would suggest some degree of conserved interaction with the host. The remaining peptide phosphorylation differences represented phosphorylation events specific to a particular MPXV clade and represent differential trends in responses (increased *versus* decreased phosphorylation).

Congo Basin MPXV Selectively Down-regulates Host Signaling Pathways As Compared With West African MPXV—To gain insight into the relation between our kinome data and differential mechanisms of host response modulation employed by either West African or Congo Basin MPXV, we employed pathway ORA with the online software InnateDB (31). Input data for the analysis was limited to significant differences in peptide target phosphorylations ($p < 0.10$) relative to the mock-infected controls to ensure that identified pathways represented conserved biological responses.

For our initial pathway analysis we focused on protein phosphorylations that were common only to Congo Basin or West African MPXV infection (Fig. 1C). Pathway ORA of protein phosphorylations common to the Congo Basin MPXV



phosphorylations common to West African MPXV infection resulted in a broader subset of pathways identified by our ORA (Table II). Up-regulated pathways were primarily related to immune activation, including interleukin 2 (IL-2) and IL-6 signaling pathways (33), and growth factor responses, including fibroblast growth factor (FGF) (34), epidermal growth factor (EGFR) (35, 36), and platelet derived growth factor beta (PDGF β). In contrast, down-regulated pathways were found to be primarily related to transforming growth factor beta (TGF β) signaling responses (Table II).

Investigation of host kinome responses to monkeypox virus

TABLE I

Pathway over representation analysis of uncommon proteins differentially phosphorylated in response to Congo basin MPXV infection

Pathway Name	Proteins in Pathway	Increased Phosphorylations	Up-Regulated Pathway P Value	Decreased Phosphorylations	Down-Regulated Pathway P Value
FoxO family signaling	4	4	0.074	0	1
Cytokine-cytokine receptor interaction	3	0	1	3	1
Growth hormone signaling pathway	3	0	1	3	1
Melanoma	7	2	0.98	5	1

TABLE II

Pathway over representation analysis of uncommon proteins differentially phosphorylated in response to West African MPXV infection

Pathway Name	Proteins in Pathway	Increased Phosphorylations	Up-Regulated Pathway P Value	Decreased Phosphorylations	Down-Regulated Pathway P Value
FGF signaling pathway	6	6	0.027	0	1
IL2	6	6	0.027	0	1
ErbB1 downstream signaling	9	8	0.034		1
Signaling events mediated by TCPTP	5	5	0.052	0	1
IL6	8	7	0.062	0	1
KitReceptor	4	4	0.099	0	1
LPA receptor mediated events	4	4	0.099	0	1
PDGFR-beta signaling pathway	4	4	0.099	0	1
Regulation of nuclear SMAD2/3 signaling	4	4	0.099	0	1
TGF-beta receptor signaling	6	1	1	5	0.027
ALK1 signaling events	3	0	1	3	0.054
Chronic myeloid leukemia	7	2	0.99	5	0.070
Colorectal cancer	7	2	0.99	5	0.070

Although these comparisons suggested that Congo Basin and West African MPXV differentially modulate host cell response following infection, the limited information from our initial pathway ORA compelled us to investigate this phenomenon further through direct comparison of the complete Congo Basin and West African MPXV kinome array data sets. We hypothesized that this comparison would provide a more detailed comparison by including protein phosphorylations that were common to both MPXV infection groups as well as those that were uncommon. As predicted, the direct comparison of the complete data sets yielded a much broader range of pathways differentially modulated by the two MPXV clades (Table III). Interestingly, Congo Basin MPXV infection resulted in the global down-regulation of host cellular responses as compared with West African MPXV following direct comparison of the two kinome data sets. As found in our initial comparative the down-regulated pathways were primarily related to growth factor signaling: including fibroblast growth factor (FGF) signaling (34), BCR-ABL-mediated signaling (17), and growth hormone signaling pathway (18)). However, pathways related to subversion of apoptotic responses were also identified, including the FAS signaling pathway (32), direct p53 effectors (37), regulation of bad phosphorylation (38), and phosphatase and tensin homolog (PTEN) dependent cell cycle arrest and apoptosis (16). Thus, our pathway ORA suggest that the Congo Basin MPXV selectively down-regulated host cell responses primarily related to growth factor signaling and apoptotic responses as compared with the less virulent West African MPXV clade.

Biological Validation of Signaling Responses Identified Through Kinome Analysis—Following the demonstration that Congo Basin MPXV infection down-regulated pathways related to growth factor signaling/cell proliferation and apoptosis as compared with West African MPXV, we sought to biologically validate these results. Importantly, we first demonstrated that the growth kinetics and level of virus replication of the two MPXV clades were similar throughout the course of our infection studies (supplemental Fig. S1).

First, our pathway ORA data for the direct comparison of Congo Basin and West African MPXV suggested that Congo Basin MPXV down-regulated cell proliferative responses as compared with West African MPXV (Table III). Thus, we monitored cell proliferation responses to the two MPXV viruses through a WST-1 assay as this assay is routinely used to investigate cell proliferation, cell viability and cytotoxicity. Our data demonstrate that Congo Basin MPXV infection resulted in a moderate but significant reduction in THP-1 cell proliferation as compared with West African MPXV (Fig. 2; data presented relative to mock-infected cells). This is consistent with the differential host responses identified through our pathway ORA.

The direct comparison of the kinome array data sets for Congo Basin and West African MPXV also suggested that West African MPXV selectively down-regulated apoptotic responses in host cells (Table I). Using fluorescence-activated cell sorting (FACS) analysis of AnnexinV staining we demonstrated a significant increase in host cell apoptosis following West African MPXV infection as compared with Congo Basin

TABLE III

Differential host cell signaling responses to Congo Basin MPXV-infected monocytes as compared to West African MPXV-infected monocytes. InnateDB is a publically available pathway analysis tool. Based on levels of differential expression or phosphorylation InnateDB is able to predict pathways that are consistent with the experimental data. Pathways are assigned a probability value (*p*) based on the number of proteins present for a particular pathway. It also provides the number of uploaded pathways associated with a particular pathway as well as the subset of individual proteins that are differentially phosphorylated. For this investigation fold change cutoffs were set at 80% confidence of the difference between the infected and mock-infected treatment

Pathway Name	Proteins in Pathway	Increased Phosphorylations	Up-Regulated Pathway P Value	Decreased Phosphorylations	Down-Regulated Pathway P Value
Agrin in postsynaptic differentiation	3	3	0.068	0	1
FGF signaling pathway	8	0	1	8	0.0018
Inhibition of cellular proliferation by gleevec	8	0	1	7	0.021
Ctcf: first multivalent nuclear factor	5	0	1	5	0.022
Signaling events activated by Hepatocyte Growth Factor Receptor (c-Met)	12	2	0.99	9	0.042
Signaling events mediated by Stem cell factor receptor (c-Kit)	12	2	0.99	9	0.042
Tpo signaling pathway	7	0	1	6	0.043
BMP2 signaling pathway(through Smad)	4	0	1	4	0.049
C-MYB transcription factor network	4	0	1	4	0.049
Calcineurin-regulated NFAT-dependent transcription in lymphocytes	4	0	1	4	0.049
Calcium signaling in the CD4+ TCR pathway	4	0	1	4	0.049
Class I PI3K signaling events mediated by Akt	4	0	1	4	0.049
Pten dependent cell cycle arrest and apoptosis	4	0	1	4	0.049
Regulation of bad phosphorylation	4	0	1	4	0.049
Direct p53 effectors	6	1	0.97	5	0.083
ErbB2/ErbB3 signaling events	6	0	1	5	0.083
FAS signaling pathway (CD95)	6	1	0.97	5	0.083
Osteopontin-mediated events	6	1	0.97	5	0.083
Role of Calcineurin-dependent NFAT signaling in lymphocytes	6	0	1	5	0.083

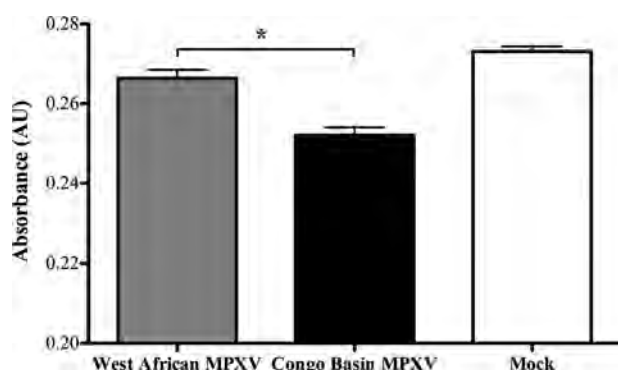


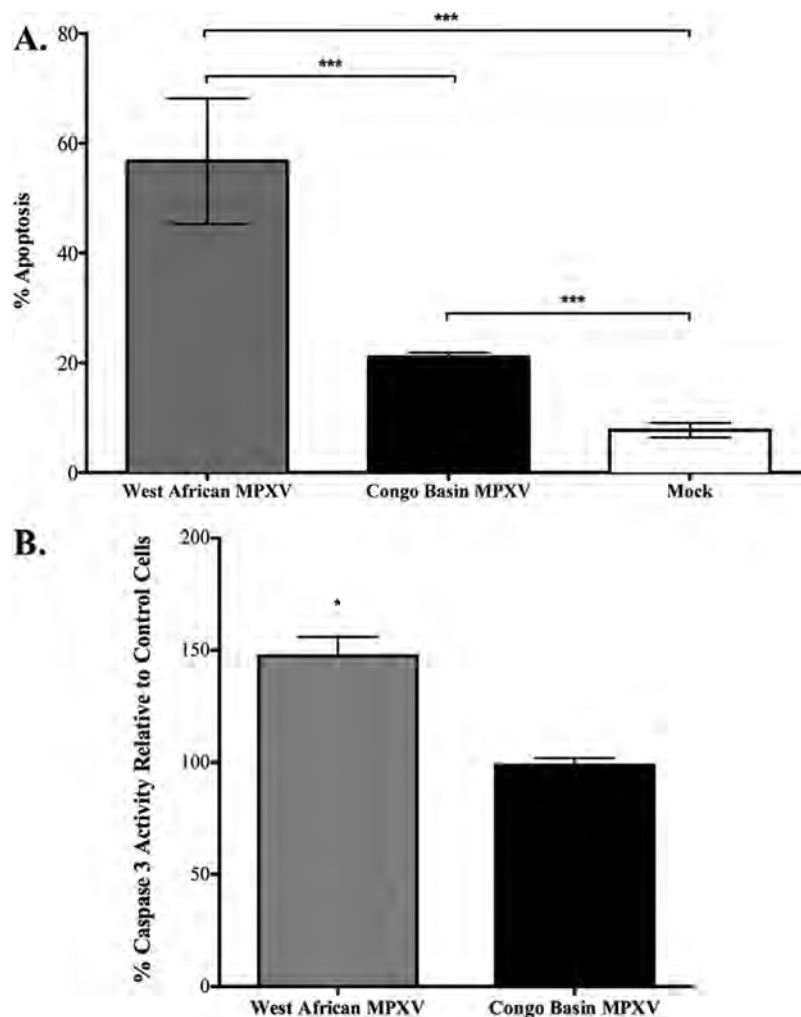
FIG. 2. Comparison of the effect of West African MPXV or Congo Basin MPXV on cell proliferation. Human THP-1 monocytes were seeded in a 96-well plate at 1×10^5 cell/well with 100 μ l of culture medium and infected at an MOI of 3 with West African or Congo Basin MPXV for 24 h. Cell proliferation was assessed through the addition of WST-1 reagent 30 min at the 24 h time point and absorbance was measured at 450 nm in a multiwell plate reader. Data is presented as the mean of three independent experiments \pm S.D. *, $p < 0.1$. A Student's *t* test was used for the comparison.

MPXV (Fig. 3A). This was further corroborated through a caspase 3 activity assay demonstrating a significant increase in caspase 3 activity in West African MPXV-infected cells relative to Congo Basin MPXV-infected cells (Fig. 3B; data presented relative to mock-infected control cells).

To further validate our kinome array data we selected a target that was common in all iterations of the pathway ORA, c-Met. c-Met-related signaling pathways were found to be repressed by Congo Basin MPXV in both Table I and Table III. We investigated the phosphorylation status of c-Met in response to both Congo Basin and West African MPXV directly through phosphospecific ELISA. Our array data demonstrated that c-Met Y1234 phosphorylation was significantly repressed (~ 1.4 -fold) in Congo Basin MPXV infected monocytes as compared with West African MPXV. Using a c-Met Y1234 phosphospecific ELISA we demonstrated that Congo Basin MPXV-infected cell lysates had a significant reduction (~ 1.4 -fold) in c-Met Y1234 phosphorylation as compared with lysates from West African MPXV-infected monocytes (Fig. 4A). Further, pharmacological inhibition of c-Met phosphorylation with 1 μ M or 10 μ M of Met Kinase Inhibitor 30 min prior to infection with the two MPXV clades (multiplicity of infection (MOI) = 3) resulted in a concentration-dependent increase in Congo Basin MPXV viral titers as compared with untreated Congo Basin MPXV-infected cells and no significant effect on West African MPXV infection (Fig. 4B). Taken together, the results of our biological validation functionally confirmed our kinome array data demonstrating the reliability and power of this approach.

FIG. 3. West African MPXV infection results in increased apoptosis as compared with Congo Basin MPXV.

Human THP-1 monocytes (1×10^6 cells) were infected at an MOI of 3 and seeded in a six-well plate with 3 ml of culture medium and incubated for 24 h. **A**, FACS analysis of THP-1 monocyte apoptosis 24 h postinfection by the two MPXV clades. Data is presented as the mean of three independent experiments \pm S.D. **B**, Caspase 3 activity of West African or Congo Basin MPXV-infected THP-1 monocyte lysates relative to the mock-infected THP-1 cells. Data is presented as the mean of three independent experiments with identical results \pm S.D. *, $p < 0.1$; ***, $p < 0.001$. A Student's *t* test was used for the comparison.



Disruption of Akt S473 and p38 α Phosphorylation, or Activation of Apoptosis, Significantly Inhibits Congo Basin MPXV Replication as Compared with West African MPXV—In addition to increasing our understanding of mechanisms of viral pathogenesis, our kinome data and pathway ORA provided the identities of specific host pathways and kinases that were differentially modulated by Congo Basin and West African MPXV. Previously, it has been demonstrated that poxviruses can selectively modulate host responses mediated by the PBK/Akt pathway for regulation of viral replication (39, 40). Soares *et al.* demonstrated that the selective pharmacological inhibition of Akt S473 phosphorylation with Akt-X or T308 phosphorylation with LY294002 reduced CPXV and VACV virus yields by 80–90% (40). Our kinome array data suggested that phosphorylation of Akt S473 was significantly increased (1.8 fold) following Congo Basin MPXV but was unaffected following West African MPXV infection. Akt T308 phosphorylation was comparably increased in both West African and Congo Basin MPXV infected cells as compared with the mock-infected controls (supplemental Table S5). Thus, we sought to investigate the effects of pharmacological inhibition

of Akt phosphorylation on West African and Congo Basin MPXV viral replication. We performed one-step viral growth curves for both MPXV clades in the presence or absence of LY294002 (20 μ M) or Akt-X (15 μ M). This concentration of inhibitors had no significant effect on cell viability (data not shown). Cells were left untreated or were pretreated with inhibitors for 30 min prior to infection at an MOI of 3 in the continued presence of inhibitors. At 24 h post-infection virus was collected and assayed for infectivity. Inhibition of Akt S308 by LY294002 had no significant inhibitory effect on virus production in monocytes infected with either MPXV clade (Fig. 5). However, inhibition of Akt S473 phosphorylation with Akt-X selectively inhibited Congo Basin MPXV virus replication (261-fold reduction in virus yield), whereas there was no significant inhibition West African MPXV infection as compared with the untreated infected controls (Fig. 5). Interestingly, pharmacological inhibition of Akt translocation with BML-257 demonstrated a similar inhibitory effect (~3.5-fold difference) on the two MPXV clades suggesting a central role for Akt in the life cycles of both MPXV clades.

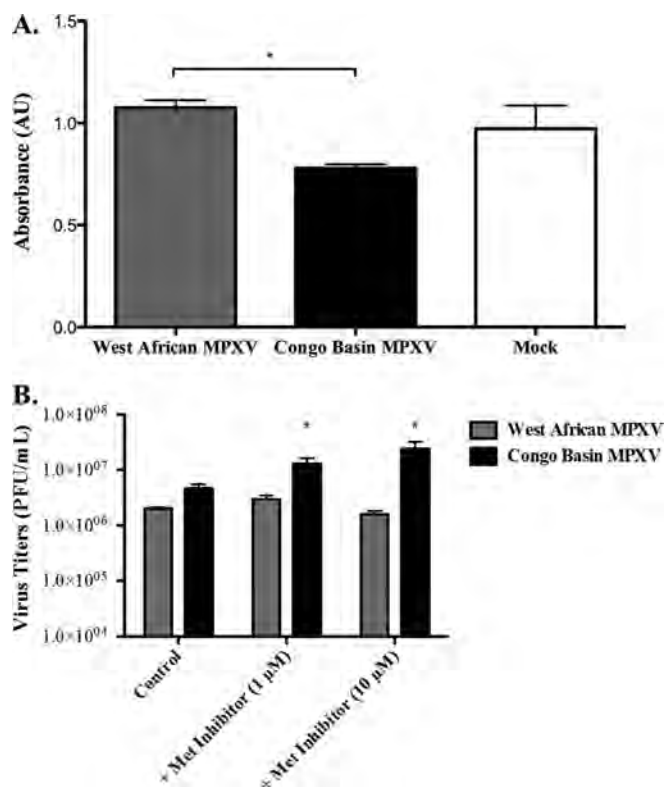


FIG. 4. West African MPXV infection increases Met phosphorylation as compared with Congo Basin MPXV. Human THP-1 monocytes (1×10^6 cells) were infected at an MOI of 3 and seeded in a six-well plate with 3 ml of culture medium and incubated for 24 h. **A**, Met PhosphoELISA analysis of West African or Congo Basin MPXV-infected THP-1 monocytes relative to the mock-infected THP-1 cells. Phosphorylated Met (Tyr1234/1235) was determined by phospho-ELISA assay as described in Methods. **B**, Effect Met phosphorylation inhibition on West African and Congo Basin MPXV virus yields. Human THP-1 monocytes were either left untreated or treated for 30 min with Met Kinase Inhibitor (1 μ M or 10 μ M) prior to virus infection. Cells were subsequently infected with West African MPXV or Congo Basin MPXV at an MOI of 3 in the absence or continued presence of inhibitor for 24 h. Viruses were then collected and viral titers were determined. Data is presented as the means of three independent experiments \pm S.D. *, $p < 0.1$. A Student's t test was used for the comparison and p values were based on comparison to the control infected conditions.

Recently, Zachos *et al.* have demonstrated that herpes simplex virus type 1 (HSV-1)-enhanced infection through stimulation of p38 MAPK signaling (41). Analysis of our kinome data sets also suggested that Congo Basin MPXV infection resulted in increased p38 phosphorylation (p38 α and p38 δ) as compared with West African MPXV (1.5-fold and 2.4 fold, respectively). We had also found that pre-treatment of HEK293 cells with SB-202190, a p38 α inhibitor, resulted in a significant inhibition of a GFP expressing Congo Basin MPXV (Data not shown) suggesting a central role for p38 in Congo Basin MPXV infection. Pretreatment of cells with SB-202190 resulted in decreased West African and Congo Basin MPXV virus yields; however, addition of the inhibitor had a 9.5-fold

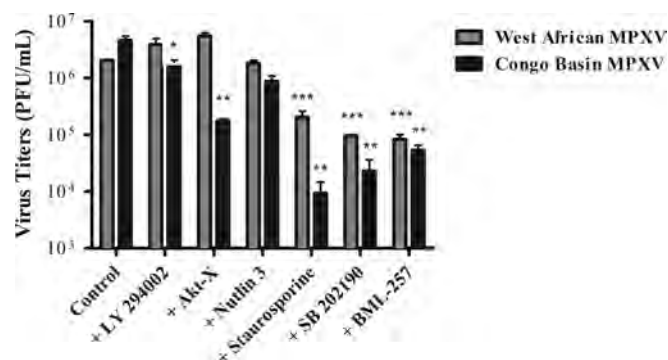


FIG. 5. Inhibitors of Akt or p38 alpha phosphorylation, or activation of apoptosis, decrease Congo Basin MPXV viral replication as compared with West African MPXV. Human THP-1 monocytes were either left untreated or treated for 30 min with LY294002 (20 μ M), Akt-X (15 μ M), nutlin 3 (10 μ M), staurosporine (10 μ M), SB-202190 (10 μ M), or BML-257 (10 μ M) prior to virus infection. Cells were subsequently infected with West African MPXV or Congo Basin MPXV at an MOI of 3 in the absence or continued presence of the pharmacological agents for 24 h. Viruses were then collected and viral titers were determined. Data are representative of three independent experiments \pm S.D. *, $p < 0.1$; **, $p < 0.01$; ***, $p < 0.001$. A Student's t test was used for the comparison and p values were based on comparison to the control infected conditions.

greater inhibitory effect on Congo Basin MPXV virus production. SB-202190 was not cytotoxic to cells at the concentration tested.

As Congo Basin MPXV selectively repressed apoptosis in infected monocytes as compared with West African MPXV, and this correlated with reduced phosphorylation of p53 in our kinome array comparison (~ 1.6 -fold), we investigated the effect of chemical antagonism of apoptosis on MPXV virus yields. We postulated that increased apoptosis in Congo Basin MPXV-infected monocytes would result in reduced virus yields as compared with West African MPXV. Cells were pre-treated with staurosporine (10 μ M) and were subsequently infected with MPXV as above. Cells treated with staurosporine were $>94\%$ viable after 24 h. Activation of apoptosis resulted in significantly reduced viral yields in both Congo Basin MPXV-infected cells (495-fold decrease) and West African MPXV-infected cells (10-fold decrease) (Fig. 5). However, the ~ 50 -fold greater inhibition of Congo Basin MPXV suggests a much stronger effect of apoptosis activation on Congo Basin MPXV virus replication. These data indicate the rapid translation of kinomic data into rational strategies for antiviral target discovery.

DISCUSSION

Although global eradication of smallpox was announced in 1980 there is a paucity of information regarding the molecular mechanisms underlying VARV disease pathogenesis. The critical importance of understanding the molecular mechanisms of poxvirus disease is further underscored by the increasing incidence of MPXV, a surrogate for VARV studies, and the accidental introduction of MPXV into the United States in

2003. Through a combination of systems kinomics and biological and functional validation assays we have demonstrated that West African and Congo Basin MPXV differentially modulate host cell responses and in particular those related to cell proliferation, cell survival and apoptosis.

Our investigation demonstrated that Congo Basin MPXV selectively downregulated pathways largely related to apoptotic events, including p53- and Fas-mediated cell signaling events, and cell proliferation, and enhanced cell survival as compared with West African MPXV. Indeed, the ability of poxviruses to subvert pro-apoptotic host cell responses, in particular through gene-encoded apoptosis inhibitors, is well documented (40, 42–45). Analysis of our kinome data sets suggested that the anti-apoptotic activities associated with Congo Basin MPXV were largely related to p53-mediated signaling apoptosis pathways and supported by FACS analysis and caspase 3 activity assays. Proteomic analysis of West African and Congo Basin MPXV has demonstrated >99% amino acid sequence conservation between the two MPXV clades; however, differences within the two sequences were sequestered to host response modifier proteins at the terminal ends of the genome (28). Interestingly, BR-203, an ortholog of myxoma virus M-T4 believed to have a role in subversion of host apoptotic responses (32, 46), is predicted to be severely truncated in West African MPXV though the full-length gene appears in Congo Basin MPXV (42). Thus, it is enticing to speculate that BR-203 plays a central role in the virulence associated with Congo Basin MPXV and may be a novel target for therapeutic investigations. Further, there is an increasing appreciation for subversion of host apoptotic responses as a means of facilitating viral replication (47). As apoptosis is an important function of innate immunity for limiting pathogen dissemination it is unsurprising that viruses have evolved diverse mechanisms for subverting host apoptotic responses.

To gain further insight into the mechanisms of MPXV-mediated host response modulation we directly compared the kinome data sets from the two MPXV clades. Pathway ORA suggested that Congo Basin MPXV-infection represses host signaling pathways largely related to growth factor signaling and cell proliferative responses as compared with the less virulent West African MPXV clade. Although it may seem counter-intuitive for a more virulent virus to reduce cell proliferative responses, investigations of vFGF, a baculovirus FGF mimic, have demonstrated that vFGF increases virus dissemination and reduces the time to death for the host (48). The ability of vFGF to bind and activate the host FGF receptor results in virus-mediated host cell proliferation. Signaling events mediated by the hepatocyte growth factor receptor c-Met were identified through pathway ORA in both the phosphorylation events common to Congo Basin MPXV and following direct comparison to the West African MPXV kinome data sets. This coupled with our phosphoELISA data and Met Kinase Inhibitor data suggested that c-Met occupied a central

role in Congo Basin MPXV infection of monocytes. This suggests that Congo Basin MPXV selectively modulates c-Met-mediated signaling pathways, and perhaps other growth factor-mediated signaling events, during infection. Indeed, the repression of monocyte cell proliferation by Congo Basin MPXV may highlight a secondary mechanism for the virus to subvert potential host cell apoptosis following enhanced, and potentially uncontrolled, cell proliferation. Recent evidence from Ryan and colleagues suggests that chronic hepatitis C infection may impede host immune responses by disabling dendritic cells as a mechanism to reduce pathogen recognition and initiation of the innate immune response (49). Moreover, pathway ORA of phosphorylation events common to Congo Basin MPXV infection suggested that the FoxO signaling pathways were distinct to infection by this MPXV clade. FoxO signaling pathways have been implicated in the delicate balance between cell survival and cell death (50). As FoxO activation can block cell proliferation and promote quiescence in many cell types it is enticing to speculate that this may reflect a vital role for the activation of FoxO signaling pathways in subversion of host immunity by Congo Basin MPXV. Thus, our data suggests that the increased virulence associated with Congo Basin MPXV as compared with West African MPXV may be a consequence of both the precise modulation of programmed cell death, cell cycle progression and promotion of cell survival. Further investigations focusing on the selective modulation of the pathways identified in our comparison of the two MPXV clade data sets may identify previously unknown roles of these pathways in viral infection.

A recent investigation by Soares *et al.* highlighted the central role of Akt phosphorylation in orthopoxvirus infection (40). Our kinome analysis demonstrated that West African and Congo Basin MPXV differentially modulate Akt S473 phosphorylation. Importantly, pharmacological inhibition of S473 phosphorylation with Akt-X significantly inhibited viral replication in Congo Basin MPXV-infected cells; however, no reduction was demonstrated for West African MPXV-infected cells. Thus, our data suggest that the two MPXV clades may utilize different host cell signaling pathways for viral replication and the precise mechanisms underlying these differences require further exploration. Interestingly, pretreatment with BML-257, an Akt translocation inhibitor, had similar inhibitory effects on West African and Congo Basin MPXV. This indicates that the modulation of Akt-mediated signaling by Congo Basin MPXV is likely related to the phosphorylation state of Akt rather than its cellular localization. Our investigation also suggests a central role for p38 α , and potentially p38-MAPK signaling, in Congo Basin MPXV infections. Our kinome data demonstrated that Congo Basin MPXV infection results in increased phosphorylation of the p38 α and treatment with the p38 α inhibitor SB-202190 resulted in a 9.5-fold greater decrease in Congo Basin MPXV virus yields as compared with West African MPXV. Although the activation of p38 MAPK signaling is classically related to stress responses and activation of cell

death (51), there is increasing evidence that under certain circumstances p38 MAPK can enhance cell survival. Indeed, p38 MAPK activation has been demonstrated to enhance cell survival responses to DNA damage (52, 53). Further, Zachos *et al.* have demonstrated that herpes simplex virus type 1 (HSV-1)-mediated stimulation of p38 MAPK resulted in enhanced viral transcription and increased virus yields (41).

Although systems kinomics has been employed extensively in cancer research (20) there has been limited application to the investigation of viral infections. Thus, molecular investigations of poxvirus disease pathogenesis have relied on gene expression studies. Rubins *et al.* demonstrated that MPXV genes related to immunomodulation were expressed throughout the course of infection (54). Alkhalil *et al.* and Rubins *et al.* recently demonstrated that Congo Basin MPXV infection down-regulated a broad range of host responses (15). More recently, Brown *et al.* demonstrated that MPXV insult resulted in reductions to host protein expression levels, most notably those participating in structural or metabolic processes (55). Although these investigations have provided important information regarding modulation of host immunity by Congo Basin MPXV, the integration of systems kinomics has provided pertinent functional information regarding the differential host response to Congo Basin MPXV and the less-virulent West African MPXV clade and identified potential host targets for therapeutic intervention.

* This study was supported, in part, by the National Institute of Allergy and Infectious Diseases, Division of Intramural Research.

§ This article contains [supplemental Fig. S1 and Tables S1 to S5](#).

§§ To whom correspondence should be addressed: National Institutes of Health (NIH), National Institute of Allergy and Infectious Diseases (NIAID), Emerging Viral Pathogens Section, 33 North Drive, Rm 2E19A, 20892. Tel.: (301) 631-7256; Fax: (301) 619-5029; E-mail: kindrachuk.kenneth@nih.gov.

REFERENCES

- Parker, S., Nuara, A., Buller, R. M., and Schultz, D. A. (2007) Human monkeypox: an emerging zoonotic disease. *Future Microbiol.* **2**, 17–34
- Von Magnus, P., Anderson, E. K., Petersen, K. B., and Birch-Andersen, A. (1959) A pox-like disease in cynomolgus monkeys. *Acta Path. Microbiol. Scand.* **46**, 156–176
- Ladnyj, I. D., Ziegler, P., and Kima, E. (1972) A human infection caused by monkeypox virus in Basankusu Territory, Democratic Republic of the Congo. *Bull World Health Organ.* **46**, 593–597
- Rimoin, A. W., Mulembakani, P. M., Johnston, S. C., Lloyd Smith, J. O., Kitalu, N. K., Kinkela, T. L., Blumberg, S., Thomassen, H. A., Pike, B. L., Fair, J. N., Wolfe, N. D., Shongo, R. L., Graham, B. S., Formenty, P., Okitolonda, E., Hensley, L. E., Meyer, H., Wright, L. L., and Muyembe, J. J. (2010) Major increase in human monkeypox incidence 30 years after smallpox vaccination campaigns cease in the Democratic Republic of Congo. *Proc. Natl. Acad. Sci. U.S.A.* **107**, 16262–16267
- Reed, K. D., Melski, J. W., Graham, M. B., Regnery, R. L., Sotir, M. J., Wegner, M. V., Kazmierczak, J. J., Stratman, E. J., Li, Y., Fairley, J. A., Swain, G. R., Olson, V. A., Sargent, E. K., Kehl, S. C., Frace, M. A., Kline, R., Foldy, S. L., Davis, J. P., and Damon, I. K. (2004) The detection of monkeypox in humans in the Western Hemisphere. *N. Engl. J. Med.* **350**, 342–350
- Jahrling, P. B., Fritz, E. A., and Hensley, L. E. (2005) Countermeasures to the bioterrorist threat of smallpox. *Curr. Mol. Med.* **5**, 817–826
- Jezek, Z., Grab, B., Paluku, K. M., and Szczeniowski, M. V. (1988) Human monkeypox: disease pattern, incidence and attack rates in a rural area of northern Zaire. *Trop. Geogr. Med.* **40**, 73–83
- Saijo, M., Ami, Y., Suzuki, Y., Nagata, N., Iwata, N., Hasegawa, H., Iizuka, I., Shiota, T., Sakai, K., Ogata, M., Fukushima, S., Mizutani, T., Sata, T., Kurata, T., Kurane, I., and Morikawa, S. (2009) Virulence and pathophysiology of the Congo Basin and West African strains of monkeypox virus in non-human primates. *J. Gen. Virol.* **90**, 2266–2271
- Osorio, J. E., Iams, K. P., Meteyer, C. U., and Rocke, T. E. (2009) Comparison of monkeypox viruses pathogenesis in mice by in vivo imaging. *PLoS One* **4**, e6592
- Hutson, C. L., Abel, J. A., Carroll, D. S., Olson, V. A., Braden, Z. H., Hughes, C. M., Dillon, M., Hopkins, C., Karem, K. L., Damon, I. K., and Osorio, J. E. (2009) Comparison of West African and Congo Basin monkeypox viruses in BALB/c and C57BL/6 mice. *PLoS One* **5**, e8912
- Hutson, C. L., Carroll, D. S., Self, J., Weiss, S., Hughes, C. M., Braden, Z., Olson, V. A., Smith, S. K., Karem, K. L., Regnery, R. L., and Damon, I. K. (2010) Dosage comparison of Congo Basin and West African strains of monkeypox virus using a prairie dog animal model of systemic orthopoxvirus disease. *Virology* **402**, 72–82
- Hutson, C. L., Olson, V. A., Carroll, D. S., Abel, J. A., Hughes, C. M., Braden, Z. H., Weiss, S., Self, J., Osorio, J. E., Hudson, P. N., Dillon, M., Karem, K. L., Damon, I. K., and Regnery, R. L. (2009) A prairie dog animal model of systemic orthopoxvirus disease using West African and Congo Basin strains of monkeypox virus. *J. Gen. Virol.* **90**, 323–333
- Sbrana, E., Xiao, S. Y., Newman, P. C., and Tesh, R. B. (2007) Comparative pathology of North American and central African strains of monkeypox virus in a ground squirrel model of the disease. *Am. J. Trop. Med. Hyg.* **76**, 155–164
- Rubins, K. H., Hensley, L. E., Relman, D. A., and Brown, P. O. (2007) Stunned silence: gene expression programs in human cells infected with monkeypox or vaccinia virus. *PLoS One* **6**, e15615
- Alkhalil, A., Hammamieh, R., Hardick, J., Ichou, M. A., Jett, M., and Ibrahim, S. (2010) Gene expression profiling of monkeypox virus-infected cells reveals novel interfaces for host-virus interactions. *Virus* **1**, 173
- Rubins, K. H., Hensley, L. E., Bell, G. W., Wang, C., Lefkowitz, E. J., Brown, P. O., and Relman, D. A. (2008) Comparative analysis of viral gene expression programs during poxvirus infection: a transcriptional map of the vaccinia and monkeypox genomes. *PLoS One* **3**, e2628
- Shenolikar, S. (2007) Analysis of protein phosphatases: toolbox for unraveling cell signaling networks. *Methods Mol. Biol.* **365**, 1–8
- Zhang, H., Zha, X., Tan, Y., Hornbeck, P. V., Mastrangelo, A. J., Alessi, D. R., Polakiewicz, R. D., and Comb, M. J. (2002) Phosphoprotein analysis using antibodies broadly reactive against phosphorylated motifs. *J. Biol. Chem.* **277**, 39379–39387
- Johnson, R. F., Dyall, J., Ragland, D. R., Huzella, L., Byrum, R., Jett, C., St Claire, M., Smith, A. L., Paragas, J., Blaney, J. E., and Jahrling, P. B. (2011) Comparative analysis of monkeypox virus infection of cynomolgus macaques by the intravenous or intrabronchial inoculation route. *J. Virol.* **85**, 2112–2125
- Piersma, S. R., Labots, M., Verheul, H. M., and Jiménez, C. R. (2010) Strategies for kinome profiling in cancer and potential clinical applications: chemical proteomics and array-based methods. *Anal. Bioanal. Chem.* **397**, 3163–3171
- Bowick, G. C., Fennewald, S. M., Scott, E. P., Zhang, L., Elsom, B. L., Aronson, J. F., Spratt, H. M., Luxon, B. A., Gorenstein, D. G., and Herzog, N. K. (2007) Identification of differentially activated cell-signaling networks associated with pichinde virus pathogenesis by using systems kinomics. *J. Virol.* **81**, 1923–1933
- Bahar, M. W., Graham, S. C., Chen, R. A., Cooray, S., Smith, G. L., Stuart, D. I., and Grimes, J. M. (2011) How vaccinia virus has evolved to subvert the host immune response. *J. Structural Biol.* **175**, 127–134
- Seet, B. T., Johnston, J. B., Brunetti, C. R., Barrett, J. W., Everett, H., Cameron, C., Sypula, J., Nazarian, S. H., Lucas, A., and McFadden, G. (2003) Poxviruses and immune evasion. *Annu. Rev. Immunol.* **21**, 377–423
- Jung, M., Finnen, R. L., Neron, C. E., and Banfield, B. W. (2011) The alphaherpesvirus serine/threonine kinase us3 disrupts promyelocytic leukemia protein nuclear bodies. *J. Virol.* **85**, 5301–5311
- Klerkx, E. P., Lazo, P. A., and Askjaer, P. (2009) Emerging biological functions of the vaccinia-related kinase (VRK) family. *Histol. Histopathol.* **24**, 749–759
- Valbuena, A., Sanz-Garcia, M., Lopez-Sanchez, I., Vega, F. M., and Lazo,

- P. A. (2011) Roles of VRK1 as a new player in the control of biological processes required for cell division. *Cell. Signal.* **23**, 1267–1272
27. Chen, N., Li, G., Liszewski, M. K., Atkinson, J. P., Jahrling, P. B., Feng, Z., Schriewer, J., Buck, C., Wang, C., Lefkowitz, E. J., Esposito, J. J., Harms, T., Damon, I. K., Roper, R. L., Upton, C., and Buller, R. M. (2005) Virulence differences between monkeypox virus isolates from West Africa and the Congo basin. *Virology* **340**, 46–63
 28. Likos, A. M., Sammons, S. A., Olson, V. A., Frace, A. M., Li, Y., Olsen-Rasmussen, M., Davidson, W., Galloway, R., Khristova, M. L., Reynolds, M. G., Zhao, H., Carroll, D. S., Curns, A., Formenty, P., Esposito, J. J., Regnery, R. L., and Damon, I. K. (2005) A tale of two clades: monkeypox viruses. *J. Gen. Virol.* **86**, 2661–2672
 29. Jalal, S., Kindrachuk, J., and Napper, S. (2007) Phosphoproteome and kinome analysis: unique perspectives on the same problem. *Curr. Anal. Chem.* **3**, 1–15
 30. Sopko, R., and Andrews, B. J. (2008) Linking the kinome and phosphorylome—a comprehensive review of approaches to find kinase targets. *Mol. Biosyst.* **4**, 920–933
 31. Goff, A. J., Chapman, J., Foster, C., Wlazlowski, C., Shamblin, J., Lin, K., Kreiselmeier, N., Mucker, E., Paragas, J., Lawler, J., and Hensley, L. (2011) A novel respiratory model of infection with monkeypox virus in cynomolgus macaques. *J. Virol.* **85**, 4898–4909
 32. Barry, M., Hnatiuk, S., Mossman, K., Lee, S. F., Boshkov, L., and McFadden, G. (1997) The myxoma virus M-T4 gene encodes a novel RDEL-containing protein that is retained within the endoplasmic reticulum and is important for the productive infection of lymphocytes. *Virology* **239**, 360–377
 33. Vassilev, L. T., Vu, B. T., Graves, B., Carvajal, D., Podlaski, F., Filipovic, Z., Kong, N., Kammlott, U., Lukacs, C., Klein, C., Fotouhi, N., and Liu, E. A. (2004) In vivo activation of the p53 pathway by small-molecule antagonists of MDM2. *Science* **303**, 844–848
 34. Reeves, P. M., Bommaris, B., Lebeis, S., McNulty, S., Christensen, J., Swimm, A., Chahroudi, A., Chavan, R., Feinberg, M. B., Veach, D., Bornmann, W., Sherman, M., and Kalman, D. (2005) Disabling poxvirus pathogenesis by inhibition of Abl-family tyrosine kinases. *Nat. Med.* **11**, 731–739
 35. Secchiero, P., Bosco, R., Celeghini, C., and Zauli, G. (2011) Recent advances in the therapeutic perspectives of nutlin-3. *Curr. Pharm. Des.* **17**, 569–577
 36. Secchiero, P., di lasio, M. G., Gonelli, A., and Zauli, G. (2008) The MDM2 inhibitor Nutlins as an innovative therapeutic tool for the treatment of haematological malignancies. *Curr. Pharm. Des.* **14**, 2100–2110
 37. Bálint, E. E., and Vousden, K. H. (2001) Activation and activities of the p53 tumour suppressor protein. *Br. J. Cancer* **85**, 1813–1823
 38. Chang, F., Steelman, L. S., Shelton, J. G., Lee, J. T., Navolanic, P. M., Blalock, W. L., Franklin, R., and McCubrey, J. A. (2003) Regulation of cell cycle progression and apoptosis by the Ras/Raf/MEK/ERK pathway (Review). *Int. J. Oncol.* **22**, 469–480
 39. Wang, G., Barrett, J. W., Stanford, M., Werden, S. J., Johnston, J. B., Gao, X., Sun, M., Cheng, J. Q., and McFadden, G. (2006) Infection of human cancer cells with myxoma virus requires Akt activation via interaction with a viral ankyrin-repeat host range factor. *Proc. Natl. Acad. Sci. U.S.A.* **103**, 4640–4645
 40. Soares, J. A., Leite, F. G., Andrade, L. G., Torres, A. A., De Sousa, L. P., Barcelos, L. S., Teixeira, M. M., Ferreira, P. C., Kroon, E. G., Souto-Padrón, T., and Bonjardim, C. A. (2009) Activation of the PI3K/Akt pathway early during vaccinia and cowpox virus infections is required for both host survival and viral replication. *J. Virol.* **83**, 6883–6899
 41. Zachos, G., Koffa, M., Preston, C. M., Clements, J. B., and Conner, J. (2001) Herpes simplex virus type 1 blocks the apoptotic host cell defense mechanisms that target Bcl-2 and manipulates activation of p38 mitogen-activated protein kinase to improve viral replication. *J. Virol.* **75**, 2710–2728
 42. Weaver, J. R., and Isaacs, S. N. (2008) Monkeypox virus and insights into its immunomodulatory proteins. *Immunol. Rev.* **225**, 96–113
 43. Sedger, L. M., Osvath, S. R., Xu, X. M., Li, G., Chan, F. K., Barrett, J. W., and McFadden, G. (2006) Poxvirus tumor necrosis factor receptor (TNFR)-like T2 proteins contain a conserved preligand assembly domain that inhibits cellular TNFR1-induced cell death. *J. Virol.* **80**, 9300–9309
 44. Wasilenko, S. T., Banadyga, L., Bond, D., and Barry, M. (2005) The vaccinia virus F1L protein interacts with the proapoptotic protein Bak and inhibits Bak activation. *J. Virol.* **79**, 14031–14043
 45. Wasilenko, S. T., Stewart, T. L., Meyers, A. F., and Barry, M. (2003) Vaccinia virus encodes a previously uncharacterized mitochondrial-associated inhibitor of apoptosis. *Proc. Natl. Acad. Sci. U.S.A.* **100**, 14345–14350
 46. Hnatiuk, S., Barry, M., Zeng, W., Liu, L., Lucas, A., Percy, D., and McFadden, G. (1999) Role of the C-terminal RDEL motif of the myxoma virus M-T4 protein in terms of apoptosis regulation and viral pathogenesis. *Virology* **263**, 290–306
 47. Best, S. M. (2008) Viral subversion of apoptotic enzymes: escape from death row. *Annu. Rev. Microbiol.* **62**, 171–192
 48. Passarelli, A. L. (2011) Barriers to success: how baculoviruses establish efficient systemic infections. *Virology* **411**, 383–392
 49. Ryan, E. J., Stevenson, N. J., Hegarty, J. E., and O'Farrelly, C. (2011) Chronic hepatitis C infection blocks the ability of dendritic cells to secrete IFN- α and stimulate T-cell proliferation. *J. Viral. Hepat.* **18**, 840–851
 50. Burgering, B. M., and Medema, R. H. (2003) Decisions on life and death: FOXO Forkhead transcription factors are in command when PKB/Akt is off duty. *J. Leukoc. Biol.* **73**, 689–701
 51. Thornton, T. M., and Rincon, M. (2009) Non-classical p38 map kinase functions: cell cycle checkpoints and survival. *Int. J. Biol. Sci.* **5**, 44–51
 52. Cappellini, A., Tazzari, P. L., Mantovani, I., Billi, A. M., Tassi, C., Ricci, F., Conte, R., and Martelli, A. M. (2005) Antiapoptotic role of p38 mitogen activated protein kinase in Jurkat T cells and normal human T lymphocytes treated with 8-methoxypsoralen and ultraviolet-A radiation. *Apoptosis* **10**, 141–152
 53. Kurosu, T., Takahashi, Y., Fukuda, T., Koyama, T., Miki, T., and Miura, O. (2005) p38 MAP kinase plays a role in G2 checkpoint activation and inhibits apoptosis of human B cell lymphoma cells treated with etoposide. *Apoptosis* **10**, 1111–1120
 54. Breman, J. G., Kalisa-Ruti, Steniowski, M. V., Zanolto, E., Gromyko, A. I., and Arita, I. (1980) Human monkeypox, 1970–79. *Bull. World Health Organ.* **58**, 165–182
 55. Brown, J. N., Estep, R. D., Lopez-Ferrer, D., Brewer, H. M., Clauss, T. R., Manes, N. P., O'Connor, M., Li, H., Adkins, J. N., Wong, S. W., and Smith, R. D. (2010) Characterization of macaque pulmonary fluid proteome during monkeypox infection: dynamics of host response. *Mol. Cell. Proteomics* **9**, 2760–2771
 56. Jalal, S., Arsenault, R., Potter, A. A., Babiuk, L. A., Griebel, P. J., and Napper, S. (2009) Genome to kinome: species-specific peptide arrays for kinome analysis. *Sci. Signal.* **2**, p1
 57. Huber, W., von Heydebreck, A., Sultmann, H., Poustka, A., and Vingron, M. (2002) Variance stabilization applied to microarray data calibration and to the quantification of differential expression. *Bioinformatics* **18** Suppl 1, S96–104
 58. Bloomfield, V. (2009) *Computer Simulation and Data Analysis in Molecular Biology and Biophysics: An Introduction Using R*, Springer, Dordrecht Heidelberg London New York



Since January 2020 Elsevier has created a COVID-19 resource centre with free information in English and Mandarin on the novel coronavirus COVID-19. The COVID-19 resource centre is hosted on Elsevier Connect, the company's public news and information website.

Elsevier hereby grants permission to make all its COVID-19-related research that is available on the COVID-19 resource centre - including this research content - immediately available in PubMed Central and other publicly funded repositories, such as the WHO COVID database with rights for unrestricted research re-use and analyses in any form or by any means with acknowledgement of the original source. These permissions are granted for free by Elsevier for as long as the COVID-19 resource centre remains active.

Vertical transmission of coronavirus disease 2019: a systematic review and meta-analysis



Alexander M. Kotlyar, MD; Olga Grechukhina, MD; Alice Chen, BS; Shota Popkhadze, MD; Alyssa Grimshaw, MSLIS; Oded Tal, PhD; Hugh S. Taylor, MD; Reshef Tal, MD, PhD

Introduction

The coronavirus disease 2019 (COVID-19) has spread from isolated cases of pneumonia in Wuhan, Hubei province, China, to become a worldwide pandemic as declared by the World Health Organization on March 11, 2020.¹ As of June 1, 2020, there have been more than 6,300,000 confirmed cases and more than 370,000 deaths worldwide. Coronaviruses are single-stranded RNA viruses. Although there are many coronaviruses, the particular coronavirus that is responsible for this pandemic is the severe acute respiratory syndrome coronavirus 2 (SARS-CoV-2).² After 2 to 7 days of incubation, most symptomatic patients typically experience fever, cough, or loss of taste or smell, with some cases developing into life-threatening pneumonia and acute respiratory distress syndrome.^{3,4} Case fatality rates range from 1% to 2%, which is substantially less than the case fatality rates for other coronavirus infections including the severe acute respiratory syndrome (SARS) and Middle East respiratory syndrome (MERS) (10% and 35%, respectively).⁵

From the Sections of Reproductive Endocrinology and Infertility (Dr Kotlyar, Ms Chen, and Drs Taylor and R. Tal) and Maternal-Fetal Medicine (Drs Grechukhina and Popkhadze), Department of Obstetrics, Gynecology, and Reproductive Sciences, Yale School of Medicine, Yale University, New Haven, CT; Harvey Cushing/John Hay Whitney Medical Library, Yale University, New Haven, CT (Ms Grimshaw); and School of Business, Conestoga College, Kitchener, Ontario, Canada (Dr O. Tal).

Received June 18, 2020; revised July 23, 2020; accepted July 29, 2020.

The authors report no conflict of interest.

Corresponding author: Alexander M. Kotlyar, MD. Alexander.kotlyar@yale.edu

0002-9378/\$36.00

© 2020 Elsevier Inc. All rights reserved.

<https://doi.org/10.1016/j.ajog.2020.07.049>

OBJECTIVE: This study aimed to conduct a systematic review of the current literature to determine estimates of vertical transmission of coronavirus disease 2019 based on early RNA detection of severe acute respiratory syndrome coronavirus 2 after birth from various neonatal or fetal sources and neonatal serology.

DATA SOURCES: Eligible studies published until May 28, 2020, were retrieved from PubMed, EMBASE, medRxiv, and bioRxiv collection databases.

STUDY ELIGIBILITY CRITERIA: This systematic review included cohort studies, case series, and case reports of pregnant women who received a coronavirus disease 2019 diagnosis using severe acute respiratory syndrome coronavirus 2 viral RNA test and had reported data regarding the testing of neonates or fetuses for severe acute respiratory syndrome coronavirus 2 immediately after birth and within 48 hours of birth. A total of 30 eligible case reports describing 43 tested neonates and 38 cohort or case series studies describing 936 tested neonates were included.

STUDY APPRAISAL AND SYNTHESIS METHODS: The methodological quality of all included studies was evaluated by a modified version of the Newcastle-Ottawa scale. Quantitative synthesis was performed on cohort or case series studies according to the neonatal biological specimen site to reach pooled proportions of vertical transmission.

RESULTS: Our quantitative synthesis revealed that of 936 neonates from mothers with coronavirus disease 2019, 27 neonates had a positive result for severe acute respiratory syndrome coronavirus 2 viral RNA test using nasopharyngeal swab, indicating a pooled proportion of 3.2% (95% confidence interval, 2.2–4.3) for vertical transmission. Of note, the pooled proportion of severe acute respiratory syndrome coronavirus 2 positivity in neonates by nasopharyngeal swab in studies from China was 2.0% (8/397), which was similar to the pooled proportion of 2.7% (14/517) in studies from outside of China. Severe acute respiratory syndrome coronavirus 2 viral RNA testing in neonatal cord blood was positive in 2.9% of samples (1/34), 7.7% of placenta samples (2/26), 0% of amniotic fluid (0/51), 0% of urine samples (0/17), and 9.7% of fecal or rectal swabs (3/31). Neonatal serology was positive in 3 of 82 samples (3.7%) (based on the presence of immunoglobulin M).

CONCLUSION: Vertical transmission of severe acute respiratory syndrome coronavirus 2 is possible and seems to occur in a minority of cases of maternal coronavirus disease 2019 infection in the third trimester. The rates of infection are similar to those of other pathogens that cause congenital infections. However, given the paucity of early trimester data, no assessment can yet be made regarding the rates of vertical transmission in early pregnancy and potential risk for consequent fetal morbidity and mortality.

Key words: COVID-19, SARS-CoV-2, transplacental transmission, vertical transmission

The presence of COVID-19 infection in a pregnant patient raises concerns given that infections with other coronaviruses such as SARS and MERS have been associated with severe maternal and neonatal morbidity and mortality and adverse pregnancy outcomes including miscarriage, preterm birth, and

stillbirth.⁶ However, the effects of COVID-19 on pregnancy and the fetus are still largely unknown because of the recent nature of the outbreak. Pregnant patients are a potentially vulnerable group to COVID-19 infection. The first and third trimesters of pregnancy can be considered periods of increased

AJOG at a Glance

Why was this study conducted?

Coronavirus disease 2019 (COVID-19) is a pandemic that has and will continue to affect many pregnant women. Knowledge regarding the possible risk of vertical transmission is very limited but is crucial for guiding patient counseling regarding COVID-19—related pregnancy risks and obstetrical care for women with COVID-19.

Key findings

The vertical transmission of COVID-19 in the third trimester is approximately 3.2% (22/936) by infant nasopharyngeal swab testing, with severe acute respiratory syndrome coronavirus 2 (SARS-CoV-2) RNA positivity in other test sites ranging from 0% (0/51) in amniotic fluid and urine (0/17), 3.6% (1/28) in the cord blood, 7.7% (2/26) by placental sample analysis, 9.7% (3/31) by rectal or anal swab, and 3.7% (3/81) by serology.

What does this add to what is known?

There is evidence of SARS-CoV-2 vertical transmission when the infection occurs in the third trimester of pregnancy.

inflammatory activity, whereas the second trimester is a period of overall decreased immune activity.^{7,8} Although initial reports of pregnant women infected with COVID-19 in the third trimester raised a concern for an increased risk for premature delivery,^{9,10} recent larger cohorts of 116 women in China and 427 women in the United Kingdom suggest that pregnant women are not at an increased risk of spontaneous abortion or spontaneous preterm birth but have higher rates of cesarean delivery (CD).^{11,12}

Vertical transmission is defined as the transmission of the infectious pathogen from the mother to the fetus during the antepartum and intrapartum periods, or to the neonate during the postpartum period via the placenta in utero, body fluid contact during childbirth, or through direct contact owing to breastfeeding after birth. Although multiple infectious vectors have been shown to be capable of vertical transmission, the possibility of vertical transmission of SARS-CoV-2 from the infected mother to the fetus or neonate has been a point of a recent debate with previous systematic reviews, albeit with a limited number of studies, concluding that there is no evidence of vertical transmission.^{13–16} No known cases of vertical transmission have been noted

with similar coronaviruses such as SARS and MERS, although the number of cases has been limited.^{17,18} COVID-19 shares 50% and 79% sequence homology with SARS and MERS, respectively; despite this homology, a similar lack of vertical transmission cannot be assumed.⁶

A concern over vertical transmission in the case of COVID-19 exists for several reasons. First is the known tissue tropism of COVID-19. The main receptor that COVID-19 binds to enter a cell is the angiotensin-converting enzyme 2 (ACE2) receptor. ACE2 is expressed in the placenta¹⁹ and is found in the syncytiotrophoblast, cytotrophoblast, endothelium, and vascular smooth muscle from both primary and secondary villi.²⁰ A recent systematic review also found evidence that ACE2 is expressed in gynecologic organs such as the ovary, uterus, and vagina.²¹ Overall, ACE2 expression is seen in numerous tissues that are in direct communication with a developing pregnancy. These data were further bolstered by a recent single-cell RNA sequencing analysis that found ACE2 expression in stromal, perivascular, placental, and decidual cells at the maternal-fetal interface.²² However, a single-cell RNA sequencing analysis looking at the coexpression of ACE2 and the transmembrane serine protein for

virus spike (S) protein priming, transmembrane serine protease 2 (TMPRSS2), showed that only a minimal number of placental cells express both proteins in any trimester. Furthermore, this group showed that chorionic membranes from the third trimester exhibit minimal coexpression of both proteins. Nonetheless, the authors suggested that viral entry into placenta cells may still occur using a combination of ACE2 and a noncanonical cell-entry mediator.²³ In addition, animal data indicated that oronasal inoculation of pregnant mice with mouse hepatitis virus (MHV), which is part of the Coronaviridae family, led to the dissemination of the virus to the fetus in each trimester. However, the dissemination was dependent on the strain of MHV and the strain of mice, with BALB/cByJ mice being the most susceptible.²⁴ In addition to this biological plausibility, there are several lines of clinical evidence concerning vertical transmission. Initial reports from China have documented immunoglobulin M (IgM) antibodies in neonates born to mothers who had positive results for COVID-19,^{25,26} raising concerns for in utero transmission because IgM cannot cross the placenta. Moreover, several recent case reports provided evidence that COVID-19 can infect the placenta as confirmed by the presence of SARS-CoV-2 viral RNA and protein in the placenta and evidence of virions found within the syncytiotrophoblast.^{27–30}

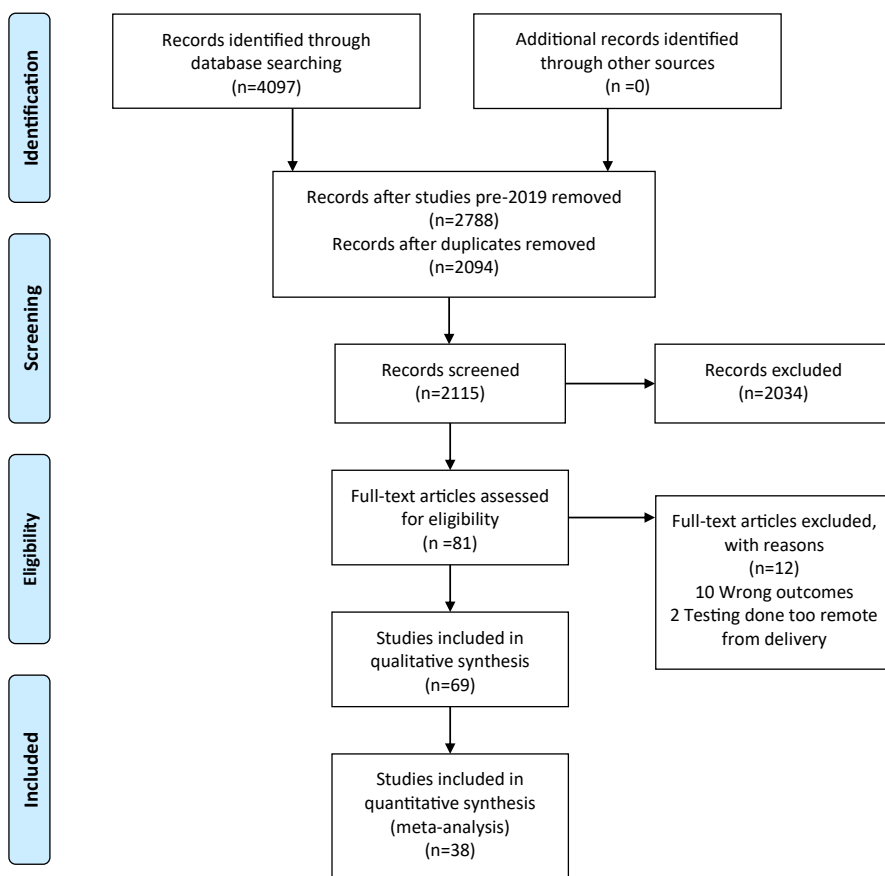
Answering the question of vertical transmission is crucial for guiding patient counseling regarding COVID-19—related risks before and during pregnancy and obstetrical care for women infected with COVID-19. Therefore, we conducted this systematic review to summarize the available evidence regarding the risk of vertical transmission.

Methods**Search strategy, study selection, and data extraction**

A medical librarian conducted a systematic search of the literature from Cochrane Library, DisasterLit, Ovid Embase, Ovid Medline, Google Scholar, LitCovid, MedRxiv, Pubmed, Scopus,

and Web of Science Core Collection databases to find relevant articles published from inception of the database to May 28, 2020, to identify cohort studies, case series, and case reports of pregnant women with COVID-19 that include information regarding fetal or neonatal COVID-19 testing. The study was conducted according to the Preferred Reporting Items for Systematic Reviews and Meta-analyses guidelines for the reporting of systematic reviews and meta-analyses and was registered in the International Prospective Register of Systematic Reviews (CRD42020190885). The databases were searched using a combination of controlled vocabulary and free-text terms for SARS-CoV-2, COVID-19, coronavirus, Coronaviridae, pregnancy, fetus, infant, mother-to-child, mother-to-infant, maternal-fetal, virus transmission, disease transmission, and vertical transmission (the full search strategy is provided in the [Supplemental Figure](#)). The search results were limited to English-language abstracts. Foreign-language articles were included only if a translation was available given the time-sensitive nature of this review. Bibliographies were cross-referenced to identify additional relevant studies. Studies were included if they were English-language articles that focused on the development of COVID-19 infection in fetuses and neonates. Citations from all databases were imported into an EndNote X9 library. Duplicates were removed from the EndNote, reducing the initial list of 4907 citations to 2904 citations. The database of 2904 citations was entered into Covidence, which is a screening and data extraction tool. Two independent screeners (A.K. and O.G.) performed a title abstract review and resolved conflicts by consensus between the 2 screeners. The screeners selected a total of 81 records for full-text review and included 68 studies that fulfilled the eligibility criteria in the qualitative synthesis ([Figure 1](#)). Cohort studies and case series (defined as having 5 or more patients) were selected for quantitative synthesis. Case series were defined as having 5 or more patients, consistent with the recommendations according to the study by Abu-Zidan et al³¹ showing that case reports have a

FIGURE 1
PRISMA flowchart outlining study selection



PRISMA, Preferred Reporting Items for Systematic Reviews and Meta-analyses.

Kothiyar. Vertical transmission of COVID-19: a systematic review and meta-analysis. *Am J Obstet Gynecol* 2021.

median number of 4 patients. Data were extracted from the article texts and tables and organized into tables in a systematic manner. The following information was extracted: author name; country; publication date; number of pregnant women; number of eligible neonates; gestational age (at onset of testing); mode of delivery; neonatal SARS-CoV-2 reverse transcription–polymerase chain reaction (RT-PCR) testing results from nasopharyngeal (NP) swab, placenta, cord blood, amniotic fluid, and any other fetal or neonatal sources; placental histology; and neonatal serology.

Eligibility criteria

Studies were included in this systematic review if they met the following criteria: (1) the study population included

women who had COVID-19 infection during pregnancy confirmed by positive viral SARS-CoV-2 RNA testing; (2) the study described results of viral RNA testing for SARS-CoV-2 infection in fetuses or neonates; (3) testing for SARS-CoV-2 infection was performed within 48 hours of delivery; and (4) any study design (cohort, case series, case report). Articles that focused on the transmission of COVID-19 outside of the perinatal period were excluded given that this was deemed out of scope for this article.

Methodological quality assessment

Each cohort or case series study selected for final inclusion in the quantitative synthesis was scored by the researchers (A.C. and R.T.) using the modified Newcastle-Ottawa scale, as previously

described (Supplemental Table).³² Items that relate to comparability and adjustment are not relevant and were removed, whereas items that focused on the selection and representativeness of cases and ascertainment of outcome and exposure were maintained. This resulted in 5 items regarding the study quality characteristics: (1) representativeness of the exposed cohort, (2) exposure assessment, (3) outcome assessment, (4) adequacy of the length of time before follow-up, and (5) adequacy of the follow-up of cohorts. We considered the quality of the report good (low risk of bias) when all 5 criteria were fulfilled, moderate when 4 were fulfilled, and poor (high risk of bias) when 3 or fewer were fulfilled.

Statistical analysis

We evaluated the positive rates of each of the explored SARS-CoV-2 testing outcomes (RT-PCR of NP swab, placenta, cord blood, rectal or anal, urine, amniotic fluid, and IgM serology). Pooled proportions of these categorical variables were calculated with percentages and 95% confidence intervals (CIs). Calculations were performed using the MedCalc Statistical Software version 19.3.1 (MedCalc Software Ltd, Ostend, Belgium; <https://www.medcalc.org; 2020>). The Cochran Q test was used to determine whether to use the fixed effects model or the random effects model ($P < .1$: random effects model). A Freeman-Tukey transformation (arcsine square root transformation)³³ was used to calculate the weighted summary proportion under the fixed and random effects models.³⁴ The random effects model was preferred because it is more conservative.

Results

Search results

A total of 81 records were selected for full-text review, and 69 studies fulfilled the eligibility criteria and were included in the qualitative synthesis. There were 30 case reports. Their characteristics and test findings are summarized in Table 1. A total of 39 additional studies were cohort studies or case series (defined as having 5 or more patients) and were

selected for quantitative synthesis. The characteristics and test findings of these cohort or case series studies are summarized in Tables 2 and 3. These were divided into reports from China (Table 2) and reports from the rest of the world (Table 3) because evidence indicates that earlier Asian viral samples were completely dominated by the original Wuhan D614 form through mid-March, and subsequently, in countries outside of China and across the globe, a different form (G614) was expanding and dominating.⁹¹ The flow diagram of the study selection strategy is presented in Figure 1. The methodological quality assessment of the cohort or case series studies included in the quantitative synthesis showed that 13 studies were of high quality, 16 studies were of moderate quality, and 10 studies were of low quality (Supplemental Figure).

Systematic review

This systematic review included 30 eligible case reports describing a total of 44 SARS-CoV-2–positive pregnant women with outcomes available for 43 neonates (Table 1) and 39 cohort or case series studies describing a total of 936 tested neonates born to SARS-CoV-2–positive pregnant women (Tables 2 and 3). Data in this review were limited to pregnant women who had laboratory-confirmed SARS-CoV-2 infection diagnosed by RT-PCR in an NP swab specimen, which is considered the gold standard for the diagnosis of COVID-19.

Because of the recent onset of the pandemic, the vast majority of data came from pregnant women in their third trimester, whereas the greatest paucity of reports involved patients in the earlier stages of pregnancy. Of the 30 case reports, 29 reports described neonatal outcomes of women in their third trimester, whereas only 2 case reports described outcomes of women in their second trimester.^{13,18,25,27–30,}

^{35–50,51–58,66} To date, no reports are available describing the assessment for the presence of SARS-CoV-2 in products of conception of a first-trimester pregnancy. Most women in case report studies (32/44) underwent CD with a

resultant CD rate of 73%. Similarly, 73% of women (659/901) in cohort or case series studies delivered via CD.

This systematic review identified 2 case reports of second-trimester fetal SARS-CoV-2 testing. Baud et al²⁸ reported a case of a patient at 19 weeks' gestation with a positive result from a SARS-CoV-2 NP swab who had a miscarriage delivering a stillborn infant. Fetal axillary, oral, meconium, and blood samples all tested negative for SARS-CoV-2 RNA. However, placental swabs from the fetal side taken immediately after expulsion were positive for SARS-CoV-2 by RT-PCR. In another case report by Hosier et al,²⁷ a COVID-19–positive patient delivered at 22 weeks' gestation because of early-onset preeclampsia with severe features. Quantitative RT-PCR tests of placental and umbilical cord samples were positive for SARS-CoV-2 RNA, and viral capsids were found within the trophoblast cells by electron microscopy, confirming infection of the fetal side of the placenta by this novel coronavirus. Although these cases do not provide evidence that placental COVID-19 infection was the cause of these adverse pregnancy outcomes, they lend support to the possibility of in utero maternal-to-fetal transmission.

Overall, the majority of COVID-19 cases of pregnant women with fetal or neonatal outcomes reported thus far involved patients in their third trimester of pregnancy. Given the plethora of studies of patients in the third trimester, we analyzed them according to the study type (case report vs cohort or case series study) and site of SARS-CoV-2 testing. Because selection bias is more likely in case reports than in cohort or case series studies, we focused our quantitative synthesis on the case series and cohort studies to reach pooled proportions regarding various parameters indicative of vertical transmission.

Severe acute respiratory syndrome coronavirus 2 reverse transcription–polymerase chain reaction testing of nasopharyngeal swab. In our review, 38 of 39 cohort or case series studies of pregnant women with COVID-19 infection had information on

TABLE 1
Case reports

Author (country)	Number of women	Number of eligible neonates	GA at onset of Sx or diagnosis (range)	Mode of delivery	RT-PCR for SARS-CoV-2							Placental histology or EM
					Neonatal NP swab	Placenta	Cord blood	Amniotic fluid	Other fetal sites or tests	Neonatal serology		
Alzamora et al (Peru) ³⁵	1	1	33 wk	CD	1/1	None	None	None	None	IgG (0/1), IgM (0/1)	None	
Chen et al (China) ³⁶	3	3	35 wk—38 wk 6 d	CD 3/3	0/3	0/3	None	None	None	None	Chorionic hemangioma (1/3), fibrin deposits in villi interstitium and around the villi (3/3), multifocal infarction (1/3)	
Dong et al (China) ²⁵	1	1	34 wk 2 d	CD	0/1	None	None	None	None	IgG and IgM elevated on delivery day and 13 d later (1/1)	None	
Fan et al (China) ¹³	2	2	36—37 wk	CD 2/2	0/2	0/2	0/2	0/2	None	None	None	
Kalafat et al (Turkey) ³⁷	1	1	35 wk 3 d	CD	0/1	0/1	0/1	None	None	None	None	
Khan et al (China) ³⁸	3	3	34 wk 6 d—39 wk 1 d	VD 3/3	0/3	None	None	None	None	None	None	
Li et al (China) ³⁹	1	1	35 wk	CD	0/1	0/1	0/1	0/1	None	None	None	
Liu et al (China) ⁴⁰	3	3	37—40 wk	VD 1/3; CD 2/3	0/3	None	0/3	None	0/3	None	None	
Lowe and Bopp (Australia) ⁴¹	1	1	40 wk 3 d	VD	0/1	None	None	None	None	None	None	
Lu et al (China) ⁴²	1	1	38 wk	CD	0/1	None	0/1	None	None	None	None	
Peng et al (China) ⁴³	1	1	34 wk 3 d	CD	0/1	0/1	0/1	0/1	Anal (0/1), serum (0/1), sputum (0/1), urine (0/1), BAL fluid (0/1)	None	None	
Schnettler et al (United States) ⁴⁴	1	1	30 wk 3 d	CD	0/1	None	None	0/1	None	None	None	
Wang et al (China) ⁴⁵	1	1	40 wk	CD	1/1	0/1	0/1	None	None	None	None	

Kotlyar. Vertical transmission of COVID-19: a systematic review and meta-analysis. *Am J Obstet Gynecol* 2021.

(continued)

TABLE 1
Case reports (continued)

Author (country)	Number of women	Number of eligible neonates	GA at onset of Sx or diagnosis (range)	Mode of delivery	RT-PCR for SARS-CoV-2							Placental histology or EM
					Neonatal NP swab	Placenta	Cord blood	Amniotic fluid	Other fetal sites or tests	Neonatal serology		
Xiong et al (China) ⁴⁶	1	1	33 wk	VD	0/1	None	None	0/1	Rectal swab (0/1)	IgG (0/1), IgM (0/1)	No inflammation	
Zamaniyan et al (Iran) ⁴⁷	1	1	32 wk	CD	0/1	0/1	0/1	1/1	None	None	None	
Baud et al (Switzerland) ²⁸	1	1	19 wk	VD	0/1	1/1	None	0/1	Fetal blood, lung, liver, thymus biopsies (all 0/1)	None	Mixed inflammatory infiltrates composed of neutrophils and monocytes in the subchorial space and increased intervillous fibrin deposition (1/1), funisitis (1/1)	
Blauvelt et al (United States) ⁴⁸	1	1	28 wk	CD	0/1	None	None	None	Rectal swab (0/1)	IgG and IgM drawn on day 5 were negative	Acute chorioamnionitis (1/1), no funisitis or histologic evidence of other placental infections	
Buonsenso et al (Italy) ⁴⁹	4	2	17–38 wk	CD 2/2	0/2	None	0/2	None	None	None	None	
Gidlöf et al (Sweden) ⁵⁰	1	2	36 wk	CD	0/2	None	None	None	None	None	None	
Hosier et al (United States) ²⁷	1	1	22 wk	D&E	N/A	1/1	1/1	None	Fetal heart, lung, kidney (0/1)	None	Diffuse perivillous fibrin and inflammatory infiltrate in intervillous space showing histiocytic intervillitis, EM showing virions noted inside syncytiotrophoblast	
Huang et al (China) ⁵¹	1	1	35 wk	CD	0/1	0/1	0/1	0/1	None	None	None	
Kirtsman et al (Canada) ²⁹	1	1	35 wk	CD	1/1	1/1	0/1	None	Plasma (1/1), stool (1/1)	None	Multiple areas of infiltration, extensive early infarction, consistent with chronic histiocytic intervillitis	
Lang and Zhao (China) ⁵²	1	1	35 wk 2 d	CD	0/1	0/1	0/1	0/1	None	None	None	
Lee et al (Republic of Korea) ⁵³	1	1	36 wk 2 d	CD	0/1	0/1	0/1	0/1	None	None	None	
Lyra et al (Portugal) ⁵⁴	1	1	39 wk 4 d	CD	0/1	Collected for future analysis	None	Collected for future analysis	None	None	None	

Kotlyar. Vertical transmission of COVID-19: a systematic review and meta-analysis. Am J Obstet Gynecol 2021.

(continued)

TABLE 1
Case reports (continued)

Author (country)	Number of women	Number of eligible neonates	GA at onset of Sx or diagnosis (range)	Mode of delivery	RT-PCR for SARS-CoV-2						Placental histology or EM
					Neonatal NP swab	Placenta	Cord blood	Amniotic fluid	Other fetal sites or tests	Neonatal serology	
Vallejo and Illagan (United States) ³⁵	1	1	36 wk	CD	0/1	None	None	None	None	None	Negative histopathologic findings
Yu et al (China) ⁵⁶	1	1	34 wk	VD	0/1	None	None	None	None	None	None
Algarroba et al (United States) ⁵⁷	1	1	28 wk	CD	0/1	None	None	None	None	None	Mature chorionic villi with focal villous edema, area of decidual vasculopathy, EM showing single virions invading a syncytiotrophoblast and also visualized in a microvillus and fibroblast processes
Vivanti et al (France) ⁵⁸	1	1	35 wk 2 d	CD	1/1	1/1	None	1/1	Rectal swab 1/1, neonatal blood 1/1	None	Diffuse perivillous fibrin deposition, infarction and acute and chronic intervillitis. SARS-CoV-2 N-protein seen within cytoplasm of perivillous trophoblastic cells

All papers are identified by author, country (unless otherwise specified), and citation number within the main text.

BAL, bronchoalveolar lavage; CD, cesarean delivery; D&E, dilation and evacuation; EM, electron microscopy; GA, gestational age; IgG, immunoglobulin G; N/A, not available; NP, nasopharyngeal; RT-PCR, reverse transcription–polymerase chain reaction; SARS-CoV-2, severe acute respiratory syndrome coronavirus 2; Sx, symptoms; VD, vaginal delivery.

Korlyar. Vertical transmission of COVID-19: a systematic review and meta-analysis. *Am J Obstet Gynecol* 2021.

neonatal NP swab testing results. There were 22 studies from China (Table 2) and 17 studies from countries outside of China (Italy, Spain, United Kingdom, and United States of America) (Table 3). In total, of 397 neonates born to mothers with COVID-19 infection in China, there were 8 who had a positive result for SARS-CoV-2 by NP swab resulting in a pooled proportion of 2.0% for vertical transmission.^{8–11,26,56,59–71,72–75} The largest cohort study from China was by Yan et al,¹¹ in which 116 COVID-19–positive pregnant patients delivered 100 infants, of whom 86 underwent testing for SARS-CoV-2. None of the 86 infants had a positive result for COVID-19 via NP swab. Among studies from outside of China, the largest cohort study thus far came from the United Kingdom involving 427 pregnant women with COVID-19 including 244 neonates tested by NP swab, 12 of whom were positive for SARS-CoV-2 (12/244).¹² An analysis of 68 women from a hospital in New York City showed that of the 55 neonates born, 48 were tested at day 0 of life with none having a positive result for COVID-19 (0/48).⁸² One Italian study that assessed 42 infants born via vaginal delivery and CD found 3 infants (3/42) who had positive results for SARS-CoV-2 via NP swabs within 48 hours after birth.⁷⁸ Pooling studies from outside of China revealed that 19 of 539 neonates born to mothers with COVID-19 infection had positive results for SARS-CoV-2 by NP swab, yielding a pooled proportion of 3.5%.^{12,18,76–90} Combining all 38 cohort or case series studies in a meta-analysis, of all 936 neonates tested, 27 had positive results for SARS-CoV-2 RNA by NP swab either immediately after birth or within 48 hours of birth, yielding a pooled proportion of 3.2% (95% CI, 2.2–4.3) (Figures 2 and 3).

Placental analysis. In our review, we identified 8 cohort or case series studies that reported on the assessment of placentas for SARS-CoV-2 by RT-PCR, 2 from China and 6 from outside of China. The placental analysis yielded the second highest pooled rate of possible vertical transmission with 7.7% (2/26) of all

TABLE 2
Cohort or case series studies from China

Author	Number of women	Number of eligible neonates	GA at onset of Sx or diagnosis (range)	Mode of delivery	RT-PCR for SARS-CoV-2						
					Neonatal NP swab	Placenta	Cord blood	Amniotic fluid	Other fetal sites or tests	Neonatal serology	Placental histology
Cao et al ⁵⁹	10	5	GA at admission: 33 wk 6 d–40 wk 5 d	VD 2; CD 8	0/5	None	None	None	None	None	None
Chen et al ¹⁰	9	6	GA at admission: 36 wk–39 wk 4 d	CD 9	0/6	None	0/6	0/6	None	None	None
Hu et al ⁶⁰	7	7	37–40 wk	VD 1; CD 6	1/7 (subsequent swabs were negative for that positive neonate)	None	None	0/7 positive	Fetal blood (0/7), feces (0/7), urine (0/7)	None	None
Khan et al ⁶¹	17	17	Date of admission: 35–41 wk	CD 17	2/17	None	None	None	None	None	None
Liu et al ⁶²	19	19	36 wk 3 d–41 wk 2 d	CD 19	0/19	None	0/10	0/10	Urine (0/10), anal swabs (0/10)	None	None
Nie et al ⁶³	33	28	3 women in the second trimester (17–26 wk), rest in the third trimester	VD 5, CD 22	1/28	0/1	0/1	None	None	1/28	None
Qiancheng et al ⁶⁴	28	23	Median GA on admission=38 wk (IQR, 36.5–39)	VD 5, CD 17	0/23	None	None	None	None	None	None
Yan et al ¹¹	116	100	37 wk 3 d–39 wk 4 d	CD 85, VD 14	0/86	None	0/10	0/10	None	None	None
Yang et al ⁶⁵	7	7	36–38 wk	CD 7	0/5	None	0/5	0/5	None	None	None
Yin et al ⁶⁶	31	17	N/A	VD 4, CD 13, TAB 3	0/17	0/2	None	0/2	Rectal swab (0/5)	None	None
Yu et al ⁵⁶	7	7	37 wk–41 wk 5 d	CD 7	1/3	None	None	None	None	None	None
Zeng et al ²⁶	6	6	N/A	CD 6	0/6	None	None	None	Fetal blood	Elevated IgM (2/6), elevated IgG (3/6)	None
Zeng et al ⁶⁷	33	33	31 wk 2 d–41 wk 4 d	VD 7, CD 26	3/33	None	None	None	Anal swab (3/33)	None	None
Zhu et al ⁹	9	10	33 wk 6 d–39 wk	VD 2, CD 7	0/9	None	None	None	None	None	None

Kotlyar. Vertical transmission of COVID-19: a systematic review and meta-analysis. Am J Obstet Gynecol 2021.

(continued)

TABLE 2
Cohort or case series studies from China (continued)

Author	Number of women	Number of eligible neonates	GA at onset of Sx or diagnosis (range)	Mode of delivery	RT-PCR for SARS-CoV-2						
					Neonatal NP swab	Placenta	Cord blood	Amniotic fluid	Other fetal sites or tests	Neonatal serology	Placental histology
Chen et al ⁶⁸	5	5	38–41 wk	VD 3, CD 2	0/5	None	None	None	None	None	No placental infarction and chorionic amniotic inflammation
Chen et al ⁶⁹	17	17	3<37 wk, 14>37 wk	CD 17	0/17	None	None	None	None	None	None
Liao et al ⁷⁰	88	10	36–40 wk	VD 10	0/7	None	None	None	None	None	None
Liu et al ⁷¹	51	51	GA at delivery: 35 wk 1 d–41 wk 2 d	VD 3, CD 48	0/51 (5 were considered false positive)	None	None	None	None	IgM and IgG (0/51)	None
Wu et al ⁷²	13	5	5–38 wk	VD 1, CD 4	0/5	None	None	None	Anal (0/4)	None	None
Wu et al ⁷³	23	21 (1 case of twins)	First trimester (6–12 wk), third trimester (31 wk 5 d–40 wk)	VD 2, CD 18	0/5 (5 negative by RT-PCR, 17 negative by clinical criteria)	None	None	None	None	None	None
Yang et al ⁷⁴	55	57 (2 cases of twins)	Average GA: 38 wk	VD 16, CD 39	0/20	None	None	None	None	None	None
Yang et al ⁷⁵	27	24 (1 case of twins)	3 women in the first trimester, rest in the third trimester (30–40 wk)	VD 5, CD 18	0/23	None	None	None	None	IgM and IgG (1/1), other 23 not tested	None

All papers are identified by author, country (unless otherwise specified), and citation number within the main text.

BAL, bronchoalveolar lavage; CD, cesarean delivery; EM, electron microscopy; GA, gestational age; IgG, immunoglobulin G; IgM, immunoglobulin G; IQR, interquartile range; N/A, not available; NP, nasopharyngeal; RT-PCR, reverse transcription–polymerase chain reaction; SARS-CoV-2, severe acute respiratory syndrome coronavirus 2; Sx, symptoms; TAB, therapeutic abortion; VD, vaginal delivery.

Kotlyar. Vertical transmission of COVID-19: a systematic review and meta-analysis. *Am J Obstet Gynecol* 2021.

TABLE 3
Cohort or case series studies from outside of China

Author (country)	Number of women	Number of eligible neonates	GA at onset of Sx or diagnosis (range)	Mode of delivery	RT-PCR for SARS-CoV-2					Neonatal serology	Placental histology
					Neonatal NP swab results	Placenta	Cord blood	Amniotic fluid	Other fetal sites or tests		
Breslin et al (United States) ⁷⁶	43	18	Median GA 37 wk (IQR, 32 wk 4 d–38 wk 6 d)	VD 10, CD 8	0/18 positive	None	None	None	None	None	None
Breslin et al (United States) ⁷⁷	7	2	26 wk 3 d–37 wk 5 d	CD 2	0/2 positive	None	None	None	None	None	None
Ferrazzi et al (Italy) ⁷⁸	42	42	Third trimester, 30 women >37 wk, 12 women <37 wk	VD 24, CD 18	3/42	None	None	None	None	None	None
Penfield et al (United States) ⁷⁹	32	10	26 wk 4 d–41 wk 2 d	VD 7, CD 4	0/10	1/1	None	None	Fetal membranes (2/10)	None	None
Pierce-Williams et al (United States) ⁸⁰	64	33 (1 set of twins)	16 wk 1 d–39 wk 1 d	VD 8/32, CD 24/32	1/33	None	None	None	None	None	None
Lokken et al (United States) ⁸¹	46	8	33 wk 0 d–38 wk 6 d	VD 3, CD 5,	0/8	0/1 (stillbirth)	None	None	Fetal autopsy sites (0/1)	None	Severe chronic villitis but no viral inclusions (1/1)
London et al (United States) ⁸²	68	48	3 in the second trimester (17 wk, 25 wk, 26 wk), the rest in the third trimester	VD 33, CD 22	0/48	None	None	None	None	None	None
Mulvey et al (United States) ⁸³	5	5	38–40 wk	VD 4/5, CD 1/5	N/A	0/5	None	None	None	None	Fetal vascular malperfusion (5/5), thrombosis (5/5), intramural fibrin deposition (4/5), meconium (3/5), avascular villi (1/5), villous stromal-vascular karyorrhexis (1/5)
Baergen and Heller (United States) ⁸⁴	20	21 (1 pair of twins)	32–40 wk	VD 15/20, CD 5/20	0/21	None	None	None	None	None	Fetal vascular malperfusion (9/20), intramural fibrin deposition (3/20), meconium macrophages (6/20), lesions of maternal vascular malperfusion (5/20), ascending infection with acute chorioamnionitis and acute funisitis (1/20), chronic villitis (4/20)

TABLE 3

Cohort or case series studies from outside of China (continued)

Author (country)	Number of women	Number of eligible neonates	GA at onset of Sx or diagnosis (range)	Mode of delivery	RT-PCR for SARS-CoV-2					Neonatal serology	Placental histology
					Neonatal NP swab results	Placenta	Cord blood	Amniotic fluid	Other fetal sites or tests		
Buonsenso et al (Italy) ⁸⁵	7	2	8 wk—37 wk 3 d	CD 2/2	0/2, on d 15 positive (1/2)	1/2	1/2	0/2	Rectal swab (0/2)	IgM negative (0/1), IgG slightly positive (1/1)	None
Govind et al (United Kingdom) ⁸⁶	9	9	27—39 wk	VD 1/9, CD 8/9	1/9	0/9	None	0/9	None	None	None
Knight et al (United Kingdom) ¹²	427	244	Median, 34 wk (IQR, 29—38), <22 wk (n=22), 22—27 wk (n=60), 28—31 wk (n=64), 32—36 wk (n=106), 37+ wk (n=142), peripartum (n=30), missing (n=3)	VD 101, CD 144	12/244 (6/244 tested positive <12 h, 6/244 tested positive >12 h)	None	None	None	None	None	None
Patanè et al (Italy) ³⁰	22	22	35—37 wk	VD 1/2, CD 1/2	2/22 (1 was negative at birth but turned positive at day 7 without contact with mother)	None	None	None	None	None	Chronic intervillitis in intervillous and the villous space (2/22)
Pereira et al (Spain) ⁸⁷	60	23	Median GA, 32 wk (range, 5—41 wk)	VD 18/23, CD 5/23	0/23	0/6	None	None	None	None	None
Shanes et al (United States) ⁸⁸	16	16	Second trimester (16 wk), third trimester (34—40 wk)	N/A	0/16	None	None	None	None	None	IUFD case pathology showed retroplacental hematoma and villous edema, maternal vascular malperfusion (12/15), central and peripheral villous infarctions (4/15), mural hypertrophy of membrane arterioles (5/15), accelerated villous maturation (2/15)

Kotlyar. Vertical transmission of COVID-19: a systematic review and meta-analysis. Am J Obstet Gynecol 2021.

(continued)

TABLE 3
Cohort or case series studies from outside of China (continued)

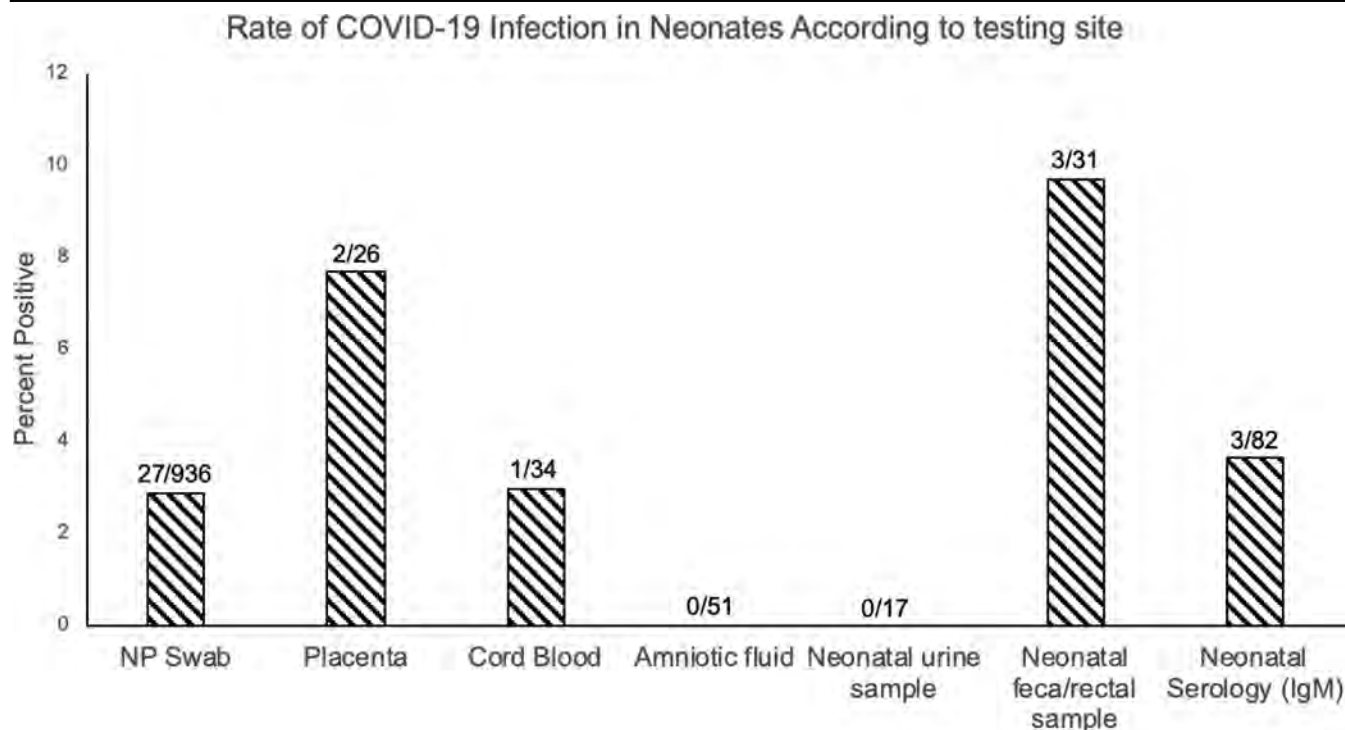
Author (country)	Number of women	Number of eligible neonates	GA at onset of Sx or diagnosis (range)	Mode of delivery	RT-PCR for SARS-CoV-2						
					Neonatal NP swab results	Placenta	Cord blood	Amniotic fluid	Other fetal sites or tests	Neonatal serology	Placental histology
Qadri and Mariona (United States) ⁸⁹	16	12	22–40 wk	VD 8/12, CD 4/12	0/12	None	None	None	None	None	None
Vintzileos et al (United States) ⁹⁰	32	29	N/A	N/A	0/29	None	None	None	None	None	None

All papers are identified by author, country (unless otherwise specified), and citation number within the main text.

BAL, bronchoalveolar lavage; CD, cesarean delivery; EM, electron microscopy; GA, gestational age; IgG, immunoglobulin G; IgM, immunoglobulin M; IQR, interquartile range; IUFD, intrauterine fetal demise; N/A, not available; NP, nasopharyngeal; RT-PCR, reverse transcription–polymerase chain reaction; SARS-CoV-2, severe acute respiratory syndrome coronavirus 2; Sx, symptoms; VD, vaginal delivery.

Korlyar. Vertical transmission of COVID-19: a systematic review and meta-analysis. *Am J Obstet Gynecol* 2021.

tested placentas of COVID-19–infected mothers having positive results for SARS-CoV-2 RNA (Figure 2). Among the case reports, 4 of 20 placentas tested for SARS-CoV-2 RNA had positive results. In 1 case, the placenta from a 19-week fetal demise had a positive result for SARS-CoV-2 RNA via PCR.²⁸ In another case mentioned earlier, a patient was diagnosed as having severe preterm preeclampsia complicated by placental abruption in the setting of COVID-19 at 22 weeks' gestation and underwent dilation and evacuation. Placental and fetal tissues were examined for the evidence of SARS-CoV-2 infection. Placenta and umbilical cord were positive for SARS-CoV-2 RNA tested by RT-PCR, whereas the fetal heart, lungs, and kidneys were negative. The sequencing of the virus isolated from the placenta confirmed it to be identical to the typical locally isolated SARS-CoV-2. Immunohistochemistry for the SARS-CoV-2 S protein and electron microscopy confirmed viral localization predominantly in the syncytiotrophoblast cells of the placenta.²⁷ The presence of SARS-CoV-2 virions in the fetal side of the placenta was similarly confirmed using electron microscopy in another case report of a woman who presented at 28 weeks' gestation and delivered by CD because of rapid maternal deterioration.⁵⁷ In this case, single virions were visible invading a syncytiotrophoblast, a single virion was also visualized in a microvillus, and virions were also noted in the mesenchymal core of terminal villus in the processes of the fibroblasts, but there was no evidence of fetal infection. In another case of a woman with a COVID-19 infection who delivered at 35 weeks' gestation by CD, placental viral testing had a positive result, which also correlated to the positive SARS-CoV-2 PCR testing of the newborn in NP, plasma, and stool samples, highly suggestive of in utero vertical transmission.²⁹ Another case of SARS-CoV-2 being detected in the placenta, which provides a particularly strong evidence for vertical transmission, was in a patient who delivered at 35 weeks and 5 days' gestation. In this case report, immunostaining of the perivillous

FIGURE 2**Rate of vertical transmission according to neonatal testing source**

COVID-19, coronavirus disease 2019; IgM, immunoglobulin M; NP, nasopharyngeal.

Kotlyar. Vertical transmission of COVID-19: a systematic review and meta-analysis. *Am J Obstet Gynecol* 2021.

trophoblastic cells showed positivity for SARS-CoV-2 N-protein. Viral RNA was also detected in placental, amniotic fluid, and neonatal blood samples taken at birth, which is indicative of transplacental transmission of SARS-CoV-2.⁵⁸

Placental histologic assessment from COVID-19–infected mothers was described in 6 cohort or case series studies showing various abnormalities that seem to have some common pathologic themes including vascular malperfusion, fibrin deposition, and chronic villitis or intervillitis. In a pathologic study of placentas from COVID-19–infected mothers, 12 of 15 placentas showed evidence of maternal vascular malperfusion, with 4 placentas demonstrating central and peripheral villous infarctions.⁸⁸ In addition, another series demonstrated the presence of placental vascular malperfusion in 10 of 20 placentas, with some showing intramural fibrin deposition (3/20) and chronic

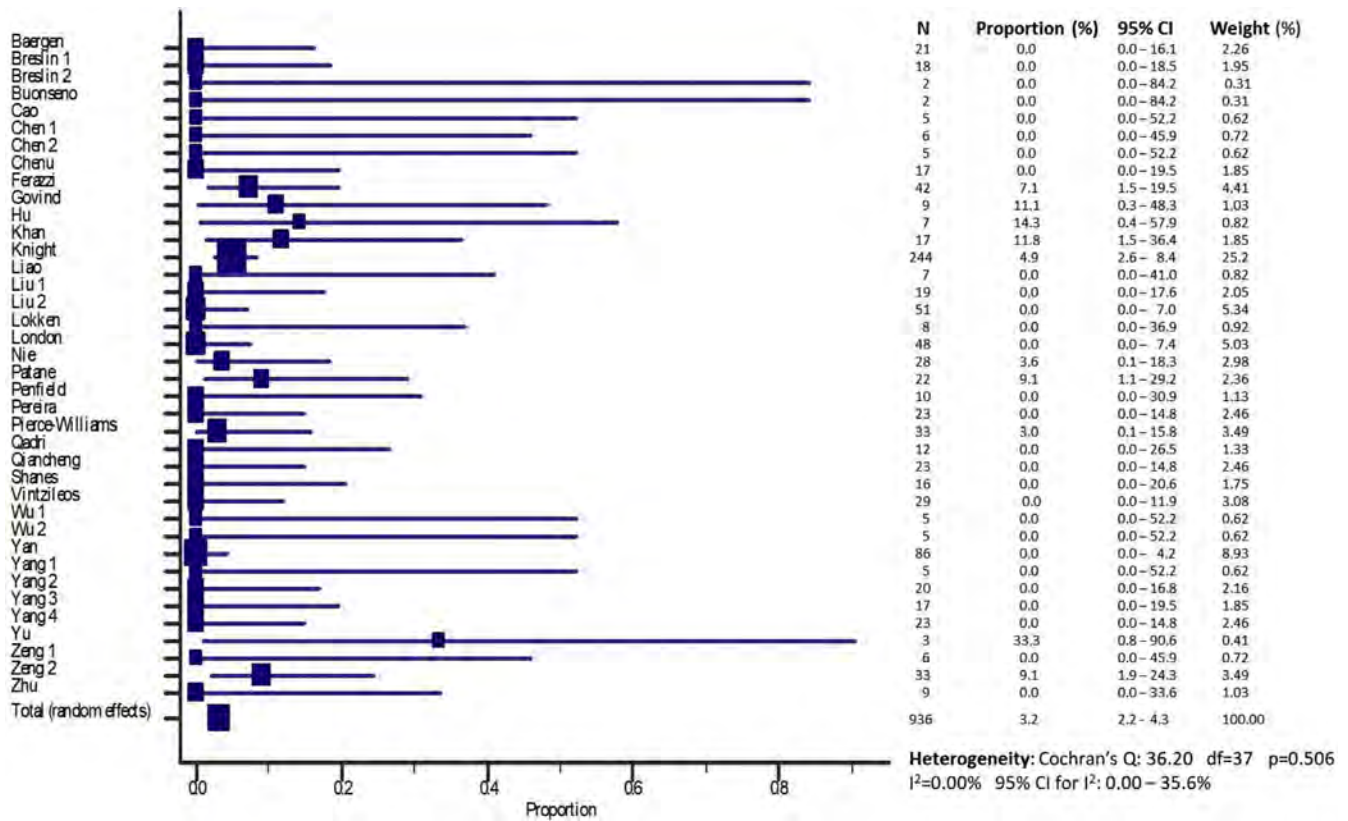
villitis (4/20).⁸⁴ In both of these studies, there was no evidence of neonatal SARS-CoV-2 infection by NP swab, and direct assessment of SARS-CoV-2 in the placenta was not performed. In another series of 5 COVID-19–positive mothers, all 5 placentas were negative for SARS-CoV-2 RNA but similarly exhibited fetal vascular malperfusion (5/5) and fibrin and complement deposition (4/5).⁸³ In a cohort of 8 COVID-19–positive patients who delivered, 1 still-born fetus delivered at 38.7 weeks' gestation did not show any SARS-CoV-2 RNA in the placenta or in fetal tissues tested at autopsy, but the placenta demonstrated evidence of severe chronic villitis.⁸¹ In another cohort study of 22 women with COVID-19, 2 neonates who were positive for SARS-CoV-2 by NP swab had placental histologic assessment revealing chronic intervillitis.³⁰ A similar evidence of chronic histiocytic intervillitis with intervillous inflammatory infiltrate consisting of mostly

CD68+ macrophages and some T cells was also seen in other reports.^{27,29,58}

Additional testing sites for severe acute respiratory syndrome coronavirus 2 by reverse transcription–polymerase chain reaction. Other neonatal sites have been tested for SARS-CoV-2 RNA. A total of 8 cohort or case series studies included in this systematic review had SARS-CoV-2 testing of the amniotic fluid (6 from China, 1 from the United Kingdom, and 1 from Italy). There were no positive cases among the 51 total amniotic fluid specimens tested (0/51) (Figure 2). However, we identified 2 case reports of positive amniotic fluid testing (Table 1). In the first case report, sterilely collected amniotic fluid (via syringe before rupturing the membranes) during a CD performed on a critically ill mother at 34 weeks' gestation was subjected to RT-PCR and had a positive result for SARS-CoV-2 RNA. The infant was immediately separated

FIGURE 3

Forest plot of meta-analysis of SARS-CoV-2 nasopharyngeal swab assessments of all case series and cohort studies



CI, confidence interval; df, degrees of freedom; SARS-CoV-2, severe acute respiratory syndrome coronavirus 2.

Kotlyar. Vertical transmission of COVID-19: a systematic review and meta-analysis. *Am J Obstet Gynecol* 2021.

from the mother, and initial testing was negative for SARS-CoV-2 RNA in the NP samples; however, the second neonatal NP swab was positive at 24 hours of life. Repeat throat swab from the neonate at 1 week of life remained positive.⁴⁷

Six cohort or case series studies (5 from China and 1 from Italy) reported cord blood testing in 34 neonates with 1 positive test result resulting in a pooled vertical transmission rate of 2.9% (Figure 2).⁸⁵ In the aforementioned case report by Vivanti et al,⁵⁸ SARS-CoV-2 RNA was also detected in the amniotic fluid and NP swab of the neonate. Furthermore, SARS-CoV-2 RNA was also detected in bronchoalveolar lavage specimens and neonatal blood, showing the presence of neonatal viremia after

transplacental transmission. Numerous case reports also assessed the cord blood for SARS-CoV-2 RNA. Of 16 case reports that tested the cord blood, none reported any positive cases (Table 1).

In adults, there has been evidence of the presence of SARS-CoV-2 in the gastrointestinal (GI) tract and persistent viral RNA identification in fecal specimens.^{92,93} In our review, among 6 cohort or case series studies (5 from China, 1 from Italy), 9.7% of neonates (3/31) had positive results for SARS-CoV-2 in the GI tract through RT-PCR testing in anal or rectal swabs and feces (Figure 2). One case report demonstrated a positive stool sample 7 days after birth.²⁹ In another study, 3 neonates of mothers with COVID-19 had positive results for SARS-CoV-2 RNA on anal swabs at day 2

of life.⁶⁷ There have been only 2 cohort or case series studies from China describing results of SARS-CoV-2 RT-PCR testing of urine samples in neonates born to women with COVID-19 infection. Of a total of 17 neonates tested, the detection rate for SARS-CoV-2 was 0% (0/17) (Figure 2).

In addition, we reviewed the articles for the presence of SARS-CoV-2 RNA in maternal body fluids that may be responsible for vertical transmission before and after delivery. There were 2 studies from China that reported on SARS-CoV-2 RT-PCR testing in vaginal swabs, demonstrating a detection rate of 0% (0/19). Our review included 6 cohort or case series studies from China that assessed for the presence of SARS-CoV-2 in breast milk by RT-PCR, revealing a

positive rate of 4.2% (2/47) in the breast milk specimens tested.^{29,72,85}

Serologic assessment. Serologic assessment was performed on neonates born to COVID-19–infected mothers in 4 cohort or case series studies from China and 1 from Italy.^{26,71,75,85} Among the total number of neonates tested in those cohort or case series studies, 3.7% of tested infants (3/82) were positive for anti–SARS-CoV-2 IgM antibodies (Figure 2). In a case report, an otherwise healthy infant was born via CD to a 29-year-old woman with an RT-PCR–confirmed COVID-19 infection. This infant was immediately placed in isolation, and a blood sample at 2 hours of age was noted to show an elevated SARS-CoV-2 immunoglobulin G (IgG) and IgM. Although the IgG can be secondary to transplacental transfer, the infant's positivity for SARS-CoV-2 IgM cannot be explained by transplacental transfer.²⁵ Furthermore, IgM antibodies usually do not appear until 3 to 7 days after infection. Paradoxically, all 5 RT-PCR tests on the infant were negative for COVID-19.²⁵ Nonetheless, the antibody profile of this infant is suggestive of fetal exposure to COVID-19 in utero. A follow-up study conducted on 6 infants born to COVID-19–positive mothers showed positive IgM antibodies in 2 infants. However, all throat swabs and blood samples from the neonates similarly tested negative for the virus.²⁶ In one of the largest studies looking at neonatal serology, Liu et al⁷¹ tested 51 infants for COVID-19 antibodies with none having a positive result for IgM and IgG. Yang et al⁷⁵ assessed 23 infants for COVID-19 infection; although none of them had positive NP swabs, 1 premature infant was found to have a positive result for anti–SARS-CoV-2 IgM within 2 hours after birth. Overall, the presence of IgM in these neonates immediately after birth is highly suggestive of in utero vertical transmission.

Comment

Main findings

In this systematic review, we aimed to summarize initial data regarding the risk of vertical transmission of COVID-19 to

help inform counseling and care of women who are pregnant or contemplating pregnancy at this time. It included 39 cohort or case series studies in the quantitative synthesis summarizing data from a total of 936 SARS-CoV-2–tested neonates to pregnant women with COVID-19 infection, spanning the initial 6 months since the disease manifested (end of December 2019). Regarding the most common method of testing for SARS-CoV-2, that is, NP swab RT-PCR testing, we determined that maternal-to-fetal transmission of the virus may occur in approximately 3.2% of infected mothers in the third trimester. Interestingly, there is a striking similarity in NP swab SARS-CoV-2 pooled positivity rates between studies from China (2%) and studies outside of China (3.5%). This rate of SARS-CoV-2 RNA positivity was also in the same range as for placental (7.7%) and cord blood samples (2.9%). The fact that IgM serology was also in the same range (3.7%) provides further support to the notion that vertical transmission is occurring in the third trimester, albeit in a minority of pregnant women. Nonetheless, these are all indirect measures of possible vertical transmission. The best evidence to date for transplacental transmission of SARS-CoV-2 was seen in the case report by Vivanti et al⁵⁸ showing not only viral RNA and protein in the placenta but also viral RNA in the amniotic fluid and neonatal blood sampled at birth. Although these studies further strengthen the case for vertical transmission occurring in utero, fetal infection could only be conclusively determined by the direct demonstration of the presence of SARS-CoV-2 in fetal tissues.

Clinical implications

Because of the teratogenicity and fetal morbidity associated with other viral infections such as Zika and Rubella, vertical transmission remains a concern with COVID-19. Compared with other known viruses leading to congenital infections, the vertical transmission rates reported in this review are consistent with those for numerous pathogens. The transmission rates for these pathogens

range from as low as 0.2% to 0.4% for cytomegalovirus and varicella zoster virus to as high as 17% to 33% for parvovirus B19.⁹⁴ Although the vast majority of infants delivered in these reports did not experience significant morbidity and mortality, nearly all of them were born in the third trimester.⁹⁴ For the aforementioned pathogens, the transplacental passage of infectious pathogens tends to occur with increasing frequency as gestational age increases, whereas detrimental effects on the fetus increase with decreasing gestational age. Therefore, we should assume that COVID-19 may also have similar detrimental effects when maternal infection occurs early in gestation.

In addition to direct fetal infection and subsequent teratogenicity, indirect fetal effects are also a major concern with the COVID-19 infection. It has recently been proposed that COVID-19 results in systemic endothelial damage that, in adults, predisposes to the development of or exacerbation of already existing hypertension and other cardiovascular diseases and results in a severe COVID-19 course.^{95,96} In particular, COVID-19 frequently induces hypercoagulability with both microangiopathy and local thrombus formation.⁹⁷ Pregnant women present an especially vulnerable population given their hypercoagulable state, with associated unique conditions. Hypertensive disorders of pregnancy are a group of conditions, the pathogenesis of which is not well understood; however, systemic endothelial dysfunction, vascular malperfusion, and a systemic proinflammatory state have been implied as potential etiologies or components of the disease pathophysiology, especially in cases of preexisting hypertension, obesity, or diabetes.⁹⁸ Of note, our systematic review found several cohort studies and case reports describing an association between maternal COVID-19 infection and placental evidence of maternal vascular malperfusion, particularly maternal vessel injury and intervillous thrombi. One may speculate that COVID-19 may result in the activation of endothelial damage pathways predisposing to the development of hypertensive disorders

of pregnancy with associated adverse maternal and neonatal outcomes (ie, prematurity, growth restriction) over the long term. This is one of the many issues that remain open for study.

Research implications

The standard for detecting COVID-19 infection is via detection of viral RNA using RT-PCR. However, this diagnostic method does exhibit variable performance. In a study assessing the performance capability of RT-PCR test in patients with COVID-19 using numerous sources for viral RNA including nasal, bronchoalveolar lavage, feces, blood, and urine specimens, sensitivities for COVID-19 detection were 63%, 93%, 29%, 1%, and 0%, respectively.⁹⁹ In our systematic review, blood similarly had one of the lowest rates of SARS-CoV-2 detection (2.9%), along with urine (0%) and amniotic fluid (0%). The lack of detection of SARS-CoV-2 in the amniotic fluid is not surprising because its source of production is fetal urine. Nevertheless, such substantial variation in SARS-CoV-2 positivity as a factor of testing site argues for specimen testing from multiple sites to increase sensitivity and reduce false-negative rates and preferably the use of complementary testing methods such as serology. In this systematic review, the rate of IgM positivity in tested neonates was 3.6%, which is quite similar to the positive rates by RT-PCR NP testing (3.2%). Patients typically develop IgG antibodies approximately 2 weeks after the onset of symptoms. Although developing fetuses can produce immunoglobulins early in gestation, the protective IgG antibodies in their circulation come from transplacental antibody transfer of maternal IgG.¹⁰⁰ Because IgM antibodies are too large to cross the placenta, the presence of IgM in a neonate during the perinatal period is suggestive of fetal production after in utero infection. The reported performance of perinatal IgM antibody testing indicates a sensitivity of 70.2% to 88.2% and specificity of 96.2% to 99%, although experience with IgM assays suggests that they are inherently limited by false-positive results in other

congenital infections.¹⁰¹ Further testing and validation of serologic assays are ongoing.

Strengths and limitations

We acknowledge that there are significant limitations to our study. Our current knowledge as reflected in this systematic review is limited to a few cohort studies and mostly case series and case reports. In addition, significant heterogeneity exists in the quality of included studies and in what data were reported. Although almost all studies reported results of SARS-CoV-2 NP testing of neonates, there was a significant variation in the performance of SARS-CoV-2 testing of other specimen sites across studies and of neonates within each study, making it challenging to aggregate the data. Moreover, because most of the included cohort or case series studies comprised pregnant patients who underwent selective testing for COVID-19 owing to symptoms, it is likely that patients with asymptomatic infections are underrepresented. Whether the risk of vertical transmission of SARS-CoV-2 may be related to symptom or disease severity is unknown, and as such, pooled rates of vertical transmission risk in this systematic review should be interpreted with caution.

Our study also has several strengths. The quantitative synthesis of this review, which was the basis for the pooled proportion results, was limited to cohort and case series studies as defined by at least 5 pregnant patients with COVID-19 infection. This significantly reduced the chance of publication bias of rare positive outcomes inherent to case reports. A second strength is that the studies included in this review were restricted to laboratory-confirmed cases of SARS-CoV-2 infection, which included both symptomatic and asymptomatic women. Diagnosis was made by RT-PCR of NP swab, which is currently the gold standard for diagnosis, thus avoiding reliance on uncertain COVID-19 diagnostic tests. Moreover, the review included only studies in which SARS-CoV-2 RT-PCR testing was performed on the fetus or neonate within 48 hours of delivery, substantially decreasing the

likelihood of a positive result arising from postpartum horizontal transmission. Another strength is that this review includes reports from multiple countries including China, the United States, the United Kingdom, Italy, and Spain, making the results more generalizable.

Conclusion and implications

Given the accumulating evidence from studies noting the presence of COVID-19 viral RNA in numerous fetal or neonatal sources and positive serology, vertical transmission of COVID-19 is indeed highly likely. This systematic review suggests that maternal COVID-19 infection in the third trimester appears to be associated with low rates of vertical transmission (approximately 3.2%) without significant consequence to the newborns. This low rate is consistent with recent transcriptomic data showing that placental cells coexpressing ACE2 and TMPRSS2 proteins, required for SARS-CoV-2 viral cell entry, are rare.²³ However, numerous questions remain to be addressed concerning vertical transmission of this novel coronavirus. These include whether the virus can cross the placenta in utero and cause an infection in fetal tissues. Furthermore, it is necessary to understand whether susceptibility varies by gestational age and whether there is a gestational age at which the virus is more likely to infect and cross the placenta. An even more crucial set of questions center around fetal development and morbidity. For example, if placental infection occurs in the first trimester, can the virus have teratogenic effects and what would those be? In addition, it would be essential to determine whether there are any non-teratogenic fetal effects that can result from viral effects on the uterine vasculature and placental tissue (ie, growth restriction; placental abruption, infarction, or stillbirth; hypertensive disorders of pregnancy). Finally, if in utero transmission indeed occurs, does the rate of transmission depend on the severity of the maternal disease and does a positive test at birth correlate with the clinical course of COVID-19 in newborns? To answer these questions, further larger-

scale studies are needed ideally across numerous countries. A cooperative system of monitoring COVID-19—positive pregnant women throughout gestation would help to answer these remaining questions to help guide patients, physicians, and policy makers. ■

REFERENCES

- Cheruiyot I, Henry BM, Lippi G. Is there evidence of intra-uterine vertical transmission potential of COVID-19 infection in samples tested by quantitative RT-PCR? *Eur J Obstet Gynecol Reprod Biol* 2020;249:100–1.
- Coronaviridae Study Group of the International Committee on Taxonomy of Viruses. The species severe acute respiratory syndrome-related coronavirus: classifying 2019-nCoV and naming it SARS-CoV-2. *Nat Microbiol* 2020;5:536–44.
- Heymann DL, Shindo N; WHO Scientific and Technical Advisory Group for Infectious Hazards. COVID-19: what is next for public health? *Lancet* 2020;395:542–5.
- Guan WJ, Ni ZY, Hu Y, et al. Clinical characteristics of coronavirus disease 2019 in China. *N Engl J Med* 2020;382:1708–20.
- Al-Omari A, Rabaan AA, Salih S, Al-Tawfiq JA, Memish ZA. MERS coronavirus outbreak: implications for emerging viral infections. *Diagn Microbiol Infect Dis* 2019;93:265–85.
- Rasmussen SA, Smulian JC, Lednicki JA, Wen TS, Jamieson DJ. Coronavirus disease 2019 (COVID-19) and pregnancy: what obstetricians need to know. *Am J Obstet Gynecol* 2020;222:415–26.
- Mor G, Aldo P, Alvero AB. The unique immunological and microbial aspects of pregnancy. *Nat Rev Immunol* 2017;17:469–82.
- Liu H, Wang LL, Zhao SJ, Kwak-Kim J, Mor G, Liao AH. Why are pregnant women susceptible to COVID-19? An immunological viewpoint. *J Reprod Immunol* 2020;139:103122.
- Zhu H, Wang L, Fang C, et al. Clinical analysis of 10 neonates born to mothers with 2019-nCoV pneumonia. *Transl Pediatr* 2020;9:51–60.
- Chen H, Guo J, Wang C, et al. Clinical characteristics and intrauterine vertical transmission potential of COVID-19 infection in nine pregnant women: a retrospective review of medical records. *Lancet* 2020;395:809–15.
- Yan J, Guo J, Fan C, et al. Coronavirus disease 2019 in pregnant women: a report based on 116 cases. *Am J Obstet Gynecol* 2020;223:111.e1–14.
- Knight M, Bunch K, Vousden N, et al. Characteristics and outcomes of pregnant women hospitalised with confirmed SARS-CoV-2 infection in the UK: a national cohort study using the UK Obstetric Surveillance System (UKOSS). *medRxiv*. Preprint posted online May 12 2020. <https://doi.org/10.1101/2020.05.08.20089268>.
- Fan C, Lei D, Fang C, et al. Perinatal transmission of COVID-19 associated SARS-CoV-2: should we worry? *Clin Infect Dis* 2020 [Epub ahead of print].
- Della Gatta AN, Rizzo R, Piliu G, Simonazzi G. Coronavirus disease 2019 during pregnancy: a systematic review of reported cases. *Am J Obstet Gynecol* 2020;223:36–41.
- Yang Z, Wang M, Zhu Z, Liu Y. Coronavirus disease 2019 (COVID-19) and pregnancy: a systematic review. *J Matern Fetal Neonatal Med* 2020 [Epub ahead of print].
- Yang Z, Liu Y. Vertical transmission of severe acute respiratory syndrome coronavirus 2: a systematic review. *Am J Perinatol* 2020;37:1055–60.
- Principi N, Bosis S, Esposito S. Effects of coronavirus infections in children. *Emerg Infect Dis* 2010;16:183–8.
- Zumla A, Hui DS, Perlman S. Middle East respiratory syndrome. *Lancet* 2015;386:995–1007.
- Levy A, Yagil Y, Bursztyn M, Barkalifa R, Scharf S, Yagil C. ACE2 expression and activity are enhanced during pregnancy. *Am J Physiol Regul Integr Comp Physiol* 2008;295:R1953–61.
- Valdés G, Neves LA, Anton L, et al. Distribution of angiotensin-(1-7) and ACE2 in human placentas of normal and pathological pregnancies. *Placenta* 2006;27:200–7.
- Jing Y, Run-Qian L, Hao-Ran W, et al. Potential influence of COVID-19/ACE2 on the female reproductive system. *Mol Hum Reprod* 2020;26:367–73.
- Li M, Chen L, Zhang J, Xiong C, Li X. The SARS-CoV-2 receptor ACE2 expression of maternal-fetal interface and fetal organs by single-cell transcriptome study. *PLoS One* 2020;15:e0230295.
- Pique-Regi R, Romero R, Tarca A, et al. Does the human placenta express the canonical cell entry mediators for SARS-CoV-2? *Elife* 2020;9:e58716.
- Barthold SW, Beck DS, Smith AL. Mouse hepatitis virus and host determinants of vertical transmission and maternally-derived passive immunity in mice. *Arch Virol* 1988;100:171–83.
- Dong L, Tian J, He S, et al. Possible vertical transmission of SARS-CoV-2 from an infected mother to her newborn. *JAMA* 2020;323:1846–8.
- Zeng H, Xu C, Fan J, et al. Antibodies in infants born to mothers with COVID-19 pneumonia. *JAMA* 2020;323:1848–9.
- Hosier H, Farhadian SF, Morotti RA, et al. SARS-CoV-2 infection of the placenta. *J Clin Invest* 2020 [Epub ahead of print].
- Baud D, Greub G, Favre G, et al. Second-trimester miscarriage in a pregnant woman with SARS-CoV-2 infection. *JAMA* 2020;323:2198–200.
- Kirtsman M, Diambomba Y, Poutanen SM, et al. Probable congenital SARS-CoV-2 infection in a neonate born to a woman with active SARS-CoV-2 infection. *CMAJ* 2020;192:E647–50.
- Patanè L, Morotti D, Giunta MR, et al. Vertical transmission of COVID-19: SARS-CoV-2 RNA on the fetal side of the placenta in pregnancies with COVID-19 positive mothers and neonates at birth. *Am J Obstet Gynecol MFM* 2020 [Epub ahead of print].
- Abu-Zidan FM, Abbas AK, Hefny AF. Clinical “case series”: a concept analysis. *Afr Health Sci* 2012;12:557–62.
- Haffar S, Bazerbachi F, Prokop L, Watt KD, Murad MH, Chari ST. Frequency and prognosis of acute pancreatitis associated with fulminant or non-fulminant acute hepatitis A: a systematic review. *Pancreatol* 2017;17:166–75.
- Freeman MF, Tukey JW. Transformations related to the angular and the square root. *Ann Math Statist* 1950;21:607–11.
- DerSimonian R, Laird N. Meta-analysis in clinical trials. *Control Clin Trials* 1986;7:177–88.
- Alzamora MC, Paredes T, Caceres D, Webb CM, Valdez LM, La Rosa M. Severe COVID-19 during pregnancy and possible vertical transmission. *Am J Perinatol* 2020;37:861–5.
- Chen S, Huang B, Luo DJ, et al. Pregnancy with new coronavirus infection: clinical characteristics and placental pathological analysis of three cases. *Zhonghua Bing Li Xue Za Zhi* 2020;49:418–23.
- Kalafat E, Yaprak E, Cinar G, et al. Lung ultrasound and computed tomographic findings in pregnant woman with COVID-19. *Ultrasound Obstet Gynecol* 2020;55:835–7.
- Khan S, Peng L, Siddique R, et al. Impact of COVID-19 infection on pregnancy outcomes and the risk of maternal-to-neonatal intrapartum transmission of COVID-19 during natural birth. *Infect Control Hosp Epidemiol* 2020;41:748–50.
- Li Y, Zhao R, Zheng S, et al. Lack of vertical transmission of severe acute respiratory syndrome coronavirus 2, China. *Emerg Infect Dis* 2020;26:1335–6.
- Liu W, Wang Q, Zhang Q, et al. Coronavirus disease 2019 (COVID-19) during pregnancy: a case series. Preprints. Preprint posted online February 25, 2020. <https://doi.org/10.1101/202002.0373.v1>.
- Lowe B, Bopp B. COVID-19 vaginal delivery – a case report. *Aust N Z J Obstet Gynaecol* 2020;60:465–6.
- Lu D, Sang L, Du S, Li T, Chang Y, Yang XA. Asymptomatic COVID-19 infection in late pregnancy indicated no vertical transmission. *J Med Virol* 2020 [Epub ahead of print].
- Peng Z, Wang J, Mo Y, et al. Unlikely SARS-CoV-2 vertical transmission from mother to child: a case report. *J Infect Public Health* 2020;13:818–20.
- Schnettler WT, Al Ahwel Y, Suhag A. Severe ARDS in COVID-19-infected pregnancy: obstetric and intensive care considerations. *Am J Obstet Gynecol MFM* 2020 [Epub ahead of print].
- Wang S, Guo L, Chen L, et al. A case report of neonatal 2019 coronavirus disease in China. *Clin Infect Dis* 2020;71:853–7.

46. Xiong X, Wei H, Zhang Z, et al. Vaginal delivery report of a healthy neonate born to a convalescent mother with COVID-19. *J Med Virol* 2020 [Epub ahead of print].
47. Zamaniyan M, Ebadi A, Aghajani-poor Mir S, Rahmani Z, Haghsheenas M, Azizi S. Preterm delivery in pregnant woman with critical COVID-19 pneumonia and vertical transmission. *Prenat Diagn* 2020 [Epub ahead of print].
48. Blauvelt CA, Chiu C, Donovan AL, et al. Acute respiratory distress syndrome in a pre-term pregnant patient with coronavirus disease 2019 (COVID-19). *Obstet Gynecol* 2020;136:46–51.
49. Buonsenso D, Raffaelli F, Tamburrini E, et al. Clinical role of lung ultrasound for diagnosis and monitoring of COVID-19 pneumonia in pregnant women. *Ultrasound Obstet Gynecol* 2020;56:106–9.
50. Gidlöf S, Savchenko J, Brune T, Josefsson H. COVID-19 in pregnancy with comorbidities: more liberal testing strategy is needed. *Acta Obstet Gynecol Scand* 2020;99:948–9.
51. Huang JW, Zhou XY, Lu SJ, et al. Dialectical behavior therapy-based psychological intervention for woman in late pregnancy and early postpartum suffering from COVID-19: a case report. *J Zhejiang Univ Sci B* 2020;21:394–9.
52. Lang G, Zhao H. Can SARS-CoV-2-infected women breastfeed after viral clearance? *J Zhejiang Univ Sci B* 2020;21:405–7.
53. Lee DH, Lee J, Kim E, Woo K, Park HY, An J. Emergency cesarean section performed in a patient with confirmed severe acute respiratory syndrome coronavirus-2 -a case report. *Korean J Anesthesiol* 2020;73:347–51.
54. Lyra J, Valente R, Rosário M, Guimarães M. Cesarean section in a pregnant woman with COVID-19: first case in Portugal. *Acta Med Port* 2020;33:429–31.
55. Vallejo V, Ilagan JG. A postpartum death due to coronavirus disease 2019 (COVID-19) in the United States. *Obstet Gynecol* 2020;136:52–5.
56. Yu N, Li W, Kang Q, et al. Clinical features and obstetric and neonatal outcomes of pregnant patients with COVID-19 in Wuhan, China: a retrospective, single-centre, descriptive study. *Lancet Infect Dis* 2020;20:559–64.
57. Algarroba GN, Rekawek P, Vahanian SA, et al. Visualization of severe acute respiratory syndrome coronavirus 2 invading the human placenta using electron microscopy. *Am J Obstet Gynecol* 2020;223:275–8.
58. Vivanti AJ, Vauloup-Fellous C, Prevot S, et al. Transplacental transmission of SARS-CoV-2 infection. *Nat Commun* 2020;11:3572.
59. Cao D, Yin H, Chen J, et al. Clinical analysis of ten pregnant women with COVID-19 in Wuhan, China: a retrospective study. *Int J Infect Dis* 2020;95:294–300.
60. Hu X, Gao J, Luo X, et al. Severe acute respiratory syndrome coronavirus 2 (SARS-CoV-2) vertical transmission in neonates born to mothers with coronavirus disease 2019 (COVID-19) pneumonia. *Obstet Gynecol* 2020;136:65–7.
61. Khan S, Jun L, Nawsherwan, et al. Association of COVID-19 with pregnancy outcomes in health-care workers and general women. *Clin Microbiol Infect* 2020;26:788–90.
62. Liu W, Wang J, Li W, Zhou Z, Liu S, Rong Z. Clinical characteristics of 19 neonates born to mothers with COVID-19. *Front Med* 2020;14:193–8.
63. Nie R, Wang S, Yang Q, et al. Clinical features and the maternal and neonatal outcomes of pregnant women with coronavirus disease 2019. medRxiv. Preprint posted online March 27 2020. <https://doi.org/10.1101/2020.03.22.20041061>.
64. Qiancheng X, Jian S, Lingling P, et al. Coronavirus disease 2019 in pregnancy. *Int J Infect Dis* 2020;95:376–83.
65. Yang P, Wang X, Liu P, et al. Clinical characteristics and risk assessment of newborns born to mothers with COVID-19. *J Clin Virol* 2020;127:104356.
66. Yin M, Zhang L, Deng G, et al. Severe acute respiratory syndrome coronavirus 2 (SARS-CoV-2) infection during pregnancy in china: a retrospective cohort study. medRxiv. Preprint posted online April 11 2020. <https://doi.org/10.1101/2020.04.07.20053744>.
67. Zeng L, Xia S, Yuan W, et al. Neonatal early-onset infection with SARS-CoV-2 in 33 neonates born to mothers with COVID-19 in Wuhan, China. *JAMA Pediatr* 2020;174:722–5.
68. Chen S, Liao E, Cao D, Gao Y, Sun G, Shao Y. Clinical analysis of pregnant women with 2019 novel coronavirus pneumonia. *J Med Virol* 2020 [Epub ahead of print].
69. Chen R, Zhang Y, Huang L, Cheng BH, Xia ZY, Meng QT. Safety and efficacy of different anesthetic regimens for parturients with COVID-19 undergoing cesarean delivery: a case series of 17 patients. *Can J Anaesth* 2020;67:655–63.
70. Liao J, He X, Gong Q, Yang L, Zhou C, Li J. Analysis of vaginal delivery outcomes among pregnant women in Wuhan, China during the COVID-19 pandemic. *Int J Gynaecol Obstet* 2020;150:53–7.
71. Liu P, Zheng J, Yang P, et al. The immunologic status of newborns born to SARS-CoV-2-infected mothers in Wuhan, China. *J Allergy Clin Immunol* 2020;146:101–9.e1.
72. Wu Y, Liu C, Dong L, et al. Coronavirus disease 2019 among pregnant Chinese women: case series data on the safety of vaginal birth and breastfeeding. *BJOG* 2020;127:1109–15.
73. Wu X, Sun R, Chen J, Xie Y, Zhang S, Wang X. Radiological findings and clinical characteristics of pregnant women with COVID-19 pneumonia. *Int J Gynaecol Obstet* 2020;150:58–63.
74. Yang H, Sun G, Tang F, et al. Clinical features and outcomes of pregnant women suspected of coronavirus disease 2019. *J Infect* 2020;81:e40–4.
75. Yang H, Hu B, Zhan S, Yang LY, Xiong G. Effects of SARS-CoV-2 infection on pregnant women and their infants: a retrospective study in Wuhan, China. *Arch Pathol Lab Med* 2020 [Epub ahead of print].
76. Breslin N, Baptiste C, Miller R, et al. Coronavirus disease 2019 in pregnancy: early lessons. *Am J Obstet Gynecol MFM* 2020;2:100111.
77. Breslin N, Baptiste C, Gyamfi-Bannerman C, et al. COVID-19 infection among asymptomatic and symptomatic pregnant women: two weeks of confirmed presentations to an affiliated pair of New York City hospitals. *Am J Obstet Gynecol MFM* 2020;2:100118.
78. Ferrazzi E, Frigerio L, Savasi V, et al. Vaginal delivery in SARS-CoV-2-infected pregnant women in Northern Italy: a retrospective analysis. *BJOG* 2020 [Epub ahead of print].
79. Penfield CA, Brubaker SG, Limaye MA, et al. Detection of SARS-COV-2 in placental and fetal membrane samples. *Am J Obstet Gynecol MFM* 2020 [Epub ahead of print].
80. Pierce-Williams RAM, Burd J, Felder L, et al. Clinical course of severe and critical COVID-19 in hospitalized pregnancies: a US cohort study. *Am J Obstet Gynecol MFM* 2020 [Epub ahead of print].
81. Lokken EM, Walker CL, Delaney S, et al. Clinical characteristics of 46 pregnant women with a severe acute respiratory syndrome coronavirus 2 infection in Washington State. *Am J Obstet Gynecol* 2020 [Epub ahead of print].
82. London V, McLaren R Jr, Atallah F, et al. The relationship between status at presentation and outcomes among pregnant women with COVID-19. *Am J Perinatol* 2020;37:991–4.
83. Mulvey JJ, Magro CM, Ma LX, Nuovo GJ, Baergen RN. Analysis of complement deposition and viral RNA in placenta of COVID-19 patients. *Ann Diagn Pathol* 2020;46:151530.
84. Baergen RN, Heller DS. Placental pathology in Covid-19 positive mothers: preliminary findings. *Pediatr Dev Pathol* 2020;23:177–80.
85. Buonsenso D, Costa S, Sanguinetti M, et al. Neonatal late onset infection with severe acute respiratory syndrome coronavirus 2. *Am J Perinatol* 2020;37:869–72.
86. Govind A, Essien S, Karthikeyan A, et al. Re: novel coronavirus COVID-19 in late pregnancy: outcomes of first nine cases in an inner city London hospital. *Eur J Obstet Gynecol Reprod Biol* 2020;251:272–4.
87. Pereira A, Cruz-Melguizo S, Adrien M, Fuentes L, Marin E, Perez-Medina T. Clinical course of coronavirus disease-2019 in pregnancy. *Acta Obstet Gynecol Scand* 2020;99:839–47.
88. Shanes ED, Mithal LB, Otero S, Azad HA, Miller ES, Goldstein JA. Placental pathology in COVID-19. *Am J Clin Pathol* 2020;154:23–32.
89. Qadri F, Mariona F. Pregnancy affected by SARS-CoV-2 infection: a flash report from Michigan. *J Matern Fetal Neonatal Med* 2020 [Epub ahead of print].

90. Vintzileos WS, Muscat J, Hoffmann E, et al. Screening all pregnant women admitted to labor and delivery for the virus responsible for coronavirus disease 2019. *Am J Obstet Gynecol* 2020;223:284–6.
91. Korber B, Fischer WM, Gnanakaran S, et al. Spike mutation pipeline reveals the emergence of a more transmissible form of SARS-CoV-2. *bioRxiv*. Preprint posted online April 30 2020. <https://doi.org/10.1101/2020.04.29.069054>.
92. Gupta S, Parker J, Smits S, Underwood J, Dolwani S. Persistent viral shedding of SARS-CoV-2 in faeces - a rapid review. *Colorectal Dis* 2020;22:611–20.
93. Tian Y, Rong L, Nian W, He Y. Review article: gastrointestinal features in COVID-19 and the possibility of faecal transmission. *Aliment Pharmacol Ther* 2020;51:843–51.
94. American College of Obstetricians and Gynecologists. Practice bulletin no. 151: cytomegalovirus, parvovirus B19, varicella zoster, and toxoplasmosis in pregnancy. *Obstet Gynecol* 2015;125:1510–25.
95. Sardu C, Gambardella J, Morelli MB, Wang X, Marfella R, Santulli G. Hypertension, thrombosis, kidney failure, and diabetes: is COVID-19 an endothelial disease? A comprehensive evaluation of clinical and basic evidence. *J Clin Med* 2020;9:1417.
96. Geng YJ, Wei ZY, Qian HY, Huang J, Lodato R, Castriotta RJ. Pathophysiological characteristics and therapeutic approaches for pulmonary injury and cardiovascular complications of coronavirus disease 2019. *Cardiovasc Pathol* 2020;47:107228.
97. Iba T, Levy JH, Levi M, Connors JM, Thachil J. Coagulopathy of coronavirus disease 2019. *Crit Care Med* 2020 [Epub ahead of print].
98. Kirollos S, Skilton M, Patel S, Arnott C. A systematic review of vascular structure and function in pre-eclampsia: non-invasive assessment and mechanistic links. *Front Cardiovasc Med* 2019;6:166.
99. Wang W, Xu Y, Gao R, et al. Detection of SARS-CoV-2 in different types of clinical specimens. *JAMA* 2020;323:1843–4.
100. Palmeira P, Quinello C, Silveira-Lessa AL, Zago CA, Carneiro-Sampaio M. IgG placental transfer in healthy and pathological pregnancies. *Clin Dev Immunol* 2012;2012:985646.
101. Kimberlin DW, Stagno S. Can SARS-CoV-2 infection be acquired in utero?: more definitive evidence is needed. *JAMA* 2020 [Epub ahead of print].

SUPPLEMENTAL FIGURE**Search strategy****Search for Ovid Embase.**

Additional database searches provided upon request: Alyssa.grimshaw@yale.edu

1. (covid-19 or COVID19 or COVID-19 or SARS-CoV-2 or SARS-CoV2 or severe acute respiratory syndrome coronavirus 2 or 2019-nCoV or 2019nCoV or coronavirus).tw,kw.
2. exp coronavirus infections/
3. exp coronavirinae/
4. 1 or 2 or 3
5. exp pregnancy/
6. exp birth/
7. exp "embryonic and placental structures"/
8. fetus/
9. exp infant/
10. (perinatal or pregnan* or maternal* or natal or prenatal or antenatal or postpartum or postnatal or neonatal or trimester* or fetomaternal*).tw,kw.
11. ((after or before) adj1 (birth* or childbirth*)).tw,kw.
12. (placenta* or placentom* or breastmilk or breast milk or mother's milk or mothers milk or breastfeed* or breastfed or breast feed* or breast fed or umbilical cord*).tw,kw.
13. (fetus* or fetal or newborn* or baby or babies or neonate* or infant* or embryo*).tw,kw.
14. or/5-13
15. exp vertical transmission/
16. exp disease transmission/
17. exp virus transmission/
18. (transmission* or transmit* or transmissibl* or transfer*).tw,kw.
19. (mother-to-child or mother-to-infant or maternal-fetal or vertical).tw,kw.
20. or/15-19
21. 4 and 14 and 20

Kotlyar. Vertical transmission of COVID-19: a systematic review and meta-analysis. Am J Obstet Gynecol 2021.

SUPPLEMENTAL TABLE

Modified Newcastle-Ottawa scale for assessing quality of cohort or case series studies

Author	Year	Representativeness of exposed cohort	Exposure assessment	Outcome assessment	Adequacy of length of time before follow-up	Adequacy of follow-up of cohorts	Methodological quality
Breslin, et al ⁷⁶	April 2020	★	★	★	★	★	High
Breslin, et al ⁷⁷	May 2020	★	★	★	★	★	High
Cao, et al ⁵⁹	April 2020		★		★		Low
Chen, et al ¹⁰	February 2020	★	★	★	★		Moderate
Ferrazzi, et al ⁷⁸	April 2020	★	★	★	★	★	High
Hu, et al ⁶⁰	April 2020		★	★	★	★	Moderate
Khan, et al ³⁸	April 2020	★	★	★	★		Moderate
Liu, et al ⁴⁰	March 2020	★		★	★		Low
Nie, et al ⁶³	March 2020	★	★	★	★		Moderate
Penfield, et al ⁷⁹	May 2020	★	★	★	★	★	High
Patane, et al ³⁰	May 2020	★	★	★	★	★	High
Pierce-Williams, et al ⁸⁰	May 2020	★	★		★	★	Moderate
Qiancheng, et al ⁶⁴	April 2020	★	★	★	★	★	High
Yan, et al ¹¹	April 2020	★	★	★	★		Moderate
Yang, et al ⁶⁵	April 2020	★	★	★	★	★	High
Yin, et al ⁶⁶	April 2020	★	★	★	★		Moderate
Yu, et al ⁵⁶	March 2020	★	★	★	★	★	High
Zeng, et al ²⁶	March 2020		★	★	★		Low
Zeng, et al ⁶⁷	March 2020	★	★	★	★	★	High
Zhu, et al ⁹	Feb 2020		★	★	★		Low
Lokken, et al ⁸¹	May 2020	★	★	★			Low
London, et al ⁸²	May 2020	★	★	★	★		Moderate
Mulvey, et al ⁸³	April 2020		★				Low
Baergen, et al ⁸⁴	May 2020	★	★	★	★		Moderate
Buonsenso, et al ⁴⁹	May 2020		★	★	★	★	Moderate
Chen, et al ⁶⁸	April 2020		★	★	★		Low
Chen, et al ⁶⁹	March 2020	★	★	★	★		Moderate
Govind, et al ⁸⁶	May 2020	★	★	★	★		Moderate
Knight, et al ¹²	May 2020	★	★	★	★	★	High
Liao, et al ⁷⁰	April 2020	★	★	★	★	★	High
Liu, et al ⁷¹	May 2020	★	★	★	★	★	High
Pereira, et al ⁸⁷	May 2020	★	★	★	★		Moderate
Qadri, et al ⁸⁹	May 2020	★	★	★	★		Moderate
Wu, et al ⁷²	May 2020	★	★	★	★	★	High
Wu, et al ⁷³	April 2020	★	★		★		Low
Yang, et al ⁷⁴	April 2020		★		★		Low

Kotlyar. Vertical transmission of COVID-19: a systematic review and meta-analysis. Am J Obstet Gynecol 2021.

(continued)

SUPPLEMENTAL TABLE

Modified Newcastle-Ottawa scale for assessing quality of cohort or case series studies (continued)

Author	Year	Representativeness of exposed cohort	Exposure assessment	Outcome assessment	Adequacy of length of time before follow-up	Adequacy of follow-up of cohorts	Methodological quality
Yang, et al ⁷⁵	May 2020	★	★	★	★		Moderate
Shanes, et al ⁸⁸	May 2020	★	★	★			Low
Vintzileos, et al ⁹⁰	April 2020	★	★	★	★		Moderate

Questions:

1. Did the patients represent the whole cases of the medical center? Cases included represented the general population of COVID-19 pregnant women.
 2. Was the diagnosis correctly made? COVID-19 was diagnosed by viral PCR.
 3. Was the outcome correctly ascertained? Clear description of adequate methodology of testing for COVID-19 in fetus or neonate was provided.
 4. Was follow-up long enough for outcomes to occur? Adequate follow-up time was reported.
 5. Were all important data cited in the report? Testing was repeated at least 2 times on 2 separate occasions.
- Methodological quality: high=5 stars, moderate=4 stars, low=3 or fewer stars.

Kotlyar. Vertical transmission of COVID-19: a systematic review and meta-analysis. *Am J Obstet Gynecol* 2021.

CORRESPONDENCE

Antibody Responses in Seropositive Persons after a Single Dose of SARS-CoV-2 mRNA Vaccine

TO THE EDITOR: The efficacy of two injections of the severe acute respiratory syndrome coronavirus 2 (SARS-CoV-2) spike messenger RNA (mRNA) vaccines (BNT162b2 [Pfizer] and mRNA-1273 [Moderna])¹ in preventing symptomatic SARS-CoV-2 infection in persons without previous coronavirus disease 2019 (Covid-19) has been shown to be high.^{2,3} We wondered what the response would be to the first vaccine dose in persons with previous Covid-19.

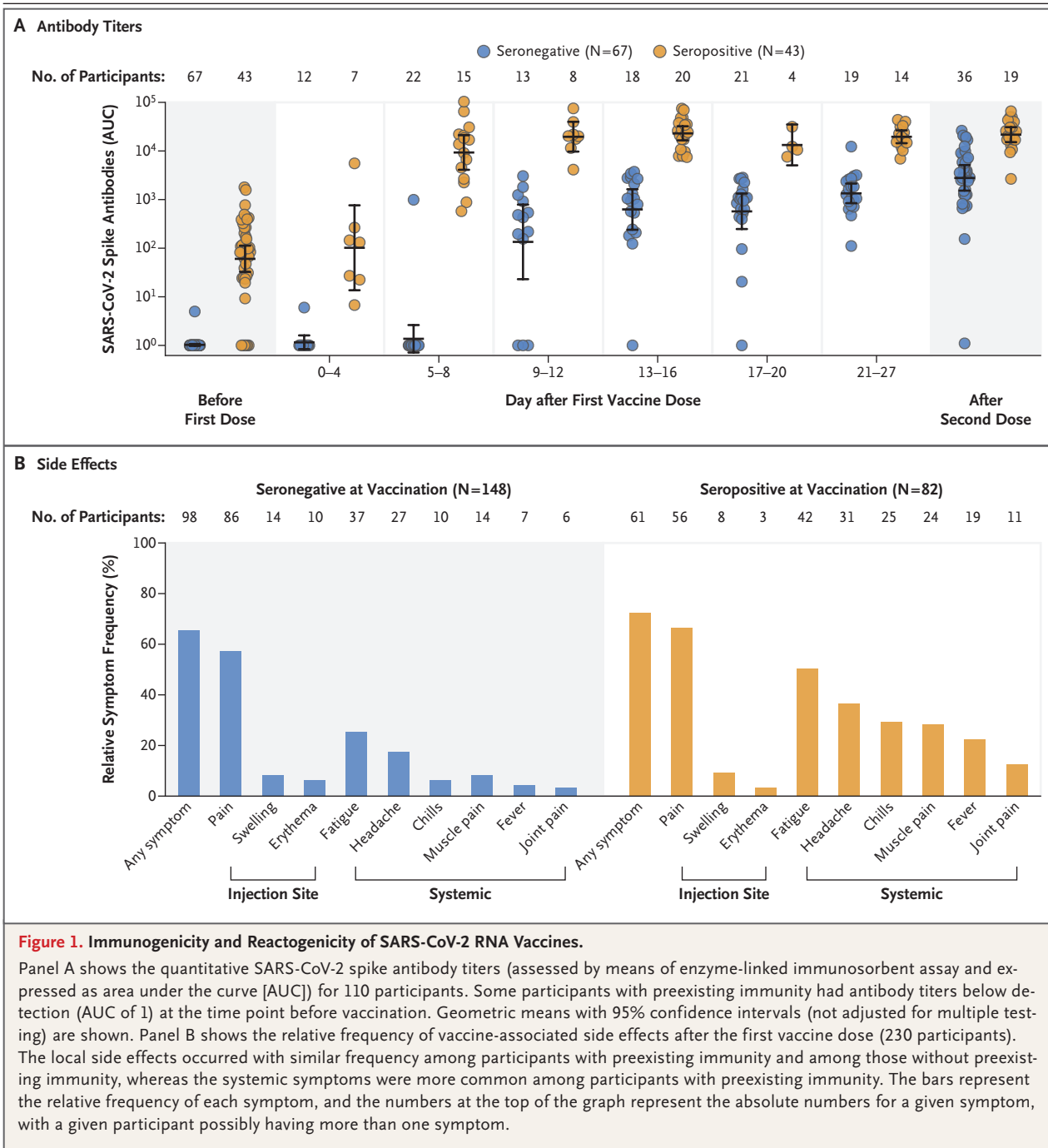
We took advantage of our ongoing institutional review board–approved, longitudinal PARIS (Protection Associated with Rapid Immunity to SARS-CoV-2) study to provide a limited snapshot of the antibody responses in 110 study participants with or without documented preexisting SARS-CoV-2 immunity (mean age overall, 40.0 years [range, 24 to 68; ≥60 years, 8%]; 67 seronegative participants [64% female] with a mean age of 41.3 years and 43 seropositive participants [59% female] with a mean age of 41.4 years) (Table S1 in the Supplementary Appendix, available with the full text of this letter at NEJM.org) who received their first spike mRNA vaccine dose in 2020 (88 received the Pfizer vaccine and 22 the Moderna vaccine). SARS-CoV-2 spike IgG was measured with the use of a previously described two-step enzyme-linked immunosorbent assay and expressed as area under the curve (AUC).^{4,5}

Repeated sampling after the first dose indicates that the majority of seronegative participants had variable and relatively low SARS-CoV-2 IgG responses within 9 to 12 days after vaccination (median AUC before vaccination, 1 [67 participants]; at 0 to 4 days, 1 [12 participants]; at 5 to 8 days, 1 [22 participants]; at 9 to 12 days, 439 [13 participants]; at 13 to 16 days, 1016 [18 participants]; at 17 to 20 days, 1037 [21 participants]; at 21 to 27 days, 1293 [19 participants]; and after the second dose, 3316 [36 participants]) (Fig. 1A). In contrast, participants with SARS-CoV-2 antibodies at baseline before the first vac-

cine injection rapidly developed uniform, high antibody titers within days after vaccination (median AUC before vaccination, 90 [43 participants]; at 0 to 4 days, 133 [7 participants]; at 5 to 8 days, 14,208 [15 participants]; at 9 to 12 days, 20,783 [8 participants]; at 13 to 16 days, 25,927 [20 participants]; at 17 to 20 days, 11,755 [4 participants]; at 21 to 27 days, 19,534 [14 participants]; and after the second dose, 22,509 [19 participants]) (Fig. 1A).

The antibody titers of vaccinees with preexisting immunity were 10 to 45 times as high as those of vaccinees without preexisting immunity at the same time points after the first vaccine dose (e.g., 25 times as high at 13 to 16 days) and also exceeded the median antibody titers measured in participants without preexisting immunity after the second vaccine dose by more than a factor of 6. Although the antibody titers of the vaccinees without preexisting immunity increased by a factor of 3 after the second vaccine dose, no increase in antibody titers was observed in the Covid-19 survivors who received the second vaccine dose. No substantial difference was noted in the dynamics of antibody responses elicited by the Pfizer and Moderna vaccines after the first dose (Fig. S1). The current analysis represents a convenience sample in which not all participants were able to provide biospecimens for antibody analysis at all the additional time intervals. Ongoing follow-up studies will show whether these early differences in immune responses are maintained over a prolonged time period.

In addition, we compared the frequency of local, injection-site-related as well as systemic reactions after the first dose of vaccine in 230 participants (mean age, 39.2 years [range, 22 to 70; ≥60 years, 8%]; 148 seronegative participants [70% female] and 82 seropositive participants [64% female]) (Fig. 1B). Overall, both vaccines (156 participants received the Pfizer vaccine and 74 the Moderna vaccine) had no side effects that



resulted in hospitalization. A total of 159 of the 230 participants (69%) who completed the PARIS study survey reported having some side effects after the first vaccine dose (46% of the seronegative survey respondents and 89% of the seropositive survey respondents). Most common were localized injection-site symptoms (pain, swelling,

and erythema), which occurred with equal frequency independently of the serostatus at the time of vaccination and resolved spontaneously within days after vaccination. Vaccine recipients with preexisting immunity had systemic side effects at higher frequencies than those without preexisting immunity (fatigue, headache, chills,

muscle pain, fever, and joint pain, in order of decreasing frequency) (Fig. 1B). Because a convenience sample was used and only participants with available data were studied, caution is needed until the full data set, including side effects occurring after the first as well as the second vaccine dose, can be assessed.

We found that a single dose of mRNA vaccine elicited rapid immune responses in seropositive participants, with postvaccination antibody titers that were similar to or exceeded titers found in seronegative participants who received two vaccinations. Whether a single dose of mRNA vaccine provides effective protection in seropositive persons requires investigation.

Florian Krammer, Ph.D.
 Komal Srivastava, M.S.
 Hala Alshammary, M.S.
 Angela A. Amoako, M.S.
 Mahmoud H. Awawda, M.S.
 Katherine F. Beach, B.S.
 Maria C. Bermúdez-González, M.P.H.
 Dominika A. Bielak, B.A.
 Juan M. Carreño, Ph.D.
 Rachel L. Chernet, B.A.
 Lily Q. Eaker, B.A.
 Emily D. Ferreri, B.S.
 Daniel L. Floda, B.A.
 Charles R. Gleason, B.S.
 Joshua Z. Hamburger, M.D.
 Kaijun Jiang, M.S.
 Giulio Kleiner, Ph.D.
 Denise Jurczynszak, Ph.D.
 Julia C. Matthews, B.A.
 Wanni A. Mendez, A.A.S.
 Ismail Nabeel, M.D.

Lubbertus C.F. Mulder, Ph.D.
 Ariel J. Raskin, B.A.
 Kayla T. Russo, B.S.
 Ashley-Beathrese T. Salimbangon, B.A.
 Miti Saksena, M.B., B.S.
 Amber S. Shin, B.S.
 Gagandeep Singh, Ph.D.
 Levy A. Sominsky, B.A.
 Daniel Stadlbauer, Ph.D.
 Ania Wajnberg, M.D.
 Viviana Simon, M.D., Ph.D.

Icahn School of Medicine at Mount Sinai
 New York, NY
 florian.krammer@mssm.edu
 viviana.simon@mssm.edu

Supported by the National Institute of Allergy and Infectious Diseases (NIAID) Collaborative Influenza Vaccine Innovation Centers (contract 75N93019C00051), the NIAID Centers of Excellence for Influenza Research and Surveillance (contract HHSN272201400008C), the JPB Foundation, the Open Philanthropy Project (research grant 2020-215611 [5384]), and anonymous donors.

Disclosure forms provided by the authors are available with the full text of this letter at NEJM.org.

This letter was published on March 10, 2021, at NEJM.org.

1. Krammer F. SARS-CoV-2 vaccines in development. *Nature* 2020;586:516-27.
2. Polack FP, Thomas SJ, Kitchin N, et al. Safety and efficacy of the BNT162b2 mRNA Covid-19 vaccine. *N Engl J Med* 2020;383:2603-15.
3. Baden LR, El Sahly HM, Essink B, et al. Efficacy and safety of the mRNA-1273 SARS-CoV-2 vaccine. *N Engl J Med* 2021;384:403-16.
4. Stadlbauer D, Amanat F, Chromikova V, et al. SARS-CoV-2 seroconversion in humans: a detailed protocol for a serological assay, antigen production, and test setup. *Curr Protoc Microbiol* 2020;57(1):e100.
5. Stadlbauer D, Tan J, Jiang K, et al. Repeated cross-sectional sero-monitoring of SARS-CoV-2 in New York City. *Nature* 2021;590:146-50.

DOI: 10.1056/NEJMc2101667

Correspondence Copyright © 2021 Massachusetts Medical Society.

Published in final edited form as:

Nature. 2020 September 01; 585(7825): 410–413. doi:10.1038/s41586-020-2293-x.

Effect of non-pharmaceutical interventions to contain COVID-19 in China

Shengjie Lai^{#1,2}, Nick W Ruktanonchai^{#1}, Liangcai Zhou³, Olivia Prosper⁴, Wei Luo^{5,6}, Jessica R Floyd¹, Amy Wesolowski⁷, Mauricio Santillana^{5,6}, Chi Zhang⁸, Xiangjun Du⁸, Hongjie Yu², Andrew J Tatem¹

¹WorldPop, School of Geography and Environmental Science, University of Southampton, UK

²School of Public Health, Fudan University, Key Laboratory of Public Health Safety, Ministry of Education, Shanghai, China

³Wuhan Center for Disease Control and Prevention, Wuhan, Hubei Province, China

⁴Department of Mathematics, University of Tennessee, Knoxville, TN, USA

⁵Computational Health Informatics Program, Boston Children's Hospital, Boston, MA, USA

⁶Department of Pediatrics, Harvard Medical School, Boston, MA, USA

⁷Department of Epidemiology, Johns Hopkins Bloomberg School of Public Health, Baltimore, MD, USA

⁸School of Public Health (Shenzhen), Sun Yat-sen University, Shenzhen, China

[#] These authors contributed equally to this work.

Summary

On March 11, 2020, the World Health Organization declared COVID-19 a pandemic¹. The outbreak containment strategies in China based on non-pharmaceutical interventions (NPIs) appear to be effective², but quantitative research is still needed to assess the efficacy of NPIs and their timings³. Using epidemiological and anonymised human movement data^{4,5}, here we develop

Users may view, print, copy, and download text and data-mine the content in such documents, for the purposes of academic research, subject always to the full Conditions of use:http://www.nature.com/authors/editorial_policies/license.html#terms

Correspondence to: Shengjie Lai; Nick W Ruktanonchai; Andrew J Tatem.

Correspondence and requests for materials should be addressed to: S.L. (Shengjie.Lai@soton.ac.uk), N.W.R. (nr1e14@soton.ac.uk), or A.J.T. (A.J.Tatem@soton.ac.uk).

Author contributions

S.L. designed the study, built the model, collected data, finalised the analysis, interpreted the findings, and wrote the manuscript. N.W.R. built the model, analysed data, interpreted the findings, and wrote the manuscript. L.Z., D.W., and J.X. collected data, interpreted the findings, commented on and revised drafts of the manuscript. J.R.F., O.P., and W.L. built the model, commented on and revised drafts of the manuscript. C.Z. collected data, interpreted the findings and commented on and revised drafts of the manuscript. A.J.T. interpreted the findings and revised drafts of the manuscript. A.W., M.S., X.D., and H.Y. interpreted the findings and commented on and revised drafts of the manuscript. All authors read and approved the final manuscript.

Ethical approval

Ethical clearance for collecting and using secondary data in this study was granted by the institutional review board of the University of Southampton (No. 48002). All data were supplied and analysed in an anonymous format, without access to personal identifying information.

Competing interests

The authors declare no competing interests.

a modelling framework that uses daily travel networks to simulate different outbreak and intervention scenarios across China. We estimated that there were a total of 114,325 COVID-19 cases (interquartile range 76,776 -164,576) in mainland China as of February 29, 2020. Without NPIs, the COVID-19 cases would likely have shown a 67-fold increase (interquartile range 44 - 94) by February 29, 2020, with the effectiveness of different interventions varying. The early detection and isolation of cases was estimated to have prevented more infections than travel restrictions and contact reductions, but combined NPIs achieved the strongest and most rapid effect. The lifting of travel restrictions since February 17, 2020 does not appear to lead to an increase in cases across China if the social distancing interventions can be maintained, even at a limited level of 25% reduction on average through late April. Our findings contribute to an improved understanding of NPIs on COVID-19 and to inform response efforts across the World.

Introduction

As of March 30, 2020 the COVID-19 outbreak has resulted in 693,282 confirmed cases and 33,106 deaths across the World⁶. As an emerging disease, effective pharmaceutical interventions are not expected to be available for months⁷, and healthcare resources will be limited for treating all cases. Nonpharmaceutical interventions (NPIs) are therefore essential components of the public health response to outbreaks^{6,8–10}. These include isolating ill persons, contact tracing, quarantine of exposed persons, travel restrictions, school and workplace closures, cancellation of mass gatherings, and hand washing, among others^{8–10}. These measures aim to reduce transmission, thereby delaying the timing and reducing the size of the epidemic peak, buying time for preparations in the healthcare system, and enabling the potential for vaccines and drugs to be used later on⁸.

Three major groups of NPIs have been implemented to contain the spread and reduce the outbreak size of COVID-19 across China¹¹. First, inter-city travel restrictions were used to prevent further seeding of the virus during the Chinese new year (CNY) holiday. A cordon sanitaire of Wuhan and surrounding cities in Hubei Province was put in place two days before CNY's day on January 25, 2020. Since CNY's day, travel restrictions in other provinces were also put in place across the country. Early identification and isolation of cases comprised the second group of NPIs, including improving the screening, identification, diagnosis, isolation, reporting, and contact tracing of suspected ill persons and confirmed cases¹¹. Along these lines, local governments across China encouraged and supported routine screening and quarantine of travellers from Hubei Province in an attempt to detect COVID-19 infections as early as possible. Highlighting how these efforts improved detection and diagnosis, the average interval from symptom onset to laboratory confirmation dropped from 12 days in the early stages of the outbreak to 3 days in early February^{3,12}. Third, contact restrictions and social distancing measures, together with personal preventive actions, such as hand washing, were implemented to reduce the community-level exposure risk. As part of these social distancing policies, the Chinese government encouraged people to stay at home as much as possible, cancelled or postponed large public events and mass gatherings, and closed libraries, museums, and workplaces^{13,14}. Additionally, school holidays were also extended, with the CNY holiday end date changed from January 30 to March 10 for Hubei province, and February 9 for many other provinces^{15,16}.

The implementation of these NPIs coincided with a rapid decline in the number of new cases across China, albeit at high economic and social costs^{3,12}. Previous studies have preliminarily explored the lockdown of Wuhan^{17,18}, travel restrictions¹⁹, airport screening²⁰, and the isolation of cases and contact tracing for containing virus transmission²¹. However, a comprehensive and quantitative comparison of the effectiveness of different NPIs in China and their timings for containing the COVID-19 outbreak is lacking. Based on epidemiological data on COVID-19 and historical and near-real time anonymised human movement data, we developed a travel network-based stochastic susceptible-exposed-infectious-removed (SEIR) modelling framework to simulate the COVID-19 spread across 340 prefecture-level cities in mainland China. Within each city, numbers of susceptible, exposed, infectious, and recovered/removed people were estimated per day since December 1, 2019. Using this modelling framework, we conducted before-and-after comparable analyses to quantify the relative effect of the three major groups of NPIs in China, including the restriction of inter-city population movement, the identification and isolation of cases, and the reduction of inner-city travel and contact to increase social distance. We also assessed the risk of COVID-19 transmission since the lifting of travel restrictions on February 17, 2020.

Results

Reconstruction of COVID-19 spread

The epidemiological parameters estimated for the early stage of the outbreak in Wuhan were initially used to parameterise the epidemic before widely implementing interventions⁵. The three major groups of NPIs outlined above were derived and measured from inter-city and inner-city population movement data, obtained from smartphone users of Baidu location-based services⁴, and data on delay from illness onset to reporting of cases across the country. Population travel and contact patterns have changed significantly since the implementation of interventions, with the timeliness of case reporting also improving (Fig. 1 and Supplementary Information Files 1 and 2). These indicators were then incorporated into the model (see Methods).

We estimated that there were a total of 114,325 COVID-19 cases (interquartile range [IQR] 76,776 – 164,576) in mainland China as of February 29, 2020, with 85% of these in Hubei Province (Extended Data Table 1). The outbreak increased exponentially prior to CNY, but the peak of epidemics across the country quickly appeared at CNY, following the implementing NPIs. The estimated epidemics and peaks were consistent with patterns of reported data by onset date, with high correlations between daily estimates and reported data found across time and regions (Extended Data Fig. 1). The overall correlation between the number of estimated cases and the reported number by province, as of February 29, 2020, was also significant ($p < 0.001$, $R^2 = 0.86$), with a high sensitivity (91%, 280/308) and specificity (69%, 22/32) in predicting cities with or without COVID-19 cases (Extended Data Fig. 1Sa and 1b).

Quantifying the effect of different NPIs

Without NPIs, as of February 29, the number of COVID-19 cases would increase rapidly across China, with a 51-fold (IQR 33 - 71) increase in Wuhan, a 92-fold (58 - 133) increase in other cities in Hubei, and a 125-fold (77 - 180) increase in other provinces. However, the apparent effectiveness of different interventions varied (Fig. 2). The lockdown of Wuhan might not have prevented the seeding of the virus from the city, as the travel ban was put in place at the latter stages of pre-CNY population movement out of the city (Fig. 1b)²². Nevertheless, if inter-city travel restrictions were not implemented, cities and provinces outside of Wuhan would have received more cases from Wuhan, and the affected geographic range would have expanded to the remote western areas of China (Extended Data Fig. 2c). Generally, the early detection and isolation of cases was estimated to quickly and substantially prevent more infections than contact reduction and social distancing across the country (5-fold versus 2.6-fold). However, without the intervention of contact reductions, in the longer term, the epidemics would increase exponentially across regions (Fig. 2c and 2f). Therefore, combined NPIs would achieve the strongest and most rapid effect on COVID-19 outbreak containment, with about a one-week interval from NPIs to epidemic peak (Extended Data Table 1).

Intervention timings

If interventions in China could have been conducted one week, two weeks, or three weeks earlier, cases could have been dramatically reduced by 66% (IQR 50% - 82%), 86% (81% - 90%), or 95% (93% - 97%), respectively (Fig. 3a). The geographical range of affected areas would also shrink from 308 cities to 192, 130, and 61 cities, respectively (Extended Data Fig. 3). However, if NPIs were conducted one week, two weeks, or three weeks later than they were, cases may have shown a 3-fold (IQR 2 - 4), 7-fold (5 - 10), or 18-fold (11 - 26) increase, respectively (Fig. 3b).

The lifting of travel restrictions

Under interventions implemented as of 17 February, 2020, the epidemics outside of Hubei province likely reached a low level (<10 cases per day, excluding imported cases from other countries) in early March, while Hubei Province might need another four weeks to reach same level as other provinces. However, if population contact resumed to the normal levels seen in previous years, the lifting of travel restrictions since February 17 might cause case numbers to rise again (Fig. 3c). Accordingly, our simulations suggest that maintaining social distancing at even a limited degree (e.g. 25% contact reduction on average) through late April would help ensure control of COVID-19 in epicentres like Wuhan.

Our estimates were sensitive to the basic reproduction number (R_0), with a higher and later peak of epidemics and longer time needed to contain the outbreak under a higher R_0 (Extended Data Fig. 3). Sensitivity analyses also suggested that our model could have robustly measured relative changes in the efficacy of interventions under different epidemiological parameters and transmission scenarios (Extended Data Figs. 4 - 9).

Extending findings

Our findings show that combined NPIs substantially reduced COVID-19 transmission across China. Earlier implementation of NPIs could have significantly reduced the magnitude and geographical range of the outbreak, but equally, a delayed response would have led to a larger outbreak. China's aggressive, multifaceted response is likely to have prevented a far worse situation, which would have accelerated spread globally. The lessons drawn from China provide robust evidence and provide a preparation window and fighting chance for containing the spread and mitigating the effects of COVID-19 in other regions around the World^{3,12}.

Our results suggest three key points. First, they support and validate the idea that population movement and close contact has a major role in the spread of COVID-19 within and beyond China^{22,23}. As the lockdown of Wuhan happened at the latter stages of the pre-CNY movement, travel restrictions did not halt the seeding of the virus from Wuhan, but did prevent cases being exported from Wuhan to a wider area. Secondly, the importance and effects of the three types of NPIs differed. Compared to travel restrictions, improved detection and isolation of cases as well as the social distancing likely had a greater impact on the containment of outbreak. The social distancing intervention reduced contact with people who travelled from the epicentre of the outbreak. This is likely to have been especially helpful in curbing the spread of an emerging pathogen to the wider community, and reduced the spread risk from asymptomatic or mild infections⁸. Third, given travel and work resuming in China, the country should consider at least the partial continuation of NPIs to ensure that the COVID-19 outbreak is sustainably controlled for the first wave of this outbreak. For example, early case identification and isolation should be maintained, which may also help to prevent and delay the arrival of a second wave, considering the increasing numbers of cases imported from other countries and the presence of asymptomatic or subclinical infections found in China²⁴.

The analyses presented here represent the most comprehensive study yet in which the effect of NPIs on COVID-19 transmission has been quantitatively assessed. The model framework accounts for daily interactions of populations, interventions between and within cities, as well as the inherent statistical uncertainty associated with a paucity of epidemiological parameters, before and after the implementation of interventions. The network-based SEIR model is methodologically robust and built on the basic SEIR models previously used to predict COVID-19 transmission in its early stages²³. Considering delays in case reporting, our approach can be used for rapid, ongoing estimation of the effectiveness of various NPIs in different countries for outbreak control decision-making.

Our study has several limitations. First, as our simulations were based on parameters estimated for symptomatic cases found in the early stage of the outbreak in Wuhan, which may not account for asymptomatic and mild infections, we may have underestimated the total number of infections. Second, our findings could be confounded by other factors that changed during the outbreak. Although we have shown that the apparent fall in incidence of COVID-19 since CNY's day in China is likely to be attributed to the interventions taken, we cannot rule out the possibility that the decrease is partially attributable to other unknown

seasonal factors, e.g. temperature and absolute humidity^{25,26}. Third, if the epidemiological parameters of COVID-19 transmission in other cities across China differed with estimates from the outbreak at the early stage where no NPIs were in place in Wuhan, then our estimates of the effectiveness of interventions in reducing COVID-19 transmission could be biased. Fourth, coverage biases in mobile phone and Baidu users likely exist. Though a high percentage (from 46.9% in 2013 to 55.3% in 2018) of the population owns smartphones in China^{27,28}, the mobile user group still does not cover specific subgroups of the population, particularly children. Therefore, our population movement data may provide an incomplete picture, and differences between the characteristics of smartphone owners and non-owners may also bias estimates in this study. Additionally, the magnitude and patterns of movements could change year by year, although previous studies have supported the consistent seasonality of travel patterns across years in China and other countries.²² Lastly, we only examined three main groups of NPIs and other interventions might also have contributed to the outbreak containment. For example, due to the data availability, we did not assess the effect of personal hygiene and protective equipment on containing COVID-19 spread. Other data sources and further investigations are needed to measure and elaborate the efficacy of each intervention.

COVID-19 has caused a substantial burden on health systems and society across many countries. From a public health standpoint, our results highlight that countries should consider proactively planning NPIs and relevant resources for containment and mitigation, given how the earlier implementation of NPIs could have lead to significant reductions in size of the outbreak in China. The results here also provide guidance for countries as to the likely effectiveness of different NPIs at different stages of an outbreak. Suspected and confirmed cases should be identified, diagnosed, isolated and reported as early as possible to control the source of infection, and the implementation of cordon sanitaires or travel restrictions for significantly affected areas may prevent seeding the virus to wider regions. Reducing contact and increasing social distance, together with improved personal hygiene can protect vulnerable populations and mitigate COVID-19 spread at the community level, and these interventions should be promoted throughout the outbreak to avoid resurgence. As called by the World Health Organization, and backed up by our findings for China here, early and integrated NPI strategies should be prepared, deployed and adjusted to maximise benefits of these interventions and minimize health, social and economic impacts around the World³.

Methods

A travel network-based stochastic susceptible-exposed-infectious-removed (SEIR) model was built to simulate the COVID-19 spread between and within all prefecture-level cities in mainland China. This model has been made openly available for further use at <https://github.com/wpgp/BEARmod>. Population movement data across the country were used to estimate the intensity of travel restrictions and contact reductions. Data from illness onset to reporting of the first index case for each county were used to infer the changing timeliness of case identification and isolation across the course of the outbreak. The outputs of the model under NPIs were validated by using daily numbers of new cases reported across all regions

in mainland China. Based on this modelling framework, the efficacy of applying or lifting non-pharmaceutical measures under various scenarios and timings were tested and quantified.

Data sources

Three population movement datasets, obtained from Baidu location-based services providing over 7 billion positioning requests per day^{4,29}, were used in this study to measure travel restrictions and social distancing across time and space. The first is an aggregated and de-identified dataset on near-real time daily relative outbound and inbound flow of smartphone users for each prefecture-level city in 2020 (340 cities in mainland China were included) to understand mobility patterns during the outbreak. The daily outflow from each city since Wuhan's lockdown and travel restrictions that were applied on January 23 were rescaled by the mean daily flow for each city during January 20 – 22 for comparing travel reductions across cities and years (Fig. 1).

The second Baidu dataset is a historical relative movement matrix with daily total number of users at city level from December 26, 2014 to May 26, 2015, aligning with the 2020 CNY holiday period, for which the corresponding period is December 1, 2019 to April 30, 2020. We assumed that the pattern of population movements was the same in years when there were no outbreaks and interventions. Adjusted by the level of travel reductions derived from the 2020 dataset where applicable, the second dataset was used to simulate the COVID-19 spread and predict future transmission via population movements under various scenarios, with or without inter-city travel restrictions. Corresponding city-level population data in 2015 for modelling were obtained from the Chinese Bureau of Statistics³⁰.

The third Baidu dataset measures daily population movements at county level (2862 counties in China) from January 26 through April 30, 2014, as described elsewhere³¹. Based on the assumption that the pattern of population contact was consistent across years when there were no interventions, it was used to estimate inner-city travel and contact reduction under the outbreak and interventions. First, we aggregated data from county to city level and rescaled the daily flows since January 29, 2014 by the mean of the daily flow for the January 26 – 28 period, aligning with the date of Wuhan's lockdown and the 2020 CNY holiday. Then, the rescaled first dataset for 2020 under interventions was compared with the 2014 dataset to derive the percentage of travel decline for each city. The percentages for cities were averaged by day to preliminarily quantify the intensity of contact reduction in China under NPIs (Supplementary Information File 2), as the policies of travel restriction and social distancing measures were implemented and occurred at the same time across the country.

We also collated data of the first case reported by county across mainland China to measure the delay from illness to case report as a reference of the improved timeliness of case identification, isolation and reporting during the outbreak (Supplementary Information File 1). The daily number of COVID-19 cases by date of illness onset in Wuhan City, Hubei Province and other provinces as of February 13, 2020 were used to further validate the epicurves estimated in this study across time. There was an abnormal increase of cases in Wuhan City and Hubei Province on February 1, 2020, based on the date of illness onset.² We interpolated the number on February 1 by using the mean of numbers of cases reported

on January 31 and February 2 in the epicurve. The number of cases reported by city across mainland China as of February 29 were used to define the predictability of our model across space. These case data were collated from the websites of national and local health authorities, news media, and publications (Supplementary Information File 3)^{2,3,32}.

Data analysis

We constructed a travel network-based SEIR modelling framework (BEARmod) for before-and-after comparable analyses on NPI efficacy. This model was extended from a typical SEIR model to specifically incorporate movement between locations that varied with each timestep. In this model, each city was represented in the model as a separate subpopulation, with its own susceptible (S), exposed (E), infected (I), and recovered/removed (R) populations.

Exposure, infection, and recovery—During each timestep, infected people first recovered or were removed at an average rate r , where r was equal to the inverse of the average infectious period, and removal represents self-isolation and effective removal from the population as a potential transmitter of disease. Explicitly, this was incorporated as a *Bernoulli* trial for each infected person with a probability of recovering $1 - \exp(-r)$. We used the median of time lags from illness onset to reported case as a proxy of the average infectious period, indicating the improving case identification and isolation under improved interventions (Supplementary Information File 1). Then, the model converted exposed people to infectious by similarly incorporating a *Bernoulli* trial for each exposed individual, where the daily probability of becoming infectious $1 - r \exp(-e)$, where e was the inverse of the average time spent exposed but not infectious, based on the estimated incubation period (5.2 days, 95% confidence interval [CI] 4.1 - 7.0).⁵ Finally, to end the exposure, infection, and recovery step of the model, newly exposed people were calculated for each city based on the number of infectious people in the city I_i , and the average number of daily contacts that lead to transmission that each infectious person has c . We simulated the number of exposed in a patch on a given day through a random draw from a *Poisson* distribution for each infectious person where the mean number of new infections per person was c , which was then multiplied by the fraction of people in the city that were susceptible. We calculated the daily contact rate c using the basic reproduction rate calculated by other studies (R_0 , 2.2, 95% CI 1.4 - 3.9) divided by the average days (5.8, 95% CI 4.3 - 7.5) from onset to first medical visit and isolation,⁵ weighted by the relative level of daily contact where relevant, based on the Baidu movement data (Supplementary Information File 2). Because simulation runs were not extended beyond five months, we did not include the addition of new susceptibles, or conversion of recovered people back to susceptible.

The infection processes within each patch therefore approximate the following deterministic, continuous-time model, where c and r through time:

$$\begin{aligned}\frac{dS}{dt} &= S - c \frac{SI}{N} \\ \frac{dE}{dt} &= c \frac{SI}{N} - \epsilon E \\ \frac{dI}{dt} &= \epsilon E - rI \\ \frac{dR}{dt} &= rI\end{aligned}$$

Movement—After the model completed the infection-related processes, we moved infectious people between cities. To do this, we moved infected people from their current location to each possible destination (including remaining in the same place) using *Bernoulli* trials for each infected person, and each possible destination city. We parameterized the probability of moving from city i to city j (p_{ij}) was equal to the proportion of smartphone users who went from city j in the corresponding day from the Baidu dataset in 2015, accounting for the travel restrictions in 2020. This included modelling the numbers of people who stayed in the same location using p_{ii} , the proportion of users who did not move to a new location on that day. This allowed us to incorporate variance in the actual composition of travellers (infected vs non-infected), but because movement numbers were generated independently, it was possible for the number of infected stayers and movers in each patch to exceed or be fewer than the number of infected people in the patch. As we only wanted to incorporate variance into relative patterns of movement and not absolute numbers (particularly because the underlying values are proportions of people who moved and therefore cannot influence the total numbers of people infected), in any case where infected movers and stayers differed from the total number of infected people in the origin patch, we rescaled values to the total number of infected people. Rescaling in this way meant the variance introduced by the *Bernoulli* trials could only influence relative movement patterns, and not actual numbers of infected people. Further, because we explicitly model the number of stayers in the same way as movers, rescaling should not introduce any bias in terms of the final relative movement patterns.

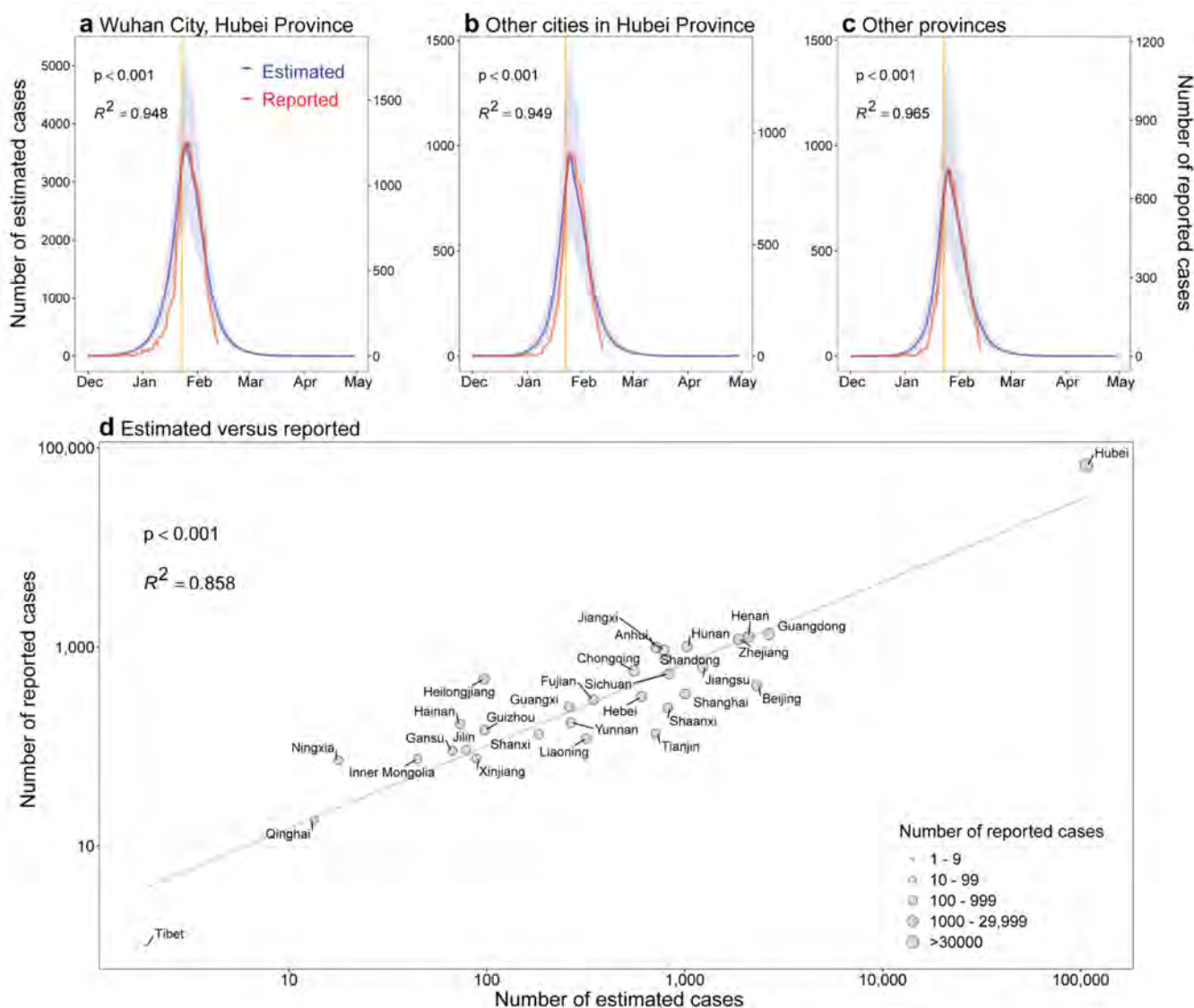
Through this model, stochasticity in the numbers and places where COVID-19 appears between simulation runs in this model through variance in numbers of people becoming exposed, infectious, and removed/recovered, as well as variance in numbers of people moving from one city to another. By modelling the COVID-19 epidemic in this way, we could simulate the incidence of COVID-19 cases, accounting for variance in recovery, infection, and movement across many simulation runs (1000). Additionally, this allowed for us to account for uncertainty in contact rates after NPIs were implemented or lifted.

Simulation runs—Using this model, we quantified how transmission of COVID-19 varied with different intervention scenarios and timings, as well as the potential of further transmission after the lifting of travel restrictions and contact distancing measures on February 17, 2020. As the earliest date of illness onset in cases was December 2, 2020³, considering the underreporting of cases and the delay from infection to onset and identification of this novel virus, we did simulations by initially infected 5 people in Wuhan on December 1, 2019 and propagating the epidemic through time, varying factors including

timing and types of interventions used, assumed contact and recovery rates, and movement. We initially infected 5 people as a minimum number of infected people that prevented stochastic extinction of the epidemic during the initial days of simulation, and found no significant difference after 3 months, over simulation runs that started with 3, 5, and 8 initially infected people (though with 3 people initially infected, 50% of runs led to zero cases over the initial week of simulation). When using data from other years we fixed the simulation dates around Chinese New Year and adjusted the start date of the epidemic accordingly.

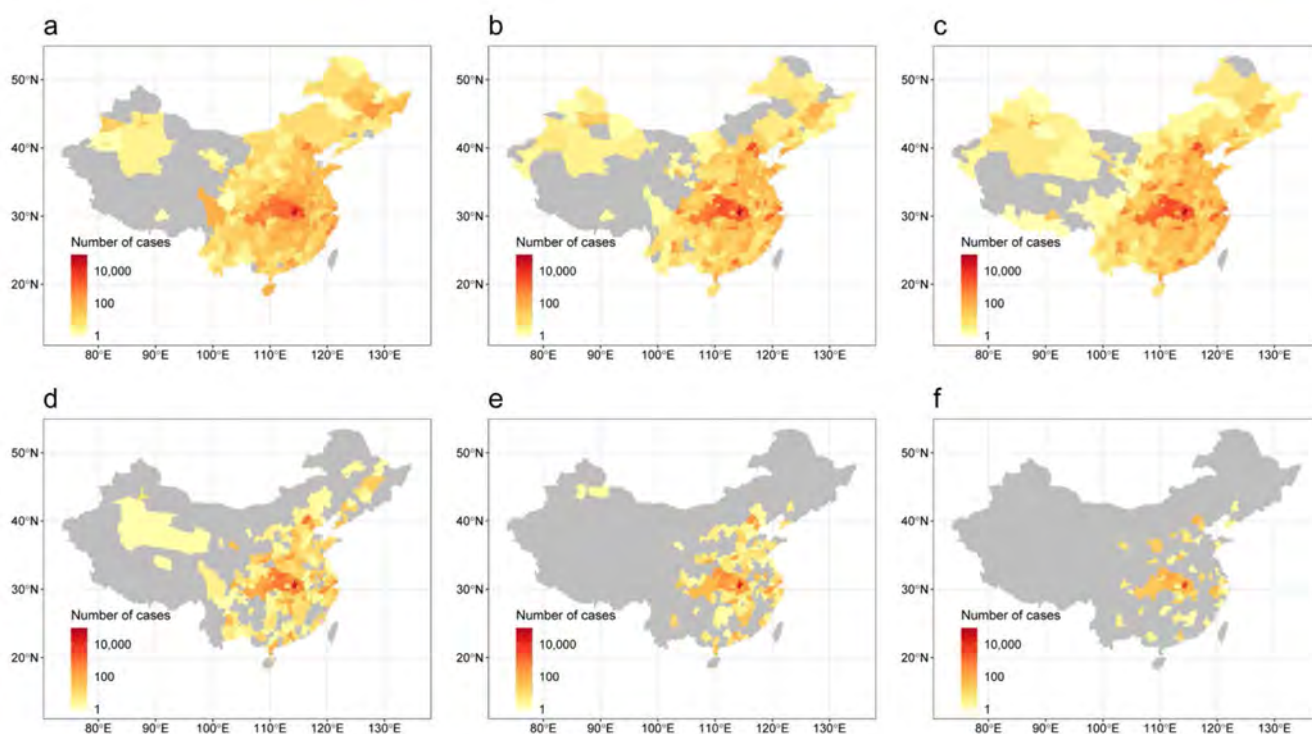
The estimates of the model for the outbreak under current NPIs as the baseline scenario were compared with reported COVID-19 cases across time and space. The sensitivity and specificity were also calculated to examine the performance of the model in predicting the occurrence of COVID-19 cases at city level across China. The relative effect of NPIs were quantitatively assessed by comparing estimates of cases under various NPIs and timings with that of the baseline scenario. We also conducted a series of sensitivity analyses to understand the impact of changing epidemiological parameters on the estimates and uncertainties of intervention efficacy. R version 3.6.1 (R Foundation for Statistical Computing, Vienna, Austria) was used to perform data collation and analyses.

Extended Data



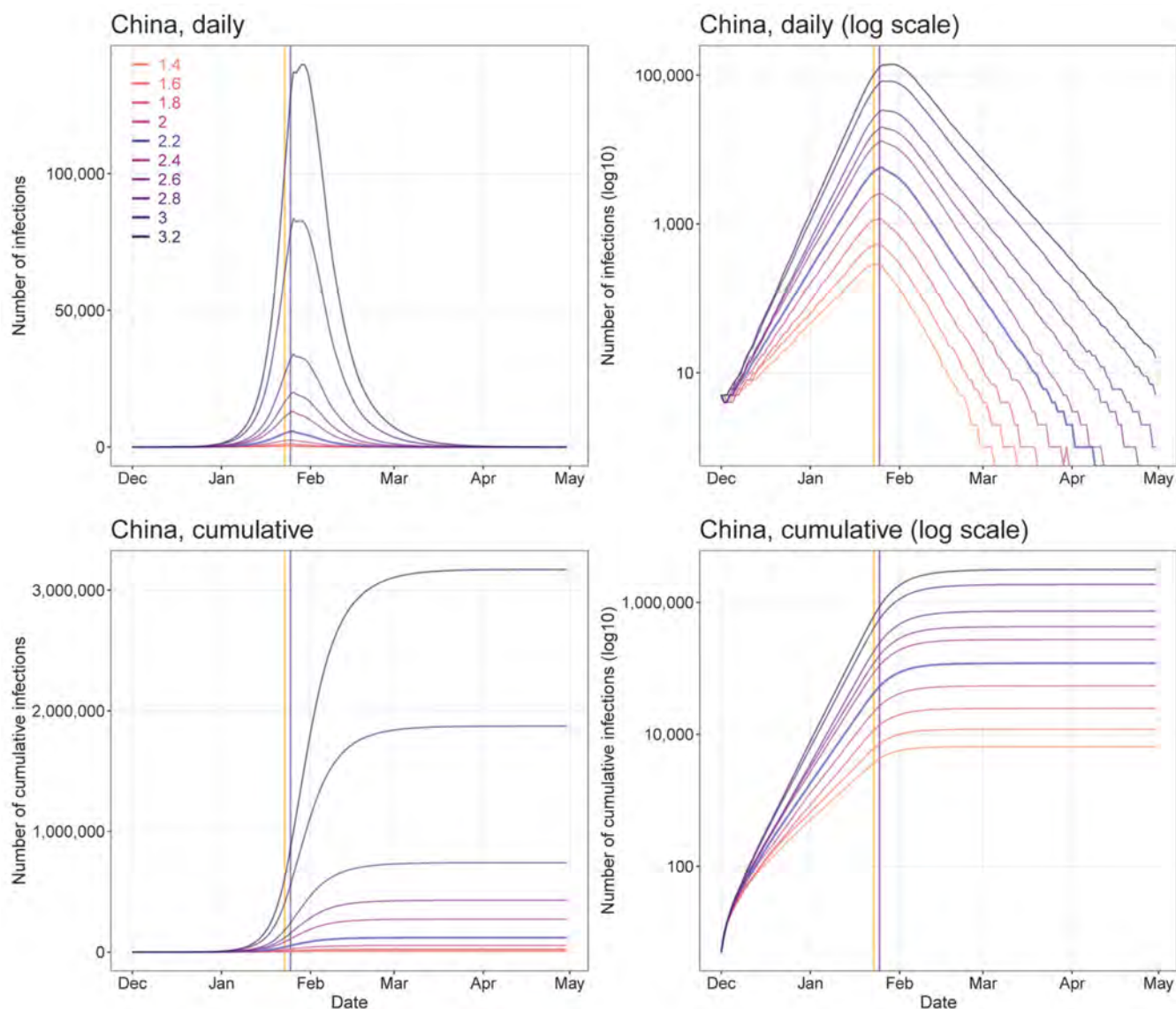
Extended Data Fig. 1. Estimated and reported epicurves of COVID-19 outbreak in mainland China.

(a) Wuhan City in Hubei Province. (b) Other cities in Hubei Province. (c) Other 30 provincial regions in mainland China. The orange vertical lines indicate Wuhan's lockdown on January 23, 2020. The estimated epicurve of COVID-19 cases presents the median (dark blue) and interquartile range (light blue) of estimates (1000 simulations), and the Pearson's correlation between the median of daily estimates and the number of daily reported cases by region as of February 13, 2020 are also presented. (d) The Pearson's correlation between the total number of estimated cases and the total number of reported cases by province as of February 29, 2020. The p values of two-sided t-test are also provided.



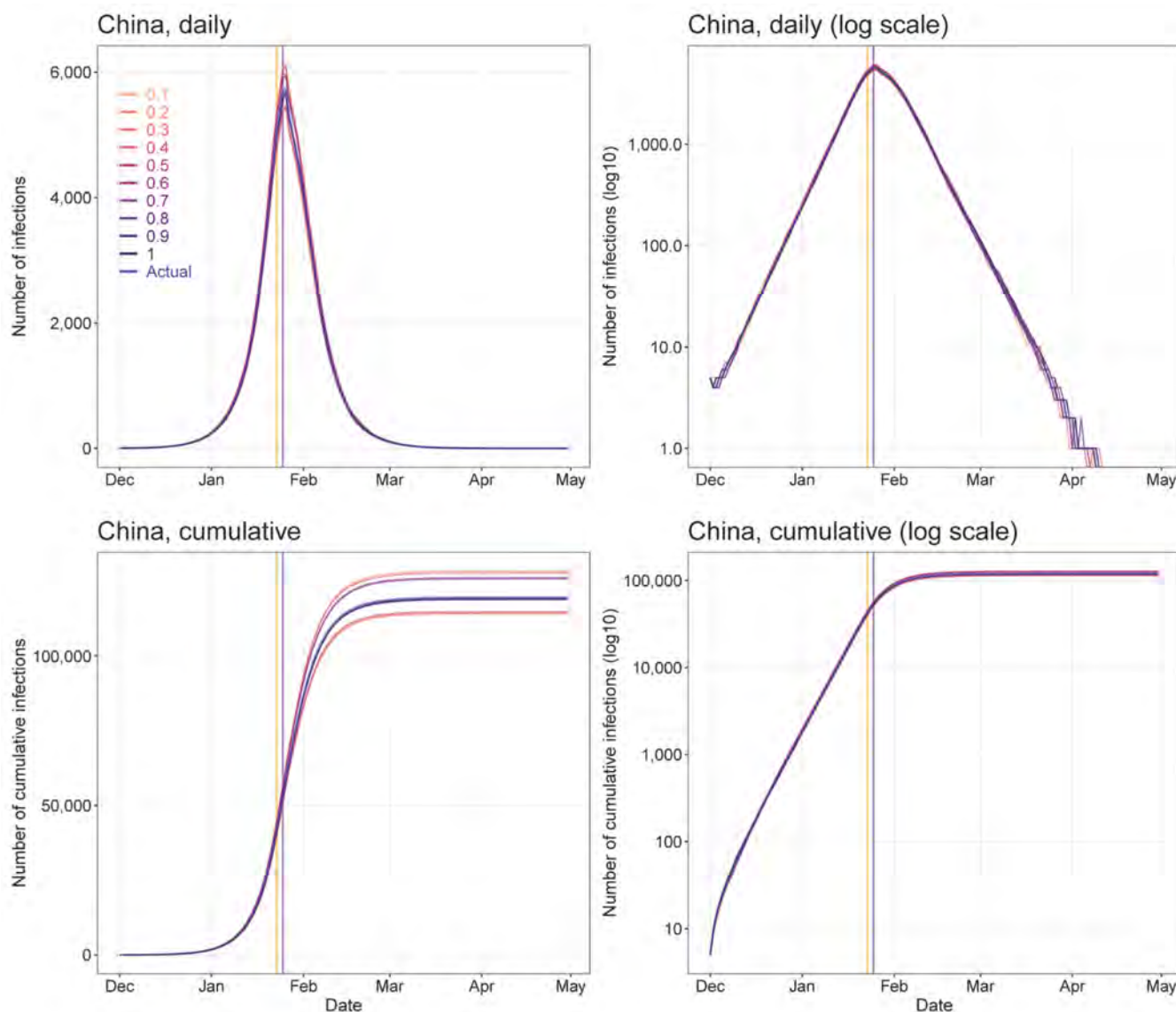
Extended Data Fig. 2. Affected areas of COVID-19 in mainland China under various intervention timings.

(a) A total of 308 cities reported COVID-19 cases, based on the data obtained from national and local health authorities, as of February 29, 2020. (b) Affected areas (298 cities) estimated by models under interventions implemented at actual timing. (c) Estimated affected areas (326 cities) under interventions at actual timing, but without inter-city travel restrictions. (d) Estimated affected areas (192 cities) under interventions at one week earlier than actual timing. (e) Estimated affected areas (130 cities) under interventions implemented at two weeks earlier than actual timing. (f) Estimated affected areas (61 cities) under interventions at three weeks earlier than actual timing. The administrative boundary maps were obtained from the National Platform of Common Geospatial Information Services of China (www.tianditu.gov.cn).



Extended Data Fig. 3. Sensitivity of estimates of COVID-19 epidemics under various values of R_0 .

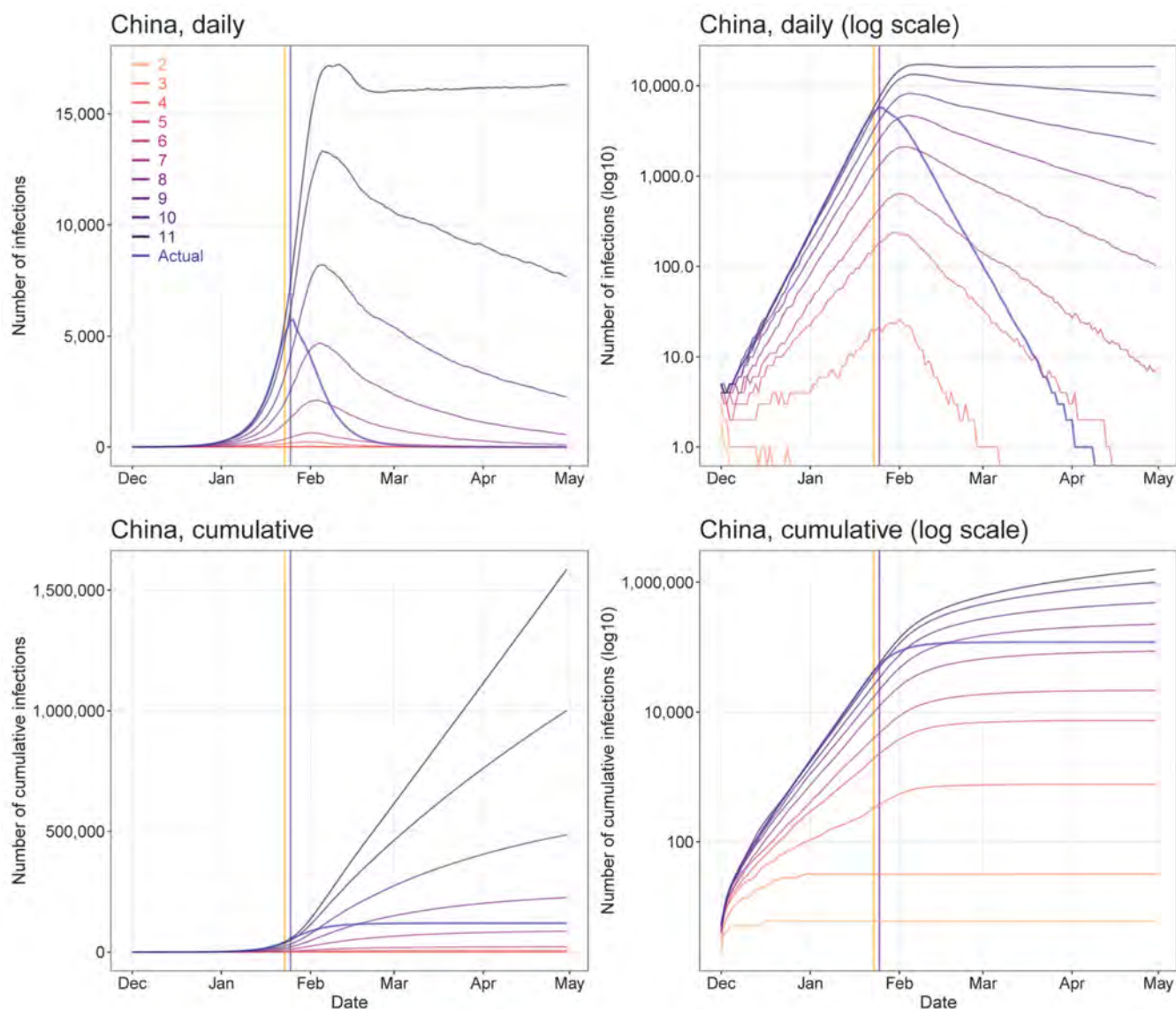
All other parameters, NPIs and input data were the same as the baseline model with $R_0 = 2.2$. Vertical lines: orange – date of Wuhan's lockdown; purple - CNY's day.



Extended Data Fig. 4. Sensitivity of estimates of COVID-19 epidemics under various levels of inter-city travel restrictions since January 23, 2020.

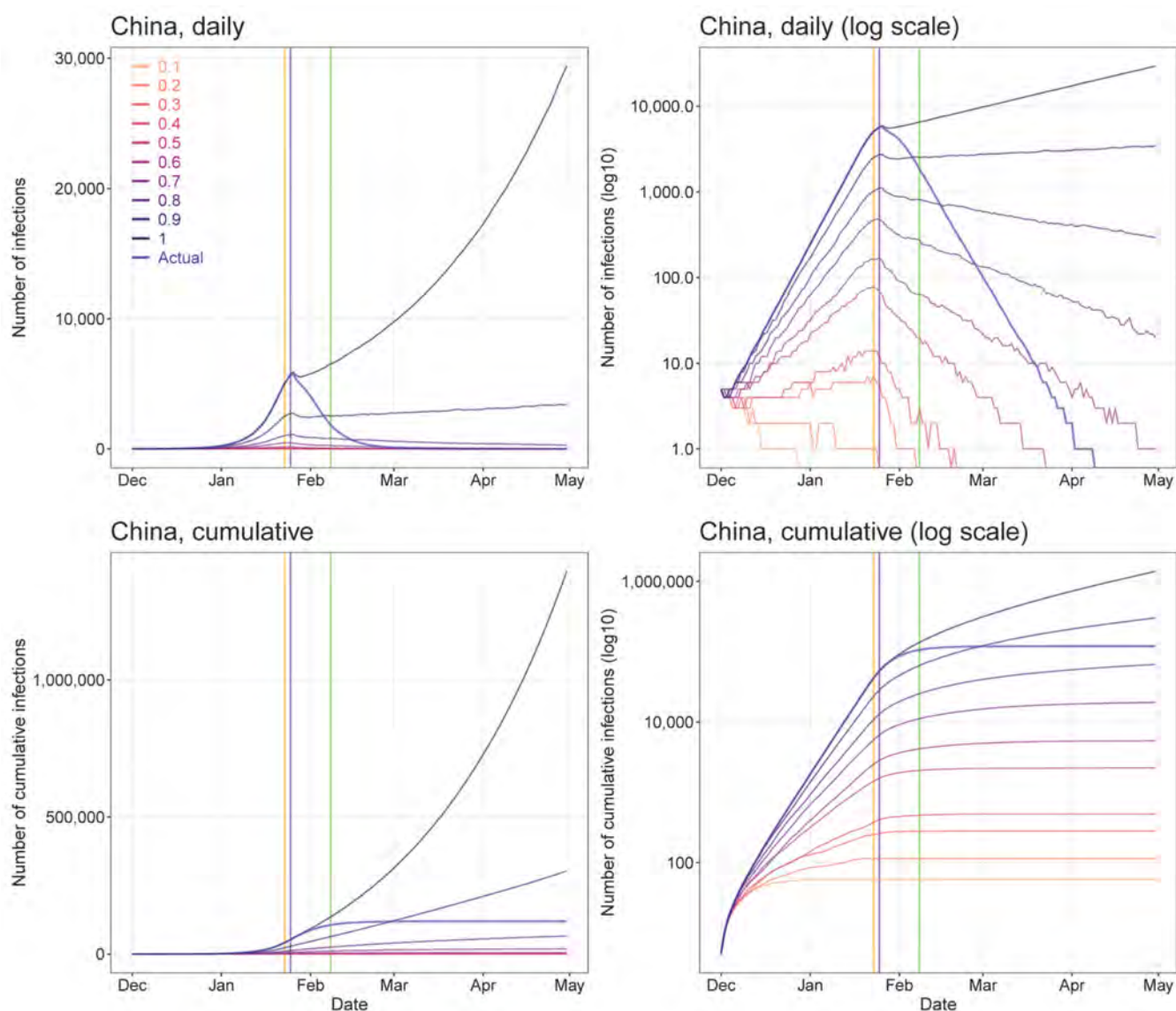
All other parameters, NPIs and input data were the same as the baseline model with $R_0 = 2.2$. The actual percentages of inter-city travel restrictions changed day-by-day across cities in China (0.1 means 90% reduction from normal travel, 1 means no travel restrictions).

Vertical lines: orange – date of Wuhan's lockdown; purple - CNY's day.



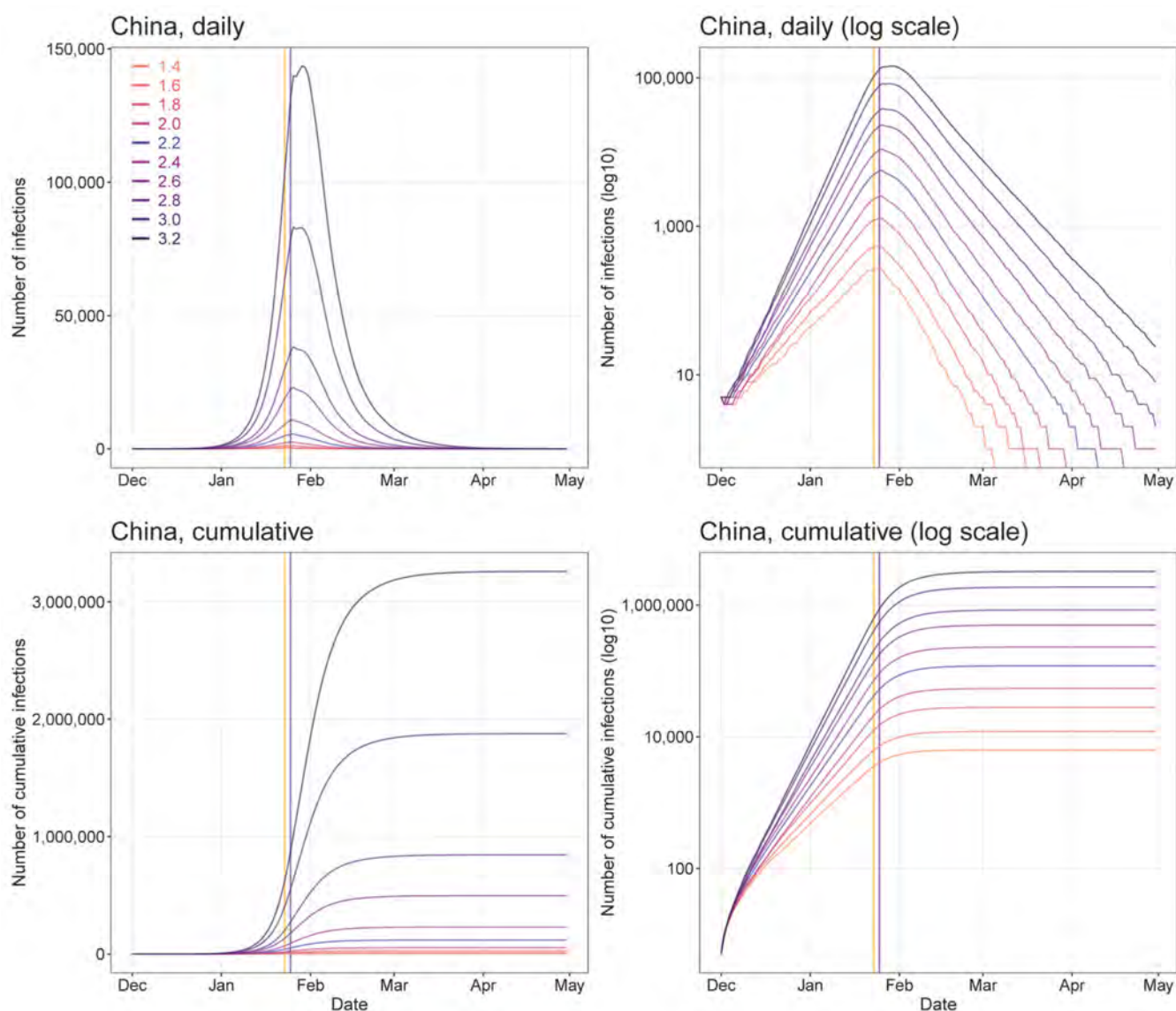
Extended Data Fig. 5. Sensitivity of estimates of COVID-19 epidemics under various numbers of days from illness onset to report/isolation.

All other parameters, NPIs and input data were the same as the baseline model with $R_0 = 2.2$. The actual delays of illness onset to report/isolation changed day-by-day (appendix Table S2). Vertical lines: orange – date of Wuhan's lockdown; purple – CNY's day.



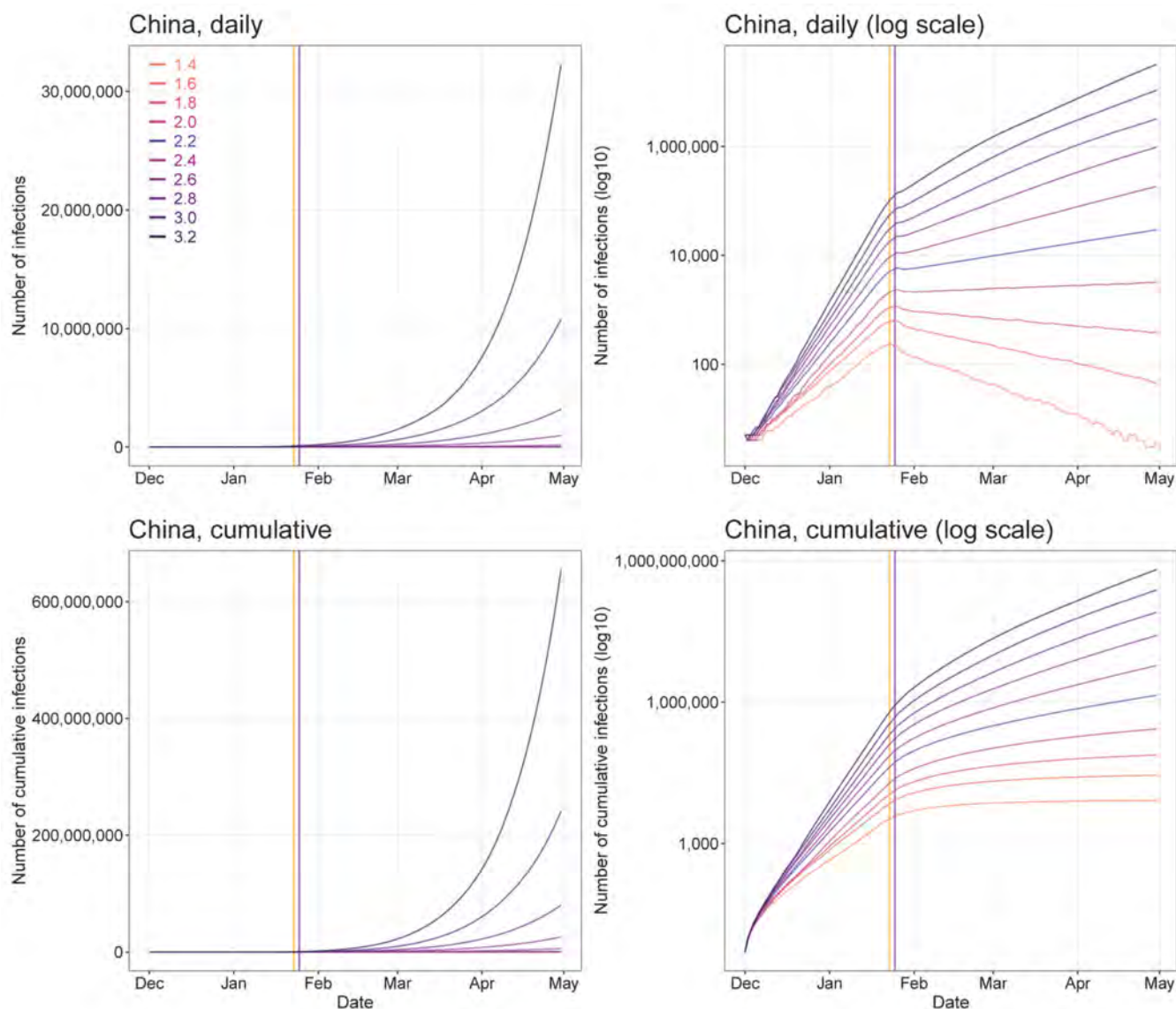
Extended Data Fig. 6. Sensitivity of estimates of COVID-19 epidemics under various contact rate values.

All other parameters, NPIs and input data were the same as the baseline model with $R_0 = 2.2$. The actual percentage of population contact (0.1 means 10% contact as usual, 1 means no contact restrictions) changed day-by-day across the country (appendix Table S1). Vertical lines: orange – date of Wuhan's lockdown; purple - CNY's day.



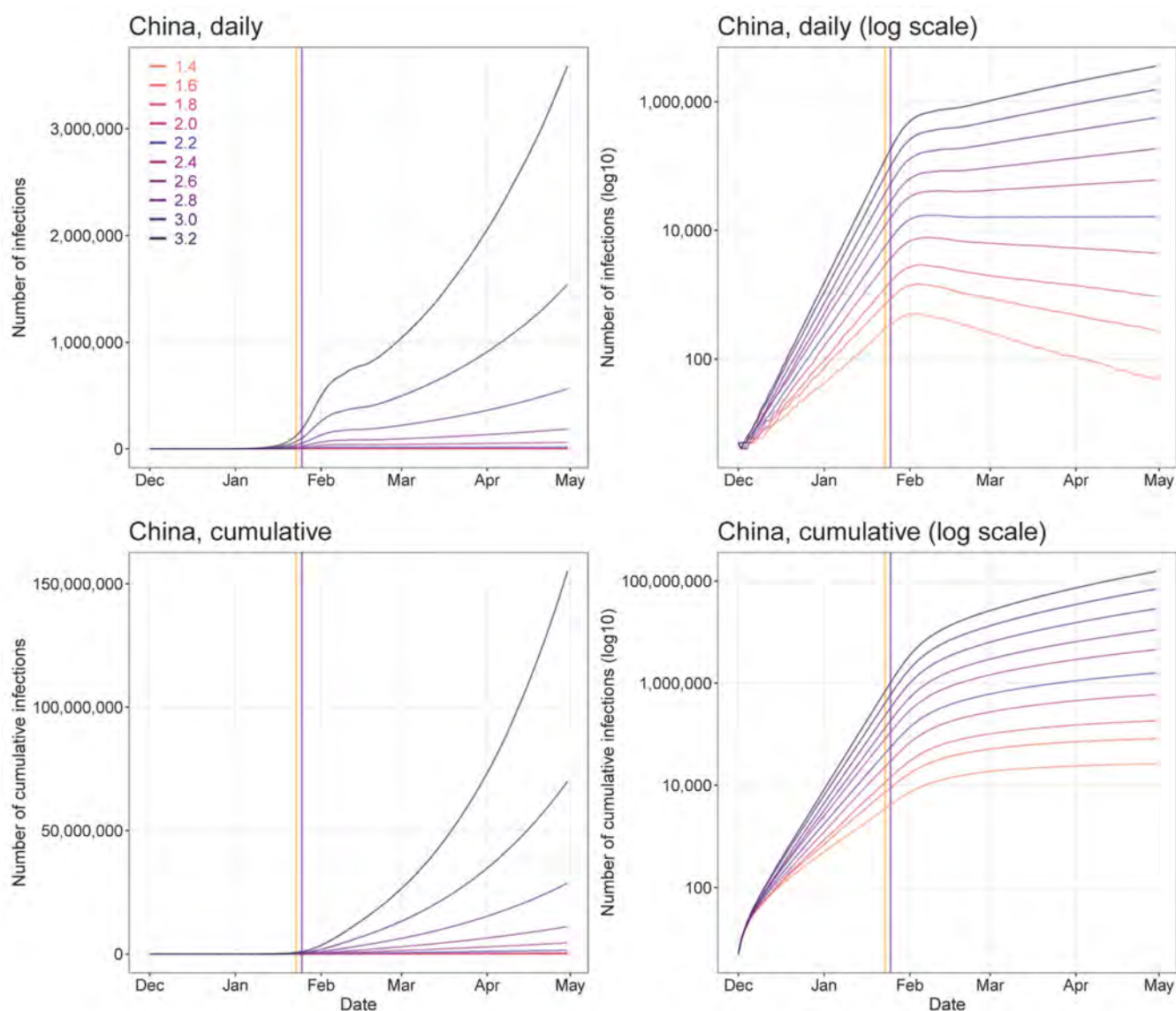
Extended Data Fig. 7. Sensitivity of estimates of COVID-19 epidemics under various values of R_0 and without inter-city travel restrictions.

All other parameters, NPIs and input data were the same as the baseline model with $R_0 = 2.2$. Vertical lines: orange – date of Wuhan's lockdown; purple - CNY's day.



Extended Data Fig. 8. Sensitivity of estimates of COVID-19 epidemics under various values of R_0 but without the intervention of inner-city contact restrictions.

All other parameters, NPIs and input data were the same as the baseline model with $R_0 = 2.2$. Vertical lines: orange – date of Wuhan's lockdown; purple - CNY's day.



Extended Data Fig. 9. Sensitivity of estimates of COVID-19 epidemics under various values of R_0 but without improved timeliness of case detection and isolation.

The delay from illness onset to detection and isolation was set as a constant of 11 days as that on January 16-18, 2020. All other parameters, NPIs and input data were the same as the baseline model with $R_0 = 2.2$. Vertical lines: orange – date of Wuhan's lockdown; purple – CNY's day

Extended Data Table 1
Reports and estimates of the COVID-19 cases in
mainland China, as of February 29, 2020.

Interventions and timing	Wuhan City, Hubei Province	Other cities in Hubei Province	Other provinces	Mainland China
Under current non-pharmaceutical interventions (NPIs)				
No. of cases reported (%) ^a	49,122 (62)	17,785(22)	12,917 (16)	79,824 (100)
Estimates of cases (%)	78,910(69)	18,503(16)	16,912 (15)	114,325(100)
Interquartile range	51,952-111,280	11,029-28,685	9,499-27,033	76,776-164,576
Dates of estimated peak	Jan 25-27	Jan 24-26	Jan 24-26	Jan 25-27
Interval between NPIs and epidemic peak ^b	7 days	6 days	6 days	7 days
Percentage (%) of cases that could have been prevented with earlier interventions				
One week ahead	61 (45-79)	71 (55-86)	78 (62-90)	66 (50-82)
Two weeks ahead	84 (78-89)	90 (82-94)	91 (84-95)	86 (81-90)
Three weeks ahead	94 (92-96)	97 (95-99)	98 (97-99)	95 (93-97)
Estimated relative no. of cases with later interventions^c				
One week delay	2.4 (1.6-3.5)	3.1 (1.8-4.6)	3.3 (2-5.4)	2.6 (1.8-3.8)
Two weeks delay	5.8 (4.0-8.6)	8.6 (5.3-12.8)	9.4 (6.1-14.6)	6.7 (4.6-10.0)
Three weeks delay	15.1 (9-21.1)	22.6 (13.5-33.9)	27.9 (17.5-42.8)	17.6(11.2-25.5)
Estimated relative no. of cases under various NPIs^c				
Without inter-city travel restriction	1.0 (0.6-1.3)	1.1 (0.7-1.7)	1.1 (0.7-1.7)	1.0(0.6-1.4)
Without inner-city contact reduction	2.5 (1.7-3.7)	2.6(1.5-4.2)	2.4(1.2-4.0)	2.6(1.7-3.7)
Without case early detection and isolation	5.0 (3.3-6.9)	5.6 (3.2-8.4)	5.1 (2.5-8.4)	5.0 (3.3-7.1)
Without all interventions above	51.4 (33.2-71.2)	91.6 (57.6-132.5)	124.7 (77.4-180)	67.3 (43.7-93.7)

^aThe reported data on COVID-19 cases were obtained from the Chinese National Health Commission as of February 29, 2020.

^bThe timeliness of case identification and reporting has been improved since January 19, 2020 and the travel restriction and social distancing were implemented from 23 January. We compared the peak dates by region with January 19 to define the interval from NPIs to epidemic peak.

^cReferring to the median of estimates under current interventions and timing. The median and interquartile range of estimates are provided here

Supplementary Material

Refer to Web version on PubMed Central for supplementary material.

Acknowledgments

We thank staff members at disease control institutions, hospitals, and health administrations across China where outbreaks occurred for field investigation, administration, and data collection. We thank Baidu Inc. sharing population movement data. We also thank Yanyan Zhu and Shuhao Lai for collating online data. This study was supported by the grants from the Bill & Melinda Gates Foundation (OPP1134076, OPP1195154); the European Union Horizon 2020 (MOOD 874850); the National Natural Science Fund of China (81773498); National Science and Technology Major Project of China (2016ZX10004222-009). AJT is supported by funding from the Bill &

Melinda Gates Foundation (OPP1106427, OPP1032350, OPP1134076, OPP1094793), the Clinton Health Access Initiative, the UK Department for International Development (DFID) and the Wellcome Trust (106866/Z/15/Z, 204613/Z/16/Z). HY is supported by funding from the National Natural Science Fund for Distinguished Young Scholars of China (No. 81525023); Program of Shanghai Academic/Technology Research Leader (No. 18XD1400300); and the United States National Institutes of Health (Comprehensive International Program for Research on AIDS grant U19 AI51915). OP is supported by funding from the National Science Foundation, USA (No. 1816075).

Role of the funding source

The funder of the study had no role in study design, data collection, data analysis, data interpretation, or writing of the report. The corresponding authors had full access to all the data in the study and had final responsibility for the decision to submit for publication.

Data and code availability

The code for the model built in this study has been made openly available for further use at <https://github.com/wpgp/BEARmod>. The data on COVID-19 cases reported by county, city, and province across China are available from the data sources listed in the Supplementary Information File 3, and the average days from illness onset to report of the first case by each county used in the modelling are detailed in Supplementary Information File 1. The mobile phone datasets analysed during the current study are not publicly available since this would compromise the agreement with the data provider, but the information on the process of requesting access to the data that support the findings of this study are available from Dr Shengjie Lai (Shengjie.Lai@soton.ac.uk), and the data on travel and contact reductions derived from the datasets and used in our model are detailed in Supplementary Information File 2.

References

1. World Health Organization. WHO Director-General's opening remarks at the media briefing on COVID-19 - 11 March 2020. 2020. <https://www.who.int/dg/speeches/detail/who-director-general-s-opening-remarks-at-the-media-briefing-on-covid-19---11-march-2020>
2. Novel Coronavirus Pneumonia Emergency Response Epidemiology Team. The epidemiological characteristics of an outbreak of 2019 novel coronavirus diseases (COVID-19) in China. *Chinese Journal of Epidemiology*. 2020; 41:145–151. [PubMed: 32064853]
3. World Health Organization. Report of the WHO-China Joint Mission on Coronavirus Disease 2019 (COVID-19). 2020. <https://www.who.int/docs/default-source/coronaviruse/who-china-joint-mission-on-covid-19-final-report.pdf>
4. Baidu Migration. 2020. <https://qianxi.baidu.com/>
5. Li Q, et al. Early Transmission Dynamics in Wuhan, China, of Novel Coronavirus-Infected Pneumonia. *N Engl J Med*. 2020; 382:1199–1207. [PubMed: 31995857]
6. World Health Organization. Novel coronavirus (2019-nCoV). 2020. <https://www.who.int/emergencies/diseases/novel-coronavirus-2019>
7. Heymann DL, Shindo N. COVID-19: what is next for public health? *The Lancet*. 2020; 395:542–545.
8. Fong MW, et al. Nonpharmaceutical Measures for Pandemic Influenza in Nonhealthcare Settings- Social Distancing Measures. *Emerg Infect Dis*. 2020; 26:976–984. [PubMed: 32027585]
9. Ryu S, et al. Nonpharmaceutical Measures for Pandemic Influenza in Nonhealthcare Settings- International Travel-Related Measures. *Emerg Infect Dis*. 2020; 26:961–966. [PubMed: 32027587]
10. Xiao J, et al. Nonpharmaceutical Measures for Pandemic Influenza in Nonhealthcare Settings- Personal Protective and Environmental Measures. *Emerg Infect Dis*. 2020; 26:967–975. [PubMed: 32027586]

11. Chen W, et al. Early containment strategies and core measures for prevention and control of novel coronavirus pneumonia in China. *Chinese Journal of Preventive Medicine*. 2020; 54:1–6.
12. World Health Organization. Press Conference of WHO-China Joint Mission on COVID-19. 2020. https://www.who.int/docs/default-source/coronaviruse/transcripts/joint-mission-press-conference-script-englishfinal.pdf?sfvrsn=51c90b9e_2
13. The State Council of the People's Republic of China. The announcement from Wuhan's headquarter on the novel coronavirus prevention and control. 2020. http://www.gov.cn/xinwen/2020-01/23/content_5471751.htm
14. The State Council of the People's Republic of China. The announcement on Strengthening Community Prevention and Control of Pneumonia Epidemic Situation of New Coronavirus Infection. 2020. http://www.gov.cn/zhengce/2020-01/27/content_5472516.htm
15. The State Council of the People's Republic of China. The State Council's announcement on extending the Lunar New Year Holiday in 2020. 2020. http://www.gov.cn/zhengce/content/2020-01/27/content_5472352.htm
16. The People's Government of Shanghai Municipality. The announcement on postponing the reoperation date of companies and the reopening date of schools. 2020. <http://www.shanghai.gov.cn/nw2/nw2314/nw2315/nw43978/u21aw1423601.html>
17. Li X, Zhao X, Sun Y. The lockdown of Hubei Province causing different transmission dynamics of the novel coronavirus (2019-nCoV) in Wuhan and Beijing. *medRxiv*. 2020
18. Kraemer MUG, et al. The effect of human mobility and control measures on the COVID-19 epidemic in China. *Science*. 2020
19. Chinazzi M, et al. The effect of travel restrictions on the spread of the 2019 novel coronavirus (COVID-19) outbreak. *Science*. 2020
20. Quilty BJ, Clifford S, Flasche S, Eggo RM, group, C. n. w. Effectiveness of airport screening at detecting travellers infected with novel coronavirus (2019-nCoV). *Euro Surveill*. 2020; 25
21. Hellewell J, et al. Feasibility of controlling COVID-19 outbreaks by isolation of cases and contacts. *The Lancet Global Health*.
22. Lai S, et al. Assessing spread risk of COVID-19 within and beyond China, January-April 2020: a travel network-based modelling study. *medRxiv*. 2020
23. Wu JT, Leung K, Leung GM. Nowcasting and forecasting the potential domestic and international spread of the 2019-nCoV outbreak originating in Wuhan, China: a modelling study. *Lancet*. 2020; 395:689–697. [PubMed: 32014114]
24. National Health Commission of the People's Republic of China. Updates on pneumonia of new coronavirus infections as of March 31 2020. 2020. <http://www.nhc.gov.cn/xcs/yqtb/202004/28668f987f3a4e58b1a2a75db60d8cf2.shtml>
25. Wang M, et al. Temperature significant change COVID-19 Transmission in 429 cities. *medRxiv*. 2020
26. Luo W, et al. The role of absolute humidity on transmission rates of the COVID-19 outbreak. *medRxiv*. 2020
27. Lai S, Farnham A, Ruktanonchai NW, Tatem AJ. Measuring mobility, disease connectivity and individual risk: a review of using mobile phone data and mHealth for travel medicine. *J Travel Med*. 2019; 26
28. List of countries by smartphone penetration. 2020. https://en.wikipedia.org/wiki/List_of_countries_by_smartphone_penetration
29. Wang X, Liu C, Mao W, Hu Z, Gu L. Tracing the largest seasonal migration on earth. *arXiv*. 2014
30. National Bureau of Statistics of China. China Statistical Yearbook 2014. 2020. <http://www.stats.gov.cn/english/Statisticaldata/AnnualData/>
31. Kraemer MUG, et al. Past and future spread of the arbovirus vectors *Aedes aegypti* and *Aedes albopictus*. *Nat Microbiol*. 2019; 4:854–863. [PubMed: 30833735]
32. Zhang J, et al. Evolving epidemiology of novel coronavirus diseases 2019 and possible interruption of local transmission outside Hubei Province in China: a descriptive and modeling study. *medRxiv*. 2020

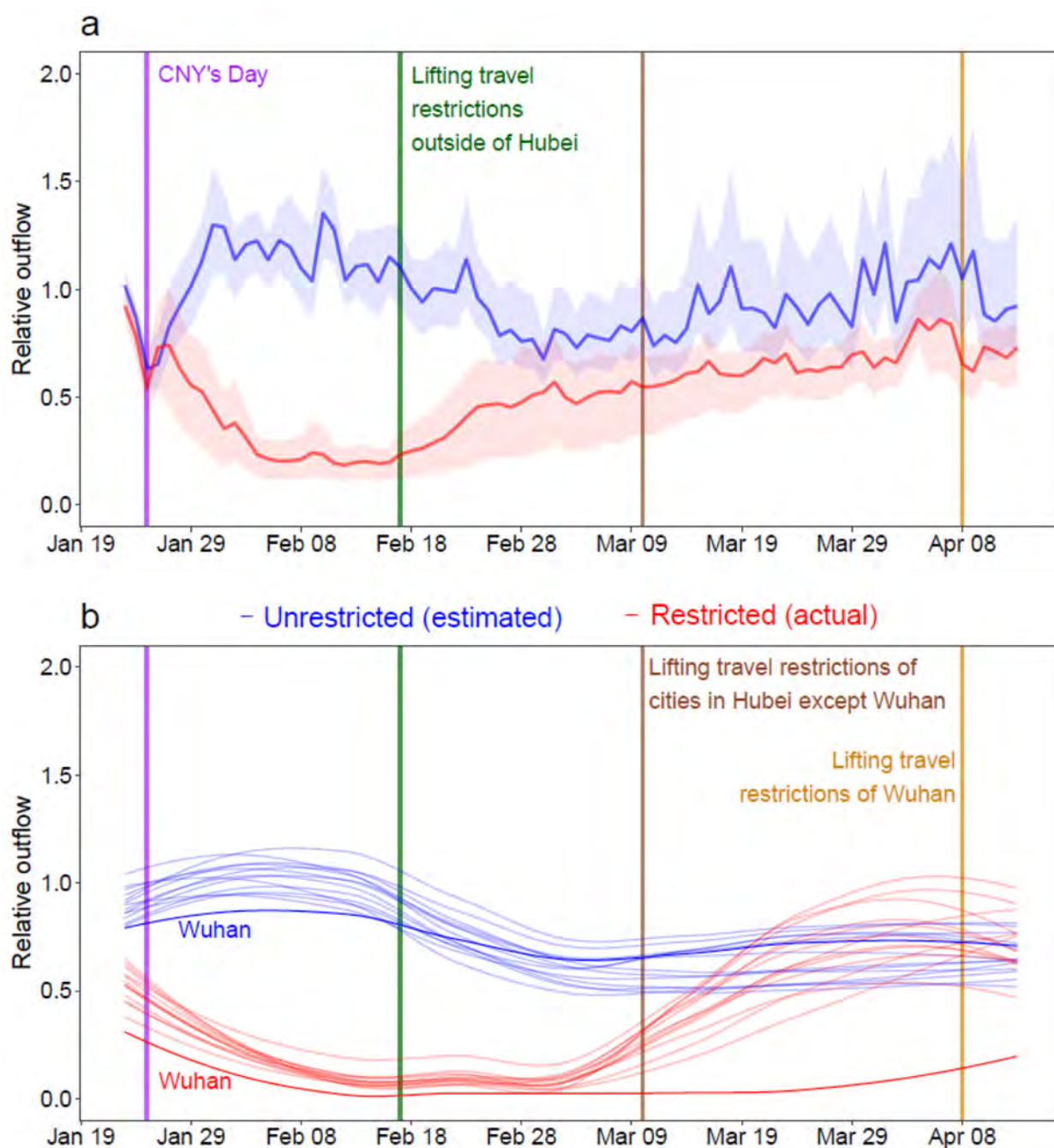


Fig. 1. Relative daily volume of outbound travellers from cities (prefecture level) across mainland China, January 23 – April 13, 2020.

(a) All cities (n=340) in mainland China, presented with the median (solid line) and interquartile range (shading) of relative outbound flows. (b) Cities in Hubei province with Wuhan highlighted by using darker colours. Each red line represents the outflow of each city in 2020, standardized by the mean of daily outflows of each city on January 20th – 22nd, 2020. Each blue line represents estimates of normal outflow by city under the scenario of no

travel restrictions, following travel in previous years. The lines of relative volume in **(b)** were smoothed by using locally estimated scatterplot smoothing (LOESS) regression.

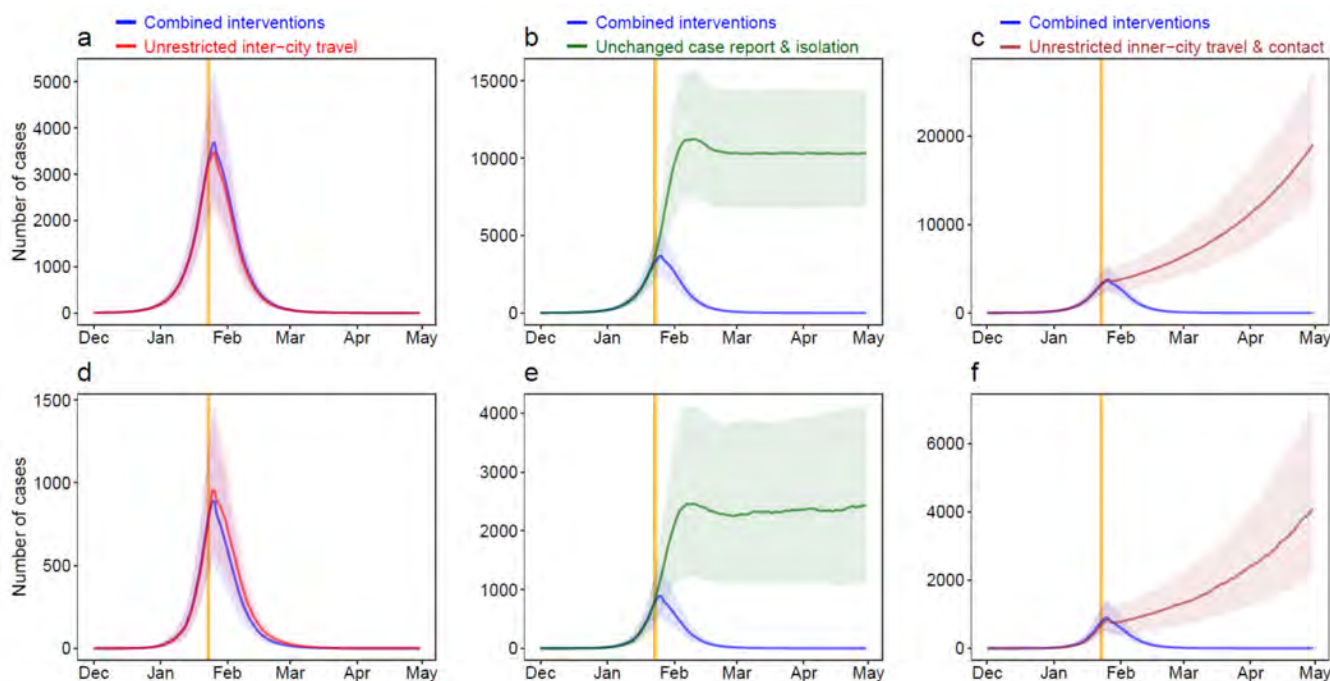


Fig. 2. Estimated epicurves of the COVID-19 outbreak under various scenarios with or without non-pharmaceutical interventions (NPIs) by region.

(a) – (c) Wuhan City. (d) – (f) Provinces outside of Hubei Province in mainland China. The blue lines present estimated transmission under current combined NPIs, and each other line represents the scenario without one type of intervention. The median and interquartile range of estimates (1000 simulations) are presented here. The orange vertical line indicates the date of Wuhan's lockdown on January 23, 2020.

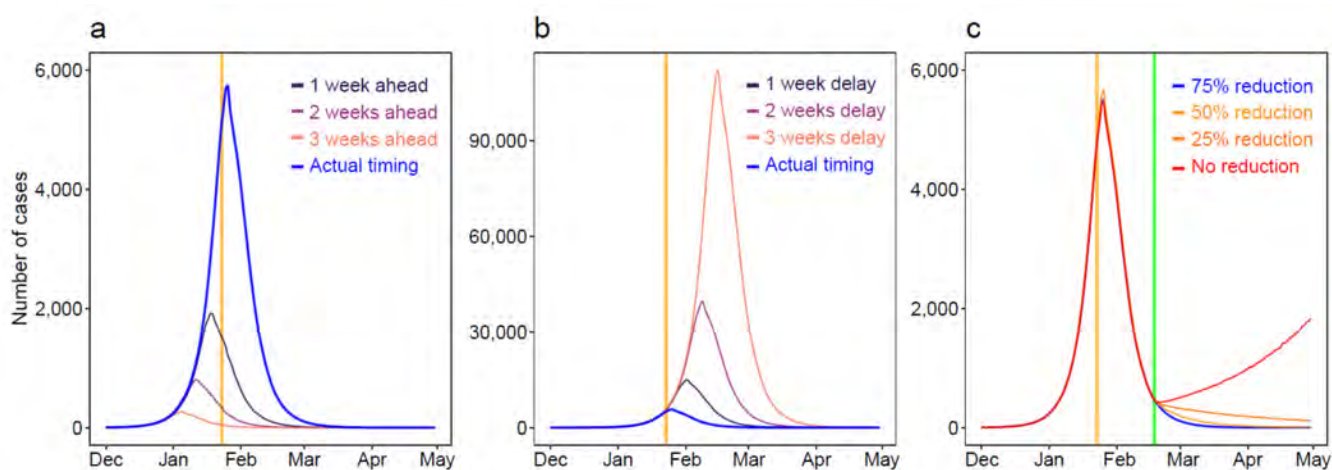


Fig. 3. Estimates of the COVID-19 outbreak under various scenarios of intervention timing and lifting of travel restrictions across China.

(a) Estimated epicurves under interventions implemented earlier than actual timing. **(b)**

Estimated epicurves under interventions implemented later than actual timing. **(c)** Estimated

COVID-19 spread under different population contact rates after lifting intercity travel

restrictions on February 17, 2020. The orange vertical lines indicate the date of Wuhan's

lockdown, and the green line shows the date of travel restrictions being lifted.

VIEWPOINT

Adam S. Luring, MD, PhD

Division of Infectious Diseases, Department of Internal Medicine and Department of Microbiology and Immunology, University of Michigan, Ann Arbor.

Emma B. Hodcroft, PhD

Institute of Social and Preventive Medicine, University of Bern, Switzerland.



Multimedia



Related article
page 522

Corresponding

Author: Adam S. Luring, MD, PhD, Division of Infectious Diseases, Department of Internal Medicine and Department of Microbiology and Immunology, University of Michigan, 1150 W Medical Center Dr, MSRB1 5510B, Ann Arbor, MI 48109-5680 (aluring@med.umich.edu).

Genetic Variants of SARS-CoV-2—What Do They Mean?

Over the course of the severe acute respiratory syndrome coronavirus 2 (SARS-CoV-2) pandemic, the clinical, scientific, and public health communities have had to respond to new viral genetic variants. Each one has triggered a flurry of media attention, a range of reactions from the scientific community, and calls from governments to either “stay calm” or pursue immediate countermeasures. While many scientists were initially skeptical about the significance of the D614G alteration, the emergence of the new “UK variant”—lineage B.1.1.7—has raised widespread concern. Understanding which variants are concerning, and why, requires an appreciation of virus evolution and the genomic epidemiology of SARS-CoV-2.

Mutations, Variants, and Spread

Mutations arise as a natural by-product of viral replication.¹ RNA viruses typically have higher mutation rates than DNA viruses. Coronaviruses, however, make fewer mutations than most RNA viruses because they encode an enzyme that corrects some of the errors made during replication. In most cases, the fate of a newly arising mutation is determined by natural selection. Those that confer a competitive advantage with

speaking, a variant is a *strain* when it has a demonstrably different phenotype (eg, a difference in antigenicity, transmissibility, or virulence).

Evaluation of a new SARS-CoV-2 variant should include assessment of the following questions: Did the variant achieve prominence through natural selection or chance events? If the evidence suggests natural selection, which mutation(s) are being selected? What is the adaptive benefit of these mutations? What effect do these mutations have on transmissibility and spread, antigenicity, or virulence?

Spike D614G

The D614G mutation in the spike glycoprotein of SARS-CoV-2 was first detected at a significant level in early March 2020 and spread to global dominance over the next month.² The mutation initially appeared to arise independently and simultaneously sweep across multiple geographic regions. This apparent convergent evolution was suggestive of natural selection and an adaptive benefit of D614G. However, subsequent sequencing efforts identified the D614G mutation in viruses in several Chinese provinces in late January. This raised the possibility that global dispersal of this mutation could have resulted from chance founder events, in which viruses harboring 614G just happened to initiate the majority of early transmission events in multiple locations.

This plausible null hypothesis led many in the evolution community to doubt that the D614G mutation was adaptive, despite in vitro data showing

Understanding which variants are concerning, and why, requires an appreciation of virus evolution and the genomic epidemiology of SARS-CoV-2.

respect to viral replication, transmission, or escape from immunity will increase in frequency, and those that reduce viral fitness tend to be culled from the population of circulating viruses. However, mutations can also increase and decrease in frequency due to chance events. For example, a “founder effect” occurs when a limited number of individual viruses establish a new population during transmission. The mutations present in the genomes of these viral ancestors will dominate the population regardless of their effects on viral fitness. This same interplay of natural selection and chance events shapes virus evolution within hosts, in communities, and across countries.

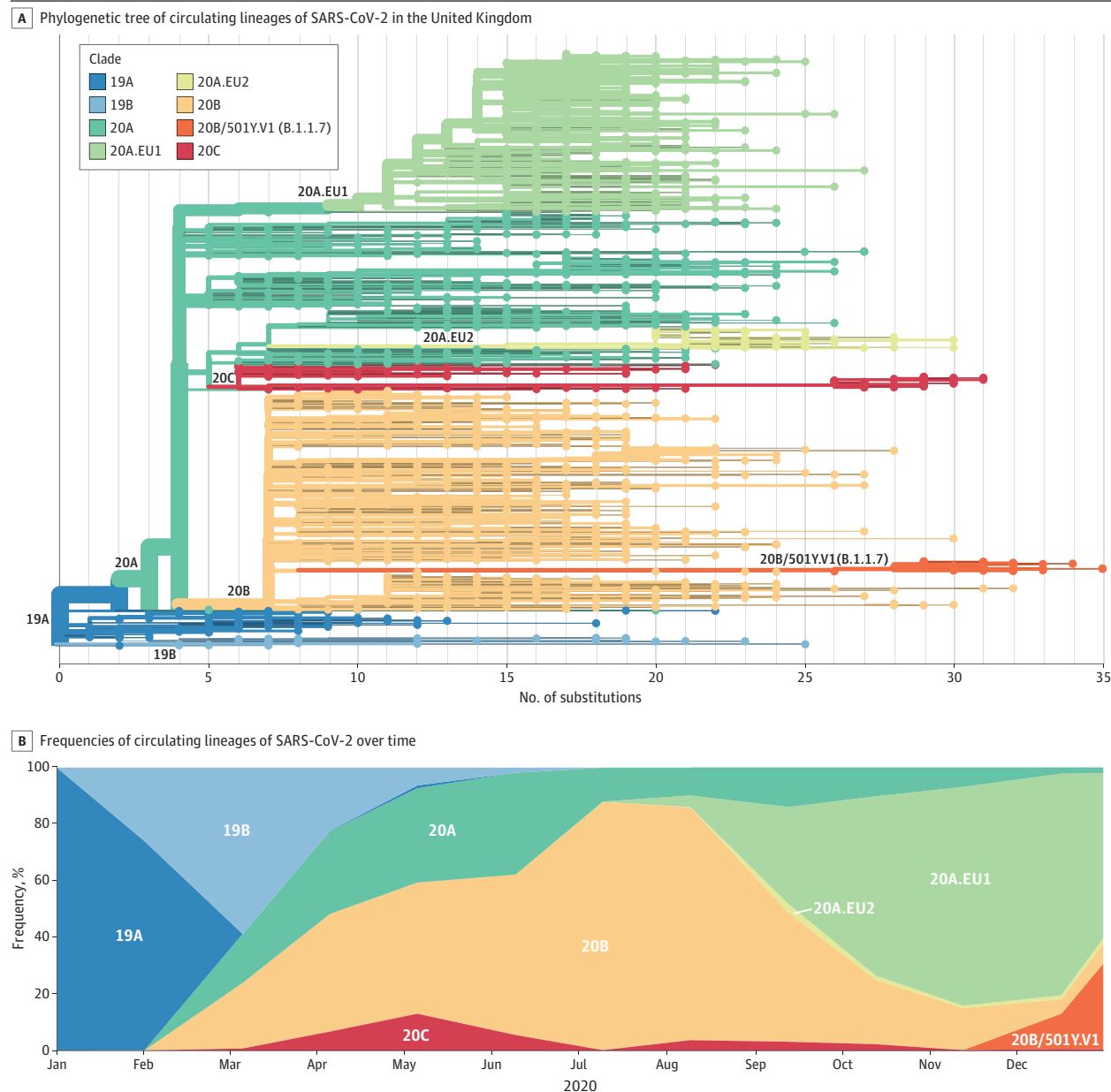
Although the terms *mutation*, *variant*, and *strain* are often used interchangeably in describing the epidemiology of SARS-CoV-2, the distinctions are important. *Mutation* refers to the actual change in sequence: D614G is an aspartic acid-to-glycine substitution at position 614 of the spike glycoprotein. Genomes that differ in sequence are often called *variants*. This term is somewhat less precise because 2 variants can differ by 1 mutation or many. Strictly

its effects on receptor binding. A recent population genetic and phylodynamic analysis of more than 25 000 sequences from the UK found that viruses bearing 614G did appear to spread faster and seed larger phylogenetic clusters than viruses with 614D.³ The effect size was modest, and the varying models did not always achieve statistical significance. More recently, complementary work in animal models indicates that 614G viruses transmit more efficiently.^{4,5}

Spike Y453F and Mink

Concerning outbreaks of SARS-CoV-2 began to emerge on mink farms in the Netherlands and Denmark in late spring and early summer 2020.⁶ Genomic and epidemiologic investigation of an early outbreak in the Netherlands demonstrated human to mink, mink to mink, and mink to human transmission.⁷ In early November 2020 Danish authorities reported 214 cases of human coronavirus disease 2019 (COVID-19) associated with mink farms. Many SARS-CoV-2 sequences from the Netherlands and Danish outbreaks had a Y453F mutation in the receptor binding domain of

Figure. Spread of a New SARS-CoV-2 Variant



A, Phylogenetic tree showing the relationship of lineage B.1.1.7 (20B/501Y.V1, orange branch and tips) to other circulating lineages. The long branch length for this lineage reflects the fact that it accumulated a significant number of

mutations prior to being discovered. B, Frequencies of circulating lineages over time. Lineages are colored as in the tree, with lineage B.1.1.7 (20B/501Y.V1) shown in orange.

spike, which might mediate increased binding affinity for mink ACE2 (angiotensin-converting enzyme 2). Eleven individuals from the Danish outbreak had a variant termed cluster 5, which had 3 additional mutations in spike (del69_70, I692V, and M1229I). An initial investigation of 9 human convalescent serum samples suggested a modest and variably statistically significant reduction in neutralization activity against cluster 5 viruses (mean, 3.58 fold; range, 0-13.5). The apparent adaptation of SARS-CoV-2 to mink was nevertheless concerning because continued evolution of the virus in an animal reservoir could potentially lead to recurrent spillover events of novel SARS-CoV-2 from mink to humans and other mam-

mals. For this reason, many countries have increased surveillance efforts and in some cases implemented large-scale culls (ie, selective slaughter) of mink on farms.

Lineage B.1.1.7 and N501Y

Lineage B.1.1.7 (also called 501Y.V1) is a phylogenetic cluster that is rapidly spreading in southeastern England⁸ (Figure). It had accumulated 17 lineage-defining mutations prior to its detection in early September, which suggests a significant amount of prior evolution, possibly in a chronically infected host. As of December 28, 2020, this variant accounted for approximately 28% of cases of

SARS-CoV-2 infection in England, and population genetic models suggest that it is spreading 56% more quickly than other lineages.⁹ Unlike D614G, which could plausibly have benefited from early chance events, lineage B.1.1.7 expanded when SARS-CoV-2 cases were widespread and has seemingly achieved dominance by out-competing an existing population of circulating variants. This is strongly suggestive of natural selection of a virus that is more transmissible at a population level. While public health interventions like masks, physical distancing, and limitations on large gatherings should remain effective, control of a more transmissible variant would likely require more stringent application and widespread adoption of these measures.

Eight of the lineage B.1.1.7 mutations are in the spike glycoprotein, including N501Y in the receptor binding domain, deletion 69_70, and P681H in the furin cleavage site. All of these mutations could plausibly influence ACE2 binding and viral replication. The 501Y spike variants are predicted to have a higher affinity for human ACE2, and a different variant, also with an N501Y mutation, is rapidly spreading in South Africa. The effects of these mutations on antigenicity are currently unclear.

Antigenicity and Vaccine Effectiveness

Genomic surveillance of SARS-CoV-2 variants has largely focused on mutations in the spike glycoprotein, which mediates attachment to cells and is a major target of neutralizing antibodies. There is intense interest in whether mutations in the spike glycoprotein mediate escape from host antibodies and could potentially

compromise vaccine effectiveness, since spike is the major viral antigen in the current vaccines. At this point, strong selection of a variant at the population level is probably not driven by host antibody because there are not sufficient numbers of immune individuals to systematically push the virus in a given direction. In contrast, if a variant has one or more mutations in spike that increase transmissibility, it could quickly outcompete and replace other circulating variants. Because current vaccines provoke an immune response to the entire spike protein, it is hoped that effective protection may still occur despite a few changes at antigenic sites in SARS-CoV-2 variants.

Separating cause from consequence is important in evaluating data on antibody neutralization of spike variants. Regardless of why the mutations were selected, it is reasonable to expect that many mutations in spike might affect neutralization by convalescent sera. It is therefore important to consider both the magnitude of the change in neutralization and the number of serum samples evaluated. Another issue is that viral glycoproteins are subject to evolutionary trade-offs. Sometimes a mutation that enhances one viral property, such as binding to a receptor, can reduce another property, such as escaping host antibody. Indeed, recent evidence suggests this could be the case for D614G.¹⁰ It is possible that mutations in spike that are “good” for the virus right now could also make it less fit in the context of population-level immunity in the future. Defining these dynamics, and their potential influence on vaccine effectiveness, will require large-scale monitoring of SARS-CoV-2 evolution and host immunity for a long time to come.

ARTICLE INFORMATION

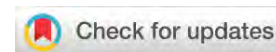
Published Online: January 6, 2021.
doi:10.1001/jama.2020.27124

Correction: This article was corrected on February 15, 2021, to fix the heading “Spike N453Y and Mink” to the correct substitution of Y453F.

Conflict of Interest Disclosures: Dr Lauring reported receiving personal fees from Sanofi as a consultant on oseltamivir and influenza and personal fees from Roche as a member of a steering committee for a clinical trial of baloxavir and influenza, outside the submitted work. No other disclosures were reported.

REFERENCES

1. Grubaugh ND, Petrone ME, Holmes EC. We shouldn't worry when a virus mutates during disease outbreaks. *Nat Microbiol*. 2020;5(4):529-530. doi:10.1038/s41564-020-0690-4
2. Korber B, Fischer WM, Gnanakaran S, et al; Sheffield COVID-19 Genomics Group. Tracking changes in SARS-CoV-2 spike: evidence that D614G increases infectivity of the COVID-19 virus. *Cell*. 2020;182(4):812-827.e19. doi:10.1016/j.cell.2020.06.043
3. Volz E, Hill V, McCrone JT, et al; COG-UK Consortium. Evaluating the effects of SARS-CoV-2 spike mutation D614G on transmissibility and pathogenicity. *Cell*. 2020;S0092867420315373.
4. Plante JA, Liu Y, Liu J, et al. Spike mutation D614G alters SARS-CoV-2 fitness. *Nature*. Published online December 23, 2020. doi:10.1038/s41586-020-2895-3
5. Hou YJ, Chiba S, Halfmann P, et al. SARS-CoV-2 D614G variant exhibits efficient replication ex vivo and transmission in vivo. *Science*. 2020;370(6523):1464-1468. doi:10.1126/science.abe8499
6. European Centre for Disease Prevention and Control. Detection of new SARS-CoV-2 variants related to mink. Posted November 12, 2020. Accessed January 3, 2021. <https://www.ecdc.europa.eu/sites/default/files/documents/RRA-SARS-CoV-2-in-mink-12-nov-2020.pdf>
7. Oude Munnink BB, Sikkema RS, Nieuwenhuijse DF, et al. Transmission of SARS-CoV-2 on mink farms between humans and mink and back to humans. *Science*. 2020;eabe5901. doi:10.1126/science.abe5901
8. Rambaut A, Loman N, Pybus O, et al; COVID-19 Genomics Consortium UK. Preliminary genomic characterisation of an emergent SARS-CoV-2 lineage in the UK defined by a novel set of spike mutations. *Virological.org*. Posted December 16, 2020. Accessed January 3, 2021. <https://virological.org/t/preliminary-genomic-characterisation-of-an-emergent-sars-cov-2-lineage-in-the-uk-defined-by-a-novel-set-of-spike-mutations/563>
9. Davies NG, Barnard RC, Jarvis CI, et al. Estimated transmissibility and severity of novel SARS-CoV-2 Variant of Concern 202012/01 in England. *CMMID*. Preprint published online December 23, 2020. Updated December 31, 2020. doi:10.1101/2020.12.24.20248822
10. Weissman D, Alameh M-G, de Silva T, et al. D614G spike mutation increases SARS CoV-2 susceptibility to neutralization. *Cell Host Microbe*. 2020;S193131282030634X.



RESEARCH ARTICLE

REVISED What settings have been linked to SARS-CoV-2

transmission clusters? [version 2; peer review: 2 approved]

Quentin J. Leclerc ^{1,2}, Naomi M. Fuller ^{1,2}, Lisa E. Knight³,
CMMID COVID-19 Working Group, Sebastian Funk ^{1,2}, Gwenan M. Knight ^{1,2}

¹Department of Infectious Disease Epidemiology, Faculty of Epidemiology and Population Health, London School of Hygiene & Tropical Medicine, London, UK

²Centre for Mathematical Modelling of Infectious Diseases, London School of Hygiene & Tropical Medicine, London, UK

³GP registrar, Brecon Surgery, Gwent Deanery, UK

v2 First published: 01 May 2020, 5:83
<https://doi.org/10.12688/wellcomeopenres.15889.1>
Latest published: 05 Jun 2020, 5:83
<https://doi.org/10.12688/wellcomeopenres.15889.2>

Abstract

Background: Concern about the health impact of novel coronavirus SARS-CoV-2 has resulted in widespread enforced reductions in people's movement ("lockdowns"). However, there are increasing concerns about the severe economic and wider societal consequences of these measures. Some countries have begun to lift some of the rules on physical distancing in a stepwise manner, with differences in what these "exit strategies" entail and their timeframes. The aim of this work was to inform such exit strategies by exploring the types of indoor and outdoor settings where transmission of SARS-CoV-2 has been reported to occur and result in clusters of cases. Identifying potential settings that result in transmission clusters allows these to be kept under close surveillance and/or to remain closed as part of strategies that aim to avoid a resurgence in transmission following the lifting of lockdown measures.

Methods: We performed a systematic review of available literature and media reports to find settings reported in peer reviewed articles and media with these characteristics. These sources are curated and made available in an editable online database.

Results: We found many examples of SARS-CoV-2 clusters linked to a wide range of mostly indoor settings. Few reports came from schools, many from households, and an increasing number were reported in hospitals and elderly care settings across Europe.

Conclusions: We identified possible places that are linked to clusters of COVID-19 cases and could be closely monitored and/or remain closed in the first instance following the progressive removal of lockdown restrictions. However, in part due to the limits in surveillance capacities in many settings, the gathering of information such as cluster sizes and attack rates is limited in several ways: inherent recall bias, biased media reporting and missing data.

Keywords

SARS-CoV-2, COVID-19, coronavirus, cluster, transmission, settings, lockdown

Open Peer Review

Reviewer Status

	Invited Reviewers	
	1	2
version 2 (revision) 05 Jun 2020	 report	 report
	↑	
version 1 01 May 2020	 report	

1 **Joël Mossong** , Laboratoire National de Santé, Dudelange, Luxembourg

2 **Samuel V. Scarpino** , Northeastern University, Boston, USA

Any reports and responses or comments on the article can be found at the end of the article.



This article is included in the [Coronavirus \(COVID-19\)](#) collection.

Corresponding authors: Quentin J. Leclerc (quentin.leclerc@lshtm.ac.uk), Gwenan M. Knight (gwen.knight@lshtm.ac.uk)

Author roles: **Leclerc QJ:** Data Curation, Formal Analysis, Investigation, Validation, Writing – Original Draft Preparation, Writing – Review & Editing; **Fuller NM:** Data Curation, Investigation, Validation, Writing – Original Draft Preparation, Writing – Review & Editing; **Knight LE:** Data Curation, Investigation, Validation, Writing – Review & Editing; **Funk S:** Conceptualization, Methodology, Supervision, Validation, Writing – Review & Editing; **Knight GM:** Conceptualization, Data Curation, Formal Analysis, Investigation, Methodology, Supervision, Validation, Writing – Original Draft Preparation, Writing – Review & Editing

Competing interests: No competing interests were disclosed.

Grant information: QJL is funded by a Medical Research Council London Intercollegiate Doctoral Training Program studentship (MR/N013638/1), NMF is funded by the Biotechnology and Biological Sciences Research Council London Interdisciplinary Doctoral Programme, SF is supported by a Wellcome Trust grant (210758), GMK is supported by a Medical Research Council grant (MR/P014658/1).

The funders had no role in study design, data collection and analysis, decision to publish, or preparation of the manuscript.

Copyright: © 2020 Leclerc QJ *et al.* This is an open access article distributed under the terms of the [Creative Commons Attribution License](#), which permits unrestricted use, distribution, and reproduction in any medium, provided the original work is properly cited.

How to cite this article: Leclerc QJ, Fuller NM, Knight LE *et al.* **What settings have been linked to SARS-CoV-2 transmission clusters?** [version 2; peer review: 2 approved] Wellcome Open Research 2020, 5:83 <https://doi.org/10.12688/wellcomeopenres.15889.2>

First published: 01 May 2020, 5:83 <https://doi.org/10.12688/wellcomeopenres.15889.1>

REVISED Amendments from Version 1

This article has been updated in response to reviewer comments, and to include 49 new transmission events which have been added to our online database. We now discuss a total of 201 transmission events (previously 152), classified into 22 setting types (previously 18).

Any further responses from the reviewers can be found at the end of the article

Introduction

The novel coronavirus SARS-CoV-2, responsible for coronavirus disease 2019 (COVID-19), was first identified in Wuhan, China at the end of 2019, and has since spread around the world (European Centre for Disease Prevention and Control, 2020). The capacity of the virus for human-to-human transmission, coupled with the lack of immunity in the population due to the novelty of SARS-CoV-2, has led to the implementation of severe reductions in people's movements in an effort to reduce disease impact. These strong measures are broadly described as "lockdowns". Due to the highly restrictive nature of lockdowns, and their impact on people's health, wellbeing and finances, it is likely that such interventions cannot be sustained for prolonged periods of time, and will have to be lifted, at least to some extent, before an effective vaccine becomes available.

To successfully remove these lockdown restrictions while avoiding a resurgence in SARS-CoV-2 transmission, we must better understand in which types of settings the virus is most likely to be transmitted. Determining particular places that are linked to clusters of cases could reveal settings that are responsible for amplifying the heterogeneity in transmission that has been reported: potentially 80% of transmission is being caused by only 10% of infected individuals (Endo *et al.*, 2020). Notably, the difference in transmission risk between households and larger communal settings is unclear, as is the difference between indoor and outdoor transmission.

Quantifying these differences in transmission can be further facilitated by the fact that, in many countries now under lockdown, intensive contact tracing of imported cases was performed in the early stages of the epidemic, resulting in the detection of clusters of cases. This data, on the first detected clusters in a country, can give knowledge of the types of settings facilitating transmission before intensive social and physical distancing took place.

The aim of our work is therefore to gather information on reported clusters of COVID-19 cases to determine types of settings in which SARS-CoV-2 transmission occurred. This could inform post-lockdown strategies by identifying places which should be kept under close surveillance and/or should still remain closed to avoid a resurgence in transmission.

Methods

Outline

We searched for scientific literature and media articles detailing clusters of SARS-CoV-2 transmission (details below) and extracted

data into a Google Sheets file (accessible at <https://bit.ly/3ar39ky>; archived as *Underlying data* (Leclerc *et al.*, 2020)). We defined "settings" as sites where transmission was recorded resulting in a cluster of cases. We restricted our definition of "cluster" to the first-generation cases that acquired the infection due to transmission in a single specific setting at a specific time. For example, if a person was infected on a cruise ship, and later infected additional people after disembarking, we would not consider that the latter were part of that "cruise ship cluster", since they were not infected on the ship. We recorded the country and further details about the type of setting, the numbers of primary and secondary cases in the cluster, cluster sizes, and attack rates. We defined a case as a person reported to be infected with the SARS-CoV-2 virus, regardless of symptoms.

Search strategy

References were found in four ways. Firstly, we performed a systematic literature review for COVID-19 clusters in PubMed on the 30th March 2020 (search term below). A total of 67 papers were found. Two reviewers (GMK and QJL) performed data extraction into the online database. We chose to only search this database and use peer reviewed articles as a quality threshold. We included data from English abstracts (where possible), but otherwise excluded non-English publications.

PubMed search: ("COVID-19"[All Fields] OR "COVID-2019"[All Fields] OR "severe acute respiratory syndrome coronavirus 2"[Supplementary Concept] OR "severe acute respiratory syndrome coronavirus 2"[All Fields] OR "2019-nCoV"[All Fields] OR "SARS-CoV-2"[All Fields] OR "2019nCoV"[All Fields] OR ("Wuhan"[All Fields] AND ("coronavirus"[MeSH Terms] OR "coronavirus"[All Fields])) AND (2019/12[PDAT] OR 2020[PDAT])) AND cluster [All Fields]

Secondly, we used the online Google search engine to find media articles detailing settings of SARS-CoV-2 transmission in general. We searched for combinations of either "COVID", "COVID-19", "COVID-2019", "severe acute respiratory syndrome coronavirus 2", "2019-nCoV", "SARS-CoV-2", "2019nCoV" or "coronavirus", and the words "transmission cluster" (e.g. "COVID transmission cluster" or "SARS-CoV-2 transmission cluster"). We only included online articles in English. From the collated list of settings, we then performed a further search for transmission in each of these settings (week beginning 6th April 2020).

Thirdly, we investigated whether information on the settings in which the first 100 "transmission events" in countries with current COVID-19 outbreaks existed by searching for publicly available data sources. As substantial investigation of cases often occurs early in an outbreak, any clusters linked to the first ~100 cases in countries outside China could give information on the transmission of SARS-CoV-2 in the absence of any social distancing measures.

Finally, following the original publication of this article on 01/05/2020, we included a "Suggested updates" tab in our publicly available database (<https://bit.ly/3ar39ky>). This allows other individuals to suggest new clusters we should include in our analysis. We review these suggestions regularly, and add

those with sufficient detail to our “Latest updated results” tab. In this revised version, we have updated our analysis to include suggestions we reviewed up to 26/05/2020.

Cluster characteristics and setting definition

With the above data, we then aimed to estimate both the final (proportion of people in that setting who became infected) and secondary (proportion of contacts of one case who became infected) attack rates in each setting. These were previously identified as key metrics, particularly within households, to estimate whether transmission is driven by a relatively small number of high-risk contacts (Liu *et al.*, 2020).

We defined a setting when several reports mentioned clusters linked to spaces with certain characteristics. For example, “Religious” includes churches and mosques, while “Public” here means public communal shared spaces such as markets or welfare centres. Where settings were a mixture of indoor and outdoor spaces, we used a mixed indoor/outdoor classification.

Results

We found evidence of SARS-CoV-2 transmission clusters for 201 events, which we classified into 22 types of settings (Table 1 and Table 2). All the studies with relevant data are compiled in an online database (accessible at <https://bit.ly/3ar39ky>; see also *Underlying data* (Leclerc *et al.*, 2020)). Many of the published reports with setting specific data came from China (47/201) and Singapore (51/201).

The vast majority of these clusters were associated with indoor or indoor/outdoor settings (21/22). Large clusters, such as those linked to churches and ships, were infrequently reported. Almost all clusters involved fewer than 100 cases (181/201), with the outliers being transmission in hospitals, elderly care, worker dormitories, food processing plants, prisons, schools, shopping and ship settings. Religious venues provided a further setting with large cluster sizes: there were separate clusters in South Korea, France, India and Malaysia (Ananthalakshmi & Sipalan, 2020; BBC, 2020; Salaün, 2020; Shin *et al.*, 2020). In addition to these settings with maximum cluster sizes of more than 100 cases per cluster, we identified five further settings with maximum cluster sizes between 50 and 100: sport (65 cases) (Korean Centre for Disease Control & Prevention, 2020), bar (80 cases) (Sim, 2020), wedding (98 cases) (Ministry of Health – New Zealand, 2020), work (97 cases) (Park *et al.*, 2020) and conference (89 cases) (Marcelo & O’Brien, 2020).

We found a notably high number of transmission events reported in worker dormitories (21/201), although all of these were from Singapore. This type of setting had the second highest total cluster size out of all the recorded events we found, with 797 cases reported in the S11 dormitory cluster in Singapore (Data Against COVID19 SG, 2020).

We found only a small number of clusters linked to schools (8/201), and there the SARS-CoV-2 cases reported were most often in teachers or other staff. For example, for two school clusters in Singapore (Ministry of Health - Singapore, 2020),

16/26 and 7/8 cases were staff. Some children were also found to be infected in these clusters, as was the case in the Salanter Akiba Riverdale school in New York, USA (Ailworth & Berzon (2020)), although testing for infection was not always universal. In a retrospective close cohort study in a French high school however, 133 children and staff were seropositive for anti-SARS-CoV-2 antibodies, 92 of whom were pupils (Fontanet *et al.*, 2020).

We identified 9 clusters linked to food processing plants in 4 different countries (USA, Germany, Canada, Netherlands). These transmission events have led to large clusters, such as in a meat processing plant in South Dakota where a total of 518 employees were infected by SARS-CoV-2 (Cannon, 2020).

The setting with the greatest number of reported clusters of SARS-CoV-2 transmission was households (36/201). Again, most were from China (25/36) with all cluster sizes being less than 10. However, for 27 out of 36 studies, we were unable to calculate either the secondary or final attack rates due to a lack of information on total household size.

We aimed to estimate secondary and final attack rates in other settings but, as for households, we found that there was substantial missing data. In particular, the number of individuals in a setting was missing, and so we were unable to perform this analysis. Where attack rates could be estimated for individual clusters, these are reported in the online database.

Although information on the index and early cases in a setting was often reported, further information on the subsequently reported 10–100 cases in a country was difficult to extract. Moreover, the index cases were often quarantined and hence not linked to further transmission in most settings.

Discussion

In this review of SARS-CoV-2 transmission events, we found that clusters of cases were reported in many, predominantly indoor, settings. Note that we restrict cluster size to only include individuals infected within a specific setting, and exclude secondary infections which occurred outside the settings. Most clusters involved fewer than 100 cases, with the exceptions being in healthcare (hospitals and elderly care), large religious gatherings, food processing plants, schools, shopping, and large co-habiting settings (worker dormitories, prisons and ships). Other settings with examples of clusters between 50–100 cases in size were weddings, sport, bar, shopping and work. The majority of our reports are from China and Singapore.

Limitations

The settings collated here are biased due to the nature of our general search for SARS-CoV-2 transmission described above. Although based on a systematic review of published peer-reviewed literature, many of the reports included came from media articles where relevant epidemiological quantities were not always reported, resulting in many missing data. Many of the more detailed studies originated from the early outbreak in China, especially those providing household information. The settings

Table 1. Summary of gathered reported events as of 20th April 2020. Where only one study for this setting is reported, the minimum, maximum and median number of secondary cases in the cluster and/or total cluster size correspond to this single reported number (if given). Total cluster size accounts for all primary and secondary cases in the cluster. For references see the online database, accessible at <https://bit.ly/3ar39ky>.

Setting type	Number of reported events	Secondary cases			Total cluster size			Total number of cases across all clusters	Countries	Indoor / outdoor
Bar	12	2	9	16	3	13	80	319	Germany, Austria, Italy, Singapore, Japan, USA, Australia, New Zealand, Brazil	Indoor / outdoor
Building site	4	/	/	/	5	20.5	49	95	Singapore	Outdoor
Conference	5	/	/	/	3	10	89	148	Canada, Singapore, Japan, USA, New Zealand	Indoor / outdoor
Elderly care	17	/	/	/	5	19	167	638	UK, Canada, Scotland, France, Germany, Italy, USA, Japan, New Zealand, Luxembourg	Indoor
Food processing plant	9	2	2	2	3	84	518	1207	USA, Germany, Canada, Netherlands	Indoor
Funeral	1	3	3	3	4	4	4	4	USA	Indoor / outdoor
Hospital	9	1	3	14	2	10	118	224	China, Singapore, Italy, Taiwan, South Korea, Japan	Indoor
Hotel	2	/	/	/	3	5	7	10	Singapore	Indoor
Household	36	1	3	11	2	4	12	168	China, Italy, Vietnam, Taiwan, South Korea, Hong Kong, France	Indoor
Meal	17	1	3	10	2	5	47	134	Singapore, USA, Vietnam, China, South Korea, Japan	Indoor
Prison	4	351	351	351	66	226	353	871	USA, Ethiopia	Indoor
Public	4	/	/	/	10	10	27	57	China, Japan	Indoor / outdoor
Religious	15	1	18	52	2	23	130	570	USA, Singapore, South Korea, US, China, India, Netherlands, Germany	Indoor / outdoor
School	8	1	1	131	2	22	133	349	Singapore, France, USA, New Zealand, Australia, Sweden	Indoor / outdoor
Ship	5	619	619	619	78	662	1156	3597	Grand Princess, Diamond Princess, Ruby Princess, USS Theodore Roosevelt, Charles de Gaulle aircraft carrier	Indoor
Shipyard	1	/	/	/	22	22	22	22	Singapore	Indoor / outdoor
Shopping	9	5	10	19	7	20	163	361	China, Singapore, Peru, Mexico	Indoor / outdoor
Sport	6	1	1	1	2	7.5	65	95	South Korea, Singapore, Italy, Japan	Indoor / outdoor
Transport	1	1	1	1	3	3	3	3	China	Indoor
Wedding	3	/	/	/	13	43	98	154	Australia, New Zealand	Indoor / outdoor
Work	12	6	7	11	4	8.5	97	198	China, Singapore, South Korea, Germany	Indoor
Worker dormitories	21	/	/	/	3	24	797	1702	Singapore	Indoor

Table 2. Definition used for each of our transmission setting types. The definitions describe in what environment transmission was deemed to occur.

Transmission setting	Definitio
Bar	Indoor space such as a bar, club, pub, small live music venues etc.
Building site	Outdoor space where construction work takes place.
Conference	Indoor professional event with many people interacting and meeting, shaking hands, eating together, team activities, etc.
Elderly Care	Care homes for the elderly; includes staff and residents. Transmission can occur between staff and residents but also from visitors.
Food processing plant	Any establishment that processes food for human consumption, such as a meat or vegetable packing plant.
Funeral	Indoor or outdoor burial ceremony; includes close contact with others such as hugging, shaking hands, eating together, singing, praying, etc.
Hospital	Any transmission that occurs within a hospital between patients and/or staff, in a COVID19 ward or not.
Hotel	Any transmission that occurs within the hotel e.g. hotel rooms, shared spaces, reception desk, etc.
Household	Transmission between individuals in a shared living space
Meal	When people eat together. Meals included took place in restaurants, hotels, cafes, home, etc. Transmission occurs over a meal by speaking, sharing foods, touching the same surfaces, etc.
Prison	Any transmission that occurs within a prison between prisoners and/or staff.
Public	Where transmission occurs on public property and does not fall into any of the other settings e.g. park, welfare centre, foodbank, etc.
Religious	Transmission occurs at a religious event such as at mass, services, prayer time, choir practice, etc.
School	Childcare or learning environments (schools, nurseries, kindergartens etc). Includes staff and children.
Ship	Any ship at sea. Includes crew and/or passengers onboard.
Shipyards	Large indoor or outdoor space where ships are made or repaired. Includes those working on the ship as well as customers
Shopping	A shop or shopping centre. Includes customers and those working in the shop.
Sport	Participation in a sporting activity indoor or outdoor e.g. gym or running.
Transport	Any means of public transportation, such as bus, plane, metro etc.
Wedding	Indoor or outdoor wedding celebration.
Work	In the workplace, typically an office.
Worker dormitories	A shared living space for workers.

we identified here therefore might not be representative of settings from a global perspective. Bias is present when relying on media coverage - a cluster is more likely to be reported if controversial or if there is an interesting social narrative. This is then compounded by the method search engines use to provide results where priority is given to high traffic stories. Overall, this can lead to some settings being overly represented in our database, which is why the numbers of clusters per settings should be compared cautiously.

Similarly, there is a bias in our reports which means that attendance in settings with many individuals is more likely to be linked to a cluster: recall bias (Spencer *et al.*, 2017). The accuracy of memories is influenced by subsequent events and experiences such that special, one-off events may be more likely to be

remembered and potentially reported. If multiple single transmission events had occurred whilst walking in a park, for example, these would be less likely to be remembered, and more difficult to detect and hence record. Networks of close contacts also tend to be small, resulting in multiple opportunities for transmission, and hence potentially increase the importance of households or workplace for transmission instead of single outstanding settings of potential transmission. Hence, we cannot determine with any reliability the relative importance of the reported different types of settings beyond the record that clusters have been linked to such places.

Other events, such as large music concert (Dalling, 2020), political (Jones, 2020) and sporting (Hope, 2020; Roan, 2020; Wood & Carroll, 2020) gatherings, could potentially have been

linked to clusters of COVID-19. But, in the absence of rigorous surveillance systems and widespread testing that would allow countries to link and report the transmissions of such events, such connections remain speculation. An example of this lack of surveillance would be the UK, where only 4/201 clusters have been recorded. The outlier for this is Singapore which appears to investigate clusters systematically and provides a well-designed online dashboard with details of all clusters detected ([Data Against COVID19 SG, 2020](#)).

In many settings, only symptomatic cases of disease severe enough to require hospitalization are tested and ultimately reported. This misses those infections that result in mildly symptomatic or asymptomatic symptoms, although there is mounting evidence for a significant proportion of infections to remain asymptomatic ([Gudbjartsson *et al.*, 2020](#); [He *et al.*, 2020](#); [Lavezzo *et al.*, 2020](#)). For some of the clusters, primarily households, all contacts were tested for infection; but for most of the data collated here, the number of COVID-19 symptomatic cases was the only information provided. These reported cases are a subset of all infections and in the absence of more comprehensive data, such as could be collated through widespread cluster investigation and community testing, we cannot conclude anything about clusters of infections, nor that we have included all relevant settings in which transmission can occur. We were also unable to estimate attack rates from the available data, meaning that comparison between rates of transmission in settings is impossible to achieve.

Settings associated with large cluster sizes

One type of setting that was associated with large numbers of eventual cases was religious venues. The common features of these meetings are the large number of attendees, confined spaces and physical contact. For example, there were eventually more than 5000 COVID-19 cases linked to transmission at the Shincheonji Church of Jesus in South Korea ([Shin *et al.*, 2020](#)). In this particular religious venue, no preventative action was taken despite knowing members were infected with SARS-CoV-2. In other venues, transmission events took place without prior knowledge of any infections and before the WHO declared pandemic status. Other large clusters in this setting type were associated with annual religious events that took place over a few days or weeks ([Ananthalakshmi & Sipalan, 2020](#); [BBC, 2020](#); [Salaün, 2020](#)). Attendees returned to their home countries where they continued to transmit. This generated many secondary cases internationally as well as locally. However, it is clear from smaller “first-generation” clusters, which our analysis focuses on, that these settings provide ideal conditions for transmission: we found 7/16 identified religious clusters had 10 cases or less, whilst 9/16 had 23 or more (see online database <https://bit.ly/3ar39ky> and *Underlying data* ([Leclerc *et al.*, 2020](#)) for more information). The number of cases in each cluster is an approximation, and little is known about the number of index cases in these religious meetings to begin with, with the exception of the South Korea cluster. Religious events are well known sources of heightened transmission; there is a focus on vaccination recommendations for attendees to the annual Hajj pilgrimage for example, which is currently being postponed for 2020 ([Aljazeera, 2020](#)).

Worker dormitories have been recognised as key places linked to transmission in Singapore, with 893 out of 942 new cases recorded on April 18th being residents in such dormitories ([Asia, 2020](#)). We found 21 reported clusters, one of which had the second largest cluster size of all the events we report here; 797 cases which from the data we believe is a first-generation cluster. Worker dormitories are similar to households ([Dalling, 2020](#)) in the sense that they are places where people live together and come in frequent close contact; however, the number of residents in dormitories is higher than in most other households. This probably contributes to the higher cluster sizes seen in this setting. Additionally, hygiene facilities can be limited in worker dormitories ([Paul *et al.*, 2020](#)), which could also explain the higher transmission. These points also apply to prisons, another type of large co-habiting setting for which we have identified 4 clusters with a maximum cluster size of 353 cases. It would be beneficial to compare attack rates across households, worker dormitories and prisons, to better understand which factors influence the risk of transmission between people who share a living space. Unfortunately, we were unable to identify the total number of residents in these dormitories and prisons, which prevented us from deriving attack rates and making this comparison.

In addition to religious events and worker homes, we also identified clusters of more than 100 cases in elderly care homes, hospitals and ships. These are all known to be at risk of clusters of infectious disease ([Blanco *et al.*, 2019](#); [Kak, 2015](#); [Lansbury *et al.*, 2017](#)). Moreover, people in these settings are often older than the general population and hence at greater risk of severe forms of COVID-19 disease ([U.S Centers for Disease Control and Prevention, 2020](#)). The increased mortality and likely dependence on availability of personal protective equipment (PPE) mean that healthcare clusters are more politically sensitive and hence more likely to be reported.

A more unexpected setting type is perhaps food processing plants, in which we identified clusters of up to 518 cases ([Cannon, 2020](#)). These plants have been the source of clusters in multiple countries. It is possible that the cold atmosphere in this setting has facilitated the spread of the virus ([Molteni, 2020](#)). Other possible explanations include the close proximity of workers for prolonged periods shared welfare spaces, as well as the need to speak loudly to communicate over the noise of the machines, which could lead to an increased projection of viral particles. Another explanation is that we may not be seeing clusters from other manufacturing settings with similar working environments, as fewer have been in operation due to lockdown guidelines during the pandemic, whereas food production has continued.

We identified seven additional setting types with cluster sizes above 50 or 100 cases (school, sport, bar, shopping, wedding, work and conference), which shared characteristics with the settings described above (see online database for more information <https://bit.ly/3ar39ky> and *Underlying data* ([Leclerc *et al.*, 2020](#))). Notably, sport, bars, shopping areas and conferences are predominantly indoor settings, where people are in close proximity. For conferences and work, like religious events, transmission within the cluster is facilitated by the duration

of the events over several days, as well as the combination of interactions there (workshops, dinners etc...). This can also apply to weddings, where transmission is further increased due to the close-proximity interactions between people (kissing, hugging, dancing etc...). As for bars and shopping areas, these are places with important fluxes of people, which increases the diversity of contacts. Finally, schools, like religious groups, can sometimes represent tightly knit communities which facilitates disease transmission amongst individuals, as was the case with the Salanter Akiba Riverdale school in New York, with a cluster size of at least 60 cases (Ailworth & Berzon (2020)).

The first 100 transmission events & under reporting

The pursuit of the first 100 transmission events revealed little on settings of transmission. This reflects the wider issue we found of under reporting and is likely to reflect the fact that many public health surveillance systems were quickly overwhelmed and could not continue outbreak investigations. An example of this is the UK where only limited information on case follow-up and cluster investigation appears to be available. The impact of such under reporting is that we cannot say with certainty what contribution each setting had to overall transmission – we do not have the denominator information on time and contact in all settings. Nor do we have universal screening for detection of all infections, many of which will be asymptomatic. The importance of such universal testing for infection in interpreting whether transmission has occurred in a setting is highlighted by the difference between the low number of clusters linked to schools and the high level of infection reported in one French high school study (Fontanet *et al.*, 2020).

Further work could pursue data from early investigation of cases where available, to explore the relative importance of different settings to transmission. Importantly, this may counter a bias towards small cluster sizes: with a lack of follow-up only some of the cases actually linked to a setting may be reported and linked. Detailed outbreak investigations should also be explored to get information on the places where transmission is unlikely to have occurred, e.g. if a COVID-19 patient reports 30 contacts at place “A”, “B” and “C”, but only contacts in “C” subsequently become infected this reflects reduced risk in settings “A” and “B”.

Implications for further work

We found that many clusters of cases were linked to indoor settings, but this may be because early spread in China was during their winter, with people naturally spending more time inside close spaces. Increasing evidence suggests that transmission of SARS-CoV-2 can occur via airborne droplets (Morawska & Cao, 2020); however, it is likely that outdoor transmission risk is lower (Nishiura *et al.*, 2020). Further work is needed to clarify this. We found only few clusters in school settings. However, there were many clusters associated with household transmission, and children could be the entry point for the virus into this setting. Although it should be noted in this context that the Report of the WHO-China Joint Mission on Coronavirus Disease 2019

(COVID-19) did not find a single instance where people recalled transmission from a child to an adult (WHO-China Joint Mission Members, 2020). More generally, the role of children in widespread transmission of the virus is unclear, and whether reopening schools could trigger increased introductions of the virus into households and further within-household spread will have to be carefully monitored.

Further investigation of settings that facilitate clusters of transmission could provide important information for containment strategies as countries lift some of the current restrictions. Previous work has suggested that there might be considerable heterogeneity in individual transmission, which would imply a disproportionate impact from preventing large transmission events from occurring (Endo *et al.*, 2020). Whilst widespread contact tracing is often considered part of future containment strategies, there is a need for this to be complemented with retrospective investigation of clusters in order to better understand the extent to which certain settings and behaviours are at particular risk of generating clusters of transmission. This could, in turn, inform contact tracing efforts and might be particularly relevant in the context of contact tracing using mobile phone apps, which has recently been suggested in support of more traditional contact tracing (Ferretti *et al.*, 2020). For example, past co-location in certain settings could be a trigger for notification of risk from an app instead of, or in addition to, individual contacts.

Online database of collected reports

The online database (accessible at <https://bit.ly/3ar39ky>) provides information on all collected reports, references and information on cluster sizes as well as notes about the study. This database will be kept as a static source linked to this report, but with an additional tab for newly reported settings. Readers can submit information in the “Suggested updates” tab and we will aim to update information if evidence for substantial new clusters are found linked to a setting that was not in this study.

Conclusions

In conclusion, we found evidence of SARS-CoV-2 transmission in many types of settings. Our results provide a basis to identify possible places that are linked to clusters of cases and could be closely monitored, for example by linking to app-based contact tracing, and/or remain closed in the first instance following the progressive removal of lockdown restrictions. However, reporting should be improved in the majority of settings, with implementation of systematic reporting on the number of potentially exposed individuals and the number of confirmed and suspected cases from these settings, to allow the estimation of attack rates.

Data availability

Underlying data

Figshare: COVID19 settings of transmission - collected reports database. <https://doi.org/10.6084/m9.figshare.12173343.v3> (Leclerc *et al.*, 2020).

This project contains 'COVID-19 settings of transmission - database.xlsx', which contains the data extracted from the initial search, as well as an updated version of the dataset from 26/05/2020.

Up to date information on all collected reports is provided in an open-access online database (accessible at <https://bit.ly/3ar39ky>).

This database provides references and information on cluster sizes as well as notes about the studies.

Data are available under the terms of the [Creative Commons Zero "No rights reserved" data waiver](#) (CC0 1.0 Public domain dedication).

Acknowledgments

We would like to thank Dr Joël Mossong for his review of our article. We would also like to thank all the anonymous individuals who suggested updates for transmission events in our online database.

The members of the LSHTM CMMID COVID-19 working group are: Graham Medley, Kevin van Zandvoort, Rein M G J Houben, Fiona Yueqian Sun, Jon C Emery, Simon R Procter, James D Munday, Hamish P Gibbs, Arminder K Deol, Mark Jit, Adam J Kucharski, Nikos I Bosse, Damien C Tully, W John Edmunds, Stefan Flasche, Christopher I Jarvis, Anna M Foss, Kathleen O'Reilly, Thibaut Jombart, Kiesha Prem, Nicholas G. Davies, Julian Villabona-Arenas, Yang Liu, Alicia Rosello, Sam Abbott, Billy J Quilty, Joel Hellewell, Petra Klepac, Carl A B Pearson, Timothy W Russell, Charlie Diamond, Rosalind M Eggo, Eleanor M Rees, Amy Gimma, Samuel Clifford, Akira Endo, Stéphane Hué, Megan Auzenberg, Katherine E. Atkins, Emily S Nightingale, Sophie R Meakin.

LSHTM CMMID COVID-19 working group funding statements: Graham Medley (Gates (OPP1184344)), Kevin van Zandvoort

(Elrha's Research for Health in Humanitarian Crises (R2HC) Programme), Rein M G J Houben (European Research Council Starting Grant (Action Number #757699)), Fiona Yueqian Sun (NIHR EPIC grant (16/137/109)), Jon C Emery (European Research Council Starting Grant (Action Number #757699)), Simon R Procter (Gates (OPP1180644)), James D Munday (Wellcome Trust (210758/Z/18/Z)), Hamish P Gibbs (NIHR (ITCRZ 03010)), Mark Jit (Gates (INV-003174), NIHR (16/137/109), European Commission (101003688)), Adam J Kucharski (Wellcome Trust (206250/Z/17/Z)), Nikos I Bosse (Wellcome Trust (210758/Z/18/Z)), W John Edmunds (European Commission (101003688)), Stefan Flasche (Wellcome Trust (grant: 208812/Z/17/Z)), Christopher I Jarvis (RCUK/ESRC (ES/P010873/1)), Kathleen O'Reilly (Gates (OPP1191821)), Thibaut Jombart (RCUK/ESRC (ES/P010873/1); UK PH RST; NIHR HPRU Modelling Methodology), Kiesha Prem (Gates (INV-003174), European Commission (101003688)), Nicholas G. Davies (NIHR (HPRU-2012-10096)), Julian Villabona-Arenas (European Research Council Starting Grant (Action Number #757688)), Yang Liu (Gates (INV-003174), NIHR (16/137/109), European Commission (101003688)), Alicia Rosello (NIHR (PR-OD-1017-20002)), Sam Abbott (Wellcome Trust (210758/Z/18/Z)), Billy J Quilty (NIHR (16/137/109)), Joel Hellewell (Wellcome Trust (210758/Z/18/Z)), Petra Klepac (Gates (INV-003174), European Commission (101003688)), Carl A B Pearson (Gates (OPP1184344)), Timothy W Russell (Wellcome Trust (206250/Z/17/Z)), Charlie Diamond (NIHR (16/137/109)), Rosalind M Eggo (HDR UK (MR/S003975/1), MRC (MC_PC 19065)), Eleanor M Rees (MRC LID Training Program studentship (MR/N013638/1)), Amy Gimma (RCUK/ESRC (ES/P010873/1)), Samuel Clifford (Wellcome Trust (208812/Z/17/Z)), Akira Endo (The Nakajima Foundation, The Alan Turing Institute), Megan Auzenberg (Gates (OPP1191821)), Katherine E. Atkins (European Research Council Starting Grant (Action Number #757688)), Emily S Nightingale (Gates (OPP1183986)), Sophie R Meakin (Wellcome Trust (210758/Z/18/Z)).

References

Ailworth E, Berzon A: **How Coronavirus Invaded One New York Community: 'We Weren't Expecting It to Be Ground Zero'**. 2020.

[Reference Source](#)

Aljazeera: **Saudi tells Muslims to wait on Hajj plans amid coronavirus crisis**. 2020.

[Reference Source](#)

Ananthakrishna A, Sipalan J: **How mass pilgrimage at Malaysian mosque became coronavirus hotspot**. 2020.

[Reference Source](#)

Asia CN: **Daily high of 942 new COVID-19 cases reported in Singapore**. 2020.

[Reference Source](#)

BBC: **Coronavirus: Search for hundreds of people after Delhi prayer meeting**. 2020.

[Reference Source](#)

Blanco N, O'Hara LM, Harris AD: **Transmission pathways of multidrug-resistant organisms in the hospital setting: a scoping review**. *Infect Control Hosp Epidemiol.* 2019; **40**(4): 447–456.

[PubMed Abstract](#) | [Publisher Full Text](#) | [Free Full Text](#)

Cannon A: **Spike in COVID-19 cases in Iowa packing plants a big part of 389**

new cases, state's largest single-day increase. 2020.

[Reference Source](#)

Dalling R: **Stereophones heavily criticised for not cancelling their gig in Cardiff**. 2020.

[Reference Source](#)

Data Against COVID19 SG: **Dashboard of the COVID-19 Virus Outbreak in Singapore**. 2020.

[Reference Source](#)

Endo A, Abbott S, Kucharski AJ, *et al.*: **Estimating the overdispersion in COVID-19 transmission using outbreak sizes outside China [version 1; peer review: 1 approved, 1 approved with reservations]**. *Wellcome Open Res.* 2020; **5**.

[Publisher Full Text](#)

European Centre for Disease Prevention and Control: **Situation update worldwide, as of 21 April 2020**. 2020.

[Reference Source](#)

Ferretti L, Wymant C, Kendall M, *et al.*: **Quantifying SARS-CoV-2 transmission suggests epidemic control with digital contact tracing**. *Science.* 2020; pii: eabb6936.

[PubMed Abstract](#) | [Publisher Full Text](#) | [Free Full Text](#)

Fontanet A, Tondeur L, Madec Y, *et al.*: **Cluster of COVID-19 in northern France: A retrospective closed cohort study.** *medRxiv.* 2020.

[Publisher Full Text](#)

Gudbjartsson DF, Helgason A, Jonsson H, *et al.*: **Spread of SARS-CoV-2 in the Icelandic Population.** *N Engl J Med.* 2020.

[PubMed Abstract](#) | [Publisher Full Text](#) | [Free Full Text](#)

He X, Lau EHY, Wu P, *et al.*: **Temporal dynamics in viral shedding and transmissibility of COVID-19.** *Nat Med.* 2020.

[PubMed Abstract](#) | [Publisher Full Text](#)

Hope R: **Coronavirus: Champions League match a 'biological bomb' that infected Bergamo, experts say.** 2020.

[Reference Source](#)

Jones S: **How coronavirus took just weeks to overwhelm Spain.** 2020.

[Reference Source](#)

Kak V: **Infections on Cruise Ships.** *Microbiol Spectr.* 2015; 3(4).

[PubMed Abstract](#) | [Publisher Full Text](#)

Korean Centre for Disease Control & Prevention: **Investigation of COVID-19 outbreaks through Zumba dance classes in Korea.** 2020.

[Reference Source](#)

Lansbury LE, Brown CS, Nguyen-Van-Tam JS: **Influenza in long-term care facilities.** *Influenza Other Res.* 2017; 11(5): 356–366.

[PubMed Abstract](#) | [Publisher Full Text](#) | [Free Full Text](#)

Lavezzo E, Franchin E, Ciavarella C, *et al.*: **Suppression of COVID-19 outbreak in the municipality of Vo, Italy.** *medRxiv.* 2020.

[Publisher Full Text](#)

Leclerc QJ, Fuller NM, Knight LE, *et al.*: **COVID19 settings of transmission - collected reports database.** *Figshare.* Dataset. 2020.

<http://www.doi.org/10.6084/m9.figshare.12173343.v3>

Liu Y, Eggo RM, Kucharski AJ: **Secondary attack rate and superspreading events for SARS-CoV-2.** *Lancet.* 2020; 395(10227): e47.

[PubMed Abstract](#) | [Publisher Full Text](#) | [Free Full Text](#)

Marcelo P, O'Brien M: **Cluster of Coronavirus Cases Tied to U.S. Biotech Meeting.** 2020.

[Reference Source](#)

Ministry of Health – New Zealand: **COVID-19 – Significant clusters,** 2020.

[Reference Source](#)

Ministry of Health - Singapore: **16 More Cases Discharged; 35 New Cases Of Covid-19 Infection Confirmed.** 2020.

[Reference Source](#)

Molteni M: **Why Meatpacking Plants Have Become Covid-19 Hot Spots.** 2020.

[Reference Source](#)

Morawska L, Cao J: **Airborne transmission of SARS-CoV-2: The world should face the reality.** *Environ Int.* 2020; 139: 105730.

[PubMed Abstract](#) | [Publisher Full Text](#) | [Free Full Text](#)

Nishiura H, Oshitani H, Kobayashi T, *et al.*: **Closed environments facilitate secondary transmission of coronavirus disease 2019 (COVID-19).** *medRxiv.* 2020.

[Publisher Full Text](#)

Park SY, Kim YM, Yi S, *et al.*: **Early Release-Coronavirus Disease Outbreak in Call Center, South Korea.** *Emerg Infect Dis.* 2020; 26(8).

[Publisher Full Text](#)

Paul R, Koustav S, Aradhana A: **The S11 dormitory: inside Singapore's biggest coronavirus cluster.** 2020.

[Reference Source](#)

Roan D: **Coronavirus: Liverpool v Atletico Madrid virus link an 'interesting hypothesis'.** 2020.

[Reference Source](#)

Salaün T: **Special Report: Five days of worship that set a virus time bomb in France.** 2020.

[Reference Source](#)

Shin Y, Berkowitz B, Kim MJ: **How a South Korean church helped fuel the spread of the coronavirus.** 2020.

[Reference Source](#)

Sim W: **Japan identifies 15 clusters as Covid-19 cases mount.** 2020.

[Reference Source](#)

Spencer EA, Brassey J, Mahtani K: **Recall bias.** 2017.

[Reference Source](#)

U.S Centers for Disease Control and Prevention: **People Who Are at Higher Risk for Severe Illness.** 2020.

[Reference Source](#)

WHO-China Joint Mission Members: **Report of the WHO-China Joint Mission on Coronavirus Disease 2019 (COVID-19).** World Health Organization. 2020.

[Reference Source](#)

Wood G, Carroll R: **Cheltenham faces criticism after racegoers suffer Covid-19 symptoms.** 2020.

[Reference Source](#)

Open Peer Review

Current Peer Review Status:  

Version 2

Reviewer Report 30 June 2020

<https://doi.org/10.21956/wellcomeopenres.17583.r39003>

© 2020 Scarpino S. This is an open access peer review report distributed under the terms of the [Creative Commons Attribution License](#), which permits unrestricted use, distribution, and reproduction in any medium, provided the original work is properly cited.



Samuel V. Scarpino 

Network Science Institute, Northeastern University, Boston, MA, USA

In this manuscript, the authors conduct a thorough literature review and identified SARS-CoV-2 transmission clusters. After assembling their data set, the authors discuss the possible similarities in settings associated with transmission. As stated, understanding how transmission risk varies across settings is critical for the safe relaxation of measures implemented to control the spread of COVID-19.

This paper provides a valuable resource and synthesis of what is currently known. I should note that this article has already been evaluated and I believe the authors have adequately addressed the points raised by the previous reviewer. However, I do have a few additional comments/questions, which I hope the authors find constructive.

1. While Google Sheets is a convenient tool for entering and sharing small data sets, it is not "permanent" and also has the potential to be corrupted or heavily modified. There is also no easy way for authors to cite the "version" of the sheet used. The authors do provide a Figshare, but that appears to date back prior to the revised version. I would strongly suggest regularly archiving a version of the data set and assigning each update a version number. At a minimum, please provide a DOI for the revised data set.
2. I am concerned that one reason we don't see more evidence for transmission at schools is that schools were closed early in nearly all locations. To my knowledge, Sweden is not reporting data on whether there have been significant transmission in their schools (as the authors know not all of which are open). I believe the authors should provide a strong disclaimer, either in the abstract or early in the discussion that we really don't have much to go on w.r.t. schools. (Of course this is my opinion and likely subject to debate).
3. The authors state, "More generally, the role of children in widespread transmission of the virus is unclear, and whether reopening schools could trigger increased introductions of the virus into households and further within-household spread will have to be carefully monitored." But, I also feel that given the uncertainty in whether children are import for ongoing transmission, there are other settings we should caveat.

4. The authors note that they, "use peer reviewed articles as a quality threshold," and, while I strongly disagree with the exclusion of pre-prints, I think the authors should at least provide some information on how many studies or clusters were excluded. Given the long (and increasing lag) between pre-print and publication, is this study missing half of all clusters that are currently published or in-review? 10% 95%? Providing information around what's been excluded is standard practice for such reviews and feels critical in this case.

Is the work clearly and accurately presented and does it cite the current literature?

Yes

Is the study design appropriate and is the work technically sound?

Partly

Are sufficient details of methods and analysis provided to allow replication by others?

Partly

If applicable, is the statistical analysis and its interpretation appropriate?

Not applicable

Are all the source data underlying the results available to ensure full reproducibility?

Partly

Are the conclusions drawn adequately supported by the results?

Yes

Competing Interests: No competing interests were disclosed.

Reviewer Expertise: Epidemiology

I confirm that I have read this submission and believe that I have an appropriate level of expertise to confirm that it is of an acceptable scientific standard.

Reviewer Report 05 June 2020

<https://doi.org/10.21956/wellcomeopenres.17583.r38985>

© 2020 Mossong J. This is an open access peer review report distributed under the terms of the [Creative Commons Attribution License](#), which permits unrestricted use, distribution, and reproduction in any medium, provided the original work is properly cited.



Joël Mossong 

Epidemiology and Microbial Genomics, Laboratoire National de Santé, Dudelange, Luxembourg

My comments and suggestions have been adequately addressed.

Is the work clearly and accurately presented and does it cite the current literature?

Yes

Is the study design appropriate and is the work technically sound?

Yes

Are sufficient details of methods and analysis provided to allow replication by others?

Yes

If applicable, is the statistical analysis and its interpretation appropriate?

Yes

Are all the source data underlying the results available to ensure full reproducibility?

Yes

Are the conclusions drawn adequately supported by the results?

Yes

Competing Interests: No competing interests were disclosed.

Reviewer Expertise: Epidemiology of infectious diseases

I confirm that I have read this submission and believe that I have an appropriate level of expertise to confirm that it is of an acceptable scientific standard.

Version 1

Reviewer Report 18 May 2020

<https://doi.org/10.21956/wellcomeopenres.17429.r38734>

© 2020 Mossong J. This is an open access peer review report distributed under the terms of the [Creative Commons Attribution License](#), which permits unrestricted use, distribution, and reproduction in any medium, provided the original work is properly cited.



Joël Mossong

Epidemiology and Microbial Genomics, Laboratoire National de Santé, Dudelange, Luxembourg

This manuscript aims to provide a descriptive analysis of transmission settings of Covid19 based on published articles or media reports, which is of major interest for controlling the epidemic.

I have several major concerns:

1. Most settings reported herein are not representative of settings from a global perspective, most are from the initial epidemic in Asia (mainly from the Singapore dashboard and <20% of settings in the manuscript are outside of Asia). This needs to be added to the discussion as a major limitation.
2. Some important and widely reported outbreaks in particular settings are missing. e.g. the outbreak of the megachurch in Mulhouse France (<https://www.dailymail.co.uk/news/article-8168819/French-megachurch-meeting-blamed-sparking->) and the Ruby Princess outbreak (reported in

<https://www1.health.gov.au/internet/main/publishing.nsf/Content/1D03BCB527F40C8BCA258503C1>) or the cluster in the french ski resort (<https://www.bbc.com/news/uk-51425702>). This somehow questions the completeness of the systematic review. The authors could have widened their search terms to include the settings (church, ship, etc.) and outbreak when searching media reports.

3. Given that this manuscript from a team in the UK, it is surprising that only 4 outbreak settings were reported for the UK. The authors need to discuss why they were not able to find more reports from the local and national media outlets in English speaking countries like UK, Ireland, and possibly also Australia, Canada and the US.
4. The authors should discuss reasons for under reporting: public health surveillance systems in many countries were quickly overwhelmed to investigate transmission settings and chains of transmissions. Transmission clusters in elderly care and hospitals homes due to political sensitivity, linked to increased mortality, lack of adequate PPE equipment
5. Meat factories and slaughter houses have recently emerged as high risk setting in the US (<https://edition.cnn.com/2020/04/08/business/meat-plant-closures-coronavirus/index.html>) and Germany (<https://www.dw.com/en/coronavirus-breaks-out-in-third-german-slaughterhouse/a-53389860>). This setting should be included separately in Table 1.

Minor comments:

1. Add the sum of cases for all clusters per setting in table 1.
2. p.3.& p. 7 "the first 100 transmission events". While this is an interesting concept, it isn't really being addressed in this article. No country presented herein has collected more than 100 events. The paragraph in the discussion on this seems therefore irrelevant and could be deleted.
3. p. 7. The authors mention that there is increasing evidence for airborne transmission. The current consensus is that most transmission occurs via airborne droplets, which is different to aerosol transmission. I suggest to replace "be airborne" by "occur via airborne droplets".

References

1. COVID-19, Australia: Epidemiology Report 9: Reporting week ending 23:59 AEDT 29 March 2020. *COVID-19 National Incident Room Surveillance Team*. 2020. [Publisher Full Text](#) | [Reference Source](#)

Is the work clearly and accurately presented and does it cite the current literature?

Yes

Is the study design appropriate and is the work technically sound?

Partly

Are sufficient details of methods and analysis provided to allow replication by others?

Yes

If applicable, is the statistical analysis and its interpretation appropriate?

Yes

Are all the source data underlying the results available to ensure full reproducibility?

Yes

Are the conclusions drawn adequately supported by the results?

Partly

Competing Interests: No competing interests were disclosed.

Reviewer Expertise: Epidemiology of infectious diseases

I confirm that I have read this submission and believe that I have an appropriate level of expertise to confirm that it is of an acceptable scientific standard, however I have significant reservations, as outlined above.

Author Response 01 Jun 2020

Quentin Leclerc, London School of Hygiene & Tropical Medicine, London, UK

This manuscript aims to provide a descriptive analysis of transmission settings of Covid19 based on published articles or media reports, which is of major interest for controlling the epidemic.

Thank you for taking the time to review our article. Please note that we have now updated our analysis to include an additional 49 transmission events (201 events total) and 4 new settings type ("Food processing plant", "Prison", "Transport" and "Wedding"; 22 setting types total). Some of these new elements overlap with your suggestions. Our Discussion section has also been updated to reflect these new results.

I have several major concerns:

- 1. Most settings reported herein are not representative of settings from a global perspective, most are from the initial epidemic in Asia (mainly from the Singapore dashboard and <20% of settings in the manuscript are outside of Asia). This needs to be added to the discussion as a major limitation.**

Thank you for raising this point. We already mentioned in the Discussion - Limitations section that many studies originated from the early outbreak in China, but have included an additional sentence there to clarify that this could prevent our results from being directly applicable to other countries. That said, please note that in our updated analysis, 98/201 (50%) events are from China and Singapore, compared to 92/152 (60%) in our original analysis, which improves the coverage of our results.

The added sentence is "The settings we identified here therefore might not be representative of settings from a global perspective."

- 1. Some important and widely reported outbreaks in particular settings are missing. e.g. the outbreak of the megachurch in Mulhouse France (<https://www.dailymail.co.uk/news/article-8168819/French-megachurch-meeting-blamed>) and the Ruby Princess outbreak (reported in <https://www1.health.gov.au/internet/main/publishing.nsf/Content/1D03BCB527F40C8BC> or the cluster in the french ski resort (<https://www.bbc.com/news/uk-51425702>). This somehow questions the completeness of the systematic review. The authors could have widened their search terms to include the settings (church, ship, etc.) and outbreak when searching media reports.**

Thank you for suggesting these additional clusters; we have now added the Ruby Princess and the French ski resort events.

Our initial analysis was focused on trying to find distinct *settings* in which transmission had occurred. Hence we were initially trying to prioritise examples of new *settings* linked to clusters rather than gathering all data on all outbreaks linked to all settings. This has changed somewhat with the open source database and we are happy to act as a gathering point for cluster data. For the outbreak in Mulhouse, this falls into the category of events that we do not include in our analysis. This because we are interested in understanding transmission only within specific settings; for example, for a cruise ship, the cluster size we report corresponds to the number of people infected on that ship only, not the people that these might have infected after disembarking. If we included people infected by passengers after disembarking, this would not reflect the “cruise ship” setting, as this additional transmission could occur in a variety of other settings (household, meal etc...).

We had already highlighted this in the Methods – Outline section, but have now repeated that point at the beginning of the Discussion to hopefully make this distinction clearer (“Note that we restrict cluster size to only include individuals infected within a specific setting, and exclude secondary infections which occurred outside the settings.”)

1. **Given that this manuscript from a team in the UK, it is surprising that only 4 outbreak settings were reported for the UK. The authors need to discuss why they were not able to find more reports from the local and national media outlets in English speaking countries like UK, Ireland, and possibly also Australia, Canada and the US.**

Our initial search was at the end of March. At that time, the number of confirmed cases in the UK was around 20,000, compared to more than 200,000 now. Therefore, there was little information at the time on clusters in these countries compared with Asia, which is why we were less likely to find media reports on that topic for the UK. For similar reasons, we had little information for English-speaking countries. In addition, because of the lack of widespread testing in the UK and/or follow-up of cases, information on clusters does not appear to be widely available in the UK. As of 26/05/2020, we have now identified 39 transmission events in English-speaking countries (19% of all the transmission events we have identified so far). Therefore, our updated analysis is more geographically balanced.

1. **The authors should discuss reasons for under reporting: public health surveillance systems in many countries were quickly overwhelmed to investigate transmission settings and chains of transmissions. Transmission clusters in elderly care and hospitals homes due to political sensitivity, linked to increased mortality, lack of adequate PPE equipment**

Thank you for this suggestion. In line with your comments on the “first 100 transmission events” we have adapted the paragraph in the discussion to discuss reasons for under reporting.

We have also added a sentence to the paragraph on healthcare clusters in the discussion to reflect the likely increased reporting of clusters linked to these settings due to political sensitivity.

1. **Meat factories and slaughter houses have recently emerged as high risk setting in the US**
<https://edition.cnn.com/2020/04/08/business/meat-plant-closures-coronavirus/index.html>
and Germany
<https://www.dw.com/en/coronavirus-breaks-out-in-third-german-slaughterhouse/a-5336161>
This setting should be included separately in Table 1.

Thank you for raising this point. Our online database had been updated to reflect this, and we have now added the “Food processing plant” setting type in our analysis, and comment on this in the Results and Discussion sections of our article.

This also applies to our new “Prison”, “Transport” and “Wedding” setting types.

Minor comments:

1. **Add the sum of cases for all clusters per setting in table 1.**

We have now implemented this suggestion in the revised article.

1. **p.3.& p. 7 "the first 100 transmission events". While this is an interesting concept, it isn't really being addressed in this article. No country presented herein has collected more than 100 events. The paragraph in the discussion on this seems therefore irrelevant and could be deleted.**

We agree it was frustrating not to find this data, which would have been an interesting angle, giving us “denominator” information. In line with the comments above we have adapted this paragraph to link to under reporting.

1. **p. 7. The authors mention that there is increasing evidence for airborne transmission. The current consensus is that most transmission occurs via airborne droplets, which is different to aerosol transmission. I suggest to replace "be airborne" by "occur via airborne droplets".**

Thank you for this suggestion, we have now rephrased this accordingly.

Competing Interests: No competing interests were disclosed.

Comments on this article

Version 2

Reader Comment 23 Jun 2020

Barney Duncan, Ex-Wellcome Biotechnology Ltd, Abermaw, Gwynedd, UK

Back in the 1980's Wellcome Biotechnology Ltd (owned & operated by the Wellcome Trust) expended much effort in trying to eliminate the use of blood fractions from nutrient media used for growing and maintenance of animal & human cell lines prior to inoculation with virus in the making of rabies and foot & mouth disease vaccines as well as interferon. At the time, it was found that without blood, cell growth and virus titres were poorer.

I have recently observed locally in North Wales 2 major clusters from the 2 Sisters Poultry processing plant on Anglesey and a meat processing plant in Wrexham. This caused me to look further into commonality of Covid outbreaks in other meat processing plants. It resulted in me coming across your paper.

I am mindful of the fact that the first outbreak was traced back to a food market in Wuhan China. The *coronavirus* likely jumped to people in a wet *market* there where meat, seafood, and live animals were handled.

I believe there may be real significance in the quantities of blood on workers overalls and working surfaces in slaughterhouses & meat processing factories. Blood deposits would surely provide a site where virus impregnated droplets from an infected worker could act as inoculum and allow virus to replicate rapidly

In consequence of these facts I would suggest the following recommendations for the next update

- 1 Add wet/cattle markets to the transmission settings list
- 2 Split food processing plant into two fractions meat and non-meat

Thank you to all participants/contributors to your paper. It is most creditable & worthwhile and I believe will prove most valuable line of research.

Barney Duncan
Chemical Engineer (ret'd)

Competing Interests: None unless you consider being a Wellcome pensioner influences my judgement but I'm sure Bill Castell (former CEO of Wellcome Biotechnology and Chairman of Wellcome Trust) could & would readily dispel any such notions !

Reader Comment 08 Jun 2020

David Henry, Bond University, Gold Coast, Queensland, Australia

This is an important topic. I am concerned about your search. I may have missed it, but I think having done this scoping exercise that you should rerun your searches with specific terms (and synonyms) for the settings of interests: schools churches, weddings, meatworks (lots of synonyms) etc. I am guessing that you will get a lot more hits. I don't think that 'transmission cluster' is a sufficiently sensitive term. I'd also like to see a PRISMA flow diagram.

Competing Interests: None

Version 1

Reader Comment 21 May 2020

María Margarita Ronderos Torres, Independent Consultant in Epidemiology, Colombia

I would like to draw to your attention the football match between Atalanta from Bergamo and Valencia from Spain on the 19th Feb at the San Siro Stadium in Milan. Aprox 40,000 fans from the Region attended the match. 35% of the Valencia team delegation when returning to Spain tested positive for COVID19. The region only went into lockdown on the 4th of March. This gave ample time (1.5 t 2 incubation periods) for household transmission with high intergeneration mix and known high elderly population. Further study is needed but this could be very well explain the explosion of cases that followed and is in line with your proposed explanation for super spread of the virus.

Competing Interests: NO competing interests



Since January 2020 Elsevier has created a COVID-19 resource centre with free information in English and Mandarin on the novel coronavirus COVID-19. The COVID-19 resource centre is hosted on Elsevier Connect, the company's public news and information website.

Elsevier hereby grants permission to make all its COVID-19-related research that is available on the COVID-19 resource centre - including this research content - immediately available in PubMed Central and other publicly funded repositories, such as the WHO COVID database with rights for unrestricted research re-use and analyses in any form or by any means with acknowledgement of the original source. These permissions are granted for free by Elsevier for as long as the COVID-19 resource centre remains active.

Household transmission of SARS-CoV-2 and risk factors for susceptibility and infectivity in Wuhan: a retrospective observational study



Fang Li*, Yuan-Yuan Li*, Ming-Jin Liu*, Li-Qun Fang, Natalie E Dean, Gary W K Wong, Xiao-Bing Yang, Ira Longini, M Elizabeth Halloran, Huai-Ji Wang, Pu-Lin Liu, Yan-Hui Pang, Ya-Qiong Yan, Su Liu, Wei Xia, Xiao-Xia Lu, Qi Liu, Yang Yang, Shun-Qing Xu

Summary

Background Wuhan was the first epicentre of COVID-19 in the world, accounting for 80% of cases in China during the first wave. We aimed to assess household transmissibility of severe acute respiratory syndrome coronavirus 2 (SARS-CoV-2) and risk factors associated with infectivity and susceptibility to infection in Wuhan.

Methods This retrospective cohort study included the households of all laboratory-confirmed or clinically confirmed COVID-19 cases and laboratory-confirmed asymptomatic SARS-CoV-2 infections identified by the Wuhan Center for Disease Control and Prevention between Dec 2, 2019, and April 18, 2020. We defined households as groups of family members and close relatives who did not necessarily live at the same address and considered households that shared common contacts as epidemiologically linked. We used a statistical transmission model to estimate household secondary attack rates and to quantify risk factors associated with infectivity and susceptibility to infection, accounting for individual-level exposure history. We assessed how intervention policies affected the household reproductive number, defined as the mean number of household contacts a case can infect.

Findings 27 101 households with 29 578 primary cases and 57 581 household contacts were identified. The secondary attack rate estimated with the transmission model was 15.6% (95% CI 15.2–16.0), assuming a mean incubation period of 5 days and a maximum infectious period of 22 days. Individuals aged 60 years or older were at a higher risk of infection with SARS-CoV-2 than all other age groups. Infants aged 0–1 years were significantly more likely to be infected than children aged 2–5 years (odds ratio [OR] 2.20, 95% CI 1.40–3.44) and children aged 6–12 years (1.53, 1.01–2.34). Given the same exposure time, children and adolescents younger than 20 years of age were more likely to infect others than were adults aged 60 years or older (1.58, 1.28–1.95). Asymptomatic individuals were much less likely to infect others than were symptomatic cases (0.21, 0.14–0.31). Symptomatic cases were more likely to infect others before symptom onset than after (1.42, 1.30–1.55). After mass isolation of cases, quarantine of household contacts, and restriction of movement policies were implemented, household reproductive numbers declined by 52% among primary cases (from 0.25 [95% CI 0.24–0.26] to 0.12 [0.10–0.13]) and by 63% among secondary cases (from 0.17 [0.16–0.18] to 0.063 [0.057–0.070]).

Interpretation Within households, children and adolescents were less susceptible to SARS-CoV-2 infection but were more infectious than older individuals. Presymptomatic cases were more infectious and individuals with asymptomatic infection less infectious than symptomatic cases. These findings have implications for devising interventions for blocking household transmission of SARS-CoV-2, such as timely vaccination of eligible children once resources become available.

Funding National Natural Science Foundation of China, Fundamental Research Funds for the Central Universities, US National Institutes of Health, and US National Science Foundation.

Copyright © 2021 Elsevier Ltd. All rights reserved.

Introduction

About a year into the COVID-19 pandemic, the global cumulative incidence of cases is still climbing, reaching more than 83.6 million as of Jan 1, 2021.¹ The resumption of economic activities depends on our understanding of important transmission venues such as households, workplaces, and schools for severe acute respiratory syndrome coronavirus 2 (SARS-CoV-2), drivers of transmission, and availability of effective control measures. Households are major transmission

venues for many respiratory pathogens. The WHO-China Joint Mission on Coronavirus Disease 2019 (COVID-19) suggested that most epidemiologically linked clusters in China were households and urged prioritisation of studies on risk factors for household transmission.² In resource-limited areas, including Wuhan in China early on in the epidemic, isolation of cases and quarantine of close contacts often occurred at home, enabling onwards transmission within households. Although children are less likely to develop

Lancet Infect Dis 2021;
21: 617–28

Published Online
January 18, 2021
[https://doi.org/10.1016/S1473-3099\(20\)30981-6](https://doi.org/10.1016/S1473-3099(20)30981-6)

For the Chinese translation of the abstract see Online for appendix 1

*Contributed equally

Wuhan Center for Disease Control and Prevention, Wuhan, Hubei, China (F Li MS, X-B Yang PhD, H-J Wang MS, P-L Liu PhD, Y-H Pang MS, Y-Q Yan PhD, S Liu MS); School of Public Health (Y-Y Li PhD, W Xia PhD, Q Liu MS, S-Q Xu PhD) and Department of Respiratory Medicine, Wuhan Children's Hospital (X-X Lu PhD), Tongji Medical College, Huazhong University of Science and Technology, Wuhan, Hubei, China; Department of Biostatistics, College of Public Health and Health Professions & Emerging Pathogens Institute, University of Florida, Gainesville, FL, USA (M-J Liu BS, N E Dean PhD, I Longini PhD, Y Yang PhD); State Key Laboratory of Pathogen and Biosecurity, Beijing Institute of Microbiology and Epidemiology, Beijing, China (L-Q Fang PhD); Department of Pediatrics, Faculty of Medicine, Chinese University of Hong Kong, Hong Kong Special Administrative Region, China (W K Wong MD); Vaccine and Infectious Diseases Division, Fred Hutchinson Cancer Research Center, Seattle, WA, USA (M E Halloran DSc); Department of Biostatistics, University of Washington, Seattle, WA, USA (M E Halloran)

Correspondence to:
Dr Shun-Qing Xu, School of Public Health, Tongji Medical College, Huazhong University of Science and Technology, Wuhan, Hubei 430030, China
xust@hust.edu.cn

or

Dr Yang Yang, Department of Biostatistics, College of Public Health and Health Professions & Emerging Pathogens Institute, University of Florida, Gainesville, FL 32611, USA
yangyang@ufl.edu

Research in context

Evidence before this study

Households offer an ideal setting for assessing person-to-person transmissibility of severe acute respiratory syndrome coronavirus 2 (SARS-CoV-2) and risk factors for infectivity and susceptibility to infection. We searched PubMed and medRxiv for articles published between Dec 1, 2019, and Aug 20, 2020, using the search terms ("COVID-19" OR "SARS-CoV-2" OR "2019-nCoV") AND ("household" OR "family") AND ("transmissibility" OR "risk factors"). We identified 22 relevant articles. Secondary attack rate estimates varied across countries from 4.6% in Taiwan to 31.6% in Zhejiang Province, China, and were mostly based on studies with fewer than 300 households. Some studies found that older age groups were associated with increased susceptibility to infection or disease, and a study in Israel identified infants as a highly susceptible group. A study in Guangzhou found no effect of age on infectivity, probably due to a small sample size. A study in South Korea reported a high infection rate among household contacts of index cases aged 10–19 years old, but not in household contacts of younger index cases. A few studies confirmed efficient presymptomatic transmission of the virus. Two studies reported much lower infectivity of asymptomatic infections than symptomatic cases, with odds ratios of 0.028 and 0.25.

Added value of this study

Based on contact-tracing records from more than 27 000 households in Wuhan up to April 18, we found that

SARS-CoV-2 was transmitted with moderate efficiency within households at the very beginning of the pandemic, with an overall secondary attack rate of 15.6% (95% CI 15.2–16.0). Children and adolescents were less susceptible to infection, but more infectious once infected, than individuals aged 20 years or older. Children's higher infectivity was affected by household size. Our study confirmed higher susceptibility of infants (aged 0–1 years) to infection than older children (≥ 2 years of age). Although children and adolescents were much less likely to have severe disease, they were as likely as adults to develop symptoms. We confirmed the high infectiousness of cases during the incubation period and found asymptomatically infected individuals were about 80% less infectious than symptomatic cases. Finally, we found isolation of cases and quarantining of household contacts away from home effectively reduced household transmission.

Implications of all the available evidence

The high infectivity of children with SARS-CoV-2 infection highlights the need for careful planning of school reopening. Additionally, the susceptibility of infants supports caregivers of infants being prioritised for vaccination. When feasible, cases could be isolated and household contacts quarantined away from their homes to prevent household transmission, particularly when presymptomatic.

severe disease than adults,² their ability to transmit to household contacts is not well characterised, yet it is highly relevant for preventing transmission in schools and households.

Households are ideal settings for assessing transmissibility of a pathogen and associated determinants of susceptibility and infectivity. The household secondary attack rate is defined as the probability that an infected person will transmit the pathogen to a susceptible household member during their infectious period. A meta-analysis estimated the household secondary attack rate for SARS-CoV-2 as approximately 15–22%,³ higher than the estimated rates of 5–10% for SARS-CoV and 1–5% for Middle East respiratory syndrome coronavirus.⁴ Most studies neither distinguished between secondary and tertiary transmissions nor controlled for exposure history. Some household studies revealed that children were less susceptible to the virus than older adults, and that the transmissibility of SARS-CoV-2 was inversely related to household size.^{4–6} Whether infectivity differs by age is less clear,³ in part because when there are coprimary cases within a household, it is not possible to resolve which resulted in secondary infections. The relative importance of the presymptomatic (incubation) period versus the symptomatic period has been noted or quantified in some studies.^{4,7} However, few studies

have assessed the relative infectivity of asymptomatic infections, although some modelling studies have used values extrapolated from viral load data of mild and severe cases.^{3,8,9}

Here, we present an analysis of a large number of households extracted from contact tracing records in Wuhan, the first epicentre of the COVID-19 pandemic, where 80% of confirmed cases in China were reported. We estimated the transmission probability of SARS-CoV-2 within households and evaluated drivers for infectivity of cases and susceptibility of their household contacts, while adjusting for measured confounders and individual-level exposure history. We assessed the infectivity levels of both presymptomatic cases and asymptomatic infections. Finally, we estimated the effectiveness of case isolation and quarantine of household contacts away from home in reducing household transmission in Wuhan.

Methods

Study population

In response to the COVID-19 outbreak, the Wuhan Center for Disease Control and Prevention (CDC) conducted epidemiological investigations to trace the close contacts of ascertained cases, following the Prevention and Control Plan for COVID-19 issued

by the National Health Commission of China.¹⁰ The retrospective cohort analysed here includes all laboratory-confirmed or clinically confirmed cases and laboratory-confirmed asymptomatic infections identified between Dec 2, 2019, and April 18, 2020, in Wuhan, China, together with their household contacts. Data on demographics, clinical symptoms, laboratory test results, and time and location of quarantine or isolation were recorded for all investigated individuals.

Written informed consent was waived by the National Health Commission of China for outbreak investigations of notifiable infectious diseases. All identifiable personal information was removed from the data by Wuhan CDC before any analysis. The study was approved by the ethics committee of Wuhan CDC (WHCDCIRB-K-2020012).

Definitions

COVID-19 cases were defined according to the National Health Commission of China's Guidelines for Diagnosis and Management of COVID-19, with seven editions released over the study period (appendix 2 pp 3–4). Clinically confirmed cases were defined as suspected cases of COVID-19 with typical pneumonia manifestations who were negative for SARS-CoV-2 nucleic acid by real-time RT-PCR. Laboratory-confirmed cases were individuals with positive detection of SARS-CoV-2 nucleic acid by real-time RT-PCR using respiratory specimens, and included asymptomatic infection (appendix 2 p 3). For this study, a household contact of an identified case was broadly defined as a family member or close relative who had unprotected contact with the case within 2 days before the symptom onset or test-positive specimen collection of the case but did not necessarily live at the same address. For each household, the date with the earliest symptom onset (symptomatic infection) or the first test-positive specimen (asymptomatic infection) was designated as day 1. Primary cases were defined as cases (including asymptomatic infections) who had symptom onset or the first test-positive specimens collected on day 1 or day 2, enabling households to have coprimary cases. Later cases were classified as secondary cases.

Statistical analysis

Households that shared common contacts were considered epidemiologically linked and were merged into a single household for all analyses, although we retained the original household size for analyses of household size as a risk factor (appendix 2 pp 7–8). We evaluated the overall household secondary attack rate in the primary analysis but also distinguished individuals who lived at the same address from those who did not in a sensitivity analysis.

Characteristics of primary cases, secondary cases, and uninfected or untested household contacts were compared using the χ^2 test for discrete variables and

Wilcoxon rank sum test for continuous variables. The observed secondary attack rate was calculated as the proportion of secondary infections among all household contacts, assuming untested contacts were uninfected. Total numbers of confirmed COVID-19 cases, proportions of confirmed cases among the population (ie, community-level attack rates), total numbers of contact-traced households, and average observed household secondary attack rates were mapped at the community level in Wuhan using ArcGIS (version 10.2; Esri, Redlands, CA, USA). Population data were obtained from the Hubei Health Statistics and Information Platform. A generalised estimating equation (GEE) regression model with a logistic link function and an exchangeable correlation structure for each household was used to assess individual-level and household-level risk factors for infection of household contacts. Both the observed secondary attack rate and GEE model were restricted to households with a single primary case. Both assumed that all secondary cases were infected by the primary case, and that all household contacts were equally exposed to the primary case. All descriptive analyses and the GEE modelling were done using R (version 3.6.1).

To account for individual-level exposure history and potential tertiary transmission, we also used a chain-binomial transmission model to estimate the secondary attack rate. This model was also used to evaluate determinants of infectivity and susceptibility to infection (appendix 2 pp 11–17). Here, both infectivity and susceptibility refer to a combination of biological effects (eg, immune response or viral shedding) and physical exposure, and our analysis cannot distinguish one mechanism from another. We assumed that each susceptible individual was exposed to any infected household members as well as a non-specific external force of infection, and that two household members had contact with each other when neither was isolated or quarantined at centralised facilities. Households with only primary cases but no exposed household contacts were excluded from the transmission analyses. A Monte Carlo expectation maximisation algorithm was used to account for uncertainties in the infection date of asymptomatic infections (appendix 2 pp 13–14).¹¹ We performed analyses under several plausible assumptions about the distributions of the incubation and infectious periods based on the literature (appendix 2 pp 9–11, 23).^{12,13} We report results assuming a mean incubation period of 5 days and a maximum infectious period of 22 days for the primary analysis. We compared household reproductive numbers, defined as the mean number of household contacts an infectious person can infect, across three time windows—before Jan 24, 2020 (before lockdown), Jan 24–Feb 10 (moderate control), and after Feb 10 (strong control)—to assess the effectiveness of general interventions such as case isolation, quarantine of close

See Online for appendix 2

Panel: Timeline of key control events during the outbreak of COVID-19 in Wuhan, China

Dec 2, 2019

Symptom onset of the earliest case recorded in surveillance.

Dec 30, 2019–Jan 1, 2020

Active case finding began, the National Health Commission and WHO were notified, and Huanan Seafood Market was closed.

Jan 23, 2020

Lockdown of Wuhan was declared. All public transportation within the city and inbound and outbound transportation were suspended.

Jan 24, 2020

Patients with fever were required to self-report to community health-care centres. Individuals with mild symptoms but not identified as suspected cases were told to isolate either at home or in designated facilities. Severe or suspected COVID-19 cases were admitted to hospital.

Feb 2, 2020

The government required district-level centralised isolation and treatment of all confirmed cases, suspected cases, and feverish patients with pneumonia symptoms; quarantine of close contacts of cases at designated facilities; and reporting of asymptomatic infections.

Feb 11–13, 2020

Tightened management of all residential communities and restricted within-community movement were initiated. Communities initiated door-to-door symptom screening.

Feb 20–22, 2020

Body temperature of each resident was monitored twice a day. Discharged patients who had been admitted with COVID-19 were told to isolate for an additional 14 days at home. A 3-day campaign was initiated on Feb 20 to test (real-time PCR) all confirmed cases, suspected cases, feverish individuals, and close contacts of cases.

April 22, 2020

Public ground transportation fully returned to normal.

April 26, 2020

National Health Commission declared no hospitalised cases in Wuhan.

contacts, and restriction of human movement in communities (panel).

From Feb 23, 2020, all household contacts were tested for SARS-CoV-2 regardless of symptom status. Before then, a substantial number of household contacts without symptoms were not tested, creating uncertainty in their infection status. We used a two-step imputation approach with the first step imputing infection status and the second step imputing a time interval that is

informative about the potential infection time of each imputed asymptomatic infection (appendix 2 pp 17–18). The imputation involves regression models based on characteristics of the household contacts, the primary cases, and the household itself that are related to whether asymptomatic household contacts were tested or not and were potentially related to the infection outcome (appendix 2 pp 24–25). For both the GEE analysis and the chain-binomial transmission analysis, the results were averaged over 300 sets of imputed data. Households with members with missing ages were excluded from all age-related analyses.

Role of the funding source

The funder of the study had no role in study design, data collection, data analysis, data interpretation, or writing of the report. All authors had full access to all the data in the study and had final responsibility for the decision to submit for publication.

Results

From Dec 2, 2019, to April 18, 2020, 29 405 households with at least one clinically confirmed or laboratory-confirmed COVID-19 case were identified. After merging epidemiologically linked households, we obtained 27 101 households with 29 578 primary cases, including coprimary cases. These primary cases had 57 581 household contacts, consisting of 10 367 secondary cases, 29 658 test-negative contacts, and 17 556 untested contacts (table 1). The median household size (before merging) was three people (IQR 2–4), and 72.7% (21 385/29 405) of the households had two or three household members. Large households tended to be younger and were more often detected later in the epidemic (appendix 2 p 26). The median age among all cases was 56 years (43–66), and 20 760 (52.0%) cases were female. Age data were missing for 1112 test-negative or untested contacts in 806 households. Primary cases and secondary cases shared similar age and sex profiles (table 1). Compared with uninfected or untested contacts, secondary cases were older, more likely to be female, and more likely to live in smaller households (table 1). Secondary cases were more likely to be laboratory confirmed than primary cases (table 1).

The cases included in this study accounted for 76.7% (39 945/52 070) of all reported cases in Wuhan as of April 18 (appendix 2 p 20). The majority of reported cases had symptom onset between Jan 24 and Feb 10 (table 1). More cases were reported and more infected households were contact traced in densely populated districts in central Wuhan such as Wu-Chang, Jiang-Han, Jiang-An, Qiao-Kou, Han-Yang, and Hong-Shan (figure). The community-level attack rates showed a similar distribution, with higher rates in central Wuhan, but average observed household secondary attack rates were spatially more evenly distributed (figure).

	All cases (n=39 945)	Primary cases (n=29 578)	Secondary cases (n=10 367)	Test-negative or untested contacts* (n=47 214)	p value
Age, years					<0.0001†
Median (IQR)	56 (43–66)	57 (44–66)	55 (39–66)	43 (28–58)	..
<20	908 (2.3%)	413 (1.4%)	495 (4.8%)	7744/46 102 (16.8%)	..
20–59	22 642 (56.7%)	16 892 (57.1%)	5750 (55.5%)	27 749/46 102 (60.2%)	..
≥60	16 395 (41.0%)	12 273 (41.5%)	4122 (39.8%)	10 609/46 102 (23.0%)	..
Sex					<0.0001†
Female	20 760 (52.0%)	15 417 (52.1%)	5343 (51.5%)	22 674 (48.0%)	..
Male	19 185 (48.0%)	14 161 (47.9%)	5024 (48.5%)	24 540 (52.0%)	..
Household size					<0.0001†
2	16 519 (41.4%)	13 115 (44.3%)	3404 (32.8%)	8857 (18.8%)	..
3–4	17 366 (43.5%)	12 550 (42.4%)	4816 (46.5%)	22 598 (47.9%)	..
5–6	4989 (12.5%)	3276 (11.1%)	1713 (16.5%)	11 864 (25.1%)	..
>6	1071 (2.7%)	637 (2.2%)	434 (4.2%)	3895 (8.2%)	..
Clinical severity‡					<0.0001§
Asymptomatic	1006 (2.5%)	567 (1.9%)	439 (4.2%)	NA	..
Mild	20 326 (50.9%)	14 928 (50.5%)	5398 (52.1%)	NA	..
Moderate	11 504 (28.8%)	8416 (28.5%)	3088 (29.8%)	NA	..
Severe	6193 (15.5%)	4895 (16.5%)	1298 (12.5%)	NA	..
Critical	916 (2.3%)	772 (2.6%)	144 (1.4%)	NA	..
Case type					<0.0001¶
Clinical	11 441 (28.6%)	8844 (29.9%)	2597 (25.1%)	NA	..
Laboratory confirmed	28 504 (71.4%)	20 734 (70.1%)	7770 (74.9%)	NA	..
Epidemic phase (based on onset of primary case)					<0.0001¶
Before Jan 24	7599 (19.0%)	7146 (24.2%)	453 (4.4%)	11 869 (25.1%)	..
Jan 24–Feb 10	25 073 (62.8%)	18 595 (62.9%)	6478 (62.5%)	27 685 (58.6%)	..
After Feb 10	7273 (18.2%)	3837 (13.0%)	3436 (33.1%)	7660 (16.2%)	..

NA=not applicable. SARS-CoV-2=severe acute respiratory syndrome coronavirus 2. *Including 8619 asymptomatic contacts who might have been tested but whose laboratory test records were missing; these individuals were treated as untested in all analyses. Age data were missing for 1112 test-negative or untested household contacts. † χ^2 test comparing secondary cases to uninfected contacts. ‡Severity categories were measured at the time of clinical assessment or laboratory testing. Mild cases include 280 cases for whom severity was missing. A total of 2060 cases died. § χ^2 test comparing proportion of asymptomatic infections between secondary and primary cases. ¶ χ^2 test comparing secondary with primary cases.

Table 1: Demographic and clinical characteristics of cases and test-negative or untested contacts of SARS-CoV-2-infected households in Wuhan, China, from Dec 2, 2019, to April 18, 2020

Secondary cases were less severe clinically than primary cases, with more asymptomatic cases (4.2% vs 1.9%) and fewer severe or critical cases (13.9% vs 19.2%; table 1). Clinical severity was missing for 280 cases and was assumed to be mild for these cases in all subsequent analyses. Among the 4903 primary and secondary cases with symptoms recorded, the most common systemic symptoms were fever (in 2970 [60.6%]), fatigue (in 1325 [27.0%]), and myalgia (in 626 [12.8%]), and the most common respiratory symptoms were dry cough (in 1776 [36.2%]), shortness of breath (in 846 [17.3%]), productive cough (in 661 [13.5%]), and chest tightness or pain (in 633 [12.9%]; appendix 2 p 27). Radiological evidence of pulmonary abnormality was confirmed in 3247 (66.2%) of 4903 cases. Secondary cases had lower rates of systemic or respiratory symptoms but a higher rate of radiological evidence than primary cases (appendix 2 p 27). Using data after Feb 22, 2020, when most household contacts

were laboratory tested, we estimated the proportion of secondary cases who developed symptoms after infection (pathogenicity) to be 84.0% (95% CI 81.7–86.1; 913/1087; appendix 2 p 28). Young adults aged 20–39 years were less likely to develop symptoms upon infection than those aged 60 years or older (78.8%, 95% CI 73.0–83.8 [186/236] vs 87.5%, 83.9–90.6 [351/401]). The pathogenicity of infection in children and adolescents (84.7%, 76.0–91.2 [83/98]) resembled that of adults aged 40 years or older, although symptomatic cases among children and adolescents were much less likely to be severe or critical than for those aged 60 years or older (2.4%, 95% CI 0.3–8.4 [two of 83] vs 18.8%, 14.9–23.3 [66/351]). Neither pathogenicity nor disease severity differed between the two sexes (appendix 2 p 28).

For the 24 985 households that had only a single primary case, the overall observed secondary attack rate was 16.0% (95% CI 15.7–16.3; table 2). The secondary

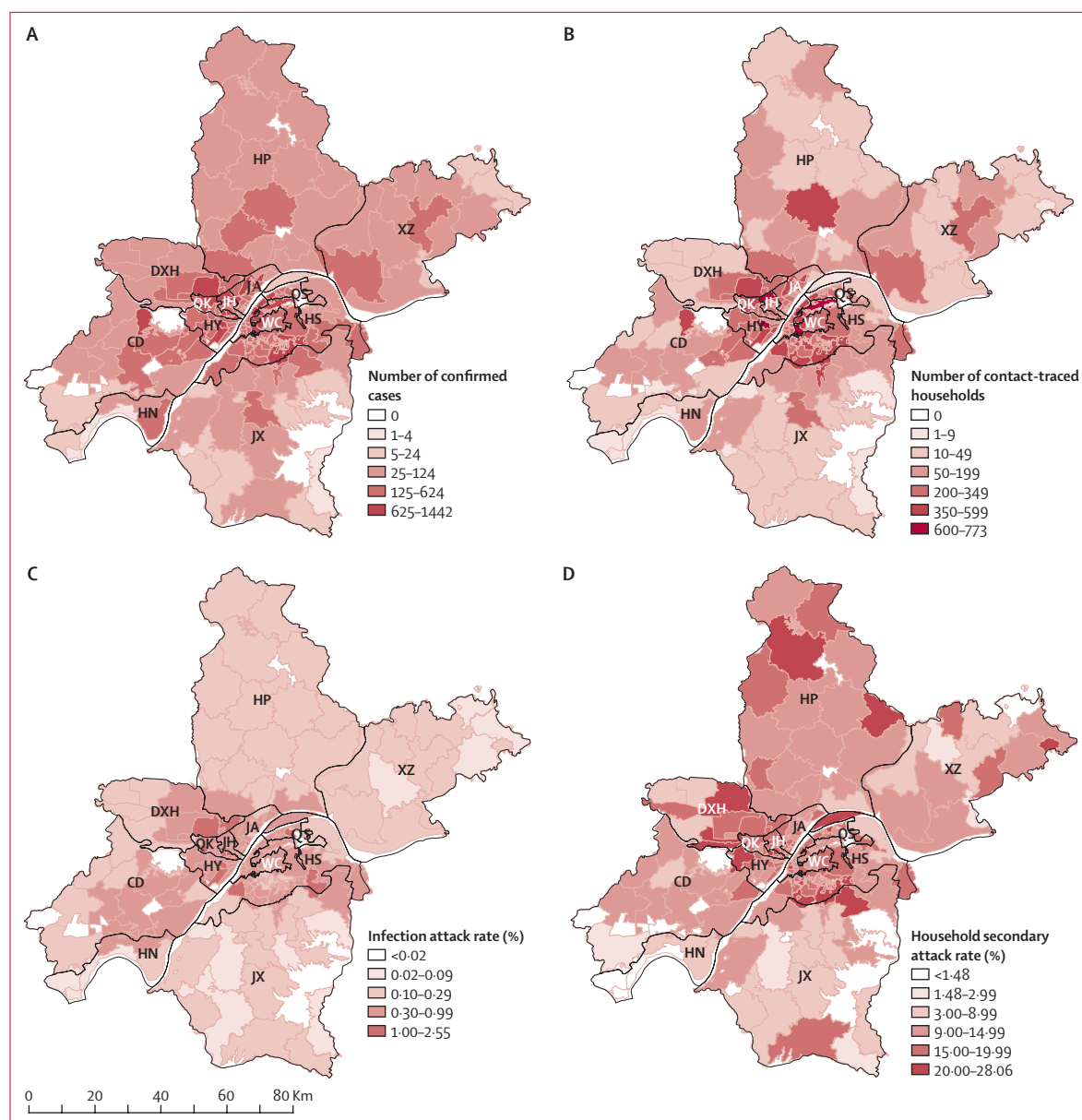


Figure: Spatial distribution of all confirmed COVID-19 cases and the retrospective cohort of contact-traced households reported during Dec 2, 2019–April 18, 2020, at the community level in Wuhan, China

(A) Distribution of all clinically or laboratory confirmed COVID-19 cases in Wuhan. (B) Distribution of all contact-traced households included in this study. (C) The community-level infection attack rate (ie, the cumulative number of confirmed cases as a percentage of the total population) in each district in Wuhan. (D) The observed household secondary attack rate (ie, the proportion of secondary infections among household contacts) among households with a single primary case included in this study. In B and D, the community of each household was determined by the community of the primary case, or the case with the earliest symptom onset if there were coprimary cases. CD=Cai-Dian. DXH=Dong-Xi-Hu. HN=Han-Nan. HP=Huang-Pi. HS=Hong-Shan. HY=Han-Yang. JA=Jiang-An. JH=Jiang-Han. JX=Jiang-Xia. QK=Qiao-Kou. QS=Qing-Shan. WC=Wu-Chang. XZ=Xin-Zhou.

attack rate estimated by the chain-binomial transmission model was similar, 15.6% (15.2–16.0), under the assumption of a mean incubation period of 5 days and a maximum infectious period of 22 days (table 3; appendix 2 p 30). The model-estimated secondary attack rate for contacts living at the same residential address was 16.1% (15.6–16.5), higher than the 12.6%

(11.4–13.9) rate estimated for contacts from the same household but living in different residences—eg, grandparents and grandchildren (appendix 2 p 31).

Based on the chain-binomial model adjusted for all covariates, household transmissibility of SARS-CoV-2 was inversely associated with household size (table 3; appendix 2 p 32). The GEE model showed a

similar household size effect (table 2). Compared with Jan 24–Feb 10, 2020, odds of daily household transmission between an infectious individual and a susceptible individual was lower after Feb 10 (table 3). A greater reduction was seen in the observed household secondary attack rate, from near 20% in the periods before Feb 10 to 4.1% after (table 2).

In general, both the observed secondary attack rate and model-estimated odds of infection (with regard to susceptibility) increased with age of the household contacts (tables 2, 3). Individuals aged 60 years or older were the most susceptible age group to SARS-CoV-2 infection. The least susceptible age group was children aged 2–5 years. The transmission model estimated that individuals younger than 20 years were about 66–84% (ORs ranging from 0.16 to 0.34) less susceptible than adults aged 60 years or older, and adults aged 20–59 years were 31–49% (ORs ranging from 0.51 to 0.69) less susceptible (table 3). Infants (aged 0–1 years) were more susceptible to infection than toddlers (2–5 years; OR 2.20, 95% CI 1.40–3.44) and elementary-school-aged children (6–12 years; 1.53, 1.01–2.34). Female contacts were slightly more susceptible than male contacts (table 3). The GEE model yielded similar ORs, although it estimated slightly larger differences in susceptibility between older contacts (≥ 60 years) and younger ones (table 2).

According to the transmission model, cases younger than 20 years were more likely to infect others than cases older than 60 years (table 3). Sex and disease severity did not seem to have an appreciable impact on infectivity, although disease severity was statistically associated with onwards transmission in the transmission model (table 3). Clinically diagnosed cases were less infectious than laboratory-confirmed cases (table 3). The GEE and transmission models produced largely concordant results regarding infectivity across age groups, except that the GEE model identified primary cases younger than 20 years old as being less infectious than older ones, whereas the transmission model suggested the opposite (tables 2, 3). The GEE model also found individuals older than 80 years to be similar to those aged 60–79 years in terms of both infectivity and susceptibility to infection (table 2), and these two age groups were thus combined for transmission modelling.

Both models found infected individuals who remained asymptomatic during the whole infection course to be much less infectious than symptomatic cases. The GEE model estimated an OR of 0.34 (95% CI 0.21–0.54) for asymptomatic individuals versus patients with mild and moderate disease (table 2). The transmission model estimated an OR of 0.42 (0.17–1.04) for asymptomatic versus symptomatic individuals up to Feb 1, which decreased to 0.21 (0.14–0.31) afterwards (table 3). Asymptomatic

	Primary cases	Household contacts	Secondary cases	Secondary attack rate (95% CI)	Odds of infection of household contacts (95% CI)*
Overall	24 985	52 822	8447	16.0% (15.7–16.3)	..
Household size					
2	11 504	12 050	3270	27.1% (26.3–27.9)	1 (ref)
3–4	10 322	24 961	3647	14.6% (14.2–15.1)	0.56 (0.53–0.59)
5–6	2669	12 076	1231	10.2% (9.7–10.8)	0.42 (0.39–0.46)
>6	490	3735	299	8.0% (7.2–8.9)	0.39 (0.34–0.46)
Epidemic phase (based on onset of primary case)					
Before Jan 24	6462	13 968	2674	19.1% (18.5–19.8)	1.14 (1.07–1.21)
Jan 24–Feb 10	15 152	31 127	5453	17.5% (17.1–18.0)	1 (ref)
After Feb 10	3371	7727	320	4.1% (3.7–4.6)	0.25 (0.22–0.29)
Age of contacts, years					
≤ 1	NA	264	16	6.1% (3.5–9.7)	0.32 (0.21–0.50)
2–5	NA	2018	55	2.7% (2.1–3.5)	0.15 (0.12–0.19)
6–12	NA	2693	125	4.6% (3.9–5.5)	0.23 (0.19–0.27)
13–19	NA	2263	141	6.2% (5.3–7.3)	0.27 (0.23–0.32)
20–39	NA	13 639	1627	11.9% (11.4–12.5)	0.48 (0.45–0.51)
40–59	NA	16 369	2828	17.3% (16.7–17.9)	0.65 (0.61–0.69)
60–79	NA	11 783	2985	25.3% (24.5–26.1)	1 (ref)
≥ 80	NA	1389	337	24.3% (22.0–26.6)	1.03 (0.90–1.17)
Sex of contacts					
Female	NA	25 682	4357	17.0% (16.5–17.4)	1.11 (1.05–1.18)
Male	NA	27 140	4090	15.1% (14.7–15.5)	1 (ref)
Age of primary case, years					
<20	327	793	46	5.8% (4.3–7.7)	0.66 (0.48–0.90)
20–39	4373	10 476	1350	12.9% (12.3–13.5)	0.97 (0.90–1.05)
40–59	9908	20 596	3114	15.1% (14.6–15.6)	0.98 (0.92–1.04)
60–79	9248	18 539	3489	18.8% (18.3–19.4)	1 (ref)
≥ 80	1129	2418	448	18.5% (17.0–20.1)	0.96 (0.84–1.09)
Sex of primary case					
Female	13 093	27 358	4259	15.6% (15.1–16.0)	0.96 (0.91–1.02)
Male	11 892	25 464	4188	16.5% (16.0–16.9)	1 (ref)
Clinical severity of primary case					
Asymptomatic	524	1367	27	2.0% (1.3–2.9)	0.34 (0.21–0.54)
Mild or moderate	19 556	41 030	6495	15.8% (15.5–16.2)	1 (ref)
Severe or critical	4905	10 425	1925	18.5% (17.7–19.2)	1.01 (0.94–1.08)
Ascertainment of primary case					
Clinical	7599	15 215	2028	13.3% (12.8–13.9)	0.72 (0.67–0.76)
RT-PCR	17 386	37 607	6419	17.1% (16.7–17.5)	1 (ref)

Untested contacts were treated as uninfected in the calculations. Secondary attack rates are not based on the transmission model. Odds ratios are calculated from a multivariable generalised estimating equation model. NA=not applicable. *Age was missing for 1027 contacts in 744 single-primary-case households; these households were excluded from the estimation of observed secondary attack rates by age group and from the multivariate generalised estimating equation model.

Table 2: Estimates of observed secondary attack rates among households with a single primary case

infections were formally required to be reported in Wuhan from Feb 1, which suggests greater ascertainment bias before Feb 1. For this reason, the estimated relative infectivity after Feb 1 is probably more accurate, implying that an asymptotically infected individual was associated with about 80% lower

	Mean incubation period: 5 days		Mean incubation period: 7 days	
	Maximum infectious period: 13 days	Maximum infectious period: 22 days*	Maximum infectious period: 13 days	Maximum infectious period: 22 days
Secondary attack rate				
Overall	10.4% (10.1–10.7)	15.6% (15.2–16.0)	12.3% (11.9–12.6)	17.1% (16.7–17.5)
Odds of household transmission				
Household size (vs two people)				
3–4	0.60 (0.57–0.63)	0.59 (0.56–0.62)	0.59 (0.56–0.62)	0.58 (0.55–0.61)
5–6	0.41 (0.38–0.43)	0.40 (0.37–0.42)	0.39 (0.37–0.42)	0.39 (0.36–0.41)
>6	0.32 (0.29–0.36)	0.31 (0.28–0.35)	0.31 (0.28–0.35)	0.30 (0.27–0.34)
Epidemic phase (vs Jan 24–Feb 10)				
Before Jan 24	0.74 (0.69–0.79)	0.72 (0.68–0.77)	0.79 (0.74–0.84)	0.77 (0.73–0.82)
After Feb 10	0.86 (0.77–0.96)	0.86 (0.77–0.95)	0.63 (0.56–0.70)	0.62 (0.56–0.69)
Odds of infection for an exposed household contact (susceptibility)				
Age group, years (vs ≥60)				
0–1	0.34 (0.23–0.51)	0.34 (0.23–0.51)	0.34 (0.23–0.51)	0.34 (0.23–0.51)
2–5	0.16 (0.13–0.19)	0.16 (0.13–0.20)	0.16 (0.13–0.19)	0.16 (0.13–0.19)
6–12	0.22 (0.19–0.26)	0.22 (0.19–0.26)	0.22 (0.19–0.26)	0.22 (0.19–0.26)
13–19	0.27 (0.23–0.31)	0.27 (0.23–0.31)	0.27 (0.23–0.31)	0.27 (0.23–0.31)
20–39	0.50 (0.48–0.53)	0.51 (0.48–0.54)	0.50 (0.48–0.53)	0.50 (0.48–0.53)
40–59	0.69 (0.65–0.72)	0.69 (0.66–0.72)	0.68 (0.65–0.72)	0.69 (0.65–0.72)
Female sex (vs male)	1.11 (1.06–1.16)	1.11 (1.07–1.16)	1.11 (1.06–1.16)	1.11 (1.06–1.16)
Odds of onwards transmission for an infective case (infectivity)				
Age group, years (vs ≥60)				
<20	1.65 (1.32–2.05)	1.58 (1.28–1.95)	1.41 (1.13–1.77)	1.38 (1.11–1.72)
20–39	1.12 (1.02–1.22)	1.10 (1.02–1.20)	1.08 (0.99–1.17)	1.07 (0.99–1.16)
40–59	1.02 (0.95–1.09)	1.02 (0.95–1.09)	1.02 (0.95–1.08)	1.02 (0.96–1.09)
Female sex (vs male)	0.97 (0.91–1.04)	0.98 (0.92–1.04)	0.97 (0.91–1.03)	0.97 (0.91–1.03)
Disease severity: severe or critical (vs mild or moderate)	0.91 (0.84–0.98)	0.92 (0.85–0.98)	0.94 (0.88–1.01)	0.94 (0.88–1.00)
Diagnosis: clinical (vs RT-PCR)	0.75 (0.70–0.80)	0.75 (0.70–0.80)	0.73 (0.69–0.78)	0.74 (0.69–0.78)
Asymptomatic infection (vs symptomatic)				
Up to Feb 1	0.88 (0.36–2.14)	0.42 (0.17–1.04)	0.61 (0.28–1.33)	0.29 (0.13–0.65)
From Feb 2	0.53 (0.38–0.76)	0.21 (0.14–0.31)	0.39 (0.27–0.56)	0.16 (0.11–0.24)
Before symptom onset (vs after symptom onset)	0.76 (0.68–0.85)	1.42 (1.30–1.55)	1.46 (1.31–1.63)	2.92 (2.67–3.19)

Data are secondary attack rate (95% CI) or odds ratio (95% CI). Overall secondary attack rates, regardless of characteristics of the infector, infectee, or household, were estimated with a separate model with fewer covariates than the model used to estimate odds ratios (appendix p 30), as some covariates will change the interpretation of the secondary attack rate. Estimates of baseline daily transmission probabilities within households and from an external source, as well as estimates of daily transmission probabilities between different age groups within households, are shown in the appendix (pp 32–33). *Primary analysis.

Table 3: Model-based estimates of secondary attack rates and odds ratios reflecting covariate effects on susceptibility and infectivity

infectivity than a symptomatic case after symptom onset. When allowing infectivity to differ before and after symptom onset among symptomatic cases, the transmission model estimated the presymptomatic (incubation) period was more infectious than the symptomatic period (table 3).

When exploring how the effective household reproductive numbers changed over the pandemic periods, we found a decrease from 0.25 (95% CI 0.24–0.26) up to Feb 10 to 0.12 (0.10–0.13) after among primary cases, marking a 52% reduction (table 4). The reduction was more substantial for secondary cases, from around 0.17 (0.16–0.18) to 0.063 (0.057–0.070), a 63% reduction.

The model-estimated secondary attack rate was moderately sensitive to assumptions around incubation and infectious periods, varying from 10.4% (95% CI 10.1–10.7) to 17.1% (16.7–17.5), with larger estimates associated with a longer incubation period or a longer infectious period (table 3). An extension of the infectious period to 27 days (21 days after symptom onset) led to a further increase in the secondary attack rate estimate to 17.8% (17.4–18.2; appendix 2 p 34). This sensitivity results from the fact that how the transmission model allocates secondary infections between the external force of infection and infectious household members depends on the durations of the incubation and infectious periods. Most findings about

	Mean incubation period: 5 days		Mean incubation period: 7 days	
	Maximum infectious period: 13 days	Maximum infectious period: 22 days*	Maximum infectious period: 13 days	Maximum infectious period: 22 days
Primary				
Before Jan 24	0.19 (0.18–0.20)	0.25 (0.24–0.26)	0.24 (0.23–0.25)	0.29 (0.28–0.30)
Jan 24–Feb 10	0.21 (0.20–0.22)	0.25 (0.24–0.26)	0.25 (0.24–0.26)	0.28 (0.27–0.28)
After Feb 10	0.12 (0.11–0.13)	0.12 (0.10–0.13)	0.10 (0.092–0.12)	0.10 (0.089–0.11)
Secondary				
Before Jan 24	0.14 (0.13–0.14)	0.17 (0.16–0.18)	0.17 (0.16–0.18)	0.20 (0.19–0.21)
Jan 24–Feb 10	0.15 (0.14–0.15)	0.17 (0.16–0.18)	0.18 (0.17–0.18)	0.19 (0.19–0.20)
After Feb 10	0.064 (0.058–0.071)	0.063 (0.057–0.070)	0.056 (0.050–0.062)	0.055 (0.049–0.061)

Data in parentheses are 95% CIs. Epidemic phases are defined by intervention policy (lockdown from Jan 23 to April 7, 2020, and tightened community management since Feb 11; panel). *Primary analysis.

Table 4: Estimates of effective household reproductive numbers for primary cases and secondary cases in different epidemic stages in 2020

risk factors are robust to varying assumptions about the natural history of disease (table 3). The estimated infectivity of asymptomatic infections versus symptomatic infections varied moderately (ORs 0.16–0.53) on or after Feb 2, whereas that of presymptomatic infections versus symptomatic infections varied more notably (ORs 0.76–2.92), between the extreme values for the incubation and infectious periods (table 3). When primary cases were defined as those with the earliest symptom onset or test-positive specimen collection date in their households (excluding the following day), the estimate of secondary attack rate increased slightly to 17.0% (16.6–17.4; appendix 2 p 35). Limiting analysis to the 15922 households with all contacts tested, which accounted for about 60% of all households, the estimates of risk factors' effects were qualitatively similar, but the estimated secondary attack rates increased—eg, to 20.6% (95% CI 20.0–21.2) under the assumption of a mean incubation period of 5 days and a maximum infectious period of 22 days—suggesting households with more secondary cases were more likely to have complete testing (appendix 2 p 36). When the effect of age on infectivity was stratified by household size, the higher infectivity of children than adults was mainly limited to households with more than three members (appendix 2 p 37). The transmission model provided satisfactory goodness-of-fit to the data, especially under the longer infectious period (appendix 2 p 22).

Discussion

We characterised the transmissibility of SARS-CoV-2 within households and associated risk factors in Wuhan, China, based on a large amount of household contact-tracing data available from early in the COVID-19 pandemic. Using a statistical transmission model, we found individuals older than 60 years were more likely to be infected than the younger population, especially those younger than 20 years. Additionally,

infants were more likely to be infected than older children. Once infected, children and adolescents were as likely as adults to develop symptoms, although much less likely to have severe disease. In addition, children and adolescents were more likely to infect others than were older age groups. Individuals with asymptomatic infection were less likely to infect others than were symptomatic cases. Symptomatic cases were more infectious during the incubation period than during the symptomatic period.

The estimated household secondary attack rate of SARS-CoV-2 in Wuhan is similar to that in Guangzhou (15.6% vs 15.5%) found by a previous study using comparable methods.⁴ Moreover, our observed household secondary attack rate in Wuhan (16.0%) was similar to that in Guangzhou (13.2%) and Shenzhen (14.9%), but lower than that in Beijing (23%) and Zhejiang province (31.6%).^{5,6,14,15} Secondary attack rate estimates in mainland China have tended to be higher than those for other locations—eg, 10.5% in the USA and 4.6% in Taiwan.^{16,17} The heterogeneity in household secondary attack rates across different regions is probably due to differences in control measures, surveillance practices, and crowdedness in households.

It has been reported that children are less, and elderly adults are more, prone to severe clinical outcomes from COVID-19,^{18,19} and several studies have found that older age groups are more likely to get infected.^{4,20,21} Similar to this study, a study in Bnei Brak, Israel, observed a higher risk of infection among infants aged 0–1 years than in older children.²⁰ A possible explanation for this finding is that infants have weaker innate immune systems and closer contact with parents than older children. We also found that SARS-CoV-2 was less likely to cause symptoms upon infection among young adults in their 20s and 30s, but its pathogenicity in children and adolescents was similar to that in adults aged 40 years or older. Similar levels of pathogenicity in children were noticed before in China and South Korea

based on a much smaller number of observations, but no comparison was made with other age groups in those studies.^{22,23}

Using the transmission model, we found that cases younger than 20 years were nearly 60% more likely to infect others than cases aged 60 years or older. This finding seems to contradict the observed secondary attack rates of the two groups and the GEE-based odds ratio estimates (table 2). The observed secondary attack rate and the GEE model did not account for individual-level exposure history and should be interpreted as unconditional results—ie, not adjusted for the amount of exposure. By contrast, the chain-binomial model evaluated how risk factors change transmission probability per daily exposure. In addition, GEE-based estimates did not consider tertiary transmissions from secondary cases to household contacts. We found children with SARS-CoV-2 infection, particularly those who were secondary cases, were more likely than adults to infect household members who were actually exposed to them during their infectious periods (appendix 2 pp 18–19, 29). This fact, together with the much faster isolation of child cases (appendix 2 p 38), which implied a short duration of exposure of contacts to infected children, supports the higher infectivity of children than adults suggested by the chain-binomial model. A survey during the early epidemic phase in Wuhan found higher contact frequency between the age groups 0–20 years and 30–50 years than between any other age groups, which could explain in part the higher infectivity of children.²⁴ The infectivity of children could be modified by other factors, which merits further investigation. For example, the higher infectivity of children than of adults was mainly limited to households with more than three members in our study. Moreover, a recent study in South Korea reported a high infection rate among household contacts of index cases aged 10–19 years but not among household contacts of younger index cases.²⁵

Using the transmission model on data available after Feb 1, we estimated that individuals with asymptomatic infections were about 80% less likely to infect others than symptomatic cases. While it has long been speculated that individuals with asymptomatic infection can transmit the disease, strong epidemiological evidence has been scarce, and a reliable assessment of the relative infectivity of asymptomatic infections versus symptomatic infections was lacking before this study.^{3,26,27} A study in Anhui province of China compared secondary attack rates among general contacts between 131 individuals with asymptomatic infections and 16 symptomatic cases, with an OR of 0.25.²⁸ All 16 symptomatic cases tested positive before symptom onset, implying the possibility of selection bias. A recent meta-analysis estimated household secondary attack rates to be 19.9% for

symptomatic index cases and 0.7% for asymptomatic ones, suggesting an OR of 0.028, which is much lower than our estimate of 0.21.³ Some modelling studies extrapolated the relative infectivity of asymptomatic or subclinical infections from viral load dynamics of mild and severe cases, and their results tended to be lower than our estimates.^{8,9}

Our results show the importance of isolating cases and quarantining household contacts outside of the home to prevent onwards transmission within households. During the period Jan 24–Feb 10, when many people with mild COVID-19 were isolated at home, the observed secondary attack rate and the model-estimated effective reproductive number within households remained essentially unchanged compared with before Jan 24 (tables 2, 4). When massive case isolation and quarantine of household contacts at designated places reached full coverage near mid-February, both the observed household secondary attack rate and household effective reproductive numbers were substantially reduced, consistent with a previous modelling study.²⁹ Such dramatic reduction in household transmissibility of the virus was mainly driven by the reduced number of days of exposure of household contacts to the cases due to the interventions (appendix 2 pp 21, 29). The daily transmission probability between an infectious case and an exposed household contact was, however, less affected by the interventions (table 3). More dramatic reduction in transmissibility for secondary cases than for primary cases was expected, as the household contacts were still exposed to primary cases during their incubation period before isolation or quarantine occurred (appendix 2 pp 21, 29).

Our study has several limitations. Although we have imputed asymptomatic infections among untested contacts in the early stage, bias cannot be ruled out as there was no protocol for laboratory testing and there could be unmeasured confounders not adjusted for in the imputation. Asymptomatic infections might still have been under-detected even after household contacts were universally tested. The overall proportion of asymptomatic infections after Feb 22 was 16%, somewhat lower than the 18% or 32% observed (depending on whether abnormal lung CT is counted as a clinical sign) in the outbreak on the *Diamond Princess* cruise.^{30,31} The GEE analysis was applied only to households with a single primary case, but these households tended to have more secondary cases aged 60 years or older (appendix 2 p 39), which might affect the generalisability of the GEE results. In addition, our data do not offer strong evidence in favour of any particular scenario of the incubation and infectious periods, and the variation in results across the different assumptions should be considered as part of the uncertainty in these estimates. Finally, we merged epidemiologically linked households, but the mixing

pattern between these households could be more complex than what was assumed.

Our study has implications for forecasting and control of the global pandemic of SARS-CoV-2. Differential susceptibility and infectivity between age groups, as well as other epidemiological parameters estimated in this study, are key inputs for modelling studies projecting the future trajectory of the pandemic. The relatively high infectivity of children in households should be considered carefully when making decisions around school reopenings, as infected children can pass the virus to their family members. Finally, given the vulnerability of infants to infection, their caregivers should be prioritised for vaccination.

Contributors

FL, X-BY, H-JW, P-LL, Y-HP, Y-QY, SL, and GL contributed to the epidemiological investigation and collected the data. YY, S-QX, and Y-YL conceived the statistical analysis plan. M-JL, Y-YL, FL, L-QF, and QL accessed, verified, and analysed data under the supervision of YY and S-QX. Y-YL and YY drafted the manuscript. All authors contributed to interpretation of results and critical revision.

Declaration of interests

We declare no competing interests

Data sharing

Data for plotting the main figure and figure S1 are available online for download. Individual-level data will not be made publicly available with this Article. Requests for sharing of deidentified individual-level data or aggregated household data for scientific research can be directed to FL (lifang@whcdc.org). All proposals will be subject to scientific review and institutional review board approval at Wuhan CDC, and all approved data requestors will need to sign a data use agreement.

Acknowledgments

S-QX and Y-YL were funded by the National Natural Science Foundation of China (91643207), the Program of Tongji-Rongcheng Center for Biomedicine (HUST), Central China Think-tank (2020HZZK018), and the Fundamental Research Funds for the Central Universities (HUST 2020kfyXGYJ004). YY and IL were supported by the US National Institutes of Health (grant R01 AI116770) and YY was supported by the US National Science Foundation (grant 2034364). We thank the staff members of all district-level CDCs and community health service centres in Wuhan for their assistance in field investigation and data collection.

References

- Dong E, Du H, Gardner L. An interactive web-based dashboard to track COVID-19 in real time. *Lancet Infect Dis* 2020; **20**: 533–34.
- WHO. Report of the WHO-China joint mission on coronavirus disease 2019 (COVID-19). 2020. [https://www.who.int/publications/i/item/report-of-the-who-china-joint-mission-on-coronavirus-disease-2019-\(covid-19\)](https://www.who.int/publications/i/item/report-of-the-who-china-joint-mission-on-coronavirus-disease-2019-(covid-19)) (accessed June 24, 2020).
- Madewell ZJ, Yang Y, Longini IM, Halloran ME. Household transmission of SARS-CoV-2: a systematic review and meta-analysis of secondary attack rate. *medRxiv* 2020; published online Aug 1. <http://doi.org/10.1101/2020.07.29.20164590> (preprint).
- Jing QL, Liu MJ, Zhang ZB, et al. Household secondary attack rate of COVID-19 and associated determinants in Guangzhou, China: a retrospective cohort study. *Lancet Infect Dis* 2020; **20**: 1141–50.
- Bi Q, Wu Y, Mei S, et al. Epidemiology and transmission of COVID-19 in 391 cases and 1286 of their close contacts in Shenzhen China: a retrospective cohort study. *Lancet Infect Dis* 2020; **20**: 911–19.
- Li W, Zhang B, Lu J, et al. The characteristics of household transmission of COVID-19. *Clin Infect Dis* 2020; **71**: 1943–46.
- Tong Z, Tang A, Li K, et al. Potential presymptomatic transmission of SARS-CoV-2, Zhejiang province, China, 2020. *Emerg Infect Dis* 2020; **26**: 1052–54.
- Moghadas SM, Fitzpatrick MC, Sah P, et al. The implications of silent transmission for the control of COVID-19 outbreaks. *Proc Natl Acad Sci USA* 2020; **117**: 17513–15.
- Ferretti L, Wymant C, Kendall M, et al. Quantifying SARS-CoV-2 transmission suggests epidemic control with digital contact tracing. *Science* 2020; **368**: eabb6936.
- National Health Commission of the People's Republic of China. Protocol of prevention and control of COVID-19 (edition 6). March 29, 2020. http://en.nhc.gov.cn/2020-03/29/c_78468.htm (accessed Jan 7, 2021).
- Yang Y, Longini IM, Halloran ME, Obenchain V. A hybrid EM and Monte Carlo EM algorithm and its application to analysis of transmission of infectious diseases. *Biometrics* 2012; **68**: 1238–49.
- Wölfel R, Corman VM, Guggemos W, et al. Virological assessment of hospitalized patients with COVID-2019. *Nature* 2020; **581**: 465–69.
- He X, Lau EHY, Wu P, et al. Temporal dynamics in viral shedding and transmissibility of COVID-19. *Nature Med* 2020; **26**: 672–75.
- Sun WW, Ling F, Pan JR, et al. Epidemiological characteristics of 2019 novel coronavirus family clustering in Zhejiang province. *Zhonghua Yu Fang Yi Xue Za Zhi* 2020; **54**: 625–29 (in Chinese).
- Wang Y, Tian H, Zhang L, et al. Reduction of secondary transmission of SARS-CoV-2 in households by face mask use, disinfection and social distancing: a cohort study in Beijing, China. *BMJ Global Health* 2020; **5**: e002794.
- Burke RM, Midgley CM, Dratch A, et al. Active monitoring of persons exposed to patients with confirmed COVID-19—United States, January–February 2020. *MMWR Morb Mortal Wkly Rep* 2020; **69**: 245–46.
- Cheng HY, Jian SW, Liu DP, et al. Contact tracing assessment of COVID-19 transmission dynamics in Taiwan and risk at different exposure periods before and after symptom onset. *JAMA Intern Med* 2020; **180**: 1156–63.
- Wu Z, McGoogan JM. Characteristics of and important lessons from the coronavirus disease 2019 (COVID-19) outbreak in China: summary of a report of 72 314 cases from the Chinese Center for Disease Control and Prevention. *JAMA* 2020; **323**: 1239–42.
- Onder G, Rezza G, Brusaferro S. Case-fatality rate and characteristics of patients dying in relation to COVID-19 in Italy. *JAMA* 2020; **323**: 1775–76.
- Dattner I, Goldberg Y, Katriel G, et al. The role of children in the spread of COVID-19: using household data from Bnei Brak, Israel, to estimate the relative susceptibility and infectivity of children (version 2). *medRxiv* 2020; published online Oct 11. <http://doi.org/10.1101/2020.06.03.20121145> (preprint).
- Davies NG, Klepac P, Liu Y, et al. Age-dependent effects in the transmission and control of COVID-19 epidemics. *Nature Med* 2020; **26**: 1205–11.
- Lu X, Zhang L, Du H, et al. SARS-CoV-2 infection in children. *N Engl J Med* 2020; **382**: 1663–65.
- Han MS, Choi EH, Chang SH, et al. Clinical characteristics and viral RNA detection in children with coronavirus disease 2019 in the Republic of Korea. *JAMA Pediatr* 2020; published online Aug 28. <https://doi.org/10.1001/jamapediatrics.2020.3988>.
- Zhang J, Litvinova M, Liang Y, et al. Changes in contact patterns shape the dynamics of the COVID-19 outbreak in China. *Science* 2020; **368**: 1481–86.
- Park Y, Choe Y, Park O, et al. Contact tracing during coronavirus disease outbreak, South Korea, 2020. *Emerg Infect Dis* 2020; **26**: 2465–68.
- Furukawa NW, Brooks JT, Sobel J. Evidence supporting transmission of severe acute respiratory syndrome coronavirus 2 while presymptomatic or asymptomatic. *Emerg Infect Dis* 2020; **26**: e201595.
- Bai Y, Yao L, Wei T, et al. Presumed asymptomatic carrier transmission of COVID-19. *JAMA* 2020; **323**: 1406–07.
- Liu Z, Chu R, Gong L, Su B, Wu J. The assessment of transmission efficiency and latent infection period on asymptomatic carriers of SARS-CoV-2 infection. *Int J Infect Dis* 2020; **99**: 325–27.

For the figure data see https://uflorida-my.sharepoint.com/:f/g/personal/yyangyang_ufl_edu/EI-U0gqXRhNDixONBcXlmBkBCtSBHdm4LhZQvdlUjh2FA

-
- 29 Lai S, Ruktanonchai NW, Zhou L, et al. Effect of non-pharmaceutical interventions to contain COVID-19 in China. *Nature* 2020; **585**: 410–13.
 - 30 Mizumoto K, Kagaya K, Zarebski A, Chowell G. Estimating the asymptomatic proportion of coronavirus disease 2019 (COVID-19) cases on board the Diamond Princess cruise ship, Yokohama, Japan, 2020. *Euro Surveill* 2020; **25**: 2000180.
 - 31 Tabata S, Imai K, Kawano S, et al. Clinical characteristics of COVID-19 in 104 people with SARS-CoV-2 infection on the *Diamond Princess* cruise ship: a retrospective analysis. *Lancet Infect Dis* 2020; **20**: 1043–50.

Viable influenza A virus in airborne particles expelled during coughs versus exhalations

William G. Lindsley,^a Francoise M. Blachere,^a Donald H. Beezhold,^a Robert E. Thewlis,^a
Bahar Noorbakhsh,^a Sreekumar Othumpangat,^a William T. Goldsmith,^a Cynthia M. McMillen,^a
Michael E. Andrew,^a Carmen N. Burrell,^b John D. Noti^a

^aHealth Effects Laboratory Division, National Institute for Occupational Safety and Health, Centers for Disease Control and Prevention, Morgantown, WV, USA. ^bDepartment of Emergency Medicine, West Virginia University, Morgantown, WV, USA.

Correspondence: William G. Lindsley, National Institute for Occupational Safety and Health, 1095 Willowdale Road, M/S 4020, Morgantown, WV 26505-2845, USA. E-mail: wlindsley@cdc.gov

Accepted 25 February 2016.

Background To prepare for a possible influenza pandemic, a better understanding of the potential for the airborne transmission of influenza from person to person is needed.

Objectives The objective of this study was to directly compare the generation of aerosol particles containing viable influenza virus during coughs and exhalations.

Methods Sixty-one adult volunteer outpatients with influenza-like symptoms were asked to cough and exhale three times into a spirometer. Aerosol particles produced during coughing and exhalation were collected into liquid media using aerosol samplers. The samples were tested for the presence of viable influenza virus using a viral replication assay (VRA).

Results Fifty-three test subjects tested positive for influenza A virus. Of these, 28 (53%) produced aerosol particles containing viable influenza A virus during coughing, and 22 (42%) produced aerosols with viable virus during exhalation. Thirteen subjects had

both cough aerosol and exhalation aerosol samples that contained viable virus, 15 had positive cough aerosol samples but negative exhalation samples, and 9 had positive exhalation samples but negative cough samples.

Conclusions Viable influenza A virus was detected more often in cough aerosol particles than in exhalation aerosol particles, but the difference was not large. Because individuals breathe much more often than they cough, these results suggest that breathing may generate more airborne infectious material than coughing over time. However, both respiratory activities could be important in airborne influenza transmission. Our results are also consistent with the theory that much of the aerosol containing viable influenza originates deep in the lungs.

Keywords Aerosols, air microbiology, airborne transmission, cough, infectious disease transmission, influenza.

Please cite this paper as: Lindsley *et al.* (2016) Viable influenza A virus in airborne particles expelled during coughs versus exhalations. *Influenza and Other Respiratory Viruses* 10(5), 404–413.

Introduction

During an influenza pandemic, measures to stop the transmission of influenza virus will be a critical part of the public health response. Although influenza is known to be transmitted through respiratory secretions containing the virus, infectious material can be passed from person to person in many different ways. The relative importance of the different pathways is uncertain and probably varies depending upon the setting, the severity of the illness, the characteristics of the viral strain, environmental conditions, and other factors.⁽¹⁾ In order to choose the appropriate interventions to block the spread of the virus, it is necessary

to understand which routes of transmission occur and when they are likely to be important.

The role of airborne transmission in the spread of influenza has been a question of particular concern to the public health community while planning for a possible pandemic.^(2,3) If patients can readily infect others via aerosols (small airborne particles) produced during coughing, speaking, sneezing, and breathing, then interventions such as patient isolation and cohorting, increased air ventilation and filtration, air disinfection, and the use of respirators or other personal protective equipment may help to protect health-care workers and other patients from the illness. On the other hand, such interventions can be costly and time-consuming

and would place additional burdens on healthcare systems when they are already under considerable strain during a pandemic. Because of these issues, organizations such as the Institute of Medicine and the World Health Organization have called for more research to provide a better understanding of influenza transmission, especially airborne transmission.^(3,4)

Several reports have provided support for the idea that airborne influenza transmission can occur.^(5–8) Influenza virus RNA has been detected in respirable airborne particles collected in healthcare facilities and other locations.^(9–16) Influenza virus RNA also has been found in aerosol particles collected directly from infected patients while they were coughing and breathing.^(17–23) Six studies have demonstrated that influenza patients expel airborne particles containing viable virus.^(13,18,19,21,24,25) Pantelic *et al.* found that subjects with influenza emitted up to 1000 viable influenza virions over 30 minutes during normal tidal breathing.⁽²⁵⁾ Lindsley *et al.* detected viable influenza A virus in airborne particles produced during coughing by 7 of 17 influenza patients (41%).⁽²⁴⁾ However, even with these reports, the likelihood of airborne transmission is still unclear, in part because many questions remain about the production of aerosols carrying infectious influenza during respiratory activities. For example, no studies have compared the production of virus-laden airborne particles between different types of respiratory activities, such as coughing and exhalation. This is an important question, because the airflow dynamics of coughs and exhalations are very different. Coughing produces a high-velocity jet that can propel a plume of aerosol particles long distances, which disperses the airborne particles widely.⁽²⁶⁾ Exhalations have much lower velocities and are likely to produce higher particle concentrations in the immediate vicinity of a patient and lower concentrations further away. Exhalations are also more common than coughs, which could affect the amount of infectious aerosol that is generated. These differences could have a significant impact on disease transmission and on the choice of interventions.

A comparison of infectious particle production during coughing and exhaling also would provide clues as to the sites of origin of influenza-laden particles from within the respiratory tract. Humans produce more aerosol particles when they cough vs. when they exhale.^(27,28) Most of the aerosol particles produced during normal breathing are thought to originate deep in the respiratory tract, while coughing may produce aerosol both from the lower airways and also from the upper airways.^(29–31) Thus, if coughing produces much more infectious aerosol than exhaling, this would suggest that much of the virus in cough-generated particles may be coming from the upper airways. Conversely, if the production of infectious aerosol particles during coughing and exhaling is similar, then that would suggest

that much of the virus-laden aerosol is originating in the bronchioles and alveoli.

The purpose of this study was to directly compare the production of aerosol particles containing viable influenza virus by infected people during coughs and exhalations. Greater knowledge about the generation of infectious aerosol particles during different respiratory maneuvers will help to better understand the likelihood and dynamics of the possible modes of influenza transmission in different scenarios and will assist in the selection and evaluation of interventions to prevent the spread of disease.

Methods

All procedures involving human subjects were reviewed and approved by the National Institute for Occupational Safety and Health (NIOSH) and West Virginia University (WVU) Institutional Review Boards. Written informed consent was obtained from all study participants.

Aerosol particle collection system

Cough- and exhalation-generated aerosols were collected using an aerosol particle collection system (Figure 1) similar to that described previously.⁽²⁴⁾ An ultrasonic spirometer (Easy One, NDD Medical Technologies) measured the volume and flow rate of each cough, and a modified 10-liter piston-style mechanical spirometer (SensorMedics model 762609) served as an accumulation chamber for the cough and exhalation aerosols. Aerosol particles were collected using an SKC BioSampler with a 5-ml vessel (#225-9593, SKC) containing 5 ml of viral transport media (VTM) consisting of Hank's balanced salt solution (HBSS;

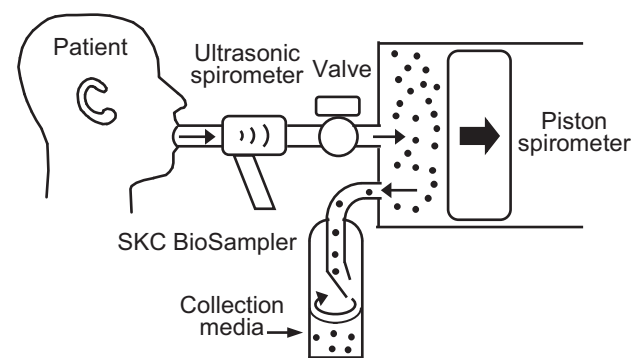


Figure 1. Collection system for airborne particles produced by subjects during coughing and exhalation. Before each respiratory activity, the piston spirometer was purged and partially filled with 4 liters of dry filtered air. The subject then sealed their mouth around the mouthpiece and coughed or exhaled as instructed. The cough or exhalation traveled through the ultrasonic spirometer, which measured the volume and flow rate, and then into the piston spirometer. When the subject was finished, the valve was closed and the SKC BioSampler was used to collect the aerosol particles produced by the subject.

Invitrogen) supplemented with 0.1% bovine serum albumin (BSA; Sigma-Aldrich), 100 units/ml penicillin G, and 100 units/ml streptomycin (Invitrogen). The particle collection efficiency for the SKC BioSampler (i.e., the percentage of particles of a given size that are collected by the sampler) is approximately 10% for particles with aerodynamic diameters of 0.1 μm ; 50% for 0.3 μm particles; 96% for 1 μm particles; 100% for 2 μm particles; and 50% for 8 μm particles.^(32–34) Particles larger than 10–15 μm are expected to be removed by the sampler elbow and not collected.

Sample collection procedure

Potential test subjects presenting with influenza-like symptoms at an outpatient clinic were recruited after they had been seen by their healthcare provider. Potential participants were excluded from the study if they reported respiratory illnesses such as severe asthma, chronic obstructive pulmonary disease, or tuberculosis; serious illnesses such as diabetes or heart disease; pregnancy; or any condition that would make it difficult or uncomfortable to inhale deeply and cough and exhale forcefully. After the study was explained to the test subject and informed consent was obtained, two nasopharyngeal swabs and an oropharyngeal swab were taken from the subject and placed in 3 ml of VTM (these will be referred to as NOP swabs). The subject's oral temperature was measured and a brief health questionnaire was administered. The subject was then asked to sit in front of the aerosol collection system. The subject was instructed to inhale as deeply as possible, seal their mouth around the mouthpiece, and cough into the machine using as much of the air in their lungs as possible. After each cough, the cough-generated aerosol was collected using the aerosol sampler. This procedure was repeated for a total of three coughs from each subject. Next, the subject was asked to repeat the procedure but to exhale as much and as rapidly as possible rather than coughing. This was also repeated three times, and the exhalation-generated aerosol was collected after each exhalation using the aerosol sampler. The order of the coughing and exhalation was alternated so that odd-numbered subjects were asked to cough three times followed by three exhalations, while even-numbered subjects were asked to exhale three times followed by three coughs. To prevent cross-contamination, the collection system was purged three times with clean dry air after each cough or exhalation, and a new mouthpiece was used for each subject. After the coughs or exhalations were completed, the VTM were removed from the SKC BioSampler and placed in a storage tube. All samples in VTM were kept on ice until the end of the day and then transported to the laboratory and stored at -80°C until analysis. Each subject was only asked to perform one test session.

Viral replication assay (VRA)

In previous studies of cough and exhalation aerosols by our group and others, the largest problem has been detecting the small amounts of viable virus present in these aerosol samples.^(13,18,19,21,24) In this study, a viral replication assay (VRA) was used to determine whether viable influenza virus was present in the samples that were collected.⁽³⁵⁾ The VRA is more sensitive and easier to use with small sample quantities than a traditional viral plaque assay or tissue culture infectious dose assay.⁽³⁵⁾ In experiments with aerosols containing viable influenza virus, the VRA amplified the amount of infectious virus in the samples by a factor of 4.6×10^5 .⁽³⁵⁾

Detection of viable influenza virus in NOP swab samples

For the NOP swab samples, Madin Darby canine kidney (MDCK) cells (CCL-34) were plated at a density of 5.0×10^4 per well in a 96-well plate (CoStar 96-well tissue culture plate, Corning). Triplicate wells were treated with 100 μl of each sample for 45 minutes. The wells were washed by adding 100 μl of phosphate-buffered saline (PBS) ml to the inoculum and removing the resulting supernatant. The cells were overlaid with 100 μl supplemented Dulbecco's modified Eagle's medium (DMEM)/F12 and incubated for 20 hours at 35°C in a humidified 5% CO_2 incubator to allow for viral replication. Total RNA was isolated from the cells and supernatant with the MagMaxTM-96 Total RNA Isolation Kit (Ambion) and transcribed into cDNA using the High Capacity cDNA Reverse Transcription Kit (Life Technologies). A 5 μl cDNA volume was analyzed using quantitative PCR (qPCR) with a custom primer/probe set specific for the matrix (M1) gene or the H3 hemagglutinin gene of influenza A virus. Details about the primers and probes are provided in the online supporting information.

Detection of viable influenza virus in cough and exhalation aerosol samples

For the cough and exhalation aerosol samples, a 6-well formatted VRA assay was used to increase the sensitivity for detecting influenza virus in the aerosol samples. MDCK cells plated at a density of 1.5×10^6 per well (CoStar 6-well tissue culture plate, Corning) were incubated at 35°C in a humidified 5% CO_2 incubator overnight. For each sample, duplicate wells with confluent cellular monolayers were next washed two times with 2 ml PBS (Invitrogen) and treated with a 1.2 ml sample volume for 45 minutes. The wells were washed by adding 1.2 ml of PBS to the inoculum and removing the resulting supernatant. One ml of supplemented Dulbecco's modified Eagle's medium (DMEM)/F12 containing 100 units/ml penicillin G/100 $\mu\text{g}/\text{ml}$ streptomycin (Invitrogen), 2 mM L-glutamine (Invitrogen), 0.2% BSA

(Sigma-Aldrich), 10 mM HEPES (Invitrogen), 0.22% sodium bicarbonate (Invitrogen), 0.01% DEAE-dextran (MP BioMedicals, LLC, Solon, OH), and 2 µg/ml N-p-tosyl-L-phenylalanine chloromethyl ketone (TPCK) (Sigma-Aldrich) was added to each well. Treated MDCK cells were subsequently incubated for 20 hours at 35°C in a humidified 5% CO₂ incubator to allow for viral replication. The treated cellular monolayer was lysed with 1 ml of MagMax™ Lysis/Binding Solution Concentrate (Ambion) and the lysate was pooled with the reserved culture supernatant (final volume of ~2 ml) and stored at -80°C until total RNA was isolated.

To account for the larger sample volume in the 6-well formatted VRA, total RNA was isolated using a modified MagMax™-96 Total RNA Isolation Kit (Ambion) protocol. A 1 ml volume of molecular-grade 2-propanol (Sigma) was mixed by inversion into each thawed, pooled sample followed by the addition of 20 µl prepared Bead Mix (Thermo Scientific). Samples were then gently shaken for 5 minutes and magnetically captured. The supernatant was discarded and the resulting RNA-bound bead pellet was resuspended in 150 µl Wash Solution 1 and transferred to a 96-well processing plate. The manufacturer's instructions were followed for the remainder of the total RNA isolation procedure. Total RNA was eluted with 30 µl of elution buffer and transcribed into cDNA using the High Capacity cDNA Reverse Transcription Kit (Life Technologies). A 5 µl cDNA volume was analyzed for the M1 gene using qPCR.

Data analysis

During the qPCR assay portion of the VRA, the samples were subjected to 45 PCR amplification cycles. The limit of quantitation (LOQ) of the qPCR assay was 15 viral copies per PCR tube, which corresponded to a threshold cycle (C_t) value of 34.1. The limit of detection (LOD) based on qPCR only was 10 viral copies per tube, which corresponded to a threshold cycle (C_t) value of 35.8. In cases where a PCR product was detected but the C_t value was higher than the C_t value for the LOQ, then the PCR product was evaluated by agarose gel electrophoresis to verify that the PCR product was the correct size (101 base pairs for the M1 matrix gene). Sample volumes of 10 µl were loaded into a 4.5% agarose gel (Nusieve GTG Agarose, Lonza) along with 10 µl of a 100-bp DNA ladder (N3231L, New England Biolabs). Electrophoresis was carried out in 1X TAE at 90 volts for approximately 90 minutes. DNA was visualized by ethidium bromide staining. The LOD with this additional step was as little as 1 viral copy per reaction tube. For additional verification, DNA sequence analysis was performed on randomly chosen cough and exhale samples by a commercial laboratory (Genewiz, Inc.) using pre-defined Sanger DNA sequencing.

Because of the low concentration of influenza virus in the cough and exhalation aerosol samples, in many cases the amount of virus detected using the qPCR assay was below the

limit of quantitation for the assay. For this reason, the results are reported here only as positive or negative for influenza A. To reduce the possibility of false-positive results, only test subjects who had NOP swabs that were positive for influenza by the M1 and H3 gene assays were considered to be confirmed to have an influenza infection and were used in the data analysis.

When analyzing the experimental data, a sample was considered to be positive for influenza if a PCR product was detected in one or more of the qPCRs and the product was confirmed to be the correct size by gel electrophoresis. For example, each cough or exhalation aerosol sample was tested by inoculating and incubating two culture wells of MDCK cells, isolating and reverse transcribing the RNA produced by the cells in each well, and conducting duplicate qPCR assays for each well. Because of the low amounts of viable influenza found in the cough and exhalation aerosols, many of the qPCRs had C_t values that were close to the maximum limit of 45 cycles for the qPCR assay. For this reason, if any one of the four qPCRs yielded a PCR product of the correct size, then that sample was considered influenza positive even if no PCR product was detected in the other three reactions. The full results from the qPCR assays are presented in the supporting information with the online version of this article.

Statistical analyses included comparison of proportion of positive coughs and exhalations using McNemar's test for paired dichotomous data.⁽³⁶⁾ The chi-square test was performed to test for differences in positive cough and exhalation proportions between the two orders of testing (cough then exhalation vs. exhalation then cough). All tests were two-tailed and performed using a 0.05 significance level.

Results

For this study, 61 adult volunteer subjects were recruited from college students presenting with influenza-like symptoms at WVU Medicine Student Health Services in Morgantown, West Virginia, USA, during January and February in 2015. A summary of the demographic information, oral temperatures, cough volume, cough peak flow rate, and symptoms reported by the test subjects in which viable influenza A virus was detected is shown in Table 1.

Nasopharyngeal and oropharyngeal (NOP) swabs were tested for viable influenza A virus using the viral replication assay (VRA) with qPCR assays for the M1 matrix gene. Fifty-three NOP swab samples (87%) were positive for viable influenza A. The H3-type hemagglutinin gene was detected in all 53 samples, consistent with the prevalence of H3N2 influenza A in the United States during the 2014-2015 influenza season. Only test subjects with influenza-positive NOP swabs were considered to be confirmed to be infected with influenza and were used in the data analysis.

Table 1. Demographic and medical information for study participants confirmed to be infected with influenza. Information for all of the patients is included in the online supporting information

# Of subjects	53	
Gender	30 Male, 23 Female	
	Mean	SD
Age (years)	21.0	3.4
Height (cm)	172	10
Weight (kg)	76.6	20.0
Temperature (°C)	37.4	0.7
# of days of symptoms	2.2	2.1
Cough volume (liters)	2.7	1.1
Peak flow rate during coughs (liters/second)	7.5	2.2
Exhalation volume (liters)	3.5	1.0
Peak flow rate during exhalation (liters/second)	4.8	2.1
Number of subjects reporting		
Fever/chills	43	
Headache	40	
Fatigue	43	
Cough	44	
Sore throat	41	
Sinus congestion	32	
Runny nose	37	
Sneezing	28	
Muscle aches	43	
Took medication for symptoms	27 yes, 26 no	
Received influenza vaccine within last 6 months	6 yes, 43 no, 4 unsure	

Viable influenza A virus was found in cough aerosol samples from 28 of 53 subjects and in exhalation aerosol samples from 22 of 52 subjects confirmed to have influenza (one exhalation aerosol sample was lost before analysis). The difference in the number of influenza-positive coughs vs. influenza-positive exhalations was not statistically significant ($P = 0.2207$). 37 subjects had influenza-positive NOP swabs and influenza-positive cough or exhalation aerosols, while for 15 subjects, influenza was detected in the NOP swabs but not in the cough or exhalation aerosols. Thirteen subjects had both cough aerosol and exhalation aerosol samples that contained viable influenza A virus, 15 had positive cough aerosol samples but negative exhalation samples, 9 had positive exhalation samples but negative cough samples, and 15 had negative cough and exhalation samples. The order in which the experiment was performed (coughs followed by exhalations, or exhalations followed by coughs) did not have a significant effect on the results ($P = 0.2499$). The influenza results for all test subjects are shown in Table 2.

To confirm that the qPCRs in the VRA were amplifying influenza virus, the size of the PCR products were verified by agarose gel electrophoresis. An example electrophoretic gel is

Table 2. Presence or absence of viable influenza A virus in NOP swabs, cough aerosol particles, and exhalation aerosol particles for each patient. H3 and M1 indicate the influenza A gene that was targeted in the PCR portion of the VRA

Patient ID	NOP swab (M1)	NOP swab (H3)	Cough (M1)	Exhalation (M1)
Subjects confirmed to have influenza				
FC134	+	+	—	—
FC135	+	+	—	—
FC136	+	+	+	+
FC137	+	+	+	—
FC138	+	+	+	+
FC139	+	+	—	+
FC140	+	+	+	+
FC141	+	+	—	—
FC142	+	+	—	—
FC143	+	+	+	+
FC144	+	+	—	—
FC145	+	+	+	—
FC146	+	+	—	+
FC150	+	+	+	+
FC151	+	+	—	+
FC152	+	+	+	—
FC153	+	+	—	+
FC154	+	+	+	—
FC155	+	+	+	—
FC157	+	+	+	—
FC158	+	+	+	—
FC159	+	+	+	+
FC160	+	+	—	—
FC161	+	+	—	+
FC162	+	+	—	—
FC163	+	+	—	—
FC164	+	+	+	+
FC165	+	+	—	+
FC166	+	+	+	—
FC167	+	+	+	+
FC168	+	+	+	—
FC171	+	+	—	—
FC172	+	+	—	+
FC173	+	+	—	—
FC174	+	+	—	—
FC175	+	+	—	+
FC176	+	+	+	—
FC177	+	+	—	—
FC178	+	+	+	+
FC179	+	+	+	+
FC180	+	+	+	—
FC181	+	+	+	—
FC182	+	+	—	—
FC183	+	+	—	—
FC184	+	+	+	+
FC185	+	+	+	—
FC186	+	+	+	—
FC187	+	+	—	Lost
FC188	+	+	+	+
FC190	+	+	—	+
FC191	+	+	—	—

Table 2. (Continued)

Patient ID	NOP swab (M1)	NOP swab (H3)	Cough (M1)	Exhalation (M1)
FC192	+	+	+	+
FC193	+	+	+	—
Positive	53	53	28	22
Negative	0	0	25	30
Total	53	53	53	52
Subjects not confirmed to have influenza				
FC133	—	+	+	—
FC147	—	—	+	—
FC148	—	—	—	—
FC149	—	—	—	—
FC156	—	—	+	—
FC169	—	—	—	—
FC170	—	+	—	—
FC189	—	—	—	+

shown in Figure 2. A total of 484 qPCRs were performed to analyze the cough and exhalation aerosol samples from the 61 subjects. Of these, a matrix gene PCR product was detected in 89 reactions. In 79 reactions (89%), gel electrophoresis of the PCR product produced a 101-base pair band, indicating the presence of influenza A. In the remaining 192 PCRs, a PCR product was not detected and no

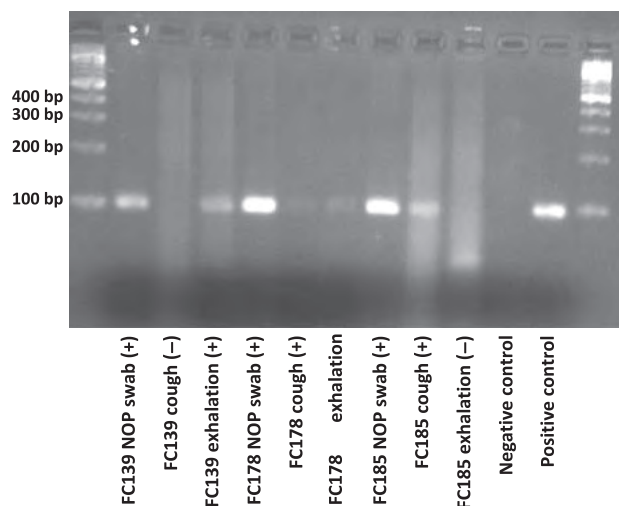


Figure 2. Electrophoretic gel used to determine the presence or absence of a 101-base pair PCR product corresponding to the influenza A M1 matrix gene. The PCR products for the NOP swabs, cough aerosols, and exhalation aerosols for three test subjects are shown. (+) indicates the sample is positive for influenza A. (—) indicates the sample is negative. The PCR products for the cough and exhalation samples for subject FC178 were confirmed to be from the influenza A M1 matrix gene by DNA sequence analysis. The negative control contained all PCR reagents, primers, and probe but no template. The positive control contained 10^4 M1 copies and was run in parallel with the experimental samples.

101-base pair bands were observed. The PCR products from 12 H3 gene analyses of the NOP swabs also were tested and found to be of the correct size (150 base pairs). As additional verification, the VRA M1 gene PCR products from 7 cough aerosol samples and 9 exhalation aerosol samples were sent to a commercial laboratory for sequence analysis. All 7 of the cough aerosol PCR products and 7 of the 9 exhalation aerosol PCR products were confirmed to match the matrix gene segment M1 from influenza A. Two of the exhalation aerosol PCR products could not be sequenced.

Discussion

Humans infected with influenza virus have been shown to expel small airborne particles containing viable virus into the environment when they cough or exhale, which suggests that the potential exists for the airborne transmission of influenza.^(13,18,19,21,24) However, it is not clear how often airborne transmission actually occurs or what factors affect the likelihood of transmission by the airborne route, in part because many questions remain about the processes involved in infectious aerosol production and the dynamics of these aerosols in the environment. Consistent with previous studies, our results show that aerosol particles containing viable influenza virus are produced by infected individuals both during coughing and during exhalation. Viable virus was detected more often in cough aerosol samples (53% of influenza-positive subjects) compared to exhalation aerosols (42% of influenza-positive subjects). However, this difference is not substantial and was not statistically significant. As people breathe constantly but cough sporadically, this suggests that patients infected with influenza may release more virus into the air over time in small airborne particles by breathing compared to coughing. On the other hand, as coughing involves much higher air velocities than breathing, coughing may spread the virus further in a given location. Thus, both mechanisms for producing infectious aerosols may be important depending upon such factors as the distance from a patient, the timescale, the infectious dose, and the air flow within a room.

Viable influenza virus was detected in the cough aerosol, exhalation aerosol, or both from 37 of 53 influenza-positive test subjects (70%), which suggests that this is a common phenomenon. It should be noted that the aerosol collection system used in these experiments does not capture particles larger than 10–15 μm in the collection media, and thus collects only small particles capable of airborne transmission and not the “large droplets” often referenced in droplet disease transmission. Viable influenza was detected in both the cough and exhalation aerosols for 35% of these subjects (13/37), while it was only detected in the cough aerosol for 41% (15/37) and only in the exhalation aerosol for 24% (9/37). These results are consistent with somewhat more

infectious aerosol being released during coughing than breathing, although they probably also reflect the fact that the airborne viable virus concentrations are quite low and are difficult to detect.

Two patients had influenza-positive cough aerosols but negative NOP swabs, while one had a positive exhalation aerosol but a negative NOP swab. One possible explanation is that, because some patients did not tolerate the nasopharyngeal swabs well, the sample obtained may not have been sufficient for detection of influenza. Alternatively, Milton *et al.*⁽¹⁹⁾ reported that the amount of influenza RNA detected in NOP swabs was only weakly correlated with the amount detected in exhaled breath; thus, it may be that these three patients had sufficient influenza virus in their lower respiratory tract to produce infectious aerosol particles but insufficient virus in their nasopharyngeal region to be detected. Finally, the possibility of a false-positive cough or breath sample or a false-negative NOP swab result cannot be excluded. For consistency and to reduce the possibility of false-positive results, only patients with positive NOP swabs were considered to be confirmed to be infected with influenza and included in our analysis.

Because of the low concentrations of airborne viable influenza virus in the cough and exhalation aerosol samples, we were not able to quantify the amount of airborne viable virus present in the original samples in our experiments. However, this should not be interpreted to mean that the risk of infection is low. Our samples were collected from only three coughs and three exhalations, while a person infected with influenza would be expected to cough dozens of times and breathe hundreds of times per hour and thus could still release a considerable amount of airborne infectious material over the course of a day. In addition, the infectious dose for airborne influenza is very low; one study found that inhalation of small aerosol particles containing only 0.7 to 3.5 plaque-forming units (PFU) of influenza was sufficient to cause seroconversion in 50% of the human subjects tested.⁽³⁷⁾

The fact that the number of aerosol samples with viable influenza was not significantly greater for coughing than for exhalation is consistent with the theory that a substantial portion of the influenza-laden aerosol produced by infected people originates in the deepest parts of the lungs rather than in the upper airways and oropharyngeal region. Smaller aerosol particles have been proposed to be produced in the alveolar and bronchial regions during both breathing and coughing by the formation and rupture of menisci as airways contract and expand. Larger particles are thought to be created by shear forces acting on fluid-covered upper airways, where air velocities are much higher than in the deeper regions. This phenomenon is thought to occur primarily during coughing because the air flow rates are much higher than during breathing.^(29–31) Since, in this

theory, deep lung particle generation occurs during both breathing and coughing while upper airway particle generation occurs only during coughing, then the modest increase in the number of positive samples seen during coughing compared to exhalation in our experiments supports the idea that much of the infectious aerosol is originating in the deep lung regions.

The ability of our system to collect cough and exhalation aerosols separately was useful for the present study, but it also significantly limited the study because of the small amount of aerosol that was collected. By comparison, the system used by Milton *et al.* collects aerosols produced by natural coughs and exhalations over a 30-minute period, and that group has reported greater success in detecting and quantifying airborne influenza virus.^(19,25,38) Thus, our results suggest that future work studying infectious aerosol production and the presence of infectious aerosols in the environment should collect sample volumes that are as large as practically possible, which would likely entail using high sample flow rates and long sample times. Unfortunately, however, maintaining high flow rates and long sample times while attempting to collect airborne viruses and maintain their viability is very challenging, especially when the viruses are contained in submicrometer aerosol particles.

Finally, it is important to acknowledge the limitations of our experiments. First, the single most difficult aspect of studying the production of aerosols containing viable influenza virus during respiratory activities is the low concentration of such viruses in the air and the difficulty in collecting enough material and maintaining viability to detect the viable virus. To maximize the sensitivity of our assays and reduce the possibility of false-negative results as much as possible, the evaluation criteria for our results were designed to provide the greatest likelihood of detecting small amounts of viable influenza virus, with steps then taken to minimize the possibility of false-positive results. However, we recognize that the possibility of some false-positive outcomes cannot be ruled out in our analysis.

Second, our test subjects were asked to inhale as deeply as possible and then cough or exhale using as much of the air in their lungs as possible. Most natural coughs and normal tidal breathing use smaller fractions of the total lung capacity, which may reduce aerosol generation. On the other hand, natural coughs are stimulated by a need to clear secretions from the airways, and thus, natural coughs may produce more aerosol particles than forced coughs. It is also possible that the ratio of the amount influenza-laden aerosol particles produced during natural coughing to that produced during natural breathing may be different than the ratio we found when comparing forced coughs to forced exhalations.

Third, the particle collection efficiency of the SKC BioSampler decreases from about 96% for 1 μm aerosol particles to about 50% for 0.3 μm particles and 10% for

0.1 μm particles.^(32–34) Thus, many of the smallest particles carrying influenza virus may not have been collected in our experiments. As noted earlier, particles larger than 10–15 μm were not collected and thus their potential contribution to disease transmission is not known. In addition, some cough aerosol particles may have deposited inside the system before they could be collected. In our previous study using the cough aerosol collection system,⁽²⁴⁾ swab samples from the face of the spirometer piston and the BioSampler elbow found little influenza, suggesting that particle losses in these locations were minimal. However, other parts of the system, such as the mouthpiece, were not tested.

Last, influenza viral shedding peaks around the first day of acute respiratory illness and then declines rapidly.^(19,21,39–41) In our study, patients presented at the clinic an average of two days after their symptoms developed (Table 1), well after the expected maximum in viral shedding. In addition, our test subjects were college-aged ambulatory outpatients with no other reported respiratory illnesses or significant health conditions. Patients who are more severely ill would generally be expected to have higher viral loads and may be more likely to produce cough and exhalation aerosols containing infectious influenza virus, especially in the early stages of illness.^(40,42) Patients who are younger or older, immunocompromised, or have underlying pulmonary illness such as asthma or chronic obstructive pulmonary disease also may have very different infectious aerosol generation patterns. This could be an important factor during an influenza pandemic, when healthcare facilities would be expected to receive large numbers of severely ill patients.

Conclusions

The purpose of this study was to directly compare the expulsion of aerosol particles containing potentially infectious influenza virus during coughing and exhalation. Our results confirm that the production of aerosols containing viable influenza virus is common among infected people. Viable virus was detected more often in cough aerosols than in exhalation aerosols, but the difference was not large. As individuals breathe more often than they cough, these results suggest that breathing may generate more airborne infectious material than coughing over time. However, both respiratory activities could be important in airborne influenza transmission. Our results are also consistent with the theory that much of the aerosol containing viable influenza originates deep in the lungs, although more direct investigation would be needed to verify this.

Acknowledgements

We would like to thank the volunteers who participated in this study and the staff of West Virginia University Medicine Student Health Services for their cheerful cooperation and

assistance. This work was funded by the Centers for Disease Control and Prevention. The authors have no competing interests to declare. The findings and conclusions in this report are those of the authors and do not necessarily represent the official position of the Centers for Disease Control and Prevention.

References

- 1 Killingley B, Nguyen-Van-Tam J. Routes of influenza transmission. *Influenza Other Respir Viruses* 2013; 7(Suppl 2):42–51.
- 2 IOM: Respiratory Protection for Healthcare Workers in the Workplace Against Novel H1N1 Influenza A: A Letter Report. Washington, DC: Institute of Medicine, 2009.
- 3 IOM: Preventing Transmission of Pandemic Influenza and Other Viral Respiratory Diseases: Personal Protective Equipment for Healthcare Personnel. Update 2010. Larson EL, Liverman CT (eds.): Washington, DC: Institute of Medicine, 2011.
- 4 WHO: WHO Public Health Research Agenda for Influenza Biannual Progress Review and Report 2010–2011. Geneva, Switzerland: World Health Organization, 2013.
- 5 Jones RM, Brosseau LM. Aerosol transmission of infectious disease. *J Occup Environ Med* 2015; 57:501–508.
- 6 Tellier R. Aerosol transmission of influenza A virus: a review of new studies. *J R Soc Interface* 2009; 6(Suppl 6):S783–S790.
- 7 Weber TP, Stilianakis NI. Inactivation of influenza A viruses in the environment and modes of transmission: a critical review. *J Infect* 2008; 57(5):361–373.
- 8 Cowling BJ, Ip DK, Fang VJ *et al.* Aerosol transmission is an important mode of influenza A virus spread. *Nat Commun* 2013; 4:1935.
- 9 Tseng CC, Chang LY, Li CS. Detection of airborne viruses in a pediatrics department measured using real-time qPCR coupled to an air-sampling filter method. *J Environ Health* 2010; 73:22–28.
- 10 Yang W, Elankumaran S, Marr LC. Concentrations and size distributions of airborne influenza A viruses measured indoors at a health centre, a day-care centre and on aeroplanes. *J R Soc Interface* 2011; 8:1176–1184.
- 11 Thompson KA, Pappachan JV, Bennett AM *et al.* Influenza aerosols in UK hospitals during the H1N1 (2009) pandemic—the risk of aerosol generation during medical procedures. *PLoS ONE* 2013; 8:e56278.
- 12 Bischoff WE, Swett K, Leng I, Peters TR. Exposure to influenza virus aerosols during routine patient care. *J Infect Dis* 2013; 207:1037–1046.
- 13 Lednicky JA, Loeb JC. Detection and isolation of airborne influenza A H3N2 virus using a Sioutas personal cascade impactor sampler. *Influenza Res Treat* 2013; 2013:656825.
- 14 Blachere FM, Lindsley WG, Pearce TA *et al.* Measurement of airborne influenza virus in a hospital emergency department. *Clin Infect Dis* 2009; 48:438–440.
- 15 Lindsley WG, Blachere FM, Davis KA *et al.* Distribution of airborne influenza virus and respiratory syncytial virus in an urgent care medical clinic. *Clin Infect Dis* 2010; 50:693–698.
- 16 Leung NH, Zhou J, Chu DK *et al.* Quantification of influenza virus RNA in aerosols in patient rooms. *PLoS ONE* 2016; 11:e0148669.
- 17 Killingley B, Grotorex J, Cauchemez S *et al.* Virus shedding and environmental deposition of novel A (H1N1) pandemic influenza virus: interim findings. *Health Technol Assess* 2010; 14:237–354.
- 18 Lindsley WG, Blachere FM, Thewlis RE *et al.* Measurements of airborne influenza virus in aerosol particles from human coughs. *PLoS ONE* 2010; 5:e15100.
- 19 Milton DK, Fabian MP, Cowling BJ, Grantham ML, McDevitt JJ. Influenza virus aerosols in human exhaled breath: particle size,

- culturability, and effect of surgical masks. *PLoS Pathog* 2013; 9: e1003205.
- 20 Gralton J, Tovey ER, McLaws ML, Rawlinson WD. Respiratory virus RNA is detectable in airborne and droplet particles. *J Med Virol* 2013; 85:2151–2159.
 - 21 Hatagishi E, Okamoto M, Ohmiya S, et al. Establishment and clinical applications of a portable system for capturing influenza viruses released through coughing. *PLoS ONE* 2014; 9:e103560.
 - 22 Fabian P, McDevitt JJ, DeHaan WH et al. Influenza virus in human exhaled breath: an observational study. *PLoS ONE* 2008; 3:e2691.
 - 23 Stelzer-Braid S, Oliver BG, Blazey AJ et al. Exhalation of respiratory viruses by breathing, coughing, and talking. *J Med Virol* 2009; 81:1674–1679.
 - 24 Lindsley WG, Noti JD, Blachere FM et al. Viable influenza A virus in airborne particles from human coughs. *J Occup Environ Hyg* 2015; 12:107–113.
 - 25 Pantelic J, Yang J, Albert B, Grantham ML, Liu F, Milton DK. Characterization of respiratory droplets from community acquired and experimental laboratory infection in humans: In Options for the Control of Influenza VIII. Cape Town, South Africa:International Society for Influenza and Other Respiratory Virus Diseases, 2013.
 - 26 Lindsley WG, King WP, Thewlis RE et al. Dispersion and exposure to a cough-generated aerosol in a simulated medical examination room. *J Occup Environ Hyg* 2012; 9:681–690.
 - 27 Gralton J, Tovey E, McLaws ML, Rawlinson WD. The role of particle size in aerosolised pathogen transmission: a review. *J Infect* 2011; 62:1–13.
 - 28 Nicas M, Nazaroff WW, Hubbard A. Toward understanding the risk of secondary airborne infection: emission of respirable pathogens. *J Occup Environ Hyg* 2005; 2:143–154.
 - 29 Johnson GR, Morawska L, Ristovski ZD et al. Modality of human expired aerosol size distributions. *J Aerosol Sci* 2011; 42:839–851.
 - 30 Fabian P, Brain J, Houseman EA, Gern J, Milton DK. Origin of exhaled breath particles from healthy and human rhinovirus-infected subjects. *J Aerosol Med Pulm Drug Deliv* 2011; 24:137–147.
 - 31 Johnson GR, Morawska L. The mechanism of breath aerosol formation. *J Aerosol Med Pulm Drug Deliv* 2009; 22:229–237.
 - 32 Willeke K, Lin X, Grinshpun SA. Improved aerosol collection by combined impaction and centrifugal motion. *Aerosol Sci Technol* 1998; 28:439–456.
 - 33 Hogan CJ Jr, Kettleson EM, Lee MH, Ramaswami B, Angenent LT, Biswas P. Sampling methodologies and dosage assessment techniques for submicrometre and ultrafine virus aerosol particles. *J Appl Microbiol* 2005; 99:1422–1434.
 - 34 Kesavan J, Schepers D, McFarland AR. Sampling and retention efficiencies of batch-type liquid-based bioaerosol samplers. *Aerosol Sci Technol* 2010; 44:817–829.
 - 35 Blachere FM, Cao G, Lindsley WG, Noti JD, Beezhold DH. Enhanced detection of infectious airborne influenza virus. *J Virol Methods* 2011; 176:120–124.
 - 36 Agresti A. *An Introduction to Categorical Data Analysis*. New York: Wiley, 1996.
 - 37 Alford RH, Kasel JA, Gerone PJ, Knight V. Human influenza resulting from aerosol inhalation. *Proc Soc Exp Biol Med* 1966; 122:800–804.
 - 38 McDevitt JJ, Koutrakis P, Ferguson ST et al. Development and performance evaluation of an exhaled-breath bioaerosol collector for influenza virus. *Aerosol Sci Technol* 2013; 47:444–451.
 - 39 Cowling BJ, Chan KH, Fang VJ et al. Comparative epidemiology of pandemic and seasonal influenza A in households. *N Engl J Med* 2010; 362:2175–2184.
 - 40 Lau LL, Cowling BJ, Fang VJ et al. Viral shedding and clinical illness in naturally acquired influenza virus infections. *J Infect Dis* 2010; 201:1509–1516.
 - 41 Loeb M, Singh PK, Fox J et al. Longitudinal study of influenza molecular viral shedding in Hutterite communities. *J Infect Dis* 2012; 206:1078–1084.
 - 42 Lee N, Chan PK, Hui DS et al. Viral loads and duration of viral shedding in adult patients hospitalized with influenza. *J Infect Dis* 2009; 200:492–500.

AUTHOR BIOGRAPHIES

William G. Lindsley, designed and constructed the aerosol collection system, coordinated the study, analyzed the data, and was the primary author of the manuscript.

Francoise M. Blachere, developed the viral replication assay and adapted it to this work, developed the qPCR assay for the H3 analysis, analyzed the samples, assisted in the data analysis, and contributed to the writing of the manuscript.

Donald H. Beezhold, helped develop the concept for the study, provided input to the methodology and analysis, and contributed to the writing of the manuscript.

Robert E. Thewlis, assisted with the development of the clinical methodology, coordinated the study with the clinic staff, provided logistical support, and recruited subjects for the study.

Bahar Noorbakhsh, assisted with the development of the clinical methodology, handled staff scheduling, and collected samples in the clinic.

Sreekumar Othumpangat, provided technical assistance on the development of the methods for analyzing the samples and collected samples in the clinic.

William T. Goldsmith, developed the equipment and methodology to collect the cough and exhalation airflow data, analyzed the data, and collected samples in the clinic.

Cynthia M. McMillen, conducted the assays for the H3 analysis, assisted with the sample processing and analysis, and analyzed the H3 data.

Michael E. Andrew, performed the statistical analysis of the data, assisted in the interpretation, and contributed to the writing of the manuscript.

Carmen N. Burrell, provided medical supervision for the study, coordinated the study with the clinic staff, and helped develop the clinical methodology for the study.

John D. Noti, helped develop the viral replication assay and adapt it to this work, provided input and advice on the sample processing and data analysis, supervised the overall research effort, and contributed to the writing of the manuscript.

Supporting Information

Additional Supporting Information may be found online in the supporting information tab for this article:

Figure S1. For the direct PCR analysis of the nasopharyngeal and oropharyngeal (NOP) swabs, viral RNA was extracted directly from 50 μ l of each NOP sample.



Since January 2020 Elsevier has created a COVID-19 resource centre with free information in English and Mandarin on the novel coronavirus COVID-19. The COVID-19 resource centre is hosted on Elsevier Connect, the company's public news and information website.

Elsevier hereby grants permission to make all its COVID-19-related research that is available on the COVID-19 resource centre - including this research content - immediately available in PubMed Central and other publicly funded repositories, such as the WHO COVID database with rights for unrestricted research re-use and analyses in any form or by any means with acknowledgement of the original source. These permissions are granted for free by Elsevier for as long as the COVID-19 resource centre remains active.



Contents lists available at ScienceDirect

International Journal of Infectious Diseases

journal homepage: www.elsevier.com/locate/ijid

Short Communication

The assessment of transmission efficiency and latent infection period in asymptomatic carriers of SARS-CoV-2 infection

Zhirong Liu^{a,c,1}, Ruilin Chu^{b,1}, Lei Gong^{a,c,1}, Bin Su^{a,c}, Jiabing Wu^{a,c,*}^a Anhui Provincial Center for Disease Control and Prevention, Hefei, China^b Department of Infectious Disease Control and Prevention, Shanghai Municipal Center for Disease Control and Prevention, Shanghai, China^c Public Health Research Institute of Anhui Province, Hefei, China

ARTICLE INFO

Article history:

Received 13 April 2020

Received in revised form 9 June 2020

Accepted 9 June 2020

Keywords:

coronavirus disease 19

SARS-CoV-2

asymptomatic infection

emerging infectious disease

ABSTRACT

Few studies have focused on the transmission efficiency of asymptomatic carriers of severe acute respiratory syndrome coronavirus 2 (SARS-CoV-2) infection. Our follow-up study was performed on 147 asymptomatic carriers in Anhui Province. Of these, 50.0% were male, 50.3% were older than 40 years, 43.8% were farmers, and 68.7% were from the north of Anhui Province. 16 of the 147 asymptomatic carriers developed symptoms in the following 14 days of isolated observation, and were subsequently diagnosed as confirmed cases. The possible latent infection period was found to range from 1–5 days before onset, with a median time of 2 days. The second attack rate for the 16 confirmed cases who had transferred from being asymptomatic carriers was 9.7% (23/236 close contacts), while for the 131 asymptomatic carriers the rate was 2.6% (24/914 close contacts), showing a significant difference in second attack rate between the two groups ($p < 0.001$). Our study indicated that COVID-19 cases are contagious during the incubation period, and that close contact screening should be extended to include the incubation period. Our results also showed that the transmission efficiency for asymptomatic carriers was lower than that for confirmed case.

© 2020 Published by Elsevier Ltd on behalf of International Society for Infectious Diseases. This is an open access article under the CC BY-NC-ND license (<http://creativecommons.org/licenses/by-nc-nd/4.0/>).

Introduction

COVID-19 is a novel infectious disease caused by severe acute respiratory syndrome coronavirus 2 (SARS-CoV-2). This disease mainly affects the lung, but can also cause damage to the intestinal tract, liver, and nervous system, with corresponding symptoms (Lu et al., 2020). The outbreak originated in Wuhan city, Hubei Province in December 2019, and quickly spread to provinces and cities across the country and aboard (Li et al., 2020; WHO, 2020; Zhu et al., 2019). As of 28 August, 2020, there were 85 022 confirmed cases in China, including 4634 deaths and 80 126 recovered cases (China NHCotPsRo, 2020a). Human-to-human transmission of SARS-CoV-2 had been demonstrated mainly through respiratory droplets and contact (Chan et al., 2020). The continuing challenges of the epidemic and research progress in China have led to emergency responses from the Chinese government, including the issuance of regulatory documents (China NHCotPsRo, 2020b; China NHCotPsRo, 2020c).

Clinical symptoms of SARS-CoV-2 infection include fever, cough, and fatigue, and in a few cases stuffy nose, runny nose, and diarrhea (China NHCotPsRo, 2020b). Severe cases result in acute respiratory distress syndrome, septic shock, and coagulopathy caused death (Huang et al., 2020). As a highly contagious infectious disease, its sources of infection include not only confirmed cases, but also asymptomatic carriers (Huang et al., 2020; Cohen, 2020). Asymptomatic carriers of SARS-CoV-2 infection are always without clinical symptoms, but positive for the viral nucleic acid test. Most are found during the screening of close contacts, and because the laboratory tests are performed at an early stage, some asymptomatic cases go on to develop illness after screening.

For this study, we conducted a follow-up study on asymptomatic carriers in Anhui Province, and analyzed the features of these infections. Our findings provide evidence for the need to modify the preventive measures.

Materials and methods

Study design

This was a follow-up study, conducted in Anhui Province, China.

* Corresponding author at. No. 12560, Fanhua Avenue, Hefei, Anhui, 230601, China.

E-mail address: wjb0386@126.com (J. Wu).

¹ These authors contributed equally to this work.

Study cases

147 asymptomatic carriers of SARS-CoV-2 infection were recruited for this study from Anhui Province. All asymptomatic carriers fulfilled the following criteria: (1) without symptoms of fever, cough, and fatigue; (2) no radiographic evidence of pneumonia; (3) with normal white cell count and normal lymphocyte count; and (4) positive nucleic acid test for SARS-CoV-2.

Data collection

A questionnaire was formulated to gather data on: (1) demographic information, such as name, age, gender, and occupation; (2) clinical symptoms, including fever, chill, cough, and fatigue if these developed during the 14-day observation period; (3) laboratory testing related to SARS-CoV-2 infection, including nucleic test result and timing of test; (4) close contact information, such as numbers, confirmed cases, and asymptomatic carriers.

Laboratory testing

Respiratory samples, including sputum and throat swab samples, were collected from all asymptomatic carriers by trained inspection personnel. Viral RNA was extracted using a TANBead nucleic acid kit (Taiwan Advanced Nanotech Inc, Taiwan, China) in a biosafety level-2 laboratory. Tests for the *ORF1ab* and *N* genes in respiratory samples were carried out using a 2019-nCoV dual fluorescent PCR kit (Shanghai BioGerm Medical Biotechnology Co., Ltd, Shanghai, China and DAAN Gene Co., Ltd, Sun Yat-sen University, Guangdong, China).

Statistical analysis

Microsoft Office software (version 2019) was employed to input and check the data, and SPSS software (version 11.0) was used to analyze the data. Categorical variables were summarized as frequencies and percentages, and continuous variables were described using medians. The frequencies of categorical variables were compared using the chi-square test, as appropriate. Tests with a *p*-value less than 0.05 were considered statistically significant.

Ethical statement

Collection of data and samples from patients was part of a routine surveillance and outbreak investigation, and was therefore

exempt from assessment by the institutional review board (IRB). The IRB of Anhui Provincial Center for Disease Control and Prevention reviewed the study.

Results

Demographic features

Table 1 shows the demographic features of the 147 asymptomatic carriers. Of these, 15.6% (23/147) were under 20 years old, and 64.6% (95/147) were aged 20–59 years. 51.7% (76/147) of the carriers were male, and 94.6% (139/147) were found by close contact screening. A total of 16 asymptomatic carriers developed symptoms during the following 14-day observation period.

Latent infectivity assessment

The results of our latent infectivity assessment are shown in Figure 1. The latent infectivity period was evaluated using the 16 confirmed cases who had transferred from being asymptomatic carriers. Two cases had tested positive 5 days before developing symptoms, one case 4 days before, three cases 3 days before, seven cases 2 days before, and three cases just 1 day prior to becoming ill. The median period was calculated as 2 days (range 1–5).

Transmission efficiency assessment

A comparison of second attack rates for asymptomatic carriers and confirmed cases is shown in Table 1. A total of 1150 close contacts was determined in relation to the 147 asymptomatic carriers. 47 close contacts tested positive for SARS-CoV-2 infection during the 14-day observation period. The 16 confirmed cases who had previously been asymptomatic accounted for 236 close contacts, with a second attack rate of 9.7%, while the remaining 131 asymptomatic carriers accounted for 914 close contacts, with a second attack rate of 2.6%. There was a significant difference between two groups (χ^2 (Li et al., 2020) = 24.257; $p < 0.001$).

Discussion

Asymptomatic infection, as part of the SARS-CoV-2 infection spectrum, has been reported in a previous study (Chan et al., 2020). An asymptomatic carrier is defined as someone with a positive SARS-CoV-2 test from respiratory samples, including sputum and throat swab, but who displays no symptoms. Some

Table 1
Demographic features and transmission efficiency assessment for asymptomatic carriers of SARS-CoV-2 infection.

Variables	n (%)			p-value
	All carriers (n = 147)	Asymptomatic carriers (n = 131)	Confirmed cases transferred from asymptomatic carriers (n = 16)	
Age				0.195
< 20 years old	23 (15.6)	23 (17.6)	0 (0.0)	
20–39 years old	50 (34.0)	43 (32.8)	7 (43.8)	
40–59 years old	45 (30.6)	41 (31.3)	4 (25.0)	
≥ 60 years old	29 (19.7)	24 (18.3)	5 (31.2)	
Gender				0.500
Male	76 (51.7)	69 (52.7)	7 (43.8)	
Female	71 (48.3)	62 (47.3)	9 (56.2)	
Source of identification				0.793
Close contact screening	139 (94.6)	123 (93.9)	16 (100.0)	
Traceability investigation	2 (1.4)	2 (1.5)	0 (0.0)	
Extended screening	6 (4.1)	6 (4.6)	0 (0.0)	
Close contact				< 0.001
Second attack rate	4.1	2.6	9.7	
Positive close contacts	47	24	23	
Total close contacts	1150	914	236	

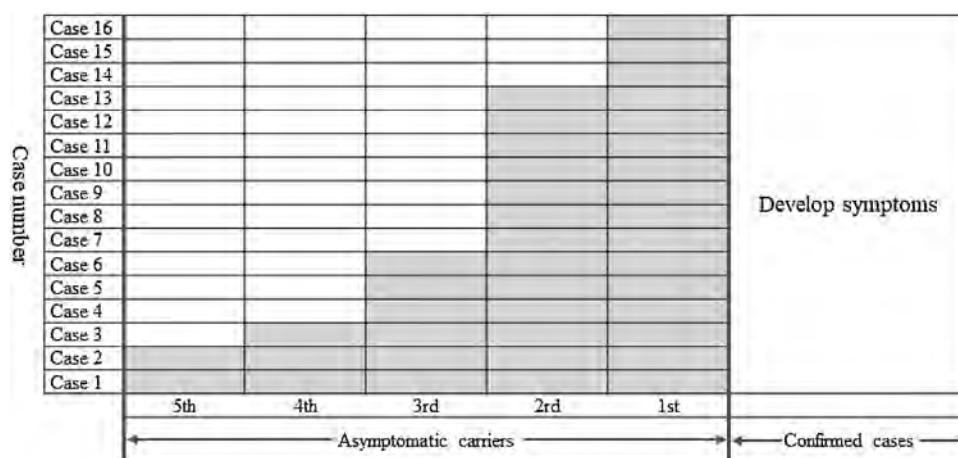


Figure 1. Assessment of latent infectivity, based on 16 confirmed cases who had transferred from being asymptomatic carriers.

studies have examined asymptomatic carriers and analyzed the incubation period (Pan et al., 2020; Wang et al., 2020). However, none has been conducted on the assessment of transmission efficiency and latent infection period with regards to asymptomatic infection. We performed this follow-up study in Anhui Province to examine these topics. Our findings could provide evidence to support the revision of control measures for SARS-CoV-2 infection.

Asymptomatic carriers can be identified in four ways. First, and most important, is active detection among close contacts. The second is based on epidemiological investigations surrounding suspected or confirmed cases. The third involves looking at the exposed population identified by tracking the SARS-CoV-2 infection source. Finally, asymptomatic carriers can be found through active surveillance in the epidemic areas. Our study confirmed that close contact screening was the main way to locate asymptomatic carriers, with the same result also being reported in a previous study (Pan et al., 2020). This revealed that close contacts identified by screening should be isolated because they are at risk of infection.

According to guidelines aimed at preventing SARS-CoV-2 infection, as potential infectious sources, asymptomatic carriers should be quarantined for 14 days from the first positive laboratory test (China NHCotPsRo, 2020d). 10.9% of the asymptomatic carriers in our study subsequently developed symptoms during the observation period to become confirmed cases. Those cases occurred during the incubation period, a median of 2 days after testing positive (range 1–5 days). Thus, close contact screening should not only focus on patients who have developed illness, but should also be extended to include asymptomatic cases during the incubation period, in order to reduce the infection risk of SARS-CoV-2 (Hu et al., 2020). Our study also assessed the transmission efficiency of asymptomatic carriers. Although the attack rate was lower than that for confirmed cases, it was shown to cause infection in 2.6% of close contacts.

In conclusion, although the transmission efficiency of asymptomatic carriers is lower than that for confirmed cases, the transmission risk from carriers should not be ignored. Second, close contacts of those infected with SARS-CoV-2 should undergo detailed observation and active laboratory screening, with these measures being included in the formulating of guidelines relating to SARS-CoV-2. Finally, close contact screening should be extended to include those present up to 5 days before the onset of illness in confirmed cases.

Funding

This study was supported by grants from Anhui Provincial Department of Science and Technology, Anhui Provincial Health Commission Emergency Research Project of Novel Coronavirus Infection (grant numbers 202004a07020002; 202004a07020004).

Conflicts of interest

The authors declare that they have no conflicts of interest.

Acknowledgements

We would like to thank the physicians and staff at the 16 municipal centers for Disease Control and prevention in Anhui Province for collecting the information of asymptomatic carriers of SARS-CoV-2 infection.

References

- Lu R, Zhao X, Li J, Niu P, Yang B, Wu H, et al. Genomic characterisation and epidemiology of 2019 novel coronavirus: implications for virus origins and receptor binding. *Lancet* 2020;395:565–74.
- Li Q, Guan X, Wu P, Wang X, Zhou L, Tong Y, et al. Early Transmission Dynamics in Wuhan, China, of Novel Coronavirus-Infected Pneumonia. *N Engl J Med* 2020;.
- WHO. Laboratory testing for 2019 novel coronavirus (2019-nCoV) in suspected human cases 2020 Geneva. 2020.
- Zhu N, Zhang D, Wang W, Li X, Yang B, Song J, et al. China Novel Coronavirus I, Research T, 2020. A Novel Coronavirus from Patients with Pneumonia in China. *N Engl J Med* 2019;382:727–33.
- China NHCotPsRo. Epidemic situation of Corona Virus Disease 19 on February 25. 2020.
- Chan JF-W, Yuan S, Kok K-H, To KK-W, Chu H, Yang J, et al. A familial cluster of pneumonia associated with the 2019 novel coronavirus indicating person-to-person transmission: a study of a family cluster. *Lancet* 2020;395:514–23.
- China NHCotPsRo. Corona Virus Disease 19 is included in the management of legal infectious diseases. 2020.
- China NHCotPsRo. Office of the State Administration of Traditional Chinese Medicine. Diagnosis and treatment of Corona Virus Disease 19 (Trial version 7). 2020.
- Huang C, Wang Y, Li X, Ren L, Zhao J, Hu Y, et al. Clinical features of patients infected with 2019 novel coronavirus in Wuhan, China. *Lancet* 2020;395:497–506.
- Cohen JND. World on alert for potential spread of new SARS-like virus found in China. 2020.
- Pan X, Chen D, Xia Y, Wu X, Li T, Ou X, et al. Asymptomatic cases in a family cluster with SARS-CoV-2 infection. *Lancet Infect Dis* 2020;20:410–1.
- Wang Y, Liu Y, Liu L, Wang X, Luo N, Ling L. Clinical outcome of 55 asymptomatic cases at the time of hospital admission infected with SARS-Coronavirus-2 in Shenzhen, China. *J Infect Dis* 2020;.
- China NHCotPsRo. The Prevention and Control Plan of Corona Virus Disease 19 (Version 5). 2020.
- Hu Z, Song C, Xu C, Jin G, Chen Y, Xu X, et al. Clinical characteristics of 24 asymptomatic infections with COVID-19 screened among close contacts in China. *Sci. China Life Sci.* 2020;.

Transmission Dynamics of COVID-19 Outbreaks Associated with Child Care Facilities — Salt Lake City, Utah, April–July 2020

Adriana S. Lopez, MHS¹; Mary Hill, MPH²; Jessica Antezano, MPA²; Dede Vilven, MPH²; Tyler Rutner²; Linda Bogdanow²; Carlene Claflin²; Ian T. Kracalik, PhD¹; Victoria L. Fields, DVM¹; Angela Dunn, MD³; Jacqueline E. Tate, PhD¹; Hannah L. Kirking, MD¹; Tair Kiphibane²; Ilene Risk, MPA²; Cuc H. Tran, PhD¹

On September 11, 2020, this report was posted as an MMWR Early Release on the MMWR website (<https://www.cdc.gov/mmwr>).

Reports suggest that children aged ≥ 10 years can efficiently transmit SARS-CoV-2, the virus that causes coronavirus disease 2019 (COVID-19) (1,2). However, limited data are available on SARS-CoV-2 transmission from young children, particularly in child care settings (3). To better understand transmission from young children, contact tracing data collected from three COVID-19 outbreaks in child care facilities in Salt Lake County, Utah, during April 1–July 10, 2020, were retrospectively reviewed to explore attack rates and transmission patterns. A total of 184 persons, including 110 (60%) children had a known epidemiologic link to one of these three facilities. Among these persons, 31 confirmed COVID-19 cases occurred; 13 (42%) in children. Among pediatric patients with facility-associated confirmed COVID-19, all had mild or no symptoms. Twelve children acquired COVID-19 in child care facilities. Transmission was documented from these children to at least 12 (26%) of 46 nonfacility contacts (confirmed or probable cases). One parent was hospitalized. Transmission was observed from two of three children with confirmed, asymptomatic COVID-19. Detailed contact tracing data show that children can play a role in transmission from child care settings to household contacts. Having SARS-CoV-2 testing available, timely results, and testing of contacts of persons with COVID-19 in child care settings regardless of symptoms can help prevent transmission. CDC guidance for child care programs recommends the use of face masks, particularly among staff members, especially when children are too young to wear masks, along with hand hygiene, frequent cleaning and disinfecting of high-touch surfaces, and staying home when ill to reduce SARS-CoV-2 transmission (4).

Contact tracing* data collected during April 1–July 10, 2020 through Utah's National Electronic Disease Surveillance System (EpiTrax) were used to retrospectively construct transmission chains from reported COVID-19 child care facility outbreaks, defined as two or more laboratory-confirmed COVID-19 cases within 14 days among staff members or attendees at the same

facility. EpiTrax maintains records of epidemiologic linkage between index patients and contacts (defined as anyone who was within 6 feet of a person with COVID-19 for at least 15 minutes ≤ 2 days before the patient's symptom onset) and captures data on demographic characteristics, symptoms, exposures, testing, and the monitoring/isolation period. A confirmed case was defined as receipt of a positive SARS-CoV-2 real-time reverse transcription–polymerase chain reaction (RT-PCR) test result. A probable case was an illness with COVID-19–compatible symptoms,[†] epidemiologically linked to the outbreak, but with no laboratory testing. For this report, the index case was defined as the first confirmed case identified in a person at the child care facility, and the primary case was defined as the earliest confirmed case linked to the outbreak. Pediatric patients were aged < 18 years; adults were aged ≥ 18 years.

Persons with confirmed or probable child care facility–associated COVID-19 were required to isolate upon experiencing symptoms or receiving a positive SARS-CoV-2 test result. Contacts were required to quarantine for 14 days after contact with a person with a confirmed case. Facility attack rates were calculated by including patients with confirmed and probable facility-associated cases (including the index patient) in the numerator and all facility staff members and attendees in the denominator. Overall attack rates include facility-associated cases (including the index case) and non-facility contact (household and nonhousehold) cases in the numerator and all facility staff members and attendees and nonfacility contacts in the denominator; the primary case and cases linked to the primary case are excluded.

During April 1–July 10, Salt Lake County identified 17 child care facilities (day care facilities and day camps for school-aged children; henceforth, facilities) with at least two confirmed COVID-19 cases within a 14-day period. This report describes outbreaks in three facilities that experienced possible transmission within the facility and had complete contact investigation information. A total of 184 persons, including 74 (40%) adults (median age = 30 years; range = 19–78 years) and 110 (60%)

* <https://www.cdc.gov/coronavirus/2019-ncov/php/contact-tracing/contact-tracing-plan/contact-tracing.html>.

[†] <https://www.cdc.gov/coronavirus/2019-ncov/symptoms-testing/symptoms.html>.

children (median age = 7 years; range = 0.2–16 years), had a known epidemiologic link to one of these three facilities with an outbreak; 54% were female and 40% were male. Among these persons, 31 confirmed COVID-19 cases occurred (Table 1); 18 (58%) cases occurred in adults and 13 (42%) in children. Among all contacts, nine confirmed and seven probable cases occurred; the remaining 146 contacts had either negative test results (50; 27%), were asymptomatic and were not tested (94; 51%) or had unknown symptoms and testing information (2; 1%).

Among the 101 facility staff members and attendees, 22 (22%) confirmed COVID-19 cases (10 adult and 12 pediatric) were identified (Table 2), accounting for 71% of the 31 confirmed cases; the remaining nine (29%) cases occurred in contacts of staff members or attendees. Among the 12 facility-associated pediatric patients with confirmed COVID-19, nine had mild symptoms, and three were asymptomatic. Among 83 contacts of these 12 pediatric patients, 46 (55%) were nonfacility contacts, including 12 (26%) who had confirmed (seven) and probable (five) COVID-19. Six of these cases occurred in mothers and three in siblings of the pediatric patients. Overall, 94 (58%) of 162 contacts of persons with facility-associated cases had no symptoms of COVID-19 and were not tested. Staff members at two of the facilities had a household contact with confirmed or probable COVID-19 and went to work while their household contact was symptomatic. These household contacts represented the primary cases in their respective outbreaks.

Facility A Outbreak

Facility A, which had been deemed an essential business and had not closed before the outbreak occurred, required daily temperature and symptom screening for the 12 staff members and children and more frequent cleaning and disinfection; staff members were required to wear masks. Two COVID-19 cases in staff members were associated with facility A (Figure). The index case at facility A (patient A1) occurred in a staff member who reported symptom onset on April 2, self-isolated on April 3, and had a positive SARS-CoV-2 RT-PCR test result from a nasopharyngeal (NP) swab specimen obtained on April 6. Three days after patient A1's symptom onset, a second staff member (patient A2) experienced symptoms and had a positive SARS-CoV-2 test result 1 day later. Ten facility contacts (nine children aged 1–5 years and one staff member) remained asymptomatic during the monitoring period and were not tested. The last reported exposure at facility A was on April 3, when the facility closed. Among the 15 nonfacility contacts of patients A1 and A2 (including four children aged 1–13 years), 10 remained asymptomatic throughout their monitoring period and were not tested, and three received negative test results; the symptom and testing information for two nonfacility contacts was unknown. The primary patient, a household contact of the index patient, reported symptom onset 9 days before

TABLE 1. Characteristics of all staff members, attendees, and their contacts associated with COVID-19 outbreaks at three child care facilities — Salt Lake County, Utah, April 1–July 10, 2020

Characteristic	No. (% with available information)		
	Total*	Adult*	Pediatric*
Facility staff members, attendees, and contacts	184 (100)	74 (100)	110 (100)
Age, yrs, median (range) [†]	9 (0.2–78)	30 (19–78)	7 (0.2–16)
Sex			
Female	100 (54)	42 (57)	58 (53)
Male	74 (40)	31 (42)	43 (39)
Unavailable	10 (5)	1 (1)	9 (8)
Linkage to facility			
Facility staff member or attendee	101 (55)	18 (24)	83 (75)
Nonfacility contact [§]	83 (45)	56 (76)	27 (25)
Confirmed[¶] COVID-19 cases			
Total	31 (17)	18 (24)	13 (12)
Symptomatic	24 (13)	15 (24)	9 (8)
Index case at facility	3 (2)	3 (4)	0 (—)
Asymptomatic	4 (2)	0 (—)	4 (4)
Probable[¶] COVID-19 cases	7 (4)	5 (7)	2 (2)
Contacts[§]			
Total	146 (79)	51 (60)	95 (86)
Contacts with a negative test result	50 (27)	27 (36)	23 (21)
Asymptomatic contacts, not tested	94 (51)	22 (30)	72 (65)
Contacts with unknown symptoms and testing	2 (1)	2 (3)	0 (—)

Abbreviation: COVID-19 = coronavirus disease 2019.

* Does not include two persons with primary cases or their six contacts; two adult contacts had unknown symptom and testing information. Percent is calculated as a percentage of the total.

[†] Age data were missing for 11 contacts.

[§] Includes pediatric and adult household and nonhousehold contacts.

[¶] A confirmed case was defined as a positive SARS-CoV-2 reverse transcription–polymerase chain reaction test result. A probable case was an illness with symptoms consistent with COVID-19 and linked to the outbreak but without laboratory testing.

symptom onset in patient A1 and received a positive SARS-CoV-2 test result from an NP specimen collected on April 6. The facility attack rate (excluding the primary case) for facility A was 17% (two of 12) and was 7% overall (including contacts) (two of 27).

Facility B Outbreak

Facility B was closed during March 13–May 4. Upon reopening, temperatures of the five staff members and children were checked daily, and more frequent cleaning was conducted; only staff members were required to wear masks. Five COVID-19 cases in three staff members and two children were associated with facility B (Figure). The index case (B1) occurred in a staff member who was tested on May 31 while presymptomatic (because of a household contact with COVID-19) and received a SARS-CoV-2-positive test result; patient B1 experienced mild COVID-19 symptoms on June 3 and last worked on May 29. A second staff member (patient B2), experienced symptoms on June 8, was tested, and received a positive test result 2 days later. Patients B3 and B4, children aged 8 months

TABLE 2. Classification of contacts with known linkage to facility-associated confirmed adult and pediatric cases* at three child care facilities — Salt Lake County, Utah, April 1–July 10, 2020

Classification	No. (%)					
	Total [†]	Adult [†]	Pediatric	Facility		
				A	B	C
COVID-19 cases at facilities [§]	22	10	12	2	5	15
Contacts [¶] linked to cases at facilities	162	79	83	25	28	109
Contacts [¶] with confirmed COVID-19	9 (6)	2 (3)	7 (8)	0 (—)	4 (14)	5 (5)
Contacts [¶] with probable COVID-19	7 (4)	2 (3)	5 (6)	0 (—)	3 (11)	4 (4)
Contacts [¶] with negative test results	50 (31)	25 (32)	25 (30)	3 (12)	13 (46)	34 (31)
Asymptomatic contacts, not tested	94 (58)	48 (61)	46 (55)	20 (80)	8 (29)	66 (61)
Contacts with unknown symptoms and testing	2 (1)	2 (3)	0 (—)	2 (1)	0 (—)	0 (—)
Interval (days)						
Facility case onset to contact onset, median (range)**	4 (1–8)	6 (4–6)	3 (1–8)	1 (1–1)	4.5 (1–6)	4 (3–8)
Facility case onset to testing, median (range) ^{††}	2.5 (0–6)	1 (0–4)	4 (1–6)	2.5 (1–4)	1 (0–3)	2 (0–10)

Abbreviation: COVID-19 = coronavirus disease 2019.

* A confirmed case was defined as a positive SARS-CoV-2 reverse transcription–polymerase chain reaction test result. A probable case was an illness with symptoms consistent with COVID-19 and linked to the outbreak but without laboratory testing.

[†] A positive adult case linked to facility attendee from Facility B is included because they were a staff member.

[§] Includes index cases.

[¶] Includes pediatric and adult household and nonhousehold contacts.

** For cases in persons who were asymptomatic, onset for contact is date of receipt of positive test result.

^{††} Does not include three pediatric facility cases in persons who were asymptomatic who did not have symptom onset dates.

and 8 years, respectively, experienced mild signs and symptoms (fever, fatigue, runny nose) 7 and 8 days, respectively, after symptom onset in patient B2; both children were tested and received positive test results the day after their symptoms commenced. A third staff member, patient B5, experienced symptoms 9 days after symptoms occurred in patient B4, was tested, and received a positive test result 1 day later. The two children likely transmitted SARS-CoV-2 to their contacts including two confirmed cases (in one child's mother and father, both symptomatic 2 and 3 days, respectively, following the child's illness onset) and three probable cases (in two adults, including one mother and a child). The index patient (B1) was a household contact of the primary patient who had symptom onset May 26, was tested on May 29, and received a positive SARS-CoV-2 test result. The facility attack rate for facility B was 100% (five of five) and the overall attack rate was 36% (12 of 33).

Facility C Outbreak

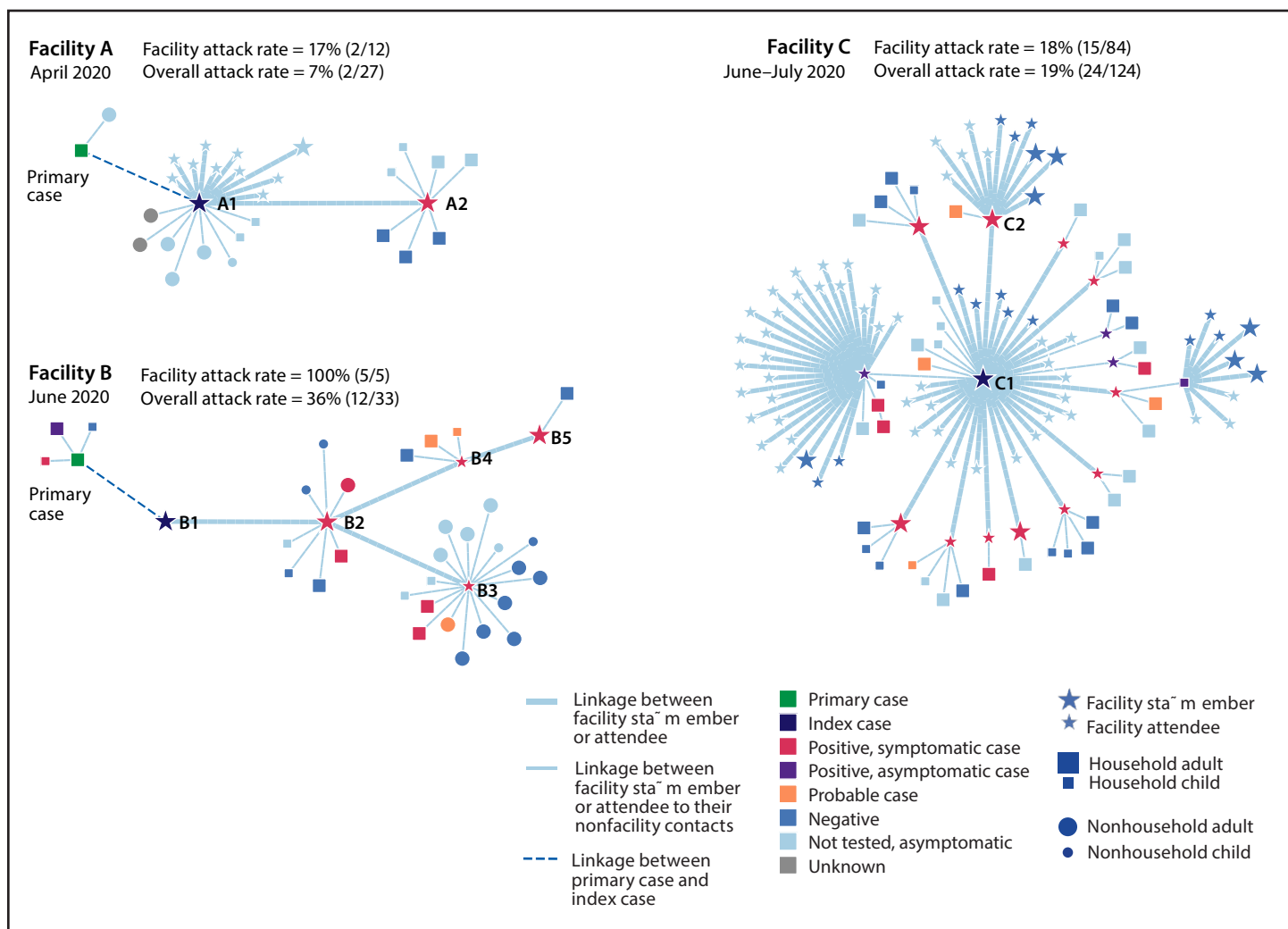
Facility C was closed during March 13–June 17. Upon reopening, the facility requested that 84 staff members and children check their temperature and monitor their symptoms daily; masks were not required for staff members or children. Fifteen COVID-19 cases (in five staff members and 10 children) were associated with facility C (Figure). Two staff members and two students reported symptoms on June 24 and self-isolated. The index case occurred in a staff member (patient C1), who had a positive test result from an NP specimen obtained on June 25.

The second staff member, patient C2, was tested 2 days later and received a positive SARS-CoV-2 test result, and the two students (aged 7 and 8 years) were tested on June 28 and 29, respectively and received positive test results. Over the subsequent 8 days, an additional eight students (aged 6–10 years), three of whom were asymptomatic, and three staff members (all symptomatic) received positive SARS-CoV-2 test results. Pediatric patients at the facility likely transmitted SARS-CoV-2 to their contacts, including five confirmed cases in household contacts (three mothers, one aunt, and one child) and two probable household cases (one mother and one child). Symptoms developed 3 and 5 days following the child's illness onset when onset date was known. One mother who was presumably infected by her asymptomatic child was subsequently hospitalized. Among the seven cases in symptomatic children, fever was the most common sign, followed by symptoms of headache and sore throat. The source for this cluster was not identified. The facility attack rate for facility C was 18% (15 of 84) and the overall attack rate was 19% (24 of 124).

Discussion

Analysis of contact tracing data in Salt Lake County, Utah, identified outbreaks of COVID-19 in three small to large child care facilities linked to index cases in adults and associated with transmission from children to household and nonhousehold contacts. In these three outbreaks, 54% of the cases linked to the facilities occurred in children. Transmission likely occurred from children with confirmed COVID-19 in a child care facility to 25% of their nonfacility contacts.

FIGURE. Transmission chains* and attack rates^{†,§} in three COVID-19 child care center outbreaks^{¶,,††} — Salt Lake County, Utah, April 1–July 10, 2020**



Abbreviation: COVID-19 = coronavirus disease 2019.

* Transmission chains developed using Microbe Trace software. <https://www.biorxiv.org/content/10.1101/2020.07.22.216275v1>.

† Facility attack rates include index cases and all facility staff members and attendees.

§ Overall attack rates include all facility staff members and attendees (including the index case) and nonfacility contacts (household and nonhousehold). It does not include the primary case or the cases linked to the primary case.

¶ A confirmed case was defined as a positive SARS-CoV-2 reverse transcription–polymerase chain reaction test result. A probable case was an illness with symptoms consistent with COVID-19 and linked to the outbreak but without laboratory testing.

** The index case was defined as the earliest confirmed case in a person at the child care facility.

†† A primary case was defined as the earliest confirmed case linked to the outbreak.

Mitigation strategies[§] could have helped limit SARS-CoV-2 transmission in these facilities. To help control the spread of COVID-19, the use of masks is recommended for persons aged ≥ 2 years.[¶] Although masks likely reduce the transmission risk (5), some children are too young to wear masks but can

transmit SARS-CoV-2, as was seen in facility B when a child aged 8 months transmitted SARS-CoV-2 to both parents.

The findings in the report are subject to at least three limitations. First, guidance for contact tracing methodology changed during the pandemic and could have resulted in differences in data collected over time. Second, testing criteria initially included only persons with typical COVID-19 signs and symptoms of fever, cough, and shortness of breath, which

[§] <https://www.cdc.gov/coronavirus/2019-ncov/if-you-are-sick/isolation.html>;
<https://www.cdc.gov/coronavirus/2019-ncov/if-you-are-sick/quarantine.html>.

[¶] <https://www.cdc.gov/coronavirus/2019-ncov/prevent-getting-sick/cloth-face-cover-guidance.html>.

Summary

What is already known about this topic?

Children aged ≥ 10 years have been shown to transmit SARS-CoV-2 in school settings.

What is added by this report?

Twelve children acquired COVID-19 in child care facilities. Transmission was documented from these children to at least 12 (26%) of 46 nonfacility contacts (confirmed or probable cases). One parent was hospitalized. Transmission was observed from two of three children with confirmed, asymptomatic COVID-19.

What are the implications for public health practice?

SARS-CoV-2 Infections among young children acquired in child care settings were transmitted to their household members. Testing of contacts of laboratory-confirmed COVID-19 cases in child care settings, including children who might not have symptoms, could improve control of transmission from child care attendees to family members.

could have led to an underestimate of cases and transmission. Finally, because the source for the outbreak at facility C was unknown, it is possible that cases associated with facility C resulted from transmission outside the facility.

COVID-19 is less severe in children than it is in adults (6,7), but children can still play a role in transmission (8–9). The infected children exposed at these three facilities had mild to no symptoms. Two of three asymptomatic children likely transmitted SARS-CoV-2 to their parents and possibly to their teachers. Having SARS-CoV-2 testing available, timely results, and testing of contacts of patients in child care settings regardless of symptoms can help prevent transmission and provide a better understanding of the role played by children in transmission. Findings that staff members worked while their household contacts were ill with COVID-19—compatible symptoms support CDC guidance for child care programs recommendations that staff members and attendees quarantine and seek testing if household members are symptomatic (4). This guidance also recommends the use of face masks, particularly among staff members, especially when children are too young to wear masks, along with hand hygiene, frequent cleaning and disinfecting of high-touch surfaces, and staying home when ill to reduce SARS-CoV-2 transmission.

Acknowledgments

Child care facility staff members and families; Dagmar Vitek and staff members, Salt Lake County Health Department and Utah Department of Health.

Corresponding author: Cuc H. Tran, ywj0@cdc.gov.

¹CDC COVID-19 Response Team; ²Salt Lake County Health Department, Utah; ³Utah Department of Health.

All authors have completed and submitted the International Committee of Medical Journal Editors form for disclosure of potential conflicts of interest. Mary Hill reports a grant from the Council of State and Territorial Epidemiologists, outside the submitted work. No other potential conflicts of interest were disclosed.

References

1. Szablewski CM, Chang KT, Brown MM, et al. SARS-CoV-2 transmission and infection among attendees of an overnight camp—Georgia, June 2020. *MMWR Morb Mortal Wkly Rep* 2020;69:1023–5. <https://doi.org/10.15585/mmwr.mm6931e1>
2. Park YJ, Choe YJ, Park O, et al.; COVID-19 National Emergency Response Center, Epidemiology and Case Management Team. Contact tracing during coronavirus disease outbreak, South Korea, 2020. *Emerg Infect Dis* 2020;26. <https://doi.org/10.3201/eid2610.201315>
3. Link-Gelles R, DellaGrotta AL, Molina C, et al. Limited secondary transmission of SARS-CoV-2 in child care programs—Rhode Island, June 1–July 31, 2020. *MMWR Morb Mortal Wkly Rep* 2020;69:1170–2. <https://doi.org/10.15585/mmwr.mm6934e2>
4. CDC. Coronavirus disease 2019 (COVID-19): guidance for child care programs that remain open. Atlanta, GA: US Department of Health and Human Services, CDC; 2020. <https://www.cdc.gov/coronavirus/2019-ncov/community/schools-childcare/guidance-for-childcare.html>
5. Hendrix MJ, Walde C, Findley K, Trotman R. Absence of apparent transmission of SARS-CoV-2 after exposure at a hair salon with a universal face covering policy—Springfield, Missouri, May 2020. *MMWR Morb Mortal Wkly Rep* 2020;69:930–2. <https://doi.org/10.15585/mmwr.mm6928e2>
6. Bialek S, Gierke R, Hughes M, McNamara LA, Pilishvili T, Skoff T; CDC COVID-19 Response Team. Coronavirus disease 2019 in children—United States, February 12–April 2, 2020. *MMWR Morb Mortal Wkly Rep* 2020;69:422–6. <https://doi.org/10.15585/mmwr.mm6914e4>
7. Dong Y, Mo X, Hu Y, et al. Epidemiological characteristics of 2143 pediatric patients with 2019 coronavirus disease in China. *Pediatrics* 2020. Epub March 16, 2020. <https://doi.org/10.1542/peds.2020-0702>
8. Stein-Zamir C, Abramson N, Shoob H, et al. A large COVID-19 outbreak in a high school 10 days after schools' reopening, Israel, May 2020. *Euro Surveill* 2020;25:2001352. <https://doi.org/10.2807/1560-7917.ES.2020.25.29.2001352>
9. Qiu H, Wu J, Hong L, Luo Y, Song Q, Chen D. Clinical and epidemiological features of 36 children with coronavirus disease 2019 (COVID-19) in Zhejiang, China: an observational cohort study. *Lancet Infect Dis* 2020;20:689–96. [https://doi.org/10.1016/S1473-3099\(20\)30198-5](https://doi.org/10.1016/S1473-3099(20)30198-5)

COVID-19 Outbreak Associated with Air Conditioning in Restaurant, Guangzhou, China, 2020

Ana M. Rule

Author affiliation: Johns Hopkins Bloomberg School of Public Health, Baltimore, Maryland, USA

DOI: <https://doi.org/10.3201/eid2611.202948>

To the Editor: In the research letter by J. Lu et al. (1), the authors claim that “The air outlet and the return air inlet for the central air conditioner were located above table C (Figure, panel B).” This sentence does not describe the actual layout depicted in the Figure, in which the air conditioner is located by table C and the exhaust fan is between tables B and D.

Furthermore, the authors do not provide evidence of why “Virus transmission in this outbreak cannot be explained by droplet transmission alone.” Their discussion does not mention the possibility that persons move around and may have been infected by touching surfaces, going to the restroom at the same time, or engaging in other close contact.

It is hard to understand how the authors conclude that “... strong airflow from the air conditioner could have propagated droplets from table C to table A, then to table B, and then back to table C.” According to the figure, air flows from table C to the exhaust fan (tables B–D). The authors do not provide evidence that the exhaust fan was not working; they ignored its presence. A simple measurement of air flow would answer this question.

The fact that “... none of the staff or other diners in restaurant X were infected” is another indication that the air conditioner was probably working. Also puzzling is the authors’ conclusion that “... the smear samples from the air conditioner were all nucleotide negative.” This finding is less consistent with aerosol transmission.”

The authors’ conclusion that “... in this outbreak, droplet transmission was prompted by air-conditioned ventilation” is not supported by the data provided. They further conclude that “The key factor for infection was the direction of the airflow” but do not follow the airflow to the exhaust fan.

Reference

1. Lu J, Gu J, Li K, Xu C, Su W, Lai Z, et al. COVID-19 outbreak associated with air conditioning in restaurant, Guangzhou, China, 2020. *Emerg Infect Dis.* 2020;26:1628–31. <https://doi.org/10.3201/eid2607.200764>

Address for correspondence: Ana M. Rule, Johns Hopkins Bloomberg School of Public Health Department of Environmental Health and Engineering, 615 N. Wolfe St. E6614, Baltimore, MD 21205; USA; email: arule1@jhu.edu

Jianyun Lu, Zhicong Yang

Author affiliation: Guangzhou Center for Disease Control and Prevention, Guangzhou, China

DOI: <https://doi.org/10.3201/eid2611.203774>

In Response: We thank Prof. Rule (1) for her comments on our letter (2). We welcome the opportunity to offer additional information on several of the points made.

We wish to explain that although she stated that, “The air outlet and the return air inlet for the central air conditioner were located above table C (Figure, panel B)” does not describe the actual layout depicted in the Figure, in which the air conditioner is located by table C and the exhaust fan is between tables B and D” (1). In fact, the air outlet and the return air inlet for the central air conditioner were located above table C (Figure 1). The central air conditioner is constructed in 2 parts: air outlet and air inlet, indicating no discrepancy between the text and the figure.

We agree that virus transmission in this outbreak could be explained by droplet transmission and the possibility that persons move around, touch surfaces, go to the restroom, or engage in other close contact. We con-



Figure 1. Inlet and outlet of air conditioner described in study of COVID-19 outbreak associated with air conditioning in restaurant, Guangzhou, China, 2020 (2).

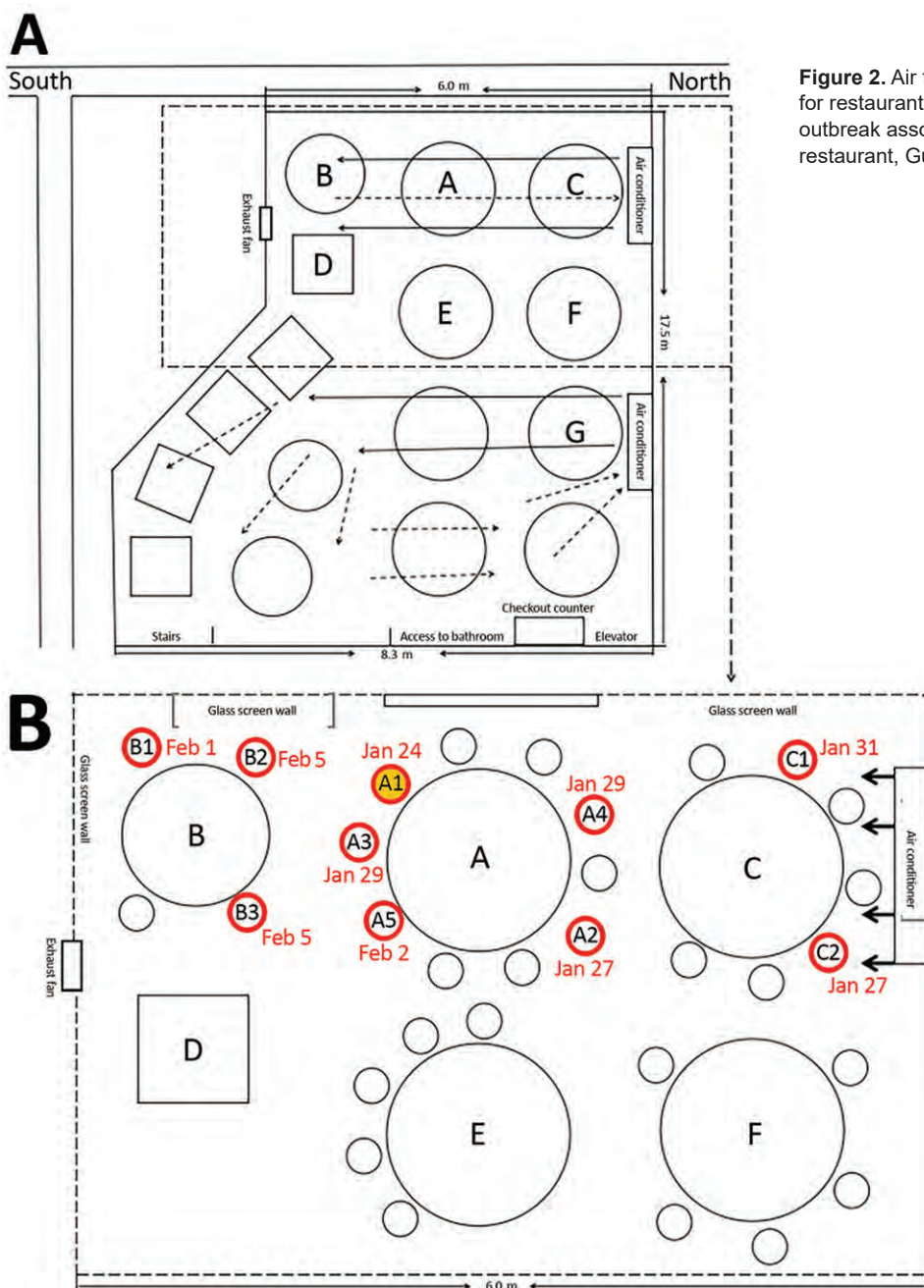


Figure 2. Air flow (A) and seating diagram (B) for restaurant described in study of COVID-19 outbreak associated with air conditioning in restaurant, Guangzhou, China, 2020 (2).

sidered these scenarios but omitted their mention in the research letter. Instead, we reported what we considered to be the most likely scenario, which is that the droplet transmission was prompted by the air blown from right to left and then across tables C, A, and B successively. The air movement facilitated dispersion of droplets containing severe acute respiratory syndrome coronavirus 2 (SARS-CoV-2) from patient A1 to the 3 patients at table B. After the air had passed over tables C, A, and B, patients C1 and C2 acquired the infection from droplets mixed with SARS-CoV-2 as they returned to the air

inlet over table C. None of the 62 persons at the other 12 tables were infected, which suggests that the alternate scenarios (touching surfaces or going to the restroom at the same time) were less likely. Furthermore, some diners and waitresses also went to the restroom and were not infected. In addition, closed-circuit television tapes did not show that the patients in our study had gone to the restroom at the same time. The tapes showed that patient C1 walked in and out several times and passed table A on the way, which might be one of the reasons for the infection of patient C1.

We did not describe the exhaust fan in the text, but we drew an exhaust fan between tables B and D in the figure. To point out the exhaust fan, we drew it bigger than actual measurements, which were only 12 × 12 inches (305 mm × 305 mm); the fan was not strong enough to remove all air produced by the central air conditioner. After the initial publication, we revised the figure to show the appropriate size of the exhaust fan and added details about its size, emphasizing that the ventilation system was not well designed (Figure 2). The main air flow is discharged from the central air conditioning outlet and then returned to the air inlet. Because of the weak exhaust system, the ventilation in the restaurant was not good. We did not ignore the presence of the exhaust fan.

We conclude that the air conditioner prompted transmission of SARS-CoV-2; the customers in the airflow were at high risk for infection with SARS-CoV-2 in the poorly ventilated environment. Because the staff and other diners were not exposed to the airflow mixed with SARS-CoV-2 transmitted by patient A1, their risk for infection was lower.

We excluded the possibility of aerosol transmission (2). It has been reported that aerosols (<5 mm) can remain in the air and disperse long distances (>1 m) (3). The potential for aerosol transmission has been reported for severe acute respiratory syndrome coronavirus (4) and Middle East respiratory syndrome coronavirus (5,6). However, in our study, none of the 62 persons at the other 12 tables were infected. Moreover, the smear samples from the air conditioner were all negative by reverse transcription PCR.

We believe that the most likely scenario for SARS-CoV-2 transmission in the restaurant was

droplet transmission prompted by the air conditioning, although other scenarios are possible. The exhaust fan was not strong enough to modify the ventilation; the main mode of air circulation was the central air conditioning outlet with air returned to the air conditioning inlet. Because of the weak exhaust system, ventilation in the restaurant was poor. We recommend that air handling systems be sufficiently powered and maintained.

References

1. Rule AM. COVID-19 outbreak associated with air conditioning in restaurant, Guangzhou, China, 2020. *Emerg Infect Dis.* 2020;26:xxx. <https://doi.org/10.3201/eid2611.202948>
2. Lu J, Gu J, Li K, Xu C, Su W, Lai Z, et al. COVID-19 outbreak associated with air conditioning in restaurant, Guangzhou, China, 2020. *Emerg Infect Dis.* 2020;26:1628–31. <https://doi.org/10.3201/eid2607.200764>
3. Fernstrom A, Goldblatt M. Aerobiology and its role in the transmission of infectious diseases. *J Pathogens.* 2013;2013:493960. <https://doi.org/10.1155/2013/493960>
4. Lee N, Hui D, Wu A, Chan P, Cameron P, Joynt GM, et al. A major outbreak of severe acute respiratory syndrome in Hong Kong. *N Engl J Med.* 2003;348:1986–94. <https://doi.org/10.1056/NEJMoa030685>
5. Kim SH, Chang SY, Sung M, Park JH, Bin Kim H, Lee H, et al. Extensive viable Middle East Respiratory Syndrome (MERS) coronavirus contamination in air and surrounding environment in MERS isolation wards. *Clin Infect Dis.* 2016;63:363–9. <https://doi.org/10.1093/cid/ciw239>
6. Tong ZD, Tang A, Li KF, Li P, Wang HL, Yi JP, et al. Potential presymptomatic transmission of SARS-CoV-2, Zhejiang Province, China, 2020. *Emerg Infect Dis.* 2020;26:1052–4. <https://doi.org/10.3201/eid2605.200198>

Address for correspondence: Zhicong Yang, Center for Disease Control and Prevention, Baiyun District, Jiahe St, Qide Rd No. 1, Guangzhou, Guangdong 510440, China; email: gdgzcdc@163.com



CORRESPONDENCE OPEN

Pathological and molecular examinations of postmortem testis biopsies reveal SARS-CoV-2 infection in the testis and spermatogenesis damage in COVID-19 patients

Xixiang Ma¹, Chuhuai Guan², Rong Chen³, Yunyun Wang², Shenglei Feng¹, Rongshuai Wang⁴, Guoqiang Qu⁴, Sijia Zhao¹, Fengli Wang¹, Xiaoli Wang¹, Dingyu Zhang^{5,6}, Liang Liu², Aihua Liao¹ and Shuiqiao Yuan¹

Cellular & Molecular Immunology _#####_; <https://doi.org/10.1038/s41423-020-00604-5>

In late December 2019, the novel severe acute respiratory syndrome coronavirus 2 (SARS-CoV-2), which causes coronavirus disease 2019 (COVID-19), was identified in Wuhan, China, and the ensuing pandemic has led to more than 50 million infected individuals and more than one million deaths by November 10, 2020 (<https://covid19.who.int/>). Pathologic investigations of autopsy tissue have focused primarily on the lung, heart, and kidney, whereas morphologic data on testis injury and the effects of SARS-CoV-2 infection on spermatogenesis are limited. Although two groups did not detect SARS-CoV-2 in the semen or testes of recovered COVID-19 patients,^{1,2} another group confirmed SARS-CoV-2 in the semen of patients.³ Therefore, it is currently unknown whether SARS-CoV-2 infection impacts spermatogenesis and male fertility. In the present study, we evaluated the effects of SARS-CoV-2 infection on spermatogenesis by examining the pathophysiology and molecular features of testes obtained from five male COVID-19 patients at autopsy.

First, the histological morphology of the testes from five COVID-19 patients and three uninfected controls was examined by periodic acid-Schiff (PAS) staining. The COVID-19 patients were aged 51, 62, 70, 78, and 83 years, and the control patients were aged 71, 78, and 80 years (Supplementary Table S1). In all five COVID-19 patients, numerous degenerated germ cells (GCs) had sloughed into the lumen of seminiferous tubules (Fig. 1a). In contrast, in the age-matched control tissues, GCs at various stages were well aligned around the whole seminiferous tubules (Fig. 1a). Strikingly, in four of the five cases, GC loss was massive, with only a few GCs left attached to the seminiferous tubules. In particular, many seminiferous tubules in the testes of patients 4 and 5 showed almost no intact GCs, similar to Sertoli cell-only syndrome. Consistent with this morphological observation, the number of DDX4 (a germ cell marker)-positive cells was dramatically reduced in all testicular specimens from the COVID-19 group (Supplementary Fig. S1a, b). Interestingly, the number of Sertoli cells in the testes of SARS-CoV-2-infected patients and uninfected controls was comparable (Supplementary Fig. S1c, d), suggesting that SARS-CoV-2 infection may not impair Sertoli cells. These morphological changes in the testes of COVID-19 patients

indicate that SARS-CoV-2 infection may impair male GC development and eventually lead to GC loss.

SARS-CoV-2 can induce cellular and humoral immune changes and destroy antiviral immunity at an early stage in COVID-19 patients.^{4,5} To ascertain how male GC loss occurs in patients with COVID-19, we investigated the presence of apoptosis and inflammatory reactions in the testicular cells. TUNEL assays revealed that the number of apoptotic cells in COVID-19 testes was significantly higher than that in control testes (Supplementary Fig. S1e, f), raising the possibility that SARS-CoV-2 damages the immune privilege and innate immune homeostasis of the testis. Indeed, immunohistochemical (IHC) staining for various immune cells revealed scattered infiltration of CD3⁺ T lymphocytes, CD20⁺ B lymphocytes, and CD68⁺ macrophages in the interstitial compartments of patients with COVID-19, whereas such infiltration was rarely detected in controls (Fig. 1b–d). In addition, we found CD38⁺ (activated B cells) and CD138⁺ (plasma cells) cells in the interstitial compartments of COVID-19 patient testes (Supplementary Fig. S2a, b). Correspondingly, extensive IgG precipitation was observed mainly in the seminiferous epithelium, interstitium, and some degenerated GCs, similar to the findings in SARS-infected testes (Fig. 1e).⁶ These data suggest that SARS-CoV-2 might trigger a secondary autoimmune response and contribute to the primary pathogenesis of viral orchitis and consequent testicular damage.

To further determine whether SARS-CoV-2 can directly attack testicular cells, we first detected the nucleic acid sequence of SARS-CoV-2 in the testes of COVID-19 patients. Through RT-qPCR-based virus nucleic acid detection, we found two testis samples (patients 1 and 3) to be positive for SARS-CoV-2 nucleic acid (Supplementary Table S2). To further confirm the presence of the virus, we examined the testes from COVID-19 patients by immunohistochemistry using an anti-SARS-CoV spike S1 antibody. As shown in Fig. 1f, the testicular sections from patients stained positively, indicating infection of testicular cells by SARS-CoV-2. (Fig. 1f) and suggesting that SARS-CoV-2 indeed infects testicular cells through the spike glycoprotein binding mechanism. Further transmission electron microscopy (TEM) analyses revealed coronavirus-like particles in the interstitial compartment of the

¹Institute of Reproductive Health, Tongji Medical College, Huazhong University of Science and Technology, Wuhan, Hubei 430030, China; ²Department of Forensic Medicine, Tongji Medical College, Huazhong University of Science and Technology, Wuhan, Hubei 430030, China; ³Department of Pathology, Wuhan Jinyintan Hospital, Wuhan, Hubei 430023, China; ⁴Hubei Chongxin Judicial Expertise Center, Wuhan, Hubei 430415, China; ⁵Research Center for Translational Medicine, Wuhan Jinyintan Hospital, Wuhan, Hubei 430023, China and ⁶Joint Laboratory of Infectious Diseases and Health, Wuhan Institute of Virology and Wuhan Jinyintan Hospital, Chinese Academy of Sciences, Wuhan, Hubei 430023, China

Correspondence: Liang Liu (907505@qq.com) or Aihua Liao (aihua_liao@sina.com) or Shuiqiao Yuan (shuiqiaoyuan@hust.edu.cn)

These authors contributed equally: Xixiang Ma, Chuhuai Guan, Rong Chen

Received: 11 November 2020 Accepted: 20 November 2020

Published online: 14 December 2020

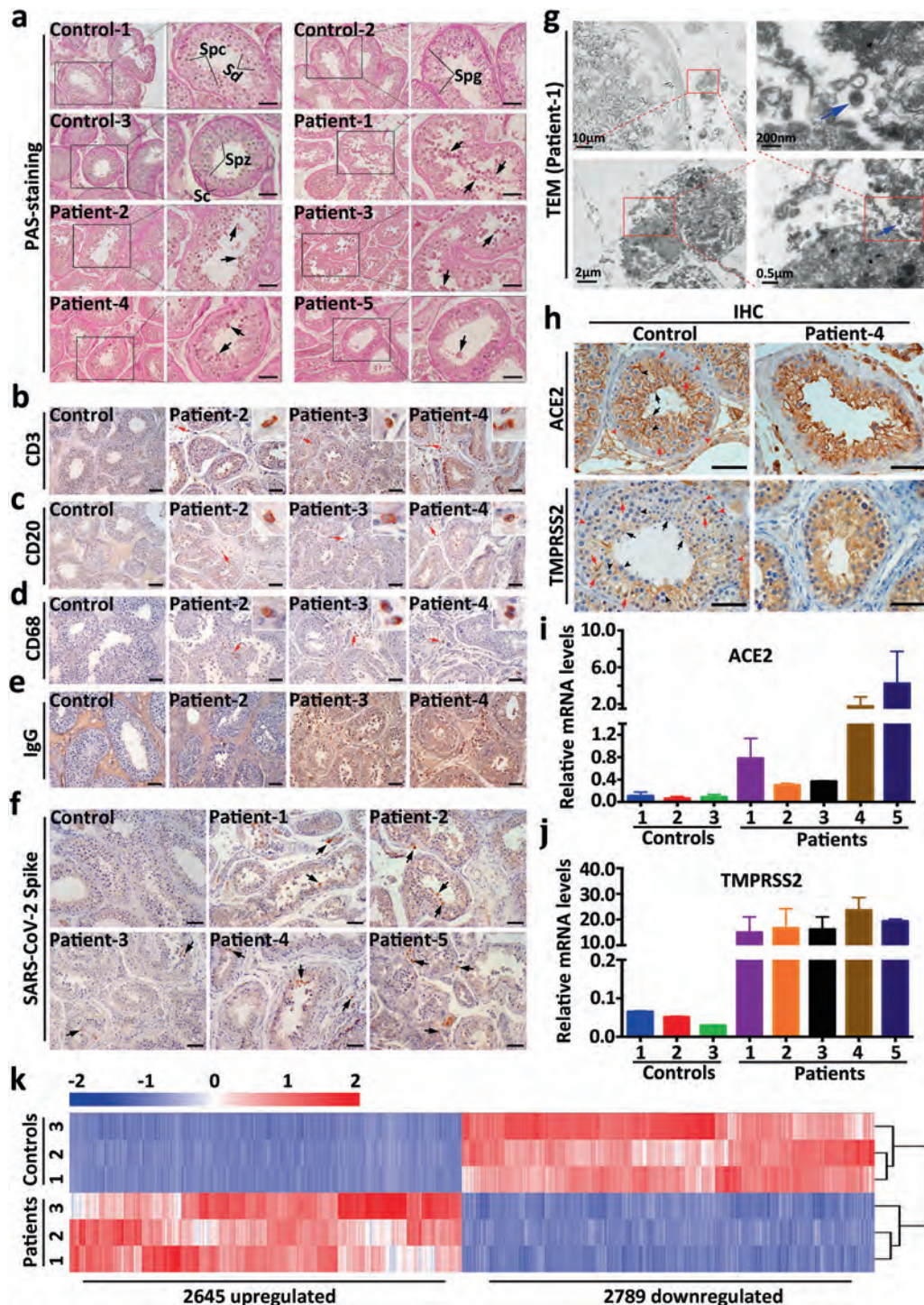


Fig. 1 Spermatogenesis damage was observed in COVID-19 patients. **(a)** Histological analyses of testicular sections from COVID-19 patients (patients 1, 2, 3, 4, and 5) and uninfected controls (controls 1, 2, and 3) showing numerous degenerated germ cells sloughing into the lumen of the seminiferous tubules of all five COVID-19 patients; normal spermatogenesis was observed in control patients. Spg spermatogonia, Spc spermatocytes, Sd spermatids, Spz spermatozoa, Sc Sertoli cells. Arrows indicate degenerated germ cells. Scale bar = 100 μ m. Representative PAS-stained images in the testicular sections of control and COVID-19 patients (patients 2, 3, and 4) are shown. Scale bar = 100 μ m. The right upper image represents a magnified inset for each positive cell stain. **(f)** Representative SARS-CoV-2 spike protein immunohistochemical staining images in the testicular sections of control and COVID-19 patients (patients 1, 2, 3, 4, and 5) are shown. Black arrows indicate SARS-CoV-2 spike S1-positive cells. Scale bar = 100 μ m. **(g)** Electron microscopy of the testis from COVID-19 patient 1, showing coronavirus-like particles suggestive of viral infection (viral particles are highlighted by blue arrows). **(h)** Representative ACE2 (upper panel) and TMPRSS2 (lower panel) immunohistochemical staining images in the testicular sections of a control and COVID-19 patient (patient 4) are shown. Black arrows indicate round spermatids; black arrowheads indicate pachytene spermatocytes; red arrows indicate Sertoli cells; red arrowheads indicate spermatogonia. Scale bar = 100 μ m. RT-qPCR analyses of relative ACE2 **(i)** and TMPRSS2 **(j)** mRNA levels in controls (controls 1, 2, and 3) and COVID-19 patients (patients 1, 2, 3, 4, and 5). Each color bar represents one sample. **(k)** Heat map of genes significantly deregulated in the testes of COVID-19 patients compared to those in the testes of controls.

testes of COVID-19 patients (Fig. 1g and Supplementary Fig. S2c), providing direct evidence that SARS-CoV-2 enters and attacks human testicular tissues.

The SARS-CoV-2 spike protein binds to the angiotensin-converting enzyme 2 (ACE2) receptor through its receptor-binding domain. In turn, ACE2 employs the serine protease TMPRSS2 to activate the S protein, allowing its HR1 and HR2 domains to interact with each other and form a six-helical bundle (6-HB) to mediate membrane fusion between the virus and a target cell.^{7–9} Therefore, we next examined the protein and mRNA levels of ACE2 and TMPRSS2 in the testes. Although both ACE2 and TMPRSS2 proteins were predominantly expressed in the cytoplasm and membrane of spermatocytes, spermatids, and Sertoli cells in control testes, elevated ACE2 and TMPRSS2 levels were observed in the seminiferous tubules of all patients with COVID-19 (Fig. 1h and Supplementary Fig. S3a, b). Consistent with the immunohistochemistry results, RT-qPCR showed significantly increased mRNA levels of ACE2 and TMPRSS2 in the testes of all COVID-19 patient compared to control patient testes (Fig. 1i, j). Together, these results indicate that the signal intensity of ACE2- and TMPRSS2-positive cells in the testes of patients with COVID-19 is higher than that in the testes of uninfected controls, which further supports the hypothesis that SARS-CoV-2 is able to attack testicular cells. However, it is not clear how SARS-CoV-2 interferes with ACE2 and TMPRSS2 expression and/or their regulation. Some common diseases (COVID-19 comorbidities) are reported to be related to ACE2 expression,¹⁰ and it is possible that higher levels of ACE2 and TMPRSS2 are observed in COVID-19 patient testes because patients with severe COVID-19 are more susceptible to SARS-CoV-2 due to underlying disease or individual differences in ACE2 and TMPRSS2 expression.

To investigate the molecular changes associated with SARS-CoV-2 infection in testes, we extracted total RNA from control (controls 1, 2, and 3) and COVID-19 patient (patients 1, 2, and 3) testes and performed RNA-seq to analyze transcriptome changes. The analysis revealed 28,801 expressed coding RNAs and lncRNAs in control and COVID-19 patient testes (Supplementary Table S3), of which 2645 were upregulated and 2789 were downregulated in COVID-19 patients compared with controls (fold change > 2, FDR < 0.001) (Fig. 1k, Supplementary Fig. S4a and Table S4). These results suggest that SARS-CoV-2 infection triggers dynamic transcriptome alterations at the molecular level in testes during specific biological processes.

To further characterize changes in the transcriptome upon SARS-CoV-2 infection in the testes, we performed Gene Ontology term analysis of the differentially regulated genes. Consistent with our virus RNA detection and IHC results, the upregulated transcripts were significantly enriched in terms related to virus invasion, such as “viral gene expression” and “viral life cycle” (Supplementary Fig. S4b). Importantly, some inflammation-related processes were activated, including the “interleukin-6-mediated signaling pathway” and “regulation of B-cell proliferation”. Consistent with our histological results (Fig. 1a), the down-regulated genes were significantly enriched in “spermatogenesis” and “reproduction” (Supplementary Fig. S4c), further illustrating the impact of SARS-CoV-2 infection on male fertility. Moreover, we found 32 inflammatory cytokines to be considerably upregulated, with a *P* value < 0.05 and fold change > 2, in COVID-19 patient testes, and 10 of these cytokines (CMTM6, FAM3C, INHBA, IL33, TNFSF10, NAMPT, CMTM4, CCL28, IL2, and TIMP1) were significantly upregulated with an FDR < 0.001 (Supplementary Fig. S4d). These bioinformatics data suggest that SARS-CoV-2 infection may lead to dysfunction of the genes that regulate spermatogenesis and inflammation-related pathways, thereby causing inflammatory immune attack in the testes and defects in spermatogenesis.

Collectively, our findings provide direct evidence that SARS-CoV-2 can infect the testis and GCs, indicating the potential

impact of the COVID-19 pandemic on spermatogenesis and male fertility. Nevertheless, further study is essential to reveal the underlying mechanism of SARS-CoV-2 infection of testicular cells and the correlation of testis infection with the clinical course of COVID-19.

ACCESSION CODES

The RNA-seq data have been submitted to the NCBI GEO database (PRJNA661970).

ACKNOWLEDGEMENTS

We thank the patients and their families for their dedication to help others understand this disease. We are also grateful for the support of the clinical staff and technicians for performing the autopsy work. This work was supported by the Strategic Collaborative Research Program of the Ferring Institute of Reproductive Medicine, Ferring Pharmaceuticals and Chinese Academy of Sciences (FIRMSCOV02), the Cultivation Plan of International Joint Research Platform of Huazhong University of Science and Technology (5001519009), and Emergency Research Funds of Ministry of Science and Technology of P.R. China (2020YFC0844700).

ADDITIONAL INFORMATION

The online version of this article (<https://doi.org/10.1038/s41423-020-00604-5>) contains supplementary material.

Competing interests: The authors declare no competing interests.

REFERENCES

- Pan, F. et al. No evidence of severe acute respiratory syndrome-coronavirus 2 in semen of males recovering from coronavirus disease 2019. *Fertil. Steril.* **113**, 1135–1139 (2020).
- Song, C. et al. Absence of 2019 novel coronavirus in semen and testes of COVID-19 patients. *Biol. Reprod.* **103**, 4–6 (2020).
- Li, D., Jin, M., Bao, P., Zhao, W. & Zhang, S. Clinical characteristics and results of semen tests among men with coronavirus disease 2019. *JAMA Netw. Open* **3**, e208292 (2020).
- Zheng, H. Y. et al. Elevated exhaustion levels and reduced functional diversity of T cells in peripheral blood may predict severe progression in COVID-19 patients. *Cell Mol. Immunol.* **17**, 541–543 (2020).
- Zheng, M. et al. Functional exhaustion of antiviral lymphocytes in COVID-19 patients. *Cell Mol. Immunol.* **17**, 533–535 (2020).
- Xu, J. et al. Orchitis: a complication of severe acute respiratory syndrome (SARS). *Biol. Reprod.* **74**, 410–416 (2006).
- Tai, W. et al. Characterization of the receptor-binding domain (RBD) of 2019 novel coronavirus: implication for development of RBD protein as a viral attachment inhibitor and vaccine. *Cell Mol. Immunol.* **17**, 613–620 (2020).
- Xia, S. et al. Fusion mechanism of 2019-nCoV and fusion inhibitors targeting HR1 domain in spike protein. *Cell Mol. Immunol.* **17**, 765–767 (2020).
- Hoffmann, M. et al. SARS-CoV-2 cell entry depends on ACE2 and TMPRSS2 and is blocked by a clinically proven protease inhibitor. *Cell* **181**, 271 (2020).
- Breidenbach, J. D. et al. Impact of comorbidities on SARS-CoV-2 viral entry-related genes. *J. Pers. Med.* **10**, E146 (2020).



Open Access This article is licensed under a Creative Commons Attribution 4.0 International License, which permits use, sharing, adaptation, distribution and reproduction in any medium or format, as long as you give appropriate credit to the original author(s) and the source, provide a link to the Creative Commons license, and indicate if changes were made. The images or other third party material in this article are included in the article's Creative Commons license, unless indicated otherwise in a credit line to the material. If material is not included in the article's Creative Commons license and your intended use is not permitted by statutory regulation or exceeds the permitted use, you will need to obtain permission directly from the copyright holder. To view a copy of this license, visit <http://creativecommons.org/licenses/by/4.0/>.

© The Author(s) 2020

Letter to the Editor

Frequency of coronavirus disease 2019 (COVID-19) symptoms in healthcare workers in a large health system

Jason H. Malenfant MD, MPH¹ , Caitlin N. Newhouse MD² and Alice A. Kuo MD, PhD, MBA³

¹Public Health & Preventive Medicine Program, David Geffen School of Medicine, University of California, Los Angeles (UCLA), Los Angeles, California,

²Division of Pediatric Infectious Diseases, David Geffen School of Medicine, University of California, Los Angeles (UCLA), Los Angeles, California and ³Division of Medicine-Pediatrics, David Geffen School of Medicine, University of California, Los Angeles (UCLA), Los Angeles, California

To the Editor—Since the early phases of the coronavirus disease 2019 (COVID-19) epidemic across the United States, identifying and tracking healthcare worker (HCW)-to-HCW transmission has been a major priority given the risk of exposing other colleagues, exposing vulnerable patients, and issues of limited staffing. Policy guidance regarding symptomatic screening for exclusion from work to mitigate transmission has not evolved much over the course of the pandemic to date.

From March 20 through April 10, 2020, a total of 2,193 severe acute respiratory coronavirus virus 2 (SARS-CoV-2) tests were ordered for HCWs in our institution, and 174 HCWs in our health system tested positive (8% positivity rate). Symptoms were not recorded for 3 individuals. Of the remaining 171 HCWs included in our symptom analysis, 69 (40%) were registered nurses, certified nursing assistants, or care partners; 31 (18%) were clinical administrative employees; 25 (15%) were physicians (of whom 11 were house staff); and 46 (27%) consisted of respiratory therapists, radiology technicians, custodial services, or other ancillary service delivery workers. In total, 119 HCWs (70%) worked in the inpatient setting, 41 (24%) worked in ambulatory clinics, and 11 (6%) had their primary workplace at an offsite office (eg, a telehealth call center).

The most common initial symptoms were cough (51%), fever (41%), and myalgia (38%). Additional common symptoms included headache (30%), nasal congestion and/or runny nose (28%), severe fatigue (26%), and sore or scratchy throat (25%). Loss of smell (16%) and loss of taste (15%) were also reported (Table 1). Variability was noted in the number of initial symptoms: 19% endorsed only 1 presenting symptom, 23% had 2 initial symptoms, 26% had 3 symptoms, and 33% had 4 symptoms or more.

Of those HCWs with only 1 initial symptom, the most common complaint was cough (47%), followed by a sore or scratchy throat (19%). Only 3 of the 32 HCWs with 1 initial symptom (9%) reported fever. Only 1 person (3%) reported loss of smell as their only initial symptom. Of those HCWs reporting 2 initial symptoms, the most common combination of initial symptoms was fever and cough (15%), followed by headache and myalgia

(10%). Approximately one-third of all HCWs did not report fever or cough as an initial presenting symptom.

Almost half (49%) of all HCWs surveyed reported working at least 1 day while symptomatic and before calling the HCW hotline to report symptoms. Of these, 57% worked for 1 day, 18% for 2 days, 10% for 3 days, and 15% for 4 or more days (maximum, 6 days).

Early reports from around the world described COVID-19 as an illness characterized primarily by fever and cough.^{1,2} Due to limited testing capacity, testing access was often initially limited to individuals who presented with these symptoms. Because of the potential for HCWs to spread SARS-CoV-2 to patients and coworkers, our health system opted for a low threshold for testing to better characterize the spectrum of disease and reduce inadvertent spread. Our data suggest that SARS-CoV-2 infection can present with a wider variety of mild symptoms than was suggested by early studies. In fact, one-third of HCWs in our study did not report fever or cough as one of their symptoms, and these individuals would have been missed by more restrictive testing guidelines. Additionally, almost half (49%) of the HCWs continued to work while experiencing symptoms, some for several days. There are several possible explanations for this. For example, it was early in the pandemic and the mild presentation of COVID-19 was not widely recognized.

Our findings have important implications for healthcare systems and other employers regarding when to test employees and when to implement mandatory stay-home-from-work policies. Employee health programs should message that early COVID-19 can present with subtle viral symptoms, including those mimicking mild upper-respiratory infections or allergies, and that individuals should have a low threshold to present for evaluation and testing.

Additionally, our data highlight the importance of universal symptom monitoring through either a daily survey or mandatory entry point at facility entrances. Screening HCWs solely for fever would have missed 60% of SARS-CoV-2-positive individuals in our sample. Health systems and other work places should consider strategies that screen for a variety of signs and symptoms of early COVID-19 infection. Universal symptom monitoring can help create a culture change in the work place, which includes being attuned to subtle changes in health and staying home from work for mild illness. This may be a difficult culture shift for various reasons including financial incentives to continue working, historical emphasis on presenteeism, and reluctance to miss work and call in a coworker for mild symptoms that may not impede one's ability to work. However, with the COVID-19 pandemic, this critical shift is

Author for correspondence: Jason H. Malenfant, E-mail: jmalenfant@mednet.ucla.edu

Cite this article: Malenfant JH, Newhouse CN, and Kuo AA. (2020). Frequency of coronavirus disease 2019 (COVID-19) symptoms in healthcare workers in a large health system. *Infection Control & Hospital Epidemiology*, <https://doi.org/10.1017/ice.2020.1297>

Table 1. Initial Signs and Symptoms Reported in HCWs Diagnosed With COVID-19

Signs and Symptoms ^a	HCWs (n=171), No. (%)
Cough	88 (51)
Fever	70 (41)
Myalgia	65 (38)
Headache	52 (30)
Nasal congestion/runny nose	48 (28)
Severe fatigue	44 (26)
Sore throat	42 (25)
Loss of smell	28 (16)
Loss of taste	26 (15)
Chills	24 (14)
Difficulty breathing	18 (11)
Chest tightness/pain	13 (8)
Diarrhea	12 (7)
Loss of appetite	9 (5)
Vomiting	2 (1)

Note. HCWs, healthcare workers.

^aHCWs could report >1 sign/symptom.

essential to stop potential transmission to vulnerable patients and other HCWs.

Health systems, school districts, and other work places can learn from this experience to develop pragmatic and effective infection control policies in the era of COVID-19. Often, areas for improvement in infection prevention can be identified to help mitigate the spread of SARS-CoV-2 within a critical work force. Especially with concern of a second and potentially multiple further waves of COVID-19, leaders can use these lessons to develop better strategies, further preparedness, and reduce burdens on our hospital systems and labor force.

Acknowledgments.

Financial support. No financial support was provided relevant to this article.

Conflicts of interest. All authors report no conflicts of interest relevant to this article.

References

1. Zhang JJ, Dong X, Cao YY, *et al*. Clinical characteristics of 140 patients infected by SARS-CoV-2 in Wuhan, China. *Allergy* 2020;75:1730–1741.
2. Chen N, Zhou M, Dong X, *et al*. Epidemiological and clinical characteristics of 99 cases of 2019 novel coronavirus pneumonia in Wuhan, China: a descriptive study. *Lancet* 2020;395:507–513.

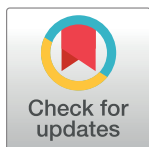
RESEARCH ARTICLE

Aerosol emission of adolescents voices during speaking, singing and shouting

Dirk Mürbe¹, Martin Kriegel², Julia Lange², Lukas Schumann², Anne Hartmann², Mario Fleischer^{1*}

¹ Department of Audiology and Phoniatrics, Charité – Universitätsmedizin Berlin, Berlin, Germany, ² Hermann-Rietschel-Institut, Technische Universität Berlin, Berlin, Germany

* mario.fleischer@charite.de



Abstract

Since the outbreak of the COVID-19 pandemic, singing activities for children and young people have been strictly regulated with far-reaching consequences for music education in schools and ensemble and choir singing in some places. This is also due to the fact, that there has been no reliable data available on aerosol emissions from adolescents speaking, singing, and shouting. By utilizing a laser particle counter in cleanroom conditions we show, that adolescents emit fewer aerosol particles during singing than what has been known so far for adults. In our data, the emission rates ranged from 16 P/s to 267 P/s for speaking, 141 P/s to 1240 P/s for singing, and 683 P/s to 4332 P/s for shouting. The data advocate an adaptation of existing risk management strategies and rules of conduct for groups of singing adolescents, like gatherings in an educational context, e.g. singing lessons or choir rehearsals.

OPEN ACCESS

Citation: Mürbe D, Kriegel M, Lange J, Schumann L, Hartmann A, Fleischer M (2021) Aerosol emission of adolescents voices during speaking, singing and shouting. PLoS ONE 16(2): e0246819. <https://doi.org/10.1371/journal.pone.0246819>

Editor: Michael Döllinger, University Hospital Erlangen at Friedrich-Alexander-University Erlangen-Nürnberg, GERMANY

Received: October 26, 2020

Accepted: January 26, 2021

Published: February 10, 2021

Copyright: © 2021 Mürbe et al. This is an open access article distributed under the terms of the [Creative Commons Attribution License](https://creativecommons.org/licenses/by/4.0/), which permits unrestricted use, distribution, and reproduction in any medium, provided the original author and source are credited.

Data Availability Statement: All relevant data are within the manuscript and its [Supporting information](#) files.

Funding: The author(s) received no specific funding for this work.

Competing interests: The authors have declared that no competing interests exist.

Introduction

Aerosols are liquid or solid particles, which are transported in the air and not influenced by gravitation usually determined by a size less than 5 µm, that escape from the respiratory system during breathing, speaking and singing. Besides droplets, they are widely accepted carriers for the transmission of SARS-CoV-2 viruses [1]. Due to the principles of voice production and the described accumulation of SARS-CoV-2-infections during choir rehearsals [2], it is assumed that singing is connected with increased aerosol emission rates. Recently, increased aerosol emissions during singing in comparison to speaking have been experimentally confirmed for adult singers [3, 4]. Further, an increased aerosol emission rate is found for raising vocal loudness [5]. This results in limitations and specific risk management strategies especially for choir singing during the COVID-19-pandemic. However, data about aerosol emission during singing for adolescents are still missing. But especially for children and young people the restrictions on ensemble and choir singing have far-reaching consequences in addition to severe cultural and financial losses. Singing together is an obligatory part of school education and an important factor for the socio-emotional development of children and young people. This applies not only to music lessons in school, but also to the extracurricular sector with music

schools and children and youth choirs. By now, the hygiene and performance concepts rely on aerosol emission rates during singing as collected from adults. For the first time, this pilot study presents data of aerosol formation when young people sing.

Materials and methods

Four girls and four boys, all 13 years old (except one girl aged 15 years), recruited in July 2020 by targeted call, participated in the study. They were members of a semiprofessional children's choir (Staats- und Domchor Berlin, Mädchenchor der Singakademie Berlin) and had perennial choir experience between five and nine years. All of them were before puberty voice changes, which was assessed by experienced choral directors. Apart from adolescent age, gender, perennial choir experience and pre-puberty voice status were no further inclusion criteria for this study.

The combination of adolescence and pre-puberty voice status allowed studying a representative group within boys' and girls' choir singers with advanced singing experience and cognitive development.

The study was conducted according to the ethical principles based on the WMA Declaration of Helsinki and was approved by the ethic committee of the Charité–Universitätsmedizin Berlin, Germany. Informed written consent was obtained from all subjects and their parents.

The investigations were carried out in a cleanroom (ISO-2-class) at the Hermann Rietschel Institute, Technische Universität Berlin, accessible through an airlock and equipped with terminal U15-filters.

To suppress the thermal plume at the subjects efficiently, the supply air in the whole cleanroom was introduced via a quasi-laminar vertical flow with a velocity of 0.3 m/s (Fig 1) [6]. Further, the room temperature was 295.15 ± 0.5 K, and the relative humidity was $46 \pm 2\%$. The static pressure in the cleanroom was about $20 \cdot (1 \pm 2\%)$ Pa greater than outside the room.

In this highly pure environment, the subjects wore cleanroom clothing and a headgear to further reduce the clothing's particle emission. To perform the experiments, subjects sat in front of the test equipment, consisting of a glass pipe with a diameter of 295 mm, through which a constant airflow of approximately $400 \text{ m}^3/\text{h}$ was generated by suction of a filter fan unit (FFU) (Ziehl-Abegg, Künzelsau, Deutschland) (Fig 1).

The vertical flow in the cleanroom and the glass-pipe construction ensured that emissions from other people (instructor, technical staff), who were necessarily in the cleanroom during measurements, were not directed to a laser particle counter (LPC) (Lighthouse Solair 3100 E, Lighthouse Worldwide Solutions, Fremont, CA).

The sampling probe (37 mm) of the LPC was placed centrally in the pipe. To reach a homogenous particle distribution at the measurement position, two baffles were inserted in the pipe to achieve a sufficient mixing of the particles at the sample point (Fig 1). The position of the LPC within the tube was based on the precedent setup of the measuring system utilizing visual (with stage fog) and quantitative (with an aerosol generator) assessments.

The particle counter was counting with a sampling flow rate of 28.3 l/min with a measuring time increment of 10 seconds. The detected particles were assigned to six size classes (>0.3 , >0.5 , >1.0 , >3.0 , >5.0 , $>10.0 \text{ }\mu\text{m}$) between $>0.3 \text{ }\mu\text{m}$ — $25.0 \text{ }\mu\text{m}$.

According to ISO 21501-4, the counting efficiency for particles of the size $0.3 \text{ }\mu\text{m}$ was $50 \pm 20\%$, and for particles of the size $0.5 \text{ }\mu\text{m}$ was $100 \pm 10\%$. An initial baseline measurement showed a count rate of <1 particles for 5 minutes. Between the trials and tasks, a time increment of 20–30 s and 60–90 s, respectively, was chosen to avoid remaining particles of the previous task. This was confirmed by the display of a zero count at the LPC.

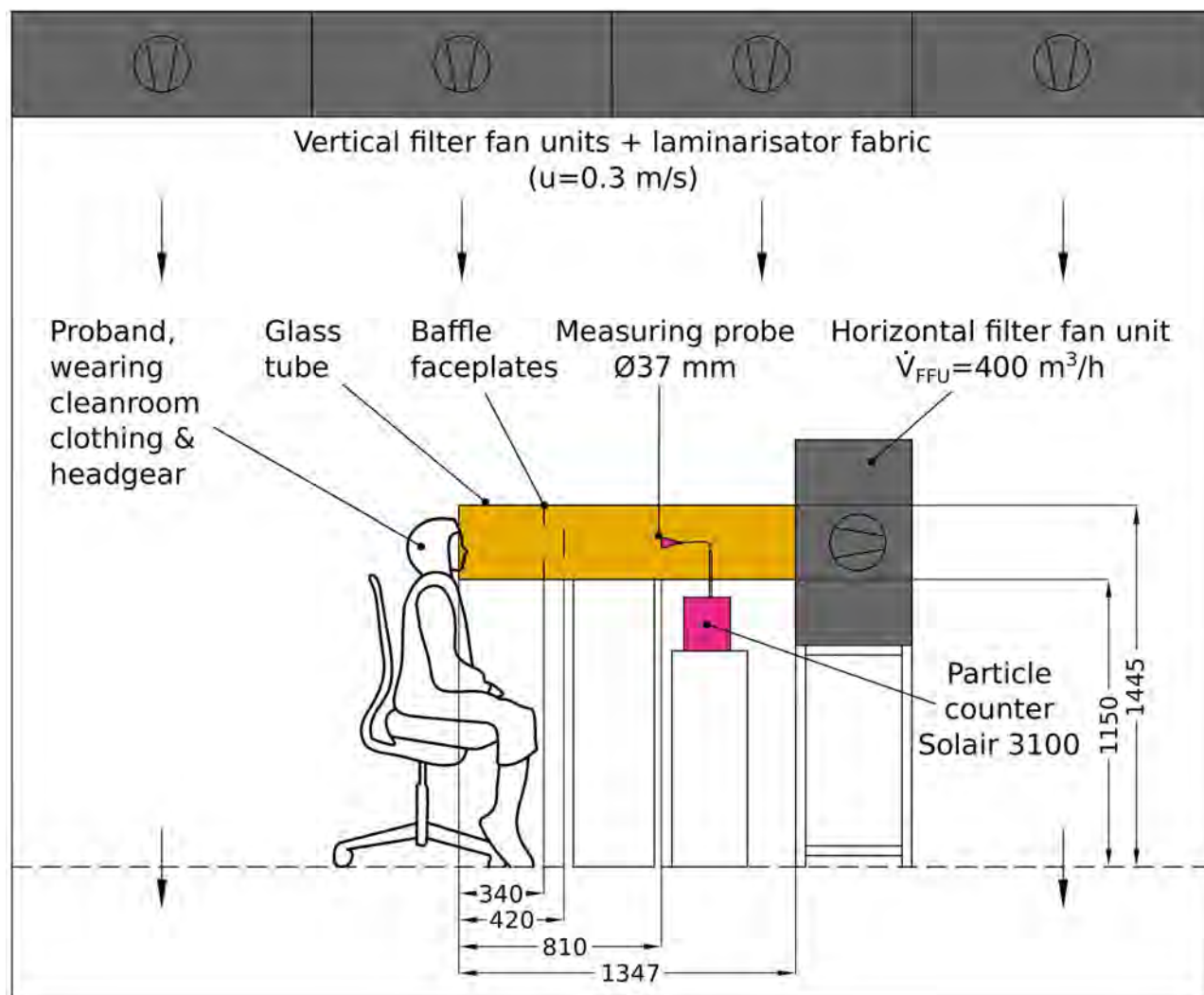


Fig 1. Experimental setup. The subjects sat frontal with their head at the free end of a glass tube (inner diameter 295 mm, length of 1347 mm) during the phonatory tasks. The suction side of a FFU that produced a horizontal volume flow of 400 m³/h on average was placed at the opposite end. To achieve a fully developed turbulent flow at the position of the LPC at 810 mm, two baffle plates at distances of 340 mm and 420 mm from the entry were applied. All length units are in mm.

<https://doi.org/10.1371/journal.pone.0246819.g001>

The emission rate P_M was computed based on scaling of the particles measured at the LPC to the volume flow of the whole glass pipe. Apart from the particle measurement, the sound pressure level $L_{AF_{MAX}}$ was measured via a calibrated sound level meter (CENTER 322_ Datalogger Sound Level Meter, Center Technologies, Houston, TX).

In the first task, the emission rates for three different vocal test conditions were compared: (a) speaking, (b) singing, and (c) shouting. Condition (a) was reading a standardized text (“Der Nordwind und die Sonne” by Åsop), a reference text for voice assessments with balanced phoneme representation. Condition (b) was singing the Swedish folk song “Vem kan segla” in key G-Major, a piece very familiar to the choir singers which could be sung reliably. For condition (c), subjects were asked to cheer enthusiastically about a soccer game goal. The time window for a measured sequence was 30 seconds for test conditions (a) and (b) and 10 seconds for test condition (c). Each test condition was repeated five times.

In the second task, sustained phonation about 10 seconds was performed to investigate the impact of vocal loudness on the emission rate. Subjects were asked to sustain the syllable /la/, pitch G4 (392 Hz), at the two loudness conditions soft voice (piano) and loud voice (forte). To facilitate the 10 seconds measurement time, the young people were allowed to take a short breath within the recording and to repeat the syllable.

The emission rates were normalized to the respective time length of the tasks (10 or 30 seconds, respectively) and are time-averaged values.

Statistical analysis, individually handled for the two tasks, was carried out by using linear mixed-effects model (LMEM) analysis in the statistical software R (<https://www.r-project.org/>) including the package lmerTest [7]. This robust and flexible statistical framework was proven to have a high accuracy for multiple observations for numerous items [8]. For this study, log-valued P_M data were incorporated as the response variable and condition as fixed effect. Further, intercepts for subject and by-subject random slopes for the effect of condition were regarded as random effects. P-values were obtained using Satterthwaite's degree of freedom method. The raw data of this study and the R-script containing statistical analyses are deposited in S1 and S2 Files.

Results

Within the measuring range between 0.3 μm and 25 μm , about 99% of all measured particles for all test conditions were smaller than 5 μm and more than 70% smaller than 1 μm (Fig 2). With regard to the common understanding to denominate particles with a size smaller than 5 μm as aerosols, the following results are cumulatively given for particles of size 0.3 μm –5 μm .

The emission rates P_M for speaking were clearly lower than for singing (Fig 3). Whereas the median values for speaking were between 16 P/s (Particles/second) and 267 P/s, this measure was between 141 P/s and 1240 P/s for singing. For shouting, P_M was still higher with values from 683 P/s up to 4332 P/s. All subjects showed a clear individual increase in P_M for all three conditions.

Linear mixed modeling showed, that these increases in condition were significant (likelihood-ratio test; $p < .00001$). On average, the ratio of P_M between singing and speaking was 5.87 ± 1.28 (standard error). For shouting and speaking, this ratio was 36.22 ± 1.28 (standard error).

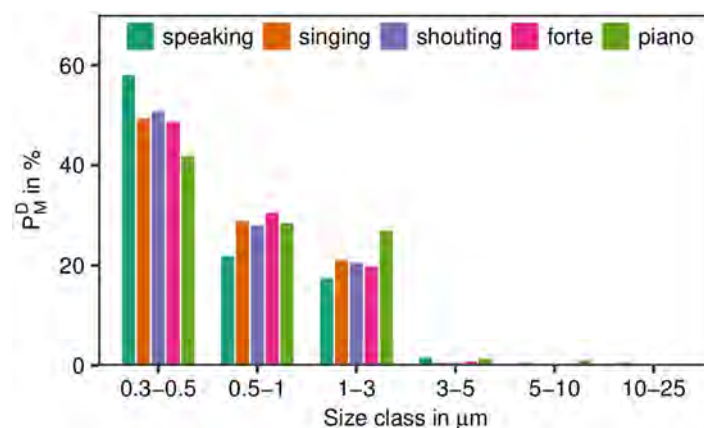


Fig 2. Size distributions. Distributions of emission rates P_M^D for different size classes and test conditions in%. These data were computed by summarizing all P_M -values for all subjects (separated by test condition) and were normalized to the sum for all size classes dependent on test condition (see S2 File for details).

<https://doi.org/10.1371/journal.pone.0246819.g002>

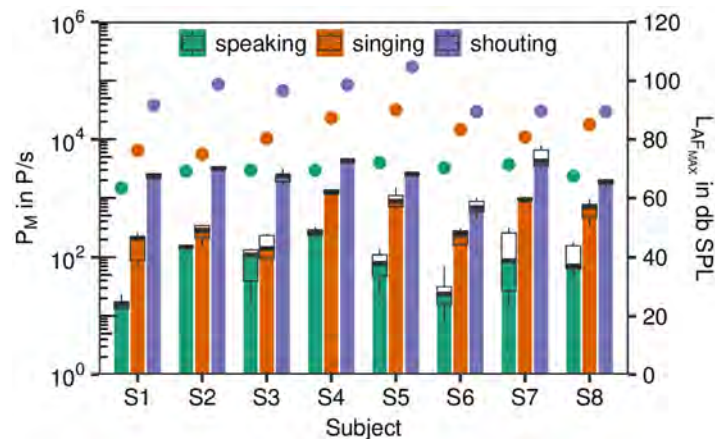


Fig 3. Emission rates. Boxplots of the emission rates (P_M in P/s, left y-axis) for the test conditions speaking, singing and shouting for subjects S1-S4 (girls) and S5-S8 (boys). The maximum sound pressure levels (L_{AF_MAX} in db SPL) are also shown (right y-axis) with different colored full circles for the test conditions.

<https://doi.org/10.1371/journal.pone.0246819.g003>

Both findings were significant ($p < .001$). Further, P_M was positively correlated with the maximum sound pressure level L_{AF_MAX} . An increase in one unit in L_{AF_MAX} resulted in an increase in 0.05 units of $\log_{10}(P_M)$. This finding was significant ($p < .001$).

For the sustained phonation task, the median values for soft phonation (piano) were between 58 P/s and 683 P/s, this measure was between 58 P/s and 1907 P/s for loud phonation (forte). In contrast to the first task, not all subjects showed a clear increase in P_M from piano to forte. This finding was mirrored by the results of the linear mixed modeling approach. The increase of P_M from piano to forte was 1.91 ± 1.47 , whereas the condition was not significant ($p = .133$). Nevertheless, a positive correlation to L_{AF_MAX} was found (Fig 4), which indicates that the emission rate increases with raising vocal loudness. Similar to the first task, an increase in one unit in L_{AF_MAX} results in an increase in 0.05 units of $\log_{10}(P_M)$, which was also significant ($p < .001$).

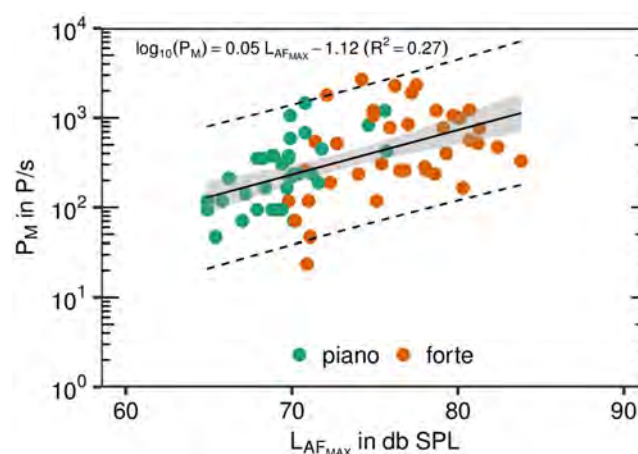


Fig 4. Emission rates vs. sound pressure level. Emission rate P_M plotted over maximum sound pressure level L_{AF_MAX} for sustained syllable /la/. All five repetitions for the two loudness conditions are represented by colored points as denoted in the legend. The black solid line represents the linear regression (see inset for details), the gray colored area represents the 95% confidence region, whereas the black dashed lines restrict the 95% prediction band.

<https://doi.org/10.1371/journal.pone.0246819.g004>

Discussion

The present study confirms higher emission rates of aerosols for singing in comparison to speaking also for adolescents. As for measurements of adult professional singers, a strong intersubject variability of aerosol emission was found for singing adolescents, too. Finally, a positive correlation of particle emission with vocal loudness was confirmed, in particular reflected by the shouting condition. It should be noted that the results obtained must be viewed critically in terms of their transferability to a larger population. One limitation, for example, is that only a limited number of children and young people are active singers, who may differ in their singing techniques. In addition, the selection of the adolescents for this study is not representative of children and young singers in general in terms of the development of vocal skills and cognitive abilities during growing up.

Comparing these values with previously published data for adult professional singers [4] (<http://doi.org/10.5281/zenodo.4011701>) using the same experimental setup, similar values for speaking, but lower values for singing were observed (Fig 5). For singing, the ratio in medians between adults and adolescents was about 3.1. Shouting values for adolescents (not available for adults) were higher than singing values for adults. Regarding sustained phonation with loud voice, the ratio in medians between adults and adolescents for the forte condition was about 6.8. It must be noted that there were slight deviations between adults and adolescents in the execution of this task, such as adolescents were allowed to shortly breathe within the recording sequence. Except for shouting, determined values for adolescents are also lower than recently published data found in professional and non-professional adult singers [3]. In this study of 12 adult subjects, emission rates of 320–2870 P/s for singing at moderate to loud volumes are determined. On the other hand, Morawska et al. [9] reported values for 15 adults of 0.322 to 1.088 P/cm³ for voiced speech and normal speaking that can be approximately converted to emission rates by multiplying these values with a mean inhalation rate for males and females of about 9.5 l/min (see [10], p.18), to about 51 to 172 P/s. In a comprehensive study with 48 adult subjects, Asadi et al. [5] found loudness correlated emission rates of 1 to 50 P/s for normal speech. Further, Gregson et al. [11] estimated also loudness dependent particle concentrations in the order of 0.1 to 1.3 and 0.19 to 2.47 P/cm³ (corresponds to an emission rate of about 15.8 to 391.1 P/s) in a study with 25 adult subjects for speaking and singing tasks.

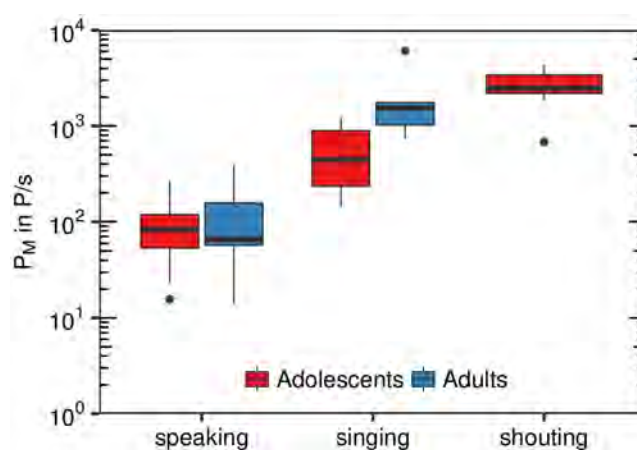


Fig 5. Comparison with data of adults singers. Boxplots of subject specific median emission rates (P_M in P/s) for the test conditions speaking, singing and shouting (adolescents only). Present data of young voices ($n = 8$) in comparison with previously measured corresponding data of professional adult singers ($n = 8$) (<http://doi.org/10.5281/zenodo.4011701>, see [4]).

<https://doi.org/10.1371/journal.pone.0246819.g005>

Quite lower values for adults in the order of 0.0049 to 0.0215 P/cm³ (corresponds to an emission rate of about 0.8 to 3.4 P/s) for talking tasks were also reported [12]. It can be summarized, that the adolescent's data for the speaking tasks presented here, are in the same order of magnitude than values reported earlier.

Regarding particle size distributions, it was found in several studies, that these distributions are mostly centered in a region of about 0.5 to 2 μm for singing [3, 11], and 0.8 to 1 μm for speaking [3, 5] and further skewed to smaller particle size. These observations were confirmed by our data for adolescents (see Fig 2).

There might be different reasons for the lower emission rates for child voices during singing. Before puberty voice changes, there are considerable differences in the vibration characteristics of the vocal folds in comparison to adults. Typical features of a child's vocal register in singing include differences in contact time and contact area of the vocal folds during each vibration cycle. There are also differences in the subglottic pressure between adults in general and young people [13, 14]. Further, there are smaller anatomical proportions of the child's airways and vocal folds are shorter before puberty voice changes. On the other hand, the fundamental frequency of the voice and accordingly the contact frequency of the vocal folds might be higher, especially in comparison with male adult voices.

Indeed, a major reason for the lower emission rates in comparison to professional singers might be the lower volume of the adolescent's voices during singing. This was especially evident in the task with intended loud singing, even if all subjects of this study had a longstanding choir experience. On the contrary, in the shouting condition, which is not related to limitations in the child's singing technique, some adolescents reached higher emission rates than adults during loud singing.

Our experimental setup uses a Laser Particle Counter (LPC) in cleanroom conditions (without a background concentration of particles) to assess the number and size of evaporated aerosols (or droplet nuclei) in their equilibrium state for different kinds of vocalisation. Estimating the precise number and size of these particles is of great interest to assess the concentration of those particles in closed rooms. Because of the great range of the exhaled air volume flow from zero (close mouth) up to at least 7.5–15 l/min for phonation [10, 15–17] and 24 l/min for blowing [18], the measurement setup must be both, highly sensitive to detect all particles and suitable to cover the whole volume flow range.

Thus, different considerations were included in designing the setup for this study. First of all, a filter fan unit with a high volume flow of 400 m³/h has been selected, whereas the flow of exhaled air is small and can be neglected. To further avoid any disturbances regarding stagnating flow at the measuring probe, this probe was positioned centrally in a glass pipe. Further, by placing a turbulence generating baffle between mouth opening and probe, there was a homogeneous particle density distribution in the cross sectional area of the glass pipe. This in turn required the choice of an adequate distance between mouth opening and LPC, which was chosen to about 0.81 m and resulted in a traveling time of the particles of about 0.14 s in maximum (see [4] for details). These experimental conditions, including a relative humidity of about 46%, result in approximately evaporated aerosols in their equilibrium state [19], which can be surveyed by the LPC with high accuracy and independently of the fluid flow at the mouth. Thus, the measured emission rates can serve as a realistic estimate for a possible carriage for viruses that propagate in the environment. Moreover, they allow a reliable comparison between the different vocalisation tasks. However, the emission rates reported in this study should not be interpreted as emitted droplets and aerosols directly at one's opened mouth [20]. Further issues with relevance for SARS-CoV-2-transmission during singing like the trajectory of larger droplets after emission from the mouth need to be studied with different methods like Particle Image Velocimetry or Phase Doppler Anemometry.

For the assessment of the risk of SARS-CoV-2-transmission during singing, both, droplets and aerosols are considered as virus carriers. While virus transmission via droplets can be mainly handled by distance and hygiene rules, the risk management of transmission through virus carrying aerosols has to be addressed with further strategies [21–23].

Activities to reduce the aerosol input in closed rooms during singing include limiting the number of singers and the rehearsal or performance time, which contributes to a lower cumulative aerosol concentration. Apart from these issues, the individual emission rates of the singers determine the aerosol input into closed rooms. For singing, an increased rate of aerosol emission compared to speaking has been found for adolescents, too. The lower aerosol emissions for adolescents' voices during singing in comparison to adult singers might contribute to develop more specific risk management strategies for different constellations of singing. Apart from singing, adolescents' aerosol emissions during shouting may be even higher than adult's emission rates during speaking. That should be considered for risk assessments in the corresponding areas, too.

Further, risk management strategies should incorporate other approaches like room size and air condition systems, which will affect the number and the concentration of potentially infectious aerosols in the room, too. Especially modern mechanical ventilation systems might significantly lower the risk of aerogenic virus transmission [24].

Based on the current prevalence of the disease, advanced risk management for singing together for instance in music lessons in school should combine the above-mentioned tools. The findings for aerosol emission for adolescent voices should be especially used to specify rehearsal and performance schedules for children's and adolescents' choirs because of the significance of education and socio-emotional development for children and young people.

Supporting information

S1 File. Raw data. R-readable data frame. In addition to data for ID, condition, cumulative PM, and SPL, the emission rates for the six size classes (C1–C6), corresponding to >0.3 – 0.5 , >0.5 – 1.0 , >1.0 – 3.0 , >3.0 – 5.0 , >5.0 – 10.0 , and >10.0 – $25\ \mu\text{m}$, are given. (CSV)

S2 File. Statistical analysis. R-script for running the statistical analyses of the data provided in [S1 File](#). (RMD)

Acknowledgments

We thank the girls and boys and the accompanying staff of the Staats- und Domchor Berlin and the Mädchenchor der Singakademie Berlin for their personal support, T. Nawka for general discussion, A. Rameau and two anonymous reviewer for their valuable comments.

Author Contributions

Conceptualization: Dirk Mürbe, Martin Kriegel, Mario Fleischer.

Data curation: Dirk Mürbe, Julia Lange, Lukas Schumann, Mario Fleischer.

Formal analysis: Dirk Mürbe, Mario Fleischer.

Writing – original draft: Dirk Mürbe, Julia Lange, Mario Fleischer.

Writing – review & editing: Martin Kriegel, Lukas Schumann, Anne Hartmann.

References

1. Morawska L, Cao J. Airborne transmission of SARS-CoV-2: The world should face the reality. *Environment International*. 2020; 139:105730 <https://doi.org/10.1016/j.envint.2020.105730> PMID: 32294574
2. Hamner L, Dubbel P, Capron I, Ross A, Jordan A, Lee J, et al. High SARS-CoV-2 Attack Rate Following Exposure at a Choir Practice—Skagit County, Washington, March 2020. *MMWR: Morbidity and Mortality Weekly Report*. 2020; 69:606–610. <https://doi.org/10.15585/mmwr.mm6919e6>
3. Alsved M, Matamis A, Bohlin R, Richter M, Bengtsson PE, Fraenkel CJ, et al. Exhaled respiratory particles during singing and talking. *Aerosol Science and Technology*. 2020; 54(11):1245–1248. <https://doi.org/10.1080/02786826.2020.1812502>
4. Mürbe D, Kriegel M, Lange J, Rotheudt H, Fleischer M. Aerosol emission is increased in professional singing; 2020. Available from: <https://doi.org/10.31219/osf.io/znjeh>.
5. Asadi S, Wexler AS, Cappa CD, Barreda S, Bouvier NM, Ristenpart WD. Aerosol emission and superemission during human speech increase with voice loudness. *Scientific Reports*. 2019; 9(1):2348. <https://doi.org/10.1038/s41598-019-38808-z>
6. Yang C, Yang X, Zhao B. The ventilation needed to control thermal plume and particle dispersion from manikins in a unidirectional ventilated protective isolation room. *Building Simulation*. 2015; 8(5):551–565. <https://doi.org/10.1007/s12273-014-0227-6>
7. Kuznetsova A, Brockhoff PB, Christensen RHB. lmerTest Package: Tests in Linear Mixed Effects Models. *Journal of Statistical Software*. 2017; 82(13):1–26. <https://doi.org/10.18637/jss.v082.i13>
8. Barr DJ, Levy R, Scheepers C, Tily HJ. Random effects structure in mixed-effects models: Keep it maximal. *Journal of Memory and Language*. 2013; 68(3):255–278. <https://doi.org/10.1016/j.jml.2012.11.001>
9. Morawska L, Johnson GR, Ristovski ZD, Hargreaves M, Mengersen K, Corbett S, et al. Size distribution and sites of origin of droplets expelled from the human respiratory tract during expiratory activities. *Journal of Aerosol Science*. 2009; 40(3):256–269. <https://doi.org/10.1016/j.jaerosci.2008.11.002>
10. Adams WC. Measurement of breathing rate and volume in routinely performed daily activities: final report, contract no. A033-205. Sacramento: California Environmental Protection Agency, Air Resources Board, Research Division. 1993;.
11. Gregson, Watson, Orton, Haddrell, McCarthy, Finnie, et al. Comparing the Respirable Aerosol Concentrations and Particle Size Distributions Generated by Singing, Speaking and Breathing. 2020; <https://doi.org/10.26434/chemrxiv.12789221.v1>
12. Papineni RS, Rosenthal FS. The Size Distribution of Droplets in the Exhaled Breath of Healthy Human Subjects. *Journal of Aerosol Medicine*. 1997; 10(2):105–116. <https://doi.org/10.1089/jam.1997.10.105>
13. McAllister A, Sundberg J. Data on subglottal pressure and SPL at varied vocal loudness and pitch in 8- to 11-year-old children. *Journal of Voice*. 1998; 12(2):166–174. [https://doi.org/10.1016/S0892-1997\(98\)80036-2](https://doi.org/10.1016/S0892-1997(98)80036-2)
14. Howard DM. Electrolaryngographically revealed aspects of the voice source in singing. *Logopedics Phoniatrics Vocology*. 2010; 35(2):81–89. <https://doi.org/10.3109/14015439.2010.482863>
15. Gupta JK, Lin CH, Chen Q. Characterizing exhaled airflow from breathing and talking. *Indoor air*. 2010; 20(1):31–39. <https://doi.org/10.1111/j.1600-0668.2009.00623.x>
16. Jiang JJ, Hanna RB, Willey MV, Rieves A. The measurement of airflow using Singing helmet that allows free movement of the jaw. *Journal of Voice*. 2016; 30(6):641–648. <https://doi.org/10.1016/j.jvoice.2015.07.018>
17. Mittal R, Erath BD, Plesniak MW. Fluid Dynamics of Human Phonation and Speech. *Annu Rev Fluid Mech*. 2013; 45:437–467. <https://doi.org/10.1146/annurev-fluid-011212-140636>
18. Amis T, O'Neill N, Wheatley J. Oral airway flow dynamics in healthy humans. *The Journal of Physiology*. 1999; 515(1):293–298. <https://doi.org/10.1111/j.1469-7793.1999.293ad.x>
19. Wei J, Li Y. Enhanced spread of expiratory droplets by turbulence in a cough jet. *Building and Environment*. 2015; 93:86–96. <https://doi.org/10.1016/j.buildenv.2015.06.018>
20. Chao CYH, Wan MP, Morawska L, Johnson GR, Ristovski ZD, Hargreaves M, et al. Characterization of expiration air jets and droplet size distributions immediately at the mouth opening. *Journal of Aerosol Science*. 2009; 40(2):122–133. <https://doi.org/10.1016/j.jaerosci.2008.10.003> PMID: 32287373
21. Hartmann A, Mürbe D, Kriegel M, Lange J, Fleischer M. Risk assessment of rehearsal rooms for choir singing regarding aerosols loaded with virus; 2020. Available from: <http://dx.doi.org/10.14279/depositonce-10388>.
22. Buonanno G, Stabile L, Morawska L. Estimation of airborne viral emission: quanta emission rate of SARS-CoV-2 for infection risk assessment. *Environment International*. 2020; 141:105794. <https://doi.org/10.1016/j.envint.2020.105794>

23. Abuhegazy M, Talaat K, Anderoglu O, Poroseva SV. Numerical investigation of aerosol transport in a classroom with relevance to COVID-19. *Physics of Fluids*. 2020; 32(10):103311. <https://doi.org/10.1063/5.0029118>
24. American Society of Heating, Refrigerating and Air-Conditioning Engineers. ASHRAE Position Document on Filtration and Air Cleaning. ASHRAE, Inc., Atlanta, GA; 2015. Available from: www.ashrae.org/about/position-documents.



Since January 2020 Elsevier has created a COVID-19 resource centre with free information in English and Mandarin on the novel coronavirus COVID-19. The COVID-19 resource centre is hosted on Elsevier Connect, the company's public news and information website.

Elsevier hereby grants permission to make all its COVID-19-related research that is available on the COVID-19 resource centre - including this research content - immediately available in PubMed Central and other publicly funded repositories, such as the WHO COVID database with rights for unrestricted research re-use and analyses in any form or by any means with acknowledgement of the original source. These permissions are granted for free by Elsevier for as long as the COVID-19 resource centre remains active.



SARS-CoV-2 seroprevalence among the general population and healthcare workers in India, December 2020–January 2021

Manoj V. Murhekar^{a,*}, Tarun Bhatnagar^a, Jeromie Wesley Vivian Thangaraj^a, V. Saravanakumar^a, Muthusamy Santhosh Kumar^a, Sriram Selvaraju^b, Kiran Rade^c, C.P. Girish Kumar^a, R. Sabarinathan^a, Alka Turuk^d, Smita Asthana^{e,1}, Rakesh Balachandrar^{f,1}, Sampada Dipak Bangar^{g,1}, Avi Kumar Bansal^{h,1}, Vishal Chopra^{i,1}, Dasarathi Das^{j,1}, Alok Kumar Deb^{k,1}, Kangjam Rekha Devi^{l,1}, Vikas Dhikav^{m,1}, Gaurav Raj Dwivedi^{n,1}, S. Muhammad Salim Khan^{o,1}, M. Sunil Kumar^{p,1}, Avula Laxmaiah^{q,1}, Major Madhukar^{r,1}, Amarendra Mahapatra^{j,1}, Chethana Rangaraju^{s,1}, Jyotirmayee Turuk^{j,1}, Rajiv Yadav^{t,1}, Rushikesh Andhalkar^{b,2}, K. Arunraj^b, Dinesh Kumar Bharadwaj^{q,2}, Pravin Bharti^{t,2}, Debduutta Bhattacharya^{j,2}, Jyothi Bhat^{t,2}, Ashrafjit S. Chahal^{i,2}, Debjit Chakraborty^{k,2}, Anshuman Chaudhury^{b,2}, Hirawati Deval^{n,2}, Sarang Dhatrak^{f,2}, Rakesh Dayal^{u,2}, D. Elantamilan^{m,2}, Prathiksha Giridharan^{b,2}, Inaamul Haq^{o,2}, Ramesh Kumar Hudda^{m,2}, Babu Jagjeevan^{q,2}, Arshad Kalliath^{p,2}, Srikanta Kanungo^{j,2}, Nivethitha N. Krishnan^{b,2}, Jaya Singh Kshatri^{j,2}, Alok Kumar^{b,2}, Niraj Kumar^{n,2}, V.G. Vinoth Kumar^{b,2}, G.G.J. Naga Lakshmi^{v,2}, Ganesh Mehta^{h,2}, Nandan Kumar Mishra^{h,2}, Anindya Mitra^{u,2}, K. Nagbhushanam^{b,2}, Arlappa Nimmathota^{q,2}, A.R. Nirmala^{s,2}, Ashok Kumar Pandey^{n,2}, Ganta Venkata Prasad^{v,2}, Mariya Amin Qurieshi^{o,2}, Sirasanambatti Devarajulu Reddy^{b,2}, Aby Robinson^{b,2}, Seema Sahay^{g,2}, Rochak Saxena^{w,2}, Krithikaa Sekar^{b,2}, Vijay Kumar Shukla^{w,2}, Hari Bhan Singh^{h,2}, Prashant Kumar Singh^{e,2}, Pushpendra Singh^{t,2}, Rajeev Singh^{n,2}, Nivetha Srinivasan^{b,2}, Dantuluri Sheethal Varma^{v,2}, Ankit Viramgami^{f,2}, Vimith Cheruvathoor Wilson^{b,2}, Surabhi Yadav^{b,2}, Suresh Yadav^{m,2}, Kamran Zaman^{n,2}, Amit Chakrabarti^{f,3}, Aparup Das^{t,3}, R.S. Dhaliwal^{m,3}, Shanta Dutta^{k,3}, Rajni Kant^{n,3}, A.M. Khan^{d,3}, Kanwar Narain^{l,3}, Somashekar Narasimhaiah^{s,3}, Chandrasekaran Padmapriyadarshini^{b,3}, Krishna Pandey^{r,3}, Sanghamitra Pati^{j,3}, Shripad Patil^{h,3}, Hemalatha Rajkumar^{q,3}, Tekumalla Ramarao^{v,3}, Y.K. Sharma^{w,3}, Shalini Singh^{e,3}, Samiran Panda^d, D.C.S. Reddy^x, Balram Bhargava^d, on behalf of ICMR Serosurveillance Group⁴

^a ICMR National Institute of Epidemiology, Chennai, Tamil Nadu, India

^b ICMR National Institute of Research in Tuberculosis, Chennai, Tamil Nadu, India

^c WHO Country Office for India, New Delhi, India

^d Indian Council of Medical Research, New Delhi, India

* Corresponding author at: ICMR National Institute of Epidemiology, Chennai 600077, India.

E-mail address: mmurhekar@nieicmr.org.in (M.V. Murhekar).

¹ Authors in alphabetical order, contributed equally.

² Authors in alphabetical order, contributed equally.

³ Authors in alphabetical order, contributed equally.

⁴ ICMR Serosurveillance Group. Epidemiology and Surveillance Working Group: Tanu Anand, Giridhara R. Babu, Himanshu Chauhan, Tanzin Dikid, Raman R Gangakhedkar, Shashi Kant, Sanket Kulkarni, J.P. Muliylil, Ravindra Mohan Pandey, Swarup Sarkar, Naman Shah, Aakash Shrivastava, Sujeet K. Singh and Sanjay Zodepy. Laboratory and Data Management Team: Anusha Hindupur, P.R. Asish, M. Chellakumar, D. Chokkalingam, Sauvik Dasgupta, M.M.E. Gowtham, Annamma Jose, K. Kalaiyarasi, N.N. Karthik, T. Karunakaran, G. Kiruthika, H. Dinesh Kumar, S. Sarath Kumar, M.P. Sarath Kumar, E. Michaelraj, Josephine Pradhan, E.B. Arun Prasath, D. Gladys Angelin Rachel, Sudha Rani, Amanda Rozario, R. Sivakumar, P. Gnana Soundari, K. Sujeetha and Arya Vinod.

^e ICMR National Institute of Cancer Prevention and Research, NOIDA, Uttar Pradesh, India^f ICMR National Institute of Occupational Health, Ahmedabad, Gujarat, India^g ICMR National AIDS Research Institute, Pune, Maharashtra, India^h ICMR National JALMA Institute for Leprosy and Other Mycobacterial Diseases, Agra, Uttar Pradesh, Indiaⁱ State TB Training and Demonstration Centre, Patiala, Punjab, India^j ICMR Regional Medical Research Centre, Bhubaneswar, Odisha, India^k ICMR National Institute of Cholera and Enteric Diseases, Kolkata, West Bengal, India^l ICMR Regional Medical Research Centre, N.E. Region, Dibrugarh, Assam, India^m ICMR National Institute for Implementation Research on Non-Communicable Diseases, Jodhpur, Rajasthan, Indiaⁿ ICMR Regional Medical Research Centre, Gorakhpur, Uttar Pradesh, India^o Government Medical College Srinagar, Srinagar, Jammu, India^p State TB Training and Demonstration Centre, Thiruvananthapuram, Kerala, India^q ICMR National Institute of Nutrition, Hyderabad, Telangana, India^r ICMR Rajendra Memorial Research Institute of Medical Sciences, Patna, Bihar, India^s National Tuberculosis Institute, Bangalore and Lady Willingdon State TB Centre, Bengaluru, Karnataka, India^t ICMR National Institute of Research in Tribal Health, Jabalpur, Madhya Pradesh, India^u State TB Training and Demonstration Centre, Ranchi, Jharkhand, India^v State TB Office, Hyderabad, Andhra Pradesh, India^w State TB Training and Demonstration Centre, Raipur, Chhattisgarh, India^x Independent Consultant, Lucknow, Uttar Pradesh, India

ARTICLE INFO

Article history:

Received 20 April 2021

Received in revised form 12 May 2021

Accepted 16 May 2021

Keywords:

SARS-CoV-2

COVID-19

IgG

Seroprevalence

India

ABSTRACT

Background: Earlier serosurveys in India revealed seroprevalence of severe acute respiratory syndrome coronavirus-2 (SARS-CoV-2) of 0.73% in May–June 2020 and 7.1% in August–September 2020. A third serosurvey was conducted between December 2020 and January 2021 to estimate the seroprevalence of SARS-CoV-2 infection among the general population and healthcare workers (HCWs) in India.

Methods: The third serosurvey was conducted in the same 70 districts as the first and second serosurveys. For each district, at least 400 individuals aged ≥ 10 years from the general population and 100 HCWs from subdistrict-level health facilities were enrolled. Serum samples from the general population were tested for the presence of immunoglobulin G (IgG) antibodies against the nucleocapsid (N) and spike (S1-RBD) proteins of SARS-CoV-2, whereas serum samples from HCWs were tested for anti-S1-RBD. Weighted seroprevalence adjusted for assay characteristics was estimated.

Results: Of the 28,598 serum samples from the general population, 4585 (16%) had IgG antibodies against the N protein, 6647 (23.2%) had IgG antibodies against the S1-RBD protein, and 7436 (26%) had IgG antibodies against either the N protein or the S1-RBD protein. Weighted and assay-characteristic-adjusted seroprevalence against either of the antibodies was 24.1% [95% confidence interval (CI) 23.0–25.3%]. Among 7385 HCWs, the seroprevalence of anti-S1-RBD IgG antibodies was 25.6% (95% CI 23.5–27.8%).

Conclusions: Nearly one in four individuals aged ≥ 10 years from the general population as well as HCWs in India had been exposed to SARS-CoV-2 by December 2020.

© 2021 The Author(s). Published by Elsevier Ltd on behalf of International Society for Infectious Diseases. This is an open access article under the CC BY-NC-ND license (<http://creativecommons.org/licenses/by-nc-nd/4.0/>).

Introduction

Population-based serosurveys are recommended to estimate the proportion of a population already infected with severe acute respiratory syndrome coronavirus-2 (SARS-CoV-2). Repeated cross-sectional serosurveys conducted in the same geographical location provide estimates to monitor trends over a period of time (World Health Organization, 2020a). Information from repeated cross-sectional surveys is valuable for public health decision makers to design and revise containment strategies. A meta-analysis undertaken by Chen et al. (2021) estimated that the overall global seroprevalence of SARS-CoV-2 was 8.0% in the general population and 17.1% among healthcare workers (HCWs).

With more than 10 million laboratory-confirmed cases and nearly 150,000 reported deaths as of 31 December 2020, India has the second highest reported number of cases of coronavirus disease 2019 (COVID-19) globally (World Health Organization, 2020b). The nationwide lockdown imposed between March and May 2020 in India was relaxed in a phased manner from June 2020, allowing interstate and interdistrict movement of people as well as restoration of economic activities (Ministry of Home Affairs, Government of India, 2020, 2021). Two population-based serial serosurveys conducted in 70 Indian districts indicated that the prevalence of SARS-CoV-2 infection among adults had increased

10-fold, from 0.73% [95% confidence interval (CI) 0.34–1.13%] in May–June 2020 to 7.1% (95% CI 6.2–8.2%) in August–September 2020 (Murhekar et al., 2020, 2021). The number of infections per reported COVID-19 case decreased from 81.6–130.1 in May–June 2020 to 26–32 in August–September 2020, mainly due to improvements in testing capacity and the number of tests performed in the country (Murhekar et al., 2020, 2021).

SARS-CoV-2 poses a high occupational risk to HCWs, who are at the forefront of management of COVID-19 cases in hospital settings. Knowledge of the burden of infection among HCWs is important to gauge the risk of within and outside hospital transmission of SARS-CoV-2, and evaluate in-hospital infection control practices and adherence to non-pharmaceutical interventions (Piccoli et al., 2021).

The number of cases of COVID-19 in India has shown a downward trend since mid-September 2020, with the reported number of cases declining from more than 90,000 per day in September 2020 to less than 20,000 cases per day in December 2020. This declining trend has been seen in all Indian states, except Kerala (FETP Network – Chennai, India, 2021). In this context, the authors conducted a third nationwide serosurvey between December 2020 and January 2021 to estimate the seroprevalence of SARS-CoV-2 antibodies in the general population, and determine the trends in infection since the previous serosurveys. In

addition, seroprevalence was estimated among HCWs working in subdistrict-level public health facilities.

Methods

Survey of general population

The third serosurvey followed the same methodology as the first and second nationwide serosurveys (Murhekar et al., 2020, 2021) (see online Supplementary material). Briefly, the third population-based serosurvey was conducted in the same 700 clusters (villages in rural areas and wards in urban areas) from 70 districts selected at random across India as in the first two serosurveys. The authors aimed to select a minimum of 400 individuals aged ≥ 10 years from each district, with a total sample size of 28,000 individuals (see online Supplementary material). The survey teams first selected four random locations from each cluster. Starting from a random household in each location, contiguous households were visited. All household members aged ≥ 10 years who were permanent residents in the area were enumerated, and consenting individuals present at the time of the visit of the survey team were included in the survey. No additional visits were made to include households which were locked or household members who were not present at the time of the first visit. In order to select at least 40 individuals from each cluster, the field teams visited a minimum of four households from each of the four random points, and enrolled at least 10 individuals per random starting location. If the teams did not identify 10 eligible individuals from the four households, more households were visited. The survey was conducted between 18 December 2020 and 6 January 2021.

Survey of HCWs

Two to three subdistrict-level public health facilities (e.g., 'taluk' or subdivisional hospital, community or primary health centre) closest to the selected cluster/s for the household survey were selected from each of the 70 districts identified for the general population survey. All consenting individuals working in these facilities were included to ensure participation of ≥ 100 HCWs from each district.

Data collection

Eligible individuals from the general population and HCWs who consented to participate were interviewed using the Open Data Kit mobile application (<https://opendatakit.org/>) to collect information on sociodemographic details, history of symptoms suggestive of COVID-19 since March 2020 (e.g., fever, cough, shortness of breath, sore throat, new loss of taste or smell, fatigue), contact with laboratory-confirmed COVID-19 cases, and history of COVID-19 illness. Venous blood (3–5 mL) was collected from each participant, and centrifuged serum samples were transported to ICMR National Institute of Epidemiology, Chennai under cold chain conditions.

Laboratory investigations

Serum samples collected from individuals from the general population were tested for the presence of immunoglobulin G (IgG) antibodies against SARS-CoV-2 on the Advia Centaur Immunoassay system using the Siemens SARS-CoV-2 IgG assay (Siemens Healthineers, India, Mumbai) and Abbott Architect i2000SR automated analyser using the Abbott SARS-CoV-2 IgG assay (Abbott Park, IL, USA). The Siemens assay detects IgG antibodies against the spike protein of the receptor binding

domain (S1-RBD), and the Abbott assay detects IgG antibodies against the nucleocapsid (N) protein of SARS-CoV-2. Serum samples from HCWs were tested only for IgG antibodies against the S1-RBD protein. Sensitivity and specificity of the Siemens IgG assay are 100% and 99.90% respectively, compared with 100% and 99.6% for the Abbott IgG assay (Center for Devices and Radiological Health, 2021). Serum samples with cut-off indices (COI) ≥ 1.0 on the Siemens IgG assay or ≥ 1.4 on the Abbott IgG assay were considered as positive for IgG antibodies against SARS-CoV-2. One hundred and fifty positive serum samples and 150 negative serum samples for each assay were retested for quality control purposes.

Statistical analysis

The characteristics of study participants are described as percentage, mean and standard deviation (SD). The reported occupations were categorized as high risk and low risk on the basis of the potential risk of exposure to a known or unknown COVID-19 case. For example, occupations such as HCWs, police or security personnel, shopkeepers, bus or taxi drivers, and bank employees were considered as high-risk occupations; and farmers, retired employees, students, information technology professionals and homemakers were considered as low-risk occupations (Murhekar et al., 2021). The weighted seroprevalence of IgG antibodies against the N protein and the S1-RBD protein were estimated separately, along with 95% CI, using a random-effects model to account for cluster sampling. Sampling weights were calculated as the product of the inverse of the sampling fraction for the selection of districts and the selection of villages or wards from each district. Weighted seroprevalence was further adjusted for the sensitivity and specificity of the respective assays (Sempos and Tian, 2021). Overall seroprevalence in the general population was estimated by considering serum samples positive on any of the assays. Weighted overall seroprevalence was adjusted for joint sensitivity and specificity of the two assays (Sempos and Tian, 2021). Seroprevalence among HCWs was considered on the basis of the anti-S1 assay alone. In addition, overall seroprevalence was calculated by age group, sex, area of residence and COVID-19-related characteristics of the study participants.

The first serosurvey was conducted among adults alone, whereas individuals aged ≥ 10 years were surveyed in the second and third surveys. The serum samples in the second serosurvey were tested only for IgG antibodies against the N protein using the Abbott assay. For comparison of seroprevalence in the three surveys, one adult per household was selected at random from the survey database, and adjusted seroprevalence of IgG antibodies against the N protein was estimated among these adults.

Overall adjusted seroprevalence in the general population aged ≥ 10 years was applied to the total population of the entire country aged ≥ 10 years to estimate the total number of cases of SARS-CoV-2 infection. Studies indicate that IgG antibodies start appearing between 7 and 14 days after symptom onset and reverse transcriptase polymerase chain reaction (RT-PCR) positivity (Long et al., 2020). The infection to case ratio was estimated by dividing the estimated number of SARS-CoV-2 infections by the number of reported COVID-19 cases detected by RT-PCR or rapid antigen test 1 week (19 December 2020) and 2 weeks (12 December 2020) before the median survey date (26 December 2020).

Sensitivity analysis

IgG antibodies against SARS-CoV-2 infection decline over time (Ripperger et al., 2020; Bolotin et al., 2021). The COI for different assays specified by manufacturers are based on ≥ 14 days convalescent sera. Lowering the COIs could improve the sensitivity of the assays used for population-based serosurveys (Bolotin et al.,

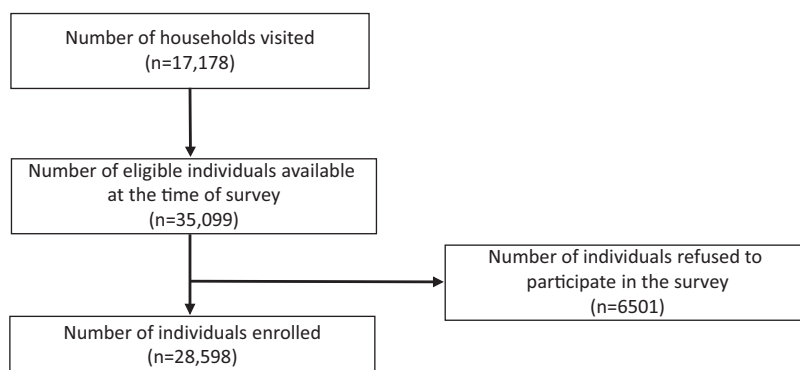


Figure 1. Flowchart of participant enrollment.

2021). In this study, seroprevalence was also calculated using lower COI of >0.54 for the Abbott assay and 0.32 for the Siemens IgG assay, as suggested by Irsara et al. (2021). In addition, seroprevalence was estimated using the lowest values of sensitivity (90.8% for the Abbott assay and 78.8% for the Siemens assay) and specificity (99.3% for Abbott assay and 100% for the Siemens assay) estimated through external validation studies (see online Supplementary material).

Protection of human participants

Written informed consent was obtained from individuals aged ≥ 18 years, and assent was obtained from children aged between 10 and 17 years, with written informed consent from their parents or guardians, before the survey (Indian Council of Medical Research, 2017). The Institutional Human Ethics Committee of ICMR National Institute of Epidemiology, Chennai approved the study protocol.

Results

Seroprevalence among the general population

In total, 17,178 households from 700 clusters in 70 districts were visited. Of the 35,099 individuals who were available at the time of the visit of the survey teams, 28,598 (81.5%) consented to participate (Figure 1).

The mean age of the study participants was 38.2 (SD 16.4) years. Nearly three-quarters of the participants ($n = 21,187$, 74.1%) were residing in rural areas, 51.6% ($n = 14,763$) were female, and 15.2% ($n = 4333$) had an occupation with a higher risk of exposure to potentially infected persons. Of the 1889 (6.6%) participants who reported history of COVID-19 symptoms since March 2020, 474 (25.1%) reported seeking medical care. The main symptoms reported by participants were cough (63.7%), fever (52.4%), tiredness/fatigue (13%), sore throat (12.4%), shortness of breath (11.2%), new loss of smell (4.2%) and new loss of taste (3.5%) (see online Supplementary material). In total, 3232 (11.4%) individuals reported having been tested for SARS-CoV-2 by RT-PCR or rapid antigen test in the past, of whom 287 (8.9%) reported a positive result (Table 1).

Of the 28,598 individuals tested, 4585 (16%) had IgG antibodies against the N protein and 6647 (23.2%) had IgG antibodies against the S1-RBD protein. Weighted and assay-characteristic-adjusted seroprevalence of IgG antibodies against the N and S1-RBD proteins were 14.3% (95% CI 13.6–15.0%) and 21.5% (95% CI 20.4–22.6%), respectively. Overall, 7436 individuals had IgG antibodies against either the N protein or the S1-RBD protein, with weighted and assay-characteristic-adjusted seroprevalence of 24.1% (95% CI

23.0–25.3%) (Table 2). Seroprevalence in districts ranged between 4.9% (20/407) in Mahisagar (Gujarat) and 44.4% (176/396) in Bijapur (Chhattisgarh) (see online Supplementary material).

Overall seroprevalence did not differ by sex (males 23.2%, 95% CI 22.1–24.5%; females 24.9%, 95% CI 23.7–26.3%). Seroprevalence was lowest among individuals aged 18–44 years and was similar among other age groups. Individuals residing in rural areas had significantly lower seroprevalence (21.4%, 95% CI 20.3–22.6%) compared with those living in urban non-slum areas (29.5%, 95% CI 27.0–32.1%) and urban slum areas (34.7%, 95% CI 31.2–38.5%) (Table 3, see online Supplementary material).

Seropositivity was higher among individuals who reported COVID-19-related symptoms (28.7%, 95% CI 26.1–31.4%), and had contact with COVID-19 cases, either within (42.5%, 95% CI 36.7–48.3%) or outside (24.9%, 95% CI 20.0–30.6) the household.

Of the 287 individuals who reported COVID-19 infection by rapid antigen test or RT-PCR, 178 (63.6%, 95% CI 57.2–69.4%) were seropositive (Table 3). Seroprevalence had a positive non-linear correlation with the cumulative incidence of reported COVID-19 cases in the 70 districts (correlation coefficient 0.352) (see online Supplementary material).

Seroprevalence among adults

In order to compare seroprevalence among adults between the three serosurveys, 16,565 adults, one per household, were selected at random from the database. Of these, 2657 had IgG antibodies against the N protein with weighted and adjusted seroprevalence of 14.3% (95% CI 13.5–15.1%). The weighted seroprevalence of IgG antibodies against either the N protein or the S-RBD protein was 24.3% (95% CI 23.1–25.6%).

Burden of SARS-CoV-2 infection in December 2020

Applying the overall seroprevalence to the population aged ≥ 10 years, it was estimated that 271,404,207 (95% CI 259,016,464–284,918,110) individuals in India had been infected by December 2020. With 10,027,311 and 10,181,165 COVID-19 cases reported by 12 December and 19 December 2020, respectively, it was estimated that there were 27.1 (95% CI 25.8–28.4) and 26.7 (95% CI 25.4–28.0) infections per reported case of COVID-19 (Table 4).

Sensitivity analysis

Using the lower cut-off values, the overall seroprevalence of SARS-CoV-2 infection was 37.4% (95% CI 35.9–38.8) (see online Supplementary material). Considering the lowest values of

Table 1
Characteristics of study participants.

Characteristics	General population <i>n</i> (%)	Healthcare workers <i>n</i> (%)
Age (years)	<i>n</i> = 28,598	<i>n</i> = 7385
10–17	2290 (8.0)	–
18–44	16,333 (57.1)	5351 (72.5)
45–60	6938 (24.3)	1956 (26.4)
>60	3037 (10.6)	78 (1.1)
Mean age (SD)	38.2 (16.4)	38.0 (10.2)
Sex	<i>n</i> = 28598	<i>n</i> = 7385
Male	13,817 (48.3)	3175 (43.0)
Female	14,763 (51.6)	4206 (56.9)
Other	18 (0.1)	4 (0.1)
Residence	<i>n</i> = 28598	–
Rural	21,187 (74.1)	–
Urban non-slum	4821 (16.9)	–
Urban slum	2590 (9.0)	–
Type of healthcare worker	–	<i>n</i> = 7382
Doctors/nurses	–	2014 (27.3)
Paramedical staff	–	2684 (36.4)
Field staff	–	2031 (27.5)
Admin staff	–	653 (8.8)
COVID-19 related symptoms	<i>n</i> = 28,598	<i>n</i> = 7385
History of COVID-19 symptoms since March 2020	1889 (6.6)	1066 (14.4)
Medical care sought by symptomatic cases	474/1889 (25.1)	557/1066 (52.3)
History of hospitalization	73/474 (15.4)	173/557 (31.1)
Occupation	<i>n</i> = 28575	–
High risk of exposure to COVID-19	4333 (15.2)	–
History of contact with known COVID-19 case	<i>n</i> = 28,576	–
Within household	598 (2.1)	–
Outside household	297 (1.0)	–
No history of contact with known COVID-19 case	27,681 (96.9)	–
History of contact with known COVID-19 case	–	<i>n</i> = 7382
Health facility	–	3120 (42.3)
Within household	–	130 (1.8)
Outside health facility/household	–	191 (2.6)
No history of contact with known COVID-19 case	–	3941 (53.3)
Ever tested for COVID-19	<i>n</i> = 28,598	<i>n</i> = 7385
RT-PCR	1028 (3.6)	1663 (22.5)
Rapid antigen test	1477 (5.2)	1509 (20.4)
RT-PCR and rapid antigen test	330 (1.2)	1402 (19.0)
Don't know the type of test	397 (1.4)	126 (1.7)
Not tested for COVID-19	25,366 (88.6)	2685 (36.4)
Results of COVID-19 testing	<i>n</i> = 3232	<i>n</i> = 4700
Reported positive for COVID-19	287 (8.9)	664 (14.1)

SD, standard deviation; COVID-19, coronavirus disease 2019; RT-PCR, reverse transcriptase polymerase chain reaction.

Table 2
Seroprevalence (%) of immunoglobulin G antibodies against severe acute respiratory syndrome coronavirus-2 infection, India, August–September 2020.

	General population aged ≥10 years			Healthcare workers
	Anti-N antibodies	Anti-S1-RBD antibodies	Anti-N or anti-S antibodies	Anti-S1-RBD antibodies
Number of individuals tested	28,598	28,598	28,598	7385
Number of positives	4585	6647	7436	1899
Unweighted prevalence ^a (%)	16.0 (15.3–16.8)	23.2 (22.2–24.3)	26.0 (25.0–27.1)	25.7 (23.7–27.9)
Weighted prevalence ^b (%)	14.6 (13.9–15.3)	21.7 (20.6–22.8)	24.6 (23.5–25.7)	–
Adjusted prevalence ^c (%)	14.3 (13.6–15.0)	21.5 (20.4–22.6)	24.1 (23.0–25.3)	25.6 (23.5–27.8)

N, nucleocapsid protein; S1-RBD, spike protein of the receptor binding domain.

^a Adjusted for clustering.^b Weighted for sampling weights.^c Adjusted for test performance.

sensitivity and specificity obtained from external validation studies, the overall seroprevalence was 24.5% (95% CI 23.4–25.7).

Seroprevalence among HCWs

In total, 7385 individuals working in 199 subdistrict-level public health facilities in 70 districts were included in the survey. Their mean age was 38 (SD 10.2) years and 4206 (56.9%) were female. Approximately one third (*n* = 2684, 36.4%) were

paramedical workers and 27.3% (*n* = 2014) were doctors/nurses (Table 1). Overall, 1066 (14.4%) reported a history of COVID-19 symptoms since March 2020, and 3441 (46.7%) reported exposure to a case of COVID-19. In all, 664 (14.1%) of the 4700 individuals who reported COVID-19 testing by rapid antigen testing or RT-PCR were positive (Table 1).

Test-performance-adjusted seroprevalence of IgG antibodies against SARS-CoV-2 infection was 25.7% (95% CI 23.7–27.9) (Table 2). Seroprevalence did not differ between different HCW

Table 3

Seroprevalence (%) of immunoglobulin G antibodies against severe acute respiratory syndrome coronavirus-2 infection by demographic characteristics, India, December 2020–January 2021.

Characteristics	General population aged ≥ 10 years ($n = 28,598$)			Healthcare workers ($n = 7385$)		
	No. tested	No. positive (anti-N/anti-S1-RBD antibodies)	Weighted and test-performance-adjusted seroprevalence % (95% CI)	No. tested	No. positive (only S1-RBD)	Test-performance-adjusted seroprevalence % (95% CI)
Sex						
Male	13,817	3503	23.2 (22.1–24.5)	3175	810	25.4 (23.5–27.3)
Female	14,763	3928	24.9 (23.7–26.3)	4206	1089	25.8 (23.0–28.7)
Other	18	5		4	0	–
Age (years)						
10–17	2290	634	27.2 (24.9–29.4)	–	–	–
18–44	16,333	3936	22.2 (21.1–23.4)	5351	1295	24.0 (21.9–26.3)
45–60	6938	2011	26.7 (25.2–28.2)	1956	587	29.9 (27.1–32.9)
>60	3037	855	26.3 (24.3–28.3)	78	17	21.6 (13.8–32.2)
Area of residence						
Rural	21,187	4997	21.4 (20.3–22.6)	–	–	–
Urban non-slum	4821	1520	29.5 (27.0–32.1)	–	–	–
Urban slum	2590	919	34.7 (31.2–38.5)	–	–	–
Occupation with high risk of exposure to COVID-19						
Yes	4333	1036	21.7 (20.1–23.3)			
No	24,242	6391	24.5 (23.4–25.8)			
Type of healthcare worker	–	–	–			
Doctors/nurses	–	–	–	2014	537	26.6 (23.5–29.7)
Paramedical staff	–	–	–	2684	681	25.3 (22.8–27.9)
Field staff	–	–	–	2031	518	25.4 (22.5–28.4)
Admin staff	–	–	–	653	162	24.6 (20.5–29.4)
History of COVID-19-related symptoms since 1 March 2020						
Yes	1889	651	28.7 (26.1–31.4)	1066	407	38.1 (32.9–43.5)
No	26,709	6785	23.8 (22.7–24.9)	6319	1492	23.4 (21.4–25.7)
History of contact with a known COVID-19 case						
Within household	598	225	42.5 (36.7–48.3)	–	–	–
Outside household	297	96	24.9 (20.0–30.6)	–	–	–
No	23,221	5850	23.4 (22.3–24.5)	–	–	–
Don't know	4460	1256	25.6 (23.4–27.8)	–	–	–
History of contact with a known COVID-19 case						
Health facility	–	–	–	3120	864	27.6 (24.8–30.4)
Within household	–	–	–	130	46	35.3 (26.7–44.9)
Outside health facility/household	–	–	–	191	57	29.7 (21.3–39.7)
No	–	–	–	3255	751	22.9 (20.2–25.9)
Don't know	–	–	–	686	180	26.1 (22.9–29.5)
Previously tested for COVID-19						
RT-PCR	1028	357	29.0 (25.9–32.2)	1663	477	28.6 (25.2–32.2)
Rapid antigen test	1477	485	26.5 (23.6–29.6)	1509	415	27.4 (23.7–31.3)
RT-PCR and rapid antigen test	330	123	29.6 (24.5–35.1)	1402	386	27.4 (23.8–31.3)
Don't know the type of test	397	128	20.3 (15.6–26.2)	126	23	18.1 (13.2–24.1)
Not tested	25,344	6334	23.8 (22.7–24.9)	2682	597	22.1 (19.7–24.7)
Results of COVID-19 testing						
Reported positive for COVID-19	287	178	63.6 (57.2–69.4)	664	395	59.4 (54.0–64.6)
Reported negative for COVID-19	2526	778	27.6 (25.2–30.2)	3982	900	22.4 (20.0–25.1)
Don't know	419	137	30.8 (25.3–36.8)	54	6	10.9 (4.2–25.4)

CI, confidence interval; COVID-19, coronavirus disease 2019; RT-PCR, reverse transcriptase polymerase chain reaction; N, nucleocapsid protein; S1-RBD, spike protein of the receptor binding domain.

Table 4Estimated number of infections among individuals aged ≥ 10 years and infection to case ratio.

	Estimate (95% CI) by N seroprevalence	Estimate (95% CI) by S seroprevalence	Estimate (95% CI) by N/S seroprevalence
Number of infections	160,556,739 (152,641,970– 168,471,508)	242,124,085 (229,736,342– 254,511,829)	271,404,207 (259,016,464– 284,918,110)
Number of reported COVID-19 cases (12 Dec)	10,027,311	10,027,311	10,027,311
Infection to case ratio (12 Dec)	16.0 (15.2–16.8)	24.1 (22.9–25.4)	27.1 (25.8–28.4)
Number of reported COVID-19 cases (19 Dec)	10,181,165	10,181,165	10,181,165
Infection to case ratio (19 Dec)	15.8 (15.0–16.5)	23.8 (22.6–25.0)	26.7 (25.4–28.0)

CI, confidence interval; COVID-19, coronavirus disease 2019; N, nucleocapsid protein; S, spike protein.

categories. Seroprevalence did not differ by age and sex. Seroprevalence was higher among HCW who reported COVID-19 symptoms in the past, those who reported contact with a COVID-19 case within the household, and those who reported a positive result on rapid antigen testing or RT-PCR (Table 3).

Discussion

The findings of the third serosurvey indicate that nearly 24% of India's population aged ≥ 10 years had been exposed to SARS-CoV-2 infection by December 2020, with an estimated 271 million infections. Seroprevalence did not differ by sex, but was lower among adults aged 18–44 years and in rural areas compared with urban areas. The results also indicate that approximately one-quarter of HCWs working in the peripheral public sector health facilities were positive for IgG antibodies.

Antibody assays were used to detect IgG against the N and S1-RBD proteins of SARS-CoV-2 in this survey. N-protein assays are reported to be more sensitive than S1 assays for the detection of antibodies in mildly infected patients that are reported to show absent or delayed, and lower SARS-CoV-2 antibody responses (Özçürümez et al., 2020; van Tol et al., 2020). It has been shown that the anti-N antibodies appear earlier than the S antibodies, and may therefore increase the clinical sensitivity of the assay if samples are drawn early (Rikhtegaran Tehrani et al., 2020). In the third serosurvey, 800 individuals were reactive for the N-protein but negative for the S1-RBD protein, possibly suggesting early infections. The IgG antibody response against different viral antigens is heterogeneous in nature and the results do not always correlate with each other (McAndrews et al., 2020). Therefore, the detection of antibodies against two different antigens, with high sensitivity and specificity, is needed to confirm the findings and avoid false-negative results in surveillance studies (Irsara et al., 2021).

Seroprevalence studies provide information about the extent of transmission in the past, and help predict the future course of the pandemic (World Health Organization, 2020a; Chen et al., 2021). Seroprevalence of IgG antibodies against SARS-CoV-2 among individuals aged ≥ 10 years in India increased from 6.6% in August 2020 to 24.1% in December 2020. The prevalence of IgG antibodies against the N protein between the two serosurveys increased at least 2.2-fold. Serum samples from the previous serosurvey were not tested for anti-S1-RBD IgG antibodies. During the same period, the reported number of COVID-19 cases in India has increased 3.5-fold. Anti-N antibody seropositivity has decreased in 15 of the 70 survey districts by 10.7% to 63.4%, with the steepest decline in Vizianagaram (Andhra Pradesh), Chennai (Tamil Nadu) and Ganjam (Odisha) districts. In the remaining 55 districts, seropositivity to anti-N antibodies has increased 1.04–76-fold (see online Supplementary material). This increase in seroprevalence is consistent with the increase in the number of COVID-19 cases reported between August and December 2020 in these districts (see online Supplementary material).

In the third serosurvey, seroprevalence was significantly lower in the 18–44 years age group, whereas in the second serosurvey, prevalence was similar across age groups. Between August and December 2020, the age-specific seroprevalence of anti-N antibodies increased 1.8-fold among individuals aged 18–44 years and 2.6–3.1-fold in the remaining age groups (see online Supplementary material).

Lower seroprevalence in the active and productive age group compared with other age groups is not consistent with the transmission pattern of COVID-19. This age group was exposed to infection early in the pandemic, as reflected by the relatively high incidence of COVID-19 among this age group between January and April 2020 (ICMR COVID Study Group, 2020). Therefore, the lower seroprevalence found in this age group could be due to relatively higher waning of IgG antibodies compared with other age groups. It is noteworthy that 81% of individuals with RT-PCR-confirmed infection were seropositive during the second survey, compared with 63% during the third serosurvey.

Higher seroprevalence of SARS-CoV-2 infection was found in urban areas compared with rural areas in the third serosurvey. Although this pattern was similar to the second serosurvey in August 2020, seroprevalence did not differ between slum and non-slum urban areas, as was observed in August 2020. Between August and December 2020, the increase in seroprevalence was highest in rural areas (2.5-fold), followed by urban non-slum areas (1.93-fold) and urban slum areas (1.07-fold), reflecting the varied distribution of susceptible populations in these areas. The declining trend in the reported number of COVID-19 cases in India from mid-September 2020 points to a reduction in transmission, which could be attributed to higher seroprevalence in urban slum and non-slum areas, considering these locations to be the drivers of the epidemic in the country (Malani et al., 2021b). The findings of the third serosurvey also indicate that a large proportion of individuals in rural areas remain susceptible to SARS-CoV-2 infection. A similar finding was observed in the recent serosurvey conducted in Karnataka and Tamil Nadu (Malani et al., 2021a; Mohanan et al., 2021).

In India, several cities and states have conducted serosurveys. Metropolitan cities such as Delhi, Mumbai, Pune, Chennai, Ahmedabad and Hyderabad have reported seroprevalence ranging between 17.6% and 56% at different timepoints (see online Supplementary material). Tamil Nadu and Kerala conducted serosurveys covering all districts in October–November 2020 and February 2021, respectively. Seroprevalence reported in Chennai, Coimbatore and Tiruvannamalai districts of Tamil Nadu were comparable to the present survey. The higher seroprevalence in Palakkad, Ernakulam and Thrissur districts of Kerala found in the present survey compared with the Kerala serosurvey could be due to the use of assays for antibodies against the N-protein alone in the Kerala serosurvey.

Seroprevalence among HCWs (25.6%) observed in this study was much higher compared with the 8.7% prevalence estimated in a systematic review and meta-analysis among HCWs (Galanis et al.,

2021). Comparable seroprevalence among clinical, paramedical, field and administrative workers in health facilities and by place of contact with known COVID-19 case suggests widespread transmission of SARS-CoV-2 in the survey areas.

This study has several limitations. First, the participation of children aged 10–17 years in this survey was lower than the census-based age distribution in India ([Office of the Registrar General and Census Commissioner, New Delhi and Government of India, 2011](#)). According to the 2011 census, approximately 21% of the population were aged 10–17 years, whereas 8% of the study population were aged 10–17 years (see online Supplementary material). The under-representation of children and over-representation of adults in the survey could lead to underestimation of the true seroprevalence if one expects a real difference in the risk of exposure to SARS-CoV-2 across age groups. Further, 26% of the study clusters in the present survey were from urban areas, whereas, according to the 2011 census, 31% of the population of India reside in urban areas. Although the proportion of clusters from urban areas in this survey was slightly lower than the national average, this survey was representative of India overall. Approximately 18.5% of eligible individuals declined to participate in this survey. If this non-response was not at random, this could introduce selection bias. Second, different assays were used to measure IgG antibodies in the three serosurveys. In the first serosurvey, a laboratory assay which detected IgG antibodies against the whole cell antigen was used, and positive sera were retested with an assay which detected antibodies against the S1 domain of the S protein of SARS-CoV-2 ([Murhekar et al., 2020](#)). In the second serosurvey, a laboratory assay which detected IgG antibodies against the N protein of SARS-CoV-2 was used ([Murhekar et al., 2021](#)). As antibodies against the N protein of SARS-CoV-2 have been shown to decline faster over a period of time, the actual seroprevalence may have been under-estimated, and thereby the actual number of infections ([Ripperger et al., 2020](#); [Bolotin et al., 2021](#)). In order to overcome these limitations, the serum samples were tested with both anti-N and anti-S1 assays in the third survey. Third, the infection to case ratio was estimated based on the reported number of cases of COVID-19. The completeness of reporting of COVID-19 cases could vary between Indian states.

In conclusion, the findings of the third nationwide serosurvey indicate that nearly one in four individuals aged ≥ 10 years from the general population as well as HCWs had been exposed to SARS-CoV-2 by December 2020 in India. Seroprevalence increased between August and December 2020, and the decline in the number of COVID-19 cases seen in India since mid-September could be on account of higher seroprevalence in urban areas. As three-quarters of the population are still susceptible, it is necessary to continue ongoing surveillance for COVID-19 cases, especially in rural areas. It is also necessary to continue implementation of non-pharmaceutical interventions, such as physical distancing, use of face masks and hand hygiene. The Government of India has initiated COVID-19 vaccination since January 2021, targeting healthcare and frontline workers in the first phase and individuals aged >60 years in the second phase ([Ministry of Health and Family Welfare, Government of India, 2020](#)). As a higher proportion of rural residents are susceptible to infection, and considering limited healthcare facilities in rural areas, especially oxygen beds ([Kumar et al., 2020](#)), elderly populations in rural areas may be prioritized for COVID-19 vaccination.

Author contributions

MVM, TB, JWVT, MSaK, KR, DCSR, SP and BB undertook the study design. TB, MSaK, JWVT, SSe, RSa, AT, SA, RB, SDB, AKB, VC,

DD, AKD, KRD, VD, GRD, SMSK, MSuK, AL, MM, AMa, CR, JT, RY, RA, KA, DKB, PB, DB, JB, ASC, DC, AC, HD, SD, RD, DE, PG, IH, RKH, BJ, AK, SK, NNN, JSK, AK, NK, VGVK, GGJN, GM, NKM, AM, KN, AN, ARN, AKP, GVP, MAQ, SDR, AR, SSa, RS, KS, VKS, HBS, PKS, PS, RSi, NS, DSV, AV, VCW, SurY, SY, KZ, AC, AD, RSD, SD, RK, AMK, KN, SN, CP, KP, SaP, ShP, HR, TR, YKS and ShS coordinated the field operations. CPGK coordinated the laboratory processing and testing of samples. VS, JWVT, MVM, RSa and MSaK performed data analysis. MVM, TB, JWVT, MSaK, KR, SP, DCSR and BB performed data interpretation. MVM, TB, VS, JWVT, RSa and MSaK accessed and verified the data. MVM, TB, MSaK and JWVT wrote the first draft of the manuscript. All authors approved the final version of the manuscript.

Conflict of interest

None declared.

Funding

This study was funded by the Indian Council of Medical Research.

Ethical approval

This study was approved by the Institutional Human Ethics Committee at ICMR National Institute of Epidemiology.

Acknowledgements

The authors acknowledge the field supervision and support provided by WHO India; the Ministry of Health and Family Welfare, Government of India; state and district health officials; and primary healthcare staff in the planning and conduct of the serosurvey. The authors thank the following team members from different Indian states.

Assam

Bibek Saikia, Ritwik Dutta, Hridoy Ranjan Gogoi, Angshuman Saikia, Dipti Kangkana Kachari, Amir Sohail Khan, Mimal Nagtey, Jiturponi Saikia, Rimpi Konwar, Tikendra Gogoi, Prahlad Das, Parmanada Upadhyay, Pullab Das, Roojali Doley, Moon Saikia, Santanu Kakoty, Gamuk Kutum, Agastin Kerketa, Gunin Mili, Tapan Kalita, Krishna Khadka, Samir Ranjan Borah, Jiban Saikia, Pranjal Das, Amit Kumar Ray, Rituraj Borgohain, Mahanta Gogol, Bidya Pegu and Ananta Bora.

Bihar

Naveen Kumar Mandal, Kumar Gautam, Sanjeev Gupta, Ujjwal Prakash, Sahdeo Mandal, Prakash Ranjan, Saurav Kumar, Santosh Kumar, Rahul Kumar, Ranjeet Kumar, Paras Kumar, Kumar Rakesh Mandal, Satish Kumar Thakur, Amit Kumar, Amit Lakra, Ashish Kumar, Binod Kumar, Amit Ranjan, Prateek Raushan, Vikas Kumar, Mumtaz Alam Khan, Baidyanath Roy, Alok Kumar, Ajeet Kumar Ram, Sakaldeep Kumar, Ajeet Kumar, Aaditya Panday, Umesh Kumar, Dharendra Kumar, Abhay Kumar, Sanjeet Kumar, Bhoop Dhakar, Vikash Kumar Roy, Kundan Kunal, Vikash Kumar, Vivek Kumar, Amrendra Kumar, Vikram Kumar Chaudhary, Mohammad Arif, Raneeta Singh, Madhu Kumari, Roushan Kumar, Deen Dayal Kushawaha, Ashish Kumar B.P. Subramanya, Ujjwal Prasad Sinha, Rajeev Chandra Kumar, Ashish Tigga, Sanjay Kumar Singh, Geetika Shankar, Anand Gautam, Susheel Gautam, Rajendra Kumar, Adarsh Varghese, Anisur Rehman Bhuiyan and Kunnal Kuvalekar.

Chhattisgarh

Archana Nagwanshi, Sunil Kumar Pankaj, Irshad Khan, Rahul Roy, Chetan Ravishankar Raut, Kunjbihari Patel, Chandra Kishore Thakre, Pekhan Kumar Sahu, Nand Kumar Modi, Nand Kumar Sahu, Champu Ratre, Bhoopendra Thakur, Awadh Baghel, Hemant Bawthande, Dev Kumar Sahu, Rajesh Kumar Soni, Devdas Joshi, Vokesh Yadu, Gulshan Sahu, Cherapalli Rao, Manish A Prasad, and Keshav Dhruw.

Gujarat

Dinkar Raval, G.C. Patel, A.M. Kadri, Harsh N. Bakshi, Pranav G. Patel, Arthur Mcwan, Anand Santoke, Monark Vyas, S.A. Aarya, Pankaj Nimawat, Shabbir Ali Dedhrotiya, Yagvalky Jani, Jitendra Patel, Hasmukh Parmar, Hardik Nakshiwal, Vaidehi Gohil, Jagdish Patel, Parulben Patel, Jigneshbhai Tadv, Priyank Gandhi, Piyushbhai Parasar, Vinodbhai Valvi, Jagdishbhai Padvi, Dhawal Patel, Divyaben Zala, Mayurbhai Vasava, Manmitbhai Solanki, Darshnaben Patel, Chetnaben Chaudhari, Aartiben Rathva, Riyaben Mistry, Nikiben Bhau, Jyotsnaben Bariya, Tejasbhai Patel, Kartikbhai Prajapati, Babita Roy, Pareshbhai Parmar, Manojbhai Bhagora, Pareshbhai Patel, Hemantbhai Kalasva, Shardaben Vankar, Divya Patel, Ravisinh Chauhan, Nimisha Patel, Misha Patel, Harsha Sadat, Puja Patel, Girish Shah, Partapsinh Taviyad, Raginiben Gosai, Krutikaben Rana, Imtiyazbhai Shaikh, Madhuben Mahera, Bhavikaben Patel, Prakashakumar Patel, Sangitaben Patel, Geetaben Patel, Pratapbhai Pagi, Bharatbhai Rana, Jinalben Patel, Archanaben Pandavi, Dilipbhai Baria, Ishavar Sinh Rathod, Sharmishtha Patel, Sunitaben Solanki, Bhavesh Vaghela, Moinuddin Mansuri, Nitesh Rathore, Purvi Nayak, Hardeep Khair, Rajendra Acharya, Vijayaben Amin, Nirmal Prajapati, V.J. Pargi, Asmitaben Kharadi, Rajubhai Patel, Komalben, Hemangini Baria, Meenaben Bamaniya, Shantaben Prajapati, Rameshbhai Patel, Imran Mansuri, Yashvantbhai Nayak, K.K. Parmar, Rahul Siroi, Krunal Darji, Mahavir Solanki, Shivani Joshi and Mahesh Gavit.

Jammu and Kashmir

Haseena Mir, Syed Arshad Rafiq, Iqra Nisar Chowdri, Tanzeela Bashir Qazi, Rafiya Kousar, Iram Sabah, Shahroz Nabi, Abdul Aziz Lone, Ishtiyaz Ahmad Sumji, Mehvish Afzal Khan, Shaista Ismail, Anjum Asma, Misbah Ferooz Kawoosa, Shifana Ayoub, Armaan Reyaz Kuchay, Saadatul Manzoor, Iftah Rafiq, Umar Wani, Tahir Zahoor Khan, Ayesha Aijaz, Masroor Gayas, Zuba Reyaz, Umar Bashir Ganaie, Nafiya Gulzar, Shazia Hafiz, Raja Salman, Tuba Riaz, Iram Jan, Mudeer Ahmad, Aadil Abdullah Bhat, Rizwana Mehmood, Sadaqat Nawaz, Zarka Arshad, Zubair Khan, Rayeesa Riyaz, Sajad Rasool Kar, Naik Sarma Bashir, S.A. Majeed, Fayaz Ahmad Wani, Milad Zahoor, Showkat Hussain Bhat, Mohammad Yusuf Rather, Syed Bilal, Qazi Tufail, Akif Manzoor, Ghulam Mohiuddin, Shabir Ahmad Dar, Feroz Ahmad, Riyaz Ahmad, Shanipal Singh, Satnam Singh, Masrat Jan, Mushtaq Ahmad and Bilquees Akhtar.

Jharkhand

Anushil Anand, Swagata Lakshmi Tarafdar, Alok Kumar, Aman Gupta, Vikash Kumar Sinha, Mukesh Kumar Aggarwal, Viresh Kumar Mishra, Nilesh Kumar, Abdul Kalam Azad, Raushan Raj, Mamta Kumari, Puja Kachhap, Soni Khatun, Sudhanshu Munda, Jayaram Mehta, Suraj Mahto, Jyoti Anant, Pratima Kumari, Ajay Kerketta and Sony Khatun.

Karnataka

Jawaid Akhtar, Pankaj Kumar Pandey, Arundathi Chandrashekar, Patil Om Prakash, Rameshchandra Reddy, Naveen Madhaiyan, K

Sarika Jain Agrawal, N. Manohar, H.P. Arundathi Das, R. Ranganath, Vivekanand Reddy, Shazia Anjum, G. Hamsaveni, Lokesh Alahari, R.S. Sreedhar, K.R. Nischit, Swathi S Aithal, Mishba Hani, Anil Talikoti, N.T. Nagraj, Satish Ghatage, Shoba Rangaswamy, G. Sandeep Reddy, Ravi Shankar, Savitha Rajesh, S. Sujatha Sridhar, Govardhan Gopal, Babu Mahendra, Vinay Kumar, Harish Raj, S. Vishwa, G. Srinivas, N. Premasudha, E.M. Vanitha, M.K. Suhail, H.R. Rakesh, S.R. Sahana, S. Sunitha, Mohammad Mustapa, M. Krishnamurthy, K.P. Rekha, Minaz-ul-Islam, Manohar Karnal, Sanjeev Patil, K. Archana, Amir Pasha, Renuka Katti, Mantappa Halamalli, Sunil Serikar, Siddu Patil, N. Nagendra, Anand Babu, N.K. Hemanth Kumar, O. Srinivasulu, H.T. Mangala Gowri, Manjunath G. Achari, K.H. Raghunandan, M.T. Ravikumara, Y.G. Srikantha, Neelakanthaayyaswamy I Hiremath, R. Hariprashanth, M.N. Prasanna, B. Dinesh Kumar, Praveen Pujar, Ullera Ashoka, A.N. Sunil, Umar Farooq M. Dalawai, N. Narasimharaju, Bheema Zakheer Hussain, Namewar Hanmanth, M. Manjunatha, Venkatesh A Millanatti, V.Sarath Kumar, M. Deepak, R. Sundara Murthi, H.S. Charan Raj Rao, J. Geetha, T.N. Basavaraju, B. Sampath and T.G. Gangadharaiah.

Kerala

P.S. Rakesh, Suja Aloysius, A.K. Anitha, Sharath G. Rao, Nikilesh Menon Ravikumar, Arun Raj, Akhila Pradeep, M.R. Abhirami, A. Shilna, T. Nikhilamol, S. Anumol Raju, A.S. Asitha, M. Manoj, R. Sindhya, Neethu Sugathan, K. Sumi, Peneena Varghese, A.L. Aravind Krishnan, M.P. Anupranam, V. Prakash Jaison, B.S. Vishnu Raj, V.S. Venoth, J. Gladson, M. Aravind Babu, D. Refic, A.R. Arima and Soniya Joseph.

Maharashtra

G.S. Ganga, Dilip Sharma, Savita Bahekar, Archana Gaikwad, Namrata Hajari, Hema Vishwakarma, Rahul Arke, Vivek Yengade, Vinod Pethkar, Pravin Dandge, Avinash Shinde, Dhiraj Panpatil, Aditya Bengale, Padmakar Kendre, Suraj Rakhunde, Prathamesh Chavan, Pramod Jamale, Anil Rathod, Akshay Phulari, Inayat Nadaf, Tejas Phale, Sunil Shirke, Ajit Buchude, Sourabh Tidake, Kartik Chitrakar, Ganesh Barate, Somnath Bangar, Kirtiraj Madankar, Sagar Rokade, N. Ramaswami, Satish Pawar, Archana Patil, Pradeep Awate, Abhijeet Raut, Deepak Madhukar Mugalikar, Vipin Itankar, Rajendra Bhosale, Rahul Rekhawar, Abhijeet Chaudhari, Rajesh Deshmukh, Nagurao S. Chavan, Balasaheb Nagargoje, Nilkanth Bhosikar, Suryankant Gite, Sunil Pokhrna, Sanjay Salunkhe, Dilip Patode, Shankar Rao Deshmukh, Balaji Shinde, Radhakrishna Pawar, Sandip Sangale, Milind Pore, Sandip Bharaswadkar, Rajabhau Yeole, Rahul Shimpi, Vikas Kokare, Chetan Khade, Harshad Lande, Avinash Borkar, Mohammad Abdul Haleem Azhar, Mujeeb Sayyed and Amol Gaikwad.

Madhya Pradesh

M.P. Sharma, Shivendra Mishra, A.S. Malviya Mahavir Khandelwal, Devendra Bhothwal, C.K. Gupta, Seema Jaiswal, Jyoti Ahirwar, Ganesh Damor, Hemant Singh Thakur, Pratipal Singh, Hemant Pancheshwar, Bhagwansingh Patil, Rameshwar Uikey, Sheetal Saryam, Akaksha Kushram, Shashibhushan Dubey, Sandip Sharma, Saurabh Bhadoriya, Himmat Singh, Yogendra Mourya, Shashank Kesharwani, Prahlad Soni, Pushpendra Rajput, Ankita Sharma, Ashish Namdeo, Jitendra Kumar, Priyanka Birha, Monu Sen, Rekha Prajapati, Priyanka Singore, Lipi Jain, Ashok Solanki and Kalpana Patel.

Odisha

Asit Mansingh, Shakti Ranjan Barik, Siba Prasad Mallik, Prashant Majhi, Deepak Sahoo, Partha Sarathi Patra, A.K. Bishoyee,

Hitesh Kumar Jain, Indurani Sagar, Santosh Kumar Sahoo, Rajesh Panda, Santosh Kumar Beuria, Sidhartha Kar, Soumya Panda, K. Sahu, Matrujyoti Pattnaik, Dasarath Majhi, Biren Kumar Padhi, Padmamohan Pradhan and Arun Padhi.

Rajasthan

P.K. Anand, S.S. Mohanty, Ramesh Kumar Sangwan, Mohendra Thakor, Anil Purohit, Pankaj Kumar, Trilok Kumar, Bhanwar Manohar, Sharwan Kumar, Jogaram Choudhary, Praveen Bhaghel, Suresh Kumar, Sandeep Kumar Yadav, Sunil Kumar, Mohan Lal Meena, Sunil Kumar, Arjun Singh and Mahaveer Singh.

Tamil Nadu

Y. John Arokyadoss, P. Kumaravel, A. Vasudevan, Magesh Kumar, J. Chitra, S. Jagannathan, Santhana Kumar, Sadham Hussain, Rajamani Sentrayan, Kuppusamy Chandrabalu, Chandra Kumar, Lal Kumar, Selvam Suresh, Nandha Kumar, Muthu Murugesan, Ranjith Kumar, Hari Vignesh, Devanga Akshitha, Dhanagopal Rajmohan, G. Preethi, Melveetil Kishor Sumitha, Rajendran Udhayakumar, Chandrasekar Tamil Mani Devi, Thanappan Selvendran, Suryanarayanan Santhosh, Annadurai Arjun, Murugesan Balakrishnan, Vel Thamizharasan, Shravan Kumar Adavath, Sahaya Mary Liza, Krishna Yadav Kattagoni, Thavamurugan Murugakaleswaran, Suresh Manickam, Govindaraj Senbagavalli and M. Thirumalai.

Telangana

R. Ananthan, Anwar Basha, P.P.S. Blessy, J.P. Deva Raj, S. Devindra, Mahesh Kumar, I.I. Meshram, Paras Sharma, Raja Sriswan, P. Raghavendra, G. Sarika, Santosh Kumar Banjara, J. Srinivas Rao, F. Sylvia, S. Sameera, Rajender Rao, A. Rajesham, B. Jagdish, R. Rajyalaxmi, Raji Reddy, N. Jhansi, B. Tulja, Venkata Ramana, B.V. Nancharamma, Hrusikesh Panda, G.L. Stephen, P. Sreenu, G. Bhavani, V. Aruna, Sree Ramakrishna, D. Narasimhulu, V. Chandrababu, G. Neeraja, Sheela Srinivas, T. Usha, K. Satyanarayana, S.P.V. Prasad, P. Sunu, Ch Anitha, D. Rani, Sai Babu, G. Vijaya Lakshmi, D. Swaroopa, G. Tulasi, Raghunadh Babu, D. Sreenu, Deepak Kumar, A. Bhagya Sri, Swetha Sarkar, Aruna Kumari, Nasar Vali, N. Anjaiah, P. Venkatamma, B. Praveen, K. Madhu, G. Subba Rao, P. Sathaiah and P. Nagender.

Uttar Pradesh

Akhileshwar Sharda, Sanidhya Bhargava, Dilip Singh, Vijay Kumar, Naresh Dhakar, Vinay Kumar, Akash Yadav, Deshdeepak Gautam, Swati Singh, Brijesh Maurya, Shaurabh Kumar, Manisha Dhakar, Sheena Singh, Nitesh Kumar, Renu Kanwar, Rahul Yadav, Narendra Yadav, Rahul Kumar, Himalaya Kumar, Raju, Balijeet Sodhi, Rajesh Jain, Shivanka Gaur, Deepak Ohari, Tikam Singh, Saubhagya Prakash, Haridutt Nemi, Dechen Yangdol, Upendra Singh, Harshit Kumar, Amit Yadav, Mohit Tiwari, Gopal Prasad, Sapna Yadav, Basudev Singh, Deepak Babu, Rahul Kumar, Chakrapani Katara, Chandra Pratap Singh, Simran Kaur Bhojwani, Manish Kumar, P. Vedival, Rahul Gond, Prabhat Kumar, Hariom Kushwah, Gani Afridi, Nistha Verma, Veer Vishal, Rakesh Sharma, K. Uday, Saurabha Yadav, Navneet Rajput, Satya Prakash, Mohit Sharma, Sunny Sharma, Santosh Kushwah, Akhalesh Yadav, Shimala Rathore, Prabha Shakya, Vikas Sabharwal, Ravinder Singh, Sushil Chander, Manoj Sharma, Ramesh Kunwar, Sukhwant Singh, Satyvrata Vaidya, Raman Sharma, Pankaj Singh, Manu Jain, Archana Srivastava, Manoj Bahukhandi, Ashish Gusain, Arjit Kumar, Dhruv Gopal, V. Mehta, Vineet Kumar Shukla, R.K. Gautam, Anil Gautam, J. S. Rawat, Bhupinder Singh, Himanshu Sharma, Madhu Kumari, Rajesh Mourya, R.S. Yadav, Surinder Singh, Agam Jain, Raju

Kumavat, Sandeep Patil, Pradhumn Katara, Namrata Soni, Prashant Upadhyaya, Praveen Pachauri, Ajay Rawat, Sanjay Chopra, Jyoti Mishra, Mohammed Husain, Debi Lal, Amit Mohan Prasad, Ghanshyam Singh, Atul Kumar Singhal, Ajay Singh Gautam, Vinay Dange, Shri Prakash Agrawal, Satish Chandra Singh, Birendra Panchal, Vishal Yadav, Mukesh Kumar Mishra, Ravi Shankar Singh, Kamlesh Sah, Sonal Rajput, Sushil Pal, Jaibardhan Siddharth, Ravi Nishad, Rohit Baghel, Punit Kumar, Abhishek Kumar Mishra, Avdhesh Kumar, Anu Gunj, Pawan Kumar, Anurag Srivastava, Vipul Kumar, Kiran, Akash Kushwaha, Vinod Kumar, Ram Poojan Yadav, Mayank Badola and Santhosh Gupta.

West Bengal

Falguni Debnath, Suman Kanungo, Gargi Dutta Bhattacharyya, Subrata Biswas, Ajay Chakraborty, Jayesh Mehta, Bandita Sengupta, Abhijit Dey, Arup Chakraborty, Subhendu Kumar Ray, Subhadip Bhunia, Amlan Datta, Debasish Roy, Shyamal Soren, Jagannath Sarkar, Somnath Mukherjee, Prakash Chandra Mridha, Girish Chandra Bera, Nitai Mandal, Santanu Sahu, Atrayee Chakraborty, Rabiul Islam Gayen, Dilip Biswas, Samudra Sengupta, Barnaman Tudu, Poulami Sen, Anjan Kumar Mallick, Saptarshi Bannerjee, Biswadeep Sengupta, Soumen Jana, Joyeeta Bhattacharyya, Medhavi Manish, Biswajit Namasharma, Chandan Ghosh, Debarati Chakraborty, Kunal Maiti, Milan Barman, Pintu Manik, Priya Rana, Purnima Roy, Rajani Kurmi, Rocky Ansari, Sanglap Maity, Somobrota Naskar, Souptik Jana, Sourav Pradhan, Bishakha Pramanik, Dipannita Sardar, Sujit Kumar Shreshta, Arpita Das, Shrikant Shankar Gawali, Sriparna Garai, Swarnendu Sasmal, Ujjal Maitra, Saiful Gazi, Joydeep Banerjee, Rupali Ghosh, Nawaid Ali, Pokhraj Dey, Chandan Ghosh, Susanta Bera, S.K. Monirul Jaman, Shrija Ghosh, Dev Kumar Dolai, Purnima Das, Wasim Reza and Rajesh Das.

Appendix A. Supplementary data

Supplementary material related to this article can be found, in the online version, at doi:<https://doi.org/10.1016/j.ijid.2021.05.040>.

References

- Bolotin S, Tran V, Osman S, Brown KA, Buchan SA, Joh E, et al. SARS-CoV-2 seroprevalence survey estimates are affected by anti-nucleocapsid antibody decline. *J Infect Dis* 2021;223:1334–8.
- Center for Devices and Radiological Health. EUA authorized serology test performance. Silver Spring, MD: FDA; 2021.
- Chen X, Chen Z, Azman AS, Deng X, Sun R, Zhao Z, et al. Serological evidence of human infection with SARS-CoV-2: a systematic review and meta-analysis. *Lancet Glob Health* 2021;9:e598–609.
- FETP Network – Chennai, India. COVID-19 Resource Center, Epicurve by state. FETP Network India; 2021 Available at: http://covidindiaupdates.in/epicurve_state.php. [Accessed 19 February 2021].
- Galanis P, Vrika I, Fragkou D, Bilali A, Kaitelidou D. Seroprevalence of SARS-CoV-2 antibodies and associated factors in healthcare workers: a systematic review and meta-analysis. *J Hosp Infect* 2021;108:120–34.
- ICMR COVID Study Group. Laboratory surveillance for SARS-CoV-2 in India: performance of testing and descriptive epidemiology of detected COVID-19, January 22–April 30, 2020. *Indian J Med Res* 2020;151:424–37.
- Indian Council of Medical Research. National ethical guidelines for biomedical and health research involving human participants. New Delhi: ICMR; 2017.
- Irsara C, Egger AE, Prokop W, Nairz M, Loacker L, Sahanic S, et al. Evaluation of four commercial, fully automated SARS-CoV-2 antibody tests suggests a revision of the Siemens SARS-CoV-2 IgG assay. *Clin Chem Lab Med* 2021;59:1143–54.
- Kumar A, Rajasekharan Nayar K, Koya SF. COVID-19: challenges and its consequences for rural health care in India. *Publ Health Pract* 2020;1:100009.
- Long Q-X, Liu B-Z, Deng H-J, Wu G-C, Deng K, Chen Y-K, et al. Antibody responses to SARS-CoV-2 in patients with COVID-19. *Nat Med* 2020;26:845–8.
- Malani A, Ramachandran S, Tandel V, Parasa R, Imad S, Sudharshini S, et al. SARS-CoV-2 seroprevalence in Tamil Nadu in October–November 2020. *MedRxiv* 2021a; 2021.02.03.21250949.
- Malani A, Shah D, Kang G, Lobo GN, Shastri J, Mohanan M, et al. Seroprevalence of SARS-CoV-2 in slums versus non-slums in Mumbai, India. *Lancet Glob Health* 2021b;9:e110–1.

- McAndrews KM, Dowlatshahi DP, Dai J, Becker LM, Hensel J, Snowden LM, et al. Heterogeneous antibodies against SARS-CoV-2 spike receptor binding domain and nucleocapsid with implications for COVID-19 immunity. *JCI Insight* 2020;5: e142386.
- Ministry of Health and Family Welfare, Government of India. COVID-19 vaccines: operational guidelines. New Delhi: MHFW; 2020.
- Ministry of Home Affairs, Government of India. Government of India issues orders prescribing lockdown for containment of COVID-19 epidemic in the country. New Delhi: MHA; 2021 Available at: <https://pib.gov.in/Pressreleaseshare.aspx?PRID=1607997>. [Accessed 12 May 2021].
- Ministry of Home Affairs, Government of India. Guidelines for phased re-opening (Unlock 1). As per the Ministry of Home Affairs Order No. 40-3/2020-DM-I (A) dated 30th May, 2020. New Delhi: MHA; 2020.
- Mohanan M, Malani A, Krishnan K, Acharya A. Prevalence of SARS-CoV-2 in Karnataka, India. *JAMA* 2021;325:1001–3.
- Murhekar MV, Bhatnagar T, Selvaraju S, Rade K, Saravanakumar V, Vivian Thangaraj JW, et al. Prevalence of SARS-CoV-2 infection in India: findings from the national serosurvey, May–June 2020. *Indian J Med Res* 2020;152:48–60.
- Murhekar MV, Bhatnagar T, Selvaraju S, Saravanakumar V, Thangaraj JWV, Shah N, et al. SARS-CoV-2 antibody seroprevalence in India, August–September, 2020: findings from the second nationwide household serosurvey. *Lancet Glob Health* 2021;9:e257–66.
- Office of the Registrar General and Census Commissioner, New Delhi and Government of India. 2011 census: age structure and marital status. Office of the Registrar General and Census Commissioner, Government of India; 2011.
- Özçürümez MK, Ambrosch A, Frey O, Haselmann V, Holdenrieder S, Kiehntopf M, et al. SARS-CoV-2 antibody testing—questions to be asked. *J Allergy Clin Immunol* 2020;146:35–43.
- Piccoli L, Ferrari P, Piumatti G, Jovic S, Rodriguez BF, Mele F, et al. Risk assessment and seroprevalence of SARS-CoV-2 infection in healthcare workers of COVID-19 and non-COVID-19 hospitals in Southern Switzerland. *Lancet Region Health Europe* 2021;1:100013.
- Rikhtegaran Tehrani Z, Saadat S, Saleh E, Ouyang X, Constantine N, DeVico AL, et al. Performance of nucleocapsid and spike-based SARS-CoV-2 serologic assays. *PLoS One* 2020;15:e0237828.
- Ripperger TJ, Uhrlaub JL, Watanabe M, Wong R, Castaneda Y, Pizzato HA, et al. Orthogonal SARS-CoV-2 serological assays enable surveillance of low-prevalence communities and reveal durable humoral immunity. *Immunity* 2020;53:925–933.e4.
- Sempos CT, Tian L. Adjusting coronavirus prevalence estimates for laboratory test kit error. *Am J Epidemiol* 2021;190:109–15.
- van Tol S, Mögling R, Li W, Godeke G-J, Swart A, Bergmans B, et al. Accurate serology for SARS-CoV-2 and common human coronaviruses using a multiplex approach. *Emerg Microbes Infect* 2020;9:1965–73.
- World Health Organization. Population-based age-stratified seroepidemiological investigation protocol for coronavirus 2019 (COVID-19) infection, 26 May 2020. Version 2.0. Geneva: WHO; 2020.
- World Health Organization. Weekly epidemiological update – 5 January 2021. Geneva: WHO; 2020 Available at: <https://www.who.int/publications/m/item/weekly-epidemiological-update-5-january-2021>. [Accessed 12 May 2021].

SARS-CoV-2 reinfection by the new Variant of Concern (VOC) P.1 in Amazonas, Brazil

paola

Jan 17

SARS-CoV-2 reinfection by the new Variant of Concern (VOC) P.1 in Amazonas, Brazil

Felipe Naveca **1,2,3**, Cristiano da Costa **2,4**, Valdinete Nascimento **1,2,3**, Victor Souza **1,2,3**, André Corado **1,2,3**, Fernanda Nascimento **1,2,3**, Ágatha Costa **1,2,3**, Débora Duarte **1,2,3**, George Silva **1,2,3**, Matilde Mejía **1,2,3**, Karina Pessoa **1,2,3**, Luciana Gonçalves **2,4**, Maria Júlia Brandão **1,2,3**, Michele Jesus **2,3,5**, Rosemary Pinto **2,4**, Marineide Silva **2,6**, Tirza Mattos **2,6**, Lígia Abdalla **7**, João Hugo Santos **8**, Rubens Costa-Filho **9**, Gabriel Luz Wallau **3,10**, Marilda Mendonça Siqueira **3,11**, Edson Delatorre*, **3,12**, Tiago Gräf*, **3,13**, Gonzalo Bello*, **3,14**, Paola Cristina Resende*, **3,11**.

*These authors contributed equally to this work.

1 Laboratório de Ecologia de Doenças Transmissíveis na Amazônia, Instituto Leônidas e Maria Deane, Fiocruz, Manaus, Amazonas, Brazil.

2 Rede Genômica de Vigilância em Saúde do Estado do Amazonas, Manaus, Amazonas, Brazil.

3 Rede Genômica Fiocruz, Brazil.

4 Fundação de Vigilância em Saúde do Amazonas, Manaus, Amazonas, Brazil.

5 Laboratório de Diversidade Microbiana da Amazônia com Importância para a Saúde, Instituto Leônidas e Maria Deane, Fiocruz, Manaus, Amazonas, Brazil.

6 Laboratório Central de Saúde Pública do Amazonas, Manaus, Amazonas, Brazil.

7 Universidade do Estado do Amazonas, Manaus, AM, Brasil.

8 Hospital Adventista de Manaus, Manaus, AM, Brasil

9 Hospital Pró-Cardíaco, Rio de Janeiro, Brazil.

10 Departamento de Entomologia e Núcleo de Bioinformática, Instituto Aggeu Magalhães, Fiocruz, Recife, Pernambuco, Brazil.

11 Laboratório de Vírus Respiratórios e Sarampo, Instituto Oswaldo Cruz, Fiocruz, Rio de Janeiro, Brazil. SARS-CoV-2 National Reference Laboratory for the Brazilian Ministry of Health (MoH) and Reference Laboratory for the World Health Organization (WHO).

12 Departamento de Biologia. Centro de Ciências Exatas, Naturais e da Saúde, Universidade Federal do Espírito Santo, Alegre, Espírito Santo, Brazil.

13 Instituto Gonçalo Moniz, Fiocruz, Salvador, Bahia, Brazil.

14 Laboratório de AIDS e Imunologia Molecular, Instituto Oswaldo Cruz, Fiocruz, Rio de Janeiro, Brazil.

Summary

The SARS-CoV-2 lineage B.1.1.28 has been evolving in Brazil since February 2020, but the recent emergence of sub-lineages with convergent mutations in the spike (S) protein raises

concern about the potential impact on viral infectivity and immune escape. The lineage P.1 (alias of B.1.1.28.1) is an emerging variant that harbours several amino acid mutations including S:K417T, S:E484K, and S:N501Y. This report describes the first confirmed case of reinfection with the P.1 lineage in a 29-years-old female resident in the Amazonas state, Brazil, previously infected with a B.1 lineage virus.

Keywords: COVID-19; SARS-CoV-2; reinfection; secondary infection; S:E484K; lineage B.1.1.28.P.1, Amazonas, Brazil

Introduction

Since the emergence of the coronavirus disease 2019 (COVID-19), a few cases of reinfection with phylogenetically distinct variants of SARS-CoV-2 have been reported **(1)**. These reinfection cases might be the consequence of a limited and transitory protective immunity induced by the primo-infection or might reflect the reinfecting virus's ability to evade the previous immune responses. The rapid spread in the United Kingdom (UK) and South Africa of emerging SARS-CoV-2 variants carrying several mutations in the receptor-binding domain (RBD) of the spike (S) protein **(2,3)** granting them the title of Variants of Concern (VOC). Among these mutations, E484K and N501Y are of particular concern since they potentially reduce antibody neutralization and increase affinity for ACE2 receptor **(4-10)**. Of note, the first official record of a reinfection case with the emerging VOC B.1.1.7 circulating in the UK **(11)** was recently published.

The SARS-CoV-2 lineage B.1.1.28 has been circulating in Brazil since February 2020 without accumulating notable amino acid changes in the S protein **(12,13)**. Nevertheless, recent genomic surveillance studies reported the emergence of two B.1.1.28 sub-clades with convergent mutations in the RBD of the S protein common to those detected in the UK and South African variants. One sub-clade, designated P.2 (alias for B.1.1.28.2), was first detected in Rio de Janeiro harboring the mutation S:E484K **(14)**. The second sub-clade, designated P.1 (alias of B.1.1.28.1), was first detected in Japanese travelers returning from the Amazonas state **(15)** and due to the presence of several important mutations in the RBD (K417T, E484K, and N501Y) was also classified as a VOC. It is currently unclear to what extent the B.1.1.28 emerging lineages are disseminating in Brazil. However, two recent reports described the first documented cases of reinfection with the emerging P.2 lineage in individuals from the Brazilian Northeast region that were primo-infected by B.1.1.33 lineage variants **(16,17)**.

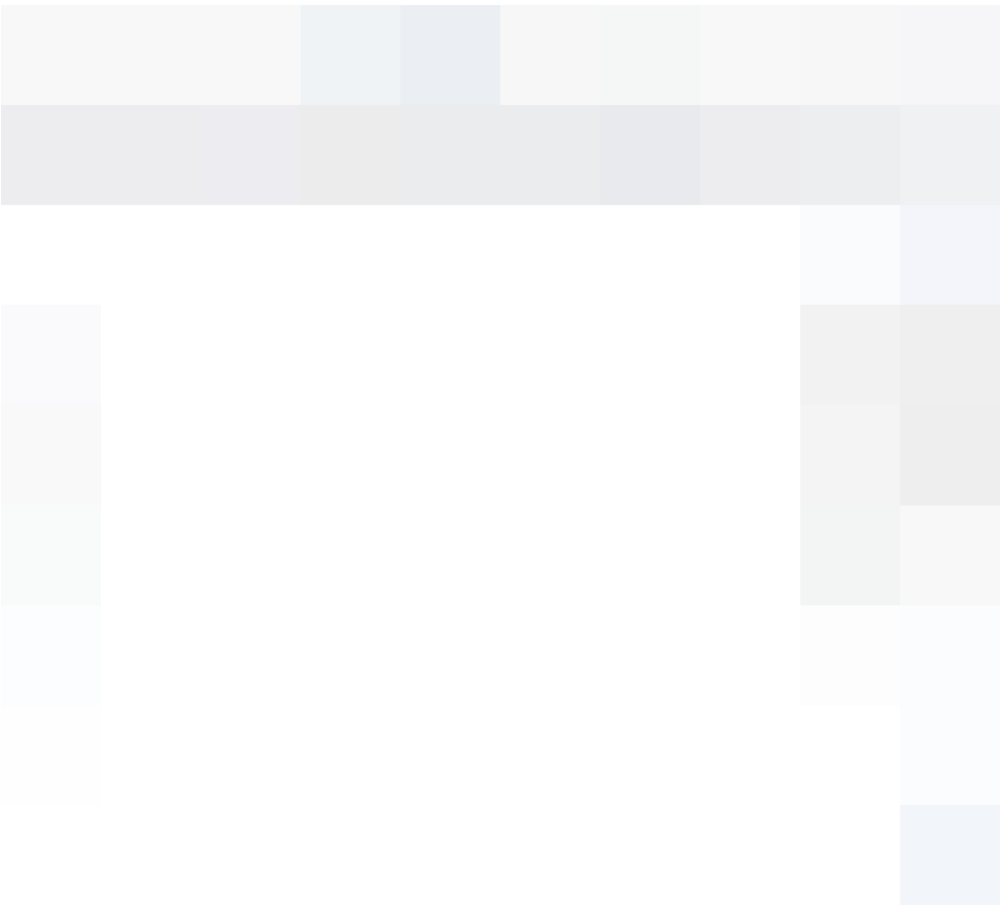
In this study, we report the first documented case of reinfection with the newly emerging P.1 lineage in a 29-years-old individual from Amazonas, a Brazilian state that was severely hit by COVID-19 at the first epidemic wave between March and July, and is currently facing a spiraling surge of deaths since November 2020. The current case report here raises questions about the role of reinfections caused by this new VOC in the Amazonas's second epidemic wave.

Case description

A 29-years-old woman resident in Manaus, Amazonas, Brazil, with no history of immunosuppression, presented two clinical episodes of COVID-19 infection with a gap interval of nine months **(Figure 1)**. In the first episode on March 16th, the patient presented long-term fever and myalgia, cough, sore throat, nausea, and back pain. The patient was classified as having mild COVID-19 with no complications regarding these clinical manifestations and imaging exams. On December 19th, the patient reported participating in an end-of-year celebration with ten other

people after testing positive in an IgG rapid test (Medlevensohn, RJ, Brazil). One of the meeting participants was RT-PCR confirmed for SARS-CoV-2 **(18)** infection on December 24th, and the patient exhibited the second symptomatic COVID-19 episode on December 27th, with fever, cough, sore throat, diarrhea, anosmia, ageusia, headache, runny nose, and resting pulse oximetry of 97%. Patient samples from the nasopharyngeal and pharyngeal swabs (NPS) were obtained on March 24th and December 30th, 2020. This study was approved by the UEA Ethics Committee CAAE: 25430719.6.0000.5016.

Figure 1. Timeline indicating the epidemiological, clinical, and laboratory events regarding the P.1 (alias of B.1.1.28.1) reinfection case in Manaus, Amazonas, Brazil. Mutation highlighted in pink indicates a new potential N-glycosylation site, and orange mutations indicate changes at the RBD.



Diagnostic Laboratory findings

The first and second NPS samples (e.g., March 24th and December 30th) were processed for diagnosis at Fiocruz Amazônia (Fiocruz/ILMD), which is part of the official network of the Ministry of Health for diagnostics and surveillance of the SARS-CoV-2 in the Amazonas state, Brazil. Briefly, total nucleic acid was extracted from the NPS specimens with Maxwell® RSC Viral Total Nucleic Acid Purification Kit (Promega, Madison, WI) and then immediately submitted to RT-qPCR detection of the SARS-CoV-2 RNA using the protocol developed by the US CDC, targeting the viral N gene, and human RNase P as the internal control **(18)**. Both RT-PCR results were positive

(mean Ct 27.5 - 1st sample; 20.5 - 2nd sample, **Figure 1**). Additionally, these samples were also positive for the DPP SARS-CoV-2 Antigen test system (Chembio Diagnostics, Medford, NY).

Genomic findings

We recovered high-quality SARS-CoV-2 whole-genomes from the two positive NPS samples from the suspected reinfection case (EPI_ISL_811148 and EPI_ISL_811149) and from other 10 subjects from Manaus that were also tested positive in December 2020 (EPI_ISL_833131 to EPI_ISL_833140). The whole-genome amplicons were generated as previously described (**19**) with a PCR scheme with nine overlapping amplicons ([Supplemental File.pdf](#)). NGS libraries were produced with Nextera XT and sequenced with MiSeq Reagent Micro Kit v2 (300-cycles). The FASTQ reads were obtained following the Illumina pipeline on BaseSpace, imported into Geneious v10.2.6, trimmed (BBduk 37.25), and mapped (BBMap 37.25) against the reference sequence EPI_ISL_402124 available in EpiCoV database from GISAID (<https://www.gisaid.org/>). Consensus sequences with a mean coverage of 3,283x and 4,663x were generated for the first infection and reinfection case, respectively, excluding duplicate reads. Sequences were genotyped with the Pangolin software v2.1.7 (**20**) that indicate the presence of two different SARS-CoV-2 lineages in each COVID-19 episode: a B.1 lineage in the primo-infection and a P.1 lineage at reinfection.

To confirm the presence of two phylogenetically different SARS-CoV-2 lineages, sequences from the suspected reinfection case were aligned with all high quality (<2% of N) SARS-CoV-2 whole-genomes (>29 kb) from Brazil available in the EpiCoV database in GISAID by January 10th, 2021. Additionally, we also selected the four Japanese whole-genomes as the first representatives of the new P.1 lineage (EPI_ISL_792680 to EPI_ISL_792683). The ML phylogenetic analysis performed with IQ-TREE v2.1.2 (**21**) confirmed that the SARS-CoV-2 sequence from primo-infection branched in a small sub-clade together with three B.1 sequences from other Brazilian states (aLRT = 79%), while the sequence from the reinfection branched together with P.1 sequences isolated in Japan in 2021 along with five new sequences isolated in Manaus in December 2020 (aLRT = 100%) (**Figure 2A**). The P.1 reinfecting virus carried all 21 lineage-defining mutations (Supplementary Table 1) and displayed 11 amino acid changes in the S protein relative to the primo-infecting B.1 virus (**Figure 1**).

To further investigate the temporal scale of the novel P.1 lineage emergence and the viral strain associated with the reinfection case, we conducted a Bayesian analysis of all 10 SARS-CoV-2 sequences that branched within such clade. The time-scaled tree was estimated using a strict molecular clock model with a uniform substitution rate prior ($8-10 \times 10^{-4}$ substitutions/site/year), the HKY nucleotide substitution model, and the Bayesian skyline coalescent prior as implemented in BEAST 1.10 (**22**). Bayesian reconstructions traced the origin of the emerging P.1 lineage to December 1st (95% High Posterior Density [HPD]: November 15th – December 4th) and the most recent common ancestor of the reinfecting virus and the closest P.1 viruses to December 23th (95% HPD: December 12th – December 29th) (**Figure 2B**). This time frame confidently excludes the possibility of long-term persistence of the P.1 virus since primo-infection and traced the second infection a few days earlier before the onset of reinfection symptoms (December 27th).



Figure 2. Evolutionary analysis of the SARS-CoV-2 genomic sequences from the reinfection case. **A.** ML phylogenetic tree of all SARS-CoV-2 whole-genome sequences from Brazil. Branches and tips were colored based on the lineage and sampling location, respectively, following the legend's color code. Branch supports (aLRT) are presented at key nodes. The first (R1) and the second (R2) genomes obtained from the reinfection case are indicated. The scale of the phylogenetic branches is given as substitutions per nucleotide site. **B.** Time-scaled Bayesian MCC tree of SARS-CoV-2 P.1 lineage. Tips are colored according to the sampling location. Colored diamonds indicate the key ancestral nodes representing the MRCA of the P.1 clade (green) and the MRCA of the reinfecting virus, and the closest P.1 sequences (purple).

Discussion

This study described the first case of reinfection with the emerging P.1 lineage (carrying mutations S:K417T, S:E484K and S:N501Y) in a young, immunocompetent woman infected with a B.1 lineage virus nine months before. Notably, the patient had equal moderate symptomatic infections during both episodes and higher viral load (SARS-CoV-2 RT-PCR Ct value) in nasopharyngeal and pharyngeal samples obtained at reinfection compared with those from primo-infection. Although samples at primo-infection were collected later relative to symptom onset compared with samples at reinfection, these findings support that natural infections do not necessarily prevent reinfection or mitigate disease at subsequent infections (11,23). Furthermore, the low Ct values (< 25) detected at reinfection suggests that the subject may have been infectious and contributed to the onward transmission of the virus in the population (24).

A recent longitudinal study in health care workers suggests that post-infection anti-SARS-CoV-2 IgG antibodies are associated with protection from reinfection for most people for at least six months (25). We may speculate that the patient here described developed a transient protective immunity after primo-infection, but the anti-SARS-CoV-2 antibodies substantially decayed by the time of reinfection nine months later (26). However, the positive IgG rapid test obtained only eight days before the onset of symptoms in the second episode suggests that reinfection probably occurred in the face of pre-existing anti-SARS-CoV-2 antibodies. Another hypothesis is that the analyzed COVID-19 convalescent individual produced total IgG antibodies with low neutralizing potency and was thus susceptible to reinfection with new viral variants (27). Finally, the cases of reinfection with the B.1.1.28-derived emerging lineages (i.e P.1 and P.2) detected here and in previous reports (16,17) might also reflect the ability of S:K484 viruses to escape from anti-SARS-CoV-2 neutralizing antibodies induced during primo-infection with S:E484 variants that predominated during the “first-wave” epidemic in Brazil (4-7).

Urgent studies are necessary to determine whether reinfection with newly emerging lineages harboring the mutation S:E484K is a widespread phenomenon or is limited to a few sporadic cases. It will also be crucial to understand the extent to which reinfection contributes to the forward transmission of SARS-CoV-2 in previously exposed populations and the rising number of SARS-CoV-2 cases observed in Amazonas and other Brazilian states during December 2020 - January 2021.

Acknowledgment

We would like to thank the funding support from CGLab/MoH (General Laboratories Coordination of Brazilian Ministry of Health), CVSLR/FIOCRUZ (Coordination of Health Surveillance and Reference Laboratories of Oswaldo Cruz Foundation), CNPq COVID-19 MCTI 402457/2020-0 and 403276/2020-9; INOVA Fiocruz VPPCB-005-FIO-20-2 and VPPCB-007-FIO-18-2-30; FAPERJ: E26/210.196/2020; FAPEAM (PCTI-EmergeSaude/AM call 005/2020 and Rede Genomica de Vigilancia em Saude - REGESAM). We also appreciate the support of all Genomic Coronavirus Fiocruz Network members, the Multi-user Research Facility of Biosafety Level 3 Platform of the Oswaldo Cruz Institute (IOC), Fiocruz, and the CGLab/MoH and Secretary of Surveillance and Health of the Brazilian MoH (SVS-MS). Additionally, we are thankful for all that contribute to the EpiCoV database from the GISAID initiative with high-quality SARS-CoV-2 genomes. All genomes used in this study are described in the acknowledgment **Supplementary Table 1** ([📄 Supplementary_table_1_acknowledgement_table_GISAID.pdf](#)).

References

1. Babiker A, Marvil C, Waggoner JJ, Collins M, Piantadosi A. The Importance and Challenges of Identifying SARS-CoV-2 Reinfections. *J Clin Microbiol* 2020.
2. Rambaut AL, N.; Pybus, O.; Barclay, W.; Barrett, J.; Carabelli, A.; Connor, T.; Peacock, T.; Robertson, D.; Volz, E.; on behalf of COVID-19 Genomics Consortium UK (CoG-UK); . Preliminary genomic characterisation of an emergent SARS-CoV-2 lineage in the UK defined by a novel set of spike mutations. *Virological.org*. <https://virological.org/2020> .
3. Tegally H, Wilkinson E, Giovanetti M, et al. Emergence and rapid spread of a new severe acute respiratory syndrome-related coronavirus 2 (SARS-CoV-2) lineage with multiple spike mutations in South Africa. *medRxiv* 2020.
4. Baum A, Fulton BO, Wloga E, et al. Antibody cocktail to SARS-CoV-2 spike protein prevents

rapid mutational escape seen with individual antibodies. *Science* 2020;369:1014-8.

5. Greaney AJ, Loes AN, Crawford KHD, et al. Comprehensive mapping of mutations to the SARS-CoV-2 receptor-binding domain that affect recognition by polyclonal human serum antibodies. *bioRxiv* 2021.

6. Liu Z, VanBlargan LA, Rothlauf PW, et al. Landscape analysis of escape variants identifies SARS-CoV-2 spike mutations that attenuate monoclonal and serum antibody neutralization. *bioRxiv* 2020.

7. Weisblum Y, Schmidt F, Zhang F, et al. Escape from neutralizing antibodies by SARS-CoV-2 spike protein variants. *Elife* 2020;9.

8. Andreano E, Piccini G, Licastro D, et al. SARS-CoV-2 escape *in vitro* from a highly neutralizing COVID-19 convalescent plasma. *bioRxiv* 2020.

9. Zahradník J, Marciano S, Shemesh M, et al. SARS-CoV-2 RBD *in vitro* evolution follows contagious mutation spread, yet generates an able infection inhibitor. *bioRxiv* 2021.

10. Nelson G, Buzko O, Spilman P, Niazi K, Rabizadeh S, Soon-Shiong P. Molecular dynamic simulation reveals E484K mutation enhances spike RBD-ACE2 affinity and the combination of E484K, K417N and N501Y mutations (501Y.V2 variant) induces conformational change greater than N501Y mutant alone, potentially resulting in an escape mutant. *bioRxiv* 2021.

11. Harrington D, Kele B, Pereira S, et al. Confirmed Reinfection with SARS-CoV-2 Variant VOC-202012/01. *Clin Infect Dis* 2021.

12. Candido DS, Claro IM, de Jesus JG, et al. Evolution and epidemic spread of SARS-CoV-2 in Brazil. *Science* 2020;369:1255-60.

13. Resende P. C. D, E., Gräf T., Mir D., Motta F.C., Appolinario L., Paixão A. C., Mendonça A. C., Ogrzewalska M., Caetano B., Wallau G. L., Docena C., Santos M. C., Ferreira J., Sousa Junior E., Silva S., Fernandes S., Vianna L. A., Souza L., Ferro J. F, Nardy V., Santos C., Riediger I., Debur M., Croda J., Oliveira, W, Abreu A, Bello G... Siqueira M. M. Evolutionary dynamics and dissemination pattern of the SARS-CoV-2 lineage B.1.1.33 during the early pandemic phase in Brazil. *Frontier in Microbiology* 2020.

14. Voloch CM, Silva F Rd, de Almeida LGP, et al. Genomic characterization of a novel SARS-CoV-2 lineage from Rio de Janeiro, Brazil. *medRxiv* 2020.

15. Japan.; NioID. ブラジルからの帰国者から検出された新型コロナウイルスの新規変異株について. *Coronavirus disease (COVID-19)*2021:4.

16. Resende PCB, J.F.; Vasconcelos, R.H.T.; Arantes I.; Appolinario L.; Mendonça, A.C.; Paixao, A.C.; Rodrigues A.C.; Silva, T.; Rocha, A.S.; Pauvolid-Corrêa, A.; Motta, F.C.; Teixeira, D.L.F.T.; Carneiro, T.F.O.; Freire Neto, F.P.F.; Herbster, I.D.; Leite, A.B.; Riediger, I.N.; Debur, M.C.; Naveca, F.G.; Almeida, W.; Livorati, M.; Bello, G.; Siqueira, M.M. Spike E484K mutation in the first SARS-CoV-2 reinfection case confirmed in Brazil, 2020. *Virologicalorg*2020.

17. Vasques Nonaka CKMF, M.; Gräf, T.; Almeida Mendes, A.V.; Santana de Aguiar, R.; Giovanetti, M.; Solano de Freitas Souza, B. Genomic Evidence of a Sars-Cov-2 Reinfection Case With E484K Spike Mutation in Brazil. *Preprints* 2021.

18. Centers for Disease Control and Prevention. CDC 2019-Novel Coronavirus (2019-nCoV) Real-Time RT-PCR Diagnostic Panel. 2020:80.

19. Nascimento VAD, Corado ALG, Nascimento FOD, et al. Genomic and phylogenetic characterisation of an imported case of SARS-CoV-2 in Amazonas State, Brazil. *Mem Inst Oswaldo Cruz* 2020;115:e200310.

20. Rambaut A, Holmes EC, O'Toole A, et al. A dynamic nomenclature proposal for SARS-CoV-2 lineages to assist genomic epidemiology. *Nat Microbiol* 2020.

21. Minh BQ, Schmidt HA, Chernomor O, et al. IQ-TREE 2: New Models and Efficient Methods for Phylogenetic Inference in the Genomic Era. *Mol Biol Evol* 2020;37:1530-4.
22. Suchard MA, Lemey P, Baele G, Ayres DL, Drummond AJ, Rambaut A. Bayesian phylogenetic and phylodynamic data integration using BEAST 1.10. *Virus Evol* 2018;4:vey016.
23. Tillett RL, Sevinsky JR, Hartley PD, et al. Genomic evidence for reinfection with SARS-CoV-2: a case study. *Lancet Infect Dis* 2021;21:52-8.
24. Bullard J, Dust K, Funk D, et al. Predicting infectious SARS-CoV-2 from diagnostic samples. *Clin Infect Dis* 2020.
25. Lumley SF, O'Donnell D, Stoesser NE, et al. Antibody Status and Incidence of SARS-CoV-2 Infection in Health Care Workers. *N Engl J Med* 2020.
26. Selhorst P, Van Iersel S, Michiels J, et al. Symptomatic SARS-CoV-2 reinfection of a health care worker in a Belgian nosocomial outbreak despite primary neutralizing antibody response. *Clin Infect Dis* 2020.
27. Robbiani DF, Gaebler C, Muecksch F, et al. Convergent antibody responses to SARS-CoV-2 in convalescent individuals. *Nature* 2020;584:437-42.

[Spike protein mutations in novel SARS-CoV-2 'variants of concern' commonly occur in ...](#)
[B.1.258Δ, a SARS-CoV-2 variant with ΔH69/ΔV70 in the Spike protein circulating in the C...](#)

arambaut  ARTIC Network

Jan 18

Hi Paola,

Rather than using the Japanese genomes which are, to my knowledge, unpublished why not use the recently released P.1 genomes from Manaus described in this post: [Genomic characterisation of an emergent SARS-CoV-2 lineage in Manaus: preliminary findings](#)

It might help put the reinfection in better context.

Andrew

paola

Jan 19

Hi Andrew,

Thank you for your comments!

The decision to not include those sequences in our reference dataset was based on the following reasons:

1. We decided to analyze genomes with high quality (>29kb) and coverage (<2% N) because this is a new lineage and all sites may be important to classify it, especially in the context of the reinfection case. The genomes deposited by the CADDE do not fulfill these criteria.

2. We also noted, however, that high quality and coverage genomes from some of the same samples were also sequenced by the Instituto Adolfo Lutz (IAL) - SP and are currently available in GISAID. We recognize the value of these genomes generated by the CADDE and IAL-SP groups as the first evidence of the circulation of the P.1 lineage in the Amazonas, but those sequences were not published yet and their inclusion in our work (that will be submitted to publication) might affect the originality of the manuscripts eventually produced by those groups. We believe it is important that groups that generated and rapidly share the primary sequences with the scientific community will be the first to publish their own data. We also modified the text to properly cite the post in the final version of our manuscript.
3. Regarding the Japanese reference sequences (which are also not published yet), we are in contact with the group that generates the sequences and they agree to be coauthors of our manuscript.
4. Because all P.1 sequences detected so far were nearly identical, the inclusion of a large number of sequences from this clade will not add much temporal information to the context of the reinfection case analyzed in our study.

Best regards,
Paola

nuno_faria

Jan 19

Hi Paola,

We are of course happy for you to use our P.1 genomes from Manaus to help to contextualize your findings regarding reinfection in Manaus. Seven of our P.1 genomes on GISAID have $\geq 95\%$ coverage so hopefully they could provide some useful context. If you do use them, just cite our virological post for now (happy to share preprint/paper citation later too).

Nuno

Article

Characterization of Host and Bacterial Contributions to Lung Barrier Dysfunction Following Co-infection with 2009 Pandemic Influenza and Methicillin Resistant *Staphylococcus aureus*

Michaela E. Nickol ¹, Justine Ciric ¹, Shane D. Falcinelli ² , Daniel S. Chertow ^{3,4}  and Jason Kindrachuk ^{1,*} 

¹ Laboratory of Emerging and Re-Emerging Viruses, Department of Medical Microbiology, University of Manitoba, Winnipeg, MB R3E 0J9, Canada; nickolm@myumanitoba.ca (M.E.N.); ciricj@myumanitoba.ca (J.C.)

² Department of Microbiology and Immunology, University of North Carolina Chapel Hill School of Medicine, Chapel Hill, NC 27599, USA; shane_falcinelli@med.unc.edu

³ Laboratory of Immunoregulation, National Institute of Allergy and Infectious Diseases, National Institutes of Health, Bethesda, MD 20892, USA; chertowd@cc.nih.gov

⁴ Critical Care Medicine Department, National Institutes of Health Clinical Center, Bethesda, MD 20892, USA

* Correspondence: Jason.Kindrachuk@umanitoba.ca; Tel.: +1-(204)-789-3807

Received: 16 January 2019; Accepted: 26 January 2019; Published: 29 January 2019



Abstract: Influenza viruses are a threat to global public health resulting in ~500,000 deaths each year. Despite an intensive vaccination program, influenza infections remain a recurrent, yet unsolved public health problem. Secondary bacterial infections frequently complicate influenza infections during seasonal outbreaks and pandemics, resulting in increased morbidity and mortality. *Staphylococcus aureus*, including methicillin-resistant *S. aureus* (MRSA), is frequently associated with these co-infections, including the 2009 influenza pandemic. Damage to alveolar epithelium is a major contributor to severe influenza-bacterial co-infections and can result in gas exchange abnormalities, fluid leakage, and respiratory insufficiency. These deleterious manifestations likely involve both pathogen- and host-mediated mechanisms. However, there is a paucity of information regarding the mechanisms (pathogen- and/or host-mediated) underlying influenza-bacterial co-infection pathogenesis. To address this, we characterized the contributions of viral-, bacterial-, and host-mediated factors to the altered structure and function of alveolar epithelial cells during co-infection with a focus on the 2009 pandemic influenza (pdm2009) and MRSA. Here, we characterized pdm2009 and MRSA replication kinetics, temporal host kinome responses, modulation of MRSA virulence factors, and disruption of alveolar barrier integrity in response to pdm2009-MRSA co-infection. Our results suggest that alveolar barrier disruption during co-infection is mediated primarily through host response dysregulation, resulting in loss of alveolar barrier integrity.

Keywords: influenza; *Staphylococcus aureus*; co-infection; 2009 pandemic; alveolar epithelial cells; kinome; virulence factors; barrier function

1. Introduction

Influenza A viruses (IAV) have posed a persistent threat to global public health for centuries, through both recurrent seasonal epidemics and sporadic pandemic outbreaks [1]. Approximately 10% of the global population is infected with an influenza virus annually, resulting in an estimated 3–5 million severe infections and 300,000–500,000 deaths [1–3]. Initial signs and symptoms include

acute onset of high fever, headache, cough, myalgias, and fatigue [4,5]. IAV is a self-limiting infection in most healthy adults, predominantly affecting the upper respiratory tract, and typically resolves within seven days of symptom onset [4,5]. However, severe infections progress to the lower respiratory tract, resulting in increased risk of respiratory failure and death. Populations at increased risk of severe influenza infection include infants, the elderly, pregnant women, and individuals with pre-existing respiratory, cardiac, neurological, or immunosuppressive conditions [5,6].

There is an increasing appreciation that a large percentage of severe or fatal influenza infections is associated with secondary bacterial infections [7]. The contribution of bacterial infection to influenza morbidity and mortality was well documented throughout the 1918 “Spanish” influenza pandemic and in all subsequent influenza pandemics over the past century [8]. Modern analyses of lung tissue and review of historical autopsy data from fatal 1918 influenza infections demonstrated that 95% of lethal cases were complicated by bacterial co-infection, primarily due to *Streptococcus pneumoniae* and *Staphylococcus aureus* [9–11]. During the 1957 and 1968 influenza pandemics, secondary bacterial pneumonia also caused significant morbidity and mortality, with *S. aureus* and *S. pneumoniae* being the predominant bacterial pathogens [9,12–16]. During the 2009 influenza pandemic, up to 34% of severe influenza infections managed in intensive care units and up to 55% of fatal cases were complicated by bacterial co-infections [17–20]. It is estimated that approximately 65,000 influenza- and pneumonia-related deaths occur in the U.S. each year [17]. *S. aureus*, including methicillin-resistant *S. aureus* (MRSA), is highly prevalent in severe IAV-bacterial co-infection in adults and infants [21–24].

Host and pathogen molecular mechanisms that contribute to severe influenza-bacterial infections in the lower respiratory tract are poorly understood. Excessive mucus production and impaired mucociliary clearance in response to IAV infection facilitates bacterial colonization of the lower respiratory tract, and respiratory epithelial cell barrier breakdown predisposes to bacterial invasion [7,17,21,25]. Influenza infection may also enhance bacterial adhesion to cells through the incorporation of hemagglutinin into the host cell membrane, promoting bacterial cell attachment [25,26]. These events, in conjunction with respiratory epithelial cell barrier breakdown, are likely critical to the development of secondary bacterial infections [25]. Type I and type II alveolar epithelial cells, responsible for physiology gas-exchange and surfactant production, respectively, become infected by influenza viruses, and altered alveolar-capillary membrane function results in impaired oxygen exchange and lung injury [27,28]. However, molecular mechanisms contributing to (1) bacterial replication, (2) bacterial virulence factor expression, and (3) host cell signaling in the context of IAV co-infection to epithelial cell barrier breakdown have not been fully elucidated [25]. Understanding the contribution of these factors to co-infection pathogenesis may yield novel therapeutic targets for treatment of IAV and bacterial co-infection.

As the pathophysiology of severe influenza-bacterial co-infections is primarily associated with the lower respiratory tract, we sought to characterize the contributions of viral-, bacterial-, and host-mediated factors to alveolar cell dysfunction. For this analysis, we employed human adenocarcinoma A549 alveolar epithelial cells to characterize host- and pathogen contributions directly in a relevant and well-characterized alveolar epithelial cell line. Further, A549 cells have been used extensively for the analysis of host responses to influenza virus infection [29–33]. We studied (1) the impact of IAV-infection on MRSA replication kinetics in A549 cell culture, (2) the host cell response to IAV, MRSA, or co-infection by analyzing temporal intracellular kinome responses, (3) the modulation of MRSA virulence factors related to adhesion and invasion in the presence or absence of IAV co-infection by RT-qPCR, and (4) alveolar epithelial barrier function and integrity during IAV, MRSA, or co-infection using electric cell-substrate impedance sensing (ECIS).

2. Materials and Methods

2.1. Virus, Bacteria, and Cell Conditions

The 2009 pandemic H1N1 Influenza A/Mexico/4108/09 (pdm2009) was kindly provided by Dr. Kevin Coombs (University of Manitoba, Canada). Virus stocks were grown in Madin–Darby canine kidney cells and concentrated following ultracentrifugation on a 35% sucrose cushion, kept at -80°C . Viral titers were determined via plaque assay [34]. MRSA USA300 (herein referred to as MRSA) was kindly provided by Dr. George Zhanel (University of Manitoba, Canada). MRSA inocula were generated following growth to mid-log phase in tryptic soy broth (TSB; Hardy Diagnostics, Santa Maria, CA, USA). Human A549 adenocarcinomic alveolar basal epithelial cells were grown in DMEM (Gibco, Grand Island, NY, USA) supplemented with 10% fetal bovine serum (Gibco, Grand Island, NY, USA) and 1% penicillin-streptomycin (HyClone Laboratories, South Logan, UT, USA) at 37°C and 5% CO_2 . Normal human bronchial epithelial cells infected with human telomerase and CDK4-expressing retrovirus (HBEC-3KT) were kindly provided by Dr. Neeloffer Mookherjee (University of Manitoba, Canada). Cells were grown in Airway Epithelial Basal Cell Medium fully supplemented with the Bronchial Epithelial Cells Growth Kit (ATCC).

2.2. Viral and Bacterial Infection of Alveolar Epithelial Cells

For infectious assays, alveolar epithelial cells were seeded at ~95% confluence in DMEM supplemented with 2% FBS 1 day prior to infection. Cells were infected with pdm2009 at a multiplicity of infection (MOI) of 0.01 or mock-infected with DMEM supplemented with 2% FBS for 1 h with gentle rocking every 15 min. Following infection, viral inocula were aspirated from cells and replenished with fresh DMEM supplemented with 2% FBS. Cells were rested for 24 h post-pdm2009 infection. Cells were then infected with mid-log phase MRSA USA300 or mock-infected 24 h post-pdm2009 addition (DMEM supplemented with 2% FBS) for 1 h with gentle rocking every 15 min to ensure equal distribution of bacteria. Bacterial MOIs of 0.1 and 0.01 were used in this investigation and were achieved by serial dilution of mid-log phase culture in DMEM supplemented with 2% FBS. Bacterial inocula were aspirated from cells and replaced with fresh DMEM supplemented with 2% FBS. Cells were harvested at 0, 1, 4, 8, 12, 16, 20, and 24 h post-MRSA infection for further investigation of bacterial replication kinetics, bacterial virulence factors' expression, and kinome analysis. Infections of HBEC-3KT cells (kindly provided by the Mookherjee laboratory) utilized the same conditions with the exception that cells were maintained in Airway Epithelial Basal Cell Medium supplemented with 6 mM L-glutamine.

2.3. Quantification of Bacterial and Viral Replication Kinetics

Enumeration of the total number of adherent and internalized bacteria was determined at 0, 1, 4, 8, 12, 16, 20, and 24 h post-MRSA infection. Media was aspirated from wells, and cells were washed at least $2\times$ with PBS prior to harvest for bacterial enumeration. Alveolar epithelial cells were lysed with 0.025% TritonX-100 (VWR Life Science, Solon, OH, USA). Cell lysates (incl. intact bacteria) were collected, and MRSA colony forming units were enumerated by standard bacterial plating on tryptic soy agar (TSA; MP Biomedicals, LLC, Solon, OH, USA). Viral replication was quantified by RT-qPCR in supernatant samples from pdm2009-MRSA-infected A549 cells. Total RNA was extracted from the supernatants with the PureLink Viral RNA/DNA Mini Kit (Life Technologies, Burlington, ON, USA) according to the manufacturer's instructions. Reverse transcription of total RNA was performed with primers specific for the pdm2009 H1N1 HA sequence using the Superscript IV first-strand cDNA synthesis kit (Life Technologies, Burlington, ON, USA). RT-qPCR was performed on an Applied Biosystems QuantStudio 6 Flex Real-Time PCR System, and each sample was run in duplicate with the PowerUp SYBR Green PCR master mix (Life Technologies, Burlington, ON, USA). Quantification of viral copy number was accomplished by comparison of RT-qPCR results to an established external standard of viral copy number.

2.4. Kinome Peptide Array Analysis

Kinome peptide array analysis was performed as previously described [35,36]. Briefly, IAV-, MRSA-, IAV-MRSA-, and mock-infected alveolar epithelial cells were scraped and pelleted by gentle centrifugation at 4, 8, 12, 16, 20, and 24 h post-MRSA addition. Cell pellets were treated with kinome lysis buffer (20 mM Tris-HCl, pH 7.5, 150 mM NaCl, 1 mM EDTA, 1 mM EGTA, 1% Triton X-100, 2.5 mM sodium pyrophosphate, 1 mM Na₃VO₄, 1 mM NaF, 1 µg/mL leupeptin, 1 µg/mL aprotinin, 1 mM phenylmethylsulfonyl fluoride) and incubated on ice for 10 min. Cell lysates were clarified by centrifugation at 14,000 rpm. Cell lysates were transferred to fresh microcentrifuge tubes, and the total protein concentrations were measured using the Pierce BCA Protein Assay Kit. Activation mix (50% glycerol, 50 µM ATP, 60 mM MgCl₂, 0.05% Brij 35, 0.25 mg/mL bovine serum albumin) was added to the equivalent amounts of total protein (100 µg) for each sample, and total sample volumes were matched by the addition of kinome lysis buffer. Samples were spotted onto kinome peptide arrays (JPT Peptide Technologies GmbH, Berlin, Germany) and incubated for 2 h at 37 °C and 5% CO₂. Following incubation, arrays were washed once with PBS containing 1% Triton X-100, followed by a single wash in deionized H₂O. Arrays were stained with PRO-Q Diamond phosphoprotein stain (Invitrogen, Carlsbad, CA, USA) for 1 h with gentle agitation. Arrays were subsequently destained (20% acetonitrile, 50 mM sodium acetate, pH 4.0) 3 times × 10 min each with the addition of fresh destain each time. A final 10 min wash was performed with deionized H₂O. Arrays were dried by gentle centrifugation. Array images were acquired using a PowerScanner microarray scanner (Tecan, Morrisville, NC, USA) with a 580-nm filter to detect dye fluorescence. Signal intensity values were collected using Array-Pro Analyzer version 6.3 software (Media Cybernetics, Rockville, MD, USA). Kinome data analysis was performed using the Platform for Integrated, Intelligent Kinome Analysis 2 (PIIKA2) software (available online: <http://saphire.usask.ca/saphire/piika>), as described previously [37]. Additional heatmaps were derived using the Heatmapper software suite [38]. Phosphorylation fold changes were validated using the Proteome Profiler Human Phospho-Kinase Array Kit according to the manufacturer's instructions (R&D Systems, Minneapolis, MN, USA).

2.5. Pathway Overrepresentation and Gene Ontology Analysis

Pathway overrepresentation and gene ontology analyses of differentially-phosphorylated proteins were performed using InnateDB software as described previously [35,36,39]. Input data were limited to peptides that demonstrated statistically-significant changes in expression as compared to their respective time-matched mock-infected controls, as described previously [40]. Protein identifiers, phosphorylation fold change values (>1), and *p*-values (<0.05) were uploaded to InnateDB.

2.6. RNA Extraction, cDNA Synthesis, and Quantitative qPCR

At each time point, samples were collected to determine the modification of bacterial virulence factors. Three biological replicates were collected per sample. Media was aspirated from the wells, and the cell monolayers were gently scraped, then pelleted via centrifugation for 10 min at 1200 rpm. The cell pellets were stored at −80 °C until RNA extraction. Bacterial RNA extraction was performed via standard TRIzol-chloroform extraction (Ambion, Carlsbad, CA, USA). Equivalent amounts of RNA from each biological replicate were used for cDNA synthesis using the QuantiNova reverse transcription kit (Qiagen, Hilden, Germany) with random primers. RT-qPCR was performed on the Applied Biosystems QuantStudio 6 Flex Real-Time PCR system (Life Technologies, Burlington, Ontario) using PowerUp SYBR Green Master Mix (Applied Biosystems, Austin, TX, USA) as a detection method. Each biological replicate was run in at least technical duplicate, and non-template controls were included during each run. Melt curve analysis was performed to ensure amplification specificity. Bacterial gene expression was quantified through comparison to the MRSA housekeeping gene 16S [41], and relative fold change in expression was calculated using the 2^{−ΔΔCT} method. Relative fold change

values represent pdm2009-MRSA (normalized to 16S)/MRSA-alone (normalized to 16S). Primer sequences are presented in Table S1.

2.7. Barrier Integrity Determination

The ECIS Z0, 96W Array Station and 96W20idf PET plates (Applied BioPhysics, Troy, NY, USA) were employed to quantify changes in the barrier integrity of alveolar epithelial cells during pdm2009-MRSA co-infection. A549 cells were seeded in 96W20idf PET plates at a concentration of 50,000 cells/mL and were rested in the 96W Array Station (Applied BioPhysics, Troy, NY, USA) for 24 h at 37 °C with 5% CO₂ prior to pdm2009 infection. Cells were subsequently infected with pdm2009 (MOI of 3.0 or 0.1) or mock-infected (DMEM supplemented with 2% FBS) followed by resting for 24 h. Viral- and mock-infected cells were subsequently infected with mid-log phase MRSA USA300 (MOI of 0.1 or 0.01) or mock-infected (DMEM supplemented with 2% FBS) 24 h post-pdm2009 infection. Resistance measurements were acquired during the duration of the entire experiment (72 h). Control conditions included: (i) cells infected with pdm2009-alone (MOI of 3.0, 0.1, or 0.01); (ii) cells infected with MRSA-alone (MOI of 0.01); (iii) mock-infected cells (background barrier resistance); and (iv) cells treated with 1% Triton-X100 (positive control for barrier dysfunction).

3. Results

3.1. MRSA Replication Kinetics Are Similar during Bacterial Infection-Alone and pdm2009-MRSA Infection

We first sought to characterize bacterial replication kinetics in human lung epithelial cells during IAV co-infection. Although IAV-bacterial co-infections can result in increased lung pathology in humans and nonhuman primates [42–44], there is little information available regarding the relation of bacterial replication kinetics to increased disease severity. To address this, we temporally-enumerated MRSA replication in alveolar epithelial cells during MRSA and pdm2009-MRSA infections. MRSA was added to mock-infected or pdm2009-infected cells 18 h post-infection. Timing was based on observational data from human patients with influenza-bacterial co-infections during the 2009 H1N1 pandemic where bacterial co-infection commonly occurred during the peak of viral infection [17]. The total number of adherent and internalized bacteria in alveolar epithelial cells was enumerated through standard bacterial plating. Although there was a trend towards faster bacterial replication in MRSA-alone infection as compared to pdm2009-MRSA infection at 4 h and 8 h post-MRSA infection, there were no statistically-significant differences in MRSA replication between the two conditions at any time point (Figure 1). Cells infected with MRSA-alone entered the exponential growth phase at 1 h post-infection and the stationary phase at 16 h post-infection. This was largely mirrored in the pdm2009-MRSA-infected cells. Bacterial colony counts began increasing exponentially at 4 h post-infection and entered the stationary phase beginning at 16 h post-infection. A similar pattern of MRSA replication in the presence or absence of pdm2009 co-infection was also found in HBEC-3KT cells (Figure S1). This suggests that bacterial replication kinetics are not impacted during influenza co-infection in anatomically- and physiologically-distinct regions of the lungs. To confirm that A549 cells were productively infected by pdm2009, supernatants were harvested from the pdm2009-MRSA-infected cells at the same time points as those used for CFU determination. Influenza virus gradually decreased throughout the course of co-infection (Figure 1B).

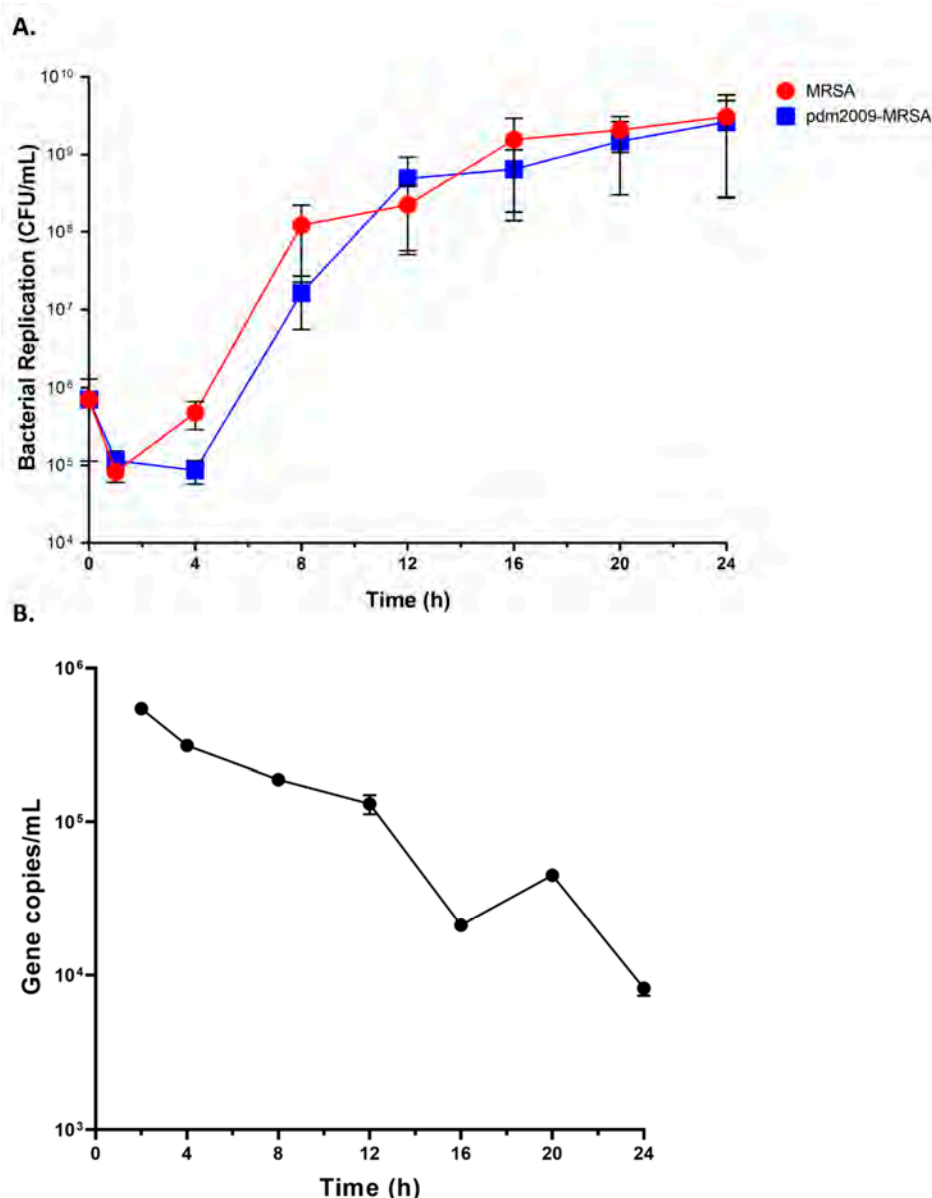


Figure 1. Pathogen replication kinetics during bacterial infection and influenza-bacterial co-infection. A549 cells were infected with 2009 pandemic influenza (pdm2009) and mock-infected, followed by MRSA infection 24 h later (MCR2009) or pdm2009-MRSA infection 24 h later (MCR2009-MRSA). Alternatively, cells were selectively infected with MRSA or pdm2009-MRSA. (A) Alveolar epithelial cells were harvested at the indicated time points, and CFU were quantified by standard bacterial plating. (B) Supernatants were harvested for isolation of viral RNA prior to quantification by RT-qPCR. Error bars represent SEM calculated from at least three biological replicates. Error bars for some of the time points are not visible due to the y-axis scale. No significant differences were found between groups as assessed by two-way ANOVA and significance testing by Tukey's test.

3.2. Temporal Analysis of Host Kinome Responses During pdm2009-MRSA Infection

As bacterial replication rates were virtually identical between the MRSA-alone infection and pdm2009-MRSA infection, we next sought to address whether aberrant cell-mediated immune responses may contribute to viral and bacterial co-infection pathogenesis. We performed temporal kinome analysis of pdm2009-, MRSA-, and pdm2009-MRSA-infected alveolar epithelial cells. We postulated that the activation state of host cell signaling responses or individual cellular kinases could provide insight into differential cellular responses found within co-infected cells as compared to pdm2009- or MRSA-alone. Time-matched mock-infected control cells served as controls. Naive

kinome analysis of pdm2009-, MRSA-, and pdm2009-MRSA-infected alveolar epithelial cells. We postulated that the activation state of host cell signaling responses or individual cellular kinases could provide insight into differential cellular responses found within co-infected cells as compared to pdm2009- or MRSA-alone. Time-matched mock-infected control cells served as controls. Naive A549 cells were initially infected with pdm2009 (MOI 0.1) or mock-infected and rested for 24 h prior to bacterial infection. MRSA addition to MRSA-infected and pdm2009-MRSA co-infected cells was designated as Time 0. Cells were harvested at various post-MRSA infection time points ranging from 4 h post-MRSA addition to 24 h post-infection. Both pdm2009-alone infected cells and mock-infected control cells were treated with MRSA-free infection inoculum at Time 0 to normalize cellular responses that may have been induced through the physical stress of the inoculum addition. Time-matched pdm2009-, MRSA-, and mock-infected control cells were collected throughout the duration of the experiment. Cell lysates were subsequently probed to quantitate host kinome responses by kinome peptide arrays. This analysis relies on the phosphorylation of specific kinase targets (immobilized peptides) on the arrays by active kinases in a cell lysate [45,46]. Data from our arrays, comprised of 309 unique kinase recognition sequences related to a broad spectrum of cell signaling pathways and processes, was analyzed using the Platform for Intelligent, Integrated Kinome Analysis 2 (PIIKA 2) software tool [37]. Hierarchical clustering analysis of the kinome data is presented in Figure 2. Overall, the kinome datasets clustered into three major clusters, which were primarily grouped based on post-MRSA infection time points. From left to right, the first cluster consisted of the 16, 20, and 24 h post-infection MRSA-alone and pdm2009-MRSA co-infection datasets (denoted as A). The second major cluster was comprised of the 4 h and 12 h MRSA-, pdm2009-, and pdm2009-MRSA-infected samples as well as the 8 h MRSA- and pdm2009-MRSA-infected samples (denoted as B). In the third cluster, all of the mock-infected datasets clustered together along with the 8, 16, 20, and 24 h post-infection pdm2009-alone infected datasets (denoted as C). Clusters B and C were more similar to each other than to the samples from Cluster A. These data suggested that the host kinome responses of the MRSA- and pdm2009-MRSA-infected samples from 16 h onwards were highly conserved between the two conditions and differentiated strongly from all other infection conditions and post-infection time points.

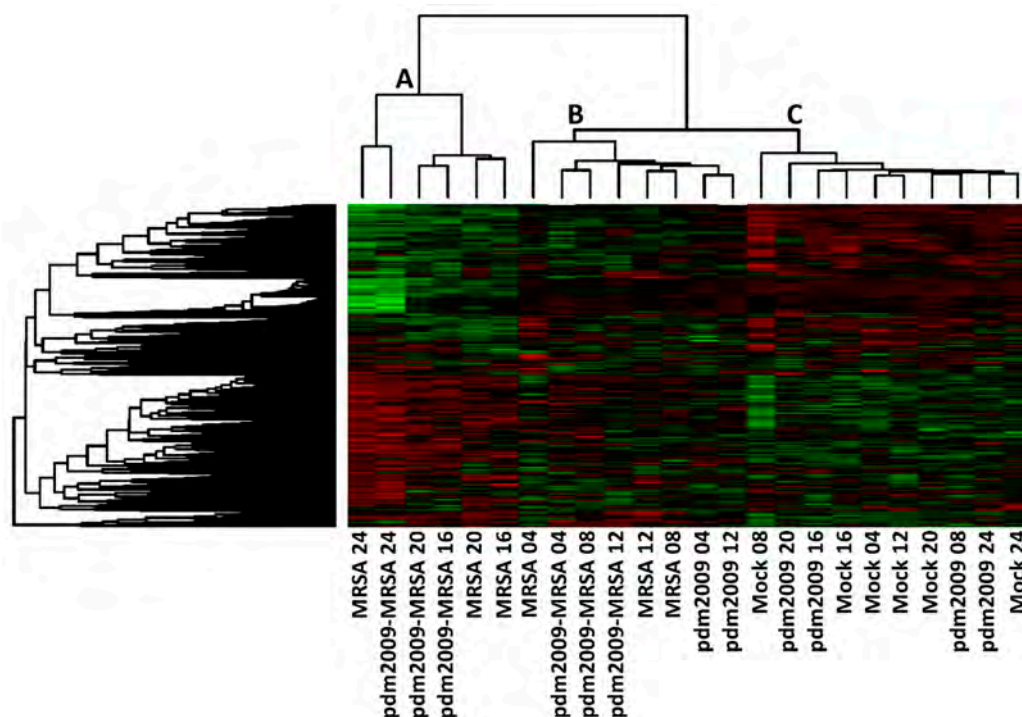


Figure 2. Hierarchical clustering of temporal kinome responses of pdm2009, MRSA, and pdm2009 MRSA-infections in alveolar epithelial cells. Cells were plated 24 h prior to initial infection with MRSA-infections in alveolar epithelial cells. Cells were plated 24 h prior to initial infection with pdm2009. Cells were infected or mock-infected with pdm2009 (MOI 0.1). Twenty four h post-pdm2009 infection, MRSA was added to cells at an MOI of 0.1. Cells were harvested for kinome analysis at the indicated time points. MRSA-alone-, pdm2009-alone-, and mock-infected time-matched samples were also collected at the indicated time points. A–C designate the three major dataset clusters as identified following hierarchical clustering.

To gain further insight into the similarities and/or differences in host kinome responses during pdm2009-MRSA co-infection as compared to infection by either pathogen alone, we performed biological subtraction of the time-matched mock-infected kinome datasets from their respective infected counterparts. Respective hierarchical clustering analysis of phosphorylation fold changes following mock-infected background subtraction is presented in Figure 3. Notably, the 16–24 h MRSA- and pdm2009-MRSA-infected datasets grouped together independent of the time-matched pdm2009-infected datasets. In contrast, at 4 h post-MRSA infection, the pdm2009-MRSA and pdm2009-alone datasets clustered together independent of the time-matched MRSA-alone dataset. However, from 8–12 h post-MRSA infection, the MRSA-alone, pdm2009-alone, and pdm2009-MRSA datasets clustered together. These data suggested that a transition phase occurred in the host cellular response from an IAV-dominated to a MRSA-dominated response. To provide additional validation of the kinome data, we performed phospho-Western blot analysis with Phospho-kinase Proteome Profiler Arrays (R&D Systems). Phosphorylation events that were conserved between the upregulated phosphorylation on the arrays (fold change ≥ 1.5 , p -value < 0.05) and the phospho-Western blots are presented in Table 1.

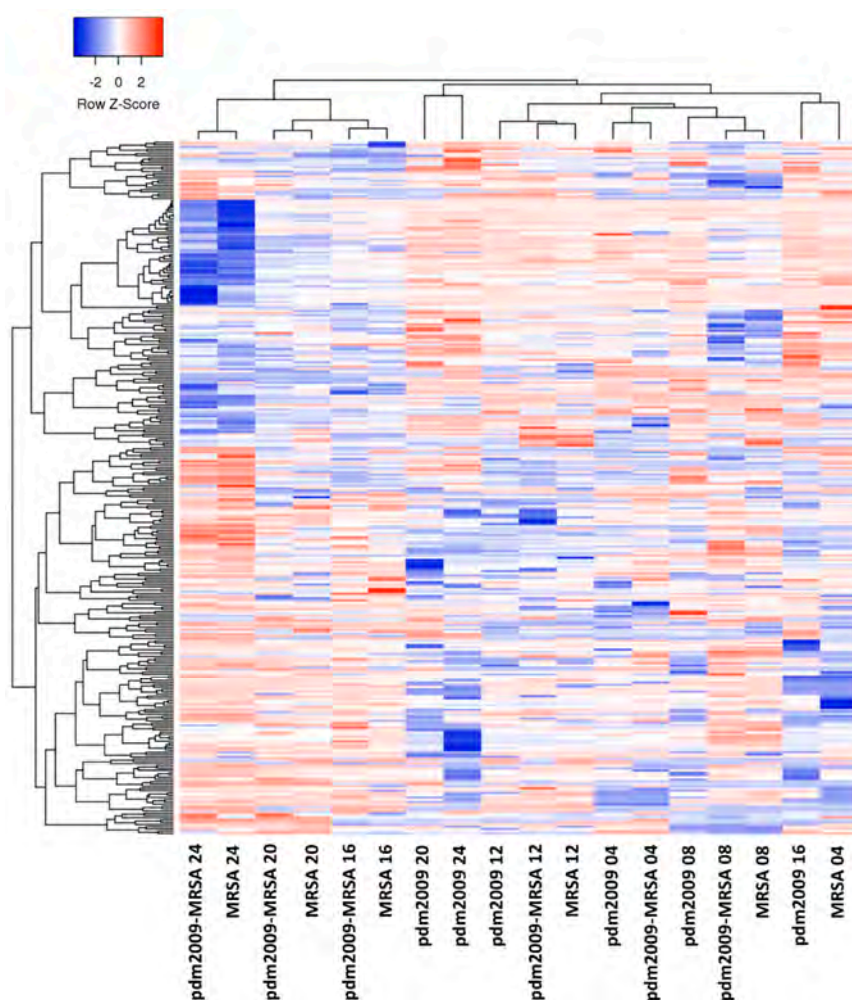


Figure 3. Background-subtracted temporal kinome responses of pdm2009, MRSA, and pdm2009-MRSA infection. Mock-infected kinome responses were subtracted from the time-matched infected samples. Fold change phosphorylation values are plotted for all kinase recognition sequences on the kinome peptide arrays. Clustering analysis was performed with the Heatmapper software suite. Z-score values represent fold change differences in phosphorylation as computed to the time-matched mock-infected control cells.

In addition, we also performed gene ontology (GO) analysis to identify biological processes that were overrepresented within our pdm2009-MRSA kinome data during the 8–12-h transition period (Table S4). While the majority of the biological processes identified mirrored those found in the pathway analysis (i.e., apoptosis- and IFN-related cellular responses) or were directly related to cellular damage responses (e.g., ATP catabolism, unfolded protein response, DNA damage), IL6- and IL8-related cellular responses were also identified, suggesting a potential role of these immune

Table 1. Conservation of phosphorylation status between kinome analysis and phospho-Western blots. pdm2009-MRSA-infected A549 cell lysates 8 h post-MRSA infection were assessed by phospho-Western blot and by peptide kinome arrays.

Target	Phosphosite	Phospho-Western Blot (Fold Change)	Kinome Analysis (Fold Change)
PDGFRb	Y751	1.81	1.61
Fyn	Y420	11.12	1.54
STAT5b	Y699	9.06	2.25
Lyn	Y397	21.30	2.11
Lck	Y394	14.42	2.03
CREB	S133	2.00	2.54
β -catenin	Y654	8.97	2.39
EGFR	Y1086	2.25	2.24
Akt	S473	9.47	3.39
p38a	T180/Y182	2.65	2.13
ERK1/2	T202/Y204; T185/Y187	29.17	2.62
GSK3a/b	S21/S9	1.75	1.73
HSP60	S70	2.02	1.83
STAT3	S727	1.36	1.87
Pyk2	Y402	1.76	2.53
PLCg1	Y783	1.67	1.31
c-Jun	S63	1.87	2.49
p53	S392	3.04	2.58

We next sought to identify host cell signaling responses or biological networks in the pdm2009-MRSA-infected alveolar cells that were selectively modulated during the 8–12 h post-MRSA infection transition phase (Figure 3). Pathway over-representation analysis at 8-h post-MRSA infection resulted in the identification of numerous pathways that were selectively upregulated as compared to the mock-infected cells (Table S2). Multiple apoptosis-related pathways were identified to be activated at this time point including p75(NTR)-, NRAGE-, NRIF-, NADE-, Tsp-1- and BH3-mediated signaling events. In addition, signaling pathways directly related to cell-cell contacts were also identified including alpha 6-beta 4 integrin-, and ephrin-mediated signaling events. Viral infection-related signaling pathways were also identified (incl. type I interferon (IFN) and inflammatory response-related signaling events). At the 12-h post-MRSA infection time point, the host response was dominated by NOTCH-related signaling and antiviral response-mediated events (incl. TRAF6-mediated IRF7 activation and IFN-related responses). As predicted from our hierarchical clustering analyses, there were strong similarities in the overrepresented signaling pathways found between the pdm2009-MRSA co-infection and MRSA-alone infection samples from 16–24 h post-MRSA addition. Upregulated pathways were primarily related to pro-apoptotic (e.g., p53- and caspase-mediated responses), cytokine signaling (e.g., TNF α ; IL1; NF κ B), innate immune response (e.g., TLR signaling; IFN β), and wound healing (e.g., TGF β -mediated signaling). In contrast, the pdm2009-alone infection samples were dominated by IFN-, JAK/STAT-, and IL4-mediated signaling during this time frame with p53-mediated signaling only being overrepresented at the 24-h time point. To provide additional clarity regarding potential differences in host responses between MRSA-alone and pdm2009-MRSA infection during the 8–12-h transition period, we directly compared the pdm2009-MRSA kinome responses to MRSA-alone responses (Table S3). At the 8-h time point, apoptosis-related signaling pathways were over-represented in pdm2009-MRSA-infected cells as compared to cells infected with MRSA-alone, suggesting that co-infection may result in an earlier activation of apoptosis in alveolar epithelial cells as compared to MRSA. At 12 h post-infection, there were fewer total differentially-upregulated pathways between the two infection conditions. Pathways related to TRAF6-, p75NTR, and apoptosis were differentially upregulated during pdm2009-MRSA infection; however, there was no clear over-representation of a particular biological response (e.g., apoptosis).

In addition, we also performed gene ontology (GO) analysis to identify biological processes that were overrepresented within our pdm2009-MRSA kinome data during the 8–12-h transition period (Table S4). While the majority of the biological processes identified mirrored those found in the pathway analysis (i.e., apoptosis- and IFN-related cellular responses) or were directly related to cellular damage

responses (e.g., ATP catabolism, unfolded protein response, DNA damage), IL6- and IL8-related cellular responses were also identified, suggesting a potential role of these immune mediators in the host response to IAV bacterial co-infections. The greatest number of significantly-modulated signaling pathways was identified at 24 h post-MRSA infection. Many of the identified pathways were related to pro-inflammatory responses (incl. TNF- and IL1-mediated signaling), general innate immune responses (incl. NF- κ B, TLR, and RIG-I/MDA5-mediated signaling), apoptosis, wound healing (e.g., TGF β signaling), and cell-cell contacts (e.g., integrin, cadherin, and gap junction signaling). Collectively, our host kinome response data demonstrated that pdm2009-MRSA infection resulted in the selective activation of host cell signaling events largely related to apoptosis, cell-cell contacts and innate immune responses. While the overall represented cell signaling pathways in the pdm2009-MRSA-infected samples resembled those found in both the pdm2009- and MRSA-alone infections during the 8–12-h time period, the cell signaling responses in the co-infections strongly resembled those of the MRSA-alone infections from 16 h onwards.

3.3. Bacterial Invasion- and Attachment-Related Virulence Factor Expression Patterns Are Modulated Early during pdm2009-MRSA Infection

As our prior analysis had focused on the potential role of selective host response modulation in IAV bacterial co-infection pathogenesis, we next sought to characterize the potential role of selective modulation of bacterial virulence factors to pathogenesis. We employed RT-qPCR to examine differential modulation of MRSA virulence factor gene expression in the presence or absence of pre-existing influenza virus infection in alveolar epithelial cells. We focused on MRSA virulence factor genes related to host-cell adhesion and invasion for our analysis. Overall, the expression of virulence factors in the pdm2009-MRSA-infected cells was largely repressed (<1) relative to MRSA-alone from 8 h onwards (Figure 4). In contrast, the expression of *hla*, *spa*, and *fmbB* was highly upregulated in the co-infected A549 cells relative to MRSA-alone at 1 h post-MRSA addition. The expression of *spa* and *fmbB* remained upregulated in the co-infected cells at 4 h post-infection, while the expression of *hla* was similar to MRSA-alone. This pattern of differential gene expression coincided with the early exponential phase of MRSA replication in infected cells (Figure 1). Taken together, our data suggest that MRSA virulence factors may contribute to pdm2009-MRSA co-infection pathogenesis during the early phase of bacterial attachment and entry in alveolar epithelial cells.

Our host kinome data suggested that pdm2009-MRSA co-infection-mediated modulation of host signaling responses shifted to a more dominant response during the exponential phase of MRSA replication in infected cells (Figure 1). Taken together, our data suggest that MRSA virulence factors may contribute to pdm2009-MRSA co-infection pathogenesis during the early phase of bacterial attachment and entry in alveolar epithelial cells. We focused on MRSA virulence factor genes related to host-cell adhesion and invasion for our analysis. Overall, the expression of virulence factors in the pdm2009-MRSA-infected cells was largely repressed (<1) relative to MRSA-alone from 8 h onwards (Figure 4). In contrast, the expression of *hla*, *spa*, and *fmbB* was highly upregulated in the co-infected A549 cells relative to MRSA-alone at 1 h post-MRSA addition. The expression of *spa* and *fmbB* remained upregulated in the co-infected cells at 4 h post-infection, while the expression of *hla* was similar to MRSA-alone. This pattern of differential gene expression coincided with the early exponential phase of MRSA replication in infected cells (Figure 1). Taken together, our data suggest that MRSA virulence factors may contribute to pdm2009-MRSA co-infection pathogenesis during the early phase of bacterial attachment and entry in alveolar epithelial cells. We focused on MRSA virulence factor genes related to host-cell adhesion and invasion for our analysis. Overall, the expression of virulence factors in the pdm2009-MRSA-infected cells was largely repressed (<1) relative to MRSA-alone from 8 h onwards (Figure 4). In contrast, the expression of *hla*, *spa*, and *fmbB* was highly upregulated in the co-infected A549 cells relative to MRSA-alone at 1 h post-MRSA addition. The expression of *spa* and *fmbB* remained upregulated in the co-infected cells at 4 h post-infection, while the expression of *hla* was similar to MRSA-alone. This pattern of differential gene expression coincided with the early exponential phase of MRSA replication in infected cells (Figure 1). Taken together, our data suggest that MRSA virulence factors may contribute to pdm2009-MRSA co-infection pathogenesis during the early phase of bacterial attachment and entry in alveolar epithelial cells.

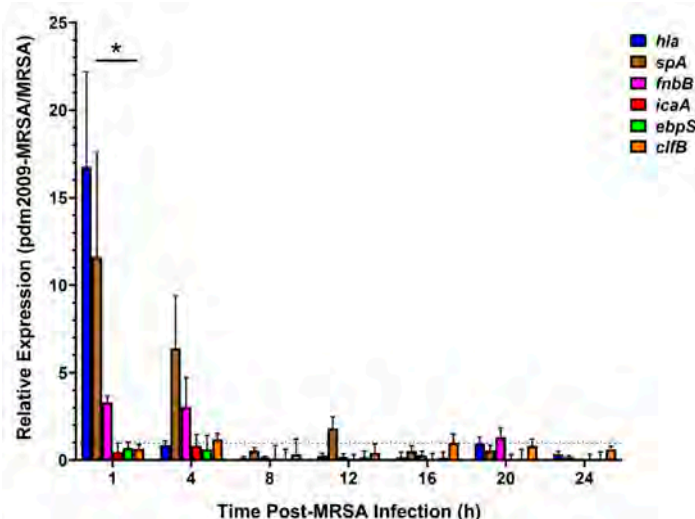


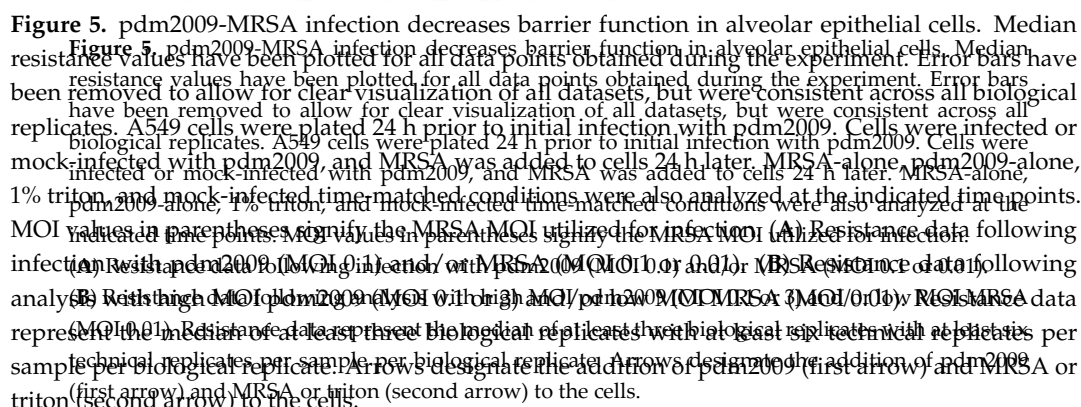
Figure 4. pdm2009-MRSA co-infection alters bacterial virulence factor expression in alveolar epithelial cells as compared to MRSA infection alone. MRSA virulence factor expression fold change values for co-infected samples relative to MRSA-alone-infected cells. Error bars represent SEM calculated from at least three biological replicates. Relative expression fold changes represent pdm2009-MRSA vs MRSA infection alone and were calculated by the $2^{-\Delta\Delta CT}$ method. Comparison between groups was assessed by two-way ANOVA and significance testing by Tukey's test, * $p < 0.05$.

3.4. MRSA-Alone and pdm2009-MRSA Infection Result in Alveolar Epithelial Cell Barrier Dysfunction

Our host kinome data suggested that pdm2009-MRSA co-infection-mediated modulation of host cell signaling responses shifted to a MRSA-dominated response during the 8–12-h post-MRSA addition period. Thus, we next examined whether the MRSA-dominated host response observed in the kinome data also dominated barrier function disruption. To assess this, we incorporated ECIS to characterize alveolar epithelial cell barrier function in response to pdm2009-MRSA infection by measuring temporal changes in resistance [47].

Alveolar epithelial cells were initially plated and rested overnight prior to pdm2009 infection (0 h). Following the overnight rest, cells were infected with pdm2009 (first arrow; Figure 5). Mock-infected control cells were treated with media alone. IAV- and mock-infected cells were subsequently infected with mid-log phase MRSA or mock-infected with media alone (second arrow; Figure 5), and resistance was continually monitored for the duration of the experiment. A summary of the data is presented in Figure 5, beginning just prior to the initial infection with pdm2009 (20 h). Mock-infected cells were left untreated throughout the duration of the experiment (negative control).

Infection of alveolar epithelial cells with pdm2009-alone at a MOI of 0.1 resulted in no changes to resistance during the first 24 h of infection. Only a small loss in resistance was found following the addition of mock-infected inoculum at 43 h (Figure 5A). The addition of MRSA (MOI 0.1) to mock-infected alveolar epithelial cells at 43 h resulted in the loss of resistance of the alveolar epithelial monolayer beginning at 57 h. Infection with pdm2009-MRSA (MOI 0.1) resulted in a nearly identical loss in resistance across the alveolar epithelial cells as that for infection with MRSA-alone. We also examined how a lower MOI of MRSA would affect the trends in resistance across our alveolar epithelial cells. Losses in resistance across the alveolar epithelial monolayers were similar between the two MOIs of MRSA tested (0.1 and 0.01). In contrast, the trend in resistance measurements differed slightly between the two MOIs of MRSA during co-infection. As these results suggested that pdm2009-MRSA co-infection-mediated disruption of alveolar epithelial barrier function largely resembled that of MRSA infection alone, we sought to expand on these observations. We examined pdm2009-MRSA co-infection using higher MOI pdm2009 and/or lower MOI MRSA inocula (Figure 5B). Infection with pdm2009-MRSA (MOI 0.1; MOI 0.01) resulted in a nearly identical loss in resistance across the alveolar epithelial cells as that for infection with MRSA-alone. We also examined how a higher MOI of pdm2009 would affect the trends in resistance across our alveolar epithelial cells. By 9 h post-pdm2009 infection (31 h; MOI 3), the resistance measurements began to decrease from the mock-infected condition and remained under 300 ohms for the duration of the experiment. Following the addition of MRSA (MOI 0.01) to the high MOI pdm2009-infected cells, resistance values across the alveolar epithelial cells began to decrease at the same time as in MRSA-alone and MOI 0.1 pdm2009-MRSA infections. However, the high MOI pdm2009-MRSA infections resulted in losses to resistance equivalent to those of the 1% triton-treated cells much more rapidly than the other infection conditions. To examine the effect of pdm2009-MRSA co-infection on distal regions of the respiratory tract, we investigated the effects of co-infection on HBEC-3KT human bronchial epithelial cells (Figure S2). The trends in loss of resistance during MRSA-alone- and pdm2009-MRSA-co-infection were largely similar to those found in A549 cells. Collectively, these data suggested that the increased damage imparted to respiratory epithelial cells by high MOI pdm2009 results in exacerbated MRSA-mediated cytotoxicity during co-infection, even at low MOIs of bacteria.



Secondary bacterial infections can complicate both seasonal and pandemic influenza virus infections, resulting in increased morbidity and mortality [7]. During the 1918 influenza pandemic, >90% of lethal infections were complicated by bacterial co-infections and were primarily associated with *S. pneumoniae* and *S. aureus* [10]. More recently, *S. aureus*, including MRSA, has been commonly associated with influenza-bacterial co-infections, including during the 2009 pandemic, where 55% of fatal cases were associated with secondary bacterial infections [18–20]. Bacteria have the ability to sense and adapt to their surrounding environment, including during infection. This includes the modulation of replication kinetics and the synthesis of virulence factors or toxins, which can enhance both adhesive and invasive properties [48]. Here, we sought to assess the roles of host and bacterial factors directly

in influenza-bacterial co-infection-mediated alveolar epithelial cell barrier dysfunction. Of note, pathophysiology associated with co-infection is thought to occur mainly in the lower respiratory tract [17]. Thus, we utilized the well-characterized alveolar epithelial adenocarcinoma A549 cells for our investigation. While it is appreciated that the potential biological implications of immortalized cell host response data must be interpreted cautiously, A549 cells provide the opportunity to assess alveolar epithelial cell responses directly in a well-characterized cell line. We have also demonstrated that the bacterial replication kinetic trends were nearly identical in the presence or absence of pdm2009 co-infection between A549 cells and HBEC-3KT cells, a normal human bronchial cell line. Further, barrier dysfunction analysis by ECIS demonstrated similar trends in loss of barrier integrity during MRSA infection alone or in conjunction with pdm2009. Future investigations will also address potential differences between non-differentiated versus differentiated/polarized A549 or primary alveolar cells.

Although we had hypothesized that pre-existing pdm2009 infection may enhance MRSA replication due to the exposure of additional bacterial binding sites on infected cells, this was not observed. Virtually identical bacterial replication kinetics were observed with no significant differences in replication at any time point. This would suggest that MRSA fitness is not altered by cellular damage or host molecule secretion (e.g., cytokines) resulting from pre-existing pdm2009 infection. This also suggests that the increased disease severity associated with influenza-bacterial co-infections is not simply due to increased bacterial burden within the lungs during co-infection.

In contrast to our replication kinetics data, the expression of MRSA virulence factors related to adhesion and invasion were selectively upregulated during the early stages of infection in pdm2009-MRSA co-infected cells as compared to bacterial infection alone. Statistical analysis demonstrated that *hla* and *spA* expression was significantly greater than all of the other virulence factors examined at 1 h post-MRSA infection; however, there were no statistically-significant differences in expression between virulence factors from 4 h onwards. Increased expression of virulence factors during pdm2009-MRSA infection as compared to MRSA-alone was inversed, as virulence factor expression in the co-infected samples was repressed as compared to MRSA-alone. This is perhaps unsurprising given that we focused on virulence factors related to bacterial adhesion and invasion. The MRSA *hla* gene codes for α -hemolysin, which forms pores in the cytoplasmic membrane of infected cells, resulting in lysis [49]. Expression of *hla* was ≥ 16 -fold higher at 1 h post-infection, but rapidly declined by the 4-h time point. This may suggest a critical role for *hla* in the immediate stages of secondary MRSA infection pathogenesis and may contribute to co-infection pathogenesis, as α -hemolysin is related to clinical pneumonia [24,50]. Similarly, *fnbB* and *spA*, which are both involved in cell adhesion, were upregulated in the co-infected cells as compared to MRSA-alone from 1–4 h post-infection. Fibronectin-binding protein B, encoded by *fnbB*, is able to bind fibronectin, fibrinogen, and elastin in order to mediate adhesion to cells, specifically for internalization of MRSA [51,52]. Protein A, the product of *spA*, mediates binding and adhesion to airway epithelial cells, while also being able to repress innate and adaptive immune responses [53]. Our data suggest that pdm2009 infection of alveolar epithelial cells results in cellular damage and subsequent exposure of host molecules (e.g., fibrinogen, elastin, and fibronectin) in the extracellular matrix and plasma membrane, resulting in the upregulation of MRSA binding factors, including FnbB and SpA. In contrast, the relative expressions of *icaA*, *ebpS*, and *clfB* were all repressed as compared to infection with MRSA-alone throughout the course of our investigation. The *ica* locus is involved in intracellular adhesion and encodes N-acetylglucosaminyltransferase [54,55]. The *ebpS* gene is able to bind elastin in injured tissues, facilitating bacterial colonization [56], and *clfB* mediates fibrinogen [57]. Our data suggest that specific bacterial adhesion and invasion factors may provide an advantage for bacterial entry into influenza-infected cells. Future investigations of the relation between targeted inhibition of *fnbB*, *hla*, and *spA* and co-infection pathogenesis in alveolar epithelial cells are warranted and may provide important information regarding novel antimicrobial therapeutic targets. However, our data also suggest that there is likely no competitive advantage for expression of adherence and invasion-related bacterial virulence factors post-entry between pdm2009-MRSA infection and MRSA-alone infection.

Further analyses of additional bacterial toxins and virulence factors may provide evidence for bacterial molecules that are related to post-bacterial adhesion/invasion co-infection pathogenesis.

Although our data suggested that the role of bacterial virulence factors in pdm2009-MRSA infection is likely important for early bacterial attachment and entry events alone, our host kinome response data suggested that host response dysregulation plays an integral role in co-infection pathogenesis. We examined this by characterizing the temporal host kinome response of alveolar epithelial cells in response to co-infection. Interestingly, the host response of co-infected cells clustered most strongly with those from pdm2009-alone infections during the early stage of infection. This was perhaps surprising, as the greatest difference in relative expression of bacterial virulence factors, including those with immunomodulatory activities (e.g., SpA), occurred early during the course of co-infection. A previous investigation by Kumar et al. demonstrated that stimulation of epithelial cells with SpA resulted in the induction of TNF α and IL8 secretion and activation of NF κ B signaling [58]. While the host response in our co-infected cells was dominated by antiviral-related signaling responses during the early course of infection, GO analysis demonstrated that IL6-, IL8-, TNF α -, and NF κ B-mediated signaling events were overrepresented in the co-infected samples, although absent in our MRSA-alone and pdm2009-alone infected cells. The upregulation of these signaling events corresponds with the upregulation of *spA* expression in the co-infected samples as compared to MRSA infection alone. This suggests that while the early host response during co-infection is largely dominated by the induction of antiviral responses, the upregulation of bacterial virulence factors might have an underlying influence on the induction of host cell cytotoxic responses. Interestingly, direct comparison of host kinome responses during pdm2009-MRSA infection to those from cells infected with MRSA-alone suggest that a stronger apoptotic response is found in co-infected cells as compared to bacteria-alone during the 8–12 h transition phase. This comparison supports the postulate that influenza-bacterial co-infections specifically alter host cellular responses as compared to either pathogen alone. Focused in vivo and in vitro investigations of the contributions of host response dysregulation, and in particular modulation of alveolar epithelial cell apoptosis, may provide important clues to the molecular mechanisms underlying the pathophysiology of influenza-bacterial co-infections. Future investigations will explore potential roles for the modulation of IFN-mediated cell signaling responses to pdm2009-MRSA infection pathophysiology. In particular, does modulation of the secretion of soluble host factors during pdm2009 infection impact downstream virulence factor expression patterns in MRSA?

In contrast, the kinome data (following background subtraction of the mock-infected samples) from co-infected cells clustered strongly with those derived from MRSA-alone infections from 16 h post-MRSA addition onwards, and this was reflected in strong upregulation of cell death responses (e.g., apoptosis-related pathways) in both infection conditions. From 8–12 h post-MRSA infection, host kinome data from the three different infection conditions clustered together. Taken together, our clustering data suggest that the host response transitions from an influenza- to bacterial-centric response during infection. Importantly, this transition phase in the host response corresponded with mid- to late-exponential MRSA growth. These data largely overlapped with the observations from our ECIS analysis of pdm2009-MRSA co-infection. The addition of pdm2009-alone to the alveolar epithelial cells at a low MOI of 0.1 did not result in a significant decrease in resistance, nor any negative repercussions in regards to barrier integrity and cell morphology. This reflects the majority of influenza infections in healthy adults, which do not generally result in severe disease [4–6]. However, the addition of high MOI pdm2009 resulted in significantly decreased barrier integrity and may reflect a relation between exacerbated disease and infectious titer of the exposure. In contrast, the addition of MRSA resulted in significant decreases in resistance and eventual loss of alveolar epithelial barrier integrity across all tested MOIs. Clinically, MRSA colonization is known to occur in healthy, young adults and may lead to overt infections, such as pneumonia [59,60]. Additionally, the development of bacterial pneumonia is known to result in inflammation of the lungs and hypoxemia, a direct result of cell barrier failure [61]. Resistance measurement trends were nearly identical between the

MRSA-alone and pdm2009-MRSA infections following the addition of MRSA. These data suggest that while pdm2009, and potentially other influenza A viruses, may provide for increased adhesion and/or attachment of bacteria to the surfaces of infected epithelial cells, disruption of alveolar epithelial cell barrier function appears highly dependent on the induction of bacterial- or host cell-mediated cytotoxicity. Although the host kinome data suggest a major host-response effect, we do not exclude the possibility that bacterial-mediated cytotoxicity may still play a direct role in alveolar epithelial cell barrier dysfunction. Future investigations will focus on comparisons of host responses between these two regions of the respiratory tract during influenza-bacterial co-infection. Although our ECIS data suggest that the differential expression of bacterial virulence factors did not augment alveolar epithelial cell barrier disruption, the roles of these virulence factors in additional post-infection processes in the lung remain to be determined. These include damage to the underlying endothelium at the alveolar-capillary barrier and the disruption or attenuation of host leukocyte recruitment and immune responses within the lung.

5. Conclusions

Although bacterial co-infections can exacerbate influenza virus infections and result in severe or fatal disease, there is a paucity of information regarding the molecular mechanisms underlying the pathogenesis of co-infections. Our data demonstrated that while bacterial replication kinetics were similar in MRSA- and pdm2009-MRSA-infected cells, the expression of bacterial virulence factors related to adhesion and invasion were significantly upregulated during the early course of co-infection. Further, our analysis of temporal host kinome responses demonstrated that host cell signaling responses shifted from viral- to bacterial-centric throughout the course of co-infection with a transition phase in the response from 8–12 h post-MRSA addition to pdm2009 infected cells. This related well to the loss of alveolar epithelial barrier function and integrity during IAV, MRSA, or co-infection as demonstrated by ECIS.

Supplementary Materials: The following are available online at <http://www.mdpi.com/1999-4915/11/2/116/s1>. Figure S1: MRSA replication kinetics during bacterial infection and influenza-bacterial co-infection in HBEC-3KT cells. Figure S2: pdm2009-MRSA infection decreases barrier function in bronchial epithelial cells. Table S1: MRSA RT-qPCR primer sequences; Table S2: Pathway overrepresentation analysis of host kinome responses in infected samples (8–12 h post-MRSA infection); Table S3: Pathway overrepresentation analysis of differentially-upregulated host kinome responses in pdm2009-MRSA infected cells vs. MRSA infection alone (8–12 h post-MRSA infection). Table S4: GO analysis of host kinome responses in infected samples (8–12 h post-MRSA infection).

Author Contributions: J.K. and D.S.C. conceived of the ideas presented herein. M.E.N., J.C., and S.D.F. performed the described experiments. M.E.N., J.C., S.D.F., D.S.C., and J.K. analyzed the data. M.E.N., J.C., S.D.F., D.S.C., and J.K. performed the drafting and revising of the manuscript.

Funding: M.E.N. is funded by a Research Manitoba Master's Studentship Award. J.K. is funded by a Tier 2 Canada Research Chair in the Molecular Pathogenesis of Emerging and Re-Emerging Viruses provided by the Canadian Institutes of Health Research (Grant No. 950-231498) and a Research Manitoba New Investigator Operating Grant (Grant No. 3531).

Conflicts of Interest: The authors declare no conflict of interest.

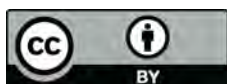
References

1. Krammer, F.; Smith, G.J.D.; Fouchier, R.A.M.; Peiris, M.; Kedzierska, K.; Doherty, P.C.; Palese, P.; Shaw, M.L.; Treanor, J.; Webster, R.G.; et al. Influenza. *Nat. Rev. Dis. Primers* **2018**, *4*, 3. [CrossRef]
2. Stephenson, I. Influenza: Molecular virology. *Expert Rev. Vaccines* **2010**, *9*, 719–720. [CrossRef]
3. Taubenberger, J.K.; Morens, D.M. Pandemic influenza—Including a risk assessment of h5n1. *Rev. Sci. Tech.* **2009**, *28*, 187–202. [CrossRef]
4. Centers for Disease Control and Prevention (CDC). Influenza. Available online: <https://www.cdc.gov/flu/index.htm> (accessed on 1 November 2018).
5. Ghebrehewet, S.; MacPherson, P.; Ho, A. Influenza. *BMJ* **2016**, *355*, i6258. [CrossRef]
6. Moghadami, M. A narrative review of influenza: A seasonal and pandemic disease. *Iran. J. Med. Sci* **2017**, *42*, 2–13.

7. McCullers, J.A. The co-pathogenesis of influenza viruses with bacteria in the lung. *Nat. Rev. Microbiol.* **2014**, *12*, 252–262. [\[CrossRef\]](#)
8. Taubenberger, J.K.; Morens, D.M. 1918 influenza: The mother of all pandemics. *Emerg Infect. Dis* **2006**, *12*, 15–22. [\[CrossRef\]](#)
9. Morens, D.M.; Taubenberger, J.K.; Fauci, A.S. Predominant role of bacterial pneumonia as a cause of death in pandemic influenza: Implications for pandemic influenza preparedness. *J. Infect. Dis.* **2008**, *198*, 962–970. [\[CrossRef\]](#)
10. Rudd, J.M.; Ashar, H.K.; Chow, V.T.; Teluguakula, N. Lethal synergism between influenza and streptococcus pneumoniae. *J. Infect. Pulm. Dis.* **2016**, *2*. [\[CrossRef\]](#)
11. Rynda-Apple, A.; Robinson, K.M.; Alcorn, J.F. Influenza and bacterial superinfection: Illuminating the immunologic mechanisms of disease. *Infect. Immun.* **2015**, *83*, 3764–3770. [\[CrossRef\]](#)
12. Louri, D.B.; Blumenfeld, H.L.; Ellis, J.T.; Kilbourne, E.D.; Rogers, D.E. Studies on influenza in the pandemic of 1957–1958. II. Pulmonary complications of influenza. *J. Clin. Investig.* **1959**, *38*, 213–265. [\[CrossRef\]](#)
13. Mark, D.D. The pathology of 1957 (asian) influenza. *Am. Rev. Tuberc.* **1959**, *79*, 440–449.
14. Oseasohn, R.; Adelson, L.; Kaji, M. Clinicopathologic study of thirty-three fatal cases of asian influenza. *N. Engl. J. Med.* **1959**, *260*, 509–518. [\[CrossRef\]](#)
15. Oswald, N.C.; Shooter, R.A.; Curwen, M.P. Pneumonia complicating asian influenza. *Br. Med. J.* **1958**, *2*, 1305–1311. [\[CrossRef\]](#)
16. Robertson, L.; Caley, J.P.; Moore, J. Importance of staphylococcus aureus in pneumonia in the 1957 epidemic of influenza a. *Lancet* **1958**, *2*, 233–236. [\[CrossRef\]](#)
17. Chertow, D.S.; Memoli, M.J. Bacterial coinfection in influenza: A grand rounds review. *JAMA* **2013**, *309*, 275–282. [\[CrossRef\]](#)
18. Louie, J.; Jean, C.; Chen, T.H.; Park, S.; Ueki, R.; Harper, T.; Chmara, E.; Myers, J.; Stoppacher, R.; Catanese, C.; et al. Bacterial coinfections in lung tissue specimens from fatal cases of 2009 pandemic influenza a (h1n1)—United states, may–august 2009. *Mmr Morb Mortal Wkly. Rep.* **2009**, *58*, 1071–1074.
19. Gill, J.R.; Sheng, Z.M.; Ely, S.F.; Guinee, D.G.; Beasley, M.B.; Suh, J.; Deshpande, C.; Mollura, D.J.; Morens, D.M.; Bray, M.; et al. Pulmonary pathologic findings of fatal 2009 pandemic influenza a/h1n1 viral infections. *Arch. Pathol. Lab. Med.* **2010**, *134*, 235–243.
20. Mauad, T.; Hajjar, L.A.; Callegari, G.D.; da Silva, L.F.; Schout, D.; Galas, F.R.; Alves, V.A.; Malheiros, D.M.; Auler, J.O., Jr.; Ferreira, A.F.; et al. Lung pathology in fatal novel human influenza a (h1n1) infection. *Am. J. Respir. Crit. Care Med.* **2010**, *181*, 72–79. [\[CrossRef\]](#)
21. Gillet, Y.; Vanhems, P.; Lina, G.; Bes, M.; Vandenesch, F.; Floret, D.; Etienne, J. Factors predicting mortality in necrotizing community-acquired pneumonia caused by *Staphylococcus aureus* containing panton-valentine leukocidin. *Clin. Infect. Dis.* **2007**, *45*, 315–321. [\[CrossRef\]](#)
22. Randolph, A.G.; Vaughn, F.; Sullivan, R.; Robinson, L.; Thompson, B.T.; Yoon, G.; Smoot, E.; Rice, T.W.; Loftis, L.L.; Helfaer, M.; et al. Critically ill children during the 2009–2010 influenza pandemic in the united states. *Pediatrics* **2011**, *128*, e1450–e1458. [\[CrossRef\]](#)
23. Rice, T.W.; Robinson, L.; Uyeki, T.M.; Vaughn, F.L.; John, B.B.; Miller, R.R., 3rd; Higgs, E.; Randolph, A.G.; Smoot, B.E.; Thompson, B.T.; et al. Critical illness from 2009 pandemic influenza a virus and bacterial coinfection in the united states. *Crit. Care Med.* **2012**, *40*, 1487–1498. [\[CrossRef\]](#)
24. Tong, S.Y.C.; Davis, J.S.; Eichenberger, E.; Holland, T.L., Jr.; Vance, G. *Staphylococcus aureus* infections: Epidemiology, pathophysiology, clinical manifestations, and management. *Clin. Microbiol. Rev.* **2015**, *28*, 603–661. [\[CrossRef\]](#)
25. Bellinghausen, C.; Rohde, G.G.U.; Savelkoul, P.H.M.; Wouters, E.F.M.; Stassen, F.R.M. Viral-bacterial interactions in the respiratory tract. *J. Gen. Virol.* **2016**, *97*, 3089–3102. [\[CrossRef\]](#)
26. Okamoto, S.; Kawabata, S.; Nakagawa, I.; Okuno, Y.; Goto, T.; Sano, K.; Hamada, S. Influenza a virus-infected hosts boost an invasive type of streptococcus pyogenes infection in mice. *J. Virol.* **2003**, *77*, 4104–4112. [\[CrossRef\]](#)
27. Herold, S.; Becker, C.; Ridge, K.M.; Budinger, G.R.S. Influenza virus-induced lung injury: Pathogenesis and implications for treatment. *Eur. Respir. J.* **2015**, *45*, 1463–1478. [\[CrossRef\]](#)
28. Short, K.R.; Kasper, J.; van der Aa, S.; Andeweg, A.C.; Zaaraoui-Boutahar, F.; Goeijenbier, M.; Richard, M.; Herold, S.; Becker, C.; Scott, D.P.; et al. Influenza virus damages the alveolar barrier by disrupting epithelial cell tight junctions. *Eur. Respir. J.* **2016**, *47*, 954–966. [\[CrossRef\]](#)

29. Chakrabarti, A.K.; Vipat, V.C.; Mukherjee, S.; Singh, R.; Pawar, S.D.; Mishra, A.C. Host gene expression profiling in influenza a virus-infected lung epithelial (a549) cells: A comparative analysis between highly pathogenic and modified h5n1 viruses. *Virol. J.* **2010**, *7*, 219. [[CrossRef](#)]
30. Dapat, C.; Saito, R.; Suzuki, H.; Horigome, T. Quantitative phosphoproteomic analysis of host responses in human lung epithelial (a549) cells during influenza virus infection. *Virus Res.* **2014**, *179*, 53–63. [[CrossRef](#)]
31. Lin, X.; Wang, R.; Zou, W.; Sun, X.; Liu, X.; Zhao, L.; Wang, S.; Jin, M. The influenza virus h5n1 infection can induce ros production for viral replication and host cell death in a549 cells modulated by human cu/zn superoxide dismutase (sod1) overexpression. *Viruses* **2016**, *8*, 13. [[CrossRef](#)]
32. Te Velthuis, A.J.W.; Long, J.C.; Bauer, D.L.V.; Fan, R.L.Y.; Yen, H.L.; Sharps, J.; Siegers, J.Y.; Killip, M.J.; French, H.; Oliva-Martin, M.J.; et al. Mini viral rnas act as innate immune agonists during influenza virus infection. *Nat. Microbiol.* **2018**, *3*, 1234–1242. [[CrossRef](#)]
33. Zhou, B.; Li, J.; Liang, X.; Yang, Z.; Jiang, Z. Transcriptome profiling of influenza a virus-infected lung epithelial (a549) cells with l-ariciresinol-4-beta-d-glucopyranoside treatment. *PLoS ONE* **2017**, *12*, e0173058.
34. Qi, L.; Kash, J.C.; Dugan, V.G.; Wang, R.; Jin, G.; Cunningham, R.E.; Taubenberger, J.K. Taubenberger. Role of sialic acid binding specificity of the 1918 influenza virus hemagglutinin protein in virulence and pathogenesis for mice. *J. Virol.* **2009**, *83*, 3754–3761. [[CrossRef](#)]
35. Kindrachuk, J.; Ork, B.; Hart, B.J.; Mazur, S.; Holbrook, M.R.; Frieman, M.B.; Traynor, D.; Johnson, R.F.; Dyall, J.; Kuhn, J.H.; et al. Antiviral potential of erk/mapk and pi3k/akt/mtor signaling modulation for middle east respiratory syndrome coronavirus infection as identified by temporal kinome analysis. *Antimicrob Agents Chemother.* **2015**, *59*, 1088–1099. [[CrossRef](#)]
36. Kindrachuk, J.; Wahl-Jensen, V.; Safronetz, D.; Trost, B.; Hoenen, T.; Arsenault, R.; Feldmann, F.; Traynor, D.; Postnikova, E.; Kusalik, A.; et al. Ebola virus modulates transforming growth factor beta signaling and cellular markers of mesenchyme-like transition in hepatocytes. *J. Virol.* **2014**, *88*, 9877–9892. [[CrossRef](#)] [[PubMed](#)]
37. Trost, B.; Kindrachuk, J.; Maattanen, P.; Napper, S.; Kusalik, A. Piika 2: An expanded, web-based platform for analysis of kinome microarray data. *PLoS ONE* **2013**, *8*, e80837. [[CrossRef](#)] [[PubMed](#)]
38. Babicki, S.; Arndt, D.; Marcu, A.; Liang, Y.; Grant, J.R.; Maciejewski, A.; Wishart, D.S. Heatmapper: Web-enabled heat mapping for all. *Nucleic Acids Res.* **2016**, *44*, W147–W153. [[CrossRef](#)] [[PubMed](#)]
39. Lynn, D.J.; Winsor, G.L.; Chan, C.; Richard, N.; Laird, M.R.; Barsky, A.; Gardy, J.L.; Roche, F.M.; Chan, T.H.; Shah, N.; et al. Innatedb: Facilitating systems-level analyses of the mammalian innate immune response. *Mol. Syst. Biol.* **2008**, *4*, 218. [[CrossRef](#)]
40. Li, Y.; Arsenault, R.J.; Trost, B.; Slind, J.; Griebel, P.J.; Napper, S.; Kusalik, A. A systematic approach for analysis of peptide array kinome data. *Sci. Signal.* **2012**, *5*, pl2. [[CrossRef](#)]
41. Atshan, S.S.; Shamsudin, M.N.; Karunanidhi, A.; van Belkum, A.; Lung, L.T.; Sekawi, Z.; Nathan, J.J.; Ling, K.H.; Seng, J.S.; Ali, A.M.; et al. Quantitative pcr analysis of genes expressed during biofilm development of methicillin resistant staphylococcus aureus (mrsa). *Infect. Genet. Evol.* **2013**, *18*, 106–112. [[CrossRef](#)]
42. Miyake, T.; Soda, K.; Itoh, Y.; Sakoda, Y.; Ishigaki, H.; Nagata, T.; Ishida, H.; Nakayama, M.; Ozaki, H.; Tsuchiya, H.; et al. Amelioration of pneumonia with streptococcus pneumoniae infection by inoculation with a vaccine against highly pathogenic avian influenza virus in a non-human primate mixed infection model. *J. Med. Primatol.* **2010**, *39*, 58–70. [[CrossRef](#)] [[PubMed](#)]
43. Smith, A.M.; McCullers, J.A. Secondary bacterial infections in influenza virus infection pathogenesis. *Curr. Top. Microbiol. Immunol.* **2014**, *385*, 327–356. [[PubMed](#)]
44. Chertow, D.S.; Kindrachuk, J.; Sheng, Z.M.; Pujanauski, L.M.; Cooper, K.; Noguee, D.; Claire, M.S.; Solomon, J.; Perry, D.; Sayre, P.; et al. Influenza a and methicillin-resistant staphylococcus aureus co-infection in rhesus macaques—A model of severe pneumonia. *Antivir. Res.* **2016**, *129*, 120–129. [[CrossRef](#)] [[PubMed](#)]
45. Kindrachuk, J.; Falcinelli, S.; Wada, J.; Kuhn, J.H.; Hensley, L.E.; Jahrling, P.B. Systems kinomics for characterizing host responses to high-consequence pathogens at the nih/niid integrated research facility-frederick. *Pathog. Dis.* **2014**, *71*, 190–198. [[CrossRef](#)]
46. Arsenault, R.; Griebel, P.; Napper, S. Peptide arrays for kinome analysis: New opportunities and remaining challenges. *Proteomics* **2011**, *11*, 4595–4609. [[CrossRef](#)] [[PubMed](#)]

47. Stolwijk, J.A.; Matrougui, K.; Renken, C.W.; Trebak, M. Impedance analysis of gpcr-mediated changes in endothelial barrier function: Overview and fundamental considerations for stable and reproducible measurements. *Pflügers Arch.* **2014**, *467*, 2193–2218. [[CrossRef](#)] [[PubMed](#)]
48. Powers, M.E.; Bubeck Wardenburg, J. Igniting the fire: Staphylococcus aureus virulence factors in the pathogenesis of sepsis. *PLoS Pathog.* **2014**, *10*, e1003871. [[CrossRef](#)] [[PubMed](#)]
49. Gouaux, E.; Hobaugh, M.; Song, L. A-hemolysin, y-hemolysin, and leukocidin from *staphylococcus aureus*: Distant in sequence but similar in structure. *Protein Sci.* **1997**, *6*, 2631–2635. [[CrossRef](#)] [[PubMed](#)]
50. Wardenburg, J.B.; Bae, T.; Otto, M.; DeLeo, F.R.; Schneewind, O. Poring over pores: A-hemolysin and panton-valentine leukocidin in *staphylococcus aureus* pneumonia. *Nat. Med.* **2007**, *13*, 1405–1406. [[CrossRef](#)]
51. Murai, M.; Moriyama, H.; Hata, E.; Takeuchi, F.; Amemura-Maekawa, J. Variation and association of fibronectin-binding protein genes fnba and fnbb in staphylococcus aureus japanese isolates. *Microbiol. Immunol.* **2016**, *60*, 312–325. [[CrossRef](#)]
52. Shinji, H.; Yosizawa, Y.; Tajima, A.; Sugimoto, S.; Seki, K.; Mizunoe, Y. Role of fibronectin-binding proteins a and b in in vitro cellular infections and in vivo septic infections by *Staphylococcus aureus*. *Infect. Immun.* **2011**, *2215*–2223. [[CrossRef](#)] [[PubMed](#)]
53. Kim, H.K.; Cheng, A.G.; Kim, H.-Y.; Missiakas, D.M.; Schneewind, O. Nontoxic protein a vaccine for methicillin-resistant *staphylococcus aureus* infections in mice. *J. Exp. Med.* **2010**, *207*, 1863–1870. [[CrossRef](#)]
54. Basanisi, M.G.; La Bella, G.; Nobili, G.; Franconieri, I.; La Salandra, G. Genotyping of methicillin-resistant *Staphylococcus aureus* (mrsa) isolated from milk and dairy products in south Italy. *Food Microbiol.* **2017**, *62*, 141–146. [[CrossRef](#)] [[PubMed](#)]
55. Ocal, D.N.; Dolapci, I.; Karahan, Z.C.; Tekeli, A. Investigation of biofilm formation properties of staphylococcus isolates. *Mikrobiyoloji Bul.* **2017**, *51*, 10–19. [[CrossRef](#)]
56. Downer, R.; Roche, F.; Park, P.W.; Mecham, R.P.; Foster, T.J. The elastin-binding protein of *Staphylococcus aureus* (ebps) is expressed at the cell surface as an integral membrane protein and not as a cell wall-associated protein. *J. Biol. Chem.* **2001**, *277*, 243–250. [[CrossRef](#)] [[PubMed](#)]
57. Ni Eidhin, D.; Perkins, S.; Francois, P.; Vaudaux, P.; Hook, M.; Foster, T.J. Clumping factor b (clfb), a new surface-located fibrinogen-binding adhesin of staphylococcus aureus. *Mol. Microbiol.* **1998**, *30*, 245–257. [[CrossRef](#)]
58. Kumar, A.; Tassopoulos, A.M.; Li, Q.; Yu, F.S. Staphylococcus aureus protein a induced inflammatory response in human corneal epithelial cells. *Biochem. Biophys. Res. Commun.* **2007**, *354*, 955–961. [[CrossRef](#)] [[PubMed](#)]
59. Davis, K.A.; Stewart, J.J.; Crouch, H.K.; Florez, C.E.; Hospenthal, D.R. Methicillin-resistant staphylococcus aureus (mrsa) nares colonization at hospital admission and its effect on subsequent mrsa infection. *Clin. Infect. Dis.* **2004**, *39*, 776–782. [[CrossRef](#)]
60. Defres, S.; Marwick, C.; Nathwani, D. Mrsa as a cause of lung infection including airway infection, community-acquired pneumonia and hospital-acquired pneumonia. *Eur. Respir. J.* **2009**, *34*, 1470–1476. [[CrossRef](#)]
61. Sarkar, M.; Niranjana, N.; Banyal, P. Mechanisms of hypoxemia. *Lung India* **2017**, *34*, 47–60. [[CrossRef](#)]



REVIEW

Open Access



A year of terror and a century of reflection: perspectives on the great influenza pandemic of 1918–1919

Michaela E. Nickol and Jason Kindrachuk^{*}

Abstract

Background: In the spring of 1918, the “War to End All Wars”, which would ultimately claim more than 37 million lives, had entered into its final year and would change the global political and economic landscape forever. At the same time, a new global threat was emerging and would become one of the most devastating global health crises in recorded history.

Main text: The 1918 H1N1 pandemic virus spread across Europe, North America, and Asia over a 12-month period resulting in an estimated 500 million infections and 50–100 million deaths worldwide, of which ~ 50% of these occurred within the fall of 1918 (*Emerg Infect Dis* 12:15–22, 2006, *Bull Hist Med* 76:105–115, 2002). However, the molecular factors that contributed to the emergence of, and subsequent public health catastrophe associated with, the 1918 pandemic virus remained largely unknown until 2005, when the characterization of the reconstructed pandemic virus was announced heralding a new era of advanced molecular investigations (*Science* 310:77–80, 2005). In the century following the emergence of the 1918 pandemic virus we have landed on the Moon, developed the electronic computer (and a global internet), and have eradicated smallpox. In contrast, we have a largely remedial knowledge and understanding of one of the greatest scourges in recorded history.

Conclusion: Here, we reflect on the 1918 influenza pandemic, including its emergence and subsequent rapid global spread. In addition, we discuss the pathophysiology associated with the 1918 virus and its predilection for the young and healthy, the rise of influenza therapeutic research following the pandemic, and, finally, our level of preparedness for future pandemics.

Keywords: Influenza, Pandemic, Pneumonia, Therapeutics, Preparedness, 1918 Spanish flu

Background

Influenza viruses have posed a continual threat to global public health since at least as early as the Middle Ages, resulting in an estimated 3–5 million cases of severe illness and 291,243–645,832 deaths annually worldwide, according to a recent estimate [1]. Regional influenza epidemics occur on an annual basis, resulting in millions of illnesses and hospitalizations despite intensive vaccination and awareness programs [2, 3]. Moreover, influenza pandemics arise sporadically due to the introduction of an antigenically-distinct influenza A virus within a population, which can result in devastating effects on global

public health and healthcare networks. The emergence of influenza subtype H1N1 in 1918, which ultimately resulted in an estimated 50–100 million deaths worldwide, would forever change the course of human history and will be discussed in detail in the following sections [4–6]. The aims of this short review are to discuss: i) the emergence and spread of the 1918 virus; ii) the unique severity of disease in young, healthy individuals; and iii) the subsequent influence of the pandemic on influenza virus therapeutic and future preparedness.

Main text

General influenza epidemiology

It is postulated that 10% of the worldwide population is infected by an influenza virus each year, resulting in a total economic burden of \$87.1 billion USD [7, 8]. As a

* Correspondence: Jason.Kindrachuk@umanitoba.ca

Laboratory of Emerging and Re-Emerging Viruses, Department of Medical Microbiology, University of Manitoba, 523-745 Bannatyne Avenue, Winnipeg, MB R3E 0J9, Canada



testament to the significant toll posed by influenza on public health and healthcare systems, the US Centers for Disease Control and Prevention (CDC) estimated that from 2010 to 2015, influenza infections resulted in 9.23–35.6 million illnesses and 139,000–707,000 hospitalizations annually in the US alone [9]. It has been suggested that children are likely the primary transmitters of influenza [10]. Lethal influenza infections are primarily associated with high risk populations, including infants (< 1 year), the elderly (> 65 years), and individuals with pre-existing comorbidities, including chronic respiratory abnormalities, cardiac disease, immunodeficiency, and pregnancy [11, 12]. Mortality in children and young adults is generally low [3]. Symptoms manifest as a sudden high fever, headache, pharyngitis, cough, myalgia, nausea, vomiting, and fatigue, which generally resolve within 7 days in healthy adults [11, 13]. Severe and/or lethal disease is typically associated with viral pneumonia or secondary bacterial infections in the lower respiratory tract [3].

A history of influenza pandemics

To be considered a pandemic, an influenza virus must: i) spread globally from a distinct location with high rates of infectivity resulting in increased mortality; and ii) the hemagglutinin (HA) cannot be related to influenza strains circulating prior to the outbreak nor have resulted from mutation [14, 15]. It should also be appreciated that prior to the first isolation of a human influenza virus in 1933, the cause of influenza outbreaks and pandemics could only be inferred based on physiological symptoms of disease, along with the speed and breadth at which illness was spread [15].

As early as 412 BC, Hippocrates, the father of modern medicine, described the first known account of an influenza-like illness in his sixth “Book of Epidemics” [16, 17]. Here, he recounted an annual recurring upper respiratory tract infection characterized by pharyngitis, coryza, and myalgia which peaked around the winter solstice [18]. This seasonal epidemic occurred in Perinthus, a northern port town located in what is now Turkey, and is referred to as the “Cough of Perinthus” [16]. It has been suggested that potential pandemics may have occurred in 1510 and 1557; however, it is unanimously agreed that the first documented influenza pandemic occurred in 1580, resulting in high morbidity [15, 19]. The virus originated in Asia, before spreading to Africa, and then simultaneously spreading from both continents to Europe. It reportedly spread across the entire European continent within 6 months, before eventually reaching the Americas [19, 20]. Two pandemics were recorded in the eighteenth century. The first began in Russia in 1729, eventually moving across the entirety of Europe within 6 months and, ultimately, across the known world

over the following 3 years [20–23]. The second pandemic began in China in 1781, before spreading to Russia and, subsequently, across all of Europe. Interestingly, this second pandemic had a high proclivity for young adults [24]. Two major pandemics also occurred throughout the nineteenth century. The first began in 1830 in China, with subsequent spread to Southeast Asia, Russia, Europe, and North America and had a low overall mortality rate [15, 19, 20, 23]. A second pandemic emerged in Russia in 1889 and spread rapidly to Europe and North America, circumnavigating the globe in just 4 months [25, 26]. The virus, suggested to be of subtype H3N8, reappeared at least 3 more times in successive years resulting in an estimated 1 million global fatalities [20, 23, 26, 27].

Four influenza pandemics have occurred over the past century (Fig. 1). The 1918–1919 Spanish flu pandemic, subtype H1N1, resulted in an estimated 50–100 million deaths worldwide and will be discussed in detail in the following sections. The 1957–1958 Asian flu pandemic, subtype H2N2, originated in China in February 1957 and spread throughout Asia and then globally by the summer. Case fatality rates were approximately 0.67% with 1–2 million deaths worldwide [20, 28–31]. Just a decade later, the 1968–1970 Hong Kong flu pandemic, subtype H3N2, emerged in China in July 1968 and spread throughout Europe, North America, and Australia by early 1969 [25]. Although mortality rates were low, the pandemic would ultimately claim between 500,000 and 2 million lives [25]. In April 2009, the 2009–2010 swine flu pandemic, subtype H1N1, began with nearly simultaneous outbreaks in Mexico and the US, before spreading globally over the next 6 weeks. While the 2009–2010 pandemic had a low associated case fatality rate, resulting in 284,000 deaths worldwide, it had devastating effects on global economies and healthcare networks [25, 32]. Conventionally, influenza pandemics result in the extinction of previously circulating virus strains; however, this view was complicated by events in 1977. Although H1N1 was replaced by H2N2 as the circulating strain following the 1957–1958 Asian flu pandemic, a descendant of the 1918 virus “re-emerged” suspiciously in 1977, likely as a result of a man-made event, and established itself as a co-circulating strain, along with the reassortant H3N2 virus (following the 1968–1970 Hong Kong flu pandemic) [4, 33]. The suspicious “re-emergence” of a descendant of the 1918 virus in 1977 has been postulated to have been the result of a man-made event. This hypothesis has gained traction, as both the HA and NA of the re-emerged virus show incredible similarity to a 1950 reference virus, and it is unlikely that this strain was maintained in an animal reservoir for almost two decades without having undergone detectable mutation [33]. In 2009, a triple

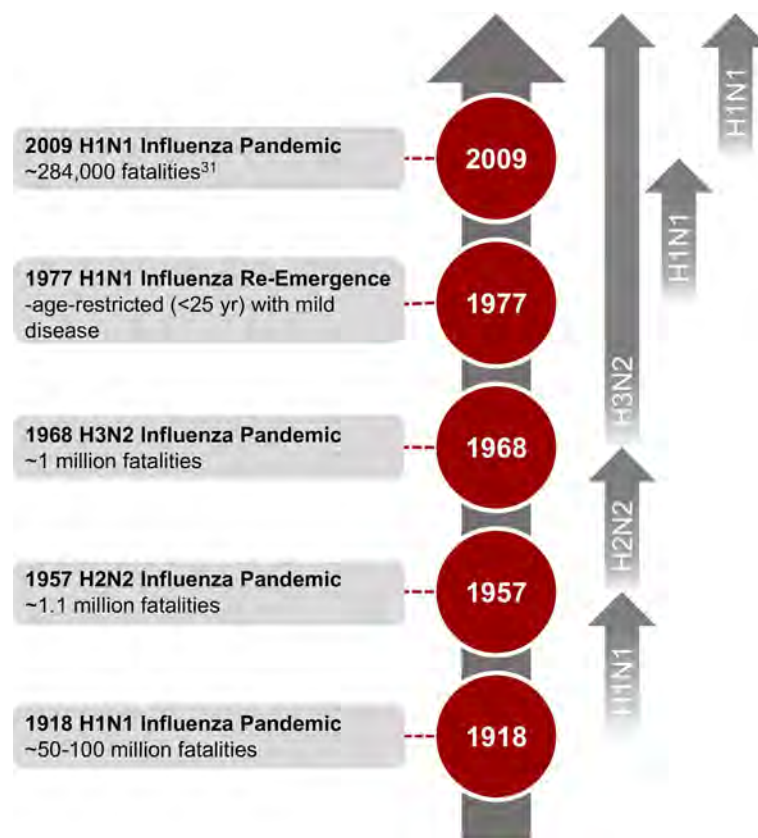


Fig. 1 Timeline of Influenza Pandemics from 1918 Onwards. Four pandemics have occurred over the last century (1918, 1957, 1968 and 2009). Circulation of H1N1 was reinitiated in 1977 and has therefore been added to this timeline. Grey arrows designate the circulating or co-circulating strains during the inter-pandemic periods

reassortment (made up of avian, swine, and human influenza genes) pandemic H1N1 jumped from pigs to humans, resulting in the co-circulation of three influenza strains [34].

The first wave of the 1918 pandemic

One hundred years following its emergence, the origin of the 1918 pandemic influenza virus remains shrouded in mystery. The 1918 pandemic began early in the final year of the First World War. Whereas prior pandemics had spread largely along trade routes, the global context of the war enabled greater viral spread facilitated by the mass mobilisation of military personnel and civilians [25, 35]. This was further augmented by the poor health and sanitation conditions found within trenches along the frontlines of the War, facilitating disease transmission [36]. Public knowledge regarding the severity of the pandemic was hindered, as many news agencies were barred from writing about the global health threat, instead reporting solely on morale boosting subjects [37]. However, as Spain was a neutral party in the War, newspapers were able to report on the devastating effects that the 1918 pandemic virus was exhibiting in Spain. Thus, it was

generally perceived that this devastating illness originated in Spain, resulting in the pandemic being incorrectly labeled as “the Spanish flu” [37].

A century following its emergence, there remains a relative paucity of knowledge regarding the ancestry and regional origin of the 1918 virus. Sequence analysis suggests that the virus was derived from an avian-like influenza virus and that all eight gene segments likely evolved in parallel [34, 38]. Analyses of influenza virus genome sequences also suggest that the initial entry of the 1918 precursor virus into human circulation began in 1915 and did not appear to have jumped directly from an avian source [4, 38, 39]. However, improved understanding regarding the emergence of the 1918 virus, as well as factors (biological, social, environmental) that contributed to viral transmission and pathogenesis, have been vital to the development of current epidemic and pandemic influenza outbreak response efforts. Descendants of the 1918 pandemic influenza virus strain have been the cause of almost every seasonal influenza A infection worldwide over the past century [4]. Additionally, each of the pandemics occurring in 1957, 1968, and 2009 were caused by descendants of the 1918 pandemic

influenza virus strain, earning the 1918 viral strain the nickname “The Mother of all Pandemics” [4].

Investigations concerning the origins of the first wave of the pandemic, beginning in March 1918, have primarily focused on the US and China, though recently it has been suggested that the origin may have been an outbreak of a respiratory disease misidentified as pneumonic plague in China [15, 36, 40]. Humphries suggests that the dissemination of labourers from China to assist Allied war efforts during this outbreak resulted in the inadvertent spread of the virus to Europe [36]. From 1916 to 1918, the route of travel to Europe for the labourers included checkpoints in Singapore, Durban, Cape Town, North Africa, and Canada. Additional reports of the first wave of the virus in the spring of 1918 suggest that the pandemic originated with Chinese workers at Camp Funston, Kansas, where the workers began suffering from 2 to 3 day fevers, gastrointestinal symptoms, and general weakness [37, 41]. Within 3 weeks 1100 soldiers had been hospitalized, and thousands more had received out-patient treatment [41]. The illness was able to spread to other military camps within the US, before traversing the Atlantic Ocean via soldiers supporting Allied operations in Europe. The US Army reported that from March–May 1918, 11.8% of US soldiers were

hospitalized due to this unidentified respiratory illness [41]. While illness rates were high during this initial wave, mortality rates were largely similar to seasonal outbreaks of influenza. Spain reported that the mortality rates for pneumonia and influenza was only 0.065% [37]. Although there was some acceptance that this new illness was indeed influenza, this was not generally accepted [37]. Radusin reported that although the physiological symptoms were similar to influenza, the illness was too mild and short-lasting with minimal complications for it to be influenza [37]. Infections began to subside in many regions by the early summer [41]. The generally accepted lines of spread of the first and second waves of the 1918 virus are provided in Fig. 2.

The second and third waves of the pandemic

In mid-August of 1918, reports suggesting a second wave of this severe illness began to surface [35]. In some regions, primarily Northern Europe, the period between the end of the first wave and the beginning of the second wave was incredibly short, making the two waves almost indistinguishable [4, 42]. This second wave, occurring from September–November 1918, was responsible for the majority of illnesses and fatalities associated with the pandemic. Although the origins of the first wave



Fig. 2 The First and Second Waves of the 1918–1919 Pandemic. First outbreaks and foci of second waves of the pandemic are labeled as red and purple circles, respectively. The lines of spread of the first and second waves of the pandemic are labeled as purple dashed lines and red solid lines, respectively. Map images were derived and/or modified from Servier Medical Arts under a Creative Commons Attribution 3.0 Unported License. Adapted from Nicholson et al. [80]

continue to be debated, the origin of the second wave is generally agreed to be the harbour town of Plymouth in Southern England, which allowed the pandemic influenza virus strain to easily spread to the rest of the world [25]. Ships from Plymouth were dispatched to Freetown, Sierra Leone in August 1918, which allowed the virus to spread across the African continent [25]. New Zealand soldiers, who stopped in Freetown on their way to and from the war front in Europe, facilitated transfer of the pandemic virus to New Zealand [25]. From Plymouth, the virus also spread to Boston, from which it was able to disseminate across the rest of North America resulting in >1 million fatalities over the ensuing four months [5, 25]. This second wave spread globally throughout the fall of 1918 with illness seen first amongst military personnel and, subsequently, within the general population [25, 35].

The second wave of the 1918 pandemic differed from the first in that much higher morbidity and mortality rates were reported, with the majority of all fatalities associated with the pandemic occurring during this wave [4]. Ultimately, the pandemic would result in an estimated 500 million infections worldwide (~1/3 of the world's population at the time) and a case fatality rate >2.5%, more than 25 times higher than any other pandemic [4, 37]. As a testament to the severity of this second wave, during the fall of 1918, the first 4–5 pages of Spanish newspapers were filled with obituaries of those who had succumbed to the pandemic virus [35]. Further, reports from Philadelphia, Pennsylvania stated that across 31 hospitals in the city, every hospital bed was occupied by patients with influenza [35]. The pandemic was especially problematic in highly isolated communities where many individuals had limited contact with prior influenza strains, thus lacking any pre-existing immunity. For example, some Inuit settlements reported case mortality rates as high as 70%, while certain communities in Africa were completely decimated [35]. Interestingly, individuals who had been infected throughout the first wave seemed to be protected against this secondary wave, and recent analyses have suggested that these individuals had up to 94% protection throughout the fall wave [4, 41].

A third and final wave of the pandemic appeared in most of the world in the early months of 1919 [4, 5, 35]. This final wave generally overlapped the first wave in terms of regional distribution; however, it seemed to spare areas where the second wave had been especially severe. Overall, morbidity rates were lower throughout this final influenza wave; however, mortality rates are believed to have been just as severe as the second wave [4, 35]. Three successive annual winter post-pandemic

recurrences occurred following the third wave of the pandemic with continually decreasing mortality rates, in particular within those 20–40 years of age [43].

Pathophysiology of the 1918 pandemic influenza virus

Classically, fatal influenza infections are primarily associated with the very young (<5 years) and the elderly (>65 years) resulting in a characteristic “U”-shaped mortality curve (Fig. 3). Interestingly, however, the 1918–1919 H1N1 influenza pandemic mortality curve exhibits a “W”-shape due to excess mortality in young adults 20–40 years of age due to influenza-related illness. It has been postulated that the increased disease severity in young adults was likely associated with immune status due to the lack of pre-existing immunity in this population [44]. Further, more than 99% of fatal infections occurred in those <65 years of age and nearly 50% of all influenza-related deaths during the 1918 pandemic were in those aged 20–40 years [4]. Influenza and pneumonia fatality rates in those aged 15–34 years were more than 20 times higher than in previous years and absolute risk of influenza-related death was higher in those <65 years of age than those >65 years old [4]. It is still not fully understood why this occurred, but it is possible that an antigenically similar influenza strain circulated prior to 1889, providing a level of protection against the novel H1N1 pandemic strain to those born prior to 1889 [4]. Additionally, archaerological and epidemiological evidence have shown that an H3 subtype influenza virus may have been responsible for the 1889 influenza pandemic, which circulated until the emergence of the 1918 pandemic virus, leaving those individuals who had not been exposed to an H1 subtype virus highly susceptible to the pandemic virus [34]. It has also been suggested that the generation of an excessive inflammatory response (“cytokine storm”) in healthy, young adults infected with the 1918 virus may have contributed to the excess mortality seen within this age group [34]. Recent in vivo studies with the 1918 virus have shown a marked upregulation of inflammatory cytokines, along with the suppression of important antiviral immune responses [34, 45]. In addition, other influenza strains, such as fatal H5N1 infections in humans, have also been associated with the deleterious consequences of an excessive inflammatory response [46]. Ultimately, the case fatality rate was so severe in young adults during the 1918–1919 pandemic that the average life expectancy rate in the US dropped by ~12 years [47].

Physiological symptoms of the 1918 pandemic virus generally lasted for 7 days and were described as feeling cold, shivering, high fever, weakness, nausea, loss of appetite, pharyngitis, cough, and bloodshot eyes [35]. In some patients, a short “rebound” to normal health would occur that was followed by an aggressive recrudescence

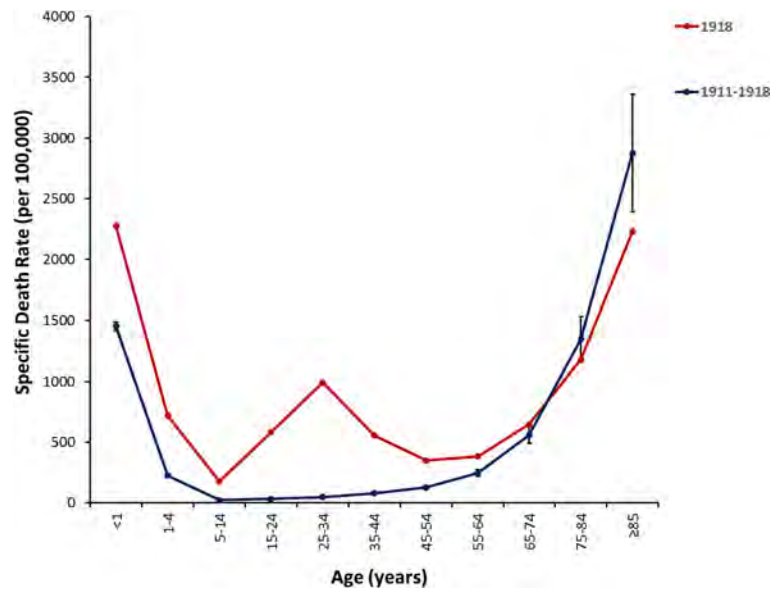


Fig. 3 Association of Age with Influenza Mortality Prior to and During the 1918–1919 pandemic. Influenza- and pneumonia-specific mortality in the United States is plotted for 1911–1917 (blue line) and for 1918 (red line) [81, 82]. Means with standard deviations are presented for the pre-pandemic mortality curve. Adapted from Taubenberger and Morens [4]

of disease and, ultimately, death [35]. Similar to the 1889 pandemic, the majority of fatal infections resulted from respiratory complications. However, it has also been demonstrated that excess influenza fatalities during the 1918–1919 pandemic were associated with an acute aggressive bronchopneumonia (including epithelial and vascular necrosis, hemorrhage, edema, and bacterial-associated variant pathology within the lungs) and a severe acute respiratory distress-like syndrome associated with severe facial cyanosis [43].

Autopsies performed on preserved lung tissues in the modern era have revealed acute pulmonary hemorrhage and secondary bacterial infections associated with pulmonary lesions in nearly all the fatal cases examined [41, 43, 47]. *Streptococcus pneumoniae* was present in many cases; however, *Staphylococcus aureus*, *Haemophilus influenzae*, and *Streptococcus pyogenes* also appeared to complicate fatal cases [48, 49]. Neutrophilic pulmonary infiltration was seen in cases of pneumococcal pneumonia, while cases of staphylococcal pneumonia were marked by multiple microabscesses infiltrated by neutrophils [48]. However, alveolar cell damage was seen in each case along with pulmonary repair and remodelling [48]. Tissues from each of the fatal cases examined had similar pathologic presentation, independent of which pandemic wave they were associated with. Despite the difference in mortality rates, each wave showed similar cellular tropism, infecting both type I and type II pneumocytes, as well as the bronchiolar respiratory epithelium [48].

The rise of vaccines and antivirals following the 1918–1919 pandemic

A multitude of scientific and technological advances have occurred over the past century, allowing for a greater understanding of the dynamic relationship between the host and influenza viruses during infection. These advances, along with access to autopsy samples and the reconstitution of the 1918 pandemic virus, have facilitated a greater understanding of how the pandemic virus differs from other seasonal and pandemic influenza virus strains. Moreover, technological advancements following the 1918–1919 influenza pandemic virus have facilitated the development of preventative measures, including vaccines and antivirals, to limit widespread illness due to influenza infections.

The determination of the genomic sequence of the 1918 pandemic virus, and the subsequent reconstruction of the virus, has provided us with the opportunity to decipher the viral- and host-specific properties that contributed to the severity of the 1918–1919 pandemic. It has been demonstrated that in contrast to other influenza viruses, the 1918 pandemic virus is highly virulent and pathogenic in multiple animal species without prior adaptation [45, 50]. While obvious knowledge gaps remain, in particular with respect to the origin of the virus and the molecular mechanisms (host and/or viral) underlying differential pathogenesis as compared to other influenza viruses, there have been considerable advances in our understanding of the 1918 pandemic virus.

Since the isolation of the first human influenza virus in 1933, researchers have worked to develop an effective influenza vaccine [16]. Current influenza vaccines are reformulated seasonally and provide protection against circulating influenza A and B viruses [13]. The World Health Organization conducts worldwide surveillance studies throughout the year on currently circulating influenza strains, and thus recommends which strains should be included in each influenza vaccine [13]. While the seasonal influenza vaccine is approximately 60% effective, this protection is dependent on the characteristics of the individual being vaccinated, including age and overall health, as well as the match between the strains included in the vaccine formulation and currently circulating strains [13]. Individuals who have been vaccinated are generally protected from illness and provide a measure of protection for those who are not able to be vaccinated due to their age or other health issues through herd immunity [13]. There has also been increasing interest in the development of “universal” influenza vaccines designed to provide protection against a wide range of antigenically-distinct influenza viruses, including those currently in circulation and those that may emerge in the future [51]. These will not be discussed in detail as recent reviews have provided excellent discussions of this topic [51–57].

Two major classes of antivirals have emerged for therapeutic treatment of severe influenza virus infections. Adamantane antivirals target the matrix-2 (M2) surface protein, while neuraminidase (NA) inhibitors target the NA viral surface protein. Adamantane compounds were the first licensed influenza antivirals and block the M2 ion channel protein from properly functioning, thus effectively blocking membrane fusion [58, 59]. Unfortunately, adamantane antivirals are only able to target influenza A viruses limiting their application for influenza B virus infections [58]. Further, more than 90% of influenza A viruses are resistant to this class of drugs due to the high mutation rate of the virus [58, 60]. Thus, the use of NA inhibitors is recommended [60]. NA inhibitors block the NA surface protein and prevent the release of progeny virus and infection of additional cells [60]. While resistance to NA inhibitors has been observed in some influenza virus strains, they are still highly effective in the majority of patients [60]. Studies have shown that both adamantane antivirals and NA inhibitors provide protection against the 1918 virus [50].

Although outside the auspice of this commentary, it should be mentioned that advances in mechanical ventilation modalities, including non-invasive positive pressure ventilation, from the 1950s onwards, have provided an additional support mechanism for treatment of severely ill patients [34]. The routine clinical use of antibiotics in the early twentieth century also heralded a new

era for combating influenza viruses. As a testament to this, excess influenza mortality declined significantly from 1942 to 1951 onwards [61–63]. However, the widespread general administration of antibiotics has resulted in an escalating public health crisis due to multi-drug resistance. This has impacted the treatment of severe influenza infections, as methicillin-resistant *S. aureus* (MRSA) is the most frequently isolated bacteria from patients with severe influenza-bacterial co-infections in the US [64, 65] and complicated up to 55% of fatalities during the 2009 pandemic [66–69].

Influenza preparedness and lessons for the future

Although it has now been a century since the start of the Spanish flu pandemic, lessons from this global health catastrophe continue to inform modern-day pandemic preparedness. Investigations of the pandemic, including those with the reconstructed virus, have allowed researchers, as well as the global public, to understand the mechanisms that underlie pandemic emergence and escalation to public health crisis. It also allows researchers to predict the potential public health risks which may be caused by new pandemic viruses. For example, sequencing of the 1918 pandemic virus revealed similarities in the H1 protein of the 2009 pandemic virus, allowing researchers to predict that a lack of protection, and thus a high mortality rate may be seen in healthy, young adults throughout the 2009 H1N1 pandemic [45]. Thus, when vaccines were limited during the early stages of the 2009 pandemic, young adults were prioritized over the elderly, who demonstrated some degree of protection to this influenza strain, resulting in a lower mortality rate in young, healthy adults [45]. The average age for laboratory-confirmed fatalities during the 2009 pandemic was 37 years in the US, supporting this vaccine prioritization initiative [70]. Additionally, the awareness of the complications caused by secondary bacterial co-infections from the 1918 pandemic ensured that the medical community was aware of this threat throughout the 2009 pandemic, likely resulting in a reduced mortality rate due to severe influenza infections with complications [45].

However, the 2009 pandemic, albeit milder than previous pandemics in terms of overall mortality, resulted in significant strains on global healthcare networks and economies [25]. In Canada, direct healthcare costs (including hospitalizations, outpatient visits, and therapeutics) related to the 2009 pandemic have been estimated at \$2 billion CAD, with \$250 million CAD related directly to hospital care [71]. A computational modeling study by Smith and colleagues suggested that direct costs related to illness would be between 0.5–4.3% of GDP in the UK for pandemics ranging from low to extreme [72]. Further, the 2002–2004 severe acute

respiratory syndrome outbreak resulted in ~\$1 billion total GDP loss in Toronto alone [73]. This highlights the importance of pandemic preparedness beyond a healthcare-centric approach to one that also includes downstream economic effects.

The 1918–1919 pandemic resulted in incredible improvements to public health as well as scientific advances. However, our current understanding of influenza viruses, and their ability to cause illness in humans is still in its infancy in many aspects, and further underlines our inherent need for continued influenza research. The identification of key molecular determinants involved in the pathophysiology of severe influenza infections will also assist drug discovery and development strategies, including insights on appropriate timing for administration of antivirals and/or antibiotics. The development of efficacious broader-spectrum or “universal” influenza vaccines is also of incredible importance. The emergence of novel highly pathogenic avian influenza (HPAI) viruses, including H5 and H7 subtypes, are of particular concern due to their pandemic potential. Circulating HPAI viruses are of potential concern to global public health [74]. Asian lineage avian influenza A (H5N1), which circulates in fowl, is rarely found in humans but has resulted in life-threatening cases when able to establish stable lineages [74] and H7N9 has resulted in sporadic human infections in China resulting in > 1500 infections with an estimated 39% case fatality rate since 2013 [75]. Because HPAI viruses can arise from previously known low-pathogenicity viruses with only minor mutations, it is important to be vigilant concerning these potential pandemic viruses [76, 77].

Conclusions

In spite of the public health advancements in the 100 years following the 1918–1919 pandemic, including widespread access in the developed world to an efficacious influenza vaccine, influenza viruses remain a global public health threat. This past year, there were > 55,000 reported influenza infections, 5155 influenza-associated hospitalizations, and 303 deaths across Canada [78]. Further, during the 2016–2017 influenza season, vaccination rates in those 18–64 years of age was only 37 and 69% in those ≥65, both below the national vaccination target of 80% [79]. These data suggest that our continued vigilance against influenza must not only include a “research”-driven focus but also include public outreach and awareness campaigns that increase the general understanding of the healthcare burden associated with influenza infections.

Acknowledgements

Not applicable.

Funding

Publication of this manuscript was supported by Research Manitoba (MEN; JK) and by the Canada Research Chairs Program (JK).

Availability of data and materials

Not applicable.

Authors' contributions

MEN and JK conceived of the ideas presented herein and made substantial contributions to the drafting and revising of the manuscript. Both authors read and approved the final manuscript.

Ethics approval and consent to participate

Not applicable.

Consent for publication

Not applicable.

Competing interests

The authors have declared that they have no competing interests.

Publisher's Note

Springer Nature remains neutral with regard to jurisdictional claims in published maps and institutional affiliations.

Received: 28 August 2018 Accepted: 28 January 2019

Published online: 06 February 2019

References

1. Iuliano AD, Roguski KM, Chang HH, Muscatello DJ, Palekar R, Tempia S, Cohen C, Gran JM, Schanzer D, Cowling BJ, et al. Estimates of global seasonal influenza-associated respiratory mortality: a modelling study. *Lancet*. 2018;391(10127):1285–300.
2. Prevention of Flu [www.canada.ca/en/public-health/services/diseases/flu-influenza/prevention-flu-influenza.html].
3. Krammer F, Smith GJD, Fouchier RAM, Peiris M, Kedzierska K, Doherty PC, Palese P, Shaw ML, Treanor J, Webster RG, et al. Influenza. *Nat Rev Dis Primers*. 2018;4(1):3.
4. Taubenberger JK, Morens DM. 1918 influenza: the mother of all pandemics. *Emerg Infect Dis*. 2006;12(1):15–22.
5. Johnson NP, Mueller J. Updating the accounts: global mortality of the 1918–1920 “Spanish” influenza pandemic. *Bull Hist Med*. 2002;76(1):105–15.
6. Tumpey TM, Basler CF, Aguilar PV, Zeng H, Solorzano A, Swayne DE, Cox NJ, Katz JM, Taubenberger JK, Palese P, et al. Characterization of the reconstructed 1918 Spanish influenza pandemic virus. *Science*. 2005;310(5745):77–80.
7. Stephenson I. Influenza: Molecular Virology. *Expert Review of Vaccines*. 2010;9(7):719–20.
8. Molinari NA, Ortega-Sanchez IR, Messonnier ML, Thompson WW, Wortley PM, Weintraub E, Bridges CB. The annual impact of seasonal influenza in the US: measuring disease burden and costs. *Vaccine*. 2007;25(27):5086–96.
9. Prevention CfDCA: Estimated Influenza Illnesses, Medical visits, and Hospitalizations Averted by Vaccination in the United States. In; 2018.
10. Cohen SA, Chui KK, Naumova EN. Influenza vaccination in young children reduces influenza-associated hospitalizations in older adults, 2002–2006. *J Am Geriatr Soc*. 2011;59(2):327–32.
11. Ghebrehewet S, MacPherson P, Ho A. Influenza. *BMJ*. 2016;355:i6258.
12. Moghadami M. A narrative review of influenza: a seasonal and pandemic disease. *Iran J Med Sci*. 2017;42(1):2–13.
13. Centers for Disease Control and Prevention: Influenza. 2018.
14. Webster RG, Laver WG. The origin of pandemic influenza. *Bull World Health Organ*. 1972;47(4):449–52.
15. Potter CW. A history of influenza. *J Appl Microbiol*. 2001;91(4):572–9.
16. Barberis I, Myles P, Ault SK, Bragazzi NL, Martini M. History and evolution of influenza control through vaccination: from the first monovalent vaccine to universal vaccines. *J Prev Med Hyg*. 2016;57(3):E115–20.
17. Pappas G, Kiriaze IJ, Falagas ME. Insights into infectious disease in the era of Hippocrates. *Int J Infect Dis*. 2008;12(4):347–50.
18. Martin PM, Martin-Granel E. 2,500-year evolution of the term epidemic. *Emerg Infect Dis*. 2006;12(6):976–80.

19. Beveridge WL. The chronicle of influenza epidemics. *Hist Philos Life Sci.* 1991;13(2):223–34.
20. Pyle GF. The diffusion of influenza: patterns and paradigms. New Jersey: Rowan & Littlefield; 1986.
21. Finkler D. Influenza in twentieth century practice. In *An International Encyclopaedia of Modern Medical Science*; Shipman TL, Ed. London: Sampson Law & Marston; 1899. p. 21–32.
22. Hirsch A. Handbook of geographical and historical pathology. London: new Sydenham Society; 1883.
23. Patterson KD. Pandemic influenza 1700–1900; a study in historical epidemiology. New Jersey: Rowan & Littlefield; 1987.
24. Pyle GF, Patterson KD. Influenza diffusion in european history: patterns and paradigms. *Ecol Dis.* 1984;2:173–84.
25. Saunders-Hastings PR, Krewski D. Reviewing the history of pandemic influenza: understanding patterns of emergence and transmission. *Pathogens.* 2016;5(4).
26. Valleron AJ, Cori A, Valtat S, Meurisse S, Carrat F, Boelle PY. Transmissibility and geographic spread of the 1889 influenza pandemic. *Proc Natl Acad Sci U S A.* 2010;107(19):8778–81.
27. Taubenberger JK, Morens DM, Fauci AS. The next influenza pandemic: can it be predicted? *JAMA.* 2007;297(18):2025–7.
28. Guan Y, Vijaykrishna D, Bahl J, Zhu H, Wang J, Smith GJ. The emergence of pandemic influenza viruses. *Protein Cell.* 2010;1(1):9–13.
29. Fukumi H. Summary report on the Asian influenza epidemic in Japan 1957. *Bull World Health Organ.* 1959;20(2–3):187–98.
30. Henderson DA, Courtney B, Inglesby TV, Toner E, Nuzzo JB. Public health and medical responses to the 1957–58 influenza pandemic. *Biosecure Bioterror.* 2009;7(3):265–73.
31. Viboud C, Simonsen L, Fuentes R, Flores J, Miller MA, Chowell G. Global mortality impact of the 1957–1959 influenza pandemic. *J Infect Dis.* 2016; 213(5):738–45.
32. Dawood FS, Iuliano AD, Reed C, Meltzer MI, Shay DK, Cheng PY, Bandaranayake D, Breiman RF, Brooks WA, Buchy P, et al. Estimated global mortality associated with the first 12 months of 2009 pandemic influenza a H1N1 virus circulation: a modelling study. *Lancet Infect Dis.* 2012;12(9):687–95.
33. Kendal AP, Noble GR, Skehel JJ, Dowdle WR. Antigenic similarity of influenza a (H1N1) viruses from epidemics in 1977–1978 to "Scandinavian" strains isolated in epidemics of 1950–1951. *Virology.* 1978;89(2):632–6.
34. Morens DM, Taubenberger JK, Harvey HA, Memoli MJ. The 1918 influenza pandemic: lessons for 2009 and the future. *Crit Care Med.* 2010;38(4 Suppl): e10–20.
35. Radusin M. The Spanish flu—part II: the second and third wave. *Vojnosanit Pregl.* 2012;69(10):917–27.
36. Humphries M. Paths of infection: the first world war and the origins of the 1918 influenza pandemic. *War Hist.* 2013;21:55–81.
37. Radusin M. The Spanish flu—part I: the first wave. *Vojnosanit Pregl.* 2012; 69(9):812–7.
38. Reid AH, Taubenberger JK, Fanning TG. Evidence of an absence: the genetic origins of the 1918 pandemic influenza virus. *Nat Rev Microbiol.* 2004;2(11): 909–14.
39. Taubenberger JK, Reid AH, Fanning TG. The 1918 influenza virus: a killer comes into view. *Virology.* 2000;274(2):241–5.
40. Barry JM. The site of origin of the 1918 influenza pandemic and its public health implications. *J Transl Med.* 2004;2(1):3.
41. Weaver PC, van Bergen L. Death from 1918 pandemic influenza during the first world war: a perspective from personal and anecdotal evidence. *Influenza Other Respir Viruses.* 2014;8(5):538–46.
42. Morens DM, Taubenberger JK. Understanding influenza backward. *JAMA.* 2009;302(6):679–80.
43. Morens DM, Fauci AS. The 1918 influenza pandemic: insights for the 21st century. *J Infect Dis.* 2007;195(7):1018–28.
44. Short KR, Kedzierska K, van de Sandt CE. Back to the future: lessons learned from the 1918 influenza pandemic. *Front Cell Infect Microbiol.* 2018;8:343.
45. Taubenberger JK, Baltimore D, Doherty PC, Markel H, Morens DM, Webster RG, Wilson IA. Reconstruction of the 1918 influenza virus: unexpected rewards from the past. *MBio.* 2012;3(5).
46. Peiris JS, Yu WC, Leung CW, Cheung CY, Ng WF, Nicholls JM, Ng TK, Chan KH, Lai ST, Lim WL, et al. Re-emergence of fatal human influenza a subtype H5N1 disease. *Lancet.* 2004;363(9409):617–9.
47. Taubenberger JK. The origin and virulence of the 1918 "Spanish" influenza virus. *Proc Am Philos Soc.* 2006;150(1):86–112.
48. Sheng ZM, Chertow DS, Ambroggio X, McCall S, Przygodzki RM, Cunningham RE, Maximova OA, Kash JC, Morens DM, Taubenberger JK. Autopsy series of 68 cases dying before and during the 1918 influenza pandemic peak. *Proc Natl Acad Sci U S A.* 2011;108(39):16416–21.
49. Rudd JM, Ashar HK, Chow VT, Teluguakula N. Lethal Synergism between Influenza and Streptococcus pneumoniae. *J Inf Secur Pulm Dis.* 2016;2(2). <http://dx.doi.org/10.16966/2470-3176.114>.
50. Palese P, Tumpey TM, Garcia-Sastre A. What can we learn from reconstructing the extinct 1918 pandemic influenza virus? *Immunity.* 2006; 24(2):121–4.
51. Park JK, Taubenberger JK. Universal influenza vaccines: to dream the possible dream? *ACS Infect Dis.* 2016;2(1):5–7.
52. Rajao DS, Perez DR. Universal vaccines and vaccine platforms to protect against influenza viruses in humans and agriculture. *Front Microbiol.* 2018;9: 123.
53. Angeletti D, Yewdell JW. Is it possible to develop a "universal" influenza virus vaccine? Outflanking antibody Immunodominance on the road to universal influenza vaccination. *Cold Spring Harb Perspect Biol.* 2018;10(7).
54. Krammer F, Garcia-Sastre A, Palese P. Is it possible to develop a "universal" influenza virus vaccine? Potential target antigens and critical aspects for a universal influenza vaccine. *Cold Spring Harb Perspect Biol.* 2018;10(7).
55. Crowe JE Jr. Is it possible to develop a "universal" influenza virus vaccine? Potential for a universal influenza vaccine. *Cold Spring Harb Perspect Biol.* 2018;10(7).
56. Andrews SF, Graham BS, Mascola JR, AB MD. Is it possible to develop a "universal" influenza virus vaccine? Immunogenetic considerations underlying B-cell biology in the development of a pan-subtype influenza a vaccine targeting the hemagglutinin stem. *Cold Spring Harb Perspect Biol.* 2018;10(7).
57. Coughlan L, Palese P. Overcoming barriers in the path to a universal influenza virus vaccine. *Cell Host Microbe.* 2018;24(1):18–24.
58. Pielak RM, Chou JJ. Influenza M2 proton channels. *Biochim Biophys Acta.* 2011;1808(2):522–9.
59. Pielak RM, Schnell JR, Chou JJ. Mechanism of drug inhibition and drug resistance of influenza a M2 channel. *Proc Natl Acad Sci U S A.* 2009;106(18): 7379–84.
60. McKimm-Breschkin JL. Influenza neuraminidase inhibitors: antiviral action and mechanisms of resistance. *Influenza Other Respir Viruses.* 2013;7(Suppl 1):25–36.
61. Deutschman Z. Trend of influenza mortality during the period 1920–51. *Bull World Health Organ.* 1953;8(5–6):633–45.
62. Viboud C, Tam T, Fleming D, Miller MA, Simonsen L. 1951 influenza epidemic, England and Wales, Canada, and the United States. *Emerg Infect Dis.* 2006;12(4):661–8.
63. Alling DW, Blackwelder WC, Stuart-Harris CH. A study of excess mortality during influenza epidemics in the United States, 1968–1976. *Am J Epidemiol.* 1981;113(1):30–43.
64. Randolph AG, Vaughn F, Sullivan R, Robinson L, Thompson BT, Yoon G, Smoot E, Rice TW, Loftis LL, Helfaer M, et al. Critically ill children during the 2009–2010 influenza pandemic in the United States. *Pediatrics.* 2011;128(6): e1450–8.
65. Rice TW, Robinson L, Uyeki TM, Vaughn FL, John BB, Miller RR 3rd, Higgs E, Randolph AG, Smoot BE, Thompson BT, et al. Critical illness from 2009 pandemic influenza a virus and bacterial coinfection in the United States. *Crit Care Med.* 2012;40(5):1487–98.
66. Chertow DS, Memoli MJ. Bacterial coinfection in influenza: a grand rounds review. *JAMA.* 2013;309(3):275–82.
67. Gill JR, Sheng ZM, Ely SF, Guinee DG, Beasley MB, Suh J, Deshpande C, Mollura DJ, Morens DM, Bray M, et al. Pulmonary pathologic findings of fatal 2009 pandemic influenza a/H1N1 viral infections. *Arch Pathol Lab Med.* 2010;134(2):235–43.
68. Mauad T, Hajjar LA, Callegari GD, da Silva LF, Schout D, Galas FR, Alves VA, Malheiros DM, Auler JO Jr, Ferreira AF, et al. Lung pathology in fatal novel human influenza a (H1N1) infection. *Am J Respir Crit Care Med.* 2010;181(1):72–9.
69. Centers for Disease C, prevention. Bacterial coinfections in lung tissue specimens from fatal cases of 2009 pandemic influenza a (H1N1) - United States, may-august 2009. *MMWR Morb Mortal Wkly Rep.* 2009;58(38):1071–4.
70. Viboud C, Miller M, Olson D, Osterholm M, Simonsen L. Preliminary estimates of mortality and years of life lost associated with the 2009 a/H1N1 pandemic in the US and comparison with past influenza seasons. *PLoS Curr.* 2010;2:RRN1153.

71. Information CifH. The impact of the H1N1 pandemic on Canadian hospitals. Ottawa, ON, Canada: CIHI; 2010.
72. Smith RD, Keogh-Brown MR, Barnett T, Tait J. The economy-wide impact of pandemic influenza on the UK: a computable general equilibrium modelling experiment. *BMJ*. 2009;339:b4571.
73. Gully PR. National Response to (SARS): Canada. In: WHO global meeting. Geneva, Switzerland: World Health Organization; 2003. p. 2003.
74. Highly Pathogenic Avian Influenza [<http://www.cfsph.iastate.edu/DiseaseInfo/disease.php?name=avian-influenza&lang=en>].
75. Centers for Disease Control and Prevention. Asian Lineage Avian Influenza A (H7N9) Virus [<https://www.cdc.gov/flu/avianflu/h7n9-virus.htm>].
76. What Will The Next Influenza Pandemic Look Like? [<https://www.scientificamerican.com/article/next-influenza-pandemic/>].
77. Monne I, Fusaro A, Nelson MI, Bonfanti L, Mulatti P, Hughes J, Murcia PR, Schivo A, Valastro V, Moreno A, et al. Emergence of a highly pathogenic avian influenza virus from a low-pathogenic progenitor. *J Virol*. 2014;88(8):4375–88.
78. Public Health Agency of Canada. FluWatch: May 20 to June 23, 2018 (Weeks 21–25) [<https://www.canada.ca/content/dam/phac-aspc/documents/services/publications/diseases-conditions/fluwatch/2017-2018/week21-25-may-20-june-23-2018/pub-wk21-25-eng.pdf>].
79. Public Health Agency of Canada. 2016/17 seasonal influenza vaccine coverage in Canada. In.; 2018.
80. Nicholson KG, Hay AJ, Webster RB, editors. Textbook of influenza. Oxford: Blackwell Science; 1998.
81. Grove RDHA. Vital statistics rates in the United States: 1940–1960. Washington: Office UGP; 1968.
82. Linder FEGR. Vital statistics rates in the United States: 1900–1940. Washington: US Government Printing Office; 1943.

Ready to submit your research? Choose BMC and benefit from:

- fast, convenient online submission
- thorough peer review by experienced researchers in your field
- rapid publication on acceptance
- support for research data, including large and complex data types
- gold Open Access which fosters wider collaboration and increased citations
- maximum visibility for your research: over 100M website views per year

At BMC, research is always in progress.

Learn more biomedcentral.com/submissions



COVID-19 vaccines dampen genomic diversity of SARS-CoV-2: Unvaccinated patients exhibit more antigenic mutational variance

Michiel J.M. Niesen¹, Praveen Anand², Eli Silvert¹, Rohit Suratekar², Colin Pawlowski¹, Pritha Ghosh², Patrick Lenehan¹, Travis Hughes¹, David Zemmour¹, John C. O'Horo³, Joseph D. Yao³, Bobbi S. Pritt³, Andrew Norgan³, Ryan T. Hurt³, Andrew D. Badley³, AJ Venkatakrishnan¹, Venky Soundararajan^{1,2*}

1. inference, inc., One Main Street, Suite 400, East Arcade, Cambridge, MA 02142, USA

2. inference Labs, Bengaluru, Karnataka, India

3. Mayo Clinic, Rochester, MN 55901, USA

* Address correspondence to: Venky Soundararajan (venky@inference.net)

Abstract

Variants of SARS-CoV-2 are evolving under a combination of immune selective pressure in infected hosts and natural genetic drift, raising a global alarm regarding the durability of COVID-19 vaccines. Here, we conducted longitudinal analysis over 1.8 million SARS-CoV-2 genomes from 183 countries or territories to capture vaccination-associated viral evolutionary patterns. To augment this macroscale analysis, we performed viral genome sequencing in 23 vaccine breakthrough COVID-19 patients and 30 unvaccinated COVID-19 patients for whom we also conducted machine-augmented curation of the electronic health records (EHRs). Strikingly, we find the diversity of the SARS-CoV-2 lineages is declining at the country-level with increased rate of mass vaccination ($n = 25$ countries, mean correlation coefficient = -0.72, S.D. = 0.20). Given that the COVID-19 vaccines leverage B-cell and T-cell epitopes, analysis of mutation rates shows neutralizing B-cell epitopes to be particularly more mutated than comparable amino acid clusters (4.3-fold, $p < 0.001$). Prospective validation of these macroscale evolutionary patterns using clinically annotated SARS-CoV-2 whole genome sequences confirms that vaccine breakthrough patients indeed harbor viruses with significantly lower diversity in known B cell epitopes compared to unvaccinated COVID-19 patients (2.3-fold, 95% C.I. 1.4-3.7). Incidentally, in these study cohorts, vaccinated breakthrough patients also displayed fewer COVID-associated complications and pre-existing conditions relative to unvaccinated COVID-19 patients. This study presents the first known evidence that COVID-19 vaccines are fundamentally restricting the evolutionary and antigenic escape pathways accessible to SARS-CoV-2. The societal benefit of mass vaccination may consequently go far beyond the widely reported mitigation of SARS-CoV-2 infection risk and amelioration of community transmission, to include stemming of rampant viral evolution.

Introduction

To date, over 175 million individuals have been infected with SARS-CoV-2 worldwide, and over 2.2 million deaths have been attributed to COVID-19. More than a year and half since the first known case of SARS-CoV-2 infection, the virus continues to evolve in different parts of the

world resulting in emerging variants of concern¹ (e.g. delta variant) with increased transmissibility. Host immune response is a key selective pressure that influences the emergence of novel strains of the SARS-CoV-2 virus in different parts of the world. Understanding the longitudinal trends of SARS-CoV-2 evolution and mapping the mutational landscape of the antigen is imperative to comprehensively combat the ongoing pandemic and future outbreaks²⁻⁴.

Accelerated development of COVID-19 vaccines and mass vaccination rollouts has led to the immunization of over 10% of the world's population (over 800 million individuals fully vaccinated⁵). Sudden immunization of a large fraction of the population at the height of the ongoing pandemic could significantly increase evolutionary pressure on the SARS-CoV-2 virus. However, to date there has been no comprehensive study on the impact of the global vaccination efforts on SARS-CoV-2 evolution. The main axes of the host immune response that have been examined in SARS-CoV-2 infection are the innate immunity⁶, the cell-mediated (i.e. T cell) and humoral or antibody-mediated responses (through B cells)⁷. B cells and T cells are two specialized cell types that undergo junctional recombination somatic hypermutation in antigen receptor genes during their differentiation, which generates extensive diversity within the immune receptor repertoire. B cells can recognize virtually any molecule (proteins, sugars, non-organic, etc.), without antigen presentation, but are largely restricted to exposed surfaces of molecules, a feature that pathogens utilize as an escape mechanism. T cells on the other hand, can generate immunity against epitopes that are buried within the antigen, but are limited to small peptides presented by complex HLA molecules. They are however essential for optimizing neutralizing antibodies through somatic hypermutation and antibody class switching in B cells during an immune response.

Since the beginning of the pandemic concerted global data sharing efforts have led to the rapid development of large-scale genomic COVID-19 resources. Over 1.8 million SARS-CoV-2 genomes from 183 countries and territories have been deposited in the GISAID database⁸. Based on this data, we and others reported that deletion mutations are enriched in the Spike protein N-terminal domain^{3,4}. Similarly, concerted efforts have led to the development of a rich immunological resource of 1.04 million peptide epitopes from over 22,000 studies⁹. Using this data we previously identified epitopes that are identical between the SARS-CoV-2 and the human proteome¹⁰. The availability of genomic and immunological data provides a timely opportunity to systematically characterize the antigenic mutational landscape of SARS-CoV-2.

In this immuno-epidemiology and clinical genomics study, we systematically analyzed the mutational burden of the known B cell and T cell epitopes and found that the prevalence of mutations in neutralizing, conformational B cell epitopes is higher than in neutralizing T cell epitopes. These results demonstrate that the SARS-CoV-2 Spike protein is presently undergoing strong B cell-driven selection pressure, with the variants of concern (particularly Beta and Gamma variants) displaying the most significant recent increases in mutations to known B-cell epitopes. Given that the Spike protein is a key antigen for COVID-19 vaccine-induced protection, as well as the emerging evidence of reasonable distinctions in B cell versus T cell activation by different COVID-19 vaccines¹¹, we prospectively conducted clinico-genomic sequencing of SARS-CoV-2 genomes from vaccinated "breakthrough infections" (n = 26) as well as unvaccinated COVID-19 patients (n = 36). We report that unvaccinated patients share significantly more genomic mutational similarity (particularly B-cell epitope mutations) to the

variants of concern than the breakthrough infection patients. This study demonstrates that mass vaccination may serve as an antigenic impediment to the evolution of fitter and more transmissible SARS-CoV-2 variants, emphasizing the urgent need to stem vaccine hesitancy as a key step to mitigate the global burden of COVID-19.

Results

Diversity of the SARS-CoV-2 lineages is declining significantly with increased rate of mass vaccination

Analysis of the 1.8 million SARS-CoV-2 genomes deposited from 183 countries and territories between Dec. 2019 and May 2021 in the GISAID database⁸ revealed a total of 1296 lineages. We quantified the monthly diversity in SARS-CoV-2 lineages within the GISAID data using Shannon entropy of the lineage probability distribution within 1-month time windows (see **Methods**). The diversity of SARS-CoV-2 lineages has declined globally (**Figure 1a, b**) and this decline appears to coincide with the onset of mass vaccination in the countries (**Figure 1b**). In order to understand the relationship between lineage diversity and mass vaccination, we compared the lineage entropy and vaccination rates, focusing on countries that had at least 25% of their population fully vaccinated, this analysis included 25 countries that had at least 100 SARS-CoV-2 genomes deposited per month for at least four different months. Analysing the relationship between vaccination rates and lineage entropy, we found that the declining diversity of SARS-CoV-2 lineages is indeed negatively correlated with increased rate of mass vaccination across the countries analyzed (**Figure 1c,d**; mean correlation coefficient = -0.72, S.D. = 0.20). Furthermore, the decline in the lineage diversity is coupled with the increased dominance of Variants of Concern: the B.1.1.7/Alpha-variant (45%), B.1.1.617/Delta-variant (21%), P.1/Gamma-variant (10%)¹², suggesting that these variants may be “fitter strains” of SARS-CoV-2.

Neutralizing B-cell epitopes of Spike glycoprotein are enriched for mutations

In order to understand how the lineage diversity is shaped by immune selection pressure, we undertook a systematic characterisation of the mutational landscape of the Spike glycoprotein. We obtained all known neutralizing B cell epitopes and MHC-I and MHC-II T cell epitopes of the Spike protein from IEDB⁹. This included 220 B cell epitopes (involving 282 of 1,273 amino acids), 262 linear MHC class I T cell epitopes (involving 1,034 amino acids), and 140 linear MHC class II T cell epitopes (involving 999 amino acids) (**Figure 2, Methods**). Analysing the 1.8 million genome sequences, a total of 10,946 distinct Spike protein amino-acid mutations were found, occurring in at least 100 genomic sequences.

Comparing the prevalence of mutation per epitope residue (defined here as mutation away from the Wuhan-Hu-1 sequence; see **Methods**) in the known conformational B cell epitopes and a control set of randomly selected amino acids shows a 4.3-fold (3.0-6.1, 95% CI) enrichment of mutations (0.021 mutations per B cell epitope residue, compared to 0.005 mutations per random control residue, over all genomic sequences) (**Figure 2b**). Additional comparisons using randomly selected distance-constrained control sets of amino acids or randomly selected control sets of

amino acids with similar solvent accessibility as B cell epitopes, show comparable enrichment of mutations in the B cell epitopes (**Figure S1**). On the other hand, both MHC class I T cell epitopes (1.0-fold; 0.7-1.5, 95% CI) and MHC class II T cell epitopes (0.9-fold; 0.6-1.3, 95% CI) show no significant enrichment in mutations compared to random control residues (**Figure 2b**). This suggests that the antibody-interfacing antigenic sites are under a stronger selection pressure compared to the T cell binding epitopes.

The rate of B cell epitope mutations has sharply increased, starting December 2021, across all 1.8 million genomic sequences (**Figure 2c**). To ensure that the observed enrichment in B cell mutations is not solely reporting on events in the countries that report the majority of sequences in the GISAID database, we have also evaluated mutations within epitopes per country and territory; a rise in B cell epitope mutations and overall enrichment in mutations within B cell epitopes is observed globally (representative countries shown in **Figure S2**). The observed increase in B cell epitope mutations can be related to the recent dominance of variants of concern. Indeed, analysis of the mutations in the known B-cell epitopes shows that variants of concern have more mutations in B-cell epitopes than sequences that are not variants of concern (**Figure 2d**). The alpha variant (pango lineage B.1.1.7), which is the dominant variant of concern in the GISAID data (**Figure 2e**), shows a 4.3-fold (2.9-6.5, 95% CI) enrichment in mutations within B cell epitopes.

To investigate how increased prevalence of variants of concern relates to the global rise in mutations within B cell epitopes and reduced lineage entropy, we compare the B cell epitope mutation patterns observed in geographical regions over time to those of the variants of concern. A monthly country-level analysis, for the 55 countries with more than 1,000 total genomic sequences deposited to GISAID, shows increased mutation of known B-cell epitopes over time (**Figure 3**). Furthermore, the specific epitopes that are mutated correspond to those that are mutated in the variants of concern. This analysis shows that different SARS-CoV-2 variants have come to dominate in different geographical regions, and that their dominance globally results in increased mutation of antigenic sites.

Whole-genome sequencing of SARS-CoV-2 genomes from unvaccinated and vaccinated individuals reveals different mutational profiles

The immuno-epidemiology analysis presented above based on publicly accessible data has shown that the diversity of the SARS-CoV-2 lineages is declining and that neutralizing B-cell epitopes of Spike glycoprotein are enriched for mutations. However, the genome sequences deposited in publicly accessible databases (e.g. GISAID) lack any clinical or phenotypic data such as vaccination status or disease severity of the linked COVID-19 patients. To address this, we performed whole genome viral sequencing in non-duplicate positive upper respiratory tract specimens 53 SARS-CoV-2 infected patients at the Mayo Clinic health system. Of these, 23 cases were vaccine breakthrough infections, with the infected individuals having been fully vaccinated for COVID-19 at the time of their positive SARS-CoV-2 test (**Figure 4a**). We find that the known B-cell epitopes exhibit more mutational diversity in the unvaccinated individuals than in the vaccinated individuals (**Figure 4b,c**). Furthermore, a larger fraction of the vaccinated (82.6%) cohort had alpha variant compared to the unvaccinated cohort (60%) (**Table S1**). Availability of a

larger number of sequenced genomes in the future can help understand whether specific variants of concern are more likely to cause breakthrough infections.

Of the 53 SARS-CoV-2 infected patients, we have complete longitudinal health records and vaccination history of 47 patients. In **Table S2**, we present the clinical characteristics of the patients with SARS-CoV-2 genomes sequenced in the Mayo Clinic with EHR data available. In the overall cohort of 47 patients, we observe high rates of comorbidities (e.g. cancer: 48.9%, chronic kidney disease: 25.5%) and cardiovascular complications (e.g. cardiac arrhythmias: 40.4%, acute kidney injury: 29.8%, venous thromboembolism: 25.5%). Comparing the vaccinated and unvaccinated cohorts, we observe that vaccinated patients generally had lower rates of comorbidities and complications compared to the overall study population, while the unvaccinated patients generally had higher rates of both comorbidities and complications. Due to the large differences in the rates of comorbidities, we cannot draw any definitive conclusions comparing complications and other clinical outcomes in the vaccinated and unvaccinated cohorts. Considering the clinical data in combination with the genomic data, we do not observe any statistically significant associations between mutation count and rates of complications recorded in clinical notes (**Figure 5**). This preliminary data suggests that the number of mutations that a patient has in the Spike protein region of the SARS-CoV-2 genome does not translate to more or less severe clinical symptoms. As a result, although unvaccinated individuals harbor more viral mutations and also exhibit more COVID-19 complications, these two factors appear to be independent.

Discussion

In summary, our analysis of 1.8 million SARS-CoV-2 genomes shows that there is a 4.3-fold enrichment in mutational prevalence in 220 known neutralizing B cell epitopes. On the other hand, T cell epitopes did not appear statistically more mutated than by chance. This suggests that the antibody-interfacing antigenic sites are under a stronger selection pressure compared to the T cell binding peptide epitopes following vaccination or infection, implying breakthrough mutations and escape mutations have a higher likelihood of occurring in neutralizing antibody-binding residues on the Spike protein.

This result does not mean that T cell immunity is not critical against SARS-CoV-2. Indeed, durable T cell responses emerge following natural infections that are closely linked with antibody responses, reflecting the helper role of T cell help to mount better neutralizing antibodies¹³. Our findings are consistent with antibody and T cell responses to multiple SARS-CoV-2 variants following vaccination with the Ad26.COV2.S adenoviral vector vaccine. A recent study reported similar CD4 and CD8 T cell responses across strains, but reduced neutralizing antibody titers of virus-specific titers for B.1.1.7, CAL.20C, P1, and B.1.351 variants¹¹. Similarly, Geers et al. reported a 2-4 fold reduction in neutralization potential of BNT162b2 mRNA vaccine-induced antibodies against the B.1.351 variant, whereas CD4+ T cell responses elicited by the wild-type Spike protein were unaffected¹⁴. In one recent study, Agerer et al. reported that mutations in CD8 T cell epitopes result in reduced association of mutant peptides with HLA class I molecules *in vitro* leading to altered T cell immune responses¹⁵. While mutation of individual T cell epitopes may alter HLA-peptide interactions and antigen presentation, our data suggest that these mutations

do not represent a common route to viral immune escape, perhaps due to recognition of additional, non-mutated viral peptides and extensive genetic heterogeneity within the HLA genes¹⁶. In our data, we observed a relative paucity of enriched mutations in T cell epitopes, which suggests that T cell responses are likely able to recognize conserved viral sequences, which are less amenable to mutation. These results suggest a greater degree of degeneracy encoded into how the T cell epitopes buffer viral evolution, and suggest an ancient mechanism for immunosurveillance that exploits the inability of mutative viruses to escape such significant host HLA affinity to a fuzzy set of peptides beyond the wildtype peptides engaged on the pathogen. Targeted experimental validation is required, of course, to validate or nullify this speculative hypothesis on how T cell response may buffer viral evolution to durably protect the host species.

Our study has a number of key limitations. First, the list of B cell and T cell epitopes in the Spike (S) glycoprotein antigen studied here may not be exhaustive as they are based on curation of studies deposited in the immune epitope database (IEDB) as of June 10, 2021 (<https://www.iedb.org/>). The immunologic analysis presented in this study consequently has to be updated regularly as more evidence emerges regarding the exhaustive T cell and B cell epitopes presented by the SARS-CoV-2 pathogen and their neutralization potential in the human population. Similarly, the SARS-CoV-2 genomes analyzed herein were deposited in the global initiative on sharing avian influenza data (GISAID) initiative as of June 10, 2021 (<https://www.gisaid.org/>). Despite having over 1 million SARS-CoV-2 genomes at the time of this analysis, GISAID still represents less than 0.60% of the 175 million COVID-19 cases reported worldwide as of June 10, 2021, thus providing only a partial representation of the genomic evolution of SARS-CoV-2. Finally, we consider any mutation away from the wild-type genomic sequence of known immunogenic epitopes as deleterious to their immunogenicity. While it is possible that mutations in the Spike protein sequence result in new immunogenic epitopes, a scan of 469,649 unique mutated peptides identified from the SARS-CoV-2 genomes reveals that only 8 of these peptides match a previously defined T cell epitopes (from IEDB), from within the SARS-CoV and SARS-CoV-2 genomes (**Table S3**). Further work is needed to confirm if any of the novel peptides, resulting from epitope mutations, are also immunogenic.

Despite these limitations, this study presents the first holistic examination, to our knowledge, of the mutational landscape of the B cell versus the T cell epitopes derived from the SARS-CoV-2 S-protein antigen, by juxtaposing the genomic mutation patterns of the pathogen onto all the known neutralizing epitopes. Our finding that T cell epitopes are significantly less mutated than B cell epitopes suggests that vaccines that predominantly rely on T cell immunity would likely bestow a more durable protection against the many SARS-CoV-2 variants of concern that continue to emerge periodically across the globe. Understanding the immunologic basis of vaccine effectiveness and durability to the genomic variations and associated perturbations to antigenic cartography will be critical to reliably inform proactive vaccine design and rollout strategies, and also better inform important public health policy decisions.

A number of recent studies have performed bioinformatic prediction of SARS-CoV-2 epitopes¹⁷. While these studies have identified viral peptide sequences that are likely immunogenic, they generally fail to account for mutational diversity in SARS-CoV-2^{17,18}. Although our work does not directly predict variant neo-epitopes, it highlights the importance of epitopes that are recurrently mutated during viral evolution in response to immune pressure. In future work,

we will more thoroughly investigate strain-level epitopes for variants of concern within these hypermutated regions. We further plan to examine the immune selection pressure across the entire SARS-CoV-2 proteome. While we have focused on viral escape from adaptive immune responses, in future work we will expand on our analysis to consider the interplay between SARS-CoV-2 sequence variation and innate immune responses¹⁹.

Methods

Calculation of SARS-CoV-2 lineage entropy

To quantify the diversity in SARS-CoV-2 genomes over time and in different geographical regions, we have calculated the entropy of the Pango lineage²⁰ probability distribution (**Figure 1a-c**). Specifically, for a given time-period, t , and geographical region, c , the lineage entropy is defined as:

Lineage entropy

$$= - \sum_{l \in \text{all lineages}} \frac{\text{Number of sequences of lineage } l(t, c)}{\text{Total number of sequences}(t, c)} \log \left[\frac{\text{Number of sequences of lineage } l(t, c)}{\text{Total number of sequences}(t, c)} \right]$$

This quantity will be valued at 0 if all genomic sequences are classified as the same lineage, and has an upper-bound of 7.17 if all 1296 possible lineages are equally probable. SARS-CoV-2 lineage data was obtained from the GISAID database⁸. Error bars shown correspond to 95% confidence intervals, obtained by bootstrap sampling of the GISAID sequence data.

Data on country vaccination rates

The percentage of fully vaccinated individuals (**Figure 1c-d**) was obtained from the OWID database²¹. When multiple values for the percentages of fully vaccinated individuals are reported for a country in a month, we use the midpoint ($0.5 \cdot \text{min} + 0.5 \cdot \text{max}$).

Prevalence of mutations per epitope

Prevalence of mutations per epitope (**Figure 2c-e**) is defined as the average probability with which a residue within that epitope is mutated with respect to the Wuhan-Hu-1 sequence (UniProt identifier: P0DTC2). Specifically, we count the total number of mutations within all epitopes of that epitope type, across the 1,844,200 sequences from the GISAID database (**Figure 2c-d**) or only sequences corresponding to variants of concern (**Figure 2e**), and divide by the total number of amino-acid residues that were summed over.

Epitope mutation fraction

The epitope mutation fraction (**Figure 3**) is defined as the fraction of sequences in which a given epitope is mutated with respect to the Wuhan-Hu-1 sequence (UniProt identifier: P0DTC2). Specifically, it is the number of sequences in which an epitope exhibits at least one

mutation, divided by the total number of sequences summed over (i.e., all sequences from a given country in a given month).

Mutational burden on T cell and B cell epitopes of SARS-CoV-2 Spike (S) protein antigen

To assess the mutational burden on T cell and B cell epitopes we have determined the prevalence of mutations per epitope for known epitopes (from IEDB), as compared to various controls. The following controls were used: unrestrained randomly selected sets of amino-acid residues that match the size of the analyzed epitopes (separate size-matched controls for T cell and B cell epitopes, **Figure 2**), randomly selected sets of co-localized residues (**Figure S2**), and randomly selected sets of surface residues (**Figure S2**). For each epitope, a random control set with the same number of amino acids as that epitope is selected. Controls with restraints on localization were generated by measuring the largest pairwise C α -C α distance between residues within a B cell epitope (using a Spike protein homology model using SWISS-MODEL²², unresolved residues were excluded), D . We then selecting a control set of residues such that all residues in the control fall within a sphere of diameter, $D + 4\text{\AA}$. Where use of a 4 \AA buffer region was found to yield a comparable C α -C α distance distribution between epitopes and controls (**Figure S2a-b**). Controls restraint to surface residues were generated by calculating the solvent accessible surface area of each residue within the Spike protein (using the Biopython SASA module). We then match each residue in a B cell epitope to a control epitope with a SASA value within 10 \AA^2 . The resulting controls yield a comparable SASA distribution to that of the B cell epitopes (**Figure S2c-d**). Sufficient sampling of the possible sets of control residues, and 95% confidence intervals were obtained via bootstrap analysis.

Amplicon sequencing of SARS-CoV-2 genomes from vaccinated and unvaccinated patients

This is a retrospective study of individuals who underwent polymerase chain reaction (PCR) testing for suspected SARS-CoV-2 infection at the Mayo Clinic and Mayo Clinic Health System care facilities. This study was reviewed by the Mayo Clinic institutional review board and determined to be exempt from human subject research. Subjects were excluded if they did not have a research authorization on file.

SARS-CoV-2 RNA-positive upper respiratory tract swab specimens from patients with vaccine breakthrough infection or reinfection were subjected to next-generation sequencing, using the commercially available Ion AmpliSeq SARS-CoV-2 Research Panel (Life Technologies Corp., South San Francisco, CA) based on the "sequencing by synthesis" method. The assay amplifies 237 sequences ranging from 125 to 275 base pairs in length, covering 99% of the SARS-CoV-2 genome. Viral RNA was first manually extracted and purified from these clinical specimens using MagMAXTM Viral / Pathogen Nucleic Acid Isolation Kit (Life Technologies Corp.), followed by automated reverse transcription-PCR (RT-PCR) of viral sequences, DNA library preparation (including enzymatic shearing, adapter ligation, purification, normalization), DNA template preparation, and sequencing on the automated GenexusTM Integrated Sequencer (Life Technologies Corp.) with the GenexusTM Software version 6.2.1. A no-template control and a positive SARS-CoV-2 control were included in each assay run for quality control purposes. Viral sequence data were assembled using the Iterative Refinement Meta-Assembler (IRMA)

application (50% base substitution frequency threshold) to generate unamended plurality consensus sequences for analysis with the latest versions of the web-based application tools: Pangolin²³ for SARS-CoV-2 lineage assignment; Nextclade²⁴ for viral clade assignment, phylogenetic analysis, and S codon mutation calling, in comparison to the wild-type reference sequence of SARS-CoV-2 Wuhan-Hu-1 (lineage B, clade 19A).

Analysis of EHR data from patients with SARS-CoV-2 genome sequencing information

For the patients with SARS-CoV-2 genome sequencing data available, we analyzed their clinical covariates from the Mayo Clinic electronic health record (EHR) database. Demographic characteristics including age at time of sample collection, sex, race, and ethnicity were obtained from structured tables. Clinical phenotypes were obtained by applying natural language processing (NLP) methods to the unstructured clinical notes, using the phenotypes and following the methodology from previous studies^{25,26}. Comorbidities were determined from clinical notes in the 5 years leading up to the sample collection date. The following comorbidity phenotypes were considered: anemia, asthma, cancer, cardiomyopathy, chronic kidney disease, chronic obstructive pulmonary disease, coronary artery disease, heart failure, hyperglycemia, hypertension, liver disease, neurologic conditions, obstructive sleep apnea, type 1 diabetes mellitus, type 2 diabetes mellitus, and solid organ transplant. Similarly, complications were determined from the clinical notes in the time period +/- 30 days relative to the sample collection date. The following complication phenotypes were considered: acute respiratory distress syndrome / acute lung injury (ARDS/ALI), acute kidney injury, anemia, cardiac arrest, cardiac arrhythmias, disseminated intravascular coagulation, heart failure, hyperglycemia, hypertension, myocardial infarction, pleural effusion, pulmonary embolism, respiratory failure, sepsis, septic shock, stroke / cerebrovascular accident, venous thromboembolism, encephalopathy / delirium, and numbness.

References

1. CDC. SARS-CoV-2 Variant Classifications and Definitions. <https://www.cdc.gov/coronavirus/2019-ncov/variants/variant-info.html> (2021).
2. McCallum, M. *et al.* N-terminal domain antigenic mapping reveals a site of vulnerability for SARS-CoV-2. *Cell* **184**, 2332–2347.e16 (2021).
3. McCarthy, K. R. *et al.* Recurrent deletions in the SARS-CoV-2 spike glycoprotein drive antibody escape. *Science* **371**, 1139–1142 (2021).
4. Venkatakrisnan, A. J. *et al.* Antigenic minimalism of SARS-CoV-2 is linked to surges in COVID-19 community transmission and vaccine breakthrough infections. (2021) doi:10.1101/2021.05.23.21257668.
5. Coronavirus (COVID-19) Vaccinations. <https://ourworldindata.org/covid-vaccinations>.
6. Kasuga, Y., Zhu, B., Jang, K.-J. & Yoo, J.-S. Innate immune sensing of coronavirus and viral evasion strategies. *Exp. Mol. Med.* **53**, 723–736 (2021).
7. Carvalho, T., Krammer, F. & Iwasaki, A. The first 12 months of COVID-19: a timeline of immunological insights. *Nat. Rev. Immunol.* **21**, 245–256 (2021).
8. Shu, Y. & McCauley, J. GISAI: Global initiative on sharing all influenza data - from vision to reality. *Euro Surveill.* **22**, (2017).
9. Vita, R. *et al.* The Immune Epitope Database (IEDB): 2018 update. *Nucleic Acids Res.* **47**, D339–D343 (2019).
10. Venkatakrisnan, A. J. *et al.* Benchmarking evolutionary tinkering underlying human-viral molecular

- mimicry shows multiple host pulmonary-arterial peptides mimicked by SARS-CoV-2. *Cell Death Discov* **6**, 96 (2020).
11. Alter, G. *et al.* Immunogenicity of Ad26.COV2.S vaccine against SARS-CoV-2 variants in humans. *Nature* 1–9 (2021).
 12. Hadfield, J. *et al.* Nextstrain: real-time tracking of pathogen evolution. *Bioinformatics* **34**, 4121–4123 (2018).
 13. Zuo, J. *et al.* Robust SARS-CoV-2-specific T cell immunity is maintained at 6 months following primary infection. *Nat. Immunol.* **22**, 620–626 (2021).
 14. Geers, D. *et al.* SARS-CoV-2 variants of concern partially escape humoral but not T-cell responses in COVID-19 convalescent donors and vaccinees. *Sci Immunol* **6**, (2021).
 15. Agerer, B. *et al.* SARS-CoV-2 mutations in MHC-I-restricted epitopes evade CD8+ T cell responses. *Sci Immunol* **6**, (2021).
 16. Haynes, W. A., Kamath, K., Lucas, C., Shon, J. & Iwasaki, A. Impact of B.1.1.7 variant mutations on antibody recognition of linear SARS-CoV-2 epitopes. *medRxiv* 2021.01.06.20248960 (2021).
 17. Sohail, M. S., Ahmed, S. F., Quadeer, A. A. & McKay, M. R. In silico T cell epitope identification for SARS-CoV-2: Progress and perspectives. *Adv. Drug Deliv. Rev.* **171**, 29–47 (2021).
 18. Crooke, S. N., Ovsyannikova, I. G., Kennedy, R. B. & Poland, G. A. Immunoinformatic identification of B cell and T cell epitopes in the SARS-CoV-2 proteome. *Sci. Rep.* **10**, 14179 (2020).
 19. Gordon, D. E. *et al.* A SARS-CoV-2 protein interaction map reveals targets for drug repurposing. *Nature* **583**, 459–468 (2020).
 20. Rambaut, A. *et al.* A dynamic nomenclature proposal for SARS-CoV-2 lineages to assist genomic epidemiology. *Nat Microbiol* **5**, 1403–1407 (2020).
 21. Coronavirus (COVID-19) Vaccinations. <https://ourworldindata.org/covid-vaccinations>.
 22. Spike glycoprotein (S glycoprotein). <https://swissmodel.expasy.org/interactive/7dVLxC/models/04>.
 23. COG-UK. <https://pangolin.cog-uk.io/>.
 24. Nextclade. <https://clades.nextstrain.org/>.
 25. Venkatakrisnan, A. J. *et al.* Mapping each pre-existing condition's association to short-term and long-term COVID-19 complications. *medRxiv* 2020.12.02.20242925 (2020).
 26. Wagner, T. *et al.* Augmented curation of clinical notes from a massive EHR system reveals symptoms of impending COVID-19 diagnosis. *Elife* **9**, (2020).

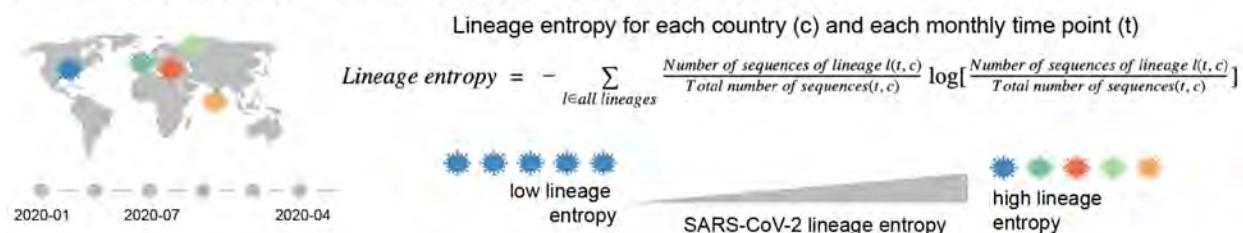
Data Availability

After publication, the data will be made available to others upon reasonable requests to the corresponding author. A proposal with detailed description of study objectives and statistical analysis plan will be needed for evaluation of the reasonability of requests.

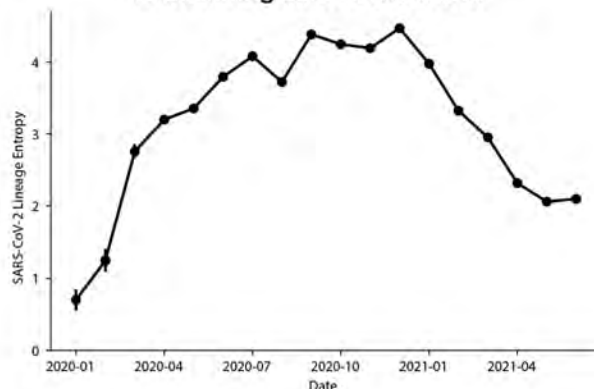
Declaration of Interests

nference collaborates with biotechnology, pharmaceutical, medical device, and diagnostics companies on data science initiatives unrelated to this study. These collaborations had no role in study design, data collection and analysis, decision to publish, or preparation of the manuscript. JCO receives personal fees from Elsevier and Bates College, and receives small grants from nference, Inc, outside the submitted work. ADB is a consultant for Abbvie and Flambeau diagnostics, is a paid member of the DSMB for Corvus pharmaceuticals, Equilibrium, and Excision biotherapeutics, has received fees for speaking for Reach MD, owns equity for scientific advisory board positions in nference and Zentalis, and is founder and President of Splissen therapeutics. JH, JCO, GJG, AWW, AV, MDS, and ADB are employees of the Mayo Clinic. The Mayo Clinic may stand to gain financially from the successful outcome of the research. nference and Mayo Clinic have filed a provisional patent application associated with this study. This research has been reviewed by the Mayo Clinic Conflict of Interest Review Board and is being conducted in compliance with Mayo Clinic Conflict of Interest policies.

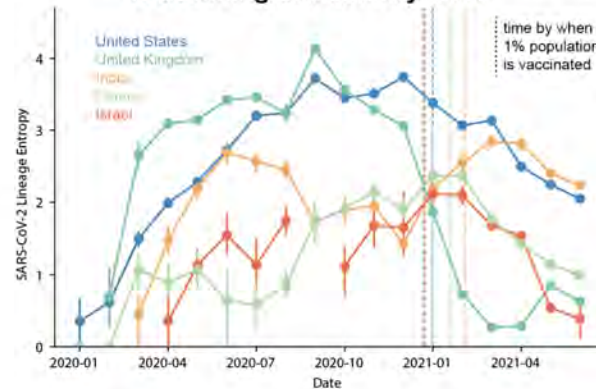
a Estimating diversity of SARS-CoV-2 genomes using lineage entropy



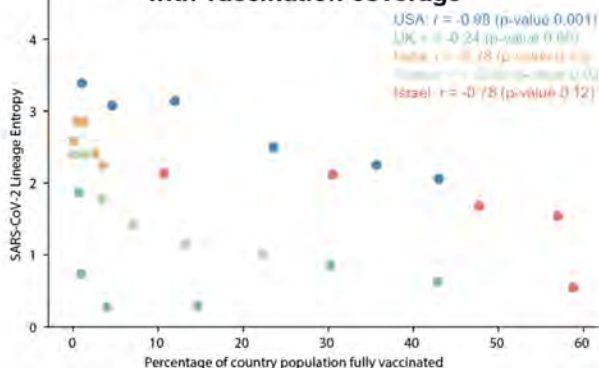
b The diversity in SARS-CoV-2 lineages is declining across the world



c The diversity in SARS-CoV-2 lineages is declining at a country level



d Lineage diversity is negatively correlated with vaccination coverage



e Lineage diversity is negatively correlated with vaccination coverage

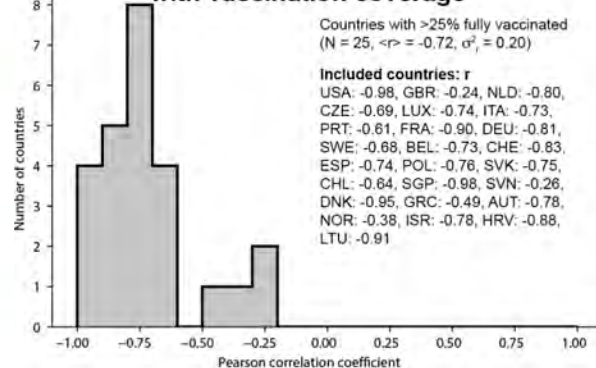
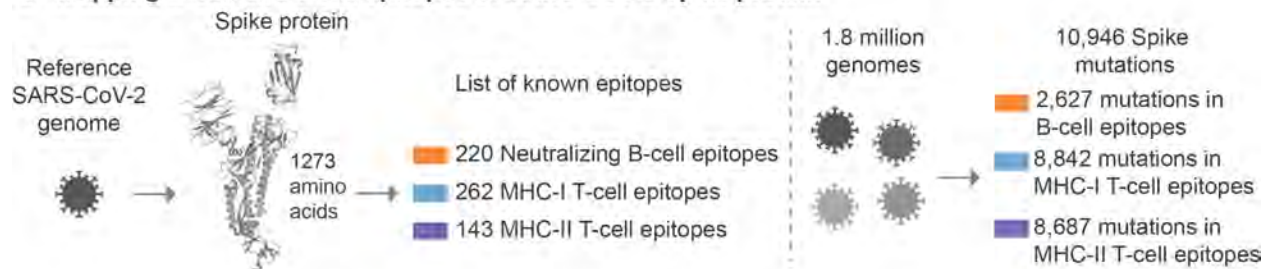
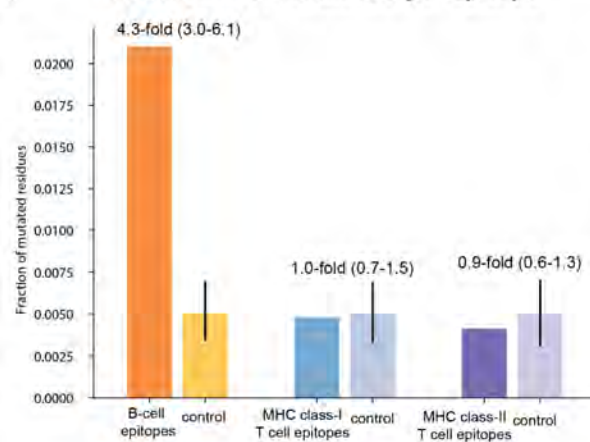


Figure 1. SARS-CoV-2 genomes show a global decline in sequence diversity coinciding with mass vaccination for COVID-19. (a) Schematic overview of estimating genomic diversity of SARS-CoV-2 (b-c) Diversity in SARS-CoV-2 lineages within the GISAID data, quantified using the entropy of the lineage probability distribution within 1-month time windows. Vertical dashed lines indicate the time at which countries reached a vaccine coverage of 1% of their total population. (d) Scatter plot showing the correlation between the country-level percentage of fully vaccinated individuals (from OWID²¹) and SARS-CoV-2 lineage entropy. (e) Distribution of the Pearson correlation coefficient between country-level percentage of fully vaccinated individuals and SARS-CoV-2 lineage entropy for all 25 countries with greater than 25% of their population fully vaccinated (as of June 26th, 2021) and at least 4-months with 100 or more sequences deposited to GISAID, after start of vaccination. The ISO 3166-1 alpha-3 code of included countries and their Pearson correlation are listed in the figure legend.

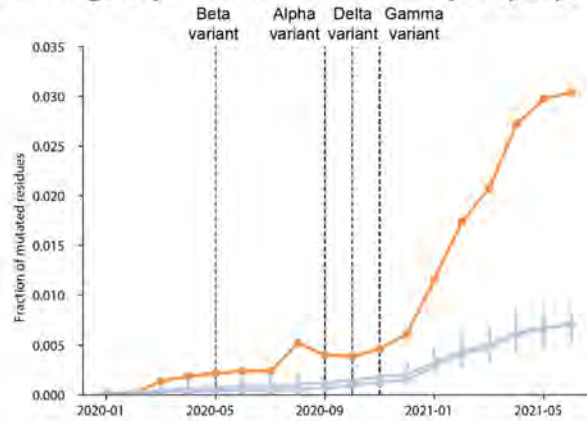
a Mapping B-cell and T-cell epitopes of SARS-CoV-2 Spike protein



b Prevalence of mutations per epitope



c Change in prevalence of mutations per epitope



d Mutations in Variants of Concern mapped to known B-cell epitopes

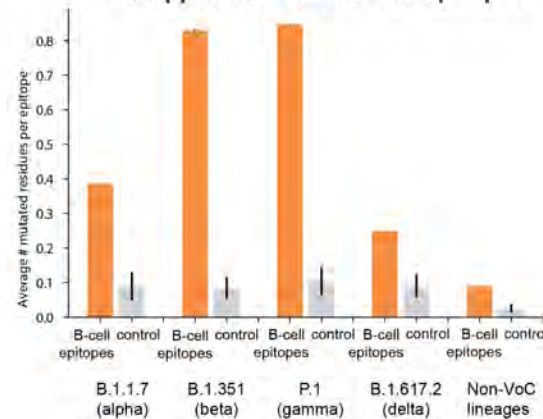


Figure 2. B cell epitopes are more mutated than CD8+ T cell epitopes across the Spike protein antigen. (a) We extracted known neutralizing epitopes of the reference SARS-CoV-2 Spike protein sequence from IEDB. Prevalence of mutations in these epitopes is determined for over 1.8 million viral genomes (GISAID). Specifically, we have quantified the average number of mutated amino acids for epitopes involved in distinct immune responses. (b) B cell epitopes (orange) show increased prevalence of mutations compared to size matched control, and T cell epitopes (blue, purple) do not show increased prevalence of mutations compared to size matched control. (c) Mutations in B cell epitopes are more prevalent and increase at a higher rate than for T cell epitopes, globally (see **Figure S3** for per country data). (d) Prevalence of mutations per B-cell epitope for SARS-CoV-2 genomic sequences of variants of concern; B.1.1.7 (alpha), B.1.531 (beta), P.1, and B.1.617.2, and Non-variant of concern sequences.

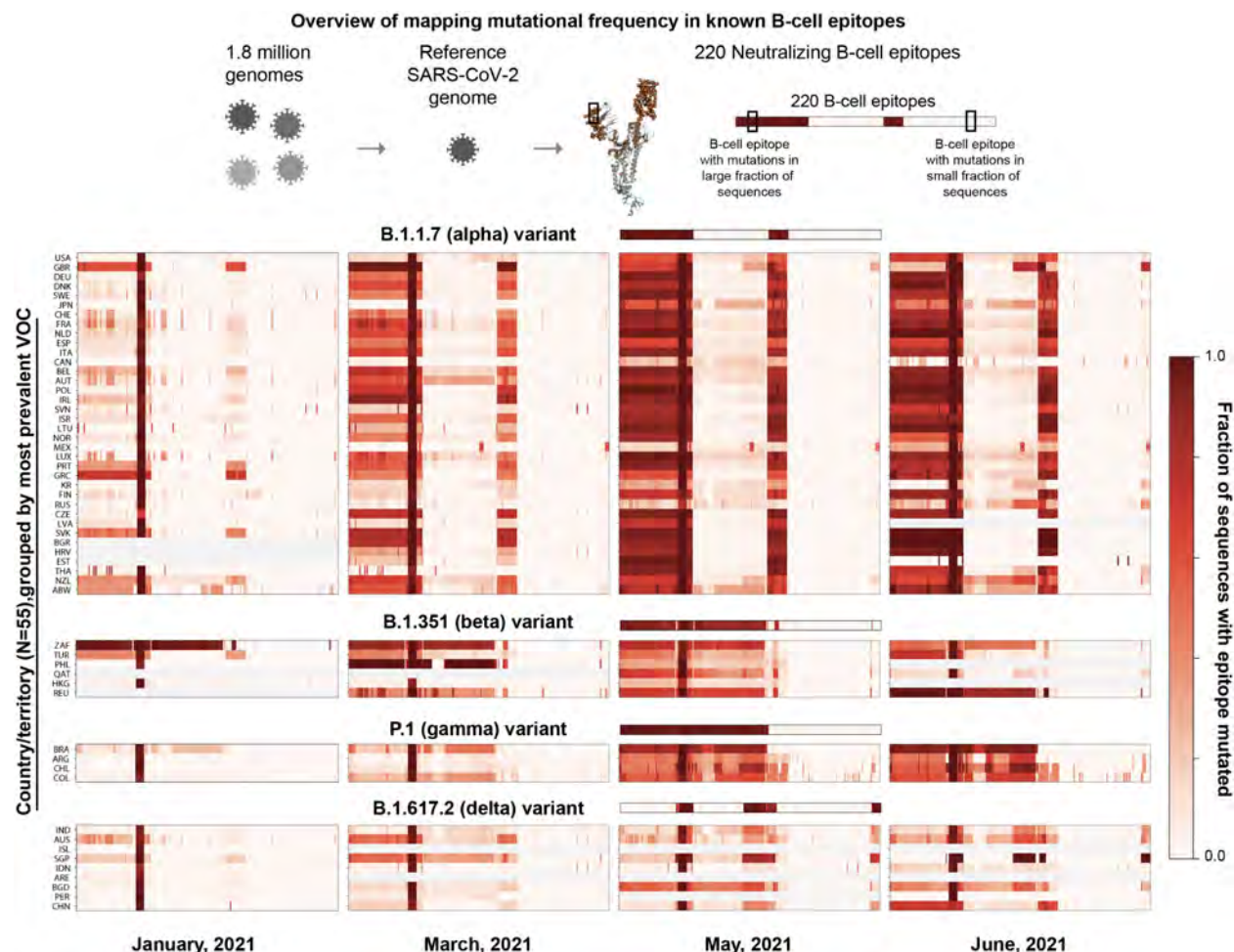
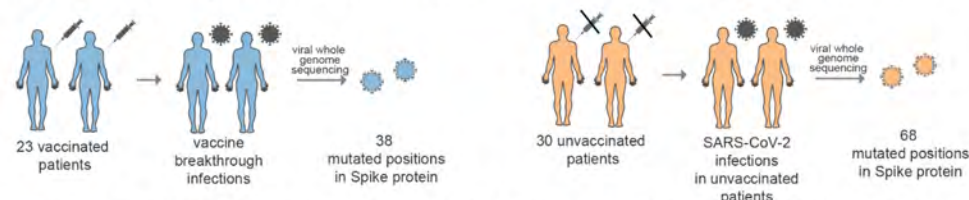
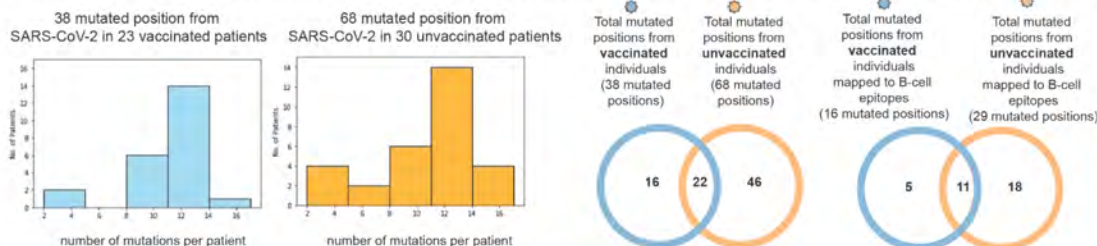


Figure 3: B-cell epitope mutation fractions for SARS-CoV-2 genomic sequences per country for 1-month time periods. Epitope mutation fractions for the variants of concern are shown as a visual guide and countries are grouped based on the most prevalent variant of concern; B.1.1.7 (alpha), B.1.531 (beta), P.1 (gamma), and B.1.617.2 (delta), in May 2021. Each row in a colormap corresponds to a country (ISO 1336-1 alpha-3 code, left; KR is South Korea) and each column corresponds to a B-cell epitope, ordering is conserved between the colormaps. Only countries with >1000 sequences deposited to GISAID are included. Rows in gray indicate countries for which no sequences were deposited in a given month.

a. Whole genome sequencing of SARS-CoV-2 from vaccinated individuals (breakthrough) and unvaccinated individuals



b. Comparison of the distributions of the number of mutated positions among the vaccinated and unvaccinated individuals



c. Comparison of the mutational profiles of SARS-CoV-2 from vaccinated and unvaccinated individuals

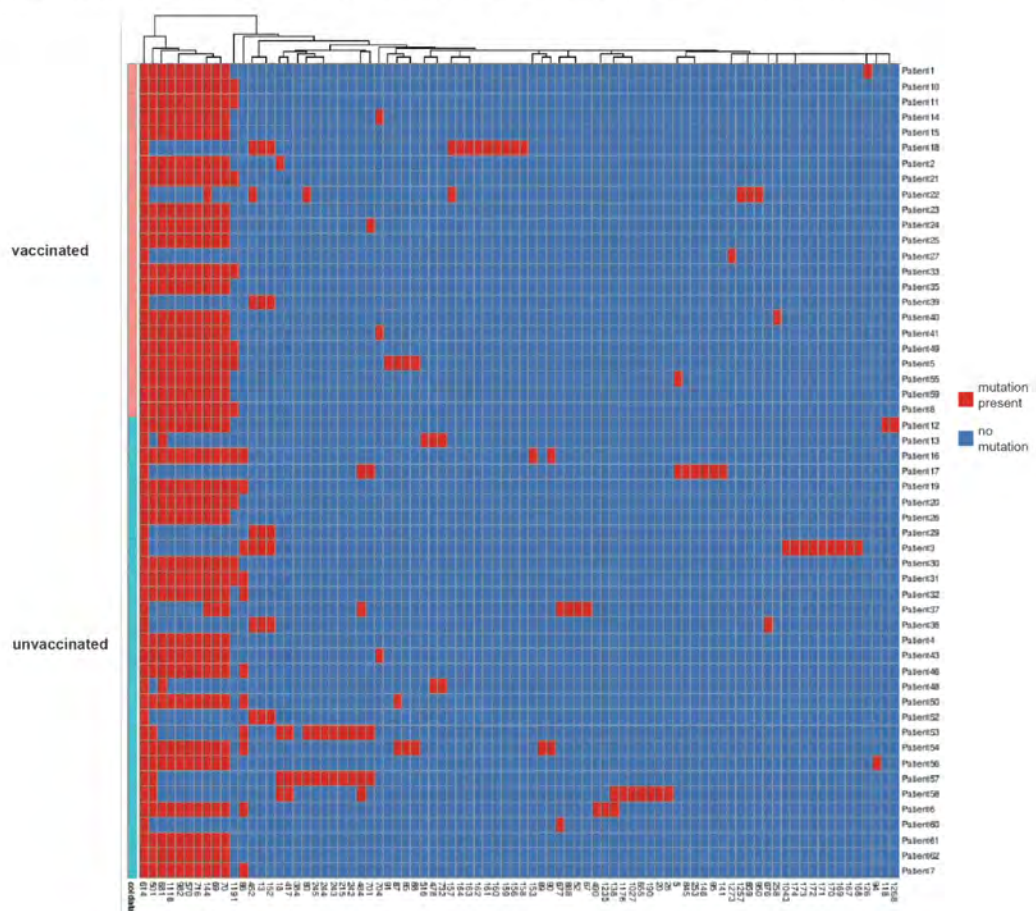


Figure 4. (a) Whole genome sequencing of SARS-CoV-2 from vaccinated individuals (breakthrough) and unvaccinated individuals (b) Comparison of the distributions of the number of mutated positions among the vaccinated and unvaccinated individuals. (c) Comparison of the mutational profiles of SARS-CoV-2 from vaccinated and unvaccinated individuals.

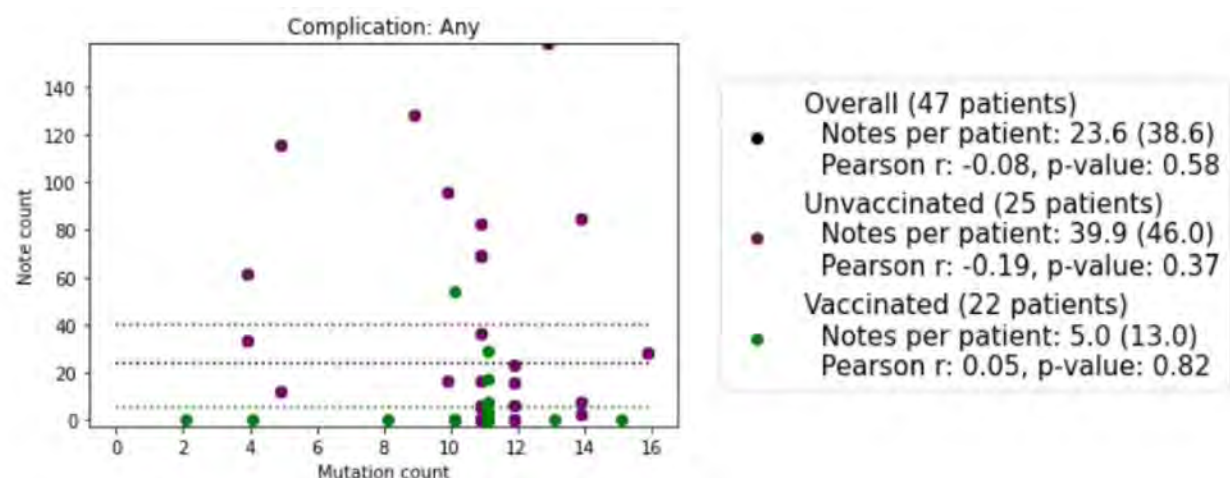


Figure 5: Scatterplot of genomic mutations vs. clinical complications for all vaccinated and unvaccinated patients. Data points representing unvaccinated patients are shown in purple, and data points representing vaccinated patients are shown in green. X-axis: The number of Spike protein mutations in the patient's SARS-CoV-2 viral genome. Y-axis: The number of clinical notes +/- 30 days from the viral sample collection date which have a positive sentiment for at least one of the following complications: acute respiratory distress syndrome / acute lung injury (ARDS/ALI), acute kidney injury, anemia, cardiac arrest, cardiac arrhythmias, disseminated intravascular coagulation, heart failure, hyperglycemia, hypertension, myocardial infarction, pleural effusion, pulmonary embolism, respiratory failure, sepsis, septic shock, stroke / cerebrovascular accident, venous thromboembolism, encephalopathy / delirium, and numbness. In the legend, we show the average number of clinical notes per patient, Pearson's r correlation coefficient, and associated p-value for the following cohorts: all sequenced patients, unvaccinated sequenced patients, and vaccinated sequenced patients. Dotted lines represent the average number of clinical notes per patient in each cohort, and the black dotted line represents the population average number of clinical notes.

Supplementary Material

Supplementary Data

Supplementary datafile S1: B-cell epitope mutation rates over all sequences and the variants of concern - B.1.1.7 (alpha), B.1.531 (beta), P.1 (gamma), and B.1.617.2 (delta).

Supplementary Table S1: Lineages of SARS-CoV-2 from infected vaccinated individuals (breakthrough infections) and unvaccinated individuals.

Variant	Percentage of vaccinated patients	Percentage of unvaccinated patients	Odds ratio	P-value
B.1.1.519	0 (0%)	2 (6.7%)	0	0.499
B.1.1.7	19 (82.6%)	18 (60%)	3.099	0.13
B.1.2	1 (4.3%)	0 (0%)	undefined	0.434
B.1.351	0 (0%)	2 (6.7%)	0	0.499
B.1.427	0 (0%)	1 (3.3%)	0	1
B.1.429	2 (8.7%)	3 (10%)	0.86	1
B.1.525	0 (0%)	1 (3.3%)	0	1
B.1.526	0 (0%)	1 (3.3%)	0	1
B.1.526.1	1 (4.3%)	0 (0%)	undefined	0.434
B.1.565	0 (0%)	1 (3.3%)	0	1
P.1	0 (0%)	1 (3.3%)	0	1

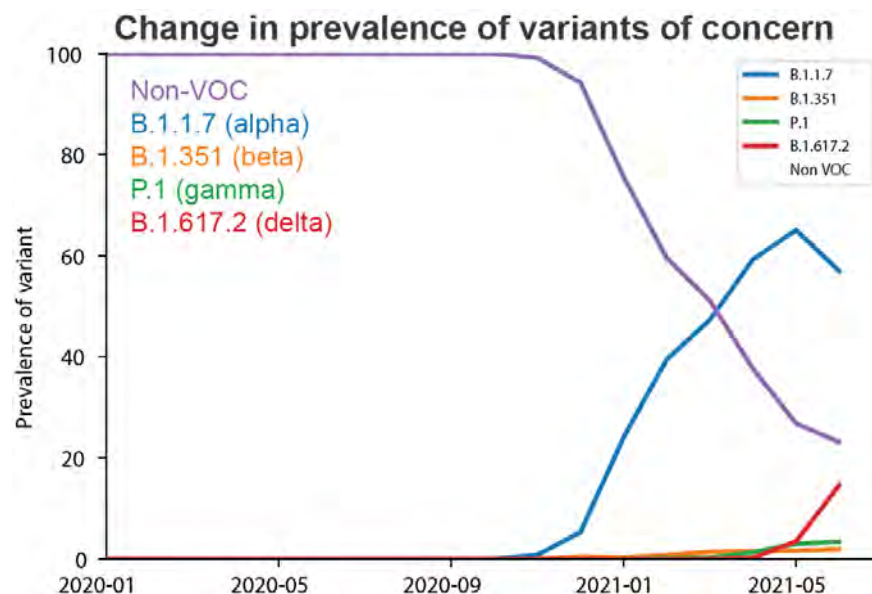
Supplementary Table S2: Clinical characteristics of patients with SARS-CoV-2 genomes sequenced in the Mayo Clinic database which have EHR data available. Comorbidities for each patient were determined from neural network models applied to the clinical notes over the past 5 years leading up to the first sample collection date. Similarly, complications for each patient were determined from neural network models applied to the clinical notes +/- 30 days relative to the first sample collection date. For continuous covariates such as age, mean and standard deviation are shown instead of patient counts and percentages. Clinical characteristics are shown for the following cohorts: (1) All sequenced patients, (2) Vaccinated patients: sequenced patients with SARS-CoV-2 infection post-vaccination, and (3) Unvaccinated patients: patients without COVID-19 vaccination or samples collected prior to vaccination date.

Clinical characteristic	All patients	Vaccinated patients	Unvaccinated patients
Total patient count	47	22	25
Age at time of sample collection (in years)			
- Mean	56.7	53.2	59.8
- Standard deviation	13.9	16.8	10.0
Sex			
- Female	34 (72.3%)	17 (77.3%)	17 (68.0%)
- Male	13 (27.7%)	5 (22.7%)	8 (32.0%)
Race			
- Black / African American	2 (4.3%)	1 (4.5%)	1 (4.0%)
- Native American	1 (2.1%)	0 (0.0%)	1 (4.0%)
- White / Caucasian	40 (85.1%)	21 (95.5%)	19 (76.0%)
- Other	2 (4.3%)	0 (0.0%)	2 (8.0%)
- Unknown	2 (4.3%)	0 (0.0%)	2 (8.0%)
Ethnicity			
- Hispanic or Latino	3 (6.4%)	2 (9.1%)	1 (4.0%)
- Not Hispanic or Latino	43 (91.5%)	20 (90.9%)	23 (92.0%)
- Unknown	1 (2.1%)	0 (0.0%)	1 (4.0%)
Comorbidities (within 5 years before sample collection date)			
- Anemia	13 (27.7%)	3 (13.6%)	10 (40.0%)
- Asthma	13 (27.7%)	6 (27.3%)	7 (28.0%)
- Cancer	23 (48.9%)	10 (45.5%)	13 (52.0%)
- Cardiomyopathy	5 (10.6%)	1 (4.5%)	4 (16.0%)
- Chronic kidney disease	12 (25.5%)	4 (18.2%)	8 (32.0%)
- Chronic obstructive pulmonary disease	5 (10.6%)	1 (4.5%)	4 (16.0%)
- Coronary artery disease	5 (10.6%)	1 (4.5%)	4 (16.0%)
- Heart failure	7 (14.9%)	2 (9.1%)	5 (20.0%)
- Hyperglycemia	4 (8.5%)	0 (0%)	4 (15.4%)
- Hypertension	29 (61.7%)	11 (50.0%)	18 (72.0%)
- Liver disease	5 (10.6%)	2 (9.1%)	3 (12.0%)
- Neurologic conditions	1 (2.1%)	0 (0%)	1 (4.0%)
- Obstructive sleep apnea	12 (25.5%)	3 (13.6%)	9 (36.0%)
- Type 1 diabetes mellitus	4 (8.5%)	1 (4.5%)	3 (12.0%)
- Type 2 diabetes mellitus	11 (23.4%)	2 (9.1%)	9 (36.0%)

- Solid organ transplant	1 (2.1%)	0 (0%)	1 (4.0%)
Complications (+/- 30 days relative to sample collection date)			
- ARDS/ALI	9 (19.1%)	0 (0.0%)	9 (36.0%)
- Acute kidney injury	14 (29.8%)	2 (9.1%)	12 (48.0%)
- Anemia	13 (27.7%)	1 (4.5%)	12 (48.0%)
- Cardiac arrest	1 (2.1%)	0 (0%)	1 (4.0%)
- Cardiac arrhythmias	19 (40.4%)	3 (13.6%)	16 (64.0%)
- Disseminated intravascular coagulation	1 (2.1%)	0 (0%)	1 (4.0%)
- Heart failure	5 (10.6%)	1 (4.5%)	4 (16.0%)
- Hyperglycemia	5 (10.6%)	0 (0.0%)	5 (20.0%)
- Hypertension	23 (48.9%)	6 (27.3%)	17 (68.0%)
- Myocardial infarction	3 (6.4%)	2 (9.1%)	1 (4.0%)
- Pleural effusion	5 (10.6%)	0 (0%)	5 (20.0%)
- Pulmonary embolism	7 (14.9%)	2 (9.1%)	5 (20.0%)
- Respiratory failure	9 (19.1%)	0 (0%)	9 (36.0%)
- Sepsis	5 (10.6%)	0 (0%)	5 (20.0%)
- Septic shock	2 (4.3%)	0 (0%)	2 (8.0%)
- Stroke/cerebrovascular accident	0 (0.0%)	0 (0.0%)	0 (0.0%)
- Venous thromboembolism	12 (25.5%)	2 (9.1%)	10 (40.0%)
- Encephalopathy/delirium	7 (14.9%)	1 (4.5%)	6 (24.0%)
- Numbness	1 (2.1%)	0 (0.0%)	1 (4.0%)
Any complication	27 (57.4%)	6 (27.3%)	21 (84.0%)
Number of notes per patient			
- Average	23.6	5.0	39.9
- Standard deviation	38.6	13.0	46.0

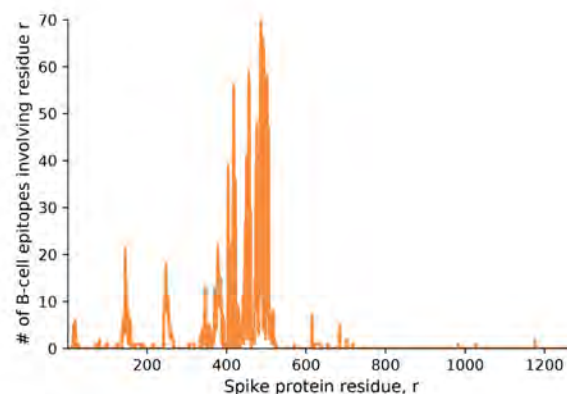
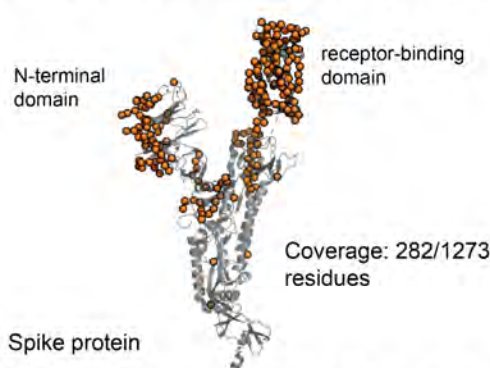
Supplementary Table S3. Scanning unique mutated n-mer peptide sequences in SARS-CoV-2 genomes for potentially new epitopes.

nmer Length	Unique no. of mutated nmers	No. of unique mutated nmers associated with surge
8	74390	2183 (2.93%)
9	84071	2453 (2.92%)
10	93839	2723 (2.9%)
11	103700	2994 (2.89%)
12	113649	3265 (2.87%)

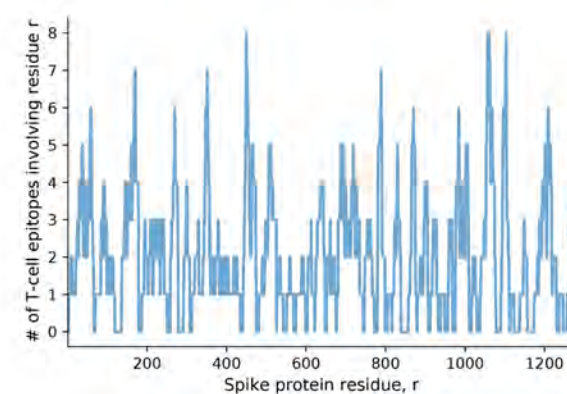
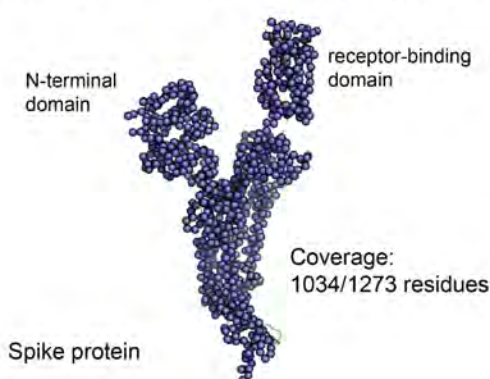


Supplementary Figure 1. Prevalence of Variants of Concern in the GISAID sequence increases over time.

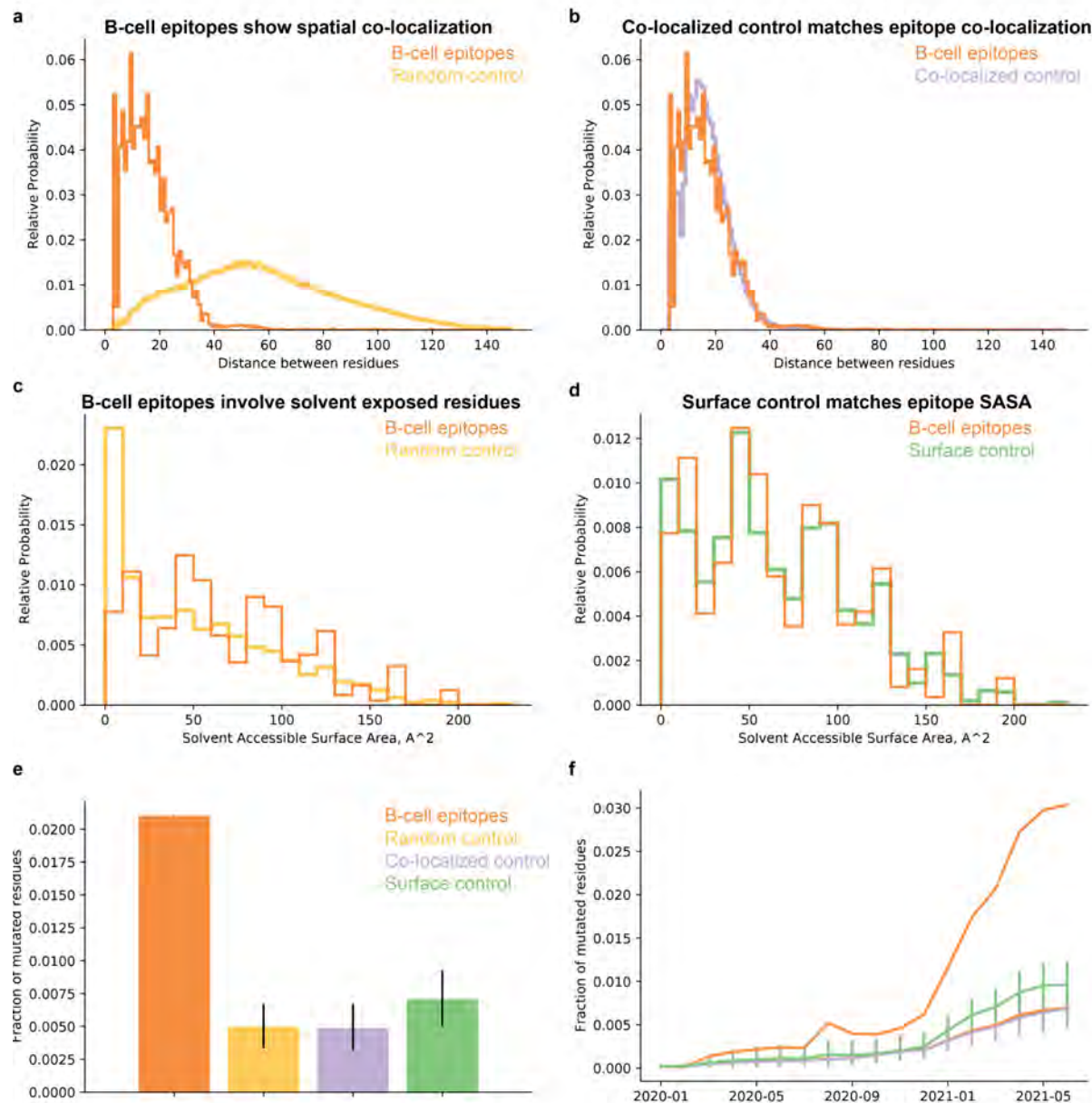
a B-cell epitope coverage of the Spike glycoprotein



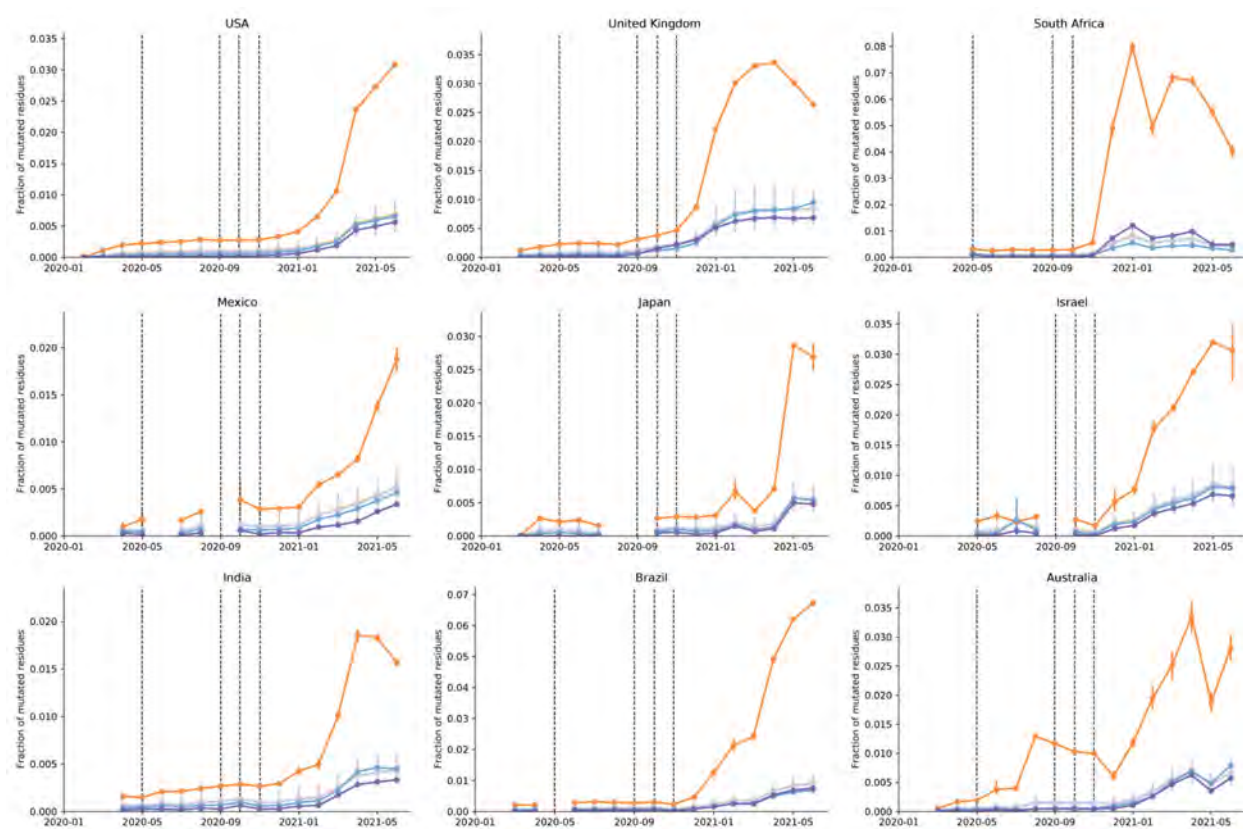
b T-cell epitope coverage of the Spike glycoprotein



Supplementary Figure 2. Neutralizing B cell and CD8⁺ T cell epitopes are unevenly distributed across the Spike protein. (a) The coverage of the Spike protein with known neutralizing B cell epitopes (from IEDB). Shown is the number of epitopes that each amino-acid residue is a part of, 280 residues are involved in at least one known B cell epitope. (b) The coverage of the Spike protein with known MHC class I T cell epitopes (from IEDB). Shown is the number of epitopes that each amino-acid residue is a part of. 1034 residues are involved in at least one known T cell epitope.



Supplementary Figure 3. B cell epitopes on the Spike antigen are more mutated than randomly selected 3-D/spatially co-localized residues and solvent-exposed surface residues. (a) Conformational B cell epitopes consist of co-localized residues, as is reflected by their low inter-residue distance distribution (orange), compared to the random control (yellow). **(b)** By selecting only residues with comparable inter-residue distance to the B cell epitopes, we have generated a co-localized residue control. **(c)** B cell epitopes consist of mainly surface residues, as is reflected by their increased solvent accessibility (orange), the random control also includes buried residues (yellow). **(d)** By selecting only residues with comparable solvent accessibility to matched residues from the B cell epitopes, we have generated a surface residue control. **(e-f)** Conformational neutralizing B cell epitopes (orange) show enhanced mutability compared both to the co-localized control (purple) and the surface residue control (green).



Supplementary Figure 4. Mutations in B cell epitopes are more prevalent and increase at a higher rate than for T cell epitopes.

Gaik C. Ooi, MD
 Pek L. Khong, MD
 Nestor L. Müller, MD, PhD
 Wai C. Yiu, MD
 Lin J. Zhou, MD
 James C. M. Ho, MD
 Bing Lam, MD
 Savvas Nicolaou, MD
 Kenneth W. T. Tsang, MD

Index terms:

Lung, CT, 60.12118
 Lung, infection, 60.21
 Severe acute respiratory syndrome (SARS)

Published online

10.1148/radiol.2303030853
 Radiology 2004; 230:836–844

Abbreviation:

SARS = severe acute respiratory syndrome

¹ From the Departments of Diagnostic Radiology (G.C.O., P.L.K., L.J.Z.) and Medicine (J.C.M.H., B.L., K.W.T.T.), University of Hong Kong, Queen Mary Hospital, Rm 405, Block K, Pokfulam Rd, Hong Kong, Special Administrative Region, China; Department of Radiology, Queen Mary Hospital, Hong Kong, Special Administrative Region, China (W.C.Y.); and Department of Radiology, Vancouver General Hospital, University of British Columbia, Canada (N.L.M., S.N.). Received June 2, 2003; revision requested June 23; final revision received September 8; accepted September 16. Address correspondence to G.C.O. (e-mail: cgcooi@hkucc.hku.hk).

Author contributions:

Guarantors of integrity of entire study, G.C.O., K.W.T.T.; study concepts and design, G.C.O., P.L.K., N.L.M., K.W.T.T.; literature research, G.C.O., P.L.K.; clinical studies, J.C.M.H., B.L., K.W.T.T.; data acquisition, W.C.Y., J.C.M.H., B.L.; data analysis/interpretation, G.C.O., P.L.K., L.J.Z., S.N., N.L.M.; statistical analysis, G.C.O.; manuscript preparation, G.C.O., P.L.K., N.L.M.; manuscript definition of intellectual content, G.C.O., P.L.K., N.L.M., K.W.T.T.; manuscript editing, G.C.O., P.L.K., N.L.M.; manuscript revision/review and final version approval, all authors

© RSNA, 2004

Severe Acute Respiratory Syndrome: Temporal Lung Changes at Thin-Section CT in 30 Patients¹

PURPOSE: To evaluate lung abnormalities on serial thin-section computed tomographic (CT) scans in patients with severe acute respiratory syndrome (SARS) during acute and convalescent periods.

MATERIALS AND METHODS: Serial thin-section CT scans in 30 patients (17 men, aged 42.5 years \pm 12.2 [SD]) with SARS were reviewed by two radiologists together for predominant patterns of lung abnormalities: ground-glass opacities, ground-glass opacities with superimposed linear opacities, consolidation, reticular pattern, and mixed pattern (consolidation, ground-glass opacities, and reticular pattern). Scans were classified according to duration in weeks after symptom onset. Longitudinal changes of specific abnormalities were documented in 17 patients with serial scans obtained during 3 weeks. Each lung was divided into three zones; each zone was evaluated for percentage of lung involvement. Summation of scores from all six lung zones provided overall CT score (maximal CT score, 24).

RESULTS: Median CT scores increased from 1 in the 1st week to 12.5 in the 2nd week. Ground-glass opacities with or without smooth interlobular septal thickening and consolidation were predominant patterns found during the 1st week. Ground-glass opacities with superimposed irregular reticular opacities, mixed pattern, and reticular opacities were noted from the 2nd week and peaked at or after the 4th week. After the 4th week, 12 (55%) of 22 patients had irregular linear opacities with or without associated ground-glass opacities and CT scores greater than 5; five of these patients had bronchial dilatation. When specific opacities were analyzed in 17 patients, consolidation generally resolved completely ($n = 4$) or to minimal residual opacities; six (55%) of 11 patients with ground-glass opacities had substantial residual disease (CT scores > 5) on final scans.

CONCLUSION: There is a temporal pattern of lung abnormalities at thin-section CT in SARS. Predominant findings at presentation are ground-glass opacities and consolidation. Reticulation is evident after the 2nd week and persists in half of all patients evaluated after 4 weeks. Long-term follow-up is required to determine whether the reticulation represents irreversible fibrosis.

© RSNA, 2004

Severe acute respiratory syndrome (SARS) is a form of pneumonia that spread from east Asia to Toronto, Ontario, Canada, through international air travel from Hong Kong and China during February to May 2003 (1). A newly discovered SARS-associated coronavirus (SARS-CoV) has been implicated in the pathogenesis of SARS (2–4). The clinical features of this syndrome have been well documented as a respiratory illness with a prodrome that starts with fever (temperature $> 38^{\circ}\text{C}$ [100.4°F]) associated with malaise and chills followed by a dry nonproductive cough and dyspnea (5–7).

The computed tomographic (CT) findings at presentation usually include unilateral or bilateral ground-glass opacities or areas of consolidation (5,6,8,9). The utility of thin-section CT in the documentation of parenchymal abnormalities in SARS when chest radiographs appear normal or show only questionable abnormalities has also been established (8,9). In their initial description of the epidemiologic, clinical, and radiologic

Longitudinal Lung Changes in 17 Patients with SARS

Patient No./ Sex/Age (y)	Features at Week 1	Features at Week 2	Features at Week 3	Features at Week 4	Features after Week 4
1/F/46	NP	Week 1, consolidation (7)	Week 1, mixed pattern (6)	NP	Week 1, resolution (0)
2/F/52	NP	Week 1, consolidation (2)	Week 1, resolution of consolidation; week 2, ground-glass opacities (15)*	Week 2, ground-glass opacities (8)*	Week 2, ground-glass opacities (6)*
3/F/45	NP	Week 1, ground-glass opacities (24)	Week 1, ground-glass opacities (16)*	Week 1, ground-glass opacities (13)*	Week 1, ground-glass opacities (13)*
4/F/34	NP	Week 1, consolidation (5)	Week 1, ground-glass opacities (5)	Week 1, reticular pattern (3)	NP
5/F/24	Week 1, ground-glass opacities (5)	NP	NP	Week 1, ground-glass opacities (9)*	Week 1, reticular pattern (3)
6/M/42	Week 1, ground-glass opacities (1)	NP	Week 1, mixed pattern; week 2, bronchial dilatation (11)	Week 1, mixed pattern (reduced); week 2, reversed; week 3, new areas of ground-glass opacities (11)	Weeks 1 and 3, reticular pattern (1)
7/M/25	Week 1, consolidation (2)	NP	NP	Week 1, resolution (0)	NP
8/M/52	Week 1, ground-glass opacities (1)	Week 1, ground-glass opacities (14)†	NP	NP	Week 1, reticular pattern; week 2, bronchial dilatation (10)
9/M/47	Week 1, ground-glass opacities (2)	Week 1, mixed pattern; week 2, bronchial dilatation (14)	Week 1, reticular pattern; week 2, bronchial dilatation (10)	Week 1, reticular pattern; week 2, bronchial dilatation (6)	Week 1, reticular pattern; week 2, bronchial dilatation (3)
10/F/48	Week 1, consolidation (8)	NP	NP	Week 1, reticular pattern (3)	NP
11/F/28	Week 1, consolidation (1)	NP	Week 1, ground-glass opacities (10)	Week 1, ground-glass opacities (3)	NP
12/M/46	NP	Week 1, ground-glass opacities (12)‡	NP	NP	Week 1, coarse reticular opacities; week 2, bronchial dilatation (6)
13/M/32	Week 1, ground-glass opacities (1)	Week 1, ground-glass opacities (3)§	NP	NP	Week 1, ground-glass opacities (1)
14/F/36	Week 1, ground-glass opacities (1)§	Week 1, ground-glass opacities; week 2, bronchial dilatation (5)*	Week 1, ground-glass opacities; week 2, bronchial dilatation (9)*	NP	Weeks 1 and 2, resolution (0)
15/M/48	Week 1, ground-glass opacities (19)	NP	NP	Week 1, ground-glass opacities (19)*	NP
16/M/55	NP	Week 1, ground-glass opacities (24)	NP	Week 1, ground-glass opacities (24)¶	Week 1, ground-glass opacities (24)¶
17/M/32	Week 1, consolidation (2)	NP	NP	Week 1, resolution (0)	

Note.—Numbers in parentheses are thin-section CT scores. NP = thin-section CT not performed.

* With irregular linear opacities.

† With smooth interlobular septal thickening, pneumomediastinum, and pneumothorax.

‡ With smooth intralobular septal thickening.

§ With smooth interlobular septal thickening.

¶ With irregular linear opacities, small effusions, pneumomediastinum, and pneumothorax.

features of the first 10 SARS patients, including the index case for Hong Kong, Tsang et al (5) alluded to radiologic features that suggest the development of fibrosis. Thin-section CT evidence of fibrosis has also recently been reported in SARS patients who have been discharged after treatment (9). The aim of this study, therefore, was to evaluate lung abnormalities on serial thin-section CT scans in patients with SARS during the acute and convalescent periods of the illness.

MATERIALS AND METHODS

Patients

All patients with clinically proved SARS who were admitted to Queen Mary Hospital, Hong Kong, China ($n = 28$), and Vancouver General Hospital, British Columbia, Canada ($n = 2$), and who underwent at least two serial thin-section CT evaluations of the thorax were included in this retrospective study. There were 30 patients (mean age, 42.5 years \pm

12.2 [SD]; median, 44 years; range, 24–72 years); 13 were women (mean age, 40.2 years \pm 10.2; median, 45 years; range, 24–56 years) and 17 were men (mean age, 43.2 years \pm 13; median, 43 years; range, 25–72 years). Diagnosis of SARS was established according to the Centers for Disease Control and Prevention and World Health Organization criteria (10,11), which included presence of high fever (temperature, $>38^{\circ}\text{C}$ [100.4°F]), respiratory symptoms (cough, shortness of

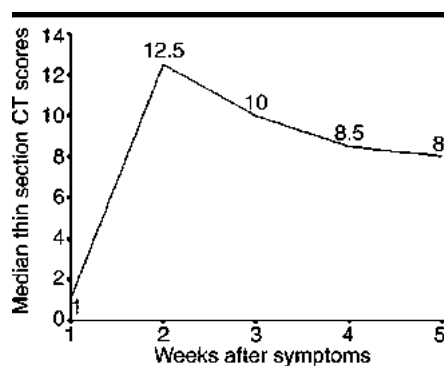


Figure 1. Line graph shows median thin-section CT scores at various time points in weeks after onset of symptoms. Scores peaked at 2nd week of illness, with a slow decline thereafter and substantial scores after the 4th week.

breath, and dyspnea), close contact within 10 days of onset of symptoms with a person who received a diagnosis of SARS, or travel within 10 days of onset of symptoms to an area with documented or suspected community transmission of SARS. Some of the researchers (J.C.M.H., B.L., S.N., K.W.T.T.) noted clinical parameters that included laboratory findings; date of onset of symptoms; indications for the scans; and presence of complications such as pneumomediastinum, pneumothorax, and superimposed infections. In the study, duration of disease refers to time in weeks from onset of symptoms. This study was conducted with institutional review board approval; patient informed consent was not required.

Thin-Section CT Scans

Thin-section CT scans were obtained with the patients in the supine position, and scanning was performed at end inspiration. One unit (HiSpeed Advantage; GE Medical Systems, Milwaukee, Wis) was used in 28 patients with the following parameters: 1.0-mm section thickness, 10-mm gap, 1- or 2-second scanning time per section, 120 kV, and 150 mA. Another unit (Lightspeed plus; GE Medical Systems) was used in one patient with the following parameters: 1.3-mm section thickness, 10-mm gap, 1-second scanning time per section, 120 kV, and 180 mA. A third unit (Toshiba Astreon; Toshiba, Tokyo, Japan) was used in one patient with the following parameters: 1.0-mm section thickness, 10-mm gap, 1-second scanning time per section, 120 kV, and 180 mA. All follow-up scans were obtained by using the same scanner as that used to obtain the initial scans. In the patient who underwent thin-section

CT with 1.3-mm section thickness, the initial scans were spiral. Spiral scans were obtained with the same scanner and the following parameters: 5-mm collimation, 120 kV, 181 mA, pitch of 0.75, scanning interval of 2.5 mm, and table feed of 11.25 mm. The thin-section CT findings at presentation in five patients in the current study were previously reported (9). In 14 of 30 patients, two CT scans were obtained; in 10 patients, three scans; in five patients, four scans; and in one patient, five scans. The images were photographed at lung (window width, 1,000–1,500 HU; window level, –700 HU) and mediastinal (window width, 350 HU; window level, 35–40 HU) settings.

Image Interpretation

Two experienced radiologists at each center (G.C.O. and P.L.K.; N.L.M. and S.N.) reviewed the thin-section CT images on hard copies and reached a decision in consensus. Three of these radiologists (N.L.M., G.C.O., S.N.) had 19, 8, and 6 years of experience in thoracic radiology, respectively, and one (P.L.K.) had 11 years of experience in radiology. The observers categorized the predominant pattern on CT scans as ground-glass opacification (hazy areas of increased attenuation without obscuration of the underlying vessels), consolidation (homogeneous opacification of the parenchyma with obscuration of the underlying vessels), reticular pattern, mixed pattern (combination of consolidation, ground glass opacities, and reticular opacities in the presence of architectural distortion), and honeycomb pattern. Presence of smooth interlobular septal thickening, intralobular lines (lacy pattern within the lobule), and irregular lines and interfaces with architectural distortion superimposed on ground-glass opacities were also noted. Reticular pattern consisted of either coarse linear or curvilinear opacities or fine subpleural reticulation without substantial ground-glass opacities. Presence of irregular or corkscrew bronchial or bronchiolar dilatation associated with any of the previously mentioned findings was noted. On the scans, presence of mediastinal lymphadenopathy (defined as a lymph node ≥ 1 cm in short-axis diameter), pneumothorax, pneumomediastinum, and pleural effusion was also noted.

The distribution of opacities was also noted as being predominantly subpleural (involving mainly the peripheral one-third of the lung), random (without predilection for subpleural or central regions), or diffuse

(continuous involvement without respect to lung segments). After evaluation, the scans were categorized according to the time between the date of onset of symptoms and the date on which the scan was obtained at 1, 2, 3, 4, and longer than 4 weeks after onset of symptoms. Patients with initial scans obtained during the first 2 weeks of the illness and with follow-up scans obtained after a minimum of 3 weeks were selected for further analysis to determine longitudinal changes of main lung abnormalities that were detected.

The extent of disease at thin-section CT was also evaluated. Each lung was divided into three lung zones: upper (above the carina), middle (below the carina up to the inferior pulmonary vein), and lower (below the inferior pulmonary vein) zones. Each lung zone (total of six lung zones) was assigned a score that was based on the following: score 0, 0% involvement; score 1, less than 25% involvement; score 2, 25% to less than 50% involvement; score 3, 50% to less than 75% involvement; and score 4, 75% or greater involvement. Summation of scores provided overall lung involvement (maximal CT score for both lungs was 24).

RESULTS

Clinical Parameters

Thin-section CT scans were obtained during a mean of 22.1 days \pm 10.7 (median, 22 days; range, 3–49 days). The indications for serial scans included clinical deterioration ($n = 7$) and requirement of a change in treatment, whether it included increased dosage of steroids ($n = 8$) or additional immunomodulation therapies ($n = 15$). In some patients, the initial thin-section CT scans were also obtained to confirm airspace disease when radiographs obtained at presentation were normal or slightly abnormal ($n = 10$). The condition in two of these patients deteriorated within 5 days after the initial thin-section CT scans were obtained, and a second thin-section CT scan was thus obtained. The mean time between the time the first and the last thin-section CT scans were obtained for the remaining 28 patients was 9.5 days \pm 2.9, 17.25 days \pm 2.05, 22.8 days \pm 1.3, and 33.4 days \pm 5.8 in four, eight, five, and 11 patients, respectively. Four patients developed pneumomediastinum, with three of them also having pneumothorax, during the 2nd and 3rd weeks of evaluation. Over the course of treatment in the 30 patients only, three patients

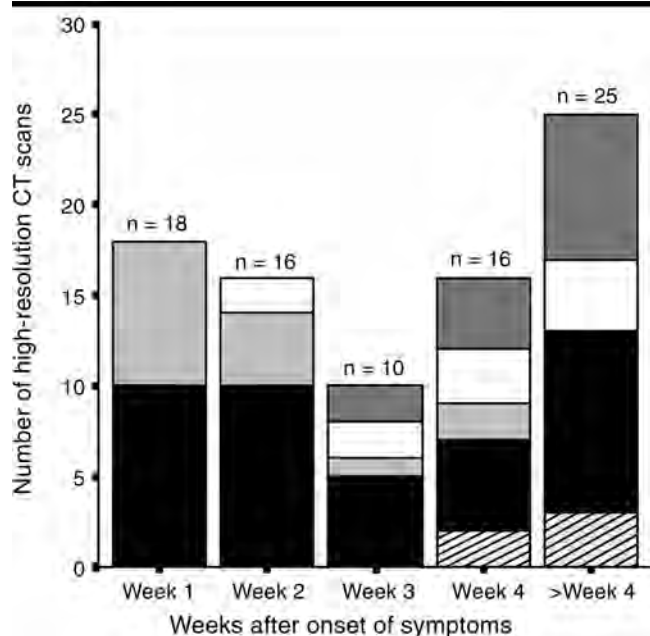


Figure 2. Stacked-bar graph shows distribution of different patterns of lung changes on thin-section CT scans at various time points from onset of symptoms. Dark gray = reticular pattern, white = mixed pattern, light gray = consolidation, black = ground-glass opacities, striped = normal.

developed oral candidiasis, one patient developed coagulase-negative staphylococcal septicemia, and another developed lower urinary tract infection.

Mean alanine aminotransferase and aspartate aminotransferase levels, total white blood cell count, and lymphocyte count at presentation for the 30 patients were $49.82 \text{ U/L} \pm 44.2$ (normal range, 6–53 U/L), $67.5 \text{ U/L} \pm 66.3$ (normal range, 13–33 U/L), $5.968 \times 10^9/\text{L} \pm 1.73$ (normal range, $4\text{--}11 \times 10^9/\text{L}$), and $0.70 \times 10^9/\text{L} \pm 0.3$ (normal range, $1.5\text{--}400.0 \times 10^9/\text{L}$), respectively. There was only one patient with a premorbid lung condition; this patient had childhood asthma. Four others had acute myelogenous leukemia treated with bone marrow transplantation, hypertension, resected renal cell carcinoma, and thyrotoxicosis controlled with medication. The other 25 patients were healthy and did not have a medical history of note prior to contraction of SARS. Coronavirus infection was confirmed in all patients from Hong Kong by means of a fourfold or greater increase in anti-SARS-CoV antibody ($n = 28$) and/or reverse transcriptase polymerase chain reaction positive for SARS-CoV RNA detected in nasopharyngeal aspirates and/or stool specimens ($n = 24$). In the two patients from Vancouver, coronavirus was isolated from respiratory secretions ($n = 1$) or fecal material ($n = 1$).

Thin-Section CT Findings

There was a marked increase in extent of disease during the 2nd week of illness, and the median CT score was 12.5 (range, 2–24). After that time, the extent decreased slowly to a median CT score of 8 (range, 0–24) during week 5, and this decrease reflected the presence of residual disease (Fig 1). The predominant patterns of abnormality changed over time (Fig 2). Within the 1st week after onset of symptoms, the main abnormalities included ground-glass opacities (10 [56%] of 18) and consolidation (eight [44%] of 18). The frequency of ground-glass opacities was highest in the 2nd week (10 [62%] of 16), and it decreased thereafter (Fig 2). Ground-glass opacities alone or with superimposed interlobular septal thickening were most commonly found in the 1st week after onset of symptoms (Figs 3, 4). At the 2nd week, smooth intralobular lines and other superimposed reticular opacities were noted in association with ground-glass opacities (Figs 3, 4). Three of 10 scans with ground-glass opacities in the 2nd week showed a combination of superimposed septal and reticular opacities. Irregular linear opacities and interfaces superimposed on ground-glass

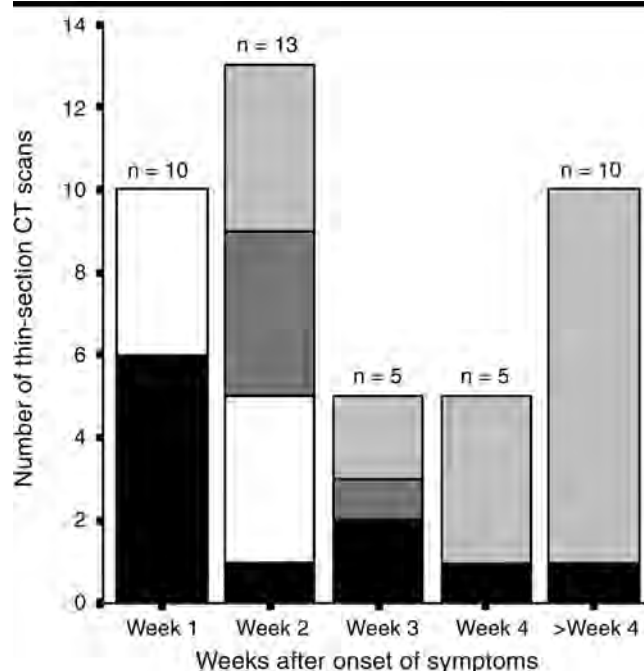


Figure 3. Stacked-bar graph shows distribution of different types of ground-glass opacities on thin-section CT scans at various time points from onset of symptoms. Light gray = ground-glass opacities plus irregular linear opacities, dark gray = ground-glass opacities plus intralobular septal thickening, white = ground-glass opacities plus smooth interlobular septal thickening, black = ground-glass opacities.

opacities accounted for 90% (nine of 10) of all ground-glass opacification found after 4 weeks (Figs 3, 4). The prevalence of consolidation as the predominant abnormality was highest within the 1st week of symptoms and decreased thereafter (Fig 2).

Mixed and predominantly reticular patterns (Fig 4c) were noted from the 2nd week of illness and reached highest proportions on or after the 4th week on three (19%) of 16 and eight (32%) of 25 scans, respectively. There were no scans with a honeycomb pattern or mediastinal lymph nodes at any time point during the evaluation. Small bilateral effusions were present in one patient. Bronchial dilatation was noted on three, three, six, and 10 scans, respectively, at the 2nd, 3rd, 4th, and after the 4th week of illness. These were associated with ground-glass opacities with superimposed irregular linear opacities in nine, mixed pattern in seven, and reticular pattern in six scans. In three scans, the bronchial dilatation was reversed on follow-up scans. Opacities were mainly sited in the subpleural regions of the lungs in the 1st week of disease (13 [72%] of 18) and became more diffuse (five [50%] of

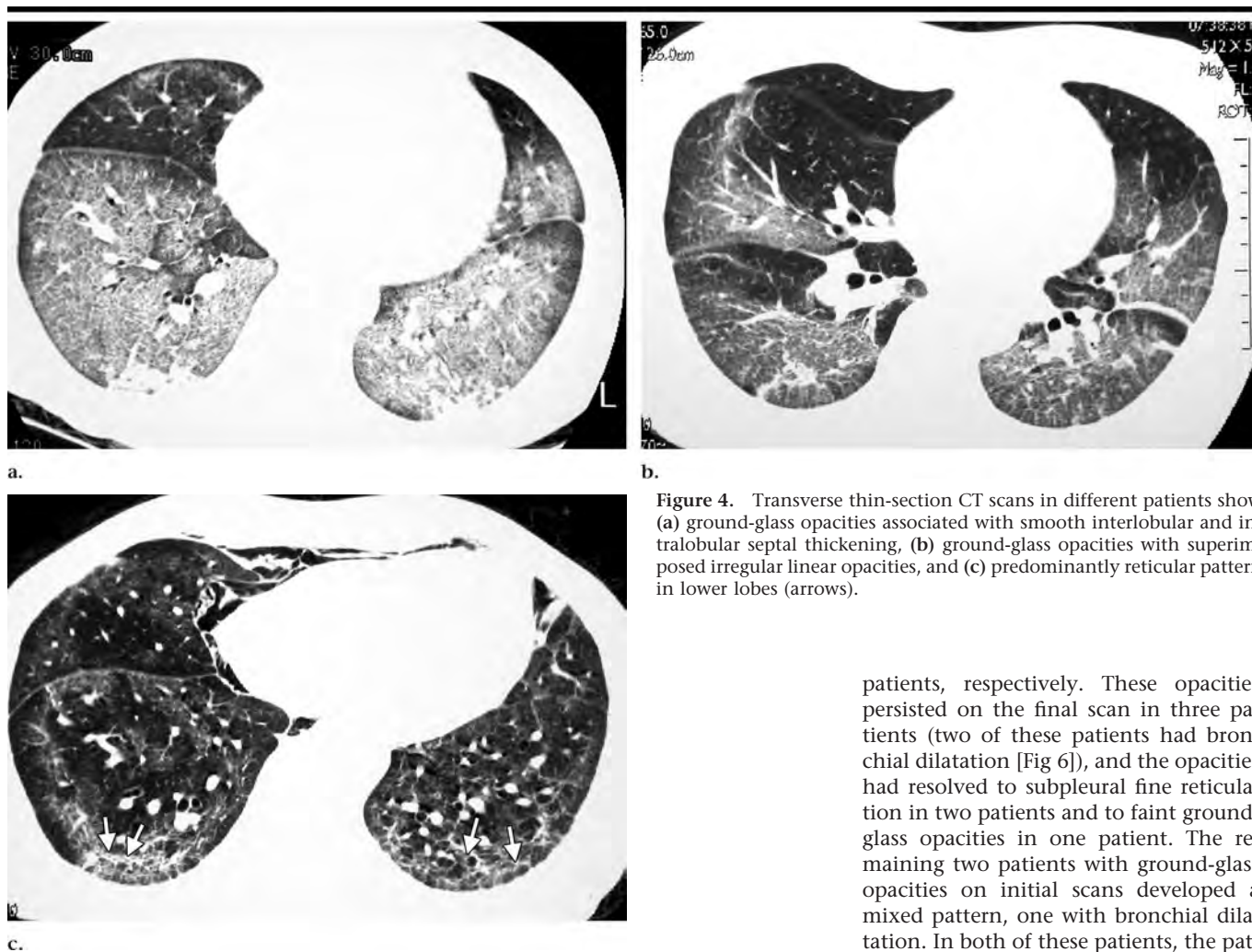


Figure 4. Transverse thin-section CT scans in different patients show (a) ground-glass opacities associated with smooth interlobular and intralobular septal thickening, (b) ground-glass opacities with superimposed irregular linear opacities, and (c) predominantly reticular pattern in lower lobes (arrows).

patients, respectively. These opacities persisted on the final scan in three patients (two of these patients had bronchial dilatation [Fig 6]), and the opacities had resolved to subpleural fine reticulation in two patients and to faint ground-glass opacities in one patient. The remaining two patients with ground-glass opacities on initial scans developed a mixed pattern, one with bronchial dilatation. In both of these patients, the pattern evolved to a reticular one, with reversal of bronchial dilatation observed on the final scans.

Of two patients with reticular opacities superimposed on ground-glass opacities on initial scans, complete resolution occurred in one, whereas a predominantly reticular pattern developed in the remaining patient and was associated with bronchial dilatation and architectural distortion (Fig 7).

In three of seven patients with predominant consolidation on the initial scans, the areas of consolidation resolved completely, although one of these patients developed extensive ground-glass opacities with reticulation in other areas of the lung. One of the seven patients developed a mixed pattern that comprised bandlike consolidation, parenchymal bands, curvilinear septal lines, and ground-glass opacities associated with architectural distortion and bronchial dilatation, and this patient had complete resolution of all features after 3 weeks (Fig 8). In two patients, the areas of consolidation were replaced by fine subpleural

10) at the 3rd week, after which opacities were sited either in the subpleural regions of the lungs or in both a diffuse and subpleural site.

In 24 patients, final thin-section CT scans were obtained at 4 weeks or longer after onset of symptoms. Of these patients, 12 had substantial residual disease (score > 5) and a mean score of 10.7 ± 5.4 (median, 9; range, 5–24), seven had minimal residual opacities (score ≤ 3) and a mean score of 2.21 ± 0.86 (median, 2.5; range, 1–3), and five had normal scans. In those with substantial residual disease, a reticular pattern was noted in five patients, a mixed pattern in two, consolidation in one, and ground-glass opacities with superimposed irregular linear opacities in four. Bronchial and/or bronchiolar dilatation was a feature in five patients. In the seven patients with minimal residual opacities, a subpleural reticular pattern was found in five patients, and small areas of ground-glass opacities with irregular linear opacities

were found in two patients. There was no zonal predominance in the distribution of the residual changes.

Longitudinal Changes of Specific Thin-Section CT Features

The Table summarizes the longitudinal changes in 17 patients in whom initial scans were obtained during the first 2 weeks of illness, and final scans were obtained at least 3 weeks later. In these patients, the initial CT scans demonstrated predominant ground-glass opacities without reticulation (eight scans), ground-glass opacities with reticulation (two scans), and consolidation (seven scans).

Serial thin-section CT scans obtained between the time that initial and final scans were obtained in the eight patients who had ground-glass opacities demonstrated that smooth interlobular septal thickening and irregular linear opacities (Figs 5, 6) had developed in the areas of ground-glass opacities in two and four

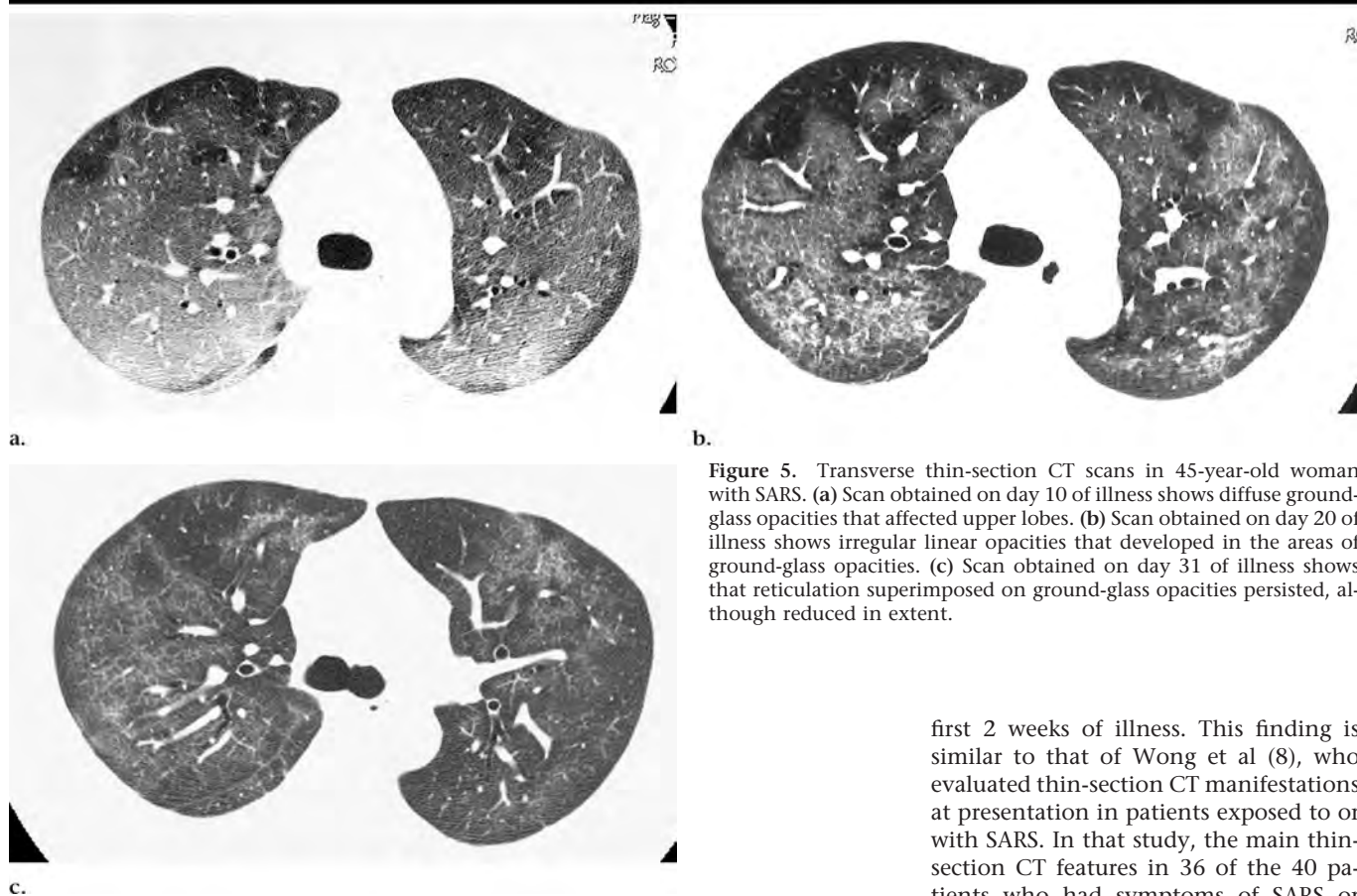


Figure 5. Transverse thin-section CT scans in 45-year-old woman with SARS. (a) Scan obtained on day 10 of illness shows diffuse ground-glass opacities that affected upper lobes. (b) Scan obtained on day 20 of illness shows irregular linear opacities that developed in the areas of ground-glass opacities. (c) Scan obtained on day 31 of illness shows that reticulation superimposed on ground-glass opacities persisted, although reduced in extent.

reticulation; in one patient, these areas were replaced by ground-glass opacities.

Consolidation in the seven patients generally resolved either completely ($n = 4$) or with minimal residual disease ($n = 3$), as denoted by scores of 3 or less. Ground-glass opacities in 11 patients (including patient 2 in whom ground-glass opacities developed in other areas of the lung at week 3) showed complete resolution in one patient, substantial residual opacities (scores > 5) in six patients, and minimal residual disease in four patients.

DISCUSSION

The serial scans obtained in our cohort provided an opportunity to study the longitudinal lung changes in SARS in the acute and convalescent periods. These scans were obtained to aid treatment and hence are heterogeneous in their timing and duration of follow-up. Nevertheless, the scans depict the lung abnormalities at specific time points in the course of the disease from onset of symptoms and allow description of temporal lung changes seen in a subgroup of patients in whom

longitudinal scans were obtained during a minimum of 3 weeks. To our knowledge, this is the first description of a longitudinal thin-section CT series in patients with clinically proved SARS in the acute and convalescent periods.

The extent of parenchymal abnormalities in our cohort of SARS patients increased markedly between the 1st and 2nd weeks after the onset of symptoms. This was followed by a slow decline in scores that reflected residual lung abnormalities at 4 weeks in 50% (12 of 24) of patients. In concordance with initial reports about lung changes in SARS, ground-glass opacities and consolidation were the predominant abnormalities found on thin-section CT scans in our cohort (5–8). These were predominantly subpleural (13 [72%] of 18) in the initial week of illness and became more diffuse (five [50%] of 10) at the 3rd week, after which opacities became distributed either in the subpleural regions of the lungs or were diffuse.

Ground-glass opacities with or without septal thickening or reticular opacities were the commonest pattern during the

first 2 weeks of illness. This finding is similar to that of Wong et al (8), who evaluated thin-section CT manifestations at presentation in patients exposed to or with SARS. In that study, the main thin-section CT features in 36 of the 40 patients who had symptoms of SARS or who were clinically suspected of having SARS were predominantly ground-glass opacities alone or in combination with consolidation. Interlobular septal thickening and intralobular lines were present in 22 and 26, respectively, of their 40 patients. In our study, the number of scans with ground-glass opacities was highest in the 2nd week (10 [63%] of 16) and decreased in the following 2 weeks, with a small upsurge in numbers after the 4th week. This upsurge was accounted for by an increase in ground-glass opacities with superimposed irregular linear opacities and interfaces.

A predominant pattern of consolidation was most common in the first 2 weeks of the illness and was not seen after the 4th week. The areas of consolidation generally either resolved completely or to small areas of fine reticulation. The reticular pattern associated with architectural distortion and bronchial or bronchiolar dilatation was noted to increase progressively from the 3rd week. In addition to this finding, 12 (50%) of 24 final scans obtained 4 weeks or longer after onset of symptoms showed substantial residual disease, consisting predominantly of a reticular pattern or of ground-glass opacities with a superim-

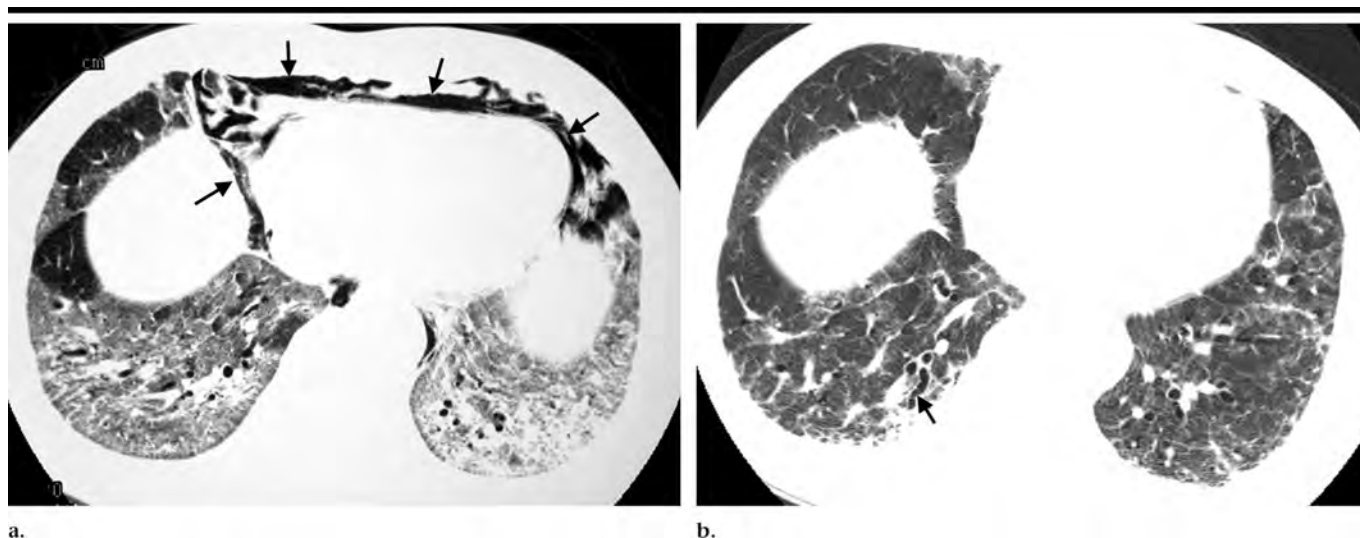


Figure 6. Transverse thin-section CT scans in 52-year-old man with SARS. (a) Scan obtained on day 12 of illness shows pneumomediastinum (arrows) and ground-glass opacities with superimposed irregular linear opacities in both lungs. (b) Follow-up scan obtained on day 37 of illness shows coarse reticular opacities with bronchial dilatation (arrow) and architectural distortion in the same areas.

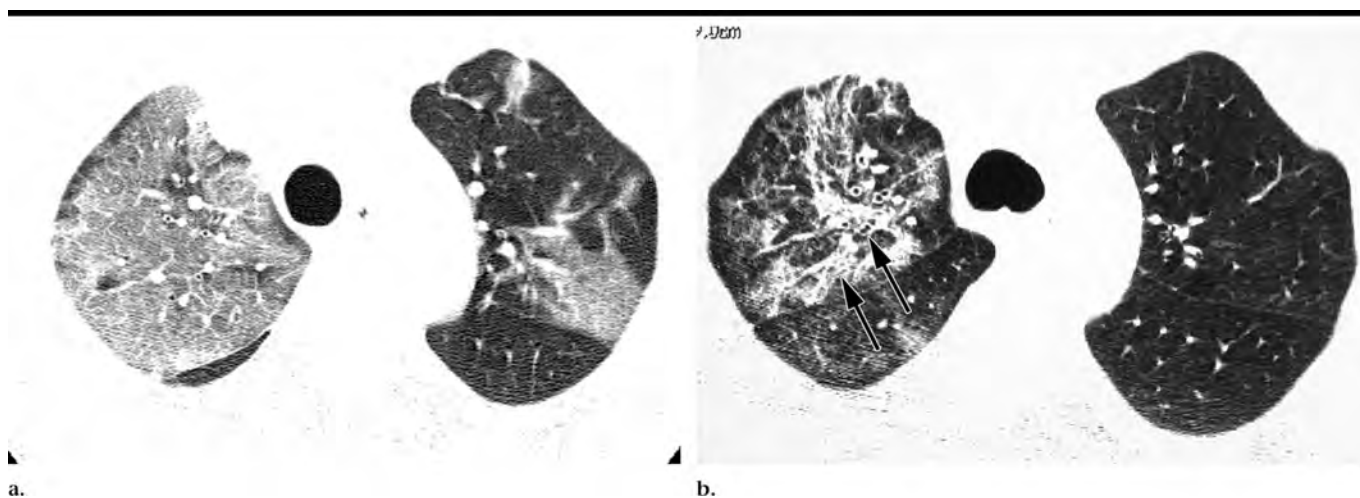


Figure 7. Transverse thin-section CT scans in 32-year-old woman with SARS. (a) Scan obtained on day 8 of illness shows ground-glass opacities predominantly in right upper lobe. (b) Scan obtained on day 30 of illness shows coarse reticular opacities that developed in right upper lobe, with bronchial dilatation (arrows) and architectural distortion.

posed reticular pattern. Bronchial or bronchiolar dilatation was an associated feature in five (42%) of these 12 scans. When specific opacities in a subgroup of 17 patients were analyzed, consolidation in general either resolved completely or decreased to minimal areas of residual opacities. However, six (55%) of 11 scans with ground-glass opacities showed a substantial amount of residual disease after 3 weeks or longer.

These findings indicate that a proportion of patients develop persistent lung changes that may suggest the development of fibrosis, although ground-glass opacities are largely reversible in SARS

(12). Antonio et al (9) studied 24 SARS patients discharged from the hospital after treatment who had undergone thin-section CT; they observed that 15 (62%) of the patients had evidence of fibrosis. These were described to be parenchymal bands, traction bronchiectasis, and irregular interfaces. However, since the natural history of SARS is as yet uncharted, it may be too early to label the lung abnormalities found as irreversible fibrosis. Features that were reversible were bandlike consolidation and parenchymal bands, terms that generally described the mixed pattern found in our patients. The parenchymal bands probably represent subseg-

mental atelectasis that was reversed with resolution of inflammation with reexpansion of alveoli. Similarly, resolution of interstitial edema and cellular infiltration, particularly of interlobular septa, could also explain resolution of subpleural curvilinear lines noted.

In a recent publication (13) about post-mortem results in six fatal cases of SARS, with mean disease duration of 16.8 days \pm 5.3 (median, 17 days; range, 8–24 days), fibrosis was not observed in the lungs, although diffuse alveolar damage was noted in cases with duration of illness longer than 10 days. Macrophages, however, featured strongly as the main

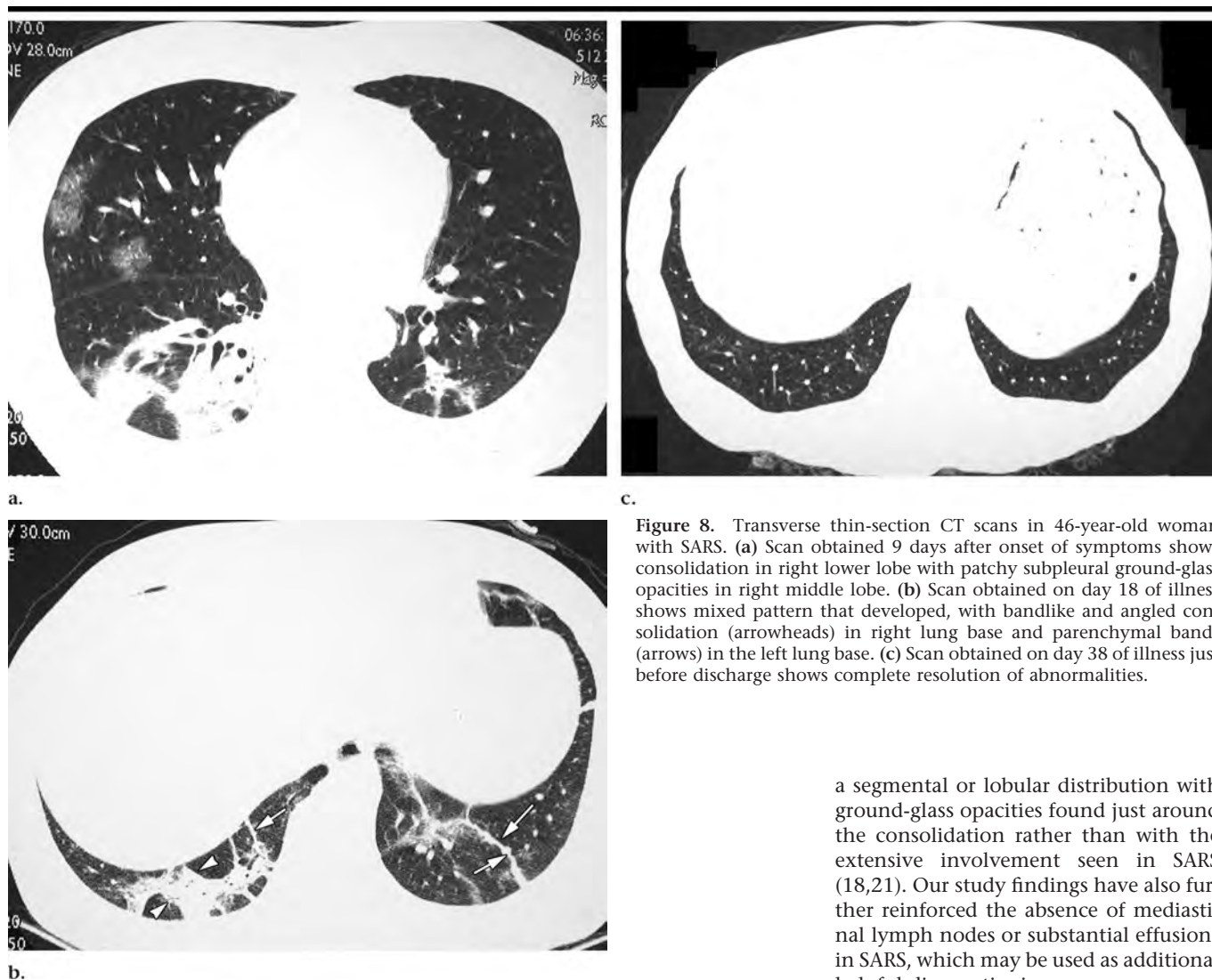


Figure 8. Transverse thin-section CT scans in 46-year-old woman with SARS. (a) Scan obtained 9 days after onset of symptoms shows consolidation in right lower lobe with patchy subpleural ground-glass opacities in right middle lobe. (b) Scan obtained on day 18 of illness shows mixed pattern that developed, with bandlike and angled consolidation (arrowheads) in right lung base and parenchymal bands (arrows) in the left lung base. (c) Scan obtained on day 38 of illness just before discharge shows complete resolution of abnormalities.

neutrophil infiltrate in the alveoli and interstitium of these fatal cases, even in those with early disease, which suggests that proinflammatory cytokines released by macrophages may underlie the pathogenesis of SARS (13). The macrophage and cellular infiltrates may also explain the predominant pattern of ground-glass opacities noted in the lungs at thin-section CT in our patients.

Thin-section CT features of SARS are not specific and could be found in other airspace diseases such as bronchiolitis obliterans organizing pneumonia, particularly in the initial phase of the illness when the ground-glass opacities and consolidation are primarily subpleural (14,15). When diffuse change develops in SARS, the thin-section CT and radiographic appearances may be indistinguishable from acute respiratory distress syndrome (5,16). Similarly the presence of smooth inter-

lobular septal thickening superimposed on extensive ground-glass opacities can also be found in other conditions—primarily alveolar proteinosis, pulmonary edema, and hemorrhage—and also in other types of bacterial or viral pneumonia, such as herpes simplex and cytomegalovirus infections (17–20).

There were no patients with peribronchiolar consolidation, bronchopneumonia, and nodules—particularly centrilobular and tree-in-bud opacities—in our cohort. The absence of these thin-section CT features may serve to distinguish SARS from other types of atypical pneumonia, particularly pneumonia of viral or *Mycoplasma* origins, and infectious bronchiolitis (17–21). The predominance of ground-glass opacities over consolidation may allow differentiation of SARS from bacterial pneumonia, which characteristically manifests as consolidation in

a segmental or lobular distribution with ground-glass opacities found just around the consolidation rather than with the extensive involvement seen in SARS (18,21). Our study findings have also further reinforced the absence of mediastinal lymph nodes or substantial effusions in SARS, which may be used as additional helpful diagnostic signs.

It should be noted, however, that our patients probably represent those at the severe end of the disease spectrum, primarily hospitalized patients, who also have developed appropriate indications or complications to justify serial evaluations with thin-section CT. Hence, natural selection bias may have been introduced into the study design. The absence of scans obtained in the prone position is another limitation of the study, particularly with reference to bandlike opacities in the lung bases, which could have represented atelectasis that may have been observed as reversible on scans obtained in the prone position had they been obtained. Other limitations include the nonuniform scanning intervals among all patients caused by the retrospective nature of this study. However, because SARS is highly infectious, it would have been inappropriate and against institutional infection-control policy to systematically evaluate all SARS patients. Thin-

section CT should be reserved for patients in whom a diagnosis is uncertain or for patients with clinical deterioration in whom further evaluation of lung abnormalities is required.

We conclude that there is a temporal pattern of lung abnormalities in SARS, and the abnormalities increased considerably at the 2nd week of illness and were observed at thin-section CT; these abnormalities resulted in substantial residual disease in 50% (12 of 24) of patients at 4 weeks or longer after disease onset. Of these 24 patients, 21% (five) had normal scans and 29% (seven) had minimal residual abnormalities. The residual abnormalities most commonly consisted of a reticular pattern with or without associated ground-glass opacities and bronchial or bronchiolar dilatation. Long-term follow-up with thin-section CT and concomitant functional studies are required to determine the long-term pulmonary sequelae of SARS.

References

1. Severe acute respiratory syndrome: travel. Available at: www.who.int/csr/sars/travel/en/. Accessed 2003.
2. Severe acute respiratory syndrome (SARS): update on SARS etiology, primers for SARS virus, laboratory testing for SARS, Archives [serial online]. April 2003. Available at: www.who.int/csr/sars/archive/en/. Accessed May 28, 2003.
3. Peiris JS, Lai ST, Poon LL, et al. Coronavirus as a possible cause of severe acute respiratory syndrome. *Lancet* 2003; 361: 1319–1325.
4. Fouchier RA, Kuiken T, Schutten M, et al. Aetiology: Koch's postulates fulfilled for SARS virus. *Nature* 2003; 423:240.
5. Tsang KW, Ho PL, Ooi GC, et al. A cluster of cases of severe acute respiratory syndrome in Hong Kong. *N Engl J Med* 2003; 348:1977–1985.
6. Lee N, Hui D, Wu A, et al. A major outbreak of severe acute respiratory syndrome in Hong Kong. *N Engl J Med* 2003; 348:1986–1994.
7. Müller NL, Ooi GC, Khong PL, Nicolaou S. Severe acute respiratory syndrome: radiographic and CT findings. *AJR Am J Roentgenol* 2003; 181:3–8.
8. Wong KT, Antonio GE, Hui DS, et al. Thin-section CT of severe acute respiratory syndrome: evaluation of 73 patients exposed to or with the disease. *Radiology* 2003; 228:395–400.
9. Antonio GE, Wong KT, Hui DSC, et al. Thin-section CT in patients with severe acute respiratory syndrome following hospital discharge: preliminary experience. *Radiology* 2003; 228:810–815.
10. Severe acute respiratory syndrome (SARS) updated interim case definition. Atlanta, Ga: Centers for Disease Control and Prevention, 2003. Available at: www.cdc.gov/ncidod/sars/casedefinition.htm. Accessed May 29, 2003.
11. Severe acute respiratory syndrome (SARS): case definitions for surveillance of severe acute respiratory syndrome (SARS) revised 1st May 2003. Available at: www.who.int/csr/sars/en/. Accessed May 29, 2003.
12. Remy-Jardin M, Giraud F, Remy J, Copin MC, Gosselin B, Duhamel A. Importance of ground-glass attenuation in chronic diffuse infiltrative lung disease: pathologic-CT correlation. *Radiology* 1993; 189:693–698.
13. Nicholls JM, Poon LL, Lee KC, et al. Lung pathology of fatal severe acute respiratory syndrome. *Lancet* 2003; 361:1773–1778.
14. Bouchardy LM, Kuhlman JE, Ball WC, Hruban RH, Askin FB, Siegelman SS. CT findings in bronchiolitis obliterans organizing pneumonia (BOOP) with radiographic, clinical and histologic correlation. *J Comput Assist Tomogr* 1993; 17: 352–357.
15. Müller NL, Guerry-Force ML, Staples CA, et al. Differential diagnosis of bronchiolitis obliterans with organizing pneumonia and usual interstitial pneumonia: clinical, functional and radiologic findings. *Radiology* 1987; 162:151–156.
16. Nicolaou S, Al-Nakshabandi NA, Müller NL. SARS: imaging of severe acute respiratory syndrome. *AJR Am J Roentgenol* 2003; 180:1247–1249.
17. Johkoh T, Itoh H, Müller NL, et al. Crazy-paving appearance at thin-section CT: spectrum of disease and pathologic findings. *Radiology* 1999; 211:155–160.
18. Tanaka N, Matsumoto T, Kuramitsu T, et al. High resolution CT findings in community-acquired pneumonia. *J Comput Assist Tomogr* 1996; 20:600–608.
19. Kim EA, Lee KS, Primack SL, et al. Viral pneumonias in adults: radiologic and pathologic findings. *RadioGraphics* 2002; 22 (special issue):S137–S149.
20. McGuinness G, Scholes JV, Garay SM, Leitman BS, McCauley DI, Naidich DP. Cytomegalovirus pneumonitis: spectrum of parenchymal CT findings with pathologic correlation in 21 AIDS patients. *Radiology* 1994; 192:451–459.
21. Reittner P, Ward S, Heyneman L, Johkoh T, Müller NL. Pneumonia: high-resolution CT findings in 114 patients. *Eur Radiol* 2003; 13:515–521.

Explosion in mortality in the Amazonian epicenter of the COVID-19 epidemic

Explosão da mortalidade no epicentro amazônico da epidemia de COVID-19

Explosión de la mortalidad en el epicentro amazónico de la epidemia de COVID-19

Jesem Douglas Yamall Orellana ¹

Geraldo Marcelo da Cunha ²

Lihsieh Marrero ³

Bernardo Lessa Horta ⁴

Iuri da Costa Leite ²

doi: 10.1590/0102-311X00120020

Abstract

Manaus, the capital of the Brazilian State of Amazonas, is the current epicenter of the COVID-19 epidemic in Amazonia. The sharp increase in deaths is a huge concern for health system administrators and society. The study aimed to analyze excess overall mortality according to Epidemiological Week (EW) in order to identify changes potentially associated with the epidemic in Manaus. Overall and cause-specific mortality data were obtained from the Central Database of the National Civil Registry and the Mortality Information System for 2018, 2019, and 2020. The study analyzed age bracket, sex, place of death, EW, calendar year, and causes of death. Ratios were calculated between deaths in 2019/2018 and 2020/2019 to estimate excess deaths, with 5% confidence intervals. No significant excess overall mortality was seen in the ratios for 2019/2018, independently of EW. Meanwhile, the ratios for 2020/2019 increased from 1.0 (95%CI: 0.9-1.3) in EW 12 to 4.6 (95%CI: 3.9-5.3) in EW 17. Excess overall mortality was observed with increasing age, especially in individuals 60 years or older, who accounted for 69.1% (95%CI: 66.8-71.4) of the deaths. The ratios for 2020/2019 for deaths at home or on public byways were 1.1 (95%CI: 0.7-1.8) in EW 12 and 7.8 (95%CI: 5.4-11.2) in EW 17. The explosion in overall mortality in Manaus and the high proportion of deaths at home or on public byways reveals the epidemic's severity in contexts of heavy social inequality and weak effectiveness of government policies, especially policies meant to deal with social inequalities and strengthen the Unified Health System.

COVID-19; Vulnerable Populations; Public Health Surveillance; Mortality

Correspondence

J. D. Y. Orellana

Instituto Leônidas e Maria Deane, Fundação Oswaldo Cruz.

Rua Teresina 476, 2º andar, sala 203, Manaus, AM

69057-070, Brasil.

jesem.orellana@fiocruz.br

¹ Instituto Leônidas e Maria Deane, Fundação Oswaldo Cruz, Manaus, Brasil.

² Escola Nacional de Saúde Pública Sergio Arouca, Fundação Oswaldo Cruz, Rio de Janeiro, Brasil.

³ Universidade do Estado do Amazonas, Manaus, Brasil.

⁴ Centro de Pesquisas Epidemiológicas, Universidade Federal de Pelotas, Pelotas, Brasil.



This article is published in Open Access under the Creative Commons Attribution license, which allows use, distribution, and reproduction in any medium, without restrictions, as long as the original work is correctly cited.

Introduction

As of May 20, 2020, two months after the World Health Organization (WHO) declared COVID-19 a pandemic, some five million cases and approximately 320,000 deaths had been reported in 216 countries/areas/territories. Even with strong evidence of underestimation of its official statistics ¹, Brazil is now the third most heavily affected country, with 280,000 cases and 18,000 deaths (World Health Organization. WHO coronavirus disease (COVID-19) dashboard. <https://covid19.who.int/>, accessed on 20/May/2020).

Distribution of COVID-19 mortality reflects Brazil's social and geographic heterogeneity, with five states accounting for 81% of the deaths: São Paulo, Rio de Janeiro, Ceará, Pernambuco, and Amazonas, the latter having the highest proportion of infected individuals, with 10.6% (95%CI: 8.8-12.1) ².

The State of Amazonas is located in the Brazilian Amazonia, a region occupying approximately 60% of Brazil's territory and whose population has been exposed historically to poverty and social inequality ³. A study on the Greater Metropolitan Area of Manaus identified extensive inequality in access to health services ⁴. This is a common reality for populations living in remote areas and on indigenous lands ⁵, whose social and economic vulnerability limits their mobility in the territory, making them more susceptible to the dramatic spread of COVID-19, especially in the more serious forms of the disease.

For more than four weeks, Manaus has shown signs of exhaustion of the public hospital network due to the rapid increase in COVID-19 cases. In the first two weeks of May alone, there were nearly 7,000 new cases, double the number identified until then. In addition, from April 19 to 28, the average daily number of burials in Manaus was 123, four times more than the daily average in the same period in 2019 ⁶. The average daily number of COVID-19 deaths confirmed by health services during the same period was only 14, suggesting extensive underreporting, a problem seen elsewhere in the world, especially in places with precarious testing and deficient health services ^{7,8}.

Despite uncertainties on COVID-19-specific mortality ⁹, indicators of excess deaths are one of the most objective and comparable parameters to assess the epidemic's impact on mortality ¹⁰. This study thus aimed to analyze excess overall mortality according to Epidemiological Week (EW) in order to identify changes in the risk of death potentially associated with the epidemic.

Methods

Study design and data sources

This was a cross-sectional study with mortality data from the Central Database of the National Civil Registry (National CRC. <https://sistema.registrocivil.org.br>) and the Mortality Information System (SIM. <http://www2.datasus.gov.br>).

Due to the pandemic scenario, the National CRC assembled a COVID-19 Registration Panel (Portal da Transparência. <https://transparencia.registrocivil.org.br/registrar-COVID>, accessed on 10/May/2020), aimed at furnishing data on causes of death from Death Certificates recorded at notary public offices, which represents the totality of natural deaths, treated here as a proxy for general mortality. The data are updated daily and comply with legal guidelines and deadlines. The time between recording of the death and its transfer to the COVID-19 Registration Panel is 14 days or less, after which the data become public.

Working definitions

According to the National CRC criteria, a suspected or confirmed death from COVID-19 is one in which the death certificate mentions the terms COVID-19, coronavirus, or novel coronavirus in sections I (lines a, b, c, d) or II (other preexisting disease conditions not directly related to the death and not recorded in the causal sequence listed in part I). Besides COVID-19, other possible causes were considered based on the National CRC: severe acute respiratory syndrome (SARS); pneumonia; septicemia; and respiratory failure. Deaths not classified in any of the above-mentioned conditions

were included in the category “other causes”. Finally, “indeterminate” deaths (causes of deaths related to respiratory causes, but inconclusive) accounted for fewer than 1% of the sample and were not presented separately.

The National CRC data were updated on May 19, 2020, 66 days after the start of EW 12 and 24 days after the last day of EW 17. The start of EW 12 corresponds to the two days after confirmation of the first case of COVID-19 and to the 15 days prior to the first death from COVID-19 in Manaus.

For purposes of comparison, we also used data on overall mortality from the SIM, furnished for the EW in question in 2018 in the city of Manaus.

Study variables

The study variables were age bracket, sex, death at home or on public byways, EW, calendar year, and causes of death. Deaths from SARS, pneumonia (PNM), and respiratory failure (RF) were aggregated in a variable called “SARS+PNM+RF”, which excludes the group of deaths suspected or confirmed by COVID-19 and according to the criteria of the National CRC.

Data analysis

We calculated the ratios between deaths in 2019 and 2018 (2019/2018) and in 2020 and 2019 (2020/2019), in EW 12 to 17 in Manaus. We also calculated the ratios between deaths in 2020/2019 in EW 14 to 17, stratified by sex, age bracket, and cause of death. For the mortality ratios, we calculated confidence intervals with 5% significance. The analyses were performed in the R program, version 3.6.1 (<http://www.r-project.org>).

Results

In 2018, according to the SIM, the mean weekly number of deaths in Manaus was 230, close to the weekly number observed in the first 70 days of 2019 and 2020 according to data from the National CRC, or 225 and 218 deaths, respectively.

As shown in Figure 1, the overall mortality ratio for 2019/2018 is very close to one, independently of EW, while the ratio 2020/2019 only showed a similar pattern (close to one) from EW 12 to 14, with a major increase in the subsequent weeks. In other words, the ratio increased from 1.0 (95%CI: 0.9-1.3) in EW 12 to 4.6 (95%CI: 3.9-5.3) in EW 17.

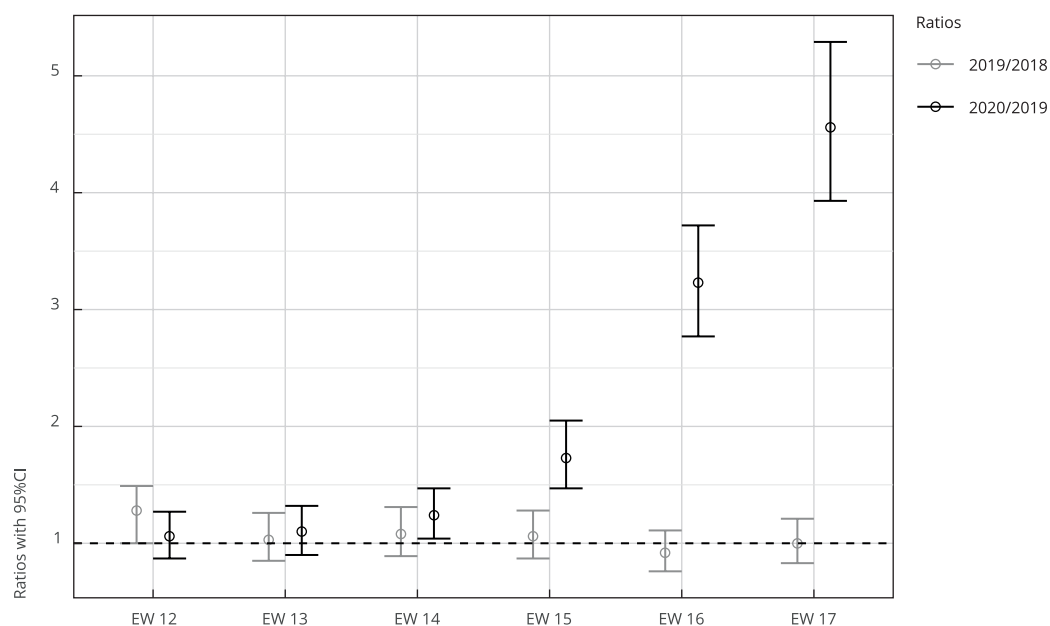
The overall mortality ratios for 2020/2019 according to age bracket were not statistically significant in males under 40 years of age or females under 30 years of age, revealing the excess mortality from those age brackets upwards in 2020, especially in males (Table 1).

When comparing the 2020/2019 mortality ratio according to groups of causes of death, the data showed a gradual increase over the weeks, especially starting in EW 15, for deaths from “SARS+PNM+RF” (Figure 2). In the group of “other causes”, the mortality ratio remained close to one until EW 14, when it increased, reaching a ratio of 3 by EW 17.

As for the distribution of deaths across age brackets, 69.1% of the deaths occurred in individuals 60 years or older (95%CI: 66.8-71.4). The ratio of deaths occurring at home or on public byways (43/38) in EW 12 was 1.1 (95%CI: 0.7-1.8). This same ratio (268/33) reached 8.1 (95%CI: 5.7-11.7) in EW 17 (data not shown).

Figure 1

Overall mortality ratios for the years 2019/2018 and 2020/2019 by Epidemiological Week (EW). Manaus, Amazonas State, Brazil.



Sources: Civil Registry National Database (National CRC. <https://sistema.registrocivil.org.br>) and Mortality Information System (SIM. <http://www2.datasus.gov.br>).

Table 1

Overall mortality and respective ratios and confidence intervals for Epidemiological Weeks (EW) 14 to 17, according to age bracket and sex. Manaus, Amazonas State, Brazil.

Sex/Age bracket (years)	2020 (n)	2019 (n)	Ratio	95%CI
Male				
0-9	51	61	0.84	0.58-1.21
10-19	9	6	1.50	0.53-4.21
20-29	35	27	1.30	0.78-2.14
30-39	54	37	1.46	0.96-2.22
40-49	110	38	2.89	2.00-4.19
50-59	195	42	4.64	3.33-6.48
60-69	315	87	3.62	2.86-4.59
70-79	332	91	3.65	2.89-4.60
80 and over	317	89	3.56	2.82-4.50
All	1,418	478	2.97	2.67-3.29

(continues)

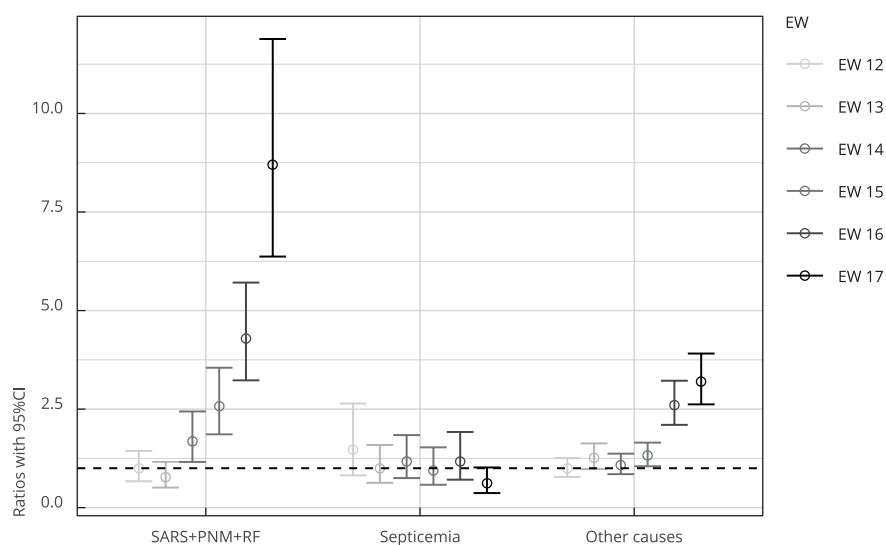
Table 1 (continued)

Sex/Age bracket (years)	2020 (n)	2019 (n)	Ratio	95%CI
Female				
0-9	48	48	1.00	0.67-1.49
10-19	3	8	0.38	0.10-1.41
20-29	15	11	1.36	0.63-2.97
30-39	30	12	2.50	1.28-4.89
40-49	65	28	2.32	1.50-3.62
50-59	94	38	2.47	1.69-3.61
60-69	175	47	3.72	2.70-5.14
70-79	185	79	2.34	1.80-3.05
80 and over	263	108	2.44	1.95-3.04
All	878	379	2.32	2.05-2.61
Both sexes				
0-9	99	109	0.91	0.69-1.19
10-19	12	14	0.86	0.40-1.85
20-29	50	38	1.32	0.86-2.01
30-39	84	49	1.71	1.21-2.43
40-49	175	66	2.65	1.99-3.50
50-59	289	80	3.61	2.82-4.63
60-69	490	134	3.66	3.02-4.43
70-79	517	170	3.04	2.56-3.62
80 and over	580	197	2.94	2.50-3.46
All	2,296	857	2.68	2.48-2.90

Source: Civil Registry National Database (National CRC. <https://sistema.registrocivil.org.br>) .

Figure 2

Mortality ratios by specific groups of causes for the years 2020/2019 by Epidemiological Week (EW). Manaus, Amazonas State, Brazil.



SARS+PNM+RF: severe acute respiratory syndrome + pneumonia + respiratory failure.

Sources: Civil Registry National Database (National CRC. <https://sistema.registrocivil.org.br>) and Mortality Information System (SIM. <http://www2.datasus.gov.br>).

Discussion

According to the results, total deaths reported in 2019 were similar to 2018, comparing EW 12 through 17 in those two years. However, the comparison between total deaths in 2020 and 2019 revealed excess mortality starting in the 15th EW of 2020, with the ratio exploding in EW 17, when the number of deaths was 200% higher than in 2019.

The increase in deaths started in EW 15, approximately 15 days after confirmation of the first 30 cases of COVID-19 in Manaus. In EW 17, the anomalous number of deaths coincided with the collapse in the public hospital system. During this period, the mean number of burials per day tripled. Deaths at home or on public byways also increased, as did COVID-19 cases in neighboring municipalities. This set of events probably resulted from a major acceleration in the epidemic in Manaus ¹¹ in the previous weeks.

The fragility of the healthcare network in Manaus and in neighboring municipalities ⁴, combined with extensive social inequality ³, help explain the critical situation with the COVID-19 epidemic. Excess mortality in the pandemic is not limited to low- and middle-income countries, but has also appeared in New York City, United States, and in the provinces of Bergamo and Brescia in northern Italy ^{9,12,13}.

In relation to age, nearly 70% of the deaths occurred in persons 60 years or older, consistent with studies in other countries ^{9,12,13,14}. In this age bracket, comorbidities are more prevalent and have been associated with worse prognosis in cases of hospitalization for COVID-19 ¹⁵.

Another key aspect involves gender differences, with a higher risk of mortality among men, corroborating findings from other studies ^{16,17}. Lower case-fatality may be associated with women's heightened perception of the symptoms and search for health services, whereas men would only tend to turn to health services in the more serious stages of COVID-19, when therapeutic possibilities are more limited. However, Zeng et al. ¹⁸ argued that higher IgG antibody levels in women could partially explain the relatively higher case-fatality in men.

There was an explosive increase in mortality from respiratory problems (SARS+PNM+RF), common complications of COVID-19 ¹⁴, during the COVID-19 pandemic. There was also a significant increase in mortality from other causes, possibly resulting from factors such as: the patient's postponement of treatment in order to avoid exposure to the virus in hospitals, health services' prioritization of care for COVID-19 patients ¹⁹.

One strength of this study was the use of the overall mortality indicator to estimate excess deaths, which appears to be a useful resource for rapid and low-cost evaluations, besides serving as a more robust and comparable indicator in a pandemic scenario ¹⁰. Unlike COVID-19-specific mortality, overall mortality does not depend on testing strategies, health systems' organization and financing, demographic structure, or the choice of denominator, which can make the case-fatality estimates vary widely ⁹. However, the interpretation of this study's results should take some limitations into account, such as the lack of standardization or review of the causes of death on the death certificates and a possible under-recording of deaths on the digital platform of the National CRC, especially in 2019, which could overestimate the ratios between total deaths in 2020 and 2019, for example. However, judging by the comparisons between total deaths in 2019 and 2018, where the ratios were always close to one, this distortion may possibly be small.

The analytical strategy adopted in this study unequivocally reveals the high excess mortality in Manaus and the epidemic's severity in contexts of great social inequality, weak effectiveness of public policies, and fragility in health services. Efforts must be stepped up by administrators at the municipal, state, and federal levels to contain or mitigate the harmful effects of COVID-19, especially in more vulnerable areas where the pandemic tends to have a heavier impact on mortality.

Contributors

J. D. Y. Orellana, G. M. Cunha and I. C. Leite participated in the study's conception, interpretation, and final drafting of the manuscript. L. Marrero and B. L. Horta participated in the interpretation and final drafting of the manuscript.

Additional informations

ORCID: Jesem Douglas Yamall Orellana (0000-0002-5607-2615); Geraldo Marcelo da Cunha (0000-0001-7128-933X); Lihsieh Marrero (0000-0002-2856-5682); Bernardo Lessa Horta (0000-0001-9843-412X); Iuri da Costa Leite (0000-0002-9136-8948).

References

1. The Lancet. COVID-19 in Brazil: "so what?". Lancet 2020; 395:1461.
2. Mellan TA, Hoeltgebaum HH, Mishra S, Whitaker C, Schnekenberg RP, Gandy A, et al. Estimating COVID-19 cases and reproduction number in Brazil. London: Imperial College London; 2020. (Report 21).
3. Waisbich LT, Shankland A, Bloom G, Coelho VSP. Introduction. The accountability politics of reducing health inequalities: learning from Brazil and Mozambique. Novos Estudos CEBRAP 2019; 38:271-89.
4. GalvãoTF, Tiguman GMB, Caicedo RM, Silva MT. Inequity in utilizing health services in the Brazilian Amazon: a population-based survey, 2015. Int J Health Plann Manage 2019; 34:e1846-53.
5. Ferrante L, Fearnside PM. Protect indigenous peoples from COVID-19. Science 2020; 368:251.
6. Prefeitura de Manaus. Manaus registra quase 2,5 mil sepultamentos em abril. <http://www.manaus.am.gov.br/noticia/manaus-registra-quase-25-mil-sepultamentos-em-abril/> (accessed on 10/May/2020).
7. Ji Y, Ma Z, Peppelenbosch MP, Pan Q. Potential association between COVID-19 mortality and health-care resource availability. Lancet Glob Health 2020; 8:e480.
8. Castro MC, Carvalho LR, Chin T, Kahn R, Franca GV, Macario EM, et al. Demand for hospitalization services for COVID-19 patients in Brazil. medRxiv 2020; 1 apr. <https://www.medrxiv.org/content/10.1101/2020.03.30.20047662v1>.
9. Onder G, Rezza G, Brusaferro S. Case-fatality rate and characteristics of patients dying in relation to COVID-19 in Italy. JAMA 2020; [Online ahead of print].
10. Leon DA, Shkolnikov VM, Smeeth L, Magnus P, Pechholdová M, Jarvis CI. COVID-19: a need for real-time monitoring of weekly excess deaths. Lancet 2020; 395:e81.
11. Programa de Pós-graduação em Ciências do Ambiente e Sustentabilidade na Amazônia, Universidade Federal do Amazonas. Atlas dos objetivos de desenvolvimento sustentável no Amazonas. (Especial COVID-19, 2). <https://edoc.ufam.edu.br/handle/123456789/3198/> (accessed on 03/May/2020).
12. Weinberger D, Cohen T, Crawford F, Mostashari F, Olson D, Pitzer VE, et al. Estimating the early death toll of COVID-19 in the United States. medRxiv 2020; 29 apr. <https://www.medrxiv.org/content/10.1101/2020.04.15.20066431v2>.
13. Ghislandi S, Muttarak R, Sauerberg M, Scotti B. News from the front: excess mortality and life expectancy in two major epicentres of the COVID-19 pandemic in Italy. medRxiv 2020; 13 may. <https://www.medrxiv.org/content/10.1101/2020.04.29.20084335v2>.
14. Shi S, Qin M, Shen B, Cai Y, Liu T, Yang F, et al. Association of cardiac injury with mortality in hospitalized patients with COVID-19 in Wuhan, China. JAMA Cardiol 2020; e200950.
15. Dietz W, Santos-Burgoa C. Obesity and its implications for COVID-19 mortality. Obesity (Silver Spring) 2020; 28:1005.
16. Ciminelli G, Garcia-Mandicó S. COVID-19 in Italy: an analysis of death registry data. VOX 2020; 22 apr. <https://voxeu.org/article/covid-19-italy-analysis-death-registry-data>.
17. Huang C, Wang Y, Li X, Ren L, Zhao J, Hu Y, et al. Clinical features of patients infected with 2019 novel coronavirus in Wuhan, China. Lancet 2020; 395:497-506.
18. Zeng F, Dai C, Cai P, Wang J, Xu L, Li J, et al. A comparison study of SARS-COV-2 IgG antibody between male and female COVID-19 patients: a possible reason underlying difference outcome between gender. medRxiv 2020; 27 mar. <https://www.medrxiv.org/content/10.1101/2020.03.26.20040709v1>.
19. Vadoros S. Excess mortality during the COVID-19 pandemic: early evidence from England and Wales. medRxiv 2020; 17 may. <https://www.medrxiv.org/content/10.1101/2020.04.14.20065706v6>.

Resumo

Manaus, capital do estado brasileiro do Amazonas, é o atual epicentro da epidemia na Amazônia com um aumento repentino de mortes que preocupa gestores e sociedade. O objetivo do estudo foi analisar o excesso na mortalidade geral, segundo Semanas Epidemiológicas (SE), visando a identificar mudanças potencialmente associadas à epidemia em Manaus. Dados de mortalidade geral e grupos de causas foram obtidos na Central de Informações do Registro Civil Nacional e no Sistema de Informações sobre Mortalidade, para 2018, 2019 e 2020. Analisou-se faixa etária, sexo, local de ocorrência do óbito, SE, ano-calendário e causas de morte. Calcularam-se razões entre as mortes ocorridas em 2019/2018 e 2020/2019 para avaliar o excesso de mortes, com intervalos de confiança no nível de 5%. Não observou-se excesso de mortalidade geral significativo nas razões 2019/2018, independentemente da SE. Já as razões de 2020/2019 passaram de 1,0 (IC95%: 0,9-1,3) na SE 12 para 4,6 (IC95%: 3,9-5,3) na SE 17. Observou-se excesso de mortalidade geral com a progressão da idade, especialmente em indivíduos com 60 anos e mais, os quais concentraram 69,1% (IC95%: 66,8-71,4) das mortes. A razão 2020/2019 para óbitos em domicílio/via pública foi de 1,1 (IC95%: 0,7-1,8) na SE 12 e de 7,8 (IC95%: 5,4-11,2) na SE 17. A explosão da mortalidade geral em Manaus e a elevada proporção de óbitos em domicílio/via pública expõe a gravidade da epidemia em contextos de grande desigualdade social e fraca efetividade de ações governamentais, em especial aquelas voltadas ao enfrentamento das desigualdades sociais e para a garantia e fortalecimento do Sistema Único de Saúde.

COVID-19; Populações Vulneráveis; Vigilância em Saúde Pública; Mortalidade

Resumen

Manaus, capital del estado brasileño del Amazonas, es el actual epicentro de la epidemia en Amazonia y el aumento repentino de muertes preocupa a gestores y a la sociedad. El objetivo del estudio fue analizar el exceso en la mortalidad general, según Semanas Epidemiológicas (SE), con el objetivo de identificar cambios potencialmente asociados a la epidemia en Manaus. Los datos de mortalidad general y grupos de causas se obtuvieron en la Central de Información del Registro Civil Nacional y en el Sistema de Información sobre Mortalidad, referentes a 2018, 2019 y 2020. Se analizó franja de edad, sexo, lugar donde se produjo el fallecimiento, SE, año-calendario y causas de muerte. Se calcularon las causas entre las muertes acaecidas en 2019/2018 y 2020/2019 para evaluar el exceso de muertes, con intervalos de confianza en el nivel de 5%. No se observó un exceso de mortalidad general significativo en las causas 2019/2018, independientemente de la SE. Ya las causas de 2020/2019 pasaron de 1,0 (IC95%: 0,9-1,3) en la SE 12 a 4,6 (IC95%: 3,9-5,3) en la SE 17. Se observó un exceso de mortalidad general con la progresión de la edad, especialmente en individuos con 60 años y más, quienes concentraron un 69,1% (IC95%: 66,8-71,4) de las muertes. La razón 2020/2019 para óbitos en domicilio/vía pública fue de 1,1 (IC95%: 0,7-1,8) en la SE 12 y de 7,8 (IC95%: 5,4-11,2) en la SE 17. La explosión de la mortalidad general en Manaus y la elevada proporción de óbitos en domicilio/vía pública expone la gravedad de la epidemia en contextos de gran desigualdad social y débil efectividad de las acciones gubernamentales, en especial aquellas dirigidas al combate de las desigualdades sociales y para la garantía y fortalecimiento del Sistema Único de Salud.

COVID-19; Poblaciones Vulnerables; Vigilancia en Salud Pública; Mortalidad

Submitted on 12/May/2020

Final version resubmitted on 21/May/2020

Approved on 23/May/2020

Contact Tracing during Coronavirus Disease Outbreak, South Korea, 2020

Young Joon Park,¹ Young June Choe,¹ Ok Park, Shin Young Park, Young-Man Kim, Jieun Kim, Sanghui Kweon, Yeonhee Woo, Jin Gwack, Seong Sun Kim, Jin Lee, Junghee Hyun, Boyeong Ryu, Yoon Suk Jang, Hwami Kim, Seung Hwan Shin, Seonju Yi, Sangeun Lee, Hee Kyoung Kim, Hyeyoung Lee, Yeowon Jin, Eunmi Park, Seung Woo Choi, Miyoung Kim, Jeongsuk Song, Si Won Choi, Dongwook Kim, Byoung-Hak Jeon, Hyosoon Yoo, Eun Kyeong Jeong, on behalf of the COVID-19 National Emergency Response Center, Epidemiology and Case Management Team

We analyzed reports for 59,073 contacts of 5,706 coronavirus disease (COVID-19) index patients reported in South Korea during January 20–March 27, 2020. Of 10,592 household contacts, 11.8% had COVID-19. Of 48,481 nonhousehold contacts, 1.9% had COVID-19. Use of personal protective measures and social distancing reduces the likelihood of transmission.

Effective contact tracing is critical to controlling the spread of coronavirus disease (COVID-19) (1). South Korea adopted a rigorous contact-tracing program comprising traditional shoe-leather epidemiology and new methods to track contacts by linking large databases (global positioning system, credit card transactions, and closed-circuit television). We describe a nationwide COVID-19 contact tracing program in South Korea to guide evidence-based policy to mitigate the pandemic (2).

The Study

South Korea's public health system comprises a national-level governance (Korea Centers for Disease Control and Prevention), 17 regional governments, and 254 local public health centers. The first case of COVID-19 was identified on January 20, 2020; by May 13, a total of 10,962 cases had been reported.

Author affiliations: Korea Centers for Disease Control and Prevention, Cheongju, South Korea (Y.J. Park, O. Park, S.Y. Park, Y.-M. Kim, J. Kim, S. Kweon, Y. Woo, J. Gwack, S.S. Kim, J. Lee, J. Hyun, B. Ryu, Y.S. Jang, H. Kim, S.H. Shin, S. Yi, S. Lee, H.K. Kim, H. Lee, Y. Jin, E. Park, S.W. Choi, M. Kim, J. Song, S.W. Choi, D. Kim, B.-H. Jeon, H. Yoo, E.K. Jeong); Hallym University College of Medicine, Chuncheon, South Korea (Y.J. Choe)

All reported COVID-19 patients were tested using reverse transcription PCR, and case information was sent to Korea Centers for Disease Control and Prevention.

We defined an index case as the first identified laboratory-confirmed case or the first documented case in an epidemiologic investigation within a cluster. Contacts in high-risk groups (household contacts of COVID-19 patients, healthcare personnel) were routinely tested; in non-high-risk groups, only symptomatic persons were tested. Non-high-risk asymptomatic contacts had to self-quarantine for 14 days and were placed under twice-daily active surveillance by public health workers. We defined a household contact as a person who lived in the household of a COVID-19 patient and a nonhousehold contact as a person who did not reside in the same household as a confirmed COVID-19 patient. All index patients were eligible for inclusion in this analysis if we identified ≥ 1 contact. We defined a detected case as a contact with symptom onset after that of a confirmed COVID-19 index patient.

We grouped index patients by age: 0–9, 10–19, 20–29, 30–39, 40–49, 50–59, 60–69, 70–79, and ≥ 80 years. Because we could not determine direction of transmission, we calculated the proportion of detected cases by the equation [number of detected cases/number of contacts traced] $\times 100$, excluding the index patient; we also calculated 95% CIs. We compared the difference in detected cases between household and nonhousehold contacts across the stratified age groups.

We conducted statistical analyses using RStudio (<https://rstudio.com>). We conducted this study as a

legally mandated public health investigation under the authority of the Korean Infectious Diseases Control and Prevention Act (nos. 12444 and 13392).

We monitored 59,073 contacts of 5,706 COVID-19 index patients for an average of 9.9 (range 8.2–12.5) days after severe acute respiratory syndrome coronavirus 2 (SARS-CoV-2) infection was detected (Table 1). Of 10,592 household contacts, index patients of 3,417 (32.3%) were 20–29 years of age, followed by those 50–59 (19.3%) and 40–49 (16.5%) years of age (Table 2). A total of 11.8% (95% CI 11.2%–12.4%) of household contacts of index patients had COVID-19; in households with an index patient 10–19 years of age, 18.6% (95% CI 14.0%–24.0%) of contacts had COVID-19. For 48,481 nonhousehold contacts, the detection rate was 1.9% (95% CI 1.8%–2.0%) (Table 2). With index patients 30–39 years of age as reference, detection of COVID-19 contacts was significantly higher for index patients >40 years of age in nonhousehold settings. For most age groups, COVID-19 was detected in significantly more household than nonhousehold contacts (Table 2).

Conclusions

We detected COVID-19 in 11.8% of household contacts; rates were higher for contacts of children than adults. These risks largely reflected transmission in the middle of mitigation and therefore might characterize transmission dynamics during school closure (3). Higher household than nonhousehold detection might partly reflect transmission during social distancing, when family members largely stayed home except to perform essential tasks, possibly creating spread within the household. Clarifying the dynamics of SARS-CoV-2 transmission will help in determining control strategies at the individual and population levels. Studies have increasingly examined transmission within households. Earlier studies on the infection rate for symptomatic household contacts in the United States reported 10.5% (95% CI 2.9%–31.4%), significantly higher than for nonhousehold contacts (4). Recent reports on COVID-19 transmission have

estimated higher secondary attack rates among household than nonhousehold contacts. Compiled reports from China, France, and Hong Kong estimated the secondary attack rates for close contacts to be 35% (95% CI 27%–44%) (5). The difference in attack rates for household contacts in different parts of the world may reflect variation in households and country-specific strategies on COVID-19 containment and mitigation. Given the high infection rate within families, personal protective measures should be used at home to reduce the risk for transmission (6). If feasible, cohort isolation outside of hospitals, such as in a Community Treatment Center, might be a viable option for managing household transmission (7).

We also found the highest COVID-19 rate (18.6% [95% CI 14.0%–24.0%]) for household contacts of school-aged children and the lowest (5.3% [95% CI 1.3%–13.7%]) for household contacts of children 0–9 years in the middle of school closure. Despite closure of their schools, these children might have interacted with each other, although we do not have data to support that hypothesis. A contact survey in Wuhan and Shanghai, China, showed that school closure and social distancing significantly reduced the rate of COVID-19 among contacts of school-aged children (8). In the case of seasonal influenza epidemics, the highest secondary attack rate occurs among young children (9). Children who attend day care or school also are at high risk for transmitting respiratory viruses to household members (10). The low detection rate for household contacts of preschool-aged children in South Korea might be attributable to social distancing during these periods. Yet, a recent report from Shenzhen, China, showed that the proportion of infected children increased during the outbreak from 2% to 13%, suggesting the importance of school closure (11). Further evidence, including serologic studies, is needed to evaluate the public health benefit of school closure as part of mitigation strategies.

Our observation has several limitations. First, the number of cases might have been underestimated because all asymptomatic patients might

Table 1. Contacts traced by age group of index coronavirus disease patients, South Korea, January 20–March 27, 2020

Index patient age, y	No. (%) index patients	No. (%) contacts traced	No. contacts traced/index patient	Average time contacts monitored, d
0–9	29 (0.5)	237 (0.4)	8.2	12.5
10–19	124 (2.2)	457 (0.8)	3.7	9.0
20–29	1,695 (29.7)	15,810 (26.8)	9.3	9.8
30–39	668 (11.7)	8,636 (14.6)	12.9	11.1
40–49	807 (14.1)	9,709 (16.4)	12.0	11.0
50–59	1,107 (19.4)	11,353 (19.2)	10.3	9.6
60–69	736 (12.9)	8,490 (14.4)	11.5	8.2
70–79	338 (5.9)	2,389 (4.0)	7.1	8.5
≥80	202 (3.5)	1,992 (3.4)	9.9	9.4
Total	5,706	59,073	10.4	9.9

Table 2. Rates of coronavirus disease among household and nonhousehold contacts, South Korea, January 20–March 27, 2020

Index patient age, y	Household		Nonhousehold	
	No. contacts positive/ no. contacts traced	% Positive (95% CI)	No. contact positive/ no. contacts traced	% Positive (95% CI)
0–9	3/57	5.3 (1.3–13.7)	2/180	1.1 (0.2–3.6)
10–19	43/231	18.6 (14.0–24.0)	2/226	0.9 (0.1–2.9)
20–29	240/3,417	7.0 (6.2–7.9)	138/12,393	1.1 (0.9–1.3)
30–39	143/1,229	11.6 (9.9–13.5)	70/7,407	0.9 (0.7–1.2)
40–49	206/1,749	11.8 (10.3–13.4)	161/7,960	2.0 (1.7–2.3)
50–59	300/2,045	14.7 (13.2–16.3)	166/9,308	1.8 (1.5–2.1)
60–69	177/1,039	17.0 (14.8–19.4)	215/7,451	2.9 (2.5–3.3)
70–79	86/477	18.0 (14.8–21.7)	92/1,912	4.8 (3.9–5.8)
≥80	50/348	14.4 (11.0–18.4)	75/1,644	4.6 (3.6–5.7)
Total	1,248/10,592	11.8 (11.2–12.4)	921/48,481	1.9 (1.8–2.0)

not have been identified. In addition, detected cases could have resulted from exposure outside the household. Second, given the different thresholds for testing policy between households and nonhousehold contacts, we cannot assess the true difference in transmissibility between households and nonhouseholds. Comparing symptomatic COVID-19 patients of both groups would be more accurate. Despite these limitations, the sample size was large and representative of most COVID-19 patients early during the outbreak in South Korea. Our large-scale investigation showed that pattern of transmission was similar to those of other respiratory viruses (12). Although the detection rate for contacts of preschool-aged children was lower, young children may show higher attack rates when the school closure ends, contributing to community transmission of COVID-19.

The role of household transmission of SARS-CoV-2 amid reopening of schools and loosening of social distancing underscores the need for a time-sensitive epidemiologic study to guide public health policy. Contact tracing is especially important in light of upcoming future SARS-CoV-2 waves, for which social distancing and personal hygiene will remain the most viable options for prevention. Understanding the role of hygiene and infection control measures is critical to reducing household spread, and the role of masking within the home, especially if any family members are at high risk, needs to be studied.

We showed that household transmission of SARS-CoV-2 was high if the index patient was 10–19 years of age. In the current mitigation strategy that includes physical distancing, optimizing the likelihood of reducing individual, family, and community disease is important. Implementation of public health recommendations, including hand and respiratory hygiene, should be encouraged to reduce transmission of SARS-CoV-2 within affected households.

Acknowledgments

We thank the Ministry of Interior and Safety, Si/Do and Si/Gun/Gu, medical staff in health centers, and medical facilities for their efforts in responding to COVID-19 outbreak.

About the Author

Dr. Young Joon Park is the preventive medicine physician leading the Epidemiology and Case Management Team for the COVID-19 National Emergency Response Center, Korea Centers for Disease Control and Prevention. His primary research interests include epidemiologic investigation of infectious disease outbreaks. Dr. Choe is an assistant professor at Hallym University College of Medicine. Her research focuses on infectious diseases epidemiology.

References

1. World Health Organization. Contact tracing in the context of COVID-19 [cited 2020 May 15]. <https://www.who.int/publications/i/item/contact-tracing-in-the-context-of-covid-19>
2. COVID-19 National Emergency Response Center. Epidemiology & Case Management Team, Korea Centers for Disease Control & Prevention. Contact transmission of COVID-19 in South Korea: novel investigation techniques for tracing contacts. *Osong Public Health Res Perspect*. 2020;11:60–3. <https://doi.org/10.24171/j.phrp.2020.11.1.09>
3. Choe YJ, Choi EH. Are we ready for coronavirus disease 2019 arriving at schools? *J Korean Med Sci*. 2020;35:e127. <https://doi.org/10.3346/jkms.2020.35.e127>
4. Burke RM, Midgley CM, Dratch A, Fenstersheib M, Haupt T, Holshue M, et al. Active monitoring of persons exposed to patients with confirmed COVID-19—United States, January–February 2020. *MMWR Morb Mortal Wkly Rep*. 2020;69:245–6. <https://doi.org/10.15585/mmwr.mm6909e1>
5. Liu Y, Eggo RM, Kucharski AJ. Secondary attack rate and superspreading events for SARS-CoV-2. *Lancet*. 2020;395:e47. [https://doi.org/10.1016/S0140-6736\(20\)30462-1](https://doi.org/10.1016/S0140-6736(20)30462-1)
6. Jefferson T, Del Mar C, Dooley L, Ferroni E, Al-Ansary LA, Bawazeer GA, et al. Physical interventions to interrupt or reduce the spread of respiratory viruses: systematic review. *BMJ*. 2009;339(sep21 1):b3675. <https://doi.org/10.1136/bmj.b3675>
7. Park PG, Kim CH, Heo Y, Kim TS, Park CW, Kim CH. Out-of-hospital cohort treatment of coronavirus disease 2019

- patients with mild symptoms in Korea: an experience from a single community treatment center. *J Korean Med Sci.* 2020;35:e140. <https://doi.org/10.3346/jkms.2020.35.e140>
8. Zhang J, Litvinova M, Liang Y, Wang Y, Wang W, Zhao S, et al. Changes in contact patterns shape the dynamics of the COVID-19 outbreak in China. *Science.* 2020;368:1481–6. <https://doi.org/10.1126/science.abb8001>
 9. Principi N, Esposito S, Marchisio P, Gasparini R, Crovari P. Socioeconomic impact of influenza on healthy children and their families. *Pediatr Infect Dis J.* 2003;22(Suppl):S207–10. <https://doi.org/10.1097/01.inf.0000092188.48726.e4>
 10. Ferguson NM, Cummings DA, Fraser C, Cajka JC, Cooley PC, Burke DS. Strategies for mitigating an influenza pandemic. *Nature.* 2006;442:448–52. <https://doi.org/10.1038/nature04795>
 11. Liu J, Liao X, Qian S, Yuan J, Wang F, Liu Y, et al. Community transmission of severe acute respiratory syndrome coronavirus 2, Shenzhen, China, 2020. *Emerg Infect Dis.* 2020;26:1320–3. <https://doi.org/10.3201/eid2606.200239>
 12. Choe YJ, Smit MA, Mermel LA. Comparison of common respiratory virus peak incidence among varying age groups in Rhode Island, 2012–2016. *JAMA Netw Open.* 2020;3:e207041. <https://doi.org/10.1001/jamanetworkopen.2020.7041>

Address for correspondence: Eun Kyeong Jeong, Korea Centers for Disease Control and Prevention, Osong Health Technology Administration Complex, 187, Osongsangmyeong 2-ro, Osong-eup, Heungdeok-gu, Cheongju, Chungcheongbuk-do, South Korea, email: jeongek@korea.kr

June 2020 Prions

- Identifying and Interrupting Superspreading Events—Implications for Control of Severe Acute Respiratory Syndrome Coronavirus 2
- Risks Related to Chikungunya Infections among European Union Travelers, 2012–2018
- Manifestations of Toxic Shock Syndrome in Children, Columbus, Ohio, USA, 2010–2017
- Genomic Epidemiology of 2015–2016 Zika Virus Outbreak in Cape Verde
- Epidemiologic Changes of Scrub Typhus in China, 1952–2016
- Pharmacologic Treatments and Supportive Care for Middle East Respiratory Syndrome
- Distribution of Streptococcal Pharyngitis and Acute Rheumatic Fever, Auckland, New Zealand, 2010–2016
- Temporary Fertility Decline after Large Rubella Outbreak, Japan
- Radical Change in Zoonotic Abilities of Atypical BSE Prion Strains as Evidenced by Crossing of Sheep Species Barrier in Transgenic Mice
- Characterization of Sporadic Creutzfeldt-Jakob Disease and History of Neurosurgery to Identify Potential Iatrogenic Cases
- Failures of 13-Valent Conjugated Pneumococcal Vaccine in Age-Appropriately Vaccinated Children 2–59 Months of Age, Spain



- Increased Risk for Carbapenem-Resistant *Enterobacteriaceae* Colonization in Intensive Care Units after Hospitalization in Emergency Department
- Antimicrobial Resistance in *Salmonella enterica* Serovar Paratyphi B Variant Java in Poultry from Europe and Latin America
- Invasive Group B *Streptococcus* Infections in Adults, England, 2015–2016
- Zoonotic Alphaviruses in Fatal and Neurologic Infections in Wildlife and Nonequine Domestic Animals, South Africa
- Effectiveness and Tolerability of Oral Amoxicillin in Pregnant Women with Active Syphilis, Japan, 2010–2018
- Endemic Chromoblastomycosis Caused Predominantly by *Fonsecaea nubica*, Madagascar
- Emergence of New Non-Clonal Group 258 High-Risk Clones among *Klebsiella pneumoniae* Carbapenemase-Producing *K. pneumoniae* Isolates, France
- Zoonotic Vectorborne Pathogens and Ectoparasites of Dogs and Cats in Eastern and Southeast Asia
- Multihost Transmission of *Schistosoma mansoni* in Senegal, 2015–2018
- Statin Use and Influenza Vaccine Effectiveness in Persons ≥ 65 Years of Age, Taiwan
- Estimating Risk for Death from Coronavirus Disease, China, January–February 2020
- Epidemiology of Coronavirus Disease in Gansu Province, China, 2020
- Severe Acute Respiratory Syndrome Coronavirus 2 from Patient with Coronavirus Disease, United States
- Syphilis in Maria Salviati (1499–1543), Wife of Giovanni de' Medici of the Black Bands
- Yaws Disease Caused by *Treponema pallidum* subspecies pertenue in Wild Chimpanzee, Guinea, 2019

**EMERGING
INFECTIOUS DISEASES**

To revisit the June 2020 issue, go to:
<https://wwwnc.cdc.gov/eid/articles/issue/26/6/table-of-contents>

Coronavirus Disease Outbreak in Call Center, South Korea

Shin Young Park, Young-Man Kim, Seonju Yi, Sangeun Lee, Baeg-Ju Na, Chang Bo Kim, Jung-il Kim, Hea Sook Kim, Young Bok Kim, Yoojin Park, In Sil Huh, Hye Kyung Kim, Hyung Jun Yoon, Hanaram Jang, Kyungham Kim, Yeonhwa Chang, Inhye Kim, Hyeyoung Lee, Jin Gwack, Seong Sun Kim, Miyong Kim, Sanghui Kweon, Young June Choe, Ok Park, Young Joon Park, Eun Kyeong Jeong

We describe the epidemiology of a coronavirus disease (COVID-19) outbreak in a call center in South Korea. We obtained information on demographic characteristics by using standardized epidemiologic investigation forms. We performed descriptive analyses and reported the results as frequencies and proportions for categorical variables. Of 1,143 persons who were tested for COVID-19, a total of 97 (8.5%, 95% CI 7.0%–10.3%) had confirmed cases. Of these, 94 were working in an 11th-floor call center with 216 employees, translating to an attack rate of 43.5% (95% CI 36.9%–50.4%). The household secondary attack rate among symptomatic case-patients was 16.2% (95% CI 11.6%–22.0%). Of the 97 persons with confirmed COVID-19, only 4 (1.9%) remained asymptomatic within 14 days of quarantine, and none of their household contacts acquired secondary infections. Extensive contact tracing, testing all contacts, and early quarantine blocked further transmission and might be effective for containing rapid outbreaks in crowded work settings.

Since the first imported case of coronavirus disease (COVID-19) was confirmed in South Korea on January 20, 2020, a sharp increase in the number of COVID-19 cases has been observed, with most infections being reported from specific clusters (1). Outbreaks of COVID-19 related to mass gathering,

religious activities, workplaces, and hospitals have accounted for the largest portion cases in the national outbreak (1).

In March 2020, the Korea Centers for Disease Control and Prevention (KCDC), South Korea's national-level public health authority, was informed about a cluster of cases of COVID-19 in a call center located in a commercial-residential mixed-use building (building X) in the capital city of Seoul. We describe the epidemiology of this COVID-19 outbreak and detail the containment efforts to limit the spread of the disease.

Materials and Methods

Setting

On March 8, the Seoul Metropolitan Government was notified of a confirmed case of COVID-19 in a person who worked in building X; the case reportedly was associated with a possible cluster of cases. On March 9, KCDC and local governments (in Seoul, the city of Incheon, and Gyeonggi Province) formed a joint response team and launched an epidemiologic investigation with contact tracing. Building X is a 19-story floor in one of the busiest urban area of Seoul. Commercial offices are located on the 1st through 11th floors, and residential apartments are located on the 13th through 19th floors. We identified and investigated 922 employees who worked in the commercial offices, 203 residents who lived in the residential apartments, and 20 visitors. The call center is located on the 7th through 9th floors and the 11th floor; it has a total of 811 employees. Employees do not generally go between floors, and they do not have an in-house restaurant for meals.

Case Definition

We defined a patient under investigation (PUI) as one who worked at, lived at, or visited building X during February 21–March 8, 2020. We defined a confirmed

Author affiliations: Korea Centers for Disease Control and Prevention, Cheongju, South Korea (S.Y. Park, Y.-M. Kim, S. Yi, S. Lee, H. Lee, J. Gwack, S.S. Kim, M. Kim, S. Kweon, O. Park, Y.J. Park, E.K. Jeong); Seoul Metropolitan Government, Seoul, South Korea (B.-J. Na, J.-i. Kim, H.S. Kim, Y.B. Kim); Seoul Health Foundation, Seoul (C.B. Kim); Seoul Center for Infectious Disease Control and Prevention, Seoul (Y. Park, I.S. Huh); Incheon Metropolitan City, Incheon, South Korea (H.K. Kim, H.J. Yoon, H. Jang); Gyeonggi Provincial Office, Suwon, South Korea (K. Kim, Y. Chang, I. Kim); Hallym University College of Medicine, Chuncheon, South Korea (Y.J. Choe)

DOI: <https://doi.org/10.3201/eid2608.201274>

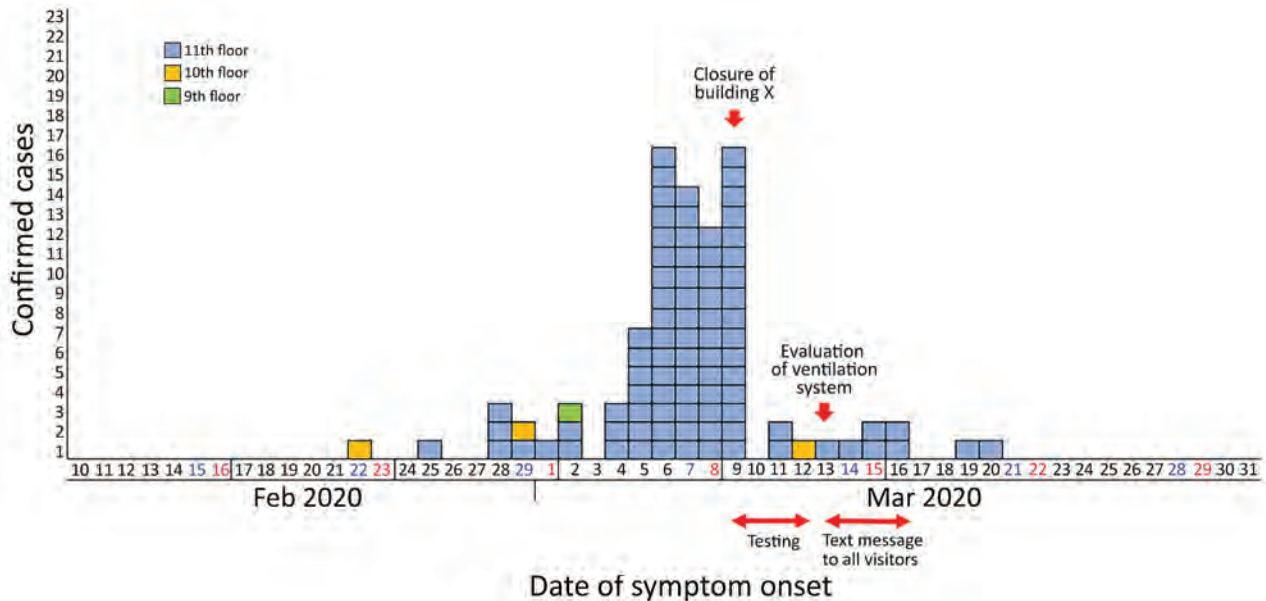


Figure 1. Epidemic curve of a coronavirus disease outbreak in a call center, by date of symptom onset, Seoul, Korea, 2020. Asymptomatic cases are excluded.

case-patient as a PUI with a positive COVID-19 laboratory test. We confirmed the diagnosis of COVID-19 by using real-time reverse transcription PCR assays. We defined a symptomatic case-patient as a confirmed case-patient with symptoms at the time of positive testing, a presymptomatic case-patient as a confirmed case-patient who was asymptomatic at the time of positive testing but later had symptoms during the 14 days of monitoring, and an asymptomatic case-patient as confirmed a case-patient with a positive COVID-19 test result who remained asymptomatic during the entire 14-day period.

Response Measures

Building X was closed on March 9, 2020, immediately after the outbreak was reported. We offered testing to all occupants (office workers and apartment residents) during March 9–12. We collected nasopharyngeal and oropharyngeal swab specimens from PUIs for immediate real-time reverse transcription

PCR testing; the average turnaround time was 12–24 hours. Confirmed case-patients were isolated, and negative case-patients were mandated to stay quarantined for 14 days. We followed and retested all test-negative case-patients until the end of quarantine. We also investigated, tested, and monitored household contacts of all confirmed case-patients for 14 days after discovery, regardless of symptoms. During March 13–16, we sent a total of 16,628 text messages to persons who stayed >5 minutes near the building X; we tracked these persons by using cell phone location data. The messages instructed the recipients to avoid contact with others and go to the nearest COVID-19 screening center to get tested.

Data Collection and Analysis

We obtained information on demographic characteristics and presence of symptoms through face-to-face interviews with case-patients, using standardized epidemiologic investigation forms. We performed

Table 1. Attack rate by location during a coronavirus disease outbreak in a call center, Seoul, South Korea, 2020

Location type and floor	Potentially exposed, no. (%)	Confirmed cases, no. (%)	Attack rate, % (95% CI)
Commercial			
1st–6th	84 (7.3)	0	0
7th (call center)	182 (15.9)	0	0
8th (call center)	207 (18.1)	0	0
9th (call center)	206 (18.0)	1 (1.0)	0.5 (0.0–3.1)
10th	27 (2.4)	2 (2.1)	7.4 (1.3–25.8)
11th (call center)	216 (18.9)	94 (96.9)	43.5 (36.9–50.4)
Residential			
13th–19th	201 (17.6)	0	0
Other	20 (1.7)	0	0
Total	1,143	97	8.5 (7.0–10.3)

SYNOPSIS

descriptive analyses reported the results as frequencies and proportions for categorical variables. The investigation was a part of public health response and was not considered research subject to institutional review board approval; therefore, written informed consent by participants was not required.

Results

Of 1,145 PUIs, we tested 1,143 (99.8%) for COVID-19 (922 employees, 201 residents, and 20 visitors) and

identified 97 (8.5%, 95% CI 7.0–10.3) confirmed case-patients (Figure 1). Of 857 patients for whom demographic information was available, 620 (72.3%) were women; mean age was 38 years (range 20–80 years). Most (94 [96.9%]) of the confirmed case-patients were working on the 11th-floor call center, which had a total of 216 employees, resulting in an attack rate of 43.5% (95% CI 36.9%–50.4%) (Table 1; Figure 2). Most of the case-patients on the 11th floor were on the same side of the building. Among the 97

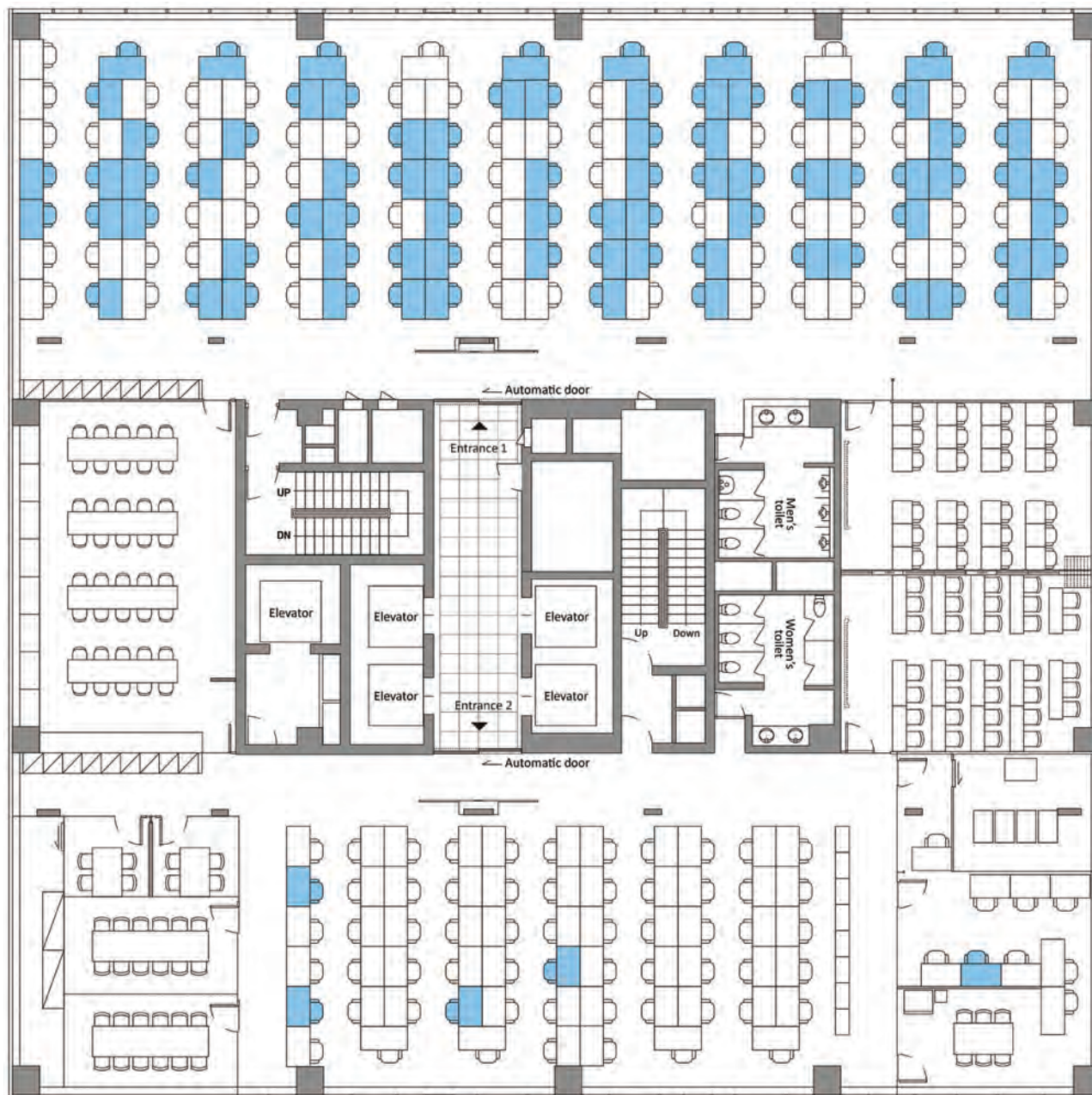


Figure 2. Floor plan of the 11th floor of building X, site of a coronavirus disease outbreak, Seoul, South Korea, 2020. Blue indicates the seating places of persons with confirmed cases.

confirmed case-patients, 89 (91.7%) were symptomatic at the time of investigation and 4 (4.1%) were presymptomatic during the time of investigation but later had onset of symptoms within 14 days of monitoring; 4 (4.1%) case-patients remained asymptomatic after 14 days of isolation.

The first case-patient with symptom onset, who worked in an office on the 10th floor (and reportedly never went to 11th floor), had onset of symptoms on February 22. The second case-patient with symptom onset, who worked at the call center on the 11th floor, had onset of symptoms on February 25. Residents and employees in building X had frequent contact in the lobby or elevators. We were not able to trace back the index case-patient to another cluster or an imported case.

We followed up on a total of 225 household contacts of confirmed COVID-19 case-patients (average 2.3 household members per confirmed case-patient). COVID-19 had occurred in 34 household members who had contact with symptomatic case-patients, translating to a secondary attack rate of 16.2% (Table 2). Among 11 household members of presymptomatic case-patients and 4 household members of asymptomatic case-patients, none had COVID-19 symptoms nor tested positive after 14 days of quarantine.

Discussion

We described the epidemiologic characteristics of a COVID-19 outbreak centered in a call center in South Korea. We identified 97 confirmed COVID-19 case-patients in building X, indicating an attack rate of 8.5%. However, if we restrict our results to the 11th floor, the attack rate was as high as 43.5%. This outbreak shows alarmingly that severe acute respiratory syndrome coronavirus 2 (SARS-CoV-2) can be exceptionally contagious in crowded office settings such as a call center. The magnitude of the outbreak illustrates how a high-density work environment can become a high-risk site for the spread of COVID-19 and potentially a source of further transmission. Nearly all the case-patients were on one side of the building on 11th floor. Severe acute respiratory syndrome coronavirus, the predecessor of SARS-CoV-2, exhibited multiple superspreading events in 2002 and 2003, in which a few persons infected others, resulting in

many secondary cases. Despite considerable interaction between workers on different floors of building X in the elevators and lobby, spread of COVID-19 was limited almost exclusively to the 11th floor, which indicates that the duration of interaction (or contact) was likely the main facilitator for further spreading of SARS-CoV-2.

Unique features of this outbreak investigation include a complete 14-day follow-up of close contacts of case-patients after containment measures were implemented. Close contact with an infected person is a well-recognized risk factor for acquiring SARS-CoV-2 (2). In a recent US study, the symptomatic secondary attack rate among 445 close contacts of COVID-19 case-patients was 10.5% among household members (3). In this outbreak in South Korea, we found that the secondary attack rate within the household was 16.5% among symptomatic index case-patients, which is consistent with other reports.

The role of asymptomatic COVID-19 case-patients in spreading the disease is of great concern. Among 97 confirmed COVID-19 case-patients in this study, 4 (4.1%) remained asymptomatic during the 14-days of monitoring. This rate is lower than the 30.8% rate estimated in previous modeling (4). A case-patient series from Beijing, China, indicated that asymptomatic case-patients accounted for 5% (13/262) of patients transferred to a designated COVID-19 hospital (5). Our data might represent the likely proportion of asymptomatic COVID-19 infections in the community setting. We also found that, among 17 household contacts of asymptomatic case-patients, none had secondary infections. Previous reports have postulated that SARS-CoV-2 in asymptomatic (or presymptomatic) case-patients might become transmissible to others (6); however, given the high degree of self-quarantine and isolation measures that were instituted after March 8 among this cohort, our analyses might have not detected the actual transmissibility in asymptomatic COVID-19 case-patients. Robust mass testing of all suspected case-patients might have prevented asymptomatic transmission because asymptomatic persons were given information about their possible infection and therefore might have self-isolated from their household members.

Table 2. Household secondary attack rate, by presence of symptoms, during a coronavirus disease outbreak in a call center, Seoul, South Korea, 2020

Symptom status of index patients	Exposed, no. (%)	Confirmed cases, no. (%)	Secondary attack rate, % (95% CI)
Symptomatic	210 (93.3)	34 (100.0)	16.2 (11.6–22.0)
Presymptomatic	11 (4.8)	0	0
Asymptomatic	4 (1.9)	0	0
Total	225	34	15.1 (10.8–20.6)

SYNOPSIS

This outbreak investigation has several limitations. First, we could not track these cases to another cluster, making it difficult to identify the actual index case-patient. Second, not all clinical information was available for all confirmed cases, prohibiting detailed description of clinical syndromes. Date of symptom onset by office seat would be informative in understanding SARS-CoV-2 transmission in close contact area. However, our findings demonstrate the power of screening all potentially exposed persons and show that early containment can be implemented and used in the middle of national COVID-19 outbreak. By testing all potentially exposed persons and their contacts to facilitate the isolation of symptomatic and asymptomatic COVID-19 case-patients, we might have helped interrupt transmission chains. In light of the shift to a global pandemic, we recommend that public health authorities conduct active surveillance and epidemiologic investigation in this rapidly evolving landscape of COVID-19.

In summary, this outbreak exemplifies the threat posed by SARS-CoV-2 with its propensity to cause large outbreaks among persons in office workplaces. Targeted preventive strategies might help mitigate the risk for SARS-CoV-2 infection in these vulnerable group.

Acknowledgments

We thank the relevant ministries (including the Ministry of Interior and Safety, Si/Do, and Si/Gun/Gu), medical staffs in health centers, and medical facilities for their efforts in responding to the COVID-19 outbreak.

The opinions expressed by authors contributing to this journal do not necessarily reflect the opinions of the Korea Centers for Disease Control and Prevention or the institutions with which the authors are affiliated.

About the Author

Ms. Park is a public health officer at the Korea Centers for Disease Control and Prevention. Her main interest is the epidemiologic investigation of infectious diseases.

References

1. COVID-19 National Emergency Response Center, Epidemiology and Case-patient Management Team, Korea Centers for Disease Control and Prevention. Early epidemiological and clinical characteristics of 28 cases of coronavirus disease in South Korea. *Osong Public Health Res Perspect*. 2020;11:8-14. <https://doi.org/10.24171/j.phrp.2020.11.1.03>
2. Bajema KL, Oster AM, McGovern OL, Lindstrom S, Stenger MR, Anderson TC, et al.; 2019-nCoV Persons Under Investigation Team; 2019-CoV Persons Under Investigation Team. Persons evaluated for 2019 novel coronavirus – United States, January 2020. *MMWR Morb Mortal Wkly Rep*. 2020;69:166-70. <https://doi.org/10.15585/mmwr.mm6906e1>
3. Burke RM, Midgley CM, Dratch A, Fenstersheib M, Haupt T, Holshue M, et al. Active monitoring of persons exposed to patients with confirmed COVID-19 – United States, January–February 2020. *MMWR Morb Mortal Wkly Rep*. 2020;69:245-6. <https://doi.org/10.15585/mmwr.mm6909e1>
4. Nishiura H, Kobayashi T, Suzuki A, Jung SM, Hayashi K, Kinoshita R, et al. Estimation of the asymptomatic ratio of novel coronavirus infections (COVID-19). *Int J Infect Dis*. 2020;S1201-9712(20)30139-9. <https://doi.org/10.1016/j.ijid.2020.03.020>
5. Tian S, Hu N, Lou J, Chen K, Kang X, Xiang Z, et al. Characteristics of COVID-19 infection in Beijing. *J Infect*. 2020;80:401-6. <https://doi.org/10.1016/j.jinf.2020.02.018>
6. Tong ZD, Tang A, Li KF, Li P, Wang HL, Yi JP, et al. Potential presymptomatic transmission of SARS-CoV-2, Zhejiang Province, China, 2020. *Emerg Infect Dis*. 2020;26:1052-4. <https://doi.org/10.3201/eid2605.200198>

Address for correspondence: Eun Kyeong Jeong, Korea Centers for Disease Control and Prevention, Osong Health Technology Administration Complex, 187, Osongsangmyeong 2-ro, Osong-eup, Heungdeok-gu, Cheongju-si, Chungcheongbuk-do, 28159, South Korea; email: jeongek@korea.kr

Accelerated Article Preview

Reduced sensitivity of SARS-CoV-2 variant Delta to antibody neutralization

Received: 26 May 2021

Accepted: 29 June 2021

Accelerated Article Preview Published
online 8 July 2021

Cite this article as: Planas, D. et al. Reduced sensitivity of SARS-CoV-2 variant Delta to antibody neutralization. *Nature* <https://doi.org/10.1038/s41586-021-03777-9> (2021).

Delphine Planas, David Veyer, Artem Baidaliuk, Isabelle Staropoli, Florence Guivel-Benhassine, Maaran Michael Rajah, Cyril Planchais, Françoise Porrot, Nicolas Robillard, Julien Puech, Matthieu Prot, Floriane Gallais, Pierre Gantner, Aurélie Velay, Julien Le Guen, Najibi Kassis-Chikhani, Dhiaeddine Edriss, Laurent Belec, Aymeric Seve, Laura Courtellemont, Hélène Péré, Laurent Hocqueloux, Samira Fafi-Kremer, Thierry Prazuck, Hugo Mouquet, Timothée Bruel, Etienne Simon-Lorière, Felix A. Rey & Olivier Schwartz

This is a PDF file of a peer-reviewed paper that has been accepted for publication. Although unedited, the content has been subjected to preliminary formatting. Nature is providing this early version of the typeset paper as a service to our authors and readers. The text and figures will undergo copyediting and a proof review before the paper is published in its final form. Please note that during the production process errors may be discovered which could affect the content, and all legal disclaimers apply.

Reduced sensitivity of SARS-CoV-2 variant Delta to antibody neutralization

<https://doi.org/10.1038/s41586-021-03777-9>

Received: 26 May 2021

Accepted: 29 June 2021

Published online: 8 July 2021

Delphine Planas^{1,2}, David Veyer^{3,4}, Artem Baidaliuk⁵, Isabelle Staropoli¹, Florence Guivel-Benhassine¹, Maaran Michael Rajah^{1,6}, Cyril Planchais⁷, Françoise Porrot¹, Nicolas Robillard⁴, Julien Puech⁴, Matthieu Prot⁵, Floriane Gallais^{8,9}, Pierre Gantner^{8,9}, Aurélie Velay^{8,9}, Julien Le Guen¹⁰, Najibi Kassis-Chikhani¹¹, Dhiaeddine Edriss⁴, Laurent Belec⁴, Aymeric Seve¹², Laura Courtellemont¹², Hélène Péré³, Laurent Hocqueloux¹², Samira Fafi-Kremer^{8,9}, Thierry Prazuck¹², Hugo Mouquet⁷, Timothée Bruel^{1,2,14}✉, Etienne Simon-Lorière^{5,14}, Felix A. Rey^{13,14} & Olivier Schwartz^{1,2,14}✉

The SARS-CoV-2 B.1.617 lineage was identified in October 2020 in India^{1–5}. It has since then become dominant in some Indian regions and UK and further spread to many countries⁶. The lineage includes three main subtypes (B.1.617.1, B.1.617.2 and B.1.617.3), harbouring diverse Spike mutations in the N-terminal domain (NTD) and the receptor binding domain (RBD) which may increase their immune evasion potential. B.1.617.2, also termed variant Delta, is believed to spread faster than other variants. Here, we isolated an infectious Delta strain from a traveller returning from India. We examined its sensitivity to monoclonal antibodies (mAbs) and to antibodies present in sera from COVID-19 convalescent individuals or vaccine recipients, in comparison to other viral strains. Variant Delta was resistant to neutralization by some anti-NTD and anti-RBD mAbs including Bamlanivimab, which were impaired in binding to the Spike. Sera from convalescent patients collected up to 12 months post symptoms were 4 fold less potent against variant Delta, relative to variant Alpha (B.1.1.7). Sera from individuals having received one dose of Pfizer or AstraZeneca vaccines barely inhibited variant Delta. Administration of two doses generated a neutralizing response in 95% of individuals, with titers 3 to 5 fold lower against Delta than Alpha. Thus, variant Delta spread is associated with an escape to antibodies targeting non-RBD and RBD Spike epitopes.

The variant Delta has been detected in many countries. It has become predominant in the state of Maharashtra and probably other Indian regions⁴ and represented 77% of sequenced viruses circulating in UK between June 2 and 9, 2021⁶. It has been classified as a Variant of Concern (VOC) and is believed to be 60% more transmissible than variant Alpha. Little is known about its sensitivity to the humoral immune response. Recent reports indicated a reduced sensitivity of members of the B.1.617 lineage to certain monoclonal and polyclonal antibodies^{1–5,7–9}.

Isolation and characterization of the variant Delta

We isolated the variant Delta from a nasopharyngeal swab of a symptomatic individual, a few days upon his return to France from India. The virus was amplified by two passages on Vero E6 cells. Sequences of the swab and the outgrown virus were identical and identified the

variant Delta (GISAID accession ID: EPI_ISL_2029113) (Extended Data Fig. 1). In particular, the Spike protein contained 9 mutations, when compared to the D614G strain (belonging to the basal B.1 lineage) used here as a reference, including five mutations in the NTD (T19R, G142D, Δ156, Δ157, R158G), two in the RBD (L452R, T478K), one mutation close to the furin cleavage site (P681R) and one in the S2 region (D950N) (Extended Data Fig. 1). This set of mutation was different from those observed in other members of the B.1.617 lineage and other VOCs (Extended Data Fig. 1). Viral stocks were titrated using S-Fuse reporter cells and Vero cells^{10,11}. Viral titers were similar in the two target cells and reached 10⁵–10⁶ infectious units/ml. Large syncytia expressing the Spike were observed in Delta-infected cells (Extended Data Fig. 2). Future work will help determining whether Delta is more fusogenic than other variants, as suggested here by the large size of Delta-induced syncytia.

¹Virus & Immunity Unit, Department of Virology, Institut Pasteur, CNRS UMR 3569, Paris, France. ²Vaccine Research Institute, Creteil, France. ³INSERM, Functional Genomics of Solid Tumors (FunGeST), Centre de Recherche des Cordeliers, Université de Paris and Sorbonne Université, Paris, France. ⁴Hôpital Européen Georges Pompidou, Laboratoire de Virologie, Service de Microbiologie, Paris, France. ⁵G5 Evolutionary genomics of RNA viruses, Department of Virology, Institut Pasteur, Paris, France. ⁶Université de Paris, Sorbonne Paris Cité, Paris, France.

⁷Laboratory of Humoral Immunology, Department of Immunology, Institut Pasteur, INSERM U1222, Paris, France. ⁸CHU de Strasbourg, Laboratoire de Virologie, Strasbourg, France. ⁹Université de Strasbourg, INSERM, IRM UMR S 1109, Strasbourg, France. ¹⁰Hôpital Européen Georges Pompidou, Service de Gériatrie, Assistance Publique des Hôpitaux de Paris, Paris, France. ¹¹Hôpital européen Georges Pompidou, Unité d'Hygiène Hospitalière, Service de Microbiologie, Assistance Publique-Hôpitaux de Paris, Paris, 75015, France. ¹²CHR d'Orléans, service de maladies infectieuses, Orléans, France. ¹³Structural Virology Unit, Department of Virology, Institut Pasteur, CNRS UMR 3569, Paris, France. ¹⁴These authors contributed equally: Timothée Bruel, Etienne Simon-Lorière, Felix A. Rey, Olivier Schwartz. ✉e-mail: timothee.brueel@pasteur.fr; olivier.schwartz@pasteur.fr

Phylogenetic analysis of the B.1.617 lineage

To contextualize the Delta isolate reported here, we inferred a global phylogeny subsampling the diversity of SARS-CoV-2 sequences available on the GISAID EpiCoV database (Extended Data Fig. 3). The B.1.617 lineage, subdivided into three sublineages according to the PANGO classification¹², derives from the B.1 lineage (D614G). The three sublineages present multiple changes in the Spike, including the L452R substitution in the RBD, already seen in other variants such as B.1.429 and P681R, located in the furin cleavage site and which may enhance Spike fusogenic activity¹³. The E484Q substitution, which may be functionally similar to the antibody-escape mutation E484K found in variants Beta and Gamma (B.1.351 and P.1), is present in B.1.617.1 and B.1.617.3, and has likely reverted in the Delta sublineage, as it was present in a sequence (B.1.617) ancestral to the three sublineages (Extended Data Fig. 1)¹⁴. Whether the absence of E484Q, the presence of T478K, other changes in the Spike or elsewhere may facilitate viral replication and transmissibility remains unknown. Interestingly, the B.1.617 lineage is not homogeneous, with multiple mutations fixed in a sublineage (e.g. Spike:T19R, G142D or D950N) also detected at lower frequencies in other sublineages. This may reflect founder effects or similar selective pressures acting on these emerging variants.

Mutational changes in variant Delta

The locations of the Spike mutations in the variant Delta showed a similar overall distribution to those that appeared in other VOCs. In particular, in addition to D614G, the D950N mutation mapped to the trimer interface (Extended Data Fig. 4a), suggesting a potential contribution in regulating Spike dynamics, as shown with D614G¹³. As with other VOCs, some mutations in Delta cluster in the NTD (Extended Data Fig. 4b). The 156-157 deletion and G158R mutation map to the same surface as the 144 and 241-243 deletions in variants Alpha and Beta (B.1.351), respectively. The T19R maps to the surface patch that has several mutations in Alpha. These altered residues lie in the NTD “supersite” targeted by most anti-NTD neutralizing antibodies¹⁵. In the RBD, mutations appearing in VOCs map to the periphery of the ACE2 binding surface (Extended Data Fig. 4c), suggesting that the virus accumulates mutations there to reduce or avoid antibody recognition while maintaining binding to ACE2. For instance, the L452R mutation found in Delta impairs neutralization by antibodies¹⁶ and is located at this periphery. The only mutation within the ACE2 patch is at location 501, which increases affinity of the RBD for ACE2 and is also involved in antibody escape¹³. The T478K mutation in the RBD is unique to Delta and falls within the epitope region of potent neutralizing mAbs categorized as “Class 1” (Extended Data Fig. 4c)¹⁷. This mutation is close to the E484K mutation that facilitates antibody escape¹³. These observations prompted us to analyze the neutralization potential of mAbs and sera from convalescents and vaccinees against variant Delta.

Neutralization of variant Delta by monoclonal antibodies

We assessed the sensitivity of Delta to a panel of human mAbs using the S-Fuse assay. We tested four clinically approved mAbs, Bamlanivimab (LY-CoV555), Etesivimab (LY-CoV016), Casirivimab (REGN10933) and Imdevimab (REGN10987) targeting the RBD^{18,19} as well as eight anti-RBD (RBD-48, RBD-85, RBD-98 and RBD-109) and anti-NTD (NTD-18, NTD-20, NTD-69 and NTD-71) mAbs derived from convalescent individuals (Planchais et al, in preparation). Neutralizing anti-RBD mAbs can be classified into 4 main categories^{17,20}. RBD-48 and RBD-85 belong to the first category (“Class 1”) and act by blocking binding of the “up” conformation of RBD to ACE2¹⁷. The precise epitopes of RBD-98 and RBD-109 are not yet defined but overlap with those of RBD-48 and RBD-85. The anti-NTD antibodies bind uncharacterized epitopes.

We measured the potency of the four therapeutic antibodies against variant Delta and included as a comparison D614G (B.1), Alpha and Beta variants. The antibodies neutralized D614G, with IC50 (Inhibitory Concentration 50%) varying from 1.2×10^{-3} to 6.5×10^{-2} $\mu\text{g/mL}$ (Fig. 1). Etesivimab displayed a 200-fold increase of IC50 against Alpha. As previously reported, Bamlanivimab and Etesivimab did not neutralize Beta²¹. Bamlanivimab lost antiviral activity against Delta, in line with previous results demonstrating that L452R is an escape mutation for this mAb¹⁶. Etesivimab, Casirivimab and Imdevimab remained active against Delta (Fig. 1).

The four other anti-RBD mAbs neutralized D614G. The IC50 of RBD-48 and RBD-98 were about 15-100-fold higher with Alpha than with D614G, whereas RBD-85 displayed increased activity against Alpha. Three mAbs inhibited Delta whereas RBD-85 was inactive (Extended Data Fig. 5).

The four anti-NTD mAbs were globally less efficient than anti-RBD mAbs. They inhibited D614G with high IC50 (1-60 $\mu\text{g/mL}$) (Extended Data Fig. 5). Three anti-NTD antibodies lost activity against Alpha and Delta, whereas the fourth (NTD-18) inhibited to some extent the two variants. Thus, Delta escapes neutralization by some antibodies targeting the RBD or NTD.

We examined by flow cytometry the binding of each mAb to Vero cells infected with the different variants. Radar plots show the binding of all antibodies tested (Extended Data Fig. 6). D614G was recognized by the 12 mAbs tested. Alpha and Delta were recognized by 9 and 7 mAb, respectively. Bamlanivimab no longer bound Delta. We also analyzed the binding of the 12 mAbs to variant Beta, which is more resistant to neutralization. Bamlanivimab and Etesivimab lost their binding to Beta and only 5 of the antibodies bound this variant (Extended Data Fig. 6). Thus, escape of Delta and other variants to neutralization is due to a reduction or loss of binding of the antibodies.

Sensitivity of variant Delta to sera from convalescent individuals

We examined the neutralization ability of sera from convalescent subjects. We first selected samples from 56 donors in a cohort of infected individuals from the French city of Orléans. All individuals were diagnosed with SARS-CoV-2 infection by RT-qPCR or serology and included critical, severe, mild-to-moderate and asymptomatic cases (Extended Data Table 1). They were not vaccinated at the sampling time. We recently characterized the potency of these sera against D614G, Alpha and Beta isolates¹¹. We analyzed individuals sampled at a median of 188 days post onset of symptoms (POS), referred to as Month 6 (M6) samples. We calculated ED50 (Effective Dose 50%) for each combination of serum and virus (Extended Data Fig. 7a). With the Alpha variant, we obtained similar ED50 values in this series of experiments than in our previous analysis¹¹ (Extended Data Fig. 7b). We thus included our published data for D614G and Beta in the comparison. With Delta, neutralization titers were significantly decreased by 4 to 6-fold when compared to Alpha and D614G strains, respectively (Extended Data Fig. 7a). This reduction in neutralizing titers was similar against Delta and Beta (Extended Data Fig. 7a).

We asked whether this neutralization profile was maintained for longer periods of time. We analyzed sera from 47 individuals from another cohort of RT-qPCR-confirmed health care workers from Strasbourg University Hospitals who experienced mild disease^{22,23}. Twenty six individuals were unvaccinated, whereas 21 received a single dose of vaccine 7-81 days before sampling. The samples were collected at a later time point (M12), with a median of 330 and 359 days for unvaccinated and vaccinated individuals, respectively (Extended Data Table 1)²³. As observed²³, the neutralization activity was globally low at M12 in unvaccinated individuals (Fig. 2a). There was a 4 fold decrease of ED50 against Beta and Delta, relative to Alpha (Fig. 2a). The 21 single-dose vaccine recipients of the M12 cohort included 9 vaccinated with AstraZeneca, 9 with Pfizer and 3 with Moderna vaccines. Sera from these vaccinated participants showed a dramatic increase in neutralizing antibody titers

against Alpha, Beta and Delta variants, as compared to unvaccinated convalescents (Fig. 2a). Therefore, as shown with other variants^{23,24}, a single dose of vaccine boosts cross-neutralizing antibody responses to Delta.

We then classified the cases as neutralizers (defined as harboring neutralizing antibodies detectable at the first serum dilution of 1/30) and non-neutralizers, for the viral variants and the two cohorts (Extended Data Fig. 7c). Between 76% and 92% of the individuals neutralized the four strains at M6. The fraction of neutralizers was lower in the second cohort at M12, a phenomenon which was particularly marked for Beta and Delta. 88% of individuals neutralized Alpha and only 47% neutralized Delta. After vaccination, 100% of convalescent individuals neutralized the four strains (Extended Data Fig. 7c).

Thus, variant Delta displays enhanced resistance to neutralization by sera from unvaccinated convalescent individuals, particularly one year after infection.

Sensitivity of variant Delta to sera from vaccine recipients

We next asked whether vaccine-elicited antibodies neutralized variant Delta in individuals that were not previously infected with SARS-CoV-2. We randomly selected 59 individuals from a cohort of vaccinated subjects established in Orléans. The characteristics of vaccinees are depicted in Extended Data Table 2. 16 individuals received the Pfizer vaccine. They were sampled at week 3 (W3) after the first dose and W8 (corresponding to week 5 after the second dose). 13 individuals were also sampled at W16. 43 individuals received the AstraZeneca vaccine. Sera from 23 individuals were sampled after one dose (W10) and from 20 other individuals after two doses (W16, corresponding to week 4 after the second dose). We measured the potency of the sera against D614G, Alpha, Beta and Delta strains (Fig. 2b,c).

With the Pfizer vaccine, after a single dose (W3), the levels of neutralizing antibodies were low against D614G, and almost undetectable against Alpha, Beta and Delta variants (Fig. 2b). Titers significantly increased after the second dose. We observed a 3-fold and 16-fold reduction in the neutralization titers against Delta and Beta, respectively, when compared to Alpha (Fig. 2b). Similar differences between strains were observed at a later time point (W16), although titers were globally slightly lower (Extended Data Fig. 7b).

A similar pattern was observed with the AstraZeneca vaccine. It induced low levels of antibodies neutralizing Delta and Beta, when compared to D614G and Alpha, after a single dose (W10) (Fig. 2c). Four weeks after the second dose (W16), neutralizing titers were strongly increased. There was however a 5-fold and 9-fold reduction in neutralization titers against Delta and Beta, respectively, relative to Alpha (Fig. 2c).

We classified the vaccine recipients as neutralizers and non-neutralizers, for the four viral strains (Extended Data Fig. 7d,e). With Pfizer, 13% of individuals neutralized the variant Delta after a single dose. 81 to 100% of individuals neutralized any of the four strains after the second dose, at W8. This fraction remained stable at W16, with the exception of variant Beta, which was neutralized by only 46% of the individuals. 74% and 61% of individuals that received a single dose of AstraZeneca vaccine neutralized D614G and Alpha strains, respectively. This fraction sharply dropped with Beta and Delta variants, which were inhibited by only 4 and 9% of the sera. Four weeks after the second dose of AstraZeneca, 95-100% of individuals neutralized the four strains.

Therefore, a single dose of Pfizer or AstraZeneca was either poorly or not at all efficient against Beta and Delta variants. Both vaccines generated a neutralizing response that efficiently targeted variant Delta only after the second dose.

Discussion

We studied the cross-reactivity of mAbs to pre-existing SARS-CoV-2 strains, sera from long-term convalescent individuals and recent

vaccine recipients against an infectious Delta isolate. Some mAbs, including Bamlanivimab, lost binding to the Spike and no longer neutralized variant Delta. We further show that Delta is less sensitive to sera from naturally immunized individuals. Vaccination of convalescent individuals boosted the humoral immune response well above the threshold of neutralization. These results strongly suggest that vaccination of previously infected individuals will be most likely protective against a large array of circulating viral strains, including variant Delta.

In individuals that were not previously infected with SARS-CoV-2, a single dose of either Pfizer or AstraZeneca vaccines barely induced neutralizing antibodies against variant Delta. About 10% of the sera neutralized this variant. However, a two-dose regimen generated high sero-neutralization levels against variants Alpha, Beta and Delta, in subjects sampled at W8 to W16 post vaccination. Neutralizing antibody levels are highly predictive of immune protection from symptomatic SARS-CoV-2 infection²⁵. A recent report analyzing all sequenced symptomatic cases of COVID-19 in England was used to estimate the impact of vaccination on infection²⁶. Effectiveness was notably lower with Delta than with Alpha after one dose of AstraZeneca or Pfizer vaccines. The two-dose effectiveness against Delta was estimated to be 60% and 88% for AstraZeneca and Pfizer vaccines, respectively²⁶. Our neutralization experiments indicate that Pfizer and AstraZeneca vaccine-elicited antibodies are efficacious against variant Delta, but about 3-5 fold less potent than against variant Alpha. There was no major difference in the levels of antibodies elicited by Pfizer or AstraZeneca vaccines.

Potential limitations of our work include a low number of vaccine recipients analyzed and the lack of characterization of cellular immunity, which may be more cross-reactive than the humoral response. Future work with more individuals and longer survey periods will help characterize the role of humoral responses in vaccine efficacy against circulating variants.

Our results demonstrate that the emerging variant Delta partially but significantly escapes neutralizing mAbs, and polyclonal antibodies elicited by previous SARS-CoV-2 infection or vaccination.

Online content

Any methods, additional references, Nature Research reporting summaries, source data, extended data, supplementary information, acknowledgements, peer review information; details of author contributions and competing interests; and statements of data and code availability are available at <https://doi.org/10.1038/s41586-021-03777-9>.

1. Yadav, P. D. et al. Neutralization of variant under investigation B.1.617 with sera of BBV152 vaccinees. *Clinical Infectious Diseases*, <https://doi.org/10.1093/cid/ciab411> (2021).
2. Ferreira, I. et al. SARS-CoV-2 B.1.617 emergence and sensitivity to vaccine-elicited antibodies. *Biorxiv*, 2021.2005.2008.443253, <https://doi.org/10.1101/2021.05.08.443253> (2021).
3. Hoffmann, M. et al. SARS-CoV-2 variant B.1.617 is resistant to Bamlanivimab and evades antibodies induced by infection and vaccination. *Biorxiv*, 2021.2005.2004.442663, <https://doi.org/10.1101/2021.05.04.442663> (2021).
4. Cherian, S. et al. Convergent evolution of SARS-CoV-2 spike mutations, L452R, E484Q and P681R, in the second wave of COVID-19 in Maharashtra, India. *Biorxiv*, 2021.2004.2022.440932, <https://doi.org/10.1101/2021.04.22.440932> (2021).
5. Edara, V.-V. et al. Infection and vaccine-induced neutralizing antibody responses to the SARS-CoV-2 B.1.617.1 variant. *Biorxiv*, 2021.2005.2009.443299, <https://doi.org/10.1101/2021.05.09.443299> (2021).
6. Public Health England. Variants distribution of cases. <https://www.gov.uk/government/publications/covid-19-variants-genomically-confirmed-case-numbers/variants-distribution-of-case-data-11-june-2021> (2021).
7. Tada, T. et al. The Spike Proteins of SARS-CoV-2 B.1.617 and B.1.618 Variants Identified in India Provide Partial Resistance to Vaccine-elicited and Therapeutic Monoclonal Antibodies. *Biorxiv*, 2021.2005.2014.444076, <https://doi.org/10.1101/2021.05.14.444076> (2021).
8. Liu, J. et al. BNT162b2-elicited neutralization of B.1.617 and other SARS-CoV-2 variants. *Nature*, <https://doi.org/10.1038/s41586-021-03693-y> (2021).
9. Wall, E. C. et al. Neutralising antibody activity against SARS-CoV-2 VOCs B.1.617.2 and B.1.351 by BNT162b2 vaccination. *The Lancet* **397**, 2331-2333, [https://doi.org/10.1016/S0140-6736\(21\)01290-3](https://doi.org/10.1016/S0140-6736(21)01290-3) (2021).
10. Buchrieser, J. et al. Syncytia formation by SARS-CoV-2 infected cells. *The EMBO Journal*, e106267, <https://doi.org/10.15252/embj.2020106267> (2020).
11. Planas, D. et al. Sensitivity of infectious SARS-CoV-2 B.1.1.7 and B.1.351 variants to neutralizing antibodies. *Nature Medicine* **27**, 917-924, (2021).

12. Rambaut, A. *et al.* A dynamic nomenclature proposal for SARS-CoV-2 lineages to assist genomic epidemiology. *Nature Microbiology* **5**, 1403-1407, (2020).
13. Plante, J. A. *et al.* The variant gambit: COVID-19's next move. *Cell Host & Microbe* **29**, 508-515, (2021).
14. CDC. SARS-CoV-2 Variant Classifications and Definitions. <https://www.cdc.gov/coronavirus/2019-ncov/cases-updates/variant-surveillance/variant-info.html> (2021).
15. McCallum, M. *et al.* N-terminal domain antigenic mapping reveals a site of vulnerability for SARS-CoV-2. *Cell* **184**, 2332-2347.e2316, (2021).
16. Starr, T. N., Greaney, A. J., Dingens, A. S. & Bloom, J. D. Complete map of SARS-CoV-2 RBD mutations that escape the monoclonal antibody LY-CoV555 and its cocktail with LY-CoV016. *Cell Reports Medicine* **2**, 100255, (2021).
17. Barnes, C. O. *et al.* SARS-CoV-2 neutralizing antibody structures inform therapeutic strategies. *Nature* **588**, 682-687, PMID - 33045718 (2020).
18. Taylor, P. C. *et al.* Neutralizing monoclonal antibodies for treatment of COVID-19. *Nature Reviews Immunology* **21**, 382-393, (2021).
19. Starr, T. N. *et al.* Prospective mapping of viral mutations that escape antibodies used to treat COVID-19. *Science* **371**, 850-854, (2021).
20. Liu, L. *et al.* Potent neutralizing antibodies against multiple epitopes on SARS-CoV-2 spike. *Nature* **584**, 450-456, (2020).
21. Wang, P. *et al.* Antibody resistance of SARS-CoV-2 variants B.1.351 and B.1.1.7. *Nature* **593**, 130-135, <https://doi.org/10.1038/s41586-021-03398-2> (2021).
22. Fafi-Kremer, S. *et al.* Serologic responses to SARS-CoV-2 infection among hospital staff with mild disease in eastern France. *EBioMedicine* **59**, <https://doi.org/10.1016/j.ebiom.2020.102915> (2020).
23. Gallais, F. *et al.* Anti-SARS-CoV-2 Antibodies Persist for up to 13 Months and Reduce Risk of Reinfection. *medRxiv*, 2021.2005.2007.21256823, <https://doi.org/10.1101/2021.05.07.21256823> (2021).
24. Krammer, F. *et al.* Antibody Responses in Seropositive Persons after a Single Dose of SARS-CoV-2 mRNA Vaccine. *New England Journal of Medicine* **384**, 1372-1374, (2021).
25. Khoury, D. S. *et al.* Neutralizing antibody levels are highly predictive of immune protection from symptomatic SARS-CoV-2 infection. *Nature Medicine*, <https://doi.org/10.1038/s41591-021-01377-8> (2021).
26. Bernal, J. L. *et al.* Effectiveness of COVID-19 vaccines against the B.1.617.2 variant. *medRxiv*, 2021.2005.2022.21257658, <https://doi.org/10.1101/2021.05.22.21257658> (2021).

Publisher's note Springer Nature remains neutral with regard to jurisdictional claims in published maps and institutional affiliations.

© The Author(s), under exclusive licence to Springer Nature Limited 2021

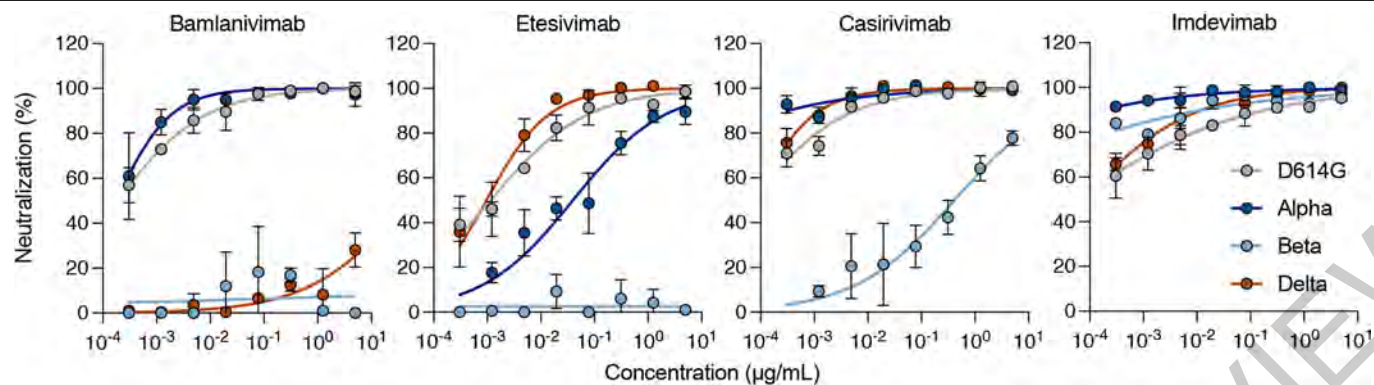


Fig. 1 | Neutralization of SARS-CoV-2 variants D614G, Alpha, Beta and Delta by therapeutic mAbs. Neutralization curves of mAbs. Dose response analysis of the neutralization by four therapeutic mAbs (Bamlanivimab, Etesivimab,

Casirivimab and Imdevimab) on D614G strain and variants Alpha, Beta and Delta. Data are mean \pm SD of four independent experiments.

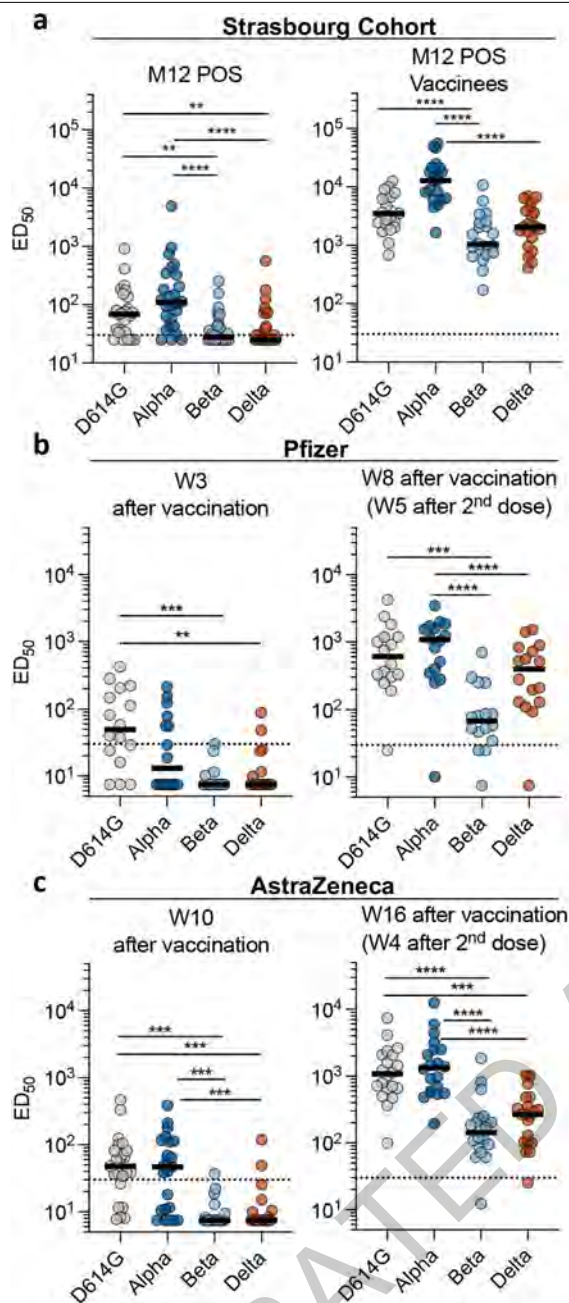


Fig. 2 | Sensitivity of SARS-CoV-2 variants D614G, Alpha, Beta and Delta to sera from convalescent individuals and vaccine recipients. Neutralization titers of the sera against the indicated viral isolates are expressed as ED₅₀.

a. Neutralizing activity of sera from the Strasbourg cohort of convalescent (n=26, left panel) and convalescent and vaccinated individuals (n=21, right panel) were sampled at Month 12 (M12) post onset of symptoms (POS).

b. Neutralizing activity of sera from Pfizer vaccinated recipients sampled at W3 (n=16) (left panel) and W8 post-vaccination (W5 after second dose) (n=16) (right panel).

c. Neutralizing activity of sera from AstraZeneca vaccinated recipients sampled at W10 (n=23) (left panel) and W16 post-vaccination (W4 post second dose) (n=20) (right panel). The dotted line indicates the limit of detection (ED₅₀=30). Data are mean from two independent experiments. Two-sided Friedman test with Dunn's multiple comparison was performed between each viral strain. **P* < 0.05, ***P* < 0.01, ****P* < 0.001, *****P* < 0.0001. M12 POS: D614G versus Beta, *P* = 0.0052; D614G versus Delta, *P* = 0.0052; Alpha versus Beta, *P* < 0.0001; Alpha versus Delta, *P* < 0.0001. M12 POS Vaccinees: D614G versus Beta, *P* < 0.0001; Alpha versus Beta, *P* < 0.0001; Alpha versus Delta, *P* < 0.0001.

Pfizer (W3): D614G versus Beta, *P* = 0.0001; D614G versus Delta, *P* = 0.0013. Pfizer (W8): D614G versus Beta, *P* = 0.0002; Alpha versus Beta, *P* < 0.0001; Alpha versus Delta, *P* = 0.0098. AstraZeneca (W10): D614G versus Beta, *P* < 0.0001; D614G versus Delta, *P* < 0.0001; Alpha versus Beta, *P* = 0.0006; Alpha versus Delta, *P* = 0.0056. AstraZeneca (W16): D614G versus Beta, *P* < 0.0001; D614G versus Delta, *P* = 0.0375; Alpha versus Beta, *P* < 0.0001; Alpha versus Delta, *P* = 0.0375.

Methods

No statistical methods were used to predetermine sample size. The experiments were not randomized and the investigators were not blinded to allocation during experiments and outcome assessment. Our research complies with all relevant ethical regulation.

Orléans Cohort of convalescent and vaccinated individuals

Since August 27, 2020, a prospective, monocentric, longitudinal, interventional cohort clinical study enrolling 170 SARS-CoV-2-infected individuals with different disease severities, and 59 non-infected healthy controls is on-going, aiming to describe the persistence of specific and neutralizing antibodies over a 24-months period. This study was approved by the ILE DE FRANCE IV ethical committee. At enrolment, written informed consent was collected and participants completed a questionnaire which covered sociodemographic characteristics, virological findings (SARS-CoV-2 RT-PCR results, including date of testing), clinical data (date of symptom onset, type of symptoms, hospitalization), and data related to anti-SARS-CoV-2 vaccination if ever (brand product, date of first and second doses). Serological status of participants was assessed every 3 months. Those who underwent anti-SARS-CoV-2 vaccination had regular blood sampling after first dose of vaccine (ClinicalTrials.gov Identifier: NCT04750720). The primary outcome was the presence of antibodies to SARS-CoV-2 Spike protein as measured with the S-Flow assay. The secondary outcome was the presence of neutralizing antibodies as measured with the S-Fuse assay. For the present study, we selected 56 convalescent and 59 vaccinated participants (16 with Pfizer and 43 with AstraZeneca). Study participants did not receive any compensation.

Strasbourg Cohort of convalescent individuals

Since April 2020, a prospective, interventional, monocentric, longitudinal, cohort clinical study enrolling 308 RT-PCR-diagnosed SARS-CoV-2 infected hospital staff from the Strasbourg University Hospitals is on-going (ClinicalTrials.gov Identifier: NCT04441684). At enrolment (from April 17, 2020), written informed consent was collected and participants completed a questionnaire which covered sociodemographic characteristics, virological findings (SARS-CoV-2 RT-PCR results including date of testing) and clinical data (date of symptom onset, type of symptoms, hospitalization). This study was approved by Institutional Review Board of Strasbourg University Hospital. The serological status of the participants has been described at Months 3 (M3) and Months 6 (M6) POS^{22,23}. Laboratory identification of SARS-CoV-2 was performed at least 10 days before inclusion by RT-PCR testing on nasopharyngeal swab specimens according to current guidelines (Institut Pasteur, Paris, France; WHO technical guidance). The assay targets two regions of the viral RNA-dependent RNA polymerase (RdRp) gene with a threshold of detection of 10 copies per reaction. The primary outcome was the presence of antibodies to SARS-CoV-2 Spike protein as measured with the S-Flow assay. The secondary outcome was the presence of neutralizing antibodies as measured with the S-Fuse assay. For the present study, we randomly selected 47 patients collected at M12 (26 unvaccinated and 21 vaccinated). Study participants did not receive any compensation.

Phylogenetic analysis

All SARS-CoV-2 sequences available on the GISAID EpiCov™ database as of May 21, 2021 were retrieved. A subset of complete and high coverage sequences, as indicated in GISAID, assigned to lineages B.1.617.1, B.1.617.2, B.1.617.3 were randomly subsampled to contain up to 5 sequences per country and epidemiological week in R with packages tidyverse and lubridate. Together with a single B.1.617 sequence this subset was included in the global SARS-CoV-2 phylogeny reconstructed with augur and visualized with auspice as implemented in the Nextstrain pipeline (<https://github.com/nextstrain/ncov>, version from 21 May 2021)²⁸. Within Nextstrain, a random subsampling approach capping

a maximum number of sequences per global region was used for the contextual non-B.1.617 sequences. The acknowledgment of contributing and originating laboratories for all sequences used in the analysis is provided in Supplementary Table 1.

3D representation of mutations on B.1.617.2 and other variants to the Spike surface

Panels in Fig. 1 were prepared with The PyMOL Molecular Graphics System, Version 2.1 Schrödinger, LLC. The atomic model used (PDB:6XR8) has been previously described²⁹.

S-Fuse neutralization assay

U2OS-ACE2 GFP1-10 or GFP 11 cells, also termed S-Fuse cells, become GFP+ when they are productively infected by SARS-CoV-2^{10,11}. Cells were tested negative for mycoplasma. Cells were mixed (ratio 1:1) and plated at 8×10^3 per well in a µClear 96-well plate (Greiner Bio-One). The indicated SARS-CoV-2 strains were incubated with serially diluted mAb or sera for 15 minutes at room temperature and added to S-Fuse cells. The sera were heat-inactivated 30 min at 56 °C before use. 18 hours later, cells were fixed with 2% PFA, washed and stained with Hoechst (dilution 1:1,000, Invitrogen). Images were acquired with an Opera Phenix high content confocal microscope (PerkinElmer). The GFP area and the number of nuclei were quantified using the Harmony software (PerkinElmer). The percentage of neutralization was calculated using the number of syncytia as value with the following formula: $100 \times (1 - (\text{value with serum} - \text{value in "non-infected"}) / (\text{value in "no serum"} - \text{value in "non-infected"}))$. Neutralizing activity of each serum was expressed as the half maximal effective dilution (ED50). ED50 values (in µg/ml for mAbs and in dilution values for sera) were calculated with a reconstructed curve using the percentage of the neutralization at the different concentrations.

Clinical history of the patient infected with B.1.617.2

A 54-year-old man was admitted April, 27, 2021 in the Emergency department of the Hôpital Européen Georges Pompidou hospital in Paris, France, for an acute respiratory distress syndrome with fever. He had no medical background and came back from India (West Bengali and few days spent in Delhi) 10 days before (April 17, 2021), where he stayed 15 days for his work. Onset of symptoms (abdominal pain and fever) was approximately April 18, 2021. The nasopharyngeal swab was tested positive for SARS-CoV-2 at his date of admission. Lung tomo-densitometry showed a mild (10-25%) COVID-19 pneumonia without pulmonary embolism. He initially received oxygen therapy 2 L/min, dexamethasone 6mg/day and enoxaparin 0,4 ml twice a day. His respiratory state worsened on day 3 (April 30, 2021). He was transferred in an intensive care unit, where he received high flow oxygen therapy (maximum 12 L/min). His respiratory condition improved, and he was transferred back in a conventional unit on day 8 (May 5, 2021). He was discharged from hospital on day 15 (May 10, 2021).

Virus strains

The reference D614G strain (hCoV-19/France/GE1973/2020) was supplied by the National Reference Centre for Respiratory Viruses hosted by Institut Pasteur (Paris, France) and headed by Pr. S. van der Werf. This viral strain was supplied through the European Virus Archive goes Global (Evag) platform, a project that has received funding from the European Union's Horizon 2020 research and innovation program under grant agreement n° 653316. The variant strains were isolated from nasal swabs using Vero E6 cells and amplified by one or two passages. B.1.1.7 originated from a patient in Tours (France) returning from United Kingdom. B.1.351 (hCoV-19/France/IDF-IPP00078/2021) originated from a patient in Creteil (France). B.1.617.2 was isolated from a nasopharyngeal swab of a hospitalized patient returning from India. The swab was provided and sequenced by the laboratory of Virology of Hôpital Européen Georges Pompidou (Assistance Publique – Hôpitaux

Article

de Paris). Both patients provided informed consent for the use of the biological materials. Titration of viral stocks was performed on Vero E6, with a limiting dilution technique allowing a calculation of TCID₅₀, or on S-Fuse cells. Viruses were sequenced directly on nasal swabs, and after one or two passages on Vero cells. Sequences were deposited on GISAID immediately after their generation, with the following IDs: D614G: EPI_ISL_414631; B.1.1.7: EPI_ISL_735391; B.1.1.351: EPI_ISL_964916; B.1.617.2: ID: EPI_ISL_2029113.

Flow Cytometry

Vero cells were infected with the indicated viral strains at a multiplicity of infection (MOI) of 0.1. Two days after, cells were detached using PBS-EDTA and transferred into U-bottom 96-well plates (50,000 cell/well). Cells were fixed in 4% PFA for 15-30 min at RT. Cells were then incubated for 15-30 min at RT with the indicated mAbs (1 µg/mL) in PBS, 1% BSA, 0.05% sodium azide, and 0.05% Saponin. Cells were washed with PBS and stained using anti-IgG AF647 (1:600 dilution) (ThermoFisher). Stainings were also performed on control uninfected cells. Data were acquired on an Attune Nxt instrument using Attune Nxt Software v3.2.1 (Life Technologies) and analysed with FlowJo 10.7.1 (Becton Dickinson).

Antibodies

The four therapeutic antibodies were kindly provided by CHR Orleans. Human anti-SARS-CoV2 mAbs were cloned from S-specific blood memory B cells of COVID-19 convalescents (Planchais et al, manuscript in preparation). Recombinant human IgG1 mAbs were produced by co-transfection of Freestyle 293-F suspension cells (Thermo Fisher Scientific) as previously described³⁰, purified by affinity chromatography using protein G sepharose 4 fast flow beads (GE Healthcare) and validated using ELISA against the trimeric S, RBD, S2 and NTD proteins (Planchais et al, in preparation).

Statistical analysis

Flow cytometry data were analyzed with FlowJo v10 software (TriStar). Calculations were performed using Excel 365 (Microsoft). Figures were drawn on Prism 9 (GraphPad Software). Statistical analysis was conducted using GraphPad Prism 9. Statistical significance between different groups was calculated using the tests indicated in each figure legend.

Reporting summary

Further information on research design is available in the Nature Research Reporting Summary linked to this paper.

Data availability

All data supporting the findings of this study are available within the article or from the corresponding authors upon request. Source data are

provided with this paper. Viral sequences are available upon request and were deposited at GISAID (<https://www.gisaid.org/>) under the following numbers: hCoV-19/France/GE1973/2020 (D614G): EPI_ISL_414631; Alpha (B.1.1.7): EPI_ISL_735391; Beta (B.1.351): EPI_ISL_964916 and Delta (B.1.617.2): EPI_ISL_2029113. Source data are provided with this paper.

27. Tzou, P. L. et al. Coronavirus Antiviral Research Database (CoV-RDB): An Online Database Designed to Facilitate Comparisons between Candidate Anti-Coronavirus Compounds. *Viruses* **12**, 1006 (2020).
28. Hadfield, J. et al. Nextstrain: real-time tracking of pathogen evolution. *Bioinformatics* **34**, 4121-4123, (2018).
29. Cai, Y. et al. Distinct conformational states of SARS-CoV-2 spike protein. *Science* **369**, 1586-1592 (2020).
30. Lorin, V. & Mouquet, H. Efficient generation of human IgA monoclonal antibodies. *J Immunol Methods* **422**, 102-110, (2015).

Acknowledgements We thank Nicoletta Casartelli for critical reading of the manuscript and Pablo Guardado Calvo for discussion. We thank patients who participated to this study, members of the Virus and Immunity Unit for discussions and help, Nathalie Aulner and the UtechS Photonic Bioluminescence (UPBI) core facility (Institut Pasteur), a member of the France Bioluminescence network, for image acquisition and analysis. The Opera system was co-funded by Institut Pasteur and the Région Île de France (DIM1Health). We thank the DRCI, CIC, Médecine du travail and Pôle de Biologie teams (CHU de Strasbourg) for the management of the Strasbourg cohort and serology testing. We thank the members of the Virus and Immunity Unit for discussion and help, the UtechS Photonic Bioluminescence (PBI) core facility (Institut Pasteur), a member of the France Bioluminescence network, for image acquisition and analysis (the Opera system was co-funded by Institut Pasteur and the Région Île de France (DIM1Health)). Work in OS lab is funded by Institut Pasteur, Urgence COVID-19 Fundraising Campaign of Institut Pasteur, Fondation pour la Recherche Médicale (FRM), ANRS, the Vaccine Research Institute (ANR-10-LABX-77), Labex IBEID (ANR-10-LABX-62-IBEID), ANR/FRM Flash Covid PROTEO-SARS-CoV-2 and IDISCOVER. Work in UPBI is funded by grant ANR-10-INSB-04-01 and Région Île-de-France program DIM1-Health. DP is supported by the Vaccine Research Institute. LG is supported by the French Ministry of Higher Education, Research and Innovation. HM lab is funded by the Institut Pasteur, the Milieu Intérieur Program (ANR-10-LABX-69-01), the INSERM, REACTing, EU (RECOVER) and Fondation de France (#00106077) grants. SFK lab is funded by Strasbourg University Hospitals (SeroCoV-HUS; PRI 7782), Programme Hospitalier de Recherche Clinique (PHRC N 2017- HUS N° 6997), the Agence Nationale de la Recherche (ANR-18-CE17-0028), Laboratoire d'Excellence TRANSPLANTEX (ANR-11-LABX-0070_TRANSPLANTEX), Institut National de la Santé et de la Recherche Médicale (UMR_S 1109). ESL lab is funded by Institut Pasteur and the French Government's Investissement d'Avenir programme, Laboratoire d'Excellence "Integrative Biology of Emerging Infectious Diseases" (grant n°ANR-10-LABX-62-IBEID). The funders of this study had no role in study design, data collection, analysis and interpretation, or writing of the article.

Author contributions Experimental strategy design, experiments: DP, DV, AB, IS, FGB, MMR, FP, TB, ESL, FR. Vital materials DV, CP, NR, JP, MP, FG, PG, AV, JLG, LC, NKC, DE, LB, AS, HP, LH, SFK, TP, HM. Manuscript writing: DP, TB, ESL, FR, OS. Manuscript editing: DV, MMR, HP, LH, SFK, TP, HM.

Competing interests C.P., H.M., O.S., T.B., F.R. have a pending patent application for the anti-RBD mAbs described in the present study (PCT/FR2021/070522).

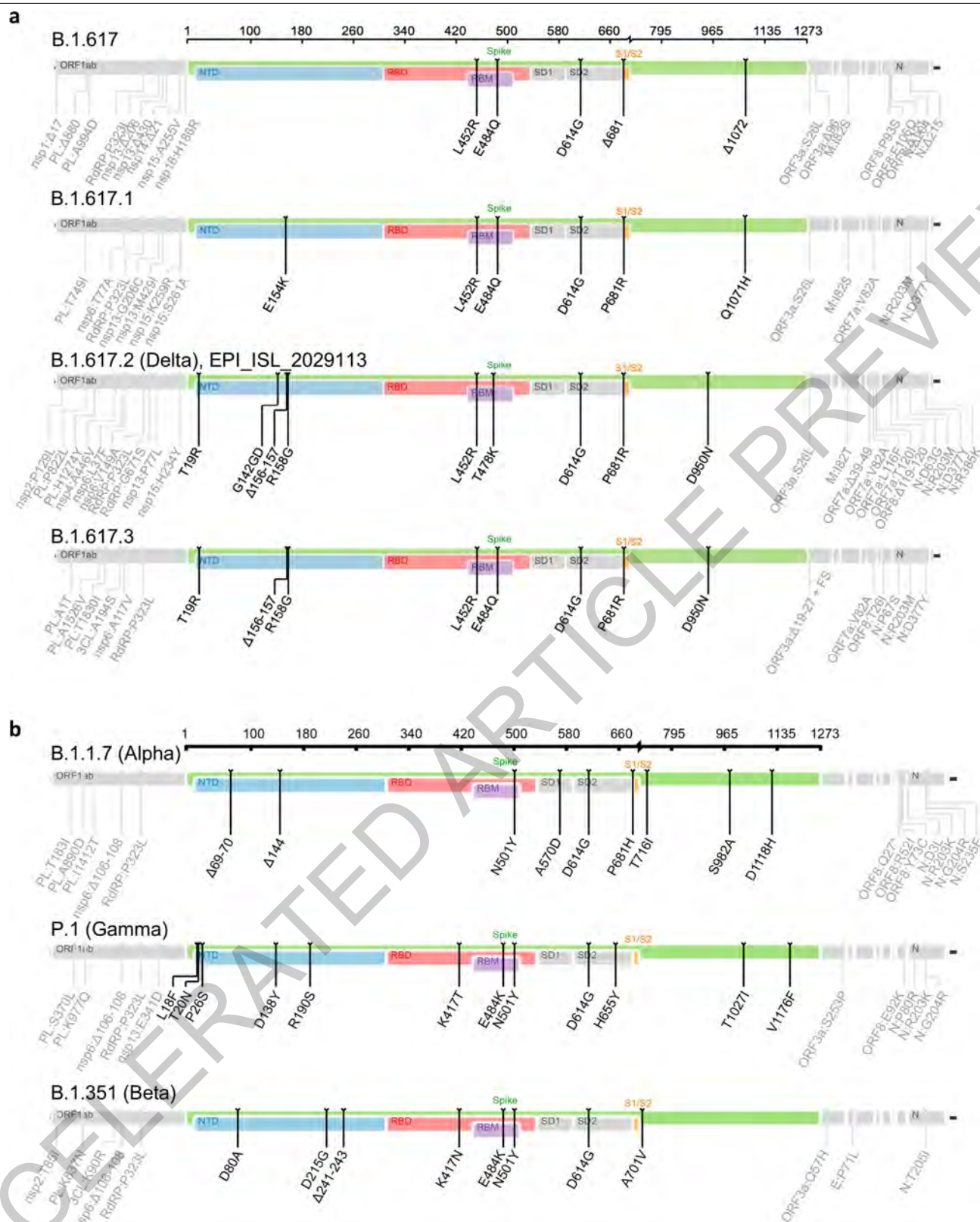
Additional information

Supplementary information The online version contains supplementary material available at <https://doi.org/10.1038/s41586-021-03777-9>.

Correspondence and requests for materials should be addressed to T.B. or O.S.

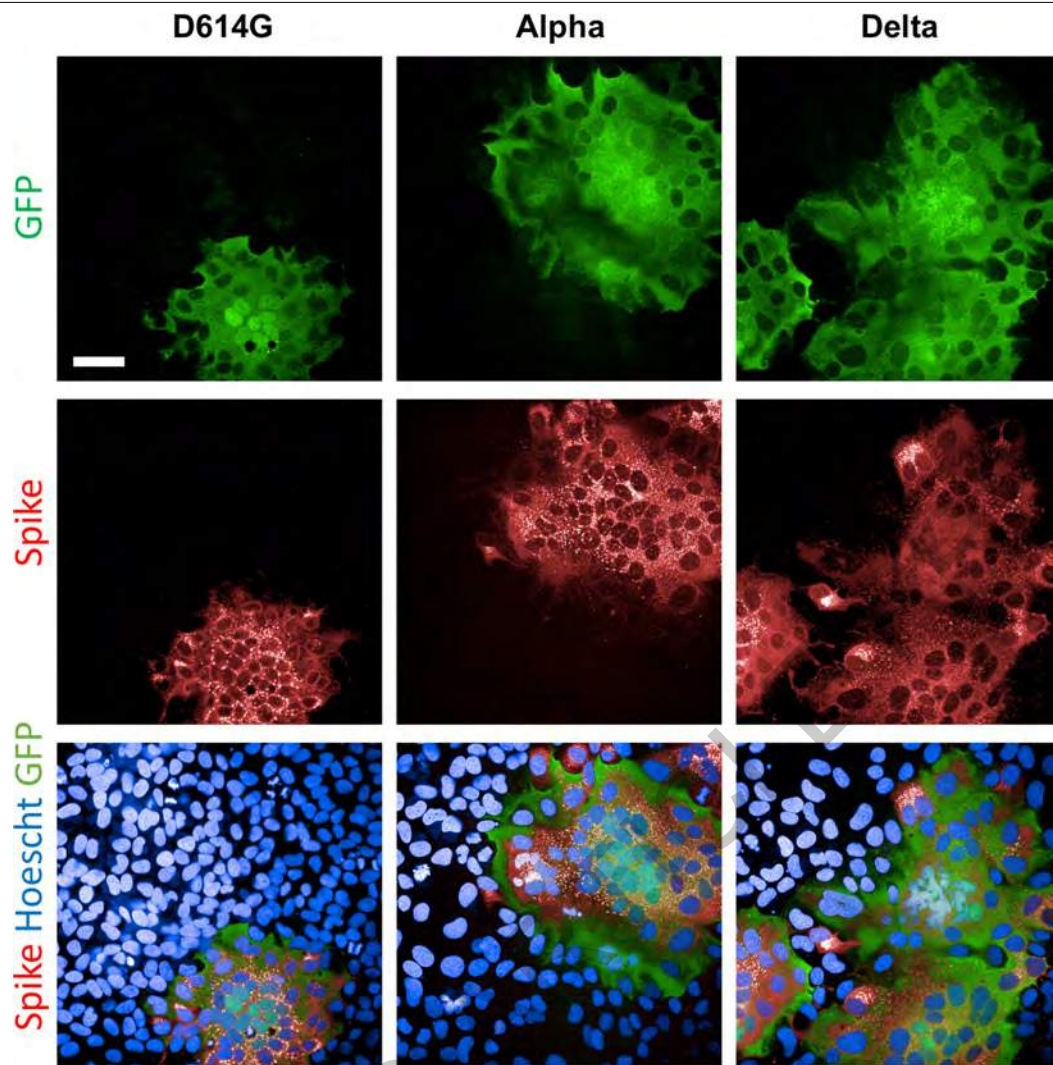
Peer review information Nature thanks the anonymous reviewers for their contribution to the peer review of this work.

Reprints and permissions information is available at <http://www.nature.com/reprints>.



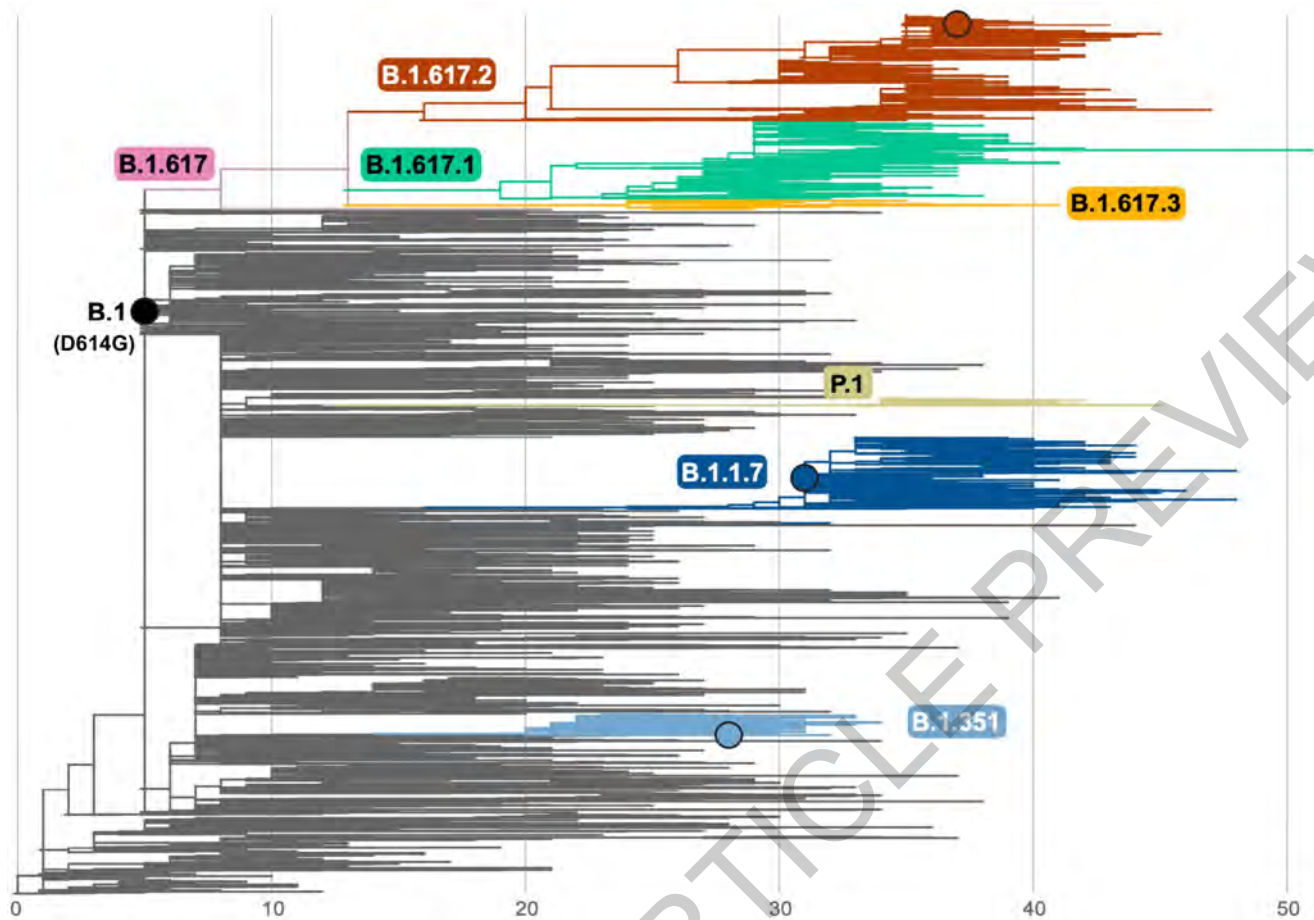
Extended Data Fig. 1 | Schematic overview of the B.1.617 sublineage and variants of concern. Schematic overview of B.1.617 sublineage (a) and variants of concern B.1.1.7 (Alpha), P.1 (Gamma) and B.1.351 (Beta) (b). Consensus

sequences with a focus on the Spike were built with the Sierra tool²⁷. Amino acid modifications in comparison to the ancestral Wuhan-Hu-1 sequence (NC_045512) are indicated.



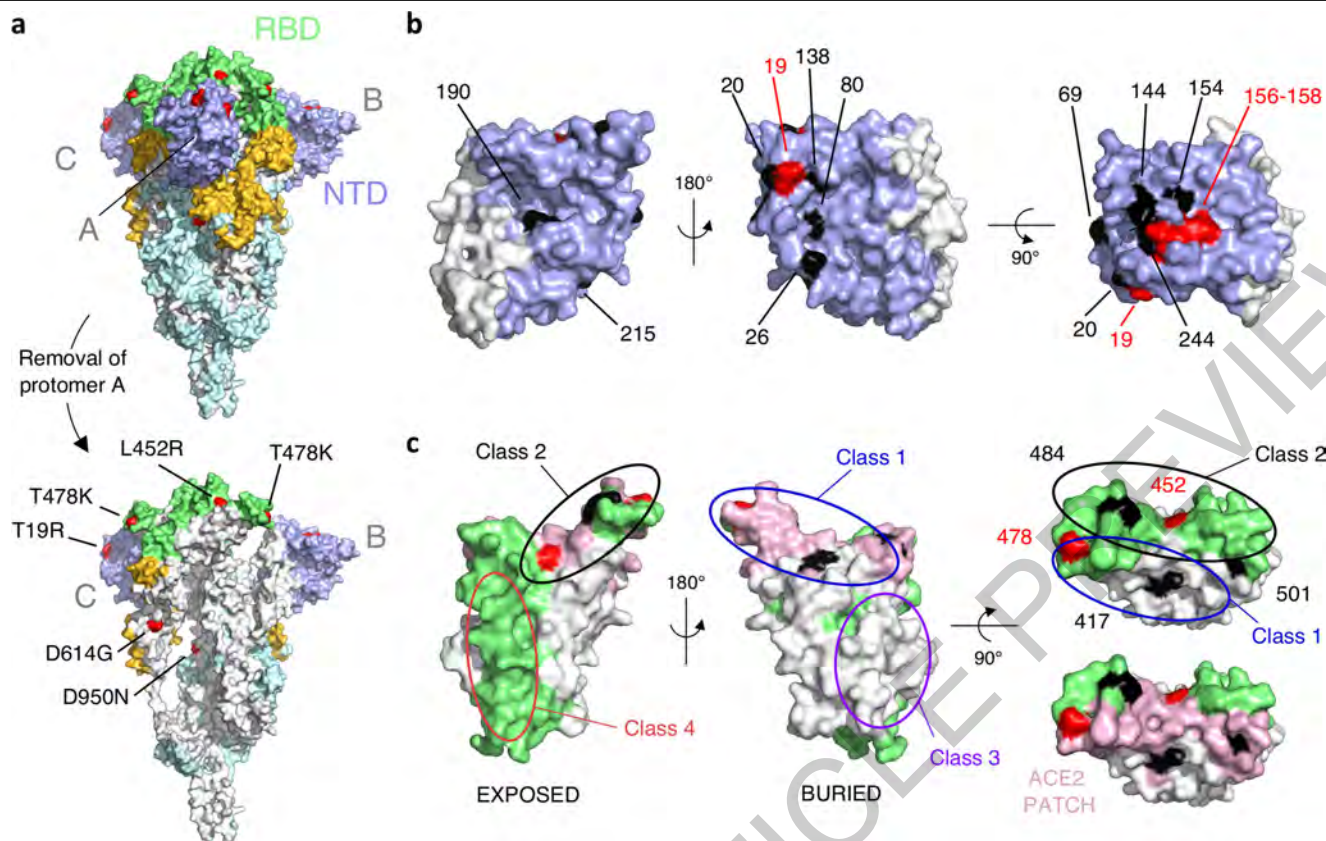
Extended Data Fig. 2 | SARS-CoV-2 variants induce syncytia in S-Fuse cells. S-Fuse cells were exposed to the indicated SARS-CoV-2 strain (MOI10³). The cells become GFP+ when they fuse together. After 20 h, infected cells were

stained with anti-Spike antibodies and Hoechst to visualize nuclei. Syncytia (green), Spike (red) and nuclei (blue) are shown. Representative images from three independent experiments are shown. Scale bar: 50 μ m.



Extended Data Fig. 3 | Global phylogeny of SARS-CoV-2 highlighting the B.1.617 lineage. The maximum likelihood tree was inferred using IQ-Tree, as implemented in the Nextstrain pipeline on a subsampled dataset of 3794 complete genomes. Branch lengths are scaled according to the number of

nucleotide substitutions from the root of the tree. The branches corresponding to key lineages are colored: B.1.1.7, dark blue; B.1.351, light blue; P.1, beige; B.1.617, pink; B.1.617.1, green; B.1.617.2, red; B.1.617.3, orange. A black circle indicates the position of the viruses studied here.

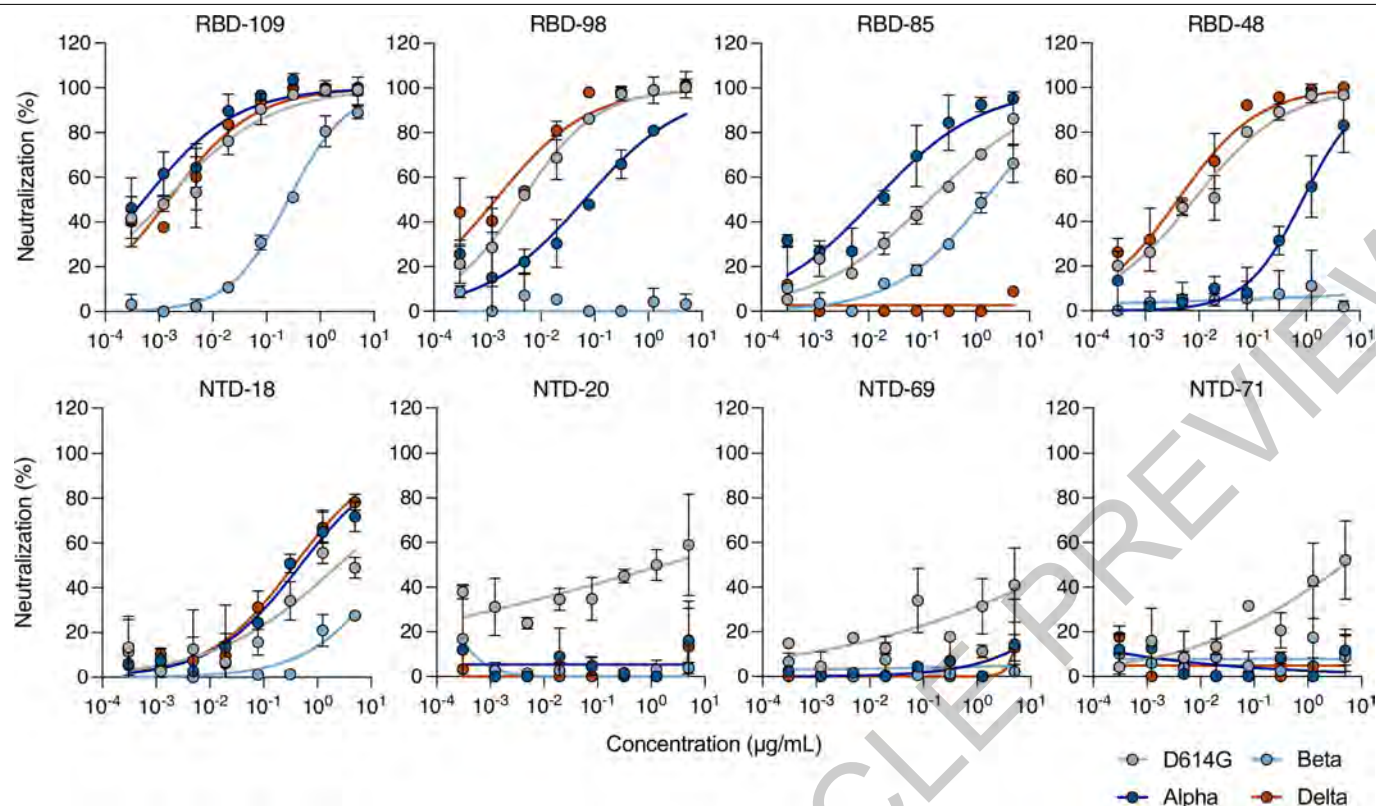


Extended Data Fig. 4 | Mapping mutations of variant Delta and other variants of concern to the Spike surface.

a. The Spike protein trimer (PDB:6XR8, corresponding to a closed spike trimer with all three RBDs in the “down” conformation) is shown with its surface colored according to domains: NTD in dark blue, RBD in green, the remainder of S1 in yellow and S2 in light blue. Interfaces between protomers were left white to help visualize the protomers’ boundaries. The three polypeptide chains in the trimer were arbitrarily defined as A, B and C. Surface patches corresponding to residues mutated in the variant Delta are colored in red. The bottom panel has the front protomer (chain A) removed to show the trimer interface (buried regions in the trimer are in white). The mutations in Delta are labelled in the bottom panel.

b. NTD shown in three orthogonal views. The left panel corresponds roughly to the orientation seen in chain B in a, and the middle panel shows a view from the

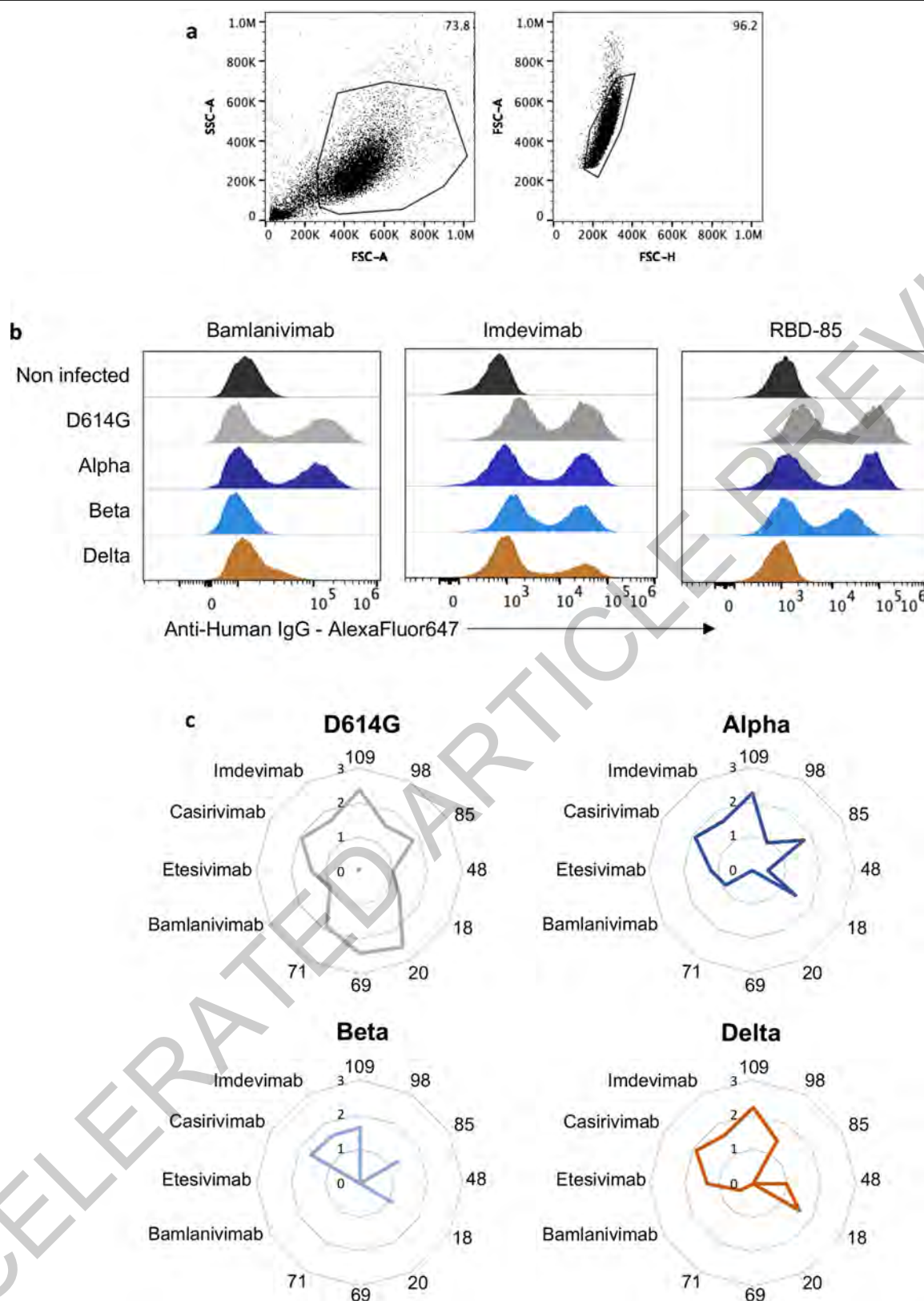
back. The right panel shows a view from the top of the trimer. Mutations found in the main variants of concern are indicated. The mutations found in variant Delta are in red. **c.** RBD shown in three orthogonal views, colored according to solvent exposure in the context of the closed spike: green and white indicate exposed and buried surfaces, as in a. The ACE2-binding surface is colored in pink. The left panel shows a view from the top of the trimer, and the middle panel a view from below. The right panels show a view down the ACE2 binding surface, highlighted in pink in the bottom panel. Mutations found in the main variants of concern are indicated. The mutations found in variant Delta are in red. The ovals indicate the epitope regions of the four main classes of anti-RBD neutralizing antibodies. Note that the mutations on the RBD cluster all around the ACE2 patch. Panels were prepared with The PyMOL Molecular Graphics System, Version 2.1 Schrödinger, LLC.



Extended Data Fig. 5 | Neutralization of SARS-CoV-2 variants D614G, Alpha, Beta and Delta by mAbs targeting the RBD and the NTD domains.

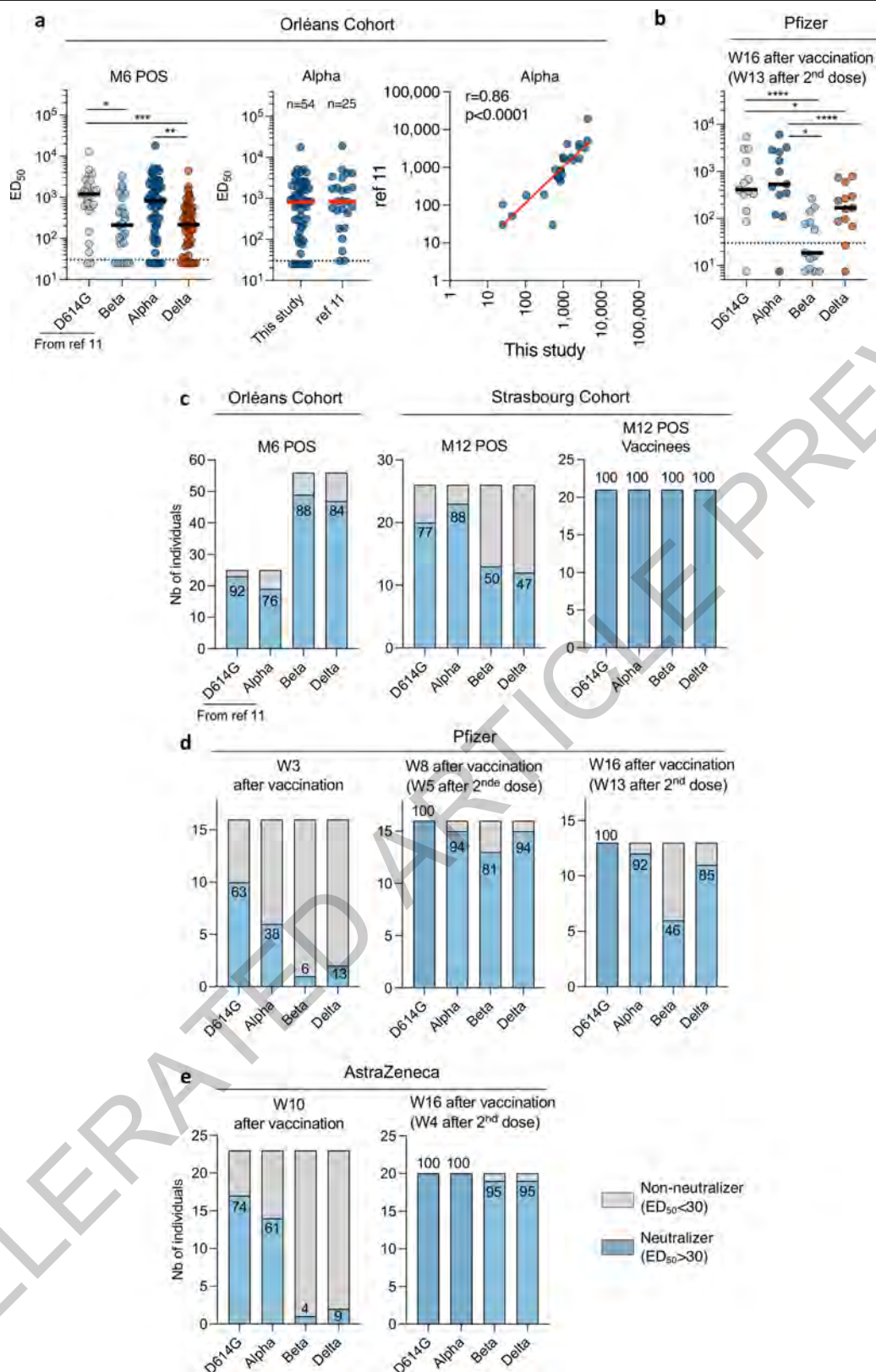
Neutralization curves of mAbs. Dose response analysis of the neutralization by

four anti-RBD and four anti-NTD on D614G strain (grey), and variants Alpha (dark blue), Beta (light blue) and Delta (orange). Data are mean \pm SD of three independent experiments.



Extended Data Fig. 6 | Binding of anti-SARS-CoV-2 mAbs to Vero cells infected with variants D614G, Alpha, Beta and Delta. Vero cells were infected with the indicated variants at a MOI of 0.1. After 48h, cells were stained with anti-SARS-CoV-2 mAbs (1 μ g/ml) and analyzed by flow-cytometry. **a.** Gating strategy. **b.** Histograms show the binding of Bamlanivimab,

Imdevimab and RBD-85 to Vero cells infected with the indicated variants. **c.** Radar charts represent for each antibody the logarithm of the mean of fluorescent intensity of the staining, relative to the non-infected condition. Data are representative of three independent experiments.



Extended Data Fig. 7 | See next page for caption.

Article

Extended Data Fig. 7 | Sensitivity of SARS-CoV-2 variants D614G, Alpha, Beta and Delta to sera from convalescent individuals and vaccine recipients. **a.** ED50 of neutralization of convalescent individuals from the Orléans cohort against the four viral variants are depicted. Samples were collected 6 months post onset of symptoms (M6 POS). Sensitivity of variants D614G and Alpha was assessed on 25 individuals previously published in ref.¹¹. Fifty six sera (including the 25 previous sera) were tested against variants Beta and Delta. Neutralization data obtained in this study and in ref.¹¹ were compared (middle panel) and correlated (right panel). Similar results were obtained, allowing to bridge the datasets. Data are mean from two independent experiments. The dotted line indicates the limit of detection (ED50=30). Two-sided Kruskal-Wallis test with Dunn's multiple comparison was performed between each viral strain. * $P < 0.05$, ** $P < 0.01$, *** $P < 0.001$, **** $P < 0.0001$. D614G versus Beta, $P = 0.0153$; D614G versus Delta, $P = 0.0008$; Alpha versus Delta, $P = 0.0014$. **b.** ED50 of neutralization of Pfizer-vaccinated individuals sampled at W16 (corresponding to W13 after the second dose). Data are mean from two independent experiments. The dotted line indicates the

limit of detection (ED50=30). Two-sided Kruskal-Wallis test with Dunn's multiple comparison was performed between each viral strain. * $P < 0.05$, ** $P < 0.01$, *** $P < 0.001$, **** $P < 0.0001$. D614G versus Beta, $P < 0.0001$; D614G versus Delta, $P = 0.0375$; Alpha versus Beta, $P < 0.0001$; Alpha versus Delta, $P = 0.0375$. **c,d,e.** Fraction of neutralizers in the cohorts of convalescent or vaccinated individuals. Individuals with an ED50 of neutralization above 30 were categorized as neutralizers and are indicated in blue. Non-neutralizers are in grey. **c.** Analysis of convalescent individuals from the Orléans cohort collected at M6 (left panel, related to Extended Data Fig. 7a.), from the Strasbourg cohort collected at M12 and unvaccinated (middle panel, related to Fig. 2a) or vaccinated (right panel, related to Fig. 2a). **c.** Sera from Pfizer vaccinated recipients were sampled at W3, W8 (left and middle panels, related to Fig. 2c), and W16 post-vaccination (related to Extended Data Fig. 7b). **e.** Sera from AstraZeneca vaccinated recipients sampled at W10 and W16 post-vaccination (related to Fig. 2c). The numbers indicate the % of neutralizers.

Extended Data Table 1 | Characteristics of the two cohorts of convalescent individuals**a.**

Orléans Cohort: M6 POS		n=56
Sex	Female	29
	Male	27
Age (Median; range)		53 (22;77)
Severity	Critical	13
	Severe	15
	Mild-Moderate	16
	Asymptomatic	12
HIV		3
PCR		53
Anti-S (S-Flow)		56
Sampling days POS (median; range)		188 (114;205)

b.

		Convalescent	Vaccinated Convalescent
Strasbourg Cohort : M12 POS		n=26	n=21
Sex	Female	21	18
	Male	5	3
Age (Median; range)		36 (24;60)	44 (23;62)
Severity	Critical	0	0
	Severe	0	0
	Mild-Moderate	26	21
	Asymptomatic	0	0
PCR		26	21
Anti-S (Abott)		26	21
Vaccine	AstraZeneca	0	9
	Pfizer	0	9
	Moderna	0	3
Sampling days (median; range)			
POS		330 (144;383)	359 (327;404)
Post Vaccine		NA	24 (7;81)

Article

Extended Data Table 2 | Characteristics of the cohort of vaccinated recipients

		Pfizer (1 or 2 doses)	AstraZeneca (1 dose)	AstraZeneca (2 doses)
Orléans cohort: Vaccinated recipients		n=16	n=23	N=20
Sex	Female	5	7	15
	Male	11	5	5
Age (Median; range)		60 (35;75)	38 (28;64)	59.5 (55;73)
Immune deficiency		0	0	0
Previous COVID-19		0	0	0
Anti-N		0	0	0
1st dose		Jan 4 – 8, 2021	Feb 8 – April 22, 2021	Feb 5 – April 7, 2021
2nd dose		Jan 20 – Feb 5, 2021	NA	May 3 – 19, 2021
Sampling days post-vaccination (Median; range)				
	W3	20 (18;25)		
	W8	57 (53;84)		
	W10		70 (41;91)	
	W16	118 (116;124)		109 (56;116)

Reporting Summary

Nature Research wishes to improve the reproducibility of the work that we publish. This form provides structure for consistency and transparency in reporting. For further information on Nature Research policies, see our [Editorial Policies](#) and the [Editorial Policy Checklist](#).

Statistics

For all statistical analyses, confirm that the following items are present in the figure legend, table legend, main text, or Methods section.

n/a Confirmed

- ☐ ☒ The exact sample size (n) for each experimental group/condition, given as a discrete number and unit of measurement
- ☐ ☒ A statement on whether measurements were taken from distinct samples or whether the same sample was measured repeatedly
- ☐ ☒ The statistical test(s) used AND whether they are one- or two-sided
Only common tests should be described solely by name; describe more complex techniques in the Methods section.
- ☐ ☒ A description of all covariates tested
- ☐ ☒ A description of any assumptions or corrections, such as tests of normality and adjustment for multiple comparisons
- ☐ ☒ A full description of the statistical parameters including central tendency (e.g. means) or other basic estimates (e.g. regression coefficient) AND variation (e.g. standard deviation) or associated estimates of uncertainty (e.g. confidence intervals)
- ☐ ☒ For null hypothesis testing, the test statistic (e.g. F , t , r) with confidence intervals, effect sizes, degrees of freedom and P value noted
Give P values as exact values whenever suitable.
- ☒ ☐ For Bayesian analysis, information on the choice of priors and Markov chain Monte Carlo settings
- ☒ ☐ For hierarchical and complex designs, identification of the appropriate level for tests and full reporting of outcomes
- ☒ ☐ Estimates of effect sizes (e.g. Cohen's d , Pearson's r), indicating how they were calculated

Our web collection on [statistics for biologists](#) contains articles on many of the points above.

Software and code

Policy information about [availability of computer code](#)

Data collection Harmony Software v4.9 (Perkin-Elmer), Attune NXT Software v3.2.1 (ThermoFischer), Flowjo Software v10.7.1, R v4.1.0, tidyverse v1.3.1, Lubridate v1.7.10

Data analysis Excel 365 v16.46 (Microsoft), Prism v9.0.2 (GraphPad Software)

For manuscripts utilizing custom algorithms or software that are central to the research but not yet described in published literature, software must be made available to editors and reviewers. We strongly encourage code deposition in a community repository (e.g. GitHub). See the Nature Research [guidelines for submitting code & software](#) for further information.

Data

Policy information about [availability of data](#)

All manuscripts must include a [data availability statement](#). This statement should provide the following information, where applicable:

- Accession codes, unique identifiers, or web links for publicly available datasets
- A list of figures that have associated raw data
- A description of any restrictions on data availability

All data are provided as supplementary tables

Field-specific reporting

Please select the one below that is the best fit for your research. If you are not sure, read the appropriate sections before making your selection.

☒ Life sciences ☐ Behavioural & social sciences ☐ Ecological, evolutionary & environmental sciences

For a reference copy of the document with all sections, see [nature.com/documents/nr-reporting-summary-flat.pdf](https://www.nature.com/documents/nr-reporting-summary-flat.pdf)

Life sciences study design

All studies must disclose on these points even when the disclosure is negative.

Sample size	162 sera from convalescent, vaccinated and vaccinated convalescent individuals were analyzed in the study. Given the explanatory nature of the study aiming at describing a phenomenon whose frequency has not yet been established we did not use statistical methods to predetermine sample size. Thus, we included between 20 and 50 patients per group to allow statistical analysis
Data exclusions	None.
Replication	All experiments were performed and verified in multiple replicates as indicated in their methods/figure legends.
Randomization	The experiments were not randomized as this is not relevant for an observational study.
Blinding	The investigators were not blinded to allocation as this is not relevant for an observational study. However, the clinical sampling and biological measurement were performed by different teams. Only the final assembly of the data revealed the global view of the results.

Reporting for specific materials, systems and methods

We require information from authors about some types of materials, experimental systems and methods used in many studies. Here, indicate whether each material, system or method listed is relevant to your study. If you are not sure if a list item applies to your research, read the appropriate section before selecting a response.

Materials & experimental systems

n/a	Involved in the study
<input type="checkbox"/>	<input checked="" type="checkbox"/> Antibodies
<input type="checkbox"/>	<input checked="" type="checkbox"/> Eukaryotic cell lines
<input checked="" type="checkbox"/>	<input type="checkbox"/> Palaeontology and archaeology
<input checked="" type="checkbox"/>	<input type="checkbox"/> Animals and other organisms
<input type="checkbox"/>	<input checked="" type="checkbox"/> Human research participants
<input type="checkbox"/>	<input checked="" type="checkbox"/> Clinical data
<input checked="" type="checkbox"/>	<input type="checkbox"/> Dual use research of concern

Methods

n/a	Involved in the study
<input checked="" type="checkbox"/>	<input type="checkbox"/> ChIP-seq
<input type="checkbox"/>	<input checked="" type="checkbox"/> Flow cytometry
<input checked="" type="checkbox"/>	<input type="checkbox"/> MRI-based neuroimaging

Antibodies

Antibodies used	The anti-S RBD-48, RBD-85, RBD-98, RBD-109, NTD-18, NTD-20, NTD-69 and NTD-71 are human anti-S monoclonal antibodies isolated and produced by Hugo Mouquet (Institut Pasteur). Bamlanivimab, Etesivimab, Casirivimab and Imdevimab are kind gifts of Thierry Prazuck and Laurent Hocqueloux. The Goat anti-Human IgG (H+L) Cross-Adsorbed Secondary Antibody, Alexa Fluor 647 (A21445) was obtained from thermoFisher Scientific.
Validation	The human anti-S RBD-48, RBD-85, RBD-98, RBD-109, NTD-18, NTD-20, NTD-69 and NTD-71 were validated using ELISAs (against the trimeric S, RBD, S2 and NTD proteins) by the team of H.Mouquet. Bamlanivimab, Etesivimab, Casirivimab and Imdevimab were validated by measuring their binding and neutralizing activity against SARS-CoV-2. Validation of the goat anti-human IgG is available from the ThermoFisher website.

Eukaryotic cell lines

Policy information about [cell lines](#)

Cell line source(s)	Vero E6 (ATCC® CRL-1586™), Freestyle 293-F (ThermoFisher) and U2OS cells (ATCC® HTB-96™), all obtained from the ATCC.
Authentication	Cell lines were not authenticated.
Mycoplasma contamination	All cells are negative for mycoplasma contamination. Tests are performed on a bi-monthly basis

Commonly misidentified lines
(See [ICLAC](#) register)

None

Human research participants

Policy information about [studies involving human research participants](#)

Population characteristics

Orleans' Cohort of convalescent and/or vaccinated individuals: since April 2020, a prospective, monocentric, longitudinal, cohort clinical study enrolling 170 SARS-CoV-2-infected individuals and 59 non-infected healthy controls is on-going, aiming to describe the persistence of specific and neutralizing antibodies over a 24-months period. Relevant co-variables are available in extended table 1a and 2.

Strasbourg Cohort of convalescent individuals: Since April 2020, a prospective, interventional, monocentric, longitudinal, cohort clinical study enrolling 308 RT-PCR-diagnosed SARS-CoV-2 infected hospital staff from the Strasbourg University Hospitals is on-going. Given the exploratory design of the two studies, the characteristics of participants were not pre-established when entering the cohorts. Relevant co-variables are available in extended table 1b.

Recruitment

Orléans cohort : Individuals admitted to the hospital for COVID-19 or with known COVID-19 consulting for a chronic disease were invited to participate.

Strasbourg Cohort : Hospital staff with PCR-confirmed COVID-19 were invited to participate.

Individuals were included without any selection other than those imposed by the entry criteria (known COVID-19 or vaccination). Under these conditions, no particular bias is envisaged.

Ethics oversight

Orléans was approved by national external committee (CPP Ile de France IV, IRB No. 00003835). Strasbourg cohort was approved by the institutional review board of Strasbourg University Hospitals. At enrolment a written informed consent was collected for all participants.

Note that full information on the approval of the study protocol must also be provided in the manuscript.

Clinical data

Policy information about [clinical studies](#)

All manuscripts should comply with the ICMJE [guidelines for publication of clinical research](#) and a completed [CONSORT checklist](#) must be included with all submissions.

Clinical trial registration

NCT04750720 and NCT04441684

Study protocol

All protocols can be accessed on [clinicaltrial.gov](#)

Data collection

Orléans and strasbourg cohorts started on April 2020 in Strasbourg Hospital (Hopitaux universitaires de Strasbourg) and Orléans Hospital (Centre hospitalier Régional Orléans) respectively, and are on-going.

Outcomes

The primary outcome of both studies was the presence of antibodies to SARS-CoV-2 Spike protein as measured with the S-Flow assay. The secondary outcome was the presence of neutralizing antibodies as measured with the S-Fuse assay.

Flow Cytometry

Plots

Confirm that:

- ☒ The axis labels state the marker and fluorochrome used (e.g. CD4-FITC).
- ☒ The axis scales are clearly visible. Include numbers along axes only for bottom left plot of group (a 'group' is an analysis of identical markers).
- ☒ All plots are contour plots with outliers or pseudocolor plots.
- ☒ A numerical value for number of cells or percentage (with statistics) is provided.

Methodology

Sample preparation

SARS-CoV-2 infected Vero cells were stained as indicated in the method section. All samples were acquired within 24h.

Instrument

Attune NxT Acoustic Focusing Cytometer, blue/red/violet/yellow (catalog number : 15360667)

Software

AttuneNxT Software v3.2.1

Cell population abundance

At least 10,000 cells were acquired for each condition.

Gating strategy

All gates were set on uninfected Vero cells.

- ☒ Tick this box to confirm that a figure exemplifying the gating strategy is provided in the Supplementary Information.

Use of Stay-at-Home Orders and Mask Mandates to Control COVID-19 Transmission — Blackfeet Tribal Reservation, Montana, June–December 2020

Caroline Q. Pratt, MSN, MPH^{1,2}; Anna N. Chard, PhD^{1,2}; Rosaula LaPine, MSN³; K. Webb Galbreath³; Cinnamon Crawford, MPH³; Albert Plant⁴; Garland Stiffarm, MPH⁴; Neil Sun Rhodes, MD⁴; Lorissa Hannon⁴; Thu-Ha Dinh, MD²

COVID-19 has disproportionately affected persons who identify as non-Hispanic American Indian or Alaska Native (AI/AN) (1). The Blackfeet Tribal Reservation, the northern Montana home of the sovereign Blackfeet Nation, with an estimated population of 10,629 (2), detected the first COVID-19 case in the community on June 16, 2020. Following CDC guidance,* and with free testing widely available, the Indian Health Service and Blackfeet Tribal Health Department began investigating all confirmed cases and their contacts on June 25. The relationship between three community mitigation resolutions passed and enforced by the Blackfeet Tribal Business Council and changes in the daily COVID-19 incidence and in the distributions of new cases was assessed. After the September 28 issuance of a strictly enforced stay-at-home order and adoption of a mask use resolution, COVID-19 incidence in the Blackfeet Tribal Reservation decreased by a factor of 33 from its peak of 6.40 cases per 1,000 residents per day on October 5 to 0.19 on November 7. Other mitigation measures the Blackfeet Tribal Reservation used included closing the east gate of Glacier National Park for the summer tourism season, instituting remote learning for public school students throughout the fall semester, and providing a Thanksgiving meal to every household to reduce trips to grocery stores. CDC has recommended use of routine public health interventions for infectious diseases, including case investigation with prompt isolation, contact tracing, and immediate quarantine after exposure to prevent and control transmission of SARS-CoV-2, the virus that causes COVID-19 (3). Stay-at-home orders, physical distancing, and mask wearing indoors, outdoors when physical distancing is not possible, or when in close contact with infected or exposed persons are also recommended as nonpharmaceutical community mitigation measures (3,4). Implementation and strict enforcement of stay-at-home orders and a mask use mandate likely helped reduce the spread of COVID-19 in the Blackfeet Tribal Reservation.

The potential effects of community mitigation measures on changes in the number and incidence of new COVID-19 cases in the Blackfeet Tribal Reservation during June 16–December 10, 2020, were assessed using deidentified

laboratory and case investigation data. The tribal health clinic, the Indian Health Service, a dialysis clinic, and a long-term care facility performed testing for SARS-CoV-2 and used various data collection tools. Local public health nurses abstracted case investigation data, including patient age, sex, race, ethnicity, test date, and exposure information. A case was defined as receipt of a positive SARS-CoV-2 result from either a nucleic acid amplification test, such as a polymerase chain reaction test, or a rapid antigen detection test by a resident of the Blackfeet Tribal Reservation. Incidence was calculated as the daily number of new COVID-19 cases per 1,000 residents. Analyses were conducted using SAS (version 9.4; SAS Institute). Population estimates for the Blackfeet Tribal Reservation and for Montana were obtained from the U.S. Census Bureau (2,5). This activity was reviewed by CDC and was conducted consistent with applicable federal law and CDC policy.†

During 2020, the Blackfeet Nation implemented three stay-at-home orders; mask use in public was required by all three orders. The first was a mandatory stay-at-home order,§ which was in place during June 29–July 31; violations of isolation or quarantine orders could result in a fine up to \$500.¶,** The second was a recommended stay-at-home order,†† which began August 19. The third was an enforced stay-at-home order,§§ which began September 28. Under this third order, breaking quarantine or isolation orders could result in up to 3 years in jail and a fine up to \$5,000.¶¶ Patients unable to isolate at home were provided temporary housing in two local hotels. A COVID-19 dispatch team delivered medications and food to community members, as needed.

† 45 C.F.R. part 46, 21 C.F.R. part 56; 42 U.S.C. Sect. 241(d); 5 U.S.C. Sect. 552a; 44 U.S.C. Sect. 3501 et seq.

§ http://www.blackfeetnation.com/wp-content/uploads/2020/07/22.-Blackfeet-Tribe-Resolution_Re-affirming-Closure-of-Blackfeet-Tribe-in-Response-to-COVID-19-Outreach_June-29_2020.pdf

¶ http://www.blackfeetnation.com/wp-content/uploads/2020/07/24.-Blackfeet-Resolution-282-200_Approving-Amende-Quarantine-Order.pdf

** http://www.blackfeetnation.com/wp-content/uploads/2020/07/27.-Blackfeet-Resolution-285-2020_Enacting-Isolation-Order.pdf

†† [http://www.blackfeetnation.com/wp-content/uploads/2020/08/20.-Blackfeet-Resolution_Extending-closure-until-further-notice.pdf#:~:text="](http://www.blackfeetnation.com/wp-content/uploads/2020/08/20.-Blackfeet-Resolution_Extending-closure-until-further-notice.pdf#:~:text=)

§§ <http://blackfeetnation.com/covid19/>

¶¶ http://www.blackfeetnation.com/wp-content/uploads/2020/10/Blackfeet-Tribe-Resolution_Continuing-Current-Fines-and-Offenses-beginning-on-October-26-2020-until-Further-Notice-Under-Current-Phase-Restrictions.pdf

* <https://www.cdc.gov/coronavirus/2019-ncov/php/contact-tracing/contact-tracing-plan/overview.html>

During June 16–December 10, 2020, a total of 1,180 COVID-19 cases were reported in the Blackfeet Tribal Reservation (Table). The median age of patients was 36 years (range = 0–96 years); 50.5% of cases occurred in females, and 91.9% of patients self-identified as AI/AN. After the first COVID-19 case was reported in the community on June 16, the Blackfeet Tribal Business Council voted not to open the east gate of Glacier National Park, which borders the reservation, through the end of the 2020 tourist season (6). The Blackfeet Tribal Reservation recorded few cases during July, when mandatory stay-at-home orders and ongoing case investigation and contact tracing were in effect, with an average daily incidence of 0.10 cases per 1,000 residents (Figure 1). On July 31, the Blackfeet Tribal Reservation opened its campgrounds to residents when the mandatory stay-at-home orders expired. In August, a slight increase in incidence was observed, to 0.19 cases per 1,000.

The second, or recommended, stay-at-home order commenced on August 19. However, the number of cases increased after gatherings at the Northwest Montana Fair and Rodeo (August 19–23) in Kalispell, outside of the reservation, and during Labor Day weekend (September 5–7). Daily incidence peaked at 6.40 cases per 1,000 residents on October 5, which was 63 times the incidence in July.

On September 28, a third stay-at-home order was issued, with strict enforcement and substantial fines for violation. Afterward, incidence decreased to 0.19 cases per 1,000 by November 7. A gradual increase in newly identified cases among persons aged 5–17 years and 30–39 years began the week of August 9, after the campgrounds opened on July 31, and peaked the week of August 16 (Figure 2). During August, the numbers of cases in these age groups were higher than those in other age groups. Incident cases among persons aged 18–39 years and 50–64 years increased after the Northwest Montana Fair and Rodeo (week of August 16) and Labor Day weekend (week of September 6), and peaked during the week of September 27, before the enforced stay-at-home order was issued.

Among 142 (12.0%) of 1,180 patients with available household exposure data, 121 (85.2%) reported at least one household contact with COVID-19. Workplace exposure data were available for 198 (16.8%) patients, 12 (6.1%) of whom reported a workplace exposure. Community exposure data were available for 133 (11.3%) patients; among these, 53 (39.8%) reported known community exposure. Twelve patients (1.0%) reported exposure in an adult congregate living facility.

TABLE. Characteristics of Blackfeet Tribal Reservation residents and COVID-19 cases — Blackfeet Tribal Reservation, Montana, June–December 2020

Characteristics	No. (%)	
	All residents* (N = 10,629)	COVID-19 patients† (N = 1,180)
Age, yrs		
Mean (SD)	N/A	37.8 (20.7)
Range	N/A	0–96
Median (IQR)	30.4	36 (21–54)
Sex		
Female	5,257 (49.5)	596 (50.5)
Male	5,372 (50.5)	564 (47.8)
Unknown	0 (—)	20 (1.7)
Race‡		
American Indian or Alaska Native	8,865 (83.4)	772 (91.9)
Asian	8 (0.1)	1 (0.1)
Black or African American	24 (0.2)	1 (0.1)
Multiple races	112 (1.1)	20 (2.4)
Other race	125 (1.2)	23 (2.7)
Unknown	0 (—)	18 (2.2)
White	1,482 (13.9)	5 (0.6)
Ethnicity¶		
Hispanic	206 (1.9)	1 (0.1)
Non-Hispanic	10,423 (98.1)	548 (74.2)
Unknown	0 (—)	190 (25.8)

Abbreviations: IQR = interquartile range; N/A = not available; SD = standard deviation.

* <https://www.census.gov/tribal/?aiaihh=0305>

† Blackfeet case investigation report.

‡ Unknown for 340 COVID-19 patients.

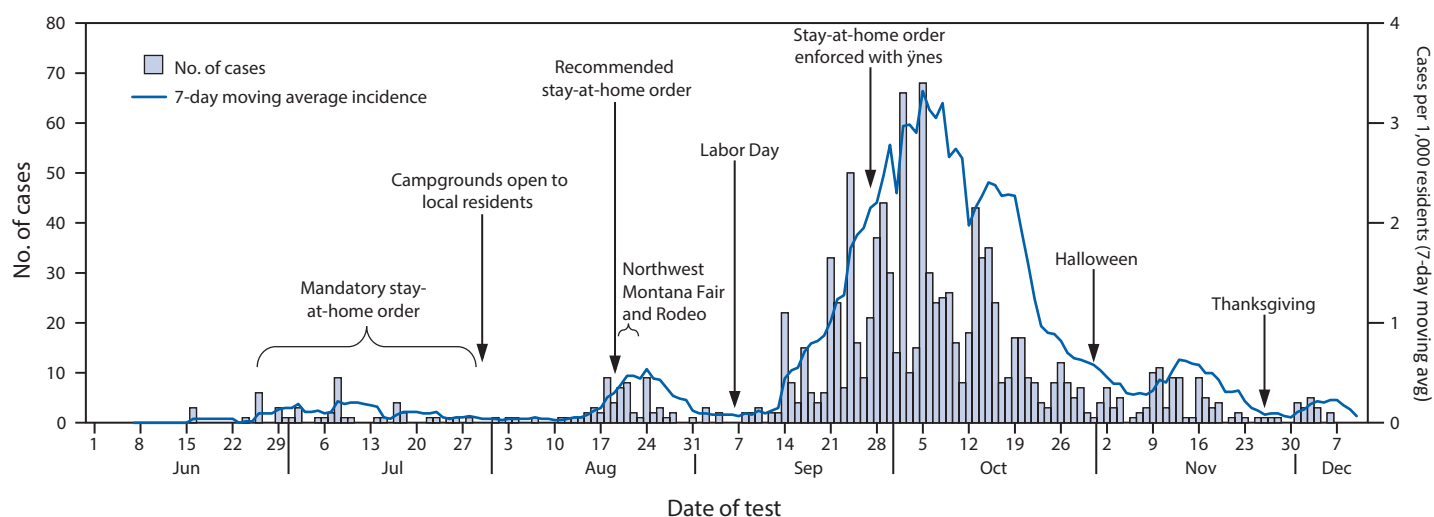
¶ Unknown for 441 COVID-19 patients.

Discussion

After implementation of mitigation measures, including case investigation, contact tracing, a mandatory stay-at-home order, and required mask use in public, the average reported daily COVID-19 incidence in the Blackfeet Tribal Reservation remained low (0.10 cases per 1,000 residents) during July. When the mandatory stay-at-home order expired on July 31, the Tribal Business Council issued a recommended stay-at-home order on August 19. After the opening of local campgrounds and Northwest Montana Fair and Rodeo and Labor Day weekend gatherings, daily COVID-19 incidence increased sharply, peaking October 5, and representing a sixty-three-fold increase over the daily average incidence in July. The continued increase in newly identified cases after September 28, when the enforced stay-at-home order commenced, reflects exposures that occurred in the preceding 2 weeks.*** The strictly enforced stay-at-home order, with increased penalties, likely contributed to the more than thirtyfold decrease in incidence by November 7.

*** <https://www.cdc.gov/coronavirus/2019-ncov/hcp/clinical-guidance-management-patients.html>

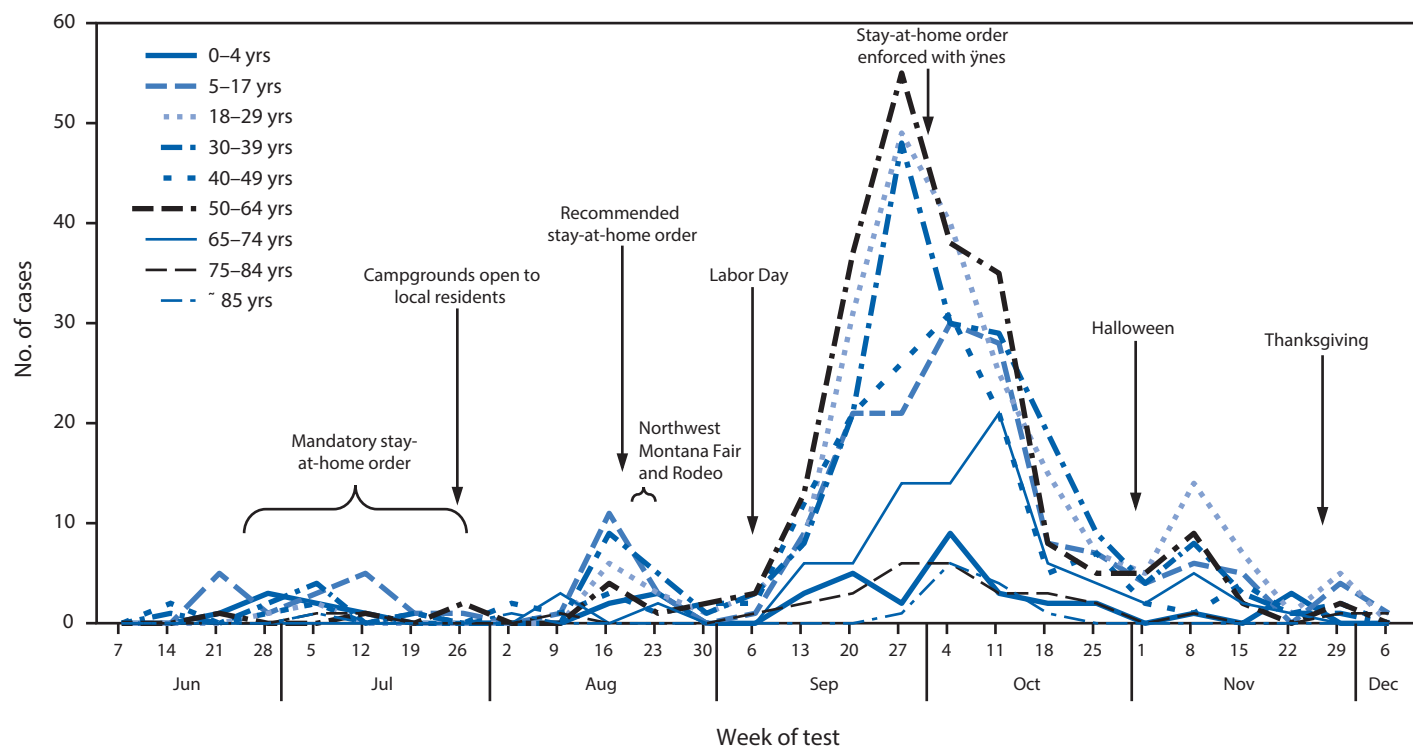
FIGURE 1. Number of COVID-19 cases, by test date and 7-day moving average incidence (N = 1,150) — Blackfeet Tribal Reservation, Montana, June 1–December 10, 2020*[†]



* Case data collected and recorded by Blackfeet and Indian Health Service public health nurses.

[†] Among 1,180 total cases, 30 were missing test date and are not included in the figure.

FIGURE 2. Number of weekly COVID-19 cases, by week of test and age group (N = 1,150) — Blackfeet Tribal Reservation, Montana, June 1–December 10, 2020*[†]



* Case data collected and recorded by Blackfeet and Indian Health Service public health nurses.

[†] Among 1,180 total cases, 30 were missing test date and are not included in the figure.

The steep declines in COVID-19 incidence in the Blackfeet Tribal Reservation might not have occurred without widespread and consistent enforcement of the mandate for mask use in public and stay-at-home orders. Wearing a mask reduces SARS-CoV-2 transmission from persons with symptomatic or asymptomatic infection and offers some protection for the wearer.^{†††} On July 15, Montana first implemented a limited mask use mandate, which only applied to counties with four or more active COVID-19 cases,^{§§§} but enforcement across the state was inconsistent (7). COVID-19 incidence in Montana increased throughout September and October, peaking November 14, at 1.54 cases per 1,000 residents (8). After the mask use mandate was applied to all Montana counties on November 17 (9), incidence in the state decreased (8).

The increases in COVID-19 cases among Blackfeet residents aged 5–17 years and 30–39 years followed relaxation of stay-at-home orders, the opening of campgrounds, and gatherings at the Northwest Montana Fair and Rodeo and during Labor Day weekend. The peaks in COVID-19 incidence in these groups were followed approximately 6 weeks later by a peak among persons aged 50–64 years. The average household size in the Blackfeet Tribal Reservation (3.4 persons) is higher than that in Montana (2.4 persons) (2,5). Using limited available household data (available for 12% of all cases), a household COVID-19 contact was reported for a larger proportion of cases among the Blackfeet (85%) than for cases among other Montana residents (22%) (10). Multigenerational households might contribute to COVID-19 transmission between age groups in the Blackfeet Tribal Reservation; however, information on multigenerational households for the Blackfeet was not available. Future planning for mitigation measures and data collection should take multigenerational households into account.

The findings in this report are subject to at least five limitations. First, the different performance characteristics of the two diagnostic tests (rapid antigen detection and molecular SARS-CoV-2 tests) created potential misclassification of cases. Second, complete standardized data were not available because the various entities conducting testing did not use the same data collection tools. Third, the lack of consistently collected data on contact tracing, exposures, order compliance, and relationships between COVID-19 cases prevented the assessment of secondary transmission. Fourth, data on household, workplace, and community exposure was limited; comparison with other populations should be made with caution. Finally, the relative contribution of each mitigation measure to the changes in COVID-19 rates could not be ascertained.

Summary

What is already known about this topic?

Community mitigation measures (e.g., stay-at-home orders and mask use), coupled with case investigation and contact tracing with immediate isolation or quarantine, are primary approaches to preventing and controlling community SARS-CoV-2 transmission.

What is added by this report?

In the Blackfeet Tribal Reservation, enforcement of stay-at-home orders and mandated use of face coverings in public, with potential fines and jail for noncompliance, were associated with a thirty-three-fold reduction in COVID-19 incidence from its peak of 6.40 cases per 1,000 residents per day on October 5 to 0.19 on November 7, 2020.

What are the implications for public health practice?

Enforcement of stay-at-home orders and mask use mandates, coupled with robust public health investigations, have been shown to reduce COVID-19 incidence.

The enforcement of stay-at-home orders, coupled with a mandate for mask use in public, likely contributed to a reduction in COVID-19 incidence, potentially helping to control the pandemic in the Blackfeet Tribal Reservation. A combination of mitigation measures, including case investigation, contact tracing, and enforced stay-at-home and mask use orders, will likely reduce COVID-19 transmission by limiting potential exposure to SARS-CoV-2. As of 2021, vaccination is available and recommended as another effective method of COVID-19 mitigation. In communities disproportionately affected by COVID-19, these mitigation strategies are likely to help reduce some COVID-19–associated health disparities.

Acknowledgments

Blackfeet Tribal Business Council; Blackfeet Tribal Health; Blackfeet Indian Health Service public health nurses; CDC COVID-19 Tribal Support Section.

Corresponding author: Caroline Pratt, yqg5@cdc.gov.

¹Epidemic Intelligence Service, CDC; ²CDC COVID-19 Emergency Response Team; ³Blackfeet Nation, Browning, Montana; ⁴Indian Health Service, Browning, Montana.

All authors have completed and submitted the International Committee of Medical Journal Editors form for disclosure of potential conflicts of interest. No potential conflicts of interest were disclosed.

^{†††} <https://www.cdc.gov/coronavirus/2019-ncov/prevent-getting-sick/cloth-face-cover-guidance.html>

^{§§§} <https://dphhs.mt.gov/aboutus/news/2020/directiverequiringfacecoverings>

References

1. Hatcher SM, Agnew-Brune C, Anderson M, et al. COVID-19 among American Indian and Alaska Native persons—23 states, January 31–July 3, 2020. *MMWR Morb Mortal Wkly Rep* 2020;69:1166–9. PMID:32853193 <https://doi.org/10.15585/mmwr.mm6934e1>
2. US Census Bureau. My tribal area. 2014–2018 American Community Survey 5-year estimates. Washington, DC: US Department of Commerce, US Census Bureau; 2020. <https://www.census.gov/tribal/?aianihh=0305>
3. Honein MA, Christie A, Rose DA, et al.; CDC COVID-19 Response Team. Summary of guidance for public health strategies to address high levels of community transmission of SARS-CoV-2 and related deaths, December 2020. *MMWR Morb Mortal Wkly Rep* 2020;69:1860–7. PMID:33301434 <https://doi.org/10.15585/mmwr.mm6949e2>
4. Moreland A, Herlihy C, Tynan MA, et al.; CDC Public Health Law Program; CDC COVID-19 Response Team. Timing of state and territorial COVID-19 stay-at-home orders and changes in population movement—United States, March 1–May 31, 2020. *MMWR Morb Mortal Wkly Rep* 2020;69:1198–203. PMID:32881851 <https://doi.org/10.15585/mmwr.mm6935a2>
5. US Census Bureau. Quick facts: Montana. Washington, DC: US Department of Commerce, US Census Bureau; 2019. <https://www.census.gov/quickfacts/fact/table/MT/PST045219>
6. Simkins JD. Blackfeet Nation shuts Glacier National Park entrance amid COVID fears. *Sunset*. Los Angeles, CA: Sunset Publishing Corporation; 2020. <https://www.sunset.com/travel/wild-lands/blackfeet-nation-glacier-national-park-covid>
7. Houghton K. Montana shifts to mask enforcement as local officials wait to see how far it goes. *Billings Gazette*. November 5, 2020. https://billingsgazette.com/news/state-and-regional/montana-shifts-to-mask-enforcement-as-local-officials-wait-to-see-how-far-it-goes/article_0cc2934f-0a3f-5280-9079-a5023402c8aa.html
8. CDC. COVID data tracker: trends in number of COVID-19 cases and deaths in the US reported to CDC, by state/territory. Atlanta, GA: US Department of Health and Human Services, CDC; 2020. https://covid.cdc.gov/covid-data-tracker/#trends_dailytrendscases
9. Office of the Governor, State of Montana. Directive implementing Executive Orders 2–2020 and 3–2020 and limiting size for public gatherings and events and limiting bar and restaurant capacity and hours. Helena, MT: Office of the Governor, State of Montana; 2020. https://covid19.mt.gov/_docs/2020-11-17_Directive-on-Group-Size-and-Capacity-FINAL.pdf
10. Montana Department of Health and Human Services. Interim analysis of COVID-19 cases in Montana (as of 10/30/2020). Helena, MT: Montana Department of Health and Human Services; 2020. Accessed March 29, 2021. <https://dphhs.mt.gov/Portals/85/publichealth/documents/CDEpi/DiseasesAtoZ/2019-nCoV/EpiProfile/COVIDEPIPROFILE10302020.pdf>

ORIGINAL ARTICLE

WILEY

Indoor transmission of SARS-CoV-2

Hua Qian¹ | Te Miao² | Li Liu³  | Xiaohong Zheng¹ | Danting Luo¹ | Yuguo Li^{2,4} ¹School of Energy and Environment, Southeast University, Nanjing, China²Department of Mechanical Engineering, The University of Hong Kong, Hong Kong, China³School of Architecture, Tsinghua University, Beijing, China⁴School of Public Health, The University of Hong Kong, Hong Kong, China

Correspondence

Yuguo Li, Department of Mechanical Engineering and School of Public Health, The University of Hong Kong, Pokfulam Road, Hong Kong, China.
Email: liyg@hku.hk

Funding information

Research Grants Council of Hong Kong, Grant/Award Number: 17202719 and C7025-16G; National Natural Science Foundation of China, Grant/Award Number: 41977370

Abstract

It is essential to understand where and how severe acute respiratory syndrome coronavirus 2 (SARS-CoV-2) is transmitted. Case reports were extracted from the local Municipal Health Commissions of 320 prefectural municipalities in China (not including Hubei Province). We identified all outbreaks involving three or more cases and reviewed the major characteristics of the enclosed spaces in which the outbreaks were reported and their associated indoor environmental aspects. Three hundred and eighteen outbreaks with three or more cases were identified, comprising a total of 1245 confirmed cases in 120 prefectural cities. Among the identified outbreaks, 53.8% involved three cases, 26.4% involved four cases, and only 1.6% involved ten or more cases. Home-based outbreaks were the dominant category (254 of 318 outbreaks; 79.9%), followed by transport-based outbreaks (108; 34.0%), and many outbreaks occurred in more than one category of venue. All identified outbreaks of three or more cases occurred in indoor environments, which confirm that sharing indoor spaces with one or more infected persons is a major SARS-CoV-2 infection risk.

KEYWORDS

COVID-19, crowding, indoor environments, indoor hygiene, outbreak, SARS-CoV-2

1 | INTRODUCTION

In less than 4 months, severe acute respiratory syndrome coronavirus 2 (SARS-CoV-2) spreads rapidly to all countries worldwide. By the end of June 2020, it had infected more than 10 million people and, by developing into coronavirus disease 2019 (COVID-19), had caused or contributed to the deaths of half a million people.¹ Understanding where and how person-to-person SARS-CoV-2 transmission occurs is essential for effective intervention.

The once-in-a-century COVID-19 pandemic has occurred in the age of artificial intelligence and big data. Many clusters/outbreaks were identified via contact tracing by local health authorities in China and elsewhere using both traditional and new technologies. The identification of these clusters allowed health authorities to quarantine close contacts for effective intervention and provided

an opportunity to study the characteristics of where and how these clusters occurred. The first COVID-19 patient was identified in Wuhan in December 2019, and the largest number of confirmed Chinese cases occurred in Hubei Province, of which Wuhan is the provincial capital.² Since January 20, 2020, the local health authorities of cities outside Hubei have reported online the details of most identified cases of infection. These were nearly only cases of SARS-CoV-2 infection that had progressed to actual disease (ie, COVID-19) and necessitated hospitalization, as by February 11, 2020, our knowledge of asymptomatic infection was non-existent.

In this study, we identified the outbreaks from these case reports from the local Municipal Health Commissions of 320 prefectural cities (municipalities) in China, not including Hubei Province, between January 4 and February 11, 2020. We also reviewed the major characteristics of the enclosed areas in which these outbreaks

Hua Qian, Te Miao and Yuguo Li contributed equally.

were determined to have occurred and their associated indoor environmental aspects.

2 | METHODS

We collected descriptions of each confirmed case from the local Municipal Health Commission website of 320 prefectural cities in mainland China, not including Hubei province. Each local Municipal Health Commission gave daily descriptions of the confirmed cases. The case descriptions generally included age, sex, venue of infection, symptoms, date of symptom onset, hospitalization, and confirmation and history of exposure. Many described cases also included patient's trajectory and relationship with other confirmed cases, and clusters had often already been identified. We consulted nationwide websites, except for those of cities in Hubei Province, and collected all available data up to February 11, 2020. Data from a few major cities—Beijing, Shanghai, and Guangzhou—were not included in our analysis due to insufficient case descriptions. Case descriptions from Hong Kong, Macao, and Taiwan were collected from their respective health authorities. We input the data into a database and conducted cross-validation to insure data reliability.

A total of 7324 cases with the minimum required descriptions (ie, the information listed above) were found; these accounted for 66.7% of the 10 980 confirmed non-Hubei cases in China by February 11, 2020.³ In this study, we defined a *cluster* as an aggregation of *three* or more cases that appeared to be linked to the same infection venue (eg, an apartment, an office, a school or a train) during a period in which people were insufficiently close proximity. We defined an *outbreak* as a cluster in which a common index patient was suspected, and we excluded tertiary and higher-generation infections in counting the number of cases involved. We also excluded outbreaks that involved only two cases, to exclude possible spouse-to-spouse transmission and to reduce the workload due to the large number of clusters or outbreaks with two cases. We also identified the index patient(s) of the identified outbreaks and their date of symptom onset.

We divided the identified outbreaks into categories for further analysis. First, the following six categories of infection venues were considered: homes (apartments and villas), transport (eg, normal and high-speed trains, private cars, buses, passenger planes, taxis, and cruise ships), restaurants and other food venues, entertainment venues (gyms, mah-jong halls, card houses, tea houses, and barbershops), and shopping venues (shopping malls and supermarkets), and an additional miscellaneous category (eg, hospitals, hotel rooms, unspecified communities, and thermal power plants). Second, the following four categories of infected individuals were considered based on their relationship: family members, family relatives, socially connected individuals, and socially non-connected individuals. A socially connected relationship was defined as one that existed between individuals who had possibly been in close contact due to friendships, acquaintances, or jobs, but did not

Practical Implication

- The indoor environments in which we live and work are the most common venues in which SARS-CoV-2 is transmitted.
- There is a need to improve the hygienic and ventilation conditions of these indoor environments to decrease the transmission of airborne infectious diseases.
- Given that there is an association between crowding and infection, in the post-pandemic future, we need to reflect deeply on the need for a healthy indoor environment.

include family connections (family members or relatives). A socially non-connected relationship was defined as one with no social connection or family connection.

3 | RESULTS

We identified 318 outbreaks involving 1,245 infected individuals in 120 cities. The top three cities (Table S2) were Shenzhen, Guangdong (24 outbreaks, 7.5%; 84 cases, 6.7%), Chongqing (16 outbreaks, 5.0%; 61 cases, 4.9%) and Bozhou, Anhui (nine outbreaks, 2.8%; 35, 2.8%). The average number (\pm standard deviation) of cases per outbreak was 3.92 ± 1.65 . More than half (171; 53.8%) of the 318 identified outbreaks involved three cases, more than a quarter (84; 26.4%) involved four cases, and only five (1.6%) outbreaks involved ten or more cases. Table S1 briefly describes four outbreaks, including the largest outbreak, which occurred in a shopping mall in Tianjin (21 cases).

Among the 318 outbreaks, 129 involved only family members, 133 involved family relatives, 29 involved socially connected individuals, 24 involved socially non-connected individuals, and only three involved multiple relationships. In addition to family members, family relatives and socially connected individuals constituted a large proportion of the infected cases (Figure 1A).

Eighty-three of the 318 identified outbreaks had multiple possible venues, which meant either that the exact venue of infection could not be identified or that more than one venue was involved in the infection. If we double- or triple-count these venues, we have a total of 416 infection venues for 318 outbreaks (Figure 1B). Among the 318 outbreaks, 254 (79.9%) occurred in a home (one in a villa; all others in apartments), 108 (34.0%) occurred on transport, 14 occurred at a restaurant or other food venue, seven occurred at an entertainment venue, and seven occurred at a shopping venue (shopping mall and supermarket), with an additional 26 occurring at a miscellaneous venue (eg, hospital, hotel room, unspecified community, and thermal power plant). Among the 235 outbreaks with an exact venue, 188 occurred in a home, 18 occurred on transport, 10 occurred at a restaurant,

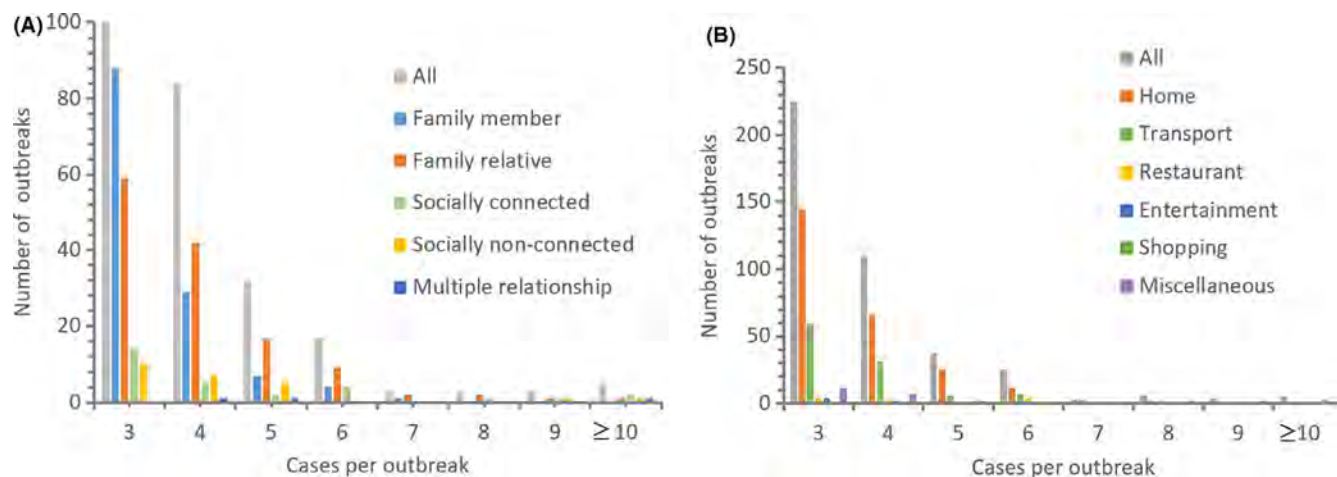
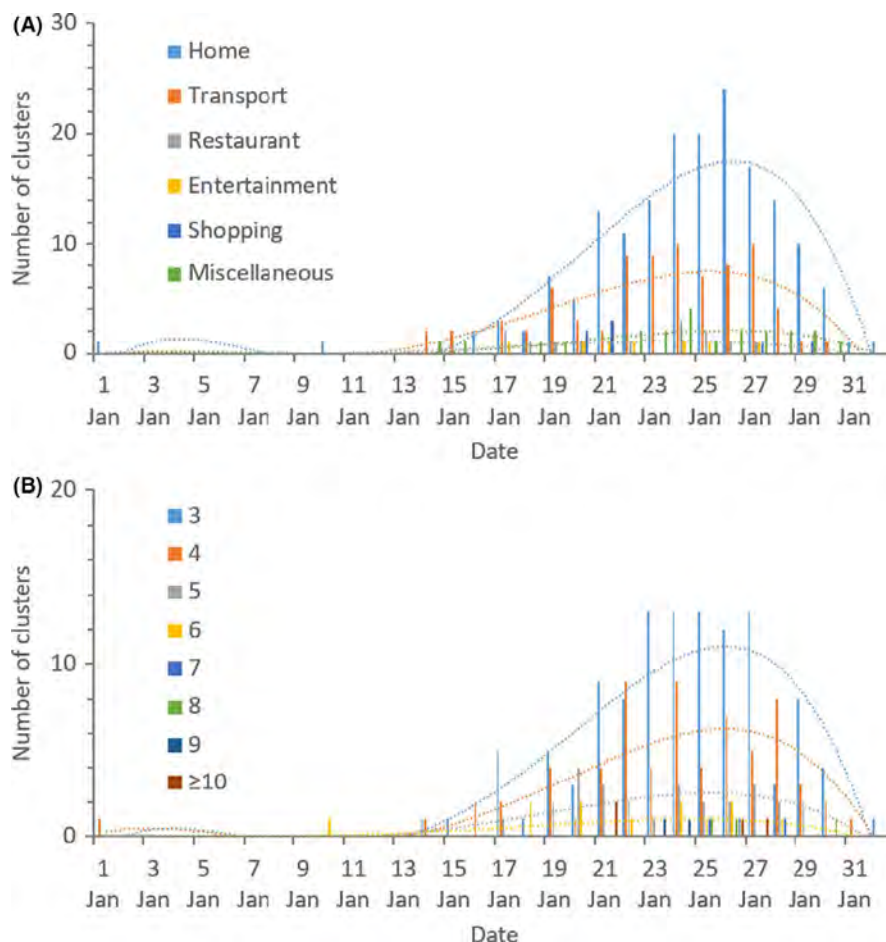


FIGURE 1 Distribution of all identified 318 outbreaks (A) involving confirmed cases of different relationships and (B) for each category of the 416 venues

FIGURE 2 Occurrence of outbreaks on median dates of infectious period for 231 actual outbreaks (A) in different categories for 300 venues and (B) with different numbers of cases in each outbreak on median dates of infectious period



six occurred at an entertainment venue, and seven occurred at a shopping venue, with an additional six occurring at a miscellaneous venue. For the 83 outbreaks with multiple possible venues, a total of 181 venues were identified (2.18 venues per outbreak). Among the 181 venues, 66 were homes, 90 were a form of transport, 4 were restaurants, 1 was an entertainment venue, and 20 were miscellaneous venues.

Most of the 254 home outbreaks comprised three to five cases (145 with three cases, 66 with four cases, and 25 with five cases). The average number of cases was 3.7 for outbreaks at homes, 3.8 for outbreaks on transport, 4.9 for outbreaks at food venues, 3.6 for outbreaks at entertainment venues, 8.7 for outbreaks at shopping venues, and 4.4 for outbreaks at miscellaneous venues. The proportion of large outbreaks was high for shops and food venues, possibly

because more susceptible individuals were present in these venues than in homes. Shopping and entertainment venues were each associated with only seven outbreaks. This suggests that it will be difficult to implement preventive measures in places that are frequented by large numbers of susceptible individuals if exact transmission routes are uncertain. In this context, it may be useful to provide further details of the seven outbreaks in shopping venues, as these had the highest average number of cases. There was one super-spreading event (outbreak) in a shopping center involving 21 cases, and there were also two outbreaks involving 10 cases (Table S1). In these three outbreaks, two of the index patients were shopping assistants in the shopping centers and one was a vegetable trimmer in the supermarket. These were all low-end shopping venues, where we suspect that the ventilation was poor or insufficient, at least for the 21-case outbreak; however, we have no direct evidence for this. In contrast, the index patient might have been a super-spreader, because the nature of the shopping assistants' job placed them in close contact with many people for a long duration. In the third case, the virus might have been present on the raw vegetables and thus been transferred to the vegetable trimmer.

Between December 29, 2019, and January 31, 2020, we also identified 231 outbreaks with known start and end dates of the suspected infectious period (Figure 2A). The identified outbreaks peaked between January 23 and 28 (Figure 2A), which coincides with the celebration period of the Chinese New Year (CNY). CNY 2020 lasted from New Year's Eve on January 24 to the Lantern Festival (ie, the 15th of Lunar January) on February 8. The official holiday in mainland China was from January 24 to 30, 2020. The peak date for the number of transport outbreaks was 1 to 2 days earlier than that for the home outbreaks as people traveled home for CNY.

Because home outbreaks dominated, the changes in the temporal profile of the number of cases (Figure 2A) closely followed that of the home outbreaks (Figure 2B). However, for outbreaks with more than six cases, no particular pattern was identified over time, which suggests a sporadic nature.

Among the 231 outbreaks with a known suspected infectious period, 126 included a known date of symptom onset for the index patient (Figure 3). We further divided those 126 outbreaks into two subgroups according to the index patient's symptom-onset date, as follows: on or before January 28 (96 outbreaks) and after January 28 (30 outbreaks). The average time from symptom onset to the end of the infectious period was 3.76 ± 4.42 days for those on and before January 28 and 0.87 ± 2.80 days for those afterward. The significant reduction in the average time from symptom onset to the end of the infectious period between these subgroups suggests the effectiveness of the early detection and isolation policy, which also explains the sharp decline in cases of infection after January 28.

Information is available on both the age and sex of the index patient for 139 outbreaks (Figure 4). Eighty-six outbreaks (62%) had a male index case, and 53 (38%) had a female index case. The average number of infected patients (excluding the index case) was approximately 3 for most age groups (3 for minors [ie, <18 years of age], with only one outbreak; 2.79 for young adults [ie, 18–35 years of age],

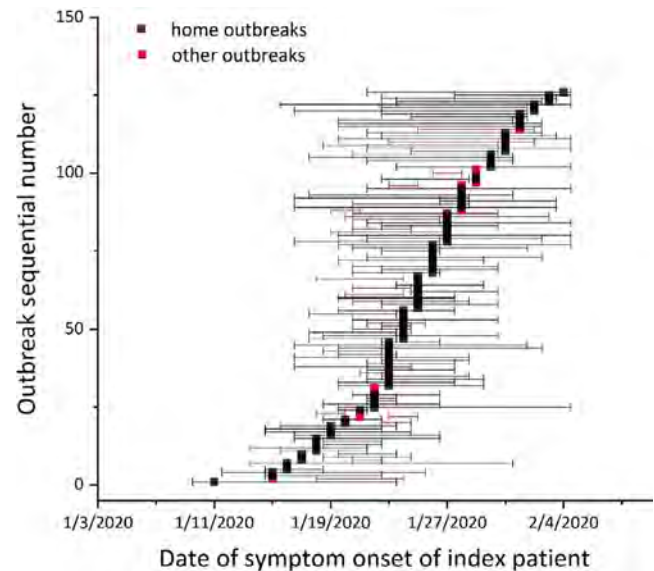


FIGURE 3 One hundred and twenty-six outbreaks with both possible starting and end infectious dates and date of symptom onset of index patient. Non-home outbreaks are shown in red

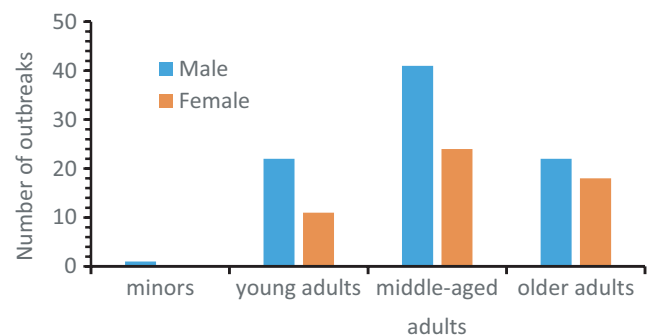


FIGURE 4 One hundred and thirty-nine outbreaks with information on the age of the index patient. Minors (<18 y old), young adults (18–35 y old), middle-aged adults (36–55 y old), senior adults (>55 y old)

in 33 outbreaks; and 3.11 for middle-aged adults [ie, 36–55 years of age], in 65 outbreaks). The average number of infected patients was 2.58 for senior adults [ie, >55 years of age], in 40 outbreaks. We were interested to note that among the outbreaks with a middle-aged index case, a female index case infected an average of 3.71 others, while a male index case infected 2.75 others. The dominant middle-aged group of reported index cases likely reflects the fact that returned migrant workers from Wuhan constituted the major pool of source patients in provinces outside Hubei.

4 | DISCUSSION

The first salient feature of the 318 identified outbreaks that involved three or more cases is that they all occurred in indoor environments. Although this finding was expected, its significance has not been

well recognized by the community or by policymakers. In a modern civilization, our lives and work are indoors. The transmission of SARS-CoV-2 from infected individuals to susceptible individuals is mainly an indoor phenomenon.

The emergence of homes as the most common COVID-19 outbreak venue in China is not surprising. During the COVID-19 epidemic in mainland China, homes became temporary quarantine places. Our estimated home dominance of 79.9% is close to the official estimate of 83% of the so-called household clusters among the nearly 1000 clusters (not outbreaks) defined by the China National Health Commission.⁴ After Wuhan announced its city lockdown on January 23, the warning message spread throughout the country. People in provinces outside Hubei also began to stay at home. Most Chinese families have one child, and some families may also include grandparents. The relatively low number of cases in these home outbreaks might be considered an advantage of the compulsory home quarantine because transmission was limited to a small number of family members. Similar stay-at-home policies have now been implemented elsewhere during the pandemic. Most urban homes are high-rise apartments, while rural homes may be single-family detached houses. Modern urban homes may be mechanically ventilated, while older homes are typically naturally ventilated. It is unfortunate that detailed characteristics of the homes in which the infections occurred are not available.

The rising trend shown before the peak period in Figure 2 was likely due to the introduction of imported cases due to the Spring Festival travel season (Chunyun in Chinese), a period around CNY during which many people leave the cities in which they work to visit their rural families. The 2020 Chunyun brought people from the epicenter Wuhan to their home cities before Wuhan's lockdown on January 23. Social and family gatherings continued after January 23 in most cities outside Hubei. Interventions such as contact tracing and confinement of estates, villages, and individual buildings were implemented gradually in most cities outside Hubei immediately after CNY, which explains the sharp declining curve after January 28. The significant reduction in the average time from symptom onset to the end of the infectious period between the before January 28 subgroup and after January 28 subgroup suggests the effectiveness of the early detection and isolation policy and explains the sharp decrease in infections after January 28.

Our study does not rule out outdoor transmission of the virus. However, among our 7324 identified cases in China with sufficient descriptions, only one outdoor outbreak involving two cases occurred in a village in Shangqiu, Henan. A 27-year-old man had a conversation outdoors with an individual who had returned from Wuhan on January 25 and had symptom onset on February 1. This outbreak involved only two cases.

The second salient feature of the 318 identified outbreaks is the relatively small number of outbreaks that involved 10 or more cases. The largest outbreak occurred in a Tianjin shopping mall and involved 21 cases, although Wu et al⁵ reported 25 cases (Table S1). This is distinct from the 2003 SARS-CoV epidemic, during which seven major super-spreading events in Hong Kong and Singapore

alone were identified to involve as many as 329 cases and super-spreading events dominated the epidemic.⁶ The occurrence of many small outbreaks (in terms of the number of cases) in the COVID-19 pandemic suggests a different transmission pattern from that of the 2003 SARS-CoV epidemic. Some viral, epidemiological, and environmental factors may have contributed to this difference between the 2003 SARS-CoV epidemic and the current COVID-19 pandemic. However, a number of large super-spreading events were later reported elsewhere in the world, including 94 people who were infected in an 11th-floor call center in Seoul with 216 employees,⁷ and 32 confirmed and 20 probable secondary cases after a 2.5-hour choir practice attended by 61 persons in Skagit County, Washington.⁸ We cannot pinpoint the exact transmission routes of these identified outbreaks. During the early phase of the pandemic, most health authorities advised that the SARS-CoV-2 was transmitted mainly by close contact and via the fomite route (eg, China NHC⁹ and US CDC¹⁰). The China NHC also suggested that long-range aerosol transmission may occur when certain conditions are met, such as in crowded enclosures or spaces with poor ventilation. By 5 November 2020, the US CDC¹¹ suggested that "It is possible that COVID-19 may spread through the droplets and airborne particles that are formed when a person who has COVID-19 coughs, sneezes, sings, talks, or breathes. There is growing evidence that droplets and airborne particles can remain suspended in the air and be breathed in by others, and travel distances beyond 6 feet (for example, during choir practice, in restaurants, or in fitness classes). In general, indoor environments without good ventilation increase this risk."

We do not have data on the hygiene conditions, such as ventilation rates and human densities, of the infection venues of the 318 outbreaks studied here. The exact location of the infection venues and the necessary parameters such as the floor area or the number of occupants were not provided in the case reports. Instead, we reviewed the current design standards of thermal and ventilation conditions, occupant density, and close-contact behavior in the various indoor environments discussed here (Table S3). The required ventilation rates vary significantly among homes, offices, trains, and buses. We note that the current ventilation rate guidelines in these environments do not consider infection control. For example, the required ventilation rate is only 3.9 L/s per person in shopping malls and 2.8 L/s per person in public buses, whereas a ventilation rate of at least 8–10 L/s is required for good indoor air quality.¹² The review showed that a rate as high as 25 L/s per person may be needed.¹² Some existing buildings are probably crowded, poorly ventilated, and unhygienic. A comprehensive review of ventilation conditions in Chinese indoor environments by Ye et al¹³ showed that the CO₂ concentration can reach 3500 pp min some buildings. The design and operation of buildings have also been under pressure to reduce energy use¹⁴ and increase human productivity. Balancing the need for energy efficiency, indoor environmental quality and health in both urban planning and building design have not been easy.¹⁵ The quality of indoor environments might be sacrificed by putting a greater focus on cost than on health.

Close-contact behavior and occupant density in the various indoor environments discussed are also reviewed in Table S3. Frequent close contact occurs indoors, and buildings have high-touch surfaces.¹⁶⁻¹⁹ Unfortunately, we do not have detailed data on surface-cleaning and hand-hygiene conditions in these indoor environments, but fomite transmission must nevertheless be considered in designing preventive approaches.

This study has limitations. We only studied outbreaks in China, where very strict intervention measures were implemented. We relied fully on the case reports of the local health authorities in each city, and variation exists in the details and the quality of their original epidemiological investigations. We also made no attempt to access any of the infection venues, and the details of each of these indoor spaces remains unknown.

This study shows that the individual indoor environments in which we live and work are the most common venues in which the virus of the once-in-a-century-pandemic is transmitted among us. An individual infected in one building may infect others in the building(s) that he or she later visits. People are in constant contact as they move from one indoor space or building to another, which creates an indoor contact network through which a virus can spread.²⁰ The buildings and transport cabins in various parts of the world are thus connected and facilitated the spread of the COVID-19 pandemic virus.

The association between crowding and infection has been known since Pringle.²¹ The most dramatic example in the current pandemic might be in the cruise ship outbreak on the crowded Diamond Princess, of which the peak basic production number was predicted to be 11²² or 14.8²³ before quarantine and much higher than elsewhere. The world's first statutory housing policy, the Artisans and Labourers Dwellings Act 1875²⁴ was developed following 19th-century empirical evidence that crowding led to a high incidence of infectious disease. A recent systematic review by the World Health Organization also found an association between crowding and infection.²⁵ A *Lancet* editorial in 2018 declared "[t]he right to a healthy home."²⁶ One WHO meeting also declared that "everyone has the right to breathe healthy indoor air"²⁷ and that "the provision of healthy indoor air should not compromise global or local ecological integrity, or the rights of future generations".²⁸ We hope that in the post-pandemic future, mankind will reflect deeply on the need for a healthy indoor environment.

ACKNOWLEDGMENTS

The authors are grateful to Shengqi Wang, Xiaoxue Cheng, Luping Ma, Ya Lei, Siying Mei, Ziyang Zhou, Yiran Lu, Mengjie Duan, Yifan Li, Qionglan He, and Ziang Xi, who helped collect the original data. The work was supported by the Research Grants Council of Hong Kong (no 17202719, C7025-16G) and National Natural Science Foundation of China (no 41977370).

CONFLICT OF INTEREST

The authors declare no conflict of interest.

AUTHORS' CONTRIBUTION

H. Qian, T. Miao, and Y. Li contributed equally. Y. Li and H. Qian contributed to study design, hypothesis formulation, and coordination. L. Liu, X. Zheng, and D. Luo contributed to data collection and initial data analyses. H. Qian and T. Miao contributed to major data analyses. Y. Li wrote the first draft of the paper, and H. Qian and T. Miao contributed to major revision. All of the other authors contributed to revision. All of the authors approved the submitted version and have agreed to be personally accountable for their own contributions.

PEER REVIEW

The peer review history for this article is available at <https://publons.com/publon/10.1111/ina.12766>.

DATA AVAILABILITY STATEMENT

Available to interested readers by contacting Dr. Li (e-mail, liyq@hku.hk).

ORCID

Li Liu  <https://orcid.org/0000-0001-8512-8676>

Yuguo Li  <https://orcid.org/0000-0002-2281-4529>

REFERENCES

1. WHO, 2020a. Coronavirus disease (COVID-2019) situation reports. Situation report – 162 by June 20, 2020. <https://www.who.int/emergencies/diseases/novel-coronavirus-2019/situation-reports>. Accessed on 1 July 2020.
2. NCPERET (The Novel Coronavirus Pneumonia Emergency Response Epidemiology Team). The epidemiological characteristics of an outbreak of 2019 Novel Coronavirus Diseases (COVID-19) – China, 2020. *China CDC Weekly*, 2020. Vol. 2 No. x.
3. WHO, 2020b. Coronavirus Disease (COVID-2019) situation reports. Situation report – 22 by Feb 11, 2020. https://www.who.int/docs/default-source/coronaviruse/situation-reports/20200211-sitrep-22-ncov.pdf?sfvrsn=fb6d49b1_2. Accessed on 17 March 2020.
4. China NHC (National Health Commission of the People's Republic of China), 2020. Transcript of press conference on 11 February 2020. <http://www.nhc.gov.cn/xcs/s3574/202002/53900c60791041e09070bca8f40f93ac.shtml>
5. Wu WS, Li YG, Wei ZF, et al. Investigation and analysis on characteristics of a cluster of COVID-19 associated with exposure in a department store in Tianjin. *Chin J Epidemiol*. 2020;41(4): 489-493.
6. Li Y, Yu IT, Xu P, et al. Predicting super spreading events during the 2003 severe acute respiratory syndrome epidemics in Hong Kong and Singapore. *Am J Epidemiol*. 2004;160(8):719-728. <https://doi.org/10.1093/aje/kwh273>
7. Park SY, Kim YM, Yi S, et al. Coronavirus disease outbreak in call center, South Korea. *Emerg Infect Dis*. 2020;26(8):1666-1670.
8. Hamner L, Dubbel P, Capron I, et al. High SARS-CoV-2 attack rate following exposure at a choir practice – Skagit County, Washington, March 2020. *Morb Mortal Wkly Rep*. 2020;69:606-610.
9. Li XH, Gao F. *Public Prevention Guidelines of Infection due to the Novel Coronavirus Pneumonia (In Chinese, 新型冠状病毒感染的肺炎公众防护指南)*. Beijing: People's Medical Publishing House; 2020.
10. United States Centers for Disease Control and Prevention, 2020. How 2019-nCoV Spreads. <https://www.cdc.gov/coronavirus/2019-ncov/about/transmission.html>. Accessed on 1 February 2020.

11. United States Centers for Disease Control and Prevention, 2020. Frequently Asked Questions. <https://www.cdc.gov/coronavirus/2019-ncov/faq.html#Spread>. Accessed on 12 November 2020.
12. Sundell J, Levin H, Nazaroff WW, et al. Ventilation rates and health: multidisciplinary review of the scientific literature. *Indoor Air*. 2011;21(3):191-204. <https://doi.org/10.1111/j.1600-0668.2010.00703.x>
13. Ye W, Zhang X, Gao J, Cao G, Zhou X, Su X. Indoor air pollutants, ventilation rate determinants and potential control strategies in Chinese dwellings: a literature review. *Sci Total Environ*. 2017;586:696-729. <https://doi.org/10.1016/j.scitotenv.2017.02.047>
14. Fisk WJ. Health and productivity gains from better indoor environments and their relationship with building energy efficiency. *Annu Rev Energy Environ*. 2000;25:537-566. <https://doi.org/10.1146/annurev.energy.25.1.537>
15. Geng Y, Ji W, Wang Z, Lin B, Zhu Y. A review of operating performance in green buildings: energy use, indoor environmental quality and occupant satisfaction. *Energ Buildings*. 2019;183:500-514. <https://doi.org/10.1016/j.enbuild.2018.11.017>
16. Glass LM, Glass RJ. Social contact networks for the spread of pandemic influenza in children and teenagers. *BMC Public Health*. 2008;8(1):61. <https://doi.org/10.1186/1471-2458-8-61>
17. King MF, Noakes CJ, Sleight PA. Modeling environmental contamination in hospital single- and four-bed rooms. *Indoor Air*. 2015;25(6):694-707. <https://doi.org/10.1111/ina.12186>
18. Zhang N, Li Y, Huang H. Surface touch and its network growth in a graduate student office. *Indoor Air*. 2018;28(6):963-972. <https://doi.org/10.1111/ina.12505>
19. Zhang N, Tang JW, Li Y. Human behavior during close contact in a graduate student office. *Indoor Air*. 2019;29(4):577-590. <https://doi.org/10.1111/ina.12554>
20. Gao X, Wei J, Lei H, Xu P, Cowling BJ, Li Y. Building ventilation as an effective disease intervention strategy in a dense indoor contact network in an ideal city. *PLoS One*. 2016;11(9):e0162481. <https://doi.org/10.1371/journal.pone.0162481>
21. John P. Observations on the diseases of the army (No. 21145). Edward Earle, 1810.
22. Mizumoto K, Chowell G. Transmission potential of the novel coronavirus (COVID-19) onboard the diamond Princess Cruises Ship, 2020. *Infect Dis Model*. 2020;5:264-270. <https://doi.org/10.1016/j.idm.2020.02.003>
23. Rocklöv J, Sjödin H, Wilder-Smith A. COVID-19 outbreak on the Diamond Princess cruise ship: estimating the epidemic potential and effectiveness of public health countermeasures. *J Travel Med*. 2020;27(3):1-7. <https://doi.org/10.1093/jtm/taaa030>
24. Britain G, Glen A. The artisans' and labourers' dwellings improvement act, 1875: With introduction, notes, appendix of statutes and forms, and index. London: [s.n.].
25. WHO (World Health Organization). *WHO Housing and Health Guidelines*. Geneva: 2018.
26. Anonymous. The right to a healthy home. *Lancet*. 2018;392(10163):2414. [https://doi.org/10.1016/S0140-6736\(18\)33113-1](https://doi.org/10.1016/S0140-6736(18)33113-1)
27. WHO (World Health Organization), 2000. The right to healthy indoor air – report on the WHO meeting.
28. Mølhave L, Krzyzanowski M. The right to healthy indoor air. *Indoor Air*. 2000;10(4):211. <https://doi.org/10.1034/j.1600-0668.2000.010004211.x>

SUPPORTING INFORMATION

Additional supporting information may be found online in the Supporting Information section.

How to cite this article: Qian H, Miao T, Liu L, Zheng X, Luo D, Li Y. Indoor transmission of SARS-CoV-2. *Indoor Air*. 2021;31:639–645. <https://doi.org/10.1111/ina.12766>



Since January 2020 Elsevier has created a COVID-19 resource centre with free information in English and Mandarin on the novel coronavirus COVID-19. The COVID-19 resource centre is hosted on Elsevier Connect, the company's public news and information website.

Elsevier hereby grants permission to make all its COVID-19-related research that is available on the COVID-19 resource centre - including this research content - immediately available in PubMed Central and other publicly funded repositories, such as the WHO COVID database with rights for unrestricted research re-use and analyses in any form or by any means with acknowledgement of the original source. These permissions are granted for free by Elsevier for as long as the COVID-19 resource centre remains active.



Contents lists available at ScienceDirect

Clinical Microbiology and Infection

journal homepage: www.clinicalmicrobiologyandinfection.com

Systematic review

The role of asymptomatic and pre-symptomatic infection in SARS-CoV-2 transmission—a living systematic review

Xuetiing Qiu^{1,†}, Ali Ihsan Nergiz^{2,†}, Alberto Enrico Maraolo³, Isaac I. Bogoch⁴, Nicola Low⁵, Muge Cevik^{6,*}¹ Center for Communicable Disease Dynamics, Department of Epidemiology, Harvard TH Chan School of Public Health, Boston, USA² Cerrahpasa Medical School, Istanbul University-Cerrahpasa, Istanbul, Turkey³ First Division of Infectious Diseases, Cotugno Hospital, AORN dei Colli, Naples, Italy⁴ Division of Infectious Diseases, Toronto General Hospital and University of Toronto, Toronto, Canada⁵ Institute of Social and Preventive Medicine, University of Bern, Bern, Switzerland⁶ Division of Infection and Global Health Research, School of Medicine, University of St. Andrews, Fife, Scotland, UK

ARTICLE INFO

Article history:

Received 25 September 2020

Received in revised form

3 January 2021

Accepted 9 January 2021

Available online 21 January 2021

Editor: M. Paul

Keywords:

Asymptomatic

Coronavirus disease 2019

Secondary attack rate

Severe acute respiratory syndrome

coronavirus 2

Transmission

ABSTRACT

Background: Reports suggest that asymptomatic individuals (those with no symptoms at all throughout infection) with severe acute respiratory syndrome coronavirus 2 (SARS-CoV-2) are infectious, but the extent of transmission based on symptom status requires further study.

Purpose: This living review aims to critically appraise available data about secondary attack rates from people with asymptomatic, pre-symptomatic and symptomatic SARS-CoV-2 infection.

Data sources: Medline, EMBASE, China Academic Journals full-text database (CNKI), and pre-print servers were searched from 30 December 2019 to 3 July 2020 using relevant MESH terms.

Study selection: Studies that report on contact tracing of index cases with SARS-CoV-2 infection in either English or Chinese were included.

Data extraction: Two authors independently extracted data and assessed study quality and risk of bias. We calculated the secondary attack rate as the number of contacts with SARS-CoV-2, divided by the number of contacts tested.

Data synthesis: Of 927 studies identified, 80 were included. Summary secondary attack rate estimates were 1% (95% CI 0%–2%) with a prediction interval of 0%–10% for asymptomatic index cases in ten studies, 7% (95% CI 3%–11%) with a prediction interval of 1%–40% for pre-symptomatic cases in 11 studies and 6% (95% CI 5%–8%) with a prediction interval of 5%–38% for symptomatic index cases in 40 studies. The highest secondary attack rates were found in contacts who lived in the same household as the index case. Other activities associated with transmission were group activities such as sharing meals or playing board games with the index case, regardless of the disease status of the index case.

Limitations: We excluded some studies because the index case or number of contacts were unclear.

Conclusion: Asymptomatic patients can transmit SARS-CoV-2 to others, but our findings indicate that such individuals are responsible for fewer secondary infections than people with symptoms.

Systematic review registration: PROSPERO CRD42020188168. **Xuetiing Qiu, Clin Microbiol Infect 2021;27:511**

© 2021 European Society of Clinical Microbiology and Infectious Diseases. Published by Elsevier Ltd. All rights reserved.

Introduction

Severe acute respiratory syndrome coronavirus 2 (SARS-CoV-2) demonstrates efficient transmission in populations without effective public health interventions; basic reproduction numbers (R_0) range between 2 and 3 [1]. Although asymptomatic transmission has been described as the ‘Achilles’ heel’ of control efforts during

* Corresponding author: Muge Cevik, Division of Infection and Global Health Research, School of Medicine, University of St Andrews, Fife, Scotland, KY16 9TF, UK.

E-mail address: mc349@st-andrews.ac.uk (M. Cevik).

† Xuetiing Qiu and Ali Ihsan Nergiz made equal contributions.

this pandemic, the extent to which transmission of SARS-CoV-2 by people without symptoms drives this pandemic remains uncertain [2]. SARS-CoV-2 infection that is asymptomatic at the time of laboratory testing is widely reported [3]; however, studies that follow infected people over time suggest that many infections are not asymptomatic throughout the entire disease course, and a large proportion of these individuals ultimately develop a diverse range of symptoms [4–7]. For instance, Sugano et al. reported a detailed cluster outbreak in music clubs in Japan, where the asymptomatic cases reported also included pre-symptomatic cases [8]. A living systematic review of studies published up to 10 June 2020 estimated that 20% (95% CI 17%–25%) of people who become infected with SARS-CoV-2 remain asymptomatic throughout infection [7].

One of the barriers to understanding the role of asymptomatic transmission is the lack of consistency in case definitions [9]. Although symptom severity exists on a spectrum, individuals infected with SARS-CoV-2 can be miscategorized as asymptomatic, when they have milder or atypical symptoms, leading to over-estimation of the proportion without symptoms [3,10]. For instance, in a detailed study of SARS-CoV-2 infections in Iceland where individuals deemed at high risk for coronavirus disease 2019 (COVID-19), including those with a consistent syndrome, were screened in a targeted manner, and other individuals were tested via a population screening mechanism, more than one-third of people in the second group reported symptoms potentially consistent with COVID-19 [3]. However, it is increasingly becoming clear that some individuals experience more diverse symptoms, including taste and smell disturbance or myalgia, either for the entire course of the illness or preceding respiratory symptoms. These symptoms can be so mild and insidious that they do not limit patients' daily activities [4,11]. The situation is further complicated by subjective patient perception and differences between studies in the elicitation and reporting of symptoms.

There are reports describing asymptomatic individuals with SARS-CoV-2 who are infectious [12] and who have infected one or more contacts [13], but the extent and significance of asymptomatic transmission requires further understanding. The aim of this review is to summarize the available evidence about secondary attack rates (defined as the probability that an infected individual will transmit the disease to a susceptible individual) among the contacts of individuals with SARS-CoV-2 with different symptom status to provide information about how contagious they are, and their role in driving the pandemic.

Materials and methods

This systematic review was registered in PROSPERO on 8 June 2020 (CRD42020188168) and will be updated in 4–6 months according to the availability of new evidence as a living systematic review [14]. The larger review aims to answer transmission dynamics of SARS-CoV-2. The analysis in this report addresses one of the review questions; to identify secondary attack rate based on symptom status.

Definitions

We defined 'asymptomatic' as an individual with laboratory-confirmed SARS-CoV-2 infection but without symptoms throughout their entire course of infection, or after 14 days of follow up; 'paucisymptomatic' as an individual with laboratory-confirmed SARS-CoV-2 infection with mild symptoms, and 'pre-symptomatic' as an individual who reports no symptoms at the time of the initial positive test result, but who subsequently develops symptoms attributable to COVID-19. We used these definitions to categorize the index cases. Secondary attack rate was

defined as the number of new SARS-CoV-2 infection cases among susceptible contacts of primary cases divided by the total number of susceptible contacts.

Search strategy

We retrieved articles about transmission of SARS-CoV-2 infection through systematic searches of eight databases: Medline, EMBASE, Europe PMC, Web of Science, SCOPUS, Chinese database (CNKI), and preprint servers (MedRxiv, BioRxiv) using relevant Medical Subject Headings (MeSH) terms (see Supplementary material, [Appendix S1](#)). The initial search was completed from 30 December 2019 to 21 May 2020, searches were repeated on 8 June 2020 and 3 July 2020, owing to the rapidly increasing number of studies.

Study selection

Studies were eligible if they met the inclusion criteria: (a) report on COVID-19 or SARS-CoV-2 infection and (b) report an outbreak investigation or contact tracing study. Exclusion criteria were: (a) review articles; (b) observational studies providing only the proportion of individuals infected; (c) studies that do not indicate the number of contacts or secondary infections; and (d) reports in media sources. We also manually screened the references of the included original studies and reviews to identify additional eligible studies.

Data extraction

Two authors (XQ and AIN) independently reviewed reports by title and abstract for relevance, with at least 20% of all reports being screened in duplicate to ensure consistency. Two authors then independently read the full-text report of all studies not excluded by title and abstract, to consider eligibility for inclusion. Any disagreements regarding study inclusion were resolved through discussion with a third author (MC). Data were extracted onto a standardized form. From each study, the following variables were extracted: the name of the first author, year of publication, country, sample size, details of index cases (categorized as asymptomatic, pre-symptomatic and symptomatic); event details such as environment, transmission details; number of contacts, number of secondary cases. If these data were not reported, we contacted authors to request them and checked with the authors about all symptoms that they sought.

Risk of bias in included studies

Two authors (XQ and AIN) independently assessed completeness of reporting and risks of bias, using an adapted version of the Joanna Briggs Institute Critical Appraisal Checklist for Case Series (see Supplementary material). Any disagreements were resolved through discussion with a third author (MC).

Data synthesis and statistical analysis

The studies are summarized in text and table form, descriptive statistics were completed for key outcome measures. Secondary attack rates were computed from raw data in each study, dividing the number of infected contacts of primary cases by the total number of susceptible exposed contacts. A pooled analysis was carried out to generate summary estimates for the secondary attack rate in each subgroup analysed (asymptomatic, pre-symptomatic and symptomatic index cases), in the framework of a random effect model. The Freeman–Tukey double-arcsine variance-

stabilizing transformation was used to combine data, because of its advantage over log and logit transformations, which do not allow computation of the proportion in the presence of zero event counts [15]. Secondary attack rates are presented as a proportion along with 95% CIs in forest plots. Heterogeneity between study estimates was gauged by means of the Cochran's Q and I^2 statistic: an I^2 value above 75% indicates high heterogeneity [16]. Moreover, a 95% prediction interval is displayed in the forest plots, which is an index of dispersion, providing information on how widely the true effect size varies. It can also provide the range of values in which a future observation will fall [17]. Analyses were performed though the software METAXL version 5.3 (Ersatz, EpiGear International, Sunrise Beach, QLD, Australia) [18].

Results

The systematic search identified 927 potentially relevant articles and 789 records were screened after removal of duplicates. Of 187 articles retrieved for full-text review and assessed for eligibility, 80 studies were included in the systematic review, and among those we identified 69 studies that indicated the symptom status of index case(s). In this analysis, we excluded 11 studies that reported asymptomatic and symptomatic index cases together or in which no symptom status of the index case was available. We re-classified three studies from asymptomatic to pre-symptomatic as the index cases developed symptoms later during the disease course after reviewing the details and contacting the authors [19–21]. The number of selected papers at each step of the screening and eligibility are reported in the flow diagram (Fig. 1).

Summary of secondary attack rates of asymptomatic index cases

Ten studies were included in the quantitative analysis (Table 1) [6,13,22–29]. Summary secondary attack rate estimate was 1% (95% CI 0%–2%) with a prediction interval range of 0%–10% (Fig. 2). All except one tested all close contacts for SARS-CoV-2, regardless of symptoms [26]. Cheng et al. only tested symptomatic cases, but they also tested high-risk populations regardless of symptoms including the household and hospital contacts [26]. Six studies reported on household contacts, two studies included hospital contacts and two studies included non-household close contacts.

Three studies identified no secondary cases after following up 17, 91 and 455 close contacts of asymptomatic index cases (asymptomatic secondary attack rate of 0%) [24–26]. Of those, two studies demonstrated higher symptomatic secondary attack rates: Cheng et al. demonstrated that mild cases had a secondary attack rate of 3.8% (95% CI 1.1%–12.8%) and severe cases had a 4% (95% CI 1.0%–15.8%) secondary attack rate [26], while Park et al. reported a household symptomatic secondary attack rate of 16.2% (95% CI 11.6%–22.0%) [24]. In another study, 305 contacts of eight asymptomatic cases were followed up, identifying one secondary case (secondary attack rate 0.3%, 95% CI 0.0%–1.8%) [28]. In the same study, attack rates from index cases with mild, moderate and severe diseases were 3.3%, 5.6% and 6.2%, respectively. Zhang et al. followed up 119 close contacts of 12 asymptomatic index cases and identified one secondary case, an asymptomatic secondary attack rate of 0.8% (95% CI 0.0%–4.6%). In the same study, the secondary attack rate was 3.5% (95% CI 1.5%–8.0%) for those with mild, 5.7% (95% CI 2.5%–12.8%) for those with moderate and 4.5% (95% CI 0.8%–21.8%) for those with severe symptoms [6]. In this study, close contacts that lived with an index case had 12 times the risk of infection as those who did not live with the index case (relative risk 12.5, 95% CI 1.6–100.8) and those who had frequent contact with an index case patient, and those who had more than five contacts had 29 times the risk of infection as those with fewer

contacts (relative risk 29.0, 95% CI 3.6–232.3). Two studies indicated an asymptomatic secondary attack rate of 1% and 1.9% [22,23]. Chaw et al. reported asymptomatic and pre-symptomatic contacts together. The authors clarified that three asymptomatic index cases and their 106 close contacts were followed up, leading to three secondary cases, a secondary attack rate of 2.8% (95% CI 0.06%–8.0%). In this study, the overall secondary attack rate was 10.6% in the household setting, which was higher for symptomatic cases (14.4%, 95% CI 8.8%–19.9%) than that of asymptomatic cases and for non-household contacts 0.7 (95% CI 0.1%–1.3) [13]. Zeng et al. conducted the largest contact tracing study, following up 753 close contacts of asymptomatic index cases and identified one secondary case, an asymptomatic secondary attack rate of 0.13% (95% CI 0.0%–0.7%) [27].

Summary of pre-symptomatic secondary attack rates

Sixteen papers reported either outbreak investigations or contact tracing studies reporting transmission from an index case during the pre-symptomatic period [13,19,21,26,30–40] (Table 2). Of those, 11 studies were included in the quantitative analysis. The summary secondary attack rate estimate was 7% (95% CI 3%–11%) with a prediction interval of 1%–40% (Fig. 3). These studies followed up 22 to 585 close contacts whose initial exposure occurred before symptom onset of the index case. Even in studies that followed up large numbers of people, including community contacts, the majority of secondary cases identified were from the same household or among gatherings of friends. In these studies, having meals together, or playing cards with the index case were exposure activities associated with transmission. The remaining one study reported an outbreak in a restaurant [40] and four studies exclusively reported family cluster outbreaks [30,32,33,39]; these investigations did not test contacts outside the household, and it is challenging to truly differentiate transmission during the pre-symptomatic period from symptomatic transmission in the household setting (see Supplementary material, Fig. S1).

Summary of symptomatic secondary attack rates

Forty-six papers reported either outbreak investigations or contact tracing studies reporting transmission from symptomatic index case(s). Of those, 40 contact tracing studies reported secondary attack rates ranging from 0% to 38.89% [13,24,27,28,38,41–75] and six reported outbreak investigation [76–80] (see Supplementary material, Table S1). Forty contact tracing studies with 44 observations were included in the quantitative analysis (Fig. 4). The summary estimate of secondary attack rate from symptomatic index subjects was 6% (95% CI 5%–8%) with a prediction interval of 5%–38%. Of those, nine studies reported less than 1% secondary attack rates, two of these were in a health-care setting, two included outdoor interaction and four included non-household contacts. Higher frequency of contacts and household contacts were reported to be higher risk than non-household contacts.

Quality assessment

All papers included a clear definition of symptomatic and asymptomatic cases, number of secondary cases and number of contacts. The majority of studies identified index cases with a clear diagnosis, had an acceptable case definition and sufficiently followed up close contacts (for a minimum of 14 days). However, in some studies the definition of close contact and setting of transmission was not provided. In addition, it was unclear in four reports whether all potential close contacts were included; therefore, the

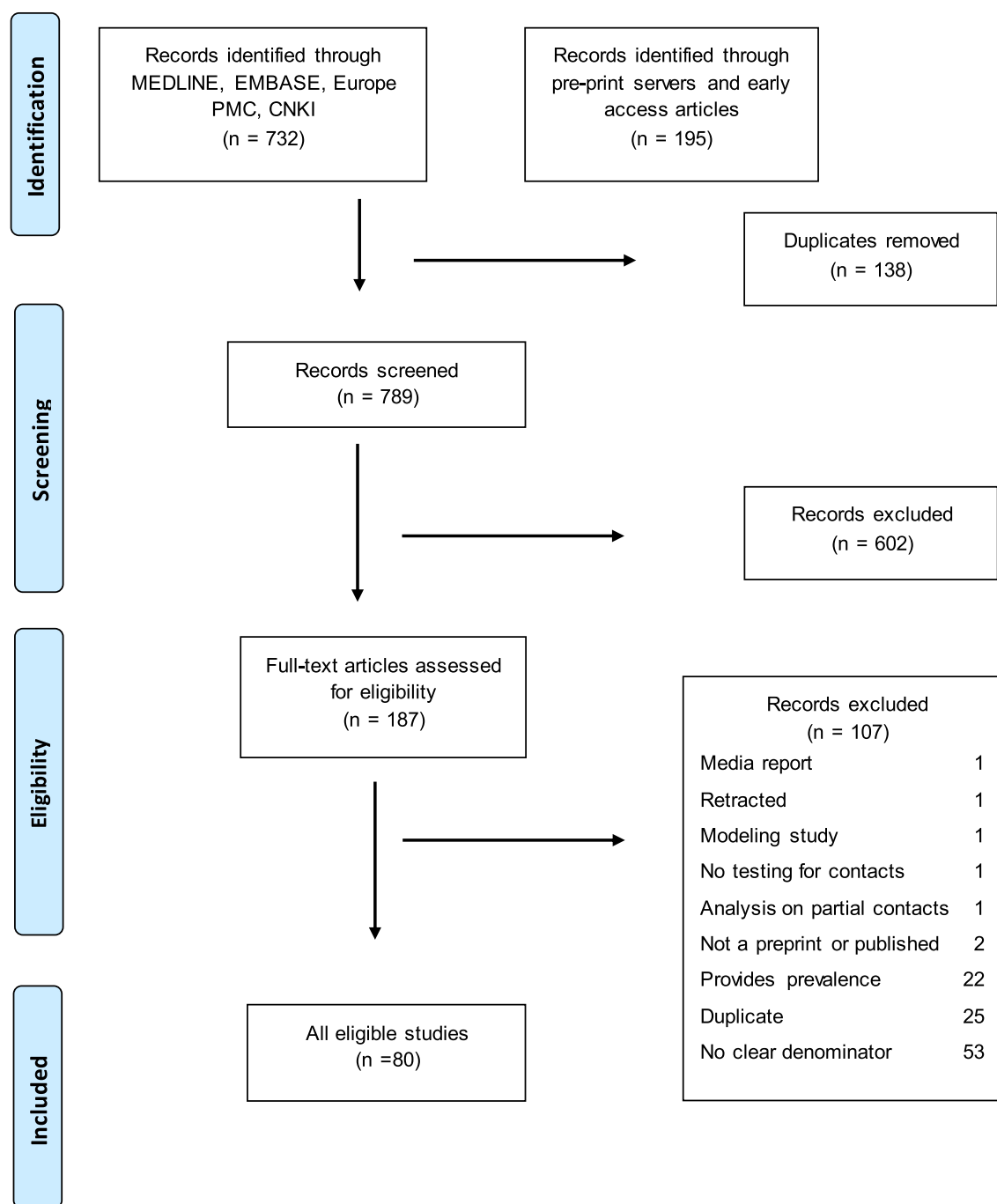


Fig. 1. Flowchart describing inclusion and exclusion of studies at each stage of the review.

direction of bias was uncertain. The quality assessment is summarized in the Supplementary material (Table S2).

Discussion

This systematic review provides comprehensive data on secondary attack rates based on symptom status of the index case(s). Although asymptomatic patients can transmit the virus to others [81], the findings from ten studies in this review found summary secondary attack rates of 1% with a prediction interval of 0%–10% for asymptomatic index cases compared with secondary attack rates of 6% with a prediction interval of 5%–38% in symptomatic

cases and 7% with a prediction interval of 1%–40% in pre-symptomatic cases. These findings suggest that individuals who are asymptomatic throughout the disease course are responsible for fewer secondary infections than symptomatic and pre-symptomatic cases. Most transmission events were associated with living with the index case or group activities such as sharing meals and playing board games.

Given the importance of transmission heterogeneity in propagating the pandemic, it is important that we learn about the various factors that contribute to transmission. According to modelling and contact tracing studies, around 80% of secondary infections can be linked to 20% of cases, which distinguishes SARS-CoV-2 from

Table 1
Transmission from truly asymptomatic index cases

	Index cases	Environment	Number of contacts	Number of secondary cases	Asymptomatic SAR (95% CI)	Symptomatic SAR (95% CI)
Chaw et al. ^a [13]	3	Household	106	3	2.8% (0.06–8.0)	14.4% (8.8–19.9)
Chen Y et al. [29]	30	Non-household	146	6	4.1% (1.7–9.1)	0.7% (0.01–1.3)
Cheng et al. [26]	9	Household	91	0	0% (0.0–4.1)	6.3% (5.3–7.5)
		Non-household				Mild 3.76 (1.1–12.8)
Gao et al. [25]	1	Household and healthcare	455	0	0% (0.0–0.08)	Severe 3.99 (1.0–15.8)
Jiang et al. [22]	3	Household	195	2	1% (0.1–3.7)	
Luo et al. [28]	8	Household and non-household	305	1	0.33% (0.0–1.8)	Mild 3.3% (OR 0.48; 0.28–0.82)
					OR (0.29 (0.04–2.2))	Mod 5.6% (OR 1.0)
Mandić-Rajčević et al. [23]	1	Healthcare	53	1	1.9% (0.0,10.0)	Sev 6.2% (OR 1.19; 0.7–2.1)
Park et al. [24]	4	Household	17	0	0% (0.0–19.5)	16.2% (11.6–22.0)
Zeng et al. [27]		All contacts	753	1	0.13% (0.0–0.7)	2.02% (1.8–2.3)
Zhang et al. [6]	12	Household	119	1	0.8% (0.0–4.6)	Mild 3.5% (1.5–8.0)
						Mod 5.7% (2.5–12.8)
						Severe 4.5% (0.8–21.8)

Abbreviations: SAR, secondary attack rate; sev, severe.

^a Authors contacted for more details.

seasonal influenza, although a similar pattern was also observed in SARS-CoV and Middle East respiratory syndrome-CoV [82–84]. There are multiple factors (environmental factors, contact patterns and socio-economic inequalities) that contribute to this heterogeneity, but some evidence is starting to emerge about the influence of individual's infectiousness on transmission dynamics. In this systematic review, we found that index cases with symptoms had a higher secondary attack rate compared with truly asymptomatic index cases. Although there is a need to better understand this difference, it may be due to shorter duration of infectiousness. In a living systematic review including studies published up to 6 June 2020, we found that asymptomatic people had a shorter duration of RNA shedding than symptomatic individuals [85]. Asymptomatic patients may therefore be contagious but for a shorter duration than symptomatic people; this might contribute to lower transmission to their contacts. However, we do not yet know the relative importance of behavioral factors by the host versus environmental

factors in determining transmission risk. It is not known whether the size of the cluster of secondary infections would be different according to index case symptom status in a high-risk environment with no mitigation measures in place.

Modelling studies suggest that it is not possible to have widespread infection without substantial pre-symptomatic transmission. Viral load dynamics of SARS-CoV-2 derived from confirmed cases suggest that peak viral loads are detected at the start of symptom onset up to day 5 of illness, indicating that the highest infectiousness occurs just before or within the first few days after symptom onset [85]. So far, several contact tracing studies emphasize that the highest risk of transmission occurs during the prodromal phase or early in the disease course [64,86]. For instance, in a prospective contact tracing study of 100 confirmed cases of COVID-19 and 2761 close contacts, no secondary cases were identified when the exposure occurred more than 5 days after symptom onset [26]. Our findings therefore have

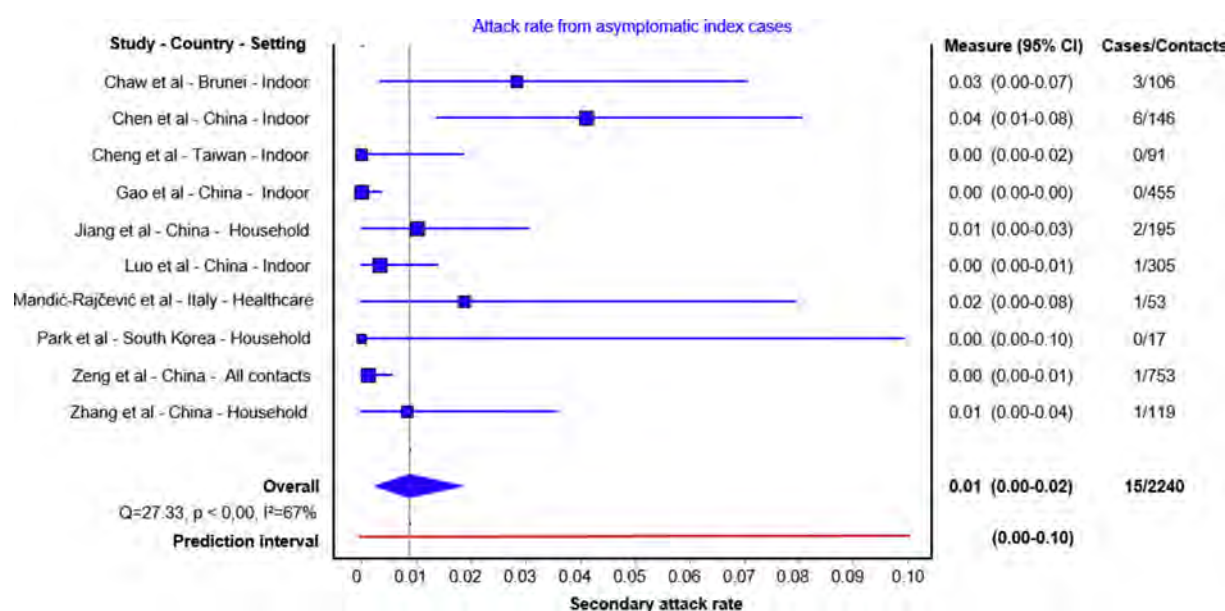


Fig. 2. Secondary attack rates from asymptomatic index cases to their contacts. For each study the secondary attack rate is reported with its 95% CI. A prediction interval at the bottom of the forest plot is depicted.

Table 2
Transmission during pre-symptomatic period

	Index cases	Environment	Number of contacts	Number of secondary cases	Pre-symptomatic SAR (95% CI)	Secondary cases
Contract tracing						
Chaw et al. ^a [13]	7	Household and non-household	585	15	2.56% (1.4–4.2)	
Cheng et al. [26]	NR	Household and non-household	299	2	0.7% (0.1–2.4)	
Hong L et al. [31]	41	Household and non-household	197	24	12.2% (8.0–17.6)	Friends, family, card-playing partners
Huang et al. [19]	1	Friends	22	7	31.8% (13.0–54.9)	Shared meal with index
Pang et al. [34]	1	Household and non-household	103	6	5.8% (2.2–12.2)	Living together or sharing meal
Park et al. [24]	4	Household	11	0	0% (0.0–2.8)	
Pung R et al. [38]	2	Religious gathering	142	3	2.1% (0.5–6.5)	
Qian et al. [35]	1	Household and non-household	137	10	7.3% (3.6–13.0)	Living together or sharing meal
Yang et al. [36]	2	Household and non-household	123	6	4.9% (1.8–10.3)	All secondary cases lived together
Ye et al. [21]	1	Family	44	4	9.1% (2.5–21.4)	Extended family
Zhao et al. [37]	1	Friends	15	4	26.7% (7.8–55.1)	Meal and Mahjong game gathering
Outbreak investigation						
Chen M et al. [30]	1	Household	3	2	66.7% (9.4–99.2)	Family cluster outbreak
Li P et al. [32]	1	Household	5	4	80% (28.4–99.5)	Family cluster outbreak
Lu J et al. [40]	1	Restaurant	82	9	11% (5.9–19.6)	
Jiang Y et al. [39]	1	Household	7	3	42.9% (11.8–79.8)	Family cluster outbreak
Qian G et al. [33]	2	Household	4	3	75% (10.4–99.4)	Family cluster outbreak

Abbreviation: SAR, secondary attack rate.

^a Authors contacted for more details.

important implications from a public health perspective. In settings such as nursing homes, homeless shelters, prisons, cruise ships and meat-packing plants in which many people spend prolonged periods of time together in the same environment including sleeping, dining and sharing common facilities, and where several outbreaks have been documented, pre-symptomatic transmission may contribute substantially to transmission [87,88]. In these settings, when infection develops, most patients are already inside the facility with high viral loads that increase the risk of onward transmission. This highlights the importance of mitigation measures and surveillance in these settings to identify those patients early in the disease course to prevent onward transmission inside the facility.

This systematic review has several strengths. First, this is a living systematic review examining the transmission of SARS-CoV-2 through contact tracing and outbreak investigation studies. Second, we only included studies with clear case definitions, which indicated the number of contacts and secondary cases. We excluded studies in which the index case was unclear, or the numbers of contacts were not provided. The estimates from individual studies are also subject to limitations, such as imprecision

resulting from small study size, and multiple sources of bias in the estimation of the true secondary attack rate, which are detailed in this paper [89]. Moreover, while the number of index cases could influence the confidence interval estimation for secondary attack rate due to heterogeneity among index cases, we have constructed a prediction interval to yield conservative confidence interval estimates.

We identified two other systematic reviews that investigated asymptomatic transmission, with different research questions, which results in different search terms and studies retrieved. One living systematic review, which included studies published up to 10 June 2020, identified five studies that directly compared secondary attack rates between asymptomatic and symptomatic index cases; all were included in our review [7]. This study only included studies that provided data to allow relative risks to be estimated. The summary risk ratios for asymptomatic versus symptomatic (0.35, 95% CI 0.10–1.27) and pre-symptomatic versus symptomatic (0.63, 95% CI 0.18–2.26) are consistent with our findings. The second review estimated only household secondary attack rates and included studies published up to 29 July

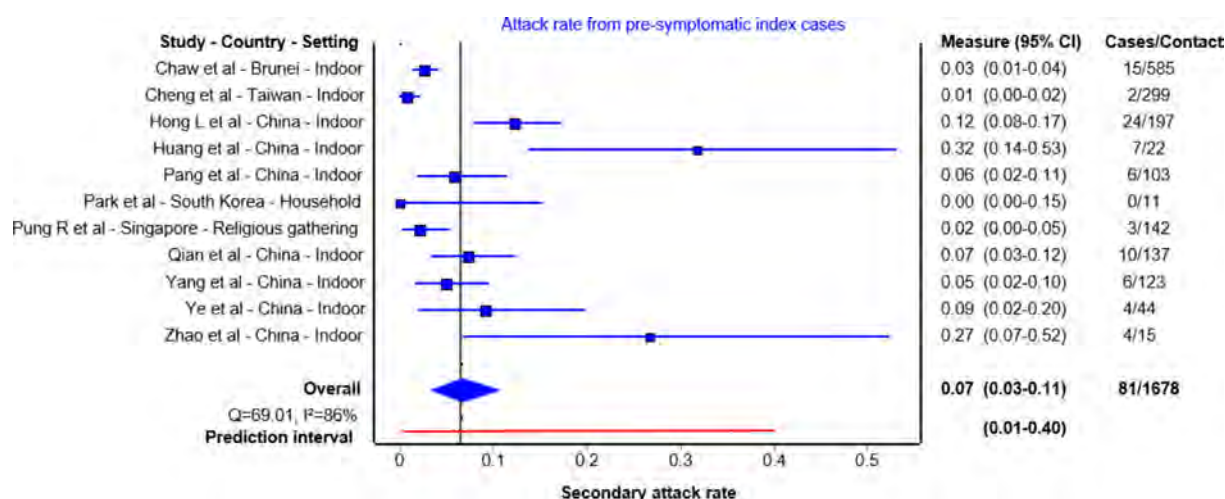


Fig. 3. Secondary attack rates from pre-symptomatic index cases to their contacts. For each study the secondary attack rate is reported with its 95% CI. A prediction interval at the bottom of the forest plot is depicted.

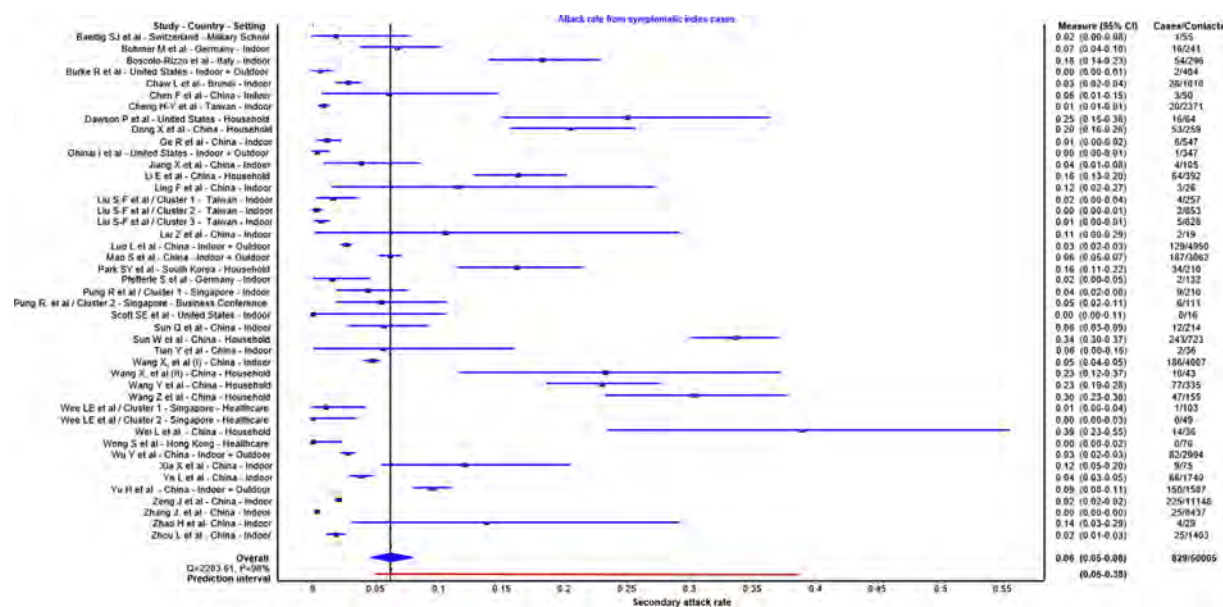


Fig. 4. Secondary attack rates from symptomatic index cases to their contacts. For each study the secondary attack rate is reported with its 95% CI. A prediction interval at the bottom of the forest plot is depicted.

2020 [90]. Of three studies that included asymptomatic index cases, two were included in our review. We excluded one of the studies because the number of contacts of asymptomatic index cases was not specified; we have not yet received details of the study after contacting the authors. Advantages of our review over these two studies are inclusion of studies published in Chinese, search terms that aimed to capture studies specifically estimating secondary attack rates.

In summary, although asymptomatic transmission is a major concern for SARS-CoV-2 community spread, secondary attack rates from those who remain asymptomatic throughout their course of infection are low, suggesting limited infectiousness. Although it is difficult to estimate the proportion of pre-symptomatic transmission, these patients are likely to be highly infectious just before and around the time of symptom onset and appear to transmit efficiently, particularly within households. Given these results, in the context of limited resources, approaches should be targeted predominantly at identifying and immediately isolating patients with prodromal or mild symptoms and their contacts, which may avert a significant number of community transmission clusters [91]. Future clinical studies should incorporate clear definitions and assess a broad range of symptoms associated with COVID-19, include longitudinal follow up of patients, and calculate secondary attack rates for a wider range of settings and populations [9].

Transparency declaration

The authors declare that there are no conflicts of interest.

Contribution statement

XQ contributed to investigation, data curation and writing the original draft; AN contributed to investigation, data curation and review and editing the article; AEM contributed to methodology, formal analysis and writing the original draft; IB and NL contributed to interpretation and to reviewing and editing the article; M.

Cevik contributed to conceptualization, methodology, investigation, writing the original draft and supervision.

Funding

No funding was received.

Acknowledgements

We would like to thank the authors of Chau et al. (Dr Tan Le Van), Mandić-Rajčević et al. (Dr Stefan Mandić-Rajčević) and Chaw et al. (Dr Liling Chaw) for providing further details about asymptomatic cases in their reports, also Prof Stephen Gillespie for his comments on the first draft of this manuscript. We would like to acknowledge Dr Shuang Jin for searching and downloading the Chinese database for this review.

Appendix A. Supplementary data

Supplementary data to this article can be found online at <https://doi.org/10.1016/j.cmi.2021.01.011>.

References

- Ruan L, Wen M, Zeng Q, et al. New measures for the coronavirus disease 2019 response: a lesson from the Wenzhou experience. *Clin Infect Dis* 2020;71: 866–9.
- Gandhi M, Yokoe DS, Havlir DV. Asymptomatic transmission, the Achilles' heel of current strategies to control Covid-19. *N Engl J Med* 2020;382:2158–60.
- Gudbjartsson DF, Helgason A, Jonsson H, et al. Spread of SARS-CoV-2 in the Icelandic population. *N Engl J Med* 2020;382:2302–15.
- Cevik M, Bamford CGG, Ho A. COVID-19 pandemic—a focused review for clinicians. *Clin Microbiol Infect* 2020;26:842–7.
- Wang Y, Liu Y, Liu L, Wang X, Luo N, Li L. Clinical outcomes in 55 patients with severe acute respiratory syndrome coronavirus 2 who were asymptomatic at hospital admission in Shenzhen, China. *J Infect Dis* 2020;221:1770–4.
- Zhang W, Cheng W, Luo L, et al. Secondary transmission of coronavirus disease from presymptomatic persons, China. *Emerg Infect Dis* 2020;26.
- Buitrago-García D, Egli-Gany D, Counotte MJ, et al. Occurrence and transmission potential of asymptomatic and presymptomatic SARS-CoV-2 infections: a living systematic review and meta-analysis. *PLoS Med* 2020;17: e1003346.

- [8] Sugano N, Ando W, Fukushima W. Cluster of severe acute respiratory syndrome coronavirus 2 infections linked to music clubs in Osaka, Japan. *J Infect Dis* 2020;222:1635–40.
- [9] Meyerowitz EA, Richterman A, Bogoch II, Low N, Cevik M. Towards an accurate and systematic characterisation of persistently asymptomatic infection with SARS-CoV-2. *Lancet Infect Dis* 2020. [https://doi.org/10.1016/S1473-3099\(20\)30837-9](https://doi.org/10.1016/S1473-3099(20)30837-9). Online ahead of print.
- [10] Lavezzo E, Franchin E, Ciavarella C, et al. Suppression of COVID-19 outbreak in the municipality of Vo, Italy. *medRxiv* 2020. 2020.04.17.20053157.
- [11] Kim ES, Chin BS, Kang CK, et al. Clinical course and outcomes of patients with severe acute respiratory syndrome coronavirus 2 infection: a preliminary report of the first 28 patients from the Korean Cohort Study on COVID-19. *J Korean Med Sci* 2020;35:e142.
- [12] Arons MM, Hatfield KM, Reddy SC, et al. Presymptomatic SARS-CoV-2 infections and transmission in a skilled nursing facility. *N Engl J Med* 2020;382:2081–90.
- [13] Chaw L, Koh W, Jamaludin S, Naing L, Alikhan M, Wong J. Analysis of SARS-CoV-2 transmission in different settings, Brunei. *Emerg Infect Dis*. 2020;26:2598–2606.
- [14] Elliott Jh, Synnot A, Turner T, et al. Living systematic review: 1. Introduction—the why, what, when, and how. *J Clin Epidemiol* 2017;91:23–30.
- [15] Lin L, Xu C. Arcsine-based transformations for meta-analysis of proportions: pros, cons, and alternatives. *Health Sci Rep* 2020;3:e178.
- [16] Sedgwick P. Meta-analyses: what is heterogeneity? *BMJ* 2015;350:h1435.
- [17] Int'Hout J, Ioannidis JPA, Rovers MM, Goeman JJ. Plea for routinely presenting prediction intervals in meta-analysis. *BMJ Open* 2016;6:e010247.
- [18] Barendregt JJ, Doi SA, Lee YY, Norman RE, Vos T. Meta-analysis of prevalence. *J Epidemiol Commun Health* 2013;67:974.
- [19] Huang L, Zhang X, Zhang X, et al. Rapid asymptomatic transmission of COVID-19 during the incubation period demonstrating strong infectivity in a cluster of youngsters aged 16–23 years outside Wuhan and characteristics of young patients with COVID-19: a prospective contact-tracing study. *J Infect* 2020;80:e1–13.
- [20] Li C, Ji F, Wang L, et al. Asymptomatic and human-to-human transmission of SARS-CoV-2 in a 2-family cluster, Xuzhou, China. *Emerg Infect Dis* 2020;26:31.
- [21] Ye F, Xu S, Rong Z, et al. Delivery of infection from asymptomatic carriers of COVID-19 in a familial cluster. *Int J Infect Dis* 2020;94:133–8.
- [22] Jiang XL, Zhang XL, Zhao XN, et al. Transmission potential of asymptomatic and paucisymptomatic SARS-CoV-2 infections: a three-family cluster study in China. *J Infect Dis* 2020;22:22.
- [23] Mandic-Rajcic S, Masci F, Crespi E, et al. Contact tracing and isolation of asymptomatic spreaders to successfully control the COVID-19 epidemic among healthcare workers in Milan (Italy). 2020. <https://doi.org/10.1101/2020.05.03.20082818>.
- [24] Park SY, Kim YM, Yi S, et al. Coronavirus disease outbreak in call center, South Korea. *Emerg Infect Dis* 2020;26:23.
- [25] Gao M, Yang L, Chen X, et al. A study on infectivity of asymptomatic SARS-CoV-2 carriers. *Respir Med* 2020;106:206.
- [26] Cheng H-Y, Jian S-W, Liu D-P, et al. Contact tracing assessment of COVID-19 transmission dynamics in Taiwan and risk at different exposure periods before and after symptom onset. *JAMA Intern Med* 2020.
- [27] 曾 晶, 邱 平, 邹 晏, et al. 四川省新型冠状病毒肺炎密切接触者分析. *中国公共卫生* 2020;36:503–6.
- [28] Luo L, Liu D, Liao X, et al. Contact settings and risk for transmission in 3410 close contacts of patients with COVID-19 in Guangzhou, China. *Ann Intern Med* 2020;173:879–87.
- [29] Chen Y, Zhang AH, Yi B, et al. Epidemiological characteristics of infection in COVID-19 close contacts in Ningbo city. *Chung Hua Liu Hsing Ping Hsueh Tsa Chih* 2020;41:667–71.
- [30] Chen M, Fan P, Liu Z, et al. A SARS-CoV-2 familial cluster infection reveals asymptomatic transmission to children. *J Infect Public Health* 2020;13:883–6.
- [31] Hong LX, Lin A, He ZB, et al. Mask wearing in pre-symptomatic patients prevents SARS-CoV-2 transmission: an epidemiological analysis. *Travel Med Infect Dis* 2020;36:101803.
- [32] Li P, Fu JB, Li KF, et al. Transmission of COVID-19 in the terminal stages of the incubation period: a familial cluster. *Int J Infect Dis* 2020;96:452–3.
- [33] Qian G, Yang N, Ma AHY, et al. A COVID-19 transmission within a family cluster by presymptomatic infectors in China. *Clin Infect Dis* 2020;71:861–2.
- [34] 庞 秋艳, 李 朋, 李 天忠, 李 化荣. 起高速服务区新型冠状病毒肺炎聚集性疫情调查. *安徽预防医学杂志* 2020;26:130–2.
- [35] 钱 丽珍, 郑 志强, 洪 万胜, 孙 芳红, 吴 方楠, 金 瑞盈. 瑞安市一起新型冠状病毒肺炎聚集性疫情调查. *预防医学* 2020;32:486–488+91.
- [36] 阳 雅兰, 李 林洪, 李 长凤, 肖 玉春, 彭 君. 重庆市一起新型冠状病毒肺炎家庭聚集性疫情调查分析. *中国公共卫生* 2020;36:285–8.
- [37] Zhao H, Li BS, Xia Y, et al. Investigation of transmission chain of a cluster COVID-19 cases. *Chung Hua Liu Hsing Ping Hsueh Tsa Chih* 2020;41:E064.
- [38] Pung R, Chiew CJ, Young BE, et al. Investigation of three clusters of COVID-19 in Singapore: implications for surveillance and response measures. *Lancet* 2020;395:1039–46.
- [39] Jiang Y, Niu W, Wang Q, Zhao H, Meng L, Zhang C. Characteristics of a family cluster of severe acute respiratory syndrome coronavirus 2 in Henan, China. *J Infect* 2020;23:23.
- [40] Lu J, Gu J, Li K, et al. COVID-19 outbreak associated with air conditioning in restaurant, Guangzhou, China, 2020. *Emerg Infect Dis* 2020;26:2.
- [41] Baettig SJ, Parini A, Cardona I, Morand GB. Case series of coronavirus (SARS-CoV-2) in a military recruit school: clinical, sanitary and logistical implications. *BMJ Mil Health* 2020;16:16.
- [42] Bohmer MM, Buchholz U, Corman VM, et al. Investigation of a COVID-19 outbreak in Germany resulting from a single travel-associated primary case: a case series. *Lancet Infect Dis* 2020;15:15.
- [43] Boscolo-Rizzo P, Borsetto D, Spinato G, et al. New onset of loss of smell or taste in household contacts of home-isolated SARS-CoV-2-positive subjects. *Eur Arch Oto-Rhino-Laryngol* 2020;277:2637–40.
- [44] Burke RM, Midgley CM, Dratch A, et al. Active monitoring of persons exposed to patients with confirmed COVID-19 – United States, January–February 2020. *MMWR Morb Mortal Wkly Rep* 2020;69:245–6.
- [45] Cheng HY, Jian SW, Liu DP, Ng TC, Huang WT, Lin HH. Contact tracing assessment of COVID-19 transmission dynamics in Taiwan and risk at different exposure periods before and after symptom onset. *JAMA Intern Med* 2020;180:1156–63.
- [46] Dawson P, Rabold EM, Laws RL, et al. Loss of taste and smell as distinguishing symptoms of coronavirus disease 2019. *Clin Infect Dis* 2021;72:682–5.
- [47] Ge R, Tian M, Gu Q, et al. The role of close contacts tracking management in COVID-19 prevention: a cluster investigation in Jiaxing, China. *J Infect* 2020;81:e71–4.
- [48] Ghinai I, McPherson TD, Hunter JC, et al. First known person-to-person transmission of severe acute respiratory syndrome coronavirus 2 (SARS-CoV-2) in the USA. *Lancet* 2020;395:1137–44.
- [49] Jiang XL, Zhang XL, Zhao XN, et al. Transmission potential of asymptomatic and paucisymptomatic severe acute respiratory syndrome coronavirus 2 infections: a 3-family cluster study in China. *J Infect Dis* 2020;221:1948–52.
- [50] Liu SF, Kuo NY, Kuo HC. Three Taiwan's domestic family cluster infections of coronavirus disease 2019. *J Med Virol* 2020;28:28.
- [51] Mao S, Huang T, Yuan H, et al. Epidemiological analysis of 67 local COVID-19 clusters in Sichuan Province, China. *Research Square*; 2020. <https://doi.org/10.21203/rs.3.rs-26119/v1>.
- [52] Pfefferle S, Guenther T, Kobbe R, et al. Low and high infection dose transmission of SARS-CoV-2 in the first COVID-19 clusters in Northern Germany. *medRxiv* 2020. <https://doi.org/10.1101/2020.06.11.20127332>.
- [53] Scott SE, Zabel K, Collins J, et al. First mildly ill, non-hospitalized case of coronavirus disease 2019 (COVID-19) without viral transmission in the United States – Maricopa County, Arizona, 2020. *Clin Infect Dis* 2020;71:807–12.
- [54] Sun WW, Ling F, Pan JR, et al. Epidemiological characteristics of 2019 novel coronavirus family clustering in Zhejiang Province. *Chung Hua Yu Fang I Hsueh Tsa Chih* 2020;54:E027.
- [55] Wang Z, Ma W, Zheng X, Wu G, Zhang R. Household transmission of SARS-CoV-2. *J Infect* 2020;81:179–82.
- [56] Wee LE, Sim JXY, Conceicao EP, et al. Containment of COVID-19 cases amongst healthcare workers: the role of surveillance, early detection and outbreak management. *Infect Control Hosp Epidemiol* 2020;1–21.
- [57] Wei L, Lv Q, Wen Y, et al. Household transmission of COVID-19, Shenzhen, January–February 2020. *medRxiv* 2020. <https://doi.org/10.1101/2020.05.11.20092692>.
- [58] Wong SCY, Kwong RT, Wu TC, et al. Risk of nosocomial transmission of coronavirus disease 2019: an experience in a general ward setting in Hong Kong. *J Hosp Infect* 2020;105:119–27.
- [59] Xia XY, Wu J, Liu HL, Xia H, Jia B, Huang WX. Epidemiological and initial clinical characteristics of patients with family aggregation of COVID-19. *J Clin Virol* 2020;127:104360.
- [60] Ye LX, Wang HB, Lu HC, et al. Investigation of a cluster epidemic of COVID-19 in Ningbo. *Chung Hua Liu Hsing Ping Hsueh Tsa Chih* 2020;41:E065.
- [61] Zhang JZ, Zhou P, Han DB, et al. Investigation on a cluster epidemic of COVID-19 in a supermarket in Liaocheng, Shandong province. *Chung Hua Liu Hsing Ping Hsueh Tsa Chih* 2020;41:E055.
- [62] Zhao H, Li BS, Xia Y, et al. Investigation of transmission chain of a cluster COVID-19 cases. *Chung Hua Liu Hsing Ping Hsueh Tsa Chih* 2020;41:E064.
- [63] Wang X, Zhou Q, He Y, et al. Nosocomial outbreak of COVID-19 pneumonia in Wuhan, China. *Eur Respir J* 2020;55:2000544.
- [64] Wang Y, Tian H, Zhang L, et al. Reduction of secondary transmission of SARS-CoV-2 in households by face mask use, disinfection and social distancing: a cohort study in Beijing, China. *BMJ Glob Health* 2020;5:e002794.
- [65] Wu Y, Song S, Kao Q, Kong Q, Sun Z, Wang B. Risk of SARS-CoV-2 infection among contacts of individuals with COVID-19 in Hangzhou, China. *Public Health* 2020;185:57–9.
- [66] Yu H-J, Hu Y-f, Liu X-x, et al. Household infection: the predominant risk factor for close contacts of patients with COVID-19. *Travel Med Infect Dis* 2020;36:101809.
- [67] Dong XC, Li JM, Bai JY, et al. Epidemiological characteristics of confirmed COVID-19 cases in Tianjin. *Chung Hua Liu Hsing Ping Hsueh Tsa Chih* 2020;41:638–42.
- [68] 凌 锋, 刘 社兰, 倪 朝荣, et al. 浙江省首例新型冠状病毒肺炎报告病例流行病学调查. *预防医学* 2020;32:109–12.

- [69] 刘 仲, 赵 梦娇, 杨 国樑, et al. 1例不明原因新型冠状病毒肺炎及其密切接触者调查分析. *山东大学学报(医学版)* 2020;58:49–53.
- [70] 周 林, 刘 晓雪, 李 战, 耿 兴义, 刘 庆皆. 新型冠状病毒肺炎病例1403例密切接触者发病分析. *山东大学学报(医学版)* 2020;58:58–61.
- [71] 孙 倩莱, 李 作超, 谭 夏林, et al. 起新型冠状病毒肺炎聚集性疫情调查. *实用预防医学* 2020;27:389–92.
- [72] 田元睿, 吴志明, 韩小亮, 王月萍, 刘泓, 扬州市首起输入性新型冠状病毒肺炎家庭聚集性疫情的流行病学调查. *上海预防医学*: 1–7.
- [73] 陈 凤阳, 李 少雄. 江西某地一起新型冠状病毒肺炎聚集性疫情调查. *江西医药* 2020;55:346–8.
- [74] Li W, Zhang B, Lu J, et al. The characteristics of household transmission of COVID-19. *Clin Infect Dis* 2020;71:1943–6.
- [75] Wang X, Pan Y, Zhang D, et al. Basic epidemiological parameter values from data of real-world in mega-cities: the characteristics of COVID-19 in Beijing, China. *BMC Infect Dis* 2020;20:526. <https://doi.org/10.1186/s12879-020-05251-9>.
- [76] Huang R, Xia J, Chen Y, Shan C, Wu C. A family cluster of SARS-CoV-2 infection involving 11 patients in Nanjing, China. *Lancet Infect Dis* 2020;20:534–5.
- [77] Li CX, Wu B, Luo F, Zhang N. Clinical study and CT findings of a familial cluster of pneumonia with coronavirus disease 2019 (COVID-19). *Sichuan Da Xue Xue Bao Yi Xue Ban* 2020;51:155–8.
- [78] Song R, Han B, Song M, et al. Clinical and epidemiological features of COVID-19 family clusters in Beijing, China. *J Infect* 2020;23:23.
- [79] Tong ZD, Tang A, Li KF, et al. Potential presymptomatic transmission of SARS-CoV-2, Zhejiang province, China, 2020. *Emerg Infect Dis* 2020;26:1052–4.
- [80] Chen D, Li Y, Deng X, et al. Four cases from a family cluster were diagnosed as COVID-19 after 14-day of quarantine period. *J Med Virol* 2020. <https://doi.org/10.1002/jmv.25849>.
- [81] Chau NVV, Thanh Lam V, Thanh Dung N, et al. The natural history and transmission potential of asymptomatic SARS-CoV-2 infection. *Clin Infect Dis* 2020;71:2679–87.
- [82] Bi Q, Wu Y, Mei S, et al. Epidemiology and transmission of COVID-19 in 391 cases and 1286 of their close contacts in Shenzhen, China: a retrospective cohort study. *Lancet Infect Dis* 2020;20:911–9.
- [83] Althouse BM, Wenger EA, Miller JC, et al. Superspreading events in the transmission dynamics of SARS-CoV-2: opportunities for interventions and control. *PLOS Biol* 2020;18:e3000897.
- [84] Adam DC, Wu P, Wong JY, et al. Clustering and superspreading potential of SARS-CoV-2 infections in Hong Kong. *Nat Med* 2020;26:1714–9.
- [85] Cevik M, Tate M, Lloyd O, Maraolo AE, Schafers J, Ho A. SARS-CoV-2, SARS-CoV, and MERS-CoV viral load dynamics, duration of viral shedding, and infectiousness: a systematic review and meta-analysis. *Lancet Microb* 2021;2:e13–22.
- [86] Böhmer MM, Buchholz U, Corman VM, et al. Investigation of a COVID-19 outbreak in Germany resulting from a single travel-associated primary case: a case series. *Lancet Infect Dis* 2020;20:920–8.
- [87] Adam DC, Wu P, Wong JY. Clustering and superspreading potential of SARS-CoV-2 infections in Hong Kong. *Nat Med* 2020;26:1714–9.
- [88] Leclerc QJFN, Knight LE. What settings have been linked to SARS-CoV-2 transmission clusters? [version 1; peer review: 1 approved with reservations]. *Wellcome Open Res* 2020;5:83.
- [89] Accorsi E, Qiu Xueting, Rumpler Eva, et al. How to detect and reduce potential sources of biases in epidemiologic studies of SARS-CoV-2. *Harvard Library*; 2020. <https://nrs.harvard.edu/URN-3:HULINSTREPOS:37366192>.
- [90] Madewell ZJ, Yang Y, Longini Jr IM, Halloran ME, Dean NE. Household Transmission of SARS-CoV-2: a systematic review and meta-analysis. *JAMA Netw Open* 2020;3:e2031756. e.
- [91] Peak CM, Kahn R, Grad YH, et al. Individual quarantine versus active monitoring of contacts for the mitigation of COVID-19: a modelling study. *Lancet Infect Dis* 2020;20:1025–33.

Outbreak

2019-nCoV (Wuhan virus), a novel Coronavirus: human-to-human transmission, travel-related cases, and vaccine readiness

Robyn Ralph^{1,2}, Jocelyne Lew¹, Tiansheng Zeng³, Magie Francis⁴, Bei Xue^{3,4}, Melissa Roux⁴, Ali Toloue Ostadgavahi⁴, Salvatore Rubino⁵, Nicholas J Dawe⁴, Mohammed N Al-Ahdal⁶, David J Kelvin^{3,4,7}, Christopher D Richardson^{4,7}, Jason Kindrachuk⁸, Darryl Falzarano^{1,2}, Alyson A Kelvin^{4,7,9}

¹ Vaccine and Infectious Disease Organization - International Vaccine Centre (VIDO-InterVac), Saskatoon, Saskatchewan, Canada

² Department of Veterinary Microbiology, University of Saskatchewan, Saskatoon, Saskatchewan, Canada

³ International Institute of Infection and Immunity, Shantou University Medical College, Shantou, Guangdong, China

⁴ Department of Microbiology and Immunology, Faculty of Medicine, Dalhousie University, Halifax, Nova Scotia, Canada

⁵ Sezione di Microbiologia Sperimentale e Clinica, Dipartimento di Scienze Biomediche, Università degli Studi di Sassari, Sassari, Italy

⁶ Department of Infection and Immunity, King Faisal Specialist Hospital and Research Center, Riyadh, Saudi Arabia

⁷ Canadian Centre for Vaccinology, IWK Health Centre, Halifax, Nova Scotia, Canada

⁸ Laboratory of Emerging and Re-Emerging Viruses, Department of Medical Microbiology, University of Manitoba, Winnipeg, Manitoba, Canada

⁹ Department of Pediatrics, Division of Infectious Disease, Faculty of Medicine, Dalhousie University, Halifax, Nova Scotia, Canada

Abstract

On 31 December 2019 the Wuhan Health Commission reported a cluster of atypical pneumonia cases that was linked to a wet market in the city of Wuhan, China. The first patients began experiencing symptoms of illness in mid-December 2019. Clinical isolates were found to contain a novel coronavirus with similarity to bat coronaviruses. As of 28 January 2020, there are in excess of 4,500 laboratory-confirmed cases, with > 100 known deaths. As with the SARS-CoV, infections in children appear to be rare. Travel-related cases have been confirmed in multiple countries and regions outside mainland China including Germany, France, Thailand, Japan, South Korea, Vietnam, Canada, and the United States, as well as Hong Kong and Taiwan. Domestically in China, the virus has also been noted in several cities and provinces with cases in all but one province. While zoonotic transmission appears to be the original source of infections, the most alarming development is that human-to-human transmission is now prevalent. Of particular concern is that many healthcare workers have been infected in the current epidemic. There are several critical clinical questions that need to be resolved, including how efficient is human-to-human transmission? What is the animal reservoir? Is there an intermediate animal reservoir? Do the vaccines generated to the SARS-CoV or MERS-CoV or their proteins offer protection against 2019-nCoV? We offer a research perspective on the next steps for the generation of vaccines. We also present data on the use of *in silico* docking in gaining insight into 2019-nCoV Spike-receptor binding to aid in therapeutic development. Diagnostic PCR protocols can be found at <https://www.who.int/health-topics/coronavirus/laboratory-diagnostics-for-novel-coronavirus>.

Key words: 2019-nCoV; coronavirus; Wuhan; human-to-human transmission; vaccine readiness.

J Infect Dev Ctries 2020; 14(1):3-17. doi:10.3855/jidc.12425

(Received 20 January 2020 – Accepted 23 January 2020)

Copyright © 2020 Ralph *et al.* This is an open-access article distributed under the Creative Commons Attribution License, which permits unrestricted use, distribution, and reproduction in any medium, provided the original work is properly cited.

Current State of emergency – Novel coronavirus outbreak in Wuhan, China

Wuhan 2019-nCoV

A novel coronavirus (CoV) has emerged in Wuhan, China (Figure 1). This virus causes pneumonia of varying severity and has resulted in a high number of hospitalizations (> 4,500) and at least 105 deaths (case-fatality rate (CFR) estimated at 1.5-3%). This virus is

currently referred to as 2019-nCoV (also Wuhan virus) and is related to Severe Acute Respiratory Syndrome coronavirus (SARS-CoV), although with only approximately 80% similarity at the nucleotide level. With a seemingly comparable chain of events as the origin of SARS-CoV, the initial infections with 2019-nCoV appears to be linked to contact with animals in wet markets. Even though human-to-human

transmission was first thought to not be a mode of transmission, there are several documented cases that support that 2019-nCoV is capable of human-to-human transmission [1].

Atypical pneumonia of unexplained cause was first reported on 30 December 2019 in Wuhan city, the capital of Hubei province in central China. Initially, four cases were noted which presented with fever (greater than 38°C), malaise, dry cough, and shortness of breath. Imaging was consistent with pneumonia or acute respiratory distress syndrome (ARDS) and patients had either reduced or normal white blood cell counts. An early link to the Wuhan South China Seafood City (also known as the South China Seafood Wholesale Market or the Huanan Seafood Market) was identified as a common factor in four of the patients. Treatment with antibiotics did not improve their condition over the next 3-5 days and a viral etiology was suspected. The patients were placed in isolation conditions. On 31 December 2020, it was announced that 27 cases of pneumonia, with 7 severe cases, had

been identified [2]. Most of the patients were stall workers at Wuhan South China Seafood City. The market is reported to contain other animals such as birds (chickens, pheasants), bats, hedgehogs, marmots, tiger frogs, and snakes, as well as organs from rabbits and other animals. The market was closed on 1 January 2020 for environmental sanitation and disinfection and has not reopened [3].

By 3 January 2020, the cumulative number of cases rose to 44, with 11 in critical condition and 121 close contacts of infected patients being monitored. At this point influenza virus, avian influenza virus, and adenovirus had been ruled out [4]. As of 5 January 2020, the number of cumulative cases increased to 59 (with onset between 8 December 2019 and 2 January 2020), and 163 close contacts being followed. At this time, SARS-CoV and MERS-CoV were ruled out as the causative agent. The number of cumulative cases increased to 59 on 5 January 2020 [5].

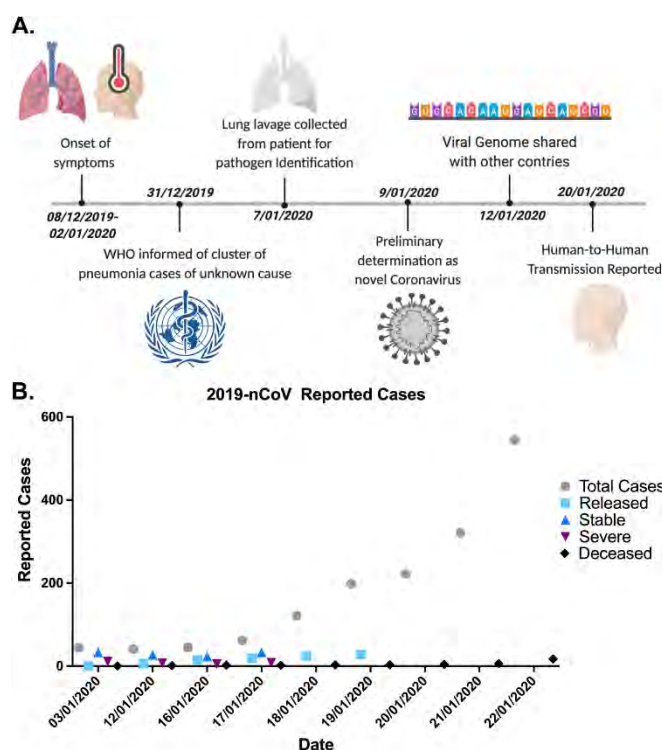
On 8 January 2020, it was reported that a novel coronavirus had been sequenced from one patient and subsequently identified in some of the other patients with pneumonia [6], later reported as 15 of the 59 patients [7]. The first report that some of the cases came from family clusters was the first suggestion that there may have been human-to-human transmission [8]. Virus isolation from one patient was reported [9]. The genome was made publicly available on 11 January 2020 on *virological.org* and later deposited into GenBank.

Additional updates should help clarify the incidence of human-to-human transmission. Given the rapid increase in case numbers, contact tracing will be vital to understanding the extent of human-to-human transmission and the possibility that 2019-nCoV mutations generate viruses with a greater potential for human-to-human transmission. It is important to note that in a Wuhan hospital cluster, 14 healthcare workers were infected by a 2019-nCoV patient [1]. This is reminiscent of several cases of healthcare workers infected by SARS-CoV and MERS-CoV patients. Hospital staff and Infectious Disease control should take necessary precautions in handling of 2019-nCoV patients (see WHO guidelines for handling of suspected and confirmed patients).

Travel-related cases

Another similarity to the SARS-CoV and the MERS-CoV epidemics is the occurrence of travel-related cases. On 13 January 2020, a single case of 2019-nCoV was reported in Thailand of a person who had travelled from Wuhan [10]. This person was not

Figure 1. Timeline of events and reported cases concerned with undiagnosed pneumonia and 2019-nCoV first identified in Wuhan, China.



The timeline of events concerning undiagnosed pneumonia, virus identification, and evidence of human-to-human transmission are shown (A). The number of reported cases plotted over time is shown (B). Case report numbers are acquired from ProMed and National Health Commission of the People's Republic of China.

reported to have been to the previously involved market, but had visited other markets [11]. The next day, a single case was reported in Japan, again following travel to Wuhan. This person reported no contact with the market, but possible contact with persons with pneumonia [12]. A second case, again originating from Wuhan, was identified in Thailand with no connection to other cases. One suspect case in Nepal with travel linked to Wuhan was also reported but not confirmed [8]. On 20 January 2020, a Chinese national, who had travelled from Wuhan, was identified as having 2019-nCoV upon arrival in South Korea and was quarantined [13]. Several airports in Asia and North America have now set up thermal screening at airports to detect possible 2019-nCoV infected individuals. On 21 January 2020, a 2019-nCoV-infected individual was identified in the state of Washington, USA [14]. This patient had also travelled to Wuhan but returned prior to the addition of thermal airport screening.

Current state of knowledge and knowledge gaps

The number of cases in Wuhan continued to increase due to retrospective testing, new cases, and changes in diagnostic evaluation for etiological agents [15]. By 28 January 2020, numerous cases had been identified in throughout China including Taiwan and Hong Kong. As of 28 January 2020, over 4,500 confirmed cases have been reported with > 100 deaths (National Health Commission of the PRC). Human-to-human transmission was suspected early in the outbreak and has now been confirmed and is the main source of infections [14] (National Health Commission of the PRC, update January 22, 2020). Many clinical questions remain unresolved at this time and await reporting and future publications. Some critical questions include: Do all infected individuals show symptoms? What is the frequency of asymptomatic infections? What is the time from exposure to onset of symptoms? Are asymptomatic individuals infectious? Is human-to-human transmission linked to specific mutations in the 2019-nCoV virus?

The extent of the outbreak geographically and epidemiologically currently remains unclear. To facilitate laboratory diagnosis of suspect cases of 2019-nCoV, the WHO has published guidelines for *Laboratory testing for 2019 novel coronavirus (2019-nCoV) in suspected human cases* (<https://www.who.int/health-topics/coronavirus/laboratory-diagnostics-for-novel-coronavirus>) [15]. At the same website PCR primer sets can be found for diagnostic testing. These primer sets

and protocols were developed by Hong Kong University and the CDC, China. An additional PCR protocol by V. Corman, T. Bleicker, S. Brünink, C. Drosten (Charité Virology, Berlin, Germany) O. Landt, (Tib-Molbiol, Berlin, Germany) M. Koopmans (Erasmus MC, Rotterdam, The Netherlands) and M. Zambon (Public Health England, London) can be found on the WHO website.

Clinical Disease and Pathogenesis of 2019-nCoV and other Coronaviruses

The clinical picture

Coronaviruses are endemic in the human population and are responsible for up to 30% of annual respiratory infections resulting in rhinitis, pharyngitis, sinusitis, bronchiolitis, and pneumonia [16,17]. While primarily associated with relatively mild, self-limiting respiratory infections, infection from these viruses can result in severe disease in neonates, the elderly, and those with underlying comorbidities [18]. However, coronaviruses are now considered potential threats to global public health following the emergence of SARS-CoV in 2002 (9% CFR), and MERS-CoV in 2012 (35% CFR).

Early clinical manifestations of MERS and SARS are largely similar. Influenza-like symptoms accompanied by fevers, chills, dry cough, headache, malaise, and dyspnea were common early in the disease course in SARS patients [19]. The mean incubation period was estimated as 4.6 days with a range of 2 to 8 days between symptom onset and hospitalization. The mean time from symptom onset to death in fatal cases was 23.7 days [20]. Fatal outcomes were most frequent in those > 60 years of age (43% CFR). No fatalities were reported in young children and adolescents and fatal disease was reported in 6.8% of patients < 60 years of age. Phase 1 of SARS was associated with increasing viral load and early disease symptoms (fever, malaise). Phase 2 was characterized by fever, hypoxemia, and decreasing viral loads, while radiographic progression of pneumonia was common. Twenty percent of patients progressed to acute respiratory distress syndrome (ARDS). Common laboratory features of SARS included lymphopenia, thrombocytopenia, disseminated intravascular coagulation, and elevated lactate dehydrogenase and creatine kinase levels [20-22]. Acute renal impairment and proteinuria were associated with 6.7% and 84% of patients, respectively [21].

Early symptoms of MERS include fever, chills, cough, shortness of breath, myalgia, and malaise following a mean incubation period of 5 days, with a range of 2 to 13 days [23]. The median times from

symptom onset to hospitalization, ICU admission, and death are 4, 5, and 11.5 days, respectively [24]. Symptomatic MERS patients present with a rapidly progressing pneumonia requiring mechanical ventilation and additional organ support within the first week of disease [20]. Severe and fatal disease is strongly linked to underlying comorbidities including diabetes mellitus, hypertension, obesity, and chronic cardiac, pulmonary, or renal disease [23]. Laboratory abnormalities include lymphopenia, leukopenia, thrombocytopenia, elevated serum creatinine levels consistent with acute kidney injury, and elevated liver enzymes [23,25-28]. High lactate levels and consumptive coagulopathy have also been reported [25,29]. Chest radiographic abnormalities are observed in most cases and the findings are consistent with viral pneumonitis, secondary bacterial pneumonia, or acute respiratory distress syndrome [23,25,28,30,31].

Therapeutics and supportive care

Currently, supportive care is the only treatment option for patients with severe SARS or MERS illness and there are no licensed therapeutics or vaccines. There are, however, several vaccine candidates as well as antiviral candidates for prophylactic and therapeutic treatment of SARS-CoV and MERS-CoV infections. Mechanical ventilation and pulmonary rescue therapy were utilized for SARS but have had limited benefit for MERS patients [32]. Extracorporeal membrane oxygenation has been employed for MERS though its use is limited due to numerous factors [26]. Renal replacement therapy has been used extensively in MERS treatment [25,33,34]. The efficacy of a variety of antiviral therapeutics has been investigated for MERS with limited success. Moderate improvements in clinical outcomes were noted in common marmosets treated with a combination of lopinavir (LPV) and ritonavir (RTV) [35]. Additional investigations of interferon (IFN) antiviral activity *in vitro* have demonstrated that IFN beta (IFN β) had superior activity as compared to other IFN types [36,37]. A randomized control trial investigating the efficacy of LPV/RTV-IFN β in MERS patients is currently ongoing [38].

Coronavirus biology and Coronavirus outbreak cycles

Molecular virology

Family *Coronaviridae* (order *Nidovirales*) is comprised of the *Coronavirinae* and *Torovirinae* subfamilies of viruses. Coronaviruses are enveloped RNA viruses with positive-sense RNA genomes ranging from 25.5 to ~32 kb in length. The spherical

virus particles range from 70-120 nm in diameter with four structural proteins. The viral envelope is covered by characteristic spike-shaped glycoproteins (S) as well as the envelope (E) and membrane (M) proteins. The S protein mediates host cell attachment and entry. The helical nucleocapsid, comprised of the viral genome encapsidated by the nucleocapsid protein (N), resides within the viral envelope. The 5' two-thirds of the coronavirus genome consists of the replicase complex (ORF1a and ORF1b) and codes for two large polyproteins, pp1a and pp1b. The viral replicase-transcriptase complex is made up of 16 non-structural proteins (nsp1-16) encoded for by the polyproteins pp1a and pp1b. Both polyproteins can be cleaved by the viral proteases PLpro (nsp3) and 3CLpro (nsp5). The non-structural proteins function in the formation of double-membrane vesicles derived from the rough endoplasmic reticulum, and are the sites of viral replication and transcription [20]. Coronaviruses also encode a unique proofreading exoribonuclease (ExoN) function of nsp14 that reduces the accumulation of mutations in the RNA genome. The remainder of the genome is transcribed into a nested set of subgenomic mRNAs. Five accessory proteins (ORF3, ORF4a, ORF4b, ORF5 and ORF8b) are also encoded; however, they are not required for replication but may play a role in pathogenesis. Remaining subgenomic RNAs encode for accessory proteins that have immunomodulatory properties or functions that remain unknown.

Coronavirus animal reservoirs and incidental hosts

Determining the animal reservoir and incidental hosts of a virus with evidence of zoonosis such as 2019-nCoV is important for controlling spillover events and limiting human infections. Although the ecological reservoir for both MERS-CoV and SARS-CoV remain undefined, evidence of viral presence in a variety of animal species has been found. Serologic evidence and the isolation of viral genomic material for SARS-CoV-related viruses have provided evidence for bats as the putative reservoir for SARS-CoV. While masked palm civets and raccoon dogs were involved in transmission to humans and initially considered potential reservoirs, they are now considered as incidental or spillover hosts [39-41]. In contrast, dromedary camels are considered to act a reservoir host for MERS-CoV, and over half of primary human infections report contact with camels, however, it is suspected that bats are likely the ancestral host for MERS-CoV or a MERS-CoV-like virus [42,43]. Zoonotic transmission of SARS-CoV likely results from direct contact with intermediate hosts [44], while human-to-human transmission of both viruses

occurs primarily through close contact and nosocomial transmission via respiratory secretions [45,46]. Considering the animals implicated as reservoir hosts for SARS-CoV and MERS-CoV, along with the conclusions from phylogenetic analyses from us and other groups, these potential reservoirs will be important starting points for investigation of the virus source.

Molecular Analysis of 2019-nCoV

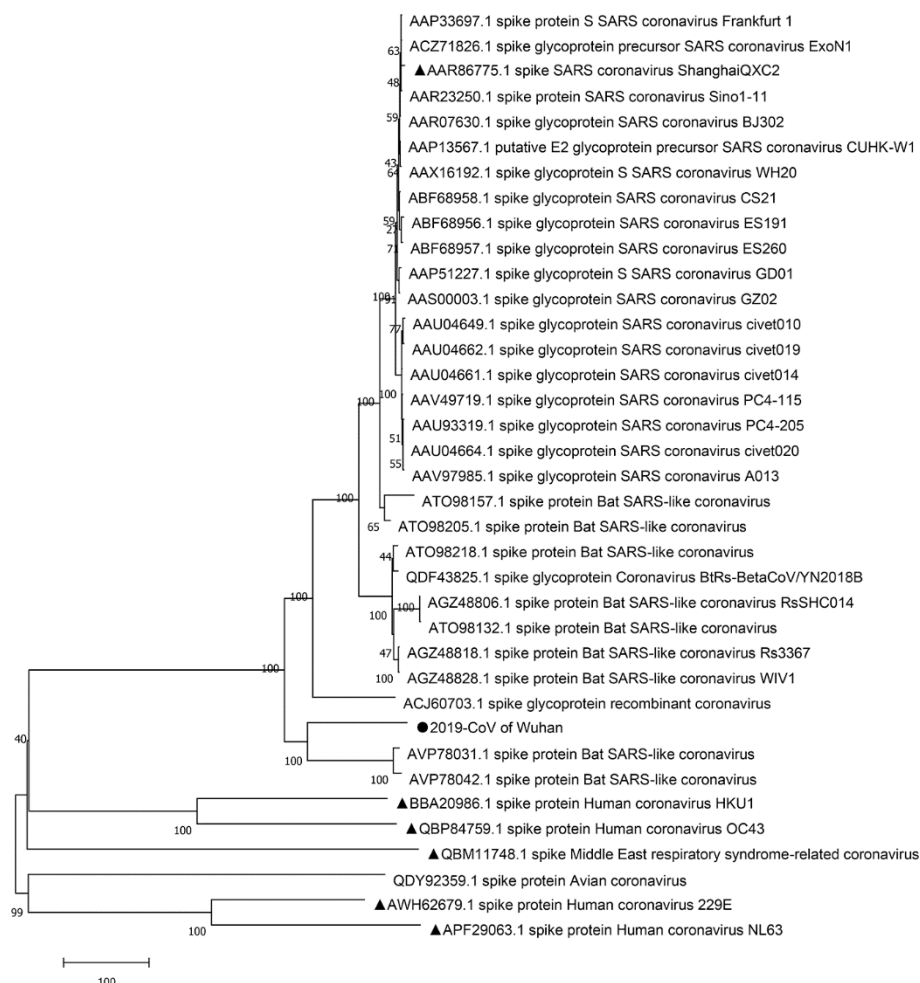
The CoV Spike protein and host receptors

The coronavirus spike protein mediates coronavirus entry into host cells. The S1 subunit of spike contains the receptor binding domain, which binds to receptors on host cells and dictates virus tropism. Viral entry is

mediated through viral and host membranes undergoing fusion via the S2 subunit of the spike protein [47]. Therefore, we analyzed and discuss the S1 domains, in particular the RBD, due to its role in determining host tropism and pathogenesis.

SARS-CoV utilizes the host ACE2 receptor for binding to host cells, including numerous respiratory epithelial cell types, alveolar macrophages, and monocytes [27,48]. Multiple cell types lacking ACE2 expression are also permissive for SARS-CoV, suggesting that additional receptors or co-receptors exist for SARS-CoV and may contribute to infection [49,50]. MERS-CoV targets DPP4 (also known as CD26), which is broadly expressed on numerous epithelial cell types and activated leukocytes.

Figure 2. Phylogenetic analysis of the Spike (S) protein of 2019-nCoV with known coronavirus S proteins.



Phylogenetic analysis of the spike protein sequences of the 2019-nCoV and some related coronaviruses. All the protein sequences used for the tree generation were downloaded from the National Center for Biotechnology Information (NCBI) and annotated by the accession number. Protein sequences were aligned using ClustalW. Then the tree was constructed with MEGA 7.0 by the neighbor-joining (NJ) method using 1,000 bootstraps. The Wuhan new coronavirus was marked by solid circle “●”. SARS coronavirus Shanghai, Human coronavirus HKU1, Human coronavirus OC43, Middle East respiratory syndrome, Human coronavirus 229E and Human coronavirus NL63 were marked by solid triangle “▲”. The NJ tree was well-constructed; the Wuhan new coronavirus showed high identity with Bat SARS-like coronavirus and separated from other coronavirus into different clusters.

Figure 3. Sequence comparison of the Spike (S) protein of 2019-nCoV to SARS-CoV and WIV-1 CoV.

Alignment of full-length S-protein from 2019-nCoV (QHD43416.1), SARS-CoV (P59594.1) and WIV1-CoV (AGZ48828.1). Red, yellow and white indicate completely conserved, functionally conserved and nonconserved residues respectively (A).

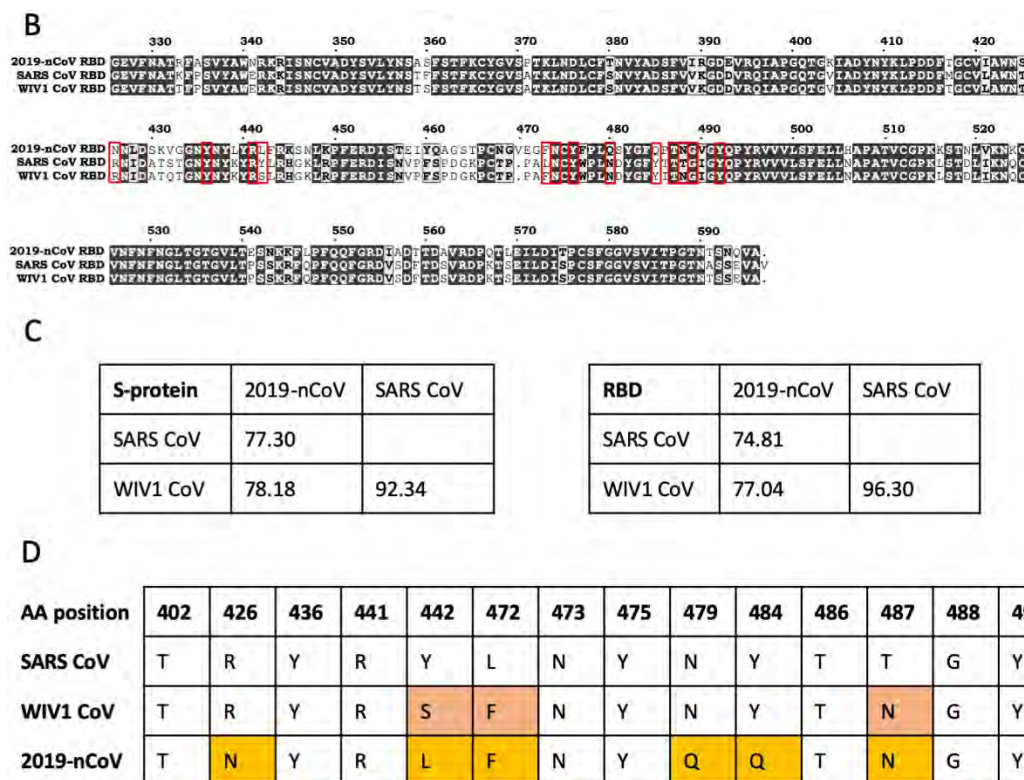
DPP4 is widely expressed in various kidney cells and likely contributes to MERS-CoV infiltration and subsequent renal dysfunction [51,52]. DCs and macrophages can also be productively infected by MERS-CoV *in vitro* [44]. The 2019-nCoV receptor(s) is currently unknown. To better understand the possible relationship of the 2019-nCoV S protein to other coronaviruses, we generated a phylogenetic tree of S protein sequences from various human and animal coronaviruses (Figure 2). Our phylogenetic data shows that 2019-nCoV S most closely resembles the S protein from a SARS-like bat CoV followed by SARS-CoV and distantly resembles other human coronaviruses including the MERS-CoV S protein.

A more in-depth analysis of S-proteins from 2019-nCoV, SARS-CoV, and WIV1-CoV, a SARS-like coronavirus that uses the ACE2 for cell entry, was conducted. An amino acid alignment of the S proteins (Figure 3A) shows high (92%) similarity between SARS-CoV and WIV1-CoV S-proteins. Lower similarity (77%) is observed between SARS-CoV and 2019-nCoV S-proteins. However, there may be

sufficient conservation in the RBD (75%) to expect that 2019-nCoV can still bind to ACE2. As a comparator, MERS-CoV S, which binds to a different receptor (dipeptidyl peptidase 4), has only 37% similarity to SARS-CoV S. Alignment of the RBD regions (Figure 3B) shows that 2019-nCoV has 6 amino acid substitutions in the 14 contact points between SARS-CoV S and ACE2 (Figure 3D). Three of these substitutions are also found in another group 2 coronavirus, WIV1-CoV, which has previously been shown to be capable of binding to human ACE2 in spite of these mutations [53].

To predict the binding affinity of 2019-nCoV to human ACE2, structural models of SARS-CoV RBD, WIV1-CoV RBD and 2019-nCoV RBD were generated to allow for comparison of amino acid side chain positions and putative binding energies (Figure 4A). Pairwise structural comparisons of the generated models to the crystalized structure of the SARS-CoV RBD complexed to ACE2 yielded RMSD values of 1.2, 0.9, and 0.9 for the SARS-CoV, WIV1-CoV, and 2019-nCoV RBDs, respectively. The low RMSD value for

Figure 3. Sequence comparison of the Spike (S) protein of 2019-nCoV to SARS-CoV and WIV-1 CoV.



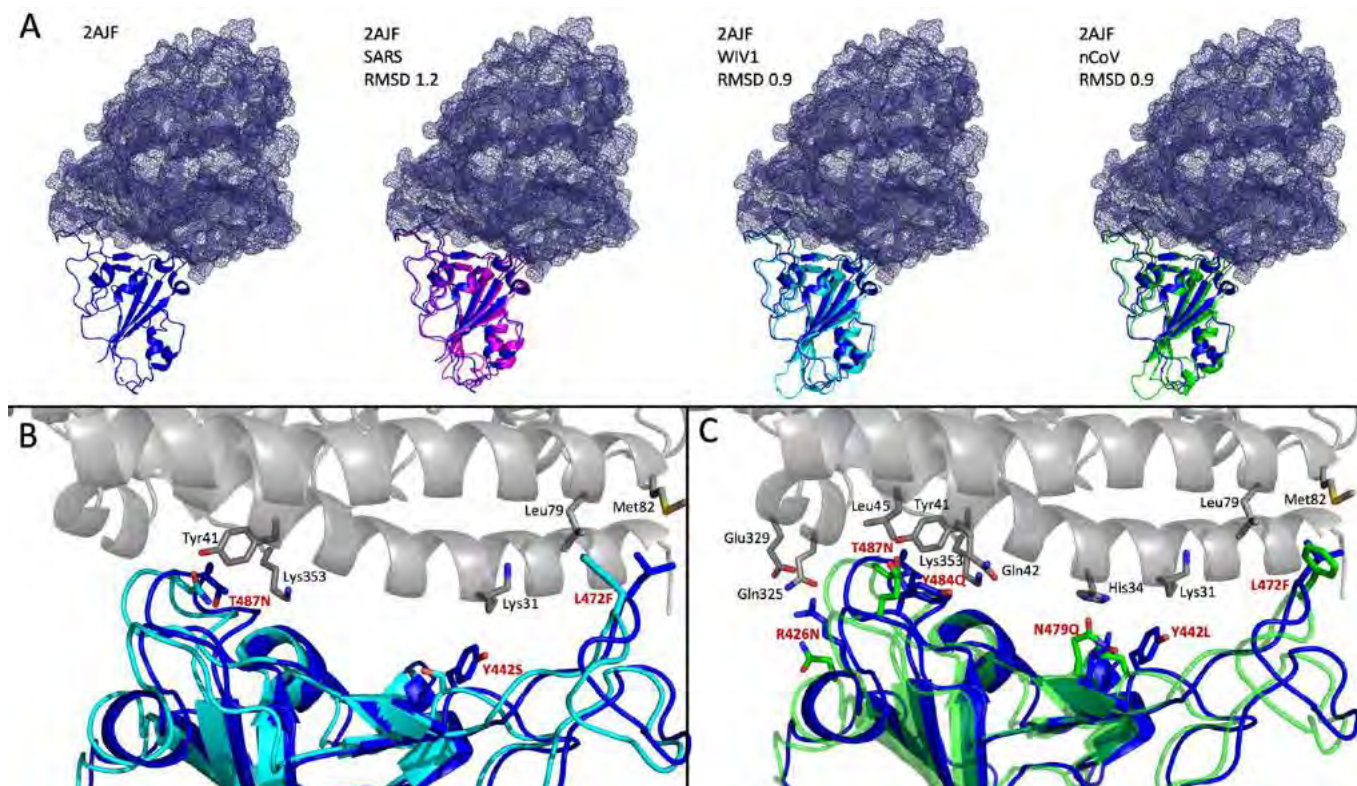
Detailed alignment of the receptor binding domain (RBD) of nCoV-2019, SARS-CoV and WIV1-CoV (B). Black, grey and white indicate 100% conserved, functionally conserved, and nonconserved residues respectively. Red boxes indicate the S protein residues in the RBD that directly interact with the ACE2 receptor. Percent identity matrices for the full-length S-protein (left) and RBD (right) provided by ClustalW (C). Residues of the SARS-CoV RBD and the corresponding WIV1-CoV and 2019-nCoV amino acids that contact the human ACE2 receptor (D). Amino acid substitutions are shown in orange for WIV1 and in yellow for nCoV-2019

the modelled SARS-CoV RBD supports the accuracy of the WIV1-CoV and 2019-nCoV RBD homology models. To observe the effects of the three additional mutations within the RBD of 2019-nCoV compared to WIV1-CoV at the binding interface (Figure 4B), the RBD models were structurally aligned to the crystal structure of the SARS-CoV RBD complexed to ACE2 [54]. The three residues mutated in RBD of WIV1-CoV – Asp487, Ser442, and Phe472 – were previously shown to have no effect on receptor binding affinity [53]. The remaining three mutations identified within the RBD of 2019-nCoV that interact with ACE2 residues have not been studied. The substitution of Arg426 to Asn426 removes the positively charged R-group of Arg but maintains the side chain's polarity and presence of an amide. Arg426 in the SARS-CoV RBD interacts with ACE2 residues Gln325 and Glu329. The structural model of 2019-nCoV RBD (Figure 4C) shows that the side chain of Gln426 is still in close

proximity to ACE2 Gln325 and Glu329, suggesting that the substitution of Arg426 to Asn426 has little effect on receptor binding. Tyr484 to Gln484, introduces a polar amino acid within a region that includes several tyrosine residues. Within the SARS-CoV RBD, Tyr484 interacts with His34 of ACE2. The R-group of Gln should not inhibit receptor binding in this region, sterically or otherwise, when compared to the R-group of Tyr484. The third substitution unique to 2019-nCoV, Asn479 to Gln479, may induce a conformational change within the RBD due to its proximity to several tyrosines. However, a hydrogen bond is located in the area between RBD Gly488 and ACE2 Lys353 is conserved. This mutation is therefore unlikely to have any negative effect on ACE2 binding.

While the structure of the 2019-nCoV RBD appears to be well conserved, we wanted to determine whether the RBD/ACE2 interaction energies were comparable to the SARS-CoV RBD. Docking was carried out using

Figure 4. Receptor binding domain (RBD) structure predictions based on homology modelling by Phyre2.



The crystal structure of the SARS-CoV RBD bound to ACE2 (PDB 2AJF), shown in dark blue, was used as a reference template for pairwise comparison with the Phyre2 models (A). Structural models generated by homology modelling for SARS-CoV RBD (magenta), WIV1-CoV RBD (cyan), and nCoV-2019 RBD (green) are shown overlaid of 2AJF (blue). RMSD values for the structural comparison of the models to 2AJF were calculated by Dali-lite and are provided for each model. Binding interface of the SARS-CoV RBD (blue)/ACE2 (grey) crystal structure with the WIV1-CoV RBD model shown in cyan (B). ACE2 amino acids that interact with RBD residues are shown as grey sticks and the corresponding amino acids of the SARS-CoV RBD and the WIV1-CoV RBD homology model are shown in blue and cyan sticks, respectively, and have red labels detailing the WIV1 mutations. Binding interface of 2AJF SARS-CoV RBD (blue) and ACE2 (grey) overlaid with the 2019-nCoV homology model (green) (C). ACE2 interface residues are shown as grey sticks, and the SARS/2019-nCoV residues are shown in blue and green stick representation, respectively. The red labels for SARS/2019-nCoV residues detail the mutations present in the 2019-nCoV RBD homology model.

the modelled RBDs and the pre-determined crystal structure of ACE2 (PDB ID: 2AJF, chain B) using HADDOCK2.2 [55]. The top models from the top cluster was selected for calculation of binding energy. The crystal structure of ACE2 complexed with SARS-CoV RBD (PDB ID: 2AJF, chain B and E) was used as a positive binding control, while the crystal structure of SARS-CoV RBD (PDB ID: 2AJF, chain E) docked to rat ACE2 served as a negative binding control [56]. The binding energy of the crystallized ACE2/SARS-CoV complex was calculated as -8.0 kcal/mol, while the crystallized RBD structure docked to modeled rat ACE2 returned a binding energy of -6.0 kcal/mol (Figure 5A). The 2.0 kcal/mol difference in binding energy would likely be larger if a crystal structure of SARS-RBD and rat ACE2 was used for comparison. The *in silico* docking strategy used here favours flexibility in the binding interface as opposed to the rigid nature of crystal structures. This effect is demonstrated with the modelled SARS-RBD and crystal ACE2 structures returning a binding energy of -12.5 kcal/mol. Additionally, WIV1-CoV binds to

ACE2 for cell entry and the modelled WIV1-RBD/ACE2 returned a binding energy of -10.3 kcal/mol. A similar binding energy, -10.2 kcal/mol was observed for the modelled RBD of 2019-nCoV and ACE2 suggesting that 2019-nCoV is capable of binding to ACE2.

Three key residues within the RBD of SARS-CoV are associated with species-specific receptor recognition, Leu472, Asn479, and Thr487 [57]. All three of these residues are substituted in the 2019-nCoV RBD to Phe472, Gln479, and Asn487 respectively. The WIV1-CoV RBD contains Phe at position 472 and Asn at position 487, but Gln479 is unique to 2019-nCoV. As shown in Figure 5, the mutation in this region does not appear to have any effect on docking energies compared to WIV1 and is not predicted to have any negative effects on the ACE2 His34 residue it likely interacts with. Leu472 to Phe472 also should have little to no effect on binding and may increase binding affinity due to the interacting ACE2 residue, Met82, since the methionine-aromatic interaction is considered to be a multifunctional motif that is involved in the

Figure 5. Binding energies of RBD homology models and their electrostatic surface potential.

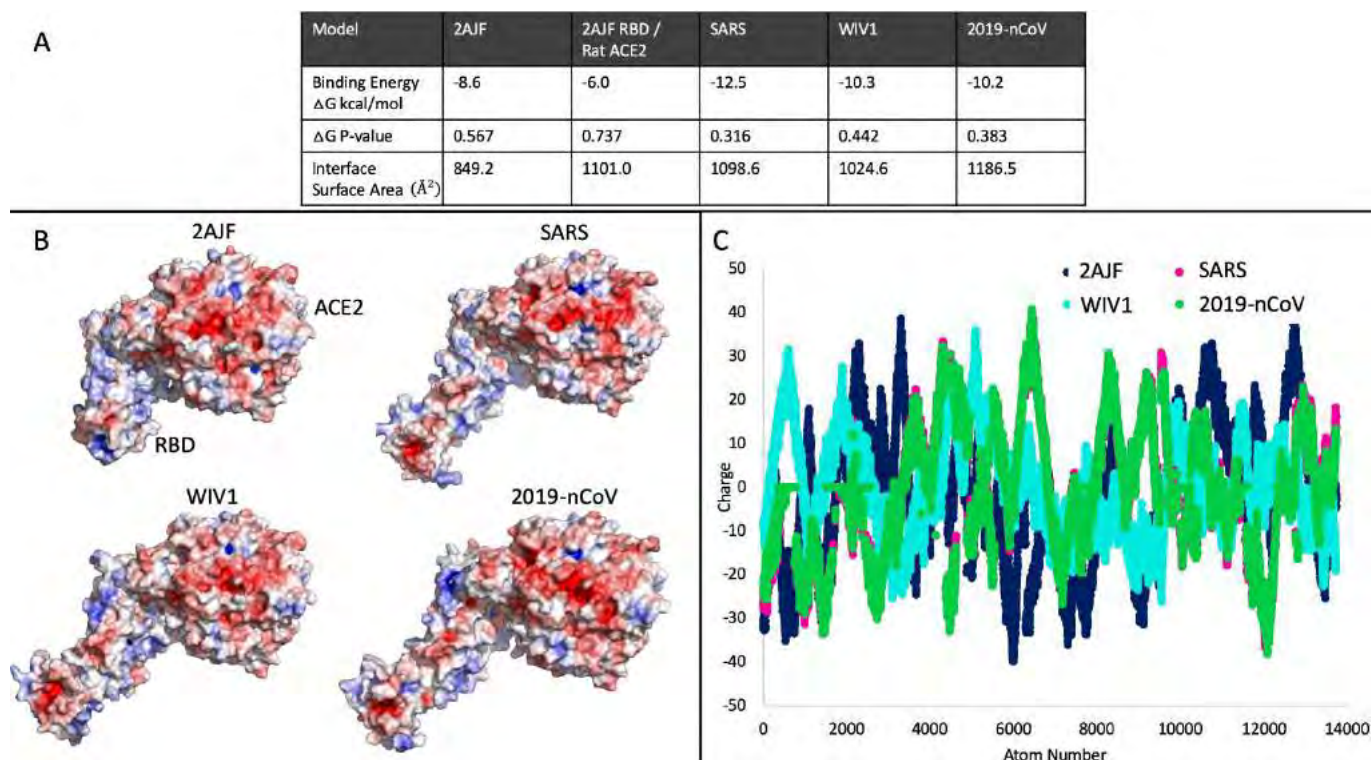


Table detailing the calculated binding energies for PDB ID 2AJF (chains B and E), the crystal structure of SARS-CoV RBD in complex with human ACE2, 2AJF chain E (SARS-CoV RBD) complexed with Rat ACE2, and the homology models complexed to ACE2 (2AJF, chain B) (A). The ΔG P-values and interface surface areas are also provided. Electrostatic potential of 2AJF and the complexed models calculated with APBS (B). The ACE2 and RBD labels on 2AJF are the same for all models. Red indicates regions of net negative charge while blue indicates a net positive charge, and white is neutral. Graphical comparison of individual atom charges for 2AJF and the models showing the individual charges of each atom (C).

stabilization of structures [58]. Thr487 to Gln487 does not inhibit binding as the substitution is also found in WIV1-CoV which can bind ACE2 for virus infection.

The electrostatic potentials of crystallized ACE2/SARS-CoV RBD and the RBD models were also determined (Figure 5C). Their atomic potential profiles are graphically represented and interestingly, 2019-nCoV traces best with the potential of the SARS-CoV RBD homology model bound to ACE2. This could indicate that the 2019-nCoV S-protein is more

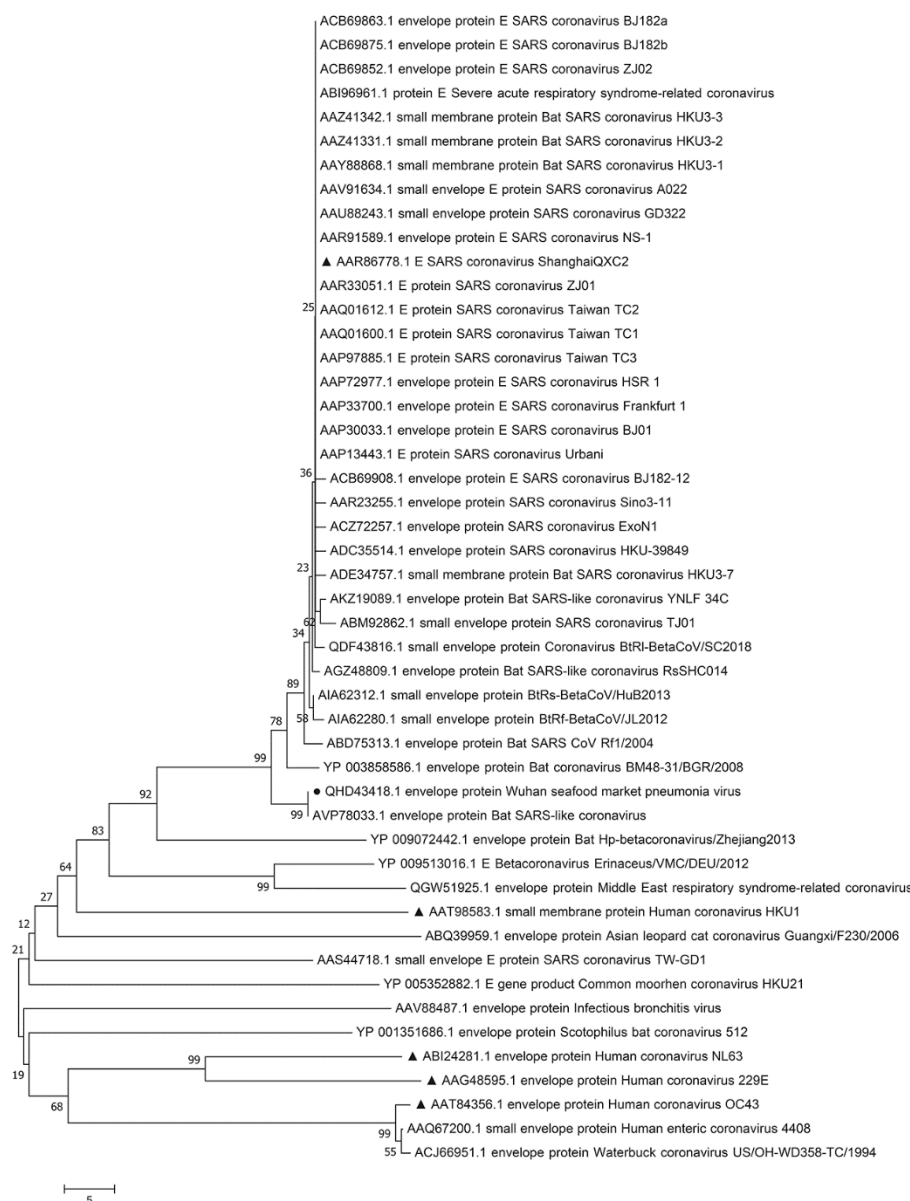
functionally similar to the SARS-CoV S-protein than initially anticipated from sequence similarities.

Vaccines and Community Readiness

Vaccine development

Vaccines provide protection from viral pathogens prior to exposure by eliciting protective immune memory with an innocuous agent. The development of neutralizing antibodies from a vaccine remains one of the hallmarks of effective vaccines although vaccines

Figure 6. Phylogenetic analysis of the envelope (E) protein sequence in novel 2019-nCoV.



All protein sequences used for tree generation were obtained from the National Center for Biotechnology Information (NCBI) and annotated by accession number. Protein sequences were then aligned using the ClustalW algorithm, and the tree was constructed with MEGA X by the neighbor-joining (NJ) method using 1,000 bootstraps. The solid black circle indicates the novel Wuhan pneumonia virus, and the solid black triangle indicates SARS coronavirus Shanghai and human coronaviruses HKU1, NL63, 229E, and OC43. The novel Wuhan coronavirus envelope protein shows high identity with Bat SARS-like coronavirus.

that induce cell-mediated immunity have also shown potential and are in development for viral pathogens such as influenza viruses. Several vaccine platforms exist with the ability to induce protective responses: killed whole virus vaccines; split-virion vaccines; subunit vaccines; live-attenuated viral vaccines; virus-like particle vaccines; nanoparticle vaccines; and nucleic acid vaccines (DNA and RNA). In regard to choosing a vaccine target and platform, the vaccine candidate must be immunogenic and immune targeting must lead to virus neutralization or potent cytotoxic responses. To date, there is not a licensed vaccine for either SARS-CoV or MERS-CoV although clinical trials have been initiated for MERS-CoV vaccines. Much of the focus for the development of a SARS-CoV or MERS-CoV vaccine has been on the S protein since it is immunogenic and antibodies targeting it can neutralize the virus [59,60]. Our analysis of the S protein (Figure 2) suggests that it has potential for vaccine development which can be related to work previously done for SARS-CoV and MERS-CoV.

The envelope protein (E) is also an attractive vaccine target that has been proposed for leverage in the development of live-attenuated vaccines [60,61]. MERS-CoV mutants with the E protein deleted are replication-competent but propagation-defective [61]. Similar results were shown for the SARS-CoV when E was removed [62]. Together this suggests that deletion of E from coronaviruses may provide a safe-single replication live viral vaccine for use in inducing a mucosal immune response. We investigated the similarity of the E protein of 2019-nCoV by phylogenetic analysis against known coronavirus E protein sequences (Figure 6) and found clustering, although somewhat distant, with human SARS-CoV. Given that vaccines have been generated for MERS- and SARS-CoVs by mutating the E protein, an E-based vaccine may represent an alternate candidate for 2019-nCoV vaccines. As vaccine candidates are identified, the requirement of animal models for vaccine development and evaluation will be essential.

Animal model development

Establishing an animal model of infection and disease pathogenesis is imperative for understanding several essential elements of viral disease in the infected host, including host tropism, immune responses, and modes of transmission, as well as for the progression of therapeutic development. Having an animal model that can recapitulate human disease is essential for vaccine and therapeutic development as well as testing. For a potential animal model to be

susceptible to infection, the virus must be able to 1.) gain entry into host cells; 2.) overcome the host's antiviral responses; and 3.) disseminate virus following infection to allow infection of other neighbouring cells and tissues. It is also of importance for the model to be able to recapitulate human disease and viral transmission modes. When evaluating the ability of an animal to be infected by a virus and serve as a model, viral shedding, clinical disease, and seroconversion should be determined. The past animal models for SARS-CoV and MERS-CoV were not universal due to the expression of the virus-specific cellular receptors for entry [63]. As SARS-CoV and MERS-CoV do not share a cellular receptor, they do not share the same host range and susceptibility, which includes research animal models [64]. *Cynomolgus* macaques, ferrets, and cats were some of the first animals to be determined susceptible to SARS-CoV [65,66]. The advantage of ferrets is that they are a smaller animal compared to non-human primates and also are able to recapitulate some of the clinical symptoms and transmission kinetics of human respiratory viruses including coughing, sneezing, fever, and weight loss [67]. Although mice can be infected with SARS-CoV, as shown by recovery of vRNA and the elicitation of neutralizing antibodies, infection does not cause severe disease [68]. However, SARS-CoV could be passaged in mice (15 times) for the establishment of a model with clinical features [69]. After the identification of MERS-CoV, it was quickly determined that typical research animal models were not susceptible to the virus including mice, Syrian hamsters, and ferrets. Larger non-human primate models, such as Rhesus macaques and common marmoset were determined susceptible. To make use of small animal models, transgenic mice have been engineered for MERS-CoV susceptibility through expression of the human DPP4 receptor [70]. Other attempts at other mouse model developments were not successful, including an immunocompromised 129/SATA1-/-1 mouse [63]. Having an understanding of the animal models and model development previously utilized for the other coronaviruses of interest will aid in the development of a model for 2019-nCoV. As is necessary, elucidation of the receptor will help guide in development, and creating a clinical picture of the acute symptoms in humans will be essential for vaccine and antiviral evaluation.

Community Readiness

Community and healthcare preparedness in response to coronavirus outbreaks remain ongoing obstacles for global public health. For example, delays

between disease development and progression and diagnosis or quarantine can severely impact both patient management and containment [21,71]. Deficiencies in outbreak preparedness and healthcare network coordination efforts must ultimately be considered in response efforts. It is strongly recommended that universal reagents be maintained and available at global repositories for future outbreaks.

Future Directions

At the time of this writing, cases continue to be reported. Furthermore, there are also many unknowns regarding this outbreak, including the reservoir host, modes of transmission/transmission potential, and the effectiveness of potential vaccine candidates. Here we have attempted to address some of these issues using foundations from previous coronavirus outbreaks as well as our own analysis. What is certain is that the numbers of reported cases are increasing and will continue to increase before the knowledge gaps surrounding 2019-nCoV are filled. Cooperation among public health officials, healthcare workers, and scientists will be key to gaining a foothold and containing virus spread. Acknowledgement of coronaviruses as a constant spillover threat is important for pandemic preparedness. Two key take-away messages are important at this time: 1) As noted by the previous lopsided cases of healthcare, healthcare workers and care givers should exercise extreme caution and use personal protective equipment (PPE) in providing care to 2019-nCoV infected patients; and 2) The research community should endeavour to compile diverse CoV reagents that can quickly be mobilized for rapid vaccine development, antiviral discovery, differential diagnosis, and specific diagnosis.

Methods

Phylogenetic Tree Analysis

The nucleotide sequence of the novel coronavirus associated with the outbreak of pneumonia in Wuhan (2019-nCoV) was downloaded from the National Center for Biotechnology Information (NCBI) (<http://www.ncbi.nlm.nih.gov>) with the accession number MN908947.3 [72]. The encoded S proteins and E proteins from additional coronaviruses were selected for the construction of a neighbor-joining tree. All sequences were downloaded from NCBI, and the accession numbers were annotated in the NJ tree. Protein sequences were aligned using ClustalW [73] and then used to construct the tree with MEGA7.0 [74] using 1,000 bootstraps.

Receptor Binding Domain (RBD) Alignment, Predictions, and Modeling

Amino acid sequences for the S protein of SARS-CoV (P59594.1), WIV1-CoV (AGZ48828.1), and 2019-nCoV (QHD43416.1), were obtained from GenBank. Alignments were completed using ClustalW with default parameters and the output was formatted with Esript [75,76]. The S protein sequences were submitted to Phyre2 for homology modelling under 'Intensive' mode and the subsequent structures were further refined using 3D refined for energy minimization [77,78]. The refined model with the lowest RMSD value was selected for use in structural comparisons and docking. The RBD models were compared to the crystal structure of SARS-CoV RBD (PDB ID:2AJF, chain E) using DaliLite v.5 pairwise comparison tool for analysis [79]. The RBD models were submitted for docking analysis to human ACE2 (PDB ID: 2AJF, chain B) using HADDOCK 2.2 [55] with residues 24, 27, 31, 34, 37, 38, 41, 42, 45, 79, 82, 83, 90, 325, 329, 330, 353, and 354 of ACE2 specified as a binding domain as well as RBD residues 402, 426, 436, 441, 442, 472, 473, 475, 479, 484, 486, 487, 488, and 491 [55]. The complex with the lowest z-score was selected and the binding energy was calculated using the PDBePISA server [80]. Electrostatics of the complexes were also determined using adaptive Poisson-Boltzmann solver (APBS) calculations and PyMol to show surface electrostatics for the docked RBD models and 2AJF [81,82]. Individual atom charges of each model and 2AJF were used for comparison of electrostatic potential between 2AJF and the models.

Acknowledgements and Funding

Research into the novel coronavirus genome (2019-nCoV) was led by Dr. Yong-Zhen Zhang at the the Shanghai Public Health Clinical Center & School of Public Health, in collaboration with the Central Hospital of Wuhan, Huazhong University of Science and Technology, the Wuhan Center for Disease Control and Prevention, the National Institute for Communicable Disease Control and Prevention, the Chinese Center for Disease Control, and the University of Sydney, Sydney, Australia. We would like to thank and acknowledge the researchers who were working to identify this pathogen and make the data publically available. Specifically, we acknowledge the National Institute for Viral Disease Control and Prevention, China CDC; Wuhan Institute of Virology, Chinese Academy of Sciences; Institute of Pathogen Biology, Chinese Academy of Medical Sciences & Peking Union Medical College; and Wuhan Jinyintan Hospital. In addition, we acknowledge GISAID (<https://www.gisaid.org/>) for providing a platform that allows data to be freely shared. J.K.

is funded by a Tier 2 Canada Research Chair in the Molecular Pathogenesis of Emerging and Re-Emerging Viruses provided by the Canadian Institutes of Health Research (Grant no. 950-231498). A.A.K. is funded by the IWK Health Centre (Grant no. 602975) and Nova Scotia Health Research Foundation (Grant no. 602932). DJK is a Tier 1 Canada Research Chair in Translational Vaccinology and Inflammation. Support for DJK was provided by LKSF, Canada Foundation for Innovation (JELF), and DMRF (Dalhousie Medical Research Foundation). VIDO-InterVac receives operational funding from the Government of Canada through Canada Foundation for Innovation – Major Science Initiatives and the Government of Saskatchewan through Innovation Saskatchewan. D.F. receives support from Canadian Institutes for Health Research (PJT 388665).

References

- China, TSCIOotPsRo. Press Conference on Pneumonia Prevention and Control of the New Coronavirus Infection held 10 am Beijing time. Available from: <https://www.scio.gov.cn/xwfbh/xwfbh/wqfbh/42311/42470/index.htm>.
- ProMed International Society for Infectious Diseases, PISfI, ProMed 20191230.6864153 Undiagnosed Pneumonia - China (Hubei): Request for Information. 2019.
- Diseases, P.I.S.f.I. 20200102.6866757 Undiagnosed Pneumonia - China (Hubei) (01): Wildlife sales, market closed, Request for Information. 2020.
- Diseases, P.I.S.f.I. 20200103.6869668 Undiagnosed Pneumonia - China (Hubei) (02): Updates, other countries responses, Request for Information. 2020.
- Diseases, P.I.S.f.I. 20200105.6872267 Undiagnosed Pneumonia - China (Hubei) (03): Updates, severe acute respiratory syndrome, Middle East Respiratory Syndrome roused roused out, WHO, Request for Information. 2020.
- Diseases, P.I.S.f.I. 20200108.6877694 Undiagnosed Pneumonia - China (Hubei) (05): Novel Coronavirus identified. 2020.
- Diseases, P.I.S.f.I. 20200108.6878869 Undiagnosed Pneumonia - China (HU) (07): official confirmation of novel coronavirus. 2020.
- Diseases, P.I.S.f.I. 20200110.6881082 Undiagnosed Pneumonia - China (Hubei) (08): Novel Coronavirus, WHO. 2020.
- Diseases, P.I.S.f.I. 20200110.6883253 Undiagnosed Pneumonia - China (Hubei) (09): Novel Coronavirus, more information, first fatality. 2020.
- Diseases, P.I.S.f.I. 20200113.6886644 Novel Coronavirus (02): Thailand ex China (Hubei) WHO. 2020.
- Diseases, P.I.S.f.I. 20200114.6889527 Novel Coronavirus (04): China (Hubei), Thailand ex China, WHO. 2020.
- Diseases, P.I.S.f.I. 20200115.6891515 Novel Coronavirus (05): China (HU), Japan ex China. 2020.
- Diseases, P.I.S.f.I. 20200120.6899007 Novel Coronavirus (11) - China (Hubei) South Korea ex China. 2020.
- Diseases, P.I.S.f.I. 20200121.6901757 Novel Coronavirus (12): China (Hubei) New fatality, healthcare workers, WHO. 2020.
- World Health Organization (WHO) (2020) Diagnostics for novel coronavirus. Available: <https://www.who.int/health-topics/coronavirus/laboratory-diagnostics-for-novel-coronavirus>. Accessed : 23 January 2020.
- Canducci F, Debiaggi M, Sampaolo M, Marinozzi MC, Berre S, Terulla C, Gargantini G, Cambieri P, Romero E, Clementi M (2008) Two-year prospective study of single infections and co-infections by respiratory syncytial virus and viruses identified recently in infants with acute respiratory disease. *J Med Virol* 80: 716-723.
- Jevsnik M, Ursic T, Zigon N, Lusa L, Krivec U, Petrovec M (2012) Coronavirus infections in hospitalized pediatric patients with acute respiratory tract disease. *BMC Infect Dis* 12: 365.
- Fehr AR, Perlman S (2015) Coronaviruses: an overview of their replication and pathogenesis. *Methods Mol Biol* 1282: 1-23.
- Donnelly CA, Ghani AC, Leung GM, Hedley AJ, Fraser C, Riley S, Abu-Raddad JL, Ho LM, Thach TQ, Chau P, Chan KP, Lam TH, Tse LY, Tsang T, Liu SH, Kong JH, Lau EM, Ferguson NM, Anderson RM (2003) Epidemiological determinants of spread of causal agent of severe acute respiratory syndrome in Hong Kong. *Lancet* 361: 1761-1766.
- de Wit E, van Doremalen N, Falzarano D, Munster VJ (2016) SARS and MERS: recent insights into emerging coronaviruses. *Nat Rev Microbiol* 14: 523-534.
- Walston S, Al-Harbi Y, Al-Omar B (2008) The changing face of healthcare in Saudi Arabia. *Ann Saudi Med* 28: 243-250.
- AL-Ahmadi H, Roland M (2005) Quality of primary health care in Saudi Arabia: a comprehensive review. *Int J Qual Health Care* 17: 331-346.
- Assiri A, Al-Tawfiq JA, Al-Rabeeah AA, Al-Rabiah FA, Al-Hajjar S, Al-Barrak A, Flemban H, Al-Nassir WN, Balkhy HH, Al-Hakeem RF, Makhdoom HQ, Zumla AI, Memish ZA (2013) Epidemiological, demographic, and clinical characteristics of 47 cases of Middle East respiratory syndrome coronavirus disease from Saudi Arabia: a descriptive study. *Lancet Infect Dis* 13: 752-761.
- Hunter JC, Nguyen D, Aden B, Al Bandar Z, Al Dhaheri W, Abu Elkheir K, Khudair A, Al Mulla M, El Saleh F, Imambaccus H, Al Kaabi N, Sheikh FA, Sasse J, Turner A, Abdel Wareth L, Weber S, Al Ameri A, Abu Amer W, Alami NN, Bunga S, Haynes LM, Hall AJ, Kallen AJ, Kuhar D, Pham H, Pringle K, Tong S, Whitaker BL, Gerber SI, Al Hosani FI (2016) Transmission of Middle East Respiratory Syndrome Coronavirus infections in healthcare settings, Abu Dhabi. *Emerg Infect Dis* 22: 647-656.
- Arabi YM, Arifi AA, Balkhy HH, Najm H, Aldawood AS, Ghabashi A, Hawa H, Alothman A, Khaldi A, Al Raiy B (2014) Clinical course and outcomes of critically ill patients with Middle East respiratory syndrome coronavirus infection. *Ann Intern Med* 160: 389-397.
- Guery B, Poissy J, el Mansouf L, Sejourne C, Ettahar N, Lemaire X, Vuotto F, Goffard A, Behillil S, Enouf V, Caro V, Mailles A, Che D, Manuguerra JC, Mathieu D, Fontanet A, van der Werf A, ME-Cs group (2013) Clinical features and viral diagnosis of two cases of infection with Middle East Respiratory Syndrome coronavirus: a report of nosocomial transmission. *Lancet* 381: 2265-2272.
- Memish ZA, Zumla AI, Al-Hakeem RF, Al-Rabeeah AA, Stephens GM (2013) Family cluster of Middle East respiratory syndrome coronavirus infections. *N Engl J Med* 368: 2487-2494.
- Zaki AM, van Boheemen S, Bestebroer TM, Osterhaus AD, Fouchier RA (2012) Isolation of a novel coronavirus from a man with pneumonia in Saudi Arabia. *N Engl J Med* 367: 1814-1820.
- Al-Tawfiq JA, Hinedi K, Ghandour J, Khairalla H, Musleh S, Ujayli A, Memish ZA (2014) Middle East respiratory

- syndrome coronavirus: a case-control study of hospitalized patients. *Clin Infect Dis* 59: 160-165.
30. Ajlan AM, Ahyad RA, Jamjoom LG, Alharthy A, Madani TA (2014) Middle East Respiratory Syndrome Coronavirus (MERS-CoV) infection: chest CT findings. *AJR Am J Roentgenol* 203: 782-787.
 31. Zumla A, Hui DS, Perlman S (2015) Middle East respiratory syndrome. *Lancet* 386: 995-1007.
 32. Chan JF, Lau SK, To KK, Cheng VC, Woo PC, Yuen KY (2015) Middle East respiratory syndrome coronavirus: another zoonotic betacoronavirus causing SARS-like disease. *Clin Microbiol Rev* 28: 465-522.
 33. Albarrak AM, Stephens GM, Hewson R, Memish ZA (2012) Recovery from severe novel coronavirus infection. *Saudi Med J* 33: 1265-1269.
 34. Omrani AS, Saad MM, Baig K, Bahloul A, Abdul-Matin M, Alaidaroos AY, Almakhlaifi GA, Albarrak MM, Memish ZA, Albarrak AM (2014) Ribavirin and interferon alfa-2a for severe Middle East respiratory syndrome coronavirus infection: a retrospective cohort study. *Lancet Infect Dis* 14: 1090-1095.
 35. Chan JF, Yao Y, Yeung ML, Deng W, Bao L, Jia L, Li F, Xiao C, Gao H, Yu P, Cai JP, Chu H, Zhou J, Chen H, Qin C, Yuen KY (2015) Treatment with lopinavir/ritonavir or interferon-beta1b improves outcome of MERS-CoV infection in a Nonhuman primate model of common marmoset. *J Infect Dis* 212: 1904-1913.
 36. Hart BJ, Dyal J, Postnikova E, Zhou H, Kindrachuk J, Johnson RF, Olinger GG Jr., Frieman MB, Holbrook MR, Jahrling PB, Hensley L (2014) Interferon-beta and mycophenolic acid are potent inhibitors of Middle East respiratory syndrome coronavirus in cell-based assays. *J Gen Virol* 95: 571-577.
 37. Chan JF, Chan KH, Kao RY, To KK, Zheng BJ, Li CP, Li PT, Dai J, Mok FK, Chen H, Hayden FG, Yuen KY (2013) Broad-spectrum antivirals for the emerging Middle East respiratory syndrome coronavirus. *J Infect* 67: 606-616.
 38. Arabi YM, Allothman A, Balkhy HH, Al-Dawood A, AlJohani S, Al Harbi S, Kojan S, Al Jeraisy M, Deeb AM, Assiri AM, Al-Hameed F, AlSaedi A, Mandourah Y, Almekhlafi GA, Sherbeen NM, Elzein FE, Memon J, Taha Y, Almotairei A, Maghrabi KA, Qushmaq I, Al Bshabshe A, Kharaba A, Shalhoub S, Jose J, Fowler RA, Hayden FG, Hussein MA, Mtg And the (2018) Treatment of Middle East Respiratory Syndrome with a combination of lopinavir-ritonavir and interferon-beta1b (MIRACLE trial): study protocol for a randomized controlled trial. *Trials* 19: 81.
 39. Chan PK, Chan MC (2013) Tracing the SARS-coronavirus. *J Thorac Dis* 5 Suppl 2: 118-121.
 40. Song HD, Tu CC, Zhang GW, Wang SY, Zheng K, Lei LC, Chen QX, Gao YW, Zhou HQ, Xiang H, Zheng HJ, Chern SW, Cheng F, Pan CM, Xuan H, Chen SJ, Luo HM, Zhou DH, Liu YF, He JF, Qin PZ, Li LH, Ren YQ, Liang WJ, Yu YS, Anderson L, Wang M, Xu RH, Wu XW, Zheng HY, Chen JD, Liang G, Gao Y, Liao M, Fang L, Jiang LY, Li H, Chen F, Di B, He LJ, Lin JY, Tong S, Kong X, Du L, Hao P, Tang H, Bernini A, Yu XJ, Spiga O, Guo ZM, Pan HY, He WZ, Manuguerra JC, Fontanet A, Danchin A, Niccolai N, Li YX, Wu CI, Zhao GP (2005) Cross-host evolution of severe acute respiratory syndrome coronavirus in palm civet and human. *Proc Natl Acad Sci USA* 102: 2430-2435.
 41. Shi Z, Hu Z (2008) A review of studies on animal reservoirs of the SARS coronavirus. *Virus Res* 133: 74-87.
 42. Memish ZA, Cotton M, Meyer B, Watson SJ, Alsahafi AJ, Al Rabeeah AA, Corman VM, Sieberg A, Makhdoom HQ, Assiri A, Al Masri M, Aldabbagh S, Bosch BJ, Beer M, Muller MA, Kellam P, Drosten C (2014) Human infection with MERS coronavirus after exposure to infected camels, Saudi Arabia, 2013. *Emerg Infect Dis* 20: 1012-1015.
 43. Alagaili AN, Briesse T, Mishra N, Kapoor V, Sameroff SC, Burbelo PD, de Wit E, Munster VJ, Hensley LE, Zalmout IS, Kapoor A, Epstein JH, Karesh WB, Daszak P, Mohammed OB, Lipkin WI (2014) Middle East respiratory syndrome coronavirus infection in dromedary camels in Saudi Arabia. *mBio* 5: e00884-14.
 44. Willman M, Kobasa D, Kindrachuk J (2019) A Comparative analysis of factors influencing two outbreaks of Middle Eastern Respiratory Syndrome (MERS) in Saudi Arabia and South Korea. *Viruses* 11: 11. pii: E1119.
 45. Anderson RM, Fraser C, Ghani AC, Donnelly CA, Riley S, Ferguson NM, Leung GM, Lam TH, Hedley AJ (2004) Epidemiology, transmission dynamics and control of SARS: the 2002-2003 epidemic. *Philos Trans R Soc Lond B Biol Sci* 359: 1091-1105.
 46. Cowling BJ, Park M, Fang VJ, Wu P, Leung GM, Wu JT (2015) Preliminary epidemiological assessment of MERS-CoV outbreak in South Korea, May to June 2015. *Euro Surveill* 20: 7-13.
 47. Li F (2016) Structure, function, and evolution of coronavirus spike proteins. *Annu Rev Virol* 3: 237-261.
 48. Qiu W, Chu C, Mao A, Wu J (2018) The impacts on health, society, and economy of SARS and H7N9 outbreaks in China: A case comparison study. *J Environ Public Health* 2018: 2710185.
 49. Gu J, Gong E, Zhang B, Zheng J, Gao Z, Zhong Y, Zou W, Zhan J, Wang S, Xie Z, Zhuang H, Wu B, Zhong H, Shao H, Fang W, Gao D, Pei F, Li X, He Z, Xu D, Shi X, Anderson VM, Leong AS (2005) Multiple organ infection and the pathogenesis of SARS. *J Exp Med* 202: 415-424.
 50. Hamming I, Timens W, Bultuis ML, Lely AT, Navis G, van Goor H (2004) Tissue distribution of ACE2 protein, the functional receptor for SARS coronavirus. A first step in understanding SARS pathogenesis. *J Pathol* 203: 631-637.
 51. Lambeir AM, Durinx C, Scharpe S, De Meester I (2003) Dipeptidyl-peptidase IV from bench to bedside: an update on structural properties, functions, and clinical aspects of the enzyme DPP IV. *Crit Rev Clin Lab Sci* 40: 209-294.
 52. Widagdo W, Raj VS, Schipper D, Kolijn K, van Leenders G, Bosch BJ, Bensaid A, Segales J, Baumgartner W, Osterhaus A, Koopmans MP, van den Brand JMA, Haagmans BL (2016) Differential expression of the Middle East Respiratory Syndrome Coronavirus receptor in the upper respiratory tracts of humans and dromedary camels. *J Virol* 90: 4838-4842.
 53. Menachery VD, Yount Jr. BL, Sims AC, Debbink K, Agnihothram SS, Gralinski LE, Graham RL, Scobey T, Plante JA, Royal SR, Swanstrom J, Sheahan TP, Pickles RJ, Corti D, Randell SH, Lanzavecchia A, Marasco WA, Baric RS (2016) SARS-like WIV1-CoV poised for human emergence. *Proc Natl Acad Sci USA* 113: 3048-3053.
 54. Li W, Zhang C, Sui J, Kuhn JH, Moore MJ, Luo S, Wong SK, Huang IC, Xu K, Vasilieva N, Murakami A, He Y, Marasco WA, Guan Y, Choe H, Farzan M (2005) Receptor and viral determinants of SARS-coronavirus adaptation to human ACE2. *EMBO J* 24: 1634-1643.
 55. van Zundert GCP, Rodrigues J, Trellet M, Schmitz C, Kastiris PL, Karaca E, Melquiond ASJ, van Dijk M, de Vries SJ, Bonvin A (2016) The HADDOCK2.2 Web server: User-friendly integrative modeling of biomolecular complexes. *J Mol Biol* 428: 720-725.
 56. Li W, Greenough TC, Moore MJ, Vasilieva N, Somasundaran M, Sullivan JL, Farzan M, Choe H (2004) Efficient replication

- of severe acute respiratory syndrome coronavirus in mouse cells is limited by murine angiotensin-converting enzyme 2. *J Virol* 78: 11429-114233.
57. Li F, Li W, Farzan M, Harrison SC (2005) Structure of SARS coronavirus spike receptor-binding domain complexed with receptor. *Science* 309: 1864-1868.
 58. Weber DS, Warren JJ (2019) The interaction between methionine and two aromatic amino acids is an abundant and multifunctional motif in proteins. *Arch Biochem Biophys* 672: 108053.
 59. Agnihothram S, Gopal R, Yount BL Jr, Donaldson EF, Menachery VD, Graham RL, Scobey TD, Gralinski LE, Denison MR, Zambon M, Baric RS (2014) Evaluation of serologic and antigenic relationships between middle eastern respiratory syndrome coronavirus and other coronaviruses to develop vaccine platforms for the rapid response to emerging coronaviruses. *J Infect Dis* 209: 995-1006.
 60. Yong CY, Ong HK, Yeap SK, Ho KL, Tan WS (2019) Recent Advances in the Vaccine Development Against Middle East Respiratory Syndrome-Coronavirus. *Front Microbiol* 10: 1781.
 61. Almazan F, DeDiego ML, Sola I, Zuniga S, Nieto-Torres JL, Marquez-Jurado S, Andres G, Enjuanes L (2013) Engineering a replication-competent, propagation-defective Middle East respiratory syndrome coronavirus as a vaccine candidate. *mBio* 4: e00650-13.
 62. DeDiego ML, Alvarez E, Almazan F, Rejas MT, Lamirande E, Roberts A, Shieh WJ, Zaki SR, Subbarao K, Enjuanes L (2007) A severe acute respiratory syndrome coronavirus that lacks the E gene is attenuated in vitro and in vivo. *J Virol* 81: 1701-1713.
 63. van Doremalen N, Munster VJ (2015) Animal models of Middle East respiratory syndrome coronavirus infection. *Antiviral Res* 122: 28-38.
 64. Li F (2015) Receptor recognition mechanisms of coronaviruses: a decade of structural studies. *J Virol* 89: 1954-1964.
 65. Kuiken T, Fouchier RA, Schutten M, Rimmelzwaan GF, van Amerongen G, van Riel D, Laman JD, de Jong T, van Doornum G, Lim W, Ling AE, Chan PK, Tam JS, Zambon MC, Gopal R, Drosten C, van der Werf S, Escriviou N, Manuguerra JC, Stohr K, Peiris JS, Osterhaus AD (2003) Newly discovered coronavirus as the primary cause of severe acute respiratory syndrome. *Lancet* 362: 263-270.
 66. Martina BE, Haagmans BL, Kuiken T, Fouchier RA, Rimmelzwaan GF, Van Amerongen G, Peiris JS, Lim W, Osterhaus AD (2003) Virology: SARS virus infection of cats and ferrets. *Nature* 425: 915.
 67. Banner D, Kelvin AA (2012) The current state of H5N1 vaccines and the use of the ferret model for influenza therapeutic and prophylactic development. *J Infect Dev Ctries* 6: 465-9.
 68. Wentworth DE, Gillim-Ross L, Espina N, Bernard KA (2004) Mice susceptible to SARS coronavirus. *Emerg Infect Dis* 10: 1293-1296.
 69. Roberts A, Deming D, Paddock CD, Cheng A, Yount B, Vogel L, Herman BD, Sheahan T, Heise M, Genrich GL, Zaki SR, Baric R, Subbarao K (2007) A mouse-adapted SARS-coronavirus causes disease and mortality in BALB/c mice. *PLoS Pathog* 3: e5.
 70. Agrawal AS, Garron T, Tao X, Peng BH, Wakamiya M, Chan TS, Couch RB, Tseng CT, (2015) Generation of a transgenic mouse model of Middle East respiratory syndrome coronavirus infection and disease. *J Virol* 89: 3659-3670.
 71. Al-Ahmadi, Roland M (2005) Quality of primary health care in Saudi Arabia: a comprehensive review. *Int J Qual Health Care* 17: 331-346.
 72. Wu F, Zhao S, Yu B, Chen YM, Wang W, Hu Y, Song ZG, Tao ZW, Tian JH, Pei YY, Yuan ML, Zhang YL, Dai FH, Liu Y, Wang QM, Zheng JJ, Xu L, Holmes EC, Zhang YZ (2020) A novel coronavirus associated with a respiratory disease in Wuhan of Hubei province, China. *NCBI*.
 73. Larkin MA, Blackshields G, Brown NP, Chenna R, McGettigan PA, McWilliam H, Valentin F, Wallace IM, Wilm A, Lopez R, Thompson JD, Gibson TJ, Higgins DG (2007) Clustal W and Clustal X version 2.0. *Bioinformatics* 23: 2947-2948.
 74. Kumar S, Stecher G, Tamura K (2016) MEGA7: Molecular evolutionary genetics analysis version 7.0 for bigger datasets. *Mol Biol Evol* 33: 1870-1874.
 75. Sievers F, Wilm A, Dineen D, Gibson TJ, Karplus K, Li W, Lopez R, McWilliam H, Remmert M, Soding J, Thompson JD, Higgins DG (2011) Fast, scalable generation of high-quality protein multiple sequence alignments using Clustal Omega. *Mol Syst Biol* 7: 539.
 76. Robert X, Gouet P (2014) Deciphering key features in protein structures with the new ENDscript server. *Nucleic Acids Res* 42: 320-324.
 77. Kelley LA, Mezulis S, Yates CM, Wass MN, Sternberg MJ (2015) The Phyre2 web portal for protein modeling, prediction and analysis. *Nat Protoc* 10: 845-858.
 78. Bhattacharya D, Nowotny J, Cao R, Cheng J (2016) 3Drefine: an interactive web server for efficient protein structure refinement. *Nucleic Acids Res* 44: 406-409.
 79. Holm L (2019) Benchmarking fold detection by DaliLite v.5. *Bioinformatics* 35: 5326-5327.
 80. Krissinel E, Henrick K (2007) Inference of macromolecular assemblies from crystalline state. *J Mol Biol* 372: 774-797.
 81. Jurrus E, Engel D, Star K, Monson K, Brandi J, Felberg LE, Brookes DH, Wilson L, Chen J, Liles K, Chun M, Li P, Gohara DW, Dolinsky T, Konecny R, Koes DR, Nielsen JE, Head-Gordon T, Geng W, Krasny R, Wei GW, Holst MJ, McCammon JA, Baker NA (2018) Improvements to the APBS biomolecular solvation software suite. *Protein Sci* 27: 112-128.
 82. Schrodinger, LLC. The PyMOL Molecular Graphics System, Version 2.1.1.

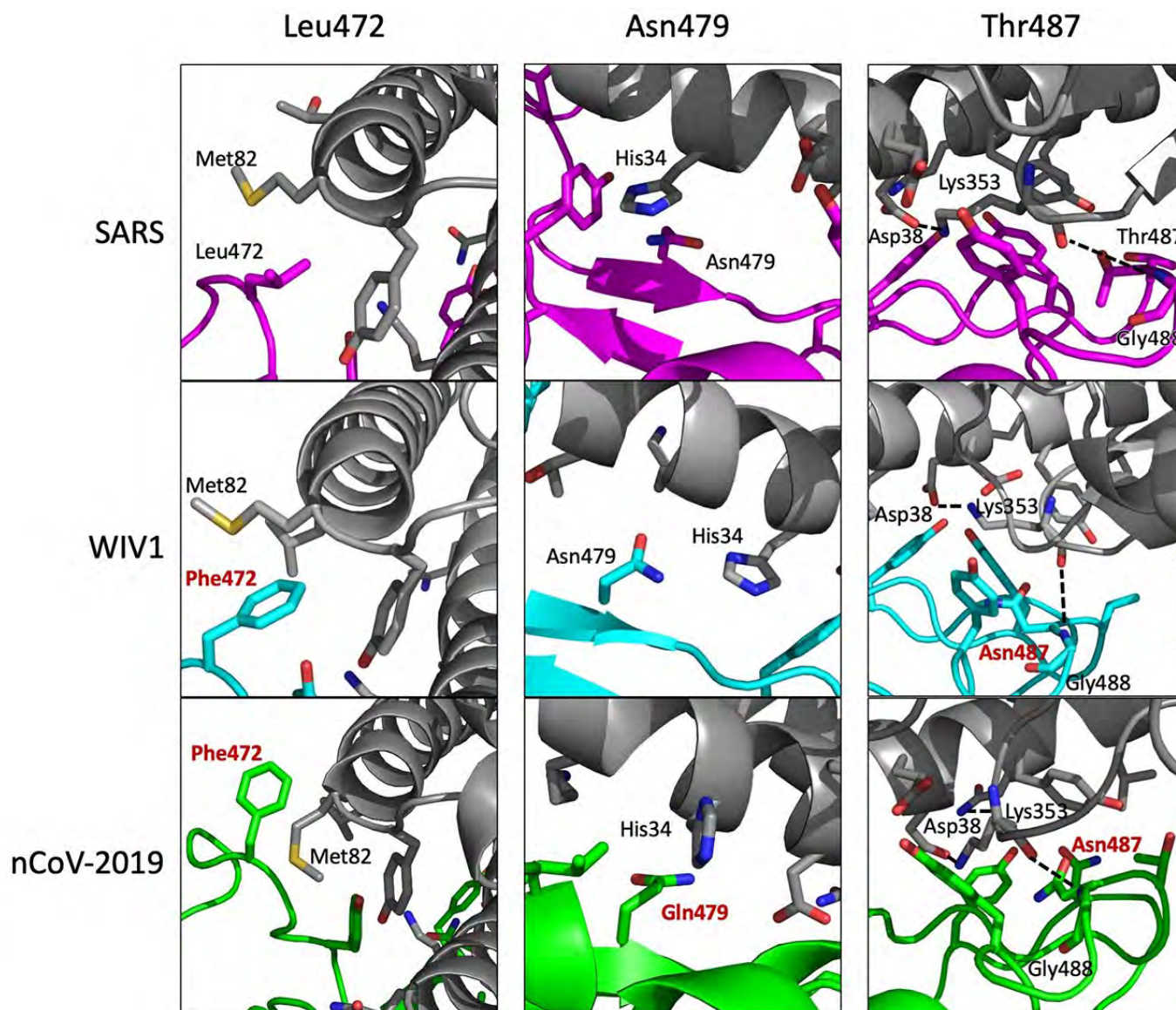
Corresponding author

Alyson Kelvin, PhD
 Assistant Professor
 Faculty of Medicine - Department of Pediatrics - Dalhousie University
 IWK Health Centre & Canadian Centre for Vaccinology
 5980 University Ave, 4th Floor, R4020
 Halifax, NS. B3K 6R8 Canada
 Phone: (902) 470-2760
 Fax: (902) 494-5125
 akelvin@dal.ca

Conflict of interests: No conflict of interests is declared.

Annex – Supplementary Items

Figure S1. Interaction of RBD residues involved in species specificity and ACE2. The RBD homology models docked to ACE2 are shown with emphasis placed on three residues associated with SARS-CoV species specificity: Leu472, Asn479, and Thr487.



ACE2 is shown in grey and ACE2 residues involved with each of the three RBD residues are shown in stick form. The SARS-CoV, WIV1-CoV, and 2019-nCoV RBD homology models are shown in magenta, cyan, and green, respectively. Amino acids involved in ACE2 binding are shown in stick representation in their respective colours. If a SARS-RBD amino acid is mutated in either WIV1-CoV RBD or 2019-nCoV, it is labelled in red. Hydrogen bonds are shown as dashed black lines.

Preliminary genomic characterisation of an emergent SARS-CoV-2 lineage in the UK defined by a novel set of spike mutations

arambaut  ARTIC Network

Dec '20

Preliminary genomic characterisation of an emergent SARS-CoV-2 lineage in the UK defined by a novel set of spike mutations

Report written by: Andrew Rambaut¹, Nick Loman², Oliver Pybus³, Wendy Barclay⁴, Jeff Barrett⁵, Alesandro Carabelli⁶, Tom Connor⁷, Tom Peacock⁴, David L Robertson⁸, Erik Volz⁴, on behalf of COVID-19 Genomics Consortium UK (CoG-UK)⁹.

1. University of Edinburgh
2. University of Birmingham
3. University of Oxford
4. Imperial College London
5. Wellcome Trust Sanger Institute
6. University of Cambridge
7. Cardiff University
8. MRC-University of Glasgow Centre for Virus Research
9. <https://www.cogconsortium.uk>



This work is licensed under a [Creative Commons Attribution-ShareAlike 4.0 International License](https://creativecommons.org/licenses/by-sa/4.0/).

Summary

Recently a distinct phylogenetic cluster (named lineage B.1.1.7) was detected within the COG-UK surveillance dataset. This cluster has been growing rapidly over the past 4 weeks and since been observed in other UK locations, indicating further spread.

Several aspects of this cluster are noteworthy for epidemiological and biological reasons and we report preliminary findings below. In summary:

The B.1.1.7 lineage accounts for an increasing proportion of cases in parts of England. The number of B.1.1.7 cases, and the number of regions reporting B.1.1.7 infections, are growing. B.1.1.7 has an unusually large number of genetic changes, particularly in the spike protein. Three of these mutations have potential biological effects that have been described previously to varying extents:

- Mutation N501Y is one of six key contact residues within the receptor-binding domain (RBD) and has been identified as increasing binding affinity to human and murine ACE2.
- The spike deletion 69-70del has been described in the context of evasion to the human immune response but has also occurred a number of times in association with other RBD changes.
- Mutation P681H is immediately adjacent to the furin cleavage site, a known location of biological significance.

The rapid growth of this lineage indicates the need for enhanced genomic and epidemiological surveillance worldwide and laboratory investigations of antigenicity and infectivity.

Background

The two earliest sampled genomes that belong to the B.1.1.7 lineage were collected on 20-Sept-2020 in Kent and another on 21-Sept-2020 from Greater London. B.1.1.7 infections have continued to be detected in the UK through early December 2020. Genomes belonging to lineage B.1.1.7 form a monophyletic clade that is well supported by a large number of lineage-defining mutations (Figure 1). As of 15th December, there are 1623 genomes in the B.1.1.7 lineage. Of these 519 were sampled in Greater London, 555 in Kent, 545 in other regions of the UK including both Scotland and Wales, and 4 in other countries.



Figure 1 | Phylogenetic tree of the B.1.1.7 lineage and its nearest outgroup sequences, for samples collected up until 30-Nov-2020. Tips from the same location have been collapsed into circles whose area is proportional to the number of genomes represented. Three large subclades are evident within the B.1.1.7 lineage, each defined by one nucleotide change. One of these clades is defined by a further stop codon in ORF8.

Lineage-defining mutations & rate of evolution

The B.1.1.7 lineage carries a larger than usual number of virus genetic changes. The accrual of 14 lineage-specific amino acid replacements prior to its detection is, to date, unprecedented in the global virus genomic data for the COVID-19 pandemic. Most branches in the global phylogenetic tree of SARS-CoV-2 show no more than a few mutations and mutations accumulate at a relatively

consistent rate over time. Estimates suggest that circulating SARS-CoV-2 lineages accumulate nucleotide mutations at a rate of about 1-2 mutations per month (Duchene et al. 2020).

A preliminary analysis of these observations is provided in Figure 2, which shows a regression of root-to-tip genetic distances against genome sampling date, for lineage B.1.1.7 and for a selection of related outgroup genomes. The rate of molecular evolution within lineage B.1.1.7 is similar to that of other related lineages. However, lineage B.1.1.7 is more divergent from the phylogenetic root of the pandemic, indicating a higher rate of molecular evolution on the phylogenetic branch immediately ancestral to B.1.1.7. Further, inferred nucleotide changes on this branch are predominantly amino acid-altering (14 non-synonymous mutations and 3 deletions). There are 6 synonymous mutations on the branch. This is suggestive of a process involving adaptive molecular evolution, although a role for increased fixation rates through relaxed selective constraint cannot be currently ruled out.



Figure 2 | Regression of root-to-tip genetic distances against sampling dates, for sequences belonging to lineage B.1.1.7 (blue) and those in its immediate outgroup in the global phylogenetic tree (brown). The regression lines are fitted to the two sets independently. The regression gradient is an estimate of the rate of sequence evolution. These rates are $5.6E^{-4}$ and $5.3E^{-4}$ nucleotide changes/site/year for the B.1.1.7 and outgroup data sets, respectively.

What evolutionary processes or selective pressures might have given rise to lineage B.1.1.7?

High rates of mutation accumulation over short time periods have been reported previously in studies of immunodeficient or immunosuppressed patients who are chronically infected with SARS-CoV-2 (Choi et al. 2020; Avanzato et al. 2020; Kemp et al. 2020). These infections exhibit detectable SARS-CoV-2 RNA for 2-4 months or longer (although there are also reports of long infections in some immunocompetent individuals). The patients are treated with convalescent plasma (sometimes more than once) and usually also with the drug remdesivir. Virus genome sequencing of these infections reveals unusually large numbers of nucleotide changes and deletion mutations and often high ratios of non-synonymous to synonymous changes. Convalescent plasma is often given when patient viral loads are high, and Kemp et al. (2020) report that intra-patient virus genetic diversity increased after plasma treatment was given.

Under such circumstances, the evolutionary dynamics of and selective pressures upon the intra-patient virus population are expected to be very different to those experienced in typical infection. First, selection from natural immune responses in immune-deficient/suppressed patients will be weak or absent. Second, the selection arising from antibody therapy may be strong due to high antibody concentrations. Third, if antibody therapy is administered after many weeks of chronic infection, the virus population may be unusually large and genetically diverse at the time that antibody-mediated selective pressure is applied, creating suitable circumstances for the rapid fixation of multiple virus genetic changes through direct selection and genetic hitchhiking.

These considerations lead us to hypothesise that the unusual genetic divergence of lineage B.1.1.7 may have resulted, at least in part, from virus evolution with a chronically-infected individual. Although such infections are rare, and onward transmission from them presumably even rarer, they are not improbable given the ongoing large number of new infections.

Although we speculate here that chronic infection played a role in the origins of the B.1.1.7 variant, this remains a hypothesis and we cannot yet infer the precise nature of this event.

Potential biological significance of mutations

Table 1 provides details of the B.1.1.7 lineage-specific non-synonymous mutations and deletions. We note that many occur in the virus spike protein. These include spike position 501, one of the key contact residues in the receptor binding domain (RBD), and experimental data suggests mutation N501Y can increase ACE2 receptor affinity (Starr et al. 2020) and P681H, one of 4 residues comprising the insertion that creates a furin cleavage site between S1 and S2 in spike. The S1/S2 furin cleavage site of SARS-CoV-2 is not found in closely related coronaviruses and has been shown to promote entry into respiratory epithelial cells and transmission in animal models (Hoffmann, Kleine-Weber, and Pöhlmann 2020; Peacock et al. 2020; Zhu et al. 2020). N501Y has been associated with increased infectivity and virulence in a mouse model (Gu et al. 2020). Both N501Y and P681H have been observed independently but not to our knowledge in combination before now.

Also present is the deletion of two amino acids at sites 69-70 in spike - this mutation is one of a number of recurrent deletions observed in the N terminal domain of Spike (McCarthy et al. 2020; Kemp et al. 2020) and has been seen in multiple lineages linked to several RBD mutations. For example, it arose in the mink-associated outbreak in Denmark on the background of the Y453F

RBD mutation, and in humans in association with the N439K RBD mutation, accounting for its relatively high frequency in the global genome data (~3000 sequences).

Table 1 | Non-synonymous mutations and deletions inferred to occur on the branch leading to lineage B.1.1.7 lineage.

gene	nucleotide	amino acid
ORF1ab	C3267T	T1001I
	C5388A	A1708D
	T6954C	I2230T
	11288-11296 deletion	SGF 3675-3677 deletion
spike	21765-21770 deletion	HV 69-70 deletion
	21991-21993 deletion	Y144 deletion
	A23063T	N501Y
	C23271A	A570D
	C23604A	P681H
	C23709T	T716I
	T24506G	S982A
	G24914C	D1118H
Orf8	C27972T	Q27stop
	G28048T	R52I
	A28111G	Y73C
N	28280 GAT->CTA	D3L
	C28977T	S235F

Outside of spike, the ORF8 Q27stop mutation truncates the ORF8 protein or renders it inactive and thus allows further downstream mutations to accrue. Early on during the pandemic multiple virus isolates with deletions leading to loss of ORF8 expression were isolated worldwide, including a large cluster in Singapore with a deletion leading to both a truncated Orf7b and ablated ORF8 expression. The Singaporean strain, which had a 382nt deletion, was associated with a milder clinical infection and less post-infection inflammation, however this cluster died out at the end of March after Singapore successfully implemented control measures (Young et al. 2020). Subsequent work has found that the ORF8 deletion has only a very modest effect on virus replication in human primary airway cells compared to viruses without the deletion, leading to a slight replication lag compared to viruses with the deletion (Gamage et al. 2020). As ORF8 is usually 121 amino acids long it is likely the stop codon at position 27 observed in lineage B.1.1.7 results in a loss of function.

Finally there are 6 synonymous mutations with 5 in ORF1ab (C913T, C5986T, C14676T, C15279T, T16176C), and one in the M gene (T26801C).

Conclusion

We report a rapidly growing lineage in the UK associated with an unexpectedly large number of genetic changes including in the receptor-binding domain and associated with the furin cleavage site. Given (i) the experimentally-predicted and plausible phenotypic consequences of some of these mutations, (ii) their unknown effects when present in combination, and (iii) the high growth rate of B.1.1.7 in the UK, this novel lineage requires urgent laboratory characterisation and enhanced genomic surveillance worldwide.

References

- Avanzato, Victoria A., M. Jeremiah Matson, Stephanie N. Seifert, Rhys Pryce, Brandi N. Williamson, Sarah L. Anzick, Kent Barbian, et al. 2020. "Case Study: Prolonged Infectious SARS-CoV-2 Shedding from an Asymptomatic Immunocompromised Individual with Cancer." *Cell*, November. <https://doi.org/10.1016/j.cell.2020.10.049>.
- Choi, Bina, Manish C. Choudhary, James Regan, Jeffrey A. Sparks, Robert F. Padera, Xueting Qiu, Isaac H. Solomon, et al. 2020. "Persistence and Evolution of SARS-CoV-2 in an Immunocompromised Host." *The New England Journal of Medicine* 383 (23): 2291–93.
- Duchene, Sebastian, Leo Featherstone, Melina Haritopoulou-Sinanidou, Andrew Rambaut, Philippe Lemey, and Guy Baele. 2020. "Temporal Signal and the Phylodynamic Threshold of SARS-CoV-2." *Virus Evolution* 6 (2): veaa061.
- Young, Barnaby E. et al. 2020. "Effects of a Major Deletion in the SARS-CoV-2 Genome on the Severity of Infection and the Inflammatory Response: An Observational Cohort Study." 2020. *The Lancet* 396 (10251): 603–11.
- Gamage, Akshamal M., Kai Sen Tan, Wharton O. Y. Chan, Jing Liu, Chee Wah Tan, Yew Kwang Ong, Mark Thong, et al. 2020. "Infection of Human Nasal Epithelial Cells with SARS-CoV-2 and a 382-Nt Deletion Isolate Lacking ORF8 Reveals Similar Viral Kinetics and Host Transcriptional Profiles." *PLoS Pathogens* 16 (12): e1009130.
- Gu, Hongjing, Qi Chen, Guan Yang, Lei He, Hang Fan, Yong-Qiang Deng, Yanxiao Wang, et al. 2020. "Adaptation of SARS-CoV-2 in BALB/c Mice for Testing Vaccine Efficacy." *Science* 369 (6511): 1603–7.
- Hoffmann, Markus, Hannah Kleine-Weber, and Stefan Pöhlmann. 2020. "A Multibasic Cleavage Site in the Spike Protein of SARS-CoV-2 Is Essential for Infection of Human Lung Cells." *Molecular Cell* 78 (4): 779–84.e5.
- Kemp, S. A., D. A. Collier, R. Datir, S. Gayed, A. Jahun, M. Hosmillo, Iatm Ferreira, et al. 2020. "Neutralising Antibodies Drive Spike Mediated SARS-CoV-2 Evasion." *Infectious Diseases (except HIV/AIDS)*. medRxiv. <https://doi.org/10.1101/2020.12.05.20241927>

McCarthy, Kevin R., Linda J. Rennick, Sham Nambulli, Lindsey R. Robinson-McCarthy, William G. Bain, Ghady Haidar, and W. Paul Duprex. 2020. "Natural Deletions in the SARS-CoV-2 Spike Glycoprotein Drive Antibody Escape." *Microbiology*. bioRxiv.

Peacock, Thomas P., Daniel H. Goldhill, Jie Zhou, Laury Baillon, Rebecca Frise, Olivia C. Swann, Ruthiran Kugathasan, et al. 2020. "The Furin Cleavage Site of SARS-CoV-2 Spike Protein Is a Key Determinant for Transmission due to Enhanced Replication in Airway Cells." Cold Spring Harbor Laboratory. <https://doi.org/10.1101/2020.09.30.318311>.

Starr, Tyler N., Allison J. Greaney, Sarah K. Hilton, Daniel Ellis, Katharine H. D. Crawford, Adam S. Dingens, Mary Jane Navarro, et al. 2020. "Deep Mutational Scanning of SARS-CoV-2 Receptor Binding Domain Reveals Constraints on Folding and ACE2 Binding." *Cell* 182 (5): 1295–1310.e20.

Zhu, Yunkai, Fei Feng, Gaowei Hu, Yuyan Wang, Yin Yu, Yuanfei Zhu, Wei Xu, et al. 2020. "The S1/S2 Boundary of SARS-CoV-2 Spike Protein Modulates Cell Entry Pathways and Transmission." Cold Spring Harbor Laboratory. <https://doi.org/10.1101/2020.08.25.266775>.

🔗 [Detection of SARS-CoV-2 P681H Spike Protein Variant in Nigeria](#)

🔗 [Transmission of SARS-CoV-2 Lineage B.1.1.7 in England: Insights from linking epidemi...](#)

🔗 [Lineage-specific growth of SARS-CoV-2 B.1.1.7 during the English national lockdown](#)

🔗 [Phylogenetic relationship of SARS-CoV-2 sequences from Amazonas with emerging Bra...](#)

🔗 [Emergence of Y453F and Δ69-70HV mutations in a lymphoma patient with long-term CO...](#)

[7 more](#)

garmstrong

Dec '20

Interesting. Note that people with B-cell deficiencies (CVID in particular, but SIgA and I think others—these deficiencies are often not diagnosed until adulthood) are well known to have chronic OPV infections (more than 5 years in several cases), which evolve over time. The viruses are considered vaccine-derived polioviruses if they're more than 1% from the original Sabin virus, and are designated iVDPV. iVDPVs can often (usually, I think) be distinguished from circulating VDPVs (cVDPVs) by a high level of non-synonymous mutations in particular parts of the capsid. cVDPVs, by contrast, arise in populations with low vaccination coverage, where the virus (usually Sabin 2) is transmitted serially, presumably with little immune pressure. cVDPVs have a much higher percentage of synonymous mutations (as you'd expect). IVIG treatment of chronically infected people with CVID may also play a role. There have been instances, in countries where polio has been eliminated, of iVDPVs have been detected and identified in wastewater. In at least a couple of those cases, I believe they attempted (unsuccessfully) to trace the individual by following up the sewage lines and testing at the branches.

Note also that a chronically infected person also would be a setup for recombination.

[🔗 Global framework for SARS-CoV-2 data analysis: Application to intrahost variation | Part 2](#)

isabel

Dec '20

Thank you for the great work.

I am concerned with the lack of monitoring of SARS-Cov-2 in animals.

COVID-19 is a zoonosis and other animals, including Syrian hamster are prone to infection .

Minks from different locations have been infected with a variant containing the S69-70deletion. It has been shown that minks can infect humans... but what was the origin of this new mink associated strain?

Now a new UK variant emerges with a mutation that increase the affinity of the spike to human and murine ACE2 ...

The mink associated SARS-CoV-2 variant has been found in wild minks...

This is not enough to take more seriously the One Health approach of this pandemics !? It's a zoonosis .

Why we still don't have monitoring plans for animals that cohabit with sars-Cov-2 positive persons ?

isabel

Dec '20

Does someone knows when the in vitro seroneutralization -SNT assays with samples obtained from vaccinated persons tested against this new strain will be available ? I am sure that they are already done. It is a pretty straightforward assay... and is a crucial assay to provide us an idea about the vaccine protection against this new strain ...

the major structural changes of the Spike could suggest a potencial failure of licensed vacines .

Do you agree ?

Or I am being too pessimist ...

isabel

Dec '20

Sorry for too many questions ... but I appreciate your work and opinion

One more ...

Faster evolutionary rate of the virus was reported in Mink associated SARS-CoV-2 in Netherlands by Munnink et al.

Do you think that spillover to new host species could speed up the evolutionary rate of SARS-CoV-2?

In HIV-1 and EIAV vaccine studies there are reports of the emergence of new variants for immune evasion. The same is associated to antivirals .

Why with SARS-CoV-2 everyone is betting in the lack of immune evasion responses to vaccines ?

What is the scientific evidence that we have that are indicating that we'll have stable and low evolutionary rates in SARS-COV-2?

- 🔗 [Mutations arising in SARS-CoV-2 spike on sustained human-to-human transmission an...](#)
- 🔗 [Spike protein mutations in novel SARS-CoV-2 'variants of concern' commonly occur in ...](#)
- 🔗 [Spike protein sequences of Cambodian, Thai and Japanese bat sarbecoviruses provide ...](#)



Since January 2020 Elsevier has created a COVID-19 resource centre with free information in English and Mandarin on the novel coronavirus COVID-19. The COVID-19 resource centre is hosted on Elsevier Connect, the company's public news and information website.

Elsevier hereby grants permission to make all its COVID-19-related research that is available on the COVID-19 resource centre - including this research content - immediately available in PubMed Central and other publicly funded repositories, such as the WHO COVID database with rights for unrestricted research re-use and analyses in any form or by any means with acknowledgement of the original source. These permissions are granted for free by Elsevier for as long as the COVID-19 resource centre remains active.

Primer

Herd Immunity: Understanding COVID-19

Haley E. Randolph¹ and Luis B. Barreiro^{1,2,3,*}¹Genetics, Genomics, and Systems Biology, University of Chicago, Chicago, IL, USA²Department of Medicine, Section of Genetic Medicine, University of Chicago, Chicago, IL 60637, USA³Committee on Immunology, University of Chicago, Chicago, IL 60637, USA*Correspondence: lbarreiro@uchicago.edu<https://doi.org/10.1016/j.immuni.2020.04.012>

The emergence of severe acute respiratory syndrome coronavirus 2 (SARS-CoV-2) and its associated disease, COVID-19, has demonstrated the devastating impact of a novel, infectious pathogen on a susceptible population. Here, we explain the basic concepts of herd immunity and discuss its implications in the context of COVID-19.

Basic Concepts of Herd Immunity

Acquired immunity is established at the level of the individual, either through natural infection with a pathogen or through immunization with a vaccine. Herd immunity (Box 1) stems from the effects of individual immunity scaled to the level of the population. It refers to the indirect protection from infection conferred to susceptible individuals when a sufficiently large proportion of immune individuals exist in a population. This population-level effect is often considered in the context of vaccination programs, which aim to establish herd immunity so that those who cannot be vaccinated, including the very young and immunocompromised, are still protected against disease. Depending on the prevalence of existing immunity to a pathogen in a population, the introduction of an infected individual will lead to different outcomes (Figure 1). In a completely naive population, a pathogen will propagate through susceptible hosts in an unchecked manner following effective exposure of susceptible hosts to infected individuals. However, if a fraction of the population has immunity to that same pathogen, the likelihood of an effective contact between infected and susceptible hosts is reduced, since many hosts are immune and, therefore, cannot transmit the pathogen. If the fraction of susceptible individuals in a population is too few, then the pathogen cannot successfully spread, and its prevalence will decline. The point at which the proportion of susceptible individuals falls below the threshold needed for transmission is known as the herd immunity threshold (Anderson and May, 1985). Above this level of immunity, herd immunity begins to take effect, and susceptible individuals benefit from indirect protection from infection (Figure 1B).

Under the simplest model, the herd immunity threshold depends on a single parameter known as R_0 , or the basic reproduction number (Figure 2A). R_0 refers to the average number of secondary infections caused by a single infectious individual introduced into a completely susceptible population (Anderson and May, 1985). If we consider a hypothetical pathogen with an R_0 of 4, this means that, on average, one infected host will infect four others during the infectious period, assuming no immunity exists in the population. Mathematically, the herd immunity threshold is defined by $1 - 1/R_0$ (e.g., if $R_0 = 4$, the corresponding herd immunity threshold is 0.75) (Anderson and May, 1985). Therefore, the more communicable a pathogen, the greater its associated R_0 and the greater the proportion of the

population that must be immune to block sustained transmission (Figure 2B). A similar parameter important for understanding population-level immunity is the effective reproduction number (R_e or R_t). R_e is defined as the average number of secondary cases generated by a single index case over an infectious period in a partially immune population (Delamater et al., 2019). Unlike R_0 , R_e does not assume a completely susceptible population and, consequently, will vary depending on a population's current immune state, which will change dynamically as an outbreak event or vaccination campaign unfolds. Ultimately, the goal of vaccination programs is to bring the value of R_e below 1. This occurs when the proportion of the population with immunity exceeds the herd immunity threshold. At this point, pathogen spread cannot be maintained, so there is a decline in the number of infected individuals within the population.

Establishing Herd Immunity within Populations

The above interpretation of R_0 and its relation to the herd immunity threshold is the simplest understanding of these terms. It relies on several key assumptions, including homogeneous mixing of individuals within a population and that all individuals develop sterilizing immunity—immunity that confers lifelong protection against reinfection—upon vaccination or natural infection. In real-world situations, these epidemiological and immunological assumptions are often not met, and the magnitude of indirect protection attributed to herd immunity will depend on variations in these assumptions.

R_0 is defined by both the pathogen and the particular population in which it circulates. Thus, a single pathogen will have multiple R_0 values depending on the characteristics and transmission dynamics of the population experiencing the outbreak (Delamater et al., 2019). This inherently implies that the herd immunity threshold will vary between populations, which is a well-documented occurrence (Delamater et al., 2019). For any infectious disease, communicability depends on many factors that impact transmission dynamics, including population density, population structure, and differences in contact rates across demographic groups, among others (Anderson and May, 1985). All of these factors will directly or indirectly impact R_0 and, consequently, the herd immunity threshold.

To establish herd immunity, the immunity generated by vaccination or natural infection must prevent onward



Box 1. Glossary

Herd immunity: the indirect protection from infection conferred to susceptible individuals when a sufficiently large proportion of immune individuals exist in a population

Herd immunity threshold: the point at which the proportion of susceptible individuals in a population falls below the threshold needed for transmission

R_0 : the average number of secondary infections caused by a single infectious individual introduced into a completely susceptible population

R_e : the average number of secondary infections generated by a single infectious individual over an infectious period in a partially immune population

Onward transmission: the effective transmission of a pathogen from an infected individual to susceptible host(s)

Case Fatality Rate (CFR): proportion of deaths attributed to a certain disease among all individuals diagnosed with that disease

Infection Fatality Rate (CFR): proportion of deaths attributed to a certain disease among all infected individuals

transmission, not just clinical disease. For certain pathogens, such as severe acute respiratory syndrome coronavirus 2 (SARS-CoV-2), clinical manifestations are a poor indicator of transmissibility, as asymptomatic hosts can be highly infectious and contribute to the spread of an epidemic. Once the herd immunity threshold is reached, the efficacy of herd immunity largely depends on the strength and duration of the immunity acquired. For pathogens in which lifelong immunity is induced, as is the case for measles vaccination or infection, herd immunity is highly effective and can prevent pathogen spread within a population. However, this situation is relatively rare, as immunity for many other infectious diseases, such as pertussis and rotavirus, wanes over time. As a consequence, herd immunity is less effective, and periodic outbreaks can still occur. Finally, if immunity is unevenly distributed within a population, clusters of susceptible hosts that frequently contact one another may remain. Even if the proportion of immunized individuals in the population as a whole surpasses the herd immunity threshold, these pockets of susceptible individuals are still at risk for local outbreaks.

Herd Immunity and SARS-CoV-2

The ongoing SARS-CoV-2 pandemic has caused over 3.5 million clinically confirmed cases of COVID-19 and has claimed more than 250,000 lives worldwide (as of May 4, 2020). Numerous clinical trials to evaluate novel vaccine candidates and drug repurposing strategies for the prevention and treatment of SARS-CoV-2 infection are currently ongoing. However, it is unknown whether these trials will produce effective interventions, and it is unclear how long these studies will take to establish efficacy and safety, although an optimistic estimate for any vaccine trial is at least 12–18 months. In the absence of a vaccine, building up SARS-CoV-2 herd immunity through natural infection is theoretically possible. However, there is no straightforward, ethical path to reach this goal, as the societal consequences of achieving it are devastating.

Since the onset of SARS-CoV-2 spread, various studies have estimated the basic reproductive number (R_0) of the virus to be in the range of 2 to 6. From an initial cohort of 425 confirmed cases in Wuhan, China, an R_0 of approximately 2.2 was estimated, meaning that, on average, each infected individual gives rise to 2.2 other infections (Li et al., 2020). More recent estimates place the R_0 higher at 5.7, although many estimates fall within this range (Sanche et al., 2020). This variation reflects the difficulty of obtain-

ing accurate R_0 estimates in an ongoing pandemic, and the current estimated SARS-CoV-2 R_0 values likely do not indicate a complete picture of the transmission dynamics across all countries.

Assuming an R_0 estimate of 3 for SARS-CoV-2, the herd immunity threshold is approximately 67%. This means that the incidence of infection will start to decline once the proportion of individuals with acquired immunity to SARS-CoV-2 in the population exceeds 0.67. As discussed above, this model relies on simplifying assumptions, such as homogeneous population mixing and uniform sterilizing immunity in recovered individuals across demographic groups, which are unlikely to hold true. Nevertheless, this basic model can give us a rough idea of the number of individuals that would need to be infected to achieve herd immunity in the absence of a vaccine given an approximate herd immunity threshold and a country's population.

Consequences of Reaching the SARS-CoV-2 Herd Immunity Threshold in the Absence of a Vaccine

One important measure to evaluate the impact of SARS-CoV-2 spread is the overall case fatality rate (CFR). The CFR is the proportion of deaths attributed to a certain disease among all individuals diagnosed with that disease (i.e., cases) over a specified period of time. It is worth noting that there is still significant uncertainty in the CFR for COVID-19 due to variation in the testing capacity per country, selection bias for which individuals receive testing, and differences in how deaths are officially attributed to COVID-19. Further, CFR is also sensitive to variation in the underlying age structure and distribution of comorbidities among populations. Consequently, CFRs may differ considerably over time and between countries. In the case of COVID-19, the initial estimate of the CFR in a small cohort of 41 individuals with laboratory-confirmed SARS-CoV-2 infection was high (15%) (Huang et al., 2020). However, this number has markedly decreased as more data have become available. Using data from all laboratory-confirmed and clinically diagnosed cases from mainland China, Verity et al. obtained an estimated overall CFR of 1.38%, adjusted for censoring, under-ascertainment, and the underlying demography in China, and similar estimates have been obtained from other groups (Verity et al., 2020; Wu et al., 2020a). Like many other infectious diseases, a non-uniform COVID-19 CFR has been reported across age groups, with the vast majority of deaths occurring among individuals 60 years old or greater.

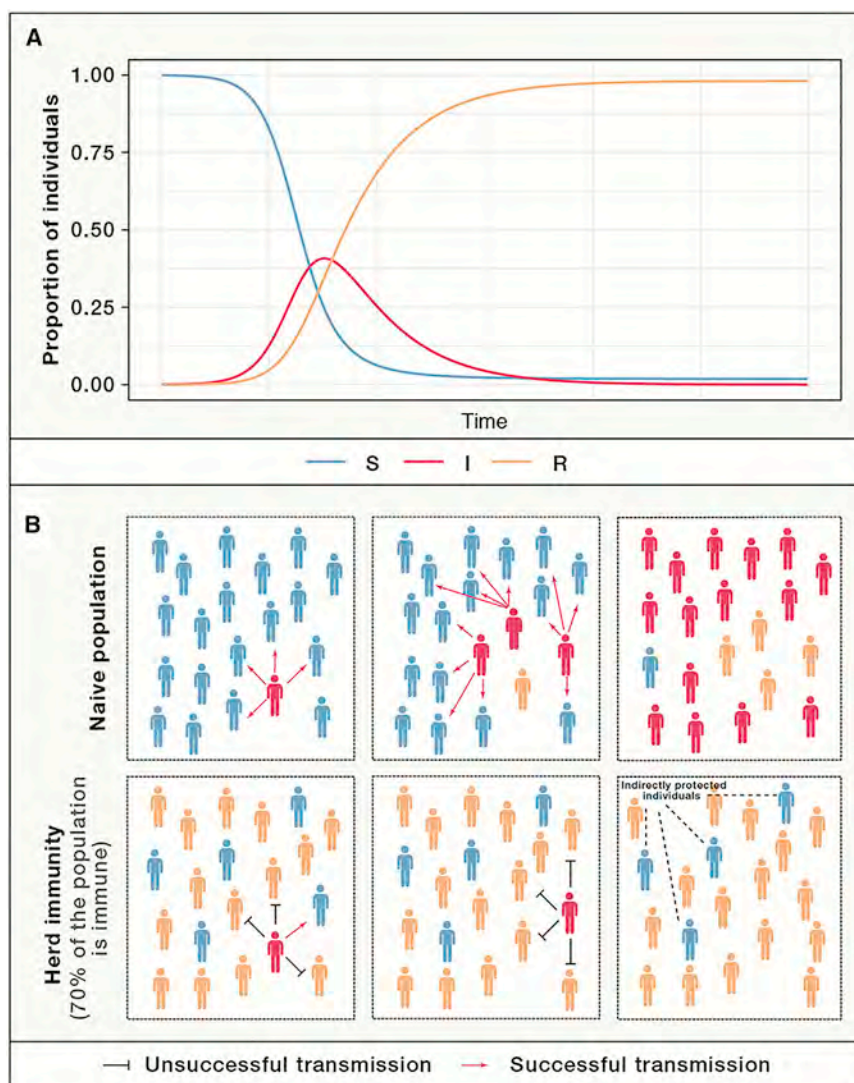


Figure 1. Herd Immunity

(A) SIR (susceptible, infectious, recovered) model for a completely immunizing infection with an $R_0 = 4$. The model assumes a closed population in which no people leave and no new cases are introduced. Following the introduction of a single infected individual, the proportion of infected individuals (red line) increases rapidly until reaching its peak, which corresponds to the herd immunity threshold. After this point, newly infected individuals infect fewer than one susceptible individual, as a sufficient proportion of the population has become resistant, preventing further spread of the pathogen (orange line).

(B) Schematic depiction of the disease propagation dynamics when one infected individual is introduced into a completely susceptible population (top panel) versus a situation in which an infected individual is introduced into a population that has reached the herd immunity threshold (bottom panel). In the naive population, an outbreak quickly emerges, whereas under the scenario of herd immunity, the virus fails to spread and persist in the population.

not vary across countries, and it does not consider factors that lead to heterogeneity in IFRs, including differences in access to healthcare resources and variation in the prevalence of comorbidities.

In reality, CFRs and IFRs vary dramatically across countries, as highlighted by the current estimates of unadjusted CFRs across the globe (Italy, 13.7%; United States, 5.77%; South Korea, 2.33%; [The Centre for Evidence-Based Medicine, 2020](#)). Although testing biases and differences in age demographics across countries account in part for these elevated regional CFRs, additional factors likely play a role, most notably a strain on

The most relevant measure to evaluate the societal cost of achieving global SARS-CoV-2 herd immunity is the overall infection fatality rate (IFR). The IFR is defined as the proportion of deaths caused by a certain disease among all infected individuals. Because some cases will not be reported, especially among asymptomatic hosts or individuals with mild symptoms, the IFR will inherently be lower than the CFR. If we combine infection fatality data with an estimate of the number of individuals that need to develop immunity to reach the herd immunity threshold, we can project the expected number of deaths as a consequence of meeting this threshold. Because of the uncertainty in the COVID-19 IFR, we use three different point estimates in our analysis: (1) an IFR of 0.2%, (2) an IFR of 0.6% that is in line with the IFR determined by Verity et al., and (3) an IFR of 1% ([Figure 2C](#)). Assuming a uniform herd immunity threshold of 67% ($R_0 = 3$) and an IFR of 0.6%, the absolute number of expected deaths across the globe would exceed 30 million people ([Figure 2C](#)). Notably, this analysis assumes that IFRs do

local healthcare systems. In Italy, a sudden influx of COVID-19 patients in March led to a shortage of intensive care unit beds and other essential medical resources, causing a substantial burden on hospitals. This outbreak underscores the importance of taking into account the limits of local healthcare infrastructure and how exceeding these limits can exacerbate negative outcomes of COVID-19.

Particularly in the context of attaining herd immunity to SARS-CoV-2, a regard for finite healthcare resources cannot be overstated, as this policy inherently relies on allowing a large fraction of the population to become infected. Unchecked, the spread of SARS-CoV-2 will rapidly overwhelm healthcare systems. A depletion in healthcare resources will lead not only to elevated COVID-19 mortality but also to increased all-cause mortality. This effect will be especially devastating for countries in which hospitals have limited surge capacity, where minimal public health infrastructure exists, and among vulnerable communities, including prison and homeless populations.

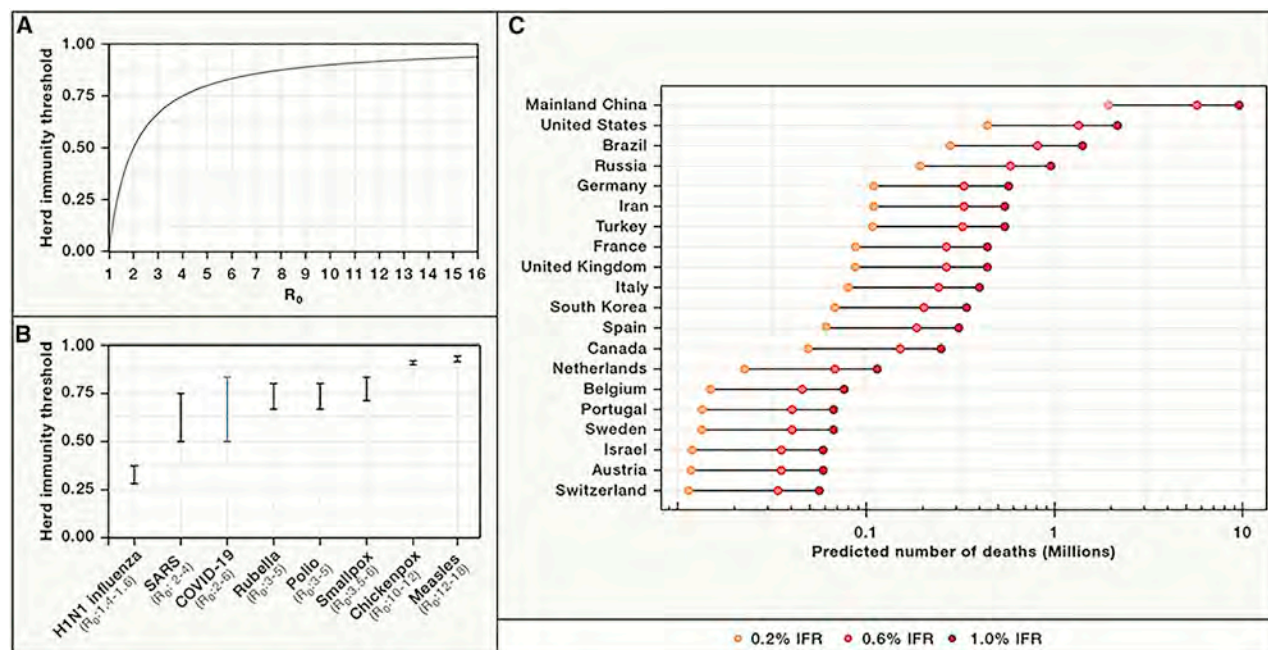


Figure 2. The Potential Health Burden of COVID-19 if Herd Immunity Is Achieved in the Absence of Vaccination

(A) Relationship between R_0 —the basic reproduction number (Box 1)—and the herd immunity threshold, which corresponds to the proportion of individuals in the population that would need to become immune for herd immunity to be established (y axis). As R_0 increases, the proportion of the population that must be immune to generate herd immunity increases ($1 - 1/R_0$).

(B) Basic reproduction numbers (R_0) and the corresponding herd immunity thresholds for various infectious diseases. R_0 estimates represent the commonly accepted R_0 range for each of the pathogens reported.

(C) Expected number of absolute deaths for the top 20 countries with the highest incidence of COVID-19 as of April 10, 2020, assuming herd immunity is established at a uniform threshold of 67% ($R_0 = 3$) in each country. Overall COVID-19 infection fatality rates (IFR) of 0.2%, 0.6%, and 1.0% are considered. We note that these numbers are necessarily underestimates given that, even after the herd immunity threshold is reached, it will take a long time until there are no more new cases, and therefore, no new deaths.

Epidemiological Considerations for SARS-CoV-2 Herd Immunity

Because SARS-CoV-2 is a novel pathogen, many features of its transmission and infection dynamics are not well characterized. Thus, our above analysis provides only a sense of the potential ramifications given a scenario in which we attain herd immunity via natural infection. We do not consider numerous complexities of viral spread and infectivity, including variation in R_0 across time and populations, heterogeneity in the attack and contact rates across demographic groups, and inter-individual variation in communicability and disease severity, although these aspects are essential to understand the full picture of SARS-CoV-2 community spread. While these epidemiological factors have important implications in the context of herd immunity, currently, they are difficult to estimate given the limited data available.

Differences in population density, cultural behaviors, population age structure, underlying comorbidity rates, and contact rates across groups influence transmission dynamics within communities, so the assumption of a uniform R_0 across populations is not realistic. Further, variation in transmissibility between individuals may play a major role in SARS-CoV-2 spread. Superspreading events occur when circumstances favorable for high rates of transmission arise. These events involve a single index case infecting a large number of secondary contacts and are known to be important in driving outbreaks of infectious diseases, including SARS, Middle East respiratory syndrome (MERS), and measles

(Lloyd-Smith et al., 2005). Reports of SARS-CoV-2 superspreading events have been documented, suggesting that heterogeneity in infectivity may significantly impact the dynamics of its transmission (Liu et al., 2020). Finally, the factors that influence inter-individual heterogeneity in COVID-19 susceptibility, clinical pathology, and disease outcome are not well understood. Reported differences in sex- and ethnicity-specific CFRs suggest that genetic, environmental, and social determinants likely underlie variation in susceptibility to COVID-19 and the severity of COVID-19 complications, although future studies are needed to explore this further (Nasiri et al., 2020).

Immunological Considerations for SARS-CoV-2 Herd Immunity

The ability to establish herd immunity against SARS-CoV-2 hinges on the assumption that infection with the virus generates sufficient, protective immunity. At present, the extent to which humans are able to generate sterilizing immunity to SARS-CoV-2 is unclear. A recent study assessing the possibility of SARS-CoV-2 reinfection in a small cohort of rhesus macaques found that reinfection was not able to occur 1 month after the first viral challenge, suggesting at least short-term sterilizing immunity in these animals (Bao et al., 2020). In a cohort of 175 recovered COVID-19 patients, SARS-CoV-2-specific serum neutralizing antibodies (NAbs) were detected at considerable, albeit variable, titers in most ($n = 165$) individuals (Wu et al., 2020b),

indicating that the production of NAb against SARS-CoV-2 is relatively common.

Whereas these findings are promising, other important questions to consider are whether NAb titers will wane over time and how long acquired immunity will last. Previous studies in confirmed SARS patients have demonstrated that NAb responses against SARS-CoV persisted for several months to 2 years, although all individuals displayed low titers after about 15 months (Mo et al., 2006). Further, elevated concentrations of specific antibodies to coronavirus 229E, one of the viruses responsible for the common cold, were found 1 year after infection, although these titers were not sufficient to prevent reinfection in all individuals (Callow et al., 1990). Together, these studies suggest that protection against reinfection with coronavirus species tends to diminish given sufficient time, although longitudinal serological studies are needed to assess the duration of SARS-CoV-2 immunity. If this proves to also be true for SARS-CoV-2, persistent herd immunity may never be attained in the absence of recurrent vaccination. Indeed, modeling of the transmission dynamics of SARS-CoV-2 predicts that short-term immunity (~10 months) would give rise to annual outbreaks, while longer-term immunity (~2 years) would lead to biennial outbreaks (Kissler et al., 2020). Mass serological testing is now needed to determine how many individuals have been infected, how many individuals are immune, and how far we are from reaching the herd immunity threshold. That said, even if reinfection can occur after sterilizing immunity wanes, enduring memory cells of the adaptive immune system would likely facilitate immune control of the virus and limit disease pathology, which would hopefully decrease the clinical severity of subsequent infections.

Recap

In a sufficiently immune population, herd immunity provides indirect protection to susceptible individuals by minimizing the probability of an effective contact between a susceptible individual and an infected host. In its simplest form, herd immunity will begin to take effect when a population reaches the herd immunity threshold, namely when the proportion of individuals who are immune to the pathogen crosses $1 - 1/R_0$. At this point, sustained transmission cannot occur, so the outbreak will decline. However, in real-world populations, the situation is often much more complex. Epidemiological and immunological factors, such as population structure, variation in transmission dynamics between populations, and waning immunity, will lead to variation in the extent of indirect protection conferred by herd immunity. Consequently, these aspects must be taken into account when discussing the establishment of herd immunity within populations. There are two possible approaches to build widespread SARS-CoV-2 immunity: (1) a mass vaccination campaign, which requires the development of an effective and safe vaccine, or (2) natural immunization of global populations with the virus over time. However, the consequences of the latter are serious and far-reaching—a large fraction of the human population would need to become infected with the virus, and millions would succumb to it. Thus, in the absence of a vaccination program, establishing herd immunity should not be the ultimate goal. Instead, an emphasis should be placed on policies that protect the most vulnerable groups in the hopes that herd immunity will eventually be achieved as a byproduct of such measures, although not the primary objective itself.

ACKNOWLEDGMENTS

We thank members of the Barreiro lab, Valerie Abadie, Sarah Cobey, Maziar Divangahi, Bana Jabri, William Koval, Joaquin Sanz, and Patrick Wilson for the constructive comments and feedback. This work was supported by grant R01-GM134376 from the National Institute of General Medical Sciences to L.B.B. H.E.R. is supported by a National Science Foundation Graduate Research Fellowship (DGE-1746045).

REFERENCES

- Anderson, R.M., and May, R.M. (1985). Vaccination and herd immunity to infectious diseases. *Nature* 318, 323–329.
- Bao, L., Deng, W., Gao, H., Xiao, C., Liu, J., Xue, J., Lv, Q., Liu, J., Yu, P., Xu, Y., et al. (2020). Reinfection could not occur in SARS-CoV-2 infected rhesus macaques. *bioRxiv*. <https://doi.org/10.1101/2020.03.13.990226>.
- Callow, K.A., Parry, H.F., Sergeant, M., and Tyrrell, D.A. (1990). The time course of the immune response to experimental coronavirus infection of man. *Epidemiol. Infect.* 105, 435–446.
- Delamater, P.L., Street, E.J., Leslie, T.F., Yang, Y.T., and Jacobsen, K.H. (2019). Complexity of the basic reproduction number (R_0). *Emerg. Infect. Dis.* 25, 1–4.
- The Centre for Evidence-Based Medicine (2020). Global COVID-19 case fatality rates. <https://www.cebm.net/covid-19/global-covid-19-case-fatality-rates>.
- Huang, C., Wang, Y., Li, X., Ren, L., Zhao, J., Hu, Y., Zhang, L., Fan, G., Xu, J., Gu, X., et al. (2020). Clinical features of patients infected with 2019 novel coronavirus in Wuhan, China. *Lancet* 395, 497–506.
- Kissler, S.M., Tedijanto, C., Goldstein, E., Grad, Y.H., and Lipsitch, M. (2020). Projecting the transmission dynamics of SARS-CoV-2 through the postpandemic period. *Science*, eabb5793.
- Li, Q., Guan, X., Wu, P., Wang, X., Zhou, L., Tong, Y., Ren, R., Leung, K.S.M., Lau, E.H.Y., Wong, J.Y., et al. (2020). Early transmission dynamics in Wuhan, China, of novel coronavirus-infected pneumonia. *N. Engl. J. Med.* 382, 1199–1207.
- Liu, Y., Eggo, R.M., and Kucharski, A.J. (2020). Secondary attack rate and superspreading events for SARS-CoV-2. *Lancet* 395, e47.
- Lloyd-Smith, J.O., Schreiber, S.J., Kopp, P.E., and Getz, W.M. (2005). Super-spreading and the effect of individual variation on disease emergence. *Nature* 438, 355–359.
- Mo, H., Zeng, G., Ren, X., Li, H., Ke, C., Tan, Y., Cai, C., Lai, K., Chen, R., Chan-Yeung, M., and Zhong, N. (2006). Longitudinal profile of antibodies against SARS-coronavirus in SARS patients and their clinical significance. *Respirology* 11, 49–53.
- Nasiri, M.J., Haddadi, S., Tahvildari, A., Farsi, Y., Arbabi, M., Hasanzadeh, S., Jamshidi, P., Murthi, M., and Mirsaedi, M. (2020). COVID-19 clinical characteristics, and sex-specific risk of mortality: Systematic Review and Meta-analysis. *medRxiv*. <https://doi.org/10.1101/2020.03.24.20042903>.
- Sanche, S., Lin, Y.T., Xu, C., Romero-Severson, E., Hengartner, N., and Ke, R. (2020). High contagiousness and rapid spread of severe acute respiratory syndrome coronavirus 2. *Emerg. Infect. Dis.* 26, <https://doi.org/10.3201/eid2607.200282>.
- Verity, R., Okell, L.C., Dorigatti, I., Winskill, P., Whittaker, C., Imai, N., Cuomo-Dannenburg, G., Thompson, H., Walker, P.G.T., Fu, H., et al. (2020). Estimates of the severity of coronavirus disease 2019: a model-based analysis. *Lancet Infect. Dis.* Published online March 30, 2020. [https://doi.org/10.1016/S1473-3099\(20\)30243-7](https://doi.org/10.1016/S1473-3099(20)30243-7).
- Wu, J.T., Leung, K., Bushman, M., Kishore, N., Niehus, R., de Salazar, P.M., Cowling, B.J., Lipsitch, M., and Leung, G.M. (2020a). Estimating clinical severity of COVID-19 from the transmission dynamics in Wuhan, China. *Nat. Med.* 26, 506–510.
- Wu, F., Wang, A., Liu, M., Wang, Q., Chen, J., Xia, S., Ling, Y., Zhang, Y., Xun, J., Lu, L., et al. (2020b). Neutralizing antibody responses to SARS-CoV-2 in a COVID-19 recovered patient cohort and their implications. *medRxiv*. <https://doi.org/10.1101/2020.03.30.20047365>.

Spike E484K mutation in the first SARS-CoV-2 reinfection case confirmed in Brazil, 2020

paola

Jan 10

Spike E484K mutation in the first SARS-CoV-2 reinfection case confirmed in Brazil

Authors

Paola Cristina Resende^{1*}, João Felipe Bezerra², Romero Henrique Teixeira de Vasconcelos², Ighor Arantes³, Luciana Appolinario¹, Ana Carolina Mendonça¹, Anna Carolina Paixão¹, Ana Carolina Duarte Rodrigues¹, Thauane Silva¹, Alice Sampaio Rocha¹, Alex Pauvolid-Corrêa^{1,4}, Fernando Couto Motta¹, Dalane Loudal Florentino Teixeira⁵, Thiago Franco de Oliveira Carneiro⁵, Francisco Paulo Freire Neto⁶, Isabel Diniz Herbst⁷, Anderson Brandão Leite⁸, Irina Nastassja Riediger⁹, Maria do Carmo Debur⁹, Felipe Gomes Naveca¹⁰, Walquiria Almeida¹¹, Mirian Livorati¹², Gonzalo Bello^{3A}, Marilda M Siqueira^{1A}

A These authors share senior authorship

Affiliations

- 1 Laboratory of Respiratory Viruses and Measles (LVRS), Oswaldo Cruz Institute, Fiocruz
- 2 Universidade Federal da Paraíba (UFPB)
- 3 Laboratório de AIDS e Imunologia Molecular, Oswaldo Cruz Institute, Fiocruz.
- 4 Department of Veterinary Integrative Biosciences, Texas A&M University, College Station, Texas, United States
- 5 Laboratório Central do Estado da Paraíba (LACEN-PB)
- 6 Institute of Tropical Medicine, Federal University of Rio Grande do Norte (UFRN)
- 7 Maternidade Escola Januário Cicco (MEJC-UFRN)
- 8 Laboratório Central do Estado do Alagoas (LACEN-AL)
- 9 Laboratório Central do Estado do Paraná (LACEN-PR)
- 10 Laboratório de Ecologia de Doenças Transmissíveis na Amazônia (EDTA), Leônidas e Maria Deane Institute, Fiocruz, on behalf of the COVIDNORTE team.
- 11 Secretary of Surveillance and Health of the Brazilian MoH (SVS-MS)
- 12 General Laboratories Coordination of the Brazilian Ministry of Health (CGLab/MoH)

Corresponding Author:

Paola Cristina Resende
paola@ioc.fiocruz.br

Summary

On December 9th, the Brazilian Ministry of Health (MoH) recognised the first case of reinfection in the country. A 37-years-old healthcare worker resident in Northeast Brazil presented two clinical episodes of COVID-19 in June and October 2020, that were confirmed by RT-PCR in samples

collected 116 days apart. Whole-genome sequencing revealed that the two infections were caused, respectively, by the two most prevalent SARS-CoV-2 Brazilian lineages B.1.1.33 (primo-infection) and B.1.1.28 (reinfection). Bayesian analysis indicates that the reinfection probably occurred between September 14th to October 11th, a few days before the second confirmed clinical episode of COVID-19, thus excluding the possibility of viral co-infection followed by long-term viral persistence. Notably, the B.1.1.28 virus detected at reinfection corresponds to a new emergent Brazilian viral lineage, initially detected in the Rio de Janeiro state, containing the mutation E484K in the Spike protein. We found this new viral variant, hereafter designated B.1.1.28(E484K), in several states from the South, Northeast, and North Brazilian regions and date its origin at August 27th, 2020 (July 14th - September 18th). These findings documented a classical SARS-CoV-2 reinfection case with the emerging Brazilian lineage B.1.1.28(E484K). Additionally, we provide evidence of this emerging Brazilian clade's geographic dissemination outside the Rio de Janeiro state.

Keywords: COVID-19; SARS-CoV-2; reinfection; secondary infection.

Introduction

The efficiency and persistence of protective immunity naturally caused by the coronavirus disease (COVID-19) or vaccination are currently unknown. Some reinfection cases have been reported in different countries **(1)**, but the differentiation between reinfection and viral persistence cases remains a challenge. The detection of two COVID-19 episodes months apart and caused by two different lineages of SARS-CoV-2 remains the most reliable evidence of a reinfection case. On December 9th, the Brazilian MoH recognised the first case of reinfection in the country **(2)**. Here, we describe this classical reinfection case and highlight details about the genomic features of the two COVID-19 episodes. Additionally, we demonstrate that the second episode's virus was related to the new viral variant, hereafter designated B.1.1.28 (E484K), circulating in several states from the South, Northeast, and North Brazilian regions.

Results

Case description

A 37-years-old woman without pre-existing comorbidities, healthcare worker (medical doctor) in Paraíba and resident in Rio Grande do Norte, neighbouring States in Brazilian Northeastern region, reported two clinical episodes of COVID-19. The first one in June and the second one in October 2020, comprising 116 days between the two episodes. On June 17th, the healthcare worker presented symptoms such as headache, runny nose, diarrhea, and myalgia, being classified as a mild COVID-19 case with no complications. The upper respiratory specimen (nasopharyngeal swabs - NPS) was collected from this patient six days later (June 23th). A second NPS was collected on 16th September as follow-up procedure. On October 11th, the patient presented new symptoms such as intense headache, ageusia, anosmia, and fatigue. This second infection was mild and evolved without complications as in the first episode, and a third NPS was collected two days later (October 13th).

This study was approved by the FIOCRUZ-IOC Ethics Committee (68118417.6.0000.5248 and CAAE 32333120.4.0000.5190) and the Brazilian Ministry of Health SISGEN (A1767C3). In addition, the patient reinfected with SARS-CoV-2 read and signed the free and informed consent form.

Diagnostic Laboratory findings

The three NPS samples collected were processed locally; the viral RNA was extracted and tested for SARS-CoV-2 using the real-time RT-PCR for the targets E (3) or N1 and N2 (4). After the diagnostic, Paraíba State Central Public Health Laboratory (LACEN-PB) sent the positive NPS and the serum specimens to the Respiratory Viruses and Measles Laboratory (LVRS) at Fiocruz (MoH National Reference Laboratory and WHO Reference Laboratory for Coronavirus) for confirmation and complementary analysis. Briefly, both positive samples were confirmed using the real-time RT-PCR protocol and the Ag-RDT Panbio COVID-19 Antigen Test (Abbott) directly from the clinical sample. According to the Brazilian MoH Technical Note, to confirm SARS-CoV-2 reinfection, two positive RT-PCR results separated by at least 90 days, independent of clinical conditions are necessary (5). The first and third clinical specimens collected on June 23th and October 13th, 2020, from the healthcare worker were positive for SARS-CoV-2 by real-time RT-PCR, while the second specimen collected on September 16th was negative. Both NPS positive specimens presented a high viral load, presumed by the low cycle threshold (Ct) values in the real time RT-PCR shown in **Table 1**.

Genomic findings

To distinguish between reinfection and long-term viral persistent hypothesis, we recovered the SARS-CoV-2 whole-genomes from the two positive NPS samples (EPI_ISL_792561 and EPI_ISL_792562) from the suspected reinfection case and 76 SARS-CoV-2 positive cases detected in the same state of Paraíba from April 6th to November 27th, 2020 (EPI_ISL_792563 to EPI_ISL_792638). The whole-genomes were recovered using Illumina or ONT Nanopore sequencing protocols previously established and used by Genomic Coronavirus Fiocruz Network to recover high-quality genomes (6,7). The FASTQ reads obtained were imported into the CLC Genomics Workbench version 20.0.4 (Qiagen A/S, Denmark), trimmed, and mapped against the reference sequence EPI_ISL_402124 available in EpiCoV database in the GISAID (<https://www.gisaid.org/>). The alignment was refined using the InDels and Structural Variants module, followed by the Local Realignment module and the final consensus obtained. Maximum Likelihood (ML) phylogenetic analysis of all SARS-CoV-2 whole-genomes from Paraíba was conducted using PhyML8 and revealed two different viral lineages in the two COVID-19 episodes. In the first episode, the lineage B.1.1.33 was detected, whereas lineage B.1.1.28 was detected in the third (second positive) one (**Figure 1**), according to Pangolin lineage classification (9). These SARS-CoV-2 lineages were also detected in other samples from Paraíba state (**Figure 1**) and represent the most prevalent viral variants circulating in Brazil during the early epidemic phase (10,11). Of note, the B.1.1.28 sequences recovered from the reinfection case and from two additional cases in the Paraíba state harbor the E484K substitution (G23012A) in the Spike protein that was recently associated with a novel SARS-CoV-2 B.1.1.28 lineage circulating in Rio de Janeiro state (12).

To better characterize the B.1.1.28 virus present in the second NPS positive sample of the reinfection case, we aligned it against all B.1.1.28 whole-genomes available in the EpiCoV database in GISAID by December 20th, 2020. Additionally, we also selected eight B.1.1.28 whole-genomes from Alagoas (n = 2), Amazonas (n = 1), and Parana (n = 5) states available at the Genomic Coronavirus Fiocruz Network database that also harbor the E484K substitution (EPI_ISL_792560, EPI_ISL_792639, EPI_ISL_792642, EPI_ISL_792645, EPI_ISL_792646, EPI_ISL_792650 to EPI_ISL_792652). The new ML phylogenetic tree revealed that the B.1.1.28

virus from the reinfection case branched in a highly supported (aLRT = 1) sub-clade with two sequences from Paraiba and 44 additional sequences recently sampled (October-December, 2020) in Brazil: 36 sequences from Rio de Janeiro recovered from the EpiCoV database in GISAID and the eight sequences from Alagoas, Parana, and Amazonas states that harbours the mutation S-E484K (Figure 2A). We identified five lineage-defining SNPs: C100U (5'UTR), T10667G (NSP5_L205V), C11824T (NSP6), G23012A (Spike_E484K), and G28628T (N_A119S) that distinguish sequences from the novel B.1.1.28 sub-clade from all other Brazilian B.1.1.28 sequences available. Because of the potential impact of the spike mutation E484K on viral phenotype (**13-16**), we designated this new emerging clade as B.1.1.28(E484K).

To further investigate the spatiotemporal emergence of the novel B.1.1.28(E484K) clade and the viral strain detected in the reinfection case, we conducted a Bayesian phylogeographic analysis of all 47 SARS-CoV-2 Brazilian sequences that branched within such clade. Time-scaled trees were estimated using a strict molecular clock model with a uniform substitution rate prior ($8-10 \times 10^{-4}$ substitutions/site/year), a GTR+I+G nucleotide substitution model, and the Bayesian skyline coalescent prior as implemented in BEAST 1.10 (**17**). Bayesian reconstructions traced the origin of the emerging B.1.1.28(E484K) lineage in the Rio de Janeiro State (PSP = 0.97) on August 27th (95% High Posterior Density [HPD]: July 14th – September 18th) and its subsequent dispersion from Rio de Janeiro to other States from the South (Parana) and Northeast (Alagoas and Paraiba) regions (**Figure 2B**). This phylogeographic reconstruction also supports a dissemination event from Paraiba State to Amazonas State and the branching of the B.1.1.28(E484K) sequence from the reinfection case with that from Amazonas with high support (PP = 1) (**Figure 2B**). The most recent common ancestor of B.1.1.28(E484K) sequences from the reinfection case and the Amazonas state was dated to September 29th (95% HPD: September 14th – October 11th), a few days earlier before the onset of reinfection symptoms (October 11th).

Discussion

We demonstrate that the first case of reinfection recognised by the Brazilian MoH on December 9th corresponds to a primoinfection with the Brazilian lineage B.1.1.33 and a reinfection with a novel emerging B.1.1.28 lineage harboring the mutation E484K in the Spike protein. The age of the common ancestor of the B.1.1.28(E484K) virus present in the second positive sample of the reinfection case and a non-related virus sampled in the Amazonas state provide a maximum limit for the reinfection episode between September 14th and October 11th, thus excluding the possibility of long-term persistence of the B.1.1.28(E484K) virus since primoinfection (before June 23rd, 2020).

Notably, the reinfection case reported here coincides with a recently reported case in the Bahia state that also described a primoinfection and reinfection with the B.1.1.33 and B.1.1.28(E484K) viral variants, respectively (**18**). These studies also confirm that the B.1.1.28(E484K) emerging variant initially described in the Rio de Janeiro state (**12**) is more widely distributed across different Brazilian states. Our analysis supports that the B.1.1.28(E484K) lineage probably emerged in the state of Rio de Janeiro around late August, but defining the precise location and time of emergence of this novel lineage will require a denser sampling from different Brazilian states during the second half of 2020.

The mutation E484K is located in the receptor-binding domain (RBD) and has also been recently described in an independent SARS-CoV-2 lineage rapidly spreading in South Africa (**19**). The rapid dissemination of these variants, combined with the ability of viruses harboring the mutation E484K to escape from neutralizing antibodies (**13-16**), and the recent cases of reinfection with the

B.1.1.28(E484K) lineage detected in Brazil should raise concern about the potential impact of this mutation on infectivity, immune escape, and reinfection.

The findings presented here support that previous exposure to SARS-CoV-2 might not guarantee immunity in all cases. It reinforces the need to maintain the non-pharmacologic protective measures not only by individuals who tested negative, but also for those who already tested positive for SARS-CoV-2. Characterization of the immune response in individuals who presented reinfection with SARS-CoV-2 will be crucial to understand better the role of viral and host factors on this, apparently, rare phenotype.

Acknowledgment

We want to thank the funding support from CGLab/MoH (General Laboratories Coordination of Brazilian Ministry of Health), CVSLR/FIOCRUZ (Coordination of Health Surveillance and Reference Laboratories of Oswaldo Cruz Foundation), CNPq COVID-19 MCTI 402457/2020-0 and 403276/2020-9; INOVA Fiocruz VPPCB-005-FIO-20-2 and VPPCB-007-FIO-18-2-30; FAPERJ: E26/210.196/2020; FAPEAM (PCTI-EmergeSaude/AM call 005/2020 and Rede Genomica de Vigilancia em Saude - REGESAM). We also appreciate the support of all Genomic Coronavirus Fiocruz Network members, the Multi-user Research Facility of Biosafety Level 3 Platform of the Oswaldo Cruz Institute (IOC), Fiocruz, and the CGLab/MoH and Secretary of Surveillance and Health of the Brazilian MoH (SVS-MS). Additionally, we are thankful for all that contribute to the EpiCoV database from the GISAID initiative with high-quality SARS-CoV-2 genomes. All genomes used in this study are described in the acknowledgment **Supplementary Table 1**.

References

1. Babiker A, Marvil C, Waggoner JJ, Collins M, Piantadosi A. The Importance and Challenges of Identifying SARS-CoV-2 Reinfections. *J Clin Microbiol* 2020.
2. Brazilian Ministry of Health. Ministério da Saúde confirma primeiro caso de reinfecção por Covid-19. 10th December, 2020 2020. <https://www.gov.br/saude/pt-br/assuntos/noticias/ministerio-da-saude-confirma-primeiro-caso-de-reinfeccao-por-covid-19> .
3. Biomanginhos FIOCRUZ. Kit Molecular SARS-CoV-2 (informações e consulta de manuais). 15th April, 2020 2020. <https://www.bio.fiocruz.br/index.php/br/produtos/reativos/testes-moleculares/novo-coronavirus-sars-cov2> .
4. Prevention. CfDCa. CDC 2019-Novel Coronavirus (2019-nCoV) Real-Time RT-PCR Diagnostic Panel. 2020; (CDC-006-00019, Revision: 06): 80.
5. Brazilian Ministry of Health Secretaria de Vigilância em Saúde. NOTA TÉCNICA Nº 52/2020-CGPNI/DEIDT/SVS/MS. In: Departamento de Imunização e Doenças Transmissíveis, Imunizações. C-GdPnd, editors. Brasília, DF; 2020. p. 4.
6. Resende PC, Motta FC, Roy S, et al. SARS-CoV-2 genomes recovered by long amplicon tiling multiplex approach using nanopore sequencing and applicable to other sequencing platforms. *bioRxiv* 2020.
7. Nascimento VAD, Corado ALG, Nascimento FOD, et al. Genomic and phylogenetic characterisation of an imported case of SARS-CoV-2 in Amazonas State, Brazil. *Mem Inst Oswaldo Cruz* 2020; 115: e200310.

8. Guindon S, Dufayard JF, Lefort V, Anisimova M, Hordijk W, Gascuel O. New algorithms and methods to estimate maximum-likelihood phylogenies: assessing the performance of PhyML 3.0. *Syst Biol* 2010; 59(3): 307-21.
9. Rambaut A, Holmes EC, O'Toole A, et al. A dynamic nomenclature proposal for SARS-CoV-2 lineages to assist genomic epidemiology. *Nat Microbiol* 2020.
10. Resende P. C. D, E., Gräf T., Mir D., Motta F.C., Appolinario L., Paixão A. C., Mendonça A. C., Ogrzewalska M., Caetano B., Wallau G. L., Docena C., Santos M. C., Ferreira J., Sousa Junior E., Silva S., Fernandes S., Vianna L. A., Souza L., Ferro J. F, Nardy V., Santos C., Riediger I., Debur M., Croda J., Oliveira, W, Abreu A, Bello G... Siqueira M. M. Evolutionary dynamics and dissemination pattern of the SARS-CoV-2 lineage B.1.1.33 during the early pandemic phase in Brazil. *Frontier in Microbiology* 2020.
11. Candido DS, Claro IM, de Jesus JG, et al. Evolution and epidemic spread of SARS-CoV-2 in Brazil. *Science* 2020; 369(6508): 1255-60.
12. Voloch CM, Silva F Rd, de Almeida LGP, et al. Genomic characterization of a novel SARS-CoV-2 lineage from Rio de Janeiro, Brazil. *medRxiv* 2020.
13. Greaney AJ, Loes AN, Crawford KHD, et al. Comprehensive mapping of mutations to the SARS-CoV-2 receptor-binding domain that affect recognition by polyclonal human serum antibodies. *bioRxiv* 2021.
14. Baum A, Fulton BO, Wloga E, et al. Antibody cocktail to SARS-CoV-2 spike protein prevents rapid mutational escape seen with individual antibodies. *Science* 2020; 369(6506): 1014-8.
15. Liu Z, VanBlargan LA, Rothlauf PW, et al. Landscape analysis of escape variants identifies SARS-CoV-2 spike mutations that attenuate monoclonal and serum antibody neutralization. *bioRxiv* 2020.
16. Weisblum Y, Schmidt F, Zhang F, et al. Escape from neutralizing antibodies by SARS-CoV-2 spike protein variants. *Elife* 2020; 9.
17. Suchard MA, Lemey P, Baele G, Ayres DL, Drummond AJ, Rambaut A. Bayesian phylogenetic and phylodynamic data integration using BEAST 1.10. *Virus Evol* 2018; 4(1): vey016.
18. Vasques Nonaka CKMF, M.; Gräf, T.; Almeida Mendes, A.V.; Santana de Aguiar, R.; Giovanetti, M.; Solano de Freitas Souza, B. Genomic Evidence of a Sars-Cov-2 Reinfection Case With E484K Spike Mutation in Brazil. *Preprints* 2021.
19. Tegally H, Wilkinson E, Giovanetti M, et al. Emergence and rapid spread of a new severe acute respiratory syndrome-related coronavirus 2 (SARS-CoV-2) lineage with multiple spike mutations in South Africa. *medRxiv* 2020.

Figures and Tables

Table 1. Epidemiological and laboratorial data of the reinfection SARS-CoV-2 case detected in Northeast of Brazil.



NPS = naso-oropharyngeal swab; Ct = cycle threshold, E = envelope protein, N1 and N2 = nucleoprotein, RP = human RNase P, NA = not applicable; ND = Not detectable.

Figure 01: ML of SARS-CoV-2 whole-genomes sequences from Paraiba. ML phylogenetic tree showing the branching pattern of SARS-CoV-2 whole genome sequences (29779 nt), from Paraiba (n = 77) classified within lineages B.1.1.28 (red), B.1.1.33 (blue), and others B.1.1 (black). Sequences derived from the primo-infection and reinfection are both highlighted with different colors as indicate in the legend at left. Nodes with high statistical (aLRT ≥ 9.0) support are marked by circular shapes.

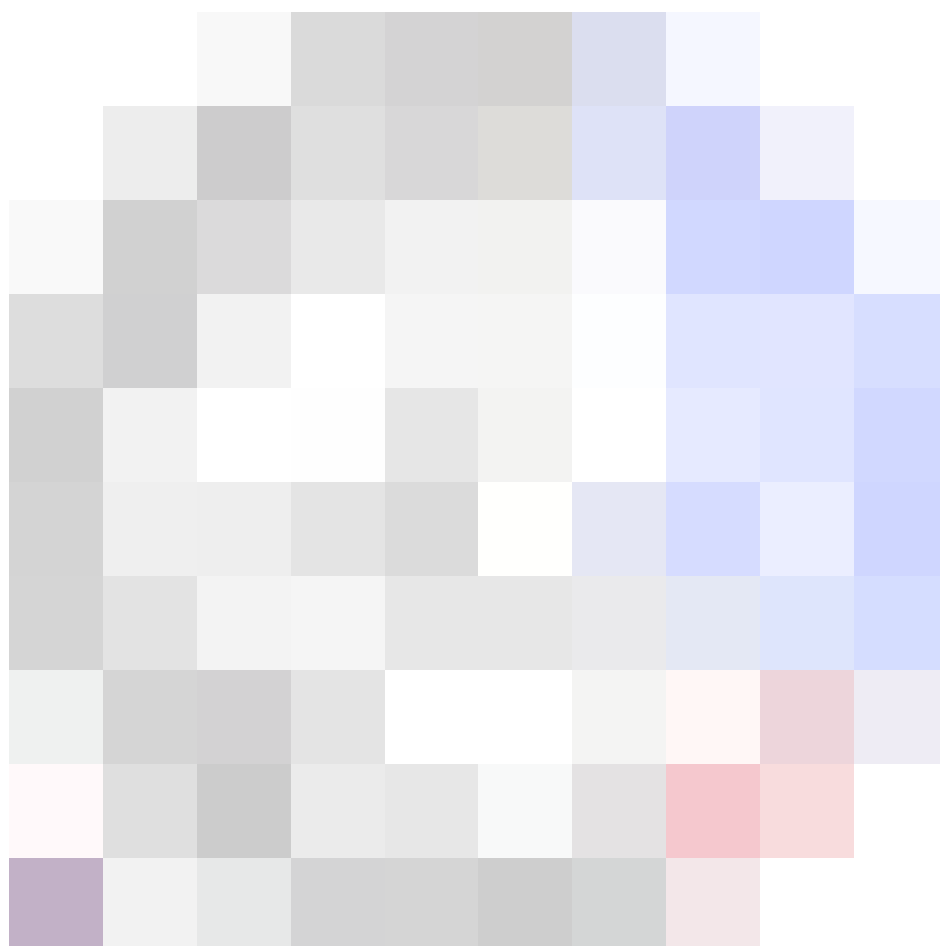


Figure 02: Emergence of the B.1.1.28(E484K) clade. **A.** ML phylogenetic tree of B.1.1.28 SARS-CoV-2 whole genome sequences (29779 nt) from Brazil (n = 376). Shaded box highlights the B.1.1.28(E484K) clade (n = 47) and its statistical support (aLRT = 1.0) is indicated in the cladogram. Sequences from Paraíba and the reinfection case are marked in orange and green, respectively. **B.** Time-scaled Bayesian MCC tree of SARS-CoV-2 whole genome sequences from the B.1.1.28(E484K) clade (n = 47). Branches are colored according to the most probable location state of their descendent nodes as indicated in the legend at right. The five lineage-defining SNPs are indicated at the MCCT root node. Circular shapes mark nodes with high statistical support (PP ≥ 9.0) and a square tip shape indicates the sequence from reinfection case.



Supplementary Materials

Supplementary Table 1. GISAID acknowledgment table [📄 Supplementary Table 1. gisaid_hcov-19_acknowledgement_table_2021_01_10_16.pdf](#) (32.3 KB)

[🔗 Phylogenetic relationship of SARS-CoV-2 sequences from Amazonas with emerging Bra...](#)











ARTICLE



<https://doi.org/10.1038/s41467-020-17367-2>

OPEN

SARS-CoV-2 is transmitted via contact and via the air between ferrets

Mathilde Richard ¹, Adinda Kok ¹, Dennis de Meulder¹, Theo M. Bestebroer¹, Mart M. Lamers ¹, Nisreen M. A. Okba ¹, Martje Fentener van Vlissingen ², Barry Rockx ¹, Bart L. Haagmans ¹, Marion P. G. Koopmans ¹, Ron A. M. Fouchier ¹ & Sander Herfst ¹✉

SARS-CoV-2, a coronavirus that emerged in late 2019, has spread rapidly worldwide, and information about the modes of transmission of SARS-CoV-2 among humans is critical to apply appropriate infection control measures and to slow its spread. Here we show that SARS-CoV-2 is transmitted efficiently via direct contact and via the air (via respiratory droplets and/or aerosols) between ferrets, 1 to 3 days and 3 to 7 days after exposure respectively. The pattern of virus shedding in the direct contact and indirect recipient ferrets is similar to that of the inoculated ferrets and infectious virus is isolated from all positive animals, showing that ferrets are productively infected via either route. This study provides experimental evidence of robust transmission of SARS-CoV-2 via the air, supporting the implementation of community-level social distancing measures currently applied in many countries in the world and informing decisions on infection control measures in healthcare settings.

¹Department of Viroscience, Erasmus University Medical Center, Rotterdam, The Netherlands. ²Erasmus Laboratory Animal Science Center, Erasmus University Medical Center, Rotterdam, The Netherlands. ✉email: s.herfst@erasmusmc.nl

In late December 2019, clusters of patients in China presenting with pneumonia of unknown etiology were reported to the World Health Organization (WHO)¹. The causative agent was rapidly identified as being a virus from the *Coronaviridae* family, closely related to the severe acute respiratory syndrome coronavirus (SARS-CoV)^{2–4}. The SARS-CoV epidemic affected 26 countries and resulted in more than 8000 cases in 2003. The newly emerging coronavirus, named SARS-CoV-2⁵, rapidly spread worldwide and was declared pandemic by the WHO on March 11, 2020⁶. The first evidence suggesting human-to-human transmission came from the descriptions of clusters among the early cases^{7,8}. Based on epidemiological data from China before measures were taken to control the spread of the virus, the reproductive number R_0 (the number of secondary cases directly generated from each case) was estimated to be between 2 and 3^{9–11}. In order to apply appropriate infection control measures to reduce the R_0 , the modes of transmission of SARS-CoV-2 need to be elucidated. Respiratory viruses can be transmitted via direct and indirect contact (via fomites), and through the air via respiratory droplets and/or aerosols. Transmission via respiratory droplets ($>5\ \mu\text{m}$) is mediated by expelled particles that have a propensity to settle quickly and is therefore reliant on close proximity between infected and susceptible individuals, usually within 1 m of the site of expulsion. Transmission via aerosols ($<5\ \mu\text{m}$) is mediated by expelled particles that are smaller in size than respiratory droplets and can remain suspended in the air for prolonged periods of time, allowing infection of susceptible individuals at a greater distance from the site of expulsion¹². Current epidemiological data suggest that SARS-CoV-2 is transmitted primarily via respiratory droplets and contact^{7–9,13,14}, which is used as the basis for mitigation of spread through physical and social distancing measures. However, scientific evidence that SARS-CoV-2 can be efficiently transmitted via the air is weak.

Previous studies have shown that ferrets were susceptible to infection with SARS-CoV^{15–19}, and that SARS-CoV was efficiently transmitted to co-housed ferrets via direct contact¹⁵. Here, we use a ferret transmission model to show that SARS-CoV-2 spreads through direct contact and through the air (via respiratory droplets and/or aerosols).

Results

Transmission of SARS-CoV-2 between ferrets. Individually housed donor ferrets were inoculated intranasally with a strain of SARS-CoV-2 isolated from a German traveller returning from China. Six hours post-inoculation (hpi), a direct contact ferret was added to each of the cages. The next day, indirect recipient ferrets were placed in adjacent cages, separated from the donor cages by two steel grids, 10 cm apart, allowing viruses to be transmitted only via the air (Fig. 1). On alternating days to prevent cross-contamination, throat, nasal and rectal swabs were collected from each ferret in the inoculated and direct contact groups and from the indirect recipient group, followed by SARS-CoV-2 detection by RT-qPCR and virus titration.

Ferrets were productively infected by SARS-CoV-2 upon intranasal inoculation, as demonstrated by the robust and long-term virus shedding from the donor ferrets (Fig. 2, Supplementary Fig. 1). SARS-CoV-2 RNA levels peaked at 3 days post-inoculation (dpi) and were detected up to 11 dpi in two animals and up to 15 and 19 dpi in the other two animals (Fig. 2, Supplementary Fig. 1). SARS-CoV-2 was transmitted to direct contact ferrets in four out of four independent experiments between 1 and 3 days post-exposure (dpe) and viral RNA was detected up to 13–15 days (i.e. 13–17 dpe) (Fig. 2, Supplementary Fig. 1). Interestingly, SARS-CoV-2 was also transmitted via the air to three out of four indirect

recipient ferrets. SARS-CoV-2 RNA was detected from 3 to 7 dpe onwards these indirect recipient ferrets and for 13–19 days (Fig. 2, Supplementary Fig. 1).

Whereas donor ferrets were inoculated with a high virus dose, direct contact and indirect recipient ferrets are likely to have received a low infectious dose via direct contact or via the air. In spite of this, the pattern of virus shedding from the direct contact and indirect recipient ferrets was similar to that of the inoculated donor ferrets, both in terms of duration and SARS-CoV-2 RNA levels, corroborating robust replication of SARS-CoV-2 upon transmission via direct contact and via the air, independent of the infectious dose. In general, higher SARS-CoV-2 RNA levels were detected in the throat swabs as compared to the nasal swabs. SARS-CoV-2 RNA levels in the rectal swabs were overall the lowest. From each SARS-CoV-2 RNA positive animal, infectious virus was isolated in VeroE6 cells from throat and nasal swabs for at least two consecutive days (Supplementary Fig. 2 and Supplementary Table 1). In contrast, no infectious virus was isolated from the rectal swabs. Infectious virus titers ranged from $10^{0.75}$ to $10^{2.75}$ TCID₅₀/ml (median tissue culture infectious dose per ml) in the donor ferrets, from $10^{0.75}$ to $10^{3.5}$ TCID₅₀/ml in the direct contact ferrets and from $10^{0.75}$ to $10^{4.25}$ TCID₅₀/ml in the indirect recipient ferrets. All SARS-CoV-2 positive ferrets seroconverted 21 dpi/dpe, and the antibody levels detected using a receptor binding domain (RBD) enzyme-linked immunosorbent assay (ELISA) were similar in donor, direct contact and indirect recipient ferrets (Fig. 3a). Plaque reduction neutralization titers (PRNT) in sera from indirect recipient ferrets were lower than that of donor and direct contact ferrets, which is probably due to the later onset of virus replication upon transmission via the air and thus a relatively earlier collection of serum after infection (Fig. 3b). The indirect recipient ferret, in which no SARS-CoV-2 was detected, did not seroconvert as expected.

Sequence analysis of viruses isolated from ferrets. MinION (Nanopore) sequencing was used to determine the whole genome consensus sequences of viruses in throat swabs collected from the four donor (all 3 dpi), the four direct contact (all 5 dpe) and three indirect recipient ferrets (7, 9 or 11 dpe). Two substitutions were detected in the consensus sequence of viruses collected from all ferrets as compared to the sequence of the original virus isolate: N501T and S686G, both in the spike protein. Residue 501 is part of the receptor binding motif that mediates contact with angiotensin-converting enzyme 2 (ACE2), the receptor of SARS-CoV-2. A threonine at position 501 (as present in the majority of SARS-CoV viruses) was previously shown to decrease the affinity of the spike protein with the receptor²⁰. Perhaps this substitution emerged in ferrets as a result of adaptation to efficient binding to ferret ACE2. Residue 686 is the first residue after the furin cleavage site. The serine to glycine substitution has not been found in human SARS-CoV-2 sequences, hence the effect of this substitution is unknown. In addition, a L260F substitution in Nsp6 was observed in the throat swab of a direct contact ferret, and two synonymous substitutions (C2910T and C7235T) were detected in an indirect recipient ferret and a direct contact ferret respectively. In order to understand whether the N501T and S686G substitutions were either positively selected in ferrets from existing minority variants in the virus isolate or had mutated in ferrets, Illumina next-generation sequencing was performed on sequential samples from the donor ferrets and on the virus stocks (Supplementary Table 2). Single nucleotide polymorphisms (SNPs) which were present in $>5\%$ of the total number of reads were called (Supplementary Table 2A). The N501T substitution was already present in all donor ferrets at 1 dpi in 14.7%–49.6% of the reads and percentages rapidly increased to 86.4%–98.7% on

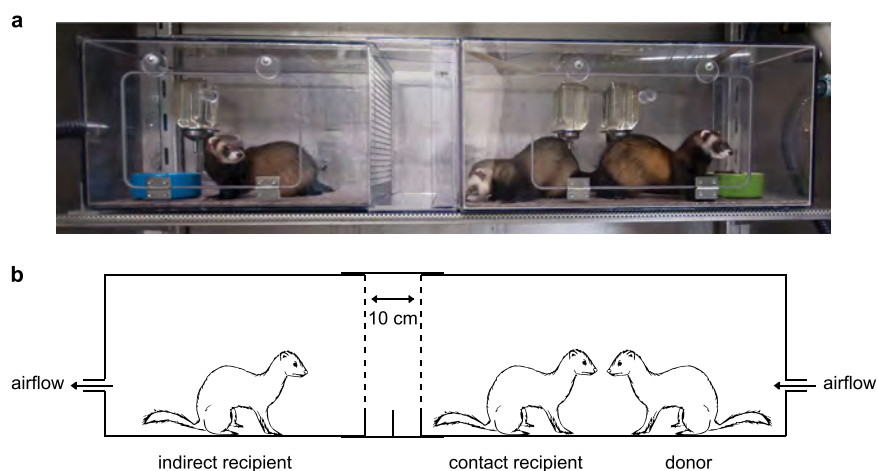


Fig. 1 The ferret transmission experimental set-up. Picture (a) and schematic representation (b) of one independent experimental set-up to assess direct contact transmission and indirect transmission via the air. One inoculated donor ferret is housed in a cage (right-hand side of the picture). Six hours later, a direct contact ferret is added to the same cage as the donor ferret. The next day, an indirect recipient ferret is placed in an opposite cage (left-hand side of the picture) separated by two steel grids, 10 cm apart, to avoid contact transmission. The direction of the air flow (100 L min^{-1}) is indicated by the arrows. The ferret transmission set-ups are placed in class III isolators in a biosafety level 3+ laboratory.

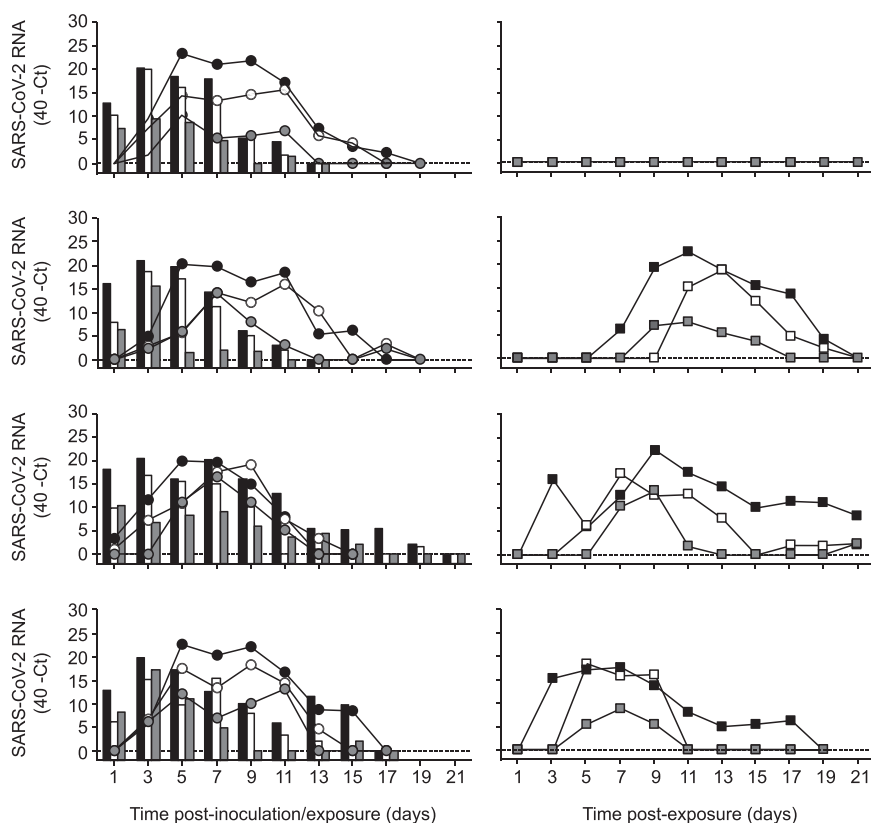


Fig. 2 SARS-CoV-2 shedding in ferrets in the transmission experiment. SARS-CoV-2 viral RNA was detected by RT-qPCR in throat (black), nasal (white) and rectal (grey) swabs collected from inoculated donor ferrets (bars; left panels), direct contact ferrets (circles; left panels) and indirect recipient ferrets housed in separate cages (squares; right panels). Swabs were collected from each ferret every other day until no viral RNA was detected in any of the three swabs. The dotted line indicates the detection limit.

3 dpi. At 7 dpi, the percentages of reads with the N501T substitution were still high, albeit lower in donor ferret 4 (66.2%). A similar trend was observed for the S686G substitution. In addition, an R685H substitution in the spike protein was detected in two ferrets and L207F and L260F substitutions in Nsp6 were detected in individual ferrets, all at low percentages (Supplementary Table 2A). SNP analysis of the virus isolates

demonstrated that S686G was the only substitution that was present in more than 5% of the reads: 8.1% in the passage 3 virus stock used to inoculate donor ferrets and 15.2% in the passage 1 virus isolate from Germany (Supplementary Table 2B). Among the other substitutions observed in the ferret samples, only the R685H substitution was detected at >1% of the reads in the original virus isolate (Supplementary Table 2B).

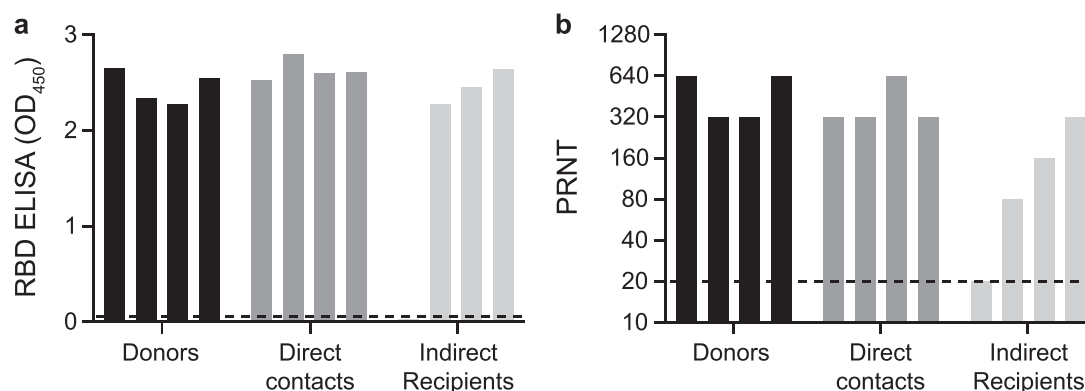


Fig. 3 Antibody responses in donor, direct contact and indirect recipient ferrets 21 dpi/dpe. Sera were collected from the donor, direct contact and indirect recipient ferrets 21 dpi/dpe and IgG responses were assessed using a SARS-CoV-2 receptor binding site (RBD) ELISA (a) and using a plaque reduction neutralization assay (b). The dotted lines indicate the detection limit of the assays. PRNT: plaque reduction neutralization titer. OD: optic density. All presera were tested negative by RBD ELISA and plaque reduction neutralization assay (OD₄₅₀ 0.02–0.05; PRNT < 20).

Discussion

Here, we show that SARS-CoV-2 is transmitted via contact and via the air between ferrets. SARS-CoV-2 transmission in experimental animal models has recently also been described by others. SARS-CoV-2 direct contact transmission between ferrets²¹ and hamsters²² was reported, with similar efficiency as observed in our study. In addition, SARS-CoV-2 was also found to be transmitted via the air in two out of six ferrets²¹, and in two out of six cats²³. However, only low levels of SARS-CoV-2 RNA were detected in nasal washes and feces of the indirect recipient ferrets, and no infectious virus was isolated²¹. Furthermore, virus shedding was shorter as compared to the donor animals and only one out of the two SARS-CoV-2 RNA positive indirect recipient ferrets seroconverted. Similarly, the transmission via the air between cats was not efficient. SARS-CoV-2 RNA was detected in the feces and tissues of one cat at 3 and 11 dpi, respectively and in nasal washes of another cat, but no infectious virus was isolated. Both SARS-CoV-2 RNA positive indirect recipient cats seroconverted. In contrast, the present study showed that SARS-CoV-2 was efficiently transmitted via the air between ferrets, as demonstrated by long-term virus shedding and the presence of infectious virus in the indirect recipient animals, which is comparable to the transmissibility of pandemic influenza viruses in the ferret model²⁴.

To date, there is no evidence of fecal-oral transmission of SARS-CoV-2 in humans. However, the prolonged detection of RNA in consecutive stool samples²⁵ and the environmental contamination of sanitary equipment²⁶ may suggest that the fecal-oral route could be a potential route of transmission of SARS-CoV-2. Here, no infectious virus was retrieved from any of the rectal swabs. Despite this, it cannot be fully excluded that SARS-CoV-2 was also transmitted from donors to direct contact ferrets partly via the fecal-oral route. In the study by Kim et al., ferret fecal material was used to inoculate ferrets, resulting in a productive infection, indicating that infectious SARS-CoV-2 was shed in fecal specimens²¹.

Our experimental system does not allow to assess whether SARS-CoV-2 was transmitted via the air through respiratory droplets, aerosols or both, as donor and indirect recipient ferret cages are placed only 10 cm apart from each other. In a recent study, SARS-CoV-2 remained infectious in aerosols for at least 3 h after aerosolization at high titers in a rotating drum, comparable to SARS-CoV²⁷. Although it is informative to compare the stability of different respiratory viruses in the air, our study provides the additional information that infectious SARS-CoV-2 particles can actually be expelled in the air and subsequently

infect recipients. In two other studies, the presence of SARS-CoV-2 in air samples collected in hospital settings was investigated. However, no SARS-CoV-2 RNA was detected in the air sampled in three isolation rooms²⁶, or 10 cm from a symptomatic patient who was breathing, coughing or speaking²⁸. Nevertheless, RNA was detected on the air exhaust outlet of one of the isolation rooms in the first study, suggesting that virus-laden droplets may be displaced by airflows²⁶.

Here we provide the first experimental evidence that SARS-CoV-2 can be transmitted efficiently via the air between ferrets, resulting in a productive infection and the detection of infectious virus in indirect recipients, as a model for human-to-human transmission. Although additional experiments on the relative contribution of respiratory droplets and aerosols to the transmission of SARS-CoV-2 are warranted, the results of this study corroborate the WHO recommendations about transmission precautions in health care settings and the social distancing measures implemented in many countries around the globe to mitigate the spread²⁹. The ferret transmission model will also be useful to understand transmission dynamics and the molecular basis of the transmissibility of SARS-CoV-2 and other betacoronaviruses, which, in the context of the current SARS-CoV-2 pandemic and future pandemic threats, is clearly of utmost importance.

Methods

Virus and cells. SARS-CoV-2 (isolate BetaCoV/Munich/BavPat1/2020; GISAID ID EPI_ISL_406862; kindly provided by Prof. Dr. C. Drosten) was propagated to passage 3 on VeroE6 cells (ATCC) in Opti-MEM I (1×) + GlutaMAX (Gibco), supplemented with penicillin (10,000 IU mL⁻¹, Lonza) and streptomycin (10,000 IU mL⁻¹, Lonza) at 37 °C in a humidified CO₂ incubator. VeroE6 cells were inoculated at an moi of 0.01. Supernatant was harvested 72 hpi, cleared by centrifugation and stored at -80 °C. The virus stock was tested mycoplasma negative and contained 3.15 × 10⁸ genome copies/ml (RdRp gene).

VeroE6 cells were maintained in Dulbecco modified Eagle medium (DMEM, Gibco) supplemented with 10% foetal calf serum (Greiner), 2 mM of L-glutamine (Gibco), 10 mM Hepes (Lonza), 1.5 mg mL⁻¹ sodium bicarbonate (NaHCO₃, Lonza), penicillin (10,000 IU/mL) and streptomycin (10,000 IU/mL) at 37 °C in a humidified CO₂ incubator. All work was performed in a Class II Biosafety Cabinet under BSL-3 conditions at the Erasmus Medical Center.

Ferret transmission experiment. All relevant ethical regulations for animal testing have been complied with. Animals were housed and experiments were performed in strict compliance with the Dutch legislation for the protection of animals used for scientific purposes (2014, implementing EU Directive 2010/63). Influenza virus, SARS-CoV-2 and Aleutian Disease Virus seronegative 6 month-old female ferrets (*Mustela putorius furo*), weighing 700–1000 g, were obtained from a commercial breeder (TripleF (USA)). Research was conducted under a project license from the Dutch competent authority (license number AVD1010020174312) and the study protocol was approved by the institutional Animal Welfare Body

(Erasmus MC permit number 17-4312-02). Animal welfare was monitored on a daily basis. Virus inoculation of ferrets was performed under anesthesia with a mixture of ketamine/medetomidine (10 and 0.05 mg kg⁻¹, respectively) antagonized by atipamezole (0.25 mg kg⁻¹). Swabs were taken under light anesthesia using ketamine to minimize animal discomfort.

Four donor ferrets were inoculated intranasally with 6×10^5 TCID₅₀ of SARS-CoV-2 virus diluted in 500 µl of phosphate-buffered saline (PBS) (250 µl instilled dropwise in each nostril) and were housed individually in a cage. Six hpi, direct contact ferrets were placed in the same cage as the donor ferrets. One day later, indirect recipient ferrets were placed in an opposite cage separated by two steel grids, 10 cm apart, to avoid contact transmission (Supplementary Fig. S1). The air flow rate from the donor to the recipient ferret was ~100 L min⁻¹ and the temperature of the room was between 21 and 22 °C. Throat, nasal and rectal swabs were collected using dry swabs (Coban, cat. 155CS01) every other day, to prevent cross-contamination, until they were negative for SARS-CoV-2 RNA or maximum for 21 dpi/dpe by determined by real-time RT-qPCR as described below. Swabs were stored at -80 °C in transport medium (Minimum Essential Medium Eagle with Hank's BSS (Lonza), 5 g L⁻¹ lactalbumine enzymatic hydrolysate (Sigma-Aldrich), 10% glycerol (Sigma-Aldrich), 200 U ml⁻¹ of penicillin, 200 mg ml⁻¹ of streptomycin, 100 U ml⁻¹ of polymyxin B sulfate (Sigma-Aldrich), and 250 mg ml⁻¹ of gentamicin (Life Technologies)) for end-point titration in VeroE6 cells as described below. Ferrets were euthanized at 21 dpi/dpe by heart puncture under anaesthesia. Therefore, the exposure duration of direct contact and indirect recipient ferrets was 21 and 20 days respectively. Blood was collected in serum-separating tubes (Greiner) and processed according to the manufacturer's instructions. Sera were heated for 1 h at 60 °C and used for the detection of specific antibodies against SARS-CoV-2 as described below. All animal experiments were performed in class III isolators in a negatively pressurized ABSL3+ facility.

RNA isolation and RT-qPCR. RNA was isolated using an in-house developed high-throughput method in a 96-well format. Sixty µl of sample were added to 90 µl of MagNA Pure 96 External Lysis Buffer (Roche). A known concentration of phocine distemper virus (PDV) was added to the sample as internal control for the RNA extraction³⁰. The 150 µl of sample/lysis buffer was added to a well of a 96-well plate containing 50 µl of magnetic beads (AMPure XP, Beckman Coulter). After thorough mixing by pipetting up and down at least 10 times, the plate was incubated for 15 minutes (min) at room temperature. The plate was then placed on a magnetic block (DynaMag™-96 Side Skirted Magnet (ThermoFisher Scientific)) and incubated for 3 min to allow the displacement of the beads towards the side of the magnet. Supernatants were carefully removed without touching the beads and beads were washed three times for 30 seconds (sec) at room temperature with 200 µl/well of 70% ethanol. After the last wash, a 10 µl multi-channel pipet was used to remove residual ethanol. Plates were air-dried for 6 min at room temperature. Plates were removed from the magnetic block and 30 µl of PCR grade water was added to each well and mixed by pipetting up and down 10 times. Plates were incubated for 5 min at room temperature and then placed back on the magnetic block for 2 min to allow separation of the beads. Supernatants were pipetted in a new plate and RNA was kept at 4 °C. Eight µl of RNA were directly pipetted into a mix for RT-qPCR, containing 0.4 µl of primers and probe mix targeting the E gene of SARS-CoV-2 (forward primer: 5'-ACAGGTACGTTAATAGTTAATAGCGT-3'; reverse primer: 5'-ATATTGCAGCAGTACGCACACA-3'; probe: 5'-FAM-ACACTAGCCATCCTTACTGCGCTTCG-BHQ-3')³¹, 0.4 µl of primers and probe mix targeting the HA gene of PDV (forward primer: 5'-CGGGTGCCCTTTTACAAGAAC-3'; reverse primer: 5'-TTCCTTCCTCAACCTCGTCC-3'; probe: 5'-Cy5-ATGCAAGGGCCAATTCTTCCAAGTT-BHQ-3'), 4 µl of TaqMan™ Fast Virus 1-Step Master Mix (ThermoFisher Scientific) and 6.2 µl of PCR grade water. Amplification and detection was performed on an ABI7700 (ThermoFisher Scientific) using the following program: 5 min 50 °C, 20" 95 °C, [3" 95 °C, 31" 58 °C] × 45 cycles.

Virus titrations. Throat, nasal and rectal swabs were titrated in quadruplicates in VeroE6 cells. Briefly, confluent VeroE6 cells were inoculated with 10-fold serial dilutions of sample in Opti-MEM I (1×) + GlutaMAX, supplemented with penicillin (10,000 IU mL⁻¹), streptomycin (10,000 IU mL⁻¹). At one hpi, the first three dilutions were washed twice with media and fresh media was subsequently added to the whole plate. At six dpi, virus positivity was assessed by reading out cytopathic effects. Infectious virus titers (TCID₅₀/ml) were calculated from four replicates of each throat, nasal and rectal swabs and from 24 replicates of the virus stock using the Spearman-Kärber method.

Serology. Pre-sera (collected before the start of the experiment) and sera collected at 21 dpi/dpe were tested for SARS-CoV-2 antibodies using a receptor binding domain (RBD) enzyme-linked immunosorbent assay (ELISA)³². ELISA plates were coated overnight at 4 °C with 100 ng/well of in-house produced SARS-CoV-2 RBD diluted in PBS. After blocking with Blocker™ BLOTTO in TBS (Life technologies) + 0.01% of Tween-20 (Sigma-Aldrich), heat-inactivated sera (diluted 1:100) were added and incubated for 1 h at 37 °C. Bound antibodies were detected using horseradish peroxidase (HRP)-labelled goat anti-ferret IgG (1:10,000; ab112770, Abcam) and 3,3',5,5'-Tetramethylbenzidine (TMB, Life Technologies) as a substrate. The absorbance of each sample was measured at 450 nm.

Additionally, pre-sera and sera collected at 21 dpi/dpe were tested for the presence of SARS-CoV-2 neutralizing antibodies using a plaque reduction neutralization test (PRNT)³². Heat-inactivated sera were two-fold serially diluted in DMEM supplemented with NaHCO₃, HEPES buffer, penicillin, streptomycin, and 1% fetal bovine serum, starting at a dilution of 1:10 in 50 µL. Fifty µL of diluted virus suspension (400 plaque-forming units) were added and the mixture was incubated for 1 h at 37 °C. The mixtures were then placed on VeroE6 cells and incubated for 8 h. After incubation, cells were fixed with 4% formaldehyde/phosphate-buffered saline (PBS) and stained with a monoclonal mouse anti-SARS-CoV nucleocapsid antibody (1:10,000; 40143-MM05, Sino Biological), and a secondary HRP-labeled goat anti-mouse IgG1 (1:2000; 1071-05, Southern Biotech). HRP was revealed using the 3,3',5,5'-tetramethylbenzidine substrate (True Blue; Kirkegaard and Perry Laboratories) and the number of infected cells per well was assessed by using ImmunoSpot Image Analyzer (CTL Europe GmbH). The plaque reduction neutralization titer (PRNT) was determined as the reciprocal of the highest dilution resulting in a reduction of >90% of the number of infected cells. The detection limit of the assay was <20.

Whole genome sequencing using MinION. A SARS-CoV-2 specific multiplex PCR was performed as recently described³³. In short, primers for 86 overlapping amplicons spanning the entire genome were designed using primal scheme (<http://primal.zibraproject.org/>) (for primer sequences, see Supplementary Table 3). The amplicon length was set to 500 bp with 75 bp overlap between the different amplicons. The libraries were generated using the native barcode kits from Nanopore (EXP-NBD104 and EXP-NBD114 and SQK-LSK109) and sequenced on a MinION R9.4 flow cell multiplexing up to 24 samples per sequence run according to the manufacturer's instructions.

The resulting raw sequence data were demultiplexed using Porechop (<https://github.com/rrwick/Porechop>). FASTQ files were then imported to the CLC Genomics Workbench v20.0.3 (QIAGEN) for analysis. First, sequences were trimmed off 33 base pairs on both the 3' and 5' ends to remove primer sequences and also using a Phred quality score threshold of 8. The trimmed sequences were mapped to the reference sequence (GISAID ID EPI_ISL_406862) with the following default parameters (match score = 1, mismatch cost = 2, insertion cost = 3, length fraction = 0.5 and similarity fraction = 8) and consensus genomes were extracted.

Next-generation sequencing. Amplicons were generated by a SARS-CoV-2 specific multiplex PCR as described above for the whole genome sequencing. Amplicons were purified with 0.8x AMPure XP beads (Beckman Coulter) and 100 ng of DNA was converted into paired-end Illumina sequencing libraries using KAPA HyperPlus library preparation kit (Roche), following the manufacturer's recommendations, to enable subsequent sequencing of multiple libraries in a single Illumina V3 MiSeq flowcell (2×300 cycles). Multiplex Adaptors (KAPA Unique Dual-Indexed Adapters Kit (Roche)) with indexes were used. FASTQ files were then imported to the CLC Genomics Workbench v20.0.3 (QIAGEN) for analysis. First, sequences were trimmed off 33 base pairs on both the 3' and 5' ends to remove primer sequences and also using a Phred quality score threshold of 20. The trimmed sequences were mapped to the reference sequence (GISAID ID EPI_ISL_406862) with the following default parameters (match score = 1, mismatch cost = 2, insertion cost = 3, length fraction = 0.5 and similarity fraction = 8). Variants were called with the Basic Variant Detection tool. Single nucleotide polymorphisms that were present in both the forward and reverse reads with a 200x minimum coverage and a minimum variant count of 10 (5%) were called.

Reporting summary. Further information on research design is available in the Nature Research Reporting Summary linked to this article.

Data availability

All data are available from the corresponding author (S.H.) on reasonable request. Porechop, which was used to demultiplex data from the MinION and Illumina sequencing, is available on github at: <https://github.com/rrwick/Porechop>. The source data underlying Figs. 2, 3, Supplementary Figs. 2 and 3 are provided as a Source data file. The sequencing raw data were deposited in the NCBI Sequence Read Archive (SRA) under the BioProject PRJNA641813. Source data are provided with this paper.

Received: 15 April 2020; Accepted: 25 June 2020;

Published online: 08 July 2020

References

1. WHO. Pneumonia of unknown cause—China. <https://www.who.int/csr/don/05-january-2020-pneumonia-of-unknown-cause-china/en/> (2020).
2. Zhu, N. et al. A Novel coronavirus from patients with pneumonia in China, 2019. *N. Engl. J. Med.* **382**, 727–733 (2020).
3. WHO. Novel Coronavirus—China. <https://www.who.int/csr/don/12-january-2020-novel-coronavirus-china/en/> (2020).

4. Zhou, P. et al. A pneumonia outbreak associated with a new coronavirus of probable bat origin. *Nature* **579**, 270–273 (2020).
5. Coronaviridae Study Group of the International Committee on Taxonomy of V. The species severe acute respiratory syndrome-related coronavirus: classifying 2019-nCoV and naming it SARS-CoV-2. *Nat. Microbiol.* **5**, 536–544 (2020).
6. WHO. WHO Director-General's opening remarks at the media briefing on COVID-19—11 March 2020. <https://www.who.int/dg/speeches/detail/who-director-general-s-opening-remarks-at-the-media-briefing-on-covid-19-11-march-2020> (2020).
7. Chan, J. F. et al. A familial cluster of pneumonia associated with the 2019 novel coronavirus indicating person-to-person transmission: a study of a family cluster. *Lancet* **395**, 514–523 (2020).
8. Huang, C. et al. Clinical features of patients infected with 2019 novel coronavirus in Wuhan, China. *Lancet* **395**, 497–506 (2020).
9. Li, Q. et al. Early Transmission Dynamics in Wuhan, China, of Novel Coronavirus-Infected Pneumonia. *N. Engl. J. Med.* **382**, 1199–1207 (2020).
10. Riou, J. & Althaus, C.L. Pattern of early human-to-human transmission of Wuhan 2019 novel coronavirus (2019-nCoV), December 2019 to January 2020. *Euro Surveill.* **25**, 2000058 (2020).
11. Wu, J. T., Leung, K. & Leung, G. M. Nowcasting and forecasting the potential domestic and international spread of the 2019-nCoV outbreak originating in Wuhan, China: a modelling study. *Lancet* **395**, 689–697 (2020).
12. Kutter, J. S., Spronken, M. I., Fraaij, P. L., Fouchier, R. A. & Herfst, S. Transmission routes of respiratory viruses among humans. *Curr. Opin. Virol.* **28**, 142–151 (2018).
13. Liu, J. et al. Community transmission of severe acute respiratory syndrome coronavirus 2, Shenzhen, China, 2020. *Emerg. Infect. Dis.* **26**, 1320–1323 (2020).
14. Burke, R. M. et al. Active monitoring of persons exposed to patients with confirmed COVID-19 - United States, January–February 2020. *MMWR Morb. Mortal. Wkly Rep.* **69**, 245–246 (2020).
15. Martina, B. E. et al. Virology: SARS virus infection of cats and ferrets. *Nature* **425**, 915 (2003).
16. ter Meulen, J. et al. Human monoclonal antibody as prophylaxis for SARS coronavirus infection in ferrets. *Lancet* **363**, 2139–2141 (2004).
17. Weingartl, H. et al. Immunization with modified vaccinia virus Ankara-based recombinant vaccine against severe acute respiratory syndrome is associated with enhanced hepatitis in ferrets. *J. Virol.* **78**, 12672–12676 (2004).
18. Chu, Y. K. et al. The SARS-CoV ferret model in an infection-challenge study. *Virology* **374**, 151–163 (2008).
19. van den Brand, J. M. et al. Pathology of experimental SARS coronavirus infection in cats and ferrets. *Vet. Pathol.* **45**, 551–562 (2008).
20. Shang, J. et al. Structural basis of receptor recognition by SARS-CoV-2. *Nature* **581**, 221–224 (2020).
21. Kim, Y.I. et al. Infection and rapid transmission of SARS-CoV-2 in ferrets. *Cell Host Microbe*. **27**, 704–709.e2 (2020).
22. Chan, J.F. et al. Simulation of the clinical and pathological manifestations of Coronavirus Disease 2019 (COVID-19) in golden Syrian hamster model: implications for disease pathogenesis and transmissibility. *Clin. Infect. Dis.* <https://doi.org/10.1093/cid/ciaa325> (2020).
23. Shi, J. et al. Susceptibility of ferrets, cats, dogs, and other domesticated animals to SARS-coronavirus 2. *Science* **368**, 1016–1020 (2020).
24. Munster, V. J. et al. Pathogenesis and transmission of swine-origin 2009 A (H1N1) influenza virus in ferrets. *Science* **325**, 481–483 (2009).
25. Wu, Y. et al. Prolonged presence of SARS-CoV-2 viral RNA in faecal samples. *Lancet. Gastroenterol. Hepatol.* **5**, 434–435 (2020).
26. Ong, S.W.X. et al. Air, surface environmental, and personal protective equipment contamination by severe acute respiratory syndrome coronavirus 2 (SARS-CoV-2) from a symptomatic patient. *JAMA* **323**, 1610–1612 (2020).
27. van Doremalen, N. et al. Aerosol and surface stability of SARS-CoV-2 as compared with SARS-CoV-1. *N. Engl. J. Med.* **382**, 1564–1567 (2020).
28. Cheng, V.C.C. et al. Escalating infection control response to the rapidly evolving epidemiology of the Coronavirus disease 2019 (COVID-19) due to SARS-CoV-2 in Hong Kong. *Infect. Control Hosp. Epidemiol.* **41**, 493–498 (2020).
29. WHO. Modes of transmission of virus causing COVID-19: implications for IPC precaution recommendations. <https://www.who.int/news-room/commentaries/detail/modes-of-transmission-of-virus-causing-covid-19-implications-for-ipc-precaution-recommendations> (2020).
30. van Doornum, G. J., Schutten, M., Voermans, J., Guldemeester, G. J. & Niesters, H. G. Development and implementation of real-time nucleic acid amplification for the detection of enterovirus infections in comparison to rapid culture of various clinical specimens. *J. Med. Virol.* **79**, 1868–1876 (2007).
31. Corman, V.M. et al. Detection of 2019 novel coronavirus (2019-nCoV) by real-time RT-PCR. *Euro Surveill.* **25**, 2000045 (2020).
32. Okba, N.M.A. et al. Severe acute respiratory syndrome coronavirus 2-specific antibody responses in coronavirus disease 2019 patients. *Emerg. Infect. Dis.* **26**, 1478–1488 (2020).
33. Oude Munnink, B.B. et al. Rapid SARS-CoV-2 whole genome sequencing for informed public health decision making in the Netherlands. Preprint at <https://www.biorxiv.org/content/biorxiv/early/2020/04/25/2020.04.21.050633.full.pdf> (2020).

Acknowledgements

We thank Prof. Dr. Christian Drosten (Charité—Universitätsmedizin Berlin) for providing the SARS-CoV-2 isolate used in this study and Drs Rik de Swart and Mathieu Sommers for their help with animal ethics and study approval and Dr. Bas Oude Munnink for providing the protocol of the Minion sequencing. This work was supported by European Union's Horizon 2020 research and innovation program VetBioNet (grant agreement No 731014) and NIH/NIAID (contract number HHSN272201400008C). S.H. was funded in part by an NWO VIDI grant (contract number 91715372).

Author contributions

M.R. and S.H. conceived, designed, analysed and performed the work. M.R. and S.H. wrote the manuscript. A.K., D.M., T.B., M.L., and N.O. helped with performing the work. M.F.V., B.R., B.H., M.K., and R.A.M.F. helped with the design of the work, interpretation of the data and manuscript revision. All authors read and approved the final manuscript.

Competing interests

The authors declare no competing interests.

Additional information

Supplementary information is available for this paper at <https://doi.org/10.1038/s41467-020-17367-2>.

Correspondence and requests for materials should be addressed to S.H.

Peer review information *Nature Communications* thanks the anonymous reviewers for their contribution to the peer review of this work. Peer reviewer reports are available.

Reprints and permission information is available at <http://www.nature.com/reprints>

Publisher's note Springer Nature remains neutral with regard to jurisdictional claims in published maps and institutional affiliations.



Open Access This article is licensed under a Creative Commons Attribution 4.0 International License, which permits use, sharing, adaptation, distribution and reproduction in any medium or format, as long as you give appropriate credit to the original author(s) and the source, provide a link to the Creative Commons license, and indicate if changes were made. The images or other third party material in this article are included in the article's Creative Commons license, unless indicated otherwise in a credit line to the material. If material is not included in the article's Creative Commons license and your intended use is not permitted by statutory regulation or exceeds the permitted use, you will need to obtain permission directly from the copyright holder. To view a copy of this license, visit <http://creativecommons.org/licenses/by/4.0/>.

© The Author(s) 2020

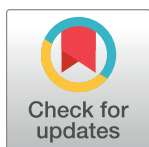
RESEARCH ARTICLE

Children's emotion inferences from masked faces: Implications for social interactions during COVID-19

Ashley L. Ruba ^{*}, Seth D. Pollak

Department of Psychology and Waisman Center, University of Wisconsin – Madison, Madison, Wisconsin, United States of America

^{*} ruba@wisc.edu



Abstract

To slow the progression of COVID-19, the Centers for Disease Control (CDC) and the World Health Organization (WHO) have recommended wearing face coverings. However, very little is known about how occluding parts of the face might impact the emotion inferences that children make during social interactions. The current study recruited a racially diverse sample of school-aged (7- to 13-years) children from publicly funded after-school programs. Children made inferences from facial configurations that were not covered, wearing sunglasses to occlude the eyes, or wearing surgical masks to occlude the mouth. Children were still able to make accurate inferences about emotions, even when parts of the faces were covered. These data suggest that while there may be some challenges for children incurred by others wearing masks, in combination with other contextual cues, masks are unlikely to dramatically impair children's social interactions in their everyday lives.

OPEN ACCESS

Citation: Ruba AL, Pollak SD (2020) Children's emotion inferences from masked faces: Implications for social interactions during COVID-19. PLoS ONE 15(12): e0243708. <https://doi.org/10.1371/journal.pone.0243708>

Editor: Zezhi Li, National Institutes of Health, UNITED STATES

Received: September 24, 2020

Accepted: November 29, 2020

Published: December 23, 2020

Peer Review History: PLOS recognizes the benefits of transparency in the peer review process; therefore, we enable the publication of all of the content of peer review and author responses alongside final, published articles. The editorial history of this article is available here: <https://doi.org/10.1371/journal.pone.0243708>

Copyright: © 2020 Ruba, Pollak. This is an open access article distributed under the terms of the [Creative Commons Attribution License](https://creativecommons.org/licenses/by/4.0/), which permits unrestricted use, distribution, and reproduction in any medium, provided the original author and source are credited.

Data Availability Statement: The raw data and analysis code are available from the Open Science Framework (doi: [10.17605/OSF.IO/7FYX9](https://doi.org/10.17605/OSF.IO/7FYX9)).

Funding: SDP was supported by the National Institute of Mental Health (R01 MH61285) and a

Introduction

COVID-19 is one of the worst pandemics in modern history. To slow the spread of the virus, both the Centers for Disease Control and the World Health Organization have recommended wearing face coverings in public spaces. This recommendation has led to speculation and concern about the ramifications of mask wearing on emotion communication [1, 2]. Of particular concern for parents and teachers is how wearing masks might impact children's social interactions [3, 4]. While much research has documented how children infer emotions from facial configurations and how this ability predicts children's social and academic competence [5–7], uncertain is how children make these inferences when part of the face is occluded by a mask. The current study explores how children draw emotional inferences from faces partially occluded by surgical masks and, as a comparison, sunglasses.

Paper and cloth “surgical” masks cover the lower half of the face, allowing the eyes, eyebrows, and forehead to remain visible. When asked to infer emotions from stereotypical facial configurations, adults tend to look at the eyes first and more frequently than other facial features (e.g., mouth, nose) [8–10], although scan patterns vary across cultures [11, 12]. Adults

core grant to the Waisman Center from the National Institute of Child Health and Human Development (U54 HD090256). ALR was supported by an Emotion Research Training Grant (T32 MH018931) from the National Institute of Mental Health. Funders did not play any role in study design, data collection and analysis, decision to publish, or preparation of the manuscript.

Competing interests: The authors have declared that no competing interests exist.

also show above-chance accuracy at inferring emotions from stereotypical facial configurations when only the eyes are visible [13–15]. (Note: Across most studies, “accuracy” refers to whether participants select the label/emotion typically associated with a particular facial configuration, such as “anger” for a face with furrowed brows and a tight mouth). Humans are particularly sensitive to eyes [16], and thus, eye musculature may convey sufficient information for adults to make reasonably accurate emotional inferences, even when masks cover the mouth and nose.

Nevertheless, focusing on the eyes alone may be insufficient for some emotion inferences [11, 17]. When facial configurations are ambiguous or subtle, adults (and children) shift their attention between the eyes and other facial features that may provide additional diagnostic information [18]. For instance, to make inferences about whether wide eyes indicate “fear” or “surprise,” adults attend to both the eyes and the mouth [19, 20]. Adults also tend to fixate on specific facial features that characterize specific emotion stereotypes, such as the mouth for happiness and the nose for disgust [8–10, 21]. Inferring emotions from these characteristic facial features (e.g., labeling a smile as “happy”) is also influenced by other parts of the face [10, 22–24]. In short, adults scan facial configurations in a holistic manner [19, 25], allowing for information to be gleaned from the mouth, nose, and other parts of the face, which are not accessible when wearing a mask.

While this research suggests how adults infer emotions when parts of the face are obscured, much less is known about how this process emerges in early childhood [7]. In the first year of life, infants shift from configural to holistic processing of faces [26, 27] and demonstrate heightened attention to eyes associated with positive affective states [28–30]. By 3-years of age, children show above-chance accuracy at inferring emotions from the eyes alone [31]. However, compared to when other parts of the face are also visible, 5- to 10-year-olds are less accurate at inferring emotions from the eyes only [32–35], although results for specific emotions have been inconsistent across studies [32, 33]. One study even found that 3- to 4-year-olds were *more accurate* at inferring happiness, sadness, and surprise from faces when the eyes were *covered* by sunglasses [35]. With respect to emotion inferences with masks, only one study has obscured the mouth (with a dark circle). Roberson et al. (2012) found that 9- to 10-year-old children and adults showed more accurate emotion inferences for uncovered faces than when the mouth was covered. However, 3- to 8-year-olds did not show these impairments. Similarly, when facial configurations are presented within a background emotion context, 12-year-olds show heightened visual attention to faces compared to 4- and 8-year-olds [18]. Thus, there may be developmental differences in children's reliance on and use of specific facial features to make emotional inferences and the impact of mask wearing on these inferences.

Current study

The current study examines how 7- to 13-year-old children draw emotional inferences from facial configurations that are partially occluded. This age range was selected because there is a shift during this time in children's use of eye information to infer others' emotions [33, 35]. Facial configurations associated with different negative emotions (i.e., sadness, anger, fear) were presented via a Random Image Structure Evolution (RISE) paradigm [36]. Facial configurations were initially presented in a highly degraded format in which children only had access to partial facial information. In a dynamic sequence, the images became less degraded at regular intervals. After each interval, children selected from an array of emotion labels to indicate their belief about how the person displaying the facial configuration was feeling. Thus, this paradigm allows for the assessment of children's emotion inferences from incomplete through

more complete facial information. This approach is more similar to daily experiences with the unfolding of others' emotions compared to a single presentation of a facial configuration at full intensity [37].

We examined how children perceived others' emotions as partial information about the face was presented, to evaluate whether masks meaningfully changed the types of inferences children made. We included sunglasses as a comparison for other types of coverings that children regularly encounter on faces in their daily lives. Together, these results shed light on how mask wearing during COVID-19 might—or might not—influence children's inferences about others' emotions and their related social interactions.

Methods

Participants

Procedures were approved by the University of Wisconsin—Madison Institutional Review Board. To test a racially diverse sample of children, participants were recruited from publicly funded after-school programs associated with the Dane County (Wisconsin) Department of Human Services. The final sample included 81 7- to 13-year-old children (37 female, $M = 9.86$ years, $SD = 1.84$ years, range = 7.06–12.98 years). Parents identified their children as Black (53%, $n = 43$), White (41%, $n = 33$), and Multi-racial (6%, $n = 5$). Three additional children participated in the study but were excluded from final analyses due to missing or corrupt data files. A power analysis confirmed that this sample size would be sufficient to detect reliable differences in a within-subjects design, assuming a medium effect size ($f = .25$) at the .05 level [36].

Stimuli

Stimuli, selected from the Matsumoto and Ekman (1988) database, were pictures of stereotypical facial configurations associated with sadness, anger, and fear posed by male and female models. These three emotions were selected given that adults tend to fixate predominantly on the eyes for these facial configurations, rather than other parts of the face (e.g., the mouth and nose, as with happiness and disgust) [8, 20]. Further, negative emotions are complex and rich in informational value [38]; yet, these emotions have received limited empirical attention in the literature on emotion perception development [39–41]. Pictures were presented in unaltered format (i.e., with no covering) or digitally altered to be (a) covered with a surgical face mask that obscured the mouth and nose, or (b) covered with sunglasses that obscured the eyes and eyebrows (see Fig 1). Pictures of each emotion (sad, anger, fear) paired with each covering type (none, mask, shades) were presented twice in a random order (i.e., 18 stimuli total). Half of the presentations were on male faces and half were on female faces.

Procedure

Parents provided written consent and children provided verbal assent prior to participation. Children were tested in a modified Random Image Structure Evolution (RISE) paradigm [36]. RISE performs pairwise exchanges of pixels in an image until the target image dissolves into an unstructured random field. These exchanges are presented in reverse order such that participants begin viewing a random visual display that gradually transforms into a fully formed, clear image (see Fig 2). Importantly, the RISE protocol holds the low-level perceptual attributes of the original image (e.g., luminance, color) constant.

Children viewed these image sequences on a high-resolution touch-sensitive color monitor. Faces were initially presented in a highly degraded format. At 14 regular 3.3-s intervals, the images became less degraded and easier to discern. After each interval, children were



Fig 1. Example stimuli by covering. From top to bottom: none, mask, shades. From left to right: sad, anger, fear. The image is from a set of photographs entitled *Japanese and Caucasian Facial Expressions of Emotion (JACFEE)* by D. Matsumoto and P. Ekman, University of California, San Francisco, 1988. Copyright 1988 by D. Matsumoto and P. Ekman. Reprinted by permission.

<https://doi.org/10.1371/journal.pone.0243708.g001>

prompted to identify the emotion depicted on the face by selecting one of the following emotion labels: “happy,” “sad,” “angry,” “surprised,” “afraid,” or “disgusted.” Labels were presented in this order on the screen, and children touched a label to indicate their response. A total of 252 responses were collected for each child (i.e., 14 trials each of 18 stimuli). Responses were coded as “accurate” if the child selected the label/emotion typically associated with a particular facial configuration (i.e., “anger” for a face with furrowed brows).

Results

All analyses were conducted in *R* [42], and figures were produced using the package *ggplot2* [43]. Alpha was set at $p < .05$. The raw data and analysis code are available on OSF: doi.org/10.17605/OSF.IO/7FYX9. Children's accuracy scores were analyzed in a 3 (Emotion: sad / anger / fear) x 3 (Covering: none / mask / shades) x 14 (Trial: 1 to 14) repeated-measures ANCOVA with child Gender as a between-subjects factor and child Age as a covariate. All significant main effects and interactions are explored below.



Fig 2. Example test sequence. Anger (no covering) is pictured. The image is from a set of photographs entitled *Japanese and Caucasian Facial Expressions of Emotion (JACFEE)* by D. Matsumoto and P. Ekman, University of California, San Francisco, 1988. Copyright 1988 by D. Matsumoto and P. Ekman. Reprinted by permission.

<https://doi.org/10.1371/journal.pone.0243708.g002>

Are children more accurate with anger, sadness, or fear?

The main effect of Emotion, $F(2, 154) = 30.46, p < .001, \eta_p^2 = .28$, showed that children were more accurate with facial configurations associated with sadness ($M = .36, SD = .48$) compared to anger ($M = .27, SD = .44, t(80) = 4.10, p < .001, d = .46, CI_{95\%} [.04, .13]$), or fear ($M = .19, SD = .39, t(80) = 7.39, p < .001, d = .82, CI_{95\%} [.12, .21]$). Children were also more accurate with facial configurations associated with anger compared to fear, $t(80) = 3.68, p < .001, d = .41, CI_{95\%} [.04, .12]$.

A similar pattern of results was seen in the Emotion x Trial interaction, $F(14, 1091) = 5.35, p < .001, \eta_p^2 = .06$, which was explored with 95% confidence intervals (estimated with bootstrapping, Fig 3). Unsurprisingly, children became more accurate with each emotion as the images became less obscured. In earlier trials, there were few differences between the stimuli. In later trials, children were more accurate with facial configurations associated with sadness compared to anger and fear, and children were more accurate with facial configurations associated with anger compared to fear.

Are children less accurate with the eyes or mouth covered?

The primary question addressed by this study is whether masks meaningfully degraded children's ability to infer others' emotions. The main effect of Covering, $F(2, 154) = 27.19, p < .001, \eta_p^2 = .26$, showed that children were more accurate when faces were uncovered ($M = .34, SD = .47$) compared to when the faces wore a mask ($M = .24, SD = .43, t(80) = 6.57, p < .001, d = .73, CI_{95\%} [.07, .13]$), or shades ($M = .24, SD = .43, t(80) = 6.24, p < .001, d = .69, CI_{95\%} [.07, .13]$). Accuracy between the faces that wore masks and shades did not differ, $t(80) = .20, p >$

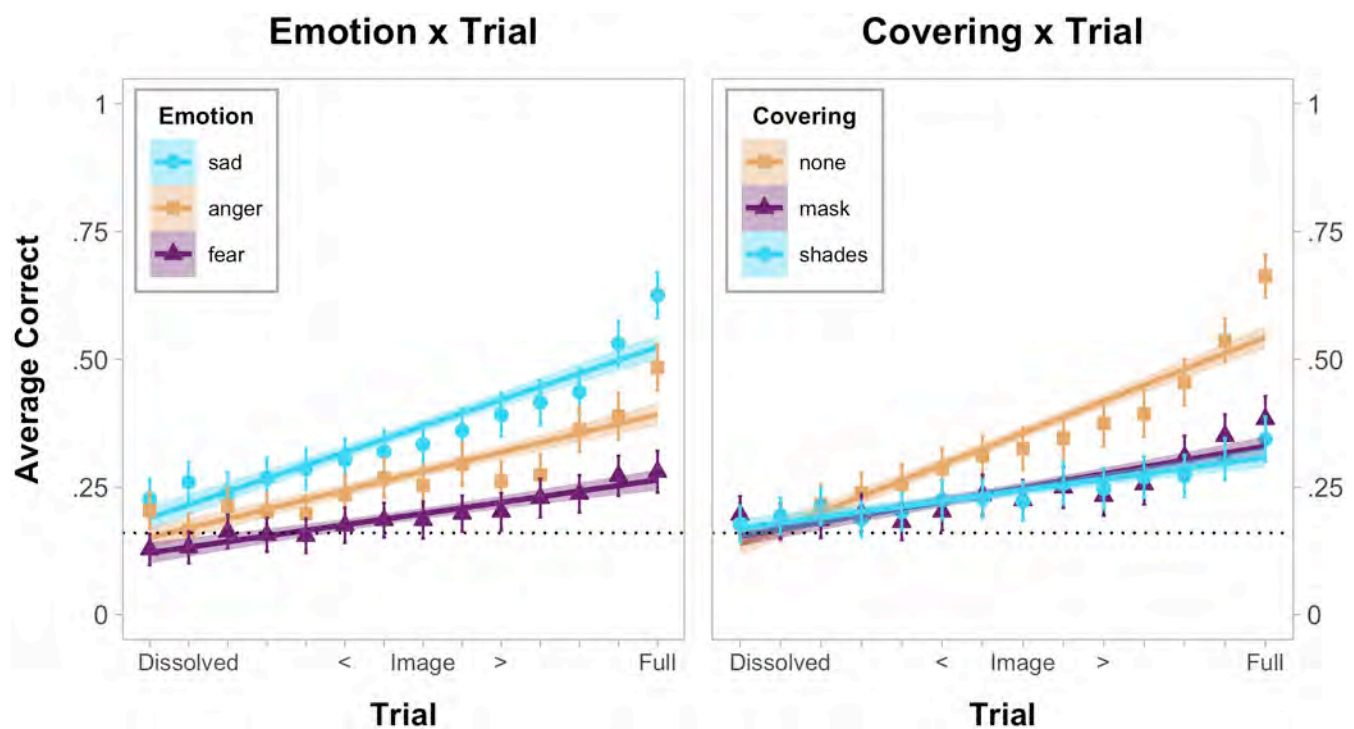


Fig 3. Linear regression and means for emotion x trial and covering x trial interactions. The dotted line indicates chance responding (1/6). Confidence intervals (95%) were estimated with bootstrapping (1,000 bootstrap estimates resampled 81 times from mean participant accuracy).

<https://doi.org/10.1371/journal.pone.0243708.g003>

.25, $d = .02$, $CI_{95\%}[-.03, .03]$. A similar pattern of results was seen in the Covering x Trial interaction, $F(18, 1372) = 10.27$, $p < .001$, $\eta_p^2 = .12$, which was also explored with 95% confidence intervals (estimated with bootstrapping, Fig 3). Yet, the overall effect of face coverings on accuracy was relatively small, especially as children gained more visual information.

How do different coverings impact children's inferences for specific emotions?

To explore the Emotion x Covering interaction, $F(4, 284) = 3.58$, $p = .009$, $\eta_p^2 = .04$, paired t -tests were conducted between each covering type, separated by emotion (Fig 4). Further, to examine if children's performance was greater than chance ($m = 1/6$) for each emotion-covering pair, additional one-sample t -tests were conducted. Bonferroni-holm corrections were applied for multiple comparisons (reported p -values are corrected).

For facial configurations associated with sadness, children were less accurate when the faces wore masks ($M = .28$, $SD = .45$) compared to when the faces had no covering ($M = .43$, $SD = .49$), $t(80) = 4.60$, $p < .001$, $d = .51$, $CI_{95\%} [.08, .21]$. Children's accuracy did not differ when the faces wore shades ($M = .37$, $SD = .48$) compared to when the faces had no covering, $t(80) = 1.91$, $p = .12$, $d = .21$, $CI_{95\%} [.00, .12]$, or wore masks $t(80) = 2.47$, $p = .063$, $d = .27$, $CI_{95\%} [.02, .16]$. Children responded with above-chance accuracy for all coverings: none, $t(80) = 10.30$, $p < .001$, $d = 1.14$, $CI_{95\%} [.38, .47]$; mask, $t(80) = 4.77$, $p < .001$, $d = .53$, $CI_{95\%} [.23, .33]$, shades, $t(80) = 7.23$, $p < .001$, $d = .80$, $CI_{95\%} [.31, .42]$.

For facial configurations associated with anger, children were less accurate when the faces wore masks ($M = .27$, $SD = .44$) compared to when the faces had no covering ($M = .34$, $SD = .48$), $t(80) = 2.72$, $p = .041$, $d = .30$, $CI_{95\%} [.02, .13]$. Children were also less accurate when the faces wore shades ($M = .20$, $SD = .40$) compared to when the faces had no covering, $t(80) = 5.01$, $p < .001$, $d = .56$, $CI_{95\%} [.09, .20]$. Children's accuracy when the faces wore masks or shades did not differ, $t(80) = 2.16$, $p = .10$, $d = .24$, $CI_{95\%} [.01, .13]$. Children only responded

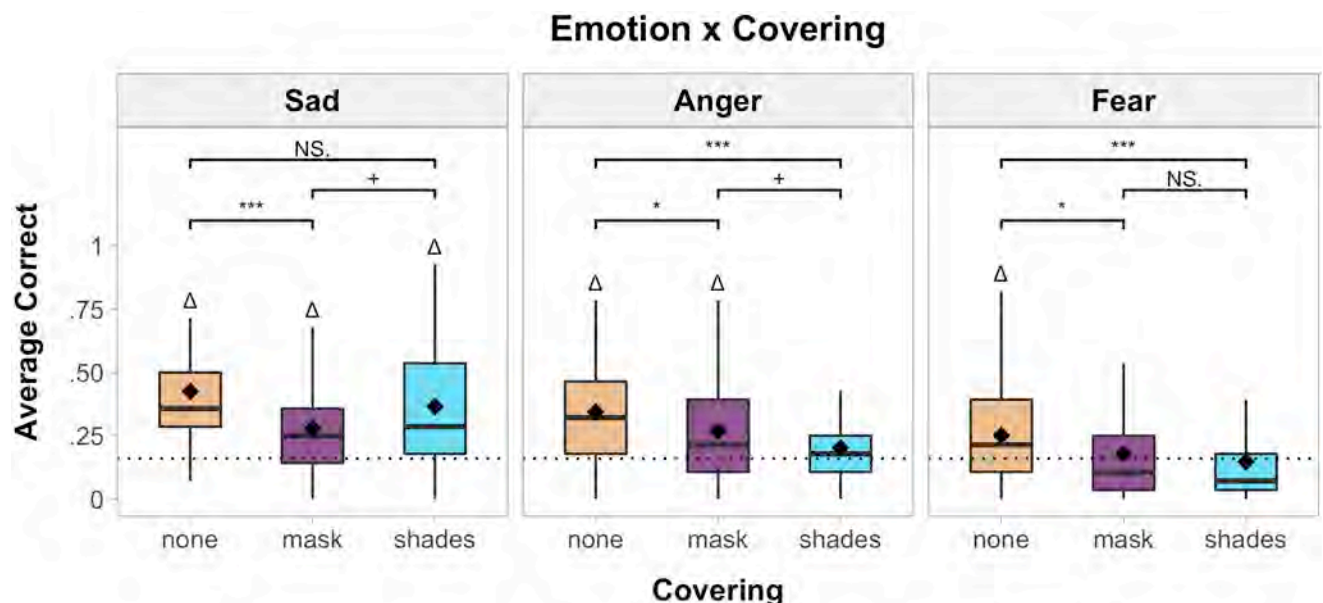


Fig 4. Boxplots for the emotion x covering interaction. * indicates comparisons between covering types for each emotion (* $p < .05$, *** $p < .001$, + $p < .10$, NS = not significant with Bonferroni-Holm corrections). The dotted line indicates chance responding (1/6). Δ indicates that accuracy was significantly greater than chance ($p < .05$ with Bonferroni-Holm corrections).

<https://doi.org/10.1371/journal.pone.0243708.g004>

with above-chance accuracy when the faces had no covering, $t(80) = 7.28, p < .001, d = .81$, $CI_{95\%} [.30, .39]$, or when the faces wore masks, $t(80) = 4.50, p < .001, d = .50$, $CI_{95\%} [.22, .31]$. Children did not respond with above-chance accuracy when the faces wore shades, $t(80) = 1.77, p = .24, d = .20$, $CI_{95\%} [.16, .24]$.

For facial configurations associated with fear, children were less accurate when the faces wore masks ($M = .18, SD = .38$) compared to when the faces had no covering ($M = .25, SD = .43$), $t(80) = 2.91, p = .028, d = .32$, $CI_{95\%} [.02, .12]$. Children were also less accurate when the faces wore shades ($M = .15, SD = .35$) compared to when the faces had no covering, $t(80) = 3.96, p < .001, d = .44$, $CI_{95\%} [.05, .16]$. Children's accuracy when the faces wore masks or shades did not differ, $t(80) = 1.09, p > .25, d = .12$, $CI_{95\%} [-.02, .09]$. Children only responded with above-chance accuracy when the faces had no covering, $t(80) = 3.85, p < .001, d = .43$, $CI_{95\%} [.21, .30]$. Children did not reach above-chance accuracy when the faces wore masks, $t(80) = .50, p > .25, d = .06$, $CI_{95\%} [.13, .22]$, or shades, $t(80) = .94, p > .25, d = .10$, $CI_{95\%} [.11, .19]$.

Thus, across all emotions, children were less accurate with faces that wore a mask compared to faces that were not covered. However, children were only less accurate with faces that wore sunglasses compared to uncovered for two emotions: anger and fear. This suggests that children inferred whether the face displayed sadness from mouth shape alone, whereas the information from the eye region was necessary for forming inferences about anger and fear (see below). Ultimately, accuracy differences between the masks and shades did not significantly differ for any emotion. Thus, while both types of coverings negatively impacted children's emotion inferences, the strongest impairments were observed for facial configurations associated with fear.

What inferences did children make for each stimulus? To further investigate why children did not reach above-chance responding for the *anger-shades*, *fear-mask*, and *fear-shades* stimuli, we examined children's responses to each stimulus. As seen in Fig 5, children tended to interpret facial configurations associated with fear as "surprised." This effect was particularly pronounced when the faces were covered by a mask. Children also tended to interpret facial configurations associated with anger as "sad" when the faces were covered by shades. In contrast, children interpreted facial configurations associated with sadness as "sad," regardless of covering.

How does children's accuracy differ based on age?

The main effect of Age, $F(1, 78) = 5.85, p = .018, \eta_p^2 = .07$, showed that accuracy improved as child age increased. The Age x Trial, $F(6, 474) = 2.40, p = .027, \eta_p^2 = .03$, interaction was explored with a simple slopes analysis. This analysis revealed that older children showed enhanced performance over the course of the experiment compared to younger children (Fig 6).

How does children's accuracy differ based on gender?

Although there was not a significant main effect of Gender, $F(1, 78) = .54, p > .25, \eta_p^2 = .01$, a Gender x Emotion interaction emerged, $F(2, 154) = 3.20, p = .044, \eta_p^2 = .04$. Follow-up comparisons showed that male participants were significantly more accurate with facial configurations associated with anger ($M = .30, SD = .46$) compared to female participants ($M = .24, SD = .42$), $t(79) = 2.28, p = .025, d = .51$, $CI_{95\%} [.01, .12]$. Accuracy for facial configurations associated with sadness, $t(79) = 1.25, p = .22, d = .28$, $CI_{95\%} [-.03, .11]$, or fear, $t(79) = .53, p > .25, d = .12$, $CI_{95\%} [-.08, .05]$, did not differ based on participant gender.

Discussion

These results highlight how children's social interactions may be minimally impacted by mask wearing during the COVID-19 pandemic. Positive social interactions are predicated on the

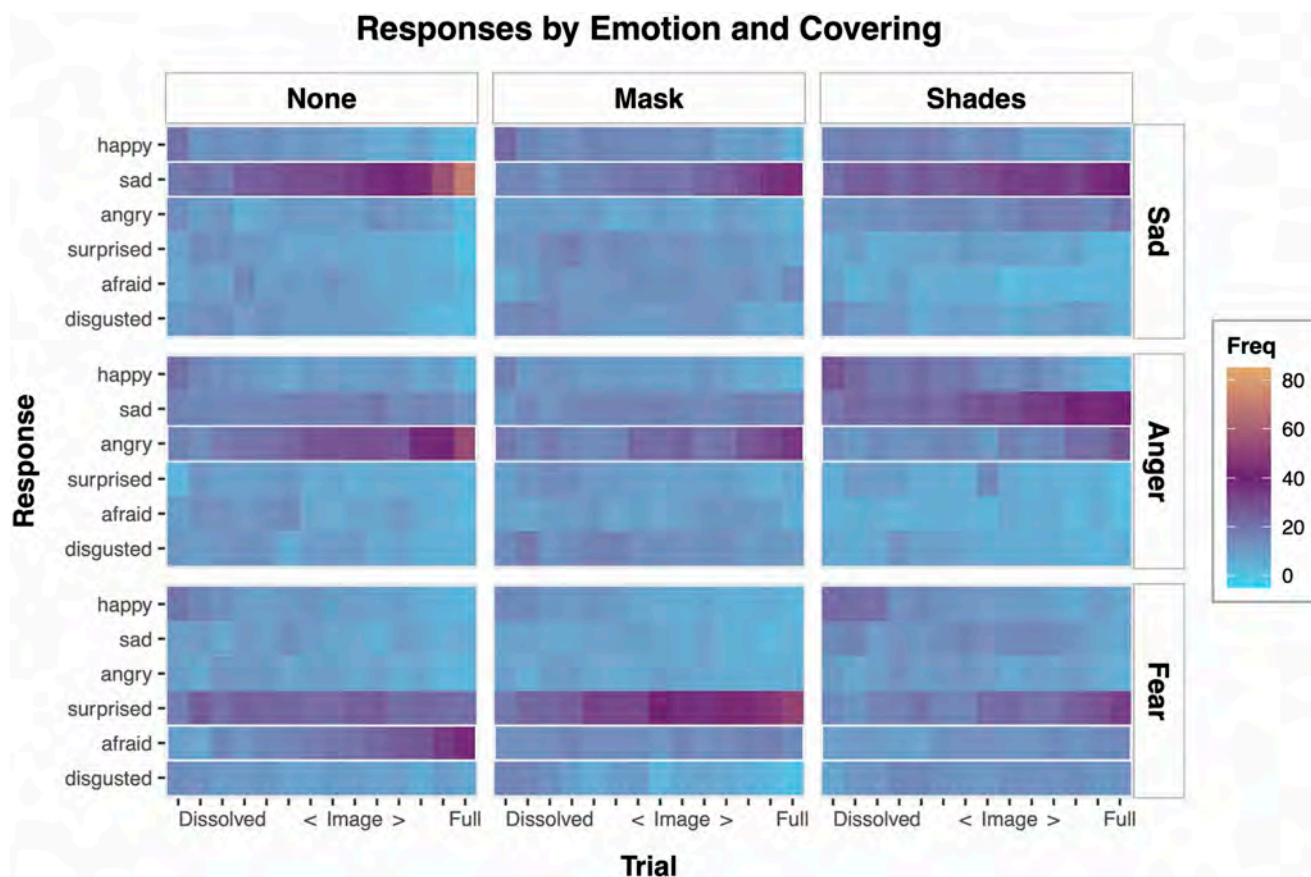


Fig 5. Average frequency of responses for each emotion and covering as a function of trial. The expected ("accurate") response for each stimulus is outlined in white.

<https://doi.org/10.1371/journal.pone.0243708.g005>

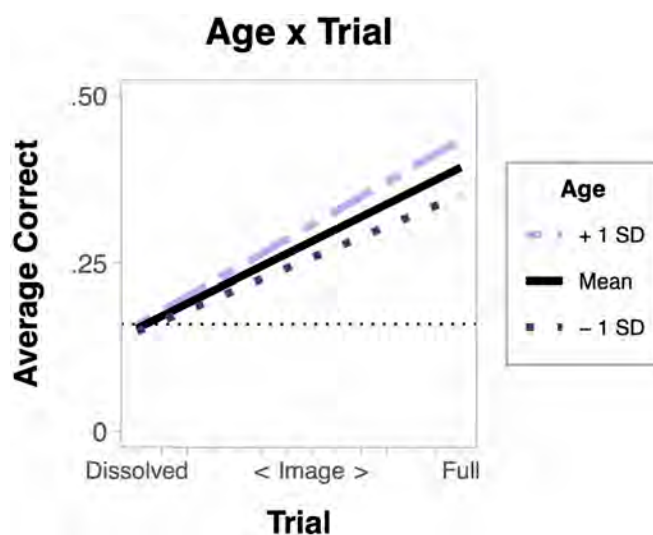


Fig 6. Simple slopes analysis for age x trial interaction. The dotted line indicates chance responding (1/6).

<https://doi.org/10.1371/journal.pone.0243708.g006>

ability to accurately infer and respond to others' emotions. In the current study, children's emotion inferences about faces that wore masks compared to when faces were not covered were still above chance. Masks seem to have the greatest effect on children's inferences about facial configurations associated with "fear," which were commonly identified as "surprised" when the mouth and nose were covered. Thus, although children may require more visual facial information to infer emotions with masks, children may reasonably infer whether someone wearing a mask is sad or angry, based on the eye region alone. In addition, children's accuracy with masked facial configurations did not significantly differ from their accuracy with facial configurations that wore sunglasses—a common accessory that children encounter in their everyday lives. Thus, it appears that masks do not negatively impact children's emotional inferences to a greater degree than sunglasses. In sum, children's ability to infer and respond to another person's emotion, and their resulting social interactions, may not be dramatically impaired by mask wearing during the COVID-19 pandemic.

Furthermore, in everyday life, it is unlikely that children draw emotional inferences from facial configurations alone. For instance, the same facial configuration may be inferred as either "anger" or "disgust" depending on background context, body posture, and facial coloration [18, 44, 45]. In addition, dynamic facial configurations and faces that are vocalizing are scanned differently than silent, static pictures of faces [46–48]. Ultimately, facial configurations displayed in everyday life are more dependent on context, less consistent, and less specific than pictures of stereotyped emotions commonly used in laboratory tasks [37]. The current paradigm improves upon these standard laboratory tasks by assessing children's emotion inferences from incomplete facial information. However, the key to children's emotional inferences is the ability to learn about and navigate the tremendous variability inherent in human emotion [7, 49]. In everyday life, children may be able to use additional contextual cues to make reasonably accurate inferences about others' variable emotional cues, even if others are wearing masks.

Future research should take these considerations into account when designing and interpreting findings on mask wearing during the COVID-19 pandemic. While the current study assessed whether children made "accurate" emotion inferences, a single facial configuration can be interpreted in many ways that are "accurate" given a particular context [37]. Researchers could explore how children make emotion inferences from a wider variety of non-stereotyped emotional cues that are presented in context. Although we did not find many age effects in the current study, future research could also explore how younger children's social interactions are impacted by mask wearing, particularly infants who are actively learning about others' emotions [50]. To conclude, while there may be some loss of emotional information due to mask wearing, children can still infer emotions from faces, and likely use many other cues to make these inferences. This suggests that children, and adults, may be able to adapt to the new reality of mask wearing to have successful interactions during this unprecedented health crisis.

Author Contributions

Conceptualization: Seth D. Pollak.

Formal analysis: Ashley L. Ruba.

Funding acquisition: Seth D. Pollak.

Investigation: Seth D. Pollak.

Methodology: Seth D. Pollak.

Project administration: Seth D. Pollak.

Resources: Seth D. Pollak.

Visualization: Ashley L. Ruba.

Writing – original draft: Ashley L. Ruba.

Writing – review & editing: Ashley L. Ruba, Seth D. Pollak.

References

- Fortin J. Masks Keep Us Safe. They Also Hide Our Smiles. [Internet]. The New York Times. 2020 [cited 2020 Jun 23]. <https://www.nytimes.com/2020/06/23/style/face-mask-emotion-coronavirus.html>
- Ong S. How face masks affect our communication [Internet]. British Broadcasting Corporation (BBC) News. 2020 [cited 2020 Jun 8]. <https://www.bbc.com/future/article/20200609-how-face-masks-affect-our-communication>
- Katz R, Hadani HS. Are you happy or sad? How wearing face masks can impact children's ability to read emotions. Brookings Inst [Internet]. 2020; <https://www.brookings.edu/blog/education-plus-development/2020/04/21/are-you-happy-or-sad-how-wearing-face-masks-can-impact-childrens-ability-to-read-emotions/>
- Klass P. Do Masks Impede Children's Development? [Internet]. The New York Times. 2020. <https://www.nytimes.com/2020/09/14/well/family/Masks-child-development.html>
- Denham SA, Bassett HH, Zinsler K, Wyatt TM. How Preschoolers' Social-Emotional Learning Predicts Their Early School Success: Developing Theory-Promoting, Competency-Based Assessments. *Infant Child Dev* [Internet]. 2014 Jul; 23(4):426–54. Available from: <http://doi.wiley.com/10.1002/icd.1840>
- Izard CE, Fine S, Schultz D, Mostow A, Ackerman BP, Youngstrom EA. Emotion knowledge as a predictor of social behavior and academic competence in children at risk. *Psychol Sci* [Internet]. 2001; 12(1):18–23. Available from: <http://journals.sagepub.com/doi/10.1111/1467-9280.00304> PMID: 11294223
- Ruba AL, Pollak SD. The development of emotion reasoning in infancy and early childhood. *Annu Rev Dev Psychol*. 2020; 2:22.1–22.29.
- Eisenbarth H, Alpers GW. Happy mouth and sad eyes: Scanning emotional facial expressions. *Emotion*. 2011; 11(4):860–5. <https://doi.org/10.1037/a0022758> PMID: 21859204
- Scheller E, Büchel C, Gamer M. Diagnostic Features of Emotional Expressions Are Processed Preferentially. Whitney D, editor. *PLoS One* [Internet]. 2012 Jul 25; 7(7):e41792. Available from: <https://dx.plos.org/10.1371/journal.pone.0041792> PMID: 22848607
- Schyns PG, Petro LS, Smith ML. Transmission of facial expressions of emotion co-evolved with their efficient decoding in the brain: Behavioral and brain evidence. *PLoS One*. 2009; 4(5). <https://doi.org/10.1371/journal.pone.0005625> PMID: 19462006
- Jack RE, Blais C, Scheepers C, Schyns PG, Caldara R. Cultural Confusions Show that Facial Expressions Are Not Universal. *Curr Biol* [Internet]. 2009; 19(18):1543–8. Available from: <http://dx.doi.org/10.1016/j.cub.2009.07.051> PMID: 19682907
- Haensel JX, Danvers M, Ishikawa M, Itakura S, Tucciarelli R, Smith TJ, et al. Culture modulates face scanning during dyadic social interactions. *Sci Rep*. 2020; 10(1):1–11. <https://doi.org/10.1038/s41598-019-56847-4>
- Kret ME, de Gelder B. Islamic headdress influences how emotion is recognized from the eyes. *Front Psychol*. 2012; 3(APR):1–13. <https://doi.org/10.3389/fpsyg.2012.00110> PMID: 22557983
- Kret ME, Fischer AH. Recognition of facial expressions is moderated by Islamic cues. *Cogn Emot*. 2018; 32(3):623–31. <https://doi.org/10.1080/02699931.2017.1330253> PMID: 28566058
- Fischer AH, Gillebaart M, Rotteveel M, Becker D, Vliek M. Veiled emotions: The effect of covered faces on emotion perception and attitudes. *Soc Psychol Personal Sci*. 2012; 3(3):266–73.
- Grossmann T. The eyes as windows into other minds: An integrative perspective. *Perspect Psychol Sci*. 2017; 12(1):107–21. <https://doi.org/10.1177/1745691616654457> PMID: 28073330
- Wegrzyn M, Vogt M, Kirecliglu B, Schneider J, Kissler J. Mapping the emotional face. How individual face parts contribute to successful emotion recognition. *PLoS One*. 2017; 12(5):1–15. <https://doi.org/10.1371/journal.pone.0177239> PMID: 28493921
- Leitzke BT, Pollak SD. Developmental changes in the primacy of facial cues for emotion recognition. *Dev Psychol* [Internet]. 2016 Apr; 52(4):572–81. Available from: <http://doi.apa.org/getdoi.cfm?doi=10.1037/a0040067> PMID: 26784383

19. Green C, Guo K. Factors contributing to individual differences in facial expression categorisation. *Cogn Emot* [Internet]. 2018; 32(1):37–48. Available from: <http://dx.doi.org/10.1080/02699931.2016.1273200> PMID: 28032518
20. Smith ML, Cottrell GW, Gosselin F, Schyns PG. Transmitting and decoding facial expressions. *Psychol Sci*. 2005; 16(3):184–9. <https://doi.org/10.1111/j.0956-7976.2005.00801.x> PMID: 15733197
21. Kanat M, Heinrichs M, Schwarzwald R, Domes G. Oxytocin Attenuates Neural Reactivity to Masked Threat Cues from the Eyes. *Neuropsychopharmacology*. 2015; 40(2):287–95. <https://doi.org/10.1038/npp.2014.183> PMID: 25047745
22. Jack RE, Garrod OGB, Schyns PG. Dynamic facial expressions of emotion transmit an evolving hierarchy of signals over time. *Curr Biol* [Internet]. 2014; 24(2):187–92. Available from: <http://dx.doi.org/10.1016/j.cub.2013.11.064> PMID: 24388852
23. Leppänen JM, Hietanen JK. Is there more in a happy face than just a big smile? *Vis cogn*. 2007; 15(4):468–90.
24. Calvo MG, Fernández-Martín A. Can the eyes reveal a person's emotions? Biasing role of the mouth expression. *Motiv Emot*. 2013; 37(1):202–11.
25. Bombari D, Schmid PC, Schmid Mast M, Birri S, Mast FW, Lobmaier JS. Emotion recognition: The role of featural and configural face information. *Q J Exp Psychol*. 2013; 66(12):2426–42. <https://doi.org/10.1080/17470218.2013.789065> PMID: 23679155
26. Cohen LB, Cashon CH. Do 7-month-old infants process independent features or facial configurations? *Infant Child Dev*. 2001; 10(1–2):83–92.
27. Schwarzer G, Zauner N, Jovanovic B. Evidence of a shift from featural to configural face processing in infancy. *Dev Sci*. 2007; 10(4):452–63. <https://doi.org/10.1111/j.1467-7687.2007.00599.x> PMID: 17552935
28. Jessen S, Altvater-Mackensen N, Grossmann T. Pupillary responses reveal infants' discrimination of facial emotions independent of conscious perception. *Cognition* [Internet]. 2016; 150:163–9. Available from: <http://dx.doi.org/10.1016/j.cognition.2016.02.010> PMID: 26896901
29. Jessen S, Grossmann T. Unconscious discrimination of social cues from eye whites in infants. *Proc Natl Acad Sci* [Internet]. 2014; 111(45):16208–13. Available from: <http://www.pnas.org/lookup/doi/10.1073/pnas.1411333111> PMID: 25349392
30. Krol KM, Monakhov M, Lai PS, Ebstein RP, Grossmann T. Genetic variation in CD38 and breastfeeding experience interact to impact infants' attention to social eye cues. *Proc Natl Acad Sci* [Internet]. 2015; 112(39):E5434–42. Available from: <http://www.pnas.org/lookup/doi/10.1073/pnas.1506352112> PMID: 26371313
31. Franco F, Itakura S, Pomorska K, Abramowski A, Nikaido K, Dimitriou D. Can children with autism read emotions from the eyes? The Eyes Test revisited. *Res Dev Disabil* [Internet]. 2014; 35(5):1015–26. Available from: <http://dx.doi.org/10.1016/j.ridd.2014.01.037> PMID: 24636022
32. Gagnon M, Gosselin P, Maassarani R. Children's ability to recognize emotions from partial and complete facial expressions. *J Genet Psychol*. 2014; 175(5):416–30. <https://doi.org/10.1080/00221325.2014.941322> PMID: 25271818
33. Guarnera M, Hichy Z, Cascio MI, Carrubba S. Facial expressions and ability to recognize emotions from eyes or mouth in children. *Eur J Psychol*. 2015; 11(2):183–96. <https://doi.org/10.5964/ejop.v11i2.890> PMID: 27247651
34. Kestenbaum R. Feeling happy versus feeling good: The Processing of discrete and global categories of emotional expressions by children and adults. *Dev Psychol*. 1992; 28(6):1132–42.
35. Roberson D, Kikutani M, Döge P, Whitaker L, Majid A. Shades of emotion: What the addition of sunglasses or masks to faces reveals about the development of facial expression processing. *Cognition* [Internet]. 2012; 125(2):195–206. Available from: <http://dx.doi.org/10.1016/j.cognition.2012.06.018> PMID: 22892280
36. Pollak SD, Sinha P. Effects of early experience on children's recognition of facial displays of emotion. *Dev Psychol* [Internet]. 2002; 38(5):784–91. Available from: <http://doi.apa.org/getdoi.cfm?doi=10.1037/0012-1649.38.5.784> PMID: 12220055
37. Barrett LF, Adolphs R, Marsella S, Martinez AM, Pollak SD. Emotional expressions reconsidered: Challenges to inferring emotion from human facial movements. *Psychol Sci Public Interes* [Internet]. 2019; 20(1):1–68. Available from: <http://journals.sagepub.com/doi/10.1177/1529100619832930> PMID: 31313636
38. Vaish A, Grossmann T, Woodward AL. Not all emotions are created equal: The negativity bias in social-emotional development. *Psychol Bull*. 2008; 134(3):383–403. <https://doi.org/10.1037/0033-2909.134.3.383> PMID: 18444702

39. Ruba AL, Repacholi BM. Do preverbal infants understand discrete facial expressions of emotion? *Emot Rev.* 2019;
40. Ruba AL, Meltzoff AN, Repacholi BM. How do you feel? Preverbal infants match negative emotions to events. *Dev Psychol* [Internet]. 2019; 55(6):1138–49. Available from: <http://doi.apa.org/getdoi.cfm?doi=10.1037/dev0000711> PMID: 30829508
41. Ruba AL, Meltzoff AN, Repacholi BM. The development of negative event-emotion matching in infancy: Implications for theories in affective science. *Affect Sci* [Internet]. 2020; 1(1):4–19. Available from: <http://dx.doi.org/10.1007/s42761-020-00005-x>
42. R Core Team. R: A language and environment for statistical computing [Internet]. Vienna, Austria: R Foundation for Statistical Computing; 2014. <http://www.r-project.org/>
43. Wickham H. *ggplot2: elegant graphics for data analysis*. New York: Springer; 2009.
44. Aviezer H, Hassin RR, Ryan J, Grady C, Susskind J, Anderson A, et al. Angry, disgusted, or afraid? Studies on the malleability of emotion perception. *Psychol Sci.* 2008; 19(7):724–32. <https://doi.org/10.1111/j.1467-9280.2008.02148.x> PMID: 18727789
45. Thorstenson CA, Pazda AD, Young SG, Elliot AJ. Face color facilitates the disambiguation of confusing emotion expressions: Toward a social functional account of face color in emotion communication. *Emotion.* 2019; 19(5):799–807. <https://doi.org/10.1037/emo0000485> PMID: 30080074
46. Blais C, Fiset D, Roy C, Régimbald CS. Supplemental Material for Eye Fixation Patterns for Categorizing Static and Dynamic Facial Expressions. *Emotion.* 2017; 17(7):1107–19.
47. Rigoulot S, Pell MD. Emotion in the voice influences the way we scan emotional faces. *Speech Commun* [Internet]. 2014; 65:36–49. Available from: <http://dx.doi.org/10.1016/j.specom.2014.05.006>
48. Morin-Lessard E, Poulin-Dubois D, Segalowitz N, Byers-Heinlein K. Selective attention to the mouth of talking faces in monolinguals and bilinguals aged 5 months to 5 years. *Dev Psychol.* 2019; 55(8):1640–55. <https://doi.org/10.1037/dev0000750> PMID: 31169400
49. Plate RC, Wood A, Woodard K, Pollak SD. Probabilistic learning of emotion categories. *J Exp Psychol Gen* [Internet]. 2019 Oct; 148(10):1814–27. Available from: <http://doi.apa.org/getdoi.cfm?doi=10.1037/xge0000529> PMID: 30570327
50. Ruba AL, Repacholi BM. Beyond language in infant emotion concept development. *Emot Reivew.* 2020;

Medical News & Perspectives

As Their Numbers Grow, COVID-19 “Long Haulers” Stump Experts

Rita Rubin, MA

For 32-year-old Hanna Lockman of Louisville, Kentucky, it all started March 12. She was at work when she suddenly felt a stabbing pain in her chest.

“It just got worse and worse and worse, to the point I was crying from the pain,” she recalled in a recent interview. At 3 AM, the pain sent her to the emergency department. “I had developed a dry cough, maybe a mild fever. I don’t remember.”

Five months, 16 emergency department trips, and 3 short hospitalizations later, Lockman can’t remember a lot of things. She places the blame squarely on coronavirus disease 2019 (COVID-19).

“I joke, ‘Well, COVID has eaten my brain, because I can’t remember how to remember words, keep track of medication,’” she said. “My brain just feels like there’s a fog.”

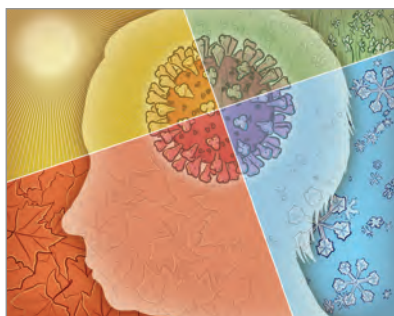
Lockman considers herself to be a “long hauler,” someone who still hasn’t fully recovered from COVID-19 weeks or even months after symptoms first arose. She serves as an administrator of 2 “Long Haul COVID Fighters” Facebook groups, whose members now number more than 8000.

The longer the pandemic drags on, the more obvious it becomes that for some patients, COVID-19 is like the unwelcome houseguest who won’t pack up and leave.

“Anecdotally, there’s no question that there are a considerable number of individuals who have a postviral syndrome that really, in many respects, can incapacitate them for weeks and weeks following so-called recovery and clearing of the virus,” Anthony Fauci, MD, director of the National Institute of Allergy and Infectious Diseases, said in July during a COVID-19 webinar organized by the International AIDS Society.

That appeared to be the case with the first severe acute respiratory syndrome (SARS), which emerged in 2002 and was also caused by a coronavirus. Some people who were hospitalized with SARS still had impaired lung function 2 years after their symptoms began, according to a prospective study of 55 patients in Hong Kong. But only 8096 people were diagnosed with SARS worldwide—a fraction of the COVID-19 cases reported each day in the US alone.

In a recent *JAMA* research letter, 125 of 143 Italian patients ranging in age from 19 to 84 years still experienced physician-confirmed COVID-19-related symptoms an average of 2 months after their first symptom emerged. All had been hospitalized, with their stays averaging about 2 weeks; 80% hadn’t received any form of ventilation.



Physicians at a Paris hospital recently reported that they saw an average of 30 long haulers every week between mid-May, when the COVID-19 lockdown ended in France, and late July. The patients’ average age was around 40 years, and women outnumbered men 4 to 1.

As with SARS, many COVID-19 long haulers are health care workers who had massive exposure to the virus early in the pandemic, neuroimmunologist Avindra Nath, MD, of the National Institute of Neurological Disorders and Stroke (NINDS), noted in a recent editorial.

Overall, approximately 10% of people who’ve had COVID-19 experience prolonged symptoms, a UK team estimated in a recently published *Practice Pointer* on postacute COVID-19 management. And yet, the authors wrote, primary care physicians have little evidence to guide their care.

Puzzling Persistence

Adults with severe illness who spend weeks in intensive care, often intubated, can experience long-lasting symptoms, but that’s not unique to patients with COVID-19. What’s unusual about the long haulers is that many initially had mild to moderate symptoms that didn’t require lengthy hospitalization—if any—let alone intensive care.

“Most of the patients that I see who are suffering from [post-COVID-19] syndrome were not hospitalized,” Jessica Dine, MD, a pulmonary specialist at the University of Pennsylvania Perelman School of Medicine, said in an interview. “They were pretty sick, but still at home.”

Why some previously healthy, often young, adults still haven’t recovered from the disease has stymied physicians.

“We in the medical field are very accustomed to taking care of respiratory syncytial virus and other pneumoviruses in young adults,” Wesley Self, MD, MPH, an emergency medicine physician at Vanderbilt University Medical Center, said in an interview. With those infections, “people feel pretty sick for 2 to 3 days, and then they feel markedly better.”

But COVID-19 is another matter, Self and his coauthors found in a recent study of 292 individuals with the disease who did not require hospitalization. “One of the goals of this particular study was to understand those with mild symptoms,” Self said. “This was an understudied group.”

More than a third of them hadn’t returned to their usual state of health 2 to 3 weeks after testing positive, the researchers wrote in the *Morbidity and Mortality Weekly Report*. The older the patients, the more likely they were to say they their pre-COVID-19 health hadn’t come back. But even a quarter of the youngest, those aged 18 to 34 years, said they had not yet regained their health.

“That certainly was a surprise to us,” Self’s coauthor and Vanderbilt colleague William Stubblefield, MD, an emergency medicine specialist, said in an interview.

Self and others say they suspect that severe acute respiratory syndrome coronavirus 2 (SARS-CoV-2) infection triggers long-lasting changes in the immune system. In some organs, especially the lungs, those changes persist far past the point at which patients have stopped shedding the virus, Self said. “Frankly, we don’t know how long that lasts.” To help answer that question, Self and his coauthors are conducting a follow-up study to assess

outpatients' health 6 months after their COVID-19 diagnosis.

Sorting Through Symptoms

Just as acute COVID-19 has been found to affect every part of the body, so, apparently, do its persistent symptoms.

In the study of Italian patients, the most common symptoms reported at follow-up were fatigue, shortness of breath, joint pain, and chest pain, in that order. None of the patients had a fever or other sign or symptom of acute illness, but about 44% of them had a worsened quality of life. As the authors pointed out, though, patients with community-acquired pneumonia can also have persistent symptoms, so the findings might not be exclusive to COVID-19.

Less formal surveys have also turned up wide-ranging lingering effects. When the [Body Politic COVID-19 Support Group](#) conducted an online survey in the spring, about 91% of 640 respondents said they hadn't fully recovered and were on day 40 of symptoms, on average. Most reported ongoing fatigue, chills and sweats, body aches, headaches, brain fog, and gastrointestinal issues. Anecdotally, some people have reported feeling better for days or weeks before relapsing with old or new symptoms, according to the organization, which started as a small Instagram group chat and has grown to more than 14 000 members.

Francis Collins, MD, PhD, director of the National Institutes of Health (NIH), [blogged](#) about the survey in September. "Because COVID-19 is such a new disease, little is known about what causes the persistence of symptoms, what is impeding full recovery, or how to help the long-haulers," Collins wrote, noting that the Body Politic and its international Patient-Led Research for COVID-19 group are now conducting a [second survey](#) of long haulers.

A recent [survey](#) by the grassroots group COVID-19 "[Survivor Corps](#)" found that fatigue was the most common of the top 50 symptoms experienced by the more than 1500 long haulers who responded, followed by muscle or body aches, shortness of breath or difficulty breathing, and difficulty concentrating.

Cough is the most common persistent symptom seen at the new [COVID-19 Recovery Clinic](#) (CORE) at Montefiore Medical Center in New York, codirector Aluko Hope, MD, MSCE, said in an interview. Between Hope, a pulmonary and critical care

specialist, and the clinic's other director, general internist Seth Congdon, MD, the clinic sees a wide range of patients, including some who were never hospitalized. What the CORE patients have in common is that they haven't yet returned to their pre-COVID-19 health. At least a few of them have been sick for 4 or 5 months, Hope said. Besides the persistent cough, which can also occur with other viruses, loss of taste and smell lingers for many long haulers.

Many of the clinic's patients are also still short of breath. This could be due to the deconditioning seen with any lengthy illness, Hope said, or to infection-specific conditions, such as postviral reactive airways disease, lung fibrosis, or viral myocarditis. Hope said that he's seen at least one patient with no history of heart disease who developed postviral heart failure.

Dine first noticed that some patients weren't getting better through Penn's [COVID Watch](#) outreach program, which texts those who are home sick with the disease twice a day until they've been symptom-free for a week to 10 days. She now sees so many people with persistent issues that she's developed a flowchart to try to narrow down the reasons for their ill health: Is this a new symptom unrelated to COVID-19? Is it a complication of the disease, like a blood clot? Or is it a side effect of treatment? If she rules those out, she said there are just 2 options left: Either the patient is still infected with SARS-CoV-2 or they have postviral syndrome.

When the Fog Doesn't Lift

Lockman and many other long haulers describe their most debilitating persistent symptom as impaired memory and concentration, often with extreme fatigue.

The effects are different from the cognitive impairment patients might experience after a critical illness, according to Hope. When it comes to COVID-19, "I do think there's a subset of patients [who] weren't even in the hospital who have a post-viral brain fog," he said.

At the end of May, Lockman took a 6-week leave of absence from her job at a human resources management company. Since that ended, she has been working part-time—4 hours on a good day. She moved her home office to her living room so she can rest on the couch. After a recent trip to the emergency department, she was so exhausted that she slept all but 3 hours the next day.

An intriguing idea is taking shape. During the July webinar, Fauci noted that some long haulers' symptoms like brain fog and fatigue are "highly suggestive" of [myalgic encephalomyelitis/chronic fatigue syndrome](#) (ME/CFS).

New York-based psychiatrist Mady Hornig, MD, a member of Columbia University Medical Center's epidemiology faculty, has long studied the role of microbial, immune, and toxic factors in the development of brain conditions such as ME/CFS, whose etiology and pathogenesis are unknown. Now she's looking at these relationships not only as a physician and scientist but also as a long hauler.

Hornig wrote off a throat tickle and cough in March as allergies. And she assumed that walking around her home shoeless caused the chilblains that later developed on her toes. It wasn't until a 4 AM fever awoke her on April 24 that she suspected she had contracted COVID-19. Although she takes 650 mg of aspirin daily for another condition, the fever persisted for 12 days, a longer stretch than any she had experienced since she had her tonsils removed at age 14, nearly 50 years ago.

Despite all the indicators, Hornig's April 27 nasal swab test was negative for SARS-CoV-2. That's likely because it was performed either [too soon or too late](#)—depending on whether the late April fever or the earlier cough or "COVID toes" were the first sign.

Her doctors told her they didn't have a better explanation than COVID-19 for her symptoms, which have also included oxygen saturation levels as low as 88% and 8- to 10-minute tachycardia episodes that still send her heart rate to 115 to 135 beats per minute at least once a day and leave her breathless, even if she's sitting down. Before COVID-19, Hornig was used to working 12- to 14-hour days. For weeks after becoming ill, tachycardia would leave her so fatigued that "I felt like I could not do anything further—my brain was just empty," she said in an interview.

About 3 out of 4 people diagnosed with ME/CFS report that it began with what appeared to be an infection, often infectious mononucleosis caused by [Epstein-Barr virus](#) (EBV), Hornig noted. One ME/CFS [International Classification of Diseases diagnosis code](#) even calls the condition "post-viral fatigue syndrome." Although EBV is a herpesvirus, not a coronavirus, Hornig speculated

that SARS-CoV-2 infection might reactivate latent EBV, triggering the fatigue.

To explore the idea, she has designed prospective studies with the Solve ME/CFS Initiative. The nonprofit in July launched a [registry](#) and biobank, funded in part by the NIH, to collect data from COVID-19 long haulers, as well as people diagnosed with ME/CFS and healthy controls.

"Because of the large number of COVID-19 cases occurring simultaneously, we have a unique scientific window and a huge responsibility to investigate any long-term consequences and disabilities that COVID-19 survivors may face," Hornig said in a [statement](#) announcing the registry and biobank. "Doing so will provide clues and potential treatment candidates for the millions of Americans already diagnosed with ME/CFS."

Hornig and other scientists point to autonomic nervous system dysregulation as the possible explanation for long-haulers' tachycardia, extreme fatigue, and other persistent symptoms. The system controls involuntary physiologic processes such as heart rate, blood pressure, respiration, and digestion.

Stanford University neurologist Mitchell Miglis, MD, who specializes in autonomic nervous system disorders such as postural orthostatic tachycardia syndrome (POTS), recently coauthored a [case report](#) about a previously healthy, 26-year-old emergency department nurse who developed classic POTS symptoms—fatigue, tachycardia—that hadn't resolved 5.5 months after she was diagnosed with COVID-19 in March.

"One of the most common symptoms of POTS is brain fog," Miglis noted. "It's not clearly related to blood flow to the brain. It's something else."

With Lauren Stiles, JD, president of [Dysautonomia International](#) and research assistant professor of neurology at Stony Brook University School of Medicine, Miglis has developed an online survey that is being shared with COVID-19 survivor social media groups to gather more infor-

mation about autonomic symptoms. He plans to resurvey respondents every 3 months for the next year to see how they progress. Miglis speculated that POTS, ME/CFS, and persistent COVID-19 may be different names for the same disorder, and patients' diagnoses depend on their physicians' subspecialty.

Nath, chief of the Section of Infections of the Nervous System at NINDS, is planning a prospective study of persistent ME/CFS-type symptoms among people who've had COVID-19. "I think we need to assure the public that we are aware of the syndrome," he said in an interview. "We're very keen to understand what it's about."

"Medical Gaslighting"

Many long haulers never had laboratory confirmation of COVID-19, which, they say, adds to some health care professionals' skepticism that their persistent symptoms have a physiological basis.

Only about a quarter of the Body Politic survey's respondents had tested positive for COVID-19, while nearly half were never tested—often because their request was denied. But everyone's answers were included in the analysis. The main difference between those who received a positive or negative result was how early in their illness they were tested. "We believe future research must consider the experiences of all people with COVID-19 symptoms, regardless of testing status, in order to better understand the virus and underscore the importance of early and widespread testing," the report's authors wrote.

Lockman was not one of the survey respondents, but she exemplifies the Body Politic's point. At her first trip to the emergency department, she was diagnosed with pneumonia and admitted to the hospital, where she received supplemental oxygen and intravenous antibiotics for 3 days. She suspected it was COVID-19 from the beginning. But she was told she wasn't sick enough or old enough to get one of the then-scarce tests for SARS-CoV-2.

Three weeks after her symptoms began, and after testing negative for influenza and respiratory syncytial virus, Lockman was finally given a SARS-CoV-2 nasal swab test. She tested negative, likely because she had low virus levels by then, she said. In June, she was hospitalized again, this time with pulmonary emboli. A physician who reviewed her chart said she had no doubt that COVID-19 explained her symptoms.

Body Politic has acknowledged that its survey sample wasn't representative of all people with COVID-19. But the organization expressed hope that the findings would inform public health professionals and future research. Toward that end, the founders of the Long Haul COVID Fighters recently launched a [Medical and Scientific Collaboration](#) group on Facebook, giving patients and researchers a place to exchange information.

One thing that's clear, Miglis said, is that "these mystery diagnoses are real, and they're not just in patients' heads."

Long haulers say they aren't always taken seriously, though, especially if they're women, harkening back to the era when "female troubles" were written off as hysteria.

"There is definitely gender bias," Dine said. Women with persistent symptoms are more likely than men to be viewed as "dramatic and anxious," she said. "One of the first steps is believing them and making them feel heard. That alone helps."

"We've experienced so much medical gaslighting, basically doctors telling us, 'That's not what you have. It's just anxiety,'" Lockman said. Despite her frustrations, she remains hopeful that her health will continue to improve, although she recognizes that there likely will be bumps along the way.

"I definitely feel better than I did a month ago," she said in early August. "But I still wake up not knowing what I'm going to deal with today." ■

Note: Source references are available through embedded hyperlinks in the article text online.



Since January 2020 Elsevier has created a COVID-19 resource centre with free information in English and Mandarin on the novel coronavirus COVID-19. The COVID-19 resource centre is hosted on Elsevier Connect, the company's public news and information website.

Elsevier hereby grants permission to make all its COVID-19-related research that is available on the COVID-19 resource centre - including this research content - immediately available in PubMed Central and other publicly funded repositories, such as the WHO COVID database with rights for unrestricted research re-use and analyses in any form or by any means with acknowledgement of the original source. These permissions are granted for free by Elsevier for as long as the COVID-19 resource centre remains active.

- 1 Wise PH, Shiel A, Southard N, et al. The political and security dimensions of the humanitarian health response to violent conflict. *Lancet* 2021; published online Jan 24. [https://doi.org/10.1016/S0140-6736\(21\)00130-6](https://doi.org/10.1016/S0140-6736(21)00130-6).
- 2 Bendavid E, Boerma T, Akseer N, et al. The effects of armed conflict on the health of women and children. *Lancet* 2021; published online Jan 24. [https://doi.org/10.1016/S0140-6736\(21\)00131-8](https://doi.org/10.1016/S0140-6736(21)00131-8).
- 3 Singh NS, Ataullahjan A, Ndiaye K, et al. Delivering health interventions to women, children, and adolescents in conflict settings: what have we learned from ten country case studies? *Lancet* 2021; published online Jan 24. [https://doi.org/10.1016/S0140-6736\(21\)00132-X](https://doi.org/10.1016/S0140-6736(21)00132-X).
- 4 Gaffey MF, Waldman RJ, Blanchet K, et al. Delivering health and nutrition interventions for women and children in different conflict contexts: a framework for decision making on what, when, and how. *Lancet* 2021; published online Jan 24. [https://doi.org/10.1016/S0140-6736\(21\)00133-1](https://doi.org/10.1016/S0140-6736(21)00133-1).
- 5 Wagner Z, Heft-Neal S, Wise PH, et al. Women and children living in areas of armed conflict in Africa: a geospatial analysis of mortality and orphanhood. *Lancet Glob Health* 2019; **7**: e1622–31.
- 6 International Rescue Committee. Where's the money? How the humanitarian system is failing to fund an end of violence against women and girls. 2019. <https://www.rescue.org/sites/default/files/document/3854/whereisthemoneyfinal.pdf> (accessed Dec 18, 2020).
- 7 Stark L, Seff I, Reis C. Gender-based violence against adolescent girls in humanitarian settings: a review of the evidence. *Lancet Child Adolesc Health* 2020; published online Nov 19. [https://doi.org/10.1016/S2352-4642\(20\)30245-5](https://doi.org/10.1016/S2352-4642(20)30245-5).
- 8 WHO. Integrated programming for better health outcomes: a multisectoral response. Global health cluster guide, 2nd edn. 2020. <https://www.who.int/health-cluster/resources/publications/hc-guide/HC-Guide-chapter-8.pdf?ua=1> (accessed Dec 15, 2020).
- 9 FP2020. Family planning's return on investment. https://www.familyplanning2020.org/sites/default/files/Data-Hub/ROI/FP2020_ROI_OnePager_FINAL.pdf (accessed Dec 18, 2020).
- 10 Sheehan P, Sweeney K, Rasmussen B, et al. Building the foundations for sustainable development: a case for global investment in the capabilities of adolescents. *Lancet* 2017; **390**: 1792–806.
- 11 WHO, UNICEF, Partnership for Maternal, Newborn and Child Health, Early Childhood Development Action Network, International Rescue Committee. Nurturing care for children living in humanitarian settings. 2021. <https://nurturing-care.org/nurturing-care-in-humanitarian-settings/> (accessed Jan 17, 2021). Ataullahjan A, Samara M, Betancourt T, Bhutta Z. Mitigating toxic stress in children affected by conflict and displacement. *BMJ* 2020; **371**: m2876.
- 12 Ataullahjan A, Samara M, Betancourt T, Bhutta Z. Mitigating toxic stress in children affected by conflict and displacement. *BMJ* 2020; **371**: m2876.
- 13 Devakumar D, Birch M, Osrin D, Sondorp E, Wells J. The intergenerational effects of war on the health of children. *BMC Med* 2014; **12**: 57.
- 14 Heckman J. There's more to gain by taking a comprehensive approach to early childhood development. https://heckmanequation.org/www/assets/2017/01/F_Heckman_CBAOnePager_120516.pdf (accessed Jan 18, 2021).
- 15 UNESCO. Global education monitoring report 2019: migration, displacement and education—building bridges, not walls. 2018. <https://unesdoc.unesco.org/ark:/48223/pf0000265866> (accessed Jan 18, 2021).
- 16 Bouchane K, Yoshikawa H, Murphy KM, Lombardi J. 2018. Early childhood development and early learning for children in crisis and conflict. Background paper prepared for global education monitoring report 2019. <https://nurturing-care.org/wp-content/uploads/2018/12/UNESCO.pdf> (accessed Jan 18, 2021).
- 17 Bhutta ZA, Gaffey MF, Spiegel PB, et al. Doing better for women and children in armed conflict settings. *Lancet* 2021; published online Jan 24. [https://doi.org/10.1016/S0140-6736\(21\)00127-6](https://doi.org/10.1016/S0140-6736(21)00127-6).
- 18 Spiegel PB. The humanitarian system is not just broke, but broken: recommendations for future humanitarian action. *Lancet* 2017; published online June 8. [http://dx.doi.org/10.1016/S0140-6736\(17\)31278-3](http://dx.doi.org/10.1016/S0140-6736(17)31278-3).



Resurgence of COVID-19 in Manaus, Brazil, despite high seroprevalence

Published Online
January 27, 2021
[https://doi.org/10.1016/S0140-6736\(21\)00183-5](https://doi.org/10.1016/S0140-6736(21)00183-5)

After initially containing severe acute respiratory syndrome coronavirus 2 (SARS-CoV-2), many European and Asian countries had a resurgence of COVID-19 consistent with a large proportion of the population remaining susceptible to the virus after the first epidemic wave.¹ By contrast, in Manaus, Brazil, a study of blood donors indicated that 76% (95% CI 67–98) of the population had been infected with SARS-CoV-2 by October, 2020.² High attack rates of SARS-CoV-2 were also estimated in population-based samples from other locations in the Amazon Basin—eg, Iquitos, Peru 70% (67–73).³ The estimated SARS-CoV-2 attack rate in Manaus would be above the theoretical herd immunity threshold (67%), given a basic case reproduction number (R_0) of 3.⁴

In this context, the abrupt increase in the number of COVID-19 hospital admissions in Manaus during January, 2021 (3431 in Jan 1–19, 2021, vs 552 in Dec 1–19, 2020) is unexpected and of concern (figure).^{5–10} After a large epidemic that peaked in late April, 2020,

COVID-19 hospitalisations in Manaus remained stable and fairly low for 7 months from May to November, despite the relaxation of COVID-19 control measures during that period (figure).

There are at least four non-mutually exclusive possible explanations for the resurgence of COVID-19 in Manaus. First, the SARS-CoV-2 attack rate could have been overestimated during the first wave, and the population remained below the herd immunity threshold until the beginning of December, 2020. In this scenario, the resurgence could be explained by greater mixing of infected and susceptible individuals during December. The 76% estimate of past infection² might have been biased upwards due to adjustments to the observed 52.5% (95% CI 47.6–57.5) seroprevalence in June, 2020, to account for antibody waning. However, even this lower bound should confer important population immunity to avoid a larger outbreak. Furthermore, comparisons of blood donors with census data showed no major

difference in a range of demographic variables,² and the mandatory exclusion of donors with symptoms of COVID-19 is expected to underestimate the true population exposure to the virus. Reanalysis and model comparison¹¹ by independent groups will help inform the best-fitting models for antibody waning and the representativeness of blood donors.

Second, immunity against infection might have already begun to wane by December, 2020, because of a general decrease in immune protection against SARS-CoV-2 after a first exposure. Waning of anti-nucleocapsid IgG antibody titres observed in blood donors² might reflect a loss of immune protection, although immunity to SARS-CoV-2 depends on a combination of B-cell and T-cell responses.¹² A study of UK health-care workers¹³ showed that reinfection with SARS-CoV-2 is uncommon up to 6 months after the primary infection. However, most of the SARS-CoV-2 infections in Manaus occurred 7–8 months before the resurgence in January, 2021; this is longer than the period covered by the UK study,¹³ but nonetheless suggests that waning immunity alone is unlikely to fully explain the recent resurgence. Moreover, population mobility in Manaus decreased from mid-November, 2020, with a sharp reduction in late December, 2020,¹⁴ suggesting that behavioural change does not account for the resurgence of hospitalisations.

Third, SARS-CoV-2 lineages might evade immunity generated in response to previous infection.¹⁵ Three recently detected SARS-CoV-2 lineages (B.1.1.7, B.1.351, and P.1), are unusually divergent and each possesses a unique constellation of mutations of potential biological importance.^{16–18} Of these, two are circulating in Brazil (B.1.1.7 and P.1) and one (P.1) was detected in Manaus on Jan 12, 2021.¹⁶ One case of SARS-CoV-2 reinfection has been associated with the P.1 lineage in Manaus¹⁹ that accrued ten unique spike protein mutations, including E484K and N501K.¹⁶ Moreover, the newly classified P.2 lineage (sublineage of B.1.128 that independently accrued the spike E484K mutation) has now been detected in several locations in Brazil, including Manaus.²⁰ P.2 variants with the E484K mutation have been detected in two people who have been reinfected with SARS-CoV-2 in Brazil,^{21,22} and there is in-vitro evidence that the presence of the E484K mutation reduces neutralisation by polyclonal antibodies in convalescent sera.¹⁵

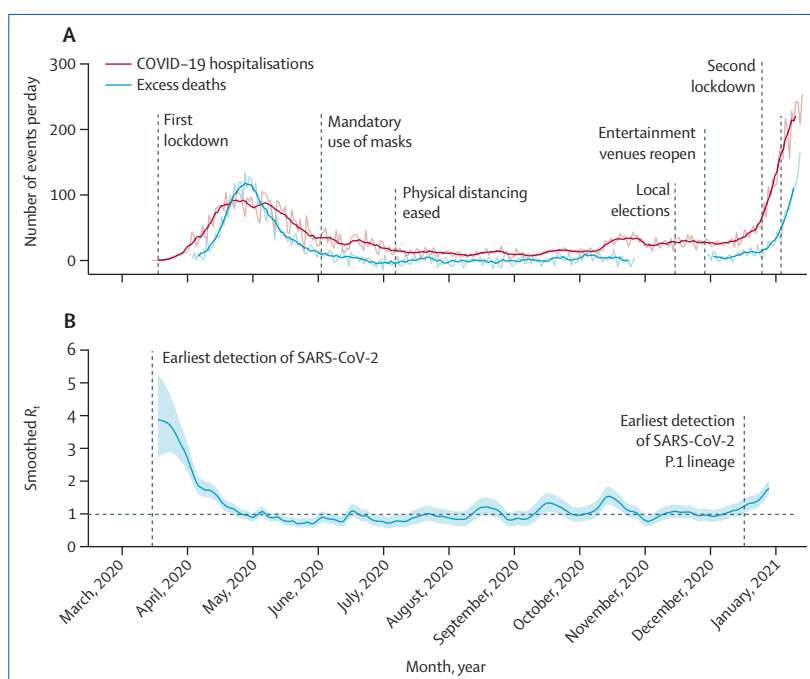


Figure: COVID-19 hospitalisations, excess deaths, and R_t in Manaus, Brazil, 2020–21

(A) Dark lines are the 7-day rolling averages and lighter lines are the daily time series of COVID-19 hospitalisations and excess deaths. Hospitalisation data are from the Fundação de Vigilância em Saúde do Amazonas.⁵ Total all-cause deaths for 2020–21 were reported initially by the Prefeitura de Manaus⁶ and subsequently in the daily COVID-19 bulletin of the Fundação de Vigilância em Saúde do Amazonas.⁷ All-cause deaths from 2019 were from Arpen/AM (Associação dos Registradores Cíveis das Pessoas Naturais do Amazonas).⁸ The compiled excess death data are from Bruce Nelson from the Instituto Nacional de Pesquisas da Amazônia.⁹ (B) R_t was calculated using the time series of COVID-19 hospitalisations after removal of the past 14 days to account for delays in notification. R_t was calculated using the EpiFilter method.¹⁰ Lines are median R_t estimates; shaded areas are the 95% CIs. R_t =Effective reproduction number. SARS-CoV-2=severe acute respiratory syndrome coronavirus 2.

Fourth, SARS-CoV-2 lineages circulating in the second wave might have higher inherent transmissibility than pre-existing lineages circulating in Manaus. The P.1 lineage was first discovered in Manaus.¹⁶ In a preliminary study, this lineage reached a high frequency (42%, 13 of 31) among genome samples obtained from COVID-19 cases in December, 2020, but was absent in 26 samples collected in Manaus between March and November, 2020.¹⁶ Thus far, little is known about the transmissibility of the P.1 lineage, but it shares several independently acquired mutations with the B.1.1.7 (N501Y) and the B.1.325 (K417N/T, E484K, N501Y) lineages circulating in the UK and South Africa, which seem to have increased transmissibility.¹⁸ Contact tracing and outbreak investigation data are needed to better understand relative transmissibility of this lineage.

The new SARS-CoV-2 lineages may drive a resurgence of cases in the places where they circulate if they have increased transmissibility compared with pre-existing circulating lineages and if they are

associated with antigenic escape. For this reason, the genetic, immunological, clinical, and epidemiological characteristics of these SARS-CoV-2 variants need to be quickly investigated. Conversely, if resurgence in Manaus is due to waning of protective immunity, then similar resurgence scenarios should be expected in other locations. Sustained serological and genomic surveillance in Manaus and elsewhere is a priority, with simultaneous monitoring for SARS-CoV-2 reinfections and implementation of non-pharmaceutical interventions. Determining the efficacy of existing COVID-19 vaccines against variants in the P.1 lineage and other lineages with potential immune escape variants is also crucial. Genotyping viruses from COVID-19 patients who were not protected by vaccination in clinical trials would help us to understand if there are lineage-specific frequencies underlying reinfection. The protocols and findings of such studies should be coordinated and rapidly shared wherever such variants emerge and spread.

Since rapid data sharing is the basis for the development and implementation of actionable disease control measures during public health emergencies, we are openly sharing in real-time monthly curated serosurvey data from blood donors through the Brazil-UK Centre for Arbovirus Discovery, Diagnosis, Genomics and Epidemiology (CADDE) Centre GitHub website and will continue to share genetic sequence data and results from Manaus through openly accessible data platforms such as GISAID and Virological.

NRF reports funding from Wellcome Trust, the Royal Society, and the UK Medical Research Council. CAP reports grants from Coordenação de Aperfeiçoamento de Pessoal de Nível Superior Brasil and FAPESP. NMF reports grants from the UK Medical Research Council, the UK National Institute of Health Research, Community Jameel, NIH NIGMS, Janssen Pharmaceuticals, the Bill & Melinda Gates Foundation, and Gavi, the Vaccine Alliance. The other authors declare no competing interests.

***Ester C Sabino, Lewis F Buss, Maria P S Carvalho, Carlos A Prete Jr, Myuki A E Crispim, Nelson A Fraiji, Rafael H M Pereira, Kris V Parag, Pedro da Silva Peixoto, Moritz U G Kraemer, Marcio K Oikawa, Tassila Salomon, Zulma M Cucunuba, Márcia C Castro, Andreza Aruska de Souza Santos, Vítor H Nascimento, Henrique S Pereira, Neil M Ferguson, Oliver G Pybus, Adam Kucharski, Michael P Busch, Christopher Dye, Nuno R Faria**
sabinoec@usp.br

Departamento de Molestias Infecciosas e Parasitárias and Instituto de Medicina Tropical da Faculdade de Medicina da Universidade de São Paulo, São Paulo, SP 05403-000, Brazil (ECS, LFB, NRF); Fundação Hospitalar de Hematologia e Hemoterapia do Amazonas, Manaus, Brazil (MPSC, MAEC, NAF); Departamento de Engenharia de Sistemas Eletrônicos, Escola Politécnica da Universidade de São Paulo, São Paulo, Brazil (CAP, VHN); Institute for Applied Economic

Research-Ipea, Brasília, Brazil (RHMP); MRC Centre for Global Infectious Disease Analysis, J-IDEA, Imperial College London, London, UK (KVP, ZMC, NMF, NRF); Institute of Mathematics and Statistics, University of São Paulo, São Paulo, Brazil (PdSP); Department of Zoology, University of Oxford, Oxford, UK (MUGK, OGP, CD, NRF); Center of Mathematics, Computing and Cognition-Universidade Federal do ABC, São Paulo, Brazil (MKO); Fundação Hemominas-Fundação Centro de Hematologia e Hemoterapia de Minas Gerais, Belo Horizonte, Brazil (TS); Faculdade Ciências Médicas de Minas Gerais, Belo Horizonte, Brazil (TS); Department of Global Health and Population, Harvard T H Chan School of Public Health, Boston, MA, USA (MCC); Oxford School of Global and Area Studies, Latin American Centre, University of Oxford, Oxford, UK (AAdSS); Centro de Ciências Ambientais, Universidade Federal do Amazonas, Manaus, Brazil (HSP); Centre for Mathematical Modelling of Infectious Diseases, London School of Hygiene & Tropical Medicine, London, UK (AK); Vitalant Research Institute, San Francisco, CA, USA (MPB); University of California, San Francisco, CA, USA (MPB)

- Lucy CO, Verity R, Watson OJ, et al. Have deaths from COVID-19 in Europe plateaued due to herd immunity? *Lancet* 2020; **395**: e110-11.
- Buss LF, Prete CA, Abraham CMM, et al. Three-quarters attack rate of SARS-CoV-2 in the Brazilian Amazon during a largely unmitigated epidemic. *Science* 2020; **371**: 288-92.
- Álvarez-Antonio C, Meza-Sánchez G, Calampa C, et al. Seroprevalence of anti-SARS-CoV-2 antibodies in Iquitos, Loreto, Peru. *MedRxiv* 2021; published online 20. <https://doi.org/10.1101/2021.01.17.21249913> (preprint).
- Fontanet A, Cauchemez S. COVID-19 herd immunity: where are we? *Nat Rev Immunol* 2020; **20**: 583-84.
- Fundação de Vigilância em Saúde do Amazonas. COVID-19 no Amazonas. Dados epidemiológicos e financeiros das ações de combate à COVID-19. Publicações. <http://www.fvs.am.gov.br/publicacoes> (accessed Jan 20, 2021).
- Prefeitura de Manaus. Publicações. COVID-19. <http://www.manaus.am.gov.br/noticia/> (accessed Jan 20, 2021).
- Fundação de Vigilância em Saúde do Amazonas. Index of media publicacao. <http://www.fvs.am.gov.br/media/publicacao> (accessed Jan 20, 2021).
- Marcelo Oliveira capyvara. Popular repositories. GitHub. 2021. <https://github.com/capyvara> (accessed Jan 20, 2021).
- Nelson BW, Instituto Nacional de Pesquisas da Amazônia (INPA). Excess deaths Manaus. 2021. <https://t.co/6g4HHEAuNY> (accessed Jan 20, 2021).
- Parag KV, Cowling BJ, Donnelly CA, et al. Deciphering early-warning signals of the elimination and resurgence potential of SARS-CoV-2 from limited data at multiple scales. *MedRxiv* 2020; published online Jan 5. <https://doi.org/10.1101/2020.11.23.20236968> (preprint).
- Tassila S, Pybus O, França R, et al. Coronavirus prevalence in Brazilian Amazon and Sao Paulo city [data set]. Dryad 2020; published online Dec 8. <https://doi.org/10.5061/dryad.c59zw3r5n>.
- Dan JM, Mateu J, Kato Y, et al. Immunological memory to SARS-CoV-2 assessed for up to 8 months after infection. *Science* 2021; published online Jan 6. <https://doi.org/10.1126/science.abb4063>.
- Lumley SF, O'Donnell D, Stoesser NE, et al. Antibody status and incidence of SARS-CoV-2 infection in health care workers. *N Engl J Med* 2020; published online Dec 23. <https://doi.org/10.1056/NEJMoa2034545>.
- ODS Atlas Amazonas. Inloco. Índice de Isolamento Social das cidades do Amazonas. Dados cedidos pela empresa Inloco. https://datastudio.google.com/s/o1rTqejYd_4 (accessed Jan 20, 2021).
- Greaney AJ, Loes AN, Crawford KHD, et al. Comprehensive mapping of mutations to the SARS-CoV-2 receptor-binding domain that affect recognition by polyclonal human serum antibodies. *BioRxiv* 2021; published online Jan 4. <https://doi.org/10.1101/2020.12.31.425021> (preprint).
- Faria NR, Claro IM, Candido D, et al. Genomic characterisation of an emergent SARS-CoV-2 lineage in Manaus: preliminary findings. *Virological*, January, 2021. <https://virological.org/t/genomic-characterisation-of-an-emergent-sars-cov-2-lineage-in-manaus-preliminary-findings/586> (accessed Jan 20, 2021).
- Rambaut A, Loman N, Pybus OG, et al. Preliminary genomic characterisation of an emergent SARS-CoV-2 lineage in the UK defined by a novel set of spike mutations. *Virological*, December, 2020. <https://virological.org/t/preliminary-genomic-characterisation-of-an-emergent-sars-cov-2-lineage-in-the-uk-defined-by-a-novel-set-of-spike-mutations/563> (accessed Jan 20, 2021).
- Tegally H, Wilkinson E, Giovanetti M, et al. Emergence and rapid spread of a new severe acute respiratory syndrome-related coronavirus 2 (SARS-CoV-2) lineage with multiple spike mutations in South Africa. *MedRxiv* 2020; published online Dec 22. <https://doi.org/10.1101/2020.12.21.20248640> (preprint).

For CADDE Centre GitHub website see <https://github.com/CADDE-CENTRE>

For GISAID see www.gisaid.org/

For Virological see <https://virological.org>

- 19 Naveca F, da Costa C, Nascimento V, et al. SARS-CoV-2 reinfection by the new variant of concern (VOC) P.1 in Amazonas, Brazil. *Virological*, Jan 18, 2021. <https://virological.org/t/sars-cov-2-reinfection-by-the-new-variant-of-concern-voc-p-1-in-amazonas-brazil/596> (accessed Jan 20, 2021).
- 20 Naveca F, Nascimento V, Souza V, et al. Phylogenetic relationship of SARS-CoV-2 sequences from Amazonas with emerging Brazilian variants harboring mutations E484K and N501Y in the Spike protein. *Virological*, Jan 11, 2021. <https://virological.org/t/phylogenetic-relationship-of-sars-cov-2-sequences-from-amazonas-with-emerging-brazilian-variants-harboring-mutations-e484k-and-n501y-in-the-spike-protein/585> (accessed Jan 20, 2021).
- 21 Nonaka VCK, Franco MM, Gräf T, et al. Genomic evidence of a SARS-CoV-2 reinfection case with E484K spike mutation in Brazil. *Preprints* 2021; published online Jan 6. <https://doi.org/10.20944/preprints202101.0132.v1> (preprint).
- 22 Resende PC, Bezerra JF, Vasconcelos RHT, et al. Spike E484K mutation in the first SARS-CoV-2 reinfection case confirmed in Brazil, 2020. *Virological*, Jan 10, 2021. <https://virological.org/t/spike-e484k-mutation-in-the-first-sars-cov-2-reinfection-case-confirmed-in-brazil-2020/584> (accessed Jan 20, 2021).

Long COVID guidelines need to reflect lived experience



Since May, 2020,¹ increasing attention has been given to the experiences of people with COVID-19 whose symptoms persist for 4 or more weeks. According to the Office for National Statistics (ONS), an estimated 186 000 people (95% CI 153 000–221 000) in private households in England currently have COVID-19 symptoms 5–12 weeks or longer after acute infection.² The ONS estimate that one in five people have symptoms that persist after 5 weeks, and one in ten have symptoms for 12 weeks or longer after acute COVID-19 infection.² Research on long COVID is growing, including into the underlying pathology, consequences, and sequelae, as well as rehabilitation for patients. Evidence suggests that a considerable proportion of people with long COVID have severe complications.^{3–5}

We have lived experiences of long COVID, with a range of symptoms lasting for more than 6 months. Staff in the UK National Health Service (NHS) have been variously supportive or disbelieving of our ongoing, often worsening, symptoms. Before our illness we were fit, healthy, and working in demanding roles, including as doctors, nurses, and other health professionals. Our symptoms of acute COVID-19 included dyspnoea, dry cough, fever, anosmia, and debilitating fatigue. Throughout 2020 we also experienced other symptoms and conditions, never experienced before our acute illnesses (panel). All of these conditions began during, or shortly after, acute COVID-19. We each are experiencing different patterns and varied severity of symptoms; we all share difficulties accessing adequate health-care services; some of us have received misguided assessment and treatment in some of the UK's recently established long COVID clinics and encountered dismissive behaviour from some health professionals.^{6–8} We share these experiences with thousands of people we engage with in rapidly growing online support groups.

We were encouraged by the announcement, on Oct 5, 2020, that the National Institute for Health and Care Excellence (NICE), the Scottish Intercollegiate Guidelines Network (SIGN), and the Royal College of General Practitioners (RCGP) were developing “a guideline on persistent effects of COVID-19 (long COVID) on patients”,⁹ consulting with a broad range of professional groups and some people with long COVID.

The final NICE–SIGN–RCGP guideline, published on Dec 18, 2020,¹⁰ should provide clear information on what is and is not known about the natural history of long COVID, provide guidance for health-care workers to identify cases, and inform clinical practice for the correct management of people with symptoms. Accurate assessment, diagnosis, treatment, and rehabilitation are especially important given the increasing evidence of organ pathology

Published Online
December 18, 2020
[https://doi.org/10.1016/S0140-6736\(20\)32705-7](https://doi.org/10.1016/S0140-6736(20)32705-7)

Panel: Conditions experienced by members of the UK doctors #longcovid group

- Myocarditis or pericarditis
- Microvascular angina
- Cardiac arrhythmias, including atrial flutter and atrial fibrillation
- Dysautonomia, including postural orthostatic tachycardia syndrome
- Mast cell activation syndrome
- Interstitial lung disease
- Thromboembolic disease (pulmonary emboli or cerebral venous thrombosis)
- Myelopathy, neuropathy, and neurocognitive disorders
- Renal impairment
- New-onset diabetes and thyroiditis
- Hepatitis and abnormal liver enzymes
- New-onset allergies and anaphylaxis
- Dysphonia

Genomic diversity of SARS-CoV-2 in Coronavirus Disease 2019 patients

Zijie Shen^{1,2#}, Yan Xiao^{3#}, Lu Kang^{1,2#}, Wentai Ma^{1,2#}, Leisheng Shi^{1,2}, Li Zhang¹, Zhuo Zhou⁴, Jing Yang^{1,2}, Jiaxin Zhong^{1,2}, Donghong Yang⁵, Li Guo³, Guoliang Zhang⁶, Hongru Li⁷, Yu Xu⁵, Mingwei Chen⁸, Zhancheng Gao⁵, Jianwei Wang³, Lili Ren^{3*}, Mingkun Li^{1,9*}.

1. Key Laboratory of Genomic and Precision Medicine, Beijing Institute of Genomics, Chinese Academy of Sciences, and China National Center for Bioinformation, Beijing, 101300, China;
2. University of Chinese Academy of Sciences, Beijing 100049, China.
3. National Health Commission of the People's Republic of China Key Laboratory of Systems Biology of Pathogens and Christophe Mérieux Laboratory, Institute of Pathogen Biology, Chinese Academy of Medical Sciences & Peking Union Medical College, Beijing 100730, China;
4. Biomedical Pioneering Innovation Center, Beijing Advanced Innovation Center for Genomics, Peking-Tsinghua Center for Life Sciences, Peking University Genome Editing Research Center, State Key Laboratory of Protein and Plant Gene Research, School of Life Sciences, Peking University, Beijing 100871, China
5. Department of Respiratory and Critical Care Medicine, Peking University People's Hospital, Beijing 100044, China
6. National Clinical Research Center for Infectious Diseases, Guangdong Key Laboratory for Emerging Infectious Diseases, Shenzhen Third People's Hospital, Southern University of Science and Technology, Shenzhen 518112, China
7. Fujian Provincial Hospital, Fujian 350000, PR China
8. Department of Respiratory and Critical Care Medicine, the First Affiliated Hospital of Xi'an Jiaotong University, Shaanxi Province 710061, P.R. China

9. Center for Excellence in Animal Evolution and Genetics, Chinese Academy of Sciences, Kunming, 650223, China;

Author Z.S., Y.X., L.K., and W.M. contributed equally to this manuscript.

* Author L.R. and M.L. contributed equally to this manuscript.

Keywords: SARS-CoV-2, COVID-19, intra-host variant, microbiota, transmission

Summary

An elevated level of viral diversity was found in some SARS-CoV-2 infected patients, indicating the risk of rapid evolution of the virus. Although no evidence for the transmission of intra-host variants was found, the risk should not be overlooked.

Corresponding author:

Mingkun Li

E-mail: limk@big.ac.cn

Beijing Institute of Genomics, Chinese Academy of Sciences

No. 1-104, Beichen West Road, Chaoyang District, Beijing, 100101, China

Tel/Fax: 86-10-84097716

Alternate corresponding author:

Lili Ren

E-mail: renliliipb@163.com

Institute of Pathogen Biology, Chinese Academy of Medical Sciences & Peking Union Medical College

Building 7, Di Sheng Bei Jie Street 1, Yizhuang District, Beijing 100730, China;

Tel/Fax: 86-10-67837321

Abstract:

Background A novel coronavirus (SARS-CoV-2) has infected more than 75,000 individuals and spread to over 20 countries. It is still unclear how fast the virus evolved and how the virus interacts with other microorganisms in the lung.

Methods We have conducted metatranscriptome sequencing for the bronchoalveolar lavage fluid of eight SARS-CoV-2 patients, 25 community-acquired pneumonia (CAP) patients, and 20 healthy controls.

Results The median number of intra-host variants was 1-4 in SARS-CoV-2 infected patients, which ranged between 0 and 51 in different samples. The distribution of variants on genes was similar to those observed in the population data (110 sequences). However, very few intra-host variants were observed in the population as polymorphism, implying either a bottleneck or purifying selection involved in the transmission of the virus, or a consequence of the limited diversity represented in the current polymorphism data. Although current evidence did not support the transmission of intra-host variants in a person-to-person spread, the risk should not be overlooked. The microbiota in SARS-CoV-2 infected patients was similar to those in CAP, either dominated by the pathogens or with elevated levels of oral and upper respiratory commensal bacteria.

Conclusion SARS-CoV-2 evolves *in vivo* after infection, which may affect its virulence, infectivity, and transmissibility. Although how the intra-host variant spreads in the population is still elusive, it is necessary to strengthen the surveillance of the viral

evolution in the population and associated clinical changes.

Abbreviations: COVID-19: Coronavirus disease 2019; CAP: Community-acquired pneumonia; SARS: Severe acute respiratory syndrome; CoV: Coronavirus; Healthy: Healthy controls; BALF: Bronchoalveolar lavage fluid; nCoV: COVID-19 patients; NC: Negative controls.

Introduction

Since the outbreak of a novel coronavirus (SARS-CoV-2) in Wuhan, China, the virus had spread to more than 20 countries, resulting in over 75,000 cases and more than 2,300 deaths (Until Feb 22, 2020) [1, 2]. The basic reproduction number was estimated to range from 2.2 to 3.5 at the early stage[3], making it a severe threat to public health. Recent studies have identified bat as the possible origin of SARS-CoV-2, and the virus likely uses the same cell surface receptor as SARS-CoV [4], namely ACE2. These studies have advanced our understanding of SARS-CoV-2. However, our knowledge of the novel virus is still limited.

The virus undergoes a strong immunologic pressure in humans, and may thus accumulate mutations to outmaneuver the immune system [5]. These mutations could result in changes in viral virulence, infectivity, and transmissibility [6]. Therefore, it is imperative to investigate the pattern and frequency of mutations occurred. Aside from the pathogen, microbiota in the lung is associated with disease susceptibility and severity [7]. Alterations of lung microbiota could potentially modify immune response against the viral and secondary bacterial infection [8, 9]. Thus, understanding the microbiota, which comprises bacteria that could cause secondary infection or exert effects on the mucosal immune system, might help to predict the outcome and reduce complications.

In our study, we conducted metatranscriptome sequencing on bronchoalveolar lavage fluid (BALF) samples from 8 subjects with Coronavirus disease 2019 (COVID-19, the disease caused by SARS-CoV-2) patients. We found that the number of intra-

host variants ranged from 0 to 51 with a median number of 4, suggesting a high evolution rate of the virus. By investigating a person-to-person spread event, we found no evidence for the transmission of intra-host variants. Meanwhile, we found no specific microbiota alteration in the BALF of COVID-19 patients comparing to CAP patients with other suspected viral causes.

Results

Data summary

By metatranscriptome sequencing, more than 20 million reads were generated for each BALF of COVID-19 patients (nCoV) as well as a negative control (nuclease-free water, NC). For comparison, the metatranscriptome sequencing data with similar number of reads from 25 virus-like community-acquired pneumonia patients (CAP, determined by at least 100 viral reads and 10-fold higher than those in the NC), 20 healthy controls without any known pulmonary diseases (Healthy), and two extra NCs (two saline solutions passing through the bronchoscope) were used in this study. Demographic and clinical information was collected and summarized in Supplementary Table 1.

After quality control, a median number of 55,571 microbial reads were generated for each sample. nCoV had the highest proportion of microbial reads compared to CAP and Healthy (nCov: median proportion of 7%, CAP: 0.8%, Healthy:0.1%, $p < 0.001$, Figure 1A), and 49% of the microbial reads could be mapped to SARS-CoV-2, which was not different from the viral proportion in CAP (Figure 1B). Only SARS-CoV-2 was identified in nCoV, and no read was mapped to other species belonging to

Betacoronavirus. Moreover, besides the detection of HCoV-OC43 in one Healthy and HCoV-NL63 in a CAP, no other samples showed any signal of *Betacoronavirus*, which proved the authenticity of the data and methods used in our analysis.

Intra-host variants in the genome of SARS-CoV-2

The sequencing depth of SARS-CoV-2 ranged from 18-fold in nCoV-5 to 32,291-fold in nCoV1, with more than 80% of the genome covered by at least 50-fold in five samples (Figure 2A, Supplementary Table 2). In total, 84 intra-host variants were identified with minor allele frequency (MAF) greater than 5%, and 25 variants were with MAF greater than 20% (Supplementary Table 3, Figure 2B, nCoV5 was excluded from the analysis due to large gaps on its genome coverage). Notably, the number of variants was not associated with the sequencing depth (Supplementary Figure 1). The overall Ka/Ks ratio was significantly smaller than 1, which was similar for intra-host variants and the polymorphisms observed in the population data, suggesting a purifying selection acting on both types of mutations (Table 1). The numbers of variants observed in the gene were proportional to gene lengths ($\text{cor} = 0.950$, $p = 8\text{E-}06$ for the intra-host variant; $\text{cor} = 0.957$, $p = 4\text{E-}06$ for the polymorphisms). Although only a small fraction of the variants was observed in multiple patients (2 out of 84, Figure 2C), some positions were more prone to mutate or variants were transmitting in the population, such as position 10779, where the mutant allele A was observed in all seven patients, with the frequency ranging from 15% to 100% (Figure 2D).

The number of intra-host variants per individual showed a large variation (0 to 51, median 4 for variants with $\text{MAF} \geq 5\%$; 0 to 19, median 1 for variants with $\text{MAF} \geq 20\%$),

which could not be explained by the batch effect, coverage variance, or contamination (Supplementary Figure 1; nCoV1-4 were in one batch, nCoV5-8 were in another batch; most mutations were not observed in the population data). We also noted that the number of variations was not relevant to the days after symptom onset or the age of patients (Supplementary Figure 2). Collectively, we did not find any reason for the extremely high level of variants in nCoV6 (51 variants). A larger population size is needed to investigate how frequent such outliers are, and whether they are associated with the level of host immune response or the viral replication rate. We also noted similar outliers for other viruses [11]. Of note, the origin of variants could be either mutation occurred *in vivo* after infection or multiple transmitted SARS-CoV-2 strains.

No evidence for transmission of intra-host variants between samples

Among the eight COVID-19 patients, nCoV4 and nCoV7 were from the same household, with dates of symptom onset differing by five days; thus a transmission from nCoV4 to nCoV7 is highly suspected, especially considering that only nCoV4 had been to the Huanan seafood market in Wuhan, which is the starting point of the outbreak and suspected to be the source. First, the consensus sequence of the virus was the same for two samples, and all four intra-host variants passing the selection criteria in nCoV4 were not detected in nCoV7 (Table 2). We further expanded the investigation to all variants with $\text{MAF} \geq 2\%$ and supported by at least 3 reads. By doing so, we detected seven variants (out of 25) shared between the two samples. However, the MAF in both nCoV4 and nCoV7 were similar to those in other samples, suggesting that these positions were either error-prone or mutation-prone; hence they cannot support the

transmission of these variants.

Meanwhile, among all 84 intra-host variants, only three of them were found to be polymorphic in the population data (position 7866 G/T; 27493 C/T; 28253 C/T). This small number of overlap also suggests that intra-host variants were rarely transmitted to other samples. However, we cannot rule out the possibility that the sequence diversity in the population is underestimated by the current database.

Missing microbiota signature associated with SARS-CoV-2 infection

Metatranscriptome data also enabled us to profile the transcriptionally active microbiota in different types of pneumonia, which is associated with the immunity response in the lung [12, 13]. In general, a significant difference in microbiota composition was observed among the nCoV, CAP, and Healthy groups ($R^2 = 0.07$, $p = 0.001$; Figure 3A). However, the clustering of some samples with NC indicated a barren microbiota in some samples. After removing the problematic samples and ambiguous components, we still found that nCoV and CAP were both different from the healthy controls (nCoV *vs.* Healthy: $R^2 = 0.45$, $p = 0.001$; CAP *vs.* Healthy: $R^2 = 0.10$, $p = 0.002$), implying a dysbiosis occurred in their lung microbiota. Microbiota could be classified into three different types (Figure 3B). In particular, the microbiota in cluster I was dominated by the possible pathogens, whereas the microorganisms in other clusters were more diverse. By further inspecting the species belonging to each cluster (Supplementary Table 4-5), we found that bacteria in Type III were mainly commensal species frequently observed in the oral and respiratory tract, whereas bacteria in Type II were mostly environmental organisms, thereby contamination was highly suspected.

Therefore, the microbiota was either pathogen-enriched (Type I) or commensal-enriched (Type III) or undetermined due to low microbial load (Type II).

The microbiota in six nCoV samples were pathogen-enriched, and the other two were commensal-enriched (Figure 3B). Moreover, two nCoV samples (2, 6) with an excess number of intra-host SARS-CoV-2 variants both possessed the pathogen-enriched microbiota. The overwhelming proportion of the virus may associate with a higher replication rate, and could also potentially stimulate the intense immune response against the virus, under which circumstance, an excess number of intra-host mutations would be expected. However, as only eight nCoV patients were included in this analysis, and the absolute microbial load was unknown, more data is needed for further investigation.

Discussion

RNA viruses have a high mutation rate due to the lack of proofreading activity of polymerases. Consequently, RNA viruses are prone to evolve resistance to drugs and escape from immune surveillance. The mutation rate of SARS-CoV-2 is still unclear. However, considering that the median number of pairwise sequence differences was 4 (Interquartile Range: 3-6) for 110 sequences collected between Dec 24, 2019 and Feb 9, 2020, the mutation rate should be at the same order of magnitude in SARS-CoV ($0.80\text{-}2.38\times 10^{-3}$ nucleotide substitution per site per year)[14]. The high mutation rate also results in a high level of intra-host variants in RNA viruses [11, 15]. The median number of intra-host variant in COVID-19 patients was 4 for variant with frequency $\geq 5\%$, and this incidence was not significantly different from that reported in a study on

Ebola (655 variants with frequency $\geq 5\%$ in 134 samples) ($p > 0.05$) [11], suggesting that the mutation rate of SARS-CoV-2 was also comparable to Ebola virus. An exoribonuclease (ExoN) has been proposed to provide proofreading activity in SARS-CoV [16, 17], and we noted that all three key motifs in the gene were identical between SARS-CoV and SARS-CoV-2 (Supplementary Figure 3). In addition, neither polymorphism nor intra-host variant was detected in these motifs, suggesting that the gene is highly conserved, and thereby it could be a potential target for antiviral therapy. Although we did not find any mutation hotspot genes in either polymorphism or intra-host variants, the observation of shared intra-host variants among different individuals implied the possibility of adaptive evolution of the virus in patients, which could potentially affect the antigenicity, virulence, and infectivity of the virus [6].

It is worth noting that the SARS-CoV-2 genome in patients could be highly diverse, which was also observed in other viruses [11]. The high diversity could potentially increase the fitness of the viral population, making it hard to be eliminated [15]. Further studies are needed to explore how this may influence the immune response towards the virus and whether there is a selection acting on different strains in the human body or during the transmission. In a single transmission event investigated in this study, we found no evidence for the transmission of multiple strains. However, it is unclear whether these intra-host variants occurred before the transmission or after the transmission, which would result in different conclusions. Additionally, a bottleneck may be involved in the transmission, which could also result in the loss of diversity [18]. Nevertheless, the observation of high mutation burden in some patients

emphasized the possibility of rapid-evolving of this virus.

Recent studies have shown that the microbiota in the lung contributed to the immunological homeostasis and potentially altered the susceptibility to viral infection. Meanwhile, the lung microbiota could also be regulated by invading viruses [9, 19]. However, besides the feature that the microbial diversity was significantly lower in pneumonia than that in healthy controls (Figure 3B), we did not identify any specific microbiota pattern shared among COVID-19 patients, neither for CAP patients. A possible reason for this could be the use of antibiotics in pneumonia patients. However, this was not true for all pneumonia samples, as a substantial proportion of bacteria were observed in some samples, including two COVID-19 patients. It is well known that a common complication of viral infection, especially for respiratory viruses, secondary bacterial infection often results in a significant increase in morbidity [20]. Thus, the elevated level of bacteria in the BALF of some COVID-19 patients might increase the risk of secondary infection. In the clinical data, the secondary infection rate for COVID-19 was between 1%-10% [2, 21]. However, the quantitative relationship between bacterial relative abundance/titer and infection is unclear.

Overall, our study has revealed the evolution of SARS-CoV-2 in the patient, a common feature shared by most RNA viruses. How these variants influence the fitness of viruses and genetic diversity in the population awaits further investigation. Currently, only limited sequences are shared in public databases (Supplementary Table 6); hence there is an urgent need to accumulate more sequences to trace the evolution of the viral genome and associate the changes with clinical symptoms and outcomes.

Methods.

Subjects and samples collection

Eight COVID-19 pneumonia samples were collected from hospitals in Wuhan from December 18 to 29, 2019; 25 virus-like community-acquired pneumonia (CAP) samples were collected from Beijing Peking University People's Hospital, The Shenzhen Third People's Hospital, Fujian Provincial Hospital, and The First-affiliated hospital of Xi'an Jiaotong University between 2014 and 2018. CAP was diagnosed following the guidelines of the Infectious Diseases Society of America and the American Thoracic Society [22]. Pneumonia patients with chronic pulmonary diseases were excluded. Meanwhile, BALF from 20 healthy volunteers were collected and used as healthy controls. Demographic information and clinical information were included in Supplementary Table 1.

For each patient, BALF samples were collected using a bronchoscope as part of normal clinical management. The volume of BALF samples ranged between 5ml and 30ml, most of which were used for bacterial culture and the remnant were aliquoted and stored at -80 °C before processing.

Metatranscriptome sequencing

A 200 ul aliquot of each SARS-CoV-2 infected whole-BALF sample was used to extract RNA using Direct-zol RNA Miniprep kit (Zymo Research, Irvine, CA, USA) and Trizol LS (Thermo Fisher Scientific, Carlsbad, CA, USA) in biosafety III laboratory, and the rest samples were operated following the same protocol in biosafety II laboratory. The

RNA was then reverse transcribed, and amplified using an Ovation Trio RNA-Seq library preparation kit (NuGEN, CA, USA) and was sequenced on an Illumina HiSeq 2500/4000 platform (Illumina, United Kingdom).

Data availability

The raw sequencing data reported in this paper have been deposited in the Genome Warehouse in National Genomics Data Center [23], under project number PRJCA002202 that is publicly accessible at <https://bigd.big.ac.cn/gsa>. Meanwhile, the data have also been submitted to NCBI Sequence Read Archive (SRA) database under project number PRJNA605907.

Data processing and taxonomic assignments

Quality control processes included adapter trimming, low quality reads removal, short reads removal by fastp (-l 70, -x, --cut-tail, --cut_tail_mean_quality 20, version: 0.20.0)[24], low complexity reads removal by Komplexity (-F, -k 8, -t 0.2, version: Nov 2019)[25], host removal by bmtagger (<ftp://ftp.ncbi.nlm.nih.gov/pub/agarwala/bmtagger>)[26, 27], and ribosomal reads removal by SortMeRNA (version:2.1b)[28].

The resultant reads were mapped against NCBI nt database (version: Jul 1 2019) using BLAST+ (version:2.9.0)(-task megablast, -evalue 1e-10, -max_target_seqs 10, -max_hsps 1, -qcov_hsp_perc 60, -perc_identity 60)[29]. Taxonomic assignment was done by MEGAN using lowest common ancestor algorithm (-ms 100, -supp 0, -me 0.01, -top 10, -mrc 60, version: 6.11.0)[30]. After performing an overall PCoA and Permanova test, samples and microorganisms were filtered for further analyses with the

following criteria. Samples with less than 5000 microbial reads were discarded. Microorganisms satisfying the following criteria were considered in the microbiota analysis, 1) archaea, bacteria, fungi, or virus; 2) with relative abundance $\geq 1\%$ in the raw data and filtered data; 3) supported by at least 100 reads; 4) abundance higher than 10-fold of that in the negative control; 5) no batch effect; 6) abundance was not negatively correlated with bacteria titer; 7) not known contamination.

Intra-individual variants detection

Clean reads were mapped to the reference genome of SARS-CoV-2 (GenBank: MN908947.3) using BWA mem (version:0.7.12)[31]. Duplicate reads were removed by Picard (<http://broadinstitute.github.io/picard>; version: 2.18.22) [32]. Mpileup file was generated by samtools (version 1.8)[33], and intra-host variants were called using VarScan (version: 2.3.9)[34] and an in-house scripts. All variants had to satisfy the following requirements: 1) Sequencing depth ≥ 50 ; 2) Minor allele frequency $\geq 5\%$; 3) Minor allele frequency $\geq 2\%$ on each strand; 4) Minor allele count ≥ 5 on each strand; 5) The minor allele was supported by the inner part of the read (excluding 10 bp on each end); 6) Both alleles could be identified in at least 3 reads that specifically assigned to genus *Betacoronavirus*.

For comparison with the polymorphism in the population, we obtained 110 sequences from GISAID (www.gisaid.org)[35, 36]. The accession number and acknowledgment were included in Supplementary Table S6.

Statistical analysis.

Pearson's chi-square test or Fisher's exact test was used for categorical variables, and

the Mann-Whitney U test or Kruskal-Wallis rank sum test was used for continuous variables that do not follow a normal distribution. A comparison of microbiota was done by Permanova test.

Ethics statement.

The study was approved by the Institutional Review Board of Beijing Peking University People's Hospital, The Shenzhen Third People's Hospital, Fujian Provincial Hospital, and The First-affiliated hospital of Xi'an Jiaotong University. The data collection for the COVID-19 patients were deemed by the National Health Commission of the People's Republic of China as the contents of the public health outbreak investigation. Written informed consent was obtained from other pneumonia patients and healthy controls.

Acknowledgments

We thank Dr. Xue Yongbiao and colleagues from National Genomics Data Center for helpful discussion and computational resource support. We thank Dr. Huang Yanyi (Peking University, Beijing, China) and Wang Jianbin (Tsinghua University, Beijing, China) for providing the sequencing platform. We also thank Dr. Huang Chaolin for assist in sample collection. We gratefully acknowledge the Authors, the Originating and Submitting Laboratories for their sequence and metadata shared through GISAID, on which some of our analysis is based, a full name list of all submitters was given in Table S6.

Funding

This work was supported by grants from Innovation Fund for Medical Sciences [2016-I2M-1-014], the National Major Science & Technology Project for Control and Prevention of Major Infectious Diseases in China [2017ZX10103004, 2018ZX10305409, 2018ZX10301401, 2018ZX10732401]; National Natural Science Foundation of China [31670169, 31871263]; and the Open Project of Key Laboratory of Genomic and Precision Medicine, Chinese Academy of Sciences.

Potential conflicts of Interests

The authors declare no competing interests.

Reference

1. Zhu N, Zhang D, Wang W, et al. A Novel Coronavirus from Patients with Pneumonia in China, 2019. *N Engl J Med* **2020**.
2. Huang C, Wang Y, Li X, et al. Clinical features of patients infected with 2019 novel coronavirus in Wuhan, China. *Lancet* **2020**.
3. Zhao S. LQ, Ran J., Musa S., Yang G., Wang W., Lou Y., Gao D., Yang L., He D., Wang M. Preliminary estimation of the basic reproduction number of novel coronavirus (2019-nCoV) in China, from 2019 to 2020: A data-driven analysis in the early phase of the outbreak. *Int J Infect Dis* **2020**.
4. Zhou P, Yang, X., Wang, X. et al. A pneumonia outbreak associated with a new coronavirus of probable bat origin. *Nature* **2020**.
5. Lucas M, Karrer U, Lucas A, Klennerman P. Viral escape mechanisms--escapology taught by viruses. *Int J Exp Pathol* **2001**; 82(5): 269-86.
6. Berngruber TW, Froissart R, Choisy M, Gandon S. Evolution of virulence in emerging epidemics. *PLoS Pathog* **2013**; 9(3): e1003209.
7. O'Dwyer DN, Dickson RP, Moore BB. The Lung Microbiome, Immunity, and the Pathogenesis of Chronic Lung Disease. *J Immunol* **2016**; 196(12): 4839-47.
8. Hanada S, Pirzadeh M, Carver KY, Deng JC. Respiratory Viral Infection-Induced Microbiome Alterations and Secondary Bacterial Pneumonia. *Front Immunol* **2018**; 9: 2640.
9. Huffnagle GB, Dickson RP, Lukacs NW. The respiratory tract microbiome and lung inflammation: a two-way street. *Mucosal Immunol* **2017**; 10(2): 299-306.

-
10. Subissi L, Imbert I, Ferron F, et al. SARS-CoV ORF1b-encoded nonstructural proteins 12-16: replicative enzymes as antiviral targets. *Antiviral Res* **2014**; 101: 122-30.
 11. Ni M, Chen C, Qian J, et al. Intra-host dynamics of Ebola virus during 2014. *Nat Microbiol* **2016**; 1(11): 16151.
 12. Ren L, Zhang R, Rao J, et al. Transcriptionally Active Lung Microbiome and Its Association with Bacterial Biomass and Host Inflammatory Status. *mSystems* **2018**; 3(5).
 13. Segal LN, Clemente JC, Tsay JC, et al. Enrichment of the lung microbiome with oral taxa is associated with lung inflammation of a Th17 phenotype. *Nat Microbiol* **2016**; 1: 16031.
 14. Zhao Z, Li H, Wu X, et al. Moderate mutation rate in the SARS coronavirus genome and its implications. *BMC Evol Biol* **2004**; 4: 21.
 15. Domingo E, Sheldon J, Perales C. Viral quasispecies evolution. *Microbiol Mol Biol Rev* **2012**; 76(2): 159-216.
 16. Minskaia E, Hertzog T, Gorbalenya AE, et al. Discovery of an RNA virus 3'->5' exoribonuclease that is critically involved in coronavirus RNA synthesis. *Proc Natl Acad Sci U S A* **2006**; 103(13): 5108-13.
 17. Smith EC, Blanc H, Surdel MC, Vignuzzi M, Denison MR. Coronaviruses lacking exoribonuclease activity are susceptible to lethal mutagenesis: evidence for proofreading and potential therapeutics. *PLoS Pathog* **2013**; 9(8): e1003565.
 18. Sigal D, Reid JNS, Wahl LM. Effects of Transmission Bottlenecks on the Diversity of Influenza A Virus. *Genetics* **2018**; 210(3): 1075-88.

-
19. Tsang TK, Lee KH, Foxman B, et al. Association between the respiratory microbiome and susceptibility to influenza virus infection. *Clin Infect Dis* **2019**.
 20. Hendaus MA, Jomha FA, Alhammadi AH. Virus-induced secondary bacterial infection: a concise review. *Ther Clin Risk Manag* **2015**; 11: 1265-71.
 21. Chen N. ZM, Dong X., Qu J., Gong F., Han Y., Qiu Y., Wang J., Liu Y., Wei Y., Xia J., Yu T., Zhang X., Zhang L. Epidemiological and clinical characteristics of 99 cases of 2019 novel coronavirus pneumonia in Wuhan, China: a descriptive study. *The Lancet* **2020**.
 22. Mandell LA, Wunderink RG, Anzueto A, et al. Infectious Diseases Society of America/American Thoracic Society consensus guidelines on the management of community-acquired pneumonia in adults. *Clin Infect Dis* **2007**; 44 Suppl 2: S27-72.
 23. National Genomics Data Center M, Partners. Database Resources of the National Genomics Data Center in 2020. *Nucleic Acids Res* **2020**; 48(D1): D24-D33.
 24. Chen S, Zhou Y, Chen Y, Gu J. fastp: an ultra-fast all-in-one FASTQ preprocessor. *Bioinformatics* **2018**; 34(17): i884-i90.
 25. Clarke EL, Taylor LJ, Zhao C, et al. Sunbeam: an extensible pipeline for analyzing metagenomic sequencing experiments. *Microbiome* **2019**; 7(1): 46.
 26. <ftp://ftp.ncbi.nlm.nih.gov/pub/agarwala/bmtagger>.
 27. Wang J, Wang W, Li R, et al. The diploid genome sequence of an Asian individual. *Nature* **2008**; 456(7218): 60-5.
 28. Kopylova E, Noe L, Touzet H. SortMeRNA: fast and accurate filtering of ribosomal RNAs in metatranscriptomic data. *Bioinformatics* **2012**; 28(24): 3211-7.

-
29. Camacho C, Coulouris G, Avagyan V, et al. BLAST+: architecture and applications. *BMC Bioinformatics* **2009**; 10: 421.
 30. Huson DH, Beier S, Flade I, et al. MEGAN Community Edition - Interactive Exploration and Analysis of Large-Scale Microbiome Sequencing Data. *PLoS Comput Biol* **2016**; 12(6): e1004957.
 31. Li H. Aligning sequence reads, clone sequences and assembly contigs with BWA-MEM. *arXiv:13033997 [q-bioGN]* **2013**.
 32. <http://broadinstitute.github.io/picard>.
 33. Li H, Handsaker B, Wysoker A, et al. The Sequence Alignment/Map format and SAMtools. *Bioinformatics* **2009**; 25(16): 2078-9.
 34. Koboldt DC, Zhang Q, Larson DE, et al. VarScan 2: somatic mutation and copy number alteration discovery in cancer by exome sequencing. *Genome Res* **2012**; 22(3): 568-76.
 35. Elbe S, Buckland-Merrett G. Data, disease and diplomacy: GISAID's innovative contribution to global health. *Glob Chall* **2017**; 1(1): 33-46.
 36. Shu Y, McCauley J. GISAID: Global initiative on sharing all influenza data - from vision to reality. *Euro Surveill* **2017**; 22(13).
 37. Zhang Z, Li J, Zhao XQ, Wang J, Wong GK, Yu J. KaKs_Calculator: calculating Ka and Ks through model selection and model averaging. *Genomics Proteomics Bioinformatics* **2006**; 4(4): 259-63.
 38. Salter SJ, Cox MJ, Turek EM, et al. Reagent and laboratory contamination can critically impact sequence-based microbiome analyses. *BMC Biol* **2014**; 12: 87.

Table 1. The number of intra-host variants and polymorphisms in the genome of SARS-CoV-2

Gene	length	Intra-host variants			Polymorphisms			P-value ²
		NS	S	Ka/Ks ¹	NS	S	Ka/Ks	
orf1a	13203	30	9	0.676	34	14	0.493*	0.627
orf1b	8088	8	5	0.355	10	8	0.277*	1
S	3822	8	3	0.599	10	6	0.375	0.692
ORF3a	828	2	1	0.561	4	2	0.561	1
E	228	0	0	NA	0	0	NA	1
M	669	2	0	NA	1	1	0.318	1
ORF6	186	1	0	NA	0	0	NA	1
ORF7a	366	2	0	NA	3	0	NA	1
ORF8	366	2	2	0.228	2	1	0.456	1
N	1260	7	2	1.048	5	7	0.214*	0.184
ORF10	117	0	0	NA	1	0	NA	1
Sum	29133	62	22	0.578*	70	39	0.368*	0.164

¹. Ka/Ks was calculated using KaKs_Calculator2.0 (MS model)[37], an asterisk is added if Ka/Ks is significantly different from 1 ($p < 0.05$).

². P-value indicating whether a significant difference of Ka/Ks ratio was observed between two types of mutations in the gene, Fisher Exact test.

Table 2. The allele frequency changes in transmission from nCoV4 to nCoV7

POS ¹	Ref_nCoV4 ²	Alt_nCoV4 ³	FRE	Ref_nCoV7	Alt_nCoV7	FRE	P-value ⁴
376	119	177	0.598	9	0	0.000	0.0003
769	777	17	0.021	16	0	0.000	1
2037	1496	33	0.022	8	0	0.000	1
3290	2249	112	0.047	17	0	0.000	1
3306	1523	137	0.083	17	0	0.000	0.389
3321	1232	29	0.023	16	0	0.000	1
4511	685	26	0.037	11	0	0.000	1
4518	710	16	0.022	8	0	0.000	1
10771	1416	185	0.116	24	3	0.111	1
10773	1467	48	0.032	24	1	0.040	0.557
10779	987	401	0.289	18	8	0.308	0.829
10814	581	53	0.084	15	1	0.063	1
11387	653	15	0.022	4	0	0.000	1
13693	1237	38	0.030	9	0	0.000	1
15682	1321	46	0.034	8	1	0.111	0.269
15685	1342	47	0.034	8	1	0.111	0.270
18499	1783	108	0.057	19	0	0.000	0.621
18699	1013	46	0.043	12	0	0.000	1
21641	520	24	0.044	5	0	0.000	1
22270	2282	55	0.024	27	2	0.069	0.153
23127	1151	176	0.133	19	0	0.000	0.159
26177	492	11	0.022	6	0	0.000	1
27493	1535	1554	0.503	40	0	0.000	1.46E-12
28253	3600	487	0.119	34	0	0.000	0.028
29398	4671	127	0.026	47	0	0.000	0.636
Sum	34842	3968	0.102	421	17	0.028	1.45E-06

- ^{1.} The four intra-host variant positions with MAF \geq 5% and passing selection criteria were highlighted in bold.
- ^{2.} Number of reads supporting the reference allele.
- ^{3.} Number of reads supporting the alternative (mutant) allele.
- ^{4.} P-value indicates whether the difference of allele frequency between nCoV4 and nCoV7 is significant or not (Fisher Exact test).

Figure legends

Figure 1. Overview of the sequencing data. (A) The proportion of microbial reads in different groups; (B) Proportion of the viral read in patients infected with different viruses.

Figure 2. Intra-host variants in SARS-CoV-2 genome. (A) Genome coverage for SARS-CoV-2. A dash line indicates coverage of 50; (B) Frequency distribution of all intra-host variants, and the frequency of different mutations in polymorphism data was shown on the right side; (C) Distribution of the intra-host variations and polymorphisms on the genome of SARS-CoV-2. The outer ring displays the structure of the genome, following by the polymorphisms distribution on the genome. The length of each bar represents the number of sequences with this mutation. Due to a large variation of the number (1-27), 5% of the bar length was added for each additional sequence. The inner rings represent the distribution of intra-host variants in different patients (ID of each patient was labeled on each ring). Red bar indicates a synonymous mutation, and blue bar indicates a nonsynonymous mutation; (D) Frequency of the mutant allele at each high level (with frequency $\geq 20\%$) intra-host variant position. Nucleotides at the position (reference allele/alternative allele), mutation type (nonsynonymous, synonymous, noncoding), gene name, amino acid change were labeled on the right side of the heatmap. The total number of variants (with frequency $\geq 20\%$) in each sample was labeled on top of the heatmap. The name of five samples with more than 80% of the genome covered by at least 50-fold was labeled in blue. An open circle was added if the sample had a sequencing depth less than 50-fold at this position.

Figure 3. Microbiota in the BALF of COVID-19 patients, CAP patients, and healthy controls. A. Principal Coordinates Analysis (PCoA) of all samples. B. Heatmap of microbiota composition after QC filter (filters were described in Methods). The CAP samples were labeled as virus names followed by numbers. COVID-19 patients were highlighted by black rectangles, and two co-occurring bacterial clusters were highlighted by red rectangles. The names of all viruses are labeled in blue, and contaminant genera reported by Salter and colleagues are labeled in red[38].

Figure 1

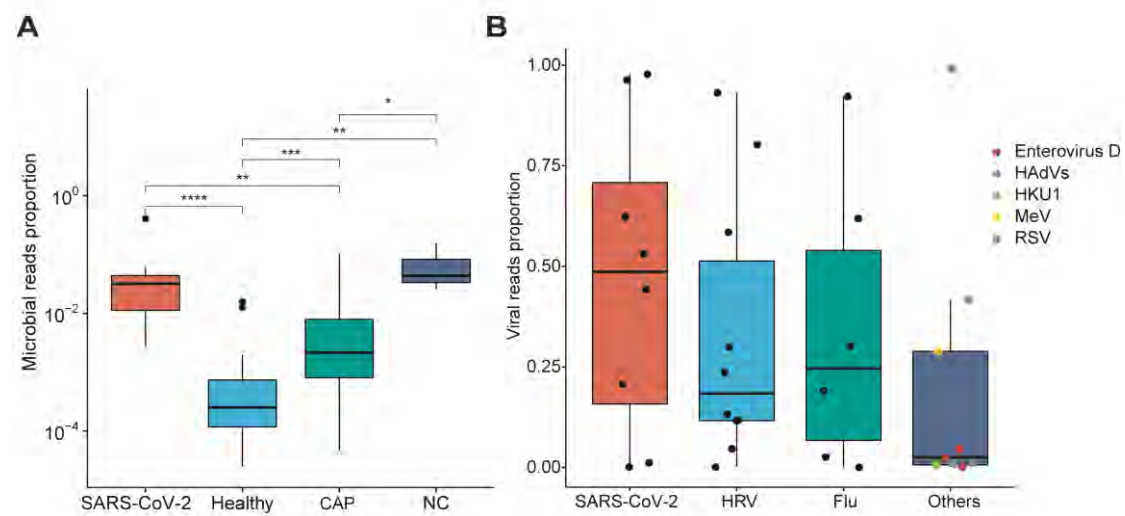
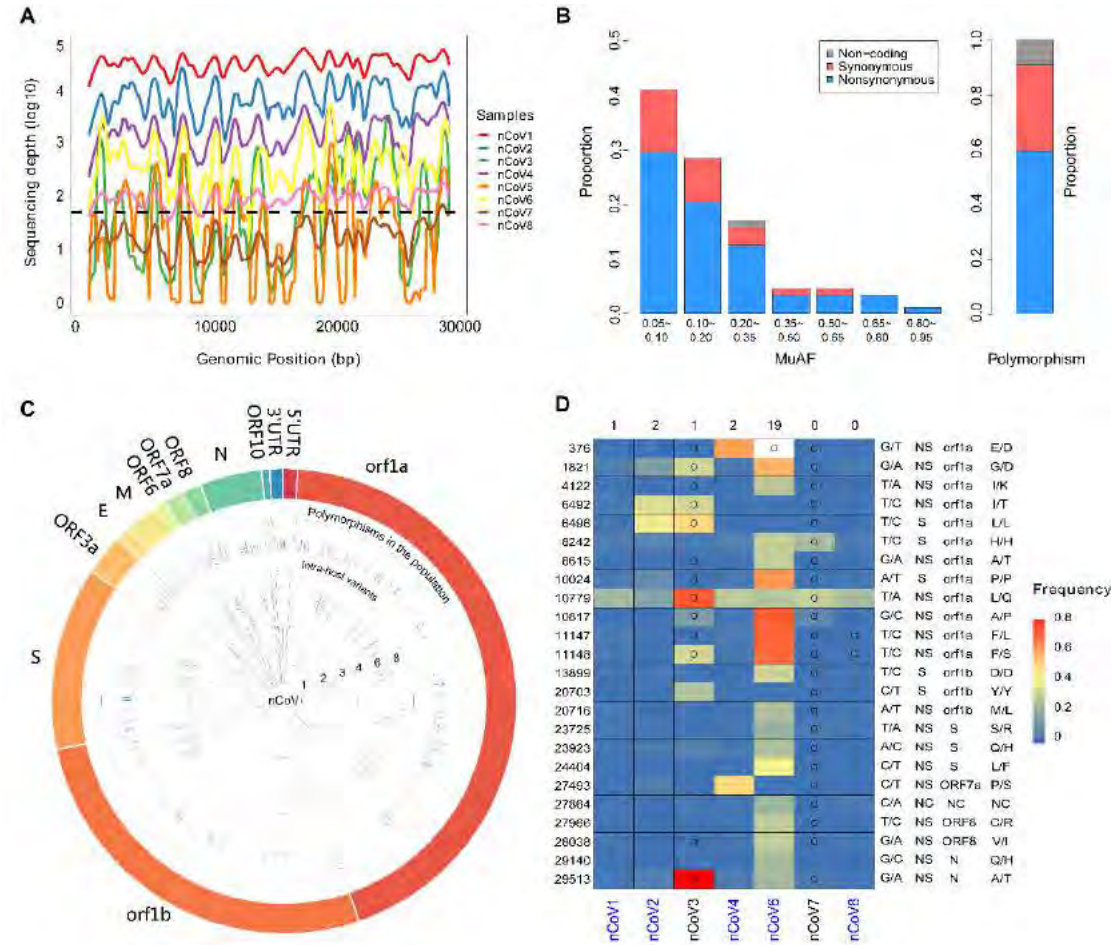


Figure 2





Contents lists available at ScienceDirect

International Journal of Infectious Diseases

journal homepage: www.elsevier.com/locate/ijidINTERNATIONAL
SOCIETY
FOR INFECTIOUS
DISEASES

Transmission potential and severity of COVID-19 in South Korea

Eunha Shim^{a,*}, Amna Tariq^b, Wongyeong Choi^a, Yiseul Lee^b, Gerardo Chowell^b^a Department of Mathematics, Soongsil University, 369 Sangdoro, Dongjak-Gu, Seoul, 06978, Republic of Korea^b Department of Population Health Sciences, School of Public Health, Georgia State University, Atlanta, GA, USA

ARTICLE INFO

Article history:

Received 4 March 2020

Received in revised form 10 March 2020

Accepted 10 March 2020

Keywords:

Coronavirus

COVID-19

Korea

Reproduction number

ABSTRACT

Objectives: Since the first case of 2019 novel coronavirus (COVID-19) identified on Jan 20, 2020, in South Korea, the number of cases rapidly increased, resulting in 6284 cases including 42 deaths as of Mar 6, 2020. To examine the growth rate of the outbreak, we present the first study to report the reproduction number of COVID-19 in South Korea.

Methods: The daily confirmed cases of COVID-19 in South Korea were extracted from publicly available sources. By using the empirical reporting delay distribution and simulating the generalized growth model, we estimated the effective reproduction number based on the discretized probability distribution of the generation interval.

Results: We identified four major clusters and estimated the reproduction number at 1.5 (95% CI: 1.4–1.6). In addition, the intrinsic growth rate was estimated at 0.6 (95% CI: 0.6, 0.7), and the scaling of growth parameter was estimated at 0.8 (95% CI: 0.7, 0.8), indicating sub-exponential growth dynamics of COVID-19. The crude case fatality rate is higher among males (1.1%) compared to females (0.4%) and increases with older age.

Conclusions: Our results indicate an early sustained transmission of COVID-19 in South Korea and support the implementation of social distancing measures to rapidly control the outbreak.

© 2020 The Author(s). Published by Elsevier Ltd on behalf of International Society for Infectious Diseases. This is an open access article under the CC BY-NC-ND license (<http://creativecommons.org/licenses/by-nc-nd/4.0/>).

Introduction

A novel coronavirus (SARS-CoV-2) that emerged out of the city of Wuhan, China, in December 2019 has already demonstrated its potential to generate explosive outbreaks in confined settings and cross borders following human mobility patterns (Mizumoto et al., 2020). While COVID-19 frequently induces mild symptoms common to other respiratory infections, it has also exhibited an ability to generate severe disease among certain groups, including older populations and individuals with underlying health issues such as cardiovascular disease and diabetes (Adler, 2020). Nevertheless, a clear picture of the epidemiology of this novel coronavirus is still being elucidated.

The number of cases of COVID-19 in the province of Hubei, the disease epicenter, quickly climbed following an exponential growth trend. The total number of COVID-19 cases is at 80,859, including 3100 deaths in China as of Mar 8, 2020 (WHO, 2020).

Fortunately, by Feb 15, 2020, the daily number of newly reported cases in China started to decline across the country, although Hubei Province reported 128 cases on average per day in the week of March 2–8, 2020 (WHO, 2020). While the epidemic continues to decline in China, 24,727 COVID-19 cases have been reported in more than 100 countries outside of China, including South Korea, Italy, Iran, Japan, Germany, and France (WHO, 2020). In particular, South Korea quickly became one of the hardest-hit countries with COVID-19, exhibiting a steadily increasing number of cases over the last few days. Hence, it is crucial to monitor the progression of these outbreaks and assess the effects of various public health measures, including the social distancing measures in real-time.

The first case in South Korea was identified on Jan 20, 2020, followed by the detection of one or two cases on average in the subsequent days. However, the number of confirmed cases of SARS-CoV-2 infection started to increase rapidly on Feb 19, 2020, with a total of 6284 confirmed COVID-19 cases including 42 deaths reported as of Mar 6, 2020, according to the Korea Centers for Disease Control and Prevention (KCDC) (KCDC, 2020) (Table 1). The epicenter of the South Korean COVID-19 outbreak has been identified in Daegu, a city of 2.5 million people, approximately 150 miles South East of Seoul. The rapid spread of COVID-19 in South Korea has been attributed to one case linked to a superspreading

* Corresponding author.

E-mail addresses: alicia@ssu.ac.kr (E. Shim), atariq1@student.gsu.edu (A. Tariq), chok10004@soongsil.ac.kr (W. Choi), yilee97@student.gsu.edu (Y. Lee), gchowell@gsu.edu (G. Chowell).

Table 1

The total number of confirmed and suspected cases as of Mar 6, 2020, as well as the case and fatality rate distribution by gender and age (KCDC, 2020).

Total	Confirmed cases				Suspected cases		
	Subtotal	Discharged	Isolated	Deceased	Subtotal	Being tested	Tested negative
164,740	6284	108	6,134	42	158,456	21,832	136,624
Classification		Cases (%)		Deaths (%)		Fatality rate (%)	
Total		6284 (100)		42 (100)		0.7	
Sex	Male	2,345 (37.3)		25 (59.5)		1.1	
	Female	3,939 (62.7)		17 (40.5)		0.4	
Age	0–9	45 (0.7)		–		–	
	10–19	292 (4.6)		–		–	
	20–29	1,877 (29.9)		–		–	
	30–39	693 (11.0)		1 (2.4)		0.1	
	40–49	889 (14.1)		1 (2.4)		0.1	
	50–59	1,217 (19.4)		5 (11.9)		0.4	
	60–69	763 (12.1)		11 (26.2)		1.4	
	70–79	340 (5.4)		14 (33.3)		4.1	
	Above 80	168 (2.7)		10 (23.8)		6.0	

event that has led to more than 3900 secondary cases stemming from church services in the city of Daegu (Kuhn, 2020; Ryall, 2020). This has led to sustained transmission chains of COVID-19, with 55% of the cases associated with the church cluster in Daegu (Bostock, 2020).

Moreover, three other clusters have been reported, including one set in Chundo Daenam hospital in Chungdo-gun, Gyeong-sangbuk-do (118 cases), one set in the gym in Cheonan, Chungcheongnam-do (92 cases), and one Pilgrimage to Israel cluster in Gyeongsangbuk-do (49 cases). These few clusters have become the primary driving force of the infection. A total of 33 cases were imported, while the four major clusters are composed of local cases, as described in Table 2.

The transmission of SARS-CoV-2 in Korea is exacerbated by amplified transmission in confined settings, including a hospital and a church in the city of Daegu. The hospital-based outbreak alone involves 118 individuals, including 9 hospital staff (News, 2020), which is reminiscent of past outbreaks of SARS and MERS (Chowell et al., 2015). To respond to the mounting number of cases of COVID-19, the Korean government has raised the COVID-19 alert level to the highest (Level 4) on Feb 23, 2020, to facilitate the implementation of comprehensive social distancing measures including enhanced infection control measures in hospitals, restricting public transportation, canceling of social events, and delaying the start of school activities (Kim, 2020).

While the basic reproduction number, denoted by R_0 , applies at the outset of an exponentially growing epidemic in the context of an entirely susceptible population and in the absence of public health measures and behavior changes, the effective reproduction number (R_t) quantifies the time-dependent transmission potential. This key epidemiological parameter tracks the average number of secondary cases generated per case as the outbreak progresses over time. Steady values of R_t above 1 indicate sustained disease

transmission, whereas values of $R_t < 1$ do not support sustained transmission, and the number of new cases is expected to follow a declining trend. In this report, using a mathematical model parameterized with case series of the COVID-19 outbreak in Korea, we investigated the transmission potential and severity of COVID-19 in Korea using preliminary data of local and imported cases reported up until Feb 26, 2020.

Methods

Data

We obtained the daily series of confirmed cases of COVID-19 in South Korea from Jan 20, 2020, to Feb 26, 2020, that are publicly available from the Korea Centers for Disease Control and Prevention (KCDC) (KCDC, 2020). Our data includes the dates of reporting for all confirmed cases, the dates of symptom onsets for the first 28 reported cases, and whether the case is autochthonous (local transmission) or imported. We also summarize the case clusters comprising one or more cases according to the source of infection, according to the field investigations conducted by the KCDC (KCDC, 2020). Accordingly, four major clusters were identified. The total number of confirmed and suspected cases as of Mar 6, 2020, as well as the crude case and fatality rate distribution by gender and age, are presented in Table 1.

Imputing the date of onset

To estimate the growth rate of the epidemic, it is ideal to characterize the epidemic curve according to dates of symptoms onset rather than dates of reporting. For the COVID-19 data in Korea, the symptom onset dates are available for only the first 28 reported cases. Moreover, all of the dates of symptoms onset are

Table 2

Characteristics of the largest COVID-19 clusters in South Korea as of Mar 8, 2020.

Cluster name	Cluster location	Cluster size	Reporting date for the first case linked to cluster	Reporting date for the last case linked to cluster
Shinchunji Church of Jesus	81, Daemyeong-ro, Nam-gu, Daegu, Republic of Korea	4482	2/18/2020	3/08/2020
Chundo Daenam hospital	79-7, Cheonghwa-ro, Hwayang-eup, Cheongdo-gun, Gyeongsangbuk-do, Republic of Korea	118	2/20/2020	2/29/2020
Cluster related to the gym in Cheonan	667, Dujong-dong, Seobuk-gu, Cheonan-si, Chungcheongnam-do, Republic of Korea	92	2/25/2020	3/08/2020
Pilgrimage to Israel	31, Guncheong-gil, Uiseong-eup, Uiseong-gun, Gyeongsangbuk-do, Republic of Korea	49	2/22/2020	3/02/2020

available for the imported cases. Therefore, we utilize this empirical distribution of reporting delays from the onset to diagnosis to impute the missing dates of onset for the remainder of the cases with missing data. For this purpose, we reconstruct 300 epidemic curves by dates of symptoms onset from which we derive a mean incidence curve of local case incidence and drop the last three data points from the analysis to adjust for reporting delays in our real-time analysis (Tariq et al., 2019).

Estimation of reproduction number from daily case incidence

We assess the effective reproduction number, R_t , which quantifies the time-dependent variations in the average number of secondary cases generated per case during an outbreak due to intrinsic factors (decline in susceptible individuals) and extrinsic factors (behavior changes, cultural factors, and the implementation of public health measures) (Anderson and May, 1991; Chowell et al., 2015; Nishiura et al., 2010). Using the Korean incidence curves for imported and local cases, we estimate the evolution of R_t for COVID-19 in Korea. First, we characterize daily local case incidence using a generalized growth model (GGM) (Viboud et al., 2016). This model describes the growth profile via two parameters: the growth rate parameter (r) and the scaling of the growth rate parameter (p). The model captures diverse epidemic profiles ranging from constant incidence ($p = 0$), sub-exponential or polynomial growth ($0 < p < 1$), and exponential growth ($p = 1$) (Viboud et al., 2016). The generation interval is assumed to follow a gamma distribution with a mean of 4.41 days and a standard deviation of 3.17 days (Nishiura et al., 2020; You et al., 2020).

Next, to estimate the most recent estimate of R_t , we simulate the progression of incident cases from GGM and apply the discretized probability distribution (ρ_i) of the generation interval

using the renewal equation (Nishiura and Chowell, 2009; Nishiura and Chowell, 2014; Paine et al., 2010) given by

$$R_{t_i} = \frac{I_i}{\sum_{j=0}^i (I_{i-j} + \alpha J_{i-j}) \rho_i}.$$

In the renewal equation, we denote the local incidence at calendar time t_i by I_i , and the raw incidence of imported cases at calendar time t_i by J_i . The parameter $0 \leq \alpha \leq 1$ quantifies the relative contribution of imported cases to secondary disease transmission (Nishiura and Roberts, 2010). The denominator represents the total number of cases that contribute to the incidence cases at time t_i . Next, we estimate R_t for 300 simulated curves assuming a Poisson error structure to derive the uncertainty bounds around the curve of R_t (Chowell, 2017).

Results

Reconstructed incidence of COVID-19

The reconstructed daily incidence curve of COVID-19 after imputing the onset dates for the Korean cases is shown in Figure 1. Between Jan 20 and Feb 18, 2020, an average of two new cases were reported each day, whereas, between February 19–26, 2020, 154 new cases were reported on average each day.

Effective reproduction number (R_t) from daily case incidence

Under the empirical reporting delay distribution from early Korean cases with available dates of onset, the intrinsic growth rate (r) was estimated at 0.6 (95% CI: 0.6, 0.7) and the scaling of growth parameter (p) was estimated at 0.8 (95% CI: 0.7, 0.8), indicating sub-exponential growth dynamics of COVID-19 in Korea (Figure 2, Table 3). The mean reproduction number R_t was estimated at 1.5

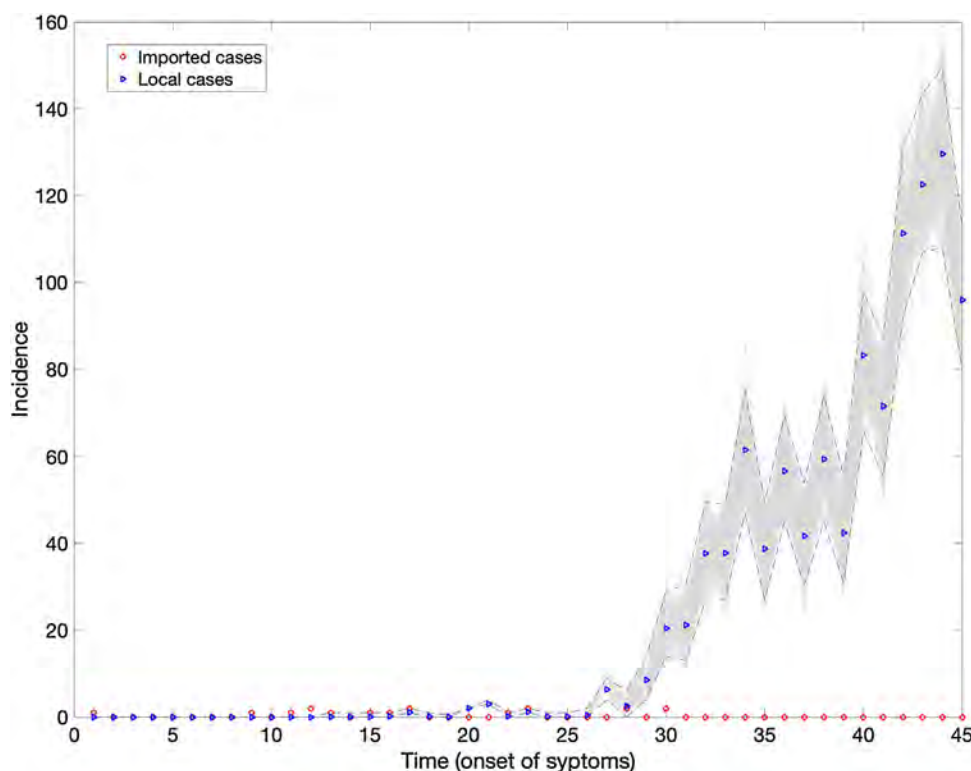


Figure 1. Reconstructed epidemic curve for the local Korean COVID-19 cases by the dates of onset as of February 26, 2020. The blue triangles represent the local cases, red triangles represent the imported cases and the gray curves correspond to the uncertainty in the local cases because of missing onset dates.

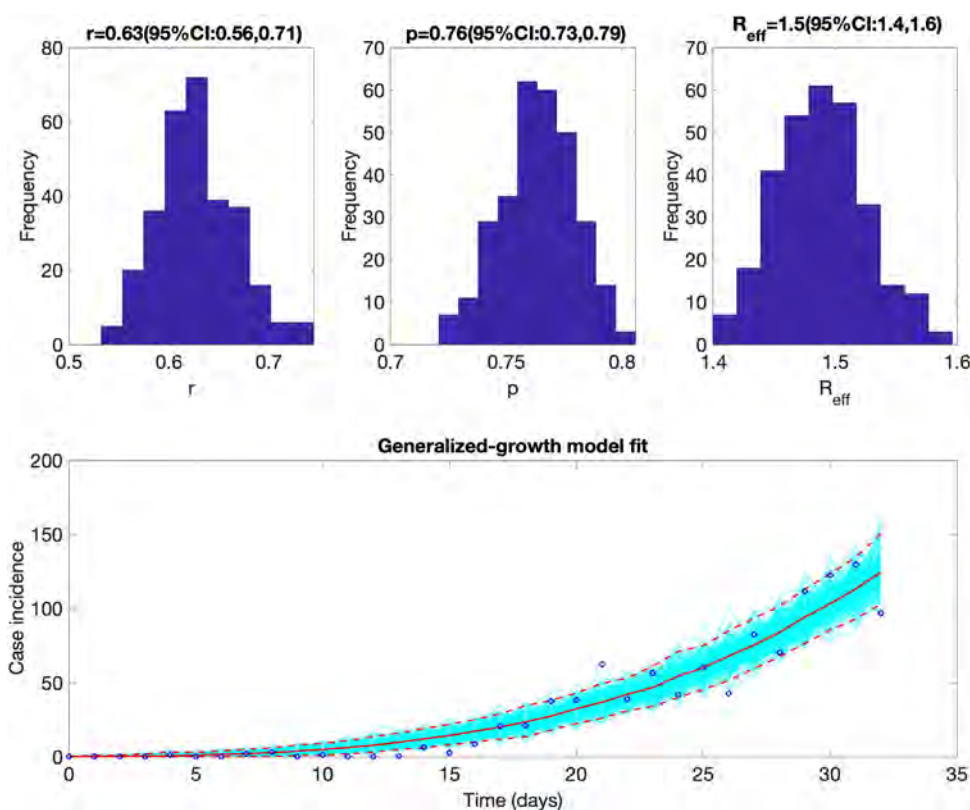


Figure 2. The mean reproduction number with 95% CI estimated by adjusting for the imported cases with $\alpha = 0.15$. Estimates for growth rate (r) and the scaling of the growth rate parameter (p) are also provided. The plot at the bottom depicts the fit of the Generalized Growth Model to the Korean data assuming Poisson error structure as of February 26, 2020.

Table 3

Mean estimates and the corresponding 95% confidence intervals for the effective reproduction number, growth rate, and the scaling of growth parameter during the early growth phase as of Feb 26, 2020.

Parameters	Estimated values
Reproduction number	1.5 (95% CI: 1.4, 1.6)
Growth rate, r	0.6 (95% CI: 0.6, 0.7)
Scaling of growth parameter, p	0.8 (95% CI: 0.7, 0.8)

(95% CI: 1.4, 1.6) as of Feb 26, 2020. Our estimates of R_t are not sensitive to changes in the parameter that modulates the contribution of the imported cases to transmission (α).

The crude case fatality rate

The crude case fatality rate is higher among males (1.1%) compared to females (0.4%) and increases with older age, from 0.1% among those 30–39 yrs to 6% among those ≥ 80 yrs as of Mar 6, 2020.

Transmission clusters

The spatial distribution of the Korean clusters is shown in Figure 3, and the characteristics of each cluster are presented in Table 2 as of Mar 8, 2020.

Shincheonji Church of Jesus cluster

As of Mar 8, 2020, 4482 confirmed cases of COVID-19 are linked to this cluster, according to the KCDC (KCDC, 2020). This largest cluster is associated with the Shincheonji Church of Jesus, with the first case (the 31st patient in the country) confirmed on Feb 18. It is

unclear how this case contracted the illness, as she does not present a recent history of travel or contact with another infected patient. However, before becoming a symptomatic case of COVID-19, she visited the hospital in Cheongdo after a minor car accident. After becoming a symptomatic case of COVID-19, she attended the Shincheonji Church of Jesus in Daegu twice. According to the KCDC, the patient had contact with 166 people, primarily at the Shincheonji Church and the hospital in Cheongdo; all those with whom the patient had contact, now placed themselves into self-quarantine. The Shincheonji church of Jesus has temporarily closed its facilities and halted the church activities as of Feb 18, 2020.

Chungdo Daenam hospital cluster

This cluster comprising 118 local cases and seven deaths is associated with Chungdo Daenam hospital, where South Korea's first coronavirus-associated case fatality occurred. Of the 118 cases, 92 were confirmed on Feb 22, 2020 (KCDC, 2020). A 63-year-old man who died of pneumonia at the hospital on Feb 19 was posthumously tested positive for COVID-19. On Feb 21, another patient at Daenam Hospital died from COVID-19, followed by another death on Feb 23. The confirmed cases were mainly from the psychiatric ward and include nine medical staff persons. The exact route of the infection is not yet known.

Cluster related to the gym in Cheonan

In the central cities of Cheonan, 92 COVID-19 patients were associated with a Zumba dance class after an instructor became the 5th confirmed case in Cheonan on Feb 25, 2020. According to the provincial government of South Chungcheong Province, everyone who attended the class in Cheonan was tested, and 27 cases were

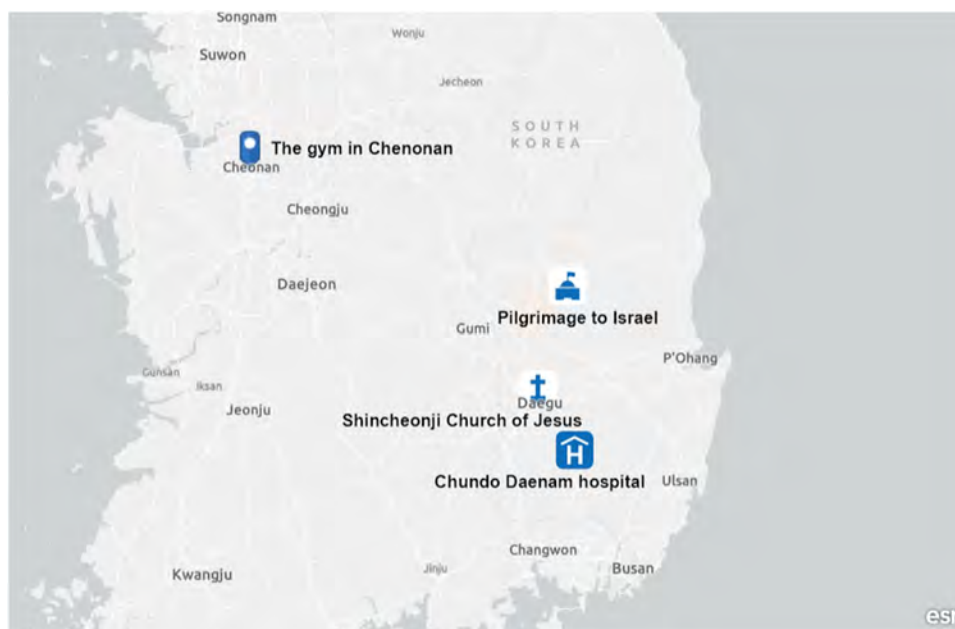


Figure 3. Map depicting the spatial distribution of the four largest clusters of COVID-19 in Korea as of March 8, 2020.

confirmed on Feb 28, 2020, with most of the cases being women in their 30's and 40's (KCDC, 2020). As of Mar 8, 2020, a total of 92 individuals were infected, including Zumba instructors and students, as well as their families and acquaintances (KCDC, 2020).

Pilgrimage tour to Israel related cluster

This cluster comprised 49 cases as of Mar 8, 2020. This cluster was identified when 31 Catholic pilgrims visited Israel between Feb 8, 2020, and Feb 16, 2020, and were subsequently confirmed to have COVID-19 (2020). Eleven individuals were diagnosed on Feb 17, 2020; twenty others were confirmed positive between February 21–25, 2020, and immediately quarantined. Of the 31 infected pilgrims, 19 came from Eiseong County, North Gyeongsang Province, while one patient, a tour guide, came from Seoul. Health authorities have traced multiple contacts by the cases of this cluster, and additional cases were confirmed after that, raising concerns about the potential risk of secondary infections.

Discussion

This is the first study to report estimates of the transmission potential of COVID-19 in Korea based on the trajectory of the epidemic, which was reconstructed by using the dates of onset of the first reported cases in Korea. The estimates of R clearly indicate the sustained transmission of the novel coronavirus in Korea; the case fatality rate appears to be higher among males and older populations (Table 1). Moreover, the imported cases contribute little to secondary disease transmission in Korea, as a majority of these cases occurred in the early phase of the epidemic, with the most recent imported case reported on Feb 9, 2020. These findings support the range of social distancing interventions that the Korean government put in place to bring the outbreak under control as soon as possible.

Our estimates of the reproduction number can be compared with earlier estimates reported for the epidemic in China, where the estimates of R lie in the range 2–7.1 (Lai et al., 2020; Li et al., 2020; Mizumoto et al., 2020; Read et al., 2020; Special Expert Group for Control of the Epidemic of Novel Coronavirus Pneumonia

of the Chinese Preventive Medicine A, 2020; Wu et al., 2020; Zhang et al., 2020; Zhou et al., 2020). Moreover, the mean R reached values as high as ~ 11 for the outbreak that unfolded aboard the Princess Cruises ship during January–February 2020 (Mizumoto and Chowell, 2020). In contrast, a recent study on Singapore's COVID-19 transmission dynamics reported lower estimates for R_t (1.1, 95% CI: 1.1, 1.3) as of Feb 19, 2020, reflecting a significant impact of the control interventions that were implemented in Singapore (Tariq et al., 2020). The estimates of the scaling of growth parameter (p) in our study indicate sub-exponential growth dynamics of COVID-19 in Korea. This aligns well with the sub-exponential growth patterns of COVID-19 in Singapore and all Chinese provinces except Hubei (Roosa et al., 2020; Tariq et al., 2020).

Since the first COVID-19 case was reported on Jan 20, 2020, the epidemic's trajectory showed a rapid upturn until Feb 18, 2020, when a superspreader (Case 31) was identified in the Shincheonji Church of Jesus in Daegu cluster. Since then, Korea's confirmed cases have risen tremendously. In fact, 55% of confirmed cases are linked to one cluster of infections, i.e., the Shincheonji Church of Jesus in Daegu (KCDC, 2020). Such superspreading events have been reported earlier for the 2015 MERS outbreak in South Korea (Cowling et al., 2015). Amplification of MERS in the hospital setting has been associated with diagnostic delays, which increase the window of opportunity for the generation of secondary cases (Chowell et al., 2015). This underscores the need for rapid testing, case detection, and active contact tracing to isolate infectious individuals.

Beyond Korea, substantial COVID-19 transmission has been reported in Italy, Iran, Germany, France, and aboard the Diamond cruise ship (Marcus, 2020; Woods, 2020). While the Chungdo Daenam hospital cluster and the cluster related to the Pilgrimage tour to Israel seem to have stabilized, the other two clusters are still being consolidated. Public health authorities are currently focused on containing the outbreak in the city of Daegu, the epicenter of the outbreak, and North Gyeongsang Province, where active contact tracing is being conducted. Nation-wide preventative measures are expected to reduce community transmission and ultimately bring R_t below one.

This is the first study to estimate the transmission potential and severity of COVID-19 in Korea. Our current findings suggest that there is a sustained disease transmission in the region, underscoring the need to implement a wide array of social distancing measures to rapidly contain the outbreak in Korea, mitigate the morbidity and mortality impact of the disease, and stem the number of case exportations to other nations.

Contributions

ES, AT, and GC analyzed the data. YS and WC retrieved and managed the data. ES, AT, and GC wrote the first draft of the paper. All authors contributed to the writing of this article.

Financial support

For ES and WC, this work was supported by the National Research Foundation of Korea (NRF) grant funded by the Korea government(MSIT) (No. 2018R1C1B6001723).

Conflict of interest

None.

Ethical approval

Not required.

References

- Adler SE. Why coronaviruses hit older adults hardest. *AARP*; 2020.
- Anderson RM, May RM. In: Oxford, editor. *Infectious Diseases of Humans*. Oxford University Press; 1991.
- Bostock B. South Korea is testing 200,000 members of a doomsday church linked to more than 60% of its coronavirus cases. *Business Insider*; 2020.
- Chowell G. Fitting dynamic models to epidemic outbreaks with quantified uncertainty: a primer for parameter uncertainty, identifiability, and forecasts. *Infect Dis Modell* 2017;2(3):379–98.
- Chowell G, Abdirizak F, Lee S, Lee J, Jung E, Nishiura H, et al. Transmission characteristics of MERS and SARS in the healthcare setting: a comparative study. *BMC Med* 2015;13(1):210.
- Cowling BJ, Park M, Fang VJ, Wu P, Leung GM, Wu JT. Preliminary epidemiological assessment of MERS-CoV outbreak in South Korea, May to June 2015. *Euro Surveill* 2015;20(25):7–13.
- Nishiura H, Chowell G. The effective reproduction number as a prelude to statistical estimation of time-dependent epidemic trends. *Math Stat Estim Approach Epidemiol* 2009;103–12 Springer D.
- KCDC. The updates on COVID-19 in Korea as of Feb 25. Seoul, Korea: Korea Centers for Disease Control and Prevention; 2020.
- Kim C. As Covid-19 cases rise, South Korea raises virus threat level to its maximum. *Vox*; 2020.
- Kuhn A. Secretive church sect at the center of South Korea's coronavirus outbreak. *NPR*; 2020.
- Lai A, Bergna A, Acciarri C, Galli M, Zehender G. Early phylogenetic estimate of the effective reproduction number Of Sars-CoV-2. *J Med Virol* 2020;.
- Li Q, Guan X, Wu P, Wang X, Zhou L, Tong Y, et al. Early transmission dynamics in Wuhan, China, of novel coronavirus-infected pneumonia. *N Engl J Med* 2020;.
- Marcus I. Chronology: Germany and Covid 19 ('Coronavirus'). *The Berlin Spectator*; 2020.
- Mizumoto K, Chowell G. Transmission potential of the novel coronavirus (COVID-19) onboard the Diamond Princess Cruises Ship, 2020. *medRxiv* 2020;2020:02.24.20027649.
- Mizumoto K, Kagaya K, Chowell G. Early epidemiological assessment of the transmission potential and virulence of 2019 Novel Coronavirus in Wuhan City: China, 2019–2020. *medRxiv* 2020;2020: 02.12.20022434.
- News B. Coronavirus: South Korea declares highest alert as infections surge. *BBC News*; 2020.
- Nishiura H, Chowell G. Early transmission dynamics of Ebola virus disease (EVD), West Africa, March to August 2014. *Euro Surveill* 2014;19(36).
- Nishiura H, Chowell G, Heesterbeek H, Wallinga J. The ideal reporting interval for an epidemic to objectively interpret the epidemiological time course. *J R Soc Interface* 2010;7(43):297–307.
- Nishiura H, Linton NM, Akhmetzhanov AR. Serial interval of novel coronavirus (2019-nCoV) infections. *medRxiv* 2020;2020: 02.03.20019497.
- Nishiura H, Roberts MG. Estimation of the reproduction number for 2009 pandemic influenza A(H1N1) in the presence of imported cases. *Eurosurveillance* 2010;15(29):19622.
- Paine S, Mercer GN, Kelly PM, Bandaranayake D, Baker MG, Huang QS, et al. Transmissibility of 2009 pandemic influenza A(H1N1) in New Zealand: effective reproduction number and influence of age, ethnicity and importations. *Euro Surveill* 2010;15(24).
- Read JM, Bridgen JR, Cummings DA, Ho A, Jewell CP. Novel coronavirus 2019-nCoV: early estimation of epidemiological parameters and epidemic predictions. *medRxiv* 2020;.
- Roosa K, Lee Y, Luo R, Kirpich A, Rothenberg R, Hyman JM, et al. Real-time forecasts of the COVID-19 epidemic in China from Feb 5 to Feb 24, 2020. *Infect Dis Modell* 2020;5:256–63.
- Ryall J. Coronavirus: Surge in South Korea virus cases linked to church 'super-spreader'. *The Telegraph*: Telegraph Media Group Limited; 2020.
- Special Expert Group for Control of the Epidemic of Novel Coronavirus Pneumonia of the Chinese Preventive Medicine A. [An update on the epidemiological characteristics of novel coronavirus pneumoniaCOVID-19]. *Zhonghua liu xing bing xue za zhi = Zhonghua liuxingbingxue zazhi* 2020;41(2):139–44.
- Tariq A, Lee Y, Roosa K, Blumberg S, Yan P, Ma S, et al. Real-time monitoring the transmission potential of COVID-19 in Singapore, February 2020. *medRxiv* 2020;2020: 02.21.20026435.
- Tariq A, Roosa K, Mizumoto K, Chowell G. Assessing reporting delays and the effective reproduction number: the Ebola epidemic in DRC, May 2018–January 2019. *Epidemics* 2019;26:128–33.
- Viboud C, Simonsen L, Chowell G. A generalized-growth model to characterize the early ascending phase of infectious disease outbreaks. *Epidemics* 2016;15:27–37.
- WHO. Coronavirus disease (COVID-2019) situation reports. 2020 Available from: <https://www.who.int/emergencies/diseases/novel-coronavirus-2019/situation-reports>. [Accessed Feb 27, 2020].
- Woods A. 44 new coronavirus cases reported on quarantined Diamond Princess cruise. *New York Post*; 2020.
- Wu JT, Leung K, Leung GM. Nowcasting and forecasting the potential domestic and international spread of the 2019-nCoV outbreak originating in Wuhan, China: a modelling study. *Lancet* 2020;.
- You C, Deng Y, Hu W, Sun J, Lin Q, Zhou F, et al. Estimation of the Time-Varying Reproduction Number of COVID-19 Outbreak in China. *medRxiv* 2020;2020:02.08.20021253.
- Zhang S, Diao M, Yu W, Pei L, Lin Z, Chen D. Estimation of the reproductive number of Novel Coronavirus (COVID-19) and the probable outbreak size on the Diamond Princess cruise ship: a data-driven analysis. *Int J Infect Dis* 2020;.
- Zhou T, Liu Q, Yang Z, Liao J, Yang K, Bai W, et al. Preliminary prediction of the basic reproduction number of the Wuhan novel coronavirus 2019-nCoV. *J Evid Based Med* 2020;.

Pathogenesis and transmission of SARS-CoV-2 in golden hamsters

<https://doi.org/10.1038/s41586-020-2342-5>

Received: 26 March 2020

Accepted: 7 May 2020

Published online: 14 May 2020

 Check for updates

Sin Fun Sia^{1,3}, Li-Meng Yan^{1,3}, Alex W. H. Chin^{1,3}, Kevin Fung², Ka-Tim Choy¹, Alvina Y. L. Wong¹, Prathanporn Kaewpreedee¹, Ranawaka A. P. M. Perera¹, Leo L. M. Poon¹, John M. Nicholls², Malik Peiris¹ & Hui-Ling Yen^{1✉}

Severe acute respiratory syndrome coronavirus 2 (SARS-CoV-2), a novel coronavirus with high nucleotide identity to SARS-CoV and to SARS-related coronaviruses that have been detected in horseshoe bats, has spread across the world and had a global effect on healthcare systems and economies^{1,2}. A suitable small animal model is needed to support the development of vaccines and therapies. Here we report the pathogenesis and transmissibility of SARS-CoV-2 in golden (Syrian) hamsters (*Mesocricetus auratus*). Immunohistochemistry assay demonstrated the presence of viral antigens in nasal mucosa, bronchial epithelial cells and areas of lung consolidation on days 2 and 5 after inoculation with SARS-CoV-2, followed by rapid viral clearance and pneumocyte hyperplasia at 7 days after inoculation. We also found viral antigens in epithelial cells of the duodenum, and detected viral RNA in faeces. Notably, SARS-CoV-2 was transmitted efficiently from inoculated hamsters to naive hamsters by direct contact and via aerosols. Transmission via fomites in soiled cages was not as efficient. Although viral RNA was continuously detected in the nasal washes of inoculated hamsters for 14 days, the communicable period was short and correlated with the detection of infectious virus but not viral RNA. Inoculated and naturally infected hamsters showed apparent weight loss on days 6–7 post-inoculation or post-contact; all hamsters returned to their original weight within 14 days and developed neutralizing antibodies. Our results suggest that features associated with SARS-CoV-2 infection in golden hamsters resemble those found in humans with mild SARS-CoV-2 infections.

SARS-CoV-2 was first detected from a cluster of patients with pneumonia in Wuhan (Hubei province, China) in December 2019. Although 55% of the initial cases were linked to one seafood wholesale market at which wild animals were also sold³, multiple viral (sustained human-to-human transmissibility by symptomatic and pre-symptomatic individuals⁴) and ecological (extensive domestic and international travel during Chinese Lunar New Year) factors have contributed to the rapid global spread of the virus. The clinical spectrum of patients with coronavirus disease 2019 (COVID-19) is wide; 19% of 44,415 confirmed patients in China progressed to severe and critical illness⁵, with an estimated 1.4% case fatality risk in symptomatic cases⁶. There is no approved vaccine or treatment against SARS-CoV-2, and the available interventions—including country lockdowns and social distancing—have severely disrupted the global supply chain and economy.

A suitable animal model is essential for understanding the pathogenesis of this disease and for evaluating vaccine and therapeutic candidates. Previous animal studies on SARS-CoV have suggested the importance of the interaction between the viral spike protein and the host angiotensin-converting enzyme 2 (ACE2) receptor^{7–10}, as well as age and innate immune status of the animals^{11–14} in pathogenesis. As with SARS-CoV, the spike protein of SARS-CoV-2 also uses ACE2 as the entry receptor¹. ACE2 is expressed on the surface

of alveolar epithelial cells and enterocytes of the small intestine and can be detected in endothelial cells and arterial smooth muscle cells¹⁵. SARS-CoV-2 showed good binding to human ACE2 but limited binding to mouse ACE2¹, which has limited the use of inbred mice for research. Macaques and transgenic ICR mice that express the human ACE2 receptor have been shown to be susceptible to infection with SARS-CoV-2^{16–18}; however, there is limited availability of these animal models. Cynomolgus macaques and rhesus macaques challenged with SARS-CoV-2 showed pneumonia with limited¹⁷ and moderate¹⁸ clinical signs, respectively. The transgenic mice challenged with SARS-CoV-2 showed pneumonia, moderate weight loss and no apparent histological changes in nonrespiratory tissues¹⁶. Previously generated transgenic mice that express the human ACE2 receptor have been reported to support the replication of SARS-CoV in the epithelial cells of the airway, but were associated with neurological-related mortality owing to high ACE2 expression in the brain^{7–10}.

The golden hamster is a widely used experimental animal model and has previously been reported to support replication of SARS-CoV^{19,20}—but not Middle Eastern respiratory syndrome coronavirus (MERS-CoV)²¹, which uses the dipeptidyl peptidase 4 (DPP4) protein as the main receptor for viral entry. A previous study of the SARS-CoV Urbani strain in 5-week-old golden hamsters

¹School of Public Health, Li Ka Shing Faculty of Medicine, The University of Hong Kong, Hong Kong, China. ²Department of Pathology, Li Ka Shing Faculty of Medicine, The University of Hong Kong, Hong Kong, China. ³These authors contributed equally: Sin Fun Sia, Li-Meng Yan, Alex W. H. Chin. [✉]e-mail: hyen@hku.hk

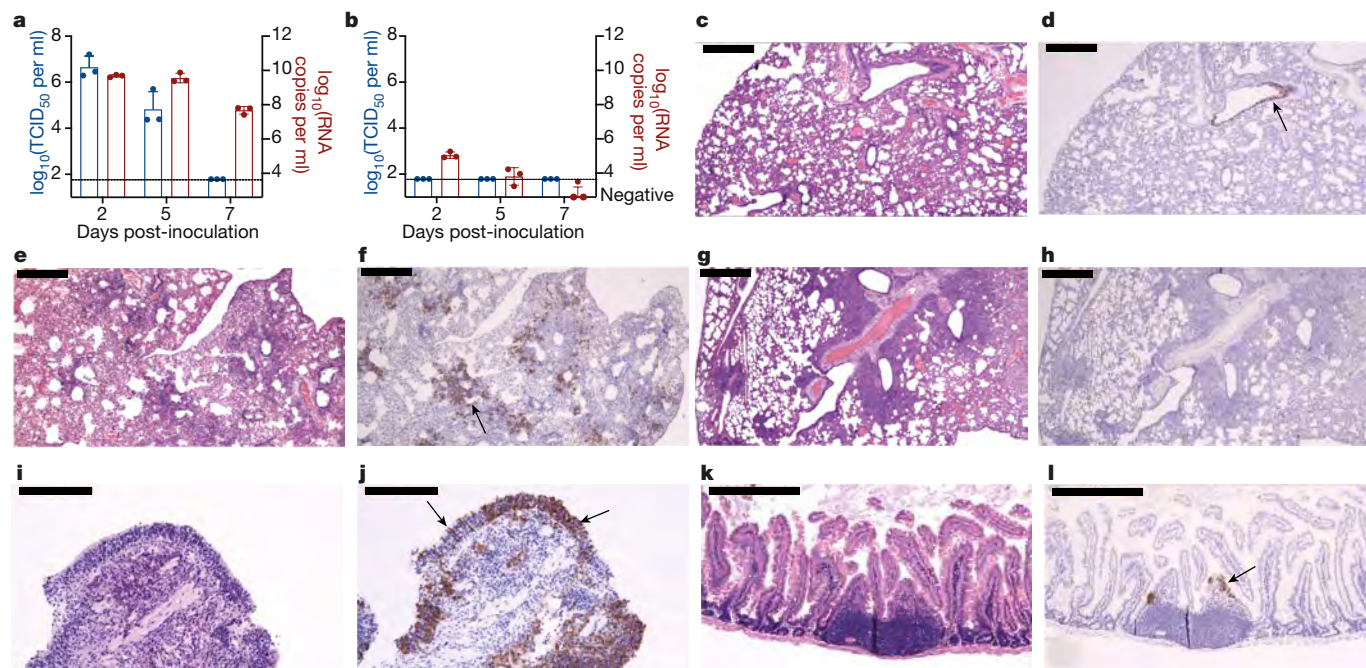


Fig. 1 | Viral load and histopathological changes in golden hamsters intranasally challenged with SARS-CoV-2. **a**, Infectious viral load ($\log_{10}(\text{TCID}_{50} \text{ per ml})$) and viral RNA ($\log_{10}(\text{RNA copies per ml})$) detected in the lungs of hamsters challenged with SARS-CoV-2 ($n=3$) at 2, 5 and 7 dpi. **b**, Infectious viral load and viral RNA detected in the kidney of hamsters challenged with SARS-CoV-2 ($n=3$) at 2, 5 and 7 dpi. Individual data points and mean \pm s.d. are shown; the detection limit ($1.789 \log_{10}(\text{TCID}_{50} \text{ per ml})$) is shown by the dotted line. **c**, Haematoxylin and eosin (H&E) staining of the lungs of hamsters challenged with SARS-CoV-2 at 2 dpi. **d**, Detection of SARS-CoV-2 N protein at bronchial epithelial cells (indicated by an arrow) by immunohistochemistry at 2 dpi. **e**, H&E staining of the lungs at 5 dpi. **f**, Detection of N protein in pneumocytes with lung consolidation (indicated by an arrow) at 5 dpi. **g**, H&E staining of the lungs at 7 dpi. **h**, The lack of detection of N

protein in the lungs at 7 dpi. **i**, H&E staining of nasal turbinate of hamsters challenged with SARS-CoV-2 at 2 dpi. **j**, Detection of N protein in nasal epithelial cells (arrow on the right) and cells morphologically resembling olfactory neurons (arrow on the left) at 2 dpi. **k**, H&E staining of duodenum of hamsters challenged with SARS-CoV-2 at 2 dpi. **l**, Detection of N protein in the duodenum epithelial cells at 2 dpi. The experiment was performed once with 9 hamsters challenged with $8 \times 10^4 \text{ TCID}_{50}$ of SARS-CoV-2, and tissues were collected from 3 hamsters for histopathology examination and immunohistochemistry at each time point. H&E staining and immunohistochemistry performed using tissues from three hamsters showed comparable results; representative images are shown. Scale bars, 200 μm (**i**, **j**), 500 μm (**c**–**h**, **k**, **l**).

showed robust viral replication, with peak viral titres detected in the lungs at 2 days post-inoculation (dpi) followed by rapid viral clearance by 7 dpi, but without weight loss or evidence of disease in the inoculated hamsters²⁰. A follow-up study that reported the testing of different strains of SARS-CoV in golden hamsters found differences in virulence between these strains; lethality was reported in hamsters challenged with the Frk-1 strain, which differs from the nonlethal Urbani strain by an L1148F substitution in the S2 domain¹⁹. Hamsters are permissive for infection by other respiratory viruses—including human metapneumovirus²², human parainfluenza virus 3²³ and influenza A virus—and may support influenza transmission by contact or airborne routes^{24,25}. Alignment of the ACE2 proteins of human, macaque, mouse and hamster suggest that the spike protein of SARS-CoV-2 may interact more efficiently with hamster ACE2 than mouse ACE2 (Extended Data Fig. 1). Here we evaluate the pathogenesis and contact transmissibility of SARS-CoV-2 in 4–5-week-old male golden hamsters.

Hamsters were infected intranasally with 8×10^4 50% tissue culture infective dose (TCID_{50}) of SARS-CoV-2 (BetaCoV/Hong Kong/VM20001061/2020; GISAID identifier EPI_ISL_412028), isolated in Vero E6 cells from the nasopharynx aspirate and throat swab of a patient from Hong Kong with a confirmed case of COVID-19. At 2, 5 and 7 dpi, the nasal turbinate, brain, lungs, heart, duodenum, liver, spleen and kidney were collected to monitor viral replication and histopathological changes. Peak viral load in the lungs was detected at 2 dpi and decreased at 5 dpi; no infectious virus was detected at 7 dpi despite of the continued detection of high copies of viral RNA (Fig. 1a). Infectious

viral load was significantly different between 2 and 7 dpi ($P = 0.019$, Dunn's multiple comparisons test), but the RNA copy number was not ($P = 0.076$). No infectious virus was detected in the kidney, although low copies of viral RNA were detected at 2 and 5 dpi (Fig. 1b).

Histopathological examination detected an increase in inflammatory cells and consolidation in 5–10% of the lungs at 2 dpi (Fig. 1c, d) and 15–35% of the lungs at 5 dpi (Fig. 1e, f). We observed mononuclear cell infiltrate in areas in which viral antigen was detected at 2 and 5 dpi. Immunohistochemistry for the nucleocapsid (N) protein of SARS-CoV-2 demonstrated viral antigen in the bronchial epithelial cells at 2 dpi (Fig. 1d), with progression to pneumocytes at 5 dpi (Fig. 1f). At 7 dpi, there was an increased consolidation in 30–60% of the lungs (Fig. 1g); however, no viral antigen was detected at this time point (Fig. 1h) and type-2 pneumocyte hyperplasia was prominent (Extended Data Fig. 2a). CD3-positive T lymphocytes were detected in the peribronchial region at 5 dpi, which may facilitate the rapid clearance of the infected cells (Extended Data Fig. 2b). There was moderate inflammatory-cell infiltration in the nasal turbinate (Fig. 1i), and viral antigen was detected in the nasal epithelial cells (Fig. 1j) and in olfactory sensory neurons at the nasal mucosa (Fig. 1j). Infection in the olfactory neurons was further confirmed in cells that express both SARS-CoV-2 N protein and neuron-specific tubulin- β III (Extended Data Fig. 2c). Compared to mock infection (Extended Data Fig. 2d, e), infection with SARS-CoV-2 leads to a reduction in the number of olfactory neurons at the nasal mucosal at 2 dpi (Extended Data Fig. 2f), prominent nasal epithelial attenuation at 7 dpi (Extended Data Fig. 2g), followed by tissue repair at 14 dpi (Extended Data Fig. 2h).

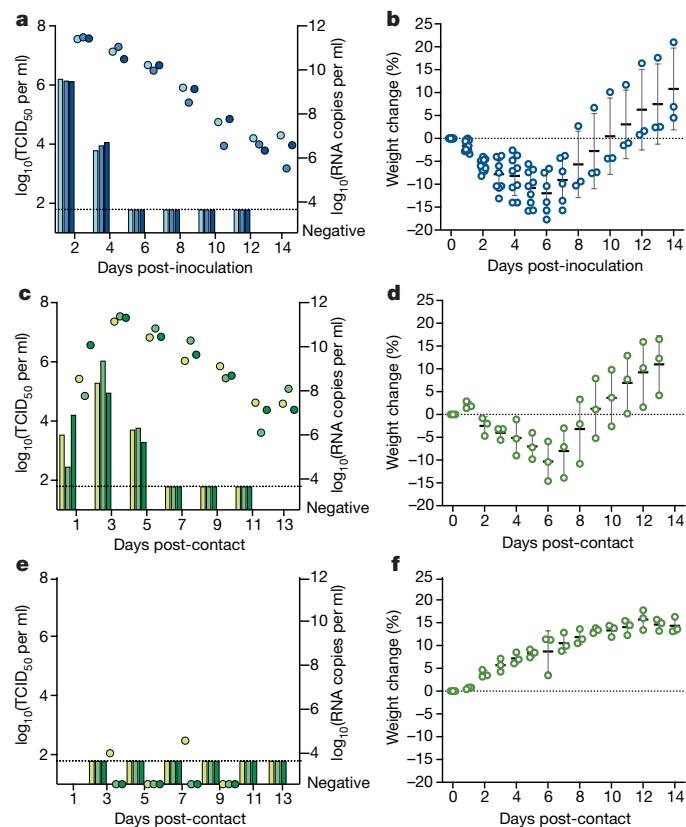


Fig. 2 | Transmission of SARS-CoV-2 in golden hamsters by direct contact.

a, Infectious viral load (\log_{10} (TCID₅₀ per ml), shown as bars) and viral RNA copy numbers (\log_{10} (RNA copies per ml), shown as dots) detected in the nasal washes of donor hamsters ($n=3$) inoculated with 8×10^4 TCID₅₀ of SARS-CoV-2. Colour-matched bars and dots represent results from the same hamster. **b**, Changes in body weight (per cent weight change compared to day 0) of hamsters inoculated with SARS-CoV-2 ($n=9$, including 3 donors and 9 hamsters challenged with SARS-CoV-2, described in Fig. 1); individual data points and mean \pm s.d. are shown. **c**, Transmission of SARS-CoV-2 to naive hamsters ($n=3$), each of which was cohoused with one inoculated donor at 1 dpi; infectious viral load and viral RNA copy numbers detected in the nasal washes of contact hamsters are shown. **d**, Changes in body weight (per cent weight change compared to the day of exposure) of contact hamsters ($n=3$) cohoused with inoculated donor at 1 dpi. **e**, Transmission of SARS-CoV-2 to naive hamsters ($n=3$), each of which was cohoused with one donor at 6 dpi; infectious viral load and viral RNA copy numbers detected in the nasal washes of contact hamsters are shown. **f**, Changes in body weight (per cent weight change compared to the day of exposure) of contact hamsters ($n=3$) cohoused with inoculated donors at 6 dpi. Direct-contact transmission experiments of cohoused donors and naive contacts at 1 dpi and 6 dpi (of the donor), respectively, were each performed once, each with three pairs of donor:direct contact at 1:1 ratio.

Though no inflammation was present (Fig. 1k), viral antigen was detected from the epithelial cells of duodenum at 2 dpi (Fig. 1l). This resembles the detection of replication of SARS-CoV in the epithelial cells of the terminal ileum and colon of patients with SARS-CoV without observing apparent architectural disruption and inflammatory infiltrate²⁶. No apparent histopathological change was observed from the brain, heart, liver and kidney at 5 dpi (Extended Data Fig. 2i–l).

To assess the transmission potential of the SARS-CoV-2 in hamsters, we intranasally inoculated three donor hamsters with 8×10^4 TCID₅₀ of the virus. At 24 hours after inoculation, each donor was transferred to a new cage and cohoused with one naive hamster. Weight changes and clinical signs were monitored daily and nasal washes were collected

every other day from donors and contacts, for 14 days. In donors, the peak infectious viral load in nasal washes was detected soon after inoculation and was followed by a rapid decline, although viral RNA was detected continuously for 14 days (Fig. 2a). Hamsters inoculated with SARS-CoV-2 showed their maximal mean weight loss (mean \pm s.d., $-11.97 \pm 4.51\%$, $n=6$) at 6 dpi (Fig. 2b). Transmission from donor to cohoused contact hamsters was efficient, and SARS-CoV-2 was detected from the cohoused hamsters at 1 day post-contact (dpc), and the peak viral load in nasal washes was detected at 3 dpc (Fig. 2c). The total viral load shed in the nasal washes was approximated by calculating the area under the curve for each hamster. The amount of virus shed in the nasal washes of contact hamsters was comparable to that of the donor hamsters ($P=0.1$, two-tailed Mann–Whitney test). Contact hamsters showed their maximal mean weight loss (mean \pm s.d., $-10.68 \pm 3.42\%$, $n=3$) at 6 dpc; all hamsters had returned to their original weight by 11 dpc (Fig. 2d). Neutralizing antibodies were detected using 90% plaque reduction neutralization (PRNT₉₀) assay from donor hamsters at 14 dpi (titres at 1:640 for all) and from contact hamsters on 13 dpc (titres at 1:160, 1:320 and 1:160). As viral RNA was continuously detected in the nasal washes of the donor for 14 days (whereas infectious virus titres decreased rapidly), we repeated the experiment and cohoused naive contact with donor hamsters at 6 dpi. A low quantity of viral RNA was detected in the nasal washes in one contact hamster at 3 and 7 dpc, without detection of infectious virus in the nasal washes (Fig. 2e); none of the contact hamsters showed weight loss (Fig. 2f). A PRNT₉₀ assay detected no neutralizing antibody ($<1:10$) from the contact hamsters at 12 dpc. The results suggest that the donor hamsters inoculated with SARS-CoV-2 have a short communicable period, of less than six days. Onward transmissibility from donor to cohoused contact hamsters was correlated with the detection of infectious virus, but not viral RNA, in the donor nasal washes.

The transmission from donor to cohoused contact hamster may have been mediated by multiple transmission routes. To investigate the transmissibility of SARS-CoV-2 among hamsters via aerosols (a collection of liquid or solid particles suspended in air and may include large droplets and fine droplet nuclei²⁷), donor hamsters and naive aerosol-contact hamsters were placed in two adjacent wire cages for 8 h at 1 dpi (of the donor) (Extended Data Fig. 3). The experiment was performed in three pairs of donor:aerosol-contact hamsters at a 1:1 ratio. The hamsters were single-housed after exposure, and were monitored daily for 14 days. Donor hamsters shed infectious virus in the nasal washes for 6 days, whereas viral RNA could be continuously detected for 14 days (Fig. 3a). Viral RNA was detected in the faecal samples of the donors at 2, 4 and 6 dpi, without detection of infectious virus (Fig. 3b). All donor hamsters showed comparable weight loss (Fig. 3c), as observed previously (Fig. 2b). Transmission via aerosols was efficient, as shown by the fact that infectious virus was detected in the nasal washes from all exposed contact hamsters at 1 dpc, with peak viral loads detected at 3 dpc (Fig. 3d). Viral RNA was continuously detected from the faecal samples of the infected aerosol-contact hamsters for 14 days, although no infectious virus was isolated (Fig. 3e). The aerosol-contact hamsters showed their maximal weight loss (mean \pm s.d., $-7.72 \pm 5.42\%$, $n=3$) at 7 dpc (Fig. 3f). The amount of virus shed in the nasal washes (approximated by area under the curve) of aerosol-contact hamsters was comparable to that of the donor hamsters ($P=0.4$, two-tailed Mann–Whitney test). Neutralizing antibodies were detected using PRNT₉₀ assay from the donor hamsters at 16 dpi (titres at 1:320, 1:640 and 1:640) and the contact hamsters at 15 dpc (titres at 1:640 for all). To evaluate the transmission potential of SARS-CoV-2 via fomites, three naive fomite-contact hamsters were each introduced to a soiled cage that had housed one donor between 0 and 2 dpi. The fomite-contact hamsters were single-housed in the soiled cages for 48 hours, and each was transferred to a new cage at 2 dpc (equivalent to 4 dpi of the donor hamster). Viral RNA was detected from different surfaces sampled

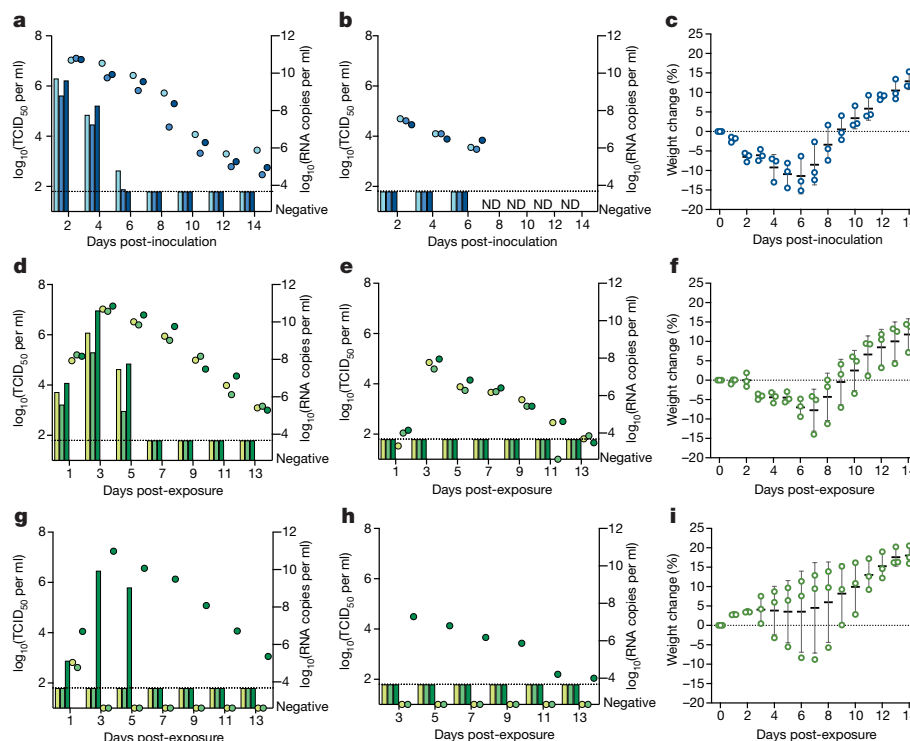


Fig. 3 | Transmission of SARS-CoV-2 in golden hamsters via aerosols and fomites. **a**, Infectious viral load (\log_{10} TCID₅₀ per ml), shown as bars and viral RNA copy numbers (\log_{10} RNA copies per ml), shown as dots detected in the nasal washes of donor hamsters ($n = 3$) inoculated with 8×10^4 TCID₅₀ of SARS-CoV-2. Colour-matched bars and dots represent results from the same hamster. **b**, Infectious virus and viral RNA detected in the faecal samples of donor hamsters ($n = 3$). ND, not determined. **c**, Changes in body weight of donor hamsters ($n = 3$); individual data points and mean \pm s.d. are shown. **d**, Aerosol transmission of SARS-CoV-2 to naive hamsters ($n = 3$) exposed to donors for 8 h at 1 dpi; infectious virus and viral RNA detected in the nasal washes of aerosol-contact hamsters are shown. **e**, Infectious virus and viral RNA detected

in the faecal samples of aerosol-contact hamsters ($n = 3$). **f**, Changes in body weight (per cent weight change compared to the day of exposure) of aerosol-contact hamsters ($n = 3$). **g**, Fomite transmission of SARS-CoV-2 to naive hamsters ($n = 3$) that were single-housed in the soiled cage of a donor for 48 h; infectious virus and viral RNA detected in the nasal washes of fomite-contact hamsters are shown. **h**, Infectious virus and viral RNA detected in the faecal samples of fomite-contact hamsters ($n = 3$). **i**, Changes in body weight (per cent weight change compared to the day of exposure) of fomite-contact hamsters ($n = 3$). Aerosol transmission and fomite transmission experiments were each performed once, with three repeats.

from the soiled cages used for housing the fomite-contact hamsters, with a low titre of infectious virus detected in the bedding (at 2 dpi), cage side surface (at 4 dpi) and water bottle nozzle (at 4 dpi) (Extended Data Table 1). One out of three fomite-contact hamsters shed infectious virus in the nasal washes starting from 1 dpc, with the peak viral load detected at 3 dpc (Fig. 3g). Viral RNA, but not infectious virus, was detected from the faecal samples (Fig. 3h). The maximal weight loss was 8.79% at 7 dpc (Fig. 3i). A PRNT₉₀ assay detected neutralizing antibody from the sera of one out of three fomite-contact hamsters at 16 dpc (titres at 1:320). Taken together, these results suggest that transmission of SARS-CoV-2 among hamsters was mediated mainly by aerosols, rather than by fomites.

Our results indicate that the golden hamster is a suitable experimental animal model for investigating infections with SARS-CoV-2, as there is apparent weight loss in the inoculated and naturally infected hamsters and evidence of efficient viral replication in the nasal mucosa and epithelial cells of the lower respiratory system. The ability of SARS-CoV-2 to infect olfactory sensory neurons at the nasal mucosa may explain the anosmia reported in patients with COVID-19. Hamsters support efficient transmission of SARS-CoV-2 from inoculated donor to naive contact hamsters by direct contact or via aerosols. We also show that transmission from the donor to naive hamsters may occur within a short period soon after inoculation; however, the donors have a short communicable period (of fewer than six days) despite of continuous detection of viral RNA in the nasal washes. Our findings are consistent with a recent report²⁸ that was published while

the current study was under peer review. Hamsters are easy to handle, and there are reagents to support immunological studies for vaccine development^{29–31}. The results also highlighted similarity and differences between the SARS-CoV and SARS-CoV-2 in the hamster model. Both viruses replicated efficiently in respiratory epithelial cells with peak viral load detected soon after inoculation, followed by an infiltration of mononuclear inflammatory cells in the lungs and rapid clearance of infectious virus by 7 dpi. Understanding the host defence mechanism that leads to rapid viral clearance in the respiratory tissues in hamsters may aid the development of effective countermeasures for SARS-CoV-2. The efficient transmission of SARS-CoV-2 to naive hamsters by aerosols also provides an opportunity to understand the transmission dynamics for this coronavirus.

Online content

Any methods, additional references, Nature Research reporting summaries, source data, extended data, supplementary information, acknowledgements, peer review information; details of author contributions and competing interests; and statements of data and code availability are available at <https://doi.org/10.1038/s41586-020-2342-5>.

1. Zhou, P. et al. A pneumonia outbreak associated with a new coronavirus of probable bat origin. *Nature* **579**, 270–273 (2020).
2. WHO. Coronavirus Disease (COVID-2019) Situation Reports. <https://www.who.int/emergencies/diseases/novel-coronavirus-2019/situation-reports> (2020).

3. Li, Q. et al. Early transmission dynamics in Wuhan, China, of novel coronavirus-infected pneumonia. *N. Engl. J. Med.* **382**, 1199–1207 (2020).
4. He, X. et al. Temporal dynamics in viral shedding and transmissibility of COVID-19. *Nat. Med.* **26**, 672–675 (2020).
5. Wu, Z. & McGoogan, J. M. Characteristics of and important lessons from the coronavirus disease 2019 (COVID-19) outbreak in China: summary of a report of 72 314 cases from the Chinese Center for Disease Control and Prevention. *J. Am. Med. Assoc.* **323**, 1239–1242 (2020).
6. Wu, J. T. et al. Estimating clinical severity of COVID-19 from the transmission dynamics in Wuhan, China. *Nat. Med.* **26**, 506–510 (2020).
7. McCray, P. B. Jr et al. Lethal infection of K18-hACE2 mice infected with severe acute respiratory syndrome coronavirus. *J. Virol.* **81**, 813–821 (2007).
8. Menachery, V. D. et al. SARS-like WIV1-CoV poised for human emergence. *Proc. Natl Acad. Sci. USA* **113**, 3048–3053 (2016).
9. Tseng, C. T. et al. Severe acute respiratory syndrome coronavirus infection of mice transgenic for the human angiotensin-converting enzyme 2 virus receptor. *J. Virol.* **81**, 1162–1173 (2007).
10. Yang, X. H. et al. Mice transgenic for human angiotensin-converting enzyme 2 provide a model for SARS coronavirus infection. *Comp. Med.* **57**, 450–459 (2007).
11. Baas, T. et al. Genomic analysis reveals age-dependent innate immune responses to severe acute respiratory syndrome coronavirus. *J. Virol.* **82**, 9465–9476 (2008).
12. Glass, W. G., Subbarao, K., Murphy, B. & Murphy, P. M. Mechanisms of host defense following severe acute respiratory syndrome-coronavirus (SARS-CoV) pulmonary infection of mice. *J. Immunol.* **173**, 4030–4039 (2004).
13. Hogan, R. J. et al. Resolution of primary severe acute respiratory syndrome-associated coronavirus infection requires Stat1. *J. Virol.* **78**, 11416–11421 (2004).
14. Roberts, A. et al. Aged BALB/c mice as a model for increased severity of severe acute respiratory syndrome in elderly humans. *J. Virol.* **79**, 5833–5838 (2005).
15. Hamming, I. et al. Tissue distribution of ACE2 protein, the functional receptor for SARS coronavirus. A first step in understanding SARS pathogenesis. *J. Pathol.* **203**, 631–637 (2004).
16. Bao, L. et al. The pathogenicity of SARS-CoV-2 in hACE2 transgenic mice. *Nature* <https://doi.org/10.1038/s41586-020-2312-y> (2020).
17. Rockx, B. et al. Comparative pathogenesis of COVID-19, MERS, and SARS in a nonhuman primate model. *Science* **368**, 1012–1015 (2020).
18. Munster, V. J. et al. Respiratory disease and virus shedding in rhesus macaques inoculated with SARS-CoV-2. *Nature* <https://doi.org/10.1038/s41586-020-2324-7> (2020).
19. Roberts, A. et al. Animal models and vaccines for SARS-CoV infection. *Virus Res.* **133**, 20–32 (2008).
20. Roberts, A. et al. Severe acute respiratory syndrome coronavirus infection of golden Syrian hamsters. *J. Virol.* **79**, 503–511 (2005).
21. de Wit, E. et al. The Middle East respiratory syndrome coronavirus (MERS-CoV) does not replicate in Syrian hamsters. *PLoS ONE* **8**, e69127 (2013).
22. MacPhail, M. et al. Identification of small-animal and primate models for evaluation of vaccine candidates for human metapneumovirus (hMPV) and implications for hMPV vaccine design. *J. Gen. Virol.* **85**, 1655–1663 (2004).
23. Buthala, D. A. & Soret, M. G. Parainfluenza type 3 virus infection in hamsters: virologic, serologic, and pathologic studies. *J. Infect. Dis.* **114**, 226–234 (1964).
24. Ali, M. J., Teh, C. Z., Jennings, R. & Potter, C. W. Transmissibility of influenza viruses in hamsters. *Arch. Virol.* **72**, 187–197 (1982).
25. Iwatsuki-Horimoto, K. et al. Syrian hamster as an animal model for the study of human influenza virus infection. *J. Virol.* **92**, e01693-17 (2018).
26. Leung, W. K. et al. Enteric involvement of severe acute respiratory syndrome-associated coronavirus infection. *Gastroenterology* **125**, 1011–1017 (2003).
27. Jones, R. M. & Brosseau, L. M. Aerosol transmission of infectious disease. *J. Occup. Environ. Med.* **57**, 501–508 (2015).
28. Chan, J. F. et al. Simulation of the clinical and pathological manifestations of coronavirus disease 2019 (COVID-19) in golden Syrian hamster model: implications for disease pathogenesis and transmissibility. *Clin. Infect. Dis.* **ciaa325** (2020).
29. Miao, J., Chard, L. S., Wang, Z. & Wang, Y. Syrian hamster as an animal model for the study on infectious diseases. *Front. Immunol.* **10**, 2329 (2019).
30. Warner, B. M., Safronetz, D. & Kobinger, G. P. in *Emerging and Re-emerging Viral Infections (Advances in Experimental Medicine and Biology)* Vol. 972 (eds Rezza, G. & Ippolito, G.) 87–101 (Springer, 2016).
31. Zivcec, M., Safronetz, D., Haddock, E., Feldmann, H. & Ebihara, H. Validation of assays to monitor immune responses in the Syrian golden hamster (*Mesocricetus auratus*). *J. Immunol. Methods* **368**, 24–35 (2011).

Publisher's note Springer Nature remains neutral with regard to jurisdictional claims in published maps and institutional affiliations.

© The Author(s), under exclusive licence to Springer Nature Limited 2020

Methods

No statistical methods were used to predetermine sample size. The hamsters were randomized from different litters into experimental groups and investigators were not blinded to allocation during experiments and outcome assessment.

Virus

The BetaCoV/Hong Kong/VM20001061/2020 virus was isolated from the nasopharyngeal aspirate and throat swab of a confirmed patient with COVID-19 in Hong Kong (GISAID identifier EPI_ISL_412028), using Vero E6 cells at the BSL-3 core facility (LKS Faculty of Medicine, University of Hong Kong). Vero E6 cells were purchased from ATCC (CRL-1586) without further authentication, and the cells routinely tested negative for *Mycoplasma* sp. by real-time PCR. Stock virus ($10^{7.25}$ TCID₅₀ per ml) was prepared after three serial passages in Vero E6 cells in Dulbecco's Modified Eagle Medium (DMEM) supplemented with 4.5 g/l D-glucose, 100 mg/l sodium pyruvate, 2% FBS, 100,000 U/l penicillin–streptomycin and 25 mM HEPES. The sequence of the stock virus was identical to the original clinical isolate.

Hamster experiments

Male golden hamsters at 4–5 weeks old were obtained from the Laboratory Animal Services Centre (Chinese University of Hong Kong). The hamsters were originally imported from Harlan (Envigo) in 1998. All experiments were performed at the BSL-3 core facility, (LKS Faculty of Medicine). The hamsters were randomized from different litters into experimental groups, and were acclimatized at the BSL-3 facility for 4–6 d before the experiments. The study protocol was reviewed and approved by the Committee on the Use of Live Animals in Teaching and Research, The University of Hong Kong (CULATR no. 5323-20). Experiments were performed in compliance with all relevant ethical regulations. For challenge studies, hamsters were anaesthetized with ketamine (150 mg/kg) and xylazine (10 mg/kg) via intraperitoneal injection and were intranasally inoculated with 8×10^4 TCID₅₀ of SARS-CoV-2 in 80 µl DMEM. On days 2, 5 and 7, three hamsters were euthanized by intraperitoneal injection of pentobarbital at 200 mg/kg. No blinding was done and a sample size of three hamsters was selected to assess the level of variation between animals. The left lungs and one kidney were collected for viral load determination and were homogenized in 1 ml PBS. Brain, nasal turbinate, right lungs, liver, heart, spleen, duodenum and kidney were fixed in 4% paraformaldehyde for histopathological examination. To collect faecal samples, hamsters were transferred to a new cage one day in advance and fresh faecal samples (10 pieces) were collected for quantitative real-time RT-PCR and TCID₅₀ assay. To evaluate SARS-CoV-2 transmissibility by direct contact, donor hamsters were anaesthetized and inoculated with 8×10^4 TCID₅₀ of SARS-CoV-2. At 1 or 6 dpi, one inoculated donor was transferred to cohousing with one naive hamster in a clean cage; the cohousing of the hamsters continued for at least 13 days. Experiments were repeated with three pairs of donors: direct contact at 1:1 ratio^{32,33}. Body weight and clinical signs of the hamsters were monitored daily. To evaluate SARS-CoV-2 transmissibility via aerosols, one naive hamster was exposed to one inoculated donor hamster in two adjacent stainless steel wired cages at 1 dpi (of the donor) for 8 h (Extended Data Fig. 3). DietGel76A (ClearH₂O) was provided to the hamsters during the 8-h exposure. Exposure was done by holding the hamsters inside individually ventilated cages (IsoCage N, Techniplast) with 70 air changes per h. Experiments were repeated with three pairs of donors: aerosol contact at 1:1 ratio. After exposure, the hamsters were single-housed in separate cages and were monitored daily for 14 d. To evaluate the transmission potential of SARS-CoV-2 virus via fomites, three naive fomite contact hamsters were each introduced to a soiled donor cage at 2 dpi. The fomite contact hamsters were single-housed for 48 h inside the soiled cages and then were each transferred to a new cage at 4 dpi

(of the donor). All hamsters were monitored daily for 14 d. For nasal wash collection, hamsters were anaesthetized using ketamine (100 mg/kg) and xylazine (10 mg/kg) via intraperitoneal injection and 160 µl of PBS containing 0.3% BSA was used to collect nasal washes from both nostrils of each hamster. Collected nasal washes were diluted 1:1 by volume and aliquoted for TCID₅₀ assay in Vero E6 cells and for quantitative real-time RT-PCR. The contact hamsters were handled first, followed by surface decontamination using 1% virkon and handling of the donor hamster.

Environmental sampling

To monitor the level of fomite contamination of SARS-CoV-2 virus in soiled cages, surface samples (5 cm × 5 cm; the whole water bottle nozzle was also swabbed) were collected using flocked polyester swabs (Puritan). Swabs were stored in 0.5 ml of viral transport medium (VTM, containing 0.45% bovine serum albumin, vancomycin, amikacin and nystatin) at −80 °C. In addition, 10 pieces of corn cob bedding were collected from the soiled cage and were soaked in 1 ml VTM for 30 min before titration of infectious virus and viral RNA extraction. Infectious viral loads were determined in Vero E6 cells, and viral RNA copy numbers were determined by quantitative real-time RT-PCR.

Viral load determination by quantitative real-time RT-PCR

RNA was extracted from 140-µl samples using QIAamp viral RNA mini kit (Qiagen) and eluted with 60 µl of water. Two µl RNA was used for quantitative real-time RT-PCR to detect and quantify the *N* gene of SARS-CoV-2 using TaqMan Fast Virus 1-Step Master Mix, as previously described³⁴.

PRNT₉₀ assay

The experiments were carried out in duplicate using Vero E6 cells seeded in 24-well culture plates. Serum samples were heat-inactivated at 56 °C for 30 min and were serially diluted and incubated with 30–40 plaque-forming units of SARS-CoV-2 for 1 h at 37 °C. The virus–serum mixtures were added to the cells and incubated 1 h at 37 °C in 5% CO₂ incubator. The plates were overlaid with 1% agarose in cell culture medium and incubated for 3 d. Thereafter, the plates were fixed and stained with 1% crystal violet. Antibody titres were defined as the highest serum dilution that resulted in >90% reduction in the number of plaques (PRNT₉₀).

Histopathology and immunohistochemistry

Tissue (hearts, livers, spleens, duodenums, brains, right lungs and kidneys) were fixed in 4% paraformaldehyde and were processed for paraffin embedding. The 4-µm sections were stained with haematoxylin and eosin for histopathological examinations. For immunohistochemistry, SARS-CoV-2 N protein was detected using monoclonal antibody (4D11)³⁵; CD3 was detected using polyclonal rabbit anti-human CD3 antibodies (DAKO); and neuron-specific β-III tubulin was detected using monoclonal antibody clone TuJ1 (R&D Systems). Images were captured using a Leica DFC 5400 digital camera and were processed using Leica Application Suite v.4.13.

Statistics and reproducibility

Kruskal–Wallis test and Dunn's multiple comparisons test were used to compare viral loads in the lungs and kidney at 2, 5 and 7 dpi. The area under the curve was calculated from the nasal washes of the donor and contact hamsters followed by Mann–Whitney test. Data were analysed in Microsoft Excel for Mac, version 16.35 and GraphPad Prism version 8.4.1. For the detection of viral replication in hamsters, 9 hamsters were inoculated and tissues were collected from hamsters at 2 ($n=3$), 5 ($n=3$) and 7 ($n=3$) dpi; the results from the three hamsters were similar (Fig. 1a, b). Inoculation of the donor hamsters was independently performed twice and the inoculated hamsters showed comparable weight loss and shed comparable amount of virus in the nasal washes (Figs. 2a, b, 3a, b).

Article

Transmissions by direct contact, aerosols or fomites were performed with three pairs of donor:contacts at 1:1 ratio.

Reporting summary

Further information on research design is available in the Nature Research Reporting Summary linked to this paper.

Data availability

The sequence of SARS-CoV-2 virus BetaCoV/Hong Kong/VM20001061/2020 can be accessed at www.gisaid.org (identifier: EPI_ISL_412028). All experimental data shown in Figs. 1–3, Extended Data Figs. 2, and Extended Data Table 1 are available from the corresponding author upon request.

32. Belser, J. A., Maines, T. R., Katz, J. M. & Tumpey, T. M. Considerations regarding appropriate sample size for conducting ferret transmission experiments. *Future Microbiol.* **8**, 961–965 (2013).
33. Nishiura, H., Yen, H. L. & Cowling, B. J. Sample size considerations for one-to-one animal transmission studies of the influenza A viruses. *PLoS ONE* **8**, e55358 (2013).
34. Chu, D. K. W. et al. Molecular diagnosis of a novel coronavirus (2019-nCoV) causing an outbreak of pneumonia. *Clin. Chem.* **66**, 549–555 (2020).
35. Nicholls, J. M. et al. Time course and cellular localization of SARS-CoV nucleoprotein and RNA in lungs from fatal cases of SARS. *PLoS Med.* **3**, e27 (2006).

36. Lan, J. et al. Structure of the SARS-CoV-2 spike receptor-binding domain bound to the ACE2 receptor. *Nature* **581**, 215–220 (2020).
37. Li, W. et al. Receptor and viral determinants of SARS-coronavirus adaptation to human ACE2. *EMBO J.* **24**, 1634–1643 (2005).

Acknowledgements We thank N. Ip for comments on the interpretation of nasal mucosal data; D. Rowlands, C. Y. H. Leung and J. Rudds for comments on hamster handling; and the Laboratory Animal Unit (University of Hong Kong) and Laboratory Animal Services Centre (Chinese University of Hong Kong) for animal husbandry support. L.L.M.P. was supported by Croucher Foundation. This study was supported by contract HHSN272201400006C from the National Institute of Allergy and Infectious Diseases of the National Institutes of Health (USA) and the theme-based research scheme (T11-705/14N) from the Research Grants Council (Hong Kong SAR, China).

Author contributions S.F.S., L.-M.Y., A.W.H.C. and H.-L.Y. designed and performed the experiments; K.-T.C., A.Y.L.W., P.K. and R.A.P.M.P. performed the experiments, K.F. and J.M.N. performed immunohistochemistry and histopathological examination; L.L.M.P., J.M.N., M.P. and H.-L.Y. analysed the data and wrote the manuscript.

Competing interests The authors declare no competing interests.

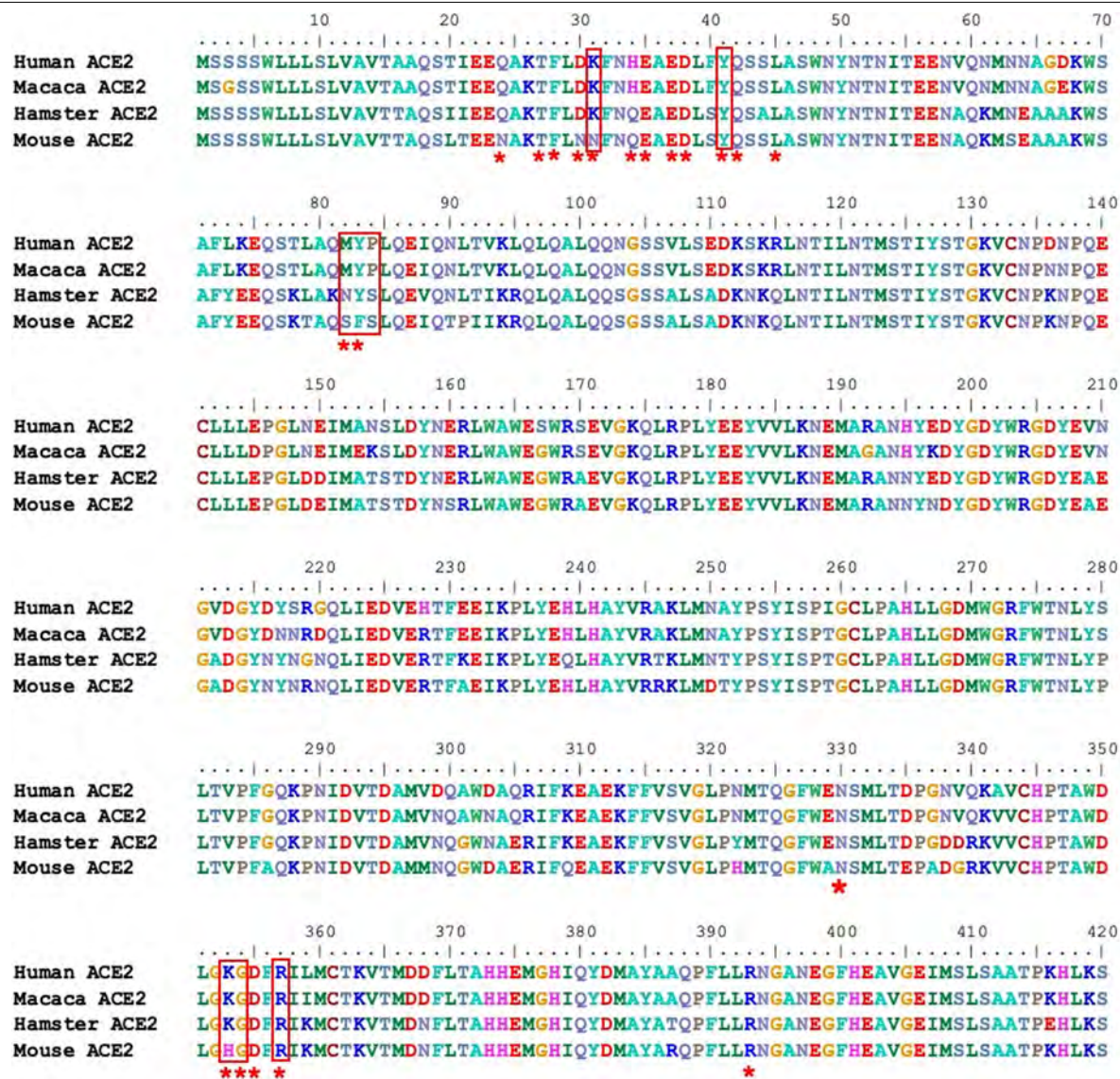
Additional information

Supplementary information is available for this paper at <https://doi.org/10.1038/s41586-020-2342-5>.

Correspondence and requests for materials should be addressed to H.-L.Y.

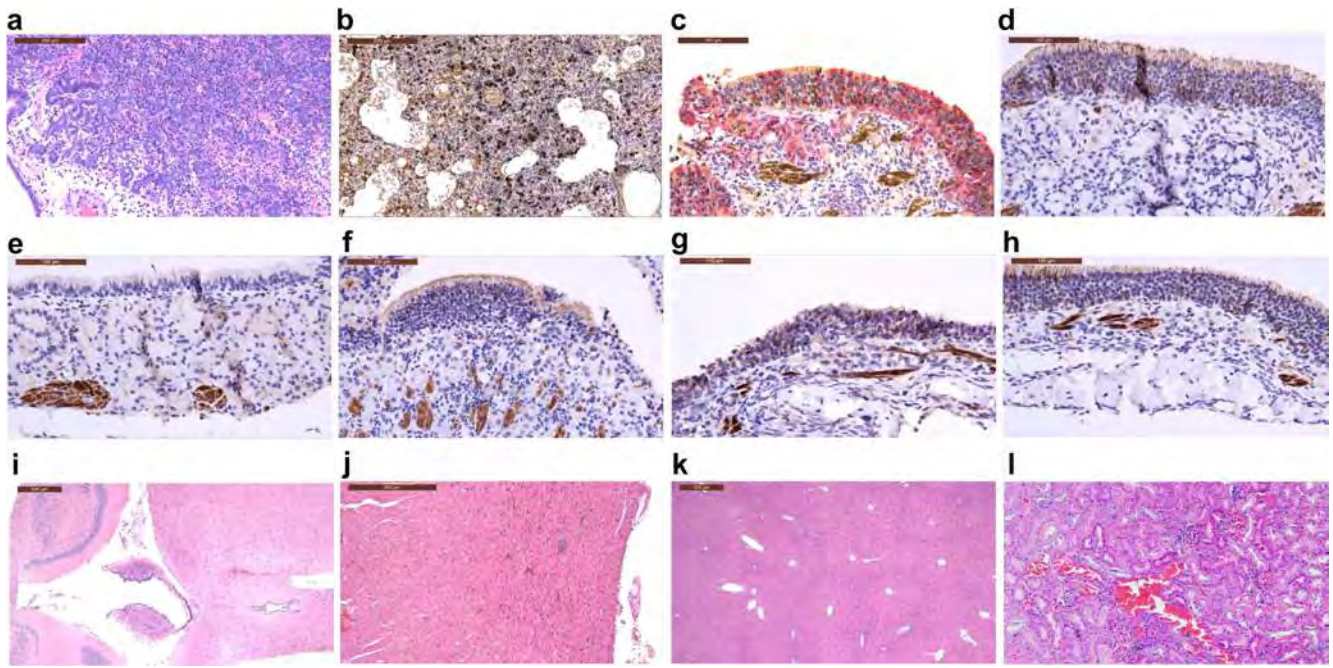
Peer review information Nature thanks Emmie de Wit, Stanley Perlman and the other, anonymous, reviewer(s) for their contribution to the peer review of this work. Peer reviewer reports are available.

Reprints and permissions information is available at <http://www.nature.com/reprints>.



Extended Data Fig. 1 | Sequence alignment of ACE2 proteins (1-420) from human, macaque, hamster and mouse. Asterisks denote amino acid residues of human ACE2 that have been shown by structural analysis to interact with the

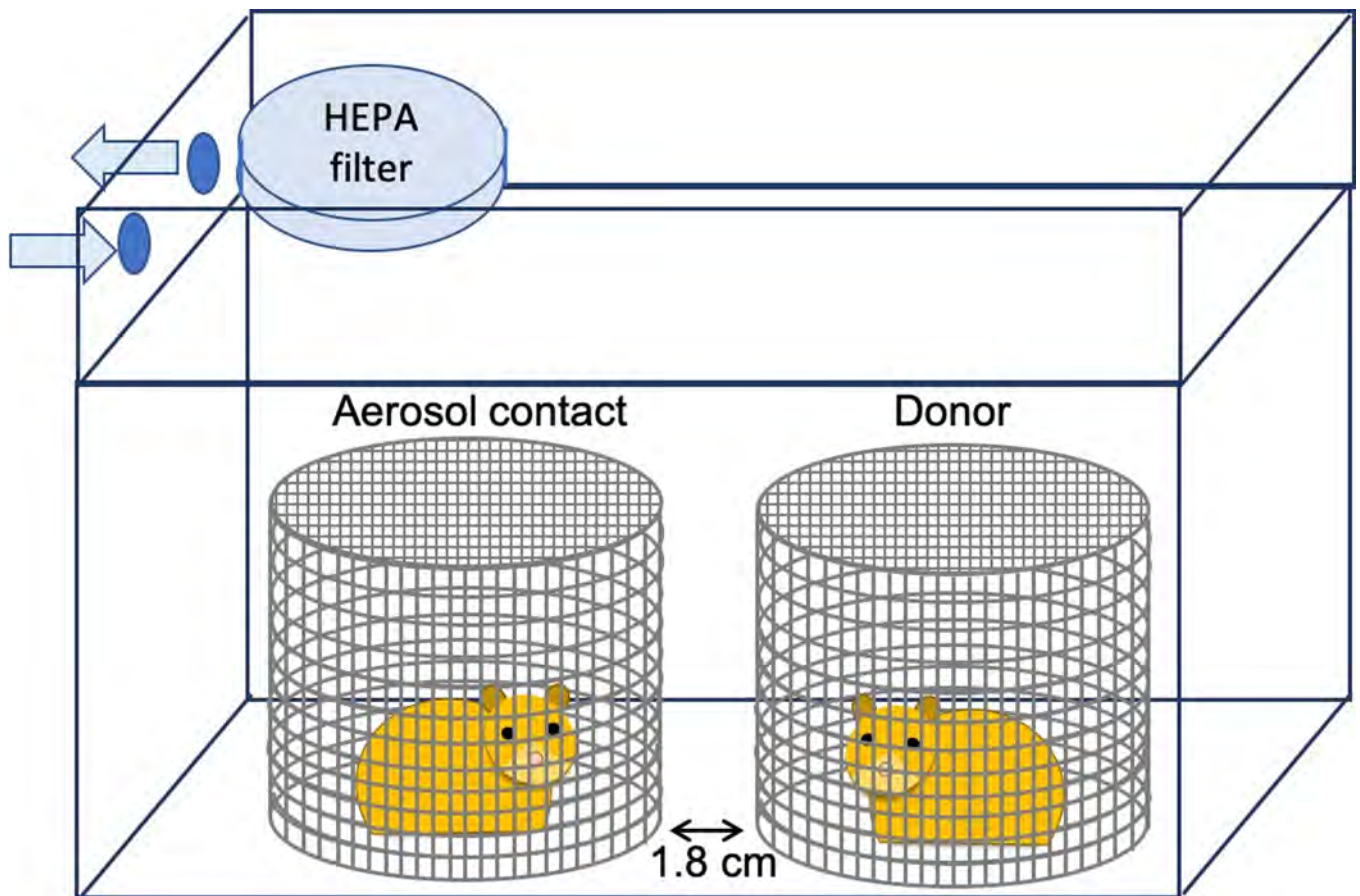
receptor-binding domain of SARS-CoV-2³⁶. Amino acid residues that are important for the interaction between human ACE2 and receptor-binding domain of SARS-CoV are highlighted by red boxes³⁷.



Extended Data Fig. 2 | Haematoxylin and eosin staining and immunohistochemistry on hamster tissues challenged with SARS-CoV-2.

a, Hyperplasia of the pneumocytes detected at 7 dpi. **b**, Detection of CD3-positive cells (using rabbit anti-human CD3 polyclonal antibody) in the lungs at 5 dpi. **c**, Detection of SARS-CoV-2 N protein (red staining, using monoclonal antibody 4D11) and olfactory neurons (brown staining, using monoclonal antibody TuJ1) from the nasal turbinate at 5 dpi. **d**, Detection of olfactory neurons (using monoclonal antibody TuJ1) from the nasal turbinate of a mock-infected hamster ($n=1$). **e**, Nasal epithelial cells from the nasal turbinate of a mock-infected hamster ($n=1$) showed negative staining for TuJ1.

f, Detection of olfactory neurons from nasal turbinate at 2 dpi. **g**, Detection of olfactory neurons from nasal turbinate at 7 dpi. **h**, Detection of olfactory neurons from nasal turbinate at 14 dpi. **i**, Haematoxylin and eosin (H&E) staining of the brain tissue at 5 dpi. **j**, H&E staining of the heart at 5 dpi. **k**, H&E staining of the liver at 5 dpi. **l**, H&E staining of the kidney at 5 dpi. Hamsters were intranasally inoculated with PBS (mock infection, $n=1$) or with 8×10^4 TCID₅₀ of SARS-CoV-2 ($n=9$), and the tissues were collected at 2 ($n=3$), 5 ($n=3$) and 7 ($n=3$) dpi. H&E and immunohistochemistry performed on tissues from three hamsters at day 2, 5 and 7 dpi showed similar results; representative results are shown.



Extended Data Fig. 3 | Experimental layout for the aerosol transmission experiment in hamsters. To evaluate SARS-CoV-2 transmissibility via aerosols, one naive hamster was exposed to one inoculated donor hamster in two adjacent stainless steel wired cages at 1 dpi for 8 h. DietGel76A (ClearH₂O) was provided to the hamsters during the 8-h exposure. Exposure was done by

holding the hamsters inside individually ventilated cages (IsoCage N, Techniplast) with 70 air changes per h. Experiments were repeated with three pairs of donors:aerosol contact at 1:1 ratio. After exposure, the hamsters were single-housed in separate cages and were monitored daily for 14 d.

Extended Data Table 1 | Detection of SARS-CoV-2 in the soiled cages

Days post-inoculation	Animal cage info	Sampled area	Material	log ₁₀ TCID ₅₀ / mL	log ₁₀ RNA copies/ mL
Day 2	donor cage A			1.79	6.70
	donor cage B	bedding	corn cobs	<	5.18
	donor cage C			<	5.79
Day 4	fomite contact cage A	cage side (in direct contact with the animals)	plastic	<	6.89
	fomite contact cage B			<	5.21
	fomite contact cage C			1.79	6.33
	fomite contact cage A	cage lid	plastic	<	3.76
	fomite contact cage B			<	4.33
	fomite contact cage C			<	4.10
	fomite contact cage A	pre-filter	paper-based	<	5.26
	fomite contact cage B			<	5.27
	fomite contact cage C			<	5.31
	fomite contact cage A	water bottle nozzle	stainless steel	<	3.64
	fomite contact cage B			<	4.20
	fomite contact cage C			2.21	6.06
	fomite contact cage A	bedding	corn cobs	<	4.84
	fomite contact cage B			<	5.27
	fomite contact cage C			<	6.06
Day 6	fomite contact cage A	cage side (in direct contact with the animals)	plastic	<	5.70
	fomite contact cage B			<	5.61
	fomite contact cage C			<	6.51
	fomite contact cage A	cage lid	plastic	<	4.75
	fomite contact cage B			<	3.46
	fomite contact cage C			<	4.24
	fomite contact cage A	pre-filter	paper-based	<	5.48
	fomite contact cage B			<	5.23
	fomite contact cage C			<	5.36
	fomite contact cage A	bedding	corn cobs	<	5.12
	fomite contact cage B			<	6.24
	fomite contact cage C			<	5.58

To evaluate transmission potential of SARS-CoV-2 virus via fomites, three naive fomite contact hamsters were each introduced to a soiled cage that was housed by a donor from 0 to 2 dpi. The fomite contact hamsters were single-housed for 48 h inside the soiled cages, and each was then transferred to a new cage (equivalent to 4 dpi of the donor). The soiled cages were left empty at room temperature and were sampled again at 6 dpi of the donor. Surface samples and corn cob bedding were collected from the soiled cages at different time points to monitor infectious viral load and viral RNA copy numbers in the samples.

Reporting Summary

Nature Research wishes to improve the reproducibility of the work that we publish. This form provides structure for consistency and transparency in reporting. For further information on Nature Research policies, see [Authors & Referees](#) and the [Editorial Policy Checklist](#).

Statistics

For all statistical analyses, confirm that the following items are present in the figure legend, table legend, main text, or Methods section.

n/a Confirmed

- ☐ ☒ The exact sample size (n) for each experimental group/condition, given as a discrete number and unit of measurement
- ☐ ☒ A statement on whether measurements were taken from distinct samples or whether the same sample was measured repeatedly
- ☐ ☒ The statistical test(s) used AND whether they are one- or two-sided
Only common tests should be described solely by name; describe more complex techniques in the Methods section.
- ☒ ☐ A description of all covariates tested
- ☒ ☐ A description of any assumptions or corrections, such as tests of normality and adjustment for multiple comparisons
- ☐ ☒ A full description of the statistical parameters including central tendency (e.g. means) or other basic estimates (e.g. regression coefficient) AND variation (e.g. standard deviation) or associated estimates of uncertainty (e.g. confidence intervals)
- ☐ ☒ For null hypothesis testing, the test statistic (e.g. F , t , r) with confidence intervals, effect sizes, degrees of freedom and P value noted
Give P values as exact values whenever suitable.
- ☒ ☐ For Bayesian analysis, information on the choice of priors and Markov chain Monte Carlo settings
- ☒ ☐ For hierarchical and complex designs, identification of the appropriate level for tests and full reporting of outcomes
- ☒ ☐ Estimates of effect sizes (e.g. Cohen's d , Pearson's r), indicating how they were calculated

Our web collection on [statistics for biologists](#) contains articles on many of the points above.

Software and code

Policy information about [availability of computer code](#)

Data collection

Experimental data were recorded in Microsoft Excel for Mac, version 16.35. Images were captured using a Leica DFC 5400 digital camera and were processed using Leica Application Suite v4.13

Data analysis

Data were analyzed in Microsoft Excel for Mac, version 16.35 and GraphPad Prism version 8.4.1.

For manuscripts utilizing custom algorithms or software that are central to the research but not yet described in published literature, software must be made available to editors/reviewers. We strongly encourage code deposition in a community repository (e.g. GitHub). See the Nature Research [guidelines for submitting code & software](#) for further information.

Data

Policy information about [availability of data](#)

All manuscripts must include a [data availability statement](#). This statement should provide the following information, where applicable:

- Accession codes, unique identifiers, or web links for publicly available datasets
- A list of figures that have associated raw data
- A description of any restrictions on data availability

The accession number for the SARS-CoV-2 virus used for the study was provided.

There are two figures that have associated raw data. All data will be provided upon request.

Field-specific reporting

Please select the one below that is the best fit for your research. If you are not sure, read the appropriate sections before making your selection.

☒ Life sciences ☐ Behavioural & social sciences ☐ Ecological, evolutionary & environmental sciences

For a reference copy of the document with all sections, see [nature.com/documents/nr-reporting-summary-flat.pdf](https://www.nature.com/documents/nr-reporting-summary-flat.pdf)

Life sciences study design

All studies must disclose on these points even when the disclosure is negative.

Sample size	This is an observational study investigates the suitability of using golden Syrian hamsters as an animal model for SARS-CoV-2. There is no comparison to be made with another virus, and a sample size of 3 was selected to evaluate the level of variation between individuals. Transmission studies are generally performed in 3-4 pairs of donor: contact at 1:1 ratio (Nishura et al., PLOS ONE 2013 and Belser et al., Future Microbiol 2013).
Data exclusions	No data was excluded in the analyses.
Replication	The challenge experiment was repeatedly performed three times. Direct contact transmission experiments were independently performed twice and naive animals were co-housed with inoculated donors on day 1 and day 6, respectively. Each experiment was performed with three pairs of donor: contact at 1:1 ratio. Aerosol transmission and fomite transmission experiments were each performed once with three pairs of donor: contact at 1:1 ratio.
Randomization	Randomization was performed while assigning the animals from different litters into experimental groups.
Blinding	Blinding was not possible for the experimental design due to the need to identify each animal (inoculated or contact) accurately.

Reporting for specific materials, systems and methods

We require information from authors about some types of materials, experimental systems and methods used in many studies. Here, indicate whether each material, system or method listed is relevant to your study. If you are not sure if a list item applies to your research, read the appropriate section before selecting a response.

Materials & experimental systems

n/a	Involved in the study
<input type="checkbox"/>	<input checked="" type="checkbox"/> Antibodies
<input type="checkbox"/>	<input checked="" type="checkbox"/> Eukaryotic cell lines
<input checked="" type="checkbox"/>	<input type="checkbox"/> Palaeontology
<input type="checkbox"/>	<input checked="" type="checkbox"/> Animals and other organisms
<input checked="" type="checkbox"/>	<input type="checkbox"/> Human research participants
<input checked="" type="checkbox"/>	<input type="checkbox"/> Clinical data

Methods

n/a	Involved in the study
<input checked="" type="checkbox"/>	<input type="checkbox"/> ChIP-seq
<input checked="" type="checkbox"/>	<input type="checkbox"/> Flow cytometry
<input checked="" type="checkbox"/>	<input type="checkbox"/> MRI-based neuroimaging

Antibodies

Antibodies used	SARS-CoV-2 N protein was detected using monoclonal antibody (4D11). CD3 was detected using polyclonal rabbit anti-human CD3 antibody purchased from DAKO. Neuron-specific beta-III tubulin was detected using monoclonal clone TuJ1 (R&D Systems).
Validation	4D11 monoclonal antibody was reported in Nicholls et al. PLoS Med. 2006 Feb;3(2):e27. PubMed PMID: 16379499 Other antibodies are available commercially.

Eukaryotic cell lines

Policy information about [cell lines](#)

Cell line source(s)	Vero E6 (ATCC CRL-1586)
Authentication	The cell line was purchased from ATCC (ATCC CRL-1586). The cell line has not been authenticated since it was purchased from ATCC.
Mycoplasma contamination	The cell line was tested negative for mycoplasma.
Commonly misidentified lines (See ICLAC register)	No commonly misidentified lines were used.

Animals and other organisms

Policy information about [studies involving animals](#); [ARRIVE guidelines](#) recommended for reporting animal research

Laboratory animals	Male golden Syrian hamsters, at 4-5 weeks old
Wild animals	This study does not involve wild animals.
Field-collected samples	This study does not involve field-collected samples.
Ethics oversight	Animal ethics was approved by the the Committee on the Use of Live Animals in Teaching and Research, The University of Hong Kong (CULATR # 5323-20).

Note that full information on the approval of the study protocol must also be provided in the manuscript.

SARS-CoV-2 Transmission and Infection Among Attendees of an Overnight Camp — Georgia, June 2020

Christine M. Szablewski, DVM^{1,2}; Karen T. Chang, PhD^{2,3}; Marie M. Brown, MPH¹; Victoria T. Chu, MD^{2,3}; Anna R. Yousaf, MD^{2,3}; Ndubuisi Anyalechi, MD¹; Peter A. Aryee, MBA¹; Hannah L. Kirking, MD²; Maranda Lumsden¹; Erin Mayweather¹; Clinton J. McDaniel, MPH²; Robert Montierth, PharmD²; Asfia Mohammed¹; Noah G. Schwartz, MD^{2,3}; Jaina A. Shah¹; Jacqueline E. Tate, PhD²; Emilio Dirlikov, PhD²; Cherie Drenzek, DVM¹; Tatiana M. Lanzieri, MD²; Rebekah J. Stewart, MSN, MPH²

On July 31, 2020, this report was posted as an MMWR Early Release on the MMWR website (<https://www.cdc.gov/mmwr>).

Limited data are available about transmission of SARS-CoV-2, the virus that causes coronavirus disease 2019 (COVID-19), among youths. During June 17–20, an overnight camp in Georgia (camp A) held orientation for 138 trainees and 120 staff members; staff members remained for the first camp session, scheduled during June 21–27, and were joined by 363 campers and three senior staff members on June 21. Camp A adhered to the measures in Georgia's Executive Order* that allowed overnight camps to operate beginning on May 31, including requiring all trainees, staff members, and campers to provide documentation of a negative viral SARS-CoV-2 test ≤12 days before arriving. Camp A adopted most† components of CDC's Suggestions for Youth and Summer Camps§ to minimize the risk for SARS-CoV-2 introduction and transmission. Measures not implemented were cloth masks for campers and opening windows and doors for increased ventilation in buildings. Cloth masks were required for staff members. Camp attendees were cohorted by cabin and engaged in a variety of indoor and outdoor activities, including daily vigorous singing and cheering. On June 23, a teenage staff member left camp A after developing chills the previous evening. The staff member was tested and reported a positive test result for SARS-CoV-2 the following day (June 24). Camp A officials began sending campers home on June 24 and closed the camp on June 27. On June 25, the Georgia Department of Public Health (DPH) was notified and initiated an investigation. DPH recommended that all attendees be tested and self-quarantine, and isolate if they had a positive test result.

A line list of all attendees was obtained and matched to laboratory results from the State Electronic Notifiable Disease Surveillance System¶ and data from DPH case investigations. A COVID-19 case associated with the camp A outbreak was

defined as a positive viral SARS-CoV-2 test** in a camp A attendee from a specimen collected or reported to DPH from the first day at camp A (June 17 for staff members and trainees; June 21 for campers) through 14 days after leaving camp A (trainees left on June 21; staff members and campers left during June 24–June 27). Out-of-state attendees (27) were excluded from this preliminary analysis. Attack rates were calculated by dividing the number of persons with positive test results by the total number of Georgia attendees, including those who did not have testing results, because negative test results are not consistently reported in Georgia.

A total of 597 Georgia residents attended camp A. Median camper age was 12 years (range = 6–19 years), and 53% (182 of 346) were female. The median age of staff members and trainees was 17 years (range = 14–59 years), and 59% (148 of 251) were female. Test results were available for 344 (58%) attendees; among these, 260 (76%) were positive. The overall attack rate was 44% (260 of 597), 51% among those aged 6–10 years, 44% among those aged 11–17 years, and 33% among those aged 18–21 years (Table). Attack rates increased with increasing length of time spent at the camp, with staff members having the highest attack rate (56%). During June 21–27, occupancy of the 31 cabins averaged 15 persons per cabin (range = 1–26); median cabin attack rate was 50% (range = 22%–70%) among 28 cabins that had one or more cases. Among 136 cases with available symptom data, 36 (26%) patients reported no symptoms; among 100 (74%) who reported symptoms, those most commonly reported were subjective or documented fever (65%), headache (61%), and sore throat (46%).

The findings in this report are subject to at least three limitations. First, attack rates presented are likely an underestimate because cases might have been missed among persons not tested or whose test results were not reported. Second, given the increasing incidence of COVID-19 in Georgia in June and July, some cases might have resulted from transmission occurring before or after camp attendance.†† Finally, it was

*<https://gov.georgia.gov/document/2020-executive-order/06112001/download>.

† Notable adopted measures included cohorting of attendees by cabin (≤26 persons), staggering of cohorts for use of communal spaces, physical distancing outside of cabin cohorts, and enhanced cleaning and disinfection, especially of shared equipment and spaces.

§ <https://www.cdc.gov/coronavirus/2019-ncov/community/schools-childcare/summer-camps.html>.

¶ <https://sendss.state.ga.us/>.

** CDC defines a viral test as one that detects SARS-CoV-2 nucleic acids (e.g., polymerase chain reaction) or antigens. <https://www.cdc.gov/coronavirus/2019-ncov/hcp/testing-overview.html>.

†† <https://dph.georgia.gov/covid-19-daily-status-report>.

TABLE. SARS-CoV-2 attack rates^{*,†} among attendees of an overnight camp, by selected characteristics — Georgia, June 2020

Characteristic	No. [§]	No. positive	Attack rate, %
Total	597	260	44
Sex			
Male	267	123	46
Female	330	137	42
Age group, yrs			
6–10	100	51	51
11–17	409	180	44
18–21	81	27	33
22–59	7	2	29
Type of attendee (dates attended camp)			
Trainee (June 17–21)	134	26	19
Staff member (June 17–27 ^{¶, **})	117	66	56
Camper (June 21–27 [¶])	346	168	49
Cabin size during camp^{††} (no. of persons/cabin)^{§§}			
Small (1–3)	13	5	38
Medium (7–13)	75	29	39
Large (16–26)	375	200	53

Abbreviation: COVID-19 = coronavirus disease 2019.

* Although positive and negative test results for Georgia residents are reportable in the state of Georgia, negative results are not consistently reported. Attack rates were calculated by dividing the number of persons with a positive test result reported to the Georgia Department of Public Health (DPH) by the total number of Georgia attendees, including those who did not provide testing results.

† A COVID-19 case associated with the camp outbreak was defined as a positive viral SARS-CoV-2 test in an attendee from a specimen collected or reported to DPH from the first day at camp A (June 17 for staff members, including trainees; June 21 for campers) through 14 days after leaving camp A (trainees left on June 21; staff members and campers left during June 24–June 27).

§ Out-of-state attendees' (n = 27; 4%) test results were not reported to DPH and therefore were not included in this analysis.

¶ Camp departures began June 24 and were completed June 27.

** Three staff members arrived June 21.

†† Among camp attendees during June 21–27 (n = 463).

§§ No cabins included 4–6 or 14–15 persons.

not possible to assess individual adherence to COVID-19 prevention measures at camp A, including physical distancing between, and within, cabin cohorts and use of cloth masks, which were not required for campers.

These findings demonstrate that SARS-CoV-2 spread efficiently in a youth-centric overnight setting, resulting in high attack rates among persons in all age groups, despite efforts by camp officials to implement most recommended strategies to prevent transmission. Asymptomatic infection was common and potentially contributed to undetected transmission, as has been previously reported (1–4). This investigation adds to the body of evidence demonstrating that children of all ages are susceptible to SARS-CoV-2 infection (1–3) and, contrary to early reports (5,6), might play an important role in transmission (7,8). The multiple measures adopted by the camp were not sufficient to prevent an outbreak in the context of substantial community transmission. Relatively large cohorts sleeping in the same cabin and engaging in regular singing and cheering likely contributed to transmission (9). Use of cloth

masks, which has been shown to reduce the risk for infection (10), was not universal. An ongoing investigation will further characterize specific exposures associated with infection, illness course, and any secondary transmission to household members. Physical distancing and consistent and correct use of cloth masks should be emphasized as important strategies for mitigating transmission in congregate settings.

Acknowledgments

Pamela Logan, Tom Campbell, Alicia Dunajcik, Amit Eichenbaum, Amanda Mohammed, Stephanie O'Conner, Zoe Schneider, Brandon Shih, Kat Topf, Stacy Thorne, Ramika Archibald, Elizabeth Dietrich, Robert Slaughter, Aron Hall, Alicia Fry, Jill Shugart, Carolina Luna-Pinto, Chastity Walker, Jennifer Fuld, Nadia Oussayef, Julie Villanueva, Dale Rose, Margaret A. Honein, CDC COVID-19 Response Team.

Corresponding author: Christine M. Szablewski, christine.szablewski@dph.ga.gov.

¹Georgia Department of Public Health; ²CDC COVID-19 Response Team; ³Epidemic Intelligence Service, CDC.

All authors have completed and submitted the International Committee of Medical Journal Editors form for disclosure of potential conflicts of interest. No potential conflicts of interest were disclosed.

References

- Bialek S, Gierke R, Hughes M, McNamara LA, Pilishvili T, Skoff T; CDC COVID-19 Response Team. Coronavirus disease 2019 in children—United States, February 12–April 2, 2020. *MMWR Morb Mortal Wkly Rep* 2020;69:422–6. <https://doi.org/10.15585/mmwr.mm6914e4>
- Dong Y, Mo X, Hu Y, et al. Epidemiology of COVID-19 among children in China. *Pediatrics* 2020;145:e20200702. <https://doi.org/10.1542/peds.2020-0702>
- Götzinger F, Santiago-García B, Noguera-Julián A, et al.; ptbnet COVID-19 Study Group. COVID-19 in children and adolescents in Europe: a multinational, multicentre cohort study. *Lancet Child Adolesc Health* 2020;S2352-4642(20):30177–2. [https://doi.org/10.1016/S2352-4642\(20\)30177-2](https://doi.org/10.1016/S2352-4642(20)30177-2)
- Huang L, Zhang X, Zhang X, et al. Rapid asymptomatic transmission of COVID-19 during the incubation period demonstrating strong infectivity in a cluster of youngsters aged 16–23 years outside Wuhan and characteristics of young patients with COVID-19: A prospective contact-tracing study. *J Infect* 2020;80:e1–13. <https://doi.org/10.1016/j.jinf.2020.03.006>
- Heavey L, Casey G, Kelly C, Kelly D, McDarby G. No evidence of secondary transmission of COVID-19 from children attending school in Ireland, 2020. *Euro Surveill* 2020;25:2000903. <https://doi.org/10.2807/1560-7917.ES.2020.25.21.2000903>
- Ludvigsson JF. Children are unlikely to be the main drivers of the COVID-19 pandemic—a systematic review. *Acta Paediatr* 2020;109:1525–30. <https://doi.org/10.1111/apa.15371>
- Park YJ, Choe YJ, Park O, et al.; COVID-19 National Emergency Response Center, Epidemiology and Case Management Team. Contact tracing during coronavirus disease outbreak, South Korea, 2020. *Emerg Infect Dis* 2020;26. <https://doi.org/10.3201/eid2610.201315>
- Stein-Zamir C, Abramson N, Shoo H, et al. A large COVID-19 outbreak in a high school 10 days after schools' reopening, Israel, May 2020. *Euro Surveill* 2020;25. Epub July 23, 2020. <https://doi.org/10.2807/1560-7917.ES.2020.25.29.2001352>

9. Hamner L, Dubbel P, Capron I, et al. High SARS-CoV-2 attack rate following exposure at a choir practice—Skagit County, Washington, March 2020. *MMWR Morb Mortal Wkly Rep* 2020;69:606–10. <https://doi.org/10.15585/mmwr.mm6919e6>
10. Hendrix MJ, Walde C, Findley K, Trotman R. Absence of apparent transmission of SARS-CoV-2 from two stylists after exposure at a hair salon with a universal face covering policy—Springfield, Missouri, May 2020. *MMWR Morb Mortal Wkly Rep* 2020;69:930–2. <https://doi.org/10.15585/mmwr.mm6928e2>

Coronavirus Disease 2019 in Children — United States, February 12–April 2, 2020

CDC COVID-19 Response Team

On April 6, 2020, this report was posted as an MMWR Early Release on the MMWR website (<https://www.cdc.gov/mmwr>).

As of April 2, 2020, the coronavirus disease 2019 (COVID-19) pandemic has resulted in >890,000 cases and >45,000 deaths worldwide, including 239,279 cases and 5,443 deaths in the United States (1,2). In the United States, 22% of the population is made up of infants, children, and adolescents aged <18 years (children) (3). Data from China suggest that pediatric COVID-19 cases might be less severe than cases in adults and that children might experience different symptoms than do adults (4,5); however, disease characteristics among pediatric patients in the United States have not been described. Data from 149,760 laboratory-confirmed COVID-19 cases in the United States occurring during February 12–April 2, 2020 were analyzed. Among 149,082 (99.6%) reported cases for which age was known, 2,572 (1.7%) were among children aged <18 years. Data were available for a small proportion of patients on many important variables, including symptoms (9.4%), underlying conditions (13%), and hospitalization status (33%). Among those with available information, 73% of pediatric patients had symptoms of fever, cough, or shortness of breath compared with 93% of adults aged 18–64 years during the same period; 5.7% of all pediatric patients, or 20% of those for whom hospitalization status was known, were hospitalized, lower than the percentages hospitalized among all adults aged 18–64 years (10%) or those with known hospitalization status (33%). Three deaths were reported among the pediatric cases included in this analysis. These data support previous findings that children with COVID-19 might not have reported fever or cough as often as do adults (4). Whereas most COVID-19 cases in children are not severe, serious COVID-19 illness resulting in hospitalization still occurs in this age group. Social distancing and everyday preventive behaviors remain important for all age groups as patients with less serious illness and those without symptoms likely play an important role in disease transmission (6,7).

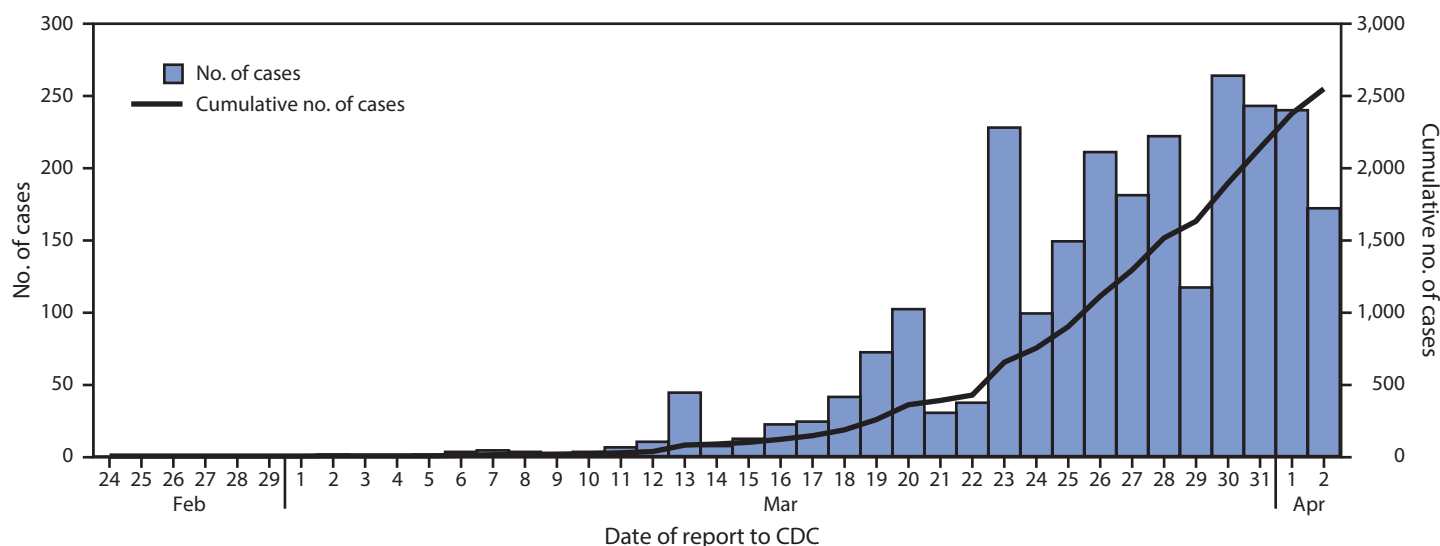
Data on COVID-19 cases were reported to CDC from 50 states, the District of Columbia, New York City, and four U.S. territories. Jurisdictions voluntarily report data on laboratory-confirmed cases using a standardized case report form.* Data on cases occurring during February 12–April 2, 2020 and submitted through an electronic case-based COVID-19

surveillance database were reviewed for this report. Data submitted to CDC are preliminary and can be updated by health departments as more data become available. At the time of this analysis, characteristics of interest were available for only a minority of cases, including hospitalization status (33%), presence of preexisting underlying medical conditions (13%), and symptoms (9.4%). Because of the high percentage of cases with missing data and because cases with severe outcomes are more likely to have hospitalization or intensive care unit (ICU) status reported, percentages of patients hospitalized, including those admitted to the ICU, were estimated as a range, for which the denominator for the lower bound included cases with both known and unknown hospitalization or ICU status, and the upper bound included only cases with known hospitalization or ICU status. For other characteristics, percentages were calculated from among the number of cases with known information for that characteristic. Demographics of COVID-19 cases were assessed among cases in children aged <18 years and adults aged ≥18 years. Because clinical severity of COVID-19 is higher among adults aged ≥65 years than in younger age groups (8), clinical features including symptoms and hospitalizations were assessed among adults aged 18–64 years and compared with those among the pediatric cases. Statistical comparisons were not performed because of the high percentage of missing data.

As of April 2, 2020, data on 149,760 laboratory-confirmed U.S. COVID-19 cases were available for analysis. Among 149,082 (99.6%) cases for which patient age was known, 2,572 (1.7%) occurred in children aged <18 years and 146,510 (98%) in adults aged ≥18 years, including 113,985 (76%) aged 18–64 years. Among the 2,572 pediatric cases, 850 (33%) were reported from New York City; 584 (23%) from the rest of New York state; 393 (15%) from New Jersey; and the remaining 745 (29%) from other jurisdictions. The distribution of reporting jurisdictions for pediatric cases was similar to that of reporting jurisdictions for cases among adults aged ≥18 years, except that a lower percentage of adult cases was reported from New York state (14%). The first pediatric U.S. COVID-19 case was reported to CDC on March 2, 2020; since March 5, pediatric cases have been reported daily (Figure 1).

Among all 2,572 COVID-19 cases in children aged <18 years, the median age was 11 years (range 0–17 years). Nearly one third of reported pediatric cases (813; 32%) occurred in children aged 15–17 years, followed by those in children aged 10–14 years (682; 27%). Among younger

* <https://www.cdc.gov/coronavirus/2019-ncov/downloads/pui-form.pdf>.

FIGURE 1. COVID-19 cases in children* aged <18 years, by date reported to CDC (N = 2,549)[†] — United States, February 24–April 2, 2020[§]

* Includes infants, children, and adolescents.

[†] Excludes 23 cases in children aged <18 years with missing report date.

[§] Date of report available starting February 24, 2020; reported cases include any with onset on or after February 12, 2020.

children, 398 (15%) occurred in children aged <1 year, 291 (11%) in children aged 1–4 years, and 388 (15%) in children aged 5–9 years. Among 2,490 pediatric COVID-19 cases for which sex was known, 1,408 (57%) occurred in males; among cases in adults aged ≥18 years for which sex was known, 53% (75,450 of 143,414) were in males. Among 184 (7.2%) cases in children aged <18 years with known exposure information, 16 (9%) were associated with travel and 168 (91%) had exposure to a COVID-19 patient in the household or community.

Data on signs and symptoms of COVID-19 were available for 291 of 2,572 (11%) pediatric cases and 10,944 of 113,985 (9.6%) cases among adults aged 18–64 years (Table). Whereas fever (subjective or documented), cough, and shortness of breath were commonly reported among adult patients aged 18–64 years (93% reported at least one of these), these signs and symptoms were less frequently reported among pediatric patients (73%). Among those with known information on each symptom, 56% of pediatric patients reported fever, 54% reported cough, and 13% reported shortness of breath, compared with 71%, 80%, and 43%, respectively, reporting these signs and symptoms among patients aged 18–64 years. Myalgia, sore throat, headache, and diarrhea were also less commonly reported by pediatric patients. Fifty-three (68%) of the 78 pediatric cases reported not to have fever, cough, or shortness of breath had no symptoms reported, but could not be classified as asymptomatic because of incomplete symptom information. One (1.3%) additional pediatric patient with a positive test result for SARS-CoV-2 was reported to be asymptomatic.

Information on hospitalization status was available for 745 (29%) cases in children aged <18 years and 35,061 (31%) cases in adults aged 18–64 years. Among children with COVID-19, 147 (estimated range = 5.7%–20%) were reported to be hospitalized, with 15 (0.58%–2.0%) admitted to an ICU (Figure 2). Among adults aged 18–64 years, the percentages of patients who were hospitalized (10%–33%), including those admitted to an ICU (1.4%–4.5%), were higher. Children aged <1 year accounted for the highest percentage (15%–62%) of hospitalization among pediatric patients with COVID-19. Among 95 children aged <1 year with known hospitalization status, 59 (62%) were hospitalized, including five who were admitted to an ICU. The percentage of patients hospitalized among those aged 1–17 years was lower (estimated range = 4.1%–14%), with little variation among age groups (Figure 2).

Among 345 pediatric cases with information on underlying conditions, 80 (23%) had at least one underlying condition. The most common underlying conditions were chronic lung disease (including asthma) (40), cardiovascular disease (25), and immunosuppression (10). Among the 295 pediatric cases for which information on both hospitalization status and underlying medical conditions was available, 28 of 37 (77%) hospitalized patients, including all six patients admitted to an ICU, had one or more underlying medical condition; among 258 patients who were not hospitalized, 30 (12%) patients had underlying conditions. Three deaths were reported among the pediatric cases included in this analysis; however, review of these cases is ongoing to confirm COVID-19 as the likely cause of death.

TABLE. Signs and symptoms among 291 pediatric (age <18 years) and 10,944 adult (age 18–64 years) patients* with laboratory-confirmed COVID-19 — United States, February 12–April 2, 2020

Sign/Symptom	No. (%) with sign/symptom	
	Pediatric	Adult
Fever, cough, or shortness of breath [†]	213 (73)	10,167 (93)
Fever [§]	163 (56)	7,794 (71)
Cough	158 (54)	8,775 (80)
Shortness of breath	39 (13)	4,674 (43)
Myalgia	66 (23)	6,713 (61)
Runny nose [¶]	21 (7.2)	757 (6.9)
Sore throat	71 (24)	3,795 (35)
Headache	81 (28)	6,335 (58)
Nausea/Vomiting	31 (11)	1,746 (16)
Abdominal pain [¶]	17 (5.8)	1,329 (12)
Diarrhea	37 (13)	3,353 (31)

* Cases were included in the denominator if they had a known symptom status for fever, cough, shortness of breath, nausea/vomiting, and diarrhea. Total number of patients by age group: <18 years (N = 2,572), 18–64 years (N = 113,985).

[†] Includes all cases with one or more of these symptoms.

[§] Patients were included if they had information for either measured or subjective fever variables and were considered to have a fever if “yes” was indicated for either variable.

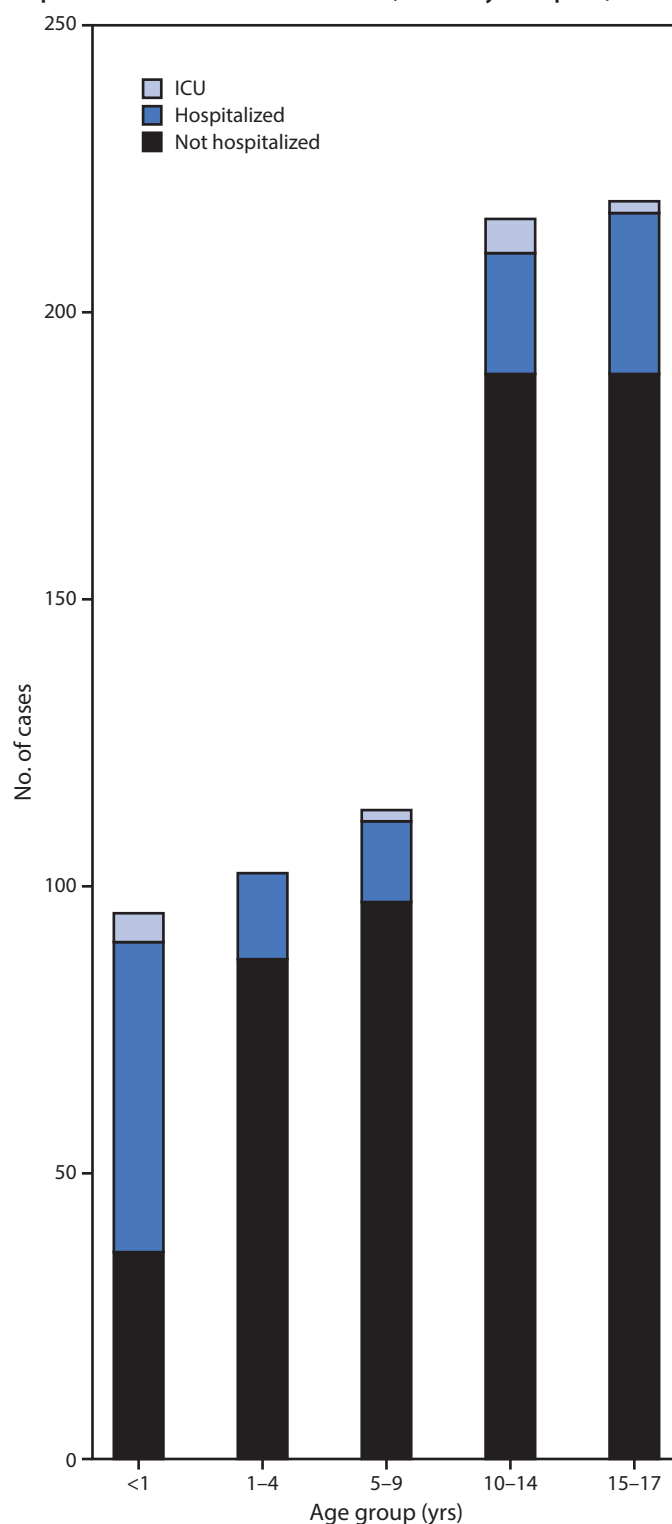
[¶] Runny nose and abdominal pain were less frequently completed than other symptoms; therefore, percentages with these symptoms are likely underestimates.

Discussion

Among 149,082 U.S. cases of COVID-19 reported as of April 2, 2020, for which age was known, 2,572 (1.7%) occurred in patients aged <18 years. In comparison, persons aged <18 years account for 22% of the U.S. population (3). Although infants <1 year accounted for 15% of pediatric COVID-19 cases, they remain underrepresented among COVID-19 cases in patients of all ages (393 of 149,082; 0.27%) compared with the percentage of the U.S. population aged <1 year (1.2%) (3). Relatively few pediatric COVID-19 cases were hospitalized (5.7%–20%; including 0.58%–2.0% admitted to an ICU), consistent with previous reports that COVID-19 illness often might have a mild course among younger patients (4,5). Hospitalization was most common among pediatric patients aged <1 year and those with underlying conditions. In addition, 73% of children for whom symptom information was known reported the characteristic COVID-19 signs and symptoms of fever, cough, or shortness of breath.

These findings are largely consistent with a report on pediatric COVID-19 patients aged <16 years in China, which found that only 41.5% of pediatric patients had fever, 48.5% had cough, and 1.8% were admitted to an ICU (4). A second report suggested that although pediatric COVID-19 patients infrequently have severe outcomes, the infection might be more severe among infants (5). In the current analysis, 59 of 147 pediatric hospitalizations, including five of 15 pediatric ICU admissions, were among children aged <1 year; however, most reported U.S. cases in infants had unknown hospitalization status.

FIGURE 2. COVID-19 cases among children* aged <18 years, among those with known hospitalization status (N = 745),[†] by age group and hospitalization status — United States, February 12–April 2, 2020



Abbreviation: ICU = intensive care unit.

* Includes infants, children, and adolescents.

[†] Number of children missing hospitalization status by age group: <1 year (303 of 398; 76%); 1–4 years (189 of 291; 65%); 5–9 years (275 of 388; 71%); 10–14 years (466 of 682; 68%); 15–17 years (594 of 813; 73%).

Summary

What is already known about this topic?

Data from China suggest that pediatric coronavirus disease 2019 (COVID-19) cases might be less severe than cases in adults and that children (persons aged <18 years) might experience different symptoms than adults.

What is added by this report?

In this preliminary description of pediatric U.S. COVID-19 cases, relatively few children with COVID-19 are hospitalized, and fewer children than adults experience fever, cough, or shortness of breath. Severe outcomes have been reported in children, including three deaths.

What are the implications for public health practice?

Pediatric COVID-19 patients might not have fever or cough. Social distancing and everyday preventive behaviors remain important for all age groups because patients with less serious illness and those without symptoms likely play an important role in disease transmission.

In this preliminary analysis of U.S. pediatric COVID-19 cases, a majority (57%) of patients were males. Several studies have reported a majority of COVID-19 cases among males (4,9), and an analysis of 44,000 COVID-19 cases in patients of all ages in China reported a higher case-fatality rate among men than among women (10). However, the same report, as well as a separate analysis of 2,143 pediatric COVID-19 cases from China, detected no substantial difference in the number of cases among males and females (5,10). Reasons for any potential difference in COVID-19 incidence or severity between males and females are unknown. In the present analysis, the predominance of males in all pediatric age groups, including patients aged <1 year, suggests that biologic factors might play a role in any differences in COVID-19 susceptibility by sex.

The findings in this report are subject to at least four limitations. First, because of the high workload associated with COVID-19 response activities on local, state, and territorial public health personnel, a majority of pediatric cases were missing data on disease symptoms, severity, or underlying conditions. Data for many variables are unlikely to be missing at random, and as such, these results must be interpreted with caution. Because of the high percentage of missing data, statistical comparisons could not be conducted. Second, because many cases occurred only days before publication of this report, the outcome for many patients is unknown, and this analysis might underestimate severity of disease or symptoms that manifested later in the course of illness. Third, COVID-19 testing practices differ across jurisdictions and might also differ across age groups. In many areas, prioritization of testing for severely

ill patients likely occurs, which would result in overestimation of the percentage of patients with COVID-19 infection who are hospitalized (including those treated in an ICU) among all age groups. Finally, this analysis compares clinical characteristics of pediatric cases (persons aged <18 years) with those of cases among adults aged 18–64 years. Severe COVID-19 disease appears to be more common among adults at the high end of this age range (6), and therefore cases in young adults might be more similar to those among children than suggested by the current analysis.

As the number of COVID-19 cases continues to increase in many parts of the United States, it will be important to adapt COVID-19 surveillance strategies to maintain collection of critical case information without overburdening jurisdiction health departments. National surveillance will increasingly be complemented by focused surveillance systems collecting comprehensive case information on a subset of cases across various health care settings. These systems will provide detailed information on the evolving COVID-19 incidence and risk factors for infection and severe disease. More systematic and detailed collection of underlying condition data among pediatric patients would be helpful to understand which children might be at highest risk for severe COVID-19 illness.

This preliminary examination of characteristics of COVID-19 disease among children in the United States suggests that children do not always have fever or cough as reported signs and symptoms. Although most cases reported among children to date have not been severe, clinicians should maintain a high index of suspicion for COVID-19 infection in children and monitor for progression of illness, particularly among infants and children with underlying conditions. However, these findings must be interpreted with caution because of the high percentage of cases missing data on important characteristics. Because persons with asymptomatic and mild disease, including children, are likely playing a role in transmission and spread of COVID-19 in the community, social distancing and everyday preventive behaviors are recommended for persons of all ages to slow the spread of the virus, protect the health care system from being overloaded, and protect older adults and persons of any age with serious underlying medical conditions. Recommendations for reducing the spread of COVID-19 by staying at home and practicing strategies such as respiratory hygiene, wearing cloth face coverings when around others, and others are available on CDC's coronavirus website at <https://www.cdc.gov/coronavirus/2019-ncov/prevent-getting-sick/prevention.html>.

Acknowledgments

State, local, and territorial health department personnel; U.S. clinical, public health, and emergency response staff members; Grace Appiah, Andrea Carmichael, Nancy Chow, Brian Emerson, Katie Forsberg, Alicia Fry, Aron Hall, Clinton McDaniel, Daniel C. Payne, Rachael Porter, Sarah Reagan-Steiner, Matt Ritchey, Katherine Roguski, Tom Shimabukuro, Ben Silk, Emily Ussery, Kate Woodworth, CDC.

CDC COVID-19 Response Team

Stephanie Bialek, CDC; Ryan Gierke, CDC; Michelle Hughes, CDC; Lucy A. McNamara, CDC; Tamara Pilishvili, CDC; Tami Skoff, CDC.

Corresponding author: Lucy A. McNamara for the CDC COVID-19 Response Team, eoevent294@cdc.gov, 770-488-7100.

All authors have completed and submitted the International Committee of Medical Journal Editors form for disclosure of potential conflicts of interest. No potential conflicts of interest were disclosed.

References

1. World Health Organization. Coronavirus disease 2019 (COVID-19) situation report – 73. Geneva, Switzerland: World Health Organization; 2020. <https://www.who.int/emergencies/diseases/novel-coronavirus-2019/situation-reports>
2. CDC. Coronavirus disease 2019 (COVID-19): cases in U.S. Atlanta, GA: US Department of Health and Human Services, CDC; 2020. <https://www.cdc.gov/coronavirus/2019-ncov/cases-updates/cases-in-us.html>
3. CDC. Bridged race population estimates. Atlanta, GA: US Department of Health and Human Services, CDC; 2020. <https://wonder.cdc.gov/bridged-race-population.html>
4. Lu X, Zhang L, Du H, et al.; Chinese Pediatric Novel Coronavirus Study Team. SARS-CoV-2 infection in children. *N Engl J Med* 2020. Epub March 18, 2020. <https://doi.org/10.1056/NEJMc2005073>
5. Dong Y, Mo X, Hu Y, et al. Epidemiological characteristics of 2143 pediatric patients with 2019 coronavirus disease in China. *Pediatrics* 2020. Epub March 16, 2020. <https://doi.org/10.1542/peds.2020-0702>
6. Hoehl S, Rabenau H, Berger A, et al. Evidence of SARS-CoV-2 infection in returning travelers from Wuhan, China. *N Engl J Med* 2020;382:1278–80. <https://doi.org/10.1056/NEJMc2001899>
7. Wei WE, Li Z, Chiew CJ, Yong SE, Toh MP, Lee VJ. Presymptomatic transmission of SARS-CoV-2—Singapore, January 23–March 16, 2020. *MMWR Morb Mortal Wkly Rep* 2020. Epub April 1, 2020.
8. Bialek S, Boundy E, Bowen V, et al.; CDC COVID-19 Response Team. Severe outcomes among patients with coronavirus disease 2019 (COVID-19)—United States, February 12–March 16, 2020. *MMWR Morb Mortal Wkly Rep* 2020;69:343–6. <https://doi.org/10.15585/mmwr.mm6912e2>
9. Ng Y, Li Z, Chua YX, et al. Evaluation of the effectiveness of surveillance and containment measures for the first 100 patients with COVID-19 in Singapore—January 2–February 29, 2020. *MMWR Morb Mortal Wkly Rep* 2020;69:307–11. <https://doi.org/10.15585/mmwr.mm6911e1>
10. The Novel Coronavirus Emergency Response Epidemiology Team. The epidemiological characteristics of an outbreak of 2019 novel coronavirus diseases (COVID-19)—China, 2020. *China CDC Weekly* 2020;2:113–22.

Symptom Duration and Risk Factors for Delayed Return to Usual Health Among Outpatients with COVID-19 in a Multistate Health Care Systems Network — United States, March–June 2020

Mark W. Tenforde, MD, PhD¹; Sara S. Kim, MPH^{1,2}; Christopher J. Lindsell, PhD³; Erica Billig Rose, PhD¹; Nathan I. Shapiro, MD⁴; D. Clark Files, MD⁵; Kevin W. Gibbs, MD⁵; Heidi L. Erickson, MD⁶; Jay S. Steingrub, MD⁷; Howard A. Smithline, MD⁷; Michelle N. Gong, MD⁸; Michael S. Aboodi, MD⁸; Matthew C. Exline, MD⁹; Daniel J. Henning, MD¹⁰; Jennifer G. Wilson, MD¹¹; Akram Khan, MD¹²; Nida Qadir, MD¹³; Samuel M. Brown, MD¹⁴; Ithan D. Peltan, MD¹⁴; Todd W. Rice, MD³; David N. Hager, MD, PhD¹⁵; Adit A. Ginde, MD¹⁶; William B. Stubblefield, MD³; Manish M. Patel, MD¹; Wesley H. Self, MD³; Leora R. Feldstein, PhD¹; IVY Network Investigators; CDC COVID-19 Response Team

On July 24, 2020, this report was posted as an MMWR Early Release on the MMWR website (<https://www.cdc.gov/mmwr>).

Prolonged symptom duration and disability are common in adults hospitalized with severe coronavirus disease 2019 (COVID-19). Characterizing return to baseline health among outpatients with milder COVID-19 illness is important for understanding the full spectrum of COVID-19–associated illness and tailoring public health messaging, interventions, and policy. During April 15–June 25, 2020, telephone interviews were conducted with a random sample of adults aged ≥18 years who had a first positive reverse transcription–polymerase chain reaction (RT-PCR) test for SARS-CoV-2, the virus that causes COVID-19, at an outpatient visit at one of 14 U.S. academic health care systems in 13 states. Interviews were conducted 14–21 days after the test date. Respondents were asked about demographic characteristics, baseline chronic medical conditions, symptoms present at the time of testing, whether those symptoms had resolved by the interview date, and whether they had returned to their usual state of health at the time of interview. Among 292 respondents, 94% (274) reported experiencing one or more symptoms at the time of testing; 35% of these symptomatic respondents reported not having returned to their usual state of health by the date of the interview (median = 16 days from testing date), including 26% among those aged 18–34 years, 32% among those aged 35–49 years, and 47% among those aged ≥50 years. Among respondents reporting cough, fatigue, or shortness of breath at the time of testing, 43%, 35%, and 29%, respectively, continued to experience these symptoms at the time of the interview. These findings indicate that COVID-19 can result in prolonged illness even among persons with milder outpatient illness, including young adults. Effective public health messaging targeting these groups is warranted. Preventative measures, including social distancing, frequent handwashing, and the consistent and correct use of face coverings in public, should be strongly encouraged to slow the spread of SARS-CoV-2.

Prolonged illness is well described in adults with severe COVID-19 requiring hospitalization, especially among older adults (1,2). Recently, the number of SARS-CoV-2 infections

in persons first evaluated as outpatients have increased, including cases among younger adults (3). A better understanding of convalescence and symptom duration among outpatients with COVID-19 can help direct care, inform interventions to reduce transmission, and tailor public health messaging.

The Influenza Vaccine Effectiveness in the Critically Ill (IVY) Network, a collaboration of U.S. health care systems, is conducting epidemiologic studies on COVID-19 in both inpatient and outpatient settings (4,5). Fourteen predominantly urban academic health systems in 13 states each submitted a list of adults with positive SARS-CoV-2 RT-PCR test results obtained during March 31–June 4, 2020, to Vanderbilt University Medical Center. Site-specific random sampling was then performed on a subset of these patients who were tested as outpatients and included patients tested in the emergency department (ED) who were not admitted to the hospital at the testing encounter and those tested in other outpatient clinics. At 14–21 days from the test date, CDC personnel interviewed the randomly sampled patients or their proxies by telephone to obtain self-reported baseline demographic, socioeconomic, and underlying health information, including the presence of chronic medical conditions. Call attempts were made for up to seven consecutive days, and interviews were conducted in several languages (4). Respondents were asked to report the number of days they felt unwell before the test date, COVID-19–related symptoms experienced at the time of testing (6), whether symptoms had resolved by the date of the interview, and whether the patient had returned to their usual state of health. For this data analysis, respondents were excluded if they did not complete the interview, if a proxy (e.g., family member) completed the interview (because of their incomplete knowledge of symptoms), if they reported a previous positive SARS-CoV-2 test (because the reference date for symptoms questions was unclear), or (because this analysis focused on symptomatic persons) if they did not answer symptoms questions or denied all symptoms at testing.

Descriptive statistics were used to compare characteristics among respondents who reported returning and not returning to their usual state of health by the date of the interview.

Summary**What is already known about this topic?**

Relatively little is known about the clinical course of COVID-19 and return to baseline health for persons with milder, outpatient illness.

What is added by this report?

In a multistate telephone survey of symptomatic adults who had a positive outpatient test result for SARS-CoV-2 infection, 35% had not returned to their usual state of health when interviewed 2–3 weeks after testing. Among persons aged 18–34 years with no chronic medical conditions, one in five had not returned to their usual state of health.

What are the implications for public health practice?

COVID-19 can result in prolonged illness, even among young adults without underlying chronic medical conditions. Effective public health messaging targeting these groups is warranted.

Generalized estimating equation regression models with exchangeable correlation structure accounting for clustering by site were fitted to evaluate the association between baseline characteristics and return to usual health, adjusting for potential a priori-selected confounders. Resolution and duration of individual symptoms were also assessed. Statistical analyses were conducted using Stata software (version 16; StataCorp).

At least one telephone call was attempted for 582 patients (including 175 [30%] who were tested in an ED and 407 [70%] in non-ED settings), with 325 (56%) interviews completed (89 [27%] ED and 236 [73%] non-ED). Among 257 nonrespondents, 178 could not be reached, 37 requested a callback but could not be reached on further call attempts, 28 refused the interview, and 14 had a language barrier. Among the 325 completed interviews, 31 were excluded: nine (3%) because a proxy was interviewed, 17 (5%) because a previous positive SARS-CoV-2 test was reported, and five (2%) who did not answer the symptoms questions. Two additional respondents were called prematurely at 7 days and were also excluded.* Among the 292 remaining patient respondents, 274 (94%) reported one or more symptoms at testing and were included in this data analysis. Following outpatient testing, 7% (19 of 262 with available data) reported later being hospitalized, a median of 3.5 days after the test date. The median age of symptomatic respondents was 42.5 years (interquartile range [IQR] = 31–54 years), 142 (52%) were female, 98 (36%) were Hispanic, 96 (35%) were non-Hispanic white, 48 (18%) were non-Hispanic black, and 32 (12%) were other non-Hispanic

race. Overall, 141 of 264 (53%) with available data reported one or more chronic medical conditions. The median interval from test to interview date was 16 days (IQR = 14–19 days); the median number of days respondents reported feeling unwell before being tested for SARS-CoV-2 was 3 (IQR = 2–7 days).

Return to Usual State of Health

Among the 270 of 274 interviewees with available data on return to usual health,[†] 175 (65%) reported that they had returned to their usual state of health a median of 7 days (IQR = 5–12 days) from the date of testing (Table 1). Ninety-five (35%) reported that they had not returned to their usual state of health at the time of interview. The proportion who had not returned to their usual state of health differed across age groups: 26% of interviewees aged 18–34 years, 32% aged 35–49 years, and 47% aged ≥50 years reported not having returned to their usual state of health ($p = 0.010$) within 14–21 days after receiving a positive test result. Presence of chronic conditions also affected return to health rates; among 180 persons with no or one chronic medical condition, 39 with two chronic medical conditions, and 44 with three or more chronic medical conditions, 28%, 46%, and 57%, respectively, reported not having returned to their usual state of health ($p = 0.003$) within 14–21 days after having a positive test result. Among respondents aged 18–34 years with no chronic medical condition, 19% (nine of 48) reported not having returned to their usual state of health. Adjusting for other factors, age ≥50 versus 18–34 years (adjusted odds ratio [aOR] = 2.29; 95% confidence interval [CI] = 1.14–4.58) and reporting three or more versus no chronic medical conditions (aOR = 2.29; 95% CI = 1.07–4.90) were associated with not having returned to usual health (Table 2). Obesity (body mass index ≥30 kg per m²) (aOR 2.31; 95% CI = 1.21–4.42) and reporting a psychiatric condition[§] (aOR 2.32; 95% CI = 1.17–4.58) also were associated with more than twofold odds of not returning to the patient's usual health after adjusting for age, sex, and race/ethnicity.

Resolution of Symptoms and Duration

Among the 274 symptomatic outpatients, the median number of symptoms was seven of 17 listed in the interview tool (IQR = 5–10), with fatigue (71%), cough (61%), and headache (61%) those most commonly reported (Figure). Among respondents who reported fever and chills on the day of testing, these resolved in 97% and 96% of respondents, respectively.

*Two patients interviewed early at 12 days and three interviewed at 13 days after testing were included. Two patients who requested interview after 21 days because they were unavailable at 14–21 days were included (interviews were conducted at 25 and 26 days). All other included respondents were interviewed 14–21 days after testing.

[†]Patients were asked the question “Would you say that you are feeling back to your usual health?”

[§]Psychiatric conditions included anxiety disorder (38), depression (21), posttraumatic stress disorder (two), paranoia (two), obsessive-compulsive disorder (one), schizophrenia (one); some patients reported more than one condition.

TABLE 1. Characteristics of symptomatic outpatients with SARS-CoV-2 real-time reverse transcription–polymerase chain reaction (RT-PCR)—positive test results (N = 270)* who reported returning to usual state of health or not returning to usual state of health at an interview conducted 14–21 days after testing — 14 academic health care systems,† United States, March–June 2020

Characteristic	Total	Returned to usual health, no. (row %)		P-value [§]
		Yes (n = 175)	No (n = 95)	
Sex				0.14
Women	140	85 (61)	55 (39)	
Men	130	90 (69)	40 (31)	
Age group (yrs)				0.010
18–34	85	63 (74)	22 (26)	
35–49	96	65 (68)	31 (32)	
≥50	89	47 (53)	42 (47)	
Race/Ethnicity				0.29
White, non-Hispanic	94	58 (62)	36 (38)	
Black, non-Hispanic	46	26 (57)	20 (43)	
Other race, non-Hispanic	32	24 (75)	8 (25)	
Hispanic	98	67 (68)	31 (32)	
Insurance (14 missing)				0.69
No	46	31 (67)	15 (33)	
Yes	210	135 (64)	75 (36)	
No. of medical conditions (7 missing)				0.003
0	123	87 (71)	36 (29)	
1	57	41 (72)	16 (28)	
2	39	21 (54)	18 (46)	
≥3	44	19 (43)	25 (57)	
Individual medical conditions (7 missing all)[¶]				
Hypertension	64	33 (52)	31 (48)	0.018
Obesity (body mass index >30 kg/m ²)	51	23 (45)	28 (55)	0.002
Psychiatric condition	49	23 (47)	26 (53)	0.007
Asthma	36	23 (64)	13 (36)	0.99
Diabetes	28	16 (57)	12 (43)	0.43
Immunosuppressive condition	15	6 (40)	9 (60)	0.047
Autoimmune condition	13	7 (54)	6 (46)	0.44
Blood disorder	8	4 (50)	4 (50)	0.47
Chronic kidney disease	7	3 (43)	4 (57)	0.26
Chronic obstructive pulmonary disease	7	4 (57)	3 (43)	0.71
Liver disease	6	4 (67)	2 (33)	1.00
Neurologic condition	6	3 (50)	3 (50)	0.48
Coronary artery disease	4	3 (75)	1 (25)	1.00
Congestive heart failure	2	2 (100)	0 (0)	0.54

* 294 patients responded to an interview 2–3 weeks after testing, did not report a previous positive SARS-CoV-2 test before the reference test, and answered questions about symptoms. Of these, 276 (94%) reported one or more symptoms at the time of SARS-CoV-2 RT-PCR testing, with 272 (99%) reporting whether they had returned to their usual state of health by the time of the interview. Two additional patients excluded who were called at 7 days, with 270 included here.

† Patients were randomly sampled from fourteen academic healthcare systems in 13 states (University of Washington [Washington], Oregon Health and Sciences University [Oregon], University of California Los Angeles and Stanford University [California], Hennepin County Medical Center [Minnesota], Vanderbilt University [Tennessee], Ohio State University [Ohio], Wake Forest University [North Carolina], Montefiore Medical Center [New York], Beth Israel Deaconess Medical Center and Baystate Medical Center [Massachusetts], Intermountain Healthcare [Utah/Idaho], University of Colorado Hospital [Colorado], and Johns Hopkins University [Maryland]).

§ Respondents who reported returning to usual health and respondents who reported not returning to usual health were compared using the chi-square test or Fisher's exact test.

¶ Excluding seven (3%) patients who did not answer questions about chronic underlying medical conditions; for those who answered questions about underlying conditions, some respondents were missing data on obesity (two), neurologic conditions (one), and psychiatric conditions (one).

Symptoms least likely to have resolved included cough (not resolved in 43% [71 of 166]) and fatigue (not resolved in 35% [68 of 192]); among 90 who reported shortness of breath at the time of testing, this symptom had not resolved in 26 (29%). The median interval to symptom resolution among those who reported individual symptoms at the time of testing but not at the time of the interview ranged from 4 to 8 days from the test date, with the longest intervals reported for loss of smell (median = 8 days; IQR = 5–10.5 days) and loss of taste (median = 8 days; IQR = 4–10 days). Among respondents who

reported returning to their usual state of health, 34% (59 of 175) still reported one or more of the 17 queried COVID-related symptoms at the time of the interview.

Discussion

Most studies to date have focused on symptoms duration and clinical outcomes in adults hospitalized with severe COVID-19 (1,2). This report indicates that even among symptomatic adults tested in outpatient settings, it might take weeks for resolution of symptoms and return to usual health.

TABLE 2. Characteristics associated with not returning to usual health among symptomatic outpatients with SARS-CoV-2 real-time reverse transcription–polymerase chain reaction (RT-PCR)–positive test results (N = 270)* reported at an interview conducted 14–21 days after testing — 14 academic health care systems,† United States, March–June 2020

Characteristic	Odds of not returning to “usual health” at 14–21 days after testing	
	Unadjusted odds ratio (95% CI) [§]	Adjusted odds ratio (95% CI) ^{§,¶}
Age group (yrs)		
18–34	Referent	Referent
35–49	1.40 (0.73–2.67)	1.38 (0.71–2.69)
≥50	2.64 (1.39–5.00)	2.29 (1.14–4.58)
Sex		
Women	Referent	Referent
Men	0.68 (0.41–1.13)	0.80 (0.46–1.38)
Race/Ethnicity		
White, non-Hispanic	Referent	Referent
Black, non-Hispanic	1.23 (0.60–2.53)	1.13 (0.53–2.45)
Other, non-Hispanic	0.53 (0.21–1.31)	0.63 (0.24–1.61)
Hispanic	0.74 (0.40–1.34)	0.83 (0.44–1.58)
No. of medical conditions		
0	Referent	Referent
1	0.94 (0.47–1.89)	0.74 (0.35–1.55)
2	2.09 (1.00–4.38)	1.50 (0.68–3.33)
≥3	3.19 (1.56–6.50)	2.29 (1.07–4.90)
Individual medical conditions**		
Hypertension	1.98 (1.12–3.52)	1.30 (0.67–2.51)
Obesity (BMI >30 kg/m ²)	2.65 (1.42–4.95)	2.31 (1.21–4.42)
Psychiatric condition	2.42 (1.29–4.56)	2.32 (1.17–4.58)
Asthma	1.00 (0.48–2.08)	1.02 (0.47–2.20)
Diabetes	1.38 (0.62–3.05)	1.06 (0.46–2.44)
Immunosuppressive condition	2.84 (0.98–8.26)	2.33 (0.77–7.04)
Autoimmune condition	1.55 (0.51–4.76)	1.05 (0.32–3.46)
Blood disorder	1.82 (0.45–7.45)	1.43 (0.33–6.24)
Chronic kidney disease	2.42 (0.53–11.05)	2.36 (0.48–11.51)
Chronic obstructive pulmonary disease	1.34 (0.29–6.12)	0.70 (0.14–3.48)
Liver disease	0.88 (0.16–4.90)	0.72 (0.12–4.25)
Neurologic condition	1.78 (0.35–9.01)	1.23 (0.23–6.62)
Coronary artery disease	0.58 (0.06–5.70)	0.48 (0.05–4.92)
Congestive heart failure	—	—

Abbreviations: BMI = body mass index; CI = confidence interval.

* 294 patients responded to 14–21-day interview, did not report a previous positive SARS-CoV-2 test before the reference test, and answered questions about symptoms; 276 (94%) of these reported one or more symptoms at the time of SARS-CoV-2 RT-PCR testing, with 272 (99%) reporting whether they had returned to their usual state of health by the time of the interview. Two additional patients who were called at 7 days were excluded, with 270 included here.

† Patients were randomly sampled from academic healthcare systems in 13 states (University of Washington [Washington], Oregon Health and Sciences University [Oregon], University of California Los Angeles and Stanford University [California], Hennepin County Medical Center [Minnesota], Vanderbilt University [Tennessee], Ohio State University [Ohio], Wake Forest University [North Carolina], Montefiore Medical Center [New York], Beth Israel Deaconess Medical Center and Baystate Medical Center [Massachusetts], Intermountain Healthcare [Utah/Idaho], University of Colorado Hospital [Colorado], and Johns Hopkins University [Maryland]).

§ For this analysis, generalized estimation equation (GEE) models with exchangeable correlation structure were used to estimate the association between characteristics and the odds of not returning to usual health by the date of the 14–21-day interview. GEE models were used to account for clustering of cases by site. 95% CIs including 1.00 are not considered statistically significant.

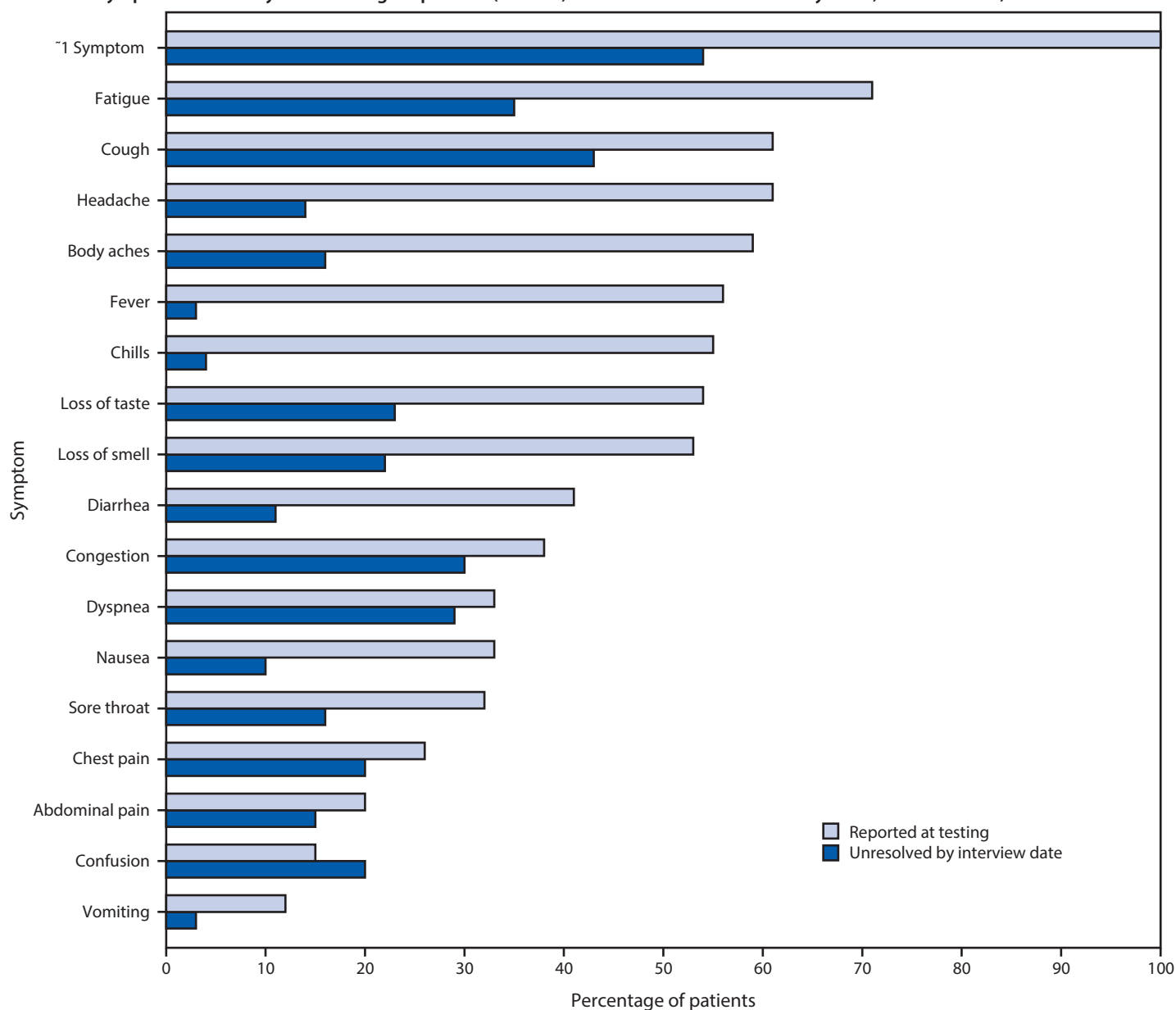
¶ In adjusted GEE models for age, sex, race/ethnicity, and number of chronic medical conditions, the other variables were used to adjust for potential confounders. Models for individual conditions (e.g., hypertension) were adjusted for age, sex, and race/ethnicity.

** Medical conditions are not exclusive and individual patients could have more than one chronic medical condition.

Not returning to usual health within 2–3 weeks of testing was reported by approximately one third of respondents. Even among young adults aged 18–34 years with no chronic medical conditions, nearly one in five reported that they had not returned to their usual state of health 14–21 days after testing. In contrast, over 90% of outpatients with influenza recover within approximately 2 weeks of having a positive test result (7). Older age and presence of multiple chronic medical conditions have previously been associated with illness severity among adults hospitalized with COVID-19 (8,9); in this study, both were also associated with prolonged illness in an

outpatient population. Whereas previous studies have found race/ethnicity to be a risk factor for severe COVID-19 illness (10), this study of patients whose illness was diagnosed in an outpatient setting did not find an association between race/ethnicity and return to usual health although the modest number of respondents might have limited our ability to detect associations. The finding of an association between chronic psychiatric conditions and delayed return to usual health requires further evaluation. These findings have important implications for understanding the full effects of COVID-19, even in persons with milder outpatient illness. Notably, convalescence can be

FIGURE. Self-reported symptoms at the time of positive SARS-CoV-2 reverse transcription–polymerase chain reaction (RT-PCR) testing results and unresolved symptoms 14–21 days later among outpatients (N = 274)* — 14 academic health care systems,[†] United States, March–June 2020



* 294 patients responded to 14–21-day interview, did not report a previous positive SARS-CoV-2 test before the reference test, and answered questions about symptoms; 276 (94%) of these reported one or more symptoms at the time of SARS-CoV-2 RT-PCR testing; those who were interviewed at 7 days were excluded, with 274 included here.

[†] Patients were randomly sampled from 14 academic health care systems in 13 states (University of Washington [Washington], Oregon Health and Sciences University [Oregon], University of California Los Angeles and Stanford University [California], Hennepin County Medical Center [Minnesota], Vanderbilt University [Tennessee], Ohio State University [Ohio], Wake Forest University [North Carolina], Montefiore Medical Center [New York], Beth Israel Deaconess Medical Center and Baystate Medical Center [Massachusetts], Intermountain Healthcare [Utah/Idaho], University of Colorado Hospital [Colorado], and Johns Hopkins University [Maryland]).

prolonged even in young adults without chronic medical conditions, potentially leading to prolonged absence from work, studies, or other activities.

The findings in this report are subject to at least three limitations. First, nonrespondents might have differed from survey respondents; for example, those with more severe illness might have been less likely to respond to telephone calls if they were

subsequently hospitalized and unable to answer the telephone. Second, symptoms that resolved before the test date or that commenced after the date of testing were not recorded in this survey. Finally, as a telephone survey, this study relied on patient self-report and might have been subject to incomplete recall or recall bias.

Nonhospitalized COVID-19 illness can result in prolonged illness and persistent symptoms, even in young adults and

persons with no or few chronic underlying medical conditions. Public health messaging should target populations that might not perceive COVID-19 illness as being severe or prolonged, including young adults and those without chronic underlying medical conditions. Preventative measures, including social distancing, frequent handwashing, and the consistent and correct use of face coverings in public, should be strongly encouraged to slow the spread of SARS-CoV-2.

IVY Network Investigators

Kimberly W. Hart, Vanderbilt University Medical Center; Robert McClellan, Vanderbilt University Medical Center.

CDC COVID-19 Response Team

Layne Dorough, CDC COVID-19 Response Team; Nicole Dzuris, CDC COVID-19 Response Team; Eric P. Griggs, CDC COVID-19 Response Team; Ahmed M. Kassem, CDC COVID-19 Response Team; Paula L. Marcet, CDC COVID-19 Response Team; Constance E. Ogokeh, CDC COVID-19 Response Team; Courtney N. Sciarratta, CDC COVID-19 Response Team; Akshita Siddula, CDC COVID-19 Response Team; Emily R. Smith, CDC COVID-19 Response Team; Michael J. Wu, CDC COVID-19 Response Team.

Corresponding author: Mark W. Tenforde, pij6@cdc.gov.

¹CDC COVID-19 Response Team; ²Oak Ridge Institute for Science and Education, Oak Ridge, Tennessee; ³Vanderbilt University Medical Center, Nashville, Tennessee; ⁴Beth Israel Deaconess Medical Center, Boston, Massachusetts; ⁵Wake Forest University Baptist Medical Center, Winston-Salem, North Carolina; ⁶Hennepin County Medical Center, Minneapolis, Minnesota; ⁷Baystate Medical Center, Springfield, Massachusetts; ⁸Montefiore Medical Center and Albert Einstein College of Medicine, Bronx, New York; ⁹Ohio State University Wexner Medical Center, Columbus, Ohio; ¹⁰University of Washington Medical Center, Seattle, Washington; ¹¹Stanford University Medical Center, Palo Alto, California; ¹²Oregon Health & Sciences University, Portland, Oregon; ¹³UCLA Medical Center, Los Angeles, California; ¹⁴Intermountain Healthcare, Salt Lake City, Utah; ¹⁵Johns Hopkins Hospital, Baltimore, Maryland; ¹⁶University of Colorado School of Medicine, Aurora, Colorado.

All authors have completed and submitted the International Committee of Medical Journal Editors form for disclosure of potential conflicts of interest. Christopher J. Lindsell reports grants from National Institutes of Health and Department of Defense, and contracts with the Marcus Foundation, CDC, Endpoint Health, Entegriion, bioMerieux, and Bioscape Digital, outside the submitted work. Daniel J. Henning reports personal fees from CytoVale and grants from Baxter, outside the submitted work. Akram Khan reports grants from United Therapeutics, Actelion Pharmaceuticals, Regeneron, and Reata Pharmaceuticals,

outside the submitted work. Samuel M. Brown reports grants from National Institutes of Health, Department of Defense, Intermountain Research and Medical Foundation, and Janssen, consulting fees paid to his employer from Faron and Sedana, and royalties from Oxford University Press, outside the submitted work. Ithan D. Peltan reports grants from National Institutes of Health, Asahi Kasei Pharma, Immunexpress Inc., Janssen Pharmaceuticals, and Regeneron, outside the submitted work. Todd W. Rice reports personal fees from Cumberland Pharmaceuticals, Inc., CytoVale, Inc., and Avisia, LLC, outside the submitted work. No other potential conflicts of interest were disclosed.

References

1. Grasselli G, Zangrillo A, Zanella A, et al.; COVID-19 Lombardy ICU Network. Baseline characteristics and outcomes of 1591 patients infected with SARS-CoV-2 admitted to ICUs of the Lombardy Region, Italy. *JAMA* 2020;323:1574–81. <https://doi.org/10.1001/jama.2020.5394>
2. Guan WJ, Ni ZY, Hu Y, et al.; China Medical Treatment Expert Group for Covid-19. Clinical characteristics of coronavirus disease 2019 in China. *N Engl J Med* 2020;382:1708–20. <https://doi.org/10.1056/NEJMoa2002032>
3. CDC. Coronavirus disease 2019 (COVID-19). COVIDView. Atlanta, GA: US Department of Health and Human Services, CDC; 2020. <https://www.cdc.gov/coronavirus/2019-ncov/covid-data/covidview/index.html>
4. Tenforde MW, Billig Rose E, Lindsell CJ, et al.; CDC COVID-19 Response Team. Characteristics of adult outpatients and inpatients with COVID-19—11 academic medical centers, United States, March–May 2020. *MMWR Morb Mortal Wkly Rep* 2020;69:841–6. <https://doi.org/10.15585/mmwr.mm6926e3>
5. Stubblefield WB, Talbot HK, Feldstein L, et al.; Influenza Vaccine Effectiveness in the Critically Ill (IVY) Investigators. Seroprevalence of SARS-CoV-2 among frontline healthcare personnel during the first month of caring for COVID-19 patients—Nashville, Tennessee. *Clin Infect Dis* 2020. Epub July 6, 2020. <https://doi.org/10.1093/cid/cia936>
6. CDC. Coronavirus disease 2019 (COVID-19). Symptoms of coronavirus. Atlanta, GA: US Department of Health and Human Services, CDC; 2020. <https://www.cdc.gov/coronavirus/2019-ncov/symptoms-testing/symptoms.html>
7. Petrie JG, Cheng C, Malosh RE, et al. Illness severity and work productivity loss among working adults with medically attended acute respiratory illnesses: US Influenza Vaccine Effectiveness Network 2012–2013. *Clin Infect Dis* 2016;62:448–55.
8. Zhou F, Yu T, Du R, et al. Clinical course and risk factors for mortality of adult inpatients with COVID-19 in Wuhan, China: a retrospective cohort study. *Lancet* 2020;395:1054–62. [https://doi.org/10.1016/S0140-6736\(20\)30566-3](https://doi.org/10.1016/S0140-6736(20)30566-3)
9. Jordan RE, Adab P, Cheng KK. Covid-19: risk factors for severe disease and death. *BMJ* 2020;368:m1198. <https://doi.org/10.1136/bmj.m1198>
10. Price-Haywood EG, Burton J, Fort D, Seoane L. Hospitalization and mortality among black patients and white patients with Covid-19. *N Engl J Med* 2020;382:2534–43. <https://doi.org/10.1056/NEJMs2011686>

Understanding how Victoria, Australia gained control of its second COVID-19 wave

James M Trauer,^{1} Michael J Lydeamore,^{2,3} Gregory W Dalton,³ David Pilcher,¹ Michael T Meehan,⁴ Emma S McBryde,⁴ Allen C Cheng,¹ Brett Sutton,³ Romain Ragonnet¹*

* Corresponding author:
A/Prof James M Trauer
Head, Epidemiological Modelling Unit
553 St Kilda Road
Melbourne
Victoria 3004
Australia
james.trauer@monash.edu

1. School of Public Health and Preventive Medicine, Monash University, Victoria
2. Central Clinical School, Monash University, Victoria
3. Department of Health, Victoria
4. Australian Institute of Tropical Health and Medicine, James Cook University, Queensland

Abstract

Victoria has been Australia's hardest hit state by the COVID-19 pandemic, but was successful in reversing its second wave of infections through aggressive policy interventions. The clear reversal in the epidemic trajectory combined with information on the timing and geographical scope of policy interventions offers the opportunity to estimate the relative contribution of each change. We developed a compartmental model of the COVID-19 epidemic in Victoria that incorporated age and geographical structure, and calibrated it to data on case notifications, deaths and health service needs according to the administrative divisions of Victoria's healthcare, termed clusters. We achieved a good fit to epidemiological indicators, at both the state level and for individual clusters, through a combination of time-varying processes that included changes to case detection rates, population mobility, school closures, seasonal forcing, physical distancing and use of face coverings. Estimates of the risk of hospitalisation and death among persons with disease that were needed to achieve this close fit were markedly higher than international estimates, likely reflecting the concentration of the epidemic in groups at particular risk of adverse outcomes, such as residential facilities. Otherwise, most fitted parameters were consistent with the existing literature on COVID-19 epidemiology and outcomes. We estimated a significant effect for each of the calibrated time-varying processes on reducing the risk of transmission per contact, with broad estimates of the reduction in transmission risk attributable to seasonal forcing (27.8%, 95% credible interval [95%CI] 9.26-44.7% for mid-summer compared to mid-winter), but narrower estimates for the individual-level effect of physical distancing of 12.5% (95%CI 5.69-27.9%) and of face coverings of 39.1% (95%CI 31.3-45.8%). That the multi-factorial public health interventions and mobility restrictions led to the dramatic reversal in the epidemic trajectory is supported by our model results, with the mandatory face coverings likely to have been particularly important.

Introduction

The COVID-19 pandemic has had an unprecedented impact on human health and society,^{1,2} with high-income, urban and temperate areas often the most severely affected.³⁻⁵ The impacts of the virus are felt through the direct effect of the virus, particularly through its considerable risk of mortality following infection^{6,7} and likely substantial post-infection sequelae,⁸ but also through the extreme lockdown measures often needed to achieve control.⁹

Australia has been relatively successful in controlling COVID-19,¹⁰ with all jurisdictions of the country achieving good control of the first wave of imported cases through March and April. However, the southern state of Victoria suffered a substantial second wave of locally-transmitted cases, reaching around 600 notifications per day, predominantly in metropolitan Melbourne in winter.

In response to the pandemic, the Victorian Government implemented a number of recommendations and policy changes with the aim of reversing the escalating case numbers that had a severe impact on social and economic activities. Specific changes included stringent restrictions on movement, increased testing rates, school closures and face covering requirements. In metropolitan Melbourne face coverings were mandated from 23rd July and significantly more stringent movement restrictions were implemented from 9th of July (moving to “stage 3”) and from 2nd August (moving from “stage 3” to “stage 4”). Case numbers peaked in the final days of July and first days of August and declined thereafter. Understanding the relative contribution of each of these interventions is complicated by several interventions being implemented within a few weeks, along with policy differences between metropolitan and regional areas. Nevertheless, the clear reversal in the trajectory of the epidemic following the implementation of these policy changes offers the opportunity to explore the contribution of these factors to the epidemic profile. Indeed, the experience of Victoria’s second wave is virtually unique in that the pattern of substantial and escalating daily community cases was reversed following these policy changes, with elimination

subsequently achieved in November. We adapted our computational model to create a unified transmission model for the state and infer the contribution of the policy interventions implemented to changing the direction of the epidemic trajectory.

Methods

We adapted the transmission dynamic model that we had used to produce forecasts of new cases, health system capacity requirements and deaths for the Victorian Department of Health and Human Services (DHHS) at the health service cluster level (henceforward “cluster”). By incorporating geographical structure to represent clusters, we built a unified model of the COVID-19 epidemic in Victoria, and fitted the model to multiple indicators of epidemic burden in order to infer the effectiveness of each component of the response to the epidemic. Full methods are provided in the Supplementary Methods, key features of the model are illustrated in Figure 1 and all code is available at <https://github.com/monash-emu/AuTuMN>.

Base model

Our model of COVID-19 epidemiology is a stratified, deterministic SEIR framework, with sequential compartments representing non-infectious and infectious incubation periods and early and late active disease (Figure 1A). The late incubation compartment and the two active compartments are stratified to simulate epidemiological considerations including asymptomatic cases,¹¹ incomplete detection of symptomatic cases, hospitalisation and ICU admission (Figure 1B). All model compartments were then stratified by age, with susceptibility, the clinical fraction, hospitalisation risk and infection fatality rate modified by age group.⁶ We introduced heterogeneous mixing by age using the synthetic mixing matrix for Australia developed by Prem *et al.* 2017 (Figure 1D).¹²

Simulation of public health interventions

We simulated movement restrictions (including school closures, business closures and working from home) by varying the relative contribution of three of four locations to the overall mixing matrix (Figure 1E) continuously over time. Using Google mobility data (<https://www.google.com/covid19/mobility/>) weighted to cluster, we scaled the work contribution with workplace mobility and the contribution from other locations (contacts outside of schools, homes, and work) with an average of mobility from the remaining Google mobility locations other than residential (Figure 1E). We simulated school closures by scaling the school contribution according to the proportion of children attending schools on site. We assumed that schools began transitioning to onsite learning from the 26th of May, at which time 400,000 of 1,018,000 students returned to onsite education. The remaining students were considered to return onsite from the 9th of June, before 90% of students moved to remote learning from the 9th of July, which continued until October.

The term “micro-distancing” is used to refer to behavioural changes that reduce the risk of transmission given an interpersonal contact and so are not captured through data on population mobility (e.g. maintaining physical distance and use of face coverings). Micro-distancing was assumed to reduce the risk of both transmission from index cases and the risk of infection of susceptible persons, with the effect of both physical distancing and face coverings applied to all three non-residential locations. Both the coverage and the effectiveness of each intervention were incorporated, with time-varying functions representing the proportion of the population complying with recommendations over time and constant calibration parameters scaling these functions to represent the effectiveness of the intervention. The profiles of compliance with these two recommendations was estimated by fitting to YouGov data, available at <https://github.com/YouGov-Data/covid-19-tracker>, with hyperbolic tan functions providing a good fit to data (Supplemental Figures 5 and 6).

Because face coverings were mandated ten days later in regional Victoria than metropolitan Melbourne, the face coverings compliance function was delayed by this period for regional clusters, while the physical distancing function was identical for all clusters.

We defined the modelled case detection rate as the proportion of all symptomatic cases that were detected (Figure 1B). We related the case detection rate (CDR, Equation 1) to the number of tests performed using an exponential function, under the assumption that a certain per capita daily testing rate is associated with a specific case detection rate, with this relationship varied during calibration (Supplemental Figure 4):

$$\text{Equation 1: } CDR(\text{time}) = 1 - e^{-\text{shape} \times \text{tests}(\text{time})}$$

Seasonal forcing was incorporated using a transposed sine function, with maximum value at the winter solstice.

Incorporation of health service clusters

We further stratified the above model to Victoria's nine health service clusters, including four clusters which together constitute metropolitan Melbourne (North, West, South, South East Metro) and five regional clusters which together constitute the rest of Victoria (Barwon South West, Gippsland, Grampians, Hume, Loddon-Mallee). We split the estimated age-specific population for Victoria (Figure 1C) according to historical patterns of accessing health service clusters provided by DHHS. The infectious seed was split across the compartments representing current infection and assigned evenly across the metropolitan clusters, with the remainder of the population assigned to the susceptible compartments. The force of infection in each cluster was calculated as a weighted average of the age-specific force of infection for each cluster, with the index cluster having the greatest weight and all non-index clusters having equal weight. The final model included 2,592 compartments interacting through a dynamic mixing matrix of dimensions 144 x 144 (16 age groups and nine geographical patches), with each matrix element scaling over time to reflect changes to population mixing in response to changes in mobility and pandemic-related policy decisions as introduced above.

Calibration

Because of the high-dimensional parameter space, we calibrated the model to reproduce local COVID-19 dynamics during Victoria's second wave using an adaptive Metropolis algorithm, which is non-Markovian but retains ergodic properties (Table 1; Supplement).¹³ For the prior distributions of epidemiological calibration parameters, we used uniform priors for highly uncertain quantities and truncated normal distributions for quantities informed by epidemiological evidence. We included adjusters in our calibration parameters to modify the proportion of symptomatic individuals, proportion of symptomatic individuals hospitalised, and the infection fatality rate. The parameters are multiplicative factors that are applied to the odds ratio equivalent to the proportion parameter, rather than directly to the parameter value itself; thus ensuring that the adjusted value lies between zero and one.

The likelihood function was constructed by first incorporating Poisson distributions with rate parameters equal to each of the state-wide daily time-series for notifications, hospitalisations, ICU admissions and deaths. This was then multiplied by terms for the daily time-series of notifications for each cluster, smoothed with a four-day moving average, using normal distributions. As there is no requirement for individuals living in a cluster catchment to attend that health service, we allocated each cluster a proportion of each notification according to the historical tendency of persons from each Local Government Area (LGA) to attend a hospital from that cluster (such that daily cluster-specific notification and death counts are not integer-valued).

Results

Calibration fit

We achieved good calibration fits to all calibration targets (Figures 2-4), along with close matches to cluster-specific indicators not used for calibration (Supplemental Figures 7-10) under the framework of a single state-wide model. The epidemic peaks in the regional clusters occurred somewhat later than in the metropolitan clusters, which is attributable to the modelled infection first being seeded in the metropolitan regions before triggering epidemics outside of Greater Melbourne and is consistent with historical reality. These fits were associated with a post-wave proportion of the population recovered of around 1-2%, with higher proportions in metropolitan regions and young adults (Figure 9).

Parameter estimation

The posterior estimates of model calibration parameters are presented in Table 1. Several epidemiological parameters with good evidence from international studies showed posteriors that were consistent with prior beliefs. This prevented overfitting, reduced the degree of freedom and provided better estimates of key free parameters including the effect of time-varying processes, allowing insights into the dynamics of the epidemic. The unadjusted risk of transmission per contact (specifically the risk of transmission per contact between a susceptible person aged 15-64 years and a symptomatic infectious person not in isolation) was estimated at 2-5%. This needed to be adjusted for each cluster modelled, with the modifiers applied to the metropolitan clusters reaching values up to double that for the regional clusters (other than Barwon South West). The extent of mixing between geographical patches was low, with around 1-2% of the total force of infection contributed by regions other than the index patch.

Estimates of the incubation period, the infectious period, the period prior to ICU admission and the duration in ICU were similar to our prior estimates derived from the literature.

Likewise, the estimated proportion of incident cases resulting in symptomatic disease was

similar to our prior estimate. However, the risk of hospitalisation (and hence ICU admission) and of death given infection were considerably greater than our age-specific prior estimates obtained from the literature. This likely reflects higher rates of exposure and infection in population groups at particularly high risk of adverse outcomes, including residents of aged care facilities.

The case detection rate associated with a testing rate of one test per 1,000 population per day was estimated at 33.0% (95%CI, 22.4-45.3), such that peak rates of detection of symptomatic infections were estimated at greater than 60%.

To understand the reasons behind the epidemic curve plateauing at the start of August and beginning to decline thereafter, we were particularly interested in parameters governing the effect of time-varying processes. We estimated that physical distancing behaviours and face coverings were both important in achieving control of Victoria's second wave, with face coverings estimated to have reduced transmission and infection risk by around 31 to 46%, while fitting to data provided little information on the effect of seasonal forcing (around 9 to 45%). Physical distancing behaviour was estimated to have reduced risk of transmission/infection by around 6 to 28%, although the smaller changes in reported adherence to this intervention (Supplemental Figure 5) meant that this had a lesser impact on the epidemic profile. For the behavioural changes in particular, the posterior probability density was substantially more informative than the prior and had negligible density around the value of zero, consistent with an effect of each of these interventions in reversing the epidemic trajectory. Additionally, the posterior probabilities of the parameters were only moderately collinear (Figure 8), supporting independent effects for each process.

Counterfactual scenarios

Figure 10 presents four counterfactual scenarios in addition to the baseline scenario. The effect of re-opening schools from 9th July (the date that stage 3 restrictions were imposed) was projected to be modest, with daily case rates peaking around 200 higher than under baseline conditions, but with the epidemic profile otherwise broadly similar. The effect of not

mandating face coverings was projected to be dramatic, with case numbers in the thousands for several months under the counterfactual of face coverings usage remaining at the baseline level of 13.0%. Returning to full mobility from 9th July resulted in a similarly poorly controlled epidemic, under the assumption that face coverings usage could not then have reached the baseline estimate of >90% compliance in all workplaces and other locations if industries such as hospitality were fully re-opened. An epidemic unmitigated by any movement and behavioural restrictions was projected to substantially overwhelm expanded ICU capacity.

Discussion

We found that the improvement in Victoria's second wave of COVID-19 cases could be well captured in our transmission model through a combination of time-variant processes that included: testing rates, population mobility, use of face coverings, physical distancing and seasonal forcing. The lower rates of COVID-19 observed in regional clusters were captured with the introduction of the infectious seed through the metropolitan clusters only, without needing to unrealistically manipulate the risk of transmission by cluster. Risk of infection in metropolitan areas was estimated to be up to double that of regional areas, consistent with international findings of a moderate correlation between population density and epidemic severity.⁵ Although Barwon South West showed transmission rates that were more comparable to metropolitan Melbourne, this region includes Victoria's second largest city of Geelong. Interaction between populations of different clusters was low in the context of significant restrictions on movement between regions. Each of the time-varying processes modelled appeared to be important to the observed dynamics, with both face coverings and behavioural changes associated with a significant reduction in transmission risk per contact. However, face coverings had a considerably greater effect on reversing the epidemic, which was observable due to the sharp transition in the extent of their use when they were mandated.

Victoria's second wave of cases was dramatically different from its first autumn wave, which was driven by importations and during which time the effective reproduction number was consistently estimated to be below one.^{14,15} Victoria's second wave was initiated by quarantine escape, from which widespread community transmission soon followed. Progressively more extensive lockdown measures were then implemented, with local targeting of specific residential blocks and then postcodes, which were insufficient to reverse the epidemic trajectory.

As noted previously, stage 3 restrictions were associated with a reduction in the effective reproduction number,¹⁶ although significant case rates persisted throughout July, and further reductions in mobility were observed with stage 4. An agent-based model with detailed social networks consideration of multiple intervention types and without geographical structure was calibrated to the Victorian epidemic.¹⁷ This model emphasised the importance of associations between individuals who would not otherwise be in regular contact to the epidemic. By contrast to previous work, our model captures the temporal and spatial implementation of the policy changes in Victoria to allow inference of the effect of each intervention. As concern increased that epidemic control had not been achieved over the course of July, policy changed rapidly in an attempt to bring the epidemic under control. Testing numbers increased following a nadir in early June and lockdown measures were implemented differently in twelve Melbourne postcodes, the remaining postcodes of Greater Melbourne, Mitchell Shire (immediately north of Greater Melbourne) and the remainder of regional Victoria. We captured these complicated geographical patterns of restriction by scaling our mixing matrices using Google mobility data, which are available at the LGA level for Victoria. School closure and face covering policy changes were captured according to the dates of policy changes.

Most of the inferred parameters were consistent with previous evidence, including a potentially important effect of seasonal forcing in terms of the absolute reduction in virus transmissibility.¹⁸ The minimal information provided on seasonal forcing is likely attributable to our simulation period spanning less than four months and so covering a small proportion

of the cycling period, such that the effect could represent other secular changes during the period modelled. Sensitivity analysis (not presented) with seasonal forcing set to zero throughout the simulations made a negligible difference to the estimates for the other parameters of interest. The effect of face coverings was greater than is typically estimated at the individual level,¹⁹ but is consistent with the dominant importance of the respiratory route to transmission.²⁰ The finding was also not unexpected given the marked shift in population use of face coverings at this time and the timing of the policy change in late July relative to the dramatic reversal in case numbers occurring around one week later. The significant estimated effect of behavioural changes suggests that reductions in interpersonal associations (macro-distancing) alone were insufficient to achieve the dramatic reversal in the epidemic trajectory observed. However, the Google mobility functions used to capture macro-distancing simulated falls in attendance at workplaces and other non-household locations to considerably below baseline values in several clusters (Figure 1), emphasising their importance. The dramatic effect of each of these interventions on the epidemic trajectory is partly attributable to our implementation of these processes as applying to both the infectious cases and the exposed individual. This approach is analogous to simulating the use of bed-nets for malaria control, where the overall effect of the intervention is quadratic, as it affects both the disease vector and the infection reservoir.²¹

Despite the complexity of our model, it is inevitably a simplification of reality. Although we assumed that asymptomatic cases were undetectable, this was addressed by varying two epidemiological parameters pertaining to these patients, and the posterior estimate of the infectiousness of asymptomatic cases suggested around threefold lower infectiousness per unit time. Our findings relating to the impact of time-varying interventions could be proxies for other effects. For example, although we considered that the effectiveness of case detection scaled with the number of tests performed, changes in the effectiveness of tracing, testing and isolation activities during the course of the epidemic wave may also have been important.

Victoria's second wave is known to have had particularly dramatic effects on residents of aged care facilities and health care workers, which we did not explicitly capture except by varying parameters relating to disease severity. Because of this, it was necessary to scale international estimates of the age-specific infection fatality rate around two- to three-fold. Although this factor seems extreme, age-specific infection fatality rate estimates increase dramatically with age,⁷ and it should be noted that the age-specific infection fatality rate parameters we used increase up to three-fold with each successive decade of age.⁶ Therefore, an age distribution of the infected population that is one decade higher than that simulated would be expected to have a comparable effect. Our age-specific estimates of the risk of hospitalisation given symptomatic COVID-19 do not fully capture the consideration that hospital admission is driven by factors other than disease severity, including infection control and workforce capacity and staff isolation requirements in residential aged care facilities, which were particularly important to this epidemic wave.

With the state's explicit objective of achieving no community transmission in Victoria (and therefore across Australia) within a few months,^{22,23} our findings emphasise that multiple interacting components of the public health interventions were required to achieve this within the modelled period.^{24,25} Consistent with findings from elsewhere,^{26–28} without reductions in contacts outside the home and mandating the use of masks, there would have been no reasonable prospect of driving transmission to zero within a time period tolerable to the community, given the starting point of the epidemiological situation in late July. The small effect of school closures was also consistent with findings from overseas,^{25,29} although if schools had remained open throughout the epidemic wave, some additional weeks would likely have been required for transmission to decline to the point that elimination was an immediate prospect. Nonetheless, it is encouraging that in a low transmission scenario, school closures are likely not necessary to gain control in the presence of other effective population-level restrictions, including masks.

In conclusion, we found that Victoria's major second wave of COVID-19 was brought under control through a combination of policy interventions that were synergistic and together

contributed substantially to the dramatic reversal in the observed epidemic trajectory. In particular the considerable individual-level effect of face coverings was critical to achieving epidemic control, and so should be a cornerstone of any public health response given the much lesser inconvenience associated with their use compared to restrictions on mobility. Rates of hospitalisation and death were higher than anticipated given international estimates of parameters pertaining to these quantities, likely reflecting the concentration of the epidemic in high-risk groups, particularly residents of aged care facilities. As vaccination is rolled out as a more targeted intervention, protection of high-risk settings, including aged care will be critical, particularly in regions with low or negligible population immunity that remain at risk of explosive epidemics.

Author declarations

BS and ACC wish to emphasise their important statutory roles during Victoria's pandemic response in 2020, as Chief Health Officer and acting Chief Health Officer respectively. MJL and GWD were also employed by DHHS during 2020. JMT provided regular advice to DHHS during this time as an independent advisor.

Funding statement

The Epidemiological Modelling Unit of Monash University provided the health system cluster-level projections for notifications, admissions and deaths under contract to the Victorian Department of Health and Human Services in 2020. JMT is a recipient of an Early Career Fellowship from the Australian National Health and Medical Research Council (APP1142638).

Acknowledgements

We gratefully acknowledge the support and advice of staff of the Victorian Department of Health and Human Services (now the Victorian Department of Health) for provision of data and assistance with its interpretation. We thank A/Prof Nicholas Golding for providing the micro-distancing compliance factors.

Contributor statement

JMT and RR constructed the model. GD, MJL and JN assisted with provision of data. JMT wrote the first draft of the manuscript, which was then revised with input from all authors.

References

- 1 Barlow P, van Schalkwyk MC, McKee M, Labonté R, Stuckler D. COVID-19 and the collapse of global trade: building an effective public health response. *Lancet Planet. Heal.* 2021; **5**: e102–7.
- 2 Nelson R. COVID-19 disrupts vaccine delivery. *Lancet Infect Dis* 2020; **20**: 546.
- 3 Walker PGT, Whittaker C, Watson OJ, *et al.* The impact of COVID-19 and strategies for mitigation and suppression in low- and middle-income countries. *Science (80-)* 2020; **369**: 413–22.
- 4 Rashed EA, Koderá S, Gomez-Tames J, Hirata A. Influence of absolute humidity, temperature and population density on COVID-19 spread and decay durations: Multi-prefecture study in Japan. *Int J Environ Res Public Health* 2020; **17**: 1–14.
- 5 Koderá S, Rashed EA, Hirata A. Correlation between COVID-19 morbidity and mortality rates in Japan and local population density, temperature, and absolute humidity. *Int J Environ Res Public Health* 2020; **17**: 1–14.
- 6 O'Driscoll M, Dos Santos GR, Wang L, *et al.* Age-specific mortality and immunity patterns of SARS-CoV-2. *Nature* 2020; published online Nov 2. DOI:10.1038/s41586-020-2918-0.
- 7 Verity R, Okell LC, Dorigatti I, *et al.* Estimates of the severity of coronavirus disease 2019: a model-based analysis. *Lancet Infect Dis* 2020; **0**. DOI:10.1016/S1473-3099(20)30243-7.
- 8 Huang C, Huang L, Wang Y, *et al.* 6-month consequences of COVID-19 in patients discharged from hospital: a cohort study. *Lancet* 2021; **397**: 220–32.
- 9 Bavli I, Sutton B, Galea S. Harms of public health interventions against covid-19 must not be ignored. *BMJ.* 2020; **371**. DOI:10.1136/bmj.m4074.
- 10 Kennedy DS, Vu V, Ritchie H, *et al.* COVID-19: Identifying countries with indicators of success in responding to the outbreak. *Gates Open Res* 2020; **4**: 62.
- 11 Davies NG, Klepac P, Liu Y, Prem K, Jit M, Eggo RM. Age-dependent effects in the transmission and control of COVID-19 epidemics. *medRxiv* 2020; : 2020.03.24.20043018.
- 12 Prem K, Cook AR, Jit M. Projecting social contact matrices in 152 countries using contact surveys and demographic data. *PLOS Comput Biol* 2017; **13**: e1005697.
- 13 Haario H, Saksman E, Tamminen J. An adaptive Metropolis algorithm. *Bernoulli* 2001. DOI:10.2307/3318737.
- 14 Adekunle A, Meehan M, Rojas-Alvarez D, Trauer J, McBryde E. Delaying the COVID-19 epidemic in Australia: evaluating the effectiveness of international travel bans. *Aust N Z J Public Health* 2020; **44**: 257–9.
- 15 Price DJ, Shearer FM, Meehan MT, *et al.* Early analysis of the australian covid-19 epidemic. *Elife* 2020; **9**: 1–14.
- 16 Saul A, Scott N, Crabb BS, Majumdar SS, Coghlan B HM. Victoria's response to a resurgence of COVID-19 has averted 9,000-37,000 cases in July 2020 | The Medical Journal of Australia. *Med J Aust* 2020. <https://www.mja.com.au/journal/2020/victorias-response-resurgence-covid-19-has-averted-9000-37000-cases-july-2020> (accessed Jan 14, 2021).
- 17 Scott N, Palmer A, Delport D, *et al.* Modelling the impact of reducing control measures on the COVID-19 pandemic in a low transmission setting. *medRxiv* 2020. DOI:10.1101/2020.06.11.20127027.
- 18 Carlson CJ, Gomez ACR, Bansal S, Ryan SJ. Misconceptions about weather and seasonality must not misguide COVID-19 response. *Nat. Commun.* 2020; **11**: 1–4.
- 19 Chu DK, Akl EA, Duda S, *et al.* Physical distancing, face masks, and eye protection to prevent person-to-person transmission of SARS-CoV-2 and COVID-19: a systematic review and meta-analysis. *Lancet* 2020; **395**: 1973–87.
- 20 Zhang R, Li Y, Zhang AL, Wang Y, Molina MJ. Identifying airborne transmission as

- the dominant route for the spread of COVID-19. *Proc Natl Acad Sci U S A* 2020; **117**: 14857–63.
- 21 Smith DL, McKenzie FE. Statics and dynamics of malaria infection in Anopheles mosquitoes. *Malar. J.* 2004; **3**: 13.
- 22 Zhang L, Tao Y, Zhuang G, Fairley CK. Characteristics Analysis and Implications on the COVID-19 Reopening of Victoria, Australia. *Innov* 2020; **1**: 100049.
- 23 Blakely T, Thompson J, Carvalho N, Bablani L, Wilson N, Stevenson M. The probability of the 6-week lockdown in Victoria (commencing 9 July 2020) achieving elimination of community transmission of SARS-CoV-2. *Med J Aust* 2020; **213**: 349-351.e1.
- 24 Giles ML, Wallace EM, Alpren C, *et al.* Suppression of SARS-CoV-2 after a second wave in Victoria, Australia. *Clin Infect Dis* 2020; published online Dec 23. DOI:10.1093/cid/ciaa1882.
- 25 Soltesz K, Gustafsson F, Timpka T, *et al.* The effect of interventions on COVID-19. *Nature*. 2020; **588**: E26–8.
- 26 Flaxman S, Mishra S, Gandy A, *et al.* Estimating the effects of non-pharmaceutical interventions on COVID-19 in Europe. *Nature* 2020; **584**: 257–61.
- 27 Dehning J, Zierenberg J, Spitzner FP, *et al.* Inferring change points in the spread of COVID-19 reveals the effectiveness of interventions. *Science (80-)* 2020; **369**. DOI:10.1126/science.abb9789.
- 28 Jarvis CI, Van Zandvoort K, Gimma A, *et al.* Quantifying the impact of physical distance measures on the transmission of COVID-19 in the UK. *BMC Med* 2020; **18**: 124.
- 29 Vlachos J, Hertegård E, Svaleryd HB. The effects of school closures on SARS-CoV-2 among parents and teachers. *Proc Natl Acad Sci U S A* 2021; **118**. DOI:10.1073/pnas.2020834118.
- 30 Litton E, Bucci T, Chavan S, *et al.* Surge capacity of intensive care units in case of acute increase in demand caused by COVID-19 in Australia. *Med J Aust* 2020; **212**: 463–7.

Parameter (units)	Prior distribution	2.5th centile	Median	97.5th centile
Unadjusted risk of transmission per contact	Uniform, support: [0.015, 0.06]	0.0254	0.0364	0.0497
Incubation period (days)	Truncated normal, mean: 5.5, standard deviation: 0.97 support: [1, infinity)	3.70	4.68	5.79
Duration of active disease (days)	Truncated normal, mean: 6.5, standard deviation: 0.77 support: [4, infinity)	4.89	5.88	7.10
Pre-ICU period (days)	Truncated normal, mean: 12.7, standard deviation: 4 support: [3, infinity)	5.47	11.2	17.9
Symptomatic proportion adjuster	Truncated normal, mean: 1, standard deviation: 0.2, support: [0.5, infinity)	0.715	0.984	1.35
Infection fatality rate adjuster	Uniform, support: [0.5, 4]	1.66	2.48	3.32
Hospitalisation rate adjuster	Uniform, support: [0.5, 3]	1.44	2.31	2.90
Infectiousness of asymptomatic persons multiplier	Uniform, support: [0.3, 0.7]	0.234	0.348	0.527
Starting infectious population (persons)	Uniform, support: [10, 30]	25.0	40.7	61.3
Seasonal forcing	Uniform, support: [0, 0.5]	0.0926	0.278	0.447
Case detection rate at one test per 1,000 per day (proportion)	Uniform, support: [0.2, 0.5]	0.224	0.330	0.453
Inter-cluster mixing (%)	Uniform, support: [0.005, 0.05]	0.67	1.41	2.88
Effect of physical distancing	Uniform, support: [0, 0.5]	0.0569	0.125	0.279
Effect of face coverings	Uniform, support: [0, 0.5]	0.313	0.391	0.458

Cluster-specific contact rate multipliers				
North Metro	Truncated normal, mean: 1, standard deviation: 0.5, support: [0.5, infinity)	0.768	1.24	1.83
West Metro		0.924	1.46	1.99
South Metro		0.659	1.07	1.55
South East Metro		0.630	1.10	1.53
Barwon South West		0.635	0.988	1.47
Other regional clusters		0.533	0.679	0.996

Table 1. Prior distributions and posterior estimates of all calibrated epidemiological model parameters.

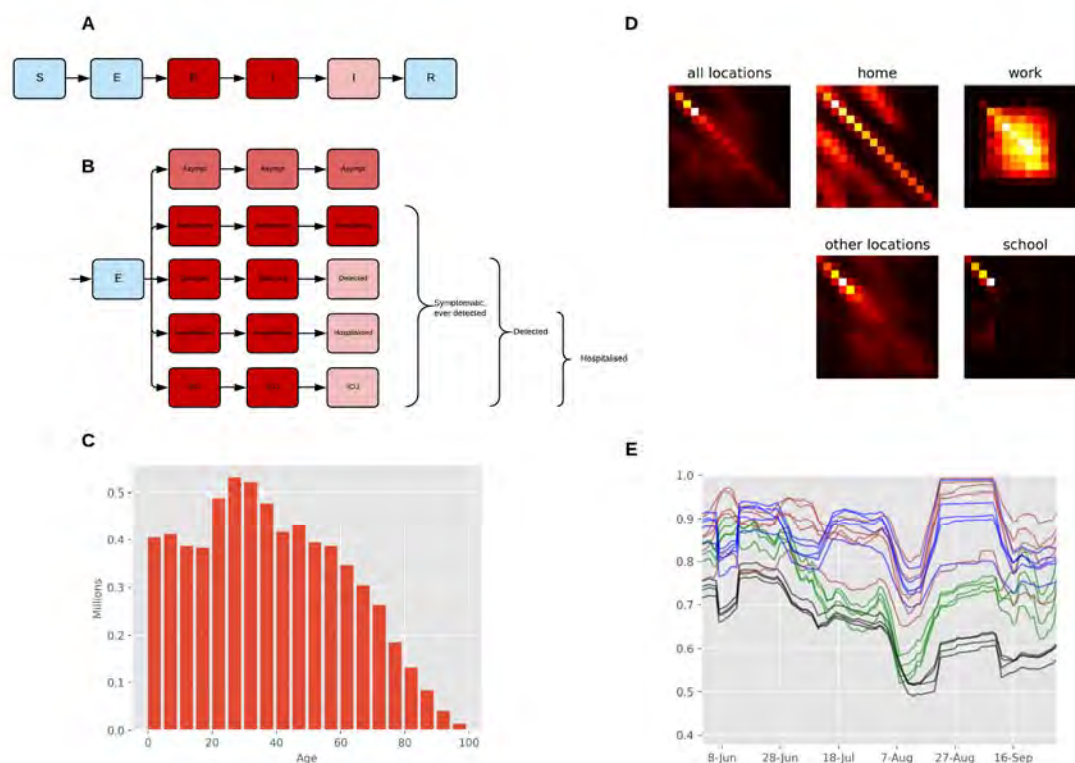


Figure 1. Age-structured COVID-19 model with population distribution, age-specific contact rates, and mobility inputs. (A) Unstratified model structure. (B) Stratification by infection and detection status. (Note that age stratification consists of further stratifying all compartments 16 times.) (C) Starting population age distribution. (D) Heterogeneous mixing matrices by age in the absence of non-pharmaceutical interventions. (E) Macro-distancing adjustments to the mixing matrices for each cluster smoothed with 7-day moving average. Black, workplace mobility for metropolitan clusters; green, other locations mobility for metropolitan clusters; blue, workplace mobility for regional clusters; brown, other locations mobility for regional clusters.

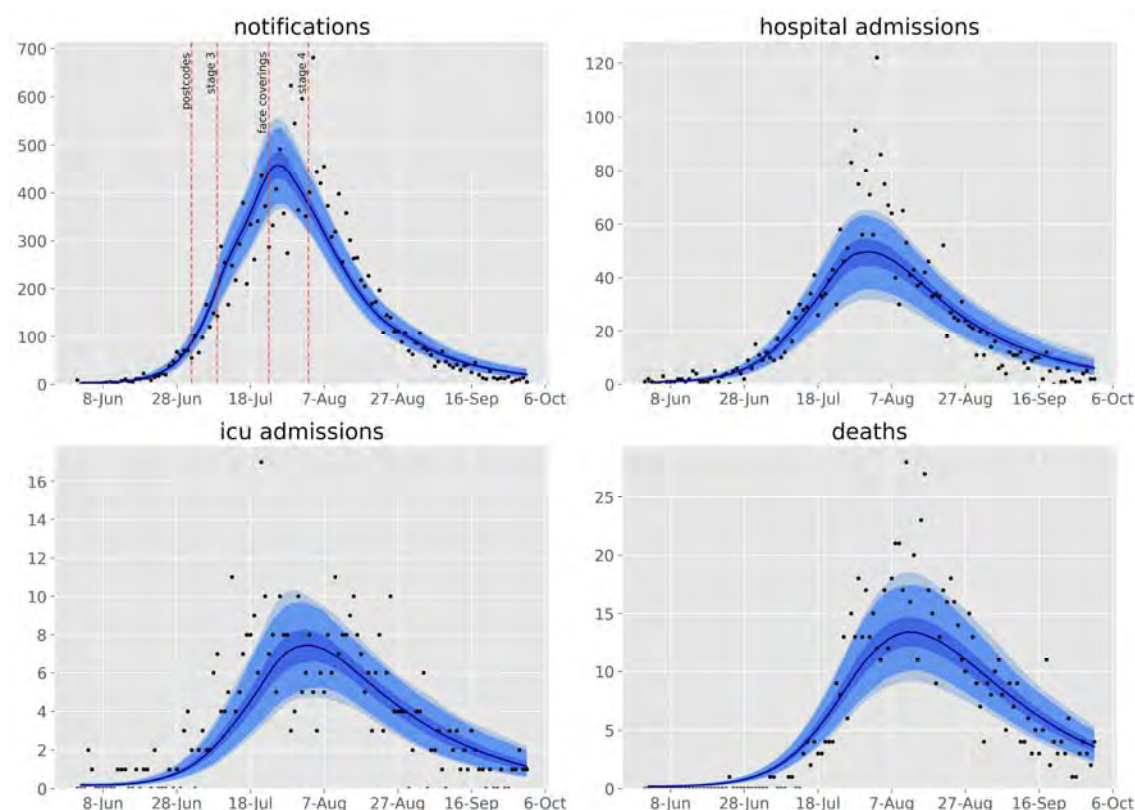


Figure 2. Calibration fits to daily state-wide time series of notifications, hospital admissions, ICU admissions and deaths. Daily confirmed cases (black dots) overlaid on the median modeled detected cases (dark blue line), with shaded areas representing the 25th to 75th centile (mid blue), 2.5th to 97.5th centile (light blue) and 1st to 99th centile (faintest blue) of estimated detected cases. Timing of restrictions applied to metropolitan Melbourne indicated in the upper left panel.

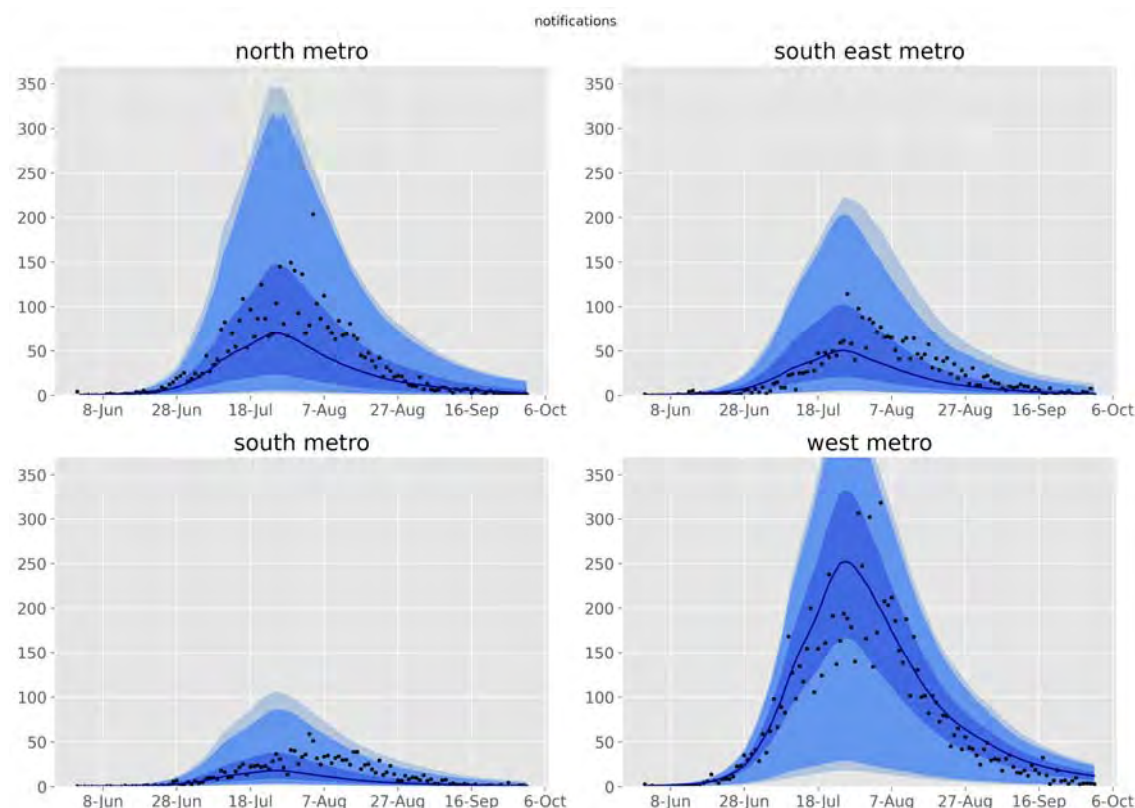


Figure 3. Calibration fits to daily time series of notifications for each metropolitan health service cluster. Daily confirmed cases (black dots) overlaid on the median modeled detected cases (dark blue line), with shaded areas representing the 25th to 75th centile (mid blue), 2.5th to 97.5th centile (light blue) and 1st to 99th centile (faintest blue) of estimated detected cases.

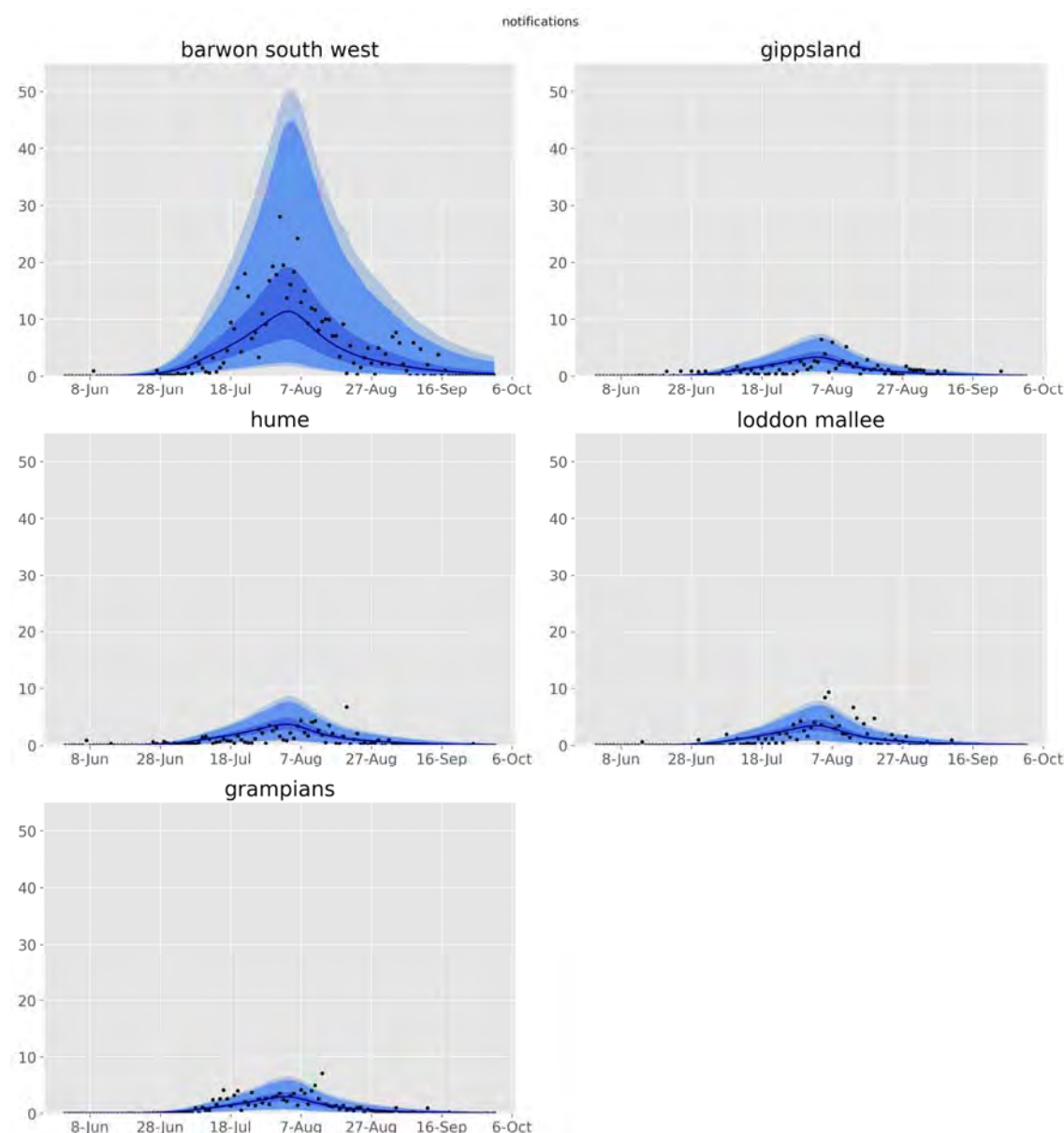


Figure 4. Calibration fits to daily time series of notifications for each regional health service cluster. Daily confirmed cases (black dots) overlaid on the median modeled detected cases (dark blue line), with shaded areas representing the 25th to 75th centile (mid blue), 2.5th to 97.5th centile (light blue) and 1st to 99th centile (faintest blue) of estimated detected cases.

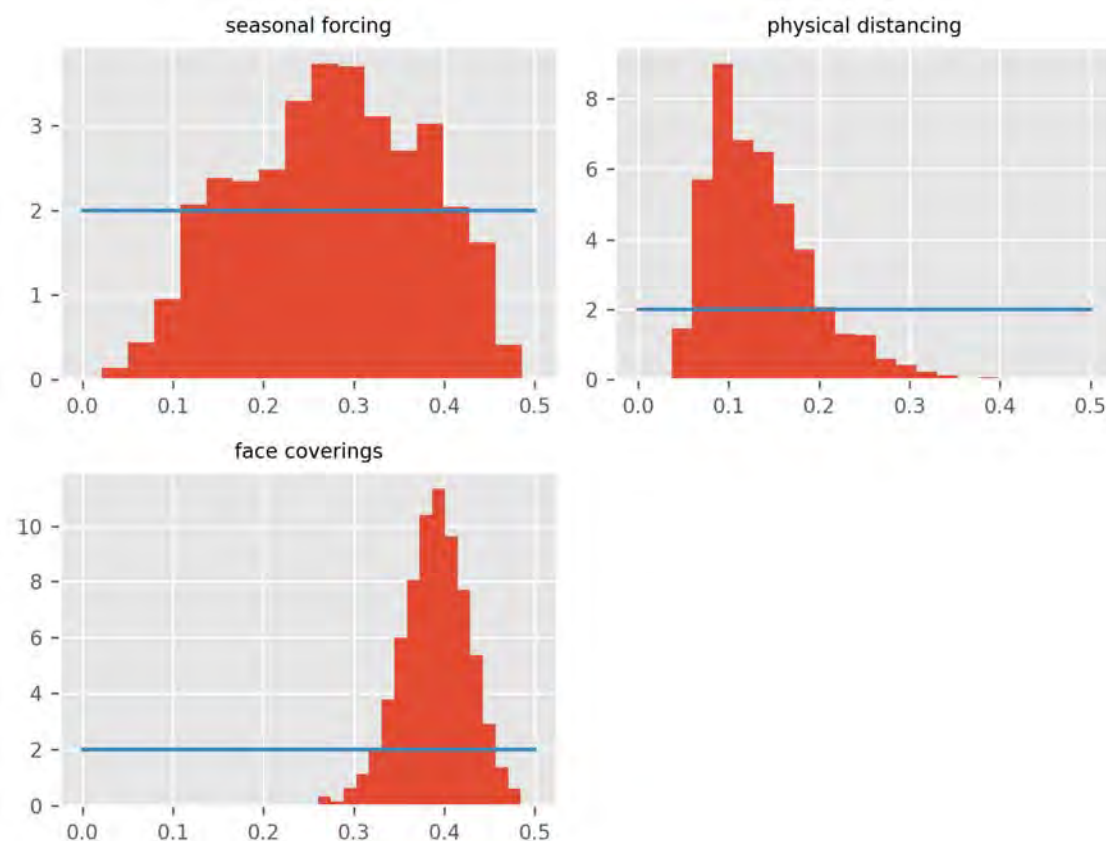


Figure 5. Posterior density histograms for key state-wide epidemiological parameters from accepted model runs. Red histograms, model posterior estimates; blue lines, prior distributions for same parameters (all are uniform or truncated normal distributions).

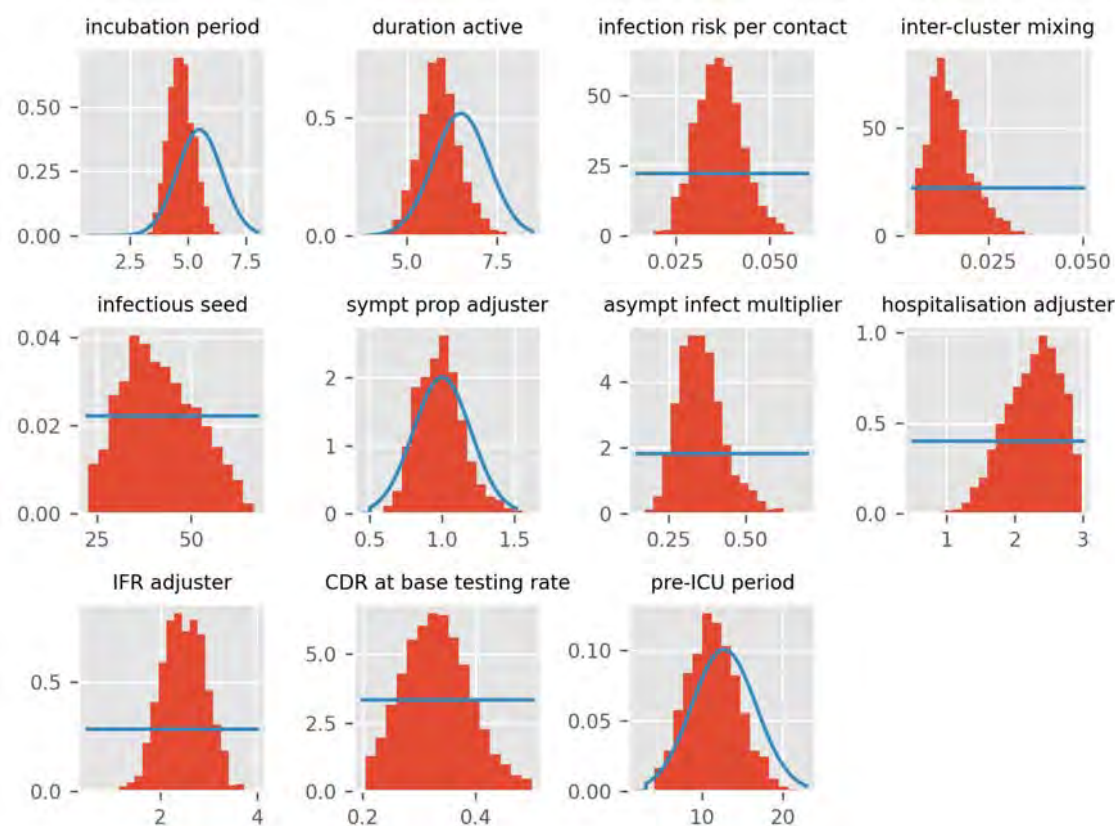


Figure 6. Posterior histograms for other state-wide epidemiological parameters. Red histograms, model posterior estimates; blue lines, prior distributions for same parameters (all are uniform or truncated normal distributions).

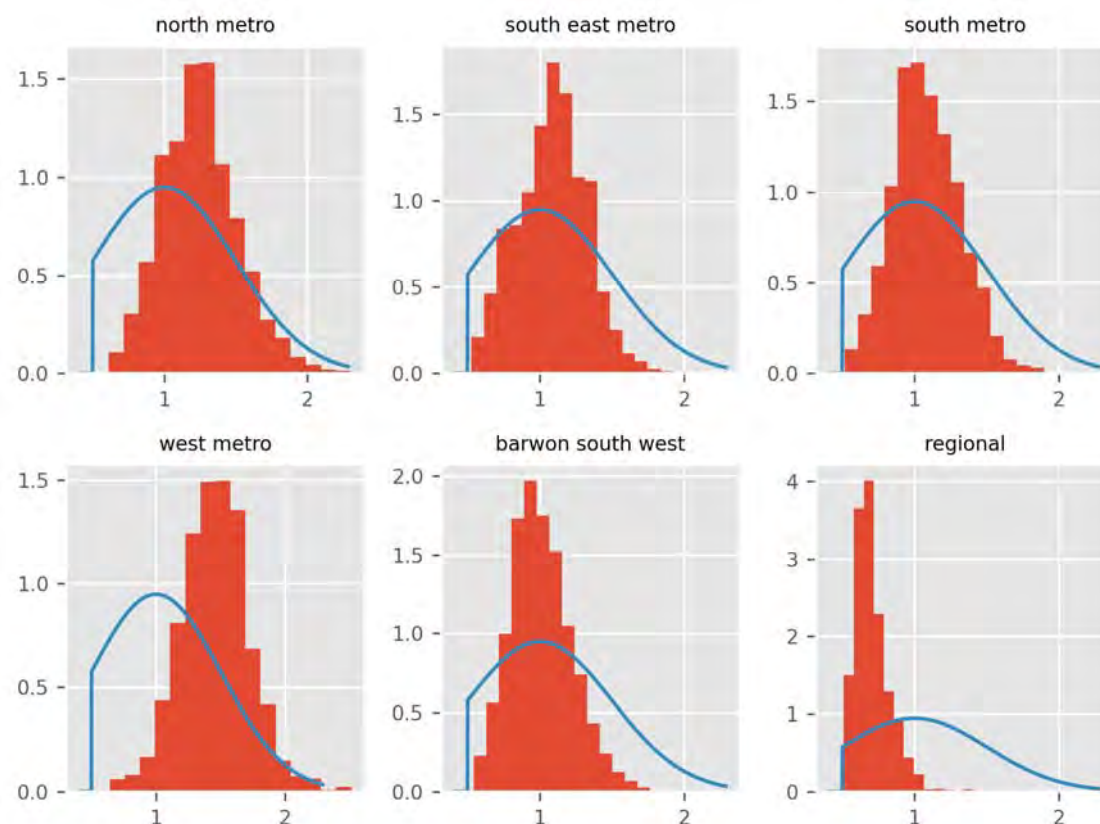


Figure 7. Posterior histograms for cluster-specific contact rate modifier parameters. Red histograms, model posterior estimates; blue lines, prior distributions for same parameters (all are uniform or truncated normal distributions).

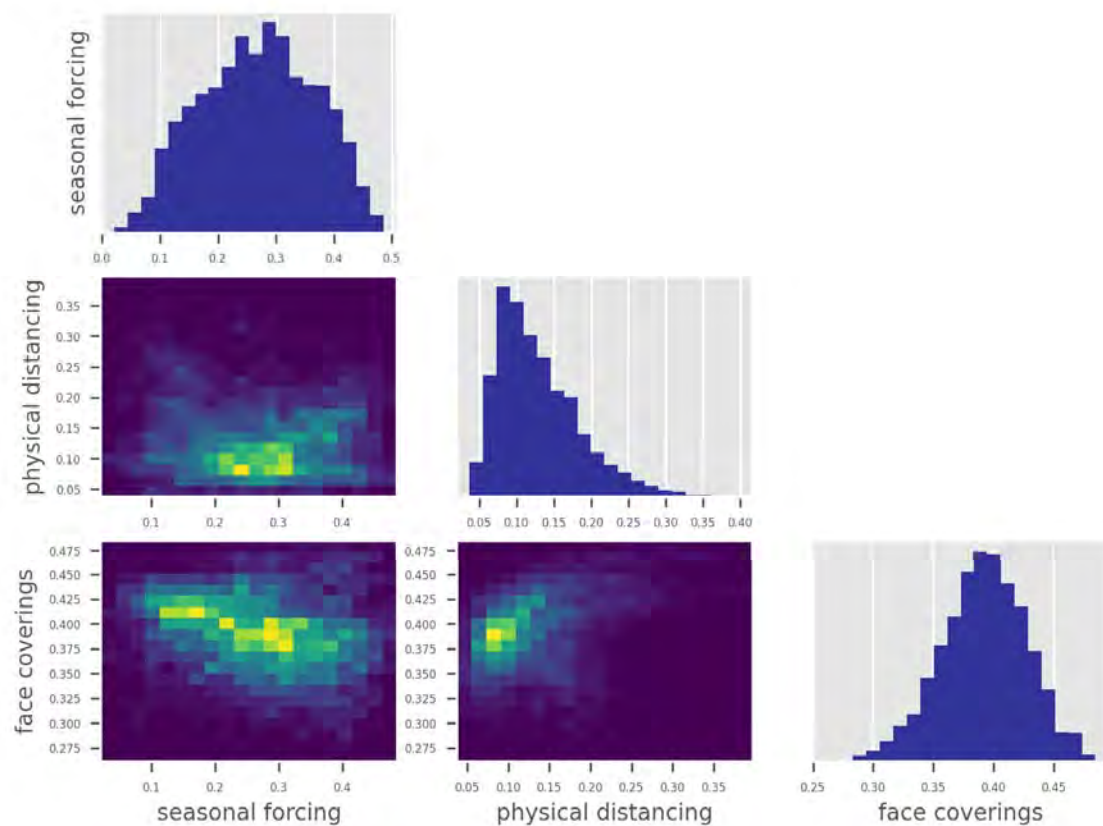


Figure 8. Correlation matrix for key state-wide epidemiological parameters.

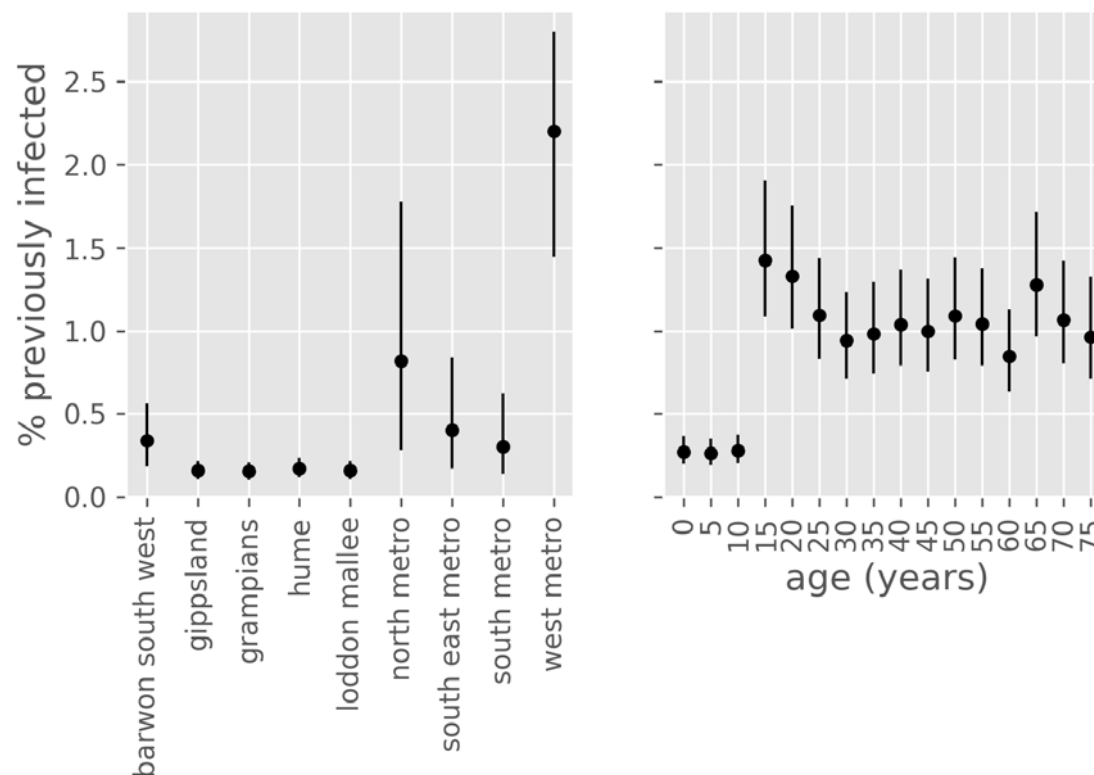


Figure 9. Estimated proportion of population recovered from COVID-19 at 1st October 2020, by age group and health service cluster. Point estimates with associated 50% credible intervals. Values are negligibly different from attack rates, except that deaths are excluded from the denominator.

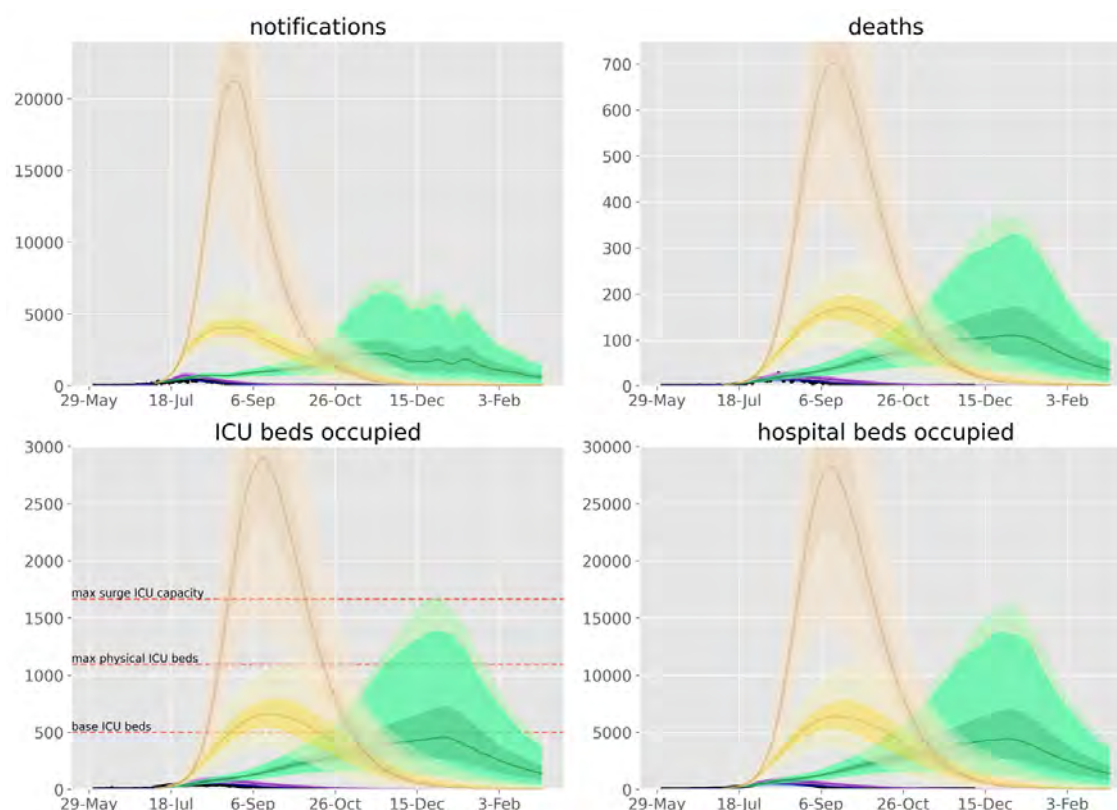
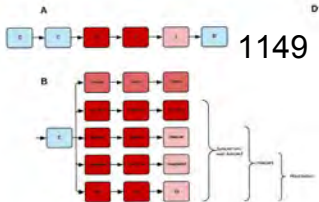
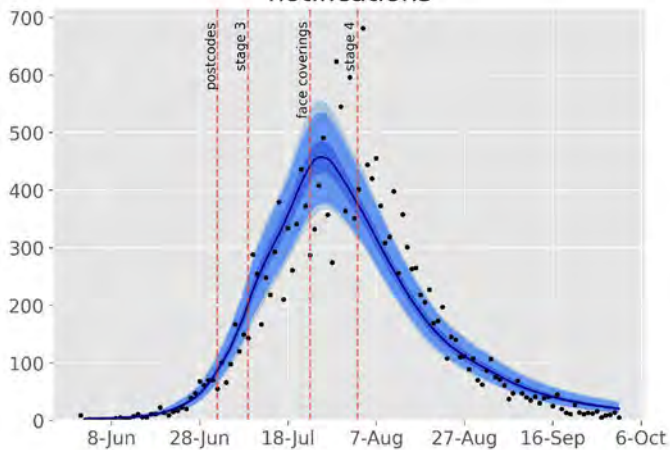


Figure 10. Counterfactual scenarios compared against baseline calibration and data. Scenarios are: purple, schools re-opened from 7th July; green, face coverings not mandated (on 23rd July); yellow, work, schools and other locations mobility return to baseline levels from 7th July with 60% face coverings compliance; brown, return to normal mobility with baseline use of face coverings. Data (black dots), median modelled estimates (lines), shaded areas 25th to 75th centile (darkest shading), 2.5th to 97.5th centile (intermediate shading depth) and 1st to 99th centile (faintest shading) of each indicator for each scenario. 7th July chosen as the date that stage 3 restrictions were imposed. We considered that full compliance with mandatory face coverings would be impractical if workplaces and other locations returned to full capacity (for example, if hospitality was fully re-opened, patrons would not wear masks in all other locations). Base and surge ICU capacity for Victoria presented on lower left panel.³⁰

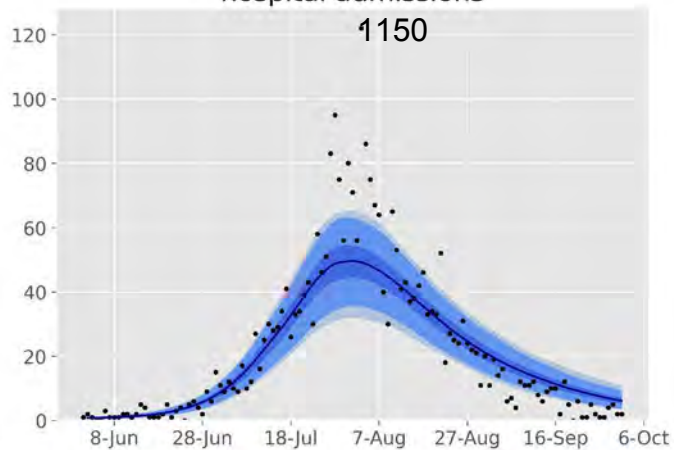


1149

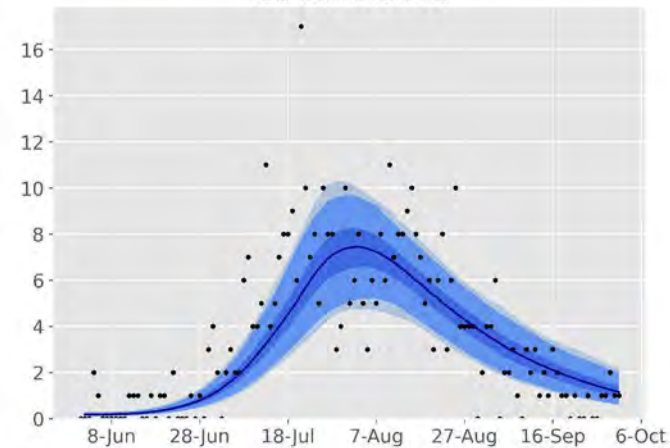
notifications



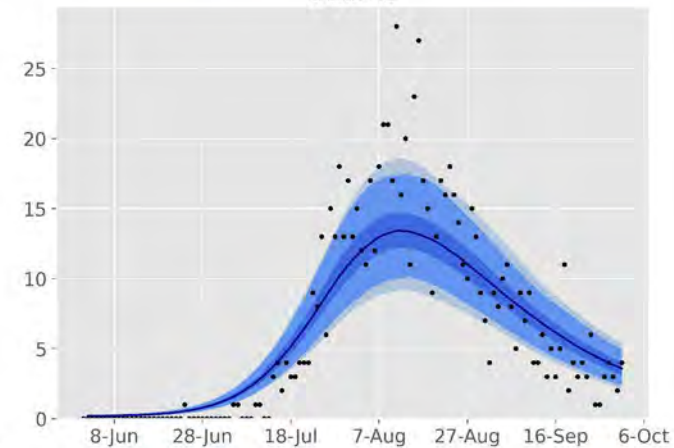
hospital admissions



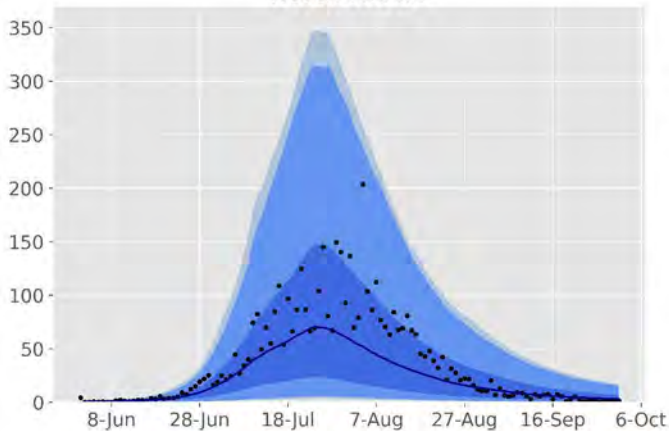
icu admissions



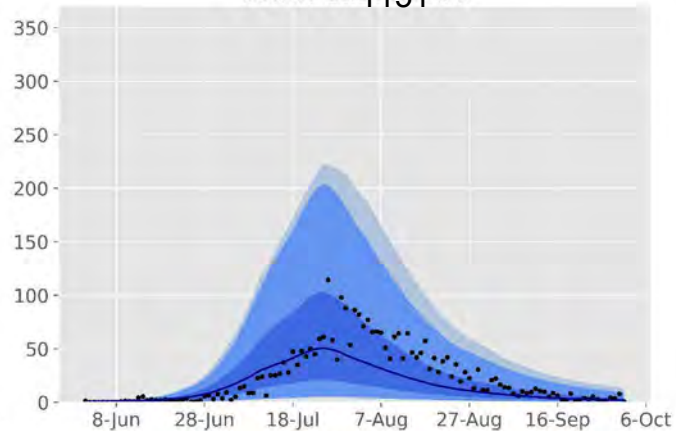
deaths



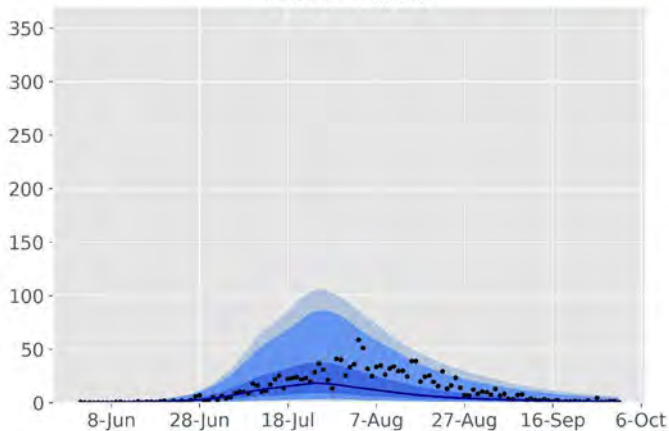
north metro



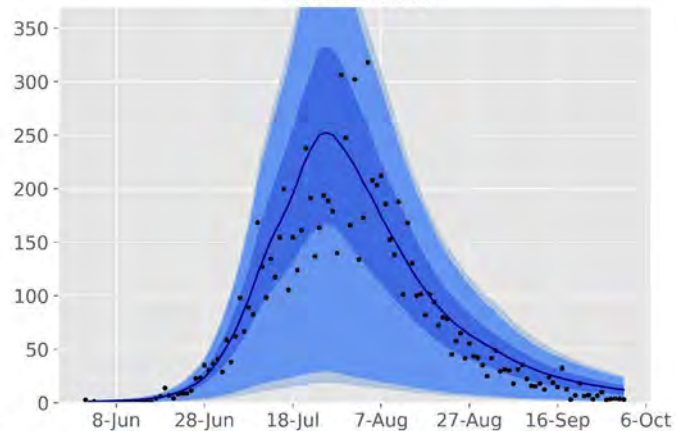
south east metro



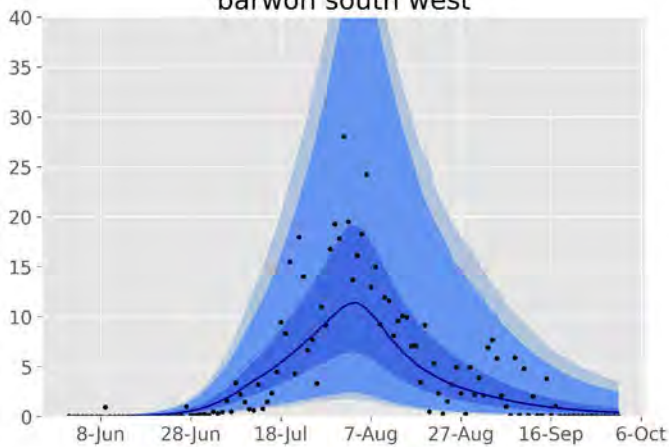
south metro



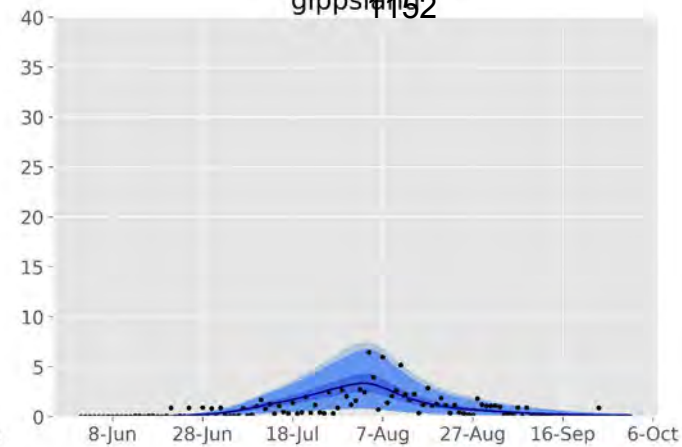
west metro



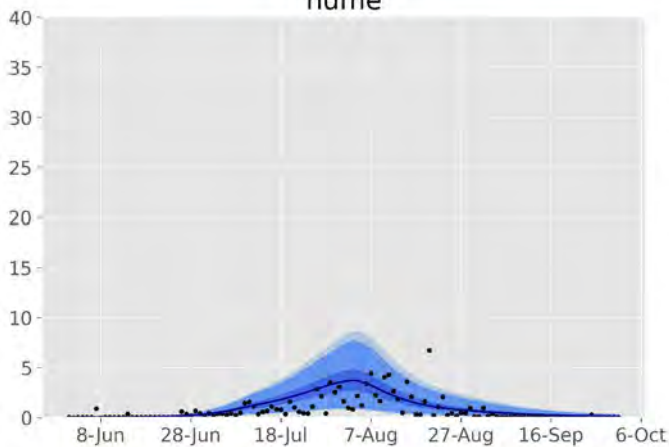
barwon south west



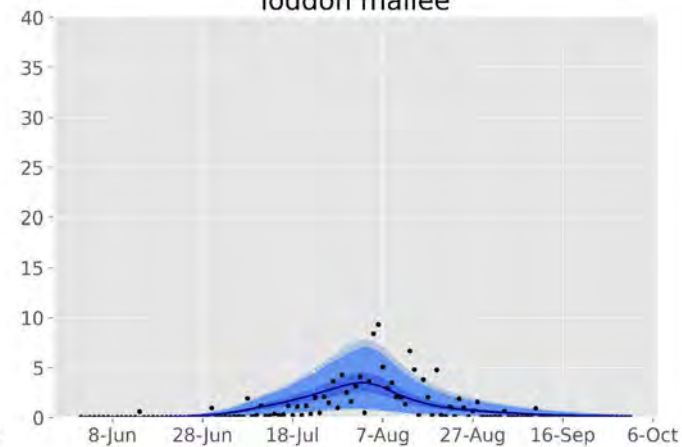
gippsland



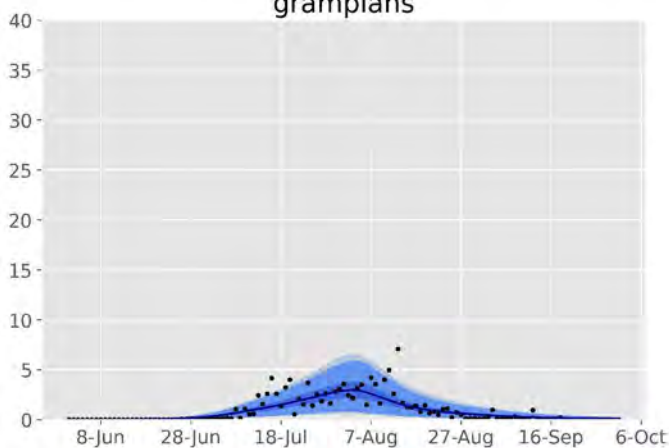
hume



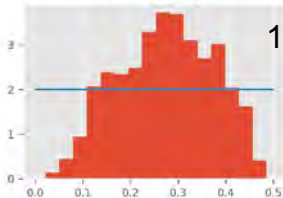
loddon mallee



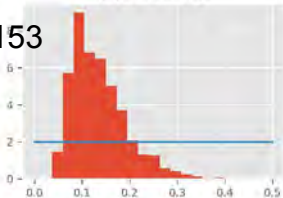
grampians



seasonal forcing

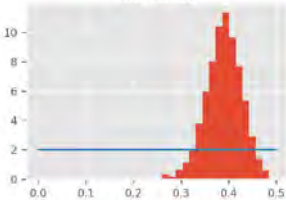


physical distancing



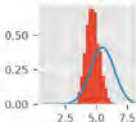
1153

face coverings

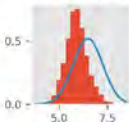


1154

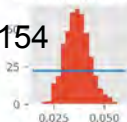
incubation period



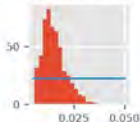
duration active



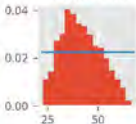
infection risk per contact



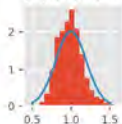
inter-cluster mixing



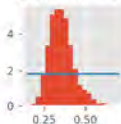
infectious seed



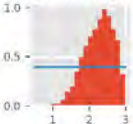
sympt prop adjuster



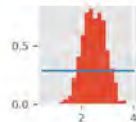
asympt infect multiplier



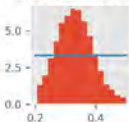
hospitalisation adjuster



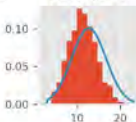
IFR adjuster



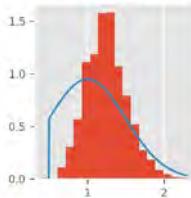
CDR at base testing rate



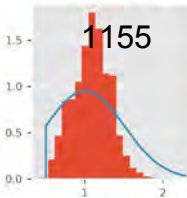
pre-ICU period



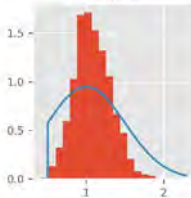
north metro



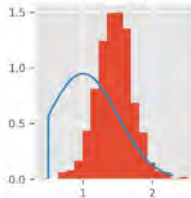
south east metro



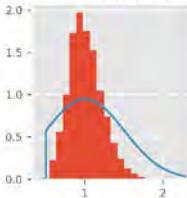
south metro



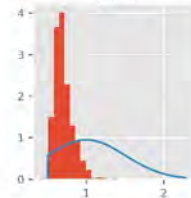
west metro



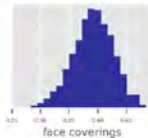
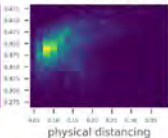
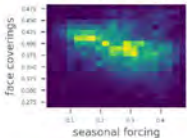
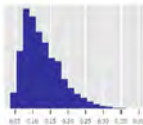
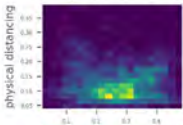
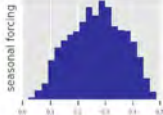
barwon south west



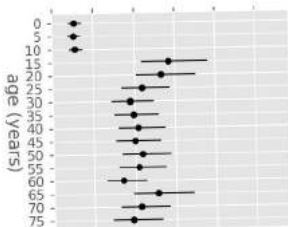
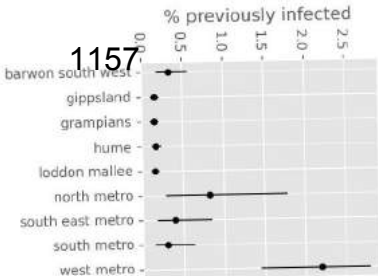
regional



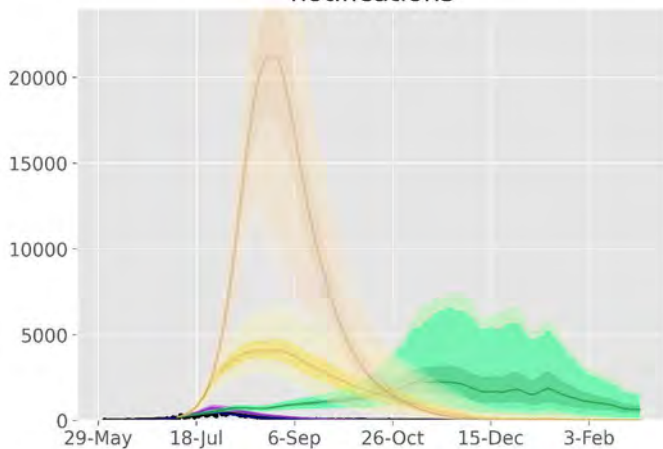
1156



1157

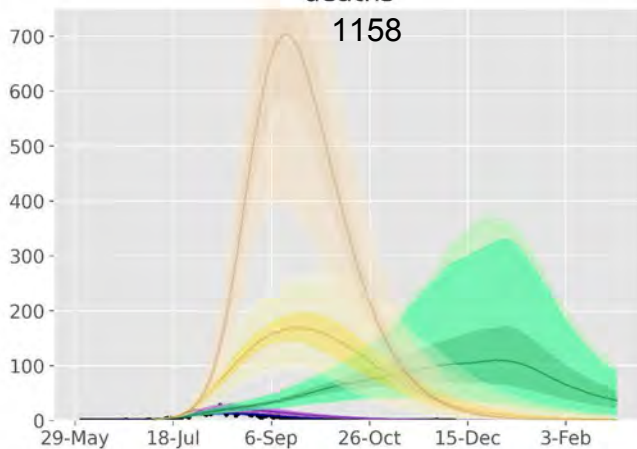


notifications

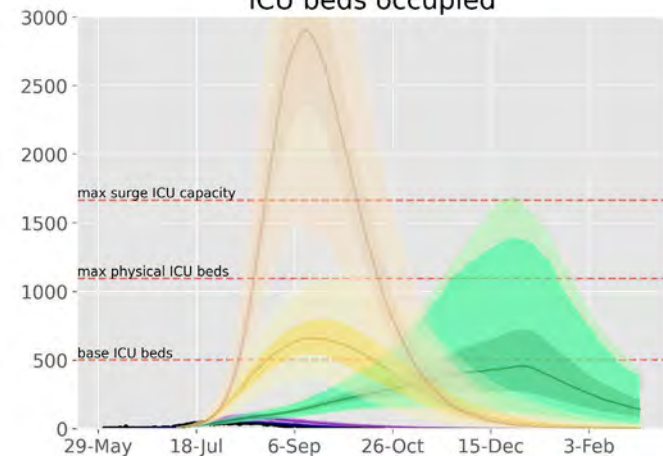


deaths

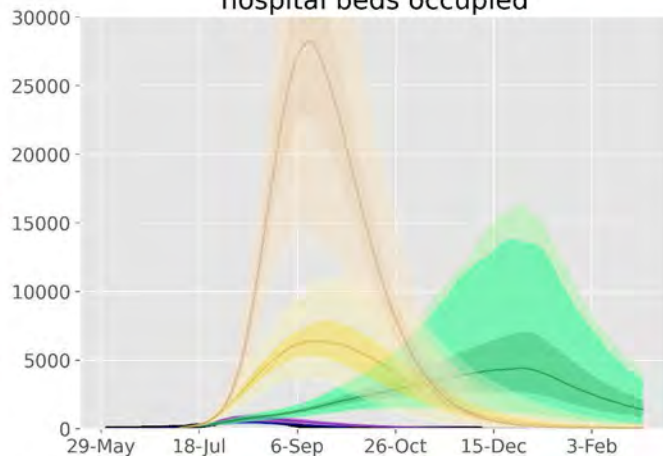
1158



ICU beds occupied



hospital beds occupied





Published in final edited form as:

J Pathol. 2016 January ; 238(1): 85–97. doi:10.1002/path.4638.

1918 pandemic influenza virus and *Streptococcus pneumoniae* coinfection results in activation of coagulation and widespread pulmonary thrombosis in mice and humans

Kathie-Anne Walters¹, Felice D'Agnillo², Zong-Mei Sheng⁴, Jason Kindrachuk³, Louis M. Schwartzman⁴, Rolf E. Keustner¹, Daniel S. Chertow^{3,4}, Basil T. Golding², Jeffery K. Taubenberger^{4,*}, and John C. Kash^{4,*}

¹Institute for Systems Biology, Seattle, WA 98109 USA

²Laboratory of Biochemistry and Vascular Biology, Division of Hematology Research and Review, Center for Biologics Evaluation and Research, Office of Blood Research and Review, Food and Drug Administration, Silver Spring, MD 20993 USA

³Critical Care Medicine Department, National Institutes of Health, Bethesda, MD 20892

⁴Viral Pathogenesis and Evolution Section, Laboratory of Infectious Diseases, National Institute of Allergy and Infectious Diseases, National Institutes of Health, Bethesda, MD 20892 USA

Abstract

To study bacterial coinfection following 1918 H1N1 influenza virus infection, mice were inoculated with the 1918 influenza virus followed by *Streptococcus pneumoniae* 72 h later. Coinfected mice exhibited markedly more severe disease, shortened survival time and more severe lung pathology, including widespread thrombi. Transcriptional profiling revealed activation of coagulation only in coinfecting mice, consistent with the extensive thrombogenesis observed. Immunohistochemistry showed extensive expression of tissue factor (F3) and prominent deposition of neutrophil elastase on endothelial and epithelial cells in coinfecting mice. Lung sections of SP-positive 1918 autopsy cases showed extensive thrombi and prominent staining for F3 in alveolar macrophages, monocytes, neutrophils, endothelial and epithelial cells, in contrast to coinfection-positive 2009 pandemic H1N1 autopsy cases. This study reveals that a distinctive feature of 1918 influenza virus and SP coinfection in mice and humans is extensive expression of tissue factor and activation of the extrinsic coagulation pathway leading to widespread pulmonary thrombosis.

* Correspondence to: John C. Kash, Ph.D., Laboratory of Infectious Diseases, NIAID, NIH, 33 North Drive, MSC 3203, Phone: 301-443-4086, Fax: 301-480-1696, kashj@niaid.nih.gov, Jeffery K. Taubenberger, M.D., Ph.D., Laboratory of Infectious Diseases, NIAID, NIH, 33 North Drive, MSC 3203, Phone: 301-443-5960, Fax: 301-480-1696, taubenbergerj@niaid.nih.gov.

Conflict of Interest: The authors declare no conflicts of interest and the research sponsors played no role in study design, in the collection, analysis and interpretation of data, in the writing of the report and in the decision to submit the report for publication

Author contributions. Conceptualization, KAW, FD, JKT, and JCK; Methodology, KAW, JKT, and JCK; Formal analysis, KAW and JCK; Investigation, KAW, FD, ZMS, JK, LMS, REK, DSC, JKT and JCK; Writing – Original Draft, KAW and JC; Writing – Review & Editing, KAW, FD, JK, DSC, BTG, JKT, and JCK; Visualization, KAW, FD, JKT, and JCK; Resources, JKT; Supervision, JKT and JCK.

Keywords

1918 influenza; *Streptococcus pneumoniae*; coinfection; inflammation; extrinsic pathway of coagulation; pulmonary thrombosis

Introduction

The 1918 influenza pandemic was responsible for the deaths of ~50 million people [1]. There is abundant evidence for secondary bacterial pneumonia being the predominant cause of death. A review of detailed epidemiology, pathology and microbiology findings in >8 000 post-mortem examinations consistently implicated secondary bacterial pneumonia, caused by common upper respiratory-tract bacteria, in most fatal influenza cases [2,3].

Enhanced pathology associated with viral-bacterial coinfection is well documented and several possible mechanisms have been proposed (reviewed in [4,5]). Specifically, viral-mediated changes in the respiratory tract, including epithelial damage, alterations in airway function and exposure of receptors, are thought to prime the upper airway for secondary bacterial infection [4]. Both enhanced and dysfunctional innate immune responses have also been implicated in the increased severity of coinfection [5]. Finally, bacteria-mediated cleavage of the viral haemagglutinin (HA) antigen has been suggested as a mechanism for increased viral replication following bacterial challenge, potentially leading to more severe lung damage and poor outcome in coinfecting mice [6,7]. Interestingly, synergism during coinfection appears to be influenced by both viral and bacterial strain-specific factors [8]. Differences in the abilities of *Streptococcus pneumoniae* (SP) strains to replicate in lungs of mice following infection with influenza was associated with differential mortality, suggesting strain specificity in the ability of SP to cause pneumonia during influenza infection [9]. Secondary infection with SP resulted in a lethal coinfection in mice inoculated with 2009 pandemic H1N1, but not seasonal H1N1, and was associated with loss of airway basal epithelial cells and lung repair responses [10]. Similar studies suggest bacterial strain-related differences also influence the synergy between *Staphylococcus aureus* and influenza virus [11].

Infection with 1918 influenza has been shown to result in severe lung pathology typified by necrotizing bronchitis, bronchiolitis, neutrophil-predominant alveolitis, and acute oedema associated with significant activation of antiviral, pro-inflammatory and cell death response genes in lung tissue in animals and humans [12-15]. The inflammatory response induced by 1918 infection has been shown to be immunopathogenic in mice and results in significant activation of reactive oxygen species (ROS) with marked oxidative damage to respiratory epithelial cells [16].

While secondary bacterial infections caused the majority of deaths during the 1918-1919 influenza pandemic, little is known about the underlying mechanisms responsible for the synergy between 1918 influenza and bacteria. In the current study, effects of secondary SP infection in mice that were infected with the 1918 influenza virus were investigated. SP was chosen because it was the most commonly identified bacteria in fatal 1918 influenza cases [2,3]. The results show that SP secondary infection greatly enhanced lung pathology in

mice; it shortened survival, increased early bacterial replication, and altered the host response to infection, with evidence including increased neutrophil activation and activation and aggregation of platelets and clotting. (AQ: please check this sentence retains your intended meaning). Histological and immunohistochemical analyses validated this thrombogenic response and showed abundant thrombi and extensive staining for F3. Importantly, staining of two SP-positive 1918 autopsy cases showed similar extensive F3 staining along with abundant thrombi. In contrast, minimal F3 staining and no thrombi was observed in SP- or *Streptococcus pyogenes*-positive 2009 pandemic H1N1 fatalities. These data support and expand observations of pulmonary thrombi observed in post mortem examinations of 1918 virus autopsies [17,18] and demonstrate that widespread pulmonary vascular thrombogenesis was a feature of 1918 pandemic H1N1 and SP coinfection, which may help explain the high death toll of the 1918 pandemic.

Materials and Methods

Viruses and bacteria

The reconstructed 1918 influenza virus, A/Brevig Mission/1/1918 (H1N1), was rescued and titred using published protocols [16,19]. SP strain A66.1 (serotype 3; x0en10; Perkin Elmer) and grown as described in [10]. All work with the reconstructed 1918 influenza virus was performed in enhanced BSL-3 and enhanced ABSL-3 laboratories at the NIH in accordance with the Biosafety in Microbiological and Biomedical Laboratories (BMBL), 5th Edition, and the Division of Select Agents and Toxins at the Centers for Disease Control and Prevention (DSAT/CDC) and the NIH and under supervision of the Biosurety Program of the NIH Department of Health and Safety.

Mouse infection studies

Groups of five 8-9 week old female BALB/c mice (Jackson Labs, Bar Harbor, ME) were placed under light anaesthesia as described in [10] and inoculated with 5×10^2 PFU of the reconstructed 1918 H1N1 influenza virus; sham inoculated with PBS at this time (day 0); or inoculated intra nasally (AQ: please check this substitution) with 10^5 colony-forming units (CFU) of SP at 3 days post-virus. Virus-alone groups were sham inoculated with PBS at day 3. Body weights were measured daily for 7-10 d post-infection and mice were humanely euthanized if they lost more than 25% of starting body weight. Lungs from three animals were collected for RNA isolation and from two animals for pathology at day 3 to 6 post-1918 (day 0 to +3 post-SP, respectively). Lungs collected for pathology were inflated with 10% neutral buffered formalin at the time of isolation. All experimental animal work was performed in accordance with United States Public Health Service (PHS) Policy on Humane Care and Use of Laboratory Mice in an enhanced ABSL-3 laboratory at NIH following approval of animal safety protocols by the NIAID Animal Care and Use Committee and in accordance with DSAT/CDC.

RNA isolation and expression microarray analysis

Total RNA was isolated from lungs and used for gene expression profiling using Agilent Mouse Whole Genome 44K microarrays as described in [10,16] and Supporting Information online. In brief, RNA from three biological replicates per condition was labelled and

hybridized to individual arrays and processed as described in [10,16]. Data normalization was performed in Analyst using central tendency followed by relative normalization using pooled RNA from mock infected mouse lung (n=4) as a reference. Transcripts showing differential expression (2-fold, $p < 0.01$) between infected and control mice were identified by standard t test. The Benjamini-Hochberg procedure was used to correct for false positive rate in multiple comparisons. Ingenuity Pathway Analysis was used for gene ontology and pathway analysis. The complete microarray dataset has been deposited in NCBI Gene Expression Omnibus [20] and is accessible through GEO Series accession number GSE70445.

Reverse Transcription Quantitative-PCR

RT-qPCR was used to estimate bacterial and viral loads in lung tissue. Reverse transcription of total lung RNA was performed with primers specific for influenza M gene, mouse *Gapdh*, SP 16S rRNA, *endA*, *nanA*, *nanB*, or *ply* using standard protocols. Primers are listed in Table S1. Quantification of each gene's C_T was graphed relative to that of the calibrator as described in [10].

Histopathology and immunohistochemistry

Mouse tissue samples were processed for histopathological examination using standard protocols. Gram staining was performed using the method of Brown and Hopps, and Movat's pentachrome staining was performed using standard protocols. Mouse immunohistochemical studies were performed using standard protocols [19] following heat-mediated antigen retrieval using antibodies specific to CD11b, ELANE, F3, MPO, thrombin, Ly6g (clone 1A8) or TPA as described in Supporting Information. Immunohistochemical studies on human 1918 and 2009 pandemic H1N1 autopsy cases used 5 μ m thick sections cut from the FFPE lung tissue blocks from cases described previously [3,21] and stained for F3 as described in Supporting Information. These samples were considered exempt for human subjects review under US Government guidelines (<http://www.hhs.gov/ohrp/policy/checklists/decisioncharts.html#c5>).

Results

Bacterial coinfection accelerated mortality of 1918 pandemic influenza virus infection

To study effects of secondary bacterial infection following primary influenza virus infection, mice were inoculated intra nasally with 5×10^2 PFU of the 1918 virus followed by inoculation with 10^5 CFU SP 72 h later. Mice inoculated with 1918- alone exhibited significant weight loss with 100% mortality by day 11 post-inoculation (Fig. 1A-B). Mice inoculated with SP-alone displayed weight loss with 100% mortality by day 7 post-SP (day 10 post-1918). Mice coinfectd with 1918 virus followed by SP 72 h later (1918+SP), showed more severe illness than mice inoculated with virus- or SP-alone, with 100% mortality by day 6 post-1918 (day +3 post-SP). Significantly, the majority of deaths in 1918+SP groups occurred in moribund mice prior to reaching 25% weight loss euthanasia criteria. The results shown are typical of three independent experiments.

Increased bacterial load and SP virulence factor expression during coinfection

Expression of influenza virus M gene RNA and bacterial 16S rRNA in lungs of infected mice was measured by RT-qPCR. The lungs of 1918 virus alone infected mice had consistent viral loads throughout the time-course (Fig. 1C). Mice exposed to 1918 virus followed by SP had similar viral levels at 4 days post-1918 (day +1 post-SP), but significantly lower levels at days five and six post-1918 inoculation compared to mice exposed to virus alone ($p < 0.05$). Bacterial levels were significantly higher in 1918+SP compared to SP-alone infected mice at days 4 and 5 post-1918 (days +1 and +2 post-SP), but equivalent at 6 d post-1918 (day +3 post-SP) (Fig. 1D). Detection of 16S rRNA in spleen tissue by RT-qPCR from both SP and 1918+SP mice provided evidence of bacteraemia on days 5 and 6 post-1918 (days +2 and +3 post-SP, respectively) (Fig. S1). The expression of several important SP virulence factor genes [22] were also measured by RT-qPCR and normalized to bacterial 16S rRNA (Fig. 1E), including pneumolysin (*ply*), endonuclease A (*endA*); and neuraminidases *nanA* and *nanB*. At day 4 to 6 post-1918 (day +1 to +3 post-SP), *ply*, *endA*, *nanA* and *nanB* RNA were detected in 1918+SP mice. In contrast, very low or undetectable levels of *endA*, *nanA* and *nanB* RNA were observed in SP-alone infected mice.

Bacterial coinfection significantly enhances lung pathology

Lungs from mice were collected at days 3-6 post-1918 (days 0 to +3 post-SP) for histopathology. A unique gross pathological feature of the 1918+SP infected mice on days 4-5 (days +2 and +3 post-SP) was the presence of extensive fibrinous pleuritis with instances of fusion of the lungs to the chest wall and diaphragm. Lung pathology was evaluated in mice at days 4 to 6 following viral infection. In infected animals, histopathological changes increased from days 4 to 6, and day 6 pathology is described in here (Fig. 2). Mock-infected mice showed no histopathological changes in their lungs (Fig. 2A-C). SP-infected mice showed mild, focal changes (Fig. 2D-F), including focal acute bronchiolitis and rare microscopic foci of acute pleuritis. Gram-positive bacteria morphologically consistent with SP were occasionally observed within the focal lesions (not shown). 1918 virus-infected mice showed a more severe pathology, affecting >25% of the lung parenchyma (Fig. 2G-I), with widespread acute bronchiolitis and multifocal areas of acute alveolitis characterized by a mixed inflammatory cell infiltrate with prominent neutrophils in both alveolar airspaces and interstitium (Fig. 2I). Coinfected mice showed very severe histopathological changes affecting >50% of lung parenchyma (Fig. 2J-L) with consolidation consisting of an acute pneumonia, featuring alveolar airspaces packed with neutrophil- and macrophage-predominant inflammatory infiltrates, extensive acute suppurative pleuritis, widespread necrotizing bronchiolitis, and abundant fibrin thrombi in veins, venules, and capillaries (Fig. 2J, arrow).

Bacterial coinfection causes perturbations in inflammation-related coagulation homeostasis

Global transcriptional profiling was performed on lung tissue mRNA at days 3-6 post-1918 (day 0 to +3 post-SP). For each experiment, mRNA from an individual infected animal was compared to mRNA from a pool of mock-infected mice ($n = 4$). Approximately 14 800

sequences showed a 2-fold change in expression ($p < 0.01$) in at least one experimental group (Fig. S2). The expression levels of 457, 1412, and 1 487 transcripts differed significantly (2-fold, $p < 0.01$) between mice infected with 1918-alone and 1918+SP at days 4, 5, and 6, respectively, correlating with increased differences in disease pathology throughout the time-course. At day 4 post-1918 (day +1 post-SP), the direction of gene expression changes were similar between 1918 alone and 1918+SP, with enhanced magnitude of change generally observed in coinfecting mice (Fig. 3A). Expression during SP-alone infection is shown for comparison. However, by days 5 and 6 post-1918 (day +2 and +3 post-SP) there were also increasingly larger groups of sequences that showed increased expression only in 1918+SP-infected mice.

Functional annotation of differentially expressed genes between 1918 and 1918+SP infected mice revealed enrichment of genes related to inflammatory response, immune cell trafficking, haematological system, and genes related to tissue injury (Fig. 3B). The distribution of enriched functional groups was generally consistent across all time points, with the exception of day 4 which showed higher enrichment of ROS scavenging and lower involvement of immune cell trafficking and inflammation, coinciding with a significantly higher bacterial burden (Fig. 1D). Examination of expression of an additional ~700 inflammatory mediators revealed that while 1918+SP coinfection was associated with increased expression of genes relative to 1918-alone, differences were modest (Fig. S3). Furthermore, many inflammation-related genes that showed higher expression levels or were specifically increased in 1918+SP mice relative to 1918-alone infected mice were not increased in SP-alone mice (Fig. S3).

Many immune response-related genes that were either more highly expressed or uniquely expressed in 1918+SP mice at day 5 are involved in neutrophil recruitment/activation, platelet aggregation/activation and coagulation (Fig. 3C-E). Levels of the mRNA for certain chemokines and adhesion molecules mediating neutrophil infiltration (e.g., *Ccl2*, *Ccl7*, *Cd177*, and *Itgam*) were significantly higher in 1918+SP-infected mice relative to 1918-alone. In contrast, those for other chemokines and adhesion molecules (e.g., *IL15*, *Ccl11*, *Ccl24*, *Itgb2*, *Ccr12*) were increased only in 1918+SP mice. Notably, many key neutrophil activation marker mRNAs were also either uniquely increased (including granule components *Mpo*, cathepsin G (*Ctsg*), *Dao*, *Mmp9*, *Fcgr3* and *Fpr2*) or more highly increased (*Mmp8*, *Fcgr1*) in 1918+SP infected mice. Certain neutrophil-related genes (including *Cleblb*, cathepsin G (*Ctsg*), *F3*, *Pf4* and *Itgb2*) also function to promote platelet aggregation/activation. Levels for Proteinase 3 (*Prtn3*), encoding a serine protease that contributes to the proteolytic generation of antimicrobial peptides and also inhibits clearance of apoptotic neutrophils, promoting inflammation, were also increased (Fig. 3C).

Expression of genes associated with platelet aggregation included those from Gp1b-IX-V/GpVI-dependent platelet activation pathway (collagen 1, *Itgb2*, and glycoproteins *Gp-1B alpha*, *Gp-1B beta*, Gp-V, Gp-VI, and Gp-IX) (**AQ: not all of these are approved mouse gene names**), which plays a critical role in collagen-induced platelet aggregation and thrombus formation at sites of vascular injury, were also significantly higher in 1918+SP infected mice (Fig. 3D). Similarly, increased mRNA levels for other genes involved in platelet aggregation were observed in 1918+SP mice including platelet-activating factor

receptor (*Ptafr*), thrombospondin s1 (*Thbs1*), platelet factor 4 (*Pf4*), a chemokine released from alpha granules of activated platelets, and purinergic receptor P2Y, G-protein coupled, 12 (*P2ry12*), a neutrophil-specific receptor. Pro-platelet basic protein (*Pbbp*), which protein activates neutrophils and stimulates the secretion of plasminogen activator, was increased only in 1918+SP mice.

Consistent with gene expression data supportive of enhanced platelet activity, increased expression of numerous coagulation cascade genes, including those for factors III, V, X, and XIII (Fig. 3E) was observed in coinfecting mice. Levels for Tissue plasminogen activator (*Plat*), encoding the key enzyme responsible for converting plasminogen to plasmin and urokinase plasminogen activator receptor (*Plaur*) were also significantly induced only in coinfecting mice. Concordantly, increased *Plat* expression was observed in 1918+SP mice by immunohistochemistry (Fig. S4). Increased expression of genes that inhibit platelets and coagulation was also observed, including tissue factor pathway inhibitor 2 (*F3pi2*), *Serpine1*, *Serpine3*, annexin A3 (*Anxa3*) and phospholipase A2 group VII (*Pla2g7*). Similar to the observations for neutrophil-related genes, expression of the majority of genes involved in platelet function and coagulation were not increased in SP-alone mice.

Neutrophil activation and deposition of elastase onto vascular endothelial cells during coinfection

To further examine the neutrophil infiltration and activation, mouse lung sections were immunostained for Ly6G, myeloperoxidase (MPO), and neutrophil elastase (ELANE), key enzyme constituents of azurophilic granules in neutrophils. 1918-SP-coinfection produced extensive and progressive infiltration of LY6G-positive neutrophils with particularly high expression in lung regions with the greatest histopathological changes, in contrast to the lower, but clearly detectable, accumulation of LY6G-positive neutrophils in mice infected with 1918- or SP-alone (Fig. 4). In coinfecting mice, cellular infiltrates expressed high levels of MPO and ELANE compared to lower expression in mice infected with 1918- or SP-alone. The 1918+SP infected mice also showed increased extracellular ELANE deposition along the endothelium of many blood vessels consistent with an enhanced degranulation response. Similarly, ELANE was also prominently expressed on alveolar and bronchiolar epithelium and neutrophils in 1918+SP infected mice (Fig. 4H). Immunohistochemical time courses for Ly6G, MPO, ELANE and the monocyte/neutrophil marker CD11b are shown in Figs. S5-S8.

Activation of coagulation and vascular thrombogenesis in lungs of coinfecting mice

Immunohistochemical staining of day 6 mouse lung sections with F3 revealed differential staining between groups (Fig. 5). SP-infected mice showed only minimal F3 staining (Fig. 5 A), especially around regions of bronchiolitis, both in respiratory epithelial cells and inflammatory cells. No evidence of vascular pathology was noted (Fig. 5 B-C). 1918-infected mice showed widespread F3 staining in areas of bronchiolitis and alveolitis (Fig. 5 D). Vessels showed prominent perivascular inflammatory cell infiltrates (Fig. 5 E-F) without evidence of thrombus formation. In marked contrast, coinfecting mice showed extensive and very prominent F3 staining throughout the lungs, especially in areas of acute pneumonia, bronchiolitis, and pleuritis (Fig. 5G & J). Unlike the other groups, there were also abundant

thrombotic lesions in small veins, venules and capillaries (Fig. 5H, I, K, L), consisting of fibrinous thrombi, sometimes with recanalization (Fig. 5 K, L). Examination of F3 expression over the infection time course revealed marked accumulation of F3 staining in the lungs of coinfecting mice, and to a lesser extent in the 1918- and SP-infected mice (Fig. S9). Similarly, 1918+SP-coinfection also resulted in prominent thrombin staining (Fig. S10).

Extensive expression of F3 and occurrence of vascular thrombi in 1918 pandemic autopsy samples with bacterial coinfection

Postmortem lung tissue sections from victims of the 1918 [3] and 2009 [21] H1N1 influenza pandemics were subsequently examined for correlative changes. F3 showed little to no immunostaining in normal lung (Fig. 6A), and only minimal levels in two 2009 pandemic autopsy cases (Fig. 6B-C). Interestingly, two 1918 pandemic autopsy cases showed marked F3 expression (Fig. 6D-F), very similar to F3 in mouse lung sections from the coinfecting group (Fig. 5G & J). As in coinfecting mouse lungs, F3 staining was observed in monocytes, macrophages, neutrophils, and also epithelial cells (Fig. 6F). Examination of ten 1918 autopsy cases showed abundant small vessel thrombosis in most cases, as previously described in 1918 [17,18]. Fibrinous thrombi were commonly observed in small veins, venules, and capillaries on examination of H&E stained lung sections (Fig. 6G-L). Some thrombi showed evidence of organization with ingrowth of fibroblasts, collagen deposition (Fig. 6J), or recanalization (Fig. 6K & L).

Discussion

In this study, SP secondary infection following 1918 pandemic virus was shown to enhance lung pathology, damage endothelial cells and activate coagulation in mice. These attributes of 1918+SP coinfection fulfil the requirements for thrombosis in Virchow's triad of reduced flow, hypercoagulability, and endothelial damage (Fig. S11). Significantly, findings from the mouse model were validated in 1918 human lung autopsy samples from two SP-positive cases. These cases showed intense and widespread F3 staining in neutrophils, monocytes, alveolar macrophages, as well as epithelial and endothelial cells accompanied by numerous small vessel thrombi. In contrast, minimal F3 staining was observed in SP- or *Streptococcus pyogenes*-positive 2009 pandemic H1N1 autopsy samples. Retrospective analysis of a previously published study from SP coinfecting 1918 and 2009 pandemic H1N1 autopsy samples [15] revealed that of 292 coagulation-related genes identified, 47% were more abundant in the 1918 samples, including, factor VIII (*F8*), von Willebrand factor (*VWF*), *PLAUR* and *PLAT*; while only 6% of these gene transcripts were more abundant in the 2009 autopsy samples. The findings of widespread thrombi and extensive expression of clotting factors strongly support activation of coagulation during 1918+SP coinfection and may explain increased fatalities associated with secondary bacterial infections during the 1918 influenza pandemic.

Increased bacterial and/or viral loads during coinfection have previously been associated with enhanced severity of influenza virus and SP coinfection [4,5,10]. Early increases in bacterial burden in 1918+SP infected mice suggests that virus-mediated damage to the respiratory epithelium increased the initial bacterial colonization, possibly by exposing

receptors for bacterial attachment [23]. Indeed, higher levels of *Ptafr*, the product of which plays a role in adhesion and invasion of *S. pneumonia*, were observed in coinfecting animals [24]. Lower levels of 1918 virus during SP coinfection are likely related to loss in tissue viability. Despite similar bacterial loads in the lungs of SP and 1918+SP infected mice at day 3 post-SP infection, there was significantly higher expression of SP virulence factors in 1918+SP mice, including *endA*, *nanA* and *nanB*, and *ply*. EndA degrades the DNA scaffold of neutrophil extracellular traps (NETs) and allow bacteria to spread from the upper airways to the lungs and into the blood-stream during pneumonia [25]; *nanA* and *nanB* play important roles in colonization [26] and *ply* has been reported to activate macrophages and neutrophils and has haemolytic and cytotoxic activities [27,28]. Differential expression of bacterial virulence factors during viral coinfection is intriguing and future studies will characterize SP virulence factor expression and roles in pathology during coinfection, which may provide insight into how viral infection-mediated immune responses modulate bacterial survival responses.

Pathology, transcript profiling, and immunohistochemical analysis of lung tissue all support perturbation of immune-related coagulation homeostasis and thrombogenesis during 1918+SP coinfection. Importantly, acute haemorrhage and thrombus formation were common findings in fatal 1918 influenza cases [3,18], suggesting the mouse model accurately reflects the underlying pathology observed in human disease. Furthermore, neutrophil transepithelial migration contributes to pulmonary oedema [29], another common finding associated with fatal 1918 infections [3]. Following 1918 influenza virus infection, the lung may be primed for perturbation of immune-related thrombosis following secondary bacterial infection. First, 1918 influenza virus is associated with enhanced damage to the respiratory epithelium relative to other influenza viruses [18]. Second, 1918 viral infection results in extensive lung infiltration of neutrophils in animals [19,30] and 1918 influenza autopsy cases [3]. It is possible that the combination of viral and bacterial stimuli result in a unique functional neutrophil phenotype, which is supported by gene expression and immunohistochemistry data of enhanced activation of neutrophils during coinfection. Increasingly, neutrophils are thought to play a key role in the interaction between inflammatory and thrombotic pathways [31-34]. The neutrophil serine proteases ELANE and cathepsin G, both of which had increased mRNA expression in 1918+SP-infected mice, are known to promote coagulation and intravascular thrombus growth through proteolysis of the coagulation suppressor tissue factor pathway inhibitor (TFPI) [34]. While infiltration of neutrophils and F3 expression is observed in mice infected with 1918 alone, there appears to be less activation of neutrophils as evidenced by less intense staining of MPO and ELANE and lower expression of numerous genes associated with neutrophil activation compared to coinfection. Exposure to SP may subsequently cause activation of extensive population of neutrophils already present in the lung, initiating the coagulation cascade, possibly through elastase/cathepsin G-mediated cleavage of TFPI. This process may further be amplified by bacteria-induced NETs, which are thought contribute to thrombosis by providing the scaffold for fibrin deposition and platelet aggregation/activation [35,36]. Therefore, while 1918-infection alone may prime the lung for thrombogenesis, in the absence of SP-induced activation of neutrophils and possibly NETs, expression of F3 and presence of neutrophils may not be sufficient for initiation of the coagulation cascade and thrombus formation. The

absence of thrombus in SP-alone infected mice can be attributed to lack of significant F3 expression and extensive infiltration of neutrophils. While SP infection alone could be associated with mortality, this may be due to different pathological mechanisms such as bacteraemia as 16S rRNA was detected in spleens of some mice as early as 2 days post-SP inoculation in both SP-alone and 1918+SP infected groups.

Secondary bacterial infections played a major role in the high mortality of the 1918 influenza pandemic, but the underlying pathophysiology responsible has not been previously investigated. While much has been learned about the genetic determinants responsible for the extreme virulence of 1918 influenza viral infection in animal models, particularly the role of the 1918 HA gene in neutrophil activation and recruitment [19,37] and the role of the viral protein PB1-F2 in susceptibility to secondary bacterial infection [38], this study represents the first investigation of the reconstructed 1918 virus and bacterial coinfection. Coinfection-induced pulmonary thrombosis would exacerbate vascular leak and alveolar oedema due to passive congestion limiting compensatory ventilation responses contributing to severe hypoxia and death (and possibly to the unusual frequency of rapid-onset cyanosis reported in 1918). Experiments evaluating efficacy of targeting neutrophil activation and/or components of the coagulation pathway to reduce severity of pneumonia during influenza viral and bacterial coinfection could open new treatment modalities.

Supplementary Material

Refer to Web version on PubMed Central for supplementary material.

Acknowledgments

This work was supported by the Intramural Research Programs of the National Institutes of Health and National Institute of Allergy and Infectious Diseases. K.A.W. and R.E.K. were supported by Defense Threat Reduction Agency contract HDTRA-1-08-C-0023. We thank Dr. David Morens at NIAID/NIH for helpful discussions. Animal care was performed by the Comparative Medicine Branch, NIH/NIAID.

References

1. Johnson NP, Mueller J. Updating the accounts: global mortality of the 1918-1920 “Spanish” influenza pandemic. *Bull Hist Med.* 2002; 76:105–115. [PubMed: 11875246]
2. Morens DM, Taubenberger JK, Fauci AS. Predominant role of bacterial pneumonia as a cause of death in pandemic influenza: implications for pandemic influenza preparedness. *J Infect Dis.* 2008; 198:962–970. [PubMed: 18710327]
3. Sheng ZM, Chertow DS, Ambroggio X, et al. Autopsy series of 68 cases dying before and during the 1918 influenza pandemic peak. *Proceedings of the National Academy of Sciences of the United States of America.* 2011; 108:16416–16421. [PubMed: 21930918]
4. McCullers JA. Insights into the interaction between influenza virus and pneumococcus. *Clin Microbiol Rev.* 2006; 19:571–582. [PubMed: 16847087]
5. McCullers JA. The co-pathogenesis of influenza viruses with bacteria in the lung. *Nat Rev Microbiol.* 2014; 12:252–262. [PubMed: 24590244]
6. Tashiro M, Ciborowski P, Klenk HD, et al. Role of *Staphylococcus* protease in the development of influenza pneumonia. *Nature.* 1987; 325:536–537. [PubMed: 3543690]
7. Tashiro M, Ciborowski P, Reinacher M, et al. Synergistic role of staphylococcal proteases in the induction of influenza virus pathogenicity. *Virology.* 1987; 157:421–430. [PubMed: 3029981]

8. McCullers JA. Do specific virus-bacteria pairings drive clinical outcomes of pneumonia? *Clin Microbiol Infect.* 2013; 19:113–118. [PubMed: 23231363]
9. McCullers JA, McAuley JL, Browall S, et al. Influenza enhances susceptibility to natural acquisition of and disease due to *Streptococcus pneumoniae* in ferrets. *J Infect Dis.* 2010; 202:1287–1295. [PubMed: 20822454]
10. Kash JC, Walters KA, Davis AS, et al. Lethal synergism of 2009 pandemic H1N1 influenza virus and *Streptococcus pneumoniae* coinfection is associated with loss of murine lung repair responses. *MBio.* 2011; 2
11. Iverson AR, Boyd KL, McAuley JL, et al. Influenza virus primes mice for pneumonia from *Staphylococcus aureus*. *J Infect Dis.* 2011; 203:880–888. [PubMed: 21278211]
12. Memoli MJ, Tumpey TM, Jagger BW, et al. An early 'classical' swine H1N1 influenza virus shows similar pathogenicity to the 1918 pandemic virus in ferrets and mice. *Virology.* 2009; 393:338–345. [PubMed: 19733889]
13. Kobasa D, Jones SM, Shinya K, et al. Aberrant innate immune response in lethal infection of macaques with the 1918 influenza virus. *Nature.* 2007; 445:319–323. [PubMed: 17230189]
14. Kash JC, Tumpey TM, Proll SC, et al. Genomic analysis of increased host immune and cell death responses induced by 1918 influenza virus. *Nature.* 2006; 443:578–581. [PubMed: 17006449]
15. Xiao YL, Kash JC, Beres SB, et al. High-throughput RNA sequencing of a formalin-fixed, paraffin-embedded autopsy lung tissue sample from the 1918 influenza pandemic. *The Journal of pathology.* 2013; 229:535–545. [PubMed: 23180419]
16. Kash JC, Xiao Y, Davis AS, et al. Treatment with the reactive oxygen species scavenger EUK-207 reduces lung damage and increases survival during 1918 influenza virus infection in mice. *Free radical biology & medicine.* 2014; 67:235–247. [PubMed: 24140866]
17. LeCount ER. Disseminated necrosis of the pulmonary capillaries in influenzal pneumonia. *J Amer Med Assoc.* 1919; 72:1519–1520.
18. Taubenberger JK, Morens DM. The pathology of influenza virus infections. *Annu Rev Pathol.* 2008; 3:499–522. [PubMed: 18039138]
19. Qi L, Davis AS, Jagger BW, et al. Analysis by single-gene reassortment demonstrates that the 1918 influenza virus is functionally compatible with a low-pathogenicity avian influenza virus in mice. *Journal of virology.* 2012; 86:9211–9220. [PubMed: 22718825]
20. Edgar R, Domrachev M, Lash AE. Gene Expression Omnibus: NCBI gene expression and hybridization array data repository. *Nucleic Acids Res.* 2002; 30:207–210. [PubMed: 11752295]
21. Gill JR, Sheng ZM, Ely SF, et al. Pulmonary pathologic findings of fatal 2009 pandemic influenza A/H1N1 viral infections. *Archives of pathology & laboratory medicine.* 2010; 134:235–243. [PubMed: 20121613]
22. Dockrell DH, Whyte MK, Mitchell TJ. Pneumococcal pneumonia: mechanisms of infection and resolution. *Chest.* 2012; 142:482–491. [PubMed: 22871758]
23. Plotkowski MC, Puchelle E, Beck G, et al. Adherence of type I *Streptococcus pneumoniae* to tracheal epithelium of mice infected with influenza A/PR8 virus. *Am Rev Respir Dis.* 1986; 134:1040–1044. [PubMed: 3777666]
24. Iovino F, Brouwer MC, van de Beek D, et al. Signalling or binding: the role of the platelet-activating factor receptor in invasive pneumococcal disease. *Cell Microbiol.* 2013; 15:870–881. [PubMed: 23444839]
25. Beiter K, Wartha F, Albiger B, et al. An endonuclease allows *Streptococcus pneumoniae* to escape from neutrophil extracellular traps. *Curr Biol.* 2006; 16:401–407. [PubMed: 16488875]
26. Brittan JL, Buckeridge TJ, Finn A, et al. Pneumococcal neuraminidase A: an essential upper airway colonization factor for *Streptococcus pneumoniae*. *Mol Oral Microbiol.* 2012; 27:270–283. [PubMed: 22759312]
27. Mitchell TJ, Dalziel CE. The biology of pneumolysin. *Sub-cellular biochemistry.* 2014; 80:145–160. [PubMed: 24798011]
28. Preston JA, Dockrell DH. Virulence factors in pneumococcal respiratory pathogenesis. *Future microbiology.* 2008; 3:205–221. [PubMed: 18366340]
29. Mayadas TN, Cullere X, Lowell CA. The multifaceted functions of neutrophils. *Annu Rev Pathol.* 2014; 9:181–218. [PubMed: 24050624]

30. Perrone LA, Plowden JK, Garcia-Sastre A, et al. H5N1 and 1918 pandemic influenza virus infection results in early and excessive infiltration of macrophages and neutrophils in the lungs of mice. *PLoS Pathog.* 2008; 4:e1000115. [PubMed: 18670648]
31. Andrews RK, Arthur JF, Gardiner EE. Neutrophil extracellular traps (NETs) and the role of platelets in infection. *Thromb Haemost.* 2014; 112:659–665. [PubMed: 25265341]
32. Gardiner EE, Andrews RK. Neutrophil extracellular traps (NETs) and infection-related vascular dysfunction. *Blood Rev.* 2012; 26:255–259. [PubMed: 23021640]
33. Kambas K, Mitroulis I, Ritis K. The emerging role of neutrophils in thrombosis-the journey of TF through NETs. *Front Immunol.* 2012; 3:385. [PubMed: 23264778]
34. Massberg S, Grahnl L, von Bruehl ML, et al. Reciprocal coupling of coagulation and innate immunity via neutrophil serine proteases. *Nat Med.* 2010; 16:887–896. [PubMed: 20676107]
35. Clark SR, Ma AC, Tavener SA, et al. Platelet TLR4 activates neutrophil extracellular traps to ensnare bacteria in septic blood. *Nat Med.* 2007; 13:463–469. [PubMed: 17384648]
36. Fuchs TA, Brill A, Duerschmied D, et al. Extracellular DNA traps promote thrombosis. *Proceedings of the National Academy of Sciences of the United States of America.* 2010; 107:15880–15885. [PubMed: 20798043]
37. Kash JC, Basler CF, Garcia-Sastre A, et al. Global host immune response: pathogenesis and transcriptional profiling of type A influenza viruses expressing the hemagglutinin and neuraminidase genes from the 1918 pandemic virus. *Journal of virology.* 2004; 78:9499–9511. [PubMed: 15308742]
38. McAuley JL, Hornung F, Boyd KL, et al. Expression of the 1918 influenza A virus PB1-F2 enhances the pathogenesis of viral and secondary bacterial pneumonia. *Cell host & microbe.* 2007; 2:240–249. [PubMed: 18005742]

Abbreviations

SP	<i>Streptococcus pneumoniae</i>
F3	tissue factor
ELANE	elastase, neutrophil expressed
HA	Hemagglutinin
IFN	Interferon
1918 virus	1918 H1N1 influenza virus
ROS	Reactive oxygen species
CFU	Colony forming units
PFU	Plaque forming units
qRT-PCR	Quantitative reverse-transcriptase polymerase chain reaction
MPO	myeloperoxidase
NETs	neutrophil extracellular traps
Ptafr	platelet-activating factor receptor

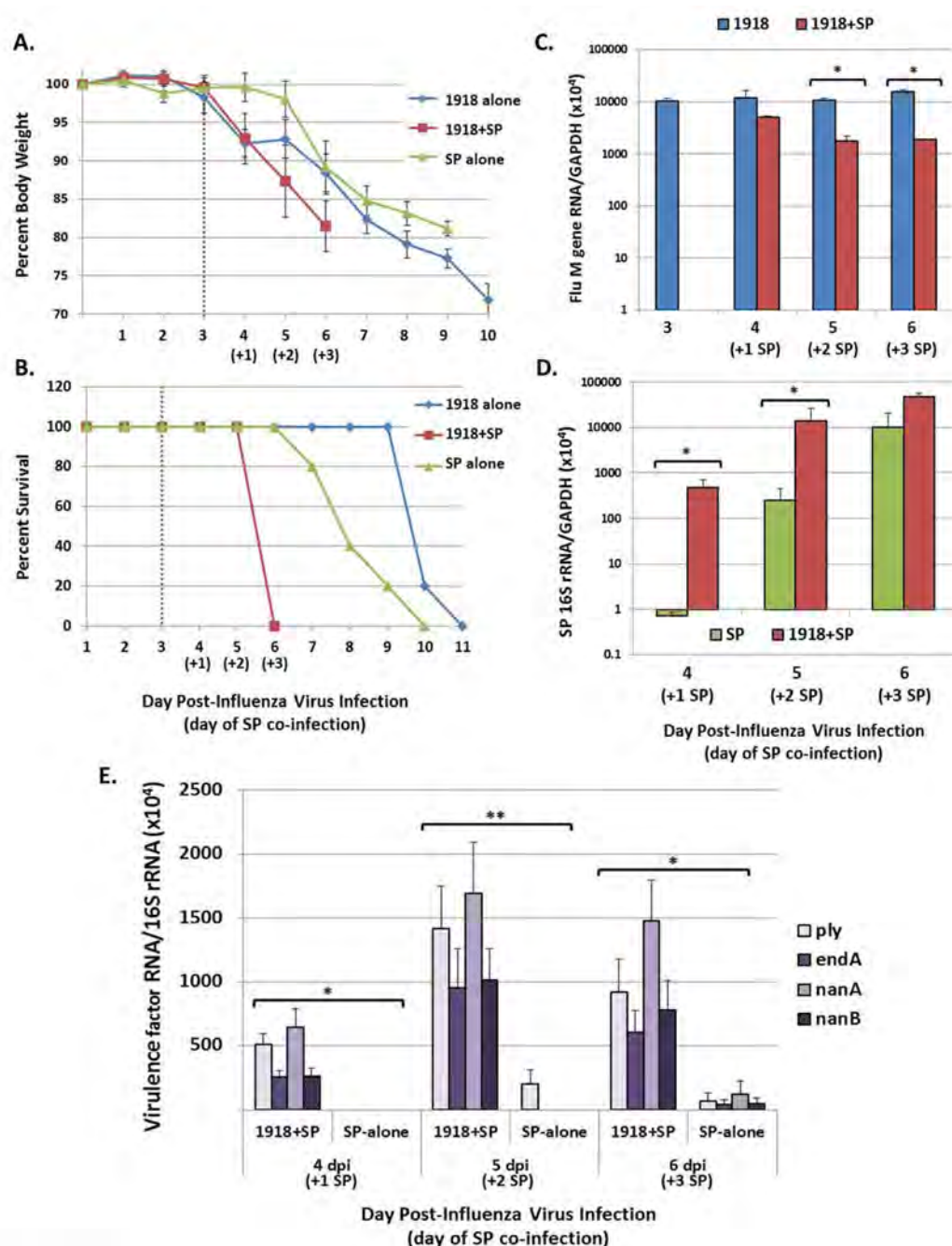


Fig. 1. Coinfection of 1918 pandemic H1N1 influenza virus and SP shortens survival and increases bacterial growth and virulence factor expression

Groups of mice were inoculated as described in Materials and methods. (A) Change in body weight following initial infection in 1918 virus-alone, SP-alone and 1918+SP infected groups. Inoculation with SP is indicated at 3 dpi following influenza virus by the dashed line. (B) Survival of 1918 virus-alone, SP-alone and 1918+SP infected mice. These data are representative of three independent experiments. (C) Quantification of influenza virus M gene mRNA expression and (D) quantification of bacterial 16S rRNA present in lung tissue using RT-qPCR. Data are presented as mean \pm standard error of the mean (SEM) of 2^{-Ct}

values relative to *Gapdh* present in RNA isolated from the lungs of three mice per group. (E) Quantification of mRNA levels of SP pneumolysin (*Ply*), endonuclease *EndA*, and neuraminidases *NanA* and *NanB* in 1918+SP and SP-alone infected lung tissue using RT-qPCR analysis. Data are presented as mean \pm SEM of 2^{-C_t} values of each virulence factor relative to 16S rRNA present in RNA isolated from the lungs of three mice per group. * $p < 0.05$ or ** $p = 0.05$ by two-tailed Mann-Whitney U-test.

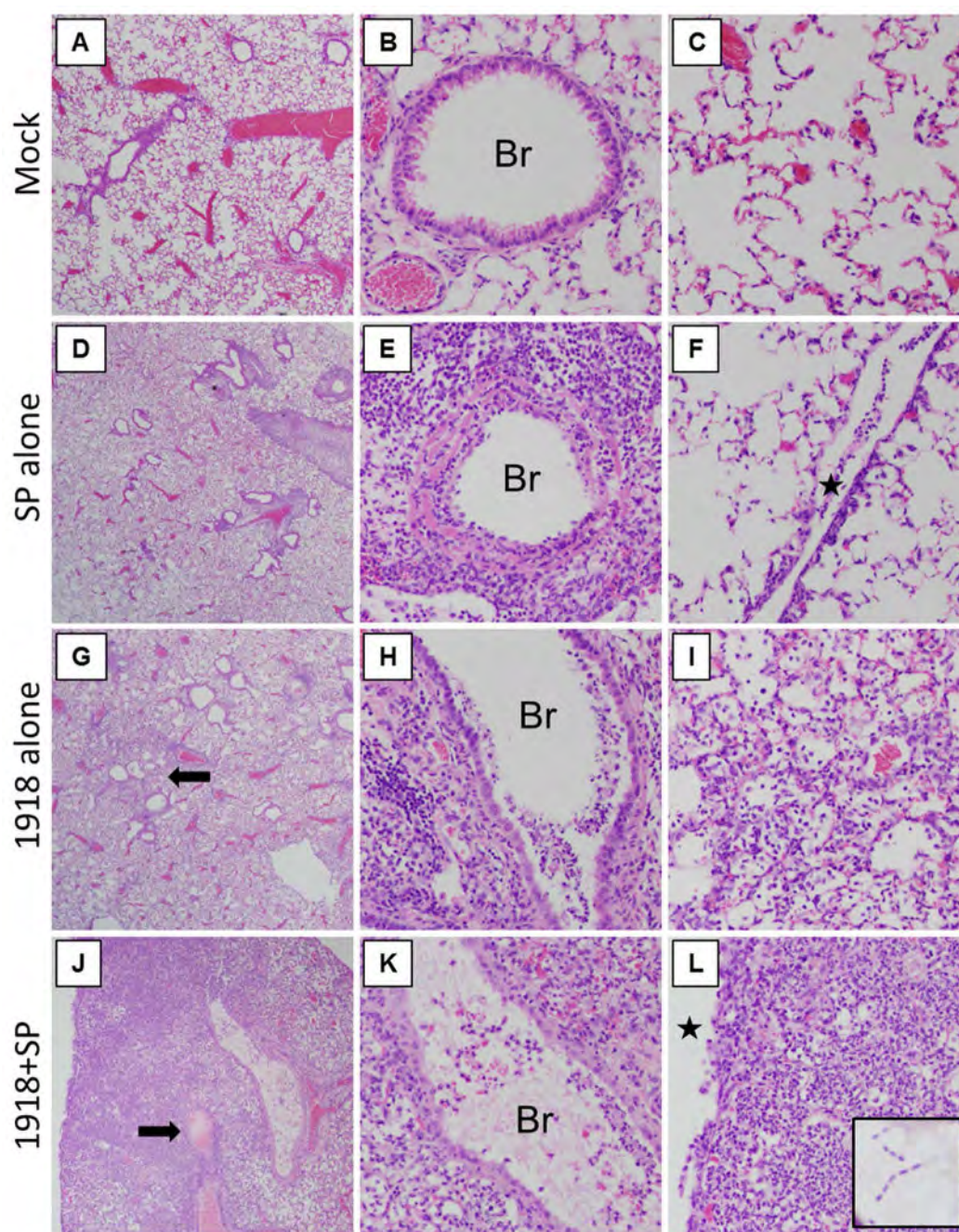


Fig. 2. 1918 and SP coinfection greatly increases severity of lung pathology

Lungs from mock and infected mice were harvested at 6 days post-1918 (3 d post-SP) and were stained with H&E. (A-C) Representative photomicrographs of mock-infected mice showing (A) no lung pathology, (B) normal bronchioles (Br), and alveoli without pathology. (D-F) Representative photomicrographs of SP-infected mice showing (D) focal, mild pathological changes, including (E) focal acute bronchiolitis (Br), and (F) rare foci of pleuritis (star). (G-I) Representative photomicrographs of 1918-infected mice showing (G) multifocal pathological changes including alveolitis (arrow) affecting >25% of lung

parenchyma, (H) multifocal acute bronchiolitis (Br), and (I) an acute alveolitis with numerous mixed inflammatory cells in the airspaces and interstitium, including abundant neutrophils. (J-K) Representative photomicrographs of 1918-SP infected mice showing (J) widespread acute pneumonia with consolidation and abundant thrombi (arrow) affecting >50% of the lung parenchyma, (K) multifocal acute bronchiolitis (Br), and (L) an acute pneumonia pattern with alveolitis with numerous mixed inflammatory cells in the airspaces and interstitium, including abundant neutrophils, and extending into an acute pleuritis (star). (A, D, G, J original magnification $\times 20$; B, C, E, F, H, I, K, L original magnification $\times 200$).

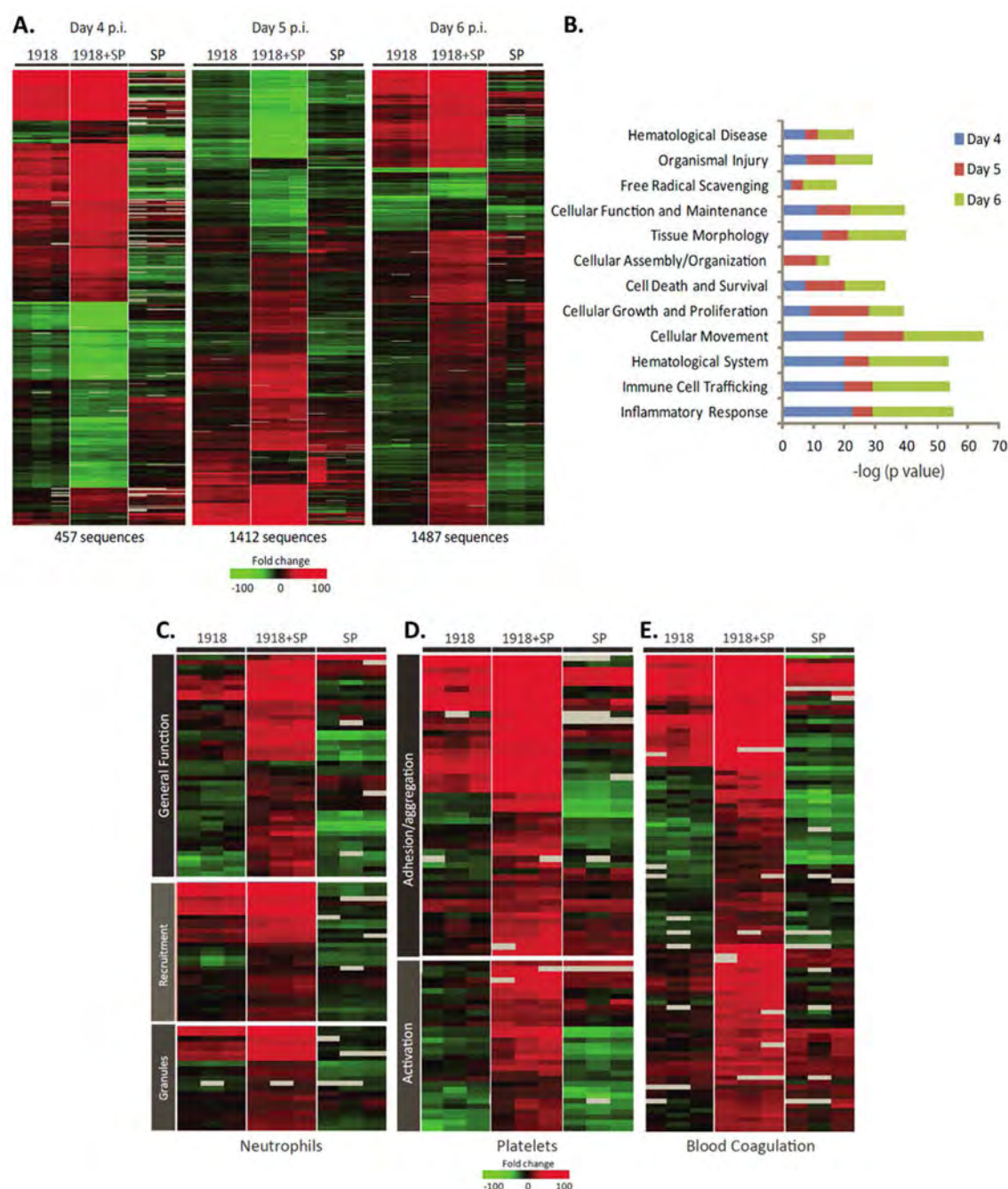


Fig. 3. Coinfection of 1918 influenza virus and SP induces a unique host response compared to either pathogen alone

(A) A standard t-test comparison was used to identify genes whose mRNA levels differed significantly (at least 2-fold difference in median expression level, $p < 0.01$) in lung tissue from 1918+SP versus 1918-infected mice. Each column represents gene expression data from an individual experiment comparing lung tissue from an infected animal relative to pooled tissue from mock infected mice ($n=9$). Red shows increased, green decreased, and black no change in mRNA levels in infected relative to uninfected mice. (B) Functional annotation analysis of genes differentially expressed between 1918+SP and 1918-infected

mice at day 4 to 6 post-1918. (C-E) Differences in host response to 1918 and SP coinfection suggest perturbations in inflammation-related coagulation homeostasis. Expression profiles of transcripts involved in (C) neutrophil infiltration and activity, (D) platelet aggregation and (E) blood coagulation that are differentially expressed in 1918, SP, and 1918+SP infected mice at day 6 post viral infection. Each column represents gene expression data from an individual experiment comparing lung tissue from an infected animal relative to pooled tissue from mock mice (n=9). Red shows increased, green decreased, and black no change in mRNA levels in infected relative to uninfected mice.

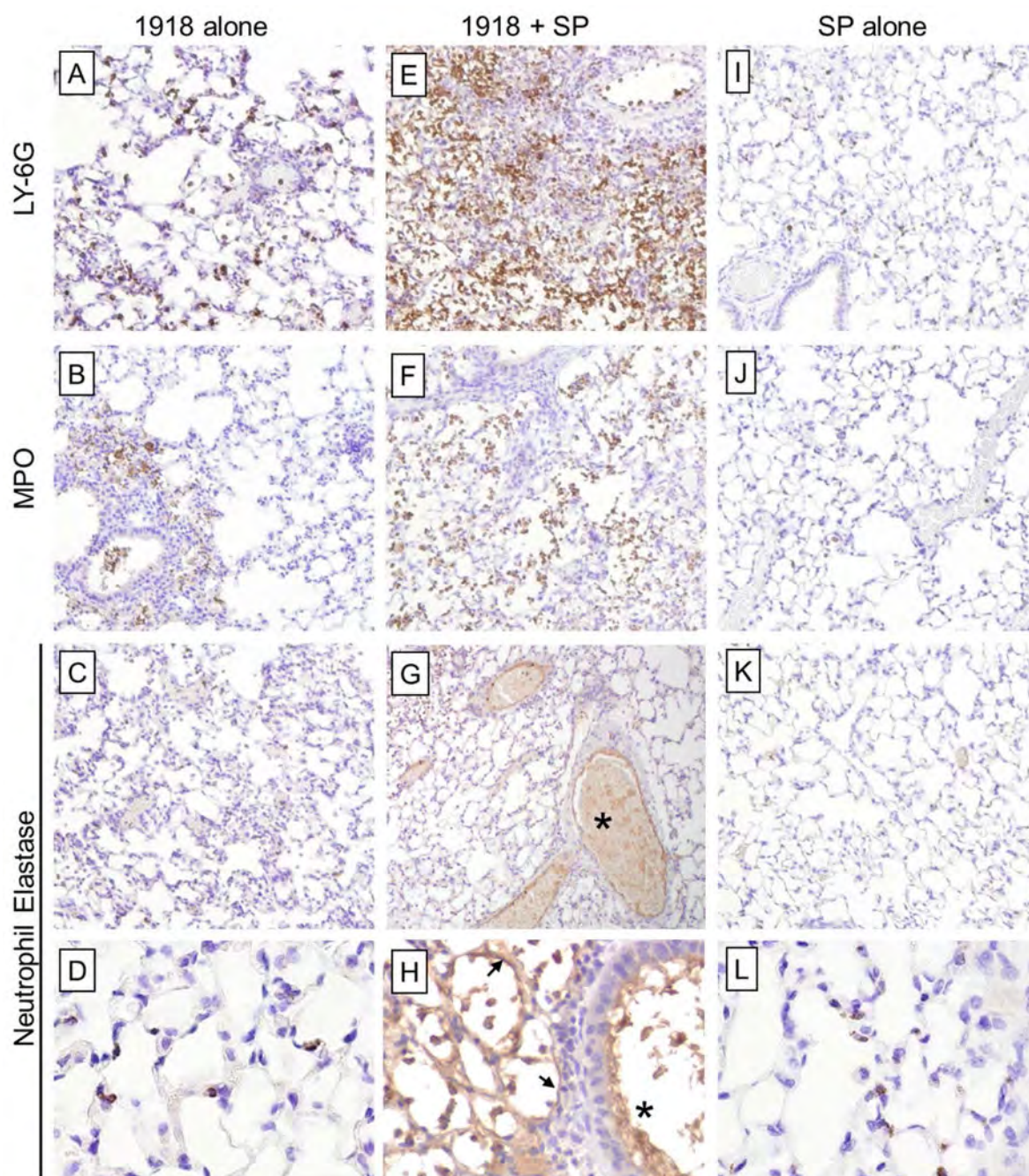


Fig. 4. 1918 and SP coinfection induces extensive neutrophil infiltration and activation

Mouse lung sections harvested at 6 d post-infection with influenza virus (3 d post-infection with SP in coinfection groups) were stained for Ly6G, a specific neutrophil marker, MPO, and neutrophil elastase (ELANE). (A-D) 1918 alone and (I-L) SP alone induced detectable increases in Ly6G-positive neutrophils with low level expression of MPO and ELANE localized primarily around large airways and blood vessels. (E-H) 1918-SP infected mice showed extensive infiltration of Ly6G-positive neutrophils with high expression levels of MPO and ELANE. Extracellular ELANE deposition was also noted on the inner lining of

many large and medium-sized blood vessels (asterisk). (H) ELANE-positive intra-alveolar neutrophils and alveolar walls (black arrows) were observed in 1918-SP infected mice whereas with (D) 1918 and (L) SP infection ELANE-positive neutrophils remained within the interstitium. (A-C, E-G, I-K original magnification $\times 100$; D, H, L original magnification $\times 600$).

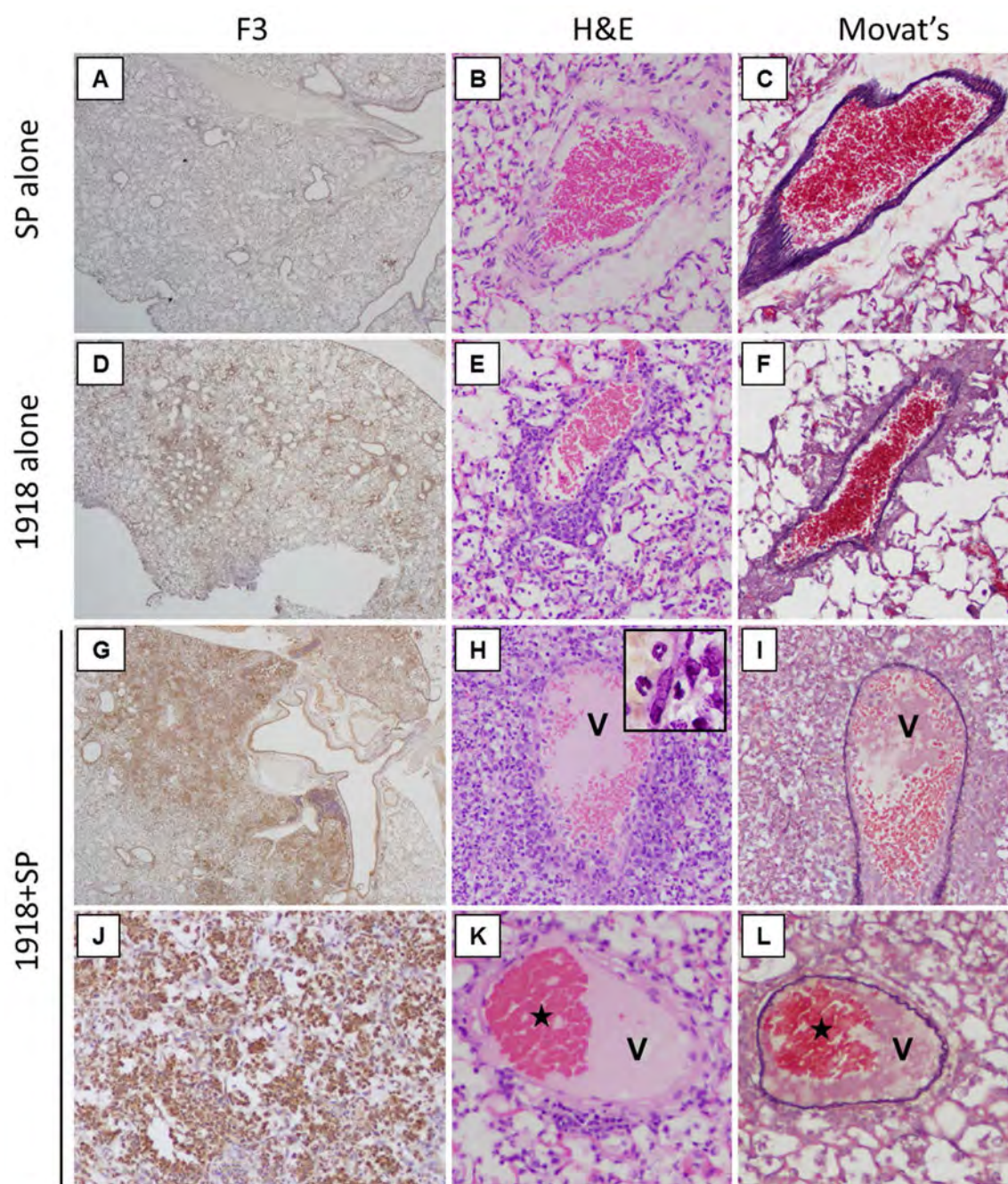


Fig. 5. 1918 and SP coinfection causes significant and widespread expression of F3 and pulmonary thrombosis in mice

Lung sections from SP-infected, 1918-infected, and coinfecting mice were immunostained for F3 and pulmonary vessels were examined for pathological changes. (A-C)

Representative photomicrographs of SP-infected mice showing (A) focal F3 staining predominantly around bronchioli, and no vascular pathology. (B-C) serial sections show (B) a normal venule without perivascular inflammation or thrombosis stained with H&E and (C) stained with Movat's stain to highlight elastin. (D-F) Representative photomicrographs of 1918-infected mice showing (D) multifocal prominent F3 staining around bronchioli and

areas of alveolitis. Vessels show perivascular inflammation but no thrombi, (E) H&E and (F) Movat's stain. (G-L) Representative photomicrographs of coinfecting mice showing (G) very prominent and diffuse F3 staining around bronchioli and (J) areas of acute pneumonia. (H, I, K, L) Abundant fibrin thrombi are seen in venules (V). Perivascular inflammation was prominent in (H) H&E stain and the thrombus was highlighted with (I) Movat's stain. Another thrombus (K, L) showed recanalization (stars) seen in both (K) H&E and (L) Movat's stain. (A, D, G original magnification $\times 20$; B, C, E, F, H, I, J, K, L original magnification $\times 200$).

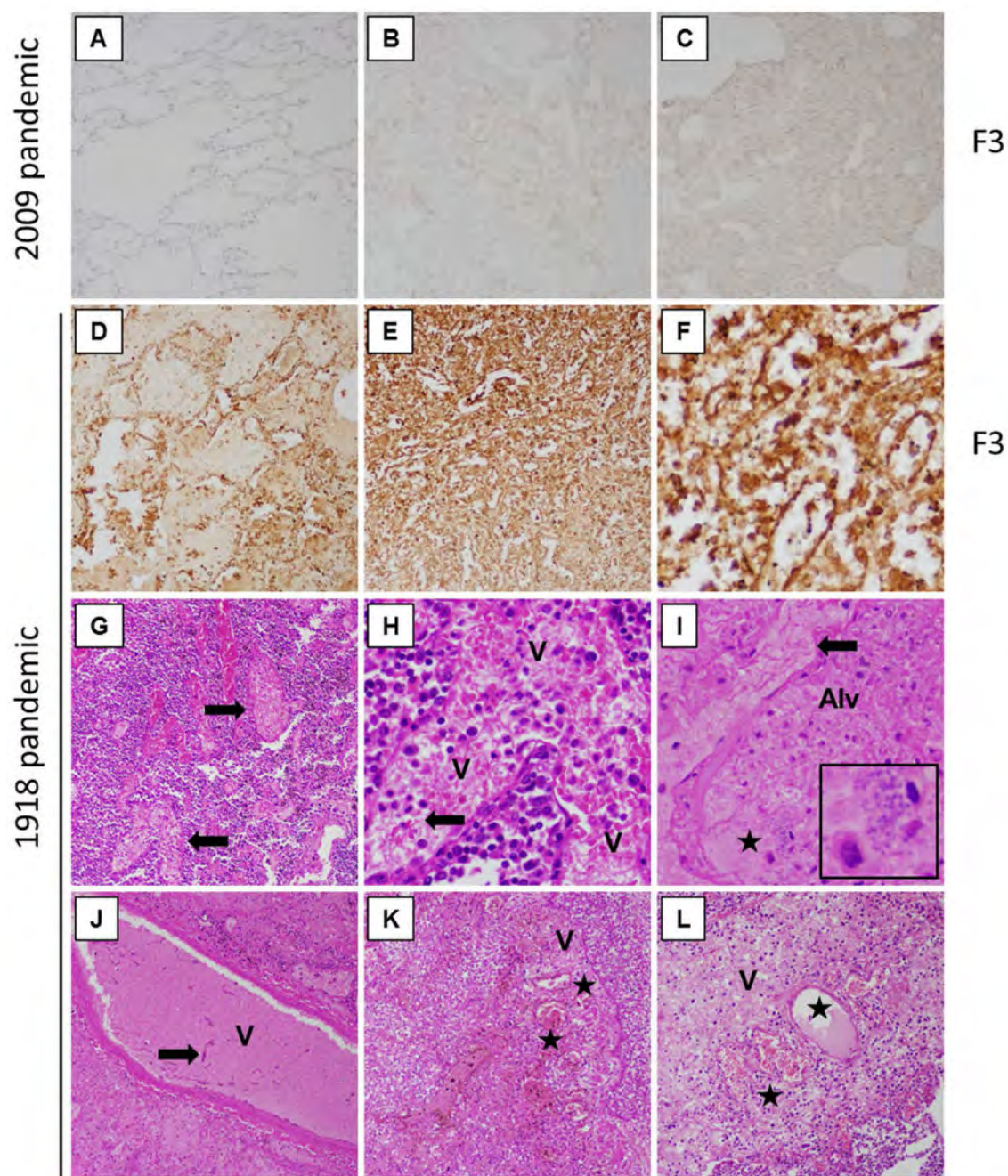


Fig. 6. Abundant and extensive expression of F3 and widespread pulmonary thrombosis in coinfecting 1918 human autopsy case material

(A-F) Post mortem lung sections were stained for F3. (A) Normal control lung showed little-to-no F3 staining. (B-C) Mild-to-moderate F3 staining was observed in two 2009 pandemic influenza post mortem cases, with staining observed in both inflammatory and epithelial cells. (B) 2009 pandemic case 14, and (C) 2009 pandemic case 1, as previously described in Gill et al. 2010 Table 2 [21]. (D-F) F3 staining of 1918 pandemic post mortem cases showing very prominent F3 staining observed in both inflammatory and epithelial cells. (D) 1918 pandemic case 19180925b, and (E-F) 1918 pandemic case 19180924d, as previously

described in Sheng et al. 2011 Supplementary Table 1 [3]. (G-L) Abundant small venule thrombi are observed 1918 pandemic post mortem cases. (G) 1918 case 19180926b showing several venules with fibrin thrombi, arrows. (H) Same case as (G) showing a venule, V, filled with thrombus consisting of erythrocytes admixed with fibrin strands, arrow). (I) 1918 case 19181017 showing an organizing thrombus with prominent fibrin in an interstitial capillary (arrow) next to an alveolus, alveoli filled with oedema, inflammatory cells, and bacteria morphologically consistent with SP (star) and inset. (J) Same case showing a venule, V, with a thrombus with early organization with fibroblasts, arrow, within the thrombus. (K) 1918 case 19180924d (same as in F) showing an organizing thrombus in a venule, denoted by V, with recanalized lumina (denoted by stars). (L) 1918 case 19181008d showing an organizing thrombus in a small vein, V, with recanalized lumina, stars. (A-E original magnification $\times 20$; G, I, J, K, L original magnification $\times 200$; F, H original magnification $\times 400$).

Reduction of secondary transmission of SARS-CoV-2 in households by face mask use, disinfection and social distancing: a cohort study in Beijing, China

Yu Wang,¹ Huaiyu Tian,² Li Zhang,¹ Man Zhang,³ Dandan Guo,⁴ Wenting Wu,¹ Xingxing Zhang,³ Ge Lin Kan,⁵ Lei Jia,¹ Da Huo,¹ Baiwei Liu,¹ Xiaoli Wang,¹ Ying Sun,¹ Quanyi Wang,¹ Peng Yang,³ C. Raina MacIntyre^{6,7}

To cite: Wang Y, Tian H, Zhang L, *et al.* Reduction of secondary transmission of SARS-CoV-2 in households by face mask use, disinfection and social distancing: a cohort study in Beijing, China. *BMJ Global Health* 2020;**5**:e002794. doi:10.1136/bmjgh-2020-002794

Handling editor Seye Abimbola

Received 1 May 2020
Revised 9 May 2020
Accepted 11 May 2020



© Author(s) (or their employer(s)) 2020. Re-use permitted under CC BY-NC. No commercial re-use. See rights and permissions. Published by BMJ.

For numbered affiliations see end of article.

Correspondence to

Dr Quanyi Wang;
wangquanyi@protonmail.com
and
Dr Peng Yang;
yangpengcdc@163.com

ABSTRACT

Introduction Transmission of COVID-19 within families and close contacts accounts for the majority of epidemic growth. Community mask wearing, hand washing and social distancing are thought to be effective but there is little evidence to inform or support community members on COVID-19 risk reduction within families.

Methods A retrospective cohort study of 335 people in 124 families and with at least one laboratory confirmed COVID-19 case was conducted from 28 February to 27 March 2020, in Beijing, China. The outcome of interest was secondary transmission of severe acute respiratory syndrome coronavirus 2 (SARS-CoV-2) within the family. Characteristics and practices of primary cases, of well family contacts and household hygiene practices were analysed as predictors of secondary transmission.

Results The secondary attack rate in families was 23.0% (77/335). Face mask use by the primary case and family contacts before the primary case developed symptoms was 79% effective in reducing transmission (OR=0.21, 95% CI 0.06 to 0.79). Daily use of chlorine or ethanol based disinfectant in households was 77% effective (OR=0.23, 95% CI 0.07 to 0.84). Wearing a mask after illness onset of the primary case was not significantly protective. The risk of household transmission was 18 times higher with frequent daily close contact with the primary case (OR=18.26, 95% CI 3.93 to 84.79), and four times higher if the primary case had diarrhoea (OR=4.10, 95% CI 1.08 to 15.60). Household crowding was not significant.

Conclusion The study confirms the highest risk of transmission prior to symptom onset, and provides the first evidence of the effectiveness of mask use, disinfection and social distancing in preventing COVID-19. We also found evidence of faecal transmission. This can inform guidelines for community prevention in settings of intense COVID-19 epidemics.

Summary box

What is already known?

- ▶ Mitigation of the COVID-19 pandemic depends solely on non-pharmaceutical interventions until drugs or vaccines are available. Transmission of COVID-19 within families and close contacts accounts for the majority of epidemic growth. Community mask wearing, hand washing and social distancing are thought to be effective but the evidence is not clear.

What are the new findings?

- ▶ The overall secondary attack rate in households was 23.0%. Face masks were 79% effective and disinfection was 77% effective in preventing transmission, while close frequent contact in the household increased the risk of transmission 18 times, and diarrhoea in the index patient increased the risk by four times. The results demonstrate the importance of the pre-symptomatic infectiousness of COVID-19 patients and shows that wearing masks after illness onset does not protect.

What do the new findings imply?

- ▶ The findings inform universal face mask use and social distancing, not just in public spaces, but inside the household with members at risk of getting infected. This further supports universal face mask use, and also provides guidance on risk reduction for families living with someone in quarantine or isolation, and families of health workers, who may face ongoing risk.

INTRODUCTION

In the absence of a vaccine for COVID-19, non-pharmaceutical interventions (NPIs) are the only available disease control measures. We have shown that population level NPIs, including travel bans and the national emergency response, were effective in flattening

the COVID-19 epidemic curve in China.¹ However, the effect of other NPIs, such as mask use and hygiene practices, have not been well studied in the COVID-19 pandemic.

In the USA, the use of face masks in the community has been recommended.² It is thought that universal face mask use (UFMU) may reduce outward transmission from asymptotically infected people and protect well people from becoming infected. However, the World Health Organization and Public Health England recommend against UFMU on the grounds that there is little evidence from randomised controlled trials to support this. Some experts suggest that in a pandemic, the precautionary principle should be used and UFMU encouraged as it is unlikely to cause harm and may result in public health gain.^{3 4} In countries where personal protective equipment is scarce, people are making their own masks.

In China, over 70% of human-to-human transmission of severe acute respiratory syndrome coronavirus 2 (SARS-CoV-2) occurred in families.^{5 6} However, data to inform COVID-19 risk reduction in households are unavailable. Given epidemic growth is dominated by household transmission,^{5 6} studying the use of NPIs, such as face masks, social distancing and disinfection in the household setting, may inform community epidemic control and prevent transmission of COVID-19 in households.

METHODS

Study population and design

We conducted a retrospective cohort study involving families of laboratory confirmed COVID-19 cases in Beijing, China. We defined family members as those who had lived with primary cases in a house for 4 days before and for more than 24 hours after the primary cases developed illness related to COVID-19. As of 21 February 2020, all laboratory confirmed COVID-19 cases reported in Beijing were enrolled in our study and followed-up. The outcome of interest was secondary transmission in the household. Families with secondary transmission were defined as those where some or all of the family members become infected within one incubation period (2 weeks) of symptom onset of the primary case.

To analyse the predictors of household transmission, we compared families with and without secondary transmission for various measured risk factors, preventive interventions and exposures.

Definition of confirmed case

According to national prevention and control guideline (fifth edition),⁷ confirmed cases were those who met the clinical, epidemiological and laboratory testing criteria for COVID-19 simultaneously.

1. Clinical criteria included: (a) fever and/or one or more respiratory symptoms; (b) radiological evidence of pneumonia; (c) white blood cell count normal or

decreased, and lymphocyte count decreased at the early stage of illness.

2. Epidemiological criteria included: (a) visits to/living in Wuhan or cities around Wuhan or other communities which had already reported COVID-19 cases in the 14 days prior to the onset of symptoms; (b) having contact with a person known to have infection with SARS-CoV-2 in the 14 days prior to onset of symptoms; (c) having contact with a person who had fever or respiratory symptoms and came from Wuhan or adjacent cities or other communities which had already reported COVID-19 cases in the 14 days prior to onset of symptoms; (d) being one of the cluster cases.

Suspected cases met one of the epidemiological criteria and any two of the clinical criteria, or met all of the clinical criteria. Confirmed cases were those suspected cases who met one of the following criteria: (a) respiratory or blood specimen tested positive for SARS-CoV-2 by real time reverse transcriptase-polymerase chain reaction; (b) virus in respiratory or blood specimen was highly homologous with known SARS-CoV-2 through gene sequencing.

Data collection

A three part structured questionnaire was developed. The first part included demographic and clinical information of the primary case. The second part was mainly focused on the primary case's knowledge about and attitudes toward COVID-19, and their self-reported practices (mask wearing, social distancing, living arrangements) and activities in the home. The third part was about self-reported behaviours of all family members, as well as the family's accommodation and household hygiene practices from 4 days before the illness onset to the day the primary case was isolated, including room ventilation, room cleaning and disinfection. Close contact was defined as being within 1 m or 3 feet of the primary case, such as eating around a table or sitting together watching TV. The frequency of contact, disinfection and ventilation was measured.

After diagnosis, the primary case was hospitalised as per standard practice in Beijing. Eligible primary cases and their family members were interviewed between 28 February and 8 March. Data on the primary case were extracted from epidemiological investigating reports from Beijing Centre for Disease Prevention and Control and supplemented by interview.

The clinical severity of the COVID-19 case was categorised as mild, severe or critical. Mild disease included non-pneumonia and mild pneumonia cases. Severe disease was characterised by dyspnoea, respiratory frequency ≥ 30 /min, blood oxygen saturation $\leq 93\%$, PaO₂/FiO₂ ratio < 300 and/or lung infiltrates $> 50\%$ within 24–48 hours. Critical cases were those who exhibited respiratory failure, septic shock and/or multiple organ dysfunction/failure.⁸

Statistical analysis

Risk factors for secondary transmission were analysed by characteristics of the primary case, characteristics of well family members and household hygiene practices. Categorical variables are presented as counts and percentages, and continuous variables as medians (IQR). The χ^2 test and Fisher exact test were applied to compare difference between groups when necessary. A composite COVID-19 knowledge score and hand hygiene score were created with multiple sub-questions. A multivariable logistic regression model was used to identify risk factors associated with SARS-CoV-2 household transmission. Univariable analysis was first performed with all measures and only those variables significant at $p < 0.1$ could be selected in the following multivariable logistic regression analysis. Backward elimination was performed to establish a final model retaining those with $p < 0.05$ in the model. Statistical analyses were performed using SAS software (V.9.4).

Ethics statement

As our study was embedded within the COVID-19 prevention and control practice within public health units, and the telephone interview was a supplementary survey of the epidemiological field investigation, ethics approval was not required. We obtained subjects' verbal informed consent before the start of the interviews.

Patient and public involvement

No patients or the public were involved in the study design, setting the research questions, interpretation or writing up of results, or reporting of the research.

RESULTS

As of 21 February 2020, 399 confirmed COVID-19 cases in 181 families were reported in Beijing. Four family clusters were excluded because we were unable to determine whether there was secondary transmission or co-exposure, leaving 177 families. After reviewing information in the epidemiological investigation reports and survey calls, 40 families were excluded as they did not meet the study inclusion criteria. A further 13 families declined to be interviewed and were also excluded, leaving 124 families for study (figure 1).

Over the 2 weeks of follow-up from onset of the primary case, secondary transmission occurred in 41/124 families (77 secondary cases), and 83/124 families had no secondary transmission. The overall secondary attack rate in families was 23.0% (77/335). In the secondary transmission group, 41 primary cases caused 77 secondary cases, with a median secondary case number in families of 2 (IQR 1–2). In the secondary transmission group, the secondary attack rate in children <18 years of age was 36.1% (13/36), compared with 69.6% (64/92) in adults, and the difference between these two age groups was significant ($\chi^2=12.08$, $p < 0.001$). The median age of the 13 secondary child cases was 3 years (IQR 2–6), 12/13 were

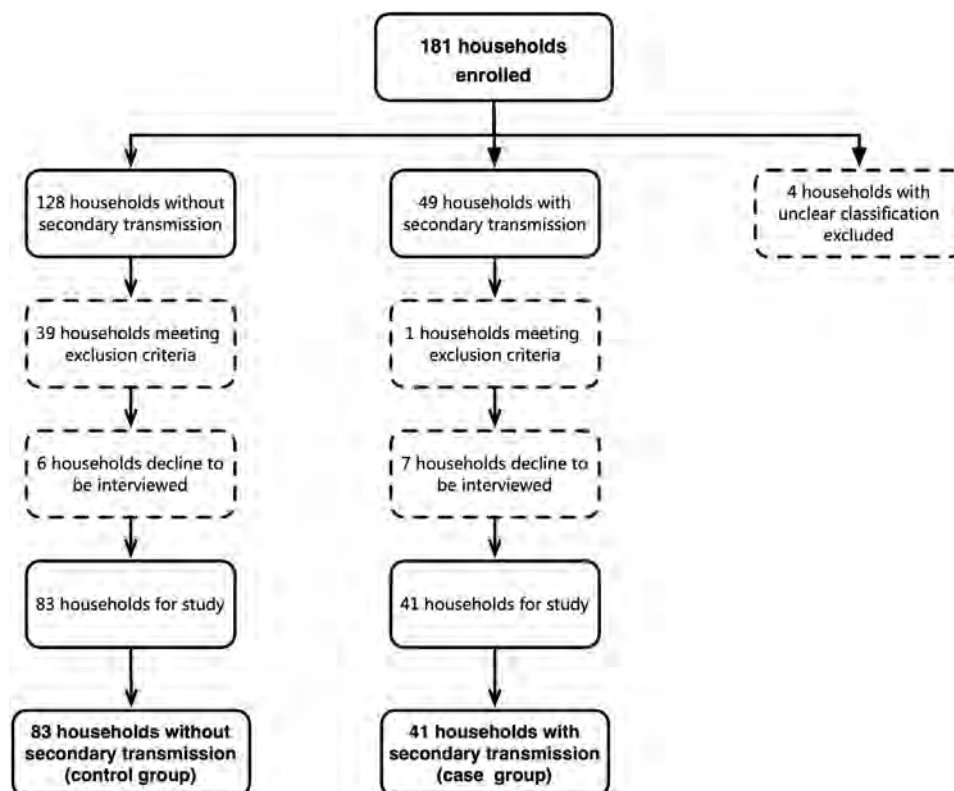


Figure 1 Selection and inclusion of interviewing subjects. Summary of household enrolment, and inclusion and interview response in the analysis of SARS-CoV-2 household transmission in Beijing, China.

Table 1 Characteristics of primary cases of COVID-19: univariable analysis

Primary cases	Total (n (%)) (n=124)	Families without transmission (n (%)) (n=83)	Families with transmission (n (%)) (n=41)	P value	Unadjusted OR (95% CI)
Age (years) (median (IQR))	45.0 (35.7–60.0)	42.0 (34.0–57.5)	52.0 (39.3–61.0)	–	–
<18	0	0	0	–	–
18–59	92 (74.2)	63 (75.9)	29 (70.7)	–	Ref
≥60	32 (25.8)	20 (24.1)	12 (29.3)	0.54	1.30 (0.56 to 3.02)
Sex	–	–	–	–	–
Men	61 (49.2)	40 (48.2)	21 (51.2)	–	Ref
Women	63 (50.8)	43 (51.8)	20 (48.8)	0.75	0.89 (0.42 to 1.87)
Education level	–	–	–	–	–
High school or lower	26 (21.0)	18 (21.7)	8 (19.5)	–	Ref
Bachelor degree	69 (55.6)	47 (56.6)	22 (53.7)	0.53	0.75 (0.30 to 1.86)
Graduate degree	29 (23.4)	18 (21.7)	11 (26.8)	0.65	0.77 (0.25 to 2.38)
Clinical severity	–	–	–	–	–
Mild	96 (77.4)	63 (75.9)	33 (80.4)	–	Ref
Severe	20 (16.1)	16 (19.3)	4 (9.8)	0.22	0.48 (0.15 to 1.54)
Critical	8 (6.5)	4 (4.8)	4 (9.8)	0.38	1.91 (0.45 to 8.13)
Fever (≥37.3°C)	–	–	–	–	–
No	18 (14.5)	9 (10.8)	9 (22.0)	–	Ref
Yes	106 (85.5)	74 (89.2)	32 (78.0)	0.11	0.43 (0.16 to 1.19)
Cough*	–	–	–	–	–
No	66 (53.2)	45 (54.2)	21 (51.2)	–	Ref
Yes	58 (46.8)	38 (45.8)	20 (48.8)	0.75	1.13 (0.53 to 2.39)
Diarrhoea†	–	–	–	–	–
No	109 (87.9)	76 (91.6)	33 (80.5)	–	Ref
Yes	15 (12.1)	7 (8.4)	8 (19.5)	0.08	2.63 (0.88 to 7.85)
Comorbidity	–	–	–	–	–
No	103 (83.1)	72 (86.7)	31 (75.6)	–	Ref
Yes	21 (16.9)	11 (13.3)	10 (24.4)	0.13	2.11 (0.81 to 5.48)
Time interval from illness onset to first hospital visit (days) (median (IQR))‡	3.0 (1.0–7.0)	3.0 (1.0–7.0)	4.0 (2.0–7.0)	–	–
≤2	47 (37.9)	35 (42.2)	12 (29.3)	–	Ref
>2	77 (62.1)	48 (57.8)	29 (70.7)	0.17	1.76 (0.79 to 3.93)
Time interval from illness onset to medical isolation (days) (median (IQR))	5.0 (2.0–7.0)	5.0 (2.0–7.0)	5.0 (3.0–9.0)	–	–
≤2	32 (25.8)	26 (31.3)	6 (14.6)	–	Ref
>2	92 (74.2)	57 (68.7)	35 (85.4)	0.05	2.66 (1.00 to 7.12)
Time interval from illness onset to laboratory confirmation (days) (median (IQR))	7.0 (4.7–10.2)	7.0 (4.4–9.9)	8.0 (5.6–12.9)	–	–
≤3	16 (12.9)	13 (15.7)	3 (7.3)	–	Ref
>3	108 (87.1)	70 (84.3)	38 (92.7)	0.20	2.35 (0.63 to 8.77)
Knowledge score on COVID-19 before illness onset (14 in total) (median (IQR))§	5 (0–9)	5 (0–9)	5 (0–10)	–	–
≥10	31 (25.0)	18 (21.7)	13 (31.7)	–	Ref
3–9	45 (36.3)	32 (38.6)	13 (31.7)	0.24	0.56 (0.22 to 1.47)
≤2	48 (38.7)	33 (39.7)	15 (36.6)	0.33	0.63 (0.25 to 1.61)
Self-awareness of being infected with SARS-CoV-2 when developed illness	–	–	–	–	–
Likely	45 (36.3)	35 (42.2)	10 (24.4)	–	Ref

Continued

Table 1 Continued

Primary cases	Total (n (%)) (n=124)	Families without transmission (n (%)) (n=83)	Families with transmission (n (%)) (n=41)	P value	Unadjusted OR (95% CI)
Unlikely	79 (63.7)	48 (57.8)	31 (75.6)	0.06	2.26 (0.98 to 5.21)
Knowledge of their own infectiousness after illness onset	–	–	–	–	–
Likely	84 (67.7)	62 (74.7)	22 (53.7)	–	Ref
Unlikely	40 (32.3)	21 (25.3)	19 (46.3)	0.02	2.55 (1.16 to 5.61)
Wear mask at home after illness onset†‡	–	–	–	–	–
Never	41 (33.1)	24 (28.9)	17 (41.5)	–	Ref
Sometimes	37 (29.8)	21 (25.3)	16 (39.0)	0.76	1.15 (0.46 to 2.87)
All the time	46 (37.1)	38 (45.8)	8 (19.5)	0.02	0.30 (0.11 to 0.82)
Self-isolated after illness onset	–	–	–	–	–
Yes	79 (63.7)	58 (69.9)	21 (51.2)	–	Ref
No	45 (36.3)	25 (30.1)	20 (48.8)	0.05	2.17 (1.00 to 4.70)
Eat separately at home after illness onset	–	–	–	–	–
Yes	70 (56.5)	54 (65.1)	16 (39.0)	–	Ref
No	54 (43.5)	29 (34.9)	25 (61.0)	0.008	2.86 (1.32 to 6.19)
Eat with separate tableware	–	–	–	–	–
Yes	81 (65.3)	58 (69.9)	23 (56.1)	–	Ref
No	43 (34.7)	25 (30.1)	18 (43.9)	0.14	1.78 (0.82 to 3.88)
Score on hand hygiene (8 in total) (with 11 missing values) (median (IQR))	8 (7–8)	8 (7–8)	7 (6–8)	–	–
≥6	103 (91.2)	68 (93.2)	35 (87.5)	–	Ref
4–5	7 (6.2)	4 (5.5)	3 (7.5)	0.63	1.46 (0.31 to 6.88)
≤3	3 (2.6)	1 (1.3)	2 (5.0)	0.28	3.88 (0.34 to 44.29)

*Primary case ever had the symptom of cough when living with others at home.

†Primary case ever had the symptom of diarrhoea (change of character of stool) when living with others at home.

‡Date on which cases self-reported the appearance of either fever ($\geq 37.3^{\circ}\text{C}$) or any respiratory symptom during epidemiological investigation. Date of hospital visit was the earliest date that cases sought medical service for COVID-19 related illness.

§A composite variable involving the primary case's knowledge on the infectivity of SARS-CoV-2, contagious population, transmission route, susceptible population, incubation period, common symptoms and preventive measures.

¶Refers to the primary case or family members wearing a face mask at home, regardless of whether it was a N95 mask, disposable surgical mask or a common mask, including cloth mask. Wearing masks all the time means the primary case wears a mask all the time except when having dinner or sleeping at home.

**A composite variable involving the primary case's hand washing practice, including using running water, washing frequency, using sanitiser and under what conditions.

mild and 1/13 was asymptomatic. Of 64 secondary adult cases, 82.8% (53/64) were mild, 10.9% (7/64) were severe, 1.6% (1/64) was critical and 4.7% (3/64) were asymptomatic. No statistically significant difference was observed in clinical severity between 41 index adult cases (table 1) and 64 secondary adult cases for the secondary transmission group ($p=0.18$).

The univariable analysis for association with secondary transmission of SARS-CoV-2 within families is shown in tables 1–3. Significant associations were:

1. Characteristics, behaviours and knowledge of the primary case: having diarrhoea, interval from illness onset to medical isolation >2 days, self-awareness of being infected with SARS-CoV-2 when the primary case developed the illness, lack of knowledge of their own infectiousness, mask wearing in the home after illness

onset, failing to self-isolate and not eating separately were associated with transmission (table 1).

2. Behaviours of family members: having daily close contact with the primary case at home, and number of family members wearing a mask in the home before and after the primary case's illness onset date were associated with transmission (table 2).
3. Household practices: frequency of using chlorine or ethanol based disinfectant for household cleaning and household ventilation duration were protective (table 3).

In multivariable logistic regression model, four factors remained significantly associated with secondary transmission. The primary case having diarrhoea in the home and daily close contact with the primary case in the home increased the risk. Transmission was significantly reduced

Table 2 Characteristics of well family members: univariable analysis

Family members	Total (n (%)) (n=121)	Families without transmission (n (%)) (n=81)	Families with transmission (n (%)) (n=40)	P value	Unadjusted OR (95% CI)
Family size (median (IQR))	4 (3–5)	3 (3–5)	4 (3–6)	–	–
≤3	56 (46.3)	41 (50.6)	15 (37.5)	–	Ref
>3	65 (53.7)	40 (49.4)	25 (62.5)	0.18	1.71 (0.79 to 3.71)
Close contact with primary cases at home (within 1 m or 3 feet) (No of times)*	–	–	–	–	–
0	41 (33.9)	36 (44.4)	5 (12.5)	–	Ref
1–3	61 (50.4)	38 (46.9)	23 (57.5)	0.005	4.55 (1.57 to 13.20)
≥4	19 (15.7)	7 (8.7)	12 (30.0)	<0.001	12.34 (3.30 to 46.23)
No of family members wearing mask at home before primary case's illness onset date (median (IQR))†	0 (0–1)	0 (0–2)	0 (0–0)	–	–
None	90 (74.4)	54 (66.7)	36 (90.0)	–	Ref
One or more	31 (25.6)	27 (33.3)	4 (10.0)	0.009	0.22 (0.07 to 0.69)
No of family members wearing mask at home after primary case's illness onset date (median (IQR))‡	1 (0–3)	2 (0–3)	0 (0–3)	–	–
None	47 (38.8)	26 (32.1)	21 (52.5)	–	Ref
Some	38 (31.4)	24 (29.6)	14 (35.0)	0.47	0.72 (0.30 to 1.73)
All	36 (29.8)	31 (38.3)	5 (12.5)	0.004	0.20 (0.07 to 0.60)

*Family members stay with the primary case at a short distance (within 1 m or 3 feet) for more than 10 min at a time. For example, they have dinner with the primary case around a table or watch TV sitting near.

†Before the primary case developed the illness, the primary case or his/her family contacts wear masks all the time at home.

‡When the primary case developed the illness, the primary case's family contacts wear masks all the time living with the primary case at home.

by frequent use of chlorine or ethanol based disinfectant in households and family members (including the primary case) wearing a mask at home before the primary case developed the illness (table 4).

DISCUSSION

This study confirms that the highest risk of household transmission is prior to symptom onset, but that precautionary NPIs, such as mask use, disinfection and social distancing in households can prevent COVID-19 transmission during the pandemic. This study is the first to confirm the effectiveness of mask use prior to symptom onset by family members, daily household disinfection and social distancing in the home. This could inform precautionary guidelines for families to reduce intrafamilial transmission in areas where there is high community transmission or other risk factors for COVID-19. Household transmission is a major driver of epidemic growth.^{5 6} Further, in countries where health system capacity is exhausted, many people with infection are required to self-isolate at home, where their household contacts will be at risk of infection. In our study, the median family size of the 124 families was 4 (range 2–9), usually with children, parents and grandparents, which is similar to the social structure of most Chinese families.⁹ Therefore, the risk of SARS-CoV-2 household transmission is high if a primary case was introduced and no measure was adopted. We showed that NPIs are effective at preventing transmission, even in homes that are

crowded and small. UFMU is a low risk intervention with potential public health benefits.^{3 4} The results suggest that community face mask use is likely to be the most effective inside the household during severe epidemics.

Almost a quarter of family members became infected, and the findings suggest that the risk was highest either before symptom onset or early in the clinical illness, as most primary cases were hospitalised after diagnosis, and interventions were not effective if applied after symptom onset. In the univariate analysis, wearing a mask after illness onset was significant, but in multivariate analysis, only wearing it before symptom onset was effective. Viral load is highest in the 2 days before symptom onset and on the first day of symptoms, and up to 44% of transmission is during the pre-symptomatic period in settings with substantial household clustering.^{10 11} This supports UFMU, probably by reducing onward transmission from people in the pre-symptomatic phase of the illness^{12 13} as well as protecting well mask users. Randomised clinical trials of face masks in the household have confirmed protection against other respiratory viruses if compliant, if used within 36 hours of the primary case symptom onset, and alone or in combination with hand hygiene.^{14 15} This study now provides specific evidence for UFMU in settings of high epidemic growth to protect against COVID-19. In our study, 91.2% (103/113) of primary cases had a high score on hand hygiene, but it was not effective, confirming the results of previous randomised clinical trials which showed hand

Table 3 Characteristics of the residence and household practices: univariable analysis between two family groups

Residence and household practices	Total (n (%)) (n=121)	Families without transmission (n (%)) (n=81)	Families with transmission (n (%)) (n=40)	P value	Unadjusted OR (95% CI)
Residential area per capita (m ²) (median (IQR))	25.0 (17.3–35.0)	28.0 (18.0–35.8)	20.0 (16.9–31.8)	–	–
≤20	50 (41.3)	30 (37.1)	20 (50.0)	–	Ref
20–40	49 (40.5)	36 (44.4)	13 (32.5)	0.16	0.54 (0.23 to 1.27)
≥40	22 (18.2)	15 (18.5)	7 (17.5)	0.51	0.70 (0.24 to 2.02)
No of bedrooms per person (median (IQR))	0.7 (0.5–1.0)	0.7 (0.5–1.0)	0.7 (0.5–1.0)	–	–
≥1	39 (32.2)	28 (34.6)	11 (27.5)	–	Ref
<1	82 (67.8)	53 (65.4)	29 (72.5)	0.49	1.34 (0.59 to 3.08)
No of washrooms (median (IQR))	1 (1–2)	1 (1–2)	1 (1–2)	–	–
2 or more	34 (28.1)	23 (28.4)	11 (27.5)	–	Ref
1	87 (71.9)	58 (71.6)	29 (72.5)	0.87	1.07 (0.46 to 2.49)
Frequency of room cleaning (wet type)	–	–	–	–	–
Once in 1–2 days	83 (68.6)	59 (72.8)	24 (60.0)	–	Ref
Once in >2 days	38 (31.4)	22 (27.2)	16 (40.0)	0.11	1.90 (0.86 to 4.19)
Frequency of chlorine or ethanol based disinfectant use for house cleaning*	–	–	–	–	–
Once in 2 or more days	86 (71.1)	50 (61.7)	36 (90.0)	–	Ref
Once a day or more	35 (28.9)	31 (38.3)	4 (10.0)	0.003	0.18 (0.06 to 0.55)
Ventilation duration per day (hours) (median (IQR))†	2.0 (1.0–6.0)	3.0 (1.5–8.0)	1.8 (1.0–4.0)	–	–
>1	85 (70.2)	62 (76.5)	23 (57.5)	–	Ref
≤1	36 (29.8)	19 (23.5)	17 (42.5)	0.02	2.55 (1.14 to 5.70)

*When cleaning the house, disinfectant which contains chlorine or ethanol is used to disinfect the floor, door and window handles, indoor air, tables and toilets.

†Ventilation means the practice of opening the window to allow convection of indoor air.

Table 4 Risk factors for SARS-CoV-2 household transmission: multivariable analysis

Risk factor	Adjusted OR	95% CI	P value
Primary case has diarrhoea	–	–	–
No	–	–	Ref
Yes	4.10	(1.08 to 15.60)	0.04
Close contact at home with primary cases (within 1 m or 3 feet) (times)	–	–	–
0	–	–	Ref
1–3	3.30	(1.05 to 10.40)	0.04
≥4	18.26	(3.93 to 84.79)	< 0.001
No of family members (including primary case) wearing a mask at home before the primary case's illness onset date	–	–	–
None	–	–	Ref
1 or more	0.21	(0.06 to 0.79)	0.02
Frequency of chlorine or ethanol based disinfectant use for house cleaning	–	–	–
Once in 2 or more days	–	–	Ref
Once a day or more	0.23	(0.07 to 0.84)	0.03

hygiene alone did not protect against respiratory transmissible viruses, but masks combined with hand hygiene did have effect.¹⁶

As the compliance of UFMU would be poor in the home, there was difficulty and also no necessity for everyone to wear masks at home. We recommended that those families with members who were at risk of getting infected with SARS-CoV-2 (such as ever having contact with a COVID-19 patient, medical workers caring for a COVID-19 patient or having a history of travelling to high risk areas) should apply UFMU to reduce the risk of household transmission.

This study showed that social distancing within the home is effective and having close contact (within 1 m or 3 feet, such as eating around a table or sitting together watching TV) is a risk factor for transmission. The study also provides evidence of effectiveness of chlorine or ethanol based household disinfection in areas with high community transmission, or where one family member is a health worker, or where there is a risk of COVID-19, such as during home quarantine, consistent with advice provided by local health authorities or organisations.¹⁷ Diarrhoea as a symptom in the primary case is also a risk factor for SARS-CoV-2 transmission within families, which highlights the importance of disinfection of the bathroom and toilet, as well as closing the toilet lid when flushing to prevent aerosolisation of the virus.

Our study has limitations. Telephone interview has inherent limitations, including recall bias. It would take about 20 min to complete an interview, and 95% (118/124) of interviews were rated as informative by the interviewers. The evaluation results of mask wearing were reliable, but we did not collect data on the concentration of disinfectant used by families. The strengths of the study were that we had complete follow-up data and were able to accurately ascertain the incidence of secondary transmission in the cohort.

CONCLUSIONS

Household transmission in the pre-symptomatic or early symptomatic period of COVID-19 is a driver of epidemic growth and any measure aimed at reducing this can flatten the curve. This study reinforces the high risk of transmission in households but importantly shows that UFMU and hygiene measures can significantly reduce the risk of household transmission of COVID-19, independent of household size or crowding. This is the first study to show the effectiveness of precautionary mask use, social distancing and regular disinfection in the household, and can inform guidelines for prevention of household transmission. The results may also be informative for families of high risk groups, such as health workers, quarantined individuals or situations where cases of COVID-19 have to be managed at home.

Author affiliations

¹Institute for Infectious Disease and Endemic Disease Control, Beijing Center for Disease Prevention and Control, Beijing Research Center for Preventive medicine, Beijing, China

²State Key Laboratory of Remote Sensing Science, College of Global Change and Earth System Science, Beijing Normal University, Beijing, China

³Office of Beijing Center for Global Health, Beijing Center for Disease Prevention and Control, Beijing Research Center for Preventive medicine, Beijing, China

⁴Institute for nutrition and food hygiene, Beijing Center for Disease Prevention and Control, Beijing Research Center for Preventive medicine, Beijing, China

⁵Department of Environmental and Occupational Health, School of Public Health, University of Nevada, Las Vegas, Nevada, USA

⁶Arizona State University College of Health Solutions, Phoenix, Arizona, USA

⁷Kirby institute, Faculty of Medicine, the University of New South Wales, Sydney, New South Wales, Australia

Acknowledgements We thank the staff members in the district and municipal Centres for Disease Prevention and Control, and medical settings in Beijing for conducting field investigation, specimen collection, laboratory detection and case reporting. We also thank all patients and families involved in the study.

Contributors All authors approved the final draft of the manuscript. The corresponding authors attest that all listed authors meet authorship criteria and that no others meeting the criteria have been omitted.

Funding This work was supported by Beijing Science and Technology Planning Project (Z201100005420010).

Competing interests None declared.

Patient and public involvement Patients and/or the public were not involved in the design, or conduct, or reporting, or dissemination plans of this research.

Patient consent for publication Not required.

Provenance and peer review Not commissioned; externally peer reviewed.

Data availability statement No additional data available.

Open access This is an open access article distributed in accordance with the Creative Commons Attribution Non Commercial (CC BY-NC 4.0) license, which permits others to distribute, remix, adapt, build upon this work non-commercially, and license their derivative works on different terms, provided the original work is properly cited, appropriate credit is given, any changes made indicated, and the use is non-commercial. See: <http://creativecommons.org/licenses/by-nc/4.0/>.

REFERENCES

- 1 Tian H, Liu Y, Li Y, *et al*. An investigation of transmission control measures during the first 50 days of the COVID-19 epidemic in China. *Science* 2020;368:638–42.
- 2 Centers for Disease Control and Prevention. Recommendation regarding the use of cloth face coverings, especially in areas of significant community-based transmission. Available: <https://www.cdc.gov/coronavirus/2019-ncov/prevent-getting-sick/cloth-face-cover.html> [Accessed 15 Apr 2020].
- 3 Greenhalgh T, Schmid MB, Czypionka T, *et al*. Face masks for the public during the covid-19 crisis. *BMJ* 2020;369:m1435.
- 4 Javid B, Weekes MP, Matheso NJ. Covid-19: should the public wear face masks? Yes—population benefits are plausible and harms unlikely. *BMJ* 2020;369:m1442.
- 5 World Health Organization. Report of the WHO-China joint mission on coronavirus disease 2019 (COVID-19), 2020. Available: https://www.who.int/docs/default-source/coronaviruse/who-china-joint-mission-on-covid-19-final-report-1100hr-28feb2020-11mar-update.pdf?sfvrsn=1a13fda0_2 [Accessed 15 Apr 2020].
- 6 Yang HY, Xu J, Li Y, *et al*. [The preliminary analysis on the characteristics of the cluster for the COVID-19]. *Zhonghua Liu Xing Bing Xue Za Zhi* 2020;41:623–8.
- 7 National Health Commission. New coronavirus pneumonia prevention and control program (5th edition) (in Chinese). Available: <http://www.nhc.gov.cn/jkj/s3577/202002/a5d6f7b8c48c451c87dba14889b30147.shtml> [Accessed 15 Apr 2020].
- 8 Zhang YP, The Novel Coronavirus Pneumonia Emergency Response Epidemiology Team. The epidemiological characteristics of an outbreak of 2019 novel coronavirus diseases (COVID-19) — China, 2020. *China CDC Weekly* 2020;2:11322.

- 9 National Bureau of Statistics. China statistical Yearbook-2019 (in Chinese). Available: <http://www.stats.gov.cn/tjsj/ndsj/2019/indexch.htm> [Accessed 3 May 2020].
- 10 Wölfel R, Corman VM, Guggemos W, *et al*. Virological assessment of hospitalized patients with COVID-2019. *Nature* 2020. doi:10.1038/s41586-020-2196-x. [Epub ahead of print: 01 Apr 2020].
- 11 He X, Lau EHY, Wu P, *et al*. Temporal dynamics in viral shedding and transmissibility of COVID-19. *Nat Med* 2020;26:672–5.
- 12 Tong Z-D, Tang A, Li K-F, *et al*. Potential presymptomatic transmission of SARS-CoV-2, Zhejiang Province, China, 2020. *Emerg Infect Dis* 2020;26:1052–4.
- 13 Bai Y, Yao L, Wei T, *et al*. Presumed asymptomatic carrier transmission of COVID-19. *JAMA* 2020. doi:10.1001/jama.2020.2565. [Epub ahead of print: 21 Feb 2020].
- 14 MacIntyre CR, Cauchemez S, Dwyer DE, *et al*. Face mask use and control of respiratory virus transmission in households. *Emerg Infect Dis* 2009;15:233–41.
- 15 Cowling BJ, Chan K-H, Fang VJ, *et al*. Facemasks and hand hygiene to prevent influenza transmission in households: a cluster randomized trial. *Ann Intern Med* 2009;151:437–46.
- 16 Wong VWY, Cowling BJ, Aiello AE. Hand hygiene and risk of influenza virus infections in the community: a systematic review and meta-analysis. *Epidemiol Infect* 2014;142:922–32.
- 17 Centers for Disease Control and Prevention. Cleaning and disinfection for households: interim recommendations for U.S. households with suspected or confirmed coronavirus disease 2019 (COVID-19). Available: https://www.cdc.gov/coronavirus/2019-ncov/prevent-getting-sick/cleaning-disinfection.html?CDC_AA_refVal=https%3A%2F%2Fwww.cdc.gov%2Fcoronavirus%2F2019-ncov%2Fprepare%2Fcleaning-disinfection.html [Accessed 15 Apr 2020].

Presymptomatic Transmission of SARS-CoV-2 — Singapore, January 23–March 16, 2020

Wycliffe E. Wei, MPH^{1,2}; Zongbin Li, MBBS¹; Calvin J. Chiew, MPH¹; Sarah E. Yong, MMed¹; Matthias P. Toh, MMed^{2,3}; Vernon J. Lee, PhD^{1,3}

On April 1, 2020, this report was posted as an MMWR Early Release on the MMWR website (<https://www.cdc.gov/mmwr>).

Presymptomatic transmission of SARS-CoV-2, the virus that causes coronavirus disease 2019 (COVID-19), might pose challenges for disease control. The first case of COVID-19 in Singapore was detected on January 23, 2020, and by March 16, a total of 243 cases had been confirmed, including 157 locally acquired cases. Clinical and epidemiologic findings of all COVID-19 cases in Singapore through March 16 were reviewed to determine whether presymptomatic transmission might have occurred. Presymptomatic transmission was defined as the transmission of SARS-CoV-2 from an infected person (source patient) to a secondary patient before the source patient developed symptoms, as ascertained by exposure and symptom onset dates, with no evidence that the secondary patient had been exposed to anyone else with COVID-19. Seven COVID-19 epidemiologic clusters in which presymptomatic transmission likely occurred were identified, and 10 such cases within these clusters accounted for 6.4% of the 157 locally acquired cases. In the four clusters for which the date of exposure could be determined, presymptomatic transmission occurred 1–3 days before symptom onset in the presymptomatic source patient. To account for the possibility of presymptomatic transmission, officials developing contact tracing protocols should strongly consider including a period before symptom onset. Evidence of presymptomatic transmission of SARS-CoV-2 underscores the critical role social distancing, including avoidance of congregate settings, plays in controlling the COVID-19 pandemic.

Early detection and isolation of symptomatic COVID-19 patients and tracing of close contacts is an important disease containment strategy; however, the existence of presymptomatic or asymptomatic transmission would present difficult challenges to contact tracing. Such transmission modes have not been definitively documented for COVID-19, although cases of presymptomatic and asymptomatic transmissions have been reported in China (1,2) and possibly occurred in a nursing facility in King County, Washington (3). Examination of serial intervals (i.e., the number of days between symptom onsets in a primary case and a secondary case) in China suggested that 12.6% of transmission was presymptomatic (2). COVID-19 cases in Singapore were reviewed to determine whether presymptomatic transmission occurred among COVID-19 clusters.

The surveillance and case detection methods employed in Singapore have been described (4). Briefly, all medical practitioners were required by law to notify Singapore's Ministry of Health of suspected and confirmed cases of COVID-19. The definition of a suspected case was based on the presence of respiratory symptoms and an exposure history. Suspected cases were tested, and a confirmed case was defined as a positive test for SARS-CoV-2, using laboratory-based polymerase chain reaction or serologic assays (5). All cases in this report were confirmed by polymerase chain reaction only. Asymptomatic persons were not routinely tested, but such testing was performed for persons in groups considered to be at especially high risk for infection, such as evacuees on flights from Wuhan, China (6), or families that experienced high attack rates.

Patients with confirmed COVID-19 were interviewed to obtain information about their clinical symptoms and activity history during the 2 weeks preceding symptom onset to ascertain possible sources of infection. Contact tracing examined the time from symptom onset until the time the patient was successfully isolated to identify contacts who had interactions with the patient. All contacts were monitored daily for their health status, and those who developed symptoms were tested as part of active case finding.

Clinical and epidemiologic data for all 243 reported COVID-19 cases in Singapore during January 23–March 16 were reviewed. Clinical histories were examined to identify symptoms before, during, and after the first positive SARS-CoV-2 test.

Records of cases that were epidemiologically linked (clusters) were reviewed to identify instances of likely presymptomatic transmission. Such clusters had clear contact between a source patient and a patient infected by the source (a secondary patient), had no other likely explanations for infection, and had the source patient's date of symptom onset occurring after the date of exposure to the secondary patient who was subsequently infected. Symptoms considered in the review included respiratory, gastrointestinal (e.g., diarrhea), and constitutional symptoms. In addition, the source patient's exposure had to be strongly attributed epidemiologically to transmission from another source. This reduced the likelihood that an unknown source was involved in the cases in the cluster.

Summary**What is already known about this topic?**

Preliminary evidence indicates the occurrence of presymptomatic transmission of SARS-CoV-2, based on reports of individual cases in China.

What is added by this report?

Investigation of all 243 cases of COVID-19 reported in Singapore during January 23–March 16 identified seven clusters of cases in which presymptomatic transmission is the most likely explanation for the occurrence of secondary cases.

What are the implications for public health practice?

The possibility of presymptomatic transmission increases the challenges of containment measures. Public health officials conducting contact tracing should strongly consider including a period before symptom onset to account for the possibility of presymptomatic transmission. The potential for presymptomatic transmission underscores the importance of social distancing, including the avoidance of congregate settings, to reduce COVID-19 spread.

Seven Clusters of COVID-19 Cases Suggesting Presymptomatic Transmission

Investigation of COVID-19 cases in Singapore identified seven clusters (clusters A–G) in which presymptomatic transmission likely occurred. These clusters occurred during January 19–March 12, and involved from two to five patients each (Figure). Ten of the cases within these clusters were attributed to presymptomatic transmission and accounted for 6.4% of the 157 locally acquired cases reported as of March 16.

Cluster A. A woman aged 55 years (patient A1) and a man aged 56 years (patient A2) were tourists from Wuhan, China, who arrived in Singapore on January 19. They visited a local church the same day and had symptom onset on January 22 (patient A1) and January 24 (patient A2). Three other persons, a man aged 53 years (patient A3), a woman aged 39 years (patient A4), and a woman aged 52 years (patient A5) attended the same church that day and subsequently developed symptoms on January 23, January 30, and February 3, respectively. Patient A5 occupied the same seat in the church that patients A1 and A2 had occupied earlier that day (captured by closed-circuit camera) (5). Investigations of other attendees did not reveal any other symptomatic persons who attended the church that day.

Cluster B. A woman aged 54 years (patient B1) attended a dinner event on February 15 where she was exposed to a patient with confirmed COVID-19. On February 24, patient B1 and a woman aged 63 years (patient B2) attended the same singing class. Two days later (February 26), patient B1 developed symptoms; patient B2 developed symptoms on February 29.

Cluster C. A woman aged 53 years (patient C1) was exposed to a patient with confirmed COVID-19 on February 26 and likely passed the infection to her husband, aged 59 years (patient C2) during her presymptomatic period; both patients developed symptoms on March 5.

Cluster D. A man aged 37 years (patient D1) traveled to the Philippines during February 23–March 2, where he was in contact with a patient with pneumonia who later died. Patient D1 likely transmitted the infection to his wife (patient D2), aged 35 years, during his presymptomatic period. Both patients developed symptoms on March 8.

Cluster E. A man aged 32 years (patient E1) traveled to Japan during February 29–March 8, where he was likely infected, and subsequently transmitted the infection to his housemate, a woman aged 27 years (patient E2), before he developed symptoms. Both developed symptoms on March 11.

Cluster F. A woman aged 58 years (patient F1) attended a singing class on February 27, where she was exposed to a patient with confirmed COVID-19. She attended a church service on March 1, where she likely infected a woman aged 26 years (patient F2) and a man aged 29 years (patient F3), both of whom sat one row behind her. Patient F1 developed symptoms on March 3, and patients F2 and F3 developed symptoms on March 3 and March 5, respectively.

Cluster G. A man aged 63 years (patient G1) traveled to Indonesia during March 3–7. He met a woman aged 36 years (patient G2) on March 8 and likely transmitted SARS-CoV-2 to her; he developed symptoms on March 9, and patient G2 developed symptoms on March 12.

Investigation of these clusters did not identify other patients who could have transmitted COVID-19 to the persons infected. In four clusters (A, B, F, and G), presymptomatic transmission exposure occurred 1–3 days before the source patient developed symptoms. For the remaining three clusters (C, D, and E), the exact timing of transmission exposure could not be ascertained because the persons lived together, and exposure was continual.

Discussion

This investigation identified seven clusters of COVID-19 in Singapore in which presymptomatic transmission likely occurred. Among the 243 cases of COVID-19 reported in Singapore as of March 16, 157 were locally acquired; 10 of the 157 (6.4%) locally acquired cases are included in these clusters and were attributed to presymptomatic transmission. These findings are supported by other studies that suggest that presymptomatic transmission of COVID-19 can occur (1–3). An examination of transmission events among cases in Chinese patients outside of Hubei province, China, suggested that

FIGURE. Seven COVID-19 clusters with evidence of likely presymptomatic SARS-CoV-2 transmission from source patients to secondary patients — Singapore, January 19–March 12, 2020

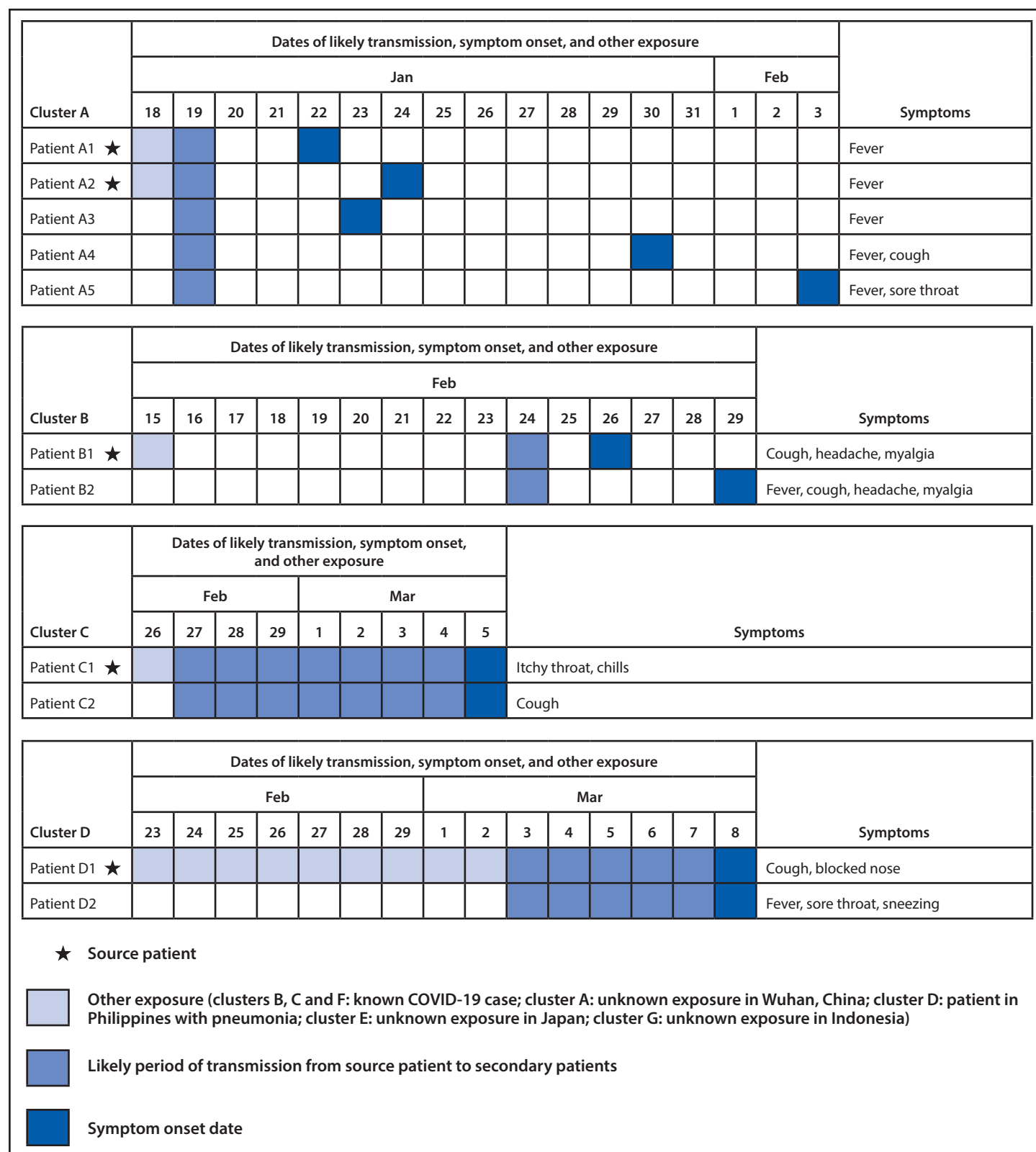


FIGURE. (Continued) Seven COVID-19 clusters with evidence of likely presymptomatic SARS-CoV-2 transmission from source patients to secondary patients — Singapore, January 19–March 12, 2020

Cluster E	Dates of likely transmission, symptom onset, and other exposure											Symptoms	
	Feb	Mar											
	29	1	2	3	4	5	6	7	8	9	10		11
Patient E1 ★													Fever
Patient E2													Cough

Cluster F	Dates of likely transmission, symptom onset, and other exposure								Symptoms
	Feb			Mar					
	27	28	29	1	2	3	4	5	
Patient F1 ★									Sore throat, blocked nose
Patient F2									Cough
Patient F3									Cough, runny nose, sore throat, myalgia

Cluster G	Dates of likely transmission, symptom onset, and other exposure										Symptoms
	Mar										
	3	4	5	6	7	8	9	10	11	12	
Patient G1 ★											Fever
Patient G2											Sore throat

★

Source patient

Other exposure (clusters B, C and F: known COVID-19 case; cluster A: unknown exposure in Wuhan, China; cluster D: patient in Philippines with pneumonia; cluster E: unknown exposure in Japan; cluster G: unknown exposure in Indonesia)

Likely period of transmission from source patient to secondary patients

Symptom onset date

12.6% of transmissions could have occurred before symptom onset in the source patient (3).

Presymptomatic transmission might occur through generation of respiratory droplets or possibly through indirect transmission. Speech and other vocal activities such as singing have been shown to generate air particles, with the rate of emission corresponding to voice loudness (7). News outlets have reported that during a choir practice in Washington on March 10, presymptomatic transmission likely played a role in SARS-CoV-2 transmission to approximately 40 of 60 choir members.*

*<https://www.latimes.com/world-nation/story/2020-03-29/coronavirus-choir-outbreak>.

Environmental contamination with SARS-CoV-2 has been documented (8), and the possibility of indirect transmission through fomites by presymptomatic persons is also a concern. Objects might be contaminated directly by droplets or through contact with an infected person's contaminated hands and transmitted through nonrigorous hygiene practices.

The possibility of presymptomatic transmission of SARS-CoV-2 increases the challenges of COVID-19 containment measures, which are predicated on early detection and isolation of symptomatic persons. The magnitude of this impact is dependent upon the extent and duration of transmissibility while a patient is presymptomatic, which, to date, have

not been clearly established. In four clusters (A, B, F, and G), it was possible to determine that presymptomatic transmission exposure occurred 1–3 days before the source patient developed symptoms. Such transmission has also been observed in other respiratory viruses such as influenza. However, transmissibility by presymptomatic persons requires further study.

The findings in this report are subject to at least three limitations. First, although these cases were carefully investigated, the possibility exists that an unknown source might have initiated the clusters described. Given that there was not widespread community transmission of COVID-19 in Singapore during the period of evaluation and while strong surveillance systems were in place to detect cases, presymptomatic transmission was estimated to be more likely than the occurrence of unidentified sources. Further, contact tracing undertaken during this period was extensive and would likely have detected other symptomatic cases. Second, recall bias could affect the accuracy of symptom onset dates reported by cases, especially if symptoms were mild, resulting in uncertainty about the duration of the presymptomatic period. Finally, because of the nature of detection and surveillance activities that focus on testing symptomatic persons, underdetection of asymptomatic illness is expected. Recall bias and interviewer bias (i.e., the expectation that some symptoms were present, no matter how mild), could have contributed to this.

The evidence of presymptomatic transmission in Singapore, in combination with evidence from other studies (9,10) supports the likelihood that viral shedding can occur in the absence of symptoms and before symptom onset. This study identified seven clusters of cases in which presymptomatic transmission of COVID-19 likely occurred; 10 (6.4%) of such cases included in these clusters were among the 157 locally acquired cases reported in Singapore as of March 16. Containment measures should account for the possibility of presymptomatic transmission by including the period before symptom onset when conducting contact tracing. These findings also suggest that to control the pandemic it might not be enough for only persons with symptoms to limit their contact with others because persons without symptoms might transmit infection. Finally, these findings underscore the importance of social distancing

in the public health response to the COVID-19 pandemic, including the avoidance of congregate settings.

Corresponding author: Vernon J. Lee, Vernon_Lee@moh.gov.sg.

¹Ministry of Health, Singapore; ²National Centre for Infectious Diseases, Singapore; ³Saw Swee Hock School of Public Health, Singapore.

All authors have completed and submitted the International Committee of Medical Journal Editors form for disclosure of potential conflicts of interest. No potential conflicts of interest were disclosed.

References

1. Qian G, Yang N, Ma AHY, et al. A COVID-19 Transmission within a family cluster by presymptomatic infectors in China. *Clin Infect Dis* 2020. Epub March 23, 2020. <https://doi.org/10.1093/cid/ciaa316>
2. Du Z, Xu X, Wu Y, Wang L, Cowling BJ, Meyers LA. Serial interval of COVID-19 among publicly reported confirmed cases. *Emerg Infect Dis* 2020. Epub March 19, 2020. <https://doi.org/10.3201/eid2606.200357>
3. Kimball A, Hatfield KM, Arons M, et al. Asymptomatic and presymptomatic SARS-CoV-2 infections in residents of a long-term care skilled nursing facility—King County, Washington, March 2020. *MMWR Morb Mortal Wkly Rep* 2020. Epub March 27, 2020. <https://doi.org/10.15585/mmwr.mm6913e1>
4. Ng Y, Li Z, Chua YX, et al. Evaluation of the effectiveness of surveillance and containment measures for the first 100 patients with COVID-19 in Singapore—January 2–February 29, 2020. *MMWR Morb Mortal Wkly Rep* 2020;69:307–11. <https://doi.org/10.15585/mmwr.mm6911e1>
5. Pung R, Chiew CJ, Young BE, et al.; Singapore 2019 Novel Coronavirus Outbreak Research Team. Investigation of three clusters of COVID-19 in Singapore: implications for surveillance and response measures. *Lancet* 2020;395:1039–46. [https://doi.org/10.1016/S0140-6736\(20\)30528-6](https://doi.org/10.1016/S0140-6736(20)30528-6)
6. Ng O-T, Marimuthu K, Chia P-Y, et al. SARS-CoV-2 infection among travelers returning from Wuhan, China. *N Engl J Med* 2020. Epub March 12, 2020. <https://doi.org/10.1056/NEJMc2003100>
7. Asadi S, Wexler AS, Cappa CD, Barreda S, Bouvier NM, Ristenpart WD. Aerosol emission and superemission during human speech increase with voice loudness. *Sci Rep* 2019;9:2348. <https://doi.org/10.1038/s41598-019-38808-z>
8. Ong SWX, Tan YK, Chia PY, et al. Air, surface environmental, and personal protective equipment contamination by severe acute respiratory syndrome coronavirus 2 (SARS-CoV-2) from a symptomatic patient. *JAMA* 2020. Epub March 4, 2020. <https://doi.org/10.1001/jama.2020.3227>
9. Hu Z, Song C, Xu C, et al. Clinical characteristics of 24 asymptomatic infections with COVID-19 screened among close contacts in Nanjing, China. *Sci China Life Sci* 2020. Epub March 4, 2020. <https://doi.org/10.1007/s11427-020-1661-4>
10. Wang Y, Liu Y, Liu L, Wang X, Luo N, Ling L. Clinical outcome of 55 asymptomatic cases at the time of hospital admission infected with SARS-Coronavirus-2 in Shenzhen, China. *J Infect Dis* 2020. Epub March 17, 2020. <https://doi.org/10.1093/infdis/jiaa119>

Review

A Comparative Analysis of Factors Influencing Two Outbreaks of Middle Eastern Respiratory Syndrome (MERS) in Saudi Arabia and South Korea

Marnie Willman ^{1,2} , Darwyn Kobasa ^{1,2}  and Jason Kindrachuk ^{2,*} 

¹ High Containment Respiratory Viruses, Special Pathogens, Public Health Agency of Canada, Winnipeg, MB R3E 3R2, Canada; hustinsm@myumanitoba.ca (M.W.); darwyn.kobasa@canada.ca (D.K.)

² Department of Medical Microbiology, University of Manitoba, Winnipeg, MB R3E 0J9, Canada

* Correspondence: Jason.Kindrachuk@umanitoba.ca; Tel.: +1-204-789-3807

Received: 6 November 2019; Accepted: 2 December 2019; Published: 3 December 2019



Abstract: In 2012, an emerging viral infection was identified in Saudi Arabia that subsequently spread to 27 additional countries globally, though cases may have occurred elsewhere. The virus was ultimately named Middle Eastern Respiratory Syndrome Coronavirus (MERS-CoV), and has been endemic in Saudi Arabia since 2012. As of September 2019, 2468 laboratory-confirmed cases with 851 associated deaths have occurred with a case fatality rate of 34.4%, according to the World Health Organization. An imported case of MERS occurred in South Korea in 2015, stimulating a multi-month outbreak. Several distinguishing factors emerge upon epidemiological and sociological analysis of the two outbreaks including public awareness of the MERS outbreak, and transmission and synchronization of governing healthcare bodies. South Korea implemented a stringent healthcare model that protected patients and healthcare workers alike through prevention and high levels of public information. In addition, many details about MERS-CoV virology, transmission, pathological progression, and even the reservoir, remain unknown. This paper aims to delineate the key differences between the two regional outbreaks from both a healthcare and personal perspective including differing hospital practices, information and public knowledge, cultural practices, and reservoirs, among others. Further details about differing emergency outbreak responses, public information, and guidelines put in place to protect hospitals and citizens could improve the outcome of future MERS outbreaks.

Keywords: coronavirus; Middle East Respiratory Syndrome (MERS), zoonosis; Middle East; Saudi Arabia; South Korea

1. Introduction

Infectious diseases pose a significant risk to the global population. The reasons behind their appearance, and how outbreaks differ are of notable interest to epidemiologists and public health professionals. Coronaviruses in particular have become a global health threat following the emergence of severe acute respiratory syndrome coronavirus (SARS-CoV) and Middle East respiratory syndrome coronavirus (MERS-CoV). While human CoVs do circulate causing mild disease year-to-year, SARS-CoV differed in its rapidity and zoonotic origin, in addition to its ability to cause severe disease [1]. SARS-CoV was the first epidemic coronavirus in decades, as well as the first highly pathogenic CoV discovered, when it appeared in Asia in 2002 [2]. This outbreak was swiftly controlled and came to an end within 8 months, in part because of excellent containment policies, limited contact between humans and the putative reservoir host, and efficient use of social media to educate affected populations on containment and protection procedures [3]. However, ten years later, a new related coronavirus emerged in Saudi Arabia in 2012, and despite the success in controlling the SARS epidemic, the new respiratory virus

Viruses 2019, 11, 1119 FOR PEER REVIEW 2 of 13
 has become an endemic problem in the Middle East. MERS-CoV has since spread to over 27 countries in Europe, North Africa, and the Middle East [4]. The global transmission of MERS-CoV is outlined in Figure 1. MERS-CoV has since spread to over 27 countries in Europe, North Africa, and the Middle East [4]. The global transmission of MERS-CoV is outlined in Figure 1.

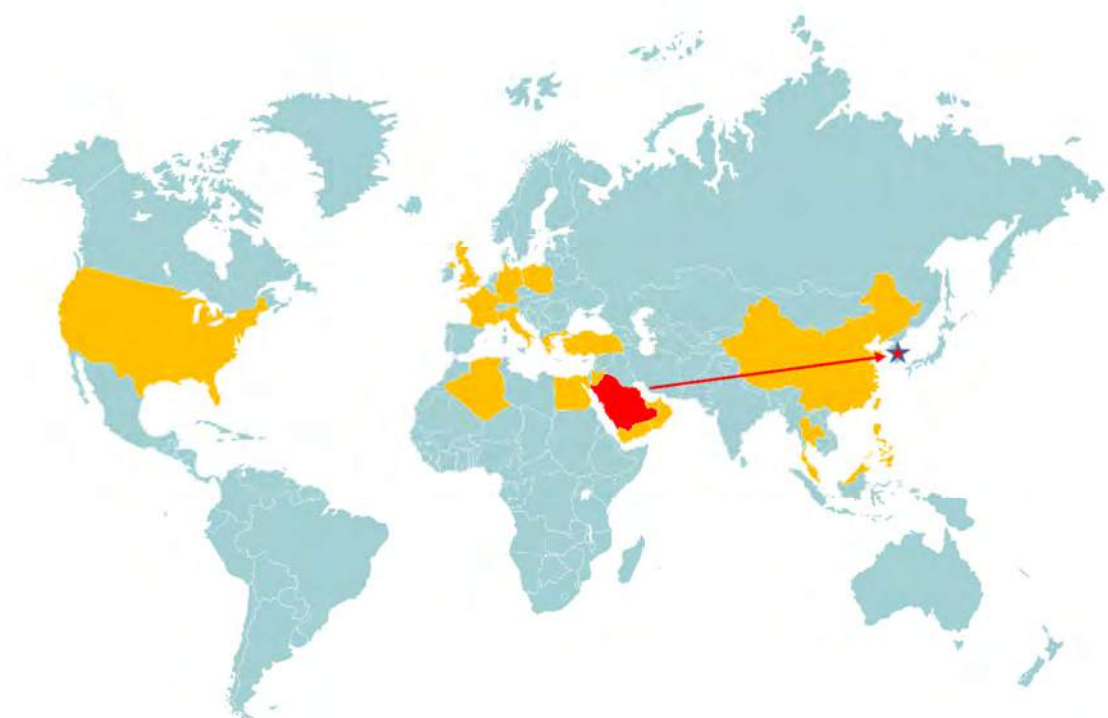


Figure 1. Global distribution of MERS-CoV outbreaks from 2012–2019. Data includes all documented occurrences of disease, including imported, nosocomial, and community cases. Highlighted in orange are countries with past or present MERS-CoV cases, while the countries of interest for the purposes of this paper, Saudi Arabia and South Korea, are shown in red. The direct importation of MERS-CoV from Saudi Arabia to South Korea is shown in red, stimulating the 2015 outbreak. Global maps were derived and/or modified from Servier Medical Art under a Creative Commons Attribution 3.0 Unported License.

In contrast to the short-lived SARS outbreak, MERS has become an endemic disease in many countries around the Middle East sustained by direct reservoir transmission leading to nosocomial infections and eventual transmission back to surrounding communities [3]. Given that MERS-CoV-like viruses have been isolated from masked palm civets, bats, and camels, these are considered some of the many reservoirs of the virus, which sustain transmission in humans and animals [2]. In fact, MERS-CoV has been detected in camels dating back several decades, and likely was endemic before it was detected by epidemiologists in 2012, as the majority of infected animals show mild or no symptoms [5]. Infection in dromedaries can result in either asymptomatic or symptomatic disease, while bats carrying SARS-like coronavirus have historically been asymptomatic [4]. Asymptomatic hosts and reservoirs can spread disease, and SARS-like coronavirus may be asymptomatic [4]. As of September 2019, 2468 laboratory-confirmed cases with 851 associated deaths have occurred with a case fatality rate of 34.4%. According to the World Health Organization (WHO) [6], here, we review differences between two geographically distinct MERS-CoV outbreaks, one short lived outbreak occurring in South Korea in 2015, and the other, an endemic MERS-CoV outbreak that has persisted in Saudi Arabia since 2013 [7,8]. We will discuss the contributions of transmission differences, potential reservoirs, containment practices, isolation procedures, levels of public education, and clinical detection and monitoring to the outcome of the outbreaks in this review.

2. MERS-CoV Virology

2. MERS-CoV Virology

MERS-CoV is a betacoronavirus with a positive, single stranded RNA genome of 27.9kb [9]. The viral structure consists of a small enveloped spherical virion, measuring approximately 90–120nm [10,11]. The MERS-CoV genome encodes two polyproteins (pp1ab and pp1b) and nested subgenomic mRNAs [2,9]. The genome of the virion is contained within the nucleocapsid, and which is responsible for RNA binding, synthesis, and translation [9]. This is surrounded by the host-derived envelope, containing the four structural proteins, spike (S), nucleocapsid (N), membrane (M), and envelope (E) [12]. The genome also encodes four nonstructural proteins (ns) in ORFs 3, 4a, 4b, and 5, which have vital functions to the virus life cycle [9,12]. The S protein is of particular interest, as it mediates virus attachment to the host cell through interaction with the dipeptidyl peptidase-4 (DPP4) receptor resulting in viral uptake [8]. In most cases, CoV S proteins are cleaved by furin-like proteases of the host into active subunits [10]. Thus, the MERS-CoV S protein is being investigated for the development of antivirals and therapeutics because of its vital role in infection and pathogenesis [13,14].

Attachment of the MERS-CoV virion to the target cell is initiated by the binding of the S1 subunit of the S protein to DPP4, which triggers conformational changes in the S2 subunit, beginning the process of fusion to the target cell [10,15]. MERS CoV was the only CoV shown to use DPP4 to gain entry to host cells [15]. Like many viruses, CoVs utilize proteases such as transmembrane protease, serine 2 (TMPRSS2) and cathepsin to activate the S protein following fusion of the viral envelope and host cell membrane [16]. This multi-step process of the S protein at multiple cleavage sites exposes the fusion peptide, stimulating the fusion process inside acidified endosomes [10]. Within the endosome, MERS-CoV disassembles, releasing the inner genomic material into the cytoplasm [15]. Once inside the cell, transcription in the cytoplasm and RNA replication in the cytoplasm proceed. During this time, coronaviruses in general, including MERS-CoV, are readily able to undergo homologous and non-homologous recombination, leading to higher rates of viral evolution and new subtypes [16]. The replication-transcription complex is formed by further protease cleavage of polyproteins pp1a and pp1ab producing nsp1 and nsp16 template genomic RNA, generating the replication complexes required for transcription and translation [17]. Viral structural and accessory proteins are translated from subgenomic co-terminal mRNAs by replication-transcription complex-mediated transcription of a full-length positive genomic RNA [15,17]. The viral envelope is added to the virion during assembly at the endoplasmic reticulum and Golgi apparatus. During assembly at the Golgi apparatus of the host cell, the S, E, and M proteins are brought together at a “budding compartment”, where the M protein likely forms the basic structure and final viral complex [10]. The fully assembled, active virion is then exocytosed to the extracellular compartment and budded from the host cell.

3. Clinical Manifestations and Diagnosis of MERS-CoV

Following exposure, the incubation period for MERS-CoV is 4–8 days [18,19]. MERS has been shown to display clusters of human-to-human direct transmission, but the R_0 , also known as the basic reproduction number, or number of people a single infected individual can in turn infect, of these events is low, typically less than 1 [20]. This makes the target of prevention a combination of reducing transmission by reservoir hosts, as well as controlling spread within a hospital or community environment. Transmission occurs primarily via dromedary camels, a large source of interaction for Middle Eastern populations [21–23].

In addition to infection of immunocompetent people, immunocompromised populations have increased susceptibility to MERS-CoV. Infection begins with symptoms that are remarkably similar to a cold, but may progress to gastrointestinal symptoms, myalgia, shortness of breath, general malaise, abdominal pain, wheezing, palpitations, and confusion [20,22–24]. Severe disease can result in hospitalization and is associated with acute respiratory distress syndrome (ARDS, a severe respiratory disease resulting from widespread sepsis), lung injury, and requirement of mechanical ventilation due to respiratory failure. Abnormal chest examination results are also commonly noted such as inflammatory lung infiltrates, alveolar collapse, or interstitial thickening of the lung lining [25].

Follow-up chest radiographs of laboratory-confirmed positive individuals have shown lung fibrosis, and pleural thickening [26]. Blood tests of these patients also showed elevated lactate dehydrogenase levels after recovery.

Once the patient has begun showing symptoms, diagnosis presents several distinct challenges. The gold standard for diagnosis of an active MERS-CoV infection is by Real Time Polymerase Chain Reactions (RT-PCR), confirming viral identity by using a well-annotated gene such as the nucleocapsid [27]. While whole blood and plasma can also show active infection of MERS-CoV, respiratory samples are typically used for nucleic acid-based tests and utilize RNA extracted from nasopharyngeal swabs, bronchoalveolar lavage, and tracheal aspirates, among others [27]. After active infection, individuals may be examined for seroconversion suggestive of MERS-CoV infection or exposure. Serology tests include Enzyme-Linked Immunosorbant Assay (i.e., ELISA), and whole virus indirect fluorescent antibody (IFA) testing [27]. Many of these isolation and identification methods begin with a viral culture grown from a clinical isolate (i.e., sputum or respiratory samples isolated from the patient), elongating the wait time for results. This long wait period makes these current diagnostics laborious and time-consuming, precluding rapid turnaround of results, which is more problematic for severely ill patients and poses further problems for nosocomial transmission. Serology tests can detect antibodies present due to previous infections, but this is less useful to identify an active infection [27,28]. Patients who have been actively infected with MERS-CoV could be tested again post-infection and documented for seroconversion, which would be helpful for contact tracing as well as future epidemiological tracking and surveillance. PCR detection and serology testing are vital components to outbreak management and epidemiological tracking, by showing infection patterns and identifying potential risk factors, which can be used by health policy makers or for disease tracking during future outbreaks. However, concerns have been raised regarding the lack of standardization of sample collection, analysis, and data availability post-outbreak, which contribute to the previously discussed information gap in MERS epidemiological analyses [29].

In the midst of an outbreak, diagnostic assay results can be back within hours, however typically, it can take significantly longer for the result to reach the attending physician during an outbreak. This means positive individuals can be left unchecked for hours to days, continuing to transmit the virus before steps are taken to quarantine and isolate them. Close contact with saliva, mucus, respiratory droplets released by coughing and sneezing, and other infected bodily fluids can transmit MERS-CoV [6].

4. MERS-CoV Ecology and Transmission

MERS-CoV was first identified in 2012 following the death of a 60-year old male from a novel respiratory virus in Saudi Arabia [30]. While MERS initially seemed to be extremely similar to its relative, SARS, the condition showed a number of differences from the start of the outbreak. Two immediately noted differences were the incubation period and reservoir transmission. The median incubation period of MERS-CoV infection is 5 days, with the average time from onset of symptoms to hospitalization of approximately 4 days [18]. However, this number varies within the literature, depending on the model utilized. Small samples size can also be a problem in this instance, from lack of documentation or records available. In contrast, SARS exhibited an incubation time of at most 10 days, with symptom onset occurring during this time, averaging 2–7 days post-exposure [28].

In addition to the length of the incubation period, another difference between MERS-CoV and SARS-CoV lies in the animal reservoir. The animal reservoir for SARS-CoV was suspected to be bats, living in large numbers in the forested area behind rural communities in SARS affected areas [8,31,32]. After the initial introduction in Hong Kong, the SARS-CoV outbreak was sustained by human-to-human transmission [28]. While MERS-like viruses have been isolated from bats, MERS-CoV is primarily transmitted by dromedary camels, a commonly farmed and heavily used animal in the Saudi Arabian region, have been suggested to be a reservoir of the virus [3,9]. However, the primary reservoir remains officially unknown. While dromedary camels can transmit the virus and be asymptomatic carriers,

many suggest that it originated in a similar manner to SARS-CoV in the bat population, and has spilled over to many animals, including camels, which are far more difficult to remove from human populations and contact [20,33]. In fact, less commonly cited animals such as llamas, pigs, horses, and sheep have been found to carry the virus in their nasal passages, and have been suggested to also be capable of being potential reservoirs [33]. This presents further problems for transmission, as many potential reservoirs are in daily contact with Middle Eastern populations.

In addition to animal-origin transmission, there are also many documented cases of nosocomial MERS-CoV infection and transmission, occasionally as a result of overcrowding and inadequate infection control measures [21]. Given that this virus is most commonly spread by respiratory droplets from infected individuals, this is not a surprising finding. While the majority of participants in a recent Saudi Arabian study among medical students were aware that infection prevention was ideally through wearing face masks and public information, 53% of participants were unaware of infection control isolation policies in their hospitals, if an outbreak arose [34]. Furthermore, nosocomial transmission is made worse by the presence of MERS-CoV “superspreaders”, who transmit the disease at a significantly higher rate than the average host [35]. There are a number of factors that can affect the interpretation of a “superspreader”, such as nearby immunodeficient patients, sharing of healthcare tools and staff, and poor hygiene in the environment. In a recent study, approximately 33.3% of laboratory-confirmed positive hospital patients were found to be superspreaders [35]. Household transmission occurred in 13–21% of cases, making nosocomial transmission and community/reservoir infections the primary targets for prevention [2].

5. MERS-CoV Pathogenesis and Clinical Manifestations

While the studies of infection control and superspreaders are all relevant to the investigation of MERS-CoV outbreaks and how they occur, there is little information available regarding pathogenesis and previous patient test results, ranging from blood tests and cytokine studies to disease progression. Many of these barriers are linked to two problems, the first being limited post-mortem findings due to religious and cultural beliefs held in the Middle Eastern regions where the outbreaks began [15]. The second is lack of publication of data and results from sample analysis of specimens from laboratory-confirmed positive patients on a global scale. The primary source of information regarding pathologies associated with MERS-CoV and disease progression come from medical imaging, which are few and open to interpretation. This gap in information makes current diagnostic trends, infection patterns, and transmission maps only partially complete, making full interpretation difficult for future infectious disease outbreaks.

The S protein of MERS-CoV targets DPP4 to access human cells [10]. DPP4 is plentiful in the respiratory tract of humans including the bronchial mucosa, but is also expressed in a variety of tissues such as bronchial epithelial cells and kidney cells [36]. This is why renal impairment is a common physiological symptom of infection in addition to lung pathologies [6,37]. However, comorbidities are extremely common in severe cases of MERS-CoV, and documentation of timing of occurrences in the literature is unclear. Therefore, more work in this area is needed before extra-pulmonary symptoms are definitively linked to severe MERS-CoV. Several studies have also shown downregulation causes severe lung pathologies in CoV models of infection, and impairment in cardiovascular health in general [38,39]. Further, progression to ARDS and subsequent cytokine expansion, including IL-8 and 6, CXCL10, and CCL2, and complications such as pulmonary fibrosis, neovascularization, and congestive heart failure due to bilateral pulmonary infiltrates have been noted for infections [2,40]. Lack of availability of samples and tests as previously described has led to a serious lack of information surrounding MERS-CoV pathogenesis, which is crucial to improving healthcare practices during an outbreak. This gap in information due to differences in testing, sample collection, and lack of standardization of collection between countries further contributes to the problem [29].

6. Introduction to the 2013 Saudi Arabian and 2015 South Korean MERS Outbreaks

Containment and clinical management of MERS presents a complicated challenge due to multiple aspects including cultural, social and healthcare practice issues. During the SARS epidemic, the quick end of the outbreak was partially attributed to efficient quarantine and isolation methods, in addition to public awareness and information distribution to affected areas [41]. This included where to seek medical attention and protective measures individuals could take to protect themselves from infection, such as face masks. In the case of MERS, there is a belief that lack of knowledge among medical staff and affected communities could be a risk factor for disease containment [34]. With a combination of hospital and community outbreaks, many have suggested that stronger implementation of proper decontamination procedures could reduce outbreak severity and length [8,42]. It has been suggested that overcrowding, and slow isolation of patients in addition to these factors may have played a role in healthcare-associated outbreaks of MERS [29].

Since 2013, MERS-CoV infections have continued to be a long-term problem for healthcare professionals across Saudi Arabia. However, the same cannot be said for a relatively short outbreak that occurred in South Korea in 2015. The South Korean outbreak was imported by a 68-year old man who had recently travelled to Saudi Arabia, where he contracted MERS, and subsequently transmitted the virus throughout a South Korean hospital following admission [43–45]. In addition, the infected patient did travel through a number of hospitals throughout his travels, likely transmitting the virus to several institutions along the way [46]. What led to the differences in handling, information availability, and ultimately severity of the outbreak in South Korea compared to the ongoing efforts in Saudi Arabia are still a topic of debate. Previous findings have suggested transmission of MERS-CoV in this case was largely determined by the number of personal contacts with the patient, and patient infectivity [47].

The case fatality rate varied significantly during the South Korean outbreak, seeing the highest spike during October 2015, with an overall case fatality rate of 21% with 39 deaths [35,45]. This was slightly lower than the mean case fatality rate of the Saudi Arabian outbreak, which has been estimated to range from 36–46% between 2012 and 2014 [48,49]. The South Korean outbreak began with a single infected individual, and lasted only 2 months, with the government declaring the epidemic over on July 6 2015 [50]. In contrast, the Saudi Arabian outbreak was maintained by a zoonotic source, which sustained the outbreak for over 6 years [51]. Comparisons are highlighted in Table 1.

6.1. Aspect 1 – Public Information and Quarantine/Isolation Practices

One major difference between the Saudi Arabian and South Korean outbreaks is the initial response by the population to declaration of the outbreak, on behalf of their government body. In Saudi Arabia, poor access to healthcare professionals at a hospital and General Practitioner level can result in delays between disease development and progression, and diagnosis or quarantine in a hospital facility [52,53]. As the Saudi Arabian outbreak continued, many individuals who relied on camels for daily living or livelihood denied the correlation between camels and MERS-CoV infections, kicking off the Kiss Your Camel campaign, which became increasingly popular in Social Media in 2015 [54]. The contribution of this to the outbreak remains unclear, but it is a prime example of the negative general reaction to the outbreak. Because of the structure of the Saudi Arabian healthcare system and lack of preparedness for an infectious disease outbreak, panic quickly followed the announcement of the outbreak, leading to the dismissal of the Saudi Arabian Health Minister, Abdullah al-Rabeeah [55]. Confusion about the outbreak and lack of coordination and organization by hospitals and healthcare centers led to loss of control and lack of public information, which further exacerbated the outbreak.

The South Korean outbreak was met with a very different mindset, with the SARS outbreak still fresh in the minds of many older adults. While the index patient denied he had travelled to Saudi Arabia, many citizens of South Korea were more open about their condition and travel during subsequent contact tracing and had a good relationship with the health care professionals in their community [56]. This is due to better universal health coverage, and flexibility to choose health care professionals compared to Saudi Arabia, where the government has more restrictions and involvement

in healthcare decisions [56,57]. From the beginning of the outbreak, South Korean patients who were MERS-positive sought and embraced medical attention much faster than did Saudi Arabian patients [58]. However, this brings about the previously discussed problem of visiting a variety of healthcare environments prior to diagnosis, exacerbating spread.

Table 1. Highlighting key social and public health differences between the 2012 Saudi Arabian and 2015 South Korean MERS outbreaks. Differences in lifestyle of citizens, personal belief systems, and healthcare response to the outbreak are all suspected to have influenced the duration of the outbreak, and the final death toll.

	Saudi Arabia	South Korea
Outbreak Timeline	2013-present	May-July 2015
Type of Outbreak	Endemic	Imported
Patient 0	60-year old resident	68-year old traveller
Case Fatality Rate	36–46%	21%
Estimated Death Toll	>400	39
Primary Source of Infection	Dromedary camels and livestock	Nosocomial
Common Nutrition Source	Dromedary camel milk and meat [59–61]	Rice, pork, and beef
Public Education During Outbreak	Poor	Good
Regulatory Boards in Place	RRT (rapid response team)	MERS-CoV Infection Prevention and Control Guideline Development Committee
Implementation of Education and Regulatory Measures	Poor, conflicted among boards	Good, standardized
Isolation/Sanitation Techniques Employed in Hospitals	Information Unavailable	Mandatory masks, gloves, gowns for visitors and staff
Government Involvement in Healthcare	High	Low
Media Coverage, Globally	High	Low

Whether due to the prior experiences of the SARS epidemic or different healthcare standards, the other unpublicized but important difference between these outbreaks was the access to information for those who may have contracted, or been in direct contact with, MERS-CoV. The South Korean outbreak had stringent decontamination and isolation practices instilled in hospitals very soon after the onset of the outbreak, such as intra-hospital isolation, mandatory masks, gloves, and gowns for workers and visitors, and rapid laboratory assessments to confirm cases [43]. By July 2015, the MERS-CoV Infection Prevention and Control Guideline Development Committee was assembled and gathered in South Korea, joined by the Korean Society of Infectious Diseases, the Korean Society of Healthcare-associated Infection, and the Korean Association of Infection Control Nurses, in a serious effort to stop nosocomial and community transmission through public information and proper isolation and decontamination procedures in hospitals [43–45]. This helped to regulate, monitor, and standardize the effort to reduce and eventually stop cases within hospitals and the surrounding community.

6.2. Aspect 2 – Personal and Cultural Belief Systems

While Saudi Arabian officials did put in place a Rapid Response Team (RRT) to combat the outbreak, a 2017 study found that, even several years after implementation, many interviewed Health Care Workers, nurses, and other hospital support staff were not fully compliant with these guidelines, putting themselves and patients at risk for MERS-CoV infections [58]. The general feeling of Saudi Arabian workers and citizens was largely that MERS was not a substantial problem, and holes in

primary care practices in addition to spread by dromedaries and humans alike in the population contributed to the continuing epidemic in the Saudi Arabian region.

In addition, a 2018 Saudi Arabian study found that many medical professionals working in hospitals with MERS-CoV infected patients were unaware of how the disease spreads, with only 25% of respondents realizing that close contact with an infected patient effectively transmits disease [36]. South Korea on the other hand, quickly implemented strict quarantine countermeasures for patients entering the hospital system [19]. This made a substantial difference in being able to counteract and reduce the number of hospital-acquired infections, sequestering outbreaks before they reached an unmanageable level.

A problem noted previously among South Korean hospital and clinic settings is visiting multiple doctors before being admitted to hospital [50]. By requiring multiple visits to multiple healthcare locations, the patient exposes many other patients who are also compromised by other ailments to the virus. For example, in the index South Korean patient's case, symptom presentation was 11 May, but it wasn't until 20 May that a diagnosis was confirmed [50]. During this time, the patient visited several outpatient clinics and healthcare environments, further contributing to viral spread.

Another contributing factor falls into the category of cultural belief systems. In a 6-country iPhone survey done in the Middle East (including hotspots of MERS-CoV outbreaks), investigators found that two-thirds of the nearly 2000 participants responded as "not concerned" or "slightly concerned" about contracting MERS [58]. Approximately 40% of those participants cited religious convictions as their reason for lack of concern. As previously discussed, cultural beliefs and practices in the Saudi Arabian region have likely contributed to incomplete containment of the outbreak, including attitudes toward personal protection and limited autopsy and post-mortem test results from Middle Eastern fatalities.

6.3. Aspect 3 – Sustained Transmission of MERS-CoV

Another major difference between South Korea and Saudi Arabia remains usage and presence of dromedary camels. A large proportion of Saudi Arabian citizens utilize on dromedary camels for entertainment (the greatest example being races, held often in the region), meat, and milk, though this may vary depending on whether the location is rural or urban [59–61]. While other livestock have been found to transmit MERS-CoV or have the potential to, camels are the only currently cited animal source of transmission to humans [33]. Thus, a primary reason for sustained transmission of MERS-CoV, in addition to previously described healthcare measures, is the constant presence and interaction with dromedary camels in Saudi Arabia. In contrast, South Korea does not utilize dromedary camels in their daily lives, limiting exposure to MERS-CoV by this route.

Another interesting finding by Park et al. is that incubation periods in South Korea were reported as being slightly longer, averaging 6 days, compared to 4.5–5 days in the Middle East [62]. This delay also contributes to sustained transmission of MERS-CoV, as continued exposure to infectious persons can contribute to sustained person-to-person transmission. Higher mortality rates in Saudi Arabia compared to South Korea are likely in part due to these differences, among others described in this review [62].

7. Conclusions and Future Directions

While there have been many treatment and prevention strategies including neutralizing monoclonal antibodies [63], antivirals [64], and orthopoxvirus-based vaccines [65], there remains no medical interventions for prevention or successful treatment of MERS. However, it is promising that an imported outbreak in South Korea was managed so effectively that it was declared over only two months after the index case. There are many lessons to be learned from the South Korean handling of the nosocomial outbreak, but one problem that remains is the cultural barrier faced in Saudi Arabia. Whether cultural, personal, or livelihood based, there are many opposing opinions that hinder the outbreak resolution effort.

Following South Korea's example, there were three major differences between the outbreaks. The first was the open relationship between healthcare professionals and patients seen in South Korea. Patients felt more comfortable with their healthcare workers, and were more willing to go to the

hospital or clinic if they felt unwell. In addition, unlike the South Korean index patient, the majority of infected individuals were truthful about their travel, and if they had been to a MERS-affected area. This allowed professionals to be involved in the isolation and treatment process much sooner than in the Saudi Arabian outbreak.

In addition, there was more stringent training for healthcare professionals in South Korea, particularly in teaching members of medical staff how to manage incoming MERS cases, whether confirmed or not. These individuals were better equipped to deal with potential cases of MERS entering the hospital environment, thus avoiding potential nosocomial spread. In the case of the start of the Saudi Arabian outbreak, some medical professionals were unaware of how to isolate and manage patients, lacking basic knowledge of transmission and viral spread, enabling the virus to travel further and faster than if the patient was isolated and protective equipment were worn by staff and visitors from the onset of treatment.

And finally, there was a notable difference in the daily interactions with camels in the two regions. Use of on dromedaries in the Saudi Arabian region is significantly higher than in South Korea, where a variety of other animals such as horses and cattle are used as well. Continual interaction with these reservoirs of MERS-CoV is the primary cited reason for the frequency and duration of the Saudi Arabian outbreak, in comparison to the South Korean outbreak.

In order to proceed forward, regulatory boards such as the grouping of the MERS-CoV Infection Prevention and Control Guideline Development Committee, among others, during the time of an outbreak is essential to swift declaration and prevention of spread. In performing this step as a unified group, standardization of knowledge, training, and practices to be upheld during an outbreak are more effectively communicated, and nosocomial transmission and infections of hospital staff can be reduced.

While the ultimate research goal remains finding a vaccine and antivirals or other therapies that improve MERS outcome, in the interim, better infection control practices, improved communication of protection knowledge to the general public, and an open, understanding relationship between healthcare providers and their patients are the primary ways to improve outbreak outcomes. MERS remains a complex virus, and has proved difficult to sequester. The future of MERS outbreak prevention is in the hands of government policy makers, hospital workers, and a well-informed general population.

Author Contributions: Conceptualization, J.K., M.W.; formal analysis, M.W., D.K. and J.K.; resources, J.K.; data curation, M.W.; writing—original draft preparation, M.W., D.K. and J.K.; writing—review and editing, M.W., D.K. and J.K.; supervision, J.K.; funding acquisition, J.K.

Funding: J.K. is funded by a Tier 2 Canada Research Chair in the Molecular Pathogenesis of Emerging and Re-Emerging Viruses provided by the Canadian Institutes of Health Research (Grant no. 950-231498).

Conflicts of Interest: The authors declare no conflicts of interest.

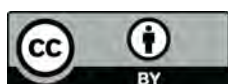
References

1. Zeng, Z.Q.; Chen, D.H.; Tan, W.P.; Qiu, S.Y.; Xu, D.; Liang, H.X.; Chen, M.X.; Li, X.; Lin, Z.S.; Liu, W.K.; et al. Epidemiology and clinical characteristics of human coronaviruses OC43, 229E, NL63, and HKU1: A study of hospitalized children with acute respiratory tract infection in Guangzhou China. *Eur. J. Clin. Microbiol. Infect. Dis.* **2018**, *37*, 363–369. [[CrossRef](#)] [[PubMed](#)]
2. De Wit, E.; van Doremalen, N.; Falzarano, D.; Munster, V.J. SARS and MERS: Recent insights into emerging coronaviruses. *Nat. Rev. Microbiol.* **2016**, *14*, 523–534. [[CrossRef](#)] [[PubMed](#)]
3. Hilgenfeld, R.; Peiris, M. From SARS to MERS: 10 years of research on highly pathogenic human coronaviruses. *Antivir. Res.* **2013**, *100*, 286–295. [[CrossRef](#)] [[PubMed](#)]
4. Wang, L.F.; Shi, Z.; Zhang, S.; Field, H.; Daszak, P.; Eaton, B.T. Review of Bats and SARS. *Emerg. Infect. Dis.* **2006**, *12*, 1834–1840. [[CrossRef](#)] [[PubMed](#)]
5. Sikkema, R.S.; Farag, E.A.B.A.; Islam, M.; Atta, M.; Reusken, C.B.E.M.; Al-Hajri, M.M.; Koopmans, M.P.G. Global status of Middle East respiratory syndrome coronavirus in dromedary camels: A systematic review. *Epidemiol. Infect.* **2019**, *147*, 84. [[CrossRef](#)] [[PubMed](#)]

6. World Health Organization. Middle East Respiratory Syndrome Coronavirus (MERS-CoV). Available online: <https://www.who.int/emergencies/mers-cov/en/> (accessed on 14 April 2019).
7. Kim, K.H.; Tandi, T.E.; Choi, J.W.; Moon, J.M.; Kim, M.S. Middle East respiratory syndrome coronavirus (MERS-CoV) outbreak in South Korea, 2015: Epidemiology, characteristics and public health implications. *J. Hosp. Infect.* **2016**, *95*, 207–213. [[CrossRef](#)] [[PubMed](#)]
8. Faridi, U. Middle East respiratory syndrome coronavirus (MERS-CoV): Impact on Saudi Arabia, 2015. *Saudi. J. Biol. Sci.* **2018**, *25*, 1402–1405. [[CrossRef](#)]
9. Rabaan, A.A.; Bazzi, A.M.; Al-Ahmed, S.H.; Al-Tawfiq, J.A. Molecular aspects of MERS-CoV. *Front. Med.* **2017**, *11*, 365–377. [[CrossRef](#)]
10. Fehr, A.R.; Perlman, S. Coronaviruses: An overview of their replication and pathogenesis. *Methods. Mol. Biol.* **2015**, *1282*, 1–23. [[CrossRef](#)]
11. Yang, Y.; Zhang, L.; Geng, H.; Deng, Y.; Huang, B.; Guo, Y.; Zhao, Z.; Tan, W. The structural and accessory proteins M, ORF 4a, ORF 4b, and ORF 5 of Middle East respiratory syndrome coronavirus (MERS-CoV) are potent interferon antagonists. *Protein Cell* **2013**, *4*, 951–961. [[CrossRef](#)]
12. Dawson, P.; Malik, M.R.; Parvez, F.; Morse, S.S. What Have We Learned About Middle East Respiratory Syndrome Coronavirus Emergence in Humans? A Systematic Literature Review. *Vector Borne Zoonotic. Dis.* **2019**, *19*, 174–192. [[CrossRef](#)] [[PubMed](#)]
13. Zhou, Y.; Yang, Y.; Huang, J.; Jiang, S.; Du, L. Advances in MERS-CoV Vaccines and Therapeutics Based on the Receptor-Binding Domain. *Viruses* **2019**, *11*, 60. [[CrossRef](#)] [[PubMed](#)]
14. Du, L.; Yang, Y.; Zhou, Y.; Lu, L.; Li, F.; Jiang, S. MERS-CoV spike protein: A key target for antivirals. *Expert Opin. Targets* **2017**, *21*, 131–143. [[CrossRef](#)] [[PubMed](#)]
15. Chan, J.F.; Lau, S.K.; To, K.K.; Cheng, V.C.; Woo, P.C.; Yuen, K.Y. Middle East respiratory syndrome coronavirus: Another zoonotic betacoronavirus causing SARS-like disease. *Clin. Microbiol. Rev.* **2015**, *28*, 465–522. [[CrossRef](#)] [[PubMed](#)]
16. Shirato, K.; Kawase, M.; Matsuyama, S. Middle East respiratory syndrome coronavirus infection mediated by the transmembrane serine protease TMPRSS2. *J. Virol.* **2013**, *87*, 12552–12561. [[CrossRef](#)] [[PubMed](#)]
17. Lokugamage, K.G.; Narayanan, K.; Nakagawa, K.; Terasaki, K.; Ramirez, S.I.; Tseng, C.T.; Makino, S. Middle East Respiratory Syndrome Coronavirus nsp1 Inhibits Host Gene Expression by Selectively Targeting mRNAs Transcribed in the Nucleus while Sparing mRNAs of Cytoplasmic Origin. *J. Virol.* **2015**, *89*, 10970–10981. [[CrossRef](#)] [[PubMed](#)]
18. Virlogeux, V.; Fang, V.J.; Park, M.; Wu, J.T.; Cowling, B.J. Comparison of incubation period distribution of human infections with MERS-CoV in South Korea and Saudi Arabia. *Sci. Rep.* **2016**, *6*, 35839. [[CrossRef](#)]
19. Ki, M. 2015 MERS outbreak in Korea: Hospital-to-hospital transmission. *Epidemiol. Health* **2015**, *37*, e2015033. [[CrossRef](#)]
20. Cotten, M.; Watson, S.J.; Zumla, A.I.; Makhdoom, H.Q.; Palser, A.L.; Ong, S.H.; Al Rabeeah, A.A.; Alhakeem, R.F.; Assiri, A.; Al-Tawfiq, J.A.; et al. Spread, circulation, and evolution of the Middle East respiratory syndrome coronavirus. *MBio* **2014**, *5*, e01062-13. [[CrossRef](#)]
21. Van Den Brand, J.M.; Smits, S.L.; Haagmans, B.L. Pathogenesis of Middle East respiratory syndrome coronavirus. *J. Pathol.* **2015**, *235*, 175–184. [[CrossRef](#)]
22. Mackay, I.M.; Arden, K.E. MERS coronavirus: Diagnostics, epidemiology and transmission. *Virol. J.* **2015**, *12*, 222. [[CrossRef](#)] [[PubMed](#)]
23. Jevšnik, M.; Uršič, T.; Zigon, N.; Lusa, L.; Krivec, U.; Petrovec, M. Coronavirus infections in hospitalized pediatric patients with acute respiratory tract disease. *BMC Infect. Dis.* **2012**, *12*, 365. [[CrossRef](#)] [[PubMed](#)]
24. Birch, C.J.; Clothier, H.J.; Seccull, A.; Tran, T.; Catton, M.C.; Lambert, S.B.; Druce, J.D. Human coronavirus OC43 causes influenza-like illness in residents and staff of aged-care facilities in Melbourne, Australia. *Epidemiol. Infect.* **2005**, *133*, 273–277. [[CrossRef](#)] [[PubMed](#)]
25. Zaki, A.M.; van Boheemen, S.; Bestebroer, T.M.; Osterhaus, A.D.; Fouchier, R.A. Isolation of a Novel Coronavirus from a Man with Pneumonia in Saudi Arabia. *N. Engl. J. Med.* **2012**, *367*, 1814–1820. [[CrossRef](#)] [[PubMed](#)]
26. Das, K.M.; Lee, E.Y.; Singh, R.; Enani, M.A.; Al Dossari, K.; Van Gorkom, K.; Larsson, S.G.; Langer, R.D. Follow-up chest radiographic findings in patients with MERS-CoV after recovery. *Indian J. Radiol. Imaging.* **2017**, *27*, 342–349. [[CrossRef](#)] [[PubMed](#)]
27. Al Johani, S.; Hajeer, A.H. MERS-CoV diagnosis: An update. *J. Infect. Public Health* **2016**, *9*, 216–219. [[CrossRef](#)] [[PubMed](#)]

28. Centers for Disease Control and Prevention. CDC Laboratory Testing for Middle East Respiratory Syndrome Coronavirus (MERS-CoV). Available online: <https://www.cdc.gov/coronavirus/mers/lab/lab-testing.html> (accessed on 10 July 2019).
29. Bernard-Stoecklin, S.; Nikolay, B.; Assiri, A.; Saeed, A.A.B.; Embarek, P.K.B.; El Bushra, H.; Ki, M.; Rahman Malik, M.; Fontanet, A.; Cauchemez, S.; et al. Comparative analysis of eleven healthcare-associated outbreaks of Middle East Respiratory Syndrome Coronavirus (MERS-CoV) from 2015 to 2017. *Sci. Rep.* **2019**, *9*, 7385. [\[CrossRef\]](#)
30. Memish, Z.A.; Zumia, A.I.; Al-Hakeem, R.F.; Al-Rabeeah, A.A.; Stephens, G.M. Family cluster of Middle East respiratory syndrome coronavirus infections. *N. Engl. J. Med.* **2013**, *368*, 2487–2494. [\[CrossRef\]](#)
31. Qiu, W.; Chu, C.; Mao, A.; Wu, J. The Impacts on Health, Society, and Economy of SARS and H7N9 Outbreaks in China: A Case Comparison Study. *J. Environ. Public Health* **2018**, 2710185. [\[CrossRef\]](#)
32. Memish, Z.A.; Mishra, N.; Olival, K.J.; Fagbo, S.F.; Kapoor, V.; Epstein, J.H.; Alhakeem, R.; Durosinloun, A.; Al Asmari, M.; Islam, A.; et al. Middle East respiratory syndrome coronavirus in bats, Saudi Arabia. *Emerg. Infect. Dis.* **2013**, *19*, 1819–1823. [\[CrossRef\]](#)
33. Vergara-Alert, J.; van den Brand, J.M.; Widagdo, W.; Muñoz, M.; Raj, S.; Schipper, D.; Solanes, D.; Cerdón, I.; Bensaid, A.; Haagmans, B.L.; et al. Livestock Susceptibility to Infection with Middle East Respiratory Syndrome Coronavirus. *Emerg. Infect. Dis.* **2017**, *23*, 232–240. [\[CrossRef\]](#) [\[PubMed\]](#)
34. Elrggal, M.E.; Karami, N.A.; Rafea, B.; Alahmadi, L.; Al Shehri, A.; Alamoudi, R.; Koshak, H.; Alkahtani, S.; Cheema, E. Evaluation of preparedness of healthcare student volunteers against Middle East respiratory syndrome coronavirus (MERS-CoV) in Makkah, Saudi Arabia: A cross-sectional study. *Z. Gesundh. Wiss.* **2018**, *26*, 607–612. [\[CrossRef\]](#) [\[PubMed\]](#)
35. Kang, C.K.; Song, K.H.; Choe, P.G.; Park, W.B.; Bang, J.H.; Kim, E.S.; Park, S.W.; Kim, H.B.; Kim, N.J.; Cho, S.I.; et al. Clinical and Epidemiologic Characteristics of Spreaders of Middle East Respiratory Syndrome Coronavirus during the 2015 Outbreak in Korea. *J. Korean Med. Sci.* **2017**, *32*, 744–749. [\[CrossRef\]](#) [\[PubMed\]](#)
36. Ohnuma, K.; Hatano, R.; Komiya, E.; Otsuka, H.; Itoh, T.; Iwao, N.; Kaneko, Y.; Yamada, T.; Dang, N.H.; Morimoto, C. A novel role for CD26/dipeptidyl peptidase IV as a therapeutic agent. *Front. Biosci.* **2018**, *23*, 1754–1779. [\[CrossRef\]](#)
37. Eckerle, I.; Müller, M.A.; Kallies, S.; Gotthardt, D.N.; Drosten, C. In-vitro renal epithelial cell infection reveals a viral kidney tropism as a potential mechanism for acute renal failure during Middle East Respiratory Syndrome (MERS) Coronavirus infection. *Virol. J.* **2013**, *10*, 359. [\[CrossRef\]](#)
38. Naskalska, A.; Dabrowska, A.; Nowak, P.; Szczepanski, A.; Jasik, K.; Milewska, A.; Ochman, M.; Zeglen, S.; Rajfur, Z.; Pyrc, K. Novel coronavirus-like particles targeting cells lining the respiratory tract. *PLoS ONE* **2018**, *13*, e0203489. [\[CrossRef\]](#)
39. Glowacka, I.; Bertram, S.; Herzog, P.; Pfefferle, S.; Steffen, I.; Muench, M.O.; Simmons, G.; Hofmann, H.; Kuri, T.; Weber, F.; et al. Differential Downregulation of ACE2 by the Spike Proteins of Severe Acute Respiratory Syndrome Coronavirus and Human Coronavirus NL63. *J. Virol.* **2010**, *84*, 1198–1205. [\[CrossRef\]](#)
40. Uhal, B.D.; Dang, M.; Dang, V.; Llatos, R.; Cano, E.; Abdul-Hafez, A.; Markey, J.; Piasecki, C.C.; Molina-Molina, M. Cell cycle dependence of ACE-2 explains downregulation in idiopathic pulmonary fibrosis. *J. Virol.* **2010**, *84*, 1198–1205. [\[CrossRef\]](#)
41. García-Laorden, M.I.; Lorente, J.A.; Flores, C.; Slutsky, A.S.; Villar, J. Biomarkers for the acute respiratory distress syndrome: How to make the diagnosis more precise. *Ann. Transl. Med.* **2017**, *5*, 283. [\[CrossRef\]](#)
42. Heymann, D.L.; Rodier, G. Global surveillance, national surveillance, and SARS. *Emerg. Infect. Dis.* **2004**, *10*, 173–175. [\[CrossRef\]](#)
43. Kim, J.Y.; Song, J.Y.; Yoon, Y.K.; Choi, S.H.; Song, Y.G.; Kim, S.R.; Son, H.J.; Jeong, S.Y.; Choi, J.H.; Kim, K.M.; et al. Middle East Respiratory Syndrome Infection Control and Prevention Guideline for Healthcare Facilities. *Infect. Chemother.* **2015**, *47*, 278–302. [\[CrossRef\]](#)
44. Park, J.W.; Lee, K.J.; Lee, K.H.; Lee, S.H.; Cho, J.R.; Mo, J.W.; Choi, S.Y.; Kwon, G.Y.; Shin, J.Y.; Hong, J.Y.; et al. Hospital Outbreaks of Middle East Respiratory Syndrome, Daejeon, South Korea, 2015. *Emerg. Infect. Dis.* **2017**, *23*, 898–905. [\[CrossRef\]](#)
45. Cho, S.Y.; Kang, J.M.; Ha, Y.E.; Park, G.E.; Lee, J.Y.; Kim, J.M.; Jang, C.I.; Jo, I.J.; Ryu, J.G.; Choi, J.R.; et al. MERS-CoV outbreak following a single patient exposure in an emergency room in South Korea: An epidemiological outbreak study. *Lancet* **2016**, *388*, 994–1001. [\[CrossRef\]](#)

46. Korea Centers for Disease Control and Prevention. Middle East Respiratory Syndrome Coronavirus outbreak in the Republic of Korea. *Osong Public Health Res. Perspect.* **2015**, *6*, 269–278. [CrossRef]
47. Kim, S.W.; Park, J.W.; Jung, H.D.; Yang, J.S.; Park, Y.S.; Lee, C.; Kim, K.M.; Lee, K.J.; Kwon, D.; Hur, Y.J.; et al. Risk factors for transmission of Middle East Respiratory Syndrome Coronavirus infection during the 2015 outbreak in South Korea. *Clin. Infect. Dis.* **2017**, *64*, 551–557. [CrossRef]
48. European Center for Disease Prevention and Control. Available online: <https://www.ecdc.europa.eu/en/news-events/epidemiological-update-middle-east-respiratory-syndrome-coronavirus-mers-cov-21-july> (accessed on 13 February 2019).
49. Majumder, M.S.; Rivers, C.; Lofgren, E.; Fisman, D. Estimation of MERS-Coronavirus Reproductive Number and Case Fatality Rate for the Spring 2014 Saudi Arabia Outbreak: Insights from Publicly Available Data. *PLoS Curr.* **2014**, *6*. [CrossRef]
50. Oh, M.D.; Park, W.B.; Park, S.W.; Choe, P.G.; Bang, J.H.; Song, K.H.; Kim, E.S.; Kim, H.B.; Kim, N.J. Middle East respiratory syndrome: What we learned from the 2015 outbreak in the Republic of Korea. *Korean J. Intern. Med.* **2018**, *33*, 233–246. [CrossRef]
51. World Health Organization. Available online: <http://www.emro.who.int/pandemic-epidemic-diseases/mers-cov/mers-situation-update-december-2018.html> (accessed on 25 May 2019).
52. Al-Ahmadi, H.; Roland, M. Quality of primary health care in Saudi Arabia: A comprehensive review. *Int. J. Qual. Health Care* **2005**, *17*, 331–346. [CrossRef]
53. Walston, S.; Al-Harbi, Y.; Al-Omar, B. The changing face of healthcare in Saudi Arabia. *Ann. Saudi Med.* **2008**, *28*, 243–250. [CrossRef]
54. Taylor, A. The Scary Reason Saudi Farmers are Kissing Camels. *The Washington Post*. Available online: https://www.washingtonpost.com/news/worldviews/wp/2014/05/16/the-scary-reason-saudi-farmers-are-kissing-camels/?utm_term=.32ceaf8016c7 (accessed on 10 March 2019).
55. Ajibaili, M. “Saudi Health Minister ‘Relieved of His Post’”. *Al Arabiya*. Available online: <http://english.alarabiya.net/en/News/middle-east/2014/04/21/Saudi-Health-Minister-relieved-of-duties-.html> (accessed on 14 March 2019).
56. Park, K.; Park, J.; Kwon, Y.D.; Kang, Y.; Noh, J.W. Public satisfaction with the healthcare system performance in South Korea: Universal healthcare system. *Health Policy* **2016**, *120*, 621–629. [CrossRef]
57. Tabekhan, A.K.; Alkhalidi, Y.M.; Alghamdi, A.K. Patients satisfaction with consultation at primary health care centers in Abha City, Saudi Arabia. *J. Family Med. Prim. Care* **2018**, *7*, 658–663. [CrossRef]
58. Alqahtani, A.S.; Rashid, H.; Basyouni, M.H.; Alhawassi, T.M.; BinDhim, N.F. Public response to MERS-CoV in the Middle East: iPhone survey in six countries. *J. Infect. Public Health* **2017**, *10*, 534–540. [CrossRef]
59. Hemida, M.G.; Elmoslemay, A.; Al-Hizab, F.; Alnaeem, A.; Almathen, F.; Faye, B.; Chu, D.K.W.; Perera, R.A.; Peiris, M. Dromedary camels and the transmission of Middle East Respiratory Syndrome Coronavirus (MERS-CoV). *Transbound Emerg. Dis.* **2018**, *64*, 344–353. [CrossRef]
60. Abrhaley, A.; Leta, S. Medicinal value of camel milk and meat. *J. Appl. Anim. Res.* **2018**, *46*. [CrossRef]
61. Elzaki Ali, R.M.; Ahmed, S.H.; Al-Mahish, M.A. Camel production in the Kingdom of Saudi Arabia: Economic and environmental impacts. *Fundam. Appl. Agric.* **2018**, *3*, 602–608. [CrossRef]
62. Park, J.E.; Jung, S.; Kim, A.; Park, J.W. MERS transmission and risk factors: A systemic review. *BMB Public Health* **2018**, *18*, 574. [CrossRef]
63. Han, H.J.; Liu, J.W.; Yu, H.; Yu, X.J. Neutralizing Monoclonal Antibodies as Promising Therapeutics against Middle East Respiratory Syndrome Coronavirus Infection. *Viruses* **2018**, *10*, 680. [CrossRef]
64. Chong, Y.P.; Song, J.Y.; Seo, Y.B.; Choi, J.P.; Shin, H.S. Rapid Response Team. Antiviral Treatment Guidelines for Middle East Respiratory Syndrome. *Infect. Chemother.* **2015**, *47*, 212–222. [CrossRef]
65. Haagmans, B.L.; van den Brand, J.M.; Raj, V.S.; Volz, A.; Wohlsein, P.; Smits, S.L.; Schipper, D.; Bestebroer, T.M.; Okba, N.; Fux, R.; et al. An orthopoxvirus-based vaccine reduces virus excretion after MERS-CoV infection in dromedary camels. *Science* **2016**, *351*, 77–81. [CrossRef]



Virological assessment of hospitalized patients with COVID-2019

<https://doi.org/10.1038/s41586-020-2196-x>

Received: 1 March 2020

Accepted: 24 March 2020

Published online: 1 April 2020

 Check for updates

Roman Wölfel^{1,6}, Victor M. Corman^{2,6}, Wolfgang Guggemos^{3,6}, Michael Seilmaier³, Sabine Zange¹, Marcel A. Müller², Daniela Niemeyer², Terry C. Jones^{2,4}, Patrick Vollmar¹, Camilla Rothe⁵, Michael Hoelscher⁵, Tobias Bleicker², Sebastian Brünink², Julia Schneider², Rosina Ehm¹, Katrin Zwirgmaier¹, Christian Drosten^{2,7} & Clemens Wendtner^{3,7}✉

Coronavirus disease 2019 (COVID-19) is an acute infection of the respiratory tract that emerged in late 2019^{1,2}. Initial outbreaks in China involved 13.8% of cases with severe courses, and 6.1% of cases with critical courses³. This severe presentation may result from the virus using a virus receptor that is expressed predominantly in the lung^{2,4}; the same receptor tropism is thought to have determined the pathogenicity—but also aided in the control—of severe acute respiratory syndrome (SARS) in 2003⁵. However, there are reports of cases of COVID-19 in which the patient shows mild upper respiratory tract symptoms, which suggests the potential for pre- or oligosymptomatic transmission^{6–8}. There is an urgent need for information on virus replication, immunity and infectivity in specific sites of the body. Here we report a detailed virological analysis of nine cases of COVID-19 that provides proof of active virus replication in tissues of the upper respiratory tract. Pharyngeal virus shedding was very high during the first week of symptoms, with a peak at 7.11×10^8 RNA copies per throat swab on day 4. Infectious virus was readily isolated from samples derived from the throat or lung, but not from stool samples—in spite of high concentrations of virus RNA. Blood and urine samples never yielded virus. Active replication in the throat was confirmed by the presence of viral replicative RNA intermediates in the throat samples. We consistently detected sequence-distinct virus populations in throat and lung samples from one patient, proving independent replication. The shedding of viral RNA from sputum outlasted the end of symptoms. Seroconversion occurred after 7 days in 50% of patients (and by day 14 in all patients), but was not followed by a rapid decline in viral load. COVID-19 can present as a mild illness of the upper respiratory tract. The confirmation of active virus replication in the upper respiratory tract has implications for the containment of COVID-19.

There is a close genetic relationship between SARS coronavirus (SARS-CoV) and the causative agent of COVID-19, SARS-CoV-2. The predominant expression of ACE2 in the lower respiratory tract is believed to have determined the natural history of SARS as an infection of the lower respiratory tract⁵. Although the positive detection of SARS-CoV-2 in clinical specimens from the upper respiratory tract has previously been described^{9,10}, these observations do not address the principal differences between SARS and COVID-19 in terms of clinical pathology. The patients who were studied here were enrolled because they acquired their infections upon known close contact to an index case, thereby avoiding representational biases owing to symptom-based case definitions. All patients were treated in a single hospital in Munich, Germany. Virological testing was done by two closely collaborating laboratories that used the same standards of technology for PCR with reverse transcription (RT-PCR) and virus isolation; these two laboratories confirmed each other's

results in almost all of the individual samples. Owing to the extremely high congruence of results, all data—except for the serological data (which are based on results from one laboratory only)—are presented together. The patients are part of a larger cluster of epidemiologically linked cases that occurred after 23 January 2020 in Munich, as discovered on 27 January (ref. ¹¹). The present study uses samples taken during the clinical course in the hospital, as well as from initial diagnostic testing before admission. In cases in which this initial diagnostic testing was done by other laboratories, the original samples were retrieved and retested under the rigorous quality standards of the present study.

RT-PCR, replication sites and infectivity

To first understand whether the described clinical presentations are solely caused by infection with SARS-CoV-2, samples from all patients

¹Bundeswehr Institute of Microbiology, Munich, Germany. ²Charité Universitätsmedizin Berlin, Berlin, Germany. ³Klinikum München-Schwabing, Munich, Germany. ⁴Center for Pathogen Evolution, Department of Zoology, University of Cambridge, Cambridge, UK. ⁵University Hospital LMU Munich, Munich, Germany. ⁶These authors contributed equally: Roman Wölfel, Victor M. Corman, Wolfgang Guggemos. ⁷These authors jointly supervised this work: Christian Drosten, Clemens Wendtner. ✉e-mail: christian.drosten@charite.de; clemens.wendtner@muenchen-klinik.de

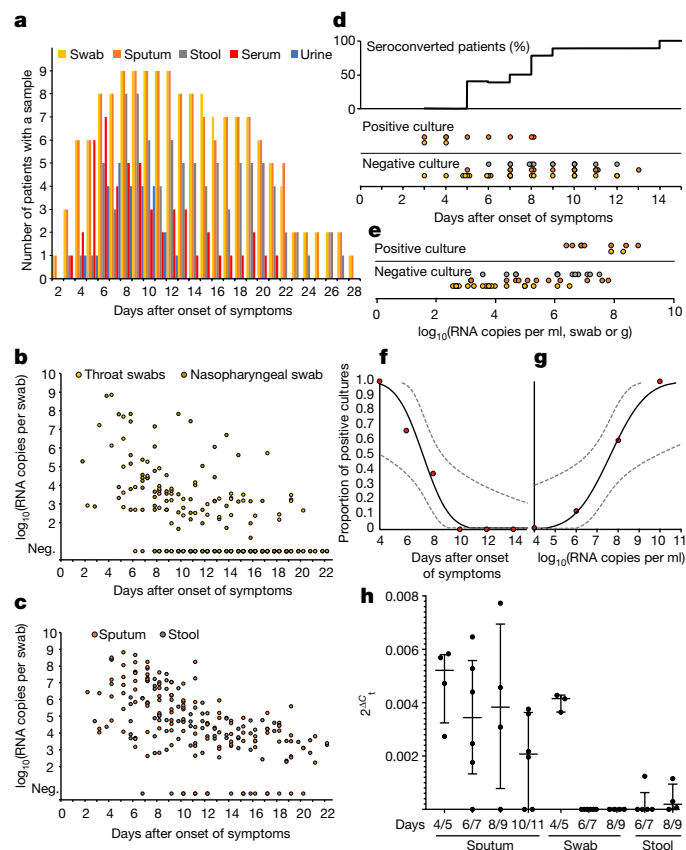


Fig. 1 | Hallmarks of viral shedding in aggregated samples. **a**, Samples and sample types per day. **b**, Viral RNA concentrations in samples from the upper respiratory tract. Neg., sample negative for RNA copies. **c**, Viral RNA concentrations in sputum and stool samples. **d**, Seroconversion and virus isolation success, dependent on day after the onset of symptoms. Top, fraction of seroconverted patients. Bottom, aggregated results of virus isolation trials. **e**, Virus isolation success, dependent on viral load. Viral loads were projected to RNA copies per ml (for sputum samples), per swab (for throat swab samples) or per g (for stool samples). **f, g**, Projected virus isolation success based on probit distributions. The inner lines are probit curves (dose–response rule). The outer dotted lines are 95% confidence interval. For a <5% isolation success, the estimated day was 9.78 (95% confidence interval 8.45–21.78) days after the onset of symptoms, and the estimated RNA concentration for <5% isolation success was estimated to be 5.40 log₁₀(RNA copies per ml) (95% confidence interval –4.11–6.51). **h**, Subgenomic viral RNA transcripts in relation to viral genomic RNA. Dots represent mean values of RT–PCR data obtained from at least two independent experiments on samples from individual patients. Plots show median values with interquartile ranges.

were tested against a panel of typical agents of respiratory viral infection, including human coronavirus (HCoV)-HKU1, HCoV-OC43, HCoV-NL63 and HCoV-229E, influenza virus A, influenza virus B, phinovirus, enterovirus, respiratory syncytial virus, human parainfluenza viruses 1–4, human metapneumovirus, adenovirus and human bocavirus. No coinfection was detected in any patient.

All patients were initially diagnosed by RT–PCR from oro- or nasopharyngeal swab specimens¹². Both types of specimen were collected over the whole clinical course in all patients. There were no discernible differences in viral loads or detection rates when comparing naso- and oropharyngeal swabs (Fig. 1b). The earliest swabs were taken on day 1 of symptoms, which were often very mild or prodromal. All swabs from all patients taken between day 1 and day 5 tested positive. The average virus RNA load was 6.76×10^5 copies per whole swab until day 5, and the maximum load was 7.11×10^8 copies per swab. Swab samples taken after day 5 had an average viral load of 3.44×10^5 copies per swab and

Table 1 | Single-nucleotide polymorphism at genome position 6446 in clinical samples from patient no. 4

	Day after onset of symptoms						
	5	6	7	8	9	10	11
Swab	A		A				
Sputum		G	G	G	G>A		
Stool			G>A	A=G	A=G	G>A	A

a detection rate of 39.93%. The last swab sample that tested positive was taken on day 28 after the onset of symptoms. The average viral load in sputum was 7.00×10^6 copies per ml, with a maximum of 2.35×10^9 copies per ml.

Because swab samples had limited sensitivity for the initial diagnosis of cases of SARS^{13,14}, we analysed the first paired swab and sputum samples taken on the same occasion from seven patients. All samples were taken between 2 and 4 days after the onset of symptoms. In two cases, swab samples had virus concentrations that were clearly higher than those in sputum samples, as indicated by a difference of >3 in the threshold cycle (C_t) value. The opposite was true in two other cases, and the remaining three cases had similar concentrations in both sample types.

None of 27 urine samples and none of 31 serum samples tested positive for RNA from SARS-CoV2.

To understand infectivity, we attempted live virus isolation on multiple occasions from clinical samples (Fig. 1d). Whereas the virus was readily isolated during the first week of symptoms from a considerable fraction of samples (16.66% of swabs and 83.33% of sputum samples), no isolates were obtained from samples taken after day 8 in spite of ongoing high viral loads.

Virus isolation from stool samples was never successful, irrespective of viral RNA concentration, on the basis of a total of 13 samples taken between day 6 and day 12 from 4 patients. The success of virus isolation also depended on viral load: samples that contained <10⁶ copies per ml (or copies per sample) never yielded an isolate. For sputum samples, interpolation based on a probit model was done to obtain laboratory-based infectivity criteria for the discharge of patients (Fig. 1f, g).

High viral loads and successful isolation from early throat swabs suggested potential virus replication in tissues of the upper respiratory tract. To obtain proof of active virus replication in the absence of histopathology, we conducted RT–PCR tests to identify viral subgenomic mRNAs directly in clinical samples (Extended Data Fig. 1). Viral subgenomic mRNA is transcribed only in infected cells and is not packaged into virions, and therefore indicates the presence of actively infected cells in samples. Levels of viral subgenomic mRNA were compared against viral genomic RNA in the same sample. In sputum samples taken on day 4 to day 9, during which time active replication in sputum was obvious in all patients as per longitudinal viral load courses (as described in ‘Viral load, antibody response and clinical course’), the ratios of mean normalized subgenomic mRNA per genome were about 0.4% (Fig. 1g). A decline occurred from day 10 to day 11. In throat swabs, all samples taken up to day 5 were in the same range, whereas no subgenomic mRNA was detectable in swabs thereafter. Together, these data indicate the active replication of SARS-CoV-2 in the throat during the first five days after the onset of symptoms. No (or only minimal) indications of replication in stool were obtained by the same method (Fig. 1g).

During our study, we sequenced full virus genomes from all patients. A G6446A exchange was first detected in one patient, and later transmitted to other patients in the cluster¹¹. In the first patient, this mutation was found in a throat swab while a sputum sample from the same day showed the original allele (G6446). The single-nucleotide

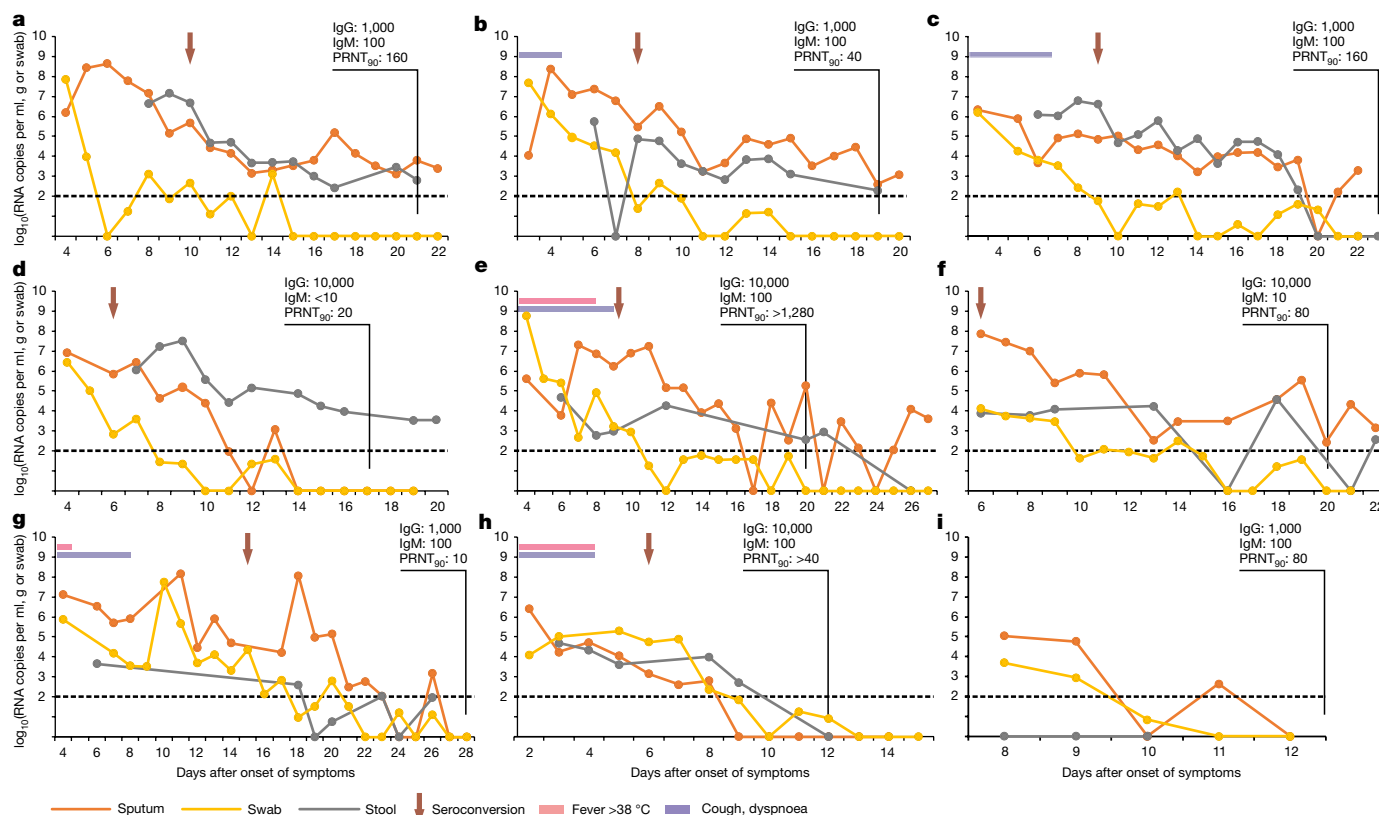


Fig. 2 | Viral load kinetics, seroconversion and clinical observations in individual cases. a–i, The panels correspond to patients no. 1 (a), 2 (b), 3 (c), 4 (d), 7 (e), 8 (f), 10 (g), 14 (h) and 16 (i) in a previous publication¹¹. Dotted lines,

limit of quantification. Experiments were performed in duplicate and the data presented are the mean of results obtained by two laboratories independently. PRNT₉₀, serum dilution that causes viral plaque reduction of 90%.

polymorphism was analysed by RT-PCR and Sanger sequencing in all sequential samples available from that patient (Table 1). The presence of separate genotypes in throat swabs and sputum strongly supported our suspicion of independent virus replication in the throat, rather than passive shedding to the throat from the lung.

Viral load, antibody response and clinical course

Daily measurements of viral load in sputum, pharyngeal swabs and stool are summarized in Fig. 2. In general, the concentrations of viral RNA were very high in initial samples. In all patients except one, the concentration of viral RNA in throat swabs seemed to be already on the decline at the time of first presentation. Viral RNA concentrations in sputum declined more slowly, with a peak during the first week of symptoms in three out of eight patients. Viral RNA concentrations in stools were also high. In many cases, the course of viral RNA concentration in stools seemed to reflect the course in sputum (Fig. 2a–c). In only one case did independent replication in the intestinal tract seem obvious from the course of stool RNA excretion (Fig. 2d). Whereas symptoms mostly waned until the end of the first week (Table 2), viral RNA remained detectable in throat swabs well into the second week. Stool and sputum samples remained RNA-positive over three weeks in six of the nine patients, in spite of full resolution of symptoms.

All cases had comparatively mild courses (Table 2). The two patients who showed some signs of lung infection were the only cases in which sputum viral loads showed a late and high peak around day 10 or 11, whereas sputum viral loads were on the decline by this time in all other patients (Fig. 2f, g). Of note, four out of nine patients showed a loss of taste and olfactory sensation, and described this loss to be stronger and more long-lasting than in common cold diseases.

Seroconversion was detected by IgG and IgM immunofluorescence using cells that express the spike protein of SARS-CoV-2 and a virus neutralization assay using SARS-CoV-2 (Table 3, Extended Data Fig. 2). Seroconversion in 50% of patients occurred by day 7, and in all patients by day 14 (Fig. 1d). No viruses were isolated after day 7. All patients showed detectable neutralizing antibodies, the titres of which did not suggest close correlation with clinical courses. Of note, patient no. 4, who showed the lowest virus neutralization titre at end of week 2, seemed to shed virus from stool over a prolonged time (Fig. 2d). Results from the differential recombinant immunofluorescence assay indicated cross-reactivity or cross-stimulation against the four endemic human coronaviruses in several patients (Extended Data Table 1).

Conclusions

The clinical courses in the patients under study—all of whom were young- to middle-aged professionals without notable underlying disease—were mild. Apart from one patient, all cases were first tested when symptoms were still mild or in the prodromal stage (a period in which most patients would present once there is general awareness of a circulating pandemic disease⁵). Diagnostic testing suggests that simple throat swabs will provide sufficient sensitivity at this stage of infection. This is in stark contrast to SARS; for instance, only 38 of 98 nasal or nasopharyngeal swab samples tested positive by RT-PCR in patients with SARS in Hong Kong¹⁵. Viral load also differs considerably between SARS and COVID-19. For SARS, it took 7 to 10 days after the onset of symptoms until peak RNA concentrations (of up to 5×10^5 copies per swab) were reached^{13,14}. In the present study, peak concentrations were reached before day 5, and were more than 1,000 times higher. Successful isolation of live virus from throat swabs is another notable difference between COVID-19 and SARS, for which such isolation was

Table 2 | Clinical characteristics of all patients

Patient ID no.	Comorbidity	Initial symptoms	Later symptoms	ANC per μ l	ALC per μ l	CRP (mg l ⁻¹)	LDH (U l ⁻¹)
1	Hypothyroidism	Cough, fever, diarrhoea	Diarrhoea	4,870	1,900	46	197
2	None	Sinusitis, cephalgia, cough	Hyposmia, ageusia	3,040	1,200	4.9	182
3	COPD	Arthralgia, sinusitis, cough	Dysosmia, dysgeusia	5,040	2,600	1.3	191
4	None	Otitis, rhinitis	Hyposmia, hypogeusia	2,420	2,220	5.9	149
7	Hypercholesterolaemia	Rhinitis, cough	Fever, dyspnoea, hyposmia, hypogeusia	4,690	900	4.9	209
8	None	Sinusitis, cough		2,500	1,600	1.7	203
10	None	Sinusitis, cough	Fever, cough	2,350	700	7.8	220
14	None	Fever, cough, diarrhoea		5,040	1,500	9.8	220
16	None	None		4,620	900	0.5	201

ALC, absolute lymphocyte count; ANC, absolute neutrophil count; CRP, C-reactive protein; COPD, chronic obstructive pulmonary disease; LDH, lactate dehydrogenase.

rarely successful^{16–18}. This suggests active virus replication in tissues of the upper respiratory tract, where SARS-CoV is not thought to replicate in spite of detectable ACE2 expression^{19,20}. At the same time, the concurrent use of ACE2 as a receptor by SARS-CoV and SARS-CoV-2 corresponds to a highly similar excretion kinetic in sputum, with active replication in the lung. SARS-CoV was previously found¹³ in sputum at mean concentrations of $1.2\text{--}2.8 \times 10^6$ copies per ml, which corresponds to observations made here.

Whereas proof of replication by histopathology is awaited, extended tissue tropism of SARS-CoV-2 with replication in the throat is strongly supported by our studies of cells that transcribe subgenomic mRNA in throat swab samples, particularly during the first 5 days of symptoms. Notable additional evidence for independent replication in the throat is provided by sequence findings in one patient, who consistently showed a distinct virus in the throat as opposed to the lung. In addition, the disturbance of gustatory and olfactory senses points at an infection of the tissues of the upper respiratory tract.

Critically, the majority of patients in the present study seemed to be beyond their shedding peak in samples from the upper respiratory tract when they were first tested, whereas the shedding of infectious virus in sputum continued throughout the first week of symptoms. Together, these findings suggest a more efficient transmission of SARS-CoV-2 than SARS-CoV, through active pharyngeal viral shedding at a time at which symptoms are still mild and typical of infections of the upper respiratory tract. Later in the disease, COVID-19 resembles SARS in terms of replication in the lower respiratory tract. Of note, the two patients who showed some symptoms of the lungs being affected showed a

prolonged viral load in sputum. Our study is limited, in that no severe cases were observed. Future studies that include severe cases should look at the prognostic value of an increase of viral load beyond the end of week 1, potentially indicating an aggravation of symptoms.

One of the most interesting hypotheses to explain the potential extension of tropism to the throat is the presence of a polybasic furin-type cleavage site at the S1–S2 junction in the SARS-CoV-2 spike protein that is not present in SARS-CoV¹⁷. The insertion of a polybasic cleavage site in the S1–S2 region in SARS-CoV has previously been shown to lead to a moderate, but discernible, gain-of-fusion activity that might result in increased viral entry in tissues with a low density of ACE2 expression²¹.

The combination of very high concentrations of virus RNA and the occasional detection of cells in stools that contain subgenomic mRNA indicate active replication in the gastrointestinal tract. Active replication is also suggested by a much higher detection rate compared to the Middle East respiratory system coronavirus (MERS-CoV), for which stool-associated RNA was found in only 14.6% of samples from 37 patients hospitalized in Riyadh (Saudi Arabia)^{22,23}. If SARS-CoV-2 was only passively present in the stool (such as after swallowing respiratory secretions), similar detection rates as for MERS-CoV would be expected. Replication in the gastrointestinal tract is also supported by analogy with SARS-CoV, which was regularly excreted in stool (from which it could be isolated in cell culture²⁴). Our failure to isolate live SARS-CoV-2 from stools may be due to the mild courses of cases, with only one case showing intermittent diarrhoea. In China, diarrhoea was seen in only 2 of 99 cases²⁵. Further studies should therefore address whether SARS-CoV-2 shed in stools is rendered noninfectious though contact with the gut environment. Our initial results suggest that measures to contain viral spread should aim at droplet-, rather than fomite-, based transmission.

The prolonged viral shedding in sputum is relevant not only for the control of infections in hospitals, but also for discharge management. In a situation characterized by a limited capacity of hospital beds in infectious disease wards, there is pressure for early discharge after treatment. On the basis of the present findings, early discharge with ensuing home isolation could be chosen for patients who are beyond day 10 of symptoms and have less than 100,000 viral RNA copies per ml of sputum. Both criteria predict that there is little residual risk of infectivity, on the basis of cell culture.

The serological courses of all patients suggest a timing of seroconversion similar to, or slightly earlier than, in SARS-CoV infection¹⁸. Seroconversion in most cases of SARS occurred during the second week of symptoms. As in SARS and MERS, IgM was not detected considerably earlier than IgG in immunofluorescence; this might in part be due to technical reasons, as the higher avidity of IgG antibodies outcompetes IgM for viral epitopes in the assay. IgG depletion can only partially alleviate this effect. Because immunofluorescence assay is a

Table 3 | IgG and IgM immunofluorescence titres against SARS-CoV-2, from all patients

Patient ID no.	Initial serum		Final serum				
	Day after onset	IgG	Day after onset	IgG	IgM	PRNT ₉₀	PRNT ₅₀
1	5	<10	21	1,000	100	160	>640
2	4	<10	19	1,000	100	40	320
3	3	<10	23	1,000	100	160	>640
4	5	<10	17	10,000	<10	20	160
7	6	<10	20	10,000	100	>1,280	>1,280
8	6	10	20	10,000	10	80	>320
10	6	<10	28	1,000	10	10	>40
14	NA	NA	12	10,000	100	>40	>40
16	NA	NA	13	1,000	100	80	>320

NA, not applicable; PRNT₅₀, serum dilution that causes viral plaque reduction of 50%.

labour-intensive method, enzyme-linked immunosorbent assay tests should be developed as a screening test. Neutralization testing is necessary to rule out cross-reactive antibodies directed against endemic human coronaviruses. On the basis of the frequently low neutralizing antibody titres observed in coronavirus infection^{26,27}, we have here developed a particularly sensitive plaque-reduction neutralization assay. Considering the titres we observed, a simpler microneutralization test format is likely to provide sufficient sensitivity in routine application and population studies.

When aligned to viral load courses, it seems there is no abrupt virus elimination at the time of seroconversion. Rather, seroconversion early in week 2 coincides with a slow but steady decline of viral load in sputum. Whether properties such as the glycosylation pattern at critical sites of the glycoprotein have a role in the attenuation of the neutralizing antibody response needs further clarification. In any case, vaccine approaches targeting mainly the induction of antibody responses should aim to induce particularly strong antibody responses to be effective.

Online content

Any methods, additional references, Nature Research reporting summaries, source data, extended data, supplementary information, acknowledgements, peer review information; details of author contributions and competing interests; and statements of data and code availability are available at <https://doi.org/10.1038/s41586-020-2196-x>.

- Zhu, N. et al. A novel coronavirus from patients with pneumonia in China, 2019. *N. Engl. J. Med.* **382**, 727–733 (2020).
- Coronaviridae Study Group of the International Committee on Taxonomy of Viruses. The species *Severe acute respiratory syndrome-related coronavirus*: classifying 2019-nCoV and naming it SARS-CoV-2. *Nat. Microbiol.* **5**, 536–544 (2020).
- WHO. Report of the WHO–China Joint Mission on Coronavirus Disease 2019 (COVID-19) <https://www.who.int/docs/default-source/coronaviruse/who-china-joint-mission-on-covid-19-final-report.pdf> (WHO, 2020).
- Hoffmann, M. et al. SARS-CoV-2 cell entry depends on ACE2 and TMPRSS2 and is blocked by a clinically proven protease inhibitor. *Cell* **181**, 271–280 (2020).
- Leung, G. M. et al. The epidemiology of severe acute respiratory syndrome in the 2003 Hong Kong epidemic: an analysis of all 1755 patients. *Ann. Intern. Med.* **141**, 662–673 (2004).
- Rothe, C. et al. Transmission of 2019-nCoV infection from an asymptomatic contact in Germany. *N. Engl. J. Med.* **382**, 970–971 (2020).
- Holshue, M. L. et al. First case of 2019 novel coronavirus in the United States. *N. Engl. J. Med.* **382**, 929–936 (2020).
- Hoehl, S. et al. Evidence of SARS-CoV-2 infection in returning travelers from Wuhan, China. *N. Engl. J. Med.* **382**, 1278–1280 (2020).
- Zou, L. et al. SARS-CoV-2 viral load in upper respiratory specimens of infected patients. *N. Engl. J. Med.* **382**, 1177–1179 (2020).
- Young, B. E. et al. Epidemiologic features and clinical course of patients infected with SARS-CoV-2 in Singapore. *J. Am. Med. Assoc.* **323**, 1488–1494 (2020).
- Böhmer, M. et al. Outbreak of COVID-19 in Germany resulting from a single travel-associated primary case. *Lancet Infect. Dis.* [https://doi.org/10.1016/S1473-3099\(20\)30314-5](https://doi.org/10.1016/S1473-3099(20)30314-5) (2020).
- Corman, V. M. et al. Detection of 2019 novel coronavirus (2019-nCoV) by real-time RT-PCR. *Euro Surveill.* **25**, 1–8 (2020).
- Drosten, C. et al. Evaluation of advanced reverse transcription-PCR assays and an alternative PCR target region for detection of severe acute respiratory syndrome-associated coronavirus. *J. Clin. Microbiol.* **42**, 2043–2047 (2004).
- Peiris, J. S. et al. Clinical progression and viral load in a community outbreak of coronavirus-associated SARS pneumonia: a prospective study. *Lancet* **361**, 1767–1772 (2003).
- Poon, L. L. et al. Detection of SARS coronavirus in patients with severe acute respiratory syndrome by conventional and real-time quantitative reverse transcription-PCR assays. *Clin. Chem.* **50**, 67–72 (2004).
- Ksiazek, T. G. et al. A novel coronavirus associated with severe acute respiratory syndrome. *N. Engl. J. Med.* **348**, 1953–1966 (2003).
- Drosten, C. et al. Identification of a novel coronavirus in patients with severe acute respiratory syndrome. *N. Engl. J. Med.* **348**, 1967–1976 (2003).
- Peiris, J. S. et al. Coronavirus as a possible cause of severe acute respiratory syndrome. *Lancet* **361**, 1319–1325 (2003).
- Bertram, S. et al. Influenza and SARS-coronavirus activating proteases TMPRSS2 and HAT are expressed at multiple sites in human respiratory and gastrointestinal tracts. *PLoS ONE* **7**, e35876 (2012).
- Xu, H. et al. High expression of ACE2 receptor of 2019-nCoV on the epithelial cells of oral mucosa. *Int. J. Oral Sci.* **12**, 8 (2020).
- Belouzard, S., Chu, V. C. & Whittaker, G. R. Activation of the SARS coronavirus spike protein via sequential proteolytic cleavage at two distinct sites. *Proc. Natl Acad. Sci. USA* **106**, 5871–5876 (2009).
- Corman, V. M. et al. Viral shedding and antibody response in 37 patients with Middle East respiratory syndrome coronavirus infection. *Clin. Infect. Dis.* **62**, 477–483 (2016).
- Zhou, J. et al. Human intestinal tract serves as an alternative infection route for Middle East respiratory syndrome coronavirus. *Sci. Adv.* **3**, eaao4966 (2017).
- Leung, W. K. et al. Enteric involvement of severe acute respiratory syndrome-associated coronavirus infection. *Gastroenterology* **125**, 1011–1017 (2003).
- Chen, N. et al. Epidemiological and clinical characteristics of 99 cases of 2019 novel coronavirus pneumonia in Wuhan, China: a descriptive study. *Lancet* **395**, 507–513 (2020).
- Drosten, C. et al. Transmission of MERS-coronavirus in household contacts. *N. Engl. J. Med.* **371**, 828–835 (2014).
- Müller, M. A. et al. Presence of Middle East respiratory syndrome coronavirus antibodies in Saudi Arabia: a nationwide, cross-sectional, serological study. *Lancet Infect. Dis.* **15**, 559–564 (2015).

Publisher's note Springer Nature remains neutral with regard to jurisdictional claims in published maps and institutional affiliations.

© The Author(s), under exclusive licence to Springer Nature Limited 2020

Article

Methods

No statistical methods were used to predetermine sample size. The experiments were not randomized and investigators were not blinded to allocation during experiments and outcome assessment.

Clinical samples and viral load conversion

Sputum and stool samples were taken and shipped in native conditions. Oro- and nasopharyngeal throat swabs were preserved in 3 ml of viral transport medium. Viral loads in sputum samples were projected to RNA copies per ml, in stool samples to copies per g and in throat swabs to copies per 3 ml, assuming that all sample components were suspended in 3 ml viral transport medium. For swab samples suspended in less than 3 ml viral transport medium, this conversion was adapted to represent copies per whole swab. An aggregated overview of samples received per day after the onset of disease from all patients is shown in Fig. 1a.

RT-PCR for SARS-CoV-2 and other respiratory viruses

RT-PCR used targets in the *E* and *RdRp* genes as previously described¹². Both laboratories used a pre-formulated oligonucleotide mixture (Tib-Molbiol) to make the laboratory procedures more reproducible. All patients were also tested for other respiratory viruses, including HCoV-HKU1, HCoV-OC43, HCoV-NL63 and HCoV-229E, influenza virus A, influenza virus B, rhinovirus, enterovirus, respiratory syncytial virus, human parainfluenza viruses 1–4, human metapneumovirus, adenovirus and human bocavirus using LightMix-Modular Assays (Roche). Additional technical details are provided in Supplementary Methods section 1.

Virus isolation

Virus isolation was done in two laboratories on Vero E6 cells. In brief, 100 µl of suspended, cleared and filtered clinical sample was mixed with an equal volume of cell culture medium. Supernatant was collected after 0, 1, 3 and 5 days and used in RT-PCR analysis. Additional technical details are provided in Supplementary Methods section 2a.

Serology

We performed recombinant immunofluorescence assays to determine the specific reactivity against recombinant spike proteins in VeroB4 cells, as previously described^{26,28}. This assay used a cloned coronavirus spike protein from HCoV-229E, HCoV-NL63, HCoV-OC43, HCoV-HKU1 or SARS-CoV-2. The screening dilution was 1:10. Plaque reduction neutralization tests were done essentially as previously described for MERS-CoV²⁶. Serum dilutions causing plaque reductions of 90% (PRNT₉₀) and 50% (PRNT₅₀) were recorded as titres. Additional technical details are provided in Supplementary Methods section 2b, c.

Statistical analyses

Statistical analyses were done using SPSS software (version 25) or GraphPad Prism (version 8).

Ethical approval statement

All patients provided informed consent for the use of their data and clinical samples for the purposes of the present study. Institutional review board clearance for the scientific use of patient data has been granted to the treating institution by the ethics committee at the Medical Faculty of the Ludwig Maximilians Universität Munich (vote 20-225 KB).

Reporting summary

Further information on research design is available in the Nature Research Reporting Summary linked to this paper.

Data availability

Sequence data are available in GISAID under accession number EPI_ISL_406862. All other data are available from C.D. upon reasonable request.

28. Corman, V. M. et al. Assays for laboratory confirmation of novel human coronavirus (hCoV-EMC) infections. *Euro Surveill.* **17**, 20334 (2012).

Acknowledgements This work was funded by grants from the German Ministry of Research (01KI1723A) and the European Union (602525) to C.D. as well as by the German Bundeswehr Medical Service Biodefense Research Program. The funders had no role in study design, data collection and analysis or decision to publish. We thank P. Mackeldanz, E. Möncke-Buchner, A. Richter, M. Schmidt and J. Beheim-Schwarzbach for technical assistance.

Author contributions R.W. and V.M.C. planned and supervised laboratory testing, and evaluated data. W.G. and M.S. managed patients and evaluated clinical data. S.Z., T.B., S.B., J.S., R.E. and K.Z. performed laboratory testing. M.A.M. managed serological laboratory testing. D.N. managed and performed virus isolation studies. T.C.J. analysed sequences and population-specific polymorphisms. P.V. managed laboratory testing. C.R. managed initial patient contacts. M.H. managed initial patient contacts and evaluated clinical data. C.D. designed and supervised laboratory studies, and wrote the manuscript. C.W. designed and supervised clinical management and clinical data.

Competing interests The authors declare no competing interests.

Additional information

Supplementary information is available for this paper at <https://doi.org/10.1038/s41586-020-2196-x>.

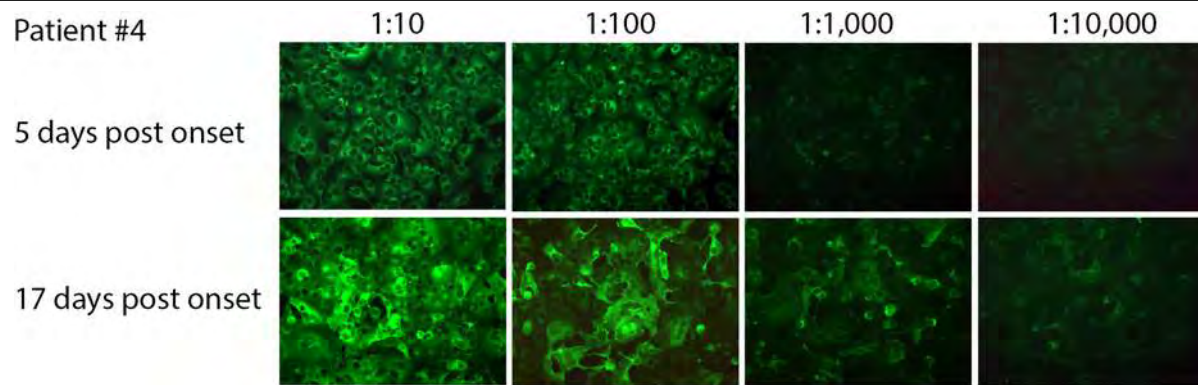
Correspondence and requests for materials should be addressed to C.D. or C.W.

Peer review information Nature thanks Peter Openshaw and the other, anonymous, reviewer(s) for their contribution to the peer review of this work.

Reprints and permissions information is available at <http://www.nature.com/reprints>.



Extended Data Fig. 1 | Sequence analysis of *E* gene subgenomic mRNA. The leader sequence (purple), putative transcription regulatory sequences (TRS) (grey) and nucleotides coding for the 5'-proximal part of the *E* gene (yellow box) are shown. PCR primer binding sites used for amplification and RT-PCR detection are shown as green arrows, and the 5'-nuclease PCR probe is shown as a red arrow.



Extended Data Fig. 2 | Recombinant SARS-CoV-2-spike-based immunofluorescence test shows seroconversion of patient no. 4.

Representative outcome of a recombinant immunofluorescence test using serum dilutions 1:10, 1:100, 1:1,000 and 1:10,000 of patient no. 4 at 5 and 17 days

after the onset of symptoms. Secondary detection was done by using a goat-anti human immunoglobulin labelled with Alexa Fluor 488 (shown in green). The experiment was performed in duplicate.

Extended Data Table 1 | IgG immunofluorescence titres against endemic human coronaviruses

Patient ID	<i>Primary serum</i>					<i>Final serum</i>				
	Day p.o.	OC43	NL63	HKU1	229E	Day p.o.	OC43	NL63	HKU1	229E
#1	5	1,000	1,000	1,000	100	15	1,000	1,000	1,000	100
#2	4	1,000	1,000	100	100	13	10,000	100	1,000	10
#3	3	10,000	100	1,000	1000	16	10,000	1,000	10,000	1,000
#4	5	1,000	100	100	100	17	10,000	10	1,000	100
#7	6	1,000	100	1,000	1000	13	10,000	1,000	10,000	10,000
#8	6	1,000	100	1,000	1000	10	10,000	1,000	10,000	100
#10	6	1,000	100	100	1000	11	10,000	1,000	100	1,000
#14	na	na	na	na	na	5	100	100	100	100
#16	na	na	na	na	na	13	10,000	1,000	1,000	100

p.o., post onset; na, not available. Increases of titre through the final serum are indicated by reciprocal titres in bold.

Reporting Summary

Nature Research wishes to improve the reproducibility of the work that we publish. This form provides structure for consistency and transparency in reporting. For further information on Nature Research policies, see [Authors & Referees](#) and the [Editorial Policy Checklist](#).

Statistics

For all statistical analyses, confirm that the following items are present in the figure legend, table legend, main text, or Methods section.

- | | |
|-------------------------------------|--|
| n/a | Confirmed |
| <input type="checkbox"/> | <input checked="" type="checkbox"/> The exact sample size (n) for each experimental group/condition, given as a discrete number and unit of measurement |
| <input type="checkbox"/> | <input checked="" type="checkbox"/> A statement on whether measurements were taken from distinct samples or whether the same sample was measured repeatedly |
| <input type="checkbox"/> | <input checked="" type="checkbox"/> The statistical test(s) used AND whether they are one- or two-sided
<i>Only common tests should be described solely by name; describe more complex techniques in the Methods section.</i> |
| <input type="checkbox"/> | <input checked="" type="checkbox"/> A description of all covariates tested |
| <input type="checkbox"/> | <input checked="" type="checkbox"/> A description of any assumptions or corrections, such as tests of normality and adjustment for multiple comparisons |
| <input type="checkbox"/> | <input checked="" type="checkbox"/> A full description of the statistical parameters including central tendency (e.g. means) or other basic estimates (e.g. regression coefficient) AND variation (e.g. standard deviation) or associated estimates of uncertainty (e.g. confidence intervals) |
| <input checked="" type="checkbox"/> | <input type="checkbox"/> For null hypothesis testing, the test statistic (e.g. F , t , r) with confidence intervals, effect sizes, degrees of freedom and P value noted
<i>Give P values as exact values whenever suitable.</i> |
| <input checked="" type="checkbox"/> | <input type="checkbox"/> For Bayesian analysis, information on the choice of priors and Markov chain Monte Carlo settings |
| <input checked="" type="checkbox"/> | <input type="checkbox"/> For hierarchical and complex designs, identification of the appropriate level for tests and full reporting of outcomes |
| <input checked="" type="checkbox"/> | <input type="checkbox"/> Estimates of effect sizes (e.g. Cohen's d , Pearson's r), indicating how they were calculated |

Our web collection on [statistics for biologists](#) contains articles on many of the points above.

Software and code

Policy information about [availability of computer code](#)

Data collection

Microsoft Excel,

Data analysis

SPSS, GraphPad Prism, Geneious

For manuscripts utilizing custom algorithms or software that are central to the research but not yet described in published literature, software must be made available to editors/reviewers. We strongly encourage code deposition in a community repository (e.g. GitHub). See the Nature Research [guidelines for submitting code & software](#) for further information.

Data

Policy information about [availability of data](#)

All manuscripts must include a [data availability statement](#). This statement should provide the following information, where applicable:

- Accession codes, unique identifiers, or web links for publicly available datasets
- A list of figures that have associated raw data
- A description of any restrictions on data availability

The data upon which figures and conclusions are based can be obtained from the corresponding author upon reasonable request. These data cannot be published in an open source because their interpretation may affect aspects of patient privacy.

Field-specific reporting

Please select the one below that is the best fit for your research. If you are not sure, read the appropriate sections before making your selection.

- ☒ Life sciences ☐ Behavioural & social sciences ☐ Ecological, evolutionary & environmental sciences

Life sciences study design

All studies must disclose on these points even when the disclosure is negative.

Sample size	Nine Patients.
Data exclusions	None.
Replication	Testing by two different laboratories.
Randomization	None.
Blinding	None.

Reporting for specific materials, systems and methods

We require information from authors about some types of materials, experimental systems and methods used in many studies. Here, indicate whether each material, system or method listed is relevant to your study. If you are not sure if a list item applies to your research, read the appropriate section before selecting a response.

Materials & experimental systems

n/a	Involved in the study
<input type="checkbox"/>	<input checked="" type="checkbox"/> Antibodies
<input type="checkbox"/>	<input checked="" type="checkbox"/> Eukaryotic cell lines
<input checked="" type="checkbox"/>	<input type="checkbox"/> Palaeontology
<input checked="" type="checkbox"/>	<input type="checkbox"/> Animals and other organisms
<input type="checkbox"/>	<input checked="" type="checkbox"/> Human research participants
<input type="checkbox"/>	<input checked="" type="checkbox"/> Clinical data

Methods

n/a	Involved in the study
<input checked="" type="checkbox"/>	<input type="checkbox"/> ChIP-seq
<input checked="" type="checkbox"/>	<input type="checkbox"/> Flow cytometry
<input checked="" type="checkbox"/>	<input type="checkbox"/> MRI-based neuroimaging

Antibodies

Antibodies used	Secondary anti-human IgG reagents (Euroimmun).
Validation	Immunofluorescence.

Eukaryotic cell lines

Policy information about [cell lines](#)

Cell line source(s)	In-house collection with reference to ATCC or DSZM.
Authentication	Functional testing for IFN locus inactivation.
Mycoplasma contamination	Regular testing.
Commonly misidentified lines (See ICLAC register)	N/A

Human research participants

Policy information about [studies involving human research participants](#)

Population characteristics	N.A.
Recruitment	Clinical admission due to symptoms, contact history, and positive initial test.
Ethics oversight	Research ethics board of Ludwig Maximillians University Munich; informed consent to scientific use and publication of anonymized data by each patient.

Note that full information on the approval of the study protocol must also be provided in the manuscript.

Clinical data

Policy information about [clinical studies](#)

All manuscripts should comply with the ICMJE [guidelines for publication of clinical research](#) and a completed [CONSORT checklist](#) must be included with all submissions.

Clinical trial registration	N.A.
Study protocol	No study protocol emergency admissions of patients with new disease.
Data collection	Data collection at treating hospital, and two laboratories as identified in affiliations list.
Outcomes	Laboratory and clinical status. No explicit outcome measure.

available at www.sciencedirect.com
journal homepage: www.europeanurology.com/eufocus



Infections

Pathological Findings in the Testes of COVID-19 Patients: Clinical Implications

Ming Yang^{a,†}, Shuo Chen^{a,†}, Bo Huang^a, Jing-Min Zhong^a, Hua Su^b, Ya-Jun Chen^a, Qin Cao^a, Lin Ma^a, Jun He^a, Xue-Fei Li^a, Xiang Li^a, Jun-Jie Zhou^a, Jun Fan^a, Dan-Ju Luo^a, Xiao-Na Chang^a, Knarik Arkun^c, Ming Zhou^{c,*}, Xiu Nie^{a,**}

^aDepartment of Pathology, Union Hospital, Tongji Medical College, Huazhong University of Science and Technology, Wuhan, China; ^bDepartment of Nephrology, Union Hospital, Tongji Medical College, Huazhong University of Science and Technology, Wuhan, China; ^cDepartment of Pathology and Laboratory Medicine, Tufts Medical Center and Tufts School of Medicine, Boston, MA, USA

Article info

Article history:

Accepted May 26, 2020

Associate Editor:

Christian Gratzke

Keywords:

COVID-19
SARS-CoV-2
Testis
Postmortem needle autopsy
Fertility

Abstract

Background: Coronavirus disease 2019 (COVID-19), caused by severe acute respiratory syndrome coronavirus 2 (SARS-CoV-2), involves multiple organs. Testicular involvement is largely unknown.

Objective: To determine the pathological changes and whether SARS-CoV-2 can be detected in the testes of deceased COVID-19 patients.

Design, setting, and participants: Postmortem examination of the testes from 12 COVID-19 patients was performed using light and electron microscopy, and immunohistochemistry for lymphocytic and histiocytic markers. Reverse transcription-polymerase chain reaction (RT-PCR) was used to detect the virus in testicular tissue.

Outcome measurements and statistical analysis: Seminiferous tubular injury was assessed as none, mild, moderate, or severe according to the extent of tubular damage. Leydig cells in the interstitium were counted in ten 400× microscopy fields.

Results and limitations: Microscopically, Sertoli cells showed swelling, vacuolation and cytoplasmic rarefaction, detachment from tubular basement membranes, and loss and sloughing into lumens of the intratubular cell mass. Two, five, and four of 11 cases showed mild, moderate, and severe injury, respectively. The mean number of Leydig cells in COVID-19 testes was significantly lower than in the control group (2.2 vs 7.8, $p < 0.001$). In the interstitium there was edema and mild inflammatory infiltrates composed of T lymphocytes and histiocytes. Transmission EM did not identify viral particles in three cases. RT-PCR detected the virus in one of 12 cases.

Conclusions: Testes from COVID-19 patients exhibited significant seminiferous tubular injury, reduced Leydig cells, and mild lymphocytic inflammation. We found no evidence of SARS-CoV-2 virus in the testes in the majority (90%) of the cases by RT-PCR, and in none by electron microscopy. These findings can provide evidence-based guidance for sperm donation and inform management strategies to mitigate the risk of testicular injury during the COVID-19 disease course.

[†] These authors contributed equally to this work.

* Corresponding author. Department of Pathology and Laboratory Medicine, Tufts Medical Center, 800 Washington Street, Boston, MA 02111, USA. Tel.: 1 617 6366147; Fax: 1 617 6367128.

E-mail address: mzhou3@tuftsmedicalcenter.org (M. Zhou).

** Corresponding author. Department of Pathology, Union Hospital, Tongji Medical College, Huazhong University of Science and Technology, 1277 Jie Fang Avenue, Wuhan, Hubei 430022, China.

E-mail address: nixiuyishi@126.com (X. Nie).

Patient summary: We examined the testes of deceased COVID-19 patients. We found significant damage to the testicular parenchyma. However, virus was not detected in testes in the majority of cases.

© 2020 European Association of Urology. Published by Elsevier B.V. This is an open access article under the CC BY-NC-ND license (<http://creativecommons.org/licenses/by-nc-nd/4.0/>).

1. Introduction

Coronavirus disease 2019 (COVID-19) is an infectious disease caused by severe acute respiratory syndrome coronavirus 2 (SARS-CoV-2). The World Health Organization (WHO) declared the COVID-19 outbreak a global pandemic on March 11, 2020. As of May 4, 2020, more than 3.43 million cases and more than 239 000 deaths have been reported worldwide [1]. Many important discoveries have been made regarding COVID-19 etiology, epidemiology, diagnosis, and treatment strategies [2]. There are also emerging data on histopathological changes in various organs [3–5], especially the lungs [6,7]. However, information on COVID-19 pathology in the testis is scarce. A recent study found that ACE2 receptor, a target for SARS-CoV-2 infection, is expressed in germ cells, Leydig cells, and Sertoli cells in the testis [8] using single-cell RNA sequencing, suggesting the testis is potentially a target for SARS-CoV-2 infection. However, an autopsy study of one patient revealed that the testis appeared normal [9]. Two studies found no SARS-CoV-2 virus in semen [10,11]. A detailed examination of the testis in COVID-19 patients is therefore warranted to ascertain whether the virus can be found in the testicular epithelium and whether there is any cytopathic effect on the testis. Such knowledge may help in determining whether SARS-CoV-2 can be transmitted via semen and the risk of testicular injury during the disease course, which may affect fertility, especially in young patients.

2. Patients and methods

2.1. Postmortem examination of the testes

This study was conducted in accordance with the principles of the Declaration of Helsinki and the guidelines of the Chinese National Health Commission, and was approved by the Ethics Committee of Union Hospital, Tongji Medical College, Huazhong University of Science and Technology. According to the Chinese regulations [12], COVID-19 diagnosis was confirmed by positive nucleic acid testing of oropharyngeal swabs or bronchoalveolar lavage fluid, radiological features of viral pneumonia, and clinical symptomatology. Postmortem examinations were carried out after consent from patients or family members and were performed within 1 h of death at Union Hospital, Tongji Medical College, Huazhong University of Science and Technology. For eight patients, a tissue sample of 1 cm × 1 cm was obtained via incisional biopsy. For the other four patients, a tissue core of 1 cm × 0.2 cm was obtained using a 14 G needle under ultrasound guidance.

2.2. Tissue processing and staining

Procured tissue was fixed in 10% formalin for hematoxylin and eosin staining or in 2.5% glutaraldehyde for electron microscopy (EM) for

48–72 h. For EM, Epon-embedded “semi-thin” sections stained with toluidine blue were examined after gradient dehydration. Selected areas were chosen for thin sections, which were then cut and stained with uranyl acetate and lead citrate. EM grids were viewed using a transmission electron microscope (HT-7800; Hitachi, Hitachinaka, Japan) [13]. Immunohistochemical stains were performed for CD3 (Dako, Copenhagen, Denmark), CD20 (Roche, Tucson, AZ, USA), CD68 (Dako), CD138 (Dako), and ACE2 (Biolyx, Hanzhou, China) according to manufacturers’ protocols on a Dako Link 48 automated stainer (for CD3, CD68, CD138, and ACE2) or a Roche Benchmark XT Ultra system (for CD20).

2.3. Reverse transcription-polymerase chain reaction (RT-PCR)

Fourteen 5-μm-thick formalin-fixed, paraffin-embedded lung and testis tissue sections were used for RNA extraction using an AmoyDx FFPE RNA extraction kit (Amoy Diagnostics, Xiamen, China). SARS-CoV-2 RNA was detected using a real-time multiplex RT-PCR kit (Liferiver Biotechnology, Shanghai, China), which detects the SARS-CoV-2 RdRp gene, E gene, and N gene simultaneously. RT-PCR was performed on an Mx3000 P real-time PCR system (Agilent Technologies, Santa Clara, CA, USA). According to the manufacturer’s protocol, a threshold cycle (Ct) of ≤43 for all three genes, or the RdRp and E genes, or the RdRp and N genes indicated the presence of SARS-CoV-2.

3. Results

3.1. Clinical characteristics

Twelve patients were included in this study. The mean age was 65 yr (range 42–87 yr; Table 1). The mean disease duration (from onset to death) was 42 d (range 23–75 d). Fever was present in ten patients. Ten patients received low-dose steroids (maximum dose 160 mg).

3.2. Pathological findings

Pathological examination was performed in 11 of the 12 cases. One case (S5) contained predominantly fibrovascular tissue with very few seminiferous tubules and was therefore not included in the pathological evaluation. Seminiferous tubules exhibited a range of changes. Sertoli cells were affected predominantly and showed swelling, vacuolation and cytoplasmic rarefaction, and detachment from tubular basement membranes (Fig. 1A and 1B). Loss and sloughing of the intratubular cell mass into the lumens was also observed (Fig. 1C). According to the extent of these changes, seminiferous tubular injury was categorized as none, mild, moderate, or severe if 0%, <10%, 10–50%, or >50% of seminiferous tubules were affected, respectively. Two (18.2%), five (45.5%), and four (36.4%) of 11 cases showed mild, moderate, and severe injury, respectively

Table 1 – Clinical features of 12 COVID-19 patients.

Case no.	Age (yr)	Disease duration (d)	Body temperature (°C)	Steroid therapy	Comorbidity	Cause of death
S20-4	87	23	37.6	No	Hypertension, chronic renal disease, coronary heart disease	COVID-19, RF
S20-5	39	30	38.7	Yes	Gastric carcinoma	COVID-19
S20-6	66	36	38.9	Yes	Hepatocellular carcinoma	COVID-19, RF
S20-7	77	27	37.7	Yes	Basal cell carcinoma of the face	COVID-19, RF, septic shock
S20-9	70	20	36.5	Yes	Lung carcinoma (histological type unknown)	COVID-19, myocardial infarction, RF
S20-12	63	44	39	Yes	Hypertension	COVID-19, pneumonia, ARDS, MODS
S20-14	61	36	39.6	Yes	None	COVID-19, RF, septic shock
S20-19	55	37	38.3	Yes	None	COVID-19, respiratory failure, MODS
S20-20	73	49	37.5	Yes	Hypertension, gastric adenocarcinoma	COVID-19, septic shock
S20-22	42	52	40	Yes	Hypertension	COVID-19, RF, septic shock, MODS
S20-23	64	75	36.6	Yes	None	RF, COVID-19 (critical type), abdominal bleeding
S20-24	57	63	37.4	Yes	None	COVID-19, DIC, lower gastrointestinal bleeding

COVID-19 = coronavirus disease 2019; RF = respiratory failure; ARDS = acute respiratory distress syndrome; MODS = multiple organ dysfunction syndrome; DIC = disseminated intravascular coagulopathy.

(Table 2). To rule out the possibility that these changes resulted from protracted severe illness, we reviewed testes from five patients who died of non-COVID-19 causes and had a disease course of at least 7 d, and found no tubular injury in two cases and mild tubular injury in three cases (Fig. 1D).

To quantify Leydig cells in the interstitium, Leydig cell and seminiferous tubule cross-sections were counted in ten 400× microscopy fields and the number of Leydig cells per tubule cross-section was calculated. As a control group, we examined five orchiectomies performed for penile cancer ($n = 1$), castration in prostate cancer ($n = 3$), and perineal trauma ($n = 1$). The mean age of patients in the control group was 66.8 yr (range 49–75 yr), which was not significantly different from the age of our COVID-19 patients ($p = 0.807$, Student t test). The mean number of Leydig cells in COVID-19 testes was 2.2 (range 0.44–5.3), which was significantly lower than in the control group (7.8, range 5.3–10; $t = -6.336$, $p < 0.001$, Student t test).

In the interstitium there was edema and mild inflammatory infiltrates composed predominantly of CD3-positive T lymphocytes (Fig. 1E) and CD68-positive histiocytes (Fig. 1F) as confirmed by immunohistochemistry. B lymphocytes and plasma cells were not found in the stroma. No inflammatory cells were found within the seminiferous tubules.

Normal spermatogenesis was observed in three cases. The other cases showed variable degrees of spermatogenic alteration (Table 2) that was in general consistent with patient age.

Immunostaining revealed that ACE2 was diffusely expressed in Sertoli cells and strongly expressed in Leydig cells (Fig. 2). It was not expressed in spermatogonia. Germ cells at other differentiation stages, including primary and secondary spermatocytes, and spermatids, are difficult to assess as they were enveloped by the cytoplasm of Sertoli cells.

Transmission EM was performed for three of the 12 cases and did not identify definite SARS-CoV-2 viral particles.

3.3. Detection of SARS-CoV-2 by RT-PCR

The target SARS-CoV-2 nucleic acid sequence was detected in lung tissue from ten of the 12 patients. It was detected in the testis from only one case (S20-5) with a threshold cycle (Ct) value of 31.68, 30.53, and 30.46 for the RdRP, E, and N genes, respectively. Of note, this patient had a high viral load: his lung, kidney, spleen, and testis were all positive for the virus on RT-PCR. The testicular tissue sampled contained predominantly fibrovascular tissue and very few seminiferous tubules.

4. Discussion

The objectives in this study were twofold. First, we investigated whether SARS-CoV-2 virus could be detected in seminiferous tubules and germ cells. Second, we sought to determine whether COVID-19 can cause injury to seminiferous tubules and Leydig cells, which may affect fertility, especially in young men. The findings could have important clinical implications.

Many viruses that infect humans can be detected in semen [14]. It has been found that SARS-CoV, a virus that belongs to the same betacoronavirus family as SARS-CoV-2 and is responsible for SARS, causes spermatogenic cell necrosis and apoptosis and induces inflammatory infiltrates in the interstitium, although viral genomic sequences were not detected in testes [15]. A recent study using single-cell RNA sequencing found that the ACE2 receptor, a target for SARS-CoV-2 infection, is expressed in germ cells, Leydig cells, and Sertoli cells in the testis [8], suggesting the testis is potentially a tropism site and reservoir for the SARS-CoV-2 virus. In a study by Pan et al [10], 19% of patients had scrotal discomfort concerning for testicular involvement around the time of their COVID-19 diagnosis. On the basis of these preliminary data, the American Society for Reproductive Medicine and the Society for Assisted Reproductive

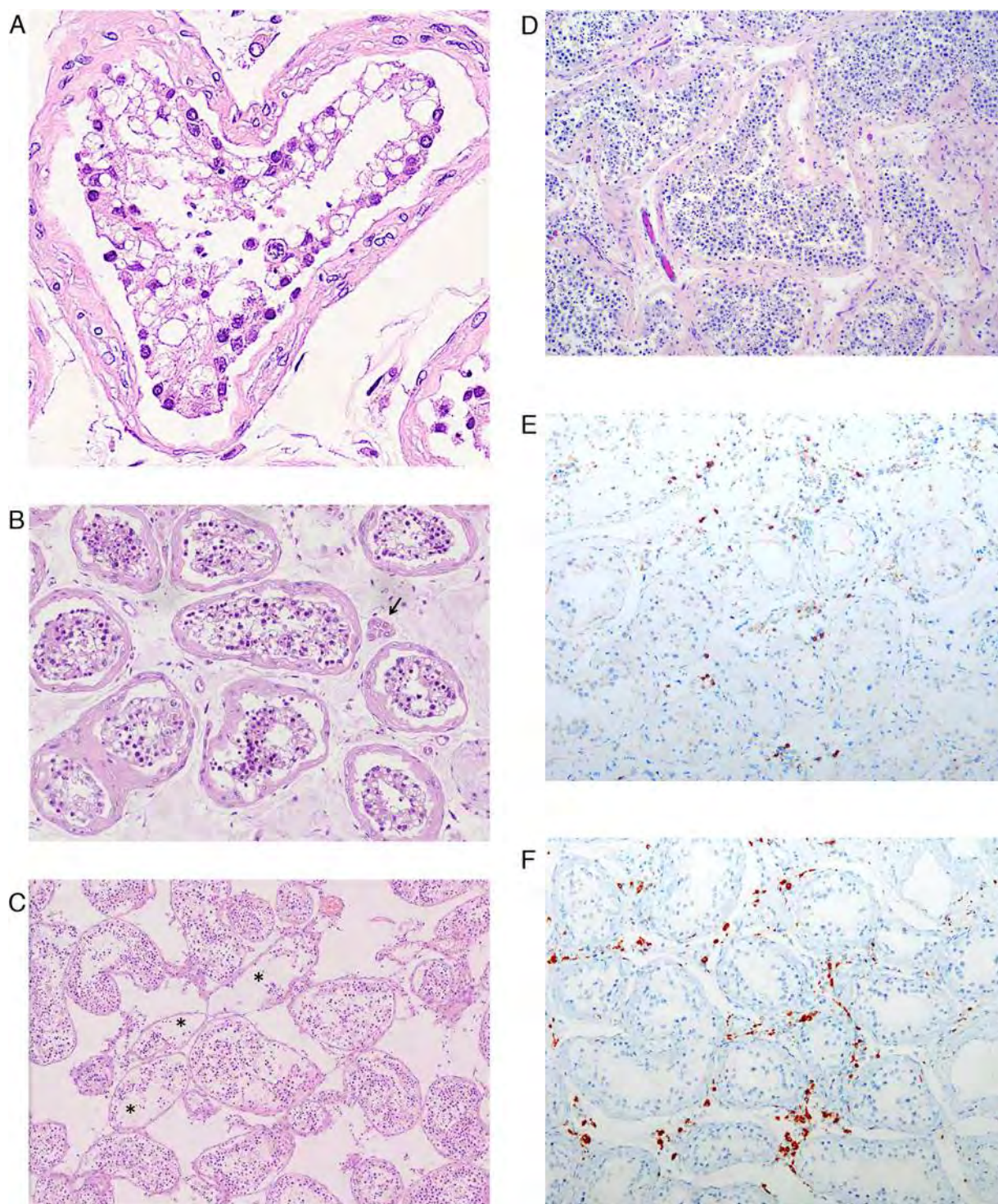


Fig. 1 – Pathology in testes from COVID-19 patients. (A) Sertoli cells shows swelling, vacuolation, and cytoplasmic rarefaction, and detachment from the tubular basement membranes. Spermatogenesis is present but reduced. **(B)** A case with severe tubular injury shows cytoplasmic vacuolation and detachment of Sertoli cells from the basement membranes. Spermatogenesis is present. Scattered Leydig cells are present (arrow). **(C)** A case with moderate tubular injury shows loss and sloughing of intratubular cells into the lumens (asterisks). There is marked interstitial edema. Note the normal spermatogenesis. **(D)** Testis from a non-COVID patient with protracted disease shows normal spermatogenesis. In the interstitium there is edema and mild inflammatory infiltrates composed predominantly of **(E)** CD3-positive T lymphocytes and **(F)** CD68-positive histiocytes according to immunohistochemistry. COVID-19 = coronavirus disease 2019.

Table 2 – Pathological findings in the testes of 12 COVID-19 patients.

Case no.	Tubular injury	Leydig cells	Spermatogenesis	SARS-CoV-2 (RT-PCR)		Electron microscopy
				Lung	Testis	
S20-4	Severe	2.0	Hypospermatogenesis, MPH	+	–	ND
S20-5	ND	ND	ND	+	+	ND
S20-6	Moderate	2.2	Hypospermatogenesis, MPH	+	–	ND
S20-7	Moderate	0.44	Maturation arrest, MPH	+	–	ND
S20-9	Moderate	1.6	Spermatogenesis appropriate for age	–	–	ND
S20-12	Mild	2.82	Hypospermatogenesis	+	–	Not detected
S20-14	Moderate	5.3	Spermatogenesis appropriate for age	+	–	Not detected
S20-19	Moderate	1.0	Spermatogenesis appropriate for age	+	–	ND
S20-20	Mild	3.6	Maturation arrest	+	–	Not detected
S20-22	Severe	ND	Maturation arrest, MPH	+	–	ND
S20-23	Severe	1.0	Hypospermatogenesis	–	–	ND
S20-24	Severe	1.5	Maturation arrest, MPH	+	–	ND

MPH = mild peritubular hyalinization; ND = not determined; RT-PCR = reverse transcription-polymerase chain reaction; SARS-CoV-2 = severe acute respiratory syndrome coronavirus 2.

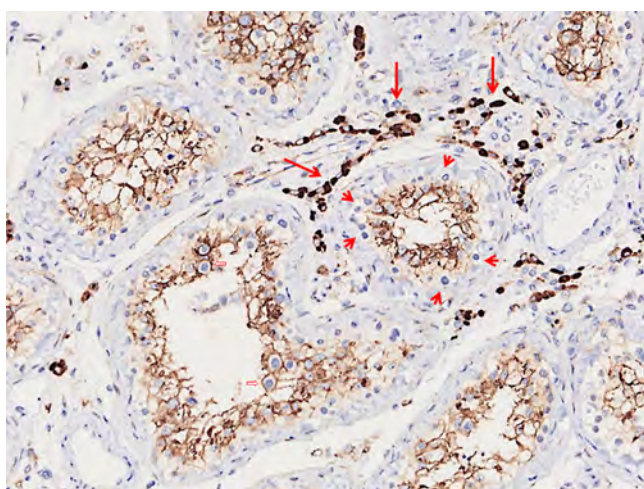


Fig. 2 – ACE2 is diffusely expressed in Sertoli cells and strongly expressed in Leydig cells (long arrows) according to immunohistochemistry. Spermatogonia are negative (short arrows). Spermatocytes of later stages are surrounded by the Sertoli cell cytoplasm (open arrows).

Technology have advised caution regarding sperm donation by COVID-19 patients [16]. However, in our study we did not find evidence of the presence of SARS-CoV-2 in testicular tissue or germ cells. Of the ten cases for whom viral RNA was detected in lung tissue by RT-PCR, nine cases were negative for the virus in testicular tissue. Only one case was positive for the virus in the testis. This patient had a high viral load and his lung, kidney, and spleen, in addition to testis, were positive for the virus by RT-PCR. The testicular tissue sampled contained predominantly fibrovascular tissue and very few seminiferous tubules. It is likely that RT-PCR detected the virus present in blood rather than in testicular tissue. We also performed electron microscopy for three of the 12 cases (S20-12, S20-14, and S20-20). Viral particles were not identified in any case. Our study supports the finding in

two recent reports that SARS-CoV-2 was not detected in semen for a total of 46 patients after a median of 31 d from COVID-19 diagnosis [10,11]. Testicular tissue from a deceased COVID-19 patient tested negative for the virus on RT-PCR [11]. However, it remains possible that the virus may attack testicular tissue early on but is cleared from the testes later during the disease course, as testicular tissue was obtained 41 d after disease onset in this study and semen was obtained 31 d after disease onset in the study by Pan et al [10]. Further studies are needed to address whether the virus can be found in the testis in the early phase of COVID-19. However, the data so far demonstrate no evidence of the virus in semen or testicular tissue later in the disease course (30–40 d after disease onset), suggesting that sperm donation or an impregnation plan could be considered during convalescence for COVID-19 patients.

We observed morphological changes suggestive of significant damage to seminiferous tubules. Sertoli cells exhibited “ballooning” changes, vacuolation, and detachment from basement membranes. There was loss and sloughing into the lumens of tubular cells. We observed interstitial edema and mild lymphocytic inflammation with predominantly T lymphocytes, consistent with viral orchitis. Furthermore, the number of Leydig cells in the interstitium was significantly reduced in COVID-19 patients. It is intriguing that both Sertoli and Leydig cells have strong expression of ACE2, a cell-surface receptor to which SARS-CoV-2 binds to gain entry into cells. Even though we did not find the virus in seminiferous tubules or Leydig cells, we speculate that viral membrane proteins, such as the spike protein, may play a role in the injury to seminiferous tubules and Leydig cells. Alternatively, hyperthermia, secondary infection, hypoxia, and steroids may play a role in the tissue damage observed in the testis of COVID-19 patients.

Our study found that spermatogenesis was not altered and was appropriate for age in COVID-19 patients during the acute phase of the disease. Sertoli cells play a critical role in the homeostasis of seminiferous tubules and spermatogenesis [17] and Leydig cells are involved in androgen production [18],

so the pathology observed may lead to seminiferous tubule damage and endocrine abnormality and eventual reduced or even absent spermatogenesis in patients who have recovered from COVID-19. Our findings suggest that studies should be undertaken to find ways to mitigate the risk of testicular injury during the COVID-19 disease course.

5. Conclusions

We reported on pathological changes in 12 testes from patients who died of COVID-19. We found no evidence of SARS-CoV-2 virus in the testes in the majority (90%) of the cases by RT-PCR, and in none of the cases by electron microscopy. However, there was significant injury to Sertoli cells and seminiferous tubules, reduction of Leydig cells, and mild inflammatory infiltrates in the interstitium. These findings can provide evidence-based guidance for sperm donation and inform management strategies to mitigate the risk of testicular injury during the COVID-19 disease course.

Author contributions: Ming Zhou had full access to all the data in the study and takes responsibility for the integrity of the data and the accuracy of the data analysis.

Study concept and design: Yang, M. Zhou, Nie.

Acquisition of data: Yang, S. Chen, Huang, Zhong, Su, Y.-J. Chen, Cao, Ma, He, X.-F. Li, X. Li, J.-J. Zhou, Fan, Luo, Chang, M. Zhou.

Analysis and interpretation of data: Yang, M. Zhou.

Drafting of the manuscript: Yang, M. Zhou, Nie.

Critical revision of the manuscript for important intellectual content: Yang, M. Zhou, Nie.

Statistical analysis: Yang.

Obtaining funding: Yang, Nie, Su.

Administrative, technical, or material support: Yang.

Supervision: M. Zhou, Nie.

Other: None.

Financial disclosures: Ming Zhou certifies that all conflicts of interest, including specific financial interests and relationships and affiliations relevant to the subject matter or materials discussed in the manuscript (eg, employment/affiliation, grants or funding, consultancies, honoraria, stock ownership or options, expert testimony, royalties, or patents filed, received, or pending) are the following: None.

Funding/Support and role of the sponsor: This work was supported by funding from a Key Special Project of the Ministry of Science and Technology of China (grant 2020YFC0845700), Fundamental Research Funds for the Central Universities (grant 2020kfyXGYJ101), and the National Natural Science Foundation of China (grant 81773022). The sponsors played a role in the design and conduct of the study; collection, management, analysis, and interpretation of the data; and preparation, review, and approval of the manuscript.

Acknowledgments: We thank Dr. Yu Yang from the Department of Pathology of Deaconess Hospital, Evansville, IN, USA for his advice on this work. Drs. Si-Hua Wang, Yi Zheng, and Cheng Yu contributed to the

postmortem biopsy work. We thank all the patients and their family members involved in the study.

References

- [1] World Health Organization. Coronavirus disease 2019 (COVID-19) situation report 105. www.who.int/docs/default-source/coronaviruse/situation-reports/20200504-covid-19-sitrep-105.pdf?sfvrsn=4cdda8af_2.
- [2] Harapan H, Itoh N, Yufika A, et al. Coronavirus disease 2019 (COVID-19): a literature review. *J Infect Public Health* 2020;13:667–73.
- [3] Yao XH, Li TY, He ZC, et al. A pathological report of three COVID-19 cases by minimally invasive autopsies. *Zhonghua Bing Li Xue Za Zhi* 2020;49:E009.
- [4] Tian S, Xiong Y, Liu H, et al. Pathological study of the 2019 novel coronavirus disease (COVID-19) through postmortem core biopsies. *Mod Pathol*. In press. <https://doi.org/10.1038/s41379-020-0536-x>.
- [5] Xu Z, Shi L, Wang Y, et al. Pathological findings of COVID-19 associated with acute respiratory distress syndrome. *Lancet Respir Med* 2020;8:420–2.
- [6] Tian S, Hu W, Niu L, Liu H, Xu H, Xiao SY. Pulmonary pathology of early-phase 2019 novel coronavirus (COVID-19) pneumonia in two patients with lung cancer. *J Thorac Oncol* 2020;15:700–4.
- [7] Zhang H, Zhou P, Wei Y, et al. Histopathologic changes and SARS-CoV-2 immunostaining in the lung of a patient with COVID-19. *Ann Intern Med* 2020;172:629–32.
- [8] Wang Z, Xu X. scRNA-seq profiling of human testes reveals the presence of the ACE2 receptor, a target for SARS-CoV-2 infection in spermatogonia, Leydig and Sertoli cells. *Cells* 2020;9:920.
- [9] Barton LM, Duval EJ, Stroberg E, Ghosh S, Mukhopadhyay S. COVID-19 autopsies, Oklahoma, USA. *Am J Clin Pathol* 2020;153:725–33.
- [10] Pan F, Xiao X, Guo J, et al. No evidence of SARS-CoV-2 in semen of males recovering from COVID-19. *Fertil Steril*. In press. <https://doi.org/10.1016/j.fertnstert.2020.04.024>.
- [11] Song C, Wang Y, Li W, et al. Absence of 2019 novel coronavirus in semen and testes of COVID-19 patients. *Biol Reprod*. In press. <https://doi.org/10.1093/biolre/iaaa050>.
- [12] National Health Commission of the People's Republic of China. New coronavirus pneumonia prevention and control program (7th edition). www.nhc.gov.cn/yzygj/s7653p/202003/46c9294a7dfe4cef80dc7f5912eb1989.shtml.
- [13] Su H, Yang M, Wan C, et al. Renal histopathological analysis of 26 postmortem findings of patients with COVID-19 in China. *Kidney Int*. In press. <https://doi.org/10.1016/j.kint.2020.04.003>.
- [14] Liu W, Han R, Wu H, Han D. Viral threat to male fertility. *Andrologia* 2018;50:e13140.
- [15] Xu J, Qi L, Chi X, et al. Orchitis: a complication of severe acute respiratory syndrome (SARS). *Biol Reprod* 2006;74:410–6.
- [16] American Society for Reproductive Medicine. SART and ASRM issue advice for infertility patients concerning the novel coronavirus (COVID-19). www.asrm.org/news-and-publications/news-and-research/press-releases-and-bulletins/sart-and-asrm-issue-advice-for-infertility-patients-concerning-the-novel-coronavirus-covid-19/.
- [17] Griswold MD. The central role of Sertoli cells in spermatogenesis. *Semin Cell Dev Biol* 1998;9:411–6.
- [18] Zirkin BR, Papadopoulos V. Leydig cells: formation, function, and regulation. *Biol Reprod* 2018;99:101–11.

RESEARCH ARTICLE

Open Access



Pregnant women with COVID-19 and risk of adverse birth outcomes and maternal-fetal vertical transmission: a population-based cohort study in Wuhan, China

Rong Yang¹, Hui Mei¹, Tongzhang Zheng², Qiang Fu³, Yiming Zhang¹, Stephen Buka², Xinan Yao⁴, Zezhong Tang⁵, Xichi Zhang⁶, Lin Qiu¹, Yaqi Zhang¹, Jieqiong Zhou¹, Jiangxia Cao¹, Youjie Wang^{7*} and Aifen Zhou^{1*}

Abstract

Background: The coronavirus disease 2019 (COVID-19) outbreak is evolving rapidly worldwide. However, little is known about the association between pregnant women with COVID-19 and the risk of adverse birth outcomes.

Method: We conducted a retrospective cohort study based on the Maternal and Child Health Information System (MCHIMS) of Wuhan, China. All pregnant women with singleton live birth recorded by the system between January 13 and March 18, 2020, were included. The adverse birth outcomes were preterm birth, low birth weight, neonatal asphyxia, premature rupture of membrane (PROM), and cesarean section delivery. Multivariate logistic regression was used to evaluate the associations between maternal COVID-19 diagnosis and adverse birth outcomes.

Results: Out of 11,078 pregnant women, 65 were confirmed with coronavirus disease 2019 (COVID-19). No deaths occurred from these confirmed cases or their newborns. Compared to pregnant women without COVID-19, pregnant women with a confirmed COVID-19 diagnosis had an increased risk of preterm birth (OR 3.34, 95% CI 1.60–7.00) and cesarean section (OR 3.63, 95% CI 1.95–6.76). There was no statistical difference in low birth weight, neonatal asphyxia, and PROM between the mothers with and without COVID-19. Among these newborns that were born to mothers with confirmed COVID-19, none was tested severe acute respiratory syndrome coronavirus 2 (SARS-CoV-2) positive or had abnormal CT results. Only one had diarrhea and three had a fever.

Conclusions: This population-based cohort study suggests that COVID-19 during the later pregnancy is associated with an increased risk of adverse birth outcomes, including iatrogenic preterm birth and cesarean section delivery. Our data provide little evidence for maternal-fetal vertical transmission of SARS-CoV-2. It is important to monitor the long-term health effects of SARS-CoV-2 infection on pregnant women and their children.

Keywords: COVID-19, Birth outcome, Maternal-fetal vertical transmission

* Correspondence: wangyoujie@mails.tjmu.edu.cn; april1972@163.com

⁷Department of Maternal and Child Health, School of Public Health, Tongji Medical College, Huazhong University of Science & Technology, 13 Hangkong Road, Wuhan 430030, China

¹Wuhan Children's Hospital (Wuhan Maternal and Child Healthcare Hospital), Tongji Medical College, Huazhong University of Science & Technology, 100 Xianggang Road, Wuhan 430030, China

Full list of author information is available at the end of the article



© The Author(s). 2020 **Open Access** This article is licensed under a Creative Commons Attribution 4.0 International License, which permits use, sharing, adaptation, distribution and reproduction in any medium or format, as long as you give appropriate credit to the original author(s) and the source, provide a link to the Creative Commons licence, and indicate if changes were made. The images or other third party material in this article are included in the article's Creative Commons licence, unless indicated otherwise in a credit line to the material. If material is not included in the article's Creative Commons licence and your intended use is not permitted by statutory regulation or exceeds the permitted use, you will need to obtain permission directly from the copyright holder. To view a copy of this licence, visit <http://creativecommons.org/licenses/by/4.0/>. The Creative Commons Public Domain Dedication waiver (<http://creativecommons.org/publicdomain/zero/1.0/>) applies to the data made available in this article, unless otherwise stated in a credit line to the data.

Background

The outbreak of SARS-CoV-2 infection has become a global epidemic threat since the end of 2019 [1–4]. As of April 14, the cumulative number of confirmed COVID-19 cases had reached 1,930,000 with 120,000 (6%) deaths worldwide. The world is now launching a forceful, focused campaign to eradicate COVID-19. Wuhan, the capital of Hubei province where COVID-19 was first reported, was the hardest-hit Chinese city and accounts for 60% of confirmed cases and 83% of COVID-19 deaths in China. SARS-CoV-2 is a new virus that results in a spectrum of illness ranging from asymptomatic to severe acute respiratory distress syndrome and death [2, 3, 5]. The consequences of infection with SARS-CoV-2 among pregnant women are currently uncertain. Several hundreds of pregnant women in Hubei province were infected with SARS-CoV-2 based on infectious disease surveillance systems in Hubei province, China. While several case series studies have analyzed the clinical symptoms and prognosis of COVID-19 cases, no population-based study so far has been conducted to examine the relationship between SARS-CoV-2 infection and adverse birth outcomes.

Several case series with small sample sizes have examined the potential for in utero vertical transmission of SARS-CoV-2 in infected pregnant women in China. In a report involving two pregnant women with confirmed COVID-19, the two newborns were reported to be negative for SARS-CoV-2 tests [6]. A study involving 9 confirmed pregnant women with COVID-19 in Wuhan found no evidence of in utero vertical transmission of SARS-CoV-2 among their newborns [7]. A study involving 6 newborns born to mothers with confirmed COVID-19 also reported negative SARS-CoV-2 tests while virus-specific antibodies IgM and IgG were detected in 2 of the newborns, suggesting a possibility of in utero SARS-CoV-2 infection [8]. A recent single case study from Wuhan also suggests the potential in utero infection of the neonate [9].

Large population-based studies are urgently needed to evaluate if SARS-CoV-2 infection during pregnancy could affect pregnancy outcomes and result in utero vertical transmission. Such data would provide key information for the protection of women and children. This population-based cohort study in Wuhan for the first time evaluated the relationship between SARS-CoV-2 infection during later pregnancy and risk of adverse birth outcomes including preterm birth, low birth weight, PROM, neonatal asphyxia, and cesarean section. It also investigated the potential in utero vertical transmission at the population level.

Methods

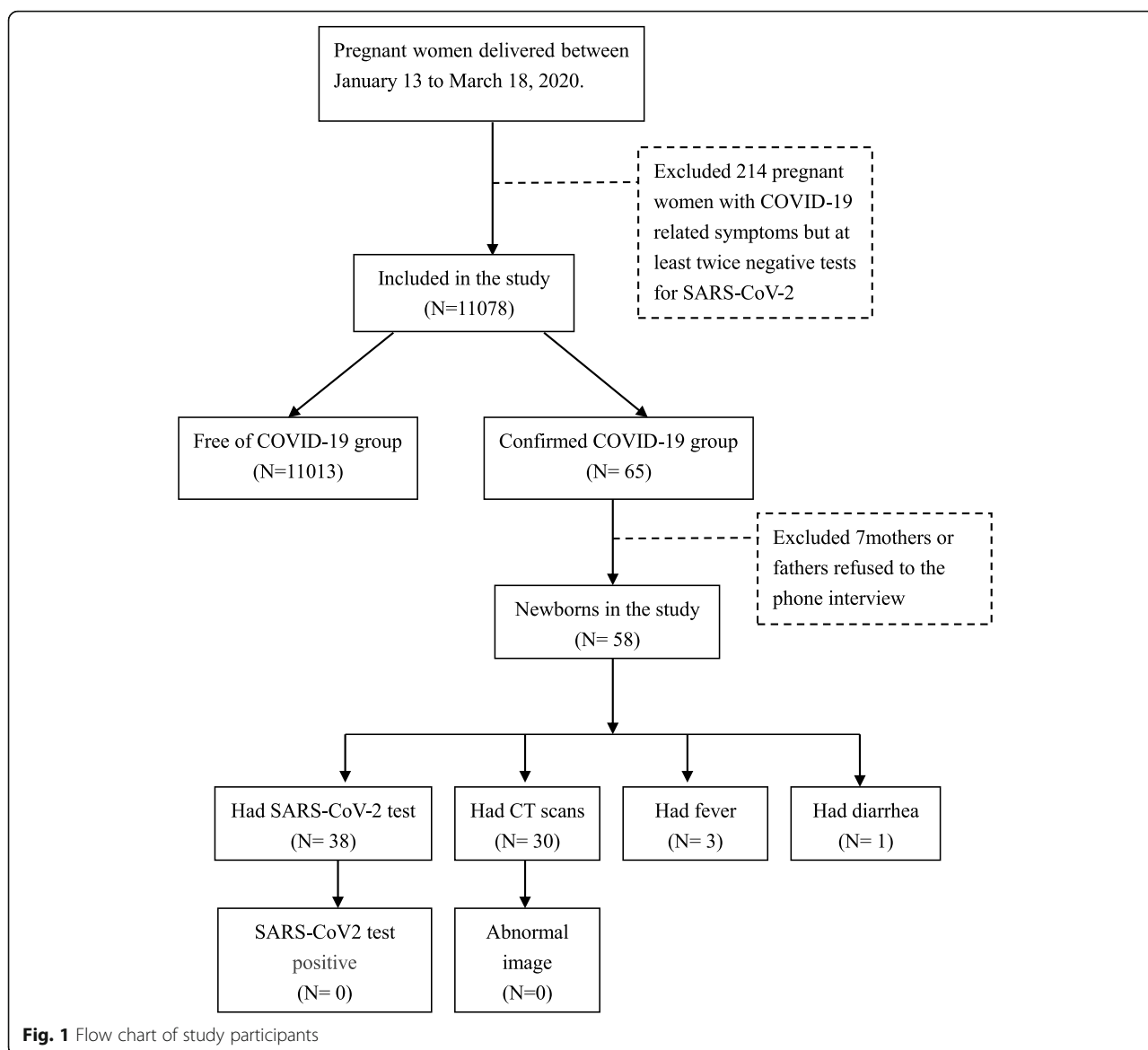
Sample

This population-based cohort study was conducted in Wuhan, the first reported city of the outbreak of

COVID-19 in China. We used the Maternal and Child Health Information Management System of Wuhan (MCHIMS) to identify the study population. The MCHIMS is used to monitor maternal and children's health by collecting information for all pregnant women and their children in the Wuhan metropolitan area. During the outbreak of COVID-19 in Wuhan, in addition to routine prenatal care data from clinical and laboratory examinations and socio-demographic information, the MCHIMS also recorded the COVID-19 diagnosis for pregnant women as part of the high-risk pregnancy surveillance during the COVID-19 pandemic in Wuhan. The pregnant women of Wuhan residents satisfying the following conditions will be included in the study: (1) gave a single live birth between January 13 and March 18, 2020 (that is, between the date of the first recorded COVID-19 case of pregnant women and the last date with available data for the study from the MCHIMS system), and (2) registered by the MCHIMS with either confirmed COVID-19 or free of COVID-19. We excluded the 214 pregnant women with COVID-19-related symptoms but at least twice tests of a negative result of SARS-CoV-2 detection. Finally, a total of 11,078 pregnant women satisfied the study criteria and were included in this study, 65 of them were recorded as confirmed cases of COVID-19. Among 11,013 women without a diagnosis of COVID-19 pregnant women, 4778 were admitted before February 3, 2020. The flow chart for the recruitment of study subjects is presented in Fig. 1.

Diagnosis of COVID-19

The study population was classified into confirmed COVID-19 group and free COVID-19 group. The diagnosis of COVID-19 was based on the clinical diagnostic criteria of the New Corona Virus Infected Pneumonia Diagnosis and Treatment Plan issued by the Chinese National Health and Health Commission in 2020 [10]. The confirmed cases of COVID-19 had taken at least twice tests for SARS-CoV-2, which used real-time RT-PCR based on a pharyngeal swab. During the outbreak, all pregnant women in Wuhan were under increased surveillance for COVID-19 and given top priority for SARS-CoV-2 testing and hospitalization. Due to the lack of available tests during the early phase of the pandemic (before February 4, 2020), only the pregnant women developing the symptoms like fever and cough or having abnormal computed tomography (CT) scan were tested for SARS-CoV-2. Since February 4, 2020, all pregnant women giving birth in hospitals were screened for the SARS-CoV-2. Pregnant women without COVID-19-related signs or symptoms were tested for the virus only once, while pregnant women with COVID-19-related signs or symptoms were tested for at least two times if the first detection was negative. Because of the



assumption from the severe acute respiratory syndrome (SARS) studies that there is no vertical transmission, all the newborns born to the infected mothers were separated from their mother immediately after delivery and were brought home unless medical observation or treatment was needed. To obtain information on COVID-19 diagnosis or SARS-CoV-2 infection status for the newborns born to these mothers with confirmed COVID-19, the study obstetricians at Wuhan Children's Hospital made follow-up phone calls. Mothers diagnosed with COVID-19 were directly transferred to specialty hospitals after delivery for treatment. After successful treatment, they were removed to facilities for quarantine for 14 days and these follow-up calls were made to their home usually after their discharge. All participants provided oral informed consent before the telephone interview.

Maternal and newborn variables

The information in the phone interviews was typically provided by the mothers, rarely by fathers. Maternal information abstracted from the MCHIMS includes age, education, employment, gestational age, gravidity, parity, pregnancy-induced hypertension, gestational diabetes mellitus, PROM, and SARS-CoV-2 infection. For the newborns, the abstracted information included sex, gestational week, preterm birth, birth weight, and neonatal asphyxia. Both maternal and newborn information was input based on the medical records by the health professionals in the delivery hospital. Primary outcomes for the newborns were preterm birth (< 37 weeks of pregnancy), low birth weight (< 2500), PROM (defined as rupture of membrane before the onset of labor), and neonatal asphyxia (defined as 1 min Apgar score ≤ 7 and umbilical arterial blood gas pH < 7.15 [11]).

Statistical analyses

Study population characteristics are presented by proportion for categorical variables. Univariate chi-square analyses were conducted to evaluate rates of birth outcomes by comparing the two groups of mothers with or without confirmed COVID-19. Multivariate logistic regression models were used to evaluate the associations between maternal COVID-19 status and adverse birth outcomes, adjusted for potential confounding variables. The following variables were included in the final models: maternal age (14–24, 25–34, 35–54), occupation (employed, housewives, part-time), education (bachelor's degree or above, high school, vocation degree, middle school or below), gravidity (1, 2, 3–10), parity (1, 2, 3–5), gestational hypertension (yes, no), preeclampsia (yes, no), gestational diabetes mellitus (yes, no), and PROM (yes, no). All analyses were performed using SAS version 9.4 (SAS Institute, Inc., Cary, North Carolina). The study was approved by the Human Ethics Committees at Wuhan Children's Hospital.

Results

Of the 11,078 pregnant women with singleton live births during the study period, 65 (0.57%) were diagnosed with COVID-19. Table 1 shows the demographic variables and pregnancy complications for these 11,078 pregnant women, and there were few differences between these pregnant women based on their COVID-19 status. Confirmed cases had higher educational attainment than the rest of the sample, with modest occupational differences as well.

Table 2 shows that the mothers with confirmed COVID-19 had a significantly higher rate of preterm birth and cesarean section. All preterm babies born to infected mothers in the present study were iatrogenic preterm birth. No significant differences in neonatal asphyxia, low birth weight, and PROM were observed between the two groups.

Figure 2 shows the multivariate logistic regression results for the associations between maternal COVID-19 status and the risk of adverse birth outcomes. Compared to mothers without COVID-19, mothers with confirmed COVID-19 had an adjusted OR of 3.34 (95% CI 1.60, 7.00) for preterm birth and an adjusted OR of 3.63 (95% CI 1.95, 6.76) for receiving cesarean section.

Table 3 presents the association between maternal COVID-19 diagnosis and preterm birth from mothers with cesarean section delivery. Compared to mothers without COVID-19, mothers with confirmed COVID-19 had an adjusted OR of 3.71 (95% CI 1.70, 8.03) for preterm birth among mothers with cesarean section delivery.

We reached 58 parents of the 65 confirmed maternal COVID-19 cases (89%) through phone calls by study

Table 1 Distribution of the characteristics of the study population by maternal COVID-19 status in Wuhan, China

Variables	COVID-19 status		P
	Free	Confirmed	
Age range, years			.60
< 25	805 (7)	4 (6)	
25–34	8610 (78)	54 (83)	
≥ 35	1598 (15)	7 (11)	
Education levels			< 0.001
Bachelor's degree or above	3179 (29)	42 (65)	
High school	1634 (15)	5 (7)	
Vocation degree	1952 (18)	7 (11)	
Middle school or below	2359 (21)	8 (12)	
Missing	1889 (17)	3 (5)	
Occupation			.04
Employed	3874 (35)	33 (51)	
Housewives	4001 (36)	20 (31)	
Part-time	3138 (29)	12 (18)	
Gravidity			.99
1	4658 (42)	27 (42)	
2	3182 (29)	19 (29)	
≥ 3	3173 (29)	19 (29)	
Parity			.36
1	6425 (58)	41 (63)	
2	4318 (39)	21 (32)	
≥ 3	27 (3)	3 (5)	
History of abortion			.57
0	6692 (61)	37 (57)	
1–2	3794 (34)	23 (35)	
≥ 3	527 (5)	5 (8)	
Gestational hypertension			.44
Yes	325 (3)	3 (5)	
No	10,688 (97)	62 (95)	
Preeclampsia			.39
Yes	83 (1)	1 (1)	
No	10,930 (99)	64 (99)	
Gestational diabetes mellitus			.07
Yes	1207 (11)	3 (5)	
No	9806 (89)	62 (95)	

obstetricians to determine the newborns' COVID-19 and/or SARS-CoV-2 infection status. As shown in Table 4, out of 58 newborns born to mothers with confirmed COVID-19, 38 newborns had the SARS-CoV-2 test and none of the newborns tested positive for SARS-CoV-2. For those who had CT scans, none of the 30 newborns born to mothers with confirmed COVID-19 was reported to have abnormal CT scan images. Three

Table 2 The birth outcomes of the newborns by maternal COVID-19 status in Wuhan, China

Variables	COVID-19 status		P
	Free	Confirmed	
Sex			.90
Male	5880 (53)	36 (55)	
Female	5124 (47)	29 (45)	
Unknown	9 (0)	0	
Asphyxia			.33
Yes	158 (1)	2 (3)	
No	10,855 (99)	63 (97)	
PROM			.15
Yes	1248 (11)	4 (6)	
No	9765 (89)	61 (94)	
Preterm birth			.01
Yes	579 (5)	9 (14)	
No	10,434 (95)	56 (86)	
Delivery mode			< 0.001
Vaginal delivery	4993 (45)	13 (20)	
Cesarean section	6020 (55)	52 (80)	

of the 58 newborns born to the mothers with confirmed COVID-19 reported to have fever, and 1 of them had diarrhea.

Discussion

Using population-based data for 11,078 pregnant women and their singleton live births in Wuhan city, we for the

Table 3 The association between maternal COVID-19 diagnosis and preterm births from mothers receiving the cesarean section

COVID-19	Preterm birth		OR [†] (95% CI)	OR [‡] (95% CI)
	Yes	No		
Free	363	5657	1.00	1.00
Confirmed	9	43	3.26 (1.58, 6.74)	3.71 (1.70, 8.03)

[†]Crude ORs

[‡]Adjusted for maternal age (14–24, 25–34, 35–54), occupation (employed, housewives, part-time), education (bachelor's degree or above, high school, vocation degree, middle school or below), gravidity (1, 2, 3–10), parity (1, 2, 3–5), gestational hypertension (yes, no), preeclampsia (yes, no), gestational diabetes mellitus (yes, no), and premature rupture of membranes (yes, no)

first time investigated if SARS-CoV-2 infection affects pregnancy outcomes and evidence for potential vertical transmission. Our study results showed that pregnant women with confirmed COVID-19 had an increased risk of adverse birth outcomes including preterm birth, and delivery with cesarean section compared to pregnant women without COVID-19. We also found no strong evidence suggesting a vertical maternal-fetal transmission of SARS-CoV-2.

Early studies have shown that physiologic and immunologic changes during pregnancy might increase the risk for pregnant women to be infected with respiratory viruses such as influenza [12, 13]. It has been reported that pregnant women are more susceptible to be infected, develop more severe complications of the disease, and have higher mortality compared to the non-pregnant population [14]. However, the infection rate of SARS-CoV-2 among pregnant women (0.57%) in the present study was comparable to that (0.50%) in the

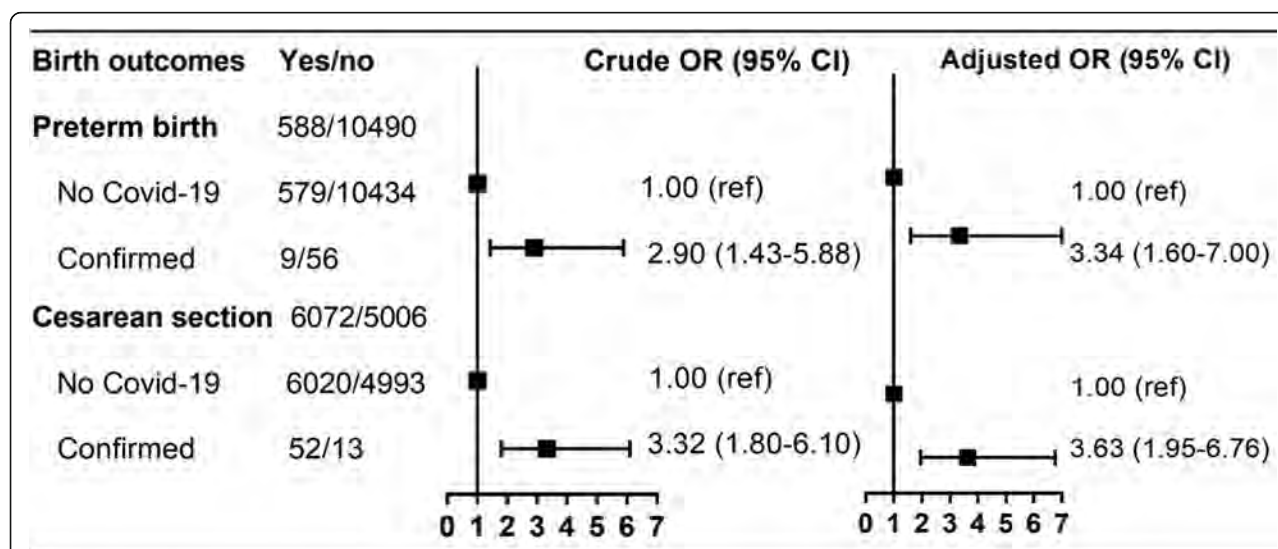


Fig. 2 Risk of adverse birth outcomes by maternal COVID-19 status in Wuhan, China. Adjusted for maternal age (14–24, 25–34, 35–54), occupation (employed, housewives, part-time), education (bachelor's degree or above, high school, vocation degree, middle school or below), gravidity (1, 2, 3–10), parity (1, 2, 3–5), gestational hypertension (yes, no), preeclampsia (yes, no), gestational diabetes mellitus (yes, no), and premature rupture of membranes (yes, no)

Table 4 The clinical manifestation and SARS-CoV2 test results for the 58 newborns born to mothers with confirmed COVID-19 in Wuhan, China

Test results or symptoms	Newborns (n = 58)
SARS-CoV2 test positive	0/38
Abnormal image of chest CT	0/30
Diarrhea	1/58
Fever	3/58

general population in Wuhan. Unlike several hospital-based studies with small sample sizes that have shown that SARS infection increases morbidity and mortality of pregnant women [15], no deaths were reported among the confirmed COVID-19 cases from the current sample of 11,078 pregnant women.

In our study, the confirmed COVID-19 mothers had higher educational attainment than mothers without the disease, with modest occupational differences as well. In China, people with higher education are more likely employed and, due to the severe traffic jam experienced in Wuhan, working people frequently used public transportation to commute to work, which increases opportunities to be exposed to the virus. Increased interpersonal contacts at the workplace further increase their risk of infection.

Our study demonstrated that pregnant women with COVID-19 were more likely to have preterm birth babies. Considering all preterm babies were born to infected mothers were iatrogenic preterm birth due to intrauterine fetal distress, we examined the possibility that the elevated risk for preterm birth resulted from higher rates of elective and early cesarean sections (Table 3), the positive association still exists among mothers with cesarean section. Previous studies have also shown that SARS and Middle East respiratory syndrome (MERS) infections are related to preterm birth, intensive care treatment for newborns, and even perinatal death [15]. A higher rate of cesarean section was found among the infected mothers in the present study; the odds of cesarean births were three times or greater among women with COVID-19 compared to those without COVID-19. However, only when there were indications posed by SARS-CoV-2 infection to pregnant women or fetuses, such as maternal breathlessness and related complications as well as fetal intrauterine distress, cesarean sections were performed as needed. Thus, those symptoms of COVID-19 have contributed to the high rate of cesarean section among the infected mothers.

It is of great concern if there is a maternal-fetal vertical transmission after SARS-CoV-2 infection. In the present study, 38 newborns born to 65 mothers with confirmed COVID-19 had tested for SARS-CoV-2, and

all of them had negative test results. Similarly, several hospital-based small case series studies conducted in Wuhan also do not support vertical transmission [16, 17]. The lack of maternal-fetal transmission was also reported in early studies of SARS and MERS infection in pregnant women [15]. However, several recent case series have suggested a possibility of vertical transmission of SARS-CoV-2, including a recently reported single case study from Wuhan that shows a neonate born to a mother with COVID-19 had elevated IgM antibody level 2 h after birth [8, 9]. Since IgM antibodies are not transferred to the fetus via the placenta [18], and usually do not appear until 3 to 7 days after infection, the observation appears to support that the neonate was infected in utero. However, the results from 5 RT-PCR tests on nasopharyngeal swabs taken from 2 h to 16 days of newborns were negative in the current study.

Conclusions

Our population-based cohort study in Wuhan shows that SARS-CoV-2 infection or diagnosis with COVID-19 during late pregnancy is associated with an increased risk of iatrogenic preterm birth and delivery with a cesarean section. In addition, our study has found little evidence to support maternal-fetal vertical transmission.

Abbreviations

COVID-19: Coronavirus disease 2019; CT: Computed tomography; MCHIMS: Maternal and Child Health Information Management System; MERS: Middle East respiratory syndrome; PROM: Premature rupture of membrane; SARS: Severe acute respiratory syndrome; SARS-CoV-2: Severe acute respiratory syndrome coronavirus 2

Acknowledgements

The authors thank the study obstetricians for their high-quality interviewing. The data used in this study were obtained from the Wuhan Maternal and Child Health Information Management System (MCHIMS). Special thanks go to Dr. Jianbo Shao at the Wuhan Children's Hospital for his support and guidance of the study.

Authors' contributions

A.F.Z. and Y.J.W. designed the study. R.Y. and F.Q. take responsibility for the data analysis. Y.J.W., R.Y., and X.A.Y. drafted the manuscript. H.M., Y.M.Z., Z.Z.T., Y.Q.Z., L.Q., J.X.C., and J.Q.Z. contributed to the data collection, data interpretation, and literature search. T.Z.Z., S.B., F.Q., and X.C.Z. had roles in revising the manuscript and editing assistance. All authors reviewed and revised the manuscript and approved the final version. The corresponding authors attest that all listed authors meet the authorship criteria and that no others meeting the criteria have been omitted.

Funding

This study is partially supported by the US National Institute of Environmental Health Science [R01ES029082].

Availability of data and materials

The datasets for the current study are available from the corresponding authors on reasonable request.

Ethics approval and consent to participate

The study protocol was approved by the Human Ethics Committee of the Wuhan Children's Hospital (Wuhan Maternal and Child Healthcare Hospital), Tongji Medical College, Huazhong University of Science & Technology. All participants provided oral informed consent before the telephone interview.

Competing interests

The authors declare no conflict of interest.

Author details

¹Wuhan Children's Hospital (Wuhan Maternal and Child Healthcare Hospital), Tongji Medical College, Huazhong University of Science & Technology, 100 Xianggang Road, Wuhan 430030, China. ²School of Public Health, Brown University, Providence, RI 02903, USA. ³Department of Epidemiology and Biostatistics, College for Public Health and Social Justice, Saint Louis University, 3545 Lafayette Ave., St. Louis, MO 63104, USA. ⁴Krannert School of Management, Purdue University, 475 Stadium Mall Drive, West Lafayette, IN 47906-2050, USA. ⁵Department of Pediatrics, Peking University First Hospital, 8 Xishiku Street, Beijing 100034, China. ⁶Rollins School of Public Health, Emory University, 1518 Clifton Rd, NE, Atlanta, GA 30322, USA. ⁷Department of Maternal and Child Health, School of Public Health, Tongji Medical College, Huazhong University of Science & Technology, 13 Hangkong Road, Wuhan 430030, China.

Received: 14 May 2020 Accepted: 25 September 2020

Published online: 19 October 2020

References

- Bar-On YM, Flamholz A, Phillips R, Milo R. SARS-CoV-2 (COVID-19) by the numbers. *Elife*. 2020;9:e57309.
- Chen N, Zhou M, Dong X, Qu J, Gong F, Han Y, et al. Epidemiological and clinical characteristics of 99 cases of 2019 novel coronavirus pneumonia in Wuhan, China: a descriptive study. *Lancet*. 2020;395(10223):507–13.
- Huang C, Wang Y, Li X, Ren L, Zhao J, Hu Y, et al. Clinical features of patients infected with 2019 novel coronavirus in Wuhan, China. *Lancet*. 2020;395(10223):497–506.
- Zhu N, Zhang D, Wang W, Li X, Yang B, Song J, et al. A novel coronavirus from patients with pneumonia in China, 2019. *N Engl J Med*. 2020;382(8):727–33.
- Wang Z, Yang B, Li Q, Wen L, Zhang R. Clinical features of 69 cases with coronavirus disease 2019 in Wuhan, China. *Clin Infect Dis*. 2020;71(15):769–77.
- Fan C, Lei D, Fang C, Li C, Wang M, Liu Y, et al. Perinatal transmission of COVID-19 associated SARS-CoV-2: should we worry? *Clin Infect Dis*. 2020; ciaa226. <https://doi.org/10.1093/cid/ciaa226>.
- Chen H, Guo J, Wang C, Luo F, Yu X, Zhang W, et al. Clinical characteristics and intrauterine vertical transmission potential of COVID-19 infection in nine pregnant women: a retrospective review of medical records. *Lancet*. 2020;395(10226):809–15.
- Zeng L, Xia S, Yuan W, Yan K, Xiao F, Shao J, et al. Neonatal early-onset infection with SARS-CoV-2 in 33 neonates born to mothers with COVID-19 in Wuhan, China. *JAMA Pediatr*. 2020;174(7):722–5.
- Dong L, Tian J, He S, Zhu C, Wang J, Liu C, et al. Possible vertical transmission of SARS-CoV-2 from an infected mother to her newborn. *JAMA*. 2020;323(18):1846–8.
- Diagnosis and treatment protocol for novel coronavirus pneumonia (trial version 7) <http://www.nhc.gov.cn/yzygj/s7653p/202003/46c9294a7dfe4cef80dc7f5912eb1989.shtml>. 3 Mar 2020.
- Neonatal Resuscitation Work Group CMA. Expert consensus on the diagnosis of neonatal asphyxia. *Chin J Perinat Med*. 2016;19(1):3–6.
- Jamieson DJ, Honein MA, Rasmussen SA, Williams JL, Swerdlow DL, Biggerstaff MS, et al. H1N1 2009 influenza virus infection during pregnancy in the USA. *Lancet*. 2009;374(9688):451–8.
- Lindsay L, Jackson LA, Savitz DA, Weber DJ, Koch GG, Kong L, et al. Community influenza activity and risk of acute influenza-like illness episodes among healthy unvaccinated pregnant and postpartum women. *Am J Epidemiol*. 2006;163(9):838–48.
- Donders F, Lonnee-Hoffmann R, Tsiakalos A, Mendling W, Martinez de Oliveira J, Judlin P, et al. ISIDOG recommendations concerning COVID-19 and pregnancy. *Diagnostics (Basel)*. 2020;10(4):243.
- Schwartz DA, Graham AL. Potential maternal and infant outcomes from (Wuhan) coronavirus 2019-nCoV infecting pregnant women: lessons from SARS, MERS, and other human coronavirus infections. *Viruses*. 2020;12(2):194.
- Li Y, Zhao R, Zheng S, Chen X, Wang J, Sheng X, et al. Lack of vertical transmission of severe acute respiratory syndrome coronavirus 2, China. *Emerg Infect Dis*. 2020;26(6):1335–6.
- Zhu H, Wang L, Fang C, Peng S, Zhang L, Chang G, et al. Clinical analysis of 10 neonates born to mothers with 2019-nCoV pneumonia. *Transl Pediatr*. 2020;9(1):51–60.
- Woo PC, Lau SK, Wong BH, Tsoi HW, Fung AM, Chan KH, et al. Detection of specific antibodies to severe acute respiratory syndrome (SARS) coronavirus nucleocapsid protein for serodiagnosis of SARS coronavirus pneumonia. *J Clin Microbiol*. 2004;42(5):2306–9.

Publisher's Note

Springer Nature remains neutral with regard to jurisdictional claims in published maps and institutional affiliations.

Ready to submit your research? Choose BMC and benefit from:

- fast, convenient online submission
- thorough peer review by experienced researchers in your field
- rapid publication on acceptance
- support for research data, including large and complex data types
- gold Open Access which fosters wider collaboration and increased citations
- maximum visibility for your research: over 100M website views per year

At BMC, research is always in progress.

Learn more biomedcentral.com/submissions



Figure 1 (facing page). Findings from a Mouse Model of Electronic-Cigarette, or Vaping, Product Use–Associated Lung Injury (EVALI).

Panel A shows levels of vitamin E acetate (VEA) quantified by isotope-dilution mass spectrometry in bronchoalveolar-lavage (BAL) fluid harvested from mice. Values are means and standard deviations for 10 mice. Panel B shows albumin levels measured in BAL fluid from mice exposed to air, a mixture of propylene glycol and vegetable glycerin (PG–VG), or VEA. Values are means and standard deviations for 10 mice. Panel C shows the total number of CD45+ cells infiltrating the lung in mice exposed to air, PG–VG, or VEA. Values are means and standard deviations for 10 mice. The P values in Panels A, B, and C were calculated by two-way analysis of variance in Tukey's post-test comparisons among the exposure groups. Panel D shows BAL fluid from a mouse exposed to VEA, containing lipid-laden macrophages (representative examples are indicated with arrows) with cytoplasmic staining by oil red O in a vesicular pattern. The macrophages are numerous and contain variable amounts of lipid. Background pneumocytes (arrowheads) show comparatively scant cytoplasm and are present as single cells or loose sheets. Panel E shows BAL fluid from a mouse exposed to PG–VG, which contained fewer identifiable macrophages and had minimal to no specific staining by oil red O. Without lipid staining, it is more difficult to distinguish between small alveolar macrophages and pneumocytes in these preparations. Panels F and G show findings in lung sections. In mice exposed to VEA (Panel F), alveolar macrophages (arrowheads and circles) in residence among pneumocytes (P) lining the alveoli (A) contained abundant oil red O–stained lipid. In mice exposed to PG–VG, tiny oil red O–stained granules in the cytoplasm of cells lining the alveoli, including pneumocytes (arrows) and alveolar macrophages (arrowheads), were observed. B denotes bronchiole.

the generated aerosols would be required to identify such by-products. Another limitation is that we did not expose animals to aerosols that contained tetrahydrocannabinol (THC) or nicotine in a dose-dependent manner. Finally, it is possible that aerosols generated from other lipophilic solvents may produce outcomes similar to the outcome seen with vitamin E acetate in this

study. Future studies are needed to address these issues. Our findings, coupled with previous research identifying vitamin E acetate in BAL fluid from patients with EVALI^{1,2} and in samples of case-associated product liquids,⁵ provide additional evidence for vitamin E acetate as a possible cause of EVALI.

Tariq A. Bhat, Ph.D.

Maciej L. Goniewicz, Ph.D., Pharm.D.

Yasmin M. Thanavala, Ph.D.

Roswell Park Comprehensive Cancer Center
Buffalo, NY

yasmin.thanavala@roswellpark.org

and Others

Dr. Blount is a member of the Lung Injury Response Lab Task Force; additional members are listed in the Supplementary Appendix, available with the full text of this letter at NEJM.org.

A complete list of authors is available with the full text of this letter at NEJM.org.

The views and opinions expressed in this letter are those of the authors and do not necessarily represent the official position of the Centers for Disease Control and Prevention, the National Institutes of Health, or the Food and Drug Administration.

Supported by grants from the National Heart, Lung, and Blood Institute of the National Institutes of Health (R01HL142511), the National Cancer Institute (NCI) (P30CA016056), and the NCI and the Center for Tobacco Products of the Food and Drug Administration (U54CA228110).

Disclosure forms provided by the authors are available with the full text of this letter at NEJM.org.

This letter was published on February 26, 2020, at NEJM.org.

1. Blount BC, Karwowski MP, Morel-Espinosa M, et al. Evaluation of bronchoalveolar lavage fluid from patients in an outbreak of e-cigarette, or vaping, product use–associated lung injury — 10 states, August–October 2019. *MMWR Morb Mortal Wkly Rep* 2019;68:1040-1.
2. Blount BC, Karwowski MP, Shields PG, et al. Vitamin E acetate in bronchoalveolar-lavage fluid associated with EVALI. *N Engl J Med* 2020;382:697-705.
3. Layden JE, Ghinai I, Pray I, et al. Pulmonary illness related to e-cigarette use in Illinois and Wisconsin — preliminary report. *N Engl J Med*. DOI: 10.1056/NEJMoa1911614.
4. Maddock SD, Cirulis MM, Callahan SJ, et al. Pulmonary lipid-laden macrophages and vaping. *N Engl J Med* 2019;381:1488-9.
5. Krishnasamy VP, Hallowell BD, Ko JY, et al. Update: characteristics of a nationwide outbreak of e-cigarette, or vaping, product use–associated lung injury — United States, August 2019–January 2020. *MMWR Morb Mortal Wkly Rep* 2020;69:90-4.

DOI: 10.1056/NEJMc2000231

SARS-CoV-2 Viral Load in Upper Respiratory Specimens of Infected Patients

TO THE EDITOR: The 2019 novel coronavirus (SARS-CoV-2) epidemic, which was first reported in December 2019 in Wuhan, China, and has been declared a public health emergency of in-

ternational concern by the World Health Organization, may progress to a pandemic associated with substantial morbidity and mortality. SARS-CoV-2 is genetically related to SARS-CoV, which

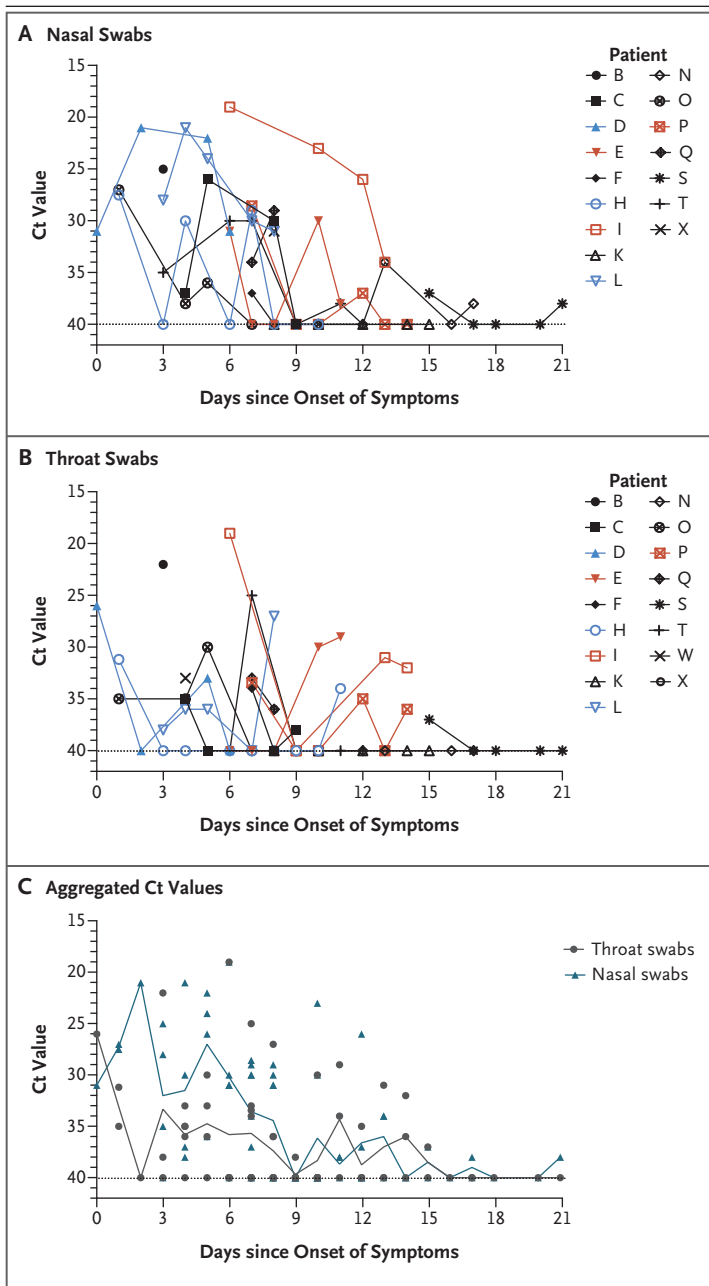


Figure 1. Viral Load Detected in Nasal and Throat Swabs Obtained from Patients Infected with SARS-CoV-2.

Panel A shows cycle threshold (Ct) values of Orf1b on reverse-transcriptase–polymerase-chain-reaction (RT-PCR) assay that were detected in nasal swabs obtained from 14 patients with imported cases and 3 patients with secondary cases, and Panel B shows the Ct values in throat swabs. Patient Z did not have clinical symptoms and is not included in the figure. Patients with imported cases who had severe illness (Patients E, I, and P) are labeled in red, patients with imported cases who had mild-to-moderate illness are labeled in black, and patients with secondary cases (Patients D, H, and L) are labeled in blue. A linear mixed-effects model was used to test the Ct values from nasal and throat swabs among severe as compared with mild-to-moderate imported cases, which allowed for within-patient correlation and a time trend of Ct change. The mean Ct values in nasal and throat swabs obtained from patients with severe cases were lower by 2.8 (95% confidence interval [CI], –2.4 to 8.0) and 2.5 (95% CI, –0.8 to 5.7), respectively, than the values in swabs obtained from patients with mild-to-moderate cases. Panel C shows the aggregated Ct values of Orf1b on RT-PCR assay in 14 patients with imported cases and 3 patients with secondary cases, according to day after symptom onset. Ct values are inversely related to viral RNA copy number, with Ct values of 30.76, 27.67, 24.56, and 21.48 corresponding to 1.5×10^4 , 1.5×10^5 , 1.5×10^6 , and 1.5×10^7 copies per milliliter. Negative samples are denoted with a Ct of 40, which was the limit of detection.

caused a global epidemic with 8096 confirmed cases in more than 25 countries in 2002–2003.¹ The epidemic of SARS-CoV was successfully contained through public health interventions, including case detection and isolation. Transmission of SARS-CoV occurred mainly after days of illness² and was associated with modest viral loads in the respiratory tract early in the illness, with viral loads peaking approximately 10 days after symptom onset.³ We monitored SARS-CoV-2 viral loads in upper respiratory specimens obtained from 18 patients (9 men and 9 women;

median age, 59 years; range, 26 to 76) in Zhuhai, Guangdong, China, including 4 patients with secondary infections (1 of whom never had symptoms) within two family clusters (Table S1 in the Supplementary Appendix, available with the full text of this letter at NEJM.org). The patient who never had symptoms was a close contact of a patient with a known case and was therefore monitored. A total of 72 nasal swabs (sampled from the mid-turbinate and nasopharynx) (Fig. 1A) and 72 throat swabs (Fig. 1B) were analyzed, with 1 to 9 sequential samples obtained from each patient. Polyester flock swabs were used for all the patients.

From January 7 through January 26, 2020, a total of 14 patients who had recently returned from Wuhan and had fever ($\geq 37.3^\circ\text{C}$) received a diagnosis of Covid-19 (the illness caused by SARS-CoV-2) by means of reverse-transcriptase–polymerase-chain-reaction assay with primers and probes targeting the N and Orf1b genes of SARS-CoV-2; the assay was developed by the Chinese Center for Disease Control and Prevention. Samples were tested at the Guangdong Provincial Center for Disease Control and Pre-

vention. Thirteen of 14 patients with imported cases had evidence of pneumonia on computed tomography (CT). None of them had visited the Huanan Seafood Wholesale Market in Wuhan within 14 days before symptom onset. Patients E, I, and P required admission to intensive care units, whereas the others had mild-to-moderate illness. Secondary infections were detected in close contacts of Patients E, I, and P. Patient E worked in Wuhan and visited his wife (Patient L), mother (Patient D), and a friend (Patient Z) in Zhuhai on January 17. Symptoms developed in Patients L and D on January 20 and January 22, respectively, with viral RNA detected in their nasal and throat swabs soon after symptom onset. Patient Z reported no clinical symptoms, but his nasal swabs (cycle threshold [Ct] values, 22 to 28) and throat swabs (Ct values, 30 to 32) tested positive on days 7, 10, and 11 after contact. A CT scan of Patient Z that was obtained on February 6 was unremarkable. Patients I and P lived in Wuhan and visited their daughter (Patient H) in Zhuhai on January 11 when their symptoms first developed. Fever developed in Patient H on January 17, with viral RNA detected in nasal and throat swabs on day 1 after symptom onset.

We analyzed the viral load in nasal and throat swabs obtained from the 17 symptomatic patients in relation to day of onset of any symptoms (Fig. 1C). Higher viral loads (inversely related to Ct value) were detected soon after symptom onset, with higher viral loads detected in the nose than in the throat. Our analysis suggests that the viral nucleic acid shedding pattern of patients infected with SARS-CoV-2 resembles that of patients with influenza⁴ and appears different from that seen in patients infected with SARS-CoV.³ The viral load that was detected in the asymptomatic patient was similar to that in the symptomatic patients, which suggests the transmission potential of asymptomatic or minimally symptomatic patients. These findings are in concordance with reports that transmission may occur early in the course of infection⁵ and suggest that case detection and isolation may require strategies different from those required for the control of SARS-CoV. How SARS-CoV-2 viral load correlates with culturable virus needs to be determined. Identification of patients with few or no symptoms and with modest levels of detectable viral RNA in the oropharynx for at least 5 days suggests that we need better data to

determine transmission dynamics and inform our screening practices.

Lirong Zou, M.Sc.

Guangdong Provincial Center for Disease Control and Prevention
Guangzhou, China

Feng Ruan, M.Med.

Zhuhai Center for Disease Control and Prevention
Zhuhai, China

Mingxing Huang, Ph.D.

Fifth Affiliated Hospital of Sun Yat-Sen University
Zhuhai, China

Lijun Liang, Ph.D.

Guangdong Provincial Center for Disease Control and Prevention
Guangzhou, China

Huitao Huang, B.Sc.

Zhuhai Center for Disease Control and Prevention
Zhuhai, China

Zhongsu Hong, M.D.

Fifth Affiliated Hospital of Sun Yat-Sen University
Zhuhai, China

Jianxiang Yu, B.Sc.

Min Kang, M.Sc.

Yingchao Song, B.Sc.

Guangdong Provincial Center for Disease Control and Prevention
Guangzhou, China

Jinyu Xia, M.D.

Fifth Affiliated Hospital of Sun Yat-Sen University
Zhuhai, China

Qianfang Guo, M.Sc.

Tie Song, M.Sc.

Jianfeng He, B.Sc.

Guangdong Provincial Center for Disease Control and Prevention
Guangzhou, China

Hui-Ling Yen, Ph.D.

Malik Peiris, Ph.D.

University of Hong Kong
Hong Kong, China

Jie Wu, Ph.D.

Guangdong Provincial Center for Disease Control and Prevention
Guangzhou, China
771276998@qq.com

Ms. Zou, Mr. Ruan, and Dr. Huang contributed equally to this letter.

Disclosure forms provided by the authors are available with the full text of this letter at NEJM.org.

This letter was published on February 19, 2020, and updated on February 20, 2020, at NEJM.org.

1. Summary of probable SARS cases with onset of illness from 1 November 2002 to 31 July 2003. Geneva: World Health Organization, 2004 (https://www.who.int/csr/sars/country/table2004_04_21/en/).

2. Lipsitch M, Cohen T, Cooper B, et al. Transmission dynamics and control of severe acute respiratory syndrome. *Science* 2003;300:1966-70.

3. Peiris JSM, Chu CM, Cheng VCC, et al. Clinical progression and viral load in a community outbreak of coronavirus-associated SARS pneumonia: a prospective study. *Lancet* 2003;361:1767-72.

4. Tsang TK, Cowling BJ, Fang VJ, et al. Influenza A virus shedding and infectivity in households. *J Infect Dis* 2015;212:1420-8.

5. Rothe C, Schunk M, Sothmann P, et al. Transmission of 2019-nCoV infection from an asymptomatic contact in Germany. *N Engl J Med* 2020;382:970-1.

DOI: 10.1056/NEJMc2001737